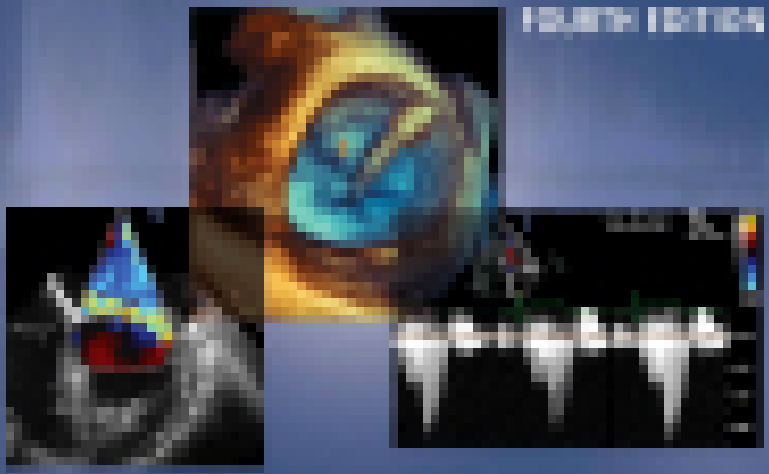
Get Full Access and More at

ExpertConsult.com

CATHERINE OTTO

# THE PRACTICE OF CLINICAL ECHOCARDIOGRAPHY

FOURTH EDITION



ELSEVIER
SAUNDERS

1600 John F. Kennedy Blvd.
Ste 1800
Philadelphia, PA 19103-2899

THE PRACTICE OF CLINICAL ECHOCARDIOGRAPHY, FOURTH EDITION ISBN: 978-1-437-72765-4
**Copyright © 2012, 2007, 2002, 1997 by Saunders, an imprint of Elsevier Inc.**

No part of this publication may be reproduced or transmitted in any form or by any means, electronic or mechanical, including photocopying, recording, or any information storage and retrieval system, without permission in writing from the publisher. Details on how to seek permission, further information about the Publisher's permissions policies and our arrangements with organizations such as the Copyright Clearance Center and the Copyright Licensing Agency, can be found at our website: www.elsevier.com/permissions.

This book and the individual contributions contained in it are protected under copyright by the Publisher (other than as may be noted herein).

**Notices**

Knowledge and best practice in this field are constantly changing. As new research and experience broaden our understanding, changes in research methods, professional practices, or medical treatment may become necessary.

Practitioners and researchers must always rely on their own experience and knowledge in evaluating and using any information, methods, compounds, or experiments described herein. In using such information or methods they should be mindful of their own safety and the safety of others, including parties for whom they have a professional responsibility.

With respect to any drug or pharmaceutical products identified, readers are advised to check the most current information provided (i) on procedures featured or (ii) by the manufacturer of each product to be administered, to verify the recommended dose or formula, the method and duration of administration, and contraindications. It is the responsibility of practitioners, relying on their own experience and knowledge of their patients, to make diagnoses, to determine dosages and the best treatment for each individual patient, and to take all appropriate safety precautions.

To the fullest extent of the law, neither the Publisher nor the authors, contributors, or editors assume any liability for any injury and/or damage to persons or property as a matter of products liability, negligence or otherwise, or from any use or operation of any methods, products, instructions, or ideas contained in the material herein.

**Library of Congress Cataloging-in-Publication Data**
The practice of clinical echocardiography / [edited by] Catherine M. Otto.—4th ed.
p. ; cm.
Includes bibliographical references and index.
ISBN 978-1-4377-2765-4 (hardcover : alk. paper)
I. Otto, Catherine M.
[DNLM: 1. Echocardiography. 2. Cardiovascular Diseases—ultrasonography. WG 141.5.E2]
616.1′207543—dc23

2012003303

*Executive Content Strategist:* Dolores Meloni
*Content Development Specialist:* Joanie Milnes
*Publishing Services Manager:* Anne Altepeter
*Project Manager:* Louise King
*Design Manager:* Steven Stave

Printed in China

Last digit is the print number: 9 8 7 6 5 4 3 2 1

Working together to grow
libraries in developing countries
www.elsevier.com | www.bookaid.org | www.sabre.org
ELSEVIER BOOK AID International Sabre Foundation

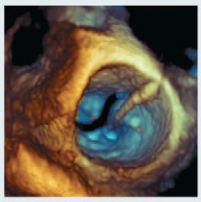
# THE PRACTICE OF CLINICAL ECHOCARDIOGRAPHY

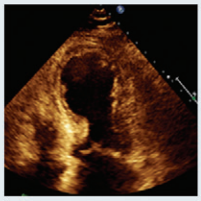
*Fourth Edition*

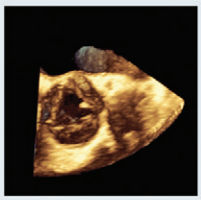
# THE PRACTICE OF CLINICAL ECHOCARDIOGRAPHY

*Fourth Edition*

**CATHERINE M. OTTO, MD**
J. Ward Kennedy-Hamilton Endowed Chair in Cardiology
Professor of Medicine
Director, Cardiology Fellowship Programs
University of Washington School of Medicine
Seattle, Washington







ELSEVIER
SAUNDERS

# PREFACE

The purpose of this book is to provide the definitive advanced reference text on the diagnostic utility of echocardiography in clinical practice. Put simply, this book reflects our role as clinicians caring for patients with cardiovascular disease. The clinical information in this book will be of value to all cardiovascular specialists, not just those focused on cardiovascular imaging. This book also will be of interest to cardiology fellows, cardiovascular anesthesiologists, and other health care providers using echocardiographic approaches in the clinical setting, including radiologists, interventional cardiologists, electrophysiologists, emergency medicine physicians, and internists with an active interest in cardiovascular disease. Cardiac sonographers, cardiovascular technologists, physician assistants, nurse practitioners, and nursing professionals who wish to go beyond the basics in echocardiographic imaging also will find this book valuable. For the clinical researcher, there are eight chapters dedicated to newer advanced echocardiographic modalities, and this information is integrated into subsequent chapters throughout the book.

Echocardiography is a key component in the evaluation of patients with suspected or known cardiovascular disease. As this technique has evolved and matured, the role of the echocardiographer has shifted from simply providing a description of the images to integrating the echocardiographic findings with other clinical data and finally to providing a diagnosis or therapeutic recommendation. Often, echocardiography supplies all the data needed for clinical decision making. When additional information is needed, the echocardiographic findings help define other imaging modalities that may be helpful. In effect, echocardiography has become a specialized type of cardiology consultation.

The information now requested by the referring physician includes not only the qualitative and quantitative interpretation of the echocardiographic images and Doppler flow data, but also a discussion of how this information may affect clinical decision making. Specific examples include decisions regarding interventional procedures (e.g., suitability for a transcatheter aortic valve implantation), medical or surgical therapy (e.g., treatment of endocarditis, surgery for aortic dissection), optimal timing of intervention in patients with chronic cardiac diseases (e.g., valvular regurgitation, mitral stenosis), prognostic implications (e.g., heart disease in pregnancy, heart failure patients), and the possible need for and frequency of periodic diagnostic evaluation (e.g., congenital heart disease, the postoperative patient). In addition, echocardiography is critical in choosing the optimal therapy for each patient (e.g., selection of patients for intracardiac defibrillator implantation) and has become essential for monitoring percutaneous interventions and the effects of medical or surgical therapy.

The clinical practice of echocardiography no longer is restricted to the full diagnostic examination performed in an imaging laboratory. Instead, echocardiography has become so integrated into cardiovascular care that specialized instruments are now used in the intensive care unit, emergency department, interventional laboratory, and operating room, as well as during electrophysiology procedures. As instruments become smaller, less expensive, and easier to use, the clinical applications of this imaging modality likely will continue to expand.

Each chapter in this book provides an advanced level of discussion, written by an expert in the field, building upon the basic material in my *Textbook of Clinical Echocardiography, Fourth Edition*. In contrast to the *Textbook,* the primary focus of this book is the role of echocardiography in clinical decision making and the impact on clinical outcomes. Emphasis is also placed on the principles of optimal data acquisition, quantitative approaches to data analysis, potential technical limitations, and areas of active research. In addition, the strengths and limitations of alternate diagnostic approaches are reviewed to put the role of echocardiography into the context of clinical practice. Detailed tables, color illustrations, echocardiographic images, Doppler tracings, and figures with key data from published outcome studies are used to provide clarity and depth. To complement the printed text, multiple choice questions at expertconsult.com provide an opportunity for readers to test their knowledge or quickly review the core material. Some highlights of the fourth edition include new chapters on echocardiographic guidance of structural heart disease interventions and echocardiographic evaluation of cardiac assist devices.

It is hoped that this book will provide the needed background to support and supplement clinical experience and expertise. Of course, competency in the acquisition and interpretation of echocardiographic and Doppler data depends on appropriate clinical education and training, as detailed in accreditation requirements for both physicians and technologists and as recommended by professional societies, including the American Society of Echocardiography, the American College of Cardiology, and the American Heart Association. I strongly support these educational requirements and training recommendations; readers of this book are urged to review the relevant documents.

Advances continue to be made both in the technical aspects of image and flow data acquisition and in our understanding of the clinical implications of specific echocardiographic findings. This book represents our knowledge base at one point in time; readers will wish to consult the current literature for the most up-to-date information. Although an extensive list of carefully selected references is provided with each chapter, the echocardiographic literature is so robust that it is impractical to include all relevant references; the reader can conduct an online medical literature search if an all-inclusive listing is desired.

Additional resources for the reader interested in achieving mastery in echocardiography include *Echocardiography Review Guide, Second Edition*, which I wrote with Becky Schwaegler and Rosario Freeman, and which provides a quick summary and self-evaluation questions for my *Textbook of Clinical Echocardiography, Fourth Edition*. These books are now complemented by the new Otto Practical Echocardiography series, all published by Elsevier and available in electronic format and online at expertconsult.com. The Practical Echocardiography series includes *Intraoperative Echocardiography*, edited by Don Oxorn; *Echocardiography in Heart Failure*, edited by Susan Wiegers and Martin St. John Sutton; *Echocardiography in Congenital Heart*

*Disease*, edited by Mark Lewin and Karen Stout; and *Advanced Echocardiographic Approaches*, which I edited with Linda Gillam. All four of these books also offer online clinical cases and video clips to enhance the learning experience.

Little time investment is needed to acquire basic skills in echocardiographic image acquisition and interpretation; the challenge lies in transitioning these skill sets from "basic" to "expert." As echocardiography becomes fully integrated into the practice of medicine in every clinical setting, each of us should be aware of our own limitations, scope of practice, and clinical practice needs. The concentrated educational content and cumulative clinical experience contained in the Otto series of textbooks and online cases not only provides a solid foundation upon which to learn the practice of echocardiography, but can also accelerate the learning curve for those who wish to challenge themselves to become a master of echocardiography.

**Catherine M. Otto**

# CONTRIBUTORS


**Jamil A. Aboulhosn, MD**
Co-Director, Ahmanson/UCLA Adult Congenital Heart Disease Center
Assistant Professor of Medicine and Pediatrics
David Geffen School of Medicine at UCLA
Los Angeles, California
Director, Children's Heart Center Nevada Adult Congenital Program
Las Vegas, Nevada

**Gerard P. Aurigemma, MD**
Professor of Medicine and Radiology
University of Massachusetts Medical School
Director, Noninvasive Cardiology
UMass Memorial Medical Center
Worcester, Massachusetts

**Thomas Bartel, MD**
Assistant Professor of Medicine
University Clinic of Internal Medicine
Medical University Innsbruck
Innsbruck, Austria

**Ann F. Bolger, MD**
William Watt Kerr Professor of Clinical Medicine
University of California, San Francisco
Director of Echocardiography
San Francisco General Hospital and Trauma Center
San Francisco, California

**Johan G. Bosch, PhD**
Associate Professor
Thoraxcenter Biomedical Engineering
Erasmus Medical Center
Rotterdam, The Netherlands

**Charles J. Bruce, MD**
Consultant in Cardiovascular Diseases
Professor of Medicine
Division of Cardiovascular Diseases
Mayo Clinic
Rochester, Minnesota

**Ian G. Burwash, MD**
Associate Professor of Medicine
University of Ottawa
Director of Echocardiography
University of Ottawa Heart Institute
Ottawa, Ontario, Canada

**John D. Carroll, MD**
Professor of Medicine
University of Colorado, Denver
Director, Interventional Cardiology
Medical Director, Cardiac and Vascular Center
University of Colorado Hospital
Denver, Colorado

**Kwan-Leung Chan, MD**
Professor of Medicine
University of Ottawa
Attending Staff
University of Ottawa Heart Institute
Ottawa, Ontario, Canada

**Michael A. Chen, MD, PhD**
Assistant Professor of Medicine
Division of Cardiology
Harborview Medical Center
University of Washington School of Medicine
Seattle, Washington

**John S. Child, MD**
Streisand/American Heart Association Professor of Medicine and Cardiology
Director, Ahmanson/UCLA Adult Congenital Heart Disease Center
Director, Ronald Reagan UCLA Medical Center Adult Non-Invasive Cardiology Laboratory
David Geffen School of Medicine at UCLA
Los Angeles, California

**Heidi M. Connolly, MD**
Professor of Medicine
Division of Cardiovascular Diseases
Mayo Clinic
Rochester, Minnesota

**Lori Croft, MD**
Associate Professor of Medicine
Zena and Michael Weiner Cardiovascular Institute
Mount Sinai School of Medicine
New York, New York

**Milind Y. Desai, MD**
Associate Professor of Medicine
Lerner College of Medicine of Case Western Reserve University
Cleveland Clinic
Cleveland, Ohio

**Marco R. Di Tullio, MD**
Professor of Medicine
Associate Director, Adult Cardiovascular Ultrasound Laboratories
Columbia University Medical Center
New York, New York

**Jean G. Dumesnil, MD**
Professor and Cardiologist
Quebec Heart and Lung Institute
Laval University
Quebec City, Quebec, Canada

**Thor Edvardsen, MD, PhD**
Professor and Co-Director
Department of Cardiology
Oslo University Hospital
Oslo, Norway

**Raimund Erbel, MD**
Professor of Medicine
West German Heart Center Essen
University Duisburg-Essen
Duisburg-Essen, Germany

**Arturo Evangelista, MD**
Head of Cardiac Imaging Department
Hospital Vall d'Hebron
Barcelona, Spain

**Kirsten E. Fleishmann, MD**
Professor of Clinical Medicine
University of California San Francisco School of Medicine
San Francisco, California

**Paul Robert Forfia, MD**
Assistant Professor of Medicine
Department of Medicine, Heart Failure/Transplant Cardiology
Director, Pulmonary Hypertension Program
Hospital of the University of Pennsylvania
Philadelphia, Pennsylvania

**Elyse Foster, MD**
Director, Echocardiography Laboratory
Professor of Clinical Medicine
Araxe Vilensky Endowed Chair in Medicine
Department of Medicine, Cardiology
University of California, San Francisco
San Francisco, California

**Rosario V. Freeman, MD**
Associate Professor of Medicine
Medical Director, Echocardiography
Associate Director, Cardiology Fellowship Program
University of Washington
Seattle, Washington

**William H. Gaasch, MD**
Professor of Medicine
Department of Cardiovascular Medicine
University of Massachusetts Medical School
Worcester, Massachusetts
Senior Consultant in Cardiology
Department of Cardiovascular Medicine
Lahey Clinic
Burlington, Massachusetts

**Ivor L. Gerber, MD**
Consultant Cardiologist
Director of Adult Echocardiography
Green Lane Cardiovascular Unit
Auckland City Hospital
Auckland, New Zealand

**Martin E. Goldman, MD**
Dr. Arthur and Hilda Master Professor of Medicine (Cardiology)
Zena and Michael Weiner Cardiovascular Institute
Mount Sinai School of Medicine
New York, New York

**Jasmine Grewal, MD**
Clinical Assistant Professor
University of British Columbia
Attending Cardiologist
St. Paul's Hospital
Vancouver, British Columbia, Canada

**Brian P. Griffin, MD**
The John and Rosemary Brown Endowed Chair in Cardiovascular Medicine
Director, Cardiovascular Medicine Fellowship Program
Cleveland Clinic
Cleveland, Ohio

**Christiane Gruner, MD**
Fellow in Hypertrophic Cardiomyopathy Research
Division of Cardiology
Toronto General Hospital
Toronto, Ontario, Canada

**Michelle Gurvitz, MD, MS**
Assistant Professor of Pediatrics
Harvard Medical School
Pediatric Cardiologist
Brigham and Women's Hospital
Children's Hospital Boston
Boston, Massachusetts

**Judy Hung, MD**
Associate Professor of Medicine
Harvard Medical School
Associate Director, Echocardiography
Division of Cardiology
Massachusetts General Hospital
Boston, Massachusetts

**Bernard Iung, MD**
Professor of Cardiology
Bichat Hospital, AP-HP
Paris, France

**Mary Etta E. King, MD**
Director of Pediatric Echocardiography
Cardiac Ultrasound Laboratory
Massachusetts General Hospital
Associate Professor of Pediatrics
Harvard Medical School
Boston, Massachusetts

**James N. Kirkpatrick, MD**
Assistant Professor of Medicine
Division of Cardiovascular Medicine
Associate Fellow, Center for Bioethics
University of Pennsylvania
Philadelphia, Pennsylvania

**Allan L. Klein, MD**
Director, Cardiovascular Imaging Research
Director, Pericardial Disease Center
Professor of Medicine, Cleveland Clinic
Lerner College of Medicine of Case Western Reserve University
Cleveland, Ohio

**Theodore J. Kolias, MD**
Associate Professor
University of Michigan
Ann Arbor, Michigan

**Thomas Konorza, MD**
Consultant
West German Heart Center Essen
University Duisburg-Essen
Duisburg-Essen, Germany

**Christopher E. Kurtz, MD**
Associate Director, Cardiovascular Disease Fellowship
Assistant Professor of Medicine
Division of Cardiology
University of Wisconsin
Madison, Wisconsin

**Mark Lewin, MD**
Professor and Chief of Pediatric Cardiology
University of Washington School of Medicine
Lab Director, Heart Center and Echocardiography
Seattle Children's Hospital
Seattle, Washington

**Akiko Maehara, MD**
Director, Intravascular Imaging and Physiology Core Laboratories
Cardiovascular Research Foundation;
Assistant Professor
Columbia University Medical Center
New York, New York

**Warren J. Manning, MD**
Section Chief, Noninvasive Cardiac Imaging and Testing
Beth Israel Deaconess Medical Center
Professor of Medicine and Radiology
Harvard Medical School
Boston, Massachusetts

**Thomas H. Marwick, MD, PhD**
Head, Cardiovascular Imaging
Heart and Vascular Institute, Cleveland Clinic
Cleveland, Ohio

**Gary S. Mintz, MD**
Chief Medical Officer
Cardiovascular Research Foundation
New York, New York

**Robert R. Moss, MB, BS**
Clinical Assistant Professor
University of British Columbia
Attending Cardiologist
St. Paul's Hospital
Vancouver, British Columbia, Canada

**Silvana Müller, MD**
Consultant
University Clinic of Internal Medicine
Medical University Innsbruck
Innsbruck, Austria

**Bradley I. Munt, MD**
Cardiologist
St. Paul's Hospital and Providence Health Care
Vancouver, British Columbia, Canada

**Tasneem Z. Naqvi, MD**
Professor of Medicine and Clinical Scholar
Director, Echocardiography and Noninvasive Diagnostic Services
Keck School of Medicine
University of Southern California, Los Angeles
Los Angeles, California

**Aaron K. Olson, MD**
Assistant Professor of Pediatrics
University of Washington
Seattle Children's Hospital
Seattle, Washington

**Donald C. Oxorn, MD**
Professor of Anesthesiology
Adjunct Professor, Medicine (Cardiology)
University of Washington
Seattle, Washington

**Philippe Pibarot, DVM, PhD**
Professor of Medicine
Laval University
Canada Research Chair in Valvular Heart Disease
Quebec Heart and Lung Institute
Quebec, Quebec, Canada

**Michael H. Picard, MD**
Professor of Medicine
Harvard Medical School
Director, Clinical Echocardiography
Massachusetts General Hospital
Boston, Massachusetts

**Juan Carlos Plana, MD**
Co-Director, Cardio-Oncology Center
Cleveland Clinic
Cleveland, Ohio
Adjunct Associate Professor
The University of Texas MD Anderson Cancer Center
Houston, Texas

**Theodore Plappert, CVT**
Manager, Quantitative Imaging Core Laboratory
University of Pennsylvania Medical Center
Philadelphia, Pennsylvania

**Thomas R. Porter, MD**
Professor of Medicine
Courtesy Professor of Radiology and Pediatric Cardiology
Director of Echocardiography Laboratories
Theodore F. Hubbard Distinguished Chair of Cardiology
University of Nebraska Medical Center
Omaha, Nebraska

**Harry Rakowski, MD**
Professor of Medicine
University of Toronto
Douglas Wigle Chair in Hypertrophic Cardiomyopathy
Director, Hypertrophic Cardiomyopathy Clinic
University Health Network
Toronto, Ontario, Canada
President, National Board of Echocardiography
Raleigh, North Carolina

**Carlos A. Roldan, MD**
Professor of Medicine
University of New Mexico School of Medicine
Director, Echocardiography Laboratory
New Mexico Veterans Affairs Health Care System
Albuquerque, New Mexico

**Raphael Rosenhek, MD**
Associate Professor of Medicine
Director, Clinic for Valvular Heart Disease
Department of Cardiology
Medical University of Vienna
Vienna, Austria

**Ernesto E. Salcedo, MD**
Professor of Medicine
University of Colorado, Denver
Director of Echocardiography
University of Colorado Hospital
Denver, Colorado

**Zainab Samad, MD**
Assistant Professor of Medicine
Duke University Medical Center
Durham, North Carolina

**Otto A. Smiseth, MD, PhD**
Professor and Division Head
Cardiovascular and Pulmonary Diseases
Oslo University Hospital
Oslo, Norway

**William J. Stewart, MD**
Professor of Medicine
Cleveland Clinic Lerner College of Medicine of Case Western Reserve University
Staff Cardiologist
Department of Cardiovascular Medicine
Cleveland Clinic
Cleveland, Ohio

**Martin St. John Sutton, MBBS**
John W. Bryfogle Professor of Cardiovascular Medicine
Director of Cardiac Imaging
University of Pennsylvania Medical Center
Philadelphia, Pennsylvania

**Marcus F. Stoddard, MD**
Professor of Medicine
Director, Noninvasive Cardiology
Division of Cardiovascular Medicine
University of Louisville
Louisville, Kentucky

**Karen K. Stout, MD**
Director, Adult Congenital Heart Disease Program
Associate Professor, Departments of Medicine and Pediatrics
University of Washington School of Medicine
Attending Cardiologist
University of Washington Medical Center and Seattle Children's Hospital
Seattle, Washington

**Pilar Tornos, MD**
Servei de Cardiologia
Hospital Universitari Vall d'Hebron
Barcelona, Spain

**Alec Vahanian, MD**
Head of Cardiology
Bichat Hospital, AP-HP
Paris, France

**Anne Marie Valente, MD**
Outpatient Director
Boston Adult Congenital Heart and Pulmonary Hypertension Program
Brigham and Women's Hospital
Children's Hospital Boston
Assistant Professor of Medicine and Pediatrics
Harvard Medical School
Boston, Massachusetts

**Andrew Wang, MD**
Associate Professor of Medicine
Duke University Medical Center
Durham, North Carolina

**Nozomi Watanabe, MD, PhD**
Cardiovascular Core Analysis Laboratory
Department of Cardiology
Kawasaki Medical School
Kurashiki, Okayama, Japan
Director, Echocardiographic Laboratory
Miyazaki Prefectural Hospital
Miyazaki, Japan

**Sarah G. Weeks, MD**
Assistant Professor
Department of Cardiac Sciences
University of Calgary
Libin Cardiovascular Institute of Alberta
Calgary, Alberta, Canada

**Rory B. Weiner, MD**
Instructor of Medicine
Harvard Medical School
Staff Cardiologist
Massachusetts General Hospital
Boston, Massachusetts

**Neil J. Weissman, MD**
President, MedStar Health Research Institute
Hyattsville, Maryland
Professor of Medicine
Georgetown University
Washington, DC

**Susan E. Wiegers, MD**
Associate Professor of Medicine
Director of Clinical Echocardiography
Hospital of the University of Pennsylvania
Philadelphia, Pennsylvania

**Lynne Williams, MB BCh, PhD**
Douglas Wigle Fellow in Hypertrophic Cardiomyopathy Research
Division of Cardiology
Toronto General Hospital
Toronto, Ontario, Canada

**Anna Woo, MD**
Director, Echocardiography Laboratory
University Health Network
Associate Professor
University of Toronto
Toronto, Ontario, Canada

**Audrey H. Wu, MD, MPH**
Clinical Assistant Professor
University of Michigan Health System
Ann Arbor, Michigan

**Feng Xie, MD**
Associate Professor of Medicine
Division of Cardiology
University of Nebraska Medical Center
Omaha, Nebraska

**Choon Hwai Yap, PhD**
Research Associate
University of Pittsburgh Medical School
Pittsburgh, Pennsylvania

**Ajit P. Yoganathan, PhD**
The Wallace H. Coulter Distinguished Faculty Chair
Associate Chair for Research
Wallace H. Coulter Department of Biomedical Engineering
Regents Professor
Georgia Institute of Technology and Emory University
Director, Center for Innovative Cardiovascular Technologies
Atlanta, Georgia

**Andrew O. Zurick III, MD**
Advanced Cardiac Imaging Fellow
Department of Cardiovascular Medicine
Heart and Vascular Institute
Cleveland Clinic
Cleveland, Ohio

# ACKNOWLEDGMENTS

My deepest gratitude is due the many individuals who made this book possible. Primary recognition goes to the chapter contributors who provided scholarly, thoughtful, and insightful discussions and integrated the clinical and echocardiographic information into a format that will benefit our readers. The support staff at each of our institutions deserves our appreciation for assisting with manuscript preparation and providing effective communication. The many research subjects who contributed to the data on which our current understanding is based certainly are worthy of acknowledgment as well. The cardiac sonographers at all our institutions are owed thanks as our partners in the clinical practice of echocardiography and as the individuals who acquired most of the images shown in this book. In addition, gratitude is due Natasha Andjelkovic, Delores Meloni, Agnes Byrne, Joanie Milnes, Louise King, and the entire editorial and production teams at Elsevier. Finally, my sincere thanks go to my colleagues in Cardiology at the University of Washington and to my family for their constant encouragement and support.

**Catherine M. Otto**

# GLOSSARY

| | |
|---|---|
| **2D** | two-dimensional |
| **3D** | three-dimensional |
| **A-long** | apical long-axis |
| **A-mode** | amplitude mode (amplitude versus depth) |
| **A** | diastolic ventricular filling velocity with atrial contraction |
| **A′** | diastolic tissue Doppler velocity with atrial contraction |
| **A2C** | apical two-chamber |
| **A4C** | apical four-chamber |
| **ABD** | automated border detection |
| **ACHD** | adult congenital heart disease |
| **ACS** | acute coronary syndrome |
| **AcT** | acceleration time |
| **AF** | atrial fibrillation |
| **AIH** | aortic intramural hematoma |
| **AMVL** | anterior mitral valve leaflet |
| **ant** | anterior |
| **Ao** | aortic or aorta |
| **AQ** | acoustic quantification |
| **Ar** | pulmonary vein atrial reversal velocity |
| **AR** | aortic regurgitation |
| **ARVD** | arrhythmogenic right ventricular dysplasia |
| **AS** | aortic stenosis |
| **ASD** | atrial septal defect |
| **ATVL** | anterior tricuspid valve leaflet |
| **AV** | atrioventricular |
| **AVA** | aortic valve area |
| **AVC** | aortic valve closure |
| **AVR** | aortic valve replacement |
| **AVSD** | atrioventricular septal defect |
| **BAV** | bicuspid aortic valve |
| **BMV** | balloon mitral valvotomy |
| **BNP** | B-type natriuretic peptide |
| **BP** | blood pressure |
| **BSA** | body surface area |
| **c** | propagation velocity of sound in tissue |
| **CABG** | coronary artery bypass graft |
| **CAD** | coronary artery disease |
| **CCTGA** | congenitally corrected transposition of the great arteries (*see* L-TGA) |
| **CCU** | coronary care unit |
| **CFR** | coronary flow reserve |
| **CO** | cardiac output |
| **COPD** | chronic obstructive pulmonary disease |
| **CPB** | cardiopulmonary bypass |
| **CRT** | cardiac resynchronization therapy |
| **CS** | coronary sinus |
| **CSA** | cross-sectional area |
| **CT** | computed tomography |
| **CTEPH** | chronic thromboembolic pulmonary hypertension |
| **CW** | continuous wave |
| **Cx** | circumflex coronary artery |
| **D** | diameter |
| **DAo** | descending aorta |
| **DCM** | dilated cardiomyopathy |
| **DICOM** | Digital Imaging and Communications in Medicine |
| **DORV** | double-outlet right ventricle |
| ***dP/dt*** | rate of change in pressure over time |
| **DSE** | dobutamine stress echocardiography |
| **DT** | deceleration time |
| **D-TGA** | complete (D or dextro) transposition of the great arteries |
| **E** | early diastolic peak velocity |
| **E′** | early diastolic tissue Doppler velocty |
| **ECG** | electrocardiogram |
| **ED** | end-diastole |
| **EDD** | end-diastolic dimension |
| **EDP** | end-diastolic pressure |
| **EDV** | end-diastolic volume |
| **EF** | ejection fraction |
| **endo** | endocardium |
| **EOA** | effective orifice area |
| **epi** | epicardium |
| **EPSS** | E-point septal separation |
| **EROA** | effective regurgitant orifice area |
| **ES** | end-systole |
| **ESD** | end-systolic dimension |
| **ESPVR** | end-systolic pressure-volume relationship |
| **ESV** | end-systolic volume |
| **ETT** | exercise treadmill test |
| **FDA** | Food and Drug Administration (USA) |
| **FL** | false lumen |
| **FPV** | flow propagation velocity |
| **FS** | fractional shortening |
| **FSV** | forward stroke volume |
| **HCM** | hypertrophic cardiomyopathy |
| **HCU** | hand-carried ultrasound |
| **HF** | heart failure |
| **HFpEF** | heart failure with preserved ejection fraction |
| **HOCM** | hypertrophic obstructive cardiomyopathy |
| **HPRF** | high pulse repetition frequency |
| **HR** | heart rate |
| **HRrEF** | heart failure with reduced ejection fraction |
| **HV** | hepatic vein |
| **IABP** | intraaortic balloon pump |
| **IAS** | interatrial septum |
| **ICD** | implanted cardiac defibrillator |
| **ICE** | intracardiac echocardiography |
| **ICU** | intensive care unit |
| **ID** | indicator dilution |
| **IE** | infective endocarditis |
| **inf** | inferior |
| **INR** | international normalized ratio |
| **IPAI** | intraaortic phased-array imaging |
| **IV** | intravenous |
| **IVC** | inferior vena cava |

**IVCT** isovolumic contraction time
**IVRT** isovolumic relaxation time
**IVUS** intravascular ultrasound

**JA** jet area

***L*** length
**LA** left atrium
**LAA** left atrial appendage
**LAD** left anterior descending coronary artery
**LAE** left atrial enlargement
**lat** lateral
**LBBB** left bundle branch block
**LCC** left coronary cusp
**LCx** left circumflex coronary artery
**LIPV** left inferior pulmonary vein
**LMCA** left main coronary artery
**LPA** left pulmonary artery
**LSPV** left superior pulmonary vein
**L-TGA** L-transposition of the great arteries (*see* CCTGA)
**LV** left ventricle
**LVAD** left ventricular assist device
**LVEDP** left ventricular end-diastolic pressure
**LVH** left ventricular hypertrophy
**LVID** left ventricular internal dimension
**LVOT** left ventricular outflow tract

**M-mode** motion display (depth versus time)
**MAC** mitral annular calcification
**MAIVF** mitral-aortic intervalvular fibrosa
**MCE** myocardial contrast echocardiography
**MFS** Marfan syndrome
**MI** myocardial infarction
**MPA** main pulmonary artery
**mPAP** mean pulmonary artery pressure
**MPI** myocardial performance index
**MR** mitral regurgitation
**MRI** magnetic resonance imaging
**MS** mitral stenosis
**MV** mitral valve
**MVA** mitral valve area
**MVL** mitral valve leaflet
**MVP** mitral valve prolapse
**MVR** mitral valve replacement

**NBTE** nonbacterial thrombotic endocarditis
**NCC** noncoronary cusp
**NPO** nothing by mouth
**NYHA** New York Heart Association (classification for heart failure symptoms)

**OM1** first obtuse marginal branch
**OM2** second obtuse marginal branch

**Δ*P*** pressure gradient
**PA** pulmonary artery
**PACS** Picture Archiving and Communications Systems
**PAH** pulmonary arterial hypertension
**pAn** pseudoaneurysm
**PAP** pulmonary artery pressure
**PAPVR** partial anomalous pulmonary venous return
**PASP** pulmonary artery systolic pressure
**PCI** percutaneous coronary intervention
**PCWP** pulmonary capillary wedge pressure
**PDA** patent ductus arteriosus or posterior descending artery (depends on context)
**PE** pericardial effusion
**PEP** preejection period
**PESDA** perfluorocarbon exposed sonicated dextrose albumin
**PET** positron-emission tomography
**PFO** patent foramen ovale
**PH** pulmonary hypertension
**PHT** pressure half time
**PISA** proximal isovelocity surface area
**PLAX** parasternal long-axis
**PM** papillary muscle
**PMVL** posterior mitral valve leaflet
**post** posterior (or inferior-lateral) ventricular wall
**PPM** patient prosthesis mismatch
**PR** pulmonic regurgitation
**PRF** pulse repetition frequency
**PRFR** peak rapid filling rate
**PS** pulmonic stenosis
**PSAX** parasternal short-axis
**PCI** percutaneous coronary intervention
**PV** pulmonary vein
**PVC** premature ventricular contraction
**PVOD** pulmonary venoocclusive disease
**PVR** pulmonary vascular resistance
**PW** pulsed wave
**PWT** posterior wall thickness

**RA** right atrium
**RAE** right atrial enlargement
**RAO** right anterior oblique
**RAP** right atrial pressure
**RCA** right coronary artery
**RCC** right coronary cusp
**RF** regurgitant fraction
**RIPV** right inferior pulmonary vein
**RJ** regurgitant jet
**ROA** regurgitant orifice area
**RPA** right pulmonary artery
**RSPV** right superior pulmonary vein
**RSV** regurgitant stroke volume
**RT3DE** real-time three-dimensional echocardiography
**RV** right ventricle
**RVAD** right ventricular assist device
**RVE** right ventricular enlargement
**RVH** right ventricular hypertrophy
**RVOT** right ventricular outflow tract
**RWT** relative wall thickness

**SAM** systolic anterior motion
**SAS** subaortic stenosis
**SC** subcostal
**SD** standard deviation
**SEE** standard error of the estimate
**SHD** structural heart disease
**SPECT** single photon emission computed tomography
**SPPA** spatial peak pulse average
**SPTA** spatial peak temporal average
**SR** strain rate
**SSN** suprasternal notch
**STE** speckle tracking echocardiography

**STJ** sinotubular junction
**STVL** septal tricuspid valve leaflet
**SV** stroke volume or sample volume (depends on context)
**SVC** superior vena cava
**SVR** systemic vascular resistance

**TAPSE** tricuspid annular plane systolic excursion
**TAPVR** total anomalous pulmonary venous return
**TAVI** transcatheter aortic valve implantation
**TDI** tissue-Doppler imaging
**TEE** transesophageal echocardiography
**TGA** transposition of the great arteries
**TGC** time gain compensation
**TIA** transient ischemic attack
**TL** true lumen
**TN** true negatives
**TOF** tetralogy of Fallot
**TP** true positives
**TPV** time to peak velocity
**TR** tricuspid regurgitation
**TS** tricuspid stenosis
**TSV** total stroke volume
**TTE** transthoracic echocardiography
**TV** tricuspid valve

**V** volume or velocity (depends on context)
**VAD** ventricular assist device
**VAS** ventriculo-atrial septum
**$V_{cf}$** velocity of circumferential shortening
**$V_{max}$** maximum velocity
**VR** ventricular contraction
**VS** ventricular septum
**VSD** ventricular septal defect
**VTI** velocity-time integral

**WPW** Wolff-Parkinson-White syndrome

***Z*** acoustic impedance

| *Symbol* | *Greek Name* | *Used For* |
|---|---|---|
| α | alpha | frequency |
| γ | gamma | viscosity |
| Δ | delta | difference |
| θ | theta | angle |
| λ | lambda | wavelength |
| μ | mu | micro- |
| π | pi | mathematical constant (approx. 3.14) |
| ρ | rho | tissue density |
| σ | sigma | wall stress |
| τ | tau | time constant of ventricular relaxation |

**Units of Measure**

| *Variable* | *Unit* | *Definition* |
|---|---|---|
| Amplitude | dB | Decibels = a logarithmic scale describing the amplitude ("loudness") of the sound wave |
| Angle | degrees | Degree = (π/180)rad. Example: intercept angle |
| Area | $cm^2$ | Square centimeters. A two-dimensional measurement (e.g., end-systolic area) or a calculated value (e.g., continuity equation valve area) |
| Frequency (*f*) | Hz<br>kHz<br>MHz | Hertz (cycles per second)<br>Kilohertz = 1000 Hz<br>Megahertz = 1,000,000 Hz |
| Length | cm<br>mm | Centimeter (1/100 m)<br>Millimeter (1/1000 m or 1/10 cm) |
| Mass | g | Grams. Example: LV mass |
| Pressure | mm Hg | Millimeters of mercury, 1 mm Hg = 1333.2 $dyne/cm^2$, where dyne measures force in $cm \cdot g \cdot s^{-2}$ |
| Resistance | $dyne{\cdot}s{\cdot}cm^{-5}$ | Measure of vascular resistance |
| Time | s<br>ms<br>μs | Second<br>Millisecond (1/1000 s)<br>Microsecond |
| Ultrasound intensity | $W/cm^2$<br>$mW/cm^2$ | Where watt (W) = joule per second and joule = $m^2 \cdot kg \cdot s^{-2}$ (unit of energy) |
| Velocity (*v*) | m/s<br>cm/s | Meters per second<br>Centimeters per second |
| Velocity-time integral (VTI) | cm | Integral of the Doppler velocity curve (cm/s) over time (s), in units of cm |
| Volume | $cm^3$<br>ml<br>L | Cubic centimeters<br>Milliliter, 1 mL = 1 $cm^3$<br>Liter = 1000 mL |
| Volume flow rate (Q) | L/min<br>mL/s | Rate of volume flow across a valve or in cardiac output<br>L/min = liters per minute<br>mL/s = milliliters per second |
| Wall stress | $dyne/cm^2$<br>$kdyn/cm^2$<br>kPa | Units of meridional or circumferential wall stress<br>Kilodynes per $cm^2$<br>Kilopascals where 1 kPa = 10 $kdyn/cm^2$ |

# 1 Transesophageal Echocardiography

IAN G. BURWASH, MD | KWAN-LEUNG CHAN, MD

**Performance of Transesophageal Echocardiography**
- Preparation of Patient
- Esophageal Intubation
- Image Format

**Standard Imaging Planes**
- Basal Views
- Four-Chamber Views
- Transgastric Views
- Aortic Views

**Three-Dimensional Imaging**

**Doppler Examination**
- Left Atrial Appendage Flow
- Pulmonary Vein Flow

**Indications for Transesophageal Echocardiography**
- Native Valve Disease
- Prosthetic Valves
- Infective Endocarditis
- Suspected Cardioembolic Event
- Atrial Septal Abnormalities
- Cardiac Tumors
- Acute Aortic Syndromes
- Atrial Fibrillation
- Congenital Heart Disease
- Coronary Artery Disease
- Pericardial Disease
- Critically Ill Patient in the Intensive Care Unit
- Monitoring During Surgical and Interventional Procedures

**Contraindications to Transesophageal Echocardiography**

**Complications of Transesophageal Echocardiography**

The role of transesophageal echocardiography (TEE) in the diagnosis and management of patients with suspected and overt cardiac disease has evolved with time as a result of refinements in technology and the addition of three-dimensional (3D) TEE.[1,2] The portable nature of the technique allows the examination to be performed in a diverse array of clinical settings that include the outpatient ambulatory clinic, intensive care unit, catheterization laboratory, and operating room. Currently, TEE accounts for approximately 5% to 10% of all echocardiography studies performed.

## Performance of Transesophageal Echocardiography

Transesophageal echocardiography is a semi-invasive procedure that should be performed only by a properly trained physician who understands the indications and potential complications of the procedure. Both technical and cognitive skills are required for the competent performance and interpretation of TEE studies (Box 1-1), and guidelines on training have been published.[2] The physician should be assisted by an experienced sonographer whose tasks are to ensure that optimal images are obtained by adjusting the controls of the echocardiographic system and to ensure safety by monitoring the responses of the patient during the procedure. Although family members or friends are usually not allowed in the room when the procedure is being performed, there are situations in which their presence can be helpful. The presence of a parent can have a calming effect when one is dealing with an apprehensive teenager. A friend or relative who speaks the same language can relieve anxiety when dealing with an anxious patient who is not fluent in English.

Transesophageal echocardiography should be performed in a spacious room that can comfortably accommodate a stretcher. The room should be equipped with an oxygen outlet and suction facilities. A pulse oximeter should be available, to be used mainly in cyanotic patients and patients with severe lung disease. The TEE probe should be carefully examined before each use. In addition to visual inspection, it is important to palpate the probe, particularly the flexion portion, to ensure that there is no unusual wear and tear of the probe.[3] Stretching of the steering cables may result in increased flexibility and mobility of the probe tip with buckling of the probe tip within the esophagus.[4] This phenomenon is associated with a poor TEE image and resistance to probe withdrawal. The probe should be advanced into the stomach and straightened by retroflexion of the extreme antiflexed probe tip. We have also detected perforation of the TEE probe sheath by a ruptured steering cable and recommend inspection of the casing for any protruding wires before probe insertion.[3] The flexion controls need to be tested on a regular basis. Anterior flexion should exceed 90°, and right and left flexion should approach 90°.

### PREPARATION OF PATIENT

Patients should be contacted at least 12 hours before the procedure and instructed to fast for at least 4 hours before the procedure. They are informed that they should be accompanied, because they will not be able to drive or return to work for several hours owing to the lingering effect of sedation. On the day of the study, the procedure is explained in detail, and informed consent is obtained. Patients are told to expect mild abdominal discomfort and gagging following the insertion of

Box 1-1

**COGNITIVE AND TECHNICAL SKILLS REQUIRED FOR THE PERFORMANCE OF TRANSESOPHAGEAL ECHOCARDIOGRAPHY**

**Cognitive Skills**

- Knowledge of appropriate indications, contraindications, and risks of TEE
- Understanding of differential diagnostic considerations in each clinical case
- Knowledge of physical principles of echocardiographic image formation and blood flow velocity measurement
- Familiarity with the operation of the ultrasonographic instrument, including the function of all controls affecting the quality of the data displayed
- Knowledge of normal cardiovascular anatomy, as visualized tomographically
- Knowledge of alterations in cardiovascular anatomy resulting from acquired and congenital heart diseases
- Knowledge of normal cardiovascular hemodynamics and fluid dynamics
- Knowledge of alterations in cardiovascular hemodynamics and blood flow resulting from acquired and congenital heart diseases
- Understanding of component techniques for general echocardiography and TEE, including when to use these methods to investigate specific clinical questions
- Ability to distinguish adequate from inadequate echocardiographic data and to distinguish an adequate from an inadequate TEE examination
- Knowledge of other cardiovascular diagnostic methods for correlation with TEE findings
- Ability to communicate examination results to patient, other health care professionals, and medical record

**Technical Skills**

- Proficiency in performing a complete standard echocardiographic examination, using all echocardiographic modalities relevant to the case
- Proficiency in safely passing the TEE transducer into the esophagus and stomach and in adjusting probe position to obtain the necessary tomographic images and Doppler data
- Proficiency in correctly operating the ultrasonographic instrument, including all controls affecting the quality of the data displayed
- Proficiency in recognizing abnormalities of cardiac structure and function as detected from the transesophageal and transgastric windows, in distinguishing normal from abnormal findings, and in recognizing artifacts
- Proficiency in performing qualitative and quantitative analysis of the echocardiographic data

From Pearlman AS, Gardin JM, Martin RP, et al: Guidelines for physician training in transesophageal echocardiography: recommendations of the American Society of Echocardiography Committee for Physician Training in Echocardiography. *J Am Soc Echocardiogr* 5:187-194, 1992.

the probe and are reassured that these responses are transient. A 20-gauge intravenous cannula is then inserted for administration of medications and contrast agents, if necessary. Lidocaine hydrochloride spray is routinely used for topical anesthesia, which should cover the posterior pharynx and tongue. We usually use diazepam 2 to 10 mg intravenously for sedation.[5] Midazolam at 0.05 mg/kg, with a total dose between 1 and 5 mg, can also be used.

Sedation is used in about 85% of our patients and should be more sparingly used in elderly patients, because they tend to be more stoic and the effect of sedation tends to be more prolonged. On the other hand, sedation is essential in young, anxious patients and when the study is expected to be protracted. We aim for light sedation so that at the end of the procedure the patients are awake and can leave with an escort. Heavy sedation is needed in situations in which blunting the hemodynamic responses to the procedure is desirable, as with a patient undergoing TEE for suspected aortic dissection.[6]

It has not been our practice to use anticholinergic agents such as glycopyrrolate to decrease salivation. In rare circumstances in which there is excessive salivation, it is usually adequate to simply instruct the patient to let the saliva dribble onto a towel placed under the chin, or remove the saliva by intermittent suction. Bacteremia is not a significant risk in TEE, and we do not use antibiotic prophylaxis to prevent endocarditis even in patients with prosthetic valves.[7,8]

## ESOPHAGEAL INTUBATION

We perform the TEE study with the patient in the left decubitus position. The physician, sonographer, and echocardiographic system are all positioned on the left-hand side of the patient.[5] Artificial teeth or dentures are routinely removed. The flexion controls should be unlocked to allow for maximum flexibility of the probe when it is being inserted. The patient's head should be in a flexed position. The tip of the probe is kept relatively straight and gently advanced to the back of the throat. It should be maintained in a central position, because deviation to either side increases the likelihood that it may become lodged in the piriform fossa. (See Fig. 2-2) The operator can facilitate this process by inserting one or two fingers into the patient's oropharynx to direct the path of the probe. Gentle pressure is exerted, and the patient is instructed to swallow. The swallowing mechanism helps guide the probe into the esophagus. In older patients, cervical spondylosis with prominent protrusion into the posterior pharynx can create difficulty with passage of the probe.[5] Manually depressing the back of the tongue provides more room, allowing the TEE probe to assume a less acute angle and facilitating intubation of the esophagus. If significant resistance is encountered when the probe is advanced, it is prudent to withdraw the probe and then initiate a new attempt. In experienced hands, the rate of failure of esophageal intubation should be less than 2%.[5,9]

A bite guard should always be used, except in edentulous patients. Our practice is to put it between the patient's teeth before the TEE probe is passed into the oropharynx and esophagus because patients with a sensitive pharynx may close their mouths involuntarily during esophageal intubation. The patient is instructed to keep the guard between the teeth throughout the procedure, and regular checks are made to ensure that it is in the proper position to prevent damage to the probe or injury to the patient.

Even when the probe is inserted without difficulties, it is not uncommon for the patient to develop nausea with or without mild retrosternal or abdominal discomfort. We find it useful to pause for 10 to 15 seconds to allow these symptoms to subside before proceeding with echocardiographic imaging. Our practice is to start with images acquired from the esophagus before advancing the probe into the stomach for the gastric views. The gastroesophageal sphincter is usually reached when the probe is advanced 40 cm from the teeth. Gentle pressure is all that is

required to advance the probe through the gastroesophageal sphincter. The patient may again experience nausea and mild discomfort, and it may be advisable to pause momentarily for these symptoms to subside. Imaging of the proximal descending thoracic aorta and aortic arch is generally reserved for the end of the study, because the probe needs to be positioned in the upper esophagus, and the patient is generally more aware of the probe at this position and tends to have more discomfort and gagging.

Inadvertent passage of the probe into the trachea can occur, particularly in deeply sedated patients. The development of stridor and incessant cough should alert the operator of this possibility. Furthermore, it would be difficult to advance the probe beyond 30 cm from the teeth, and the image quality is usually poor.[5]

In patients on mechanical ventilation, esophageal intubation is more difficult. We usually introduce the probe with the patient lying supine, because the airway is protected and aspiration is unlikely. The probe is positioned behind the endotracheal tube and gently advanced. It is helpful to have the patient's mandible pulled forward when the probe is being advanced. If there is undue resistance at about 25 to 30 cm from the teeth, slight deflation of the endotracheal tube cuff can be considered to ease passage of the probe. We do not usually remove the gastric tube, which can be used as a guide to help in proper positioning and passage of the TEE probe. In a minority of intubated patients, successful esophageal intubation may be achieved only with direct laryngoscopy.

### IMAGE FORMAT

There is no general agreement on how the imaging planes should be displayed. Our preference is to orient the images such that the right-sided structures are on the left side of the screen and the left-sided on the right. The apex of the imaging plane with the electronic artifact is at the top of the screen. Thus, in longitudinal views, superior structures are to the right of the screen and the inferior to the left.[10]

## Standard Imaging Planes

The TEE probe should be capable of multiplane imaging and preferably also real-time 3D imaging. The imaging plane is steered electronically from 0° to 180° by means of a pressure-sensitive switch, providing views that are unobtainable using monoplane and biplane probes. The following discussion focuses only on standard imaging views routinely performed at the University of Ottawa Heart Institute using multiplane TEE (Table 1-1). These views are considered "standard" because they have important clinical relevance and can be obtained in most patients with specific imaging planes. Further advances in image quality and image analysis of 3D TEE will likely facilitate the rapid acquisition of these imaging planes.

Four basic maneuvers are used to obtain specific tomographic views with TEE.[11] The first relates to the positioning of the probe by advancement or withdrawal of the probe. Although this is a simple maneuver, it is the most crucial, and the imaging views can be conveniently categorized according to the location of the TEE probe within the esophagus or stomach into four groups: basal, four-chamber, transgastric, and aortic views (Fig. 1-1). The second maneuver involves rotation of the probe from side to side. This is particularly useful when using longitudinal imaging planes, which provide a better demonstration of the continuity between vertically aligned structures such as the superior vena cava and the arch vessels (Fig. 1-2).[10,11] Steering the imaging plane using the pressure-sensitive switch is the third maneuver to obtain different tomographic views (Fig. 1-3). The accompanying images in Figures 1-1, 1-2, and 1-3 represent the typical images obtained with one of the basic maneuvers and provide the starting points for further adjustment of the imaging plane to obtain optimal long- or short-axis views of specific structures. This may be achieved using the fourth maneuver, which involves manipulation of the anterior-posterior and right-left flexion control knobs. The availability of a steerable imaging plane has drastically reduced the need to use the flexion knobs, but there are situations in which these knobs play a crucial role in obtaining proper tomographic views.[11] These maneuvers provide an almost infinite number of imaging planes. Table 1-1 summarizes the standard imaging planes and the cardiac structures evaluated in these four groups of views.

**TABLE 1-1 Standard Imaging Planes with Multiplane Transesophageal Echocardiography***

| *Imaging View* | *Standard Imaging Plane* | *Angle of Imaging Array (°)* | *Main Cardiac Structures* |
|---|---|---|---|
| Basal | Aortic valve | 0-60 | Aortic valve, coronary arteries, LA appendage, pulmonary veins |
| | Atrial septum | 90-120 | Fossa ovalis, superior vena cava, inferior vena cava |
| | Pulmonary bifurcation | 0-30 | Pulmonic valve, main and right pulmonary arteries, proximal left pulmonary artery |
| Four-chamber | LV | 0-180 | LV (regional and global function), RV, tricuspid valve |
| | Mitral valve | 0-180 | Anterior and posterior mitral leaflets, papillary muscles, chords |
| | LV outflow tract | 120-160 | Aortic valve, ascending aorta, LV and RV outflow tracts, pulmonic valve, main pulmonary artery |
| Transgastric | LV | 0-150 | LV, RV, tricuspid valve |
| | Mitral valve | 0-150 | Anterior and posterior mitral leaflets, papillary muscles, chords |
| | Coronary sinus | 0 | Coronary sinus, tricuspid valve |
| Aortic | Descending thoracic aorta | 0 | Entire descending thoracic aorta |
| | Aortic arch | 90 | Aortic arch, arch vessels, left pulmonary artery |

*At the University of Ottawa Heart Institute.

### BASAL VIEWS

The basal group of views is obtained with the TEE probe located in the midesophagus. The base of the heart, particularly the aortic valve, is well seen. The relationship of the two great arteries can be very well defined and followed cephalad to at least the level of the pulmonary bifurcation. Beyond this level, the interposing trachea makes imaging impossible. Three tomographic planes are found to be particularly useful and are routinely performed at our laboratory.

#### *Aortic Valve*

A short-axis view of the aortic valve can be obtained with the probe at about 30 to 35 cm from the teeth. The left coronary cusp often appears to have nodular thickening if the aortic valve

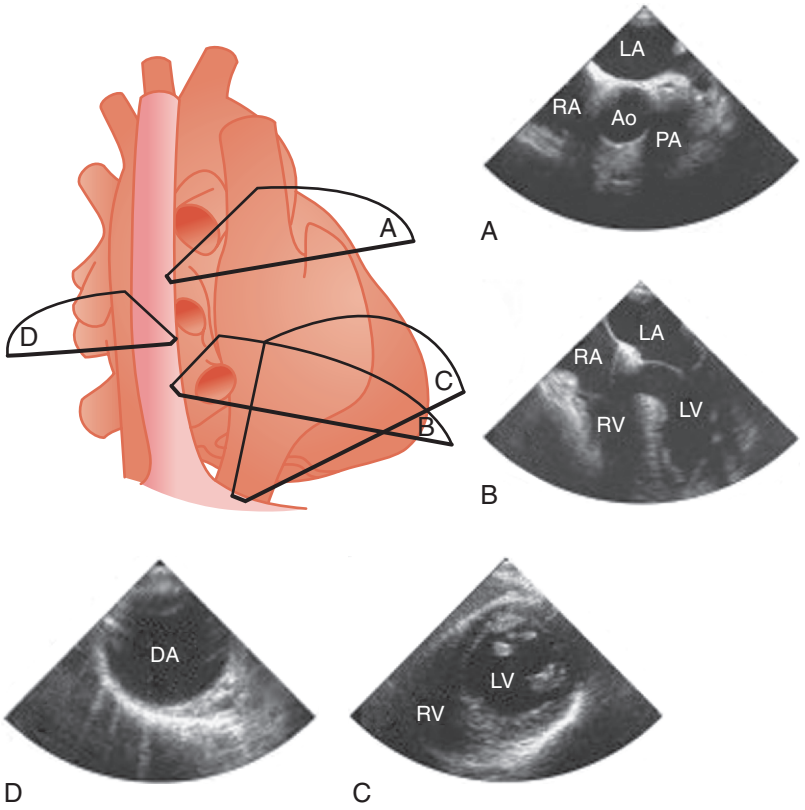



**Figure 1-1** Diagram showing the transesophageal echocardiography transducer locations for the four standard imaging views: basal (**A**), four-chamber (**B**), transgastric (**C**), and aortic (**D**). *Ao*, Aorta; *DA*, descending aorta; *PA*, pulmonary artery.

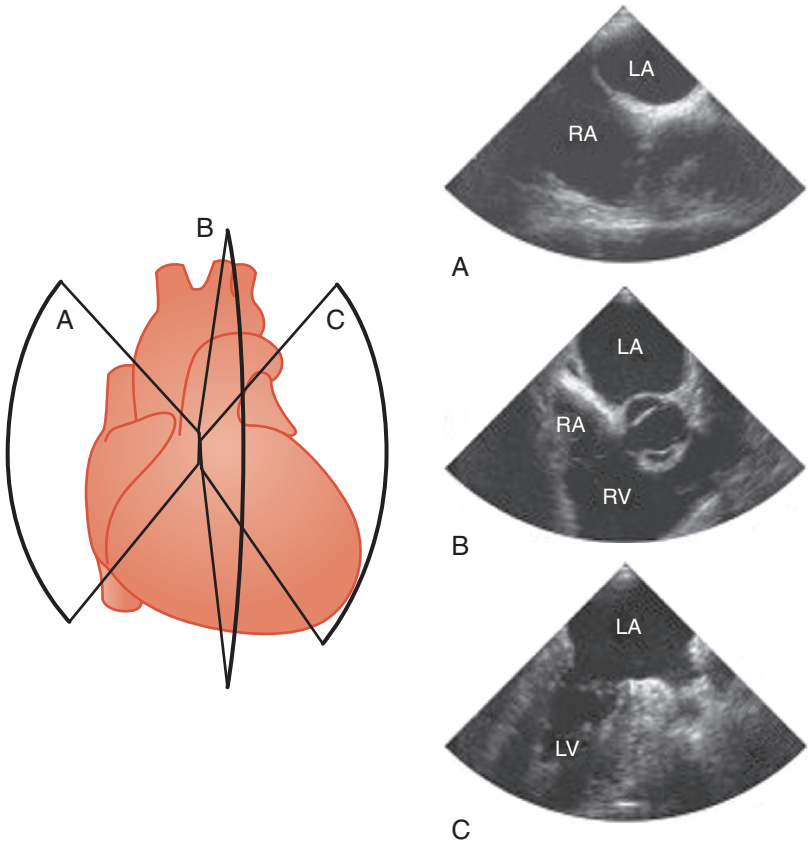



**Figure 1-2** Diagram showing the transesophageal echocardiography longitudinal imaging planes obtained by rotation of probe: atrial septum (**A**), RV outflow tract (**B**), and two-chamber view (**C**).

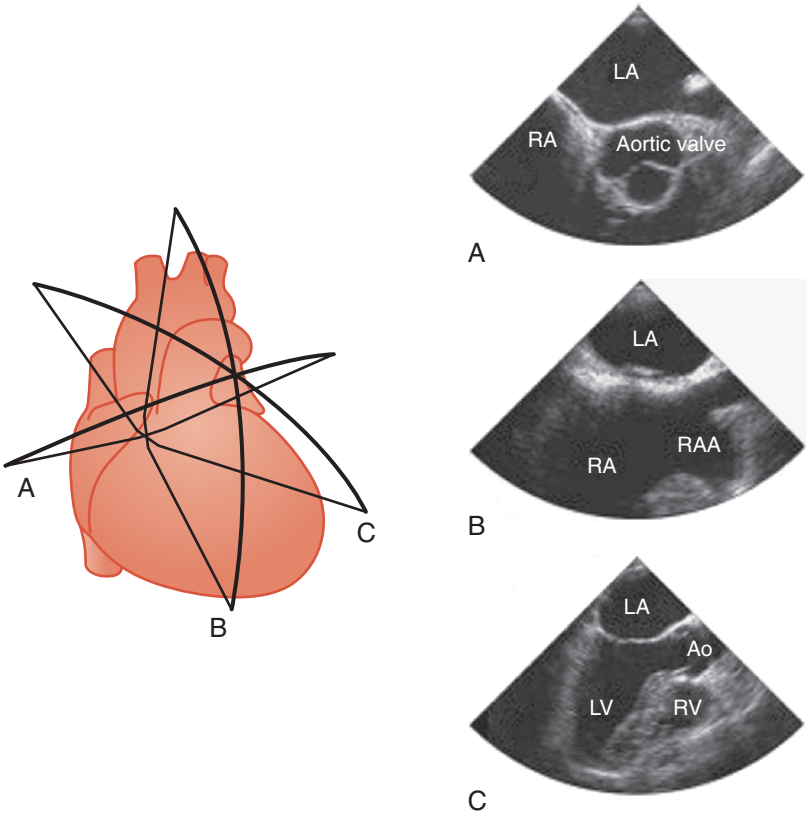



**Figure 1-3** Diagram showing the transesophageal echocardiography rotational imaging planes (0°-180°): aortic valve (**A,** 40°), superior vena cava (**B,** 100°), and LV outflow tract (**C,** 140°). *RAA*, Right atrial appendage.

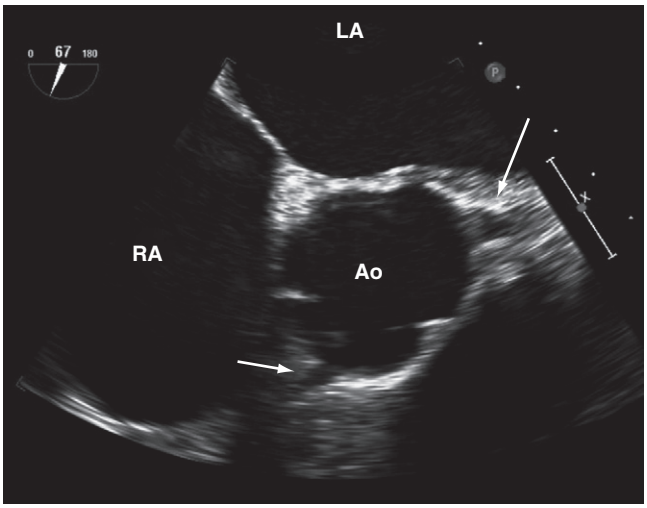



**Figure 1-4** The right (*short arrow*) and left (*long arrow*) coronary arteries can be imaged. The latter can frequently be followed to the bifurcation such that the proximal portions of the left anterior descending and the circumflex arteries can also be imaged. *Ao*, Aorta.

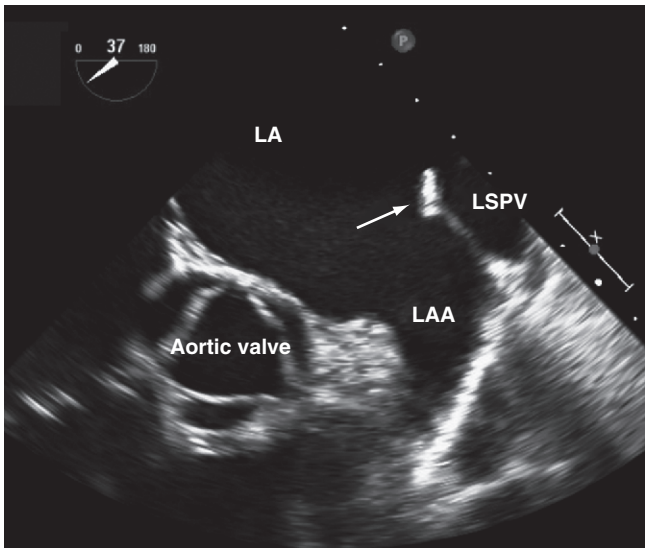



**Figure 1-5** The bulbous partition (*arrow*) between the left upper pulmonary vein and the left atrial appendage (*LAA*) is demonstrated. *LSPV*, Left superior pulmonary vein.

is cut obliquely, which is often the case at 0°.[10] Steering the imaging plane to 30° to 60° should eliminate this artifact by providing an optimal short-axis view of the aortic valve (see Fig. 1-3, *A*).[11] A slight pull-back of the transducer should allow visualization of both the left and right coronary arteries (Fig. 1-4). The left coronary artery can be followed to its bifurcation into the left anterior descending and circumflex arteries. The right coronary artery is more difficult to display, and only the proximal 2 to 3 cm is usually seen. Other structures well seen in this view are the left atrial appendage and left pulmonary veins. The partition between these structures can be quite bulbous and should not be confused with an abnormal intracardiac mass (Fig. 1-5).[12] Rotating the probe to the right should reveal the right pulmonary veins.

We like the horizontal plane in imaging the four pulmonary veins. The left and right pulmonary veins are imaged separately. When one pulmonary vein is identified, a slight translational movement of the probe should bring out the other, because the orifices of the superior and inferior pulmonary veins are in close proximity. The inferior pulmonary veins run horizontal

to the imaging plane, whereas the superior veins are more anterior and at an obtuse angle, making them more suitable for Doppler assessment. It is feasible to image the superior and inferior pulmonary veins, left or right, in the same view using the vertical plane and imaging can be facilitated with the use of color flow imaging (Figs. 1-6 and 1-7). The right and left atrial appendages wrap around the great arteries anteriorly. The left atrial appendage is more prominent and can consist of multiple lobes (Fig. 1-8).[13]

A comprehensive interrogation using multiple imaging planes should be performed to exclude left atrial appendage thrombus in the appropriate clinical setting. The right atrial appendage is smaller and triangular in shape (see Fig. 1-3, *B*). The endocardial surfaces of both appendages are corrugated and should not be confused with small thrombi.[12] A long-axis view of the aorta can be achieved with the imaging plane at about 120° (Fig. 1-9). A more rightward imaging plane, such as 150°, may be needed if the ascending aorta is dilated and tortuous. This view allows the visualization of a longer length of the ascending aorta and thus significantly reduces the blind spot caused by the interposing trachea.

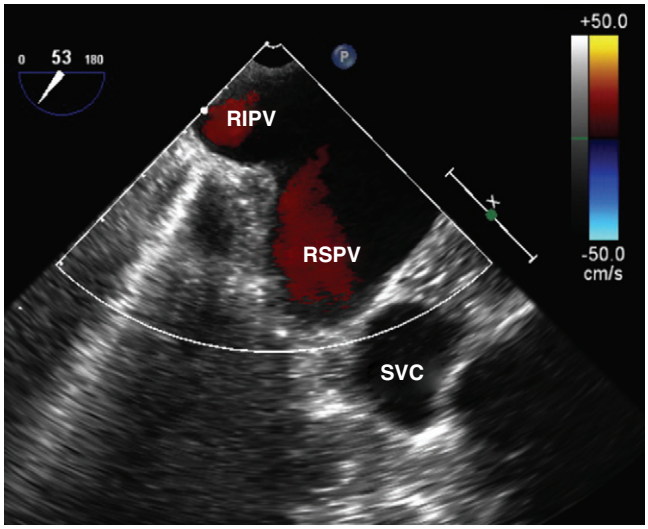



**Figure 1-6** The two right pulmonary veins are demonstrated using the longitudinal plane, and their identification can be facilitated by color flow imaging. The superior vein provides better Doppler spectral signal due to its parallel alignment with the ultrasound. *RIPV*, Right inferior pulmonary vein; *RSPV*, right superior pulmonary vein; *SVC*, superior vena cava.

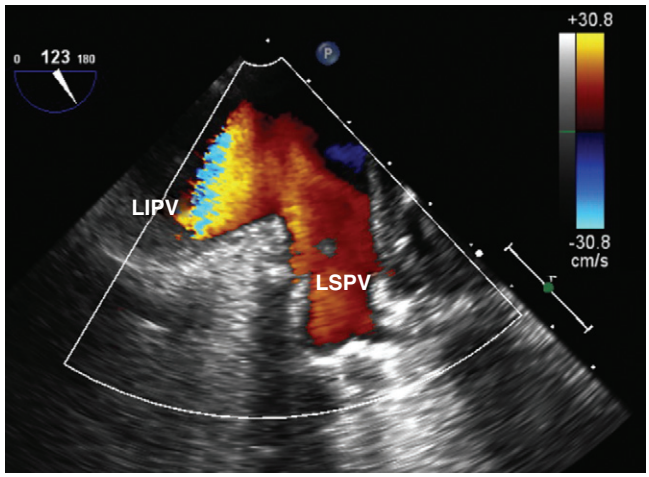



**Figure 1-7** The two left pulmonary veins are demonstrated using the longitudinal imaging plane. As with the right-sided counterparts, the superior vein is preferred for Doppler interrogation. *LIPV*, Left inferior pulmonary vein; *LSPV*, left superior pulmonary vein.

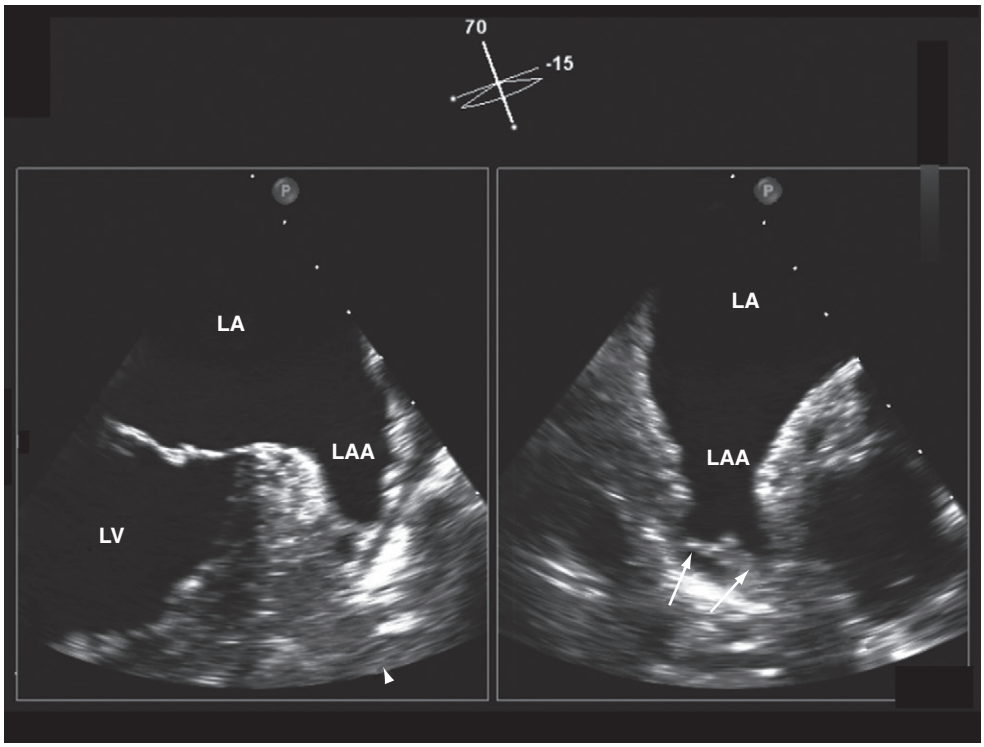



**Figure 1-8** The left atrial appendage (*LAA*) can have multiple lobes that can be readily assessed using X-plane imaging with the 3D transesophageal probe. Two lobes (*arrows*) are demonstrated at –15° (and not at 70°).

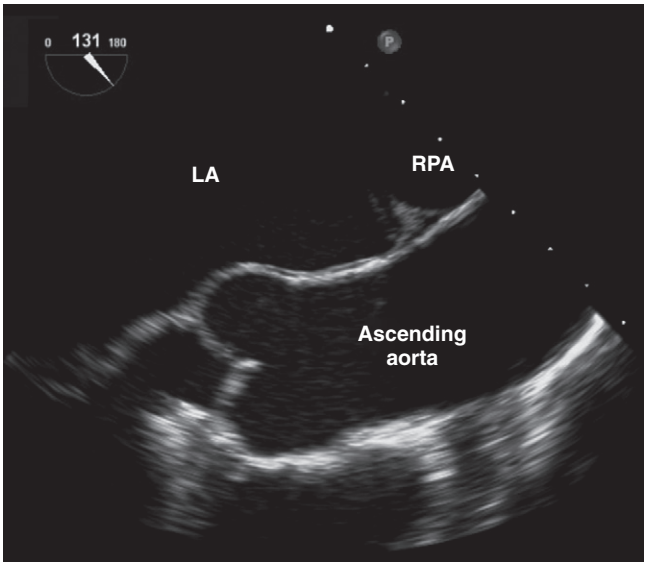



**Figure 1-9** Slight withdrawal of the probe relative to the probe position used to acquire the image shown in Figure 1-3, C, shows the right pulmonary artery (*RPA*) in short axis and more of the ascending aorta.

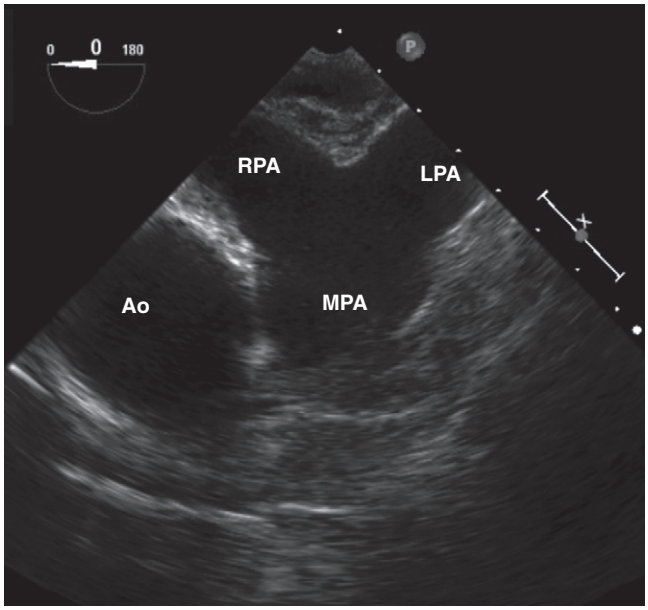



**Figure 1-10** The bifurcation of the main pulmonary artery (*MPA*) into the right (*RPA*) and left (*LPA*) pulmonary arteries is shown using the transverse plane. *Ao*, Aorta.

### *Atrial Septum*

We prefer to image the atrial septum using the longitudinal plane at 90° to 120°. The fossa ovalis, which is the thinnest part of the atrial septum, and the continuity of the superior vena cava with the RA are very well demonstrated in this view (see Fig. 1-3, *B*). This view is particularly valuable in demonstrating the sinus venosus atrial septal defect, which is usually located just inferior to the entrance of the superior vena cava.[14,15] The foramen ovale, if present, is located at the superior aspect of the fossa ovalis and is readily seen in this view. It is important to advance the probe to the level of the inferior vena cava so as not to neglect the inferior aspect of the atrial septum.[16] Careful sweep of the atrial septum with left-right rotation is needed to visualize the entire atrial septum. Continuous rotation from right to left will sequentially demonstrate the left ventricular (LV) outflow tract and the right ventricular (RV) outflow tract (see Fig. 1-2, *B*).

### *Pulmonary Bifurcation*

The pulmonary bifurcation view is achieved by withdrawal of the probe with the imaging plane at 0°. The pulmonic valve and main pulmonary artery are best seen slightly superior to the aortic valve (Fig. 1-10). The pulmonic valve is thinner than the aortic valve and is usually difficult to image in true cross section. Further slight withdrawal allows imaging of the pulmonary bifurcation. The entire length of the right pulmonary artery, but only the very proximal portion of the left pulmonary artery, can be seen. The right pulmonary artery can usually be followed to its first bifurcation by rotation of the probe rightward, but this maneuver is better performed with the longitudinal plane at 90°. Gradual rotation from left to right provides good visualization in cross section of the entire right pulmonary artery and its first bifurcation. This is an important view in the detection of proximal pulmonary emboli.[17,18]

## FOUR-CHAMBER VIEWS

Four-chamber views are obtained with the transducer within the middle to lower esophagus (see Fig. 1-1, *B*). It is difficult to image the left ventricle in its true long axis. Excessive anterior flexion should be avoided to prevent foreshortening of the ventricles. Indeed, to optimize visualization of the left ventricle, it is advisable to withdraw the probe slightly and at the same time attempt gentle retroflexion while maintaining adequate contact between the imaging surface and the esophagus. In the setting of a dilated and unfolded aorta, rotating the imaging plane to about 20° to 30° may be necessary to obtain the four-chamber view without the aorta obscuring the tricuspid valve and part of the RV.

### *Left Ventricle*

The inferior septum and anterolateral wall are usually seen in the four-chamber view (see Fig. 1-1, *B*). The LV apex is difficult to visualize, particularly in patients with a dilated LV. In addition to retroflexion, rightward flexion can often be helpful to minimize foreshortening of the LV. Far-field imaging can be improved by decreasing the transmission frequency or by using harmonic imaging. A continuous sweep from 0° to 180° should be performed to examine the different left ventricular segments so as to have a comprehensive assessment of left ventricular global and regional function (see Fig. 1-2, *C*).

### *Mitral Valve*

The mitral valve is well seen using the four-chamber view, but the depth of the imaging plane should be reduced to enhance the resolution of the image (see Figs. 1-1, *B*, and 1-2, *C*). To identify the individual scallops of the anterior and posterior mitral leaflets, a careful sweep from 0° to 180° should be made. The technique of visualizing specific scallops of the mitral leaflets has been published,[19] but patient-to-patient variation should be kept in mind. The presence of a good long-axis view of the aortic valve and proximal ascending aorta, usually at 120°, is a good indication that the middle scallops of both the anterior and the posterior mitral leaflets are imaged and provides the internal reference for the analysis of the other imaging planes. Both papillary muscles can be imaged, but usually not in the same plane. The subvalvular chords are seldom completely imaged because they are frequently obscured

by the mitral leaflets. The morphologic information obtained from this view should be corroborated by the short-axis view of the mitral valve obtained from the transgastric view, which also allows a better assessment of the subvalvular structures, including the papillary muscles and chords. Four-chamber views are ideal for the assessment of mitral regurgitation in relation to the number of regurgitant jets, the direction of the jets, and the severity of regurgitation.[20,21]

### *Left Ventricular Outflow Tract*

We like to image the left ventricular outflow tract at 120° to 160°, because the outflow tract has a horizontal alignment in this plane that may allow optimal imaging even in the setting of a prosthetic aortic valve (see Fig. 1-3, *C*). The opening and closing of the aortic valve as well as the presence or absence of aortic regurgitation can be well visualized. The proximal ascending aorta is present in this view. A slight withdrawal of the probe will allow more of the ascending aorta to be visualized (see Fig. 1-9). A slight rotation to the left will show the RV outflow tract with the thin pulmonic valve. The motion of the pulmonic valve and the presence or absence of pulmonic regurgitation can be adequately assessed using this view.

## TRANSGASTRIC VIEWS

There is slight resistance during the passage of the TEE probe through the gastroesophageal junction, and the appearance of the liver is a clear indication that the probe is in the stomach. Anterior flexion, often with leftward rotation and flexion, is required to achieve good contact between the imaging surface and the gastric wall. Extreme anterior flexion with further advancement of the probe can sometimes produce images similar to the five-chamber view obtained from the subxiphoid surface approach.

### *Left Ventricle*

Multiple cross sections of the LV can usually be obtained using the transgastric approach (see Fig. 1-1, *C*, and Fig. 1-11). These are the views commonly used in the intraoperative assessment of LV function.[19] Optimization of the short-axis views of the left ventricle can be achieved with leftward rotation accompanied by leftward flexion. To visualize the LV apex, gentle advancement of the probe is required together with slight retroflexion. In our experience, the short-axis view of the LV apex can be obtained in about 60% of cases. Another way to visualize the LV apex is to use the longitudinal plane at about 90° (see Fig. 1-11). Careful lateral rotation can be used to obtain comprehensive regional assessment of the LV. Leftward rotation of this imaging plane can yield a good alignment with the LV outflow tract and aortic valve to allow accurate measurement of the transaortic pressure gradients in the setting of aortic stenosis (Fig. 1-12).[22] The RV can be seen with rightward rotation of the probe. Both short- and long-axis views of the tricuspid valve are achievable, although the tricuspid valve and its papillary muscles are better assessed with the long-axis plane.

### *Mitral Valve*

The mitral valve can be best assessed using the horizontal imaging plane with the transducer brought up to near the gastroesophageal junction (Fig. 1-13). Anterior flexion and leftward flexion are usually required to optimize this view. Adjusting the imaging plane to about 20° will help to bring out the lateral commissure. This view provides unambiguous assessment of the individual scallops of both the anterior and posterior mitral leaflets and thus should be attempted in all patients with myxomatous mitral valve degeneration. In our experience, this view is achievable in about 70% of patients. Both papillary muscles and chords can be demonstrated, and the continuity between these structures and the mitral leaflets is best seen in the long-axis plane.

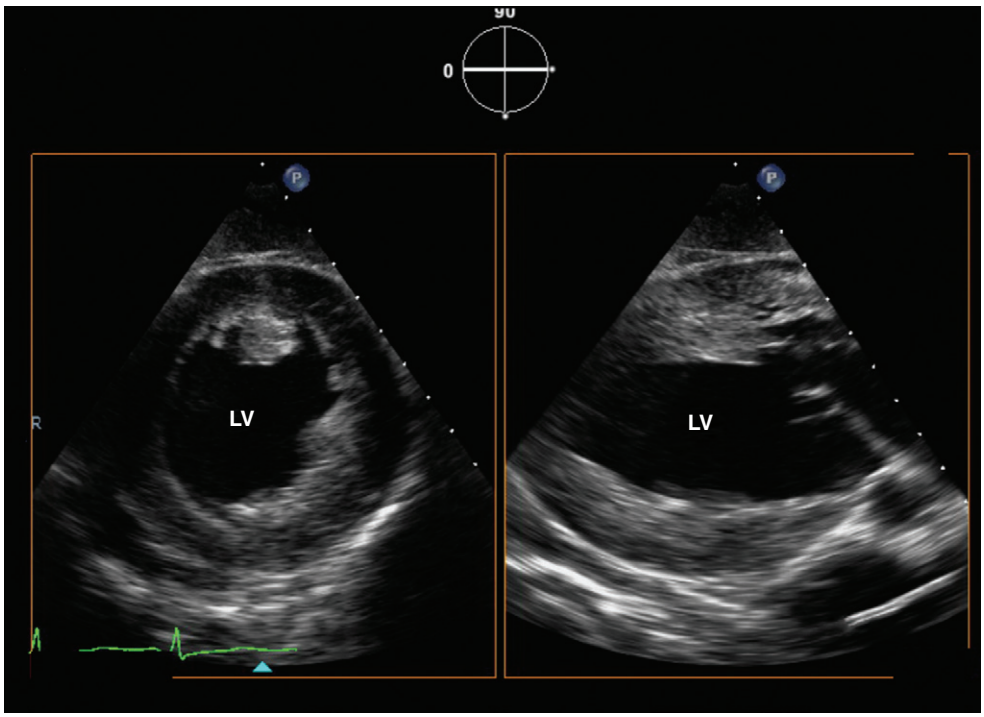



**Figure 1-11** The short- and long-axis views of the LV are demonstrated using X-plane imaging from the transgastric window.

### *Coronary Sinus*

The coronary sinus comes into view when the probe is withdrawn to near the gastroesophageal junction and the flexion knobs are in relatively neutral positions (Fig. 1-14). This view can also be achieved by retroflexion with the probe in the lower esophagus. The coronary sinus is seen as a vascular structure located posterior to the LV at the atrioventricular groove draining into the RA. The tricuspid valve can be visualized to the right and anterior. A dilated coronary sinus should raise the possibility of the presence of a persistent left superior vena cava, which is the most common cause. Leftward rotation while following the coronary sinus may sometimes demonstrate this anomalous vein.[23] In the esophageal views, the left superior vena cava is usually sandwiched between the left atrial (LA) appendage and left superior pulmonary vein.[24]

## AORTIC VIEWS

The thoracic aorta is well assessed by TEE because of its close proximity to the esophagus.

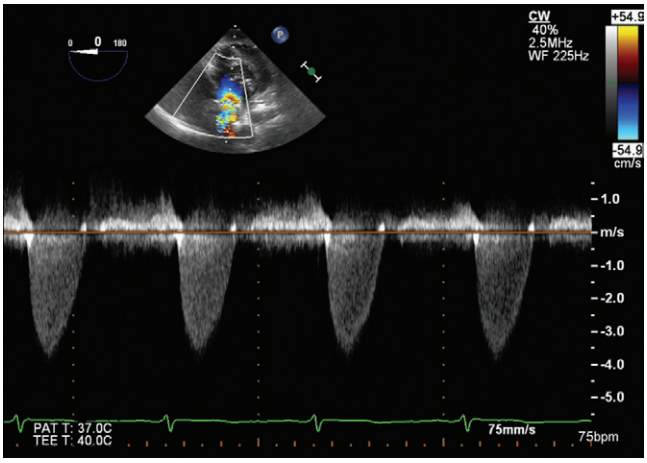



**Figure 1-12** Transgastric window is used to assess the severity of aortic stenosis using CW Doppler echocardiography.

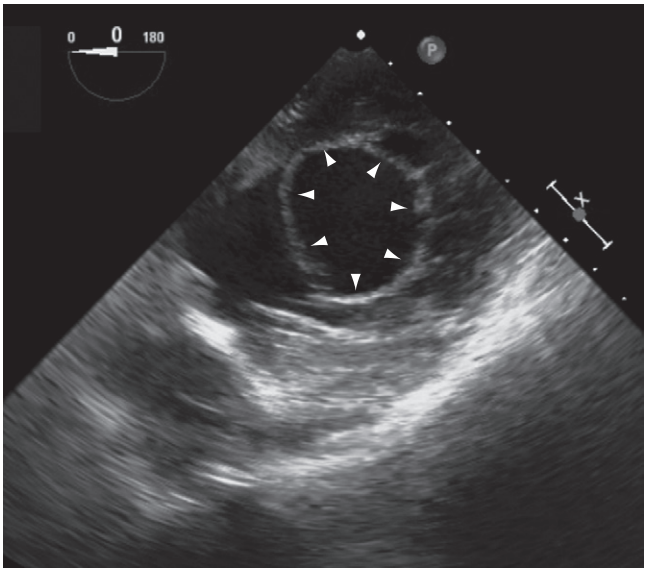


**Figure 1-13** Transgastric view of the mitral valve (*arrowheads*) in the short axis showing the circular orifice of the mitral valve in early diastole.

### *Descending Thoracic Aorta*

The best way to assess the descending thoracic aorta is to use the horizontal imaging plane with the transducer rotated leftward and posterior, followed by slow withdrawal from the level of the diaphragm to the aortic arch (see Fig. 1-1, *D*).[12] Because of the relationship between the esophagus and aorta, slight rotational adjustment is required to visualize the entire circumference of the aortic wall as the probe is slowly withdrawn.[24] If the aorta is dilated or tortuous, proper short-axis views of the descending aorta will require adjustment of the imaging plane by 0° to 90°.

### *Aortic Arch*

The longitudinal imaging plane at 90° is preferred in imaging the aortic arch because it allows visualization of the entire circumference of the aorta (Fig. 1-15).[24] Anterior rotation of the longitudinal plane should visualize the entire aortic arch, but the proximal aortic arch may not be visualized when the aortic arch is unfolded. The transducer will need to be withdrawn slightly to image the arch vessels, which course superiorly. In

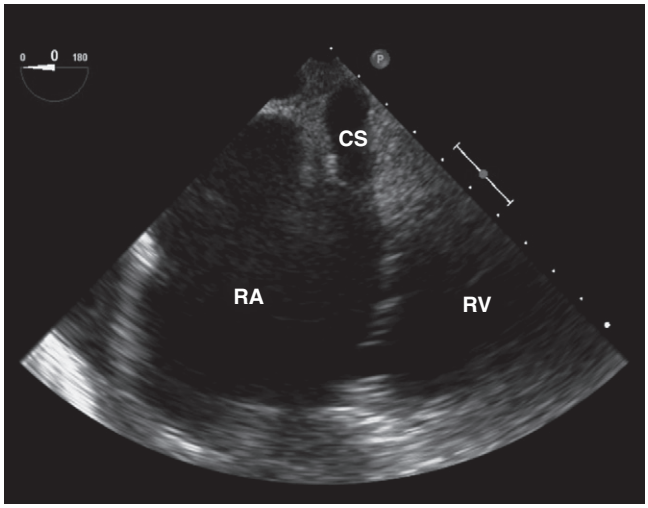



**Figure 1-14** The coronary sinus (*CS*) is demonstrated with the probe at the gastroesophageal junction.

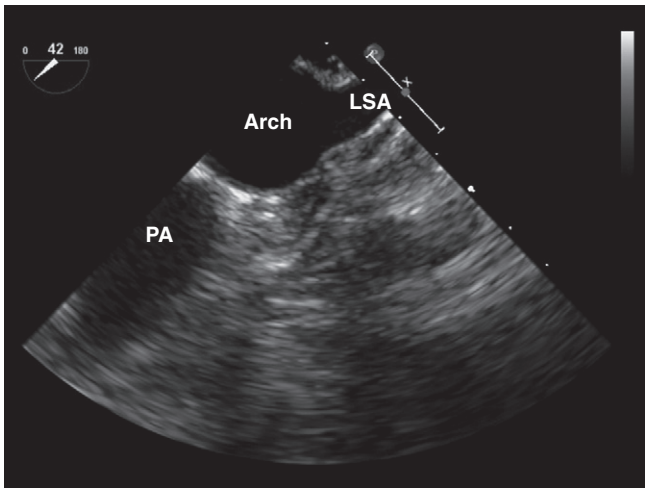



**Figure 1-15** The aortic arch is imaged using the longitudinal plane, showing the origin of the left subclavian artery (*LSA*). *PA*, Pulmonary artery.

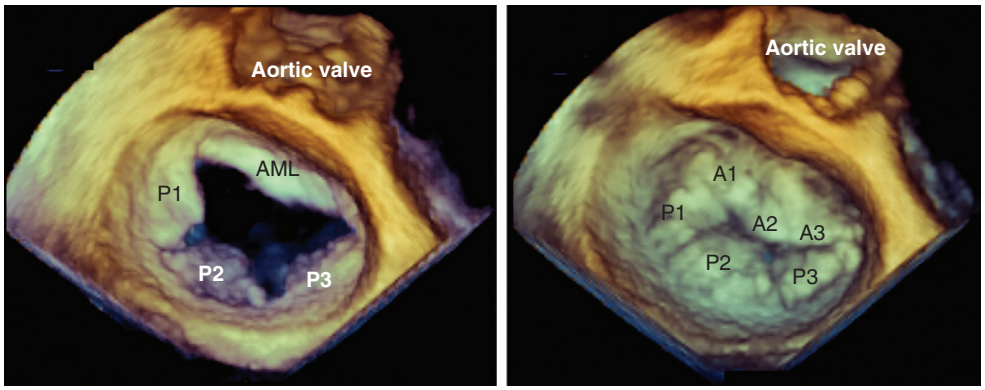



**Figure 1-16** The individual scallops of the anterior (*A1*, lateral scallop; *A2*, middle scallop; *A3*, medial scallop) and posterior mitral leaflets (*P1*, lateral scallop; *P2*, middle scallop; *P3*, medial scallop) in diastole (*left* panel) and systole (*right* panel) are shown using the 3D zoom mode. *AML*, Anterior mitral leaflet.

one third of patients, all three arch vessels can be imaged, but in the other two thirds of patients, only the two distal arch vessels can be imaged. It is rare not to be able to image at least one arch vessel. As a rule, the brachiocephalic artery, which is anterior and more rightward, is the most difficult to image because of the interposing trachea. The transverse plane in a more superior location may sometimes show the three arch vessels in their short axis. Advancing the probe by 1 to 2 cm so that the imaging plane is just inferior to the aortic arch can frequently image the proximal left pulmonary artery. It is sometimes possible to follow it to the first bifurcation. This view should be sought in patients suspected of having pulmonary embolism.

## Three-Dimensional Imaging

Advances in transducer technology have enabled the incorporation of real-time 3D-imaging capacity into the commercially available TEE probe, such that 3D imaging can be readily performed during a conventional two-dimensional (2D) TEE study providing unique anatomic perspectives in a number of clinical situations.[25-32] (See Chapter 4.) The current clinical indications of 3D TEE are summarized in Table 1-2, and the indications are likely to increase with time. In our opinion, 3D TEE imaging should be routinely performed in patients with mitral valve disease and congenital heart disease (Fig. 1-16).

The currently available 3D TEE probe can perform 3D imaging in several modes: 3D full volume, 3D zoom, 3D live, 3D color-flow imaging, and X-plane imaging. We find 3D zoom and X-plane imaging to be the most useful. To acquire 3D full volume, the full pyramidal volume is obtained by stitching together four subvolumes gated to the R-wave of the electrocardiogram. To minimize the stitch artifact between the subvolumes, it is best to acquire the images during a breath hold (Fig. 1-17). In this mode, frame rates are relatively low. Although analysis of the volumetric data set can be performed online, it is frequently performed offline so as not to prolong the study. In the full-volume mode, the semiautomatic multiple parallel slice display can be a quick and useful format in the assessment of LV topography, such as in patients with regional wall motion abnormalities or ventricular aneurysms.

In the real-time live 3D mode, the 3D data set is displayed in real time. It is important to minimize the sector angle so as to increase the frame rate, which is considerably reduced compared to 2D imaging. We find the 3D zoom mode to be the most

**TABLE 1-2 Common Indications for Using Real-time Three-Dimensional Transesophageal Echocardiography**

| *Cardiac Structure* | *Information from 3D TEE* | *Clinical Situations* |
|---|---|---|
| Mitral valve | En-face view of mitral valve | Assessment of the location of prolapsing or flail mitral leaflet scallops for potential mitral valve repair; intraoperative assessment of mitral valve clip repair. |
| Prosthetic valve | Number, size, and location of perivalvular regurgitant jets | Preoperative and intraoperative assessment for device closure of perivalvular regurgitation |
| Atrial septum | Number, size, and location of atrial septal defect | Preoperative and intraoperative assessment for device closure of atrial septal defect |
| Intracardiac baffle or conduit | Better anatomic perspective of intracardiac abnormalities | Assessment of naïve and postoperative complex congenital heart disease |

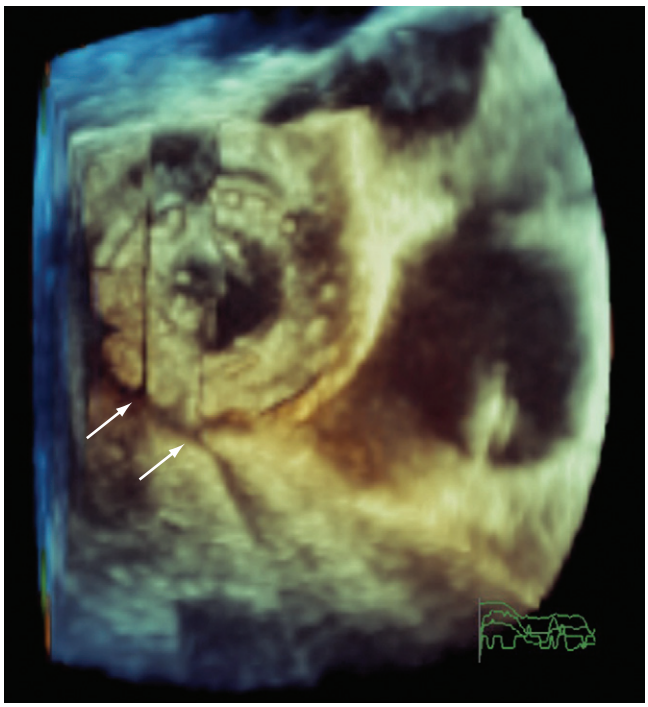


**Figure 1-17** Transesophageal 3D view of the bioprosthetic mitral valve in the full volume mode shows the stitch artifact (*arrows*) between the subvolumes.

versatile. In the 3D zoom mode, the area of interest is identified and encompassed by the zoom box, generally in two orthogonal planes. The height and width of the zoom box are adjusted to include the entire area of interest and at the same time streamlined as much as possible in order to enhance the frame rate. Indeed, the 3D zoom mode is our preferred display format when using the 3D live mode. The availability of the X-plane is a very welcome addition to TEE imaging. It allows the simultaneous display of an additional plane during standard 2D imaging. The orientation of the additional plane is usually orthogonal but can be easily adjusted to any specific orientation. The availability of the X-plane provides a quick and comprehensive assessment of complex structures. One example is the LA appendage, which frequently has multiple lobes (see Fig. 1-8). The use of the X-plane allows rapid assessment of the multiple lobes. Similarly, when multiple mitral regurgitant jets are present, X-plane imaging can readily identify the number and orientations of the regurgitant jets.

Real-time 3D color flow imaging can also be performed to provide a 3D assessment of the color flow jet, but the volume of interest is small, and the frame rate is quite limited in this mode.[33,34] In vitro and early clinical studies have suggested that 3D color flow imaging gives a more accurate assessment of the shape and size of the vena contracta and flow convergence, both of which are important measures of mitral regurgitation severity. Its clinical usefulness, however, remains unclear.

In order to obtain a high-quality 3D image, the 2D image needs to be optimized in terms of gain and compression settings. A slightly higher gain setting generally provides better 3D images. In both the 3D zoom and 3D live modes, the zoom box should be streamlined to focus on the area of interest to maximize the frame rate. Because the best 3D imaging is obtained with the structure close to the transducer and orthogonal to the ultrasound beam, the TEE transducer should be manipulated to achieve these two objectives. For instance, the transgastric window is superior to the transesophageal window in 3D imaging of the LV papillary muscles. The mitral valve is well suited for 3D TEE imaging precisely for these reasons (see Fig. 1-16). On the other hand, it is much more difficult to obtain a good 3D image of the aortic valve because the valve plane is frequently parallel to the ultrasound beam.

## Doppler Examination

Transesophageal echocardiography can be used to assess the flow patterns across the four cardiac valves, but it does not provide additional information to transthoracic echocardiography (TTE). Furthermore, good ultrasound beam alignment with the transvalvular flow may not be feasible because of the anatomic confines of the esophagus. However, accurate Doppler assessment of aortic stenosis can often be obtained from the transgastric window (see Fig. 1-12).[22] On the other hand, intracardiac flows such as pulmonary vein flow and LA appendage flow are better and more consistently obtained by TEE and provide important insight into intracardiac hemodynamics.

### LEFT ATRIAL APPENDAGE FLOW

The LA appendage can be imaged from the midesophagus aortic valve short-axis view (30° to 60°) or the midesophagus two-chamber view (80° to 100°). LA appendage flow should be recorded by positioning the color flow sector over the LA appendage and placing the pulsed-Doppler sample volume at the site of maximal flow velocity. This usually occurs in the proximal or middle third of the LA appendage. Velocity recordings from the distal third of the LA appendage frequently have wall motion artifacts and are usually unsatisfactory. Wall filters should be set low, because low-velocity flow may be present.

The pattern of LA appendage flow is dependent on cardiac rhythm.[35,36] In atrial fibrillation, a regular atrial contraction wave is absent. (See Chapter 42.) In atrial flutter, the velocity waves are more regular and tend to be of greater velocity because of the slower atrial rate. The normal LA appendage velocities are as follows: contraction, 60 ± 14 cm/s; filling, 52 ± 13 cm/s; and early diastolic filling, 20 ± 11 cm/s.[35,37]

The potential clinical utility of measuring LA appendage velocities relates to their association with LA spontaneous echo contrast and LA thrombus.[35,36,38,39] Patients with atrial fibrillation and a LA appendage emptying velocity less than 20 cm/s are more likely to have LA thrombus and have a 2.6-fold greater risk of ischemic stroke compared to patients with a velocity greater than 20 cm/s.[38,39] Lower LA appendage velocities have also been observed in stroke patients in normal sinus rhythm.[40] LA appendage velocities may predict successful cardioversion of atrial fibrillation[41] and the maintenance of sinus rhythm at 1 year.[35,36,42]

### PULMONARY VEIN FLOW

Pulmonary venous flow patterns provide unique and ancillary information for evaluating LV diastolic function, measuring LV filling pressure, assessing mitral regurgitation severity, differentiating constrictive pericarditis from restrictive cardiomyopathies, and identifying pulmonary vein stenosis after radiofrequency ablation of atrial fibrillation.[43-45] TTE can obtain pulmonary vein flow in up to 90% of patients; however, TEE allows a more consistent and reliable acquisition of high-quality laminar Doppler signals.[43,46]

The pulmonary veins are imaged from the midesophagus, and flow is evaluated by placing the pulsed-Doppler sample volume 1.0 to 2.0 cm into the pulmonary veins. The ultrasound beam can be aligned parallel to flow in the left and right superior pulmonary veins; however, this alignment is often not achievable with the inferior pulmonary veins.

## Indications for Transesophageal Echocardiography

In general, TTE should be the initial diagnostic investigation, because it is noninvasive and imparts no risk to the patient. However, patient factors (i.e., obesity, emphysema, chest deformities, or subcutaneous emphysema) and the clinical setting (i.e., surgical bandages, mechanical ventilation, or traction) frequently limit ultrasound penetration or proper patient positioning, resulting in a nondiagnostic TTE. TEE can provide excellent cardiac visualization in these situations and should be considered to obtain the necessary diagnostic information.

TEE can also visualize cardiac structures not usually seen by TTE (i.e., the superior vena cava, pulmonary veins, and descending thoracic aorta) and can provide improved anatomic and spatial resolution to both diagnose cardiac pathology and guide patient management. Common clinical indications for TEE are listed in Box 1-2.

Box 1-2

**COMMON INDICATIONS FOR TRANSESOPHAGEAL ECHOCARDIOGRAPHY**

Nondiagnostic transthoracic echocardiogram
Evaluation of native valve disease
Evaluation of prosthetic valves
Evaluation of suspected and definite infective endocarditis
Evaluation of a suspected cardioembolic event
Evaluation of cardiac tumors or masses
Evaluation of an atrial septal abnormality
Evaluation of an acute aortic syndrome or aortic disease
Atrial fibrillation (TEE-guided strategy for "early" cardioversion)
Evaluation of naïve and surgically corrected congenital heart disease
Detection of coronary artery anomalies and coronary artery disease
Evaluation of postoperative cardiac tamponade and pericardial disease
Evaluation of the critically ill patient
Intraoperative monitoring
Guidance of interventional procedures

## NATIVE VALVE DISEASE

The close proximity of the mitral valve to the posteriorly positioned TEE transducer allows excellent visualization of the mitral annulus, leaflets, chordal structures, and papillary muscles. (See Chapters 18 and 19.) Ruptured chordae tendinae can be visualized, and prolapsing or flail scallops can be localized, to predict the potential for successful mitral valve repair.[20,47-49] Abnormalities of the papillary muscles, such as a partial or complete rupture, are better visualized by TEE than TTE.[50] 3D TEE provides superior delineation of the mitral valve anatomy and can more precisely characterize and localize mitral valve pathology compared to 2D TEE.[26,30,31,51]

The severity of mitral valve regurgitation can be quantified by TEE using the same methods employed for TTE[52]; however, color Doppler regurgitant jet areas tend to be larger on TEE than on TTE.[53] 3D color Doppler imaging provides additional information on the mechanism and severity of mitral regurgitation that may not be apparent from 2D TEE.[33,51,54,55] Pulmonary vein flow can be assessed in nearly all patients and provides a valuable measure of mitral regurgitation severity.[43,56] The vena contracta width and regurgitant orifice area, derived by the proximal flow convergence method, can be measured using TEE and can provide prognostic information in patients with asymptomatic mitral regurgitation.[57-59] The accuracy of these latter measures to quantify mitral regurgitation severity can be improved using 3D TEE.[33,55]

In mitral stenosis, TEE can assess valve mobility and leaflet thickening, but subvalvular disease and calcification may be underestimated in the esophageal views due to a shadowing effect from the thickened and calcified mitral valve leaflets and annulus.[60] (See Chapter 21.) Effective orifice area can be derived by the pressure half-time method, proximal flow convergence method, or orifice planimetry.[61,62] Accurate orifice planimetry requires a tomographic cut of the distal, most narrowed portion of the mitral orifice. Optimal alignment of the image is frequently not possible using 2D TEE, but may be achievable by 3D TEE.[31] The suitability of a patient for percutaneous balloon mitral valvuloplasty usually incorporates a TEE evaluation of the LA chamber and appendage to identify thrombus, an assessment of the mitral valve morphology score, and an evaluation of mitral regurgitation severity. Mitral valve morphology on TEE is predictive of the prognosis of patients following percutaneous balloon mitral valvuloplasty; however, TTE is preferred to evaluate valve morphology because of the limitations of TEE in evaluating calcification and subvalvular thickening.[60,63] TEE can be used during transcatheter mitral commissurotomy to guide the transseptal puncture and balloon placement and to identify potential procedural complications (i.e., severe mitral regurgitation, cardiac tamponade, or significant atrial septal defect).[64] (See Chapter 5.) 3D TEE may provide incremental information during the procedure by confirming the coaxial trajectory of the balloon through the stenotic mitral valve and by better evaluating commissural opening postdilation.[65,66]

Subaortic membranes frequently require TEE for definitive diagnosis.[67] Anatomic valve area of a stenotic aortic valve can be measured using multiplane TEE by planimetry of the maximum systolic orifice area in the esophageal short-axis (30° to 60°) view.[22,68] Proper transducer position should be confirmed by rotating to the longitudinal plane and verifying that the leaflet tips are being imaged. However, dynamic movements of the aortic valve can cause misalignment of the imaging plane with the narrowest cross-sectional area and result in an inaccurate measurement of the anatomic valve area. 3D TEE can avoid this potential pitfall.[69] Unfortunately, valve calcification can affect the accuracy of TEE-measured orifice areas using either 2D or 3D techniques.[70]

TEE is rarely necessary to evaluate aortic regurgitation severity. The standard methods used during TTE to quantify aortic regurgitation severity can be used during TEE.[52,71] Color jet areas on TEE tend to be larger than those obtained during TTE.[53] Vena contracta width on TEE correlates well with the regurgitant fraction and regurgitant volume.[72] Aortic regurgitation severity can also be quantified using the proximal flow convergence method.[73] Holo-diastolic flow reversal in the descending aorta can be detected by TEE using pulsed Doppler.[74]

The tricuspid and pulmonic valves can be visualized on TEE; however, TTE generally provides better visualization because of the anterior position of these valves. 3D TEE appears to be of limited value in evaluating these valves. In one study, 3D TEE provided optimal visualization of the tricuspid valve in only 11% of patients.[75] However, TEE may provide clinically relevant information about the tricuspid and pulmonic valves in patients with poor TTE images.

## PROSTHETIC VALVES

TEE is more sensitive for detecting abnormalities of bioprosthetic and mechanical prostheses when compared to TTE.[76] (See Chapter 25.) Leaflet thickening and calcification, flail leaflets, vegetations, thrombi, filamentous strands, and motion of the occluding device are better appreciated on TEE.[76-83] TEE can distinguish pannus from thrombus formation and guide the use of thrombolytic therapy.[84-87] TEE is especially valuable in assessing a mitral prosthesis, because the transducer's posterior position provides excellent visualization of vegetations and thrombi that usually locate on the LA aspect of the prosthesis.[76,78] However, the ventricular aspect of a mitral prosthesis may not be adequately seen on TEE, and TTE should be performed to complete the assessment.[88] 3D TEE can provide excellent visualization of a mitral prosthesis ring, leaflets, or strut (mechanical or bioprosthesis).[27] The aortic prosthesis ring can also be

well seen on 3D TEE; however, visualization of the leaflets can be suboptimal.[27]

TEE should be performed if significant prosthetic mitral regurgitation is suspected clinically, but not seen on TTE. TEE can distinguish normal variant from pathological prosthetic valve regurgitation and determine whether the regurgitation is paravalvular or transvalvular in origin, potentially modifying the surgical procedure.[77-80,89] 3D TEE may provide better delineation of the site and extent of paravalvular regurgitation or mitral prosthesis dehiscence compared to 2D TEE.[27] The incremental benefit of TEE in assessing prosthetic aortic regurgitation severity is less clear, because the regurgitant jet is usually well seen on TTE, and TEE visualization may be compromised by partial shadowing of the regurgitation jet by either the aortic or mitral prosthesis when imaged in the esophageal views.[80]

All bioprostheses and mechanical prostheses are inherently stenotic, the severity dependent on the prosthesis type and size and the presence of associated pathology such as leaflet calcification, pannus formation, or valve thrombosis. In general, TTE is sufficient to assess the hemodynamic severity of a stenotic aortic or mitral prosthesis, but only TEE has sufficient resolution to distinguish these pathologic conditions.[84,85] In patients with an inadequate TTE, TEE can be used to quantify the stenosis severity, as described for native valve stenoses.[22,62,68,90]

## INFECTIVE ENDOCARDITIS

Identification of a vegetation in the clinical setting of suspected endocarditis confirms the diagnosis.[91] Studies comparing TTE and TEE for detecting a vegetation in native valve endocarditis report a sensitivity of 28% to 70% for TTE, substantially lower than the 86% to 100% sensitivity reported for TEE.[92-97] (See Chapter 22.) Smaller vegetations are better detected by TEE because of the improved spatial resolution of this technique.[93] However, TTE and TEE have a similar specificity that exceeds 90% when strict criteria for diagnosing a vegetation are used.[92,93,95,97] Pulmonic valve vegetations are better detected by TEE than TTE, despite the anterior position of the pulmonic valve.[98] In contrast, TEE has not been reported to have a better sensitivity for detecting tricuspid valve vegetations compared to TTE.[99] However, we would recommend a TEE if there is a clinical suspicion of tricuspid valve endocarditis but the TTE is negative.

Prosthetic valve endocarditis is more difficult to diagnose by either TTE or TEE. The sensitivity of TTE for detecting vegetations ranges from 0% to 43% and increases to 33% to 86% using TEE.[76,94,100,101] Clearly, TEE can identify a vegetation in a significant number of patients with a negative TTE and should be performed in patients with suspected prosthetic valve endocarditis if the TTE does not identify a vegetation.[102]

Although TEE provides a greater sensitivity than TTE for detecting vegetations in native and prosthetic-valve endocarditis, TEE has the greatest impact on diagnosis in patients with suspected endocarditis and an intermediate clinical probability of endocarditis.[102,103] The absence of a vegetation on TEE in this setting makes the diagnosis of endocarditis unlikely (less than 10%), and alternative diagnoses should be considered.[101,104] However, a negative TEE does not supplant a clinical and microbiological diagnosis, because false-negative studies have been reported. Patients with a negative TEE study may benefit from a follow-up TEE in 7 to 10 days if there is a high index of suspicion of endocarditis, a prosthetic valve, or persistent bacteremia.[101-104] TEE is likely not warranted in patients with a low clinical probability of endocarditis, because the diagnostic yield is small.[103]

Complications of infective endocarditis, including abscess formation, leaflet diverticula, leaflet perforation, fistula tracts, mycotic aneurysms, and pseudoaneurysm formation, are significantly better detected by TEE than TTE.[94,105-108] TTE has a low sensitivity (less than 30%) for detecting an abscess,[105] so a patient with a suspected abscess on clinical grounds or persistent bacteremia should undergo TEE despite a negative TTE. TEE can be falsely negative in up to half of patients with an abscess.[108] This often occurs when the abscess cavity is localized on the posterior aspect of a calcified mitral annulus or when a prosthesis is present.[108]

The potential utility of TEE in uncomplicated confirmed endocarditis remains to be defined. Large (greater than 10 to 15 mm) or severely mobile vegetations on TEE are associated with systemic embolization, and vegetation size is an independent predictor of survival.[96,109,110] Furthermore, complications are more likely to occur in patients in whom a vegetation fails to decrease in size with therapy.[111] Although we routinely perform a TTE in follow-up of patients with uncomplicated confirmed endocarditis to reevaluate vegetation size and valve function, we do not routinely perform a follow-up TEE.

## SUSPECTED CARDIOEMBOLIC EVENT

Cardiogenic embolism accounts for approximately 15% to 30% of ischemic strokes and should be considered as a potential cause of cerebral ischemia, especially in those patients without significant cerebrovascular disease.[112] (See Chapter 41.) Potential cardioembolic sources encompass conditions that have a propensity for thrombus formation, intracardiac or intraaortic masses, and potential passageways for paradoxical emboli. Cardiac abnormalities having a strong association with cardioembolic events include atrial fibrillation, LA or LV thrombi, vegetations, intracardiac tumor, mitral stenosis, mechanical valves, recent myocardial infarction, dilated cardiomyopathy, ischemic LV dysfunction (ejection fraction less than 28%), and intraaortic debris.[113,114] Minor risk sources with weaker associations include atrial septal aneurysms, patent foramen ovale, spontaneous echo contrast, mitral annular calcification, mitral valve prolapse, and calcified aortic stenosis.[113-115] Although many of these conditions can be diagnosed clinically, echocardiography is frequently necessary to diagnose anatomic abnormalities.[116] In general, TEE is superior to TTE at identifying major and minor risk sources.

LA thrombus is usually located in the LA appendage, a region poorly visualized on TTE. TTE has a sensitivity for detecting LA thrombi of only 0% to 53%, whereas TEE has a sensitivity of 93% to 100% and a specificity exceeding 95%.[117,118] Care must be taken not to mistake the pectinate muscles for LA appendage thrombus. LA spontaneous echo contrast is rarely appreciated on TTE but is well seen on TEE. LV thrombi can usually be detected by TTE (sensitivity and specificity approaching or exceeding 90%), and contrast echocardiography can improve the diagnostic accuracy.[119] In general, TEE adds no incremental sensitivity unless the TTE is inconclusive, because the apex is located in the far-field position and apical foreshortening is common.[120,121] TEE may better detect small myxomas or papillary fibroelastomas.[122,123] Similarly, TEE is superior to TTE for detecting an atrial septal aneurysm and patent foramen ovale, although the addition of harmonic imaging to TTE has improved the sensitivity of TTE for detecting a patent foramen ovale.[124-126]

The cardioembolic risk of a patent foramen ovale is related to the defect size, which can be better appreciated by TEE.[127,128] Aortic arch atheroma can be detected by TTE; however, TEE is required to adequately assess the extent, degree of lumen protrusion, and morphological features (i.e., mobility, ulceration, calcification) that characterize the potential embolic risk.[38,129-131]

The indication for performing a TEE in a patient with a suspected cardioembolic event is controversial.[113,132,133] Although TEE has a better sensitivity than TTE for detecting potential cardioembolic sources,[134,135] the yield for identifying a major risk source is limited. An analysis of pooled data suggested an overall detection rate for intracardiac masses of only 4% for TTE and 11% for TEE.[113] The yield was greater in patients with cardiac disease (TTE, 13%; TEE, 19%), but small in patients without cardiac disease (TTE, 0.7%; TEE, 1.6%). Of importance, the identification of minor risk source by TEE may not significantly alter patient management. Therefore, TEE should only be performed if the results have a reasonable chance of altering patient management or therapy. In this regard, TEE likely has the greatest potential impact on management when the TTE fails to identify a cardioembolic source in a patient with (1) unexplained cerebral ischemia before 55 years of age, (2) recurrent events or events in multiple cerebrovascular territories, (3) occlusion of a large peripheral or visceral artery, or (4) suspected endocarditis.

## ATRIAL SEPTAL ABNORMALITIES

Atrial septal defects, atrial septal aneurysms, and patent foramen ovale are identified more frequently by TEE than TTE.[14,124,126] Sinus venosus defects and associated anomalous pulmonary venous drainage are easily detected on TEE, but frequently missed on TTE.[14,15] Therefore, a TEE should be considered in a patient with unexplained right heart dilation despite a negative TTE for intracardiac shunting. (See Chapter 44.) TEE can delineate the morphological details of an atrial septal defect and patent foramen ovale, determine the size of the defect and severity of left-to-right shunting, determine the potential for percutaneous closure, and assist with proper device placement during percutaneous closure.[32,127,128,136,137] The en-face view of the atrial septum using 3D TEE and multiplanar reconstruction provides a better appreciation of the defect (i.e., size, presence of multiple defects, septal rim length) and spatial relationships among the defect, occluding device, and surrounding cardiac structures such as the mitral valve and aortic root.[32,75,138,139]

## CARDIAC TUMORS

The sensitivity of TTE and TEE for detecting atrial myxomas has been reported to be 95% and 100%, respectively.[140] (See Chapter 46.) Similar high sensitivities have been reported when detecting nonmyxomatous intracardiac tumors.[140] However, the sensitivities of TTE and TEE are dependent on tumor size and may be as low as 62% and 77%, respectively, for detecting papillary fibroelastomas smaller than 2 mm.[123] TEE is superior to TTE for characterizing features of an intracardiac tumor that are important for diagnosis and management, such as the involvement of multiple chambers, site of attachment, presence of multiple tumors, infiltration of adjacent structures, and presence of tumor calcification or cyst formation.[122,140] TEE can be used to guide percutaneous biopsy of an intracardiac tumor.[141] 3D TEE may provide incremental information relevant to deciding the optimal surgical approach.[142]

Pericardial or paracardial tumors are better detected using TEE than TTE.[140] TEE appears especially valuable for detecting tumors located at the base of the heart, adjacent to the great vessels, or adjacent to the right heart.[122,140] However, the size and extent of paracardial involvement is not usually well delineated using TTE or TEE. Magnetic resonance imaging and computed tomography have a wider field of view and provide a superior evaluation of extracardiac involvement.

## ACUTE AORTIC SYNDROMES

Aortic dissection can be detected by TEE with a high degree of accuracy and is the diagnostic investigation of choice for suspected aortic dissection in many institutions.[143] (See Chapter 36.) The presence of an intimal flap is diagnostic of aortic dissection and can be distinguished from reverberation artifacts commonly seen in the ascending aorta by using M-mode echocardiography.[144] A small segment of the superior ascending aorta may not be visualized by TEE because of the interposition of the air-filled trachea and bronchus. Multiplane TEE has a sensitivity of 98% to 100% and a specificity of 94% to 95%[145] and can be performed at the bedside of hemodynamically unstable patients. TEE can determine the extent of the dissection and involvement of arch vessels or coronary arteries, differentiate the true and false lumen, identify thrombus within the false lumen, locate the site of the intimal tear, detect signs of rupture, and evaluate for aortic valve involvement and the potential for valve repair.[143,146] TEE can also guide stent graft implantation for descending thoracic aorta dissections and identify complications following surgical repair.[147,148]

Intramural hematoma and penetrating aortic ulcers have a similar presentation to aortic dissection.[149,150] TEE has a sensitivity and specificity that exceed 90% for identifying intramural hematoma[145] and can be performed serially to assess for hematoma regression or progression or the development of classic dissection.[151] The diagnostic accuracy of TEE for detecting penetrating aortic ulcers is unclear; however, one study reported a sensitivity of 83%.[152] The presence, depth, and diameter of a penetrating ulcer are predictive of disease progression and prognosis.[153]

Traumatic aortic rupture and blunt aortic trauma can be diagnosed by TEE with a sensitivity of 63% to 100% and a specificity of 84% to 100%.[130,154] TEE can guide the acute management and triage patients for conservative therapy, immediate surgery, or postponed surgical repair.[155] However, TEE cannot consistently visualize the superior ascending aorta and aortic arch branch vessels, a frequent site of traumatic injury.

## ATRIAL FIBRILLATION

Atrial fibrillation predisposes the LA to contractile dysfunction, chamber dilation, and thrombus formation in approximately 13% of patients with nonrheumatic atrial fibrillation of more than 2 days' duration.[156] TEE is clearly superior to TTE for detecting LA thrombus and has a sensitivity ranging from 93% to 100% and a specificity greater than 95%.[117,118] In addition, LA appendage velocity less than 55 cm/s on TEE identifies patients at increased risk for thrombus formation.[157] The presence of LA thrombus, spontaneous echo contrast, LA appendage velocity below 20 cm/s, or complex aortic atheroma on TEE identifies patients with atrial fibrillation at higher risk of thromboembolism.[38,158]

A TEE-guided strategy can be used in patients with atrial fibrillation of more than 2 days' duration to permit "early" cardioversion without a preceding 3 weeks of therapeutic anticoagulation.[159] (See Chapter 42.) This approach provides a therapeutic option for patients at increased risk of a hemorrhagic complication with anticoagulation therapy or who are not tolerating their atrial fibrillation. In the TEE-guided approach, LA thrombus is ruled out by TEE and followed by "early" cardioversion. The TEE-guided strategy had a similar incidence of embolic events, stroke, or transient ischemic attack, but fewer hemorrhagic events, compared to the conventional management strategy.[159] The costs of the two strategies are similar.[160]

LA appendage velocity may predict the likelihood of maintaining sinus rhythm post cardioversion[41,42]; however, we do not perform TEE studies in patients with atrial fibrillation solely for this purpose.

## CONGENITAL HEART DISEASE

The potential indications for TEE in patients with congenital heart disease are extensive and encompass the preoperative, interventional, intraoperative, and postoperative management of these patients.[161-163] (See Chapters 43-45.) TEE better appreciates abnormalities of the atrial septum and pulmonary veins.[14,15,32,75,137,162] The atrioventricular valves and site of chordal insertion are better visualized using TEE if surgical valvuloplasty is being considered for an atrioventricular canal defect.[164] TEE can better appreciate a baffle stenosis or leak, or complication of a Fontan procedure such as obstruction or thrombosis.[165,166] TEE can characterize outflow tract obstructions[67,162] or abnormalities of the aorta, such as aortic coarctation or a patent ductus arteriosus.[167,168] 3D TEE provides incremental information beyond 2D TEE, including a better delineation of the shape of an intracardiac defect, anatomic position, extent of an atrial rim, and potential presence of multiple or fenestrated defects.[32,139,169,170]

## CORONARY ARTERY DISEASE

Stress echocardiography with TTE imaging is a widely used technique for evaluating patients with suspected or confirmed coronary artery disease, and the addition of a contrast agent can improve the diagnostic accuracy when endocardial definition is limited.[171,172] (See Chapters 15 and 16.) In specific clinical situations, TEE can be used to diagnose coronary artery disease by either (1) visualizing coronary stenoses in the proximal vessels, or (2) detecting stress-induced regional wall motion abnormalities.

The left main coronary artery can be visualized in more than 85% of patients using TEE. The proximal left anterior descending artery and left circumflex artery can also be visualized in most patients. The proximal right coronary artery is more difficult to visualize but may be seen in more than 50% of patients. In patients with visualized vessels, TEE has a sensitivity and specificity of greater than 90% for identifying a significant left main coronary artery stenosis.[173,174] The sensitivity of TEE for detecting significant proximal disease in the left anterior descending artery, left circumflex artery, or right coronary artery is 78% to 100%, 50% to 89%, and 82% to 100%, respectively, but significantly decreases when nonvisualized segments are included in the analysis.[173,174] However, TEE should not replace coronary angiography in the diagnosis of proximal coronary artery disease, but rather should be potentially used when an angiographic stenosis of the left main or left anterior descending artery is of questionable severity and intravascular ultrasound is unavailable.[175]

Stress TEE can be performed using either transesophageal atrial pacing or pharmacologic stimulation with dobutamine or dipyridamole infusion. These techniques are accurate in detecting and risk-stratifying patients with coronary artery disease and can be performed safely in morbidly obese patients.[176-179] However, TEE is an invasive procedure with potential risks and should be reserved for patients with poor TTE images.

Additional applications of TEE include the detection of anomalous coronary arteries, coronary artery aneurysms, and coronary artery fistulas.[173]

## PERICARDIAL DISEASE

Cardiac tamponade can be challenging to diagnose early after cardiac surgery. (See Chapter 29.) Localized compression of a cardiac chamber (usually the RA) may not be apparent on TTE because the thrombus is located posteriorly; image quality is poor because of suboptimal patient positioning, surgical bandages, and drainage tubes; and the findings of RA or RV diastolic collapse are frequently absent. TEE circumvents many of these problems and can better detect extracardiac compression.[180] In constrictive pericarditis, TEE with respiratory monitoring can be helpful in patients with a nondiagnostic TTE.[181,182] Pericardial thickening, pericardial metastases, intrapericardial thrombus, and pericardial cysts are better seen by TEE than TTE.[180,183] However, computed tomography and magnetic resonance imaging are better techniques for evaluating pericardial thickness, pericardial calcification, localized pericardial abnormalities, and tissue characterization of a pericardial mass.[182]

## CRITICALLY ILL PATIENT IN THE INTENSIVE CARE UNIT

TTE image quality in an intensive care unit is frequently inadequate, and in this setting TEE can provide rapid access to diagnostic information that alters patient management.[184,185] TEE can evaluate myocardial function, valve function, volume status, hemodynamics, and intracardiac shunting, which are critical components for the diagnosis and management of patients with unexplained hypotension, pulmonary edema, or hypoxia.[17,18,184-187]

## MONITORING DURING SURGICAL AND INTERVENTIONAL PROCEDURES

A comprehensive intraoperative TEE can evaluate global and segmental LV function; detect intraoperative myocardial ischemia; monitor hemodynamics including cardiac output, LV filling pressures, and volume status; determine the potential cause of hemodynamic disturbances; and evaluate the adequacy of surgical repairs, replacements or reconstructions before leaving the operating room.[188] (See Chapter 2.) The American Society of Anesthesiologists and the Society of Cardiovascular Anesthesiologists recently updated their guidelines on the use of perioperative TEE, recommending that intraoperative TEE be used in all open heart and thoracic aorta surgical procedures and be considered during coronary artery bypass graft surgery.[163] Intraoperative TEE was recommended during noncardiac surgery when the patient has known or suspected cardiovascular pathology that might result in hemodynamic, pulmonary, or neurologic compromise.[163]

TEE is routinely used during percutaneous closure of an atrial septal defect or patent foramen ovale to exclude multiple defects, size the defect, guide positioning of the occluding device, and determine the presence of residual shunting.[137,170] (See Chapter 5.) 3D TEE can provide additional information relevant to the procedure.[32,170] Percutaneous closure of a ventricular septal defect is usually performed under 2D or 3D TEE guidance.[32,170] During percutaneous mitral valvuloplasty, TEE can direct the transseptal puncture, assist with proper balloon placement, evaluate the result, identify any complications, and shorten procedure and fluoroscopy times.[189] For transcatheter aortic valve implantation, TEE can guide proper prosthesis positioning and identify periprocedural complications.[190] During transcatheter closure of a periprosthetic valve leak, TEE can delineate the precise location and extent of any paravalvular jets.[170] 3D TEE can improve spatial appreciation of the regurgitant jets (i.e., number, location, extent), better identify complications, and improve procedural efficiency.[27,33] TEE can assist with the proper positioning of a LA appendage occluding device, which is essential to avoid complications.[32] TEE has also been used to guide catheter ablation of arrhythmias, alcohol septal ablation for hypertrophic cardiomyopathy, and biopsy of the RV or an intracardiac mass.[32,141]

## Contraindications to Transesophageal Echocardiography

There are few absolute contraindications to performing a TEE (Box 1-3); however, relative contraindications are more frequently encountered in clinical practice. Thus, a critical analysis of the risk-benefit ratio is required based on available information and potential discussion with the attending physician.

An elective TEE should be postponed if the patient has not been fasting for 4 to 6 hours before the procedure because of the risk of vomiting and aspiration. However, an urgent TEE can be performed with minimal risk of vomiting and aspiration if only clear fluids were taken up to 2 hours before the procedure.[191] TEE should not be performed in an uncooperative patient who is not heavily sedated or paralyzed to minimize the chance of injury. Patients with a tenuous cardiorespiratory status should be intubated and ventilated to avoid decompensation during the procedure. TEE should not be attempted in a patient with an esophageal obstruction (stricture or mass) because of the potential for esophageal rupture. Upper endoscopy should be considered before performing a TEE if the patient has a history of dysphagia or odynophagia. An esophageal diverticulum is a relative contraindication to TEE because the probe can potentially enter and perforate the diverticulum. Fluoroscopic balloon guidance or a fiberoptic endoscope and overtube can be used to allow a TEE examination in the presence of a Zenker diverticulum.[192] TEE should not be performed in patients with an unrepaired tracheoesophageal fistula, esophagectomy, perforated viscus, or active gastrointestinal bleed. A history of esophageal varices is not an absolute contraindication to TEE; however, the small risk of major bleeding needs to be weighed against the potential for important incremental information. A severe coagulopathy is a relative contraindication to TEE; however, TEE can safely be performed in patients on anticoagulation therapy. Severe cervical arthritis or dislocation of the atlantoaxial joint, where neck flexion is severely limited, is a relative contraindication.

**Box 1-3**

**CONTRAINDICATIONS TO TRANSESOPHAGEAL ECHOCARDIOGRAPHY**

**Absolute**
Uncooperative patient
Severe respiratory depression
Tenuous cardiorespiratory status
Esophageal obstruction (stricture, mass)
Esophagectomy or esophagogastrectomy
Tracheoesophageal fistula
Perforated viscus
Active upper gastrointestinal bleed

**Relative**
Esophageal diverticulum
Esophageal varices
Previous esophageal surgery
History of dysphagia
Recent upper gastrointestinal bleed
Severe cervical arthritis with restricted mobility
Atlantoaxial joint disease with restricted mobility
Severe coagulopathy

## Complications of Transesophageal Echocardiography

TEE is a relatively safe procedure with a low risk of serious complications. In up to 1.9% of TEE studies, the esophagus cannot be successfully intubated.[193] Procedural complications occur in up to 3.5% of patients and predominantly involve the gastrointestinal, cardiovascular, or respiratory systems.[193] The vast majority of complications are minor (Box 1-4), with approximately 0.2% to 0.5% of patients suffering a major complication.[5,9,193,194] TEE-related mortality has been estimated at less than 0.01%.[194] A recent review of 17 studies encompassing 42,355 patients identified four TEE procedural deaths.[193]

**Box 1-4**

**PROCEDURAL COMPLICATIONS WITH TRANSESOPHAGEAL ECHOCARDIOGRAPHY**

**Major Complications**
Death
Esophageal rupture/perforation
Upper gastrointestinal bleed (Mallory-Weiss tear, mucosal laceration/ulceration, etc.)
Laryngospasm or bronchospasm
Congestive heart failure or pulmonary edema
Sustained ventricular tachycardia

**Minor Complications**
Excessive retching or vomiting
Sore throat
Hoarseness
Minor pharyngeal or lip bleeding
Nonsustained or sustained supraventricular tachycardia/atrial fibrillation
Nonsustained ventricular tachycardia
Bradycardia or heart block
Transient hypotension or hypertension
Angina
Transient hypoxia
Tracheal intubation
Dental injury (loose/chipped tooth)

Perforation of the esophagus and major upper gastrointestinal bleeding are serious gastrointestinal complications that occur in up to 0.01% and 0.03% of TEE studies, respectively.[194] Minor gastrointestinal complications include lip and pharyngeal bleeding due to mucosal trauma and excessive retching or vomiting that can require premature termination of the examination.[9] Dental injuries occur in up to 0.03% of patients.[194] A minor sore throat may be present for 24 hours after the procedure. Approximately 0.1% of patients have persistent odynophagia that requires further investigation.[194]

Cardiac complications are rare and include nonsustained and sustained supraventricular tachycardias or atrial fibrillation, nonsustained and sustained ventricular tachycardia, bradycardia, transient hypotension or hypertension, angina pectoris, congestive heart failure, and pulmonary edema.[193,194]

Respiratory complications include laryngospasm (less than 0.02%), accidental tracheal intubation, transient hypoxia, and blood-tinged sputum.[193,194]

Adverse reactions may occur from intravenous sedation or topical anesthesia. Intravenous sedation can cause respiratory depression, hypoxia, hypotension, or paradoxical reactions. Topical anesthesia with benzocaine or lidocaine can cause acute toxic methemoglobinemia, a rare but potentially lethal condition that manifests clinically in approximately 0.115% of TEE studies.[195] In this condition, the topical anesthesia agent oxidizes hemoglobin and prevents oxygen delivery to the tissues, potentially resulting in cyanosis, lethargy, tachycardia, dyspnea, and death.[195-197] Methylene blue administration is indicated if the methemoglobin levels are above 30%, or if the patient has cyanosis, central nervous system depression, or cardiopulmonary compromise.[195]

Intraoperative TEE has a morbidity rate of 0.2% to 1.2%, similar to that reported in the nonoperative setting.[194] The complication rates for TEE in pediatric patients are variable.[194] The largest case series of predominantly intraoperative TEE reported a complication rate of 2.4% (excluding failed intubations).[198]

## KEY POINTS

- TTE and TEE are complementary modalities with distinctly different advantages and limitations for the evaluation of patients with suspected cardiac disease.
- TEE is a relatively safe semi-invasive procedure with a small but definite risk of gastrointestinal, cardiac, and respiratory complications.
- The performance of a TEE requires the echocardiographer to have knowledge of cardiac anatomy and pathology, as well as proficiency in manipulating the transducer imaging plane and ultrasound machine image controls.
- TEE is an essential component of the pre- and perioperative evaluation of the patient being considered for mitral valve repair.
- TEE is a valuable modality to detect and quantify prosthetic mitral valve dysfunction.
- TEE has a high sensitivity and specificity for identifying a vegetation in patients with suspected endocarditis. Alternative diagnoses should be considered if the TEE is negative.
- TEE should only be performed in the patient with a potential cardioembolic event if the results will alter management. The greatest impact of TEE on management resides in the young patient with unexplained cerebral ischemia, recurrent events, or events in multiple vascular distributions.
- TEE can be considered the diagnostic investigation of choice for the diagnosis of thoracic aortic dissection.
- A TEE-guided strategy can be used in patients with atrial fibrillation of more than 2 days' duration to allow "early" cardioversion without a preceding 3 weeks of therapeutic anticoagulation.
- TEE has an integral role in monitoring patients undergoing open heart or aortic surgery and guiding catheter-based intracardiac procedures.
- 3D TEE currently provides important incremental information in the evaluation of patients with mitral valve disease, prosthetic valve regurgitation, atrial septal defects, and congenital heart disease. The applications of 3D TEE will likely continue to expand with technological refinements.

## REFERENCES


1. Frazin L, Talano JV, Stephanides L, et al: Esophageal echocardiography. *Circulation* 54:102-108, 1976.
2. Pearlman AS, Gardin JM, Martin RP, et al: Guidelines for physician training in transesophageal echocardiography: recommendations of the American Society of Echocardiography Committee for physician training in echocardiography. *J Am Soc Echocardiogr* 5:187-194, 1992.
3. Chan K, Burwash I: Unusual structural abnormality in a biplane transesophageal transducer with normal imaging function. *J Am Soc Echocardiogr* 11:310-312, 1998.
4. Kronzon I, Cziner DG, Katz ES, et al: Buckling of the tip of the transesophageal echocardiography probe: a potentially dangerous technical malfunction. *J Am Soc Echocardiogr* 5:176-177, 1992.
5. Chan KL, Cohen GI, Sochowski RA, et al: Complications of transesophageal echocardiography in ambulatory adult patients: analysis of 1500 consecutive examinations. *J Am Soc Echocardiogr* 4:577-582, 1991.
6. Chan K: Impact of transesophageal echocardiography on the management of patients with aortic dissection. *Chest* 101:406-410, 1991.
7. Steckelberg JM, Khandheria BK, Anhalt JP, et al: Prospective evaluation of the risk of bacteremia associated with transesophageal echocardiography. *Circulation* 84:177-180, 1991.
8. Melendez L, Chan K, Cheung P, et al: Incidence of bacteremia in transesophageal echocardiography: a prospective study of 140 consecutive patients. *J Am Coll Cardiol* 18:1650-1654, 1991.
9. Daniel WG, Erbel R, Kasper W, et al: Safety by transesophageal echocardiography: a multicenter survey of 10,419 examinations. *Circulation* 83:817-821, 1991.
10. Cohen G, Chan K: Biplane transesophageal echocardiography: clinical applications of the long-axis plane. *J Am Soc Echocardiogr* 4:155-163, 1991.
11. Seward JB, Khandheria BK, Freeman WK, et al: Multiplane transesophageal echocardiography: image orientation, examination technique, anatomic correlations, and clinical applications. *Mayo Clin Proc* 68:523-551, 1993.
12. Seward JB, Khandheria BK, Oh JK, et al: Transesophageal echocardiography: technique, anatomic correlations, implementation, and clinical applications. *Mayo Clin Proc* 63:649-680, 1988.
13. Veinot JP, Harrity PJ, Gentile F, et al: Anatomy of the normal left atrial appendage: a quantitative study of age-related changes in 500

autopsy hearts. Implications for echocardiographic examination. *Circulation* 96:3112-3115, 1997.
14. Kronzon I, Tunick PA, Freedberg RS, et al: Transesophageal echocardiography is superior to transthoracic echocardiography in the diagnosis of sinus venosus atrial septal defect. *J Am Coll Cardiol* 17:537-542, 1991.
15. Pascoe RD, Oh JK, Warnes CA, et al: Diagnosis of sinus venosus atrial septal defect with transesophageal echocardiography. *Circulation* 94: 1049-1055, 1996.
16. Fagan S, Veinot JP, Chan KL: Residual sinus venosus atrial septal defect following surgical closure of atrial septal defect. *J Am Soc Echocardiogr* 14:738-741, 2001.
17. Wittlich N, Erbel R, Eichler A, et al: Detection of central pulmonary artery thromboemboli by transesophageal echocardiography in patients with severe pulmonary embolism. *J Am Soc Echocardiogr* 5:515-524, 1992.
18. Pruszczyk P, Torbicki A, Pacho R, et al: Noninvasive diagnosis of suspected severe pulmonary embolism: transesophageal echocardiography vs spiral CT. *Chest* 112:722-728, 1997.
19. Shanewise JS, Cheung AT, Aronson S, et al: ASE/SCA guidelines for performing a comprehensive intraoperative multiplane transesophageal echocardiography examination: recommendations of the American Society of Echocardiography Council for Intra-operative Echocardiography and the Society of Cardiovascular Anesthesiologists Task Force for Certification in Perioperative Transesophageal Echocardiography. *J Am Soc Echocardiogr* 12:884-900, 1999.
20. Enriquez-Sarano M, Freeman WK, Tribouilloy CM, et al: Functional anatomy of mitral regurgitation: accuracy and outcome implications of transesophageal echocardiography. *J Am Coll Cardiol* 34:1129-1136, 1999.
21. Pieper EP, Hellemans IM, Hamer HP, et al: Additional value of biplane transesophageal echocardiography in assessing the genesis of mitral regurgitation and the feasibility of valve repair. *Am J Cardiol* 75:489-493, 1995.
22. Blumberg FC, Pfeifer M, Holmer SR, et al: Transgastric Doppler echocardiographic assessment of the severity of aortic stenosis using multiplane transesophageal echocardiography. *Am J Cardiol* 79:1273-1275, 1997.
23. Catoire P, Beydon L, Delaunay L, et al: Persistent left superior vena cava diagnosed by transesophageal echocardiography. *J Cardiothorac Vasc Anesth* 7:375-379, 1993.
24. Seward JB, Khandheria BK, Edwards WD, et al: Biplanar transesophageal echocardiography: anatomic correlations, image orientation, and clinical applications. *Mayo Clin Proc* 65:1193-1213, 1990.
25. Flachskampf FA, Badano L, Daniel WG, et al: European Association of Echocardiography; Echo Committee of the European Association of Cardiothoracic Anaesthesiologists. recommendations for transoesophageal echocardiography: update 2010. *Eur J Echocardiogr* 11:557-576, 2010.
26. Pepi M, Tamborini G, Maltagliati A, et al: Head-to-head comparison of two- and three-dimensional transthoracic and transesophageal echocardiography in the localization of mitral valve prolapse. *J Am Coll Cardiol* 48:2524-2530, 2006.
27. Sugeng L, Shernan SK, Weinert L, et al: Real-time three-dimensional transesophageal echocardiography in valve disease: comparison with surgical findings and evaluation of prosthetic valves. *J Am Soc Echocardiogr* 21:1347-1354, 2008.
28. Saric M, Perk G, Purgess JR, et al: Imaging atrial septal defects by real-time three-dimensional transesophageal echocardiography: step-by-step approach. *J Am Soc Echocardiogr* 23:1128-1135, 2010.
29. García-Fernández MA, Cortés M, García-Robles JA, et al: Utility of real-time three-dimensional transesophageal echocardiography in evaluating the success of percutaneous transcatheter closure of mitral paravalvular leaks. *J Am Soc Echocardiogr* 23:26-32, 2010.
30. Kwak J, Andrawes A, Garvin S, et al: 3D transesophageal echocardiography: a review of recent literature 2007-2009. *Curr Opin Anaesthesiol* 23:80-88, 2010.
31. Vegas A, Meineri M: Three-dimensional transesophageal echocardiography is a major advance for intraoperative clinical management of patients undergoing cardiac surgery: A core review. *Anesth Analg* 110:1548-1573, 2010.
32. Lee AP, Lam Y, Yip GW, et al: Role of real time three-dimensional transesophageal echocardiography in guidance of interventional procedures in cardiology. *Heart* 96:1485-1493, 2010.
33. Skaug TR, Hergum T, Amundsen BH, et al: Quantification of mitral regurgitation using high pulse repetition frequency three-dimensional color Doppler. *J Am Soc Echocardiogr* 23:1-8, 2010.
34. Little SH, Pirat B, Kumar R, et al: Three-dimensional color Doppler echocardiography for direct measurement of vena contracta area in mitral regurgitationin vitro validation and clinical experience. *JACC Cardiovasc Imaging* 1:695-704, 2008.
35. Agmon Y, Khandheria BK, Gentile F, et al: Echocardiographic assessment of the left atrial appendage. *J Am Coll Cardiol* 34:1867-1877, 1999.
36. Donal E, Yamada H, Leclercq C, et al: The left atrial appendage, a small, blind-ended structure: a review of its echocardiographic evaluation and its clinical role. *Chest* 128:1853-1862, 2005.
37. Tabata T, Oki T, Fukuda N, et al: Influence of aging on left atrial appendage flow velocity patterns in normal subjects. *J Am Soc Echocardiogr* 9:274-280, 1996.
38. The Stroke Prevention in Atrial Fibrillation Investigators Committee on Echocardiography: Transesophageal echocardiographic correlates of thromboembolism in high-risk patients with nonvalvular atrial fibrillation. *Ann Intern Med* 128:639-647, 1998.
39. Goldman ME, Pearce LA, Hart RG, et al: Pathophysiologic correlates of thromboembolism in nonvalvular atrial fibrillation: I. Reduced flow velocity in the left atrial appendage (The Stroke Prevention in Atrial Fibrillation [SPAFF-III] study). *J Am Soc Echocardiogr* 12:1080-1087, 1999.
40. Kamalesh M, Copeland TB, Sawada S: Severely reduced left atrial appendage function: A cause of embolic stroke in patients in sinus rhythm? *J Am Soc Echocardiogr* 11:902-904, 1998.
41. Palinkas A, Antonielli E, Picano E, et al: Clinical value of left atrial appendage flow velocity for predicting of cardioversion success in patients with non-valvular atrial fibrillation. *Eur Heart J* 22:2201-2208, 2001.
42. Antonielli E, Pizzuti A, Palinkas A, et al: Clinical value of left atrial appendage flow for prediction of long-term sinus rhythm maintenance in patients with nonvalvular atrial fibrillation. *J Am Coll Cardiol* 39:1443-1449, 2002.
43. Tabata T, Thomas JD, Klein AL: Pulmonary venous flow by Doppler echocardiography: revisited 12 years later. *J Am Coll Cardiol* 41:1243-1250, 2003.
44. Nishimura RA, Tajik AJ: Evaluation of diastolic filling of left ventricle in health and disease: Doppler echocardiography is the clinician's Rosetta stone. *J Am Coll Cardiol* 30:8-18, 1997.
45. Klein AL, Burstow DJ, Tajik AJ, et al: Effects of age on left ventricular dimensions and filling dynamics in 117 normal persons. *Mayo Clin Proc* 69:212-224, 1994.
46. Jensen JL, Williams FE, Beilby BJ, et al: Feasibility of obtaining pulmonary venous flow velocity in cardiac patients using transthoracic pulsed wave Doppler technique. *J Am Soc Echocardiogr* 10:60-66, 1997.
47. Agricola E, Oppizzi M, De Bonis M, et al: Multiplane transesophageal echocardiography performed according to the guidelines of the American Society of Echocardiography in patients with mitral valve prolapse, flail, and endocarditis: diagnostic accuracy in the identification of mitral regurgitant defects by correlation with surgical findings. *J Am Soc Echocardiogr* 16:61-66, 2003.
48. Grewal KS, Malkowski MJ, Kramer CM, et al: Multiplane transesophageal echocardiographic identification of the involved scallop in patients with flail mitral valve leaflet: Intraoperative correlation. *J Am Soc Echocardiogr* 11:966-971, 1998.
49. Omran AS, Woo A, David TE, et al: Intraoperative transesophageal echocardiography accurately predicts mitral valve anatomy and suitability for repair. *J Am Soc Echocardiogr* 15:950-957, 2002.
50. Moursi MH, Bhatnagar SK, Vilacosta I, et al: Transesophageal echocardiographic assessment of papillary muscle rupture. *Circulation* 94:1003-1009, 1996.
51. Salcedo EE, Quaife RA, Seres T, et al : A Framework for systematic characterization of the mitral valve by real-time three-dimensional transesophageal echocardiography. *J Am Soc Echocardiogr* 22:1087-1089, 2009.
52. Zoghbi WA, Enriquez-Sarano M, Foster E, et al: Recommendations for evaluation of the severity of native valvular regurgitation with two-dimensional and Doppler echocardiography. *J Am Soc Echocardiogr* 16:777-802, 2003.
53. Smith MD, Harrison MR, Pinton R, et al: Regurgitant jet size by transesophageal compared with transthoracic Doppler color flow imaging. *Circulation* 83:79-86, 1991.
54. Sugeng L, Spencer KT, Mor-Avi V, et al: Dynamic three-dimensional color flow Doppler: an improved technique for the assessment of mitral regurgitation. *Echocardiography* 20:265-273, 2003.
55. Shanks M, Siebelink HM, Delgado V, et al: Quantitative assessment of mitral regurgitation: comparison between three-dimensional transesophageal echocardiography and magnetic resonance imaging. *Circ Cardiovasc Imaging* 3:694-700, 2010.
56. Hynes MS, Tam JL, Burwash IG, et al: Predictive value of pulmonary venous flow patterns in detecting mitral regurgitation and left ventricular abnormalities. *Can J Cardiol* 15:665-670, 1999.
57. Grayburn PA, Fehske W, Omran H, et al: Multiplane transesophageal echocardiographic assessment of mitral regurgitation by Doppler

color flow mapping of the vena contracta. *Am J Cardiol* 74:912-917, 1994.
58. Pu M, Vandervoort PM, Griffin BP, et al: Quantification of mitral regurgitation by the proximal convergence method using transesophageal echocardiography: Clinical validation of a geometric correction for proximal flow constraint. *Circulation* 92:2169-2177, 1995.
59. Enriquez-Sarano M, Avierinos JF, Messika-Zeitoun D, et al: Quantitative determinants of the outcome of asymptomatic mitral regurgitation. *N Engl J Med* 352:875-883, 2005.
60. Marwick TH, Torelli J, Obarski T, et al: Assessment of the mitral valve splitability score by transthoracic and transesophageal echocardiography. *Am J Cardiol* 68:1106-1107, 1991.
61. Stoddard MF, Prince CR, Tuman WL, et al: Angle of incidence does not affect accuracy of mitral stenosis area calculation by pressure half-time: Application to Doppler transesophageal echocardiography. *Am Heart J* 127:1562-1572, 1994.
62. Degertekin M, Basaran Y, Gencbay M, et al: Validation of flow convergence region method in assessing mitral valve area in the course of transthoracic and transesophageal echocardiographic studies. *Am Heart J* 135:207-214, 1998.
63. Levin TN, Feldman T, Bednarz J, et al: Transesophageal echocardiographic evaluation of mitral valve morphology to predict outcome after balloon mitral valvotomy. *Am J Cardiol* 73:707-710, 1994.
64. Park SH, Kim MA, Hyon MS: The advantages of on-line transesophageal echocardiography guide during percutaneous balloon mitral valvuloplasty. *J Am Soc Echocardiogr* 13:26-34, 2000.
65. Gill EA, Kim MS, Carroll JD: 3D TEE for evaluation of commissural opening before and during percutaneous mitral commissurotomy. *J Am Coll Cardiol Imag* 2:1034-1035, 2009.
66. Eng MH, Salcedo EE, Quaife RA, et al: Implementation of real time three-dimensional transesophageal echocardiography in percutaneous mitral balloon valvuloplasty and structural heart disease interventions. *Echocardiography* 26:958-966, 2009.
67. Essop MR, Skudicky D, Sareli P: Diagnostic value of transesophageal versus transthoracic echocardiography in discrete subaortic stenosis. *Am J Cardiol* 70:962-963, 1992.
68. Hoffmann R, Flachskampf FA, Hanrath P: Planimetry of orifice area in aortic stenosis using multiplane transesophageal echocardiography. *J Am Coll Cardiol* 22:529-534, 1993.
69. Nakai H, Takeuchi M, Yoshitani H, et al: Pitfalls of anatomical aortic valve area measurements using two-dimensional transoesophageal echocardiography and the potential of three-dimensional transoesophageal echocardiography. *Eur J Echocardiogr* 11:369-376, 2010.
70. Cormier B, Iung B, Porte JM, et al: Value of multiplane transesophageal echocardiography in determining aortic valve area in aortic stenosis. *Am J Cardiol* 77:882-885, 1996.
71. Meyerowitz CB, Jacobs LE, Kotler MN, et al: Assessment of aortic regurgitation by transesophageal echocardiography: Correlation with angiographic determination. *Echocardiography* 10:269-278, 1993.
72. Willett DL, Hall SA, Jessen ME, et al: Assessment of aortic regurgitation by transesophageal color Doppler imaging of the vena contracta: validation against an intraoperative aortic flow probe. *J Am Coll Cardiol* 37:1450-1455, 2001.
73. Sato Y, Kawazoe K, Kamata J, et al: Clinical usefulness of the effective regurgitant orifice area determined by transesophageal echocardiography in patients with eccentric aortic regurgitation. *J Heart Valve Dis* 6:580-586, 1997.
74. Sutton DC, Kluger R, Ahmed SU, et al: Flow reversal in the descending aorta: A guide to intraoperative assessment of aortic regurgitation with transesophageal echocardiography. *J Thorac Cardiovasc Surg* 108:576-582, 1994.
75. Sugeng L, Shernan SK, Salgo IS, et al: Live 3-dimensional transesophageal echocardiography initial experience using the fully-sampled matrix array probe. *J Am Coll Cardiol* 52:446-449, 2008.
76. Daniel WG, Mugge A, Grote J, et al: Comparison of transthoracic and transesophageal echocardiography for detection of abnormalities of prosthetic and bioprosthetic valves in the mitral and aortic positions. *Am J Cardiol* 71:210-215, 1993.
77. Daniel LB, Grigg LE, Weisel RD, et al: Comparison of transthoracic and transesophageal assessment of prosthetic valve dysfunction. *Echocardiography* 7:83-95, 1990.
78. Khandheria BK, Seward JB, Oh JK, et al: Value and limitations of transesophageal echocardiography in the assessment of mitral valve prosthesis. *Circulation* 83:1956-1968, 1991.
79. Chaudhry FA, Herrera C, DeFrino PF, et al: Pathologic and angiographic correlations of transesophageal echocardiography in the prosthetic heart valve dysfunction. *Am Heart J* 122:1057-1064, 1991.
80. Karalis DG, Chandrasekaran K, Ross JJ, Jr, et al: Single-plane transesophageal echocardiography for assessing function of mechanical or bioprosthetic valves in the aortic valve position. *Am J Cardiol* 69:1310-1315, 1992.
81. Gueret P, Vignon P, Fournier P, et al: Transesophageal echocardiography for the diagnosis and management of nonobstructive thrombosis of mechanical mitral prosthesis. *Circulation* 91:103-110, 1995.
82. Orsinelli DA, Pearson AC: Detection of prosthetic valve strands by transesophageal echocardiography: Clinical significance in patients with suspected cardiac source of embolism. *J Am Coll Cardiol* 26:1713-1718, 1995.
83. Muratori M, Montorsi P, Teruzzi G, et al: Feasibility and diagnostic accuracy of quantitative assessment of mechanical prostheses leaflet motion by transthoracic and transesophageal echocardiography in suspected prosthetic valve dysfunction. *Am J Cardiol* 97:94-100, 2006.
84. Barbetseas J, Nagueh SF, Pitsavos C, et al: Differentiating thrombus from pannus formation in obstructed mechanical prosthetic valves: An evaluation of clinical, transthoracic and transesophageal echocardiographic parameters. *J Am Coll Cardiol* 32:1410-1417, 1998.
85. Girard SE, Miller FA, Orszulak TA, et al: Reoperation for prosthetic aortic valve obstruction in the era of echocardiography: trends in diagnostic testing and comparison with surgical findings. *J Am Coll Cardiol* 37:579-584, 2001.
86. Lengyl M: Management of prosthetic valve thrombosis. *J Heart Valve Dis* 13:329-334, 2004.
87. Tong AT, Roudaut R, Ozkan M, et al: Transesophageal echocardiography improves risk assessment of thrombolysis of prosthetic valve thrombosis: results of the international PRO-TEE registry. *J Am Coll Cardiol* 43:77-84, 2004.
88. Tenenbaum A, Fisman EZ, Vered Z, et al: Failure of transesophageal echocardiography to visualize a large mitral prosthesis vegetation detected solely by transthoracic echocardiography. *J Am Soc Echocardiogr* 8:944-946, 1995.
89. Flachskampf FA, Hoffmann R, Franke A, et al: Does multiplane transesophageal echocardiography improve the assessment of prosthetic valve regurgitation? *J Am Soc Echocardiogr* 8:70-78, 1995.
90. Gorscan J III, Kenny WM, Diana P, et al: Transesophageal continuous-wave Doppler to evaluate mitral prosthetic stenosis. *Am Heart J* 121:911-914, 1991.
91. Baddour LM, Wilson WR, Bayer AS, et al: Infective endocarditis: diagnosis, antimicrobial therapy, and management of complications: a statement for healthcare professionals from the Committee on Rheumatic Fever, Endocarditis, and Kawasaki Disease, Council on Cardiovascular Disease in the Young, and the Councils on Clinical Cardiology, Stroke, and Cardiovascular Surgery and Anesthesia, American Heart Association—executive summary: endorsed by the Infectious Diseases Society of America. *Circulation* 111:3167-3184, 2005.
92. Birmingham GD, Rahko PS, Ballantyne F: Improved detection of infective endocarditis with transesophageal echocardiography. *Am Heart J* 123:774-781, 1992.
93. Erbel R, Rohmann S, Drexler M, et al: Improved diagnostic value of echocardiography in patients with infective endocarditis by transesophageal approach: A prospective study. *Eur Heart J* 9:43-53, 1988.
94. Taams MA, Gussenhoven EJ, Bos E, et al: Enhanced morphologic diagnosis in infective endocarditis by transoesophageal echocardiography. *Br Heart J* 63:109-113, 1990.
95. Shively BK, Gurule FT, Roldan CA, et al: Diagnostic value of transesophageal compared with transthoracic echocardiography in infective endocarditis. *J Am Coll Cardiol* 18:391-397, 1991.
96. Mügge A, Daniel WG, Frank G, et al: Echocardiography in infective endocarditis: Reassessment of prognostic implications of vegetation size determined by the transthoracic and the transesophageal approach. *J Am Coll Cardiol* 14:631-638, 1989.
97. Shapiro SM, Young E, De Guzman S, et al: Transesophageal echocardiography in diagnosis of infective endocarditis. *Chest* 105:377-382, 1994.
98. Ramadan FB, Beanlands DS, Burwash IG: Isolated pulmonic valve endocarditis in healthy hearts: a case report and review of the literature. *Can J Cardiol* 16:1282-1288, 2000.
99. San Roman JA, Vilacosta I, Zamorano JL, et al: Transesophageal echocardiography in right-sided endocarditis. *J Am Coll Cardiol* 21:1226-1230, 1993.
100. Zabalgoitia M, Herrera CJ, Chaudhry FA, et al: Improvement in the diagnosis of bioprosthetic valve dysfunction by transesophageal echocardiography. *J Heart Valve Dis* 2:595-603, 1993.
101. Lowry RW, Zoghbi WA, Baker WB, et al: Clinical impact of transesophageal echocardiography in the diagnosis and management of infective endocarditis. *Am J Cardiol* 73:1089-1091, 1994.
102. Roe MT, Abramson MA, Li J, Heinle SK, et al: Clinical information determines the impact of transesophageal echocardiography on the diagnosis of infective endocarditis by the Duke criteria. *Am Heart J* 139:945-951, 2000.

103. Lindner JR, Case RA, Dent JM, et al: Diagnostic value of echocardiography in suspected endocarditis: An evaluation based on the pretest probability of disease. *Circulation* 93:730-736, 1996.
104. Sochowski RA, Chan KL: Implication of negative results on a monoplane transesophageal echocardiographic study in patients with suspected infective endocarditis. *J Am Coll Cardiol* 21:216-221, 1994.
105. Daniel WG, Mugge A, Martin RP, et al: Improvement in the diagnosis of abscesses associated with endocarditis by transesophageal echocardiography. *N Engl J Med* 324:795-800, 1991.
106. de Castro S, Cartoni D, d'Amati G, et al: Diagnostic accuracy of transthoracic and multiplane transesophageal echocardiography for valvular perforation in acute infective endocarditis: Correlation with anatomic findings. *Clin Infect Dis* 30:825-826, 2000.
107. Tingleff J, Egeblad H, Gotzsche CO, et al: Perivalvular cavities in endocarditis: Abscesses versus pseudoaneurysms? A transesophageal Doppler echocardiographic study in 118 patients with endocarditis. *Am Heart J* 130:93-100, 1995.
108. Hill EE, Herijgers P, Claus P, et al: Abscess in infective endocarditis: the value of transesophageal echocardiography and outcome: a 5-year study. *Am Heart J* 154:923-928, 2007.
109. Di Salvo G, Habib G, Pergola V et al: Echocardiography predicts embolic events in infective endocarditis. *J Am Coll Cardiol* 37:1069-1076, 2001.
110. Thuny F, Di Salvo G, Belliard O, et al: Risk of embolism and death in infective endocarditis: prognostic value of echocardiography: a prospective multicenter study. *Circulation* 112:69-75, 2005.
111. Rohmann S, Erhel R, Darius H, et al: Effect of antibiotic treatment on vegetation size and complication rate in infective endocarditis. *Clin Cardiol* 20:132-140, 1997.
112. Ferro JM: Cardioembolic stroke: an update. *Lancet Neurol* 2:177-188, 2003.
113. Kapral MK, Silver FL, with the Canadian Task Force on Preventive Health Care: Preventive health care, 1999 update: 2. Echocardiography for the detection of a cardiac source of embolus in patients with stroke. *Can Med Assoc J* 161:989-996, 1999.
114. Ay H, Furie KL, Singhal A, et al: An evidence-based causative classification system for acute ischemic stroke. *Ann Neurol* 58:688-697, 2005.
115. Overell JR, Bone I, Lees KR: Interatrial septal abnormalities and stroke: a meta-analysis of case-control studies. *Neurology* 55:1172-1179, 2000.
116. Pepi M, Evangelista A, Nihoyannopoulos P, et al: Recommendations for echocardiography use in the diagnosis and management of cardiac sources of embolism. *Eur J Echocardiogr* 11: 461-476, 2010.
117. Hwang JJ, Chen JJ, Lin SC, et al: Diagnostic accuracy of transesophageal echocardiography for detecting left atrial thrombi in patients with rheumatic heart disease having undergone mitral valve operations. *Am J Cardiol* 72:677-681, 1993.
118. Manning WJ, Weintraub RM, Wakomonski CA, et al: Accuracy of transesophageal echocardiography for identifying left atrial thrombi. A prospective intraoperative study. *Ann Intern Med* 123:817-822, 1995.
119. Senior R, Becher H, Monaghan M, et al: Contrast echocardiography: evidence-based recommendations by European Association of Echocardiography. *Eur J Echocardiogr* 10:194-212, 2009.
120. Mugge A, Daniel WG, Haverich A, et al: Diagnosis of noninfective cardiac mass lesions by two-dimensional echocardiography: Comparison of the transthoracic and transesophageal approaches. *Circulation* 83:70-78, 1991.
121. Chen C, Koschyk D, Hamm C, et al: Usefulness of transesophageal echocardiography in identifying small left ventricular apical thrombus. *J Am Coll Cardiol* 21:208-215, 1993.
122. Mügge A, Daniel WG, Haverich A, et al: Diagnoses of noninfective cardiac mass lesions by two-dimensional echocardiography: Comparison of the transthoracic and transesophageal approaches. *Circulation* 83:70-78, 1991.
123. Sun JP, Asher CR, Yang XS, et al: Clinical and echocardiographic characteristics of papillary fibroelastomas. A retrospective and prospective study in 162 patients. *Circulation* 103:2687-2693, 2001.
124. Siostrzonek P, Zangeneh M, Gössinger H, et al: Comparison of transesophageal and transthoracic contrast echocardiography for detection of a patent foramen ovale. *Am J Cardiol* 68:1247-1249, 1991.
125. Clarke NR, Timperley J, Kelion AD, et al: Transthoracic echocardiography using second harmonic imaging with Valsalva manoeuvre for the detection of right to left shunts. *Eur J Echocardiogr* 5:176-181, 2004.
126. Mugge A, Daniel WG, Angermann C, et al: Atrial septal aneurysm in adult patients: A multicenter study using transthoracic and transesophageal echocardiography. *Circulation* 91:2785-2792, 1995.
127. Hausmann D, Mügge A, Daniel WG: Identification of patent foramen ovale permitting paradoxical embolism. *J Am Coll Cardiol* 26:1030-1038, 1995.
128. Schuchlenz HW, Weihs W, Horner S, et al: The association between the diameter of a patent foramen ovale and the risk of embolic cerebrovascular events. *Am J Med* 109:456-462, 2000.
129. Tunick PA, Kronzon I: Atheromas of the thoracic aorta: Clinical and therapeutic update. *J Am Coll Cardiol* 35:545-554, 2000.
130. Willens HJ, Kessler KM: Transesophageal echocardiography in the diagnosis of diseases of the thoracic aorta: Part II—atherosclerotic and traumatic diseases of the aorta. *Chest* 117:233-243, 2000.
131. Di Tullio MR, Sacco RL, Savoia MT, et al: Aortic atheroma morphology and the risk of ischemic stroke in a multiethnic population. *Am Heart J* 139:329-336, 2000.
132. Warner MF, Momah KI: Routine transesophageal echocardiography for cerebral ischemia: is it really necessary? *Arch Intern Med* 156:1719-1723, 1996.
133. McNamara RL, Lima JA, Whelton PK, et al: Echocardiographic identification of cardiovascular sources of emboli to guide clinical management of stroke: a cost-effective analysis. *Ann Intern Med* 127:775-787, 1997.
134. Pearson AC, Labovitz AJ, Tatineni S, et al: Superiority of transesophageal echocardiography in detecting cardiac source of embolism in patients with cerebral ischemia of uncertain etiology. *J Am Coll Cardiol* 17:66-72, 1991.
135. Labovitz AJ for the STEPS Investigators: Transesophageal echocardiography and unexplained cerebral ischemia: A multicenter follow-up study. *Am Heart J* 137:1082-1087, 1999.
136. Rittoo D, Sutherland GR, Shaw TR: Quantification of left-to-right shunting and defect size after balloon mitral commissurotomy using biplane transesophageal echocardiography, color flow Doppler mapping, and the principle of proximal flow convergence. *Circulation* 87:1591-1603, 1993.
137. Ewert P, Berger F, Daehnert I, et al: Transcatheter closure of atrial septal defects without fluoroscopy: Feasibility of a new method. *Circulation* 101:847-849, 2000.
138. Martin-Reyes R, Lopez-Fernandez T, Moreno-Yanguela M, et al: Role of real-time three-dimensional transoesophageal echocardiography for guiding transcatheter patent foramen ovale closure. *Eur J Echocardiogr* 10:148-150, 2009.
139. Taniguchi M, Akagi T, Watanabe N, et al: Application of real-time three-dimensional transesophageal echocardiography using a matrix array probe for transcatheter closure of atrial septal defect. *J Am Soc Echocardiogr* 22:1114-1120, 2009.
140. Engberding R, Daniel WG, Erbel R, et al: Diagnosis of heart tumours by transoesophageal echocardiography: A multicentre study in 154 patients. *Eur Heart J* 14:1223-1228, 1993.
141. Beaver TA, Robb JF, Teufel EJ, et al: Right ventricular outflow tract obstruction in an older woman: Facilitated diagnosis with transesophageal echocardiography-guided biopsy. *J Am Soc Echocardiogr* 13:622-625, 2000.
142. Müller S, Feuchtner G, Bonatti J, et al: Value of transesophageal 3D echocardiography as an adjunct to conventional 2D imaging in preoperative evaluation of cardiac masses. *Echocardiography* 25:624-631, 2008.
143. Nienaber CA, Eagle KA: Aortic dissection: new frontiers in diagnosis and management: Part I: from etiology to diagnostic strategies. *Circulation* 108:628-635, 2003.
144. Vignon P, Spencer KT, Rambaud G, et al: Differential transesophageal echocardiographic diagnosis between linear artifacts and intraluminal flap of aortic dissection or disruption. *Chest* 119:1778-1790, 2001.
145. Willens HJ, Kessler KM: Transesophageal echocardiography in the diagnosis of diseases of the thoracic aorta: Part I—aortic dissection, aortic intramural hematoma, and penetrating atherosclerotic ulcer of the aorta. *Chest* 116:1772-1779, 2000.
146. Movsowitz HD, Levine RA, Hilgenberg AD, et al: Transesophageal echocardiographic description of the mechanisms of aortic regurgitation in acute type A aortic dissection: Implications for aortic valve repair. *J Am Coll Cardiol* 36:884-890, 2000.
147. Rocchi G, Lofiego C, Biagini E, et al: Transesophageal echocardiography-guided algorithm for stent-graft implantation in aortic dissection. *J Vasc Surg* 40:880-885, 2004.
148. Masani ND, Banning AP, Jones RA, et al: Follow-up of chronic thoracic aortic dissection: Comparison of transesophageal echocardiography and magnetic resonance imaging. *Am Heart J* 131:1156-1163, 1996.
149. Evangelista A, Mukherjee D, Mehta RH, et al: Acute intramural hematoma of the aorta: a mystery in evolution. *Circulation* 111:1063-1070, 2005.
150. Tsai TT, Nienaber CA, Eagle KA: Acute aortic syndromes. *Circulation* 112;3802-3813, 2005.
151. Kaji S, Akasaka T, Katayama M, et al: Long-term prognosis of patients with type B aortic intramural hematoma. *Circulation* 108(Suppl 1):II307-II311, 2003.

152. Vilacosta I, San Roman JA, Aragoncillo P, et al: Penetrating atherosclerotic aortic ulcer: Documentation by transesophageal echocardiography. *J Am Coll Cardiol* 32:83-89, 1998.
153. Ganaha F, Miller DC, Sugimoto K, et al: Prognosis of aortic intramural hematoma with and without penetrating atherosclerotic ulcer: a clinical and radiological analysis. *Circulation* 106:342-348, 2002.
154. Goarin JP, Cluzel P, Gosgnach M, et al: Evaluation of transesophageal echocardiography for diagnosis of traumatic aortic injury. *Anesthesiology* 93:1373-1377, 2000.
155. Vignon P, Martaille JF, Francois B, et al: Transesophageal echocardiography and therapeutic management of patients sustaining blunt aortic injuries. *J Trauma* 58:1150-1158, 2005.
156. Weigner MJ, Thomas LR, Patel U, et al : Early cardioversion of atrial fibrillation facilitated by transesophageal echocardiography: short-term safety and impact on maintenance of sinus rhythm at 1 year. *Am J Med* 110:694-702, 2001.
157. Handke M, Harloff A, Hetzel A, et al: Left atrial appendage flow velocity as a quantitative surrogate parameter for thromboembolic risk: determinants and relationship to spontaneous echocontrast and thrombus formation—a transesophageal echocardiographic study in 500 patients with cerebral ischemia. *J Am Soc Echocardiogr* 18:1366-1372, 2005.
158. Zabalgoitia M, Halperin JL, Pearce LA, et al: Transesophageal echocardiographic correlates of clinical risk of thromboembolism in nonvalvular atrial fibrillation. Stroke Prevention in Atrial Fibrillation III Investigators. *J Am Coll Cardiol* 31:1622-1626, 1998.
159. Klein AL, Grimm RA, Murray RD, et al: Use of transesophageal echocardiography to guide cardioversion in patients with atrial fibrillation. *N Engl J Med* 344:1411-1420, 2001.
160. Klein AL, Murray RD, Becker ER, et al: Economic analysis of a transesophageal echocardiography-guided approach to cardioversion of patients with atrial fibrillation: the ACUTE economic data at eight weeks. *J Am Coll Cardiol* 43:1217-1224, 2004.
161. Ayres NA, Miller-Hance W, Fyfe DA, et al: Indications and guidelines for performance of transesophageal echocardiography in the patient with pediatric acquired or congenital heart disease: report from the task force of the Pediatric Council of the American Society of Echocardiography. *J Am Soc Echocardiogr* 18:91-98, 2005.
162. Warnes CA, Williams RG, Bashore TM, et al: ACC/AHA 2008 guidelines for the management of adults with congenital heart disease: a report of the American College of Cardiology/American Heart Association Task Force on Practice Guidelines (Writing Committee to Develop Guidelines on the Management of Adults With Congenital Heart Disease). Developed in collaboration with the American Society of Echocardiography, Heart Rhythm Society, International Society for Adult Congenital Heart Disease, Society for Cardiovascular Angiography and Interventions, and Society of Thoracic Surgeons. *J Am Coll Cardiol* 52:e1-121, 2008.
163. Thys DM, Abel MD, Brooker RF, et al: Practice guidelines for perioperative transoesophageal echocardiography: An updated report by the American Society of Anesthesiologists and the Society of Cardiovascular Anesthesiologists Task Force on Transesophageal Echocardiography. *Anesthesiology* 112:1084-1096, 2010.
164. Sreeram N, Stumper OF, Kaulitz R, et al: Comparative value of transthoracic and transesophageal echocardiography in the assessment of congenital abnormalities of the atrioventricular junction. *J Am Coll Cardiol* 16:1205-1214, 1990.
165. Kaulitz R, Stümper OFW, Geuskens R, et al: Comparative values of the precordial and transesophageal approaches in the echocardiographic evaluation of atrial baffle function after an atrial correction procedure. *Am J Coll Cardiol* 16:686-694, 1990.
166. Stümper O, Sutherland GR, Geuskens R, et al: Transesophageal echocardiography in evaluation and management after a Fontan procedure. *J Am Coll Cardiol* 17:1152-1160, 1991.
167. Engvall J, Sjoqvist L, Nylander E, et al: Biplane transoesophageal echocardiography, transthoracic Doppler, and magnetic resonance imaging in the assessment of coarctation of the aorta. *Eur Heart J* 10:1399-1409, 1995.
168. Andrade A, Vargas-Barron J, Rijlaarsdam M, et al: Utility of transesophageal echocardiography in the examination of adult patients with patent ductus arteriosus. *Am Heart J* 130:543-546, 1995.
169. Baker GH, Shirali G, Ringewald JM, et al: Usefulness of live three-dimensional transesophageal echocardiography in a congenital heart disease center. *Am J Cardiol* 103:1025-1028, 2009.
170. Hudson PA, Eng MH, Kim MS, et al: A comparison of echocardiographic modalities to guide structural heart disease interventions. *J Interv Cardiol* 21:535-546, 2008.
171. Olszewski R, Timperley J, Szmigielski C, et al: The clinical applications of contrast echocardiography. *Eur J Echocardiogr.* 8:S13-S23, 2007.
172. Sicari R, Nihoyannopoulos P, Evangelista A, et al: Stress echocardiography expert consensus statement: European Association of Echocardiography (EAE) (a registered branch of the ESC). *Eur J Echocardiogr* 9:415-437, 2008.
173. Youn HJ, Foster E: Transesophageal echocardiography (TEE) in the evaluation of the coronary arteries. *Cardiol Clin* 18:833-848, 2000.
174. Biederman RW, Sorrell VL, Nanda NC, et al: Transesophageal echocardiographic assessment of coronary stenosis: a decade of experience. *Echocardiography* 18:49-57, 2001.
175. Firstenberg MS, Greenberg NL, Lin SS, et al: Transesophageal echocardiography assessment of severe ostial left main coronary stenosis. *J Am Soc Echocardiogr* 13:696-698, 2000.
176. Noguchi Y, Nagata-Kobayashi S, Stahl JE, et al: A meta-analytic comparison of echocardiographic stressors. *Int J Cardiovasc Imaging* 21:189-207, 2005.
177. Legault S, Sénéchal M, Bergeron S, et al: Usefulness of an accelerated transoesophageal stress echocardiography in the preoperative evaluation of high risk severely obese subjects awaiting bariatric surgery. *Cardiovasc Ultrasound* 8:30, 2010.
178. Siddiqui TS, Stoddard MF: Safety of dobutamine stress transesophageal echocardiography in obese patients for evaluation of potential ischemic heart disease. *Echocardiography* 21:603-608, 2004.
179. Kamalesh M, Matorin R, Sawada S, et al: Comparative prognostic significance of transesophageal versus transthoracic stress echocardiography. *Echocardiography* 19:313-318, 2002.
180. Hutchison SJ, Smalling RG, Albornoz M, et al: Comparison of transthoracic and transesophageal echocardiography in clinically overt or suspected pericardial heart disease. *Am J Cardiol* 74:962-965, 1994.
181. Klein AL, Cohen GI, Pietrolungo JF, et al: Differentiation of constrictive pericarditis from restrictive cardiomyopathy by Doppler transesophageal echocardiographic measurements of respiratory variations in pulmonary venous flow. *J Am Coll Cardiol* 22:1935-1943, 1993.
182. Verhaert D, Gabriel RS, Johnston D, et al: The role of multimodality imaging in the management of pericardial disease. *Circ Cardiovasc Imaging* 3:333-343, 2010.
183. Ling LH, Oh JK, Tei C, et al: Pericardial thickness measured with transesophageal echocardiography: Feasibility and potential clinical usefulness. *J Am Coll Cardiol* 29:1317-1323, 1997.
184. Vignon P: Hemodynamic assessment of critically ill patients using echocardiography Doppler. *Curr Opin Crit Care* 11:227-234, 2005.
185. Porembka DT: Importance of transesophageal echocardiography in the critically ill and injured patient. *Crit Care Med* 35(Suppl 8):S414-S430, 2007.
186. Heidenreich PA, Stainback RF, Redberg RF, et al: Transesophageal echocardiography predicts mortality in critically ill patients with unexplained hypotension. *J Am Coll Cardiol* 26:152-158, 1995.
187. Hoole SP, Falter F: Evaluation of hypoxemic patients with transesophageal echocardiography. *Crit Care Med* 35(Suppl 8):S408-S413, 2007.
188. Oxorn DC: Intraoperative echocardiography. *Heart* 94:1236-1243, 2008.
189. Park SH, Kim MA, Hyon MS: The advantages of on-line transesophageal echocardiography guide during percutaneous balloon mitral valvuloplasty. *J Am Soc Echocardiogr* 13:26-34, 2000.
190. Jayasuriya C, Moss RR, Munt B: Transcatheter aortic valve implantation in aortic stenosis: the role of echocardiography. *J Am Soc Echocardiogr* 24:15-27, 2011.
191. Greenfield SM, Webster GJ, Brar AS, et al: Assessment of residual gastric volume and thirst in patients who drink before gastroscopy. *Gut* 39:360-362, 1996.
192. Fergus I, Bennett ES, Rogers DM et al: Fluoroscopic balloon-guided transesophageal echocardiography in a patient with Zenker's diverticulum. *J Am Soc Echocardiogr* 17:483-486, 2004.
193. Côté G, Denault A: Transesophageal echocardiography-related complications. *Can J Anaesth* 55:622-647, 2008.
194. Hilberath JN, Oakes DA, Shernan SK , et al: Safety of transesophageal echocardiography. *J Am Soc Echocardiogr* 23:1115-1127, 2010.
195. Novaro GM, Aronow HD, Militello MA et al: Benzocaine-induced methemoglobinemia: experience from a high-volume transesophageal echocardiography laboratory. *J Am Soc Echocardiogr* 16:170-175, 2003.
196. Moore TJ, Walsh CS, Cohen MR et al: Reported adverse event cases of methemoglobinemia associated with benzocaine products. *Arch Intern Med* 164:1192-1196, 2004.
197. BheemReddy S, Messineo F, Roychoudhury D: Methemoglobinemia following transesophageal echocardiography: a case report and review. *Echocardiography* 23:319-321, 2006.
198. Stevenson JG: Incidence of complications in pediatric transesophageal echocardiography: experience in 1650 cases. *J Am Soc Echocardiogr* 12:527-532, 1999.



# 2 Monitoring Ventricular Function in the Operating Room: Impact on Clinical Outcome

DONALD C. OXORN, MD

**Evaluation of Intraoperative Ventricular Function**
Left Ventricular Filling
Global Systolic Function
Regional Wall Motion
**Use of Transesophageal Echocardiography to Monitor Intraoperative Cardiac Function in Specific Clinical Entities**
Separation from Cardiopulmonary Bypass
Off-Pump Coronary Bypass Surgery
Cardiac Function in Noncardiac Surgery
Positioning of Intravascular Devices
Transplant Surgery
**Alternate Techniques**
Epicardial/Epiaortic Echocardiography
**Transesophageal Echocardiography as a Monitor of Intraoperative Ventricular Function: Impact on Postoperative Outcomes and Cost-Effectiveness**

In this chapter, the focus is on the use of transesophageal echocardiography (TEE) in the assessment of cardiac function in the setting of both cardiac and noncardiac surgery. In addition, the impact intraoperative TEE has had on the quality of perioperative care is discussed. Intraoperative assessments of valvular function, chamber size, masses, and great vessels are covered in other sections of the book. The milieu of the operating room is unique and is not always conducive to obtaining TEE images of high quality. Dim the lights in the room as much as possible to avoid the necessity for "overgaining." Try to get the important parts of the study completed before the surgical incision is made. Set the loop cycle to a time-based rather than a beat-based mode, as this will prevent premature looping when electrocautery is used. The TEE probe is placed under general anesthesia so that the patient is not able to complain if insertion is too forceful; this makes the understanding of the difficulties of probe insertion and manipulation especially important (Figs. 2-1, 2-2, and 2-3).

## Evaluation of Intraoperative Ventricular Function

### LEFT VENTRICULAR FILLING

Using TEE, the clinician can assess left ventricular filling with Doppler estimation of left atrial (LA) pressure, and two-dimensional (2D) measurement of left ventricular (LV) cross-sectional area, calculation of LV volume, and assessment of diastolic function.

#### *Left Atrial Pressure*

LA pressure can be estimated with Doppler TEE by several methods. If mitral regurgitation is present, measurement of the peak velocity of the regurgitant jet and application of the modified Bernoulli equation allows calculation of the left ventricular to atrial pressure gradient; in the absence of aortic stenosis, subtraction of this number from the peak systolic blood pressure yields LA pressure. Certain mitral inflow and pulmonary venous variables also correlate with LA pressure; in patients undergoing cardiovascular surgery, Kuecherer and colleagues[1] found that changes in the systolic fraction of the pulmonary venous tracing correlated inversely and strongly with pulmonary capillary wedge pressure and theorized that this related to decreased atrial compliance. Nomura and associates[2] found that in patients with ejection fractions less than 35%, the deceleration time of the early velocity of mitral inflow correlated with pulmonary capillary wedge pressure and that a deceleration time greater than 150 msec was strongly predictive of a pulmonary capillary wedge pressure of less than 10 mm Hg. Arguing that the aforementioned Doppler parameters were overly influenced by loading conditions, Kinnaird and colleagues[3] proposed that examining the deceleration slope of the diastolic component of pulmonary venous flow allowed the left atrium to be treated as a receiving chamber in its own right and showed that this deceleration time was inversely correlated with LA pressure. The ratio of early to atrial LV diastolic filling velocity (E/A ratio) has also been used to predict fluid responsiveness in cardiac surgical patients. Patients with higher E/A ratios tended to have a more rightward position on the diastolic pressure volume curve (Fig. 2-4) and thereby were less likely to increase their cardiac output with an infusion of colloid.[4]

There are a number of caveats related to the intraoperative estimation of LA pressure with TEE. Patients with a rhythm other than sinus or with valvular regurgitation were excluded in most studies; these are the patients in whom preload estimates are often crucial. In suitable patients, correlations but not absolute values of LA pressure are usually yielded. Use of the mitral regurgitation jet to calculate LA pressure dictates that mitral regurgitation must be present. Finally, an estimate of LA pressure, whether obtained by Doppler echocardiography or by

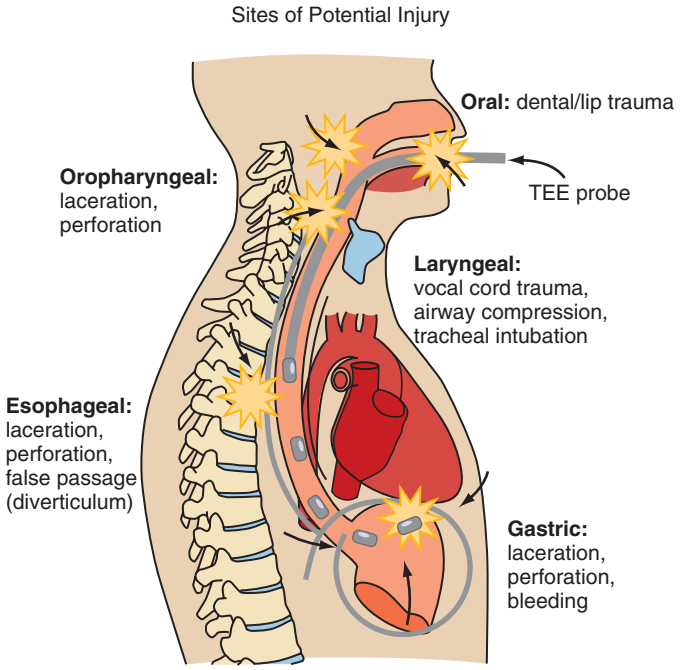



**Figure 2-1** Sites of potential injury with TEE probe placement. *(From Hilberath JN, Oakes DA, Shernan SK, et al: Safety of transesophageal echocardiography.* J Am Soc Echocardiogr *23:1115-1127, 2010.)*

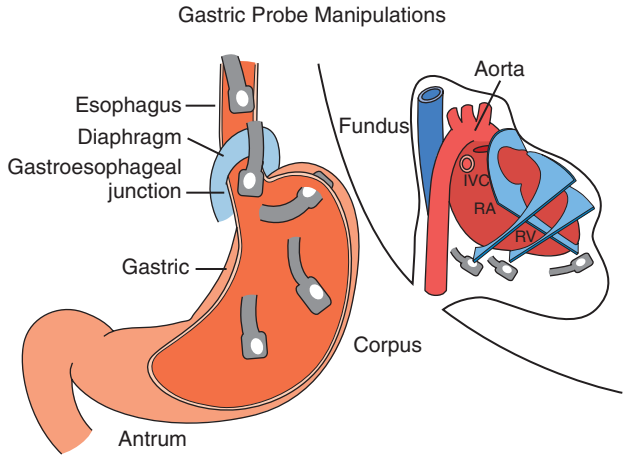



**Figure 2-3 Gastric probe manipulations.** Gastric injury typically occurs in the gastric fundus during deep transgastric probe manipulation, especially when requiring extreme anteflexion to bring the probe inline and in contact with the apex of the heart (e.g., deep transgastric aortic outflow view). The gastroesophageal junction is a vulnerable zone because probe manipulation at this level may place the relatively fixed tissues under considerable tension. *(From Hilberath JN, Oakes DA, Shernan SK, et al: Safety of transesophageal echocardiography.* J Am Soc Echocardiogr *23:1115-1127, 2010.)*

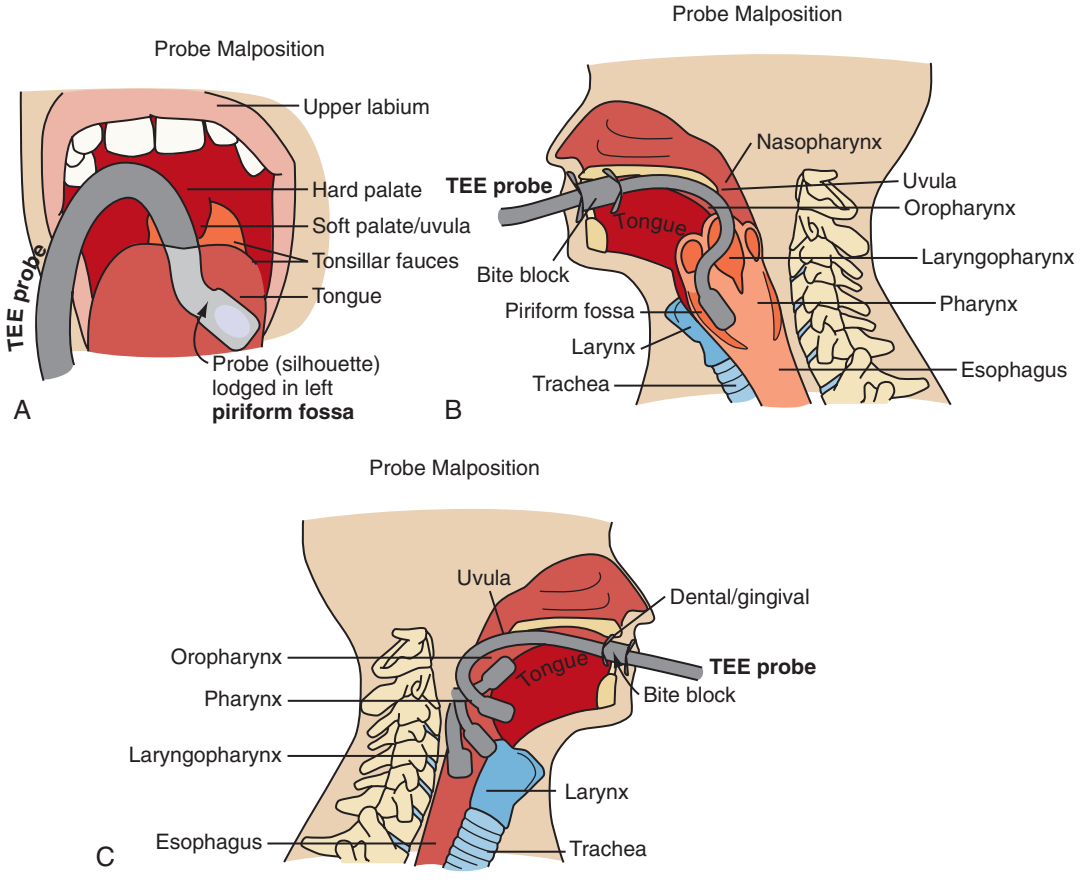



**Figure 2-2 Probe malposition. A** and **B,** Difficulty during probe insertion can be encountered if the TEE probe is lodged into one of the pyriform sinuses. **C,** In addition to causing mucosal injury to the oropharynx, the TEE probe can occasionally become distorted in extreme flexion. Attempts to withdraw a TEE probe in this configuration before advancing into the stomach and unfolding the kink can lead to severe esophageal injury. *(From Hilberath JN, Oakes DA, Shernan SK, et al: Safety of transesophageal echocardiography.* J Am Soc Echocardiogr *23:1115-1127, 2010.)*

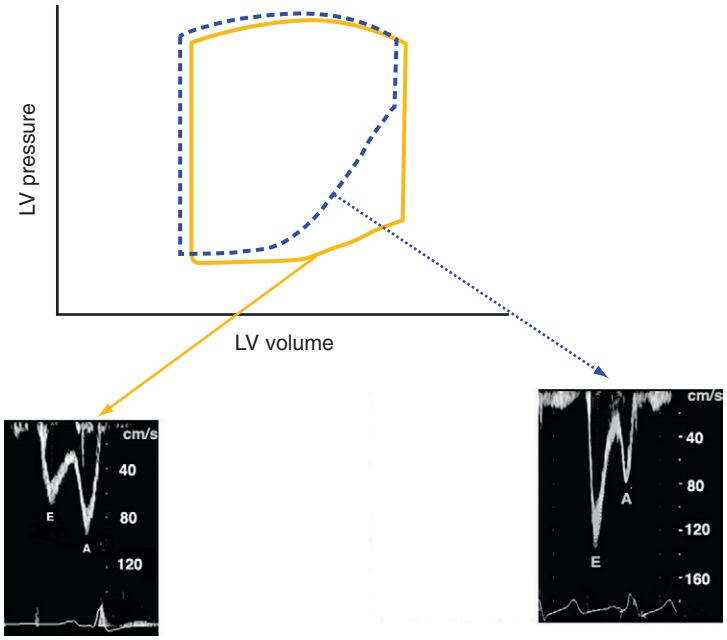



**Figure 2-4 Schematic representation of the pressure/volume relationship of the left ventricle.** Measurement of the E/A (E and A waves of the transmitral flow) ratio gives information on the position of the diastolic pressure/volume curve of the left ventricle. Lower ratios suggest a leftward position on this curve, and higher ratios, a rightward position, in which left ventricle compliance is reduced. Patients with low E/A ratios are more likely to increase cardiac output after volume infusion than patients with high E/A ratios.

pulmonary artery catheter, may still yield inaccurate estimates of preload in patients with decreased ventricular compliance[5]; this is the case in many patients following cardiopulmonary bypass.[6]

Measurements of LA size and volume by TEE are underestimates of the values obtained by transthoracic echocardiography (TEE)[7] but are most accurate when obtained using Simpson's biplane technique.[7]

### *Left Ventricular Diastolic Function*

In patients with impaired diastolic function, LV filling in the period following separation from cardiopulmonary bypass is especially tenuous as both systolic and diastolic function are further reduced.[8-10] In addition to the standard parameters of mitral inflow and pulmonary venous flow velocities, newer techniques may be used to better define problems with ventricular filling.

Tissue Doppler imaging of the mitral annulus has been proposed as a descriptor of LV relaxation that is less affected by changes in loading conditions and ventricular function than more traditional Doppler parameters.[11] The E′ velocity relates directly to LV relaxation; thus this parameter has been used to correct for LV relaxation and render the E wave of mitral inflow more accurate in the estimation of LV filling pressure (E/E′ ratio). There is a paucity of data, however, regarding the usefulness of tissue Doppler of the mitral annulus in the intraoperative setting. Many factors other than LA pressure influence the E/E′ ratio,[12] and in reality many of these conditions are present in the intraoperative population, limiting the usefulness of this parameter.

Color M-mode flow propagation velocity is another less load-dependent measure of diastolic function and is attractive in that it examines simultaneous pulsed-wave (PW) Doppler measurements throughout the LV cavity (Fig. 2-5). Djaiani[13] has shown that in patients undergoing coronary artery bypass graft, a value less than 50 cm/sec identifies abnormal diastolic function.

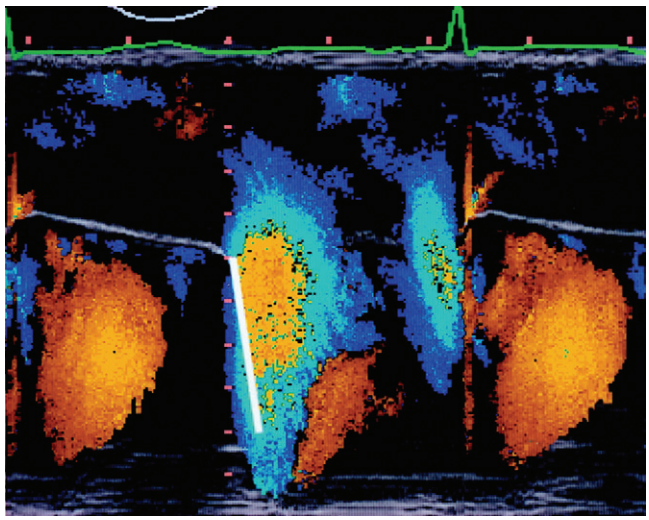


**Figure 2-5** Color M-mode propagation velocity shown as the slope of the first aliasing velocity during early filling of the ventricle. *(From Djaiani GN, McCreath BJ, Ti LK, et al: Mitral flow propagation velocity identifies patients with abnormal diastolic function during coronary artery bypass graft surgery.* Anesth Analg *95:524-530, 2002.)*

### *End-Diastolic Area and End-Systolic Area*

The American Society of Echocardiography's guidelines and standards committee have published recommendations for chamber quantification by both TTE and TEE. The normal ranges for dimension and volume are comparable between the two techniques.[14]

A number of authors have examined the intraoperative relationship between end-diastolic area or end-systolic area measured at the transgastric midpapillary level and cardiac volume status. In a classic paper, Cheung and associates[15] performed an elegant study examining the effect of graded hypovolemia produced by autologous blood collection on hemodynamic- and TEE-derived indices of LV preload in patients undergoing

coronary artery bypass surgery. Patients with valvular insufficiency, rhythms other than sinus, and overt congestive heart failure were excluded. End-diastolic area, end-systolic area, pulmonary capillary wedge pressure, and measures of end-diastolic and end-systolic wall stress decreased linearly as blood volume was reduced by 0% to 15% in all patients; however, in patients with impaired LV function, only the TEE-derived indices maintained linearity. As the authors acknowledge, estimation of ventricular volume in the patient with asymmetric ventricular dysfunction may be problematic, because hypokinetic or akinetic areas may not be represented in the area of the 2D cut.

It must also be remembered that the presence of a small end-diastolic area or end-systolic area does not always reflect decreased intravascular volume. Small LV volumes can be seen with restrictions to filling, as in pericardial disease, or decreased right-sided heart function (Fig. 2-6), for example, owing to right ventricular (RV) infarction or a large pulmonary embolus. Other causes of a small LV volume include increased inotropy or redistribution of blood out of the thoracic cavity.

### *Left Ventricular Volumes*

The generally accepted method for volume measurement is the biplane method of disks (Simpson's rule). Smith and colleagues[16] found that measurement of LV volume was underestimated by TEE when compared to ventriculography and attributed this to underestimation of ventricular length; more recent studies using multiplane probes[17] have shown that volumetric data obtained by TTE and TEE show minor or no differences. Notwithstanding its accuracy, this technique is rarely used in the intraoperative setting because of the high frequency and rapidity of hemodynamic shifts.

The use of real-time three-dimensional (3D) TEE in the operating room has increased dramatically. Although real-time 3D TTE assessment of LV volume has shown promise, this experience has not been replicated with real-time 3D TEE[18] and cannot be recommended for routine use in the operating room.

### *Conclusion*

The assessment of preload with intraoperative TEE is in most cases a semiquantitative estimate based on visual inspection of end-diastolic area and end-systolic area and supported by an array of Doppler indices. Confounding conditions, such as RV failure, vasodilation, or the administration of inotropic agents, must be considered.

## GLOBAL SYSTOLIC FUNCTION

### *Cardiac Output*

Doppler TEE has the potential to be used in the intraoperative setting for the continuous measurement of cardiac output. These methods use the concept that the cross-sectional area of a conduit within the cardiovascular system multiplied by the Doppler-derived time-velocity integral yields the stroke volume through that conduit. When the result is multiplied by heart rate, the product is cardiac output.

Several important assumptions are inherent to this approach. Valid area formulas must be applicable to the anatomic site being analyzed. The velocity profile across the valve must be flat and devoid of skew.[19,20] Whichever anatomic area is chosen, the ability to consistently obtain the image and to interrogate parallel to flow is mandatory.

### Transesophageal Doppler Technology

With this technique, Doppler data is obtained and used to calculate hemodynamic parameters in a fashion similar to the techniques described later.[21] Because no 2D imaging is used, the probe is considerably smaller than a standard TEE probe, can be placed orally or nasally, and can be left in for longer periods of time. The probe is placed in the esophagus in order to measure velocities in the descending thoracic aorta. A number of assumptions are inherent in the technique, and they may be violated in the intraoperative setting; these include the diameter of the aorta at the point of Doppler interrogation, the presence of a flat velocity profile, and the angle of insonation. Perhaps most importantly, the technique assumes that the amount of blood flowing in the descending aorta as a fraction of total cardiac output is constant. This may be a reasonable assumption in clinically static situations[22]; however, in the dynamic environment of cardiac surgery, this may not be the case.[23] At the present time, trending of hemodynamic variables appears possible, although reliance on esophageal Doppler for the absolute determination of hemodynamic variables does not appear to be justified.[24]

### Left Ventricular Outflow Tract

This Doppler technique has been extensively studied and found to be extremely accurate when applied to a group of patients before and after cardiopulmonary bypass.[25] With the probe in the stomach, turned leftward, in the flexed position, and at low imaging frequency, the aortic valve and LV outflow tract can

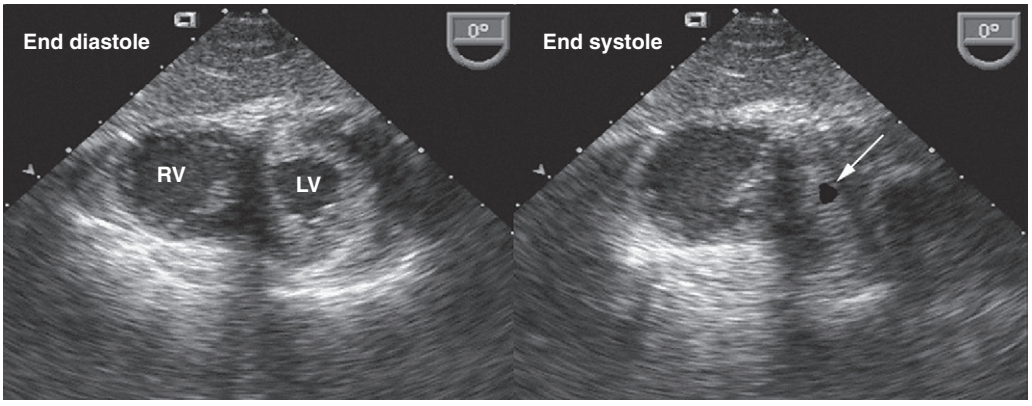



**Figure 2-6** Transgastric image of a transesophageal echocardiography scan obtained in a patient with pulmonary hypertension secondary to cystic fibrosis. Although the end-systolic area of the left ventricle is exceedingly small (*arrow*), this was secondary to right-sided heart failure and not absolute hypovolemia.

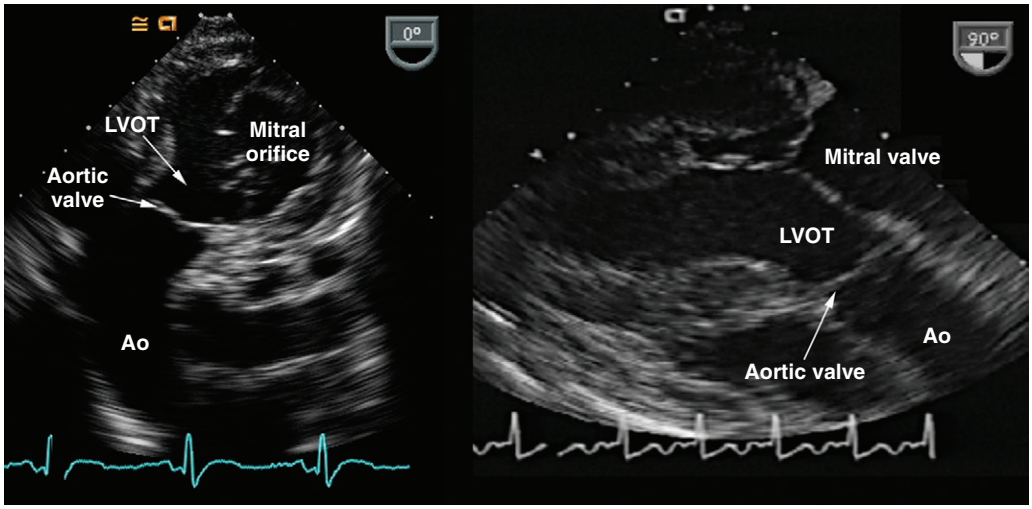



**Figure 2-7** Transesophageal echocardiography imaging from the stomach allows parallel alignment with the ascending aorta (*Ao*). *Left* panel, the deep transgastric long-axis view; *right* panel, the transgastric long-axis view. *LVOT*, Left ventricular outflow tract.

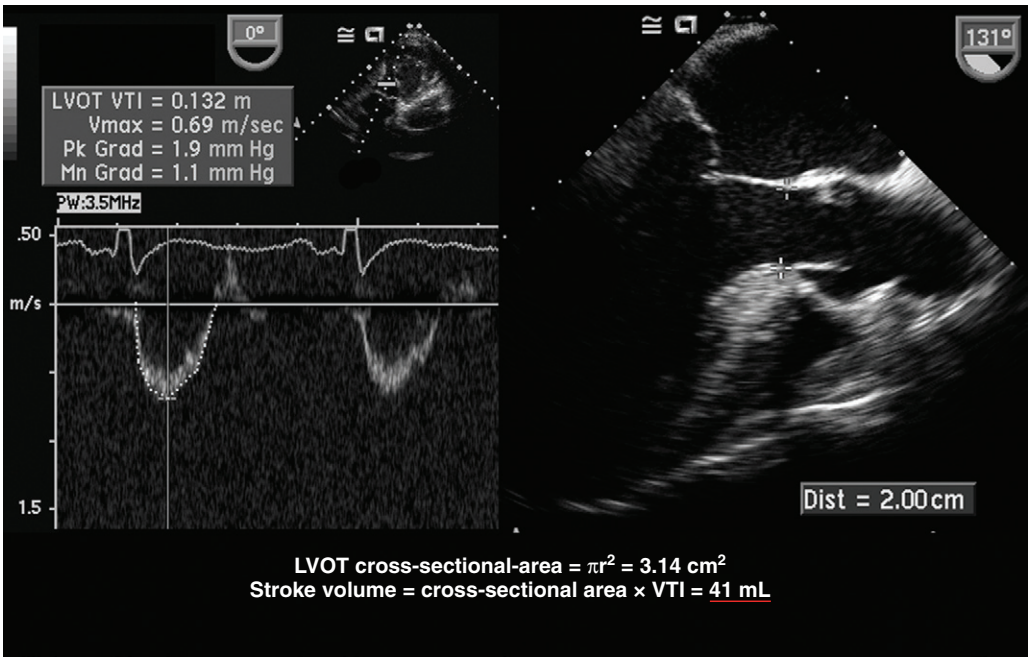



**Figure 2-8** Transgastric imaging of the left ventricular outflow tract (*LVOT*). The ascending aorta is well visualized, and the Doppler intercept angle is small. Pulsed-Doppler velocity time integral and diameter measurement (obtained in a mide sophageal long axis) are used to calculate stroke volume. *Mn Grad*, Mean gradient; *Pk Grad*, peak gradient; *Vmax*, maximum velocity; *VTI*, velocity time integral.

usually be imaged between 0° and 140° (Fig. 2-7). Imaging from the stomach allows parallel pulsed-Doppler interrogation of the LV outflow tract; its diameter can be obtained from either the stomach or the midesophageal long-axis view. Calculation of the cross-sectional area and cardiac output follow the standard formula (Fig. 2-8). To avoid contamination of the Doppler signal by the region of flow acceleration adjacent to the aortic valve orifice, the sample volume must be placed precisely in the LV outflow tract. In the presence of outflow tract obstruction, the validity of the measurement may be compromised.

### Pulmonary Artery

With the probe at 0° and retroflexed, the main pulmonary artery and pulmonic valve can be imaged at the base of the heart (Fig. 2-9). In a study by Gorcsan and colleagues[26] using both PW and continuous-wave (CW) methodologies, pulmonary artery diameter was measured just distal to the pulmonic valve. Interobserver variability was low in all studies, and correlation with thermodilution was strong. Alternatively, the main pulmonary artery may be imaged at 60° to 90° using the aortic arch as a window (Fig. 2-10).

### Right Ventricular Outflow Tract

From the transgastric approach, the probe is turned rightward and flexed to image the RV outflow tract at a rotation angle between 0° and 120°. Imaging frequency must usually be reduced to ensure optimal penetration. Maslow and colleagues[27] found excellent correlation between cardiac output calculated with PW Doppler and thermodilution. Patients with pulmonary hypertension, significant tricuspid

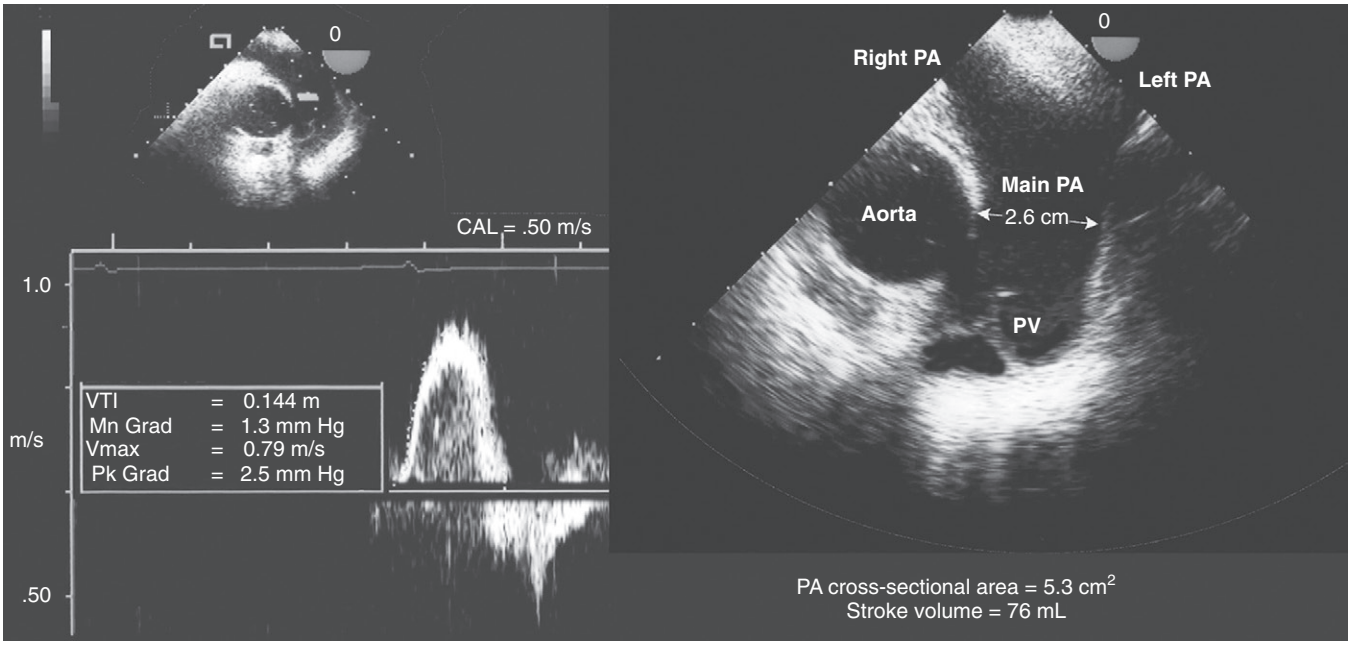



**Figure 2-9** Imaging at the base of the heart of the main pulmonary artery (*PA*) and its branches. Pulsed-Doppler velocity time integral (VTI) and diameter measurement are used to calculate stroke volume. *Mn Grad*, Mean gradient; *Pk Grad*, peak gradient; *PV*, pulmonary valve; *Vmax*, maximum velocity.

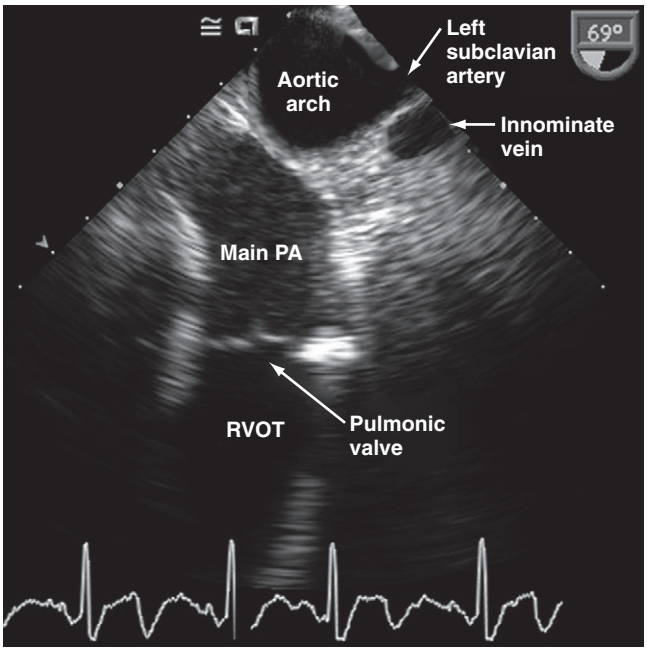



**Figure 2-10** Using the aortic arch as a window, the high esophageal aortic arch short-axis view is obtained. The main pulmonary artery (*PA*), pulmonic valve, left subclavian artery, and innominate vein are seen. This view is suitable for Doppler interrogation. *RVOT*, Right ventricular outflow tract.

regurgitation, and nonsinus rhythms were excluded. In a significant percentage (16%) of patients, the 2D image was not suitable.

## Mitral Valve

Using the mitral valve for calculation of cardiac output has the advantages of consistent imaging and parallel Doppler alignment. However, the saddle shape of the mitral annulus makes the area measurement unpredictable, and the cross-sectional velocity skew is of concern when using PW Doppler.

## Practical Considerations

For intraoperative transesophageal Doppler calculation of cardiac output, the LV outflow tract method is the most reproducible. Adjustments in the degree of probe flexion and imaging angle should be made to ensure that the aortic valve and ascending aorta are clearly visualized and that the Doppler intercept angle is small (see Fig. 2-8). Several measurements should be made and averaged, this being especially important when dealing with rhythms other than sinus. In practical terms, Doppler measurement of cardiac output is used when a pulmonary artery catheter is not in place or when conditions, such as severe tricuspid regurgitation, render thermodilution inaccurate. When right- and left-sided outputs are obtained simultaneously, shunt fraction may be calculated. There is a need for further validation of this approach in patients with a spectrum of cardiovascular diseases.

### *Ejection Fraction and Stroke Volume*

Although it is somewhat load dependent and therefore not a pure index of "contractility," ejection fraction is often assumed to reflect ventricular contractility. During intraoperative TEE, the fractional area of change measured at the transgastric midpapillary level is often used interchangeably with ejection fraction, although gauging volume in a potentially asymmetric chamber based on a measure of area has obvious limitations. In an elegant study, Royse and colleagues[28] demonstrated that fractional area of change when corrected for afterload was closely related to preload recruitable stroke work, a relatively load-independent measure of contractility. $dP/dT$ was more load dependent and less reliable. The patient group was quite diverse in terms of overall ventricular function. As mentioned previously, the most common and generally accepted method for volume measurement is the biplane method of disks, Simpson's rule (Fig. 2-11).

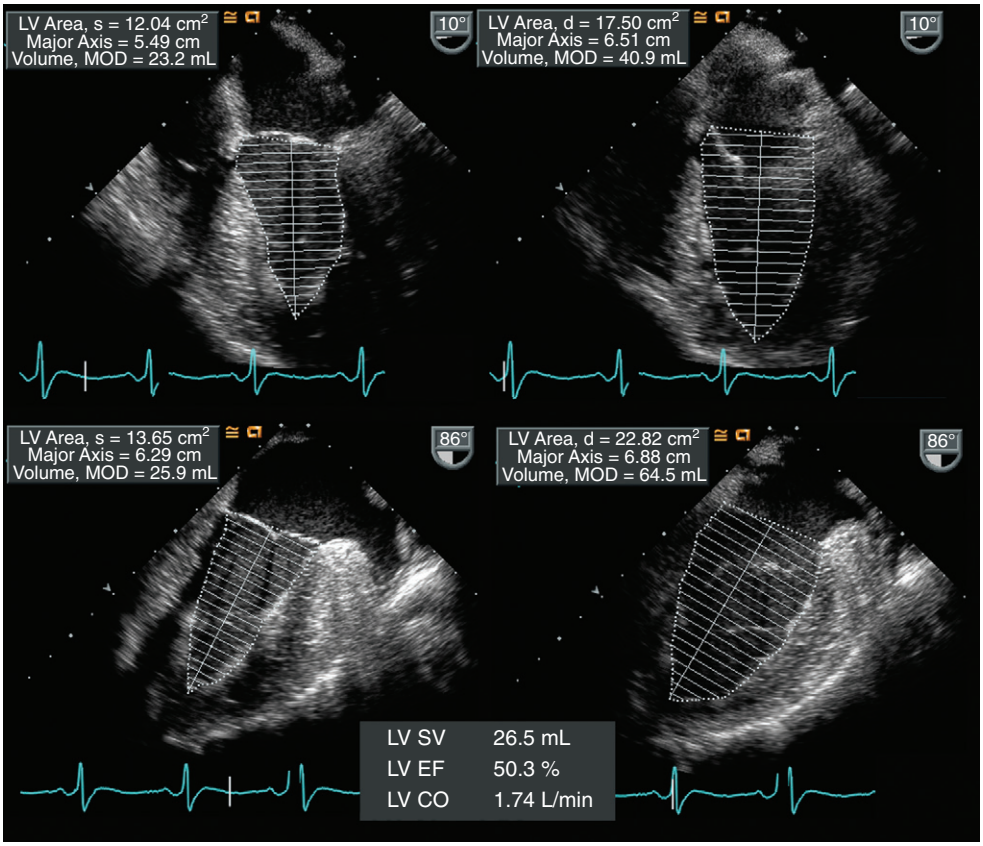



**Figure 2-11** Measurements of systolic (*s*, left) and diastolic (*d*, right) area made in the four-chamber (*upper* panels) and two-chamber (*lower* panels) views are used to obtain volumetric data by the method of disks (*MOD*). From these measurements, stroke volume (*SV*), ejection fraction (*EF*), and cardiac output (*CO*) can be calculated.

Practically, intraoperative ejection fraction is still most often visually estimated or is measured by single plane fractional area change. Concern remains that fractional area change underestimates ejection fraction in patients in whom hypokinetic areas are not represented in the measurement. The use of TEE-derived volumetric data to estimate ejection fraction is more accurate, though manual tracing is tedious; however, software that comes with many TEE machines allows rapid calculation. Real-time 3D TEE, although seemingly attractive, does not at present have a routine place in the intraoperative assessment of ventricular volumes and ejection fraction.

### *Contractility*

Ejection fraction and myocardial thickening, although largely affected by contractility, are not independent of the influence of loading conditions. The end-systolic pressure-volume relationship and resultant end-systolic elastance defines contractility in a load-independent fashion as described in the classic paper by Sagawa.[29] At present, however, the methods for intraoperative data analysis that involve a number of surrogates for invasive measurements are prohibitively complex.

## *Other Indices of Left Ventricular Function*

### Tissue Doppler Imaging

The use of tissue Doppler imaging in the assessment of diastolic function has already been described. Systolic myocardial velocity at the lateral mitral annulus is a measure of longitudinal systolic function that correlates with ejection fraction.[30] One of the major limitations of this technique is that lack of movement of myocardial tissue secondary to tethering is not readily distinguished from hypokinesis owing to ischemia. In order to circumvent this issue, the use of strain and strain rate imaging has been extensively studied and is discussed in several excellent reviews.[31,32] (See Chapter 10.) In essence, strain rate represents the local rate of myocardial deformation and is estimated by spatial velocity gradients obtained by tissue Doppler imaging. Because Doppler is used, the angle of insonation is a limitation; however, strain rate may also be measured by the Doppler-independent technique of speckle tracking.[31] By acquiring high-quality 2D echo images and identifying unique acoustic markers in the image to track specific areas of myocardium over time, strain rate can be calculated.

Simmons and colleagues[32] showed the feasibility of using TEE to obtain radial and longitudinal LV wall velocities; there was consistency between TTE and TEE measurements, and regional reduction in S′ correlated with decreased regional wall motion. Skarvan and colleagues[33] used tissue Doppler imaging of the anterior wall as a complement to visual assessment of systolic wall thickening.

More recently, several authors have done feasibility studies of intraoperative strain analysis using both tissue Doppler imaging[34] and speckle tracking[35] (Fig. 2-12). Intraoperative strain analysis shows promise for the analysis of global and regional systolic function.

### *dP/dt*

The rate of pressure rise at the onset of ventricular contraction (*dP/dt*) is a load-dependent index of systolic performance. Measurement of dP/dt using CW Doppler of the mitral regurgitation jet has been validated against measurements in the cardiac

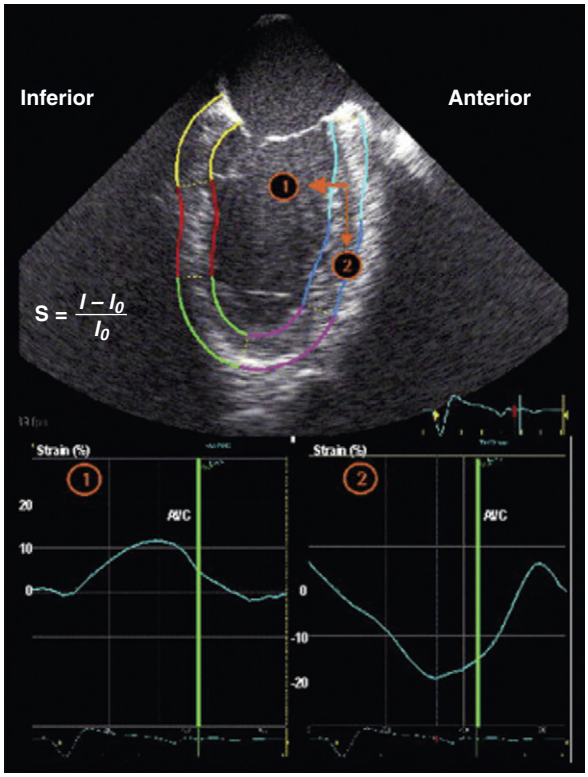



**Figure 2-12** *Top:* Midesophageal two-chamber view of the LV with the anterior (*right*) and inferior wall (*left*). The different colors indicate the separation into, from top to bottom, basal, mid, and apical segments. *Bottom*: Radial (*1*) and longitudinal (*2*) strain from the anterobasal segment in this view. *AVC*, Aortic valve closure; *l*, instantaneous length; $l_0$, original length; *S*, strain. *(From Kukucka M, Nasseri B, Tscherkaschin A, et al: The feasibility of speckle tracking for intraoperative assessment of regional myocardial function by transesophageal echocardiography.* J Cardiothorac Vasc Anesth *23:462-467, 2009.)*

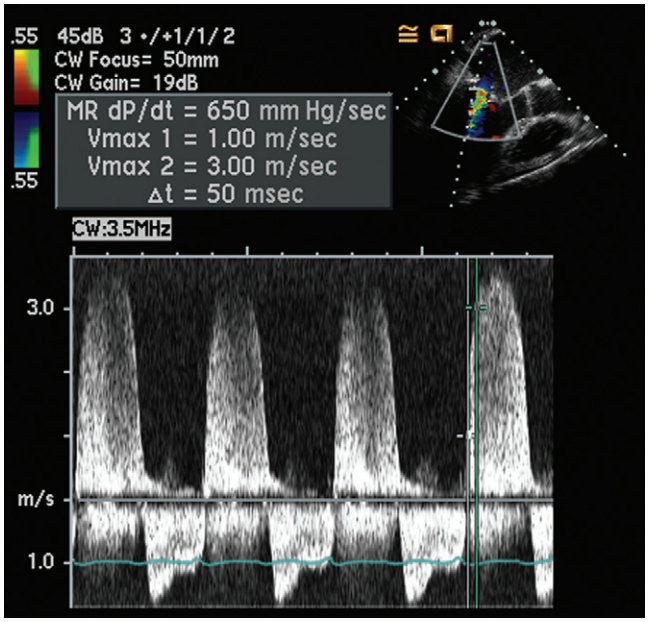



**Figure 2-13** Measurement of *dP/dt* is taken from the mitral regurgitation jet obtained by CW Doppler. The duration of time required for the velocity to increase from 1 to 3 m/sec (or the pressure to rise from 4 to 36 mm Hg) is measured. *MR*, Mitral regurgitation; *Vmax*, maximum velocity.

catheterization laboratory.[36] The time in seconds required for an increase of the pressure gradient from 4 to 36 mm Hg (or an increase of velocity from 1 to 3 m/sec) is divided by the pressure difference of 32 mm Hg for calculation of dP/dt. Normal values are 800 to 1200 mm Hg/sec (Fig. 2-13).[37] The presence of mitral stenosis contraindicates the technique. It has not been adequately tested in the intraoperative environment.

### *Right Ventricular Function*

In the setting of cardiopulmonary bypass, the evaluation of RV function is important. RV dysfunction often occurs secondary to the inadequate delivery of cardioplegia[38] and to the embolization of intracardiac air down the right coronary artery following separation from cardiopulmonary bypass (Fig. 2-14). The triangular shape of the right ventricle makes its global function hard to quantitate with TEE, although the modified method of disks has been used in offline analysis in the setting of coronary bypass grafting.[39] The abnormal septal motion often seen following cardiopulmonary bypass makes analysis more difficult. Standards for the measurement of RV volumes with TEE have been published.[14]

Tricuspid annular velocity measurement by tissue Doppler imaging has been used to quantitate RV function, with excursions less than 1.5 cm associated with poor prognosis in a variety of cardiovascular diseases.[40] The technique is feasible during cardiac surgery using modified transgastric imaging.[40]

Right ventricular speckle tracking was shown to be feasible in the operating room[41] and compared well with other indices such as tricuspid annular plane systolic excursion and fractional area of change. The technology is complex and at present is still in evolution.

TEE assessment of intraoperative RV function is best accomplished by visual inspection and semiquantitative assessment in both the transgastric and the four-chamber views.

## REGIONAL WALL MOTION

The link between perioperative myocardial ischemia and cardiac morbidity[42] has led to an intensive search for accurate methods of its intraoperative detection (Fig. 2-15). Visual inspection of the electrocardiogram for ST segment changes has been the foundation on which the newer technologies of automated ST analysis and TEE detection of regional wall motion abnormalities have been added. There are several points on which to judge the merits of TEE: applicability, accuracy, reproducibility, cost, expertise required for interpretation, and prognostic importance.

Segmental analysis is most frequently undertaken using the 16-segment model first proposed by Schiller and colleagues[43] and later modified for TEE by Shanewise and co-workers.[44] In 2002, a 17th segment, the apical cap, was added.

The recognition that coronary occlusion leads to the immediate development of regional wall motion abnormalities[45] and their frequent regression following revascularization[44] has prompted investigators to examine the usefulness of intraoperative TEE as a monitor of ischemia. The paucity of contraindications to TEE means that it can be used in most patients undergoing general anesthesia. The midpapillary view is generally easy to obtain and demonstrates areas of myocardium subtended by the three major coronary arteries. Interpretation is

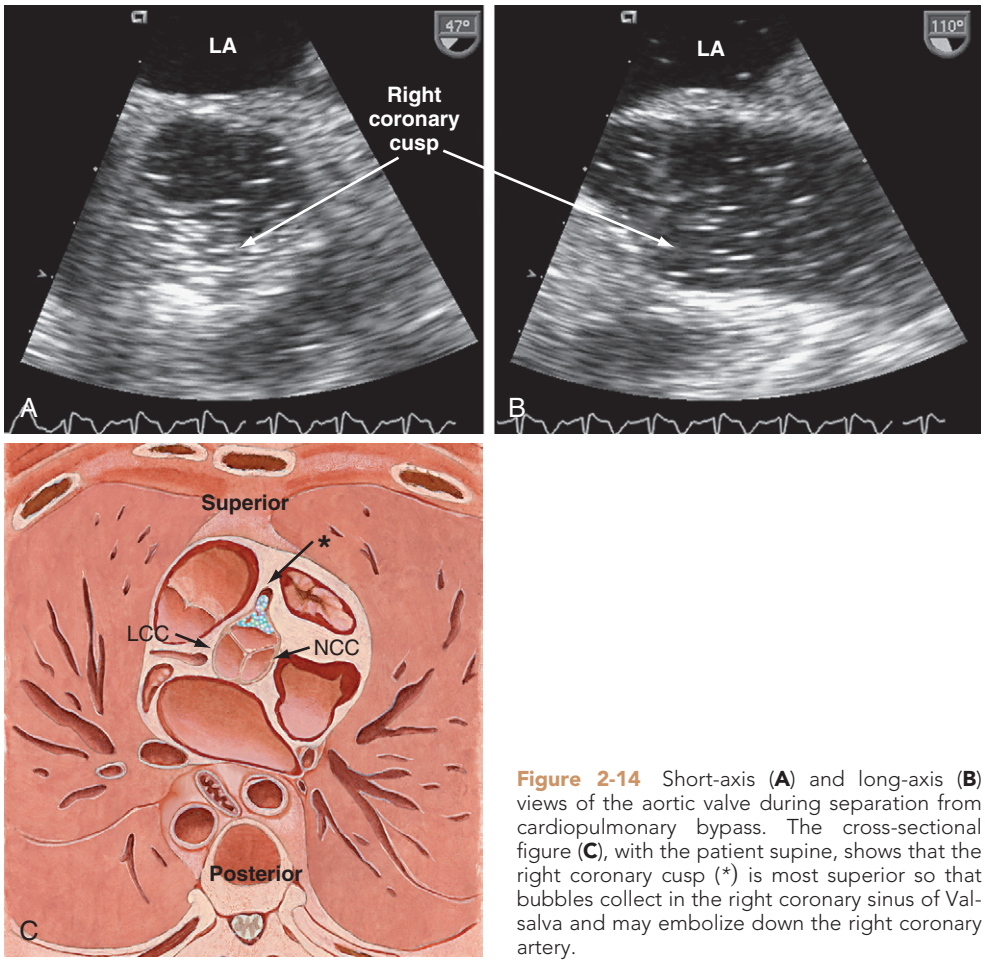



**Figure 2-14** Short-axis (**A**) and long-axis (**B**) views of the aortic valve during separation from cardiopulmonary bypass. The cross-sectional figure (**C**), with the patient supine, shows that the right coronary cusp (*) is most superior so that bubbles collect in the right coronary sinus of Valsalva and may embolize down the right coronary artery.

rarely confounded by rhythm disturbances, as is the case for automated ST analysis. TEE cannot be used, however, in patients receiving regional anesthesia, and because the probe is not inserted until after anesthetic induction, it cannot detect changes during this vulnerable period.

Conflicting studies regarding the prognostic importance of regional wall motion abnormalities were subsequently published. In a study by London and colleagues,[46] 156 patients undergoing noncardiac surgery who were at high risk for coronary artery disease were studied. Specific clinical, electrocardiographic, or hemodynamic events prompted analysis of stored images. The number of new wall motion abnormalities detected was low, and discordance with electrocardiographic findings was significant . The number of postoperative cardiac complications was low. In the study by Leung and associates,[47] patients undergoing coronary artery bypass were examined with electrocardiography and TEE. Although prebypass ischemia was rare, postbypass ischemia was more common, and postoperative cardiovascular complications were associated more closely with TEE findings than with electrocardiography alone.

It is now accepted that regional wall motion abnormalities, although often the result of myocardial ischemia, also may result from hypovolemia, tethering of nonischemic myocardium, and myocardial stunning after cardiopulmonary bypass. Abnormal interventricular septum abnormalities are seen after cardiopulmonary bypass, with right-sided chamber overload, ventricular pacing, and bundle branch blocks. Off-line analysis has been employed in most of the large-scale studies involving comparison of TEE with other methods of ischemia detection, but extrapolation to the accuracy of real-time TEE analysis should not be assumed. Regional wall motion abnormalities that subtend the anatomic distribution of coronary artery flow are more often a result of ischemia than those that do not.

Comunale and colleagues[48] also documented the poor concordance between the TEE and electrocardiography and attributed this finding to the lack of standard definitions of significant regional wall motion abnormalities and ischemic ST changes, the exclusion of longitudinal TEE views, and the use of different models of segment nomenclature.

TEE is the most sensitive test for intraoperative myocardial ischemia and has therefore been adapted by many practitioners as cutting-edge technology in this regard. Conditions that lead to its lack of specificity, as mentioned, must be taken into account. The ability to monitor additional tomographic planes; the use of cine loops for comparison; and the advent of new technologies, such as tissue Doppler imaging and speckle tracking with strain imaging and real-time 3D TEE, should improve accuracy. Regional wall motion abnormalities precede electrocardiographic changes,[49] and once ischemia is diagnosed, TEE can be used to directly monitor the effects of intervention.

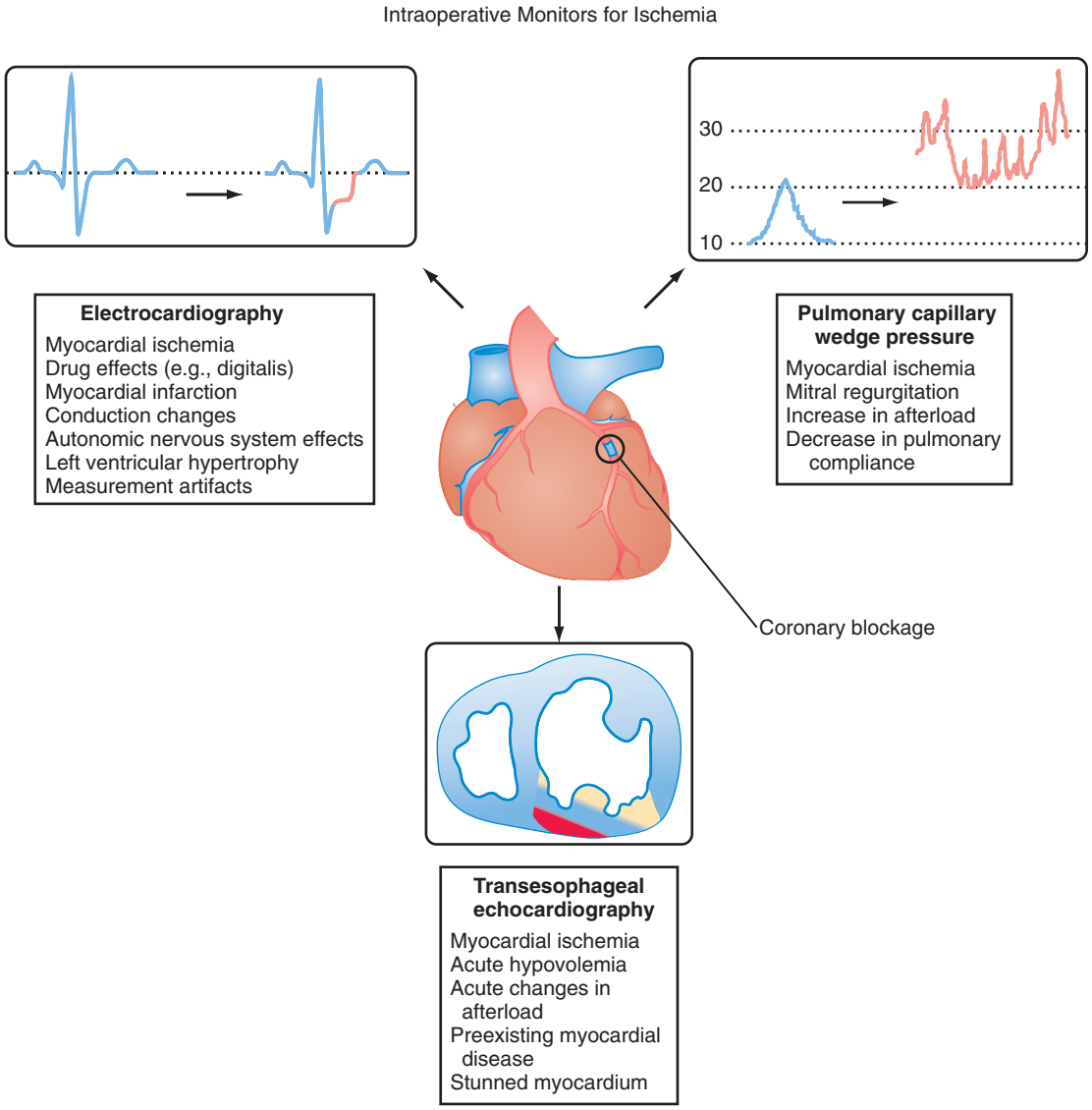



**Figure 2-15** Causes of ischemic changes on intraoperative monitors. *(From Fleisher LA: Real-time intraoperative monitoring of myocardial ischemia in noncardiac surgery.* Anesthesiology *92:1183-1188, 2000.)*

## Use of Transesophageal Echocardiography to Monitor Intraoperative Cardiac Function in Specific Clinical Entities

The use of TEE has improved our ability to intelligently manage post–cardiopulmonary bypass instability. It has allowed us to understand the intraoperative changes that occur during some of the newer techniques in coronary revascularization and can guide us in placement of numerous intracardiac and intravascular devices. Its use in monitoring cardiac function during noncardiac surgery is most advantageous in the diagnosis of sudden and unexplained hemodynamic instability.

### SEPARATION FROM CARDIOPULMONARY BYPASS

At the time of separation of the patient from cardiopulmonary bypass, the use of TEE may guide the anesthesiologist in the use of pharmacologic and nonpharmacologic therapies and can maximize the likelihood of a smooth transition.

#### *Intracardiac Air*

Left-sided intracardiac air is ubiquitous following procedures in which left-sided chambers have been open to atmosphere and is identified by its characteristic "firefly" appearance. Air is often seen entering the left atrium from the pulmonary veins or enmeshed in the mitral subvalvular apparatus (Fig. 2-16). Echocardiographic inspection is carried out in the four-chamber and transgastric long-axis views. Careful evacuation by the surgeon is important and involves suctioning on the aortic root vent or needle aspiration of the LV apex to evacuate trapped pockets. In addition to guiding evacuation, TEE is useful in diagnosing the consequences of embolization through the right coronary ostium, which results in ventricular dysfunction in a right coronary distribution (see Fig. 2-14).

#### *Cardiac Output*

There are a number of potential causes of low cardiac output immediately following cardiopulmonary bypass: perioperative infarction,[50] coronary air emboli, metabolic abnormalities, hypovolemia, LV outflow tract obstruction, and inadequate myocardial protection. It seems intuitive that the

yield of TEE, when it is used during hemodynamic instability during and after cardiac surgery, would be high. Two published series have demonstrated the myriad diagnoses that have been made and the ability to intervene on many patients (Table 2-1).[51,52] No attempt was made to compare TEE with other diagnostic modalities, although the speed with which information is made available appears hard to supersede. The prebypass TEE-derived wall motion score index was found to independently predict the need for postbypass inotropic support.[53]

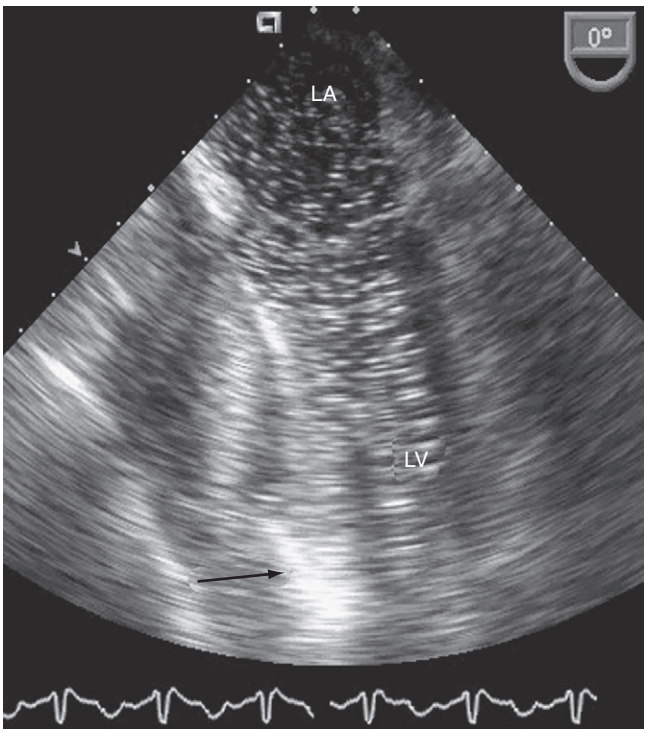



**Figure 2-16 Four-chamber midesophageal view.** As the patient is being separated from cardiopulmonary bypass, a pocket of air enmeshed in the left ventricular subvalvular apparatus is noted (*arrow*), with numerous bubbles emanating from it.

## OFF-PUMP CORONARY BYPASS SURGERY

One of the major controversies in cardiac surgery is the performance of coronary revascularization without cardiopulmonary bypass, the off-pump bypass or "beating heart" operation. The major criticism is that incomplete revascularization leads to repeat interventions, and in addition, coexistent pathology such as mitral regurgitation cannot be dealt with. Shroyer's[54] pivotal study showed that at 1 year, the off-pump strategy led to worse composite outcomes, although the accompanying editorial emphasized that in certain patient subsets benefits may still exist,[55] such as in those with atheromatous disease of the aorta.[56]

Hemodynamic instability can occur both from intraoperative ischemia and from cardiovascular deformation by the device used to stabilize the heart during coronary anastomoses (Fig. 2-17).[57] Although the number of readable myocardial segment decreases during cardiac displacement, TEE can adequately detect regional wall motion abnormalities in most patients.[58] and may help guide revascularization strategy.[59] It has been suggested that displacing the heart with a saline bag posteriorly aids in transgastric image quality.[60]

## CARDIAC FUNCTION IN NONCARDIAC SURGERY

The most recent guidelines published jointly by the American Society of Anesthesiologists and Society of Cardiovascular Anesthesiologists Task Force on Transesophageal Echocardiography[61] and by the European Association of Echocardiography[62] are summarized in Table 2-2.

Regardless of the type of noncardiac surgery being undertaken, the greatest diagnostic yield for intraoperative TEE is obtained when sudden and unexplained hypotension occurs.[60] Memtsoudis and colleagues[63] examined the use of TEE in cardiac arrest during noncardiac surgery. In 18 of 22 patients, the etiology was detected by TEE and helped guide subsequent management.

As the use of intraoperative TEE for cardiac surgery continues to proliferate, so will its use in unstable patients undergoing noncardiac surgery.[64]

**TABLE 2-1 Relevant Intraoperative Transesophageal Echocardiographic Findings Categorized by Indication**

| | Indication, *n* | | | | |
|---|---|---|---|---|---|
| *Finding* | *Hemodynamic Instability* | *Surgical Planning* | *Trauma* | *Hypoxemia* | *Total Number of Patients* |
| Severe left ventricular dysfunction ± regional wall motion abnormality | 15 | 2 | — | — | 17 |
| Aortic dissection ± aortic regurgitation | 1 | 13 | — | — | 14 |
| Significant mitral regurgitation | 4 | 2 | — | — | 6 |
| Intracardiac/great vessel shunt | 1 | 1 | — | 2 | 4 |
| Hyperdynamic left ventricular function | 2 | — | 1 | — | 3 |
| Severe right ventricular dysfunction | 2 | — | 1 | — | 3 |
| Extracardiac clot | 2 | — | — | — | 2 |
| Significant aortic regurgitation | 2 | — | — | — | 2 |
| Significant tricuspid regurgitation | 1 | — | — | — | 1 |
| Pericardial tamponade | 1 | — | — | — | 1 |
| No relevant findings | 5 | 1 | 4 | 3 | 13 |

From Brandt RR, Oh JK, Abel MD, et al: Role of emergency intraoperative transesophageal echocardiography. *J Am Soc Echocardiogr* 11(10):972-977, 1998.

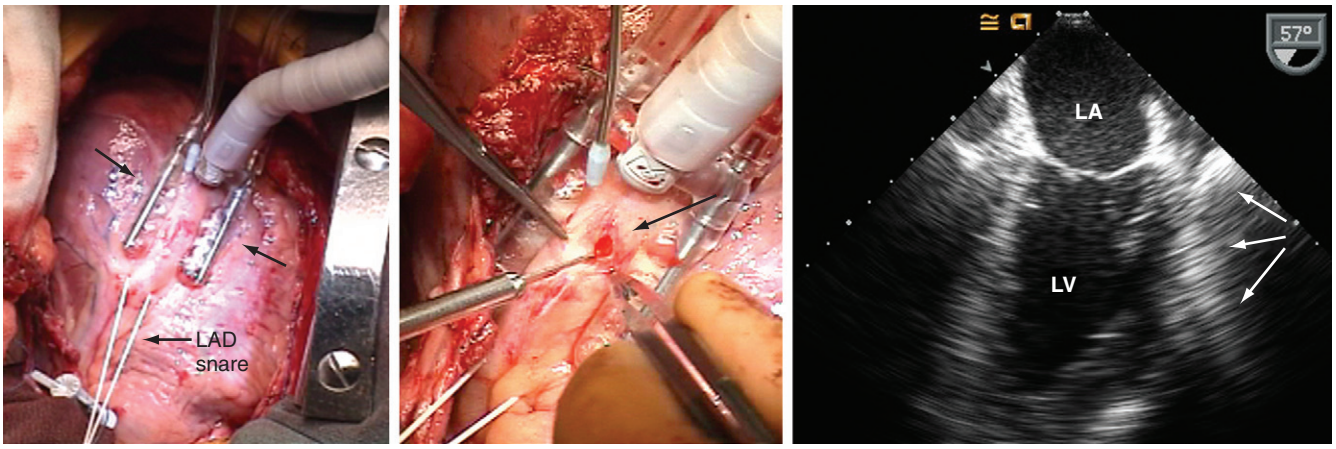



**Figure 2-17** In the *left* panel, the *two arrows* indicate the stabilizing device, which, through suction, lifts and immobilizes a portion of the anterior cardiac wall. The two limbs of the device straddle the left anterior descending artery (*LAD*), which has a snare around it. In the *center* panel, an arteriotomy has been made in the LAD (*arrow*). In the *right* panel, the stabilizer (*arrows*) deforms the anterior wall of the left ventricle.

**TABLE 2-2 Recommendations for the Use of Perioperative TEE in Adults**

| *Clinical Situation* | *Recommendations (ASA/SCA Task Force)*[60] | *Recommendations (European Association of Echocardiography)*[61] |
|---|---|---|
| Cardiac (non-CABG) and thoracic aortic surgery | Should be used in all adults without contraindications to TEE | TEE should be used in adult patients undergoing cardiac surgery or surgery to the thoracic aorta under general anesthesia, in particular, in valvular repair procedures. |
| CABG | Should be considered in CABG surgeries as well<br>• to confirm and refine the preoperative diagnosis,<br>• to detect new or unsuspected pathology,<br>• to adjust the anesthetic and surgical plan accordingly, and<br>• to assess the results of the surgical intervention. | |
| Transcatheter intracardiac procedures | May be used | |
| Noncardiac surgery | TEE may be used when the nature of the planned surgery or the patient's known or suspected cardiovascular pathology might result in severe hemodynamic, pulmonary, or neurologic compromise.<br>• If equipment and expertise are available, TEE should be used when unexplained life-threatening circulatory instability persists despite corrective therapy. | TEE may be used in patients undergoing specific types of major surgery where its value has been repeatedly documented. These include neurosurgery at risk from venous thromboembolism, liver transplantation, lung transplantation, and major vascular surgery, including vascular trauma.<br>TEE may be used in patients undergoing major noncardiac surgery in whom severe or life-threatening hemodynamic disturbance is either present or threatened.<br>TEE may be used in major noncardiac surgery in patients who are at a high cardiac risk, including severe cardiac valve disease, severe coronary heart disease, or heart failure. |
| Critical care | For critical care patients, TEE should be used when diagnostic information that is expected to alter management cannot be obtained by transthoracic echocardiography or other modalities in a timely manner. | TEE may be used in the critical care patient in whom severe or life-threatening hemodynamic disturbance is present and unresponsive to treatment, or in patients in whom new or ongoing cardiac disease is suspected and who are not adequately assessed by transthoracic imaging or other diagnostic tests. |

*CABG*, Coronary artery bypass graft.

## POSITIONING OF INTRAVASCULAR DEVICES

Intraoperative TEE can be used to guide the positioning of a number of intravascular devices.

### *Pulmonary Artery Catheters*

Right heart dysfunction, tricuspid regurgitation, and atrial fibrillation are entities in which proper placement of a pulmonary artery catheter may be challenging. Guidance with TEE helps facilitate passage through the tricuspid valve. It also allows determination of the depth of advancement into the pulmonary artery (Fig. 2-18); this may be important in instances where the pulmonary artery may be transected, such as lung transplantation.

### *Central Venous Pressure Air Aspiration Catheters*

Specialized central venous catheters are often used during sitting craniotomies to aspirate air that has gained access to the venous circulation. Correct positioning is at the right atrial-superior vena caval junction, and imaging is best in the mid-esophagus with rightward rotation and a transducer angle of approximately 90° to 100° (Fig. 2-19).

### *Intraaortic Balloon Pump*

The intraaortic balloon pump is best imaged in the descending aorta in a vertical TEE plane. Correct positioning of the catheter tip is at the inferior border of the transverse aortic arch.[65] Once the tip of the balloon is visualized at a transducer angle of

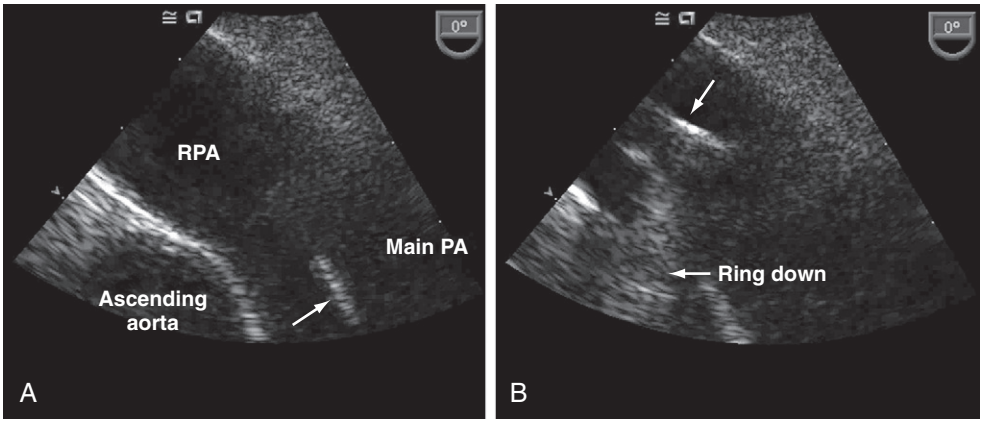



**Figure 2-18** **A,** In this high esophageal short axis, the tip of the pulmonary artery (*PA*) catheter (*arrow*) is seen in the main pulmonary artery. **B,** The balloon is inflated (with resultant ring down artifact) and the pulmonary artery catheter advances into the right pulmonary artery (*RPA*).

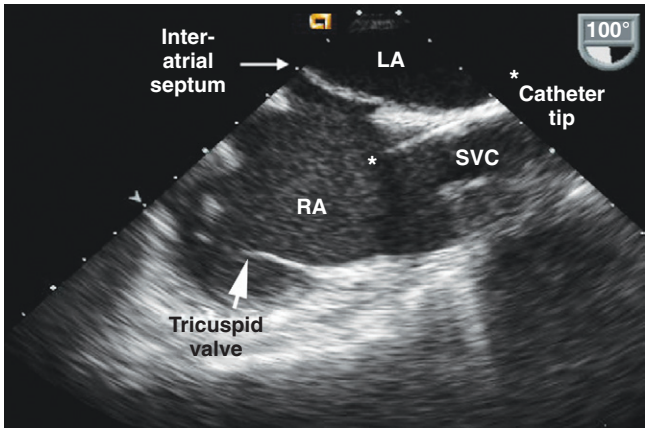



**Figure 2-19** A catheter inserted from the arm is positioned at the junction of the right atrium and superior vena cava (*SVC*) to evacuate any air that gains access to the venous circulation during sitting craniotomy.

approximately 90°, the probe marking at the teeth is noted. The probe is slowly withdrawn until the left subclavian artery orifice is seen; the marking is again noted. The distance between the balloon and the subclavian orifice should be approximately 5 cm (Fig. 2-20).

### *Left Ventricular Assist Device*

As the left ventricular assist device withdraws blood from the left ventricle, LA pressure falls below right atrial pressure. (See Chapter 31.) It is important to determine whether a patent foramen ovale is present, because right-to-left shunting will invariably occur. Any thrombi detected on the left side of the heart must be dealt with before instituting flow through the device. A mechanical aortic valve, even if functional, should be replaced with a bioprosthetic valve to minimize the increased risk of valvular thrombosis and possible embolization. Mitral stenosis, if significant, may limit the ability of blood to be removed to the device by the inflow cannula. The orifice of the

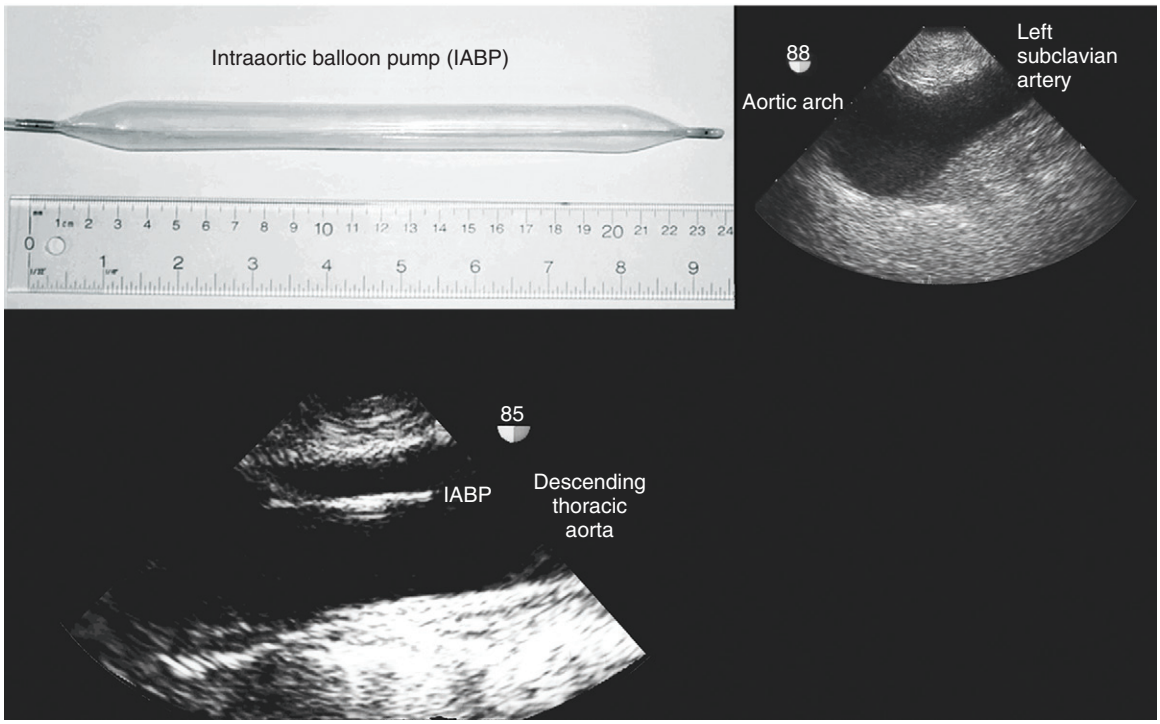



**Figure 2-20** Intraaortic balloon pump (*IABP*) positioned in the descending thoracic aorta. The left subclavian artery is visualized to ensure the IABP does not encroach on the vessel orifice.

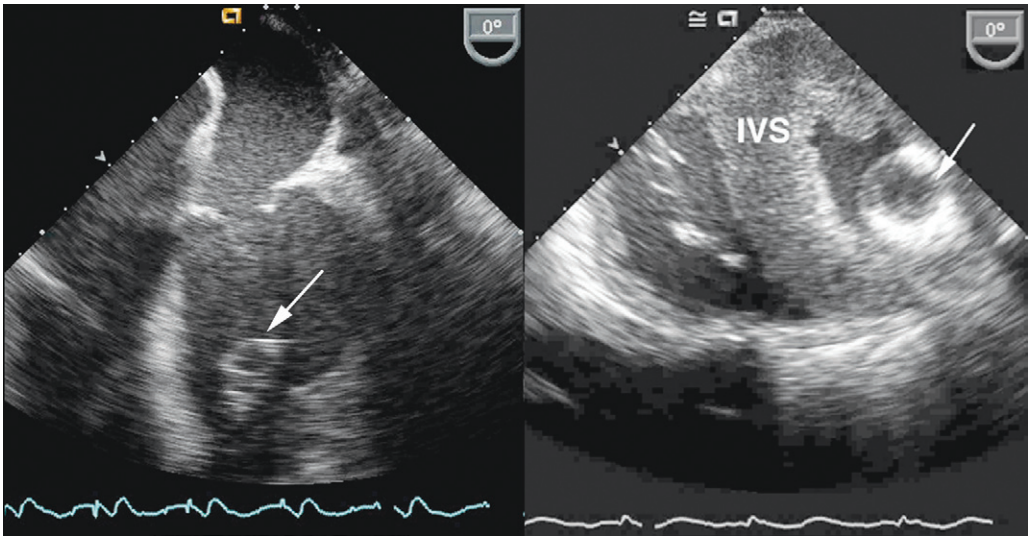



**Figure 2-21** The inflow cannula of the left ventricular assist device (*arrow*) is seen to freely enter the apical region of the left ventricle and not abut the interventricular septum (*IVS*). *Left* panel, four-chamber view; *right* panel, transgastric short-axis view.

ventricular apical cannula (inflow cannula) should be imaged in the four- and two-chamber views, and the lack of obstruction by adjacent walls should be ascertained (Fig. 2-21). On occasion, the inflow cannula is placed in the left atrium via one of the pulmonary veins. Because the outflow cannula terminates in the ascending aorta (Fig. 2-22), it is important to rule out significant aortic regurgitation; this would lead to LV distension during aortic flow. Patients may return to the OR because of left ventricular assist device malfunction. The TEE exam should focus on possible causes: intracardiac thrombi, or problems with the cannulae themselves[66] (Fig. 2-23).

### *Right Ventricular Assist Device*

In positioning the right ventricular assist device, it is preferable to avoid impingement on the tricuspid valve.

### *Coronary Sinus Cannulation*

The coronary sinus is cannulated through blind right atrial puncture for the purposes of administering retrograde cardioplegia. Occasionally, TEE guidance is required, especially in minimally invasive surgical procedures (Fig. 2-24).

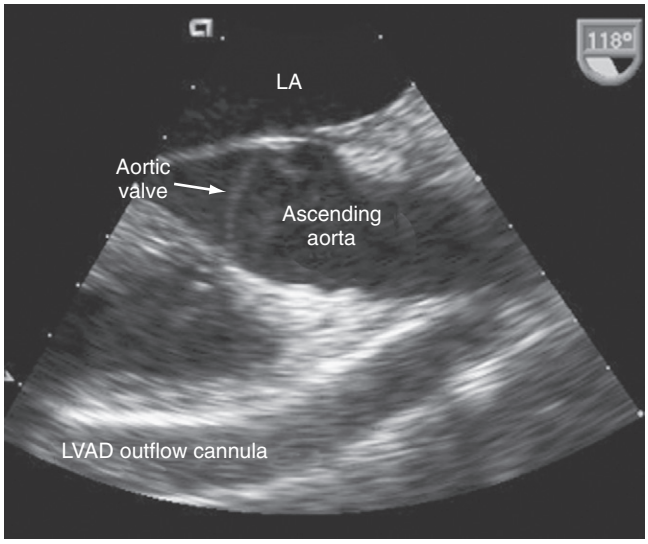



**Figure 2-22** The outflow cannula of the left ventricular assist device (*LVAD*) terminates in the ascending aorta.

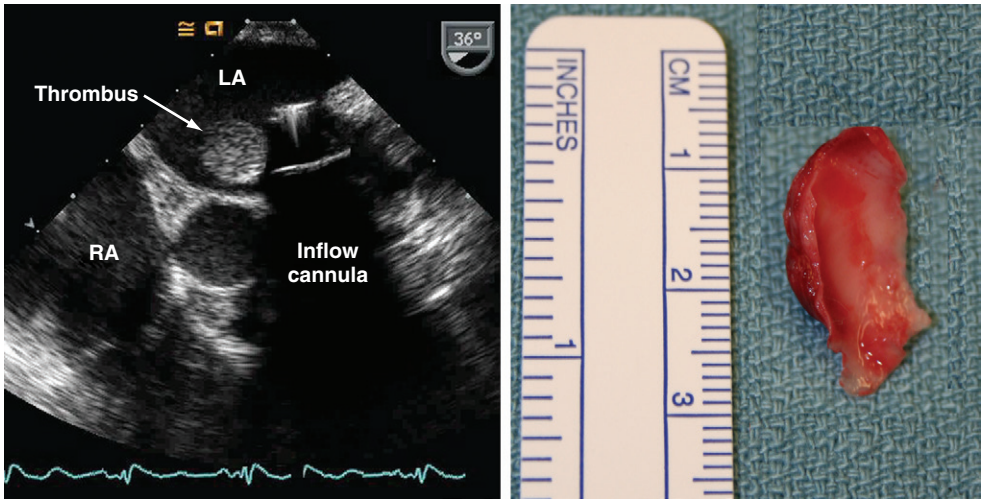



**Figure 2-23** Because of left ventricular assist device malfunction, this patient returned to the operating room for left ventricular assist device exploration. Intraoperative TEE (*left*) revealed a thrombus impinging on the inflow cannula in the left atrium. The surgical specimen is seen at *right*.

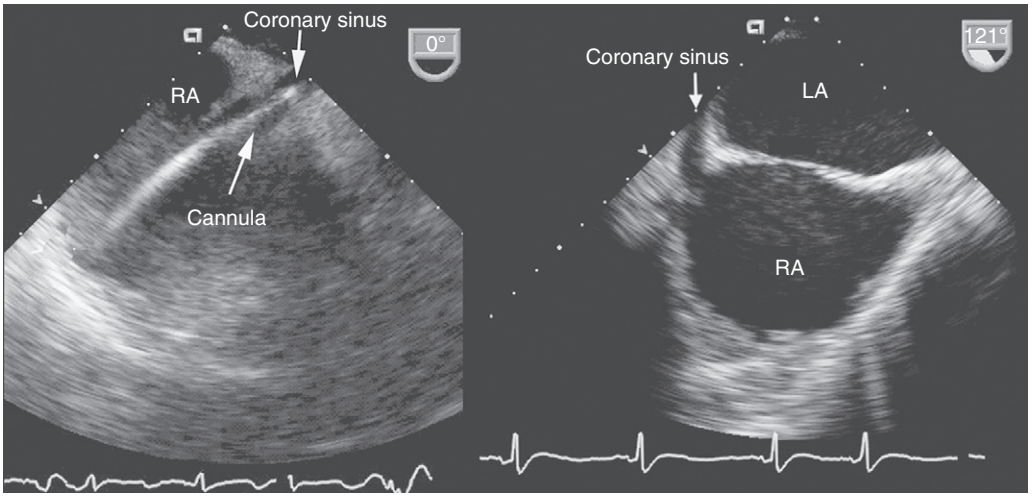



**Figure 2-24** The coronary sinus, visualized in a low esophageal view (*left*) and a bicaval view (*right*). In the left panel, the catheter is seen traversing the right atrium (*RA*) and entering the coronary sinus orifice.

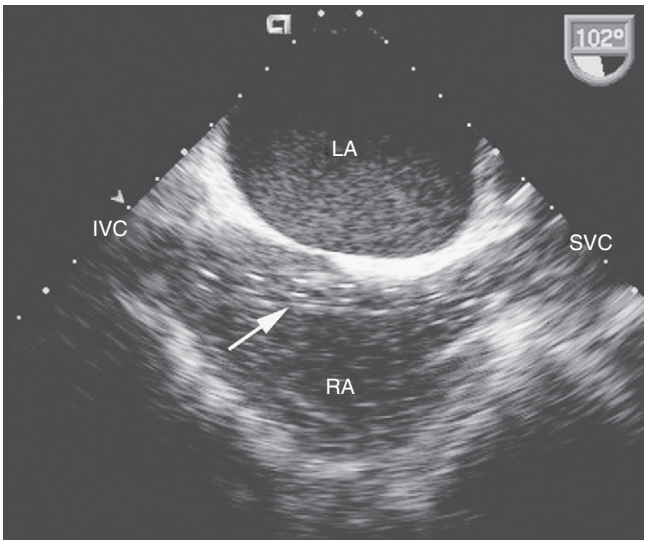



**Figure 2-25** The multiorifice femoral venous cannula is seen entering the right atrium from the inferior vena cava (*IVC*). *SVC*, Superior vena cava.

### *Left Ventricular Vent*

An LV vent is placed through the right superior pulmonary vein into the left atrium and advanced through the mitral valve into the left ventricle to drain excess ventricular volume on bypass.

### *Femoral Venous Cannula*

Occasionally venous drainage on bypass is achieved through femoral venous cannulation with advancement into the right atrium (Fig. 2-25).

## TRANSPLANT SURGERY

### *Heart Transplantation*

TEE is used to examine the native heart for LV thrombi and to assess the function of the donor heart before procurement and after the recipient is separated from cardiopulmonary bypass, when the effects of the ischemic time may become evident. In addition, the anastomoses may be examined if obstruction is suspected, such as in the pulmonary artery anastomosis (Fig. 2-26).

### *Lung Transplantation*

During lung transplantation, the use of TEE has been described in the evaluation of vascular anastomoses. The pulmonary venous anastomoses are generally well seen, and velocities are usually less than 1 m/sec in the absence of significant obstruction.[67,68]

The right pulmonary artery anastomoses (and less likely the left) may be visualized in the midesophageal ascending aortic short-axis view, although the angle of flow usually precludes Doppler interrogation of the anastomosis (Fig. 2-27).

If the recipient's heart exhibits right ventricular hypertrophy, right ventricular outflow tract obstruction may develop when the new lungs are reperfused.

### *Liver Transplantation*

During reperfusion of the transplanted liver, significant right-sided embolization can occur, with resultant hemodynamic instability. TEE can aid in this diagnosis and guide treatment.

# Alternate Techniques

## EPICARDIAL/EPIAORTIC ECHOCARDIOGRAPHY

On occasion there may be contraindications to TEE, or the images obtained may be suboptimal. Using a high-frequency ultrasound probe in a sterile sheath, the cardiac surgeon can image the heart by placing it on the epicardial surface and obtain standard surface echocardiographic images[69] (Fig. 2-28). Similarly, the ascending aorta may be scanned for regions of atheromatous disease, which should be avoided during aortic cross clamping[70] (Fig. 2-29).

# Transesophageal Echocardiography as a Monitor of Intraoperative Ventricular Function: Impact on Postoperative Outcomes and Cost-Effectiveness

The recommendations of the American Society of Anesthesiologists and the Society of Cardiovascular Anesthesiologists task force for the use of perioperative TEE[71] and the European Association of Echocardiography for the use of intraoperative TEE in cardiac and noncardiac surgery[72] are presented in Table 2-2.

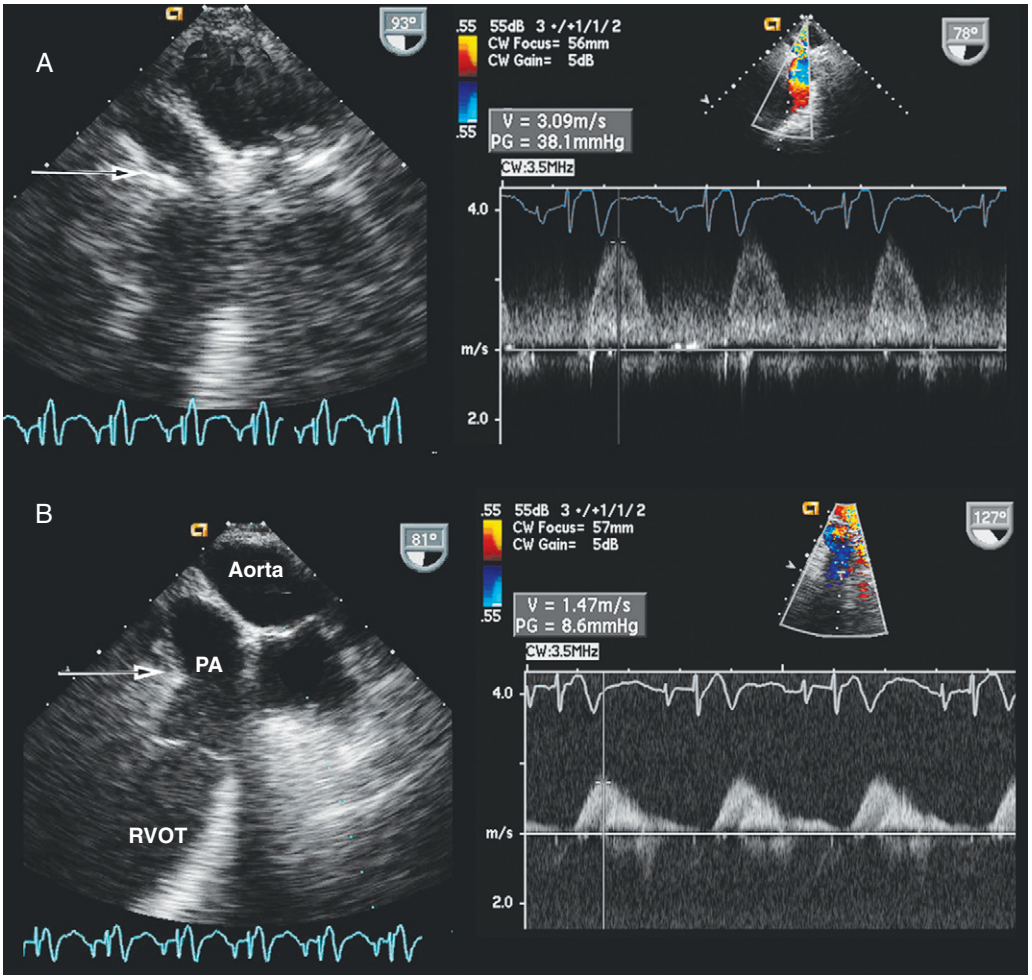



**Figure 2-26** **Images obtained from a high esophageal window. A,** Pressure gradient (*PG*) of 38 mm Hg across the pulmonary artery led to the diagnosis of an anastomotic obstruction (*arrow*). **B,** Anastomosis was revised with resolution of the gradient. *PA*, Pulmonary artery; *RVOT*, right ventricular outflow tract; *V*, velocity.

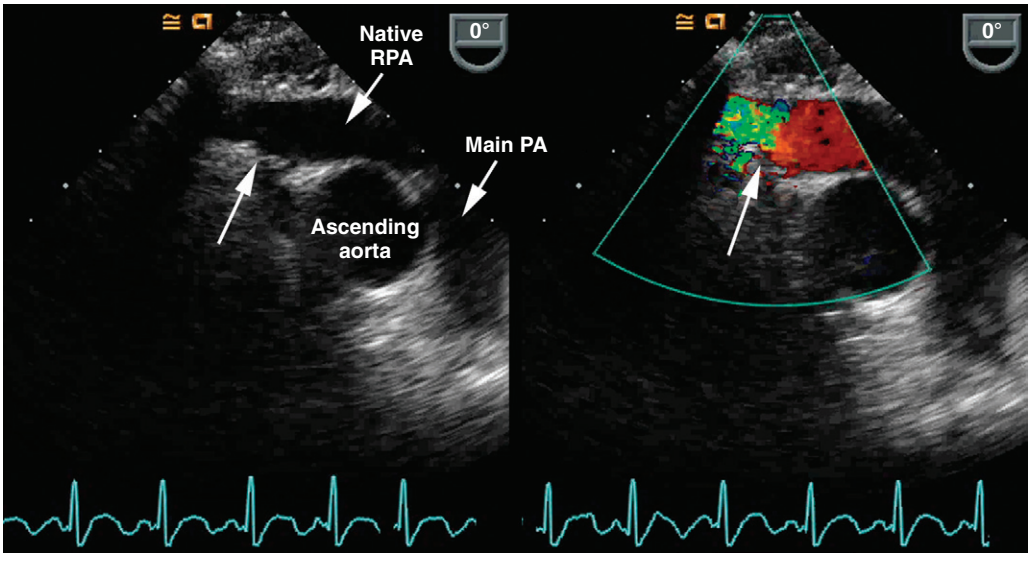



**Figure 2-27** **Midesophageal ascending aortic short-axis view in a patient who received a right-sided lung transplant.** In the *left* panel, the arrow indicates the slight narrowing of the anastomotic site. In the *right* panel, aliasing in the color Doppler signal is seen at the anastomosis. *PA*, Pulmonary artery; *RPA*, right pulmonary artery.

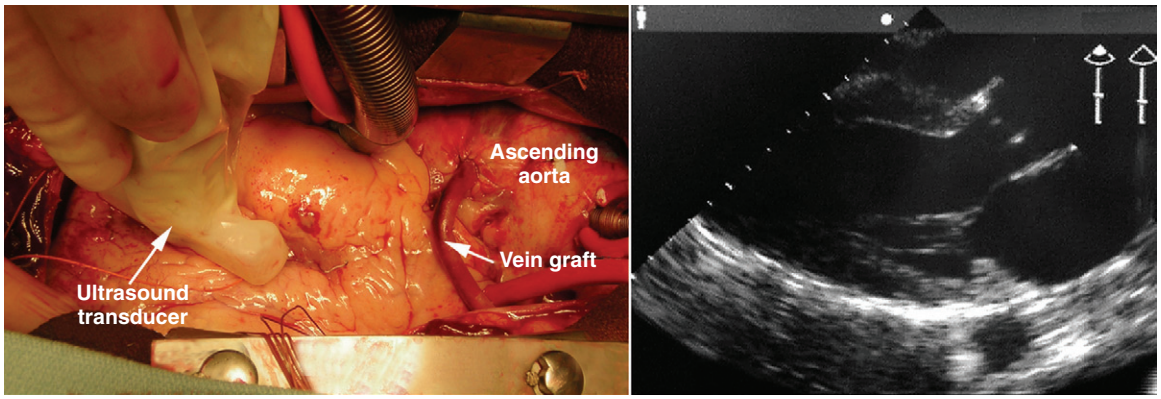



**Figure 2-28** In the *left panel,* the surgeon places an ultrasound probe directly on the epicardial surface after protecting it with a sterile sheath. In the *right panel,* a parasternal long-axis view is obtained.

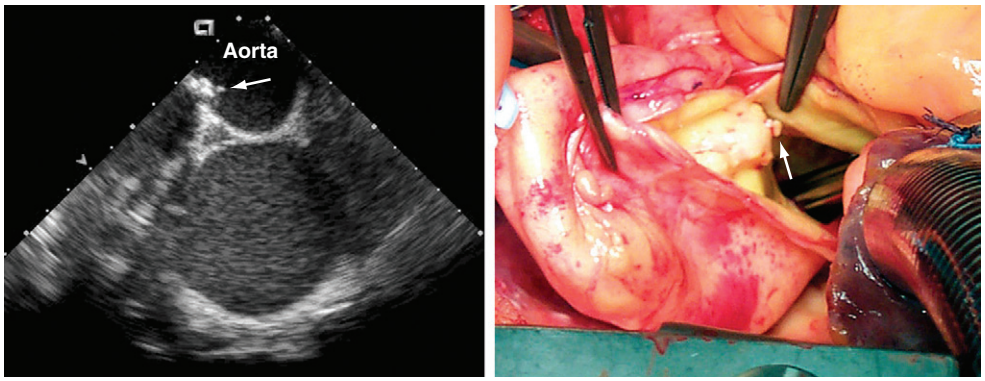



**Figure 2-29** In the *left panel,* epiaortic scanning reveals a mobile atheroma in the ascending aorta, which led to a modification of cannulation strategy. In the *right panel,* the mobile atheroma is seen in the open aortic root (*arrow*).

Several studies have addressed the impact of intraoperative TEE monitoring of ventricular function during coronary bypass surgery. In all instances, benefits must be weighed against the reported complication rate of TEE of approximately 0.2%.[71]

In a study conducted at the Mayo Clinic, Click and colleagues[72] prospectively analyzed the effect of intraoperative TEE on surgical management. TEE use (and thus inclusion in the study) was determined by the treating physicians. Of the 292 patients having coronary artery bypass graft surgery, there were 97 new TEE findings (33% of all cases) prebypass and 24 new TEE findings (8% of all cases) postbypass. This large number probably reflects a selection bias, because more complex cases were more apt to be selected for TEE.

In a series of unselected and consecutive cardiac surgical patients having exclusively coronary artery bypass graft with TEE monitoring, Qaddoura and co-workers,[73] also at the Mayo Clinic, noted new prebypass findings in 52 patients, resulting in alterations of the surgical procedure in 21 of them; the most common occurrence was a previously undiagnosed patent foramen ovale (Table 2-3). Postbypass there were 19 new findings in 15 patients, resulting in 15 surgical interventions in 10 patients (see Table 2-3). In a retrospective review of 2343 unselected patients having cardiac surgery, Forrest and assosiates[74] found a surgical impact of TEE findings of 4.5%. When the data for coronary artery bypass graft patients was analyzed, the surgical impact was 6.7% of high-risk patients versus 2.8% of low-risk patients. What would be difficult to determine given the designs of these two studies is whether the additional procedures performed led to improved outcome. Bergquist and colleagues[75,76] studied the concordance between real-time intraoperative TEE interpretation by five cardiac anesthesiologists and offline analysis by two blinded investigators in the assessment of LV filling, ejection fraction area, and regional wall motion. Results obtained by the two methods were within 10% of each other 75% of the time with respect to ejection fraction and filling. The accuracy of regional assessment was variable: more accurate for normal than for abnormal wall motion and better in anesthesiologists with more advanced echocardiographic training. In the second part of the study, TEE was found to be the most important factor in guiding hemodynamic interventions in 17% of cases examined. What is lacking is a clear demonstration that the TEE assessments were correct and that the same interventions would not have been undertaken if guided by more traditional monitors. Cost and outcome were not examined. Mathew and colleagues[77] demonstrated that cardiac anesthesiologists interpret TEE examinations at a level comparable to physicians whose primary practice is echocardiography.

At the Cleveland Clinic, Savage and co-workers[78] examined the use of intraoperative TEE monitoring in a group of high-risk patients undergoing coronary artery bypass graft. In addition to documenting numerous management changes related to TEE-derived information (Table 2-4), they documented lower short-term morbidity and mortality rates as compared with a

**TABLE 2-3 New Findings in 474 Coronary Artery Bypass Graft Patients and Surgical Impact by Intraoperative Transesophageal Echocardiography**

| *New Findings Prebypass (46 Patients)* | n | *Surgical Impact of Prebypass Findings (16 Patients)* | n | *New Findings Postbypass (15 Patients)* | n | *Surgical Impact of Postbypass Findings (10 Patients)* | n |
|---|---|---|---|---|---|---|---|
| PFO | 22 | PFO closed | 7 | Significant MR | 3 | MV Repair | 2 |
| MVP with MR | 3 | No surgical impact | — | Altered cardiac function | | Graft flow evaluation | 3 |
| Significant MR (5), TR (4), AR (3) | 12 | MV (2), TV (2), aortic valve (1) repair | 5 | Depressed LVF | 6 | Graft revision | 5 |
| Aortic valve disease (Lambl, mild AS) | 2 | Aortic valve explored (Lambl excised) | 2 | New RWMA | 7 | IABP inserted | 5 |
| Subvalvular AS | 1 | Myomectomy | 1 | New RWMA and depressed LV or RV function | 2 | | |
| Improved LVF | 4 | No IABP | 4 | Dynamic obstruction | 1 | Medical treatment | — |
| Aortic atheroma | 5 | OPCAB | 2 | Total | 19 | Total | 15 |
| Depressed LVF and RVF | 2 | No surgical impact | — | | | | |
| New RWMA | 1 | No surgical impact | — | | | | |
| Total | 52 | Total | 21 | | | | |

From Qaddoura FE, Abel MD, Mecklenburg KL, et al: Role of intraoperative transesophageal echocardiography in patients having coronary artery bypass graft surgery. *Ann Thorac Surg* 78:1586-1590, 2004.

*AR*, Aortic regurgitation; *AS*, aortic stenosis; *AV*, aortic valve; *EF*, ejection fraction; *IABP*, intraaortic balloon pump; *LVF*, left ventricular function; *MR*, mitral regurgitation; *MV*, mitral valve; *MVP*, mitral valve prolapse; *OPCAB*, off-pump coronary artery bypass; *PFO*, patent foramen ovale; *RVF*, right ventricular function; *RWMA*, regional wall motion abnormality; *TR*, tricuspid regurgitation; *TV*, tricuspid valve.

**TABLE 2-4 Surgical Management Alterations during Coronary Artery Bypass Grafting Based on Transesophageal Echocardiographic Findings**

| *Alteration* | *Before CPB*, n | *Before CPB Separation*, n | *After CPB Separation*, n | *After CC*, n | *Total Number of Patients* |
|---|---|---|---|---|---|
| Rush to CPB | 2 | — | — | — | 2 |
| Return to CPB | — | — | 3 | 1 | 4 |
| Reopen | — | — | — | 2 | 2 |
| LVAD/ECMO | 0 | 0 | 0 | 1 | 1 |
| Additional redo grafts | 8 | 2 | 3 | 1 | 12 |
| IABP | 4 | 3 | 2 | 0 | 9 |

From Savage RM, Lytle BW, Aronson S, et al: Intraoperative echocardiography is indicated in high-risk coronary artery bypass grafting. *Ann Thorac Surg* 64(2):368-373, 1997.

*CC*, Chest closure; *CPB*, cardiopulmonary bypass; *ECMO*, extracorporeal membrane oxygenation; *IABP*, intraaortic balloon pump; *LVAD*, left ventricular assist device.

**TABLE 2-5 Patient Outcomes with and without Intraoperative Transesophageal Echocardiography**

| *Variable* | *Management with TEE* | *Management without TEE* |
|---|---|---|
| Patients, *n* | 82 | 478 |
| Age, yr | 68.4 | 64.8 |
| Severity score | 6.1 | 5.9 |
| Hospital deaths, *n* (%) | 1 (1.2) | 18 (3.8) |
| Myocardial infarction, *n* (%) | 1 (1.2) | 14 (3.5) |
| Cardiac morbidity, *n* (%) | 1 (1.2) | 7 (1.5) |
| ICU CNS morbidity, *n* (%) | 3 (3.6) | 18 (3.8) |
| Hospital CNS morbidity, *n* (%) | 1 (1.2) | 16 (3.3) |

From Savage RM, Lytle BW, Aronson S, et al: Intraoperative echocardiography is indicated in high-risk coronary artery bypass grafting. *Ann Thorac Surg* 64(2):368-373, 1997.

*CNS*, Central nervous system; *ICU*, intensive care unit.

historical group of patients with similar severity scores[79] who were not monitored with TEE (Table 2-5). An individual not part of the anesthetic or surgical team read the TEE scan; it is uncertain whether someone involved in direct patient management would have as readily garnered the information.

In studies from Australia,[80] Europe,[81,82] Canada,[83] and India,[84] the real-time accrual of information with TEE was demonstrated to be of value in the management of hemodynamic perturbations and the planning of the surgical procedure in coronary artery bypass graft and other cardiac surgical procedures (Tables 2-6 and 2-7). No assessment of the effect of intraoperative TEE monitoring on patient outcome was made. These studies and others are summarized in Table 2-8.

Cost effectiveness has been demonstrated by studies of the use of TEE in congenital cardiac surgery,[85] preparation for elective cardioversion,[86] and determination of antibiotic treatment duration in endocarditis.[87] Similar data for routine TEE monitoring in coronary artery bypass graft are lacking.

Fanshawe and colleagues[88] showed substantial savings with the routine use of TEE in cardiac surgical patients but not specifically coronary artery bypass graft. In a number of instances, surgery was either cancelled or newly recommended based on the findings of intraoperative TEE; whether these alterations of treatment were beneficial was not determined in follow-up. The claim of improved patient outcome must be tempered by the fact that most surgical changes involved closure of an asymptomatic patent foramen ovale. Their findings are summarized in Table 2-9.

In the largest series to date of the impact of intraoperative TEE on decision making in cardiac surgery, Eltzschig and colleagues[89] retrospectively examined 12,566 patients. From 1990 to 2004, the frequency with which intraoperative TEE was performed increased steadily (Fig. 2-30). The major findings, presented in Table 2-10, reveal that a large number of procedures were affected by TEE findings both before and after cardiopulmonary bypass. As pointed out in the accompanying commentary,[90] changes in therapeutic management are not, as endpoints, as convincing as morbidity, mortality, and cost, but nonetheless the study and its magnitude were commended as an "excellent resource for the design of future, randomized, controlled trials examining the potential benefits of intraoperative TEE on clinical outcome."

The impact of monitoring of ventricular function during noncardiac surgery has not been studied as closely. In a

**TABLE 2-6 Influence of Intraoperative Transesophageal Echocardiography as the Driving Force on Interventions Compared with Other Monitors**

| | Monitor | | | | | |
|---|---|---|---|---|---|---|
| *Intervention,* n *(%)* | *TEE* | *ECG* | *Arterial Catheter* | *PA Catheter* | *Other** | *Total* |
| Fluid bolus | 275 (28) | 0 | 129 (13) | 73 (7) | 519 | 996 |
| Antiischemic therapy | 207 (56) | 114 (31) | 11 (3) | 31 (8) | 9 | 372 |
| Vasopressor or inotrope therapy | 56 (16) | 3 (1) | 183 (51) | 27 (7) | 92 | 361 |
| Change in anesthetic depth | 4 (2) | 0 | 164 (78) | 2 (1) | 41 | 211 |
| Vasodilator therapy | 6 (4) | 9 (6) | 96 (68) | 13 (9) | 18 | 142 |
| Antiarrhythmic therapy | 0 | 55 (89) | 0 | 0 | 7 | 62 |
| Surgical intervention | 9 (17) | 17 (33) | 12 (23) | 0 | 14 | 52 |
| Miscellaneous | 3 (8) | 2 (6) | 27 (75) | 3 (8) | 1 | 36 |
| Total | 560 (25) | 200 (9) | 622 (28) | 149 (7) | 701 | 2232 |

From Kolev N, Brase R, Swanevelder J, et al: The influence of transoesophageal echocardiography on intraoperative decision making: a European multicentre study. *Anaesthesia* 53(8):767-773, 1998.

*ECG*, Electrocardiography; *PA*, pulmonary artery.

*Indicates that the interventions were not based on information from the four monitors studied. More than half of these interventions were transfusion of blood for low hematocrit.

**TABLE 2-7 Summary of Surgical Modifications Related to the Intraoperative Use of Transesophageal Echocardiography**

| *Modification* | *Number* |
|---|---|
| Return on bypass for revision of coronary artery bypass graft | 4 |
| **Modification of Planned Surgery** | |
| Valvular replacement cancelled | 5 |
| Valvular replacement or repair | 11 |
| Pleural drainage | 3 |
| Detection of air emboli before aortic unclamping | 2 |
| Surgical exploration for hemodynamic instability | 7 |
| Femoral artery bypass for aortic dissection | 2 |
| **Others** | |
| Ventricular aneurysm resection | 1 |
| Aortoplasty | 1 |
| Cancellation of aortic dissection (diagnostic error) | 1 |
| Left ventricular assist device | 1 |
| Total | 38 |

From Couture P, Denault AY, McKenty S, et al: Impact of routine use of intraoperative transesophageal echocardiography during cardiac surgery. *Can J Anaesth* 47(1):20-26, 2000.

**TABLE 2-9 A Retrospective Analysis of the Costs and Benefits Related to Alterations in Cardiac Surgery from Routine Intraoperative Transesophageal Echocardiography Procedures (Other Than PFO) Changed by TEE**

| *Procedure Proposed* | *Procedure Performed* | *TEE Findings* | *Number of Patients* |
|---|---|---|---|
| CABG | CABG + TVR | TR + 4 | 1 |
| MVR | MV repair | P2 prolapse | 1 |
| CABG | CABG + MVR | MR + 4 | 1 |
| CABG + MVR | CABG | MR + 1 | 1 |
| MVR | — | MR + 1 | 2 |

Estimated costs (in US$) for yearly TEE service per four operating rooms: machine, 100,000; service contract, 25,000; probe replacement/repair 64,000; cleaning, 1200; storage/video, 3600; total cost 193,800.

From Fanshawe M, Ellis C, Habib S, et al: A retrospective analysis of the costs and benefits related to alterations in cardiac surgery from routine intraoperative transesophageal echocardiography. *Anesth Analg* 95:824-827, 2002.

*CABG*, Coronary artery bypass grafting; *MR*, mitral regurgitation; *MV* repair, mitral valve repair; *MVR*, mitral valve replacement; *P2*, middle scallop of posterior mitral valve leaflet; *PFO*, patent foramen ovale; *TR*, tricuspid regurgitation; *TVR*, tricuspid valve replacement.

**TABLE 2-8 Summary of Studies Examining the Alterations in Therapy during Cardiac Surgery with the Use of Intraoperative Transesophageal Echocardiography**

| *Study* | *Population* | *Surgery* | *Altered Therapy,* n/% | *Outcome Reported* |
|---|---|---|---|---|
| Bergquist and colleagues[73,74] | $n = 75$, 584 interventions | C-revasc | 98/17% of all interventions | No |
| Savage and colleagues[77] | $n = 82$, "high risk" | C-revasc | Surgical change: 27/33% of patients | Compared to historical controls |
| Savage and colleagues[77] | $n = 82$, "high risk" | C-revasc | Hemodynamic change: 42/51% of patients | Compared to historical controls |
| Sutton and Kluger[75] | $n = 120$ | C-revasc | 16/13% of all patients | No |
| Kolev and colleagues[79] | $n = 224$, 2232 interventions | C-all NC | 560/25% of all interventions | No |
| Couture and colleagues[81] | $n = 851$ | C-all | 125/15% of all patients | No |
| Mishra and colleagues[82] | $n = 5016$ | C-all | 1146/23% of all patients | No |
| Click and colleagues[70] | $n = 3245$ | C-all | 441/14% of all patients pre-bypass<br>121/4% of all patients post-bypass | No |
| Qaddoura and colleagues[71] | $n = 474$ | C-revasc | 21/4% of all patients pre-bypass | No |
| Qaddoura and colleagues[71] | $n = 474$ | C-revasc | 19/4% of all patients post-bypass | No |
| Forrest and colleagues[72] | $n = 1785$<br>low risk $n = 821$<br>medium risk $n = 696$<br>high risk $n = 268(140)$ | C-revasc | 62/3.5% of all patients<br>2.8%<br>2.9%<br>6.7% | No |

*C-all*, Coronary and noncoronary cardiac surgery; *C-revasc*, coronary revascularizations; *NC*, noncardiac surgery.

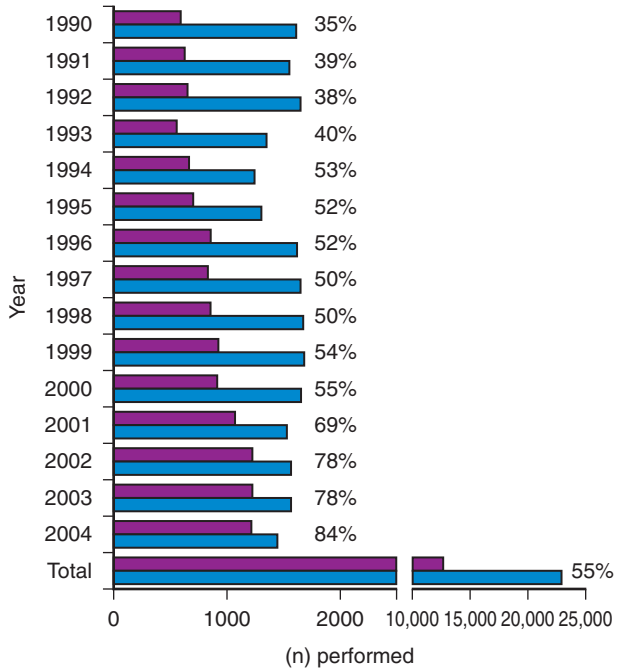



**Figure 2-30** Percent transesophageal echocardiography performed per year. Overview of TEE (*purple bars*) performed per year in 12,566 cardiac surgical patients who underwent intraoperative TEE examination. (*Blue bars*, number of surgeries.) *(From Eltzschig HK, Rosenberger P, Loffler M, et al: Impact of intraoperative transesophageal echocardiography on surgical decisions in 12,566 patients undergoing cardiac surgery.* Ann Thorac Surg *85:845-853, 2008.)*

**TABLE 2-10 Influence of TEE on Surgical Decision Making**

| *Surgical Subset* | *Pre CPB-TEE Influenced Surgical Decisions (%)* | *Post CPB-TEE Influenced Surgical Decisions (%)* |
|---|---|---|
| All patients ($n$ = 12,566) | 7 | 2.2 |
| CABG only ($n$ = 3835) | 5.4 | 1.5 |
| Valve only ($n$ = 3840) | 6.3 | 3.3 |
| CABG + valve ($n$ = 2944) | 12.3 | 2.2 |

From Eltzschig HK, Rosenberger P, Loffler M, et al: Impact of intraoperative transesophageal echocardiography on surgical decisions in 12,566 patients undergoing cardiac surgery. *Ann Thorac Surg* 85: 845-853, 2008.

*CABG*, Coronary artery bypass graft; *CPB*, cardiopulmonary bypass.

retrospective review by Suriani and colleagues,[91] the use of TEE was associated with some alterations in anesthetic and surgical management in most cases. However, the indications for TEE were subjective, and neither the cost effectiveness nor the effect on outcome was studied. Hofer and co-workers[92] prospectively examined patients at "high risk" for myocardial ischemia who were having major noncardiac surgery. A large number of patients had therapeutic changes based on TEE findings (Table 2-11), but outcome data were lacking. Other studies have also described the changes in intraoperative management during noncardiac surgery,[93,94] but cost-effectiveness or outcome data were not provided. The authors acknowledge that randomized controlled clinical trials to evaluate outcome with intraoperative TEE are difficult to perform.

Although data showing improved outcomes is lacking, intraoperative TEE has become an essential tool in the assessment of ventricular function during cardiac surgery and in the monitoring of specific clinical entities, such as device placement and organ transplantation. It must be emphasized that appropriate physician training and quality assurance are crucial to the correct interpretation of data. Numerous technologic advances are on the horizon and may improve intraoperative applicability.

**TABLE 2-11 Preoperative Cardiovascular Diagnoses and Intraoperative Transesophageal Echocardiography: Incidence of Therapeutic Consequences**

| | *Total*, N | *Vasodilator*, n (%) | *Vasopressor*, n (%) | *Fluid*, n (%) |
|---|---|---|---|---|
| CAD | 61 | 36 (59) | 28 (46) | 11 (18) |
| CAD + valve | 13 | 7 (54) | 5 (39) | 5 (39) |
| Valve | 11 | 4 (36) | 3 (27) | 2 (18) |
| SWMA | 28 | 26 (93)* | 20 (71)* | 9 (32) |
| EF <40% | 15 | 8 (53) | 6 (40) | 1 (7) |
| LHF | 10 | 8 (80)* | 3 (30) | 1 (10) |
| PAH | 11 | 8 (73)* | 8 (73)* | 4 (36) |
| RHF | 10 | 7 (70)* | 5 (50) | 2 (20) |
| Total | 99 | 54 (55) | 43 (43) | 24 (24) |

Vasodilator/vasopressor/fluid, new therapy, or changes of therapy with respect to vasodilator/vasopressor and fluid management.

From Hofer CK, Zollinger A, Rak M, et al: Therapeutic impact of intra-operative transoesophageal echocardiography during noncardiac surgery. *Anaesthesia* 59:3-9, 2004.

*CAD*, Coronary artery disease; *EF*, ejection fraction; *LHF*, left-sided heart failure; *PAH*, pulmonary arterial hypertension; *RHF*, right-sided heart failure; *SWMA*, systolic wall motion abnormality; *Valve*, valve diseases.

*$P$ <0.05.

## KEY POINTS

- TEE is an essential tool for monitoring cardiac function in the operating room.
- TEE allows evaluation of ventricular function and filling pressures.
- Doppler-derived cardiac output is best calculated using velocity and diameter obtained from the left ventricular outflow tract.
- Although the calculation of left ventricular contractility using TEE is prohibitively complex, the fractional area of change provides a useful surrogate and is suited to the rapidly changing environment of the operating room.
- TEE assessment of intraoperative RV function is best accomplished by visual inspection and semiquantitative assessment in both the transgastric and the four-chamber views.
- Knowledge of the coronary circulation allows the echocardiographer to inform the surgeon of culprit vessels in the setting of ischemic wall motion abnormalities.
- Using TEE, the echocardiographer can guide the surgeon in placement of the coronary sinus cardioplegia cannula, the intraaortic balloon pump, and other intravascular devices.
- After heart or lung transplantation, TEE is important in the assessment of overall graft function and anastomotic integrity.
- Using TEE, the echocardiographer can guide the surgeon in evacuating air from the left ventricle following cardiopulmonary bypass.
- TEE is particularly useful for in determining the etiology of failure to wean from cardiopulmonary bypass.

## REFERENCES


1. Kuecherer HF, Muhiudeen IA, Kusumoto FM, et al: Estimation of mean left atrial pressure from transesophageal pulsed Doppler echocardiography of pulmonary venous flow. *Circulation* 82:1127-1139, 1990.
2. Nomura M, Hillel Z, Shih H, et al: The association between Doppler transmitral flow variables measured by transesophageal echocardiography and pulmonary capillary wedge pressure. *Anesth Analg* 84:491-496, 1997.
3. Kinnaird TD, Thompson CR, Munt BI: The deceleration [correction of declaration] time of pulmonary venous diastolic flow is more accurate than the pulmonary artery occlusion pressure in predicting left atrial pressure. *J Am Coll Cardiol* 37:2025-2030, 2001.
4. Lattik R, Couture P, Denault AY, et al: Mitral Doppler indices are superior to two-dimensional echocardiographic and hemodynamic variables in predicting responsiveness of cardiac output to a rapid intravenous infusion of colloid. *Anesth Analg* 94:1092-1099, 2002.
5. Swenson JD, Bull D, Stringham J: Subjective assessment of left ventricular preload using transesophageal echocardiography: corresponding pulmonary artery occlusion pressures. *J Cardiothorac Vasc Anesth* 15:580-583, 2001.
6. Groban L, Dolinski SY: Transesophageal echocardiographic evaluation of diastolic function. *Chest* 128:3652-3663, 2005.
7. Eshoo S, Ross DL, Thomas L: Evaluation of left atrial size on transoesophageal echocardiography: what is the best measure? *Heart Lung Circ* 17:100-106, 2008.
8. Tsang MW, Davidoff R, Korach A, et al: Diastolic dysfunction after coronary artery bypass grafting: the effect of glucose-insulin-potassium infusion. *J Card Surg* 22:185-191, 2007.
9. Pauliks LB, Undar A, Clark JB, et al: Segmental differences of impaired diastolic relaxation following cardiopulmonary bypass surgery in children: a tissue Doppler study. *Artif Organs* 33:904-908, 2009.
10. Denault AY, Couture P, Buithieu J, et al: Left and right ventricular diastolic dysfunction as predictors of difficult separation from cardiopulmonary bypass. *Can J Anaesth* 53:1020-1029, 2006.
11. Ho CY, Solomon SD: A clinician's guide to tissue Doppler imaging. *Circulation* 113:e396-e398, 2006.
12. Masutani S LW, Hasegawa H, Cheng HJ, Cheng CP: Restrictive left ventricular filling pattern does not result from increased left atrial pressure alone. *Circulation* 117:1550-1554, 2008.
13. Djaiani GN, McCreath BJ, Ti LK, et al: Mitral flow propagation velocity identifies patients with abnormal diastolic function during coronary artery bypass graft surgery. *Anesth Analg* 95:524-530, 2002.
14. Lang RM, Bierig M, Devereux RB, et al: Recommendations for chamber quantification: a report from the American Society of Echocardiography's Guidelines and Standards Committee and the Chamber Quantification Writing Group, developed in conjunction with the European Association of Echocardiography, a branch of the European Society of Cardiology. *J Am Soc Echocardiogr* 18:1440-1463, 2005.
15. Cheung AT, Savino JS, Weiss SJ, et al: Echocardiographic and hemodynamic indexes of left ventricular preload in patients with normal and abnormal ventricular function. *Anesthesiology* 81:376-387, 1994.
16. Smith MD, MacPhail B, Harrison MR, et al: Value and limitations of transesophageal echocardiography in determination of left ventricular volumes and ejection fraction. *J Am Coll Cardiol* 19:1213-1222, 1992.
17. Colombo PC, Municino A, Brofferio A, et al: Cross-sectional multiplane transesophageal echocardiographic measurements; Comparison with standard transthoracic values obtained in the same setting. *Echocardiography* 19:383-390, 2002.
18. Vegas A, Meineri M: Core review: three-dimensional transesophageal echocardiography is a major advance for intraoperative clinical management of patients undergoing cardiac surgery: a core review. *Anesth Analg* 110:1548-1573, 2010.
19. Savino JS, Troianos CA, Aukburg S, Weiss R, Reichek N: Measurement of pulmonary blood flow with transesophageal two-dimensional and Doppler echocardiography. *Anesthesiology* 75: 445-451,1991.
20. Samstad SO, Torp HG, Linker DT, et al: Cross sectional early mitral flow velocity profiles from colour Doppler. *Br Heart J* 62:177-184, 1989.
21. Schober P, Loer SA, Schwarte LA: Perioperative hemodynamic monitoring with transesophageal Doppler technology. *Anesth Analg* 109:340-353, 2009.
22. Bein B, Worthmann F, Tonner PH, et al: Comparison of esophageal Doppler, pulse contour analysis, and real-time pulmonary artery thermodilution for the continuous measurement of cardiac output. *J Cardiothorac Vasc Anesth* 18:185-189, 2004.
23. Leather HA, Wouters PF: Oesophageal Doppler monitoring overestimates cardiac output during lumbar epidural anaesthesia. *Br J Anaesth* 86:794-797, 2001.
24. Knirsch W, Kretschmar O, Tomaske M, et al: Comparison of cardiac output measurement using the CardioQP oesophageal Doppler with cardiac output measurement using thermodilution technique in children during heart catheterisation. *Anaesthesia* 63:851-855, 2008.
25. Parra V, Fita G, Rovira I, et al: Transoesophageal echocardiography accurately detects cardiac output variation: a prospective comparison with thermodilution in cardiac surgery. *Eur J Anaesthesiol* 25:135-143, 2008.
26. Gorcsan JD, Diana P, Ball BA, et al: Intraoperative determination of cardiac output by transesophageal continuous wave Doppler. *Am Heart J* 123:171-176, 1992.
27. Maslow A, Comunale ME, Haering JM, et al: Pulsed wave Doppler measurement of cardiac output from the right ventricular outflow tract. *Anesth Analg* 83:466-471, 1996.
28. Royse CF, Connelly KA, MacLaren G, et al: Evaluation of echocardiography indices of systolic function: a comparative study using pressure-volume loops in patients undergoing coronary artery bypass surgery. *Anaesthesia* 62:109-116, 2007.
29. Sagawa K: The end-systolic pressure-volume relation of the ventricle: definition, modifications and clinical use. *Circulation* 63:1223-1227, 1981.
30. Galiuto L, Ignone G, DeMaria AN: Contraction and relaxation velocities of the normal left ventricle using pulsed-wave tissue Doppler echocardiography. *Am J Cardiol* 81:609-614, 1998.
31. Maclaren G, Kluger R, Prior D, et al: Tissue Doppler, strain, and strain rate echocardiography: principles and potential perioperative applications. *J Cardiothorac Vasc Anesth* 20:583-593, 2006.
32. Simmons LA, Weidemann F, Sutherland GR, et al: Doppler tissue velocity, strain, and strain rate imaging with transesophageal echocardiography in the operating room: a feasibility study. *J Am Soc Echocardiogr* 15:768-776, 2002.
33. Skarvan K, Filipovic M, Wang J, et al: Use of myocardial tissue Doppler imaging for intraoperative monitoring of left ventricular function. *Br J Anaesth* 91:473-480, 2003.
34. Lee CH, Yang MM, Ho AC, et al: Evaluation of the longitudinal contraction of the ventricle septum in patients undergoing off-pump coronary artery bypass graft surgery by strain rate imaging. *Acta Anaesthesiol Taiwan* 44:11-18, 2006.
35. Kukucka M, Nasseri B, Tscherkaschin A, et al: The feasibility of speckle tracking for intraoperative assessment of regional myocardial function by transesophageal echocardiography. *J Cardiothorac Vasc Anesth* 23:462-467, 2009.
36. Bargiggia GS, Bertucci C, Recusani F, et al: A new method for estimating left ventricular dP/dt by continuous wave Doppler-echocardiography. Validation studies at cardiac catheterization. *Circulation* 80:1287-1292, 1989.
37. Poelaert JI, Schupfer G: Hemodynamic monitoring utilizing transesophageal echocardiography: the relationships among pressure, flow, and function. *Chest* 127:379-390, 2005.
38. Winkelmann J, Aronson S, Young CJ, et al: Retrograde-delivered cardioplegia is not distributed equally to the right ventricular free wall and septum. *J Cardiothorac Vasc Anesth* 9:135-139, 1995.
39. Samad BA, Alam M, Jensen-Urstad K: Prognostic impact of right ventricular involvement as assessed by tricuspid annular motion in patients with acute myocardial infarction. *Am J Cardiol* 90:778-781, 2002.
40. David JS, Tousignant CP, Bowry R: Tricuspid annular velocity in patients undergoing cardiac operation using transesophageal echocardiography. *J Am Soc Echocardiogr* 19:329-334, 2006.
41. Tousignant C, Desmet M, Bowry R, et al: Speckle tracking for the intraoperative assessment of right ventricular function: a feasibility study. *J Cardiothorac Vasc Anesth* 24:275-279, 2010.
42. Swaminathan M, Morris RW, De Meyts DD, et al: Deterioration of regional wall motion immediately after coronary artery bypass graft surgery is associated with long-term major adverse cardiac events. *Anesthesiology* 107:739-745, 2007.
43. Schiller NB, Shah PM, Crawford M, et al: Recommendations for quantitation of the left ventricle by two-dimensional echocardiography. American Society of Echocardiography Committee on Standards, Subcommittee on Quantitation of Two-Dimensional Echocardiograms. *J Am Soc Echocardiogr* 2:358-367, 1989.
44. Shanewise JS, Cheung AT, Aronson S, et al: ASE/SCA guidelines for performing a comprehensive intraoperative multiplane transesophageal echocardiography examination: recommendations of the American Society of Echocardiography Council for Intraoperative Echocardiography and the Society of Cardiovascular Anesthesiologists Task Force for Certification in Perioperative Transesophageal Echocardiography. *J Am Soc Echocardiogr* 12:884-900, 1999.
45. Tennant R, Wiggers CJ: The effect of coronary occlusion on myocardial contraction. *Am J Physiol* 112:351-361, 1935.
46. London MJ, Tubau JF, Wong MG, et al: The "natural history" of segmental wall motion

abnormalities in patients undergoing noncardiac surgery. S.P.I. Research Group. *Anesthesiology* 73:644-655, 1990.
47. Leung JM, O'Kelly B, Browner WS, et al: Prognostic importance of postbypass regional wall-motion abnormalities in patients undergoing coronary artery bypass graft surgery. SPI Research Group. *Anesthesiology* 71:16-25, 1989.
48. Comunale MEHP, Body SC, Ley C, et al: The concordance of intraoperative left ventricular wall-motion abnormalities and electrocardiographic S-T segment changes: association with outcome after coronary revascularization. Multicenter Study of Perioperative Ischemia (McSPI) Research Group. *Anesthesiology* 88:945-954, 1998.
49. Hauser AM, Gangadharan V, Ramos RG, et al: Sequence of mechanical, electrocardiographic and clinical effects of repeated coronary artery occlusion in human beings: echocardiographic observations during coronary angioplasty. *J Am Coll Cardiol* 5:193-197, 1985.
50. Nakajima H, Ikari Y, Kigawa I, et al: Rapid diagnosis and management of intraoperative myocardial infarction during valvular surgery: using intraoperative transesophageal echocardiography followed by emergency coronary artery bypass grafting without coronary angiography. *Echocardiography* 22:834-838, 2005.
51. Chan KL: Transesophageal echocardiography for assessing cause of hypotension after cardiac surgery. *Am J Cardiol* 62:1142-1143, 1988.
52. Brandt RR, Oh JK, Abel MD, et al: Role of emergency intraoperative transesophageal echocardiography. *J Am Soc Echocardiogr* 11:972-977, 1998.
53. McKinlay KH, Schinderle DB, Swaminathan M, et al: Predictors of inotrope use during separation from cardiopulmonary bypass. *J Cardiothorac Vasc Anesth* 18:404-408, 2004.
54. Shroyer AL, Grover FL, Hattler B, et al: On-pump versus off-pump coronary-artery bypass surgery. *N Engl J Med* 361:1827-1837, 2009.
55. Peterson ED: Innovation and comparative-effectiveness research in cardiac surgery. *N Engl J Med* 361:1897-1899, 2009.
56. Mishra M, Malhotra R, Karlekar A, et al: Propensity case-matched analysis of off-pump versus on-pump coronary artery bypass grafting in patients with atheromatous aorta. *Ann Thorac Surg* 82:608-614, 2006.
57. Kapoor PM, Chowdhury U, Mandal B, et al: Trans-esophageal echocardiography in off-pump coronary artery bypass grafting. *Ann Card Anaesth* 12:176, 2009.
58. Wang J, Filipovic M, Rudzitis A, et al: Transesophageal echocardiography for monitoring segmental wall motion during off-pump coronary artery bypass surgery. *Anesth Analg* 99:965-973, 2004.
59. Gurbuz AT, Hecht ML, Arslan AH: Intraoperative transesophageal echocardiography modifies strategy in off-pump coronary artery bypass grafting. *Ann Thorac Surg* 83:1035-1040, 2007.
60. Kim SH, Yeo JS, Yoon TG, et al: Placing a saline bag underneath the displaced heart enhances transgastric transesophageal echocardiographic imaging during off-pump coronary artery bypass surgery. *Anesth Analg* 109:1038-1040, 2009.
61. Practice guidelines for perioperative transesophageal echocardiography. An updated report by the American Society of Anesthesiologists and the Society of Cardiovascular Anesthesiologists Task Force on Transesophageal Echocardiography. *Anesthesiology* 112:1084-1096, 2010.
62. Flachskampf FA, Badano L, Daniel WG, et al: Recommendations for transoesophageal echocardiography: update 2010. *Eur J Echocardiogr* 11:557-576, 2010.
63. Memtsoudis SG, Rosenberger P, Loffler M, et al: The usefulness of transesophageal echocardiography during intraoperative cardiac arrest in noncardiac surgery. *Anesth Analg* 102:1653-1657, 2006.
64. Mahmood F, Christie A, Matyal R: Transesophageal echocardiography and noncardiac surgery. *Semin Cardiothorac Vasc Anesth* 12:265-289, 2008.
65. Shanewise JS, Sadel SM: Intraoperative transesophageal echocardiography to assist the insertion and positioning of the intraaortic balloon pump. *Anesth Analg* 79:577-580, 1994.
66. Chumnanvej S, Wood MJ, MacGillivray TE, et al: Perioperative echocardiographic examination for ventricular assist device implantation. *Anesth Analg* 105:583-601, 2007.
67. Michel-Cherqui M, Brusset A, Liu N, et al: Intraoperative transesophageal echocardiographic assessment of vascular anastomoses in lung transplantation. A report on 18 cases. *Chest* 111:1229-1235, 1997.
68. Huang YC, Cheng YJ, Lin YH, et al: Graft failure caused by pulmonary venous obstruction diagnosed by intraoperative transesophageal echocardiography during lung transplantation [In Process Citation]. *Anesth Analg* 91:558-559, 2000.
69. Reeves ST, Glas KE, Eltzschig H, et al: Guidelines for performing a comprehensive epicardial echocardiography examination: recommendations of the American Society of Echocardiography and the Society of Cardiovascular Anesthesiologists. *J Am Soc Echocardiogr* 20:427-437, 2007.
70. Glas KE, Swaminathan M, Reeves ST, et al: Guidelines for the performance of a comprehensive intraoperative epiaortic ultrasonographic examination: recommendations of the American Society of Echocardiography and the Society of Cardiovascular Anesthesiologists; endorsed by the Society of Thoracic Surgeons. *J Am Soc Echocardiogr* 20:1227-1235, 2007.
71. Kallmeyer IJ, Collard CD, Fox JA, et al: The safety of intraoperative transesophageal echocardiography: A case series of 7200 cardiac surgical patients. *Anesth Analg* 92:1126-1130, 2001.
72. Click RL, Abel MD, Schaff HV: Intraoperative transesophageal echocardiography: 5-year prospective review of impact on surgical management. *Mayo Clin Proc* 75:241-247, 2000.
73. Qaddoura FE, Abel MD, Mecklenburg KL, et al: Role of intraoperative transesophageal echocardiography in patients having coronary artery bypass graft surgery. *Ann Thorac Surg* 78:1586-1590, 2004.
74. Forrest AP, Lovelock ND, Hu JM, et al: The impact of intraoperative transoesophageal echocardiography on an unselected cardiac surgical population: a review of 2343 cases. *Anaesth Intensive Care* 30:734-741, 2002.
75. Bergquist BD, Leung JM, Bellows WH: Transesophageal echocardiography in myocardial revascularization: I. Accuracy of intraoperative real-time interpretation. *Anesth Analg* 82:1132-1138, 1996.
76. Bergquist BD, Bellows WH, Leung JM: Transesophageal echocardiography in myocardial revascularization: II. Influence on intraoperative decision making. *Anesth Analg* 82:1139-1145, 1996.
77. Mathew JP, Fontes ML, Garwood S, et al: Transesophageal echocardiography interpretation: a comparative analysis between cardiac anesthesiologists and primary echocardiographers. *Anesth Analg* 94:302-309, 2002.
78. Savage RM, Lytle BW, Aronson S, et al: Intraoperative echocardiography is indicated in high-risk coronary artery bypass grafting [see comments]. *Ann Thorac Surg* 64:368-373, 1997.
79. Higgins TL, Estafanous FG, Loop FD, et al: Stratification of morbidity and mortality outcome by preoperative risk factors in coronary artery bypass patients. A clinical severity score. *JAMA* 267:2344-2348, 1992.
80. Sutton DC, Kluger R: Intraoperative transoesophageal echocardiography: impact on adult cardiac surgery. *Anaesth Intensive Care* 26:287-293, 1998.
81. Kolev N, Brase R, Swanevelder J, et al: The influence of transoesophageal echocardiography on intra-operative decision making. A European multicentre study. European Perioperative TOE Research Group. *Anaesthesia* 53:767-773, 1998.
82. Mahdy S, Brien BO, Buggy D, et al: The impact of intraoperative transoesophageal echocardiography on decision-making during cardiac surgery. *Middle East J Anesthesiol* 20:199-206, 2009.
83. Couture P, Denault AY, McKenty S, et al: Impact of routine use of intraoperative transesophageal echocardiography during cardiac surgery. *Can J Anaesth* 47:20-26, 2000.
84. Mishra M, Chauhan R, Sharma KK, et al: Real-time intraoperative transesophageal echocardiography—how useful? Experience of 5,016 cases. *J Cardiothorac Vasc Anesth* 12:625-632, 1998.
85. Bettex DA, Pretre R, Jenni R, et al: Cost-effectiveness of routine intraoperative transesophageal echocardiography in pediatric cardiac surgery: a 10-year experience. *Anesth Analg* 100:1271-1275, 2005.
86. Seto TB, Taira DA, Tsevat J, et al: Cost-effectiveness of transesophageal echocardiographic-guided cardioversion: a decision analytic model for patients admitted to the hospital with atrial fibrillation. *J Am Coll Cardiol* 29:122-130, 1997.
87. Rosen AB, Fowler VG, Jr, Corey GR, et al: Cost-effectiveness of transesophageal echocardiography to determine the duration of therapy for intravascular catheter-associated *Staphylococcus aureus* bacteremia [see comments]. *Ann Intern Med* 130:810-820, 1999.
88. Fanshawe M, Ellis C, Habib S, et al: A retrospective analysis of the costs and benefits related to alterations in cardiac surgery from routine intraoperative transesophageal echocardiography. *Anesth Analg* 95:824-827, 2002.
89. Eltzschig HK, Rosenberger P, Loffler M, et al: Impact of intraoperative transesophageal echocardiography on surgical decisions in 12,566 patients undergoing cardiac surgery. *Ann Thorac Surg* 85:845-853, 2008.
90. Greilich PE: Invited commentary. *Ann Thorac Surg* 85:852-853, 2008.
91. Suriani RJ, Neustein S, Shore-Lesserson L, et al: Intraoperative transesophageal echocardiography during noncardiac surgery. *J Cardiothorac Vasc Anesth* 12:274-280, 1998.
92. Hofer CK, Zollinger A, Rak M, et al: Therapeutic impact of intra-operative transoesophageal echocardiography during noncardiac surgery. *Anaesthesia* 59:3-9, 2004.
93. Canty DJ, Royse CF: Audit of anaesthetist-performed echocardiography on perioperative management decisions for non-cardiac surgery. *Br J Anaesth* 103:352-358, 2009.
94. Schulmeyer MC, Santelices E, Vega R, et al: Impact of intraoperative transesophageal echocardiography during noncardiac surgery. *J Cardiothorac Vasc Anesth* 20:768-771, 2006.



# Contrast Ultrasound Imaging: Technical Aspects and Clinical Applications

THOMAS R. PORTER, MD | FENG XIE, MD

**Left Ventricular Ultrasonic Contrast Agents**
Characteristics of Microbubbles
Clinical Contrast Agents
**Perfusion Imaging Techniques**
Harmonic High–Mechanical-Index Intermittent Imaging (Harmonic) Power Doppler
Low–Mechanical-Index Imaging Schemes
**Qualitative and Quantitative Methods of Analysis**
Continuous Infusion Imaging
Technical Equipment, Image Processing, and Artifacts
**Safety of Ultrasound Contrast**
**Clinical Applications of Contrast Enhanced Ultrasound**
Detecting Acute Ischemia/Risk Area in the Emergency Setting
Assessment of Myocardial Viability in the Acute and Chronic Setting
Detection of Coronary Artery Disease
**Other Diagnostic Applications of Microbubbles**
Improved Left Ventricular Cavity Opacification
Doppler Enhancement
Contrast Perfusion Imaging of Other Organs
Molecular Imaging with Contrast Ultrasound
Detection of Carotid Artery Atherosclerosis
**Therapeutic Applications of Ultrasound and Microbubbles**
Drug and Gene Delivery
Thrombolysis

The use of intravenous microbubbles for real-time perfusion imaging is now a reality. There is a consensus throughout the ultrasound community that ultrasound contrast is safe and effective for improving endocardial border delineation and should be used for improving left ventricular (LV) wall motion and detecting LV apical hypertrophy, noncompaction, thrombus, endomyocardial fibrosis, takotsubo, LV aneurysm, or pseudoaneurysm.[1] Furthermore, multicenter studies have demonstrated perfusion imaging with ultrasound contrast is comparable to radionuclide imaging, with the potential to improve spatial resolution, detect subendocardial ischemia, and reduce ionizing radiation exposure to the patient. Single-center studies have consistently demonstrated the incremental clinical benefit of myocardial perfusion imaging during dobutamine, vasodilator, or bicycle stress echocardiography, and in the evaluation of acute coronary syndromes. Intravenous targeted microbubbles also have a potential role in molecular imaging of arteriogenesis and transplant rejection, as well as in the detection of remote ischemia. Ultrasound-mediated microbubble destruction serves as a mechanism for targeting drug and gene delivery. Image-guided targeted microbubble destruction with ultrasound is being used to noninvasively dissolve intravascular and microvascular thrombi in ischemic stroke and acute myocardial infarction animal models either with reduced-dose fibrinolytic agents or in the absence of fibrinolytic agents. The actual clinical role of contrast echocardiography in these areas remains uncertain, but clearly the potential exists for tremendous advances in both the detection of cardiovascular disease and prompt noninvasive therapies.

## Left Ventricular Ultrasonic Contrast Agents

### CHARACTERISTICS OF MICROBUBBLES

Microbubbles must meet numerous physical and chemical standards to reach the LV cavity and myocardium following venous injection. The first requirement is size. Microbubbles greater than 8 μm in diameter are filtered from the pulmonary circulation and will not reach the LV cavity.[2] The scattering cross section of a microbubble is related to the sixth power of its radius, and thus the smaller bubbles that reach the LV are less reflective than the bubbles filtered by the pulmonary circulation. To detect the comparatively weak echoes of the bubbles small enough for transpulmonary passage, imaging modalities have been developed that register the more "microbubble-specific" resonant frequencies. The resonant frequency of a microbubble is inversely related to its diameter.[3]

Another problem arising with the small microbubble size is surface tension. The internal pressure of gases within microbubbles is increased dramatically as the size of a microbubble decreases to less than 7 μm. Therefore, the gases within the microbubbles are at very high concentration and rapidly diffuse into blood. This immediately reduces their size and hence their contrast effect, a limitation that becomes most evident when attempts are made to obtain myocardial ultrasonographic contrast from an intravenous injection. Therefore, a second requirement for intravenous microbubbles is to have a method of preventing dissolution after exposure to blood. The gas composition is one of the most important factors for retention of microbubble size in circulation. First-generation contrast agents

**TABLE 3-1 Recent Microbubble Formulations (Approved and Not Approved by the U.S. Food and Drug Administration)**

| *Name* | *Manufacturer* | *Size, μm* | *Concentration* | *Shell Composition* | *Indication* | *Gas Content* | *Availability* |
|---|---|---|---|---|---|---|---|
| AI-700 | Acusphere | 2.9 | — | Synthetic polymer | Myocardial perfusion | Perfluorocarbon | Not approved |
| CARDIOsphere | Point BioMedical | 4.0 | — | Polymer bilayer | Myocardial perfusion | Nitrogen | Not approved |
| Definity | Bristol-Myers Squibb | 1.1-3.3 | $1.2 \times 10^{10}$ | Lipid encapsulated | LV opacification | Perfluoropropane | USA |
| Optison7 | GE Healthcare | 2.0-4.5 | $5\text{-}8 \times 10^{8}$ | Denatured albumin | LV opacification | Perfluoropropane | |
| SonoVue | Bracco | 2.5 | $1.0\text{-}5.0 \times 10^{8}$ | Phospholipids | LV opacification and myocardial perfusion | Sulfur hexafluoride | Europe, Asia |

contained room air, which is 78% nitrogen. Because nitrogen rapidly diffuses, these microbubbles survived only seconds.[4] To overcome this problem, slowly diffusing, high–molecular-weight insoluble gases were incorporated into the microbubbles. The diffusivity of a gas is inversely proportional to the square root of its molecular weight (Graham's law). When less soluble gases with a higher molecular weight were incorporated inside the microbubble, the microbubbles became more stable so that myocardial contrast could be visualized following intravenous injections. Perfluorocarbons have the added advantage of preferentially remaining a gas instead of becoming a liquid at higher temperatures (low Ostwald coefficient). Several types of microbubble solutions containing high–molecular-weight gases have been developed for potential clinical use (Table 3-1).

### CLINICAL CONTRAST AGENTS

Optison (GE Healthcare, Princeton, N.J.) was the first perfluorocarbon-containing intravenous ultrasonographic contrast agent approved for use in humans. Its indication was enhancement of LV opacification from intravenous injection. Perfluorocarbon-exposed sonicated dextrose albumin (PESDA) is a contrast agent formulated on-site by sonicating 5% dextrose with 5% human serum albumin (3:1 mixture) after hand agitating this mixture with the perfluorocarbon decafluorobutane. Intravenously injected perfluorocarbon-containing sonicated albumin microbubbles appear to have a rapid transit through the myocardium and do not affect LV function, coronary and systemic hemodynamics, or pulmonary gas exchange. Both PESDA and Optison have proven to be capable of creating consistent myocardial contrast enhancement in animal and human studies when used with newer imaging techniques.[5-7]

Definity (Lantheus Medical Imaging, North Billerica, Mass.) has also received U.S. Food and Drug Administration (FDA) approval for endocardial border detection. Definity is a lipid-coated microbubble that is formed from two components: a long-chain lipid and an emulsifier. This is typically a saturated diacyl phosphatidylcholine and a polyethylene glycol spacer. To create stable microbubbles, this mixture must be activated with a Vialmix device. In Europe, Sonovue (Bracco Diagnostics, Milan, Italy) has been approved as a contrast agent for limited clinical applications. This microbubble has a phospholipid shell surrounding a sulfur hexafluoride gas.

Two recent ultrasound contrast agents sought FDA approval as myocardial perfusion imaging agents. One agent was formulated by altering microbubble shell thickness (CARDIOsphere; Point BioMedical, San Carlos, Calif.). This agent has an albumin and polylactide shell that is of sufficient thickness that it remains stable in the bloodstream even though the encapsulated gas is nitrogen. Although it was never approved by the FDA, multicenter clinical trials were performed with this unique microbubble to detect myocardial perfusion abnormalities during dipyridamole stress echocardiography.[8] Another fluorocarbon-based microbubble, Imagify (Acusphere Inc., Lexington, Mass.) also sought FDA approval for a myocardial perfusion indication, but also was denied despite completing multicenter trials showing accuracy for detecting coronary artery disease equivalent to radionuclide imaging.[9] This agent was used to improve LV opacification and assess myocardial perfusion (Fig. 3-1) and had receiver operator characteristics identical to those of radionuclide imaging in detecting coronary artery disease (Fig. 3-2).

## Perfusion Imaging Techniques

Although high–molecular-weight gases have rendered thin-shelled microbubbles more stable, their detection in the myocardium with echocardiographic equipment is limited with conventional imaging techniques. The development of harmonic imaging, intermittent imaging, harmonic power Doppler, and, more recently low mechanical-index (MI) real-time detection techniques has dramatically enhanced the myocardial contrast produced from intravenously injected microbubbles.

### HARMONIC HIGH–MECHANICAL-INDEX INTERMITTENT IMAGING

Microbubbles in an ultrasonic field have the ability to scatter ultrasound not only linearly but also nonlinearly. At peak incident pressures (above 0.1 megapascals), the microbubbles respond in a nonlinear manner. This physical property is attributable to the fact that gas bubbles are compliant and react to insonation at diagnostic frequencies with compression and rarefaction, thus emitting radial oscillations. However, the magnitude of compression and rarefaction is not the same with each oscillation, and therefore both linear and nonlinear returning waves occur.[10] The nonlinear responses occur in both the fundamental and harmonic frequencies and can be received and filtered by an appropriate echocardiography system. Because tissue and side lobes exhibit a significantly smaller nonlinear response to ultrasound, ultrasonic transducers that selectively receive the nonlinear responses produce a much better signal-to-noise ratio and more sensitive detection of microbubbles than conventional imaging.[11]

Microbubbles are destroyed by real-time ultrasound when it is transmitted at diagnostic intensities (MIs greater than 0.3). Destruction can be reduced by selecting one frame out of every one to several cardiac cycles, usually with triggering the frame to the electrocardiogram. This has been referred to as intermittent imaging. When the intermittent ultrasound impulse is at a

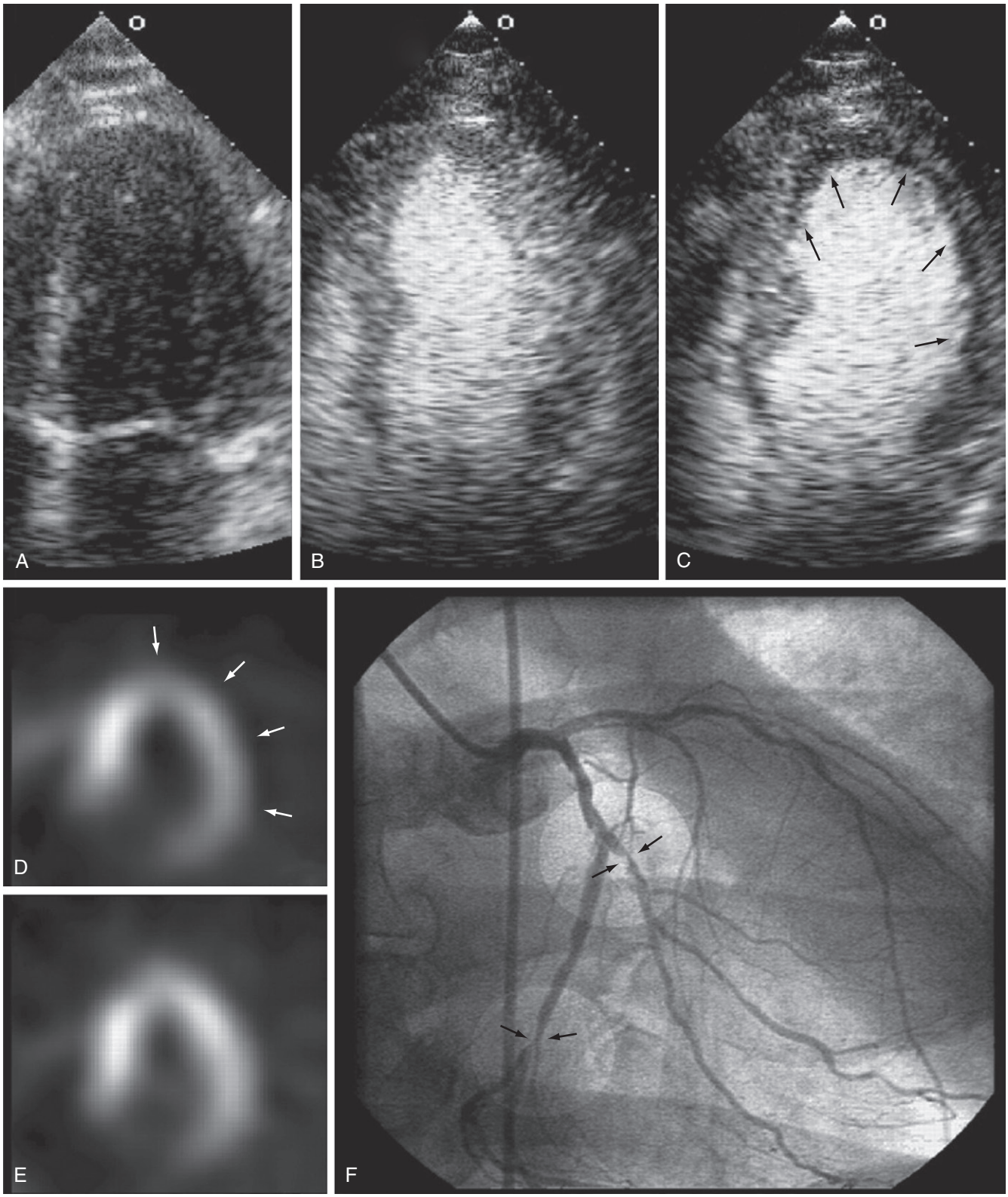



**Figure 3-1 Example of a myocardial perfusion defect.** These images were produced with the Acusphere contrast agent (Imagify) in a multicenter trial, comparing perfusion imaging with real-time perfusion echocardiography precontrast (**A**), at rest (**B**), and with stress (**C**), which shows a decrease in apical and lateral myocardial perfusion (*arrows*), with radionuclide stress (**D**) and rest (**E**) images, which show lateral ischemia, and the corresponding angiogram (**F**) showing circumflex artery stenosis (*arrow*). *(Reprinted, with permission, from Senior R, Monaghan M, Main ML, et al: Detection of coronary artery disease with perfusion stress echocardiography using a novel ultrasound imaging agent: two phase 3 international trials in comparison with radionuclide perfusion imaging.* Eur J Echocardiogr *10:26-35, 2009.)*

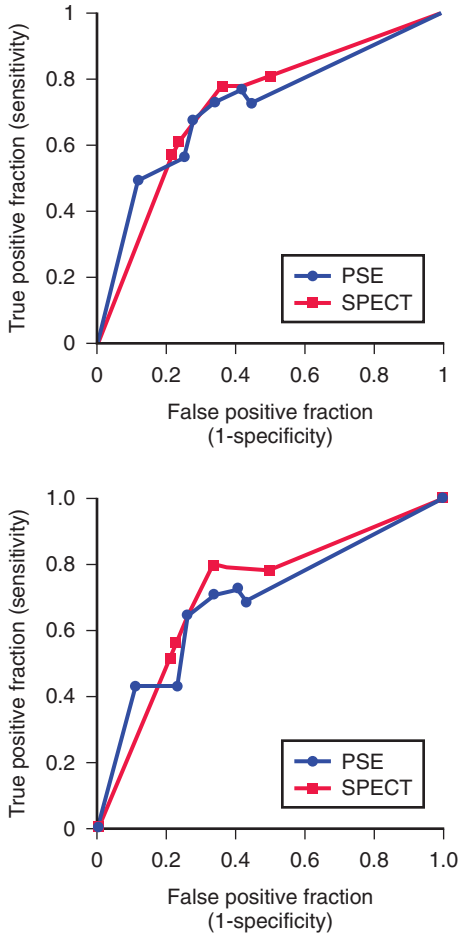



**Figure 3-2** Receiver operator characteristic curve for myocardial perfusion imaging with the Acusphere contrast agent and radionuclide single photon emission computed tomography (SPECT) imaging compared to quantitative coronary angiography in 622 chronic, stable, chest pain patients (*top*) and in the 492 patients without prior myocardial infarction (*bottom*). The points on the curves indicate the results for each reader (4 for SPECT and 6 for PSE). *(Reprinted, with permission, from Senior R, Monaghan M, Main ML, et al: Detection of coronary artery disease with perfusion stress echocardiography using a novel ultrasound imaging agent: two phase 3 international trials in comparison with radionuclide perfusion imaging.* Eur J Echocardiogr *10:26-35, 2009.)*

high intensity (MIs above 0.9), there is a strong and brief nonlinear echo. This transient scattering produces a large contrast signal from the microbubbles.[12,13] Interrupting the high-intensity ultrasound for a short period of time allows for replenishment of microbubbles, which serve to produce contrast enhancement for the subsequent triggered frame. When microbubbles are administered as a continuous infusion and the ultrasound pulsing interval is incrementally varied, the reappearance of bubbles in the myocardium permits the calculation of mean microbubble velocity and plateau (or peak) myocardial signal intensity.[14] Because the background subtracted plateau intensity correlates with capillary cross-sectional area, multiplying the contrast replenishment rate and plateau intensity allows one to quantify myocardial blood flow changes. Therefore, with a combination of second harmonic and intermittent imaging, it has become possible to noninvasively examine myocardial perfusion in animals and humans using a wide variety of intravenous higher molecular-weight microbubbles.[3,15-18]

## (HARMONIC) POWER DOPPLER

Power Doppler images are based on the integrated power in the Doppler signal instead of its mean frequency shift, as used in conventional color Doppler.[19] The amplitude of the Doppler signal is related to the concentration of moving scatterers at a particular location. This amplitude is much greater in the presence of microbubbles when compared with the signal of red blood cells.[20] This type of Doppler signal is more sensitive, not subject to aliasing, and independent of the angle of insonation. Intermittent harmonic power Doppler, therefore, can be used just like intermittent harmonic imaging to examine myocardial blood flow changes. It is, however, subject to flash artifacts, which occur with movement of the heart. Harmonic power Doppler has been successfully employed in animal[21] and human myocardial perfusion studies, showing satisfactory concordance in the comparison between echocardiographic and $^{99m}$Tc-sestamibi single-photon emission computed tomography (SPECT) stress imaging.[22,23]

## LOW–MECHANICAL-INDEX IMAGING SCHEMES

Significant achievements have been made in low-MI real-time visualization of myocardial function and perfusion. Pulse inversion Doppler is a multipulse technique that separates linear and nonlinear scattering using the radiofrequency domain. The concept is an extension of pulse inversion, in which alternating positive and negative pulses of identical amplitude are transmitted into the tissue, the sum signal of which is equal to 0 (Fig. 3-3). The responses of linear scatterers to this kind of pulse, therefore, will be canceled. On the other hand, the signal from nonlinear scatterers (which do not react to positive and negative pressures in the same way) will not be equal to 0 and can be registered as a bubble-specific response.[24] Pulse inversion Doppler overcomes motion artifacts by sending multiple pulses of alternating polarity into the myocardium. This allows one to visualize wall thickening and contrast enhancement simultaneously at very low MIs (less than 0.2) while maintaining an excellent signal-to-noise ratio. Since it can receive only even order harmonics, however, there is significant attenuation, especially in basal myocardial segments in apical windows. Initial studies using this technique in humans have demonstrated brilliant myocardial opacification from very small bolus injections of intravenous Optison.[25,26]

Power modulation is another technique that improves the signal-to-noise ratio at very low MIs. This technique, developed by Philips (Andover, Mass.), is also a multipulse cancellation technique, only here the power of each pulse is varied. The low-power pulses create a linear response, whereas the slightly higher power pulse results in a linear response from tissue but a nonlinear response from bubbles. The linear responses from the two different pulses (the amplified low-power pulse and the slightly higher power pulse) can be subtracted from each other. The transducer then sees only the nonlinear behavior, which emanates exclusively from the microbubbles. Both pulse inversion Doppler and power modulation can be used at very low MIs to assess myocardial contrast in real time with excellent spatial resolution at higher bandwidths.

Contrast pulse sequencing (Siemens Acuson Sequoia; Mountain View, Calif.) extends these multipulse techniques by interpulse phase and amplitude modulation.[27] An example of the excellent myocardial tissue rejection and increased microbubble signal intensity with contrast pulse sequencing in a normal

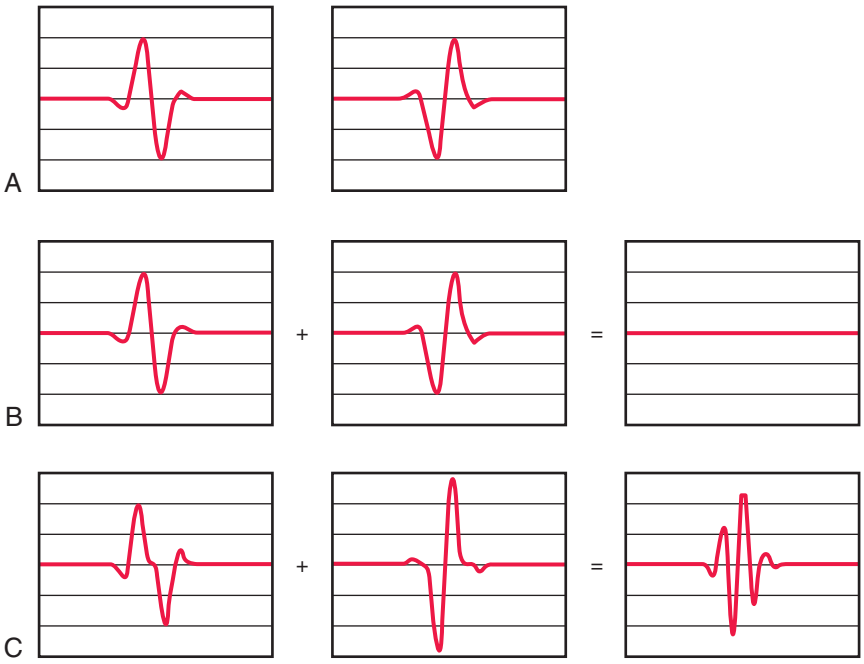



**Figure 3-3 How pulse inversion is used to suppress nonlinear responses from tissue and elicit nonlinear responses from microbubbles.** Pulses of alternating polarity (**A**), when transmitted to tissue, will cancel each other out with the summed response shown in **B**. However, because microbubbles respond nonlinearly to these pulses of alternating polarity, there is actually a nonlinear response (**C**) at twice the transmitted frequency. *(With permission from Rafter P, Phillips P, Vannan MA: Imaging technologies and techniques.* Cardiol Clin *22:181-197, 2004.)*

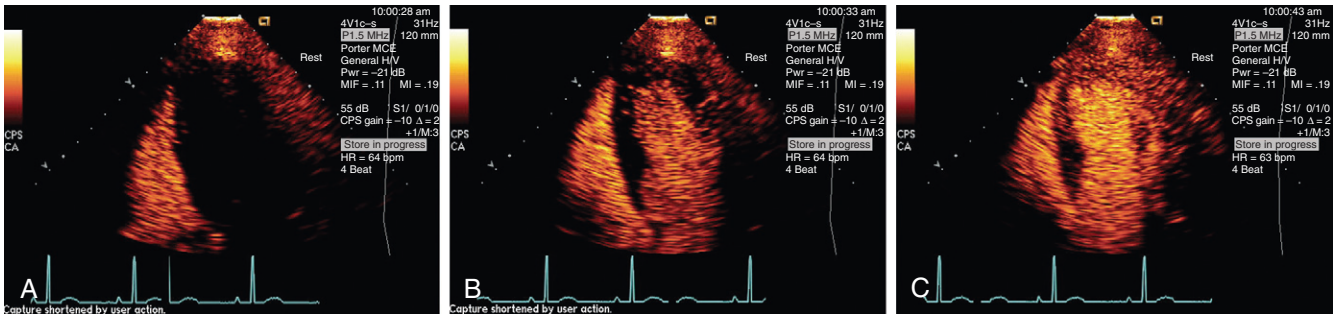



**Figure 3-4 Contrast pulse sequencing images.** Example of the absence of tissue signal from the LV cavity or muscle (apical four-chamber view prior to contrast in panel **A**) and the bright LV cavity (**B**) and myocardial contrast enhancement (**C**) in a patient being imaged with the interpulse phase and amplitude modulation scheme. *(With permission from Contrast Pulse Sequencing; Siemens Acuson Sequoia.)*

**TABLE 3-2 Different Low–Mechanical-Index Imaging Techniques**

| *Name* | *Company Manufacturer* | *Tissue Cancellation* | *Nonlinear Activity* | *Advantages/Disadvantages* |
|---|---|---|---|---|
| Pulse inversion Doppler | Philips | Alternating polarity | Even order harmonics | Spatial resolution/<br>Attenuation and low sensitivity |
| Power modulation | Philips Agilent | Alternating amplitude | Fundamental | Sensitivity/<br>Sensitivity<br>Poor resolution |
| Contrast pulse sequencing | Siemens<br>Acuson | Alternating amplitude/polarity | Fundamental and harmonics | Sensitivity and resolution/<br>Sensitivity |

The methods by which the pulse sequence schemes cancel tissue and the frequency in which enhanced nonlinear response is detected is also shown.

patient from the apical four-chamber view is displayed in Figure 3-4. Table 3-2 summarizes the various perfusion imaging techniques and lists their advantages and disadvantages.

## Qualitative and Quantitative Methods of Analysis

Regardless of the route of microbubble injection, an accurate definition of microbubble concentration in the myocardium requires that the relationship between concentration and signal intensity be linear. This precondition is fulfilled at low intramyocardial microbubble concentrations; with an increase of the concentration, however, echocardiographic systems normally reach a saturation point, where videointensity is no longer proportional to the microbubble concentration.[28] This becomes a factor with bolus injections of microbubbles, in which transient high concentrations can be reached even in regions with reduced myocardial blood flow, leading to a brief period during which contrast enhancement falsely appears normal in these regions. It is not until microbubble concentration falls during the washout period that differences in microbubble concentration are visually evident. It is during this time period that there is a linear relationship between concentration and signal

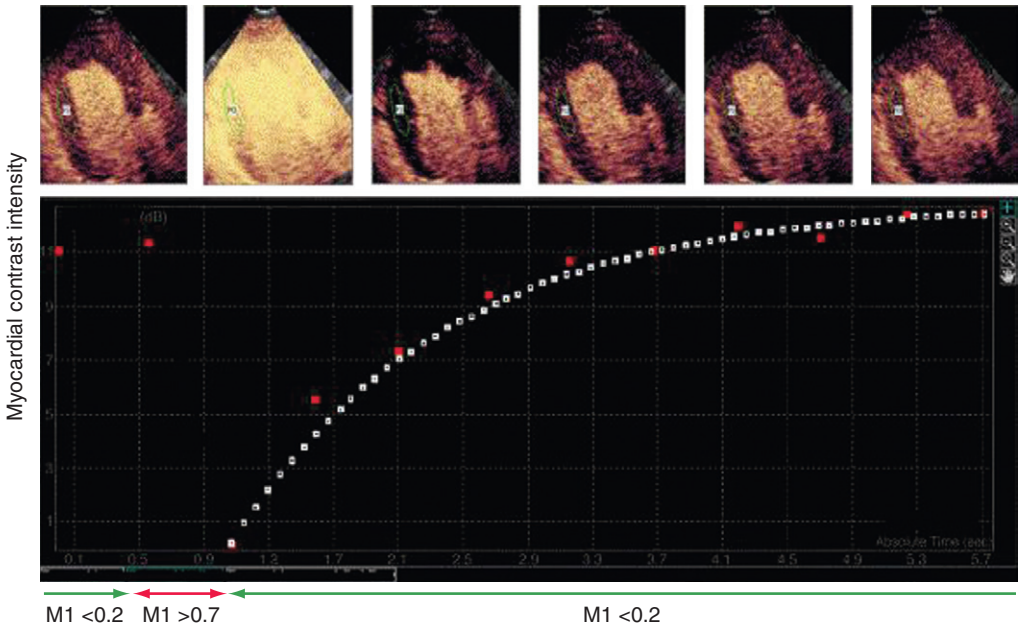



**Figure 3-5 Example of myocardial contrast replenishment.** After a high-mechanical-index (MI) impulse (depicted as the bright flash in the second apical three-chamber image in the *top* panels) the time curve of myocardial contrast intensity is shown (*bottom panel*). using a typical low-MI pulse sequence scheme. Note that after the high-MI impulse, there is replenishment of myocardial contrast while imaging at a low MI (0.2). This can be plotted and fitted to the one-exponential function. *(With permission from Rafter P, Phillips P, Vannan MA: Imaging technologies and techniques.* Cardiol Clin *22:181-197, 2004.)*

intensity. With bolus intravenous injections of microbubbles, the myocardial contrast intensity during this washout period is a reflection of myocardial blood volume. Estimates of myocardial blood flow cannot be ascertained from bolus injections, because mean transit times cannot be obtained from time intensity curves as a result of dispersion of the bolus by intrapulmonary filtering. Therefore, with intravenous injections, myocardial blood volume (peak intensity) can be estimated, but quantification of myocardial blood flow is not possible.

## CONTINUOUS INFUSION IMAGING

The difficulties arising with thresholding effect and saturation point of echocardiography systems can partly be avoided by using a continuous peripheral venous infusion for microbubbles instead of a bolus injection. This method assumes that the input of microbubbles into the myocardium is constant. The practical advantage of a continuous infusion is that attenuation artifacts due to high contrast intensity in the LV cavity can be reduced.[29,30] Moreover, the contrast dosage administered can easily be adjusted depending on the individual imaging conditions of different patients.[31]

Starting from the presumption that a true continuous venous infusion of a constant number of microbubbles can be achieved, a quantitative assessment of myocardial blood flow is possible. The ultrasound beam destroys these microbubbles when a high MI is used, so that insonation at high MIs results in almost complete bubble destruction with every pulse. Triggering ultrasound to one frame timed to end-systole in the cardiac cycle at a sequence of incrementally longer cardiac cycles allows a replenishment of contrast agent corresponding to flow to the given region during that time sequence. The longer the triggering intervals are set, the more microbubbles refill the capillaries and the higher the signal intensity to be registered in the tissue, until finally a plateau phase is reached. Alternatively, if one is imaging at low MI in real time, brief high-MI impulses can be applied to the imaging plane, following which replenishment can be visualized in real time at a low MI (Fig. 3-5). The plateau background-subtracted myocardial contrast intensity of a respective myocardial region is related to the capillary cross-sectional area. The rate at which this plateau stage is achieved (slope) is proportional to the blood flow velocity in that region. Because the peak background-subtracted myocardial videointensity is directly related to capillary cross-sectional area, the slope times peak or plateau myocardial videointensity represents a measure of myocardial blood flow.[13] Although this methodology holds much promise, incomplete destruction of microbubbles in the ultrasound field could lead to significant underestimation of myocardial blood flow abnormalities.[32] Models have been proposed and validated that correct the plateau myocardial signal intensity (which is subject to regional ultrasound beam inhomogeneities) by dividing this value by the adjacent LV cavity intensity (Fig. 3-6). The replenishment versus time curve fits a one-exponential curve function and has been useful for quantifying myocardial blood flow. The normalized plateau intensities multiplied by the rate of contrast replenishment and divided by tissue density are used to compute myocardial blood flow.[33,34] Continuous infusion techniques can be done with infusion pumps or handheld infusions. With either of the commercially available contrast agents, one can mix them at the bedside with saline and infuse them either as a continuous drip or as a handheld infusion.

## TECHNICAL EQUIPMENT, IMAGE PROCESSING, AND ARTIFACTS

Processing and analysis play a major role in the quantitative, reproducible assessment of echocardiographic myocardial perfusion. In most cases, myocardial signal intensity in one or more

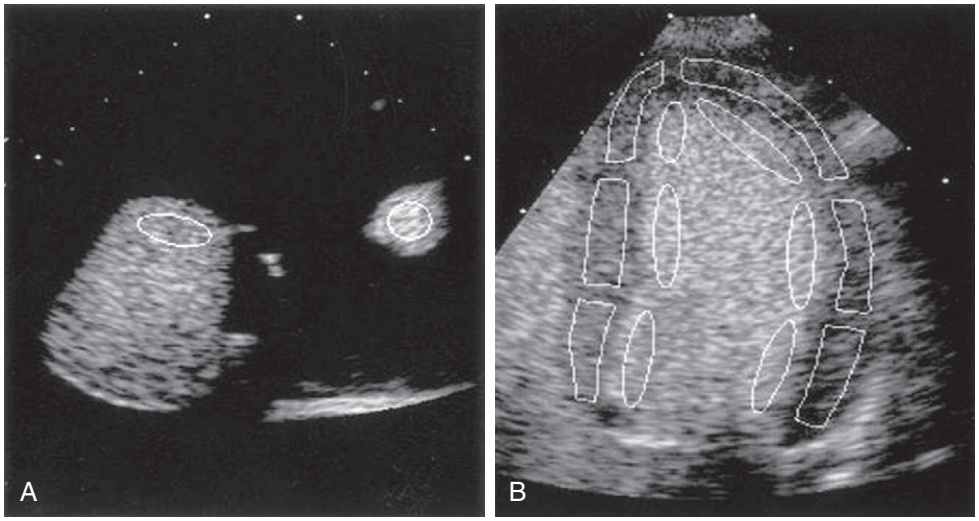



**Figure 3-6 Normalization of myocardial signal intensity for quantitation of myocardial blood flow.** Regions of interest are shown in a perfusion phantom (**A**) and normal human (**B**). Quantification of myocardial blood flow is performed by normalizing each myocardial signal intensity with the adjacent LV cavity to compensate for regional beam inhomogeneities and beam attenuation. *(With permission from Vogel R, Indermuhle A, Reinhardt J, et al: The quantification of absolute myocardial perfusion in humans by contrast echocardiography.* J Am Coll Cardiol *45:754-762, 2005.)*

regions of interest per frame is specified. The regions of interest have to be maintained in a constant position, large enough to provide the highest signal-to-noise ratio, but without including any parts of the brighter endocardial or epicardial border. The alignment, manually or by a computer algorithm, should be performed at or near end-systole, to reduce contributions from contrast in larger intramyocardial arterioles.[35] Regions of interest should also corrected by using background subtraction,[36] performed by subtracting any background intensity post high-MI impulses from contrast-enhanced pictures. If the signal intensity in the regions of interest is measured from video data, it can be displayed in a dynamic range of 256 pixels, the different values related to the pixel that contains the highest signal intensity. Because the ability of the human eye to distinguish among many shades of gray is relatively poor, color coding is a helpful tool for better detection of perfusion abnormalities.[36,37] To prevent the loss of information that comes from analyzing video images, digital intensity obtained from returning signals before postprocessing is more commonly used today. This information is unprocessed and not affected by the postprocessing functions of the imaging chain. All quantitative analyses to date have been shown to be time consuming and technically demanding.[38] Nonetheless, there is general agreement that visual analysis of myocardial perfusion data will be inadequate when quantifying myocardial contrast enhancement from venous infusions of contrast.

Commercially available ultrasound systems and digital review stations are now equipped with quantitative signal intensity systems that can measure contrast intensity as well as myocardial blood flow changes using the one-exponential function. Quantification of myocardial contrast enhancement will require that we understand what normal variations in contrast enhancement exist within different regions. Animal and human studies have demonstrated that there is a regional heterogeneity in myocardial contrast enhancement from microbubbles.[33,34,39] A recent metaanalysis of quantitative stress myocardial contrast echocardiography (MCE) has demonstrated the potential for both the rate of replenishment (beta) and the product of plateau intensity and rate of replenishment (A × beta) to detect coronary artery disease.[40]

Three-dimensional real-time perfusion concepts have been developed, which attempt to quantify myocardial blood flow changes using volumetric acquisition protocols.[41] In this setting, high-MI impulses to destroy microbubbles during continuous infusions of microbubbles cover a volume of interest (as opposed to a single imaging plane). Care must be taken with this approach to prevent LV cavity destruction, and thus maintain a constant input function. The feasibility and accuracy of this approach have yet to be determined.

## Safety of Ultrasound Contrast

In October 2007, the FDA issued a Box Warning regarding the use of Definity and Optison, stating that deaths had occurred within 30 minutes of contrast administration (http://www.fda.gov/Drugs/DrugSafety/PostmarketDrugSafetyInformationforPatientsandProviders/ucm110260.htm). The echocardiographic community was obviously concerned and perplexed with this warning, as it seemed to be inconsistent with what was observed in routine practice. To study this, several single and multicenter experiences were reported, and no such increase in mortality was observed when compared with an equivalent patient population not receiving contrast (Table 3-3). As can be seen in the table, there was no increased risk associated with contrast use in well over 100,000 patients, including patients in the intensive care setting, patients with potential acute coronary syndromes undergoing resting or stress echocardiography, or patients following acute myocardial infarction.[42-54] A rare anaphylactoid reaction may occur in response to Definity; this is estimated to occur with a frequency of 0.006%.[50] More recent publications focusing on the use of contrast within the first 24 hours of hospital admission have demonstrated that patients receiving contrast may have a reduced mortality rate compared to patients not receiving contrast, suggesting that the increased diagnostic accuracy afforded by the use of contrast may lead to earlier correct diagnoses and

**TABLE 3-3 Safety of Ultrasound Contrast Agents**

| Study | Year | Contrast Agent | Study Nature | Total No. of Patients | No. of Contrast Patients | No. of Noncontrast Patients | Contrast | | Noncontrast | |
|---|---|---|---|---|---|---|---|---|---|---|
| | | | | | | | Death | MI | Death | MI |
| Exuzide et al[a] | 2010 | Optison | Critically ill | 14,500 | 2900 | 11,600 | 38 (1.3%) | NA | 129 (1.1%) | NA |
| Abdelmoneim et al[b] | 2010 | Definity Optison | Elevated RVSP | 16,434 | 6164 | 10,270 | 1 (0.016%) | 3 (0.03%) | 2 (0.03%) | 5 (0.05%) |
| Abdelmoneim et al[c] | 2009 | Definity Optison | | 26,774 | 10,792 | 15,982 | 1 (0.009%) | 3 (0.028%) | 2 (0.013%) | 7 (0.044%) |
| Dolan et al[d] | 2009 | Definity Optison | Stress echo Resting echo | 48,308 | 42,408 | 5900 (rest echo) | 0 (0%) within 30 min 2 (0.01%) within 24 hr | 0 (0%) within 30 min 8 (0.019%) within 24 hr | 0 (0%) within 30 min 1 (0.017%) within 24 hr Only rest echo | 0 (0%) within 30 min 7 (0.01%) within 24 hr Only rest echo |
| Gaibazzi et al[e] | 2009 | SonoVue | | 500 | 500 | NA | 0 (0%) | 0 (0%) | 0 (0%) | 2 (0.1%) |
| Anantharam et al[f] | 2009 | SonoVue Luminity | | 2775 | 689 | 2086 | 0 (0%) | 0 (0%) | 0 (0%) | 2 (0.1%) |
| Main et al[g] | 2008 | Definity | Hospitalized patients | 4,300,966 | 58,254 | 4,242,712 | 616 (1.06%) | NA | 45,789 (1.08%) | NA |
| Gabriel et al[h] | 2008 | Definity Optison | | 9798 | 4786 | 5012 | 2 (0.04%) | NA | 3 (0.06%) | NA |
| Wei et al[i] | 2008 | Definity Optison | | 78,383 | 78,383 | NA | 0 (0%) | NA | NA | NA |
| Kusnetzky et al[j] | 2008 | Definity | Hospitalized patients | 18,671 | 6196 | 12,475 | 26 (0.42%) | NA | 46 (0.37%) | NA |
| Shaikh et al[k] | 2008 | Definity Optison | | 5069 | 2914 | 2155 | 0 | 1 (0.03%) | 0 | 0 |
| Timperley et al[l] | 2005 | SonoVue Optison | | 751 | 751 | NA | 0 (0%) | NA | NA | NA |
| Tsutsui et al[m] | 2005 | Definity Optison | | 2498 | 1486 | 1012 | 0 (0%) | 0 (0%) | 0 (0%) | 0 (0%) |

References:

[a]Exuzide A, Main ML, Coby C, et al: A retrospective comparison of mortality in critically ill hospitalized patients undergoing echocardiography with and without an ultrasound contrast. *JACC Cardiovasc Imaging* 3:578-585, 2010.

[b]Abdelmoneim SS, Bernier M, Scott CG, et al: Safety of contrast agent used during stress echocardiography in patients with elevated right ventricular systolic pressure a cohort study. *Circ Cardiovasc Imaging* 3:240-248, 2010.

[c]Abdelmoneim SS, Bernier M, Scott CG, et al: Safety of contrast agents use during stress echocardiography; a 4-year experience form a single center cohort study of 26,774 patients. *JACC Cardiovasc Imaging* 2:1048-1056, 2009.

[d]Dolan MS, Gala S, Dodla S, et al: Safety and efficacy of commercially available ultrasound contrast agents for rest and stress echocardiography: a multicenter experience. *J Am Coll Cardiol* 53:32-38, 2009.

[e]Gaibazzi N, Squeri A, Ardissino D, Reverberi C: Safety of contrast flash-replenishment stress echocardiography in 500 patients with a chest pain episode of undetermined origin within the last 5 days. *Eur J Echocardiogr* 10:726-732, 2009.

[f]Anantharam B, Chahal N, Chelliah R, et al: Safety of contrast in stress echocardiography in stable patients and in patients with suspected acute coronary syndrome but negative 12-hour troponin. *Am J Cardiol* 104:14-18, 2009.

[g]Main ML, Ryan AC, Davis TE, et al: Acute mortality in hospitalized patients undergoing echocardiography with and without an ultrasound contrast agent (multicenter registry results in 4,300,966 consecutive patients). *Am J Cardiol* 102:1742-1746, 2008.

[h]Gabriel RS, Smyth YM, Menon V, et al: Safety of ultrasound contrast agents in stress echocardiography. *Am J Cardiol* 102:1269-1272, 2008.

[i]Wei K, Mulvagh SL, Carson L, et al: The safety of Definity and Optison for ultrasound image enhancement: a retrospective analysis of 78,383 administered contrast doses. *J Am Soc Echocardiogr* 11:1202-1206, 2008.

[j]Kusnetzky LL, Khalid A, Khumri TM, et al: Acute mortality in hospitalized patients undergoing echocardiography with and without an ultrasound contrast agent: results in 18,671 consecutive patients. *J Am Coll Cardiol* 51:1704-1706, 2008.

[k]Shaikh K, Chang SM, Peterson L, et al: Safety of contrast administration for endocardial enhancement during stress echocardiography compared with noncontrast stress. *Am J Cardiol* 102:1444-1450, 2008.

[l]Timperley J, Mitchell ARJ, Thibault H, et al: Safety of contrast dobutamine stress echocardiography: a single center experience. *J Am Soc Echocardiogr* 18:163-167, 2005.

[m]Tsutsui JM, Elhendy A, Xie F, et al: Safety of dobutamine stress real-time myocardial contrast echocardiography. *J Am Coll Cardiol* 45:1235-124, 2005.

*echo*, Echocardiography; *NA*, not available; *RVSP*, right ventricular systolic pressure.

subsequent reduced mortality.[48] These publications have also demonstrated the significant value that contrast has even when just being used for enhancing LV opacification, where more than 35% of patients evaluated had a change in diagnosis when contrast was added to the echocardiographic examination or a change in medications.[55]

Although diagnostic ultrasound MIs do have the potential to disrupt capillaries and induce both hemorrhage and hemolysis, these studies have still only been done in settings where minimal attenuation of the ultrasound beam exists.[56] Much larger human trials using ultrasound and contrast during stress echocardiography have confirmed no significant adverse effects occur.[54,57] High-MI impulses (MI up to 1.9) applied during dobutamine stress echocardiography (DSE) have the potential to elicit isolated ventricular premature depolarizations, but no sustained arrhythmias induced by these transient high-MI impulses from diagnostic transducers have been observed.[58]

## Clinical Applications of Contrast Enhanced Ultrasound

### DETECTING ACUTE ISCHEMIA/RISK AREA IN THE EMERGENCY SETTING

In several animal and human investigations, intracoronary ultrasound contrast injections have successfully delineated the area at risk after acute myocardial infarction, which is defined as the complete transmural extent of the perfusion bed supplied

by an occluded coronary artery.[59-61] These studies have shown that area at risk measured with intracoronary contrast is superior to clinical, electrocardiographic, hemodynamic, or angiographic data in determining actual risk area. Intravenous microbubbles encapsulating high–molecular-weight gases in combination with new imaging techniques have made the rapid noninvasive assessment of risk area possible in an acute setting. In several animal experiments, the spatial distribution of hypoperfusion after coronary artery occlusion and reperfusion has been accurately quantified with intravenous myocardial contrast echocardiography.[5,62-64] Perfusion defects delineated by ultrasound contrast have correlated with the extent of wall motion abnormality in the corresponding myocardial segment and postmortem measurements of risk area.[62] Continuous infusions of microbubbles have been employed to quantify reductions in myocardial blood flow using the destruction-replenishment techniques described previously.[14]

Resting MCE data have been used in the emergency department in a large number of patients with chest pain and nondiagnostic electrocardiograms. In patients with low or moderate clinical risk scores, myocardial perfusion assessed with intermittent high-MI ultraharmonic or harmonic power Doppler imaging provided incremental prognostic information to the clinical assessment of risk (Thrombolysis in Myocardial Infarction [TIMI] Risk Score). Patients with both abnormal regional wall motion and abnormal myocardial perfusion in these single-center studies had a significantly worse event-free survival when compared to patients with abnormal regional function but normal myocardial perfusion.[65]

## ASSESSMENT OF MYOCARDIAL VIABILITY IN THE ACUTE AND CHRONIC SETTING

Identification of patients with the "no-reflow" phenomenon has proven to be an important clinical application for myocardial contrast echocardiography. This phenomenon, described first in an animal setting by Kloner and associates[66] in 1974, is characterized by a lack of recovery in microvascular perfusion, although the occluded coronary artery is successfully reopened by percutaneous intervention or thrombolysis. Ito and co-workers[67] were the first to systematically examine myocardial microvascular perfusion with intracoronary microbubbles in patients with acute anteroseptal myocardial infarction immediately following restoration of antegrade flow in the left anterior descending artery. Using intracoronary sonicated radiographic contrast, they demonstrated that 23% of the patients had persistent contrast defects (i.e., no reflow) in the area at risk after recanalization. The long-term prognosis of these no-reflow patients was impaired, and there was significant deterioration in regional and global systolic function at follow-up. These findings have been confirmed by other investigators. Several investigators have succeeded in detecting the no-reflow phenomenon from intravenous administration of microbubbles in patients with acute myocardial infarction following revascularization. Lepper and colleagues[68] studied myocardial contrast enhancement in patients with acute infarction undergoing angioplasty immediately before and 24 hours after recanalization using intravenous perfluorocarbon-containing microbubbles and intermittent harmonic imaging. An improvement of myocardial perfusion within 24 hours after intervention was predictive of functional recovery verified at 4-week follow-up.[69] In patients undergoing primary coronary stenting, homogenous myocardial contrast enhancement within the infarct zone by continuous infusion intravenous MCE was highly predictive of regional recovery of function.[70] Restoration of microvascular perfusion was most likely to occur if patients demonstrated at least partial perfusion to the risk area before primary stenting. In recent comparative studies between nitroglycerin-enhanced SPECT and MCE, the assessment of myocardial viability by MCE was superior to that by SPECT in predicting patient outcome.[71] Multicenter studies have recently demonstrated that the extent of microvascular damage, assessed on day 1 following reperfusion therapy in acute myocardial infarction, is the most powerful independent predictor of whether LV remodeling will occur.[72] Furthermore, MCE performed during dipyridamole infusion 1 week after acute myocardial infarction in patients receiving primary fibrinolytic therapy has been shown to be useful in both detecting a significant residual stenosis within the infarct vessel and predicting when multivessel coronary disease is present.[73]

Visualization of collateral myocardial blood flow to the risk area before and after revascularization following acute myocardial infarction has been demonstrated with intracoronary contrast. In patients with occluded vessels, injection of ultrasonographic contrast material into adjacent coronary arteries can produce myocardial contrast enhancement in the perfusion bed subtended by the occluded vessel.[74,75] This phenomenon is clinically relevant because it indicates viability of the perfusion bed subtended by the occluded coronary artery.[76] Sabia and associates[77] demonstrated that revascularization of an occluded coronary artery after myocardial infarction resulted in improved function only when myocardial contrast enhancement was observed following ultrasound contrast injection into the opposite coronary artery.[78] The spatial extent of collateral blood flow as defined by contrast echocardiography correlated closely with improvement in regional function within the infarct zone. Table 3-4 summarizes the clinical studies performed evaluating the ability of MCE to detect myocardial viability, both in the post–myocardial infarction setting and in the evaluation for hibernating myocardium.

In patients with chronic coronary artery disease and LV dysfunction, both the visual and quantitative assessment of MCE during a continuous infusion of intravenous microbubbles has provided significant independent data on the effects of revascularization to that segment, exceeding that which can be obtained with radionuclide imaging.[79] In this setting, the product of the slope of myocardial replenishment and plateau myocardial contrast intensity (an index of myocardial blood flow) in dysfunctional segments correlated with contractile reserve by low-dose dobutamine, as well as greater than 60% thallium uptake with radionuclide SPECT. More importantly, this index of myocardial blood flow by MCE was able to identify viable myocardium in segments that did not exhibit contractile reserve by DSE.[80] However, these studies have all had small patient numbers and have yet to be verified in multicenter studies.

## DETECTION OF CORONARY ARTERY DISEASE

### *With Vasodilator Stress Perfusion Imaging*

Until the past few years, radionuclide scintigraphy has been the diagnostic tool to address myocardial perfusion during stress testing. This method, especially when performed with $^{99m}$Tc rather than $^{201}$Tl, provides high sensitivity in identifying patients with coronary artery disease. It is limited, however, by poor spatial resolution and frequent attenuation artifacts. With

**TABLE 3-4 Predictive Value of MCE for Detection of Myocardial Viability within 7 Days After Acute Myocardial Infarction, and for Identification of Hibernating Myocardium**

| *Study* | *N* | *Follow-up (months)* | *Sensitivity* | *Specificity* | *Reference Standard* |
|---|---|---|---|---|---|
| **Detection of Myocardial Viability Post Myocardial Infarction** | | | | | |
| Swinburn et al[a] | 96 | 3-6 | 59% | 76% | RF |
| Main et al[b] | 34 | 2 | 77% | 83% | RF |
| Hillis et al[c] | 37 | 2 | 80% | 67% | RF |
| Janardhana et al[d] | 50 | 3 | 87% | 78% | RF |
| Korosoglou et al[e] | 32 | 1 | 81% | 88% | RF |
| Huang et al[f] | 34 | 4 | 83% | 82% | RF |
| Nunes Sbano et al[g] | 50 | 6 | 95% | 52% | RF |
| Abe et al[h] | 21 | 6 | 98% | 32% | RF |
| Dwivedi et al[i] | 95 | 46 | 80% | 76% | CO |
| Galiuto L et al[j] | 110 | 6 | 70% | 74% | RF |
| **Detection of Hibernating Myocardium** | | | | | |
| Korosoglou et al[k] | 43 | 3 | 86% | 64% | RF |
| Chelliah et al[l] | 39 | 3 | 88% | 61% | RF |
| Korosoglou et al[m] | 34 | 3-6 | 88% | 66% | RF |
| Shimoni et al[n] | 20 | 3-4 | 82% | 69% | RF |

The reference standard was either recovery of regional function (RF) or clinical outcome (CO, defined as death or nonfatal myocardial in farction).

References:

[a]Swinburn JM, Lahiri A, Senior R. Intravenous myocardial contrast echocardiography predicts recovery of dyssynergic myocardium early after acute myocardial infarction. *J Am Coll Cardiol* 2001;38:19-25.

[b]Main ML, Magalski A, Chee NK, et al: Full-motion pulse inversion power Doppler contrast echocardiography differentiates stunning from necrosis and predicts recovery of left ventricular function after acute myocardial infarction. *J Am Coll Cardiol* 38:1390-1394, 2001.

[c]Hillis GS, Mulvaugh SL, Gunda M, et al: Contrast echocardiography using intravenous octafluoropropane and real-time perfusion imaging predicts function recovery after acute myocardial infarction. *J Am Soc Echocardiogr* 16:638-645, 2003.

[d]Janardhana R, Swinburn JM, Greaves K, et al: Usefulness of myocardial contrast echocardiography using low-power continuous imaging early after acute myocardial infarction to predict late functional left ventricular recovery. *Am J Cardiol* 92:493-497, 2003.

[e]Korosglou G, Labadze N, Giannitsis E, et al: Usefulness of real-time myocardial perfusion imaging to evaluate tissue level perfusion in patients with non ST-elevation myocardial infarction. *Am J Cardiol* 95:1033-1038, 2005.

[f]Haung WC, Chiou KR, Liu CP, et al: Comparison of real-time contrast echocardiography and low-dose dobutamine stress echocardiography in predicting the left ventricular functional recovery in patients after acute myocardial infarction under different therapeutic intervention. *Int J Cardiol* 104:81-91, 2005.

[g]Sbano JC, Tsutsui JM, Andrade JL, et al: Detection of functional recovery using low-dose dobutamine and myocardial contrast echocardiography after acute myocardial infarction treated with successful thrombolytic therapy. *Echocardiography* 22:496-502, 2005.

[h]Abe Y, Muro T, Sakanoue Y, et al: Intravenous myocardial contrast echocardiography predicts regional and global left ventricular remodeling after acute myocardial infarction: comparison with low dose dobutamine stress echocardiography. *Heart* 91:1578-1583, 2005.

[i]Dwivedi G, Janardhanan R, Hayat SA, Swinburn JM, Senior R. Prognostic value of myocardial viability detected by myocardial contrast echocardiography early after acute myocardial infarction. *J Am Coll Cardiol* 50:327-334, 2007.

[j]Galiuto L, Garramone B, Scara A, et al: The extent of microvascular damage during myocardial contrast echocardiography is superior to other known indexes of post-infarct perfusion in predicting left ventricular remodeling. *J Am Coll Cardiol* 51:552-559, 2008.

[k]Korosoglou G, Hansen A, Hoffend J, et al: Comparison of real-time myocardial contrast echocardiography for the assessment of myocardial viability fluorodeoxyglucose-18 positron emission tomography and dobutamine stress. *Am J Cardiol* 94:570-576, 2004.

[l]Chelliah RK, Hickman M, Kinsey C, et al: Myocardial contrast echocardiography versus single photon emission computed tomography fro assessment of hibernating myocardium in ischemic cardiomyopathy: preliminary qualitative and quantitative results. *J Am Soc Echocardiogr* 23:840-847, 2010.

[m]Korosoglou G, Hansen A, Bekerdejian R, et al: Usefulness of myocardial parametric imaging to evaluate myocardial viability in experimental and in clinical studies. *Heart* 92:350-365, 2006.

[n]Shimoni S, Grangogiannis NG, Aggeli CJ, et al: Identification of hibernating myocardium with quantitative intravenous myocardial contrast echocardiography. Comparison with dobutamine echocardiography and thallium-201 scintigraphy. *Circulation* 107:538-544, 2003.

intravenous perfluorocarbon contrast agents and nonlinear ultrasonographic techniques, detection of underperfused myocardial segments during stress echocardiography has become feasible. Initial studies deployed intermittent harmonic or power Doppler imaging techniques to detect coronary stenoses during vasodilator stress.[23,81] Real-time perfusion and other lower MI imaging techniques have been applied to vasodilator stress as well. Multicenter studies comparing MCE with radionuclide SPECT during dipyridamole stress have demonstrated a similar sensitivity and specificity between the two techniques, regardless of stenosis severity.[82,83] Prognostically, real-time perfusion during dipyridamole stress has been shown to be superior to SPECT in predicting patient outcome.[84]

Both adenosine and the selective A2A receptor antagonist regadenoson have been used as vasodilator stress agents with real-time perfusion imaging and have demonstrated excellent sensitivity and specificity for detection of coronary artery disease.[85,86] Regadenoson has the advantage that it can be given as a 400-mcg bolus, with immediate real-time perfusion imaging, resulting in a 10-minute stress test. An example of an inducible perfusion defect following a regadenoson bolus injection is demonstrated in Figure 3-7. More recently, adenosine stress real-time perfusion has been compared with 3-tesla cardiac magnetic resonance imaging as a reference standard for the detection of functionally significant coronary artery disease. It was found to have sensitivity of 85% and specificity 74%.[87] Table 3-5 summarizes all recent studies using vasodilator stress MCE to detect coronary artery disease and predict patient outcome.

### *During Dobutamine or Exercise Stress Echocardiography*

Real-time perfusion techniques have been used to detect coronary stenoses during exercise and DSE. In predominately single-center studies, real-time perfusion echocardiography has been shown to increase the sensitivity of the dobutamine stress test

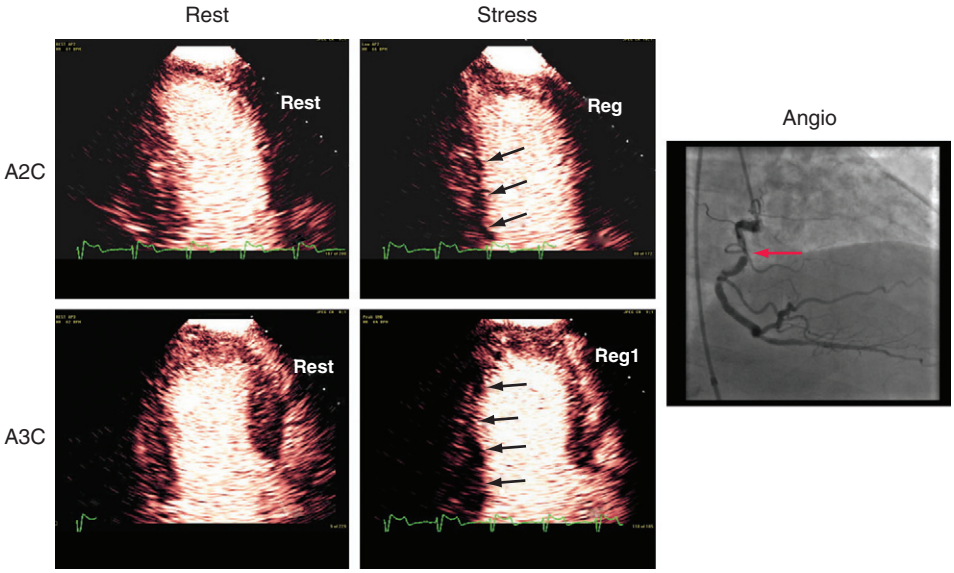



**Figure 3-7 Inducible perfusion defect in the inferior wall (*arrows*) following a regadenoson (*Reg*) bolus injection.** Contrast images at reat with stress (*left*) are shown in the apical two-chamber (*A2C*) and long-axis (*A3C*) views. Angiography (*Angio*) shows a severe stenosis (*arrow*) in the proximal right coronary artery.

**TABLE 3-5 Vasodilator Myocardial Perfusion Stress Imaging Studies Performed with Intravenous Ultrasound Contrast during Stress Echocardiography in the Past 5 Years**

| *Study* | *Year* | *Test* | *N* | *Bolus or CI* | *Mode* | *Sensitivity* | *Specificity* | *Accuracy* | *Standard Reference* |
|---|---|---|---|---|---|---|---|---|---|
| Tsutsui[54] | 2005 | Dipy or Adeno | 36 | Bolus | TRI and RT | — | — | TRI 81%<br>RT 85% | SPECT |
| Winter[a] | 2005 | Adeno | 36 | CI | RT | 81% | 67% | 79% | Angio |
| Jeetley[82] | 2006 | Dipy | 123 | CI | TRI | 80% | 63% | — | Angio |
| Toledo[b] | 2006 | Dipy | 34 | CI | TRI | 83% | 67% | 75% | Angio |
| Gudmundsson[c] | 2006 | Adeno | 35 | CI | RT | 83% | 93% | 92% | SPECT |
| Korosoglou[106] | 2006 | Dipy or Adeno | 89 | CI | RT | 83% | 72% | — | Angio |
| Malm[d] | 2006 | Adeno | 43 | CI | RT | 77% | 69% | 73% | Angio |
| Xie[85] | 2007 | Adeno | 40 | CI | RT | 73% | 90% | 84% | Angio |
| Wasmeier[e] | 2008 | Adeno | 24 | Bolus | RT | 67% | 67% | — | Angio |
| Lipiec[f] | 2008 | Dipy | 103 | Bolus | RT | 67% | 86% | 70% | Angio |
| Mor-Avi[g] | 2008 | Adeno | 16 | CI | RT | 71% | 94% | 90% | Angio |
| Hayat[106] | 2008 | Dipy | 63 | CI | RT | 92% | 95% | — | Angio |
| Senior[9] | 2009 | Dipy | 285*<br>377* | CI<br>CI | RT<br>RT | 61%<br>71% | 74%<br>64% | 68%<br>69% | Angio<br>Angio |
| Gudmundsson[h] | 2009 | Adeno | 50 | CI | RT | 92% | 93% | 93% | SPECT |
| Abdelmoneim[i] | 2009 | Adeno | 79 | CI | RT | 78% | 73% | 72% | Angio |
| Gaibazzi[j] | 2010 | Dipy | 150 | CI | RT | 96% | 38-69% | 61-87% | Angio |
| Arnold[87] | 2010 | Adeno | 65 | CI | RT | 85% | 76% | 82% | CMR |
| Gaibazzi[k] | 2010 | Dipy | 400 | Bolus | RT | 96% | 66% | 86% | Angio |

References:

[a]Winter R, Gudmundsson P, Willenheimer R: Real-time perfusion adenosine stress echocardiography in the coronary care unit: a feasible bedside tool for predicting coronary artery stenosis in patients with acute coronary syndrome. *Eur J Echocardiogr* 6:31-40, 2005.

[b]Toledo E, Jacobs LD, Lodato JA, et al: Quantitative diagnosis of stress-induced myocardial ischemia using analysis of contrast echocardiography parametric perfusion images. *Eur J Echocardiogr* 7:217-225, 2006.

[c]Gudmundsson P, Winter R, Dencker M, et al: Real-time perfusion adenosine stress echocardiography versus myocardial perfusion adenosine scintigraphy for the detection of myocardial ischaemia in patients with stable coronary artery disease. *Clin Physiol Funct Imaging* 26:32-38, 2006.

[d]Malm S, Frigstad S, Torp H, et al: Quantitative adenosine real-time myocardial contrast echocardiography for detection of angiographically significant coronary artery disease. *J Am Soc Echocardiogr* 19:365-372, 2006.

[e]Wasmeier GH, Asmussen S, Voigt JU, et al: Real-time myocardial contrast stress echocardiography using bolus application. *Ultrasound Med Biol* 34:1724-1731, 2008.

[f]Lipiec P, Wejner-Mik P, Krzeminska-Pakula M, et al: Accelerated stress real-time myocardial contrast echocardiography for the detection of coronary artery disease: comparison with $^{99m}$Tc single photon emission computed tomography. *J Am Soc Echocardiogr* 21:941-947, 2008.

[g]Mor-Avi V, Koch R, Holper EM, et al: Value of vasodilator stress myocardial contrast echocardiography and magnetic resonance imaging for the differential diagnosis of ischemic versus nonischemic cardiomyopathy. *J Am Soc Echocardiogr* 21:425-432, 2008.

[h]Gudmundsson P, Shahgaldi K, Winter R, et al: Head to Head comparison of two modalities of perfusion adenosine stress echocardiography with simultaneous SPECT. *Cardiovasc Res* 7:19-27, 2009.

[i]Abdelmoneim SS, Dhoble A, Bernier M, et al: Absolute myocardial blood flow determination using real-time myocardial contrast echocardiography during adenosine stress: comparison with single-photon emission computed tomography. *Heart* 95:1662-1668, 2009.

[j]Gaibazzi N, Rigo F, Squeri A, et al: Incremental value of contrast myocardial perfusion to detect intermediate versus severe coronary artery stenosis during stress-echocardiography. *Cardiovasc Ultrasound* 8:16-23, 2010.

[k]Gaibazzi N, Rigo F, Reverberi C: Detection of coronary artery disease by combined assessment of wall motion, myocardial perfusion and coronary flow reserve: a multiparametric contrast stress-echocardiography study. *J Am Soc Echocardiogr* 2010;23:1242-1250, 2010.

*Adeno*, Adenosine; *Angio*, angiography; *CI*, continuous infusion; *Dipy*, dipyridamole; *EX*, exercise; *RT*, real time; *SPECT*, single-photon emission computed tomography; *TRI*, triggered.

when compared to wall motion analysis[88,89] and to improve the ability of the test to predict death or nonfatal myocardial infarction.[90] Lonnebaken and co-workers[91] has also shown the value of dobutamine-induced perfusion abnormalities at intermediate stress levels in detecting coronary artery disease. The improved detection of coronary artery disease with real-time perfusion over conventional stress echocardiography appears to be due to the induction of perfusion defects in the absence of wall motion abnormalities, but also to the ability of real-time perfusion to delineate subendocardial wall thickening abnormalities that were detectable only because of the coexistent perfusion defect.[92] Examples of inducible perfusion defects within single vessel territories (the left anterior descending and left circumflex) are displayed in Figures 3-8 and 3-9, whereas a multivessel inducible perfusion defect is displayed in Figure 3-10.

Clinical studies have also demonstrated the incremental value of myocardial perfusion assessment using low-MI imaging during exercise testing.[93] Similar to dobutamine stress, the improved detection appears to be related to the ability of real-time perfusion to detect subendocardial ischemia.[94] Prognostically, the addition of perfusion analysis to wall motion during supine bicycle stress has enhanced the power of the test to predict cardiac events.[95] Table 3-6 lists the clinical studies that have been performed in the previous 5 years examining the sensitivity and specificity of MCE in detecting coronary artery disease during dobutamine and exercise stress echocardiography.[8,54,73,93,96-105]

### *Artifacts in Myocardial Perfusion Assessments*

One must be able to differentiate potential artifacts that create the appearance of perfusion defects. The most comment artifact is that due to attenuation. This typically occurs in basal segments and is differentiated from true defects by its location. Attenuation typically masks not only the myocardium but adjacent epicardial and endocardial borders as well. Attenuation is usually present both at rest and during stress, whereas inducible defects are present only during stress and typically involve just the subendocardium. Other potential artifacts are lung shadows, which will often mask an entire region (e.g., the anterior wall in the apical two-chamber view). This can be overcome by purposefully foreshortening these views, cutting out the apex but permitting better delineation of contrast replenishment within the basal to mid segments (Fig. 3-11). A third location where artifacts tend to occur is in the apical region. If the near-field gains (time gain compensation) are set too low, the apex will appear hypoperfused (Fig. 3-12, *A*). Unlike true defects, this can be corrected by increasing the near-field potentiometers (Fig. 3-12, *B*). One must be sure under resting conditions and in the presence of normal wall motion that apical contrast enhancement is similar to basal and mid segments (using adjustment of near-field gain settings) and that the myocardial contrast disappearance is observed after a high-MI impulse so that replenishment can be visualized. Near-field destruction of microbubbles can also cause the false appearance of perfusion defects in the apex. This can be corrected by moving the focus

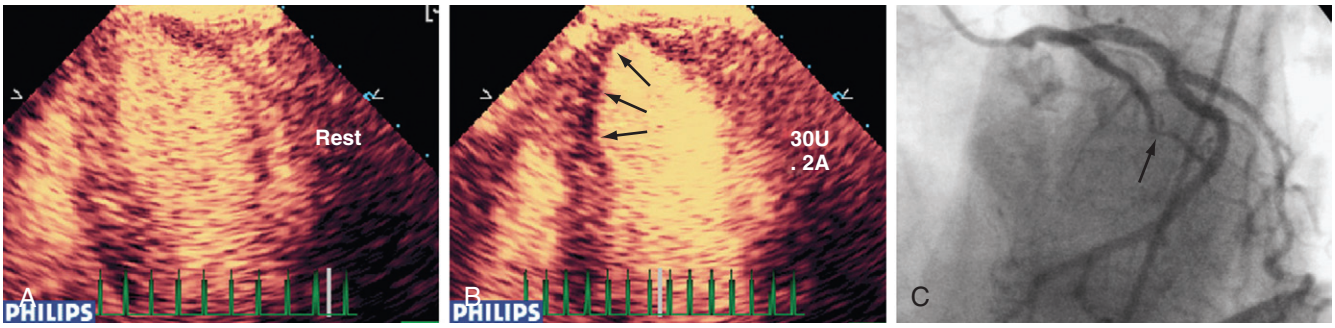



**Figure 3-8 Inducible septal and apical perfusion defect during DSE using real-time contrast echocardiography.** In the apical four-chamber view, resting images (*left*) show normal wall motion and myocardial perfusion. With dobutamine (*center*, 30 mcg/kg per minute plus atropine 0.2 mg), akinesis, and decreased myocardial perfusion of the apical septum is seen (*arrows*). Coronary angiography showed severe stenosis (*arrow*) in the left anterior descending coronary artery.

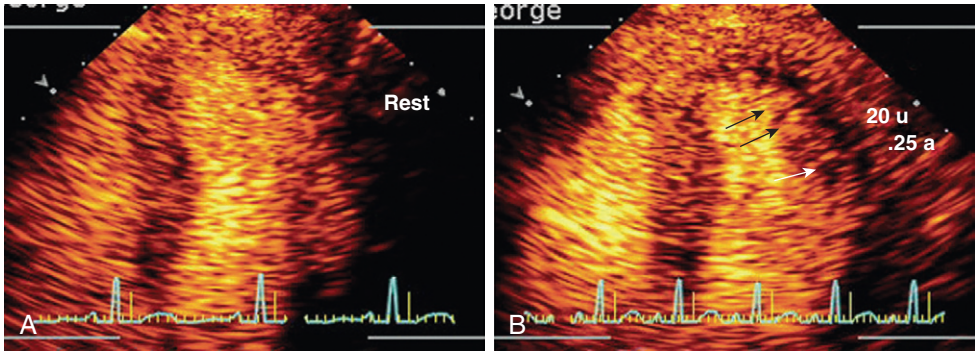



**Figure 3-9 Lateral wall perfusion defect detected with real-time contrast echocardiography during DSE.** Resting images in a four-chamber view (*left*) show normal myocardial perfusion, but with stress (*right*) decreased perfusion in the lateral wall is seen (*arrows*).

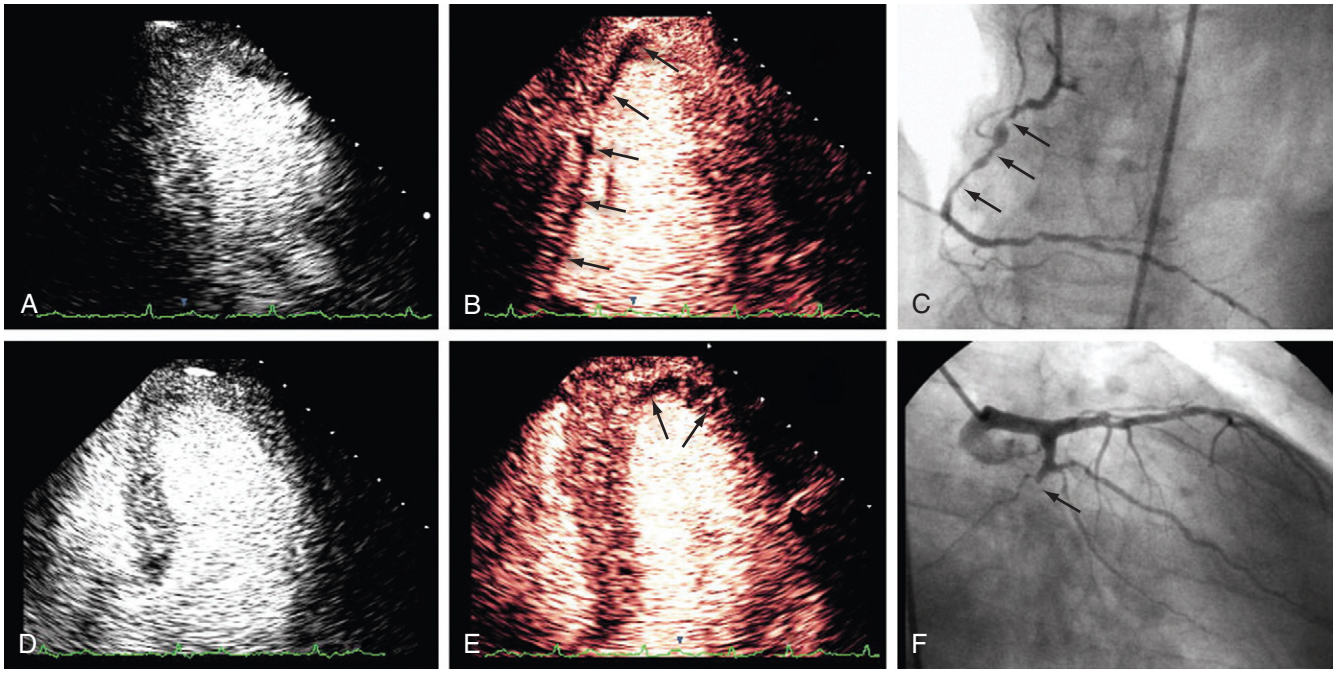



**Figure 3-10 Multivessel pattern of inducible perfusion defect during DSE in which subendocardial defects are seen in multiple coronary artery territories.** At rest, the apical long-axis (**A**) and four-chamber (**D**) views show normal wall motion and myocardial perfusion. With stress, the same views show reduced myocardial perfusion (arrows) in the inferior (**B**) and lateral apical (**E**) walls. Coronary angiography shows right coronary (**C**) and left circumflex (**F**) disease corresponding to the contrast stress study results.

**TABLE 3-6 Dobutamine or Exercise Myocardial Perfusion Stress Imaging Studies Performed with Intravenous Ultrasound Contrast during the Past 5 Years**

| *Study* | *Year* | *Test* | *N* | *Bolus or CI* | *Mode* | *Sensitivity* | *Specificity* | *Accuracy* | *Standard Reference* |
|---|---|---|---|---|---|---|---|---|---|
| Tsutsui[90] | 2005 | Dob | 1351 | Bolus | RT | — | — | 84% | Angio |
| Elhendy[101] | 2005 | Dob | 128 | Bolus | RT | 89% | 53% | 81% | Angio |
| Xie[103] | 2005 | Dob | 27 | Bolus | RT | 66% | 50% | 65% | Angio |
| Elhendy[a] | 2006 | Dob | 64 | Bolus and CI | RT | 74% | 79% | 77% | Angio |
| Miszalski-Jamka[b] | 2007 | EX | 42 | CI | RT | 88% | 88% | — | Angio |
| Hacker[c] | 2008 | Dob | 32 | CI | RT | 86% | 91% | — | Angio |
| Xie[92] | 2008 | Dob | 94 | CI | RT | 91 | 49 | 73 | Angio |
| Miszalski-Jamka[95] | 2009 | EX | 103 | CI | RT | 88% | 86% | 87% | Angio |
| Lønnebakken[91] | 2009 | Dob | 37 | CI | RT | 70% | 87% | — | Angio |
| Dodla[94] | 2010 | EX | 99 | CI | RT | 97% | 73% | 85% | Angio |
| Dodla[94] | 2010 | Dob | 155 | CI | RT | 85% | 64% | 75% | Angio |

References:

[a]Elhendy A, Tsutsui KM, O'Leary EL, et al: Noninvasive diagnosis of coronary artery bypass graft disease by dobutamine stress real-time myocardial contrast perfusion imaging. *J Am Soc Echocardiogr* 19:1482-1487, 2006.

[b]Miszalski-Jamka T, Kuntz-Hehner S, Schmidt H, et al: Real time myocardial contrast echocardiography during supine bicycle stress and continuous infusion of contrast agent. Cutoff values for myocardial contrast replenishment discriminating abnormal myocardial perfusion. *Echocardiography* 24:638-648, 2007.

[c]Hacker M, Hoyer HX, Uebleis C, et al: Quantitative assessment of cardiac allograft vasculopathy by real-time myocardial contrast echocardiography: a comparison with conventional echocardiographic analyses and [Tc99m] sestamibi SPECT. *Eur J Echocardiogr* 9:494-500, 2008.

*Angio*, Angiography; *CI*, continuous infusion; *Dob*, dobutamine; *EX*, exercise; *RT*, real time; *TRI*, triggered.

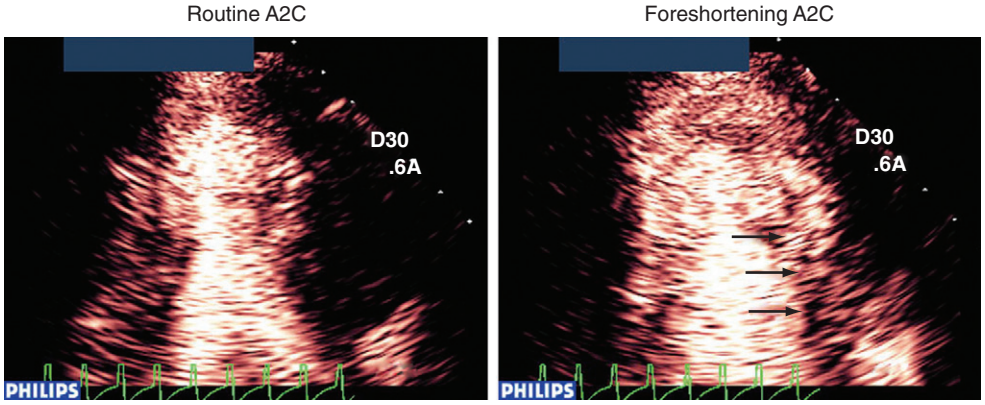



**Figure 3-11** Purposefully foreshortening an apical two-chamber image can improve the delineation of myocardial contrast enhancement within the basal to mid segments of the anterior wall (*arrows*).

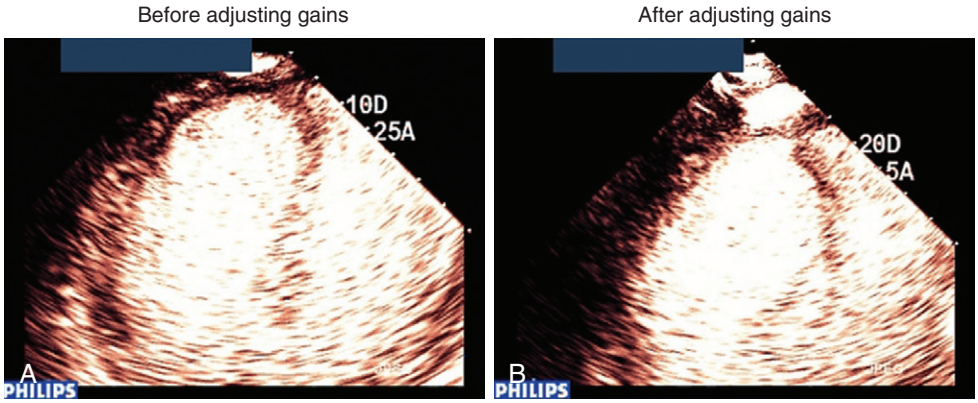



**Figure 3-12** Slightly increasing the time gain compensation in the near field can permit more homogenous myocardial contrast in the apical segments during real-time perfusion imaging. Before (**A**) and after (**B**) adjusting near-field gains.

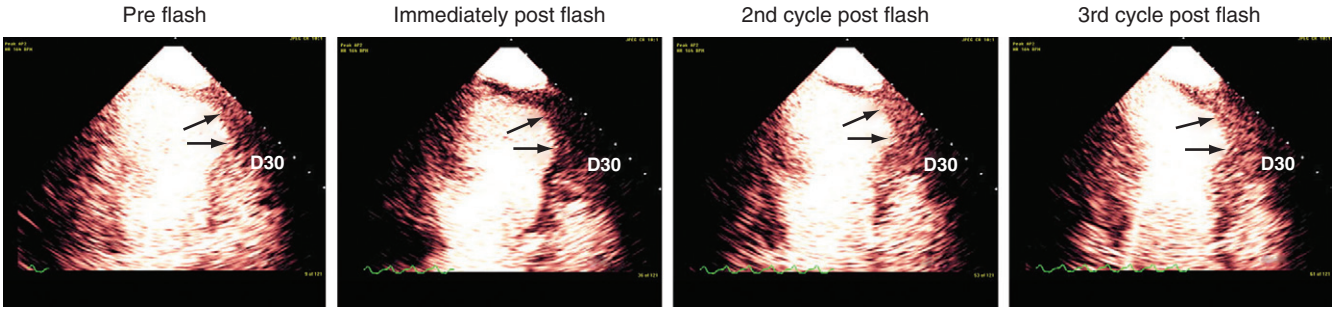



**Figure 3-13** Normal myocardial contrast replenishment within hypokinetic thinned septal and apical segments during DSE in a patient who was chronically paced. Therefore, no significant coronary artery disease was present despite the regional wall motion abnormality.

to the near field, which decreases the scan-line density in this region and reduces destruction.

### *Real-Time Myocardial Contrast Echocardiography in Specific Clinical Scenarios*

Patients with left bundle branch block and pacemaker-dependent patients represent clinical scenarios which both the assessment of wall thickening and conventional myocardial perfusion imaging with radionuclide SPECT are not helpful in the detection of coronary artery disease.[106] In these patients, there are difficulties with interpretation of wall thickening in the septum (in left bundle branch block) or, in pacemaker-dependent patients, in the septum and entire apex. In patients with left bundle branch block, perfusion defects in the interventricular septum are seen on radionuclide SPECT despite normal myocardial blood flow with real-time perfusion and no significant coronary artery disease by angiography. The reason for this appears to be the partial volume effect, as the false-positive perfusion defects seen with radionuclide SPECT had a normal perfusion appearance with higher resolution real-time MCE and were independently associated with smaller septal systolic wall thickness measurements.[106] Similar wall thickness abnormalities encompassing a larger territory (the septum and apex) are seen in pacemaker-dependent patients. An example of normal perfusion despite septal and apical hypokinesis and wall thinning due to chronic right ventricular pacing is shown in Figure 3-13.

### *Large Arteriolar Contrast Imaging*

If a higher MI is used in real time, microbubbles within capillaries are destroyed, but those transiting faster through larger arterioles (greater than 300 μm) can still be visualized. These larger arterioles are not involved with autoregulation, and their contrast intensity exhibits a predominately diastolic component under normal conditions. As the smaller arterioles (150 to 300 μm) involved with autoregulation dilate in response to a coronary stenosis, a correspondingly greater concentration of microbubbles from these arterioles is injected retrograde into the larger arterioles during systole. Wei and colleagues[35,107] have demonstrated that this increase in systolic contrast intensity (or increase in the systolic-to-diastolic signal ratio) from these larger arterioles can detect when significant stenoses are present in the left anterior descending artery under resting conditions.

## Other Diagnostic Applications of Microbubbles

### IMPROVED LEFT VENTRICULAR CAVITY OPACIFICATION

The only currently approved indication for the use of ultrasound contrast is to improve LV opacification. Several different intravenous ultrasound contrast agents have demonstrated their ability to improve the diagnostic value of echocardiographic examinations in patients with suboptimal imaging

conditions. In routine ultrasonographic examinations of patients with poor echocardiographic windows, contrast enhancement of the LV cavity provides better delineation of the endocardial border. Clinically, this could give information regarding regional and global systolic function that could not be assessed with routine echocardiography. Tissue harmonic imaging by itself has significantly improved endocardial border definition, often eliminating the need for intravenous ultrasonographic contrast agents filled with room air.[108] During the past few years, however, studies have shown that intravenous perfluorocarbon-containing microbubbles, because of their consistent LV opacification, have improved border definition in the LV of patients with suboptimal tissue harmonic images. Although the use of contrast may increase the costs for routine transthoracic echocardiograms, substantial cost savings could still be achieved in the examination of patients with poor baseline harmonic image quality because contrast would eliminate the need for additional diagnostic studies in these situations.[109] Indeed, recent clinical studies have shown that if contrast were used for suboptimal windows, downstream testing would be reduced by 33%, resulting in an average cost savings of $122 per patient.[55]

Reilly and co-workers[110] studied the effect of intravenous Optison injections in harmonic transthoracic echocardiography in the intensive care unit. Their results indicated a significant increase in interpreter confidence in evaluating myocardial segments that could not be analyzed without contrast application. Furthermore, the ability to estimate LV ejection fraction was clearly improved with Optison. Kurt and associates[55] recently demonstrated that significant changes in patient management occurred when contrast was used in intensive care unit patients, and Main and colleagues[48] discovered that acutely hospitalized patients receiving contrast to enhance LV opacification had 24% lower mortality than patients not receiving contrast. Malhotra and co-workers[111] compared stress echocardiograms performed with both fundamental and harmonic imaging modalities with and without intravenous Optison contrast in 200 patients. They reported that the combination of harmonic ultrasonography with Optison resulted in the most consistent endocardial border delineation, which significantly exceeded the quality of either fundamental contrast imaging or tissue harmonic imaging alone. Interobserver agreement with Optison and harmonic imaging in this study was 95%. A recent multicenter study compared the reproducibility and accuracy of contrast-enhanced cardiac magnetic resonance imaging, contrast-enhanced and unenhanced echocardiography, and cineventriculography in quantifying ejection fraction using biplane methods. The echocardiographic settings for contrast-enhanced imaging were an MI of 0.3, gain settings of 60%, and compression of 15% (Sonos 5500; Philips, Andover, Mass.). These studies demonstrated that the most reproducible method (lowest intraclass coefficient) for quantifying ejection fraction was contrast-enhanced echocardiography.[112] Contrast-enhanced echocardiography also had the highest interobserver agreement for analyzing regional wall motion.[113]

Contrast-induced homogeneous opacification of the LV cavity could also assist physicians in detecting LV thrombi or tumors[114,115] and complications of acute myocardial infarction such as myocardial rupture and LV pseudoaneurysm.[116] This technique has also been used during transesophageal echocardiography to delineate false and true lumen in patients with aortic dissection.[117] Using a continuous infusion of microbubbles, one can examine the replenishment patterns of contrast within cardiac masses following high-MI impulses to differentiate among malignant tumors, stromal tumors, and thrombi.[118]

## DOPPLER ENHANCEMENT

Intravenous microbubbles affect Doppler recordings because the scatter from them is much greater than from red blood cells. Microbubbles therefore can markedly increase the signal strength in a Doppler examination, which may be helpful in patients with suboptimal imaging quality. Von Bibra and associates[119] described a significant enhancement of spectral and color Doppler and an increase in the signal-to-noise ratio in the quantitative assessment of aortic stenosis, pulmonary venous flow, and mitral regurgitation by intravenous injection of Levovist. Transthoracic pulmonary venous flow velocities have been improved by intravenous contrast enhancement to the point that they are comparable to those obtained with transesophageal imaging.[120] Moreover, intravenous microbubble ultrasound contrast was successful in providing a clear spectral signal across stenotic aortic valves in cases in which the echocardiogram would have been nondiagnostic without contrast enhancement.[121] The gradients determined using contrast-enhanced Doppler signals correlated well with catheterization calculations.[121] Okura and colleagues[122] studied the effect of Albunex in 45 patients with prosthetic aortic valves. They found a significant improvement in transvalvular continuous-wave Doppler signal intensity with intravenous Albunex, increasing the frequency of satisfactory Doppler signals from 64% to 93% of patients. More recently, Jeon and co-workers[123] have demonstrated that a 10% air, 10% blood, 80% saline hand-agitated mixture is more optimal than the traditional agitated air-saline mixture in Doppler enhancement of the tricuspid regurgitant jet. They found that brief premixture of the patient's own blood with air and saline produces greater concentrations of small microbubbles, which improved the accuracy of the pulmonary artery pressure measurement.

## CONTRAST PERFUSION IMAGING OF OTHER ORGANS

The replenishment curves following microbubble destruction that have been used to detect myocardial blood flow changes can be applied to solid organs as well. The time versus acoustic intensity curve following ultrasound-mediated destruction of microbubbles has been validated as a method of measuring blood flow changes within the cerebral microcirculation.[124] This has been applied in traumatic brain injury to document the beneficial effect of early decompressive surgery on cerebral microvascular blood flow.[125] Contrast-enhanced ultrasound has also been shown to accurately quantify renal cortical blood flow changes in response to flow-limiting stenoses or during dopamine infusion.[126]

Quantitative measurements with contrast-enhanced ultrasound in skeletal muscle have also been used to demonstrate that physiologic increases in insulin alter microvascular blood volume without altering muscle blood flow.[127] Womack and colleagues[128] used high-resolution contrast-enhanced ultrasound to examine forearm skeletal muscle capillary blood flow responses to hand grip exercise in diabetic patients. A defective capillary blood volume response was observed almost exclusively in the diabetic patients who had developed microvascular disease. Unlike microvascular complications, however, this

defective capillary response was unrelated to the duration of disease. This indicates a potential role for defective capillary blood flow responses in the pathogenesis of microvascular complications in diabetes.

### MOLECULAR IMAGING WITH CONTRAST ULTRASOUND

Several potential applications for attaching ligands to the microbubble shell (polymer, albumin, or lipid) exist. Ligands include monoclonal antibodies, peptides, and glycoproteins,[129] which are typically conjugated to the microbubble shell in a manner that attaches them to a molecular spacer that projects the ligand away from the shell surface.

Lindner and associates[130] hypothesized that during the early inflammatory response after reperfusion, activated leukocytes adherent to the venular endothelial surface may bind microbubbles and therefore may be responsible for their prolonged transit. Using tumor necrosis factor-α injection in an animal setting, they showed that both lipid and albumin microbubbles attach to activated leukocytes. The binding of the albumin microbubbles was mediated by $\beta_2$-integrins, whereas the interaction between leukocytes and lipid microbubbles involved the complement pathway.[130] In a subsequent investigation, the leukocytes involved were identified to be mostly neutrophils and monocytes. Both lipid and albumin microbubbles were phagocytosed by these cells, remained acoustically active for up to 30 minutes, and could be detected in vivo after microbubbles from the blood pool had already vanished.[131]

Microbubbles also can be conjugated with disintegrins, which serves to target the microbubbles to $\alpha_v$ integrins that are expressed on neovascular endothelium.[132] Unlike unlabeled microbubbles that pass freely through the microcirculation, these microbubbles are retained within regions of increased arteriogenesis that occur in response to prolonged hindlimb ischemia.[133] The arteriogenic effects of certain agents, such as fibroblast growth factor-2, used to treat ischemic regions can therefore be assessed noninvasively by measuring signal intensity following intravenous injections of microbubbles targeted to $\alpha_v$ integrins. Similarly, phosphatidylserine has been incorporated into the shells of microbubbles to increase complement-mediated avidity to activated leukocytes. These microbubbles have been shown to be retained within reperfused myocardium, and the signal intensity derived from these microbubbles correlates closely with the severity and extent of postischemic inflammation.[134] The retained signal intensity from microbubbles targeted to activated leukocytes or to upregulated leukocyte adhesion molecules on the endothelial surface has also been used in animal studies to detect rejection following cardiac transplantation.[135,136] Microbubbles targeted to both $\alpha_v\beta_3$ integrins and activated leukocytes have been used to assess the effects of agents that inhibit endothelial integrin and platelet glycoprotein IIb/IIIa receptors in reducing myocardial infarct size.[137]

Microbubble targeting imaging has the potential to image myocardial regions where there has been remote ischemia. P-selectin is externalized by endothelium within minutes of ischemic territories and persists for up to hours. Therefore, it can be detected by microbubbles targeted to P-selectin, and preclinical studies have demonstrated ultrasound contrast retention within recently ischemic myocardium of rats and mice.[138,139] In the setting of heart transplant rejection, microbubbles targeted to intracellular adhesion molecules (e.g., ICAM-1) have been used to detect endothelial activation within the myocardium.[140] Detection of inflammatory plaque has also recently been demonstrated with contrast-enhanced ultrasound. Targeted microbubbles have demonstrated vascular endothelial adhesion molecule (VCAM-1) upregulation in apolipoprotein-deficient mice with differing degrees of plaque inflammation.[141] Early detection of plaque in animal models has been shown with microbubbles targeted to VCAM-1 and P-selectin.[142] One question that remains is whether the sensitivity of current surface ultrasound systems will be able to detect retained microbubbles in larger animal models and humans. Retention fractions need to be improved, which may require that microbubbles be targeted to multiple ligands.

### DETECTION OF CAROTID ARTERY ATHEROSCLEROSIS

Contrast-enhanced ultrasound has been used in two particular areas of carotid imaging. First, it has been used to better define intimal medial thickness as well as severity of plaque stenosis.[143] More importantly, contrast-enhanced ultrasound has been used to detect the adventitial vasa vasorum and intraplaque neovascularization.[144] The presence and extent of vasa vasorum–derived intraplaque neovascularization has recently been correlated with plaque stability and clinical cardiovascular outcome, indicating the potential for the assessment of carotid plaque neovascularity to identify the vulnerable patient.[145]

## Therapeutic Applications of Ultrasound and Microbubbles

A number of studies indicate that ultrasound-mediated microbubble destruction may also be used for therapeutic purposes. These applications include targeted drug and gene delivery, stimulation of arteriogenesis, and thrombus dissolution.

### DRUG AND GENE DELIVERY

The fact that microbubbles are destroyed by the ultrasound beam has led to the study of their potential role in depositing conjugated drugs or genes to an "ultrasound-targeted" organ.[146] Skyba and co-workers[147] studied the intravascular destruction of perfluorocarbon-containing microbubbles and the bioeffects of this process in the isolated spinotrapezius muscle of rats. With just one frame of ultrasound from a diagnostic ultrasound transducer (2.3 MHz at 1.1 MI), microbubble destruction was observed that caused local microvessel rupture. When the bubbles were mixed with colloidal particles, these particles were "microinjected" into the interstitial space. The degree of microbubble destruction and resulting "drug delivery" was directly related to the MI used.[148] Before these observations, it was demonstrated that large quantities of synthetic DNA, in the form of antisense oligonucleotides, adhere to perfluorocarbon-exposed sonicated dextrose albumin microbubbles.[149] These antisense oligonucleotides are synthetic gene products that can be used to inhibit the translation of messenger RNA into proteins and enzymes that regulate pathologic processes such as neointimal hyperplasia following vascular injury. In these studies, external diagnostic ultrasound released the synthetic antisense into the insonified kidney if the antisense oligonucleotide was given intravenously bound to microbubbles. Subsequently, it was shown that recombinant adenovirus containing β-galactosidase

could be conjugated to the surface of intravenously injected perfluorocarbon-containing albumin microbubbles and successfully targeted to the myocardium of rats by diagnostic ultrasound at a high MI (1.5). Postmortem analysis showed β-galactosidase transgene expression in the myocardium after ultrasound antigen delivery, but no expression of the transgene in the control groups that had received microbubbles alone, virus alone, or virus plus ultrasound.[150] Targeted intramyocardial gene delivery has also been reported in vivo with lipid-encapsulated microbubbles.[151] The simultaneous imaging of microbubbles appears to be important in targeted delivery, in that the highest quantity of delivered agent occurs when high-MI delivery impulses are applied only when maximal signal intensity from the microbubbles within the region of interest is present[152] (Fig. 3-14). Current diagnostic transducers are equipped with the ability to switch from sensitive low-MI pulse sequence schemes, which image the microbubbles, to high-MI impulses that destroy drug-carrying microbubbles. Low-frequency, high-MI impulses have been shown to create transient, temporary micropores in the endothelial cells.[153] This has led to the observation of "microinjections" of drugs conjugated to the microbubbles into the subendothelial spaces, even across the blood-brain barrier with transcranial ultrasound.[154] Ultrastructural observations following ultrasound-mediated destruction of microbubbles in the brain has demonstrated increased numbers of intracytoplasmic vacuoles within the brain capillary endothelium following ultrasound-mediated destruction of circulating intracerebral microbubbles.[155] Low-MI pulse sequence schemes, therefore, have the advantage of guiding when to apply high-MI impulses, and thus could significantly reduce unwanted bioeffects of hemorrhage or permanent endothelial injury. Most of these therapeutic effects of diagnostic ultrasound transducers are at peak negative pressures and pulse durations that fall within current FDA guidelines.[156]

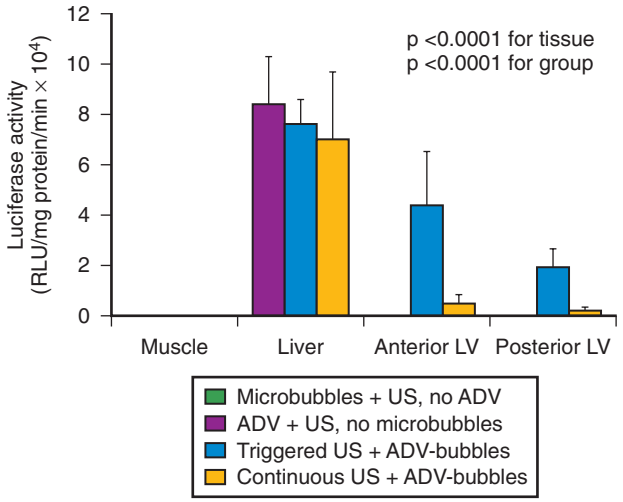



**Figure 3-14 Luciferase activity in the anterior and posterior myocardium following intravenous microbubble injections that are conjugated with the adenovirus (ADV) encoding the luciferase gene.** When diagnostic ultrasound (US) application is in a continuous mode (*yellow bars*), there is minimal deposition of the gene into the myocardium. However, when US is delivered only when a maximum quantity of microbubbles is present (triggered US; *blue bars*), there is a significant increase in gene transfer. The liver uptake is maximal (*purple bar*) when the ADV is administered without microbubbles. Activity is so low with microbubbles but no ADV (absent green bars) that no signal is detected. *(With permission from Chen S, Shohet RV, Bekeredjian R, et al: Optimization of ultrasound parameters for cardiac gene delivery of adenoviral or plasmid deoxyribonucleic acid by ultrasound-targeted microbubble destruction.* J Am Coll Cardiol *42:301-308, 2003.)*

Targeted delivery of genes has been explored as a method to cure type 1 diabetes. Recent work by Chai and associates[157] has demonstrated that a modified rat insulin promoter gene can be specifically delivered to beta cells in the pancreas using guided high-MI impulses from a diagnostic transducer. Specifically, using image-guided diagnostic ultrasound targeted destruction, these investigators have shown that plasmids containing a modified rat insulin promoter (termed RIP 3.1) are more effective than the full-length rat insulin promoter or a cytomegalovirus promoter in delivering the insulin gene to beta and alpha cells of the pancreas. Another area where guided ultrasound targeted microbubble destruction may be effective is in transiently altering blood-brain barrier permeability. Transcranial ultrasound and intravenous microbubbles have been used in mice to target delivery of antibodies directed against the amyloid-beta peptide and specifically remove the amyloid-beta plaques that are considered pathogenetic in Alzheimer disease.[158]

## THROMBOLYSIS

Several investigators have examined the potential of high-energy ultrasound alone to dissolve thrombi in vitro as well as in an animal setting. Transcatheter ultrasound has been shown to reduce thrombus weight and possibly recanalize occluded femoral arteries.[159] Because this process involves cavitation, more recent investigations have focused on whether microbubbles could potentiate this phenomenon. When combined with intravenous perfluorocarbon microbubbles, low-intensity, high-frequency ultrasound significantly increased the thrombolytic effect of urokinase in vitro. Even more importantly, ultrasound plus perfluorocarbon-containing microbubbles (PESDA) alone proved to be equivalent to urokinase in degree of thrombus dissolution. Therefore, it appeared that ultrasound and microbubbles could produce a localized clot lysis similar to a fibrinolytic agent without a systemic lytic state.[160] To demonstrate the potential for this in vivo, acutely thrombosed iliofemoral arteries in 10 rabbits received transcutaneous ultrasound treatment on one side and no ultrasound treatment on the other following intravenous PESDA injections. After ultrasound treatment, all arteries that had received PESDA and ultrasound were recanalized by angiography, but none of the arteries treated with PESDA alone were patent. Ultrasound alone also was unable to recanalize any of the thrombosed vessels.[161]

More recent work has focused on the potential clinical applications of using ultrasound and intravenous microbubbles to recanalize acutely thrombosed arteriovenous grafts, as well as restoring flow in acute intracoronary or intracerebral thrombi.[162-164] Effectiveness may be reduced in the setting of attenuation, but recanalization may still be feasible if platelet targeted microbubbles are used (Fig. 3-15). In a porcine model, the use of guided high-MI impulses from a diagnostic transthoracic ultrasound transducer and both nontargeted and platelet-targeted microbubbles in acute ST segment elevation myocardial infarction improved microvascular recovery and regional wall thickening independent of whether epicardial recanalization occurred.[165] The mechanism for improved microvascular flow in the absence of epicardial recanalization may be related to nitric-oxide–mediated stimulation of collateral flow.[166]

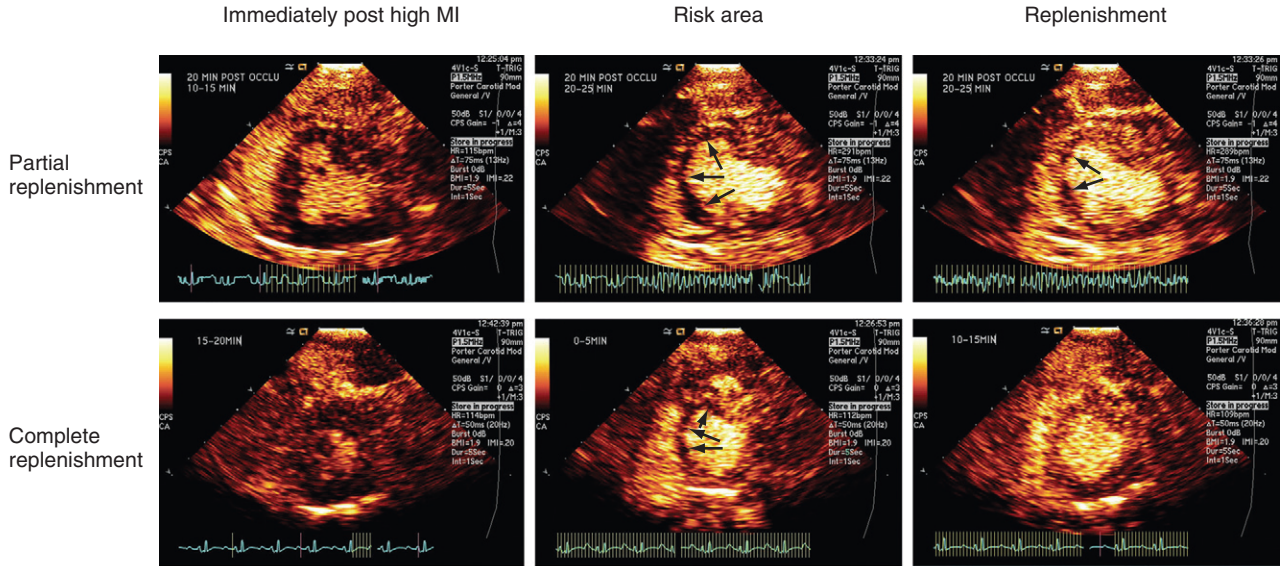



**Figure 3-15** Microvascular flow within the risk area improves following acute left anterior descending artery thrombotic occlusion, when the risk area is treated with a continuous infusion of platelet-targeted microbubbles and guided high-mechanical-index impulses from a diagnostic transducer. Improvements in microvascular flow and regional function were observed even in the absence of epicardial recanalization. *(With permission from Xie F, Lof J, Matsunaga T, et al: Diagnostic ultrasound combined with glycoprotein IIb/IIIa-targeted microbubbles improves microvascular recovery after acute coronary thrombotic occlusions.* Circulation *119:1378-1385, 2009.)*

## KEY POINTS

- Ultrasound contrast agents are produced by electromechanical sonification or as lipid-encapsulated microbubbles.
- High-MI MCE uses intermittent ranging.
- Low-MI MCE uses pulse inversion or power modulation.
- Contrast agents may be given as bolus injections or as a continuous infusion.
- Myocardial contrast imaging can be evaluated in a qualitative or quantitative manner.
- Contrast echocardiographic evaluation of myocardial ischemia has been used to detect acute coronary syndromes.
- MCE can be used to detect myocardial viability.
- MCE demonstrates areas of inducible ischemia during stress testing.
- Intravenous contrast echocardiography also can be used to detect blood flow in other organs and in tumors.
- Thrombolysis and targeted drug delivery may be possible in the future using microbubbles and ultrasound.

## REFERENCES


1. Mulvagh SL, Rakowski H, Vannan MA, et al: American Society of Echocardiography consensus statement on the clinical applications of ultrasonic contrast agents in echocardiography. *J Am Soc Echocardiogr* 21:1179-1201, 2008.
2. Meltzer RA, Tickner EG, Popp RL: Why do the lungs clear ultrasound contrast? *Ultrasound Med Biol* 6:263-269, 1980.
3. Strauss AL, Beller KD: Persistent opacification of the left ventricle and myocardium with a new echo contrast agent. *Ultrasound Med Biol* 25:763-769, 1999.
4. Porter TR, Xie F: Visually discernible myocardial echocardiographic contrast following intravenous injection of sonicated dextrose albumin microbubbles containing high molecular weight less soluble gases. *J Am Coll Cardiol* 25:509-515, 1995.
5. Meza M, Greener Y, Hunt R, et al: Myocardial contrast echocardiography: reliable, safe, and efficacious myocardial perfusion assessment after intravenous injection of a new echocardiographic contrast agent. *Am Heart J* 132:871-881, 1996.
6. Colon PJ, 3rd, Richards DR, Moreno CA, et al: Benefits of reducing the cardiac cycle-triggering frequency of ultrasound imaging to increase myocardial opacification with FSO69 during fundamental and second harmonic imaging. *J Am Soc Echocardiogr* 10:602-607, 1997.
7. Porter TR, Xie F, Kricsfeld A, et al: Noninvasive identification of acute myocardial ischemia and reperfusion with contrast ultrasound using intravenous perfluoropropane-exposed sonicated dextrose albumin. *J Am Coll Cardiol* 26:33-40, 1995.
8. Wei K, Crouse l, Weiss J, et al: Comparison of usefulness of dipyridamole stress myocardial contrast echocardiography to technetium-99m sestamibi single-photon emission computed tomography for detection of coronary artery disease (PB127 Multicenter Phase 2 Trial Results). *Am J Cardiol* 91:1293-1298, 2003.
9. Senior R, Monaghan M, Main ML, et al: Detection of coronary artery disease with perfusion stress echocardiography using a novel ultrasound imaging agent: two phase 3 international trials in comparison with radionuclide perfusion imaging. *Eur J Echocardiogr* 10:26-35, 2009.
10. de Jong N, Ten Cate FJ, Lancee CT: Principles and recent developments in ultrasound contrast agents. *Ultrasonics* 29:324-330, 1991.
11. Chang PH, Shung KK, Levene HB: Quantitative measurements of second harmonic Doppler using ultrasound contrast agents. *Ultrasound Med Biol* 22(9):1205-1214, 1996.
12. Burns PN, Wilson ST, Muradali D et al: Microbubble destruction is the origin of harmonic signals from FS069. *Radiology* 201:158-159, 1996.
13. Burns PN, Wilson SR, Muradali D, et al: Intermittent ultrasound harmonic contrast enhanced imaging and Doppler improves sensitivity and longevity of small vessel detection. *Radiology* 201:159-163, 1996.
14. Wei K, Jayaweera AR, Firoozan S, et al: Quantification of myocardial blood flow with ultrasound-induced destruction of microbubbles administered as a constant venous infusion. *Circulation* 97:473-483, 1998.

15. Porter TR, Xie F, Kricsfeld D, et al: Improved myocardial contrast with perfluorocarbon-exposed sonicated dextrose albumin. *J Am Coll Cardiol* 27:1497-1501, 1996.
16. Binder T, Assayag P, Baer F, et al: NC100100, a new echo contrast agent for the assessment of myocardial perfusion: Safety and comparison with technetium-99m sestamibi single-photon emission computed tomography in a randomized multicenter study. *Clin Cardiol* 22:273-282, 1999.
17. Main ML, Escobar JF, Hall SA, et al: Detection of myocardial perfusion defects by contrast echocardiography in the setting of acute myocardial ischemia with residual antegrade flow. *J Am Soc Echocardiogr* 11:228-235, 1998.
18. Porter TR, Li S, Kricsfeld D, et al: Detection of myocardial perfusion in multiple echocardiographic windows with one intravenous injection of microbubbles using transient response second harmonic imaging. *J Am Coll Cardiol* 29:791-799, 1997.
19. Macsweeny JE, Cosgrove DO, Arenson J: Colour Doppler energy (power) mode ultrasound. *Clin Radiol* 51:387-391, 1996.
20. Powers JE, Burns PN, Souquet J: Imaging instrumentation for ultrasound contrast agents. In Nanda NC, Schlief R, Goldberg BB, editors: *Advances in echo imaging using contrast enhancement*, ed 2. Dordrecht, The Netherlands, 1997, Kluwer Academic, p 139.
21. Broillet A, Puginier J, Ventrone R, et al: Assessment of myocardial perfusion by intermittent harmonic power Doppler using SonoVue, a new ultrasound contrast agent. *Invest Radiol* 33:209-215, 1998.
22. Senior R, Kaul S, Soman P, et al: Power Doppler harmonic imaging: a feasibility study of a new technique for the assessment of myocardial perfusion. *Am Heart J* 139:245-251, 2000.
23. Heinle SK, Noblin J, Goree-Best P, et al: Assessment of myocardial perfusion by harmonic power Doppler imaging at rest and during adenosine stress: comparison with $^{99m}$Tc-sestamibi SPECT imaging. *Circulation* 102:55-60, 2000.
24. Simpson DH, Burns PN: Pulse inversion Doppler: a new method for detecting nonlinear echoes from microbubble contrast agents. *Proc IEEE Ultrason Symp* 2:1597-1600, 1997.
25. Burns PN, Wilson SR, Simpson DH: Pulse inversion imaging of liver blood flow: improved method for characterizing focal masses with microbubble contrast. *Invest Radiol* 35:58-71, 2000.
26. Albrecht T, Hoffmann CW, Schettler S, et al: B-mode enhancement at phase-inversion US with air-based microbubble contrast agent: initial experience in humans. *Radiology* 216: 273-278, 2000.
27. Rafter P, Phillips P, Vannan MA: Imaging technologies and techniques. *Cardiol Clin* 22:181-197, 2004.
28. Skyba DM, Jayaweera AR, Goodman NC, et al: Quantification of myocardial perfusion with myocardial contrast echocardiography during left atrial injection of contrast: implications for venous injection. *Circulation* 90:1513-1521, 1994.
29. Lindner JR, Villanueva FS, Dent JM, et al: Assessment of resting perfusion with myocardial contrast echocardiography: theoretical and practical considerations. *Am Heart J* 139:231-240, 2000.
30. Weissman NJ, Mylan CC, Hack TC, et al: Infusion versus bolus contrast echocardiography: a multicenter, open-label, crossover trial. *Am Heart J* 139:399-404, 2000.
31. Wei K, Jayaweera AR, Firoozan S, et al: Basis for detection of stenosis using venous administration of microbubbles during myocardial contrast echocardiography: bolus or continuous infusion? *Circulation* 32:252-260, 1998.
32. Porter TR, Xie F, Li S, et al: Effect of transducer standoff on the detection, spatial extent, and quantification of myocardial contrast defects caused by coronary stenosis. *J Am Soc Echocardiogr* 12:951-956, 1999.
33. Vogel R, Indermuhle A, Reinhardt J, et al: The quantification of absolute myocardial perfusion in humans by contrast echocardiography. *J Am Coll Cardiol* 45:754-762, 2005.
34. Yano A, Ito H, Iwakura K, Kimura R, et al: Myocardial contrast echocardiography with a new calibration method can estimate myocardial viability in patients with myocardial infarction. *J Am Coll Cardiol* 43:1799-1806, 2004.
35. Wei K, Tong KL, Belcik T, et al: Detection of coronary stenoses at rest with myocardial contrast echocardiography. *Circulation* 112: 1154-1160, 2005.
36. Pasquet A, Greenberg N, Brunken R, et al: Effect of color coding and subtraction on the accuracy of contrast echocardiography. *Int J Cardiol* 70:223-231, 1999.
37. Jayaweera AR, Sklenar J, Kaul S: Quantification of images obtained during myocardial contrast echocardiography. *Echocardiography* 11:385-396, 1994.
38. Angermann CE, Krueger TM, Junge R, et al: Intravenous Albunex during transoesophageal echocardiography: quantitative assessment by videodensitometry and integrated backscatter analysis from unprocessed radiofrequency signals. *J Am Soc Echocardiogr* 8:839-853, 1995.
39. Jiang L, Lu P, Khankirawatana B, et al: Heterogeneity of segmental myocardial video-intensity increments during intermittent harmonic imaging with continuous intravenous infusion of perfluorocarbon microbubbles. *J Am Coll Cardiol* 31:438A:1179, 1998.
40. Abdelmoneim SS, Dhoble A, Bernier M, et al: Quantitative myocardial contrast echocardiography during pharmacological stress for diagnosis of coronary artery disease: a systematic review and meta-analysis of diagnostic accuracy studies. *Eur J Echocardiogr* 10:813-825, 2009.
41. Toledo E, Lang RM, Collins KA, et al: Imaging and quantification of myocardial perfusion using real-time three-dimensional echocardiography. *J Am Coll Cardiol* 47:146-154, 2006.
42. Exuzide A, Main ML, Coby C, et al: A retrospective comparison of mortality in critically ill hospitalized patients undergoing echocardiography with and without an ultrasound contrast. *JACC Cardiovasc Imaging* 3:578-585, 2010.
43. Abdelmoneim SS, Bernier M, Scott CG, et al: Safety of contrast agent used during stress echocardiography in patients with elevated right ventricular systolic pressure a cohort study. *Circ Cardiovasc Imaging* 3:240-248, 2010.
44. Abdelmoneim SS, Bernier M, Scott CG, et al: Safety of contrast agents use during stress echocardiography; a 4-year experience form a single center cohort study of 26,774 patients. *JACC Cardiovasc Imaging* 2:1048-1056, 2009.
45. Dolan MS, Gala S, Dodla S, et al: Safety and efficacy of commercially available ultrasound contrast agents for rest and stress echocardiography: a multicenter experience. *J Am Coll Cardiol* 53:32-38, 2009.
46. Gaibazzi N, Squeri A, Ardissino D, Reverberi C: Safety of contrast flash-replenishment stress echocardiography in 500 patients with a chest pain episode of undetermined origin within the last 5 days. *Eur J Echocardiogr* 10:726-732, 2009.
47. Anantharam B, Chahal N, Chelliah R, et al: Safety of contrast in stress echocardiography in stable patients and in patients with suspected acute coronary syndrome but negative 12-hour troponin. *Am J Cardiol* 104:14-18, 2009.
48. Main ML, Ryan AC, Davis TE, et al: Acute mortality in hospitalized patients undergoing echocardiography with and without an ultrasound contrast agent (multicenter registry results in 4,300,966 consecutive patients). *Am J Cardiol* 102:1742-1746, 2008.
49. Gabriel RS, Smyth YM, Menon V, et al: Safety of ultrasound contrast agents in stress echocardiography. *Am J Cardiol* 102:1269-1272, 2008.
50. Wei K, Mulvagh SL, Carson L, et al: The safety of Definity and Optison for ultrasound image enhancement: a retrospective analysis of 78,383 administered contrast doses. *J Am Soc Echocardiogr* 11:1202-1206, 2008.
51. Kusnetzky LL, Khalid A, Khumri TM, et al: Acute mortality in hospitalized patients undergoing echocardiography with and without an ultrasound contrast agent: results in 18,671 consecutive patients. *J Am Coll Cardiol* 51:1704-1706, 2008.
52. Shaikh K, Chang SM, Peterson L, et al: Safety of contrast administration for endocardial enhancement during stress echocardiography compared with noncontrast stress. *Am J Cardiol* 102:1444-1450, 2008.
53. Timperley J, Mitchell ARJ, Thibault H, et al: Safety of contrast dobutamine stress echocardiography: a single center experience. *J Am Soc Echocardiogr* 18:163-167, 2005.
54. Tsutsui JM, Elhendy A, Xie F, et al: Safety of dobutamine stress real-time myocardial contrast echocardiography. *J Am Coll Cardiol* 45:1235-1242, 2005.
55. Kurt M, Shaikh KA, Peterson, L, et al: Impact of contrast echocardiography on evaluation of ventricular function and clinical management in a large prospective cohort. *J Am Coll Cardiol* 53:802-810, 2009.
56. Miller DL, Driscoll EM, Dou C, et al: Microvascular permeabilization and cardiomyocyte injury provoked by myocardial contrast echocardiography in a canine model. *J Am Coll Cardiol* 47:1464, 2006.
57. Timperley J, Mitchell ARJ, Thibault H, et al: Safety of contrast dobutamine stress echocardiography: a single center experience. *J Am Soc Echocardiogr* 18:163-167, 2005.
58. Chapman S, Windle J, Xie F, et al: Incidence of cardiac arrhythmias with therapeutic versus diagnostic ultrasound and intravenous microbubbles. *J Ultrasound Med* 24:1099-1107, 2005.
59. Ito H, Tomooka T, Sakai N, et al: Time course of functional improvement in stunned myocardium in risk area in patients with reperfused anterior infarction. *Circulation* 87: 355-362, 1993.
60. Kaul S, Pandian NG, Okada RD, et al: Contrast echocardiography in acute myocardial ischemia: In-vivo determination of total left ventricular "area at risk." *J Am Coll Cardiol* 4:1272-1282, 1984.
61. Touchstone DA, Nygaard TW, Kaul S. Correlation between left ventricular risk area and clinical, electrocardiographic, hemodynamic,

and angiographic variables during acute myocardial infarction. *J Am Soc Echocardiogr* 3:106-117, 1990.
62. Dittrich HC, Bales GL, Kuvelas T, et al: Myocardial contrast echocardiography in experimental coronary artery occlusion with a new intravenously administered contrast agent. *J Am Soc Echocardiogr* 8:465-474, 1995.
63. Grauer SE, Pantely GA, Xu J, et al: Myocardial imaging with a new transpulmonary lipid-fluorocarbon echo contrast agent: Experimental studies in pigs. *Am Heart J* 132:938-945, 1996.
64. Firschke C, Lindner JR, Wei K, et al: Myocardial perfusion imaging in the setting of coronary artery stenosis and acute myocardial infarction using venous injection of a second-generation echocardiographic contrast agent. *Circulation* 96:959-967, 1997.
65. Tong KL, Kaul S, Wang XQ, et al: Myocardial contrast echocardiography versus thrombolysis in myocardial infarction score in patients presenting to the emergency department with chest pain and a nondiagnostic electrocardiogram. *J Am Coll Cardiol* 46:920-927, 2005.
66. Kloner RA, Ganote CE, Jennings RB: The "no-reflow" phenomenon after temporary coronary occlusion in the dog. *Clin Invest* 54:1496-1508, 1974.
67. Ito H, Tomooka T, Sakaii N, et al: Lack of myocardial perfusion immediately after successful thrombolysis: A predictor of poor recovery of left ventricular function in anterior myocardial infarction. *Circulation* 85:1699-1705, 1992.
68. Lepper W, Hoffmann R, Kamp O, et al: Assessment of myocardial reperfusion by intravenous myocardial contrast echocardiography and coronary flow reserve after primary percutaneous transluminal coronary angiography in patients with acute myocardial infarction. *Circulation* 101:2368-2374, 2000.
69. Firschke C, Lindner JR, Goodman NC, et al: Myocardial contrast echocardiography in acute myocardial infarction using aortic root injections of microbubbles: potential application in the cardiac catheterization laboratory. *J Am Coll Cardiol* 29:207-216, 1997.
70. Balcells E, Powers ER, Lepper W, et al: Detection of myocardial viability by contrast echocardiography in acute infarction predicts recovery of resting function and contractile reserve. *J Am Coll Cardiol* 41:827-833, 2003.
71. Dwivedi G, Janardhanan R, Hayat SA, Lim TK, Senior R: Comparison between myocardial contrast echocardiography (99m) technetium sestamibi single photon emission computed tomography determined myocardial viability in predicting hard cardiac events following acute myocardial infarction. *Am J Cardiol* 104:1184-1188, 2009.
72. Galiuto L, Garramone B, Scara A, et al: The extent of microvascular damage during myocardial contrast echocardiography is superior to other known indexes of post-infarct reperfusion in predicting left ventricular remodeling: results of the multicenter AMICI study. *J Am Coll Cardiol* 51:552-559, 2008.
73. Janardhanan R, Senior R: Accuracy of dipyridamole myocardial contrast echocardiography for the detection of residual stenosis of the infarct-related artery and multivessel disease early after acute myocardial infarction. *J Am Coll Cardiol* 43:2247-2252, 2004.
74. Lim YJ, Nanto S, Masuyama T, et al: Discrepancies between wall motion abnormalities and regional myocardial perfusion in patients with myocardial infarction: Evaluation by myocardial contrast echocardiography. *J Cardiol* 19:343-350, 1989.
75. Lim YJ, Nanto S, Masuyama T, et al: Coronary collaterals assessed with myocardial contrast echocardiography in healed myocardial infarction. *Am J Cardiol* 66:556-561, 1990.
76. Grill HP, Brinker JA, Taube JC, et al: Contrast echocardiographic mapping of collateralized myocardium in humans before and after coronary angioplasty. *J Am Coll Cardiol* 16: 1594-1600, 1990.
77. Sabia PJ, Powers ER, Ragosta M, et al: An association between collateral blood flow and myocardial viability in patients with recent myocardial infarction. *N Engl J Med* 327:1825-1831, 1992.
78. Kaul S, Jayaweera AR, Glasheen WP, et al: Myocardial contrast echocardiography and the transmural distribution of flow: a critical appraisal during myocardial ischemia not associated with infarction. *J Am Coll Cardiol* 20:1005-1016, 1992.
79. Chelliah RK, Hickman M, Kinsey C, et al: Myocardial contrast echocardiography versus single photon emission computed tomography for the assessment of hibernating myocardium in ischemic cardiomyopathy: preliminary qualitative and quantitative results. *J Am Soc Echocardiogr* 23:840-847, 2010.
80. Shimoni S, Fragogiannis NG, Aggeli CJ, et al: Identification of hibernating myocardium with quantitative intravenous myocardial contrast echocardiography: comparison with dobutamine echocardiography and thallium-201 scintigraphy. *Circulation* 107:538-844, 2003.
81. Kaul S, Senior R, Dittrich H, et al: Detection of coronary artery disease with myocardial contrast echocardiography: Comparison with $^{99m}$Tc-sestamibi single-photon emission computed tomography. *Circulation* 96:785, 1997.
82. Jeetley P, Hickman M, Kamp O et al: Myocardial contrast echocardiography for the detection of coronary artery stenosis: a prospective multicenter study in comparison with single-photon emission computed tomography. *J Am Coll Cardiol* 47:141-145, 2006.
83. Senior R, Monaghan M, Main ML, et al: Detection of coronary artery disease with perfusion stress echocardiography using a novel ultrasound imaging agent: two phase 3 international trials in comparison with radionuclide perfusion imaging. *Eur J Echocardiogr* 10:26-35, 2009.
84. Dawson D, Kaul S, Peters D, et al: Prognostic value of dipyridamole stress myocardial contrast echocardiography: comparison with single photon emission computed tomography. *J Am Soc Echocardiogr* 22:954-960, 2009.
85. Xie F, Hankins J, Mahrous HA, Porter TR: Detection of coronary artery disease with a continuous infusion of Definity ultrasound contrast during adenosine stress real time perfusion echocardiography. *Echocardiography* 24:1044-1050, 2007.
86. Porter TR, Xie F, Adolphson M, et al: Abstract 10419: Safety and accuracy of regadenoson bolus real time perfusion stress echocardiography. *Circulation* 122:A10419, 2010.
87. Arnold JR, Karamitsos TD, Pegg TJ, et al: Adenosine stress myocardial contrast echocardiography for the detection of coronary artery disease: a comparison with coronary angiography and cardiac magnetic resonance. *JACC Cardiovasc Imaging* 3:934-943, 2010.
88. Cwajg J, Xie F, O'Leary E, et al: Detection of angiographically significant coronary artery disease with accelerated intermittent imaging after intravenous administration of ultrasound contrast material. *Am Heart J* 139:675-683, 2000.
89. Elhendy A, O'Leary EL, Xie F, et al: Comparative accuracy of real-time myocardial contrast perfusion imaging and wall motion analysis during dobutamine stress echocardiography for the diagnosis of coronary artery disease. *J Am Coll Cardiol* 44:2185-2191, 2004.
90. Tsutsui JM, Elhendy A, Anderson JR, et al: Prognostic value of dobutamine stress myocardial contrast perfusion echocardiography. *Circulation* 112:1444-1450, 2005.
91. Lonnebakken MT, Bleie O, Strand E, et al: Myocardial contrast echocardiography in assessment of stable coronary artery disease at intermediate dobutamine-induced stress level. *Echocardiography* 26:52-60, 2009.
92. Xie F, Dodla S, O'Leary E, Porter TR: Detection of subendocardial ischemia in the left anterior descending coronary artery territory with real-time myocardial contrast echocardiography during dobutamine stress echocardiography. *JACC Cardiovasc Imaging* 1:271-278, 2008.
93. Shimoni S, Zoghbi WA, Xie F, et al: Real-time assessment of myocardial perfusion and wall motion during bicycle and treadmill exercise echocardiography: comparison with single photon emission computed tomography. *J Am Coll Cardiol* 37:741-747, 2001.
94. Dodla S, Xie F, Smith M, et al: Real-time perfusion echocardiography during treadmill exercise and dobutamine stress testing. *Heart* 96:220-225, 2010.
95. Miszalski-Jamka T, Kuntz-Hehner S, Schmidt H, et al: Myocardial contrast echocardiography enhances long-term prognostic value of supine bicycle stress two-dimensional echocardiography. *J Am Soc Echocardiogr* 22:1220-1227, 2009.
96. Porter TR, Xie F, Silver M, et al: Real-time perfusion imaging with low mechanical index pulse inversion Doppler imaging. *J Am Coll Cardiol* 37:748-753, 2001.
97. Olszowska M, Kostkiewicz M, Tracz W, Przewlocki T: Assessment of myocardial perfusion in patients with coronary artery disease. Comparison of myocardial contrast echocardiography and 99mTc MIBI single photon emission computed tomography. *Int J Cardiol* 90:49-55, 2003.
98. Peltier M, Vancraeynest D, Pasquet A, et al: Assessment of the physiologic significance of coronary disease with dipyridamole real-time myocardial contrast echocardiography. Comparison with technetium-99m sestamibi single-photon emission computed tomography and quantitative coronary angiography. *J Am Coll Cardiol* 43:257-264, 2004.
99. Yu EH, Skyba DM, Leong-Poi H, et al: Incremental value of parametric quantitative assessment of myocardial perfusion by triggered low-power myocardial contrast echocardiography. *J Am Coll Cardiol* 43:1807-1813, 2004.
100. Moir S, Haluska BA, Jenkins C, et al: Incremental benefit of myocardial contrast to combined dipyridamole-exercise stress echocardiography for the assessment of coronary artery disease. *Circulation* 110:1108-1113, 2004.
101. Elhendy A, Tsutsui JM, O'Leary EL, et al: Noninvasive diagnosis of coronary artery disease in patients with diabetes by dobutamine stress real-time myocardial contrast perfusion imaging. *Diabetes Care* 28:1662-1667, 2005.
102. Tsutsui JM, Xie F, McGrain AC, et al: Comparison of low-mechanical index pulse sequence

schemes for detecting myocardial perfusion abnormalities during vasodilator stress echocardiography. *Am J Cardiol* 95:565-570, 2005.
103. Xie F, Tsutsui JM, McGrain AC, et al: Comparison of dobutamine stress echocardiography with and without real-time perfusion imaging for detection of coronary artery disease. *Am J Cardiol* 96:506-511, 2005.
104. Jeetley P, Hickman M, Kamp O, et al: Myocardial contrast echocardiography for the detection of coronary artery stenosis. *J Am Coll Cardiol* 47:141-145, 2005.
105. Korosoglou G, Dubart AE, DaSilva KG, Jr, et al: Real-time myocardial perfusion imaging for pharmacologic stress testing: added value to single photon emission computed tomography. *Am Heart J* 151:131-138, 2006.
106. Hayat SA, Dwivedi G, Jacobsen A, et al: Effects of left bundle-brank block on cardiac structure, function, perfusion, and perfusion reserve: implications for myocardial contrast echocardiography versus radionuclide perfusion imaging for the detection of coronary artery disease. *Circulation* 117:1832-1841, 2008.
107. Wei K, Le E, Jayaweera AR, et al: Detection of noncritical coronary stenosis at rest without recourse to exercise or pharmacological stress. *Circulation* 105:218-223, 2002.
108. Main ML, Asher CR, Rubin DN, et al: Comparison of tissue harmonic imaging with contrast (sonicated albumin) echocardiography and Doppler myocardial imaging for enhancing endocardial border resolution. *Am J Cardiol* 83:218-222, 1999.
109. Shaw LJ, Gillam L, Feinstein S, et al: Use of an intravenous contrast agent (Optison) to enhance echocardiography: Efficacy and cost implications. Optison Multicenter Study Group. *Am J Manag Care* 25:169-176, 1998.
110. Reilly JP, Tunick PA, Timmerman RJ, et al: Contrast echocardiography clarifies uninterpretable wall motion in intensive care unit patients. *J Am Coll Cardiol* 35:485-490, 2000.
111. Malhotra V, Nwogu J, Bondmass MD, et al: Is the technically limited echocardiographic study an endangered species? Endocardial border definition with native tissue harmonic imaging and Optison contrast: a review of 200 cases. *J Am Soc Echocardiogr* 13:771-773, 2000.
112. Hoffmann R, von Bardeleben S, ten Cate F, et al: Assessment of systolic left ventricular function: a multi-centre comparison of cineventriculography, cardiac magnetic resonance imaging, unenhanced and contrast-enhanced echocardiography. *Eur Heart J* 26:607-616, 2005.
113. Hoffmann R, von Bardeleben S, Kasprzak JD, et al: Analysis of regional left ventricular function by cineventriculography, cardiac magnetic resonance imaging, and unenhanced and contrast-enhanced echocardiography. *J Am Coll Cardiol* 47:121-128, 2006.
114. Nagai T, Atar S, Luo H, et al: The usefulness of second generation ultrasound contrast agent to identify intracardiac thrombus [abstract]. *J Am Coll Cardiol* 33:408A, 1999.
115. Thanigaraj S, Schechtman KB, Perez JE: Improved echocardiographic delineation of left ventricular thrombus with the use of intravenous second-generation contrast image enhancement. *J Am Soc Echocardiogr* 12:1022-1026, 1999.
116. Waggoner AD, Williams GA, Gaffron D, et al: Potential utility of left heart contrast agents in diagnosis of myocardial rupture by 2-dimensional echocardiography. *J Am Soc Echocardiogr* 12:272-274, 1999.
117. Kimura BJ, Phan JN, Housman LB: Utility of contrast echocardiography in the diagnosis of aortic dissection. *J Am Soc Echocardiogr* 12:155-159, 1999.
118. Kirkpatrick JN, Wong T, Bednarz JE, et al: Differential diagnosis of cardiac masses using contrast echocardiographic perfusion imaging. *J Am Coll Cardiol* 43:1412-1419, 2004.
119. von Bibra H, Sutherland G, Becher H, et al: Clinical evaluation of left heart Doppler contrast enhancement by a saccharide-based transpulmonary contrast agent. The Levovist Cardiac Working Group. *J Am Coll Cardiol* 25:500-508, 1995.
120. Lambertz H, Schuhmacher R, Tris HP, et al: Improvement of pulmonary venous flow Doppler signal after intravenous injection of Levovist. *J Am Soc Echocardiogr* 10:891-898, 1997.
121. Nakatani S, Imanishi T, Terawawa A, et al: Clinical application of transpulmonary contrast-enhanced Doppler technique in the assessment of severity of aortic stenosis. *J Am Coll Cardiol* 20:973-978, 1992.
122. Okura H, Yoshida K, Akasaka T, et al: Improved transvalvular continuous-wave Doppler signal intensity after intravenous Albunex injection in patients with prosthetic aortic valves. *J Am Soc Echocardiogr* 10:608-612, 1997.
123. Jeon DS, Huai L, Iwami T, et al: The usefulness of a 10% air-10% blood-80% saline mixture for contrast echocardiography: Doppler measurement of pulmonary artery systolic pressure. *J Am Coll Cardiol* 39:124-128, 2002.
124. Rim SJ, Leong-Poi H, Lindner JR, et al: Quantification of cerebral perfusion with "real-time" contrast-enhanced ultrasound. *Circulation* 104:2582-2587, 2001.
125. Heppner P, Ellegala DB, Durieux M, et al. Contrast ultrasonographic assessment of cerebral perfusion in patients undergoing decompressive craniectomy for traumatic brain injury. *J Neurosurg* 104:738-745, 2006.
126. Wei K, Le E, Bin JP, et al: Quantification of renal blood flow with contrast-enhanced ultrasound. *J Am Coll Cardiol* 37:1135-1140, 2001.
127. Coggins M, Linder J, Rattigan S, et al: Physiologic hyperinsulinemia enhances human skeletal muscle perfusion by capillary recruitment. *Diabetes* 50:2682-2690, 2001.
128. Womack L, Peters D, Barrett EJ, et al: Abnormal skeletal muscle capillary recruitment during exercise in patients with type 2 diabetes mellitus and microvascular complications. *J Am Coll Cardiol* 53:2175-2183, 2009.
129. Linder JR: Molecular imaging of myocardial and vascular disorders with ultrasound. *JACC Cardiovasc Imaging* 3:204-211, 2010.
130. Lindner JR, Coggins MP, Kaul S, et al: Microbubble persistence in the microcirculation during ischemia/reperfusion and inflammation is caused by integrin- and complement-mediated adherence to activated leukocytes. *Circulation* 101:668-675, 2000.
131. Lindner JR, Dayton PA, Coggins MP, et al: Noninvasive imaging of inflammation by ultrasound detection of phagocytosed microbubbles. *Circulation* 102:2745-2750, 2000.
132. Leong-Poi H, Christiansen J, Klibanov AL, et al: Noninvasive assessment of angiogenesis by ultrasound and microbubbles targeted to $\alpha_v$-integrins. *Circulation* 107:455-460, 2003.
133. Leong-Poi H, Christiansen J, Heppner P, et al: Assessment of endogenous and therapeutic arteriogenesis by contrast ultrasound molecular imaging of integrin expression. *Circulation* 111:3248-3254, 2005.
134. Christiansen JP, Leong-Poi H, Klibanov AL, et al: Noninvasive imaging of myocardial reperfusion injury using leukocyte-targeted contrast echocardiography. *Circulation* 105:1764-1767, 2002.
135. Weller GER, Lu E, Csikari MM, et al: Ultrasound imaging of acute cardiac transplant rejection with microbubbles targeted to intercellular adhesion molecule-1. *Circulation* 108:218-224, 2003.
136. Kondo I, Ohmori K, Oshita A, et al: Leukocyte-targeted myocardial contrast echocardiography can assess the degree of acute allograft rejection in a rat cardiac transplantation model. *Circulation* 109:1056-1061, 2004.
137. Sakuma T, Sari I, Goodman CN, et al: Simultaneous integrin $\alpha_v\beta_3$ and glycoprotein IIb/IIIa inhibition causes reduction in infarct size in a model of acute coronary thrombosis and primary angioplasty. *Cardiovasc Res* 66:552-561, 2005.
138. Kaufmann BA, Lewis C, Xie A, Mirza-Mohd A, Lindner JR: Detection of recent myocardial ischaemia by molecular imaging of P-selectin with targeted contrast echocardiography. *Eur Heart J* 28:2011-2017, 2007.
139. Villanueva FS, Lu E, Bowry S, et al: Myocardial ischemic memory imaging with molecular echocardiography. *Circulation* 115:345-352, 2007.
140. Kondo I, Ohmori K, Oshita A, et al: Leukocyte-targeted myocardial contrast echocardiography can assess the degree of acute allograft rejection in a rat cardiac transplantation model. *Circulation* 109:1056-1061, 2004.
141. Kaufmann BA, Sanders JM, Davis C, et al: Molecular imaging of inflammation in atherosclerosis with targeted ultrasound detection of vascular cell adhesion molecule-1. *Circulation* 116:276-284, 2007.
142. Kaufmann BA, Carr CL, Belcik JT, et al: Molecular imaging of the initial inflammatory response in atherosclerosis: implication for early detection of disease. *Arterioscler Thromb Vasc Biol* 30:54-59, 2010.
143. Feinstein SB. Contrast ultrasound of the carotid artery vasa vasorum and atherosclerotic plaque neovascularization. *J Am Coll Cardiol* 48:236-243, 2006.
144. Staub D, Schinkel AF, Coll B, et al: Contrast-enhanced ultrasound imaging of the vasa vasorum: from early atherosclerosis to the identification of unstable plaques. *JACC Cardiovasc Imaging* 3:761-771, 2010.
145. Staub D, Patel MB, Tibrewala A, et al: Vasa vasorum and plaque neovascularization on contrast-enhanced carotid ultrasound imaging correlates with cardiovascular disease and past cardiovascular events. *Stroke* 41:41-7.151, 2010.
146. Wei K, Skyba DM, Firschke C, et al: Interaction between microbubbles and ultrasound: in vitro and in vivo observations. *J Am Coll Cardiol* 29:1081-1088, 1997.
147. Skyba AM, Price RJ, Linka AZ, et al: Direct in vivo visualization of intravascular destruction of microbubbles by ultrasound and its local effects on tissue. *Circulation* 98:290-293, 1998.
148. Price RJ, Skyba DM, Kaul S, et al: Delivery of colloidal particles and red blood cells to tissue through microvessel ruptures created by

targeted microbubble destruction with ultrasound. *Circulation* 98:1264-1267, 1998.
149. Porter TR, Iversen PL, Li S, et al: Interaction of diagnostic ultrasound with synthetic oligonucleotide-labeled perfluorocarbon-exposed sonicated dextrose albumin microbubbles. *J Ultrasound Med* 15:577-584, 1996.
150. Shohet RV, Chen S, Zhou Y-T, et al: Echocardiographic destruction of albumin microbubbles directs gene delivery to the myocardium. *Circulation* 101:2554-2556, 2000.
151. Unger EC, McCreery TP, Sweitzer RH, et al: In vitro studies of a new thrombus-specific ultrasound contrast agent. *Am J Cardiol* 81:58G-61G, 1998.
152. Chen S, Shohet RV, Bekeredjian R, et al: Optimization of ultrasound parameters for cardiac gene delivery of adenoviral or plasmid deoxyribonucleic acid by ultrasound-targeted microbubble destruction. *J Am Coll Cardiol* 42:301-308, 2003.
153. Taniyama Y, Tachibana K, Hiraoka K, et al: Local delivery of plasmid DNA into rat carotid artery using ultrasound. *Circulation* 105:1233-1239, 2002.
154. Kinoshita M, McDannold N, Jolesz FA, Hynynen K: Targeted delivery of antibodies through the blood-brain barrier by MRI-guided focused ultrasound. *Biochem Biophys Res Commun* 340:1085-1090, 2006.
155. Sheikov N, McDannold N, Vykhodtseva N, et al: Cellular mechanisms of the blood-brain barrier opening induced by ultrasound in presence of microbubbles. *US Med Biol* 30:979-989, 2004.
156. FDA: *Information for manufacturers seeking marketing clearance of diagnostic ultrasound systems and transducers*. HHS Publication, FDA, Center for Devices and Radiological Health) Food and Drug Administration, 9200 Corporate Blvd., Rockville, MD 20850, 1997.
157. Chai R, Chen S, Ding J, Grayburn PA: Efficient, glucose responsive and islet-specific transgene expression by a modified rat insulin promoter. *Gene Ther* 16:1202-1209, 2009.
158. Jordao JF, Ayala-Grosso CA, Markham K, et al: Antibodies targeted to the brain with image-guided focused ultrasound reduces amyloid-beta plaque load in the TgCRND8 mouse model of Alzheimer's disease. *PLoS One* 5:e10549, 2010.
159. Rosenschein U, Bernstein JJ, DiSegni E, et al: Experimental ultrasonic angioplasty: Disruption of atherosclerotic plaques and thrombi in vitro and arterial recanalization in vivo. *J Am Coll Cardiol* 15:711-717, 1990.
160. Porter TR, LeVeen RF, Fox R, et al: Thrombolytic enhancement with perfluorocarbon-exposed sonicated dextrose albumin microbubbles. *Am Heart J* 132:964-968, 1996.
161. Birnbaum Y, Luo H, Nagai T, et al: Noninvasive in vivo clot dissolution without a thrombolytic drug. *Circulation* 97:130-134, 1998.
162. Xie F, Tsutsui JM, Lof J, et al: Effectiveness of lipid microbubbles and ultrasound in declotting thrombosis. *US Med Biol* 31:979-985, 2005.
163. Tsutsui JM, Grayburn PA, Xie F, Porter TR: Drug and gene delivery and enhancement of thrombolysis using ultrasound and microbubbles. *Cardiol Clin* 22:299-312, vii, 2004.
164. Culp WC, Porter TR, Lowery J, et al: Intracranial clot lysis with intravenous microbubbles and transcranial ultrasound in swine. *Stroke* 25:2407-2411, 2004.
165. Xie F, Lof J, Matsunaga T, et al: Diagnostic ultrasound combined with glycoprotein IIb/IIIa-targeted microbubbles improves microvascular recovery after acute coronary thrombotic occlusions. *Circulation* 119:1378-1385, 2009.
166. Siegel RJ, Suchkova VN, Miyamoto T, et al: Ultrasound energy improves myocardial perfusion in the presence of coronary occlusion. *J Am Coll Cardiol* 44:1454-1458, 2004.



# Three-Dimensional Echocardiography

RORY B. WEINER, MD | MICHAEL H. PICARD, MD

**Technical Considerations**
Advantages and Disadvantages of Three-Dimensional Acquisition Techniques
**Three-Dimensional Echocardiographic Work Flow**
**Evidence-Based Applications of Three-Dimensional Echocardiography**
Left Ventricular Volume and Function
Left Ventricular Mass
Right Ventricular Volume
Atrial Volume
Valvular Heart Disease
Congenital Heart Disease
Guidance of Intracardiac Catheter-Based Interventions
Other Selected Applications
**Technology Diffusion**
**Future Considerations**
**Summary**

For a full understanding of cardiac structures, the user of two-dimensional (2D) echocardiography must be able to mentally integrate a series of these views in order to understand the three-dimensional (3D) structure of the heart and the spatial relations between its components. For example, when performing 2D echocardiography on a patient with prolapse of a portion of the posterior mitral valve leaflet, the echocardiographer individually examines each portion of the valve from a series of 2D images and mentally reconstructs the entire valve to determine which portion of the valve is prolapsing. To accurately perform this task, one must know the precise relationship of each 2D image to the others. In addition, when quantifying cardiac chamber volumes, mass, or function with 2D echocardiography, one relies on assumptions about the geometry of the chamber to apply specific formulas for calculation of these and other parameters. As chambers become distorted in shape, the geometric assumptions about shape become less accurate, as do the calculated values using these formulas.

3D echocardiography from both transthoracic (TTE) and transesophageal (TEE) approaches eliminates the need for cognitive 3D reconstruction of image planes and the need to use geometric assumptions about shape of structures for cardiac quantitation (Fig. 4-1). This is particularly applicable to complex shapes, such as the right ventricle, an aneurysmal left ventricle, an asymmetrically stenotic or regurgitant valve orifice, eccentrically directed regurgitant jets assessed by color Doppler, valve annuli, and the complex structural relationships observed in congenital heart lesions. The 3D echocardiographic technique has the potential to decrease the time required for complete image acquisition of the heart. Also, the 3D echocardiogram can be viewed from various projections by rotation of the images, and thus an improved appreciation of the relationships between various cardiac structures can be obtained.

Advances in transducer technology and image processing power have helped improve 3D echocardiography acquisition, display, and image quality. Whereas initial 3D echocardiography required transducer locating systems and labor-intensive offline reconstruction, current approaches enable 3D ultrasound (US) imaging in real time.

## Technical Considerations

The 3D US data set can be acquired either (1) as a series of 2D images and then reconstructed into a 3D image (reconstruction technique) or (2) as a 3D volume of US data (volumetric technique). The earliest 3D echocardiograms were obtained using the reconstruction technique[1,2] and required that the precise location and timing of the each image be known to facilitate the integration of the images. Whereas the reconstruction method is time consuming because of image acquisition, spatial registration, offline reconstruction, and image rendering and display, this approach has proven accurate and valuable for quantitation of left ventricular (LV) size and function,[3] right ventricular (RV) size and function,[4] pericardial effusions,[5] and valve disease.[6] In fact, early 3D echocardiographic reconstructions demonstrated that the mitral valve annulus is saddle shaped, and thus prolapse of the leaflets below the low points of the annulus into the left atrium (LA) can only be observed in 2D echocardiographic views that display these low points, typically the anterior and posterior portions of the annulus as seen in the parasternal and apical long-axis views.[6] The 3D reconstruction approach has mostly been replaced by the volumetric 3D techniques that are the focus of this chapter. More detailed information about reconstruction techniques can be found in earlier editions of this textbook.[7]

The volumetric approach requires a specialized transducer to collect a pyramidal (or 3D) volume of image data. The resultant image can then be displayed in many fashions. The surface of the structure can be displayed as a solid object. Alternatively, the volume can be displayed with varying degrees of transparency and shading to show different depths, thus allowing visualization of various structures within the volume (Fig. 4-2).

The development of complex TTE and TEE US transducers has enabled acquisition of 3D volume data sets in real time or "near" real time. To achieve this goal, the transducer elements are typically arranged in a rectangular grid or matrix array, and advanced electronics enable beam steering in multiple directions. To scan a volume of adequate size and at a reasonable frame rate, multiple US pulses must be emitted from this matrix array at the same time and processed in parallel. The earliest

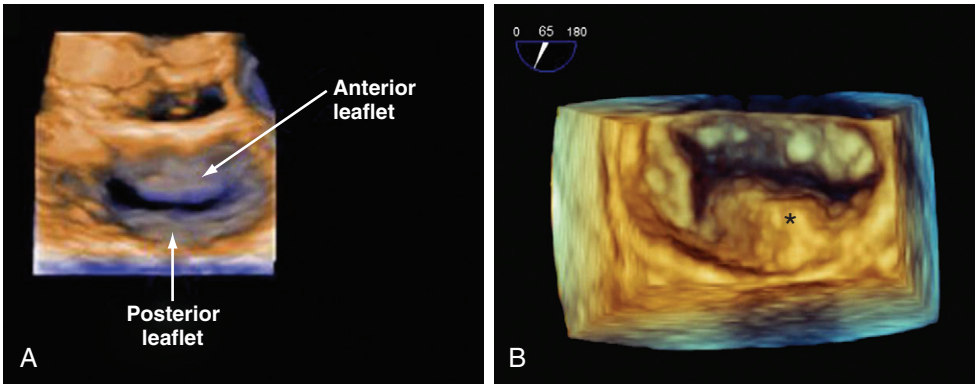



**Figure 4-1** **A,** Diastolic frame of a 3D TTE of mitral valve viewed from the LA demonstrating myxomatous anterior leaflet in a patient with anterior mitral valve prolapse. **B,** Diastolic frame of a 3D TEE of mitral valve viewed from the LA demonstrating myxomatous posterior leaflet (*) in a patient with posterior mitral valve prolapse.

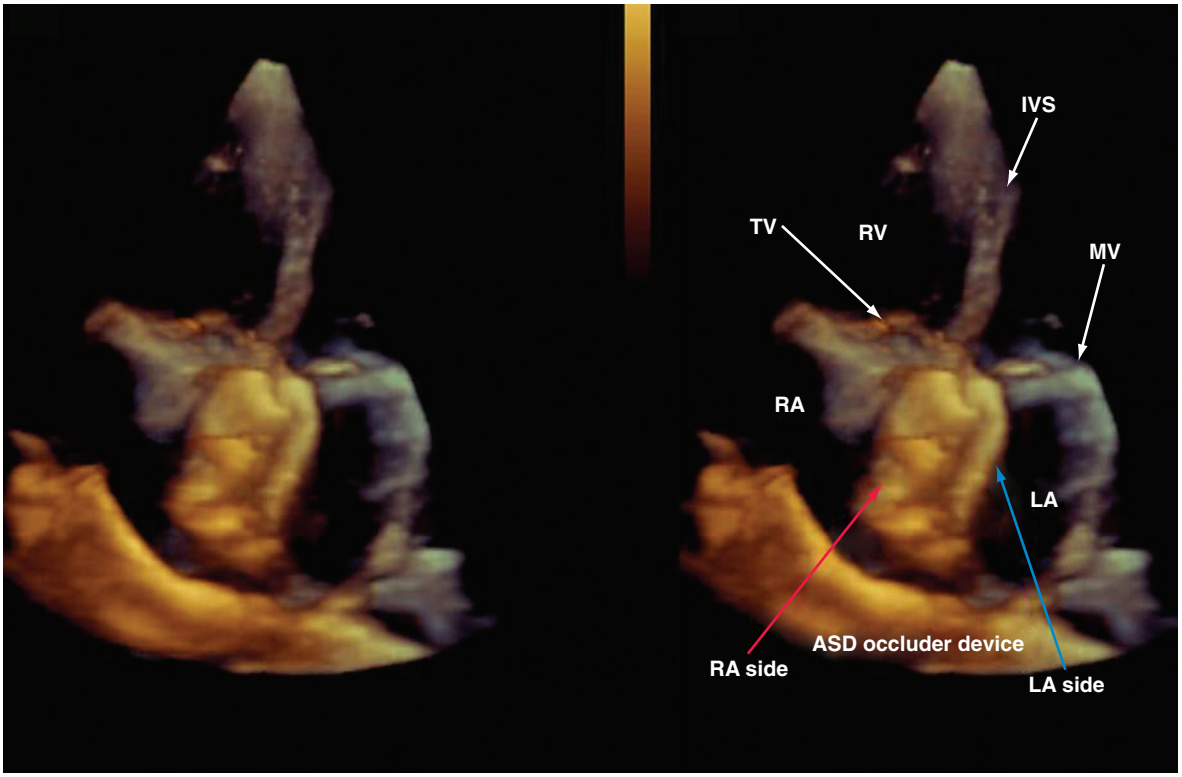



**Figure 4-2** Real-time 3D TTE from an apical view demonstrating an atrial septal defect (*ASD*) occluder device. The 3D depth is depicted by varying degrees of transparency and brightness. Structures closest to the viewer are brightest. *IVS*, Interventricular septum; *MV*, mitral valve; *TV*, tricuspid valve.

device utilized a sparse-array matrix transducer with 256 elements and acquired a pyramid-shaped volume of US data within a single cardiac cycle.[8-10] Although this provided real-time 3D images, the spatial and temporal resolution were not ideal, and volume rendering was not performed on the machine.

Current real-time 3D (RT3D) TTE systems utilize matrix array transducers with approximately 3000 elements, whereas 3D TEE matrix array transducers have a lower number of elements. A pyramid-shaped 3D US volume of about 30° by 50° can be acquired and displayed in real time. With a volume of this size, only a portion of the adult heart can typically be displayed in real time and three dimensions. However, this is large enough to display valves, the RV, complex defects, masses, color Doppler jets, the infant LV, or portions of the adult LV. To optimally visualize this RT3D US image, one rotates the image to view from all perspectives (Fig. 4-3). Display of a larger volume can be obtained from a single-beat acquisition on specific echocardiographic devices. However, for most devices, it typically requires acquisition of component volumes from a series of consecutive cardiac cycles, and these are then combined to yield a 90° by 90° image set. Color Doppler flow mapping by the 3D volumetric technique typically requires acquisition of a larger number of component volumes. To reduce artifacts that may appear in these "fused" images

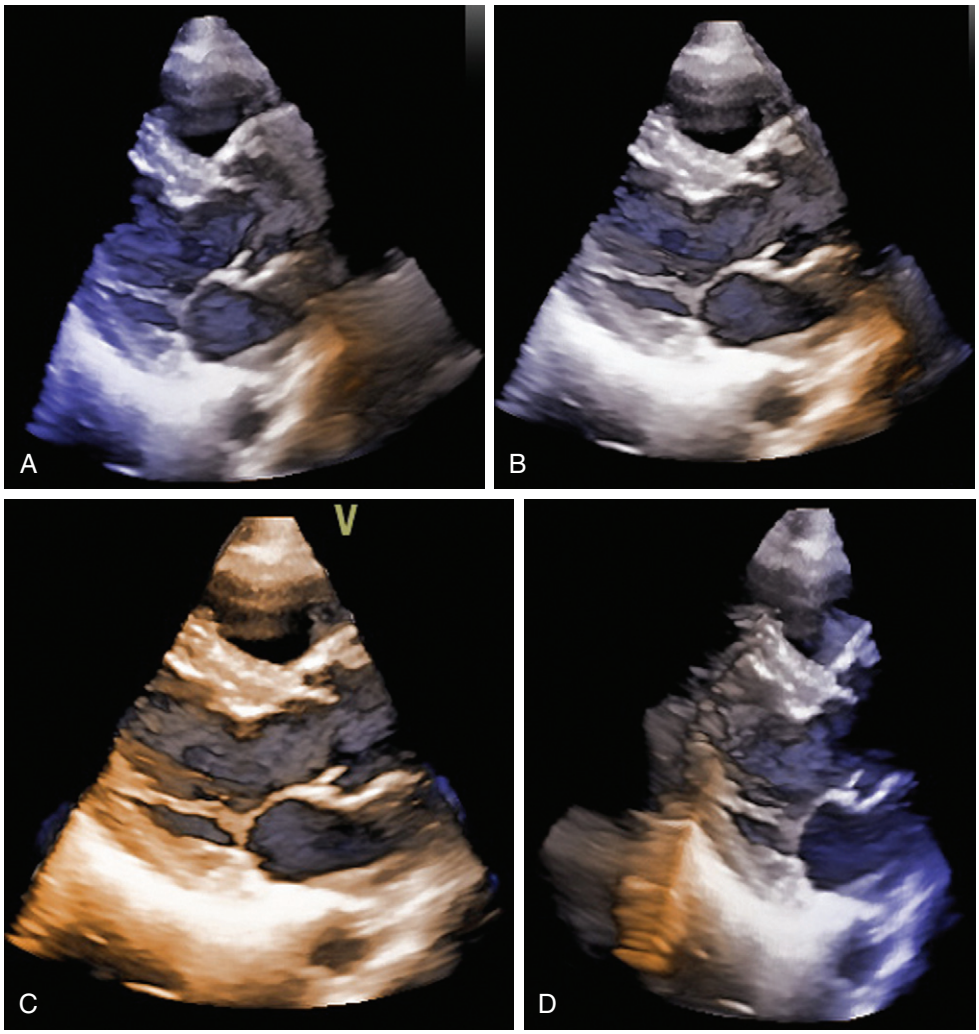



**Figure 4-3** Parasternal long-axis view of a real-time 3D TTE demonstrating that for optimal review, the structures included in the volume can be viewed from various perspectives (**A-D**).

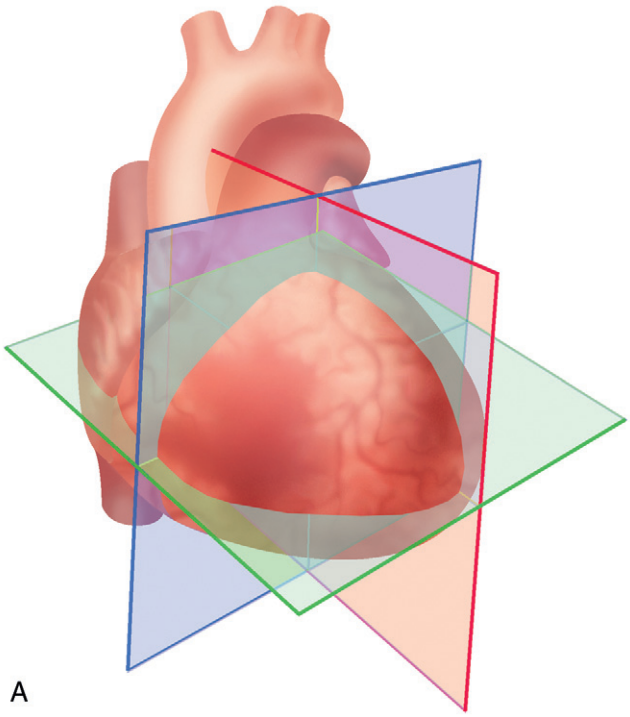
resulting from changes in position of the heart during the image acquisition, it is best if the images are acquired with held respiration. The frame rates at which these "full-volume" images are obtained typically vary from 20 to 40 Hz for both 3D TTE and 3D TEE. The full-volume frame rate will vary as a function of depth and size of the volume. Even though transducer position is more limited for RT3D TEE compared to RT3D TTE, image quality is superior much as 2D TEE image quality is typically superior to 2D TTE, and for similar reasons. In addition to 3D imaging, matrix array transducers can provide unique 2D acquisitions. For example, from a single transducer position, the 2D US plane can be adjusted in a fashion similar to a multiplane TEE transducer so that multiple 2D image planes can be obtained over *multiple* cardiac cycles without moving the transducer. This can be of particular value when tracking the circumferential extent of a prosthetic-valve paravalvular leak.[11] Also, multiple image planes of a structure can be obtained during the *same* cardiac cycle. In this scenario, rather than transmit and receive from the transducer elements to obtain a volume of US data, the pattern of firing of the elements can be configured to transmit and receive a series of 2D planes. This real-time multiplane imaging is of particular interest for quantitation. For example, the endocardial borders from a series of simultaneous apical views of the LV can be automatically or manually traced to calculate the LV volume and systolic function. This is similar to the approach with 3D reconstruction methods, except that all images of the heart are obtained in the same cycle, and the processing is faster. This real-time multiplane approach can be used to ensure that 2D images are on axis. For example, while visualizing a parasternal long-axis view as a guide, a second imaging plane can be directed that is perpendicular to the narrowest opening of the leaflet tips of a stenotic mitral valve.

When the 3D US full-volume image is first displayed on the echocardiographic machine or a workstation, only an outer surface of the pyramidal data set is seen, and it provides little information. To visualize the cardiac structures within this volume, layers of it must be removed—a process referred to as "cropping" (Fig. 4-4). Multiple cropping planes can be created to display structures of interest and the relationship of several structures to one another.

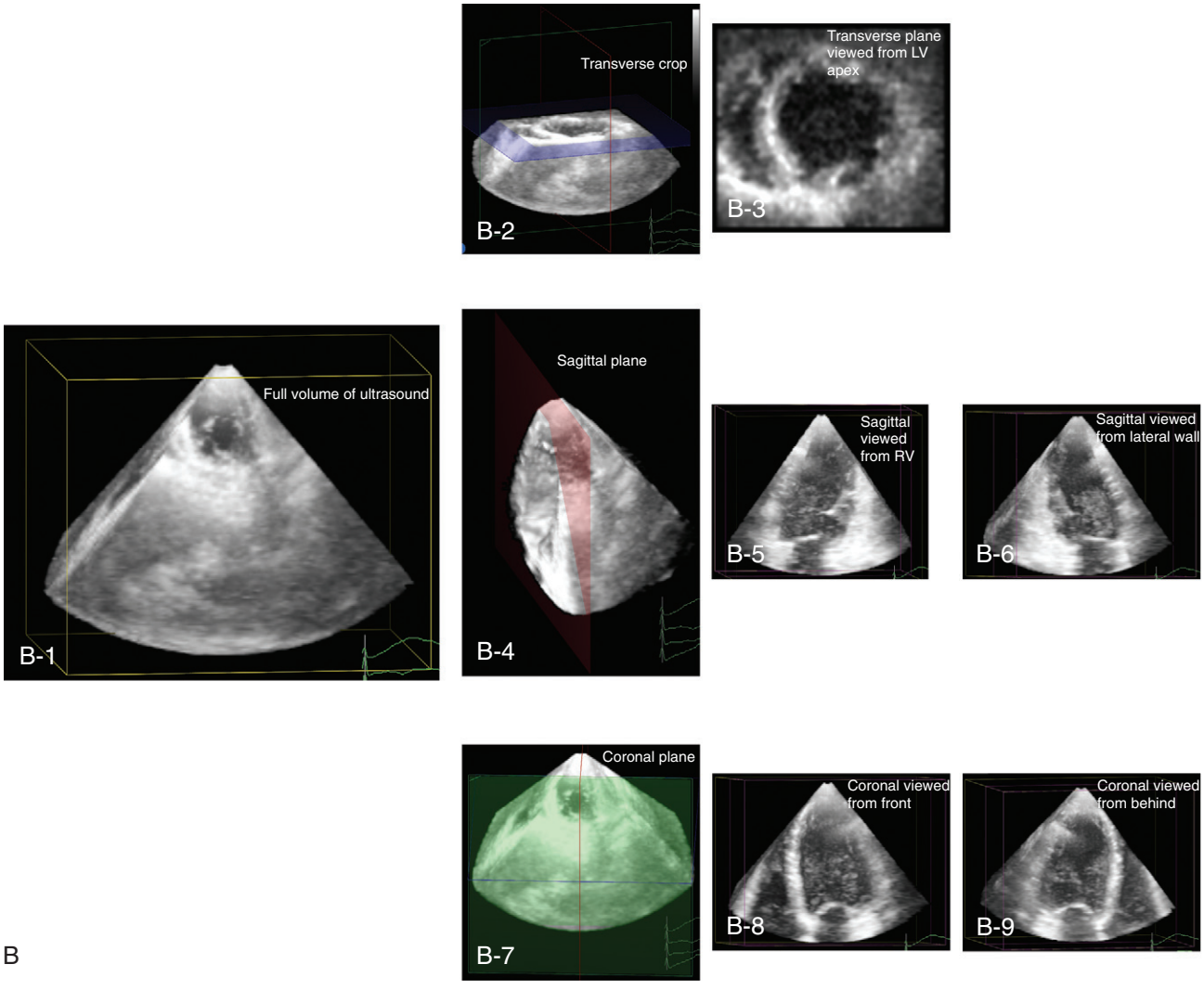
3D color flow Doppler is acquired in a similar fashion with the volumetric technique and displayed in real time simultaneously with the gray-scale images[12,13] (Fig. 4-5).

In general, the RT3D image is used for visualization of structures, whereas the offline cropping of the larger or composite 3D volume sets is used for quantitation or improved resolution of structures.

**Figure 4-4 Cropping of a full-volume ultrasound data set. A,** Schematic of standard cropping in transverse, sagittal, and coronal planes is shown with the colors corresponding to the image planes shown below; however, any 3D cropping plane can be created. **B,** Individual cropping planes through an ultrasound volume collected from the apical transducer position demonstrate cardiac structures from various perspectives. To visualize structures within the 3D ultrasound volume (**B-1**), cropping is performed. The transverse plane in *blue* (**B-2**) yields a short-axis view (**B-3**) viewed from the LV apex; the sagittal plane in *red* (**B-4**) yields either an apical two-chamber view viewed from the RV (**B-5**) or viewed from the lateral wall (**B-6**) or long-axis view depending on depth and angle of the cropping plane; and the coronal plane in *green* (**B-7**) yields an apical four-chamber view viewed from the front (**B-8**) or from behind (**B-9**).



A




B

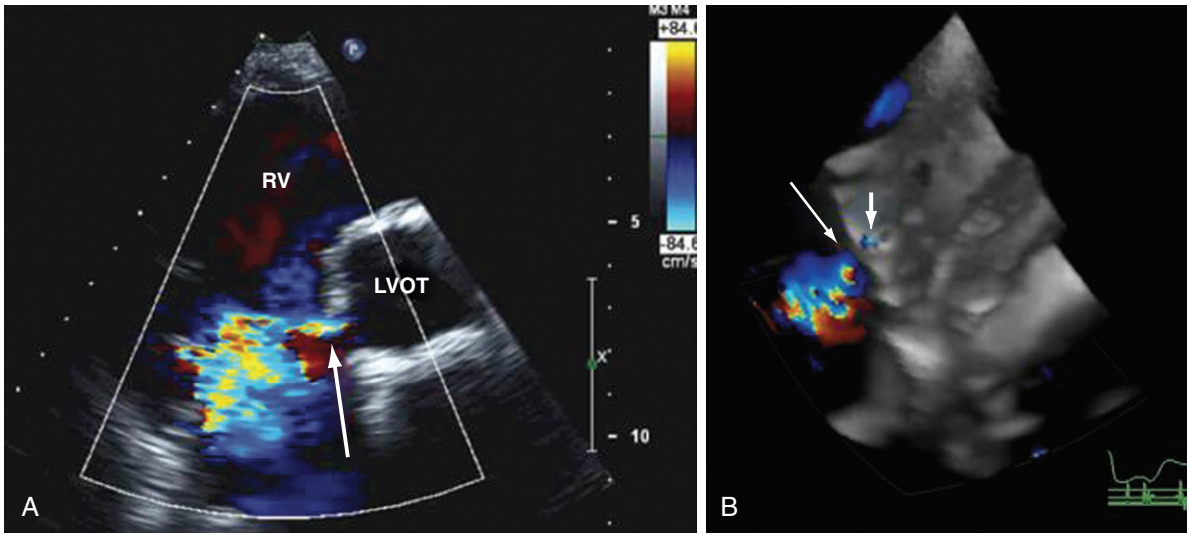



**Figure 4-5** Color flow Doppler demonstrating left to right shunting through a membranous ventricular septal defect (*arrows*) on 2D (**A**) and 3D (**B**) TTEs. The 3D image is viewed from the LV outflow tract or lateral wall perspective looking "en face" at the defect. Proximal flow convergence area (*short arrow*). *LVOT*, Left ventricle outflow tract.

### ADVANTAGES AND DISADVANTAGES OF THREE-DIMENSIONAL ACQUISITION TECHNIQUES

Compared to the reconstruction technique, image acquisition with the volumetric method is simpler and potentially faster. With the RT3D and the real-time multiplane 2D display, there is no time needed for offline reconstruction and display. For the "near real-time, full-volume" method, offline manipulation (cropping) is required, but typically the amount of time required compared to reconstruction techniques is short. Image quality of the RT3D and full-volume 3D images is a function of matrix array transducer characteristics such as frame rate and number of transducer elements. The image quality, however, continues to improve with advances in transducer technology.

For some of the 3D US methods, quantitation from the 3D image requires transfer to a special workstation. Because both reconstruction techniques and most of the current full-volume method combine multiple images gated to the cardiac and respiratory cycle, accurate image display can be challenging when the heart rate is irregular, such as during arrhythmias and when the patient is breathing at a rapid rate or with varying effort. The motion artifacts that may result will be most apparent in the cropped views that include the interfaces of the combined component images. For example, if the LV imaging volume is acquired by fusing four sequential volume sets from a parasternal short-axis view (medial to lateral) during which the patient coughs, when the images are cropped and viewed from the perspective of the LA or the LV apex, one will see the motion artifact with the appearance that the images are not stitched together well. However, if one crops and views this same image set from the perspective of the ventricular septum to observe a long-axis of the valve (sagittal plane), display of such artifacts would be minimized because the stitch artifact would not be in the plane displayed (Fig. 4-6).

3D color Doppler has some limitations. For example, Doppler interrogation with the volumetric method is subject to low frame rates, although this is improving. Importantly, pulsed-wave and continuous-wave Doppler capabilities have recently become available on some matrix array transducers, allowing all TTE or TEE imaging to be performed with one transducer.

In clinical practice, most 3D TTE and TEE US imaging is performed with matrix array transducers and the volumetric methods. Because quantitation of cardiac structure and function is accurate with the reconstruction approach, it is still used in some research applications with both TTE and TEE modalities. Although dimensions, volumes, and areas can be calculated from cropped 3D US volumes, deriving linear dimensions that extend out of these cropped planes remains a challenge.

## Three-Dimensional Echocardiographic Work Flow

The images obtained and cropped from a 3D US volume should focus on the goals of the imaging. Assessments of ventricular function, aortic valve function, or an atrial septal defect with 3D TTE require reconstructions or volume acquisitions of different parts of the heart. With 3D LV volume quantitation, for example, the 3D volume is obtained from an apical window to ensure that the entire LV is within the volume of acquisition while for a 3D assessment of the aortic valve the 3D volume is obtained from a parasternal window so that the valve is in the near field and frame rate and resolution are optimized. In the past, whether or not the 3D US image set was adequate could only be determined after cropping. Enhancements are now available that display examples of cropped 2D planes during acquisitions of the US volume so that image adequacy can be assessed in real time. Such modifications increase the likelihood that the 3D US volume obtained will contain the structure of interest, be free of artifacts, and be of adequate image quality.

It is likely that in the future, specific imaging protocols will be developed. Ideally this approach will include a rapid acquisition of the 3D US volume, and then the majority of image preparation time will be spent cropping the volume to display and quantify cardiac structures, function, and pathology. This cropping may be standardized to demonstrate all cardiac structures in specific orientations. For example, the cardiac volume can be cropped in planes sagittal (apical two-chamber or

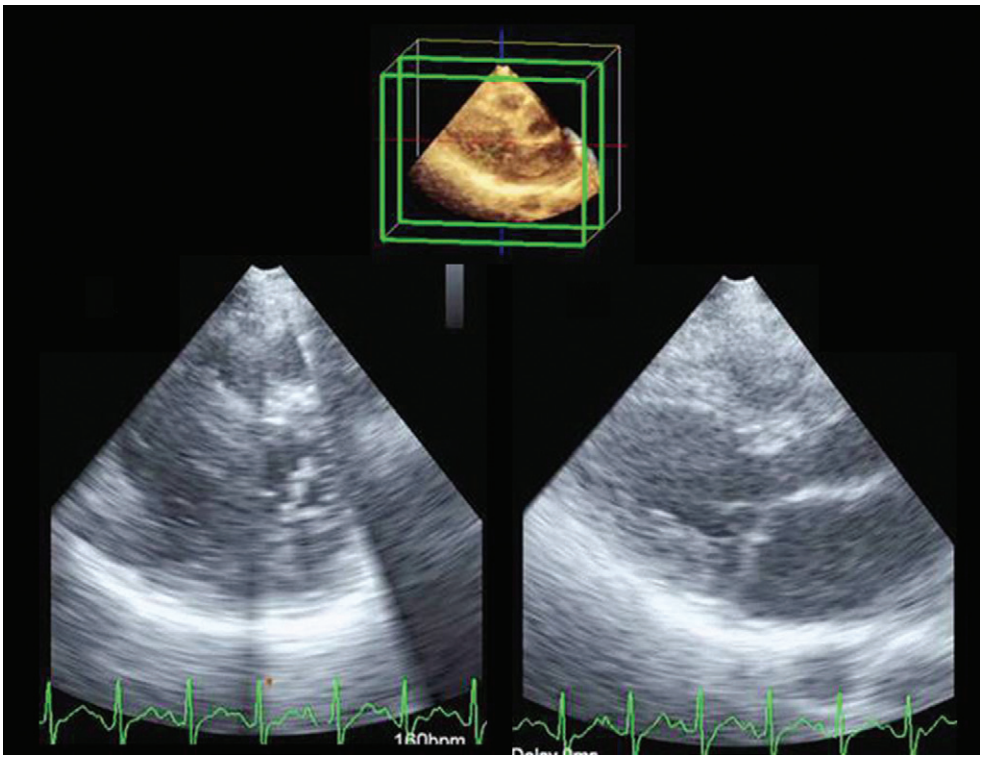


**Figure 4-6** Example of stitch artifact that occurs from patient motion during acquisition of the component subvolumes that are combined for the full-volume 3D ultrasound image. The artifact is noted (*left*) when the cropping plane includes more than one subvolume. If the cropping plane does not include multiple subvolumes (*right*), the artifact is not seen.

long-axis depending on angle and depth of plane), coronal (apical four-chamber), and transverse (short-axis) relative to the heart (Fig. 4-7). Although predetermined or automated cropping planes can be used to rapidly display and quantify structures of interest, in many cases of cardiac pathology the anatomic relationships may be altered, and thus it is critical to individualize the cropping process to optimize the views of each cardiac structure. This is particularly true for color flow Doppler assessment in which the paths of regurgitant jets do not respect standardized planes.

## Evidence-Based Applications of Three-Dimensional Echocardiography

### LEFT VENTRICULAR VOLUME AND FUNCTION

Validation studies using a variety of reference standards have demonstrated the improved accuracy of 3D echocardiography-derived LV volume compared to LV volumes measured from 2D echocardiograms in humans.[14] (See Chapter 9.) Initial 3D echocardiographic studies of LV volume involved the reconstruction method, and more recent studies have utilized the volumetric method. Selected validation studies of 3D LV volume are highlighted in Table 4-1.

3D echocardiography provides a more accurate representation of the LV endocardial surface than the 2D echocardiogram. The volume calculation with 2D echocardiograms relies on assumptions of the symmetry and geometry of the LV, whereas the volume of the LV by 3D echocardiography is calculated from the 3D LV endocardial surface without assumptions of shape. Also, methods used with 2D echocardiography are at risk to yield underestimations if the images used for the quantitation are foreshortened (Fig. 4-8). With 3D echocardiographic data sets transferred to an offline workstation, the volume can be calculated by several methods. First is a method of disks, in which multiple short-axis planes are derived to create a series of component volumes of the LV, which are summed from base to apex. This measurement is more accurate when a larger number of short-axis planes is used. A second method is to directly sum the volumetric picture elements (voxels) enclosed by the endocardial borders of the 3D structure (see Fig. 4-8, *B*). Compared to reference standards, the accuracy of 3D echocardiographic LV volume by the *reconstruction* method is a function of the number of component images used because this determines the extent of interpolation of the endocardial surface between images.[15] The accuracy of the 3D echocardiographic LV volume by the *volumetric* method is a function of the number of elements in the matrix array transducer, the voxel size, and the spatial resolution of the image.

Compared to cardiac magnetic resonance imaging (MRI), both end-diastolic and end-systolic LV volumes of normal subjects and patients with cardiac disease are smaller when calculated from 3D echocardiography regardless of the 3D echocardiographic acquisition technique. Images obtained from the apical transducer position may underestimate the LV cavity slightly because of the US point-spread function and beam width.[16-18] In many of the validation studies, the volume of the 3D echocardiogram was calculated from apical (or long-axis) images, whereas the cardiac MRI used short-axis images; this may account for some differences. Another explanation for

**TABLE 4-1 Left Ventricular Volume Quantitation in Humans by Three-Dimensional Echocardiography Compared to Cardiac Magnetic Resonance Imaging**

| *Study* | *3D Technique* | *Subjects Studied* | n | *Pearson Linear Correlation Coefficient (r)* | *SEE (mL)* | *Mean Difference ± 1 SD of the Difference (Bland-Altman Analysis, mL)* | *Interobserver Variability (%)* |
|---|---|---|---|---|---|---|---|
| Gopal[a] | Reconstruction, freehand scanning, spark gap transducer locator | Normal | 15 | EDV 0.92<br>ESV 0.81 | 7<br>4 | — | 5<br>8 |
| Buck[b] | Reconstruction, rotational scanning | Patients with CAD and aneurysms | 23 | EDV 0.97<br>ESV 0.97 | 15<br>12 | −11 ± 15<br>−3 ± 13 | — |
| Nosir[c] | Reconstruction, rotational scanning | Patients with CAD (31) and normal (15) | 46 | EDV 0.98<br>ESV 0.98 | — | −1 ± 14<br>−2 ± 11 | — |
| Lee[d] | Volumetric | Patients with "various cardiac disorders" | 25 | EDV 0.99<br>ESV 0.99 | 11<br>10 | 1 ± 12<br>4 ± 10 | — |
| Kühl[e] | Volumetric, semiautomated border detection | Patients with cardiomyopathy (14) and normal (10) | 24 | EDV 0.98<br>ESV 0.98 | 18<br>18 | −14 ± 19<br>−13 ± 21 | — |
| Jenkins[f] | Volumetric | Patients referred for echocardiography | 50 | EDV—<br>ESV— | —<br>— | -4 ± 29<br>-3 ± 18 | — |
| Corsi[g] | Volumetric | Normal and patients with CAD, dilated cardiomyopathy and other cardiac diseases | 16 | EDV 0.99<br>ESV 0.99 | — | 3 ± 6<br>3 ± 4 | — |
| Jacobs[h] | Volumetric, semiautomated border detection | Patients referred for cardiac MRI | 50 | EDV 0.96<br>ESV 0.97 | — | −14 ± 17<br>−7 ± 16 | 10<br>11 |
| Bu[i] | Volumetric | Children | 19 | EDV 0.97<br>ESV 0.97 | 9<br>3 | −7 ± 10<br>−2 ± 3 | 3<br>0 |
| Caiani[j] | Volumetric | Patients referred for MRI: normal (7), cardiomyopathy (9), CAD (15), other (15) | 46 | EDV 0.97<br>ESV 0.97 | 17<br>16 | −4 ± 15<br>−4 ± 17 | 8<br>13 |
| van den Bosch[k] | Volumetric | Patients with congenital heart disease referred for MRI | 29 | EDV 0.97<br>ESV 0.98 | 9<br>5 | −3 ± 12<br>1 ± 10 | — |
| Gutierrez-Chico[l] | Volumetric | Patients with cardiomyopathy | 35 | EDV 0.99<br>ESV 0.99 | — | −13 ± 11<br>−10 ± 8 | — |
| Sugeng[m] | Volumetric | Patients referred for clinical CT angiography | 31 | EDV 0.94 ($r^2$)<br>ESV 0.93 ($r^2$) | — | −4 ± 50<br>−6 ± 60 | 11.2 ± 8.6<br>14.2 ± 11.8 |
| Mor-Avi[n] | Volumetric | Multicenter study, patients referred for LV size/function evaluation | 92 | EDV 0.91<br>ESV 0.93 | — | −67 ± 46<br>−41 ± 46 | 8 ± 8<br>13 ± 14 |
| Nikitin[o] | Volumetric | Cardiac patients LVEF < 45% (40), cardiac patients LVEF > 45% (14), normal (10) | 64 | EDV 0.97<br>ESV 0.98 | — | 7 ± 14<br>3 ± 11 | 4<br>6 |
| Jenkins[p] | Volumetric | Patients with past MI | 50 | EDV 0.70-0.91<br>ESV 0.84-0.95 | — | — | 7 ± 53<br>2 ± 23 |
| Soliman[q] | Volumetric, semiautomated border detection | Patients with ischemic cardiomyopathy (10), dilated cardiomyopathy (10), normal (7) | 27 | EDV 0.98 ($r^2$)<br>ESV 0.98 ($r^2$) | — | −7.1 ± 19.8<br>−4.2 ± 8.3 | 5.2<br>6.4 |

*CAD*, Coronary artery disease; *CT*, computed tomography; *EDV*, end-diastolic left ventricular volume; *ESV*, end-systolic left ventricular volume; *LVEF*, left ventricular ejection fraction; *MI*, myocardial infarction; *MRI*, magnetic resonance imaging; *SD*, standard deviation; *SEE*, standard error of the estimate.


[a]Gopal AS, Keller AM, Rigling R, et al: Left ventricular volume and endocardial surface area by three-dimensional echocardiography: comparison with two-dimensional echocardiography and nuclear magnetic resonance imaging in normal subjects. *J Am Coll Cardiol* 22(1):258-270, 1993.

[b]Buck T, Hunold P, Wentz KU, et al: Tomographic three-dimensional echocardiographic determination of chamber size and systolic function in patients with left ventricular aneurysm: comparison to magnetic resonance imaging, cineventriculography, and two-dimensional echocardiography. *Circulation* 96(12):4286-4297, 1997.

[c]Nosir YF, Lequin MH, Kasprzak JD, et al: Measurements and day-to-day variabilities of left ventricular volumes and ejection fraction by three-dimensional echocardiography and comparison with magnetic resonance imaging. *Am J Cardiol* 82(2):209-214, 1998.

[d]Lee D, Fuisz AR, Fan PH, et al: Real-time 3-dimensional echocardiographic evaluation of left ventricular volume: correlation with magnetic resonance imaging—a validation study. *J Am Soc Echocardiogr* 14(10):1001-1009, 2001.

[e]Kühl HP, Schreckenberg M, Rulands D, et al: High-resolution transthoracic real-time three-dimensional echocardiography: quantitation of cardiac volumes and function using semi-automatic border detection and comparison with cardiac magnetic resonance imaging. *J Am Coll Cardiol* 43(11):2083-2090, 2004.

[f]Jenkins C, Bricknell K, Hanekom L, Marwick TH: Reproducibility and accuracy of echocardiographic measurements of left ventricular parameters using real-time three-dimensional echocardiography. *J Am Coll Cardiol* 44(4):878-886, 2004.

[g]Corsi C, Lang RM, Veronesi F, et al: Volumetric quantification of global and regional left ventricular function from real-time three-dimensional echocardiographic images. *Circulation* 112(8):1161-1170, 2005.

[h]Jacobs LD, Salgo IS, Goonewardena S, et al: Rapid online quantification of left ventricular volume from real-time three-dimensional echocardiographic data. *Eur Heart J* 27(4):460-468, 2006.

[i]Bu L, Munns S, Zhang H, et al: Rapid full volume data acquisition by real-time 3-dimensional echocardiography for assessment of left ventricular indexes in children: a validation study compared with magnetic resonance imaging. *J Am Soc Echocardiogr* 18(4):299-305, 2005.

[j]Caiani EG, Corsi C, Zamorano J, et al: Improved semiautomated quantification of left ventricular volumes and ejection fraction using 3-dimensional echocardiography with a full matrix-array transducer: comparison with magnetic resonance imaging. *J Am Soc Echocardiogr* 18(8):779-788, 2005.

[k]van den Bosch AE, Robbers-Visser D, Krenning BJ, et al: Real-time transthoracic three-dimensional echocardiographic assessment of left ventricular volume and ejection fraction in congenital heart disease. *J Am Soc Echocardiogr* 19(1):1-6, 2006.

[l]Gutierrez-Chico JL, Zamorano JL, Perez de Isla L, et al: Comparison of left ventricular volumes and ejection fractions measured by three-dimensional echocardiography versus by two-dimensional echocardiography and cardiac magnetic resonance in patients with various cardiomyopathies. *Am J Cardiol* 95(6):809-813, 2005.

[m]Sugeng L, Mor-Avi V, Weinert L, et al: Quantitative assessment of left ventricular size and function: side-by-side comparison of real-time three-dimensional echocardiography and computed tomography with magnetic resonance reference. *Circulation* 114(7):654-661, 2006.

[n]Mor-Avi V, Jenkins C, Kühl, et al: Real-time 3-dimensional echocardiographic quantification of left ventricular volumes. *J Am Coll Cardiol Img* 1(4):413-423, 2008.

[o]Nikitin NP, Constantin C, Loh PH, et al: New generation 3-dimensional echocardiography for left ventricular volumetric and functional measurements: comparison with cardiac magnetic resonance. *Eur J Echocardiogr* 7(5):365-372, 2006.

[p]Jenkins C, Bricknell K, Chan J, et al: Comparison of two- and three-dimensional echocardiography with sequential magnetic resonance imaging for evaluating left ventricular volume and ejection fraction over time in patients with healed myocardial infarction. *Am J Cardiol* 99(3):300-306, 2007.

[q]Soliman OI, Kirschbaum SW, van Dalen BM, et al: Accuracy and reproducibility of quantitation of left ventricular function by real-time three-dimensional echocardiography versus cardiac magnetic resonance. *Am J Cardiol* 102(6):778-783, 2008.

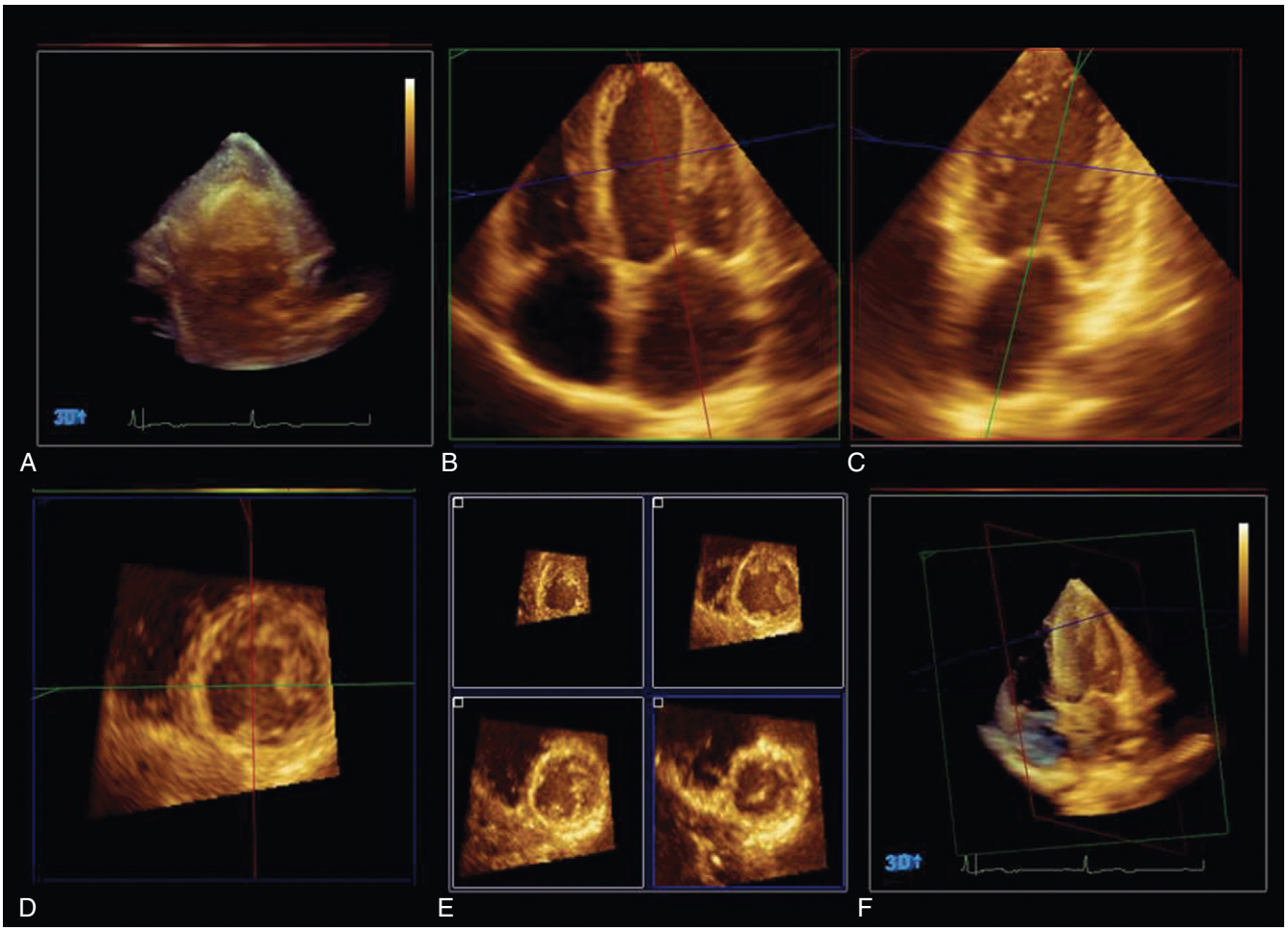



**Figure 4-7 Example of a cropping protocol that yields prespecified standard imaging planes. A,** Full volume of data. **B,** Coronal plane crop that results in an apical four-chamber view. **C,** Sagittal plane crop that results in an apical two-chamber view. **D,** Transverse plane crop at mid-LV level that results in a short-axis view. **E,** Four simultaneous short-axis images obtained when four transverse cropping planes are placed through the volume simultaneously. **F,** 3D image from the volume.

the discrepancy between 3D echocardiography and cardiac MRI is the difference in definition of the endocardial border. For echocardiography, the inner border of the endocardial trabeculations is traced, whereas on MRI the outer border of the trabeculations is commonly traced (i.e., trabeculae are included in the LV cavity), and so a larger volume is measured in the same patient.[19] A multicenter study examining the differences between LV volume by 3D echocardiography and cardiac MRI has shown that a 1-mm difference in the position of the endocardial surface resulted in a 10% difference in volume.[20]

Because the LV volumes calculated from 3D echocardiograms are accurate, it follows that the derivations of LV stroke volume and ejection fraction from these volumes are also accurate.[21] The advantages of this technique for assessment of LV function is most noticeable in subjects with wall motion abnormalities or distorted ventricles such as LV aneurysms.[22] LV volume can be calculated from either manual or automated border tracing throughout the cardiac cycle with the generation of volume-time curves as a measure of systolic and diastolic function.[23,24] Observer variability is low, and change in LV volume, stroke volume, and ejection fraction are also more precisely determined with 3D echocardiography compared to other echocardiographic techniques. Thus, the 3D echocardiographic technique has shown value in clinical situations in which accurate characterization of changes of these parameters is critical, such as heart failure risk stratification in post–myocardial infarction patients[25] and LV volume determination to guide decisions for valve surgery.[26]

The use of contrast enhancement in 3D echocardiography and acquisitions that reduce stitch artifact may further improve volume and ejection-fraction measurements. Contrast-enhanced 3D echocardiography has shown improved agreement with ejection fraction as measured by cardiac MRI.[27] Two-beat acquisitions of the LV volume yield similar LV volumes and ejection fraction as 4-beat acquisitions with fewer artifacts, but the current low temporal resolution of single-beat acquisition underestimates LV end-diastolic volume and LV ejection fraction.[28]

## LEFT VENTRICULAR MASS

LV mass is an important predictor of prognosis. (See Chapter 9.) It is calculated as the product of the volume of the LV myocardium and the myocardial density (g/cm$^3$). The specific gravity of cardiac muscle, a ratio of its density relative to water, is often substituted for density. The myocardial volume is calculated with 3D echocardiography as the space between the epicardial and endocardial borders of the LV. This can be calculated directly

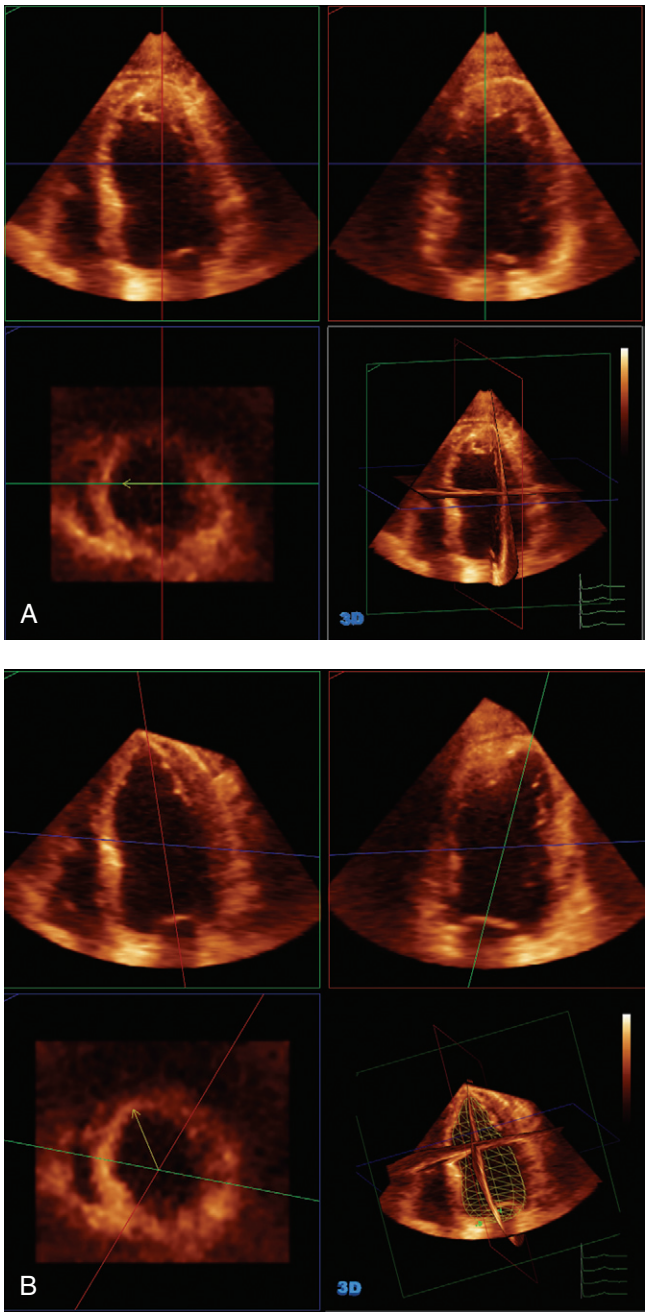



**Figure 4-8** The full-volume transthoracic ultrasound data set enables positioning of cropping planes so that the true length of the left ventricle is visualized and measured. **A,** Typical 2D imaging planes for the four-chamber (coronal plane, *upper left*) and two-chamber (sagittal plane, *upper right*) views fail to include an aneurysm at the anterior apex of the left ventricle. **B,** Coronal (*green*) and sagittal (*red*) cropping planes adjusted through the true long axis of the left ventricle in the same full-volume data set. The endocardial borders are then detected and an accurate left ventricular volume quantified. End-diastolic volume (*yellow shell*) is shown (*lower right*).

as a sum of the voxels in this enclosed space or derived from the difference of the epicardial and endocardial volumes. Initial 3D quantitative LV mass analysis relied on manual tracing of endocardial and epicardial borders or semiautomated border detection of multiple 2D long-axis planes extracted from volumetric data. These processes were time consuming and required geometric modeling to convert the multiplanar area measurements into volumes. Subsequently, the development of rapid algorithms for the detection of the 3D endocardial surface allows for direct quantification of LV volumes and has been applied to the epicardial (in addition to the endocardial) surface to calculate LV mass. Using such algorithms, LV mass is quickly calculated and compares favorably to MRI.[29]

Potential sources of error with 3D echocardiographic measures of LV mass include the need to include the entire epicardial surface of the LV within the image sector and exact tracing of endocardial trabeculations. However, human studies document close correlation of 3D echocardiographic measurements compared to cardiac MRI LV mass measurements (Table 4-2). These studies have been conducted in various patient populations, including left ventricular hypertrophy,[30] various forms of cardiomyopathy,[31] wall motion abnormalities,[32] and congenital heart disease.[33] Furthermore, regression of 3D echocardiographically measured LV mass with pharmacologic therapy has been demonstrated in a small study of hypertensive patients.[34] Because LV mass derived from 3D echocardiography is more accurate, more precise, and less variable than that from 2D echocardiography, it is expected that fewer subjects will be required in clinical trials of LV mass regression using this technique compared to trials that have used 2D echocardiography to measure LV mass change.

## RIGHT VENTRICULAR VOLUME

The RV has a complex geometrical shape, and the RV inflow, outflow, and apex do not all align within a single 2D plane. This makes calculation of total RV area or volume challenging by 2D echocardiography. 3D echocardiography can eliminate the need for geometric assumptions used in the calculation of RV volume. The methods for calculating RV volume from the 3D image are the same as described previously for LV volume. The RV is typically smaller and more heavily trabeculated than the LV surface, and therefore one might expect lower accuracy of volume quantitation compared to the LV. However, initial validation studies for RV volume performed mainly in nonhuman models showed correlation coefficients, standard errors, biases, precision, and percent interobserver variability similar to those for LV volume quantitation.[7] Additionally, the accuracy of RV volume determination in humans is improving as technical factors are optimized[35] and new software programs specific for volumetric analysis are utilized.[36] Selected validation and clinical studies of RV volume assessment by 3D echocardiography are highlighted in Table 4-3. For healthy male and female adults with a wide age range, the normal reference values for indexed RV end-diastolic volume, indexed RV end-systolic volume, and RV ejection fraction by 3D echocardiography are 49 ± 10 mL/m$^2$, 16 ± 6 mL/m$^2$, and 67 ± 8%, respectively.[37]

As measurement techniques and software programs have improved, RV volume assessment with 3D echocardiography is being applied in disease states that affect the RV. Specifically, 3D echocardiographic quantification of RV volume and function has been applied to a small number of patients with arrhythmogenic RV dysplasia/cardiomyopathy.[38] Although the correlations with cardiac MRI are lower than noted in other validation studies, patients with pathologic RVs could be discriminated from normal controls and unaffected family members. 3D echocardiographic quantitation of RV volume has also been used to assess RV remodeling in secondary pulmonary hypertension[39] and has shown that RV volumes are largest and RV ejection fraction lowest in patients with pulmonary hypertension compared to healthy volunteers or patients with other

**TABLE 4-2 Left Ventricular Mass Quantification by Three-Dimensional Echocardiography Compared to Cardiac Magnetic Resonance Imaging**

| *Study* | *3D Technique* | *Subjects Studied* | n | *Pearson Linear Correlation Coefficient (r)* | *SEE (g)* | *Mean Difference ± 1 SD of the Difference (Bland-Altman Analysis, mL)* | *Interobserver Variability (%)* |
|---|---|---|---|---|---|---|---|
| Gopal[a] | Reconstruction | Normal | 15 | 0.90 | 11 | — | 13 |
| Lee[b] | Volumetric | Patients with "various cardiac disorders" | 25 | 0.95 | 6 | 5±26 | — |
| Mor-Avi[c] | Volumetric | Patients referred for echocardiography | 21 | 0.90 | — | 4±14 | 0-23 |
| Oe[d] | Volumetric | Patients referred for MRI for LV hypertrophy | 21 | 0.95 | 20 | −14±29 | 11 |
| van den Bosch[e] | Volumetric | Patients with congenital heart disease | 20 | 0.94 | 19 | 10±19 | — |
| Bu[f] | Volumetric | Children | 19 | 0.97 | 9 | 2±10 | 5 |
| Qin[g] | Volumetric | Patients with cardiomyopathy (25) or aortic regurgitation (2) | 27 | 0.92 | 29 | −9±33 | — |
| Caiani[h] | Volumetric, semi-automated border detection | Patients referred for MRI | 21 | 0.96 | — | −2.1±11.5 | 12.5 |
| Yap[i] | Volumetric (using biplane and multiplane) | Adult patients with congenital aortic stenosis and concentric LV hypertrophy | 18 | 0.84 biplane 0.90 multiplane | — | — | — |
| Pouleur[j] | Volumetric, semi-automated border detection | Patients with aortic valve disease (20), severe mitral regurgitation (10), previous MI (33); Normal (20) | 83 | 0.94 | — | 1 ± 28 | 3 ± 27 |
| Takeuchi[k] | Volumetric, surface detection algorithm | Patients referred for MRI | 55 | 0.95 | — | −1.8 ± 19.9 | 12 ± 9 |

*MI*, Myocardial infarction; *MRI*, magnetic resonance imaging; *SD*, standard deviation; *SEE*, standard error of the estimate.

[a]Gopal AS, Keller AM, Shen Z, et al: Three-dimensional echocardiography: in vitro and in vivo validation of left ventricular mass and comparison with conventional echocardiographic methods. *J Am Coll Cardiol* 24(2):504-513, 1994.

[b]Lee D, Fuisz AR, Fan PH, et al: Real-time 3-dimensional echocardiographic evaluation of left ventricular volume: correlation with magnetic resonance imaging—a validation study. *J Am Soc Echocardiogr* 14(10):1001-1009.

[c]Mor-Avi V, Sugeng L, Weinert L, et al: Fast measurement of left ventricular mass with real-time three-dimensional echocardiography: comparison with magnetic resonance imaging. *Circulation* 110(13):1814-1818, 2004.

[d]Oe H, Hozumi T, Arai K, et al: Comparison of accurate measurement of left ventricular mass in patients with hypertrophied hearts by real-time three-dimensional echocardiography versus magnetic resonance imaging. *Am J Cardiol* 95(10):1263-1267, 2005.

[e]van den Bosch AE, Robbers-Visser D, Krenning BJ, et al: Comparison of real-time three-dimensional echocardiography to magnetic resonance imaging for assessment of left ventricular mass. *Am J Cardiol* 97(1):113-117, 2006.

[f]Bu L, Munns S, Zhang H, et al: Rapid full volume data acquisition by real-time 3-dimensional echocardiography for assessment of left ventricular indexes in children: a validation study compared with magnetic resonance imaging. *J Am Soc Echocardiogr* 18(4):299-305, 2005.

[g]Qin JX, Jones M, Travaglini A, et al: The accuracy of left ventricular mass determined by real-time three-dimensional echocardiography in chronic animal and clinical studies: a comparison with postmortem examination and magnetic resonance imaging. *J Am Soc Echocardiogr* 18(10):1037-1043, 2005.

[h]Caiani EG, Corsi C, Sugeng L, et al: Improved quantification of left ventricular mass based on endocardial and epicardial surface detection with real time three dimensional echocardiography. *Heart* 92(2):213-219. 2006.

[i]Yap SC, van Geuns RJ, Nemes A, et al: Rapid and accurate measurement of LV mass by biplane real-time 3D echocardiography in patients with concentric LV hypertrophy: comparison to CMR. *Eur J Echocardiogr* 9(2):255-260, 2008.

[j]Pouleur AC, le Polain de Waroux JB, Pasquet A, et al: Assessment of left ventricular mass and volumes by three-dimensional echocardiography in patients with or without wall motion abnormalities: comparison against cine magnetic resonance imaging. *Heart* 94(8):1050-1057, 2008.

[k]Takeuchi M, Nishikage T, Mor-Avi V, et al: Measurement of left ventricular mass by real-time three-dimensional echocardiography: validation against magnetic resonance and comparison with two-dimensional and M-mode measurements. *J Am Soc Echocardiogr* 21(9):1001-1005, 2008.

cardiac disease.[36] In patients with various complex and/or surgically repaired congenital heart diseases, 3D echocardiographic assessment of RV size and function was reproducible and had good accuracy compared to MRI.[40] Further studies in patients with a wider range of conditions affecting the RV are warranted to confirm the results of these initial studies and to define the role of 3D echocardiography in the clinical diagnosis and management of these patients. (See Chapters 32 and 33.)

## ATRIAL VOLUME

LA size is not only a marker of diastolic function but has also been shown to be a predictor of adverse outcomes including atrial fibrillation, stroke, and cardiac events. In these assessments, LA volume has been shown to be a stronger risk factor than LA area or linear dimension,[41] thus LA volume calculations derived from 2D planes are recommended as the standard measurement technique.[42] However, because of lack of symmetry of the atria, 3D echocardiography is better suited for accurate quantitation of left and right atrial volumes, and the methods are similar to that for calculation of ventricular volume by 3D echocardiography. LA volume measurement by 3D echocardiography compares well against traditional 2D echocardiographic measurements,[43] and although the number of studies is limited, accuracy appears comparable to MRI.[44,45] By providing a detailed analysis of the phasic changes of LA volume throughout the cardiac cycle, 3D echocardiography enables the assessment of the reservoir, conduit, and active contraction functions of the LA.[46,47]

3D echocardiographically derived LA volume measurement has been shown to be more sensitive to changes in volume than 2D echocardiographic measurements[48] and is a predictor of cardiac events in patients with severe LV dysfunction.[49] In a study of 178 outpatients, LA minimum volume by 3D echocardiography provided prognostic information for the occurrence of major cardiovascular events.[50] Additionally, 3D echocardiography for LA volume and function has been evaluated in specific clinical contexts, including hypertrophic cardiomyopathy and evaluation of the LA appendage.[51,52]

**TABLE 4-3 Right Ventricular Volume Quantitation by Three-Dimensional Echocardiography Compared to a Reference Standard**

| Study | 3D Technique | Subjects Studied | n | Reference Standard | Pearson Linear Correlation Coefficient (r) | SEE (mL) | Mean Difference ± 1 SD of the Difference (Bland-Altman Analysis, mL) | Interobserver Variability (%) |
|---|---|---|---|---|---|---|---|---|
| Vogel[a] | Reconstruction, rotational and fan | Patients with repaired congenital heart disease (13); | 16 | MRI | EDV 0.95<br>ESV 0.75 | — | 5 ± 4<br>6 ± 5 | 4<br>5 |
| Fujimoto[b] | Reconstruction, rotational scanning | Normal | 15 | MRI | EDV 0.94<br>ESV 0.97 | — | 0 ± 10<br>0 ± 6 | 8<br>7 |
| Leibundgut[c] | Volumetric | Patients referred for MRI | 100 | MRI | EDV 0.84<br>ESV 0.83 | — | 10.2 ± 21.2<br>4.5 ± 14.5 | 2.7 ± 11.6<br>1.9 ± 8.3 |
| Gopal[d] | Volumetric | Normal | 71 | MRI | EDV 0.9<br>ESV 0.8 | 4.3<br>8.1 | — | — |
| Jenkins[e] | Volumetric | Patients with LV wall motion abnormalities and possible | 50 | MRI | EDV 0.91<br>ESV 0.90 | — | −3 ± 10<br>−4 ± 7 | 0 ± 10<br>1 ± 3 |
| Niemann[f] | Volumetric | Patients with congenital heart disease (16); normal (14) | 30 | MRI | EDV 0.99<br>ESV 0.98 | — | 0.91 ± 2.0<br>0.71 ± 2.1 | — |
| van der Zwaan[g] | Volumetric | Patients with congenital heart disease | 50 | MRI | EDV 0.93<br>ESV 0.91 | — | 34 ± 65<br>11 ± 54 | 1 ± 15<br>6 ± 17 |
| Grewal[h] | Volumetric | Patients with severe pulmonic regurgitation | 25 | MRI | EDV 0.88<br>ESV 0.89 | — | — | — |
| Sugeng[i] | Volumetric | Patients with heart failure (9), pulmonary hypertension (12), | 28 | MRI, cardiac | EDV 0.87<br>ESV 0.89 | — | −14 ± 73<br>−9 ± 53 | 7 ± 5<br>10 ± 9 |

*CAD*, Coronary artery disease; *CT*, computed tomography; *EDV*, end-diastolic left ventricular volume; *ESV*, end-systolic left ventricular volume; *MRI*, magnetic resonance imaging; *SD*, standard deviation; *SEE*, standard error of the estimate.

[a]Vogel M, Gutberlet M, Dittrich S, et al: Comparison of transthoracic three dimensional echocardiography with magnetic resonance imaging in the assessment of right ventricular volume and mass. *Heart* 78(2):127-130, 1997.

[b]Fujimoto S, Mizuno R, Nakagawa Y, et al: Estimation of the right ventricular volume and ejection fraction by transthoracic three-dimensional echocardiography. A validation study using magnetic resonance imaging. *Int J Cardiovasc Imaging* 14(6):385-390, 1998.

[c]Leibundgut G, Rohner A, Grize L, et al: Dynamic assessment of right ventricular volumes and function by real-time three-dimensional echocardiography: a comparison study with magnetic resonance imaging in 100 adult patients. *J Am Soc Echocardiogr* 23(2):116-126, 2010.

[d]Gopal AS, Chukwu EO, Iwuchukwu CJ, et al: Normal values of right ventricular size and function by real-time 3-dimensional echocardiography: comparison with cardiac magnetic resonance imaging. *J Am Soc Echocardiogr* 20(5):445-455, 2007.

[e]Jenkins C, Chan J, Bricknell K, et al: Reproducibility of right ventricular volumes and ejection fraction using real-time three-dimensional echocardiography: comparison with cardiac MRI. *Chest* 131(6):1844-1851, 2007.

[f]Niemann PS, Pinho L, Balbach T, et al: Anatomically oriented right ventricular measurements with dynamic three-dimensional echocardiography validated by 3-tesla magnetic resonance imaging. *J Am Coll Cardiol* 50(17):1668-1676, 2007.

[g]van der Zwaan HB, Helbing WA, McGhie JS, et al: Clinical value of real-time three-dimensional echocardiography for right ventricular quantification in congenital heart disease: validation with cardiac magnetic resonance imaging. *J Am Soc Echocardiogr* 23(2):134-140, 2010.

[h]Grewal J, Majdalany D, Syed I, et al: Three-dimensional echocardiographic assessment of right ventricular volume and function in adult patients with congenital heart disease: comparison with magnetic resonance imaging. *J Am Soc Echocardiogr* 23(2):127-133, 2010.

[i]Sugeng L, Mor-Avi V, Weinert L, et al: Multimodality comparison of quantitative volumetric analysis of the right ventricle. *J Am Coll Cardiol Img* 3(1):10-18, 2010.

3D echocardiographic evaluation of the right atrium (RA) has been studied less than that of the LA; however the feasibility of RA volume assessment with 3D echocardiography and its superiority over 2D echocardiographic measurements have been demonstrated.[53] Detailed knowledge of RA anatomic features (i.e., crista terminalis, cavotricuspid isthmus) is of particular interest to electrophysiologists performing catheter ablation procedures, and 3D TEE is being studied for this application.[54] A current limitation of studies of 3D echocardiographically derived atrial volumes is the paucity of comparisons to reference standards such as cardiac MRI and CT imaging.

## VALVULAR HEART DISEASE

3D echocardiography is especially suited for assessment of valve disease because of its ability to image nonplanar valve leaflets, demonstrate the spatial relationships of all components of the valve and surrounding structures, and depict color Doppler flow in three dimensions. Its use is emerging in the preoperative and intraoperative US evaluation of patients being considered for or undergoing repair and replacement of valves.[55] (See Chapter 5.)

### *Mitral Valve*

As previously discussed, since its early development, 3D echocardiographic approaches have been used to understand the complex geometry of the mitral valve (MV) and improve the echocardiographic diagnosis of MV prolapse.[6] The delineation of the nonplanar shape of the mitral annulus has led to identification of imaging planes and 2D echocardiographic views from which it can be seen that the mitral leaflets truly prolapse below the annulus into the LA. Studies suggest that with RT3D TTE, visualization of the MV is feasible in the majority of patients and that the anterior mitral leaflet is visualized better than the posterior mitral leaflet.[56] RT3D TEE has been shown to provide excellent visualization of the MV, as all scallops of both leaflets were visualized in approximately 90% of patients.[57]

### Mitral Stenosis

Characterization of mitral stenosis is a strength of 2D echocardiography. (See Chapter 21.) Whereas planimetry and pressure half-time methods with 2D echocardiography and Doppler typically provide equivalent assessments of the MV area, there are situations, particularly immediately after percutaneous

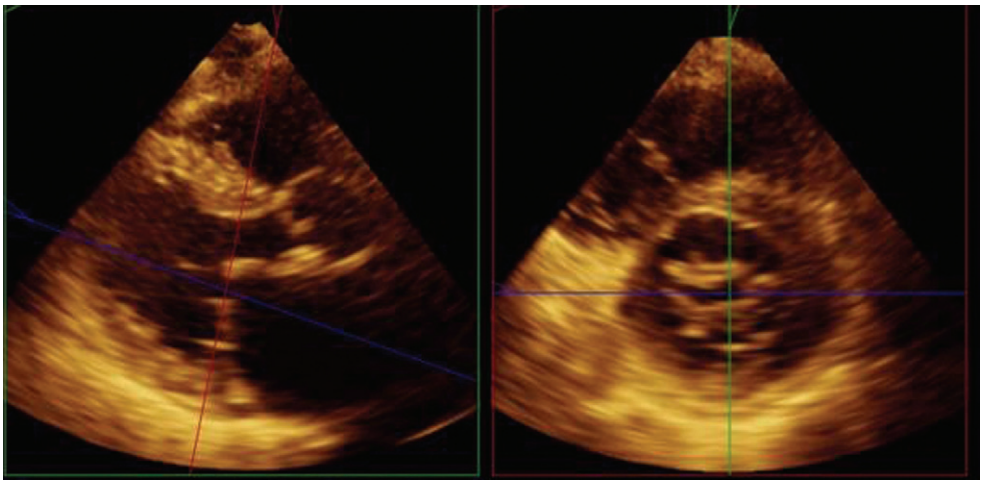


**Figure 4-9 Two images from a full-volume TTE of a patient with mitral stenosis.** Sagittal (long-axis) plane through the middle of the LV (*left*). The stenotic mitral valve is viewed from a lateral perspective. A transverse cropping plane (*red*) is then positioned orthogonally at the smallest mitral valve orifice at the leaflet tips. The resultant short-axis view (*right*) displays the stenotic mitral valve orifice viewed from the LV perspective.

mitral valvuloplasty,[58] in which only planimetry provides an accurate measure. Accurate planimetry of MV area requires a parasternal image plane that is perpendicular to the long axis of the smallest mitral orifice. This is a time-consuming task, especially when the valve orifice is asymmetrically narrowed. Deviations from the ideal image plane positioning will lead to significant overestimations of the valve area.[59] With 3D echocardiographic reconstruction techniques, a series of parallel short-axis planes through the MV is used to identify the smallest MV area for direct planimetry.[60] With the 3D volumetric technique, the best image of the valve can be cropped and rotated to display the best plane for planimetry[61] (Figs. 4-9, 4-10). Because multiple US planes can be created simultaneously with a matrix array probe, another method for planimetry of the MV area is to obtain a long-axis view of the MV and then position a second intersecting imaging plane that is perpendicular to the limiting orifice.[62] Investigations have shown MV area by 3D TTE to be more precise than 2D measures and comparable to that of the pressure half-time technique when compared to invasive measures of valve area.[61] In such comparisons, the 3D measurement frequently changed the classification of mitral stenosis severity. For experienced sonographers, there may not be a significant difference in valve area calculation compared with 2D echocardiography; however, the time required to acquire the view of the MV for planimetry is reduced. The benefits will be observed by less experienced personnel. The Wilkins morphology valve score by the 3D approach demonstrates less interobserver variability than the 2D echocardiographic technique,[61] and efforts are underway to develop novel scoring systems using 3D echocardiography that provide prognostic information that is additive to the Wilkins score.[63] Studies suggest that 3D echocardiography may better quantify the degree of commissural fusion before percutaneous mitral valvuloplasty, the leaflet morphology after the procedure,[64] and the MV area in the period immediately following.[65] The presence of atrial fibrillation, especially when the ventricular response is variable, continues to pose a challenge for the application of 3D echocardiography in mitral stenosis.

## Mitral Regurgitation

3D echocardiography has been used for several different aspects of mitral regurgitation (MR) (Fig. 4-11). First, it can quantify the severity of MR. (See Chapter 18.) Second, it can delineate specific anatomic lesions responsible for MR resulting from degenerative disease, myxomatous valve disease, congenital lesions, or endocarditis. Third, it can provide insights into the mechanisms responsible for functional and ischemic MR. Last, by better understanding the mechanisms of the regurgitation and the shape and anatomical relationships of surrounding supporting structures, such as annulus and papillary muscles, 3D echocardiography can assist in the design of valve repair techniques and prosthetic supports, such as annular rings. (See Chapter 19.)

3D echocardiographic quantification of MR can be performed either by the proximal isovelocity surface area (PISA) method or the vena contracta area method.[13,66,67] For the PISA method, the 3D color Doppler image of the flow convergence zone is examined to find the true shape of this region. The true radius and the convergence angle correction factor are then measured and used in the equations for MR volume and regurgitant orifice area. Alternatively, the true flow convergence area can be quantified free of assumptions of geometry and used in the calculations (Fig. 4-12). This approach is of particular value for quantitation of regurgitation from MV prolapse in which the jet may be eccentrically directed in the LA and the shape of the flow convergence zone may not be a symmetric hemiellipse.[68] In recent studies, both 3D TTE and TEE approaches have demonstrated accurate calculations of regurgitant orifice area and regurgitant volume when compared to MRI.[69,70] For the calculation of vena contracta area, the best image of the vena contracta is obtained, the full-volume color Doppler image set is then cropped in a plane parallel to the leaflets, the image is rotated to view the vena contracta enface, and finally the previously cropped portion of the image is added back until the largest vena contracta area is depicted. With the improved quantification of the complex geometry of the vena contracta and flow convergence areas, it is not unexpected that the 3D technique has produced more accurate measurements than 2D echocardiography[71] and has shown better correlations with invasive measurements of regurgitant severity than 2D echocardiography.[13,66] The direct measurement of the regurgitant orifice area by 3D echocardiography is feasible when image quality permits and may overcome some of the limitations of the calculation of this area by the PISA method.[12]

Another application of 3D echocardiography has been the direct visualization and localization of prolapsed segments of

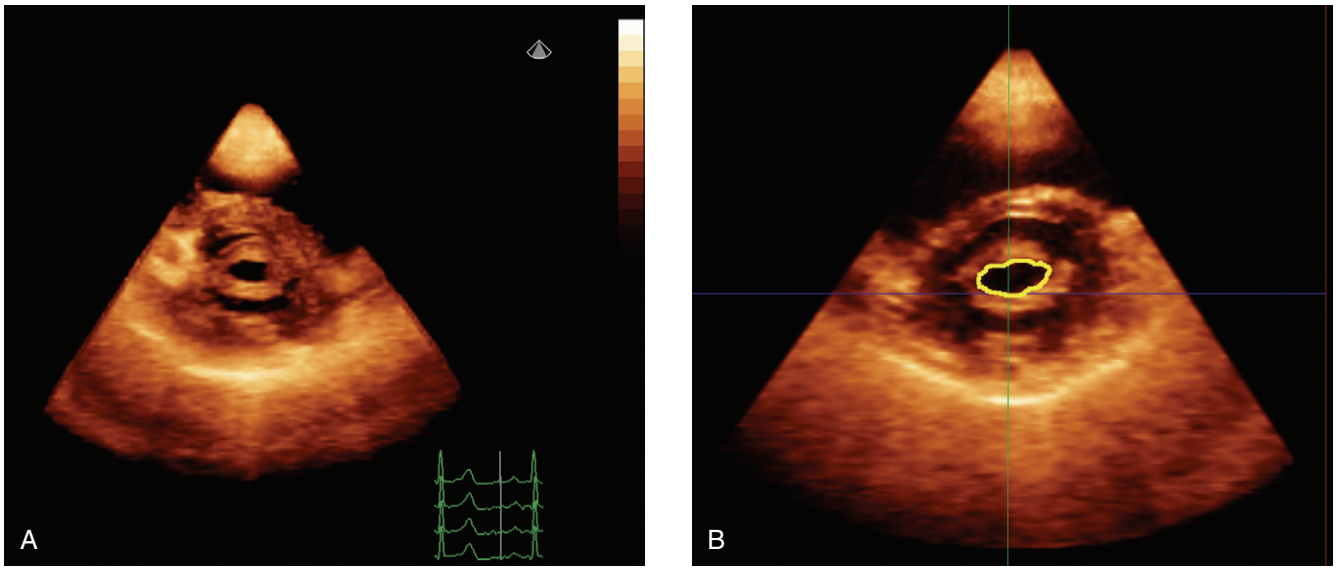



**Figure 4-10 Full-volume 3D transthoracic echocardiography of mitral stenosis. A,** Transverse (short-axis) plane through a stenotic mitral valve viewed from the LA perspective. **B,** Same plane viewed from the LV perspective with planimetry of the orifice in *yellow* (1.5 $cm^2$).

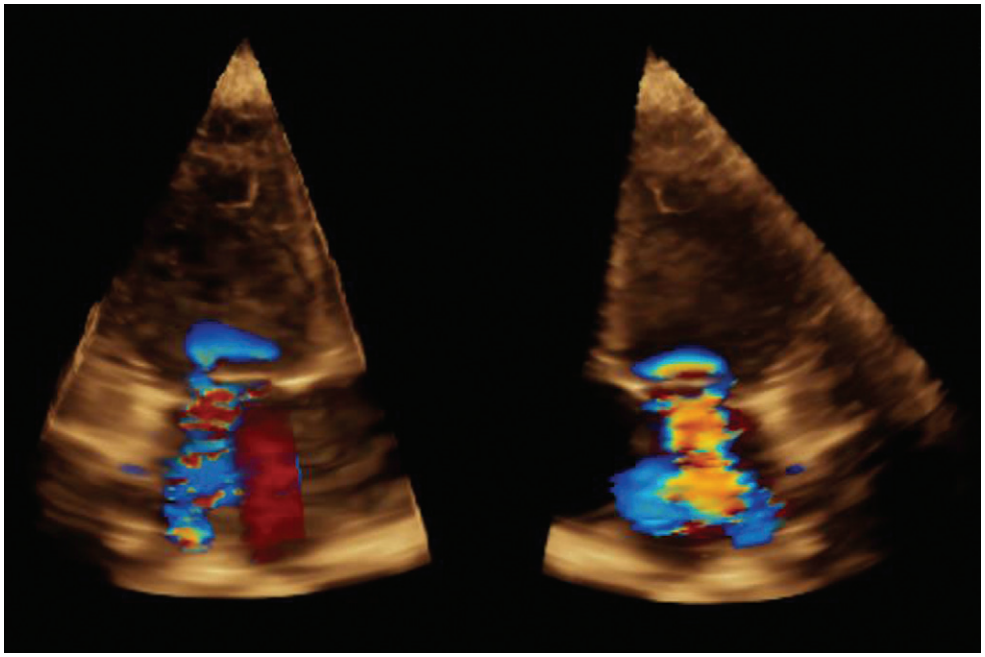
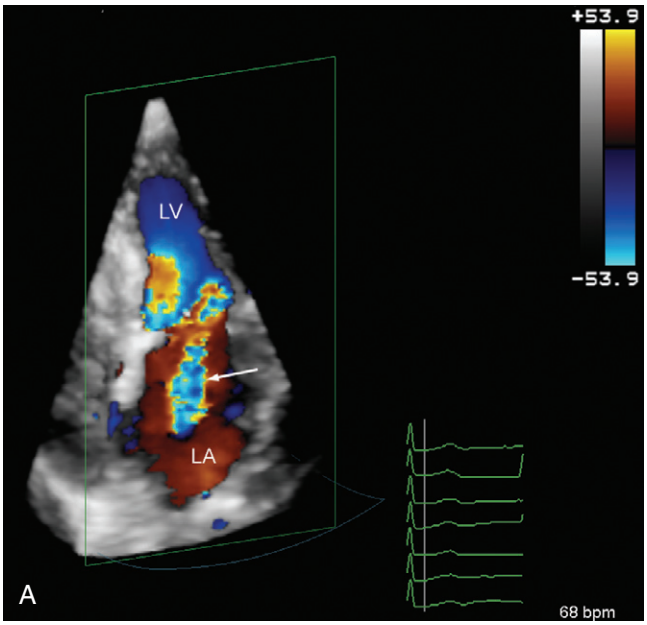


**Figure 4-11 Mitral regurgitation on 3D TTE as seen from cropping planes that best depict the jet direction.** Whereas the mitral regurgitation jet appears central *at right*, which approximates the apical four-chamber view, the eccentric inferior regurgitant jet direction is noted *at left*, which approximates an apical two-chamber view. The asymmetric natures of the proximal flow convergence zone and the vena contracta are also appreciated from the 3D echocardiogram. *(Courtesy Siemens Medical Solutions USA Inc., Ultrasound.)*

mitral leaflets before surgical repair[72,73] (Fig. 4-13). Recent evaluations with 3D TTE have demonstrated a comparative accuracy to 2D TEE for localizing the prolapsing segment.[74,75] A major determinant of this accuracy is image quality. With this technique, the most accurate detection has been for pathology of the central portion of the leaflets. For 3D TTE with current matrix array transducers, the parasternal transducer position typically provides better visualization of the leaflets compared to the apical window: The structure of interest is closer to the transducer, and thus scan line density will be greater and beam spread artifact will be less. 3D TEE improves the detection and localization of prolapsing mitral leaflet segments. In patients undergoing MV repair for MR, 3D TEE was superior to 2D TEE in the diagnosis of bileaflet disease and some specific leaflet portions such as P1, A2, and A3 valve segments.[76] The use of 3D TEE for a systematic characterization of the mitral valve is becoming more common, and protocols for a complete evaluation have been published.[77] Despite the improved performance of both 3D TTE and TEE for the morphologic evaluation of the MV, studies documenting improved patient outcomes with this



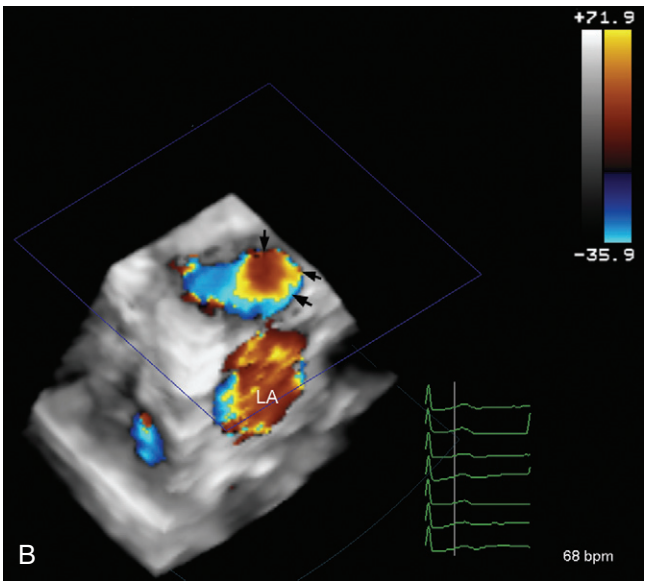
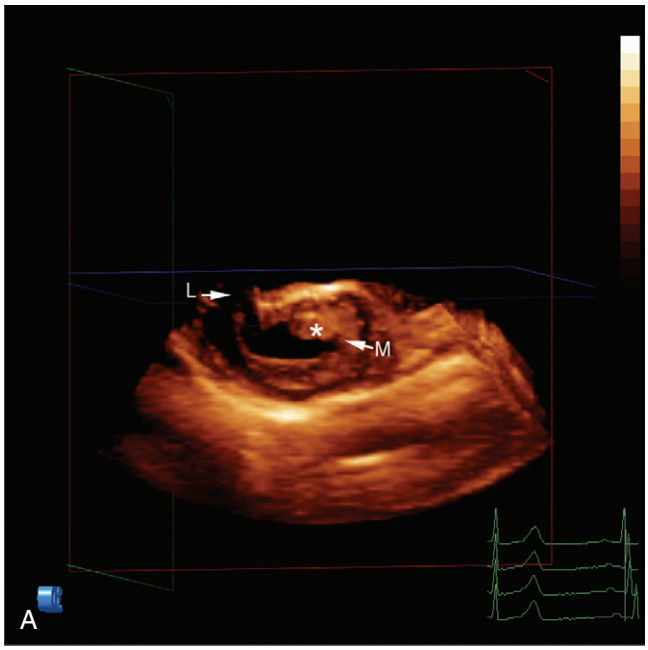




**Figure 4-12** **Full-volume 3D TTE of mitral regurgitation. A,** Cropping of the full-volume image set to display the full extent of an eccentrically directed jet of mitral regurgitation (*white arrow*) as viewed from the anterior aspect of the RV and similar to an apical five-chamber view but with the right heart cut away. **B,** Transverse plane above the mitral valve viewed from the perspective of the LV to display the proximal isovelocity surface area (orange-blue interface, *black arrows*).



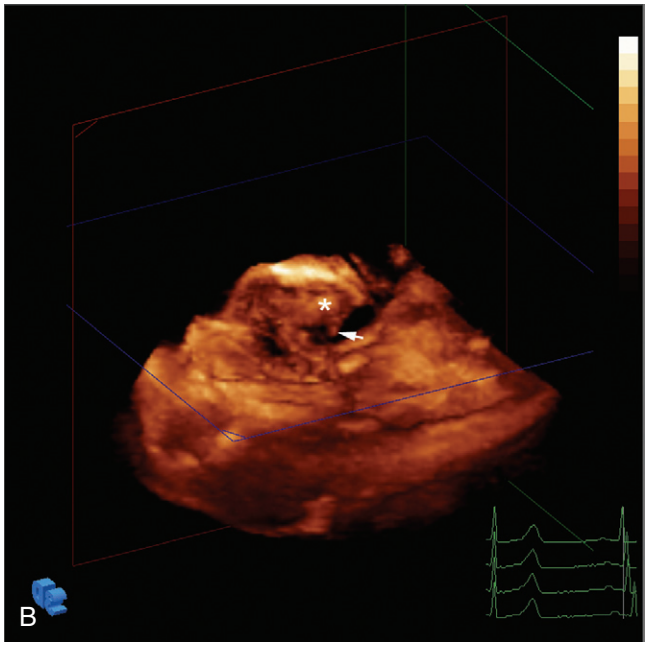




**Figure 4-13** **3D TTE of mitral valve prolapse. A,** Mitral valve viewed from the LA demonstrating prolapse (*) of the midportion of the anterior leaflet of the mitral valve. **B,** Same valve viewed from the LV cavity. The LV perspective allows visualization of a ruptured chord to the prolapsed segment (*white arrow*). *L*, Lateral commissure; *M*, medial commissure.

technique are required to help establish the clinical role of this modality.

Quantitative analysis of the geometry of the mitral apparatus represents another application of 3D echocardiography. Measurements of annular size by 3D TTE in patients with various forms of cardiomyopathy have been shown to correlate well with MRI.[78] In addition, observations from 3D echocardiography have provided important insights into mechanisms responsible for both functional and ischemic MR.[79-82] 3D echocardiography has shown that as the LV dilates, it leads to displacement of normal papillary muscle position such that the mitral leaflets are apically tethered (increased MV tenting area), and the resulting *functional* MR occurs through incompletely closing leaflets. 3D echocardiography has also shown that, in contrast, regional distortion of wall motion and/or distortion of the wall shape, such as aneurysm formation, adjacent to a papillary muscle will lead to a disruption of the normal spatial relationships between a papillary muscle and MV, resulting in disruption of normal coaptation and *ischemic* MR. 3D TTE quantification of papillary muscle anatomy can also discriminate the pathologies of MR, with preservation of papillary muscle symmetry occurring in functional MR and unequal papillary muscle tethering lengths occurring in ischemic MR.[83] Clinical studies with 3D echocardiography have confirmed prior experimental studies and demonstrated that with

ischemia and infarction, as the mitral annulus flattens, it enlarges predominantly in the anterior-posterior direction and annular motion during the cardiac cycle is reduced, especially compared to that of the posterior segments.[84,85] Based on these observations, repair techniques that reduce anterior-posterior annular diameter,[86] decrease tenting area,[87] restore normal ventricular geometry,[67,88] and reposition papillary muscles[89] have each been proposed for treatment of ischemic MR. In contrast, maneuvers that reduce global LV dilation and enhance reverse LV remodeling are being tested for functional MR.[90]

Experience with 3D echocardiography for evaluation of prosthetic valves is increasing, and the technique appears most accurate for the mitral position.[91] In a study of 18 patients with mitral valve dehiscence, 3D TEE provided additional information about the exact anatomic characteristics of the dehiscence and origin of the MR and was used to help plan the most appropriate corrective intervention.[92] 3D TEE to help guide percutaneous procedures, such as percutaneous valve repairs and paravalvular leak closure, is gaining increased use (See Chapter 5).

### *Aortic Valve*

3D echocardiography may have value in the assessment of aortic valve disease because all aspects of the three leaflets of the aortic valve cannot be visualized in a single 2D plane, and the 2D US imaging plane often is oblique through the stenotic or regurgitant aortic orifice. Direct planimetry of the aortic valve in aortic stenosis, description of valve morphology (i.e., number of leaflets) (Fig. 4-14), localization and description of subvalvular obstruction (both discrete membranes and hypertrophic septum/LV outflow tract [LVOT] obstruction), quantification of aortic regurgitation, and assessment of aortic root pathology have all been demonstrated with 3D echocardiography.[93-101]

#### Aortic Stenosis

Planimetry of aortic valve area by volumetric 3D TTE and by intraoperative 3D TEE (reconstruction technique) compares favorably with both invasive and by 2D TEE valve area measurements.[95,102] Studies of aortic valve planimetry by volumetric 3D TEE suggest similar benefits.[103,104] As noted for mitral stenosis, the advantage of 3D imaging in aortic stenosis centers on its ability to optimally define an imaging plane through the stenotic orifice.[105] As the technique continues to evolve, 3D TEE aortic valve planimetry is likely to have a role in the assessment of aortic stenosis in the operating room, because Doppler methods are more difficult there. However, because planimetry of the aortic valve from standard 2D TEE is accurate in many cases, further studies are necessary to determine in which subsets of patients and clinical situations the 3D approach is of additive value.

The 3D echocardiographic approach for aortic valve area measurement is also expected to be beneficial for continuity equation–based measurements, as a growing body of literature has documented that the LVOT is elliptical in shape.[106] This may be a source of inaccuracy in standard continuity equation–based measurements that assume a circular shape for the LVOT.[107] Additionally, direct measurements of stroke volume derived from 3D LV volumes yield more accurate continuity equation–based measurements of aortic valve area than the traditional 2D approach.[108]

#### Aortic Regurgitation

The vena contracta and PISA methods described for assessment of MR can be applied to aortic regurgitation, though experience is more limited.[109,110] In in vitro models, direct measurement of PISA with 3D TTE has been validated and calculation of aortic regurgitation volumes with 3D color Doppler has been shown to be more accurate than the conventional 2D method that uses the hemispheric assumption of flow convergence.[111] Furthermore, in the absence of other regurgitant valves, aortic regurgitation can also be accurately quantified as the difference in LV and RV stroke volumes calculated by 3D TTE.[112] Aortic valve repair is feasible for certain etiologies of aortic regurgitation.[113] Measurements of the ascending aorta, the sinotubular junction, the perpendicular distance from annulus to coaptation point of the leaflet tips, the distance from annulus to sinotubular junction, and the distance from the sinotubular junction to leaflet

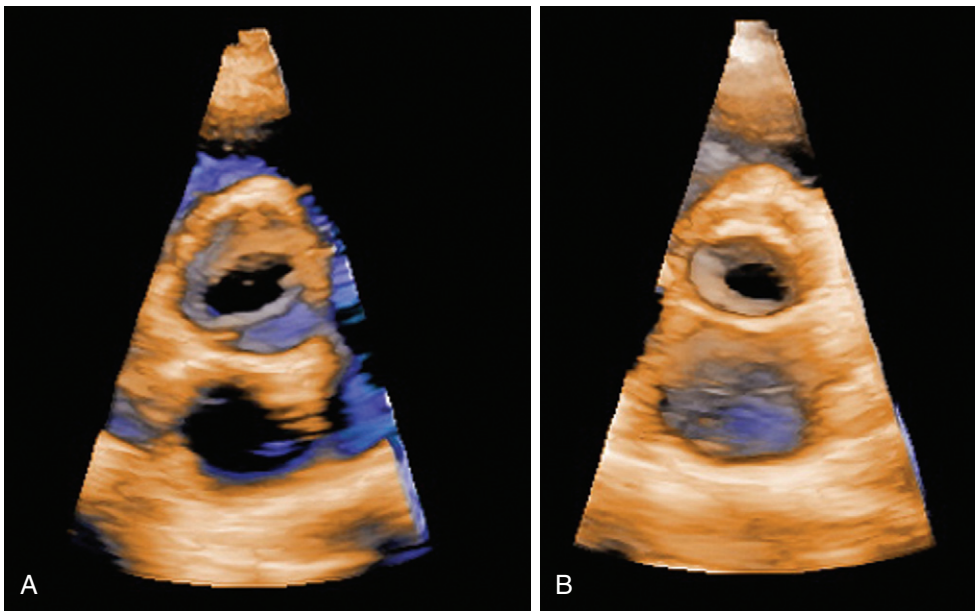



**Figure 4-14** Bicuspid aortic valve on 3D transthoracic echocardiography viewed from the aortic perspective (**A**) and LV perspective (**B**).

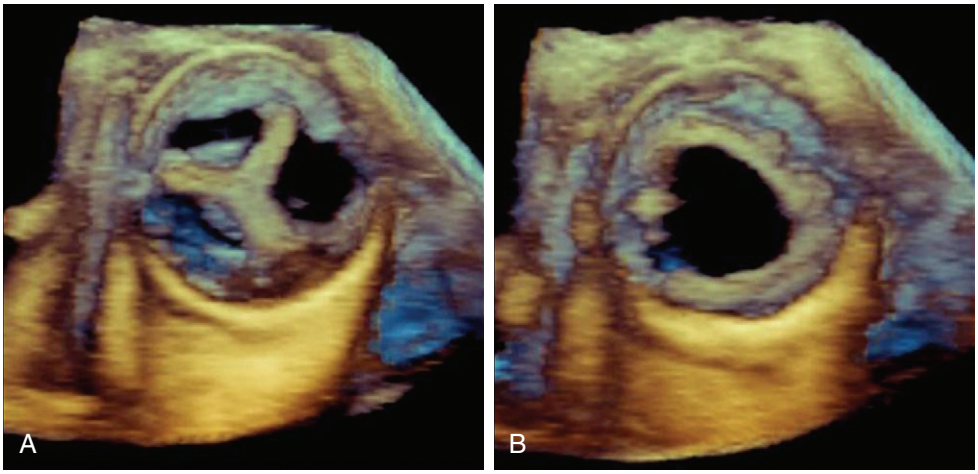



**Figure 4-15** 3D TEE of a pericardial aortic prosthetic valve demonstrating diffuse leaflet thickening, as viewed from the ascending aorta. **A,** Diastole (leaflets closed). **B,** Systole (leaflets open).

coaptation point can provide insights into the mechanisms responsible for aortic regurgitation and incomplete aortic valve closure.[101] These measurements are feasible with 3D TEE and may facilitate the development of new repair techniques and the assessment of the success of aortic valve repair.

### Aortic Prostheses

Similar to the mitral valve, studies investigating the use of 3D echocardiography in the assessment of prosthetic aortic valves are currently limited, although the clinical experience is increasing[114] (Fig. 4-15). The use of 3D TEE for transcatheter aortic valve implantation (TAVI) is evolving[115] (See Chapter 5).

### *Tricuspid and Pulmonic Valves*

The utility of 3D echocardiography for evaluation of the right-sided valves has not been as well-studied as the left-sided valves (Fig. 4-16). Initial reports for 3D echocardiography of the tricuspid valve were in the form of case reports, although a recent study comparing 3D TTE to MRI found that measurements of the tricuspid annulus are comparable between the two techniques.[116] 3D echocardiographic studies have shown that the tricuspid valve annulus is less saddle shaped and more round or oval than the MV annulus.[117] This may have implications for annuloplasty and/or repair of the tricuspid valve.[118] 3D echocardiography has also been used to evaluate the tricuspid valve in pulmonary hypertension,[119] rheumatic disease,[120] carcinoid heart disease,[121] and complex congenital heart lesions.[122] For example, quantitative 3D TTE has shown that following Fontan procedures, bidirectional cavopulmonary shunts, and Norwood procedures, significant tricuspid regurgitation can result from enlarged annular area, reduced systolic annulus area change, systolic annular flattening, and papillary muscle displacement.[123] Observations that the tricuspid regurgitation results predominantly from annular and ventricular abnormalities, rather than from the valve, may facilitate modification of surgical techniques.

Studies of the pulmonic valve are even more limited, but reports are emerging describing the 3D echocardiographic assessment of the anatomy of the RV outflow tract and pulmonic valve,[124] the vena contracta and regurgitant volume in pulmonic regurgitation,[125] and the pulmonic valve in carcinoid heart disease.[126]

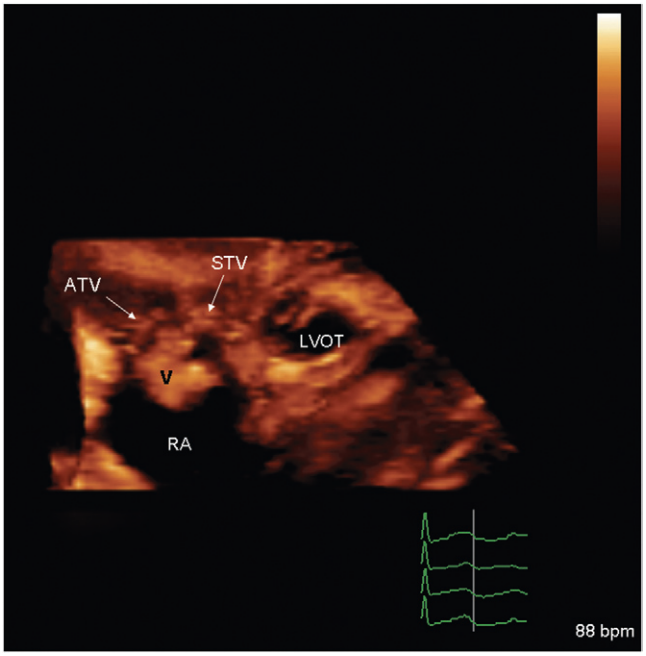



**Figure 4-16 Transverse crop from a 3D full-volume TTE of a tricuspid valve vegetation.** The vegetation is seen to arise from the atrial surface of the septal leaflet. *ATV,* Anterior leaflet of tricuspid valve; *LVOT,* left ventricular outflow tract; *STV,* septal leaflet of tricuspid valve; *V,* vegetation.

## CONGENITAL HEART DISEASE

3D echocardiography has a potential impact on diagnosis and treatment of patients with congenital heart disease because of the ability to define and display the complex spatial relationships seen in many of these pathologies. In addition, the shorter time for image acquisition with volumetric 3D echocardiography improves the probability of complete

cardiac US imaging assessment of children. A study of 75 patients with suspicion of congenital heart defects reported that 3D TTE image sets were obtained in all cases in less than 5 minutes, and sedation of infants and children was never required.[127] In a more recent report of 3D TTE in 70 patients with simple and complex congenital heart disease, improved depiction of cardiac and lesion morphology compared to 2D imaging was noted regardless of the experience level of the echocardiographer.[128] In this study, in at least 30% of the cases, the 3D echocardiogram added new information compared to the 2D imaging. Other investigators have confirmed that in about one third of patients with congenital heart disease, 3D TTE provided anatomic information not seen on 2D echocardiography that was helpful in clinical decision making.[129] This additive benefit was most prominent in patients with atrial septal defect, ventricular septal defect, atrioventricular septal defect, and L-transposition of the great vessels. In another 29% of this population, the 3D technique provided additional information compared to 2D echocardiography, but it was deemed not critical to decision making, and in 36% of the patients the information was equivalent for the two techniques.

Validation studies and evidence supporting the use of 3D echocardiography in congenital heart disease are now available for numerous measures of cardiac structure and function, including LV volume, mass and ejection fraction,[130] RV volume and function,[131] and single ventricle measurements.[132] 3D echocardiography has also been used to evaluate the mechanisms and sites of regurgitation in congenital abnormalities of the atrioventricular valves.[133] Additionally, there are case reports describing the successful use of 3D echocardiography for assessment of cleft MV[134] and Ebstein's anomaly.[135]

The detection and quantification of atrial septal defects is a particular strength of 3D TTE and TEE[136,137] (Fig. 4-17). The area or diameters of the defect can be measured from an enface view from either the RA or LA perspective.[138] Calculation of atrial septal defect shunt volume from 3D TEE reconstructions of Doppler color flow through the defect compares favorably to other methods.[139] Visualization of the extent of septal rim and assessment of the proximity of other structures is necessary when considering if a patient with an atrial septal defect is a candidate for percutaneous closure device, and 3D echocardiography may provide value in this assessment (See Chapter 5). In addition to secundum atrial septal defect, 3D TTE has been utilized to assess sinus venosus defects,[140] unroofed coronary sinus,[141] atrioventricular septal defects,[142] and ventricular septal defects.[143]

Currently the role of 3D echocardiography in patients with congenital heart disease is still being defined. It is likely that a paradigm that integrates 2D and 3D echocardiography in the evaluation and treatment of patients with congenital heart disease will produce the best patient outcomes.[144] Continued refinement of 3D technology, including development of higher frequency TTE matrix array transducers with smaller footprints and faster frame rates, and smaller 3D TEE probes will allow this technique to reach its full potential in this unique patient population.

## GUIDANCE OF INTRACARDIAC CATHETER-BASED INTERVENTIONS

Percutaneous catheter-based noncoronary procedures are gaining acceptance and becoming more commonplace in cardiac catheterization and electrophysiology laboratories.

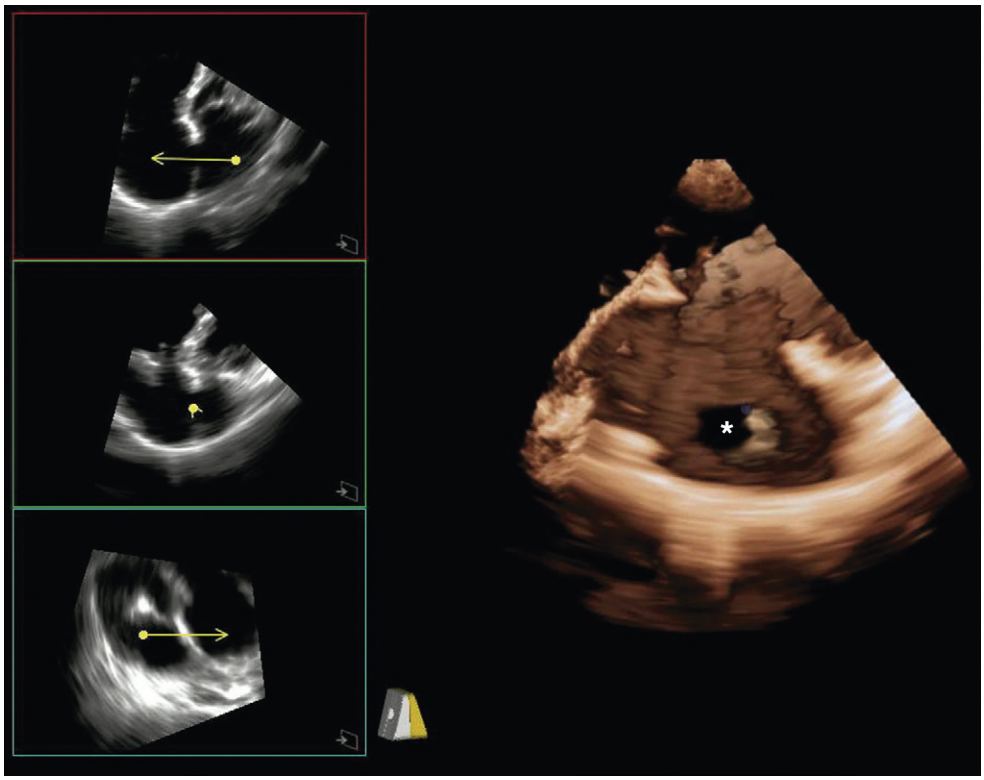



**Figure 4-17 3D TTE of a secundum atrial septal defect.** *Left*, Views from three cropping planes. *Right*, en-face view of the defect from the RA perspective. The 3D en-face view clearly depicts the shape of the atrial septal defect (*) and the adequacy of the surrounding septal tissue. *(Courtesy Siemens Medical Solutions USA Inc., Ultrasound.)*

Imaging guidance of such procedures has traditionally utilized fluoroscopy, which results in radiation exposure and, unless large volumes of radiologic contrast are used, has limited ability to depict complex anatomy and defects. Intracardiac echocardiography and 2D TEE are established modalities to help guide catheter-based procedures, although they have limitations. RT3D TEE has emerged as a powerful imaging tool because it allows the interventionalist a real-time 3D appreciation of cardiac anatomy, location of defects, and position of devices and catheters relative to the defects. Although these can be assessed with 2D TEE, it is easier with 3D imaging to rapidly understand the spatial relationships. The feasibility of 3D TTE and TEE has been demonstrated for closure of secundum atrial septal defect (see Fig. 4-2) and patent foramen ovale (Fig. 4-18), MV repair, mitral balloon valvuloplasty for mitral stenosis, TAVI, closure of prosthetic valve paravalvular regurgitation, closure of ventricular septal defects, LA appendage obliteration, and pulmonary vein ablation for atrial fibrillation.[145-147] In a multicenter evaluation of RT3D TEE for guidance of such catheter-based interventions, several distinct advantages of RT3D TEE were found.[147] Specifically, RT3D TEE allowed for visualization of the entire length of intracardiac catheters, including the tips of all catheters and the balloons and devices they carry, along with clear depiction of their positions in relation to other cardiac structures. Another advantage of RT3D TEE is the ability to demonstrate certain structures in an en face view, allowing appreciation of the exact shape of the lesion undergoing intervention.

Compared with 2D TTE and fluoroscopy, RT3D TTE has demonstrated efficacy in helping to guide RV biopsy, by providing improved visualization and localization of the bioptome tip in the RV.[148]

Recent evaluations support the use of RT3D echocardiography, both TTE[149] and TEE,[150] for guiding closure of atrial septal defects and detection of complications of this procedure, such as a torn interatrial septum.[151] There is also evidence that use of RT3D TEE to assist percutaneous closure of interatrial communications can result in lower radiation exposure for patients.[152] A true representation of atrial septal defect shape with 3D TEE enables more accurate measurement of defect size compared to 2D TEE. This can guide selection of the appropriate closure device and reduce residual shunting.[137]

Catheter-based therapy of valvular heart disease represents another major area where RT3D echocardiography is being utilized. In addition to mitral stenosis, RT3D echocardiography also has uses in guiding the treatment of MR. RT3D echocardiography has been used to evaluate the impact of a coronary sinus-based percutaneous transvenous mitral annuloplasty on dynamic changes of mitral annular geometry, demonstrating a reduction in mitral annular area and dimensions.[153] Percutaneous edge-to-edge repair of the MV to reduce MR is a promising technology, and RT3D echocardiography may guide perpendicular alignment of the therapy catheter to the MR jet and help position devices along leaflet edges.[154] Additionally, RT3D echocardiography may help detect the complications that can occur in the setting of percutaneous MV repair.[155] Paravalvular regurgitation in the setting of prosthetic MV dehiscence is another clinical situation in which RT3D echocardiography is being utilized to select patients and guide percutaneous therapy.[156] In this setting, the imaging requirements include visualization of location and size of the leak, guiding wire position through the leak, and determining of the size and number of devices required to close the leak(s) (Fig. 4-19). The incremental value of RT3D over 2D echocardiography for device closure of paravalvular leak needs to be established.

TAVI has been shown to reduce mortality in patients with severe aortic stenosis who are not suitable candidates for surgery.[157] TEE is relied on during the TAVI procedure to assist in device sizing, device positioning, adequacy of device deployment and function, and identification of complications. As with guidance of other procedures, RT3D TEE provides better display of device and cardiac structures such as the aortic annulus compared with 2D TEE.[158]

Atrial fibrillation is another disease in which RT3D echocardiography is used to guide catheter-based therapies. RT3D TEE can be used to help guide transseptal puncture in patients undergoing atrial fibrillation ablation, allowing for fast and safe transatrial access with a single puncture attempt.[159] For patients with atrial fibrillation who have contraindications to anticoagulation, LA appendage occlusion devices may represent a novel treatment option.[160] In a study of 66 patients, RT3D TEE for visualization and quantitation of LA appendage orifice areas was feasible and correlated well with 64-slice cardiac computed tomography.[52] Thus, RT3D TEE may help select patients suitable for LA appendage occlusion, determine device size, and assess position during deployment. In addition, color Doppler from an en face view of the implanted device as seen from the LA perspective can rapidly identify residual flow around the

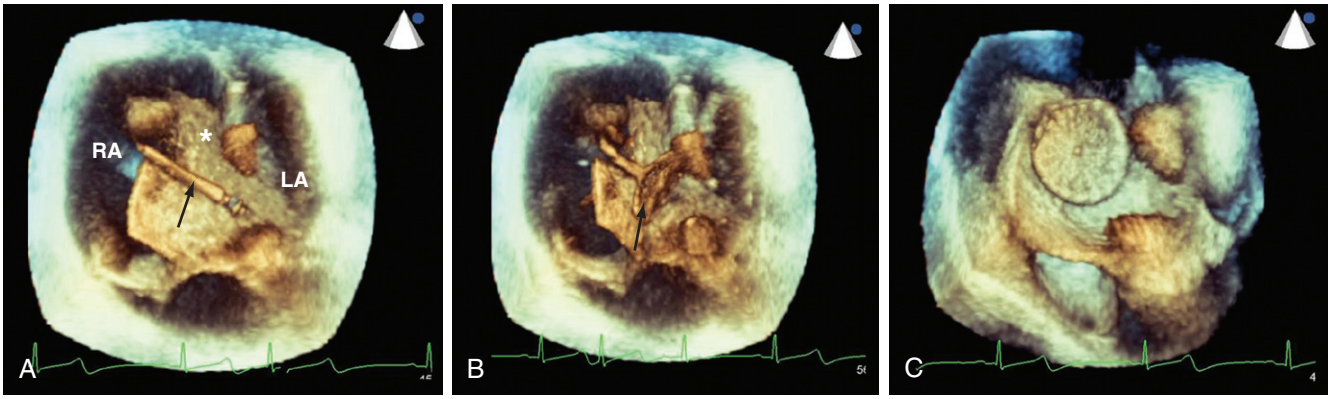



**Figure 4-18** 3D TEE obtained during percutaneous closure of a patent foramen ovale, as viewed from an LA perspective. **A,** Guiding catheter (*arrow*) seen traversing the patent foramen ovale. Interatrial septum viewed en face (*). **B,** LA septal occluder disk opened (*arrow*) and in the process of being pulled against the LA side of the interatrial septum. **C,** LA septal occluder disk apposed to the LA side of the interatrial septum.

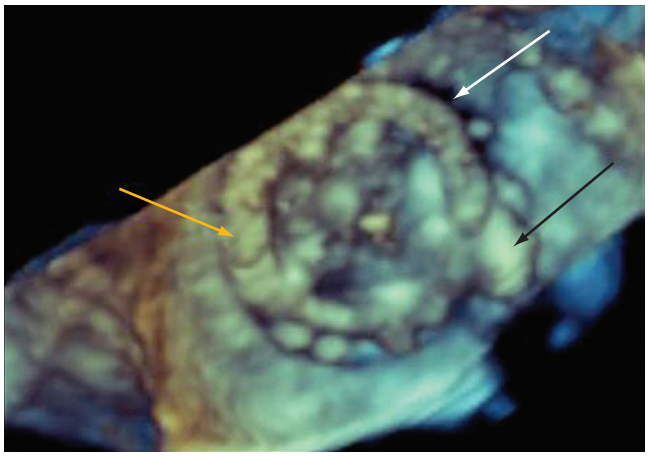


**Figure 4-19** 3D TEE obtained during percutaneous closure of a paravalvular leak associated with a single-tilting disk prosthetic mitral valve. An occluder device (*black arrow*) is positioned in a portion of the gap between valve and cardiac tissue. An area of residual paravalvular leak (*white arrow*) is also seen. The sewing ring of the valve is noted (*yellow arrow*). The highly reflective spot in the middle of the valve is its central strut.

margin of the device, which may prompt repositioning or change in device sizing.

## OTHER SELECTED APPLICATIONS

As would be expected, 3D echocardiography can be applied to almost any current use of 2D echocardiography. Several of these situations are described in this section. When assessing its additive value, important questions include whether the technology provides additional information that alters diagnosis or outcome and whether the information is obtained in a simpler or faster fashion.

### *Stress Echocardiography*

The use of single cardiac cycle multiplane 2D imaging or 3D echocardiography during stress echocardiography offers several advantages over the current practice. First, all ventricular segments are imaged rapidly at each stage, which is particularly important at peak stress, so that all myocardial segments are visualized before reduction in workload and the resolution of transient ischemia-induced wall motion abnormalities (Fig. 4-20). Second, if image acquisition is performed properly, the entire LV is imaged, and the risk of not evaluating the true LV apex due to foreshortening of the 2D view is reduced. Third, function of all myocardial segments is assessed at the same point in time, enabling accurate comparisons. Fourth, cropping of the images enables display and interpretation of image planes that are on-axis, thus reducing errors that occur with interpretation of oblique cuts of the ventricular walls or rotational motion. Last, cropping of the 3D images from each stage allows comparison of reproducible and identical myocardial segments at each stage, even if the heart has changed size or shape. However, if wall motion of all segments of the LV is accurately visualized and interpreted during 2D stress echocardiography, then it is unlikely that 3D imaging will improve the accuracy of the test.

The feasibility of the integration of 3D echocardiography with treadmill and pharmacologic stress echocardiography has been demonstrated.[161-163] Comparisons of 2D and 3D stress echocardiography have shown variable results, with some reporting comparable sensitivity and specificity for the two imaging methods during dobutamine[164] while others reported a lower sensitivity but higher specificity for the 3D stress echocardiogram during treadmill exercise.[165] One study comparing multiplane apical views to multislice short-axis views obtained from 3D TTE during dobutamine stress echo has demonstrated comparable sensitivity but enhanced specificity of the multiple simultaneous short-axis views. The improvement appears to be due to increased specificity for disease of the right coronary artery.[166] The time required to perform the 3D imaging during both pharmacologic and exercise stress has been reported to be approximately 50% shorter than that needed to acquire the comparable 2D images.[164,167]

With present-day 3D echocardiographic systems, several factors may influence test accuracy. The low frame rate of current 3D images might reduce detection of wall motion abnormalities, especially when images of rapidly beating ventricles are obtained. In addition, poor image quality has been noted in up to 9% of the 3D image sets.[165] Several 3D image acquisitions from different transducer positions may be necessary to acquire adequate-quality images of all myocardial segments. For example, 3D volumes from the standard apical transducer position will provide high-resolution images of the apical portions of the LV compared to more basal portions, because the resolution of the structures in the far field is influenced by the increasing scan line separation. However, 3D images from the parasternal transducer position can provide higher-resolution images of those basal portions. The large size of some matrix array transducers has contributed to difficulties in visualizing the anterior and lateral walls of the LV due to variable contact of the entire transducer footprint on the chest wall, thus resulting in a lack of the anterolateral regions of the LV in the volume acquired.[168] However, improvements in the technology are resulting in smaller transducers that should resolve this issue. The limitations of image quality during stress have been reduced with the addition of intravenous contrast for LV opacification.[169] The fusion of component images from multiple cardiac cycles may lead to image artifacts, particularly during stress and recovery when the heart rate is changing and patients are breathing rapidly. These artifacts can lead to the false impression of dyssynchrony or wall motion abnormality.[168]

Although 3D imaging is ideally suited for stress echocardiography, several enhancements are necessary before widespread clinical application. These include increases in frame (volume) rates that enable visualization of ventricular wall motion at the increased heart rates encountered at peak stress and additional methods that allow flexibility in the side-by-side display of cropped images from different stages.

### *Left Ventricular Dyssynchrony*

In randomized trials of advanced systolic heart failure, cardiac resynchronization therapy (CRT) has resulted in a reduction in symptoms and improved survival.[170] Echocardiography, specifically tissue Doppler imaging, has been used to assess LV mechanical dyssynchrony (LVMD) in an effort to select patients and predict response to CRT. (See Chapter 26.) However, results from a multicenter trial highlight the limitations of current tissue Doppler imaging–based measures of LVMD for patient selection for CRT, particularly those due to interpreter variability.[171] Efforts are focused on identifying echocardiographic methods for assessment of LVMD that have

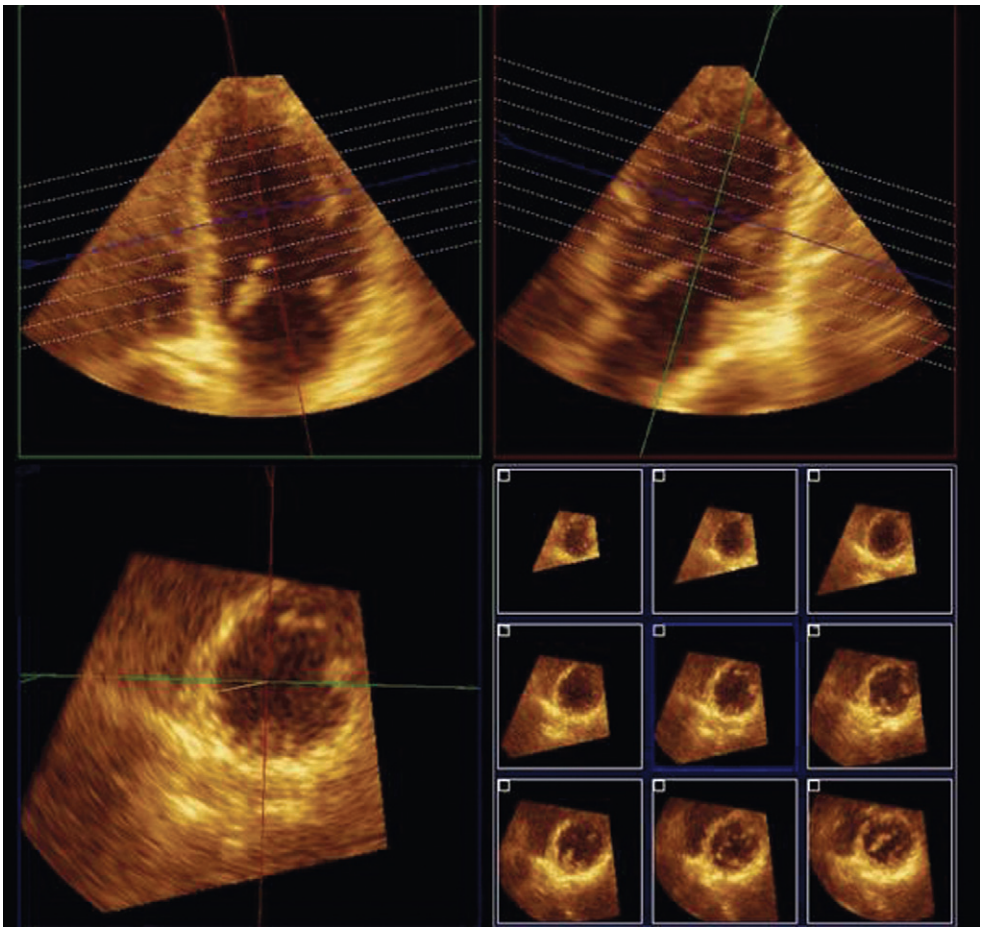


**Figure 4-20 One type of display of full-volume 3D stress echocardiogram.** Nine simultaneous short-axis views (*inset*) from apex (*upper left*) to base (*lower right*) of the LV. The distance between each adjacently displayed short-axis image is equal, and positions of these transverse cropping planes are shown (*white lines*) on the coronal and sagittal crops.

reduced measurement variability. 3D echocardiography is being studied this context.[172-174] The advantages of 3D echocardiography for the assessment of LVMD and the response to CRT in heart failure patients are similar to those noted earlier for stress echocardiography—all segments can be assessed simultaneously. Specifically, a full-volume data set is acquired and is imported into analysis software in which the complete LV endocardial border is tracked through the cardiac cycle. The LV volume is then divided into a series of subvolumes, the change in each subvolume during the cardiac cycle is calculated, and time-volume curves are generated. In LVMD, there is dispersion of the timing of the minimum volume point for all the subvolumes (Fig. 4-21). A systolic dyssynchrony index can be derived by calculating the standard deviation of the time to minimum volume in each of the subvolumes; this index is expressed as a percentage of the duration of the cardiac cycle.[175] In a recent study of 187 patients at two centers, LVMD quantification by 3D TTE was reproducible between centers and systolic dyssynchrony index was a predictor of response to CRT.[176] 3D TTE to quantify LV reverse remodeling and predict response to CRT has also been demonstrated.[177,178] Despite these promising results, limitations of 3D echocardiography for assessment of LVMD do exist.[179] Another potential role for 3D echocardiography is in the creation of color-coded parametric images that provide a spatial display illustrating which LV segments are most delayed.[180] When incorporated with information about coronary venous anatomy, this provides a visual display of how one may position the LV pacing lead adjacent to the most delayed segment. Additionally, techniques such as 3D speckle tracking are beginning to be studied for LVMD.[181]

### *Hypertrophic Cardiomyopathy*

In hypertrophic cardiomyopathy, 3D echo has shown improved identification of systolic anterior motion of the MV, improved localization of the predominant septal hypertrophy,[182,183] and usefulness for measurement of LVOT area and quantification of LVOT obstruction at rest and after provocation.[184] 3D echocardiography may also have value in the identification and quantification of LVOT and septal remodeling after surgical myomectomy and percutaneous alcohol septal ablation.[98]

### *Endocarditis*

Case reports have highlighted the value of 3D echocardiography in infectious endocarditis (Fig. 4-22). These reports suggest that 3D echocardiographic assessment may improve the detection of valve perforations, in addition to identifying the number and location of vegetations on both native and prosthetic valves[185,186] as well as on pacemaker leads.[187] Additional studies suggest that vegetation size measured on 3D TTE is more accurate than on 2D TTE.[188] A recent case series of 13 patients showed that intraoperative 3D TEE provided more information about complications of endocarditis such as

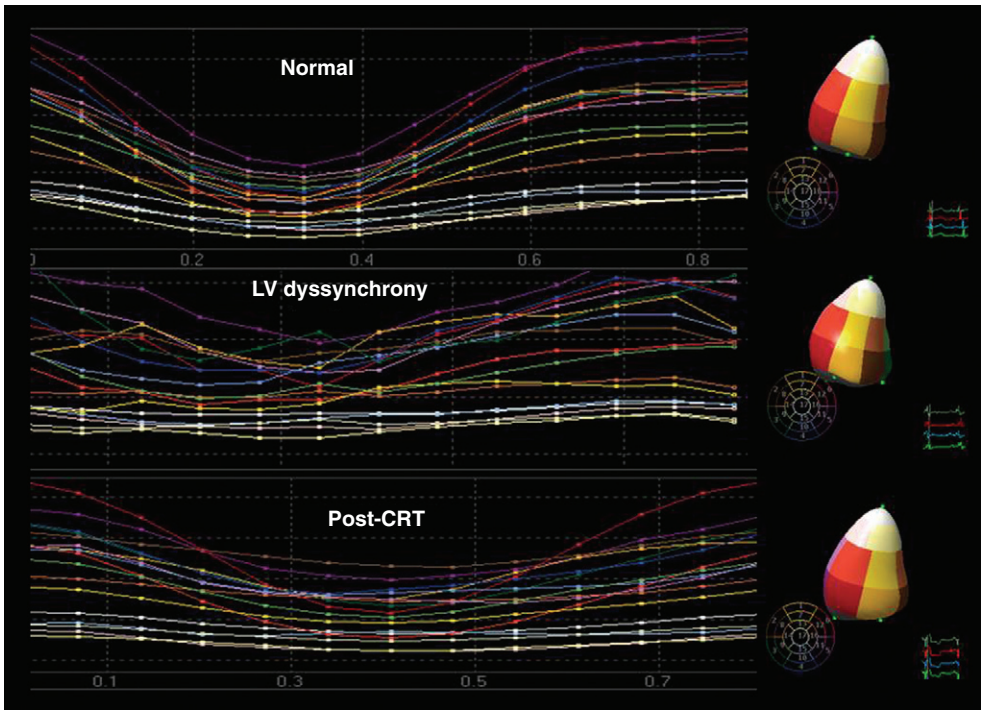



**Figure 4-21** **Intraventricular mechanical dyssynchrony of the LV can be assessed by 3D transthoracic echocardiography.** LV volume throughout a single cardiac cycle (*top*) is derived from a full-volume acquisition. All segments achieve their minimum volume at approximately the same time in the cardiac cycle. The same LV volume calculations in a patient with left bundle branch block and New York Heart Association class III heart failure (*middle*). A wide dispersion of time to minimum volume is observed for the segments representing intraventricular mechanical dyssynchrony. A follow-up 3D echocardiogram was performed 1 month after a cardiac resynchronization device was implanted, and the pattern of LV volume over time (*bottom*) now shows synchronous motion of the LV segments. *CRT*, Cardiac resynchronization therapy.

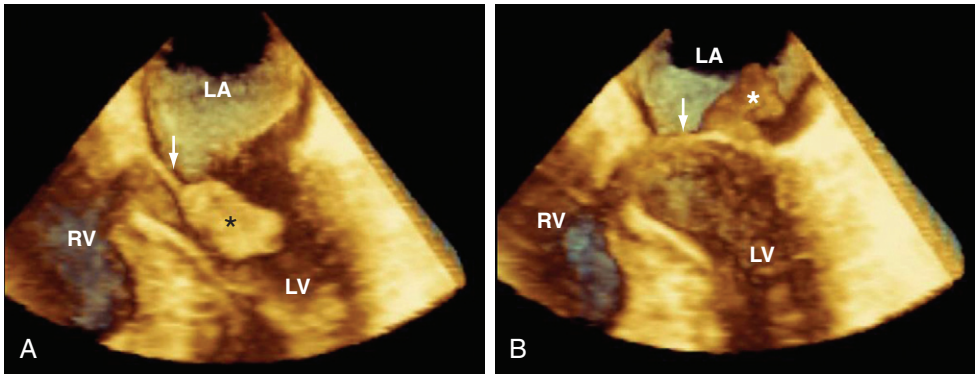



**Figure 4-22** Full-volume 3D TEE of a mitral valve vegetation in a patient with *Enterococcus faecalis* bacteremia. The vegetation (*) is seen to arise from the atrial surface of the anterior mitral leaflet. *Arrow* designates base of anterior mitral valve leaflet. **A,** Valve open in diastole. **B,** Valve closed in systole.

abscesses, perforations, and ruptured chordae and that this information may be helpful in planning the cardiac surgical procedure.[189] Systematic studies comparing 3D echocardiography (TEE and TTE) to the 2D echocardiographic modalities are still required to determine if vegetation detection rate is improved and if 3D echocardiography has incremental value to guide clinical decision making.

### *Aortic Dissection*

Case reports have demonstrated aortic dissection by 3D echocardiography,[190] and a study in a small number of patients suggests that the diagnosis of type A aortic dissection by TTE can be dramatically enhanced with 3D echocardiography.[191] In a more recent study, comparing 3D and 2D TEE, the assessment of entry-site tear size in chronic aortic dissection was enhanced and compared favorably to CT.[192] Case reports suggest that 3D echocardiography can be useful for the imaging follow-up of patients with surgically repaired aortic dissection.[193]

### *Myocardial Perfusion*

3D echocardiographic imaging enables display of myocardial contrast perfusion zones in a single cardiac cycle rather than reliance on a single image plane as is the common practice of 2D myocardial contrast echocardiography. The extent of

perfusion defect and quantification of myocardial perfusion have been demonstrated in both experimental preparations and humans with volumetric 3D echocardiography.[194] 3D myocardial contrast echocardiography has been used to assess subendocardial perfusion abnormalities after percutaneous intervention for myocardial infarction and was more precise than the 2D technique in this setting.[195] A potential impediment to use of RT3D TTE for myocardial perfusion is that the high intensity acoustic power and large number of scan lines that the current matrix array transducers transmit enhance premature microbubble destruction.

### *Pericardial Effusion*

The size of pericardial effusions can be more accurately quantified by 3D echocardiography than by 2D techniques. The 3D technique does not rely on the assumption that the fluid is symmetrically distributed. With the 3D echocardiographic method, the pericardial fluid volume is calculated as the difference between the volume of the outer pericardial sac (parietal pericardium) and the outer surface of the heart. Experimental studies using the reconstruction technique have shown excellent accuracies compared to true volume ($r = 0.98$; SEE 7.7 mL; mean error $1.1 \pm 7.8$ mL),[5] and more recent clinical experiences with volumetric TTE have confirmed its benefits.[196] For accurate quantitation of the fluid, the entire parietal pericardium or outer border of the effusion must be obtained in the image volume.

### *Intracardiac Masses*

The detection of masses, including thrombi and tumors, within the heart by 3D echocardiography has been documented in several case series.[188,197,198] 3D echocardiography may improve the detection of the site of attachment of the mass and the size of the mass. (See Chapter 46.) As image quality improves, it may have the potential to provide additive information over 2D echocardiography to help guide surgical procedures.[199] Studies are required to determine if serial quantification of thrombus volume with 3D echocardiography is an accurate and reproducible method to assess response to therapy.

## Technology Diffusion

Among the impediments to the widespread clinical use of 3D echocardiography are availability and cost of equipment, unfamiliarity with the technique, and image quality. Studies have shown that short, intensive, interactive sessions that incorporate supervised training in the cropping of 3D data sets and the interpretation of 3D echocardiograms lead to significant improvements in user expertise.[200] Thus, in addition to identifying specific indications where 3D TTE and TEE are critical, continued efforts at sonographer and physician "hands-on" training are necessary. Although 3D TTE image quality has not always been comparable to that of 2D TTE, the excellent image quality of 3D TEE has led to its rapid acceptance for specific indications such as assessment of mitral valve disease and guidance of intracardiac catheter-based interventions.

## Future Considerations

The key to the future of 3D echocardiographic imaging is continued technologic enhancements. Enhancements to transducer technology and computer processing will enable higher frame (volume) rate acquisitions with smaller matrix array transducers, and this should lead to improved image quality and color Doppler display. Such advances have already led to larger volume data acquisitions during a single cardiac cycle, and thus the current integration of several cardiac cycles for full cardiac 3D volume display will be a transition phase for the technique. The single cardiac cycle method will remove the artifacts observed with arrhythmias, respirations, and patient motion.

As 3D echocardiographic full-volume data acquisition becomes a routine part of the clinical work flow, there is the potential for shortened image acquisition time because a 3D volume of US containing all cardiac structures should be able to be imaged within just a few cardiac cycles from a few imaging windows. Additional time would then be spent on preparing the image sets for interpretation, mainly by cropping the views into image planes that best display the various cardiac structures. Efforts are now being focused on developing 3D TTE and TEE imaging protocols and standardized image cropping planes, and on training personnel for this image preparation and quantitation. In addition, enhancements to the 3D image display should lead to development of novel ways to view the images and the ability to perform "virtual dissections" through the image set both offline and in real time. Because echocardiography has superior temporal resolution compared to other noninvasive cardiac imaging modalities (some of which have superior spatial resolution), there is the potential to enhance noninvasive diagnostic and therapeutic cardiac imaging through fusion of modalities, such as cardiac MRI, computed tomographic imaging, or angiography with 3D echocardiography[201] (Fig. 4-23).

Clinical investigations comparing 2D echocardiography and 3D echocardiography continue to be required in order to demonstrate where there is incremental value of 3D

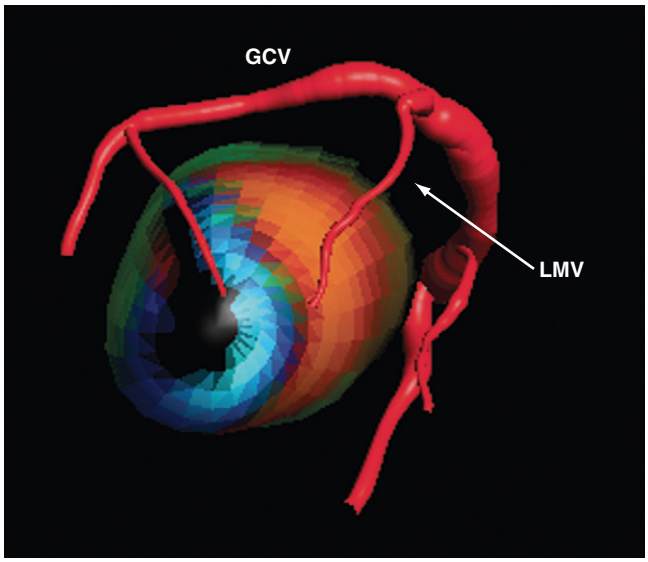



**Figure 4-23** An image integrating 3D TTE and 3D rotational coronary venous angiography viewed from the lateral apex of the LV. This example displays the LV dyssynchrony map (on a 3D echocardiographic volume of the LV) and the coronary venous anatomy before placement of pacing wires for cardiac resynchronization therapy. The most delayed myocardial segments are coded on the LV volume in *orange*, and the earliest contracting segments are in *green*. *GCV*, Great cardiac vein; *LMV*, lateral marginal vein. *(Courtesy Francois Tournoux, MD, Massachusetts General Hospital.)*

echocardiography for detection and quantification of specific cardiac pathologies and for improved patient care.

## Summary

3D echocardiography has many advantages over 2D echocardiography, including improved visualization of complex shapes and spatial relations between cardiac structures; improved quantitation of cardiac volumes, mass, and function; improved visualization of color Doppler flow fields; improved display and assessment of valve dysfunction and some structural cardiac lesions; and decreased time for image acquisition. Technical improvements, including enhanced TTE transducer design for better image quality from volumetric data sets and more automation of the image processing (cropping) protocol, are required for its widespread clinical use and for it to replace 2D TTE. 3D TEE by the volumetric method is relatively new, but because its image quality is superior to that of 3D TTE, it is being incorporated into clinical practice. 3D echocardiography continues to undergo dynamic evolution.

## KEY POINTS

- Understanding the complex shapes and spatial relationships of various cardiac structures is enhanced with 3D echocardiography.
- 3D echocardiography eliminates the need to assume a specific geometric shape of the LV or RV when quantifying volume and ejection fraction.
- 3D echocardiography has the potential to reduce the time required for echocardiographic image acquisition.
- 3D US can be acquired as either a series of 2D images requiring reconstruction into a 3D image or more commonly as a 3D volume of ultrasound.
- The volumetric technique requires a rectangular (matrix) array transducer. A small RT3D volume or a larger 3D full-volume composed of component images from several cardiac cycles can be displayed.
- Multiple 2D image planes can be obtained simultaneously with a matrix array transducer.
- 3D echocardiographic quantitation of LV volume, ejection fraction, mass, and RV volume are more accurate than the 2D approaches, and these measurements derived from 3D echocardiography have reduced measurement variability.
- In congenital heart disease, significant benefits of 3D echocardiography compared to 2D echocardiography have been noted in patients with atrial septal defect, ventricular septal defect, atrioventricular septal defects, and L-transposition of the great vessels.
- Continued enhancements to the current 3D technology will include higher volume or frame rate acquisitions to improve image quality and resolution. These are required for broader clinical application of the technology.
- 3D TEE has a role in real-time guidance of intracardiac catheter-based interventions such as patent foramen ovale/atrial septal defect closures, ventricular septal defect closures, LA appendage occlusion, transcatheter aortic valve implantation, and transcatheter mitral valve repair.

## REFERENCES


1. Dekker DL, Piziali RL, Dong E, Jr: A system for ultrasonically imaging the human heart in three dimensions. *Comput Biomed Res* 7(6):544-553, 1974.
2. Moritz WE, Shreve PL: A microprocessor-based spatial locating system for use with diagnostic ultrasound. *Proc IEEE* 64:966-974, 1976.
3. Siu SC, Rivera JM, Guerrero JL, et al: Three-dimensional echocardiography. In vivo validation for left ventricular volume and function. *Circulation* 88(4 Pt 1):1715-1723, 1993.
4. Jiang L, Vazquez de Prada JA, et al: Three-dimensional echocardiography: in vivo validation for right ventricular free wall mass as an index of hypertrophy. *J Am Coll Cardiol* 23(7):1715-1722, 1994.
5. Vazquez de Prada JA, Jiang L, Handschumacher MD, et al: Quantification of pericardial effusions by three-dimensional echocardiography. *J Am Coll Cardiol* 24(1):254-259, 1994.
6. Levine RA, Handschumacher MD, Sanfilippo AJ, et al: Three-dimensional echocardiographic reconstruction of the mitral valve, with implications for the diagnosis of mitral valve prolapse. *Circulation* 80(3):589-598, 1989.
7. Picard MH: Three-dimensional echocardiography. In Otto CM, editor: *The practice of clinical echocardiography*, ed 3, Philadelphia, 2007, Saunders Elsevier.
8. Snyder JE, Kisslo J, von Ramm O: Real-time orthogonal mode scanning of the heart. I. System design. *J Am Coll Cardiol* 7(6):1279-1285, 1986.
9. von Ramm OT, Smith SW: Real time volumetric ultrasound imaging system. *J Digit Imaging* 3(4):261-266, 1990.
10. Sheikh K, Smith SW, von Ramm O, Kisslo J: Real-time, three-dimensional echocardiography: feasibility and initial use. *Echocardiography* 8(1):119-125, 1991.
11. Foster GP, Isselbacher EM, Rose GA, et al: Accurate localization of mitral regurgitant defects using multiplane transesophageal echocardiography. *Ann Thorac Surg* 65(4):1025-1031, 1998.
12. Iwakura K, Ito H, Kawano S, et al: Comparison of orifice area by transthoracic three-dimensional Doppler echocardiography versus proximal isovelocity surface area (PISA) method for assessment of mitral regurgitation. *Am J Cardiol* 97(11):1630-1637, 2006.
13. Khanna D, Vengala S, Miller AP, et al: Quantification of mitral regurgitation by live three-dimensional transthoracic echocardiographic measurements of vena contracta area. *Echocardiography* 21(8):737-743, 2004.
14. Siu SC, Levine RA, Rivera JM, et al: Three-dimensional echocardiography improves noninvasive assessment of left ventricular volume and performance. *Am Heart J* 130(4):812-822, 1995.
15. Siu SC, Rivera JM, Handschumacher MD, et al: Three-dimensional echocardiography: the influence of number of component images on accuracy of left ventricular volume quantitation. *J Am Soc Echocardiogr* 9(2):147-155, 1996.
16. Weyman AE: Cross-sectional scanning: Technical principles and instrumentation (Ch 2). In Weyman AE, editor: *Principles and practice of echocardiography*, ed 2, Philadelphia, 1993, Lea & Febiger.
17. Erbel R, Schweizer P, Lambertz H, et al: Echoventriculography-a simultaneous analysis of two-dimensional echocardiography and cineventriculography. *Circulation* 67(1):205-215, 1983.
18. Schnittger I, Fitzgerald PJ, Daughters GT, et al: Limitations of comparing left ventricular volumes by two dimensional echocardiography, myocardial markers and cineangiography. *Am J Cardiol* 50(3):512-519, 1982.
19. Mannaerts HF, Van Der Heide JA, Kamp O, et al: Quantification of left ventricular volumes and ejection fraction using freehand transthoracic three-dimensional echocardiography:

Comparison with magnetic resonance imaging. *J Am Soc Echocardiogr* 16(2):101-109, 2003.
20. Mor-Avi V, Jenkins C, Kühl, et al: Real-time 3-dimensional echocardiographic quantification of left ventricular volumes. *J Am Coll Cardiol Img* 1(4):413-423, 2008.
21. Fleming SM, Cumberledge B, Kiesewetter C, et al: Usefulness of real-time three-dimensional echocardiography for reliable measurement of cardiac output in patients with ischemic or idiopathic dilated cardiomyopathy. *Am J Cardiol* 95(2):308-310, 2005.
22. Qin JX, Jones M, Shiota T, et al: Validation of real-time three-dimensional echocardiography for quantifying left ventricular volumes in the presence of a left ventricular aneurysm: in vitro and in vivo studies. *J Am Coll Cardiol* 36(3):900-907, 2000.
23. Zeidan Z, Erbel R, Barkhausen J, et al: Analysis of global systolic and diastolic left ventricular performance using volume-time curves by real-time three-dimensional echocardiography. *J Am Soc Echocardiogr* 16(1):29-37, 2003.
24. Corsi C, Lang RM, Veronesi F, et al: Volumetric quantification of global and regional left ventricular function from real-time three-dimensional echocardiographic images. *Circulation* 112(8):1161-1170, 2005.
25. Gopal AS, Chukwu EO, Mihalatos DG, et al: Left ventricular structure and function for post myocardial infarction and heart failure risk stratification by three-dimensional echocardiography. *J Am Soc Echocardiogr* 20(8):949-958, 2007.
26. Hare JL, Jenkins C, Nakatani S, et al: Feasibility and clinical decision-making with 3D echocardiography in routine practice. *Heart* 94(4):440-445, 2008.
27. Jenkins C, Moir S, Chan J, et al: Left ventricular volume measurement with echocardiography: a comparison of left ventricular opacification, three-dimensional echocardiography, or both with magnetic resonance imaging. *Eur Heart J* 30(1):98-106, 2009.
28. Macron L, Lim P, Bensaid A, et al: Single-beat versus multibeat real-time 3D echocardiography for assessing left ventricular volumes and ejection fraction: a comparison study with cardiac magnetic resonance. *Circ Cardiovasc Imaging* 3(4):450-455, 2010.
29. Takeuchi M, Nishikage T, Mor-Avi V, et al: Measurement of left ventricular mass by real-time three-dimensional echocardiography: validation against magnetic resonance and comparison with two-dimensional and m-mode measurements. *J Am Soc Echocardiogr* 21(9):1001-1005, 2008.
30. Oe H, Hozumi T, Arai K, et al: Comparison of accurate measurement of left ventricular mass in patients with hypertrophied hearts by real-time three-dimensional echocardiography versus magnetic resonance imaging. *Am J Cardiol* 95(10):1263-1267, 2005.
31. Qin JX, Jones M, Travaglini A, et al: The accuracy of left ventricular mass determined by real-time three-dimensional echocardiography in chronic animal and clinical studies: a comparison with postmortem examination and magnetic resonance imaging. *J Am Soc Echocardiogr* 18(10):1037-1043, 2005.
32. Pouleur AC, le Polain de Waroux JB, Pasquet A, et al: Assessment of left ventricular mass and volumes by three-dimensional echocardiography in patients with or without wall motion abnormalities: comparison against cine magnetic resonance imaging. *Heart* 94(8):1050-1057, 2008.
33. Van den Bosch AE, Robbers-Visser D, Krenning BJ, et al: Comparison of real-time three-dimensional echocardiography to magnetic resonance imaging for assessment of left ventricular mass. *Am J Cardiol* 97(1):113-117, 2006.
34. Galzerano D, Tammaro P, Cerciello A, et al: Freehand three-dimensional echocardiographic evaluation of the effect of telmisartan compared with hydrochlorothiazide on left ventricular mass in hypertensive patients with mild-to-moderate hypertension: A multicentre study. *J Hum Hypertens* 18(1):53-59, 2004.
35. Hoch M, Vasilyev NV, Soriano B, et al: Variables influencing the accuracy of right ventricular volume assessment by real-time 3-dimensional echocardiography: an in vitro validation study. *J Am Soc Echocardiogr* 20(5):456-461, 2007.
36. Tamborini G, Brusoni D, Torres Molina JE, et al: Feasibility of new generation three-dimensional echocardiography for right ventricular volumetric and functional measurements. *Am J Cardiol* 102(4):499-505, 2008.
37. Tamborini G, Marsan NA, Gripari P, et al: Reference values for right ventricular volumes and ejection fraction with real-time three-dimensional echocardiography: evaluation In a large series of normal subjects. *J Am Soc Echocardiogr* 23(2):109-115, 2010.
38. Prakasa KR, Dalal D, Wang J, et al: Feasibility and variability of three dimensional echocardiography in arrhythmogenic right ventricular dysplasia/cardiomyopathy. *Am J Cardiol* 97(5):703-709, 2006.
39. Sukmawan R, Akasaka T, Watanabe N, et al: Quantitative assessment of right ventricular geometric remodeling in pulmonary hypertension secondary to left-sided heart disease using real-time three-dimensional echocardiography. *Am J Cardiol* 94(8):1096-1099, 2004.
40. Van der Zwaan HB, Helbing WA, McGhie JS, et al: Clinical value of real-time three-dimensional echocardiography for right ventricular quantification in congenital heart disease: validation with cardiac magnetic resonance imaging. *J Am Soc Echocardiogr* 23(2):134-140, 2010.
41. Tsang TS, Abhayaratna WP, Barnes ME, et al: Prediction of cardiovascular outcomes with left atrial size: Is volume superior to area or diameter? *J Am Coll Cardiol* 47(5):1018-1023, 2006.
42. Lang RM, Bierig M, Devereux RB, et al: Recommendations for chamber quantification: a report from the American Society of Echocardiography's Guidelines and Standards Committee and the Chamber Quantification Writing Group, developed in conjunction with the European Association of Echocardiography, a branch of the European Society of Cardiology. *J Am Soc Echocardiogr* 18(12):1440-1463, 2005.
43. Maddukuri PV, Vieira ML, DeCastro S, et al: What is the best approach for the assessment of left atrial size? Comparison of various unidimensional and two-dimensional parameters with three-dimensional echocardiographically determined left atrial volume. *J Am Soc Echocardiogr* 19(8):1026-1032, 2006.
44. Keller AM, Gopal AS, King DL: Left and right atrial volume by freehand three-dimensional echocardiography: In vivo validation using magnetic resonance imaging. *Eur J Echocardiogr* 1(1):55-65, 2000.
45. Poutanen T, Ikonen A, Vainio P, et al: Left atrial volume assessed by transthoracic three dimensional echocardiography and magnetic resonance imaging: Dynamic changes during the heart cycle in children. *Heart* 83(5):537-542, 2000.
46. Spencer KT, Mor-Avi V, Gorcsan J, III, et al: Effects of aging on left atrial reservoir, conduit, and booster pump function: a multi-institution acoustic quantification study. *Heart* 85(3):272-277, 2001.
47. Anwar AM, Geleijnse ML, Soliman OI, et al: Left atrial Frank-Starling law assessed by real-time, three-dimensional echocardiographic left atrial volume changes. *Heart* 93(11):1393-1397, 2007.
48. Anwar AM, Soliman OI, Geleijnse ML, et al: Assessment of left atrial volume and function by real-time three-dimensional echocardiography. *Int J Cardiol* 123(2):155-161, 2008.
49. Suh IW, Song JM, Lee EY, et al: Left atrial volume measured by real-time 3-dimensional echocardiography predicts clinical outcomes in patients with severe left ventricular dysfunction and in sinus rhythm. *J Am Soc Echocardiogr* 21(5):439-445, 2008.
50. Caselli S, Canali E, Foschi ML, et al: Long-term prognostic significance of three-dimensional echocardiographic parameters of the left ventricle and left atrium. *Eur J Echocardiogr* 11(3):250-256, 2010.
51. Eshoo S, Semsarian C, Ross DL, et al: Left atrial phasic volumes are modulated by the type rather than the extent of left ventricular hypertrophy. *J Am Soc Echocardiogr* 23(5):538-544, 2010.
52. Shah SJ, Bardo DM, Sugeng L, et al: Real-time three-dimensional echocardiography of the left atrial appendage: initial experience in the clinical setting. *J Am Soc Echocardiogr* 21(12):1362-1368, 2008.
53. Muller H, Burri H, Lerch R: Evaluation of right atrial size in patients with atrial arrhythmias: comparison of 2D versus real time 3D echocardiography. *Echocardiography* 25(6):617-623, 2008.
54. Faletra FF, Ho SY, Auricchio A: Anatomy of right atrial structures by real-time 3D transesophageal echocardiography. *J Am Coll Cardiol Img* 3(9):966-975, 2010.
55. Jungwirth B, Mackensen GB: Real-time 3-dimensional echocardiography in the operating room. *Semin Cardiothorac Vasc Anesth* 12(4):248-264, 2008.
56. Sugeng L, Coon P, Weinert L, et al: Use of real-time 3-dimensional transthoracic echocardiography in the evaluation of mitral valve disease. *J Am Soc Echocardiogr* 19(4):413-421, 2006.
57. Sugeng L, Shernan SK, Salgo IS, et al: Live 3-dimensional transesophageal echocardiography initial experience using the fully-sampled matrix array probe. *J Am Coll Cardiol* 52(6):446-449, 2008.
58. Thomas JD, Wilkins GT, Choong CY, et al: Inaccuracy of mitral pressure half-time immediately after percutaneous mitral valvotomy: Dependence on transmitral gradient and left atrial and ventricular compliance. *Circulation* 78(4):980-993, 1988.
59. Binder TM, Rosenhek R, Porenta G, et al: Improved assessment of mitral valve stenosis by volumetric real-time three-dimensional echocardiography. *J Am Coll Cardiol* 36(4):1355-1361, 2000.
60. Chen Q, Nosir YF, Vletter WB, et al: Accurate assessment of mitral valve area in patients with

mitral stenosis by three-dimensional echocardiography. *J Am Soc Echocardiogr* 10(2):133-140, 1997.
61. Zamorano J, Cordeiro P, Sugeng L, et al: Real-time three-dimensional echocardiography for rheumatic mitral valve stenosis evaluation: An accurate and novel approach. *J Am Coll Cardiol* 43(11):2091-2096, 2004.
62. Sebag IA, Morgan JG, Handschumacher MD, et al: Usefulness of three-dimensionally guided assessment of mitral stenosis using matrix-array ultrasound. *Am J Cardiol* 96(8):1151-1156, 2005.
63. Anwar AM, Attia WM, Nosir YF, et al: Validation of a new score for the assessment of mitral stenosis using real-time three-dimensional echocardiography. *J Am Soc Echocardiogr* 23(1):13-22, 2010.
64. Langerveld J, Valocik G, Plokker HW, et al: Additional value of three-dimensional transesophageal echocardiography for patients with mitral valve stenosis undergoing balloon valvuloplasty. *J Am Soc Echocardiogr* 16(8):841-849, 2003.
65. Zamorano J, Perez de Isla L, Sugeng L, et al: Non-invasive assessment of mitral valve area during percutaneous balloon mitral valvuloplasty: role of real-time 3D echocardiography. *Eur Heart J* 25(23):2086-2091, 2004.
66. Sitges M, Jones M, Shiota T, et al: Real-time three-dimensional color Doppler evaluation of the flow convergence zone for quantification of mitral regurgitation: Validation experimental animal study and initial clinical experience. *J Am Soc Echocardiogr* 16(1):38-45, 2003.
67. Yosefy C, Levine RA, Vaturi M, et al: Real-time 3D echo can enhance assessment of the vena contracta width: overcoming the problem of oblique measurement in eccentric jets. *Circulation* 110(Suppl III):746, 2004.
68. Yosefy C, Levine RA, Solis-Martin J, et al: Proximal flow convergence region as assessed by real-time 3D echocardiography: Challenging the hemispherical assumption. *J Am Soc Echocardiogr* 20(4):389-396, 2007.
69. Marsan NA, Westenberg JJ, Ypenburg C, et al: Quantification of functional mitral regurgitation by real-time 3D echocardiography: comparison with 3D velocity-encoded cardiac magnetic resonance. *J Am Coll Cardiol Img* 2(11):1245-1252, 2009.
70. Shanks M, Siebelink HM, Delgado V, et al: Quantitative assessment of mitral regurgitation: comparison between three-dimensional transesophageal echocardiography and magnetic resonance imaging. *Circ Cardiovasc Imaging* 3(6):694-700, 2010.
71. Little SH, Pirat B, Kumar R, et al: Three-dimensional color Doppler echocardiography for direct measurement of vena contracta area in mitral regurgitation: in vitro validation and clinical experience. *J Am Coll Cardiol Img* 1(6):695-704, 2008.
72. Salustri A, Becker AE, van Herwerden L, et al: Three-dimensional echocardiography of normal and pathologic mitral valve: A comparison with two-dimensional transesophageal echocardiography. *J Am Coll Cardiol* 27(6):1502-1510, 1996.
73. Chauvel C, Bogino E, Clerc P, et al: Usefulness of three-dimensional echocardiography for the evaluation of mitral valve prolapse: An intraoperative study. *J Heart Valve Dis* 9(3):341-349, 2000.
74. Sharma R, Mann J, Drummond L, et al: The evaluation of real-time 3-dimensional transthoracic echocardiography for the preoperative functional assessment of patients with mitral valve prolapse: a comparison with 2-dimensional transesophageal echocardiography. *J Am Soc Echocardiogr* 20(8):934-940, 2007.
75. Gutierrez-Chico JL, Zamorano Gomez JL, Rodrigo-Lopez JL, et al: Accuracy of real-time 3-dimensional echocardiography in the assessment of mitral prolapse. Is transesophageal echocardiography still mandatory? *Am Heart J* 155(4):694-698, 2008.
76. Grewal J, Mankad S, Freeman WK, et al: Real-time three-dimensional transesophageal echocardiography in the intraoperative assessment of mitral valve disease. *J Am Soc Echocardiogr* 22(1):34-41, 2009.
77. Salcedo EE, Quaife RA, Seres T, et al: A framework for systematic characterization of the mitral valve by real-time three-dimensional transesophageal echocardiography. *J Am Soc Echocardiogr* 22(10):1087-1099, 2009.
78. Anwar AM, Soliman OI, Nemes A, et al: Assessment of mitral annulus size and function by real-time 3-dimensional echocardiography in cardiomyopathy: comparison with magnetic resonance imaging. *J Am Soc Echocardiogr* 20(8):941-948, 2007.
79. Otsuji Y, Handschumacher MD, Schwammenthal E, et al: Insights from three-dimensional echocardiography into the mechanism of functional mitral regurgitation: Direct in vivo demonstration of altered leaflet tethering geometry. *Circulation* 96(6):1999-2008, 1997.
80. Otsuji Y, Handschumacher MD, Liel-Cohen N, et al: Mechanism of ischemic mitral regurgitation with segmental left ventricular dysfunction: Three-dimensional echocardiographic studies in models of acute and chronic progressive regurgitation. *J Am Coll Cardiol* 37(2):641-648, 2001.
81. Hung J, Guerrero JL, Handschumacher MD, et al: Reverse ventricular remodeling reduces ischemic mitral regurgitation: Echo-guided device application in the beating heart. *Circulation* 106(20):2594-2600, 2002.
82. Kwan J, Shiota T, Agler DA, et al: Geometric differences of the mitral apparatus between ischemic and dilated cardiomyopathy with significant mitral regurgitation: Real-time three-dimensional echocardiography study. *Circulation* 107(8):1135-1140, 2003.
83. Veronesi F, Corsi C, Sugeng L, et al: Quantification of mitral apparatus dynamics in function and ischemic mitral regurgitation using real-time 3-dimensional echocardiography. *J Am Soc Echocardiogr* 21(4):347-354, 2008.
84. Ahmad RM, Gillinov AM, McCarthy PM, et al: Annular geometry and motion in human ischemic mitral regurgitation: Novel assessment with three-dimensional echocardiography and computer reconstruction. *Ann Thorac Surg* 78(6):2063-2068; discussion 8, 2004.
85. Watanabe N, Ogasawara Y, Yamaura Y, et al: Geometric deformity of the mitral annulus in patients with ischemic mitral regurgitation: A real-time three-dimensional echocardiographic study. *J Heart Valve Dis* 14(4):447-452, 2005.
86. Daimon M, Shiota T, Gillinov AM, et al: Percutaneous mitral valve repair for chronic ischemic mitral regurgitation: A real-time three-dimensional echocardiographic study in an ovine model. *Circulation* 111(17):2183-2189, 2005.
87. Messas E, Bel A, Szymanski C, et al: Relief of mitral leaflet tethering following chronic myocardial infarction by chordal cutting diminishes left ventricular remodeling. *Circ Cardiovasc Imaging* 3(6):679-686, 2010.
88. Qin JX, Shiota T, McCarthy PM, et al: Importance of mitral valve repair associated with left ventricular reconstruction for patients with ischemic cardiomyopathy: A real-time three-dimensional echocardiographic study. *Circulation* 108(Suppl 1):11241-11246, 2003.
89. Langer F, Rodriguez F, Ortiz S, et al: Subvalvular repair: The key to repairing ischemic mitral regurgitation? *Circulation* 112(9 Suppl):I383-I389, 2005.
90. Acker MA, Bolling S, Shemin R, et al: Mitral valve surgery in heart failure: Insights from the Acorn Clinical Trial. *J Thorac Cardiovasc Surg* 132(3):568-577, 77 e1-e4, 2006.
91. Sugeng L, Shernan SK, Weinert L, et al: Real-time three-dimensional transesophageal echocardiography in valve disease: comparison with surgical findings and evaluation of prosthetic valves. *J Am Soc Echocardiogr* 21(12):1347-1354, 2008.
92. Kronzon I, Sugeng L, Perk G, et al: Real-time 3-dimensional transesophageal echocardiography in the evaluation of post-operative mitral annuloplasty ring and prosthetic valve dehiscence. *J Am Coll Cardiol* 53(17):1543-1547, 2009.
93. Nanda NC, Roychoudhury D, Chung SM, et al: Quantitative assessment of normal and stenotic aortic valve using transesophageal three-dimensional echocardiography. *Echocardiography* 11(6):617-625, 1994.
94. Menzel T, Mohr-Kahaly S, Kolsch B, et al: Quantitative assessment of aortic stenosis by three-dimensional echocardiography. *J Am Soc Echocardiogr* 10(3):215-223, 1997.
95. Ge S, Warner JG, Jr, Abraham TP, et al: Three-dimensional surface area of the aortic valve orifice by three-dimensional echocardiography: Clinical validation of a novel index for assessment of aortic stenosis. *Am Heart J* 136(6):1042-1050, 1998.
96. Fyfe DA, Ludomirsky A, Sandhu S, et al: Left ventricular outflow tract obstruction defined by active three-dimensional echocardiography using rotational transthoracic acquisition. *Echocardiography* 11(6):607-615, 1994.
97. Miyamoto K, Nakatani S, Kanzaki H, et al: Detection of discrete subaortic stenosis by 3-dimensional transesophageal echocardiography. *Echocardiography* 22(9):783-784, 2005.
98. Sitges M, Qin JX, Lever HM, et al: Evaluation of left ventricular outflow tract area after septal reduction in obstructive hypertrophic cardiomyopathy: A real-time 3-dimensional echocardiographic study. *Am Heart J* 150(4):852-858, 2005.
99. Acar P, Jones M, Shiota T, et al: Quantitative assessment of chronic aortic regurgitation with 3-dimensional echocardiographic reconstruction: Comparison with electromagnetic flowmeter measurements. *J Am Soc Echocardiogr* 12(2):138-148, 1999.
100. Shiota T, Jones M, Tsujino H, et al: Quantitative analysis of aortic regurgitation: Real-time 3-dimensional and 2-dimensional color Doppler echocardiographic method—a clinical and a chronic animal study. *J Am Soc Echocardiogr* 15(9):966-971, 2002.
101. Sato Y, Kamata J, Izumoto H, et al: Morphological analysis of aortic root in eccentric aortic regurgitation using anyplane two-dimensional images produced by transesophageal three-dimensional echocardiography. *J Heart Valve Dis* 12(2):186-196, 2003.

102. Goland S, Trento A, Iida K, et al: Assessment of aortic stenosis by three-dimensional echocardiography: an accurate and novel approach. *Heart* 93(7):801-807, 2007.
103. Nikai H, Takeuchi M, Yoshitani H, et al: Pitfalls of anatomical aortic valve area measurements using two-dimensional transoesophageal echocardiography and the potential of three-dimensional transoesophageal echocardiography. *Eur J Echocardiogr* 11(4):369-376, 2010.
104. de la Morena G, Saura D, Oliva MJ, et al: Real-time three-dimensional transoesophageal echocardiography in the assessment of aortic valve stenosis. *Eur J Echocardiogr* 11(1):9-13, 2010.
105. Blot-Souletie N, Hebrard A, Acar P, et al: Comparison of accuracy of aortic valve area assessment in aortic stenosis by real time three-dimensional echocardiography in biplane mode versus two-dimensional transthoracic and transesophageal echocardiography. *Echocardiography* 24(10):1065-1072, 2007.
106. Doddamani S, Bello R, Friedman MA, et al: Demonstration of left ventricular outflow tract eccentricity by real time 3D echocardiography: implications for the determination of aortic valve area. *Echocardiography* 24(8):860-866, 2007.
107. Poh KK, Levine RA, Solis J, et al: Assessing aortic valve area in aortic stenosis by continuity equation: a novel approach using real-time three-dimensional echocardiography. *Eur Heart J* 29(20):2526-2535, 2008.
108. Gutierrez-Chico JL, Zamorano JL, Prieto-Moriche E, et al: Real-time three-dimensional echocardiography In aortic stenosis: a novel, simple, and reliable method to improve accuracy in area calculation. *Eur Heart J* 29(10): 1296-1306, 2008.
109. Fang L, Hsiung MC, Miller AP, et al: Assessment of aortic regurgitation by live three-dimensional transthoracic echocardiographic measurements of vena contracta area: Usefulness and validation. *Echocardiography* 22(9): 775-781, 2005.
110. Chin CH, Chin CH, Lo HS: The correlation between three-dimensional vena contracta area and aortic regurgitation index in patients with aortic regurgitation. *Echocardiography* 27(2):161-166, 2010.
111. Pirat B, Little SH, Igo SR, et al: Direct measurement of proximal isovelocity surface area by real-time three-dimensional color Doppler for quantitation of aortic regurgitant volume: an in vitro validation. *J Am Soc Echocardiogr* 22(3):306-313, 2009.
112. Li X, Jones M, Irvine T, et al: Real-time 3-dimensional echocardiography for quantification of the difference in left ventricular versus right ventricular stroke volume in a chronic animal model study: Improved results using C-scans for quantifying aortic regurgitation. *J Am Soc Echocardiogr* 17(8):870-875, 2004.
113. Alsoufi B, Borger MA, Armstrong S, et al: Results of valve preservation and repair for bicuspid aortic valve insufficiency. *J Heart Valve Dis* 14(6):752-758; discussion 8-9, 2005.
114. Gonzalez-Ferrer JJ, Fernandez-Jimenez R, Perez de Isla L, et al: Rocking aortic valve prosthesis: a 3-dimensional transesophageal echocardiography view. *J Am Coll Cardiol* 55(17):e135, 2010.
115. Bagur R, Rodes-Cabau J, Doyle D, et al: Usefulness of TEE as the primary imaging technique to guide transcatheter transapical aortic valve implantation. *J Am Coll Cardiol Img* 4(2):115-124, 2011.
116. Anwar AM, Geleijnse ML, Soliman OI, et al: Assessment of normal tricuspid valve anatomy in adults by real-time three dimensional echocardiography. *Int J Cardiovasc Imaging* 23(6):717-724, 2007.
117. Kwan J, Kim GC, Jeon MJ, et al: 3D geometry of a normal tricuspid annulus during systole: a comparison study with the mitral annulus using real-time 3D echocardiography. *Eur J Echocardiogr* 8(5):375-383, 2007.
118. Ton-Nu TT, Levine RA, Handschumacher MD, et al: Geometric determinants of functional tricuspid regurgitation: insights from 3-dimensional echocardiography. *Circulation* 114(2):143-149, 2006.
119. Sukmawan R, Watanabe N, Ogasawara Y, et al: Geometric changes of tricuspid valve tenting in tricuspid regurgitation secondary to pulmonary hypertension quantified by a novel system with transthoracic real-time 3-dimensional echocardiography. *J Am Soc Echocardiogr* 20(5):470-476, 2007.
120. Anwar AM, Geleijnse ML, Soliman OI, et al: Evaluation of rheumatic tricuspid valve stenosis by real-time three-dimensional echocardiography. *Heart* 93(3):363-364, 2007.
121. Bhattacharyya S, Toumpanakis C, Burke M, et al: Features of carcinoid heart disease identified by 2- and 3-dimensional echocardiography and cardiac MRI. *Circ Cardiovasc Imaging* 3(1):103-111, 2010.
122. Takahashi K, Inage A, Rebeyka IM, et al: Real-time 3-dimensional echocardiography provides new insight into mechanisms of tricuspid valve regurgitation in patients with hypoplastic left heart syndrome. *Circulation* 120(12):1091-1098, 2009.
123. Nii M, Guerra V, Roman KS, et al: Three-dimensional tricuspid annular function provides insight into the mechanisms of tricuspid valve regurgitation in classic hypoplastic left heart syndrome. *J Am Soc Echocardiogr* 19(4):391-402, 2006.
124. Anwar AM, Soliman O, van den Bosch AE, et al: Assessment of pulmonary valve and right ventricular outflow tract with real-time three-dimensional echocardiography. *Int J Cardiovasc Imaging* 23(2):167-175, 2007.
125. Pothineni KR, Wells BJ, Hisung MC, et al: Live/real time three-dimensional transthoracic echocardiographic assessment of pulmonary regurgitation. *Echocardiography* 25(8):911-917, 2008.
126. Lee KJ, Connolly HM, Pellikka PA: Carcinoid pulmonary valvulopathy evaluated by real-time 3-dimensional transthoracic echocardiography. *J Am Soc Echocardiogr* 21(4): 407.e1-2, 2008.
127. Balestrini L, Fleishman C, Lanzoni L, et al: Real-time 3-dimensional echocardiography evaluation of congenital heart disease. *J Am Soc Echocardiogr* 13(3):171-176, 2000.
128. Seliem MA, Fedec A, Cohen MS, et al: Real-time 3-dimensional echocardiographic imaging of congenital heart disease using matrix-array technology: Freehand real-time scanning adds instant morphologic details not well delineated by conventional 2-dimensional imaging. *J Am Soc Echocardiogr* 19(2):121-129, 2006.
129. De Castro S, Caselli S, Papetti F, et al: Feasibility and clinical impact of live three-dimensional echocardiography in the management of congenital heart disease. *Echocardiography* 23(7): 553-561, 2006.
130. Riehle TJ, Mahle WT, Parks WJ, et al: Real-time three-dimensional echocardiographic acquisition and quantification of left ventricular indices in children and young adults with congenital heart disease: comparison with magnetic resonance imaging. *J Am Soc Echocardiogr* 21(1):78-83, 2008.
131. Grison A, Maschietto N, Reffo E, et al: Three-dimensional echocardiographic evaluation of right ventricular volume and function in pediatric patients: validation of the technique. *J Am Soc Echocardiogr* 20(8):921-929, 2007.
132. Soriano BD, Hoch M, Ithuralde A, et al: Matrix-array 3-dimensional echocardiographic assessment of volumes, mass, and ejection fraction in young pediatric patients with a functional single ventricle: a comparison study with cardiac magnetic resonance. *Circulation* 117(14):1842-1848, 2008.
133. Takahashi K, Mackie AS, Rebeyka IM, et al: Two-dimensional versus transthoracic real-time three-dimensional echocardiography in the evaluation of the mechanisms and site of atrioventricular valve regurgitation in a congenital heart disease population. *J Am Soc Echocardiogr* 23(7):726-734, 2010.
134. Ozkan M, Kava H, Duran NE, et al: Depiction of a cleft mitral valve by real time three-dimensional transesophageal echocardiography. *Echocardiography* 27(3):356-358, 2010.
135. Bharucha T, Anderson RH, Lim ZS, et al: Multiplanar review of three-dimensional echocardiography gives new insights into the morphology of Ebstein's malformation. *Cardiol Young* 20(1):49-53, 2010.
136. Marx GR, Fulton DR, Pandian NG, et al: Delineation of site, relative size and dynamic geometry of atrial septal defects by real-time three-dimensional echocardiography. *J Am Coll Cardiol* 25(2):482-490, 1995.
137. Johri AM, Witzke C, Solis J, et al: Real-time three dimensional transesophageal echocardiography in patients with secundum atrial septal defects: outcomes following transcatheter closure. *J Am Soc Echocardiogr* 24(4):431-437, 2011 .
138. Mehmood F, Vengala S, Nanda NC, et al: Usefulness of live three-dimensional transthoracic echocardiography in the characterization of atrial septal defects in adults. *Echocardiography* 21(8):707-713, 2004.
139. Hofmann T, Franzen O, Koschyk DH, et al: Three-dimensional color Doppler echocardiography for assessing shunt volume in atrial septal defects. *J Am Soc Echocardiogr* 17(11):1173-1178, 2004.
140. Nanda NC, Ansingkar K, Espinal M, et al: Transesophageal three-dimensional echo assessment of sinus venosus atrial septal defect. *Echocardiography* 16(8):835-837, 1999.
141. Vargas-Barron J, Espinola-Zavaleta N, Romero-Cardenas A, et al: Two- and three-dimensional echocardiographic unroofed coronary sinus. *J Am Soc Echocardiogr* 14(7):742-744, 2001.
142. Barrea C, Levasseur S, Roman K, et al: Three-dimensional echocardiography improves the understanding of left atrioventricular valve morphology and function in atrioventricular septal defects undergoing patch augmentation. *J Thorac Cardiovasc Surg* 129(4):746-753, 2005.
143. Van den Bosch AE, Ten Harkel DJ, McGhie JS, et al: Feasibility and accuracy of real-time 3-dimensional echocardiographic assessment of ventricular septal defects. *J Am Soc Echocardiogr* 19(1):7-13, 2006.

144. Ge S: How can we best image congenital heart defects? Are two-dimensional and three-dimensional echocardiography competitive or complementary? *J Am Soc Echocardiogr* 23(7):722-725, 2010.
145. Rana BS, Thomas MR, Calvert PA, et al: Echocardiographic evaluation of patent foramen ovale prior to device closure. *J Am Coll Cardiol Img* 3(7):749-760, 2010.
146. Halpern DG, Perk G, Ruiz C, et al: Percutaneous closure of a post-myocardial infarction ventricular septal defect guided by real-time three-dimensional echocardiography. *Eur J Echocardiogr* 10(4):569-571, 2009.
147. Perk G, Lang RM, Garcia-Fernandez MA, et al: Use of real time three-dimensional transesophageal echocardiography In intracardiac catheter based interventions. *J Am Soc Echocardiogr* 22(8):865-882, 2009.
148. Amitai ME, Schnittger I, Popp RL, et al: Comparison of three-dimensional echocardiography to two-dimensional echocardiography and fluoroscopy for monitoring of endomyocardial biopsy. *Am J Cardiol* 99(6):864-866, 2007.
149. Chen FL, Hsiung MC, Hsieh KS, et al: Real time three-dimensional transthoracic echocardiography for guiding Amplatzer septal occlude device deployment in patients with atrial septal defect. *Echocardiography* 23(9):763-770, 2006.
150. Taniguchi M, Akagi T, Watanabe N, et al: Application of real-time three-dimensional transesophageal echocardiography using a matrix array probe for transcatheter closure of atrial septal defect. *J Am Soc Echocardiogr* 22(10):1114-1120, 2009.
151. Kijima Y, Taniguchi M, Akagi T, et al: Torn atrial septum during transcatheter closure of atrial septal defect visualized by real-time three-dimensional transesophageal echocardiography. *J Am Soc Echocardiogr* 23(11):1222.e5-8, 2010.
152. Balzer J, van Hall S, Rassaf T, et al: Feasibility, safety, and efficacy of real-time three-dimensional transoesophageal echocardiography for guiding device closure of interatrial communications: initial clinical experience and impact on radiation exposure. *Eur J Echocardiogr* 1(11):1-8, 2010.
153. Sack S, Kahlert P, Bilodeau L, et al: Percutaneous transvenous mitral annuloplasty: initial human experience with a novel coronary sinus implant device. *Circ Cardiovasc Interv* 2(4):277-284, 2009.
154. Naqvi TZ: Echocardiography in percutaneous valve therapy. *J Am Coll Cardiol Img* 2(10):1226-1237, 2009.
155. Pedrazzini GB, Klimusina J, Pasotti E, et al: Complications of percutaneous edge-to-edge mitral valve repair: the role of real-time three-dimensional transesophageal echocardiography. *J Am Soc Echocardiogr* 24(6):706.e5-e7, 2010.
156. Garcia-Fernandez MA, Cortes M, Garcia-Robles JA, et al: Utility of real-time three-dimensional transesophageal echocardiography in evaluating the success of percutaneous closure of mitral paravalvular leaks. *J Am Soc Echocardiogr* 23(1):26-32, 2010.
157. Leon MB, Smith CR, Mack M, et al: Transcatheter aortic-valve implantation for aortic stenosis in patients who cannot undergo surgery. *N Engl J Med* 363(17):1597-1607, 2010.
158. Ng AC, Delgado V, van der Kley F, et al: Comparison of aortic root dimensions and geometries before and after transcatheter aortic valve implantation by 2- and 3-dimensional transesophageal echocardiography and multislice computed tomography. *Circ Cardiovasc Imaging* 3(1):94-102, 2010.
159. Chierchia GB, Capulzini L, de Asmundis C, et al: First experience with real-time three-dimensional transoesophageal echocardiography-guided transseptal in patients undergoing atrial fibrillation ablation. *Europace* 10(11):1325-1328, 2008.
160. Reddy VY, Holmes D, Doshi SK, et al: Safety of percutaneous left atrial appendage closure: results from the Watchman left atrial appendage system for embolic protection in patients with AF (PROTECT AF) clinical trial and the continued access registry. *Circulation* 123(4):417-424, 2011.
161. Zwas DR, Takuma S, Mullis-Jansson S, et al: Feasibility of real-time 3-dimensional treadmill stress echocardiography. *J Am Soc Echocardiogr* 12(5):285-289, 1999.
162. Pulerwitz T, Hirata K, Abe Y, et al: Feasibility of using a real-time 3-dimensional technique for contrast dobutamine stress echocardiography. *J Am Soc Echocardiogr* 19(5):540-545, 2006.
163. Badano LP, Muraru D, Rigo F, et al: High volume-rate three-dimensional stress echocardiography to assess inducible myocardial ischemia: a feasibility study. *J Am Soc Echocardiogr* 23(6):628-635, 2010.
164. Aggeli C, Giannopoulos G, Misovoulos P, et al: Real-time three-dimensional dobutamine stress echocardiography for coronary artery disease diagnosis: validation with coronary angiography. *Heart* 93(6):672-675, 2007.
165. Jenkins C, Haluska B, Marwick TH: Assessment of temporal heterogeneity and regional motion to identify wall motion abnormalities using treadmill exercise stress three-dimensional echocardiography. *J Am Soc Echocardiogr* 22(3):268-275, 2009.
166. Yoshitani H, Takeuchi M, Mor-Avi V, et al: Comparative diagnostic accuracy of multiplane and multislice three-dimensional dobutamine stress echocardiography in the diagnosis of coronary artery disease. *J Am Soc Echocardiogr* 22(5):437-442, 2009.
167. Peteiro J, Pinon P, Perez R, et al: Comparison of 2- and 3-dimensional exercise echocardiography for the detection of coronary artery disease. *J Am Soc Echocardiogr* 20(8):959-967, 2007.
168. Takeuchi M, Otani S, Weinert L, et al: Comparison of contrast-enhanced real-time live 3-dimensional dobutamine stress echocardiography with contrast 2-dimensional echocardiography for detecting stress-induced wall-motion abnormalities. *J Am Soc Echocardiogr* 19(3):294-299, 2006.
169. Nemes A, Geleijnse ML, Krenning BJ, et al: Usefulness of ultrasound contrast agent to improve image quality during real-time three-dimensional stress echocardiography. *Am J Cardiol* 99(2):275-278, 2007.
170. Cleland JG, Daubert JC, Erdmann E, et al: The effect of cardiac resynchronization on morbidity and mortality In heart failure. *N Engl J Med* 352(15):1539-1549, 2005.
171. Chung ES, Leon AR, Tavazzi L, et al: Results of the predictors of response to CRT (PROSPECT) trial. *Circulation* 117(20):2608-2616, 2008.
172. Takeuchi M, Jacobs A, Sugeng L, et al: Assessment of left ventricular dyssynchrony with real-time 3-dimensional echocardiography: comparison with Doppler tissue imaging. *J Am Soc Echocardiogr* 20(12):1321-1329, 2007.
173. Liodakis E, Sharef OA, Dawson D, et al: The use of real-time three-dimensional echocardiography for assessing mechanical synchronicity. *Heart* 95(22):1865-1871, 2009.
174. Soliman OI, van Dalen BM, Nemes A, et al: Quantification of left ventricular systolic dyssynchrony by real-time three-dimensional echocardiography. *J Am Soc Echocardiogr* 22(3):232-239, 2009.
175. Kapetanakis S, Kearney MT, Siva A, et al: Real-time three-dimensional echocardiography: a novel technique to quantify global left ventricular mechanical dyssynchrony. *Circulation* 112(7):992-1000, 2005.
176. Kapetanakis S, Bhan A, Murgatroyd F, et al: Real-time 3D echo in patient selection for cardiac resynchronization therapy. *J Am Coll Cardiol Img* 4(1):16-26, 2011.
177. Marsan NA, Bleeker GB, Ypenburg C, et al: Real-time three-dimensional echocardiography as a novel approach to assess left ventricular and left atrium reverse remodeling and to predict response to cardiac resynchronization therapy. *Heart Rhythm* 5(9):1257-1264, 2008.
178. Soliman OI, Geleijnse ML, Theuns DA, et al: Usefulness of left ventricular systolic dyssynchrony by real-time three-dimensional echocardiography to predict long-term response to cardiac resynchronization therapy. *Am J Cardiol* 103(11):1586-1591, 2009.
179. Sonne C, Sugeng L, Takeuchi M, et al: Real-time 3-dimensional echocardiographic assessment of left ventricular dyssynchrony: pitfalls in patients with dilated cardiomyopathy. *J Am Coll Cardiol Img* 2(7):802-812, 2009.
180. Tournoux F, Chan RC, Manzke R, et al: Integrating functional and anatomical information to guide cardiac resynchronization therapy. *Eur J Heart Fail* 12(1):52-57, 2010.
181. Tanaka H, Hara H, Saba S, et al: Usefulness of three-dimensional speckle tracking strain to quantify dyssynchrony and the site of latest mechanical activation. *Am J Cardiol* 105(2):235-242, 2010.
182. Qin JX, Shiota T, Asher CR, et al: Usefulness of real-time three-dimensional echocardiography for evaluation of myectomy in patients with hypertrophic cardiomyopathy. *Am J Cardiol* 94(7):964-966, 2004.
183. Song JM, Fukuda S, Lever HM, et al: Asymmetry of systolic anterior motion of the mitral valve in patients with hypertrophic obstructive cardiomyopathy: a real-time three-dimensional echocardiographic study. *J Am Soc Echocardiogr* 19(9):1129-1135, 2006.
184. Fukuda S, Lever HM, Stewart WJ, et al: Diagnostic value of left ventricular outflow tract area in patients with hypertrophic cardiomyopathy: a real-time three-dimensional echocardiographic study. *J Am Soc Echocardiogr* 21(7):789-795, 2008.
185. Nemes A, Lagrand WK, McGhie JS, ten Cate FJ: Three-dimensional transesophageal echocardiography in the evaluation of aortic valve destruction by endocarditis. *J Am Soc Echocardiogr* 19(3):355. e13-e14, 2006.
186. Kort S: Real-time 3-dimensional echocardiography for prosthetic valve endocarditis: Initial experience. *J Am Soc Echocardiogr* 19(2):130-139, 2006.
187. Naqvi TZ, Rafie R, Ghalichi M: Real-time 3D TEE for the diagnosis of right-sided endocarditis in patients with prosthetic devices. *J Am Coll Cardiol Img* 3(3):325-327, 2010.
188. Asch FM, Bieganski SP, Panza JA, Weissman NJ: Real-time 3-dimensional echocardiogra-

phy evaluation of intracardiac masses. *Echocardiography* 23(3):218-224, 2006.
189. Hansalia S, Biswas M, Dutta R, et al: The value of live/real time three-dimensional transesophageal echocardiography in the assessment of valvular vegetations. *Echocardiography* 26(10):1264-1273, 2009.
190. Nemes A, McGhie JS, ten Cate FJ: Real-time 3-dimensional echocardiographic evaluation of aortic dissection. *J Am Soc Echocardiogr* 19(1):108.e3, 2006.
191. Htay T, Nanda NC, Agrawal G, et al: Live three-dimensional transthoracic echocardiographic assessment of aortic dissection. *Echocardiography* 20(6):573-577, 2003.
192. Evangelista A, Aguilar R, Cuellar H, et al: Usefulness of real-time three-dimensional transoesophageal echocardiography in the assessment of chronic aortic dissection. *Eur J Echocardiogr* 12(4):272-277, 2011.
193. Muraru D, Badano LP, Del Mestre L, et al: Real-time three dimensional echocardiography in the postoperative follow-up of type-A aortic dissection—a case report. *J Am Soc Echocardiogr* 23(6):682.e1-e4, 2010.
194. Toledo E, Lang RM, Collins KA, et al: Imaging and quantification of myocardial perfusion using real-time three-dimensional echocardiography. *J Am Coll Cardiol* 47(1):146-154, 2006.
195. Iwakura K, Ito H, Okamura A, et al: Comparison of two- versus three-dimensional myocardial contrast echocardiography for assessing subendocardial perfusion abnormality after percutaneous coronary intervention in patients with acute myocardial infarction. *Am J Cardiol* 100(10):1502-1510, 2007.
196. Hernandez CM, Singh P, Hage FG, et al: Live/real time three-dimensional transthoracic echocardiographic assessment of pericardial disease. *Echocardiography* 26(10):1250-1263, 2009.
197. Chamoun AJ, McCulloch M, Xie T, et al: Real-time three-dimensional echocardiography versus two-dimensional echocardiography in the diagnosis of left ventricular apical thrombi: preliminary findings. *J Clin Ultrasound* 31(8):412-418, 2003.
198. Anwar AM, Nosir YF, Ajam A, et al: Central role of real-time three-dimensional echocardiography in the assessment of intracardiac thrombi. *Int J Cardiovasc Imaging* 26(5):519-526, 2010.
199. Müller S, Feuchtner G, Bonatti J, et al: Value of transesophageal 3D echocardiography as an adjunct to conventional 2D imaging in preoperative evaluation of cardiac masses. *Echocardiography* 25(6):624-631, 2008.
200. Jenkins C, Monaghan M, Shirali G, et al: An intensive interactive course for 3D echocardiography: is "crop till you drop" an effective learning strategy? *Eur J Echocardiogr* 9(3):373-380, 2008.
201. Mansour M, Rasche V, Picard MH, et al: Integration of three-dimensional coronary venous angiography with three-dimensional echocardiography for biventricular device implantation. *Heart Rhythm* 3(11):1391-1392, 2006.

# 5 Echocardiographic Guidance of Structural Heart Disease Interventions

ERNESTO E. SALCEDO, MD | JOHN D. CARROLL, MD

**Structural Heart Disease**
Definition
Structural Heart Disease Interventions
Fluoroscopy and Cineangiography
**Echocardiographic Guidance of Structural Heart Disease Interventions**
Echocardiographic Modalities
**Assisting with Access Routes**
**Transseptal Catheterization**
**Transapical Catheterization**
**Recognizing and Analyzing Catheters and Devices with Echocardiography**
**Specific Structural Heart Disease Interventions**
Closure of Intracardiac Communications
Aortic Valve Interventions
Balloon Mitral Valvotomy
Mitral Regurgitation
Prosthetic Valves
Transcatheter Mitral Valve Replacement
Right Heart Valve Disease
Percutaneous Interventions in the Left Ventricle
Percutaneous Closure of Left Atrial Appendage
Percutaneous Closure of Aortic Pseudoaneurysms
**Procedures Not Covered in this Chapter**
**Limitations and Alternate Approaches**
Intracardiac Ultrasound
Computed Tomography
Cardiac Magnetic Resonance Imaging
Multimodality Imaging
**The Catheterization Laboratory of the Future**

In the past few years, percutaneous interventions have been developed as alternatives to open heart surgery for the treatment of many structural heart diseases. Cardiac imaging plays a major role in patient selection, procedure guidance, and the short- and long-term follow-up of these patients. Both transthoracic (TTE) and transesophageal echocardiography (TEE) have unique attributes that facilitate their application in the catheterization laboratory, and they have become the main imaging tools in the management of most patients with structural heart disease (SHD).

Guidance of structural heart disease interventions requires that the echocardiographer understand the morphology and physiopathology of the SHD abnormality, be familiar with the catheterization laboratory environment, and recognize the echocardiographic and fluoroscopic appearance of the catheters and devices being used for the intervention. Images are obtained following structured protocols, ensuring completeness of the evaluation and facilitating the flow of the intervention. The echocardiographer must anticipate the imaging needs at each point of the intervention.

Echocardiographic imaging planes are frequently different from the fluoroscopic or angiographic planes used in the catheterization laboratory. Therefore, a common language needs to be established between the interventionalist and echocardiographer to designate directionality of the catheters and devices as they are advanced and deployed.

In this chapter we emphasize the role of echocardiography for guidance of SHD interventions.

## Structural Heart Disease

### DEFINITION

In its broadest definition, SHD refers to all cardiac disorders that are marked by abnormal cardiac structure and function. Thus, SHD encompasses valvular heart disease, congenital heart disease, and acquired disorders characterized by abnormalities of heart chambers, valves, myocardium, and cardiac function such as left ventricular (LV) aneurysm/pseudoaneurysm, pericardial disease, and all forms of myocardial disease[1-5] (Fig. 5-1).

### STRUCTURAL HEART DISEASE INTERVENTIONS

SHD interventions are distinguished from the two other large areas of interventional cardiology: coronary artery intervention (percutaneous coronary intervention, or PCI) and peripheral artery intervention. SHD intervention is a useful grouping for the specialty because these interventions require technical, imaging, and hemodynamic knowledge and skills that are distinctive from PCI and other vascular interventional skills. Training programs in interventional cardiology now describe SHD interventions as a unique component, continuing medical education conferences have separate sessions, and textbooks have emerged that are focused on SHD interventions,[6] all as a consequence of this uniqueness in clinical practice, knowledge base, and interventional skills.

SHD interventions involve image guidance that is fundamentally different from that used in PCI and other vascular

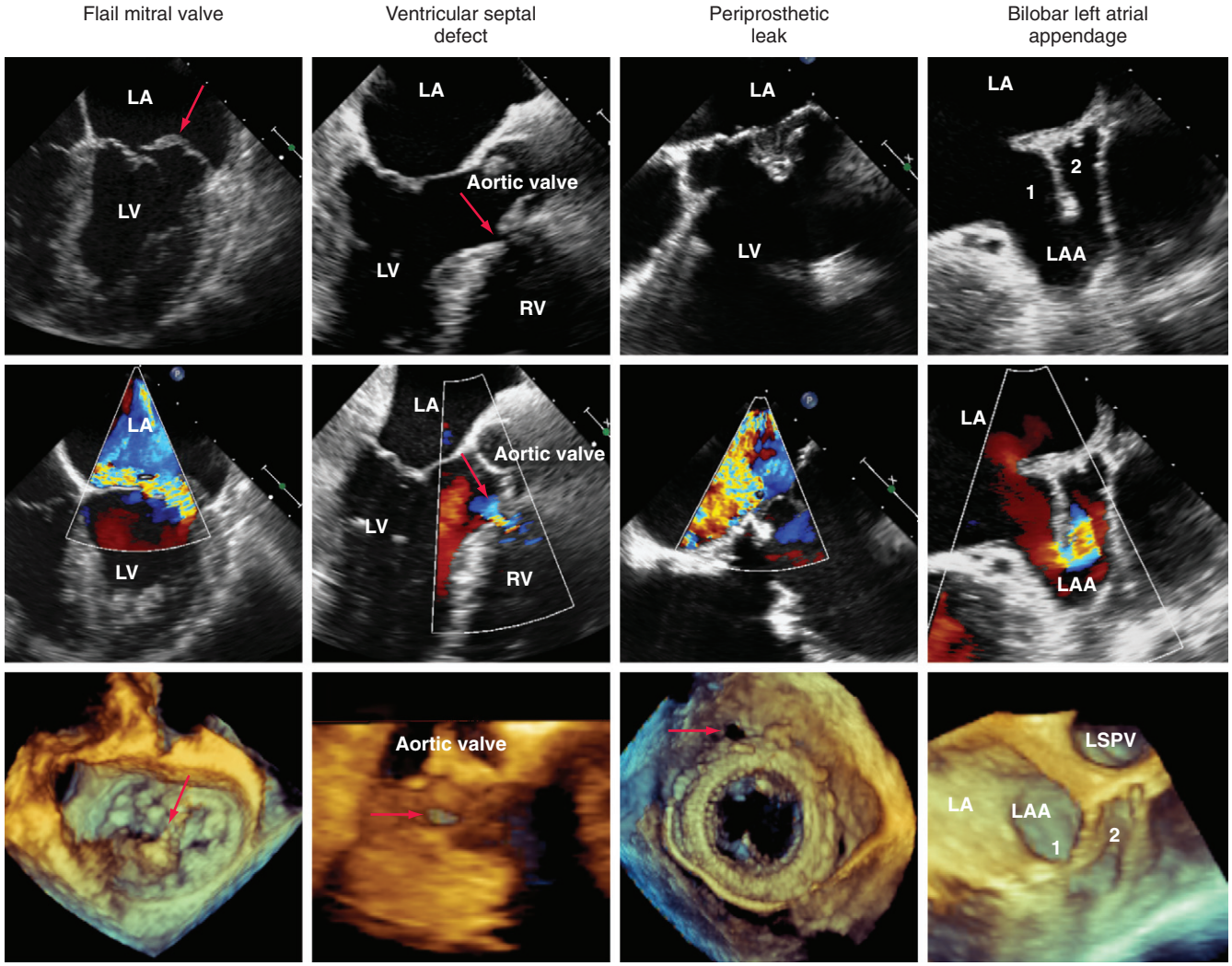



**Figure 5-1 Structural heart disease.** Typical examples of patients with structural heart disease referred for percutaneous interventions. The first patient has a flail posterior mitral leaflet (*arrows*) and was referred for mitral clip repair. The second patient has a perimembranous ventricular septal defect (VSD) (*arrows*) and was referred for percutaneous VSD repair. The third patient has a periprosthetic mitral valve leak (*arrow*) and two prior open heart surgeries and was referred for percutaneous repair. The fourth patient illustrates an anatomic variant of the left atrial appendage (*LAA*), in this case bilobar (*1,* primary lobe; *2,* secondary lobe), this being an important consideration for the use of an LAA occluder. *LSPV,* Left superior pulmonary vein.

interventions. PCI is solely guided by x-ray fluoroscopy and coronary angiography. On the other hand, image guidance of SHD interventions often requires an additional modality—typically cardiac ultrasound (Table 5-1). The form of ultrasound varies by the procedure being performed, but also by local expertise, experience, and the techniques available. TEE and intracardiac echocardiography (ICE) are the two forms of cardiac ultrasound commonly used, whereas TTE is a third form used less frequently in adults because of suboptimal image quality in many patient undergoing SHD interventions.

During an intervention, ultrasound imaging and Doppler hemodynamic assessment are used diagnostically to assess the abnormal structure and function before and after the intervention and assess other relevant structures and physiologic parameters. Both techniques are also critical to manage complications.[7] In the flow of most SHD interventions, imaging makes the transition back and forth from its diagnostic utility to its true image guidance use.

**TABLE 5-1 Cardiac Ultrasound Properties That Promote Its Use in SHD Interventions**

| *Cardiac Ultrasound Properties* | *Importance to SHD Interventions* |
|---|---|
| Excellent temporal and spatial resolution of soft tissue | The target of many interventions is soft tissue (valves, chamber walls), and these are not visualized by x-ray except during angiography, which cannot be repeatedly used. |
| No harmful effects of ultrasound energy | Efforts to minimize the use of ionizing radiation from x-ray are facilitated by substituting ultrasound guidance for various tasks performed during the procedure. |
| Doppler and echocardiographic visualization and quantification of flow abnormalities, chamber function, and valve function are accurate and broadly accepted as gold standards | Intraprocedure assessments of cardiac function, shunts, and valve function are required in most interventions; need to be repeated; and may replace or complement catheter-based pressure measurements, oximetric determination of shunt location and quantification, and thermodilution measurement of cardiac output. |

*SHD,* Structural heart disease.

**TABLE 5-2 Main Imaging Modalities Used to Assist Structural Heart Disease Interventions**

| | *Frequency of Use* | *Advantages* | *Disadvantages* |
|---|---|---|---|
| Fluoroscopy and cineangiography | ++++ | Current gold standard | Radiation<br>No soft tissue characterization |
| Intracardiac echocardiography (ICE) | ++ | No radiation<br>High-resolution soft tissue characterization | Poor resolution in far fields<br>No 3D rendering |
| Transthoracic echocardiography (TTE) | ++ | Noninvasive<br>No radiation<br>Soft tissue characterization | Limited echo windows<br>Adds complexity to procedure<br>Additional personnel required |
| Transesophageal echocardiography (TEE) | +++ | No radiation<br>High-resolution soft tissue characterization<br>3D imaging rendering possible | Semiinvasive<br>Adds complexity to procedure<br>Additional personnel required |

### FLUOROSCOPY AND CINEANGIOGRAPHY

Fluoroscopy is the major real-time imaging modality used in all SHD interventions. Transcatheter or percutaneous interventions of the heart require the interventional cardiologist to first access the circulation via a peripheral artery or vein and then navigate wires, catheters, delivery systems, and other specialized tools to the heart. These procedural tasks are almost exclusively performed with fluoroscopy. Once the heart is reached, image guidance often becomes a multimodality affair for SHD interventions. Fluoroscopy and echocardiography are used together or in an alternating fashion (Table 5-2).

Fluoroscopy remains the major imaging modality for SHD interventions for multiple reasons, starting with its ability to provide global or large-field guidance for the navigation of equipment. With table panning and large field-of-view flat detectors, the interventional cardiologist can track the course of catheters and devices from the distal access point to any place within the heart. In addition, fluoroscopy is essential because all diagnostic and interventional supplies are radiopaque. The design and choice of material for equipment has historically been done to optimize x-ray visualization. Fluoroscopy is also the principal imaging modality because it is so widely available, physicians have been trained and gained extensive experience using it, and the x-ray system has many features and imaging tools that further enhance the utility of x-ray imaging.

As an imaging modality, fluoroscopy has many strong features. It is real time and provides the continuous feedback essential for performing an intervention. It has a high spatial and temporal resolution critical for cardiac work. Although fluoroscopy is two-dimensional (2D) and produces a projection or "shadow" image, in skilled hands it allows the determination of device position relative to anatomic landmarks and interventional targets. Certain SHD targets are in fact apparent on fluoroscopy (e.g., a calcified aortic valve). Finally, it is a modality that is simple to set up and use in the procedure room.

Cineangiography has been used for decades in the diagnosis and quantification of many forms of SHD. Ventriculography, aortography, and other selective chamber/vessel injections have been the first techniques used to diagnose all of SHD. In the era of SHD interventions, cineangiography is still used in a focused fashion but does not have a central role because of several key facts. First, angiographic contrast dye is an acute osmotic load, may be nephrotoxic, and must be injected in large volumes to clearly show the features of SHD. Second, it cannot be repeated numerous times. Third, it produces 2D projection images that often misrepresent the complex three-dimensional (3D) relationships of key structures in SHD.

The focused use of cineangiography is still common in certain interventions such as left atrial appendage occlusion, transcatheter aortic and pulmonic valve implantation, and ventricular septal defect closure. Cineangiography is intertwined with the use of fluoroscopy to perform certain tasks of the intervention. Cineangiographic images provide a road map for fluoroscopic guidance and also help determine the optimal projection that is needed for a specific step of an intervention. Note that this function of cineangiography is not readily replaced by using ultrasound.

Cineangiography is not a static technique, and important developments are leading to a rebirth of angiography in general.[8] Rotational angiography is a new acquisition technique that has now been coupled with 3D reconstruction algorithms. The traditional 2D x-ray tools of fluoroscopy and cineangiography are being supplemented by C-arm computed tomographic (CT) techniques that convert the imaging system into a CT scanner capable of imaging soft tissue. These volumetric 3D data sets or preprocedure acquired cardiac CT scan data can be registered or fused with fluoroscopy to provide a more powerful imaging guidance tool for SHD interventions.[9] These developments have profoundly changed neurointerventions and many interventional radiology procedures.[10] The cardiac applications are emerging later because of the challenge of imaging the heart's rapid motion and the precision needed in interventions within this complex structure.[11]

## Echocardiographic Guidance of Structural Heart Disease Interventions

### ECHOCARDIOGRAPHIC MODALITIES

All of the echocardiographic methods used in the echocardiographic laboratory[7,12-16] can be used in the catheterization laboratory for the guidance of SHD interventions. The approach to obtain this information is through either TTE or TEE. The selection of either approach depends on the intervention to be performed, the need for endotracheal intubation, and the quality of the TTE windows. Because of the increased spatial resolution of TEE, we favor its use for all patients who require endotracheal intubation and in all patients with suboptimal transthoracic windows. The development of real-time 3D echocardiography has opened a new window into the heart and has been particularly useful in the guidance of SHD interventions; currently all of our TEE-guided interventions are performed with 3D TEE. The new 3D TEE technology allows for switching from 2D to 3D and color imaging, which is of great value to obtain all required information immediately preceding the intervention and for procedural guidance (Fig. 5-2).

## Assisting with Access Routes

The initial role of echocardiography in the catheterization laboratory for guidance of SHD interventions is in facilitating the access of guidewires, catheters, and devices into the appropriate vessel and cardiac chamber. Although fluoroscopy is the main imaging tool for this purpose, real-time ultrasound guidance

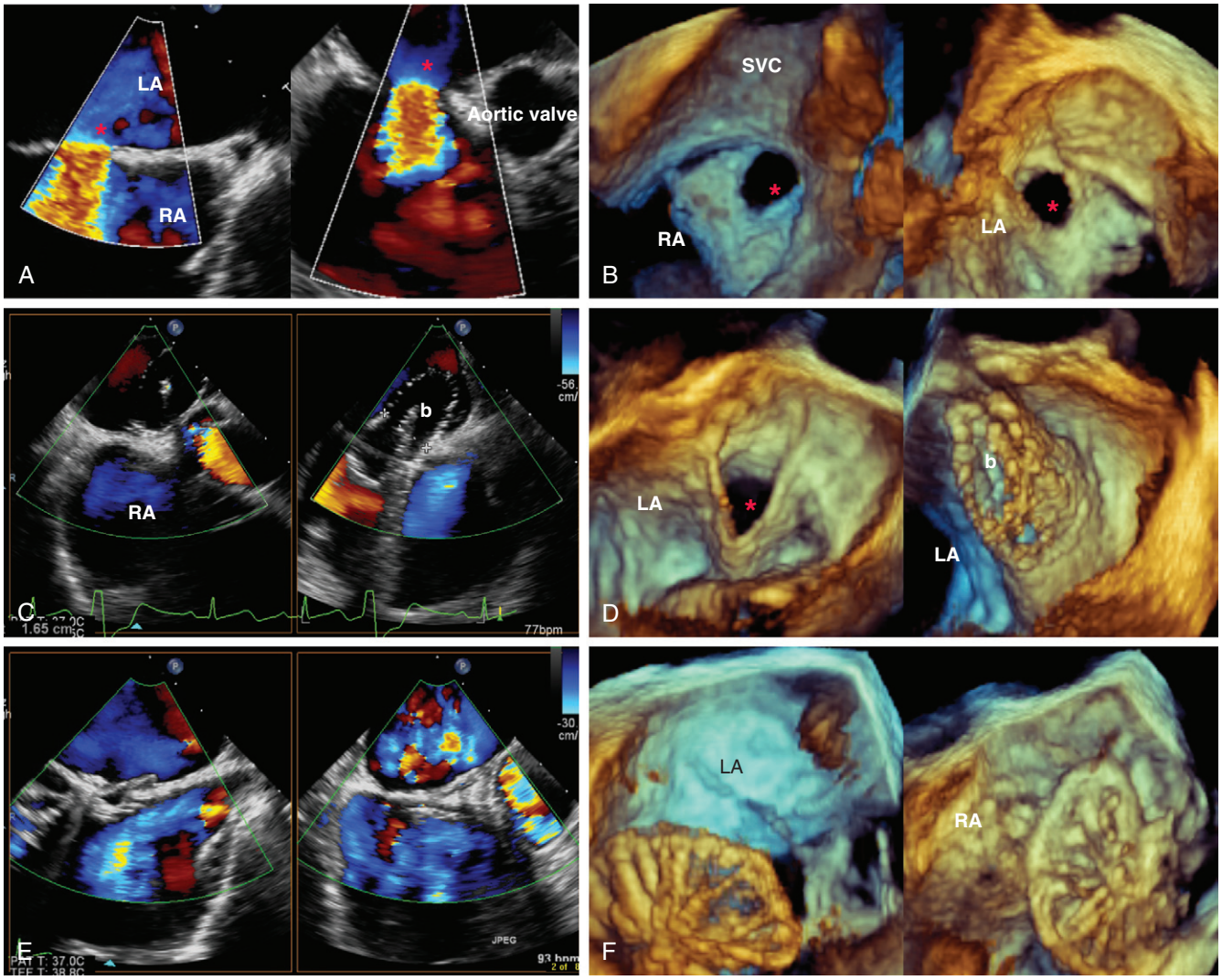



**Figure 5-2 TEE applications in structural heart disease interventions.** With real-time 3D TEE, it is now possible to alternate 2D (x-biplane) and 3D presentations. In this patient undergoing percutaneous closure of a secundum atrial septal defect (*), simultaneous biplane color images are presented in panels **A,** preprocedure, **C,** balloon sizing, and **E,** post–device deployment. Presentations on 3D are illustrated in panels **B,** preprocedure, **D,** balloon sizing, and **F,** post–device deployment. *b*, Balloon; *SVC*, superior vena cava.

reduces time to access, number of attempts, and complications in central venous access, as well as providing improved common and superficial femoral artery cannulation.[17,18]

## Transseptal Catheterization

Since the original description of transseptal left heart catheterization as a new diagnostic method by Ross[19] more than 50 years ago, transseptal catheterization has become an integral part of SHD interventions.[20,21] The technical aspects on how to perform a successful transseptal catheterization have been well described in the literature[22,23]; the role of echocardiography in assisting this initial step of SHD interventions has also been demonstrated and is illustrated in Figure 5-3.

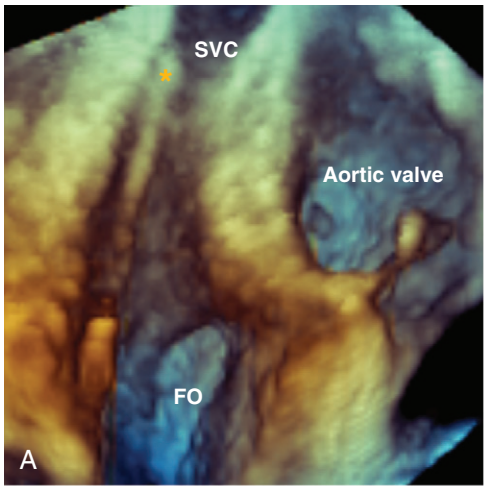
## Transapical Catheterization

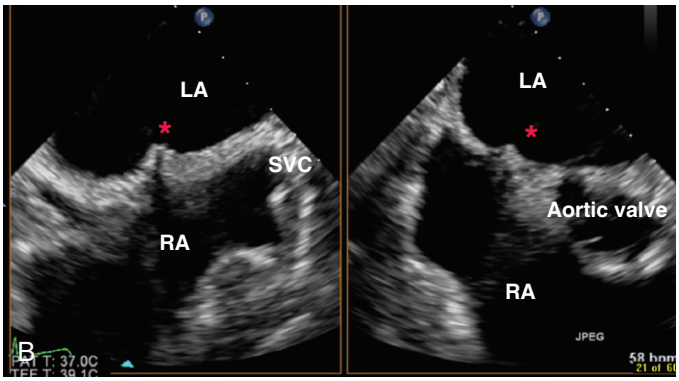
Direct cardiac puncture to access the LV has been traditionally used when operators were concerned about crossing the native aortic or mitral valves,[24] or more recently in the presence of simultaneous mechanical aortic and mitral prosthesis.[25] Patients with SHD who are candidates for transapical catheterization include those undergoing percutaneous aortic valve replacement and those with paravalvular mitral prosthetic leaks.[26]

## Recognizing and Analyzing Catheters and Devices with Echocardiography

The echocardiographer assisting with structural heart disease interventions needs to be familiar with the equipment required for the intervention. A complete description of each piece of equipment required for the performance of SHD interventions is beyond the scope of this chapter; however, a general understanding of the types, function, and fluoroscopic and echocardiographic appearance of these catheters and devices is essential for successfully assisting SHD interventions. Table 5-3 summarizes the main items used in percutaneous SHD interventions, and Figures 5-4 and 5-5 illustrate the fluoroscopic and echocardiographic appearance of selected catheters and devices.

It is also important to recognize pitfalls and common echocardiographic artifacts seen during structural heart disease interventions, as illustrated in Figure 5-6.



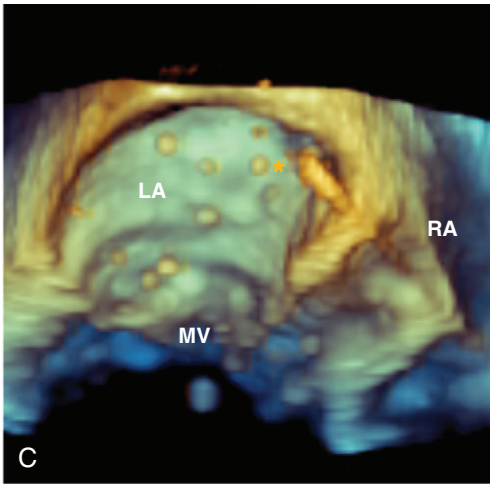




**Figure 5-3 Septal puncture.** Both 2D and 3D methods can be used to provide septal puncture guidance. **A,** 3D TEE view of the interatrial septum as seen from the right atrium. The tip of the guiding catheter (*yellow asterisk*) is in the superior vena cava (*SVC*) and will need to be withdrawn to the level of the fossa ovalis (*FO*). Once in the fossa ovalis, biplane 2D imaging (**B**) permits visualization of the "tenting" (*red asterisk*) and puncture of the membrane of the FO—inferior to the SVC and posterior to the aorta. **C,** 3D imaging illustrates the dilator (*yellow asterisk*) in the LA and microbubbles in the LA cavity, confirming correct positioning of the catheter.

## Specific Structural Heart Disease Interventions

The general classification of structural heart disease interventions, the approval status of different devices in use, and common image guidance modalities are shown in Tables 5-4, 5-5, and 5-6.

**TABLE 5-3 Common Equipment Used in Structural Heart Disease Interventions**

| | |
|---|---|
| Guidewires | Soft J-tipped wires<br>Stiff wires<br>Glide wires<br>Steerable wires |
| Sheath/dilator sets | Introductory sheath/dilator sets<br>Long delivery sheath/dilator sets |
| Diagnostic catheters | Extruded catheters<br>Floating balloon catheters<br>Woven Dacron catheters |
| Transseptal catheterization apparatus | Guidewire<br>Mullins introducer (sheath and dilator)<br>Brockenbrough needle and stylet |
| Balloon dilation catheters | Inoue balloon |
| Endovascular stents | Large vessel stents (>12 mm)<br>Medium size vessel stent (6-12 mm) |
| Closure devices | Amplatzer ASD, PFO, PDA,VSD, and vascular plug (AGA Medical, Plymouth, Minn.)<br>CArdioSEAL, STARFlex and BioSTAR (NMT Medical, Boston)<br>Helex (W.L. Gore Associates, Flagstaff, Ariz.)<br>Premere (St Jude Medical, St. Paul, Minn.) |
| Retrieval devices | Snare retrieval devices<br>Basket retrieval devices |

*ASD,* Atrial septal defect; *PDA,* patent ductus arteriosus; *PFO,* patent foramen ovale; *VSD,* ventricular septal defect.

**TABLE 5-4 SHD Interventions of Septal Defects**

| *SHD Intervention Category* | *Status 2011* | *Image Guidance Modalities Commonly Used* |
|---|---|---|
| **Interatrial Septum Interventions** | | |
| Secundum atrial septal defect | Approved devices | Fluoroscopy and TEE or ICE |
| Fenestrated atrial septum | Approved device | Fluoroscopy and TEE or ICE |
| Patent foramen ovale | Approved devices OUS, off-label use of approved devices in US | Fluoroscopy and TEE or ICE |
| Atrial balloon septostomy | Off-label use of approved balloon catheters | Fluoroscopy alone or with TEE, TTE, or ICE |
| Transseptal catheterization | Approved catheters, needles, and RF ablation catheters | Fluoroscopy alone or with TEE or ICE |
| **Interventricular Septum Interventions** | | |
| Congenital muscular VSD | Approved device | Fluoroscopy and TEE |
| Congenital perimembranous VSD | Experimental, predominantly preclinical | Fluoroscopy and TEE |
| Post–myocardial infarction VSD | Approved device OUS, IDE device in US available for compassionate use | Fluoroscopy and TEE |

*ICE,* Intracardiac echocardiography; *IDE,* investigational device exemption; *OUS,* outside United States; *RF,* radio frequency; *VSD,* ventricular septal defect.

## CLOSURE OF INTRACARDIAC COMMUNICATIONS

### *Atrial Septal Defects*

The presence of symptoms, echocardiographic findings of right ventricular (RV) volume overload, or the presence of shunt-related pulmonary hypertension are accepted indications for atrial septal defect (ASD) closure.[27,28] Surgical closure is required for patients with ostium primum and sinus venosus ASDs, as well as for patients with secundum ASDs whose anatomy is unsuitable for device closure. (See Chapter 44.)

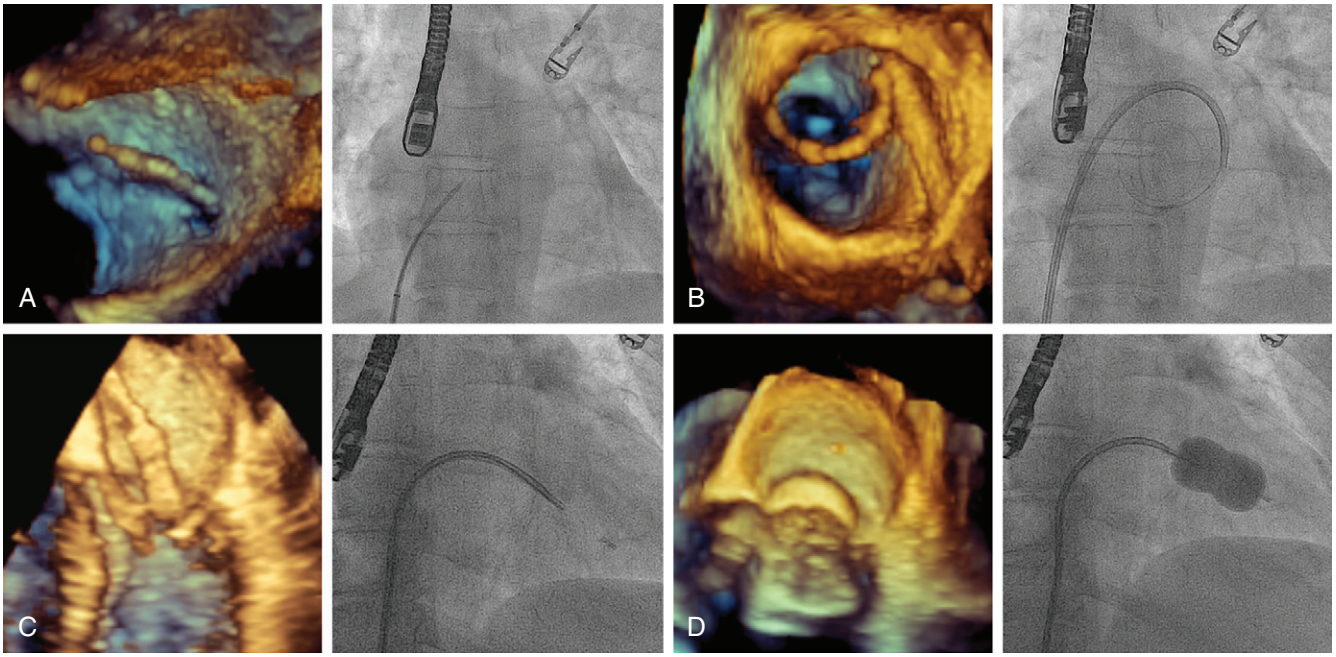



**Figure 5-4 Echo (3D TEE) and fluoroscopic appearance of catheters and devices in mitral valve balloon valvotomy. A,** Guidewire entering the left atrium. Note the lack of soft tissue characterization of the fluoroscopic image. **B,** Delivery catheter and a guidewire have been advanced and rolled into LA. **C,** Deflated balloon is near the orifice of the mitral valve. **D,** Inflated balloon is seen dilating the mitral valve orifice.

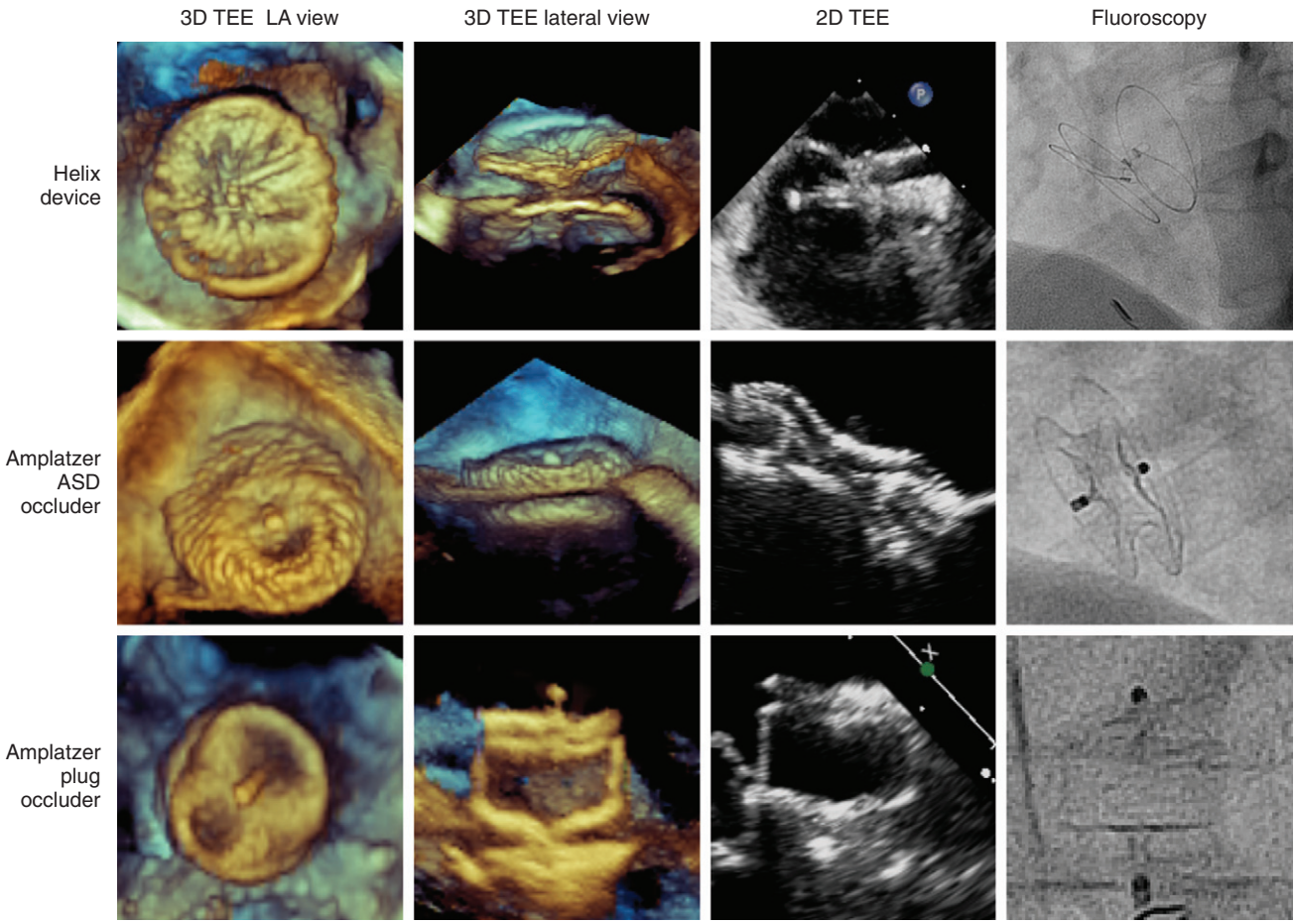



**Figure 5-5 Occluders.** For three different occluder devices, the enhanced spatial resolution of the 3D TEE images is contrasted with the 2D images provided by 2D TEE and fluoroscopy.

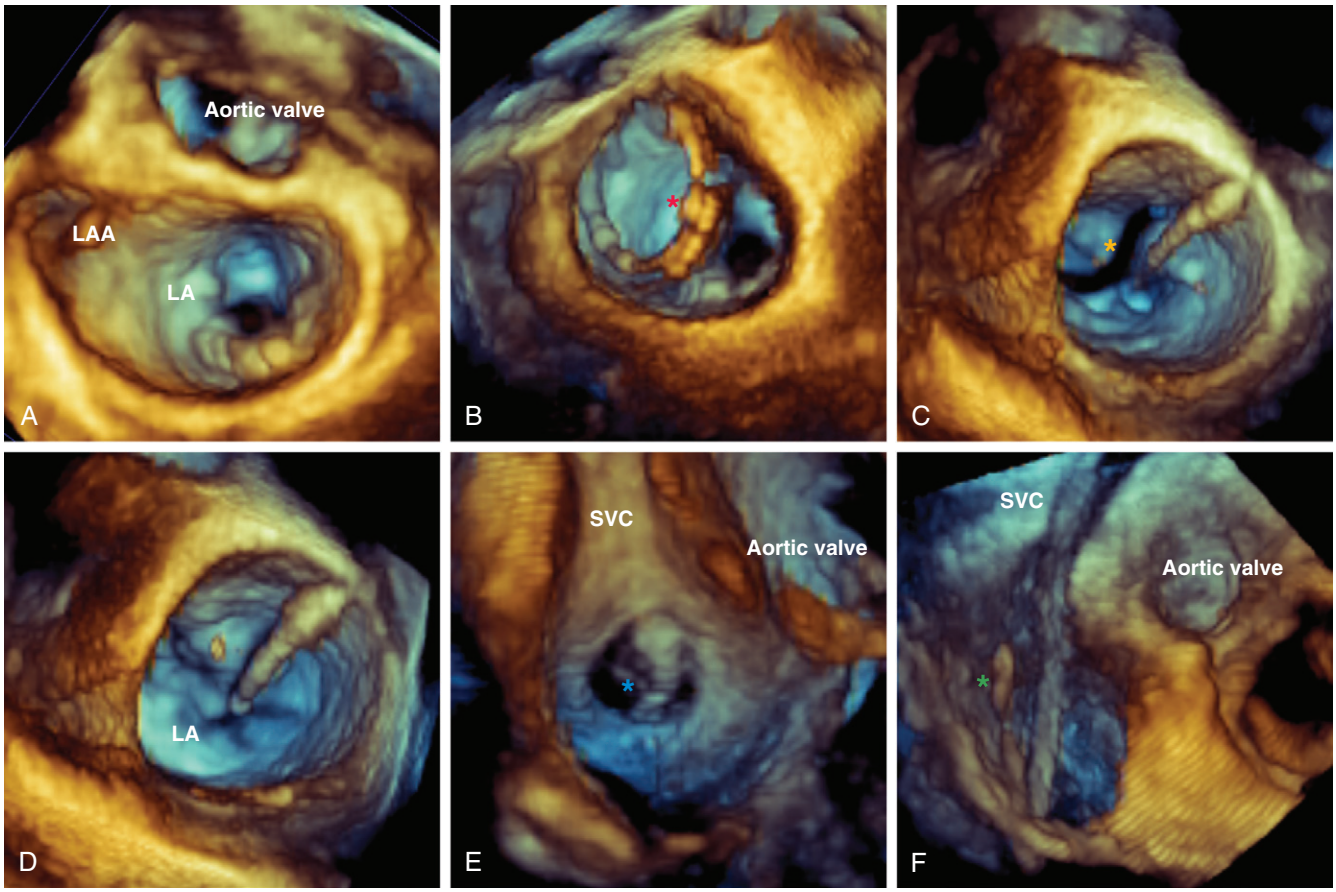



**Figure 5-6** **3D TEE artifacts during structural heart disease interventions. A,** En face view of a stenotic mitral valve. Guidewire in the LA is not seen because it is in a plane superior to the selected plane of view. **B,** By slightly withdrawing the TEE probe, the guidewire comes into view and is easily identified (*red asterisk*). **C,** Black S-shaped line (*yellow asterisk*) that on motion appears as a large fissure in the mitral valve, but in reality represents a shadowing artifact from a catheter in the LA. **D,** A slight rotation of the tomographic plane eliminates the artifact. **E,** The membrane of the fossa ovalis appears to have a hole (*blue asterisk*), giving the illusion of an atrial septal defect when in reality there is none. Changing the gain or looking from a different perspective clarifies the problem. **F,** "Ghost" artifact (*green asterisk*) with the appearance of two catheters in the RA when in reality there was only one. *LAA*, Left atrial appendage; *SVC*, superior vena cava.

The first percutaneous ASD closure was reported by King and colleagues[29] in 1976; this method has now become the preferred treatment for hemodynamically significant secundum-type ASD. Percutaneous ASD closure can be performed safely and with minimal risk even in elderly patients.[30] They profit in terms of symptom reduction, improvement of exercise capacity, and right-heart remodeling.[31]

Echocardiography provides substantial information regarding the characteristics of ASDs.[32] TEE is the favored imaging tool to select patients for percutaneous ASD closure and to guide the intervention. Of particular relevance to ASD closure is the characterization of the ASD rims, defined as the interatrial tissue surrounding the ASD and named after the cardiac structure adjacent to it: superior vena cava rim (superior), aortic rim (anterosuperior), coronary sinus rim (anteroinferior), inferior vena cava rim (inferior), and posterior rim. Inferior rims less than 5 mm in length make patients unsuitable for device closure. Likewise, an ASD more than 35 to 36 mm in diameter has a higher incidence of device embolization, and surgical closure is preferred. ASD sizing is an important aspect of intraprocedural TEE evaluation and is usually accomplished by direct measurement of the defect or by measuring the "waist" diameter of an ASD sizing balloon inflated until the color flow determines absence of shunt.

The TEE protocol we currently use for transcatheter ASD closure guidance include 2D imaging, 2D imaging with color, and 3D imaging. We use the "zoom 3D" mode to guide catheters and the device through the ASD as well as for guidance of the initial deployment of the left atrium hemidisk. For the deployment of the right atrium hemidisk, we use 2D imaging or simultaneous biplane (x-plane) 3D imaging. Color 2D imaging is used to verify absence of residual shunting before releasing the device (Figs. 5-7 and 5-8).

Cardiac CT angiography is an accurate and useful technique for preprocedural assessment of ASDs and may be superior to conventional TEE in large defects that have deficient inferior rims.[33]

### *Patent Foramen Ovale*

A large body of circumstantial evidence, including reports showing an actual embolus traversing the patent foramen ovale (PFO), epidemiologic association, and case-control series, links PFO to cryptogenic strokes.[34] (See Chapter 41.) The echocardiographic diagnosis of PFO and the characterization of "high-risk" subgroups including PFO size and presence of interatrial septal aneurysm and embryonic recesses have been well described in the literature.[35] Recently the added value of 3D TEE to define the morphologic phenotypes of PFO has been

**TABLE 5-5 SHD Interventions of Valves**

| *SHD Intervention Category* | *Status 2011* | *Image Guidance Modalities Commonly Used* |
|---|---|---|
| **Aortic Valve Interventions** | | |
| Balloon valvuloplasty | Approved balloon catheters and widely performed | Fluoroscopy |
| Transcatheter prosthetic valve implantation | Approved OUS, pending approval in US | Fluoroscopy and TEE<br>CTA-fluoroscopy overlay |
| Paravalvular leak closure | | Fluoroscopy and TEE<br>CTA-fluoroscopy overlay |
| **Mitral Valve Interventions** | | |
| Balloon valvotomy | Approved balloon catheter system | Fluoroscopy and TEE, TTE, or ICE |
| Mitral valve repair with Alfieri edge-to-edge technique | Approved device OUS, pending approval in US | Fluoroscopy and TEE |
| Annular reduction techniques | Experimental, some technologies in clinical trials | Fluoroscopy and, depending on specific technology, TTE or TEE |
| Percutaneous LV and mitral annulus remodeling | Experimental, some technologies in clinical trials | Fluoroscopy and, depending on specific technology, TTE or TEE |
| Transcatheter prosthetic valve implantation | Experimental, predominantly preclinical | Fluoroscopy and TEE<br>CTA-fluoroscopy overlay |
| Paravalvular leak closure | No FDA-approved devices, off-label use of approved devices | Fluoroscopy and TEE<br>CTA-fluoroscopy overlay |
| **Pulmonic Valve Interventions** | | |
| Balloon valvotomy | Approved balloon catheters and widely performed | Fluoroscopy |
| Transcatheter prosthetic valve implantation | Approved in US (Melody Valve) | Fluoroscopy and TEE<br>CTA-fluoroscopy overlay |
| **Tricuspid Valve Interventions** | | |
| Balloon valvuloplasty | Off-label use of approved balloon catheter system | Fluoroscopy and TTE or ICE |
| Transcatheter prosthetic valve implantation | Experimental, predominantly preclinical | TBD |

*CTA*, Computed tomographic angiography; *FDA*, U.S. Food and Drug Administration; *ICE*, intracardiac echocardiography; *OUS*, outside United States; *SHD*, structural heart defect; *TBD*, to be determined.

**TABLE 5-6 SHD Interventions for Other Abnormalities**

| *SHD Intervention Category* | *Status 2011* | *Image Guidance Modalities Commonly Used* |
|---|---|---|
| **Myocardial Interventions** | | |
| Alcohol septal ablation in HCM | Involves no investigative devices or drugs | Fluoroscopy and TEE or TTE |
| Stem cell implantation in cardiomyopathy | Experimental cell-based therapy | Fluoroscopy and TEE or TTE<br>CTA-fluoroscopy overlay |
| **Pericardial Interventions** | | |
| Balloon pericardiotomy | Off-label use of approved balloon | Fluoroscopy |
| **Miscellaneous Chamber Interventions** | | |
| Left atrial appendage | Approved OUS, active clinical trials in US for two devices | Fluoroscopy and TEE |
| Left ventricular aneurysm | Experimental, predominantly preclinical | Fluoroscopy and TEE<br>CTA-fluoroscopy overlay |
| Left ventricular pseudoaneurysm | Experimental, some rare off-label use of approved devices | Fluoroscopy and, depending on specific technology, TTE or TEE |
| Percutaneous LV assist devices | Approved devices, one inserted transseptally, the other retrogradely | Fluoroscopy alone or with TEE or ICE |
| **Miscellaneous Great Vessels Interventions** | | |
| Coarctation of aorta | Off-label use of approved stents | Fluoroscopy |
| Patent ductus arteriosus | Approved devices | Fluoroscopy |
| Aortic pseudoaneurysm | Off-label use of approved devices and coils | Fluoroscopy and TTE, TEE, or ICE<br>CTA-fluoroscopy overlay |
| Pulmonary artery stenosis | Off-label use of approved stents | Fluoroscopy<br>CTA-fluoroscopy overlay |

*CTA*, Computed tomographic angiography; *HCM*, hypertrophic cardiomyopathy; *ICE*, intracardiac echocardiography; *OUS*, outside United States.

described.[36] A PFO is categorized as "complex" when any of the following findings is present: long tunnel length (8 mm or more), multiple openings into left atrium, atrial septal aneurysm, hybrid defect (PFO and additional defects in the fossa ovalis), thick secondary septum (10 mm or more), presence of a Eustachian ridge or valve, and presence of a Chiari network. If none of these findings is present, the PFO is categorized as "simple."[36] In addition, the importance of a structured and systematic echocardiographic evaluation of the interatrial septum, in patients being considered for percutaneous PFO closure, has been described.[37,38] The percutaneous closure of a PFO can be guided with fluoroscopy, with ICE, or with TTE or TEE. At our institution, most PFO closures are done under fluoroscopic and ICE imaging. In patients with large or complex PFO, TEE is used to define interatrial septal anatomy (Fig. 5-9), to determine the size and type of the device to be used, and to assist with device deployment.

The TEE protocol we use for PFO closure is similar to the one described for ASD closure. Echocardiography also plays an important role in detecting and managing periprocedural complications such as cardiac perforation, device embolization, device thrombosis, device erosion, and arm fracture.[39]

### *Ventricular Septal Defects*

Ventricular septal defects (VSDs) are common congenital heart defects in children and adults. The majority (70% to 80%) involves the membranous septum and the adjacent portion of the muscular septum and are called perimembranous VSDs (see Chapter 44). Muscular VSDs account for 10% to 15% of all VSDs and can be apical, midseptal, anterior, or posterior defects. Although the standard treatment for perimembranous VSD is open heart surgery, catheter-based approaches for their closure have been shown to be an attractive alternative to surgical closure with acceptable mortality and morbidity as well as encouraging results.[40,41] Yang and co-workers recently reported their experience with percutaneous perimembranous VSD closure in 848 patients, 110 of whom were more than 20 years of age.[42] All patients were screened by conventional 2D and color Doppler TTE. These authors noted that although TEE is the imaging modality most frequently used to guide transcatheter perimembranous VSD closure, TEE was used only in the early stages of their experience and was gradually replaced by TTE combined with angiography.

Development of a VSD is a rare (1% to 2%) but serious complication of transmural myocardial infarction. The incidence of post–myocardial infarction VSD has decreased significantly with thrombolytic therapy,[43] yet morbidity and mortality

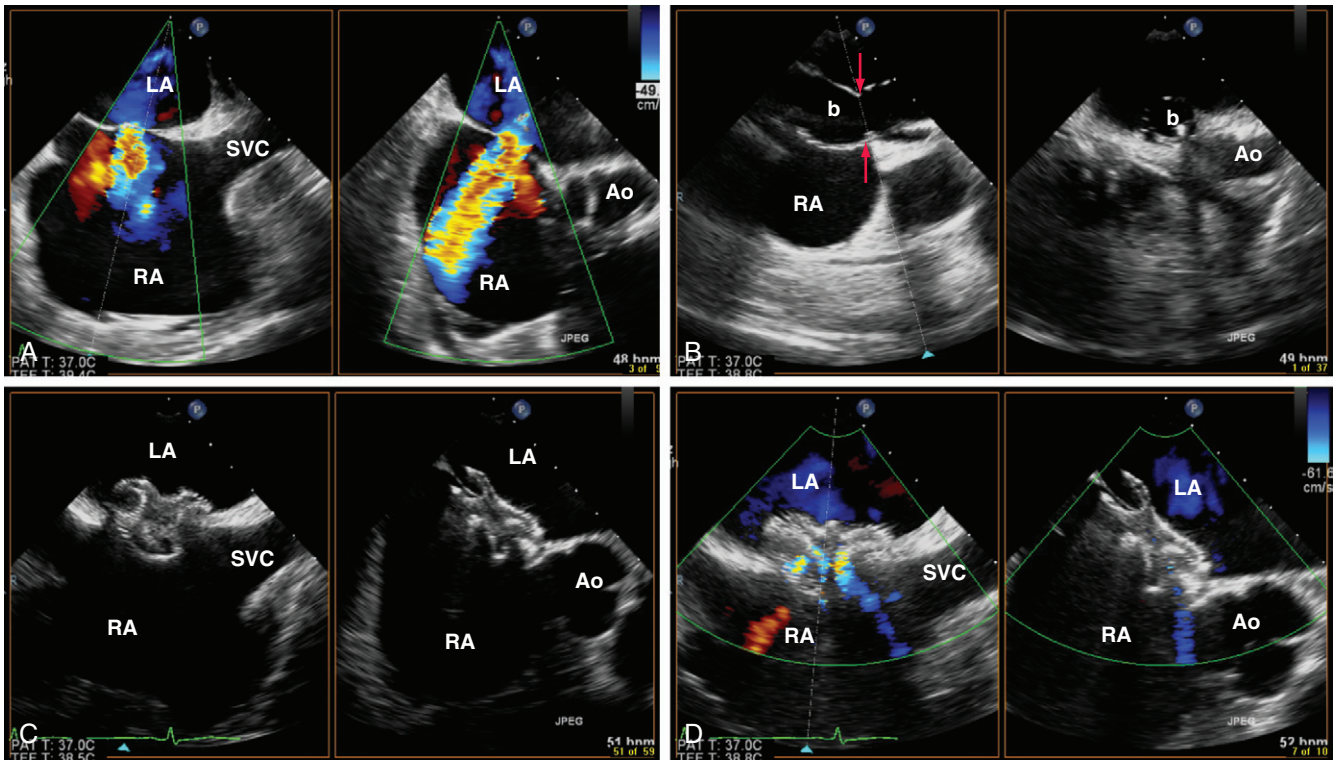



**Figure 5-7 Biplane 2D TEE atrial septal defect device (ASD) closure.** Real-time x-plane TEE (biplane images derived from 3D data sets) during a percutaneous ASD closure. **A,** *Color:* Shunt from the LA to the RA. **B,** The inflated sizing balloon (*b*) is seen in long and short axis with the "waist" marked by *arrows*. This dimension is used to estimate the device size to be used. **C,** Both hemidisks of the Amplatzer device have been deployed. **D,** Color Doppler shows small degree of shunting through the device (normal finding) and absence of peridevice shunt. *Ao*, Aorta; *SVC*, superior vena cava.

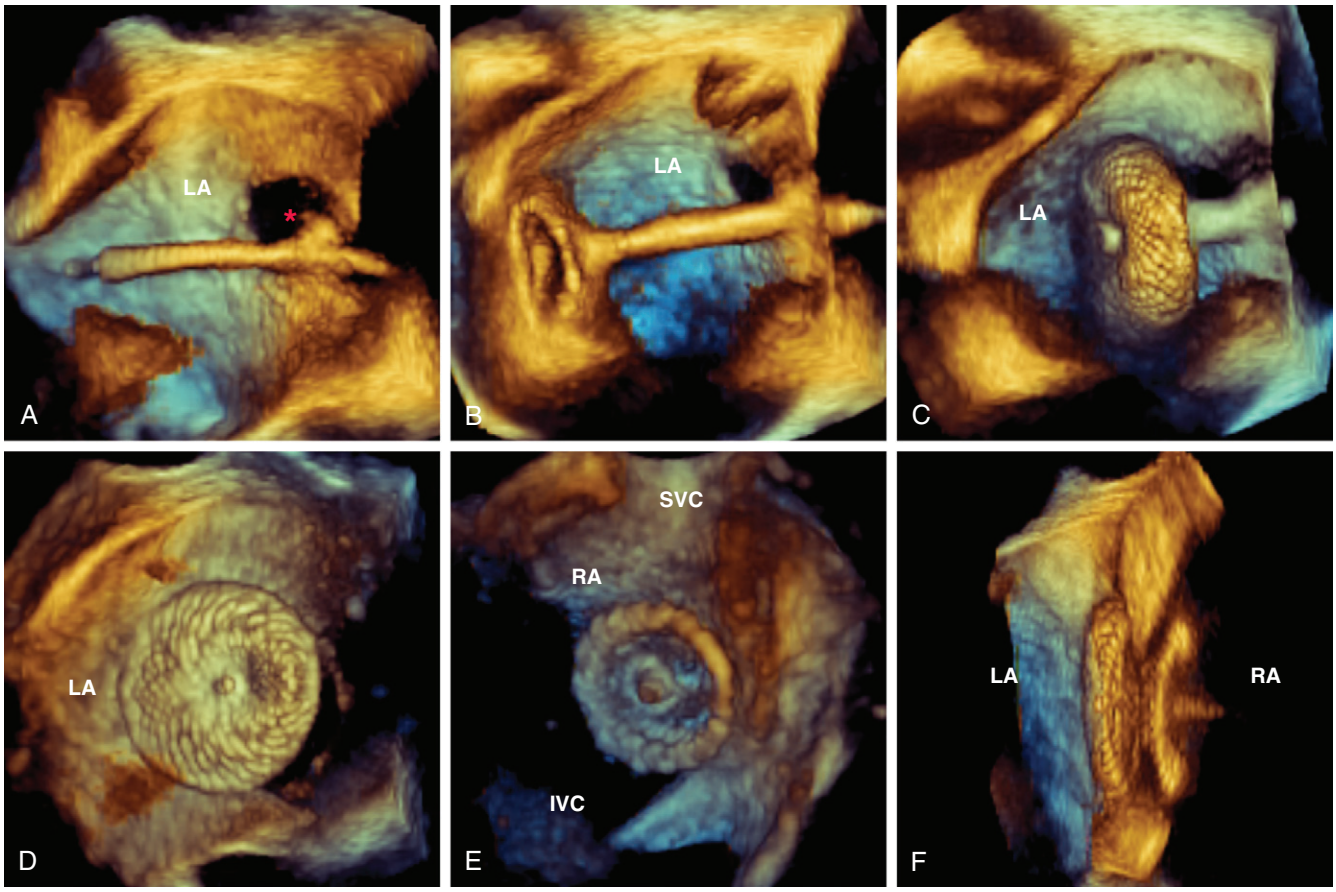



**Figure 5-8 3D TEE guidance of Amplatzer atrial septal defect (ASD) closure device.** All views are zoom 3D images of the interatrial septum as seen from the LA (panels **A** through **D**), from the RA (**E**), or from an anteroposterior perspective (**F**). **A,** Delivery catheter is seen in the LA entering through the ASD (*red asterisk*). **B,** LA disk is being deployed. **C,** LA disk is fully deployed and catheter is pulled back. **D,** Catheter is pulled back until the left hemidisk abuts the interatrial septum. **E,** Right hemidisk is deployed and sits in the RA inferiorly to the superior vena cava (*SVC*) and superiorly and anteriorly to the inferior vena cava (*IVC*). **F,** Device is seen in profile with one hemidisk in the LA and the other in the RA.

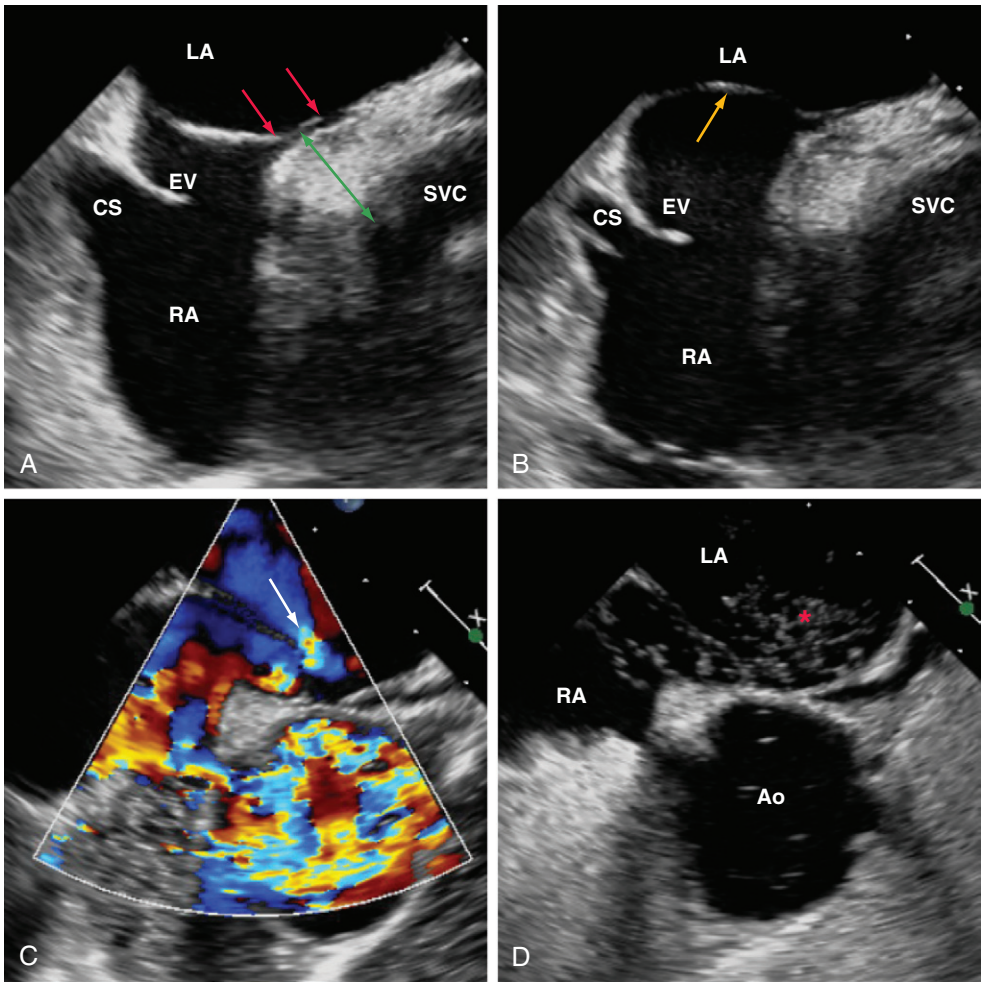



**Figure 5-9 TEE evaluation of patent foramen ovale (PFO).** Key points to be noted in the evaluation of PFOs being considered for device closure. **A,** *Red arrows* demark the length of the PFO tunnel. A thickened septum secundum (*green arrow*) next to the superior vena cava (*SVC*). A prominent Eustachian valve (*EV*) is seen next to the coronary sinus (*CS*). **B**, Interatrial septum (*yellow arrow*) as it moves into the LA. This excessive excursion denotes the presence of an interatrial septum aneurysm. **C,** Interatrial shunt (*white arrow*) as seen with color Doppler. **D,** Microbubbles (*) entering the LA from the RA through the PFO. *Ao*, Aorta.

remain high. (See Chapter 14.) Surgical repair[44] is difficult because of friable and necrotic tissue and can be complicated by persistent shunt or a recurrent VSD. Percutaneous catheter-based closure techniques have therefore been developed and are now frequently used to treat these patients.[45-47] The aim of the percutaneous procedure should be complete closure or at least a major reduction in the left-to-right shunt with normalization of hemodynamics.[48]

The deployment of a VSD closure device requires the creation of an arteriovenous wire loop. A guidewire is introduced in a femoral artery; it is advanced trough the aorta and aortic valve into the LV. Through the VSD, the wire is advanced into the RV and right atrium, and it is finally steered into the superior vena cava and pulled out through the internal jugular vein. TEE complements fluoroscopy in guiding the wire to create the arteriovenous loop and then advancing the delivery catheter and deploying the closure device. TEE is particularly helpful in aligning the closing device parallel to the long axis of the interventricular septum and outside of the VSD tract. We have found that 3D TEE helps clarifying the complex morphology of post–myocardial infarction VSDs and currently is our preferred imaging tool to guide percutaneous VSD closures.

## AORTIC VALVE INTERVENTIONS

### *Balloon Aortic Valvuloplasty*

Surgical aortic valve replacement is the treatment of choice for severe symptomatic calcific aortic stenosis in adults. (See Chapter 23.) However, patients with advanced age, hemodynamic instability, or multiple comorbidities often carry an unacceptably high operative risk and can be considered for balloon aortic valvuloplasty. There are two different approaches to reach the aortic valve for balloon aortic valvuloplasty—the retrograde approach by arterial access through the aorta (most commonly used) and the antegrade approach by venous transseptal access.[49]

Balloon aortic valvuloplasty has long been used as a treatment modality in children and adolescents with valvular aortic stenosis.[50] In addition, in children and young adults, the

systematic use of Doppler echocardiography guidance for balloon aortic valvuloplasty interventions is feasible and is associated with high success and very low complication rates. Compared to historical series of balloon aortic valvuloplasty guided by angiography, patients who undergo balloon aortic valvuloplasty with echocardiographic guidance have a significant reduction of fluoroscopic time and a tendency to a lower incidence of significant aortic regurgitation.[51]

In adults, balloon aortic valvuloplasty is useful as palliative treatment for symptomatic relief in elderly patients with severe calcific aortic stenosis who are deemed inoperable.[52,53] Balloon aortic valvuloplasty can be used as a palliation or bridge to definitive therapy in patients with severe aortic stenosis who are poor candidates for surgery.[54] It is associated with good medium-term outcomes in this very high-risk population group and enables some patients to receive definitive therapy in the future.[55] In these patients, echocardiography provides information regarding preprocedure and postprocedure LV ejection fraction, mean gradients, and presence and severity of aortic regurgitation.

### *Transcatheter Aortic Valve Implantation*

Transcatheter aortic valve implantation (TAVI) is maturing as an interventional technique for the treatment of severe symptomatic aortic stenosis.[56-63] The procedural results continue to improve, in part through the use of multidisciplinary teams, including cardiac surgeons, interventional cardiologists, and cardiac imaging specialists. The anatomy of the aortic valvar complex and its implications for TAVI have recently been reviewed.[64]

Two TAVI systems are currently in use: the self-expandable CoreValve ReValving (CoreValve, Irvine, Calif.) and the balloon-expandable Edwards valve (Edwards Lifesciences, Irvine, Calif.). Retrograde transarterial or antegrade transapical approaches are used to implant the aortic valve. To facilitate passage of the prosthesis through the stenotic native valve, balloon aortic valvuloplasty is performed before valve insertion. With the balloon expandable valve, burst ventricular pacing is used to decrease transvalvular flow and avoid expulsion of the system toward the aorta on deployment.

The central role that echocardiography plays in TAVI has recently been reviewed by Jayasuriya and colleagues.[65] In addition, the usefulness and limitations of echocardiography in optimizing the outcome of percutaneous aortic valve implantation have been recently evaluated by Moss and co-workers.[66] In this study, candidates for percutaneous aortic valve implantation were evaluated with transthoracic echocardiography to assess aortic annular dimension and aortic valve hemodynamics. TTE was found useful in guiding correct device sizing. Fifty consecutive patients were deemed suitable for percutaneous aortic valve implantation. Seventy-four percent (37 of 50) of patients underwent TEE during the procedure. TEE was used for the early detection of paravalvular aortic regurgitation and complemented fluoroscopy in the detection of complications. These authors felt that echocardiography played an important role in case selection, in guiding device placement, and in detecting complications of percutaneous aortic valve implantation. The use of 2D and 3D TEE to aid in the positioning and deployment of TAVI has been recently reported, demonstrating that TEE can be an important adjunct to fluoroscopy for guiding percutaneous aortic valve implantation and, therefore, can improve the safety and efficacy of the TAVI procedure.[67] The use of balloon aortic valvotomy sizing of the aortic annulus has been described as an important adjunct to TEE when selecting valve size.[68]

Masson and colleagues[69] have recently reviewed the clinical experience of multiple centers with different valve implantation systems and techniques and highlighted the recognition and management of potential complications. Echocardiography was found to be of particular use in the identification of aortic dissection, detection of annular and root rupture, recognition of mitral valve injury, and detection of paravalvular regurgitation and acute structural valve failure. Bagur and co-workers recently reported their experience in 100 patients in whom TEE was used as the primary imaging technique to guide transapical aortic valve implantation.[70] They found that TEE provided acute and midterm results similar to those of angiography-guided procedures and significantly reduced use of contrast during the procedure.

## BALLOON MITRAL VALVOTOMY

Mitral stenosis occurs from commissural fusion, leaflet thickening, and chordal shortening and fusion, usually as the result of rheumatic fever. Because mitral stenosis is primarily a mechanical obstruction to forward flow through the mitral valve orifice, the only definitive therapy is mechanical relief of this obstruction. The current procedures that are effective in providing such therapy are balloon mitral valvotomy (BMV) (most commonly used approach), open mitral commissurotomy (rarely used), and mitral valve replacement (used in patients who are not candidates for BMV).[71]

Suitability for BMV is determined by valve morphology and the presence and severity of mitral regurgitation. (See Chapter 21.) Patients with moderate or severe mitral regurgitation are usually not candidates for BMV. The Wilkins score[72,73] addresses the morphologic suitability of the mitral valve for BMV and is useful in patient selection with a lower score (less than 9), predicting a favorable outcome with BMV.

The basic steps for BMV are[74] (1) characterize mitral valve morphology and hemodynamics before BMV (to evaluate the degree and location of commissural fusion, determine presence and severity of mitral regurgitation and measure mean mitral valve gradient); (2) guide the transseptal puncture (see Fig. 5-3); (3) locate and define relationships of atrial appendage and mitral orifice and perform visual biofeedback calibration with catheters while inside the left atrium (catheter navigation); (4) ensure coaxial trajectory orientation while navigating the catheter through the mitral orifice (balloon catheter alignment); (5) perform precise position and exclude subvalvular chordal apparatus involvement before inflation and monitor balloon inflation; (6) inspect postinflation commissurotomy results (commissure splitting, mean mitral valve gradient); and (7) search for potential complications (iatrogenic valvular damage, atrial septal defect at site of septal puncture, or pericardial effusion) (Fig. 5-10).

## MITRAL REGURGITATION

Surgery is currently the standard of care for patients with severe mitral regurgitation. Mitral repair has a distinct advantage over mitral replacement because it preserves LV systolic function, obviates the need for anticoagulation, and improves survival (see Chapter 18). Unfortunately, surgical repair is not always feasible, because of advanced age and comorbidities or lack of local surgical expertise. This has promoted the development of

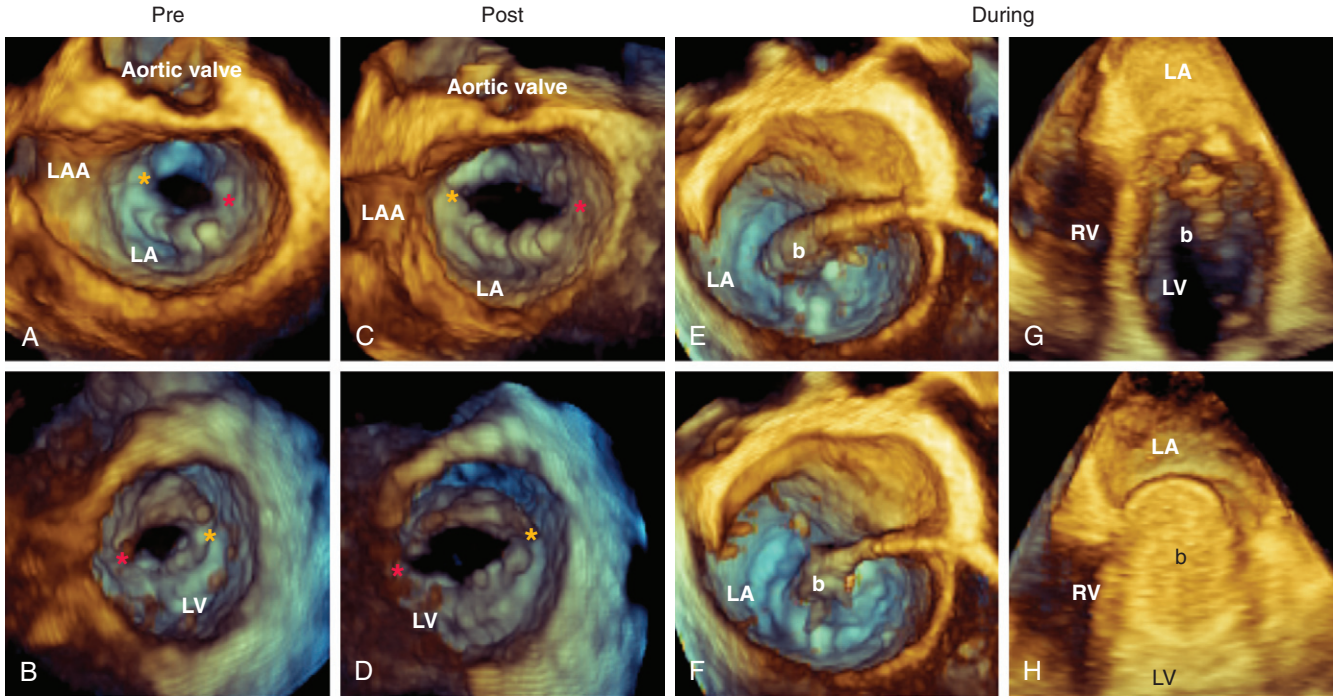



**Figure 5-10** **3D TEE guided mitral valve balloon valvotomy (BMV). A** and **B,** Stenotic mitral valve orifice in a patient with severe mitral stenosis before MVBV. **A,** Mitral valve as seen from the LA. **B,** Stenotic mitral valve as seen from the LV. Fused posteromedial commissure (*red asterisk*); fused anterolateral commissure (*yellow asterisk*). **C** and **D,** Commissural splitting produced by the balloon valvotomy. Note the significant enlargement of the mitral valve area and the splitting of the commissures. **E** to **H,** 3D TEE images obtained during MVBV guidance. **E,** Deflated balloon (*b*) has been advanced through the interatrial septum and is directed to the mitral orifice. **F,** Deflated balloon has been advanced through the mitral orifice into the LV. **G,** Deflated balloon is seen along the long axis of the LV. **H,** Inflated balloon is seen in its longitudinal cross section stretching and splitting the mitral valve commissures. *LAA,* Left atrial appendage.

a variety of transcatheter technologies to treat mitral regurgitation. Echocardiography plays a central role not only in characterizing the cause and severity of mitral regurgitation, but also in determining timing for intervention, providing procedural guidance, and evaluating short- and long-term results. (See Chapter 19.) In addition to fluoroscopy, TEE is the main imaging tool used to assist transcatheter interventions for mitral regurgitation.

### *Percutaneous Edge-to-Edge Mitral Repair*

The Alfieri edge-to-edge mitral repair is a surgical technique to treat mitral regurgitation by approximating the middle scallops of the mitral leaflets, creating a double orifice with improved leaflet coaptation.[75-77] A percutaneous method to create the same type of repair is now available. A transseptal approach is used to deliver a clip device (MitraClip, Abbott Vascular, Menlo Park, Calif.) that grasps the mitral leaflet edges to improve leaflet coaptation and reduce or eliminate mitral regurgitation.[78,79] Echocardiographic and hemodynamic measurements after percutaneous mitral valve repair with this technique show a decrease in mitral valve area, but no evidence of clinically significant mitral stenosis.[80]

TEE plays a central role in guiding the percutaneous edge-to-edge repair. It helps in determining the best site for septal puncture for delivery of catheters to the central area of the mitral valve orifice. TEE permits correct positioning of the clip device over the mitral orifice perpendicular to the line of leaflet coaptation. This step is essential to prevent clip disengagement and to obtain an acceptable reduction in regurgitant severity. The added value of 3D TEE imaging for optimal guidance during the procedure and to evaluate the anatomic result and residual mitral regurgitation has been reported,[81] and 3D TEE is our preferred imaging tool for edge-to-edge mitral valve repair (Figs. 5-11 and 5-12).

The MOBIUS Leaflet Repair system (Edwards Lifesciences) is another catheter-based edge-to-edge technique for the percutaneous treatment of mitral regurgitation. In contrast to the MitraClip, this system uses a catheter to stitch the free edges of the anterior and the posterior mitral leaflets, creating a double-orifice mitral valve. A suction catheter is used to adhere the leaflets together and facilitate stitch placement. This is accomplished under fluoroscopic and echocardiographic guidance.[82,83]

### *Annuloplasty Approaches Using the Coronary Sinus*

In patients with functional mitral regurgitation, the surgical implantation of an annuloplasty ring reshapes the circumference of the annulus and reduces the medial-lateral annular dimension. By moving the posterior annulus and posterior valve leaflet closer to the anterior leaflet, better systolic leaflet coaptation is accomplished.[84] Several biomedical companies are exploring transcatheter approaches that imitate surgical annuloplasty.[85-87] The coronary sinus runs just outside and roughly in the same plane as the posterior mitral annulus; therefore, a device that is placed in the coronary sinus can deform

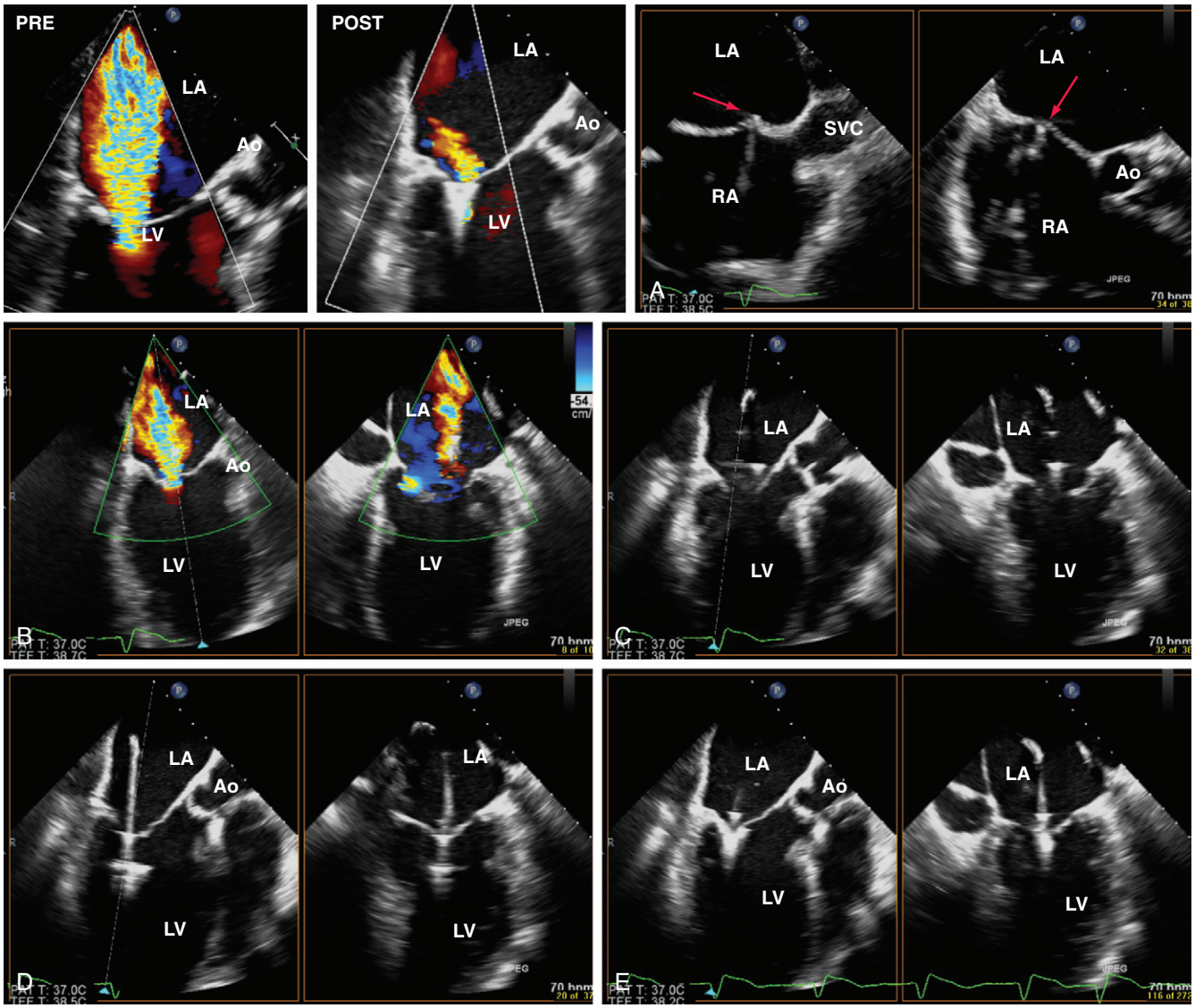



**Figure 5-11** **TEE guidance of mitral clip repair.** (*Top left*) TEE color Doppler images before (*PRE*) and after (*POST*) mitral valve clip repair. Note the presence of severe mitral regurgitation before the procedure and only mild mitral regurgitation after clip repair. **A,** Point of septal puncture, chosen to optimize device delivery. **B,** Guiding catheter and device delivery system are directed to the area of mitral regurgitation by following the mitral regurgitant jet. **C,** Clip approximates the coaptation point of the mitral valve. **D,** Device is advanced into the LV near the tips of the mitral leaflets. **E,** Catheter has been withdrawn, and the clip is grasping the free edges of the leaflets. *Ao*, Aorta; *SVC*, superior vena cava.

the mitral annulus, decrease the intercommissural distance, and, by approximating the mitral leaflets, decrease or obliterate the presence of mitral regurgitation. Currently there are three coronary sinus annuloplasty devices undergoing clinical trials: (1) the Percutaneous Transvenous Mitral Annuloplasty device (Viacor, Wilmington, Mass.), which consists of three straight and rigid nitinol rods seated in a multilumen catheter, which is introduced in the coronary sinus in to the interventricular groove[85]; (2) the Carillon device (Cardiac Dimensions, Kirkland, Wash.), which consists of a curved nitinol arc connecting a proximal and a distal anchor[86]; and (3) the Edwards MONARC system (Edwards Lifesciences), which is a nitinol assembly with a small distal anchor, a larger proximal anchor, and a springlike bridging segment.[87]

In all of these trials, TTE and TEE are used for patient selection and procedural guidance. TTE with 3D imaging is used to characterize the mitral annulus; TEE is used to measure quantitative procedural baseline mitral regurgitation and the septal-lateral annular dimension.

### *Percutaneous Left Ventricular and Mitral Annulus Remodeling*

Current treatments for functional mitral regurgitation, secondary to LV dysfunction, include medical therapy and surgery—consisting of either mitral valve repair or mitral valve replacement. An integrated approach directed to reshape the remodeled LV and annulus to treat functional mitral regurgitation is being developed (Coapsys-Myocor, Maple Grove, Minn.). Coapsys reshapes the ventricle, compressing the mitral annulus and subvalvular apparatus to decrease functional mitral regurgitation.[88] A surgical trial (RESTOR-MV) with this device supports the concept of the ventricular reshaping strategy to reduce mitral regurgitation.[89] Echocardiography was an integral part of the protocol in the RESTOR-MV trial. 2D and 3D TEE provided

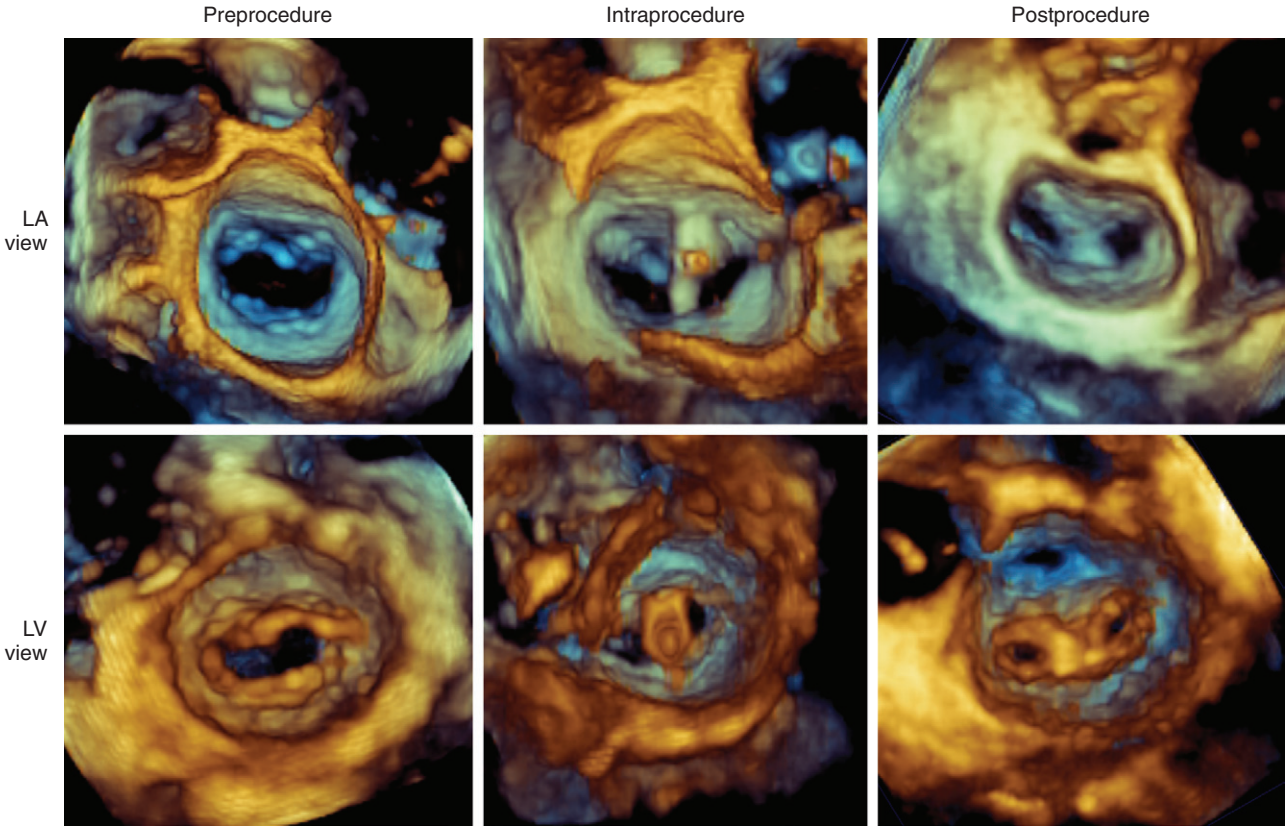



**Figure 5-12 3D TEE guidance of mitral clip repair.** These 3D TEE zoom images depict the mitral valve as seen from the LA and LV before, during, and after mitral valve clip repair. Note how the 3D imaging facilitates placing the device in the center of the mitral valve orifice and perpendicular to the coaptation line. After the device is implanted, a two-orifice mitral valve is noted.

real-time imaging of the LV mitral annulus and presence and severity of existing mitral regurgitation. To further reduce the invasiveness of the procedure, a percutaneous implantation system has been developed [88](iCoapsys, Maple Grove, Minn.). A clinical trial (VIVID: Valvular and Ventricular Improvement via iCoapsys Delivery) has been launched. The implantation has four stages: pericardial access, site identification, device implantation and sizing, and therapeutic evaluation. Echocardiography plays a central role in each of these stages.

## PROSTHETIC VALVES

### *Prosthetic Paravalvular Leaks*

Paravalvular leaks are a rare but serious complication of valve replacement surgery. Most paravalvular leaks follow a benign clinical course, but occasionally, and especially if leaks are large, patients develop heart failure, endocarditis, or hemolysis. (See Chapter 25.) Most clinically significant paravalvular leaks occur in association with prosthetic mitral valves, but prosthetic valves in any position can be affected. Surgical reintervention is associated with high morbidity and mortality; therefore, there has been a compelling interest in developing percutaneous transcatheter closure procedures. Both LV puncture and retrograde transfemoral approaches are used with fluoroscopic and transesophageal guidance. Mahjoub and colleagues[90] have recently described a reference method for TEE and fluoroscopic localization and guidance of mitral paraprosthetic transcatheter leak reduction.

In our laboratory, we use real-time 3D TEE both to define defect anatomy and to guide transcatheter paravalvular leak closure.[91] When combined with the information derived from existing 2D imaging modalities (echocardiography and fluoroscopy), 3D echocardiography enhances catheter navigation by defining the location of the defect relative to surrounding intracardiac structures. With real-time 3D TEE guidance, we facilitate both catheter navigation and defect crossing without the need for time-intensive offline reconstruction. In addition, 3D echocardiography can be used immediately after paravalvular leak closure to assess device stability and interaction with prosthetic valve struts and prosthetic leaflets. The added value of 3D TEE guidance for paravalvular mitral leak closure has also been reported by other laboratories.[92,93]

### *Transcatheter Valve-in-Valve Implants*

The valve-in-valve implant concept is a novel therapeutic option for patients with degenerative failure of bioprosthesis. The transcatheter valve-in-valve implantation does not need reoperation, potentially reducing morbidity and mortality. However, this requires accurate sizing of the transcatheter valve, which is currently available in only two sizes. Therefore, 3D imaging techniques, particularly CT and potentially 3D TEE, are used to provide a more exact sizing of the xenograft ring. Transatrial, transcatheter mitral valve-in-valve implantation has been shown to be feasible off pump in an experimental sheep mode.[94,95] Two recent case reports have demonstrated the feasibility of using this approach in humans.[96,97]

## TRANSCATHETER MITRAL VALVE REPLACEMENT

Several companies are developing percutaneous mitral valve replacement devices. A stent-based bioprosthesis inserted via a transseptal or transapical approach is favored. Lozonschi and co-workers[98] have recently reported an experimental model of a self-expanding valved stent created for transapical replacement of the mitral valve. It houses a trileaflet glutaraldehyde-preserved porcine valve provided with atrial and ventricular fixation systems. Ten pigs underwent transapical mitral valved stent implantation through a lower ministernotomy. The valved stent function was assessed by TEE and contrast left ventriculogram. All animals exhibited normal hemodynamics immediately after mitral valved stent implantation and maintained stability for the entire period of monitoring.[98]

Endovalve (Micro Interventional Devices Inc., Langhorne, Penn.) is developing a mitral valve replacement system with a foldable nitinol structure that attaches to the native valve apparatus with a gripper and is fully valve sparing. Initially this will be used with a minithoracotomy approach. A subsequent truly percutaneous delivery catheter using the same valve design is planned for later development. Again, TEE will likely play an important role in supporting this new technology.

## RIGHT HEART VALVE DISEASE

### *Tricuspid Balloon Valvotomy*

Tricuspid stenosis is usually secondary to rheumatic heart disease and most commonly occurs in association with mitral stenosis (see Chapter 34). Surgical commissurotomy and valve replacement are the standard surgical approaches to correct it. Percutaneous tricuspid balloon valvotomy can now be used to treat tricuspid stenosis in a fashion similar to that used to treat mitral stenosis.

Balloon valvotomy for tricuspid stenosis appears to be effective and associated with low morbidity.[99-102] Thus, in symptomatic patients refractory to medical therapy, balloon valvotomy of the stenotic tricuspid valve should be considered. Echocardiography is used to determine the presence and severity of tricuspid stenosis, as well as to document the degree of associated tricuspid regurgitation. The echocardiographic guidance for tricuspid valvotomy is similar to the one described for BMV.

### *Pulmonic Valvotomy*

Congenital pulmonic valve stenosis comprises 7% to 9% of all congenital heart defects. In the past, surgical valvotomy was the treatment of choice; more recently, balloon valvuloplasty has become the preferred option for the management of congenital pulmonic valve stenosis. Balloon dilatation is usually performed only in patients with a peak-to-peak gradient greater than 50 mm Hg.[103] Echo/Doppler methods play an important role in the diagnosis and determination of pulmonic stenosis severity, as well as in short- and long-term follow-up. Procedural guidance is usually done with fluoroscopy and cineangiography.

### *Percutaneous Pulmonic Valve Implantation*

The most common consideration for percutaneous pulmonic valve implantation is in patients who have previously undergone surgery of the RV outflow tract during repair of congenital heart disease and have symptoms related to RV outflow tract dysfunction.[104]

The RV outflow tract gradient and severity of pulmonic regurgitation are evaluated using standard approaches (see Chapter 34). Echocardiography performed 24 hours after percutaneous pulmonic valve implantation shows a reduction in RV pressure and RV outflow tract gradient along with a significant reduction in the degree of pulmonic regurgitation.[105] Pulmonic valve implantation is usually done with fluoroscopic and angiographic guidance.

## PERCUTANEOUS INTERVENTIONS IN THE LEFT VENTRICLE

### *Alcohol Septal Ablation for Hypertrophic Cardiomyopathy*

Hypertrophic cardiomyopathy is a clinically heterogeneous autosomal dominant genetic heart disease characterized by unexplained LV hypertrophy (see Chapter 27). It is the most common cause of sudden cardiac death in the young and is an important substrate for heart failure disability at any age.

Alcohol septal ablation is an effective method to treat symptomatic hypertrophic cardiomyopathy (HCM) refractory to medical therapy.[106,107] Guidance of the procedure by contrast TTE or TEE facilitates choosing the appropriate septal perforator artery to infuse with alcohol and avoid acute complications that cannot be anticipated by angiography alone.[108] The commonly accepted indications for alcohol septal ablation in patients with HCM include symptoms that interfere substantially with lifestyle despite optimal medical therapy; septal thickness of at least 15 to 16 mm; systolic anterior motion of the mitral valve; LV outflow tract gradient of 30 mm Hg at rest or 50 mm Hg on provocation; accessible septal branch; absence of intrinsic abnormality of the mitral valve; and absence of proximal left anterior descending coronary artery stenosis.

Echocardiographic guidance of septal ablation for HCM starts with characterization of the degree and location of septal hypertrophy, demonstration of systolic anterior motion of the mitral valve leaflet, outlining the degree and direction of the associated mitral regurgitation jet, and measurement of the resting or provocable (amyl nitrite or catheter-induced premature ventricular contractions) LV outflow tract gradient. In general we use TTE guidance unless transthoracic windows are suboptimal, in which case we use TEE. The objective of septal ablation is to safely administer 100% ethanol into the area of septal hypertrophy responsible for outflow obstruction and systolic anterior motion of the mitral valve. Therefore, it is critical to identify the septal branches of the left anterior descending coronary artery that supply the septal myocardium responsible for the obstruction. This is best accomplished by the use of myocardial contrast echocardiography. A wire is passed into the septal perforator estimated to supply the area of septal hypertrophy responsible for outflow obstruction, and then a short balloon is advanced over the wire into the proximal part of the target vessel. The balloon is inflated to completely obstruct the septal artery as demonstrated by the absence of reflux of contrast around the balloon. About 1 mL of a mixture of radiographic contrast agent mixed with blood and agitated saline is injected through the balloon catheter and visualized by TTE showing contrast enhancement in the thickened septum. Multiple views (apical 4, apical 5, apical long-axis view, and short-axis LV views) allow characterization of the extent of the contrast enhancement and permit recognition of undesirable areas of blood supply of the selected septal perforator such as the free wall of the right ventricle and the anterolateral wall of the LV and papillary muscles.

Once the appropriate septal perforator is selected, 1 to 5 mL of alcohol is slowly injected through the central lumen of the

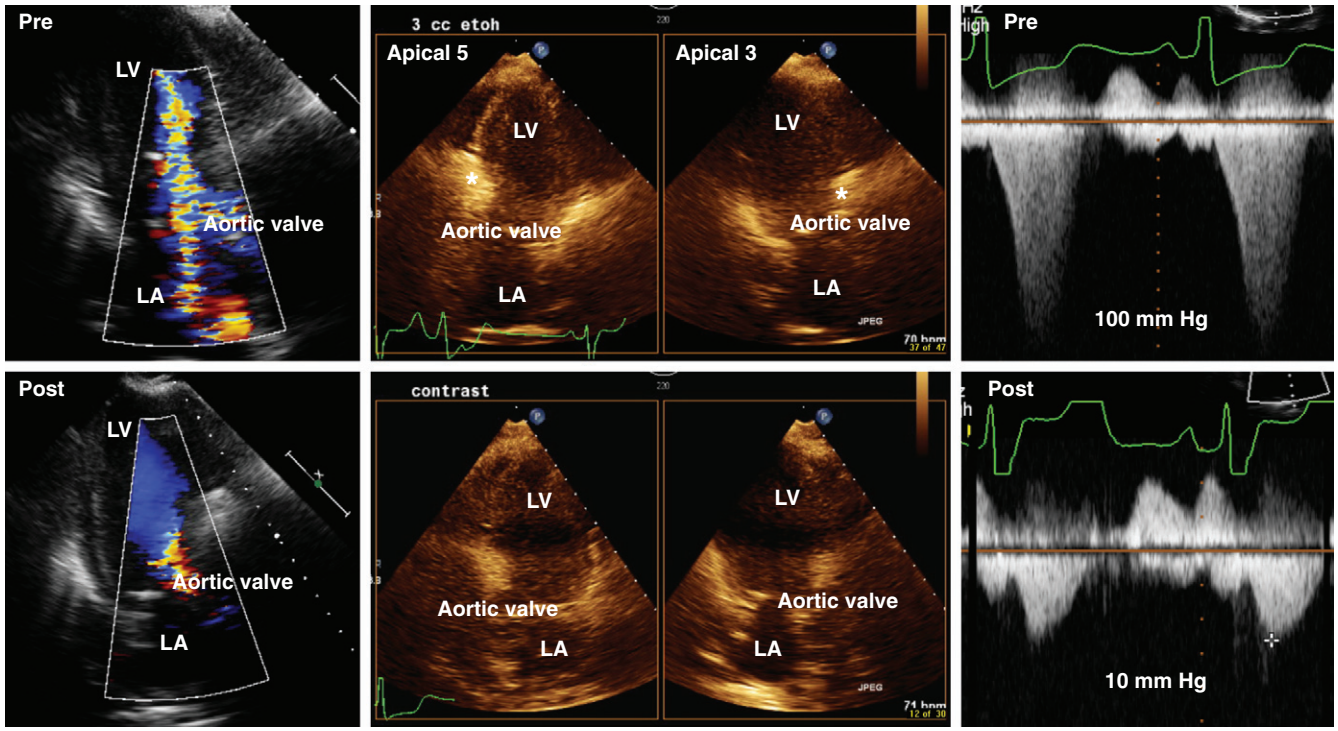



**Figure 5-13 Alcohol septal ablation for hypertrophic cardiomyopathy (HCM).** Resolution of mitral regurgitation (*left panels*) immediately post alcohol septal ablation in this patient with HCM. Drop of left ventricular outflow tract gradient from 100 mm Hg to 10 mm Hg (*right panels*) with alcohol septal ablation. Simultaneous biplane views of the LV (*middle* panels) from the apical 5 and apical 3 chambers. These planes permit visualizing the area of the interventricular septum (*) that is enhanced with the injection of contrast and, later on, alcohol in the appropriate septal perforator.

balloon catheter under echocardiographic guidance. After each milliliter of alcohol is injected, the presence and severity of systolic anterior motion and mitral regurgitation are recorded. In addition, the outflow gradient is measured and the degree of basal septal hypokinesis is noted. It is very important to continuously monitor the entire myocardium with echocardiography to watch for hypokinesis and myocardial enhancement in undesirable areas, which can represent alcohol in those areas. The immediate postinjection Doppler gradient is used to confirm satisfactory results. The goal is to reduce the resting gradient to less than 10 mm Hg or 50% of the preprocedure provocable gradient. If this is not achieved, a second potential septal perforator is searched for and the process is repeated. At the end of the procedure, the presence and degree of systolic anterior motion and mitral regurgitation are noted, and a final resting and post–premature ventricular contraction gradient is recorded (Fig. 5-13).

Echocardiography also plays an important role in detecting and managing potential complications during septal ablation for HCM. In addition to recognizing wall-motion abnormalities in inappropriate locations, echocardiography is ideally suited to detect a new pericardial effusion suggesting cardiac perforation, increased degree of mitral regurgitation suggesting papillary muscle compromise, and the presence of a new ventricular defect suggesting a large transmural septal infarct.

### *Percutaneous Closure of Pseudoaneurysm of Left Ventricle*

LV pseudoaneurysm is an uncommon, often fatal complication associated with myocardial infarction, cardiothoracic surgery, trauma, and, occasionally, infective endocarditis. LV pseudoaneurysms form when cardiac rupture is contained by adherent pericardium or scar tissue (see Chapter 14). LV pseudoaneurysms are not common, the diagnosis is difficult, and they are prone to rupture.[109] Most investigators support surgery as the appropriate treatment for LV pseudoaneurysm,[110] because untreated pseudoaneurysms have a 30% to 45% risk of rupture. However, surgery for repair of LV pseudoaneurysm still carries high morbidity and mortality. There are now several reports of percutaneous closure of LV pseudoaneurysms with encouraging results.[111-113]

## PERCUTANEOUS CLOSURE OF LEFT ATRIAL APPENDAGE

Patients with atrial fibrillation have a fivefold higher risk of stroke, making this the primary cause of long-term disability and one of the leading causes of death in patients with atrial fibrillation. (See Chapter 42.) Antithrombotic therapy to prevent thromboembolism is recommended for most patients with atrial fibrillation, using the CHAD2 guidelines for nonvalvular atrial fibrillation and the ACC/AHA guidelines for management in those with coexisting valve disease.[114]

In patient with atrial fibrillation, most thromboemboli arise from the left atrial appendage (LAA). Percutaneous device LAA closure has now been developed as an adjunct and as an alternative to pharmacotherapy in patients with atrial fibrillation.[115] Encouraging randomized data is available with the WATCHMAN device[116,117] (Atritech, Plymouth, Minn.), and several other devices are in various stages of clinical development. These include the Amplatzer Septal Occluder and cardiac plug (AGA Medical, Plymouth, Minn.), PLAATO (ev3 endovascular, Plymouth, Minn.) and the transcatheter patch (Custom Medical Devices, Athens, Greece). The deployment in all the devices is fairly similar. The left atrium is accessed through a standard septal puncture, the sheath is advanced up to the LAA orifice,

and a pigtail catheter is inserted into the LAA. The morphology of the LAA is characterized by TEE, paying special attention to its orifice shape and size, angulation of the orifice and body of the LAA, and presence and number of lobules. The device is sized, advanced, and deployed into the LAA orifice.[118] After device deployment, TEE is used to determine device stability and presence of any residual flow in the LAA. TEE is also the principal modality to evaluate for procedural complications such as structural damage, pericardial effusion, and residual atrial septal defects.

### PERCUTANEOUS CLOSURE OF AORTIC PSEUDOANEURYSMS

Pseudoaneurysms of the ascending aorta usually follow previous aortic dissection repair, aortic valve replacement, coronary artery bypass graft surgery, and cardiac transplantation. Surgical repair is the standard form of therapy, but it is associated with significant morbidity and mortality. Percutaneous closure of aortic pseudoaneurysms is therefore an attractive alternative, and now there are several reports with successful outcomes using this modality.[119-121] Transthoracic and TEE provide useful imaging guidance for percutaneous closure of aortic pseudoaneurysms.

## Procedures Not Covered in This Chapter

There are several other echocardiographic applications in the catheterization laboratory that we have not covered in this chapter. This is because they are not, strictly speaking, SHD interventions, or they are covered in other chapters of this book. We do provide some references for the interested reader to review. These include use of echocardiography to guide myocardial biopsy[7,122,123]; cardiac electrophysiology–related procedures[7,124-127]; balloon pericardiotomy[128,129]; and uncommon congenital heart disease interventions.[130]

## Limitations and Alternate Approaches

Although echocardiography is the most commonly used imaging technique to supplement fluoroscopy during SHD interventions, it has some limitations that need to be recognized. Image quality may be compromised by having the patient in the supine position instead of the usual left lateral decubitus. This problem can be partially corrected by the use of a rotating table with mild lateral rotation, or by the use of a pillow under the patient's right shoulder. If image quality remains nondiagnostic, an alternative imaging approach, such as TEE or ICE, should be considered. An additional shortcoming of TTE during interventions for SHD is that not all the standard echocardiographic windows are available during the intervention. The easiest window to use is the apical window; the left parasternal, subcostal, and suprasternal windows tend to be less accessible because they interfere with fluoroscopic imaging.

Because of these problems with TTE, TEE is favored in many SHD interventions. Unless general anesthesia is planned for other reasons, TEE can be performed under conscious sedation, with the added complexity and potential for complications this brings to the procedure. To decrease the chances of aspiration, the table needs to be somewhat rotated, and a pillow under the patient's right shoulder is used. Continuous oral suction also decreases the chances of aspiration. In addition to the standard conscious sedation regimen, we favor the use of intravenous antiemetic agents to decrease the gagging and vomiting that can significantly impair the safe performance of an intervention. Although image quality with TEE usually is excellent, suboptimal images may be seen in patients with a large esophagus or with a hiatal hernia that precludes adequate probe-to-esophagus contact. In prolonged procedures, there is also the potential for dryness in the esophageal mucosa and image deterioration. Adding a lubricant to the esophageal probe at 30- to 60-minute intervals decreases this problem.

Another limitation of TEE is the relative narrow field of view, especially in the near-field structures such as the posterior left atrium. Frequently catheters or devices are not visualized because they are out of the imaging field. The probe position can be adjusted as needed to bring the catheters into view, or, if this is not possible, the device or catheter can be advanced under fluoroscopic guidance alone until it comes into the echocardiographic field of view.

### INTRACARDIAC ULTRASOUND

Echocardiographic guidance of SHD interventions has been significantly affected by the development of intracardiac echocardiography.[131,132] ICE is now a standard tool in centers performing catheter therapies for SHD (See Chapter 6). The impact of ICE has been affected by multiple facets, including the unique aspects of the images, the ability of the interventionalist to perform ICE, the special skills needed, the costs and reuse of the catheter, and the vascular access issues (Fig. 5-14). In addition, the list of specific procedures for which ICE has been used continues to grow and includes both diagnostic use as well as image guidance, typically combined in the same procedure. Finally, the future of ICE is likely to include more widespread use, the addition of real-time 3D imaging, enhanced integration into the procedure room, and a variety of new catheter designs.

There are four areas in SHD interventions where ICE has had its greatest impact. These include the performance of transseptal catheterization, closure of interatrial defects (Figs. 5-15 and 5-16), mitral interventions, and atrial fibrillation ablation. ICE provides in-depth understanding of the anatomy, is used during balloon sizing of defects, guides the placement of the device, and then allows conformation of proper device placement, completeness of closure, and absence of complications.[133] ICE guidance in the performance of transseptal catheterization has become routine. With the probe in the right atrium, all key structures are visualized by ICE. This has increased the safety of the procedure, but also allowed the site of transseptal crossing to be more precisely determined.[134] Valvular interventions may also be guided by ICE (Fig. 5-17). Mitral balloon commissurotomy for mitral stenosis can be greatly facilitated by the use of ICE. After guiding the transseptal puncture, ICE can provide unique assessment of the subvalvular apparatus, assess the placement of the balloon, and monitor the result.[135] Atrial fibrillation ablation has been a procedure that has moved ICE into being a necessary technology in the electrophysiology laboratory. ICE provides guidance for the transseptal catheterization, but also for the subsequent visualization of ablation in the left atrium and pulmonary veins.[136]

### COMPUTED TOMOGRAPHY

SHD interventions can often be planned using cardiac CT angiography. Comprehensive fine resolution of cardiac structure and display of 3D relationships to adjacent structures in combination with a full field of view are the strengths of

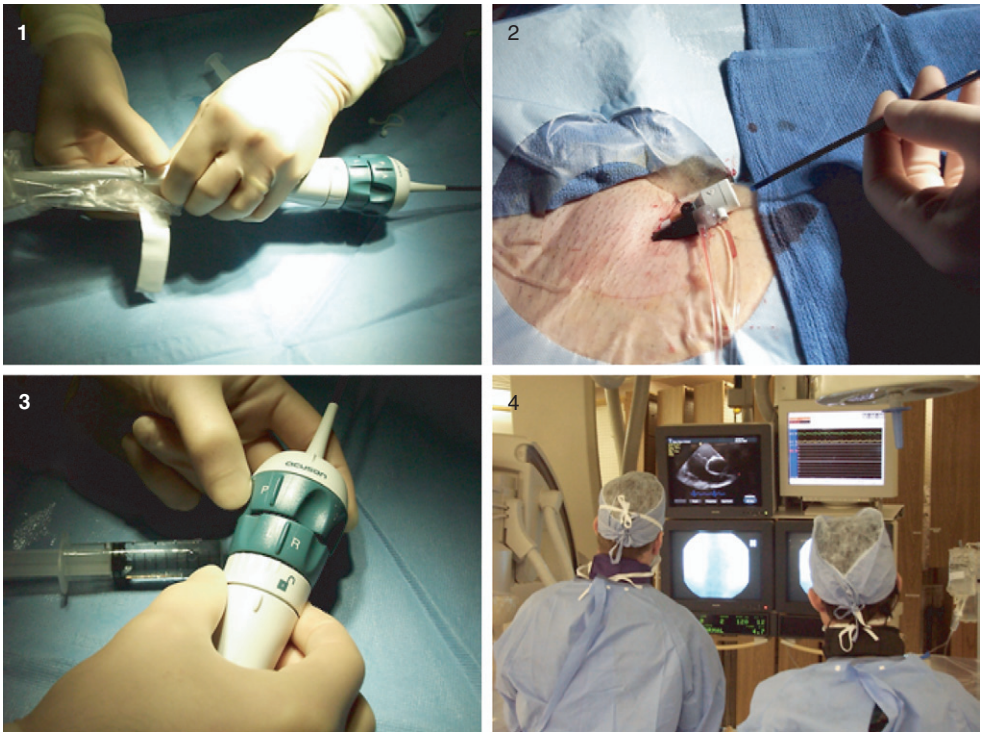



**Figure 5-14 Steps in intracardiac echocardiography (ICE).** The four steps in using ICE to guide structural heart disease interventions. *1*, Preparation of ICE catheter for plug and play. *2*, Insertion into vascular access point and navigation to the heart using fluoroscopic guidance. *3*, Navigation within the heart for visualization of structures of interest for the intervention. *4*, Display and interpretation of images during intervention.

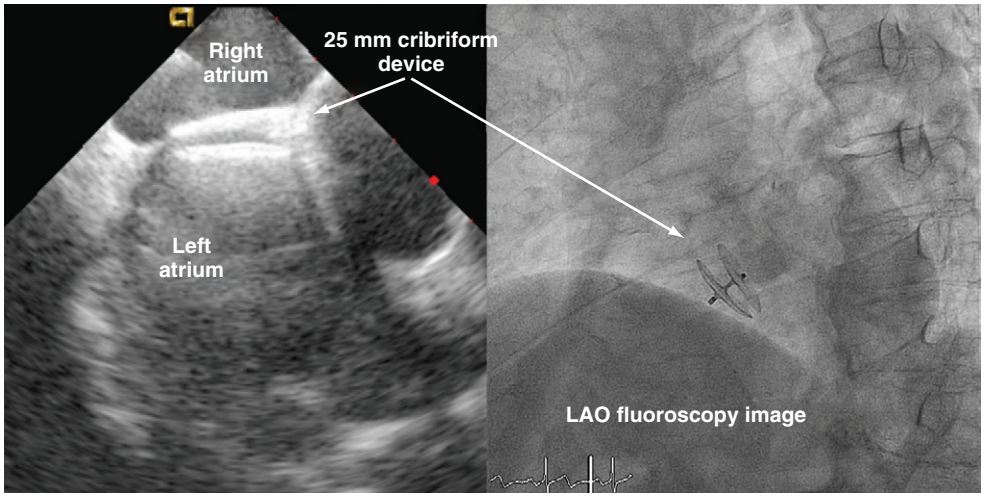



**Figure 5-15 Device visualization using both intracardiac echocardiography (ICE) and fluoroscopy.** Appearance of a nitinol mesh device used to close a multifenestrated atrial septal defect using ICE (*left*) and fluoroscopy (*right*) visualization. *LAO*, left anterior oblique.

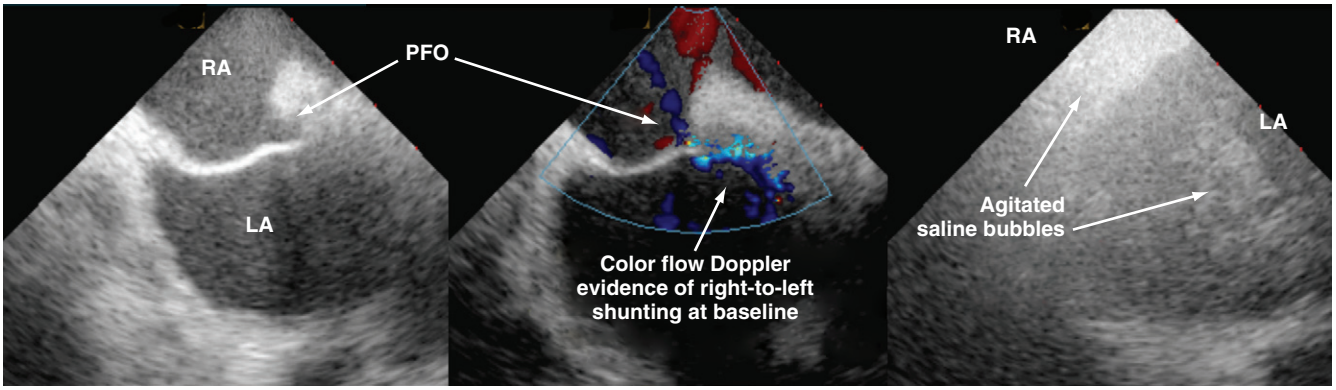



**Figure 5-16 Intracardiac echocardiography (ICE) assessment of patent foramen ovale (*PFO*) immediately before closure.** Intraprocedure assessment of a PFO in a patient with systemic hypoxemia from right-to-left shunting. ICE placement in the RA is straightforward and yields excellent image quality of interatrial septum. (*Left panel*) Visualization of the thin septum primum and septum secundum, which is thick, i.e., lipomatous. The PFO tunnel length and width at any point of the tunnel can be measured. (*Middle panel*) Color flow Doppler visualization of the right-to-left flow in the PFO. (*Right panel*) Dense opacification of both the RA and LA from a peripheral injection of agitated saline that immediately traversed the PFO. These three findings provide the evidence for the need for closure, including the large volume of shunting producing systemic hypoxemia, and the measurements needed for device sizing.

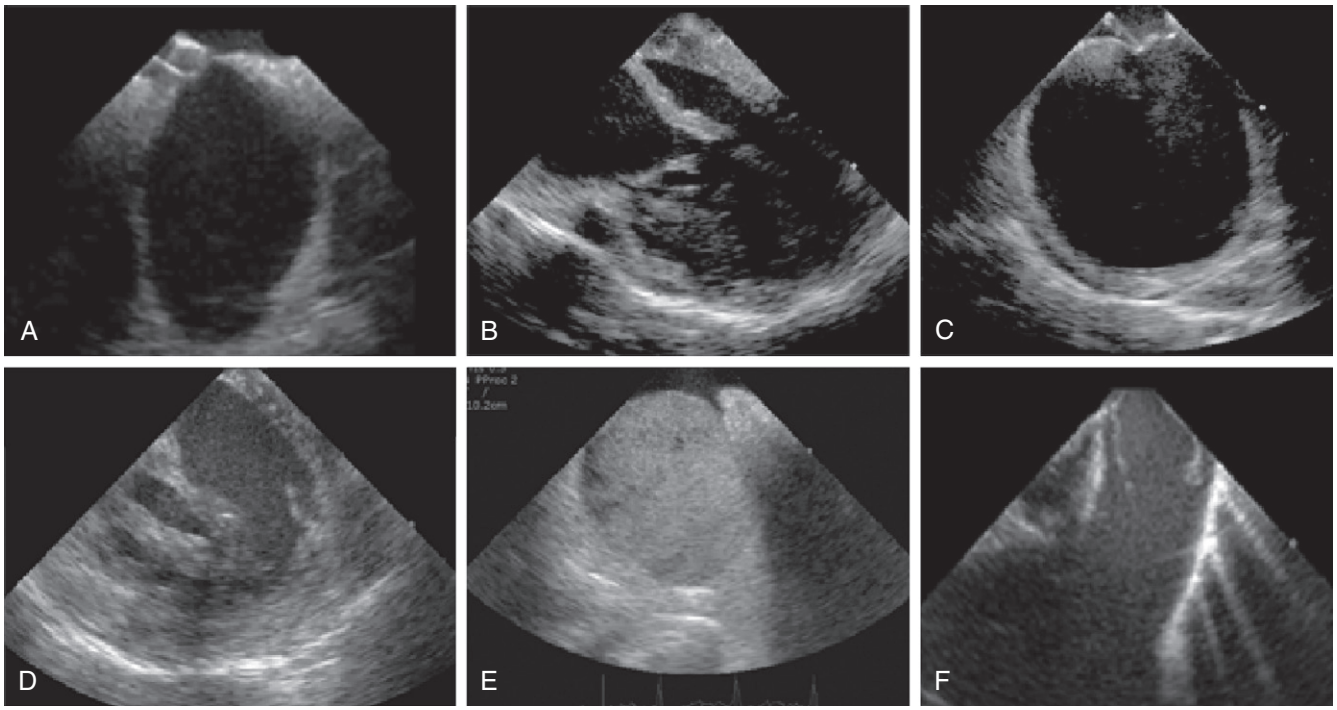



**Figure 5-17 Six panels of intracardiac echocardiography (ICE) findings during structural heart disease interventions. A,** ICE catheter in the RA visualizes the interatrial septum with a "j" wire being navigated to cross a patent foramen ovale before closure. **B,** ICE catheter in the RV visualizes the mitral leaflets during a mitral balloon valvotomy. Note the thickened anterior leaflet. **C,** ICE catheter in the RA visualizes the interatrial septum, showing "tenting" due to engagement of a transseptal catheter before needle puncture. **D,** ICE catheter in the RV visualizes the mitral subvalvular apparatus, which is severely thickened, contracted, and matted. The mitral balloon valvotomy was aborted because of this finding. **E,** ICE catheter in the RA visualizes the LA, which is opacified by bubbles from agitated saline being injected in the left pulmonary artery to document a large pulmonary arteriovenous fistula during a closure procedure. **F,** ICE catheter in the RV visualizes the pulmonic valve immediately after inflation of a balloon in a congenitally stenotic valve. The thin valve leaflets now open widely and no longer dome.

tomographic imaging techniques such as cardiac CT angiography and magnetic resonance. Multislice CT scanners have become useful in SHD intervention because of faster gantry rotation speeds, increased numbers of detectors and dual sources, and improved spatial and temporal resolution. CT angiography can provide the information to describe the target of the intervention, help size the device, and potentially plan the pathway to the target and the needed delivery system. Currently CT angiography is used for planning TAVI,[137] paravalvular leak closure, large ASD closure,[138] and VSD closure, and whenever any other cardiac structural defect is poorly characterized by echocardiography.

### CARDIAC MAGNETIC RESONANCE IMAGING

Cardiac magnetic resonance imaging is a valuable technique used in SHD interventions,[139-143] but less useful than cardiac CT angiography because of the length of acquisition and analysis, the somewhat reduced spatial resolution, and the wider availability of CT angiography. That being said, cardiac magnetic resonance is more common in the pediatric patient population and has the ability to quantify shunts, regurgitant volumes, and many aspects of cardiac function relevant to SHD. Cardiac gating and breath-holding are needed.

### MULTIMODALITY IMAGING

Preprocedure CT angiography and cardiac magnetic resonance can now be imported, segmented, and registered with fluoroscopy in the SHD interventional lab as well as in the hybrid operating room. This advanced multimodality approach requires an image workstation and applications on the workstation that allow the CT angiography and MR images to be manipulated and segmented to optimize their use for the intervention. A new team approach must be developed in hospitals performing SHD interventions that includes physicians with training in advanced imaging modalities and echocardiographers with specialized knowledge and TEE skills specific for image-guided interventions.[3]

Echocardiography joins fluoroscopy and preprocedure CT angiography and cardiac magnetic resonance as the multimodality imaging approaches to SHD interventions. Each brings advantages and disadvantages. The available technologies as well as expertise at an institution often determine which modalities are used. As the new SHD interventions become available, there is a new emphasis on determining the image guidance strategy that is optimal for the intervention. Furthermore, the multiple modalities used include the differing needs of planning for the intervention versus its real-time image guidance.

## The Catheterization Laboratory of the Future

3D imaging has emerged as an important tool to aid in SHD interventions. Not only are the 3D relationships between structures of critical importance to understand before an intervention, but the navigation of delivery systems and the deployment of devices are greatly aided by real-time 3D imaging. New approaches to 3D imaging will include 3D ICE and also the

ability to generate and immediately use 3D images from other modalities.[144,145]

An important technology development relevant to SHD interventions is the C-arm CT approach.[146] The standard flat detector rotating around the patient with or without contrast injection transforms this x-ray machine into a CT scanner capable of soft-tissue visualization. This in-room capability may be especially useful in TAVI in providing annulus measurements for device sizing, root anatomy to avoid coronary obstruction complications during valve implantation, and orientation information for proper device deployment to avoid embolization.

Optimization of image display includes large flat screens with very high resolution to allow the display and manipulation of images from multiple modalities. For preprocedure planning, image display on the monitor has been replaced by the ability of rapid prototyping[147] to take imaging data from CT angiography, cardiac magnetic resonance, or 3D echocardiography and transform images into physical heart models. The physicality of a model allows the interventional team to examine the patient's heart in a unique fashion and simulate the intervention by trying different device sizes, for example.

SHD interventions have stimulated the development of novel devices and interventional techniques, and these unique interventions have also fundamentally transformed medical imaging, including diagnostic imaging, planning for interventions, and the actual image guidance process. This chapter on SHD interventions has emphasized the important role echocardiography plays in procedural guidance and highlights the transformation of echocardiography, both the technology and the echocardiographer, to support these interventions. This has occurred in a short period of time.

## KEY POINTS

- SHD has come into use in the interventional cardiology community to designate a group of disorders potentially amenable to catheter-based therapies, often involving unique devices that act to close defects, plug communications, and modify cardiac function.
- SHD interventions is a useful grouping for the specialty because these interventions require technical, imaging, and hemodynamic interpretation knowledge and skills that are distinct from those required by percutaneous coronary interventions and other vascular interventional skills.
- The main imaging tools to guide SHD interventions include fluoroscopy, cineangiography, intracardiac echocardiography, and transthoracic and transesophageal echocardiography.
- All of the usual echocardiographic methods used in the echocardiographic laboratory, including 2D and 3D echocardiography, spectral Doppler, color Doppler, and contrast echocardiography, are used in the catheterization laboratory to support SHD interventions. Both TTE and TEE approaches can be used.
- Echocardiography plays a central role in guiding structural heart disease interventions by facilitating access to the target vessel or chamber and by assisting with catheter navigation and device delivery.
- The SHD interventions that have benefited the most from echocardiographic guidance include closure of septal defects, alcohol septal ablation for hypertrophic cardiomyopathy, balloon valvuloplasty, edge-to-edge mitral valve repair, closure of paravalvular leaks, left atrial appendage occlusion, and, more recently, transcutaneous aortic valve implantation.
- Advanced imaging modalities to assist in the management of patients with SHD include computed tomography and cardiac magnetic resonance imaging.
- The cardiac catheterization laboratory of the future will have integrated multimodality imaging to assist in SHD interventions.

## REFERENCES


1. Cubeddu RJ, Inglessis I, Palacios IF: Structural heart disease interventions: an emerging discipline in cardiovascular medicine. *J Invasive Cardiol* 21:478-482, 2009.
2. Herrmann HC, Baxter S, Ruiz CE, et al: Results of the Society of Cardiac Angiography and Interventions survey of physicians and training directors on procedures for structural and valvular heart disease. *Catheter Cardiovasc Interv* 76(4):E106-E110, 2010.
3. Hilliard AA, Nishimura RA: The interventional cardiologist and structural heart disease: the need for a team approach. *JACC Cardiovasc Imaging* 2:8-10, 2009.
4. Ruiz CE, Feldman TE, Hijazi ZM, et al: Interventional fellowship in structural and congenital heart disease for adults. *JACC Cardiovasc Interv* 3:e1-15, 2010.
5. Salem DN, O'Gara PT, Madias C, Pauker SG: Valvular and structural heart disease: American College of Chest Physicians evidence-based clinical practice guidelines, ed 8. *Chest* 133:593S-629S, 2008.
6. Carroll J, Weber J: *Manual of structural heart disease interventions*, 2011, Lippincott Williams & Wilkins.
7. Silvestry FE, Kerber RE, Brook MM, et al: Echocardiography-guided interventions. *J Am Soc Echocardiogr* 22:213-231; quiz 316-7, 2009.
8. Carroll JD: The death or the rebirth of the left ventriculogram? *Catheter Cardiovasc Interv* 73:241-242, 2009.
9. Garcia JA, Eng MH, Wink O, et al: Image guidance of percutaneous coronary and structural heart disease interventions using a computed tomography and fluoroscopy integration. *Vascular Disease management* 4:89-97, 2007.
10. Wallace MJ, Kuo MD, Glaiberman C, et al: Three-dimensional C-arm cone-beam CT: applications in the interventional suite. *J Vasc Interv Radiol* 19:799-813, 2008.
11. Glatz AC, Zhu X, Gillespie MJ, Hanna BD, Rome JJ: Use of angiographic CT imaging in the cardiac catheterization laboratory for congenital heart disease. *JACC Cardiovasc Imaging* 3:1149-1157, 2010.
12. Salcedo EE, Quaife RA, Seres T, Carroll JD: A framework for systematic characterization of the mitral valve by real-time three-dimensional transesophageal echocardiography. *J Am Soc Echocardiogr* 22:1087-1099, 2009.
13. Lang RM, Bierig M, Devereux RB, et al: Recommendations for chamber quantification: a report from the American Society of Echocardiography's Guidelines and Standards Committee and the Chamber Quantification Writing Group, developed in conjunction with the European Association of Echocardiography, a branch of the European Society of Cardiology. *J Am Soc Echocardiogr* 18:1440-1463, 2005.
14. Hudson PA, Eng MH, Kim MS, et al: A comparison of echocardiographic modalities to guide structural heart disease interventions. *J Interv Cardiol* 21:535-546, 2008.
15. Flachskampf FA, Badano L, Daniel WG, et al: Recommendations for transoesophageal echocardiography: update 2010. *Eur J Echocardiogr* 11:557-576, 2010.

16. Baumgartner H, Hung J, Bermejo J, et al: Echocardiographic assessment of valve stenosis: EAE/ASE recommendations for clinical practice. *Eur J Echocardiogr* 10:1-25, 2009.
17. Seto AH, Abu-Fadel MS, Sparling JM, et al: Real-time ultrasound guidance facilitates femoral arterial access and reduces vascular complications: FAUST (Femoral Arterial Access With Ultrasound Trial). *JACC Cardiovasc Interv* 3:751-758, 2010.
18. Gutzeit A, Schoch E, Sautter T, et al: Antegrade access to the superficial femoral artery with ultrasound guidance: feasibility and safety. *J Vasc Interv Radiol* 21:1495-1500, 2010.
19. Ross J, Jr, Braunwald E, Morrow AG: Transseptal left heart catheterization: a new diagnostic method. *Prog Cardiovasc Dis* 2:315-318, 1960.
20. Ross J, Jr: Transseptal left heart catheterization a 50-year odyssey. *J Am Coll Cardiol* 51:2107-2115, 2008.
21. Babaliaros VC, Green JT, Lerakis S, Lloyd M, Block PC: Emerging applications for transseptal left heart catheterization old techniques for new procedures. *J Am Coll Cardiol* 51:2116-2122, 2008.
22. Tzeis S, Andrikopoulos G, Deisenhofer I, Ho SY, Theodorakis G: Transseptal catheterization: considerations and caveats. *Pacing Clin Electrophysiol* 33:231-242, 2010.
23. Earley MJ: How to perform a transseptal puncture. *Heart* 95:85-92, 2009.
24. Braunwald: Cooperative study on cardiac catheterization. Percutaneous left ventricular puncture. *Circulation* 37:III80, 1968.
25. Ommen SR, Higano ST, Nishimura RA, Holmes DR, Jr: Summary of the Mayo Clinic experience with direct left ventricular puncture. *Cathet Cardiovasc Diagn* 44:175-178, 1998.
26. Lim DS, Ragosta M, Dent JM: Percutaneous transthoracic ventricular puncture for diagnostic and interventional catheterization. *Catheter Cardiovasc Interv* 71:915-918, 2008.
27. Rigatelli G, Cardaioli P, Hijazi ZM: Contemporary clinical management of atrial septal defects in the adult. *Expert Rev Cardiovasc Ther* 5:1135-1146, 2007.
28. Webb G, Gatzoulis MA: Atrial septal defects in the adult: recent progress and overview. *Circulation* 114:1645-1653, 2006.
29. King TD, Thompson SL, Steiner C, Mills NL: Secundum atrial septal defect. Nonoperative closure during cardiac catheterization. *JAMA* 235:2506-2509, 1976.
30. Khan AA, Tan JL, Li W, et al: The impact of transcatheter atrial septal defect closure in the older population: a prospective study. *JACC Cardiovasc Interv* 3:276-281, 2010.
31. Jategaonkar S, Scholtz W, Schmidt H, Horstkotte D: Percutaneous closure of atrial septal defects: echocardiographic and functional results in patients older than 60 years. *Circ Cardiovasc Interv* 2:85-89, 2009.
32. Huang X, Shen J, Huang Y, et al: En face view of atrial septal defect by two-dimensional transthoracic echocardiography: comparison to real-time three-dimensional transesophageal echocardiography. *J Am Soc Echocardiogr* 23:714-721, 2010.
33. Quaife RA, Chen MY, Kim M, et al: Preprocedural planning for percutaneous atrial septal defect closure: transesophageal echocardiography compared with cardiac computed tomographic angiography. *J Cardiovasc Comput Tomogr* 4:330-338, 2010.
34. Overell JR, Bone I, Lees KR: Interatrial septal abnormalities and stroke: a meta-analysis of case-control studies. *Neurology* 55:1172-1179, 2000.
35. Fazio G, Ferro G, Carita P, et al: The PFO anatomy evaluation as possible tool to stratify the associated risks and the benefits arising from the closure. *Eur J Echocardiogr* 11:488-491, 2010.
36. Rana BS, Shapiro LM, McCarthy KP, Ho SY: Three-dimensional imaging of the atrial septum and patent foramen ovale anatomy: defining the morphological phenotypes of patent foramen ovale. *Eur J Echocardiogr* 11:i19-i25, 2010.
37. Rana BS, Thomas MR, Calvert PA, Monaghan MJ, Hildick-Smith D: Echocardiographic evaluation of patent foramen ovale prior to device closure. *JACC Cardiovasc Imaging* 3:749-760, 2010.
38. Davison P, Clift PF, Steeds RP: The role of echocardiography in diagnosis, monitoring closure and post-procedural assessment of patent foramen ovale. *Eur J Echocardiogr* 11:i27-i34, 2010.
39. Yared K, Baggish AL, Solis J, et al: Echocardiographic assessment of percutaneous patent foramen ovale and atrial septal defect closure complications. *Circ Cardiovasc Imaging* 2:141-149, 2009.
40. Zheng Q, Zhao Z, Zuo J, et al: A comparative study: Early results and complications of percutaneous and surgical closure of ventricular septal defect. *Cardiology* 114:238-243, 2009.
41. Al-Kashkari W, Balan P, Kavinsky CJ, Cao QL, Hijazi ZM: Percutaneous device closure of congenital and iatrogenic ventricular septal defects in adult patients. *Catheter Cardiovasc Interv* 2010.
42. Yang J, Yang L, Wan Y, et al: Transcatheter device closure of perimembranous ventricular septal defects: mid-term outcomes. *Eur Heart J* 31:2238-2245, 2010.
43. Ledakowicz-Polak A, Polak L, Zielinska M: Ventricular septal defect complicating acute myocardial infarction-still an unsolved problem in the invasive treatment era. *Cardiovasc Pathol* 2010.
44. Papadopoulos N, Moritz A, Dzemali O, et al: Long-term results after surgical repair of postinfarction ventricular septal rupture by infarct exclusion technique. *Ann Thorac Surg* 87:1421-1425, 2009.
45. Ahmed J, Ruygrok PN, Wilson NJ, et al: Percutaneous closure of post-myocardial infarction ventricular septal defects: a single centre experience. *Heart Lung Circ* 17:119-123, 2008.
46. Martinez MW, Mookadam F, Sun Y, Hagler DJ: Transcatheter closure of ischemic and posttraumatic ventricular septal ruptures. *Catheter Cardiovasc Interv* 69:403-407, 2007.
47. Thiele H, Kaulfersch C, Daehnert I, et al: Immediate primary transcatheter closure of postinfarction ventricular septal defects. *Eur Heart J* 30:81-88, 2009.
48. Holzer R, Balzer D, Amin Z, et al: Transcatheter closure of postinfarction ventricular septal defects using the new Amplatzer muscular VSD occluder: Results of a U.S. Registry. *Catheter Cardiovasc Interv* 61:196-201, 2004.
49. Cubeddu RJ, Jneid H, Don CW, et al: Retrograde versus antegrade percutaneous aortic balloon valvuloplasty: immediate, short- and long-term outcome at 2 years. *Catheter Cardiovasc Interv* 74:225-231, 2009.
50. Fratz S, Gildein HP, Balling G, et al: Aortic valvuloplasty in pediatric patients substantially postpones the need for aortic valve surgery: a single-center experience of 188 patients after up to 17.5 years of follow-up. *Circulation* 117:1201-1206, 2008.
51. Bourgault C, Rodes-Cabau J, Cote JM, et al: Usefulness of Doppler echocardiography guidance during balloon aortic valvuloplasty for the treatment of congenital aortic stenosis. *Int J Cardiol* 128:30-37, 2008.
52. Pedersen WR, Klaassen PJ, Boisjolie CR, et al: Feasibility of transcatheter intervention for severe aortic stenosis in patients ≥90 years of age: aortic valvuloplasty revisited. *Catheter Cardiovasc Interv* 70:149-154, 2007.
53. Don CW, Witzke C, Cubeddu RJ, et al: Comparison of procedural and in-hospital outcomes of percutaneous balloon aortic valvuloplasty in patients >80 years versus patients < or =80 years. *Am J Cardiol* 105:1815-1820, 2010.
54. Ben-Dor I, Pichard AD, Satler LF, et al: Complications and outcome of balloon aortic valvuloplasty in high-risk or inoperable patients. *JACC Cardiovasc Interv* 3:1150-1156, 2010.
55. Hamid T, Eichhofer J, Clarke B, Mahadevan VS: Aortic balloon valvuloplasty: is there still a role in high-risk patients in the era of percutaneous aortic valve replacement? *J Interv Cardiol* 23:358-361, 2010.
56. Webb JG, Lichtenstein S: Transcatheter percutaneous and transapical aortic valve replacement. *Semin Thorac Cardiovasc Surg* 19: 304-310, 2007.
57. Webb JG: Percutaneous aortic valve replacement. *Curr Cardiol Rep* 10:104-109, 2008.
58. Walther T, Kasimir MT, Doss M, et al: One-year interim follow-up results of the TRAVERCE trial: the initial feasibility study for trans-apical aortic-valve implantation. *Eur J Cardiothorac Surg* 2010.
59. Walther T, Dewey T, Borger MA, et al: Transapical aortic valve implantation: step by step. *Ann Thorac Surg* 87:276-283, 2009.
60. Thomas M: The global experience with percutaneous aortic valve replacement. *JACC Cardiovasc Interv* 3:1103-1109, 2010.
61. Grube E, Buellesfeld L, Mueller R, et al: Progress and current status of percutaneous aortic valve replacement: results of three device generations of the CoreValve Revalving system. *Circ Cardiovasc Interv* 1:167-175, 2008.
62. Eltchaninoff H, Zajarias A, Tron C, et al: Transcatheter aortic valve implantation: technical aspects, results and indications. *Arch Cardiovasc Dis* 101:126-132, 2008.
63. Carroll JD: The benefits from TAVI: mortality and beyond. *Catheter Cardiovasc Interv* 75:1127-1128, 2010.
64. Piazza N, de Jaegere P, Schultz C, et al: Anatomy of the aortic valvar complex and its implications for transcatheter implantation of the aortic valve. *Circ Cardiovasc Interv* 1:74-81, 2008.
65. Jayasuriya C, Moss RR, Munt B: Transcatheter aortic valve implantation in aortic stenosis: the role of echocardiography. *J Am Soc Echocardiogr* 24:15-27, 2011.
66. Moss RR, Ivens E, Pasupati S, et al: Role of echocardiography in percutaneous aortic valve implantation. *JACC Cardiovasc Imaging* 1:15-24, 2008.
67. Lerakis S, Babaliaros VC, Block PC, et al: Transesophageal echocardiography to help position and deploy a transcatheter heart valve. *JACC Cardiovasc Imaging* 3:219-221, 2010.

68. Babaliaros VC, Junagadhwalla Z, Lerakis S, et al: Use of balloon aortic valvuloplasty to size the aortic annulus before implantation of a balloon-expandable transcatheter heart valve. *JACC Cardiovasc Interv* 3:114-118, 2010.
69. Masson JB, Kovac J, Schuler G, et al: Transcatheter aortic valve implantation: review of the nature, management, and avoidance of procedural complications. *JACC Cardiovasc Interv* 2:811-820, 2009.
70. Bagur R, Rodes-Cabau J, Doyle D, et al: Usefulness of TEE as the Primary Imaging Technique to Guide Transcatheter Transapical Aortic Valve Implantation. *JACC Cardiovasc Imaging* 4:115-124, 2011.
71. Carabello BA: Modern management of mitral stenosis. *Circulation* 112:432-437, 2005.
72. Wilkins GT, Weyman AE, Abascal VM, Block PC, Palacios IF: Percutaneous balloon dilatation of the mitral valve: an analysis of echocardiographic variables related to outcome and the mechanism of dilatation. *Br Heart J* 60:299-308, 1988.
73. Abascal VM, Wilkins GT, Choong CY, et al: Echocardiographic evaluation of mitral valve structure and function in patients followed for at least 6 months after percutaneous balloon mitral valvuloplasty. *J Am Coll Cardiol* 12:606-615, 1988.
74. Eng MH, Salcedo EE, Quaife RA, Carroll JD: Implementation of real time three-dimensional transesophageal echocardiography in percutaneous mitral balloon valvuloplasty and structural heart disease interventions. *Echocardiography* 26:958-966, 2009.
75. Alfieri O, Maisano F, De Bonis M, et al: The double-orifice technique in mitral valve repair: a simple solution for complex problems. *J Thorac Cardiovasc Surg* 122:674-681, 2001.
76. Bhudia SK, McCarthy PM, Smedira NG, et al: Edge-to-edge (Alfieri) mitral repair: results in diverse clinical settings. *Ann Thorac Surg* 77:1598-1606, 2004.
77. Kuduvalli M, Ghotkar SV, Grayson AD, Fabri BM: Edge-to-edge technique for mitral valve repair: medium-term results with echocardiographic follow-up. *Ann Thorac Surg* 82:1356-1361, 2006.
78. Feldman T, Wasserman HS, Herrmann HC, et al: Percutaneous mitral valve repair using the edge-to-edge technique: six-month results of the EVEREST Phase I Clinical Trial. *J Am Coll Cardiol* 46:2134-2140, 2005.
79. Mauri L, Garg P, Massaro JM, et al: The EVEREST II Trial: design and rationale for a randomized study of the Evalve Mitraclip system compared with mitral valve surgery for mitral regurgitation. *Am Heart J* 160:23-29, 2010.
80. Herrmann HC, Rohatgi S, Wasserman HS, et al: Mitral valve hemodynamic effects of percutaneous edge-to-edge repair with the MitraClip device for mitral regurgitation. *Catheter Cardiovasc Interv* 68:821-828, 2006.
81. Swaans MJ, Van den Branden BJ, Van der Heyden JA, et al: Three-dimensional transoesophageal echocardiography in a patient undergoing percutaneous mitral valve repair using the edge-to-edge clip technique. *Eur J Echocardiogr* 10:982-983, 2009.
82. Webb JG, Maisano F, Vahanian A, et al: Percutaneous suture edge-to-edge repair of the mitral valve. *EuroIntervention* 5:86-89, 2009.
83. Naqvi TZ, Buchbinder M, Zarbatany D, et al: Beating-heart percutaneous mitral valve repair using a transcatheter endovascular suturing device in an animal model. *Catheter Cardiovasc Interv* 69:525-531, 2007.
84. Daimon M, Fukuda S, Adams DH, et al: Mitral valve repair with Carpentier-McCarthy-Adams IMR ETlogix annuloplasty ring for ischemic mitral regurgitation: early echocardiographic results from a multi-center study. *Circulation* 114:I588-93, 2006.
85. Sack S, Kahlert P, Bilodeau L, et al: Percutaneous transvenous mitral annuloplasty: initial human experience with a novel coronary sinus implant device. *Circ Cardiovasc Interv* 2:277-284, 2009.
86. Schofer J, Siminiak T, Haude M, et al: Percutaneous mitral annuloplasty for functional mitral regurgitation: results of the CARILLON Mitral Annuloplasty Device European Union Study. *Circulation* 120:326-333, 2009.
87. Webb JG, Harnek J, Munt BI, et al: Percutaneous transvenous mitral annuloplasty: initial human experience with device implantation in the coronary sinus. *Circulation* 113:851-855, 2006.
88. Pedersen WR, Block P, Leon M, et al: iCoapsys mitral valve repair system: Percutaneous implantation in an animal model. *Catheter Cardiovasc Interv* 72:125-131, 2008.
89. Grossi EA, Patel N, Woo YJ, et al: Outcomes of the RESTOR-MV Trial (Randomized Evaluation of a Surgical Treatment for Off-Pump Repair of the Mitral Valve). *J Am Coll Cardiol* 56:1984-1993, 2010.
90. Mahjoub H, Noble S, Ibrahim R, et al: Description and assessment of a common reference method for fluoroscopic and transesophageal echocardiographic localization and guidance of mitral periprosthetic transcatheter leak reduction. *JACC Cardiovasc Interv* 4:107-114, 2011.
91. Kim MS, Casserly IP, Garcia JA, et al: Percutaneous transcatheter closure of prosthetic mitral paravalvular leaks: are we there yet? *JACC Cardiovasc Interv* 2:81-90, 2009.
92. Hamilton-Craig C, Boga T, Platts D, et al: The role of 3D transesophageal echocardiography during percutaneous closure of paravalvular mitral regurgitation. *JACC Cardiovasc Imaging* 2:771-773, 2009.
93. Horton KD, Whisenant B, Horton S: Percutaneous closure of a mitral perivalvular leak using three dimensional real time and color flow imaging. *J Am Soc Echocardiogr* 23:903 e5-e7, 2010.
94. Kempfert J, Blumenstein J, Chu MW, et al: Minimally invasive off-pump valve-in-a-ring implantation: the atrial transcatheter approach for re-operative mitral valve replacement after failed repair. *Eur J Cardiothorac Surg* 35:965-969; discussion 969, 2009.
95. Kempfert J, Blumenstein JM, Borger MA, et al: Minimally invasive off-pump valve-in-a-valve implantation: the atrial transcatheter approach for re-operative mitral valve replacement. *Eur Heart J* 29:2382-2387, 2008.
96. Cheung A, Webb JG, Wong DR, et al: Transapical transcatheter mitral valve-in-valve implantation in a human. *Ann Thorac Surg* 87:e18-20, 2009.
97. de Weger A, Tavilla G, Ng AC, et al: Successful transapical transcatheter valve implantation within a dysfunctional mitral bioprosthesis. *JACC Cardiovasc Imaging* 3:222-223, 2010.
98. Lozonschi L, Quaden R, Edwards NM, et al: Transapical mitral valved stent implantation. *Ann Thorac Surg* 86:745-748, 2008.
99. Ashraf T, Pathan A, Kundi A: Percutaneous balloon valvuloplasty of coexisting mitral and tricuspid stenosis: single-wire, double-balloon technique. *J Invasive Cardiol* 20:E126-E128, 2008.
100. Boccuzzi G, Gigli N, Cian D, et al: Percutaneous transcatheter balloon valvuloplasty for severe tricuspid valve stenosis in Ebstein's anomaly. *J Cardiovasc Med (Hagerstown)* 10:510-515, 2009.
101. Harle T, Kronberg K, Motz R, Elsasser A: Balloon valvuloplasty of a tricuspid valve stenosis in double balloon technique. *Clin Res Cardiol* 99:203-205, 2010.
102. Yeter E, Ozlem K, Kilic H, Ramazan A, Acikel S: Tricuspid balloon valvuloplasty to treat tricuspid stenosis. *J Heart Valve Dis* 19:159-160, 2010.
103. Rao PS: Percutaneous balloon pulmonary valvuloplasty: state of the art. *Catheter Cardiovasc Interv* 69:747-763, 2007.
104. Kumar A, Kavinsky C, Amin Z, Hijazi ZM: Percutaneous pulmonic valve implantation. *Curr Treat Options Cardiovasc Med* 11:483-491, 2009.
105. Khambadkone S, Coats L, Taylor A, et al: Percutaneous pulmonary valve implantation in humans: results in 59 consecutive patients. *Circulation* 112:1189-1197, 2005.
106. Agarwal S, Tuzcu EM, Desai MY, et al: Updated meta-analysis of septal alcohol ablation versus myectomy for hypertrophic cardiomyopathy. *J Am Coll Cardiol* 55:823-834, 2010.
107. Alam M, Dokainish H, Lakkis NM: Hypertrophic obstructive cardiomyopathy-alcohol septal ablation vs. myectomy: a meta-analysis. *Eur Heart J* 30:1080-1087, 2009.
108. Himbert D, Brochet E, Ducrocq G, Vahanian A: Contrast echocardiography guidance for alcohol septal ablation of hypertrophic obstructive cardiomyopathy. *Eur Heart J* 31:1148, 2010.
109. Frances C, Romero A, Grady D: Left ventricular pseudoaneurysm. *J Am Coll Cardiol* 32:557-561, 1998.
110. Bolooki H: Surgical treatment of complications of acute myocardial infarction. *JAMA* 263:1237-1240, 1990.
111. Clift P, Thorne S, de Giovanni J: Percutaneous device closure of a pseudoaneurysm of the left ventricular wall. *Heart* 90:e62, 2004.
112. Prakash S, Garg N, Xie GY, Dellsperger KC: Giant left ventricular pseudoaneurysm. *J Cardiovasc Comput Tomogr* 4:284-285, 2010.
113. Romaguera R, Slack MC, Waksman R, et al: IMAGE CARDIO MED: Percutaneous closure of a left ventricular outflow tract pseudoaneurysm causing extrinsic left coronary artery compression by transseptal approach. *Circulation* 121:e20-e22, 2010.
114. Fuster V, Ryden LE, Cannom DS, et al: ACC/AHA/ESC 2006 Guidelines for the Management of Patients with Atrial Fibrillation: a report of the American College of Cardiology/American Heart Association Task Force on Practice Guidelines and the European Society of Cardiology Committee for Practice Guidelines (Writing Committee to Revise the 2001 Guidelines for the Management of Patients With Atrial Fibrillation): developed in collaboration with the European Heart Rhythm Association and the Heart Rhythm Society. *Circulation* 114:e257-e354, 2006.
115. Ussia GP, Mule M, Cammalleri V, et al: Percutaneous closure of left atrial appendage to prevent embolic events in high-risk patients with chronic atrial fibrillation. *Catheter Cardiovasc Interv* 74:217-222, 2009.
116. Fountain RB, Holmes DR, Chandrasekaran K, et al: The PROTECT AF (WATCHMAN Left

Atrial Appendage System for Embolic PROTECTion in Patients with Atrial Fibrillation) trial. *Am Heart J* 151:956-961, 2006.
117. Holmes DR, Reddy VY, Turi ZG, et al: Percutaneous closure of the left atrial appendage versus warfarin therapy for prevention of stroke in patients with atrial fibrillation: a randomised non-inferiority trial. *Lancet* 374:534-542, 2009.
118. Singh IM, Holmes DR, Jr: Left atrial appendage closure. *Curr Cardiol Rep* 12:413-421, 2010.
119. Bashir F, Quaife R, Carroll JD: Percutaneous closure of ascending aortic pseudoaneurysm using Amplatzer septal occluder device: the first clinical case report and literature review. *Catheter Cardiovasc Interv* 65:547-551, 2005.
120. Muraki S, Inguu A, Baba M, Izumiyama O, Hasegawa T: [A case report of a pseudoaneurysm of the thoracic aorta (thrombotic closure type) showing like a mediastinal tumor–value of endoscopic ultrasonography in differential diagnosis]. *Nippon Kyobu Geka Gakkai Zasshi* 44:1917-1920, 1996.
121. Stasek J, Polansky P, Bis J, et al: The percutaneous closure of a large pseudoaneurysm of the ascending aorta with an atrial septal defect Amplatzer occluder: two-year follow-up. *Can J Cardiol* 24:e99-e101, 2008.
122. Sloan KP, Bruce CJ, Oh JK, Rihal CS: Complications of echocardiography-guided endomyocardial biopsy. *J Am Soc Echocardiogr* 22: 324 e1-4, 2009.
123. Mortensen SA, Egeblad H: Endomyocardial biopsy guided by cross-sectional echocardiography. *Br Heart J* 50:246-251, 1983.
124. Stec S, Zaborska B, Sikora-Frac M, Krynski T, Kulakowski P: First experience with microprobe transoesophageal echocardiography in non-sedated adults undergoing atrial fibrillation ablation: feasibility study and comparison with intracardiac echocardiography. *Europace* 2010.
125. Dello Russo A, Casella M, Pelargonio G, et al: Intracardiac echocardiography in electrophysiology. *Minerva Cardioangiol* 58:333-342, 2010.
126. Priester R, Bunting T, Usher B, et al: Role of transesophageal echocardiography among patients with atrial fibrillation undergoing electrophysiology testing. *Am J Cardiol* 104:1256-1258, 2009.
127. Dravid SG, Hope B, McKinnie JJ: Intracardiac echocardiography in electrophysiology: a review of current applications in practice. *Echocardiography* 25:1172-1175, 2008.
128. Swanson N, Mirza I, Wijesinghe N, Devlin G: Primary percutaneous balloon pericardiotomy for malignant pericardial effusion. *Catheter Cardiovasc Interv* 71:504-507, 2008.
129. Hsu KL, Tsai CH, Chiang FT, et al: Percutaneous balloon pericardiotomy for patients with recurrent pericardial effusion: using a novel double-balloon technique with one long and one short balloon. *Am J Cardiol* 80:1635-1637, 1997.
130. Hijazi ZM, Awad SM: Pediatric cardiac interventions. *JACC Cardiovasc Interv* 1:603-611, 2008.
131. Asrress KN, Mitchell AR: Intracardiac echocardiography. *Heart* 95:327-331, 2009.
132. Kim SS, Hijazi ZM, Lang RM, Knight BP: The use of intracardiac echocardiography and other intracardiac imaging tools to guide noncoronary cardiac interventions. *J Am Coll Cardiol* 53:2117-2128, 2009.
133. Mullen MJ, Dias BF, Walker F, et al: Intracardiac echocardiography guided device closure of atrial septal defects. *J Am Coll Cardiol* 41:285-292, 2003.
134. Cafri C, de la Guardia B, Barasch E, Brink J, Smalling RW: Transseptal puncture guided by intracardiac echocardiography during percutaneous transvenous mitral commissurotomy in patients with distorted anatomy of the fossa ovalis. *Catheter Cardiovasc Interv* 50:463-467, 2000.
135. Green NE, Hansgen AR, Carroll JD: Initial clinical experience with intracardiac echocardiography in guiding balloon mitral valvuloplasty: technique, safety, utility, and limitations. *Catheter Cardiovasc Interv* 63:385-394, 2004.
136. Knight BP, Kim SS: Use of intracardiac echocardiography during ablation for atrial fibrillation. In Sylvestry F, Wiegers SE, editors: *Intracardiac Echocardiography*, London, UK, 2005, Martin-Dunitz.
137. Ng AC, Delgado V, van der Kley F, et al: Comparison of aortic root dimensions and geometries before and after transcatheter aortic valve implantation by 2- and 3Dimensional transesophageal echocardiography and multislice computed tomography. *Circ Cardiovasc Imaging* 3:94-102, 2010.
138. Quaife RA, Carroll JD: CT evaluation of the interatrial septum in atrial septal defects. In Hijazi ZM, Feldman T, Abdullah Al-Qbandi MH, Horst S, editors: *Transcatheter Closure of Atrial Septal Defects & Patent Foramen Ovale: A Comprehensive Assessment*, Minneapolis, 2010, Cardiotext.
139. Holmvang G, Palacios IF, Vlahakes GJ, et al: Imaging and sizing of atrial septal defects by magnetic resonance. *Circulation* 92:3473-3480, 1995.
140. Low SC, Oliveira GR, Maki JH: Magnetic resonance imaging of unroofed coronary sinus. *Heart* 95:720, 2009.
141. Moore P: MRI-guided congenital cardiac catheterization and intervention: the future? *Catheter Cardiovasc Interv* 66:1-8, 2005.
142. Teo KS, Disney PJ, Dundon BK, et al: Assessment of atrial septal defects in adults comparing cardiovascular magnetic resonance with transoesophageal echocardiography. *J Cardiovasc Magn Reson* 12:44, 2010.
143. Quaife RA, Carroll JD: Cardiac CT and MRI in Patient Assessment and Procedural Guidance in Structural Heart Disease Interventions. In: Carroll JD, editor: *Manual of Structural Heart Disease Interventions (in press)*, Lippincott, 2011, Williams & Wilkins.
144. Carroll JD: The future of image guidance of cardiac interventions. *Catheter Cardiovasc Interv* 70:783, 2007.
145. Chen SYJ, Hansgen A, Carroll JD: The Future Cardiac Catheterization Laboratory. In Carroll JD, SY C, editors: *Cardiology Clinics: Advances in Coronary Angiography*, 2009.
146. Schwartz J, Neubauer A, Fagan T, Grass M, Carroll JD: Potential role of three-dimensional rotational angiography and C-arm CT for valvular repair and implantation (in press). *Int J Cardiac Imaging* 2011.
147. Kim MS, Hansgen AR, Wink O, Quaife RA, Carroll JD: Rapid prototyping: a new tool in understanding and treating structural heart disease. *Circulation* 117:2388-2394, 2008.

# 6 Intracardiac Echocardiography

THOMAS BARTEL, MD | SILVANA MÜLLER, MD |
THOMAS KONORZA, MD | RAIMUND ERBEL, MD

Equipment and Handling Procedures
Guiding Device Closure of Interatrial Communications
Monitoring of Percutaneous Left Atrial Appendage Closure
Guiding Radiofrequency Pulmonary Vein Ablation
Monitoring Transcatheter Aortic Valve Implantation
Perioperative and Periinterventional Imaging of the Ascending Aorta
Periinterventional Imaging of the Descending Thoracic Aorta
Periinterventional Imaging of the Mitral Valve
Limitations

During the past decade, intracardiac echocardiography (ICE) has become a standard guiding approach in interventional treatment of structural heart disease,[1] such as in device closure of interatrial communications, percutaneous transluminal septal myocardial ablation, pulmonary vein ablation, percutaneous left atrial appendage closure, and recently in transcatheter aortic valve implantation (TAVI). With the introduction of the 8F AcuNav catheter (Acuson Siemens, Mountain View, Calif.), which is also used for ICE,[2] intraaortic phased-array imaging (IPAI) became feasible. Guidance by fluoroscopy alone is limited because it cannot distinguish soft tissues and does not allow cross-sectional imaging. Consequently accurate positioning of devices can be difficult without echocardiographic guidance.[2a] On the other hand, distant posterior areas are difficult to depict with transthoracic echocardiography, especially when the patient is supine. Although transesophageal echocardiography (TEE) including real-time three-dimensional (3D) imaging is a well established diagnostic tool and provides exceptional high-resolution images, TEE's usefulness for interventional procedures is not always ideal (see Chapter 5). However, evidence that ICE guidance can improve the safety of these procedures is still lacking.

Miniaturized ultrasound-tipped catheter devices were primarily introduced for intravascular use. The first attempts to percutaneously introduce intravenous probes with built-in echo transducers for in vivo intracardiac imaging were reported in the late 1960s. During the following two decades, several intracardiac echocardiographic catheters were developed. Later, intravascular ultrasound (IVUS) was employed to image coronary arteries as well as the aorta and peripheral vessels (see Chapter 7). IVUS-based intracardiac imaging was also used for guiding electrophysiologic procedures. Nevertheless, intracardiac IVUS lacks Doppler capabilities and is further limited by inadequate ultrasound penetration. For current noncoronary percutaneous interventions in structural heart disease, high-quality near-field images as well as Doppler flow analysis are a prerequisite for optimal results and also aid in avoiding and detecting complications. Thus, technical advances led from IVUS to the development of ICE and IPAI. Using these methods as a guiding tool in noncoronary percutaneous interventions is justifiable on the basis of improved procedural success and reduced complications, although costs of the catheter and reimbursement are problematic in many countries. In particular, progress in electrophysiologic ablation is clearly linked to the advances made with ICE.[3] ICE and IPAI are also exciting research tools. Transfer of the methodology from the realm of research to routine clinical use is ongoing, such as in TAVI.[4]

## Equipment and Handling Procedures

Current devices (Acuson, Mountain View, Calif.) are multimodal, phased-array transducer-tipped intracardiac echocardiographic catheters. Nowadays, the 8 F AcuNav catheter has become the tool of choice for ICE. Other devices have been introduced[5] but have gained only limited acceptance (Table 6-1).

Just like conventional echocardiography, the miniaturized AcuNav transducer provides a 90°-sector image. The ICE probe can be connected to standard ultrasound units (Siemens and General Electric) through the SwiftLink Catheter Connector, which attaches to the ultrasound unit like any probe. After the SwiftLink Catheter Connector is covered with a sterile jacket, it is placed into the sterile field at the catheter table, where it is connected to the sterile intracardiac echocardiographic probe. The catheter steering mechanism and the function of the transducer should be checked in a water bath before insertion.

In comparison to the 10-Fr version, the 8-Fr AcuNav catheter has facilitated ICE and increased patient comfort and probably safety as well. After its introduction in pediatric cardiology,[2] the 8-Fr ICE catheter now is also used in adult interventional cardiology. The catheter possesses the unlimited echocardiographic capabilities of its predecessor but is available with more insertable length and in a shorter version. Besides two-dimensional (2D) and M-mode imaging, the ICE catheter also permits functional analysis. It possesses complete Doppler capabilities, including pulsed wave, continuous wave, color flow, and tissue Doppler modalities (Table 6-2).

An access sheath is required for introducing the ultrasound catheter into the femoral vessels or the right jugular vein. The disposable ICE catheter can be navigated through the inferior vena cava (femoral venous access) or the superior vena cava (SVC) (jugular venous access) into the right atrium (RA). This

**TABLE 6-1 Presently Available Intracardiac Echocardiographic Devices**

| *Catheters* | *Company* | *Features* |
|---|---|---|
| UltraICE | Boston Scientific | Rotational, nonsteerable |
| EP Med View Flex | St. Jude Medical | Side-looking, 10 Fr, 2-8 MHz |
| ClearICE | St. Jude Medical | Side-looking, steerable, 3D localization |
| AcuNav | Siemens/Biosense-Webster | Side looking, steerable, 8 Fr and 10 Fr |
| SoundStar | Siemens/Biosense-Webster | Side-looking, steerable, 10 Fr, 3D localization |

**TABLE 6-2 Doppler Imaging Modes and Frequencies of the Intracardiac Echocardiographic Catheter Family**

| | | |
|---|---|---|
| Catheter versions | 10 F | 8 F |
| Insertable length | 90 cm | 90 cm (formerly 110 cm) |
| Steering | Four-way | Four-way |
| 2D imaging frequency | 5.0-10.0 MHz | 5.0-10.0 MHz |
| Color Doppler frequency | 4.0-7.0 MHz | 4.0-7.0 MHz |
| CW Doppler | 5.0 MHz | 5.0-5.2 MHz |
| PW Doppler | 4.0-5.0 MHz | 4.0-5.0 MHz |
| Recommended access sheaths | 11 Fr | 8 or 9 Fr |
| Penetration | 15 cm | 15 cm |

*PW*, Pulsed wave.

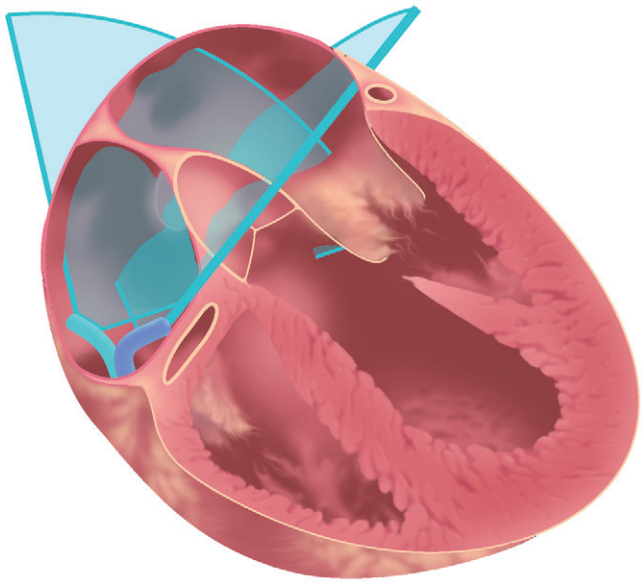


**Figure 6-1 Standard transatrial views for intracardiac imaging are obtained with the catheter tip in the RA.** Two image planes are shown in blue—a short-axis view of the aortic valve and interatrial septum atrium, and a longitudinal view through the interatrial septum.

may present a potential risk, although most patients undergo ICE as part of an interventional procedure, so the additional risk remains minimal. Special caution is needed when navigating the ICE catheter through the pelvic veins. Although the risk of venous injury or perforation is very low, isolated pelvic vein perforation and inferior vena cava dissection have been described. Adequate handling of the catheter device includes use of a long access sheath and fluoroscopy, two recommended precautions that enhance patient safety. The long access sheath in particular spares the examiner problems associated with pelvic vein navigation, thereby increasing patient safety. In addition, it is recommended to infuse saline solution before ICE. This increases venous pressure and dilates the central veins, facilitating venous puncture and insertion of access sheaths and the ICE catheter. Even intracardiac navigation becomes easier if the heart is well filled. The intracardiac probe does not accommodate a guidewire and is therefore fundamentally different from IVUS catheters. These require guidewires and are therefore relatively safe to manipulate. Obtaining arbitrary views may be difficult, however, especially in the near field. Particularly in the vicinity of the RA, the guidewire can restrict full visualization of lumen and wall, and it will frequently not allow adequate views of structures of interest, such as the transition into other chambers or vessel orifices.

## PRACTICAL TIPS

- Use long access sheaths to avoid injuring the pelvic veins during navigation.
- Use fluoroscopy as a precaution to safely advance the bidirectionally steerable (but guidewireless) catheter into the heart.
- Infuse 500 mL saline solution to dilate the veins and to facilitate catheter passage. Added benefit: reduced tendency for vagal responses when both the left and the right femoral veins need to be punctured.

To permit adequate imaging of the interatrial septum and its neighboring structures, two standardized views are used: (1) a transatrial longitudinal view showing the extent of the atrial septum from cranial to its distal margins—this view is seen with the catheter retroflexed inside the RA; and (2) a perpendicular transatrial short-axis view for visualizing the anterior part of the atrial septum and the transition to the aortic valve and the ascending aorta (Fig. 6-1).

The aortic valve is visualized by turning the catheter toward the aorta. One may need to straighten or even slightly anteflect the catheter. The tricuspid valve and the right ventricle (RV) are best displayed in a longitudinal view by anteflexing the probe after positioning the tip in the high RA. The left and right pulmonary veins as well as the left atrial appendage (LAA) are each visualized in a modified transatrial longitudinal view. For depicting the left pulmonary veins and the LAA, the catheter is angulated inferiorly; to visualize the right pulmonary veins, it is turned clockwise and advanced superiorly.

Clockwise rotation of the straightened ICE catheter permits visualization of the smallest anatomic details in the near field as well as to a depth of up to 12 cm. In order to enter the right ventricle, the tip of the probe is positioned in the mid to upper RA with the piezoelectric crystal facing the free wall of the RA, before the probe is gradually deflected anteriorly. From the right ventricle, the transventricular long-axis view of the left ventricle (LV) is obtained, which shows the interventricular septum proximally, the LV outflow tract, and the mitral valve apparatus. When the catheter tip is tilted to the right, the transventricular short-axis view of the LV comes into view (Figs. 6-2 and 6-3).

Interpretation of LV wall motion from transventricular views requires care because the catheter is moving inside the RV. By tilting the catheter tip away from the transventricular long-axis view, the RV outflow tract and pulmonary valve can be visualized as well (Fig. 6-4).

To avoid ventricular arrhythmias, the catheter has to be carefully navigated inside the RV cavity. The catheter should not be advanced beyond the pulmonary valve. When using the SVC

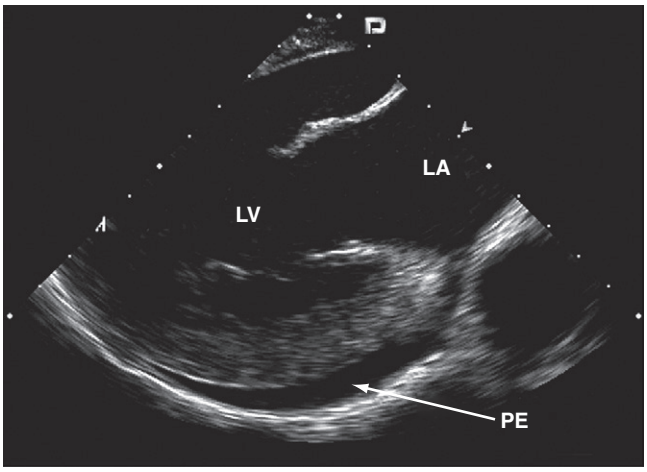



**Figure 6-2** Transventricular long-axis view of the LV and the LA in patient with pericardial effusion. *PE*, Pericardial effusion.

**TABLE 6-3 Standardized Views**

| *Window* | *Catheter Position* | *Standardized Cut Plane* |
|---|---|---|
| Transatrial | RA | Longitudinal, craniocaudal view of IAS, LA, LAA |
| | RA | Short-axis view of the anterior IAS, aortic valve, and ascending aorta |
| | RA | Longitudinal view of the RV, showing TV, RV |
| Transventricular | RV | Long-axis view of the LV, IVS, LVOT, LA including LAA |
| | RV | Short-axis view of the LV |
| Transvenous | IVC | Aortic view of the abdominal aorta and its side branches |
| | SVC/RA | Aortic view of the ascending aorta and aortic valve |
| Intraaortic | Aorta | Imaging from inside the whole aorta including aortic arch |
| | Aorta | Long-axis view of the aortic valve seen from the aortic arch |

*IAS*, Interatrial septum; *IVC*, inferior vena cava; *IVS*, interventricular septum; LAA, left atrial appendage; *LVOT*, left ventricular outflow tract; *TV*, tricuspid valve.

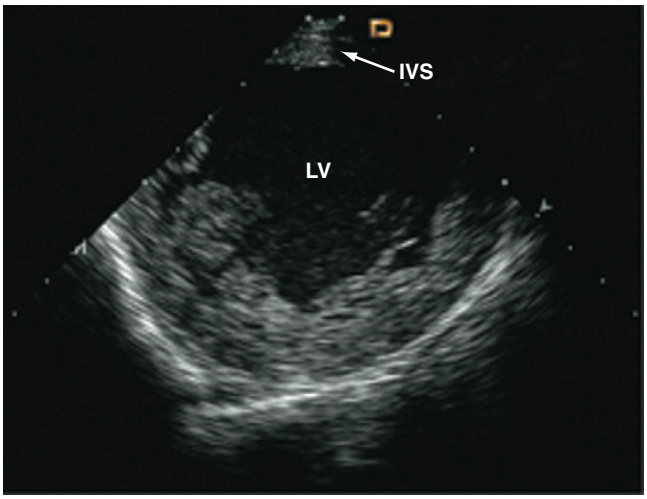



**Figure 6-3** Transventricular short-axis view of the LV. *IVS*, Interventricular septum.

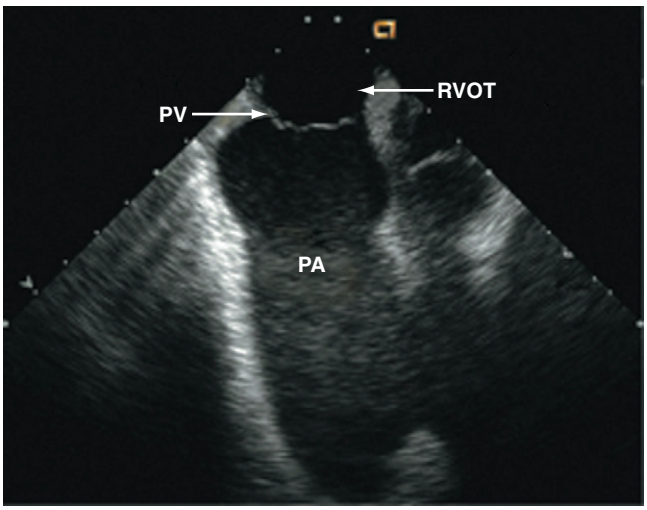



**Figure 6-4** Catheter positioned in the RV provides a view of the right ventricular outflow tract (*RVOT*) and the pulmonic valve (*PV*). *PA*, Pulmonary artery.

approach, inadvertent catheter passage into the coronary sinus has to be avoided by all means. A certain expertise in intracardiac catheter manipulation is essential to safely advance the catheter into the right heart, to orient oneself inside the heart, to obtain standardized views, and to adequately visualize the cardiac anatomy[6] (Table 6-3; also see Fig. 6-1).

Although the diagnostic potential and limitations of this imaging modality have not been fully evaluated, ICE may find an adequate place in operating rooms and catheterization laboratories for online monitoring of complex intracardiac interventions. Nonsurgical cardiac procedures require real-time, high-quality, and near-field views for optimal results. Moreover, continuous progress in the field of percutaneous interventions warrants more effective imaging guidance without compromise to patient comfort and safety. ICE has been proven an important diagnostic tool for depicting expected or unanticipated aberrant anatomy in patients with congenital heart disease. Tissue motion, intracardiac devices, and their relation to the surrounding structures can be very clearly delineated.

## Guiding Device Closure of Interatrial Communications

Device closure of interatrial communications is performed for treatment of severe left-to-right shunts associated with atrial septal defects (ASDs) (see Chapter 44) and for prevention of recurrent paradoxical embolism in patients with a patent foramen ovale (see Chapter 41). Some complications with closure of interatrial communications are due to suboptimal device performance.[7] Others, however, may be related to discontinuous echocardiographic monitoring, because supine patients do not tolerate continuous monitoring with TEE well unless they are sedated or under general anesthesia. More than 10 years of experience make us believe that some specific complications of transcatheter closure can potentially be avoided with improved echocardiographic monitoring. In that respect, ICE can be recommended as the method of choice for guiding percutaneous device closure, especially of ASDs.

Before passing instrumentation through the interatrial communication, the ICE catheter is advanced through the inferior vena cava into the RA. The transducer is aimed at the left atrium (LA) to obtain the transatrial longitudinal view. As a first step,

adequate position of a long guidewire in the left superior pulmonary vein is demonstrated. The left superior pulmonary veins are depicted by angulating the probe from the longitudinal view inferiorly. The stretched size of ASDs can be adequately measured by ICE; however, sizing balloons must still be used—a mandatory step for estimating the size of the communication before ASD device closure.[8]

Next, the long access sheath required for occluder device application is inserted over the guidewire. Fluoroscopic imaging during that part of the procedure can be reduced to very short intermittent checks because placement of the tip of the sheath into the LA can be primarily guided and documented by ICE. Simultaneous echocardiographic and fluoroscopic viewing is recommended during deployment of the closure device.

## PRACTICAL TIPS

- ICE displays release of the left-sided counteroccluder opening in the LA.
- The whole system including the long access sheath with the delivery cable inside and the opened left-sided counteroccluder is slightly pulled back until the open counteroccluder applies some traction on the atrial septum. ICE depicts the moment when the left-sided counteroccluder is closely aligned with the atrial septum.
- With the delivery cable still under traction, the long access sheath is further withdrawn to release the right-sided counteroccluder. ICE demonstrates release of the right-sided counteroccluder inside the RA and the left-sided counteroccluder remaining on the left side of the septum.
- While monitoring the opening of the right-sided counteroccluder, the delivery cable is carefully pushed forward until the counteroccluder also fits tightly into the atrial septum, but from the right side. Viewing two perpendicular cut planes (transatrial longitudinal and short-axis views) is mandatory to confirm the result and to rule out jamming of one of the counteroccluders in the interatrial communication (Fig. 6-5).

With the occluder device positioned but still connected to the delivery cable, the "wriggle maneuver" is monitored. Aiming to ensure that the counteroccluder cannot tilt or slip to the contralateral side, the occluder device is pushed and pulled before release. This will guarantee that the atrial septum is optimally engaged. Details of this maneuver, which is considered the best technique to avoid unsatisfactory device orientation or embolization, can be nicely shown by ICE. The wriggle maneuver should be visualized in the transatrial longitudinal view and again in the transatrial short-axis view. In the short-axis view, any compression of the aortic bulb by the occluder device can be ruled out. It is sensible to also use ICE for monitoring device disconnection from the delivery cable.

Once it is released, the device lines up with the atrial septum, reaching its definitive orientation. The final position of the device should be visualized to ensure that the counteroccluder completely encloses the rims of the interatrial communication. After device deployment, color flow imaging can depict any residual shunt. During deployment of the occluder device, the device and the intracardiac echocardiographic catheter do not interfere with each other. As a precaution, the intracardiac echocardiographic catheter should be kept at least 1 cm from the occluder device. A closer position would impair optimal imaging of the occluder device. As elucidated, continuous ICE imaging during each stage of the procedure allows optimal device positioning, a prerequisite for safe percutaneous closure of interatrial communications. Real-time 3D ICE imaging will be available soon.

Several investigators demonstrated that ICE can safely guide interventional therapy in interatrial communications and that ICE monitoring is superior to conventional TEE.[9-12] TEE requires general anesthesia with or without endotracheal intubation, whereas ICE permits unlimited echocardiographic viewing in fully conscious and compliant patients. This is of utmost importance, because malposition and migration of the device into the systemic or pulmonary circulation or perforation of the cardiac wall and rapid thrombus formation on the device are known to happen on occasion.[7,13,14] ICE provides better image resolution than TEE and therefore facilitates the procedure, particularly when long continuous or repeated

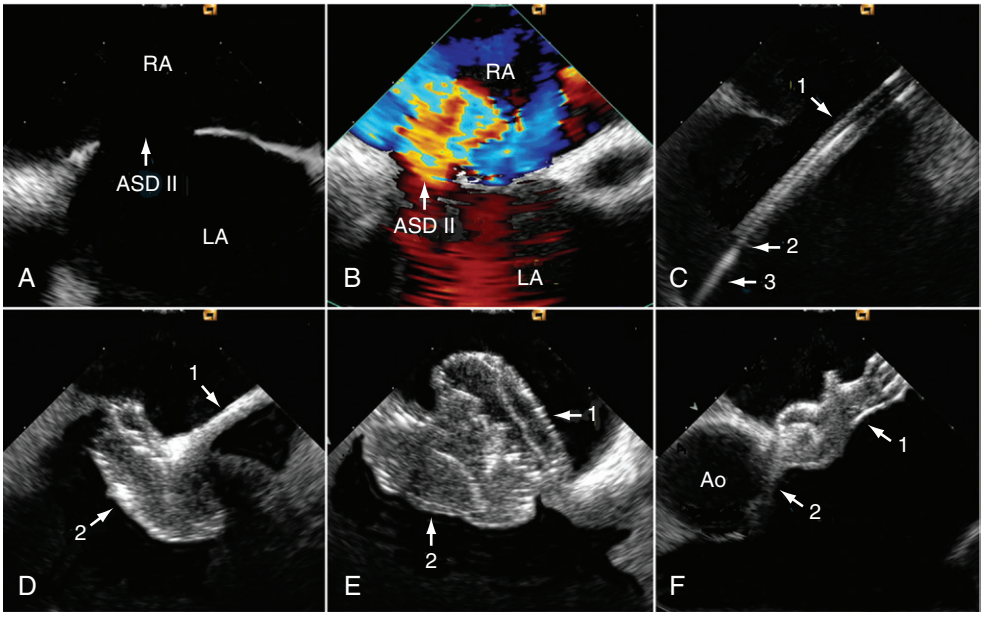



**Figure 6-5** Device closure of an atrial septal defect (*ASD*) guided by intracardiac echocardiography. **A,** ASD. *ASD II,* Secundum atrial septal defect. **B,** Significant left-to-right shunt. **C,** Long access sheath with indwelling wire. *1,* Long sheath crossing the septum; *2,* tip of long sheath; *3,* wire. **D,** Unfolded left-sided counteroccluder. *1,* Sheath with folded right-sided counteroccluder inside; *2,* unfolded left-sided counteroccluder. **E,** Unfolded counteroccluders with the device being pulled. *1,* Unfolded right-sided counteroccluder; *2,* left-sided counteroccluder. **F,** Final device position. *1,* Device after release from the delivery cable; *2,* aorta (*Ao*) is shown to be unaffected.

echocardiographic viewing is required or when complications begin to develop. ICE results in much less procedural stress to the patient, and fluoroscopic and procedural times can be shortened.[9,12] Because many patients with interatrial communications are of reproductive age or younger, reduction of radiation exposure has to be considered a major advantage of ICE. In that respect, patients who undergo ASD closure benefit more from ICE than patients undergoing closure of a patent foramen ovale, because ASD closure is more complex and more time consuming. Employing ICE in the pediatric population is also recommended. Several years' experience show that ICE is a practical and straightforward approach for guiding device closure in children and adolescents.[2,11] The overall risk related to ICE appears to be low. Moreover, it is likely that ICE improves the safety of interventional device closure in interatrial communications. From an economic point of view, savings from shorter procedural time and from avoiding general anesthesia need to be weighed against the cost of the ICE catheter. After a brief learning curve, interventional cardiologists who are familiar with echocardiography can fully benefit from the advantages of ICE.

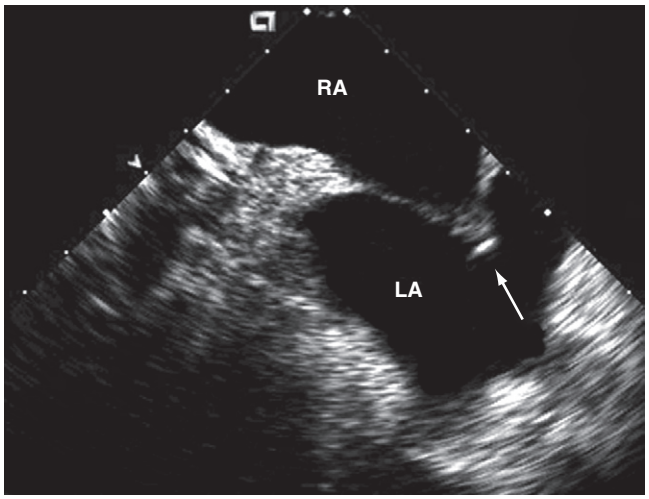



**Figure 6-6** Intracardiac echocardiographic imaging depict "tenting" of the fossa ovalis (*arrow*) while a Brockenbrough needle is advanced from the RA.

## Monitoring of Percutaneous Left Atrial Appendage Closure

ICE guidance for LAA device closure has only been described in a few cases.[15,16] It is an option in patients with atrial fibrillation in whom oral anticoagulation is contraindicated. Anatomical variation of the LAA, exclusion of thrombi, and the diameter of the ostium are usually assessed by TEE, which is also used for intraprocedural monitoring. As in any other percutaneous transseptal catheter interventions, one needs to establish access to the atrial appendage by septal puncture before LAA closure. This is best done under ICE guidance. Before atrial septal puncture, anatomic anomalies should be ruled out. When tenting of the fossa ovalis identifies contact with the transseptal needle, the pressure on the needle can be slightly increased until the needle perforates the atrial septum. For device closure, using novel placement of an intracardiac echo probe via a Mullins sheath in the RV outflow tract and pulmonary artery[16] seems to be advantageous over viewing from the LA. This allows near-field visualization of device deployment in the LAA. This technique may increase the spectrum of patients who benefit from the procedure by decreasing procedure time, fluoroscopy, and procedure-related morbidity (Fig. 6-6).

Transseptal crossover and advancement of the dilator and sheath are adequately imaged and the ostium of the LAA is easily delineated and measured by ICE. Device positioning, release, potential periprosthetic leaks, and especially the spatial relation of the device to the surrounding structures can be continuously monitored in the transatrial longitudinal view. In some patients, the transventricular long-axis view can represent an alternative (see Table 6-3).

## Guiding Radiofrequency Pulmonary Vein Ablation

The rapidly evolving field of interventional electrophysiology creates a demand for guidance by imaging. This is particularly true in view of the fact that currently available techniques, such as fluoroscopy and endocardial ECG, may be helpful but have

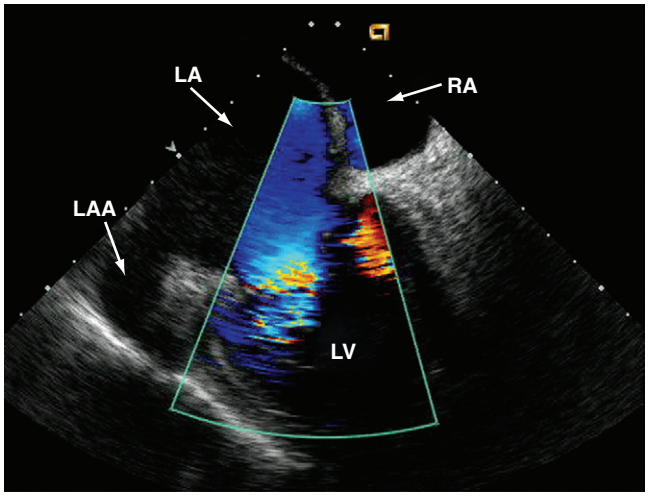



**Figure 6-7 Transatrial longitudinal view.** Left atrial appendage (*LAA*) and transmitral flow into the LV.

certain limitations. In many cases, angiographic guidance of circular mapping catheters is not sufficiently accurate. After initial puncture of the interatrial septum, high-quality images provided by ICE are capable of guiding transseptal pulmonary vein ablation, a treatment option in atrial fibrillation. Delineation of the endocardium and direct visualization of the pulmonary venous ostium facilitate mapping and radiofrequency ablation by depicting the target area, ensuring electrode-tissue contact, and helping with energy titration (Fig. 6-7).

Angiography-guided placement can result in poor contact between the ablation catheter and the endocardial surface. Inadequate contact reduces heat transfer to the tissue and allows convective heat loss into the circulating blood.

In the transatrial longitudinal view, the left pulmonary veins can be imaged by advancing the probe without tension or steering forces. Clockwise rotation of the catheter and insertion into the SVC allows the right pulmonary veins to be visualized in a cross-sectional view. Left or right steering permits longitudinal views of the right pulmonary veins. Thus, accurate anatomical

positioning of the ablation catheter tip in relation to adjacent endocardial structures is supported[17] (Fig. 6-8).

Doppler measurements of pulmonary vein flow velocities before and after ablation are recommended. During the procedure, the ablation zone can be directly visualized, including the evolving tissue injury. Visualization permits assessment of shape, cross-sectional area, wall thickness, and lesion formation[18] and depicts lesion size and continuity.[19] ICE is also useful for monitoring bubble formation during the phase of radiofrequency energy delivery, allowing radiofrequency dose titration to prevent overheating of the catheter tip. After effective ablation, transvenous flow velocities should be interrogated using continuous-wave Doppler in order to identify the potential presence of a gradient,[20] which can occur as a complication. This illustrates that ICE contributes to the safety of the ablation procedure and to prevention or early detection of potential complications associated with electrophysiologic interventions, that is, thrombus formation[21] and development of pulmonary vein stenosis.[20] Periinterventional monitoring depicts each step of the ablation process, improves efficacy, and also reduces early and late complications.[22] As demonstrated for device closure of interatrial communications, ICE can lower fluoroscopy time and shorten the ablation procedure.

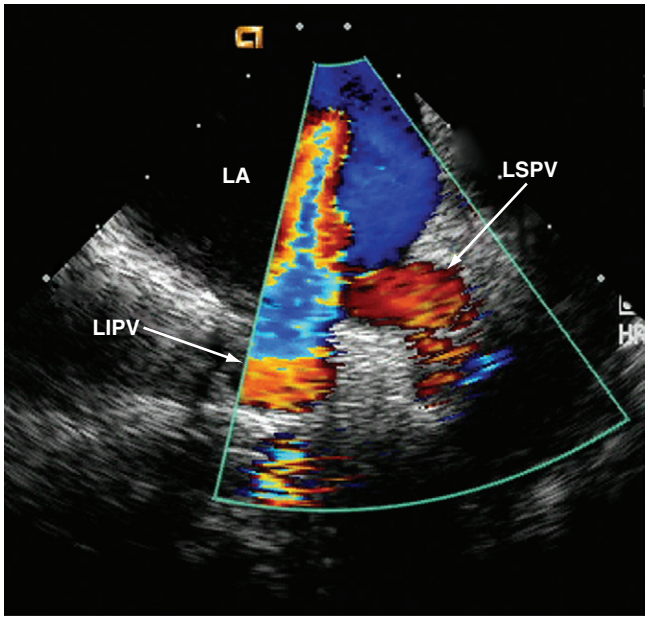



**Figure 6-8** **Modified transatrial longitudinal view.** Flow from left-sided pulmonary veins into the LA. *LIPV*, Left inferior pulmonary vein; *LSPV*, left superior pulmonary vein.

## Monitoring Transcatheter Aortic Valve Implantation

Generally, potential alternative sound windows are available for ICE-based intrainterventional assessment in TAVI. These include the transaortic window for viewing from inside the ascending aorta[23] and the transventricular window for transseptal viewing from the right ventricle.[24] Views from inside the aorta are inconvenient because the ICE catheter is prone to interfere with procedural catheters. In many individuals, it is also challenging to keep the ICE catheter stabilized in the RV (transventricular approach) throughout the procedure. However, longitudinal views from the lower SVC and the upper RA supplemented by RA short-axis views seem to be most suitable for continuous guidance, because the catheter position remains stable and the catheter does not interfere with the TAVI procedure[24a] (Figs. 6-9 and 6-10).

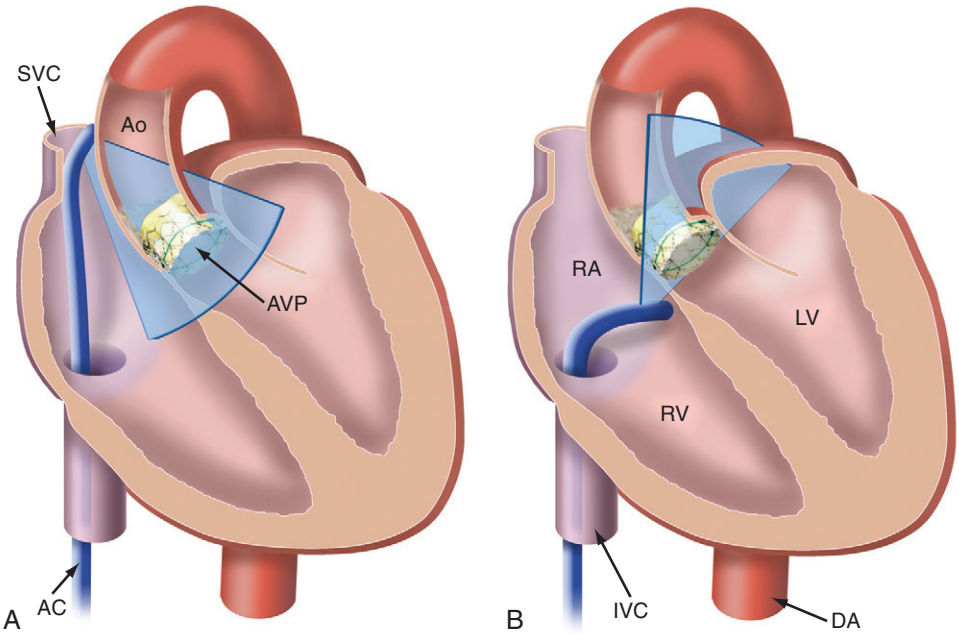



**Figure 6-9** Longitudinal transcaval/transatrial (**A**) and short-axis transatrial (**B**) standard intracardiac echocardiographic views for transcatheter aortic valve implantation. *Ao*, Ascending aorta; *AC*, AcuNav catheter; *AVP*, aortic valve prosthesis; *DA*, descending aorta; *IVC*, inferior vena cava; *SVC*, superior vena cava. *(From Bartel T, Bonaros N, Müller L, et al: Intracardiac echocardiography: a new guiding tool for transcathter aortic valve replacement.* J Am Soc Echocardiogr *24:966-57, 2011).*

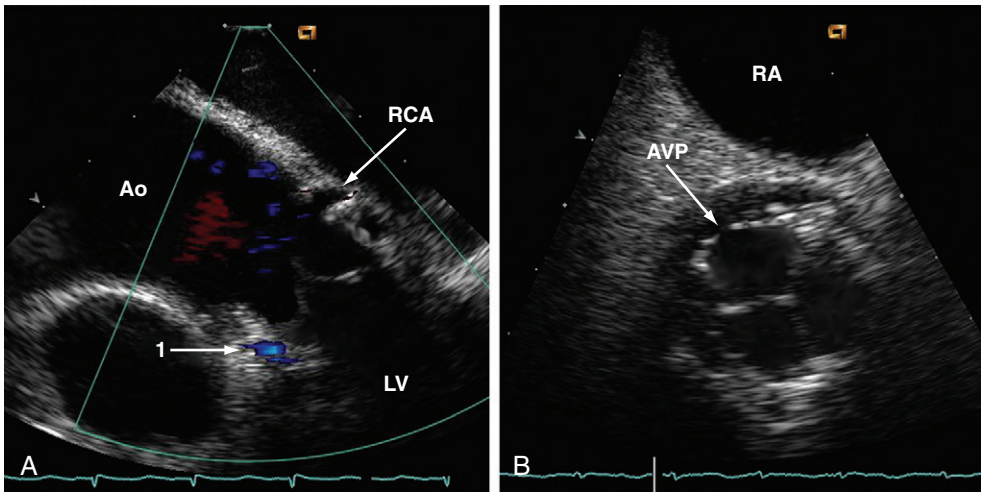



**Figure 6-10** Longitudinal transcaval (**A**) and short-axis (**B**) intracardiac echocardiographic views of aortic valve prosthesis after deployment and at end-diastole. *1*, Minimal paravalvular leak; *Ao*, aorta; *AVP*, aortic valve prosthesis; *RCA*, right coronary artery. *(From Bartel T, Bonaros N, Müller L, et al: Intracardiac echocardiography: a new guiding tool for transcathter aortic valve replacement.* J Am Soc Echocardiogr *24:966-57, 2011).*

Even in asymptomatic patients, aortic stenosis is known to be associated with a poor prognosis.[25] An increasing number of patients cannot undergo surgical aortic valve replacement owing to high perioperative risk due to comorbidities and advanced age.[26] The periinterventional risk of TAVI must be weighed against these facts.[27] Especially in extremely high-risk patients, each step of the procedure can cause life-threatening complications.[28] Although periprocedural echocardiography is regarded as an important means of lowering the rate of complications, and although TEE monitoring is frequently used in those patients exposed to extreme risks to assist with the interventional steps and to detect complications, current guidelines for TAVI do not include any detailed methodologic suggestions for intraprocedural use of echocardiography.[29]

Echocardiography also qualifies as a tool for guiding TAVI with the purpose of increasing its benefit-to-risk ratio.[30] Intraprocedural TEE has become an established method,[29] although it is not necessarily an ideal guiding tool, one reason being the difficulty of aligning the Doppler beam with transvalvular flow in the deep transgastric view. Transgastric measurement of aortic valve blood flow cannot be considered a routine approach and is known to require a significant learning curve. It also may not depict the maximum transvalvular or transprosthetic gradient because the TEE approach results in a non-parallel Doppler angle. In contrast, the Doppler beam can be nicely aligned with transvalvular flow in the transcaval/transatrial longitudinal ICE view, and determination of transvalvular pressure gradients is therefore much easier than with TEE. The gradient not only gives an estimate of the effectiveness of predilatation, but helps to avoid unnecessary additional dilatations. This is meaningful for risk management because each balloon dilatation is associated with the risk of annulus dissection and significant aortic regurgitation.

When positioned at the level of the aortic valve, the TEE probe impedes posterior-to-anterior fluoroscopic viewing, which is mandatory for angiography, balloon dilatation, final adjustment of the prosthesis, and its subsequent implantation. This is another drawback of TEE. The only workaround is repeated TEE probe withdrawal at crucial points of TAVI work flow, subsequent repositioning of the probe, and new alignment to obtain appropriate TEE views. Consequently, TEE provides only episodic monitoring on the one hand. On the other hand, repeated repositioning of the TEE probe may cause several interruptions of TAVI work flow. Although real-time 3D TEE represents a feasible guiding tool and may improve spatial orientation, it nevertheless remains a variant of TEE with all disadvantages inherent in this technique when applied to TAVI.

In contrast to TEE, the ICE catheter can be left in place with the probe aimed at the aortic valve during the entire TAVI procedure. Slight readjustments of the catheter may be occasionally required. Simultaneous and uninterrupted echocardiographic guidance by ICE is an ideal method for assisting predilatation, final adjustment, and deployment of the valve prosthesis; for ruling out potential complications as early as possible; for confirming proper prosthetic valve function without a need for repeated angiography; and for checking LV function immediately after implantation. Decreased use of contrast agents is meaningful, because renal failure has been reported to be the commonest short-term complication after TAVI.[31] In comparison to TEE, ICE provides a more coaxial view of the ascending aorta and may therefore help to improve coaxiality between the valve-balloon system and the ascending aorta. ICE also assists wire crossing of the native valve in the majority of patients and better depicts the coronary ostia than TEE, which helps to rapidly exclude any obstruction by displaced debris from the calcified native valve (Fig. 6-11).

Both ICE and TEE approaches can be considered equivalent with respect to determining annulus size and LV function. Measuring annulus size is particularly critical and essential for selecting the correct size valve prosthesis. The ICE catheter is maneuverable by the interventional operator, who can adjust the transducer as needed and independently from a noninvasive cardiologist or anesthetist, while the ultrasound unit is operated by an ultrasonographic technician. Operated by an interventional cardiologist also experienced in echocardiography and especially in ICE application, this tool has some potential in minimizing procedural risks by avoiding and, whenever possible, detecting TAVI complications[32] at the earliest possible time.

TAVI can also be completed under local anesthesia and moderate sedation,[33,34] provided patients are selected accordingly.

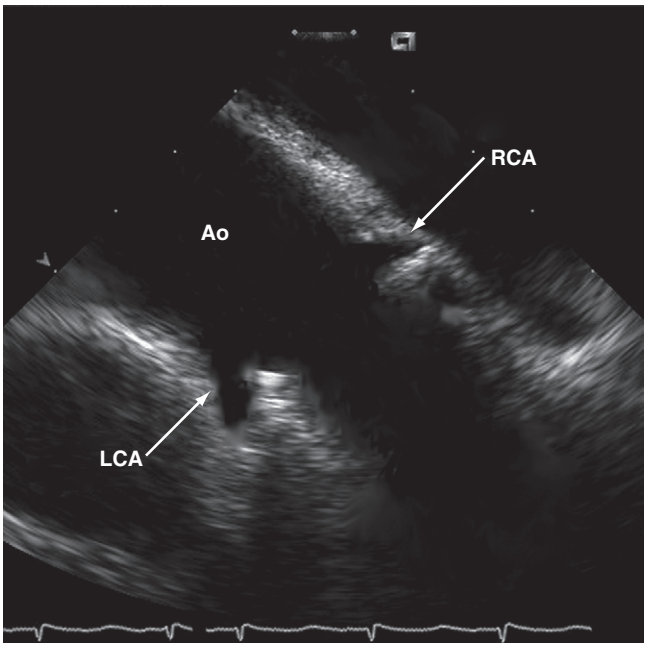



**Figure 6-11** Longitudinal intracardiac echocardiographic view demonstrates both coronary arteries branching off above the opened aortic valve prosthesis. *Ao*, Aorta; *LCA*, left coronary artery, *RCA*, right coronary artery. *(From Bartel T, Bonaros N, Müller L, et al: Intracardiac echocardiography: a new guiding tool for transcathter aortic valve replacement.* J Am Soc Echocardiogr *24:966-57, 2011).*

However, prolonged TEE imaging requires deeper sedation. The availability of ICE as an adjunct for TAVI lets the operator decide whether to use local anesthesia plus sedation or general anesthesia independently of the need for echocardiographic guidance.

## Perioperative and Periinterventional Imaging of the Ascending Aorta

When a high transesophageal image plane—also known as "banana view"—is used, TEE depicts the caudal part of the ascending aorta anteriorly to the right pulmonary artery. Unfortunately, ascending aortic flow is not aligned with the Doppler beam in this plane. For that reason, perioperative functional assessment of the aortic valve and the ascending aorta by TEE is limited to regurgitant flow detection. Perioperative IPAI and ICE from the RA and the SVC may become alternative approaches for complete morphologic assessment of the ascending aorta and functional evaluation of the aortic valve. In order to display the proximal ascending aorta, the ICE catheter is used as described for TAVI. Alternatively, it can be inserted via a jugular venous access and advanced through the SVC into the upper RA. In contrast to transfemoral access, no fluoroscopic guidance is needed with the jugular venous approach because the access sheath guides the catheter sufficiently, making direct catheter navigation superfluous. From the superior RA, the aortic bulb and aortic valve can be displayed in the long-axis view and, after tilting the tip of the catheter, also in a short-axis view. After the catheter is pulled back into the SVC, a longitudinal cut plane of the whole ascending aorta reaching up to the innominate artery can be obtained. In contrast to TEE, systolic flow is mostly aligned with the Doppler beam of the catheter, permitting color flow and pressure gradient recordings of highest image quality. Therefore, ICE might be of clinical interest immediately after aortic valve surgery or surgery of the ascending aorta (Fig. 6-12).

Intraoperative cannulation of the ascending aorta with surgical devices can also be monitored with IPAI views from the SVC. Further development of right-heart assist devices could create another potential application. Nevertheless, clinical experience with the transjugular approach is limited.

## Periinterventional Imaging of the Descending Thoracic Aorta

TEE adds incremental information, improving the safety of stent-graft placement in type B aortic dissection. In addition, IVUS is considered helpful in patients with complex dissection including abdominal extension.[35] With respect to aortic diseases, the main limitation of IVUS is attributable to its inability to perform Doppler analysis. Flow detection by TEE is also limited if the flow is not aligned with the Doppler beam. In consequence, detecting flow from true to false lumen and vice versa by TEE depends on the alignment of the dissection flap. Therefore, TEE has a low sensitivity for detecting small entries and reentries (Fig. 6-13).

On the other hand, sonographic approaches may help lower the current complication rate of percutaneous stent-graft implantation,[36] thus opening up new opportunities for monitoring interventional therapy in aortic diseases using IPAI. In that respect, IPAI not only combines advantages of TEE and IVUS, but adds capabilities.

The descending thoracic aorta cannot be viewed from any venous approach. Periinterventional sonographic diagnostic methods need to clarify which lumen supplies the side branches, a difficult feat with TEE and even with IVUS images. Thus, the need to navigate the aorta with the echocardiographic catheter turns from a disadvantage into an advantage, because the Doppler beam can be aligned with any flow between true and false lumen and with blood flow into small branches. Thus, intraaortic monitoring by IPAI has great potential to become a tool for the effective guidance of aortic stent-graft implantation, in such a manner that all entries are closed. First case reports also suggest that IPAI is capable of safely guiding other diagnostic intraaortic procedures in aortic diseases.[37]

Since the approval of the 8-Fr ICE catheter, its intraaortic use has added to the diagnostic spectrum in aortic disease.[37] For intraaortic employment of the echocardiographic catheter, a very long access sheath is definitely recommended so that only the tip of the catheter with the transducer sticks out of the sheath. Sheath and indwelling catheter are then jointly pulled back while imaging is performed. The catheter can be rotated intermittently and aimed at the region of interest by tilting its tip.

In type B aortic dissection, the echocardiographic catheter is placed into the true lumen and IPAI performed carefully. IPAI provides scans of the dissection flap when the device is rotated and withdrawn. Detection and precise localization of tears in the dissection membrane must be considered important for therapeutic decision making. In most cases, there are obviously more entries than are demonstrable by angiography, IVUS, or TEE. The fact that such data form the basis for optimal stent-graft placement, which aims to close all entries to the false

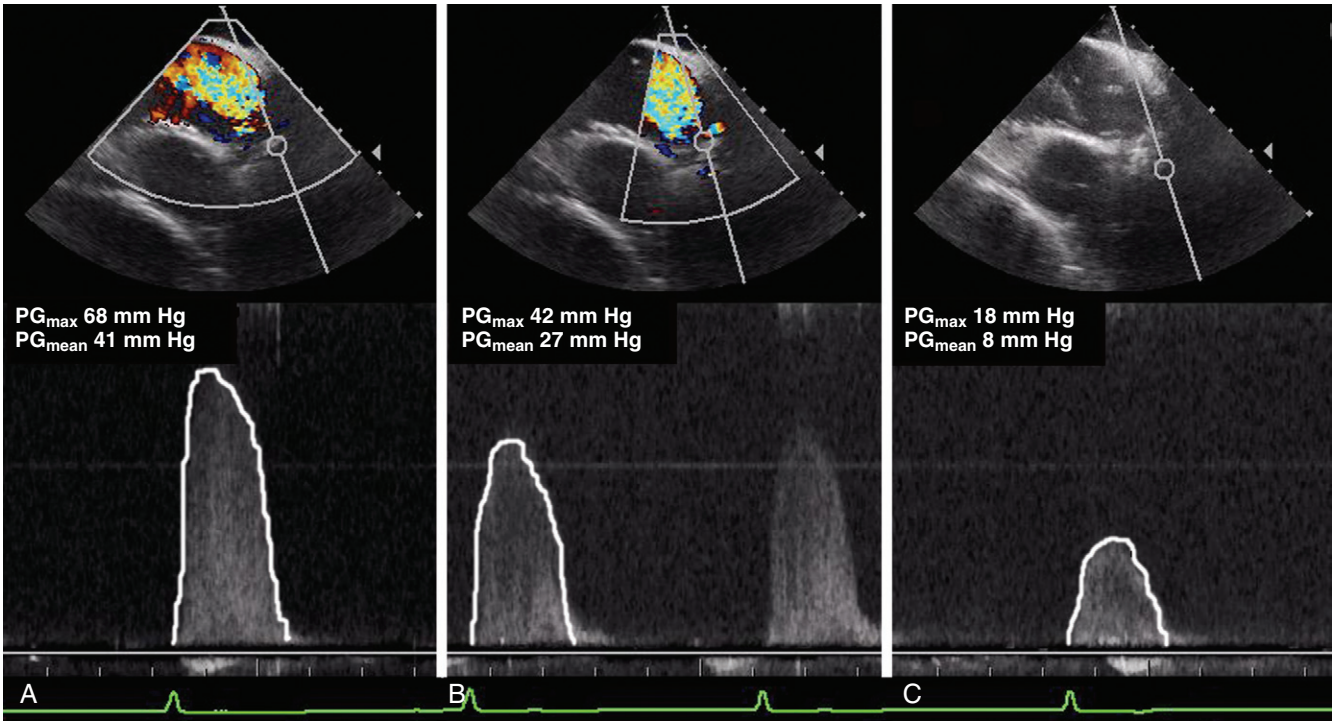



**Figure 6-12** **Aortic valve and ascending aorta seen from the superior vena cava:** measurement of pressure gradients (*PG*) before transcatheter aortic valve replacement (**A**), after predilatation (**B**), and after valve deployment (**C**). This approach allows full intraoperative hemodynamic assessment as well.

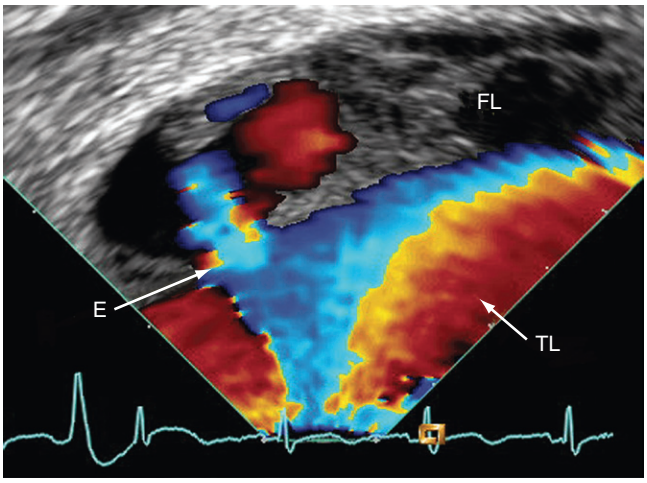



**Figure 6-13** Intraluminal phased-array imaging from the true lumen (*TL*) to the false lumen (*FL*): thrombus formation in type B aortic dissection. *E*, Entry.

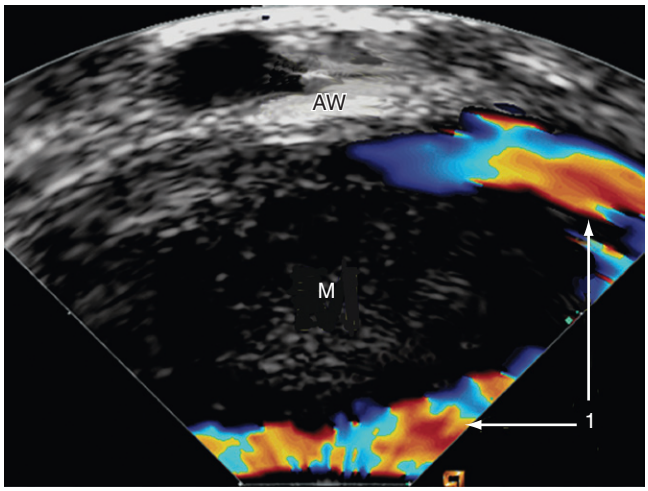



**Figure 6-14** Intraluminal phased-array imaging of an intraaortic mass (*M*). *1*, Flow around the mass; *AW*, aortic wall.

lumen, mandates a detailed analysis of the sensitivity of conventional diagnostic approaches. If overlooked or not properly closed by interventional treatment, even small tears can lead to significant flow into and inside the false lumen, impairing the desired thrombus formation in the false lumen and thereby impeding healing of the dissection. IPAI depicts more entries than one would expect from conventional diagnostics and demonstrates which abdominal vessels originate from the true and the false lumen. Thrombus formation in the false lumen, a result of effective pressure separation between true and false lumen, can be also displayed.

IPAI can also be used to safely guide percutaneous biopsies of intraaortic masses suspected to be tumors. To accomplish that, the transducer is aimed at the mass and the radial-jaw biopsy forceps (Fig. 6-14).

Under continuous ultrasonographic imaging, targeted biopsies are taken from the depth of the mass. Opening, pushing, and closure of the biopsy forceps can be precisely guided and

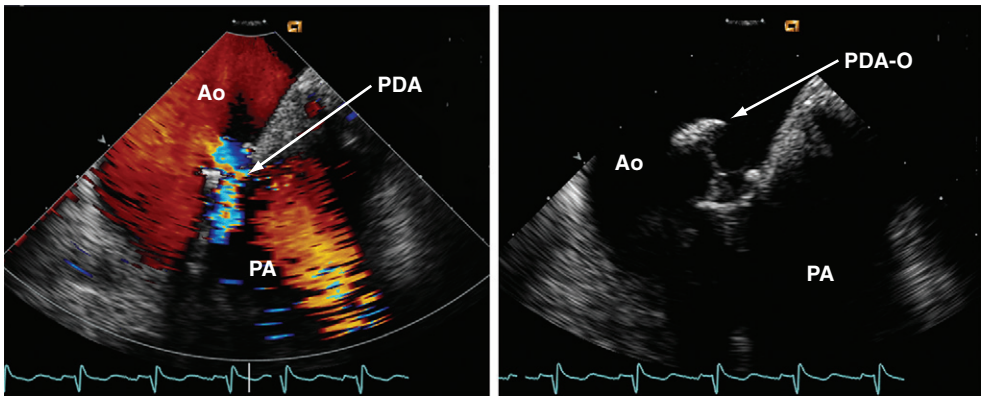



**Figure 6-15** Intraaortic viewing: device closure of patent ductus arteriosus (*PDA*). *Ao*, Aorta; *PA*, pulmonary artery; *PDA-O*, patent ductus arteriosus occluder.

documented.[37] With careful handling, interference between the echocardiographic catheter and the lesion can be avoided. Nevertheless, there is some risk of peripheral embolization during the procedure.

Percutaneous device closure of patent ductus arteriosus is another interventional approach nicely guidable by use of IPAI. It may help to reduce procedural time, limit radiation exposure, and lower the amount of contrast agent administered. It is conceivable that IPAI can contribute to the safety and success of this nonroutine procedure[38] (Fig. 6-15).

## Periinterventional Imaging of the Mitral Valve

Percutaneous transseptal balloon mitral valvotomy (BMV) (see Chapter 21) can be performed in concentric stenosis when the commissures are fused because of rheumatic heart disease without significant calcification and mitral regurgitation. Suitability of mitral stenosis for BMV can be assessed using the Wilkins score and a commissural score. As described for interventional left atrial appendage closure, atrial septal puncture is guided by the ICE transatrial longitudinal view. In that view, tool positioning in the LA can also be monitored. After introduction of a special guidewire into the LA, the transventricular long-axis view of the LV is obtained. Mitral ring diameter and intercommissural distance are measured, and the fused commissures are visualized. A balloon of appropriate size is selected. The same view is also useful for guiding a balloon through the stenotic mitral valve into the LV. Adhering to the double balloon technique, the distal balloon is inflated. Inflation should be monitored with ICE and fluoroscopy simultaneously. The next steps must be completed quickly to avoid prolonged LV inflow occlusion. Simultaneous echocardiographic and fluoroscopic viewing and documentation are recommended to accomplish this goal. The distal balloon is first inflated, and then pulled back toward the stenotic valve. Not until this step is completed is the proximal balloon inflated and valvotomy performed. At this time, ICE demonstrates that the balloon fits tightly into the stenotic valve orifice. The newer single-balloon technique[39] may require even closer echocardiographic guidance to precisely position the cylindrical balloon into the stenosis.

After balloon deflation and withdrawal, immediate two-dimensional and Doppler analyses are recommended to show the split commissures and to exclude any injury of the commissures or the mitral valve apparatus. In addition, the degree of mitral regurgitation is reassessed. Intraprocedural ICE viewing may be considered an optional imaging modality, especially if the transthoracic acoustic window is very poor. It allows analysis of the valvular anatomy and is ideal when enhanced views are required.[40] ICE is capable of providing excellent imaging and guidance, which results in low radiation exposure and minimizes the need for contrast angiography.[15]

One would expect the more sophisticated interventional procedures to derive more benefits from ICE. Thus, there is great potential for ICE in percutaneous valve implantation techniques and other catheter-based "valvular repair" procedures currently under development. Another future application may arise from the increasing importance of minimally invasive and reconstructive mitral valve surgery.

## Limitations

Adequate handling of the ICE catheter requires a learning curve, even for an interventionalist familiar with left and right heart catheterization and IVUS. Additionally, the relatively large probe may limit its use in infants. In addition, the multifrequency probe does not provide harmonic imaging capability. ICE does, however, eliminate the need for general anesthesia and intubation, thereby lowering costs and increasing patient comfort. On the other hand, the high price for one AcuNav catheter remains an important shortcoming. Today, the catheter is no longer a disposable device. The lumenless catheter can be resterilized with gas. Vanguard AG Medical Services for Europe (Berlin, Germany) is an approved CE-certified company licensed to resterilize ICE catheters. Technical and medical safety and compliance with appropriate legal regulations governing health care products are guaranteed. After more than 2 years of experience, we can recommend resterilization as a safe procedure that permits each catheter to be reused approximately three times. Although the image quality may slightly deteriorate from resterilization, each catheter can eventually be used four times, markedly lowering the costs for each use, even when the cost of resterilization is accounted for.

**TABLE 6-4 Usefulness and Effectiveness of Intracardiac and Intravascular Imaging**

| *Procedure* | *Clinical Benefit* |
|---|---|
| Device closure of atrial septal defect | Very high |
| Device closure of patent foramen ovale | Moderate |
| Left atrial appendage closure | Moderate |
| Radiofrequency pulmonary vein ablation | Very high |
| PTSMA | Moderate |
| Transcatheter aortic valve implantation | High |
| Surgery of the ascending aorta | Undetermined |
| Interventional therapy of the descending aorta | Potentially high |
| Balloon mitral valvotomy | High |
| Surgical/interventional mitral valve repair | Undetermined |

*PTSMA*, Percutaneous transluminal septal myocardial ablation.

Finally, the relation between advantages and disadvantages of using ICE and IPAI depends mainly on the expenditure and the risk of the specific interventional procedures. Increasing familiarity of interventional cardiologists with this technique may also affect its use in clinical practice (Table 6-4).

## KEY POINTS

As an alternative to TEE and IVUS and in conjunction with fluoroscopy, ICE can guide a variety of noncoronary percutaneous interventional therapeutic interventions:

| **Interventional Procedure** | **Guidance by ICE** |
|---|---|
| 1. Device closure of interatrial communications | View from the RA |
| 2. LAA occlusion | View from the RA (and RV) |
| 3. Radiofrequency pulmonary vein ablation | View from the RA |
| 4. Percutaneous transluminal septal myocardial ablation in hypertrophic cardiomyopathy | View from the RV |
| 5. Imaging of the ascending aorta and aortic valve | View from the SVC and RA |
| 6. Imaging of the descending thoracic aorta | Intraaortic view |
| 7. Imaging of the abdominal aorta | View from the IVC |
| 8. Mitral valve angioplasty and repair | View from the RA and RV |

## REFERENCES


1. Silvestry FE, Kerber RE, Brook MM, et al: Echocardiography-guided interventions. *J Am Soc Echocardiogr* 22:213-231, 2009.
2. Luxenberg DM, Silvestry FE, Herrmann HC, et al: Use of a new 8 French intracardiac echocardiographic catheter to guide device closure of atrial septal defects and patent foramen ovale in small children and adults: initial clinical experience. *J Invasive Cardiol* 17:540-545, 2005.

2a. Zamorano JL, Badano LP, Bruce C, et al: EAE/ASE recommendations for the use of echocardiography in new transcatheter interventions for valvular heart disease. *Eur Heart J* 32:2189-2214, 2011.

3. Olgin JE, Kalman JM, Chin M, et al: Electrophysiological effects of long, linear atrial lesions placed under intracardiac ultrasound guidance. *Circulation* 96:2715-2721, 1997.
4. Bartel T, Müller L, Müller S: Intra-aortic phased-array imaging: new guiding tool for transcatheter aortic valve implantation. *Eur Heart J* 30:2368, 2009.
5. Hijazi ZM, Shivkumar K, Sahn DJ: Intracardiac echocardiography during interventional and electrophysiological cardiac catheterization. *Circulation* 119:587-596, 2009.
6. Bartel T, Müller S, Caspari G, Erbel R: Intracardiac and intraluminal echocardiography: indications and standard approaches. *Ultrasound Med Biol* 28:997-1003, 2002.
7. Chessa M, Carminati M, Butera G, et al: Early and late complications associated with transcatheter occlusion of secundum atrial septal defect. *J Am Coll Cardiol* 39:1061-1065, 2002.
8. Bartel T, Konorza T, Barbieri V, et al: Single-plane balloon sizing of atrial septal defects with intracardiac echocardiography: an advantageous alternative to fluoroscopy. *J Am Soc Echocardiogr* 21:737-740, 2008.
9. Bartel T, Konorza T, Arjumand J, et al: Intracardiac echocardiography is superior to conventional monitoring for guiding closure of interatrial communications. *Circulation* 107:795-797, 2003.
10. Mullen MJ, Dias BF, Walker F, et al: Intracardiac echocardiography guided device closure of atrial septal defects. *J Am Coll Cardiol* 41:285-292, 2003.
11. Koenig P, Cao QL, Heitschmidt M, et al: Role of intracardiac echocardiographic guidance in transcatheter closure of atrial septal defects and patent foramen ovale using the Amplatzer device. *J Interv Cardiol* 16:51-62, 2003.
12. Bartel T, Konorza T, Neudorf U, et al: Intracardiac echocardiography: an ideal guiding tool for device closure of interatrial communications. *Eur J Echocardiogr* 6:92-96, 2005.
13. Nkomo VT, Theuma P, Maniu VC, et al: Patent foramen ovale transcatheter closure device thrombosis. *Mayo Clin Proc* 76:1057-1061, 2001.
14. Martin F, Sánchez PL, Doherty E, et al: Percutaneous transcatheter closure of patent foramen ovale in patients with paradoxical embolism. *Circulation* 106:1121-1126, 2002.
15. Vaina S, Ligthart J, Vijayakumar M, et al: Intracardiac echocardiography during interventional procedures. *Eurointervention* 1:454-464, 2006.
16. Macdonald ST, Newton JD, Ormerod OJ: Intracardiac echocardiography off piste? Closure of the left atrial appendage using ICE and local anesthesia. *Catheter Cardiovasc Interv* 77:124-127, 2011.
17. Epstein LM, Mitchell MA, Smith TW, Haines DE: Comparative study of fluoroscopy and intracardiac echocardiographic guidance for the creation of linear atrial lesions. *Circulation* 98:1796-1801, 1998.
18. Tardif JC, Groeneveld PW, Wang PJ, et al: Intracardiac echocardiographic guidance during microwave catheter ablation. *J Am Soc Echocardiogr* 12:41-47, 1999.
19. Roithinger FX, Steiner PR, Goseki Y, et al: Low-power radiofrequency application and intracardiac echocardiography for creation of continuous left atrial linear lesions. *J Cardiovasc Electrophysiol* 10:680-691, 1999.
20. Callans DJ, Ren JF, Schwartzman D, et al: Narrowing of the superior vena cava-right atrium junction during radiofrequency catheter ablation for inappropriate sinus tachycardia: analysis with intracardiac echocardiography. *J Am Coll Cardiol* 33:1667-1670, 1999.
21. Ren JF, Marchlinski FE, Callans DJ: Left atrial thrombus associated with ablation for atrial fibrillation: identification with intracardiac echocardiography. *J Am Coll Cardiol* 43:1861-1867, 2004.
22. Marrouche NF, Martin DO, Wazni O, et al: Phased-array intracardiac echocardiography monitoring during pulmonary vein isolation in patients with atrial fibrillation: impact on outcome and complications. *Circulation* 107:2710-2716, 2003.
23. Bartel T, Müller L, Müller S: Intra-aortic phased-array imaging: new guiding tool for transcatheter aortic valve implantation. *Eur Heart J* 30:2368, 2009.
24. Vaina S, Ligthart J, Vijayakumar M, et al: Intracardiac echocardiography during interventional procedures. *Eurointervention* 1:454-464, 2006.

24a. Bartel T, Bonaros N, Müller L, et al: Intracardiac echocardiography: a new guiding tool for transcathter aortic valve replacement. *J Am Soc Echocardiogr* 24:966-957, 2011.

25. Rosenhek R, Zilberszac R, Schemper M, et al: Natural history of severe aortic stenosis. *Circulation* 121:151-156, 2010.
26. Iung B, Baron G, Butchart EG, et al: A prospective survey of patients with valvular heart disease in Europe: the Euro Heart Survey on Valvular Heart Disease. *Eur Heart J* 24:1231-1243, 2003.
27. Vahanian A, Otto CM: Risk stratification of patients with aortic stenosis. *Eur Heart J* 31:416-423, 2010.

28. Tuzcu EM, Kapadia SR, Svensson LG: "SOURCE" of enthusiasm for transcatheter aortic valve implantation. *Circulation* 122:8-10, 2010.
29. Vahanian A, Alfieri O, Al-Attar N, et al: Transcatheter valve implantation for patients with aortic stenosis: a position statement from the European Association of Cardio-thoracic Surgery (EACTS) and the European Society of Cardiology (ESC), in collaboration with the European Association of Percutaneous Cardiovascular Interventions (EAPCI). *Eur Heart J* 29:1462-1470, 2008.
30. Moss RR, Ivens E, Pasupati S, et al: Role of echocardiography in percutaneous aortic valve implantation. *JACC Cardiovasc Imaging* 1:25-28, 2008.
31. Dworakowski R, MacCarthy PA, Monaghan M, et al: Transcatheter aortic valve implantation for severe aortic stenosis—a new paradigm for multidisciplinary intervention: a prospective cohort study. *Am Heart J* 160:237-243, 2010.
32. Masson JB, Kovac J, Schuler G, Ye J, Cheung A, Kapadia S, et al: Transcatheter aortic valve implantation: review of the nature, management, and avoidance of procedural complications. *JACC Cardiovasc Intervention* 2:811-820, 2009.
33. Behan M, Haworth P, Hutchinson N, Trivedi U, Laborde JC, Hildick-Smith D: Percutaneous aortic valve implants under sedation: Our initial experience. *Catheter Cardiovasc Interv* 72:1012-1015, 2008.
34. Covello RD, Ruggeri L, Landoni G, Guarracino F, Bignami E, Gonfalini M, et al: Transcatheter implantation of an aortic valve: anesthesiological management. *Minerva Anesthesiol* 76:100-108, 2010.
35. Koschyk DH, Nienaber CA, Knap M, et al: How to guide stent-graft implantation in type B aortic dissection? *Circulation* 122(suppl I):I-260-I-264, 2005.
36. Eggebrecht H, Nienaber CA, Neuhäuser M, et al: Endovascular stent-graft placement in aortic dissection: a meta-analysis. *Eur Heart J* 27:489-498, 2006.
37. Bartel T, Eggebrecht H, Erbel R: Safe biopsy of aortic masses guided by intraluminal two-dimensional ultrasonography. *Heart* 90:974, 2004.
38. Bartel T, Gliech V, Müller S: Device closure of patent ductus arteriosus: optimal guidance by transaortic phased-array imaging. *Eur J Echocardiogr* 12:E9, 2011.
39. Joseph G, Chandy S, George P, et al: Evaluation of a simplified transseptal mitral valvuloplasty technique using over-the-wire single balloons and complementary femoral and jugular venous approaches in 1,407 consecutive patients. *J Invasive Cardiol* 17:132-138, 2005.
40. Salem MI, Makaryus AN, Kort S, et al: Intracardiac echocardiography using the AcuNav ultrasound catheter during percutaneous balloon mitral valvuloplasty. *J Am Soc Echocardiogr* 15:1533-1537, 2002.



# Intravascular Ultrasound: Principles and Clinical Applications

AKIKO MAEHARA, MD | GARY S. MINTZ, MD | NEIL J. WEISSMAN, MD

**Technical Background**
- Gray-Scale Intravascular Ultrasound
- Image Formation
- Image Interpretation
- Radiofrequency IVUS
- IVUS versus Angiography

**Clinical Applications**
- Integration into Practice
- Standard IVUS Acquisition Protocol
- Safety
- Assessment of Stenosis Severity
- Assessment of LMCA Disease
- Lesion Length and Reference Dimensions
- Unusual Lesion Morphology
- Assessment of Vulnerable Plaque
- Prediction of No-Reflow During Interventional Procedures
- Assessment of Interventional Complications
- Restenosis, Late Malapposition, Stent Fracture, and Stent Thrombosis
- Treatment of In-Stent Restenosis
- Bioabsorbable Stents
- Does IVUS Guidance Reduce Stent Restenosis and Thrombosis?
- Practical Recommendations

## Technical Background

### GRAY-SCALE INTRAVASCULAR ULTRASOUND

Gray-scale intravascular ultrasound (IVUS) utilizes one or more miniaturized transducers secured at the end of a flexible catheter that is inserted into arteries for in vivo tomographic visualization of vascular anatomy. Intracoronary ultrasound has become the most commonly used form of intravascular imaging and is regularly employed to delineate plaque morphology and distribution, to assess angiographically ambiguous lesions, to assess atherosclerosis progression and regression, to guide transcatheter coronary intervention, and to assess mechanisms of restenosis (Fig. 7-1).[1-2] The IVUS catheter is attached to either a portable or installed ultrasound machine through an interface that ensures sterility of the catheter and allows for motorized pullback. Motorized pullback of the IVUS catheter (or of the transducer within the catheter) at 0.5 mm/s or 1.0 mm/s allows calculation of lesion length and plaque volumes (necessary for progression/regression studies), ensures adequate time to visualize the lesion, and allows comparison between IVUS "runs" done at different times but with similar pullback speeds.

There are two types of transducers used in IVUS catheters: mechanical and phased array. The mechanical catheter uses a single transducer that is mounted at the tip of the catheter and rotated quickly (at 1800 rotations per minute [rpm]). Because the IVUS transducer is oriented at a 90° angle to the length of the catheter, the images are displayed as cross-sectional views of the artery. The mechanical transducer has the advantage of a simple design and a greater signal-to-noise ratio. These properties account for its high image quality with an overall resolution (with current 40- to 45-MHz transducers) of approximately 100 to 120 μm. The primary disadvantage of mechanical transducers is that they require a central drive shaft to rotate the transducer on the tip of the catheter. This drive shaft decreases catheter flexibility. If a mechanical transducer is placed within a tortuous vessel, the drive shaft may be constricted, resulting in nonuniform rotation of the distal transducer, thus creating an artifact of the image termed nonuniform rotational distortion.

The phased array transducer uses multiple, tiny transducer elements. Each transducer element is permanently mounted around the circumference of the catheter tip and sends and receives ultrasound from a small sector. The multiple imaging sectors are then "added together" to produce a cross-sectional image of the artery. Because the phased array transducer is permanently fixed with no moving parts, it is more flexible and transverses torturous vessels more easily. These transducers do not produce nonuniform rotational distortion artifacts. However, the 20-MHz phased array transducer does require more complex programming to add the sectors together and thus has a lower temporal resolution (a function of computational speed) and lower spatial resolution.

### IMAGE FORMATION

An IVUS image is formed when ultrasound bounces off the multiple layers of the artery and returns to the transducer.[3] The coronary artery is a muscular vessel composed of three basic layers: intima, media, and adventitia (Fig. 7-2). The intima, only a few cells thick at birth, is the site of atherosclerotic plaque accumulation. The intima is directly surrounded by the media, a layer of predominately homogeneous smooth muscle cells that provides the artery with its vascular tone. The outermost layer is the adventitia. Each of these layers tends to have a different acoustic property, allowing each to be visualized separately. When ultrasound encounters the intima, there is a large change in acoustic impedance; and much of it is bounced back

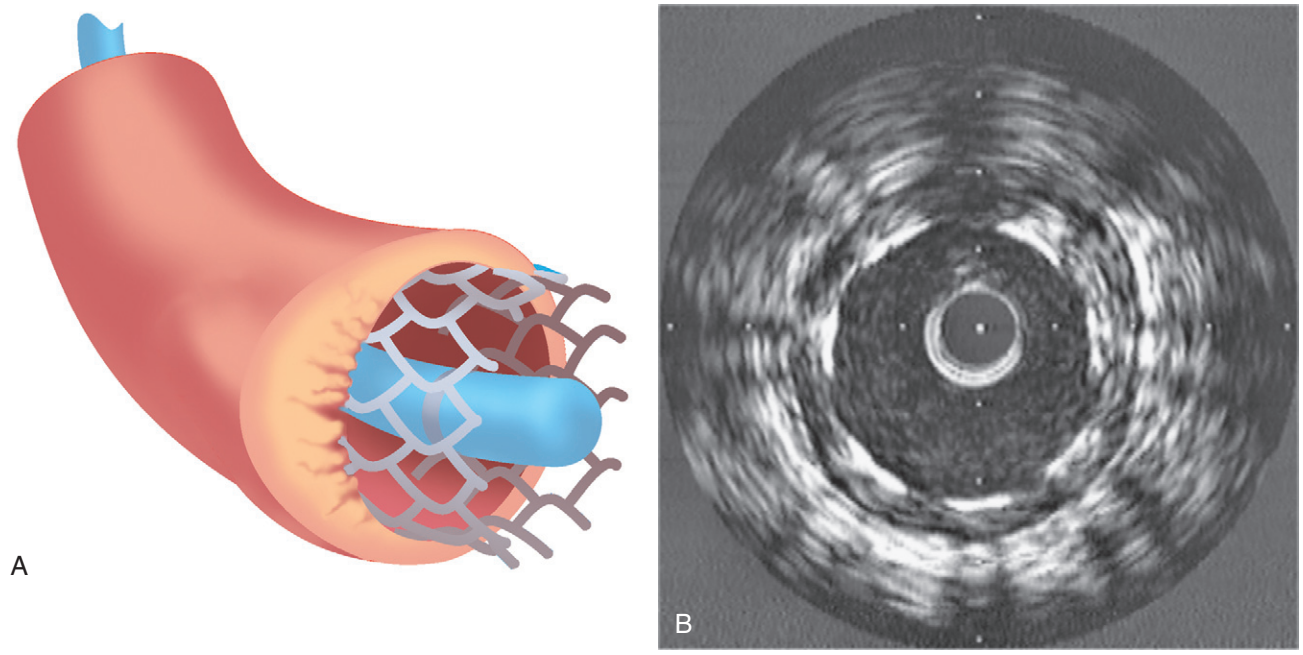



**Figure 7-1** **A,** Pictorial representation of an intravascular ultrasound catheter inserted into a coronary artery after stent deployment. **B,** Actual intravascular ultrasound image of a well-deployed coronary stent.

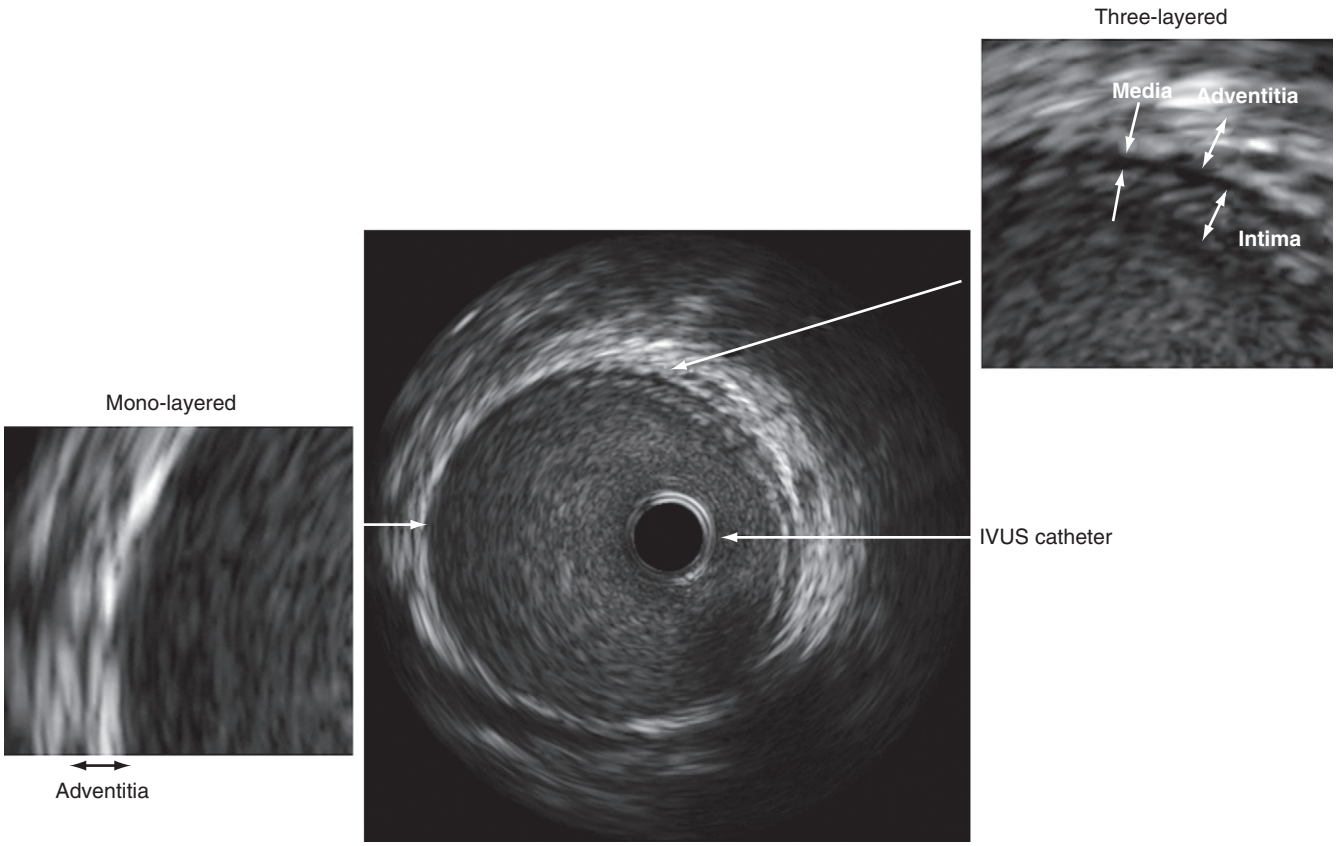



**Figure 7-2** *Center* image was magnified and displayed at right and left. (*Right*) Typical "three-layered" appearance indicating intima, media (dark band), and adventitia. (*Left*) "Mono-layered" appearance indicating very thin intima below intravascular ultrasound resolution, media (not visible), and adventitia.

to the transducer and displayed as a single concentric echo. Unless the intima becomes extremely hard, such as with the formation of a calcified plaque, some ultrasound penetrates through to the media. Because the media is composed of homogeneous smooth muscle cells, it passes through with minimal reflection; thus the media appears as a dark zone devoid of echoes. The adventitia has numerous layers of collagen fibers and therefore is a highly reflective structure that appears bright. As a result of the different acoustic properties of each layer, the normal coronary artery has a three-layered appearance, which

includes (1) a bright echo from the intima, (2) a dark zone from the media, and (3) bright echoes from the adventitia. Because the resolution of IVUS is approximately 100 to 120 μm, the intima has to be at least this thick to be visualized as a distinct structure. In Western society, most patients presenting to the cardiac catheterization laboratory have some diffuse thickening of the intima. But if the intima is truly disease free, as in a newborn, child, or adolescent, then the intima will be much thinner and below the resolution of IVUS so that the artery will appear as a monolayer (see Fig. 7-2).

## IMAGE INTERPRETATION

The interpretation of an IVUS image involves only a few simple steps: (1) identify the IVUS catheter in the center of the screen, keeping in mind that the IVUS catheter is traveling down the blood-filled lumen; (2) identify the dark stripe of the media that tells the size of the artery in the absence atherosclerotic disease; (3) remember that all of the echoes within the media stripe represent intima or intimal (atherosclerotic) disease and (4) all of the echoes outside the media are adventitia (see Fig. 7-2).

The amount of ultrasound that reflects off of tissue depends on the acoustic impedance (density) of the tissue. This property provides IVUS with some ability to differentiate plaque of different compositions. Hard material (calcium or fibrotic plaque) will reflect more ultrasound and appear brighter, whereas soft plaque (fat) will not reflect the ultrasound and will appear dark. Calcium is so dense that no ultrasound penetrates to the deeper tissues and, thus, produces acoustic shadows; shadowing, along with the bright echoes is the hallmark of calcification. A conventional approach is to compare the overall brightness of the plaque to the surrounding adventitia. Plaque is typically characterized as hypoechoic if less dense than the adventitia, hyperechoic if more dense than the adventitia, calcified if bright with acoustic shadowing, or mixed. IVUS can detect dense calcium with high sensitivity and specificity,[4-6] but its accuracy in identifying high-risk lipid rich plaque or even thrombus formation is poor.[7] As shown in Figure 7-3, gray-scale IVUS can also detect two other types of high-risk plaques: (1) noncalcified attenuated plaque (which correlates with fibroatheroma) and (2) calcium nodules (calcium with a convex shape and irregular surface).[8-10]

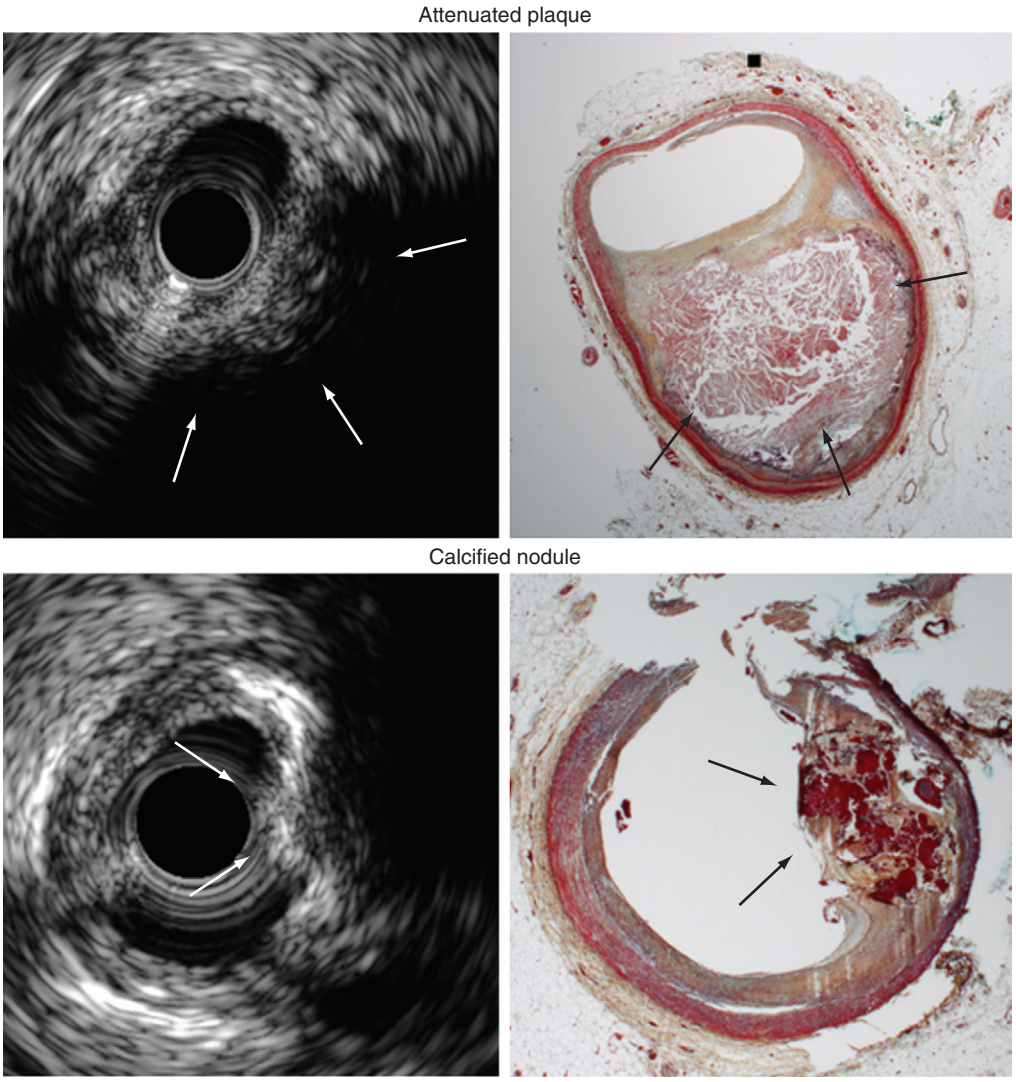



**Figure 7-3** Both intravascular ultrasound (IVUS) and corresponding histology (Russell-Movat's pentachrome staining) are shown. (*Top*) IVUS image shows typical "attenuated plaque"—non-hyperechoic plaque with attenuation. Corresponding histology shows advanced fibroatheroma (*black arrows*). Intravascular ultrasound image (*bottom*) shows "calcified nodule," which has convex irregular surface with acoustic shadow. Corresponding histology shows cluster of calcified nodules (*black arrows*).

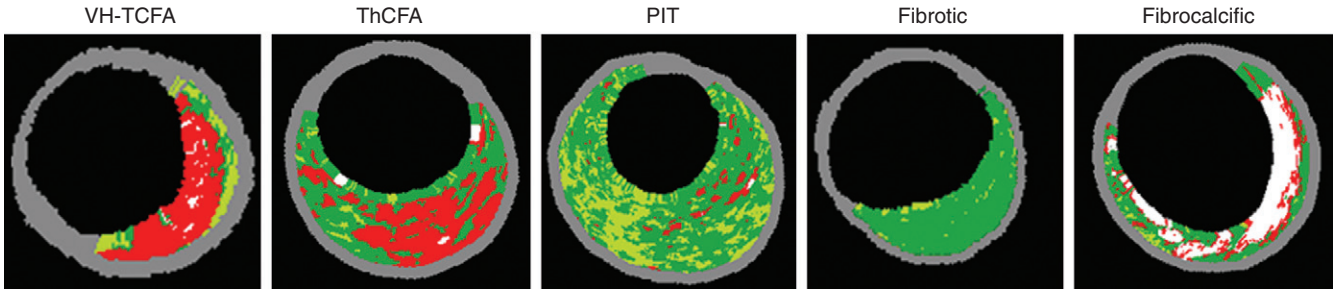



**Figure 7-4 Virtual histology (VH) IVUS classification.** (*red*, necrotic core; *white*, dense calcium; *light green*, fibrofatty; *dark green*, fibrous tissue) *VH-TCFA*, VH thin-cap fibroatheroma; *ThCFA*, thick-cap fibroatheroma; *PIT*, pathologic intimal thickening; fibrotic plaque; and fibrocalcific plaque.

## RADIOFREQUENCY IVUS

Standard gray-scale IVUS is limited, in part, because it uses only the amplitude of reflected ultrasound to formulate the image. In an effort to improve on the qualitative assessment of the reflected ultrasound signal, Kawasaki and coworkers developed a plaque characterization algorithm called integrated backscatter IVUS using time domain information directly from the radiofrequency signal. This process has resulted in improved plaque characterization with a reported in vitro sensitivity of 90% and specificity or 92% for lipid-rich plaque.[11]

In a similar effort to improve plaque characterization, spectral analysis (virtual histology [VH]-IVUS) combines signal frequency and amplitude analysis to create an algorithm that detects fibrous tissue (dark green), fibrofatty (light green), necrotic core (red), and dense calcium (white). Reported sensitivity and specificity of VH-IVUS are 91.7% and 96.6% for identification of the lipid-rich necrotic core.[12-14] However, VH-IVUS cannot detect thrombus (in fact, thrombus appears as either fibrotic or fibrofatty plaque depending on the age of the thrombus) and has not been validated for assessment of stent metal or intimal hyperplasia. VH-IVUS lesion phenotype has been classified as (1) VH thin-cap fibroatheroma, (2) thick-cap fibroatheroma, (3) pathologic intimal thickening, (4) fibrotic plaque, and (5) fibrocalcific plaque (Fig. 7-4). Fibrotic plaque has mainly fibrous tissue with less than 10% confluent necrotic core, less than 10% confluent dense calcium, less than 15% fibrofatty. Fibrocalcific plaque has mainly fibrous tissue with greater than 10% confluent dense calcium, but less than 10% confluent necrotic core. Pathologic intimal thickening has a mixture of all plaque components, but dominantly fibrofatty with less than 10% confluent necrotic core and less than 10% confluent dense calcium. Fibroatheroma (both VH thin-cap fibroatheroma and thick-cap fibroatheroma) has greater than 10% confluent necrotic core. Because the resolution of VH-IVUS is 150 to 250 μm, it is not possible to detect fibrous cap thickness less than 65 μm (the typical pathologic definition of a thin fibrous cap). Therefore, if there is greater than 30° of necrotic core abutting to the lumen in three consecutive slices, the fibroatheroma is classified as VH thin-cap fibroatheroma; otherwise, it is classified as thick-cap fibroatheroma.[15]

## IVUS VERSUS ANGIOGRAPHY

Angiography permits the measurement of only luminal diameters and typically in only two or three views. Because of its tomographic presentation and high resolution, IVUS is far more accurate than angiography in assessing atherosclerotic plaque extent, morphology, and distribution.

To appreciate and apply IVUS in clinical practice, one needs to have a full understanding of how IVUS and angiography differ. Angiography is often referred to as a "shadowogram" of the lumen because a silhouette of the arterial lumen is obtained by injecting radiopaque dye into the lumen and projecting the shadow from the dye on to cineangiographic film. The shadow-o-gram is then used to extrapolate a luminal narrowing to a plaque accumulation. It is common to detect atherosclerosis in an artery that appears "normal" by angiography. Although it may appear to be a discrepancy at first, it is not, and both the angiography and the IVUS studies are providing complementary and accurate information. The primary difference is that angiography is visualizing just the lumen, whereas IVUS visualizes both the lumen and arterial walls. If the assumption is that all angiographic stenoses are from plaque, then it would make sense to conclude that an angiogram displaying a lumen without any narrowing is free of plaque. However, that may not be true (and usually is not). Conversely, an angiogram of an artery can be free of any stenosis, but that artery can still have many areas of plaque. This is true because of three phenomena: (1) atherosclerotic plaque is often diffusely distributed, (2) arteries can undergo vascular remodeling, and (3) complex atherosclerotic plaques are not appreciated by the two-dimensional silhouette.

It has been verified in autopsy studies and other IVUS studies of healthy donors that most people have diffuse atherosclerotic disease throughout their arteries by midlife, and this disease often remains angiographically silent because of its diffuse nature. In addition to diffuse plaque, vascular remodeling is also responsible for the high prevalence of angiographically silent disease. Both pathology and IVUS studies have documented that coronary arteries will enlarge to accommodate focal plaque deposition in an attempt to maintain luminal integrity. Compensatory dilation of the arterial wall occurs in direct response to the accumulation of atherosclerotic plaque. An absolute reduction in lumen dimensions typically does not occur until the lesion occupies approximately 40% to 50% of the area within the internal elastic membrane (40% to 50% cross-sectional narrowing).[16] As a result, most of the atherosclerotic burden is contained within angiographically normal reference segments.[17]

Complex luminal shapes can result from irregular plaques or the disruption of a plaque (from balloon angioplasty). Although such a lesion may appear hazy, it may not demonstrate a luminal stenosis when viewed from only one or two views and projected as a silhouette. This may be similar to an eccentric lesion, which can fool inexperienced angiographers, unless a large number and variety of views are obtained, each displaying a different

severity. However, a lumen with highly irregular borders may not be fully appreciated, even in multiple views. The tomographic images of IVUS are necessary to appreciate the true luminal shape. Therefore, diffuse plaque, vascular remodeling, and irregular plaque can all lead to an inability of angiography to appreciate the plaque that is seen on IVUS. This is predominately because angiography only visualizes the lumen and does so in limited views using silhouettes of the dye.

Finally, angiography may contain areas that are hazy or lesions that are ambiguous. These hazy or ambiguous lesions may result from irregular plaque, a focal area of calcium, a dissection, or an intraluminal thrombus. IVUS is particularly useful for ambiguous lesions because each of the causes (plaque irregularities, calcium, dissection, or thrombus) appear different on IVUS.

## Clinical Applications

The concepts involved in the use of IVUS to guide coronary interventions are not different from the concepts involved in the use of angiography to guide interventional procedures. From a practical standpoint, the primary uses of IVUS are to assess the severity of a coronary artery stenosis including left main coronary artery (LMCA) disease, to measure lesion length, to measure reference vessel size, to identify complications, to optimize final results, and to assess causes of stent failure (including stent underexpansion, stent fracture, and late acquired stent malapposition).

### INTEGRATION INTO PRACTICE

Many practical aspects of IVUS imaging are facilitated by designating specific IVUS technologists who become responsible for all practical aspects of IVUS imaging: (1) equipment and catheter setup, (2) image optimization, (3) proper recording of IVUS imaging runs, (4) accurate voice and onscreen alphanumeric documentation, (5) patient and procedure logs, and (6) equipment maintenance. With time, technologists can be trained to interpret images accurately, to provide the iterative feedback necessary for IVUS-based decision making, and to answer questions posed by the primary operators. Measurements should be made offline (from hard drive after the imaging run is complete), not when the catheter is in the vessel; this saves procedure time and minimizes patient ischemia.

The angiographic (i.e., "road-map") monitors can be "wired" to display IVUS images. Angiographic monitors offer superior resolution, are convenient and readily visible to the operator, and allow the IVUS machine to be placed in a position away from the patient table and out of the way of the nurses providing patient care.

In a busy laboratory with multiple operators, it is important to standardize image acquisition and analysis. The use of a motorized transducer pullback device aids (in fact, enforces) discipline and acquisition standards; there is no question whether the transducer is being advanced or withdrawn. The preferred pullback speed is 0.5 mm/s; this is the fastest rate at which the trained eye can assimilate the information. Standardization of image acquisition facilitates offline image analysis and comparison of serial (preintervention versus postintervention or postintervention versus follow-up) studies; it is essential for multicenter studies.

### STANDARD IVUS ACQUISITION PROTOCOL

IVUS imaging should include careful uninterrupted imaging of (1) at least 10 mm of distal reference, (2) the lesion site(s), and (3) the entire proximal reference back to the aorta. Advantages of motorized pullback are (1) controlled catheter withdrawal so no segment of the vessel is skipped or imaged too quickly by pulling the catheter back too rapidly, (2) the ability to concentrate on the images without having to simultaneously pay attention to catheter manipulation, (3) the ability to make length and volumetric measurements, and (4) uniform and reproducible image acquisition for multicenter and serial studies. Disadvantages of motorized pullback are the following: (1) even at slow pullback speeds, it is possible to skip over focal lesions; (2) not enough attention may be paid to important regions of interest; and (3) it is not possible to have the transducer "sit" at one specific site in the vessel.

However, motorized transducer pullback does not preclude the addition of careful, manually controlled interrogation of the lesion. Manual transducer pullback should be at a slow rate similar to motorized pullback. Advantages are that it is possible to concentrate on specific regions of interest by having the transducer sit at a specific site in the vessel. Disadvantages include the following: (1) it is easy to skip over significant pathology by pulling the transducer back too quickly or unevenly, (2) length and volume measurements cannot be performed, and (3) antegrade and retrograde manual catheter movement can be confusing when the study is reviewed at a later date.

When interrogating ostial lesions, it is important that the guiding catheter be disengaged from the ostium. If not, the true ostial lumen dimensions may not be identified. In all cases, at least one continuous uninterrupted imaging run should be performed from approximately 10 mm beyond the target lesion to the ostial junction of the ostium with the aorta.

### SAFETY

Three large studies have evaluated the safety of IVUS. Other than transient spasm, complications appear to be rare (Table 7-1).[18-20]

### ASSESSMENT OF STENOSIS SEVERITY

Coronary angiography underestimates stenosis severity most markedly in vessels with 50% to 75% plaque burden (plaque area divided by arterial area) at necropsy and in patients with multivessel disease.[21-25] Clinical events are determined by lumen size, not by the amount of plaque. Therefore, it is important to focus on accurate measurement of lumen dimensions and not to be distracted by the plaque burden. Plaque burden in patients with atherosclerosis tends to be large even in the absence of lumen compromise.

**TABLE 7-1 Studies Evaluating the Safety of Intravascular Ultrasound**

| *Study* | *Number of Patients* | *Number of Centers* | *Transient Vessel Spasms* | *Major Complications* |
|---|---|---|---|---|
| Hausmann and colleagues[18] | 2207 | 28 | 2.9% | 0.4% |
| Batkoff and Linker[19] | 718 | 12 | 0.6% | 0.6% |
| Gorge and colleagues[20] | 7085 | 51 | 3.0% | 0.14% |

Data from references 18, 19, and 20.




Figure 7-5 Normal left main coronary artery (LMCA) compared to LMCA with severe disease.

Studies performed more than 10 years ago suggested that an IVUS minimum lumen area (MLA) greater than 4 $mm^2$ was a valid criterion for deferring an intervention based both on comparisons to physiologic measures and on follow-up data.[26-29] This cutoff only applied to major epicardial vessels excluding the LMCA and excluding saphenous vein grafts. However, it was necessary to interrogate the lesion carefully to identify the image slice with the smallest lumen, especially in very focal stenoses. Once the smallest lumen is identified, careful measurement was required. Recently this cutoff has come under criticism for a number of reasons including the size of the vessels (studies were done mostly in large 3.5-mm vessels), the average MLA of the intermediate lesions studied (4 $mm^2$), and the fact that these studies have been misinterpreted to suggest that lesions with an MLA below 4 $mm^2$ justify stent implantation. For this reason, it is recommended that for major epicardial vessels excluding the LMCA, physiologic lesion assessment (using an intracoronary pressure wire and maximum hyperemia with intravenous adenosine to measure the fractional flow reserve) is a complementary approach to assess lesion severity.[30]

## ASSESSMENT OF LMCA DISEASE

A high percentage of patients with angiographically "normal" LMCA with only nonsignificant stenosis have substantial disease by IVUS.[31-34] Reasons for the discrepancy between angiography and necropsy or IVUS assessment of LMCA disease include the following: (1) diffuse atherosclerotic involvement affects the angiographic diameter stenosis (DS) calculation because of the lack of a normal reference segment; (2) a short LMCA also makes identification of a normal reference segment difficult; (3) unique geometric issues exist in LMCA disease (the correlation between angiography and necropsy or IVUS appears to be somewhat better in non-LMCA stenoses); and (4) there is significant interobserver and intraobserver variability in the angiographic assessment of LMCA disease.[35-42] In fact, the LMCA is the coronary arterial segment with the greatest variability in angiographic assessment.

We reported 122 patients who underwent angiographic and IVUS assessment of the severity of LMCA disease, who did not have subsequent catheter or surgical intervention, and who were followed for 1 year.[43] There were three distinct predictors of these cardiac events: diabetes; a major epicardial vessel or bypass graft with a quantitative angiography (QCA) DS greater than 50% that was left untreated; and LMCA lesion site minimal lumen diameter measured by IVUS. An example is shown in Figure 7-5.

Jasti and colleagues reported that an IVUS MLA of 5.9 $mm^2$ or a minimal lumen diameter of 2.8 mm corresponded to physiologic ischemia (fractional flow reserve less than 0.75) in the LMCA.[44] Hernandez and co-workers evaluated 354 angiographically intermediate (diameter of stenosis 25% to 60%) unprotected LMCA lesions by IVUS. Of the patients evaluated, 186 had an MLA of at least 6 $mm^2$, and only 7 patients were revascularized.[45] In 2 years, percentages for survival free of cardiac death (97.7%) and revascularization (96.5%) were very high, suggesting a MLA of 6 $mm^2$ or greater as a safety cutoff to defer the revascularization of LMCA disease.

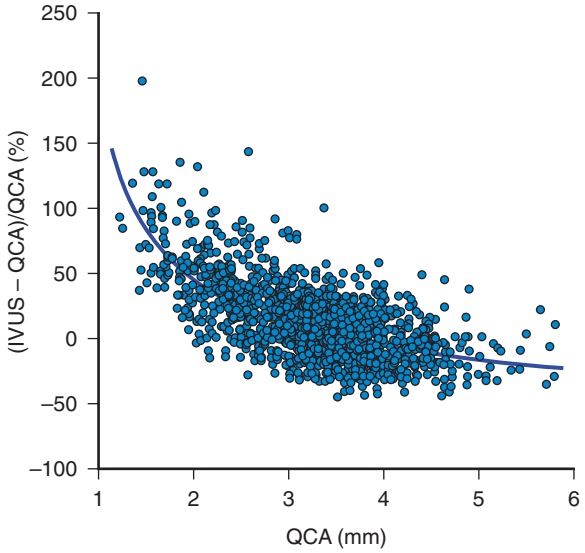



**Figure 7-6 Correlation between reference diameter by quantitative angiography (QCA) and intravascular ultrasound (IVUS).** At smaller vessel sizes, IVUS dimensions are larger than QCA; at larger vessel sizes, the difference is small.

## LESION LENGTH AND REFERENCE DIMENSIONS

The two most important measurements for stent size selection are lesion length and reference dimension. Motorized transducer pullback is essential for length measurements and has been validated in vivo.[46] A comparison of IVUS and QCA reference lumen measurements in 3311 nonostial native coronary arteries or saphenous vein graft lesions showed a QCA proximal reference lumen diameter of 3.05 ± 0.68 mm and an IVUS proximal reference lumen diameter of 3.41 ± 0.62 mm ($p$ less than 0.0001 versus QCA). The difference between the IVUS and QCA measurements was 0.36 ± 0.64 mm or 15 ± 24%. This difference was greatest in the smallest vessels, decreased asymptotically with increasing vessel size, and was zero at a QCA reference of approximately 4 mm shown in Figure 7-6.

This analysis suggests that, especially in the smaller arteries (which have higher restenosis rates), (1) the angiographic assessment of reference lumen dimensions is flawed and (2) an IVUS measurement would indicate that a larger device could be used that could result in larger final lumen dimensions without having to resort to midwall or media-to-media device/vessel sizing.[47,48] Alternatively, some authorities have advocated the use of IVUS "true vessel," "media-to-media," or midwall dimensions for device sizing; however, this should only be done by highly experienced IVUS users because it carries a greater risk of acute complications such as stent edge dissection.

## UNUSUAL LESION MORPHOLOGY

IVUS is useful in understanding lesions with an unusual angiographic appearance including filling defects, haziness, aneurysms, ulceration, myocardial bridge, and spontaneous dissection.[49-53] Examples are summarized in Figure 7-7 and shown in Figures 7-8 through 7-11.

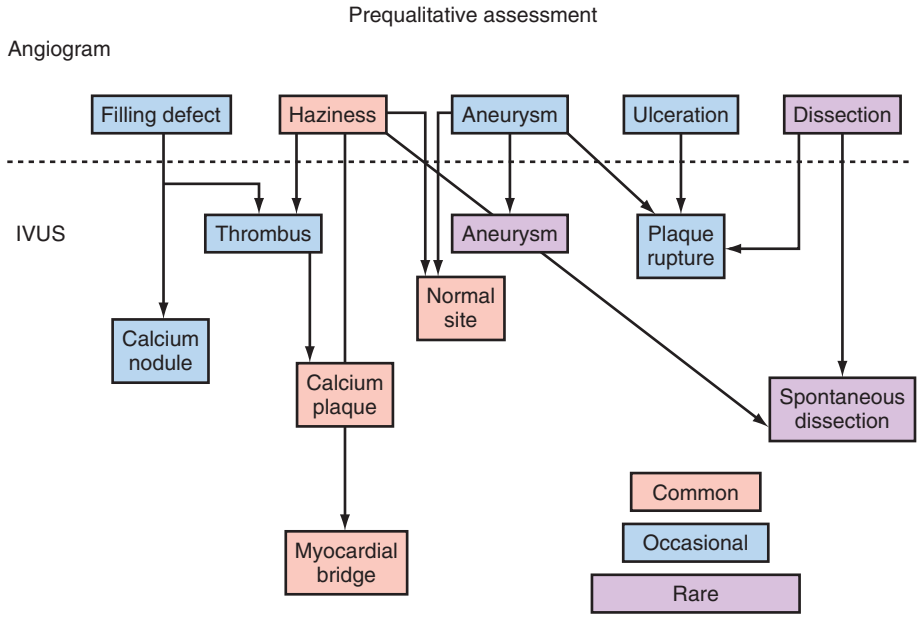



**Figure 7-7** Summary of preintervention qualitative assessment by intravascular ultrasound (IVUS). If the angiogram shows a filling defect, IVUS will show either thrombus or calcium nodule. If the angiogram shows haziness, IVUS will show thrombus, calcified plaque, myocardial bridge, normal site, or spontaneous dissection. Causes of an angiographic aneurysm include true aneurysm, false aneurysm, plaque rupture, or just a normal site that appears aneurysmal.

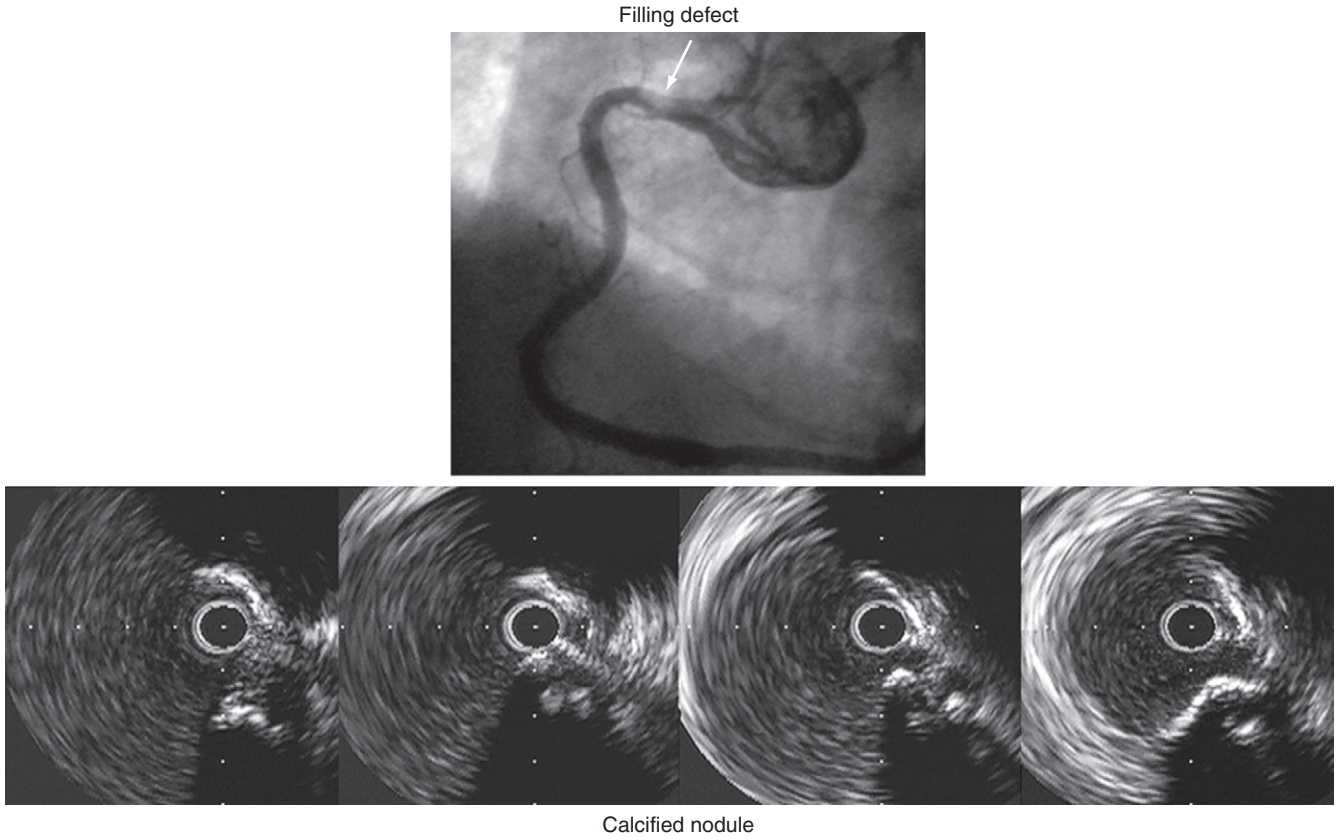



**Figure 7-8 Angiogram shows filling defect in the proximal right coronary artery.** Intravascular ultrasound shows calcified nodule.

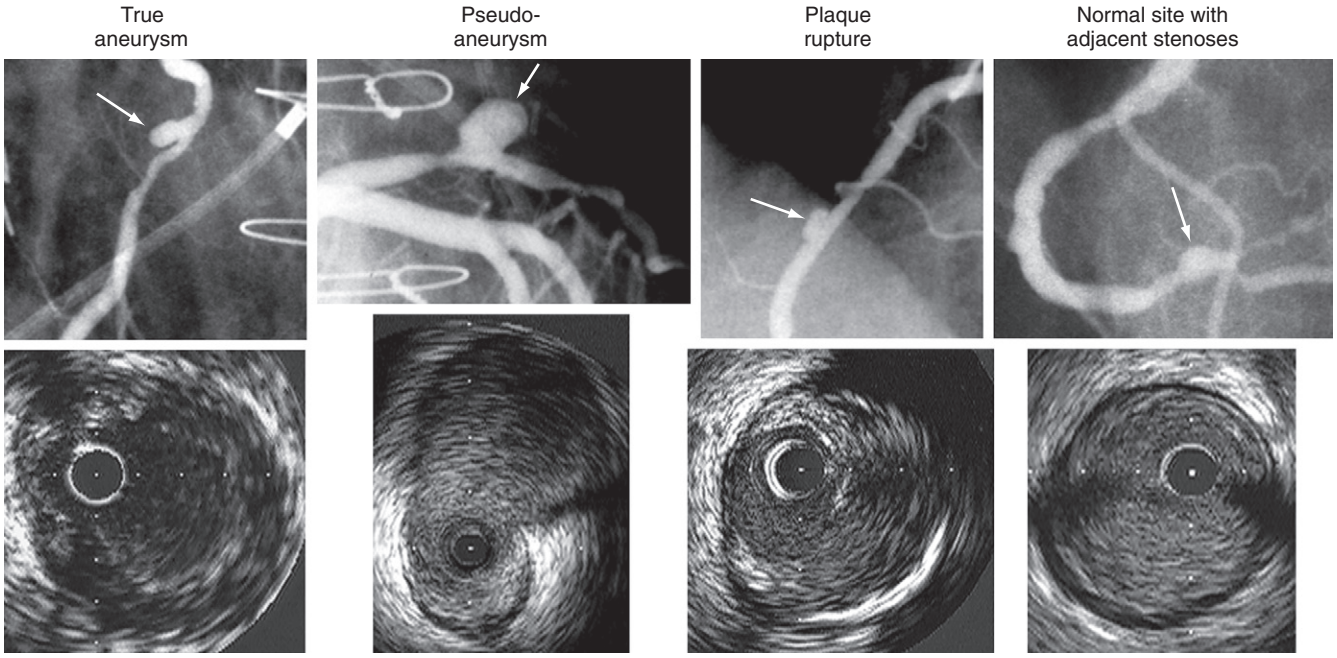



**Figure 7-9 All angiograms have the appearance of an aneurysm.** Intravascular ultrasound can differentiate true (three-layered) or pseudoaneurysm, plaque rupture, or just normal segments with adjacent stenoses.

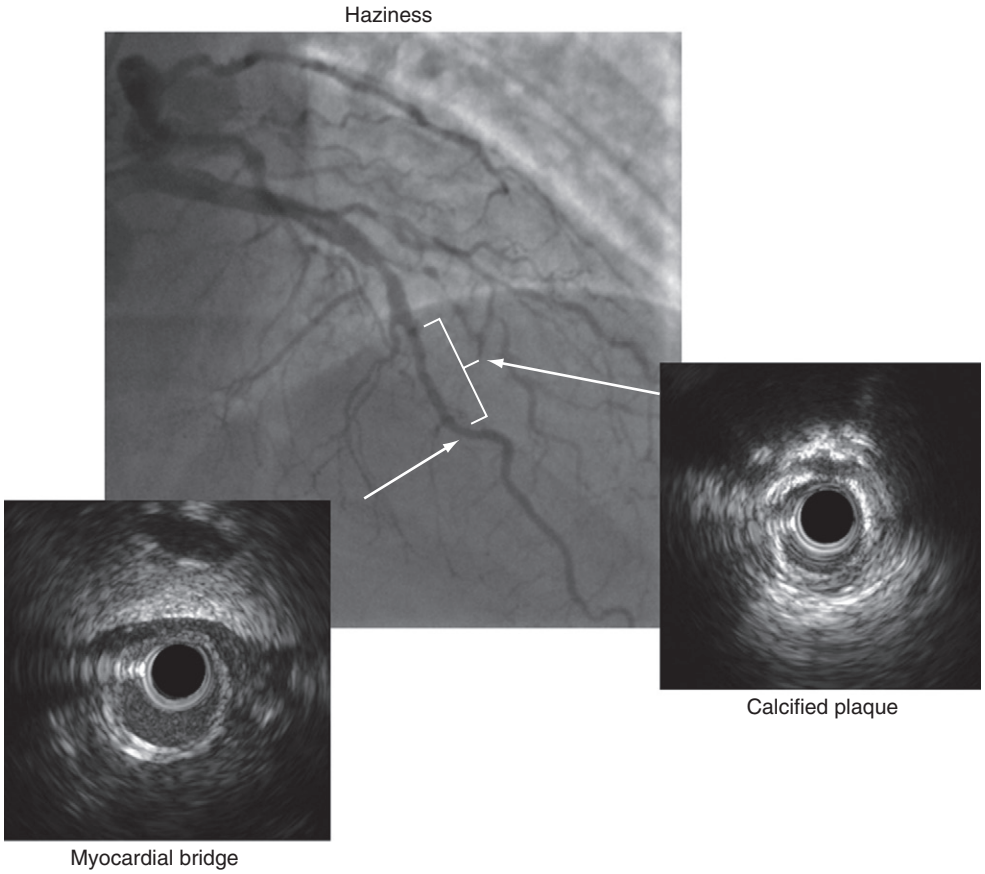



**Figure 7-10 Angiogram shows diffuse stenosis with haziness in mid to distal left descending artery.** Proximal segment of haziness appears as calcified plaque, and distal end appears as myocardial bridge by intravascular ultrasound (surrounded by low echoic band).

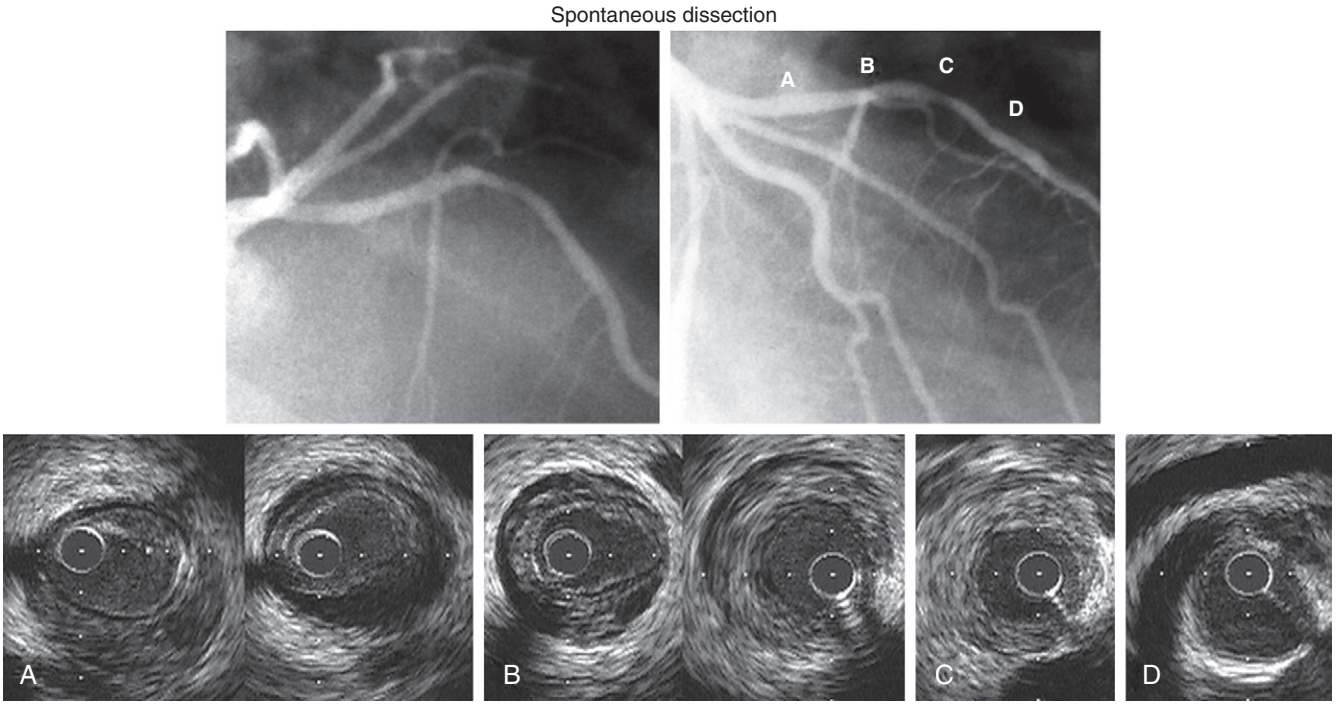



**Figure 7-11** Angiogram shows diffuse mild stenosis in mid to distal left descending artery (*A-D*). Corresponding intravascular ultrasound images shows spontaneous dissection (with intramural hematoma).

An IVUS classification of angiographic coronary artery aneurysms has also been created.[50] Of 77 aneurysm-containing lesions, 21 (27%) were classified as true aneurysm; 3 (4%) were classified as pseudoaneurysms (all having previous intervention); 12 (16%) were complex plaques; and the other 41 (53%) were normal arterial segments adjacent to one or more stenoses. Examples are shown in Figure 7-9. In a study of 300 consecutive IVUS-defined plaque ruptures, 91% were categorized as complex by angiography: ulceration in 81%, intimal flap in 40%, thrombus in 7%, and coronary aneurysm in 7%.[51] Approximately one quarter of patients had IVUS-detectable myocardial bridges in the LAD coronary artery; only 3% (11 of 331) were diagnosed by angiography. In 13% of cases, IVUS-detectable myocardial bridges appeared as mild (diameter of stenosis less than 25%) fixed lesions and/or angiographic haziness (see Fig. 7-10).[52] Spontaneous dissections are an intramural process that appears as a medial dissection with an intramural hematoma occupying the dissected false lumen without intimal tears and without a communication between the true and false lumens.[53] An example is shown in Figure 7-11.

## ASSESSMENT OF VULNERABLE PLAQUE

PROSPECT (Providing Regional Observations to Study Predictors of Events in the Coronary Tree) was a prospective study of the natural history of coronary atherosclerosis using angiography and VH-IVUS to identify the clinical and lesion-related factors that predicted future coronary events.[15] It was performed at 37 sites in the United States and Europe. Patients with acute coronary syndromes were enrolled after undergoing successful percutaneous coronary intervention of all culprit lesions responsible for the acute event. Angiography was performed of the entire coronary tree followed by gray-scale and VH-IVUS of the proximal 6 to 8 cm of all epicardial arteries. All baseline angiograms and gray-scale and VH-IVUS images were prospectively analyzed without knowledge of subsequent events using prespecified definitions and methodology. Plaque burden and luminal area as prospectively measured by gray-scale IVUS and plaque composition (thin-cap fibroatheroma) as assessed by VH-IVUS were determined to be independent predictors of future adverse cardiovascular events (Fig. 7-12).

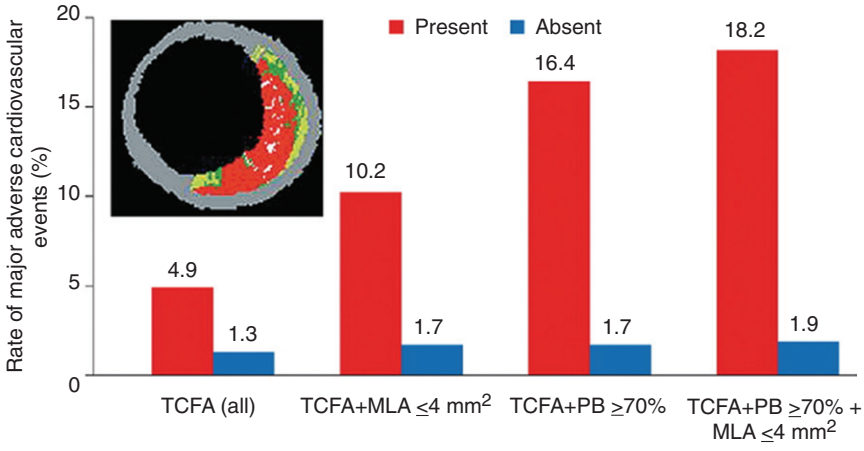
## PREDICTION OF NO-REFLOW DURING INTERVENTIONAL PROCEDURES

IVUS guidance may also be useful to identify high-risk lesions before intervention, such as those that cause no-reflow or periprocedural myocardial infarction, particularly noncalcified attenuated plaque.[54-57] Noncalcified attenuated plaque may be a gray-scale indication of a larger necrotic core and/or fibroatheroma (96% of attenuated plaques contained a fibroatheroma vs. 52.3% on nonattenuated plaques, $p < 0.0001$).[9] In support of this, multiple VH-IVUS studies have shown that a larger necrotic core is related to distal embolization during percutaneous coronary intervention in both acute coronary syndromes and stable angina patients.[58-61]

## ASSESSMENT OF INTERVENTIONAL COMPLICATIONS

IVUS detects poststent dissections or other complications more often than angiography.

One type of dissection, intramural hematoma, appears as an angiographic dissection in 60%, as newly developed stenosis that does not disappear after nitroglycerin (i.e., not a spasm) in 11%, and as no angiographic abnormality in 29%.[62] Similarly, perivascular trauma appears as an angiographic perforation in 24%, as angiographic dissection in 33%, as new stenosis in 5%, and as no abnormality in 38%. Angiographic "haziness" at the stent edge may demonstrate an edge dissection or residual plaque, especially a calcified eccentric plaque, when studied by IVUS.




| | | | | |
|---|---|---|---|---|
| Lesion hazard ratio (95%) | 3.90 (2.25–6.76) | 6.55 (3.43–12.51) | 10.83 (5.55–21.10) | 11.05 (4.39–27.82) |
| *p* value | <0.001 | <0.001 | <0.001 | <0.001 |
| Prevalence (%) | 46.7 | 15.9 | 10.1 | 4.2 |

**Figure 7-12** Event rates for lesions with and without thin-cap fibroatheromas (TCFAs) at a median follow-up of 3.4 years. *MLA*, minimum lumen area; *PB*, plaque burden. *(From Stone GW, Maehara A, Lansky AJ, et al: A prospective natural-history study of coronary atherosclerosis.* N Eng J Med *364:226-235, 2011.)*

## RESTENOSIS, LATE MALAPPOSITION, STENT FRACTURE, AND STENT THROMBOSIS

In the bare metal stent (BMS) era, serial IVUS studies in humans showed (1) that tubular-slotted stent designs exhibit almost no chronic recoil, (2) that in-stent restenosis was almost entirely neointimal hyperplasia, (3) that there was no predilection for tissue accumulation within any one segment, and (4) that neointimal thickness was independent of stent size.[63,64] It is for these reasons that many studies have reported that the absolute minimum stent area (MSA) by IVUS was the strongest quantitative predictor of clinical and angiographic in-stent restenosis.[65-67]

Because drug-eluting stents (DES) have less neointimal hyperplasia, the MSA necessary to minimize restenosis can be smaller than with BMS. Using the data from SIRIUS, Sonoda and coworkers reported that the best cutoff to predict an MLA at follow-up of 4 $mm^2$ was an MSA of 5 $mm^2$ for sirolimus-eluting stents (SES) and 6.5 $mm^2$ for BMS.[68] A similar study by Hong and colleagues showed that the MSA that best separated angiographic restenosis from no restenosis was 5.5 $mm^2$ in SES.[69] We combined various TAXUS studies and reported that the best cutoff to predict angiographic binary restenosis for the paclitaxel-eluting stent (PES) was 5.7 $mm^2$.[70] However, "bigger is better" is still true; also, (1) a larger MSA is still associated with a lower restenosis rate, whereas (2) an MSA of 5.0 to 5.5 $mm^2$ may not be achievable in small vessels that are increasingly stented.

On the other hand, full lesion coverage may be more important in the DES era than in the BMS era. Costa and colleagues reported that longitudinal geographic miss (GM)—injured or diseased segment not covered by SES—was observed in 47.6%,; axial GM—balloon-artery size ratio less than 0.9 or greater than 1.3—was observed in 35.2%; and both GM in 16.5%.[71] One-year target vessel revascularization rates were 6.1% in the longitudinal GM group versus 2.6% in the no-longitudinal GM group ($p = 0.001$); the GM was the independent predictor for target vessel revascularization. In support of this, Liu and co-workers reported that the stent edge plaque burden that best separated restenosis from no restenosis was approximately 50%.[72]

Figure 7-13 summarizes the percentage of neointimal hyperplasia (%NIH = NIH volume divided by stent volume) and late acquired malapposition in various multi-center randomized trials.[73-83] In BMS, %NIH averaged (approximately) 30% of stent volume, and %NIH was consistently greater in diabetes than nondiabetes.[84] In the DES era, %NIH was reported as 2.7% to 3.1% in SES, 2.5% to 6.9% in everolimus-eluting stents, 7.4% to 12.2% in PES, and 16.1% to 17.6% in zotarolimus-eluting stents. Though NIH varied among DES, the clinical efficacy (target vessel revascularization) and safety (stent thrombosis) were similar in noncomplex lesions.

IVUS predictors of either drug-eluting acute/subacute stent thrombosis or restenosis are stent underexpansion and residual edge "problems," such as GM, adjacent secondary plaques, or significant edge dissections—but not acute malapposition.[85-87] Stent underexpansion was more diffuse in stent thrombosis than restenosis.[88]

IVUS studies have documented late-acquired stent malapposition in approximately 5% of BMS in non-STEMI (ST elevation myocardial infarction) patients, about 5% to 15% of BMS in STEMI patients and DES in non-STEMI patients, and about 25% to 30% of DES in STEMI patients.[73-83,89-92] Late-acquired stent malapposition is typically the result of positive vessel wall remodeling and/or thrombus dissolution behind the stent struts (especially in myocardial infarction patients). Cook and colleagues reported that 10 of 13 very late stent thrombosis patients (mean 1.8 years after stent implantation) had stent malapposition with a malapposition area twice as large as in control patients with malapposition, but without very late stent thrombosis (mean = 8.3 vs. 4.0 $mm^2$).[93] Alfonso and co-workers reported 15 (1.3%) patients with an angiographic aneurysm 9 months post-DES implantation; subsequently, 3 patients (with significantly larger aneurysms than others) suffered late stent thrombosis.[94] One metaanalysis suggested that there was an increased frequency of very late stent thrombosis in the setting of large areas of late malapposition.[95] In a second report, Cook and colleagues correlated the presence and size of the malapposition area with inflammatory cells from intracoronary aspirates, suggesting that it was not just the malapposition, but malapposition in the setting of vessel wall inflammation, that

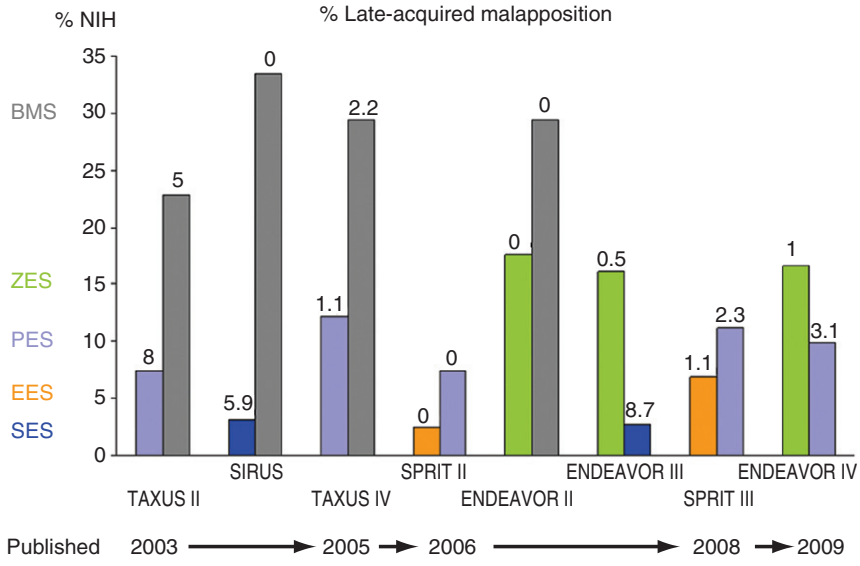



**Figure 7-13** Summary of %NIH (neointimal hyperplasia volume divided by stent volume) in various drug-eluting stent randomized trials. *BMS*, bare metal stent (*gray*); *ZES*, zotarolimus-eluting stent (*green*); *PES*, paclitaxel-eluting stent (*lavender*); *EES*, everolimus-eluting stent (*orange*); *SES*, sirolimus-eluting stent (*dark blue*). The numeric values above each bar indicate the incidence of late-acquired malapposition.

contributed to very late stent thrombosis.[96] In addition, in-stent neoatherosclerosis and subsequent rupture causing very late stent thrombosis has been reported by IVUS, VH-IVUS, optical coherent tomography, and coronary angioscopy.[97-100]

More recently, stent fracture is being implicated as a cause of DES failure, especially with SES. In a prior retrospective IVUS study of 17 non-STEMI patients with 20 stent strut fractures, 18 (90%) occurred in SES and 2 (10%) in BMS, but none in PES.[101] Of note, 5 of 20 stent fractures were accompanied by coronary aneurysm formation with two very late stent thromboses (Fig. 7-14). It has been proposed that biologic reactions to the eluted drug cause positive vessel remodeling with aneurysm formation and malapposition that allow motion and/or kinking of the stent within the aneurysm, leading to strut fracture. Angiographic data from three PES trials in nonacute coronary syndromes revealed a 1.1% rate of stent fracture associated with restenosis and/or stent thrombosis.[102] In the Nordic IVUS study, stent malapposition and stent fracture were found in 43% (37 of 87) and 16% (14 of 87) of DES thrombosis cases and 27% (10 of 37) and 27% (10 of 37) of BMS thrombosis cases.[103]

## TREATMENT OF IN-STENT RESTENOSIS

The uses of IVUS in evaluating patients with in-stent restenosis include (1) determining whether in-stent restenosis is severe enough to treat, (2) identifying occult mechanical problems with the stent that (presumably) occurred at the time of implantation, (3) assessing the patterns of in-stent restenosis, and (4) assessing the acute results. Using integrated TAXUS data (331 treated with PES and 304 treated with BMS who did not require revascularization in the first 9 months postintervention), we reported that the optimal thresholds of MLA that best predicted subsequent target vessel revascularization-free survival during the subsequent 3 years were 4.2 $mm^2$ for PES and 4.0 $mm^2$ for BMS.[104]

There are a number of technical and mechanical complications of stent implantation that can remain unrecognized until the patient presents with in-stent restenosis. These include (1) missing the lesion, (2) stent underexpansion, (3) stent "crush," and (4) having the stent stripped off the balloon during the implantation procedure. Because most stents are radiolucent, some lesions, especially aortoostial lesions, can be missed. Incomplete stent expansion during implantation can be missed angiographically because stents are porous and contrast can flow through and around them. Chronic stent recoil is rare.[63,105] If the guidewire is accidentally removed and, in recrossing the freshly placed (and presumably not fully implanted) stent, it courses adjacent to the stent and enters the stent through one of the diamonds, subsequent adjunct balloon dilation can crush part of the stent against the vessel wall. These mechanical problems constitute a minority of in-stent restenoses. However, the treatment of in-stent restenosis must begin by excluding these problems and, if they are present, by correcting them. Examples are shown in Figures 7-15 and 7-16. In an analysis of more than 1000 consecutive in-stent restenosis lesions, the frequency of these mechanical complications was found to be 4% to 5%.[106]

## BIOABSORBABLE STENTS

The first generation of bioabsorbable everolimus-eluting stents (BVS) implanted in 30 simple de novo lesions showed higher acute recoil than conventional metallic platform stents. At 6 months, the 11.8% reduction in scaffold area (chronic recoil) and a small neointimal response of 5.5% resulted in a total 24.3% decrease in MLA by IVUS.[107] However, at 2 years, the lumen area increased because of decrease in plaque size without change in vessel size.[108] The second-generation BVS had an improved scaffold that had only a 2% chronic recoil.[109]

## DOES IVUS GUIDANCE REDUCE STENT RESTENOSIS AND THROMBOSIS?

A number of randomized and nonrandomized studies compared IVUS versus angiographic guidance of BMS implantation.[110-112] A metaanalysis of the seven randomized IVUS versus angiography trials showed that IVUS improved final BMS dimensions to reduce BMS restenosis and repeat revascularization.[112] In the DES era, Roy and co-workers reported that IVUS guidance reduced stent thrombosis both within 1 month and from 1 to 12 months (0.7% vs. 2.0% at

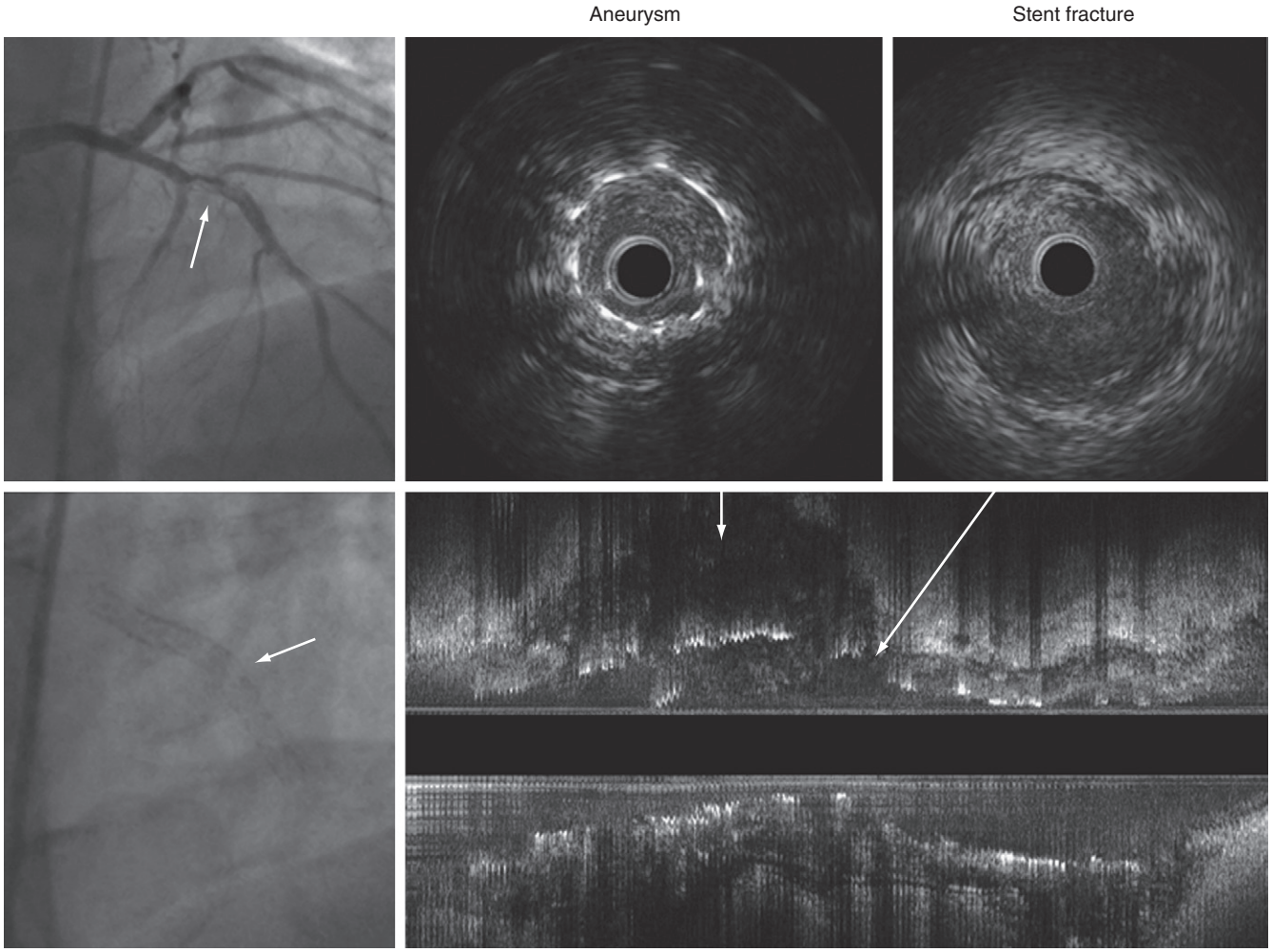



**Figure 7-14** An example of late-acquired aneurysm with stent fracture and very late stent thrombosis.

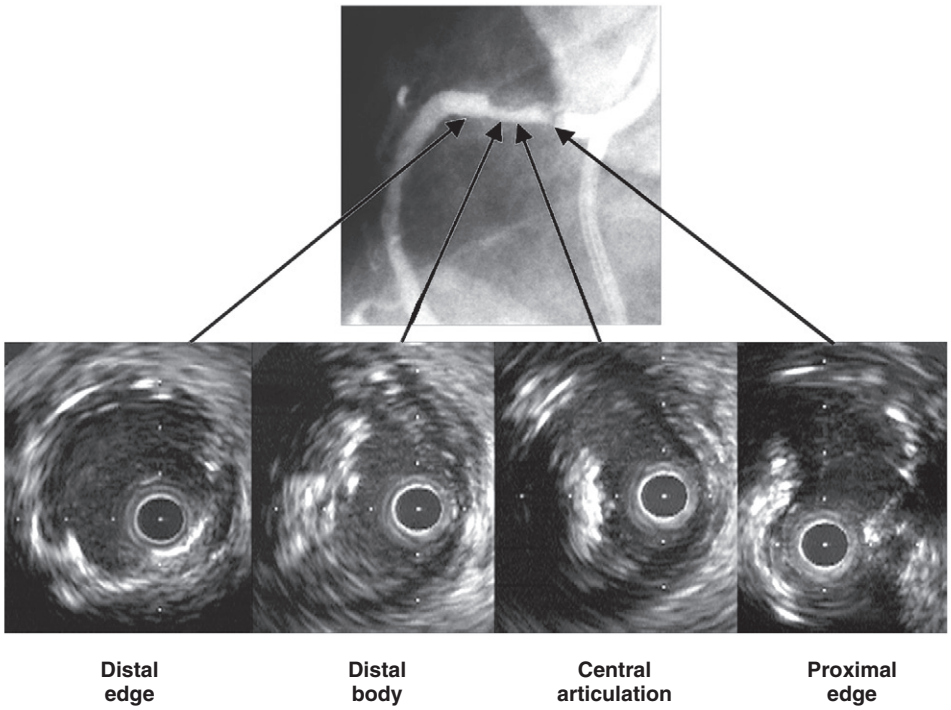



**Figure 7-15** The implanted stent is crushed against the vessel wall.

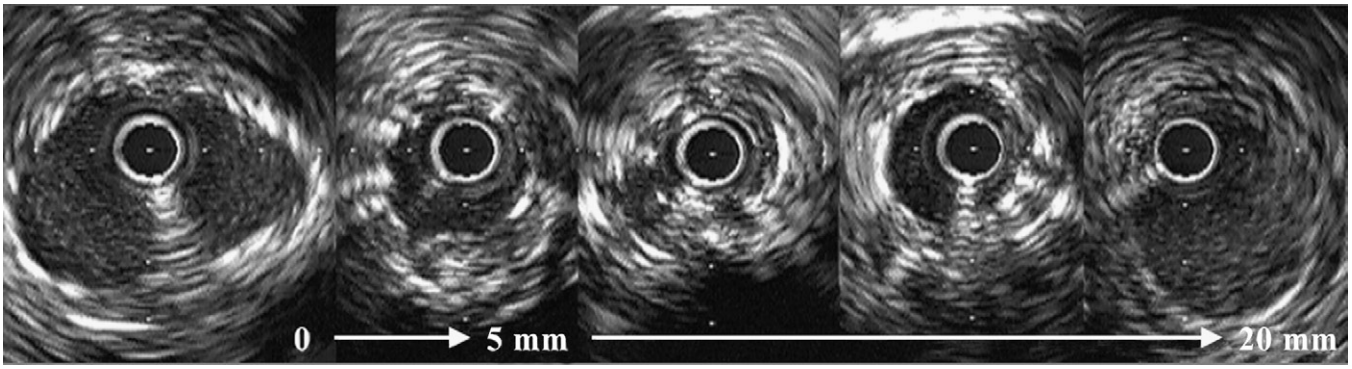



**Figure 7-16** Chronic stent underexpansion in a saphenous vein graft.

1 year, p = 0.014), supporting the use of IVUS during interventional procedures.[113] The improvement of major adverse cardiac events, particularly mortality, has been supported by Park and colleagues in unprotected LMCA-treated arteries.[114]

## PRACTICAL RECOMMENDATIONS

In practical day-to-day terms, how should IVUS be used during stenting procedures? The following is one suggested algorithm for routine use of IVUS. It begins with preintervention IVUS and concludes with iterative IVUS to optimize the final result. Perform preintervention IVUS to assess lesion characteristics and measure reference vessel size and lesion length. From the maximum reference lumen diameter, determine the maximum achievable stent dimension. Select stent length based on distance between proximal and distal references.

After the stent is implanted, repeat IVUS imaging to assess the MSA. If the MSA is adequate, stop. If the MSA is inadequate, perform additional high-pressure inflations, if necessary using a larger balloon. If additional balloon inflations are performed, recheck the IVUS results. If IVUS detects a complication such as a major dissection, an intramural hematoma, or perforation, treat appropriately and repeat IVUS to ensure that the complication is corrected. Conversely, if, despite the angiographic appearance, IVUS imaging shows a good acute result, stop.

If the interventional cardiologist wants to selectively used IVUS, it will be especially useful in the following three situations: (1) when you expect a good result, but flow is limited (IVUS can identify a correctable cause such as flow-limiting dissection or intramural hematoma); (2) any patient presenting with stent failure in which IVUS may identify a mechanical problem such as simple stent underexpansion or a crushed stent; and (3) with LMCA lesions or small-vessel stenting.

### KEY POINTS

- IVUS provides a unique, tomographic view of the artery from the inside out with high resolution.
- Standardization improves the clinical utilization of IVUS.
- IVUS images all components of the arterial wall, providing information beyond the luminal profile displayed by angiography to include plaque burden and distribution, remodeling, true vessel size, high-risk plaque morphology, and so forth.
- IVUS can guide stent implantation to optimize the acute results and reduce late complications.
- The added information from IVUS is particularly helpful for angiographically ambiguous lesions, unusual lesions, and complex clinical scenarios.

## REFERENCES

1. Mintz GS, Nissen SE, Anderson WD, et al: ACC clinical expert consensus document on standards for the acquisition, measurement and reporting of intravascular ultrasound studies: a report of the American College of Cardiology Task Force on Clinical Expert Consensus Documents (Committee to Develop a Clinical Expert Consensus Document on Standards for Acquisition, Measurement and Reporting of Intravascular Ultrasound Studies [IVUS]). *J Am Coll Cardiol* 37:1478-1492, 2001.
2. Di Mario C, Görge G, Peters R, et al: Clinical application and image interpretation in intracoronary ultrasound. *Eur Heart J* 19:207-229, 1998.
3. Fitzgerald PJ, Goar FG, Connolly AJ, et al: Intravascular ultrasound imaging of coronary arteries. Is three layers the norm? *Circulation* 86:154-158, 1992.
4. Friedrich GJ, Moes NY, Mühlberger VA, et al: Detection of intralesional calcium by intracoronary ultrasound depends on the histologic pattern. *Am Heart J* 128:435-441, 1994.
5. Kostamaa H, Donovan J, Kasaoka S, et al: Calcified plaque cross-sectional area in human arteries: correlation between intravascular ultrasound and undecalcified histology. *Am Heart J* 137:482-488, 1999.
6. Mintz GS, Popma JJ, Pichard AD, et al: Patterns of calcification in coronary artery disease. A statistical analysis of intravascular ultrasound and coronary angiography in 1155 lesions. *Circulation* 91:1959-1965, 1995.
7. Prati F, Arbustini E, Labellarte A, et al: Intravascular ultrasound insights into plaque composition. *Z Kardiol* 89(Suppl 2):117-123, 2000.
8. Bridal SL, Forenès P, Bruneval P, Berger G: Correlation of ultrasonic attenuation (30 to 50 MHz) and constituents of atherosclerotic plaque. *Ultrasound Med Biol* 23:691-703, 1997.
9. Wu X, Maehara A, Mintz GS, et al: Virtual histology intravascular ultrasound analysis of non-culprit attenuated plaque detected by grayscale intravascular ultrasound in patients with acute coronary syndromes. *Am J Cardiol* 105:48-53, 2010.
10. Lee JB, Mintz GS, Lisauskas JB, et al: Histolopathologic validation of intravascular ultrasound diagnosis of a calcified coronary nodule, a type of plaque suspected to be vulnerable (abstract). *Circulation* 122:A21455, 2010.
11. Okubo M, Kawasaki M, Ishihara Y, et al: Development of integrated backscatter intravascular ultrasound for tissue characterization of coronary plaques. *Ultrasound Med Biol* 34:655-663, 2008.

12. Watson RJ, McLean CC, Moore MP, et al: Classification of arterial plaque by spectral analysis of in vitro radio frequency intravascular ultrasound data. *Ultrasound Med Biol* 26:73-80, 2000.
13. Nair A, Kuban BD, Tuzcu EM, et al: Coronary plaque classification with intravascular ultrasound radiofrequency data analysis. *Circulation* 106:2200-2206, 2002.
14. Nair A, Margolis MP, Kuban BD, Vince GD: Automated coronary plaque characterization with intravascular ultrasound backscatter: ex vivo validation. *EuroInterv* 3:113-120, 2007.
15. Stone GS, Maehara A, Lansky AJ, et al: A prospective natural-history study of coronary atherosclerosis. *N Eng J Med* 364:226-235, 2011.
16. Glagov S, Weisenberg E, Zarins CK, et al: Compensatory enlargement of human atherosclerotic coronary arteries. *N Engl J Med* 316:1371-1375, 1987.
17. Mintz GS, Painter JA, Pichard AD, et al: Atherosclerosis in angiographically "normal" coronary artery reference segments: an intravascular ultrasound study with clinical correlations. *J Am Coll Cardiol* 25:1479-1485, 1995.
18. Hausmann D, Erbel R, Alibelli-Chemarin M-J, et al: The safety of intracoronary ultrasound: A multicenter survey of 2207 examinations. *Circulation* 91:623-630, 1995.
19. Batkoff BW, Linker DT: The safety of intracoronary ultrasound: Data from a multicenter European registry. *Catheter Cardiovasc Diagn* 38:238-241, 1996.
20. Görge G, Peters RJG, Pinto F, et al: Intravascular ultrasound: Safety and indications for use in 7085 consecutive patients studied in 32 centers in Europe and Israel. *J Am Coll Cardiol* 27:155A, 1996.
21. Arnett EN, Isner JM, Redwood DR, et al: Coronary artery narrowing in coronary artery disease: Comparison of cineangiographic and necropsy findings. *Ann Intern Med* 91:350-356, 1979.
22. Waller BF: Anatomy, histology, and pathology of the major epicardial coronary arteries relevant to echocardiographic imaging techniques. *J Am Soc Echocardiogr* 2:232-252, 1989.
23. Isner JM, Donaldsen RF: Coronary angiographic and morphologic correlation. In Waller BF, editor: *Cardiac morphology*, Philadelphia, 1984, Saunders, pp 571-592.
24. Marcus ML, Skorton DJ, Johnson MR, et al: Visual estimates of percent diameter coronary stenosis: "A battered gold standard." *J Am Coll Cardiol* 11:882-885, 1988.
25. Hutchins GM, Bulkley BH, Ridolfi RL, et al: Correlation of coronary arteriograms and left ventriculograms with postmortem studies. *Circulation* 56:32-37, 1977.
26. Abizaid A, Mintz GS, Pichard AD, et al: Clinical, intravascular ultrasound, and quantitative angiographic determinants of the coronary flow reserve before and after percutaneous transluminal coronary angioplasty. *Am J Cardiol* 82:423-428, 1998.
27. Nishioka T, Amanullah AM, Luo H, et al: Clinical validation of intravascular ultrasound imaging for assessment of coronary stenosis severity: Comparison with stress myocardial perfusion imaging. *J Am Coll Cardiol* 33:1870-1878, 1999.
28. Takagi A, Tsurumi Y, Ishii Y, et al: Clinical potential of intravascular ultrasound for physiological assessment of coronary stenosis: Relationship between quantitative ultrasound tomography and pressure-derived fractional flow reserve. *Circulation* 100:250-255, 1999.
29. Abizaid AS, Mintz GS, Mehran R, et al: Long-term follow-up after percutaneous transluminal angioplasty was not performed based on intravascular ultrasound findings: importance of lumen dimensions. *Circulation* 100:256-261, 1999.
30. Tonino PA, De Bruyne B, Pijls NH, et al: Fractional flow reserve versus angiography for guiding percutaneous coronary intervention. *N Eng J Med* 360:213-224, 2009.
31. Hermiller JB, Buller CE, Tenaglia AN, et al: Unrecognized left main coronary artery disease in patients undergoing interventional procedures. *Am J Cardiol* 71:173-176, 1993.
32. Yamagishi M, Hongo Y, Goto Y, et al: Intravascular ultrasound evidence of angiographically undetected left main coronary artery disease and associated trauma during interventional procedures. *Heart Vessels* 11:262-268, 1996.
33. Gerber TC, Erbel R, Görge G, et al: Extent of atherosclerosis and remodeling of the left main coronary artery determined by intravascular ultrasound. *Am J Cardiol* 73:666-671, 1994.
34. Ge J, Liu F, Görge G, et al: Angiographically "silent" plaque in the left main coronary artery detected by intravascular ultrasound. *Coron Artery Dis* 6:805-810, 1995.
35. Fisher LD, Judkins MP, Lesperance J, et al: Reproducibility of coronary arteriographic reading in the Coronary Artery Surgery Study (CASS). *Catheter Cardiovasc Diagn* 8:565-575, 1982.
36. Isner JM, Kishel J, Kent KM, et al: Accuracy of angiographic determination of left main coronary arterial narrowing: Angiographic-histologic correlative analysis in 28 patients. *Circulation* 63:1056-1064, 1981.
37. Detre KM, Wright E, Murphy ML, et al: Observer agreement in evaluating coronary angiograms. *Circulation* 52:979-986, 1975.
38. DeRouen TA, Murray JA, Owen W: Variability in the analysis of coronary arteriograms. *Circulation* 55:324-328, 1977.
39. Zir LM, Miller SW, Dinsmore RE, et al: Interobserver variability in coronary angiography. *Circulation* 53:627-632, 1976.
40. Sanmarco ME, Brooks SH, Blankenhorn DH: Reproducibility of a consensus panel in the interpretation of coronary angiograms. *Am Heart J* 96:430-437, 1978.
41. Cameron A, Kemp HG, Jr, Fisher LD, et al: Left main coronary artery stenosis: angiographic determination. *Circulation* 68:484-489, 1983.
42. Flemming RM, Kirkeeide RL, Smalling RW, et al: Patterns in visual interpretation of coronary arteriograms as detected by quantitative coronary arteriography. *J Am Coll Cardiol* 18:945-951, 1991.
43. Abizaid AS, Mintz GS, Abizaid A, et al: One year follow-up after intravascular ultrasound assessment of moderate left main coronary artery disease in patients with ambiguous angiograms. *J Am Coll Cardiol* 34:707-715, 1999.
44. Jasti V, Ivan E, Yalamanchilli V, et al: Correlations between fractional flow reserve and intravascular ultrasound in patients with an ambiguous left main coronary artery stenosis. *Circulation* 110: 2831-2836, 2004.
45. Hernandez JT, Hernandez FH, Runoroso JR, et al: Prospective application of predefined intravascular ultrasound criteria for revascularization of intermediate left main coronary artery lesions: results at 2 years from the LITRO study. http://ww3.aievolution.com/tct1001/files/content/abstracts/1615/344_DelaTorreHernandez.pps. Accessed January 23, 2011.
46. Fuessl RT, Mintz GS, Pichard AD, et al: In vivo validation of intravascular ultrasound length measurements using a motorized transducer pullback device. *Am J Cardiol* 77:1115-1118, 1996.
47. Stone GW, Hodgson JMcB, Goar FG, et al: For the CLOUT Investigators. Improved procedural results of coronary angioplasty with intravascular ultrasound guided balloon sizing: The CLOUT Pilot Trial. *Circulation* 95:2044-2052, 1997.
48. Abizaid A, Pichard AD, Mintz GS, et al: Acute and long-term results of an IVUS-guided PTCA/provisional stent implantation strategy. *Am J Cardiol* 84:1381-1384, 1999.
49. Duissaillant GD, Mintz GS, Pichard AD, et al: Intravascular ultrasound identification of calcified intraluminal lesions misdiagnosed as thrombi by coronary angiography. *Am Heart J* 132:687689, 1996.
50. Maehara A, Mintz GS, Ahmed JM, et al: An intravascular ultrasound classification of angiographic coronary artery aneurysms. *Am J Cardiol* 88:365-370, 2001.
51. Maehara A, Mintz GS, Bui AB, et al: Morphologic and angiographic features of coronary plaque rupture detected by intravascular ultrasound. *J Am Coll Cardiol* 40:904-910, 2002.
52. Tsujita K, Maehara A, Mintz GS, et al: Comparison of angiographic and intravascular ultrasonic detection of myocardial bridging of the left anterior descending coronary artery. *Am J Cardiol* 102:1608-1613, 2008.
53. Maehara A, Mintz GS, Castagna MT, et al: Intravascular ultrasound assessment of spontaneous coronary artery dissection. *Am J Cardiol* 89:466-468, 2002.
54. Lee SY, Mintz GS, Kim SY, et al: Attenuated plaque detected by IVUS: Clinical, angiographic, and morphological features and post-percutaneous coronary intervention complications in patients with acute coronary syndrome. *J Am Coll Cardiol Interv* 2:65-72, 2009.
55. Okura H, Taguchi H, Kubo T, et al: Atherosclerotic plaque with ultrasonic attenuation affects coronary reflow and infarct size in patients with acute coronary syndrome. *Circ J* 71:648-653, 2007.
56. Endo M, Hibi K, Shimizu T, et al: Impact of ultrasound attenuation and plaque rupture as detected by intravascular ultrasound on the incidence of no-reflow phenomenon after percutaneous coronary intervention in ST-segment elevation myocardial infarction. *J Am Coll Cardiol Interv* 3:540-549, 2010.
57. Wu X, Mintz GS, Xu K, et al: Relationship between attenuated plaque identified by intravascular ultrasound and no-reflow after stenting in acute myocardial infarction: The HORIZONS-AMI trial. *J Am Coll Cardiol Interv* 4:495-502, 2011.
58. Higashikuni Y, Tanabe K, Tanimoto S, et al: Impact of culprit plaque composition on the no-reflow phenomenon in patients with acute coronary syndrome. An intravascular ultrasound radiofrequency analysis. *Circ J* 72:1235-1241, 2008.
59. Kawaguchi R, Oshima S, Jingu M, et al: Usefulness of virtual histology intravascular ultrasound to predict distal embolization for ST-segment elevation myocardial infarction. *J Am Coll Cardiol* 50:1641-1646, 2007.

60. Kawamoto T, Okura H, Koyama Y, et al: The relationship between coronary plaque characteristics and small embolic particles during coronary stent implantation. *J Am Coll Cardiol* 50:1635-1640, 2007.
61. Hong YJ, Jeong MH, Choi YH, et al: Impact of plaque components on no-reflow phenomenon after stent deployment in patients with acute coronary syndrome: a virtual histology-intravascular ultrasound analysis. *Eur Heart J* 32:2059-2066, 2011.
62. Maehara A, Mintz GS, Bui AB, et al: Incidence, morphology, angiographic findings, and outcomes of intramural hematomas after percutaneous coronary interventions. *Circulation* 105:2037-2042, 2002.
63. Hoffmann R, Mintz GS, Dussaillant GR, et al: Patterns and mechanisms of in-stent restenosis. A serial intravascular ultrasound study. *Circulation* 94:1247-1254, 1996.
64. Hoffmann R, Mintz GS, Pichard AD, et al: Intimal hyperplasia thickness at follow-up is independent of stent size: A serial intravascular ultrasound study. *Am J Cardiol* 82:1168-1172, 1998.
65. Hoffmann R, Mintz GS, Mehran R, et al: Intravascular ultrasound predictors of angiographic restenosis in lesions treated with Palmaz-Schatz stents. *J Am Coll Cardiol* 31:43-49, 1997.
66. Kasaoka S, Tobis JM, Akiyama T, et al: Angiographic and intravascular ultrasound predictors of in-stent restenosis. *J Am Coll Cardiol* 32:30-35, 1998.
67. Moussa I, Moses J, Di Mario C, et al: Does the specific intravascular ultrasound criterion used to optimize stent expansion have an impact on the probability of stent restenosis? *Am J Cardiol* 83:1012-1017, 1999.
68. Sonoda S, Morino Y, Ako J, et al: Impact of final stent dimensions on long-term results following sirolimus-eluting stent implantation. *J Am Coll Cardiol* 43:1959-1963, 2004.
69. Hong MK, Mintz GS, Lee CW, et al: Intravascular ultrasound predictors of angiographic restenosis after sirolimus-eluting stent implantation. *Eur Heart J* 27:1305-1310, 2006.
70. Doi H, Maehara A, Mintz GS, et al: Impact of post-intervention minimal stent area on 9-month follow-up patency of paclitaxel-eluting stents: An integrated intravascular ultrasound analysis from the TAXUS IV, V, and VI and TAXUS ATLAS Workhorse, Long lesion, and direct stent trials. *J Am Coll Cardiol Interv* 2:1269-1275, 2009.
71. Costa MA, Angiolillo DJ, Tannenbaum M, et al: Impact of stent deployment procedural factors on long-term effectiveness and safety of sirolimus-eluting stents (final results of the multicenter prospective STLLR trial). *Am J Cardiol* 101:1704-1711, 2008.
72. Liu J, Maehara A, Mintz GS, et al: An integrated TAXUS IV, V, and VI intravascular ultrasound analysis of the predictors of edge restenosis after bare metal or paclitaxel-eluting stents. *Am J Cardiol* 103:501-506, 2009.
73. Colombo A, Drzewiecki J, Banning A, et al: Randomized study to assess the effectiveness of slow- and moderate-release polymer-based paclitaxel-eluting stents for coronary artery lesions. *Circulation* 108:788-794, 2003.
74. Tanabe K, Serruys PW, Degertekin M, et al: Incomplete stent apposition after implantation of paclitaxel-eluting stents or bare metal stents: Insights from the randomized TAXUS II trial. *Circulation* 111:900-905, 2005.
75. Moses JW, Leon MB, Popma JJ, et al: Sirolimus-eluting stents versus standard stents in patients with stenosis in a native coronary artery. *N Eng J Med* 349:1315-1323, 2003.
76. Ako J, Morino Y, Honda Y, et al: Late incomplete stent apposition after sirolimus-eluting stent implantation. *J Am Coll Cardiol* 46:1002-1005, 2005.
77. Weissman NJ, Koglin J, Cox DA, et al: Polymer-based paclitaxel-eluting stents reduce in-stent neointimal tissue proliferation. *J Am Coll Cardiol* 45:1201-1205, 2005.
78. Weissman NJ, Ellis SG, Grube E, et al: Effect of the polymer-based, paclitaxel-eluting TAXUS Express stent on vascular tissue responses: a volumetric intravascular ultrasound integrated analysis from the TAXUS IV, V, and VI trials. *Eur Heart J* 2007;28:1574-1582.
79. Serruys PW, Ruygrok P, Neuzner J, et al: A randomized comparison of an everolimus-eluting coronary stent with a paclitaxel-eluting coronary stent: the SPRIT II trial. *EuroInterv* 2:286-294, 2006.
80. Sakurai R, Bonneau HN, Honda Y, et al: Intravascular ultrasound findings in ENDEAVOR II and ENDEAVOR III. *Am J Cardiol* 100:71M-76M, 2007.
81. Miyazawa A, Ako J, Hongo Y, et al: Comparison of vascular response to zotarolimus-eluting stent versus sirolimus-eluting stent: Intravascular ultrasound results from ENDEAVOR III. *Am Heart J* 155:108-113, 2008.
82. Stone GW, Midei M, Newman W, et al: Comparison of an everolimus-eluting stent and a paclitaxel-eluting stent in patients with coronary artery disease. *JAMA* 299:1903-1913, 2008.
83. Waseda K, Miyazawa A, Ako J, et al: Intravascular ultrasound results from the ENDEAVOR IV trial. *J Am Coll Cardiol Interv* 2:779-784, 2009.
84. Kornowski R, Mintz GS, Kent KM, et al: Increased restenosis in diabetes mellitus after coronary interventions is due to exaggerated intimal hyperplasia: A serial intravascular ultrasound study. *Circulation* 95:1366-1369, 1997.
85. Cheneau E, Leborgne L, Mintz GS, et al: Predictors of subacute stent thrombosis. Results of a systematic intravascular ultrasound study. *Circulation* 108:43-47, 2003.
86. Fujii K, Carlier SG, Mintz GS, et al: Stent underexpansion and residual reference segment stenosis are related to stent thrombosis after sirolimus-eluting stent implantation. *J Am Coll Cardiol* 45:995-998, 2005.
87. Okabe T, Mintz GS, Buch AN, et al: Intravascular ultrasound parameters associated with stent thrombosis after drug-eluting stent deployment. *Am J Cardiol* 100:615-620, 2007.
88. Liu X, Doi H, Maehara A, et al: A volumetric intravascular ultrasound comparison of early drug-eluting stent thrombosis versus restenosis. *J Am Coll Cardiol Interv* 2:428-434, 2009.
89. Hong MK, Mintz GS, Lee CW, et al: Incidence, mechanism, predictors, and long-term prognosis of late stent malapposition after bare-metal stent implantation. *Circulation* 109:881-886, 2004
90. Hong MK, Mintz GS, Lee CW, et al: Late stent malapposition after drug-eluting stent implantation. An intravascular ultrasound analysis with long-term follow-up. *Circulation* 113:414-419, 2006
91. van der Hoeven BL, Liem SS, Jukema JW, et al: Sirolimus-eluting stents versus bare-metal stents in patients with ST-segment elevation myocardial infarction: 9-month angiographic and intravascular ultrasound results and 12-months clinical outcome. *J Am Coll Cardiol* 51:618-626, 2008
92. Guo N, Maehara A, Mintz GS, et al: Incidence, mechanisms, predictors, and clinical impact of acute and late stent malapposition after primary intervention in patients with acute myocardial infarction. *Circulation* 122:1077-1084, 2010.
93. Cook S, Wenaweser P. Togni M, et al: Incomplete stent apposition and very late stent thrombosis after drug-eluting stent implantation. *Circulation* 115:2426-2434, 2007.
94. Alfonso F, Pérez-Vizcayno MJ, Ruiz M, et al: Coronary aneurysm after drug-eluting stent implantation. Clinical, angiographic, and intravascular ultrasound findings. *J Am Coll Cardiol* 53:2053-2060, 2009.
95. Hassan AKM, Bergheanu SC, Stijnen T, et al: Late stent malapposition risk is higher after drug-eluting stent compared with bare-metal stent implantation and associates with late stent thrombosis. *Eur Heart J* 31:1172-1180, 2010.
96. Cook S, Ladich E, Nakazawa G, et al: Correlation of intravascular ultrasound findings with histopathological analysis of thrombus aspiration in patients with very late drug-eluting stent thrombosis. *Circulation* 120:391-399, 2009.
97. Lee CW, Kang SJ, Park DW, et al: Intravascular ultrasound findings in patients with very late stent thrombosis after either drug-eluting or bare-metal stent implantation. *J Am Coll Cardiol* 55:1936-1942, 2010.
98. Kang SJ, Mintz GS, Park DW, et al: Tissue characterization of in-stent neointimal using intravascular ultrasound radiofrequency data analysis. *Am J Cardiol* 106:1561-1565, 2010.
99. Takano M, Yamamoto M, Inami S, et al: Appearance of lipid-laden intima and neovascularization after implantation of bare-metal stents. *J Am Coll Cardiol* 55:26-32, 2010.
100. Kashiwagi M, Kitabata H, Tanaka A, et al: Very late clinical cardiac event after MBS implantation: In vivo optical coherence tomography examination. *J Am Coll Cardiol Imaging* 3:525-527, 2010.
101. Doi H, Maehara A, Mintz GS, et al: Classification and potential mechanisms of intravascular ultrasound patterns of stent fracture. *Am J Cardiol* 103: 818-823, 2009.
102. Popma JJ: Strut fractures after DES: Definitions, frequency, timing, device specificity, and associated clinical events. Transcatheter cardiovascular therapeutics. www.tctmd.com/txshow.aspx?tid=2532&id=73192&trid=2380. Accessed April 8, 2009.
103. Kosonen P: Stent fracture, strut malapposition common in stent thrombosis cases. www.tctmd.com/Show.aspx?id=90294. Accessed January 23, 2011.
104. Doi H, Maehara A, Mintz GS, et al: Impact of in-stent minimal lumen area at 9 months post-stent implantation on 3-year target lesion revascularization free survival: A serial intravascular ultrasound analysis from the TAXUS IV, V, and VI trials. *Circ Cardiovasc Interv* 1:111-118, 2008.
105. Hong M-K, Park S-W, Lee CW, et al: Intravascular ultrasound comparison of chronic recoil among different stent designs. *Am J Cardiol* 84:1247-1250, 1999.
106. Castagna MT, Mintz GS, Weissman NJ, et al: The contribution of "mechanical" problems to in-stent restenosis. An intravascular ultrasound analysis of 1090 consecutive in-stent

restenosis lesions. *Am Heart J* 142:970-974, 2001.
107. Ormiston JA, Serruys PW, Regar E, et al: A bioabsorbable everolimus-eluting coronary stent system for patients with single de-novo coronary artery lesions (ABSORB): a prospective open-label trial. *Lancet* 371:899-907, 2008.
108. Serruys PW, Ormiston JA, Onuma Y, et al: A bioabsorbable everolimus-eluting coronary stent system (ABSORB): 2-year outcomes and results from multiple imaging methods. *Lancet* 373:897-910, 2009.
109. Serruys PW, Onuma Y, Ormiston JA, et al: Evaluation of the second generation of a bioabsorbable everolimus drug-eluting vascular scaffold for treatment of de novo coronary artery stenoses. *Circulation* 122:2301-2312, 2010.
110. Fitzgerald PJ, Oshima A, Hayase M, et al: Final results of the Can Routine Ultrasound Influence Stent Expansion (CRUISE) study. *Circulation* 102:523-530, 2000.
111. Russo RJ, Silva PD, Teirstein PS, et al: A randomized controlled trial of angiography versus intravascular ultrasound-directed bare-metal coronary stent placement (The AVID trial). *Circ Cardiovasc Interv* 2:113-123, 2009.
112. Parise H, Maehara A, Stone GW, et al: A meta-analysis of randomized studies comparing intravascular ultrasound versus angiographic guidance of percutaneous coronary intervention in the pre-drug eluting era. *Am J Cardiol* 107:374-382, 2011.
113. Roy P, Steinberg DH, Sushinsky SJ, et al: The potential clinical utility of intravascular ultrasound guidance in patients undergoing percutaneous coronary intervention with drug-eluting stents. *Eur Heart J* 29:1851-1857, 2008.
114. Park SJ, Kim YH, Park DW, et al: Impact of intravascular ultrasound guidance on long-term mortality in stenting for unprotected left main coronary artery stenosis. *Circ Cardiovasc Interv* 2:167-177, 2009.



# Handheld Echocardiography

MARTIN E. GOLDMAN, MD | LORI CROFT, MD

**Background**
Types of Echocardiographic Instruments
Reliability and Accuracy
**Ultrasound "Stethoscope"**
**Education and Training Guidelines and Requirements**
Medical Students
Medical Residents
Emergency Physicians
Intensivists
Recommendations
**Clinical Applications**
Emergency Department
Intensive Care Unit
Internal Medicine
Cardiology
**Future Directions**

Although technology has transformed almost all aspects of our daily lives, the bedside cardiac physical examination uses technology that is almost 200 years old. In 1816, embarrassed to examine an obese young woman by putting his head to her chest, René Théophile-Hyacinthe Laennec rolled a sheet of paper, then placed one end over her precordium and the other to his ear. Thus, the stethoscope was born.[1] The sphygmomanometer for measurement of blood pressure dates back to 1881, when it was invented by Samuel Siegfried Karl Ritter von Basch. It is with these two ancient tools that most physicians approach a patient at the bedside to this day. In the interim, the explosive growth of medical technology has spawned relatively inexpensive, miniature ultrasound machines, which can be taken to the bedside and allow immediate imaging across several medical specialties.

Smaller ultrasound systems are now routinely used, and often required, for safe placement of central venous lines, as well as for applications such as bladder size determination, wound loculations, paracentesis, thoracentesis, and arthrocentesis. Some smaller ultrasound devices are also configured to allow cardiac examination. These hand-carried cardiac ultrasound (HCU) devices are being used for diagnostic cardiac imaging in many different locations, in and out of the hospital, by cardiologists and noncardiologists alike. Because of their relative ease of use, portability, and affordable cost, HCU systems have made point-of-care (bedside) echocardiography available to all medical personnel as an "ultrasound-stethoscope." Currently, the appropriate training, scope of practice, and credentialing for point-of-care echocardiography by various health care providers is an area of active investigation and ongoing discussion.

## Background

In 1978, J. R. Roelandt proposed the first miniaturized HCU system.[2] Since that time, bulky keyboards, large monitors, and video recorders have now been replaced by touch pads, flat screens, and digital storage devices. The American Society of Echocardiography defines an HCU device as a small ultrasound machine typically weighing less than 6 pounds that can obtain images and data.[3] Since that publication in 2002, advances in ultrasound technology have incorporated all the capabilities expected of a full sized system into these small machines (Fig. 8-1).[4-6]

### TYPES OF ECHOCARDIOGRAPHIC INSTRUMENTS

Currently, there are four basic types of echocardiographic systems (Table 8-1):

1. Large, very expensive systems carrying the most advanced instrumentation, capable of two-dimensional (2D), M-mode imaging, designated contrast settings, color flow Doppler, pulsed-wave (PW) and continuous-wave (CW) Doppler, tissue Doppler imaging, tissue harmonic imaging, speckle strain imaging, stress echocardiography formats, and broadband multifrequency imaging with image processing and digital storage, as well as volumetric (three-dimensional [3D], four-dimensional [4D]) imaging and transesophageal, intravascular, and intracardiac echocardiography. These systems typically are based in a hospital echocardiography laboratory or large office practice, with an instrument cost over $250,000.
2. Compact, smaller version of the full-sized systems that are more portable and less expensive, but have most of the features available on larger systems. Some are capable of transesophageal echocardiography (TEE) but lack volumetric (3D) imaging. With a compact system, resolution and penetration may be less robust with a lower cost between $100,000 and $150,000. These systems are usually located in an echocardiography laboratory or cardiology office but also are offered in smaller, battery-powered options that can be attached to a cart or separated and carried for portability.
3. Handheld or hand-carried ultrasound (HCU) devices are small, light, battery powered, less expensive systems with good 2D imaging quality and full Doppler capabilities, often with digital and wireless communication, some with stress and TEE options. These systems can be cart mounted or hand carried and may be in an office, emergency department, or hospital setting to provide "point-of-care" ultrasound with multiprobe capability. HCU systems cost between $50,000 and $100,000, depending on options.

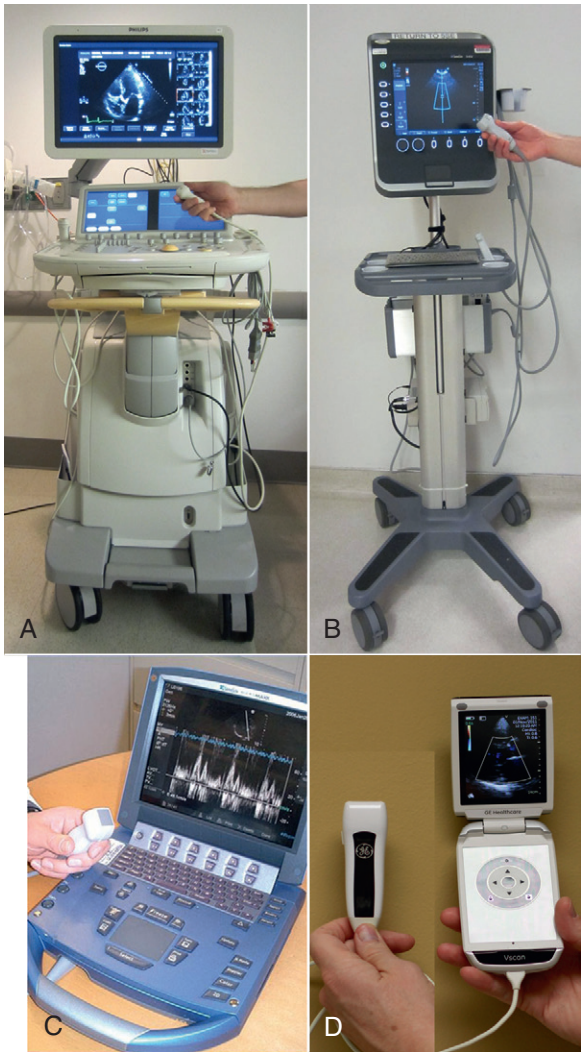



**Figure 8-1** **A,** A complete echocardiographic system (Philips iE33, Philips Healthcare, Andover, Mass.), which allows advanced imaging modalities such as 3D imaging but is relatively large and expensive. This type of system is used both in the echocardiography laboratory and for portable inpatient studies. **B,** A compact system (S-ICU system, Sonosite, Inc., Bothell, Wash.) that is more portable and lower in cost but lacks some features of a complete system. These systems may also include transducers for noncardiac imaging. **C,** A hand-carried system (MicroMaxx, Sonosite, Inc., Bothell, Wash.) that can be carried to the bedside. **D,** A palm-sized ultrasound device (Vscan, GE Healthcare, Waukesha, Wisc.) with limited functions but a relatively low cost and small size that fits in a pocket.

4. Palm-sized devices are very small. They can truly be held in one hand and viewed on a small screen and have potential as a smartphone application. These devices can image in 2D, with a caliper for measurement, usually with no or limited color flow Doppler and no electrocardiographic gating. They are relatively inexpensive for their size and capability, around $10,000, and can be used for point-of-care screening or as a true "echo-stethoscope."

These echocardiographic systems can be separated on the basis of performance capability, size, weight, and cost. Some of the smaller systems can perform a full examination, whereas the palm-sized units can be applied for screening of left ventricular (LV) function, wall thickness, chamber size, hypertrophy, pericardial effusions, and abdominal aortic aneurysms (Fig. 8-2). Ultimately, the choice of system to use will vary with the goal of the examination, the skill and experience of the persons performing the imaging, and its interpretation (Table 8-2). Typically, complete and compact echocardiography systems are used by cardiologists in the context of an echocardiography laboratory. The focus of this chapter is the use of hand-carried and palm-sized echocardiography systems outside the echocardiography laboratory by health care providers in other specialties. The two most important considerations in the clinical use of these smaller, readily accessible, heavily promoted systems are (1) the technical performance of the imaging device and (2) the appropriate level of skill and training to acquire and interpret the images.

**TABLE 8-1 Classification of Currently Available Echocardiography Machines According to Size and Function**

| *Echocardiography Machines* | *Capabilities* |
|---|---|
| Stationary high-end systems | Full range of standard echocardiographic modalities and measurements (MM, 2D, PW, CW, Color, TDI, TEE), and advanced modalities (3D, contrast) |
| Mobile (smaller machines on wheels, middle range technology) | Full range of standard echocardiographic modalities and measurements (MM, 2D, PW, CW, Color, TDI, TEE) |
| Portable (small machines that can be carried by a person) | Basic, standard echocardiographic modalities and measurements (MM, 2D, PW, CW, Color) |
| Handheld or pocket-size imaging devices | Limited functions (2D, Color) and measurement package |

From Sicari R, Galderisi M, Voigt JU, et al: The use of pocket-size imaging devices: a position statement of the European Association of Echocardiography. *Eur J Echocardiogr* 12:85-87, 2011.

*Color*, Color Doppler; *MM*, M-mode; *PW*, pulsed ware; *TDI*, tissue Doppler imaging.

## RELIABILITY AND ACCURACY

The reliability and accuracy of the hand-carried ultrasound devices have been validated in studies comparing their performance to full-size systems with images obtained by skilled technicians or physicians. Vourvouri and colleagues[7,8] demonstrated greater than a 90% concordance between results using an HCU and a standard full-size system in the echocardiographic evaluation of LV size and function with older-generation hand-carried devices including the OptiGo (Philips Healthcare, Andover, Mass.) and Sono-heart (Sonosite, Bothell, Wash.). Vourvouri and co-workers[9] also imaged 300 consecutive patients referred to a cardiologist with a hand-carried device. Agreement between the HCU device (OptiGo) and the standard system for the detection of major abnormalities was excellent (98%). However, even this level of agreement may be suboptimal in the clinical setting, because the HCU did miss 4% of the major findings.

Because of limitations in penetration and resolution, HCUs may underestimate severity of wall motion abnormalities in patients with poor ultrasound tissue penetration, which is often a problem in overweight or obese patients. In general, the quality of the images obtained with an HCU device correlates directly with the skill and experience of the personnel acquiring and interpreting the images. Cardiology fellows had 100% agreement between HCU and conventional echocardiography on qualitative assessment of LV systolic function and a 94% concordance for LV end-diastolic dimension and interventricular septal thickness, with an ultrasound imaging time of only 6 ± 2 minutes.[10] Therefore, with proper training, HCU devices

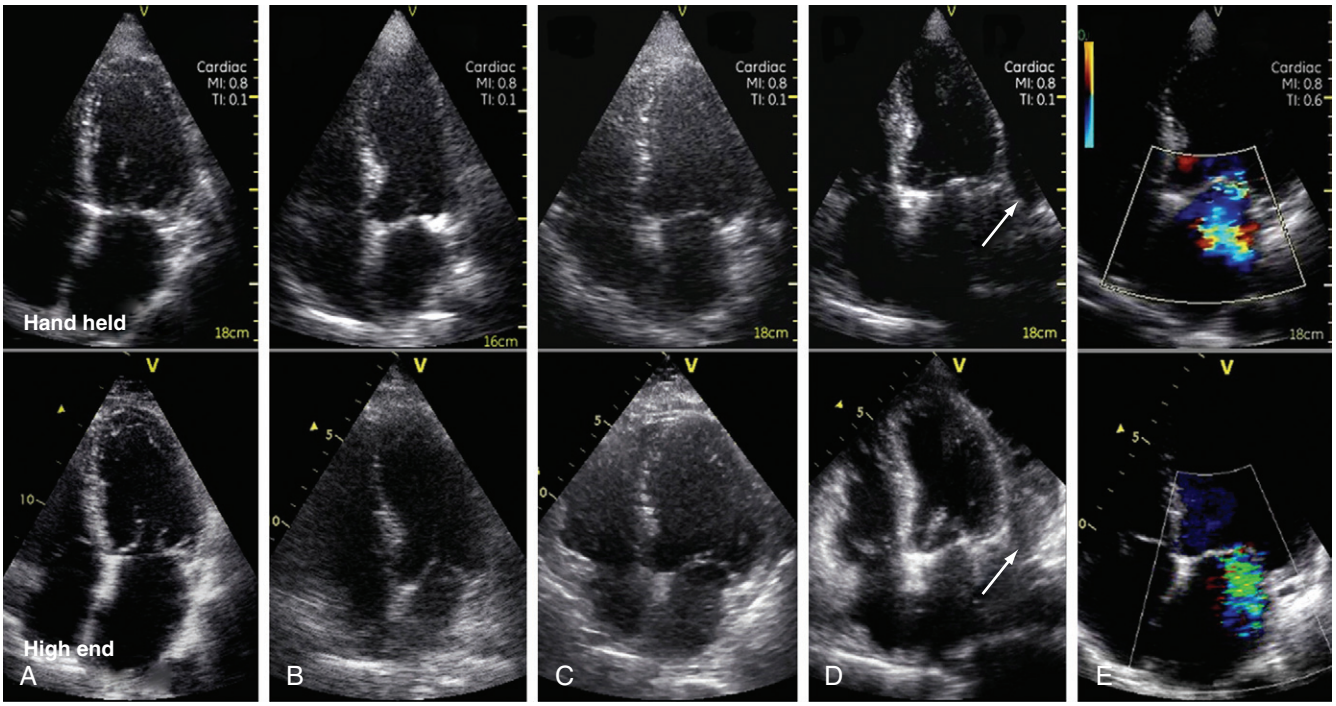



**Figure 8-2** Comparison of image quality of the handheld device (*top*) and a high-end device (*bottom*). **A,** Echogenic patient. **B,** Patient with suboptimal echogenicity. **C,** Patient with very poor echogenicity. **D,** Patient with pericardial effusion (*arrow*). **E,** Patient with mitral regurgitation. The pathology is somewhat more easily detected with the wider image sector of the high-end device. *(From Prinz C, Voigt JU: Diagnostic accuracy of a handheld ultrasound scanner in routine patients referred for echocardiography.* J Am Soc Echocardiogr *24:111-116, 2011.)*

**TABLE 8-2 Echocardiography Modalities Needed by Various Health Care Providers**

| | *2D Imaging* | *M-Mode* | *Color Flow Imaging* | *Doppler Velocity* | *TEE* | *3D* | *Stress* | *Perfusion* | *Strain* | *TDI* | *Quant* |
|---|---|---|---|---|---|---|---|---|---|---|---|
| Echocardiographer | ✓ | ✓ | ✓ | ✓ | ✓ | ✓ | ✓ | ✓ | ✓ | ✓ | ✓ |
| Cardiologist | ✓ | ✓ | ✓ | ✓ | ✓ | ✓ | | | | ✓ | ✓ |
| Anesthesiologist* | ✓ | | ✓ | ✓ | ✓ | ✓ | | | | | |
| Internist | ✓ | | ✓ | | | | | | | | |
| Intensivist | ✓ | | ✓ | | | | | | | | |
| Emergency department MD or emergency medical technician | ✓ | | ✓ | | | | | | | | |
| Medical student | ✓ | | ✓ | | | | | | | | |
| Nurse, advanced registered nurse practitioner, or physicians assistant | ✓ | | ✓ | | | | | | | | |

*Doppler*, Continuous/pulsed-Doppler spectral velocity data; *M-mode*, M-mode imaging; *Quant*, quantification; *Stress*, stress echocardiography; *Strain*, strain and strain rate imaging; *TDI*, tissue-Doppler imaging.
*Required echo-related skills will vary if a general anesthesiologist or cardiac subspecialist is used.

represent a valuable alternative to standard echocardiographic systems for well-trained personnel in some specific clinical applications.

Even the smallest palm-sized devices, potentially true cardiac "stethoscopes," have been evaluated against more sophisticated echocardiographic systems. Dalla Pozza and colleagues[11] used three small ultrasound devices in a pediatric population. The two larger HCU systems (a laptop-sized Philips p50 and a compact Philips CX 50) had excellent image accuracy (93%) compared to full echocardiography instruments; however, the palm-sized device (ACUSON P10, Siemens Healthcare, Malvern, Pa.) had only a 64.5% accuracy. Prinz and Voigt[12] compared the diagnostic accuracy of a palm-sized device (Vscan, GE Healthcare), used for imaging by an experienced cardiologist in 349 routine patients with varying LV function, to that of two laptop-sized HCU systems (either a Vivid 7 or E9, GE Healthcare). The palm-sized HCU showed excellent correlation in the evaluation of regional wall motion, visual ejection fraction, LV wall thickness and dimensions, and valve regurgitation (Fig. 8-3). These studies corroborate that HCUs and even palm-sized devices can be used by experienced, qualified sonographers and physicians for routine clinical cardiac imaging and may represent a valuable alternative to standard echocardiographic systems, for certain applications.

## Ultrasound "Stethoscope"

The concept of a stethoscope is that the physician listens to the patient's heart sounds to deduce clinical and hemodynamic information from the noise created by blood flow and valve

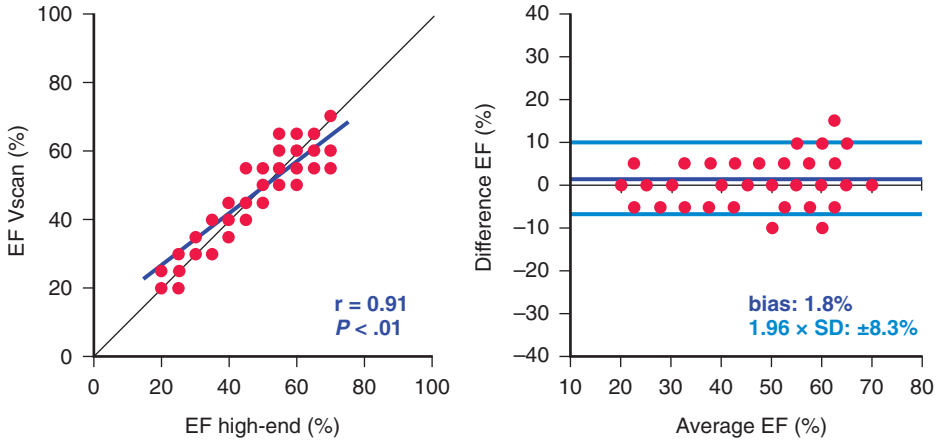



**Figure 8-3** *Left*: Good correlation (r = 0.91, *P* < .01) between ejection fraction calculations with a handheld device (Vscan) versus a high-end echocardiography system. *Right*: Bland-Altman plot shows no relevant bias and normal variation of assessments. Data points of several patients are clustered because of ejection fraction assessment in prespecified levels of 5%. *(From Prinz C, Voigt JU: Diagnostic accuracy of a handheld ultrasound scanner in routine patients referred for echocardiography.* J Am Soc Echocardiogr *24:111-116, 2011.)*

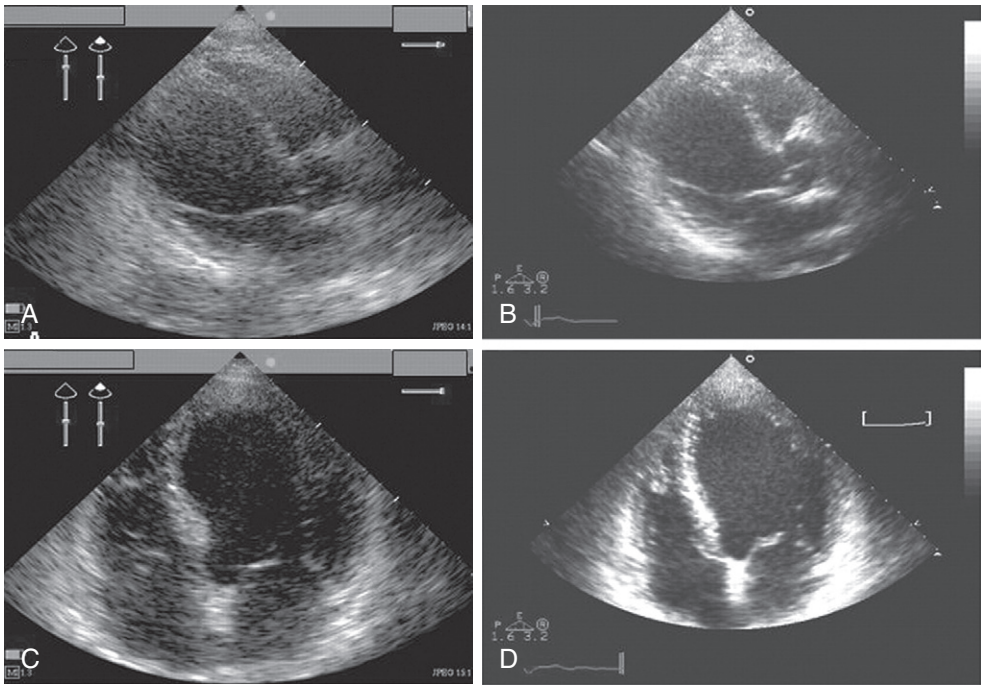



**Figure 8-4** Parasternal long-axis (*top*) and apical four-chamber views (*bottom*) acquired with hand-carried ultrasound (**A, C**) and standard echocardiography (**B, D**) showing dilated LV in a 67-year-old man with history of stroke. A neurologist had referred this patient to the outpatient cardiology clinic for electrocardiographic abnormalities and dyspnea on effort. *(From Trambaiolo P, Papetti F, Posteraro A, et al: A hand-carried cardiac ultrasound device in the outpatient cardiology clinic reduces the need for standard echocardiography.* Heart *93:470-475, 2007.)*

motion. Echocardiography has the potential to work like a stethoscope by using (ultra)sound waves to create images of the heart and visualization of blood flow that provide more accurate data than can be obtained from the acoustic sounds appreciated with a conventional stethoscope. Integrated into the physical examination, the HCU or palm device, as an ultrasound stethoscope, facilitates rapid identification of cardiac abnormalities (e.g., valve disease, chamber dilation, hypertrophy, pericardial effusion, or wall motion abnormalities). This can eliminate more sophisticated, costly studies and expedite appropriate therapeutic interventions (Figs. 8-3 to 8-5).[13-15] The Naples Ultrasound Stethoscope in Cardiology study[16] demonstrated that whereas the physical examination diagnosed cardiac abnormalities in 38.2% of patients, the addition of a palm-sized echocardiography examination increased the detection of cardiac abnormalities to 69.7%. The goal of promoting these very portable palm-sized or HCU systems is not to replace the comprehensive, carefully done Doppler echocardiographic examination, a detailed anatomic and hemodynamic evaluation, but to complement and improve the physical examination.[17]

The European Society of Echocardiography recommended indications for palm-size echocardiography devices reflect this approach (Box 8-1).[18] In addition to this limited list of indications, they further recommend:

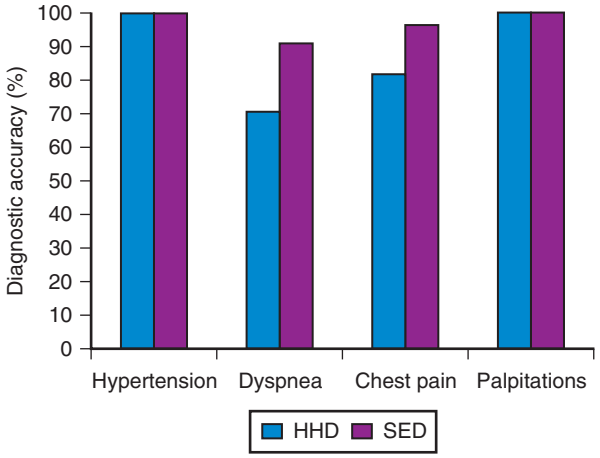



**Figure 8-5 Ability of echocardiographic examination to resolve the referral question.** Handheld device (HHD) showed good reliability in examination of patients referred for hypertension or palpitations, but was less accurate than standard echocardiographic device (SED) for those who presented with dyspnea or chest pain, as a result of biases in measurements of wall thicknesses and in assessment of valvular diseases and regional wall motion. *(From Giannotti G, Mondillo S, Galderisi M, et al: Handheld echocardiography: added value in clinical cardiological assessment.* Cardiovasc Ultrasound *3:7, 2005.)*

**Box 8-1**

**SUMMARY OF INDICATIONS FOR POCKET-SIZE DEVICES**

1. Complement to a physical examination in the coronary and intensive care unit
2. Tool for a fast initial screening in an emergency setting
3. Cardiologic counselling in outpatient health care facilities and hospitals
4. First cardiac evaluation in ambulances
5. Screening programs in schools, industry, and community activities
6. Triaging candidates for a complete echocardiographic examination
7. Teaching tool
8. Semi-quantification of extravascular lung water

From Sicari R, Galderisi M, Voigt JU, et al: The use of pocket-size imaging devices: a position statement of the European Association of Echocardiography. *Eur J Echocardiogr* 12:85-87, 2011.

- HCU imaging results should be included in the physical examination documentation and the images stored according to rules for other imaging data at each institution.
- Training and certification in HCU is recommended for all users, specific to the scope of practice for each user.
- Patients should be made aware that an HCU examination does not replace a complete echocardiogram.

## Education and Training Guidelines and Requirements

Both the American Society of Echocardiography (ASE) and the American College of Emergency Physicians (ACEP) have produced written guidelines and documents on the training of physicians using cardiac ultrasound and echocardiography. Comprehensive echocardiography training guidelines have been described by the ASE and are documented in a position paper, the American College of Cardiology/American Heart Association Clinical Competence Statement on Echocardiography.[19] These training guidelines are applicable for those physicians and practitioners who perform comprehensive echocardiography. However, the training requirements for comprehensive echocardiography exceed the training needed for point-of-care echocardiography in many clinical situations. For example, the requirements for emergency physicians who are performing focused ultrasound in the emergent setting are limited to the specific diagnoses being evaluated.[20] Similarly, intensivists have a limited scope of practice compared to a comprehensive echocardiographic examination with a correspondingly limited training scope and duration.[21]

For specific HCU training, the ASE recommends at least Level 1 training (performing 75 examinations and personally interpreting 150 examinations). However, this time commitment is usually practical only for cardiology training programs. There is no consensus on the appropriate training protocols required for HCU for noncardiologist and non–emergency department use. Various focused transthoracic echocardiography (TTE) training programs for intensivists, emergency-department physicians, anesthesiologists, hospitalists, and other medical specialties have been proposed, varying from a few hours to a few days.[22-24] As expected, a meta-analysis found that the accuracy of hand-carried echocardiography depended on the training time allocated and level of skill of the personnel performing the echocardiogram, ranging from medical students to cardiologists.[25] Ultimately, each professional specialty society will be responsible for maintaining the integrity of their training protocols and for ensuring the responsible practice and use of these imaging techniques.

### MEDICAL STUDENTS

The use of HCU by medical students completing abbreviated training programs has been evaluated in several studies and has been found to be additive to the history and physical examination. Diagnoses by medical students trained on an HCU system (OptiGo) for 18 hours were compared with those of a board-certified, experienced cardiologist using a standard physical examination.[26] Medical students performing echocardiography correctly identified 75% of abnormal findings compared with 49% by a cardiologist's physical examination as adjudicated by findings using a standard echocardiographic system. Another study showed that a medical student echocardiography curriculum, which included 60 hours of didactics and 40 hours of supervised imaging, resulted in a significant improvement in the accuracy of bedside diagnosis.[27]

### MEDICAL RESIDENTS

In a formal training program of noncardiologists using HCU by Alexander at Duke, 20 medical house officers participated in a standardized 3-hour HCU training program (30 minutes of introduction to ultrasound and the HCU device, 75 minutes of case reviews, and 75 minutes of hands-on practice).[28] The study demonstrated that the HCU substantially improved the assessment of LV function and pericardial effusion over history and physical examination, but was less effective for aortic valve disease. This study suggested that despite having only a 3-hour

training period, medical residents can use HCU echocardiography to substantially improve their assessment of LV function and pericardial effusion with an acceptable level of accuracy compared with standard echocardiography. Kimura and associates[10] devised an HCU curriculum consisting of a 1-hour lecture on cardiac physical examination and a 1-hour session of echocardiogram instruction for internal medicine residents and successfully improved their ability to accurately determine LV function.

### EMERGENCY PHYSICIANS

The ACEP Recommendations for Emergency Physicians who are performing Focused Ultrasound in the Emergent Setting (FOCUS)[20] are available online (http://www.acep.org/) and include both a training-based and a practice-based pathway. Residency training in ultrasound should include appropriate verification. The practice-based pathway includes didactic education plus performance of 25 ultrasound studies with confirmatory studies for each primary indication or a total of 150 studies for general emergency medicine ultrasound privileges. The ACEP also encourages point-of-care ultrasound for many other organ systems other than the heart. Their guidelines recommend 80 hours of general ultrasound instruction throughout residency and performance of 25 to 50 cardiac ultrasound examinations.[29] Wright and colleagues[30] suggest that because of the steep learning curve for echocardiography, emergency-department physicians with an interest in TTE at point of care should establish a quality assurance relationship with the cardiology echocardiography section of their institution.

### INTENSIVISTS

Intensivists who supervise care of a hospital's most complex and unstable patients have also integrated general and cardiac ultrasound into their armamentarium. Manasia and co-workers[31] found that after ten 1-hour tutorial sessions, intensivists who performed limited echocardiograms to assess LV function, volume status, and source of hypotension in 90 patients in the intensive care unit successfully performed a diagnostic limited TTE in 94% of patients and interpreted them correctly independently in 84% of patients. Importantly, new cardiac information provided a change of management in 37% of patients and additionally useful information was found in 41% of patients.

### RECOMMENDATIONS

All of these studies on the type and duration of training needed for HCU examination by physicians at various levels of training and in various specialties will be helpful in defining the standards for the use of HCU by health care providers. Clearly we need evidence-based recommendations for education and training of health care providers, tailored to the scope of practice in each specialty. We also need to work toward methods of competency testing and credentialing of practitioners as HCU becomes more widespread. In a recent editorial in *Chest*,[32] Schmidt calls for all intensivist training programs to incorporate a formal ultrasound curriculum for their fellows, including hands-on guidance. He cautions that "with the coming boom in ICU [intensive care unit] ultrasound, it is essential that skills spread as fast as the machines."

## Clinical Applications

The application of HCU is undergoing active investigation in several clinical settings. The goals of HCU in each setting depend on the specific clinical issues, and the long-term effect of point-of-care ultrasound is in evolution (Fig. 8-4). However, studies already support the use of HCU to improve the diagnosis, treatment, and risk stratification of heart failure in outpatient and inpatient settings and to improve the use of full echocardiographic examinations (Table 8-3).[12,21,22,33-37]

### EMERGENCY DEPARTMENT

The ASE and ACEP recently published a consensus statement that defines the important role of focused cardiac ultrasound (FOCUS).[20] FOCUS is a time-sensitive evaluation of the symptomatic patient that includes assessment for pericardial effusion and evaluation of chamber size, global cardiac function, and patient volume status. Intravascular volume may be assessed by chamber size, function, inferior vena cava size, and respiratory change. The examination may also guide emergency pericardiocentesis and transvenous pacemaker placement. The consensus statement emphasizes the complementary role of FOCUS to that of comprehensive echocardiography. HCU can supplement the physical examination, as well as facilitate the rapid triage of emergency department or intensive care patients (Box 8-2).

### INTENSIVE CARE UNIT

The general indications for performing an echocardiographic or ultrasound examination in the ICU include hemodynamic instability, suspected pulmonary embolism, infective endocarditis, aortic dissection or rupture, unexplained hypoxemia, source of embolus, central line placement, and assessment of pleural effusion and intraabdominal fluid collections.

The FREE (focused rapid echocardiography evaluation) examination, which incorporates a rapid assessment of LV and RV function and relative inferior vena cava size and its respiratory change to assess overall volume status and cardiac status, was feasible in 80% of 53 patients in a trauma unit, 85% of whom were mechanically ventilated.[38] Overall, 54% had a change in clinical management based on the FREE examination.

**Box 8-2**

**GOALS OF FOCUSED CARDIAC ULTRASOUND IN THE SYMPTOMATIC EMERGENCY-DEPARTMENT PATIENT**

- Assessment for the presence of pericardial effusion
- Assessment of global cardiac systolic function
- Identification of marked right ventricular and LV enlargement
- Intravascular volume assessment
- Guidance of pericardiocentesis
- Confirmation of transvenous pacing wire placement

From Labovitz AJ, Noble VE, Bierig M, et al: Focused cardiac ultrasound in the emergent setting: a consensus statement of the American Society of Echocardiography and American College of Emergency Physicians. *J Am Soc Echocardiogr* 23:1225-1230, 2010.

**TABLE 8-3 Selected Studies of Point-of-Care Echocardiography**

| Year of Publication | Clinical Setting | Study Group | Comparison | Outcomes | Reference |
|---|---|---|---|---|---|
| 2007 | Cardiology outpatient clinic | 222 consecutive patients with echocardiography in 108 | HCU by a cardiologist vs. complete TTE | Overall agreement between POC and TTE was 73%, and a definite diagnosis was established by HCU in 31% | 36 |
| 2008 | Heart failure inpatients | 75 adults with decompensated HF | Clinical evaluation, BNP levels, and echocardiography of IVC | Larger IVC diameter at discharge predicted 30-day readmission rates | 34 |
| 2009 | Medical ICU | 44 ICU patients | LV function HCU vs. formal TTE | Correct agreement for normal vs. abnormal LV systolic function in 86% with agreement on severity of LV dysfunction in 82% | 22 |
| 2009 | Medicine inpatients | 10 hospitalists evaluating 354 patients | Cardiac physical exam vs. HCU with full TTE as reference standard | Compared to physical exam, HCU improved hospitalists estimate of LV function but did not improve evaluation of valve dysfunction | 35 |
| 2011 | General medicine outpatient clinic | 175 adults with heart failure | Internist HCU vs. BNP levels | HCU was the only independent predictor of death or hospitalization for cardiac disease (hazard ratio 5.55, 95%CI 2.04-14.28) at 48 ± 7 month follow-up | 33 |
| 2011 | Echocardiography lab | 349 adults referred for a diagnostic study | HCU versus high-end echocardiography | No significant differences in assessment of LV size, ejection fraction or regional wall motion between HCU and high-end echocardiography. Agreement for pericardial effusion, valve stenosis, and regurgitation also was very good | 12 |
| 2011 | Cardiology outpatient clinic | 189 patients at initial consultation | Physical exam vs. HCU by cardiologist | HCU was diagnostic in 75% and indicated that no further cardiac evaluation was needed in an additional 20% | 37 |
| 2011 | ICU | 201 ICU patients | HCU by recently trained resident vs. experienced intensivist | After 12 hours of training, residents adequately assessed global LV function, LV dilation, dilated IVC, and pericardial effusion | 21 |

*BNP*, Brain natriuretic peptide; *Echo*, echocardiography; *HCU*, hand-carried ultrasound; *HF*, heart failure; *ICU*, intensive care unit; *IVC*, inferior vena cava; *POC*, point-of-care ultrasound.

## INTERNAL MEDICINE

In a general community outpatient clinic, 175 patients with suspected heart failure were examined using an HCU device (OptiGo, Philips, Andover, Mass.) by an internist who had received 4 weeks of training in HCU. The examination included assessment of LV size and systolic function, left atrial size, and valve dysfunction. In the 90 patients (55%) with an abnormal baseline HCU study, 25% were hospitalized for cardiac indication over the next 48 months. On multivariate analysis, an abnormal HCU examination was a strong predictor of clinical outcome with a hazard ratio of 5.55 (95% confidence interval 2.04-14.28, $P = .0004$) and was more predictive than serum BNP levels (Fig. 8-5).[33]

## CARDIOLOGY

A limited examination on a relatively inexpensive HCU system can be time efficient and cost effective. In a cardiology clinic, a hand-carried ultrasound system (OptiGo, Philips) was compared to a standard echocardiographic system with a mean examination time of 6.7 ± 1.5 minutes using an HCU versus 13.6 ± 2.4 minutes using the standard echocardiographic system.[6] The HCU was considered satisfactory in 85% of patients, and the data were concordant with the standard echocardiographic system in 83.8% of patients. Certainly, a cardiologist could incorporate an HCU examination as part of the bedside evaluation with great utility and impact on clinical management (Fig. 8-6).

Because of its time saving and ability to eliminate unnecessary examinations, screening and triaging with HCU or palm-sized systems is cost effective to eliminate unnecessary full examinations. One analysis estimated a 29% reduction in departmental workload, at a significant cost savings if all patients with a complete echocardiogram requested for LV function assessment underwent HCU initially and only those with abnormal scans underwent complete standard echocardiography.[39] HCU's high accuracy for detection of normal

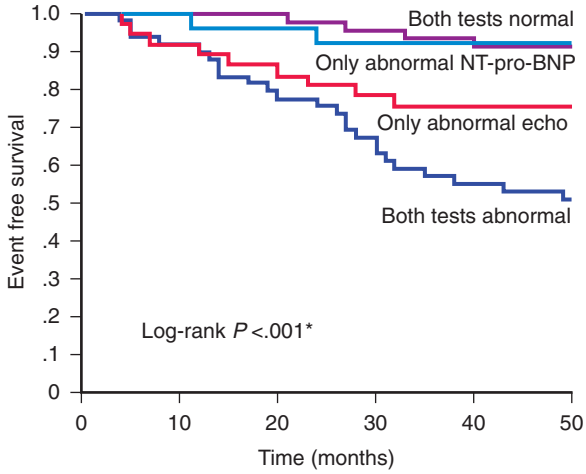



**Figure 8-6** Kaplan-Meier event-free survival curves for 175 outpatients with heart failure symptoms or risk factor, stratified according to hand-carried echocardiographic results and N-terminal pro–brain natriuretic peptide (*NT-pro-BNP*) in combination: both normal, only abnormal NT-pro-BNP, only abnormal hand-carried echocardiographic results, and both abnormal. *Difference statistically significant for both abnormal echocardiographic results and NT-pro-BNP versus others. *(From Lipczyńska M, Szymański P, Klisiewicz A, Hoffman P: Hand-carried echocardiography in heart failure and heart failure risk population: a community based prospective study.* J Am Soc Echocardiogr *24:125-131, 2011.)*

cardiac anatomy and function also is an efficient tool in eliminating unnecessary examinations.

## Future Directions

Point-of-care ultrasonography has become state-of-the-art care provided by several different medical specialties as well as primary care providers. In their *New England Journal of Medicine* article, Moore and Copel[40] note that ultrasonography is a user-dependent technology, and as usage spreads, there is a need to ensure competence, define the benefits of appropriate use, and limit unnecessary imaging and its consequences. They focus on procedural guidance, diagnostic assessment, the e-FAST examination (focused assessment with sonography for trauma, extended to include an examination of the chest for pneumothorax), and screening, especially for abdominal aortic aneurysms. There is minimal mention of cardiac imaging. Although they state that point-of-care ultrasound may be particularly cost effective by eliminating more expensive imaging tests, appropriate training and quality assurance as well as outcome and clinical effectiveness studies are needed.[41] True point-of-care ultrasound and echocardiographic examinations will be performed in the emergency department as well as by hospitalists and medical house staff. The same caution for adequate training and interpretation should be applied to the propagation of point-of-care cardiac echocardiographic imaging by noncardiologists.

William Zoghbi, in his capacity as president of the American Society of Echocardiography, editorialized that point-of-care echocardiography fulfills the mandate of the Patient Protection and Affordable Care Act of 2010 that rewards value, quality, and outcomes over quantity. HCU is poised to deliver cost-effective quality care.[39,42] With the graying and aging of Americans, there will be an increased incidence of valvular heart disease and murmurs on physical examination.[43] Inexpensive HCU cardiac examinations may provide effective triage for those patients requiring full echocardiographic examinations, thereby expediting care, ensuring appropriate use of expensive technologies, and reducing health care costs. Integration of hand-carried or palm-sized ultrasound devices into the medical school physical examination curriculum could empower future clinicians with the basic skills for image acquisition and interpretation and improve medical care, expediting critical decisions at significant savings to the health care system.

### KEY POINTS

- Hand-carried ultrasound (HCU) refers to small, lightweight systems with basic 2D imaging capability.
- Palm-sized devices are best suited as an adjunct to supplement the bedside physical examination.
- HCU is ideal for inexpensive screening of large populations with low prevalence of disease.
- Training guidelines for image acquisition and interpretation vary by specialty and need.
- Small but technologically complete laptop-sized systems are also available but require the same level of training and expertise as larger complete echocardiography systems.

## REFERENCES


1. Cheng TO: How Laennec invented the stethoscope. *Int J Cardiol* 118:281-285, 2007.
2. Roelandt J, Wladimiroff JW, Baars AM: Ultrasonic real time imaging with a handheld-scanner. Part II—initial clinical experience. *Ultrasound Med Biol* 4:93-97, 1978.
3. Seward JB, Douglas PS, Erbel R, et al: Hand-carried cardiac ultrasound (HCU) device: recommendations regarding new technology. A report from the Echocardiography Task Force on New Technology of the Nomenclature and Standards Committee of the American Society of Echocardiography. *J Am Soc Echocardiogr* 15:369-373, 2002.
4. Mondillo S, Giannotti G, Innelli P, et al: Handheld echocardiography: its use and usefulness. *Int J Cardiol* 111:1-5, 2006.
5. Mondillo S, Galderisi M: [Handheld echocardiography in clinical practice]. *Ital Heart J Suppl* 6:265-271, 2005.
6. Giannotti G, Mondillo S, Galderisi M, et al: Handheld echocardiography: added value in clinical cardiological assessment. *Cardiovasc Ultrasound* 3:7, 2005.
7. Vourvouri EC, Poldermans D, de Sutter J, et al: Experience with an ultrasound stethoscope. *J Am Soc Echocardiogr* 15:80-85, 2002.
8. Vourvouri EC, Schinkel AFL, Roelandt JRTC, et al: Screening for left ventricular dysfunction using a hand-carried cardiac ultrasound device. *Eur J Heart Fail* 5:767-774, 2003.
9. Vourvouri EC, Poldermans D, Deckers JW, et al: Evaluation of a hand carried cardiac ultrasound device in an outpatient cardiology clinic. *Heart* 91:171-176, 2005.
10. Kimura BJ, Amundson SA, Willis CL, et al: Usefulness of a handheld ultrasound device for bedside examination of left ventricular function. *Am J Cardiol* 90:1038-1039, 2002.
11. Dalla Pozza R, Loeff M, Kozlik-Feldmann R. Netz H: Hand-carried ultrasound devices in pediatric cardiology: clinical experience with three different devices in 110 patients. *J Am Soc Echocardiogr* 23:1231-1237, 2010.
12. Prinz C, Voigt JU: Diagnostic accuracy of a handheld ultrasound scanner in routine patients referred for echocardiography. *J Am Soc Echocardiogr* 24:111-116, 2011.
13. Bloch A, Crittin J, Jaussi A: Should functional cardiac murmurs be diagnosed by auscultation or by Doppler echocardiography? *Clin Cardiol* 24:767-769, 2001.
14. Shry EA, Smithers MA, Mascette AM: Auscultation versus echocardiography in a healthy population with precordial murmur. *Am J Cardiol* 87:1428-1430, 2001.
15. Salustri A, Trambaiolo P: Point-of-care echocardiography: small, smart and quick. *Eur Heart J* 23:1484-1487, 2002.
16. Galderisi M, Santoro A, Versiero M, et al: Improved cardiovascular diagnostic accuracy by pocket size imaging device in non-cardiologic outpatients: the NaUSiCa (Naples Ultrasound Stethoscope in Cardiology) study. *Cardiovasc Ultrasound* 8:51, 2010.
17. Salustri A, Trambaiolo P: The "ultrasonic stethoscope": is it of clinical value? *Heart* 89:704-706, 2003.
18. Sicari R, Galderisi M, Voigt JU, et al: The use of pocket-size imaging devices: a position statement of the European Association of Echocardiography. *Eur J Echocardiogr* 12:85-87, 2011.
19. Douglas PS, Khanderia B, Stainback RF, et al: ACCF/ASE/ACEP/ASNC/SCAI/SCCT/SCMR 2007 appropriateness criteria for transthoracic and transesophageal echocardiography: a report of the American College of Cardiology Foundation Quality Strategic Directions Committee Appropriateness Criteria Working Group, American Society of Echocardiography, American College of Emergency Physicians, American Society of Nuclear Cardiology, Society for Cardiovascular Angiography and Interventions, Society of Cardiovascular Computed Tomography, and the Society for Cardiovascular Magnetic Resonance. Endorsed by the American College of Chest Physicians and the Society of Critical Care Medicine. *J Am Soc Echocardiogr* 20:787-805, 2007.
20. Labovitz AJ, Noble VE, Bierig M, et al: Focused cardiac ultrasound in the emergent setting: a consensus statement of the American Society of Echocardiography and American College of

Emergency Physicians. *J Am Soc Echocardiogr* 23:1225-1230, 2010.
21. Vignon P, Mücke F, Bellec F, et al: Basic critical care echocardiography: validation of a curriculum dedicated to noncardiologist residents. *Crit Care Med* 39(4):636-642, 2011.
22. Melamed R, Sprenkle MD, Ulstad VK, et al: Assessment of left ventricular function by intensivists using handheld echocardiography. *Chest* 135:1416-1420, 2009.
23. Breitkreutz R, Uddin S, Steiger H, et al: Focused echocardiography entry level: new concept of a 1-day training course. *Minerva Anestesiol* 75:285-292, 2009.
24. Khasawneh FA, Smalligan RD: Focused transthoracic echocardiography. *Postgrad Med* 122:230-237, 2010.
25. Kobal SL, Atar S, Siegel RJ: Hand-carried ultrasound improves the bedside cardiovascular examination. *Chest* 126:693-701, 2004.
26. Kobal SL, Trento L, Baharami S, et al: Comparison of effectiveness of hand-carried ultrasound to bedside cardiovascular physical examination. *Am J Cardiol* 96:1002-1006, 2005.
27. Decara JM, Kirkpatrick JN, Spencer JT, et al: Use of hand-carried ultrasound devices to augment the accuracy of medical student bedside cardiac diagnoses. *J Am Soc Echocardiogr* 18:257-263, 2005.
28. Alexander JH, Peterson ED, Chen AY, et al: Feasibility of point-of-care echocardiography by internal medicine house staff. *Am Heart J* 147:476-481, 2004.
29. Emergency ultrasound guidelines. *Ann Emerg Med* 53:550-570, 2009.
30. Wright J, Jarman R, Connolly J, Dissmann P: Echocardiography in the emergency department. *Emerg Med J* 26:82-86, 2009.
31. Manasia AR, Nagaraj HM, Kodali RB, et al: Feasibility and potential clinical utility of goal-directed transthoracic echocardiography performed by noncardiologist intensivists using a small hand-carried device (SonoHeart) in critically ill patients. *J Cardiothorac Vasc Anesth* 19:155-159, 2005.
32. Schmidt GA: ICU ultrasound. The coming boom. *Chest* 135:1407-1408, 2009.
33. Lipczyńska M, Szymański P, Klisiewicz A, Hoffman P: Hand-carried echocardiography in heart failure and heart failure risk population: a community based prospective study. *J Am Soc Echocardiogr* 24:125-131, 2011.
34. Goonewardena SN, Gemignani A, Ronan A, et al: Comparison of hand-carried ultrasound assessment of the inferior vena cava and N-terminal pro-brain natriuretic peptide for predicting readmission after hospitalization for acute decompensated heart failure. *JACC Cardiovasc Imaging* 1:595-601, 2008.
35. Martin LD, Howell EE, Ziegelstein RC, et al: Hand-carried ultrasound performed by hospitalists: does it improve the cardiac physical examination? *Am J Med* 122:35-41, 2009.
36. Trambaiolo P, Papetti F, Posteraro A, et al: A hand-carried cardiac ultrasound device in the outpatient cardiology clinic reduces the need for standard echocardiography. *Heart* 93:470-475, 2007.
37. Cardim N, Fernandez Golfin C, Ferreira D, et al: Usefulness of a new miniaturized echocardiographic system in outpatient cardiology consultations as an extension of physical examination. *J Am Soc Echocardiogr* 24(2):117-124, 2011 Feb.
38. Ferrada P, Murthi S, Anand RJ, et al: Transthoracic focused rapid echocardiographic examination: real-time evaluation of fluid status in critically ill trauma patients. *J Trauma* 70:56-62; discussion 62-54, 2011.
39. Greaves K, Jeetley P, Hickman M, et al: The use of hand-carried ultrasound in the hospital setting—a cost-effective analysis. *J Am Soc Echocardiogr* 18:620-625, 2005.
40. Moore CL, Copel JA: Point-of-care ultrasonography. *N Engl J Med* 364:749-757, 2011.
41. Kimura BJ, Amundson SA, Shaw DJ: Hospitalist use of hand-carried ultrasound: preparing for battle. *J Hosp Med* 5:163-167, 2010.
42. Zoghbi WA: Echocardiography at the point of care: an ultra sound future. *J Am Soc Echocardiogr* 24:132-134, 2011.
43. Croft LB, Donnino R, Shapiro R, et al: Age-related prevalence of cardiac valvular abnormalities warranting infectious endocarditis prophylaxis. *Am J Cardiol* 94:386-389, 2004.



# Quantitative Evaluation of Left Ventricular Structure, Wall Stress, and Systolic Function

GERARD P. AURIGEMMA, MD | WILLIAM H. GAASCH, MD

**Definitions and Theoretical Considerations**
**Assessment of Left Ventricular Mass, Volume, and Geometry**
M-Mode Echocardiography
Two-Dimensional Echocardiography
Alternative Methods for Quantitation of Left Ventricular Structure and Function
**Assessment of Left Ventricular Systolic Function**
Ejection Fraction
Fractional Shortening and Related Indices
Stress-Shortening Relations
Pressure-Volume Analysis
**Potential Limitations**

The quantitation of left ventricular (LV) systolic function, size, and geometry is critical to the proper evaluation and management of patients with all types of heart disease.[1] For example, the assessment of LV function in patients with coronary artery disease provides better prognostic information than does knowledge of the number of diseased vessels (Fig. 9-1). Even when only one or two vessels are diseased, a low ejection fraction (EF) is associated with a higher mortality than that seen in patients with three-vessel disease and a normal EF.[2] Large LV systolic and diastolic volumes are also associated with a poor prognosis; thus, a patient with a reduced EF after a myocardial infarction can be categorized according to subsequent risk based on the absolute end-systolic volume (ESV) (Fig. 9-2).[3] Furthermore, information concerning LV size and geometry has important therapeutic implications, in view of the salutary effects of therapy with angiotensin-converting enzyme inhibitors on postinfarction remodeling and prognosis in patients with a reduced EF.[4,5]

Similarly, in cardiomyopathy of any cause, mortality remains high in patients with an EF less than 35%,[1,6] even with medical therapy. A depressed EF is uniformly present in patients with idiopathic dilated cardiomyopathy and results from a combination of afterload excess and depressed contractility. In this setting, indices of LV geometry, such as the relative wall thickness (RWT) or the mass/volume ratio (Fig. 9-3), provide prognostic information that is independent of the EF. Conversely, it is important to identify the significant percentage of patients with heart failure symptoms who have a normal EF (Fig. 9-4).[7,8]

Measurement of LV volume, mass, and function can provide data that are necessary to define the optimal time for surgery in patients with volume overload hypertrophy owing to chronic, severe mitral regurgitation or aortic regurgitation. In this regard, the prognostic usefulness of ventricular end-diastolic volume (EDV) and ESV, the EF, the ratio of EDV to mass, systolic stress-shortening relations, and end-systolic pressure-volume (P-V) relations has been tested in a variety of clinical studies. The ESV and EF appear to provide the most useful clues to prognosis.[9-15] Certainly, a most important determinant of postoperative survival is the level of LV systolic function (Fig. 9-5).

In pressure overload hypertrophy due to aortic stenosis, an assessment of systolic function is perhaps less important than in the regurgitant lesions. Although severe depression of the EF may indicate an increased surgical risk, patients with an EF as low as 20% to 25% can show substantial clinical improvement after aortic valve replacement.[16-18] In such patients, excessive systolic loads are usually responsible for the low EF; this situation is termed *inadequate hypertrophy* or *afterload excess.* Alternatively, *excessive* or *inappropriate hypertrophy,* indicated by a high RWT, appears to identify a group of patients having a high perioperative risk[19,20]; in this situation, a normal or high EF does not seem to be beneficial. In aortic stenosis, therefore, indices of LV geometry[20] (RWT) appear to provide prognostic clues that are not reflected in the EF.

It is well established that increased LV mass is a strong predictor of cardiovascular morbidity and cardiovascular and all-cause mortality, even when age, blood pressure, and other risk factors are considered.[21-27] Some investigators have suggested that LV geometry provides prognostic information that is incremental to the extent of LV hypertrophy.[24-26] For example, an increased ratio of LV wall thickness to cavity dimension[27] identifies patients at higher risk for cardiovascular morbidity and mortality (Table 9-1).

Thus, a substantial body of clinical research has demonstrated the prognostic value of indices of LV volume, mass, geometry, and function. Most if not all of these indices are routinely available to the clinician from standard M-mode and two-dimensional (2D) and Doppler echocardiography. In this chapter the echocardiographic techniques for evaluating LV geometry, stress, and systolic function are reviewed. Principles and methods are discussed, and clinical applications to patients with pressure and volume overload hypertrophy are emphasized.

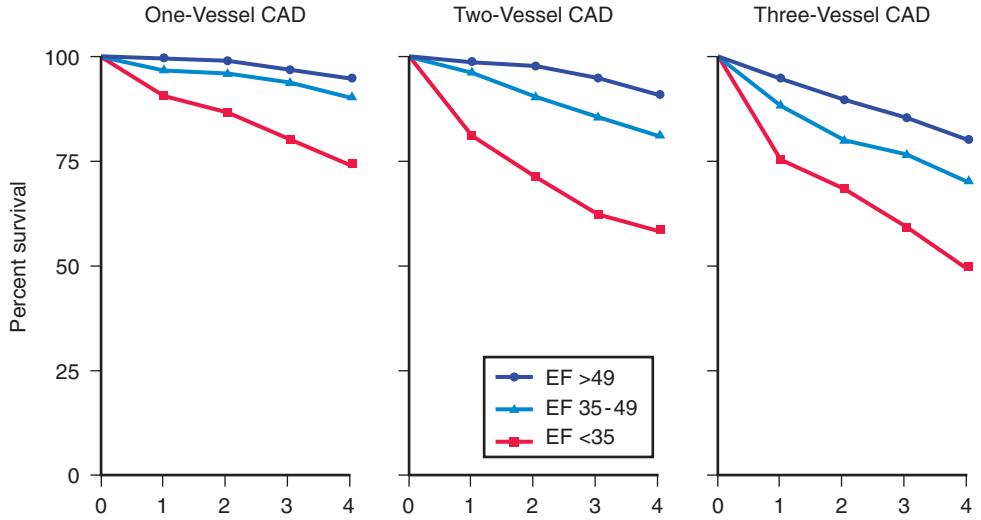



**Figure 9-1 The relation between LV ejection fraction (*EF*) and survival in patients with single-, double-, and triple-vessel coronary artery disease.** The negative impact of a low EF is seen in all three groups. Survival is better in patients with three-vessel coronary artery disease (*CAD*) and a normal EF than in those with one- or two-vessel disease and a low EF. *(Adapted from Mock MB, Rindqvist I, Fisher LD, et al: Survival of medically treated patients in the coronary artery surgery (CASS) registry.* Circulation *66:562-567, 1982. In Aurigemma GP, Gaasch WH, Villegas B, Meyer TE:* Curr Probl Cardiol *20:368, 1995.)*

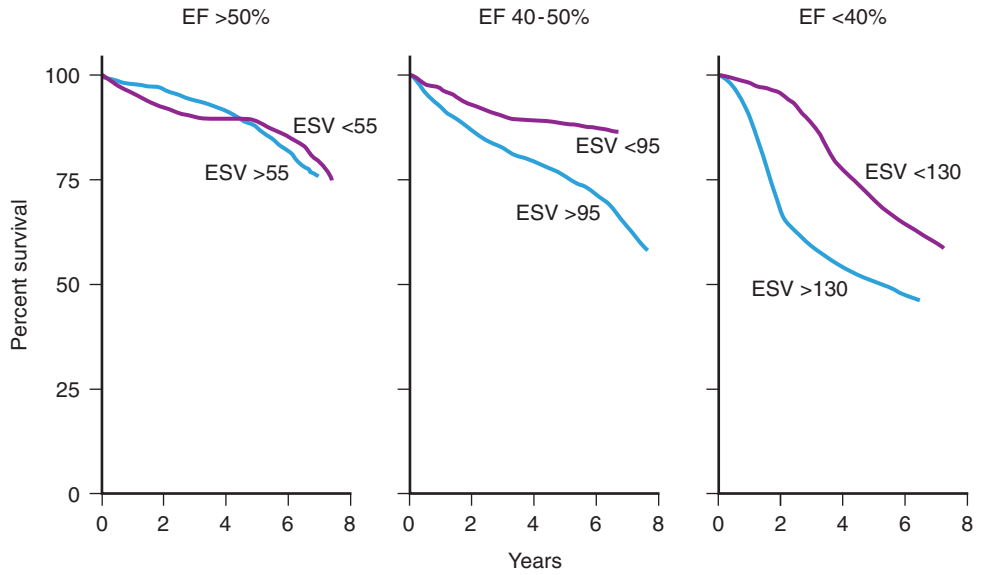



**Figure 9-2 The relation between LV end-systolic volume and survival in patients with normal, near-normal, and abnormal ejection fraction (*EF*).** Data were obtained from patients with a history of myocardial infarction. End-systolic volume (*ESV*) is a major predictor of survival when the EF is less than 50%. *(Adapted from White HD, Norris RM, Brown MA, et al: Left ventricular end systolic volume as the major determinant of survival after recovery from myocardial infarction.* Circulation *76:44-51, 1987. In Aurigemma GP, Gaasch WH, Villegas B, Meyer TE:* Curr Probl Cardiol *20:369, 1995.)*

## Definitions and Theoretical Considerations

The systolic pumping of the LV is a complex process that involves a coordinated contraction of subendocardial, midwall, and subepicardial muscle fibers. These fibers are arranged in a complex, helical fashion (See Fig. 10-16). At the equator of the ventricle, midwall fibers are oriented circumferentially; contraction of these fibers mainly contributes to a decrease in the minor axis (or dimension) of the ventricle and is responsible for generation of much of the stroke volume (SV) (Fig. 9-6). Longitudinally oriented fibers in the subendocardium and subepicardium contribute to shortening of the long axis of the ventricle, also contributing to SV. In addition to circumferential and long-axis shortening, the apex of the LV rotates counterclockwise during systolic contraction, and the base rotates clockwise (as viewed from the apex).[28,29] Such "twist," like fiber shortening, appears to be influenced by the contractile state of the myocardium (see Fig. 10-14). In concert with these shortening and twisting motions, wall thickening contributes to volume displacement and generation of the SV. Preload, afterload, contractility, and geometry influence shortening and thickening.[30]

The pumping activity of the LV provides oxygenated blood to the tissues of the body; therefore, the SV can be used as a parameter of the pump performance of the ventricle (Box 9-1). Because LV systolic pressure and SV are inversely related, using

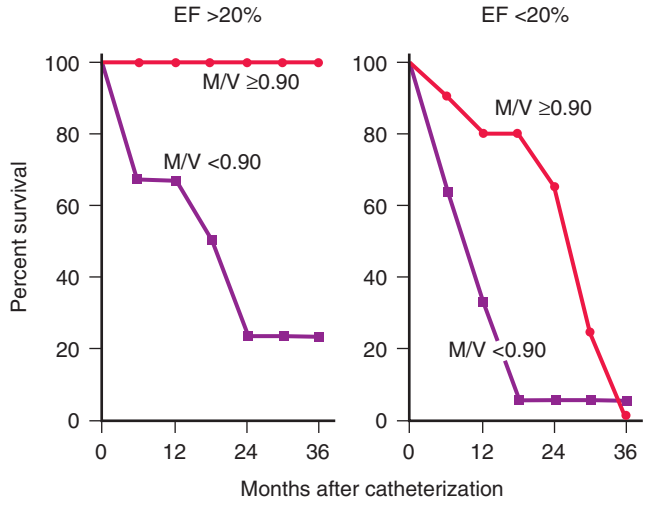



**Figure 9-3 The relation between LV mass/volume ratio (*M/V*) and survival in patients with an ejection fraction (*EF*) greater than and less than 20%.** Data were obtained from patients with dilated cardiomyopathy. Patients with a normal M/V ratio exhibit better survival than those with a low ratio; this trend is seen in EF categories. *(Adapted from Feild BJ, Baxley WA, Russell RO Jr, et al: Left ventricular function and hypertrophy in cardiomyopathy with depressed ejection fraction.* Circulation *47:1022-1031, 1973. In Aurigemma GP, Gaasch WH, Villegas B, Meyer TE:* Curr Probl Cardiol *20:370, 1995.)*

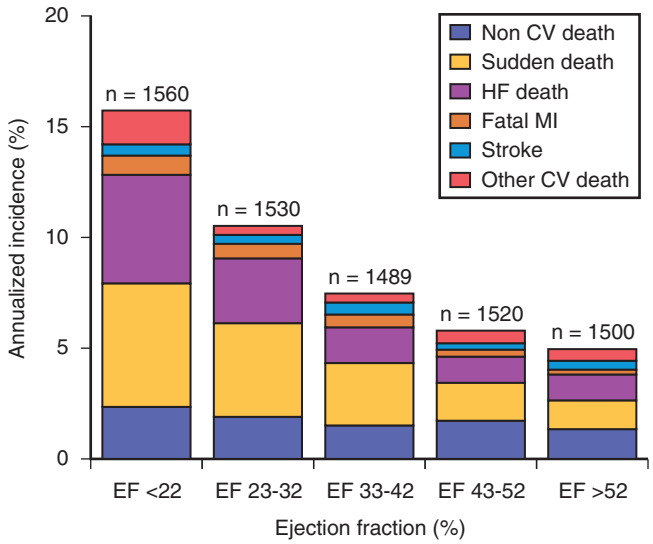



**Figure 9-4 The utility of ejection fraction (*EF*) data in patients with heart failure (*HF*) and preserved EF.** Data from 7599 patients with a broad spectrum of symptomatic HF enrolled in the Candesartan in Heart failure: Assessment of Reduction in Mortality and morbidity (CHARM) Program; mean LVEF in patients enrolled in CHARM was 38.8 ± 14.9%. These data demonstrate that EF is a powerful predictor of cardiovascular outcome in heart failure patients across a broad spectrum of ventricular function. However, above 45%, EF does not further contribute to assessment of cardiovascular risk in heart failure patients. *CV*, Cardiovascular; *MI*, myocardial infarction.

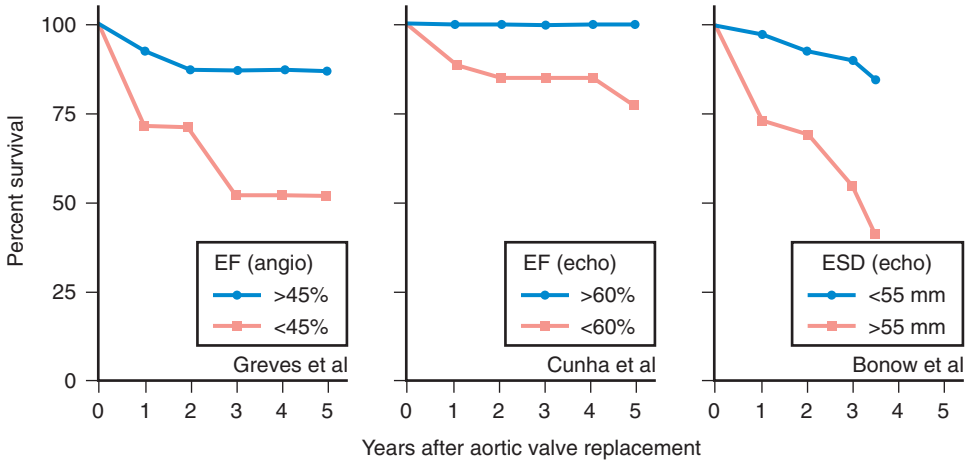



**Figure 9-5 Relation of preoperative ventricular function to postoperative survival.** These and other published data (see text) indicated that preoperative ventricular function is an important determinant of postoperative survival. *EF (angio)*, Ejection fraction by angiography; *EF (echo)*, systolic ejection fraction by echocardiography; *ESD (echo)*, end-systolic dimension by echocardiography. *(Adapted from Hoshino PK, Gaasch WH: When to intervene in chronic aortic regurgitation.* Arch Intern Med *146:349-352, 1986. Copyright © 1986 American Medical Association. In Aurigemma GP, Gaasch WH, Villegas B, Meyer TE:* Curr Probl Cardiol *20:371, 1995.)*

**TABLE 9-1 Relation between Morbid Events and the Pattern of Left Ventricular Geometry**

| | Normal LV Mass | | LV Hypertrophy | | |
|---|---|---|---|---|---|
| | *RWT < 0.45 (n = 150)* | *RWT ≥ 0.45 (n = 34)* | *RWT < 0.45 (n = 40)* | *RWT ≥ 0.45 (n = 29)* | *P* |
| CV deaths (%) | 0 | 3 | 10 | 21 | <0.001 |
| CV events (%) | 11 | 15 | 23 | 31 | 0.03 |
| All deaths (%) | 1 | 6 | 10 | 24 | <0.01 |

The prognostic value of LVH for morbid events in men (at an average of 10.2 years of follow-up) is striking. For all endpoints, the RWT provides incremental value for assessing risk. P-value obtained by analysis of variance.

From Koren M, Devereux R, Casale PN, et al: Relation of left ventricular mass and geometry to morbidity and mortality in uncomplicated essential hypertension. *Ann Intern Med* 114:345-352, 1991.

*CV*, Cardiovascular; *LVH*, left ventricular hypertrophy; *RWT*, relative wall thickness.

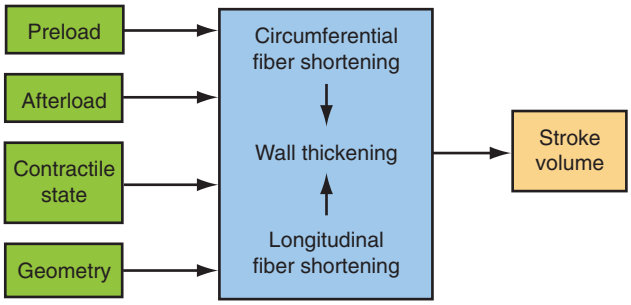



**Figure 9-6 Circumferential and longitudinal fibers contribute to wall thickening and volume displacement.** These functions are influenced by LV preload, afterload, contractile state, and geometry. *(From Aurigemma GP, Gaasch WH, Villegas B, Meyer TE:* Curr Probl Cardiol *20:374, 1995.)*

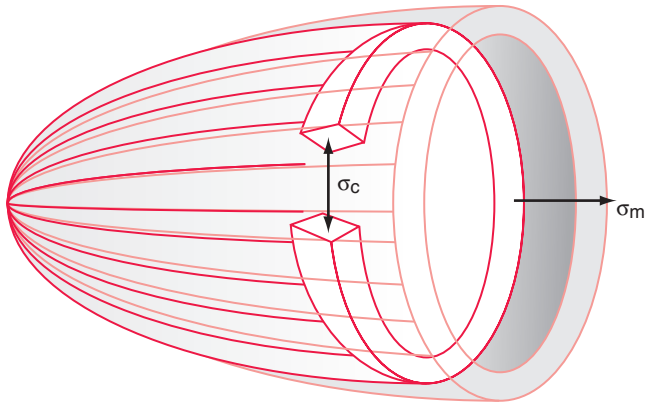



**Figure 9-7 Schematic of the LV (represented as a truncated ellipsoid) illustrating the major stress vectors.** Meridional stress ($\sigma_m$) is the force acting along the long axis of the LV; meridional stress opposes long-axis shortening. Circumferential stress ($\sigma_c$) is the force acting in the equatorial direction; circumferential stress opposes circumferential fiber shortening, and circumferentially oriented fibers are located in the midwall of the LV. The inner shell represents the LV in systole, and the outer, the ventricle in diastole. *(From Aurigemma GP, Gaasch WH, Villegas B, Meyer TE:* Curr Probl Cardiol *20:375, 1995.)*

**Box 9-1**

## ASPECTS OF VENTRICULAR FUNCTION

**Pump Performance**
The pumping activity of the LV that results in the delivery of oxygenated blood to the tissues. Stroke volume and stroke work are parameters of pump performance.

**Ventricular Function**
LV performance assessed relative to end-diastolic fiber length (or related parameter).

**Myocardial Contractility**
A basic property of the myocardium that reflects its active state, rather than loading conditions.

**Contractile Function**
A descriptor of ventricular performance or function that is affected by inotropic state, fiber length, or load.

stroke work as an index of ventricular performance can be more appropriate; a stroke work parameter credits the ventricle for the development of pressure and for shortening. When performance is assessed relative to end-diastolic fiber length or a related parameter, ventricular function can be described. Thus, a ventricular function curve can be generated by plotting stroke work against end-diastolic pressure, diameter, volume, or wall stress. Volume loading therefore produces an increment in stroke work (i.e., performance) through use of the Frank-Starling mechanism. By contrast, increased myocardial contractility also can produce an increment in stroke work, but in this case performance is augmented through a change in inotropic state rather than by a change in end-diastolic fiber length. In other words, contractility refers to a basic property of the myocardium that reflects the intensity of its active state. The use of the term *contractility* should be restricted to situations in which a change in performance or EF cannot be ascribed to a change in preload or afterload. *Contractile function* is a more general term used to describe changes in performance or function that could be affected by changes in inotropic state, fiber length, or loads. Thus, a change in the EF might best be classified as a change in contractile function; this term is often used interchangeably with *systolic function*. To fully describe the ventricle, it is necessary to define several additional terms that refer to its mechanical properties.[30]

*Stress* is defined as the force per unit cross-sectional area (CSA) of a material. It is an engineering term used to compare loads borne by different-sized elements of a material; the total load is less important than the load per unit of material. If the same load is borne by a smaller amount of material, the stress on that material is higher. In a spherical model of the LV, wall stress ($\sigma$) is directly proportional to the transmural pressure ($P$) and inversely proportional to the product of chamber radius ($R$) and wall thickness ($Th$):

$$\sigma = PR/2Th$$

In the LV, geometry is much more complex, and several components of stress exist within the wall (Fig. 9-7). Of these, meridional and circumferential stresses have most commonly been used in the analysis of LV mechanics. The meridional stress vector is oriented in the longitudinal or apex-to-base direction and represents the component of the load resisting long-axis shortening; circumferential stress is oriented along the equator, perpendicular to the long axis, and represents the component of the load resisting minor-axis shortening. Meridional stress ($\sigma_m$) can be calculated as

$$\sigma_m = P \times LVID/[4 \times Th(1 + LVID/Th)]$$

in which $P$ is pressure (mm Hg), $Th$ is wall thickness, and $LVID$ is cavity dimension.[31] This stress parameter does not require measurement of the long axis of the LV cavity. Circumferential stress ($\sigma_c$) can be calculated as

$$\sigma_c = P \times a^2[1 + (b^2/r^2)]/(b^2 - a^2)$$

in which $P$ is end-systolic pressure (mm Hg), $a$ is the internal (endocardial) radius, $b$ is the external (epicardial) radius, and $r$ is the midwall radius.[32] Other approaches to the calculation of circumferential stress, using minor- and major-axis dimensions, have been evaluated.[32] Formulas for calculation of meridional and circumferential stress using 2D echocardiographic data are as follows[33]:

$$\sigma_m = 1.33P\ A_m/A_c \times 10^3\ \text{kdyn/cm}^2$$

in which $A_t$ is the short-axis area subtended by the LV epicardium and right side of the septum, $A_c$ is the cavity (endocardial) area, $A_m = A_t - A_c$ or myocardial area, and $L$ is the LV cavity

length, obtained from the apical four-chamber view. 2D and M-mode methods yield somewhat different results, with M-mode–derived $\sigma_m$ being higher than 2D-derived values, even in normal subjects. In spherical ventricles, $\sigma_m$ by any method tends to overestimate afterload.[34]

The determination of wall stress requires assessment of LV pressure. Invasively determined values may be combined with echocardiographic dimensions, but they are often not available or simultaneously obtained. Three methods have been proposed for using noninvasive recordings to ascertain LV systolic pressures; LV diastolic pressures (and therefore diastolic stress) cannot be reliably determined noninvasively. Although these methods assume that there is no LV outflow gradient, the first and easiest method assumes that end-systolic LV pressure can be approximated by peak arterial pressure.[30] Thus, cuff systolic blood pressure is substituted for LV end-systolic pressure. The second method involves calibration of an externally recorded pulse recording using cuff systolic and diastolic pressures, with calculation of arterial pressures at the dicrotic notch.[35] The third involves the substitution of mean arterial pressure, derived from cuff recording, for end-systolic pressure, given the close correlation between these two values, as shown by Rozich.[36]

Because wall stress parameters incorporate appropriate size normalization, they allow comparison among the mechanical properties of different hearts. End-systolic wall stresses, calculated using end-systolic pressures (or the surrogates discussed earlier) and dimensions, are taken as indices of LV afterload, whereas end-diastolic wall stress, calculated using end-diastolic pressure and dimension, is a measure of LV preload.

*Preload* is the force (i.e., load) acting to stretch the resting myofibril. Preload is commonly estimated as the LV end-diastolic pressure, diameter, or volume, but to be more precise, this force should be normalized for each unit CSA of muscle and expressed as end-diastolic wall stress. In this manner, LV preload is analogous to the preload on a strip of isolated cardiac muscle in a myograph. This force, which acts to stretch the myocardium, is resisted by the stiffness of the muscle. Thus, the extent to which the myocardial fiber is stretched depends on an interaction between preload and muscle stiffness.[37] Because preload influences initial fiber length, it affects LV systolic performance. This phenomenon, which operates on a beat-to-beat basis, is generally referred to as *Starling's law of the heart* or the *Frank-Starling mechanism*.

The preload reserve of the ventricle depends on the baseline hemodynamic conditions and the stiffness of the myocardium. Thus, in the upright posture, normal human subjects exhibit a substantial preload reserve, whereas in the recumbent posture they may exhibit a minimal preload reserve. The difference in preload reserve is related to difference in the baseline EDV, which is lower in the upright posture than it is when the subject is recumbent, owing to the differences in venous return. This fact should be kept in mind when interpreting exercise studies; the EDV of the normal LV generally increases during upright exercise, but it may not during recumbent exercise. Moreover, the ability to recruit the Frank-Starling mechanism may also be limited in hypertrophied ventricles that have abnormal ventricular compliance characteristics (Fig. 9-8). Thus, in patients with aortic stenosis or hypertensive heart disease, there may be little or no increment in LV EDV during exercise, and consequently the EF may not increase normally.[38-40] Such limited preload reserve occurs as a result of a steep diastolic PV relation in which large changes in filling pressure cause only small changes in volume. This mechanism may even underlie marginal LV function in the basal state.

Despite a low EF, many dilated hearts (particularly those with compensated mitral or aortic regurgitation) generate a normal or high SV. In this instance, although the Frank-Starling mechanism may be a contributing factor, the large SV is primarily a function of the large EDV. In other words, the presence of a large LV chamber does not necessarily indicate use of preload reserve at the fiber level. Many such hearts retain the ability to use preload reserve to augment SV. By contrast, in end-stage heart failure, preload reserve may be exhausted.

*Afterload* can be thought of as the force (i.e., stress) developed by the myocardium after the onset of contraction. As described by the Laplace relation, afterload (systolic wall stress) is directly related to LV systolic pressure and radius and inversely related to wall thickness. Afterload varies with time, and thus it can be

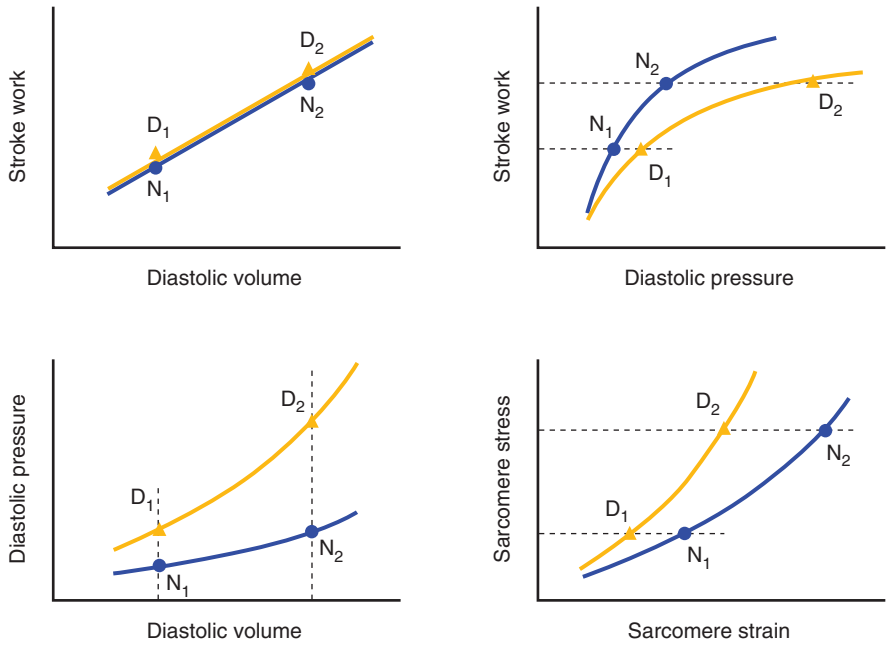



**Figure 9-8 The effect of diastolic dysfunction on the relation between LV systolic performance and preload.** Classic ventricular function curves relating stroke work to end-diastolic volume are shown in the *top left* panel; stroke work is related to end-diastolic pressure in the *top right* panel; diastolic pressure-volume curves are shown *below*. When the LV end-diastolic pressure is used as an index of preload, ventricular systolic function in diastolic heart failure ($D_1$, $D_2$) appears to be less than normal ($N_1$, $N_2$). These results are extrapolated to sarcomere stress-shortening relations. For a given level of sarcomere stress (point *1* to point *2*), there is much less sarcomere strain in patients with diastolic failure ($D_1$, $D_2$) than in normal ($N_1$, $N_2$). *(From Aurigemma GP, Zile MR, Gaasch WH: Contractile behavior of the left ventricle in diastolic heart failure: with emphasis on regional systolic function.* Circulation *113:296-304, 2006.)*

calculated at the instant of aortic valve opening, at the end of ejection, or at any instant throughout systole. Whereas LV systolic pressure and systemic vascular resistance can affect afterload, neither of these should be considered the equivalent of afterload.[41-43] Likewise, aortic input impedance influences systolic pressure and stress, but impedance is not the equivalent of afterload.[44]

In aortic stenosis, the LV systolic pressure may exceed 250 mm Hg, but if there is an appropriate increase in LV wall thickness, the force borne by each unit of heart muscle might remain near normal (i.e., afterload is normal).[30] On the other hand, an acute increase in systolic pressure or chamber size can result in an increased afterload.[45] By virtue of the inverse relation between load and shortening, an acute increase in afterload generally causes a decrease in shortening, and vice versa.

Contractility can be defined as the quality of cardiac muscle that determines performance independent of loading conditions. Contractility is easiest to study and define in isolated heart muscles when loading conditions are held constant. For example, if resting length is held constant, the addition of digitalis or norepinephrine to an isolated muscle preparation results in an increase in the extent and velocity of force development and shortening; such increased performance under constant loading conditions reflects an augmented inotropic state (i.e., increased contractility). In many cardiac diseases, abnormal LV pump function may be caused by disordered loading conditions, depression of contractility, or both. For this reason, it may be difficult to determine the exact cause of decreased fiber shortening. Accordingly, there has been considerable interest in the development of a sensitive index of contractility that is not affected by changes in loading conditions.[46,47] Unfortunately, there is no completely load-independent index of basal contractile state.[30] Thus, directional changes in contractility (during acute hemodynamic interventions) are relatively easy to demonstrate, but it is not possible to define a basal level of contractility in patients with chronic heart disease.

## Assessment of Left Ventricular Mass, Volume, and Geometry

Remodeling of the LV in valvular heart disease, heart failure, and hypertensive heart disease is characterized by changes in LV mass and geometry. Descriptors of LV geometry include the RWT, short-axis/long-axis ratio, and mass/volume ratio. These descriptors are easily obtained by M-mode and 2D echocardiography. As suggested earlier, alterations in LV geometry have been used to assist risk stratification in a variety of diseases and to describe more completely remodeling changes effected by valve replacement. In patients with idiopathic dilated cardiomyopathy, for example, a poorer survival is associated with larger short-axis dimension and a greater ratio of short/long axes (i.e., a more spherical LV geometry).[48,49]

### M-MODE ECHOCARDIOGRAPHY

#### *Mass*

Whereas newer and more costly tomographic methods, such as ultrafast computed tomography and magnetic resonance imaging (MRI), permit more precise quantitation, echocardiography remains the most commonly used technique for estimating LV mass and geometry. This subject has been reviewed by the Chamber Quantification Writing Group of the American Society of Echocardiography (ASE).[50] M-mode echocardiography is universally available and relatively low cost, and there is a considerable body of evidence supporting its accuracy in LV mass quantitation.[51,52] Quantitation of mass is based on the geometric assumption that the ventricle is a prolate ellipsoid with a 2:1 long-axis/short-axis ratio.[51,52] In practical terms, LV mass estimates are most accurate in ventricles with normal shape, specifically, a long-axis/short-axis ratio that approximates 2:1. It is assumed, of course, that minor-axis dimensions are measured in a region free of wall motion abnormalities. This assumption is invalidated in ischemic heart disease with focal wall motion abnormality or in right ventricular overload. Estimates of myocardial mass and volume are derived from LV minor-axis dimensions obtained with the transducer in the parasternal position (Fig. 9-9). Under 2D echocardiographic guidance, the ultrasound beam is aligned so that it is perpendicular to the interventricular septum and posterior wall at a

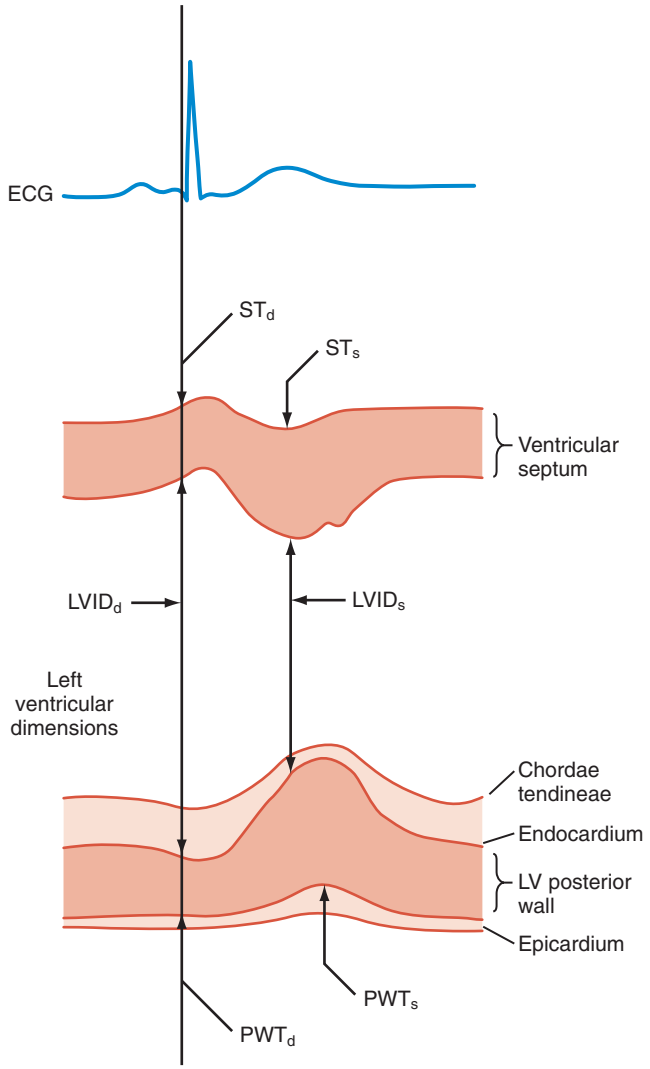



**Figure 9-9 Schematic of an M-mode echocardiogram obtained using 2D echocardiographic guidance.** Measurements are made coincident with the Q wave of the simultaneous electrocardiogram. *ECG*, Electrocardiogram; *$LVID_d$*, left ventricular internal dimensions in diastole; *$LVID_s$*, left ventricular internal dimensions in systole; *$PWT_d$*, posterior wall thickness in diastole; *$PWT_s$*, posterior wall thickness in systole; *$ST_d$*, ventricular septal thickness in diastole; *$ST_s$*, ventricular septal thickness in systole. *(From Aurigemma GP, Gaasch WH, Villegas B, Meyer TE:* Curr Probl Cardiol *20:381, 1995.)*

level slightly below the mitral leaflet tips; the chamber dimension is obtained from the parasternal long-axis view.[49-51] This approach maximizes the LV cavity dimension and ensures that proper beam orientation with respect to the papillary muscles is obtained. LV mass is estimated from measurements of septal and posterior wall thickness and LV cavity dimensions at end-diastole using the anatomically validated cube formula[51,52]:

$$\text{LV mass} = 0.8[1.04(\text{ST}_\text{d} + \text{LVID}_\text{d} + \text{PWT}_\text{d})^3 - \text{LVID}_\text{d}^3] + 0.6\ \text{g}$$

in which $ST_d$ is the diastolic septal thickness, $LVID_d$ is the diastolic LV cavity dimension, $PWT_d$ is the diastolic posterior wall thickness, and 1.04 is the specific gravity of myocardium. The measurements are made using the leading-edge ASE standard technique.[50] As shown by Devereux and colleagues,[1,52] LV mass estimates made with ASE measurements overestimate true anatomic LV weights by 20%, necessitating a correction factor of 0.8. The chamber quantification recommendations note that direct measurements by 2D echocardiography may be substituted for 2D-derived M-mode measurements.[50] It is important to note, however, that direct 2D measurements will yield lower values than 2D-directed M-mode measurements.[50] The accuracy of three-dimensional (3D) methods for calculating LV mass has been demonstrated (see Chapter 4).

### Volume

A simple estimate of LV volume may be obtained from the LV minor-axis internal dimension (LVID), derived by M-mode echocardiography as

$$\text{V} = \text{LVID}^3$$

The geometric assumptions are similar to those used for LV mass calculation. However, in the dilated, spherical LV encountered in long-standing valvular regurgitation or dilated cardiomyopathy, the ratio of length to minor-axis dimension decreases, leading to significant overestimation of LV volumes by this simple method. Teichholz and colleagues[53] derived a formula that attempts to correct for this problem:

$$\text{V}_\text{d} = [7/(2.4 + \text{LVID}_\text{d})] \times \text{LVID}_\text{d}^3$$

LV volumes derived with this formula correlate well with single-plane angiographic estimates.[53] Because M-mode echocardiography provides minor-axis dimensions of the LV in systole and diastole, the Teichholz method may be used to compute LV volumes at end-systole and end-diastole and thus to derive SV and cardiac output (Table 9-2). A compelling advantage of this method is that LV volume can be determined rapidly from easily obtained M-mode measurements. However, given the required geometric assumptions, 2D and 3D methods will always be preferable to M-mode estimates of ventricular volumes.[50]

**TABLE 9-2 Relationship between Chamber Size and Stroke Volume**

| | $LVID_d$ (cm) | EF (%) | SV (mL) |
|---|---|---|---|
| Normal | 5 | 65 | 81 |
| LVH | 4.4 | 75 | 63 |
| DCM | 7.5 | 20 | 84 |

This table illustrates the relationship between chamber size and resting stroke volume (SV). End-diastolic volumes are estimated from the $LVID_d$ using the Teichholz method[53] and SV calculated as the product of end-diastolic volume and ejection fraction (EF). Note that resting SV may be normal in dilated cardiomyopathy (DCM) and less than normal in extreme hypertrophic remodeling. Depending on heart rate, resting cardiac output in patients with extreme LVH or hypertrophic cardiomyopathy may be lower than normal. This table suggests the teleologic reason for chamber dilation.

*LVH*, Left ventricular hypertrophy; $LVID_d$, left ventricular internal dimensions in diastole.

### Relative Wall Thickness

M-mode estimates of myocardial mass and volume are derived from LV minor-axis dimensions obtained with the transducer in the parasternal position (see Fig. 9-9). These same measurements are used to describe LV geometry. Although the amount of LV mass is an important predictor of subsequent cardiac events in hypertensive disease, the geometry and pattern of LV hypertrophy also provide insight into the pathophysiology of hypertensive hypertrophy[49] and may confer prognostic information (see Chapter 34).[24-26] The most commonly used index of the pattern of hypertrophy is the RWT,[27] which is calculated as

$$\text{RWT} = 2 \times \text{PWT/LVID}$$

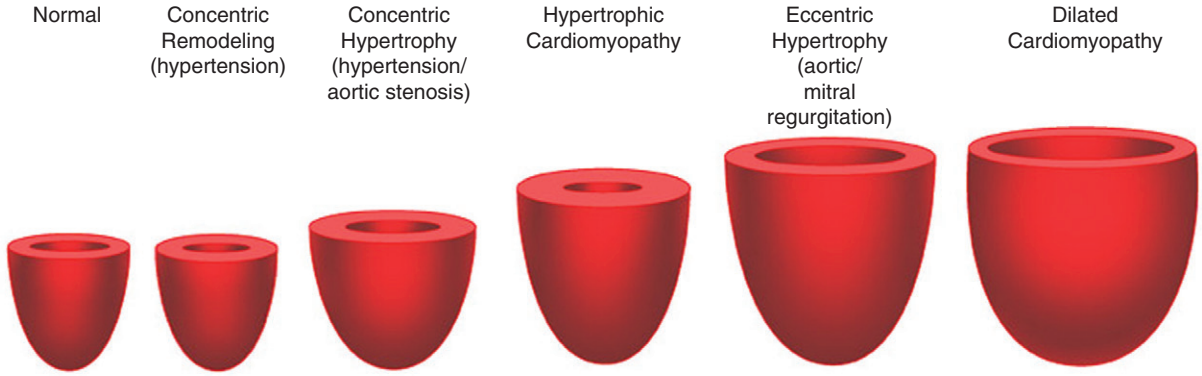
in which *PWT* is the posterior wall thickness and *LVID* is the LV internal dimension, respectively; RWT may be measured in diastole or systole. RWT also has been expressed as $h/R$, in which $h$ is wall thickness and $R$ is cavity radius. In the normal or compensated ventricle, the RWT increases in direct proportion to elevations in systolic pressure.

In untreated hypertensive patients, LV mass and relative wall thickness determinations may be used to subdivide the population into four general categories (Fig. 9-10):

1. Concentric hypertrophy (elevations in both LV mass and RWT),
2. Eccentric hypertrophy (elevation in LV mass with normal RWT),
3. Concentric remodeling (normal mass but abnormally high RWT), and
4. Normal LV mass and RWT.

In a population of untreated hypertensive patients, the majority had normal LV mass and normal RWT; concentric hypertrophy was the least common abnormal pattern observed.[27] More recently, Khouri and associates[54] have used MRI to refine this original paradigm and added a subclassification of geometric subtypes (see Fig. 9-9; Figs. 9-10 and 9-11). These authors suggest that concentric or eccentric LVH can each be subclassified into two subgroups, yielding four distinct geometric patterns.[54,55] In this and another large, population-based study utilizing MRI, there was a strong association between obesity and concentric LVH, helping to dispel the notion that LVH in this condition is exclusively eccentric.[56]

What is the clinical relevance of the mass and geometry subcategories? Patients with concentric hypertrophy have a relatively high incidence of adverse cardiovascular and noncardiovascular events compared with patients with eccentric hypertrophy.[25-27] In addition, concentric geometry, even without hypertrophy, appears to be associated with adverse consequences during follow-up (see Table 9-1). Thus, in hypertensive disease, as noted earlier, incremental information regarding risk for both cardiovascular and noncardiovascular events is provided by assessing geometry and LV mass. The RWT may provide insight into the appropriateness of hypertrophy.[49] There is occasionally more muscle mass than would be required for the observed pressure; thus, a high RWT, such as is encountered in hypertrophic cardiomyopathies, "hypertensive hypertrophic cardiomyopathy of the elderly,"[57] uncommonly in hypertension, and not infrequently in aortic stenosis,[58] indicates excessive or inappropriate LV hypertrophy. In our experience, RWT values



| | Normal | Concentric Remodeling (hypertension) | Concentric Hypertrophy (hypertension/ aortic stenosis) | Hypertrophic Cardiomyopathy | Eccentric Hypertrophy (aortic/ mitral regurgitation) | Dilated Cardiomyopathy |
|---|---|---|---|---|---|---|
| Mass | N | N | ↑ | ↑ | ↑↑ | ↑↑ |
| Volume | N | N-↓ | N | N-↓ | ↑↑ | ↑↑↑ |
| RWT | N | ↑ | ↑ | ↑↑ | N-↓ | ↓ |
| M/V | N | ↑ | ↑ | ↑↑ | N-↓ | ↓ |
| Systolic stress | N | N-↓ | V | ↓ | ↑↑ | ↑↑↑ |
| Systolic shortening | | | | | | |
| Endocardial | N | N | N-↓ | ↑↑ | N | ↓ |
| Midwall | N | N-↓ | ↓ | – | N | ↓ |

**Figure 9-10 LV volume, mass, and geometry, stress, and systolic shortening in various cardiac disorders.** Different cardiac disorders are classified with respect to LV mass, volume, relative wall thickness (*RWT*), and mass/volume (*M/V*) ratio, and stress and shortening as normal (*N*), increased (*up arrows*), or decreased (*down arrows*). *(Redrawn from Aurigemma GP, Gaasch WH, Villegas B, Meyer TE:* Curr Probl Cardiol *20:385, 1995.)*

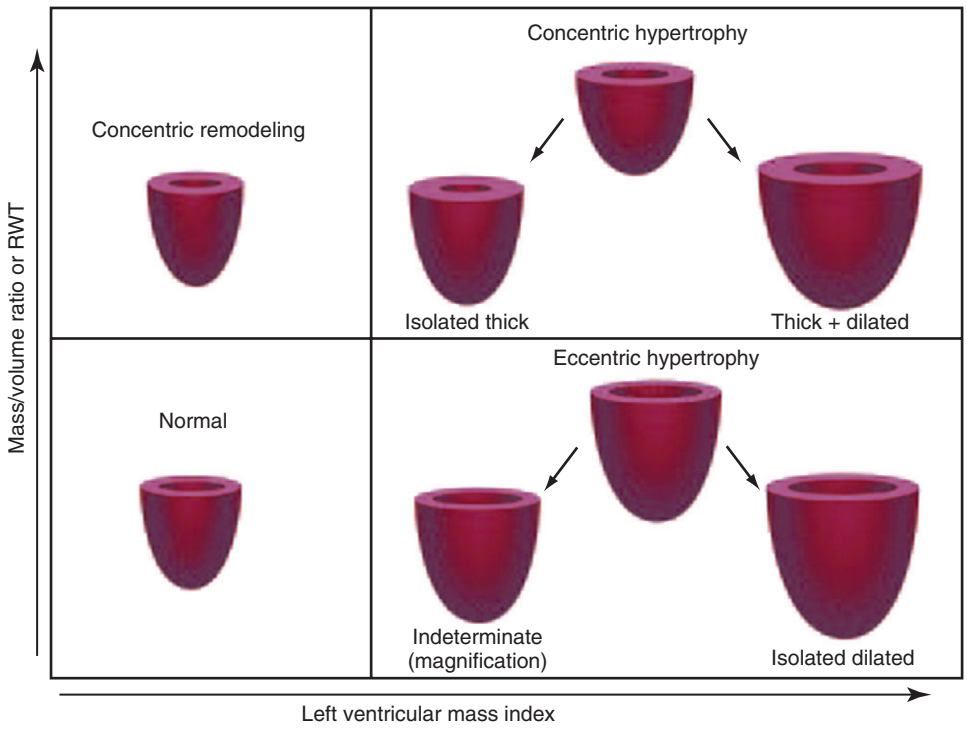



**Figure 9-11 Remodeling subtypes.** Individuals may be classified by presence or absence of LVH (horizontal axis) and by geometry (vertical axis), depending on mass-to-volume ratio. If mass-to-volume ratio is high, geometry is classified as concentric. The paradigm of Khouri and colleagues[54] subdivides the two LVH classes by whether chamber dilation is present. *RWT*, Relative wall thickness.

greater than 0.8 are uncommon in aortic stenosis, but when present, they appear to represent inappropriate hypertrophy.

The interaction among shape, load, and function is complex and important because each one may influence the others. A decompensated heart clearly demonstrates abnormalities of all three—low RWT, high afterload, and reduced function—yet it is not possible to state which abnormality is primary. Does the ventricle dilate, thereby raising afterload and reducing pump performance, or is shortening impaired first, leading to dilation, which then raises afterload? Human studies shed little light because of the lengthy time course of disease and other confounding factors; animal studies suggest that all three events may occur in concert.[58]

## TWO-DIMENSIONAL ECHOCARDIOGRAPHY

2D echocardiography permits acquisition of data with excellent spatial orientation because the LV can be sampled in real time at multiple levels. In many laboratories, therefore, 2D echocardiography is the principal noninvasive means for quantitation of LV volume and for the assessment of global and regional systolic function. LV mass and volume quantitation by 2D echocardiography requires high-quality images and true long- and short-axis images of the LV. A variety of geometric models are used to approximate the shape of the LV and to compute LV volumes, including the prolate ellipse model, the hemiellipse model, and others that represent a combination of geometric shapes. Detailed review of the geometric principles underlying these volumes for formulas may be found elsewhere.[49] This chapter emphasizes the applications most suited for clinical use.

### *Mass*

Theoretically, 2D echocardiographic assessment of LV mass can improve on the limitations of M-mode methods; mean wall thickness can be back-calculated from planimetered short-axis myocardial area, which helps avoid reliance on single-dimensional determinations. One of the most practical 2D methods for mass calculation, the area-length method, approximates the LV as a cylinder-hemiellipsoid; volume is calculated for both the inner and outer "shells" (the LV cavity and total myocardial area, respectively):

$$V = 5/6\ A \times L$$

in which *A* is planimetered short-axis area obtained at the high papillary muscle level, and *L* is the LV length obtained from the apical four-chamber view; area and length measurements are made at end-diastole. In this way, total LV and internal (LV cavity) volume are determined; myocardial volume is the difference between the inner and outer shells.[59] Myocardial volume is then multiplied by the specific gravity of myocardium (1.04 g/mL) to compute myocardial mass. The model has been validated by comparing echocardiographic and anatomic LV mass in 21 patients who underwent 2D echocardiographic studies shortly before death[60]; there was an excellent correlation between anatomic and echocardiographic mass (r = 0.93, standard error = 31 g). It is important to note that phantom-generated regression equations were used to correct clinical mass measurements for each 2D echocardiographic machine. Although more complicated 2D and 3D echocardiographic methods provide greater accuracy for LV mass determination, the 2D cylinder-hemiellipsoid area-length method represents a relatively simple and practical approach that yields acceptable results.[49]

### *Volume*

A variety of geometric approaches have been described for the quantitation of LV volume from 2D echocardiography. There are theoretical advantages for use of the Simpson's rule algorithm, and this approach is preferable when ventricular shape is distorted, such as with an apical aneurysm. The Simpson's rule approach, also known as the *method of disks,* is predicated on the fact that the volume of the whole LV (or of any object) may be computed as the sum of individual "slice" volumes. In general, the accuracy of the measurement varies directly with the number of slices:

$$V = \sum_{i=1}^{n} A_i T$$

*V* is total volume (cavity or myocardial), *A* is planimetered area, and *T* is slice thickness. Myocardial volume is then multiplied by the specific gravity of myocardium to estimate myocardial mass. It is best to compute LV volume from two orthogonal apical views with the LV length divided equally along that length[50,61]; apical four- and two-chamber views at end-diastole should be recorded to maximize ventricular length. The use of the cylinder-hemiellipsoid (area-length) method for calculating the volume component represents a reasonable alternative to the method of disks.

### *Geometry*

Compared with M-mode echocardiography, 2D echocardiography offers improved spatial orientation because the LV can be sampled in real time at multiple levels. Accordingly, 2D echocardiography may be used to quantify the LV mass and chamber volumes of abnormally shaped ventricles, and because measurements of LV length are possible, this technique provides more extensive description of LV geometry. Estimates of both the short-axis/long-axis ratio and the volume/mass ratio[62] are possible with 2D echocardiography. In patients with normal LV mass and function, the short-axis/long-axis ratio ranges from 0.45 to 0.62.[62-64] In untreated hypertensive patients with normal LV ejection fraction, the short-axis/long-axis ratios range from 0.52 ± 0.04 in patients with concentric remodeling to 0.63 ± 0.03 in patients with eccentric hypertrophy. The short-axis/long-axis ratio also provides information regarding ventricular compensation in valvular heart disease. As in patients with dilated cardiomyopathy, in whom the ventricle becomes more spherical, patients with poorly compensated aortic stenosis and aortic regurgitation (those with low EFs) tend to have higher short-axis/long-axis ratios.[64] A high ratio in turn alters the relationship of meridional to circumferential stresses, a change in the distribution of afterload that may affect overall pump performance.[64]

The end-diastolic volume/mass ratio in normal men and women, as defined by 2D echocardiography, is approximately 0.8.[63] It has been traditionally assumed that the ratio of LV volume to mass is relatively constant from the most basal to the most apical slices of the LV. A study using the technique of ultrafast computed tomography, which can provide approximately eight tomographic slices through the LV, showed that in normal subjects, the volume/mass ratio decreased from approximately 0.8 at the most basal slice, a finding consistent with results of 2D echocardiography, to approximately 0.25 at the most apical slice. LV mass exceeds LV volume at each slice location.[65]

It is important to emphasize that 2D echocardiographic methods have problems that limit their routine use for quantitation in the clinical setting[49] (Box 9-2). M-mode echocardiography samples at approximately 1000 frames per second, whereas the frame rate for 2D echocardiography is orders of magnitude less: 30 to 60 frames per second under optimal conditions. There is considerable image degradation when stop frames are used, making precise endocardial definition problematic. Near-field artifact and poor lateral resolution make it difficult to reliably identify endocardium around the entire ventricular perimeter. Apical views often do not yield images of sufficient quality for manual tracing, and computations tend to be tedious. The use of intravenous contrast has improved the accuracy of LV volume determinations. 3D echocardiography (see Chapter 4) has been shown to provide the most accurate ultrasound determination of LV volume, mass, and EF, largely because the need for geometric assumptions and on-axis views will be eliminated.[50,64-68]

**Box 9-2**

**LIMITATIONS OF ULTRASOUND METHODS FOR MASS AND VOLUME QUANTITATION**

**General**
- All methods require high-quality images with good endocardial definition.
- Most methods require geometric assumptions about LV shape and are applicable only to normally shaped hearts.

**M-Mode Echocardiography**
- Small errors in measurement may lead to large errors in mass/volume determinations.
- May be insensitive to small changes in mass (20 to 40 g) observed in response to antihypertensive treatment.

**Two-Dimensional Echocardiography**
- Limited frame rate, making timing of cardiac events difficult.
- Considerable degradation when images are stop-framed.
- Apical images may foreshorten true LV length.
- Tedious, labor-intensive computations.

## ALTERNATIVE METHODS FOR QUANTITATION OF LEFT VENTRICULAR STRUCTURE AND FUNCTION

In addition to cardiac ultrasound, the clinician may use other noninvasive and invasive techniques to measure LV size and function. A brief review of some of the more commonly used techniques is therefore appropriate.

### *Doppler Echocardiography*

Routine Doppler measurements of flow velocity may be combined with echocardiographic dimensional data to determine SV and cardiac output.[69,70] This technique is known as the velocity-time integral (VTI) method. The appeal of this method is that, unlike M-mode and 2D echocardiographic measurements, VTI measurements do not require geometric assumptions about cardiac shape.

To compute SV using the VTI method, an integral of the systolic pulsed-wave flow envelope in the aortic outflow tract is computed (Fig. 9-12). To obtain this velocity spectrum, the transducer is placed in the apical position with the sample volume positioned at the level of the aortic-valve annulus. Although the VTI may be obtained in other locations, such as the pulmonary artery or LV inflow across the mitral valve, accuracy seems to be best with measurements made in the proximal ascending aorta. The cross-sectional linear dimension of the proximal ascending aorta is obtained in the same approximate location where the pulsed- or continuous-wave Doppler velocity spectrum is recorded, using the parasternal long-axis window. SV is then the product of the VTI and CSA of the aortic annulus, which is assumed to be circular:

$$CSA = \pi(D/2^2)$$

$$SV = CSA \times VTI$$

in which *CSA* is the cross-sectional area of the aortic annulus, *D* is the linear dimension of the annulus, and *VTI* is the

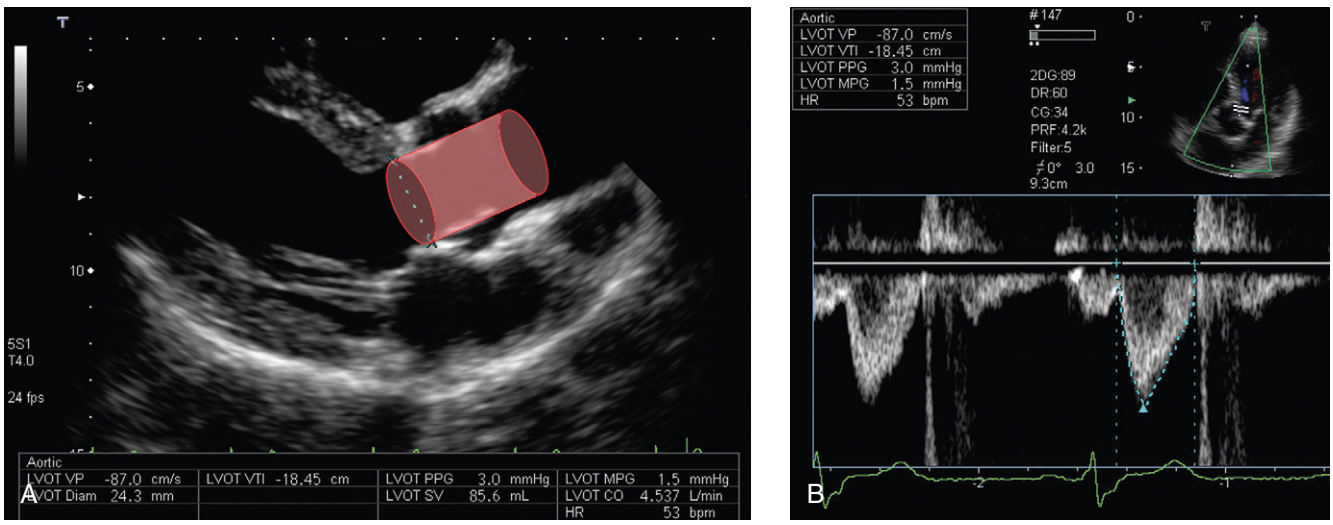



**Figure 9-12 Calculation of cardiac output using the velocity-time integral (VTI) method.** The pulsed-wave Doppler-derived VTI is displayed. The LV outflow tract (*LVOT*) dimension is approximately 24 mm, and radius 12 mm. π times the square of the annular radius yields the LVOT cross-sectional area, and the VTI is 18.5 cm by planimetry. The stroke volume is 84 mL per beat (LVOT cross-sectional area multiplied by the VTI) and yields a cardiac output of 4.5 L/min at the patient's heart rate of 53 bpm.

velocity-time integral. SV and cardiac output obtained by the VTI method correlate well with results of concurrent thermodilution cardiac output determinations in patients who were without left-sided valvular regurgitation.[69,70] The Doppler VTI method is highly dependent on accurate measurements of aortic annular diameter because the CSA formula involves squaring the annular dimension; it is also assumed that the Doppler beam is oriented parallel to flow. This method also requires that there be no significant aortic or mitral valve disease. This method can be particularly useful for following changes in a single patient—beat to beat, or over weeks to months.

Doppler echocardiographic assessments of LV function do not depend on measurements of ventricular size (and thus avoid the attendant geometric assumptions and sources of error); they rely on information derived from flow velocities.[71] This information includes measurement of LV SV, cardiac output, and peak flow velocity of aortic ejection, all of which, being ejection phase indices, are dependent on afterload. Another Doppler approach to evaluation of systolic function is to measure the rate of rise of ventricular pressure ($dP/dt$) from the continuous-wave profile of the mitral regurgitant flow.[72]

### *Magnetic Resonance Imaging*

In many respects, MRI is the ideal method to quantitate LV mass and volume and is considered the reference standard for LV quantitation.[66,73] It combines the attributes of ultrafast computed tomography (noninvasive and permitting true tomographic imaging throughout the entire cardiac volume) with several unique advantages. MRI does not require contrast administration or ionizing radiation, and there is no limitation to image plane selection; thus, the heart may be imaged not only in the familiar contrast ventriculography views but also in the long- and short-axis planes used in standard transthoracic echocardiography. MRI usually provides images with excellent contrast between myocardium and the blood pool so that manual or even semiautomated computerized mass and volume quantitation is possible.[74,75] For these reasons, MRI has provided the most accurate noninvasive estimates of LV mass and volume to date, even in ventricles distorted by myocardial infarction.[76] Gradient echocardiographic techniques display the heart in cineloop fashion at up to 64 frames per cardiac cycle. This technique can be used to quantitate EF and regional function and to estimate the severity of valvular regurgitation.[77]

## Assessment of Left Ventricular Systolic Function

The major factors affecting LV systolic performance and function are preload, afterload, myocardial contractile (or inotropic) state, and heart rate. Nonuniform contraction can also be important; thus, regional variations in mechanical function, as occur in coronary heart disease or even with electronic ventricular pacing, can affect SV. Only if synchronous contraction is present, heart rate is stable, and loading conditions are constant does a change in performance indicate a change in contractility. These traditional concepts relating preload, afterload, and contractility are generally considered in the assessment of an acute response to altered hemodynamic conditions. Thus, an isolated increase in preload is said to produce an increment in performance through the Frank-Starling mechanism, whereas an isolated increase in afterload is said to produce a decrease in the SV (or EF) by virtue of the inverse force-shortening relation. Unfortunately, in the intact heart, especially in patients with chronic heart disease, it is virtually impossible to produce an *isolated* change in preload or afterload. For example, nitrates are classified as vasodilators and agents that primarily affect preload, but the associated decrease in LV volume and arterial pressure leads to a reduction in afterload. Likewise, a pure arterial vasodilator also reduces heart size (and preload) by augmenting the SV. It is apparent, therefore, that preload and afterload are intimately related, and that it is an oversimplification to assume that isolated changes in preload or afterload occur in patients with chronic heart disease.

Most interventions that produce an acute change in preload or afterload also result in a length-dependent change in intrinsic myocardial contractility,[78] which further complicates the assessment of global systolic function. Therefore, acute changes in preload produce changes in performance through the Frank-Starling mechanism *and* through this length-dependent activation. The importance of this phenomenon in the chronically enlarged or diseased heart is unknown.

It is usually not difficult to detect an acute change in LV performance or contractile function, but it is harder to determine the major mechanism or mechanisms responsible for the change. Chronic changes in LV volume, mass, and geometry are even more difficult to interpret because such changes tend to limit our use of the traditional interrelationships of preload, afterload, and contractility. Indeed, there is no acceptable index of basal contractility that can be used in patients with chronic heart disease, nor can LV end-diastolic pressure or even absolute EDV be used as a surrogate for fiber stretch in chronically diseased hearts. For these and other reasons, the evaluation of contractile function and the distinction between a compensated and a decompensated ventricle often rest on empiric observations coupled with analyses based on physiologic principles. In the following section, the use and limitations of several clinically useful approaches to the evaluation of contractile function are discussed (Box 9-3).

### EJECTION FRACTION

The EF is the most widely used measure of LV systolic function. This parameter is defined as the change in LV volume (i.e., SV) divided by the initial volume (i.e., EDV):

$$EF = (EDV - ESV)/EDV$$

in which *EDV* is end-diastolic volume and *ESV* is end-systolic volume; these may be obtained by either M-mode or 2D echocardiography.[50] The EF, representing volume strain, is appropriately normalized; it can be used as an index of systolic function that is independent of the size of the patient or the ventricle.

The normal ventricle ejects more than half of its EDV; the average EF, as determined by 2D echocardiography, varies from 63% to 69%.[50] In patients with coronary disease or idiopathic

**Box 9-3**

**CLINICAL METHODS USED TO EVALUATE SYSTOLIC FUNCTION**

Ejection fraction
Fractional shortening at endocardium and midwall
Stress-shortening relations
Pressure-volume analysis

cardiomyopathy, it is generally conceded that values in the range of 40% to 50% are abnormal but of little clinical significance.[6] However, in patients with mitral regurgitation, an EF in this range may denote significant depression in contractile function.[79]

### *Hemodynamic Determinants of the Ejection Fraction*

Acute changes in LV loading conditions are known to exert a major influence on the EF. Thus, an acute increase in preload and/or a decrease in afterload results in a higher EF. By contrast, an acute decrease in preload and/or an increase in afterload reduces the EF. Under such circumstances, it can be difficult to decide whether a change in contractility has occurred. If, however, alterations in load are associated with a change in the EF that is opposite to the expected result, it is possible to conclude that a simultaneous change in contractility (i.e., inotropic state) also occurred. For example, an increased EF in the presence of increased afterload likely represents increased contractility because an increase in afterload would normally be expected to cause a lower EF. Despite its load sensitivity, the EF can therefore provide useful information, even during acute hemodynamic interventions. In this regard, the concept of preload reserve is important.

In patients with chronic heart disease, the EF can be an important index of contractile function, in part because of its sensitivity to increased afterload. As LV dysfunction develops and dilation occurs, afterload tends to increase, as dictated by the Laplace relationship, and the EF falls. Such a decline in the EF can be useful in identifying LV dysfunction early in the course of a disease; it does not, however, identify the underlying mechanism or mechanisms. Therefore, in patients with chronic heart disease, the EF must be interpreted with consideration of the magnitude and time course of changes in loading conditions that evolve during progression of the disease. For example, early in the course of aortic regurgitation, LV preload and afterload tend to be increased; these changes affect the EF in opposite directions, and it remains within the normal range. As the ventricle remodels and eccentric hypertrophy develops, the loads normalize despite LV enlargement; if myocardial contractility is preserved, the EF remains normal. As the hemodynamic burden increases (or contractile dysfunction develops), the afterload increases and the EF decreases. Thus, even a modest decline in the EF can be an important early marker of LV dysfunction.

In decompensated aortic stenosis, LV systolic pressures increase in parallel with an increase in wall stress, as predicted by the Laplace relationship. As wall stress progressively rises, EF decreases. Carabello and colleagues[16] have shown that patients with critical aortic stenosis, congestive heart failure, and decreased EF owing to high levels of wall stress ("afterload mismatch") may anticipate improvement in systolic function following afterload reduction associated with valve replacement[16,79,80]. By contrast, those patients whose reduction in EF is out of proportion to the high levels of wall stress are thought to have developed cardiomyopathic changes in addition to excess afterload; such patients generally do not experience functional improvement after valve replacement.[16,80] This subgroup of patients may be identifiable by a low transvalvular gradient (usually less than 30 mm Hg) in association with severe stenosis of the aortic valve.[16] In the clinical setting, making the proper diagnosis can be challenging. Because the Gorlin equation is flow dependent, patients with primary LV dysfunction and coexistent (mild) calcific aortic stenosis can be difficult to distinguish from those with LV dysfunction caused by unrelieved severe aortic stenosis (See Chapter 23.) Dobutamine echocardiography is used to help make this distinction and to assess prognosis.[81]

## FRACTIONAL SHORTENING AND RELATED INDICES

The fractional change (percentage) in minor-axis dimension is a widely used index of systolic performance; fractional shortening is usually derived from M-mode echocardiographic tracings (Fig. 9-13). This measurement is particularly useful because LV circumferential fiber shortening is responsible for most of the SV. In this regard, fractional shortening is similar to the EF; in the absence of focal wall motion abnormalities, the two indices correlate closely, although the absolute values for fractional

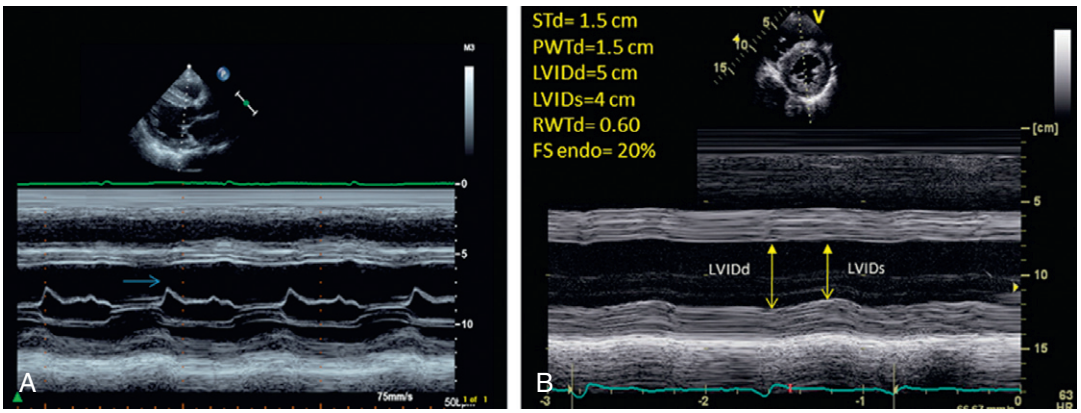



**Figure 9-13 M-mode echocardiographic findings in systolic dysfunction.** Although M-mode is not currently used as the principal means to assess LV systolic function, it can furnish important data. **A,** M-mode obtained in a patient with dilated cardiomyopathy. Poor stroke volume shown by exaggerated separation between the most anterior excursion of the anterior leaflet of the mitral valve and the interventricular septum (E-point septal separation—*arrow*). **B,** From a patient with systemic amyloidosis. Image shows thick walls, high ratio of wall thickness to cavity dimension (relative wall thickness, RWT), and reduced endocardial fractional shortening. The constellation of thick walls, high RWT, nondilated LV cavity, and poor fractional shortening should always prompt consideration of amyloid cardiomyopathy.

shortening are obviously less than those for EF. Fractional shortening, measured at the endocardium ($FS_{endo}$ [%]), is calculated as

$$FS_{endo} = 100 \times (LVID_d - LVID_s)/(LVID_d)$$

Normal values for $FS_{endo}$ exceed 25%.[49] As is the case with EF, $FS_{endo}$ is influenced by factors in addition to contractile state and should be interpreted in the light of loading conditions; increases in preload and decreases in afterload increase fractional shortening.

A refinement of fractional shortening, the velocity of circumferential shortening ($V_{cf}$) reflects the mean velocity of ventricular shortening at the level of the LV minor axis, and it is also calculated from M-mode echocardiographic dimensions:

$$V_{cf} = FS_{endo}/ET$$

in which *ET* is the ejection time derived from the duration of aortic valve opening, from the period of aortic forward flow (pulsed-wave or continuous-wave Doppler), or from a carotid pulse tracing. The $V_{cf}$ is expressed in circumferences per second (the lower limit of normal is 1.1 c/s). Because $V_{cf}$ measures the velocity rather than the extent of shortening, it is theoretically a more sensitive index of contractility than $FS_{endo}$ and may be an earlier marker of abnormality in chronic disease states. As with the EF and fractional shortening, this parameter is normalized for LV chamber size and may be used to make comparisons between patients. $V_{cf}$ has been shown to be relatively insensitive to acute changes in preload.[82,83] However, it is also possible that this preload insensitivity may be a result of acute elevations in preload increasing heart size (and pressure) and thus increasing afterload. Thus, augmentation in afterload may offset the increased shortening caused by the increased preload. A further refinement in $V_{cf}$, the rate-corrected $V_{cf}$,[84] may be obtained by dividing $V_{cf}$ by the square root of the preceding RR interval. This index is designed to allow comparison between patients with differing heart rates. The incremental value of velocity of shortening methods (e.g., $V_{cf}$, rate-corrected $V_{cf}$) compared with extent of shortening (e.g., fractional shortening) may be marginal.[85]

Standard M-mode measurements also may be used to estimate circumferential fractional shortening at the midwall ($FS_{mw}$ [%]), using the same standard M-mode echocardiographic measurements. $FS_{mw}$ is calculated using a modified two-shell cylindrical model.[86] This method assumes constant LV mass throughout the cardiac cycle and does not require the assumption that inner and outer wall thickening fractions are equal.[74,87] Most important, in contrast to $FS_{endo}$, $FS_{mw}$ is not influenced by LV geometry (RWT) and therefore has particular use in the evaluation of the hypertrophied heart with increased RWT.

Normal systolic function includes the excursion of the mitral annulus toward the relatively immobile apex; thus, the long axis of the LV shortens during systole. An assessment of the longitudinal (or long-axis) shortening of the LV can be made using M-mode measurements under 2D echocardiographic guidance.[88] Using the apical window, the transducer is oriented to maximize apical endocardial to mitral annular distance. M-mode tracings are made with the cursor directed through the lateral aspects of the mitral annulus; recordings of multiple cardiac cycles are made on strip chart paper,[88] and mitral annular excursion is normalized for initial diastolic length.

Several investigators have used mitral annular excursion and long-axis shortening as a descriptor of ventricular systolic function. Keren and LeJemtel[71] showed that the principal systolic mitral annular excursion toward the apex coincides with the systolic component of pulmonary venous flow; this systolic phase of mitral annular motion is markedly attenuated in patients with dilated cardiomyopathy. Jones and Gibson[88] showed that in the normal LV mitral annular excursion toward the apex precedes circumferential shortening, which leads to a more spherical LV shape early in systole.[88] These investigators also showed that mitral annular descent was reduced in patients with mitral disease who had undergone valve replacement.[71] In patients with "compensated" hypertensive heart disease, that is, LV hypertrophy and normal EF, long-axis shortening is depressed compared with normal controls.[71] Similar findings have been reported using the technique of strain imaging and MRI tagging, as will be described later.[89,90]

Other ultrasound techniques have been employed in recent years to investigate LV systolic and diastolic function. The timing of ventricular ejection and relaxation can be used to derive a combined index of ventricular function (Fig. 9-14).[89] Doppler tissue imaging applies a modification of pulsed Doppler methods to the assessment of myocardial systolic motion.[91,92] In this way, the velocity of myocardial tissue or of the mitral annulus, and not just the total excursion, may be measured. The velocity of the diastolic mitral annular motion has been applied to the study of LV diastolic function (see Chapter 11). This technique is now being employed to evaluate the extent of systolic dyssynchrony and to evaluate the appropriateness of biventricular pacemaker implantation, as described in Chapters 10 and 26.

## STRESS-SHORTENING RELATIONS

On the basis of extensive experimental and clinical experience, the myocardial force-velocity relation provides a framework for evaluating the contractile state and function of the LV. A most important advantage of assessing function with a stress-shortening analysis is that it avoids afterload dependency, the major limitation of the EF alone. Unfortunately, end-diastolic

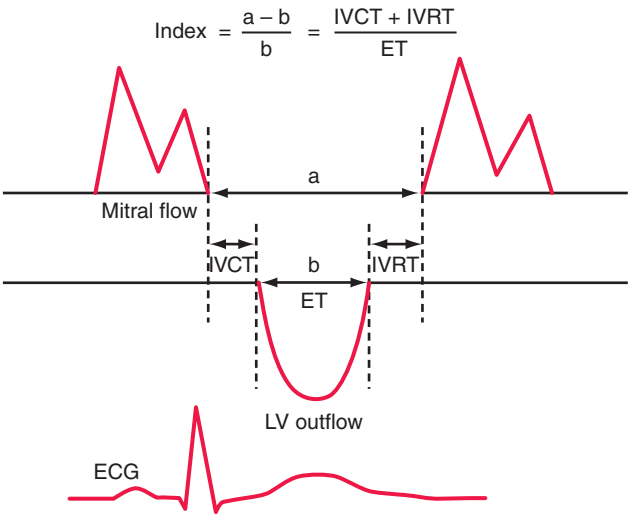



**Figure 9-14 Principle of the Tei (myocardial performance) index.** The index is calculated as the sum of isovolumic contraction time (*IVCT*) and isovolumic relaxation time (*IVRT*) divided by ejection time (*ET*). In the extreme, a heart that has very long isovolumic times compared to the ET has very poor performance. *ECG*, Electrocardiogram. *(From Tei C. New non-invasive index for combined systolic and diastolic ventricular function. J Cardiol 26:135-136, 1995.)*

fiber length (or the degree to which the resting fiber is stretched) is difficult if not impossible to measure; LV end-diastolic pressure, EDV, or even wall stress fails to provide an absolute measure of fiber length. For this reason, length is generally omitted and the simpler force-velocity or stress-shortening relation is used as a substitute for the force-length-velocity relation.

Both systolic stress (the force per unit CSA of myocardium) and shortening (fractional change in length or volume) are appropriately normalized and allow accurate comparisons among hearts of different sizes.[75] Therefore, contractile function in pressure overload hypertrophy, volume overload hypertrophy, and dilated and hypertrophic cardiomyopathies may be assessed within the framework of the stress-shortening relation (Fig. 9-15).

A major limitation of the simple stress-shortening analysis is the assumption that differences in resting length do not substantially influence the stress-shortening relation. In this regard, a distinction must be made between acute interventions and chronic steady-state conditions. Changes in fiber length and appropriate use of preload reserve certainly occur during acute or short-term hemodynamic interventions. However, under chronic conditions (e.g., chronic compensated volume overload), this may not be the case.[93] After the acute or subacute phase, when the compensatory remodeling process is complete and chronic changes in LV volume and mass are established, end-diastolic fiber length may not be substantially different from normal.[94] In pressure overload or concentric hypertrophy, end-diastolic sarcomere lengths may even be less than normal.[95,96] In such hearts, high chamber stiffness apparently limits use of the preload reserve. It appears, therefore, that assumptions about chronic changes in fiber length are unwarranted.

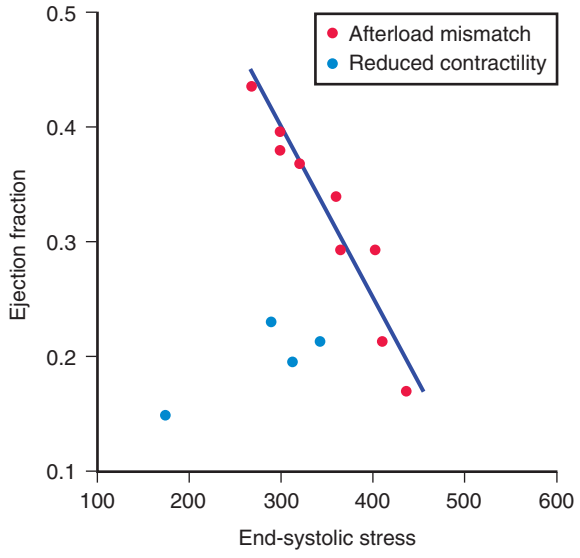



**Figure 9-15 Relationship between ejection fraction (EF) and end-systolic stress in patients undergoing cardiac catheterization for critical aortic stenosis and severe congestive heart failure.** All patients were free of significant coronary artery disease. Patients falling close to the regression line relating EF to stress (*red circles*) are thought to have LV dysfunction owing to excessive wall stress (afterload). These patients experienced a gratifying functional recovery after aortic valve replacement. In contrast, the four subjects who fell below the regression line (*blue circles*) have depressed EF beyond that predicted by the level of afterload and are considered to have depressed contractility as well. These patients did not experience functional recovery after valve replacement. *(Adapted from Carabello BA, Green LH, Grossman W, et al: Hemodynamic determination of prognosis of aortic valve replacement in critical aortic stenosis and advanced congestive heart failure.* Circulation *62:42, 1980. In Aurigemma GP, Gaasch WH, Villegas B, Meyer TE:* Curr Probl Cardiol *20:416, 1995.)*

## *Midwall Stress-Shortening Analysis*

The analysis of midwall stress-shortening relations may be superior to that of endocardial stress-shortening relations, especially for comparison of contractile state between hearts differing in LV geometry (Figs. 9-16 and 9-17). The first advantage

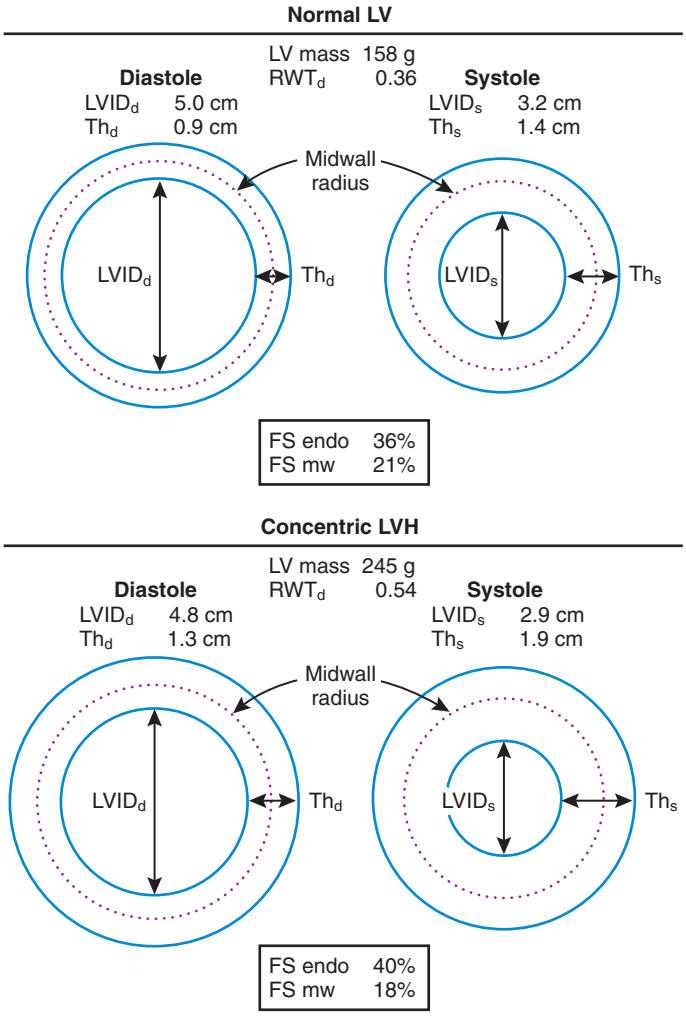



**Figure 9-16 Relationship between LV shortening and LV hypertrophy.** LV shortening in a normal LV (*top*) and with concentric LV hypertrophy (*LVH*) (*bottom*), illustrating the added insight into systolic function provided by midwall shortening. LV endocardial dimension (*LVID*), wall thickness (*Th*), relative wall thickness (*RWT*), and LV mass are measured in diastole (*d*). Systolic dimensions (*s*) are shown at *right*. Midwall circumference indicated by *dotted line*. Systolic shortening refers to percent reduction in circumference that occurs from diastole to systole. *FS endo*, percent reduction of endocardial circumference (*dark inner circle*), and *FS mw*, percent reduction of midwall circumference (*dotted line*), are in normal range. However, concentric LVH (elevated relative wall thickness dimension *RWTd* and LV mass) is associated with an increased value for FS endo, but a diminution in FS mw, compared with normal LV, owing to the nonuniformity of systolic thickening. Myocardial fibers in the inner (subendocardial) layers contribute more to systolic thickening than those in the outer (epicardial) layers; this effect is exaggerated when concentric geometry is present.

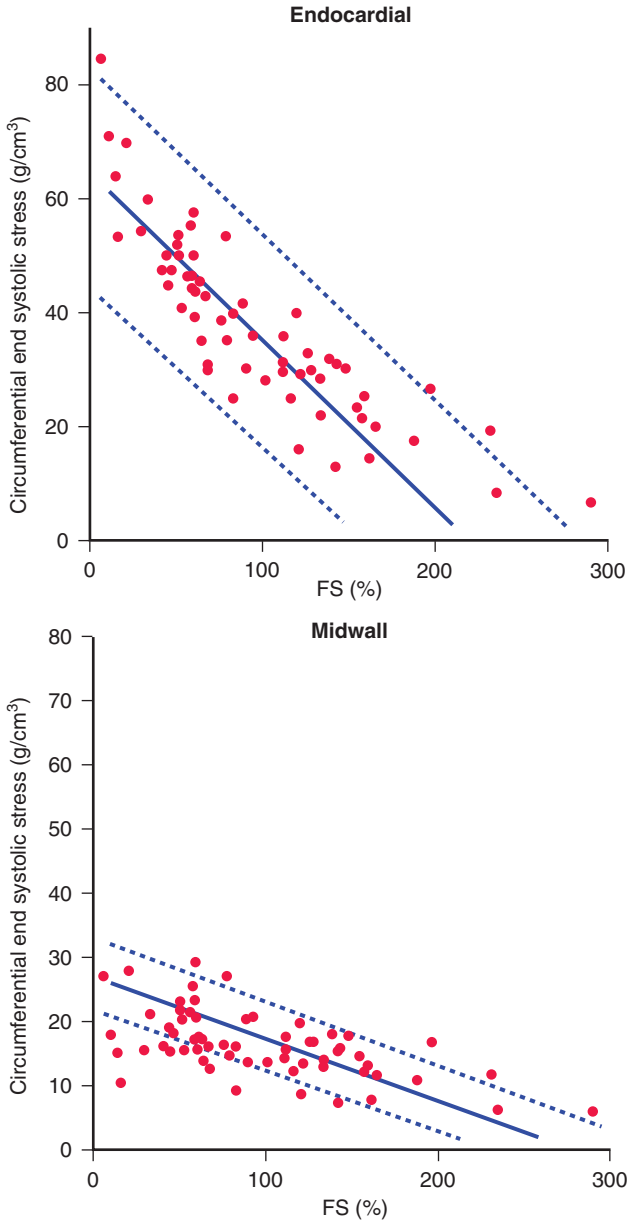



**Figure 9-17 Endocardial and midwall stress-shortening relations in pressure overload hypertrophy.** *Top* panel: Fractional shortening (FS) at the endocardium versus circumferential stress in a consecutive series of patients with severe, symptomatic aortic stenosis who were free of segmental wall motion abnormalities. All patients fall within the 95% confidence intervals of the stress-shortening relationship, suggesting normal contractile function. In contrast, the *bottom* panel shows midwall shortening versus circumferential stress in the same population. A substantial portion (approximately one third) of these patients demonstrates a diminution in contractility by midwall analysis.

of midwall measurements is that the (circumferential) stress vector and the shortening transient are oriented in the same direction because circumferential fibers predominate in the midwall of the LV.[30]

Second, the values for midwall (but not endocardial) shortening are consonant with experimental data indicating that myocardial fibers shorten by approximately 15% to 20%. Circumferential midwall strain ranges from 9% ± 2% in the anesthetized, open-chest dog (implanted markers)[97] to 30% ± 7% in conscious humans (MRI tagging).[97a] We believe that the experimental results represent an underestimate of strain, but MRI techniques likely overestimate true myocardial shortening. All methods indicate that circumferential shortening at the endocardium exceeds that seen at the midwall. We believe that studies designed to assess myocardial contractile function should ideally be based on midwall stress-shortening data and not on endocardial shortening parameters, which may be contaminated by altered ventricular geometry.

An example of the usefulness of a midwall stress-shortening analysis is shown in Figure 9-18. The endocardial stress-shortening relation is normal in patients with pressure overload hypertrophy owing to aortic stenosis; thus, LV function is normal. By contrast, the midwall stress-shortening relation is abnormal in approximately one third of the patients, indicating a subtle depression of myocardial function in these individuals.[74]

In the past decade, there have been many studies of strain imaging techniques[91,92,98-101] (see Fig. 9-18). A variety of techniques are now in use for the assessment of regional and global systolic and diastolic function and are covered in detail in Chapter 10. Strain imaging has as a principal virtue the ability to assess regional systolic function and may be one day be used to lessen the subjectivity involved in gauging wall motion in the clinical arena. Normal strain values have been derived—and there have also been applications to systemic disease, such as hypertensive disease. It is important to realize that, like all systolic function parameters, systolic strain is inversely proportional to the level of afterload (Figs. 9-19 and 9-20).

## PRESSURE-VOLUME ANALYSIS

By plotting LV pressure against volume throughout the entire cardiac cycle, a P-V loop can be generated (Fig. 9-21). The height of the loop is determined by systolic pressure, and its width is determined by SV; thus, the area within the loop is a measure of stroke work. By definition, such loops incorporate EDV and ESV; thus, the SV and the EF are displayed. The bottom limb of the loop (i.e., the diastolic P-V curve) describes ventricular diastolic compliance. Therefore, the P-V loop can provide a simple yet comprehensive description of ventricular pump function.[102] Such loops can be generated from a variety of techniques that provide ventricular volume data in conjunction with LV pressure.[84,103,104] Online, beat-to-beat determinations of LV volumes with automated edge detection can be combined with LV pressure measurements to yield real-time pressure-volume loops, useful in both clinical and research settings[104,105] (Fig. 9-22).

By manipulating LV volume and/or arterial pressure, multiple coordinates of the maximal ratio of pressure to volume or dimension (which occurs near end-ejection) can be obtained; these coordinates exhibit a nearly linear direct relation. The slope of this relation ($E_{max}$) is relatively insensitive to acute changes in loading conditions. The relation shifts upward and to the left during positive inotropic interventions, and it shifts downward to the right when the ventricle is depressed; the slope of the relation generally increases with the former and decreases with the latter (Figs. 9-23 and 9-24).

This end-systolic index of contractility is sensitive to acute changes in contractility, but its reliability is diminished in chronically diseased hearts, especially dilated hearts. In large ventricles, the end-systolic P-V curve can be displaced down and to the right (depressed $E_{max}$), in the absence of a depressed

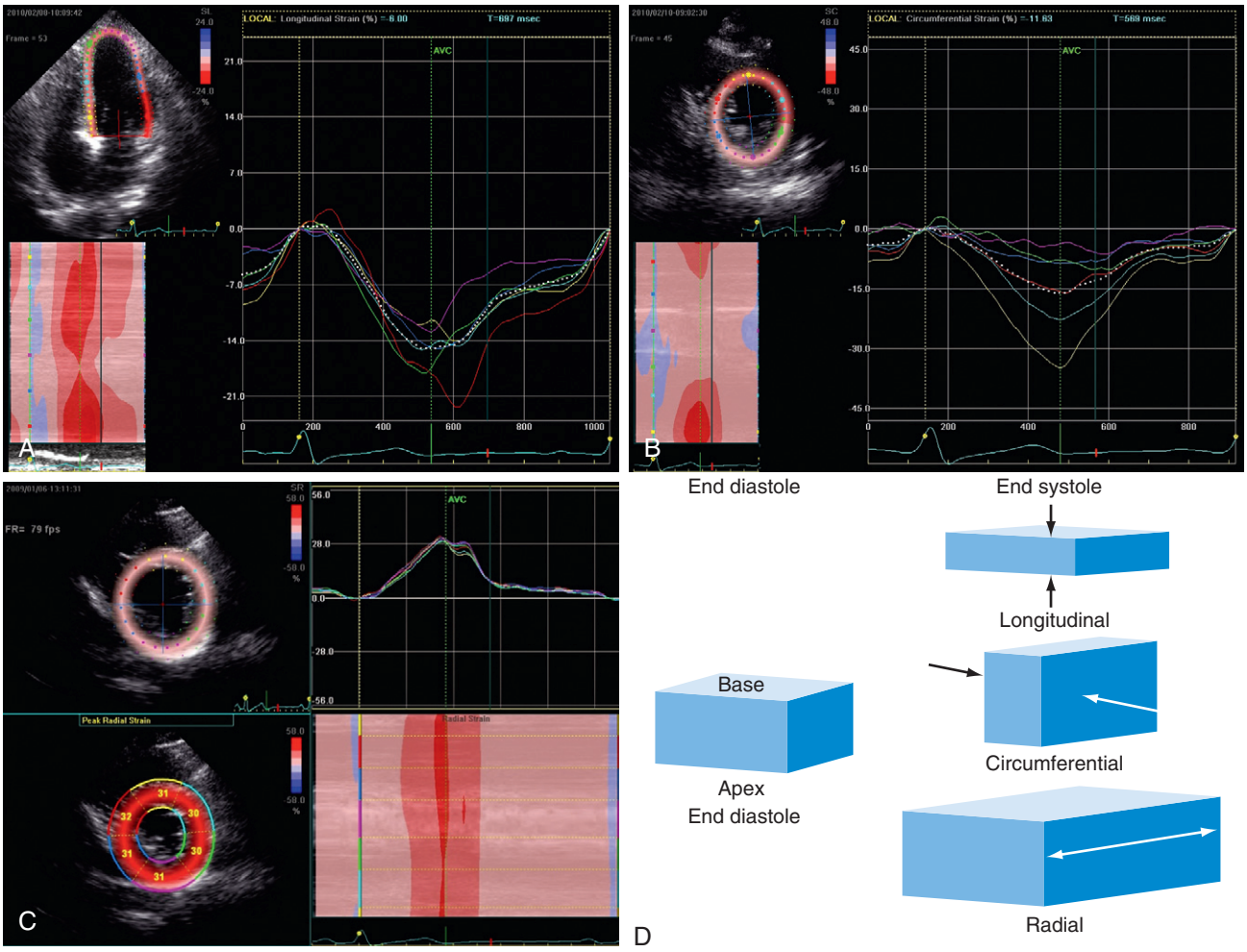



**Figure 9-18** **Principal strains.** Three principal systolic strains from a normal subject. **A,** Typical longitudinal strains related to long-axis shortening. Average systolic longitudinal strain in this example is 15%, though there is regional heterogeneity. Each colored curve represents average longitudinal strain in that segment. Parametric display shows that this strain is negative, indicating compression of myocardium in systole. **B,** Circumferential strain, which, like longitudinal strain, is negative, indicating compression of myocardium in circumferential plane. Average circumferential strain is likewise 15% in this normal individual. **C,** Radial strain, which represents wall thickening and is therefore positive in this parametric display. **D,** Schematic showing the three principal strains. During systole, a cube of myocardium deforms along its long axis (longitudinal shortening), along its circumference (circumferential shortening) and therefore the cube thickens along its endocardial to epicardial axis (radial strain, or thickening).

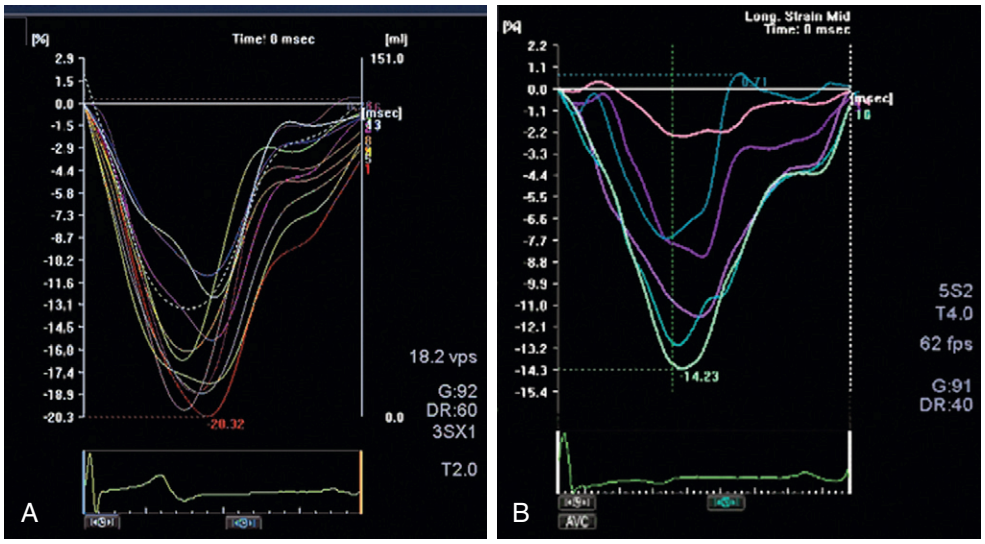



**Figure 9-19** **Strain imaging in hypertensive heart disease. A,** Normal longitudinal strain contrasted with (**B**) strain display from a 43-year-old hypertensive man. LV mass index was elevated as was relative wall thickness; ejection fraction was estimated at 45% by modified Simpson's rule. Strain curves display mild global depression in longitudinal shortening with some regional heterogeneity. Patient underwent subsequent magnetic resonance imaging, which showed scattered areas of delayed hyperenhancement. Catheterization demonstrated no obstructive coronary artery disease and myocardial biopsy was consistent with hypertensive heart disease. *(Adapted from Bogaert J, Rademahers F: Regional non-uniformity of normal adult left ventricle.* Am J Physiol Circ Physiol *280:H610-H620, 2001.)*

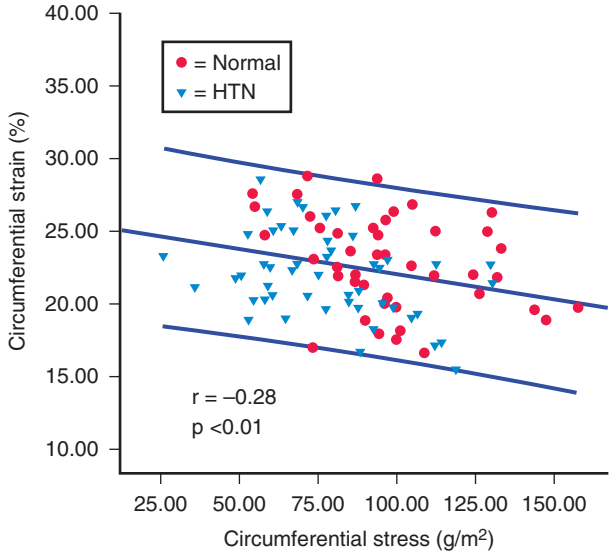



**Figure 9-20** **Load dependency of strain.** Relationship between circumferential strain and circumferential end-systolic stress. As expected, there is a negative correlation, indicating that strain is not load independent. *HTN*, Hypertension. *(From Narayanan A, Aurigemma GP, Chinali M, et al: Cardiac mechanics in mild hypertensive heart disease: a speckle-strain imaging study.* Circ Cardiovasc Imaging *2:382-390, 2009.)*

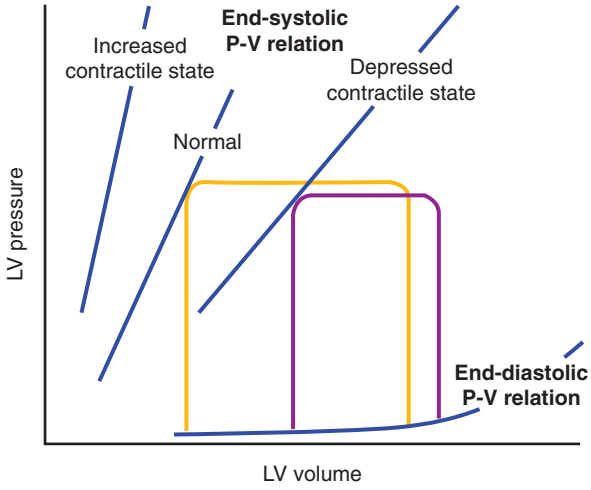



**Figure 9-21** **LV pressure-volume (P-V) loops.** *Yellow* loop indicates normal ventricle. Acute decrease in contractile state shown in *purple*; the loop is displaced to the right, and the end-systolic P-V line shifts downward and to the right. Effect of an acute increase in contractile state is illustrated by the line at *left*; slope of the end-systolic P-V line is increased (corresponding loop is not shown). *(From Aurigemma GP, Gaasch WH, Villegas B, Meyer TE:* Curr Probl Cardiol *20:418, 1995.)*

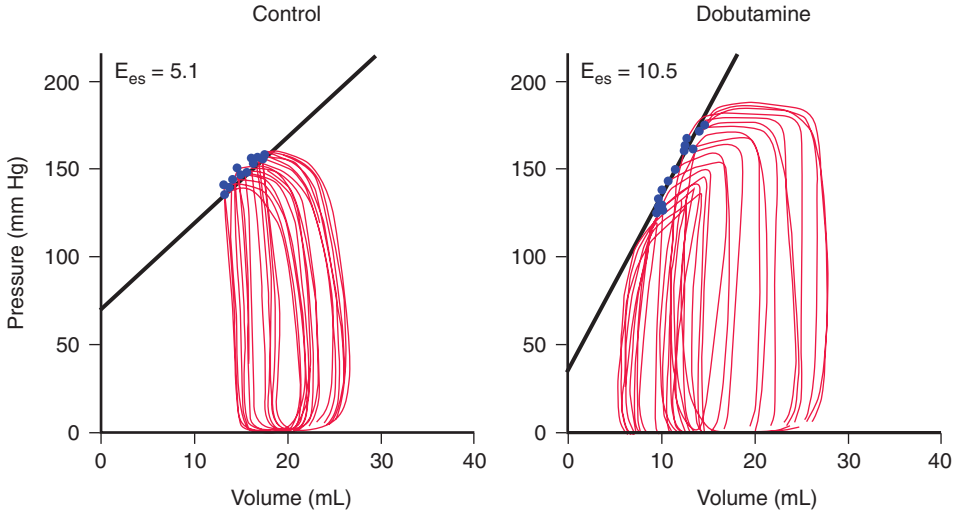



**Figure 9-22** **Pressure-volume loops with inferior vena caval occlusion at baseline and with 3 µg/kg/min of dobutamine infusion in an intact canine model.** Volume assessed online with transesophageal echocardiographic border detection using a Simpson's rule algorithm. End-systolic elastance ($E_{es}$) or the slope of the end-systolic pressure-volume (P-V) relation, increased with positive inotropic modulation, which is consistent with increased contractility. *(Courtesy Dr. John Gorcsan III.)*

contractility. For this reason, $E_{max}$ should be normalized for heart size,[106,107] as illustrated in Figure 9-23. In this example of chronic aortic regurgitation, there is modest LV enlargement, the ESV is less than 60 mL/m$^2$, the EF is normal, and the total SV is high. Such data indicate that the ventricle is compensated, albeit larger than normal. However, the depressed slope of the end-systolic P-V relation inappropriately suggests depressed contractility. These disparate conclusions can be reconciled if the effect of chamber dilation on $E_{max}$ is considered.[107] Thus, if the slope is normalized for chamber size, it approximates that seen in the normal heart.

Recognizing this limitation, end-systolic stress-volume or stress-dimension relations should not be a major criterion for the diagnosis of chronic contractile dysfunction. Certainly, they are not useful as a measure of basal contractility, and they have limited applicability in comparisons among normal and diseased hearts. The raw P-V or stress-dimension data provide important diagnostic information, and, with few exceptions, the simple measurement of the ESV or dimension identifies a depressed ventricle.

An example of the usefulness of echocardiography pressure-dimension loops is shown in Figure 9-24. This example

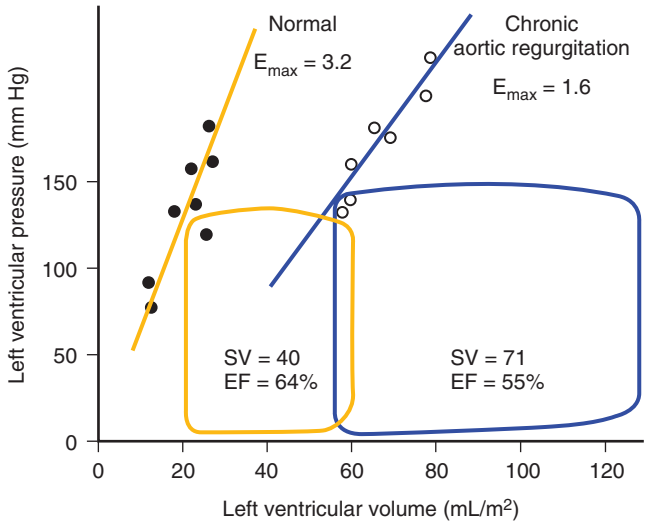



**Figure 9-23 LV pressure-volume loops and end-systolic pressure-volume lines illustrate effects of chronic aortic regurgitation on ventricular size and function.** Moderate ventricular enlargement is present, ejection fraction (*EF*) is normal, and stroke volume (*SV*) is high. Data are consistent with compensated aortic regurgitation. However, slope of the end-systolic pressure-volume relation ($E_{max}$) is reduced. This apparent inconsistency may be resolved by considering the effect of chamber size on $E_{max}$. If slope is normalized for chamber size (end-diastolic volume), result indicates that $E_{max}$ is similar in the two ventricles. *(Adapted from Shen WF, Roubin G, Choong CYP, et al: Evaluation of relationship between myocardial contractile state and left ventricular function in patients with aortic regurgitation.* Circulation *71:31-38, 1985. In Aurigemma GP, Gaasch WH, Villegas B, Meyer TE:* Curr Probl Cardiol *20:420, 1995.)*

illustrates the effect of mitral valve replacement on LV size and function in compensated and decompensated chronic mitral regurgitation. In compensated mitral regurgitation, the chamber is enlarged but the end-systolic dimension is only 42 mm, systolic stress is minimally increased, and the fractional shortening is normal (35%). After valve replacement, the stress-dimension loop returns to near normal. In decompensated mitral regurgitation, the EDV and ESV are markedly increased and fractional shortening is low (26%). After mitral valve replacement, there is persistent LV enlargement and a further decline in shortening. A similar analysis has been used in patients with aortic regurgitation.[108] (See Chapter 20.)

## Potential Limitations

It is worthwhile to briefly reiterate some of the practical limitations of echocardiographic evaluation of LV structure and function. It is axiomatic that quantitation of mass and volumes requires high-quality echocardiographic images, with good endocardial definition. For a variety of reasons, such high-quality images may not be available in many patients encountered in clinical practice. As noted previously, M-mode (and most 2D) quantitative methods require that the ventricle not have major shape distortion. Meticulous attention to beam orientation is also imperative for M-mode quantitation of the LV. Every millimeter of inaccuracy in LV chamber dimension results in an 8-g difference in LV mass[109]; a 1-mm inaccuracy in LV wall thickness measurement results in a 15-g difference in LV mass. Moreover, experience with the technique of 3D echocardiography[109] raises significant questions about whether ultrasound beam orientation is truly orthogonal to the long axis of the LV in routine clinical practice. These findings may help to explain why, for the individual patient, serial M-mode echocardiographic studies may be insensitive to the 20- to 40-g changes in

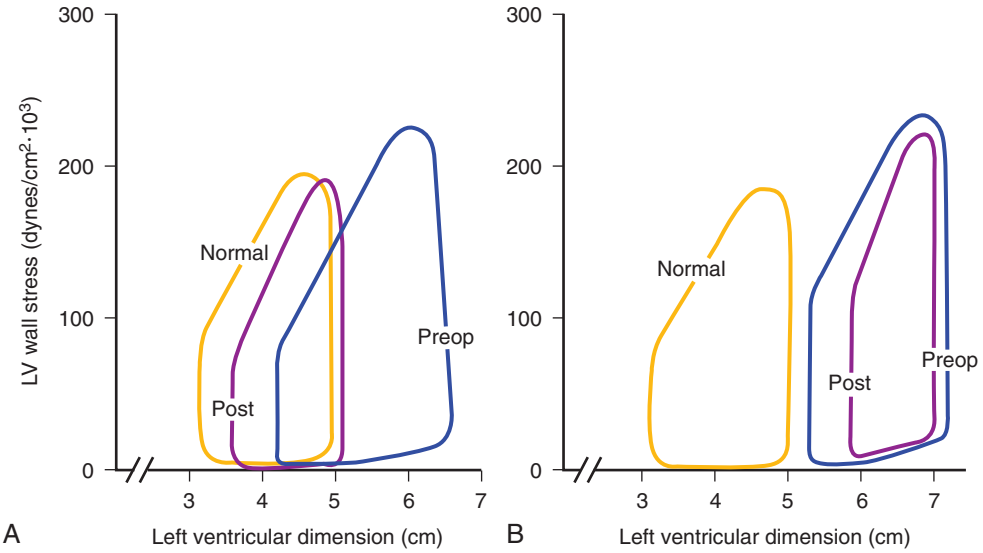



**Figure 9-24 LV response to mitral valve replacement in compensated and decompensated mitral regurgitation.** LV stress-dimension loops in two cases of mitral regurgitation, before (*Preop*) and after (*Post*) mitral valve replacement. **A,** Preoperative loop indicates compensated ventricular function; end-diastolic dimension is 6.5 cm, end-systolic dimension is 4.2 cm, systolic stress is minimally elevated, and fractional shortening is normal (35%). After valve replacement the end-diastolic dimension and end-systolic wall stress return to normal but fractional shortening decreases (29%). **B,** Preoperative loop indicates a decompensated ventricle; end-diastolic and end-systolic dimensions are markedly increased (7.3 cm and 5.4 cm, respectively) and fractional shortening is low (26%). After valve replacement there is persistent LV enlargement and a further decline in fractional shortening. *(From Aurigemma GP, Gaasch WH, Villegas B, Meyer TE:* Curr Probl Cardiol *20:421, 1995.)*

LV mass that are observed, on average, in response to antihypertensive treatment.[110,111]

As noted previously, 2D echocardiographic methods also have limitations, including limited frame rate (which renders precise timing of cardiac events difficult), near-field artifacts, and poor lateral resolution. Apical views often do not yield images of sufficient quality for manual tracing, and foreshortening of the long axis of the LV leads, in part, to volume estimates lower than those obtained by contrast ventriculography. Despite these important limitations, however, quantitative ultrasound techniques find widespread clinical and research applications because of their portability and low cost, and because results are immediately obtainable.

## KEY POINTS

- Assessment of LV mass, volume, and geometry is critical for the management of patients and the assessment of prognosis.
- Current noninvasive methods, M-mode echocardiography, 2D echocardiography, and 3D echocardiography are utilized for assessment of mass, volume, and shape. Each has strengths and limitations.
- Assessment of LV systolic function generally involves computation of the EF, but other aspects of systolic function, such as SV and cardiac output, can be calculated as well.
- A major limitation of EF is its dependence on load; this limitation is particularly important in the assessment of systolic function in valvular heart disease.
- There are compelling advantages to use of midwall shortening as an index of systolic function when the LV has undergone hypertrophic remodeling in response to hypertension.

## REFERENCES


1. Gaasch WH: Diagnosis and treatment of heart failure based on LV systolic or diastolic dysfunction. *JAMA* 271:1276-1280, 1994.
2. Mock MB, Rindqvist I, Fisher LD, et al: Survival of medically treated patients in the coronary artery surgery (CASS) registry. *Circulation* 66:562-567, 1982.
3. White HD, Norris RM, Brown MA, et al: Left ventricular end systolic volume as the major determinant of survival after recovery from myocardial infarction. *Circulation* 76:44-51, 1987.
4. Pfeffer MA, Braunwald E, Moye LA, et al: Effect of captopril on mortality and morbidity in patients with left ventricular dysfunction after myocardial infarction: results of the survival and ventricular enlargement trial. *N Engl J Med* 327:669-677, 1992.
5. The SOLVD Investigators: Effect of enalapril on survival in patients with reduced left ventricular ejection fractions and congestive heart failure. *N Engl J Med* 325:293-302, 1991.
6. Solomon SD, Anavekar N, Skali H, et al: Influence of ejection fraction on cardiovascular outcomes in a broad spectrum of heart failure patients. *Circulation* 112:3738-3744, 2005.
7. Aurigemma GP, Gottdiener JS, Shemanski L, et al: Predictive value of systolic and diastolic function for incident congestive heart failure in the elderly: the Cardiovascular Health Study. *J Am Coll Cardiol* 37:1042-1048, 2001.
8. Gottdiener JS, McClelland RL, Marshall R, et al: Outcome of congestive heart failure in elderly persons: influence of left ventricular systolic function. The Cardiovascular Health Study. *Ann Intern Med* 137:31-39, 2002.
9. Bonow RO, Carabello BA, Chatterjee K, et al: ACC/AHA 2006 guidelines for the management of patients with valvular heart disease: a report of the American College of Cardiology/American Heart Association Task Force on Practice Guidelines (writing committee to revise the 1998 guidelines for the management of patients with valvular heart disease) developed in collaboration with the Society of Cardiovascular Anesthesiologists endorsed by the Society for Cardiovascular Angiography and Interventions and the Society of Thoracic Surgeons. *J Am Coll Cardiol* 48:e1-e148, 2006.
10. Schuler G, Peterson KL, Johnson A, et al: Temporal response of left ventricular performance to mitral valve surgery. *Circulation* 59:1218-1231, 1979.
11. Gaasch WH, Carroll JD, Levine HJ, et al: Chronic aortic regurgitation: prognostic value of left ventricular end-systolic dimension and end-diastolic radius/thickness ratio. *J Am Coll Cardiol* 1:775-782, 1983.
12. Zile MR, Gaasch WH, Carroll JD, et al: Chronic mitral regurgitation: predictive value of preoperative echocardiographic indexes of left ventricular function and wall stress. *J Am Coll Cardiol* 3:235-242, 1984.
13. Bonow RO, Lakatos E, Maron BJ, Epstein SE: Serial long-term assessment of the natural history of asymptomatic patients with chronic aortic regurgitation and normal left ventricular systolic function. *Circulation* 84:625-635, 1991.
14. Carabello BA, Usher BW, Hendrix GH, et al: Predictors of outcome for aortic valve replacement in patients with aortic regurgitation and left ventricular dysfunction: a change in the measuring stick. *J Am Coll Cardiol* 10:991-997, 1987.
15. Crawford MH, Souchek J, Oprian CA, et al: Determinants of survival and left ventricular performance after mitral valve replacement. *Circulation* 81:1173-1181, 1990.
16. Carabello BA, Green LH, Grossman W, et al: Hemodynamic determination of prognosis of aortic valve replacement in critical aortic stenosis and advanced congestive heart failure. *Circulation* 62:42, 1980.
17. Connolly HM, Oh JK, Schaff HV, et al: Severe aortic stenosis with low transvalvular gradient and severe left ventricular dysfunction: result of aortic valve replacement in 52 patients. *Circulation* 101:1940-1946, 2000.
18. Collinson J, Henein M, Flather M, et al: Valve replacement for aortic stenosis in patients with poor left ventricular function: comparison of early changes with stented and stentless valves. *Circulation* 100(19 suppl):II1-5, 1999.
19. Orsinelli DA, Aurigemma GP, Battista S, et al: Left ventricular hypertrophy and mortality after aortic valve replacement for aortic stenosis: a high risk subgroup identified by preoperative relative wall thickness. *J Am Coll Cardiol* 22:1679-1683, 1993.
20. Aurigemma G, Battista S, Orsinelli D, et al: Abnormal left ventricular intracavitary flow acceleration in patients undergoing aortic valve replacement for aortic stenosis: a marker for high postoperative morbidity and mortality. *Circulation* 86:926-936, 1992.
21. Mathew J, Sleight P, Lonn E, et al: Reduction of cardiovascular risk by regression of electrocardiographic markers of left ventricular hypertrophy by the angiotensin-converting enzyme inhibitor ramipril. *Circulation* 104:1615-1621, 2001.
22. Levy D, Garrison RJ, Savage D, et al: Prognostic implications of echocardiographically determined left ventricular mass in the Framingham Heart Study. *N Engl J Med* 322:1561-1566, 1990.
23. Levy D, Garrison RJ, Savage D, et al: Left ventricular mass and incidence of coronary heart disease in an elderly cohort. *Ann Intern Med* 110:101-107, 1990.
24. Devereux RB, Dahlof B, Gerdts E, et al: Regression of hypertensive left ventricular hypertrophy by losartan compared with atenolol: the Losartan Intervention for Endpoint Reduction in Hypertension (LIFE) trial. *Circulation* 110:1456-1462, 2004.
25. Verdecchia P, Schillaci G, Borgioni C, et al: Adverse prognostic significance of concentric remodeling of the left ventricle in hypertensive patients with normal left ventricular mass. *J Am Coll Cardiol* 25:871-878, 1995.
26. Devereux R: Left ventricular geometry, pathophysiology and prognosis. *J Am Coll Cardiol* 25:885-887, 1995.
27. Ganau A, Devereux RB, Roman MJ, et al: Patterns of left ventricular hypertrophy and geometric remodeling in essential hypertension. *J Am Coll Cardiol* 19:550-558, 1992.
28. Buchalter MB, Weiss JL, Rogers WJ, et al: Noninvasive quantification of left ventricular

rotational deformation in normal humans using magnetic resonance imaging myocardial tagging. *Circulation* 81:1236-1244, 1990.
29. Notomi Y, Setser RM, Shiota T, et al: Assessment of left ventricular torsional deformation by Doppler tissue imaging: validation study with tagged magnetic resonance imaging. *Circulation* 111(9):141-147, 2005.
30. Aurigemma GP, Zile MR, Gaasch WH: Contractile behavior of the left ventricle in diastolic heart failure: with emphasis on regional systolic function. *Circulation* 113:296-304, 2006.
31. St. John Sutton M, Plappert T, Hirshfeld JW, et al: Assessment of left ventricular mechanics in patients with asymptomatic aortic regurgitation: a two-dimensional echocardiographic study. *Circulation* 69:259-270, 1984.
32. Gaasch WH, Zile MR, Hoshino PK, et al: Stress-shortening relations and myocardial blood flow in compensated and failing canine hearts with pressure overload hypertrophy. *Circulation* 79:872-883, 1989.
33. Mirsky I: Review of the various theories for evaluation of left ventricular wall stress. In Mirsky I, Chiston DN, Sandler H, editors: *Cardiac mechanics: physiological, chemical, and mathematical considerations*, New York, 1974, Wiley.
34. Douglas PS, Reichek N, Plappert T, et al: Comparison of echocardiographic methods for assessment of left ventricular shortening and wall stress. *J Am Coll Cardiol* 9:945-951, 1987.
35. Colan SD, Borow KM, Neumann A: Use of the calibrated carotid pulse tracing for calculation of left ventricular pressure and wall stress throughout ejection. *Am Heart J* 109:1306-1310, 1985.
36. Rozich JD, Carabello BA, Usher BW, et al: Mitral valve replacement with and without chordal preservation in patients with chronic mitral regurgitation. *Circulation* 86:1718-1726, 1992.
37. Gaasch WH, Battle WE, Oboler AD, et al: Left ventricular stress and compliance in man: With special reference to normalized ventricular function curves. *Circulation* 45:746-762, 1972.
38. Clyne CA, Arrighi JA, Maron BJ, et al: Systemic and LV responses to exercise stress in asymptomatic patients with valvular aortic stenosis. *Am J Cardiol* 68:1469-1476, 1991.
39. Cuocolo A, Sax F, Brush J, et al: Left ventricular hypertrophy and impaired diastolic filling in essential hypertension. *Circulation* 81:978-986, 1990.
40. Kitzman D, Higginbotham M, Cobb F, et al: Exercise intolerance in patients with heart failure and preserved LV systolic function. *J Am Coll Cardiol* 7:1065-1072, 1991.
41. Schwinger RH, Bohm M, Koch A, et al: The failing heart is unable to use the Frank-Starling mechanism. *Circ Res* 74:959-969, 1994.
42. Ross J Jr: Afterload mismatch and preload reserve: A conceptual framework for the analysis of ventricular function. *Prog Cardiovasc Dis* 18:255-264, 1976.
43. Grossman W, Jones D, McLaurin LP: Wall stress and patterns of hypertrophy in the human left ventricle. *J Clin Invest* 56:56-64, 1975.
44. Pouleur H, Covell JW, Ross J Jr: Effects of alterations in aortic input impedance on the force-velocity-length relationship in the intact canine heart. *Circ Res* 45:126-135, 1979.
45. Goldfine H, Aurigemma GP, Zile MR, Gaasch WH: Left ventricular length-force-shortening relations before and after surgical correction of chronic mitral regurgitation. *J Am Coll Cardiol* 31:180-185, 1998.
46. Carabello BA, Spann JF: The uses and limitations of end-systolic indices of left ventricular function. *Circulation* 69:1058-1064, 1984.
47. Sagawa K: The end-systolic pressure-volume relationship of the ventricle: Definitions, modifications, and clinical use. *Circulation* 61:1223-1227, 1981.
48. Douglas PS, Morrow R, Ioli A, et al: Left ventricular shape, afterload and survival in idiopathic dilated cardiomyopathy. *J Am Coll Cardiol* 13:311-315, 1989.
49. Gaasch WH, Zile MR: Left ventricular structural remodeling in health and disease: with special emphasis on volume, mass, and geometry. *J Am Coll Cardiol* 58(17):1733-1740, 2011.
50. Lang RM, Bierig M, Devereux RB, et al: Recommendations for chamber quantification: a report from the American Society of Echocardiography's Guidelines and Standards Committee and the Chamber Quantification Writing Group, developed in conjunction with the European Association of Echocardiography, a branch of the European Society of Cardiology. *J Am Soc Echocardiogr* 18:1440-1463, 2005.
51. Devereux R, Reichek N: Echocardiographic determination of left ventricular mass in man. Anatomic validation of the method. *Circulation* 55:613-618, 1977.
52. Devereux RB, Alonso D, Lutas E, et al: Echocardiographic assessment of left ventricular hypertrophy: comparison to necropsy findings. *Am J Cardiol* 57:450-458, 1986.
53. Teichholz LE, Kreulen T, Herman MV, et al: Problems in echocardiographic volume determinations: echocardiographic-angiographic correlations in the presence or absence of asynergy. *Am J Cardiol* 37:7-12, 1976.
54. Khouri MG, Peshock RM, Ayers CR, et al: A 4-tiered classification of left ventricular hypertrophy based on left ventricular geometry: the Dallas heart study. *Circ Cardiovasc Imaging* 3:164-171, 2010.
55. Chinali M, Aurigemma GP: Refining patterns of left ventricular hypertrophy using cardiac MRI: "brother, can you spare a paradigm?" *Circ Cardiovasc Imaging* 3:129-131, 2010.
56. Turkbey EB, McClelland RL, Kronmal RA, et al: The impact of obesity on the left ventricle: the Multi-Ethnic Study of Atherosclerosis (MESA). *JACC Cardiovasc Imaging* 3:266-274, 2010.
57. Topol E, Traill T, Fortuin N: Hypertensive hypertrophic cardiomyopathy of the elderly. *N Engl J Med* 312:277-283, 1985.
58. Litwin SE, Katz SE, Weinberg EO, et al: Serial echocardiographic Doppler assessment of left ventricular geometry and function in rats with pressure-overload hypertrophy: Chronic angiotensin converting enzyme inhibition attenuates the transition to heart failure. *Circulation* 91:2642-2649, 1995.
59. Schiller N, Shah P, Crawford M, et al: Recommendations for quantitation of the left ventricle by two-dimensional echocardiography. *J Am Soc Echocardiogr* 2:358-367, 1989.
60. Reichek NR, Helak J, Plappert T, et al: Anatomic validation of left ventricular mass from clinical two-dimensional echocardiography: Initial results. *Circulation* 67:348-352, 1983.
61. Wahr DW, Schiller NB: Left ventricular volumes determined by two-dimensional echocardiography in a normal adult population. *J Am Coll Cardiol* 1:863-868, 1983.
62. St. John Sutton MG, Plappert T, Crosby L, et al: Effects of reduced left ventricular mass on chamber architecture, load, and function: A study of anorexia nervosa. *Circulation* 72:991-1000, 1985.
63. Byrd BF, Wahr D, Wang YS, et al: Left ventricular mass and volume/mass ratio determined by two-dimensional echocardiography in normal adults. *J Am Coll Cardiol* 6:1021-1025, 1985.
64. Douglas PS, Reichek N, Hackney K, et al: Contribution of afterload, hypertrophy, and geometry to left ventricular ejection fraction in aortic valve stenosis, pure aortic regurgitation and idiopathic dilated cardiomyopathy. *Am J Cardiol* 59:1398-1404, 1987.
65. Feiring A, Rumberger J, Reiter S, et al: Determination of left ventricular mass in dogs with rapid-acquisition cardiac computed tomographic scanning. *Circulation* 72:1355-1364, 1985.
66. Takeuchi M, Nishikage T, Mor-Avi V, et al: Measurement of left ventricular mass by real-time three-dimensional echocardiography: validation against magnetic resonance and comparison with two-dimensional and m-mode measurements. *J Am Soc Echocardiogr* 21:1001-1005, 2008.
67. Mor-Avi V, Sugeng L, Lang RM: Real-time 3-dimensional echocardiography: an integral component of the routine echocardiographic examination in adult patients? *Circulation* 119:314-329, 2009.
68. Mor-Avi V, Sugeng L, Weinert L, et al: Fast measurement of left ventricular mass with real-time three-dimensional echocardiography: Comparison with magnetic resonance imaging. *Circulation* 110:1814-1818, 2004.
69. Gardin JM, Tomasso CL, Talano JV: Evaluation of dilated cardiomyopathy by pulsed Doppler echocardiography. *Am Heart J* 106:1057-1065, 1983.
70. Lewis JF, Kuo LC, Nelson JG, et al: Pulsed Doppler echocardiographic determination of stroke volume and cardiac output: Clinical validation of two new methods using the apical window. *Circulation* 70:425-431, 1984.
71. Keren G, LeJemtel T: Mitral annulus motion: relation to pulmonary venous and transmitral flows in normal subjects and in patients with dilated cardiomyopathy. *Circulation* 78:621-629, 1988.
72. Bargiggia GS, Bertucci C, Recusani F, et al: A new method for estimating left ventricular dP/dt by continuous wave Doppler-echocardiography: Validation studies at cardiac catheterization. *Circulation* 80:1287-1292, 1989.
73. Aurigemma GP, Reichek N, Venugopal R, et al: Automated left ventricular mass, volume, and shape from 3D MRI: In vitro validation. *Am J Card Imaging* 5:257-263, 1991.
74. Aurigemma GP, Silver KH, Fox MA, et al: Depressed midwall and long axis shortening in hypertensive left ventricular hypertrophy with normal ejection fraction. *J Am Coll Cardiol* 26:195-202, 1995.
75. Mirsky I, Pasternac A, Ellison RC: General index for the assessment of cardiac function. *Am J Cardiol* 30:483-491, 1972
76. Shapiro EP, Rogers WJ, Beyar R, et al: Determination of left ventricular mass by magnetic resonance imaging in hearts deformed by acute infarction. *Circulation* 79:706-711, 1989.
77. Lima JAC, Desai MY: Cardiovascular magnetic resonance imaging: Current and emerging applications. *J Am Coll Cardiol* 44:1164-1171, 2004.

78. Allen DG, Kentish JC: The cellular basis of the length tension relation in cardiac muscle. *J Mol Cell Cardiol* 17:821-828, 1985.
79. Ross J, Jr: Afterload mismatch in aortic and mitral valve disease: Implications for surgical therapy. *J Am Coll Cardiol* 5:811-826, 1985.
80. Sutton M, Plappert T, Spiegel A, et al: Early postoperative changes in left ventricular chamber size, architecture, and function in aortic stenosis and aortic regurgitation and their relation to intraoperative changes in afterload: a prospective two-dimensional echocardiographic study. *Circulation* 76:77-89, 1987.
81. DeFilippi CR, Willett DL, Brickner ME, et al: Usefulness of dobutamine echocardiography in distinguishing severe from nonsevere valvular aortic stenosis in patients with depressed left ventricular function and low transvalvular gradients. *Am J Cardiol* 75:191-194, 1995.
82. Colan SD, Borow KM, Neuman AS: The left ventricular end-systolic wall stress-velocity of fiber shortening relation: A load independent index of myocardial contractility. *J Am Coll Cardiol* 4:715-724, 1984.
83. Quinones MA, Gaasch WH, Alexander JK: Influences of acute changes in preload, afterload, contractile state, and heart rate on ejection and isovolumic indices of myocardial contractility in man. *Circulation* 53:293-300, 1976.
84. McKay RG, Aroesty JM, Heller GV, et al: Left ventricular pressure-volume diagrams and end-systolic pressure-volume relations in human beings. *J Am Coll Cardiol* 3:301-312, 1984.
85. Aurigemma GP, Meyer TE, Sharma M, et al: Evaluation of extent of shortening versus velocity of shortening at the endocardium and midwall in hypertensive heart disease. *Am J Cardiol* 83:792-794, 1999.
86. Shimizu G, Zile M, Blaustein AS, Gaasch WH: Left ventricular chamber filling and midwall fiber lengthening in patients with left ventricular hypertrophy: Overestimation of fiber velocities by conventional midwall measurements. *Circulation* 71:266-272, 1985.
87. deSimone G, Devereux RB, Roman MJ, et al: Assessment of left ventricular function by the midwall fractional shortening/end systolic stress relation in human hypertension. *J Am Coll Cardiol* 23:1444-1451, 1994.
88. Jones CR, Gibson D: Functional importance of the long axis dynamics of the human left ventricle. *Br Heart J* 65:215-220, 1990.
89. Tei C: New non-invasive index for combined systolic and diastolic ventricular function. *J Cardiol* 26:135-136, 1995.
90. Palmon L, Reichek N, Yeon S, et al: Intramural myocardial shortening in hypertensive left ventricular hypertrophy with normal pump function. *Circulation* 89:122-131, 1994.
91. Sutherland GR, Stewart MJ, Groundstroem KWE, et al: Color Doppler myocardial imaging: A new technique for the assessment of myocardial function. *J Am Soc Echocardiogr* 7:441-458, 1994.
92. Abraham TP, Nishimura RA: Myocardial strain: can we finally measure contractility? *J Am Coll Cardiol* 37:731-734, 2001.
93. Ross J, Jr: Adaptations of the left ventricle to chronic valvular overload. *Circ Res* 35:64-70, 1974.
94. Ross J, Jr, Sonnenblick EH, Taylor RR, et al: Diastolic geometry and sarcomere lengths in the chronically dilated canine left ventricle. *Circ Res* 28:49-56, 1971.
95. Sonnenblick EH: Correlation of myocardial ultrastructure and function. *Circulation* 38:29-44, 1968.
96. Laks MM, Morady F, Swan HJC: Canine right and left ventricular cell and sarcomere lengths after banding the pulmonary artery. *Circ Res* 24:705-710, 1969.
97. Villareall FJ, Lew WYW, Waldman LK et al: Transmural myocardial deformation in the ischemic canine left ventricle. *Circ Res* 68:368-381, 1991.
97a. Clark NR, Reichek N, Bergey P, et al: Circumferential myocardial shortening in the normal human left ventricle. Assessment by MRI using spatial modulation of magnetization. *Circulation* 84:67-74, 1991.
98. Edvardsen T, Gerber BL, Garot J, et al: Quantitative assessment of intrinsic regional myocardial deformation by Doppler strain rate echocardiography in humans: validation against three-dimensional tagged magnetic resonance imaging. *Circulation* 106:50-56, 2002.
99. Amundsen BH, Helle-Valle T, Edvardsen T, et al: Noninvasive myocardial strain measurement by speckle tracking echocardiography: validation against sonomicrometry and tagged magnetic resonance imaging. *J Am Coll Cardiol* 47:789-793, 2006.
100. Hurlburt HM, Aurigemma GP, Hill JC, et al: Direct ultrasound measurement of longitudinal, circumferential, and radial strain using 2-dimensional strain imaging in normal adults. *Echocardiography* 24:723-731, 2007.
101. Narayanan A, Aurigemma GP, Chinali M, et al: Cardiac mechanics in mild hypertensive heart disease: a speckle-strain imaging study. *Circ Cardiovasc Imaging* 2:382-390, 2009.
102. Sagawa K, Maughan L, Suga H, Sunagawa K: *Cardiac contractility and the pressure-volume relationship*, New York, 1988, Oxford University Press.
103. Magorien DJ, Shaffer P, Bush CA, et al: Assessment of left ventricular pressure-volume relations using gated radionuclide angiography, echocardiography and micromanometer pressure recordings. *Circulation* 67:844-852, 1983.
104. Gorcsan J, III, Gasior TA, Mandarino WA: Assessment of the immediate effects of cardiopulmonary bypass on left ventricular performance by on-line pressure-area relations. *Circulation* 89:180-190, 1994.
105. Gorcsan J, III, Denault A, Gasior TA, et al: Rapid estimation of LV contractility from end systolic relations by echocardiographic automated border detection and femoral artery pressure. *Anesthesiology* 81:553-562, 1994.
106. Sagawa K: The ventricular pressure-volume diagram revisited. *Circ Res* 43:677-680, 1978.
107. Berko B, Gaasch WH, Tanigawa N, et al: Disparity between ejection and end systolic indexes of left ventricular contractility in mitral regurgitation. *Circulation* 75:1310-1319, 1987.
108. Gaasch WH, Carroll JD, Levine HJ, et al: Chronic aortic regurgitation: Prognostic value of left ventricular end-systolic dimension and end-diastolic radius/thickness ratio. *J Am Coll Cardiol* 1:775-782, 1983.
109. King DL: Three-dimensional echocardiography: Use of additional spatial data for measuring left ventricular mass. *Mayo Clin Proc* 69:293-295, 1994.
110. Gottdiener JS, Livengood SV, Meyer PS, et al: Should echocardiography be performed to assess the effects of antihypertensive therapy? Test-retest reliability of echocardiography for measurement of left ventricular mass and function. *J Am Coll Cardiol* 25:424-430, 1995.
111. Dahloff B, Pennert K, Hanson L: Reversal of left ventricular hypertrophy in hypertensive patients: A meta-analysis of 109 treatment studies. *Am J Hypertens* 5:95-110, 1992.



# Myocardial Mechanics: Velocity, Strain, Strain Rate, Cardiac Synchrony, and Twist

OTTO A. SMISETH, MD, PhD | THOR EDVARDSEN, MD, PhD

**Physical Principles of Tissue Doppler Echocardiography**
Velocity and Displacement Imaging
Deformation Imaging
Strain Rate and Strain by Tissue Doppler Imaging
**Physical Principles of Speckle Tracking Echocardiography**
Basic Principles
LV Rotation and Twist by Speckle Tracking Echocardiography
**Normal Physiology of the Left Ventricle**
Isovolumic Contraction
Ejection
Isovolumic Relaxation
Diastole
**Myocardial Ischemia**
**Cardiac Synchrony**
Mechanisms of LV Mechanical Dyssynchrony
Effect of Left Bundle Branch Block on LV Function
**Mechanical Dispersion**
**Right Ventricular Function**

In daily clinical practice, left ventricular (LV) function is commonly evaluated by two-dimensional (2D) and M-mode echocardiography. Despite all obvious advantages, visual evaluation of LV function by 2D echo suffers from being subjective and provides only semiquantitative data. Furthermore, visual assessment has limited ability to detect subtle changes in function and changes in timing of myocardial motion throughout systole and diastole. M-mode echocardiography provides quantitative data, but does not allow comprehensive evaluation of regional LV function. Tissue-Doppler imaging (TDI) and speckle tracking echocardiography (STE) have been introduced as quantitative and more objective methods to quantify regional and global LV systolic and diastolic function.[1]

This chapter explains the technical principles behind TDI and STE and the physiologic meaning of the different parameters. The clinical application of the methodologies is reviewed. Finally, synchronization of ventricular contraction is addressed.

## Physical Principles of Tissue Doppler Echocardiography

### VELOCITY AND DISPLACEMENT IMAGING

#### *Velocities by Color Doppler*

The Doppler principle has traditionally been used to measure blood flow velocities, but may also be used to measure myocardial and other tissue velocities. Separation between velocities in myocardium and blood is possible because of different signal amplitudes and Doppler frequencies. The myocardium is moving at a much lower speed than blood, and therefore Doppler frequencies are lower. Furthermore, the amplitude of myocardial signals is much higher than for blood. These differences allow myocardial velocities to be separated from blood flow velocities by using filters that reject echoes originating from the blood pool (Fig. 10-1). Velocities can be recorded using color Doppler or pulsed Doppler mode.

Myocardial velocity imaging was first introduced in the early 1990s[2,3] and is now an established clinical method for quantifying LV systolic and diastolic function. Similar to color flow imaging, TDI utilizes an autocorrelator technique to calculate and display multigated points of color-coded velocities along a series of ultrasound scan lines within a 2D sector. As illustrated in Figure 10-2, myocardial motion can be imaged as color-coded velocities superimposed on a 2D gray-scale image in real time. The frame rate for 2D color Doppler is typically from 80 to 200 frames per second, depending on the width of the ultrasound sector, and is usually set higher than for the simultaneous gray-scale images. Myocardial velocities are automatically decoded into numeric values that can be stored digitally for later offline analyses.[4] By convention, velocities toward the transducer are color-coded red and velocities away from the transducer are coded blue. Figure 10-3 shows 2D images from a normal person and from a patient with acute myocardial infarction.

During normal LV systole the base of the ventricle descends toward the apex, and moves back during diastole, while the apex is relatively stationary. Therefore, from apical views, long-axis motion is dominated by red-encoded velocities in systole and blue-encoded velocities during early filling and atrial-induced filling. Dysfunctional myocardium, however, may show grossly abnormal motion with reversed longitudinal velocities during systole. Assessment of myocardial function by the 2D color display, however, is not very useful in practical diagnostics, and velocity analysis should be done as postprocessing. In some cases it may be helpful to use the curved M-mode format, which provides a quick view of direction and timing of

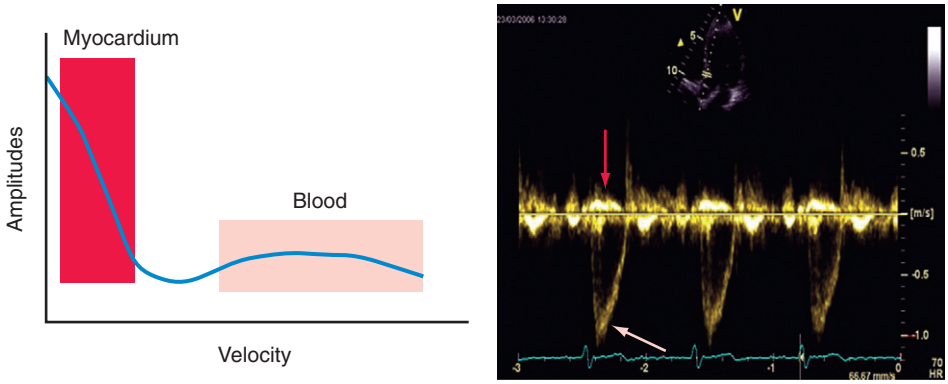



**Figure 10-1 Principle for separation of myocardial velocities from blood flow velocities.** (*Left* panel) The difference in velocity and amplitude between myocardial and blood velocities. (*Right* panel) A recording in the LV outflow tract that samples both myocardial and blood flow velocities. High-intensity signals from the myocardium (*red arrow*); low-intensity but high-velocity signals from the blood (*white arrow*).

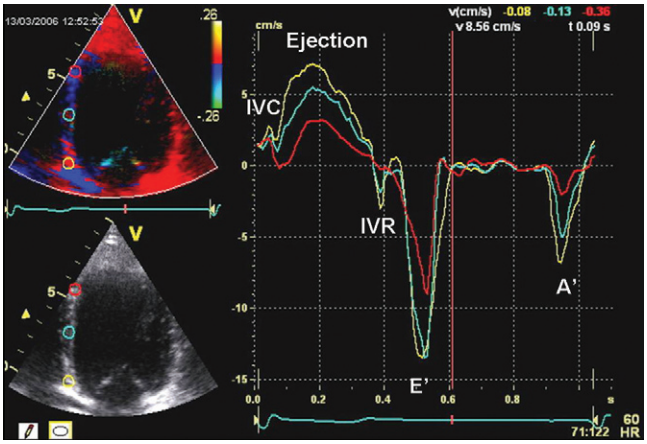



**Figure 10-2 Normal myocardial velocities.** Tissue Doppler velocities from the anterior wall of the LV in a healthy individual. *A'*, Velocity during atrial-induced filling; *E'*, velocity during early diastolic filling; *IVC*, isovolumic contraction; *IVR*, isovolumic relaxation.

velocities in different segments (Fig. 10-4). The standard approach, however, is analysis of velocity traces from multiple regions within a 2D image, as illustrated in Figure 10-2. This analysis allows direct comparison of velocities in different segments on the same image. The most important measures from the velocity traces are peak systolic ejection velocity (S) and peak early-diastolic lengthening velocity (E′). One should be aware that a velocity obtained with the autocorrelation method used in TDI in 2D color mode represents the mean value of an instantaneous velocity spectrum recorded from the same location.[4,5] A schematic presentation of all tissue Doppler modalities (tissue velocities, displacement, strain rate, and strain) from the apical four-chamber view is demonstrated in Figure 10-5.

Assessment of LV function from the parasternal short axis is possible, but only a very limited number of segments can be imaged (Fig. 10-6). Therefore most often apical views are preferred when assessing LV function by TDI.

### *Velocities by Pulsed Doppler*

Another approach is to use spectral tissue Doppler with pulsed Doppler activated, which is applied mainly to measure mitral and tricuspid annular velocities. It is important to be aware that the pulsed Doppler mode presents the peaks of the instantaneous velocity spectrum, whereas the color mode provides mean velocities. This implies that velocities measured by the 2D color method described earlier are lower than velocities by pulsed Doppler—typically about 25% lower.[6,7] The difference, however, depends on the band width of the velocity spectrum, which is determined by sample volume and by acoustical noise. Figure 10-7 illustrates the difference between velocities by color Doppler and pulsed Doppler modes. Disadvantages of the pulsed Doppler method are (1) limited spatial resolution and (2) the fact that velocities are obtained from only one region at a time.

### *Limitations of Velocity Imaging*

#### Angle Dependency

Like all other Doppler modalities, velocity imaging is angle dependent, because only velocity components in the beam direction are recorded. Therefore it is essential that the ultrasound beam be aligned parallel to the LV wall in long-axis imaging and perpendicular to the wall for radial measurements in the short axis. In longitudinal views, velocities should not be measured near the apex because the apical curvature gives large angle problems.

#### Movement of Sample Volume Relative to Myocardium

Tissue Doppler measures velocity within a fixed area in space, but not within a defined piece of myocardium. Because of cardiac motion, the difference between the two may be significant. This limitation, which applies to all TDI modalities, can in part be compensated for by using tracking algorithms that move the sample volume continuously or in steps during the heart cycle.

#### Reverberations

Reverberations are echoes due to multiple reflections within the body, and in transthoracic imaging they are often caused by relatively motionless tissue layers close to the body surface. In gray-scale imaging, they are seen as false echoes or reduced contrast. For color TDI, the reverberations may cause a bias in the mean velocity estimate, and often the bias is toward zero velocity. The amount of bias depends on the intensity of the reverberation signal relative to the tissue velocity signal. Still, the sign of the velocity is seldom affected, so it might be difficult to detect reverberations when using the color display.

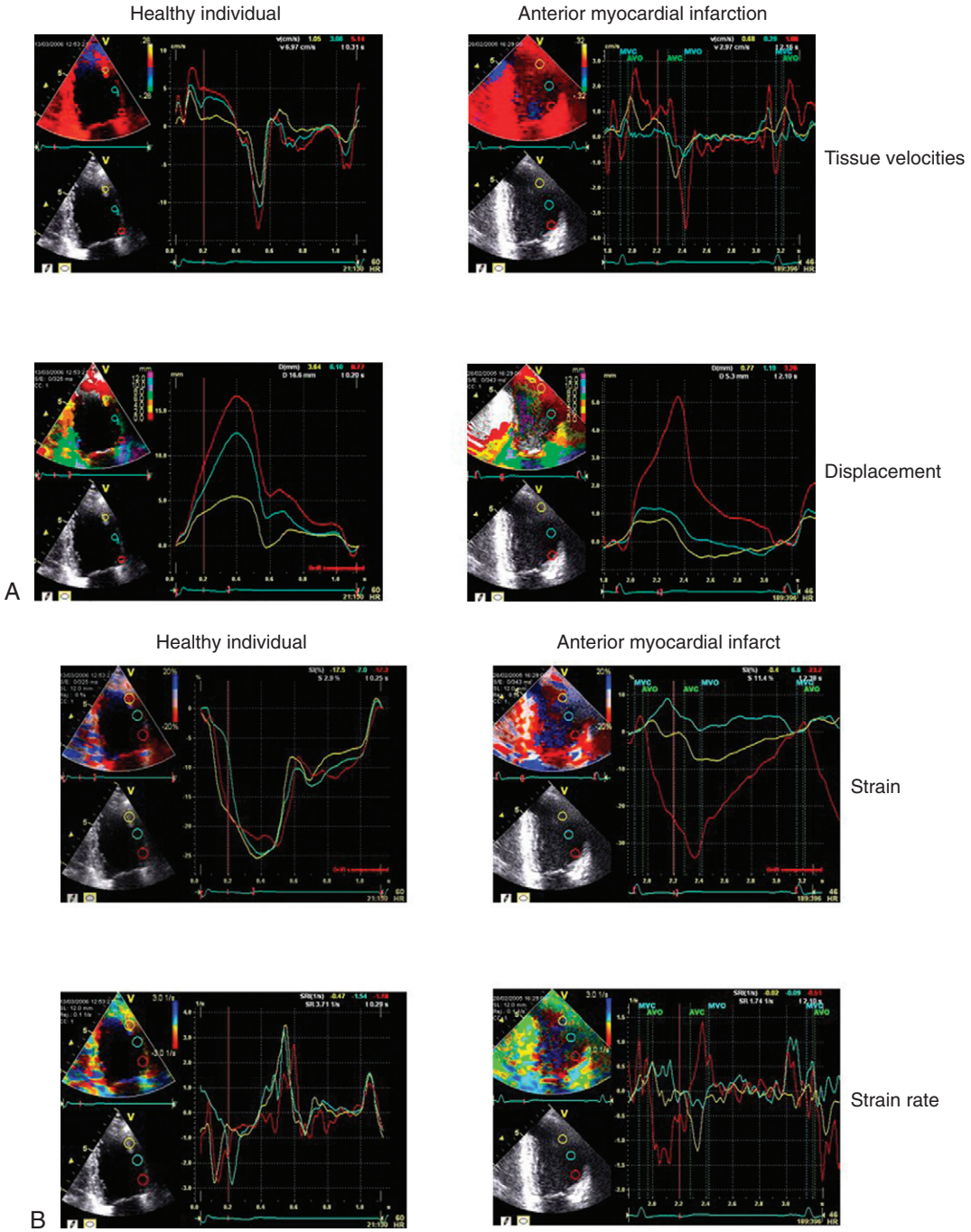



**Figure 10-3** **Acute myocardial infarction.** Recordings from a healthy individual (*left*) and from a patient with anterior myocardial infarction (*right*; be aware of different scales). All tissue Doppler modalities are sampled from three identical levels along the anterior left ventricular wall. In ischemic myocardium, systolic velocities and displacement are typically reduced (**A**), and there are reductions in systolic strain and strain rate (**B**).

## Tethering Effects and Cardiac Translation

Because myocardium in one region of the ventricle is tethered to neighboring myocardium, velocities in one region are affected by motion in adjacent tissue. In addition, regional velocities may be due to motion of the entire heart (translation).[8-10] Therefore myocardial velocities demonstrate marked regional nonuniformity in the normal ventricle.[11,12] These factors are not limitations of the TDI methodology, but reflect a limitation of velocity to serve as a parameter of regional contractility.

## Load Dependency

Similar to global ejection fraction, all regional ejection phase indices are load dependent.[9,11] This problem, however, is less important than for ejection fraction, because the TDI parameters are used primarily to diagnose regional myocardial dysfunction, and regional differences are likely to persist even when there are changes in global ventricular loading. This is not a limitation of the technology, but reflects a fundamental relationship between myocardial fiber shortening and load.

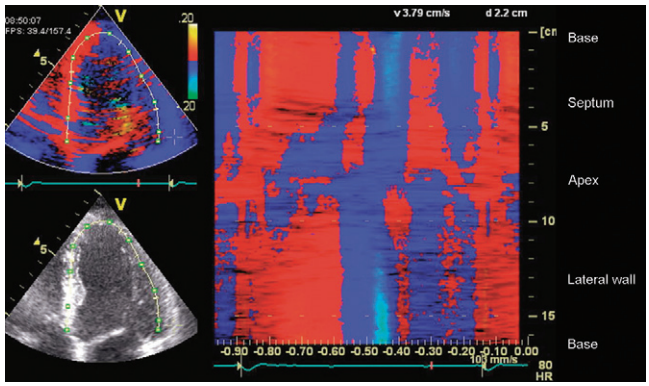



**Figure 10-4 Curved M-mode display of myocardial velocities.** Tissue Doppler imaging velocities in 2D display in systole from a normal heart (*left*) and as curved M-mode (*right*).

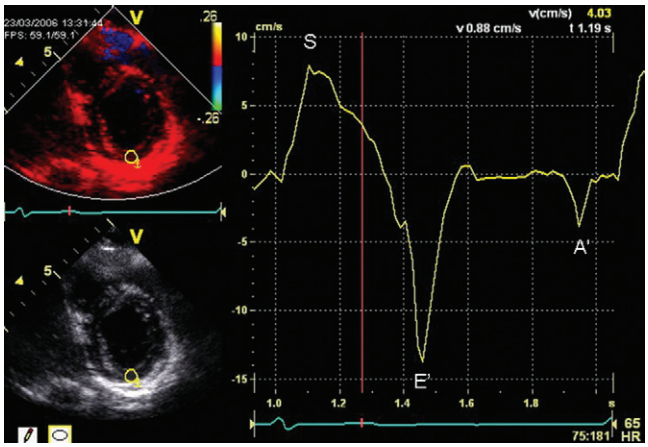



**Figure 10-6** Myocardial velocities from the posterior LV segment in a parasternal short-axis view. *A'*, Velocity during atrial-induced filling; *E'*, velocity during early diastolic filling; *S*, systolic ejection velocity.

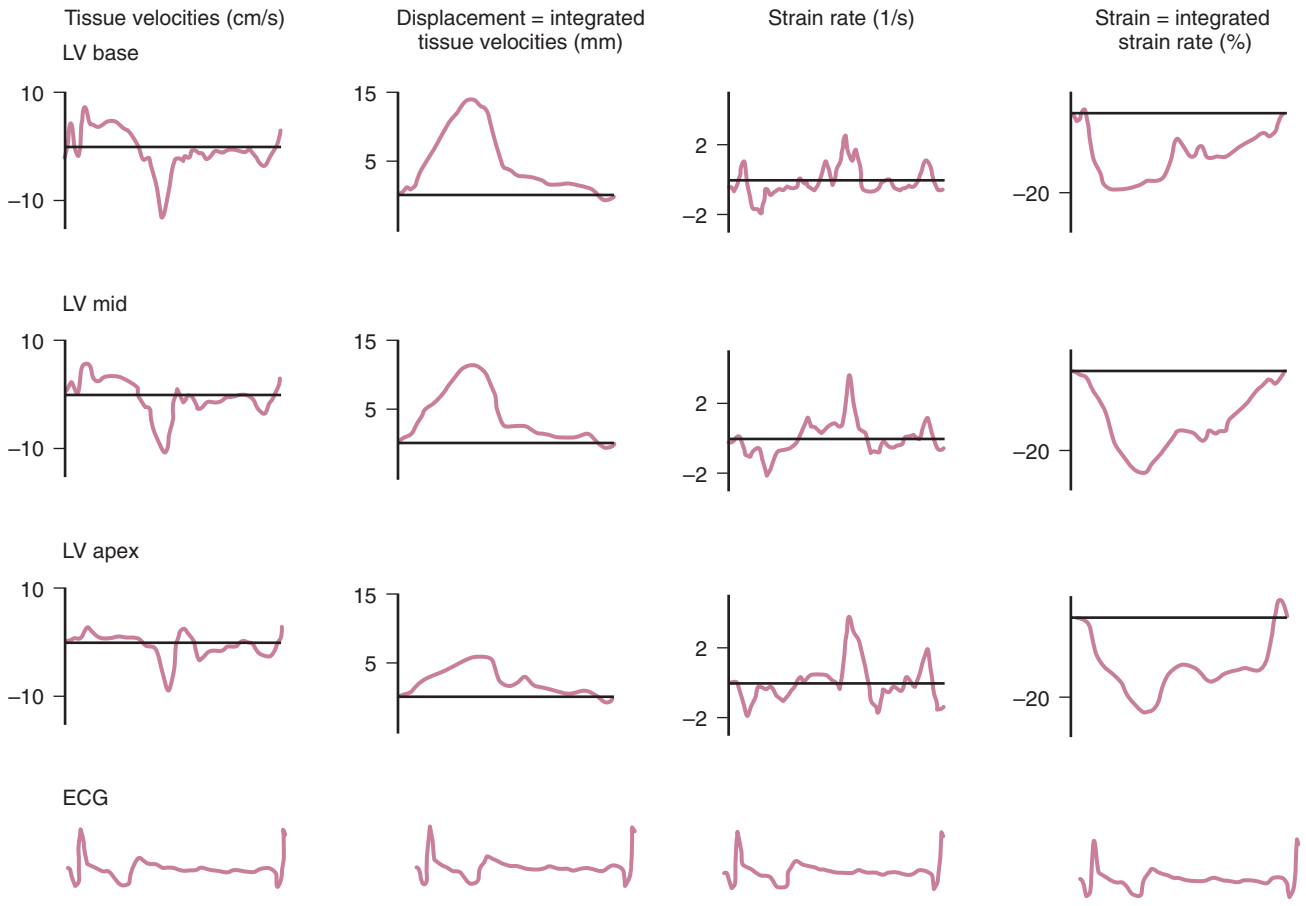



**Figure 10-5 Tissue Doppler recordings from the septum of a normal subject in a long-axis view.** The *first* column shows velocity tracings, with positive velocities (toward the apex) in systole, and negative velocities (away from the apex) in diastole. The *second* column shows displacement curves obtained by temporal integration of the velocities. The *third* column shows strain rate, obtained by a spatial derivation of velocity data. Strain rate is negative in systole (shortening) and positive in diastole (lengthening). The *fourth* column shows strain, obtained by temporal integration of strain rate. The time axis is the same for all modalities. Velocity and displacement decrease from base to apex, whereas strain and strain rate are relatively similar in magnitude at all levels. *(From Smiseth OA, Stoylen A, Ihlen H: Tissue Doppler imaging for the diagnosis of coronary artery disease.* Curr Opin Cardiol *19[5]:421-429, 2004.)*

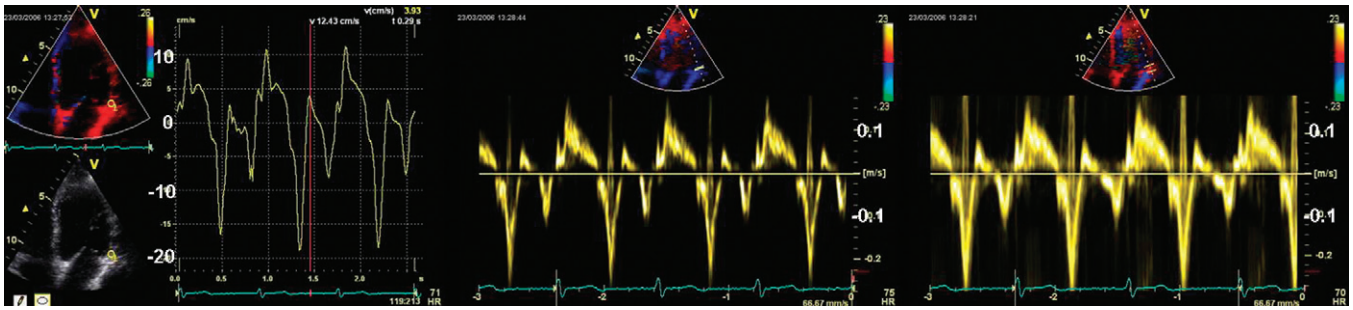


**Figure 10-7 Comparison between myocardial velocities by color Doppler and pulsed Doppler modes.** All images are recorded from identical position in the same LV. Myocardial color Doppler (*left panel*); pulsed Doppler (*middle* and *right panels*). Because the color mode gives mean velocities, amplitudes are smaller than with pulsed Doppler mode. The recording in the *right* panel is performed with a larger sample volume (12 mm) and higher gain than for the *middle* panel (5 mm). Please note the effect of sample volume and gain on signal amplitudes in systolic and diastolic velocities.

### *Displacement Imaging*

By performing temporal integration of velocities from a particular region, one obtains *displacement* curves (see Figs. 10-3 and 10-5). In long-axis views, velocity and displacement increase progressively from apex toward base. Displacement can be displayed in real time as color-coded bands or measured offline from displacement curves. At the present time, this modality has not proven to provide added diagnostic value to velocity imaging.[11] The limitations that are listed for velocity imaging also apply to displacement imaging.

## DEFORMATION IMAGING

*Strain* means deformation and is an excellent parameter for quantification of myocardial function. Analogous to LV ejection fraction, which quantifies global contractility, myocardial strain quantifies regional contractility. In principle, strain may also be used to quantify diastolic function, but this application has not been well developed.

Quantification of myocardial function in terms of strain and strain rate has been available for a long time in cardiac physiology using implanted myocardial markers.[13] The first clinical method that could measure myocardial strain was magnetic resonance imaging with tissue tagging, but complexity and cost have limited this methodology to research protocols.[14] More recently, strain-rate imaging by TDI and that by STE have been introduced as bedside, clinical methods.[9,15-18]

### *Definitions of Strain and Strain Rate*

Strain is a measure of how much an object has been deformed, and several formulas can be used to calculate different types of strain. In cardiac mechanics, we use the simple approach proposed by Mirsky and Parmley[19,20] and calculate strain as percent or fractional change in dimension. This implies that systolic strain is a measure of percentage shortening when measurements are done in the long axis, and percent thickening for radial measurements in the short axis. This strain measure is named Lagrangian strain and is given by Equation A. The Greek letter epsilon (ε) is used as the symbol of Lagrangian strain. In the formula, L is the current length and $L_0$ is the original length.

$$\text{Strain} = \frac{L - L_0}{L} = \frac{\Delta L}{L_0} \qquad \text{(A)}$$

Figure 10-8 illustrates schematically the principles for calculation of Lagrangian strain, and Figure 10-9 shows a typical myocardial strain trace recorded from implanted myocardial markers in an anesthetized dog. By convention, lengthening and

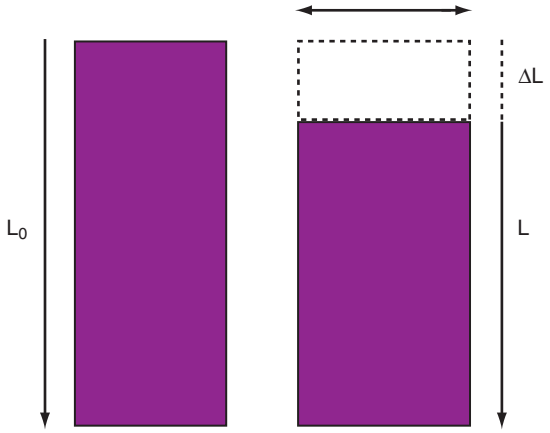



**Figure 10-8 Schematic illustration of myocardial strain.** Lagrangian strain equals $\Delta L/L_0$. *L*, Current length; $L_0$, original length.

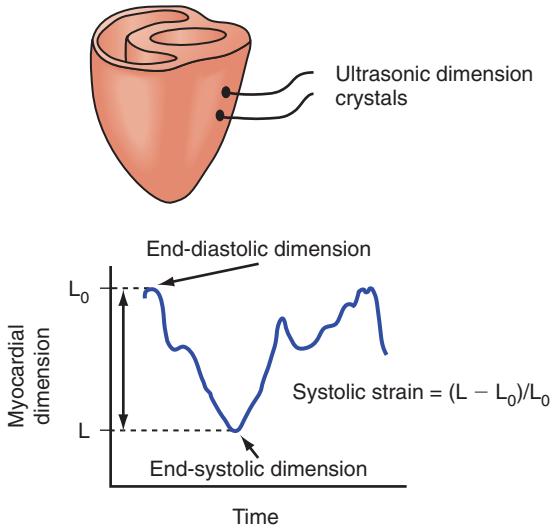



**Figure 10-9 Typical longitudinal myocardial strain trace.** The recording shows strain by sonomicrometry in an anesthetized dog. Strain was recorded between two ultrasonic crystals implanted into the myocardium. The figure illustrates calculation of systolic strain. Please note that peak systolic strain equals systolic shortening fraction. *L*, Current length; $L_0$, original length.

thickening strains are assigned positive values and shortening and thinning strains negative values. This implies that systolic shortening results in negative strains, and systolic thickening in positive strains.

When strain is measured in one dimension, there will only be shortening and lengthening strains or thickening and thinning strains, respectively. During the heart cycle, however, the LV myocardium goes through a complex three-dimensional (3D) deformation that leads to shear strains, when one border is displaced relative to another. In a clinical context, however, we only assess the one-dimensional myocardial strains.

## STRAIN RATE AND STRAIN BY TISSUE DOPPLER IMAGING

### *Basic Principles*

It was proposed by Fleming and associates[21] that myocardial Doppler velocity gradients may be used to assess myocardial contractility. The theoretical basis for measuring strain by TDI is that myocardial velocity gradient is an estimate of strain rate, and therefore strain can be calculated as the temporal integral of strain rate. Using these concepts, Heimdal and co-workers[16] introduced real-time strain-rate imaging based on myocardial Doppler velocities. Strain rate, commonly abbreviated SR, can be estimated by TDI as a velocity gradient between two spatial points ($x$ and $x + \Delta x$) as shown in Equation B.

$$SR \approx \frac{v(x) - v(x + \Delta x)}{\Delta x} \quad (B)$$

Temporal integration of the velocity gradient gives the logarithmic strain estimate denoted *natural strain* ($\varepsilon_N$) shown in Equation C. The name refers to the use of the natural logarithm function, ln. Lagrangian strain ($\varepsilon$) can be derived from natural strain using the mathematical conversion in Equation D. To accurately determine strain, it is necessary to track and follow the motion of the material points (fixed particles) within the myocardium through time. This is not feasible with TDI, and therefore only estimates, not direct measures, of strain can be obtained by this imaging modality.

$$\varepsilon_N = \ln(L / L_0) \quad (C)$$

$$\varepsilon = \exp(\varepsilon_N) - 1 \quad (D)$$

The rationale for using spatial velocity gradient as a marker of myocardial function is that a velocity difference between two adjacent regions implies either compression or lengthening of the tissue in between, and the spatial velocity gradient equals strain rate. When LV systolic function is studied in the LV long axis, strain rate measures regional shortening rate, and strain measures regional shortening fraction. In the LV short axis, strain rate measures systolic thickening rate. During diastole, strain rate measures myocardial lengthening and thinning rates, respectively. Because strain is dimensionless, strain rate has units of 1/s.

In principle, strain rate is not influenced by overall motion of the heart (translation) or by motion caused by contraction in adjacent segments. This is in contrast to *velocity* within a myocardial segment, which is the net result of motion caused by contractions in that segment, motion due to tethering to other segments, and cardiac translation.[9,22] The effect of tethering explains why LV longitudinal velocities measured from an apical window increase progressively from the apex toward the base. Strains and strain rates, however, are essentially similar between apex and base. Therefore strain and strain rate in principle are superior to velocity as markers of regional contractility. However, there are technical issues that make strain-rate imaging more challenging than velocity imaging.

### *Limitations of Strain and Strain-Rate Imaging by Tissue Doppler Imaging*

#### Signal Noise

Strain rate by TDI has significant problems with random noise. This reflects an effect of measuring a difference between velocities, because the error is the sum of the errors of the two velocities. The signal-to-noise ratio for strain rate can be improved by increasing the spatial offset (strain length) for the velocity points, which increases the velocity difference but will reduce the spatial resolution. The problem with random noise can also be reduced by temporal averaging within a heart cycle and by averaging multiple heart cycles. However, these methods for noise reduction represent compromises between optimal signal-to-noise ratio and requirements for high spatial and temporal resolution. The spatial offset for measurement of longitudinal strain and strain rate is typically between 5 and 12 mm but can be defined by the operator. For transmural strain, wall thickness and translational motion restrict the range for adjustment of strain length. As a rule of thumb, the strain length should be set to approximately half the systolic thickness of the wall.[23] Strain-rate imaging has limited lateral resolution, which limits the ability to measure separately from subendocardial and subepicardial wall layers in long-axis views. Furthermore, when the sample volume is at the inner or outer LV wall layers, the signal may in part represent velocities in the blood pool and pericardium, respectively. Fortunately, measurement of strain is associated with fewer noise problems than measurement of strain rate, because integration tends to eliminate random noise. In the strain signal, however, there may be significant drift within a given heart cycle.

#### Angle Dependency

Another problem with strain-rate imaging is strong sensitivity to misalignment between the cardiac axis and the ultrasound beam. Similar to measurement of blood flow velocity, myocardial velocity is reduced in proportion to the cosine of the angle between the velocity vector and the ultrasound beam. Furthermore, because myocardium is virtually uncompressible, shortening in one axis is always accompanied by thickening in the other axis, and this increases measurement problems due to misalignement.[9] Therefore care should be taken to align the ultrasound beam parallel to all myocardial segments of interest. It is of special importance to avoid misinterpretation in myocardial areas close to the LV apex because of the apical curvature. Angle problems can be reduced by using the smallest possible sector and recording from one wall at a time. Some reports indicate that the problem with misalignment might be less than anticipated.[11,24]

#### Reverberations

Reverberations are a major source of error in strain-rate imaging. A small local bias in the velocity will cause large changes in the spatial velocity gradient and therefore in the strain rate. The only way to avoid reverberation noise is to get a better scanning window. When analyzing the strain-rate data, it is important to recognize the reverberation artifacts and to

avoid the regions affected. Curved anatomic M-mode can be an effective tool to identify larger reverberation artifacts and, for the experienced user, can be seen as "unphysiologic" color patterns.

### Movement

Movement of the myocardium relative to the sampling volume and load dependency are limitations as discussed in the section on limitations of velocity imaging.

#### *Preferred Tissue Doppler Imaging Modalities in Clinical Routine*

In spite of theoretical advantages of strain rate and strain relative to velocity,[25] there are unresolved technical limitations of these modalities. Therefore, with the present state of the technologies, velocity imaging is preferred as the primary TDI methodology for assessing regional function. Strain and strain-rate imaging may be used as a supplementary method for exploring changes in regional function. Strain by STE appears more robust and is preferable to TDI-based strain. Displacement imaging needs more validation before it can be recommended for routine clinical use. Normal values for mitral annular velocities by TDI are presented in Table 10-1.[26] Velocities measured in 2D color mode are lower than by pulsed wave Doppler, and this needs to be taken into account when interpreting E′ in a clinical context. In adults, E′ velocity decreases with age; therefore age-based normal values should be utilized when applying these measures of LV diastolic function in clinical practice.

## Physical Principles of Speckle Tracking Echocardiography

### BASIC PRINCIPLES

Speckle tracking echocardiography (STE) measures local myocardial displacement in echocardiographic images and may be used to quantify myocardial function in terms of velocity and strain. Furthermore, STE may be used to assess LV rotation and twist. The speckles are created by interference of ultrasound beams in the myocardium and are seen in gray-scale B-mode images as a characteristic speckle pattern (Fig. 10-10). The speckles are the result of constructive and destructive interference of ultrasound that is back-scattered from structures smaller than the wavelength of ultrasound. Random noise is filtered out by the computer algorithm, yielding small segments of myocardium with temporarily stable and unique speckle patterns.[27] These segments, or "kernels," serve as acoustic markers that can be tracked from frame to frame within an image plane using block matching. Figure 10-11 shows recordings from a normal heart. It is also possible to calculate myocardial velocity vectors that are displayed superimposed on the dynamic gray-scale images (Fig. 10-12).[28] Because of the relatively low frame rate of STE, this imaging modality is not optimal for measuring strain rate.

#### *Strain by Speckle Tracking Echocardiography*

In contrast to tissue Doppler–based strain, which measures velocities from a fixed point in space with reference to an external probe, STE measures instantaneous distance between two kernels. This implies that STE is relatively angle independent and can measure strain in different directions in the same image, including circumferential and radial strains in multiple segments from LV short-axis images and longitudinal strain from myocardial areas close to the LV apex. However,

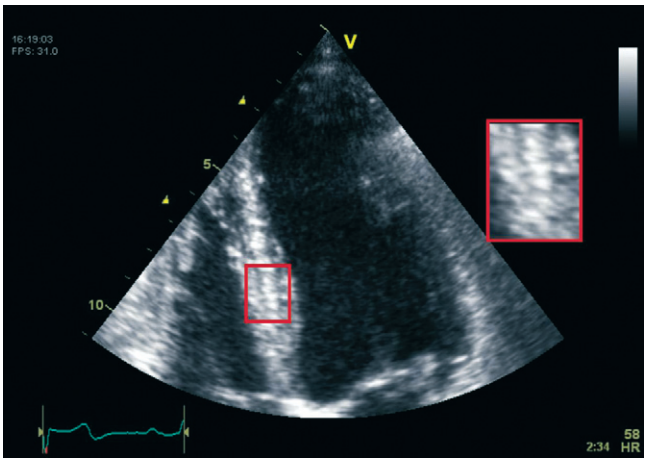



**Figure 10-10 Myocardial speckles.** Speckle tracking echocardiography measures strain by tracking speckles in gray-scale echocardiographic images. A part of the septum (*red box*) from a four-chamber view is enlarged.

**TABLE 10-1 Normal Values for Mitral Annular Velocities by TDI in 1266 Healthy Individuals**

| | LV (Mean of Four Walls) | | | | RV (Free Wall) | | |
|---|---|---|---|---|---|---|---|
| | *S′ (pwTDI)* | *S′ (cTDI)* | *E′ (pwTDI)* | *A′ (pwTDI)* | *S′ (pwTDI)* | *E′ (pwTDI)* | *A′ (pwTDI)* |
| **Female Sex** | | | | | | | |
| Feasibility, no. (%) | 652 (98%) | 657 (99%) | 652 (98%) | 652 (98%) | 648 (98%) | 648 (98%) | 648 (98%) |
| <40 y, cm/s | 8.9 ± 1.1 | 7.2 ± 1.0 | 14.6 ± 2.3 | 8.8 ± 1.9 | 13.0 ± 1.8 | 14.7 ± 2.9 | 12.4 ± 3.5 |
| 40-60 y, cm/s | 8.1 ± 1.2 | 6.5 ± 1.0 | 11.3 ± 2.4 | 10.0 ± 1.9 | 12.4 ± 1.9 | 13.1 ± 2.9 | 15.0 ± 3.5 |
| >60 y, cm/s | 7.2 ± 1.2 | 5.7 ± 1.1 | 8.2 ± 3.2 | 10.6 ± 1.9 | 11.8 ± 2.0 | 11.0 ± 2.3 | 16.1 ± 3.1 |
| All, cm/s | 8.2 ± 1.3 | 6.6 ± 1.1 | 11.8 ± 3.2 | 9.7 ± 2.0 | 12.5 ± 1.9 | 13.3 ± 3.0 | 14.4 ± 3.7 |
| **Male Sex** | | | | | | | |
| Feasibility, no. (%) | 590 (98%) | 601 (99%) | 590 (98%) | 590 (98%) | 586 (97%) | 586 (97%) | 586 (97%) |
| <40 y, cm/s | 9.4 ± 1.4 | 7.6 ± 1.2 | 14.1 ± 2.7 | 9.1 ± 1.7 | 13.2 ± 2.0 | 14.5 ± 2.9 | 12.3 ± 3.5 |
| 40-60 y, cm/s | 8.6 ± 1.3 | 6.9 ± 1.3 | 10.7 ± 2.3 | 10.4 ± 1.6 | 12.8 ± 2.2 | 12.5 ± 3.2 | 14.3 ± 3.7 |
| >60 y, cm/s | 8.0 ± 1.3 | 6.4 ± 1.2 | 8.2 ± 1.9 | 11.1 ± 1.6 | 12.5 ± 2.3 | 11.0 ± 3.0 | 15.8 ± 4.2 |
| All, cm/s | 8.6 ± 1.4 | 6.9 ± 1.3 | 10.8 ± 3.0 | 10.3 ± 1.7 | 12.8 ± 2.2 | 12.5 ± 3.3 | 14.2 ± 3.9 |

Modified from Dalen H, Thorstensen A, Vatten LJ, et al: Reference values and distribution of conventional echocardiographic Doppler measures and longitudinal tissue Doppler velocities in a population free from cardiovascular disease. *Circ Cardiovasc Imaging* 3(5):614-622, 2010.
*cTDI*, Color tissue-Doppler imaging; *pwTDI*, pulsed-wave tissue-Doppler imaging.

STE is not totally angle independent, because ultrasound images have better resolution along the ultrasound beam than perpendicular to the beam direction. Therefore, in principle, speckle tracking works better for measurements of motion and deformation in the direction along the ultrasound beams than for other directions. The ability of STE to measure strain had been documented in studies that have used both sonomicrometry and magnetic resonance imaging as reference methods.[17,29]

When applying STE, it is important to optimize image quality of the gray-scale image. This includes keeping the focus position at intermediate depth and adjusting the sector depth and width to include little but the region of interest. Assessment of 2D strain by STE is a semiautomatic method that requires a brief manual definition of a few points along the endocardial border. Furthermore, the sampling region of interest needs to be adjusted to ensure that most of the wall thickness is incorporated in the analysis and to avoid the pericardium. When automated tracking does not fit with the visual impression of wall motion, regions of interest need to be adjusted manually. End-systole is defined by aortic valve closure in the apical long-axis view, and this view should therefore always be analyzed first.

In most patients, 2D strain can be successfully assessed by STE in multiple LV segments. Strain values are calculated for each segment (segmental strain), for each of the theoretical vascular distribution areas (territorial strain), and as the average value of all segmental strains (global strain).[18] Feasibility is best for longitudinal and circumferential strain and is more challenging for radial strain.[30] One explanation for the lower feasibility for radial assessment of strain is that fewer speckles are present in this direction. Figure 10-13 shows segmental and

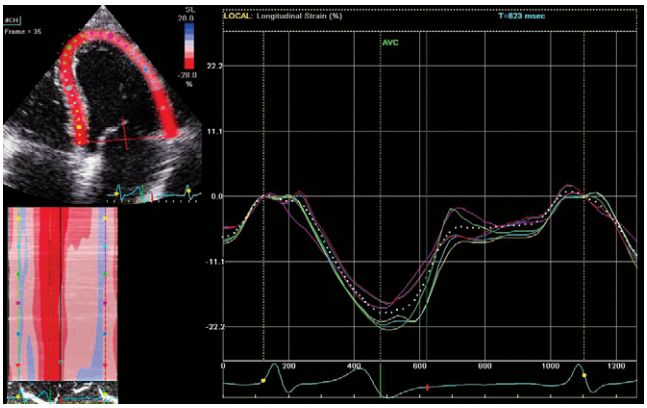



**Figure 10-11 Speckle tracking echocardiography showing long-axis strains.** The figure demonstrates a typical strain pattern from a normal LV. The colors in each strain trace correspond to the colorized LV segments in the 2D display at *upper left*. *AVC*, Aortic valve closure; *T*, time.

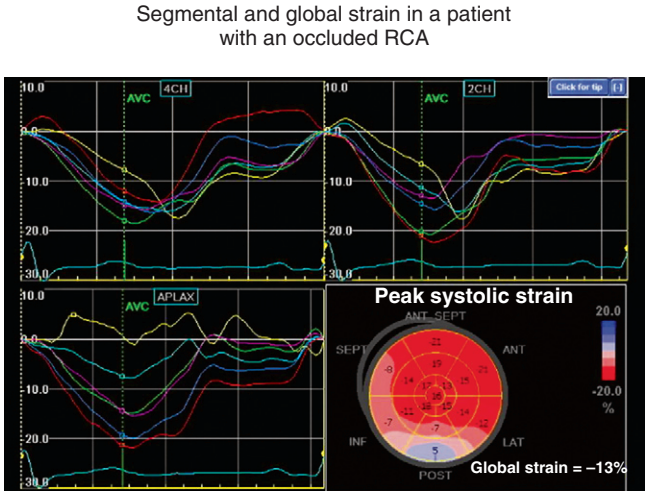



**Figure 10-13 Segmental longitudinal strain curves from all 16 LV segments in a patient with a myocardial infarction caused by an occlusion in the right coronary artery.** The bull's-eye plot at *lower right* demonstrates peak systolic strain value in each segment. *Red* color indicates shortening strains and *blue* indicates lengthening strains (see scale in *lower right panel*). The longitudinal global strain is the average value of peak systolic strain in all 16 LV segments and is –13% in this example.

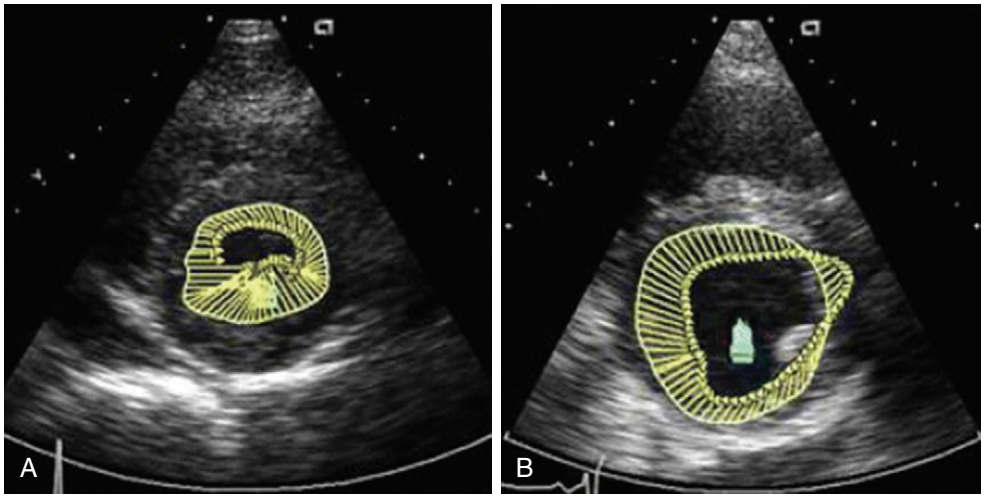



**Figure 10-12 Instantaneous myocardial velocity vectors can be calculated and displayed on dynamic gray-scale images.** This figure shows radial velocity vectors in the apical short-axis view from a normal patient (**A**) and a patient with left bundle branch block (LBBB) (**B**). In the normal patient, in late systole, the radial vectors show a synchronous pattern. In LBBB, in late systole, the septal vectors have peaked, whereas the lateral wall vectors are directed in the opposite direction (dyssynchronous). *(Modified from Vannan MA, Pedrizzetti G, Li P, et al: Effect of cardiac resynchronization therapy on longitudinal and circumferential left ventricular mechanics by velocity vector imaging: description and initial clinical application of a novel method using high-frame rate B-mode echocardiographic images.* Echocardiography *22[10]:826-830, 2005.)*

**TABLE 10-2 Normal Values for STE-Derived Longitudinal Strain and Strain Rates**

| Parameter | Peak Systolic Strain (%) | Peak Systolic Strain Rate (1/s) | Early Diastolic (E′) (1/s) |
|---|---|---|---|
| Mean ± SEM | −18.6 ± 0.1 | −1.10 ± 0.01 | 1.55 ± 0.01 |
| Lower 95% limit | 18.5 | −1.09 | 1.54 |
| Upper 95% limit | −18.7 | −1.11 | 1.56 |

Modified from Marwick TH, Leano RL, Brown J, et al: Myocardial strain measurement with 2-dimensional speckle-tracking echocardiography: definition of normal range. *JACC Cardiovasc Imaging* 2(1):80-84, 2009.

global strain in a patient with myocardial infarction. Normal global longitudinal strain values are reported between 18% and 25% in healthy individuals.[18,31] Measurements of longitudinal and circumferential LV deformation appear to be superior to LV ejection fraction as measures of LV function in patients with myocardial infarction.[30,32]

When evaluating LV systolic function, strain can be measured as peak systolic strain (positive or negative), as peak strain at end-systole (at time of aortic valve closure), or as peak strain regardless of timing (in systole or early diastole). There is no consensus regarding which time point should be used to measure peak strain in the assessment of systolic function.[33] Table 10-2 shows normal ranges for longitudinal strain and strain rates.[31]

It is also feasible to measure right ventricular (RV) and atrial strain by STE. However, because of the thin walls of these structures, signal quality may be suboptimal.

More recently, real-time 3D STE has been introduced as a method to measure LV volume, and preliminary results are promising.[34] In contrast to 2D STE, which cannot track motion occurring out of plane, 3D STE can track motion of speckles within the scan volume, irrespective of its direction. One limitation of the 3D STE technique is its dependency on image quality and in particular its ability to define the endocardial border. Furthermore, 3D STE is limited by random noise and relatively low temporal and spatial resolution.

### *Limitations of Strain Imaging by Speckle Tracking Echocardiography*

#### Inadequate Tracking

Like other 2D imaging techniques, STE relies on the assumption that morphologic details can be tracked from one frame to the next—that is, that they can be identified in consecutive frames. Because of the complex motion of the LV, this assumption may not always be valid.

Suboptimal tracking of the endocardial border may be a problem, in particular when image quality is poor. Because of the spatial smoothing, an erroneous segmental tracking might influence neighboring segmental strain values. When strain traces appear unphysiologic, one should evaluate signal quality and suboptimal tracking as potential causes. The global strain might be misjudged if too many segmental strain values are discarded because of suboptimal tracking. This is particularly true in localized myocardial diseases where strain values are unevenly distributed.

#### Spatial and Temporal Resolution

Raw tracking data are often quite noisy, so temporal and spatial averaging is needed to extract useful information. The smoothing is often performed using a spline method, which gives a good fit to the raw data while preventing too-rapid fluctuations. Frame rates of 40 to 80 frames per second are recommended. Too low a frame rate may cause the speckles to move out of plane or beyond the search area in successive frames. Too high a frame rate is not recommended because this is normally achieved by reducing the number of ultrasound beams in each frame, and thereby reducing the image quality. However, higher frame rates than 80/s may be needed to avoid undersampling in tachycardia. The relatively low temporal resolution of STE is a limitation in particular in regard to assessment of peak velocities and strain rates, because accurate measurement of these variables may require higher frame rates.

#### Reverberations

Reverberation with resulting underestimation of the true deformation represents an important and very common source of error. Furthermore, any artifacts that resemble speckles will influence the speckle tracking quality, and care should be taken to avoid these.

#### Off-Axis Image Plane

Because the polarity of radial strain is opposite to that of longitudinal and circumferential strains, it is essential that measurements be taken with optimal orientation of image planes. If the image plane intersects the ventricular wall at an angle intermediate between the long and the short axes, the measurement will underestimate true strain in the main axis. This implies that foreshortening might affect the 2D STE results and should be reduced to a minimum. Similarly, the short-axis views should be circular to assess the deformation in the true circumferential or radial planes.

## LV ROTATION AND TWIST BY SPECKLE TRACKING ECHOCARDIOGRAPHY

Left ventricular twist is the relative rotation of the apex around the LV long axis with respect to the base during the cardiac cycle. When viewed from apex to base, the apex rotates counterclockwise during systole and the base rotates in the opposite direction (Fig. 10-14). This is visualized in the simulation in Cines 1 and 2 (at ExpertConsult.com). The *rotation* and the apex-to-base difference in rotation, referred to as LV *twist* angle, are both expressed in degrees. The term *torsion* is a normalized value and refers to the base-to-apex gradient in rotation angle, expressed in degrees per centimeter (°/cm). It has been demonstrated that STE can measure LV rotation and twist (Fig. 10-15).[35,36] Because echocardiography does not provide accurate measures of the distance between the two image planes, it is difficult to measure torsion. Therefore the echocardiographic measures are limited to rotation and twist.

### *Limitations of LV Rotation and Twist by Speckle Tracking Echocardiography*

When using STE to measure LV twist, image quality of basal LV short-axis recordings represents a limitation. This is in part due to acoustic problems related to the depth of the basal part of the ventricle and to the wide sector angle that is needed to visualize the entire LV base. Furthermore, measurements are complicated by out-of-plane motion when the base descends toward the apex in systole. Because the twist increases toward the apex, it is important to standardize the apical short-axis view. It is often easiest to find the correct circular apical short-axis view by tilting the probe from the apical four-chamber view

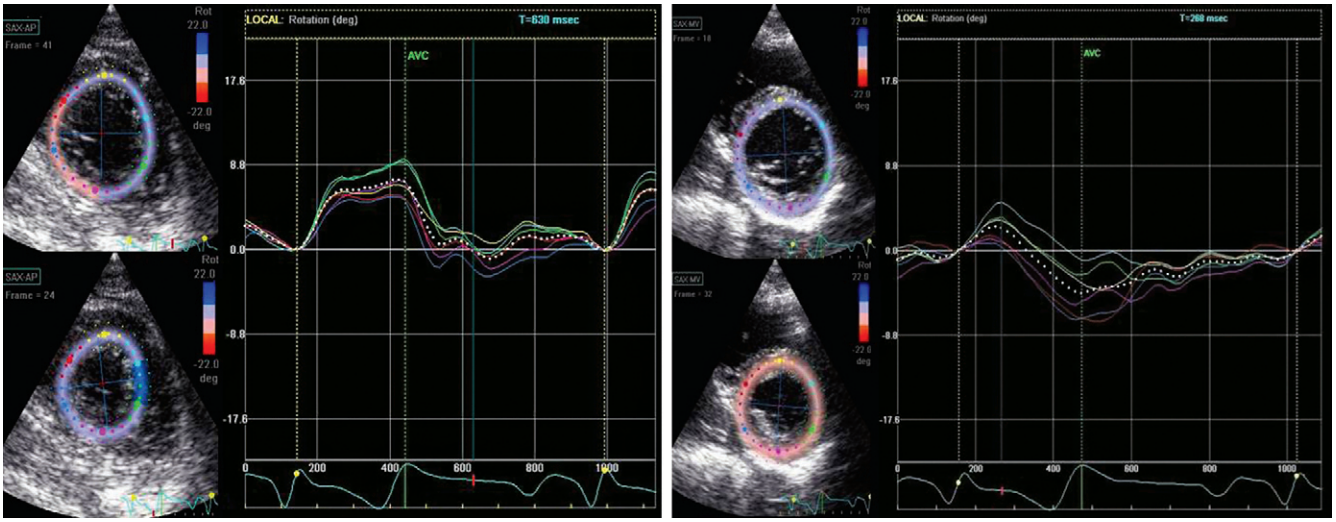



**Figure 10-14 LV rotation by speckle tracking echocardiography.** Apical rotation (*left panel*); basal rotation (*right panel*). The LV short axis in the *upper* windows of both panels represents end-diastole; *lower windows* represent the beginning of diastole and end of rotation. Note that when viewed from the apex, apical rotation is counterclockwise and basal rotation, clockwise, as shown by the *crosses* in the short-axis views. Clockwise rotation is represented by negative numbers in the scales, and counterclockwise rotation is represented by positive numbers.

rather than moving the probe in the apical direction from the parasternal short-axis view. This also increases the chance of capturing a circular apical short-axis view where the endocardium nearly closes at end-systole.[35]

The lack of standardization of imaging planes and different speckle tracking algorithms among vendors make it difficult at the present time to implement LV twist as a clinical measure. More documentation is needed before clinical recommendations can be given regarding assessment of LV twist as a diagnostic modality.

## Normal Physiology of the Left Ventricle

In order to interpret echocardiographic recordings by myocardial velocity and deformation imaging, it is important to understand the physiology of LV function. During normal systole, longitudinal myocardial shortening causes the LV base to descend toward the apex,[31,32,37] and there is circumferential shortening. Systolic thickening is a result of both longitudinal and circumferential shortening. The systolic descent of the base is approximately 12 to 15 mm in healthy people,[37] whereas the apex is relatively stationary, moving only a few millimeters. During diastole, there is myocardial lengthening during early diastole and during atrial-induced filling.

In addition, there is a twisting motion (torsion) of the left ventricle about its long axis, reflecting the fact that apex and base rotate in opposite directions (see Fig. 10-15). Left ventricular twist and untwist appear to play an important role for normal LV function.[38-42] Left ventricular untwist is associated with release of restoring forces, which contributes to diastolic suction and thereby facilitates early diastolic filling.[42] The twisting during systole and untwisting during early diastole have been referred to as a wringing motion of the left ventricle. The structural basis for LV twist is the spiral architecture of myocardial fiber orientation (Fig. 10-16). The subendocardial fibers are arranged in a right-handed helix and the subepicardial fibers in a left-handed helix.[36,43,44]

The magnitude and characteristics of LV twist have been described in various clinical and experimental studies, and it is well established that LV rotation is sensitive to changes in both regional and global LV function.[45-57] Therefore assessment of LV rotation represents an interesting approach for quantifying LV function. However, until recently magnetic resonance tagging has been the only clinical method available.[47,53-56,58-61] It has recently been shown that LV rotation and twist can be measured with STE.[35,36]

In LV short-axis images, TDI shows that the subendocardium moves faster than the subepicardium, which results in a transmural velocity gradient. Figure 10-17 illustrates that this velocity gradient reflects a progressive increase in strain (thickening fraction) when moving the sample volume from the epicardium toward the endocardium. More thickening in subendocardium than subepicardium does not represent a difference in contractility between wall layers, but is just a consequence of geometry and tissue incompressibility. As illustrated in Figure 10-18, the transmural gradient in thickening is consistent with the behavior of wall layers in simple spherical and ellipsoidal models.[62,63] Therefore a similar transmural strain gradient would occur with a noncontracting structure when compressed from the outside. In the LV long axis, there are also higher velocities and strains in the inner than in the outer wall layers, but the differences are smaller than for radial measurements and are difficult to measure by current technology.[64]

During the cardiac cycle, the LV velocity trace has three major velocity spikes (see Fig. 10-2).[4] In the long axis, the dominant systolic velocity component is directed toward the LV apex and represents the ejection phase. There are two major velocity components during diastole: an early diastolic velocity and an atrial-induced velocity, both directed toward the LV base. In addition, there are well-defined velocity spikes during isovolumic contraction and isovolumic relaxation.[65] All these velocity spikes are distinct features of the velocity trace and can be seen in virtually any imaging projection, but magnitude and direction of the velocities depends on projection.

### ISOVOLUMIC CONTRACTION

As illustrated in Figure 10-3, there is a sharp but brief velocity spike during isovolumic contraction. This velocity spike is caused by shortening that starts before mitral valve closure

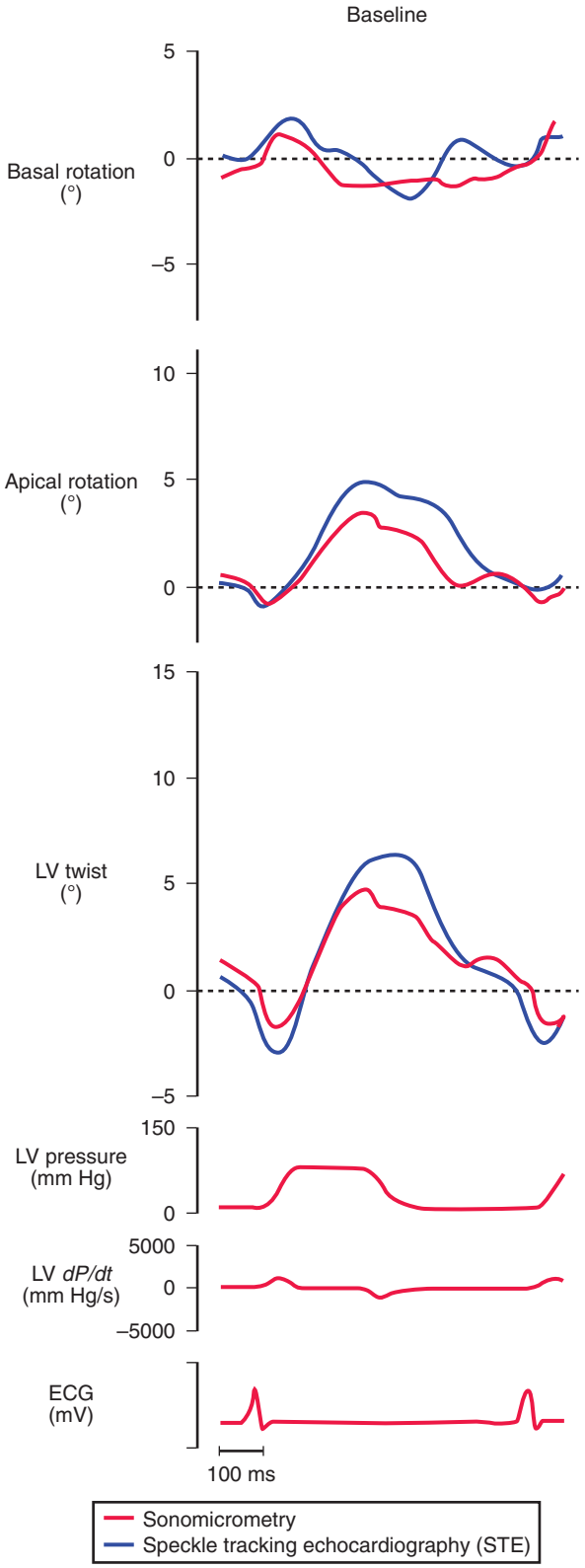



**Figure 10-15** Representative traces from an experimental study showing LV rotation and twist by sonomicrometry (*red lines*) and STE (*blue lines*). Twist is calculated as the difference between apical and basal rotation. Counterclockwise rotation is represented by positive numbers. *ECG*, Electrocardiogram. *(Modified from Opdahl A, Helle-Valle T, Remme EW, et al: Apical rotation by speckle tracking echocardiography: a simplified bedside index of left ventricular twist.* J Am Soc Echocardiogr *21[10]:1121-1128, 2008.)*

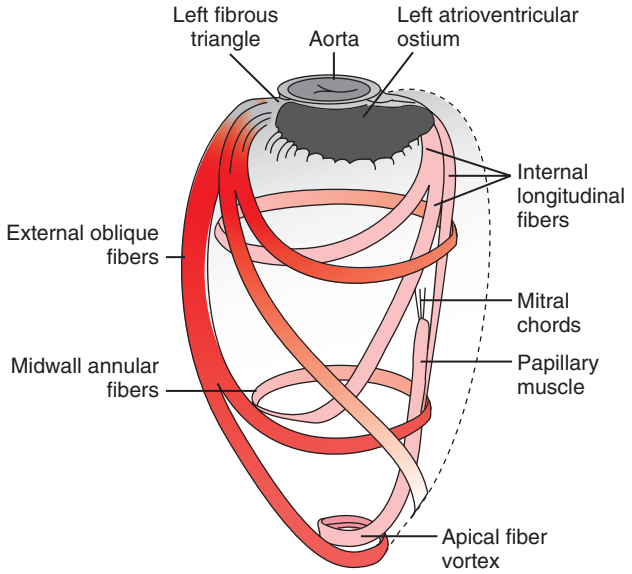



**Figure 10-16 Schematic drawing of fiber orientation in the left ventricle.** The subendocardial fibers have an approximately longitudinal orientation and the midwall fibers approximately circumferential orientation. The subepicardial fibers are oriented about 60° relative to the circumferential direction. *(From http://biomed.brown.edu/Courses/BI108/2006-108websites/group05ventrestoration/Website/cardiac_geometry.htm.)*

and is temporarily arrested when the mitral valve reaches its final closing position.[66] Myocardial shortening during isovolumic contraction can occur because blood is displaced toward the LV base and into the bulging mitral leaflets, which causes reduction in LV long and short axis, but no real change in LV volume. In some cases there is a small negative velocity component at the end of isovolumic contraction (see Fig. 10-2), which may reflect slight normal asynchrony in electromechanical activation.

The high frame rate of TDI enables measurement of myocardial acceleration, and studies of mitral and tricuspid ring motion suggest that isovolumic contraction acceleration can serve as an index of contractility.[67,68] This is an interesting concept and may be valid for studies of global LV function. However, regional myocardial acceleration does not reflect regional contractility during ischemia.[69] More studies are needed before isovolumic contraction acceleration can be recommended as a clinical tool to measure contractility.

## EJECTION

Peak systolic ejection velocity (S) has proven to be a marker of regional systolic function.[5,10,70-72] Myocardial velocity reaches a peak during the early phase of ejection and then decreases gradually. In some cases a second, smaller peak occurs later during ejection. Longitudinal velocities are more reproducible than radial velocities and can be measured in virtually all vascular territories of the LV. Therefore longitudinal velocities are recommended in the assessment of LV function. Table 10-1 presents normal ejection velocities from the LV long axis as assessed by TDI.

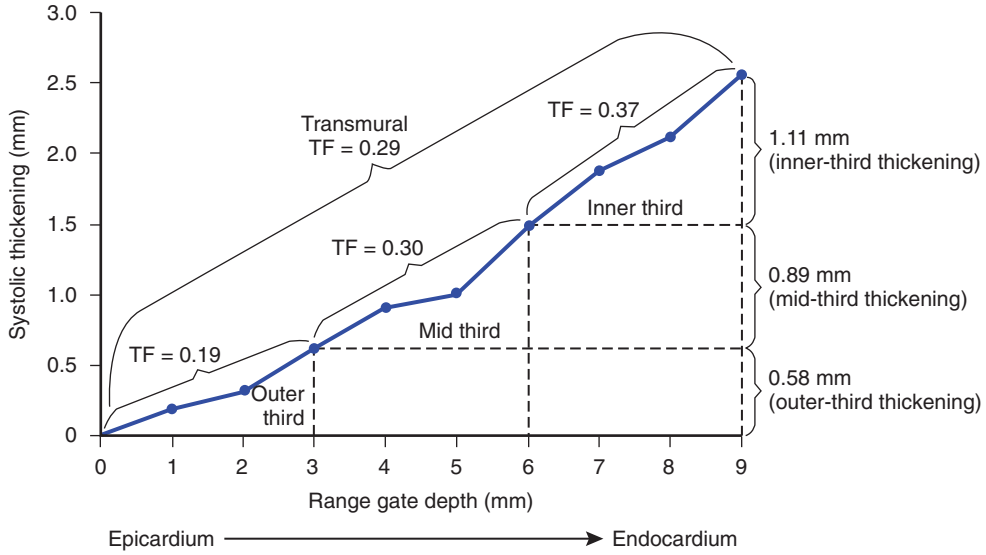



**Figure 10-17 Demonstration of transmural gradient in myocardial strain (thickening fraction) between inner and outer LV wall layers in a canine study.** The LV wall was divided into three layers, each 3 mm thick. Systolic thickening was measured by a 10-MHz miniaturized Doppler probe that was sutured to the epicardium. The figure displays systolic thickening fraction layer by layer and demonstrates that the inner layer thickens more than the outer layer. *TF,* Thickening fraction. *(Reproduced from Zhu WX, Myers ML, Hartley CJ, et al: Validation of a single crystal for measurement of transmural and epicardial thickening.* Am J Physiol *251[5 Pt 2]:H1045-H1055, 1986.)*

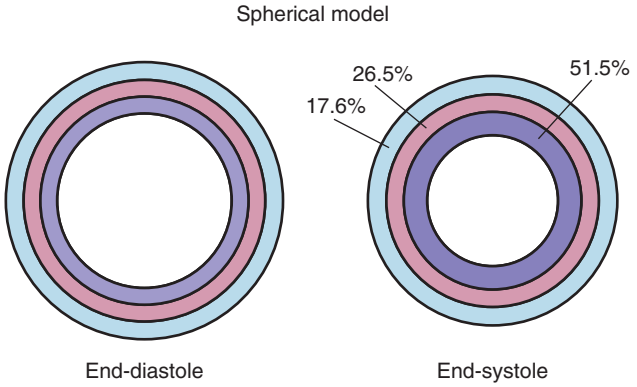



**Figure 10-18 Explanation of transmural strain gradient in LV short-axis strain.** A spherical model in which the wall is divided into equally spaced layers. The model assumes homogeneity of regional function and conservation of mass. In this model, there are no contractile elements, and therefore the difference in thickening between layers is only a geometric effect. The starting position (*left*) simulates end-diastole. At *right*, systole is simulated by reducing inner radius by 25%. Note the marked differences in the thickening of the inner (51.5%), middle (26.5%), and outer layers (17.6%). The same principle applies to cylindrical models, but the magnitude of the gradient is smaller. *(Reproduced from Hexeberg E, Homans DC, Bache RJ: Interpretation of systolic wall thickening. Can thickening of a discrete layer reflect fibre performance?* Cardiovasc Res *29[1]:16-21, 1995.)*

## ISOVOLUMIC RELAXATION

In the LV long axis, there is a negative velocity spike during isovolumic relaxation, which starts near end-systole and is temporarily interrupted by aortic valve closure[66] reflecting myocardial lengthening (see Fig. 10-2). This is analogous to the mechanism for the isovolumic contraction velocity and is attributed to a slight increase in LV volume associated with aortic valve closure and bulging of the valve leaflets into the LV. The volume increase at the end of systole is smaller than the volume decrease at the beginning of systole, consistent with the smaller cusps of the aortic valve compared with the mitral valve leaflets. At the end of isovolumic relaxation, there is normally a small positive velocity component that represents slight postsystolic shortening.[73] The etiology of this velocity component is not known, but it may reflect normal intraventricular asynchrony of relaxation.[74] In the diseased ventricle, and in particular during myocardial ischemia, there may be marked postsystolic shortening, and the postsystolic velocity may extend into the diastolic filling phase. Postsystolic velocities and strains in healthy subjects, however, are of low amplitude and occur before mitral valve opening.[73]

## DIASTOLE

Assessment of mitral annulus velocities by TDI plays an important role in the evaluation of patients with suspected diastolic dysfunction. Measurements are done from apical views, and velocities may be measured at septal, lateral, anterior, and inferior mitral annular areas. However, most often mitral annulus velocities are measured from an apical four-chamber view, and the septal, the lateral, or an average value of septal and lateral mitral annulus velocities is used. There are two main velocity waves, which reflect early-diastolic (E′) and atrial-induced (A′) myocardial lengthening (see Fig. 10-2). The E′ wave is often followed by an oppositely directed wave of low amplitude (E″) during early diastasis, which reflects changes in geometry associated with redistribution of blood within the LV cavity. In patients with markedly elevated LV filling pressure and delayed apical filling, E″ may be reduced or eradicated. Similar to systolic velocities, diastolic velocities decrease progressively from base toward apex.

Normal values for mitral annular velocities by TDI are presented in Table 10-1. Velocities measured in 2D color mode are lower than those measured by pulsed wave Doppler, and this needs to be taken into account when interpreting E′ in a clinical

context. In adults, E′ velocity decreases with age; therefore age-based normal values should be used when applying these measures of LV diastolic function in clinical practice.[75]

The magnitude of E′ is closely related to myocardial relaxation as indicated by its correlation with the time constant of LV isovolumic relaxation.[76-79] In addition to relaxation, which reflects the decay rate of active fiber force, E′ is determined by LV restoring forces, which represent release of energy that is stored in the myocardium when the ventricle has contracted below its resting length.[80] During early diastole, the restoring forces recoil the fibers back to their resting length, analogous to the recoil of a spring that has been compressed below its unstressed length. Restoring forces increase progressively when end-systolic volume is reduced and are therefore dependent on LV contractility. This illustrates the tight coupling between systolic shortening and diastolic lengthening and implies that E′ is determined by systolic as well as diastolic function. In the failing heart, however, when LV end-systolic volume is increased, restoring forces are essentially abolished, and systolic function has less influence on E′.

In addition to LV relaxation and restoring forces, E′ is also determined by early-diastolic load, which is LV pressure at onset of filling.[80] Strictly speaking, it is not LV intracavitary pressure, but LV transmural pressure (LV pressure minus pericardial pressure) that represents the distending force during filling.[81] Therefore the early-diastolic transmural LV pressure represents the load that causes LV lengthening and is named *LV lengthening load*.[80] In general, LV lengthening load will track changes in LV preload because changes in early-diastolic pressure are accompanied by changes in end-diastolic pressure. Thus the three main determinants of E′ are rate of relaxation, restoring forces, and lengthening load. In addition, LV diastolic stiffness may modulate E′.

In the failing ventricle, E′ is much less load dependent than are transmitral flow velocities.[79,82-84] Thus, when LV filling pressure becomes elevated in a failing ventricle, E increases more than E′, and the E/E′ ratio becomes elevated. This relative load independency of E′ forms the basis for using the E/E′ ratio as a marker of elevated LV filling pressure.[77,78,83,85]

It is also possible to measure diastolic strain rates and strains by TDI or STE. As shown in Figure 10-19, there are diastolic strain rates that correspond to the E′ and A′ velocity spikes, and strains that reflects early-diastolic and atrial-induced lengthening. In contrast to velocities, strain rates and strains are relatively similar at all measurement levels between base and apex. Strain rate and strain by TDI, however, have not proven to give added diagnostic value in routine assessment of diastolic function.

Therefore, at the present time, TDI-derived mitral annulus velocities by pulsed wave Doppler are recommended for the routine clinical evaluation of LV diastolic function.[79,86] Measurement of diastolic function by strain and strain rate needs more validation before recommendations can be made with regard to routine clinical use. Given the current state of the technologies, strain imaging by STE appear more robust than strain imaging by tissue Doppler.

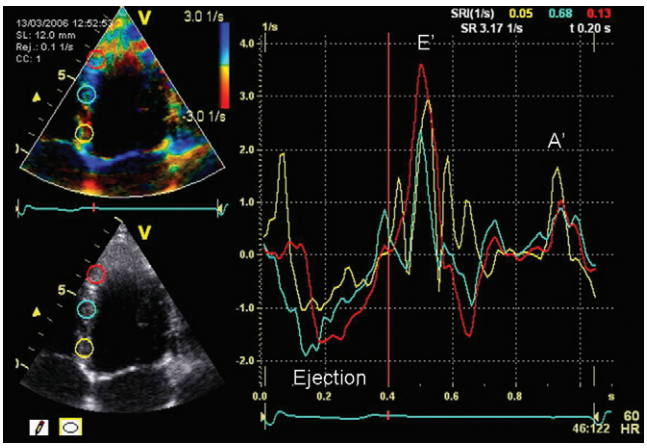



**Figure 10-19 Strain rates from the septum in a healthy individual.** The dominant negative trace during systole corresponds to ejection. The two dominant positive spikes are during early diastolic filling (*E′*) and during atrial-induced filling (*A′*).

## Myocardial Ischemia

Myocardial ischemia may be caused by either a reduction in coronary blood flow, as in acute coronary syndrome, or by an increase in myocardial oxygen demand during stress in patients with coronary artery stenosis. In either case, ischemia leads to reduction in regional myocardial function, which ranges from reduced systolic shortening (hypokinesia) to systolic lengthening (dyskinesia). Furthermore, myocardial ischemia leads to postsystolic shortening, that is, segmental shortening after end of LV ejection. Reduced systolic shortening and postsystolic shortening, which are the two hallmarks of ischemic dysfunction, can be quantified both by velocity and by deformation imaging.[9,16,72,87-91] Typical velocity and strain traces in acute myocardial ischemia are shown in Figure 10-3.

The main advantage of strain relative to velocity imaging is that measurements are less influenced by translational motion and tethering, and this makes strain more specific with regard to segmental localization of ischemia.[9,92] Therefore, in patients with acute infarctions, strain better defines the transitional zone between intact and dysfunctional myocardium and is superior to velocity imaging for defining anatomical extension of dysfunctional myocardium.[11]

In principle, strain is better than ejection velocity to quantify myocardial function, and in particular to differentiate between degrees of ischemic dysfunction. Whereas ejection velocity differentiates well between normal and ischemic myocardium, it has limited ability to differentiate between hypokinetic and dyskinetic myocardium. As demonstrated in Figure 10-20, systolic ejection velocity approaches zero in hypokinetic segments and becomes slightly negative in dyskinetic segments, but the difference between hypokinesis and dyskinesis is only minor. The strain trace in dyskinetic myocardium, however, is strikingly different from that in hypokinetic myocardium.

By extending velocity analysis to the isovolumic phases, however, velocity imaging may also identify dyskinetic myocardium. In ventricles with preserved systolic function, there is a dominantly positive longitudinal velocity during isovolumic contraction, with only a minor negative velocity component. With severe ischemia, the positive velocity component diminishes, and the negative component increases.[65,93] In dyskinetic myocardium, the positive velocity component is replaced by a large negative isovolumic contraction velocity (see Fig. 10-20). Furthermore, dyskinesia is associated with enhanced postsystolic velocity due to postsystolic shortening. Therefore a typical velocity trace from dyskinetic myocardium has a large negative velocity spike during isovolumic contraction and a large positive velocity during isovolumic relaxation, with velocities near

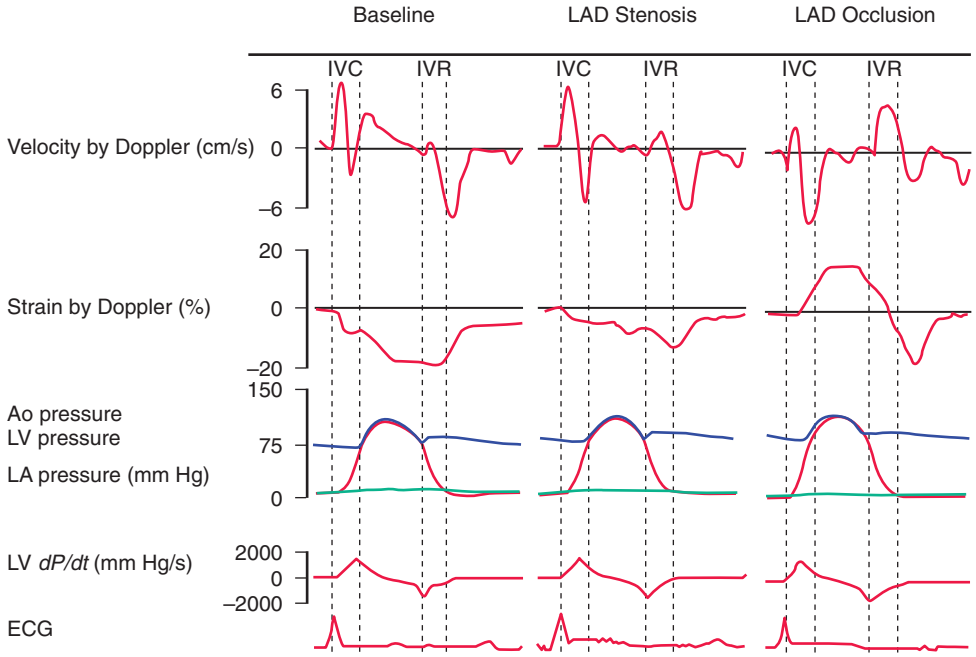



**Figure 10-20** Representative traces at baseline, during left anterior descending (*LAD*) stenosis and occlusion in an anesthetized dog showing myocardial Doppler velocities, strain, and pressure traces. Note that the ejection velocities are relatively similar during LAD stenosis and LAD occlusion, whereas the isovolumic contraction (*IVC*) and isovolumic relaxation (*IVR*) velocities are markedly different. During LAD occlusion, the large negative velocity spike during isovolumic contraction corresponds to systolic lengthening, as demonstrated in the strain trace. Furthermore, the marked postsystolic velocity during isovolumic relaxation corresponds to late systolic and postsystolic shortening in the strain trace. *(Modified from Skulstad, Urheim S, Edvardsen T, et al: Grading of myocardial dysfunction by tissue Doppler echocardiography: a comparison between velocity, displacement, and strain imaging in acute ischemia.* J Am Coll Cardiol *47:1672-1682, 2006.)*

zero during ejection. One should be aware that myocardial lengthening may not occur in nontransmural infarcts, because of shortening of intact subepicardial fibers.

Postsystolic shortening by TDI (Fig. 10-21) can be used as a marker of acute as well as stress-induced myocardial ischemia.[4,65,89,94] The mechanism of postsystolic shortening can be delayed active contraction, passive recoil of dyskinetic myocardium, or a combination of active contraction and passive recoil.[95] When postsystolic shortening occurs in entirely passive or necrotic myocardium, it is analogous to the behavior of a stretched elastic spring that recoils passively when the stretching force is removed. In moderately ischemic myocardium, postsystolic shortening is due to delayed active contraction.[95] Postsystolic shortening is not a specific sign for tissue viability because it occurs in actively contracting as well as in necrotic myocardium. Experimental work suggests that postsystolic shortening that far exceeds systolic lengthening may be a marker of tissue viability,[96] but the validity of this concept needs to be tested clinically. Clinically, postsystolic shortening, measured either as a postsystolic velocity or postsystolic strain, serves as a marker of ischemia, although low-magnitude postsystolic shortening can be present in some patients with a normal LV velocity pattern.[73,97]

Ischemia is also associated with changes in diastolic myocardial velocities, which could improve the ability of TDI to identify ischemic regions.[72,95,98] The clinical value of assessing diastolic velocities other than isovolumic relaxation velocities during ischemia, however, remains to be determined.

Displacement imaging and strain-rate imaging can also be used for assessing ischemic dysfunction. In clinical practice, however, they have no proven added value. The most robust TDI methodology is velocity imaging, which is recommended as the primary method; strain imaging may be used as a supplementary method.

In this section we have mainly discussed longitudinal TDI measures, because apical views give the most extensive imaging of the LV. Similar findings during ischemia can be observed with radial measurements in short-axis images, but are restricted to anteroseptal and posterior segments. Some authors present radial measurements as *velocity gradient* instead of strain rate.[26,99] This is a valid approach but is not used very much clinically.

In summary, myocardial ischemia is characterized by reduction in systolic ejection velocity and a postsystolic shortening velocity. Furthermore, in dyskinetic myocardium there is a marked negative velocity during isovolumic contraction representing systolic lengthening. Strain measurement can be used to verify changes in tissue velocities and is very useful to confirm dyskinesia. Furthermore, strain imaging provides a more site-specific measure.

## Cardiac Synchrony

Normal ventricular activation spreads rapidly through the conduction system, and the result is a synchronized ventricular contraction. In patients with severe heart failure, however, there is often prolonged inter- or intraventricular conduction, which leads to inter- or intraventricular mechanical dyssynchrony, resulting in ineffective ventricular function. Approximately one third of patients with low LV ejection fraction and class III to IV heart failure have a QRS duration longer than 120 ms. In addition, heart failure patients may have prolonged

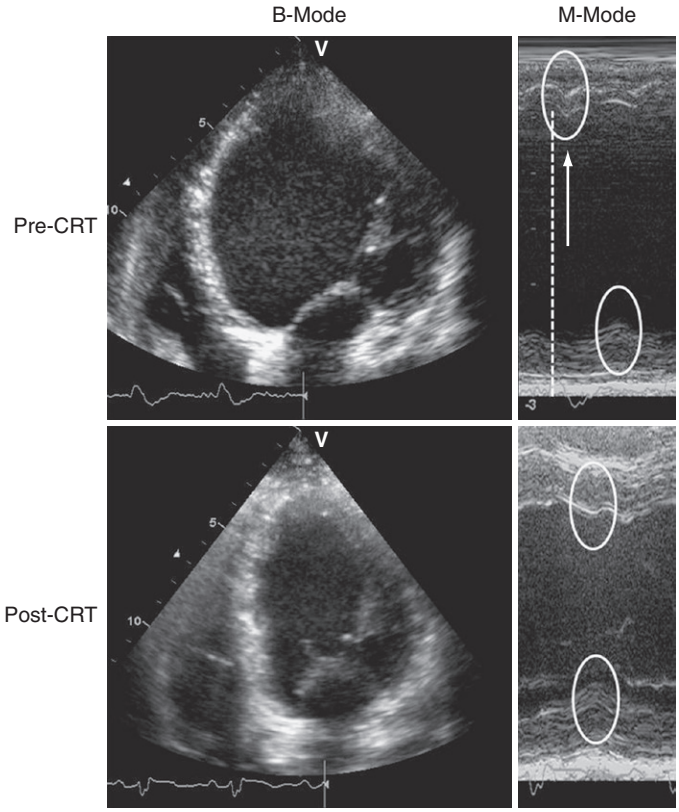



**Figure 10-21** B-mode and M-mode images from a patient responding to cardiac resynchronization therapy (*CRT*). *Upper panels* show LV before CRT and *lower panels* after 6 months of treatment. The M-mode recording demonstrates a typical septal beaking (*arrow*). This is seen as abnormal rapid leftward motion of the septum during preejection followed by rightward (paradoxical) motion. After CRT, a postsystolic septal displacement is observed. Peak systolic displacements (*ovals*) are dyssynchronous during left bundle branch block, but become more synchronous after CRT. *Dotted vertical line* indicates onset R in electrocardiogram. *(Courtesy Ola Gjesdal.)*

atrioventricular interval and therefore atrioventricular dyssynchrony. Of the three types of cardiac dyssynchrony, it is LV intraventricular dyssynchrony that appears to be the principal factor associated with development of heart failure.

## MECHANISMS OF LV MECHANICAL DYSSYNCHRONY

In principle, LV mechanical dyssynchrony has three possible etiologies: (1) delay in electrical conduction, (2) regional prolongation of electromechanical coupling time, and (3) different timing of myocardial shortening due to ischemia or nonuniform loading conditions. However, there is little evidence that disturbances in electromechanical coupling cause LV dyssynchrony. Therefore the clinical challenge is to differentiate between dyssynchrony that is caused by electrical conduction delay (electrical dyssynchrony) and dyssynchrony that is due to load or ischemia (primary mechanical dyssynchrony). This differentiation is important, because presumably only electrical dyssynchrony can be treated with biventricular pacing. Therefore, when patients are evaluated as candidates for biventricular pacing, it is essential to determine whether there is LV electrical dyssynchrony. A method that combines invasive LV pressure and myocardial strain by echocardiography has been proposed to differentiate between the two etiologies of dyssynchrony, but the method has not been clinically tested.[100] At present, QRS width in the electrocardiogram (ECG) is the only routine method that is used to identify electrical dyssynchrony, and the left bundle branch block pattern is the QRS morphology that best predicts success of cardiac resynchronization therapy. Chapter 26 discusses how to apply echocardiography in selection of candidates for cardiac resynchronization therapy.

## EFFECT OF LEFT BUNDLE BRANCH BLOCK ON LV FUNCTION

The most prominent echocardiographic feature of left bundle branch block (LBBB) is abnormal systolic motion of the interventricular septum.[101] (See Cine 3 at ExpertConsult.com.) The abnormal motion starts with rapid leftward motion of the septum during preejection, followed by rightward (paradoxical) motion, and is referred to as *septal beaking* when imaged by M-mode echocardiography[102] (see Fig. 10-21) and as *septal flash* (Fig. 10-22) when using myocardial velocity imaging.[103]

When using strain imaging, the abnormal systolic shortening pattern during LBBB can be assessed in more detail. In the normal heart the septum, similar to the LV free wall, shortens continuously during the LV ejection phase. In patients with LBBB, the septum has two phases with systolic shortening, one during preejection and one during midejection, and is followed by two phases of systolic lengthening.[104] This is illustrated in Figure 10-23.[104] The two phases of shortening are followed by early- and late-systolic lengthening. The preejection shortening and relengthening correspond to septal beaking and flash. The result of the abnormal motion is that net septal shortening, measured at the time of aortic valve closure, is markedly reduced compared to a normal heart. Therefore intraventricular dyssynchrony results in reduced contribution from the septum to LV stroke volume, and there is significant waste of myocardial work.[104-106] Reduced septal contribution is partly compensated for by increased shortening of the late-activated LV free wall, which is prestretched by the early septal contraction[107] (see Fig. 10-23). Strain analysis suggests that early-systolic septal shortening in LBBB causes a pressure rise that stretches the lateral wall and increases regional shortening via the Frank-Starling mechanism.[108] This in turn leads to increased work in the LV lateral wall and is a stimulus to regional hypertrophy and remodeling.[109] The pattern of septal strains, however, may be different in patients with septal dysfunction due to ischemia or other causes.

The mechanism of abnormal preejection motion of the septum in LBBB has been debated, but a recent study concludes that septal beaking during LBBB is caused by active septal contraction that is unopposed by the late-activated lateral LV wall.[110] It was previously proposed that preejection leftward septal motion occurs because the RV is activated first, causing RV pressure to transiently exceed LV pressure, thereby pushing the septum leftward like a passive membrane.[111,112] As shown recently, this mechanism may contribute to septal beaking but plays a minor role.[110] Therefore onset of preejection septal shortening represents timing of septal activation.

The early systolic lengthening of the septum can be attributed to forceful contraction of the hyperextended, late-activated LV lateral wall, which increases the transseptal pressure gradient and thereby pushes the septum rightward. The late-systolic

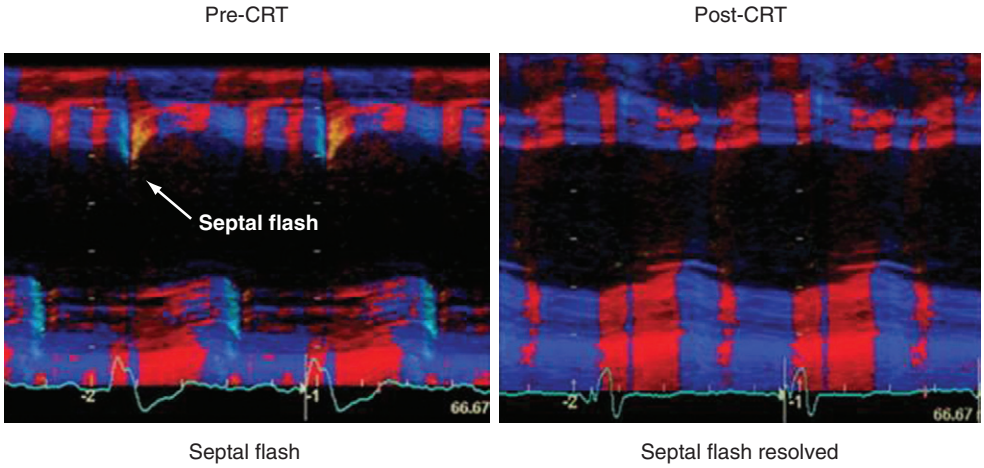



**Figure 10-22 Septal flash during left bundle branch block.** In dyssynchrony (*left*), the septum shows an early and fast thickening (*blue* color) and thinning (*red* color) during preejection. *CRT*, Cardiac resynchronization therapy. *(Modified from Parsai C, Bijnens B, Sutherland GR, et al: Toward understanding response to cardiac resynchronization therapy: left ventricular dyssynchrony is only one of multiple mechanisms.* Eur Heart J *30[8]:940-949, 2009.)*

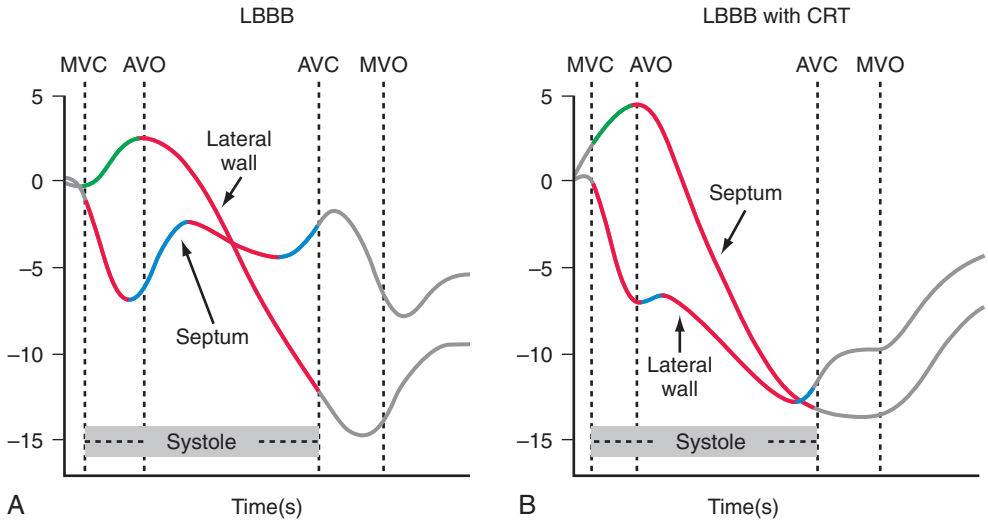



**Figure 10-23** The figure demonstrates systolic strain traces from septum and lateral wall in a patient with left bundle branch block (*LBBB*) before (*left*) and after (*right*) treatment with cardiac resynchronization therapy (*CRT*). During LBBB without CRT, there is a marked septal shortening (*red lines*) during preejection, and there is shortening during midejection. Each shortening is followed by lengthening (*blue lines*), resulting in both early- and late-systolic lengthening. The lateral wall shows preejection stretch (*green lines*) before treatment. These changes are reverted after treatment. A preejection stretch has appeared in the septum after treatment with CRT, indicating that there is also slight dyssynchrony during CRT. *AVC*, Aortic valve closure; *AVO*, aortic valve opening; *MVC*, mitral valve closure; *MVO*, mitral valve opening. *(Modified from De Boeck BW, Teske AJ, Meine M, et al: Septal rebound stretch reflects the functional substrate to cardiac resynchronization therapy and predicts volumetric and neurohormonal response.* Eur J Heart Fail *11(9):863-871, 2009.)*

lengthening of the septum probably reflects that the early activated septal segments start relaxing earlier than the late-activated lateral wall segments.[112]

## Mechanical Dispersion

In this section we describe a recently introduced application of velocity and deformation imaging that quantifies temporal nonuniformity of myocardial contraction: *mechanical dispersion*. This variable has turned out to be a promising marker of risk for ventricular arrhythmias and sudden death.[113,114] Mechanical dispersion can be assessed by either velocity or strain imaging and is calculated as the standard deviation of the time from onset of the Q-wave on the ECG to maximum myocardial shortening in 16 LV segments. Figure 10-24 shows typical recordings by strain imaging in a healthy individual and in a patient who has experienced ventricular arrhythmias. In the healthy heart, there is essentially similar timing of end of shortening in all myocardial segments. In the patient with arrhythmia, however, there is marked variability between segments in timing of end of shortening, and this variability is termed *mechanical dispersion*.

In patients with ischemic heart disease, increased mechanical dispersion has been associated with risk of arrhythmic events, independently of LV ejection fraction.[113] Because the majority of patients who suffer from malignant arrhythmias have ejection fractions above 35%, there is a need for new methods to identify risk.

Mechanical dispersion can also be demonstrated in patients with long QT syndrome (LQTS).[114,115] Until recently, LV function

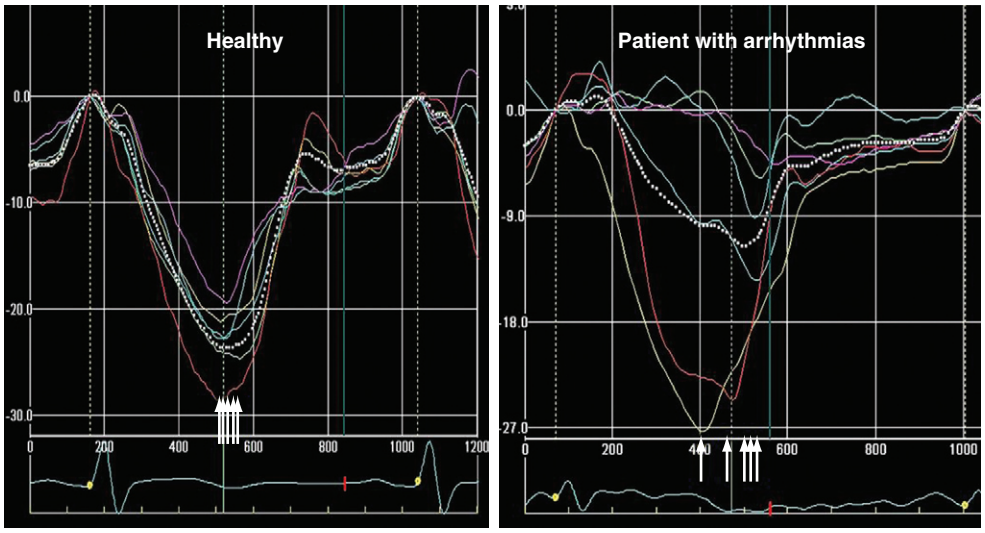



**Figure 10-24** Mechanical dispersion by strain echocardiography in a healthy individual (*left*) and a patient with previous ventricular arrhythmias (*right*). *Arrows* indicate the timing of peak strain in each of the myocardial LV segments as seen from the apical four-chamber view. The patient who has experienced previous ventricular arrhythmia has markedly dispersed timing of peak strain compared to the healthy individual. *(Modified from Haugaa KH, Smedsrud MK, Steen T, et al: Mechanical dispersion assessed by myocardial strain in patients after myocardial infarction for risk prediction of ventricular arrhythmia.* JACC Cardiovasc Imaging *3[3]:247-256, 2010.)*

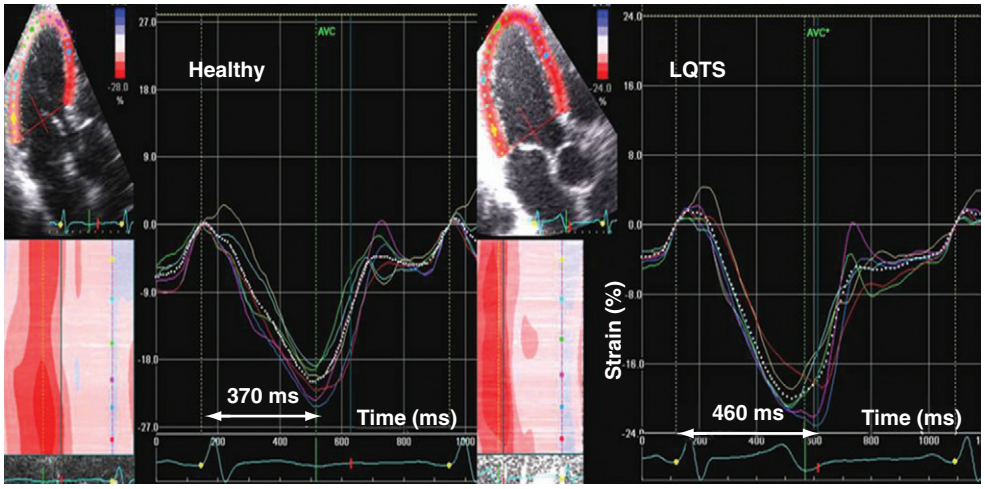



**Figure 10-25** Mechanical dispersion in a healthy individual (*left*) and a symptomatic long QT syndrome (*LQTS*) patient (*right*). Septal segments (*red, violet,* and *blue* curves) from apical long-axis view in the LQTS patient show prolonged myocardial shortening. The timing of peak strain in the LQTS patient is markedly dispersed compared to the healthy individual. *(Modified from Haugaa KH, Amlie JP, Berge KE, et al: Transmural differences in myocardial contraction in long-QT syndrome: mechanical consequences of ion channel dysfunction.* Circulation *122[14]:1355-1363, 2010.)*

was regarded as normal in these patients. Assessment of myocardial function by myocardial velocity and strain imaging, however, has revealed that LQTS patients have mechanical dispersion, that is, regional differences in duration of myocardial contraction (Fig. 10-25). The presence of mechanical dispersion was associated with a higher risk of cardiac arrhythmias in LQTS patients.[115] Potentially, mechanical dispersion in LQTS patients is related to the prolonged action potential duration and dispersion of action potential repolarization that are part of the syndrome. Both prolonged action potential duration with development of early after depolarizations and dispersion of electrical repolarization are considered to be important mechanisms of ventricular arrhythmias in these patients.

Mechanical dispersion as a clinical measure of risk of ventricular arrhythmias and sudden death is currently undergoing further testing. At the present time, assessment of mechanical dispersion is not established as a clinical routine method and should be considered a research tool.

## Right Ventricular Function

The RV has a complex anatomical structure. The RV is functionally divided into two parts, the inflow tract and the outflow tract, separated by the crista supraventricularis. Echocardiographic imaging of RV function and measurement of ejection fraction have been difficult because of the complex form and motion pattern of the RV and problems with defining the endocardial surface of the thin RV free wall. Another important factor that complicates the interpretation of RV function is the varying loading conditions. In daily cardiology practice, RV function is usually evaluated qualitatively by 2D echocardiography (see Chapter 32).

During systolic contraction there is longitudinal shortening of the RV, with the base descending toward the apex, while the apical part is relatively stationary. In addition, there is circumferential shortening that squeezes the ventricle. The interventricular septum contributes to RV as well as to LV function, and the relative contribution can be different in the normal and the diseased heart. The precise role of the septum remains to be determined.

RV (fractional area change) is also widely used as a measure of RV function.[116] It can be regarded as an area-based measure of RV function and is calculated from a four-chamber view.

Tricuspid annular plane systolic excursion (TAPSE) can be measured by M-mode echocardiography. TAPSE is a relatively fast and accurate measure of RV function. TAPSE correlates well with RV ejection fraction measured by radionuclide angiography.[117-119] A similar measure is obtained by TDI measurements of displacement.

The RV long-axis function can be expressed as velocity, strain, and strain rate along the lateral RV wall. All these measurements are helpful for quantifying RV longitudinal motion and will provide useful information in terms of quantification.

## KEY POINTS

- TDI provides measures of myocardial velocity, displacement, strain rate, and strain but is angle dependent.
- STE provides angle-independent measures of myocardial strain in multiple directions and can also be used to measure LV rotation and twist.
- TDI and STE provide unique diagnostic information in a number of cardiac diseases, but also have significant technical limitations.
- Assessment of mitral annulus velocities by TDI plays an important role in the evaluation of patients with suspected diastolic dysfunction.
- Myocardial velocity and strain imaging can be applied clinically to diagnose myocardial ischemia.
- Myocardial velocity and strain imaging can be used to quantify methods for quantification of LV dyssynchrony.
- Assessment of LV mechanical dispersion by velocity and strain imaging is a promising approach for prediction of risk of ventricular arrhythmias.

## REFERENCES


1. Marwick TH: Measurement of strain and strain rate by echocardiography: ready for prime time? *J Am Coll Cardiol* 47(7):1313-1327, 2006.
2. McDicken WN, Sutherland GR, Moran CM, Gordon LN: Colour Doppler velocity imaging of the myocardium. *Ultrasound Med Biol* 18(6-7):651-654, 1992.
3. Sutherland GR, Stewart MJ, Groundstroem KW, et al: Color Doppler myocardial imaging: a new technique for the assessment of myocardial function. *J Am Soc Echocardiogr* 7(5):441-458, 1994.
4. Edvardsen T, Aakhus S, Endresen K, et al: Acute regional myocardial ischemia identified by 2-dimensional multiregion tissue Doppler imaging technique. *J Am Soc Echocardiogr* 13(11):986-994, 2000.
5. Wilkenshoff UM, Hatle L, Sovany A, et al: Age-dependent changes in regional diastolic function evaluated by color Doppler myocardial imaging: a comparison with pulsed Doppler indexes of global function. *J Am Soc Echocardiogr* 14(10):959-969, 2001.
6. Dokainish H: Tissue Doppler imaging in the evaluation of left ventricular diastolic function. *Curr Opin Cardiol* 19(5):437-441, 2004.
7. Stoylen A, Skjaerpe T: Systolic long axis function of the left ventricle. Global and regional information. *Scand Cardiovasc J* 37(5):253-258, 2003.
8. Kerber RE, Marcus ML, Wilson R, et al: Effects of acute coronary occlusion on the motion and perfusion of the normal and ischemic interventricular septum. *Circulation* 54(6):928-935, 1976.
9. Urheim S, Edvardsen T, Torp H, et al: Myocardial strain by Doppler echocardiography. Validation of a new method to quantify regional myocardial function. *Circulation* 102(10):1158-1164, 2000.
10. Wilkenshoff UM, Sovany A, Wigstrom L, et al: Regional mean systolic myocardial velocity estimation by real-time color Doppler myocardial imaging: a new technique for quantifying regional systolic function. *J Am Soc Echocardiogr* 11(7):683-692, 1998.
11. Skulstad H, Urheim S, Edvardsen T, et al: Grading of myocardial dysfunction by tissue Doppler echocardiography: a comparison between velocity, displacement, and strain imaging in acute ischemia. *J Am Coll Cardiol* 47(8):1672-1682, 2006.
12. Galiuto L, Ignone G, DeMaria AN: Contraction and relaxation velocities of the normal left ventricle using pulsed-wave tissue Doppler echocardiography. *Am J Cardiol* 81(5):609-614, 1998.
13. Ellis RM, Franklin DL, Rushmer RF: Left ventricular dimensions recorded by sonocardiometry. *Circ Res* 4(6):684-688, 1956.
14. Zerhouni EA, Parish DM, Rogers WJ, et al: Human heart: tagging with MR imaging—a method for noninvasive assessment of myocardial motion. *Radiology* 169(1):59-63, 1988.
15. Edvardsen T, Gerber BL, Garot J, et al: Quantitative assessment of intrinsic regional myocardial deformation by Doppler strain rate echocardiography in humans: validation against three-dimensional tagged magnetic resonance imaging. *Circulation* 106(1):50-56, 2002.
16. Heimdal A, Stoylen A, Torp H, Skjaerpe T: Real-time strain rate imaging of the left ventricle by ultrasound. *J Am Soc Echocardiogr* 11(11):1013-1019, 1998.
17. Amundsen BH, Helle-Valle T, Edvardsen T, et al: Noninvasive myocardial strain measurement by speckle tracking echocardiography: validation against sonomicrometry and tagged magnetic resonance imaging. *J Am Coll Cardiol* 47(4):789-793, 2006.
18. Gjesdal O, Hopp E, Vartdal T, et al: Global longitudinal strain measured by two-dimensional speckle tracking echocardiography is closely related to myocardial infarct size in chronic ischaemic heart disease. *Clin Sci (Lond)* 113(6):287-296, 2007.
19. Mirsky I, Pasternac A, Ellison RC: General index for the assessment of cardiac function. *Am J Cardiol* 30(5):483-491, 1972.
20. Mirsky I, Parmley WW: Assessment of passive elastic stiffness for isolated heart muscle and the intact heart. *Circ Res* 33(2):233-243, 1973.
21. Fleming AD, Xia X, McDicken WN, et al: Myocardial velocity gradients detected by Doppler imaging. *Br J Radiol* 67(799):679-688, 1994.
22. Uematsu M, Nakatani S, Yamagishi M, et al: Usefulness of myocardial velocity gradient derived from two-dimensional tissue Doppler imaging as an indicator of regional myocardial contraction independent of translational motion assessed in atrial septal defect. *Am J Cardiol* 79(2):237-241, 1997.
23. Matre K, Fannelop T, Dahle GO, et al: Radial strain gradient across the normal myocardial wall in open-chest pigs measured with Doppler strain rate imaging. *J Am Soc Echocardiogr* 18(10):1066-1073, 2005.
24. Storaa C, Aberg P, Lind B, Brodin LA: Effect of angular error on tissue Doppler velocities and strain. *Echocardiography* 20(7):581-587, 2003.
25. Weidemann F, Jamal F, Kowalski M, et al: Can strain rate and strain quantify changes in regional systolic function during dobutamine infusion, B-blockade, and atrial pacing—implications for quantitative stress echocardiography. *J Am Soc Echocardiogr* 15(5):416-424, 2002.
26. Dalen H, Thorstensen A, Vatten LJ, et al: Reference values and distribution of conventional echocardiographic Doppler measures and longitudinal tissue Doppler velocities in a population free from cardiovascular disease: clinical perspective. *Circ Cardiovasc Imaging* 3(5):614-622, 2010.
27. Leitman M, Lysyansky P, Sidenko S, et al: Two-dimensional strain—a novel software for real-time quantitative echocardiographic assessment of myocardial function. *J Am Soc Echocardiogr* 17(10):1021-1029, 2004.
28. Kim DH, Kim HK, Kim MK, et al: Velocity vector imaging in the measurement of left ventricular twist mechanics: head-to-head one way comparison between speckle tracking

echocardiography and velocity vector imaging. *J Am Soc Echocardiogr* 22(12):1344-1352, 2009.
29. Korinek J, Wang J, Sengupta PP, et al: Two-dimensional strain—a Doppler-independent ultrasound method for quantitation of regional deformation: validation in vitro and in vivo. *J Am Soc Echocardiogr* 18(12):1247-1253, 2005.
30. Gjesdal O, Helle-Valle T, Hopp E, et al: Noninvasive separation of large, medium, and small myocardial infarcts in survivors of reperfused ST-elevation myocardial infarction: a comprehensive tissue Doppler and speckle-tracking echocardiography study. *Circ Cardiovasc Imaging* 1(3):189-196, 2008.
31. Marwick TH, Leano RL, Brown J, et al: Myocardial strain measurement with 2-dimensional speckle-tracking echocardiography: definition of normal range. *JACC Cardiovasc Imaging* 2(1):80-84, 2009.
32. Becker M, Hoffmann R, Kuhl HP, et al: Analysis of myocardial deformation based on ultrasonic pixel tracking to determine transmurality in chronic myocardial infarction. *Eur Heart J* 27(21):2560-2566, 2006.
33. Sjoli B, Orn S, Grenne B, et al: Diagnostic capability and reproducibility of strain by Doppler and by speckle tracking in patients with acute myocardial infarction. *JACC Cardiovasc Imaging* 2(1):24-33, 2009.
34. Nesser HJ, Mor-Avi V, Gorissen W, et al: Quantification of left ventricular volumes using three-dimensional echocardiographic speckle tracking; comparison with MRI. *Eur Heart J* 30:1565-1573, 2009.
35. Helle-Valle T, Crosby J, Edvardsen T, et al: New noninvasive method for assessment of left ventricular rotation: speckle tracking echocardiography. *Circulation* 112(20):3149-3156, 2005.
36. Notomi Y, Lysyansky P, Setser RM, et al: Measurement of ventricular torsion by two-dimensional ultrasound speckle tracking imaging. *J Am Coll Cardiol* 45(12):2034-2041, 2005.
37. Pai RG, Bodenheimer MM, Pai SM, et al: Usefulness of systolic excursion of the mitral annulus as an index of left ventricular systolic function. *Am J Cardiol* 67(2):222-224, 1991.
38. Wang J, Khoury DS, Yue Y, et al: Left ventricular untwisting rate by speckle tracking echocardiography. *Circulation* 116(22):2580-2586, 2007.
39. McDonald IG: The shape and movements of the human left ventricle during systole: a study by cineangiography and by cineradiography of epicardial markers. *Am J Cardiol* 26(3):221-230, 1970.
40. Rademakers FE, Buchalter MB, Rogers WJ, et al: Dissociation between left ventricular untwisting and filling. Accentuation by catecholamines. *Circulation* 85(4):1572-1581, 1992.
41. Gibbons Kroeker CA, Ter Keurs HE, Knudtson ML, et al: An optical device to measure the dynamics of apex rotation of the left ventricle. *Am J Physiol Heart Circ Physiol* 265(4):H1444-H1449, 1993.
42. Moon MR, Ingels NB Jr, Daughters GT, et al: Alterations in left ventricular twist mechanics with inotropic stimulation and volume loading in human subjects. *Circulation* 89(1):142-150, 1994.
43. Wu MT, Tseng WY, Su MY, et al: Diffusion tensor magnetic resonance imaging mapping the fiber architecture remodeling in human myocardium after infarction: correlation with viability and wall motion. *Circulation* 114(10):1036-1045, 2006.
44. Sengupta PP, Tajik AJ, Chandrasekaran K, Khandheria BK: Twist mechanics of the left ventricle: principles and application. *JACC Cardiovasc Imaging* 1(3):366-376, 2008.
45. Hansen DE, Daughters GT, Alderman EL, et al: Effect of volume loading, pressure loading, and inotropic stimulation on left ventricular torsion in humans. *Circulation* 83(4):1315-1326, 1991.
46. Yun KL, Niczyporuk MA, Daughters GT, et al: Alterations in left ventricular diastolic twist mechanics during acute human cardiac allograft rejection. *Circulation* 83(3):962-973, 1991.
47. Maier SE, Fischer SE, McKinnon GC, et al: Evaluation of left ventricular segmental wall motion in hypertrophic cardiomyopathy with myocardial tagging. *Circulation* 86(6):1919-1928, 1992.
48. Buchalter MB, Rademakers FE, Weiss JL, et al: Rotational deformation of the canine left ventricle measured by magnetic resonance tagging: effects of catecholamines, ischaemia, and pacing. *Cardiovasc Res* 28(5):629-635, 1994.
49. DeAnda A Jr, Komeda M, Nikolic SD, et al: Left ventricular function, twist, and recoil after mitral valve replacement. *Circulation* 92(9):458-466, 1995.
50. Gibbons Kroeker CA, Tyberg JV, Beyar R: Effects of load manipulations, heart rate, and contractility on left ventricular apical rotation: an experimental study in anesthetized dogs. *Circulation* 92(1):130-141, 1995.
51. Gibbons Kroeker CA, Tyberg JV, Beyar R: Effects of ischemia on left ventricular apex rotation: an experimental study in anesthetized dogs. *Circulation* 92(12):3539-3548, 1995.
52. Knudtson ML, Galbraith PD, Hildebrand KL, et al: Dynamics of left ventricular apex rotation during angioplasty: a sensitive index of ischemic dysfunction. *Circulation* 96(3):801-808, 1997.
53. Stuber M, Scheidegger MB, Fischer SE, et al: Alterations in the local myocardial motion pattern in patients suffering from pressure overload due to aortic stenosis. *Circulation* 100(4):361-368, 1999.
54. Nagel E, Stuber M, Lakatos M, et al: Cardiac rotation and relaxation after anterolateral myocardial infarction. *Coron Artery Dis* 11(3):261-267, 2000.
55. Sandstede JJW, Johnson T, Harre K, et al: Cardiac systolic rotation and contraction before and after valve replacement for aortic stenosis: a myocardial tagging study using MR imaging. *Am J Roentgenol* 178(4):953-958, 2002.
56. Fuchs E, Muller MF, Oswald H, et al: Cardiac rotation and relaxation in patients with chronic heart failure. *European Journal of Heart Failure* 6(6):715-722, 2004.
57. Tibayan FA, Rodriguez F, Langer F, et al: Alterations in left ventricular torsion and diastolic recoil after myocardial infarction with and without chronic ischemic mitral regurgitation. *Circulation* 110(11 Suppl 1):II 109-114, 2004.
58. Buchalter MB, Weiss JL, Rogers WJ, et al: Noninvasive quantification of left ventricular rotational deformation in normal humans using magnetic resonance imaging myocardial tagging. *Circulation* 81(4):1236-1244, 1990.
59. Fogel MA, Weinberg PM, Hubbard A, Haselgrove J: Diastolic biomechanics in normal infants utilizing MRI tissue tagging. *Circulation* 102(2):218-224, 2000.
60. Nagel E, Stuber M, Burkhard B, et al: Cardiac rotation and relaxation in patients with aortic valve stenosis. *Eur Heart J* 21(7):582-589, 2000.
61. Setser RM, Kasper JM, Lieber ML, et al: Persistent abnormal left ventricular systolic torsion in dilated cardiomyopathy after partial left ventriculectomy. *J Thorac Cardiovasc Surg* 126(1):48-55, 2003.
62. Hexeberg E, Homans DC, Bache RJ: Interpretation of systolic wall thickening. Can thickening of a discrete layer reflect fiber performance? *Cardiovasc Res* 29(1):16-21, 1995.
63. Arts T, Reneman RS, Veenstra PC: A model of the mechanics of the left ventricle. *Ann Biomed Eng* 7(3-4):299-318, 1979.
64. Hashimoto I, Li X, Hejmadi BA, Jones M, Zetts AD, Sahn DJ: Myocardial strain rate is a superior method for evaluation of left ventricular subendocardial function compared with tissue Doppler imaging. *J Am Coll Cardiol* 42(9):1574-1583, 2003.
65. Edvardsen T, Urheim S, Skulstad H, et al: Quantification of left ventricular systolic function by tissue Doppler echocardiography: added value of measuring pre- and postejection velocities in ischemic myocardium. *Circulation* 105(17):2071-2077, 2002.
66. Remme EW, Lyseggen E, Helle-Valle T, et al: Mechanisms of preejection and postejection velocity spikes in left ventricular myocardium: interaction between wall deformation and valve events. *Circulation* 118(4):373-380, 2008.
67. Vogel M, Schmidt MR, Kristiansen SB, et al: Validation of myocardial acceleration during isovolumic contraction as a novel noninvasive index of right ventricular contractility: comparison with ventricular pressure-volume relations in an animal model. *Circulation* 105(14):1693-1699, 2002.
68. Vogel M, Cheung MM, Li J, et al: Noninvasive assessment of left ventricular force-frequency relationships using tissue Doppler-derived isovolumic acceleration: validation in an animal model. *Circulation* 107(12):1647-1652, 2003.
69. Lyseggen E, Rabben SI, Skulstad H, et al: Myocardial acceleration during isovolumic contraction: relationship to contractility. *Circulation* 111(11):1362-1369, 2005.
70. Isaaz K, Munoz del RL, Lee E, Schiller NB: Quantitation of the motion of the cardiac base in normal subjects by Doppler echocardiography. *J Am Soc Echocardiogr* 6(2):166-176, 1993.
71. Pai RG, Gill KS: Amplitudes, durations, and timings of apically directed left ventricular myocardial velocities: I. Their normal pattern and coupling to ventricular filling and ejection. *J Am Soc Echocardiogr* 11(2):105-111, 1998.
72. Derumeaux G, Ovize M, Loufoua J, et al: Doppler tissue imaging quantitates regional wall motion during myocardial ischemia and reperfusion. *Circulation* 97(19):1970-1977, 1998.
73. Voigt JU, Lindenmeier G, Exner B, et al: Incidence and characteristics of segmental postsystolic longitudinal shortening in normal, acutely ischemic, and scarred myocardium. *J Am Soc Echocardiogr* 16(5):415-423, 2003.
74. Sengupta PP, Khandheria BK, Korinek J, et al: Apex-to-base dispersion in regional timing of left ventricular shortening and lengthening. *J Am Coll Cardiol* 47(1):163-172, 2006.
75. Nagueh SF, Appleton CP, Gillebert TC, et al: Recommendations for the evaluation of left ventricular diastolic function by echocardiography. *J Am Soc Echocardiogr* 22(2):107-133, 2009.

76. Firstenberg MS, Greenberg NL, Main ML, et al: Determinants of diastolic myocardial tissue Doppler velocities: influences of relaxation and preload. *J Appl Physiol* 90(1):299-307, 2001.
77. Nagueh SF, Middleton KJ, Kopelen HA, et al: Doppler tissue imaging: a noninvasive technique for evaluation of left ventricular relaxation and estimation of filling pressures. *J Am Coll Cardiol* 30(6):1527-1533, 1997.
78. Ommen SR, Nishimura RA, Appleton CP, et al: Clinical utility of Doppler echocardiography and tissue Doppler imaging in the estimation of left ventricular filling pressures: A comparative simultaneous Doppler-catheterization study. *Circulation* 102(15): 1788-1794, 2000.
79. Sohn DW, Chai IH, Lee DJ, et al: Assessment of mitral annulus velocity by Doppler tissue imaging in the evaluation of left ventricular diastolic function. *J Am Coll Cardiol* 30(2):474-480, 1997.
80. Opdahl A, Remme EW, Helle-Valle T, et al: Determinants of left ventricular early-diastolic lengthening velocity. Independent contributions from left ventricular relaxation, restoring forces, and lengthening load. *Circulation* 2009.
81. Smiseth OA, Frais MA, Kingma I, et al: Assessment of pericardial constraint in dogs. *Circulation* 71(1):158-164, 1985.
82. Hasegawa H, Little WC, Ohno M, et al: Diastolic mitral annular velocity during the development of heart failure. *J Am Coll Cardiol* 41(9):1590-1597, 2003.
83. Nagueh SF, Mikati I, Kopelen HA, et al: Doppler estimation of left ventricular filling pressure in sinus tachycardia. A new application of tissue doppler imaging. *Circulation* 98(16):1644-1650, 1998.
84. Nagueh SF, Sun H, Kopelen HA, et al: Hemodynamic determinants of the mitral annulus diastolic velocities by tissue Doppler. *J Am Coll Cardiol* 37(1):278-285, 2001.
85. Nagueh SF, Lakkis NM, Middleton KJ, et al: Doppler estimation of left ventricular filling pressures in patients with hypertrophic cardiomyopathy. *Circulation* 99(2):254-261, 1999.
86. Nagueh SF, Bhatt R, Vivo RP, et al: Echocardiographic evaluation of left ventricular hemodynamics in patients with decompensated heart failure. *Circ Cardiovasc Imaging* 4(3):220-227, 2011.
87. Edvardsen T, Skulstad H, Aakhus S, et al: Regional myocardial systolic function during acute myocardial ischemia assessed by strain Doppler echocardiography. *J Am Coll Cardiol* 37(3):726-730, 2001.
88. Gorcsan J III, Strum DP, Mandarino WA, Pinsky MR: Color-coded tissue Doppler assessment of the effects of acute ischemia on regional left ventricular function: comparison with sonomicrometry. *J Am Soc Echocardiogr* 14(5):335-342, 2001.
89. Voigt JU, Exner B, Schmiedehausen K, et al: Strain-rate imaging during dobutamine stress echocardiography provides objective evidence of inducible ischemia. *Circulation* 107(16): 2120-2126, 2003.
90. Madler CF, Payne N, Wilkenshoff U, et al: Non-invasive diagnosis of coronary artery disease by quantitative stress echocardiography: optimal diagnostic models using off-line tissue Doppler in the MYDISE study. *Eur Heart J* 24(17):1584-1594, 2003.
91. Smiseth OA, Stoylen A, Ihlen H: Tissue Doppler imaging for the diagnosis of coronary artery disease. *Curr Opin Cardiol* 19(5):421-429, 2004.
92. Stoylen A, Heimdal A, Bjornstad K, et al: Strain rate imaging by ultrasonography in the diagnosis of coronary artery disease. *J Am Soc Echocardiogr* 13(12):1053-1064, 2000.
93. Pislaru C, Bruce CJ, Belohlavek M, et al: Intracardiac measurement of pre-ejection myocardial velocities estimates the transmural extent of viable myocardium early after reperfusion in acute myocardial infarction. *J Am Coll Cardiol* 38(6):1748-1756, 2001.
94. Kukulski T, Jamal F, Herbots L, et al: Identification of acutely ischemic myocardium using ultrasonic strain measurements. A clinical study in patients undergoing coronary angioplasty. *J Am Coll Cardiol* 41(5):810-819, 2003.
95. Skulstad H, Edvardsen T, Urheim S, et al: Postsystolic shortening in ischemic myocardium: active contraction or passive recoil? *Circulation* 106(6):718-724, 2002.
96. Lyseggen E, Skulstad H, Helle-Valle T, et al: Myocardial strain analysis in acute coronary occlusion: a tool to assess myocardial viability and reperfusion. *Circulation* 112(25):3901-3910, 2005.
97. Pislaru C, Anagnostopoulos PC, Seward JB, et al: Higher myocardial strain rates during isovolumic relaxation phase than during ejection characterize acutely ischemic myocardium. *J Am Coll Cardiol* 40(8):1487-1494, 2002.
98. Gorcsan J III, Strum DP, Mandarino WA, et al: Quantitative assessment of alterations in regional left ventricular contractility with color-coded tissue Doppler echocardiography. Comparison with sonomicrometry and pressure-volume relations. *Circulation* 95(10): 2423-2433, 1997.
99. Derumeaux G, Ovize M, Loufoua J, et al: Assessment of nonuniformity of transmural myocardial velocities by color-coded tissue Doppler imaging: characterization of normal, ischemic, and stunned myocardium. *Circulation* 101(12):1390-1395, 2000.
100. Russell K, Opdahl A, Remme EW, et al: Evaluation of left ventricular dyssynchrony by onset of active myocardial force generation: a novel method which differentiates between electrical and mechanical etiologies. *Circ Cardiovasc Imaging* 2010.
101. McDonald IG: Echocardiographic demonstration of abnormal motion of the interventricular septum in left bundle branch block. *Circulation* 48(2):272-280, 1973.
102. Dillon JC, Chang S, Feigenbaum H: Echocardiographic manifestations of left bundle branch block. *Circulation* 49(5):876-880, 1974.
103. Parsai C, Bijnens B, Sutherland GR, et al: Toward understanding response to cardiac resynchronization therapy: left ventricular dyssynchrony is only one of multiple mechanisms. *Eur Heart J* 30(8):940-949, 2009.
104. Gjesdal O, Remme EW, Opdahl A, et al: Mechanisms of abnormal systolic motion of the interventricular septum during left bundle-branch block. *Circ Cardiovasc Imaging*, in press.
105. Nelson GS, Curry CW, Wyman BT, et al: Predictors of systolic augmentation from left ventricular preexcitation in patients with dilated cardiomyopathy and intraventricular conduction delay. *Circulation* 101(23):2703-2709, 2000.
106. Prinzen FW, Vernooy K, Deboeck BW, Delhaas T: Mechano-energetics of the asynchronous and resynchronized heart. *Heart Fail Rev* 2010.
107. Prinzen FW, Hunter WC, Wyman BT, McVeigh ER: Mapping of regional myocardial strain and work during ventricular pacing: experimental study using magnetic resonance imaging tagging. *J Am Coll Cardiol* 33(6):1735-1742, 1999.
108. Breithardt OA, Stellbrink C, Herbots L, et al: Cardiac resynchronization therapy can reverse abnormal myocardial strain distribution in patients with heart failure and left bundle branch block. *J Am Coll Cardiol* 42(3):486-494, 2003.
109. Spragg DD, Leclercq C, Loghmani M, et al: Regional alterations in protein expression in the dyssynchronous failing heart. *Circulation* 108(8):929-932, 2003.
110. Gjesdal O, Remme E, Opdahl A, et al: Preejection tug of war between early-activated septum and late-activated lateral wall in left bundle branch block (abstract). *Eur Heart J* 31:407, 2010.
111. Kingma I, Tyberg JV, Smith ER: Effects of diastolic transseptal pressure gradient on ventricular septal position and motion. *Circulation* 68(6):1304-1314, 1983.
112. Little WC, Reeves RC, Arciniegas J, et al: Mechanism of abnormal interventricular septal motion during delayed left ventricular activation. *Circulation* 65(7):1486-1491, 1982.
113. Haugaa KH, Smedsrud MK, Steen T, et al: Mechanical dispersion assessed by myocardial strain in patients after myocardial infarction for risk prediction of ventricular arrhythmia. *JACC Cardiovasc Imaging* 3(3):247-256, 2010.
114. Haugaa KH, Amlie JP, Berge KE, et al: Transmural differences in myocardial contraction in long-QT syndrome: mechanical consequences of ion channel dysfunction. *Circulation* 122(14):1355-1363, 2010.
115. Haugaa KH, Edvardsen T, Leren TP, et al: Left ventricular mechanical dispersion by tissue Doppler imaging: a novel approach for identifying high-risk individuals with long QT syndrome. *Eur Heart J* 30(3):330-337, 2009.
116. Lopez-Candales A, Rajagopalan N, Saxena N, et al: Right ventricular systolic function is not the sole determinant of tricuspid annular motion. *Am J Cardiol* 98(7):973-977, 2006.
117. Meluzin J, Spinarova L, Bakala J, et al: Pulsed Doppler tissue imaging of the velocity of tricuspid annular systolic motion; a new, rapid, and non-invasive method of evaluating right ventricular systolic function. *Eur Heart J* 22(4):340-348, 2001.
118. Badano LP, Ginghina C, Easaw J, et al: Right ventricle in pulmonary arterial hypertension: haemodynamics, structural changes, imaging, and proposal of a study protocol aimed to assess remodelling and treatment effects. *Eur J Echocardiogr* 11(1):27-37, 2010.
119. Kaul S, Tei C, Hopkins JM, Shah PM: Assessment of right ventricular function using two-dimensional echocardiography. *Am Heart J* 107(3):526-531, 1984.



# Assessment of Diastolic Function by Echocardiography

JUAN CARLOS PLANA, MD | MILIND Y. DESAI, MD | ALLAN L. KLEIN, MD

**Basic Principles**
Physiology of Diastole
Determinants of Diastolic Function
Definition of Diastolic Dysfunction
**Echocardiographic Evaluation of Diastolic Function**
Doppler Techniques in Assessment of Diastolic Filling Patterns
LA Volume Index
Strain Imaging in Evaluation of Diastolic Function
Torsion Echocardiography
New ASE/EAE Guidelines
**Clinical Utility of Diastolic Function Assessment**
Myocardial Diseases
Hypertension and Hypertensive Heart Disease
Ischemic Cardiac Disease
Pericardial Disease
Restrictive versus Constrictive Physiology

Heart failure (HF) is a major public health problem in the Western world. Over the years, our understanding of the natural history of HF has evolved to recognize that cardiovascular disease can result in systolic and or diastolic dysfunction of the heart.[1,2] To date, echocardiography remains the most robust and widely used technique in the evaluation of diastolic function.[3] This chapter discusses the state-of-the-art echocardiographic techniques used in the optimal assessment of diastolic function. The role of echocardiography in specific cardiac diseases, that cause diastolic dysfunction, is then highlighted.

## Basic Principles

### PHYSIOLOGY OF DIASTOLE

The cardiac cycle is broadly divided into two phases: systole and diastole. Diastole is the time period that extends from the closure of the aortic valve to the termination of the mitral inflow (closure of the mitral valve). It is divided into four phases: isovolumic relaxation, early rapid filling, diastasis, and atrial systole. These phases are shown relating the aorta, left ventricle (LV), left atrium (LA), and LV volumes[4] (Fig. 11-1).

#### *Isovolumic Relaxation*

By definition, this period extends from the time of aortic valve closure to mitral valve opening and occurs without a change in LV volume.[5] It is an energy-dependent process, which occurs until middiastole. Ventricular pressure ($P_v$) decay during the isovolumic period follows an approximately exponential curve that can be characterized by its starting pressure ($P_o$) and its time constant ($\tau$).[6] This curve can be fitted with the assumption of either a zero asymptote $P_v = (P_o e^{-t/\tau})$, or a nonzero asymptote $P_v = (P_o e^{-t/\tau} + P_b)$ (to account for subatmospheric pressure and the effects of pericardial pressure), where $P_b$ is the LV pressure at the time of aortic closure or peak negative $dp/dt$, t is the time after the onset of relaxation, and $\tau$ is the time constant of relaxation.

A low $\tau$ value is suggestive of fast relaxation, whereas a high value represents slow relaxation. Isovolumic relaxation ends when the LV pressure falls below the LA pressure, resulting in mitral valve opening and the beginning of the rapid filling phase.[7]

#### *Rapid Filling*

The rapid filling phase starts with the opening of the mitral valve.[7] Left ventricular suction, continued LV relaxation, and elastic recoil leads to a continuous fall in LV pressure, resulting in the development of an LA-to-LV pressure gradient, with subsequent blood acceleration.[7] This gradient is influenced by the level of LA pressure at mitral valve opening, and the rate of decline of LV pressure.[8] Blood rapidly enters the LV from the LA during the early filling period with approximately 70% of the stroke volume received by the LV during the first third of diastole.[9] Active ventricular suction plays an important role in the rapid filling phase.[10] It occurs as a result of the recoil of the compressed elastic myocardial fibers during contraction.[11] Rapid filling ends in the moment that atrial and ventricular pressures equilibrate.[7]

#### *Diastasis*

Diastasis occurs between the rapid filling and the atrial contraction phases. After rapid filling, LA and LV pressures equilibrate, yielding no forward driving gradient.[7]

#### *Atrial Systole*

The atrial filling phase of diastole occurs when the LA pressure rises above the LV pressure. This late diastolic transmitral flow increases ventricular end-diastolic volume by 25% in normal individuals, with only a small rise in mean pulmonary venous pressure. Diastole ends with the onset of ventricular systole, when the rapid increase in ventricular pressure closes the mitral valve.[7]

### DETERMINANTS OF DIASTOLIC FUNCTION

The following are the major determinants of diastolic function: (1) active myocardial relaxation; (2) LV compliance; (3) LA function; (4) heart rate; and (5) the pericardium.[7,11]

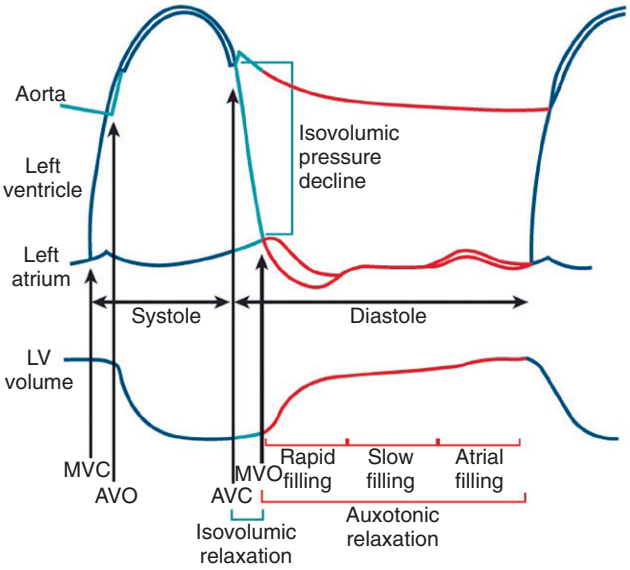



**Figure 11-1** Changes in left ventricular pressure and volume throughout the cardiac cycle. The cardiac cycle is divided into systole, the time period from mitral valve closure (*MVC*) to aortic valve closure (*AVC*), and diastole. Diastole is further divided into isovolumic relaxation (the time period from AVC to mitral valve opening (*MVO*) during which the LV pressure declines with no change in volume) and autoxonic relaxation (the time period from MVO to MVC during which the LV volume increases at variable pressure. *AVO,* Aortic valve opening. *(Adapted from Bonnema DD, Baicu C, Zile MR. Pathophysiology of diastolic heart failure: relaxation and stiffness. In: Klein AL, Garcia MJ, editors:* Diastology: clinical approach to diastolic heart failure. *Philadelphia, 2008, Saunders, pp 11-25.)*

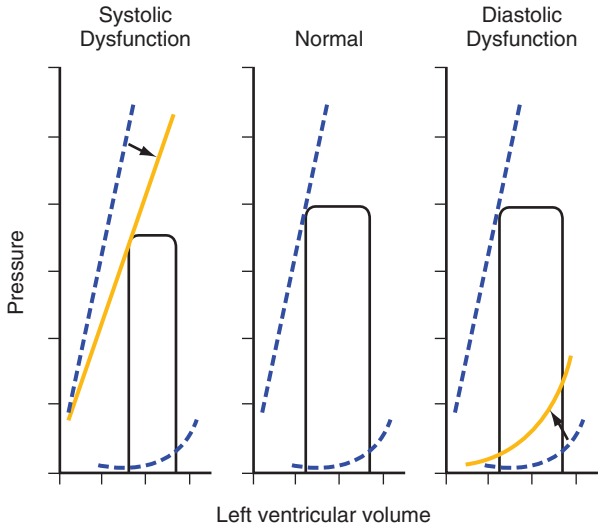



**Figure 11-2** Schematic representation of ventricular pressure-volume loops. The *center* panel demonstrates the normal situation. Note the exponential nature of the curve through late diastole. In systolic dysfunction (*left*), the end-systolic pressure line is displayed downward and is manifested by a decreased ability of the LV to generate high pressures for a given volume. Diastolic dysfunction (*right*) involves an upward and leftward shift of the exponential curve, a result of elevated filling pressures for a given volume. *(From Katz AM: Influence of altered inotropy and lusitropy on ventricular pressure-volume loops.* Am Coll Cardiol *11:438-445, 1988.)*

Myocardial relaxation, which occurs during isovolumic relaxation and early diastolic filling, is an active process involving the use of intracellular adenosine triphosphate and calcium by the myocardium.[12] Several factors affect isovolumic relaxation, including internal loading forces (cardiac fiber), external loading factors (wall stress, arterial impedance), and reduced or inhibited myocardial contractility (metabolic, neurohormonal, or pharmacologic).

Ventricular compliance is the ratio of change in volume to change in pressure ($dV/dP$), and stiffness is the mathematical inverse of compliance ($dP/dV$). From a conceptual standpoint, we can divide it into two components: intrinsic myocardial and chamber compliance. Compliance is the net result of a variety of factors: viscoelastic nature of the myocardium; chamber size, shape, and wall thickness; right ventricular (RV) and LV pressure-volume interactions; pleural pressure; and pericardial characteristics.[13] Intrinsic myocardial stiffness relates to the amount of collagen within the myocardium. Collagen plays an essential role in converting the contractile force of the myocytes into intraventricular pressure and determining the overall ventricular size and shape.[14,15] Pressure-induced hypertrophy is associated with increased collagen content deposition, with secondary increase in overall chamber stiffness. Evaluation of LV ventricular compliance has been studied and quantified extensively using pressure-volume loops, which demonstrate the degree to which pressure and volume change vis-à-vis each other over a wide range of physiologic pressures and volumes[16-18] (Fig. 11-2). The volume of blood that enters the LV is largely determined by the characteristics of the pulmonary veins, the LA, and the mitral valve .[7] The pressure gradient between the pulmonary veins or LA and the LV, the rate of myocardial relaxation, and ventricular suction are responsible for early rapid filling.[10,19] Hence, diseases of the mitral valve, such as mitral stenosis, delay LV filling and prevent early rapid filling.[7]

The LA predominantly acts as a passive reservoir of blood during early LV filling, and as an active pump at end-diastole.[20] Atrial systolic function (active phase) may be essential to maintain the cardiac output in disease states.[21,22] In young and healthy normal individuals, the atrial contribution is less than 20% of the total volume, whereas in older normal subjects, the atrial "kick" accounts for a greater proportion of the total LV filling.[23] Atrial contractile function has delayed recoery (stunning) following electrical cardioversion.[24] Decreased atrial systolic function as a result of infiltration plays a role in the reduction in forward transmitral atrial contraction wave by Doppler echocardiography as seen in advanced cardiac amyloidosis.[25]

*Heart rate* has a direct impact on cardiac output in cases of diastolic dysfunction.[26,27] As heart rate increases, the diastolic filling period preferentially decreases with respect to the systolic ejection period. As ventricular filling is functionally delayed, adequacy of inflow deteriorates and cardiac output paradoxically falls. Catecholamines may enhance relaxation and increase heart rate, thus decreasing the diastolic period.[28]

Other factors that affect diastolic function include neurohormonal activation, conduction abnormalities, and the stiffness of the pericardium. LV relaxation may be impaired by conduction abnormalities that cause segmental asynchrony.[29] This may contribute to decreased exercise tolerance in patients with left bundle branch block or RV paced rhythms. The pericardium considerably affects diastolic function as commonly seen in constrictive pericarditis.[30]

## DEFINITION OF DIASTOLIC DYSFUNCTION

Heart failure can be divided in two groups: heart failure with a reduced ejection fraction (HFrEF), and heart failure with a preserved ejection fraction (HFpEF), or diastolic HF. A study from

the Mayo Clinic evaluated a total of 4596 consecutive patients admitted with decompensated HF. Of these, 53% had a reduced ejection fraction. The proportion of patients with HFpEF increased over the period from 1987 to 2001. There are several differences between HFrEF and HFpEF from the structural and functional standpoint. In HFrEF, there is LV cavity enlargement, eccentric LV remodeling with low LV mass/volume ratio, and abnormal systolic and diastolic function; whereas in HFpEF, there is normal cavity size, concentric hypertrophy with high LV mass/volume ratio, and abnormal diastolic function. Myocardial structure follows a similar trend with cardiomyocyte hypertrophy in HFpEF and loss of myofilaments in HFrEF.[31-34]

Bhatia et al evaluated the epidemiology and outcomes of patients with HFpEF in a population-based study. Patients with HFpEF were more likely to be older and female and to have a history of hypertension and atrial fibrillation. The presenting symptoms and clinical presentation were similar to patients with reduced ejection fraction. The survival of patients with HFpEF was similar to those of patients with reduced ejection fraction (Fig. 11-3).[35] As a result of modern evidence-based HF therapy, the prognosis of patients with HFrEF has improved progressively over the past three decades. Conversely, despite frequent use of similar pharmacologic agents, the prognosis of patients with HFpEF remained unaltered over the same time period.[36]

Because diastolic dysfunction is common as an isolated disease in the elderly and also increases the burden of HF among patients with systolic dysfunction, these results have major public health implications for the future, particularly given the increasing age of our population.

Differentiation between HFrEF and HFpEF cannot be made on the basis of history, physical examination, electrocardiogram, or chest radiograph alone, because these clinical markers have the same frequency of occurrence in these two forms of HF.[37] The following criteria (Table 11-1) for HFpEF were proposed by the Working Group for the European Society of Cardiology: (1) presence of signs or symptoms of HF; (2) LV ejection fraction greater than 50%; and (3) evidence of LV diastolic dysfunction.[38] These diagnostic criteria have three major problems. The first is the requirement that there be signs *or* symptoms of HF. It is well recognized that the mere presence of breathlessness and fatigue is not specific for the presence of HF. It would be more prudent to use specific diagnostic criteria, such as the Framingham criteria. Second is the requirement that a measurable abnormality in diastolic function be present. Similar to measurements of systolic function, measurements of ventricular relaxation, filling, and compliance are load dependent. Therefore, their poor specificity, sensitivity, and predictive accuracy limit the application of this requirement in the clinical setting. Vasan and Levy have refined these criteria and divided

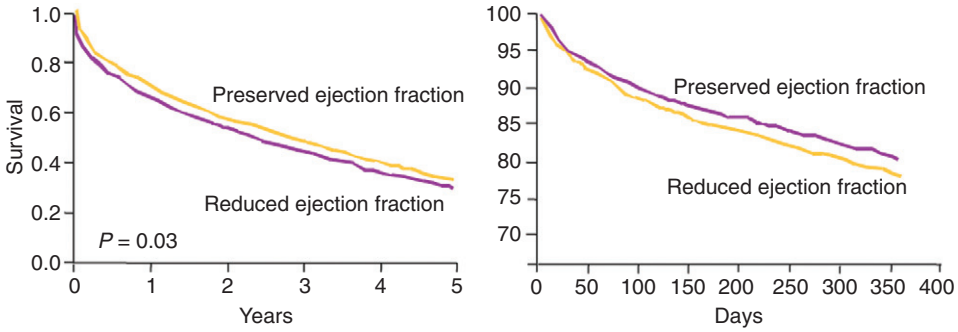



**Figure 11-3** Kaplan-Meier survival curve for patients with heart failure and preserved or reduced ejection fraction. (Left panel *adapted from Owan TE, Hodge DO, Herges RM, et al: Trends in prevalence and outcome of heart failure with preserved ejection fraction.* N Engl J Med *355:251-259, 2006.* Right panel *adapted from Bhatia RS, Tu JV, Lee DS, et al: Outcome of heart failure with preserved ejection fraction in a population-based study.* N Engl J Med *355:260-269, 2006.)*

**TABLE 11-1 Overview of Diagnostic Guidelines for HFpEF**

| | HFpEF Guidelines Year Published (Ref. No.) | | | |
|---|---|---|---|---|
| | *ESC 1998* | *NHLBI 2000* | *Lahey 2005* | *ESC 2007* |
| HF signs and symptoms (other criteria) | Present | Present | Present | Present |
| Normal LV systolic function | LVEF >45%<br>LVEDVI <102 mL/m$^2$ | LVEF >50% within 72 hr HF episode | LVEF >50%<br>LVEDVI <97 mL/m$^2$ | LVEF >50%<br>LVEDVI <97 mL/m$^2$ |
| LV diastolic dysfunction | LVEDP >16 mm Hg<br>PCWP >12 mm Hg<br>E/A <0.5<br>DT >280 ms<br>IVRT >105 ms<br>Ar >0.35 m/s<br>$Ar_{dur}$-$A_{dur}$ > 20 ms | LVEDP >16 mm Hg<br>PCWP >12 mm Hg | LVEDP >16 mm Hg<br>PCWP >12 mm Hg<br>E/A <0.5<br>DT >280 ms<br>IVRT >105 ms<br>LA enlargement<br>LVH | LVEDP >16 mm Hg<br>PCWP >12 mm Hg<br>E/E′ >15<br>E/E′ >8 + NT-proBNP >220 pg/mL |

Adapted from Paulus WJ, van Ballegoij JJ: Treatment of heart failure with normal ejection fraction: an inconvenient truth! *J Am Coll Cardiol* 55:526-537, 2010.

All four sets of guidelines require the simultaneous presence of HF signs and/or symptoms and normal LV systolic function and diastolic LV dysfunction. Criteria for normal LV systolic function are comparable, but criteria for diastolic LV dysfunction are variable.

*A*, Atrial wave mitral flow velocity; $A_{dur}$, duration of atrial wave mitral flow velocity; *Ar*, pulmonary vein atrial reversal velocity; $Ar_{dur}$, duration of reverse pulmonary vein systole flow velocity; *DT*, deceleration time; *E*, early mitral flow velocity; *E′*, early tissue Doppler lengthening velocity; *HF*, heart failure; *HFpEF*, heart failure with preserved LV ejection fraction; *IVRT*, isovolumic relaxation time; *LVEF*, left ventricular ejection fraction; *LVH*, left ventricular hypertrophy; *NT-proBNP*, N-terminal pro-B-type natriuretic peptide; *PCWP*, pulmonary capillary wedge pressure.

them into definite, probable, and possible diastolic HF.[39] Definite diastolic HF requires definitive evidence of HF; objective evidence of normal systolic function, with an ejection fraction greater than 50% within 72 hours of the HF event; and objective evidence of diastolic dysfunction on cardiac catheterization. If objective evidence of diastolic dysfunction is lacking, but the first two criteria are present, this fulfills the criteria for probable diastolic HF. If the first criterion is present and ejection fraction is greater than 50% but not assessed within 72 hours of the HF event, this fulfills the criteria for possible diastolic HF. Possible diastolic HF can be upgraded to probable diastolic HF if one of a number of additional criteria is present. The clinical application of these guidelines is limited, because they are both complex and empiric. Controversy exists whether measurements of LV relaxation or compliance by cardiac catheterization or Doppler echocardiography are actually needed when LV hypertrophy or concentric remodeling is present.[33] Recently, further definitions of diastolic HF or HF with preserved ejection fraction (HFpEF) have been proposed.[40]

## Echocardiographic Evaluation of Diastolic Function

Echocardiography has been the mainstay for understanding the physiology of diastolic function, and identifying the pathophysiology of diastolic dysfunction. In current practice, the clinician has a number of techniques in the evaluation of diastolic function, including the traditional Doppler techniques, which include mitral inflow and pulmonary vein flow and the newer modalities, such as tissue Doppler imaging and color M-mode Doppler. Table 11-2 provides the common diastolic filling variables that can be measured in clinical practice. Table 11-3 provides the clinical utility and technical limitations of various

**TABLE 11-2 Criteria Used to Define the Grade of Diastolic Dysfunction**

| *Criteria* | *Normal Young* | *Normal Adult* | *Impaired Relaxation (Grade 1)* | *Pseudonormal (Grade 2)* | *Restrictive Reversible (Grade 3)* | *Restrictive Irreversible (Grade 4)* |
|---|---|---|---|---|---|---|
| E/A ratio | 1-2 | 1-2 | <1.0 | 1-1.5 (reverses with Valsalva maneuver) | >1.5 | 1.5-2.0 (Doppler values similar to grade 3 except no change with Valsalva maneuver) |
| Deceleration time (ms) | <240 | 150-240 | ≥240 | 150-200 | <150 | <150 |
| IVRT (ms) | 70-90 | 70-90 | >90 | <90 | <70 | <70 |
| PV $S_2$/D ratio | <1 | ≥1 | ≥1 | <1 | <1 | <1 |
| $Ar_{dur} - A_{dur}$ (ms) | ≥30 | ≤0 | ≤0 or ≥30 | ≥30 | ≥30 | ≥30 |
| Ar velocity (cm/s) | <35 | <35 | <35 | ≥35 | ≥35 | ≥35 |
| Propagation velocity (cm/s) | >55 | >55 | >45 | <45 | <45 | <45 |
| Mitral E′ velocity (cm/s) | >10 | >8 | <8 | <8 | <8 | <8 |
| Left atrium | Normal | Normal | Normal or mildly enlarged LA | Mild to moderate LA enlargement | Severe LA enlargement | Severe LA enlargement |

Adapted from Bursi F, Weston SA, Redfield MM: Systolic and diastolic heart failure in the community. *JAMA* 296:2209-2216, 2006; Garcia MJ, et al: New Doppler echocardiographic applications for the study of diastolic function. *J Am Coll Cardiol* 32:865-875, 1998; and Yamada H, Klein AL. Diastology 2010: Clinical approach to diastolic heart failure. *J Echocardiogr* 8:65-79, 2010.

$A_{dur}$, Duration of transmitral atrial velocity; *Ar,* pulmonary vein atrial reversal velocity; $Ar_{dur}$, duration of pulmonary vein atrial reversal velocity; *D,* diastolic wave; *E/A,* ratio of early to late diastolic filling velocities; *IVRT,* isovolumic relaxation time; *PV,* pulmonary vein; *S,* systolic wave.

**TABLE 11-3 Utility of Different Echocardiographic Techniques in Assessment of Diastolic Function**

| | *Clinical Utility* | *Technical Points* | *Limitations* |
|---|---|---|---|
| Mitral inflow | Can assess LV compliance, relaxation, filling pressures.<br>Short DT associated with poor prognosis.<br>Best used with combined systolic and diastolic heart failure. | Sample volume between 1 and 2 mm, velocity filter at 200 Hz, sweep speed between 50 and −100 mm/s.<br>Can measure E and A waves, DT, IVRT.<br>A duration can be measured at mitral annulus. | Preload dependent<br>E/A ratio can be pseudonormalized. |
| Pulmonary vein flow | Can assess LV compliance, relaxation, filling pressures.<br>Blunted systolic/diastolic velocities associated with poor prognosis.<br>Best used with combined systolic and diastolic heart failure.<br>$PV_a$ used to assess pseudonormalization. | Sample volume box between 3 and 4 mm, velocity placed 1-2 cm into the PV, filter at 200 Hz, sweep speed between 50 and 100 mm/s.<br>Can measure S, D, and $PV_a$ waves. | Preload dependent<br>Technically difficult to obtain in all patients<br>Blunted S/D from other conditions including atrial fibrillation and mitral regurgitation |
| Tissue Doppler imaging | Can assess LV compliance, relaxation, filling pressures.<br>E/E′ >15 associated with elevated filling pressures.<br>Best used with primary diastolic heart failure. | Sample volume box between 4 and 5 mm at all four mitral annuli, filter at 200 Hz, sweep speed between 50 and 100 mm/s.<br>Can measure S′, E′, and A′ waves. | Relatively preload independent<br>Angle and translation dependent<br>Different velocities at annuli (lateral > medial) |
| Color M-mode | Can assess LV compliance, relaxation, filling pressures.<br>E/Vp >1.5 associated with elevated filling pressures.<br>Best used with primary diastolic heart failure. | Slope of flow propagation (first aliasing velocity) for 4 cm into LV.<br>The 2D depth is reduced to 16 cm.<br>The color velocity scale is set for color aliasing by moving the baseline up so that it is in the 40 cm/s range.<br>The M-mode sweep should be recorded at a speed of 100 mm/s.<br>Can measure Vp slope. | Relatively preload independent<br>Technically difficult to obtain in all patients<br>Influenced by LV geometry |

*A*, Filling wave due to atrial contraction; *Ar,* pulmonary vein atrial reversal; *D*, diastolic PV flow; *DT*, deceleration time; *E*, early diastolic filling velocity; *IVRT*, isovolumic relaxation time; *PV*, pulmonary vein; *S*, systolic PV flow; *Vp*, velocity of propagation.

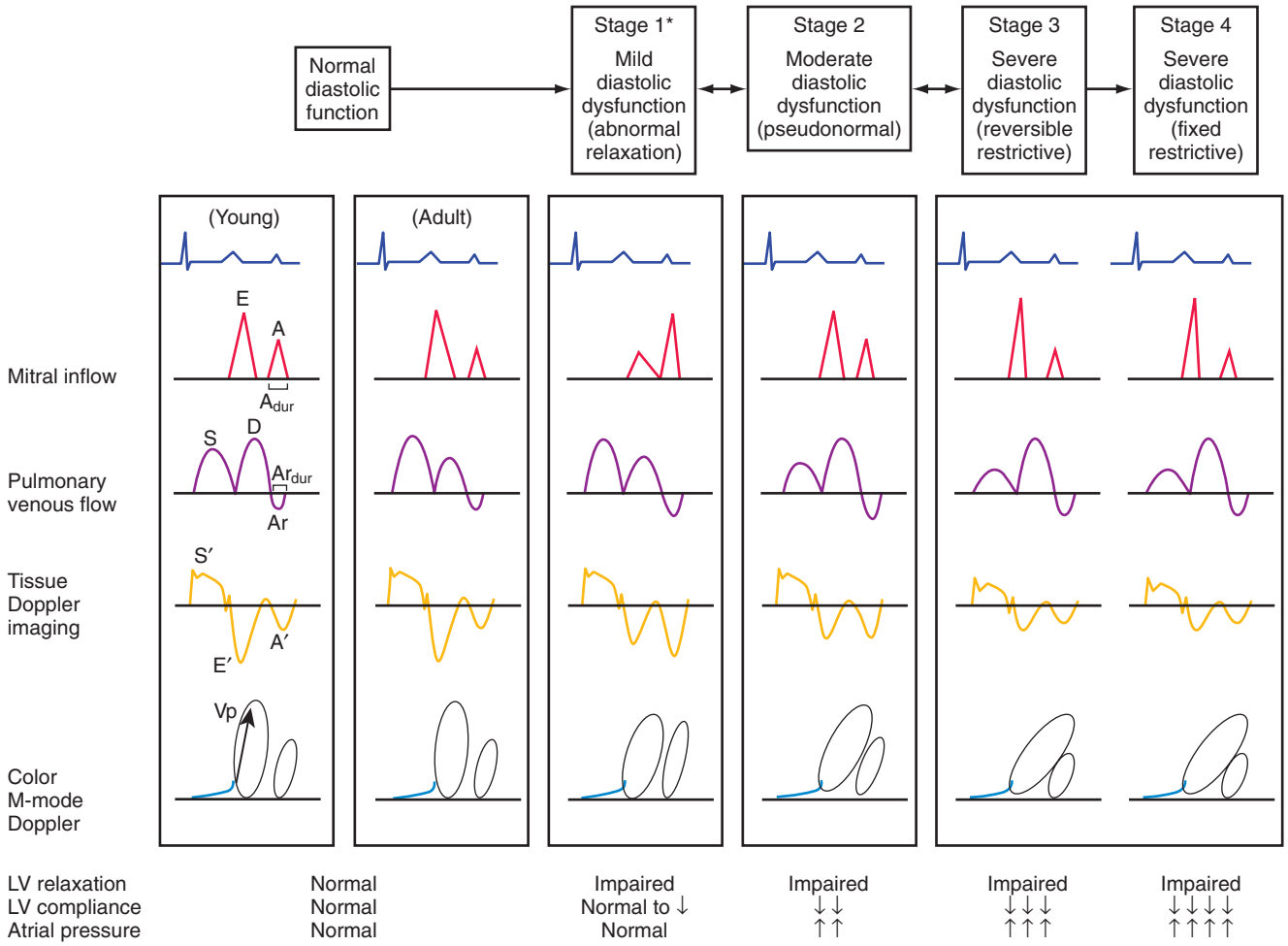



**Figure 11-4** Stages of diastolic function. Schematic representation of the typical patterns seen with mitral inflow, pulmonary venous flow, tissue Doppler echocardiography, and color M-mode propagation velocity (*Vp*) for normal (young and adult), impaired relaxation, pseudonormal, and restrictive diastolic function. The stages of diastolic dysfunction can be determined using an integrated approach with these four different modalities for assessment of diastolic flow pattern. *A*, Late mitral filling; *A′*, tissue Doppler atrial velocity; *Ar*, pulmonary vein atrial reversal velocity; $Ar_{dur}$, duration of pulmonary vein Ar; *D*, pulmonary vein diastolic filling; *E*, early mitral filling; *E′*, tissue Doppler early diastolic velocity; *S*, pulmonary vein systolic filling; *S′*, tissue Doppler systolic velocity; *Vp*, propagation velocity.
*Stage 1 can be divided into stage 1A and stage 1B depending on an elevated LV end-diastolic pressure. *(Adapted from Garcia MJ, Thomas JD, Klein AL: New Doppler echocardiographic applications for the study of diastolic function.* J Am Coll Cardiol *32:865-875, 1998.)*

echocardiographic techniques in assessment of diastolic function. A framework of the different imaging modalities is shown in Figure 11-4 in normal subjects and in patients with different stages of diastolic dysfunction.

## DOPPLER TECHNIQUES IN ASSESSMENT OF DIASTOLIC FILLING PATTERNS

There is a large body of scientific evidence validating the typical patterns of diastolic filling in normal subjects, and those with diastolic dysfunction. These filling patterns are generally not characteristic of a particular disease process, but represent the end product of a complex set of pathophysiologic events. Furthermore, these patterns can also be affected by operator-related issues (e.g., precise placement of the sample volume) and physiologic factors (e.g., heart rate and volume status) and are not a reflection of true diastolic function.[33]

### *Transmitral Flow Assessment*

The most traditional technique of assessment of LV filling patterns involves using pulsed-wave Doppler mitral flow velocity recordings.[41] The following are the variables derived from mitral inflow interrogation: peak early diastolic transmitral flow velocity (E), peak late diastolic transmitral flow velocity (A), early filling deceleration time (DT), and A-wave duration ($A_{dur}$). Normal mitral flow velocity curves vary with loading conditions, age, and heart rate.

Normal individuals demonstrate a rapidly accelerating E wave, relatively rapid deceleration, and an A wave significantly smaller than the E wave. The E/A ratio is greater than 1, the mitral DT (reflecting LV compliance) is typically between 160 and 240 ms, and the isovolumic relaxation time (IVRT) is between 70 and 90 ms. With normal aging, there is slowing of LV relaxation and, hence, a gradual decrease of the peak E wave velocity, and an increase of A wave peak velocity. In most individuals, E and A waves become approximately equal in the sixth decade of life.[42]

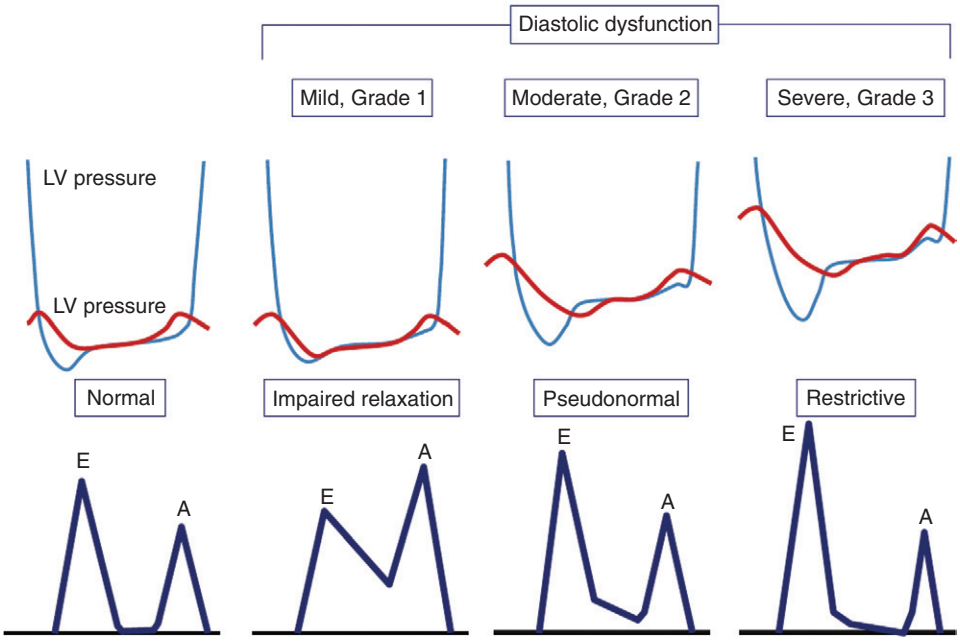



**Figure 11-5** Schematic representation of LV and LA pressures (*upper*) and transmitral flow velocity patterns (*lower*) in normal patients and in different types of diastolic dysfunction. This schema divides patients into four filling patterns: normal pattern of relaxation and filling; impaired relaxation, or grade 1 mild diastolic dysfunction; pseudonormal relaxation, or grade 2 moderate diastolic dysfunction; and restrictive filling pattern, or grade 3 severe diastolic dysfunction. *(Adapted from Yamada H, Klein AL: Diastology 2010: clinical approach to diastolic heart failure.* J Echocardiogr *8:65-79, 2010.)*

The evolution of traditional diastolic parameters with progressively worsening diastolic function, occurs in the following manner: For patients with diastolic dysfunction, three abnormal filling patterns are initially recognized[26,43] (Fig. 11-5). In stage 1 diastolic dysfunction (abnormal relaxation), there is a low E wave and a high A wave, resulting in an E/A ratio less than 1. DT is prolonged and is usually greater than 240 ms and IVRT is greater than 90 ms. Stage 2 diastolic dysfunction, or pseudonormal pattern, is associated with a normal appearance of the transmitral inflow with an E/A ratio between 1 and 1.5, a DT between 160 and 240 ms, and an IVRT between 60 and 100 ms. With disease progression (stage 3 diastolic dysfunction or restrictive filling), there is a very high E wave, a low A wave, and a significantly decreased DT. The E/A ratio is usually greater than 2 with a DT less than 160 ms, and IVRT less than 70 ms.

Further observations have subcategorized this last pattern to either reversible or fixed restrictive pattern (stage 4) depending on the response to the Valsalva maneuver or other preload reducing maneuvers.[44] The major challenge in the interpretation of Doppler mitral inflow patterns is in distinguishing the normal from the pseudonormal pattern. To accurately assess and stratify the degree of diastolic abnormality, further measurements are generally necessary. There are several traditional methods that are useful in distinguishing normal from pseudonormal patterns, including the Valsalva maneuver, pulmonary venous (PV) flow measurements, and the tissue Doppler annular velocities (E′).

### *Mitral Inflow at Peak Valsalva Maneuver*

Because preload affects interpretation of diastolic dysfunction, the Valsalva maneuver is another supplement to the measurement of mitral inflow parameters (Fig. 11-6). The strain phase of the Valsalva maneuver is a simple approach used to decrease LA pressure. During this phase, E wave velocity normally decreases by 20% with a smaller decrease in A velocity.[41] In patients with pseudonormal mitral inflow patterns, Valsalva strain lowers LA pressure and unmasks the underlying impaired LV relaxation, resulting in a measured E/A less than 1.[45] Patients with restrictive filling patterns or individuals who are preload sensitive will revert to a pseudonormal or even impaired relaxation pattern. Patients with restrictive filling patterns without any change with Valsalva have severe irreversible or fixed diastolic dysfunction. The primary limitation in the use of Valsalva to assess diastology is obtaining adequate signals for measurement. Ommen and colleagues[45] were able to obtain satisfactory Doppler data in only 61% of patients during a Valsalva maneuver. In addition, the inherent limitations in performance of an adequate Valsalva maneuver limit its utility in routine practice.

### *Pulmonary Venous Flow*

PV flow velocity variables provide an integrated approach with mitral inflow in the evaluation of diastolic dysfunction. The four useful variables from the PV flow interrogation are peak systolic PV flow velocity (S), peak diastolic PV flow velocity (D), peak PV atrial reversal flow velocity ($PV_a$), and $PV_a$ duration ($a_{dur}$). Figure 11-5 shows a schematic representation of the PV variables in normal diastolic function and in various stages of diastolic dysfunction.[43]

The flow from the PV to the LA occurs in three phases: systolic phase (peak early and late systolic PV flow velocity); early diastolic phase (peak diastolic PV flow velocity); and retrograde flow during the late diastole with atrial contraction. With a normal LA pressure, the majority of the flow into LA occurs in systole. However, when the mean LA pressure increases, the majority of the antegrade flow occurs in diastole with a concomitant reduction in systolic flow. A decreased systolic fraction of less than 40% is associated with an elevated mean LA pressure greater than 15 mm Hg.[46] Similar to mitral inflow, the pulmonary vein flow demonstrates a U-shaped curve,

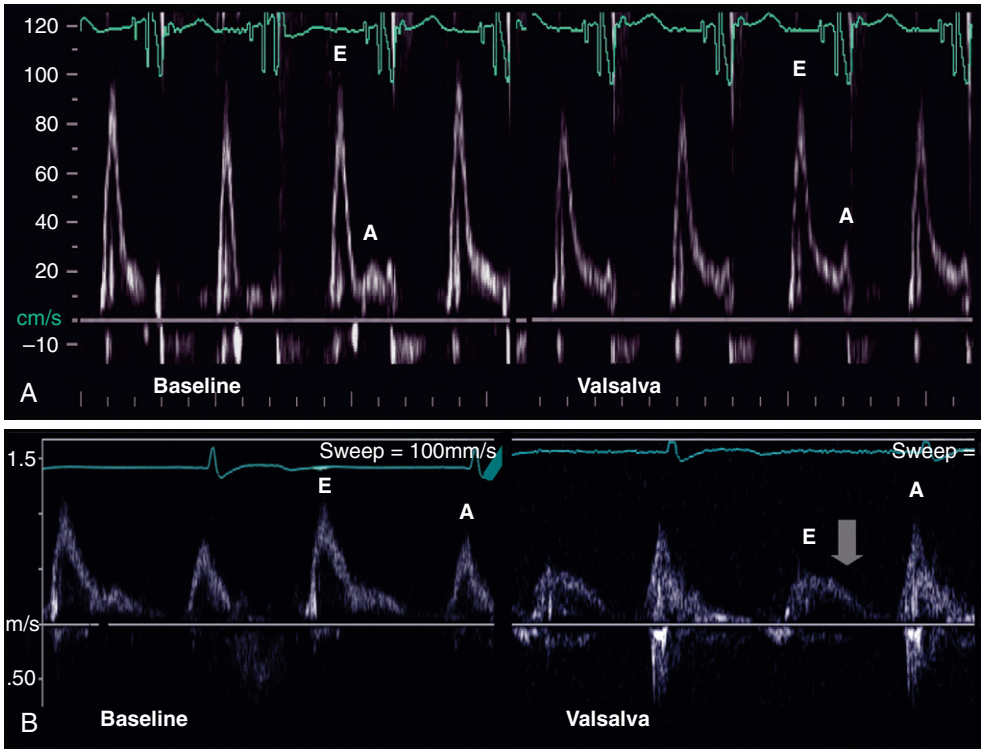



**Figure 11-6** Effect of Valsalva maneuver on mitral inflow in a patient with different stages of diastolic dysfunction. **A,** Patient with stage 3 diastolic dysfunction. Notice that after Valsalva maneuver, the E wave remains the same, consistent with irreversible diastolic dysfunction (stage 4). **B,** Patient with stage 2 diastolic dysfunction. With Valsalva, there is blunting of the E wave and appearance of stage 1 diastolic dysfunction. *A*, Atrial component of diastolic filling; *E*, early diastolic filling.

suggesting preload dependence. Pulmonary vein atrial reversal velocity and duration provides incremental value in assessing diastolic function. An atrial reversal velocity greater than 35 cm/s and an duration of 30 ms longer than the mitral inflow A-wave duration is predictive of an LV end-diastolic pressure greater than 15 mm Hg.[47] For multiple reasons, however, it may be difficult to optimally assess PV flow. A frequent reason is inadequate PV flow profiles, commonly seen as a result of body habitus and operator dependence. Blunting of PV systolic waves may be present in young healthy individuals as a result of rapid diastolic "suction," and atrial reversal may be absent in advanced diastolic dysfunction as a result of the loss of atrial function.[25,48] Therefore, newer modalities, including color M-mode Doppler and tissue-Doppler imaging (TDI), have evolved to provide additional information for the assessment of diastolic function and evaluation of LV filling pressures[45] (Fig. 11-7).

### *Evaluation of the Right Heart by Doppler*

Diastolic function of the right-sided heart can be evaluated by the interrogation of the tricuspid inflow, hepatic veins, and superior vena cava flows.[49] The Doppler flow patterns in the hepatic veins and superior vena cava are somewhat similar to the PV flow patterns.[50,51] In addition to the systole (S), diastole (D), and atrial waves, a second reversed flow is often seen between the S and the D wave at the end of ventricular contraction.[23] Right-sided flow velocities normally increase during inspiration and decrease with Valsalva.[23,52] As with the PV flow, the S wave is related to right atrial (RA) relaxation and tricuspid annular descent, and the D is related to early RV filling velocity (E). The magnitude of atrial reversal and ventricular contraction varies according to RV stiffness, RA contractility, and central venous pressure.[53] The effect of respiration of the right-sided flows is useful in differentiating constriction from restriction and estimating right-sided filling pressures.[50,51]

### *Tissue-Doppler Imaging for Evaluation of Diastolic Function*

The Doppler principle states that the velocity of a moving object will alter the frequency of a reflected sound wave. Ultrasonic Doppler technique is a direct application of this effect and is based on the analysis of the amount of frequency shift of ultrasound waves reflected by a moving object. This ultrasound principle has been applied in cardiovascular medicine for many years, predominantly for blood flow velocity measurements within the heart and great vessels.[54] In conventional Doppler color imaging, wall filters are employed to eliminate high-amplitude, low-frequency signals reflected from myocardium in favor of the low-amplitude, high-frequency signals reflected from moving red blood cells. These low Doppler frequency shifts are produced by the contracting myocardium and provide information for the assessment of myocardial function during systole and diastole. TDI is an echocardiographic technique that directly measures myocardial velocities. In TDI, wall filters are bypassed to specifically measure the velocities of the myocardium, which typically range from 0 to 20 cm/s. Doppler gain settings also must be increased to adequately visualize the TDI waveforms (see Chapter 10).

TDI was first described in 1989 by Isaaz and colleagues,[55] who demonstrated that low myocardial velocities at the posterior mitral annulus correlated with abnormal posterior wall motion on LV angiography.

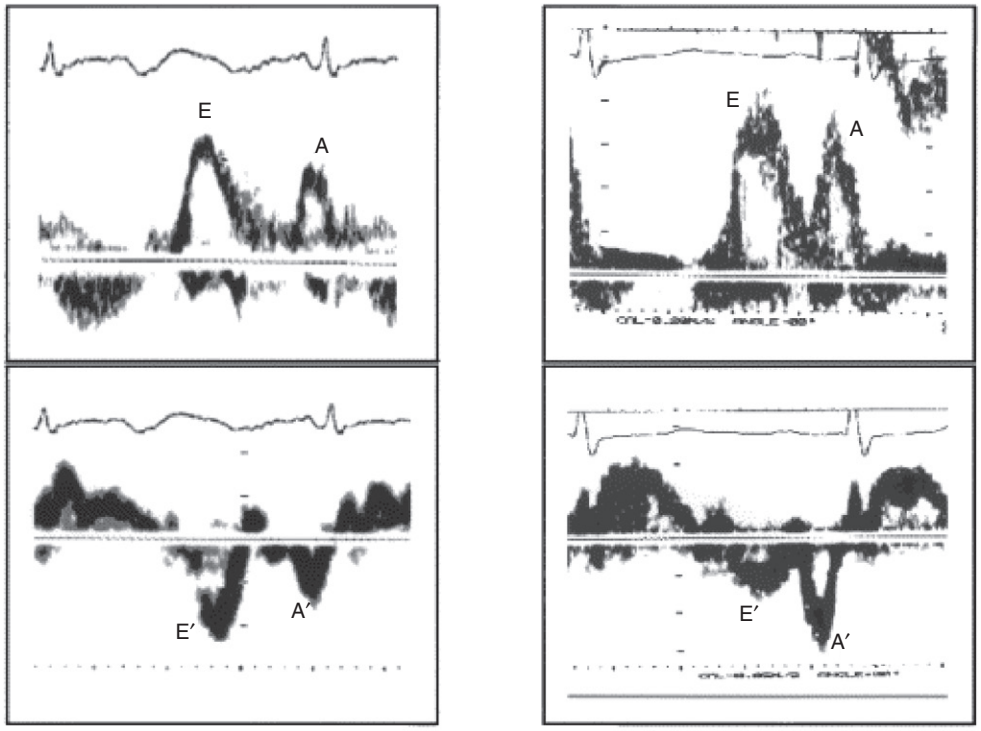



**Figure 11-7** Standard pulsed Doppler transmitral inflow (*upper panels*) showing the early (*E′*) and atrial (*A*) filling velocities, and myocardial axial velocities (*lower panels*) recorded at the basal lateral wall in a healthy volunteer and in a patient with severe aortic stenosis, LV hypertrophy, and elevated filling pressures (pseudonormal). Early diastolic myocardial velocity (*E′*) is significantly reduced, as well as the early-to-atrial velocity ratio (*E′/A′*) in the pseudonormal patient. *(From Garcia MJ, Thomas JD, Klein AL: New Doppler echocardiographic applications for the study of diastolic function.* J Am Coll Cardiol *32[4]:865-875, 1998.)*

## Techniques of Tissue-Doppler Imaging

Pulsed and color TDI have been used for the assessment of myocardial function; however, both techniques show advantages and disadvantages. Using pulsed Doppler techniques we can (1) obtain high-quality Doppler signals, (2) measure mean and instantaneous local acceleration, and (3) obtain quantitative wall motion information (i.e., velocity, acceleration, and displacement). However, the pulsed Doppler technique has many shortcomings, including (1) the need for manual mapping, (2) a limited spatial resolution making it difficult to distinguish subendocardial from subepicardial myocardial velocities, (3) difficulty in simultaneous recording of different ventricular wall segments, and (4) recognition that important qualitative differences exist between the various echocardiographic machines in terms of obtained signals. On the other hand, using color TDI of the myocardium, we can superimpose wall motion velocity on the two-dimensional (2D) echocardiographic imaging by velocity color coding. 2D color Doppler imaging of the myocardium (1) enables rapid visual qualitative assessment of wall dynamics, (2) provides a good spatial resolution to differentiate between velocity profiles of subendocardial and subepicardial layers, and (3) allows simultaneous analysis of various myocardial regions. However, it is limited by poor temporal resolution. In contrast, M-mode color-coded tissue imaging is characterized by a high spatial and temporal resolution, but sampling is performed only along a single line.

In the assessment of diastolic function, velocities typically are measured at the annuli or myocardium in the longitudinal axis to minimize the effect of cardiac translation.[56] From either the apical four-chamber or two-chamber acoustic windows, the region of interest is placed at the level of the mitral annulus on the septal, lateral, anterior, or posterior aspects of the annulus. Recordings are obtained during apnea to minimize translation-induced motion artifacts. In clinical TDI applications, three waveforms are visualized per cardiac cycle: the peak systolic wave (S′), early diastolic wave (E′), and end-diastolic wave produced by atrial contraction (A′).

In evaluation of velocities in healthy subjects, the annular early diastolic wave velocities recorded in the short-axis view were higher at the posterior wall than at the anteroseptal wall.[57] Garcia and colleagues[57] found an average value of 6.3 ± 1.7 cm/s for E′ at the anteroseptal wall versus 9.3 ± 3 cm/s at the posterior wall. In the apical view, myocardial diastolic velocities recorded by TDI are higher at the base than at the mid-LV or at the apex.[58,59] Although TDI velocities decrease with age, a healthy 50-year-old adult has spectral TDI values of 10 cm/s or greater and color TDI values of generally 6 cm/s or greater for S′, E′, and A′.

## Relationship of E′ to Active Relaxation

E′ is a relatively preload-independent measure of myocardial relaxation in patients with cardiac disease, whereas it appears load dependent in patients with normal systolic function.[56,60] It has been shown that in patients with abnormal relaxation, saline loading led to a pseudonormal transmitral pattern, whereas TDI E′ and E′/A′ remained unchanged. Also, the authors showed that the time constant of relaxation (τ) was better linearly related to E′ and E′/A′ than to transmitral velocity variables.[56] A value of E′ less than 8.5 cm/s with a ratio E′/A′

less than 1 identified a pseudonormalized transmitral velocity pattern with a 88% sensitivity and 67% specificity (Fig. 11-8). Another study[60] included three groups of patients: 34 normal subjects, 40 asymptomatic patients with normal ejection fraction and transmitral E/A less than 1 (abnormal relaxation), and 51 patients with HF and E/A ratio greater than 1 (pseudonormal). It was shown that E′ was lower with a decreased E′/A′ in both impaired relaxation and pseudonormal compared with normals; the ratio E/E′ was similar between normals and patients with impaired relaxation but was significantly higher in the patients with pseudonormal transmitral pattern.

## Estimation of LV Filling Pressures

Sohn and colleagues demonstrated that E′, correlated with invasive indices of myocardial relaxation (τ).[56] Nagueh and colleagues[60] showed that the pulsed Doppler peak early mitral inflow velocity (E) divided by TDI early diastolic mitral annular velocity (E′) resulted in a ratio (E/E′) that correlated with pulmonary capillary wedge pressure (PCWP). In their study, they evaluated 60 patients in whom the mean PCWP was measured (Fig. 11-8), finding a good correlation between the E/E′ ratio and the mean PCWP (correlation coefficient $r = 0.87$).[60]An E/E′ ratio greater than 10 indicated a PCWP greater than 12 mm Hg with a 91% sensitivity and a 81% specificity of 62%. Ommen and colleagues[45] corroborated their work, demonstrating that the E/E′ is useful in estimating mean LV filling pressures. The E/E′ ratio has since been demonstrated to be useful in estimating LV filling pressures in patients with hypertrophic cardiomyopathy (HCM),[61] sinus tachycardia,[61] atrial fibrillation,[62] and postcardiac transplantation.[63]

However, there are certain situations where E/E′ may not provide an accurate assessment of pulmonary capillary wedge pressure. First, in the normal heart, E′ behaves as a load-dependent variable. As a result, E/E′ actually decreases in response to massive fluid loading, as seen in experimental animal models.[64] Nevertheless, this finding is of very little clinical importance, because the LA pressure is rarely elevated in patients with normal hearts.[65] Second, E/E′ does not increase in patients with constrictive pericarditis, despite elevated PCWP. E′ increases as constriction gets worse. As a result, the E/E′ ratio decreases as diastolic filling pressures increase (annulus paradoxus).[65] Third, E/E′ may not provide an accurate calculation of filling pressures in patients with mitral valve disease (mitral annular calcification, mitral stenosis, mitral regurgitation) or after mitral valve surgery (mitral valve annuloplasty or mitral valve replacement).

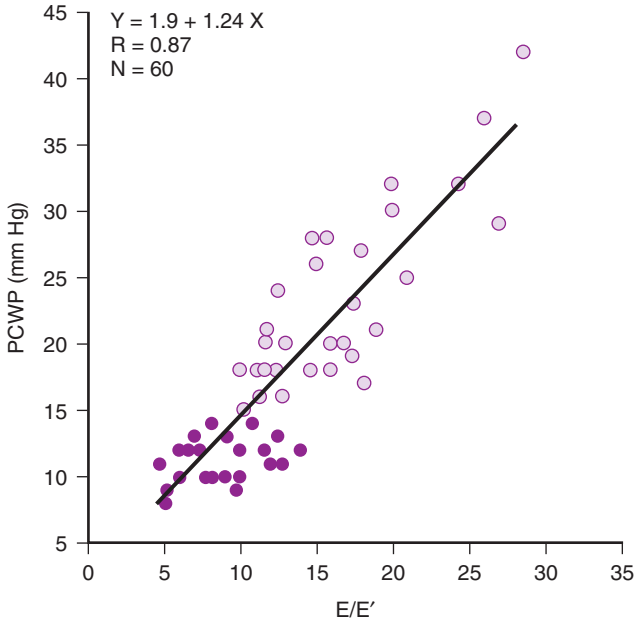



**Figure 11-8** Relation of early transmitral velocity to tissue Doppler mitral annular early diastolic velocity (E/E′) to pulmonary capillary wedge pressure (PCWP) in 60 patients. The *solid dots* indicate patients with impaired LV relaxation. The *open dots* indicate patients with a pseudonormalized pattern of diastolic filling. *(From Nagueh S, Middleton JK, Kopelen HA, et al: Doppler tissue imaging: a noninvasive technique for evaluation of left ventricular relaxation and estimation of filling pressures.* J Am Coll Cardiol *30[6]:1527-1533,1997.)*

More recently, concerns have been raised in terms of the ability of E/E′ to estimate LV filling pressures in the patients with decompensated HF. Mullens and co-workers[66] prospectively evaluated a cohort of patients with advanced decompensated HF (ejection fraction less than 30%, NYHA class III or IV symptoms) who underwent simultaneous echocardiographic and hemodynamic evaluation on admission, and after 48 hours of intensive medical therapy. They concluded that in decompensated patients with advanced systolic HF, TDI-derived mitral E/E′ ratio may not be as reliable in predicting intracardiac LV filling pressures, particularly in those with larger LV volumes and more impaired cardiac indices, and in the presence of cardiac resynchronization therapy.[66] In a follow-up article addressing the controversy, Little and Oh[67] stated that the failure of E/E′ to perform adequately may result at least partially from the characteristics of the patients studied. Significant mitral regurgitation was present in nearly a quarter of the patient population, where, as mentioned previously, E/E′ may not correlate well with PCWP. Additionally, half of the patients had undergone cardiac resynchronization therapy, and most had a prolonged QRS with variable degrees of mechanical dyssynchrony.[68] In contrast, a recent paper by Nagueh and associates[68] found that Doppler echocardiography provided good accuracy in the assessment of hemodynamics in 79 patients with decompensated heart failure.

Given that in patients with elevated LV filling pressures the cardiac myocytes are under strain, B-type natriuretic peptide (BNP) levels can be useful in determining the presence of elevated filling pressures. A recent study demonstrated that BNP had a significant correlation ($r = 0.51$) with mitral E/E′. Other investigators have shown that BNP and mitral E/E′ are similarly accurate in diagnosing clinical HF in patients hospitalized for dyspnea; however, a comprehensive Doppler assessment using 2D, conventional Doppler, and TDI variables appeared more specific than BNP.[69] In patients with indwelling pulmonary artery catheters, E/E′ and BNP were highly and equally sensitive for PCWP greater than 15 mm Hg, but E/E′ was more specific.

## Tissue Doppler Assessment of Diastolic Function and Prognosis

Recently, there has been tremendous interest in the prognostic implications of TDI diastolic variables. One study demonstrated that after first acute myocardial infarction, E′ and E/E′ were univariate predictors of death or hospital readmission. Another population-based study[70] showed that patients with increasing degrees of diastolic dysfunction (using a comprehensive Doppler-echocardiography assessment including TDI variables) have increasingly worse outcome. E/E′ has been demonstrated to be a strong multivariate predictor of patient outcome when assessed a mean of 1.6 days after acute myocardial infarction.[71] In a study of 225 patients who had symptomatic

HF, E/E′ predicted mortality, transplantation, and hospitalization for HF and was incremental to deceleration time and ejection fraction.[72]

### *Color M-Mode Doppler*

During isovolumic relaxation, the LV pressure drops without LV filling. The time constant of LV pressure decline (τ) is an index of LV relaxation that is relatively independent of heart rate and preload. After mitral valve opening, LV filling occurs with variable LV pressures (auxotonic relaxation). Measurements made during auxotonic relaxation are determined both by active relaxation and passive chamber stiffness, with the latter becoming increasingly important toward the end of ventricular filling.[73] The active processes during early diastole lead to a rapid LV pressure drop during isovolumic relaxation and fast active filling at low pressures during early auxotonic relaxation. As early as the 1930s, normal ventricular relaxation was thought to result in "active suction" of the blood into the LV. However, only in the early 1980s, the presence of diastolic intraventricular pressure gradients were confirmed.[74-76] The gradients between the ventricular base (mitral valve) and apex were suggested to exert a suction effect ("recoil"). It was later demonstrated that these gradients were diminished by ischemia and related to systolic function.[76] With the demonstration of intraventricular pressure gradients during early diastole in filling and in nonfilling heartbeats, their potential role as an index for isovolumic and early auxotonic ventricular relaxation was established.[77] Because pressure gradients in fluids imply fluid acceleration and fluid currents, a noninvasive index of fluid acceleration would, in theory, reflect these intraventricular pressure gradients. The color M-mode velocity propagation index (Vp) can potentially fulfill this promise.

#### Acquisition of Color M-Mode Images

Color M-mode Doppler is a pulsed Doppler technique in which mean velocities are color encoded and displayed in time (on the horizontal axis) and depth along the entire scan line (on the vertical axis). Acquisition is made in the four-chamber view. To visualize the direction of the inflowing blood, a large color box is placed from the mitral valve to the apex. The scan line should ideally go through the center of the mitral valve and along the central part of the blood column.[78,79] Switching to M-mode and with the chart recorder set at a sweep rate of 100 mm/s, an M-mode spatial-temporal velocity map with the shape of a flame is displayed (see Fig. 11-5). By digital processing, for each pixel of the displayed color M-mode map, time, depth, and numerical velocity can be determined. The Euler equation enables the calculation of instantaneous pressure gradients along the inflow tract in a noninvasive way; however, it is too cumbersome for routine practice.[79] Therefore, for clinical practice, the spatial-temporal velocity information is expressed as distance-to-time ratios (cm/s) and is known as the flow propagation velocity because it has the dimensions of velocity and it has been interpreted as the distance the flow-wave (E-wave) propagates into the LV as a function of time. The following techniques have been proposed for determining flow propagation velocity: (1) Stugaard and colleagues[80] measured the time delay between onset of maximal flow velocity at the mitral valve tips and at 3.7 cm toward the apex. This technique requires offline postprocessing using dedicated software to decode the color of each pixel into numerical values. It depends on two individual pixels, and the reliance on accurate measurement of apical flow constitutes its primary limitation.[81] (2) Brun and colleagues[82] measured slopes of the isovelocity lines formed by transition of no color to color (black to red). The technique was later modified by Garcia and colleagues,[83] who traced the slope of the first "aliasing" velocity (red to blue) from the mitral valve plane to 4 cm distal in the LV (Vp in cm/s) (see Fig. 11-10, later). The latter technique only requires online adaptation of the Nyquist range limit or baseline to obtain aliasing. Both techniques rely on a large number of pixels, and the measurements can be performed online. (3) The Takatsuji method of flow propagation velocity calculation depends on offline, progressive scaling down of the Nyquist range by specific software. The slope between the site of the highest velocity at the mitral valve connected with the point in which aliasing becomes apparent when the Nyquist range is further scaled down by 30% (regardless of the depth of this point) is defined as Vp (Fig. 11-9).[84]

#### Flow Propagation Velocity and Hemodynamics

It has been demonstrated that despite worsening relaxation, E wave increases as a result of increasing filling pressures (pseudonormalization), but Vp does not rise.[84] This indirectly suggests preload independence. In invasive canine studies, significant preload alteration[80,85] did not induce significant change in propagation velocity. Recently, preload independence has also been demonstrated in human patients with and without LV systolic dysfunction.[85,86] There is an inverse relationship between Vp and the isovolumetric time constant of relaxation (τ). In dogs, Stugaard and colleagues showed a significant reduction of Vp in parallel with an increase in τ during induction of diastolic failure with regional[80] or global ischemia and with high-dose propranolol.[87] Similar highly significant correlations between Vp and changes in τ during esmolol and dobutamine infusion were obtained in dogs by Garcia and colleagues.[85] Invasive studies in humans also show a consistent high inverse correlation between tau and the propagation rate Vp. Takatsuji and colleagues[84] found a strong inverse relation in 40 patients undergoing cardiac catheterization ($r = -0.82$; $P$ less than

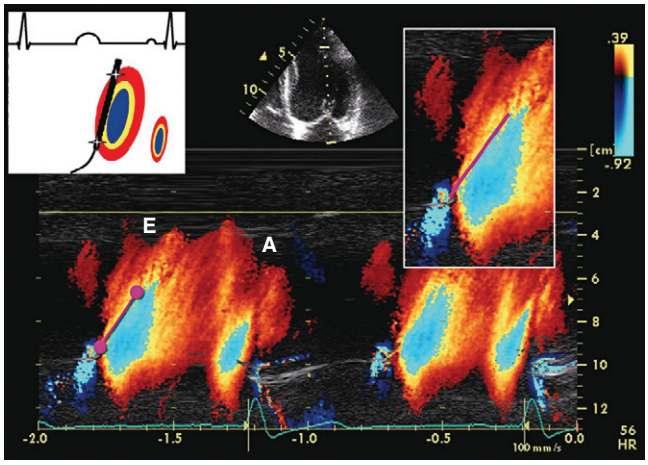



**Figure 11-9** Example of color M-mode of LV inflow propagation velocity (Vp). Measure Vp from the intersection of the anterior mitral valve leaflet M-mode extending along the first edge of uniform color or aliasing velocity approximately 4 cm into the left ventricle. Schematic diagram (*upper left* corner) represents color M-mode measurement of inflow propagation. *A*, Late filling or atrial contribution; *E*, early filling. *(Adapted from Morehead AJ: Sonographer's perspective of evaluating diastolic function. In Klein AL, Garcia MJ, editors:* Diastology: clinical approach to diastolic heart failure. *Philadelphia, 2008, Saunders, pp 215-229).*

0.001), similar to values reported by Garcia and colleagues ($r = -0.86$; $P$ less than 0.001),[83] and Brun and colleagues ($r = -0.73$; $P$ less than 0.0001).[82]

### Clinical Use of Color M-Mode Doppler

In normal adults, little loss in blood velocity occurs between the basal ventricle and the apical region. The color M-mode flame appears at the apical region before early flow at the mitral valve level has stopped. The slope of the displayed filling wave is relatively steep. With impaired relaxation, the slope of the first filling wave is less steep; velocity loss makes the maximal velocities reside at the level of the mitral tips, and they mostly do not reach the apical region. With further reduction in diastolic relaxation and elevation of filling pressures as a result of reduced compliance, the slope of the early filling wave will stay reduced; the wave usually gets blurry as a result of low flow velocities in the apical region, which can continue after early mitral inflow has stopped or even after mitral valve closure. Brun and colleagues[82] have been the first to show that velocity propagation is related to wall relaxation. The progressive decrease of Vp runs in parallel with the increase of the isovolumic relaxation constant $\tau$, irrespective of rising filling pressures.[84] Nishihara and colleagues[88] have confirmed that the strong correlation between $\tau$ and Vp is also valid in HCM. Using his acquisition method, Garcia and colleagues[89] have proposed a cutoff value of 55 cm/s and 45 cm/s to define impaired relaxation in young and middle-aged adults, respectively.

### Estimation of Filling Pressures and Prognosis

Combined indices of 1/Vp, as a preload-independent surrogate for $\tau$, with preload and relaxation-dependent mitral inflow parameters, provide close prediction of mean PCWP.[83,86,90,91] PCWP can be predicted accurately using a combination of IVRT and Vp with an r-value of 0.89 ($P$ less than 0.0001), and the regression equation: $PCWP = 4.5 \times (10^3/[\{2 \times IVRT\} + Vp]) - 9$ (in mm Hg, 1 SEE = 3.3).[90] Reported positive and negative predictive values for $(10^3/[\{2 \times IVRT\} + Vp])$ greater than 5.5 to predict PCWP greater than 15 are 100% and 94%, respectively.[90] However, E/Vp is the most widely used index. In a heterogeneous group comprising normal, ischemic, hypertrophic, and dilated hearts, PCWP was calculated as follows: $PCWP = [5.27 \times E/Vp] + 4.6$ (in mm Hg, SEE = 3.1) ($r = 0.80$, $P$ less than 0.001).[83] Reported positive and negative predictive values for E/Vp greater than 1.5 to predict PCWP greater than 12 mm Hg are 93% and 70%, respectively.[86] Correlation between E/Vp and PCWP outperforms correlations with maximal E ($r = 0.62$) and E/A ($r = 0.52$), independent of ejection fraction. Nagueh and colleagues[61,92] have confirmed that the same formula is valid in HCM. The E/Vp ratio has also been applied to assess filling pressures in atrial fibrillation with reasonable accuracy: averaged over three heartbeats, E/Vp yields a 100% specificity and 72% sensitivity in predicting a PCWP greater than 15 mm Hg.[93] It favorably corresponds to NYHA-class and elevated values of brain natriuretic peptide in this group.[94]

### Limitations of Vp as a Preload Independent Index for Relaxation

Reliability and reproducibility of the three different acquisition and reading methods constitute a major limitation for the application of Vp. In a direct comparison of the three methods, large differences in obtained numerical values and in interobserver and intraobserver reproducibility of Vp were generated.[81] The method described by Garcia and colleagues[83] is advocated because of the acceptable and superior reproducibility compared to the other methods.[81] Reported intraobserver and interobserver variability varies from less than 10%; in the lower (pathologic) ranges of Vp and up to 20% in the "higher" (normal) range of Vp and for TEE acquisitions.[83,85,90,93] Moreover, it does not require dedicated software and therefore is the most feasible technique for rapid, online measurements.

All conditions associated with altered intraventricular flow patterns giving rise to significant turbulence or significant local pressure gradient formation constitute a limitation to the application of the technique: significant aortic regurgitation, mitral stenosis, artificial mitral valves, and intracavity obstructions. Merging of early and late inflow as a result of tachycardia or atrioventricular conduction delay could lead to erroneous measurements. Marked variations on both transmitral inflow and Vp recordings can be seen during atrial fibrillation and in some patients during respiration. In these patients, it should be recommended to average more than three cardiac cycles.

## LA VOLUME INDEX

The measurement of LA volume is highly feasible and reliable in most echocardiograms, with the most accurate measurements obtained from the apical four-chamber and two-chamber views.[95] This measurement is very relevant clinically, as there is a significant relationship between LA volume and echocardiographic indexes of diastolic function.[96] The E/E′ ratio is a reflection of the filling pressures at the time of the examination. In contrast, the LA volume is a reflection of the cumulative effects of filling pressures over time. Some echocardiographers have compared the LA volume in diastology with the hemoglobin A1c of diabetology. Observational studies including 6657 patients without history of atrial fibrillation or valvular heart disease have shown that an LA volume index of 34 $nL/m^2$ or greater is an independent predictor of death, HF, atrial fibrillation, and ischemic stroke.[97] However, it is important to recognize that a dilated LA may be seen in athletes and in patients with bradycardia and four-chamber enlargement, anemia, and other high-output states; atrial flutter or fibrillation; and significant mitral valve disease, in the absence of cardiovascular disease.[67] Normal values of the left atrial volume index (LA volume/BSA) are shown in Table 11-4.

## STRAIN IMAGING IN EVALUATION OF DIASTOLIC FUNCTION

### *Assessment of Diastolic Function by Strain Echocardiography*

One advantage of the new ultrasound deformation strain indices for the study of diastolic events is that they offer high real-time temporal resolution of deformation (sampling rates greater than 200 frames/s) compared with other noninvasive imaging modalities (Fig. 11-10). This is important when studying diastole, because high-amplitude, short-lived deformations occur during this time period.[98,99] SR imaging has shown the normal sequence of regional changes in deformation during diastole to be complex.[98] Regional lengthening begins in the midinferior septal segment, might happen before aortic valve closure, and may have propagated to the apex by the time of mitral valve opening. The basal segments are the last to start to lengthen in early diastole. Their lengthening is associated with the onset of flow into the LV. On the other hand, in the free walls, changes in deformation are more

**TABLE 11-4 Reference Limits and Partition Values for Left Atrial Dimension and Volume**

| | Women | | | | Men | | | |
|---|---|---|---|---|---|---|---|---|
| | *Reference Range* | *Mildly Abnormal* | *Moderately Abnormal* | *Severely Abnormal* | *Reference Range* | *Mildly Abnormal* | *Moderately Abnormal* | *Severely Abnormal* |
| **Atrial Dimension** | | | | | | | | |
| LA diameter, cm | 2.7-3.8 | 3.9-4.2 | 4.3-4.6 | ≥4.7 | 3.0-4.0 | 4.1-4.6 | 4.7-5.2 | ≥5.2 |
| LA diameter/BSA, cm/m$^2$ | 1.5-2.3 | 2.4-2.6 | 2.7-2.9 | ≥3.0 | 1.5-2.3 | 2.4-.2.6 | 2.7-2.9 | ≥3.0 |
| RA minor-axis dimension, cm | 2.9-4.5 | 4.6-4.9 | 5.0-5.4 | ≥5.5 | 2.9-4.5 | 4.6-4.9 | 5.0-5.4 | ≥5.5 |
| RA minor-axis dimension/BSA, cm/m$^2$ | 1.7-2.5 | 2.6-2.8 | 2.9-3.1 | ≥3.2 | 1.7-2.5 | 2.6-2.8 | 2.9-3.1 | ≥3.2 |
| **Atrial Area** | | | | | | | | |
| LA area, cm$^2$ | ≤20 | 20-30 | 30-40 | >40 | ≤20 | 20-30 | 30-40 | >40 |
| **Atrial Volumes** | | | | | | | | |
| LA volume, mL | 22-52 | 53-62 | 63-72 | ≥73 | 18-58 | 59-68 | 69-78 | ≥79 |
| LA volume/BSA, mL/m$^2$ | 22 ± 6 | 29-33 | 34-39 | ≥40 | 22 ± 6 | 29-33 | 34-39 | ≥40 |

Adapted from Lang RM et al: Recommendation for chamber quantification: a report from the American Society of Echocardiography's Guidelines and Standards Committee and the Chamber Quantification Writing Group, developed in conjunction with the European Association of Echocardiography, a branch of the European Society of Cardiology. *J Am Soc Echocardiogr* 18:1440-1463, 2005.
*BSA*, Body surface area.

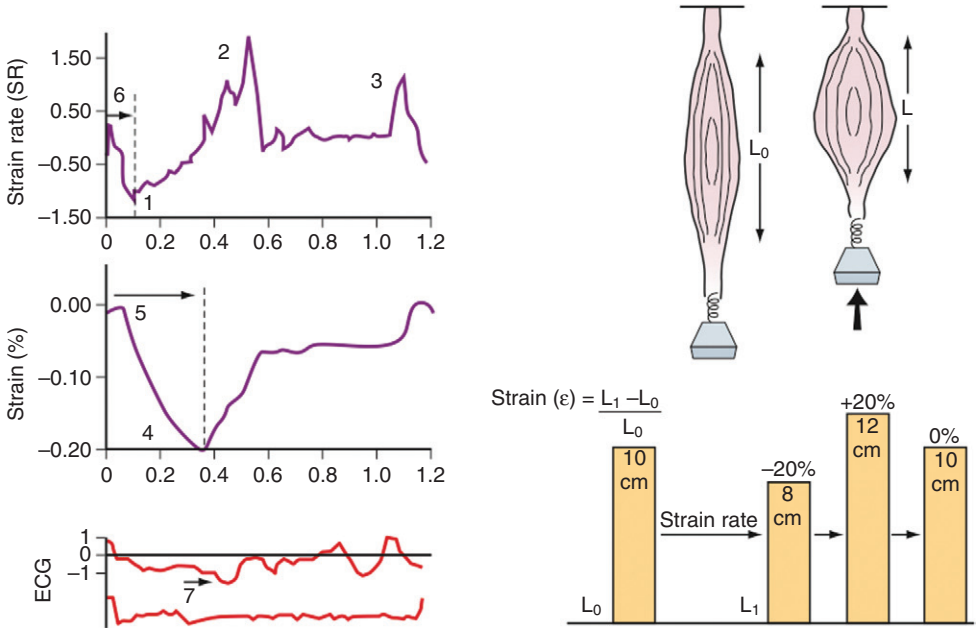



**Figure 11-10** Schematic representation of potential quantitative parameters obtained from echocardiography derived strain rate (SR) tracing (*left*). Both amplitude and timing of mechanical events can be used to assess regional function by SR imaging. SR tracing (*upper*): *1*, Peak systolic SR; *2*, peak early diastolic SR; *3*, peak late diastolic SR; *6*, time to peak systolic SR. Strain tracing (*middle*) is obtained by integrating the SR signal. This procedure is automatic in most custom or commercially available analysis packages. *4*, Peak systolic strain; *5*, time to peak. *7*, SR signal showing low systolic SR but presence of postsystolic SR (*lower*). Schematic illustrating concept of strain and SR (*right*). Strain (ε) is change in length normalized to initial length of muscle (*upper right*). Thus, decrease in length (such as occurring in muscle contraction) would result in negative strain, increase in length (muscle relaxation) would result in positive strain, and rate at which length changes occur would be SR. *(From Yip G, Abraham T, Belohlavek M, Khandheria BK:* J Am Soc Echocardiogr *16[12]:1334-1342, 2003.)*

variable. After the cessation of early lengthening as a result of early filling, there is a reverse lengthening wave caused by passive recoil, which starts at the apex and spreads toward the base. During diastasis there are usually no measurable changes in deformation. Diastasis is followed by a base-apex wave of lengthening that is caused by atrial filling of the ventricle. This normal pattern may be markedly altered in disease. However, in describing regional deformation changes during filling, not only must regional radial and longitudinal deformation be examined, but also an attempt should be made to resolve regional twisting/untwisting occurring during IVRT. To do this, circumferential shear strain must be measured. Circumferential radial shear strain can be shown to be abnormal in diseased segments. Diastolic strain rate measurements that comprise all LV segments are advantageous over myocardial velocities for the assessment of diastolic function. The ratio of mitral early diastolic velocity (E) to strain rate during the isovolumic relaxation (SRivr) can be used to estimate LV filling pressures. Wang and collaborators used these parameters in the evaluation of 50 patients with simultaneous right heart catheterization and echocardiographic imaging. Mitral E/SRivr ratio had the best correlation with mean wedge pressure. E/SRivr was most useful in patients with an E/E′ ratio of 8 to 15 and was more accurate than E/E′ in patients with normal ejection fraction and evidence of regional LV dysfunction.[100]

### Left Atrial Strain

Analogous to assessing LV mechanics by strain (ε) and strain rate (SR) imaging, measures of myocardial deformation have been increasingly adapted to study LA mechanics. Both echocardiographic methods of measuring strain and SR, color TDI,[101-104] and 2D speckle tracking imaging[105-108] have been adapted to the measurement of LA deformation. In both methods, different measures of myocardial deformation, tissue velocity (V), strain ε, and strain rate SR can be derived at the three respective phases of the LA phasic cycle (conduit, reservoir, and contractile phases). The advantage of analyzing LA myocardial mechanics with strain and SR imaging is the insight that can be obtained about each component of LA phasic function. One could use this method to resolve the exact change in LA phasic function with different disease states and investigate the effect after treatment. Research in this field remains sparse but shows promise. The reasons for the transition from asymptomatic diastolic dysfunction to symptomatic diastolic HF are not fully understood. A recent study has drawn attention to the presence of a lower atrial contractile reserve in patients with diastolic HF.[109] Kurt and colleagues[110] concluded in their study that LA strain La(ε) is significantly reduced and that LA stiffness is the most accurate index in identifying patients with diastolic HF.

## TORSION ECHOCARDIOGRAPHY

LV torsion (or twist) plays an important role with respect to LV ejection and filling.[111] During the cardiac cycle, there is a systolic twist, followed by an early diastolic untwist of the LV over its long axis due to oppositely directed apical and basal rotations. As viewed from the LV apex, the base of the heart rotates clockwise, while the apex rotates in a counterclockwise direction. LV rotation is sensitive to changes in both regional and global LV function.[112-114] Therefore, assessment of LV rotation represents an interesting approach for quantifying global LV function during systole and diastole. Historically, magnetic resonance imaging (MRI) tagging was the first clinically available method,[114,115] and as a result, implementation of the evaluation of LV torsion was limited by the complexity and cost of the technique.

Speckle tracking imaging (STI) has provided the possibility of evaluating the deformation mechanics of the myocardial fibers during the different parts of the cardiac cycle[116] (see Chapter 10). This non-Doppler assessment of cardiac mechanics could rival MRI or TDI in measuring LV torsion and may prove more versatile in assessing patients in clinical and research settings. Motion analysis by speckle tracking has been attempted using block matching and autocorrelation search algorithms.[117] Speckle motion has been closely linked to underlying tissue motion when small displacements are involved. On the basis of this displacement estimation technique, LV rotation (angle displacement about the central axis of LV in the short-axis view) for assessment of LV torsion can be measured.[72]

### Validation of Torsion Calculated by Speckle Tracking

The accuracy and consistency of speckle tracking imaging method for LV torsion measurement was assessed in comparison with tagged MRI and TDI in 15 patients.[117,118] LV torsion was defined as the net difference of LV rotation at the basal and apical planes. Data on 13 of 15 patients could be used to perform speckle tracking analysis. The LV torsion profiles estimated by STI strongly correlated with those obtained by tagged MRI. The STI torsional velocity profiles also correlated well with those obtained by the TDI method.

In another study, apical and basal rotation by speckle tracking was measured from short-axis images by automatic frame-to-frame tracking of gray-scale speckle patterns in mongrel dogs and healthy humans and compared to sonomicrometry (dogs) and MRI (humans).[119,120] In dogs, the mean peak apical rotation was $-3.7 \pm 1.2°$ and $-4.1 \pm 1.2°$, and basal rotation was $1.9 \pm 1.5°$ and $2.0 \pm 1.2°$ by sonomicrometry and speckle tracking, respectively. Apical rotation by both methods decreased during left anterior descending coronary artery occlusion ($P$ less than 0.007), whereas basal rotation was unchanged. In healthy humans, apical rotation was $-11.6 \pm 3.8°$ and $-10.9 \pm 3.3°$, and basal rotation was $4.8 \pm 1.7°$ and $4.6 \pm 1.3°$ by MRI tagging and speckle tracking echocardiography, respectively. Torsion measurement by speckle tracking echocardiography showed good correlation and agreement with sonomicrometry ($r = 0.94$; $P$ less than 0.001) and MRI ($r = 0.85$; $P$ less than 0.001).

### Left Ventricular Untwisting Rate by Speckle Tracking Echocardiography

As mentioned previously, LV filling results from the positive early diastolic transmitral pressure gradient and depends on both the LV pressure drop during isovolumic relaxation and the LA driving pressure.[65,100] The rapid decline in LV pressure during this phase is caused by active myocardial relaxation and LV elastic recoil. LV elastic recoil/untwisting generates the suction force for LV filling. Accordingly, LV untwisting rate may provide an additional noninvasive insight into LV diastolic dysfunction. Previous work with MRI in an animal model, has shown that LV untwisting rate correlates closely with the time constant of LV relaxation.[121]

In a recent study, Wang and collaborators[122] conducted a study evaluated 67 patients with simultaneous right heart catheterization and echocardiographic imaging. Patients with LV systolic dysfunction had a significantly lower untwisting rate, in comparison with the control group, and the patients with normal ejection fraction. The determinants for untwisting rate were twist, end-systolic volume (ESV), and τ. In patients with diastolic dysfunction and normal ejection fraction, twist and ESV were the independent predictors. A recent study by the same group[123] showed that the untwisting rate calculation method that best reflects LV relaxation is the peak negative time derivative of twist during early diastole.

### Comprehensive Integration of Systolic and Diastolic Mechanics

Wang and colleagues[124] examined myocardial deformation and rotation in patients with HF aiming at elucidating the mechanisms that account for normal ejection fraction in patients with diastolic HF. LV longitudinal and radial strains are reduced, but circumferential deformation and twist are normal in diastolic HF patients. On the other hand, in patients with systolic HF, longitudinal, radial, circumferential, and twist are all reduced. Multivariate regression analysis suggests that preserved LV twist and circumferential strain may contribute to normal ejection fraction, in patients with diastolic HF.[124]

### NEW ASE/EAE GUIDELINES

In 2009, Nagueh and colleagues[3] published recommendations for the evaluation of LV diastolic function by echocardiography, which represents a big leap forward in the field. The guidelines present an organized approach for grading the degree of diastolic dysfunction, and for calculation of filling pressures in the patient with normal or depressed systolic function. Using the guidelines, the first step is to grade the diastolic dysfunction. The grading scheme is mild or grade 1 (impaired relaxation pattern), moderate or grade 2 (pseudonormal), and severe or grade 3 (restrictive pattern) (Fig. 11-11). The next step is the estimation of LA pressures, which can be accomplished by following the algorithms provided depending on the systolic function of the patient (normal or depressed) (Figs. 11-12 and 11-13, respectively). When grading the degree of diastolic dysfunction, it is important to realize that patients would not necessarily fulfill all the criteria mentioned in a given grade. In these situations, judgment must be exercised as to what is the grade that best characterizes the patient, after carefully evaluating and balancing the parameters obtained and the predominance of the criteria during the comprehensive evaluation of the patient.

## Clinical Utility of Diastolic Function Assessment

The clinical utility of echocardiographic assessment of diastolic function in specific diseases is discussed in this section.

### MYOCARDIAL DISEASES

#### *Dilated Cardiomyopathy*

Dilated cardiomyopathy manifests with a multitude of diastolic filling patterns. Differences in diastolic function may explain differences in clinical symptoms between patients with similar degrees of systolic dysfunction. When systolic dysfunction is

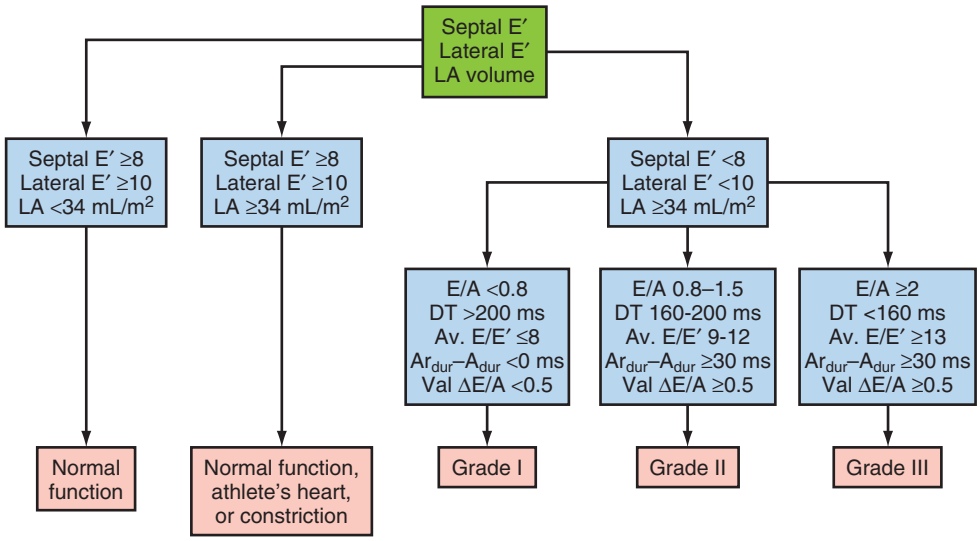



**Figure 11-11** Scheme for grading diastolic dysfunction. *Av.*, Average; *Val*, Valsalva. *(Adapted from: Nagueh SF, Appleton CP, Gillebert TC, et al: Recommendations for the evaluation of left ventricular diastolic function by echocardiography.* J Am Soc Echocardiogr *22:107-133, 2009.)*

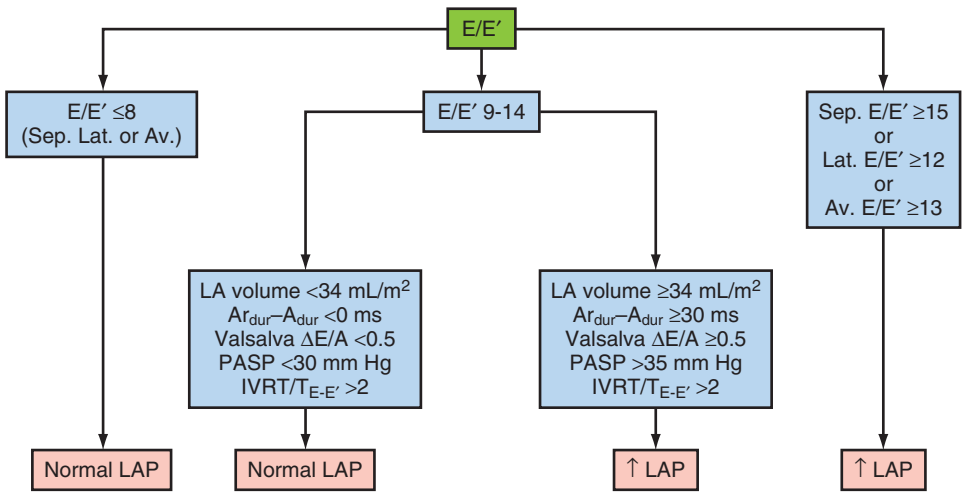



**Figure 11-12** Diagnostic algorithm for the estimation of LV filling pressures in patients with normal ejection fraction. *Av*, Average; *LAP*, left atrial pressure; *Lat*, lateral; *PASP*, pulmonary artery systolic pressure; *Sep*, septal. *(Adapted from Nagueh SF, Appleton CP, Gillebert TC, et al: Recommendations for the evaluation of left ventricular diastolic function by echocardiography.* J Am Soc Echocardiogr *22:107-133, 2009.)*

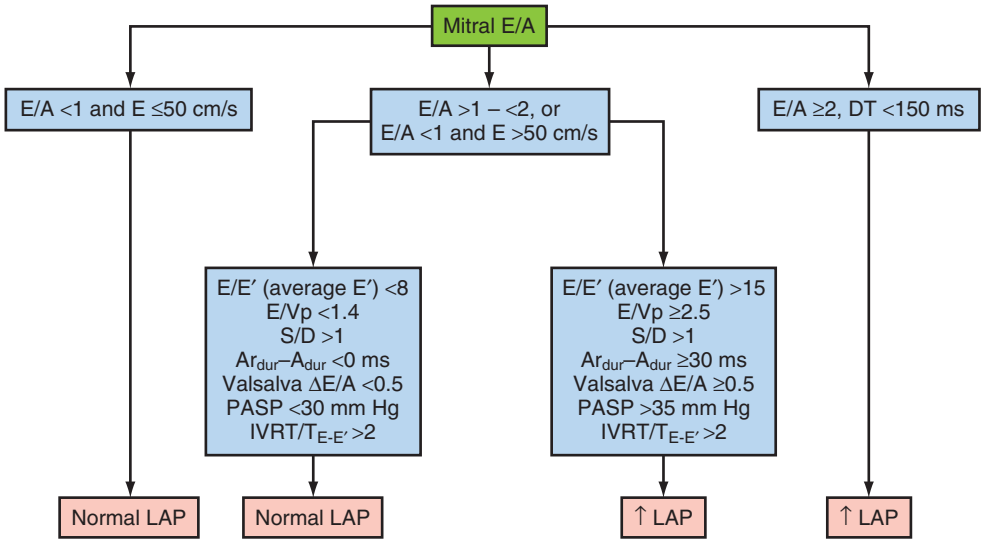



**Figure 11-13** Diagnostic algorithm for the estimation of pressures in patients with depressed ejection fraction. *(Adapted from Nagueh SF, Appleton CP, Gillebert TC, et al: Recommendations for the evaluation of left ventricular diastolic function by echocardiography. J Am Soc Echocardiogr 22:107-133, 2009.)*

present, the elevated ESV results in a shift along the pressure-volume curve to a steeper segment. This means that for a given diastolic pressure-volume relationship, compliance is reduced at higher LV volumes. Thus, the expected pattern of diastolic filling in advanced dilated cardiomyopathy is that of reduced compliance: a high E velocity, rapid deceleration slope, low A velocity, and E/A ratio greater than 1 (stage 3).

### *Amyloidosis*

Cardiac amyloidosis is associated with abnormal LV and RV diastolic function (see Chapter 28). As the disease process worsens following impaired relaxation, there is worsening of compliance, resulting in pseudonormal and restrictive patterns associated with a progressive decrease in compliance with progressive deposition of amyloid fibrils in the myocardium.[125] The prognosis of cardiac amyloidosis is generally poor, but it depends on the type of disease, with AL (primary) amyloidosis having the worst prognosis.[126] In a serial study of more than 800 patients with primary amyloidosis over a 10-year period, the median survival was 2.1 years, and less than 6 months once congestive HF had occurred.[127] Mean LV wall thickness and LV impairment have been suggested as useful variables in the assessment of cardiac involvement and prognosis. In a study of 132 patients with biopsy-proven amyloidosis, those with a wall thickness of 15 mm or greater had a median survival of 0.4 years compared with 2.4 years for those with a mean wall thickness of greater than12 mm but less than 15 mm.[128] There are associated abnormalities of RV diastolic function.[49] In patients with RV free wall thickness of less than 7 mm, there is abnormal relaxation, and when the RV wall is greater than 7 mm in thickness, restrictive physiology is present. Doppler echocardiography has also been shown to be useful in the prognostic stratification of patients with amyloidosis. Patients with a DT of the mitral early filling wave at baseline study of 150 ms or less had a significantly reduced survival compared to those whose DT was greater than 150 ms.[129] (Fig. 11-14) A Doppler index combining systolic and diastolic performance (Tei index) has shown significant prognostic importance in cardiac amyloidosis.[130] RV enlargement has also been identified as an independent predictor of poor outcomes among patients with primary amyloidosis.[131] Newer diagnostic tools, including strain and SR imaging, have been used to characterize patients with cardiac amyloidosis before the onset of congestive symptoms and with preserved LV function and tissue Doppler velocities.[132] Among patients with AL amyloidosis, the mean basal strain, a measure of longitudinal LV function, was a powerful predictor of outcome and was superior to standard 2D echocardiography, Doppler flow measurements, and simple tissue Doppler velocity indexes.[133]

### *Hypertrophic Cardiomyopathy*

Patients with HCM often have a pattern of LV diastolic filling consistent with impaired relaxation. (See Chapter 27.) Some studies have suggested that Doppler evaluation of LV diastolic filling can be used to assess the effects of medical therapy (e.g., beta-blockers or calcium channel blockers) on diastolic function in this disease.

SR imaging indices have been shown to be better than regional velocity profile data in detecting regional abnormalities in patients with asymmetric septal hypertrophy and in discriminating HCM from physiologic hypertrophy. SR imaging has also been shown to be better than either gray-scale M-mode or velocity data either in detecting changes in regional function after septal ablation[134] or in detecting the regression of hypertrophy after antioxidant treatment for HCM.

## HYPERTENSION AND HYPERTENSIVE HEART DISEASE

In left ventricular hypertrophy, the predominant abnormality is impaired relaxation, resulting in a pattern of reduced early diastolic filling and an enhanced atrial contribution to filling. The Doppler velocity curve typically shows a prolonged IVRT, reduced acceleration to a reduced E velocity, prolonged early diastolic deceleration slope, an increased A velocity, and an E/A ratio less than 1. When LV systolic dysfunction supervenes, the elevated LV end-diastolic pressure and elevated LA pressure may result in pseudonormalization of this pattern with an enhanced E velocity (related to a higher mitral valve opening gradient) and reduced A velocity (resulting from the elevated LV end-diastolic pressure).

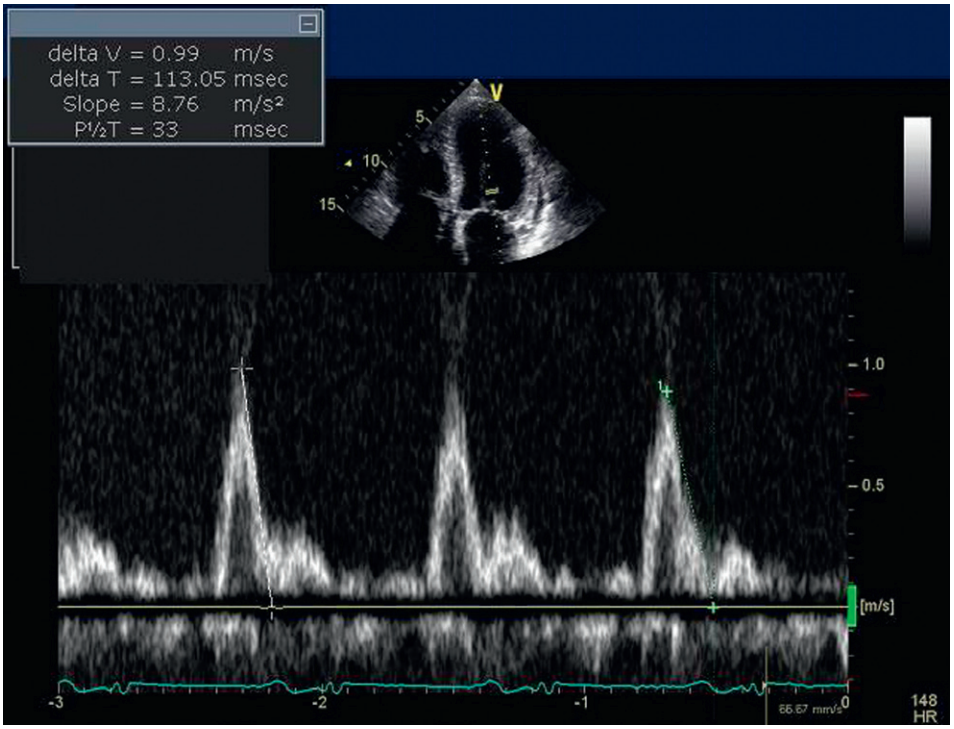



**Figure 11-14 Survival Curves in Cardiac etc.** Survival in 63 patients with cardiac amyloidosis subdivided on the basis of the deceleration time (DT) of 150 msec. Patients with a shortened deceleration time of less than 150 msec (*blue line*) had significantly reduced survival compared with patients with a deceleration time of greater than 150 msec. (*From Klein AL, Hatle LK, Taliercio CP, et al:* Circulation *83:808-816, 1991.*)

TDI has been demonstrated as a better discriminator between normal controls and patients with primary or secondary LV hypertrophy with a decrease in E′ and in ratio E′/A′ and with a prolonged time from the electrocardiogram Q wave to the onset of E′ in pathologic groups.[58] Differences in the onset of diastolic myocardial velocity waves between the different myocardial components of the cardiac base have been reported in both primary and secondary LV hypertrophy.[135] The etiology of LV volume overload leading to LV hypertrophy may result in different TDI velocity patterns.[135] Abe and colleagues[135a] have reported lower E′ and prolonged time to E′ onset in patients with chronic aortic regurgitation when compared with those with mitral regurgitation. Myocardial early diastolic velocities have been demonstrated to decrease with age.[135,136] However, it has been shown that the difference between normal controls and patients with LV hypertrophy remained significant even after accounting for age.[136]

Recently, strain imaging has been shown to differentiate between control subjects and patients with hypertension and among patients with hypertension, to differentiate between those with and without diastolic dysfunction.[137]

## ISCHEMIC CARDIAC DISEASE

In patients with coronary artery disease and no prior myocardial infarction, induction of ischemia results in diastolic dysfunction before systolic dysfunction. Diastolic filling curves with ischemia induced by balloon inflation during percutaneous transluminal angioplasty show rapid onset of a reduced E velocity, with resolution of these changes as ischemia is relieved. In acute myocardial infarction, a pattern of delayed relaxation is seen acutely. At follow-up, one of several patterns of LV filling may be observed. With successful reperfusion and little myocardial damage, LV diastolic filling returns to normal. With an infarction but preserved LV systolic function, the pattern of impaired relaxation often persists. (See Chapter 14.) With a large infarction and significant LV systolic dysfunction, the pseudonormalized pattern of high E velocity and low A velocity as a result of a combination of reduced compliance, a high LV end-diastolic pressure, and a shift along the diastolic pressure volume curve (increased ESV) can be seen.

Many patients with ischemic heart disease demonstrate abnormal diastolic function recorded by pulsed Doppler TDI despite having normal systolic function.[55] Recent studies have also shown a reduced E′ and E′/A′ ratio in ischemic or infarcted segments.[138,138a] One study also showed that the number of segments with abnormal E′/A′ ratio was higher in ischemic patients with a decreased transmitral Doppler E/A ratio compared with those with a normal transmitral E/A ratio. Recording diastolic TDI has also been shown to be a sensitive method for detecting transient myocardial ischemia—for example, during inflation of an angioplasty balloon.[139,140]

## PERICARDIAL DISEASE

With both pericardial tamponade and pericardial constriction, cardiac filling is impaired by pericardial extrinsic constraint, and there is marked reciprocal respiratory variation of LV and RV filling. In the case of tamponade physiology, filling is impaired in both early and late diastole. With constrictive pericarditis, early diastolic filling tends to be normal, with marked impairment of filling late in diastole when the heart has expanded to the maximum allowed by the fibrotic pericardial encasement. TDI is useful in separating restrictive from constrictive physiology (see Chapters 28 and 29).

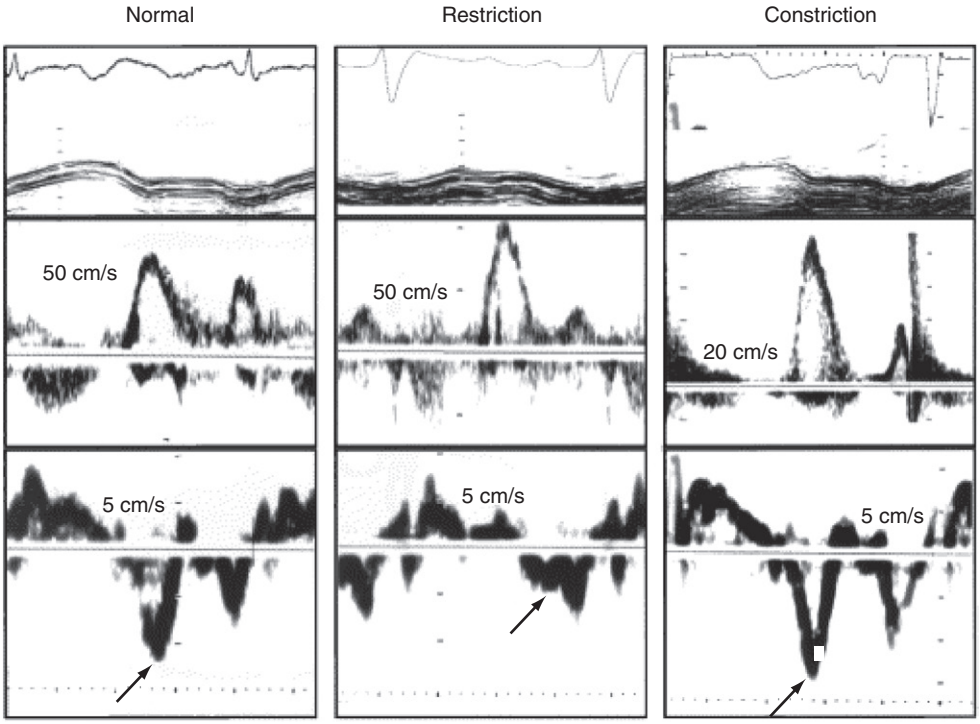



**Figure 11-15** Representative samples of the mitral annular M-mode tracings, tissue Doppler imaging velocities in the longitudinal axis, and transmitral Doppler flow velocities in a normal volunteer, a patient with restrictive cardiomyopathy, and a patient with constrictive pericarditis. A marked difference in early diastolic longitudinal axis velocities, despite similar early transmitral flow velocities, is appreciated. *(Adapted from Garcia MJ, Thomas JD, Klein AL: New Doppler echocardiographic applications for the study of diastolic function.* J Am Coll Cardiol *32[4]:865-875, 1998.)*

## RESTRICTIVE VERSUS CONSTRICTIVE PHYSIOLOGY

Hearts encased with the constrictive process have normal or enhanced relaxation (thus increased E′ velocity and color M-mode slope) and could fill mainly in a longitudinal fashion. In contrast, hearts with restrictive diseases showed marked impairment of relaxation due to the myopathic process and had decreased E′ velocities and decreased annular E′ velocities.[141] As a result E′ can also be used to distinguish between restrictive and constrictive physiology[142] (Fig. 11-15). It has been demonstrated that E′ measured by pulsed Doppler at the level of the lateral part of the mitral annulus was significantly lower in 7 patients with restrictive cardiomyopathy than in 15 normal subjects and 8 patients with constrictive pericarditis. In another study, abnormal pulsed TDI velocity pattern was reported in 12 patients with constrictive pericarditis versus a group of 20 normal subjects.[143] A cutoff of E′ of 8 cm/s or greater was useful in separating constrictive pericarditis from restriction in another study.[144]

Reuss and coworkers found that in control patients mitral lateral E′ velocity is 25% higher than the septal one. Whereas in constrictive pericarditis, averaged lateral E′ velocity was 2% lower than septal E′ velocity. This reversal of the relationship between the velocities is called annulus reversus.[145]

Recently, Choi and colleagues performed a study comparing E′ of the septal annulus (sE′), lateral mitral annulus (lE′), and right lateral tricuspid annulus (rlE′) in patients with constrictive pericarditis and restrictive cardiomyopathy. They concluded that the ratio between lateral and septal E′ is significantly reduced in constrictive pericarditis compared to normal controls and restrictive cardiomyopathy. The reduced lE′/sE′ , and rE′/sE′ appear to be useful diagnostic parameters for the diagnosis of constrictive pericarditis. Moreover, reduced lE′ is correlated with pericardial thickness on the respective side.[146]

However, E/E′ fails to characterize the filling pressure in this group of patients, a phenomenon called annulus paradoxus. There is an inverse relationship between E/E' and LV filling pressure.[147]

## KEY POINTS

- Diastolic HF is as common as systolic HF and is associated with significant morbidity and mortality.
- The major parameters of diastolic function include active myocardial relaxation, LV compliance, LA function, pulmonary vein flow, mitral valve characteristics, and heart rate.
- Echocardiographic techniques for evaluation of diastolic function include mitral inflow, pulmonary venous flow, tissue Doppler imaging, and color M-mode Doppler and LA volume index.
- For patients with diastolic dysfunction, four abnormal filling patterns are recognized: stage 1 (mild) or abnormal relaxation, stage 2 (moderate) or pseudonormal, stage 3 (severe) or restrictive, and stage 4 (severe) or irreversible restrictive.

## KEY POINTS—cont'd

- TDI and color M-mode Doppler evaluation of LV diastolic filling are less preload dependent than mitral inflow or PV flow.
- The ratio of peak early mitral inflow velocity divided by TDI early diastolic mitral annular velocity (E/E′) correlates with PCWP. Similarly, the ratio of peak early mitral inflow velocity divided by color M-mode flow propagation (E/Vp) correlates with PCWP.
- An E/E′ ratio greater than 15 or E/Vp greater than 1.5 suggests elevated LV filling pressures.
- Mitral inflow and PV flow can adequately assess LV filling pressures in patients with systolic HF. TDI and color M-mode are needed when there is primary diastolic HF (with a normal ejection fraction).
- A short mitral inflow DT is associated with a poor prognosis in most diseases, except for hypertrophic cardiomyopathy.
- Strain and strain rate (SR) are measures of myocardial mechanical properties. Myocardial strain is a dimensionless index of change in myocardial length in response to an applied force and is expressed as fractional or percentage of change. SR is the time derivative of strain with unit of per second ($s^{-1}$).

## REFERENCES


1. Brogan WCD, Hillis LD, Flores ED, Lange RA: The natural history of isolated left ventricular diastolic dysfunction. *Am J Med* 92:627-630, 1992.
2. Gaasch WH: Diagnosis and treatment of heart failure based on left ventricular systolic or diastolic dysfunction [see comments]. *JAMA* 271:1276-1280, 1994.
3. Nagueh SF, Appleton CP, Gillebert TC, et al: Recommendations for the evaluation of left ventricular diastolic function by echocardiography. *J Am Soc Echocardiogr* 22:107-133, 2009.
4. Bonnema DD, Baicu C, Zile MR: Pathophysiology of diastolic heart failure: relaxation and stiffness. In Klein AL, Garcia MJ, editors: *Diastology: clinical approach to diastolic heart failure*, Philadelphia, 2008, Saunders Elsevier, pp 11-25.
5. Thomas JD, Flachskampf FA, Chen C, et al: Isovolumic relaxation time varies predictably with its time constant and aortic and left atrial pressures: implications for the noninvasive evaluation of ventricular relaxation. *Am Heart J* 124:1305-1313, 1992.
6. Weiss JL, Frederikson JW, Weisfeldt JL: Hemodynamic determinants of the time-course of fall in canine left ventricular pressure. *J Clin Invest* 58:751-776, 1976.
7. Little WC, Downes TR: Clinical evaluation of left ventricular diastolic performance. *Prog Cardiovasc Dis* 32:273-290, 1990.
8. Choong CY, Abascal VA, Thomas JD, et al: Combined influence of ventricular loading and relaxation in the transmitral flow velocity profile in dogs measured by Doppler echocardiography. *Circulation* 78:672-683, 1988.
9. Thomas JD, Weyman AE: Echo-Doppler evaluation of ventricular diastolic function: physics and physiology. *Circulation* 77:977-990, 1991.
10. Robinson T, Factor S, Sonnenblick E: The heart as a suction pump. *Sci Am* 254:84, 1986.
11. Klein AL, Asher CR: Diseases of the pericardium, restrictive cardiomyopathy, and diastolic dysfunction. In: Topol EJ, Califf RM, Prystowsky EN, editors: *Textbook of cardiovascular medicine*, Philadelphia, 2007, Lippincott Williams & Wilkins, pp 420-459.
12. Pouleur H: Diastolic dysfunction and myocardial energetics. *Eur Heart J* 11(Suppl C. P):30-34, 1990 May.
13. Gaasch WH, Quinones MA, Waisser E, et al: Diastolic compliance of the left ventricle in man. *Am J Cardiol* 36:193-201, 1975.
14. Janicki JS: Myocardial collagen remodeling and left ventricular diastolic function. *Braz J Med Biol Res* 25:975-982, 1992.
15. Matsubara B, Hennigar J, Janicki J: Structural and functional role of myocardial collagen. *Circulation* 84:II-212, 1991.
16. Gilbert JC, Glantz SA: Determinants of left ventricular filling and of the diastolic pressure-volume relation. *Circ Res* 64:827-852, 1989.
17. Cheng CP, Igarashi Y, Little WC: Mechanism of augmented rate of left ventricular filling during exercise. *Circ Res* 70:9-19, 1992.
18. Tyberg JV, Misbach GA, Glantz SA, et al: A mechanism for shifts in the diastolic, left ventricular, pressure-volume curve: the role of the pericardium. *Eur J Cardiol* 7:163-175, 1978.
19. Suga H, Goto Y, Igarashi Y, et al: Ventricular suction under zero source pressure for filling. *Am J Physiol* 251:H47-H55, 1986.
20. Toutouzas P, Stefanadis C, Boudoulas H: 1st international symposium on left atrial function: Introduction. *Eur Heart J Suppl* 2(supplement K):K1-K3, 2000.
21. Ito T, Suwa M, Hirota Y, et al: Influence of left atrial function on Doppler transmitral and pulmonary venous flow patterns in dilated and hypertrophic cardiomyopathy: evaluation of left atrial appendage function by transesophageal echocardiography. *Am Heart J* 131:122-130, 1996.
22. Pollick C, Taylor D: Assessment of left atrial appendage function by transesophageal echocardiography. Implications for the development of thrombus. *Circulation* 84:223-231, 1991.
23. Klein AL, Burstow DJ, Tajik AJ, et al: Effects of age on left ventricular dimensions and filling dynamics in 117 normal persons. *Mayo Clin Proc* 69:212-224, 1994.
24. Grimm RA, Leung DY, Black IW, et al: Left atrial appendage "stunning" after spontaneous conversion of atrial fibrillation demonstrated by transesophageal Doppler echocardiography. *Am Heart J* 130:174-176, 1995.
25. Plehn JF, Southworth J, Cornwell GGD: Brief report: Atrial systolic failure in primary amyloidosis [see comments]. *N Engl J Med* 327:1570-1573, 1992.
26. Appleton CP, Carucci MJ, Henry CP, Olajos M: Influence of incremental changes in heart rate on mitral flow velocity: Assessment in lightly sedated, conscious dogs. *J Am Coll Cardiol* 17:227-236, 1991.
27. Harrison MR, Clifton GD, Pennell AT, DeMaria AN: Effect of heart rate on left ventricular diastolic transmitral flow velocity patterns assessed by Doppler echocardiography in normal subjects. *Am J Cardiol* 67:622-627, 1991.
28. Walsh RA: Sympathetic control of diastolic function in congestive heart failure (Review). *Circulation* 82:I52-I58, 1990.
29. Tanabe A, Mohri T, Ohga M, et al: The effects of pacing-induced left bundle branch block on left ventricular systolic and diastolic performances. *Jpn Heart J* 31:309-317, 1990.
30. Hatle LK, Appleton CP, Popp RL: Differentiation of constrictive pericarditis and restrictive cardiomyopathy by Doppler echocardiography [see comments]. *Circulation* 79:357-370, 1989.
31. Kitzman DW, Little WC, Brubaker PH, et al: Pathophysiological characterization of isolated diastolic heart failure in comparison to systolic heart failure. *JAMA* 288:2144-2150, 2002.
32. Brucks S, Little WC, Chao T, et al: Contribution of left ventricular diastolic dysfunction to heart failure regardless of ejection fraction. *Am J Cardiol* 95:603-606, 2005.
33. Zile MR, Gaasch WH, Carroll JD, et al: Heart failure with a normal ejection fraction: is measurement of diastolic function necessary to make the diagnosis of diastolic heart failure? *Circulation* 104:779-782, 2001.
34. van Heerebeek L, Borbely A, Niessen HW, et al: Myocardial structure and function differ in systolic and diastolic heart failure. *Circulation* 113:1966-1973, 2006.
35. Bhatia RS, Tu JV, Lee DS, et al: Outcome of heart failure with preserved ejection fraction in a population-based study. *N Engl J Med* 355:260-269, 2006.
36. Owan TE, Hodge DO, Herges RM, et al: Trends in prevalence and outcome of heart failure with preserved ejection fraction. *N Engl J Med* 355:251-259, 2006.
37. Echeverria HH, Bilsker MS, Myerburg RJ, Kessler KM: Congestive heart failure: Echocardiographic insights. *Am J Med* 75:750-755, 1983.
38. Paulus WJ, Tschope C, Sanderson JE, et al: How to diagnose diastolic heart failure: a consensus statement on the diagnosis of heart failure with normal left ventricular ejection fraction by the Heart Failure and Echocardiography Associations of the European Society of Cardiology. *Eur Heart J* 28:2539-2550, 2007.

39. Vasan RS, Levy D: Defining diastolic heart failure: a call for standardized diagnostic criteria [see comments]. *Circulation* 101:2118-2121, 2000.
40. Hunt SA, Abraham WT, Chin MH, et al: ACC/AHA 2005 guideline update for the diagnosis and management of chronic heart failure in the adult: A report of the American College of Cardiology/American Heart Association Task Force on Practice Guidelines (Writing Committee to Update the 2001 Guidelines for the Evaluation and Management of Heart Failure): developed in collaboration with the American College of Chest Physicians and the International Society for Heart and Lung Transplantation: endorsed by the Heart Rhythm Society. *Circulation* 112:e154-235, 2005.
41. Appleton CP, Firstenberg MS, Garcia MJ, Thomas JD: The echo-Doppler evaluation of left ventricular diastolic function. A current perspective. *Cardiol Clin* 18:513-546, ix, 2000.
42. Yamada H, Klein AL: Diastology 2010: Clinical approach to diastolic heart failure. *J Echocardiogr* 8:65-79, 2010.
43. Appleton CP, Gonzalez MS, Basnight MA: Relationship of left atrial pressure and pulmonary venous flow velocities: importance of baseline mitral and pulmonary venous flow velocity patterns studied in lightly sedated dogs. *J Am Soc Echocardiogr* 7:264-275, 1994.
44. Nishimura RA, Housmans PR, Hatle LK, Tajik AJ: Assessment of diastolic function of the heart: background and current applications of Doppler echocardiography. Part I. Physiologic and pathophysiologic features. *Mayo Clin Proc* 64:71-81, 1989.
45. Ommen SR, Nishimura RA, Appleton CP, et al: Clinical utility of Doppler echocardiography and tissue Doppler imaging in the estimation of left ventricular filling pressures: a comparative simultaneous Doppler-catheterization study. *Circulation* 102:1788-1794, 2000.
46. Kuecherer HF, Muhiudeen IA, Kusumoto FM, et al: Estimation of mean left atrial pressure from transesophageal pulsed Doppler echocardiography of pulmonary venous flow. *Circulation* 82:1127-1139, 1990.
47. Rossvoll O, Hatle LK: Pulmonary venous flow velocities recorded by transthoracic Doppler ultrasound: relation to left ventricular diastolic pressures. *J Am Coll Cardiol* 21:1687-1696, 1993.
48. Appleton CA, Hatle LK, Popp RL: Relation of transmitral flow velocity patterns to left ventricular diastolic function: new insights from a combined hemodynamic and Doppler echocardiographic study. *J Am Coll Cardiol* 12:426-440, 1988.
49. Klein AL, Hatle LK, Burstow DJ, et al: Comprehensive Doppler assessment of right ventricular diastolic function in cardiac amyloidosis. *J Am Coll Cardiol* 15:99-108, 1990.
50. Klein AL, Cohen GI: Doppler echocardiographic assessment of constrictive pericarditis, cardiac amyloidosis, and cardiac tamponade. *Cleve Clin J Med* 59:278-290, 1992.
51. Cohen GI, Pietrolungo JF, Thomas JD, et al: A practical guide to assessment of ventricular diastolic function using Doppler echocardiography. *J Am Coll Cardiol* 27:1753-1760, 1996.
52. Appleton CP, Hatle LK, Popp RL: Superior vena cava and hepatic vein Doppler echocardiography in healthy adults. *J Am Coll Cardiol* 10:1032-1039, 1987.
53. Zoghbi WA, Habib GB, Quinones MA: Doppler assessment of right ventricular filling in a normal population. Comparison with left ventricular filling dynamics. *Circulation* 82:1316-1324, 1990.
54. Hatle L, Angelsen B: *Doppler ultrasound in cardiology: physical principles and clinical applications*, Philadelphia, 1982, Lea & Febiger.
55. Isaaz K, Thompson A, Ethevenot G, et al: Doppler echocardiographic measurement of low velocity motion of the left ventricular posterior wall. *Am J Cardiol* 64:66-75, 1989.
56. Sohn DW, Chai IH, Lee DJ, et al: Assessment of mitral annulus velocity by Doppler tissue imaging in the evaluation of left ventricular diastolic function. *J Am Coll Cardiol* 30:474-480, 1997.
57. Garcia MJ, Rodriguez L, Ares M, et al: Myocardial wall velocity assessment by pulsed Doppler tissue imaging: characteristic findings in normal subjects. *Am Heart J* 132:648-656, 1996.
58. Pai RG, Gill KS: Amplitudes, durations, and timings of apically directed left ventricular myocardial velocities: II. Systolic and diastolic asynchrony in patients with left ventricular hypertrophy. *J Am Soc Echocardiogr* 11:112-118, 1998.
59. Galiuto L, Ignone G, DeMaria AN: Contraction and relaxation velocities of the normal left ventricle using pulsed-wave tissue Doppler echocardiography. *Am J Cardiol* 81:609-614, 1998.
60. Nagueh SF, Middleton KJ, Kopelen HA, et al: Doppler tissue imaging: a noninvasive technique for evaluation of left ventricular relaxation and estimation of filling pressures. *J Am Coll Cardiol* 30:1527-1533, 1997.
61. Nagueh SF, Lakkis NM, Middleton KJ, et al: Doppler estimation of left ventricular filling pressures in patients with hypertrophic cardiomyopathy. *Circulation* 99:254-261, 1999.
62. Sohn DW, Song JM, Zo JH, et al: Mitral annulus velocity in the evaluation of left ventricular diastolic function in atrial fibrillation. *J Am Soc Echocardiogr* 12:927-931, 1999.
63. Sundereswaran L, Nagueh SF, Vardan S, et al: Estimation of left and right ventricular filling pressures after heart transplantation by tissue Doppler imaging. *Am J Cardiol* 82:352-357, 1998.
64. Masutani S, Little WC, Hasegawa H, et al: Restrictive left ventricular filling pattern does not result from increased left atrial pressure alone. *Circulation* 117:1550-1554, 2008.
65. Oh JK, Hatle L, Tajik AJ, Little WC: Diastolic heart failure can be diagnosed by comprehensive two-dimensional and Doppler echocardiography (Comment). *J Am Coll Cardiol* 47:500-506, 2006.
66. Mullens W, Borowski AG, Curtin RJ, et al: Tissue Doppler imaging in the estimation of intracardiac filling pressure in decompensated patients with advanced systolic heart failure. *Circulation* 119:62-70, 2009.
67. Little WC, Oh JK: Echocardiographic evaluation of diastolic function can be used to guide clinical care. *Circulation* 120:802-809, 2009.
68. Nagueh SF, Bhatt R, Vivo RP, et al: Echocardiographic evaluation of hemodynamics in patients with decompensated systolic heart failure. *Circ Cardiovasc Imaging* 4:220-227, 2011.
69. Dokainish H, Zoghbi WA, Ambriz E, et al: Comparative cost-effectiveness of B-type natriuretic peptide and echocardiography for predicting outcome in patients with congestive heart failure. *Am J Cardiol* 97:400-403, 2006.
70. Redfield MM, Jacobsen SJ, Burnett JC, Jr, et al: Burden of systolic and diastolic ventricular dysfunction in the community: appreciating the scope of the heart failure epidemic. *JAMA* 289:194-202, 2003.
71. Hillis GS, Moller JE, Pellikka PA, et al: Noninvasive estimation of left ventricular filling pressure by E/E′ is a powerful predictor of survival after acute myocardial infarction. *J Am Coll Cardiol* 43:360-367, 2004.
72. Thomas JD, Popovic ZB: Assessment of left ventricular function by cardiac ultrasound. *J Am Coll Cardiol* 48:2012-2025, 2006.
73. Zile MR, Brutsaert DL: New concepts in diastolic dysfunction and diastolic heart failure: Part I: Diagnosis, prognosis, and measurements of diastolic function. *Circulation* 105:1387-1393, 2002.
74. Ling D, Rankin JS, Edwards CD, et al: Regional diastolic mechanics of the left ventricle in the conscious dog. *Am J Physiol* 236, 1979.
75. Courtois M, Kovacs SJ, Jr, Ludbrook PA: Transmitral pressure-flow velocity relation. Importance of regional pressure gradients in the left ventricle during diastole. *Circulation* 78:661-671, 1988.
76. Courtois M, Kovacs SJ, Ludbrook PA: Physiological early diastolic intraventricular pressure gradient is lost during acute myocardial ischemia. *Circulation* 81:1688-1696, 1990.
77. Nikolic SD, Feneley MP, Pajaro OE, et al: Origin of regional pressure gradients in the left ventricle during early diastole. *Am J Physiol* 268:H550-H557, 1995.
78. Greenberg NL, Castro PL, Drinko J, et al: Effect of scanline orientation on ventricular flow propagation: assessment using high frame-rate color Doppler echocardiography. *Biomed Sci Instrum* 36:203-208, 2000.
79. Greenberg NL, Vandervoort PM, Firstenberg MS, et al: Estimation of diastolic intraventricular pressure gradients by Doppler M-mode echocardiography. *Am J Physiol Heart Circ Physiol* 280:H2507-H2515, 2001.
80. Stugaard M, Smiseth OA, Risoe C, Ihlen H: Intraventricular early diastolic filling during acute myocardial ischemia: assessment by multigated color M-mode Doppler echocardiography. *Circulation* 88:2705-2713, 1993.
81. Sessoms MW, Lisauskas J, Kovacs SJ: The left ventricular color M-mode Doppler flow propagation velocity V(p): In vivo comparison of alternative methods including physiologic implications. *J Am Soc Echocardiogr* 15:339-348, 2002.
82. Brun P, Tribouilloy C, Duval AM, et al: Left ventricular flow propagation during early filling is related to wall relaxation: a color M-mode Doppler analysis. *J Am Coll Cardiol* 20:420-432, 1992.
83. Garcia MJ, Ares MA, Asher C, et al: An index of early left ventricular filling that combined with pulsed Doppler peak E velocity may estimate capillary wedge pressure. *J Am Coll Cardiol* 29:448-454, 1997.
84. Takatsuji H, Mikami T, Urasawa K, et al: A new approach for evaluation of left ventricular diastolic function: spatial and temporal analysis of left ventricular filling flow propagation by color M-mode Doppler echocardiography. *J Am Coll Cardiol* 27:365-371, 1996.
85. Garcia MJ, Smedira NG, Greenberg NL, et al: Color M-mode Doppler flow propagation velocity is a preload insensitive index of left ventricular relaxation: animal and human validation. *J Am Coll Cardiol* 35:201-208, 2000.
86. Firstenberg MS, Levine BD, Garcia MJ, et al: Relationship of echocardiographic indices to

pulmonary capillary wedge pressures in healthy volunteers. *J Am Coll Cardiol* 36:1664-1669, 2000.
87. Stugaard M, Risoe C, Ihlen H, Smiseth OA: Intracavitary filling pattern in the failing left ventricle assessed by color M-mode Doppler echocardiography. *J Am Coll Cardiol* 24:663-670, 1994.
88. Nishihara K, Mikami T, Takatsuji H, et al: Usefulness of early diastolic flow propagation velocity measured by color M-mode Doppler technique for the assessment of left ventricular diastolic function in patients with hypertrophic cardiomyopathy. *J Am Soc Echocardiogr* 13:801-808, 2000.
89. Garcia MJ, Thomas JD, Klein AL: New Doppler echocardiographic applications for the study of diastolic function. *J Am Coll Cardiol* 32:865-875, 1998.
90. Gonzalez-Vilchez F, Ares M, Ayuela J, Alonso L: Combined use of pulsed and color M-mode Doppler echocardiography for the estimation of pulmonary capillary wedge pressure: an empirical approach based on an analytical relation. *J Am Coll Cardiol* 34:515-523, 1999.
91. Gonzalez-Vilchez F, Ayuela J, Ares M, et al: Comparison of Doppler echocardiography, color M-mode Doppler, and Doppler tissue imaging for the estimation of pulmonary capillary wedge pressure. *J Am Soc Echocardiogr* 15:1245-1250, 2002.
92. Nagueh SF, Lakkis NM, Middleton KJ, et al: Changes in left ventricular diastolic function 6 months after nonsurgical septal reduction therapy for hypertrophic obstructive cardiomyopathy. *Circulation* 99:344-347, 1999.
93. Nagueh SF, Kopelen HA, Quinones MA: Assessment of left ventricular filling pressures by Doppler in the presence of atrial fibrillation. *Circulation* 94:2138-2145, 1996.
94. Oyama R, Murata K, Tanaka N, et al: Is the ratio of transmitral peak e-wave velocity to color flow propagation velocity useful for evaluating the severity of heart failure in atrial fibrillation? *Circ J* 68:1132-1138, 2004.
95. Lang RM, Bierig M, Devereux RB, et al: Recommendations for chamber quantification. *Eur J Echocardiogr* 7:79-108, 2006.
96. Tsang TS, Barnes ME, Gersh BJ, et al: Left atrial volume as a morphophysiologic expression of left ventricular diastolic dysfunction and relation to cardiovascular risk burden. *Am J Cardiol* 90:1284-1289, 2002.
97. Abhayaratna WP, Seward JB, Appleton CP, et al: Left atrial size: physiologic determinants and clinical applications. *J Am Coll Cardiol* 47:2357-2363, 2006.
98. Stoylen A, Slordahl S, Skjelvan GK, et al: Strain rate imaging in normal and reduced diastolic function: comparison with pulsed Doppler tissue imaging of the mitral annulus. *J Am Soc Echocardiogr* 14:264-274, 2001.
99. Voigt JU, Lindenmeier G, Werner D, et al: Strain rate imaging for the assessment of preload-dependent changes in regional left ventricular diastolic longitudinal function. *J Am Soc Echocardiogr* 15:13-19, 2002.
100. Wang J, Khoury DS, Thohan V, et al: Global diastolic strain rate for the assessment of left ventricular relaxation and filling pressures. *Circulation* 115:1376-1383, 2007.
101. Quintana M, Lindell P, Saha SK, et al: Assessment of atrial regional and global electromechanical function by tissue velocity echocardiography: a feasibility study on healthy individuals. *Cardiovasc Ultrasound* 3:4, 2005.
102. Sirbu C, Herbots L, D'Hooge J, et al: Feasibility of strain and strain rate imaging for the assessment of regional left atrial deformation: a study in normal subjects. *Eur J Echocardiogr* 7:199-208, 2006.
103. Thomas L, Levett K, Boyd A, et al: Changes in regional left atrial function with aging: evaluation by Doppler tissue imaging. *Eur J Echocardiogr* 4:92-100, 2003.
104. Zhang Q, Kum LC, Lee PW, et al: Effect of age and heart rate on atrial mechanical function assessed by Doppler tissue imaging in healthy individuals. *J Am Soc Echocardiogr* 19:422-428, 2006.
105. Saraiva RM, Demirkol S, Buakhamsri A, et al: Left atrial strain measured by two-dimensional speckle tracking represents a new tool to evaluate left atrial function. *J Am Soc Echocardiogr* 23:172-180, 2010.
106. Cameli M, Caputo M, Mondillo S, et al: Feasibility and reference values of left atrial longitudinal strain imaging by two-dimensional speckle tracking. *Cardiovasc Ultrasound* 7:6, 2009.
107. Vianna-Pinton R, Moreno CA, Baxter CM, et al: Two-dimensional speckle-tracking echocardiography of the left atrium: feasibility and regional contraction and relaxation differences in normal subjects. *J Am Soc Echocardiogr* 22: 299-305, 2009.
108. Kim DG, Lee KJ, Lee S, et al: Feasibility of two-dimensional global longitudinal strain and strain rate imaging for the assessment of left atrial function: a study in subjects with a low probability of cardiovascular disease and normal exercise capacity. *Echocardiography* 26:1179-1187, 2009.
109. Melenovsky V, Borlaug BA, Rosen B, et al: Cardiovascular features of heart failure with preserved ejection fraction versus nonfailing hypertensive left ventricular hypertrophy in the urban Baltimore community: the role of atrial remodeling/dysfunction. *J Am Coll Cardiol* 49:198-207, 2007.
110. Kurt M, Wang J, Torre-Amione G, Nagueh SF: Left atrial function in diastolic heart failure. *Circ Cardiovasc Imaging* 2:10-15, 2009.
111. Rademakers FE, Buchalter MB, Rogers WJ, et al: Dissociation between left ventricular untwisting and filling. Accentuation by catecholamines. *Circulation* 85:1572-1581, 1992.
112. Gibbons Kroeker CA, Tyberg JV, Beyar R: Effects of load manipulations, heart rate, and contractility on left ventricular apical rotation. An experimental study in anesthetized dogs. *Circulation* 92:130-141, 1995.
113. Hansen DE, Daughters GT, 2nd, Alderman EL, et al: Effect of volume loading, pressure loading, and inotropic stimulation on left ventricular torsion in humans. *Circulation* 83:1315-1326, 1991.
114. Buchalter MB, Rademakers FE, Weiss JL, et al: Rotational deformation of the canine left ventricle measured by magnetic resonance tagging: effects of catecholamines, ischaemia, and pacing. *Cardiovasc Res* 28:629-635, 1994.
115. Stuber M, Scheidegger MB, Fischer SE, et al: Alterations in the local myocardial motion pattern in patients suffering from pressure overload due to aortic stenosis. *Circulation* 100:361-368, 1999.
116. Leitman M, Lysyansky P, Sidenko S, et al: Two-dimensional strain—a novel software for real-time quantitative echocardiographic assessment of myocardial function. *J Am Soc Echocardiogr* 17:1021-1029, 2004.
117. Notomi Y, Setser RM, Shiota T, et al: Assessment of left ventricular torsional deformation by Doppler tissue imaging: validation study with tagged magnetic resonance imaging. *Circulation* 111:1141-1147, 2005.
118. Notomi Y, Lysyansky P, Setser RM, et al: Measurement of ventricular torsion by two-dimensional ultrasound speckle tracking imaging. *J Am Coll Cardiol* 45:2034-2041, 2005.
119. Amundsen BH, Helle-Valle T, Edvardsen T, et al: Noninvasive myocardial strain measurement by speckle tracking echocardiography: validation against sonomicrometry and tagged magnetic resonance imaging. *J Am Coll Cardiol* 47:789-793, 2006.
120. Helle-Valle T, Crosby J, Edvardsen T, et al: New noninvasive method for assessment of left ventricular rotation: speckle tracking echocardiography. *Circulation* 112:3149-3156, 2005.
121. Dong SJ, Hees PS, Siu CO, et al: MRI assessment of LV relaxation by untwisting rate: a new isovolumic phase measure of tau. *Am J Physiol Heart Circ Physiol* 281:H2002-H2009, 2001.
122. Wang J, Khoury DS, Yue Y, et al: Left ventricular untwisting rate by speckle tracking echocardiography. *Circulation* 116:2580-2586, 2007.
123. Wang J, Khoury DS, Kurrelmeyer K, et al: Assessment of left ventricular relaxation by untwisting rate based on different algorithms. *J Am Soc Echocardiogr* 22:1040-1046, 2009.
124. Wang J, Khoury DS, Yue Y, et al: Preserved left ventricular twist and circumferential deformation, but depressed longitudinal and radial deformation in patients with diastolic heart failure. *Eur Heart J* 29:1283-1289, 2008.
125. St John Sutton MG, Reichek N, Kastor JA, Giuliani ER: Computerized M-mode echocardiographic analysis of left ventricular dysfunction in cardiac amyloid. *Circulation* 66:790-799, 1982.
126. Kyle RA: Amyloidosis. *Circulation* 91:1269-1271, 1995.
127. Gertz MA, Kyle RA: Amyloidosis: prognosis and treatment. *Semin Arthritis Rheum* 24:124-138, 1994.
128. Cueto-Garcia L, Reeder GS, Kyle RA, et al: Echocardiographic findings in systemic amyloidosis: spectrum of cardiac involvement and relation to survival. *J Am Coll Cardiol* 6:737-743, 1985.
129. Klein AL, Hatle LK, Taliercio CP, et al: Prognostic significance of Doppler measures of diastolic function in cardiac amyloidosis. A Doppler echocardiography study. *Circulation* 83:808-816, 1991.
130. Tei C, Dujardin KS, Hodge DO, et al: Doppler index combining systolic and diastolic myocardial performance: clinical value in cardiac amyloidosis. *J Am Coll Cardiol* 28:658-664, 1996.
131. Patel AR, Dubrey SW, Mendes LA, et al: Right ventricular dilation in primary amyloidosis: an independent predictor of survival. *Am J Cardiol* 80:486-492, 1997.
132. Koyama J, Ray-Sequin PA, Falk RH: Longitudinal myocardial function assessed by tissue velocity, strain, and strain rate tissue Doppler echocardiography in patients with AL (primary) cardiac amyloidosis. *Circulation* 107:2446-2452, 2003.
133. Koyama J, Falk RH: Prognostic significance of strain Doppler imaging in light-chain amyloidosis. *JACC Cardiovasc Imaging* 3:333-342, 2010.
134. Abraham TP, Nishimura RA, Holmes DR, Jr, et al: Strain rate imaging for assessment of regional myocardial function: results from a

clinical model of septal ablation. *Circulation* 105:1403-1406, 2002.
135. Naqvi TZ, Neyman G, Broyde A, et al: Comparison of myocardial tissue Doppler with transmitral flow Doppler in left ventricular hypertrophy. *J Am Soc Echocardiogr* 12(1): 15-21, 1999.
135a. Abe M, Oki T, Tabata T, et al: Difference in the diastolic left ventricular wall motion velocities between aortic and mitral regurgitation by pulsed tissue Doppler Imaging. *J Am Soc Echocardiogr* 12(1):15-21, 1999.
136. Rodriguez L, Garcia M, Ares M, et al: Assessment of mitral annular dynamics during diastole by Doppler tissue imaging: comparison with mitral Doppler inflow in subjects without heart disease and in patients with left ventricular hypertrophy. *Am Heart J* 131:982-987, 1996.
137. Marwick TH: Measurement of strain and strain rate by echocardiography: ready for prime time? *J Am Coll Cardiol* 47:1313-1327, 2006.
138. Alam M, Wardell J, Andersson E, et al: Effects of first myocardial infarction on left ventricular systolic and diastolic function with the use of mitral annular velocity determined by pulsed wave Doppler tissue imaging. *J Am Soc Echocardiogr* 13:343-352, 2000.
138a. Garcia-Fernandez MA, Azevedo J, Moreno M, et al: Regional diastolic function in ischaemic heart disease using pulsed wave Doppler tissue imaging. *Eur Heart J* 20:496-505, 1999.
139. Bach DS, Armstrong WF, Donovan CL, Muller DW: Quantitative Doppler tissue imaging for assessment of regional myocardial velocities during transient ischemia and reperfusion. *Am Heart J* 132:721-725, 1996.
140. Derumeaux G, Loufoua J, Pontier G, et al: Tissue Doppler imaging differentiates transmural from nontransmural acute myocardial infarction after reperfusion therapy. *Circulation* 103:589-596, 2001.
141. Klein AL, Dahiya A: Annular velocities in constrictive pericarditis—annulus and beyond. *JACC Cardiovasc Imaging* 2011.
142. Garcia MJ, Rodriguez L, Ares M, et al: Differentiation of constrictive pericarditis from restrictive cardiomyopathy: assessment of left ventricular diastolic velocities in longitudinal axis by Doppler tissue imaging. *J Am Coll Cardiol* 27:108-114, 1996.
143. Oki T, Tabata T, Yamada H, et al: Right and left ventricular wall motion velocities as diagnostic indicators of constrictive pericarditis. *Am J Cardiol* 81:465-470, 1998.
144. Rajagopalan N, Garcia MJ, Rodriguez L, et al: Comparison of new Doppler echocardiographic methods to differentiate constrictive pericardial heart disease and restrictive cardiomyopathy. *Am J Cardiol* 87:86-94, 2001.
145. Reuss CS, Wilansky SM, Lester SJ, et al: Using mitral "annulus reversus" to diagnose constrictive pericarditis. *Eur J Echocardiogr* 10:372-375, 2009.
146. Choi JH, Choi JO, Ryu DR, et al: Mitral and tricuspid annular velocities in constrictive pericarditis and restrictive cardiomyopathy: correlation with respective pericardial thickness in computed tomography. *JACC Cardiovasc Imaging* 4:567-575, 2011.
147. Ha JW, Oh JK, Ling LH, et al: Annulus paradoxus: transmitral flow velocity to mitral annular velocity ratio is inversely proportional to pulmonary capillary wedge pressure in patients with constrictive pericarditis. *Circulation* 104:976-978, 2001.



# Digital Image Processing and Automated Image Analysis in Echocardiography

JOHAN G. BOSCH, PhD

**Digital Image Processing and Automated Analysis: Definition and Motivation**
**Digital Image Storage, Communication, and Compression**
Digital Images
Storage Formats and Image Communication
Image Compression
**Medical Image Processing**
Image Enhancement: Level Manipulations, Filtering
Image Interpretation: The Interpretation Pyramid
**Automated Border Detection in Echocardiography**
Problems and Pitfalls of Border Detection in Echography
Practical Considerations for Automated Border Detection
**Overview of Automated Border Detection Methods**
Feature-Driven Methods
Structure-Based Method: Tissue Tracking
Object-Based Methods: Geometric Modeling
Pattern Matching
3D Active Surface Detection
Population-Model Based Method: Active Appearance Models
Classification and Automated Localization
**Future Promise**
Intelligent Ultrasound Systems

Digital image processing techniques nowadays can be found in any ultrasound machine or offline analysis system. Moreover, ultrasound systems have evolved into fully digital, computerized systems. Digital image storage and digital processing of echocardiographic images, both for image enhancement and for analysis, have become standard techniques. Several automated image analysis tools are commercially available for two-dimensional (2D) and three-dimensional (3D) echocardiographic data, and more advanced automated analysis techniques are appearing rapidly.

Such automated approaches include automated structure localization, automated border detection (ABD) techniques, tissue tracking, and tissue/function classification or computer-aided diagnosis. Automated analyses can potentially supply the echocardiologist with quantitative and more objective tools for research and clinical practice. However, ultrasound is a difficult imaging modality for interpretation, for both humans and machines. In this chapter, we want to provide the clinician with an overview of available tools, some insight into the background of different techniques with their possibilities and limitations, and some practical guidelines for the choice and use of techniques. We concentrate on ABD.

## Digital Image Processing and Automated Analysis: Definition and Motivation

*Digital image processing* concerns manipulation of images by a computer. More specifically, it refers to enhancement or analysis of images. *Image enhancement* aims at improvement of images, for visual interpretation or for further automated analysis. This can range from a simple contrast adjustment to sophisticated filtering. *Image analysis* generally involves the derivation of some quantitative measures or parameters from images. In a narrower sense, this often refers to automatic localization and outlining (border detection) of certain structures, or to the tracking of the motion of such structures. In echocardiography, the left ventricular (LV) myocardium is of prime interest. Outlining of the LV endocardial border allows quantitative measurements of LV cavity area, shape, volume, and so on. Combination with the epicardial border allows calculation of wall thickening and LV mass. Tracking the motion of tissue or borders over the cardiac cycle allows the calculation of local wall displacement, velocity, relative shortening (strain), etc. Similar analyses may be applied to other structures such as the right ventricle (RV), atria, and valves.

In clinical practice, quantitative measurements are still underemployed: Visual estimation of parameters such as ejection fraction or semiquantitative classification (e.g., wall motion scoring for stress echocardiography) still plays a dominant role. Such *eyeballing* can be done fast, without much ado, and some experts reach an admirable accuracy. In general, however, it is inaccurate, irreproducible, subjective, and hard to learn.[1] Visual estimation of quantifiable measures should be discouraged for any purpose beyond a rough classification, whenever a quantitative alternative is present. Quantitative analysis is advisable when repetitive interpretations are done, when more subtle differences are sought, when interpretation experience is limited, and whenever scientific research is the goal.

The classic method of outlining the borders is *manual drawing*. Any ultrasound machine or offline analysis system has facilities for this, using a mouse or trackball. Manual drawing, however, is known to have high inter- and intraobserver variability; it is strenuous and time consuming for the operator and requires expertise and dexterity. Concerning consistency and workload, manual drawing is especially hard to perform practically when large sets of images are involved: for example,

analyzing one or more complete cardiac cycles, for several cross sections, and over multiple stages (as in stress echocardiography); or analyzing the hundreds of 2D frames in a full-cycle 3D data set. ABD can provide solutions to these problems. Moreover, if ABD can be performed fully automatically and fast, it allows real-time monitoring of clinical parameters.

Procedures such as stress echocardiography that currently rely on visual scoring of wall motion could benefit enormously from automated analysis; the lack of quantification and the large inter- and intraobserver and interinstitution variabilities[2] are perceived as important limitations. The potential of real-time 3D echocardiography for volume estimation and regional wall motion quantification also depends largely on automated analysis.

## Digital Image Storage, Communication, and Compression

### DIGITAL IMAGES

Inside any modern ultrasound system, images are created as *digital* images. The generation of the ultrasound images (ultrasound physics, signal processing, and instrumentation) is beyond the scope of this chapter. Excellent descriptions can be found in many handbooks.[3-5] Digital images consist of *pixels* whose brightness or color is represented by a numeric (digital) value. *Brightness level* is also referred to as *intensity* or *gray value*. A *cineloop* or movie is a sequence of such images, typically at a *frame rate* of 20 to 200 images per second. The digital representation makes it possible to store and process images in a computer—hence, digital image processing. Modern ultrasound systems are totally digitized and support the storage and communication of digital images and cineloops. For display on a monitor and recording on VCR, these digital images are converted into an analog video signal. The use of analog video output or VCR tape should be strongly discouraged for analysis purposes. Although it is possible to redigitize the analog video with devices such as frame grabbers, this results in severe, irreversible loss of information and image quality: spatial resolution, frame rate, and intensity accuracy will be degraded; separation among image, graphics, and color overlays is lost; and calibration and patient information disappears.

### STORAGE FORMATS AND IMAGE COMMUNICATION

#### *DICOM*

The method of choice for digital image storage and exchange is *DICOM* (Digital Imaging and Communications in Medicine[6]). DICOM is a generally accepted international standard for medical images of all modalities, including all types of ultrasound imaging. The DICOM standard (current version: 2009) is still being extended and improved to better support new developments in medical imaging. As its name implies, DICOM is a communication standard rather than a file format—it defines how medical imaging devices such as ultrasound systems, Picture Archiving and Communications Systems (PACS) servers, and printers communicate to transport, store, retrieve, find, or print images and associated patient information. All major manufacturers have committed themselves to support DICOM. Ultimately, this should lead to the integrated electronic patient record, which contains the full patient file, including patient history, laboratory reports, images of all modalities, and other information. Therefore, DICOM is a very complicated standard: the full description covers several thousand pages.[6] A very readable explanation of DICOM for echocardiographers is given by Thomas.[7]

Note that if a device is labeled "DICOM compliant," this does *not* mean that it will automatically work with every other DICOM device: DICOM defines a multitude of services and imaging modalities. For every device, a *DICOM Conformance Statement* defines precisely which services are supplied and supported for what modalities and to what extent. To verify interoperability between devices, their conformance statements should be compared—not a simple job for a novice in DICOM. In particular, interoperability between vendors is rather limited for ultrasound, because many essential parameters are stored in vendor-specific "private tags" that are not accessible to others. Also, there is as yet no standardized format for 3D data storage.

#### *General-Purpose Formats*

Other widely used *general-purpose image formats* such as BMP, TIF, GIF, and JPEG are often used for export of screen shots or single images for use in reports, presentations, and publications. For movies, AVI, MPEG, and QuickTime are popular formats. These general-purpose formats usually cannot store additional patient information and can lead to significant image quality degradation because of lossy compression (see later discussion). Therefore, they should not be used for primary image storage or archiving.

### IMAGE COMPRESSION

To reduce data storage requirements, *image compression* can be employed. *Lossless* compression techniques (such as run-length encoding [RLE], lossless JPEG) can reduce file sizes by a factor of 2 to 5, and uncompressing will produce a perfect copy of the original image. *Lossy* compression reaches much higher compression ratios (up to 20 to 100) by eliminating information for which the eye is least sensitive, at the cost of some irreversible image degradation. This degradation is acceptable visually (JPEG factor 20 has been found to produce no diagnostically significant degradation[8]) and is marginal compared to the degradation associated with VCR storage. However, the compression artifacts may certainly influence digital image processing and analysis. Severely lossy compression is not advisable for archiving or when digital image postprocessing is foreseen. Lossy compression techniques include lossy JPEG, fractal and wavelet compression, and MPEG. DICOM currently[6] supports RLE, JPEG (lossless and lossy), JPEG2000, and MPEG2 compression schemes.

## Medical Image Processing

Medical image processing is a thriving subdiscipline of digital image processing.[9,10] Several good handbooks on medical image processing, with special attention to ultrasound, are available.[11,12]

### IMAGE ENHANCEMENT: LEVEL MANIPULATIONS, FILTERING

Image enhancement deals with the improvement of images, either for visual interpretation or as a preprocessing for analysis. Image-enhancement techniques used by ultrasound machines and analysis programs are similar to those used by most

general-purpose image manipulating programs (such as photo editors). The simplest class of such operations includes *level manipulations* or *lookup-table operations*: these change the brightness level (or color or transparency) of each pixel without considering any neighboring pixels. The original brightness of the pixel is simply used to look up the new value in a conversion table. Lookup-table operations include *brightness level manipulations* and *pseudocoloring*. In 3D visualization, such operations are the main tools to control the appearance of the volume rendering, in terms of brightness, transparency, and surface extraction.

*Brightness level manipulations* include all one-to-one conversions of image brightness levels (input) to display brightness levels (output), either linear or nonlinear. Examples are digital contrast/brightness adjustments, image inversion, and gamma correction. Some examples are given in Figure 12-1. Note that many level manipulations may result in *clipping* (see Fig. 12-1, *C*, *D*, and *E*) and in reduction of the effectively used number of brightness levels. The extreme example is *thresholding* (see Fig. 12-1, *E*), in which all brightness levels above a threshold are set to white, and all below to black.

*Pseudocoloring* involves a direct conversion of brightness levels to a color scale, generally labeled with names such as Rainbow, Ocean, or Harvest. Because the eye is more sensitive to color differences than to intensities, this may reveal subtle intensity differences. It can be visually pleasing but may also be highly suggestive, as it clusters similar gray values into color groups. Because brightness levels in ultrasound are highly dependent on signal attenuation and local gain settings, the borders that are suggested visually by these colors have little practical significance.[13] Pseudocoloring is also sometimes applied to highlight brightness differences with respect to some baseline value (e.g., increase above the local brightness level in a baseline image) with a color (e.g., to visualize the arrival of contrast agents in perfusion imaging). This is an effective tool, but one should be aware that tissue motion may also induce a brightness change and show up as color.

*Filtering* entails image operations that consider pixels within their neighborhood and deal with the spatial or temporal aspects of the image. Filtering operations include smoothing (noise reduction), and sharpening (edge enhancement). Smoothing or low-pass filtering (e.g., uniform, Gaussian) is used in many ABD methods (see later discussion) to reduce the speckle noise and get more or less homogeneous regions; high-pass edge enhancing or detection filters (e.g., Sobel, Laplacian) are often used to find (candidate) border points. Note that most smoothing methods slightly change the positions of edges and differentiate poorly between noise and weak signals. High-pass filters tend to be very sensitive to noise. In general, filtering does not improve the appearance of ultrasonographic images without simultaneously removing valuable information. Smoothing and sharpening filters may be available on your 3D ultrasound machine for real-time use: keep the caveats just mentioned in mind when using this option.

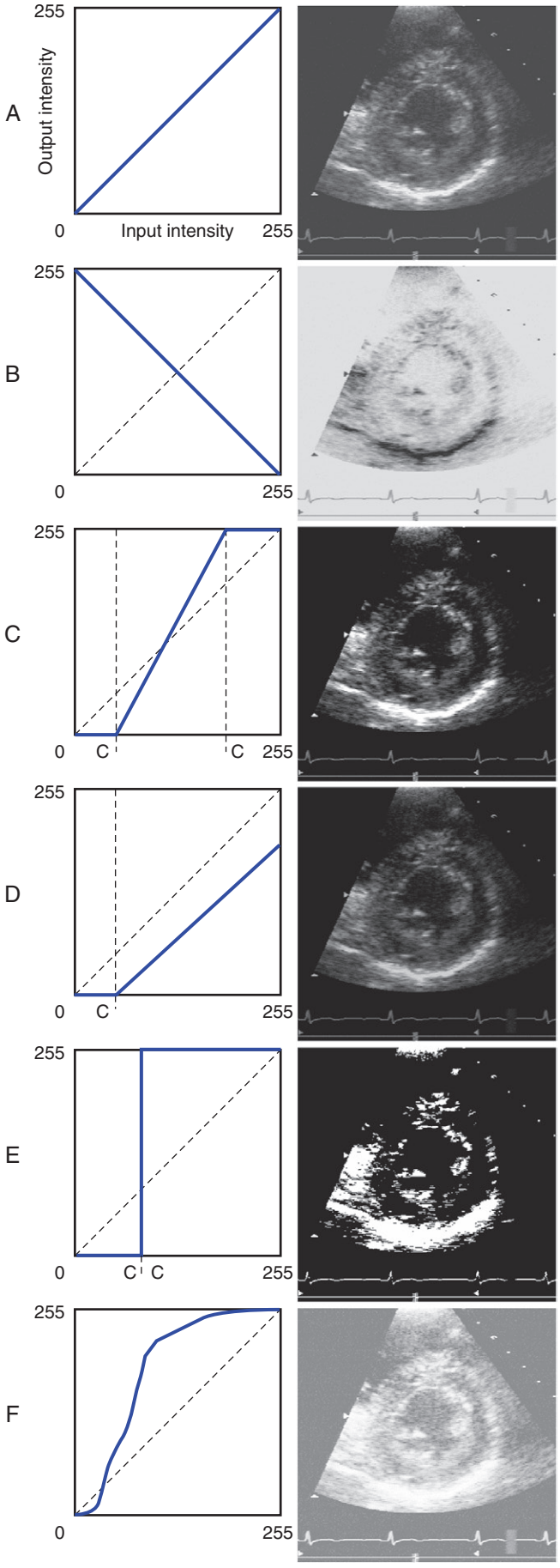



**Figure 12-1 Image brightness conversions (lookup-table operations) and their results. A,** Identity: no change. **B,** Inversion. **C,** Increased contrast (note clipping, *C*). **D,** Decreased brightness. **E,** Thresholding. **F,** Histogram equalization.

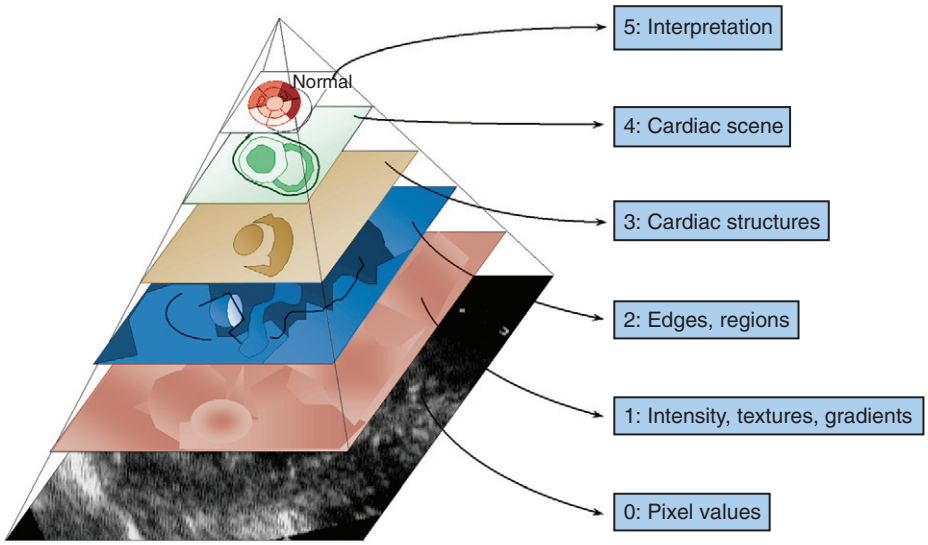



**Figure 12-2** The image interpretation pyramid.

**TABLE 12-1 Abstraction Level Hierarchy**

| *Level* | *General* | *Speech* | *Image* | *Cardiac* | *Associated Operations* |
|---|---|---|---|---|---|
| 0 | Raw data | Samples | Pixels | Pixels | Image generation |
| 1 | Features | Amplitude, frequency | Intensity, textures, gradients | Intensity, textures, gradients | Preprocessing, filtering, feature extraction |
| 2 | Structures | Phonemes | Edges, regions | Edges, regions | Linking, merging, matching, clustering |
| 3 | Objects | Words | World entities, borders, objects | Cardiac structures (lumen, endocardium valve) | Model relaxation, border finding, classification |
| 4 | Object sets | Sentences | Scene | Cardiac scene | Scene modeling, interobject relationships |
| 5 | Interpretation | Significance | Scene interpretation | Interpretation and diagnosis | High-level interpretation, expert systems, rules |

## IMAGE INTERPRETATION: THE INTERPRETATION PYRAMID

The interpretation of medical images is an extremely complicated task that is very hard to transfer into a computer. For us humans, vision is a natural task that we perform instantly and automatically. From the study of human perception however, we know that vision is anything but a simple, straightforward process. Think of the many well-known optical illusions: there is a lot of hidden interpretation going on. In the interpretation of images, several information abstraction levels can be distinguished. This is generally known as the *image interpretation pyramid* (Fig. 12-2). The levels of this pyramid give us more insight into the mechanisms of different automated techniques and their limitations. A good analogy is found in the interpretation of handwriting or spoken language. This analogy is described in Table 12-1. For interpretation of a written text, one has to know about the alphabet, spelling, vocabulary, syntax, and semantics, and ultimately about the subject of the text, the intentions of the source, and adornments such as humor, sarcasm, and metaphors. These last aspects are not about language—they refer to the real-world domain that the text is discussing. Interpretation is not a simple bottom-up process of combining letters into words into sentences into significance. Text can be fragmented; there are imperfections, such as misspellings and ambiguities, and missing domain knowledge that necessitate feedback between all levels, and even guessing, to come to a consistent interpretation.

### *Cardiac Image Interpretation*

In image interpretation, we have a similar hierarchy. At the base, we find the raw image information (pixels). Going up, we encounter image *features* such as local texture and gradients; *structures* such as regions (groups of adjacent pixels with similar properties) and edges (lines of sudden change, between regions); *objects* such as a square or a person; and a *scene*, such as a football match. At the top we have *significance*, such as finding out who's winning; this requires very specific knowledge of the behavior of players and audience, rules of play, and so on.

Interpretation of cardiac images is still more difficult, because it requires expert knowledge about the 3D anatomic structures in the heart, their dynamic behavior, pathology and anatomic variability between patients, and the intricacies of the imaging modality involved. This last point specifically is not to be underestimated for ultrasound. Furthermore, missing or ambiguous information, noise and artifacts, and higher-level knowledge of anatomy, physiology, and pathology are involved and necessitate feedback and interactions between levels.

Clearly, very different sorts of knowledge are applied at each level to come to a valid interpretation, and only the lower levels have to do with image properties: higher levels concern anatomical models of the heart, physiology, congenital or pathologic conditions, and so on. ABD systems generally have very limited knowledge at the higher interpretation levels and resolve this in one of three ways:

1. They use simplifying assumptions regarding the objects. For example, the LV is considered to be a dark, round object in the middle of the image; the endocardial contour is convex, the endocardium is the strongest edge in the image, and the cardiac wall will not move more than *x* pixels per frame. Most of such assumptions will hold only to some extent or are overly general.
2. They limit themselves to a subset of the problem domain, such as certain standard views (e.g., only short-axis at mid-papillary level), image quality (no dropouts, low noise), anatomy (e.g., no congenital defects), or imaging equipment type or settings (scale, gain, frequency).
3. They require the user to handle the high-level aspects by initializing, guiding, or correcting the system.

### *Rules for a Well-Behaved Automated Border Detection Method*

No practical system can do without the intervention of the user. Ideally, there is only one desired and necessary interaction: when multiple interpretations could be correct, the user should have the final decision. In practice, a computer system can never have all the high-level knowledge that the physician has, and it requires the physician's intervention to handle such blind spots. Systems with little high-level knowledge and models, however, rely heavily on the user to handle their shortcomings and mistakes—which most users find deeply irritating.

With these limitations in mind, we can formulate a few criteria for a good and well-behaved ABD method.

1. The method should generate "correct" contours. Because this judgment may be subjective (in the light of multiple possible interpretations), a system should preferably be able to adapt to the expert user's general ideas about correct contours.
2. The contours should be reproducible. This seems obvious for an automatic system, but almost all systems require some type of user interaction (parameter choices, indicating a start point or region, corrections), which will lead to some variability in results. This inter- and intraobserver difference should possibly be smaller than the inter- and intraobserver variabilities associated with similar manual work.
3. The method should be user friendly. It should only address the user for high-level expert decisions, not for handling "stupid" mistakes or do repetitive corrections. This implies:
   - It should not generate physically or anatomically impossible solutions; unlikely solutions should be marked as such. It should supply alternative solutions when relevant.
   - It should not override user-drawn contours (apart from cleanup of minor imperfections).
   - It should allow for easy, intelligent, minimized control and correction (e.g., by applying the intent of the correction throughout the whole image set).

## Automated Border Detection in Echocardiography

### PROBLEMS AND PITFALLS OF BORDER DETECTION IN ECHOGRAPHY

Ultrasound is a particularly difficult imaging modality for interpretation. Inexperienced users mostly find it harder to interpret than other tomographic modalities such as computed tomography and magnetic resonance imaging. Ultrasound exhibits several specific properties that impede automated analysis.

1. Pixel intensity does not directly reflect any physical property of the tissue visualized, in contrast to the Lambert-Beer law for radiography or the Hounsfield units for computed tomography. In ultrasound, images are formed by sound reflection and scattering, resulting in a combination of interference patterns (ultrasound speckle patterns) and reflections at tissue transitions or inhomogeneities. Different tissues are often distinguishable only by subtle differences in texture (speckle patterns) or by the coherent behavior of this texture over time, rather than by different intensity values.
2. Ultrasonographic image information is very *anisotropic* and position-dependent. Reflection intensity, lateral and radial point-spread functions, and signal-to-noise ratio are strongly dependent on both the depth and the angle of incidence of the ultrasound beam, as well as on the user-controlled time gain compensation settings.
3. Image disturbances (*artifacts*) are caused by factors such as side lobes, reverberations, clutter, and aberration. Many of these problems are especially prominent with high gain settings, which are often necessary in obese or older patients.
4. Parts of the anatomy are not imaged, because of *dropouts* (for structures parallel to the ultrasound beam), *shadowing* (behind acoustically impermeable structures such as bone or lung), scan sector limitations, and limited echocardiographic windows. Still-frame images generally miss some information; the human eye compensates for this when viewing a sequence of images. It resolves ambiguities and interpolates the missing parts by exploiting the temporal coherence of structures and speckle, which allows discrimination among noise, artifacts, and anatomy.
5. In specific cases (especially in 3D imaging) the limited temporal resolution and the scanning process may introduce artifacts. The sequential scanning of lines combines information from different moments into one image. For quickly moving structures, this may lead to spatial distortion. Sharp transitions between "older" and "newer" image parts may appear. This is particularly prominent in real-time 3D ultrasound, where information from different heartbeats is stitched together to include a complete object (such as the LV).
6. In 2D ultrasound, the exact spatial localization of the cross-sectional plane is generally not known. This in contrast to 3D techniques (3D ultrasound, magnetic resonance imaging, or computed tomography), where the 3D context is known, and this information is often employed in model positioning for detection. In 2D cardiac ultrasound, the choice of the imaged cross section depends both on the skill and precision of the sonographer and on the available echocardiographic window, which is limited by ribs, lungs, and so on. Apart from volume measurement errors, this may also result in detection problems if the ABD method relies on assumptions of shape and the presence or absence of other structures such as valves or papillary muscles.

### PRACTICAL CONSIDERATIONS FOR AUTOMATED BORDER DETECTION

Practical considerations for appropriate border detection (either automatic or manual) are listed in Box 12-1, subdivided into three categories. A few explanations follow.

#### *Acquisition and Image Quality*

The primary requirement for automated analysis is *optimal image quality.* For ABD this is even more crucial than for manual tracing or visual analysis. If the border cannot be seen, an intelligent guess or interpolation is the only option (for computer

BOX 12-1

**PRACTICAL CONSIDERATIONS FOR AUTOMATED BORDER DETECTION**

**Acquisition and Image Quality**
Optimize border visualization
Limit variation in system settings (gain, power, time gain control, lateral gain control)
Limit variation in cross sections (use landmarks)
Proper region of interest/depth
High frame-rate
Digital storage (preferably lossless); no filtering
No spatial/temporal subsampling or small regions of interest for storage

**Contour Definitions and Consistency**
Inventory of desired calculations
Standardize border drawing definitions:
  Inclusion or exclusion of papillary muscles, trabecular structures, valves, etc.
  Position of edges: leading, peak, trailing
Exclusion criteria and special cases:
  Image quality: foreshortening, dropouts, artifacts, noise
  Pathologies: hypertrophy, dilation, cardiac masses, etc.
  Congenital deformations, etc.
Assess inter- and intraobserver variabilities:
  To test standardization
  To check errors against study goal, estimate patient population size for significance
Include acquisition protocol?

**Choice of Detection Technique**
Check specifics of technique against problem:
  Views/cross sections
  Cardiac objects (LV, RV, endocardium, epicardium)
  Border definitions
  Single frame, end-diastolic/end-systolic, full-cycle, multicycle
  Real-time online or offline with corrections
  Dependence on image quality, artifacts, settings
  Amount and types of user interaction
Is manual analysis a practical alternative?

*and* human). Therefore, one should take every precaution to optimize image quality, standardize system settings, and reduce variability in settings and cross sections.

Select a view and depth such that the object of interest is in focus, fits well inside the scan sector, and fills most of it. Try to adjust acoustic power, overall gain, and time gain control such that the endocardium is best and most homogeneously visualized. Remember that stop-frame images are much harder to interpret than moving sequences; individual frames may be much less pleasing than the cineloop suggests.

A high frame rate (at least 25 frames per second) is advisable, both for full-cycle analysis and for proper selection of end-diastolic (ED) and end-systolic (ES) frames in case of ED/ES analysis. For most tissue tracking or speckle tracking techniques, a higher frame rate (above 50) is advised, because such techniques rely on local correlation between consecutive frames, which quickly degrades for lower frame rates.

### *Contour Definitions and Consistency*

Before attempting manual or automated detection, make sure that proper criteria are defined for the desired contours. This may depend on the desired calculations to be performed from the contour. Trabecular structures, papillary muscles, or valves can either be included or excluded for certain calculations (LV volume, regional wall motion, LV mass). Many topics need to be standardized: whether leading, mid, or trailing edges are drawn; and what to trace in case of foreshortening, dropout, and so on.[13] When possible, perform inter- and intraobserver comparisons and try to reach consensus between observers *before* starting a large study. In some cases, this should include the image acquisition protocol, to assess inter- and intraoperator variability in the choice of cross section, ultrasonographic system settings, and other factors.

### *Choice of Detection Technique*

When considering an automated technique for border detection, it is wise to thoroughly check the specifications of the automated method with respect to the purpose of your study, and familiarize yourself with its peculiarities on the broadest possible range of images. Most methods are tailored to an application or have distinct restrictions in their applicability: the imaging modes involved (M-mode, B-mode, 3D, contrast, etc.); the views or cross sections involved; the object to be detected (e.g., LV, RV, atrium); the type of contour to be found (blood-tissue border or other, such as epicardium); single-frame, ED/ES, full-cycle or multicycle analysis; the brand and type of echocardiographic machine used, and online or offline availability of the detection; possibilities for user correction of the boundaries; dependency on system gain, image quality, and common artifacts such as dropouts or noise; and amount of user interaction needed. If no suitable automated technique is found for a certain analysis, manual measurements might provide the only practical alternative.

## Overview of Automated Border Detection Methods

Ever since the invention of echocardiography, methods have been devised for the automated analysis of these images. Literally hundreds of methods have been reported,[14,15] most of which have only academic value. An excellent overview was recently published by Noble and Boukerroui.[14] We limit ourselves to the main directions of research, based on the levels of the interpretation described above. We refrain from any comparisons of reported success scores, as there are no standard test data sets (yet) for this purpose, nor standard test criteria. Detected contours are generally compared with contours manually drawn by one or more experts, or derived values such as area or volume are compared with an alternative measurement. Most of these results are hard to compare between studies. Note that good results on one or two cases do not prove a method's merit: no matter how naive the method, one can always find some images on which it will work. Robustness can only be assessed by applying the method on large sets of clinical-quality images.

A listing of representative techniques is given in Table 12-2. We pay special attention to modern 3D approaches.

### FEATURE-DRIVEN METHODS

This class of ABD methods relies principally on image intensity values and basic features (levels 0 and 1 of the image pyramid) without making strict assumptions on shapes of borders and so forth. Such techniques are typically useful for finding irregular or topologically undetermined shapes (tumors, lesions) and less useful when detecting objects of

**TABLE 12-2 Overview of Automated Border Detection Methods at Different Abstraction Levels**

| *Level Name* | *Basic Technique(s)* | *Advanced Techniques* |
|---|---|---|
| 1. Preprocessing | Heavy smoothing for noise/speckle reduction<br>Contrast stretching, histogram equalization | Integrated backscatter thresholding (AQ)[16]<br>Speckle suppression: anisotropic diffusion,[76] adaptive filtering,[37] morphologic filters,[77] wavelet transforms[78]; Fourier-based filters[20] |
| 2. Edge or region detection | Global or local thresholding[37]<br>Simple edge detectors [39,54]<br>Temporal continuity | Advanced edge detectors: Marr-Hildreth[79]; Canny[44,80]<br>Pattern or profile matching[38,60]<br>Region detection: region growing[20]; clustering based on Gaussian[17] or Rayleigh distribution[18]; resolution pyramids; neural nets; Markov random fields, level sets[21,22,81]<br>Tracking: optical flow,[24-27] block similarity[29-36]<br>Registration,[28] Kalman-based temporal prediction[55-58,67] |
| 3. Geometric objects or models | Implicit models: e.g., radial search for candidate points, interpolation/linking,[79] smoothing/shape filtering[37] | Dynamic programming optimization[38,39,44]<br>Snakes/balloons/active contours/deformable models[48,49,54,80]<br>Active shape models (ASM)[60,61] |
| 4. Anatomic structure or scene models | None or implicit:<br>Hard-coded<br>Manually positioned models<br>User-drawn initial shape/ROI | Model positioning/landmark finding techniques: row/column sums, template matching; Hough transform[82]; fuzzy logic[78]<br>Composite geometric shape models—2D, 2D+T, 3D, 3D+T: Point distribution models,[61] 3D shape neural nets,[79] multiple active contours[80] |
| 5. Interpretation, high-level knowledge | None<br>User intervention: correction of contours, etc. | Adaptation of models to image and user[38,67]<br>Use of patient group–derived models: appearance eigenvariations (AAM)[59-68]<br>Learning behavior over all cases analyzed: marginal space learning, probabilistic boosting networks[70-73]<br>Rule-based analysis,[75] multiple hypothesis generation<br>Pathology awareness, automated classification[74]<br>Analysis-based acquisition, automated scan assistants[56-58] |

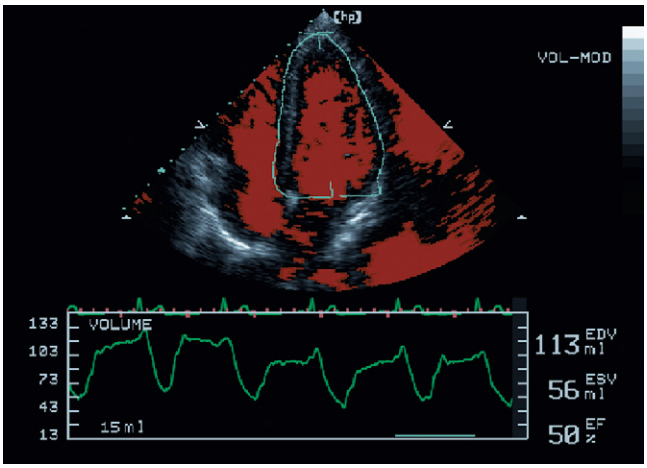



**Figure 12-3** Acoustic quantification on Philips (Hewlett-Packard) equipment. *(Courtesy Philips Medical Systems Ultrasound, Andover, Mass.)*

well-defined shape in an imperfect image (such as LV segmentation in echocardiograms). Thresholding, clustering, region growing, and level set techniques can be placed in this class. Thresholding uses a fixed level of intensity to separate different tissues, such as blood and myocardium. One of the earliest commercial automated analysis techniques, Acoustic Quantification[16] (Fig. 12-3), was based on thresholding of the integrated backscatter level of the radiofrequency signal to separate blood from tissue. In clustering techniques, pixels of similar properties are categorized into groups (e.g., blood or myocardium) based on some statistical distribution, such as Gaussian[17] or Rayleigh[18] distributions. Most clustering approaches use pixel intensity, but they may also be edge or phase based.[19] In classical region growing,[20] an object is segmented by iteratively adding similar neighboring pixels to a region and/or removing dissimilar pixels. Level set approaches[21,22] are related to region growing but mathematically similar to deformable models (described later). The contour is implicitly described by an evolution equation, and the detected objects can take any shape and topology. As mentioned earlier, all of these methods pose no or few restrictions on shapes of the found regions; this makes them vulnerable to typical ultrasound artifacts such as dropouts or clutter. Therefore, these methods are often integrated into methods with explicit models to handle such artifacts.[23]

## STRUCTURE-BASED METHOD: TISSUE TRACKING

A good example of a structure-based method can be found in the various 2D tissue tracking methods. Such approaches track the motion of certain structures by finding correspondence between regions in consecutive images. Most approaches rely on straightforward block similarity measures such as normalized cross correlation or sum of absolute differences. An alternative approach, optical flow, was already proposed in an early stage for 2D tissue tracking[24,25] and recently has gained new interest.[26,27] Also, tissue tracking can be formulated as a deformation problem, and image registration can be applied.[28] In general, such tissue tracking techniques can provide motion information in the form of displacement of a set of points (generally along a user-drawn line) or calculate a complete 2D displacement vector field. Recently, several 3D tissue tracking approaches have been realized as well.[29-33] By calculating time integrals, total relative deformation (strain) can be calculated in all directions. As a 2D or 3D approach, tissue tracking can overcome the principal limitation of tissue Doppler imaging (TDI[34]). TDI supplies a direct physical (Doppler) velocity measurement that can be performed with high temporal resolution, but it can only give a one-dimensional motion estimate (in the direction of the ultrasound beam).

As an example of a structure-based tracking method, we describe the approach of Lysyansky, Friedman, and colleagues[35,36] for 2D tissue tracking. This method forms the basis of the 2D speckle tracking software in the EchoPAC analysis system (GE-Vingmed Medical Systems, Horten, Norway) (Fig. 12-4).

The user loosely traces an approximate endocardial contour in one frame of a cycle. A band outside this contour is used as the region of interest. Within this region (Fig. 12-4, *A*), the

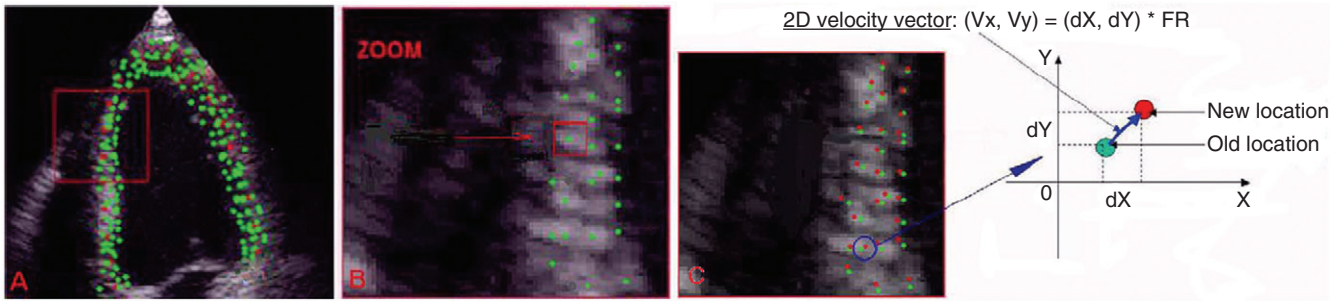



**Figure 12-4** **2D strain imaging. A,** In a region defined by a loosely drawn endocardial contour (*red dots*), natural acoustic markers are identified in the myocardium (*green dots*). **B,** Zoomed display of found acoustic markers (*green dots*: center of each marker). **C,** These markers are tracked from frame to frame, and their displacements define 2D velocity vectors. *(Modified from Leitman M, Lysyansky P, Sidenko S, et al: Two-dimensional strain—a novel software for real-time quantitative echocardiographic assessment of myocardial function.* J Am Soc Echocardiogr *17:1021-1029, 2004.)*

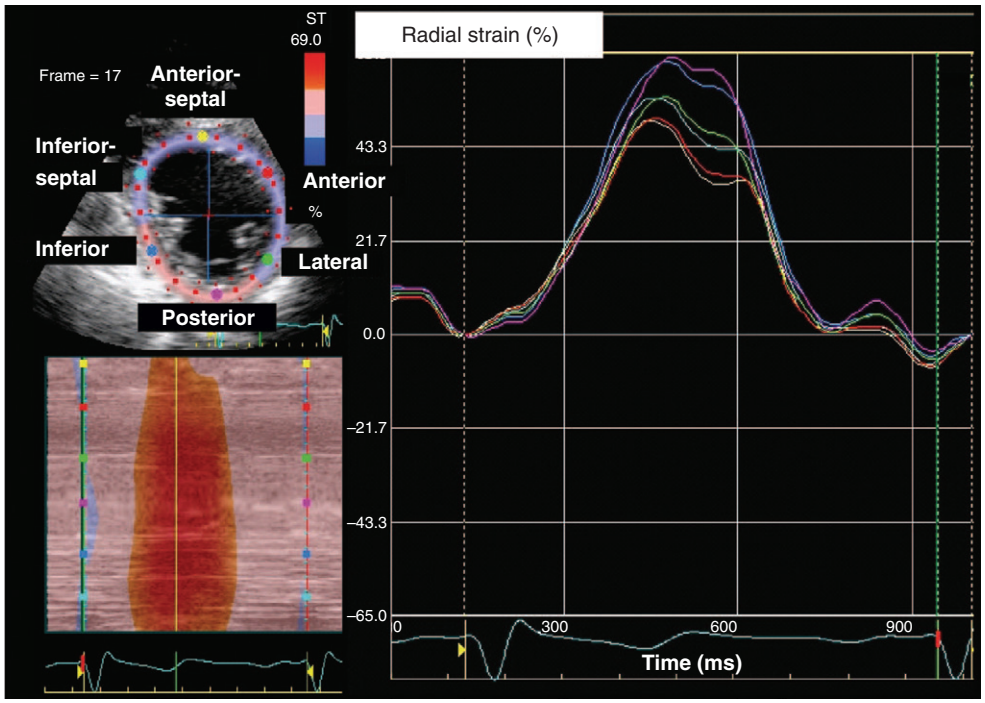



**Figure 12-5** **An example of radial time-strain curves in a normal control subject from the midventricular short-axis view.** Radial strain was calculated by speckle tracking from multiple circumferential points over a cardiac cycle. These data were averaged to six time-strain plots to represent standard segments. Note that time to peak strain in a normal subject occurs synchronously over a very narrow time range. *(From Suffoletto MS, Dohi K, Cannesson M, et al: Novel speckle-tracking radial strain from routine black-and-white echocardiographic images to quantify dyssynchrony and predict response to cardiac resynchronization therapy.* Circulation *113:960-968, 2006.)*

speckle structure is analyzed and speckles of high intensities are identified as natural targets (see Fig. 12-4, *A* and *B*). These targets are tracked over consecutive frames (see Fig. 12-4, *C*) by block matching with a sum of absolute differences similarity criterion.[34,36] From the resulting velocity field, local displacement and strain are calculated (Fig. 12-5).

Similar speckle tracking approaches from other vendors are available. A prerequisite for successful application is a sufficiently high frame rate and good image quality.

## OBJECT-BASED METHODS: GEOMETRIC MODELING

Several popular border detection techniques are based on deformable geometric models. In these methods (known under names such as active contours, snakes, and balloons), the border is represented as a geometric object: a curved line or surface that should separate blood from tissue. This object obeys geometric constraints: it should resemble a certain shape, it should be smooth, and so on. For detection, the model is initialized somewhere in the image and deformed iteratively to best fit the image data. Mostly this involves minimizing some energy terms, related to the amount of deformation applied to the model (internal energy) and the quality of fit to the image data (external energy). The latter can be represented by, for example, edge strength on the border, or contrast between inner and outer regions. Methods of this class can vary widely in the type of image features, the shape or motion model, their shape constraints, and their initialization and optimization strategies.

These methods operate mainly on levels 1 and 2 of the image pyramid, employing a geometric model (level 2), driven by image features (level 1). They are especially useful if much variation in borders is expected for different patients, such as if congenital defects are present.[37] However, it can be difficult to

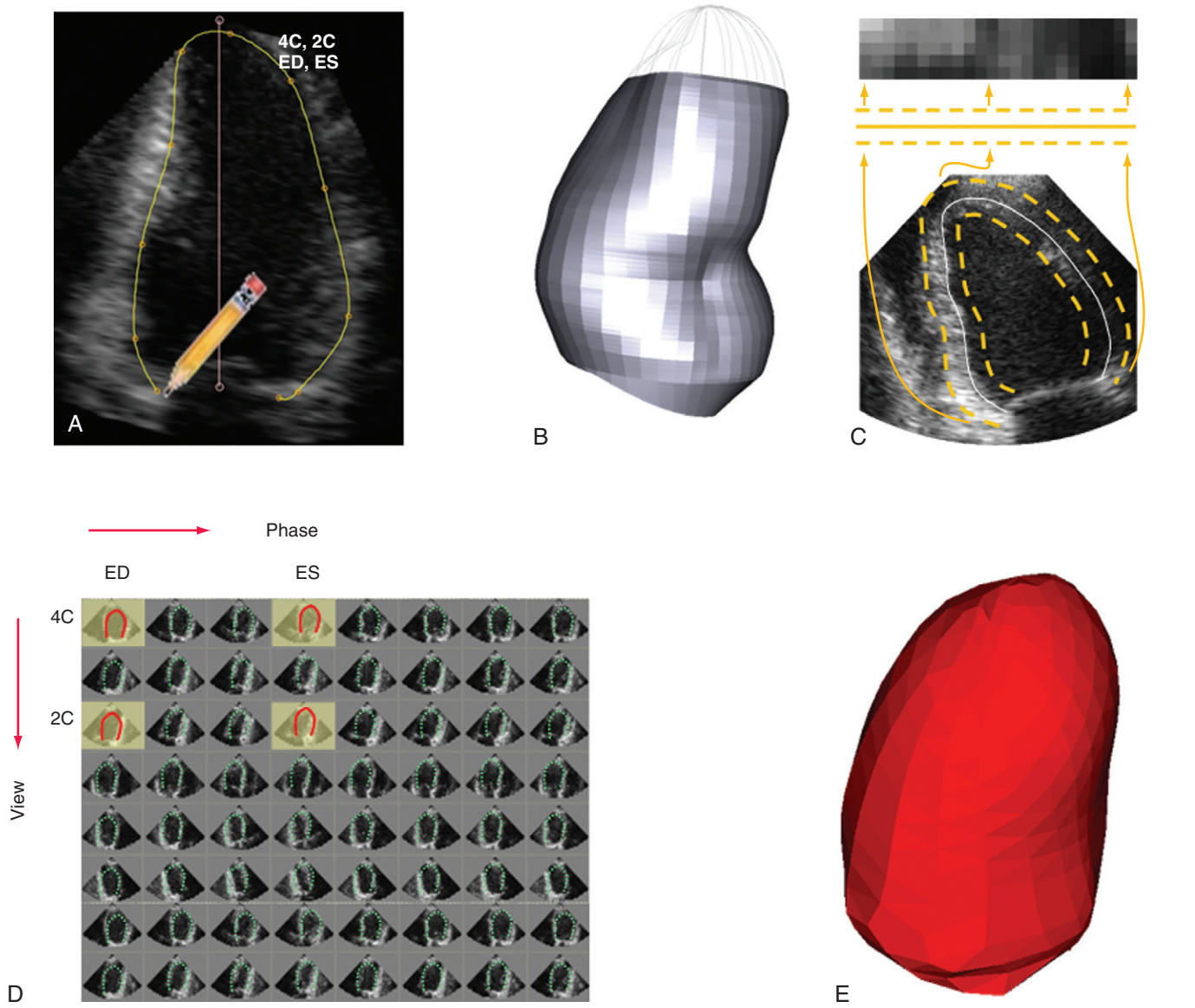



**Figure 12-6** **Semiautomatic four-dimensional (4D) border detection based on geometric models and pattern matching. A,** The method is initialized by manual delineation in four- (*4C*) and two-chamber (*2C*), in end-diastole (*ED*) and end-systole (*ES*). From these borders, a geometric model (**B**) and edge patterns (**C**) are obtained. **D,** These are matched to the remaining cross sections and cardiac phases by dynamic programming. **E,** One of the 3D endocardial borders automatically detected over the full cycle. *(Modified from Van Stralen M, Bosch JG, Voormolen MM, et al: Left ventricular volume estimation in cardiac 3D ultrasound: a semi-automatic border detection approach.* Acad Radiol *12:1241-1249, 2005.)*

achieve a balance here: preventing entirely implausible solutions while allowing for a range of normal and pathological shapes.

## PATTERN MATCHING

A four-dimensional (4D) semiautomatic model-based approach[38] was developed in our lab based on pattern matching and dynamic programming, which can derive a 4D segmentation with very limited user interaction. It was based on the earlier Echo-CMS system[39] for 2D image analysis that has been applied in studies on wall motion patterns for cardiac resynchronization therapy by biventricular pacing[40] and regional wall motion quantification for myocardial viability,[41] stress echocardiography,[42] and LV remodeling.[43]

Each 3D image of the 4D sequence is represented as a (cylindrical) set of long-axis 2D image slices. To initialize, one ED and ES contour are manually drawn in the four-chamber and two-chamber slices (Fig. 12-6). These shapes are interpolated spatiotemporally to form a 4D geometric model. In addition, a 4D pattern of the intensities is created by spatiotemporal interpolation of the image intensity patterns close to the manually delineated borders. This 4D "edge pattern" is thus a user-defined description of the borders. The intensities close to the interpolated 4D geometric model are then matched with the edge pattern. Optimal connective borders are determined using dynamic programming.[44] After detection of all contours (see Fig. 12-6, *D*), the user may apply any corrections by overdrawing part of a contour. Consecutively, all models are updated with the extra user-defined information, which is interpolated and extrapolated over the sequence, followed by a redetection of all nonmanual contours. The detected borders will resemble the user's definition of the border, and the method is thus suitable for different delineation protocols, not limited to intensity

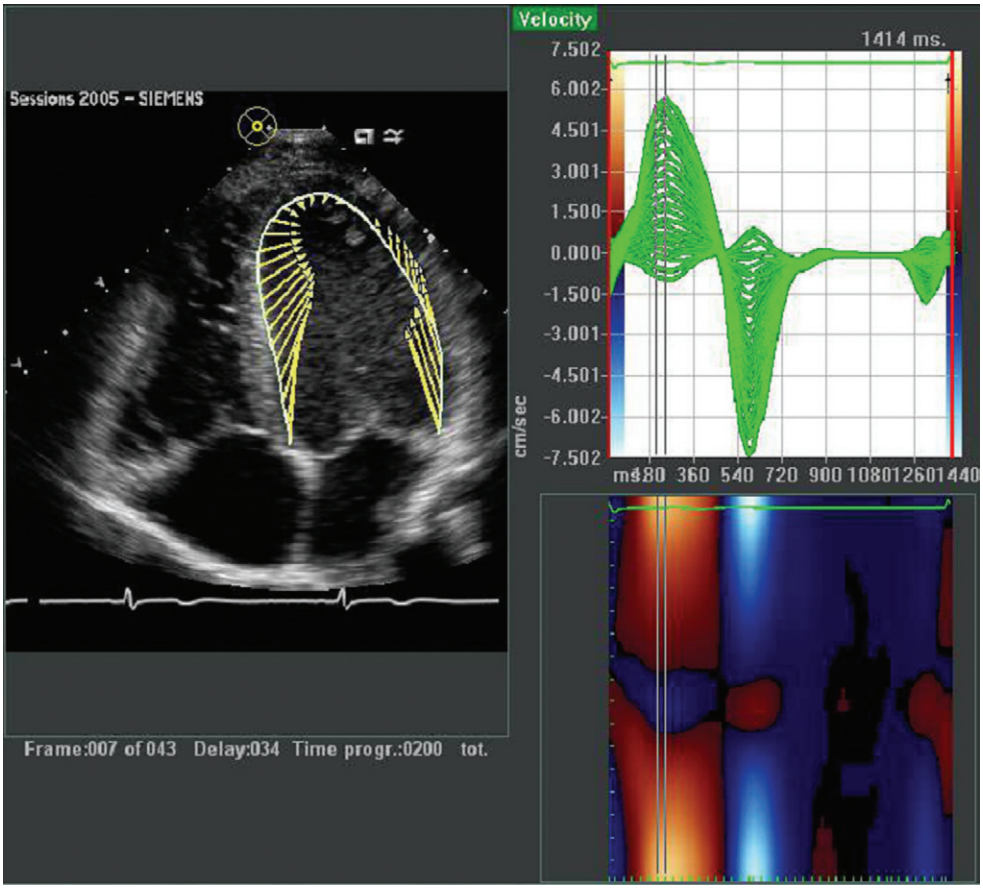



**Figure 12-7** Siemens Axius Velocity Vector Imaging. Border with *arrows* showing the local direction of border motion (*left*). Velocity for all points on border as function of time and displayed as a tissue Doppler imaging–style color map (*right*). *(Courtesy Siemens Medical Solutions, Malvern, Pa.)*

transitions, and including contrast-enhanced images. For research purposes, it has been shown to be a valuable tool, especially since it allows effective, smooth 4D corrections with little interaction.

Similar techniques are available for 2D analysis, such as the Axius Velocity Vector Imaging[45,46] approach commercialized by Siemens Medical Solutions (Malvern, Pa.). This technique, based on the work of Pedrizzetti and Tonti,[47] requires a user-drawn initial border and tracks the points of this border over one or more heart cycles. It applies template matching by cross correlation along lines perpendicular to the initial border and finds a one-dimensional path in the temporal direction for each point, by searching a maximum likelihood over its neighborhood in the subsequent frames. Consecutively, it tracks the motion of all points along the direction of the border (tangential) as well. Combining these perpendicular and tangential displacements supplies a 2D velocity vector in each point (Fig. 12-7, *left*). From the resulting borders, volumes are calculated, but TDI-like velocity, strain and strain rate plots are also generated (Fig. 12-7, *right*). The technique does not rely on speckle tracking or radiofrequency information and can be applied online or offline on B-mode images of most transducers and systems. Initial clinical validation shows promising results especially for cardiac resynchronization therapy.[45,46]

## 3D ACTIVE SURFACE DETECTION

Several practical methods for segmentation of 4D (3D + time) ultrasound images are now available. Semiautomatic analysis tools such as 4D-LV-Analysis (TomTec Imaging Systems GmbH, Unterschleissheim, Germany) are widely used and have shown good results in comparison to MRI.[48-50] This method uses manually traced borders in three views (the four-chamber view, and views at 60° and 120° rotation) in end-diastole and end-systole as initialization. A 3D spline-based spatiotemporal deformable model is then applied,[51,52] which ensures that the surface is smooth in time and space. The TomTec 4D RV-Function software (Fig. 12-8) uses essentially the same approach for detecting borders in the RV, initialized by manual delineation of the borders in two perpendicular long-axis views.[53]

Another example is the semiautomatic 4D detection as implemented in the Philips QLAB analysis package. This method is based on the active surface detection technique described by Gérard and co-workers.[54] A deformable surface is described as a two-simplex mesh; for each mesh vertex, the internal energy is determined by the local surface smoothness, and external energy by nearby image gradients combined with image intensity. The 3D mesh is initialized in the ED and ES 3D images by manually indicating five markers for mitral valve and apex in the two-chamber and four-chamber cross sections. A standard LV 3D shape is fitted affinely to the manual points to define an initial mesh, and the active surface optimization is started from there in a coarse-to-fine manner. First, rigid-body and affine transforms are applied, then local mesh deformations and mesh refinement.

After ED and ES surfaces have been found, the detection can be extended over the full cycle. For all remaining phases, an initial mesh is generated by propagating the ED and ES shapes using a 4D statistical heart motion model. The active surface optimization is then applied in each 3D image separately (Fig. 12-9). The found shapes can be manually edited conveniently by 3D mesh dragging. A wide range of analytical parameters is

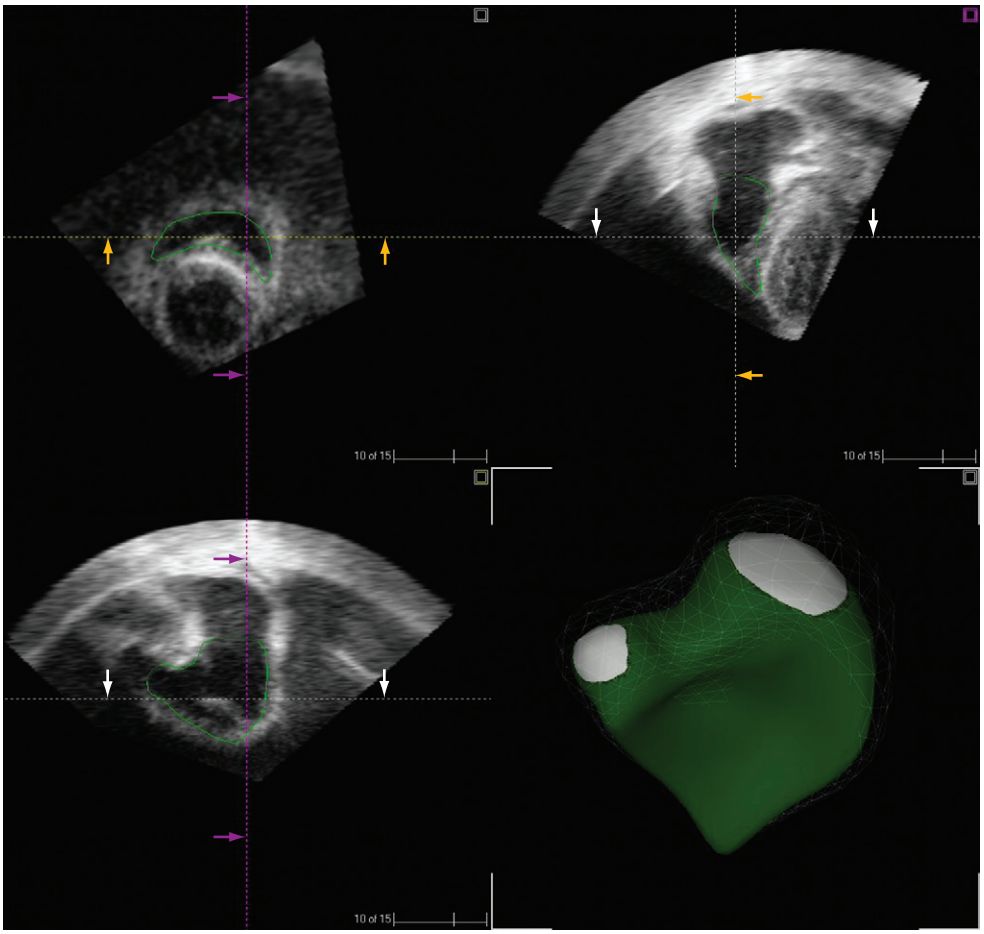



**Figure 12-8 Tomtec 4D RV-function, semiautomated segmentation of RV from 4D echocardiograms.** *Bottom right*: 3D representation of segmented RV lumen. *Other views*: Three orthogonal cross sections showing the RV endocardial contour in *green*. *(Courtesy Tomtec Imaging Systems, Unterschleissheim, Germany.)*

derived from the 3D shapes, concerning global and regional volumes and wall motion indexes. This method has been validated successfully against several other modalities.[50,54]

The method is fast and reasonably robust and supplies a practical tool for analysis of the 3D endocardial volume. One should note that because of the nature of the detection approach and its spatiotemporal smoothness constraints, the found surfaces and graphs are always relatively rounded and smooth. Furthermore, it may be hard to apply manual corrections, because this disturbs the nice temporal continuity of shapes and graphs: such corrections are not propagated over the temporal sequence.

Recently, GE introduced the 4D LVQ tool in the EchoPAC software[55] (Fig. 12-10), an active surface technique that uses 18 manually placed points as initialization (mitral valve annulus and apex on three apical views, in end-diastole and end-systole).

Orderud and colleagues[33] have combined 3D deformable models with a very efficient Kalman filter update scheme, which allows fast convergence of the model to the data and subsequent fully automated real-time segmentation of 3D echocardiographic data. Not only does this supply real-time quantification possibilities, it may also allow real-time optimal view extraction[56,57] or feedback on imaging system settings.[58]

## POPULATION-MODEL BASED METHOD: ACTIVE APPEARANCE MODELS

A relatively new class of techniques called *active appearance models* (AAMs) holds great promise. These techniques were originally developed by Cootes and co-workers[59] for facial recognition and medical image analysis, as an extension of the active shape model[60,61] approach. AAMs have been applied to magnetic resonance imaging[62,63] and 2D and 3D echocardiography[63-65] with very promising results. These techniques derive the typical shape and appearance of an echocardiogram from a large set of example images with expert-drawn contours. Principal component analysis (PCA) on a point distribution model extracts the average organ shape and the principal variations (*eigenvariations*) of shape. By warping all examples to the average shape, an average image and principal image variations can be found. By applying another PCA, simultaneous shape and intensity, eigenvariations are modeled in an *appearance model* (Fig. 12-11, *A*). Such an appearance model can synthetically generate "probable" echocardiographic images (see Fig. 12-11, *C*) similar to the variations shown in Figure 12-11, *A*. By deforming the model along the characteristic model eigenvariations, using a gradient descent minimization of the difference between the synthetic and the real image, the desired structure can be found (see Fig. 12-11, *B*). This can be done fast and fully automatically with good results.[66]

This technique has some significant advantages: it models both average organ shape and all variations over a population of examples; it models the complete organ appearance, including typical artifacts; it captures the expert's definition of proper border definition; it can model complex shapes (e.g., LV endocardium plus LV epicardium, RV, valves); it is not limited to blood-tissue borders; and it is easily customizable for different types of images. Limitations of this technique are its dependence on the training data, the selected population of examples, and the quality of the expert contours.

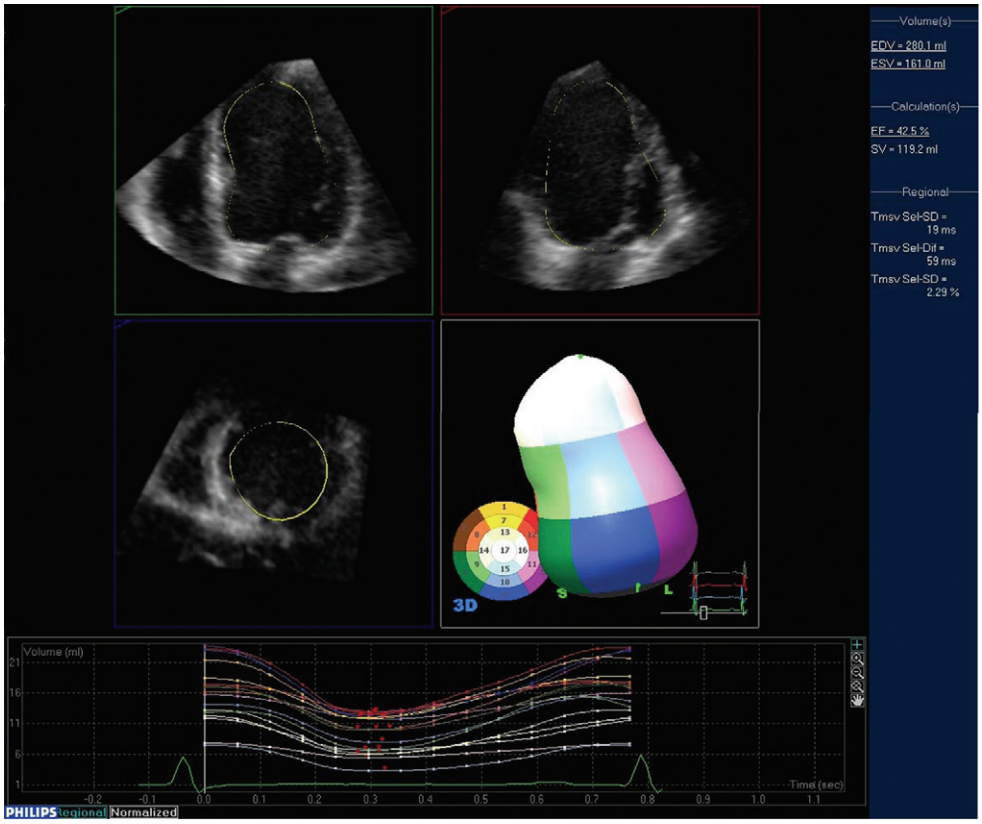



**Figure 12-9** Semiautomatic 3D active surface border detection (Philips QLAB 3DQ advanced). *(Courtesy Philips Medical Systems Ultrasound, Andover, Mass.)*

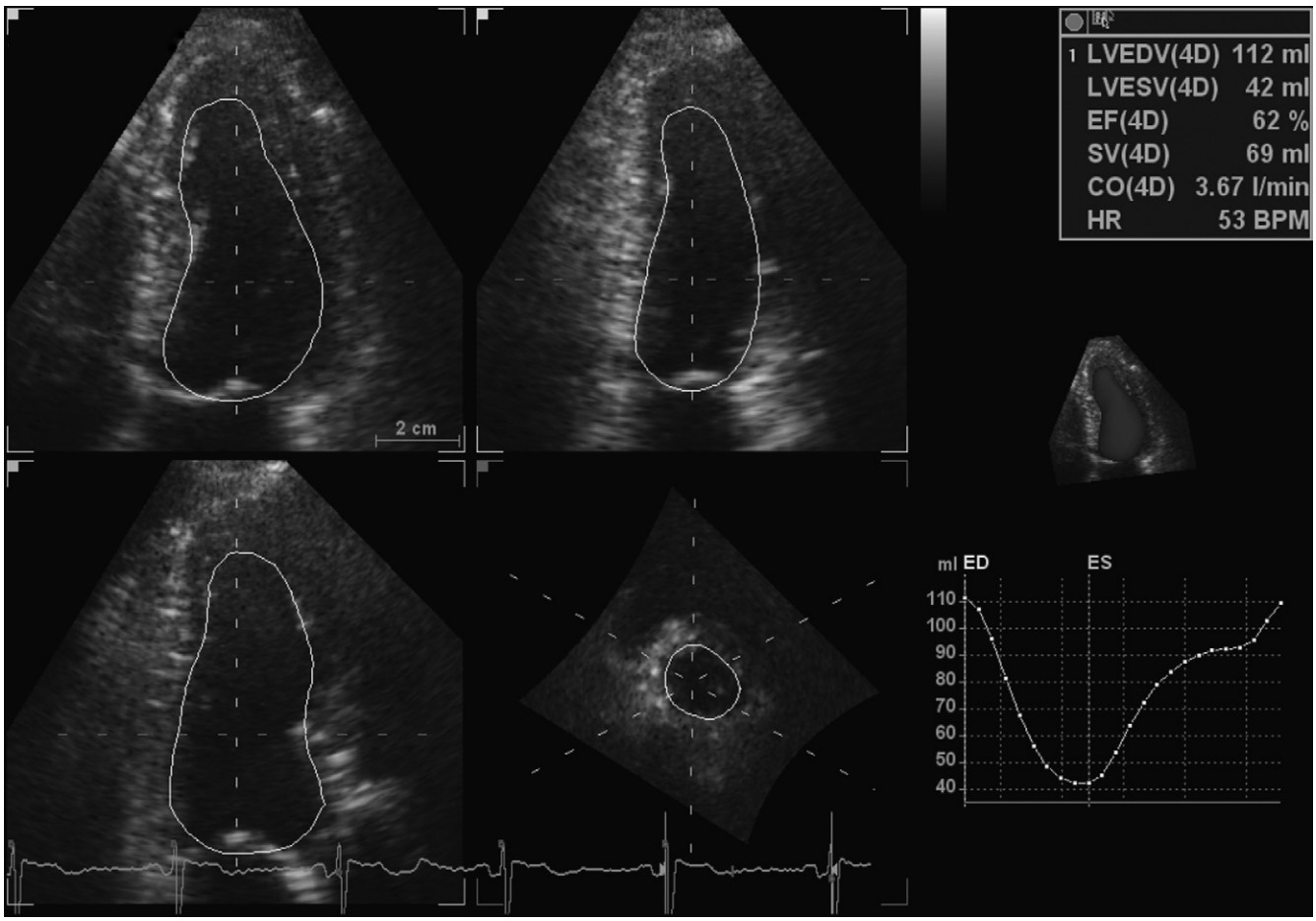



**Figure 12-10** **LV surface detection using 4DLVQ in GE Vingmed EchoPAC software.** Borders are initialized by manual annotation of mitral valve annulus and apex in the standard apical views. The complete 4D surface is detected; 3D ES volume is shown with time-volume curve. *(Courtesy J. Hansegard, GE Vingmed Ultrasound, Horten, Norway.)*

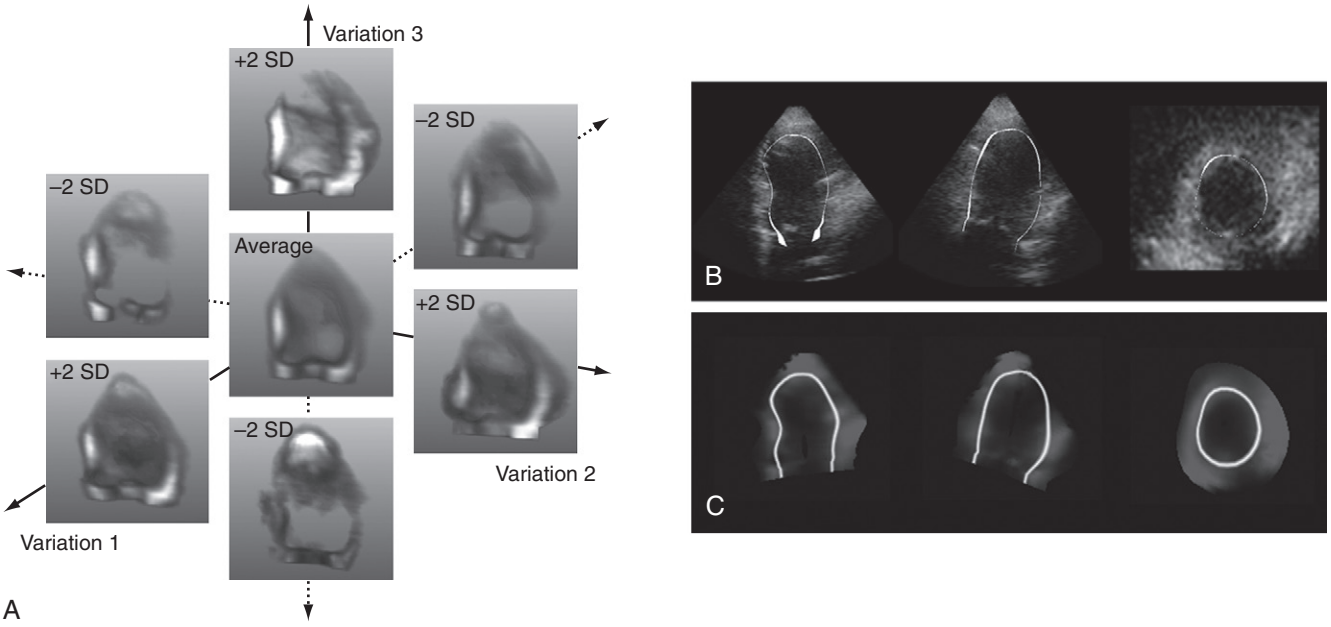



**Figure 12-11** **3D active appearance model segmentation. A,** 3D appearance model of the LV at end-diastole, showing the average appearance and the first three main variations. **B,** Four-chamber, two-chamber, and short-axis cross sections of a 3D image with manually delineated borders. **C,** Corresponding image and borders, synthesized by the appearance model. *(Courtesy K.Y.E. Leung, Rotterdam, The Netherlands.)*

A recent commercial application that employs a similar approach is the Axius Auto Ejection Fraction software (Auto EF) by Siemens Medical Solutions (Malvern, Pa.). Auto EF is based on the work of Comaniciu and colleagues[67,68] It comprises a fully automated endocardial contour detection approach for the apical four-chamber and two-chamber cross sections, which employs a population-based statistical model of endocardial shape and appearance in end-diastole and end-systole. After a rough determination of the position of the ventricle, the appearance model matches to the image and finds the endocardial contour for the estimated end-diastolic and end-systolic frame. Using a robust information fusion approach, the contour is tracked over the complete sequence from both frames, merging the motion estimated from the images (by an optical flow approach) with a dynamics model. The PCA-based shape model is strongly adapted to the current patient, and the motion estimates and their varying confidence (Fig. 12-12) are combined with expected shape dynamics using a Kalman filter–based tracking. From the found contours, ED and ES volumes and EF are calculated, along with a full-cycle volume curve. Initial clinical evaluations show promising results.[69]

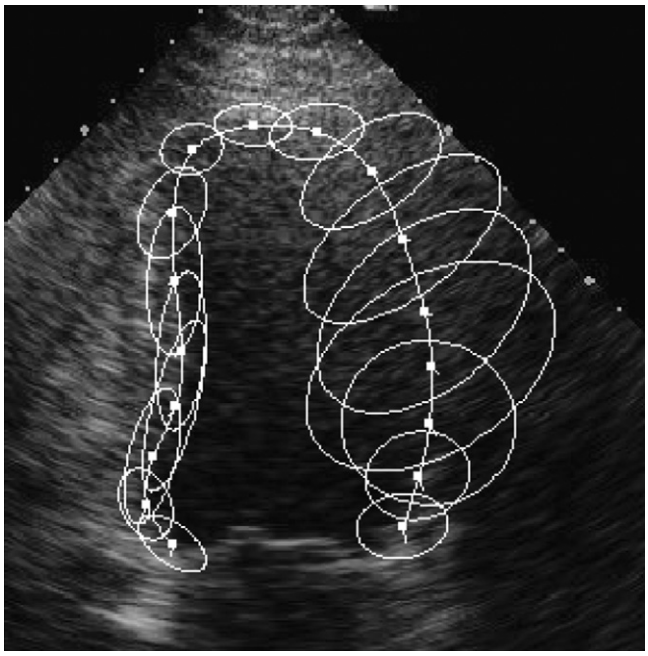


**Figure 12-12** Siemens Axius AutoEF detection process: border point candidates with 95% confidence ellipses corresponding to the local measurement uncertainty. *(From Comaniciu D, Zhou XS, Krishnan S: Robust real-time tracking of myocardial border: an information fusion approach.* IEEE Trans Med Imaging *23[7]:849-860, 2004.)*

## CLASSIFICATION AND AUTOMATED LOCALIZATION

A novel approach for image analysis is the use of large databases of expert-analyzed example data to train classifiers.[70-73] The intent is to use automated classification to find positions of certain structures in the image, or generate a view classification or even a diagnosis by image similarity. The principle is very much like the automated face localization in digital cameras and uses large numbers of simple structural image features generated from a selected region. By feeding a classifier many positive and negative examples, it can be trained to select a signature of such features that robustly identifies the sought structure. Such signatures can be calculated very effectively for many candidate positions and allow fast localization of typical structures (Fig. 12-13).

## Future Promise

In recent years, several instrumental developments have had important beneficial effects on the feasibility of ABD, and the ABD methods themselves have improved considerably. Recently,

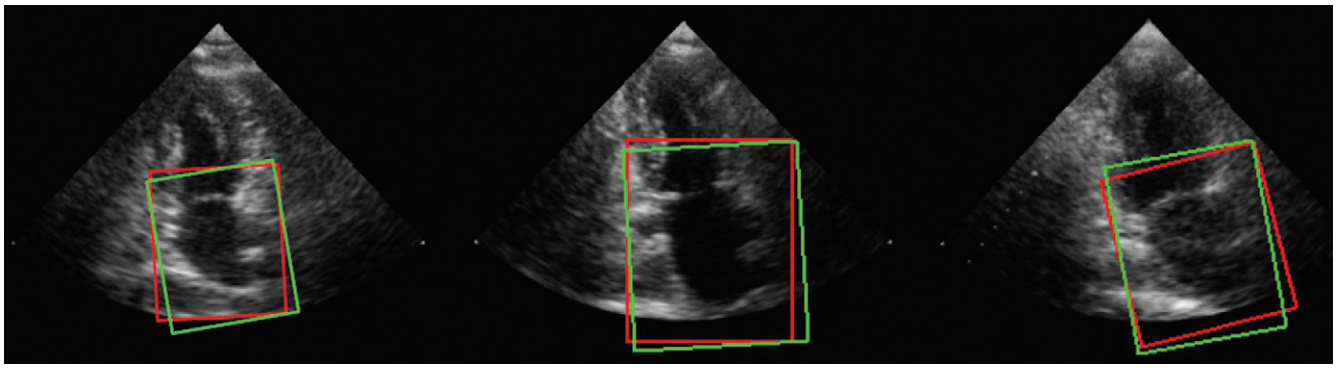


**Figure 12-13 Three examples of automatic localization and pose estimation of left atrium (LA) in apical two-chamber images by a Probabilistic Boosting Network (PBN) classifier.** Ground truth pose of LA (*red box*); automatically detected by PBN (*green box*). *(Modified from Zhang J, Zhou SK, McMillan L, Comaniciu D: Joint real-time object detection and pose estimation using probabilistic boosting network. In* Proceedings of the IEEE Conference on Computer Vision and Pattern Recognition, *Minneapolis, Minn., June 2007, pp 1-8.)*

several useful tools for ABD have become available commercially,[30,36,45,48,53-55,68] and in the near future, further improvements in the applicability of ABD can be expected.

The complete digitization of image formation and storage has improved image quality considerably. Front-end improvements resulting in clutter reduction, higher frame rates, and other benefits have also contributed considerably. The advent of real-time 3D imaging turned ultrasound into a truly 3D modality and also has greatly boosted development toward automated analysis. The continuous increase in computing power and the advent of novel algorithms have enabled such developments. In general, any further improvement in image quality is likely to enhance ABD as well.

## INTELLIGENT ULTRASOUND SYSTEMS

As discussed earlier, there are several important developments that together may bring automated echocardiographic image analyses to a new level of intelligence. Robust classification approaches[70-73] seem to offer solutions for the automated localization of structures and may replace manual initialization of segmentation. More realistic models (such as statistical models of object shape or appearance[59-67]) can capture patient variability and typical artifacts and thus provide more natural and realistic segmentations and even classification.[74] Modeling of the complete 3D anatomy will allow handling of view variability. Integration of tissue tracking and segmentation offers mutual improvements.[31] The advent of real-time tracking, segmentation, and classification allows great opportunities for direct quantification and image-guided feedback on probe position and image optimization. Significant research is already taking place in this field, especially aimed toward handheld and pocket-sized ultrasound devices, which are targeted at users who are less experienced in echocardiographic acquisition. Automated scan assistants that can derive information such as cardiac phase[58] or judge the correctness or quality of an acquired view in real time[57] can significantly improve the applicability and user friendliness of such small devices.

Especially for diagnosis, contributions from the realm of artificial intelligence[75] and computer-aided diagnosis are desirable: formal reasoning from rule-based expert knowledge; generating multiple hypotheses with measures of confidence; reasoning with pathologic or congenital conditions during detection; checking overall consistency of an interpretation and taking action to resolve conflicts; opportunistically choosing an optimal detection strategy for the image data presented; and learning from operator corrections and actions. Ultimately, such developments should lead to an intelligent "automated image interpretation assistant" for echocardiographers.

## KEY POINTS

- ABD plays an increasingly important role in 2D and 3D clinical echocardiography and allows a more quantitative use of echocardiography.
- Optimal image quality and rigorous standardization of image acquisition and analysis are essential for reliable ABD.
- Digital image storage with lossless or no compression is highly recommended.
- Application of ABD in clinical research should be applied with care. The user should be aware of the possibilities and limitations of the technique, should be able to distinguish imaging and detection artifacts from pathology, and should remain critical about the outcome.
- Modeling of anatomical and pathological variability over patient groups plays an increasingly important role in ABD techniques.
- 2D tissue tracking approaches complement tissue-Doppler imaging applications as well as wall motion analysis by border detection. 3D tracking is gaining importance and will soon allow assessment of the true 3D contraction patterns of the myocardium.
- Instrumental hardware improvements, more elaborate 3D and 4D modeling/analysis techniques and artificial intelligence approaches have boosted, and will further improve, clinical feasibility of ABD.

## REFERENCES


1. Foster E, Cahalan MK: The search for intelligent quantitation in echocardiography: "eyeball," "trackball" and beyond. *J Am Coll Cardiol* 22:848-850, 1993.
2. Hoffman R, Lethen H, Marwick TH, et al: Analysis of interinstitutional observer agreement in interpretation of dobutamine stress echocardiograms. *J Am Coll Cardiol* 27:330-336, 1996.
3. Feigenbaum H, Armstrong WF, Ryan T: Physics and instrumentation. In *Feigenbaum's echocardiography*, ed 7, Philadelphia, 2009, Lippincott Williams & Wilkins, pp 9-38.
4. Szabo T: *Diagnostic ultrasound imaging: inside out*, Burlington, Mass., 2004, Elsevier Academic Press.
5. Cobbold RSC: *Foundations of biomedical ultrasound*, New York, 2007, Oxford University Press.
6. DICOM Standards Committee: *Digital Imaging and Communications in Medicine (DICOM), 2009 edition*, Rosslyn, Va., 2009, National Electrical Manufacturers Association. ftp://medical.nema.org/medical/dicom/2009.
7. Thomas JD: The DICOM image formatting standard: what it means for echocardiographers. *J Am Soc Echocardiogr* 8:319-327, 1995.
8. Karson TH, Chandra S, Morehead AJ, et al: JPEG compression of digital echocardiographic images: impact on image quality. *J Am Soc Echocardiogr* 8:306-318, 1995.
9. Gonzalez RC, Woods RE: *Digital image processing*, ed 3, Englewood Cliffs, N.J., 2007, Prentice-Hall.
10. Sonka M, Hlavac V, Boyle R: *Image processing, analysis and machine vision*, ed 3, Pacific Grove, Calif., 2007, Thomson Engineering.
11. Bankman I: *Handbook of medical image processing and analysis*, ed 2, Burlington, Mass., 2008, Academic Press.
12. Sonka M, Fitzpatrick JM: *Handbook of medical imaging, vol 2. Medical image processing and analysis*, Bellingham, Wash., 2000, SPIE—The International Society for Optical Engineering.
13. Lang RM, Bierig M, Devereux RB, et al: Recommendations for chamber quantification: a report from the American Society of Echocardiography's Guidelines and Standards Committee and the Chamber Quantification Writing Group, developed in conjunction with the European Association of Echocardiography, a branch of the European Society of Cardiology. *J Am Soc Echocardiogr* 18:1440-1463, 2005.
14. Noble JA, Boukerroui D: Ultrasound image segmentation: a survey. *IEEE Trans Med Imaging* 25:987-1010, 2006.
15. Leung KYE, Bosch JG: Automated border detection in three-dimensional echocardiography: principles and promises. *Eur J Echocardiogr* 11(2):97-108, 2010.
16. Perez JE, Waggoner AD, Barzilai B, et al: Online assessment of ventricular function by automatic boundary detection and ultrasonic backscatter imaging. *J Am Coll Cardiol* 19:313-320, 1992.
17. Papademetris X, Sinusas AJ, Dione DP, Duncan JS: Estimation of 3D left ventricular deformation from echocardiography. *Med Image Anal* 5:17-28, 2001.
18. Sarti A, Corsi C, Mazzini E, Lamberti C: Maximum likelihood segmentation of ultrasound images with Rayleigh distribution. *IEEE Trans Ultrason Ferroelectr Freq Control* 52:947-960, 2005.
19. Boukerroui D, Basset O, Baskurt A, Gimenez G: A multiparametric and multiresolution segmentation algorithm of 3-D ultrasonic data. *IEEE Trans Ultrason Ferroelectr Freq Control* 48:64-77, 2001.
20. Verlande M, Flachskampf FA, Schneider W, et al: 3D reconstruction of the beating left ventricle and mitral valve based on multiplanar TEE. In *Proceedings, Computers in Cardiology*, Los Alamitos, Calif., 1991, IEEE Computer Society Press, p 285.
21. Lin N, Yu W, Duncan JS: Combinative multiscale level set framework for echocardiographic image segmentation. *Med Image Anal* 7:529-537, 2003.
22. Corsi C, Saracino G, Sarti A, Lamberti C: Left ventricular volume estimation for real-time three-dimensional echocardiography. *IEEE Trans Med Imaging* 21:1202-1208, 2002.
23. Sanchez-Ortiz GI, Wright GJT, Clarke N, et al: Automated 3-D echocardiography analysis compared with manual delineations and SPECT MUGA. *IEEE Trans Med Imaging* 21:1069-1076, 2002.
24. Mailloux GE, Langlois F, Simard PY, Bertrand M: Restoration of the velocity field of the heart from two-dimensional echocardiograms. *IEEE Trans Med Imaging* 8:143-153, 1989.
25. Meunier J: Tissue motion assessment from 3D echographic speckle tracking. *Phys Med Biol* 43:1241-1254, 1998.
26. Sühling M, Arigovindan M, Jansen C, et al: Myocardial motion analysis from B-mode echocardiograms. *IEEE Trans Image Processing* 14(4):525-536, 2005.
27. Leung KYE, Danilouchkine MG, Van Stralen M, et al: Tracking left ventricular borders in 3D echocardiographic sequences using motion-guided optical flow. *Proc SPIE Med Imaging* 7259:72590W, 2009.
28. Elen A, Choi HF, Loekx D, et al: Three-dimensional cardiac strain estimation using spatio-temporal elastic registration of ultrasound images: a feasibility study. *IEEE Trans Med Imaging* 27:1580-1591, 2008.
29. Kawagishi T: Speckle tracking for assessment of cardiac motion and dyssynchrony. *Echocardiography* 25:1167-1171, 2008.
30. Perez de Isla L, Balcones DV, Fernandez-Golfin C, et al: Three-dimensional-wall motion tracking: a new and faster tool for myocardial strain assessment: comparison with two-dimensional-wall motion tracking. *J Am Soc Echocardiogr* 22:325-330, 2009.
31. Nillesen MM, Lopata RGP, de Boode W, et al: 3D cardiac segmentation using temporal correlation of radiofrequency ultrasound data. Proc Med Image *Comput Comput Assist Interv* (1):927-934, 2009.
32. Duncan JS, Yan P, Zhu Y, et al: LV strain estimation from 4D echocardiography. *Proc. ISBI* 696-699, 2007.
33. Orderud F, Kiss G, Langeland S, et al: Combining edge detection with speckle-tracking for cardiac strain assessment in 3D echocardiography. *Proc. IEEE Ultrasonics Symp* 1959-1962, 2008.
34. Suffoletto MS, Dohi K, Cannesson M, et al: Novel speckle-tracking radial strain from routine black-and-white echocardiographic images to quantify dyssynchrony and predict response to cardiac resynchronization therapy. *Circulation* 113:960-968, 2006.
35. Behar V, Adam D, Lysyansky P, Friedman Z: The combined effect of nonlinear filtration and window size on the accuracy of tissue displacement estimation using detected echo signals. *Ultrasonics* 41:743-753, 2004.
36. Leitman M, Lysyansky P, Sidenko S, et al: Two-dimensional strain—a novel software for real-time quantitative echocardiographic assessment of myocardial function. *J Am Soc Echocardiogr* 17:1021-1029, 2004.
37. Nillesen MM, Lopata RGP, Gerrits IH, et al: Segmentation of the heart muscle in 3-D pediatric echocardiographic images. *Ultrasound Med Biol* 33:1453-1462, 2007.
38. Van Stralen M, Bosch JG, Voormolen MM, et al: Left ventricular volume estimation in cardiac 3D ultrasound: a semi-automatic border detection approach. *Acad Radiol* 12:1241-1249, 2005.
39. Bosch JG, Savalle LH, van Burken G, Reiber JHC: Evaluation of a semiautomatic contour detection approach in sequences of short-axis two-dimensional echocardiographic images. *J Am Soc Echocardiogr* 8:810-821, 1995.
40. Breithardt OA, Stellbrink C, Kramer AP, et al: Echocardiographic quantification of left ventricular asynchrony predicts an acute hemodynamic benefit of cardiac resynchronization therapy. *J Am Coll Cardiol* 40(3):536-545, 2002.
41. Nijland F, Kamp O, Verhorst PMJ, et al: Myocardial viability: impact on left ventricular dilatation after acute myocardial infarction. *Heart* 87(1):17-22, 2002.
42. Cain P, Short L, Baglin T, et al: Development of a fully quantitative approach to the interpretation of stress echocardiography using radial and longitudinal myocardial velocities. *J Am Soc Echocardiogr* 15(8):759-767, 2002.
43. Warda HM, Bax JJ, Bosch JG, et al: Effect of intracoronary aqueous oxygen on left ventricular remodeling after anterior wall ST-elevation acute myocardial infarction. *Am J Cardiol* 96(1):22-24, 2005.
44. Dong L, Pelle G, Brun P, Unser M: Model-based boundary detection in echocardiography using dynamic programming technique. In *Proceedings, SPIE Medical Imaging V*, Bellingham, Wash., 1991, SPIE—The International Society for Optical Engineering, pp 178-189.
45. Vannan MA, Pedrizzetti G, Li P, et al: Effect of cardiac resynchronization therapy on longitudinal and circumferential left ventricular mechanics by velocity vector imaging: description and initial clinical application of a novel method using high-frame rate b-mode echocardiographic images. *Echocardiography* 22(10):826-830, 2005.
46. Cannesson M, Tanabe M, Suffoletto MS, et al: Velocity vector imaging to quantify ventricular dyssynchrony and predict response to cardiac resynchronization therapy. *Am J Cardiol* 98(7):949-953, 2006.
47. Pedrizzetti G, Tonti G: Method of tracking position and velocity of objects' borders in two or three dimensional digital images, particularly in echographic images. U.S. Patent 2005/0074153, April 2005.
48. Kühl HP, Schreckenberg M, Rulands D, et al: High-resolution transthoracic real-time three-dimensional echocardiography. Quantitation of cardiac volumes and function using semi-automatic border detection and comparison with cardiac magnetic resonance imaging. *J Am Coll Cardiol* 43:2083-2090, 2004.
49. Nikitin NP, Constantin C, Loh PH, et al: New generation 3-dimensional echocardiography for left ventricular volumetric and functional

measurements: comparison with cardiac magnetic resonance. *Eur J Echocardiogr* 7:365-372, 2006.
50. Jenkins C, Chan J, Hanekom L, Marwick TH: Accuracy and feasibility of online 3-dimensional echocardiography for measurement of left ventricular parameters. *J Am Soc Echocardiogr* 19:1119-1128, 2006.
51. Soliman OI, Krenning BJ, Geleijnse ML, et al: Quantification of left ventricular volumes and function in patients with cardiomyopathies by real-time three-dimensional echocardiography: a head-to-head comparison between two different semiautomated endocardial border detection algorithms. *J Am Soc Echocardiogr* 20:1042-1049, 2007.
52. Chukwu EO, Barasch E, Mihalatos DG, et al: Relative importance of errors in left ventricular quantitation by two-dimensional echocardiography: insights from three-dimensional echocardiography and cardiac magnetic resonance imaging. *J Am Soc Echocardiogr* 21:990-997, 2008.
53. Gopal AS, Chukwu EO, Iwuchukwu CJ, et al: Normal values of right ventricular size and function by real-time 3-dimensional echocardiography: comparison with cardiac magnetic resonance imaging. *J Am Soc Echocardiogr* 20:445-455, 2007.
54. Gérard O, Billon AC, Rouet JM, et al: Efficient model-based quantification of left ventricular function in 3-D echocardiography. *IEEE Trans Med Imaging* 21(9):1059-1068, 2002.
55. Hansegård J, Urheim S, Lunde K, et al: Semi-automated quantification of left ventricular volumes and ejection fraction by real-time three-dimensional echocardiography. *Cardiovasc Ultrasound* 7:18, 2009.
56. Orderud F, Torp H, Rabben SI: Automatic alignment of standard views in 3D echocardiograms using real-time tracking. *Proc SPIE Med Imaging* 7265(72650D):1-12, 2009.
57. Snare SR, Aase SA, Mjolstad OC, et al: Automatic real-time view detection. *Proc. IEEE Ultrasonics Symp* 2304-2307, 2009.
58. Aase SA, Snare SR, Dalen H, et al: Echocardiography without electrocardiogram. *Eur J Echocardiogr* 12(1):3-10, 2011.
59. Cootes TF, Taylor CJ: Statistical models of appearance for medical image analysis and computer vision. Proc. SPIE Medical Imaging 2001, Image Processing, Vol 4322. Bellingham WA, 2001, SPIE, pp 236-248.
60. Cootes TF, Hill A, Taylor CJ, Haslam J: Use of active shape models for locating structures in medical images. *Image Vision Computing* 12:355, 1994.
61. Parker AD, Hill A, Taylor CJ, et al: Application of point distribution models to the automated analysis of echocardiograms. In *Proceedings, Computers in Cardiology*, Los Alamitos, Calif., 1994, IEEE Computer Society Press, p 25.
62. Mitchell SC, Lelieveldt BPF, van der Geest RJ, et al: Multistage hybrid active appearance model matching: Segmentation of left and right ventricles in cardiac MR images. *IEEE Trans Med Imaging* 20(5):415-423, 2001.
63. Mitchell SC, Bosch JG, Lelieveldt BPF, et al: 3-D active appearance models: segmentation of cardiac MR and ultrasound images. *IEEE Trans Med Imaging* 21(9):1167-1178, 2002.
64. Bosch JG, Mitchell SC, Lelieveldt BPF, et al: Automatic segmentation of echocardiographic sequences by active appearance motion models. *IEEE Trans Med Imaging* 21(11):1374-1383, 2002.
65. Leung KYE, van Stralen M, Voormolen MM, et al: Improving 3D active appearance model segmentation of the left ventricle with Jacobian tuning. *Proc SPIE Med Imaging* 6914:69143B, 2008.
66. Leung KYE, van Stralen M, van Burken G, et al: Automatic active appearance model segmentation of 3D echocardiograms. *Proc IEEE Int Symp Biomed Imaging* 320-323, 2010.
67. Comaniciu D, Zhou XS, Krishnan S: Robust real-time tracking of myocardial border: an information fusion approach. *IEEE Trans Med Imaging* 23(7):849-860, 2004.
68. Georgescu B, Zhou XS, Comaniciu D, Rao B: Real-time multi-model tracking of myocardium in echocardiography using robust information fusion. Medical Image Computing and Computer-Assisted Intervention—MICCAI 2004. *Lecture Notes in Computer Science* 3216:777-785, 2004.
69. Cannesson M, Suffoletto MS, Tanabe M, et al: A novel two-dimensional echocardiographic image analysis system using artificial intelligence shape and pattern recognition for rapid automated ejection fraction (Abstract). *J Am Coll Cardiol* 47:251A, 2006.
70. Georgescu B, Zhou XS, Comaniciu D, Gupta A: Database-guided segmentation of anatomical structures with complex appearance. *Proc Comput Vis Pattern Recogn* 2:429-436, 2005.
71. Carneiro G, Georgescu B, Good S, Comaniciu D: Detection of fetal anatomies from ultrasound images using a constrained probabilistic boosting tree. *IEEE Trans Med Imaging* 27(9):1342-1355, 2008.
72. Lu X, Georgescu B, Zheng Y, et al: Autompr: Automatic detection of standard planes in 3D echocardiography. *Proc Int Symp Biomed Imaging* 1279-1282, 2008.
73. Zhang J, Zhou SK, McMillan L, Comaniciu D: Joint real-time object detection and pose estimation using probabilistic boosting network. In *Proceedings of the IEEE Conference on Computer Vision and Pattern Recognition*, Minneapolis, Minn., June 2007, pp 1-8.
74. Bosch JG, Nijland F, Mitchell SC, et al: Computer-aided diagnosis via model-based shape analysis: Automated classification of wall motion abnormalities in echocardiograms. *Acad Radiol* 12(3):358-367, 2005.
75. Bovenkamp EGP, Dijkstra J, Bosch JG, Reiber JHC: Multi-agent segmentation of IVUS images. *Pattern Recognition* 37(4):647-663, 2004.
76. Montagnat J, Sermesant M, Delingette H, et al: Anisotropic filtering for model-based segmentation of 4D cylindrical echocardiographic images. *Pattern Recogn Lett* 24:815-828, 2003.
77. Klingler JW, Vaughan CL, Fraker TD, Andrews LT: Segmentation of echocardiographic images using mathematical morphology. *IEEE Trans Biomed Eng* 35:925-934, 1988.
78. Setarehdan SK, Soraghan JJ: Automatic left ventricular feature extraction and visualisation from echocardiographic images. In *Proceedings, Computers in Cardiology*, Los Alamitos, Calif., 1996, IEEE Computer Society Press, p 9.
79. Coppini G, Poli R, Valli G: Recovery of the 3-D shape of the left ventricle from echocardiographic images. *IEEE Trans Med Imaging* 14:301-317, 1995.
80. Chalana V, Linker DT, Haynor DR, Kim Y: A multiple active contour model for cardiac boundary detection on echocardiographic sequences. *IEEE Trans Med Imaging* 15:290-298, 1996.
81. Angelini ED, Homma S, Pearson G, et al: Segmentation of real-time three-dimensional ultrasound for quantification of ventricular function: A clinical study on right and left ventricles. *Ultrasound Med Biol* 31:1143-1158, 2005.
82. Stralen M van, Leung KYE, Voormolen MM, et al: Time continuous detection of the left ventricular long axis and the mitral valve plane in 3-D echocardiography. *Ultrasound Med Biol* 34(2):196-207, 2008.

13

# The Role of Echocardiographic Evaluation in Patients Presenting with Acute Chest Pain to the Emergency Department

KIRSTEN E. FLEISHMANN, MD | SARAH G. WEEKS, MD

**Background and Principles**
**Echocardiography and the Physiology of Acute Ischemia**
**Technical Aspects of Echocardiography in the Emergency Department**
Image Acquisition
Stress Echocardiography
Image Interpretation
Myocardial Contrast Echocardiography
**Clinical Applications**
Triage of Patients with Chest Pain
Clinical Use of Myocardial Contrast Echocardiography
Use of Echocardiography in Chest Pain Units and Clinical Algorithms
Cost Effectiveness
Assessment of the Need for Urgent Coronary Angiography
Risk Stratification and Analysis of Long-Term Clinical Outcome
Evaluation of Other Causes of Chest Pain
**Limitations**
Ischemia Evaluation
Image Quality
Personnel Availability
**Future Developments**
Tele-echocardiography
Strain Analysis for Regional Function
**Summary**

## Background and Principles

Coronary artery disease (CAD) accounted for 4.0 million hospital discharges in 2007 with more than 8 million patients presenting each year to emergency departments in the United States with a chief complaint of chest pain.[1] The challenge for the clinician is to identify those patients with a serious cause of chest pain requiring intervention. Acute coronary syndrome (ACS) often presents with atypical symptoms and a lack of diagnostic changes in the electrocardiogram (ECG) or cardiac markers. Time is critical when it comes to a patient with chest pain. Early treatment of myocardial injury, as well as other serious diagnoses, improves morbidity and mortality rates. Patients without a clear diagnosis are often admitted for observation as well as further cardiac testing, resulting in significant expense. Of patients presenting with chest pain, fewer than 30% are eventually diagnosed with ACS.[2,3] Efficient diagnosis not only aids the patient, but reduces hospitalization time and costs.

The diagnosis of myocardial infarction is based on evidence of myocardial necrosis in a clinical setting consistent with myocardial ischemia.[4] Most commonly this involves a change in cardiac biomarkers in conjunction with symptoms, ECG changes, or abnormal cardiac imaging. Use of serum cardiac markers (troponin, CK-MB) is central to the evaluation of chest pain and/or dyspnea in the emergency department. Unfortunately, these markers often take hours from symptom onset to exceed the normal range and are not elevated in acute coronary syndromes that are not associated with frank myocardial necrosis. Depending on the particular cardiac marker, levels can also be elevated in the absence of acute coronary syndrome, such as in the setting of renal insufficiency.[5] Electrocardiographic changes are frequently nonspecific.

Given these limitations, echocardiography can be a useful adjunct in assessing the emergency-department patient with chest pain. The evaluation of left ventricular (LV) systolic function, specifically wall thickening, with myocardial perfusion can aid in the diagnosis and triage of patients with chest pain. Echocardiography may also be useful in the diagnosis of other etiologies of chest pain, including aortic dissection, aortic stenosis, hypertrophic cardiomyopathy, and pericardial effusion (Box 13-1). This chapter focuses on the current application of echocardiography for early diagnosis of ACS.

## Echocardiography and the Physiology of Acute Ischemia

Acute ischemia is associated with a number of biochemical and physiologic changes in myocardial tissue.[6] The ischemic cascade begins with biochemical changes causing subsequent abnormalities in diastolic and systolic function. These abnormalities typically precede the development of symptoms, electrocardiographic changes, or the increase in cardiac biomarker levels.[7] The ability to detect myocardial ischemia earlier in the cascade of events by assessment of global and regional function has led to an interest in the use of echocardiography in patients presenting with chest pain without a clear diagnosis of ACS.

**Box 13-1**

**GOALS OF ECHOCARDIOGRAPHY IN EVALUATION OF PATIENTS WITH ACUTE CHEST PAIN**

Diagnosis of acute coronary syndrome
- Determination of coronary vascular territory involved
- Assessment of the area of myocardium at risk
- Evaluation of global ventricular function

Exclusion of other causes of chest pain
- Aortic dissection
- Pericarditis (with effusion)
- Aortic stenosis
- Hypertrophic cardiomyopathy

In addition, while coronary blood flow is maintained at a constant rate over a wide range of coronary pressure through autoregulation, myocardial contrast echocardiography (MCE) may also be helpful in assessing suspected CAD. Only once a coronary vessel is more than 85% obstructed does the flow fall below a normal threshold.[8] However, MCE evaluates myocardial perfusion and thereby may detect severely stenotic lesions noninvasively as well.

## Technical Aspects of Echocardiography in the Emergency Department

### IMAGE ACQUISITION

The emergency department environment often makes the echocardiogram more challenging than in the controlled environment of the echocardiography lab. Transthoracic echocardiographic (TTE) examination of patients with chest pain should focus on the evaluation of biventricular function and the presence of regional wall motion abnormalities (lack of normal wall thickening, particularly if in a vascular territory). It may also include assessment of myocardial blood flow using echocardiographic contrast (if available). The study should also serve to screen for nonischemic causes of cardiac chest pain such as aortic stenosis, hypertrophic cardiomyopathy, pericardial effusion, and aortic dissection (although sensitivity for the last diagnosis is limited, and a negative TTE is not sufficient to rule it out).

The standard two-dimensional (2D)-TTE views necessary for assessment of wall thickening are the parasternal long- and short-axis views and the apical four-chamber, two-chamber and three-chamber views (Fig. 13-1 demonstrates the apical two-chamber and short-axis views). If adequate image quality cannot be achieved from the parasternal or apical views, subcostal views can be extremely helpful. Off-axis or foreshortened views make the interpretation of regional wall motion abnormalities difficult and increase the likelihood of error. Images should be analyzed in accordance with the American Society of Echocardiography guidelines.[9]

The use of echocardiographic contrast agents can be invaluable in defining endocardial borders for wall motion analysis (see Chapter 3). Commercially available intravascular echocardiographic contrast agents contain gas-filled microbubbles, which are small enough to pass through the pulmonary circulation, resulting in opacification of the LV. This results in enhancement of endocardial borders (Fig. 13-2).

A well-trained, experienced sonographer or echocardiographer is essential in the emergency setting. The sonographer should acquire necessary images in an efficient manner with attention to proper patient positioning, transducer selection, and technical settings. The technical settings may vary depending on the patient characteristics, such as the use of lower-frequency imaging in obese patients. Second harmonic imaging increases the signal-to-noise ratio, resulting in clearer imaging. The use of echocardiographic contrast requires changes in technical settings for endocardial definition versus myocardial perfusion, particularly in mechanical index.

The advancement of echocardiographic technology has substantially reduced the number of patients with inadequate echocardiographic images. In an early study by Horowitz and colleagues on the use of echocardiography in patients with acute chest pain, adequate images were obtained in 81% of patients.[10] A recent study evaluated patients with technically difficult imaging and found that the addition of contrast agent improved the percentage of myocardial segments visualized from 68% to 99%. This improvement had a direct impact on patient care.[11]

### STRESS ECHOCARDIOGRAPHY

Echocardiographic imaging in conjunction with exercise or pharmacologic stress to assess for ischemia is safe and effective in detecting inducible wall-motion abnormalities. Exercise stress can be performed using a standard treadmill protocol (i.e., Bruce) or a supine bicycle protocol. The advantage of bicycle protocols is the ability to image wall motion throughout exercise, as the patient exercises on an echocardiographic table that can be tilted into a left lateral position. The supine bicycle protocol increases the energy expenditure, typically in 30-watt increments every 3 minutes. This allows for image comparison at low, medium, and high workload. Additional Doppler information including pulmonary artery systolic pressure estimate, transaortic stroke volume, and valvular gradients can be obtained.

Treadmill studies image patients at baseline and just after peak exercise only. For maximum sensitivity, it is essential that the echocardiographic imaging begin immediately after exercise terminates, before significant heart rate decrease. This stress modality is primarily for assessment of global and regional systolic function (see Chapter 15).

For patients unable to exercise adequately, pharmacologic stress testing can be performed (see Chapter 16). Dobutamine is the agent most studied and, therefore, most commonly used in North America. Dobutamine stress echocardiography (DSE) has demonstrated excellent negative predictive value for the presence of obstructive CAD (96% at 6 months).[12] Baseline images are obtained, followed by the infusion of dobutamine at incremental levels (usually 5, 10, 20, 30, 40 mcg/kg/min) of 3 minutes' duration. The test is terminated when the patient's heart rate reaches 85% of maximum predicted heart rate, or there is evidence of myocardial ischemia, hypotension, significant arrhythmia, significant LV outflow tract obstruction, or drug-related side effects. Patients who do not reach target heart rate despite 40 mcg/kg/min of dobutamine can perform handgrip maneuvers or be given intravenous atropine in doses of 0.1 to 0.25 mg up to a total of 1 mg.

Endocardial definition is essential for reliable wall motion assessment. Images during stress decrease in quality because of the cardiac movement and hyperventilation. The use of second harmonic imaging has increased the sensitivity for the diagnosis of CAD from 64% to 92% in patients with poor image quality.

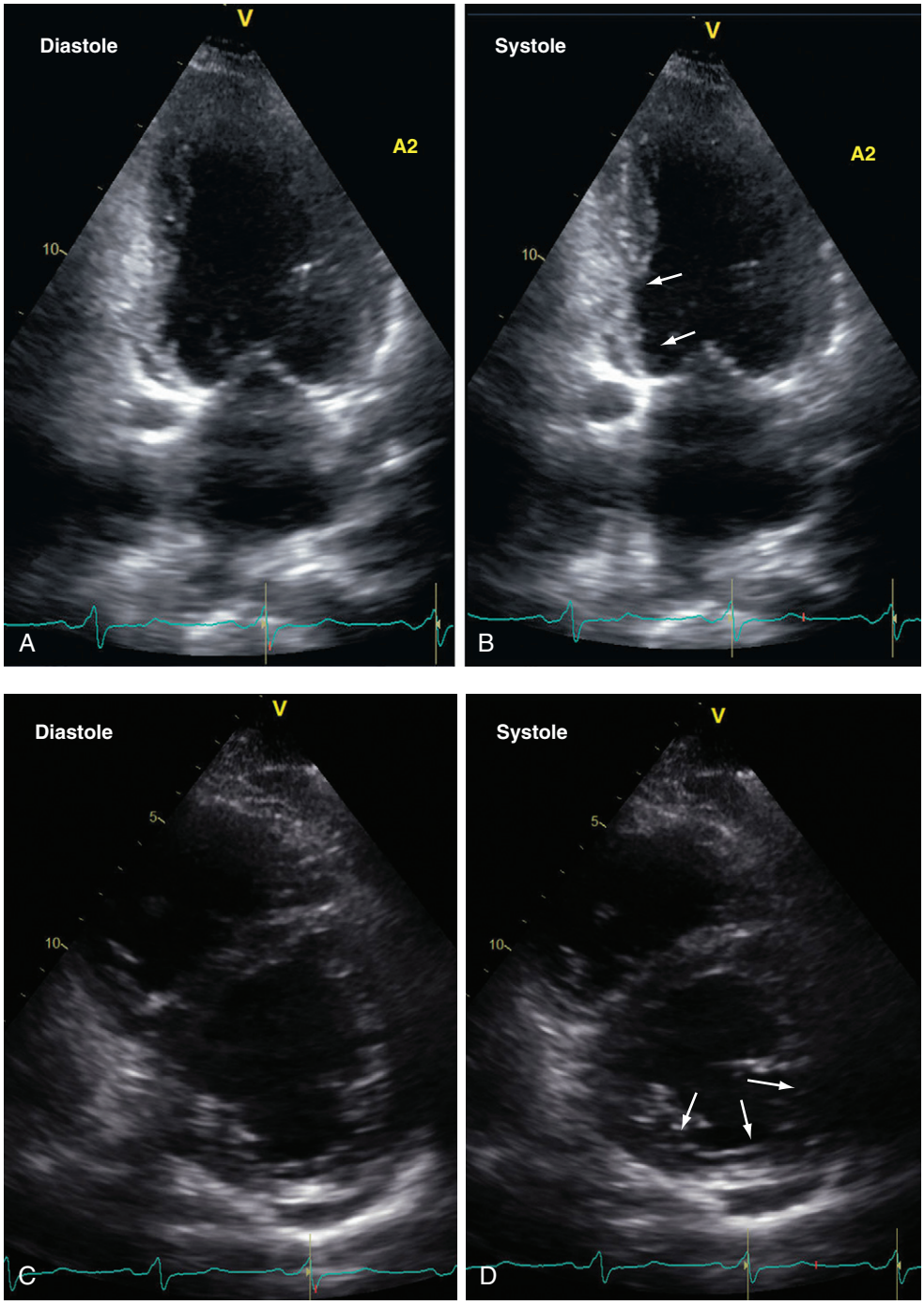



**Figure 13-1** Still frames from the echocardiogram of a patient with acute chest pain, showing akinesis (*arrows*) of the basal inferior and inferolateral segments, in the apical two-chamber view (**A,** diastole; **B,** systole) and the basal parasternal short axis (**C,** diastole; **D,** systole).

Specificity is unchanged with second harmonic imaging.[13] The use of echocardiographic contrast agents has also increased the sensitivity of stress echocardiography for the diagnosis of CAD. Rainbird and colleagues[14] analyzed 300 consecutive patients undergoing DSE. The percentage of wall segments visualized increased from 94.4% to 99.8% with the use of LV opacification during peak exercise (*P* less than 0.01). There was no decrease in segment visualization at peak exercise, as was the case if an echocardiographic contrast agent was not used.

This technique has been safely used when performed by specially trained nurses and sonographers, with images electronically transferred to the cardiologist for interpretation.[15,16]

## IMAGE INTERPRETATION

Accurate interpretation of regional wall motion also requires an experienced echocardiographer. Wall thickening and systolic endocardial motion are evaluated for each LV segment, leading to its classification as hyperkinetic, normal, hypokinetic, akinetic, or dyskinetic.

The American Society of Echocardiography recommends a 16-segment model of regional wall motion evaluation (Fig. 13-3).[9] This model is consistent with the models used in nuclear and magnetic resonance imaging. Each segment is assigned a score based on visual assessment of contractility: normal = 1, hypokinesis = 2, akinesis = 3, dyskinesis = 4, and

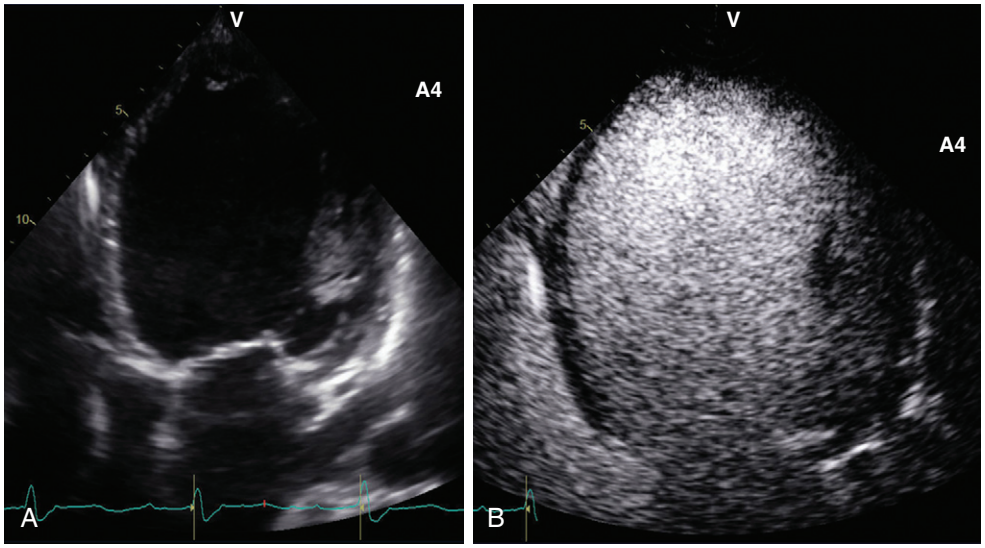



**Figure 13-2** Improvement in LV endocardial border delineation, particularly at the apex, with the use of intravenous echocardiographic contrast and second harmonic imaging (**A,** without contrast; **B,** with contrast).

aneurysmal = 5. The wall motion score index, a semiquantitative measure of regional wall motion abnormality, is calculated by averaging wall motion scores for visualized segments. An LV with normal systolic function has a wall motion score index of 1, whereas a dysfunctional ventricle will have an increasing wall motion score index proportional to the severity. This score correlates with myocardial infarct size on pathologic studies[17] and to perfusion defect size on single photon emission computed tomographic (SPECT) imaging.[18] A similar 14-segment wall motion index predicts long-term survival in patients with chest pain.[19]

Evaluation of stress-induced regional wall motion abnormalities is based on detailed comparison of rest and stress images, which is facilitated by simultaneous, synchronized display of images.

Recent refinements in tissue Doppler/speckle tracking imaging and the measurement of myocardial velocity allow for quantitative analysis of regional function.[20,21] Although not routine at present, these quantitative measures have been shown to distinguish between patients with non–ST-elevation myocardial infarction and unstable angina or noncoronary chest pain.[22]

### MYOCARDIAL CONTRAST ECHOCARDIOGRAPHY

MCE allows for the assessment of myocardial perfusion with the use of intravenous echocardiographic contrast agents, as well as assessment of wall thickening. Myocardial perfusion is assessed by the injection of microbubbles at the bedside, in real time, with rapid image acquisition. These inert, intravascular microbubbles are delivered to the capillary bed in territories with normal perfusion. Areas that are hypoperfused lack the echocardiographic enhancement generated by the contrast agent (perfusion defect). The difference in areas with and without adequate perfusion is highlighted by destruction of the bubbles at timely intervals, allowing for image acquisition as the areas of normal perfusion increase in signal intensity faster compared to areas with hypoperfusion. The destruction of bubbles occurs with the use of high-intensity pulses (mechanical index 1.0) synchronized to end-systole, whereas imaging occurs at a mechanical index of approximately 0.5 (Fig. 13-4).

**TABLE 13-1 Chest Pain in the Emergency Department**

| *Suspected Cause of Chest Pain* | *Alternate Imaging Techniques* |
|---|---|
| Dissection | Transesophageal echocardiography, CT angiography, MR angiography, aortogram |
| Coronary artery disease | CT angiography, nuclear perfusion imaging, left heart catheterization |
| Pericarditis/myocarditis | Cardiac MRI |
| Pulmonary embolus | Ventilation/perfusion scan, CT angiography, pulmonary angiography |

*CT*, Computed tomography; *MR*, magnetic resonance; *MRI*, magnetic resonance imaging.

## Clinical Applications

### TRIAGE OF PATIENTS WITH CHEST PAIN

Ischemia-induced regional wall motion abnormalities develop quickly once myocardial blood flow falls below a critical level. Rest echocardiography has therefore been used in the assessment of patients with symptoms suggestive of ACS. The diagnostic accuracy has, however, varied vastly between studies, likely because of the following factors: timing in relation to symptoms, infarct size, and technical variation. A recent study of emergency department patients with symptoms suggestive of ACS reported TTE to have a negative predictive value of 97%; however, the positive predictive valve was only 24%.[23] Although normal systolic function at rest is reassuring, it is insufficient to exclude the diagnosis of ACS (Table 13-1). The evaluation of wall thickening by TTE is deemed appropriate in patients with suspected ACS but nondiagnostic initial testing.[24]

### CLINICAL USE OF MYOCARDIAL CONTRAST ECHOCARDIOGRAPHY

The ability to analyze perfusion has added a potential new dimension to the echocardiographic assessment. A multicenter study by Kang and colleagues[25] enrolled 114 consecutive patients presenting to the emergency department with chest pain on exertion or at rest. Patients with ST elevation or Q waves on ECG were excluded. Echocardiography and MCE were performed to evaluate regional wall motion as well as myocardial perfusion. The sensitivity and specificity of a myocardial perfusion defect for the diagnosis of acute myocardial infarction were

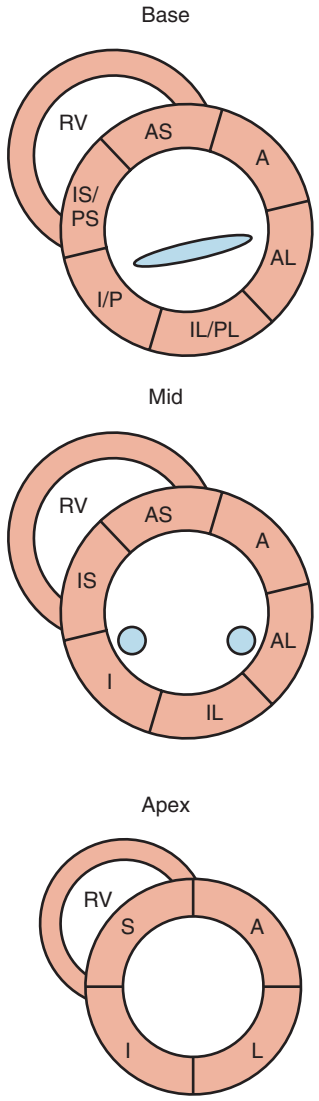



**Figure 13-3** A 16-segment model for evaluation of regional wall motion as recommended by the American Society of Echocardiography. *A*, Anterior; *AL*, anterolateral; *AS*, anteroseptal; *I*, inferior; *IL*, inferolateral; *IS*, inferoseptal; *PL*, posterolateral; *PS*, posteroseptal. *(Adapted from Schiller NB, Shah PM, Crawford M, et al: Recommendations for quantification of the left ventricle by two-dimensional echocardiography.* J Am Soc Echocardiogr *2:358-367, 1989.)*

93% and 63%, respectively. For the diagnosis of unstable angina, the sensitivity was 59% with a specificity of 96%. The authors concluded that the use of MCE to predict clinically confirmed acute coronary syndrome was more sensitive than the use of ECG, cardiac troponins, or echocardiographic assessment of regional wall motion abnormalities alone.

MCE has been compared to the use of the TIMI (Thrombolysis In Myocardial Infarction) risk score for risk stratification of patients presenting with chest pain.[26] More than 900 patients with suspected cardiac chest pain and a nondiagnostic ECG underwent MCE for perfusion and regional wall motion. Only 2 of 523 patients with normal regional function had a primary event. In patients with abnormal regional function, myocardial perfusion was better able to differentiate patients between intermediate- and high-risk groups.

MCE and SPECT were found to be equivalent in their ability to diagnose acute myocardial infarction in the emergency department in a multicenter study. MCE provided a 17%

**Box 13-2**

**ESSENTIAL FEATURES OF A SUCCESSFUL CHEST PAIN UNIT**

1. Telemetry capabilities
2. Timely serial cardiac marker measurements and electrocardiographic testing
3. Access to timely investigations such as: treadmill testing, echocardiography, computed tomography, nuclear imaging, and angiography
4. Bed availability to hold majority of patients 6 to 12 hours

increase in ability to predict future events.[27] In a large, single-center study, wall thickening and myocardial perfusion were significant predictors of cardiac events in patients presenting with chest pain and no ST-segment elevation[28] (Fig. 13-5).

A predictive model for chest pain patients with nondiagnostic initial testing has been developed. Abnormal regional function with or without abnormal myocardial perfusion was found to be an independent predictor of nonfatal myocardial infarction and cardiac death.[29]

## USE OF ECHOCARDIOGRAPHY IN CHEST PAIN UNITS AND CLINICAL ALGORITHMS

Chest pain units specializing in evaluation of patients presenting with acute chest pain have become widely used (Box 13-2). Use of clinical algorithms has been evaluated by clinical outcomes. For example, Gibler and colleagues[30] developed a "Heart ER Program," a diagnostic and treatment program for patients with chest pain in an urban tertiary-care emergency department. More than 1000 patients with symptoms suggestive of ACS were enrolled. Patients with known CAD, acute ST segment shift, hemodynamic instability, or clinical presentation consistent with unstable angina were admitted directly. Two-dimensional echocardiography and graded exercise testing were performed on all patients at the end of a 9-hour observation period. The results determined the disposition of the patient. The vast majority of patients were discharged from the emergency department (82.1%); only 15% were admitted for further evaluation. Of patients admitted, 34% were found to have a cardiac etiology for their symptoms. Stress echocardiography can be safely used in those patients at low risk, after an initial 6-hour observation period.[31]

DSE has also been studied in a clinical algorithm for chest pain assessment in the emergency department.[32,33] Patients with normal ECG and cardiac markers underwent rest 2D echocardiograms. If the rest images were normal, a DSE protocol was used with a trained nurse and sonographer. The test was completed in an average time of 5.4 hours from presentation. Using clinical follow-up and cardiac catheterization data for comparison, the protocol was found to have a sensitivity of 89.5%, a specificity of 88.9%, and a negative predictive value of 98.5%.[32]

The prognostic valve of predischarge DSE in chest pain patients with negative cardiac markers was evaluated in 377 patients by Bholasingh and co-workers.[12] Cardiac events occurred in 30% of patients with a positive DSE versus 4% of those with a negative DSE (odds ratio [OR] 10.7, *P* less than 0.0001).

A group in Italy evaluated 6723 intermediate-risk patients in the emergency department presenting with chest pain and a

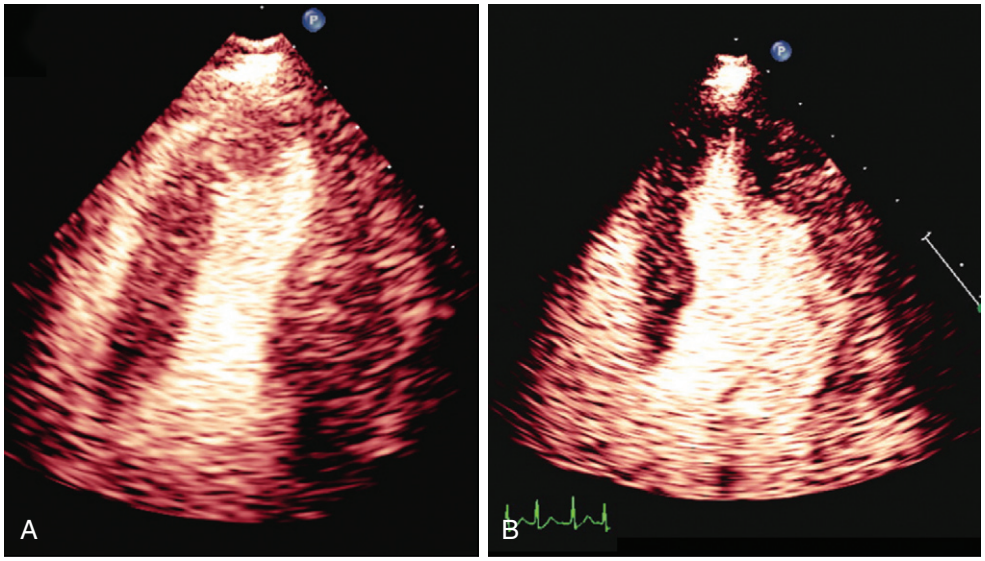



**Figure 13-4** **An example of a normal and a positive stress echocardiogram using intravenous echocardiographic contrast material for assessment of myocardial perfusion. A,** Apical four-chamber view with normal myocardial perfusion septum and basal lateral wall (myocardium appearing dark); **B,** apical four-chamber view with an inducible perfusion defect of the septum and apex at stress (myocardium appears dark when compared to the lateral wall).

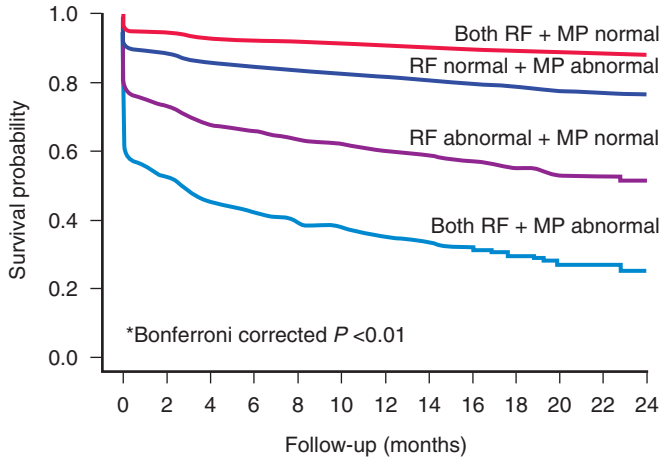



**Figure 13-5** Survival probabilities for patients presenting to the emergency department with chest pain and no ST segment elevation on electrocardiogram (ECG) with different combinations of regional function (*RF*) and myocardial perfusion (*MP*) after adjustment for age, hypertension, diabetes, hypercholesterolemia, smoking status, and ECG. *(From Rinkevich D, Kaul S, Wang XQ, et al., Regional LV perfusion and function in patients presenting to the emergency department with chest pain and no ST-segment elevation.* Eur Heart J *26:1606-1611, 2005.)*

nondiagnostic ECG.[34] In general, older patients or those with multiple risk factors or nondiagnostic ECGs had SPECT imaging, younger patients and those with fewer than two risk factors and normal ECGs underwent treadmill exercise testing, and those unable to exercise or with uncertain or nondiagnostic ETT or SPECT results had DSEs. Although the multiple types of testing performed make interpretation of this group's results more difficult, this protocol enabled them to make the early diagnosis of CAD in 22% of their chest pain unit patients, with early discharge in 78%.

A subsequent manuscript reported on approximately 500 patients with recent chest pain, but without ischemic ECG changes or definite evidence of CAD after a 6-hour workup including troponin levels. Patients unable to exercise and those with left bundle-branch block or poor echocardiographic windows were excluded. Patients had exercise echocardiography and exercise sestamibi nuclear stress imaging within 24 hours and patients with abnormal troponin levels at any time or positive stress tests were recommended for angiography. Endpoints for the study were greater than 50% stenosis on catheterization or cardiovascular events at 6 months. The exercise echocardiogram was positive in 20% of the cohort, the exercise sestamibi study in 24%. Fourteen patients with negative exercise echocardiograms were ultimately diagnosed with CAD versus 13 patients with negative exercise sestamibi studies. The sensitivity of exercise echocardiography and exercise sestamibi imaging for the ultimate diagnosis of CAD in this study was similar (85% vs. 86%), whereas the specificity of exercise echocardiography was slightly higher (95% vs. 90%), leading to a higher likelihood ratio for a positive exercise echocardiography test.[35]

## COST EFFECTIVENESS

Cost-effectiveness analyses of diagnostic strategies for patients with chest pain have found the preferred initial strategy to be noninvasive testing for patients with low to intermediate pretest probability of CAD, and coronary angiography for those with high pretest probability.

For example, in one study,[36] the incremental cost of exercise echocardiography compared with exercise electrocardiography in 55-year old men with atypical angina was $41,900 per quality-adjusted life-year (QALY), a range generally considered cost-effective in comparison to other accepted interventions. In comparison, exercise SPECT cost $54,800 per QALY as compared with exercise electrocardiography for these patients. However, in higher risk patients, such as 55-year-old men with typical angina, the incremental cost-effectiveness ratio of routine coronary angiography compared with exercise echocardiography was only $36,400 per QALY saved, making angiography an attractive strategy from a cost-effectiveness standpoint. The incremental cost-effectiveness ratio of exercise electrocardiography compared with no testing was $57,700 per QALY saved for 55-year-old men with nonspecific chest pain. The authors concluded that exercise electrocardiography or exercise

echocardiography resulted in reasonable cost-effectiveness ratios for patients at mild to moderate risk for CAD.

The cost effectiveness of MCE in the emergency department was evaluated by Wyrick and colleagues.[37] Patients with a nondiagnostic ECG, cardiac sounding chest discomfort and a normal MCE had a very low 24-hour event rate (0.6%). Using MCE would have negated the admission of 45% of those patients admitted, with an average cost savings of $900 per patient.

## ASSESSMENT OF THE NEED FOR URGENT CORONARY ANGIOGRAPHY

Coronary angiography is still generally regarded as the gold standard test for diagnosing obstructive epicardial CAD. Patients with a nondiagnostic ECG and a high pretest probability of CAD often proceed directly to angiography and possible percutaneous coronary intervention. This technique leads to prompt diagnosis; in most cases, however, it does not yield information about the functional significance of stenosis found. Functionality of lesions can be assessed in the catheterization suite with the use of pressure wires, but this is often time consuming and costly. Echocardiographic findings may assist in the decision regarding the need for urgent coronary angiography. Normal global and regional function could lead to a more conservative approach, with later stress imaging to rule out significant coronary stenosis. Conversely, the finding of a new wall motion abnormality may prompt more urgent coronary angiography.

MCE for perfusion assessment may also be beneficial in determining the need for and timing of coronary angiography. Angiographic flow does not necessitate the presence of tissue perfusion. Several studies have evaluated the use of contrast echocardiography to assess microvascular reperfusion after acute myocardial infarction. Greaves and co-workers[38] performed contrast echocardiography in 15 patients post primary percutaneous coronary intervention for acute myocardial infarction. Analysis showed that a perfused hypokinetic or akinetic segment was 50 times more likely to recover function than a nonperfused segment. MCE predicted segmental myocardial recovery with a sensitivity of 88%, a specificity of 74%, and positive and negative predictive values of 83% and 81%, respectively. MCE outperformed other known modalities such as TIMI frame rate, myocardial blush grade, and percentage of ST segment resolution.

Myocardial viability post acute myocardial infarction determined by MCE and SPECT imaging were compared in 99 patients. Only MCE-determined viability was found to be an independent multivariate predictor of morbidity and mortality.[39]

## RISK STRATIFICATION AND ANALYSIS OF LONG-TERM CLINICAL OUTCOME

A number of studies have demonstrated incremental utility of echocardiography, beyond clinical assessment and electrocardiography in predicting clinical outcome of patients with acute chest pain.[40,41] In a prospective study of patients visiting a large urban emergency department, Fleischmann and colleagues[40] identified echocardiographic predictors of serious predischarge complications (significant recurrent myocardial ischemia, heart failure, and arrhythmia) in patients with chest pain. Doppler echocardiograms performed an average of 21 hours after presentation assessed biventricular, regional, and valvular function. In univariate analysis, LV function (OR 2.9), right ventricular (RV) function (OR 2.7), LV end-diastolic dimension (OR 1.6), LV end-systolic dimension (OR 1.4), and wall motion index (OR 3.0) predicted complications. Wall motion index was an independent predictor of complications beyond clinical and electrocardiographic variables.

The long-term survival of 448 patients in this study was examined.[13] Over a follow-up period of 35 ± 12 months, independent predictors of survival were moderate or severe LV dysfunction and more than mild valvular regurgitation. These echocardiographic findings offered incremental prognostic value over clinical and ECG findings in patients presenting with acute chest pain. Kaplan-Meier survival curves stratified by LV function and the grade of mitral regurgitation in this study are shown in Figures 13-6 and 13-7, respectively.

DSE has been shown to predict subsequent cardiac events in patients with known or suspected CAD.[42] A cohort of 860 patients was assessed using the 16-segment model for wall motion and followed for 52 months. The independent

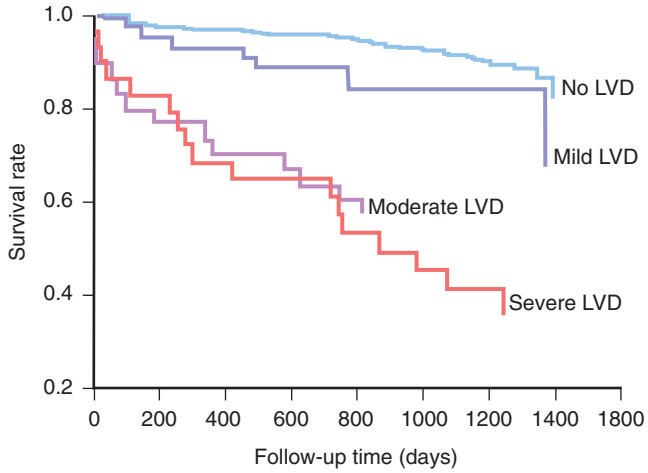



**Figure 13-6** Kaplan-Meier survival curves for patients presenting with chest pain stratified by LV dysfunction (*LVD*). *(From Fleischmann KE, Lee RT, Come PC, et al: Impact of valvular regurgitation and ventricular dysfunction on long term survival in patients with chest pain.* Am J Cardiol *80:1266-1272, 1997. From Excerpta Medica Inc.)*

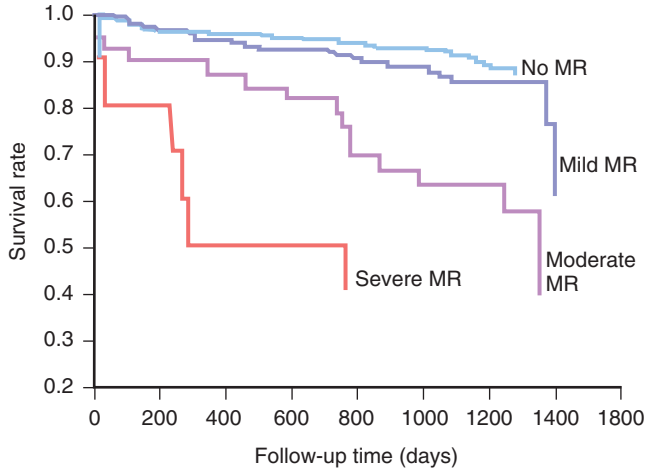



**Figure 13-7** Kaplan-Meier survival curves for patients presenting with chest pain stratified by grade of mitral regurgitation (*MR*) (on a 4+ scale). *(From Fleischmann KE, Lee RT, Come PC, et al: Impact of valvular regurgitation and ventricular dysfunction on long term survival in patients with chest pain.* Am J Cardiol *80:1266-1272, 1997. From Excerpta Medica Inc.)*

predictors of cardiac events were history of congestive heart failure (hazard ratio 2.51), percentage of abnormal segments at peak stress (hazard ratio 1.23), and abnormal LV end-systolic volume response to stress (hazard ratio 1.98). The noninvasive diagnosis of CAD in women has been historically more difficult than in men. DSE may be the diagnostic test of choice in this patient population given its higher specificity.[43]

The use of exercise over pharmacologic stress has the advantage of accurately assessing functional capacity, an important prognostic indicator. Exercise echocardiography has been compared to DSE for the detection of CAD. A study by Dagianti and co-workers[44] compared dipyridamole echocardiography and dobutamine echocardiography with exercise echocardiography for the detection of CAD in 100 patients. Diagnostic accuracy was equal for exercise and dobutamine echocardiography at 87%, which was higher than that for dipyridamole (78%).

### EVALUATION OF OTHER CAUSES OF CHEST PAIN

Although the assessment of global and regional ventricular function is the core of the echocardiogram for the patient presenting with chest pain, it is essential to also provide a rapid screen for other nonischemic causes of chest pain.

Aortic dissection is a life-threatening diagnosis that may be detected on TTE, although sensitivity is limited (see Chapter 36). An intimal flap may be identified in the aortic root, proximal ascending aorta, arch, or descending abdominal aorta. It is important to note that the sensitivity of TTE imaging for aortic dissection is only 79%, compared to 99% for transesophageal echocardiograms.[45] Therefore, a negative TTE is not sufficient to exclude the diagnosis if clinical suspicion exists. Other potential clues to aortic dissection would include aortic regurgitation, a dilated proximal aorta, and the presence of a pericardial effusion.

Pericardial effusion can be diagnosed on TTE. The subcostal window is especially useful in patients with limited apical and parasternal image quality (Fig. 13-8). The potential hemodynamic consequences of a pericardial effusion may be evaluated by scanning for signs of right atrial collapse, RV collapse, exaggerated respiratory variation in tricuspid and/or mitral valve inflow velocities, and inferior vena cava size and respiratory variation. (See Chapter 29.) The use of echocardiographic guidance for pericardiocentesis has been shown to enhance the safety of the procedure.[46]

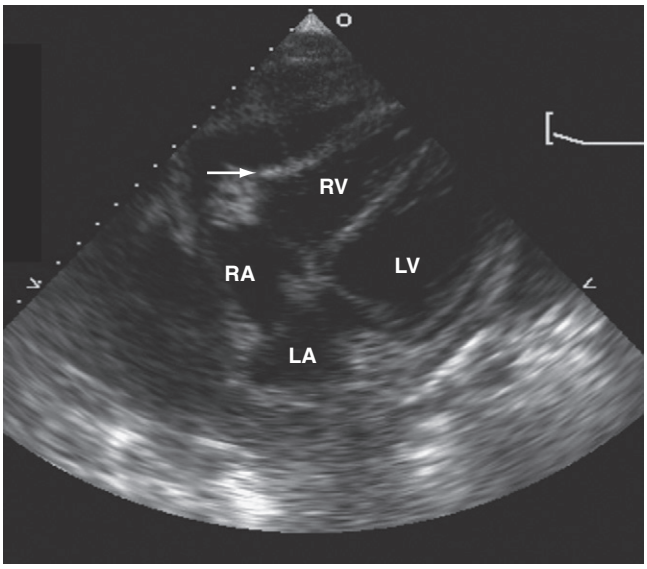



**Figure 13-8 Transthoracic images of a patient presenting to the emergency department with atypical chest pain.** This subcostal view shows a small pericardial effusion (*arrow*). The patient was diagnosed with pericarditis.

Screening for aortic stenosis involves 2D imaging for calcification and restricted movement of the valve, as well as Doppler measurement of transvalvular gradients (see Chapter 23). Similarly, signs of hypertrophic obstructive cardiomyopathy include hypertrophy (asymmetric), the presence of systolic anterior motion of the anterior mitral valve leaflet, and Doppler evidence of a dynamic gradient in the LV outflow tract (see Chapter 27).

## Limitations

### ISCHEMIA EVALUATION

Echocardiographic evaluation of patients with suspected acute coronary syndrome has several limitations. Between episodes of cardiac ischemia, the wall thickening may be completely normal, so normal LV systolic function in a pain-free patient cannot rule out cardiac ischemia as the cause of the patient's symptoms. In addition, small areas of ischemic myocardium, particularly in the subendocardium, may not result in a discernible wall motion abnormality, leading to false negatives. Using MCE to evaluate perfusion provides better risk stratification in these patients. Additional testing as appropriate to the patient's risk should be considered after infarction is ruled out.

The presence of preexisting LV dysfunction makes the evaluation of new regional wall motion abnormalities more difficult and may decrease the specificity of this technique.

### IMAGE QUALITY

Detection of regional wall motion abnormalities requires adequate visualization of endocardial borders, which may be difficult in patients with morbid obesity, chest wall deformity, chest trauma, or recent thoracic surgery. The use of second harmonic imaging with echocardiographic contrast administration may improve endocardial border delineation in such patients and make echocardiographic evaluation in the emergency department more feasible.

### PERSONNEL AVAILABILITY

Ready availability of skilled sonographers and echocardiographers is essential to expanding the use of echocardiography in the evaluation of patients with chest pain in the emergency department. Both sonographers and echocardiographers are generally available during usual working hours in most hospitals. However, it may not be economically practical to have personnel on site 24 hours a day for many medical centers. Contacting "on-call" sonographers and echocardiographers outside the hospital is inevitably associated with delays in the management of such patients. The national shortage of sonographers complicates the situation further.[45]

Digital tele-echocardiography systems, which allow transmission of digital images over a high-speed network to an experienced echocardiographer outside the hospital for immediate evaluation, may aid in ensuring adequate image interpretation.

**TABLE 13-2 A Sampling of Clinical Studies for Use of Echocardiography in the Assessment of Chest Pain**

| *Year* | *Study* | *Sample Size* | *Population* | *Result* |
|---|---|---|---|---|
| 1984 | Nishimura[a] | 61 | Patients within 12 hours of an acute MI | Increased wall motion score index was predictive of in-hospital complications |
| 1990 | Peels[b] | 43 | Acute chest pain with non diagnostic ECG and no history of CAD | 88% sensitive<br>78% specific for diagnosis of ischemia when compared to angiography |
| 1991 | Sabia[c] | 171 | Patients presenting with cardiac symptoms | LV systolic dysfunction predicts both short- and long-term cardiac events |
| 1994 | Fleischmann[d] | 513 | Patients presenting with chest pain | Moderate LV systolic dysfunction and significant valvular regurgitation independently predict survival |
| 1997 | Trippi[e] | 163 | Patients presenting with chest pain, normal markers and nondiagnostic ECG | DSE has a negative predictive value of 98.5% for coronary artery ischemia |
| 2003 | Bholasingh[f] | 377 | Patient with chest pain and nondiagnostic ECG, negative markers | DSE was an independent predictor of cardiac events |
| 2005 | Kang[g] | 114 | Patients presenting with chest pain at rest | Myocardial perfusion defect on contrast echocardiography was associated with an odds ratio of 21 for the diagnosis of acute MI |
| 2005 | Tong[h] | 957 | Patients with chest pain and nondiagnostic ECG | Contrast echocardiography provides short- and long-term prognostic information before results of cardiac markers |
| 2005 | Rinkevich[i] | 1017 | Patients with chest pain, no ST elevation | Wall thickening and myocardial perfusion predicted cardiac events |
| 2010 | Wei[j] | 720 | Patients with chest pain and no ST elevation | Regional wall motion abnormality ± abnormal perfusion was an independent predictor of nonfatal MI and cardiac death |

References:

[a]Nishimura RA, Tajik AJ, Shub C, et al: Role of two-dimensional echocardiography in the prediction of in-hospital complications after acute myocardial infarction. *J Am Coll Cardiol* 4:1080-1087, 1984.

[b]Peels CH, Visser CA, Kupper AJ, et al: Usefulness of two-dimensional echocardiography for immediate detection of myocardial ischemia in the emergency room. *Am J Cardiol* 65:687-691, 1990.

[c]Sabia P, Abbott RD, Afrookteh A, et al: Importance of two-dimensional echocardiographic assessment of left ventricular systolic function in patients presenting to the emergency room with cardiac-related symptoms. *Circulation* 84:1615-1624, 1991.

[d]Fleischmann KE, Goldman L, Robiolio PA, et al: Echocardiographic correlates of survival in patients with chest pain. *J Am Coll Cardiol* 23:1390-1396, 1991.

[e]Trippi JA, Lee KS, Kopp G, et al: Dobutamine stress tele-echocardiography for evaluation of emergency department patients with chest pain. *J Am Coll Cardiol* 30:627-632, 1997.

[f]Bholasingh R, Cornel JH, Kamp O, et al: Prognostic value of predischarge dobutamine stress echocardiography in chest pain patients with a negative cardiac troponin T. *J Am Coll Cardiol* 41:596-602, 2003.

[g]Kang D, Kang S, Song J, et al: Efficacy of myocardial contrast echocardiography in the diagnosis and risk stratification of acute coronary syndrome. *Am J Cardiol* 96:1498-1502, 2005.

[h]Tong KL, Kaul S, Wang XQ, et al: Myocardial contrast echocardiography versus thrombolysis in myocardial infarction score in patients presenting to the emergency department with chest pain and a nondiagnostic electrocardiogram. *J Am Coll Cardiol* 46:920-927, 2005.

[i]Rinkevich D, Kaul S, Wang XQ, et al., Regional left ventricular perfusion and function in patients presenting to the emergency department with chest pain and no ST-segment elevation. *Eur Heart J* 26:1606-1611, 2005.

[j]Wei K, Peters D, Belcik T, et al: A predictive model for patients presenting to the emergency department with chest pain and a non-diagnostic electrocardiogram. *J Am Soc Echocardiogr* 23:636-642, 2010.

*CAD*, Coronary artery disease; *ECG*, electrocardiogram; *MI*, myocardial infarction.

## Future Developments

### TELE-ECHOCARDIOGRAPHY

Electronic transmission of images has been used successfully in a variety of telemedicine projects (Table 13-2). Successful use in nonemergent settings has been reported in the difficult diagnostic cases, such as patients with congenital heart disease requiring special expertise.[47-49] Trippi and colleagues[15] (described previously) used DSE in the emergency department to determine which patients presenting with chest pain could be safely discharged. In this study, echocardiograms were digitized into a quad-screen systolic eight-frame cineloop format (resolution 320 by 240 pixels), then transmitted to the interpreting physician over the standard telephone line using a proprietary "lossless" format predating current DICOM standards.[50,51]

Technologic developments since that time, including higher memory capacity, faster microprocessors, and network connections via the Internet or dedicated lines, may result in more widespread use. Of course, transmission of patient-specific data also requires proper encryption and adequate safeguards to ensure patient privacy.

### STRAIN ANALYSIS FOR REGIONAL FUNCTION

Tissue-Doppler imaging[52-54] and speckle tracking have been shown to increase the sensitivity of regional function assessment (Fig. 13-9). Currently used for research purposes, these techniques have potential to aid in evaluation of regional wall motion once techniques are simplified for use on a routine clinical basis. (See Chapter 10.)

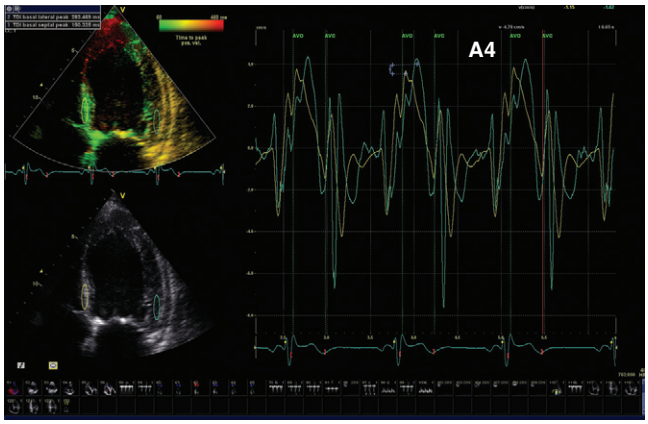



**Figure 13-9 Tissue-Doppler imaging of the LV in the apical four-chamber view in a patient with ischemia-induced LV dysfunction.** Areas of interest are highlighted at the basal septum and basal lateral wall. Results on the right represent the tissue velocities in the two areas of interest throughout the cardiac cycle.

## Summary

TTE can provide useful information in the diagnosis and triage of patients presenting with acute chest pain. Depending on the situation, stress echocardiography or transesophageal

echocardiography may provide additional information. The echocardiogram elicits information about global function, regional function, valvular function, and pericardial effusion. This not only helps in triage of patients with suspected acute coronary syndrome, but also can provide information on both short- and long-term outcomes. Newer techniques using echocardiographic contrast agents for LV opacification and myocardial perfusion have further enhanced the bedside echocardiographic assessment of patients with chest pain.

## KEY POINTS

- Acute chest pain results in millions of emergency department visits annually. Early diagnosis improves patient outcomes as well as reduces hospital costs.
- Echocardiography can help screen for the presence of myocardial ischemia with the assessment of wall motion. Wall motion abnormalities occur before the onset of symptoms or ECG changes in the ischemic cascade.
- The presence of aortic valve disease, LV or RV dysfunction, elevated pulmonary systolic pressure, or pericardial effusion could all be helpful in diagnosis of the patient with chest pain.
- Myocardial contrast agents are now commonly used not only for LV opacification and better endocardial definition, but also for perfusion assessment. MCE has a sensitivity of greater than 90% for the presence of acute myocardial infarction.
- Stress echocardiography is a safe and cost-effective way to assess for the presence of significant CAD.
- Treadmill stress echocardiograms require rapid acquisition of images after peak exercise to maintain sensitivity.
- Bicycle echocardiography can assess for evidence of inducible ischemia, as well as the effect of exercise on valvular disease, shunt or pulmonary artery pressure.
- Dobutamine echocardiograms have been used for the assessment of chest pain in patients with normal cardiac markers and normal ECG. The negative predictive valve has been shown to be greater than 98%.
- For patients at intermediate risk of CAD, stress echocardiography has been shown to be cost effective over routine treadmill testing or SPECT imaging.
- Echocardiograms performed early in the evaluation of patients with chest pain are prognostic for in-hospital complications as well as long-term prognosis.

## REFERENCES


1. Pitts SR, Niska RW, Xu J, Burt CW: National Hospital Ambulatory Medical Care Survey: 2006 Emergency Department Summary. *Natl Health Stat Report* 7:1-138, 2008.
2. Gibler WB, Young CP, Hedges JR, et al: Acute myocardial infarction in chest pain patients with non-diagnostic ECG's: serial CK-MB sampling in the emergency department. *Ann Emerg Med* 21:504-512, 1992.
3. Stussman BJ: National Hospital Ambulatory Medicine Care Survey: 1995 emergency department summary. *Adv Data* 285:1-18, 1997.
4. Alpert JS, Thygesen KA, Antman E, Bassand JP: Myocardial infarction redefined—a consensus document of The Joint European Society of Cardiology/American College of Cardiology Committee for the Redefinition of Myocardial Infarction. *J Am Coll Cardiol* 36:959-969, 2000.
5. Frankel WL, Herold DA, Ziegler TW, et al: Cardiac troponin T is elevated in asymptomatic patients with chronic renal failure. *Am J Clin Pathol* 106:118-123, 1996.
6. Tennant R, Wiggers CJ: The effect of coronary artery occlusion on myocardial contraction. *Am J Physiol* 112:351-361, 1935.
7. Hauser AM, Gangadharan V, Ramos RG, et al: Sequence of mechanical, electrocardiographic and clinical effects of repeated coronary artery occlusion in human beings: echocardiographic observations during coronary angioplasty. *J Am Coll Cardiol* 5:193-197, 1985.
8. Gould KL, Lipscomb K: Effects on coronary stenoses on coronary flow reserve and resistance. *Am J Cardiol* 34:48-55, 1974.
9. Lang RM, Bierig M, Devereux RB, et al: Recommendations for Chamber Quantification: A report from the American Society of Echocardiography's Guidelines and Standards Committee and the Chamber Quantification Writing Group, developed in conjunction with the European Association of Echocardiography, a branch of the European Society of Cardiology. *J Am Soc Echocardiogr* 18:1440-1463, 2005.
10. Horowitz RS, Morganroth J, Parrotto C, et al: Immediate diagnosis of acute myocardial infarction by two-dimensional echocardiography. *Circulation* 65:323-329, 1982.
11. Kurt M, Shaikh KA, Peterson L, et al: Impact of contrast echocardiography on evaluation of ventricular function and clinical management in a large prospective cohort. *J Am Coll Cardiol* 53:802-810, 2009.
12. Bholasingh R, Cornel JH, Kamp O, et al: Prognostic value of predischarge dobutamine stress echocardiography in chest pain patients with a negative cardiac troponin T. *J Am Coll Cardiol* 41:596-602, 2003.
13. Franke A, Hoffman R, Keuhl HP, et al: Non-contrast second harmonic imaging improves interobserver agreement and accuracy of dobutamine stress echocardiography in patients with impaired image quality. *Heart* 83:133-140, 2000.
14. Rainbird AJ, Mulvagh SL, Oh JK, et al: Contrast dobutamine stress echocardiography: clinical practice assessment in 300 consecutive patients. *J Am Soc Echocardiogr* 14:378-385, 2001.
15. Trippi JA, Lee KS: Dobutamine stress tele-echocardiography as a clinical service in the emergency department to evaluate patients with chest pain. *Echocardiography* 16:179-185, 1999.
16. Trippi JA, Lee KS, Kopp G, et al: Dobutamine stress tele-echocardiography for evaluation of emergency department patients with chest pain. *J Am Coll Cardiol* 30:627-632, 1997.
17. Shen WK, Khandheria BK, Edwards WD, et al: Value and limitations of two-dimensional echocardiography in predicting myocardial infarct size. *Am J Cardiol* 68:1143-1149, 1991.
18. Oh JK, Gibbons RJ, Christian TF, et al: Correlation of regional wall motion abnormalities detected by two-dimensional echocardiography with perfusion defect determined by technetium-99m sestamibi imaging in patients treated with reperfusion therapy during acute myocardial infarction. *Am Heart J* 131:32-37, 1996.
19. Fleischmann KE, Lee RT, Come PC, et al: Impact of valvular regurgitation and ventricular dysfunction on long term survival in patients with chest pain. *Am J Cardiol* 80:1266-1272, 1997.
20. Abraham TP, Dimaano VL, Liang HY: Role of tissue Doppler and strain echocardiography in current clinical practice. *Circulation* 116: 2597-2609, 2007.
21. Blessberger H, Binder T: Non-invasive imaging: two dimensional speckle tracking echocardiography: basic principles. *Heart* 96: 716-722, 2010.
22. Grenne B, Eek C, Sjøli B, et al: Changes of myocardial function in patients with non-ST-elevation acute coronary syndrome awaiting coronary angiography. *Am J Cardiol* 105:1212-1218, 2010.
23. Hickman M, Swinburn JM, Senior R: Wall thickening assessment with tissue harmonic echocardiography results in improved risk stratification for patients with non-ST-segment elevation acute chest pain. *Eur J Echocardiogr* 5:142-148, 2004.
24. Douglas PS, Khandheria B, Strainback RF, et al: ACCF/ASE/ACEP/ASNC/SCAI/SCCT/SCMR 2007 appropriateness criteria for transthoracic and transesophageal echocardiography. *J Am Coll Cardiol* 50:187-204, 2007.
25. Kang D, Kang S, Song J, et al: Efficacy of myocardial contrast echocardiography in the diagnosis and risk stratification of acute coronary syndrome. *Am J Cardiol* 96:1498-1502, 2005.

26. Tong KL, Kaul S, Wang XQ, et al: Myocardial contrast echocardiography versus Thrombolysis In Myocardial Infarction score in patients presenting to the emergency department with chest pain and a nondiagnostic electrocardiogram. *J Am Coll Cardiol* 46:920-927, 2005.
27. Kaul S, Senior R, Harrel FE, et al: Incremental value of cardiac imaging in patients presenting to the emergency department with chest pain and without ST-segment elevation: a multicenter study. *Am Heart J* 148:129-136, 2004.
28. Rinkevich D, Kaul S, Wang XQ, et al: Regional left ventricular perfusion and function in patients presenting to the emergency department with chest pain and no ST-segment elevation. *Eur Heart J* 26:1606-1611, 2005.
29. Wei K, Peters D, Belcik T, et al: A predictive model for patients presenting to the emergency department with chest pain and a nondiagnostic electrocardiogram. *J Am Soc Echocardiogr* 23:636-642, 2010.
30. Gibler WB, Runyon JP, Levy RC, et al: A rapid diagnostic and treatment center for patients with chest pain in the emergency department. *Ann Emerg Med* 25:1-8, 1995.
31. Lewis WR, Amsterdam EA, Turnipseed S, et al: Immediate exercise testing of low risk patients with known coronary artery disease presenting to the emergency department with chest pain. *J Am Coll Cardiol* 33:1843-1847, 1999.
32. Savonitto S, Ardissino D, Granger CB, et al: Prognostic value of the admission electrocardiogram in acute coronary syndromes. *JAMA* 281:707-713, 1999.
33. Dribben WH, Kirk MA, Trippi JA, Cordell WH. A pilot study to assess the safety of dobutamine stress echocardiography in the emergency department evaluation of cocaine-associated chest pain. *Ann Emerg Med* 38:42-48, 2001.
34. Conti A, Paladini B, Magazzini S, et al: Chest pain unit management of patients at low and not low-risk for coronary artery disease in the emergency department. A 5-year experience in the Florence area. *Eur J Emerg Med* 9:31-36, 2002.
35. Conti A, Sammicheli L, Gallini C, et al: Assessment of patients with low-risk chest pain in the emergency department: head-to-head comparison of exercise stress echocardiography and exercise myocardial SPECT. *Am Heart J* 149:894-901, 2005.
36. Kuntz KM, Fleischmann KE, Hunink MG, et al: Cost-effectiveness of diagnostic strategies for patients with chest pain. *Ann Intern Med* 130:709-718, 1999.
37. Wyrick J, Kalvaitis S, McConnell J, et al: Cost-efficiency of myocardial contrast echocardiography in patients presenting to the emergency department with chest pain of suspected cardiac origin and a non-diagnostic electrocardiogram. *Am J Cardiol* 102: 649-652, 2008.
38. Greaves K, Dixon SR, Fejka M, et al: Myocardial contrast echocardiography is superior to other known modalities for assessing myocardial reperfusion after acute myocardial infarction. *Heart* 89:139-144, 2003.
39. Dwivedi G, Janardhanan R, Hayat SA, et al: Comparison between myocardial contrast echocardiography and 99m-technetium sestamibi single photon emission computed tomography determined myocardial viability in predicting hard cardiac events following acute myocardial infarction. *Am J Cardiol* 104:1184-1188, 2009.
40. Fleischmann KE, Lee TH, Come PC, et al: Echocardiographic prediction of complications in patients with chest pain. *Am J Cardiol* 79:292-298, 1997.
41. Kontos MC, Arrowood JA, Paulsen WH, et al: Early echocardiography can predict cardiac events in emergency department patients with chest pain. *Ann Emerg Med* 31:550-557, 1998.
42. Chuah SC, Pellikka PA, Roger VL, et al: Role of dobutamine stress echocardiography in predicting outcome in 860 patients with known or suspected coronary artery disease. *Circulation* 97:1474-1480, 1998.
43. Geleijnse ML, Krenning BJ, Soliman OI, et al: Dobutamine stress echocardiography for the detection of coronary artery disease in women. *Am J Cardiol* 99:714 -717, 2007.
44. Dagianti A, Penco M, Agati L, et al: Stress echocardiography: comparison of exercise, dipyridamole, and dobutamine in detecting and predicting the extent of coronary artery disease. *J Am Coll Cardiol* 26:18-25, 1995.
45. Erbel R, Daniel W, Visser C, et al: Echocardiography in the diagnosis of aortic dissection. *Lancet* 333:457-461, 1989.
46. Callahan JA, Seward JB, Nishimura R, et al: Two-dimensional echocardiographically guided pericardiocentesis: experience in 117 consecutive patients. *Am J Cardiol* 55:476-479, 1985.
47. Fisher JB, Alboliras ET, Berdusis K, et al: Rapid identification of congenital heart disease by transmission of echocardiograms. *Am Heart J* 131:1225-1227, 1996.
48. Caldwell MA, Miles R, Barrington W: Long distance transmission of diagnostic cardiovascular information. *Biomed Sci Instrum* 32:1-6, 1996.
49. Scholz TD, Kienzle MG: Optimizing utilization of pediatric echocardiography and implications for telemedicine. *Am J Cardiol* 83:1645-1648, 1999.
50. Trippi JA, Kopp G, Lee KS, et al: The feasibility of dobutamine stress echocardiography in the emergency department with telemedicine interpretation. *J Am Soc Echocardiogr* 9:113-118, 1996.
51. Trippi JA, Lee KS, Kopp G, et al: Emergency echocardiography telemedicine: an efficient method to provide 24-hour consultative echocardiography. *J Am Coll Cardiol* 27:1748-1752, 1996.
52. Uematsu M, Miyatake K, Tanaka N, et al: Myocardial velocity gradient as a new indicator of regional left ventricular contraction: detection by a two-dimensional tissue Doppler imaging technique. *J Am Coll Cardiol* 26:217-223, 1995.
53. McDicken WN, Sutherland GR, Moran CM, et al: Colour Doppler velocity imaging of the myocardium. *Ultrasound Med Biol* 18:651-654, 1992.
54. Miyatake K, Yamagishi M, Tanaka N, et al: New method for evaluating left ventricular wall motion by color-coded tissue Doppler imaging: in vitro and in vivo studies. *J Am Coll Cardiol* 25:717-724, 1995.



# 14 Echocardiography in the Coronary Care Unit: Management of Acute Myocardial Infarction, Detection of Complications, and Prognostic Implications

IVOR L. GERBER, MD, MBCHB | ELYSE FOSTER, MD

**Applicable Modes of Echocardiography in the Coronary Care Unit**
**Echocardiography in the Diagnosis and Localization of Acute Myocardial Infarction**
Diagnostic Role of Echocardiography
Localization of Infarction
Right Ventricular Infarction
**Detecting Complications of Acute Myocardial Infarction**
Hemodynamic Classification of Myocardial Infarction Using Doppler Echocardiography
Postinfarction Pericarditis and Pericardial Effusion
Acute Mitral Regurgitation
Ventricular Septal Rupture
Rupture of the Ventricular Free Wall
Pseudoaneurysm
Infarct Expansion and True Aneurysm Formation
Left Ventricular Thrombus
**Risk Stratification after Myocardial Infarction**
Left Ventricular Systolic Function
Regional Wall Motion Score
Left Ventricular Diastolic Function
Left Atrial Volume
Left Ventricular Remodeling
Stress Echocardiography
Coronary Flow Reserve
Mitral Regurgitation
**Summary**

## Applicable Modes of Echocardiography in the Coronary Care Unit

Echocardiography is ideally suited for cardiac imaging in the coronary care unit, with major advantages compared to other imaging modalities including its portability, ease of use, relative low cost, and the wealth of anatomic, hemodynamic, and functional information able to be obtained rapidly at the bedside. Soon after its earliest introduction, the use of transthoracic echocardiography (TTE) was extended to routine use in the coronary care unit, where it provides rapid bedside assessment of all stages of ischemic heart disease, ranging from presentations with undifferentiated acute chest pain, confirmation of acute myocardial infarction (MI), acute MI mechanical complications and heart failure, and the management of chronic ischemic heart disease.[1]

In the patient presenting with chest pain who has a nondiagnostic electrocardiogram (ECG), identification of a segmental wall motion abnormality assists in the determination of definitive therapy. High-quality two-dimensional (2D) imaging obtained either during chest pain or shortly thereafter has a negative predictive value of approximately 95% for the identification of acute MI. In the patient with an established MI, early evaluation of left ventricular (LV) ejection fraction, regional wall motion, diastolic function, and mitral regurgitation greatly assists with management. When recurrent chest pain complicates reperfusion therapy, electrocardiographic changes may be nonspecific. In this situation, echocardiography helps differentiate between recurrent ischemia and pericarditis. The cause of hemodynamic instability in patients with MI, including pump failure and mechanical complications, often can be established by bedside TTE without invasive monitoring.

Despite advances in echocardiographic imaging, assessment of regional wall motion remains a challenge with interobserver variability. The use of left-sided contrast agents for LV opacification improves interobserver agreement and has been shown to be superior to routine evaluation for the detection of acute coronary syndromes.[2] Because perfusion abnormalities precede wall motion abnormalities in the ischemic cascade, myocardial contrast echocardiography has a higher sensitivity for the detection of coronary artery disease.[3] Myocardial contrast echocardiography also has a significant role in the evaluation of myocardial viability.[4] Quantitation with myocardial strain techniques is a further significant step forward to reduce interobserver variability in the assessment of regional wall motion abnormalities. Myocardial strain was initially based on tissue Doppler, with the main limitation of angle dependence, and has been largely replaced by the development of speckle-tracking techniques.[5-7]

Progressive improvements and miniaturization of handheld echocardiographic instruments have resulted in their increasing use as an adjunct to the physical examination. They are particularly useful for targeted evaluation of global and regional LV and right ventricular (RV) systolic function and for the detection of pericardial effusion. Several studies have shown the utility of these systems,[8-10] but they are not yet comparable to

full-service systems, and care should be exercised to ensure that clinicians using and reporting studies with these instruments are appropriately trained. (See Chapter 8.)

In patients with severe hemodynamic compromise, TTE may be limited by mechanical ventilation, recent cardiac surgery, and an inability to adequately position the patient. Whereas the use of contrast agents has reduced the need for alternative imaging modalities in this situation, transesophageal echocardiography (TEE) has proven to be efficacious, especially in ruling out complications related to cardiac rupture and for the assessment of global and regional ventricular function. With careful sedation and close monitoring, TEE can be performed safely early after acute MI.

Stress echocardiography has an important role in the postinfarction period for the assessment of myocardial viability and inducible myocardial ischemia. (See Chapters 15 and 16.) Dobutamine stress echocardiography (DSE), using low doses that do not significantly alter hemodynamics, improves function in viable but not in nonviable myocardial segments. Higher doses of dobutamine and exercise echocardiography can be used to detect residual ischemia. DSE should be used with caution early after MI as a result of reports of free wall rupture in association with high-dose dobutamine stress testing within the first week following MI.[11] Cardiac magnetic resonance imaging (MRI) is increasingly used for the assessment of myocardial viability as well as ischemia and may provide improved image quality. However, MRI is not as readily available as TTE in most cardiac centers, is not portable, and is not suitable in certain patients, including patients with a pacemaker or implanted cardiac defibrillator, and those with certain arrhythmias.

Three-dimensional (3D) echocardiography has evolved from a research tool with limited clinical applicability to widespread clinical use. (See Chapter 4.) Recent reports have demonstrated the clinical feasibility of volumetric analysis of real-time 3D echocardiographic data that allows fast, semiautomated, dynamic measurement of LV volume and ejection fraction; automated detection of regional wall motion abnormalities[12]; and real-time 3D echocardiographic perfusion imaging.[13] It is likely that real-time 3D echocardiography will continue to play a prominent role in the comprehensive assessment of patients with coronary artery disease.

## Echocardiography in the Diagnosis and Localization of Acute Myocardial Infarction

### DIAGNOSTIC ROLE OF ECHOCARDIOGRAPHY

The accuracy of an echocardiographic diagnosis of an MI is dependent on its ability to detect wall motion abnormalities in the involved segment. The severity of the wall motion abnormality depends on the transmural extent of the infarction, and the circumferential limits depend on the arterial distribution and collateral blood supply. Images of the left ventricle (LV) adequate for segmental analysis of wall motion can be obtained in more than 90% of patients by skilled sonographers, and the use of left-sided contrast agents has increased the percentage of patients in whom technically adequate images can be obtained.[14,15] The most widely used scoring system for grading the severity of a wall motion abnormality is that recommended by the American Society of Echocardiography,[16] as shown in Table 14-1. Several studies have examined the specificity of echocardiographic wall motion abnormalities for diagnosis of acute coronary syndromes, showing a higher specificity for infarction than for ischemia. Other causes of segmental dysfunction must be recognized, and a false-positive diagnosis can often be avoided if wall thickening is examined in addition to endocardial motion. The inward motion of the endocardial surface may be delayed or paradoxical owing to abnormal conduction in the presence of Wolff-Parkinson-White syndrome,[17] a left bundle branch block,[18] or RV pacing.[19] Paradoxical septal motion also is present in RV volume overload and following open-heart surgery.[20] In these conditions, the systolic thickening of the septum or other involved segment (e.g., posterolateral wall in Wolff-Parkinson-White syndrome) should be preserved. Nonischemic causes of segmental dysfunction that result in reduced systolic thickening and endocardial motion include focal myocarditis, idiopathic cardiomyopathy, and the apical ballooning syndrome (takotsubo cardiomyopathy).[21] TTE is valuable in the diagnosis of takotsubo cardiomyopathy, with characteristic acute features of LV impairment in a noncoronary distribution and early improvement of LV function on serial echo consistent with myocardial stunning rather than MI.[22] Tong and colleagues[23] reported on the diagnostic and prognostic value of myocardial contrast echocardiography in 957 patients presenting to the emergency department with suspected cardiac chest pain and a nondiagnostic ECG. Only 2 of 523 patients with normal regional function had an early primary event, and regional function provided incremental prognostic value for predicting intermediate and late events. In patients with abnormal regional function, myocardial perfusion further classified patients into intermediate- and high-risk groups. The authors suggested that patients with both abnormal regional function and abnormal myocardial perfusion are at high risk for early cardiac events and could be triaged even before cardiac serum markers become available. Although this is a promising technology, expertise in the acquisition and interpretation of the images may not be widely available, and the cost effectiveness requires further study. Newer techniques for the evaluation of regional wall motion, including myocardial strain rate imaging and tissue characterization, are discussed in more detail in Chapter 10.

**TABLE 14-1 Scoring System for Grading Wall Motion[16]**

| *Score* | *Wall Motion* | *Endocardial Motion** | *Wall Thickening** |
|---|---|---|---|
| 1 | Normal | Normal | Normal (>30%) |
| 2 | Hypokinesis | Reduced | Reduced (<30%) |
| 3 | Akinesis | Absent | Absent |
| 4 | Dyskinesis | Outward | Thinning |
| 5 | Aneurysmal | Diastolic deformity | Absent or thinning |

*In systole.

### LOCALIZATION OF INFARCTION

The classification of acute MI according to electrocardiographic patterns has been based largely on comparing autopsy findings with the distribution of pathologic Q waves during the chronic phase of infarction. Echocardiographic localization has significant advantages over electrocardiographic localization, particularly for apical and lateral wall infarction.

In 1989, the American Society of Echocardiography recommended a 16-segment model for LV segmentation.[16] More recently, in an attempt to establish segmentation standards applicable to all types of imaging, including echocardiography,

nuclear perfusion imaging, cardiovascular MRI, and cardiac computed tomography (CT), a 17-segment model has been proposed.[24] This new model includes the apical cap, which is the segment beyond the end of the LV cavity, and is generally only seen with some contrast and myocardial perfusion studies. With routine echocardiographic studies, the 16-segment model can be used, without the apical cap. The LV segments and the approximate and most common coronary arterial distribution in relation to these segments are depicted in Figures 14-1 and 14-2, respectively. The anterior, anterolateral, anteroseptal, and

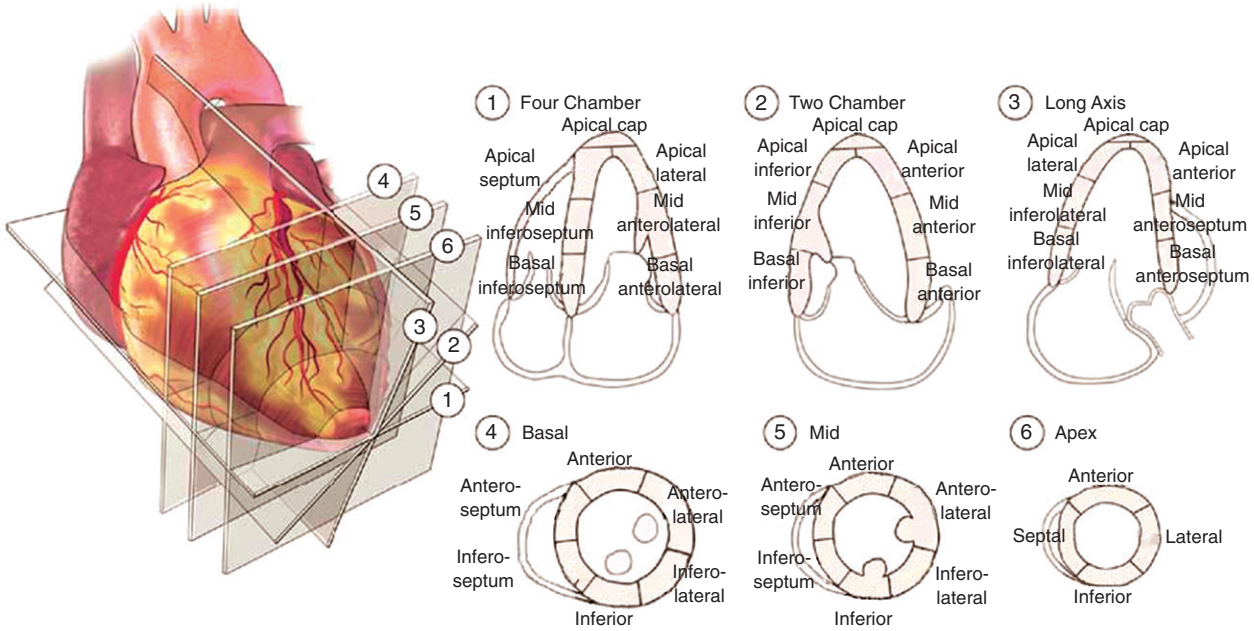



**Figure 14-1** Segmental analysis of LV walls, based on schematic views, in parasternal and apical views. *(From Lang RM, Bierig M, Devereux RB, et al: Chamber Quantification Writing Group; American Society of Echocardiography's Guidelines and Standards Committee; European Association of Echocardiography. Recommendations for chamber quantification: a report from the American Society of Echocardiography's Guidelines and Standards Committee and the Chamber Quantification Writing Group, developed in conjunction with the European Association of Echocardiography, a branch of the European Society of Cardiology.* J Am Soc Echocardiogr *18[12]:1440-1463, 2005.)*

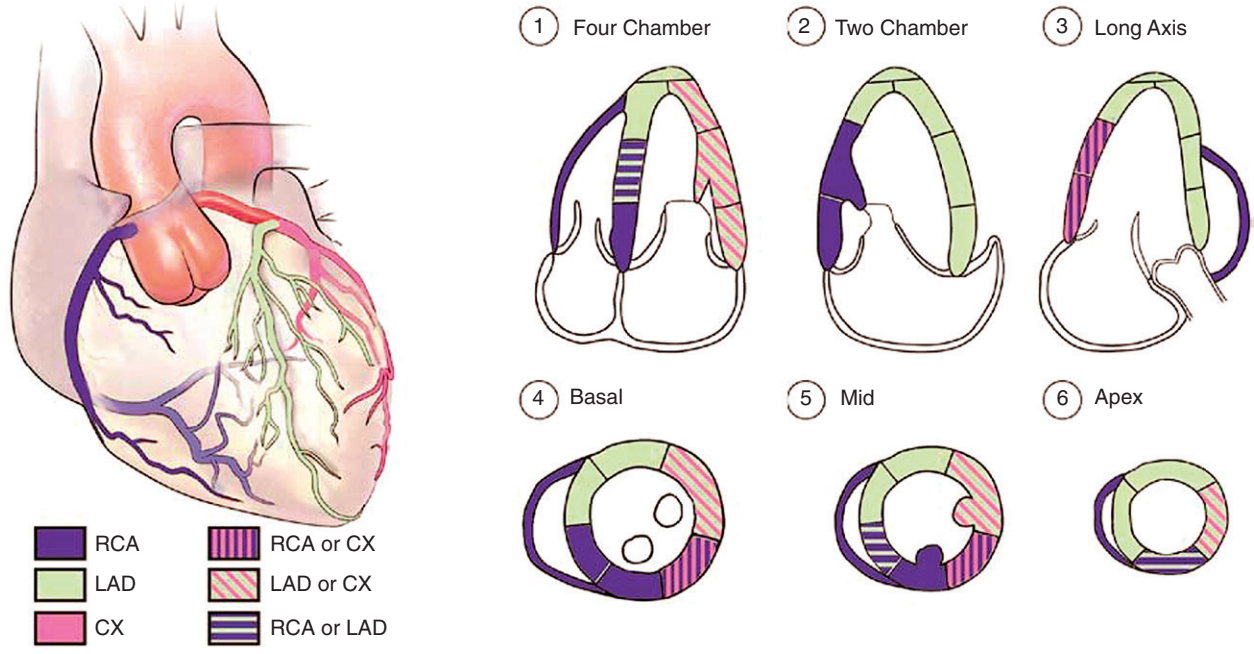



**Figure 14-2 Typical coronary artery distribution of blood flow shown in the apical and parasternal short-axis views.** *CX*, Circumflex; *LAD*, left anterior descending; *RCA*, right coronary artery. *(From Lang RM, Bierig M, Devereux RB, et al: Chamber Quantification Writing Group; American Society of Echocardiography's Guidelines and Standards Committee; European Association of Echocardiography. Recommendations for chamber quantification: a report from the American Society of Echocardiography's Guidelines and Standards Committee and the Chamber Quantification Writing Group, developed in conjunction with the European Association of Echocardiography, a branch of the European Society of Cardiology.* J Am Soc Echocardiogr *18[12]:1440-1463, 2005.)*

apical (anterior and septal) segments correspond to the left anterior descending (LAD) artery distribution. Isolated disease in a diagonal branch of the LAD artery results in a discrete wall motion abnormality in the portion of the anterolateral wall supplied by that vessel. The lateral wall and lateral apex are in the distribution of the left circumflex artery. The inferolateral wall is supplied by the posterior descending artery. In 80% of the population, the posterior descending artery arises from the right coronary artery and supplies the inferolateral wall and the inferior free wall and inferior septum (right dominant). In the other 20% of patients, the posterior descending artery arises from the circumflex artery (left dominant system). The right ventricle (RV) is supplied by the right coronary artery via its acute marginal branches. In general, infarctions in the LAD distribution tend to be more apically situated, whereas those in the right coronary artery and the circumflex distribution are more basal in their location. The extent of apical involvement and its distribution depends, to a degree, on the relative supply from the left anterior and posterior descending arteries. It should be noted that the extent of the segmental wall motion is related to the exact coronary anatomy in an individual patient, which may be variable. In addition, the presence of collaterals and previous bypass surgery alters the distribution of ischemia and infarction relative to the involved arterial supply.

Direct visualization of the ostia of the left main coronary artery and right coronary artery and the proximal LAD artery in adults may be achieved using TTE and TEE, and this may be useful to exclude anomalous coronary artery origins. (See Chapter 17.) Transthoracic Doppler echocardiography may also be useful to determine coronary artery flow. Otsuka and colleagues[25] recently showed that the detection of reverse flow in the distal right coronary artery and the inferior septal branches using transthoracic Doppler echocardiography detected an occluded right coronary artery with a sensitivity and specificity of 100% and 98%, respectively. Lee and colleagues[26] showed in a study of 46 consecutive patients with first acute anterior MI that diastolic peak distal LAD artery flow velocity equal to 25 cm/s by transthoracic Doppler echocardiography could distinguish TIMI 3 flow in the LAD coronary artery from TIMI 2 flow with a sensitivity, specificity, and accuracy of 77%, 94%, and 89%, respectively. The use of contrast agents may expand the feasibility of this technology to localize a coronary artery stenosis and quantify coronary flow.

## RIGHT VENTRICULAR INFARCTION

Although RV infarction was first described in the 1930s, it was only after the hemodynamic consequences were recognized in the 1970s that RV infarction was considered a clinical entity.

RV infarction occurs in up to 50% of inferior MI, but hemodynamic compromise develops in fewer than half of such cases.[27] The RV is predominantly supplied by acute marginal branches of the right coronary artery, and occlusion of the right coronary artery proximal to the origin of these branches results in ischemic dysfunction of the RV. When the occlusion is distal to the right atrial (RA) branches, augmented RA contractility enhances RV function and cardiac output. Conversely, more proximal occlusions result in ischemic depression of RA contractility, which impairs RV filling and function, resulting in more severe hemodynamic compromise. Much less commonly, RV infarction occurs in association with acute anteroseptal MI as a result of a variation of coronary artery anatomy in which RV branches arise from the LAD artery.[28] In addition, the anterior apex of the RV may be supplied by the LAD "wrapping" around the apex of the heart. Isolated RV infarction has been reported to occur in fewer than 3% of autopsy studies of acute MI.[28]

**Box 14-1**

### ECHOCARDIOGRAPHIC SIGNS OF RIGHT VENTRICULAR INFARCTION

**Primary**
RV dilation
Segmental wall motion abnormality of the RV free wall
Decreased descent of the RV base
Tricuspid valve annulus peak systolic velocity <12 cm/s

**Secondary**
Paradoxic septal motion
Tricuspid regurgitation
Tricuspid papillary muscle rupture
Pulmonary regurgitant jet pressure half-time <150 ms
Dilated inferior vena cava
Right-to-left interatrial septal bowing
Right-to-left shunting across patent foramen ovale

The diagnosis of RV infarction should be suspected in a patient with jugular venous distention and clear lung fields in the setting of an inferior MI. The clinical importance of RV infarction is emphasized by the much higher incidence of hemodynamic compromise, arrhythmias, and in-hospital mortality than MI involving only the LV.[29] The electrocardiographic sign of 1-mm ST segment elevation in $V_{4R}$ is sensitive and specific for the diagnosis, but these changes may resolve within 12 hours and do not provide information as to the extent of involvement or its hemodynamic impact.[30]

Echocardiography plays a vital role in the evaluation of patients with suspected RV infarction[31] (Box 14-1). In an early report, Sharpe and colleagues[32] described the M-mode echocardiographic findings of RV infarction including RV enlargement and paradoxical septal motion. The 2D echocardiographic signs of RV infarction include RV dilation, decreased RV function, segmental wall motion abnormalities, and paradoxical septal motion.[33] In many cases, the inferior wall motion abnormality may be relatively small with preserved overall LV function. Tissue Doppler echocardiography may provide complementary evidence for RV infarction. In a study of 60 patients with a first acute inferior MI, a tricuspid valve annulus peak systolic velocity less than 12 cm/s had a sensitivity, specificity, and negative predictive value of 81%, 82%, and 92%, respectively, for RV infarction.[34] Tricuspid annular plane systolic excursion of 14 mm or less is a useful objective measure of RV dysfunction and should be measured in patients with suspected RV infarction. Reduced RV compliance may be detected by an increased A wave velocity on the hepatic vein flow signal and by a short pressure half-time of the pulmonary regurgitant jet (less than 150 ms). The latter has been shown to be a predictor of in-hospital events in patients with RV infarction.[35] Characteristic echocardiographic features of RV failure with high RA pressures include bowing of the interatrial septum into the left atrium (LA) and dilation of the inferior vena cava with lack of inspiratory collapse. These echocardiographic indicators of RV function correlate with clinical status and prognosis.[36]

Echocardiography also plays a crucial role in detecting complications of RV infarction, including ventricular septal rupture,

severe tricuspid regurgitation (as a result of papillary muscle ischemic dysfunction or rupture) and functional regurgitation resulting from tricuspid valve annular dilatation. In addition, severe hypoxemia resulting from right-to-left shunting across a patent foramen ovale may occur with large RV infarction associated with elevated RA pressures.

In most cases of RV infarction, RV function improves and returns to near normal within 3 to 12 months regardless of the patency of the infarct-related artery, although the improvement may not be complete when compared to a control group.[37] Experimental evidence suggests that this unique feature of RV functional recovery is a result of the beneficial effects of collaterals and the more favorable oxygen supply-demand characteristics compared to the LV.[37] Because the acutely ischemic dysfunctional RV represents predominantly viable myocardium, which may spontaneously recover or respond favorably to successful reperfusion even late after the onset of occlusion, it has been suggested that the term *RV infarction* is largely a misnomer and that the term *RV ischemic dysfunction* should be used.[38] However, it is important to recognize that RV infarction is associated with high in-hospital mortality, and early pharmacologic[39] or mechanical[33] reperfusion enhances recovery of RV function with an improved clinical course and survival. Although relatively uncommon, cardiogenic shock due to RV infarction has similar poor outcomes to patients with cardiogenic shock due to LV infarction.[40]

## Detecting Complications of Acute Myocardial Infarction

The prognosis of MI markedly improved with the advent of thrombolysis and primary percutaneous coronary intervention (PCI), and survival is excellent for most patients who receive timely restoration of flow of the culprit vessel. A large MI, typically due to prolonged occlusion of the LAD resulting in a large territory of severely hypokinetic myocardium, may be complicated early and late by pump failure. In the acutely hemodynamically unstable patient, it is critical to exclude cardiac rupture, a situation that is potentially amenable to surgery, before concluding that cardiogenic shock is on the basis of pump failure (Box 14-2). In most cases, TTE (supplemented when necessary by TEE) is sufficient to exclude papillary muscle, free wall, and ventricular septal rupture. Most of the earlier published studies on the incidence of mechanical complications of acute MI were performed in the prethrombolytic era, when TTE was in its relative infancy with respect to image quality and expertise in reporting. Table 14-2 compares the incidence of mechanical complications after acute MI before and in the reperfusion era.

### HEMODYNAMIC CLASSIFICATION OF MYOCARDIAL INFARCTION USING DOPPLER ECHOCARDIOGRAPHY

In 1967, Killip and coworkers[41] classified patients with acute MI into four groups depending on the clinical manifestations of cardiac failure on admission. In 1977, Forrester et al[42] classified patients with acute MI using right heart catheterization into four groups based on cardiac index and pulmonary capillary wedge pressure (PCWP). Both classifications predicted in-hospital mortality independently of the patient's age, gender, precipitating factors, and location of the MI. Although invasive measurement of PCWP and cardiac output may be performed in patients with acute MI complicated by cardiac failure or cardiogenic shock, recent data suggest that the use of invasive catheters in critically ill patients may be associated with increased mortality.[43]

A carefully performed Doppler echocardiographic study can provide sufficient information to determine a patient's hemodynamic category after infarction. The noninvasive measurement of cardiac output and PCWP in patients with acute MI and cardiac failure is useful to guide therapy and for prognosis.

A simple echocardiographic method of estimating cardiac output is to measure the velocity-time integral of aortic flow by pulsed-wave or continuous-wave Doppler. In patients with acute MI, various measures of LV diastolic function have been shown to accurately estimate PCWP when compared to invasive measurements. Earlier studies demonstrated the value of transmitral Doppler to estimate PCWP. In a study of postinfarction patients with LV ejection fraction less than 35%, a mitral deceleration time of less than 120 ms was highly predictive of a PCWP greater than 20 mm Hg.[44]

Subsequent studies showed the value of pulmonary venous flow Doppler to estimate PCWP. In subjects older than 40 years of age with normal filling pressures, pulmonary venous peak velocities and velocity-time integrals are higher during systole

**Box 14-2**

### ECHOCARDIOGRAPHY IN COMPLICATIONS OF MYOCARDIAL INFARCTION

**Hemodynamic States**
Hypovolemia
RV infarction
Globally reduced LV contractility

**Mechanical Complications**
Papillary muscle rupture and severe mitral regurgitation
Ventricular septal rupture
Free wall rupture and tamponade

**Other**
LV aneurysm
Mural thrombus
Pericardial effusion

**TABLE 14-2 Comparison of the Incidence of Mechanical Complications after Acute Myocardial Infarction before and in the Reperfusion Era**

| *MI Complication* | *Before Reperfusion Era (Average)* | *In Reperfusion Era* |
|---|---|---|
| Pericardial effusion | 25% | 6.6% |
| LV thrombus (anterior MI) | 35-40% | 5.5% |
| Mitral regurgitation | 53% | 28% |
| Infarct expansion | 30% | 4% |
| Septal rupture | 1-3% | 0.6% |
| Free wall rupture | 2% | 0.8% |

Adapted from Guereta P, Khalifeb K, Jobicc Y, et al: Echocardiographic assessment of the incidence of mechanical complications during the early phase of myocardial infarction in the reperfusion era: a French multicenter prospective registry. *Arch Cardiovasc Dis* 101:41-47, 2008.
*MI*, Myocardial infarction.

than during diastole, and the duration of the pulmonary venous A wave is less than that of the mitral A wave. With high filling pressures, diastolic filling predominates and the A wave duration exceeds that of the mitral A wave. In patients with acute MI, a systolic fraction of pulmonary venous flow less than 45% was highly associated with a PCWP greater than 18 mm Hg.[45] In a study comparing pulmonary venous flow Doppler to transmitral Doppler to estimate PCWP in patients with acute MI, the deceleration time of the diastolic component of pulmonary venous flow had a better correlation with PCWP than the mitral deceleration time. The sensitivity and specificity of a diastolic component pulmonary venous deceleration time less than 160 ms in predicting a PCWP greater than or equal to 18 mm Hg were 97% and 96%, respectively, compared with 86% and 59%, respectively, for a mitral deceleration time of less than 130 ms.[45]

Several newer parameters of LV diastolic function have been studied in postinfarction patients. Tissue Doppler imaging measuring mitral annular velocities is a well-validated method for estimating PCWP.[46] The Tei index, defined as the sum of isovolumic contraction and relaxation times divided by ejection time, expresses global LV function. In patients with acute MI, the Tei index has been shown to correlate significantly with the PCWP and the cardiac index. A Tei index of 0.60 or greater diagnosed impaired hemodynamics (PCWP of at least 18 mm Hg and/or cardiac index of 2.2 L/min/$m^2$ or less) with a sensitivity, specificity, and accuracy of 86%, 82%, and 83%, respectively.[47] In addition, a Tei index of 0.55 or greater can distinguish pseudonormal/restrictive mitral flow from normal mitral flow with a sensitivity, specificity, and accuracy of 84%, 100%, and 88%, respectively.[48]

Elevated pulmonary artery systolic pressure is associated with increased mortality in acute MI.[49] Doppler echocardiographic measurement of pulmonary artery systolic pressure using tricuspid regurgitant jets has been well validated, and the size and respiratory dynamics of the inferior vena cava can be used to estimate RA pressure.

Combining these parameters with measurements (quantitative or qualitative) of LV and RV function, color flow Doppler interrogation for mitral regurgitation, and assessment of mechanical complications results in a comprehensive evaluation of the hemodynamic state after infarction. When the data from a transthoracic examination are incomplete, one should not hesitate to employ TEE given its established safety even in the critically ill patient. Of course, the hemodynamic information available from an echocardiographic examination is available only at a single point in time, and continued invasive monitoring may be necessary in patients with ongoing instability.

## POSTINFARCTION PERICARDITIS AND PERICARDIAL EFFUSION

Postinfarction pericarditis occurs within the first 4 days following an ST segment elevation MI treated with early thrombolysis or primary PCI.[50,51] The reported frequency of postinfarction pericarditis is variable depending on the definition used, with most studies basing the diagnosis on the presence of one or more of the following: pericardial chest pain, pericardial friction rub, and/or typical ECG changes. Regardless of the definition used, the incidence of postinfarction pericarditis has markedly decreased from up to 25% in the prethrombolytic era to approximately 5% in large studies of patients treated with thrombolytics and/or primary PCI, with a prevalence related to the timing of restoring patency of the culprit vessel.[52] Colchicine may be used for the treatment of pericarditis in this setting, and early postinfarction pericarditis is usually self-limiting after a few days. Late cardiac tamponade and constrictive pericarditis are not recognized complications. Onset after 10 days is usually considered Dressler syndrome, which also has a much lower incidence in the modern era of early reperfusion, of 0.5% with thrombolysis and 0.1% with primary PCI.

A pericardial effusion that occurs after an MI is not pathognomonic of pericarditis, and there is only a weak association between pericarditis and pericardial effusion in this setting. Several investigators have reported on the incidence of pericardial effusion following infarction, with an average incidence of approximately 25%.[53] In these studies, pericardial effusion was associated with larger infarctions as measured by wall motion scores or degree of creatine kinase elevation. The incidence of congestive heart failure and mortality is higher in those patients with effusions apparent on echocardiography. These earlier reports of a high incidence of pericardial effusion after an MI were mostly in the prethrombolytic era in the 1980s. In a contemporary large study of 908 patients from 25 French hospitals,[54] a pericardial effusion was noted in 6.6% of patients when assessed by ECG at admission and at discharge. In most cases the effusion was small and hemodynamically insignificant. Infarct-associated pericardial effusion usually occurs within the first 5 days but may occur at anytime during the first 3 weeks. The effusion is usually small, and circumferential effusions are rare. Spontaneous resolution of the effusion is usually slow, ranging up to 6 to 18 months. Moderate to large pericardial effusion (10 mm or more) after an MI is uncommon. Although most often associated with LV free wall rupture, it can also occur with heart failure or pericarditis. In the largest published study on moderate to large pericardial effusion after an MI, the overall 30-day mortality rate was 43% and was higher in those with cardiac tamponade and electromechanical dissociation (89%) than in those with cardiac tamponade and hypotension (22%) and those without initial tamponade (17%). Even in the absence of electromechanical dissociation or tamponade, mortality was twice that of patients with a moderate to large pericardial effusion.[55]

Although cardiac rupture is the most common cause of a moderate to large pericardial effusion early after acute MI, the differential diagnosis in the acute setting must include aortic dissection and perimyocarditis. In addition, iatrogenic pericardial effusion may occur after coronary stenting with vessel rupture, after implantation of a temporary pacemaker with perforation of the RV, after cardiac biopsy, and after a transseptal puncture for interventional procedures.

## ACUTE MITRAL REGURGITATION

Acute mitral valve incompetence in the setting of MI is usually a result of necrosis and rupture of papillary muscle tissue (Fig. 14-3). Incomplete coaptation of the mitral valve leaflets secondary to LV remodeling and distortion of ventricular architecture may also cause mitral regurgitation, and this is discussed in more detail later.

The clinical recognition of mitral regurgitation in the setting of MI may be confounded by several variables. Up to 50% of patients with hemodynamically significant mitral regurgitation do not have an audible murmur owing to rapid equalization of LV and LA pressures (especially in a low output state) or because

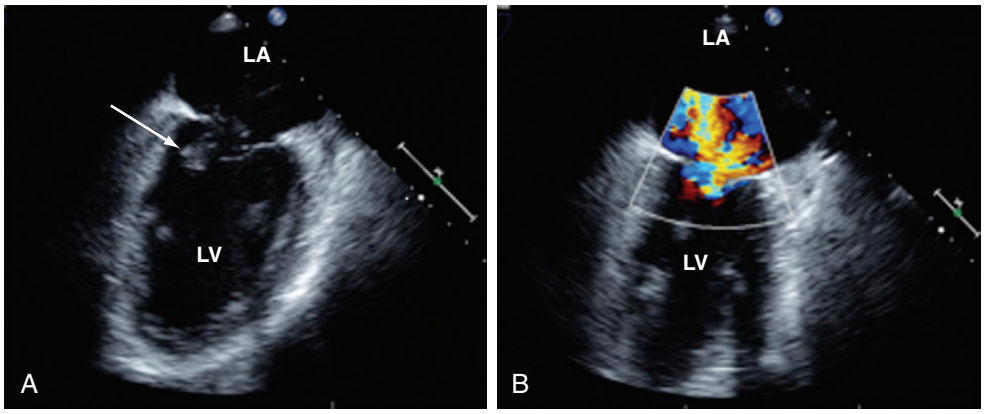



**Figure 14-3** TEE (65° view) showing (**A**) papillary muscle rupture (*arrow*) and (**B**) severe mitral regurgitation due to papillary muscle rupture.

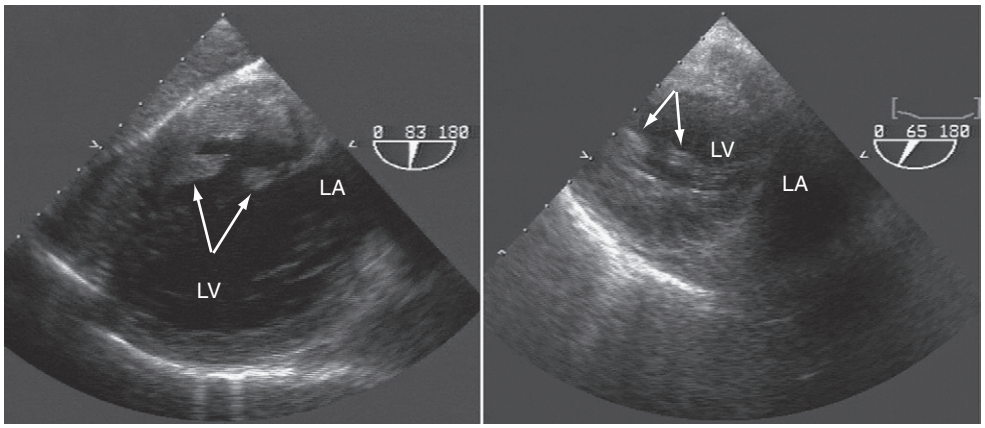



**Figure 14-4** TEE (transgastric views) of posteromedial papillary muscle rupture (*left*), which is more common as a result of its single blood supply, and anterolateral papillary muscle rupture (*right*), which is less common as a result of a dual blood supply.

the murmur is obscured by lung sounds in a patient with pulmonary edema or mechanical ventilation. In those patients with a new systolic murmur and evidence of cardiac failure, the main differential diagnosis is papillary muscle rupture and acute ventricular septal rupture. In this situation, TTE is highly accurate in establishing the cause, but TEE may be necessary to determine the precise anatomic defect.

Detection and grading of mitral regurgitation is accomplished with 2D, M-mode, color, and spectral Doppler techniques. 2D imaging may detect abnormalities in the mitral valve apparatus, including flail leaflets and/or ruptured papillary muscle. Even if not clearly visualized, papillary muscle rupture should be suspected when there is an eccentric jet of mitral regurgitation with a relatively normal-sized LA. Although color flow parameters are those most often used, accurate grading of mitral regurgitation severity should encompass other Doppler-echocardiographic signs as well.[56] In the patient with pulmonary edema, the unexpected findings of a small infarction, a hyperdynamic LV, or increased early mitral inflow velocity[57] should prompt a careful search for mitral regurgitation even when color flow Doppler mapping is unrevealing.

Papillary muscle necrosis with rupture and acute severe mitral regurgitation is a life-threatening complication of MI that almost always requires urgent surgical intervention. In a review of papillary muscle rupture, 15 of 17 cases occurred in patients with inferior infarction and rupture of the posteromedial papillary muscle.[58] The more frequent involvement of the posteromedial papillary muscle is due to its blood supply from a single coronary artery (posterior descending artery) compared to the dual coronary artery supply of the anterolateral papillary muscle (LAD and circumflex arteries) (Fig. 14-4). Chordae to both leaflets arise from each of the papillary muscles, so that in cases of "complete" rupture of the entire trunk of a papillary muscle, both leaflets are affected. In less severe cases, the rupture is "incomplete" and only a single head is torn. The 2D echocardiographic findings include prolapse of one or both leaflets, a flail leaflet, and liberation of a portion of the papillary muscle. In some patients, the ruptured muscle may remain tethered to the chordae, and chaotic motion is present. Spectral and color flow Doppler imaging of the jet is usually easily accomplished with surface imaging, but an eccentric path of flow may complicate its identification. TEE is superior in this regard.

When only a single head of the papillary muscle is affected (incomplete rupture), medical stabilization often is possible. When rupture is complete, involving the main trunk of the papillary muscle, the complication is uniformly fatal without immediate recognition and prompt surgical repair.

## VENTRICULAR SEPTAL RUPTURE

Ventricular septal defect owing to myocardial rupture had a reported incidence during the prethrombolytic era of 1% to 2% of all acute MIs and up to 5% of all fatal infarctions.[59] In the GUSTO-1 trial, the incidence of ventricular septal rupture was only 0.2% (84 of 41,021 enrolled patients), suggesting that

thrombolytic therapy reduced the incidence of rupture.[60] Primary PCI has also reduced the incidence of ventricular septal rupture to 0.2% to 0.5%. In the largest published series, of 408 patients with ventricular septal rupture complicating acute MI between 1990 and 2007, the rate of rupture remained unchanged at 0.25% to 0.31%, and the mortality rate remained high and relatively constant. The survival benefit associated with surgical repair was seen only in hospital but not at 30 days or 1 year. Overall in-hospital, 30-day, and 1-year mortality rates were 50%, 54%, and 65%, respectively, similar to previous reports.[59]

Ruptures occur only in the presence of transmural infarction and result from hemorrhage within the necrotic zone. Independent risk factors for the development of a ventricular septal defect include first infarction, advanced age (older than 65 years), hypertension, female gender, and chronic renal disease.[61] In addition, there is a higher incidence in patients without a history of prior angina and with infarcts in the distribution of a single vessel. Thus, septal rupture is more likely following abrupt occlusion of a single artery that vascularizes a territory for which there is little collateral flow. Unlike papillary muscle rupture, ventricular septal rupture occurs with equal frequency among patients with anterior (LAD) and inferior (right coronary artery) infarctions but less frequently in those with lateral (left circumflex artery) infarctions.[62]

In the prethrombolytic era, ventricular septal rupture usually presented 3 to 6 days after acute MI, whereas most ventricular septal ruptures associated with early thrombolytic therapy or primary PCI occur at a peak incidence time within 24 hours after treatment.[60] Thus, although timely restoration of culprit vessel patency reduces the rate of rupture, it tends to occur earlier. Thrombolytic therapy that is delayed more than 12 hours following the onset of chest pain may increase the incidence of ventricular septal rupture.[63]

Patients with ventricular septal rupture usually present with recurrent chest pain, dyspnea, and sudden hypotension or shock. A new harsh pansystolic murmur is present in approximately 50% of patients but may be difficult to distinguish clinically from acute severe mitral regurgitation and may be relatively soft with LV failure or pulmonary hypertension. Particular ECG changes may be associated with an increased likelihood of septal rupture. It has recently been shown that in patients with anterior MI with ST-segment elevation in all inferior ECG leads in addition to anterior leads, ventricular septal rupture occurred in 9 of 21 patients (43%), but those ECG changes were present in only 10 of 275 patients (3.6%) of those who did not have septal rupture.[64]

Bedside echocardiography is highly sensitive and specific in the diagnosis of ventricular septal rupture. Simple ventricular septal rupture is a discrete defect with a direct through-and-through communication between the LV and RV, with ventricular entry and exit sites located at a similar horizontal level. Complex ventricular septal rupture has entry and exit sites at different levels along the ventricular septum through a dissecting hemorrhage. A dissecting hematoma is seen as intramyocardial echocardiographic lucent defects. Ventricular septal ruptures may be multiple, and there may be associated LV free wall or papillary muscle rupture. Infarct expansion is readily diagnosed by echocardiography and typically occurs before rupture. Ventricular septal rupture due to occlusion of the right coronary artery usually occurs in the basal inferior septum (Fig. 14-5), and ventricular septal rupture after acute anterior MI most often occurs in the distal one third of the septum (Fig. 14-6). When ventricular septal rupture is clinically suspected, it is often necessary to use nonconventional imaging planes, first with color Doppler to locate the defect, and then with 2D imaging. The width of the jet by color flow Doppler correlates with the size of the defect as measured at surgery. Although the peak gradient across the ventricular septal defect measured with continuous wave Doppler allows an estimate of RV systolic pressure, the measurement should be used with caution in patients with complex defects involving indirect tracts through the myocardium. Associated echocardiographic findings of elevated RV pressure include RV dilation, decreased RV systolic function, and paradoxical septal motion. Signs of increased RA pressure include RA dilation, bowing of the interatrial septum toward the left throughout the cardiac cycle, and plethora of the inferior vena cava. When TTE is suboptimal, TEE is highly accurate with improved delineation of the site of defect, morphology, presence of multiple defects, and extent of RV involvement.

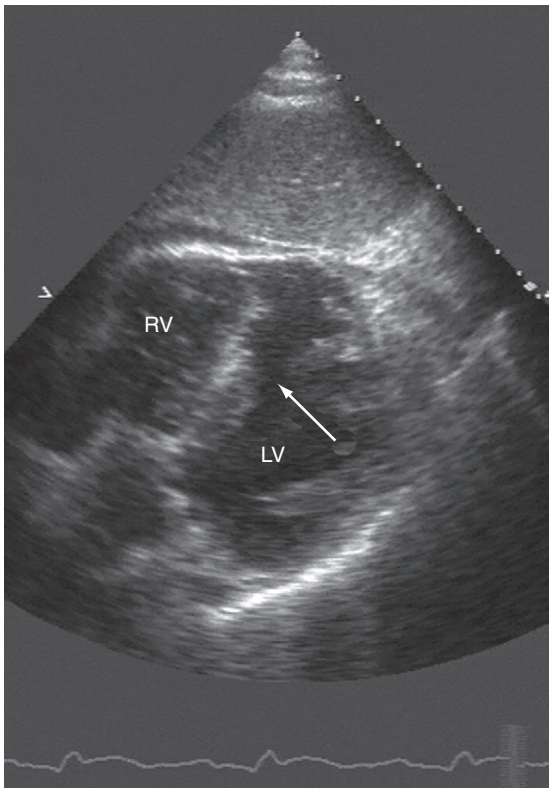



**Figure 14-5** TTE (subcostal view) showing a large ventricular septal defect resulting from a rupture in a patient with a large inferior myocardial infarction. The area of discontinuity can be visualized as a large, irregularly shaped area of myocardial dropout (*arrow*). Note the dilated RV consistent with RV infarction or RV volume/pressure overload.

Although ventricular septal rupture carries a very high mortality rate, with and without urgent surgery, echocardiography may risk stratify patients. Complex septal ruptures and RV involvement are significant determinants of adverse clinical outcome.[65] Rupture of the posterior septum after inferior MI is associated with a higher mortality rate, related to the degree of associated RV dysfunction. Moreover, posterior septal ruptures tend to be more complex and associated with remote myocardial involvement. In contrast, anterior septal defects more often have a direct course and involve a discrete myocardial region. The strongest indicator of poor prognosis is the development of cardiogenic shock associated with as much as a 90%

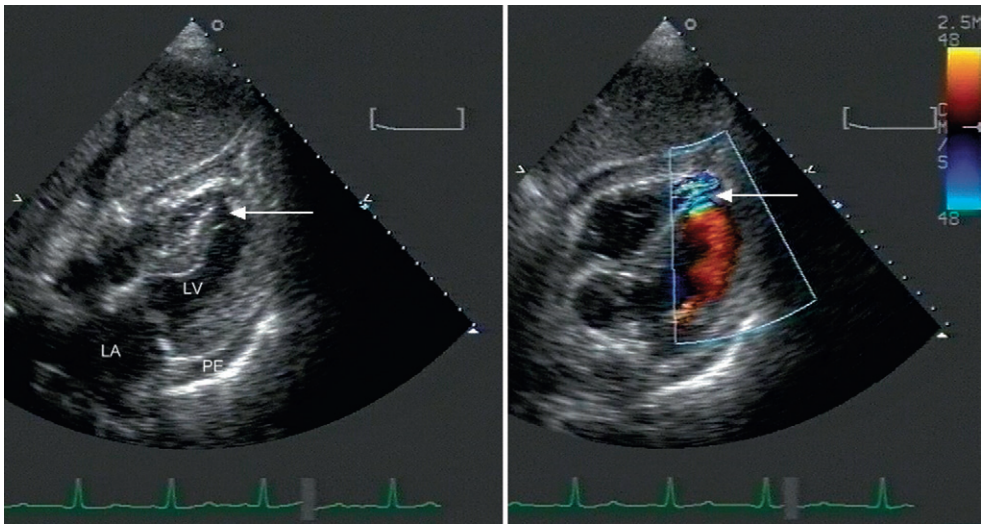



**Figure 14-6** TTE (subcostal view) showing a ventricular septal defect resulting from rupture involving the apical septum (*left*). Color flow Doppler demonstrates left-to-right shunting across the septal defect (*right*). Also note the small circumferential pericardial effusion (*PE*).

mortality rate. Early surgery appears to improve survival when cardiogenic shock is present, with the SHOCK trial investigators reporting a survival rate of 19% in the surgically treated group compared to 5% in the medically treated group.[66] When the patient can be stabilized medically, operative mortality may be improved when surgical repair is delayed until 6 weeks following the event. In select patients, a conservative approach may be appropriate and associated with a good midterm outcome. A recent report described 7 patients of 27 with post-MI ventricular septal rupture who did not undergo surgery and were followed up for a mean of approximately 3 years. All 7 patients had single-vessel disease, small defect size (on average 9.8 mm), minimal left-to-right shunt, and preserved RV function.[65] Although early definitive surgical correction remains the gold standard for treatment, percutaneous device closure should be considered in certain cases (Fig. 14-7). Potentially suitable candidates for a transcatheter approach include simple defects that are smaller than 15 mm, either in the acute setting when the surgical risk is considered prohibitively high, or in the subacute and chronic setting with comparable mortality to surgery.[67]

## RUPTURE OF THE VENTRICULAR FREE WALL

Rupture of the free wall of the LV is the second most common mechanical cause of death in acute ST segment elevation MI after cardiogenic shock due to pump failure and is usually, although not invariably, a fatal event.[68] Risk factors for free wall rupture are similar to those for papillary muscle and ventricular septal rupture; however, this complication is more likely to occur in patients with a transmural MI involving the inferolateral wall associated with a left circumflex occlusion or with a LAD occlusion.[69] Early successful reperfusion appears to decrease the risk of rupture. In a study of 1300 patients, the overall incidence of cardiac rupture was lower in those receiving thrombolytic therapy (1.7%) than in those in the conventional therapy group (2.7%). Among patients who received thrombolytic therapy, patients older than 70 years and women had higher rates of rupture.[70] Moreover, patients in whom reperfusion was unsuccessful have a significantly higher rate of rupture than those who were successfully reperfused (5.9% versus 0.5%).[71] Conversely, late reperfusion appears to increase the risk of myocardial rupture though decreasing overall mortality.[72] Nonrandomized, retrospective studies comparing primary PCI with thrombolysis have shown a significantly lower risk of free wall rupture in patients treated with primary PCI.

Ventricular free wall rupture usually presents clinically as an acute catastrophic event rapidly leading to death. However, recent pathologic and clinical studies have suggested that some cases may take a subacute or chronic course when a small rupture is temporarily sealed by fibrinous pericardial adhesions or thrombus. Intramural hematoma or hemorrhage at the junction of the necrotic and the normal myocardium results in a small endocardial rent. The tear usually takes a circuitous pathway through the myocardium, ending in a small epicardial opening. A prodrome of persistent or recurrent chest pain (in the absence of an elevation in creatinine kinase), repetitive large-volume emesis, unexplained agitation, hypotension, or syncope may be associated with the initial small tear. A small amount of hemorrhage into the pericardial space may precede the final catastrophic event. Patients diagnosed during this subacute phase and taken promptly to surgery have a greater chance of survival. In a prospective study of 608 consecutive patients with acute MI, subacute free wall rupture (death occurring 30 minutes to a few days after the first clinical indication of the event) was identified in 2.5%, whereas acute free wall rupture (death within 30 minutes) occurred in 4.1% cases. The long-term outcome of survivors who underwent urgent surgery was good.[73]

Echocardiography has a high sensitivity for diagnosing rupture. An echocardiographic feature of risk for rupture is infarct expansion with significant wall thinning at the infarct site. A small pericardial effusion is a common finding after an uncomplicated transmural MI, but increasing size of a pericardial effusion and the presence of thrombus in the pericardial space significantly increases the specificity for rupture (greater than 98%), as shown in Figure 14-8. The absence of pericardial effusion virtually excludes rupture. An intrapericardial thrombus appears as an echo-dense mass; it may be mobile, undulating within the pericardial space, or immobile, impinging on the cardiac chambers.[73] Direct visualization of the myocardial tear

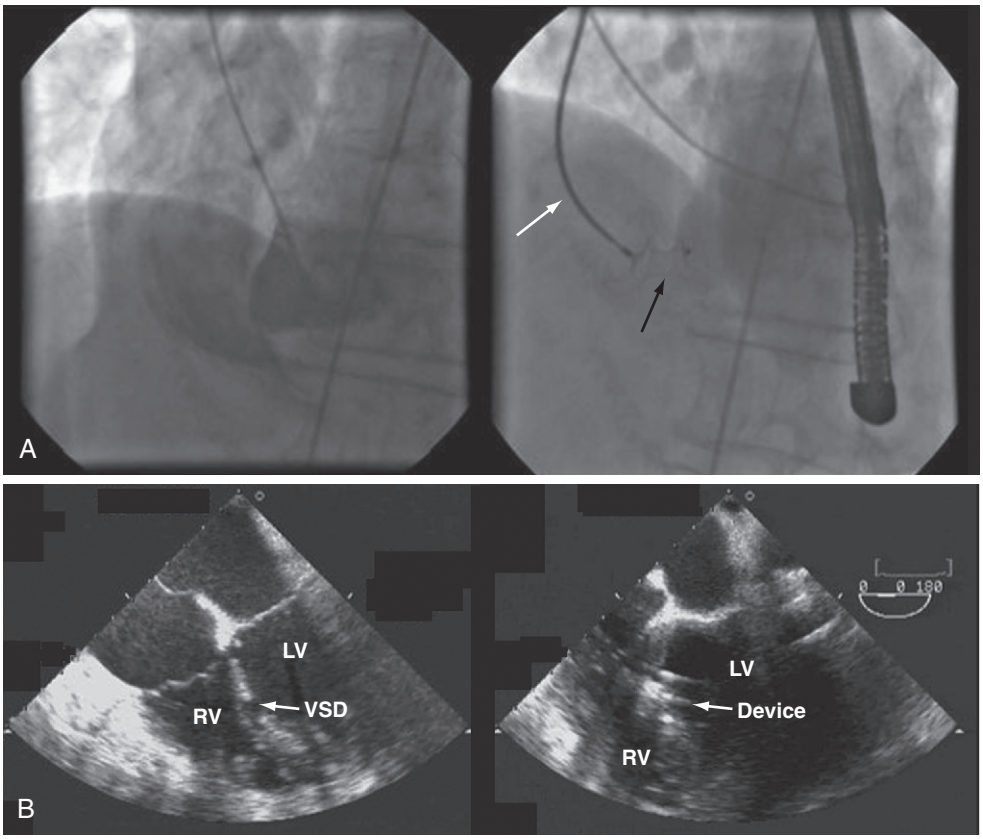



**Figure 14-7** **A,** Left ventriculography before closure of postinfarction ventricular septal defect showing left-to-right shunt (*left panel*) and angiographic image (*right panel*) showing the Amplatzer device in position (*black arrow*), before release from delivery cable (*white arrow*). **B,** TEE images at 0° showing a postinfarction ventricular septal defect (*VSD*) located in the mid inferior septum (*left panel*) and postprocedure showing device placement in the mid inferior septum (*right panel*). *(From Ahmed A, Ruygrok P, Wilson N, et al. Percutaneous closure of post-myocardial infarction ventricular septal defects: a single centre Experience.* Heart Lung Circ *17:119-123, 2008.)*

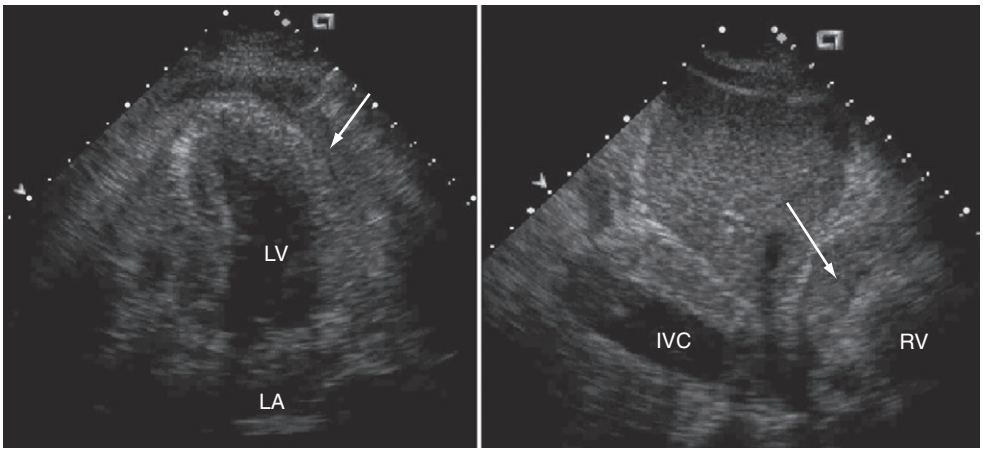



**Figure 14-8** TTE showing hemorrhagic pericardial effusion with thrombus within pericardial space (*arrow*) in apical four-chamber view (*left*) and subcostal view (*right*). Note the dilated and plethoric inferior vena cava (*IVC*).

with TTE is relatively uncommon, reported in up to 40% of patients. When the diagnosis is uncertain, the use of left heart contrast may clearly delineate the tear.[74]

The mortality rate of free wall rupture in the absence of surgical intervention has been reported to be very high, although recent series report as much as a 50% survival rate in patients who underwent pericardiocentesis and conservative medical management.[75] The in-hospital mortality rate for those who undergo surgical repair is in the range of 40%. Those who survive until hospital discharge appear to have a good long-term prognosis.[68] Thus, early echocardiographic diagnosis with prompt surgical or percutaneous drainage is mandatory in patients who develop postinfarction myocardial rupture.

## PSEUDOANEURYSM

A pseudoaneurysm is a contained rupture of the LV free wall. It usually represents a complication of an acute MI, but it may also occur after cardiac surgery, chest trauma, and endocarditis. An LV pseudoaneurysm is not uncommonly diagnosed

incidentally, with 48% (25 of 52 patients with LV pseudoaneurysm) diagnosed incidentally in a series from the Mayo Clinic. The majority of pseudoaneurysms are located in the inferoposterior or inferolateral regions (associated with right coronary or left circumflex coronary occlusions) and rarely occur within the ventricular septum.[76]

It is important to distinguish a pseudoaneurysm, which has a high likelihood of spontaneous rupture, from a true aneurysm, which seldom ruptures. The walls of the pseudoaneurysm are composed of organizing thrombus from hemorrhage into the pericardial space after cardiac rupture, and varying amounts of the epicardium and parietal pericardium. In contrast, the wall of a true aneurysm consists of dense fibrous tissue with excellent tensile strength (Fig. 14-9). An often-described distinguishing echocardiographic feature of a pseudoaneurysm is the narrow neck, with a ratio of neck diameter to maximum aneurysm diameter less than 0.5, compared with the broader "entrance" to the body of a true aneurysm. However, this sign may not always be reliable and has been reported to be only 60% sensitive in distinguishing a pseudoaneurysm from a true aneurysm.[76] This is particularly the case with aneurysms at the base of the heart, most commonly after inferior MI. Spectral and color Doppler imaging demonstrate characteristic flow in and out of the pericardial cavity at the site of the tear (Fig. 14-10), as well as abnormal flow within the pseudoaneurysm.

Surgical repair is the preferred treatment, although conservative medical treatment in certain high-risk patients may not be associated with an increased risk of cardiac rupture.[77] Percutaneous closure of a pseudoaneurysm is a potential approach in carefully selected patients and is performed with TEE guidance (Fig. 14-11).

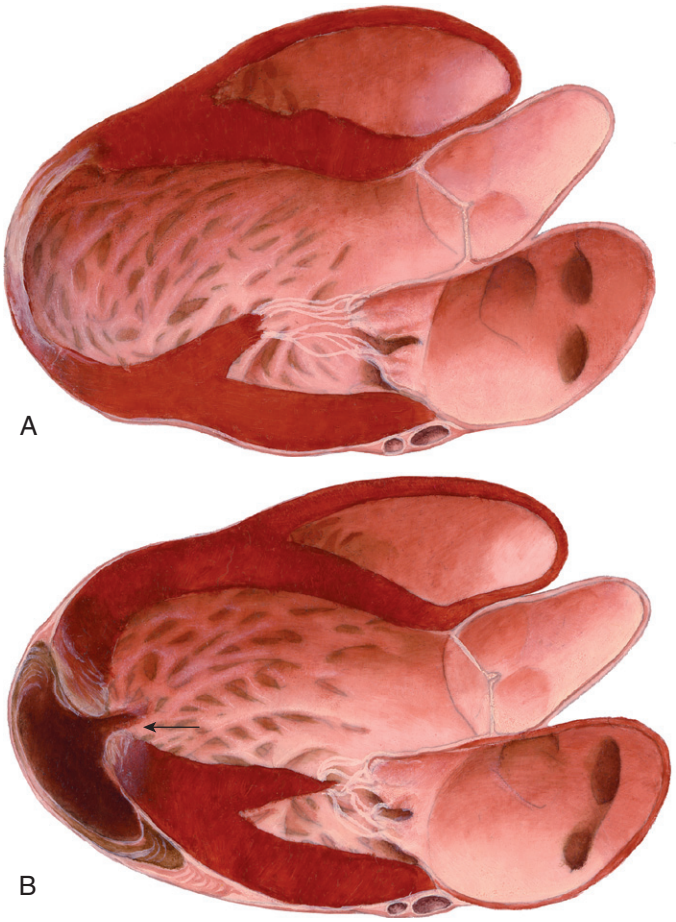



**Figure 14-9** Difference between true aneurysm (**A**) and false aneurysm (**B**). Note that in true aneurysm there is continuity of myocardium in the region of dilation (*arrows*), in contrast to loss of this continuity in pseudoaneurysm with abrupt area of rupture (*arrow*). *(Modified from MacKenzie JW, Lemole GM: Pseudoaneurysm of the left ventricle.* Tex Heart Inst J *21:296-301, 1994.)*

## INFARCT EXPANSION AND TRUE ANEURYSM FORMATION

Infarct expansion represents acute remodeling with an increase in the circumferential extent of the area of infarction that results from stretching and thinning of the infarcted zone. This process typically occurs 24 to 72 hours after acute transmural MI. Early

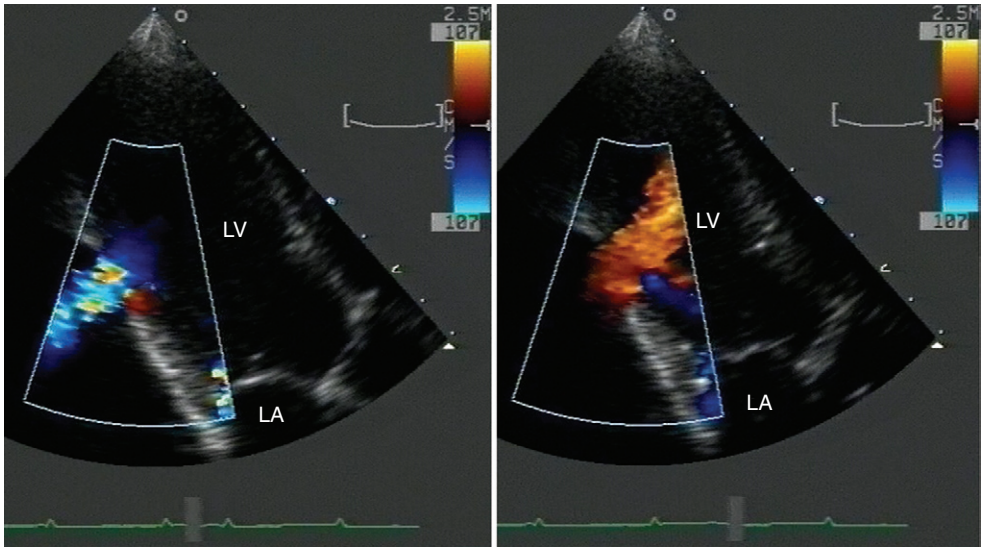



**Figure 14-10** TTE in apical three-chamber view demonstrating rupture of midinferolateral wall with flow from LV cavity into pseudoaneurysm in systole (*left*) and from pseudoaneurysm into LV cavity in diastole (*right*). Wall of pseudoaneurysm is not shown.

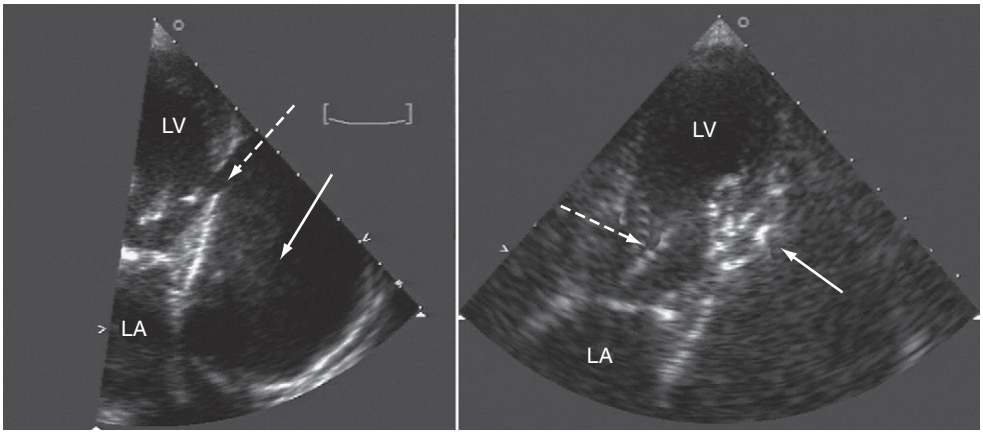



**Figure 14-11** TTE in apical four-chamber view demonstrating large pseudoaneurysm of midinferolateral wall (*left*). *Solid arrow*, pseudoaneurysm; *dashed arrow*, site of free wall rupture. Appearance after transcatheter closure is shown at *right*. *Solid arrow*, Amplatzer device; *dashed arrow*, catheter.

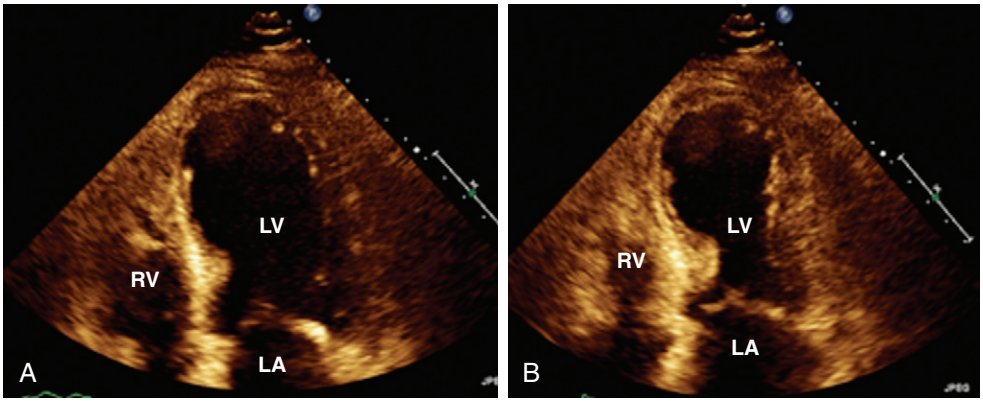



**Figure 14-12** **A,** Apical four-chamber view at end-diastole. Note thin-walled and expanded apex compared to basal and mid-LV segments. There is no diastolic deformity of apex; thus this is not a true apical aneurysm. **B,** Apical four-chamber view at end-systole. Note augmented contractility of basal and mid-LV segments, and akinetic and expanded apex.

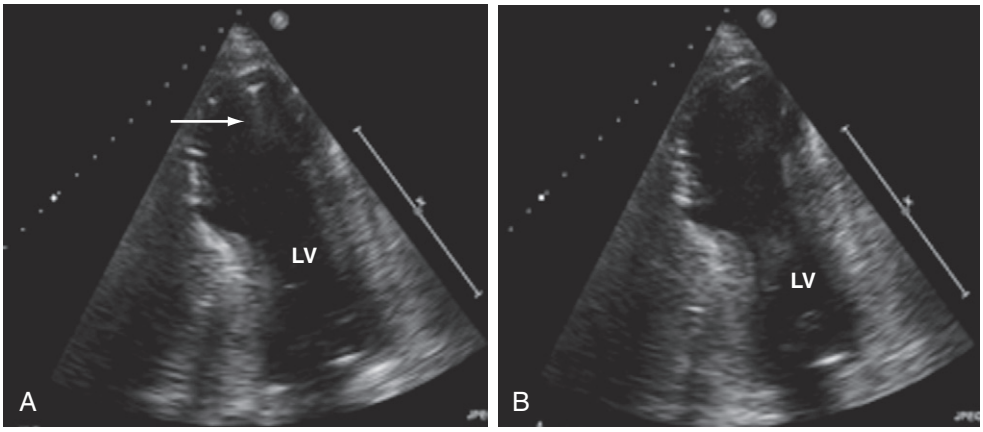



**Figure 14-13** **A,** Apical four-chamber view of LV at end-diastole. Note aneurysmal apex (*arrow*) with characteristic deformity of true apical aneurysm. **B,** Apical four-chamber view of LV at end-systole. Note augmented contractility of basal and mid-LV segments, but not of aneurysmal apex.

clinical studies demonstrated that infarct expansion with a consequent increase in LV volume and wall stress was associated with an in-hospital mortality rate up to 40%. Although any region of the LV may be affected, it is more common after anteroapical MI. Echocardiographic features of infarct expansion include an aneurysmal bulge of the myocardium with reduced local wall thickness (Fig. 14-12). This thin necrotic wall has low tensile strength and typically precedes mechanical complications including ventricular septal rupture, free wall rupture, and papillary muscle rupture.

In the absence of rupture, the final expression of infarct expansion is aneurysm formation, which occurs only with transmural infarction and a full-thickness scar. A true aneurysm is defined as a deformity of the thinned infarct segment that is apparent during diastole as well as during systole and demonstrates a diastolic contour abnormality (Fig. 14-13). In contrast,

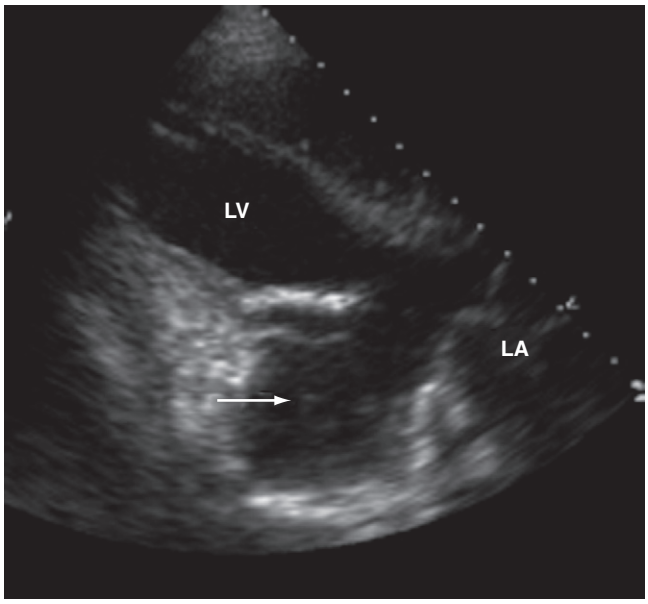



**Figure 14-14** Parasternal long-axis view showing massive basal inferior wall aneurysm (*arrow*). Note wide neck of aneurysm consistent with true aneurysm, rather than pseudoaneurysm.

a dyskinetic myocardial segment deforms during systole, extending beyond the normal contour of the myocardium. The involved myocardial segment is scarred with thin walls (less than 7 mm) and increased echogenicity owing to the increased collagen content. The wall of the aneurysm may eventually calcify. Most aneurysms occur in the LV apex and anterior wall, and less commonly in the inferior wall (Fig. 14-14). Aneurysms of the lateral wall are very uncommon. The reported incidence of aneurysm formation after acute MI before the reperfusion era is quite variable, with an average of 30%[78,79] Although the use of thrombolytic therapy per se has not been convincingly shown to reduce the frequency of aneurysm formation, a study of 205 patients presenting with acute MI reported a significantly reduced incidence of aneurysm formation in those patients receiving thrombolytic therapy and exhibiting a patent infarct-related artery compared to those who received thrombolytic therapy but without a patent infarct-related artery.[78] A similar reduced incidence of LV aneurysm formation of primary PCI has been reported.

Serial 2D echocardiographic studies show that aneurysmal dilation is present as early as 5 days after MI. New aneurysms after 3 months are unlikely. Spontaneous rupture of an acute aneurysm is rare, and late rupture virtually never occurs. Aneurysms may vary in size; very small aneurysms may be difficult to visualize by echocardiography. Technically, the detection of an apical aneurysm is highly dependent on the skill of the operator. Routine employment of high-frequency transducers with a shallow focal point enhances near-field resolution and aids examination of the LV apex. Left-sided contrast agents also may enable detection of small apical aneurysms. Using these methods, the sensitivity of TTE for detection of apical aneurysms should approach 100%. It should be noted that TEE may not provide adequate visualization of the LV apex and therefore, in our experience, is less sensitive than surface imaging.

Echocardiographic recognition of a LV aneurysm is clinically relevant for the following reasons: First, the early formation of an aneurysm adversely affects early (in-hospital) and late (1 year) mortality and is associated with an increased incidence of cardiac failure. Second, thrombi are frequently found within aneurysms and are associated with systemic embolization. Third, aneurysms may cause life-threatening ventricular arrhythmias. In patients with heart failure or ventricular arrhythmias, aneurysmectomy may be recommended, and echocardiography plays an important role in patient selection. When considering aneurysmectomy, it is important to ensure that the basal portions of the LV have normal function. A basal (residual) shortening fraction or ejection fraction greater than 18% or 40%, respectively, is more likely to be associated with a satisfactory result. Newer surgical approaches to managing ventricular aneurysms include reduction myoplasty and Dor myoplasty.[80] Echocardiography also plays an important role in assessing the feasibility of these techniques.

## LEFT VENTRICULAR THROMBUS

Studies in the prethrombolytic era reported incidence rates of thrombus formation after anterior MI, especially those involving the apex, of up to 60%, and rarely in inferior infarction.[81] LV thrombus tends to develop on the endocardium of akinetic, nonviable segments. The peak timing of thrombus formation after acute MI is 3 days, but thrombus may occur as early as within a few hours in large areas of apical akinesis and may occur a few weeks after an MI. In general, thrombolytic therapy has decreased the rate of mural thrombus development, but thrombus formation may still occur after lytic therapy and concurrent antithrombin and antiplatelet agents. In the GISSI-2 trial there was no significant difference between the four treatment groups (recombinant tissue plasminogen activator with or without heparin, streptokinase with or without heparin), with respect to thrombus formation with an overall incidence of 28%.[82] The overall tendency for reperfusion therapy to decrease the size of the infarction is likely to lower the risk of thrombus formation. The incidence of LV thrombus is also reduced by primary PCI for acute MI. In a recent study of 100 consecutive patients with acute anterior ST-elevation MI (excluding patients who presented with cardiogenic shock) treated with stenting of the LAD within 2 to 12 hours of symptom onset, LV thrombus was diagnosed by echocardiography in 13 patients and by cardiac MRI in 2 patients. All patients underwent echocardiography within the first 1 to 3 days, 4.5 ± 1.1 days post-MI, and after 3 months.[83] All patients were treated with aspirin 75 mg/day and clopidogrel 75 mg/day, 50% were treated with a glycoprotein IIb/IIIa inhibitor, and 20% received thrombolysis before stenting. Of the 15 patients (15%) diagnosed with LV thrombus, 10 were diagnosed within the first week, 4 were diagnosed between 1 and 4 weeks, and 1 was diagnosed between 4 and 12 weeks. Other studies have reported a lower prevalence of LV thrombus in patients with acute MI treated with primary stenting,[84,85] but these studies included patients with lower-risk nonanterior MIs, were retrospective, and did not utilize serial echocardiograms or MRI. Thus, LV thrombus remains a common complication of anterior MI treated with contemporary intervention. The major focus of the currently used pharmacologic agents after acute MI is the antiplatelet effects, and antiplatelet treatment has little or no influence on thrombin generation, which plays a key role in the development of LV thrombus. The major mechanism of the reduced prevalence of LV thrombus in the reperfusion era is rapid restoration of culprit vessel patency and limited myocardial damage.

The echocardiographic appearance of a mural thrombus is that of a mass distinct from the endocardium and protruding to a variable extent into the LV cavity (Fig. 14-15). Under ideal conditions, the surface of the thrombus can be distinguished clearly from the underlying endocardium and the mass can be visualized in two different imaging planes. The tissue characteristics of an acute thrombus are usually similar to those of the myocardium. A chronic thrombus may have increased reflectivity, demonstrate a layered appearance corresponding to the lines of Zahn, and contain areas of calcification. The base of attachment to the wall may be broad in the case of a sessile thrombus and narrow in a pedunculated thrombus. Occasionally, thrombus may have a cystic appearance with a relative echolucency to the center of the thrombus. False-positive echocardiographic diagnoses are usually a result of pseudotendons (i.e., false chordae) spanning the LV apex, coarse trabeculations associated with LV hypertrophy, or near-field artifacts (commonly present with low-frequency transducers). High-frequency transducers with a short focus point can sometimes differentiate true thrombus from these other phenomena. Left-sided contrast agents may outline the contours of the thrombus, creating a filling defect with improved detection of thrombus (Fig. 14-16).

The greatest clinical concern of a mural thrombus is the potential for systemic embolization, especially stroke. The likelihood of an embolic event is highest in the first 2 weeks after an acute MI and decreases over the following 6 weeks. After this time, there is endothelialization of the thrombus associated with reduced embolic potential. When multiple characteristics of the thrombus are analyzed, mobility of the thrombus is most closely associated (positive predictive value 85%) with embolic events, and when both mobility and protrusion of the thrombus into the LV cavity occur, embolic rates of up to 40% have been reported. Anticoagulant therapy appears to decrease the risk of embolic events and enhances the resolution of thrombus, but there are no prospective randomized studies confirming this. Spontaneous resolution of LV thrombus may occur. In any given patient on anticoagulation, the morphology may spontaneously change from sessile to pedunculated and vice versa; mobility may resolve spontaneously.[86] This emphasizes the need to follow patients with LV thrombus with serial echocardiography. Thrombectomy should be considered in selected patients in whom a very high-risk thrombus morphology is detected.

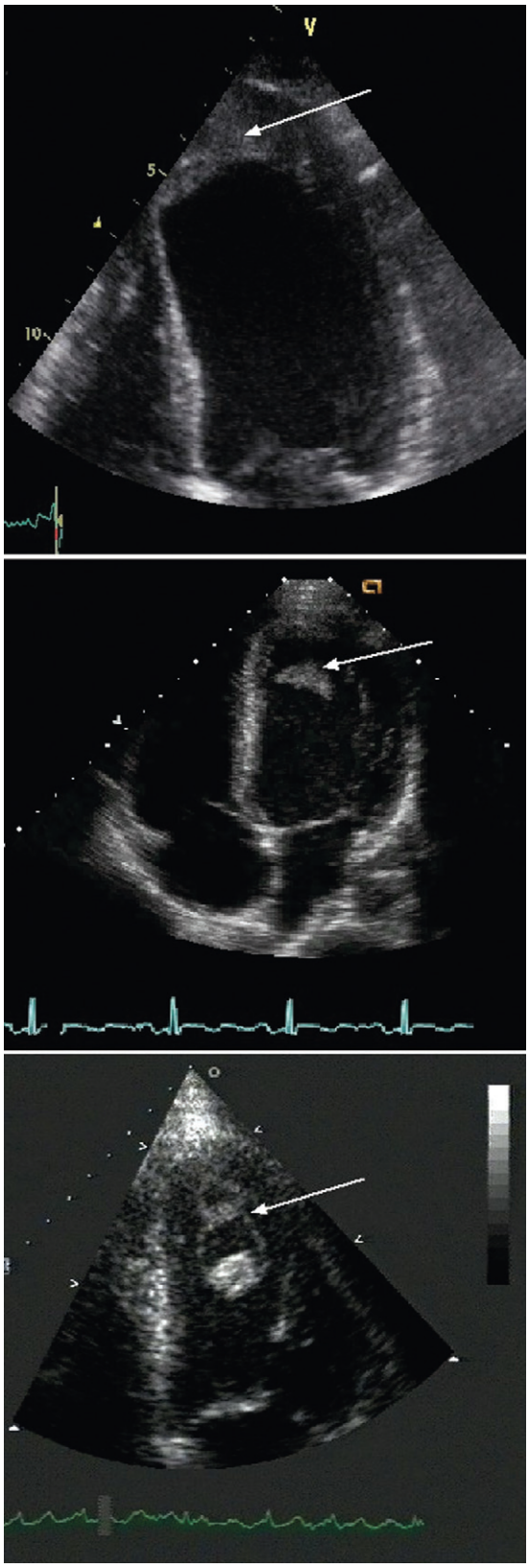


**Figure 14-15** *Top*, Acute thrombus (*arrow*) in LV apex. Note that thrombus is homogeneous in texture, without evidence of calcification. *Middle*, Protruding thrombus (*arrow*), a feature associated with increased embolic risk. *Bottom*, Uncommonly, thrombus may be cystic in appearance (*arrow*).

## Risk Stratification after Myocardial Infarction

Despite advances in the management of acute MI, patients who survive are at increased risk of cardiac morbidity and mortality. Routine echocardiographic measures after acute MI include assessment of LV volume, systolic and diastolic function, regional wall motion abnormalities, and the presence and degree of mitral regurgitation. In addition, evaluation of myocardial viability and residual ischemia guides revascularization strategies.

### LEFT VENTRICULAR SYSTOLIC FUNCTION

Echocardiographic measures of global LV systolic function including LV ejection fraction and LV end-systolic volume are well established predictors of prognosis after acute MI and can be accurately measured by echocardiography in the vast

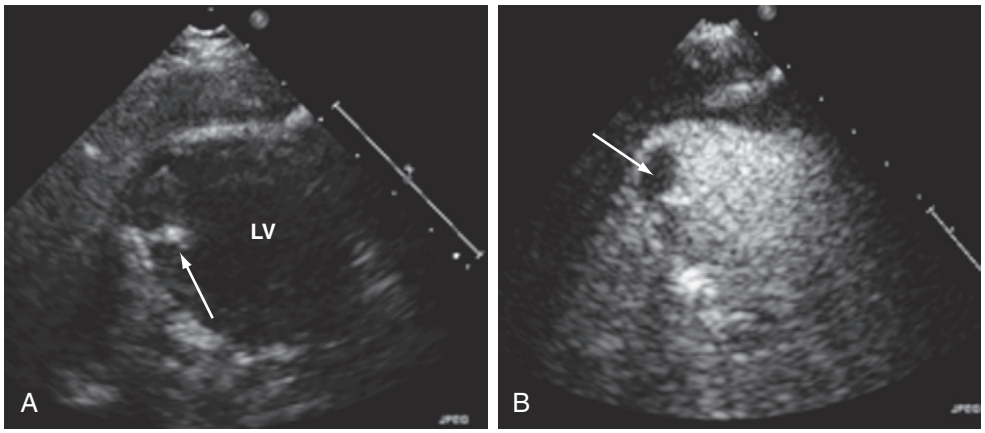



**Figure 14-16** **A,** Apical four-chamber view of LV showing nonspecific echodensity at apical septum (*arrow*). **B,** With use of myocardial contrast, apical thrombus (*arrow*) is now more obviously visible as a filling defect.

majority of patients. Although LV ejection fraction is a powerful predictor of outcome, the ejection fraction may be normal as a result of compensatory regional hyperkinesis in the noninfarcted segments despite extensive myocardial damage, such as in inferior MI.[87] In a study of 605 patients with acute MI, White and colleagues[88] showed that LV end-systolic volume was the single best prognostic indicator for survival, and superior to LV ejection fraction in patients with LV ejection fraction less than 50%.

## REGIONAL WALL MOTION SCORE

Semiquantitative assessment of regional systolic function using wall motion score index is an alternative to ejection fraction for the assessment of LV systolic function.[89] An echocardiographic wall motion score has been the most widely used measure of functional infarct size in clinical practice. The total score is derived by assigning a grade of 1 through 5 (see Table 14-1) to each myocardial segment that is adequately visualized. For a segment to be scored, the majority of the endocardium within that segment must be apparent, and wall thickening and endocardial motion should be examined. The scores for each segment are added and then divided by the number of segments graded for a total wall motion score. Several studies have demonstrated that a higher wall motion score index (12 to 24 hours after admission) is associated with a higher rate of in-hospital complications, including malignant arrhythmias, pump failure, and death.[89,90] A higher wall motion score index also predicts a higher rate of complications, including free wall rupture, ventricular septal rupture, papillary muscle rupture, and death from cardiogenic shock. A higher wall motion score, signifying a more extensive infarction, also is predictive of late mortality. In a study of 767 patients with acute MI, echocardiography was performed at a median of 1 day after admission, and patients were followed for a median of 19 months. Whereas both LV ejection fraction and wall motion score index were powerful predictors of all-cause mortality by univariate analysis, wall motion score index was an independent predictor of death, primarily in patients with non–ST segment elevation MI. In addition, mortality was high in patients with extensive regional wall motion abnormalities but relatively preserved ejection fraction, most likely as a result of compensatory regional hyperkinesis.[91]

Wall motion abnormalities remote from the infarction site may be present early in the course of the infarction or may develop in the presence of postinfarction angina, suggesting de novo ischemia. The echocardiographic finding of remote asynergy at or soon after clinical presentation is strong evidence of multivessel disease. Abnormal wall motion in a second (or even third) coronary distribution is possibly a result of (1) previous infarction, (2) increased myocardial oxygen demands placed on the noninfarcted segment as a result of increased wall stress outstripping its oxygen supply, or (3) a cessation in its collateral blood supply that originated from the newly occluded vessel.

**TABLE 14-3 The Role of Diastolic Functional Parameters in Prognosis after Myocardial Infarction**

| *Study* | *n* | *Comment* |
|---|---|---|
| MeRGE AMI (2008)[93] | 3396 | Restrictive filling is independent predictor of mortality after acute MI regardless of LV ejection fraction, LV end-systolic volume index, and Killip class. |
| Kruszewski (2010)[92] | 400 | Ratio of mitral E wave to early mitral annulus diastolic velocity (E/E′) >15 measured day 1 after acute MI associated with increased risk of adverse events within first year and medium-term mortality. |
| Whalley (2006)[95] | 3855 | Mortality is four times higher in patients with restrictive filling pattern than in those with nonrestrictive filling patterns after acute MI. |
| Moller (2003)[94] | 110 | Patients with a persistently abnormal or a deterioration of LV filling pattern as opposed to improved or normal filling are at increased risk of cardiac death and readmission as a result of heart failure. |
| Moller (2000)[96] | 125 | Restrictive filling and pseudonormal filling independently predicted death. |
| Hillis (2004)[97] | 250 | Ratio of mitral E wave to early mitral annulus diastolic velocity (E/E′) >15 was the most powerful independent predictor of survival. |
| Moller (2001)[98] | 67 | Ratio of mitral E wave velocity to color M-mode flow propagation velocity ≥1.5 was a significant predictor of the composite of cardiac death and readmission for heart failure. |

*MeRGE*, Meta-analysis Research Group in Echocardiography.

## LEFT VENTRICULAR DIASTOLIC FUNCTION

Doppler echocardiography for the assessment of LV diastolic function provides accurate prognostic information in the early phase after acute MI[92-98] (Table 14-3). The ratio of early (E

wave) to late (A wave) transmitral peak velocities and a shortened deceleration time of early transmitral flow were one of the earliest measures of LV diastolic function shown to be powerful predictors of outcome. In a study of 125 consecutive patients with acute MI, Moller and colleagues[96] demonstrated that pseudonormal and restrictive filling patterns were related to progressive LV dilatation and predicted cardiac mortality. Specifically, 1-year survival was 100% in patients with normal filling, 89% in those with impaired relaxation, 50% in those with a pseudonormal pattern, and 35% in those with a restrictive pattern. The Meta-Analysis Research Group in Echocardiography (MeRGE)[93] is the largest study published to date on the Doppler echocardiography in acute MI. This study showed that a restrictive filling pattern occurs in approximately 20% of patients with acute MI and when present is associated with a nearly threefold increase in mortality. This relationship is independent of age, LV size, LV ejection fraction, and Killip class. In a tissue Doppler study of 250 patients with acute MI, an E/E′ ratio greater than 15 predicted all-cause mortality incremental to LV ejection fraction, age, and a restrictive filling transmitral filling pattern.[97] In addition, this study showed that measurement of E/E′ allowed risk stratification among patients with normal and reduced LV systolic function. The value of serial echocardiography after MI is emphasized by the finding that patients with a persistently abnormal or deteriorating LV filling pattern as opposed to improved or normal filling are at increased risk of cardiac death and readmission as a result of heart failure after acute MI.[98]

## LEFT ATRIAL VOLUME

In contrast to Doppler indices of LV diastolic function, LA volume is a more stable parameter integrating the effects of elevated left filling pressures from preexisting cardiovascular conditions and acute disease. Beinart and colleagues[99] demonstrated that LA volume index (corrected for body surface area) measured within 48 hours of an acute MI is an independent predictor of 5-year mortality and was a more powerful predictor than LV volumes and the presence of mitral regurgitation. Similarly, Moller and colleagues[100] showed that LA volume index was a powerful predictor of mortality and remained an independent predictor after adjustment for clinical factors, LV systolic function, and Doppler-derived parameters of diastolic function.

## LEFT VENTRICULAR REMODELING

After transmural MI, alterations in LV structure and function occur, commonly referred to as LV remodeling.[101] The early phase of LV remodeling is confined to the infarct zone and consists primarily of infarct expansion, whereas the late phase involves changes in the entire myocardium and may continue for months. The major factors that determine the magnitude and duration of the remodeling process include the size and location of the initial infarct (usually a complication of a larger anterior infarction), the patency and time to restoration of flow in the infarct-related artery, neurohormonal activation, and the ability of the extracellular matrix to form a stable, mature collagen scar.[102] The major clinical significance of remodeling is the resultant ventricular dilatation with reduced contractility, associated with an increased incidence of cardiac failure, arrhythmias, and death. In addition, remodeling may also cause mitral regurgitation as a result of apical and lateral displacement of the papillary muscles, a process that is associated with increased mortality and risk of cardiac failure. The use of beta-blockers and angiotensin-converting enzyme inhibitors after acute MI has been shown to prevent or retard remodeling.

Echocardiography, including 3D echocardiography, plays a major role in predicting ventricular remodeling and functional recovery. Although thrombolysis and percutaneous coronary artery interventions frequently restore patency of the infarct-related artery, myocardial perfusion may be absent, which is associated with adverse outcomes. Myocardial contrast echocardiography is an accurate measure of reperfusion at a microvascular level, has been shown in multiple studies to predict LV function after MI,[103,104] and may predict functional recovery after acute MI.[105-108] Echocardiography during low-dose dobutamine infusion is used to detect myocardial viability in segments that have persistent dysfunction following reperfusion. Low-dose DSE can detect contractile reserve of dysfunctional myocardium and predict LV dilatation[109,110] and functional recovery.[111] LV strain and strain rate quantified using tissue-Doppler or speckle-tracking imaging after acute MI can differentiate between transmural and nontransmural MI and thus reflect the extent of nonviable myocardium.[112] In addition to this useful diagnostic information, the LV strain parameters have been shown to independently predict death or the development of heart failure during follow-up after acute MI and may provide incremental prognostic information beyond LV ejection fraction.[113,114] Studies utilizing color-coded tissue Doppler imaging and speckle-tracking radial strain analysis for the assessment of LV dyssynchrony after acute MI have shown that the presence of LV dyssynchrony at baseline was significantly related to the extent of LV dilatation at 6 months follow-up.[115] Additional larger studies are needed to determine the prognostic valve of measures of LV dyssynchrony after acute MI.

## STRESS ECHOCARDIOGRAPHY

Echocardiography during higher-dose dobutamine infusion or with dynamic stress can be used to detect residual ischemia and provides prognostic value superior to that of exercise electrocardiography in the postinfarction period. A normal stress echo provides favorable prognostic information in patients with preserved ejection fraction after MI, with a reported 5-year survival of 94%. In addition, a 95% 1-year survival after acute MI was reported in patients with a negative stress echocardiogram compared with 85% and 75% in those with high- and low-dose ischemia, respectively.[116] Caution should be exercised in the first week after a transmural infarction because cases of myocardial rupture during high-dose dobutamine infusion have been reported.[11] Improvement of wall motion during low-dose dobutamine infusion (contractile reserve) indicates the presence of viable (stunned) myocardium that improves spontaneously in function after acute MI and is associated with an improved outcome. Stress echocardiography is discussed in further detail in Chapters 15 and 16.

## CORONARY FLOW RESERVE

Coronary flow reserve is defined as the ratio between the hyperemic diastolic flow velocity (after intravenous adenosine infusion) and the resting diastolic flow velocity. Noninvasive assessment of coronary flow reserve, especially of the LAD

artery, has been shown to provide prognostic information in patients with stable coronary artery disease and in patients early after acute MI.[117] In a study of 329 patients with known or suspected coronary artery disease and a negative stress echocardiogram, a coronary flow reserve of 1.92 or less was the best predictor of future cardiac events, with a sensitivity of 77% and specificity of 85%. The optimal cutoff ratio for predicting myocardial viability was 1.5 for coronary flow velocity reserve 24 hours after acute PCI for acute anterior MI, with a sensitivity and specificity of 94% and 91%, respectively.[118] In a further study of 15 patients with first acute anterior MI who underwent PCI, a diastolic deceleration time of the LAD artery flow velocity less than 190 ms was always related to nonviable myocardium.[119]

## MITRAL REGURGITATION

Mitral regurgitation is common among patients presenting with acute MI, and the prevalence increases twofold in patients with heart failure.[120] Earlier studies reported a prevalence of mitral regurgitation in acute MI by angiography of 2% to 19%,[121] whereas echocardiographic studies report a widely varying prevalence of 8% to 74%.[122] The different reported prevalences of mitral regurgitation may be a result of different sensitivities of the two imaging modalities and the timing of imaging. In addition, some recent studies included patients with troponin-positive acute coronary syndromes, which previously may not have been considered an acute MI.

Mitral regurgitation diagnosed in acute MI may be a result of preexisting mitral regurgitation, for example as a result of structural leaflet disease (such as mitral valve prolapse), which needs to be differentiated from ischemic causes directly related to the MI, such as papillary muscle rupture (discussed in detail previously). Ischemic mitral regurgitation can be defined as valvular incompetence associated with myocardial ischemia or infarction in the absence of primary leaflet or chordal pathology and may vary from trivial to severe[123] (Fig. 14-17). Papillary muscle dysfunction represents malfunction of the scarred papillary muscle and of the underlying ventricular wall. This results in retraction of the anterior or posterior leaflet and malcoaptation. The LV remodeling process that occurs after a transmural MI may also result in apical and posterior displacement of the LV wall supporting the papillary muscle and the papillary muscle itself, with abnormal mitral leaflet coaptation and mitral regurgitation. In addition, dilatation of the mitral annulus to varying degrees usually also contributes to the regurgitation. It is important to realize that, depending on the site of the infarction and the degree of remodeling, one mitral leaflet may be more involved than the other (the posterior leaflet is more commonly involved) and the regurgitation jet may therefore be eccentric, which is a common cause for underestimating the severity of mitral regurgitation.

The presence of ischemic mitral regurgitation in acute MI is associated with an adverse prognosis and increases mortality even when mild, with a graded relationship between severity and reduced survival.[124] In a study of 417 patients with acute MI, mild mitral regurgitation (present in 29%) and moderate or severe mitral regurgitation (present in 6%) diagnosed by echocardiography were independently associated with increased 1-year mortality.[125]

In patients requiring surgical myocardial revascularization, it is generally accepted that mitral valve surgery is necessary for severe ischemic regurgitation and not for mild regurgitation, but it is controversial how to treat moderate ischemic mitral regurgitation.[126] A recent study demonstrated that coronary artery bypass graft surgery alone may be sufficient to correct moderate mitral regurgitation when regurgitant severity decreases during DSE.[127]

## Summary

Early experimental models employing echocardiography for the detection and quantitation of ischemia and infarction helped investigators elucidate the pathophysiology. This work was directly transferable into the coronary care unit and provided the basis for the clinical, diagnostic, and prognostic role of echocardiography. Advances in echocardiography, especially color flow Doppler imaging, increased the capabilities of echocardiography in detecting the occurrence of complications, such as ventricular septal defect and papillary muscle rupture. Newer modalities, including myocardial contrast echocardiography, speckle-tracking radial strain analysis, and 3D

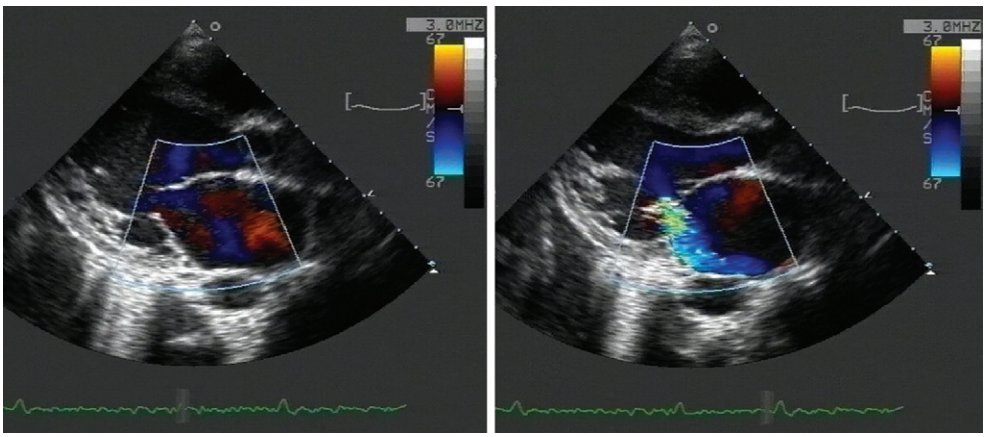


**Figure 14-17 Ischemic mitral regurgitation in patient with inferolateral myocardial infarction.** Note normal thickening in systole of anterior interventricular septum compared to lack of thickening of akinetic inferolateral wall (systolic frame at *right* compared with end-diastolic frame at *left*), with resultant posteriorly directed jet of mitral regurgitation.

echocardiography, continue to show promise in the comprehensive evaluation of patients admitted to the coronary care unit, including accurate assessment of LV systolic and diastolic function, regional wall motion abnormalities, and myocardial perfusion and viability. Based on a wealth of accumulated data on the diagnostic and prognostic value of echocardiography in the coronary care unit, its portability and noninvasive nature, and continuing advances in technology, will ensure that echocardiography remains the noninvasive imaging modality of choice in the coronary care unit.

## KEY POINTS

- The principal advantages of TTE in the coronary care unit include its portability, noninvasive nature, and the wealth of anatomic and hemodynamic information provided.
- The use of left-sided contrast agents has increased the percentage of patients in whom technically adequate images can be obtained.
- TTE provides key prognostic information after MI.
- All mechanical complications of MI can be detected by echocardiography.
- Echocardiography is the gold-standard imaging modality for the evaluation of ischemic mitral regurgitation.
- Provided proper precautions are taken, TEE is safe in the early postinfarction period and provides complementary information to TTE when needed.
- Pharmacologic stress echocardiography with dobutamine allows the identification of viable myocardium and residual ischemia after MI, which helps determine optimal revascularization strategies.
- Handheld echocardiographic instruments provide a rapid bedside assessment of wall motion, global ventricular function, and pericardial effusion.
- Myocardial contrast echocardiography allows a comprehensive assessment of global and regional LV function, myocardial perfusion, and myocardial viability and can predict functional recovery after MI.
- Myocardial strain with speckle-tracking techniques allows accurate quantification of regional wall motion.
- Ongoing advances in echocardiographic imaging, including 3D echocardiography, will see real-time 3D echocardiography play an increasing role in the assessment of patients with coronary artery disease.

## REFERENCES


1. Marwick TH: The future of echocardiography. *Eur J Echocardiogr* 10:594-601, 2009.
2. Kaul S, Senior R, Firschke C, et al: Incremental value of cardiac imaging in patients presenting to the emergency department with chest pain and without ST-segment elevation: a multicenter study. *Am Heart J* 148:129-136, 2004.
3. Lepper W, Belcik T, Wei K, et al: Myocardial contrast echocardiography. *Circulation* 109: 3132-3135, 2004.
4. Khumri TM, Nayar S, Idupulapati M, et al: Usefulness of myocardial contrast echocardiography in predicting late mortality in patients with anterior acute myocardial infarction. *Am J Cardiol* 98:1150-1155, 2006.
5. Pellerin D, Sharma R, Elliott P, et al: Tissue Doppler, strain, and strain rate echocardiography for the assessment of left and right systolic ventricular function. *Heart* 89(Suppl 3):iii9-iii17, 2003.
6. Serri K, Reant P, Lafitte M, et al: Global and regional myocardial function quantification by two-dimensional strain: application in hypertrophic cardiomyopathy. *J Am Coll Cardiol* 47:1175-1181, 2006.
7. Amundsen BH, Helle-Valle T, Edvardsen T, et al: Noninvasive myocardial strain measurement by speckle tracking echocardiography: validation against sonomicrometry and tagged magnetic resonance imaging. *J Am Coll Cardiol* 47:789-793, 2006.
8. Mondillo S, Giannotti G, Innelli P, et al: Handheld echocardiography: its use and usefulness. *Int J Cardiol* 111:1-5, 2006.
9. Hellmann DB, Whiting-O'Keefe Q, Shapiro EP, et al: The rate at which residents learn to use hand-held echocardiography at the bedside. *Am J Med* 118:1010-1018, 2005.
10. Giannotti G, Mondillo S, Galderisi M, et al: Hand-held echocardiography: added value in clinical cardiological assessment. *Cardiovasc Ultrasound* 3:7, 2005.
11. Orlandini AD, Tuero EI, Diaz R, et al: Acute cardiac rupture during dobutamine-atropine echocardiography stress test. *J Am Soc Echocardiogr* 13:152-153, 2000.
12. Corsi C, Lang RM, Veronesi F, et al: Volumetric quantification of global and regional left ventricular function from real-time three-dimensional echocardiographic images. *Circulation* 112:1161-1170, 2005.
13. Toledo E, Lang RM, Collins KA, et al: Imaging and quantification of myocardial perfusion using real-time three-dimensional echocardiography. *J Am Coll Cardiol* 47:146-154, 2006.
14. Malm S, Frigstad S, Sagberg E, et al: Accurate and reproducible measurement of left ventricular volume and ejection fraction by contrast echocardiography: a comparison with magnetic resonance imaging. *J Am Coll Cardiol* 44:1030-1035, 2004.
15. Reilly JP, Tunick PA, Timermans RJ, et al: Contrast echocardiography clarifies uninterpretable wall motion in intensive care unit patients. *J Am Coll Cardiol* 38: 485-490, 2000.
16. Schiller NB, Shah PM, Crawford M, et al: Recommendations for quantitation of the left ventricle by two-dimensional echocardiography. American Society of Echocardiography Committee on Standards, Subcommittee on Quantitation of Two-Dimensional Echocardiograms. *J Am Soc Echocardiogr* 2:358-367, 1989.
17. Kuecherer HF, Abbott JA, Botvinick EH, et al: Two-dimensional echocardiographic phase analysis. Its potential for noninvasive localization of accessory pathways in patients with Wolff-Parkinson-White syndrome [see comments]. *Circulation* 85:130-142, 1992.
18. Shah KD, Daxini BV: Noninvasive and invasive evaluation of left bundle branch block (LBBB). *Acta Cardiol* 45:125-131, 1990.
19. Xiao HB, Brecker SJ, Gibson DG: Differing effects of right ventricular pacing and left bundle branch block on left ventricular function. *Br Heart J* 69:166-173, 1993.
20. Force T, Bloomfield P, O'Boyle JE, et al: Quantitative two-dimensional echocardiographic analysis of motion and thickening of the interventricular septum after cardiac surgery. *Circulation* 68:1013-1020, 1983.
21. Movahed M, Donohue D: Review: transient left ventricular apical ballooning, broken heart syndrome, ampulla cardiomyopathy, atypical apical ballooning, or Tako-Tsubo cardiomyopathy. *Cardiovasc Revasc Med* 8:289-292, 2007.
22. Prasad A, Lerman A, Rihal C: Apical ballooning syndrome (Tako-Tsubo or stress cardiomyopathy): A mimic of acute myocardial infarction. *Am Heart J* 155:408-417, 2008.
23. Tong KL, Kaul S, Wang XQ, et al: Myocardial contrast echocardiography versus Thrombolysis In Myocardial Infarction score in patients presenting to the emergency department with chest pain and a nondiagnostic electrocardiogram. *J Am Coll Cardiol* 46:920-927, 2005.
24. Lang RM, Bierig M, Devereux RB, et al: Chamber Quantification Writing Group; American Society of Echocardiography's Guidelines and Standards Committee; European Association of Echocardiography. Recommendations for chamber quantification: a report from the American Society of Echocardiography's Guidelines and Standards Committee and the Chamber Quantification

Writing Group, developed in conjunction with the European Association of Echocardiography, a branch of the European Society of Cardiology. *J Am Soc Echocardiogr* 18:1440-1463, 2005.
25. Otsuka R, Watanabe H, Hirata K, et al: A novel technique to detect total occlusion in the right coronary artery using retrograde flow by transthoracic Doppler echocardiography. *J Am Soc Echocardiogr* 18:704-709, 2005.
26. Lee S, Otsuji Y, Minagoe S, et al: Noninvasive evaluation of coronary reperfusion by transthoracic Doppler echocardiography in patients with anterior acute myocardial infarction before coronary intervention. *Circulation* 108: 2763-2768, 2003.
27. Goldstein JA: Pathophysiology and management of right heart ischemia. *J Am Coll Cardiol* 40:841-853, 2002.
28. Tahirkheli NK, Edwards WD, Nishimura RA, et al: Right ventricular infarction associated with anteroseptal myocardial infarction: a clinicopathologic study of nine cases. *Cardiovasc Pathol* 9:175-179, 2000.
29. Hamon M, Agostini D, Le Page O, et al: Prognostic impact of right ventricular involvement in patients with acute myocardial infarction: meta-analysis. *Crit Care Med* 36:2023-2033, 2008.
30. Fijewski TR, Pollack ML, Chan TC, et al: Electrocardiographic manifestations: right ventricular infarction. *J Emerg Med* 22:189-194, 2002.
31. Kozakova M, Palombo C, Distante A: Right ventricular infarction: the role of echocardiography. *Echocardiography* 18:701-707, 2001.
32. Sharpe DN, Botvinick EH, Shames DM, et al: The noninvasive diagnosis of right ventricular infarction. *Circulation* 57:483-490, 1978.
33. Kakouros N, Cokkinos D: Right ventricular myocardial infarction: pathophysiology, diagnosis, and management. *Postgrad Med J* 86:719-728, 2010.
34. Ozdemir K, Altunkeser BB, Icli A, et al: New parameters in identification of right ventricular myocardial infarction and proximal right coronary artery lesion. *Chest* 124:219-226, 2003.
35. Cohen A, Logeart D, Costagliola D, et al: Usefulness of pulmonary regurgitation Doppler tracings in predicting in-hospital and long-term outcome in patients with inferior wall acute myocardial infarction. *Am J Cardiol* 81:276-281, 1998.
36. Ketikoglou DG, Karvounis HI, Papadopoulos CE, et al: Echocardiographic evaluation of spontaneous recovery of right ventricular systolic and diastolic function in patients with acute right ventricular infarction associated with posterior wall left ventricular infarction. *Am J Cardiol* 93:911-913, 2004.
37. Laster SB, Shelton TJ, Barzilai B, et al: Determinants of the recovery of right ventricular performance following experimental chronic right coronary artery occlusion. *Circulation* 88:696-708, 1993.
38. Goldstein JA: Right versus left ventricular shock: a tale of two ventricles. *J Am Coll Cardiol* 41:1280-1282, 2003.
39. Mattioli AV, Fini M, Mattioli G: Right ventricular dysfunction after thrombolysis in patients with right ventricular infarction. *J Am Soc Echocardiogr* 13:655-660, 2000.
40. Pfisterer M: Right ventricular involvement in myocardial infarction and cardiogenic shock. *Lancet* 362:392-394, 2003.
41. Killip T, 3rd, Kimball JT: Treatment of myocardial infarction in a coronary care unit. A two year experience with 250 patients. *Am J Cardiol* 20:457-464, 1967.
42. Forrester JS, Diamond GA, Swan HJ: Correlative classification of clinical and hemodynamic function after acute myocardial infarction. *Am J Cardiol* 39:137-145, 1977.
43. Dalen JE, Bone RC: Is it time to pull the pulmonary artery catheter? *JAMA* 276:916-918, 1996.
44. Giannuzzi P, Imparato A, Temporelli PL, et al: Doppler-derived mitral deceleration time of early filling as a strong predictor of pulmonary capillary wedge pressure in postinfarction patients with left ventricular systolic dysfunction. *J Am Coll Cardiol* 23:1630-1637, 1994.
45. Yamamuro A, Yoshida K, Hozumi T, et al: Noninvasive evaluation of pulmonary capillary wedge pressure in patients with acute myocardial infarction by deceleration time of pulmonary venous flow velocity in diastole. *J Am Coll Cardiol* 34:90-94, 1999.
46. Ommen SR, Nishimura RA, Appleton CP, et al: Clinical utility of Doppler echocardiography and tissue Doppler imaging in the estimation of left ventricular filling pressures: a comparative simultaneous Doppler-catheterization study. *Circulation* 102:1788-1794, 2000.
47. Takasaki K, Otsuji Y, Yoshifuku S, et al: Noninvasive estimation of impaired hemodynamics for patients with acute myocardial infarction by Tei index. *J Am Soc Echocardiogr* 17:615-621, 2004.
48. Abd-El-Rahim AR, Otsuji Y, Yuasa T, et al: Noninvasive differentiation of pseudonormal/restrictive from normal mitral flow by Tei index: a simultaneous echocardiography-catheterization study in patients with acute anteroseptal myocardial infarction. *J Am Soc Echocardiogr* 16:1231-1236, 2003.
49. Moller JE, Hillis GS, Oh JK, et al: Prognostic importance of secondary pulmonary hypertension after acute myocardial infarction. *Am J Cardiol* 96:199-203, 2005.
50. Aydinalp A, Wishniak A, van den Akker-Berman L, et al: Pericarditis and pericardial effusion in acute ST-elevation myocardial infarction in the thrombolytic era. *Isr Med Assoc J* 3:181-183, 2002.
51. Imazio M, Negro A, Belli R, et al: Frequency and prognostic significance of pericarditis following acute myocardial infarction treated by primary percutaneous intervention. *Am J Cardiol* 103:1525-1529, 2009.
52. Dorfman T, Aqel R: Regional Pericarditis: A review of the pericardial manifestations of acute myocardial infarction. *Clin Cardiol* 32: 115-120, 2009.
53. Galve E, Garcia-del-Castillo H, Evangelista A, et al: Pericardial effusion in the course of myocardial infarction: incidence, natural history, and clinical relevance. *Circulation* 73:294-299, 1986.
54. Guereta P, Khalifeb K, Jobicc Y, et al: Echocardiographic assessment of the incidence of mechanical complications during the early phase of myocardial infarction in the reperfusion era: a French multicenter prospective registry. *Arch Cardiovasc Dis* 101:41-47, 2008.
55. Figueras J, Barrabes J, Serra V, et al: Hospital outcome of moderate to severe pericardial effusion complicating ST-elevation acute myocardial infarction. *Circulation* 122:1902-2909, 2010.
56. Zoghbi WA, Enriquez-Sarano M, Foster E, et al: Recommendations for evaluation of the severity of native valvular regurgitation with two-dimensional and Doppler echocardiography. *J Am Soc Echocardiogr* 16:777-802, 2003.
57. Thomas L, Foster E, Hoffman JI, et al: The Mitral Regurgitation Index: an echocardiographic guide to severity. *J Am Coll Cardiol* 33:2016-2022, 1999.
58. Nishimura RA, Schaff HV, Shub C, et al: Papillary muscle rupture complicating acute myocardial infarction: analysis of 17 patients. *Am J Cardiol* 51:373-377, 1983.
59. Moreyra A, Huang M, Wilson A, et al: Trends in incidence and mortality rates of ventricular septal rupture during acute myocardial infarction. *Am J Cardiol* 106:1095-1100, 2010.
60. Crenshaw BS, Granger CB, Birnbaum Y, et al: Risk factors, angiographic patterns, and outcomes in patients with ventricular septal defect complicating acute myocardial infarction. GUSTO-I (Global Utilization of Streptokinase and TPA for Occluded Coronary Arteries) Trial Investigators. *Circulation* 101:27-32, 2000.
61. Vargas-Barron J, Molina-Carrion M, Romero-Cardenas A, et al: Risk factors, echocardiographic patterns, and outcomes in patients with acute ventricular septal rupture during myocardial infarction. *Am J Cardiol* 95: 1153-1158, 2005.
62. Menon V, Webb JG, Hillis LD, et al: Outcome and profile of ventricular septal rupture with cardiogenic shock after myocardial infarction: a report from the SHOCK Trial Registry. Should we emergently revascularize occluded coronaries in cardiogenic shock? *J Am Coll Cardiol* 36(3 suppl A):1110-1116, 2000.
63. Keeley EC, de Lemos JA: Free wall rupture in the elderly: deleterious effect of fibrinolytic therapy on the ageing heart. *Eur Heart J* 26: 1693-1694, 2005.
64. Hayashi T, Hirano Y, Takai H, et al: Usefulness of ST-segment elevation in the inferior leads in predicting ventricular septal rupture in patients with anterior wall acute myocardial infarction. *Am J Cardiol* 96:1037-1041, 2005.
65. Sivadasan Pillai H, Tharakan J, Titus T, et al: Ventricular septal rupture following myocardial infarction. Long-term survival of patients who did not undergo surgery. Single-centre experience. *Acta Cardiol* 60:403-407, 2005.
66. Slater J, Brown RJ, Antonelli TA, et al: Cardiogenic shock due to cardiac free-wall rupture or tamponade after acute myocardial infarction: A report from the SHOCK Trial Registry. Should we emergently revascularize occluded coronaries for cardiogenic shock? *J Am Coll Cardiol* 36(3 suppl A):1117-1122, 2000.
67. Attia R, Blauth C: Which patients might be suitable for a septal occluder device closure of postinfarction ventricular septal rupture rather than immediate surgery? *Interact Cardiovasc Thorac Surg* 11:626-629, 2010.
68. Haddadin S, Milano A, Faggian G, et al: Surgical treatment of postinfarction left ventricular free wall rupture. *J Card Surg* 24:624-631, 2009.
69. Lopez-Sendon J, Gurfinkel E, Lopez de Sa E, et al: Factors related to heart rupture in acute coronary syndromes in the Global Registry of Acute Coronary Events. *Eur Heart J* 31:1449-1456, 2010.
70. Bueno H, Martinez-Selles M, Perez-David E, et al: Effect of thrombolytic therapy on the risk of cardiac rupture and mortality in older patients with first acute myocardial infarction. *Eur Heart J* 26:1705-1711, 2005.

71. Nakamura F, Minamino T, Higashino Y, et al: Cardiac free wall rupture in acute myocardial infarction: Ameliorative effect of coronary reperfusion. *Clin Cardiol* 15:244-250, 1992.
72. Honan MB, Harrell F, Jr, Reimer KA, et al: Cardiac rupture, mortality and the timing of thrombolytic therapy: A meta-analysis [see comments]. *J Am Coll Cardiol* 16:359-367, 1990.
73. Purcaro A, Costantini C, Ciampani N, et al: Diagnostic criteria and management of subacute ventricular free wall rupture complicating acute myocardial infarction. *Am J Cardiol* 80:397-405, 1997.
74. Wilkenshoff UM, Ale Abaei A, Kuersten B, et al: Contrast echocardiography for detection of incomplete rupture of the left ventricle after acute myocardial infarction. *Z Kardiol* 93: 624-629, 2004.
75. Figueras J, Cortadellas J, Evangelista A, et al: Medical management of selected patients with left ventricular free wall rupture during acute myocardial infarction. *J Am Coll Cardiol* 29:512-518, 1997.
76. Yeo TC, Malouf JF, Oh JK, et al: Clinical profile and outcome in 52 patients with cardiac pseudoaneurysm. *Ann Intern Med* 128:299-305, 1998.
77. Tuan J, Kaivani F, Fewins H: Left ventricular pseudoaneurysm. *Eur J Echocardiogr* 9:107-109, 2008.
78. Tikiz H, Balbay Y, Atak R, et al: The effect of thrombolytic therapy on left ventricular aneurysm formation in acute myocardial infarction: relationship to successful reperfusion and vessel patency. *Clin Cardiol* 24:656-662, 2001.
79. Tikiz H, Ramazan A, Balbay Y, et al: Left ventricular aneurysm formation after anterior myocardial infarction: clinical and angiographic determinants in 809 patients. *Int J Cardiol* 82:7-14; discussion 14-6, 2002.
80. Sartipy U, Albage A, Lindblom A: The Dor procedure for left ventricular reconstruction. Ten-year clinical experience. *Eur J Cardiothorac Surg* 27:1005-1010, 2005.
81. Greaves SC, Zhi G, Lee RT, et al: Incidence and natural history of left ventricular thrombus following anterior wall acute myocardial infarction. *Am J Cardiol* 80:442-448, 1997.
82. Turpie AG, Robinson JG, Doyle DJ, et al: Comparison of high-dose with low-dose subcutaneous heparin to prevent left ventricular mural thrombosis in patients with acute transmural anterior myocardial infarction [see comments]. *N Engl J Med* 320:352-357, 1989.
83. Solheim S, Seljeflot I, Lunde K, et al: Frequency of left ventricular thrombus in patients with anterior wall acute myocardial infarction treated with percutaneous coronary intervention and dual antiplatelet therapy. *Am J Cardiol* 106:1197-1200, 2010.
84. Osherov A, Borovik-Raz M, Aronson D, et al: Incidence of early left ventricular thrombus after acute anterior wall myocardial infarction in the primary coronary intervention era. *Am Heart J* 157:1074-1080, 2009.
85. Zielinska M, Kaczmarek K, Tylkowski M: Predictors of left ventricular thrombus formation in acute myocardial infarction treated with successful primary angioplasty with stenting. *Am J Med Sci* 335:171-176, 2008.
86. Domenicucci, S, Chiarella, F, Bellotti, P, et al: Long-term prospective assessment of left ventricular thrombus in anterior wall acute myocardial infarction and implications for a rational approach to embolic risk. *Am J Cardiol* 839:519-524, 1999.
87. Mollema S, Nucifora G, Bax J: Prognostic value of echocardiography after acute myocardial infarction. *Heart* 95:1732-1745, 2009.
88. White HD, Norris RM, Brown MA, et al: Left ventricular end-systolic volume as the major determinant of survival after recovery from myocardial infarction. *Circulation* 76:44-51, 1987.
89. Galasko G, Basau S, Lahiri A, et al: A prospective comparison of echocardiographic wall motion score index and radionuclide ejection fraction in predicting outcome following acute myocardial infarction. *Heart* 86:271-276, 2001.
90. Carluccio E, Tommasi S, Bentivoglio M, et al: Usefulness of the severity and extent of wall motion abnormalities as prognostic markers of an adverse outcome after a first myocardial infarction treated with thrombolytic therapy. *Am J Cardiol* 85:411-415, 2000.
91. Moller JE, Hillis GS, Oh JK, et al: Wall motion score index and ejection fraction for risk stratification after acute myocardial infarction. *Am Heart J* 151:419-425, 2006.
92. Kruszewski K, Scott A, Barclay J, et al: Noninvasive assessment of left ventricular filling pressure after acute myocardial infarction: a prospective study of the relative prognostic utility of clinical assessment, echocardiography, and B-type natriuretic peptide. *Am Heart J* 159:47-54, 2010.
93. Meta-Analysis Research Group in Echocardiography (MeRGE) AMI Collaborators: Independent prognostic importance of a restrictive left ventricular filling pattern after myocardial infarction. *Circulation* 117:2591-2598, 2008.
94. Moller J, Poulsen S, Sondergaard E, et al: Impact of early changes in left ventricular filling pattern on long-term outcome after acute myocardial infarction. *Int J Cardiol* 89: 207-215, 2003.
95. Whalley G, Gamble G, Doughty R: Restrictive diastolic filling predicts death after acute myocardial infarction: systematic review and meta-analysis of prospective studies. *Heart* 92: 1588-1594, 2006.
96. Moller JE, Sondergaard E, Poulsen SH: Pseudonormal and restrictive filling patterns predict left ventricular dilation and cardiac death after a first myocardial infarction: a serial color M-mode Doppler echocardiographic study. *J Am Coll Cardiol* 36:1841-1846, 2000.
97. Hillis G, Moller J, Pellika P, et al: Noninvasive estimation of left ventricular filling pressure by E/e′ is a powerful predictor of survival after acute myocardial infarction. *J Am Coll Cardiol* 43:360-367, 2004.
98. Moller JE, Sondergaard E, Poulsen SH: Color M-mode and pulsed wave tissue Doppler echocardiography: powerful predictors of cardiac events after first myocardial infarction. *J Am Soc Echocardiogr* 14:757-763, 2001.
99. Beinart R, Bovko V, Schwamm E, et al: Long-term prognostic significance of left atrial volume in acute myocardial infarction. *J Am Coll Cardiol* 44:327-334, 2004.
100. Moller JE, Hillis GS, Oh JK, et al: Left atrial volume: a powerful predictor of survival after acute myocardial infarction. *Circulation* 107: 2207-2212, 2003.
101. Giannuzzi P, Temporelli P, Bosimi E, et al: Heterogeneity of left ventricular remodeling after acute myocardial infarction: results of the Gruppo Italiano per lo Studio della Sopravvivenza nell'Infarto Miocardico-3 Echo Substudy. *Am Heart J* 141:131-138, 2001.
102. St John Sutton M, Scott CH: A prediction rule for left ventricular dilatation post-MI? *Eur Heart J* 23:509-511, 2002.
103. Greaves K, Dixon SR, Fejka M, et al: Myocardial contrast echocardiography is superior to other known modalities for assessing myocardial reperfusion after acute myocardial infarction. *Heart* 89:139-144, 2003.
104. Balcells E, Powers ER, Lepper W, et al: Detection of myocardial viability by contrast echocardiography in acute infarction predicts recovery of resting function and contractile reserve. *J Am Coll Cardiol* 41:827-833, 2003.
105. Hillis GS, Mulvagh SL, Pellikka PA, et al: Comparison of intravenous myocardial contrast echocardiography and low-dose dobutamine echocardiography for predicting left ventricular functional recovery following acute myocardial infarction. *Am J Cardiol* 92:504-508, 2003.
106. Main ML, Magalski A, Morris BA, et al: Combined assessment of microvascular integrity and contractile reserve improves differentiation of stunning and necrosis after acute anterior wall myocardial infarction. *J Am Coll Cardiol* 40:1079-1084, 2002.
107. Mengozzi G, Rossini R, Palagi C, et al: Usefulness of intravenous myocardial contrast echocardiography in the early left ventricular remodeling in acute myocardial infarction. *Am J Cardiol* 90:713-719, 2002.
108. Jeetley P, Swinburn J, Hickman M, et al: Myocardial contrast echocardiography predicts left ventricular remodelling after acute myocardial infarction. *J Am Soc Echocardiogr* 17:1030-1036, 2004.
109. Coletta C, Sestili A, Seccareccia F, et al: Influence of contractile reserve and inducible ischaemia on left ventricular remodelling after acute myocardial infarction. *Heart* 89:1138-1143, 2003.
110. Nijland F, Kamp O, Verhorst PM, et al: Myocardial viability: impact on left ventricular dilatation after acute myocardial infarction. *Heart* 87:17-22, 2002.
111. Bolognese L, Buonamici P, Cerisano G, et al: Early dobutamine echocardiography predicts improvement in regional and global left ventricular function after reperfused acute myocardial infarction without residual stenosis of the infarct-related artery. *Am Heart J* 139:153-163, 2000.
112. Vartdal T, Brunvand H, Pettersen E, et al: Early prediction of infarct size by strain Doppler echocardiography after coronary reperfusion. *J Am Coll Cardiol* 49:1715-1721, 2007.
113. Park Y, Kang S, Song J, et al: Prognostic value of longitudinal strain after primary reperfusion therapy in patients with anterior-wall acute myocardial infarction. *J Am Soc Echocardiogr* 21:262-267, 2008.
114. Hung C, Shin S, Hassanein A, et al: Strain and strain rate imaging are independent predictors of mortality after high-risk myocardial infarction [abstract]. *J Am Coll Cardiol* 10:A142, 2008.
115. Mollema S, Liem S, Suffoletto M, et al: Left ventricular dyssynchrony immediately after acute myocardial infarction predicts left ventricular remodelling. *J Am Coll Cardiol* 50: 1532-1540, 2007.
116. Sicari R, Landi P, Picano E, et al: Exercise-electrocardiography and/or pharmacological stress echocardiography for non-invasive risk stratification early after uncomplicated

myocardial infarction. A prospective international large scale multicentre study. *Eur Heart J* 23:1030-1037, 2002.
117. Pizzuto F, Voci P, Mariano E, et al: Assessment of flow velocity reserve by transthoracic Doppler echocardiography and venous adenosine infusion before and after left anterior descending coronary artery stenting. *J Am Coll Cardiol* 38:155-162, 2001.
118. Rigo F, Cortigiani L, Pasanisi E, et al: The additional prognostic value of coronary flow reserve on left anterior descending artery in patients with negative stress echo by wall motion criteria. A Transthoracic Vasodilator Stress Echocardiography Study. *Am Heart J* 151:124-130, 2006.
119. Saraste A, Koskenvuo J, Saraste M, et al: Coronary artery flow velocity profile measured by transthoracic Doppler echocardiography predicts myocardial viability after acute myocardial infarction. *Heart* 93:456-457, 2007
120. Trichon BH, Felker GM, Shaw LK, et al: Relation of frequency and severity of mitral regurgitation to survival among patients with left ventricular systolic dysfunction and heart failure. *Am J Cardiol* 91:538-543, 2003.
121. Bursi F, Enriquez-Sarano M, Jacobsen SJ, et al: Mitral regurgitation after myocardial infarction: a review. *Am J Med* 119:103-112, 2006.
122. Bursi F, Enriquez-Sarano M, Nkomo VT, et al: Heart failure and death after myocardial infarction in the community: the emerging role of mitral regurgitation. *Circulation* 111: 295-301, 2005.
123. Marwick T, Lancellotti P, Pierard L: Ischaemic mitral regurgitation: mechanisms and diagnosis. *Heart* 95:1711-1718, 2009.
124. Levine RA, Schwammenthal E: Ischemic mitral regurgitation on the threshold of a solution: from paradoxes to unifying concepts. *Circulation* 112:745-758, 2005.
125. Feinberg MS, Schwammenthal E, Shlizerman L, et al: Prognostic significance of mild mitral regurgitation by color Doppler echocardiography in acute myocardial infarction. *Am J Cardiol* 86:903-907, 2000.
126. Gorman RC, Gorman JH, 3rd: Why should we repair ischemic mitral regurgitation? *Ann Thorac Surg* 81:785; author reply 785-786, 2006.
127. Roshanali F, Mandegar MH, Yousefnia MA, et al: Low-dose dobutamine stress echocardiography to predict reversibility of mitral regurgitation with CABG. *Echocardiography* 23:31-37, 2006.

# 15 Exercise Echocardiography

ROSARIO V. FREEMAN, MD, MS

**Physiologic Principles of Exercise Echocardiography**
**Exercise Stressors Used for Stress Echocardiography**
**Methodology**
Equipment
Procedure
Imaging
Doppler
Room Layout
Personnel
Interpretation
**Diagnostic Accuracy of Exercise Echocardiography**
**Comparison with Other Stress Modalities**
Cost Effectiveness
Safety
Appropriate Use and Quality Assurance
**Applications**
Coronary Artery Disease: Initial Diagnosis
Coronary Artery Disease: Known Coronary Artery Disease
Coronary Artery Disease: Prognosis
Coronary Disease Diagnosis in Women
Risk Stratification Prior to Noncardiac Surgery
Hypertrophic Cardiomyopathy
Dilated Cardiomyopathy and Cardiac Transplantation
Valvular Heart Disease
Other Applications
**Future Directions**

Stress echocardiography integrates echocardiographic imaging with exercise electrocardiographic (ECG) testing to aid in real-time evaluation of ischemic, valvular, and cardiopulmonary heart disease. Accuracy for stress echocardiography to detect extent and location of myocardial ischemia is excellent, particularly when baseline ECG abnormalities render standard exercise ECG testing nondiagnostic.[1,2] In addition to initial coronary disease diagnosis, stress echocardiography is used to monitor disease progression in patients with known disease and assess clinical response to medical therapy. Stress echocardiography provides valuable information on myocardial viability, risk stratification, and prognostication. Nonischemia applications of stress echocardiography include evaluation and clinical management of cardiopulmonary, congenital, and valvular heart disease. Future advances include three-dimensional (3D) imaging, spectral Doppler interrogation with stress, myocardial strain and strain rate analysis, and integration of coronary flow reserve data using myocardial perfusion images.

The premise of stress echocardiography is provocation of transient myocardial ischemia by one of various cardiac stressors.[3-6] Nonexercise cardiac stressors include pharmacologic and pacing protocols (see Chapter 16). Pharmacologic stressors include agents that increase myocardial contractility and oxygen demand (dobutamine) and agents that induce transient regional hypoperfusion via coronary vasodilation (dipyridamole). Exercise stress is generally preferred over pharmacologic stress, as it allow for evaluation of exercise tolerance, symptom provocation, and prognostication.[7] Exercise stressors include treadmill and bicycle ergometry protocols. Images are acquired during peak exercise or, because of imaging difficulty due to patient motion, immediately after exercise cessation. Imaging data are then integrated with ECG data, exercise tolerance, and patient symptoms for final interpretation.

Capability for echocardiography to detect myocardial ischemia was shown more than three decades ago in animal models demonstrating concordance between severity and duration of coronary perfusion impairment and visualized regional wall motion abnormalities.[8,9] Early corroborating human studies using M-mode imaging demonstrated left anterior descending artery territory ischemia via reduced interventricular septal motion.[10] In one of the earliest descriptions of inducible ischemia during bicycle exercise, septal wall motion abnormalities, visualized by M-mode imaging, correlated with occlusion of the left anterior descending artery.[11] However, inability to image more than a discrete portion of the heart with M-mode imaging limited its overall utility as a diagnostic tool. Subsequent development of two-dimensional (2D) imaging allowed tomographic cardiac imaging, increasing utility for ischemia assessment.[12] Advances in transducer performance and development of harmonic imaging and digital loop grabbers have dramatically improved image quality and simplified interpretation. Stress echocardiography is now widely available.[13] Clinical guidelines provide recommendations regarding application of stress echocardiography as a first-line diagnostic tool.[5,6]

## Physiologic Principles of Exercise Echocardiography

During exercise, increases in myocardial oxygen demand results in augmented systolic function with increased myocardial thickening. With a hemodynamically significant coronary stenosis, the relative disparity in oxygen delivery to the distal coronary bed cannot meet increases in myocardial oxygen demand. Transient hypoperfusion results in mechanical dysfunction of affected myocardium. Stress echocardiography is well suited to assess this ischemic response by visualizing global and regional myocardial motion, allowing for localization of coronary lesions, given that coronary artery anatomy and myocardial distribution are relatively similar among patients (see Chapter 13).[14]

Myocardial ischemia generally progresses in a defined sequence of events, termed the *ischemic cascade*.[15] Ischemia is initiated by regional hypoperfusion of a distal coronary bed. After resultant metabolic changes within affected myocardium, alterations in function occur; initially with abnormalities in myocardial relaxation (diastolic dysfunction), and subsequently with systolic dysfunction of affected segments. Only in the later stages of ischemia are characteristic ECG changes, such as ST segment depression, and frank angina manifest (Fig. 15-1).[16,17] Propagation of ischemia generally proceeds from the subendocardium outward to the subepicardial layer in cases of more severe or prolonged ischemia.[18] However, because endocardial myocardial oxygen demand is higher, only moderate ischemia is needed to produce visually identifiable contractile dysfunction. With exercise ECG testing, ischemia diagnosis occurs with onset of angina or ECG changes, occurring in the later stages of the ischemic cascade (Fig. 15-2), contributing to acknowledged limitations in diagnostic accuracy for exercise ECG testing. In contrast, stress testing with integrated cardiac imaging identifies ischemia earlier, at onset of regional hypoperfusion (nuclear perfusion stress) or with systolic dysfunction (echocardiography). With stressor cessation and restoration of adequate coronary flow, induced abnormalities typically recover rapidly, but may persist if ischemia is severe. Early studies using echocardiographic imaging during angioplasty balloon inflation demonstrate onset of regional systolic dysfunction as early as 19 seconds after balloon inflation, with subsequent ischemic ECG changes and angina occurring 30 to 40 seconds after inflation. These abnormalities typically resolved within 10 to 20 seconds after balloon deflation.[17,19,20] Angioplasty balloon inflation models represent ischemia from a dynamic obstruction; imaging during provoked ischemia with a fixed coronary obstruction has shown a similar temporal progression with mechanical dysfunction preceding ECG changes and angina.[21,22]

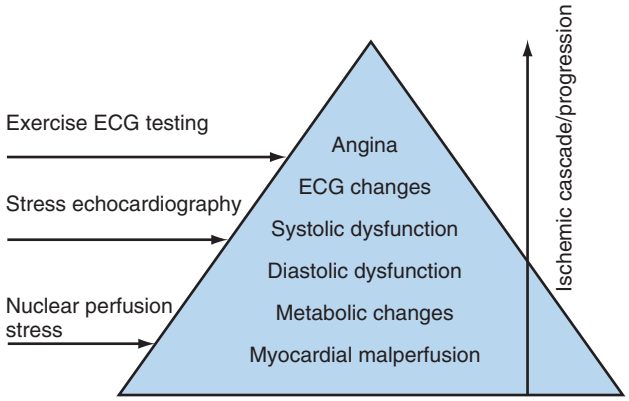



**Figure 15-1 Ischemic cascade.** Ischemia is initiated by myocardial hypoperfusion. Following metabolic changes within affected myocardium, alterations in function occur; initially with diastolic dysfunction, then progressing to systolic dysfunction. In the later stages of ischemia, characteristic electrocardiographic (*ECG*) changes and frank angina manifest.

In the absence of a physiologically significant coronary narrowing, the myocardial response to stress is augmented systolic function with increased inward *hyperdynamic* motion. In the presence of ischemia, myocardial responses include the following:

1. *Hypokinesis*, myocardial thickening with inward motion less than 5 mm or relatively less than the rest of the myocardium
2. *Akinesis*, absence of thickening or inward motion
3. *Dyskinesis*, thinned myocardium with paradoxical outward systolic motion, a passive myocardial response to increased intraventricular pressure[23]

In absence of disease, baseline systolic function is generally normal and myocardial response to exercise is hyperdynamic (Fig. 15-3). In ischemic but noninfarcted myocardium, the stress response is concordant with ischemia severity: hypokinesis in mild cases progressing to akinesis in more severe cases. Chronically infarcted regions with permanent transmural injury appear thinned and akinetic or dyskinetic. Acutely infarcted myocardium appears hypokinetic or akinetic with normal wall thickness as postinfarction remodeling has not yet occurred. If blood flow is rapidly restored to acutely infarcted

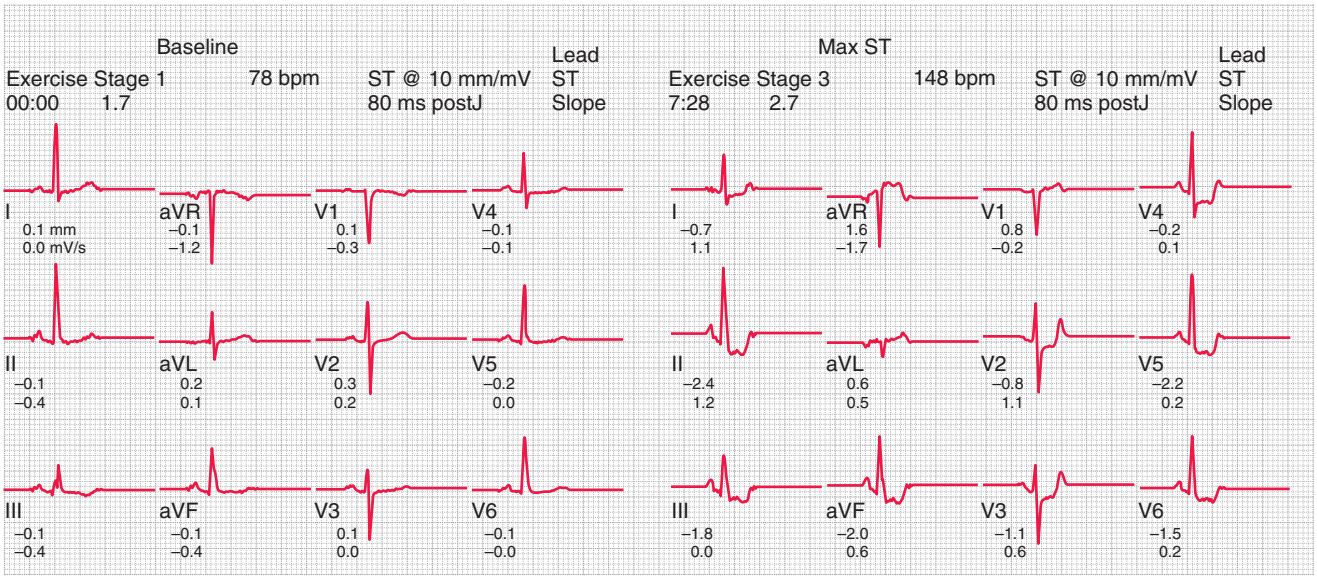



**Figure 15-2 Treadmill exercise ECG stress study.** This patient exercised 7 minutes and 28 seconds on a standard Bruce protocol (9 METs) and experienced chest discomfort and presyncope at peak stress. Baseline electrocardiogram (ECG) showed normal sinus rhythm with T wave inversion in lead III (*left*). Peak stress ECG showed horizontal ST depression in leads II, III, aVF, and V4-V6. Subsequent angiography revealed a proximal 80% left anterior descending artery lesion and moderate disease in the left circumflex artery.

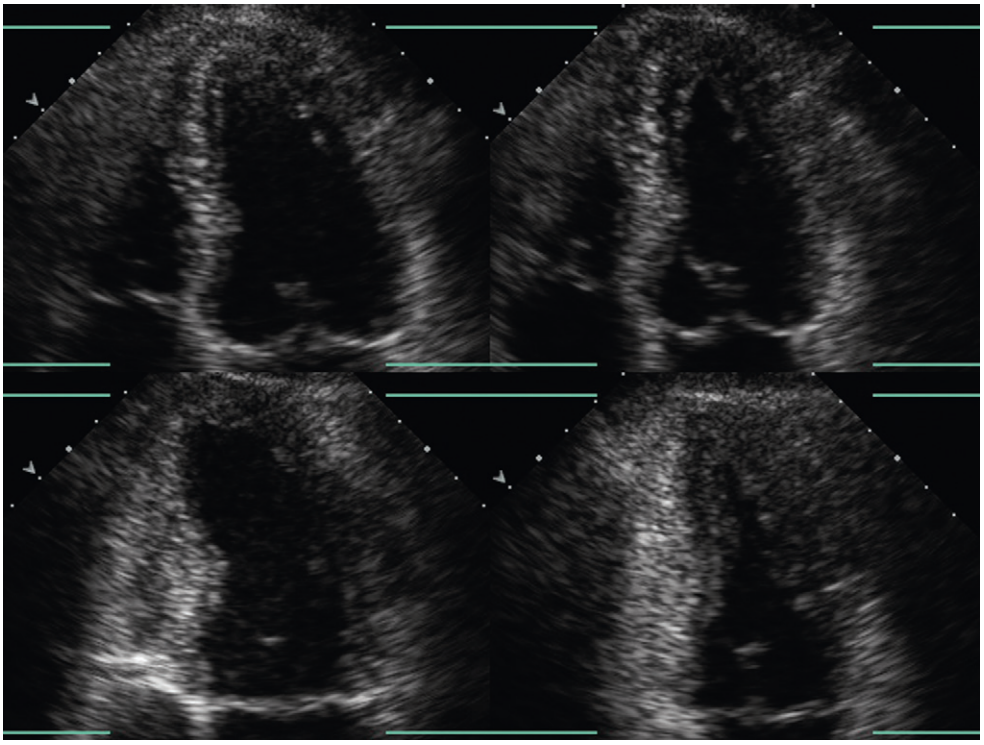


**Figure 15-3 Images from a normal exercise echocardiogram study taken at rest and immediately after cessation of treadmill exercise.** *Upper left*: Apical four-chamber view during rest. *Upper right*: Apical four-chamber view after exercise stress, *Lower left*: Apical four-chamber view during rest. *Lower right*: Apical four-chamber view after exercise stress. At rest, LV chamber size is normal. After exercise, there is hyperdynamic function of all segments with a decrease in chamber size.

myocardium, return of function is variable temporally and spatially. Regions of transmural infarct resulting from prolonged ischemia typically remain hypocontractile, but tissue subjected to only a short duration of coronary flow limitation typically regains contractility. Time duration of myocardial recovery after an infarction varies from days to months and is termed *stunned myocardium*. Prediction of functional recovery stunned segments may be accomplished with low dose dobutamine stress echocardiography or other modalities of viability testing (see Chapter 16).

The effect of ischemic on myocardial wall motion and thickening is proportional to the severity of impaired coronary blood flow.[22,24] For intermediate-range lesions (50% to 60% stenosis of the epicardial vessel) or single-vessel disease where only a few myocardial segments are affected, abnormalities during ischemia are typically subtle and transient or may be absent altogether. Assuming use of an adequate stressor, the severity of coronary narrowing where systolic dysfunction is perceptible is approximately 60% stenosis, with progression to akinesis when greater than 80% stenosis is present (Fig. 15-4). Note that visual estimates of stenosis severity based on planar angiographic images may not necessarily correlate with physiologically significant occlusions.[24-26] In the absence of significant coronary stenoses, exercise-induced reductions in relative coronary flow reserve may occur in patients with microvascular disease or increased myocardial mass, as occurs in left ventricular hypertrophy. In these cases, although a stressor may produce characteristic ECG changes or anginal symptoms, frank regional wall motion abnormalities may not be evident.[27,28]

## Exercise Stressors Used for Stress Echocardiography

In individuals able to exercise maximally, exercise stress is preferred over nonexercise stressors, as it allows for a contextual understanding of results relative to patient symptoms and functional capacity.[29] Metabolic equivalents (METs) are a measure of oxygen ($O_2$) consumption where 1 MET (resting metabolic state) equals 3.5 mL $O_2$ per kg/min. Exercise stressors should be used unless the patient is unable to achieve at least 5 METs or use the exercise equipment. Exercise protocols most widely used are treadmill and bicycle ergometry (upright or supine). In the United States, treadmill protocols are more common, unless the patient has neurologic, vascular, or orthopedic constraints that limit treadmill exercise performance.

Regardless of exercise stress type, an adequate workload is necessary to provide a diagnostic study. The most common hemodynamic target used is achievement of a heart rate goal based on patient age and gender, calculated as 85% of the maximal predicted heart rate: (estimated 220 − patient's age − For men and 210 − patient age for women). If necessary, workload can be augmented with other measures such as hyperventilation or handgrip exercise.[30] During the stress study, patients should subjectively report exertion level, using standardized scales, such as the Borg rating of perceived exertion (Box 15-1).[31] It is institution and physician dependent whether exercise is discontinued once hemodynamic targets are achieved, or whether the patient continues to maximum exercise capacity.

With treadmill exercise protocols, baseline echocardiographic images are obtained in a left lateral decubitus position to facilitate acoustic windows (Table 15-1). Exercise then commences according to standardized protocols.[31] Most patients who are reasonably active perform the Bruce protocol. However, in patients with mobility restrictions or limited exercise tolerance, the Cornell or Naughton protocols are other options to allow for at least 6 to 12 minutes of continuous exercise. Systolic blood pressure is monitored throughout the study and should increase by at least 20 mm Hg with exercise. The treadmill portion is halted for:

(1) concerning symptoms (severe angina, ataxia, dizziness, pallor,

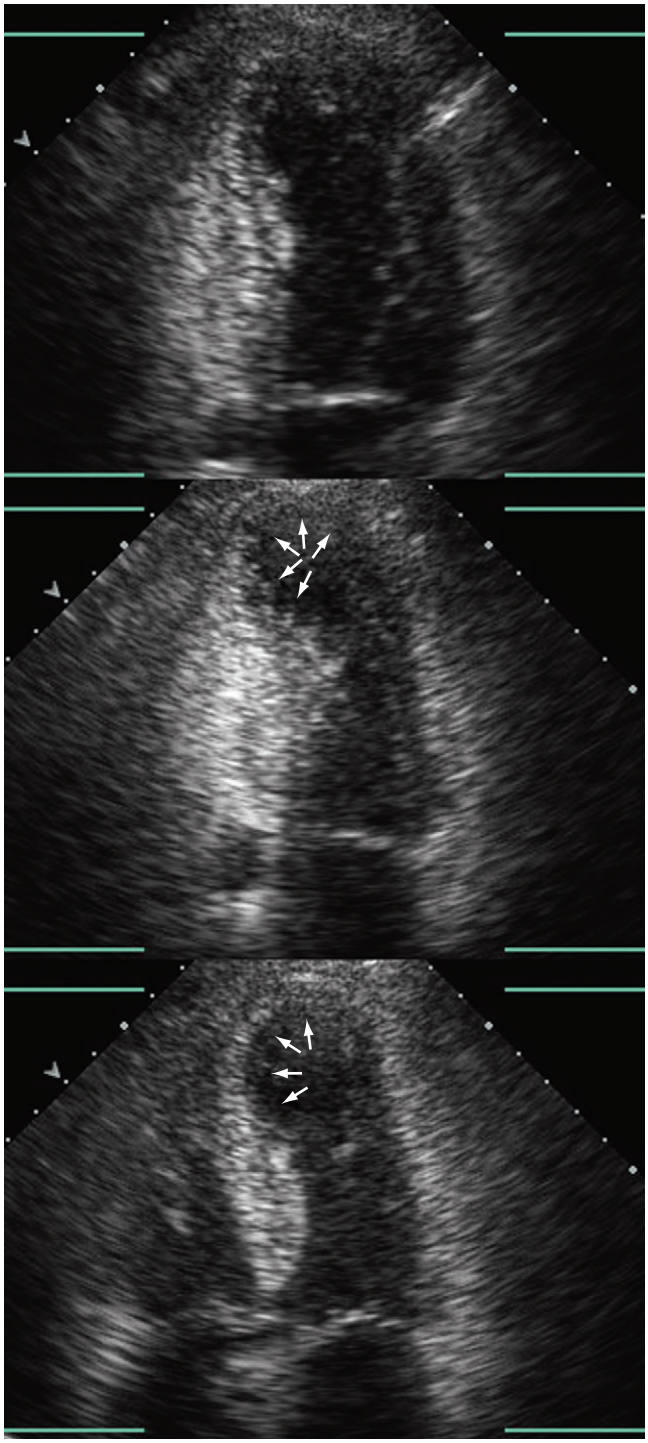


**Figure 15-4 Abnormal treadmill stress echocardiogram.** The patient exercised 7 minutes and 30 seconds on a standard Bruce protocol and developed angina at peak stress. *Top*: Apical two-chamber view atrest during systole. *Middle*: After exercise, there is thinning and hypokinesis of the entire apex and distal inferior wall in the apical two-chamber view (*arrows*). *Bottom*: On the apical four-chamber stress view, there is thinning and dyskinesis of the entire apex and distal inferoseptum (*arrows*). All other segments became hyperdynamic.

(2) severe hypertension (systolic blood pressure greater than 220 mm Hg),
(3) hypotensive response (more than 10 mm Hg drop in systolic blood pressure),
(4) concerning ECG changes or arrhythmias, or

**Box 15-1**

**BORG RATING OF PERCEIVED EXERTION**

6 No exertion at all
7 Extremely light
8
9 Very light
10
11 Light
12
13 Somewhat hard
14
15 Hard (heavy)
16
17 Very hard
18
19 Extremely hard
20 Maximal exertion

(5) hemodynamic targets are achieved.[31] Based on total exercise duration, a nomogram based on age, gender, and degree of physical conditioning provides an estimate of functional aerobic impairment.[32]

Because patient motion limits imaging during active treadmill use, "stress" imaging is performed immediately after exercise cessation without a cool-down period. The duration of ischemia induced abnormalities is variable, dependent on coronary occlusion severity, number of vessels affected, presence of collateral blood flow, and achieved workload.[33] Although ischemic abnormalities can persist for some time after exercise cessation, most reverse within minutes. Therefore, expeditious imaging is critical; image acquisition within 60 to 90 seconds after exercise completion is generally adequate. Reasonable patient agility is required to transition to the imaging table, reassume a left lateral decubitus position, and allow imaging within this time window (see Table 15-1). If prolonged delays in patient transfer occur or acoustic windows are suboptimal, transient ischemia may be missed. This is particularly true with intermediate-range occlusions or single-vessel disease where induced abnormalities are often fleeting. Although feasibility of peak stress imaging on the treadmill has been demonstrated, the minimal incremental benefit attributable to time savings while scanning upright coupled with difficulties in obtaining reproducible results limits widespread use.[34]

For bicycle ergometry, baseline images are obtained in a left lateral decubitus position (see Table 15-1). Patients perform either upright or supine bicycle exercise with a goal of achieving increases in wattage, 2 to 3 minutes per stage. At each stage, pedal resistance increases in a stepwise manner and the patient must maintain a constant cadence (about 60 rpm). Because workload is effort driven, achievement of maximal workload is more patient dependent than in treadmill protocols. After completion of exercise, the patient reassumes a left lateral decubitus position for further imaging. If apical windows are not easily accessible, subcostal views provide an alternative. During upright or supine ergometry, most myocardial segments can be well visualized.[35] However, care must be taken to avoid apical foreshortening as can occur with even mild head elevation. For supine bicycle ergometry, integrated imaging stretchers allow patient rotation and positioning such that transition to a separate imaging bed is obviated, resulting in time savings (see Table 15-1). Bicycle protocols allow for a relatively stationary position for simultaneous image acquisition during active exercise.[36,37]

**TABLE 15-1 Exercise Stress Protocols for Echocardiography**

| *Treadmill* | *Upright Bicycle* | *Supine Bicycle* |
|---|---|---|
| 1. Patient on imaging bed<br>Image parasternal long-axis view<br>Image parasternal short-axis view<br>Image apical four-chamber<br>Image apical two-chamber | 1. Patient on imaging bed<br>Image parasternal long-axis view<br>Image parasternal short-axis view<br>Image apical four-chamber<br>Image apical two-chamber | 1. Patient on integrated imaging bed<br>Image parasternal long-axis view<br>Image parasternal short-axis view<br>Image apical four-chamber<br>Image apical two-chamber |
| 2. Patient moves to treadmill | 2. Patient moves to bicycle | 2. Patient remains on integrated bed |
| 3. Exercise commences | 3. Image apical rest views | 3. Exercise commences |
| 4. Exercise cessation | 4. Exercise commences | 4. Imaging at each stage end |
| 5. Patient moves to imaging bed<br>Postexercise imaging | 5. Imaging at each stage end | 5. Exercise cessation |
| | 6. Exercise cessation | 6. Postexercise imaging |
| | 7. Patient moves to imaging bed<br>Postexercise imaging | |

Imaging concurrent with peak stress, as opposed to immediate posttreadmill imaging, increases sensitivity for detecting transient ischemia.[36,38,39]

In the United States, treadmill stress is favored over bicycle ergometry because of widespread availability of treadmills in hospital settings and familiarity of walking as a form of exercise. Treadmill ECG testing, as an established diagnostic modality, is well validated, providing a wealth of prognostic information referenced to exercise duration and ECG response to exercise. With treadmill exercise, patients generally achieve higher workloads than with bicycle exercise, increasing likelihood of attaining hemodynamic targets. Supine ergometry stress typically produces a lower heart rate increase and a systolic blood pressure response about 20 mm Hg higher than that of upright exercise because of physiologic differences in preload. Additionally, maximum oxygen uptake tends to be lower with bicycle ergometry (10% to 20%) and should be considered during study interpretation.[31] Last, with supine ergometry, where the lower extremities must be supported against gravity, if quadriceps fatigue precedes maximal workload, patients may prematurely discontinue exercise.

In Europe, where bicycling is a more common form of exercise, bicycle protocols are favored. Guided by real-time wall motion evaluation, bicycle protocols allow for ischemia detection at onset, allowing identification of the ischemic threshold, in contrast to treadmill protocols that use ECG changes or symptom onset as a time point to discontinue exercise. Real-time ischemia identification allows for increased detection of subtle or transient ischemia with single-vessel disease or intermediate-severity lesions. Bicycle protocols allows imaging without the "all-or nothing" constraints of a narrow immediate poststress imaging window, as seen in treadmill protocols. The choice of which stressor to employ should be individualized to the ability of the patient to perform exercise, experience level of the personnel administering the study, and availability of equipment. Published reports demonstrate comparable accuracy between different exercise protocols.[39-41] As long as an adequate workload is achieved, overall accuracy is likely equivalent regardless of the stressor employed.[42]

# Methodology

## EQUIPMENT

The standard for laboratories performing exercise echocardiography includes high-quality instruments with a digital frame grabber, harmonic imaging capability, and an offline analysis system. Appropriate equipment (treadmill or bicycle ergometer) should be available, as should imaging beds with lateral cutouts to facilitate apical imaging. A cardiac arrest cart and defibrillator should be easily accessible.[5,6]

Digital frame grabbers and split-screen displays allow side-by-side comparison of rest and stress images to facilitate identification of regional wall motion abnormalities. Digital frame capture rates ranging from 20- to 100-ms intervals are looped and replayed continuously for analysis.[43,44] These intervals allow for variable capture within the cardiac cycle ranging from systole alone to the entire cardiac cycle. Most systems acquire eight frame digital loops per view with about 50 ms for each frame. However, if heart rate exceeds 150 bpm, image quality may be improved by reducing the capture interval to 30 to 40 ms. Digital clips of about 10 to 20 seconds per view are needed for adequate wall motion analysis. Gating of baseline and stress images to the ECG allows comparative analysis of endocardial motion at the same point in the cardiac cycle, optimizing identification of interval changes in regional function. A videotaped backup recording of the study is helpful to ensure that digital loops accurately reflect myocardial motion.[45]

## PROCEDURE

A brief history is taken to document symptoms, atherosclerosis risk factors, and current medications and to review basic laboratory findings. Written informed consent should be obtained before the procedure. An activity-specific questionnaire may aid in predicting peak exercise capacity.[46] Patients should refrain from oral intake 3 to 4 hours before the procedure.[31] Medications that may affect maximal workload (i.e., atrioventricular nodal blocking agents) should be held for one or two doses, unless the study purpose is to diagnose ischemia while on active therapy or risk of an adverse event off medication is deemed too high. Telemetry leads are placed at standard limb and precordial sites, slightly displacing leads that interfere with acoustic windows. One ECG lead is concurrently displayed on the echocardiography monitor to allow image gating and correlate changes in wall motion with ECG abnormalities. Information on heart rate, rhythm, exercise capacity, and blood pressure is recorded (Box 15-2).[29] Common ECG criteria for ischemia are greater than 1 mm horizontal or down-sloping ST depression at least 60 ms after the end of the QRS complex in anatomically contiguous leads.[29] Patients should be intermittently asked for presence or severity of symptoms. If severe symptoms occur or ischemia develops, the study should be discontinued. Monitoring should continue until blood pressure, heart rate, and ECG have returned to near-baseline levels and any induced symptoms have resolved. Study results should be conveyed to the

referring provider promptly, with immediate discussion when the stress test is strongly positive.

Optimal acoustic windows are located and baseline echocardiographic images obtained. If baseline abnormalities are seen, a brief transthoracic study should be performed to evaluate ventricular dysfunction, significant valvular abnormalities, or pericardial effusion. If baseline image quality is suboptimal (up to 20% of cases), transpulmonary contrast aids endocardial border definition (Fig. 15-5). Transpulmonary contrast is particularly helpful for assessing anterior and lateral wall motion, regions that may be more difficult to see in larger patients or those with underlying pulmonary disease. However, because contrast lasts only 1 to 2 minutes after injection, separate injections are needed for baseline and stress images. For treadmill studies, contrast is injected during peak exercise so it is in place during poststress imaging.

**Box 15-2**

**EXERCISE ECG TESTING MEASUREMENT PARAMETERS**

**Hemodynamic and Symptomatic Parameters**
1. Heart rate (last 10 seconds of each minute)
2. Blood pressure (last 30 seconds of each stage)
3. Exercise duration
4. Heart rate recovery after exercise cessation
5. Time to onset/resolution of angina
6. Subjective level of perceived exertion
7. Other cardiopulmonary symptoms (presyncope, dyspnea)

**ECG Parameters**
1. ST segment elevation/depression and slope
2. Arrhythmias
3. Number leads involved
4. Time to onset and resolution ST abnormalities

Adapted from Gibbons L, Balady GJ, Bricker JT, et al: ACC/AHA Guideline update for exercise testing: a report of the American College of Cardiology/American Heart Association Task Force on Practice Guidelines. *J Am Coll Cardiol* 40:1431-1440, 2002.
*ECG*, Electrocardiography.

## IMAGING

Myocardial segments are evaluated in multiple views to avoid misdiagnosis due to an oblique image plane. Prestress optimization of image planes and views is critical to maximize diagnostic accuracy. The four basic views used are concordant with standard transthoracic tomographic planes: the parasternal short- and long-axis views and the apical four- and two-chamber views. Subcostal views are not commonly used but may be substituted in the rare instance when they provide better images, such with intervening lung tissue due to chronic pulmonary disease.[35] Once baseline images are obtained, acoustic windows are identified and marked to minimize transducer repositioning on poststress imaging. Because induced ischemia may normalize quickly, sequencing for poststress imaging typically starts with apical windows, moving to parasternal windows. Several digital loops are acquired in each view in rapid sequence to optimize loop selection for comparison. Vigorous cardiac contraction, tachycardia, and exaggerated respiration increases translational and rotational movement of the heart. Patients with excessive cardiac motion should briefly halt respiration at

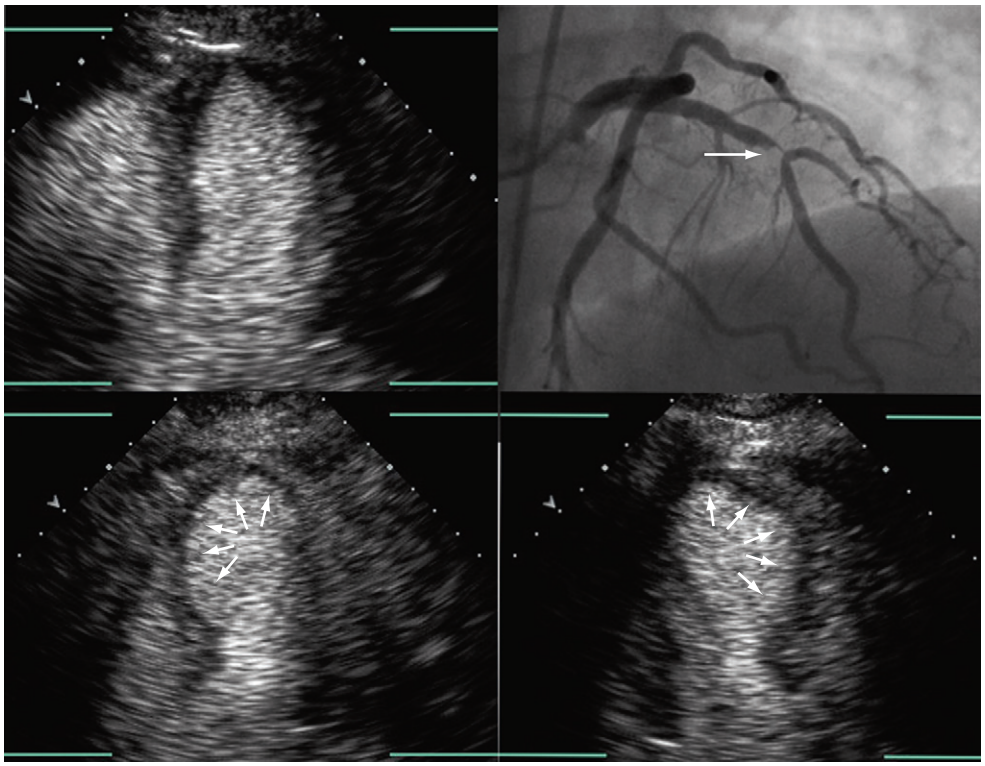


**Figure 15-5** Abnormal treadmill stress echocardiogram with transpulmonary contrast to enhance the endocardial border. *Upper left*: Resting four-chamber view shows normal LV cavity size with symmetric systolic wall motion. *Bottom left* and *right*: After exercise, aneurysmal dilation and hypokinesis are seen in the entire apex, distal inferoseptum, and distal anterior wall (*arrows*). Other segments are hyperdynamic. *Upper right*: Subsequent angiography revealed mid-90% left anterior descending artery lesion (*arrow*).

end- or midexpiration to aid in maintaining a relatively constant imaging plane. With normalization of heart rate near to baseline, an additional set of images should be obtained to evaluate for late-onset ischemia.

## DOPPLER

Doppler echocardiography is not routinely performed during stress echocardiography for ischemia evaluation. Rapid heart rate and additional time requirements for imaging do not allow for reliable data acquisition. Doppler-derived indicators of myocardial response to stress include left ventricular (LV) ejection velocity, aortic systolic ejection rates, transmitral filling velocities, and tissue Doppler interrogation of myocardial velocities. Although research-based applications using Doppler interrogation during peak stress suggest some additive value, the additional time demands of Doppler interrogation in its current state, coupled with relatively small incremental gain in information, limit routine use. In patients with valve lesions who have equivocal symptoms or are asymptomatic, tailored Doppler interrogation during exercise echocardiography provides objective data on exercise tolerance, symptom provocation, hemodynamic effects of exercise, and pulmonary pressure response to exercise (see later discussion).[47]

## ROOM LAYOUT

Room layout is critical to success of the procedure. The narrow time window between exercise cessation and recording of post-stress images necessitates spatial optimization to maximize time savings and facilitate image acquisition. A typical floor plan minimizes the number of steps and impediments for patient transfers (Fig. 15-6).[48] Adequate space around the imaging bed for the ECG and echocardiography instruments, sonographer, and medical professionals is necessary. Patients should receive clear instructions on maneuvers required after exercise termination to avoid introducing unnecessary delay. Often, it helps to have a "practice" transition from the treadmill to the imaging bed so the patient knows what is expected. Emergency medical equipment, drugs, and supplies should be readily available.

## PERSONNEL

Staffing for exercise echocardiography requires at least two people: a sonographer and a medical professional to monitor the patient and evaluate for symptom onset.[6] A physician trained in advanced cardiac life support should be in the immediate vicinity of the stress laboratory and available for emergencies.[29,49] In many laboratories, physician supervision is a requirement, either physically or more remotely, observing from a monitor. However, several studies document the safety of exercise supervision by properly trained allied health professionals such as physician assistants, exercise physiologists, or registered nurses.[50,51] Regardless of the personnel used, considerable skill on the part of the medical supervisor, sonographer, and/or technician is needed to facilitate an adequate study and recognize signs and symptoms of ischemic heart disease.

There is a significant learning curve associated with the technical challenges of image acquisition, study implementation, and interpretation. To optimize imaging, sonographers should have completed training in standard transthoracic imaging with an additional 3 months of training in exercise echocardiography and should possess basic knowledge of coronary anatomy and myocardial distribution. It is recommended that sonographers complete more than 50 stress studies to claim proficiency and perform more than 10 studies per month to maintain appropriate skill level. Physicians responsible for supervision and interpretation should be at least level II trained in echocardiography (Box 15-3). Supervised overreading of at least 100 studies by a level III–trained echocardiographer with independent interpretation of 200 studies is recommended to attain a minimum competence level for independent interpretation, and additional interpretation of more than 15 studies per month is recommended to maintain skills.[6,52] Although these volumes are reasonable for routine study interpretation, more specialized applications, such as evaluation of valvular heart

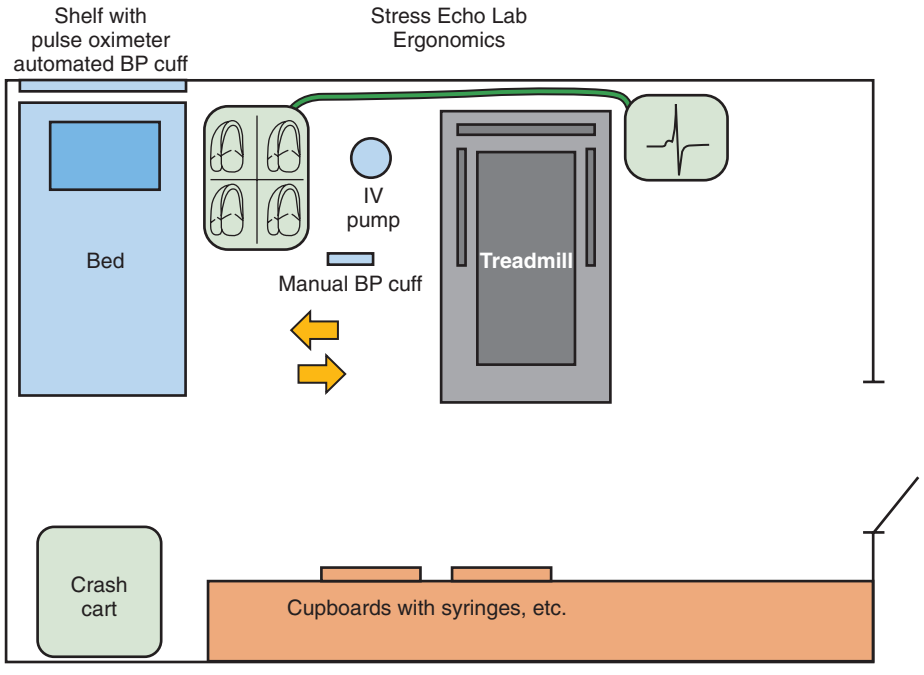



**Figure 15-6 Room layout.** Stress echocardiography laboratory equipment set-up. Beginning at the bottom of the figure and moving clockwise: storage cupboards with intravenous (*IV*) equipment, crash cart, imaging bed with shelf above for pulse oximeter and automated blood pressure (*BP*) cuff, echocardiography machine with frame grabber, IV pump for pharmacologic stress echocardiography, manual BP cuff, treadmill, electrocardiography (ECG) machine. The patient moves between the imaging bed and the treadmill, requiring no more than two steps in each direction (*yellow arrows*).

**Box 15-3**

**RECOMMENDED PHYSICIAN KNOWLEDGE FOR PERFORMANCE AND INTERPRETATION OF STRESS ECHOCARDIOGRAPHY[6]**

- Understand indications and limitations of exercise echocardiography with knowledge of alternative diagnostic procedures
- Knowledge of cardiovascular drugs and effects on stress response
- Understand study endpoints and indications for study termination
- Understand diagnostic accuracy and prognostic value of stress echocardiography in different patient populations
- Identify LV wall segments, recognize wall motion abnormalities, and interpret digitally acquired images
- Understand conditions and circumstances for indeterminate or false test results
- Competence in cardiopulmonary resuscitation
- Apply Doppler data to physiologic changes occurring during stress (hemodynamic studies)

**TABLE 15-2 Interpretation of Myocardial Response to Stress**

| *Resting Myocardial Appearance* | *Myocardial Response to Exercise* | *Interpretation* |
|---|---|---|
| Normal | Hyperdynamic | Nonischemic |
| Normal | Hypokinetic or akinetic | Ischemic |
| Normal | Unchanged (lack of hyperdynamic response) | Microvascular ischemia or balanced ischemia |
| Hypokinetic | Akinetic | Infarcted myocardium |
| Akinetic | Dyskinetic | Transmural infarct |

disease, warrant more clinical expertise and volume.[53] Continuous quality-improvement practices should be employed to ensure consistency and accuracy of interpretations.[54]

## INTERPRETATION

A normal study is one where there is normal resting wall motion with a hyperdynamic response to exercise (see Fig. 15-3). With abnormal studies, location, extent, and severity of interval changes are noted and recorded (Table 15-2). During interpretation, provoked abnormalities concordant with a coronary artery distribution should be noted. More detailed segmental analysis using the 16-segment LV model (see Figure 13-3) and standard wall motion analysis scale (normal, hypokinetic, akinetic, dyskinetic) may be used for reporting.[14] Several factors affect myocardial appearance and response to stress:

1. Compensatory hyperdynamic function of nonischemic regions
2. Tethering of nonischemic regions
3. Balanced ischemia
4. Lack of hyperdynamic response to stress

With prolonged ischemia, compensatory hyperdynamic function in regions remote to ischemic zones occurs because of a physiologic response of the ventricle to maintain overall cardiac output.[55] If pronounced, this may mask stress induced abnormalities in ischemic segments. Nonischemic segments adjacent to ischemic myocardium may show decreased motion despite the presence of adequate blood flow because of *tethering* from akinetic regions, leading to overestimation of ischemic burden.[56] Stress-induced global hypokinesis, or a lack of hyperdynamic response to exercise, may be seen in patients with disease in all major epicardial coronary arteries, or "balanced" ischemia. However, other markers of coronary artery disease are usually identifiable, such as decreased exercise tolerance, ischemic ECG changes, or angina. Rarely, a lack of hyperdynamic response occurs in absence of major coronary artery obstruction, such as in left ventricular hypertrophy, diabetes, severe arterial hypertension, and hypertrophic cardiomyopathy. Angiographic studies in these subsets suggest a reduction in coronary flow reserve due to microvascular disease, with smaller regions of ischemia failing to manifest in frank mechanical dysfunction. Because heterogeneity in wall motion is absent, diagnostic accuracy to identify ischemia is lowered.[57,58] Although current diagnostic testing does not allow for definitive diagnosis of microvascular ischemia, advances in myocardial contrast perfusion imaging may increase understanding of this disease process in the future.

Interpretation of stress echocardiography remains largely qualitative, with visualized wall motion abnormalities the core marker of ischemia. This approach is generally adequate for patient management. Reliability and reproducibility of study interpretation are largely dependent on interpreter experience.[59] Adequate physician and sonographer training and conservative interpretation criteria improve diagnostic sensitivity, consistency, reliability and validity.[60,61] A logical approach to interpretation is essential. Echocardiographers should be cognizant of the patient's clinical history. For example, in patients with prior coronary bypass surgery, wall motion analysis may suggest collateralized vessels, not a typical pattern for patients without coronary disease. Similarly, in individuals with prior infarcts, tethering effects on adjacent nonischemic regions should be considered.

Interpreters should be vigilant for induced wall motion changes that do not actually signify ischemia. Such "false-positive" findings include abnormal septal motion with ventricular pacing, an intrinsic conduction abnormality, or postoperative changes. Another false-positive septal abnormality is early relaxation of the anteroseptal region relative to other segments. "Early relaxation" can usually be timed in the cardiac cycle to just before mitral valve opening and is not indicative of ischemia.[62] Other commonly misdiagnosed regions include the basal inferior wall. Without prior bypass revascularization, an isolated basal wall motion abnormality should be scrutinized closely, given the unlikelihood of an isolated proximal wall abnormality with hyperdynamic mid and distal segments.[59] Falsely negative studies are most commonly due to procedural difficulties, such as inadequate workload, performance below the ischemic threshold, inexperienced interpreters, poor endocardial border definition, and inferior image quality. Myocardial regions more subject to "false negatives" or missed ischemia include the lateral wall, particularly in obese patients, and those where interposed lung tissue hinders imaging.

With residual coronary occlusion and chronic ischemia, stress echocardiography can be used to evaluate for viable myocardium. Viable myocardium is hypokinetic, as minimally adequate blood flow meets basal metabolic needs but is insufficient to support normal function. Distinguishing between viable or infarcted myocardium has been applied to coronary revascularization, based on the premise that revascularization of viable tissue improves systolic function and reduces ischemic burden.[4] For stress echocardiography, a "biphasic" response is

the hallmark of viable myocardium where mild augmentation in wall motion occurs following a low-level stressor, but with higher stressor doses, segments become frankly ischemic and decrease contractility, again becoming hypokinetic or akinetic. Because of the subtlety in wall motion assessment during viability testing, exercise stressors have not proven reliable, and conventional protocols use pharmacologic stressors (see Chapter 16). The future role of viability testing is not clear. A recent substudy of the Surgical Treatment for Ischemic Heart Failure Trial found that identification of substantial viable myocardium did significantly affect 5-year mortality comparing medical therapy with and without bypass surgery, implying that viability assessment alone should not be the deciding factor in determining treatment strategy.[63]

More quantitative approaches to exercise echocardiography provide standardized interpretation but are labor intensive to implement. The most commonly used semiquantitative application is the *wall motion score index*, in which the LV is divided into segments and regional wall motion of each segment is assessed (see Chapter 13, page 239).[14] Wall motion is graded between 1 and 4 depending on abnormality severity (0 hyperkinetic, 1 normal motion, 2 hypokinetic, 3 akinetic, and 4 dyskinetic). The summed total is divided by the number of segments evaluated to calculate a global wall motion score index. Alternatively, individual coronary artery distributions can be assigned to obtain a regional wall motion score index. Similar to qualitative interpretation, overscoring of nonischemic segments "tethered" to ischemic myocardium overestimates ischemic burden.

Computer-driven algorithms offer the potential for decreasing time demands for quantitative analysis. The *centroid* and *centerline* algorithms gauge wall motion referenced to a "baseline" within the LV. With the centroid method, multiple radii extending from a geometric center of mass to the endocardial and epicardial surfaces of the LV are generated and relative differences in wall motion between rest and stress images are compared. With the centerline method, distance measurements of the endocardium and epicardium perpendicular to the midpoint of the myocardium are compared. However, subjective decision making by the interpreter is still needed in marking endocardial and epicardial borders. (See Chapter 12.) Availability of automated endocardial border recognition algorithms is increasing. However, the need for superior image quality for accurate border delineation is paradoxic, because excellent qualitative interpretation is usually possible without the time demands of quantitative measurement. Moreover, most available analysis packages rely on radial motion analysis and do not reliably account for torsional or translational movement. Although a quantitative tool is an attractive concept to increase ease and reliability of interpretation, with the added labor requirements no currently available tools supplant standard qualitative analysis.[64]

## Diagnostic Accuracy of Exercise Echocardiography

Diagnostic accuracy of cardiac stress testing is generally reported as sensitivity and specificity to detect angiographically identified lesions. However, consideration of stenosis severity that denotes disease presence should be made. Stenosis thresholds create artificial distinctions (disease present versus not present) in a process that actually represents a spectrum. If the "set point" is higher (use of greater than 70% versus greater than 50% coronary artery stenosis used as the definition of disease presence), patients with true ischemia but less severe occlusion would be erroneously labeled "false positive." Higher set points increase sensitivity by increasing true positive likelihood and reducing false negatives.[24,65-70] Additionally, there are acknowledged limitations of 2D angiography in measuring hemodynamic significance of lesions.[71,72] However, limited data using quantitative angiography demonstrate excellent correlation with stress echocardiography results.[22,25]

Diagnostic accuracy is affected by factors that introduce bias.[73,74] Early exercise echocardiography studies suffered from reporting bias, where newer modalities are favored over old. For example, if echocardiographic stress test accuracy is compared with standard ECG testing, the exercise ECG portion is the same. Echocardiographic imaging is only additive with impossibility for a "worse" performance. Validation studies for exercise echocardiography tended to be performed at higher-volume centers with increased clinical expertise, drawing from patient groups with prior myocardial infarction or known disease, where higher pretest probability increased test sensitivity. With acceptance of test validity of a modality, posttest referral bias is introduced (Fig. 15-7), where only positive tests are referred for confirmatory testing (in this case, angiography), and negative tests are accepted as correct without verification.[75] Last, with accepted use of a modality and more widespread application, pretest disease probability drops with drifts in sensitivity and specificity. This has been documented with nuclear perfusion stress, for which larger-cohort data are available.[76]

Diagnostic accuracy depends on disease prevalence in the tested population, definition of disease "presence," and criteria used to define a positive test. Inclusion of borderline or equivocal findings (i.e., identifying a lack of a hyperdynamic response as ischemia) increases likelihood of identifying disease, raising sensitivity at the expense of specificity by increasing false positives. If image quality is suboptimal or with delay in poststress imaging, diagnostic accuracy suffers (Table 15-3).[36,38,39,42,70] With single-vessel disease, the ischemic zone is relatively smaller and

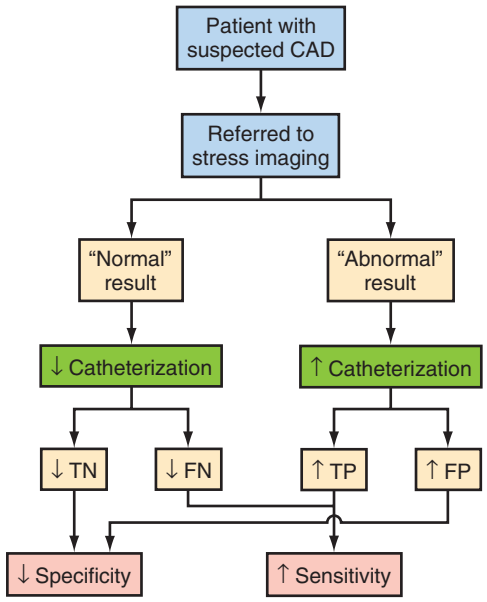



**Figure 15-7 Posttest referral bias.** Because abnormal test results lead to increased referral for confirmatory coronary catheterization, studies evaluating diagnostic accuracy have relatively higher true positive and false positive rates, which result in higher sensitivity and lower specificity.[74]

**TABLE 15-3 Factors Affecting Exercise Echocardiography Interpretation and Accuracy**

| *Lowered Specificity (False-Positive Errors)* | *Lowered Sensitivity (False-Negative Errors)* |
|---|---|
| Hypertensive response to stress as abnormal | Poor image quality |
| Basal inferior wall abnormalities as abnormal | Excessive postexercise delay to imaging |
| Tethered segments as abnormal | Single-vessel disease |
| Lack of hyperdynamic response as abnormal | Testing patients with lower pretest disease probability |
| Early septal relaxation as abnormal | Lateral wall abnormalities |
| Interventricular conduction delay or paced rhythms | Inadequate workload (suboptimal effort or medications) |
| Valvular heart disease with loss of contractile reserve | Multivessel disease with balanced ischemia |
| Cardiomyopathies | Mild or intermediate-severity stenoses |
| Inexperienced personnel | Inexperienced personnel |

ischemia is more difficult to detect, lowering sensitivity by increasing false-negative studies, approximately 75% compared to overall sensitivity of 84% in all patients with coronary disease.[70,77] Patients unable to achieve a high workload are less likely to reach an ischemic threshold, as can occur in patients on medications that lower heart rate response to exercise (i.e., atrioventricular nodal blocking agents). Last, interpreter experience is critical, with increased diagnostic accuracy seen for higher-volume, more experienced readers. Overall, exercise echocardiography is both sensitive and specific for ischemia identification (accuracy 85% to 90%) (Table 15-4). A meta-analysis of more than 2600 patients drawing from 24 studies reported overall sensitivity of 85% and specificity of 77%.[78]

## Comparison with Other Stress Modalities

Exercise ECG testing is the most established stress modality, widely available and well validated for initial coronary artery disease diagnosis, cardiac risk assessment, and prognostication. In a review of 58 exercise ECG studies involving nearly 12,000 patients undergoing both coronary angiography and exercise testing, mean sensitivity was 67% with mean specificity of 72%.[29] The greatest diagnostic value for exercise ECG testing is its negative predictive value. However, if baseline ECG abnormalities are present, sensitivity and specificity decline.[57] Additionally, ECG ST segment changes during exercise can be effected by factors other than ischemia, such as endogenous estrogen, which can have a digoxin-like effect on the ECG, and hyperventilation, which can cause diffuse ST segment abnormalities.[79] For patients with baseline ST-T segment abnormalities, left bundle branch block, left ventricular hypertrophy, and paced rhythms, imaging cardiac stress testing (echocardiography or nuclear perfusion stress) is preferred over exercise ECG testing. Although overall diagnostic accuracy for ischemia is improved with the addition of imaging, additional equipment, space, and personnel with specialized expertise are needed. With the added time demands and costs, it is logistically impossible and cost ineffective to replace all exercise ECG tests with imaging studies. Exercise imaging studies should therefore be targeted in those with nondiagnostic ECGs, either at baseline or anticipated during stress (Table 15-5).

**TABLE 15-4 Selected Studies: Diagnostic Accuracy for Exercise Echocardiography**

| *Study* | *Mode* | *Number of Patients* | *Criteria for Significant Occlusion* | *Sensitivity* | *Specificity* | *Accuracy* |
|---|---|---|---|---|---|---|
| Armstrong (1986)[1] | TME | 95 | >50% | 88% | 87% | 87% |
| Armstrong (1987)[65] | TME | 123 | >50% | 88% | 86% | 88% |
| Ryan (1988)[67] | TME | 64 | >50% | 78% | 100% | 86% |
| Pozzoli (1991)[69] | UBE | 75 | >50% | 71% | 96% | 80% |
| Marwick (1992)[70] | TME | 150 | >50% | 84% | 86% | 85% |
| Quinones (1992)[81] | TME | 112 | >50% | 74% | 88% | 78% |
| Hecht (1993)[38] | SBE | 180 | >50% | 93% | 86% | 91% |
| Ryan (1993)[37] | UBE | 309 | >50% | 91% | 78% | 87% |
| Mertes (1993)[110] | SBE | 79 | >50% | 84% | 85% | 85% |
| Marangelli (1994)[66] | TME | 80 | >75% | 89% | 91% | 90% |
| Marwick (1994)* | BE | 86 | >50% | 88% | 80% | 85% |
| Williams (1994)* | UBE | 70 | >50% | 88% | 84% | 86% |
| Marwick (1995)[149] | TME/ UBE | 161 | >50% | 80% | 81% | 81% |
| Dagianti (1995)[41] | SBE | 60 | >70% | 76% | 94% | 87% |
| Luotolahti (1996)* | UBE | 118 | >50% | 94% | 70% | 92% |
| Roger (1997)[75] | TME | 340 | >50% | 78% | 41% | 69% |

*SBE*, Supine bicycle ergometry; *TME*, treadmill echocardiography; *UBE*, upright bicycle ergometry.

*References:

Luotolahti M, Saraste M, Hartiala J: Exercise echocardiography in the diagnosis of coronary artery disease. *Ann Med* 28:73-77, 1996.

Marwick TH, D'Hondt AM, Mairesse GH, et al: Comparative ability of dobutamine and exercise stress in inducing myocardial ischaemia in active patients. *Br Heart J* 72:31-38, 1994.

Williams MJ, Marwick TH, O'Gorman D, Foale RA: Comparison of exercise echocardiography with an exercise score to diagnose coronary artery disease in women. *Am J Cardiol* 74:435-438, 1994.

**TABLE 15-5 Comparison: Different Exercise Test Modalities**

| *Exercise ECG* | *Exercise Nuclear Perfusion* | *Exercise Echocardiography* |
|---|---|---|
| Largest historical database | Additional time requirement (~4 hr) | Additional time requirement (~30 min) |
| Versatile | Increased personnel training | Increased personnel training |
| Limited accuracy with baseline ECG abnormalities | Increased expertise | Increased expertise |
| | Equipment requirements | Equipment requirements |
| | Most sensitive modality | Most specific modality |
| | Significant increase in cost (~5× higher than ECG) | Significant increase in cost (~2.5× higher than ECG) |
| | | Directly visualizes wall motion |

*ECG*, Electrocardiography.

Stress echocardiography and nuclear perfusion stress provide reasonably comparable information with regard to ischemia diagnosis, diagnosis of myocardial viability, and prognostication.[78,80] Accuracy for both modalities is improved with multivessel disease, increased disease severity, a higher ischemic workload achieved, and more experienced readers. However, because echocardiographic imaging is performed in real time, stress echocardiography can provide concurrent data on valvular function and pulmonary pressures during testing and offers

additional information and safety by identifying preexisting conditions that may affect testing, such as valvular heart disease. For exercise echocardiography, radiation exposure is absent and, unless transpulmonary contrast is needed, intravenous access is not needed. Stress echocardiography can be performed within 1 to 2 hours, whereas nuclear perfusion stress requires, at a minimum, several hours to complete.

Comparative studies between echocardiography and nuclear perfusion stress modalities tend to occur in centers where expertise in a particular modality is favored. Earlier comparative studies with nuclear modalities used thallium scintigraphy. Contemporary practice currently uses sestamibi or thallium single photon emission computed tomography (SPECT), which reduces imaging artifacts. Studies document comparable performance between echocardiography and nuclear modalities.[69,81-83] Summary receiver operating characteristic curves show superiority of exercise echocardiography to exercise ECG testing, with comparable sensitivity to exercise SPECT. When specificity is reduced (higher sensitivity valued), nuclear perfusion stress modalities tend to perform better (Fig. 15-8).[84] A meta-analysis drawing from 44 studies confirmed comparable sensitivity between echocardiography (85%) and nuclear testing (87%).[78] For both modalities, sensitivity for single-vessel disease is lower than for multivessel disease (in one study, sensitivity for single-vessel disease was 61% for nuclear versus 58% for echocardiography).[81]

Stress echocardiography differs from nuclear perfusion stress by assessing functional consequences of ischemia rather than alterations in regional myocardial perfusion. Therefore, if resting wall motion abnormalities are present, subtle ischemia may be more difficult to interpret, resulting in slight advantages in sensitivity seen with nuclear perfusion stress. Overall, nuclear perfusion stress tends to offer higher sensitivity, higher technical success rate, less interobserver variability, and better accuracy for detecting ischemia when resting wall motion abnormalities are present. Advantages for stress echocardiography include shorter test time, greater patient convenience, higher specificity, versatility, the absence of radiation exposure, and lower cost. In most centers, the choice is driven by local personnel expertise and facility accommodation.

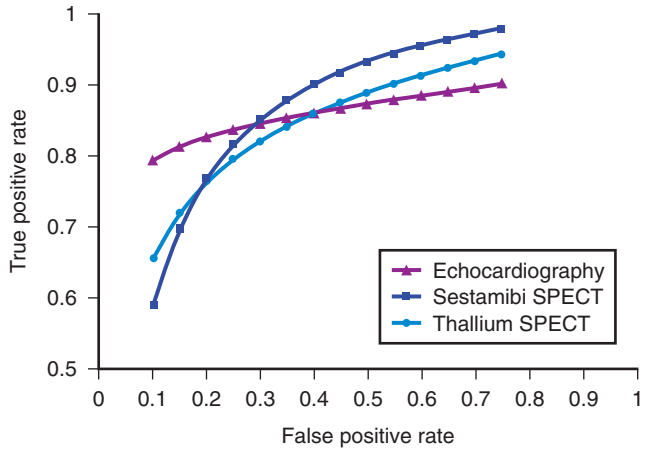



**Figure 15-8 Receiver operator characteristic curves for exercise echocardiography compared to nuclear perfusion stress testing.** True positive rate (sensitivity) is plotted on the y-axis and false positive rate (1-specificity) is plotted on the *x*-axis. When specificity is valued, echocardiography tends to perform better.[84] *SPECT*, Single photon emission computed tomography.

## COST EFFECTIVENESS

Care providers should be aware of, and incorporate into their clinical practice, relative costs of procedures. Cost considerations for various cardiac stress modalities include the patient's incurred costs, Medicare and insurer reimbursement charges, and additional costs of downstream diagnostic testing prompted by the study. Prior comparative cost analyses highlight the importance of pretest disease probability assessment in selecting diagnostic modality type. For example, with high pretest probability, the most cost-effective course may be to proceed directly to angiography.

Several papers comment on cost effectiveness for cardiac stress testing.[85-87] Medicare fees provide comparative and relative costs for professional and technical fees.[29] The "test-only" relative value units for exercise ECG testing are least, with imaging additive, approximately 2.3× higher for echocardiography and 5.3× higher for nuclear perfusion stress.[29] However, test-only costs do not account for increased accuracy and reduced confirmatory downstream testing that imaging confers. When this is accounted for, cost-based analyses favor stress imaging studies, particularly when the likelihood of a nondiagnostic stress ECG study is high.[85-89]

The diagnostic value of any testing modality is greatest when it significantly increases (based on a positive result) or lowers (based on a negative result) coronary artery disease suspicion. Thus, the greatest value is in patients with intermediate range pretest probability (range 20% to 80%). In patients with a low pretest probability, such as those with few cardiovascular risk factors, a positive result is more likely "false positive." Similarly, in individuals with high pretest probability, a negative result may be looked on with skepticism, and direct coronary angiography should be considered. Providers should be aware of direct and downstream costs of different diagnostic options and relative expertise in the various modalities at their institutions. Current diagnostic schemes and pathways have not yet incorporated routine use of newer diagnostic technologies such as cardiac magnetic resonance imaging or multislice computed tomographic angiography.

## SAFETY

There are no adverse effects with exercise echocardiography other than those associated with physical exercise and risk incurred from provoked ischemia. Unlike other forms of diagnostic testing, such as angiography or nuclear perfusion stress, radiation exposure is absent. Major complications are rare, with myocardial infarction reported in approximately 1 in 2500 tests and death in approximately 1 in 10,000.[29,31,90] Contraindications include those normally associated with exercise ECG testing (Box 15-4).

## APPROPRIATE USE AND QUALITY ASSURANCE

Cardiac imaging studies comprise about 50% of medical diagnostic testing. However, recent studies suggest that about 10% to 15% of these studies are either inappropriate or noncontributory.[91] With impending concerns around Medicare solvency, there is now increased scrutiny on appropriate use of cardiac imaging modalities.[92,93] Implications of appropriate use are critical, because such testing often dictates downstream use of other tests, such as coronary angiography. The American College of Cardiology has published appropriateness criteria to

Box 15-4

**CONTRAINDICATIONS FOR EXERCISE ECHOCARDIOGRAPHY**

| Absolute Contraindications | Relative Contraindications |
|---|---|
| Acute myocardial infarction (within 48 hr) | Left main coronary stenosis |
| High-risk unstable angina | Severe arterial hypertension (SBP >200 mm Hg, DBP >110 mm Hg) |
| Uncontrolled cardiac arrhythmias | Poor acoustic windows/image quality (not aided by transpulmonary contrast) |
| Symptomatic severe aortic stenosis | Mental or physical impairment with inability to exercise |
| Symptomatic heart failure | Tachyarrhythmias or bradyarrhythmias |
| Acute pulmonary embolus | Atrioventricular nodal blocking agents |
| Acute aortic dissection | Hypertrophic cardiomyopathy |
| Acute myocarditis or pericarditis | |

*DBP*, Diastolic blood pressure; *SBP*, systolic blood pressure.

provide expert consensus–guided recommendations for cardiac imaging, drawing from clinical scenarios; a score is assigned to clinical scenarios ranging from 1 (inappropriate) to 9 (appropriate).[94] For example, an "appropriate" stress echocardiography indication would be in a patient with an intermediate pretest probability of coronary artery disease and an uninterpretable ECG, versus an "inappropriate" indication such as routine transpulmonary contrast use despite adequate visualization of all segments on noncontrast images. Recent studies evaluating these developed criteria suggest that approximately 10% to 15% of studies may be classified as "inappropriate."[95] Future refinement should aid in altering clinical practice to guide individual patient care and maximize cardiac imaging utility by educating care providers and influencing policy making regarding payer coverage. Additional recent publications have also addressed quality assurance for stress echocardiography.[54]

## Applications

### CORONARY ARTERY DISEASE: INITIAL DIAGNOSIS

The primary application of exercise echocardiography is in diagnosing and managing coronary disease.[5,6] In patients with angina symptoms and moderate pretest probability, stress testing should be performed within 3 to 7 days of symptom onset as long as the patient is asymptomatic at the time of the study. Symptomatic patients with higher pretest disease probability (ischemic ECG change or positive cardiac biomarkers) should proceed directly to coronary angiography. Exercise echocardiography is also valuable for distinguishing between ischemic and nonischemic cardiopulmonary disease such as pulmonary hypertension or valvular heart disease.[96]

Historically, initial evaluation for chest discomfort was in the emergency department, with hospital admission to rule out acute infarction prior to risk stratification. Now, intermediate- and lower-risk patients are increasingly managed with emergency department "chest pain units" that perform triage and risk stratify patients and provide expedited stress testing once an acute coronary syndrome has been excluded.[97,98] (See Chapter 13.) This approach has been effective in identifying higher-risk individuals while concurrently reducing inpatient stays.[99] Although test modality is institution dependent, reports demonstrate improved accuracy with exercise echocardiography over exercise ECG testing, with comparable performance compared to nuclear perfusion stress.[100,101] Given this, exercise echocardiography is an attractive option for an initial diagnostic study, especially considering shorter test duration, absence of radiation exposure, cost savings, and patient convenience.

Exercise testing in asymptomatic individuals for coronary disease diagnosis is not recommended.[102] Although functional capacity and hemodynamic response to exercise are gauged, there is no evidence that results from such testing affect clinical outcome, especially given that prognosis in low-risk patients is excellent and false-positive findings may instigate unnecessary additional testing. However, judicious testing in certain asymptomatic high-risk subsets, such as those with diabetes or vascular disease, is often considered, particularly for those contemplating higher-risk activities such as a new vigorous exercise regimen.[102]

### CORONARY ARTERY DISEASE: KNOWN CORONARY ARTERY DISEASE

Cardiac stress testing after a recent myocardial infarction allows assessment of injury extent and residual ischemia, potentially aiding in decision making for future therapies. Although now rare in contemporary practice, if a patient with a recent infarction did not undergo angiography, a *submaximal* predischarge stress test 3 to 7 days after the event is recommended for risk assessment.[103] Submaximal protocols have lower hemodynamic endpoints (goal only 5 METs or 70% predicted maximum heart rate).[104] As early as 2 to 3 weeks after an infarction, a *symptom-limited* stress test can be performed reasonably safely, with incidence of infarction less than 1%.[29,105] Given ECG abnormalities frequently present, the sensitivity of exercise ECG testing in this population is poor, in the range of 50% to 70%.[81] As with other applications, overall diagnostic accuracy for cardiac imaging stress studies is significantly improved over exercise ECG testing, with visual localization of ischemic territory.

In individuals under consideration for revascularization (percutaneously or surgically), echocardiography viability protocols are well established for pharmacologic stressors (i.e., dobutamine) (see Chapter 16).[106] Viability testing with exercise stressors is not routinely performed. Although limited data using low-level bicycle ergometry demonstrates feasibility, accuracy is not as high as with pharmacologic applications, and tethering from resting wall motion abnormalities increases difficulty of interpretation.[107,108] In 52 postinfarction patients who underwent low-level supine bicycle exercise and low-dose dobutamine echocardiography, sensitivity for predicting functional recovery with exercise was only 81%, compared to 91% for dobutamine.[109]

Following percutaneous revascularization, stress echocardiography can document improvement in exercise tolerance and regional function.[110,111] Echocardiographic imaging provides improved diagnostic accuracy for restenosis over exercise ECG, with one study showing sensitivity for exercise echocardiography 83% compared to only 42% for exercise ECG.[110-113] As with other comparative studies, exercise echocardiography performs similarly to nuclear perfusion stress for restenosis diagnosis, with 89% concordance.[114] Exercise echocardiography after surgical coronary revascularization allows assessment of graft patency and evaluation for residual ischemia.[115-117] However, in clinical practice, cardiac stress testing surveillance in any asymptomatic individual is controversial, considering the lack of impact on clinical outcomes.

## CORONARY ARTERY DISEASE: PROGNOSIS

Presence of resting wall motion abnormalities, ejection fraction, and location and severity of regional wall motion abnormalities identified by echocardiography are well-validated predictors of cardiovascular events in patients with coronary disease, chest discomfort, or congestive heart failure.[118-121] Prognostic factors derived from exercise ECG testing include exercise duration, achieved workload, induced ST segment abnormalities, and hemodynamic response to exercise, including heart rate recovery.[122-124] With visual assessment of ventricular function, ischemic response, and additional information gained from the exercise ECG portion of the study, exercise echocardiography is well suited to allow prognostication.[125-128] Poorer outcome is seen in patients with resting wall motion abnormalities, larger ischemic regions, and shorter exercise duration and time onset to ischemia.[129-135] In an observational study of 4004 patients undergoing exercise echocardiography, 16.7% of patients developed echocardiographic evidence of ischemia despite symptom absence or ischemic ECG changes and were more likely to suffer a major adverse cardiac event or death in the following 5 years.[136] Exercise echocardiography has also demonstrated prognostic value in patients with baseline systolic dysfunction. In 1107 patients with ejection fraction less than 50%, 5-year mortality was significantly higher in those with who developed ischemia during stress echocardiography (Fig. 15-9).[137] The positive predictive value for myocardial infarction and death for stress echocardiography ranges from 63% to 80%, with negative predictive value 78% to 95%, and is uniformly improved over exercise ECG testing, particularly in patients with resting ECG abnormalities.[136,138,139]

In patients without known coronary disease, the negative predictive value of exercise echocardiography is excellent, with likelihood of a major cardiac event over the next several years less than 1%.[140-142] A meta-analysis evaluating the prognostic value of stress imaging showed comparable results between exercise echocardiography and exercise nuclear perfusion stress. For exercise echocardiography, negative predictive value for primary outcomes (infarction or cardiac death) was 98.4% with an estimated annualized rate for a primary outcome of only 0.54% per year.[141]

## CORONARY DISEASE DIAGNOSIS IN WOMEN

Women with coronary disease tend to have fewer obstructive coronary lesions and less single-vessel disease, are older at the time of presentation, and have more comorbidities and functional debilitation, leading to acknowledged limitations in cardiac stress testing. Moreover, there is a relative paucity of female representation in cardiovascular studies that evaluate different diagnostic modalities. Poor study representation and inadequate test validation adversely affect diagnostic accuracy. In a metaanalysis of studies published between 1966 and 1995, only 27 studies included at least 50 women who underwent exercise testing and angiography, and only 3 used exercise echocardiography.[143]

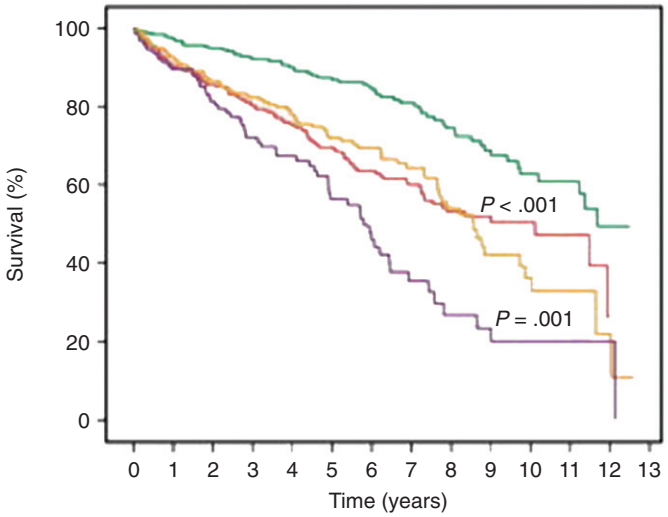



**Figure 15-9** All-cause mortality according to severity of baseline systolic dysfunction and ischemia presence during exercise echocardiography.[137] Survival curves are shown for patients with mild LV dysfunction and no ischemia (*green line*), mild LV dysfunction and ischemia (*red line*), moderate to severe LV dysfunction and no ischemia (*yellow line*), and moderate to severe LV disjunction with ischemia (*purple line*).

Exercise ECG testing in women is associated with increased false-positive findings, often due to resting ST-T wave abnormalities or hypertension-induced abnormalities.[29,144] Studies document false-positive ST segment depressions in as many as 40% of women compared to less than 10% of men.[145,146] Because of isotope scatter and attenuation, nuclear imaging also has limitations; accuracy of thallium-201 perfusion imaging is reduced with obscuration of the inferior wall in obese patients and of the anterior wall in large-breasted women. This has been ameliorated, in part, with use of technecium-99m, a higher-energy radioisotope that provides better tissue penetration.[147]

In a meta-analysis of 19 exercise ECG studies which included at least 50 women, weighted mean sensitivity was only 61% with specificity of 70%.[143] Imaging increases diagnostic accuracy with a weighted mean sensitivity of 86% and specificity of 79% for stress echocardiography and 78% and 64%, respectively, for nuclear perfusion stress.[143] Published diagnostic accuracy of exercise echocardiography in women is presented in Table 15-6. Because likelihood of a nondiagnostic exercise ECG study is higher in women, some studies support imaging stress studies as an initial diagnostic modality.[148] A cost analysis balancing cost with the lowest number of false negatives and fewest inappropriate angiography referrals found that exercise echocardiography provided the best accuracy at the lowest cost.[149] However, uniform referral for imaging stress studies would be logistically difficult and impractical, particularly given that the negative predictive value of a normal exercise ECG study remains high.

Concordant with the general population, stress echocardiography provides prognostic information in women.[150-153] In a

**TABLE 15-6 Diagnostic Accuracy of Exercise Echocardiography in Women**

| Study | Mode | Number of Patients | Sensitivity | Specificity | Accuracy |
|---|---|---|---|---|---|
| Sawada (1989)* | TME or UBE | 57 | 86% | 86% | 86% |
| Williams (1994)* | UBE | 70 | 88% | 84% | 86% |
| Marwick (1995)[149] | TME or UBE | 161 | 80% | 81% | 81% |
| Roger (1997)[75] | TME or UBE | 96 | 79% | 37% | 63% |

*TME*, Treadmill echocardiography; *UBE*, upright bicycle ergometry.

*References:

Sawada SG, Ryan T, Fineberg NS, et al: Exercise echocardiographic detection of coronary artery disease in women. *J Am Coll Cardiol* 14:1440-1447, 1989.

Williams MJ, Marwick TH, O'Gorman D, Foale RA: Comparison of exercise echocardiography with an exercise score to diagnose coronary artery disease in women. *Am J Cardiol* 74:435-438, 1994.

community-based study of 1188 women, resting wall motion abnormalities or exercise-induced ischemia predicted higher rates of myocardial infarction and death.[151] Prospective, female-specific investigations for coronary disease diagnosis remain sparse. The NHLBI's Women Ischemia Syndrome Evaluation study is the largest prospective female-specific study to date, studying different modalities of cardiac diagnostic testing and evaluating influence of menopausal status and hormones on diagnostic test results in nearly 1000 women.[144] Future results will shed light on the gender-specific issues that effect variances on diagnostic accuracy or all cardiac stress testing modalities.

## RISK STRATIFICATION PRIOR TO NONCARDIAC SURGERY

Given the hemodynamic burden associated with surgery, preoperative risk stratification in intermediate- to high-risk asymptomatic individuals such as those with vascular disease, diabetes, prior ischemic heart disease, or congestive heart failure, may aid in decision making, particularly where surgery is elective.[154] Patients with vascular disease typically carry significant cardiovascular risk factors. Therefore, diagnosis of vascular disease provides the opportunity to identify coronary disease in asymptomatic patients and initiate earlier medical therapy to limit long-term atherosclerotic disease sequelae. The greatest published experience in preoperative risk stratification is in patients with vascular disease, given that cardiac events are the main source of perioperative morbidity and mortality (death or myocardial infarction in approximately 10%). Pharmacologic stress is more commonly used, because exercise is usually obviated due to lower extremity claudication. A positive stress test is associated with 10% to 20% risk of a cardiac event perioperatively or in subsequent years. The benefit of routine preoperative stress testing in asymptomatic patients is questionable. Rather, empiric risk factor modification, as in any patient, should be prescribed. Studies suggest that preemptive revascularization for asymptomatic coronary disease is not beneficial, irrespective of a positive stress study result, given procedural risks and risk associated with perioperative discontinuance of antiplatelet therapy. The exception to this is in patients with proximal left anterior descending or left main artery equivalent disease, most of whom would be symptomatic regardless.[155,156]

## HYPERTROPHIC CARDIOMYOPATHY

Echocardiography is a critical diagnostic tool in patients with hypertrophic cardiomyopathy (see Chapter 27). Resting transthoracic imaging allows evaluation of septal wall thickness, gauging of left ventricular outflow tract (LVOT) obstruction severity via continuous-wave Doppler–derived pressure gradients taken, and assessment of associated mitral regurgitation due to systolic anterior motion of the mitral valve and/or subvalvular apparatus. Studies drawing from hypertrophic cardiomyopathy cohorts demonstrate association of resting LVOT gradients with adverse cardiovascular events and heart failure.[157] During stress, changes in ventricular loading may provoke dynamic outflow obstruction; LVOT obstruction is present in about 30% of hypertrophic cardiomyopathy patients at rest, but approximately an additional 33% develop LVOT obstruction with exercise. Exercise-induced LVOT gradients are a predictor of developing heart failure symptoms. Current expert consensus recommendations support septal reduction (surgical myomectomy or alcohol septal ablation) in patients with severe heart failure symptoms or with an LVOT gradient greater than 50 mm Hg at rest or provoked during exercise.[158] Exercise echocardiography for hypertrophic cardiomyopathy patients primarily involves LVOT gradient assessment, but also includes assessment of mitral regurgitation severity.[159] Exercise stress testing should not be performed in symptomatic patients or patients with peak LVOT gradient greater than 90 mm Hg.

During exercise testing, standard exercise protocols are used, with cessation of exercise if symptoms develop or a gradient greater than 50 mm Hg is provoked (Fig. 15-10). Because of the ability to image at peak stress, supine bicycle stress is preferred over treadmill protocols where provoked gradients may have returned to baseline by the time imaging is completed. LVOT velocity should be recorded at baseline and at each stage of stress. After recording LVOT velocity, mitral regurgitation severity (vena contracta) is recorded. It is often difficult to identify separate peak velocities for LVOT and mitral regurgitant jets, and care must be taken to differentiate Doppler signals. Because mitral regurgitation velocity reflects the transmitral pressure difference and LVOT velocity reflects the LV-to-aortic pressure difference, mitral regurgitation peak velocity is always higher than LVOT velocity, and the LVOT signal is typically later peaking than the mitral regurgitation signal because of dynamic LVOT obstruction (Fig. 15-10). Exercise-induced regional wall motion abnormalities that develop in absence of coronary disease are thought to be due to microvascular ischemia. After septal reduction intervention, stress echocardiography is used to document reduction in LVOT gradient and monitor treatment efficacy.

## DILATED CARDIOMYOPATHY AND CARDIAC TRANSPLANTATION

Both pharmacologic and exercise stress echocardiography have been safely used in patients with dilated cardiomyopathy, but pharmacologic testing is predominantly used, such as in identification of viable myocardium after an infarction. Exercise echocardiography for earlier identification of patients at risk for systolic dysfunction, such as those with myocarditis or cancer survivors exposed to cardiotoxic agents, has also been examined.[159,160] Exercise echocardiography had been proposed as an approach to identify candidates for resynchronization therapy, with exercise dyssynchrony correlating with declines in cardiac

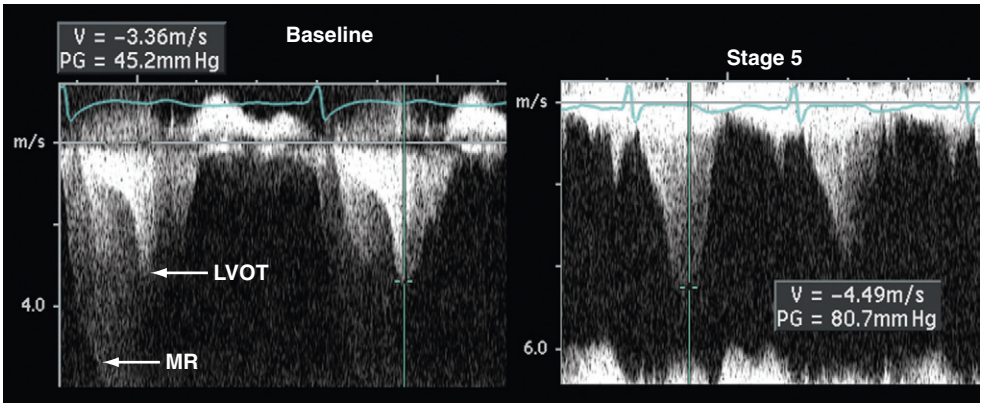



**Figure 15-10 Spectral Doppler tracings taken during supine bicycle exercise stress in a patient with hypertrophic cardiomyopathy.** *Left*: At baseline, superimposed Doppler tracings for mitral regurgitation (*MR*) and the left ventricular outflow tract (*LVOT*) are shown. Peak LVOT velocity is measured at 3.4 m/s (*arrows*). Care must be taken to ensure that correct Doppler signal is interrogated to accurately reflect severity of LVOT obstruction. With increasing workload, peak LVOT velocity increased to 3.9 m/s in stage 3 and 4.1 m/s in stage 4. With exaggerated respiratory effort and patient motion during ergometry, peak measured velocities may underestimate severity of LVOT obstruction because of transiently less optimal Doppler interrogation angle. In this example, peak velocity was measured at 4.5 m/s in stage 5; in the same clip, second heartbeat was discarded because of its underestimation of peak LVOT velocity.

output and worsening mitral regurgitation.[161] However, recent studies, such as PROSPECT, have not shown echocardiographic markers of dyssynchrony, such as M-mode, Doppler tissue velocities, strain, and wall motion timing, to be predictive of clinical response to resynchronization therapy.[162,163]

Allograft vasculopathy after cardiac transplantation is typically asymptomatic. Surveillance testing for allograft vasculopathy primarily uses pharmacologic (dobutamine) stress testing and coronary angiography with intravascular ultrasound. Diagnostic accuracy of dobutamine echocardiography for allograft vasculopathy is reasonable and provides prognostic information for subsequent cardiac events.[164] Limited data with exercise echocardiography demonstrate reasonable specificity (range 86% to 95%), but poor sensitivity (approximately 25%), likely due in part to poor autonomic heart rate response of the denervated heart.[165,166]

## VALVULAR HEART DISEASE

Stress echocardiography is an adjunct in management of patients with valvular heart disease by gauging disease severity and aiding in understanding dynamic response of valve function to physiologic demand.[167,168] Stress echocardiography allows evaluation of:

1. Exercise tolerance and contextual evaluation of a patient's clinical status
2. Hemodynamic response to exercise (blood pressure, heart rate)
3. Pulmonary hypertension
4. Ventricular function
5. Direct evaluation of stenosis or regurgitant severity
6. Exercise-induced arrhythmias

Patients with significant valve lesions (stenotic or regurgitant) should have a complete standard transthoracic echocardiogram documenting severity of cardiac and valve function, evaluating coexisting valve lesions, and providing pulmonary pressure estimates. Exercise testing for valvular heart disease should not be performed in symptomatic patients because of increased risk of hemodynamic compromise and arrhythmia. Clinical guidelines recommend valve intervention for symptomatic valve disease, such as surgery, without need for exercise testing.[47,169] In asymptomatic patients or those with equivocal symptoms, stress testing is useful for clinical decision making, such as optimizing timing of intervention, given that physiologic effects of valve lesions may not be present at rest, but may be provoked during exercise.

Indicators of increased hemodynamic significance of valve lesions include failure to augment flow across a stenotic valve during stress or abnormal stress-induced increases in pulmonary pressure. For regurgitant lesions, changes in ventricular loading resulting from exercise may alter ventricular geometry, resulting in increased regurgitation severity. Exercise stress is preferred over pharmacologic stress because it provides data regarding symptom provocation, exercise tolerance, and hemodynamic response to exercise. Intervention should be considered with provocation of cardiopulmonary symptoms (exertional dyspnea, heart failure, arrhythmias, angina, or syncope).[47] Concurrent ischemia evaluation is often suboptimal because of underlying ventricular structural abnormalities, such as left ventricular hypertrophy, arrhythmia, or patient inability to achieve target workload.

In patients with aortic stenosis, if symptom status is not clear or there has been an unexplained decline in activity level, exercise stress testing allows gauging of exercise tolerance and exertional symptoms.[170,171] (See Chapter 23.) Transaortic valve velocities and gradients may be taken during exercise echocardiography, but are difficult to reliably record because of exaggerated respiratory cardiac motion and time limitations of data acquisition for poststress treadmill protocols. Exercise testing can be safely performed if supervised by an experienced physician, but should be ended promptly if there is a hypotensive response or only a minimal increase in blood pressure, or greater than 4 mm of horizontal ST depression in contiguous leads, or if the patient experiences cardiopulmonary symptoms such as dyspnea, dizziness, or angina.[172-174] Exercise-induced ST segment changes do not correlate well with coronary artery disease presence or severity. Reduced exercise tolerance, symptom provocation, an abnormal exercise response (rise in transvalvular gradient greater than 20 mm Hg), or a relative limitation in contractile reserve suggests a worse prognosis; these patients should be considered for valve replacement.[174-176] In a study of 69 patients with severe aortic stenosis, exercise

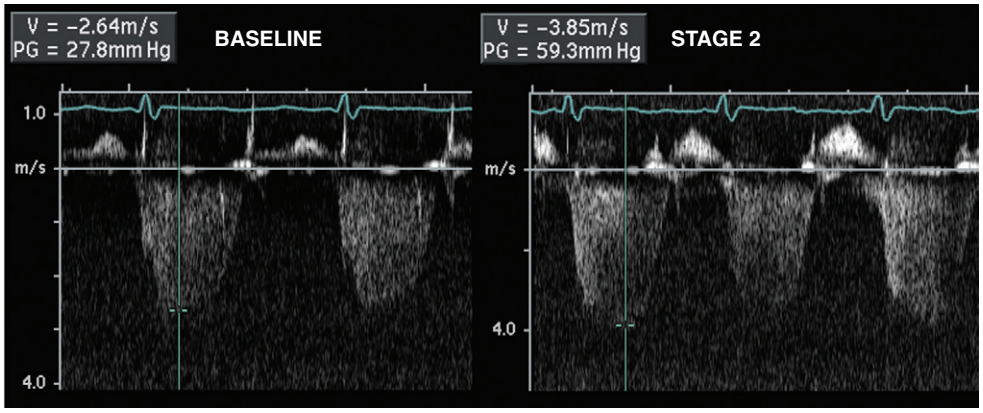



**Figure 15-11 Spectral Doppler tricuspid regurgitant tracings during supine bicycle exercise stress in a patient with prior posterolateral myocardial infarction, normal volume status, and exertional dyspnea.** Nuclear perfusion stress did not show new ischemia. *Left*: At rest, LV chamber size is normal with thinning of the inferolateral segments. There is moderate, functional mitral regurgitation. Resting pulmonary systolic pressure is normal at 28 to 33 mm Hg (TR jet velocity 2.6 m/s). *Right*: During exercise, patient developed dyspnea. Mitral regurgitation severity was comparable by color mapping, but pulmonary systolic pressure increased to 59 to 64 mm Hg (TR jet velocity of 3.9 m/s). *TR*, Tricuspid regurgitation.

increases in transaortic pressure gradient over 18 mm Hg were an independent predictor of symptom onset in the ensuing 15 months.[174] The role of exercise stress for low-flow, low-gradient aortic stenosis evaluation is limited. In these patients, low-dose dobutamine stress is typically used to augment cardiac output for evaluation of LV contractile reserve and aortic valve hemodynamics.

For patients with mitral stenosis and equivocal symptoms, echocardiographic evaluation with exercise focuses on pulmonary arterial systolic pressure estimate, but should also include assessment of central venous pressure (inferior vena cava diameter), valve anatomy, mitral valve area, and concurrent mitral regurgitation. (See Chapter 21.) Intervention, such as mitral valvuloplasty, should be considered when pulmonary systolic pressure exceeds 50 mm Hg (rest) or 60 mm Hg (with exercise), or if transmitral mean gradient increases to over 15 mm Hg.[47] During stress, mitral valve area measurements from Doppler transmitral tracings are technically difficult to acquire because of increased heart rate and alterations in the atrial-ventricular filling with rapid deceleration of LV filling velocity and decreases in pressure half-time. The continuity equation provides an alternative method for mitral valve area calculation.[167,177,178] For patients with rheumatic valve disease and only mild regurgitation at rest, exercise echocardiography may unmask significant mitral regurgitation during exercise, suggesting a mechanism for symptoms in patients not normally be expected to be symptomatic.[179]

Disease progression in chronic regurgitation can be insidious. Timing of surgical intervention in asymptomatic patients is predicated on evidence of adverse hemodynamic effect on the LV, such as impaired systolic function or ventricular enlargement.[47,169] (See Chapter 18.) In asymptomatic patients with normal indices at rest, significance of valve lesions may manifest with decreased exercise tolerance, increase in pulmonary pressure, or worsening of regurgitation with changes in ventricular loading (Fig. 15-11).[47,167] Symptom provocation, worsening pulmonary hypertension (greater than 60 mm Hg with exercise), decreased exercise capacity, or loss of contractile reserve should prompt earlier consideration of surgical intervention.[180-182] Echocardiographic evaluation during stress focuses on pulmonary systolic pressures, but also includes assessment of ventricular size and function, as well as simpler measures of regurgitation severity, such as vena contracta. Early stress applications evaluating mitral regurgitation severity via quantitative Doppler echocardiography show feasibility, but this is technically difficult to implement and is not yet widely used.[168] A prospective, multicenter registry to evaluate the potential role of exercise echocardiography in assessing ischemic mitral regurgitation in patients referred for coronary bypass surgery is currently underway.[183]

Patients with a prosthetic valve area that is small relative to body habitus may experience symptoms consistent with valve stenosis, such as decreased exercise tolerance or heart failure symptoms. (See Chapter 25.) There is an emerging role for exercise stress testing for evaluation of prosthetic valve-patient mismatch. During exercise, a significant increase in transvalvular gradient greater than 20 mm Hg for an aortic prosthesis or greater than 12 mm Hg for a mitral prosthesis in an otherwise normally functioning valve or provocation of cardiopulmonary symptoms is consistent with severe patient-prosthesis mismatch and should prompt consideration of redo valve replacement.[168]

### OTHER APPLICATIONS

Exercise protocols in the pediatric population are adjusted to account for decreased stature with similar indices of exercise tolerance, ECG monitoring, and identification of regional wall motion abnormalities.[184] However, ischemic heart disease is less prevalent in children, and therefore exercise echocardiography is primarily targeted at arrhythmia evaluation and assessment of hemodynamic significance of valvular and congenital abnormalities.

In patients with chronic pulmonary or systemic inflammatory disease, pulmonary arterial hypertension is associated with significant morbidity and mortality. (See Chapters 33 and 37.) However, early diagnosis may be hindered if resting pulmonary pressures are normal. Assessment of patients during exercise may enable earlier identification of patients to target earlier instigation of potentially beneficial therapies.[185-187]

## Future Directions

Quantitative approaches to interpretation should increase reproducibility and accuracy for stress echocardiography, particularly for less experienced readers. Historically, significant

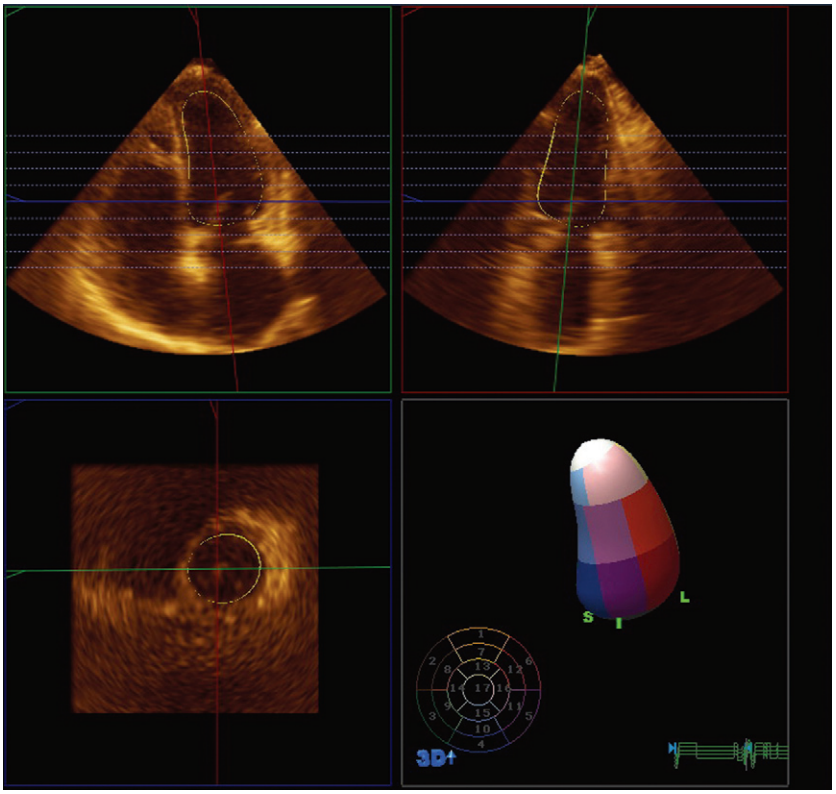



**Figure 15-12 Semiautomated border recognition to assess LV volume.** Marks are placed at the mitral annulus and apex, and LV volumes are estimated. Several image planes can be concurrently displayed. Regional wall motion can be assessed by segmenting the volume into the standard 16 segments, which can be viewed from multiple angles (*bottom right*). In this case, end-diastolic volume (*EDV*) is 65 mL, end-systolic volume (*ESV*) is 30 mL, and ejection fraction is 54%. Horizontal lines on apical views represent multislice short-axis image planes that can be simultaneously shown (see Fig. 15-14).

subjective input was needed to define cardiac borders for quantitative methods, which was time consuming. Advances in semiautomated border recognition algorithms and acoustic quantification now allow for more streamlined analysis of systolic and diastolic LV volumes, decreasing interpretation time with improved diagnostic accuracy, particularly for more inexperienced readers (Fig. 15-12).[188] Addition of echocardiographic diagnostic aids, such as transpulmonary contrast, to quantitative approaches may likely further improve diagnostic accuracy, allowing assessment of coronary flow reserve integrated with wall motion analysis.[189-193] In a study using parametric still images taken from contrast-enhanced echocardiograms, feasibility of automated quantitative regional wall motion analysis was demonstrated, with improved diagnostic accuracy for inexperienced readers over standard qualitative visual evaluation (specificity increased from 58% to 79% and accuracy increased from 74% to 84%).[194]

Assessment of diastolic function during stress may be beneficial in identifying ischemia earlier in the ischemic cascade. (See Chapter 11.) Strategies include evaluation of increased LV filling pressure (Doppler mitral inflow and mitral annular tissue velocity, E/E′ ratio) and identifying delayed relaxation via myocardial strain imaging.[195-197] As with any Doppler application, limitations include underestimation of velocities with nonparallel intercept angles, individual heterogeneity in velocities, and inaccurate velocity measurement due to increased translational cardiac motion. Although evaluation of diastolic function during stress echocardiography is feasible, individual variability in diastolic indices and time constraints of image acquisition during stress limit utility of diastolic function assessment to only supplemental to conventional systolic evaluation.

Tissue Doppler interrogation evaluates myocardial tissue velocity referenced to the transducer, identifying temporal abnormalities in regional contraction. (See Chapter 10.) This allows for differentiation of normal and hypokinetic motion, offering an adjunct to qualitative assessment of regional wall motion.[198-201] *Speckle tracking* allows simultaneous tracking of two or more adjacent points, or "speckles," evaluating relative velocity between points, rather than referenced to the transducer, and does not require a parallel interrogation angle. Strain and strain rate imaging are quantitative measures derived from tissue Doppler velocities or speckle tracking.[202] Strain rate refers to speed of myocardial deformation (m/s or cm/s), and strain represents relative deformation of a given myocardial segment (dimensionless), measured in three directions: radial, circumferential, and longitudinal. Alterations in these measures during stress suggest interval changes in function.[203] In the regional evaluation of systolic function, for segments with an appearance of systolic motion adjacent to hypokinetic or akinetic segments, abnormal strain indices may identify tethered motion rather than normal motion. Strain analysis can also be applied to ischemia assessment during diastole, where normal decreases in myocardial strain are delayed (Fig. 15-13).[204] With background imaging noise and respiratory artifact, strain and strain rate imaging have been difficult to implement during exercise stress, with one study documenting noninterpretable data in as many as 36% of subjects.[205] Available systems allow offline analysis of prerecorded samples, but analysis remains technically

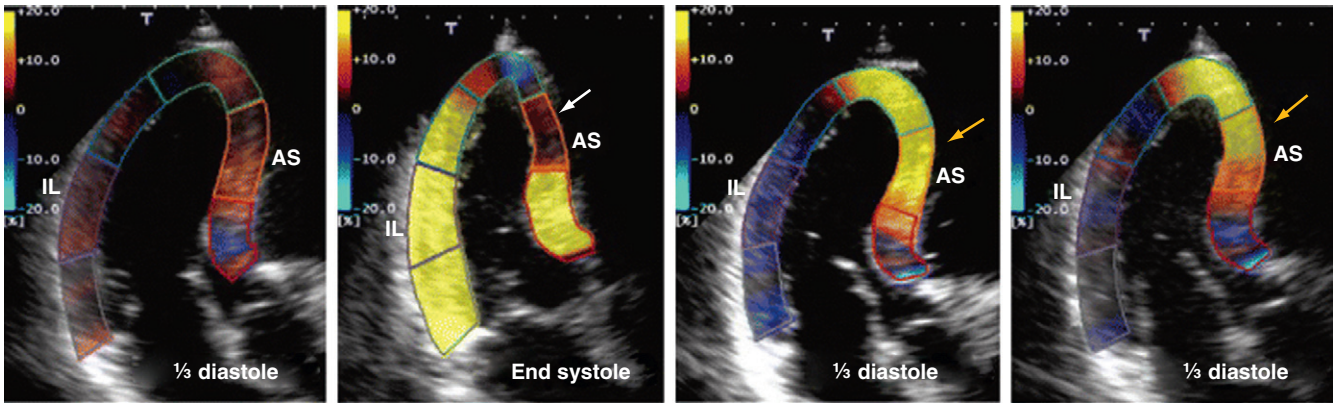



**Figure 15-13 Apical long-axis images in a patient with 70% left anterior descending coronary artery stenosis.** 2D speckle-tracking is superimposed on images taken at baseline, immediately poststress, and during recovery after treadmill exercise; *yellow* represents increasing strain. On immediate poststress images, decrease in peak systolic strain is seen in mid-anteroseptum (*white arrow*). Five minutes after exercise, high strain level due to delayed relaxation (*yellow arrow*) is seen in the midanteroseptal segment one third into diastole. Ten minutes after cessation of exercise, this was less pronounced (*yellow arrow*), but did persist.[204]

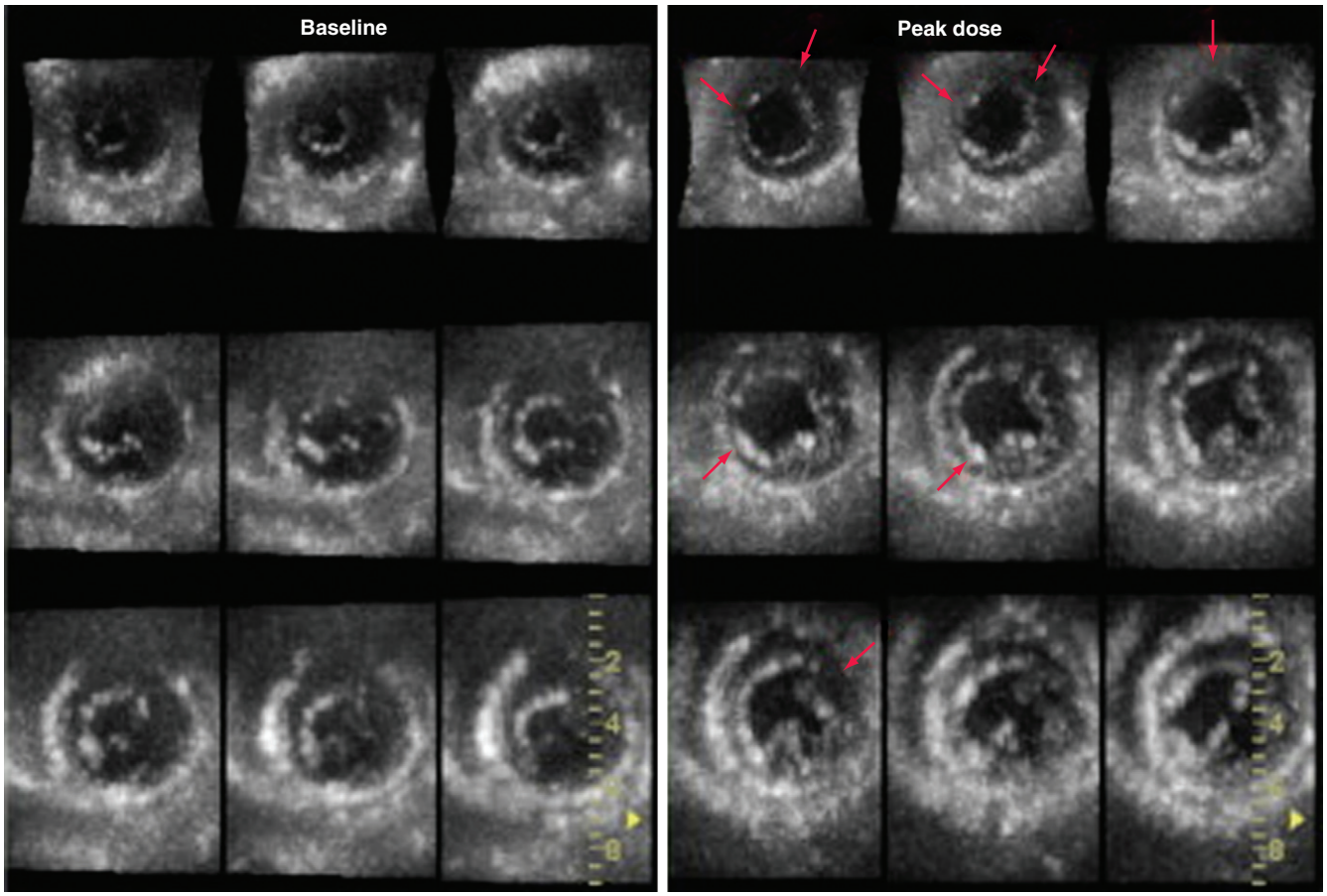



**Figure 15-14 Multislice short-axis views of heart at baseline and at peak dobutamine infusion.** For each stage (baseline and peak dobutamine dose infusion), short-axis cuts are shown from apex (*upper left*) progressing toward base of heart (*lower right*). In this example, new stress-induced regional wall motion abnormalities were seen in the apex, inferoseptum, and lateral wall (*red arrows*).[209]

challenging with a lengthy time requirement, prohibiting routine clinical use. There has been recent progress in automating strain data and abbreviating time for image analysis.[201]

Advantages of 3D echocardiography for LV function assessment include the ability to use and optimize infinite image planes within an acquired 3D volume, leading to improved accuracy by decreasing assumptions on ventricular shape and avoiding LV foreshortening (see Chapter 4).[206] Initially, single-beat 3D volume acquisitions were restricted by pyramidal volume size, limiting imaging of larger ventricles. Relative to 2D imaging, image resolution for 3D was significantly inferior. Spatial imaging was poor because of inadequate line density, and temporal resolution was poor because of decreased frame rate. Time requirements for offline analysis made 3D imaging

prohibitive for mainstream use. Newer real-time 3D matrix-array transducers have an increased number of imaging elements within a smaller transducer footprint, providing considerably improved image resolution. Temporal resolution and spatial resolution have significantly improved. Full volumes are now generated via sequential image synchronization over several cardiac cycles (about four to seven), combining subvolumes into one image volume.[207] However, alignment of subvolumes may be limited in patients underlying arrhythmia ("stitch" artifact).

Rather than drawing from an entire 3D volume set, matrix-array transducers display concurrent images from biplanar (orthogonal planes) or triplanar modes, providing the ability to match image planes for resting and stress images within a volume, typically to planes concordant with standard apical two-chamber, four-chamber, and long-axis views (triplanar mode).[208] Because exercise echocardiography sensitivity decreases with longer time intervals from exercise cessation, a shorter image acquisition time point allows evaluation of LV function at higher workload. Display of multislice cuts through a single volume allows evaluation of concurrent multiple segments (Fig. 15-14).[209] Pretest optimization of image planes to reduce LV foreshortening is also beneficial given that even the most experienced sonographers require about 30 seconds for image acquisition with standard 2D protocols, and optimal image planes may be difficult to obtain.

Early studies demonstrate feasibility of real-time 3D stress imaging.[210-213] Most studies use pharmacologic stress (dobutamine), given that exercise-induced translational cardiac motion and exaggerated respiratory motion limit image quality during volume acquisition because of stitch artifact.[214] Feasibility of 3D stress echocardiography in patients with enlarged ventricles or poor image quality (where transpulmonary contrast would typically be used) has not been adequately assessed. Advantages of real-time 3D stress testing include reduction of scanning time and reduced operator dependence. However, manipulation of images and planes offline significantly increases analysis time.[207,215,216] Further applications of 3D stress echocardiography using quantitative measures for endocardial excursion and fractional area change have shown feasibility.[217]

In its current state, real-time 3D stress echocardiography provides relatively limited spatial resolution with lower frame rates compared to standard 2D imaging. Additionally, standardized 3D stress protocols are not yet available, making it difficult to justify use of 3D echocardiography independent from standard 2D imaging. However, with potential to provide real-time quantitative measures of LV volume, systolic function, and regional wall motion, advances will likely allow for future application.[206]

## KEY POINTS

- Exercise echocardiography integrates real-time echocardiography with exercise (ECG) testing to aid in evaluation of ischemic, valvular, and cardiopulmonary heart disease.
- For bicycle ergometry protocols, images are acquired during peak exercise, or, because of difficulties due to patient motion, images are acquired immediately after exercise for treadmill protocols. Imaging data is integrated with ECG data, exercise tolerance, and patient symptoms for final interpretation.
- When image quality is poor, transpulmonary contrast aids endocardial border definition.
- Stress echocardiography and stress nuclear studies provide comparable information on ischemia diagnosis, myocardial viability, and prognostication. Advantages of stress echocardiography include widespread availability, shorter test times, greater patient convenience, versatility, absence of radiation exposure, and lower cost.
- Future advances in stress echocardiography include real-time 3D imaging, spectral Doppler interrogation with stress, myocardial strain and strain rate analysis, and integration of coronary flow reserve data using myocardial perfusion images.

## REFERENCES


1. Armstrong WF, O'Donnell J, Dillon JC, et al: Complementary value of two-dimensional exercise echocardiography to routine treadmill exercise testing. *Ann Intern Med* 105:829-835, 1986.
2. Marwick TH, Shaw L, Case C, et al: Clinical and economic impact of exercise electrocardiography and exercise echocardiography in clinical practice. *Eur Heart J* 24:1153-1163, 2003.
3. Ross J Jr: Assessment of ischemic regional myocardial dysfunction and its reversibility. *Circulation* 74:1186-1190, 1986.
4. Marwick TH: Stress echocardiography. *Heart* 89:113-118, 2003.
5. Sicari R, Nihoyannopoulos P, Evangelista A, et al: Stress echocardiography expert consensus statement European Association of Echocardiography (EAE) (a registered branch of the ESC). *Eur J Echocardiogr* 9:415-437, 2008.
6. Pellikka PA, Nagueh SF, Elhendy AA, et al: American Society of Echocardiography recommendations for performance, interpretation, and application of stress echocardiography. *J Am Soc Echocardiogr* 20:1022-1041, 2007.
7. Lauer MS: The "exercise" part of exercise echocardiography. *J Am Coll Cardiol* 39:1353-1355, 2002.
8. Kerber RE, Marcus ML, Abboud FM: Echocardiography in experimentally-induced myocardial ischemia. *Am J Med* 63:21-28, 1977.
9. Kerber RE, Marcus ML, Ehrhardt J, et al: Correlation between echocardiographically demonstrated segmental dyskinesis and regional myocardial perfusion. *Circulation* 52:1097-1104, 1975.
10. Gordon MJ, Kerber RE: Interventricular septal motion in patients with proximal and distal left anterior descending coronary artery lesions. *Circulation* 55(2):338-341, 1977.
11. Mason SJ, Weiss JL, Weisfeldt ML, et al: Exercise echocardiography: detection of wall motion abnormalities during ischemia. *Circulation* 59:50-59, 1979.
12. Wann LS, Faris JV, Childress RH, et al: Exercise cross-sectional echocardiography in ischaemic heart disease. *Circulation* 60:1300-1308, 1979.
13. Picano E: Stress echocardiography: a historical perspective. *Am J Med* 114:126-130, 2003.
14. Lang RM, Bierig M, Devereux RB, et al: Recommendations for chamber quantification: a report from the American Society of Echocardiography's Guidelines and Standards Committee and the Chamber Quantification Writing Group. *J Am Soc Echocardiogr* 18:1440-1463, 2005.
15. Battler A, Froelicher VF, Gallagher KP, et al: Dissociation between regional myocardial dysfunction and ECG changes during ischemia in the conscious dog. *Circulation* 62:735-744, 1980.
16. Nesto RW, Kowalchuk GJ: The ischemic cascade: temporal sequence of hemodynamic, electrocardiographic, and symptomatic expressions of ischemia. *Am J Cardiol* 57:23, 1987.

17. Hauser AM, Gangadharan V, Ramos RG, et al: Sequence of mechanical, electrocardiographic and clinical effects of repeated coronary artery occlusion in human beings: echocardiographic observations during coronary angioplasty. *J Am Coll Cardiol* 5:193-197, 1985.
18. Ross J: Mechanisms of regional ischaemia and antianginal drug action during exercise. *Prog Cardiovasc Dis* 31:455-466, 1989.
19. Visser CA, David GK, Kan G, et al: Two-dimensional echocardiography during percutaneous transluminal coronary angioplasty. *Am J Cardiol* 111:1035, 1986.
20. Wohlgelernter D, Cleman M, Highman HA, et al: Regional myocardial dysfunction during coronary angioplasty: evaluation by two-dimensional echocardiography and 12 lead electrocardiography. *J Am Coll Cardiol* 7:1245-1254, 1986.
21. Sugishita Y, Koseki S, Matsuda M, et al: Dissociation between regional myocardial dysfunction and ECG changes during myocardial ischemia induced by exercise in patients with angina pectoris. *Am Heart J* 106:1, 1983.
22. Sheikh KH, Bengtson JR, Helmy S, et al: Relation of quantitative coronary lesion measurements to the development of exercise-induced ischemia assessed by exercise echocardiography. *J Am Coll Cardiol* 15:1043-1051, 1990.
23. Arnese M, Fioretti PM, Cornel JH, et al: Akinesis becoming dyskinesis during high-dose dobutamine stress echocardiography: a marker of myocardial ischaemia or a mechanical phenomenon? *Am J Cardiol* 73:896-899, 1994.
24. Beleslin BD, Ostojic M, Djordjevic-Dikic A, et al: Integrated evaluation of relation between coronary lesion features and stress echocardiography results: the importance of coronary lesion morphology. *J Am Coll Cardiol* 33:717-726, 1999.
25. Salustri A, Arnese M, Boersma E, et al: Correlation of coronary stenosis by quantitative coronary arteriography with exercise echocardiography. *Am J Cardiol* 75:287-290, 1995.
26. Agati L, Arata L, Luongo R, et al. Assessment of severity of coronary narrowings by quantitative exercise echocardiography and comparison with quantitative arteriography. 67:1201-1207, 1991.
27. Pálinkás A, Tóth E, Amyot R, et al: The value of ECG and echocardiography during stress testing for identifying systemic endothelial dysfunction and epicardial artery stenosis. *Eur Heart J* 23:1587-1595, 2002.
28. Nihoyannopoulos P, Kaski J-C, Crake T, Maseri A: Absence of myocardial dysfunction during stress in patients with syndrome X. *J Am Coll Cardiol* 18:1463-1470, 1991.
29. Gibbons L, Balady GJ, Bricker JT, et al: ACC/AHA Guideline update for exercise testing: a report of the American College of Cardiology/American Heart Association Task Force on Practice Guidelines. *J Am Coll Cardiol* 40:1431-1440, 2002.
30. Strizik B, Chiu S, Ilercil A, et al: Usefulness of isometric handgrip during treadmill exercise stress echocardiography. *Am J Cardiol* 90:420-422, 2002.
31. Myers J, Arena R, Franklin B, et al: Recommendations for clinical exercise laboratories: a scientific statement from the American Heart Association. *Circulation* 119:3144-3161, 2009.
32. Gulati M, Black HR, Shaw LJ, et al: The prognostic value of a nomogram for exercise capacity in women. *N Engl J Med* 353:468, 2005.
33. Kloner RA, Allen J, Cox TA, et al: Stunned left ventricular myocardium after exercise treadmill testing in coronary artery disease. *Am J Cardiol* 68:329-334, 1991.
34. Peteiro J, Garrido I, Monserrat L, et al: Comparison of peak and post-exercise treadmill echocardiography with the use of harmonic imaging acquisition. *J Am Soc Echocardiogr* 17:1044-1049, 2004.
35. Ginzton LE, Conant R, Brizendine M, et al: Exercise subcostal two-dimensional echocardiography: A new method of segmental wall motion analysis. *Am J Cardiol* 53:805, 1984.
36. Presti CF, Armstrong WF, Feigenbaum H: Comparison of echocardiography at peak exercise and after bicycle exercise in evaluation of patients with known or suspected coronary artery disease. *J Am Soc Echocardiogr* 1:119-126, 1988.
37. Ryan T, Segar DS, Sawada DG, et al: Detection of coronary artery disease with upright bicycle exercise echocardiography. *J Am Soc Echocardiogr* 6:186-197, 1993.
38. Hecht HS, DeBord L, Sotomayor N, et al: Supine bicycle stress echocardiography: peak exercise imaging is superior to postexercise imaging. *J Am Soc Echocardiogr* 6:265-271, 1993.
39. Badruddin SM, Ahmad A, Mickelson J, et al: Supine bicycle versus post-treadmill exercise echocardiography in the detection of myocardial ischemia: a randomized single-blind crossover trial. *J Am Coll Cardiol* 33:1485-1490, 1999.
40. Applegate RJ, Dell'Italia LJ, Crawford MH: Usefulness of two-dimensional echocardiography during low-level exercise testing early after uncomplicated acute myocardial infarction. *Am J Cardiol* 60:10-14, 1987.
41. Dagianti A, Penco M, Agati L, et al: Stress echocardiography: comparison of exercise, dipyridamole and dobutamine in detecting and predicting the extent of coronary artery disease. *J Am Coll Cardiol* 26:18-25, 1995.
42. Modesto K, Rainbird A, Klarich et al: Comparison of supine bicycle exercise and treadmill exercise Doppler echocardiography in evaluation of patients with coronary artery disease. *Am J Cardiol* 91:1245-1248, 2003.
43. West SR, Feigenbaum H, Armstrong WF, et al: Split-screen simultaneous digital imaging of rest and stress echocardiogram: a new method for evaluation of exercise induced wall motion abnormalities. *J Am Coll Cardiol* 3:563, 1984.
44. Hecht HS, DeBord L, Shaw R, et al: Digital supine bicycle stress echocardiography: a new technique for evaluating coronary artery disease. *J Am Coll Cardiol* 21:950-956, 1993.
45. Attenhofer CH, Pellikka PA, Oh JK, et al: Is review of videotape necessary after review of digitized cine-loop images in stress echocardiography? A prospective study in 306 patients. *J Am Soc Echocardiogr* 10:179-184, 1997.
46. Myers J, Bader D, Madhavan R, Froelicher V: Validation of a specific activity questionnaire to estimate exercise tolerance in patients referred for exercise testing. *Am Heart J* 142:1041-1046, 2001.
47. Bonow RO, Carabello BA, Chatterjee K, et al: 2008 focused update incorporated into the ACC/AHA 2006 guidelines for the management of patients with valvular heart disease. *Circulation* 118:e523-e661, 2008.
48. Freeman RV: Exercise echocardiography. In Otto CM, editor: *The practice of clinical echocardiography*, ed 3, Philadelphia, 2007, WB Saunders, pp 326-352.
49. Ali B, Zafari AM: Narrative review: cardiopulmonary resuscitation and emergency cardiovascular care: review of the current guidelines. *Ann Intern Med* 147:171-179, 2007.
50. Kane GC, Hepinstall MJ, Kidd GM, et al: Safety of stress echocardiography supervised by registered nurses: results of a 2-year audit of 15,404 patients. *J Am Soc Echocardiogr* 21:337-341, 2008.
51. Franklin BA, Gordon S, Timmis GC, O'Neill WW: Is direct physician supervision of exercise stress testing routinely necessary? *Chest* 111:262-265, 1997.
52. Quiñones MA, Douglas PS, Foster E, et al: American College of Cardiology/American Heart Association clinical competence statement on echocardiography: a report of the American College of Physicians—American Society of Internal Medicine Task Force on Clinical Competence. *Circulation* 107:1068-1089, 2003.
53. Imran MB, Pálinkás A, Pasanisi EM, et al: Optimal reading criteria in stress echocardiography. *Am J Cardiol* 90:444-445, 2002.
54. Picard MH, Adams D, Bierig SM, et al: American Society of Echocardiography recommendations for quality echocardiography laboratory operations. *J Am Soc Echocardiogr* 24:1-10, 2011.
55. Buda AJ, Lefkowitz CA, Gallagher KP: Augmentation of regional function in nonischemic myocardium during coronary occlusion measured with two-dimensional echocardiography. *J Am Coll Cardiol* 16:175, 1990.
56. Guth BD, White FC, Gallagher KP, Bloor CM: Decreased systolic wall thickening in myocardium adjacent to ischemic zones in conscious swine during brief coronary artery occlusion. *Am Heart J* 107:458, 1984.
57. Cortigiani L, Bigi R, Rigo F, et al: Diagnostic value of exercise electrocardiography and dipyridamole stress echocardiography in hypertensive and normotensive chest pain patients with right bundle branch block. *J Hypertens* 21:2189-2194, 2003.
58. Picano E, Pálinkás A, Amyot R: Diagnosis of myocardial ischemia in hypertensive patients. *J Hypertens* 19:1177-1183, 2001.
59. Hoffmann R, Lethen H, Marwick T, et al: Analysis of interinstitutional observer agreement in interpretation of dobutamine stress echocardiograms. *J Am Coll Cardiol* 27:330-336, 1996.
60. Picano E, Lattanzi F, Orlandini A, et al: Stress echocardiography and the human factor: the importance of being expert. *J Am Coll Cardiol* 17:666-669, 1991.
61. Varga A, Picano E, Dodi C, et al: Madness and method in stress echo reading. *Eur Heart J* 20:1271-1275, 1999.
62. Obeidat O, Arida M, Al-Mallah M, et al: Segmental early relaxation phenomenon: incidence, clinical characteristics, and significance in stress echocardiography. *Chest* 125:1218-1223, 2004.
63. Bonow RO, Maurer G, Holly TA, et al: Myocardial viability and survival in ischemic left ventricular dysfunction. *N Engl J Med* 364: 1617-1625, 2011.
64. Pellikka PA: Stress echocardiography for the diagnosis of coronary artery disease: progress towards quantification. *Curr Opin Cardiol* 20:395-398, 2005.
65. Armstrong WF, O'Donnell J, Ryan T, Feigenbaum H: Effect of prior myocardial infarction and extent and location of coronary disease on accuracy of exercise echocardiography. *J Am Coll Cardiol* 10:531-538, 1987.

66. Marangelli V, Iliceto S, Piccinni G, et al: Detection of coronary artery disease by digital stress echocardiography: comparison of exercise, transesophageal atrial pacing and dipyridamole echocardiography. *J Am Coll Cardiol* 24:117-124, 1994.
67. Ryan T, Vasey CG, Presti CF, et al: Exercise echocardiography: detection of coronary artery disease in patients with normal left ventricular wall motion at rest. *J Am Coll Cardiol* 11:993-999, 1988.
68. Crouse LJ, Harbrecht JJ, Vacek JL, et al: Exercise echocardiography as a screening test for coronary artery disease and correlation with coronary arteriography. *Am J Cardiol* 67:1213-1218, 1991.
69. Pozzoli MM, Fioretti PM, Salustri A, et al: Exercise echocardiography and technecium-99 m MIBI single photon emission computed tomography in the detection of coronary artery disease. *Am J Cardiol* 67:350-355, 1991.
70. Marwick TH, Nemec JJ, Pashkow FJ, et al: Accuracy and limitations of exercise echocardiography in a routine clinical setting. *J Am Coll Cardiol* 19:74-81, 1992.
71. White CW, Wright CB, Doty DB, et al: Does visual interpretation of the coronary arteriogram predict the physiological importance of a coronary stenosis? *N Engl J Med* 310:819-824, 1984.
72. Topol EJ, Nissen S: Our preoccupation with coronary luminology: the dissociation between clinical and angiographic findings in ischemic heart disease. *Circulation* 92:2333, 1995.
73. Hachamovitch RDCM: Methods and limitations of assessing new noninvasive tests: Part II: outcomes-based validation and reliability assessment of noninvasive testing. *Circulation* 117:2793-2801, 2008.
74. Hachamovitch R, Di Carli MF: Methods and limitations of assessing new noninvasive tests: Part I: Part I: Anatomy-Based Validation of Noninvasive Testing. *Circulation* 117:2684-2690, 2008.
75. Roger VL, Pellikka PA, Bell MR, et al: Sex and test verification bias. Impact on the diagnostic value of exercise echocardiography. *Circulation* 95:405-410, 1997.
76. Detrano R, Janosi A, Lyons KP, et al: Factors affecting sensitivity and specificity of a diagnostic test: the exercise thallium scintigram. *Am J Med* 84:699-710, 1988.
77. Ryan T, Armstrong WF, O'Donnell JA, Feigenbaum H: Risk stratification after acute myocardial infarction by means of exercise two-dimensional echocardiography. *Am Heart J* 1144:1305-1316, 1987.
78. Fleischmann KE, Hunink MG, Kuntz KM, Douglas PS: Exercise echocardiography or exercise SPECT imaging? A meta-analysis of diagnostic test performance. *JAMA* 280:913-920, 1998.
79. Detrano R, Gianrossi R, Froelicher V: The diagnostic accuracy of the exercise electrocardiogram: a meta-analysis of 22 years of research. *Prog Cardiovasc Dis* 32:173-206, 1989.
80. Lee TH, Boucher CA: Clinical practice. Noninvasive tests in patients with stable coronary artery disease. *N Engl J Med* 244:1840-1845, 2001.
81. Quinones MA, Verani MS, Haichin RM, et al: Exercise echocardiography versus $^{201}$Tl single-photon emission computed tomography in evaluation of coronary artery disease. Analysis of 292 patients. *Circulation* 85:1026-1031, 1992.
82. Geleijnse ML, Elhendy A: Can stress echocardiography compete with perfusion scintigraphy in the detection of coronary artery disease and cardiac risk assessment? *Eur J Echocardiogr* 1:12-21, 2000.
83. O'Keefe JH, Barnhart CS, Bateman TM: Comparison of stress echocardiography and stress myocardial perfusion scintigraphy for diagnosing coronary artery disease and assessing its severity. *Am J Cardiol* 75:25-34, 1995.
84. Kymes SM, Bruns DE, Shaw LJ, et al: Anatomy of a meta-analysis: a critical review of "Exercise echocardiography or exercise SPECT imaging? A meta-analysis of diagnostic test performance." *J Nucl Cardiol* 7:599-615, 2000.
85. Shaw LJ, Heller GV, Travin MI, et al: Cost analysis of diagnostic testing for coronary artery disease in women with stable chest pain. *J Nucl Cardiol* 6:559, 1999.
86. Garber AM, Solomon NA: Cost-effectiveness of alternative test strategies for the diagnosis of coronary artery disease. *Ann Intern Med* 130:719-728, 1999.
87. Kuntz KM, Fleischmann KE, Hunink MG, et al: Cost effectiveness of diagnostic strategies for patients with chest pain. *Ann Intern Med* 130:719, 1999.
88. Kim C, Kwok YS, Saha S, et al: Diagnosis of suspected coronary artery disease in women: a cost-effectiveness analysis. *Am Heart J* 137:1019, 1999.
89. Marwick TH: Cost-effectiveness of stress echocardiography for assessment of coronary artery disease: What we know and what we need to know. *Eur J Echocardiogr* 1:22-31, 2000.
90. Gibbons L, Blair SN, Kohl HW, Cooper K: The safety of maximal exercise testing. *Circulation* 80:846, 1989.
91. Mitka M: New tools assess need for cardiac tests. *JAMA* 301:2084, 2009.
92. Picano E, Pasanisi E, Brown J, Marwick TH: A gatekeeper for the gatekeeper; inappropriate referrals to stress echocardiography. *Am Heart J* 154:126-132, 2007.
93. Sengupta PP, Khandheria BK: A rising paradigm of appropriateness. *J Am Soc Echocardiogr* 11:1205-1206, 2010.
94. Douglas PS, Khandheria B, Stainback RF, et al: ACCF/ASE/ACEP/AHA/ASNC/SCAI/SCCT/SCMR 2008 appropriateness criteria for stress echocardiography. *Circulation* 117:1478-1497, 2008.
95. Mansour IN, Lang RM, Aburuwaida WM, et al: Evaluation of the clinical application of the ACCF/ASE appropriateness criteria for stress echocardiography. *J Am Soc Echocardiogr* 23:1199-1204, 2010.
96. Bergeron S, Ommen SR, Bailey KR, et al: Exercise echocardiographic findings and outcome of patients referred for evaluation of dyspnea. *J Am Coll Cardiol* 43:2242-2246, 2004.
97. Anderson JL, Adams CD, Antman EM, et al: ACC/AHA 2007 guidelines for the management of patients with unstable angina/non-ST-elevation myocardial infarction: a report of the American College of Cardiology/American Heart Association Task Force on Practice Guidelines (writing committee to revise the 2002 guidelines for the management of patients with unstable angina/non-ST-elevation myocardial infarction). *Circulation* 116:e148-e304, 2007.
98. Anderson JL, Adams CD, Antman EM, et al: 2011 ACCF/AHA focused update incorporated into the ACC/AHA 2007 guidelines for the management of patients with unstable angina/non–ST-elevation myocardial infarction. *Circulation* 123:e426-e579, 2011.
99. Bedetti G, Pasanisi EM, Tintori G, et al: Stress echo in chest pain unit: the SPEED trial. *Int J Cardiol* 102:461-467, 2005.
100. Jeetley P, Burden L, Senior R: Stress echocardiography is superior to exercise ECG in the risk stratification of patients presenting with acute chest pain with negative troponin. *Eur J Echocardiogr* 7:155-164, 2006.
101. Conti A, Sammicheli L, Gallini C, et al: Assessment of patients with low-risk chest pain in the emergency department: head-to-head comparison of exercise stress echocardiography and exercise myocardial SPECT. *Am Heart J* 149:894-901, 2005.
102. Lauer M, Froelicher ES, Williams M, Kligfield P: Exercise testing in asymptomatic adults: a statement for professionals from the American Heart Association Council on Clinical Cardiology, Subcommittee on Exercise, Cardiac Rehabilitation, and Prevention. *Circulation* 223:771-776, 2005.
103. Braunwald E, Antman EM, Beasley JW, et al: ACC/AHA 2002 guideline update for the management of patients with unstable angina and non-ST-segment elevation myocardial infarction. *J Am Coll Cardiol* 40:366-374, 2002.
104. Hamm LF, Crow RS, Stull GA, Hannan P: Safety and characteristics of exercise testing early after acute myocardial infarction. *Am J Cardiol* 63:1193-1197, 1989.
105. Jain A, Myers GH, Sapin PM, O'Rourke RA: Comparison of symptom limited and low level exercise tolerance tests early after myocardial infarction. *J Am Coll Cardiol* 22:1816-1820, 1993.
106. Armstrong WF, Zoghbi WA: Stress echocardiography: current methodology and clinical applications. *J Am Coll Cardiol* 45:1739-1747, 2005.
107. Haghani K, Shapiro S, Ginzton LE: Low-level exercise echocardiography identifies contractile reserve in patients with a recent myocardial infarction: comparison with dobutamine stress echocardiography. *J Am Soc Echocardiogr* 15:671-677, 2002.
108. Lancellotti P, Hoffer EP, Pierard LA: Detection and clinical usefulness of a biphasic response during exercise echocardiography early after myocardial infarction. *J Am Coll Cardiol* 41:1142-1147, 2003.
109. Hoffer EP, Dewé W, Celentano C, Pierard LA: Low-level exercise echocardiography detects contractile reserve and predicts reversible dysfunction after acute myocardial infarction: comparison with low-dose dobutamine echocardiography. *J Am Coll Cardiol* 34:989-997, 1999.
110. Mertes H, Erbel R, Nixdorff U, et al: Exercise echocardiography for the evaluation of patients after nonsurgical coronary artery revascularization. *J Am Coll Cardiol* 21:1087, 1993.
111. Broderick T, Sawada S, Armstrong WF, et al: Improvement in rest and exercise-induced wall motion abnormalities after coronary angioplasty: an exercise echocardiographic study. *J Am Coll Cardiol* 15:591-599, 1990.
112. Hecht HS, DeBord L, Shaw R, et al: Usefulness of supine bicycle stress echocardiography for detection of restenosis after percutaneous transluminal coronary angioplasty. *Am J Cardiol* 71:293-296, 1993.
113. Crouse LJ, Vacek JL, Beauchamp GD, Kramer PH: Use of exercise echocardiography to evaluate patients after coronary angioplasty. *Am J Cardiol* 78:1163-1166, 1996.

114. Fioretti PM, Pozzi MM, Ilmer B, et al: Exercise echocardiography versus thallium-201 SPECT for assessing patients before and after PTCA. *Eur J Cardiology* 13:213, 1992.
115. Sawada SG, Judson WE, Ryan T, et al: Upright bicycle exercise echocardiography after coronary artery bypass grafting. *Am J Cardiol* 64:1123-1129, 1989.
116. Crouse LJ, Vacek JL, Beauchamp GD, et al: Exercise echocardiography after coronary artery bypass grafting. *Am J Cardiol* 70:572-576, 1992.
117. Kafka HK, Leach AJ, Fitzgibbon GM: Exercise echocardiography after coronary artery bypass surgery: correlation with coronary angiography. *J Am Coll Cardiol* 25:1019, 1995.
118. Stein JH, Neumann A, Preston LM, et al: Improved risk stratification in unstable angina: identification of patients at low risk for in-hospital cardiac events by admission echocardiography. *Clin Cardiol* 21:725-730, 1998.
119. Ryan T, Armstrong W, O'Donnell JA, Feigenbaum H: Risk stratification after acute myocardial infarction by means of exercise two-dimensional echocardiography. *Am Heart J* 114:1305-1316, 1987.
120. Cicala S, de Simone G, Roman G, et al: Prevalence and prognostic significance of wall-motion abnormalities in adults without clinically recognized cardiovascular disease. The Strong Heart Study. *Circulation* 116:143-150, 2007.
121. Carluccio E, Tommasi S, Bentivoglio M, et al: Usefulness of the severity and extent of wall motion abnormalities as prognostic markers of an adverse outcome after a first myocardial infarction treated with thrombolytic therapy. *Am J Cardiol* 85:411-415, 2000.
122. Chen MS, Blackstone EH, Pothier CE, Lauer MS: Heart rate recovery and impact of myocardial revascularization on long-term mortality. *Circulation* 110:2851-2857, 2004.
123. Vivekananthan DP, Blackstone EH, Pothier CE, Lauer MS: Heart rate recovery after exercise is a predictor of mortality, independent of the angiographic severity of coronary disease. *J Am Coll Cardiol* 42:831-838, 2003.
124. Watanabe J, Thamilarasan M, Blackstone EH, et al: Heart rate recovery immediately after treadmill exercise and left ventricular systolic dysfunction as predictors of mortality: the case of stress echocardiography. *Circulation* 104: 1911-1916, 2001.
125. Peteiro J, Monserrat L, Piñeiro M, et al: Comparison of exercise echocardiography and the Duke treadmill score for risk stratification in patients with known or suspected coronary artery disease and normal resting electrocardiogram. *Am Heart J* 151:1324e1-10, 2006.
126. Elhendy A, Arruda AM, Mahoney DW, Pellikka PA: Prognostic stratification of diabetic patients by exercise echocardiography. *J Am Coll Cardiol* 37:1551-1557, 2001.
127. Mazur W, Rivera JM, Khoury AF, et al: Prognostic value of exercise echocardiography: validation of a new risk index combining echocardiographic, treadmill, and exercise electrocardiographic parameters. *J Am Soc Echocardiogr* 16:318-325, 2003.
128. Elhendy A, Mahoney DW, McCully RB, et al: Use of a scoring model combining clinical, exercise test, and echocardiographic data to predict mortality in patients with known or suspected coronary artery disease. *Am J Cardiol* 93:1223-1228, 2004.
129. Sicari R, Pasanisi E, Venneri L, et al: Stress echo results predict mortality: a large-scale multicenter prospective international study. *J Am Coll Cardiol* 41:589-595, 2003.
130. Arruda AM, Das MK, Roger VL, et al: Prognostic value of exercise echocardiography in 2,632 patients > or = 65 years of age. *J Am Coll Cardiol* 37:1036-1041, 2001.
131. Biagini E, Elhendy A, Bax JJ, et al: The use of stress echocardiography for prognostication in coronary artery disease: an overview. *Curr Opin Cardiol* 20:386-394, 2005.
132. McCully RB, Roger VL, Mahoney DW, et al: Outcome after abnormal exercise echocardiography for patients with good exercise capacity: prognostic importance of the extent and severity of exercise-related left ventricular dysfunction. *J Am Coll Cardiol* 39:1345-1352, 2002.
133. Olmos LI, Dakik H, Gordon R, et al: Long-term prognostic value of exercise echocardiography compared with exercise $^{201}$Tl, ECG, and clinical variables in patients evaluated for coronary artery disease. *Circulation* 98:2679-2686, 1998.
134. Yao SS, Qureshi E, Sherrid MV, Chaudhry FA: Practical applications in stress echocardiography: risk stratification and prognosis in patients with known or suspected ischemic heart disease. *J Am Coll Cardiol* 42:1084-1090, 2003.
135. Elhendy A, Mahoney DW, Khandheria BK, et al: Prognostic significance of the location of wall motion abnormalities during exercise echocardiography. *J Am Coll Cardiol* 40:1623-1629, 2002.
136. Bouzas-Mosquera A, Peteiro J, Alvarez-Garcia N, et al: Prediction of mortality and major cardiac events by exercise echocardiography in patients with normal exercise electrocardiographic testing. *J Am Coll Cardiol* 53:1981-1990, 2009.
137. Peteiro J, Bouzas-Mosquera A, Pazos P, et al: Prognostic value of exercise echocardiography in patients with left ventricular systolic dysfunction and known or suspected coronary artery disease. *Am Heart J* 160:301-307, 2010.
138. Quintana M, Lindvall K, Ryden L, et al: Prognostic value of predischarge exercise stress echocardiography after acute myocardial infarction. *Am J Cardiol* 76:1115-1121, 1995.
139. Bouzas-Mosquera A, Peteiro J, Alvarez-García N, et al: Prognostic value of exercise echocardiography in patients with left bundle branch block. *JACC Cardiovasc Imaging* 2:251-259, 2009.
140. McCully RB, Roger VL, Mahoney DW, et al: Outcome after normal exercise echocardiography and predictors of subsequent cardiac events: follow-up of 1,325 patients. *J Am Coll Cardiol* 31:144-149, 1998.
141. Metz LD, Beattie M, Hom R, et al: The prognostic value of normal exercise myocardial perfusion imaging and exercise echocardiography: a meta-analysis. *J Am Coll Cardiol* 49:227-237, 2007.
142. Sawada SG, Ryan T, Conley MJ, et al: Prognostic value of a normal exercise echocardiogram. *Am Heart J* 120:49-55, 1990.
143. Kwok Y, Kim C, Grady D, et al: Meta-analysis of exercise testing to detect coronary artery disease in women. *Am J Cardiol* 83:660, 1999.
144. Shaw LJ, Bairey Merz CN, Pepine CJ, et al: Insights from the NHLBI-Sponsored Women's Ischemia Syndrome Evaluation (WISE) Study: Part I: gender differences in traditional and novel risk factors, symptom evaluation, and gender-optimized diagnostic strategies. *J Am Coll Cardiol* 47:s4-s20, 2006.
145. Cox JL, Teskey RK, Lalonde LD, Iles SE: Noninvasive testing in women presenting with chest pain: evidence for diagnostic uncertainty. *Can J Cardiol* 11:885-890, 1995.
146. Curzen N, Patel D, Clarke D, et al: Women with chest pain: as exercise testing worthwhile? *Heart* 76:156-160, 1996.
147. Shaw LJ, Miller DD, Romeis JC, et al: Gender differences in the noninvasive evaluation of patients with suspected coronary artery disease. *Ann Intern Med* 120:559-566, 1994.
148. Mieres JH, Shaw LJ, Arai A, et al: Role of noninvasive testing in the clinical evaluation of women with suspected coronary artery disease. *Circulation* 111:682-696, 2005.
149. Marwick TH, Anderson T, Williams MJ, et al: Exercise echocardiography is an accurate and cost-efficient technique for detection of coronary artery disease in women. *J Am Coll Cardiol* 26:335-341, 1995.
150. Arruda-Olson AM, Juracan EM, Mahoney DW, et al: Prognostic value of exercise echocardiography in 5,798 patients: is there a gender difference? *J Am Coll Cardiol* 39:625-631, 2002.
151. Vasey CG, Usedom JE, Allen SM, Koch GG: Prognostic value of exercise echocardiography in women in the community setting. *Am J Cardiol* 85:258-260, 2000.
152. Shaw LJ, Vasey C, Sawada S, et al: Impact of gender on risk stratification by exercise and dobutamine stress echocardiography long-term mortality in 4234 women and 6898 men. *Eur Heart J* 26:447-456, 2005.
153. Heupler S, Mehta R, Lobo A, et al: Prognostic implications of exercise echocardiography in women with known or suspected coronary artery disease. *J Am Coll Cardiol* 30:414-420, 1997.
154. Eagle KA, Berger PB, Calkins H, et al: ACC/AHA guideline update for perioperative cardiovascular evaluation for noncardiac surgery. *J Am Coll Cardiol* 39:542-553, 2002.
155. Poldermans D, Schouten O, Vidakovic R, et al: A clinical randomized trial to evaluate the safety of a noninvasive approach in high-risk patients undergoing major vascular surgery: the DECREASE-V Pilot Study. *J Am Coll Cardiol* 49:1763-1769, 2007.
156. Schouten O, van Dornburg RT, Bax JJ, et al: Noncardiac surgery after coronary stenting: early surgery and interruption of antiplatelet therapy are associated with an increase in major adverse cardiac events. *J Am Coll Cardiol* 49:122-124, 2007.
157. Maron BJ, Maron MS, Wigle ED, Braunwald E: The 50-year history, controversy, and clinical implications of left ventricular outflow tract obstruction in hypertrophic cardiomyopathy: from idiopathic hypertrophic subaortic stenosis to hypertrophic cardiomyopathy. *J Am Coll Cardiol* 54:191-200, 2009.
158. Maron BJ, McKenna WJ, Danielson GK, et al: ACC/ESC clinical expert consensus document on hypertrophic cardiomyopathy: a report of the American College of Cardiology Task Force on Clinical Expert Consensus Documents and the European Society of Cardiology Committee for Practice Guidelines. *J Am Coll Cardiol* 42:1687-1713, 2003.
159. Wu WC, Bhavsar JH, Aziz GF, Sadaniantz A: An overview of stress echocardiography in the study of patients with dilated or hypertrophic cardiomyopathy. *Echocardiography* 21:467-475, 2004.
160. De Caro E, Smeraldi A, Trocchio G, et al: Subclinical cardiac dysfunction and exercise

performance in childhood cancer survivors. *Pediatr Blood Cancer* 56:122-126, 2011.
161. Lafitte S, Bordachar P, Lafitte M, et al: Dynamic ventricular dyssynchrony: an exercise-echocardiography study. *J Am Coll Cardiol* 47: 2253-2259, 2006.
162. Chung ES, Leon AR, Tavazzi L, et al: Results of the Predictors of Response to CRT (PROSPECT) Trial. *Circulation* 117:2608-2616, 2008.
163. Miyazaki C, Redfield MM, Powell BD, et al: Dyssynchrony indices to predict response to cardiac resynchronization therapy: a comprehensive prospective single-center study. *Circ Heart Fail* 3:565-573, 2010.
164. Cai Q, Rangasetty UC, Barbagelata A, et al: Cardiac allograft vasculopathy: advances in diagnosis. *Cardiol Rev* 19:30-35, 2011.
165. Cohn JM, Wilensky RL, O'Donnell JA, et al: Exercise echocardiography, angiography and intracoronary ultrasound after cardiac transplantation. *Am J Cardiol* 77:1216-1219, 1996.
166. Collings CA, Pinto FJ, Valantine HA, et al: Exercise echocardiography in heart transplant recipients: a comparison with angiography and intracoronary ultrasonography. *J Heart Lung Transplant* 13:604-613, 1994.
167. Wu WC, Aziz GF, Sadaniantz A: The use of stress echocardiography in the assessment of mitral valvular disease. *Echocardiography* 21:451-458, 2004.
168. Picano E, Pibarot P, Lancelloti P, et al: The emerging role of exercise testing and stress echocardiography in valvular heart disease. *J Am Coll Cardiol* 54:2251-2260, 2009.
169. Vahanian A, Baumgartner H, Bax J, et al: Guidelines on the management of valvular heart disease: The Task Force on the Management of Valvular Heart Disease of the European Society of Cardiology. *Eur Heart J* 28:230-268, 2007.
170. Ennezat PV, Maréchaux S, Iung B, et al: Exercise testing and exercise stress echocardiography in asymptomatic aortic valve stenosis. *Heart* 95:877-884, 2009.
171. Maréchaux S, Hachicha Z, Bellouin A, et al: Usefulness of exercise-stress echocardiography for risk stratification of true asymptomatic patients with aortic valve stenosis. *Eur Heart J* 31:1390-1397, 2010.
172. Chambers J: Exercise testing to guide surgery in aortic stenosis. *Heart* 82:7-8, 1999.
173. Alborino D, Hoffman JL, Fournet PC, Bloch A: Value of exercise testing to evaluate the indication for surgery in asymptomatic patients with valvular aortic stenosis. *J Heart Valve Dis* 11:204-209, 2002.
174. Lancellotti P, Lebois F, Simon M, et al: Prognostic importance of quantitative exercise Doppler echocardiography in asymptomatic valvular aortic stenosis. *Circulation* 112(9 Suppl):I377-I382, 2005.
175. Lancellotti P, Karsera D, Tumminello G, et al: Determinants of an abnormal response to exercise in patients with asymptomatic valvular aortic stenosis. *Eur J Echocardiogr* 9:338-343, 2008.
176. Leurent G, Donal E, de Place C, et al: Argument for a Doppler echocardiography during exercise in assessing asymptomatic patients with severe aortic stenosis. *Eur J Echocardiogr* 10:69-73, 2009.
177. Leavitt JI, Coats MH, Falk RH: Effects of exercise on transmitral gradient and pulmonary artery pressure in patients with mitral stenosis or a prosthetic mitral valve: a Doppler echocardiographic study. *J Am Coll Cardiol* 17:1520-1526, 1991.
178. Schwammenthal E, Vered Z, Agranat O, et al: Impact of atrioventricular compliance on pulmonary artery pressure in mitral stenosis: an exercise echocardiographic study. *Circulation* 102:2378-2384, 2000.
179. Tischler MD, Battle RW, Saha M, et al: Observations suggesting a high incidence of exercise-induced severe mitral regurgitation in patients with mild rheumatic mitral valve disease at rest. *J Am Coll Cardiol* 25:128-133, 1995.
180. Leung DY, Griffin BP, Stewart WJ, et al: Left ventricular function after valve repair for chronic mitral regurgitation: predictive value of preoperative assessment of contractile reserve by exercise echocardiography. *J Am Coll Cardiol* 28:1198-1205, 1996.
181. Lancellotti P, Cosyns B, Zacharakis D, et al: Importance of left ventricular longitudinal function and functional reserve in patients with degenerative mitral regurgitation: assessment by two-dimensional speckle tracking. *J Am Soc Echocardiogr* 21:1331-1336, 2008.
182. Supino PG, Borer JS, Schuleri K, et al: Prognostic value of exercise tolerance testing in asymptomatic chronic nonischemic mitral regurgitation. *Am J Cardiol* 100:1274-1281, 2007.
183. Lancellotti P, Donal E, Cosyns B, et al: Effects of surgery on ischaemic mitral regurgitation: a prospective multicentre registry (SIMRAM registry). *Eur J Echocardiogr* 9:26-30, 2008.
184. Pahl E, Duffy CE, Chaudhry FA: The role of stress echocardiography in children. *Echocardiography* 17:507-512, 2000.
185. Alkotob ML, Soltani P, Sheatt MA, et al: Reduced exercise capacity and stress-induced pulmonary hypertension in patients with scleroderma. *Chest* 130:176-181, 2006.
186. Steen V, Chou M, Shanmugam V, et al: Exercise-induced pulmonary arterial hypertension in patients with systemic sclerosis. *Chest* 134:146-151, 2008.
187. Collins N, Bastian B, Jones C, et al: Abnormal pulmonary vascular responses in patients registered with a systemic autoimmunity database: Pulmonary Hypertension Assessment and Screening Evaluation using stress echocardiography (PHASE-I). *Eur J Echocardiogr* 7:439-446, 2006.
188. Mor-Avi V, Jacobs LD, Weiss RJ, et al: Color encoding of endocardial motion improves the interpretation of contrast-enhanced echocardiographic stress tests by less-experienced readers. *J Am Soc Echocardiogr* 19:48-54, 2006.
189. Shimoni S, Zoghbi WA, Xie F, et al: Real-time assessment of myocardial perfusion and wall motion during bicycle and treadmill exercise echocardiography: comparison with single photon emission computed tomography. *J Am Coll Cardiol* 37:741-747, 2001.
190. Laskar R, Grayburn PA: Assessment of myocardial perfusion with contrast echocardiography at rest and with stress: an emerging technology. *Prog Cardiovasc Dis* 43:245-258, 2000.
191. Moir S, Marwick TH: Combination of contrast with stress echocardiography: a practical guide to methods and interpretation. *Cardiovasc Ultrasound* 2:15, 2004.
192. Mulvagh SL, DeMaria AN, Feinstein SB, et al: Contrast echocardiography: current and future applications. *J Am Soc Echocardiogr* 13:331-342, 2000.
193. Jeetley P, Hickman M, Kamp O, et al: Myocardial contrast echocardiography for the detection of coronary artery stenosis: a prospective multicenter study in comparison with single-photon emission computed tomography. *J Am Coll Cardiol* 47:141-145, 2006.
194. Kachenoura N, Mor-Avi V, Frouin F, et al: Diagnostic value of parametric imaging of left ventricular wall motion from contrast-enhanced echocardiograms in patients with poor acoustic windows. *J Am Soc Echocardiogr* 22:273-283, 2009.
195. Burgess MI, Jenkins C, Sharman JE, Marwick TH: Diastolic stress echocardiography: hemodynamic validation and clinical significance of estimation of ventricular filling pressure with exercise. *J Am Coll Cardiol* 47:1891-1900, 2006.
196. Shaikh KA, Quinones M: The diastolic stress test: a new approach to an old problem. *Heart Fail Rev* 2010.
197. Ha JW, Oh JK, Pellikka PA, et al: Diastolic stress echocardiography: a novel noninvasive diagnostic test for diastolic dysfunction using supine bicycle exercise Doppler echocardiography. *J Am Soc Echocardiogr* 18:63-68, 2005.
198. Reuss CS, Moreno CA, Appleton CP, Lester SJ: Doppler tissue imaging during supine and upright exercise in healthy adults. *J Am Soc Echocardiogr* 18:1343-1348, 2005.
199. Pasquet A, Armstrong G, Beachler L, et al: Use of segmental tissue Doppler velocity to quantitate exercise echocardiography. *J Am Soc Echocardiogr* 12:901-912, 1999.
200. Mädler CF, Payne N, Wilkenshoff U, et al: Noninvasive diagnosis of coronary artery disease by quantitative stress echocardiography: optimal diagnostic models using off-line tissue Doppler in the MYDISE study. *Eur Heart J* 24:1584-1594, 2003.
201. Smiseth O, Stoylen A, Halfdan I: Tissue Doppler imaging for the diagnosis of coronary artery disease. *Curr Opin Cardiol* 19:421-429, 2004.
202. Sutherland GR, Di Salvo G, Claus P, et al: Strain and strain rate-imaging: a new clinical approach to quantifying regional myocardial function. *J Am Soc Echocardiogr* 17:788-802, 2004.
203. Ingul CB, Rozis E, Slordahl SA, Marwick TH: Incremental value of strain rate imaging to wall motion analysis for prediction of outcome in patients undergoing dobutamine stress echocardiography. *Circulation* 115:1252-1259, 2007.
204. Ishii K, Imai M, Suyama T, et al: Exercise-induced post-ischemic left ventricular delayed relaxation or diastolic stunning: is it a reliable marker in detecting coronary artery disease? *J Am Coll Cardiol* 53:698-705, 2009.
205. Davidavicius G, Kowalski M, Williams I, et al: Can strain and strain rate measurement be performed during both dobutamine and exercise echocardiography, and do regional deformation responses differ with different forms of stress testing? *J Am Soc Echocardiogr* 16:299-308, 2003.
206. Hung J, Lang R, Flachskampf F, et al: 3D echocardiography: a review of the current status future directions. *J Am Soc Echocardiogr* 20: 213-233, 2007.
207. Yang HS, Bansal RC, Mookadam F, et al: Practical guide for three-dimensional transthoracic echocardiography using a fully sampled matrix array transducer. *J Am Soc Echocardiogr* 21:979-989, 2008.
208. Eroglu E, D'hooge J, Herbots L, et al: Comparison of real-time tri-plane and conventional 2D dobutamine stress echocardiography for the assessment of coronary artery disease. *Eur Heart J* 27:1719-1724, 2006.

209. Yoshitani H, Takeuchi M, Mor-Avi V, et al: Comparative diagnostic accuracy of multiplane and multi-slice three dimensional dobutamine stress echocardiography in the diagnosis of coronary artery disease. *J Am Soc Echocardiogr* 22:437-442, 2009.
210. Takuma S, Cardinale C, Homma S: Real-time three-dimensional stress echocardiography: a review of current applications. *Echocardiography* 17:791-794, 2000.
211. Badano L, Muraru D, Rigo F, et al: High volume-rate three-dimensional stress echocardiography to assess inducible myocardial ischemia: a feasibility study. *J Am Soc Echocardiogr* 23:628-635, 2010.
212. Pratali L, Molinaro S, Corciu AI, et al: Feasibility of real-time three-dimensional stress echocardiography: pharmacological and semisupine exercise. *Cardiovasc Ultrasound* 8:1-10, 2010.
213. Pulerwitz T, Hirata K, Abe Y, et al: Feasibility of using a real-time 3-dimensional technique for contrast dobutamine stress echocardiography. *J Am Soc Echocardiogr* 19:540-545, 2006.
214. Ahmad M: Real-time three-dimensional dobutamine stress echocardiography: a valuable adjunct or a superior alternative to two-dimensional stress echocardiography? *J Am Soc Echocardiogr* 5:443-444, 2009.
215. Varnero S, Santagata P, Pratali L, et al: Head to head comparison of 2D vs. 3D dipyridamole stress echocardiography. *Cardiovasc Ultrasound* 6:31, 2008.
216. Sawada AG, Thomaides A: Three-dimensional stress echocardiography: the promise and limitations of volumetric imaging. *Curr Opin Cardiol* 24:426-432, 2009.
217. Walimbe V, Garcia M, LaLude O, et al: Quantitative real-time 3-dimensional stress echocardiography: a preliminary investigation of feasibility and effectiveness. *J Am Soc Echocardiogr* 20:13-22, 2007.



# Stress Echocardiography with Nonexercise Techniques: Principles, Protocols, Interpretation, and Clinical Applications

THOMAS H. MARWICK, MD, PhD

**Background**
Indications
Choice and Mechanism of Action of Nonexercise Stressors
**Basic Principles**
Pharmacology and Physiopathology
Echocardiographic Approach
**Technical Aspects**
General Considerations
Exercise-Simulating Agents
Vasodilator Stress Protocols
Vasoconstrictor Protocols
Pacing Stress
**Accuracy for Diagnosis of Coronary Artery Disease**
Dobutamine Stress Echocardiography
Dipyridamole Stress Echocardiography
Vasodilator Stress with Adenosine Echocardiography
Pacing Stress Echocardiography
Comparison between Nonexercise Stressors for the Diagnosis of Coronary Artery Disease
**Assessment of Disease Significance**
Prognostic Evaluation and Prediction of Cardiac Events in Patients Undergoing Major Noncardiac Surgery
Prognostic Evaluation of Patients with Stable Coronary Disease
Prognostic Evaluation of Patients after Myocardial Infarction
**Evaluation of Therapy**
Medical Therapy
Follow-up after Coronary Interventions
**Assessment of Myocardial Viability**
Clinical Significance
Use of Dobutamine Echocardiography for the Diagnosis of Viable Myocardium
Prediction of Recovery of Global Function and Outcome
**New Technologies**
Image Quality
Quantitative Approaches to Interpretation
Stress Doppler Echocardiography
**Alternatives**
Exercise Stress Testing
Pharmacologic Stress Echocardiography versus Perfusion Scintigraphy
**The Future of Pharmacologic Stress Echocardiography**

## Background

### INDICATIONS

The performance of a maximal level of stress is a critical determinant of the sensitivity of all stress modalities for the detection of coronary artery disease. Unfortunately, many patients—fully 30% to 40% at some tertiary centers—either cannot exercise at all or cannot exercise maximally, but may still need to undergo stress testing for diagnostic, decision-making, or prognostic purposes. The most common causes of limited exercise capacity are vascular disease and orthopedic problems. Other situations warranting nonexercise stress testing include severe cardiopulmonary disease and general debility, especially among the elderly, in whom pharmacologic testing has been shown to be well tolerated and reliable.

Although the inability of a patient to exercise maximally constitutes the main indication for the use of nonexercise stressors, such stressors are also indicated in other situations (Box 16-1). The most important of these situations include circumstances in which pharmacologic stress may offer diagnostic dimensions that are not available from exercise stress, for example, the diagnosis of coronary spasm using ergonovine testing. Although newer and simpler methods such as contrast-enhanced magnetic resonance imaging (MRI) have assumed a major role in viability assessment (see later discussion), stress echocardiography may be helpful in selected patients early or late after myocardial infarction, after which left ventricular (LV) dysfunction may not be permanent. The diagnostic challenge in this situation is that although stunned myocardium improves spontaneously, the revascularization of hibernating myocardium has implications for functional capacity and prognosis. Echocardiography can be used with dobutamine or dipyridamole stress, or both, for the identification of viable myocardium. A more historical role relates to the use of pharmacologic stress echocardiography in the cardiac catheterization laboratory—the functional evaluation of coronary stenoses having evolved to the evaluation of fractional flow reserve. Likewise, although use in the operating room was a legitimate reason to select pharmacologic stress, this is rarely performed in practice.

Finally, because of their relative technical ease, nonexercise methods have been used in preference to exercise echocardiography even in patients who are able to exercise. The incremental nature of these stressors means that the time course of ischemia can be identified; these data are difficult to gather using treadmill stress[1] or bicycle exercise testing, although it is possible.

**Box 16-1**

**INDICATIONS FOR NONEXERCISE STRESSORS**

| Unable to Exercise | Able to Exercise |
|---|---|
| Inability to exercise maximally | Specific indications |
| *Diagnosis of coronary artery disease, decision making* | *Coronary spasm* |
| *Risk stratification* | *Myocardial viability* |
| Situations preventing exercise | Developing indications |
| *Angiography laboratory, operating room* | *Onset of ischemia* |
| | *New technologies (TDI, CK, contrast)* |

*CK*, Color kinesis; *TDI*, tissue-Doppler imaging.

The decision to use a nonexercise stress still may not be justifiable with routine echocardiographic imaging at present. However, the facilitation of adjunctive techniques (which may be less feasible during exercise than nonexercise stress)—such as strain and contrast perfusion echocardiography—could in the future justify the use of nonexercise techniques in patients who are able to exercise.

## CHOICE AND MECHANISM OF ACTION OF NONEXERCISE STRESSORS

The two general groups of nonexercise stress agents induce ischemia by increasing myocardial work and oxygen consumption (exercise-simulating agents) or by influencing coronary perfusion and therefore myocardial oxygen supply (vasoactive agents). The latter include the coronary vasodilators dipyridamole and adenosine, which cause ischemia by altering regional flow, and ergonovine, which can be used to provoke coronary spasm. In addition, nonpharmacologic approaches including hand-grip and the cold pressor test have been used. Hand-grip testing is often combined with dobutamine-atropine testing, but the cold pressor test has not been widely adopted clinically because of limited efficacy and patient discomfort.

### *Exercise-Simulating Agents*

The exercise simulators include dobutamine and other sympathomimetic agents, pacing, and atropine (usually used as an adjunct to the other approaches), all of which increase cardiac work and myocardial oxygen requirement. The induction of ischemia and regional dysfunction reflects the inability of the diseased coronary circulation to respond to this increased oxygen demand, a process that parallels the response to exercise. Because increased cardiac workload and oxygen demand is the usual mechanism underlying ischemia in most ambulatory situations, the exercise-simulating agents are often considered to be a more physiologic means of stressing the heart. However, additional mechanisms include effects on cardiac metabolism producing an "oxygen-wasting" effect[2] and concurrent "supply" ischemia due to reduction of subendocardial perfusion and maldistribution of coronary flow.

### *Vasoactive Agents*

The use of dipyridamole in combination with myocardial perfusion imaging is based on the induction of maximal coronary vasodilation in all territories. Flow heterogeneities (and therefore apparent perfusion defects) develop if a coronary stenosis limits the regional hyperemic response.[3] Of note, this process may not involve the provocation of ischemia in a functional or metabolic sense. In contrast, the development of regional wall motion abnormalities at stress echocardiography necessitates the induction of ischemia.

The mechanism of vasodilator-induced wall motion abnormalities has been attributed to coronary steal.[3] Traditionally, horizontal steal involves blood flowing to nonstenosed from stenosed territory, owing to reduced collateral flow into the stenosed territory because of depressurization of vessels supplying the collaterals due to increased runoff. Vertical steal occurs because vasodilator-induced depressurization of the microcirculation causes subendocardial vessels to collapse under the greater extravascular pressure in this region and "steal" flow to the subepicardium from the subendocardium. However, in experimental studies, steal appears less important than previously proposed, and vasodilator-induced ischemia has been attributed to the combination of reduced endocardial myocardial blood flow reserve with increased myocardial oxygen demand caused by hypotension and reflex tachycardia.[4] The administration of atropine or increased sympathetic activity secondary to angina may augment this process. Systemic hypotension may certainly accentuate hypoperfusion, as driving pressure is the main determinant of myocardial perfusion when vasodilator reserve is exhausted. Stenosis "collapse" may be provoked if profound microcirculatory vasodilation causes a reduction of lateral pressure induced by increased flow.

### *Agents Used to Identify Myocardial Viability*

In the presence of dysfunctional but viable myocardium, regional function is enhanced by the inotropic effect of low-dose dobutamine. This appears to require both recruitable perfusion and an increment in metabolism. Viable myocardium supplied by a patent infarct-related vessel (generally corresponding to stunned myocardium) demonstrates a sustained improvement during the infusion, which then reverses after the test. Viable tissue supplied by a stenosed infarct-related artery (which may involve stunned or chronically malperfused tissue) is characterized by an initial improvement, occurring at low doses (less than 20 mcg/kg/min), or low heart rates, or both, followed by deterioration of regional function as the chronotropic effect becomes more prominent and myocardial work increases. If the region is supplied by a critically stenosed artery, however, it may be possible for the territory to become ischemic before there is a noticeable enhancement of contractility. Moreover, the ability of the myocardium to thicken is determined by the amount of infarcted tissue within the segment.

Myocardial viability may also be inferred from the contractile response to dipyridamole. The mechanism of this is also putative but probably relates to myocardial congestion with interstitial fluid due to vasodilation. A so-called mini-Starling effect may be caused by this congestive process, producing additional tension on the myofibrils.

# Basic Principles

## PHARMACOLOGY AND PHYSIOPATHOLOGY

### *Exercise-Simulating Agents*

The exercise-simulating agents include dobutamine, dopamine, epinephrine, and isoproterenol. Of these, dobutamine has become the most commonly administered exercise-simulating

agent, and the majority of published data on pharmacologic stress echocardiography have involved this agent. Although other sympathomimetic agents have been used for stress testing, dopamine may cause localized limb ischemia due to vasoconstriction, and epinephrine and isoproterenol are probably the more arrhythmogenic.

Dobutamine is predominantly a beta-1 agonist; normal areas of myocardium become hyperkinetic in response to its inotropic effect. Segments supplied by a stenosed coronary artery may become akinetic or dyskinetic, but more subtly, and are unable to augment their thickening and excursion. Vasodilation and chronotropy appear at higher doses, usually at the 20 mcg/kg/min level of the routine dobutamine stress protocols, reflecting the stimulation of other receptors to a lesser degree. This chronotropic response appears to be the most important factor in terms of precipitating ischemia. Most dobutamine stress protocols cause a mean heart rate increment of 40 to 50 beats per minute and mean peak heart rates of 110 to 120 beats per minute.[5] However, reflex bradycardia may occur in response to hypertension. Blood pressure normally rises in response to the inotropic effect of the drug, but high doses cause vasodilation and therefore cause blood pressure to fall at peak doses. Increases in myocardial oxygen demand due to increased cardiac work, as well as a weak vasodilator effect, lead to the development of coronary hyperemia in territories supplied by normal coronary arteries. Although this response is probably less than that induced by coronary vasodilators, the coronary hyperemic response to dobutamine stress permits its use with perfusion imaging, both scintigraphic and with microbubbles.[6] The detection of myocardial perfusion defects in the presence of coronary disease may be augmented by partial volume effects due to thinning of the ischemic wall.

### *Vasoactive Agents*

The principal coronary vasodilators are dipyridamole, adenosine, and regadenoson, which differ with respect to the onset and duration of their effects. Dipyridamole increases endogenous adenosine levels by reducing cellular reuptake and metabolism, and thereby acts indirectly.[3] This indirect mechanism causes some delay between the administration of this agent and the timing of peak vasodilation, and this indirect action may account for interindividual variations in the magnitude of its effects. Adenosine acts directly on the vasculature, its vasodilator efficacy being equivalent to that of papaverine. The potency and speed of onset of adenosine cause its side effects to be more intense but also more short-lived than those of dipyridamole. By comparison to adenosine, the new A(2A)-specific receptor agonists have fewer complications but a similar mechanism of action.[7] As with adenosine, however, their primary vasodilator role makes them more attractive for perfusion imaging than for wall motion assessment.

Ergonovine stress echocardiography is not widely practiced, although its use as a test for coronary spasm is well validated. This agent has a direct effect on the vessel; responsiveness to acetylcholine may be related to loss of nitric oxide production at the site of disease.

### *Exercise Simulation Using Pacing Stress*

Several nonpharmacologic stressors have been used, including "physiologic" stresses such as the cold pressor test, which are poorly tolerated. Pacing is an alternative means of increasing cardiac work; pacing-induced tachycardia increases myocardial oxygen consumption and causes myocardial ischemia in the setting of significant coronary stenoses. The reduction of subendocardial perfusion with pacing may also contribute to the development of ischemia.

Ventricular pacing is not favored, as it causes both abnormal regional contractility and abnormal perfusion, so that pacing stress techniques generally involve atrial stimulation, either transvenously or via the esophagus. Of the transesophageal pacing approaches, the "pill" electrode is effective but may cause significant discomfort. Attachment of pacing electrodes to transesophageal echocardiography (TEE) probes has been reported in trials but has not moved into commercial production. A small esophageal pacing catheter offers enhanced contact between the electrodes and the esophagus. The technique causes less discomfort than other pacing techniques because of the presence of smaller pacing thresholds but is not widely used.

Pacing stress may be useful in patients in whom the pharmacologic approaches are contraindicated or associated with side effects. Additional attractions that might justify its use in preference to pharmacologic testing include the capacity to achieve a target heart rate in virtually all patients, the potential to immediately terminate the tachycardia if the patient develops complications (in contrast to pharmacologic methods, which require a period of time for the effects to dissipate), and the ability to perform measurements in the ischemic ventricle at a low heart rate (after cessation of pacing). Using atrial pacing stress, ischemic myocardium has been shown to have reduced ventricular compliance. Sudden termination of stress during ischemia may also be of value in the combination of stress testing with color flow Doppler, as the use of low frame rates may pose a problem at high heart rates. However, despite the benefits of transesophageal atrial pacing, its availability for many years, and recent data showing correlation with dobutamine stress echocardiography (DSE) despite a shorter test duration and better patient tolerance, this technique has not become widely used because it remains somewhat invasive.

### *Combined Approaches*

Atropine reduces the depressant effect of vagal stimulation on heart rate and may be particularly useful when reflex reduction of the heart rate occurs in response to blood pressure elevation. Atropine is combined with dobutamine in patients who fail to develop an adequate degree of tachycardia in response to dobutamine, the most common situation involving patients taking beta receptor antagonists. Tachycardia (and therefore ischemia due to increased oxygen demand) may be obtained by combining atropine with dipyridamole.[8,9] In both circumstances, the addition of atropine to other stressors has been associated with an increment in sensitivity. Indeed, there is a trend toward earlier use of atropine during the dobutamine protocol, especially in beta-blocked patients. Early administration of atropine should not be allowed to interfere with the assessment of the low-dose response, so we do not administer this agent before the end of the 20 mcg/kg/min dose. A simple guide is that patients who fail to attain a heart rate of 70 beats per minute, or fail to increase heart rate by 5 beats per minute at this dose, rarely achieve target heart rate and might as well have the atropine early so as to avoid a prolonged test.

Combinations of dobutamine and dipyridamole have been described but are not used, because although the combination has afforded higher levels of sensitivity than the individual tests can provide, this is obtained at the cost of an unacceptably long stress protocol.

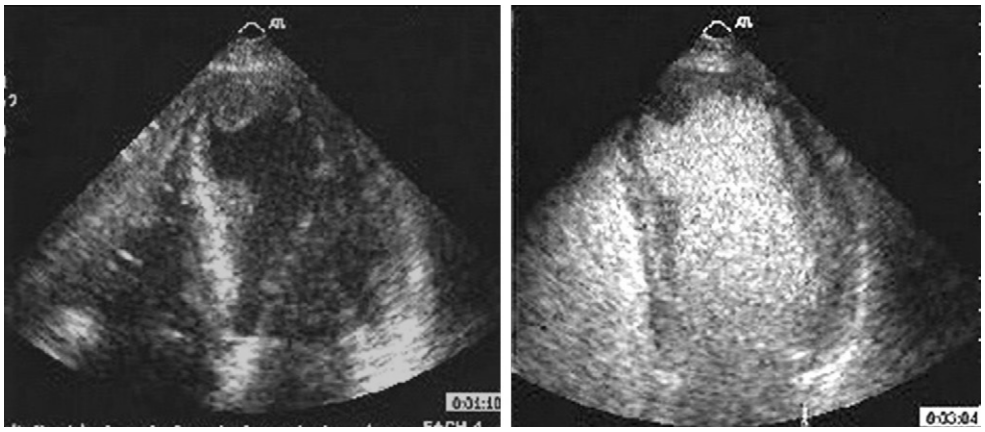


**Figure 16-1 Use of myocardial contrast for LV opacification during stress echocardiography.** Compared with harmonic imaging (**A**), the postcontrast end-diastolic apical four-chamber image (**B**) shows significant improvement of lateral wall resolution.

## ECHOCARDIOGRAPHIC APPROACH

### *Image Acquisition*

The technical challenges of pharmacologic and pacing stress, although less extreme than those posed by exercise echocardiography, mandate the use of the best available equipment. The development of harmonic imaging has had a major impact on endocardial visualization[10] and therefore on the feasibility of stress echocardiography.[11] Although very few patients (less than 2%) have completely uninterpretable images, failure to detect the endocardium in every myocardial segment is very common, and contrast is indicated if two segments are obscured (Fig. 16-1).

Typically, transthoracic images are obtained in the standard views (parasternal long- and short-axis and apical four- and two-chamber). Two additional views are helpful—an apical long-axis view, which may overcome technical problems with parasternal imaging, and an apical short-axis view. Of the complementary imaging techniques, including contrast, strain, and three-dimensional (3D) imaging (see later section), the evaluation of coronary flow reserve in the left anterior descending artery is the simplest addition, although this seems to be most feasible in combination with adenosine.[12]

TEE has been employed in combination with both pharmacologic and pacing stress, usually for patients with inadequate transthoracic images. During transesophageal imaging with pharmacologic stress, we approximate the standard imaging planes as closely as possible by recording transverse and longitudinal esophageal and transgastric short- and long-axis views. During pacing with electrodes attached to the TEE probe, the need to stimulate the esophagus inhibits the ability to move the transducer, so that imaging is performed in the transgastric planes only.

Although the constraints of a busy stress echocardiography schedule may preclude the performance of a detailed examination in every patient, a "screening" M-mode, pulsed wave (especially for LV inflow), and color Doppler echocardiographic examination should be performed at the beginning of every study. According to the setting, tissue Doppler images maybe helpful at baseline for the assessment of filling pressure[13] and dyssynchrony.[14] Time should also be taken to optimize two-dimensional (2D) echocardiographic images and gain settings (for endocardial detection) and to zoom on the ventricles (to obtain the best spatial resolution and frame rate). During the stress, the patient is imaged continuously, and the images are stored in digital clips. When the study is performed for the diagnosis of coronary disease, we favor a multiscreen display to show as many stages as possible, as changes may be transient. Many types of viewing software do not permit this. If so, the minimum default quad-screen display should include a resting image, a low-dose image (10 mcg/kg/min dobutamine, 0.56 mg/kg dipyridamole, or a small heart rate increment with pacing), a high-dose image (40 mcg/kg/min dobutamine or 0.84 mg/kg dipyridamole with or without atropine), and an early poststress image. The ability to save images at multiple stages enables easy alteration of this display. For example, when the clinical question pertains to the possibility of viable myocardium, the display could include two low-dose images (5 and 10 mcg/kg/min dobutamine) and one high-dose image.

### *Image Processing*

Digital techniques are critical for successful interpretation and archiving of stress echocardiograms. Digital image processing facilitates image display and interpretation by allowing a side-by-side display of resting, low-dose, and high-dose images, as well as the ability to review individual frames (which is useful to evaluate the temporal sequence of contraction). However, all studies should also be recorded in continuous format. Traditionally, this involved use of videotape, to provide a backup in case technical problems with the digital capture (especially triggering) or corruption of the archived data threaten loss of the study. Indeed, routine review of tape has a significant impact on diagnosis, probably by permitting review of off-axis images and regions that are not adequately represented by saving a single cardiac cycle. Although videotape is now rarely available in the echocardiography lab, continuous digital capture is an alternative.

### *Qualitative Interpretation*

The interpretation of stress echocardiograms for clinical purposes is based on a qualitative evaluation of regional function at rest and stress.[15] Some standardization is obtained by scoring regional wall motion and thickening in a number of segments. The American Heart Association has proposed a unified 17-segment model that includes the apical cap, to facilitate comparison between imaging modalities.[16] Although this template ignores the small but important detail that the true apex

is often not identified at echocardiography, its role as the standard should make its use preferred to the older 16-segment model (anterior, septal, lateral, and inferior at the apex, with these segments as well as anteroseptal and posterior segments at the base and midpapillary muscle level). Despite this standardization, however, the expertise of the physician interpreting the test is critical, and even accomplished echocardiographers require a significant learning period. In a study of echocardiographers learning dipyridamole stress echocardiography, Picano and colleagues reported that 100 supervised studies were required to bring the accuracy of "novices" to the level of "experts." Despite many technical advances in stress echocardiography in the past two decades, this learning curve remains important.

The standard qualitative algorithm for interpretation of pharmacologic stress echocardiography is summarized in Table 16-1. With the exception of the low-dose responses, which denote myocardial viability, it may also be applied to pacing or other stressors.

Regional wall motion at rest may be classified as normal, hypokinetic, akinetic, or dyskinetic. Severe hypokinesia may be difficult to distinguish from akinesia; a useful guide is based on endocardial excursion, with less than 2 mm identifying akinesia and less than 5 mm indicating hypokinesia. Regions that fail to thicken or that move only in late systole (after movement of the adjacent myocardium) may be moving passively and should be considered akinetic, irrespective of endocardial excursion. Segments with resting akinesis or dyskinesis are most likely composed of infarcted myocardium if the wall is thinned and dense, but in the absence of thinning are likely to consist of viable tissue. Indeed, hypokinetic segments are not identified as being infarcted, on the basis that residual contraction implies the presence of residual viability. Because the process of thinning and fibrosis takes some time after infarction, myocardium of normal thickness is commonly seen after recent or nontransmural infarction. Improvement of abnormal function in response to low doses of dobutamine (5 or 10 mcg/kg/min) or dipyridamole (0.28 or 0.56 mg/kg) suggests the presence of viable myocardium (Fig. 16-2). This finding is more reliable if the segment subsequently deteriorates, which indicates ischemia.

**TABLE 16-1 Interpretation of Myocardial Viability and Ischemia Using Dobutamine Echocardiography**

| *Diagnosis* | *Resting Function* | *Low-Dose* | *Peak/Poststress Function* |
|---|---|---|---|
| Normal | Normal | Normal | Hyperkinetic |
| Ischemic | Normal | Normal (unless severe CAD) | Reduction vs. rest<br>Reduction vs. other segments<br>Delayed contraction |
| Viable, patent IRA | Hypo/akinetic | Improvement | Sustained improvement |
| Viable, stenosed IRA | Hypo/akinetic | Improvement | Reduction (c/w low-dose) |
| Infarction | A/dyskinetic | No change | No change |

*CAD*, Coronary artery disease; *c/w*, compared with; *IRA*, infarct-related artery.

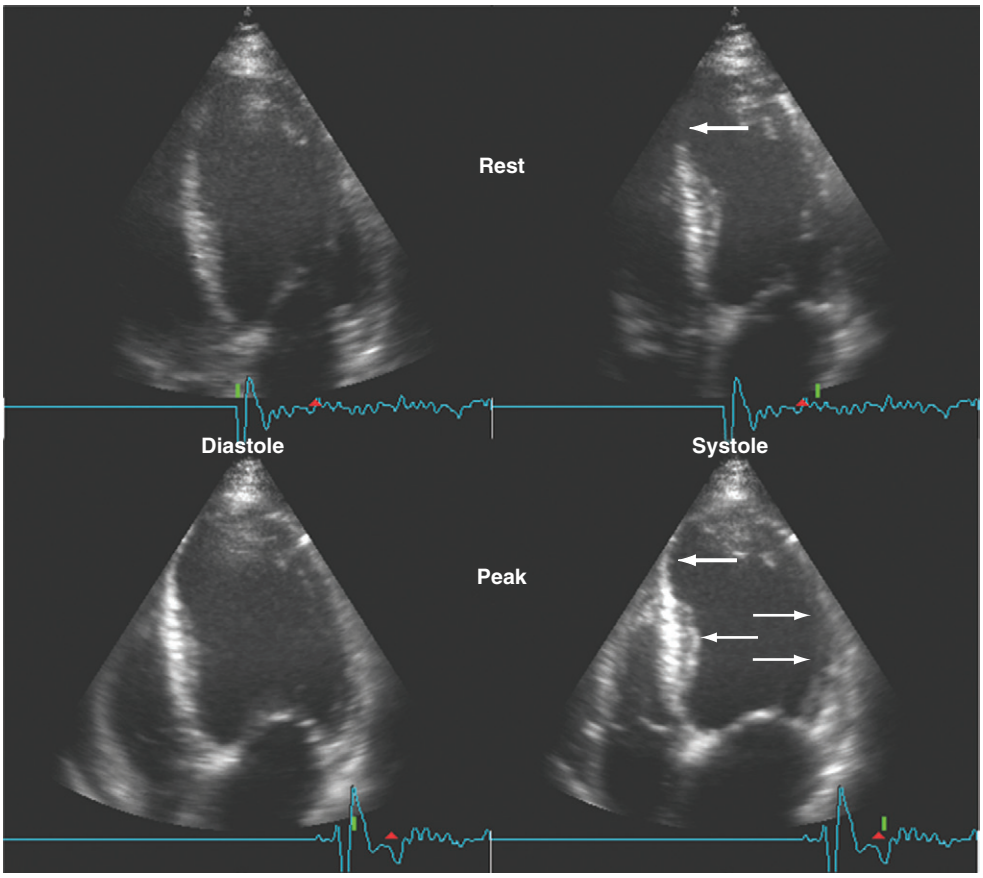



**Figure 16-2 End-diastolic and end-systolic freeze-frame images illustrating LV enlargement on DSE in a patient with LV dysfunction and multivessel coronary artery disease.** There is a resting wall motion abnormality in the apex (*large arrow*), which is unchanged with stress. At peak stress, there is LV enlargement with reduction of systolic motion and thickening of the lateral (and to a lesser degree the septal) wall.

The global LV responses to dobutamine stress include a reduction of cavity size and an increase in cardiac output—mainly due to increased heart rate rather than stroke volume after intermediate dose (e.g., 20 mcg/kg/min), a point that is pertinent to the LV strain response (see later discussion). LV dilation implies multivessel or left main coronary artery disease (see Fig. 16-2), but this is less commonly seen with pharmacologic than with exercise stress, probably because of reduction of loading. Together with an extreme inotropic response, this afterload reduction may produce cavity obliteration (Fig. 16-3) and even outflow obstruction—which is not meaningful. Although the LV cavity obliteration response is favorable prognostically (presumably reflecting a low probability of multivessel disease),[17] it may impair sensitivity both because of reduced transmural wall stress and because endocardial excursion is reduced and small areas of wall motion are unrecognized.[18] Use of intravenous beta-blockade allows the heart rate to slow rapidly after stress, filling the LV cavity and revealing wall motion abnormalities that were unidentified at peak stress.[19] A similar outcome can be obtained by poststress imaging.

The normal response to inotropic stress is to increase endocardial excursion, speed of contraction, and degree of myocardial thickening. A deterioration of function from rest, or after an initial enhancement of function, indicates ischemia (Fig. 16-4). Variants of overt deterioration include delayed contraction ("tardokinesis") and reduced myocardial thickening. Caution should be applied in the assessment of periinfarct zones, which may fail to improve function with stress, or even appear dyskinetic if the infarct bulges due to tethering by the infarcted zone. Examination of wall thickening may assist in distinguishing periinfarct ischemia and tethering.

The evaluation of segments with abnormal resting function is more difficult. Akinetic or even dyskinesic segments may still be viable if they augment in response to either low-dose dipyridamole or dobutamine. Care must be taken to avoid misinterpretation based on differences in image planes, especially if the wall motion abnormality is localized. Deterioration of augmenting myocardium identifies ischemia, but in the absence of augmentation, a deterioration of function probably reflects increased loading rather than ischemia. Segments with resting hypokinesia often reflect nontransmural infarction, although some normal segments may be mildly hypokinetic, and it is important to be wary of overinterpretation, especially in the posterior wall. Analysis of myocardial deformation using 2D strain techniques has suggested that the pattern of impaired longitudinal function with preserved radial or rotational motion may be used to identify nontransmural infarction, as measured by gadolinium-enhanced MRI. Hypokinetic segments are also the most challenging for the identification of ischemia; those demonstrating a stress-induced improvement are classified as normal, and those showing a deterioration (compared with either rest or low-dose) are identified as ischemic. However, differentiation between degrees of hypokinesia may be difficult, even with side-by-side cineloop analysis. Some caution needs to be applied in the interpretation of regional variations in the degree of hyperkinesis, as these may occur in normal patients. There is a risk of overinterpretation of hypokinetic regions that fail to improve function in response to stress, even if adjacent segments mount a hyperkinetic response. A decision to characterize these as ischemic should be made in the context of the rest of the study.

The greatest limitations of the current application of stress echocardiography are concerns related to subjectivity and reproducibility. Although single-center studies have suggested that the interobserver variation in interpretation is small, interinstitution variability (although similar to that of other imaging techniques) is significant.[20] Interinstitution variability is particularly a problem in studies of poor image quality and in patients with mild ischemia. This discordance has been progressively reduced by definition of standard reading criteria[21] and

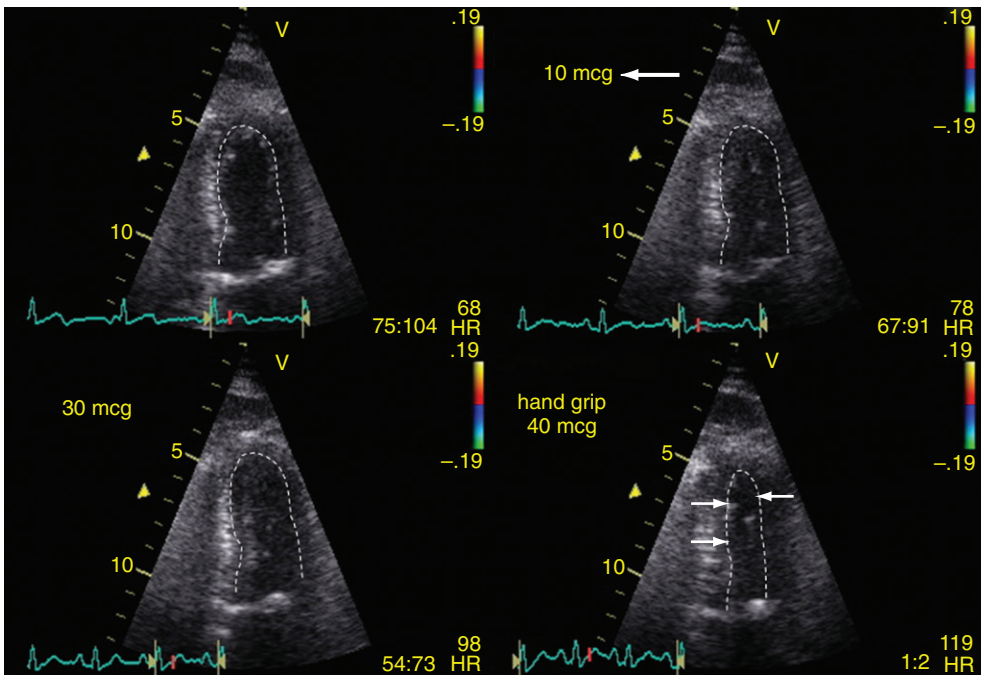



**Figure 16-3 End-systolic freeze-frame images of apical four-chamber views illustrating marked reduction in LV volume at peak stress, with close to cavity obliteration.** The resulting low transmural wall stress may prevent the induction of ischemia despite the presence of coronary artery disease.

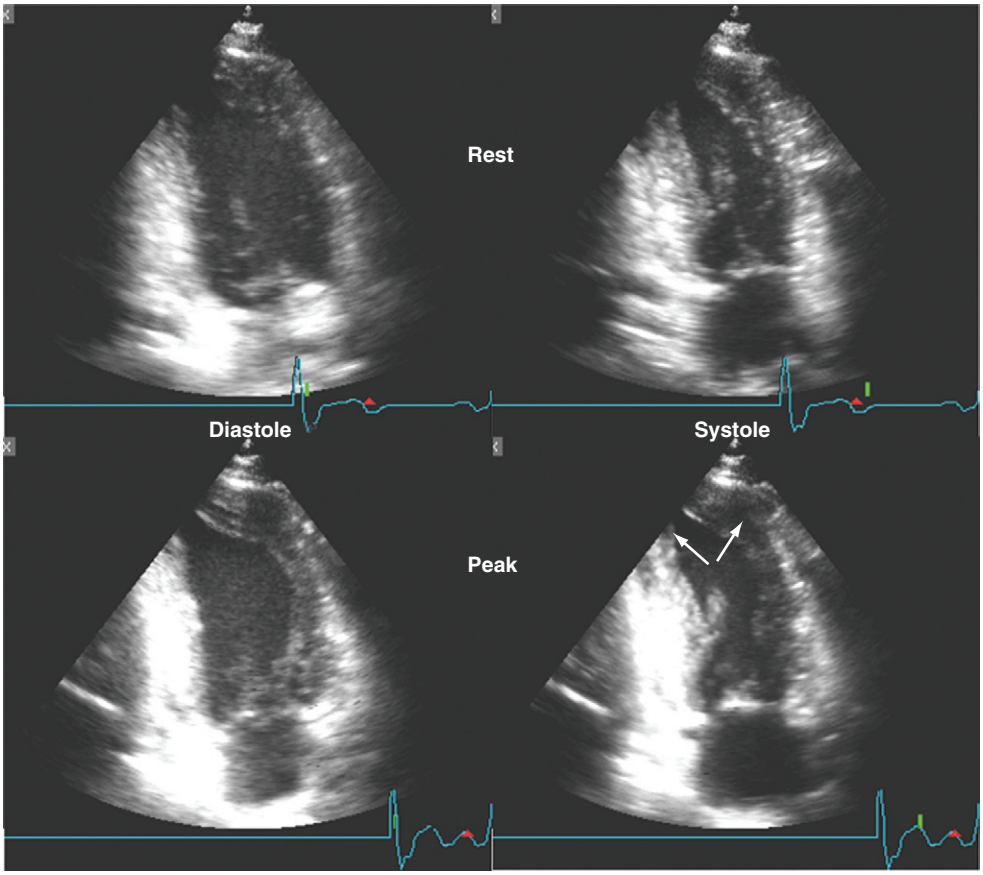



**Figure 16-4 Apical two-chamber views illustrating the development of myocardial ischemia (reduced wall thickening, *arrows*) of the apex during DSE.** End-diastolic images are given on the *left* and systolic images on the *right*, with resting images *above* and peak dose *below*.

the adoption of harmonic imaging.[22] The following reading guidelines are useful for controlling variation: Minor degrees of hypokinesia are not identified as ischemia (especially if only apparent at peak and not at poststress readings); focal abnormalities that do not follow angiographic territories are ignored; abnormalities are corroborated whenever possible with another view; basal inferior and septal segments are not identified as abnormal in the absence of a neighboring abnormal segment; studies are read by multiple observers whenever possible; and reading is blinded to all other data.

Finally, a standard sequence is of value in the interpretation of stress echocardiograms. We first review the resting data or previous transthoracic echocardiography (TTE) for non–wall-motion data that may color our interpretation, including M-mode and Doppler components. On the digital images, we first check that images are triggered correctly and that the prestress, peak stress, and poststress views are comparable. We then briefly review all of the side-by-side displays to see if there are new wall motion abnormalities or obvious changes in cavity size (suggesting multivessel disease) or cavity shape. Segmental analysis is carried out by careful comparison of regional function in each of the 16 segments, comparing the same site at rest and at stress. Both wall motion and thickening are compared, using both cineloop and frame-by-frame review of the digital images. Freezing the images and stepping through one frame at a time is invaluable—delayed contraction is a hallmark of ischemic tissue that is not apparent to the unaided eye, but is often recognizable when images are reviewed frame by frame. The reader should think twice about identifying resting- or stress-induced wall motion abnormalities in segments that move rapidly and smoothly in early systole. Focusing on the first part of systole may minimize the contribution of rotational or translational movement, and assessing the timing of contraction may also avoid false positive interpretations provoked by early relaxation (Fig. 16-5). The ability to save multiple cycles in each view has reduced the need to review continuous capture stress images, but these remain of value for nonstandard views and to check on uncertainties arising from the digitized images. The site, extent (number of abnormal segments), severity (segmental wall motion score), and time of onset and offset of ischemia, as well as the effect of ischemia on global LV function, should be recorded.

## Technical Aspects

### GENERAL CONSIDERATIONS

Patients are instructed to fast, partly because nausea is a side effect with some agents (especially dipyridamole and adenosine), and in case complications ensue, with attending aspiration risks. For dipyridamole stress testing, coffee, tea, and cola drinks should be avoided for 12 hours before the examination, as xanthines antagonize the effects of dipyridamole on adenosine metabolism, as well as by direct competitive inhibition of adenosine.

For diagnostic testing, patients should be instructed to stop antiischemic drugs on the day of the procedure, but medications may be continued if testing is being performed to assess

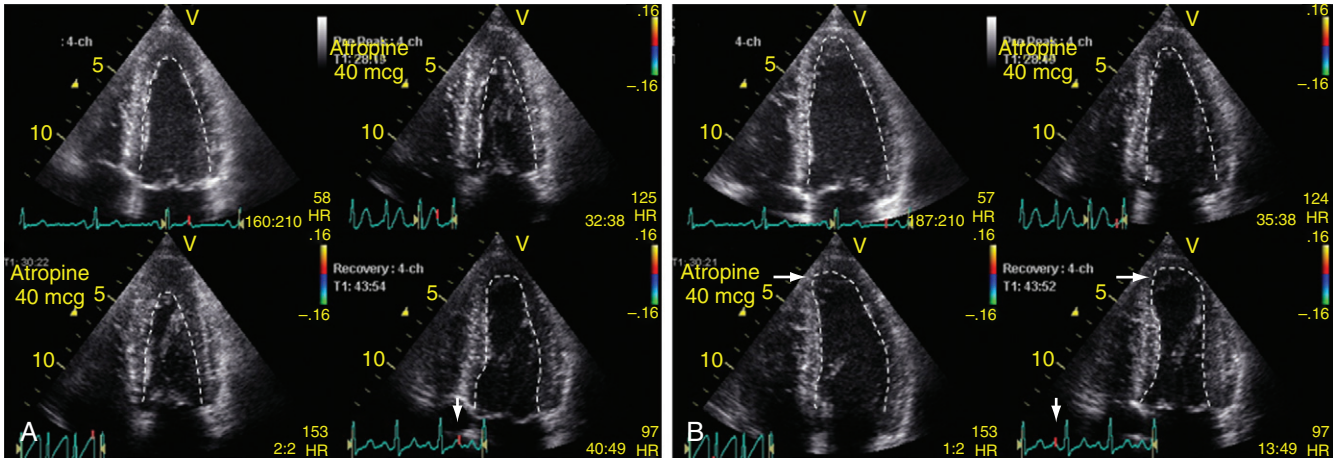



**Figure 16-5** **Apical four-chamber views illustrating the phenomenon of early relaxation. A,** Homogeneous contraction with reduction of apical cavity volume. **B,** Apical shape change after end of systole (*broad arrow* on electrocardiogram).

the adequacy of therapy. Intravenous access is secured, and monitoring electrodes may be moved away from the echocardiographic windows. Two personnel are mandatory for performance of these protocols, usually a sonographer and nurse, with a physician in close proximity. Clinical and electrocardiographic monitoring during the tests parallels the monitoring undertaken during exercise stress testing. In addition to the usual resuscitation equipment, intravenous beta-blocking agents and nitrates should be available to treat severe ischemia. For dipyridamole stress, aminophylline should be available for the treatment of severe ischemia.

## EXERCISE-SIMULATING AGENTS

### *Protocols for Administration of Sympathomimetic Agents*

Dobutamine has been administered using various empiric regimens, but none is clearly superior to the others. The most widely used is an incremental administration from 5 to 40 mcg/kg/min in 2- or 3-minute stages.[5] Variants include maximal doses of up to 50 mcg/kg/min; lower dose-rates administered over longer periods are able to attain hemodynamic effects similar to those achieved by the high-dose protocols. New accelerated dobutamine protocols that have been used to reduce the duration of the test appear to be safe[23] but may sacrifice the ability to identify a biphasic response. Whichever regimen is applied, a reasonable (i.e., 2- to 3-minute) period at peak heart rate is desirable, as ischemic wall motion abnormalities may take a short time to become apparent. If atropine is added to induce an increase in heart rate, the usual dose is 1 to 2 mg total in 0.25-mg increments.

### *Hemodynamic Responses to Sympathomimetics*

Low doses of dobutamine enhance LV contractility, usually without the development of tachycardia. At doses greater than 20 mcg/kg/min, systolic blood pressure increases and heart rate augments to more than 100 beats per minute. Heart rate can be expected to increase to about 120 beats per minute in most patients, reflecting a increment of 40 to 50 beats per minute. In normotensive patients, systolic blood pressure usually increases to about 170 mm Hg (i.e., by 30 to 40 mm Hg)—less during dobutamine than during exercise. The systolic pressure response may be marked in hypertensive patients and blunted in patients with LV dysfunction or multivessel coronary disease. The peak rate-pressure product is usually about 20,000—less than with exercise,[24-29] which has important implications for the relative sensitivity of dobutamine and exercise echocardiography. Although the development of ischemia at lower dobutamine doses and cardiac workloads indicates the presence of more extensive coronary disease, there is too much overlap for the hemodynamic response to be a reliable predictor of one-, two-, or three-vessel disease. The hemodynamic response to dobutamine shows significant variability between patients. Beta blockade may attenuate the physiologic response, with a significantly lower heart rate response (usually about 100 beats per minute), and a lower double-product (to levels of around 14,000), although this may be avoided by use of atropine.

### *Side Effects of Stress Testing with Sympathomimetic Agents*

Other than the development of myocardial ischemia, dose-limiting side effects generally reflect intense adrenergic stimulation. Consequently, dobutamine stress is contraindicated in patients with severe hypertension and serious arrhythmias. Serious side effects are rare during DSE, with death, myocardial infarction, or sustained tachyarrhythmias in about 3 per 1000.[8,30] Nonetheless, case reports of fatalities have been reported from ventricular fibrillation and cardiac rupture,[31] and safety in patients at highest risk—those with severe LV dysfunction—has been described only in small populations.[32] Nonetheless, considering that the sickest patients (those unable to exercise and with questions of myocardial viability) undergo the test, this safety profile is reasonable. This may reflect the detection of ischemia by online imaging, permitting termination before serious problems arise.

Less serious complications include palpitations (atrial and ventricular extra systoles), hypertension, anxiety (sometimes manifested as dyspnea or vagal reactions), tremor, and urinary urgency. Hypotension may arise from the vasodilator effect of high-dose dobutamine, the development of outflow tract obstruction, or the development of severe ischemia.[33] Unlike hypotension during exercise testing, it does not denote the presence of serious coronary disease or LV dysfunction. In particular, the finding of an LV outflow tract gradient does not appear

to be prognostically meaningful. The frequency of these side effects has varied from 5%, if only serious, dose-limiting side effects are considered, to 82%, if all side effects are included. Variability also relates to the type of stress protocol, the incidence being lower if the test is terminated for attainment of a target heart rate or at detection of ischemia or if submaximal test responses are excluded.

## VASODILATOR STRESS PROTOCOLS

### *Stress Protocols*

Dipyridamole is administered into a large proximal arm vein to minimize local discomfort from this strongly alkaline compound. Various dipyridamole administration regimens have been used. For myocardial perfusion imaging, the most commonly administered dose is 0.56 mg/kg IV, but the sensitivity of dipyridamole echocardiography is optimal if 2 minutes of infusion are added if the initial response is negative and no major side effects have appeared. Because the time of onset of ischemia correlates with the severity of coronary disease and prognosis, images are recorded every 2 minutes from the conclusion of the first dose until 18 minutes from the start. Digital images are saved at rest, before the start of the second dose (8 minutes), after the second dose (12 minutes, which is the most common time for the onset of ischemia), and at 16 minutes. Aminophylline (in aliquots of 50 to 75 mg intravenously) is used to reverse the effects of dipyridamole if severe ischemia or side effects arise; the threshold for using this agent is influenced by the overall LV function and the clinical state of the patient.

Because exogenous adenosine is able to act directly, it rapidly achieves steady state, and its biologic effects are of rapid onset. A fixed dose schedule of 0.14 or 0.17 mg/kg/min or incremental protocols (3-minute stages starting at 0.10 mg/kg/min, increasing to 0.14 and 0.18 mg/kg/ minute) been used for echocardiographic studies.[34,35] The use of aminophylline is rarely required for side effects, as these resolve within 1 minute of stopping the infusion.

### *Hemodynamic Responses to Vasodilators*

The mechanism of ischemia with of vasodilator agents is chiefly through coronary steal. There is a small contribution of increasing oxygen demand from tachycardia, which may be a response to angina and side effects rather than arising from the agents themselves. Similarly, blood pressure is usually little changed by these stressors, which may cause hypotension. The addition of atropine leads to an augmentation of heart rate and cardiac work,[9] effectively combining reduced coronary supply with increased oxygen demand.

### *Side Effects of Vasodilators*

Side effects during dipyridamole stress usually follow completion of the infusion, rarely preclude completion of the study, and usually resolve spontaneously. Minor side effects, including flushing and headache, occur in about two thirds of patients studied with high-dose dipyridamole. Severe or prolonged myocardial ischemia is infrequent but can be treated with nitrates or aminophylline. Serious side effects are very rare—probably less frequent than with dobutamine[8,36]—but severe myocardial ischemia and infarction, bronchospasm, complete heart block, and even death have been reported. Dipyridamole stress is contraindicated with atrioventricular block and bronchospasm, although patients with chronic obstructive airway disease with no or minimal airway reactivity may undergo the test.

The side-effect profile of adenosine is similar to that of dipyridamole, and although the intensity and frequency of side effects with adenosine is greater, they are of shorter duration. Some form of side effect occurs in most patients undergoing adenosine stress.[37] In a high-dose protocol,[35] side effects prevented about one third of patients from achieving peak dose, a comparable frequency to that found with dobutamine. Because the effect of adenosine is very transient, cessation of the infusion is usually the only treatment required for side effects. The use of regadenoson minimizes the risk of bronchospasm and heart block, is convenient because of a single dose, and has the same coronary vasodilator effect as dipyridamole,[38] but regadenoson is suited to study of perfusion rather than wall motion responses.

## VASOCONSTRICTOR PROTOCOLS

Ergonovine stress may be useful for the diagnosis of coronary spasm, the frequency of which is greater in smokers and patients with some coronary disease. Ergonovine testing has been most widely used in the angiography laboratory, because spasm can be visualized directly and intracoronary nitrates infused to treat severe spasm. However, ergonovine stress appears to be safe when applied noninvasively in patients without significant stenoses, and the test has been applied to some patient groups without previous angiography. The standard protocol involves repeated bolus doses of ergonovine maleate at 5-minute intervals up to a total cumulative dose of 0.35 mg, unless ischemia is detected.

## PACING STRESS

### *Stress Protocols*

The use of an implanted pacemaker to alter the heart rate during testing is often necessary to achieve target heart rate in the presence of atrioventricular block, even if pharmacologic stress is being used. Ventricular stimulation produces dyssynchronous contraction, but interpretable images are obtainable if image quality is sufficient to evaluate thickening, and atrial pacing poses no problems for interpretation.[39] The test endpoints are the same as those for other nonexercise stressors; in the absence of these endpoints, pacing at peak heart rate is continued for 3 minutes. No protocol has been uniformly accepted. We use pacing in combination with dobutamine in order to obtain the inotropic response to stress, and therefore maintain a 3-minute incremental protocol when pacing is added, usually starting at 100 beats per minute.

Transesophageal pacing requires topical pharyngeal anesthesia and mild sedation and is rarely used. Use of a short protocol minimizes the risk of electrode movement and loss of capture. Atropine is often required to overcome atrioventricular block.

### *Hemodynamic Responses*

The hemodynamic response to pacing is more controllable than with pharmacologic agents. Heart rates of 160 beats per minute are attainable, but systolic blood pressure is stable, giving a rate-pressure product of less than 20,000. Use of transesophageal pacing in an awake patient may itself provoke hemodynamic changes and hence ischemia, so that "resting" transesophageal echocardiographic images may not be truly acquired at rest.

### *Side Effects*

Fewer side effects occur during transesophageal pacing than with pharmacologic stress. Esophageal discomfort, gagging, or nausea are uncommon with modern pacing electrodes. Angina may be provoked by stress but is usually self-limiting after cessation of pacing. Atrial flutter or fibrillation may also be precipitated. Esophageal injury is theoretically possible in response to high levels of stimulation over a prolonged period, but this has not been reported.

## Accuracy for Diagnosis of Coronary Artery Disease

### DOBUTAMINE STRESS ECHOCARDIOGRAPHY

The comparative sensitivity and specificity of DSE for the detection of coronary artery disease has been well summarized in two meta-analyses. Kim and colleagues[40] reported an 80% (95% confidence interval [CI], 77% to 83%) sensitivity and 84% (95% CI, 80% to 86%) specificity in 82 pharmacologic stress studies between 1974 and 1999. In nearly 7000 patients from 62 DSE studies between 1991 to 2006, reported by Geleijnse and co-workers,[41] the sensitivity was 81% and specificity was 82%. No single feature accounts for false-positive results, although the most frequent site of false-positive results is the basal inferior wall. The correlates of false negative results are a matter of discussion. The meta-analysis just mentioned did not show an effect from a variety of features conventionally associated with enhanced sensitivity—use of a coronary stenosis cutoff of 70% (rather than 50%), higher achieved heart rate, cessation of beta-blockers at the time of testing, the use of atropine, and the incorporation of a biphasic response. Armstrong[42] has argued that these observations likely reflect the heterogeneity of testing in the meta-analysis, ranging from diagnostic testing for coronary artery disease, through evaluation of ischemia on therapy, to functional evaluation of coronary stenoses.

The use of a 50% or 70% stenosis cutoff is arbitrary and does not take into account stenosis location or vessel size, both of which clearly influence the likelihood of an abnormal response. This concern has been addressed in several studies that have compared the results of DSE with stenosis diameter at quantitative coronary angiography.[43] The angiographic cutoff value with the best predictive value for a positive dobutamine test was a luminal diameter of 1.07 mm, percent diameter stenosis of 52%, and percent area stenosis of 75%, of which minimal lumen diameter was found to have the best predictive value for a positive dobutamine stress test (odds ratio, 51; sensitivity, 94%; specificity, 75%). Stenoses less than 1 mm in diameter can be identified with a sensitivity of 86%.[43]

The use of myocardial fractional flow reserve (the ratio of mean hyperemic distal coronary to aortic pressure) as a functional index of coronary stenosis severity takes into account collateral flow and overcomes the limitations of comparing stress echocardiography with the anatomic severity of stenosis. The degree of dobutamine-induced dyssynergy correlates significantly better with myocardial fractional flow reserve than percent stenosis or minimal lumen diameter, and the sensitivity of DSE is significantly lower for lesions in vessels smaller than 2.6 mm than for larger vessels.

The existence of a regional wall motion abnormality identifies the presence of coronary disease, so DSE demonstrates higher sensitivities in patients with myocardial infarction. In patients with single-vessel disease, the sensitivity of DSE (40% to 70%) is lower than in multivessel disease. Because dobutamine produces a less potent stress on the heart than exercise (see earlier discussion), DSE is probably more susceptible to external influences than exercise echocardiography or myocardial perfusion scintigraphy. This may be pertinent to the extrapolation of results from clinical trials (in which patients were carefully supervised and tested under optimal conditions, off therapy), to routine clinical practice, in which patients are often tested on therapy and are more likely to have a "suboptimal" test result because of inability to complete the protocol or interference by beta-blocker therapy.[5]

### DIPYRIDAMOLE STRESS ECHOCARDIOGRAPHY

The sensitivity and specificity of vasodilator stress echocardiography have been reported as 80% (95% CI, 77% to 83%) and 84% (95% CI, 80% to 86%) in a recent meta-analysis.[40] The low-dose (0.56 mg/kg) protocol is associated with lower sensitivity than the high-dose regimen. Atropine appears to enhance sensitivity, although this is only about 50% in patients with single-vessel disease. TEE imaging enhances the accuracy of this test. The greater variation in the sensitivity of stress echocardiography with vasodilators than dobutamine and exercise stress seems to relate to patient selection and the definition of "significant" disease; many of the more favorable results pertain to populations with a high percentage of patients with more severe coronary disease. The specificity is excellent.

Investigators have sought to address the accuracy of dipyridamole stress with physiologic rather than anatomic criteria of significant stenosis. In 30 patients with isolated stenoses of the left anterior descending coronary artery, predictors of an abnormal dipyridamole echocardiogram were a stenotic flow reserve of less than 2.8, stenosis diameter greater than 59%, lumen diameter less than 1.35 mm, and coronary flow reserve less than 2.0, of which stenotic flow reserve was the only independent predictor of ischemia. This study was interesting on two grounds: First, it implies that dipyridamole identifies fewer mild stenoses than DSE, and second, it identified angiographic variables of stenosis severity to relate to dipyridamole echocardiographic results better than intracoronary Doppler variables. Other studies have confirmed that the optimal angiographic cutoff point for dipyridamole stress echocardiography is 60%, as compared with 58% for dobutamine and 54% for exercise echocardiography.[44]

### VASODILATOR STRESS WITH ADENOSINE ECHOCARDIOGRAPHY

The reported accuracy of adenosine stress echocardiography is variable. A recent meta-analysis[45] gave it a sensitivity of 68% and specificity of 81%, after weighting for study size. Favorable results are more likely with multivessel disease or prior infarction; the sensitivity is 60% or less in patients with a normal electrocardiogram or without prior infarction.[35] The intense coronary vasodilation induced by adenosine or dipyridamole[46] permits the comparison of rest and hyperemic images using contrast echocardiography. Similarly, coronary flow reserve may be measured at adenosine stress TTE or TEE.[47] The longer time course and less predictable peak flow with dipyridamole make this a less attractive agent; if dipyridamole is selected, a high dose is certainly required.[12]

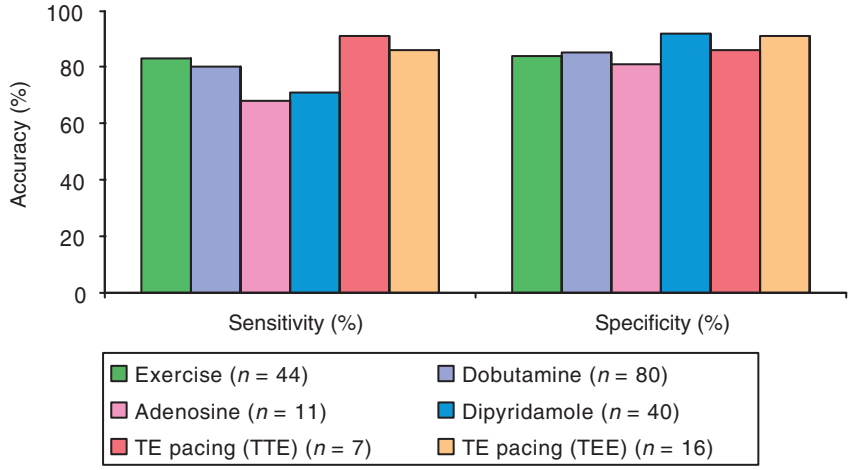



**Figure 16-6** **Meta-analysis of sensitivity and specificity of stress echocardiography performed with various stress modalities.** *(From Noguchi Y, Nagata-Kobayashi S, Stahl JE, Wong JB: A meta-analytic comparison of echocardiographic stressors.* Int J Cardiovasc Imaging *21:189-207, 2005.)*

**TABLE 16-2 Studies Comparing Sensitivity and Specificity of Dobutamine and Vasodilator Stress Echocardiography (>100 patients)**

| *Study* | *Patients,* N | *CAD,* n *(%)* | *Multivessel Disease,* n *(% All CAD)* | *Myocardial Infarction,* n *(% All CAD)* | *Sensitivity: Dobutamine, %* | *Sensitivity: Dipyridamole, %* | *Specificity: Dobutamine, %* | *Specificity: Dipyridamole, %* |
|---|---|---|---|---|---|---|---|---|
| Beleslin[27] | 136 | 119 (88) | 11 (9) | 41 (34) | 82 | 74 | 77 | 94 |
| Ostojic[49] | 150 | 131 (87) | 16 (12) | 38 (29) | 75 | 71 | 79 | 89 |
| Anthopoulos[50]* | 120 | 89 (74) | 48 (40) | 38 (30) | 87 | 66 | 84 | 90 |
| San Roman[51] | 102 | 63 (62) | 34 (54) | 0 (0) | 77 | 77 | 95 | 97 |
| Fragasso[52] | 101 | 56 (56) | 37 (65) | 0 (0) | 88 | 61 | 80 | 91 |

*CAD*, Coronary artery disease.
*Adenosine used instead of dipyridamole.

## PACING STRESS ECHOCARDIOGRAPHY

Studies that have combined atrial pacing with echocardiography show very favorable results. A meta-analysis from the limited number of studies (and patients within studies) proposed a sensitivity and specificity of 91% and 86% for TTE and 86% and 91% for TEE.[45] The accuracy of both transesophageal imaging and pacing probably reflects the benefits of high-quality images as much as the role of pacing stress, as similar favorable findings have been obtained using TEE with dobutamine and dipyridamole. The discrepancy between the reported accuracy, feasibility, and patient acceptance of pacing stress contrasts with the limited application of the test. The following are important issues that influence our continued use of pharmacologic stress. First, the evidence base for diagnostic, management, and prognostic information using pharmacologic agents is greater than with pacing stress. Second, the pacing test is unlikely to be useful for the detection of viable myocardium, and even when this is not needed from a clinical standpoint, the biphasic response has been shown to facilitate the distinction of ischemia in the setting of resting wall motion abnormalities. Third, most patients and some clinicians look on the test as being excessively invasive. This test has several "niche" applications: patients with hypertension or rhythm contraindications to dobutamine, potentially unstable patients (because the stress can be stopped suddenly), or patients with chronotropic incompetence of various causes.

## COMPARISON BETWEEN NONEXERCISE STRESSORS FOR THE DIAGNOSIS OF CORONARY ARTERY DISEASE

### *Selection of the Optimal Pharmacologic Stress*

The comparative sensitivity and specificity of DSE and vasodilator stress echocardiography for the detection of coronary artery disease have been well summarized in the meta-analysis of Picano and associates.[48] Both tests are effective for the diagnosis of coronary artery disease. However, variations in the study groups make it difficult to compare the relative efficacy of the stressors by merely comparing the results of individual studies, and the limitations of meta-analyses for assessment of therapies likely applies to their application to diagnostic testing.

Figure 16-6[45] summarizes the accuracy of stress echocardiography with a variety of stressors and Table 16-2 summarizes large head-to-head comparisons of the tests in the same patients, under the same conditions.[27,49-52] The feasibility of dobutamine and vasodilator stress are similar. The sensitivity of DSE exceeds that of vasodilator stress; the main source of discrepancy appears to be patients with single-vessel coronary disease, among whom dobutamine appears to be superior. This difference parallels a significantly greater cardiac workload with dobutamine compared with vasodilator stress.

The contraindications to inotropes and vasodilators vary, so their selection may be individualized; patients with hypertension or arrhythmias should undergo a vasodilator stress, and

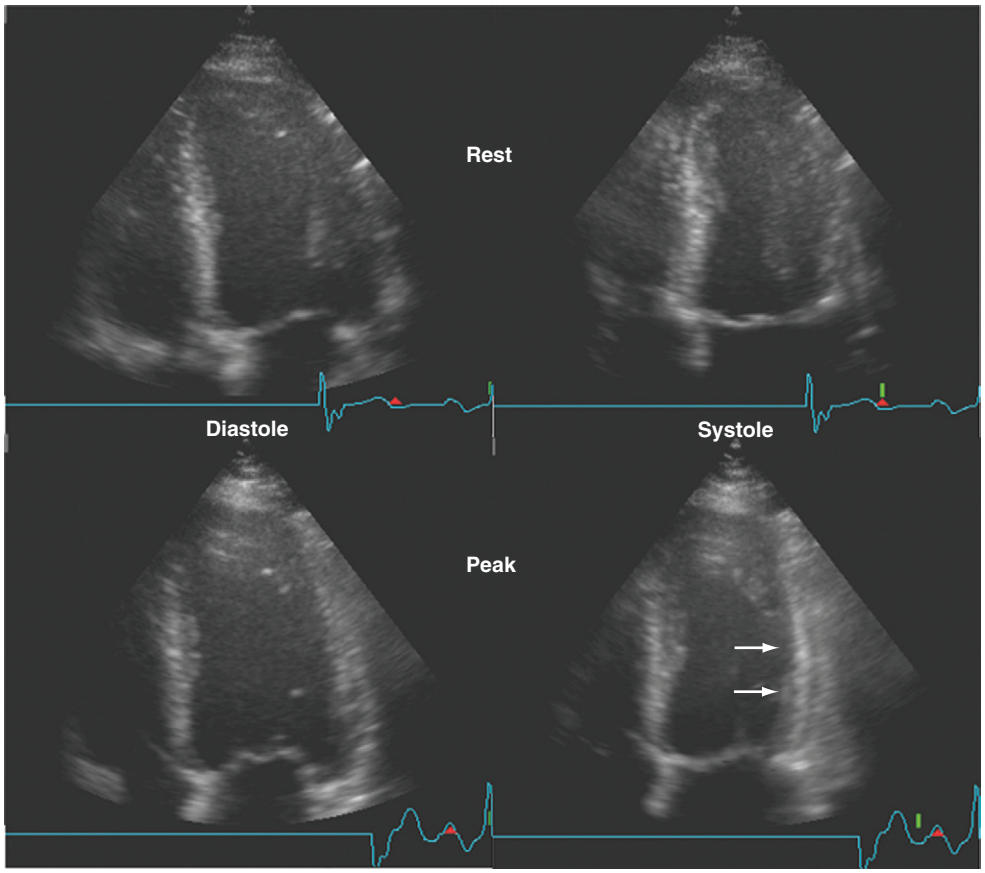



**Figure 16-7 Lateral wall ischemia.** Freeze-frame images in the apical four-chamber view demonstrate normal thickening at rest (*above*), with reduced thickening at peak stress (*below, arrows*).

patients with bronchospasm or conduction disorders should be submitted to inotropic stress. However, in the majority of patients who do not have these contraindications, dobutamine appears to be the most sensitive agent for pharmacologic stress echocardiography.

### *Selection of Pacing Rather Than Other Nonexercise Stress*

There are few comparative data between pacing and pharmacologic stress. Pacing is reportedly less feasible (77% versus 96%, $p$ less than .0001), but more sensitive (83% versus 43%, $p = .0005$) than dipyridamole echocardiography. Atrial pacing showed more favorable safety, duration, and patient acceptance than DSE.

## Assessment of Disease Significance

The use of stress echocardiography for identification of the "culprit" coronary lesion is often constrained by the assumptions inherent in allocating territories of the heart to individual coronary vessels. The most ambiguous areas in this respect are the apex (usually supplied by the left anterior descending coronary artery) and the posterior wall (usually supplied by the left circumflex artery). Because of the equivocal involvement of the right coronary or left circumflex vessels in the posterior territory, investigators have examined the ability to discern the presence of coronary disease in the anterior and posterior circulations. Although in the preharmonic imaging era the lateral wall was a source of false-negative results, the accuracy of DSE in this area has improved (Fig. 16-7).

The recognition of multivessel disease at stress echocardiography may be important in planning revascularization rather than medical therapy. The ability of stress echocardiography to predict multivessel disease is greatest in patients with a history of previous myocardial infarction. In these circumstances, its sensitivity for the correct identification of disease is 80% to 85% and its specificity is 88%. In contrast, the sensitivity for multivessel disease in patients without previous infarction is approximately 70%, exceeding the levels reported in this situation using exercise echocardiography. A close correlation has been demonstrated between the extent of ischemia defined by DSE and that defined by perfusion scintigraphy. Both, however, underestimate the angiographic extent of disease,[5] a reflection of the difficulties of assessing the functional implications of disease extent on anatomic grounds.

In addition to the "space coordinate" (extent of abnormal segments),[3] another indication of the extent of coronary disease is the "time coordinate" (ischemic threshold). Multivessel disease may be predicted if ischemia has an early onset (similar to the "ischemia-free" time at exercise testing), corresponding to its occurrence at a low dose or provocation at a low heart rate and rate-pressure product.[53] This corresponds to a lower ischemic threshold at exercise testing[54] as well as a worse prognosis.

## PROGNOSTIC EVALUATION AND PREDICTION OF CARDIAC EVENTS IN PATIENTS UNDERGOING MAJOR NONCARDIAC SURGERY

Coronary artery disease is highly prevalent in elderly patients undergoing major surgery, especially those with vascular disease. In addition to unstable coronary syndromes, particularly high-risk settings include severe valvular disease, decompensated heart failure, and significant cardiac arrhythmias. Indeed, cardiac events are the leading cause of perioperative complications at vascular surgery, as well as accounting for many late deaths after vascular surgery. However, although postoperative unstable angina and heart failure are frequent in these patients, perioperative "hard" endpoints (death, myocardial infarction) occur in less than 10%, and fewer among patients undergoing nonvascular procedures. In addition, apart from in patients with left main disease (where revascularization is linked to improved survival in unselected groups), the weight of evidence suggests that coronary revascularization before noncardiac surgery does not reduce morbidity and mortality. Because of these observations, and the realization that perioperative testing is among the most frequent inappropriate indications for testing, the current guidelines emphasize how important it is for the ordering physician to consider the likelihood that that an ordered test would influence patient management.

The selection of patients for evaluation before noncardiac surgery should be based on patient-specific factors and the risk of the surgery. The first step in preoperative risk stratification is clinical evaluation.[55] Patients with unstable coronary syndromes within the previous 6 months constitute a high-risk group and warrant careful functional testing or possibly angiography and preoperative intervention. The nature of the planned surgery is important; extensive risk evaluation is best directed toward vascular, major orthopedic, and major abdominal operations that engender significant cardiac risk. Those with previous bypass surgery (within 5 years) or negative coronary investigations within 2 years are at low risk and do not require reinvestigation in the absence of recurrent symptoms. Finally, the patient history has an important influence on risk; in more than 4300 patients[56] undergoing high-risk surgery, history of ischemic heart disease, congestive heart failure or cerebrovascular disease, insulin treatment, and preoperative serum creatinine level greater than 2.0 mg/dL were markers of risk; patients with none, one, two, or three or more of these factors had approximate major cardiac complication rates of 0.5%, 1%, 5%, and 10%, respectively. Inactive patients are usually asymptomatic even in the presence of significant coronary disease, so nonexercise stress imaging techniques are required if screening is to be undertaken.

Reports of functional testing with pharmacologic stress echocardiography and other noninvasive tests published between 1975 and 2001 has been subjected to meta-analysis.[57] In that study, the prediction of perioperative cardiac death and nonfatal myocardial infarction was accomplished with the greatest weighted sensitivity (85%; 95% CI: 74% to 97%) with DSE, although this test had modest specificity (70%; 95% CI: 62% to 79%). This result follows the general behavior of predictive testing in this setting—a negative test is a very reassuring feature (event rate with a negative test should be less than 5%), but the predictive value of a positive test is intermediate (from 20% to 70%)—reflecting the role of not only coronary stenoses but also medical treatment and anesthetic intervention in the genesis of events at surgery. Positive tests may be further stratified by paying attention to the ischemic threshold and the clinical risk factor status (Fig. 16-8). In the preceding meta-analysis,[57] receiver operating characteristic curve analysis showed DSE to be superior to other tests, especially myocardial perfusion scintigraphy (relative odds ratio 5.5, 95% CI: 2.0 to 14.9).

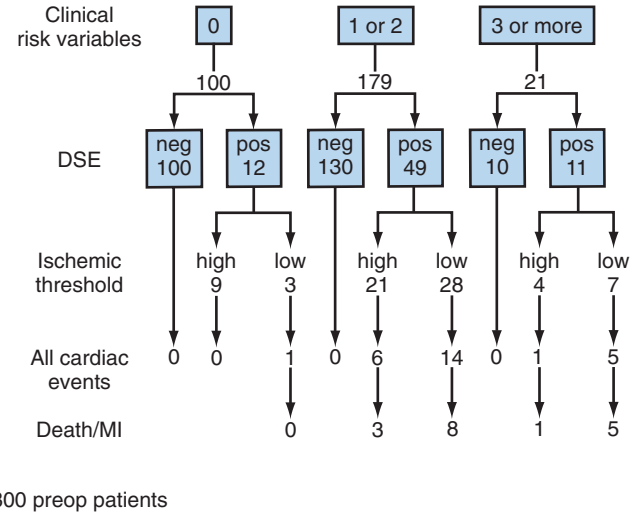



**Figure 16-8 Evaluation of risk in patients undergoing vascular surgery.** Patients without clinical predictors of risk rarely have a positive DSE study, are unlikely to suffer events, and usually do not require testing. The presence of ischemia is predictive of events, especially if the patient has multiple clinical risk factors or a low ischemic threshold. *MI*, Myocardial infarction; *neg*, negative; *pos*, positive; *preop*, preoperative. *(From Poldermans D, Arnese M, Fioretti PM, et al: Improved cardiac risk stratification in major vascular surgery with dobutamine-atropine stress echocardiography.* J Am Coll Cardiol *26:648-653, 1995.)*

Although beta adrenoceptor blockers protect against cardiac events at the time of major surgery, the universal use of beta blockade is also not without risk.[58] On the other hand, noninvasive evaluation before surgery is a frequent scenario of inappropriate testing[59] and should not be used in patients with low cardiac risk or those undergoing low-risk surgery. Exactly how to respond to a positive test is controversial—it does not appear that coronary revascularization is effective for the control of risk.[60]

## PROGNOSTIC EVALUATION OF PATIENTS WITH STABLE CORONARY DISEASE

Major cardiac events are infrequent in stable chronic coronary disease (less than 1% per year), but some patients have a more favorable prognosis with intervention. The detection of left main or multivessel disease at coronary angiography is often used to identify subgroups likely to benefit from revascularization, but this procedure is too costly and invasive to be used in all patients. As in the case of preoperative risk stratification, clinical data (including the severity of angina, prior infarction, heart failure, and diabetes) may identify high- and low-risk subgroups, and additional investigations are of most value in those at intermediate or greater risk. Exercise capacity and ST segment depression at exercise testing offer important prognostic information in patients who are able to exercise,[61] and exercise single photon emission computed tomography (SPECT)[62] or exercise echocardiography has been shown to provide incremental data in many patients.[63]

**TABLE 16-3 Use of Stress Echocardiography to Predict Events in Patients with Chronic Stable Coronary Disease**

| Study | Stress | Patients, N | Mean Follow-up, Mo | Predictive Value, % | | Comments |
|---|---|---|---|---|---|---|
| | | | | Positive Test | Negative Test | |
| Poldermans[65] | Dobutamine | 430 | 17 | 26 | 87 | |
| Kamaran[66] | Dobutamine | 210 | 16 | 43 | 92 | |
| Marcovitz[67] | Dobutamine | 291 | 15 | 10-17 | 99 | |
| Schroder[64] | Dobutamine | 134 | 19 | 31 | 94 | |
| Steinberg[72] | Dobutamine | 120 | 60 | 67<br>13 | 67<br>95 | All events<br>Hard events |
| Senior[68] | Dobutamine | 121 | 15 | 45 | 88 | |
| Chuah[69] | Dobutamine | 860 | 52 | 14 | 96 | |
| Poldermans[70] | Dobutamine | 1659 | 36 | 8-20 | 96 | Hard events |
| Picano[71] | Dipyridamole (high dose)<br>Dipyridamole (low dose) | 539<br>539 | 36<br>36 | 26<br>41 | 94<br>94 | |
| Schroder[64] | Dipyridamole | 134 | 19 | 27 | 92 | |

The prognostic implications[64] of pharmacologic stress echocardiography are summarized in Table 16-3.[64-72] Ischemia is an independent predictor of adverse outcomes, incremental to clinical and resting echocardiographic data. Ischemic threshold adds significantly to simple assessment of test positivity. For example, cardiac events occurred in 41% of patients with wall motion abnormalities occurring at low-dose dipyridamole, and 26% of those with high-dose responses. Ischemia is a better predictor of cardiac events than is coronary anatomy.[71] The prognostic value of pharmacologic stress appears to be preserved within various subgroups, including hypertensive patients.[73]

Dobutamine and dipyridamole offer comparable risk stratification in patients at low to moderate risk of cardiac events[74] and similar to that of SPECT.[74] The prognostic components of both tests include the presence, severity, and extent of induced ischemia. Perhaps the most important aspect of the prognostic literature is that a negative test portends extremely low risk, evidenced by an event rate of 1% or less per year. However, there are some exceptions—patients with diabetes are a high-risk group, among whom even patients with a negative test retain some risk, especially in the subset who are unable to exercise.[75] Likewise, the protection from ischemia provided by antianginal drug therapy does not necessarily translate to protection against subsequent cardiac events, so the predictive value of a negative test on treatment is less than in patients off treatment.[76]

### PROGNOSTIC EVALUATION OF PATIENTS AFTER MYOCARDIAL INFARCTION

Although the current era of early intervention has led to a reduction in the use of stress echocardiography following myocardial infarction, there is little to choose between the efficacy of invasive and noninvasive strategies. If the latter is chosen, clinical features such as age and the presence of heart failure should be used in the initial risk assessment. The extent of infarcted and ischemic myocardium are major determinants of outcome. Stress echocardiography permits the assessment of ischemia as homozonal dyssynergy (periinfarct ischemia) or heterozonal dyssynergy (multivessel disease), and infarction may also be estimated.

Table 16-4 summarizes the prognostic implications of positive and negative nonexercise stress echocardiography after infarction.[77-82] The presence of ischemia and its time of onset are important predictors of cardiac events[79]; in elderly patients, ischemia was an independent predictor of mortality.[83] All tests have proven to be effective for the detection of multivessel disease[77] and predictive for the subsequent development of cardiac events.

## Evaluation of Therapy

### MEDICAL THERAPY

The dependence of stress echocardiography on the development of ischemia is a disadvantage to the extent that antianginal therapy reduces its sensitivity, particularly with dipyridamole stress. Patients on beta-blockers account for most patients who fail to attain a heart rate greater than 85% of age-predicted maximum. With DSE, the interaction between dobutamine and beta-blockers involves competitive inhibition, and if enough dobutamine is administered, this effect may be overcome.[84] A similar role is relevant to atropine. The interaction between medical therapy and the development of ischemia may be of use in evaluating the adequacy of therapy.[85-87] Sequential testing is limited by the subjectivity of wall motion scoring, and this application requires a reliable quantitative approach.

### FOLLOW-UP AFTER CORONARY INTERVENTIONS

Stress echocardiography performed before and after angioplasty has been shown to confirm resolution of ischemia.[88] However, there is little justification for the routine use of a stress imaging test in *asymptomatic* patients within 2 years of percutaneous and 5 years of surgical revascularization.[89,90] Chest wall pains may be difficult to distinguish from recurrent symptoms due to restenosis or graft closure after angioplasty and bypass surgery. Stress echocardiography can be used effectively *in symptomatic patients* for the diagnosis of restenosis, progressive disease, and graft closure.[91-94]

## Assessment of Myocardial Viability

### CLINICAL SIGNIFICANCE

LV dysfunction after myocardial infarction is due not only to scarring but also to stunned and hibernating myocardium. Stunning shows spontaneous resolution of dysfunction,[95] but

**TABLE 16-4 Application of Nonexercise Stressors to Postinfarction Risk Evaluation (>100 Patients)**

| Study | Year | Patients, N | Timing | Stress | Follow-up, Months | Outcomes | Predictive Value, % | | Relative Risk | p |
|---|---|---|---|---|---|---|---|---|---|---|
| | | | | | | | Positive | Negative | | |
| Bolognese[77] | 1992 | 217 | | Dipyridamole | 24 | Cardiac death | 30 | 99 | 2.78 | NS |
| | | | | | | Cardiac death, reinfarction | 80 | 98 | 3.47 | NS |
| | | | | | | Cardiac death, reinfarction, angina | 33 | 90 | 3.24 | 0.0001 |
| Sclavo[78] | 1992 | 103 | 5-8 days | Dipyridamole | 14.5 | Cardiac death | 0 | 97 | | NS |
| | | | | | | Cardiac death, reinfarction | 0 | 96 | | NS |
| | | | | | | Cardiac death, reinfarction, angina | 22 | 89 | 1.94 | NS |
| Picano[79] | 1993 | 925 | 10 days | Dipyridamole | 14 | Cardiac death | 6 | 98 | 3.05 | <0.002 |
| Chiarella[80] | 1994 | 251 | 70 hours | Dipyridamole | 13 days | Cardiac death | 2 | 99 | 2.05 | NS |
| | | | | | | Cardiac death, reinfarction | 8 | 98 | 4.11 | <0.04 |
| | | | | | | Cardiac death, reinfarction, angina | 40 | 97 | 13.46 | <0.0001 |
| Picano[81] | 1995 | 1080 | 10 days | Dipyridamole | 14 | Reinfarction | 6 | 97 | 1.91 | <0.02 |
| | | | | | | Cardiac death, reinfarction | 11 | 98 | 5.15 | <0.02 |
| | | | | | | Cardiac death, reinfarction, angina | 24 | 88 | 2.08 | <0.03 |
| | | | | | | Cardiac death, reinfarction | 11 | 100 | | <0.02 |
| | | | | | | Cardiac death, reinfarction, angina | 54 | 79 | 2.55 | <0.0001 |
| Picano[82] | 1998 | 314 | 12 days | Dobutamine | 9 | Cardiac death | 5 | 98 | 2.24 | NS |
| | | | | | | Cardiac death, reinfarction | 7 | 96 | 1.76 | NS |
| | | | | | | Cardiac death, reinfarction, angina | 15 | 90 | 1.45 | NS |

*NS*, Not significant.

hibernating tissue requires myocardial revascularization to resume normal function. The benefit of assessing myocardial viability has become more controversial in the light of the STICH trial, which showed no survival benefit from the interaction of viability testing and revascularization in an observational substudy of the use of these tests.[96] Previous studies showed that patients with viable myocardium may improve cardiac function or overall functional capacity, as well as avoid subsequent cardiac events from this inherently unstable tissue. Clinical decisions about whether to revascularize, which vessel to revascularize, and how to do it may be influenced by the detection of viable myocardium.

The recovery of function is an imperfect gold standard for defining viability (and thereby the performance of noninvasive testing), as it is influenced by the adequacy of revascularization, bypass graft closure, and restenosis. However, it has the attraction of having direct clinical relevance. Positron emission tomography and thallium scintigraphy using rest-redistribution or stress-redistribution-reinjection protocols are alternative markers of viability, as they have a high negative predictive value. On the other hand, they may be "too sensitive" a reference standard, because their high sensitivity for small regions of viable myocardium means that revascularization of some fails to improve regional function.

## USE OF DOBUTAMINE ECHOCARDIOGRAPHY FOR THE DIAGNOSIS OF VIABLE MYOCARDIUM

The typical response of viable myocardium is to increase thickening in response to low doses of dobutamine; in the presence of a stenosed infarct-related artery, function subsequently deteriorates as the tissue becomes ischemic. Indeed, there is a balance between the recovery of function and the development of ischemia—the latter may compromise the functional recovery of areas that are marginally perfused at rest. The high-dose response (greater than 20 mcg/kg/min) has been shown to be a less reliable predictor of recovery. Although some investigators start at lower doses, or use only a low-dose protocol for the assessment of viability, and others use 5-minute rather than 3-minute increments,[97] there does not appear to be a clear benefit in favor of any of these alternatives.

Dipyridamole enhances both segmental shortening and load-independent indices of ventricular function in stunned myocardium. The mechanism of this phenomenon is unclear, but a "local Frank-Starling response" (whereby augmentation of myocardial blood volume leads to increased sarcomere separation) appears to be the most likely explanation. In addition, an indirect sympathomimetic response to dipyridamole-induced ischemia may contribute to improvement of regional function, as may resolution of ischemia secondary to improvement of coronary perfusion. Dipyridamole is used for this purpose in low-dose and "infralow-dose" protocols; the choice of agent is dependent on local expertise and preference.

Viable segments are characterized by reduced resting function, which augments in response to low-dose dobutamine (usually 7.5 to 10 mcg/kg/min, although we extend this to 20 mcg/kg/min if long-acting beta-blockers such as carvedilol are being used). There is continued augmentation if there is a patent infarct-related artery or the tissue is well collateralized. In the presence of a stenosed infarct-related artery, an increasing proportion of segments become ischemic as the heart rate increases.[98] This initial improvement followed by deterioration in function constitutes the "biphasic response," which is strongly predictive of eventual functional recovery of the tissue.[98] A uniphasic response or a classic ischemic response is less predictive of the recovery of resting function. Because the biphasic response is the most reliable finding (Fig. 16-9), our preference is to induce ischemia whenever possible by proceeding to maximal stress (i.e., 40 mcg/kg/min dobutamine with or without atropine), rather than using a separate "viability" or low-dose protocol. In patients with severe LV dysfunction, this approach warrants caution, and early termination may be needed if ischemia is progressive or if other responses might induce instability. Finally, viability studies are the most difficult to interpret; we usually compare multiple low doses, using continuous videotape recording if there is uncertainty.

The response of regional function to dobutamine is influenced by the extent of viable tissue, the degree of residual stenosis, the extent and magnitude of collaterals, the size of the risk area (which influences tethering), and the presence of drug therapy.[99] The uniphasic response is ambiguous—it may be caused by part of the wall augmenting (i.e., admixture of scar

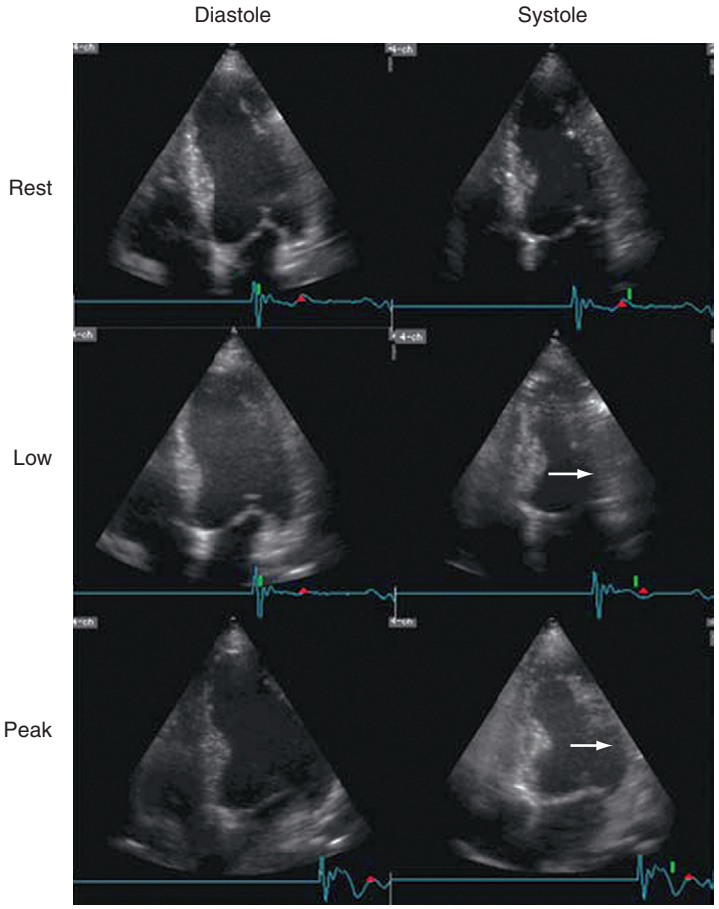



**Figure 16-9 Biphasic response to dobutamine stress.** Apical four-chamber diastolic (*left*) and systolic (*right*) views at rest (*top*), with low-dose dobutamine (*middle*), and with peak-dose dobutamine (*bottom*), illustrating reduced systolic thickening at rest, increment with low dose, and deterioration at peak dose in the lateral wall.

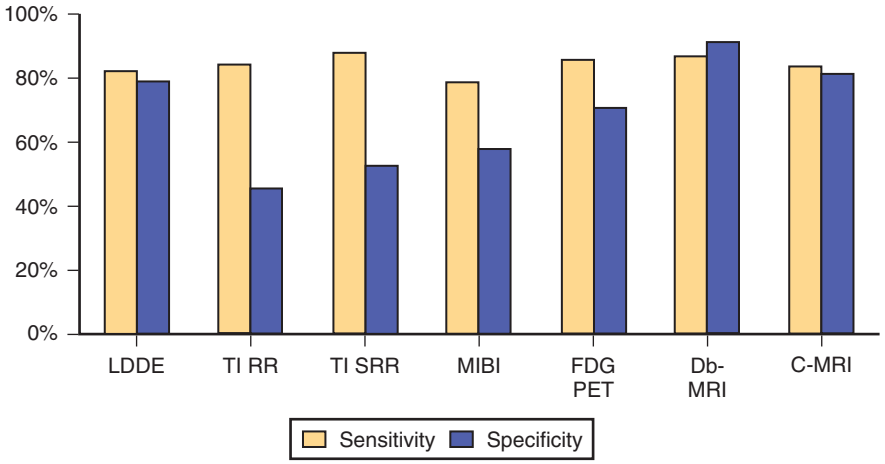



**Figure 16-10 Meta-analysis of sensitivity and specificity of different techniques for assessing viability.** *C-MRI*, Contrast magnetic resonance imaging; Db-MRI, dobutamine stress magnetic resonance imaging; *FDG PET*, fluorodeoxyglucose positron emission tomography; *LDDE*, low-dose dobutamine echocardiography; *MIBI*, [$^{99m}$Tc] methoxyisobutylisonitrile; *SPECT*, single photon emission computed tomography; *Tl RR*, thallium rest-redistribution; *Tl SRR*, thallium stress-rest-redistribution.

and normal tissue) or all of the wall mounting a partial response (i.e., viable myocardium). The ability to discriminate the extent of subendocardial damage, with its implications for the likelihood of subsequent functional recovery, is poor. The augmentation of function is dependent on delivery of more substrate; thus, tissue supplied by more severe stenosis may become ischemic before it augments function, which may compromise the recognition of viability.

The accuracy of dobutamine for prediction of regional functional recovery has been studied in a number of small trials, which Schinkel and colleagues[100] have combined in a meta-analysis of 1421 patients from 41 studies, showing a sensitivity of 80% and a specificity of 78%. The overall sensitivity of dobutamine appears greater than that of dipyridamole stress (approximately 60%), although the specificity of the former is less (78% versus 87%). Nuclear approaches are more sensitive but less specific than these techniques (Fig. 16-10).

## PREDICTION OF RECOVERY OF GLOBAL FUNCTION AND OUTCOME

Improvements in ejection fraction, exercise capacity, and outcome are goals of revascularization, whereas most studies have focused on improvement of LV function within individual

segments. Stress echocardiography can be used to predict improved global LV function after revascularization. Earlier work on this topic proposed that the identification of 4 of 16 viable (biphasic) segments at DSE gave 89% sensitivity and 81% specificity for prediction of a significant (5%) improvement in ejection fraction.[101] However, the meta-analysis just mentioned[100] showed that a variety of thresholds (13% to 25% of the LV showing a viable response) produced a sensitivity of 57% and specificity of 73%. The global ventricular response to low-dose dobutamine may be a better predictor of global functional recovery.[102] A large number of thinned and akinetic segments or large ventricular volumes imply a low likelihood of recovery.[103] The revascularization of patients with adequate amounts of viable myocardium (usually greater than 25% of LV mass) is associated with improved functional class. A recent meta-analysis of 4167 patients in 29 studies showed that the threshold extent of viability for association with improved outcome was 36% (95% CI: 32% to 40%) by stress echocardiography, 39% (95% CI: 28% to 50%) by SPECT, and 26% (95% CI: 17% to 35%) by positron emission tomography.[104] Viable myocardium may influence survival in two ways. First, revascularized viable tissue may lead to improved function and thereby improved outcome.[105] Second, nonrevascularized viable tissue may be unstable and act as a substrate for recurrent events,[106] including mortality.[105]

The clinical value of viability assessment has recently been questioned in the light of the STICH trial, funded by the National Institutes of Health.[96] This nonrandomized substudy of patients with coronary artery disease and LV dysfunction, participating in a randomized trial of medical therapy with or without coronary artery bypass graft, showed nearly 50% of patients to have evidence of extensive viability by either SPECT or DSE. Mortality was less common among patients with extensive viable myocardium (37 versus 51%; hazard ratio for death among patients with viable myocardium, 0.64; 95% CI: 0.48 to 0.86; $p = 0.003$), but there was no significant interaction between viability and treatment ($p = 0.53$). It is unclear to what extent these findings will alter the use of viability testing, which is often used to better understand the balance of risk and benefit of intervention, in the context of a variety of other variables. The results of these nonrandomized findings from STICH are balanced by a multicenter study showing that in patients with coronary artery disease and severe LV dysfunction who demonstrated myocardial viability, revascularization improved survival compared with medical therapy.[105]

## New Technologies

### IMAGE QUALITY

#### *Contrast Echocardiography for LV Opacification*

Although perfect image quality is certainly not essential for a stress echocardiographic study to be interpretable, it certainly favors concordance between observers[20] and facilitates an accurate diagnosis of disease extent and distinction of ischemia and scar. The use of contrast echocardiography may facilitate not only delineation of the endocardial border,[11] but provision of accurate results.[107] The implications of this finding are addressed in another chapter.

#### *Contrast Echocardiography for Assessment of Myocardial Perfusion*

The comparison of myocardial perfusion at rest and during hyperemia is now possible with either high or low mechanical index imaging.[108] The low mechanical index approach allows real-time imaging, which is probably easier during stress than intermittent imaging, and bubble destruction with a high-energy flash allows appreciation of refill, which depends on perfusion (Fig. 16-11). All stressors produce coronary

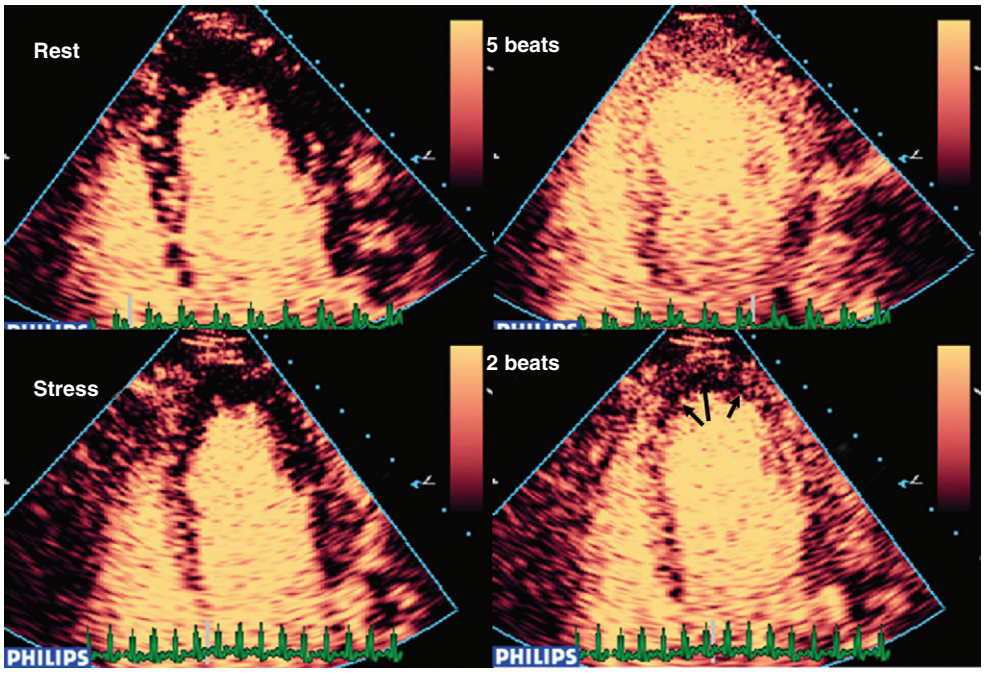



**Figure 16-11 Use of destruction-replenishment imaging to identify evidence of ischemia from perfusion as well as wall motion.** *Left*, Immediate postdestruction image (note lack of myocardial contrast) at rest (*above*) and at peak stress (*below*). *Right*, Return of contrast after sufficient time to allow for refill of myocardium. Note apical subendocardial perfusion defect (LV apex, *arrows*) in this patient who did not demonstrate abnormal wall motion.

**TABLE 16-5 Sensitivity and Specificity of Myocardial Contrast Echocardiography for the Detection of Significant Coronary Stenoses**

| | Myocardial Contrast | | Wall Motion | | | |
|---|---|---|---|---|---|---|
| *Study* | *Sensitivity (CAD)* | *Specificity (no CAD)* | *Sensitivity (CAD)* | *Specificity (no CAD)* | *Stress* | *Angio* |
| Cwaig[109] | 87% (32) | — (13) | | | Db/Ex | All 45 |
| Shimoni[110] | 75% (28) | 100% (16) | 75% | | Ex | 44/101 |
| Heinle[111] | 75% (12) | 67% (3) | — | — | Adeno | 15/123 |
| Wei[112] | 100% (15) | — | — | — | Adeno | 15/54 |
| Rocchi[113] | 89% (12) | 88% (N segts) | 68% | 100% | Dipy | 12/25 |
| Olszowska[114] | 97% (44) | 93% (N segts) | 89% | 94% | Db | All 44 |
| Moir[115] | 91% (43) | 70% (27) | 74% | 81% | Dipy-Ex | 70/85 |
| Elhendy[116] | 91% (127) | 51% (43) | 70% | 74% | Db | All 170 |
| Peltier[117] | 86% (22) | 69% (13) | — | — | Dipy | All 35 |

*Adeno*, Adenosine; *CAD*, coronary artery disease; *Db*, dobutamine; *Ex*, excercise.

hyperemia to some degree, although the vasodilator stressors have the most marked effect, and the lack of tachycardia with these agents facilitates imaging. The use of myocardial contrast for LV chamber opacification increase the sensitivity of wall motion assessment (Table 16-5)[109-117] and provide accuracy that is comparable to that of SPECT.[118] In addition, there are limited data to show an improvement of prognostic assessment.[119]

### *Three-Dimensional Echocardiography*

3D echocardiography resolves technical problems introduced by off-axis images and foreshortening of the apex as well as permitting interrogation of subsegmental areas (Fig. 16-12). The feasibility of this technique may be enhanced by the use of contrast for LV opacification.[120,121] The accuracy of stress 3D echocardiography is supported by a limited evidence base,[122,123] and despite major advances, the current version of this technology has limitations in temporal and spatial resolution.[124] Thus, the most prudent strategy is to use 3D echocardiography as an adjunct to standard stress echocardiography.

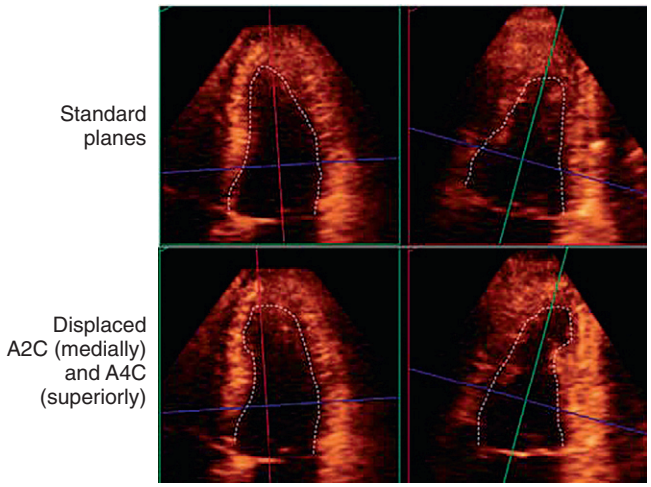



**Figure 16-12 Potential benefit of 3D echocardiography to stress echocardiography by identifying subsegmental wall motion abnormalities.** *Upper* panels, Peak-stress end-systolic freeze-frame images in conventional apical four-chamber and two-chamber views demonstrate homogeneous contraction. *Lower* panels, Off-axis images, with septal displacement of apical two-chamber (*red axis marker* on four-chamber view) and slight superior displacement of apical four-chamber (*green axis marker* on two-chamber view), demonstrate apical shape change consistent with left anterior descending territory ischemia.

## QUANTITATIVE APPROACHES TO INTERPRETATION

The current qualitative algorithm for interpretation of stress echocardiograms requires a significant level of expertise on the part of the observer. A less subjective means of interpretation could improve feasibility and reproducibility. Either semiquantitative or fully quantitative strategies of examining wall motion can be used to evaluate global and regional LV function. Global indices (ejection fraction or end-systolic volume) are insensitive to mild degrees of ischemia and are not an answer to the shortcomings of qualitative interpretation. Wall motion scoring offers a semiquantitative regional approach, which may improve the reproducibility of observers, but this does not constitute a major deviation from the regional approach used by most experienced readers and does not measure function independent of the observer.

The simplest approach to quantitation of regional function involves tracing of endocardial (and/or epicardial) interfaces and their superimposition using a fixed or floating reference system with measurement of endocardial excursion or myocardial thickening. The feasibility and accuracy of this approach has now been documented in several studies,[125] and the tedious and time-consuming process of tracing multiple systolic and diastolic frames has been automated by developments in contrast echocardiography and edge tracking.[126] However, failure to compensate for rotational or translational cardiac movement remains associated with false-positive results, and the method has not found broad clinical use.

Myocardial tissue Doppler may provide another means of quantifying regional function. It has the attraction of quantifying motion in the longitudinal (base-apex) direction, which corresponds to the contribution of longitudinal subendocardial muscle fibers. Peak velocity correlates with wall motion interpretation,[127] ischemia at dual isotope SPECT,[128] and angiographically defined coronary disease.[129] However, problems pertaining to angle dependency and susceptibility to tethering and translational movement make it unsuitable for clinical use.

Strain-rate and strain imaging overcomes the problems of tethering and translation. The measurement of myocardial shortening by this site-specific technique has been extensively validated,[130,131] and it appears that strain is an analog of regional ejection fraction, whereas strain rate corresponds to $dP/dt$.[132] The most successful application of strain rate has been to the assessment of augmentation at low-dose DSE (Fig. 16-13)[133-135]—a low-dose strain rate greater than 1.2/s or an increment of

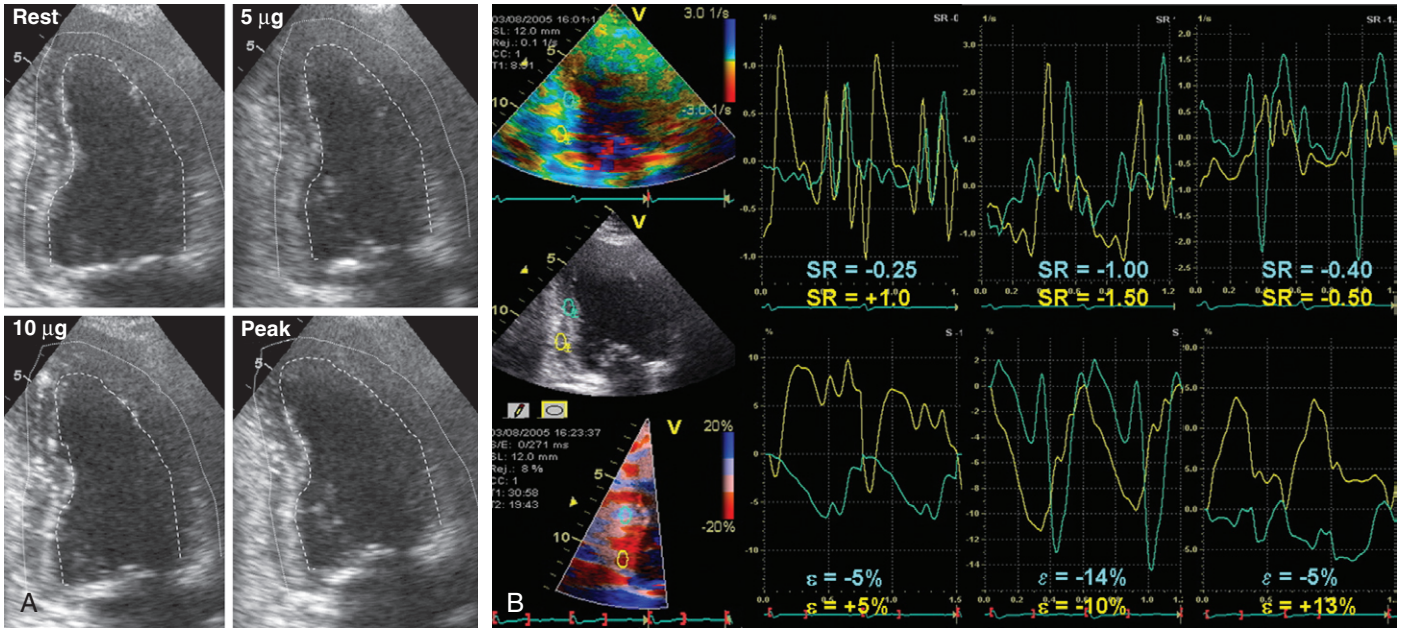



**Figure 16-13 Application of myocardial deformation imaging to stress echocardiography.** End-systolic freeze-frame images in apical two-chamber view (**A**) show less thickening in inferior wall at rest, which improves with low-dose and deteriorates again at peak. However, these changes are subtle; response is more readily identified from deformation imaging (**B**). Basal inferior segment (*yellow*) shows positive strain (ε) and strain rate (*SR*) (lengthening) at rest, shortening at low dose, and lengthening again at peak.

0.6/s is associated with recovery after revascularization. Signal noise is a particular problem for its application with peak-dose dobutamine. Only one small study has suggested it to be superior to wall motion assessment.[136] Others suggest that there may be some value for improving concordance or for less expert readers, without a major increment of accuracy.[137]

The use of speckle tracking (2D strain) offers smoother curves and avoids angle dependency,[138] but it operates at low frame rate and is dependent on good image quality. Limited results suggest it to be inferior to tissue velocity based strain for the assessment of viability.[139] Despite limited encouraging reports, low frame rate appears to limit its role in the diagnosis of ischemia, and image quality in the far field also appears to pose problems for tracking.[140]

## STRESS DOPPLER ECHOCARDIOGRAPHY

The use of Doppler to evaluate coronary flow permits the measurement of coronary flow reserve, effectively adding a marker of perfusion or vascular function to wall motion. The information provided can improve the sensitivity for detection of ischemia, as well as providing information about disorders of coronary vasomotor function and heart failure.[135,141,142] The technique seems most feasible with vasodilator stress but can be performed with dobutamine and after exercise.

Doppler responses to stress can examine systolic or diastolic blood flow alterations caused by ischemia. Unfortunately, this information is of limited value—changes in stroke volume occur mainly in the presence of extensive ischemia, and stress-induced alterations in global cardiac function are not specific for coronary disease. Similarly, ischemia-induced mitral regurgitation is uncommon.[143] However, the use of Doppler to assess low-output aortic stenosis is potentially useful in discriminating the relative contribution of impaired LV function and a stenosed valve; generally, the presence of LV contractile reserve is the most reassuring finding.[144] A stenotic valve usually demonstrates an increment of aortic valve gradient with a stable valve area (Fig. 16-14).

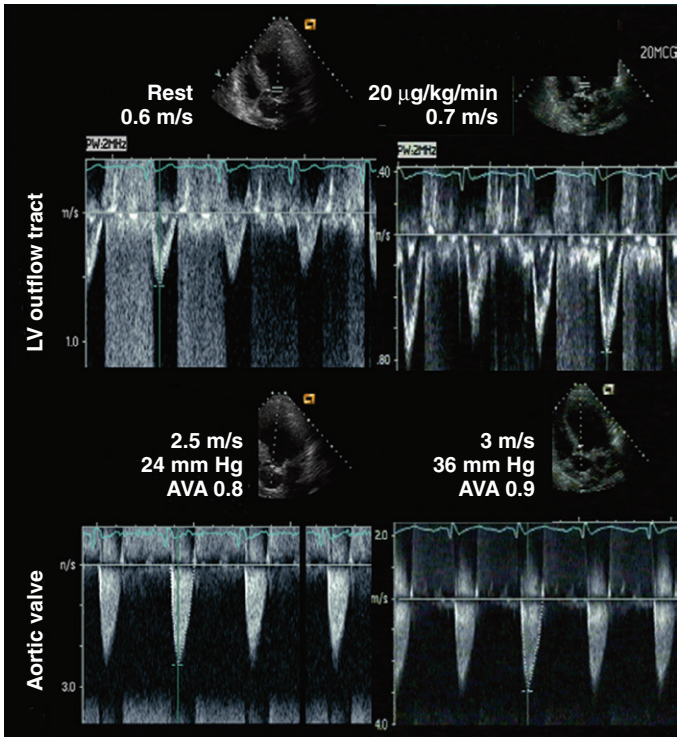



**Figure 16-14 Use of Doppler imaging with low-dose dobutamine stress to evaluate low-output aortic stenosis in a patient with contractile reserve.** Note stable outflow tract velocity with increment of valvular velocity. *AVA*, Aortic valve area.

LV relaxation may be altered by the development of myocardial ischemia. Reductions in passive LV filling (i.e., impaired relaxation secondary to ischemia) may be identified during

**TABLE 16-6 Sensitivity and Specificity of Echocardiography with Exercise and Nonexercise Methodologies**

| Study | Patients, N | CAD, n | CAD Diameter, % | Multivessel, n (% all CAD) | Myocardial Infarction, n (% all CAD) | Sensitivity, % | | | | Specificity, % | | | | Comments |
|---|---|---|---|---|---|---|---|---|---|---|---|---|---|---|
| | | | | | | Ex | Dob | DP | Atrial Pacing | Ex | Dob | DP | Atrial Pacing | |
| Picano[148] | 55 | 34 | >70 | 18 (53) | 6 (18) | 76 | — | 72 | — | 81 | — | 100 | — | Exercise and dipyridamole comparable |
| Hoffman[29] | 66 | 50 | >70 | 21 (42) | 0 (0) | 80 | 79 | — | — | 87 | 81 | — | — | Exercise and dobutamine comparable |
| Cohen[24] | 52 | 37 | >70 | 21 (57) | 11 (30) | 78 | 86 | — | — | 87 | 87 | — | — | Exercise and dobutamine comparable |
| Beleslin[27] | 136 | 119 | >50 | 11 (9) | 41 (34) | 80 | 82 | 74 | — | 82 | 77 | 94 | — | Exercise, dobutamine and dipyridamole comparable |
| Marangelli[149] | 60 | 35 | >75 | 19 (54) | — | 89 | — | 43 | 83 | 91 | — | 92 | 76 | Exercise has best balance of sensitivity and specificity |
| Marwick[25] | 86 | 56 | >50 | 34 (61) | 0 (0) | 88 | 54 | — | — | 80 | 83 | — | — | Exercise superior with submaximal dobutamine |
| Dagianti[150] | 60 | 25 | >70 | 15 (60) | 0 (0) | 76 | 72 | 52 | — | 94 | 97 | 97 | — | Myocardial infarction excluded |
| Rallidis[151] | 85 | 85 | >70 | 40 (47) | 42 (49) | 77 | 67 | — | — | — | — | — | — | Only known CAD |

*CAD*, Coronary artery disease; *Dob*, dobutamine; *DP*, dipyridamole; *Ex*, exercise.

DSE[145] but are more feasible with stressors that provoke ischemia without tachycardia, such as dipyridamole and pacing. Tissue-Doppler assessment may be of value in examining regional diastolic function with less influence from left atrial pressure.[146] Changes of diastolic function in response to stress are not specific for ischemia and may be due to LV hypertrophy. An increment of filling pressure with exercise may be a means of identifying the contribution of increased filling pressure to dyspnea, but the value of assessing this during pharmacologic stress is undefined.

## Alternatives

### EXERCISE STRESS TESTING

In patients who are unable to exercise maximally, a nonexercise stressor is mandatory, as the sensitivity of exercise echocardiography is low. In patients who *are* able to exercise, exercise echocardiography is increasingly used instead of the stress electrocardiogram. Although this strategy is contrary to the ACC/AHA guidelines,[90] it may be cost effective.[147] The advantages of pharmacologic approaches are feasibility, better image quality, and ability to image the heart during stepwise increments of stress as well as at peak stress. Pharmacologic stressors probably give accuracy similar to that of exercise stress (Table 16-6).[24,25,27,29,148-151] The reported greater feasibility of nonexercise techniques may be colored by greater expertise in pharmacologic than in exercise echocardiography at some centers. The greater extent of ischemia with exercise than with dobutamine may reflect the greater cardiac workload imposed by exercise—this more extensive ischemia may lead the observer to be more confident in the results of exercise, despite the image quality being better with dobutamine. Electrocardiographic data are useful with exercise stress and less so with pharmacologic stressors, and data about exercise are readily extrapolated to everyday life. Exercise capacity data are prognostically important. Because exercise echocardiography offers more data than the nonexercise approaches, we limit the use of exercise-simulating techniques to patients who are unable to perform maximal exercise. However, the new techniques that are adjunctive to stress echocardiography (for example, contrast, tissue Doppler, and acoustic quantification echocardiography) are more easily performed in the stationary patient and may lead to an increase in the number of nonexercise studies in the future. The sensitivity and specificity of the tests in meta-analyses are compared in Figure 16-15.

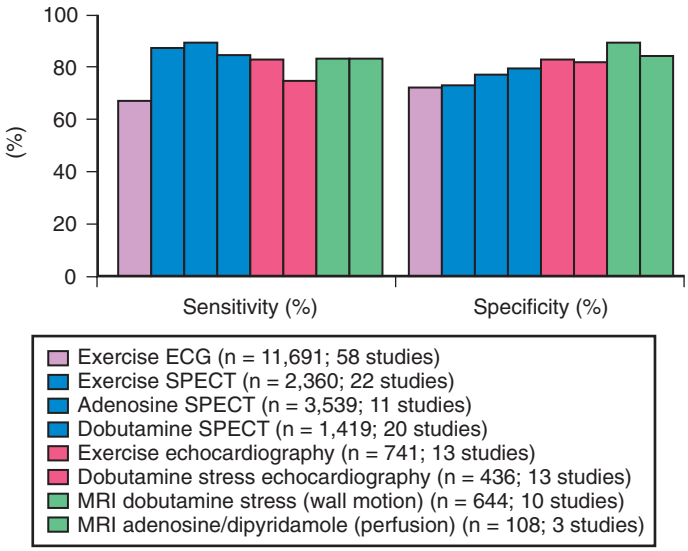



**Figure 16-15 Comparison of stress echocardiography techniques (*red*) with nuclear (*blue*) and magnetic resonance imaging (*green*) in meta-analyses of each technique.** *(Data obtained from O'Rourke RA, Fuster V, Alexander W, et al, editors:* Hurst's the heart: manual of cardiology, *ed 11. New York, 2005, McGraw-Hill.)*

### PHARMACOLOGIC STRESS ECHOCARDIOGRAPHY VERSUS PERFUSION SCINTIGRAPHY

Nuclear perfusion imaging is the most widely used technique for the noninvasive diagnosis of coronary artery disease and is technically easier to perform and interpret than stress echocardiography. However, nuclear imaging has disadvantages pertaining to specificity, cost, and patient convenience. Because there is a substantial variation in the reported accuracy of both stress echocardiography and nuclear imaging, based on variations in the population studied, their relative accuracy in those

who are unable to exercise can best be addressed by direct comparison.

### Diagnosis of Coronary Artery Disease

Scintigraphy and echocardiography have a concordance rate of 80% to 90% for the presence or absence of disease in most studies. A meta-analysis of vasodilator or dobutamine stress with either echocardiography or SPECT showed a consistent message of higher sensitivity with SPECT (especially for vasodilator stress) and higher specificity with echocardiography.[40] Studies comparing stress echocardiography and scintigraphy using dipyridamole, adenosine, dobutamine, or atrial pacing stress are summarized in Table 16-7.[5,35,152-156] Using dobutamine or pacing stress, the sensitivities are comparable, with most studies showing slightly greater sensitivity with scintigraphy. This difference is most evident in patients with single-vessel disease,[157] a finding that might be expected from the identification of flow heterogeneity with perfusion imaging, which is an earlier event in the ischemic cascade than regional dysfunction, identified by echocardiography. Similarly, antianginal therapy may compromise the results of echocardiography because it prevents the development of ischemia with less effect on perfusion scintigraphy. Vasodilator stress echocardiography is significantly less sensitive than perfusion scintigraphy. This difference is most marked in patients with single-vessel coronary disease and reflects failure to develop coronary steal in the absence of extensive coronary disease. This difference is less prominent in patients with multivessel disease.

The specificities of stress echocardiography and perfusion scintigraphy are comparable, with most series showing a small benefit for echocardiography. Two important sources of false-positive results are patients with left bundle branch block and patients with LV hypertrophy. Stress echocardiography appears to show greater specificity in patients with left bundle branch block.[158] Patients with hypertensive hypertrophy are prone to false-positive results with SPECT but not stress echocardiography.[52] Good scintigraphy is always better than poor stress echocardiography, and good stress echocardiography is always better than poor scintigraphy.

Stress MRI is an exciting technique that permits high-resolution imaging of both perfusion (including subendocardial perfusion) and wall motion. However, cost and availability make it seem unlikely that this will become a serious alternative to stress echocardiography for most patients in the near future. Although ischemia detection with MRI and echocardiography has a concordance rate of 80% to 90%, reports of higher accuracy with MRI are based on avoidance of nondiagnostic studies.[159] The evaluation of perfusion with MRI allows the detection of subendocardial abnormalities and may be helpful in the evaluation of disorders of the coronary microcirculation.

### Prognostic Assessment

Although a substantial amount of literature regarding the individual predictive abilities of echocardiography and perfusion imaging is available, comparative data are sparse. In patients undergoing surgery for vascular disease, dipyridamole stress thallium imaging has been shown to have a negative predictive value of more than 90% in most studies.[55] The occurrence of unexpected cardiac events in some patients is probably due to plaque instability at the site of nonsignificant stenoses (which do not cause abnormal perfusion results). The predictive value of ischemia at scintigraphy ranges from 30% to 50%, this result being attributable to positive perfusion studies in the context of mild (prognostically benign) coronary disease and false-positive results. Overall, these results are comparable to those of pharmacologic stress echocardiography (see Table 16-7). Direct comparisons of stress echocardiography and SPECT for the prediction of perioperative cardiac events have shown their prognostic value to be similar.[160,161] A meta-analysis of published work concluded that DSE and SPECT (mainly with dipyridamole stress) had comparable levels of accuracy, with cost effectiveness in favor of echocardiography.[162]

In patients with chronic stable coronary disease and after myocardial infarction, the relative prognostic roles of stress echocardiography and myocardial perfusion scintigraphy appear comparable. Ischemia may be difficult to identify within segments having abnormal resting function, and this is a source of discrepancy from the findings of perfusion scintigraphy.

### Diagnosis of Viable Myocardium

The comparison of positron emission tomography, thallium reinjection techniques, and DSE from meta-analyses is summarized in Figure 16-10; Table 16-8 summarizes matched data.[163-174] Most comparative studies show SPECT techniques to be more sensitive but of lower specificity for the prediction of functional recovery.

**TABLE 16-7 Comparison of Pharmacologic Stress Echocardiography and Single Photon Emission Computed Tomography for Diagnosis of Coronary Artery Disease (>50 patients)**

| Study | Patients, N | Stress | Dose | Sensitivity, % | | Single-Vessel Disease | | Specificity | |
|---|---|---|---|---|---|---|---|---|---|
| | | | | Echocardiography | Nuclear Imaging | Echocardiography | Nuclear Imaging | Echocardiography | Nuclear Imaging |
| Marwick[35] | 97 | Adenosine | 0.18 mg/kg/min | 58 | 86 | 52 | 81 | 87 | 71 |
| Marwick[5] | 217 | Dobutamine | 40 mcg | 72 | 76 | 66 | 74 | 83 | 67 |
| Senior[152] | 61 | Dobutamine | 40 mcg | 93 | 95 | 86 | 86 | 94 | 71 |
| Ho[153] | 54 | Dobutamine | 40 mcg | 93 | 98 | — | — | 73 | 73 |
| Huang[154] | 93 | Dobutamine | 40 mcg | 93 | 90 | — | — | 77 | 81 |
| Santoro[155] | 60 | Dobutamine | 40 mcg | 61 | 91 | — | — | 96 | 81 |
| San Roman[156] | 102 | Dobutamine | 40 mcg + atropine | 78 | 87 | — | — | 88 | 70 |
| Santoro[155] | 60 | Dipyridamole | 0.84 mg/kg | 55 | 97 | — | — | 96 | 89 |
| San Roman[156] | 102 | Dipyridamole | 0.84 mg/kg | 81 | 87 | — | — | 94 | 70 |

**TABLE 16-8 Comparison of Nuclear and Stress Echocardiographic Techniques for Prediction of Viability (Evidenced by Improvement of Regional LV Function)***

| | | | Sensitivity, % | | Specificity | |
|---|---|---|---|---|---|---|
| *Study* | *Thallium Technique* | *Dobutamine Protocol, mcg/kg/min* | *Thallium SPECT* | *Dobutamine Echocardiography* | *Thallium SPECT* | *Dobutamine Echocardiography* |
| Marzullo[163] | Rest-redistribution | Low-dose, 10 | 86 | 82 | 92 | 92 |
| Charney[164] | Rest-redistribution | Low-dose, 10 | 95 | 71 | 85 | 93 |
| Kostopoulos[165] | Rest-redistribution | Low-dose, 10 | 90 | 87 | 69 | 94 |
| Qureshi[166] | Rest-redistribution | High-dose, 40 | 90 | 74 | 56 | 89 |
| Nagueh[167] | Rest-redistribution | High-dose, 40 | 91 | 68 | 43 | 83 |
| Senior[168] | Stress (dobutamine)-rest/NTG | Low-dose, 10 | 92 | 87 | 78 | 82 |
| Arnese[169] | Stress (dobutamine) reinjection | Low-dose, 10 | 89 | 74 | 48 | 95 |
| Perrone-Filardi[170] | Stress (dobutamine) reinjection | Low-dose, 10 | 100 | 79 | 22 | 83 |
| Bax[171] | Stress (dobutamine) reinjection | Low-dose, 10 | 93 | 85 | 43 | 63 |
| Haque[172] | Stress (exercise) reinjection | Low-dose, 20 | 100 | 94 | 40 | 80 |
| Vanoverschelde[173] | Stress (exercise) reinjection | High-dose, 40 | 72 | 88 | 73 | 77 |
| Elsasser [174] | Stress (dobutamine) reinjection | High-dose, 40 | 87 | 95 | 98 | 80 |

*NTG*, Nitroglycerin; *SPECT*, single photon emission computed tomography.
*Average ejection fraction 38%.

## The Future of Pharmacologic Stress Echocardiography

Just like the rest of echocardiography, pharmacologic stress echocardiography continues to evolve, and the only certainty in prediction of the future is that it will be different. The major themes of this evolution are likely to be efficacy, quality, and cost factors on one side, and new technologies on the other. As discussed in the chapter, the latter are likely to include perfusion, quantitation, and 3D imaging, with the intent of increasing accuracy, reproducibility, and reading speed. The more pressing (and less predictable) need relates to how the current cost pressures influence pharmacologic stress echocardiography. Part of this process will relate to the application of appropriateness criteria.[89] It will also relate in part to the development of standardized management algorithms, and stress echocardiography is likely to be favored over alternative techniques if quality is maintained.

### KEY POINTS

- Nonexercise stress tests with dobutamine, vasodilators, and pacing are all feasible, although interest in pacing has not been sustained, and all demonstrate satisfactory levels of accuracy.
- Despite greater ease in gathering images, pharmacologic stress is less potent than exercise stress. The resulting lesser extent of ischemia may paradoxically make the interpretation of these studies more difficult than that of exercise.
- The adoption of new technologies such as myocardial contrast, 3D, and myocardial deformation techniques is easier with pharmacologic than with exercise stress.
- Subjective interpretation remains the Achilles heel of stress echocardiography—perhaps even more so with pharmacologic stress echocardiography because of the subtleties of interpreting augmentation of function in viability studies. Measurement of myocardial velocity and deformation offers potential support to interpretation but remains in evolution.

## REFERENCES


1. Peteiro J, Bouzas-Mosquera A: Peak treadmill exercise echocardiography. *Rev Recent Clin Trials* 5:94-102, 2010.
2. Mairesse GH, Vanoverschelde JL, Robert A, et al: Pathophysiologic mechanisms underlying dobutamine-induced myocardial ischemia. *Am Heart J* 136:63-70, 1998.
3. Picano E, Lattanzi F: Dipyridamole echocardiography. A new diagnostic window on coronary artery disease [Review]. *Circulation* 83:III19-III26, 1991.
4. Bin JP, Le E, Pelberg RA, et al: Mechanism of inducible regional dysfunction during dipyridamole stress. *Circulation* 106:112-117, 2002.
5. Marwick T, D'Hondt AM, Baudhuin T, et al: Optimal use of dobutamine stress for the detection and evaluation of coronary artery disease: combination with echocardiography or scintigraphy, or both? *J Am Coll Cardiol* 22:159-167, 1993.
6. Dodla S, Xie F, Smith M, O'Leary E, Porter TR: Real-time perfusion echocardiography during treadmill exercise and dobutamine stress testing. *Heart* 96:220-225, 2010.
7. Botvinick EH: Current methods of pharmacologic stress testing and the potential advantages of new agents. *J Nucl Med Technol* 37:14-25, 2009.
8. Picano E, Mathias W, Jr, Pingitore A, et al: Safety and tolerability of dobutamine-atropine stress echocardiography: a prospective, multicentre study. Echo Dobutamine International Cooperative Study Group [see comments]. *Lancet* 344:1190-1192, 1994.
9. Pingitore A, Picano E, Colosso MQ, et al: The atropine factor in pharmacologic stress echocardiography. Echo Persantine (EPIC) and Echo Dobutamine International Cooperative (EDIC) Study Groups. *J Am Coll Cardiol* 27:1164-1170, 1996.
10. Caidahl K, Kazzam E, Lidberg J, et al: New concept in echocardiography: harmonic imaging of tissue without use of contrast agent [see comments]. *Lancet* 352:1264-1270, 1998.
11. Franke A, Hoffmann R, Kuhl HP, et al: Non-contrast second harmonic imaging improves interobserver agreement and accuracy of dobutamine stress echocardiography in patients with impaired image quality. *Heart* 83:133-140, 2000.
12. Lim HE, Shim WJ, Rhee H, et al: Assessment of coronary flow reserve with transthoracic Doppler echocardiography: comparison among adenosine, standard-dose dipyridamole, and high-dose dipyridamole. *J Am Soc Echocardiogr* 13:264-270, 2000.
13. Ommen SR, Nishimura RA, Appleton CP, et al: Clinical utility of Doppler echocardiography and tissue Doppler imaging in the estimation of left ventricular filling pressures: a

comparative simultaneous Doppler-catheterization study. *Circulation* 102:1788-1794, 2000.
14. Bleeker GB, Bax JJ, Schalij MJ, van der Wall EE: Tissue Doppler imaging to assess left ventricular dyssynchrony and resynchronization therapy. *Eur J Echocardiogr* 6:382-384, 2005.
15. Armstrong WF, Pellikka PA, Ryan T, et al: Stress echocardiography: recommendations for performance and interpretation of stress echocardiography. Stress Echocardiography Task Force of the Nomenclature and Standards Committee of the American Society of Echocardiography. *J Am Soc Echocardiogr* 11:97-104, 1998.
16. Cerqueira MD, Weissman NJ, Dilsizian V, et al: Standardized myocardial segmentation and nomenclature for tomographic imaging of the heart: a statement for healthcare professionals from the Cardiac Imaging Committee of the Council on Clinical Cardiology of the American Heart Association. *Circulation* 105:539-542, 2002.
17. Secknus MA, Niedermaier ON, Lauer MS, Marwick TH: Diagnostic and prognostic implications of left ventricular cavity obliteration response to dobutamine echocardiography. *Am J Cardiol* 81:1318-1322, 1998.
18. Yuda S, Khoury V, Marwick TH. Influence of wall stress and left ventricular geometry on the accuracy of dobutamine stress echocardiography. *J Am Coll Cardiol* 40:1311-1319, 2002.
19. Mathias W, Jr, Tsutsui JM, Andrade JL, et al: Value of rapid beta-blocker injection at peak dobutamine-atropine stress echocardiography for detection of coronary artery disease. *J Am Coll Cardiol* 41:1583-1589, 2003.
20. Hoffmann R, Lethen H, Marwick T, et al: Analysis of interinstitutional observer agreement in interpretation of dobutamine stress echocardiograms. *J Am Coll Cardiol* 27:330-336, 1996.
21. Hoffmann R, Lethen H, Marwick T, et al: Standardized guidelines for the interpretation of dobutamine echocardiography reduce interinstitutional variance in interpretation. *Am J Cardiol* 82:1520-1524, 1998.
22. Hoffmann R, Marwick TH, Poldermans D, et al: Refinements in stress echocardiographic techniques improve inter-institutional agreement in interpretation of dobutamine stress echocardiograms. *Eur Heart J* 23:821-829, 2002.
23. San Roman JA, Sanz-Ruiz R, Ortega JR, et al: Safety and predictors of complications with a new accelerated dobutamine stress echocardiography protocol. *J Am Soc Echocardiogr* 21:53-57, 2008.
24. Cohen JL, Ottenweller JE, George AK, Duvvuri S: Comparison of dobutamine and exercise echocardiography for detecting coronary artery disease. *Am J Cardiol* 72:1226-1231, 1993.
25. Marwick TH, D'Hondt AM, Mairesse GH, et al: Comparative ability of dobutamine and exercise stress in inducing myocardial ischaemia in active patients. *British Heart Journal* 72:31-38, 1994.
26. Previtali M, Lanzarini L, Fetiveau R, et al: Comparison of dobutamine stress echocardiography, dipyridamole stress echocardiography and exercise stress testing for diagnosis of coronary artery disease. *Am J Cardiol* 72:865-870, 1993.
27. Beleslin BD, Ostojic M, Stepanovic J, et al: Stress echocardiography in the detection of myocardial ischemia. Head-to-head comparison of exercise, dobutamine, and dipyridamole tests. *Circulation* 90:1168-1176, 1994.
28. Rallidis L, Cokkinos P, Tousoulis D, Nihoyannopoulos P: Comparison of dobutamine and treadmill exercise echocardiography in inducing ischemia in patients with coronary artery disease. *J Am Coll Cardiol* 30:1660-1668, 1997.
29. Hoffmann R, Lethen H, Kleinhans E, et al: Comparative evaluation of bicycle and dobutamine stress echocardiography with perfusion scintigraphy and bicycle electrocardiogram for identification of coronary artery disease. *Am J Cardiol* 72:555-559, 1993.
30. Secknus MA, Marwick TH: Evolution of dobutamine echocardiography protocols and indications: safety and side effects in 3,011 studies over 5 years. *J Am Coll Cardiol* 29:1234-1240, 1997.
31. Orlandini AD, Tuero EI, Diaz R, et al: Acute cardiac rupture during dobutamine-atropine echocardiography stress test. *J Am Soc Echocardiogr* 13:152-153, 2000.
32. Cornel JH, Balk AH, Boersma E, et al: Safety and feasibility of dobutamine-atropine stress echocardiography in patients with ischemic left ventricular dysfunction. *J Am Soc Echocardiogr* 9:27-32, 1996.
33. Marcovitz PA, Bach DS, Mathias W, et al: Paradoxic hypotension during dobutamine stress echocardiography: clinical and diagnostic implications. *J Am Coll Cardiol* 21:1080-1086, 1993.
34. Tawa CB, Baker WB, Kleiman NS, et al: Comparison of adenosine echocardiography, with and without isometric handgrip, to exercise echocardiography in the detection of ischemia in patients with coronary artery disease. *J Am Soc Echocardiogr* 9:33-43, 1996.
35. Marwick T, Willemart B, D'Hondt AM, et al: Selection of the optimal nonexercise stress for the evaluation of ischemic regional myocardial dysfunction and malperfusion. Comparison of dobutamine and adenosine using echocardiography and 99mTc-MIBI single photon emission computed tomography [see comments]. *Circulation* 87:345-354, 1993.
36. Picano E, Marini C, Pirelli S, et al: Safety of intravenous high-dose dipyridamole echocardiography. The Echo-Persantine International Cooperative Study Group. *Am J Cardiol* 70: 252-258, 1992.
37. Cerqueira MD, Verani MS, et al: Safety profile of adenosine stress perfusion imaging: results from the Adenoscan Multicenter Trial Registry [see comments]. *J Am Coll Cardiol* 23:384-389, 1994.
38. Goudarzi B, Fukushima K, Bravo P, et al: Comparison of the myocardial blood flow response to regadenoson and dipyridamole: a quantitative analysis in patients referred for clinical (82)Rb myocardial perfusion PET. *Eur J Nucl Med Mol Imaging* 38:1908-1916, 2011.
39. Picano E, Alaimo A, Chubuchny V, et al: Noninvasive pacemaker stress echocardiography for diagnosis of coronary artery disease: a multicenter study. *J Am Coll Cardiol* 40:1305-1310, 2002.
40. Kim C, Kwok YS, Heagerty P, Redberg R: Pharmacologic stress testing for coronary disease diagnosis: a meta-analysis. *Am Heart J* 142:934-944, 2001.
41. Geleijnse ML, Krenning BJ, van Dalen BM, et al: Factors affecting sensitivity and specificity of diagnostic testing: dobutamine stress echocardiography. *J Am Soc Echocardiogr* 22:1199-1208, 2009.
42. Armstrong WF: Dobutamine stress echocardiography: single center studies vs. meta-analysis vs. the real world. *J Am Soc Echocardiogr* 22:1209-1211, 2009.
43. Segar DS, Brown SE, Sawada SG, et al: Dobutamine stress echocardiography: correlation with coronary lesion severity as determined by quantitative angiography. *J Am Coll Cardiol* 19:1197-1202, 1992.
44. Beleslin BD, Ostojic M, Djordjevic-Dikic A, et al: Integrated evaluation of relation between coronary lesion features and stress echocardiography results: the importance of coronary lesion morphology. *J Am Coll Cardiol* 33:717-726, 1999.
45. Noguchi Y, Nagata-Kobayashi S, Stahl JE, Wong JB: A meta-analytic comparison of echocardiographic stressors. *Int J Cardiovasc Imaging* 21:189-207, 2005.
46. Kaul S, Senior R, Dittrich H, et al: Detection of coronary artery disease with myocardial contrast echocardiography: comparison with 99mTc-sestamibi single-photon emission computed tomography. *Circulation* 96:785-792, 1997.
47. Hamouda MS, Kassem HK, Salama M, et al: Evaluation of coronary flow reserve in hypertensive patients by dipyridamole transesophageal Doppler echocardiography. *Am J Cardiol* 86:305-308, 2000.
48. Picano E, Molinaro S, Pasanisi E: The diagnostic accuracy of pharmacological stress echocardiography for the assessment of coronary artery disease: a meta-analysis. *Cardiovasc Ultrasound* 6:30, 2008.
49. Ostojic M, Picano E, Beleslin B, et al: Dipyridamole-dobutamine echocardiography: a novel test for the detection of milder forms of coronary artery disease. *J Am Coll Cardiol* 23:1115-1122, 1994.
50. Anthopoulos LP, Bonou MS, Kardaras FG, et al: Stress echocardiography in elderly patients with coronary artery disease: applicability, safety and prognostic value of dobutamine and adenosine echocardiography in elderly patients. *J Am Coll Cardiol* 28:52-59, 1996.
51. San Roman JA, Vilacosta I, Castillo JA, et al: Dipyridamole and dobutamine-atropine stress echocardiography in the diagnosis of coronary artery disease. Comparison with exercise stress test, analysis of agreement, and impact of antianginal treatment. *Chest* 110:1248-1254, 1996.
52. Fragasso G, Lu C, Dabrowski P, et al: Comparison of stress/rest myocardial perfusion tomography, dipyridamole and dobutamine stress echocardiography for the detection of coronary disease in hypertensive patients with chest pain and positive exercise test. *J Am Coll Cardiol* 34:441-447, 1999.
53. Poldermans D, Arnese M, Fioretti PM, et al: Improved cardiac risk stratification in major vascular surgery with dobutamine-atropine stress echocardiography. *J Am Coll Cardiol* 26:648-653, 1995.
54. Severi S, Picano E, Michelassi C, et al: Diagnostic and prognostic value of dipyridamole echocardiography in patients with suspected coronary artery disease. Comparison with exercise electrocardiography. *Circulation* 89: 1160-1173, 1994.
55. Eagle KA, Brundage BH, Chaitman BR, et al: Guidelines for perioperative cardiovascular evaluation for noncardiac surgery. Report of the American College of Cardiology/American Heart Association Task Force on Practice Guidelines. Committee on Perioperative Cardiovascular Evaluation for Noncardiac Surgery. *Circulation* 93:1278-1317, 1996.
56. Lee TH, Marcantonio ER, Mangione CM, et al: Derivation and prospective validation of a

simple index for prediction of cardiac risk of major noncardiac surgery. *Circulation* 100: 1043-1049, 1999.
57. Kertai MD, Boersma E, Bax JJ, et al: A meta-analysis comparing the prognostic accuracy of six diagnostic tests for predicting perioperative cardiac risk in patients undergoing major vascular surgery. *Heart* 89:1327-1334, 2003.
58. Devereaux PJ, Yang H, Yusuf S, et al: Effects of extended-release metoprolol succinate in patients undergoing non-cardiac surgery (POISE trial): a randomised controlled trial. *Lancet* 371:1839-1847, 2008.
59. Gibbons RJ, Miller TD, Hodge D, et al: Application of appropriateness criteria to stress single-photon emission computed tomography sestamibi studies and stress echocardiograms in an academic medical center. *J Am Coll Cardiol* 51:1283-1289, 2008.
60. McFalls EO, Ward HB, Moritz TE, et al: Coronary-artery revascularization before elective major vascular surgery. *N Engl J Med* 351:2795-2804, 2004.
61. Shaw LJ, Peterson ED, Shaw LK, et al: Use of a prognostic treadmill score in identifying diagnostic coronary disease subgroups. *Circulation* 98:1622-1630, 1998.
62. Berman DS, Hachamovitch R, Kiat H, et al: Incremental value of prognostic testing in patients with known or suspected ischemic heart disease: a basis for optimal utilization of exercise technetium-99m sestamibi myocardial perfusion single-photon emission computed tomography. *J Am Coll Cardiol* 26:639-647, 1990.
63. Marwick TH, Mehta R, Arheart K, Lauer MS: Use of exercise echocardiography for prognostic evaluation of patients with known or suspected coronary artery disease. *J Am Coll Cardiol* 30:83-90, 1997.
64. Schroder K, Wieckhorst A, Voller H: Comparison of the prognostic value of dipyridamole and dobutamine stress echocardiography in patients with known or suspected coronary artery disease. *Am J Cardiol* 79:1516-1518, 1997.
65. Poldermans D, Fioretti PM, Boersma E, et al: Dobutamine-atropine stress echocardiography and clinical data for predicting late cardiac events in patients with suspected coronary artery disease. *Am J Med* 97:119-125, 1994.
66. Kamaran M, Teague SM, Finkelhor RS, et al: Prognostic value of dobutamine stress echocardiography in patients referred because of suspected coronary artery disease. *Am J Cardiol* 76:887-891, 1995.
67. Marcovitz PA, Shayna V, Horn RA, et al: Value of dobutamine stress echocardiography in determining the prognosis of patients with known or suspected coronary artery disease. *Am J Cardiol* 78:404-408, 1996.
68. Senior R, Soman P, Khattar RS, Lahiri A: Prognostic value of dobutamine stress echocardiography in patients undergoing diagnostic coronary arteriography. *Am J Cardiol* 79:1610-1614, 1997.
69. Chuah SC, Pellikka PA, Roger VL, et al: Role of dobutamine stress echocardiography in predicting outcome in 860 patients with known or suspected coronary artery disease. *Circulation* 97:1474-1480, 1998.
70. Poldermans D, Fioretti PM, Boersma E, et al: Long-term prognostic value of dobutamine-atropine stress echocardiography in 1737 patients with known or suspected coronary artery disease: a single-center experience. *Circulation* 99:757-762, 1999.
71. Picano E, Severi S, Michelassi C, et al: Prognostic importance of dipyridamole-echocardiography test in coronary artery disease. *Circulation* 80:450-457, 1989.
72. Steinberg EH, Madmon L, Patel CP, et al: Long-term prognostic significance of dobutamine echocardiography in patients with suspected coronary artery disease: results of a 5-year follow-up study. *J Am Coll Cardiol* 29:969-973, 1997.
73. Cortigiani L, Paolini EA, Nannini E: Dipyridamole stress echocardiography for risk stratification in hypertensive patients with chest pain. *Circulation* 98:2855-2859, 1998.
74. Pingitore A, Picano E, Varga A, et al: Prognostic value of pharmacological stress echocardiography in patients with known or suspected coronary artery disease: a prospective, large- scale, multicenter, head-to-head comparison between dipyridamole and dobutamine test. Echo-Persantine International Cooperative (EPIC) and Echo-Dobutamine International Cooperative (EDIC) Study Groups. *J Am Coll Cardiol* 34:1769-1777, 1999.
75. Marwick TH, Case C, Sawada S, et al: Use of stress echocardiography to predict mortality in patients with diabetes and known or suspected coronary artery disease. *Diabetes Care* 25:1042-1048, 2002.
76. Sicari R, Cortigiani L, Bigi R, et al: Prognostic value of pharmacological stress echocardiography is affected by concomitant antiischemic therapy at the time of testing. *Circulation* 109:2428-2431, 2004.
77. Bolognese L, Sarasso G, Aralda D, et al: High dose echocardiography test early after uncomplicated acute myocardial infarction: correlation with exercise testing and coronary angiography. *J Am Coll Cardiol* 14:357-363, 1989.
78. Sclavo MG, Noussan P, Pallisco O, Presbitero P: Usefulness of dipyridamole-echocardiographic test to identify jeopardized myocardium after thrombolysis. Limited clinical predictivity of dipyridamole-echocardiographic test in convalescing acute myocardial infarction: correlation with coronary angiography. *Eur Heart J* 13:1348-1355, 1992.
79. Picano E, Landi P, Bolognese L, et al: Prognostic value of dipyridamole echocardiography early after uncomplicated myocardial infarction: a large-scale, multicenter trial. The EPIC Study Group. *Am J Med* 95:608-618, 1993.
80. Chiarella F, Domenicucci S, Bellotti P, et al: Dipyridamole echocardiographic test performed 3 days after an acute myocardial infarction: feasibility, tolerability, safety and in-hospital prognostic value. *Eur Heart J* 15:842-850, 1994.
81. Picano E, Pingitore A, Sicari R, et al: Stress echocardiographic results predict risk of reinfarction early after uncomplicated acute myocardial infarction: large- scale multicenter study. Echo Persantine International Cooperative (EPIC) Study Group. *J Am Coll Cardiol* 26:908-913, 1995.
82. Picano E, Sicari R, Landi P, et al: Prognostic value of myocardial viability in medically-treated patients with global left ventricular dysfunction early after acute uncomplicated myocardial infarction: a dobutamine stress echocardiographic study. *Circulation* 98:1078-1084, 1998.
83. Camerieri A, Picano E, Landi P, et al: Prognostic value of dipyridamole echocardiography early after myocardial infarction in elderly patients. Echo Persantine Italian Cooperative (EPIC) Study Group. *J Am Coll Cardiol* 22:1809-1815, 1993.
84. Salustri A, Fioretti PM, McNeill AJ, et al: Pharmacological stress echocardiography in the diagnosis of coronary artery disease and myocardial ischaemia: a comparison between dobutamine and dipyridamole. *Eur Heart J* 13:1356-1362, 1992.
85. Lombardi M, Morales MA, Michelassi C, et al: Efficacy of isosorbide-5-mononitrate versus nifedipine in preventing spontaneous and ergonovine-induced myocardial ischaemia. A double-blind, placebo-controlled study. *Eur Heart J* 14:845-851, 1993.
86. Dodi C, Pingitore A, Sicari R, et al: Effects of antianginal therapy with a calcium antagonist and nitrates on dobutamine-atropine stress echocardiography. Comparison with exercise electrocardiography. *Eur Heart J* 18:242-247, 1997.
87. Varga A, Preda I: Pharmacological stress echocardiography for exercise independent assessment of anti-ischaemic therapy [editorial; comment]. *Eur Heart J* 18:180-181, 1997.
88. Akosah KO, Porter TR, Simon R, et al: Ischemia-induced regional wall motion abnormality is improved after coronary angioplasty: demonstration by dobutamine stress echocardiography. *J Am Coll Cardiol* 21:584-589, 1993.
89. Douglas PS, Khandheria B, Stainback RF, et al: ACCF/ASE/ACEP/AHA/ASNC/SCAI/SCCT/SCMR 2008 appropriateness criteria for stress echocardiography: a report of the American College of Cardiology Foundation Appropriateness Criteria Task Force, American Society of Echocardiography, American College of Emergency Physicians, American Heart Association, American Society of Nuclear Cardiology, Society for Cardiovascular Angiography and Interventions, Society of Cardiovascular Computed Tomography, and Society for Cardiovascular Magnetic Resonance endorsed by the Heart Rhythm Society and the Society of Critical Care Medicine. *J Am Coll Cardiol* 51:1127-1147, 2008.
90. Gibbons RJ, Abrams J, Chatterjee K, et al: ACC/AHA 2002 guideline update for the management of patients with chronic stable angina–summary article: a report of the American College of Cardiology/American Heart Association Task Force on Practice Guidelines (Committee on the Management of Patients With Chronic Stable Angina). *Circulation* 107:149-158, 2003.
91. Pirelli S, Danzi GB, Alberti A, et al: Comparison of usefulness of high-dose dipyridamole echocardiography and exercise electrocardiography for detection of asymptomatic restenosis after coronary angioplasty. *Am J Cardiol* 67: 1335-1338, 1991.
92. Heinle SK, Lieberman EB, Ancukiewicz M, et al: Usefulness of dobutamine echocardiography for detecting restenosis after percutaneous transluminal coronary angioplasty. *Am J Cardiol* 72:1220-1225, 1993.
93. Bjoernstad K, Aakhus S, Lundbom J, et al: Digital dipyridamole stress echocardiography in silent ischemia after coronary artery bypass grafting and/or after healing of acute myocardial infarction. *Am J Cardiol* 72:640-646, 1993.
94. Elhendy A, Geleijnse ML, Roelandt JR, et al: Assessment of patients after coronary artery bypass grafting by dobutamine stress echocardiography. *Am J Cardiol* 77:1234-1236, 1996.
95. Kloner RA, Bolli R, Marban E, et al: Medical and cellular implications of stunning, hiberna-

tion and preconditioning: an NHLBI workshop. *Circulation* 97:1848-1867, 1998.
96. Bonow RO, Maurer G, Lee KL, et al: Myocardial viability and survival in ischemic left ventricular dysfunction. *N Eng J Med* 364:1617-1625, 2011.
97. Weissman NJ, Rose GA, Foster GP, Picard MH: Effects of prolonging peak dobutamine dose during stress echocardiography. *J Am Coll Cardiol* 29:526-530, 1997.
98. Afridi I, Kleiman NS, Raizner AE, Zoghbi WA: Dobutamine echocardiography in myocardial hibernation. Optimal dose and accuracy in predicting recovery of ventricular function after coronary angioplasty. *Circulation* 91:663-670, 1995.
99. Kaul S: Response of dysfunctional myocardium to dobutamine. "The eyes see what the mind knows". *J Am Coll Cardiol* 27:1608-1611, 1996.
100. Schinkel AF, Bax JJ, Poldermans D, et al: Hibernating myocardium: diagnosis and patient outcomes. *Curr Probl Cardiol* 32:375-410, 2007.
101. Cornel JH, Bax JJ, Elhendy A, et al: Biphasic response to dobutamine predicts improvement of global left ventricular function after surgical revascularization in patients with stable coronary artery disease: implications of time course of recovery on diagnostic accuracy. *J Am Coll Cardiol* 31:1002-1010, 1998.
102. Pasquet A, Lauer MS, Williams MJ, et al: Prediction of global left ventricular function after bypass surgery in patients with severe left ventricular dysfunction. Impact of pre-operative myocardial function, perfusion, and metabolism. *Eur Heart J* 21:125-136, 2000.
103. Marwick TH, Zuchowski C, Lauer MS, et al: Functional status and quality of life in patients with heart failure undergoing coronary bypass surgery after assessment of myocardial viability. *J Am Coll Cardiol* 33:750-758, 1999.
104. Inaba Y, Chen JA, Bergmann SR: Quantity of viable myocardium required to improve survival with revascularization in patients with ischemic cardiomyopathy: a meta-analysis. *J Nucl Cardiol* 17:646-654, 2010.
105. Afridi I, Grayburn PA, Panza JA, et al: Myocardial viability during dobutamine echocardiography predicts survival in patients with coronary artery disease and severe left ventricular systolic dysfunction. *J Am Coll Cardiol* 32:921-926, 1998.
106. Williams MJ, Odabashian J, Lauer MS, et al: Prognostic value of dobutamine echocardiography in patients with left ventricular dysfunction. *J Am Coll Cardiol* 27:132-139, 1996.
107. Plana JC, Mikati IA, Dokainish H, et al: A randomized cross-over study for evaluation of the effect of image optimization with contrast on the diagnostic accuracy of dobutamine echocardiography in coronary artery disease The OPTIMIZE Trial. *JACC Cardiovasc Imaging* 1:145-152, 2008.
108. Moir S, Marwick TH: Combination of contrast with stress echocardiography: a practical guide to methods and interpretation. *Cardiovasc Ultrasound* 2:15, 2004.
109. Cwajg J, Xie F, O'Leary E, et al: Detection of angiographically significant coronary artery disease with accelerated intermittent imaging after intravenous administration of ultrasound contrast material. *Am Heart J* 139:675-683, 2000.
110. Shimoni S, Zoghbi WA, Xie F, et al: Real-time assessment of myocardial perfusion and wall motion during bicycle and treadmill exercise echocardiography: comparison with single photon emission computed tomography. *J Am Coll Cardiol* 37:741-747, 2001.
111. Heinle SK, Noblin J, Goree-Best P, et al: Assessment of myocardial perfusion by harmonic power Doppler imaging at rest and during adenosine stress: comparison with (99m) Tc-sestamibi SPECT imaging. *Circulation* 102:55-60, 2000.
112. Wei K, Crouse L, Weiss J, et al: Comparison of usefulness of dipyridamole stress myocardial contrast echocardiography to technetium-99m sestamibi single-photon emission computed tomography for detection of coronary artery disease (PB127 Multicenter Phase 2 Trial results). *Am J Cardiol* 91:1293-1298, 2003.
113. Rocchi G, Fallani F, Bracchetti G, et al: Noninvasive detection of coronary artery stenosis: a comparison among power-Doppler contrast echo, 99Tc-Sestamibi SPECT and echo wall-motion analysis. *Coron Artery Dis* 14:239-245, 2003.
114. Olszowska M, Kostkiewicz M, Tracz W, Przewlocki T: Assessment of myocardial perfusion in patients with coronary artery disease. Comparison of myocardial contrast echocardiography and 99mTc MIBI single photon emission computed tomography. *Int J Cardiol* 90:49-55, 2003.
115. Moir S, Haluska BA, Jenkins C, et al: Incremental benefit of myocardial contrast to combined dipyridamole-exercise stress echocardiography for the assessment of coronary artery disease. *Circulation* 110:1108-1113, 2004.
116. Elhendy A, O'Leary EL, Xie F, et al: Comparative accuracy of real-time myocardial contrast perfusion imaging and wall motion analysis during dobutamine stress echocardiography for the diagnosis of coronary artery disease. *J Am Coll Cardiol* 44:2185-2191, 2004.
117. Peltier M, Vancraeynest D, Pasquet A, et al: Assessment of the physiologic significance of coronary disease with dipyridamole real-time myocardial contrast echocardiography. Comparison with technetium-99m sestamibi single-photon emission computed tomography and quantitative coronary angiography. *J Am Coll Cardiol* 43:257-264, 2004.
118. Jeetley P, Hickman M, Kamp O, et al: Myocardial contrast echocardiography for the detection of coronary artery stenosis: a prospective multicenter study in comparison with single-photon emission computed tomography. *J Am Coll Cardiol* 47:141-145, 2006.
119. Tsutsui JM, Elhendy A, Anderson JR, et al: Prognostic value of dobutamine stress myocardial contrast perfusion echocardiography. *Circulation* 112:1444-1450, 2005.
120. Pulerwitz T, Hirata K, Abe Y, et al: Feasibility of using a real-time 3-dimensional technique for contrast dobutamine stress echocardiography. *J Am Soc Echocardiogr* 19:540-545, 2006.
121. Takeuchi M, Otani S, Weinert L, et al: Comparison of contrast-enhanced real-time live 3-dimensional dobutamine stress echocardiography with contrast 2-dimensional echocardiography for detecting stress-induced wall-motion abnormalities. *J Am Soc Echocardiogr* 19:294-299, 2006.
122. Matsumura Y, Hozumi T, Arai K, et al: Noninvasive assessment of myocardial ischaemia using new real-time three-dimensional dobutamine stress echocardiography: comparison with conventional two-dimensional methods. *Eur Heart J* 26:1625-1632, 2005.
123. Ahmad M, Xie T, McCulloch M, et al: Real-time three-dimensional dobutamine stress echocardiography in assessment stress echocardiography in assessment of ischemia: comparison with two-dimensional dobutamine stress echocardiography. *J Am Coll Cardiol* 37:1303-1309, 2001.
124. Jenkins C, Haluska B, Marwick TH. Assessment of temporal heterogeneity and regional motion to identify wall motion abnormalities using treadmill exercise stress three-dimensional echocardiography. *J Am Soc Echocardiogr* 22:268-275, 2009.
125. Koch R, Lang RM, Garcia MJ, et al: Objective evaluation of regional left ventricular wall motion during dobutamine stress echocardiographic studies using segmental analysis of color kinesis images. *J Am Coll Cardiol* 34:409-419, 1999.
126. Perez JE, Miller JG, Holland MR, et al: Ultrasonic tissue characterization: integrated backscatter imaging for detecting myocardial structural properties and on-line quantitation of cardiac function. *Am J Card Imaging* 8:106-112, 1994.
127. Wilkenshoff UM, Sovany A, Wigstrom L, et al: Regional mean systolic myocardial velocity estimation by real-time color Doppler myocardial imaging: a new technique for quantifying regional systolic function. *J Am Soc Echocardiogr* 11:682-692, 1998.
128. Pasquet A, Armstrong G, Rimmerman CM, Marwick TH: Correlation of myocardial Doppler velocity response to exercise with independent evidence of myocardial ischemia by dual isotope single photon emission computed tomography. *Am J Cardiol* 85:536-542, 2000.
129. Cain P, Baglin T, Case C, et al: Application of tissue Doppler to interpretation of dobutamine echocardiography: comparison with quantitative coronary angiography. *Am J Cardiol* 87:525-531, 2001.
130. Urheim S, Edvardsen T, Torp H, et al: Myocardial strain by Doppler echocardiography. Validation of a new method to quantify regional myocardial function. *Circulation* 102:1158-1164, 2000.
131. Edvardsen T, Gerber BL, Garot J, et al: Quantitative assessment of intrinsic regional myocardial deformation by Doppler strain rate echocardiography in humans: validation against three-dimensional tagged magnetic resonance imaging. *Circulation* 106:50-56, 2002.
132. Greenberg NL, Firstenberg MS, Castro PL, et al: Doppler-derived myocardial systolic strain rate is a strong index of left ventricular contractility. *Circulation* 105:99-105, 2002.
133. Hoffmann R, Altiok E, Nowak B, et al: Strain rate measurement by Doppler echocardiography allows improved assessment of myocardial viability inpatients with depressed left ventricular function. *J Am Coll Cardiol* 39:443-449, 2002.
134. Hanekom L, Jenkins C, Jeffries L, et al: Incremental value of strain rate analysis as an adjunct to wall-motion scoring for assessment of myocardial viability by dobutamine echocardiography: a follow-up study after revascularization. *Circulation* 112:3892-3900, 2005.
135. Vitarelli A, Montesano T, Gaudio C, et al: Strain rate dobutamine echocardiography for prediction of recovery after revascularization in patients with ischemic left ventricular dysfunction. *J Card Fail* 12:268-275, 2006.
136. Voigt JU, Exner B, Schmiedehausen K, et al: Strain-rate imaging during dobutamine stress echocardiography provides objective evidence

of inducible ischemia. *Circulation* 107:2120-2126, 2003.
137. Bjork Ingul C, Rozis E, Slordahl S, Marwick TH: Incremental value of strain rate imaging to wall motion analysis for prediction of outcome in patients undergoing dobutamine stress echocardiography. *Circulation* 115:1252-1259, 2007.
138. Leitman M, Lysyansky P, Sidenko S, et al: Two-dimensional strain-a novel software for real-time quantitative echocardiographic assessment of myocardial function. *J Am Soc Echocardiogr* 17:1021-1029, 2004.
139. Bansal M, Jeffriess L, Leano R, et al: Assessment of myocardial viability at dobutamine echocardiography by deformation analysis using tissue velocity and speckle-tracking. *JACC Cardiovasc Imaging* 3:121-131, 2010.
140. Ingul CB, Stoylen A, Slordahl SA, et al: Automated analysis of myocardial deformation at dobutamine stress echocardiography: an angiographic validation. *J Am Coll Cardiol* 49:1651-1659, 2007.
141. Rigo F, Ciampi Q, Ossena G, et al: Prognostic value of left and right coronary flow reserve assessment in nonischemic dilated cardiomyopathy by transthoracic Doppler echocardiography. *J Card Fail* 17:39-46, 2011.
142. Sicari R, Rigo F, Gherardi S, et al: The prognostic value of Doppler echocardiographic-derived coronary flow reserve is not affected by concomitant antiischemic therapy at the time of testing. *Am Heart J* 156:573-579, 2008.
143. Heinle SK, Tice FD, Kisslo J: Effect of dobutamine stress echocardiography on mitral regurgitation. *J Am Coll Cardiol* 25:122-127, 1994.
144. Monin JL, Quere JP, Monchi M, et al: Low-gradient aortic stenosis: operative risk stratification and predictors for long-term outcome: a multicenter study using dobutamine stress hemodynamics. *Circulation* 108:319-324, 2003.
145. el-Said ES, Roelandt JR, Fioretti PM, et al: Abnormal left ventricular early diastolic filling during dobutamine stress Doppler echocardiography is a sensitive indicator of significant coronary artery disease. *J Am Coll Cardiol* 24:1618-1624, 1994.
146. von Bibra H, Tuchnitz A, Klein A, et al: Regional diastolic function by pulsed Doppler myocardial mapping for the detection of left ventricular ischemia during pharmacologic stress testing: a comparison with stress echocardiography and perfusion scintigraphy. *J Am Coll Cardiol* 36:444-452, 2000.
147. Marwick TH, Shaw L, Case C, et al: Clinical and economic impact of exercise electrocardiography and exercise echocardiography in clinical practice. *Eur Heart J* 24:1153-1163, 2003.
148. Picano E, Lattanzi F, Masini M, et al: Comparison of the high-dose dipyridamole-echocardiography test and exercise two-dimensional echocardiography for diagnosis of coronary artery disease. *Am J Cardiol* 59:539-542, 1987.
149. Marangelli V, Iliceto S, Piccinni G, et al: Detection of coronary artery disease by digital stress echocardiography: comparison of exercise, transesophageal atrial pacing and dipyridamole echocardiography. *J Am Coll Cardiol* 24:117-124, 1994.
150. Dagianti A, Penco M, Agati L, et al: Stress echocardiography: comparison of exercise, dipyridamole and dobutamine in detecting and predicting the extent of coronary artery disease [published erratum appears in J Am Coll Cardiol 1995 Oct;26(4):1114] [see comments]. *J Am Coll Cardiol* 26:18-25, 1995.
151. Rallidis L, Cokkinos P, Tousoulis D, Nihoyannopoulos P: Comparison of dobutamine and treadmill exercise echocardiography in inducing ischemia in patients with coronary artery disease. *J Am Coll Cardiol* 30:1660-1668, 1997.
152. Senior R, Sridhara BS, Anagnostou E, et al: Synergistic value of simultaneous stress dobutamine sestamibi single-photon-emission computerized tomography and echocardiography in the detection of coronary artery disease. *American Heart Journal* 128:713-718, 1994.
153. Ho FM, Huang PJ, Liau CS, et al: Dobutamine stress echocardiography compared with dipyridamole thallium- 201 single-photon emission computed tomography in detecting coronary artery disease. *Eur Heart J* 16:570-575, 1995.
154. Huang PJ, Ho YL, Wu CC, et al: Simultaneous dobutamine stress echocardiography and thallium-201 perfusion imaging for the detection of coronary artery disease. *Cardiology* 88: 556-562, 1997.
155. Santoro GM, Sciagra R, Buonamici P, et al: Head-to-head comparison of exercise stress testing, pharmacologic stress echocardiography, and perfusion tomography as first-line examination for chest pain in patients without history of coronary artery disease [see comments]. *J Nucl Cardiol* 5:19-27, 1998.
156. San Roman JA, Rollan MJ, Vilacosta I, et al: [Echocardiography and MIBI-SPECT scintigraphy during dobutamine infusion in the diagnosis of coronary disease]. *Rev Esp Cardiol* 48:606-614, 1995.
157. Pozzoli MM, Fioretti PM, Salustri A, et al: Exercise echocardiography and technetium 99m MIBI single photon emission computed tomography in the detection of coronary artery disease. *Am J Cardiol* 67:350-355, 1991.
158. Mairesse GH, Marwick TH, Arnese M, et al: Improved identification of coronary artery disease in patients with left bundle branch block by use of dobutamine stress echocardiography and comparison with myocardial perfusion tomography. *Am J Cardiol* 76:321-325, 1995.
159. Nagel E, Lehmkuhl HB, Bocksch W, et al: Noninvasive diagnosis of ischemia-induced wall motion abnormalities with the use of high-dose dobutamine stress MRI: comparison with dobutamine stress echocardiography. *Circulation* 99:763-770, 1999.
160. Van Damme H, Pierard L, Gillain D, et al: Cardiac risk assessment before vascular surgery: a prospective study comparing clinical evaluation, dobutamine stress echocardiography, and dobutamine Tc-99m sestamibi tomoscintigraphy. *Cardiovascular Surgery* 5:54-64, 1997.
161. Pasquet A, D'Hondt AM, Verhelst R, et al: Comparison of dipyridamole stress echocardiography and perfusion scintigraphy for cardiac risk stratification in vascular surgery patients. *Am J Cardiol* 82:1468-1474, 1998.
162. Shaw LJ, Eagle KA, Gersh BJ, Miller DD: Meta-analysis of intravenous dipyridamole-thallium-201 imaging (1985 to 1994) and dobutamine echocardiography (1991 to 1994) for risk stratification before vascular surgery [see comments]. *J Am Coll Cardiol* 27:787-798, 1996.
163. Marzullo P, Parodi O, Reisenhofer B, et al: Value of rest thallium-201/technetium-99m sestamibi scans and dobutamine echocardiography for detecting myocardial viability. *Am J Cardiol* 71:166-172, 1993.
164. Charney R, Schwinger ME, Chun J, et al: Dobutamine echocardiography and resting-redistribution thallium- 201 scintigraphy predicts recovery of hibernating myocardium after coronary revascularization. *Am Heart J* 128:864-869, 1994.
165. Kostopoulos KG, Kranidis AI, Bouki KP, et al: Detection of myocardial viability in the prediction of improvement in left ventricular function after successful coronary revascularization by using the dobutamine stress echocardiography and quantitative SPECT rest-redistribution-reinjection 201TI imaging after dipyridamole infusion. *Angiology* 47: 1039-1046, 1996.
166. Qureshi U, Nagueh SF, Afridi I, et al: Dobutamine echocardiography and quantitative rest-redistribution 201Tl tomography in myocardial hibernation. Relation of contractile reserve to 201Tl uptake and comparative prediction of recovery of function. *Circulation* 95:626-635, 1997.
167. Nagueh SF, Vaduganathan P, Ali N, et al: Identification of hibernating myocardium: comparative accuracy of myocardial contrast echocardiography, rest-redistribution thallium-201 tomography and dobutamine echocardiography. *J Am Coll Cardiol* 29:985-993, 1997.
168. Senior R, Glenville B, Basu S, et al: Dobutamine echocardiography and thallium-201 imaging predict functional improvement after revascularisation in severe ischaemic left ventricular dysfunction. *British Heart Journal* 74:358-364, 1995.
169. Arnese M, Cornel JH, Salustri A, et al: Prediction of improvement of regional left ventricular function after surgical revascularization. A comparison of low-dose dobutamine echocardiography with 201Tl single-photon emission computed tomography. *Circulation* 91:2748-2752, 1995.
170. Perrone-Filardi P, Pace L, Prastaro M, et al: Assessment of myocardial viability in patients with chronic coronary artery disease. Rest-4-hour-24-hour 201Tl tomography versus dobutamine echocardiography [see comments]. *Circulation* 94:2712-2719, 1996.
171. Bax JJ, Cornel JH, Visser FC, et al: Prediction of recovery of myocardial dysfunction after revascularization. Comparison of fluorine-18 fluorodeoxyglucose/thallium-201 SPECT, thallium-201 stress-reinjection SPECT and dobutamine echocardiography. *J Am Coll Cardiol* 28:558-564, 1996.
172. Haque T, Furukawa T, Takahashi M, Kinoshita M: Identification of hibernating myocardium by dobutamine stress echocardiography: comparison with thallium-201 reinjection imaging. *American Heart Journal* 130:553-563, 1995.
173. Vanoverschelde JL, D'Hondt AM, Marwick T, et al: Head-to-head comparison of exercise-redistribution-reinjection thallium single-photon emission computed tomography and low dose dobutamine echocardiography for prediction of reversibility of chronic left ventricular ischemic dysfunction. *J Am Coll Cardiol* 28:432-442, 1996.
174. Elsasser A, Muller KD, Vogt A, et al: Assessment of myocardial viability: dobutamine echocardiography and thallium-201 single-photon emission computed tomographic imaging predict the postoperative improvement of left ventricular function after bypass surgery. *Am Heart J* 135:463-475, 1998.

# 17 Echocardiographic Evaluation of Coronary Blood Flow: Approaches and Clinical Applications

NOZOMI WATANABE, MD

**Coronary Anatomy**
**Doppler Evaluation of Coronary Flow**
Technical Aspects
Detection
**Assessment of Coronary Flow Profile**
**Clinical Applications**
Coronary Flow Velocity Reserve Measurement
Noninvasive Diagnosis of Coronary Stenosis
Coronary Flow Measurements in Acute Coronary Syndrome
Coronary Flow in the No-Reflow Phenomenon
Impaired Coronary Circulation in Hypertrophic Cardiomyopathy
Coronary Flow Reserve in Syndrome X and Chest Pain Syndrome
**Alternative Approaches**

Coronary flow velocity and coronary flow velocity reserve measurements provide useful clinical and physiologic information. Previously, coronary flow velocity has been assessed invasively by Doppler flow wire technique in the cardiac catheterization lab. Recent technologic advances in Doppler echocardiography provide noninvasive coronary flow detection by Doppler transthoracic echocardiography (TTE).[1,2] The accuracy of these new noninvasive transthoracic coronary flow and coronary flow reserve (CFR) measurements has been validated compared to Doppler flow wire.[3-7] Doppler TTE is widely available in the clinical setting, and this technique can be performed in an outpatient setting.[8,9] The majority of the clinical data regarding this technique has been reported by European and Japanese groups, but Takeuchi and colleagues[10] did a unique investigation testing the feasibility of transthoracic coronary flow detection in the relatively obese U.S. population and found a similar success rate for recording coronary flow and CFR. Intravenous contrast injection helps in detection of the coronary signal.[11-14] This new, noninvasive imaging technique of the coronary arteries promises to expand the field of diagnostic echocardiography and bring new insight into the pathophysiology of ischemic heart disease.

## Coronary Anatomy

It is important to understand the coronary arterial anatomy for assessment of coronary flow by Doppler TTE (Fig. 17-1). The left and right coronaries originate from the left and right coronary sinuses of the aortic root. The left main coronary artery bifurcates into the left anterior descending (LAD) artery, which runs over the anterior interventricular sulcus, and the left circumflex (LCx) artery in the left atrioventricular sulcus. The LAD artery often around beyond the apex. In this situation, the LAD artery extends up the posterior interventricular sulcus. The septal branches arise at an acute angle from the LAD artery, coursing close to the endocardium on the right side of the interventricular septum. The LCx artery is the other principal vessel originating from the left main coronary artery. It is covered by the left atrial (LA) appendage in its proximal portion, and then courses along the left atrioventricular sulcus. The right coronary artery (RCA) has its origin at the right coronary aortic sinus and follows the right atrioventricular sulcus. The posterior descending artery lies in the posterior interventricular sulcus.

## Doppler Evaluation of Coronary Flow

### TECHNICAL ASPECTS

There are some important technical issues for detecting coronary flow signals. First, a good high-resolution and high-sensitivity ultrasound system with a high-frequency transducer is required (7 to 12 MHz for mid to distal LAD artery; 2 to 5 MHz for proximal LAD artery, RCA, and LCx artery). Second, in color Doppler imaging, the Doppler velocity range should be set in the range of 10 to 30 cm/s to detect the coronary flow signal because the blood flow velocity is relatively slow. In cases in which it is difficult to detect a coronary flow signal, intravenous injection of contrast agent enhances the Doppler signal intensity.[5,11] The contrast enhancer used in the most studies was Levovist (Schering AG, Berlin, Germany). Levovist, at a concentration of 300 mg/mL, was administered intravenously by using an infusion pump. The infusion rate is adjusted from 0.5 to 2 mL/min, according to the quality and intensity of the Doppler signal enhancement achieved. By positioning the Doppler sample volume in the coronary flow stream under the guidance of color Doppler flow imaging, the characteristic coronary flow spectrum, with biphasic predominantly diastolic flow velocities, can be recorded. In the pulsed Doppler technique, angle correction is required depending on the direction of coronary flow.

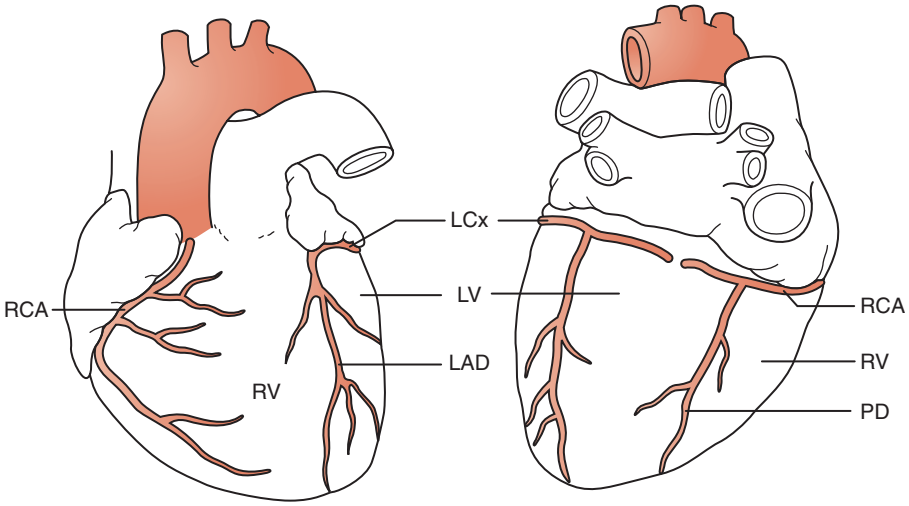



**Figure 17-1 Anatomic position of epicardial coronary arteries.** Left and right coronary arteries originate from the left and right coronary sinuses, respectively. Left anterior descending artery (*LAD*) runs over the anterior interventricular sulcus toward apex. Left circumflex artery (*LCx*) runs along the left atrioventricular sulcus. Right coronary artery (*RCA*) runs along the right atrioventricular sulcus, and the posterior descending artery (*PD*) runs in the posterior interventricular sulcus. Thus, landmarks for searching coronary flow by TTE are interventricular sulcus and atrioventricular sulcus.

## DETECTION

### *Left Main and Proximal Coronary Arteries*

Patients should be examined in the left lateral decubitus position. To visualize the left main trunk and proximal left anterior descending artery, start with the image plane at the level of the aortic root, in a short-axis view (Fig. 17-2, *A*). This part of the exam can be performed using a relatively low-frequency transducer (2 to 4 MHz). The left main trunk is identified as a tubular structure that originates from the left coronary sinus. By adjusting the orientation of the ultrasound beam toward the distal side of the left main trunk, the proximal LAD artery, which runs from the bifurcation toward the anterior wall of the heart, can be visualized using color Doppler flow mapping. At the level of the left main bifurcation, the proximal circumflex artery is detected by rotating the transducer clockwise.

The proximal RCA, which originates from right coronary sinus, can be identified at the aortic root, in short-axis or long-axis views (Fig. 17-3).

### *Left Anterior Descending Coronary Artery*

In the short-axis images of the left ventricle (LV), the midportion of the LAD artery can be identified as a cross section of the tubular structure containing the color Doppler flow signal, located in the anterior interventricular sulcus (see Fig. 17-2, *B* and *C*). The color Doppler signal in the LAD artery, which typically appears as a red color, is mainly seen in diastole. After confirming its position, rotate the transducer counterclockwise to image the LV in a long-axis view aligned with the intraventricular sulcus under the guidance of color Doppler flow imaging. To visualize the distal portion of the LAD artery, image the LV in a long-axis view starting from the apex and searching for the coronary flow signal around the intraventricular sulcus. In this view, pericardial fluid may appear similar to a coronary flow signal near the epicardium. However, pericardial fluid is seen mainly in systole and can easily be discriminated by pulsed Doppler recording. The coronary flow pattern by pulsed Doppler is biphasic, but pericardial fluid generally has a systolic, bidirectional signal. Once the LAD artery is found as a cross section of the tubular structure containing the color Doppler flow signal, rotate the transducer clockwise (toward the two-chamber view position) to detect the flow signal in the long-axis view (Fig. 17-4). Coronary flow detection in the distal portion of the LAD artery is important, as CFR should be measured distal to any stenosis. Coronary blood flow velocity profiles are recorded by positioning a pulsed sample volume on the color flow signal. The incident angle between the Doppler beam and direction of blood flow should be used to correct the velocity scale.

### *Posterior Descending Coronary Artery*

The posterior descending coronary artery usually is the distal extension of the RCA and runs along the posterior interventricular sulcus toward the apex. After obtaining an apical two-chamber image of the LV, angle the ultrasound beam superiorly to image the posterior interventricular sulcus (see Fig. 17-2, *C*). In this situation a lower frequency probe is recommended because this area is far from the transducer, compared to the anterior interventricular sulcus. Carefully examine this area using color Doppler flow imaging to locate the right posterior descending coronary artery (Fig. 17-5). Though the success rate in detecting coronary flow velocity profile in the right posterior descending coronary artery is lower compared with the LAD artery, a contrast-enhanced Doppler technique improves the success rate.[15]

### *Left Circumflex Coronary Artery*

The LCx artery can be found in the modified four-chamber view (see Fig. 17-2, *D*). It is normally distinguished as a color flow signal running along the basal lateral wall[16] (Fig. 17-6). However, visualization of circumflex arteries is relatively difficult because of their anatomic variations, and furthermore, these vessels are distant from the transducer.

## Assessment of Coronary Flow Profile

Doppler spectral tracings of coronary flow velocity can be recorded by the pulsed-Doppler technique by positioning a sample volume (1.5 to 2.5 mm wide) on the color Doppler signal. Angle correction is needed in each examination. Coronary flow profile provides some useful clinical information, such as coronary flow direction, coronary flow velocity, and coronary flow pattern. Normal coronary flow is characterized by a biphasic flow profile, which consists of a small systolic and a large diastolic flow signal (Fig. 17-7). It should be noted that pulsed-Doppler recording provides coronary flow velocity and not the absolute volume of coronary blood flow. CFR by

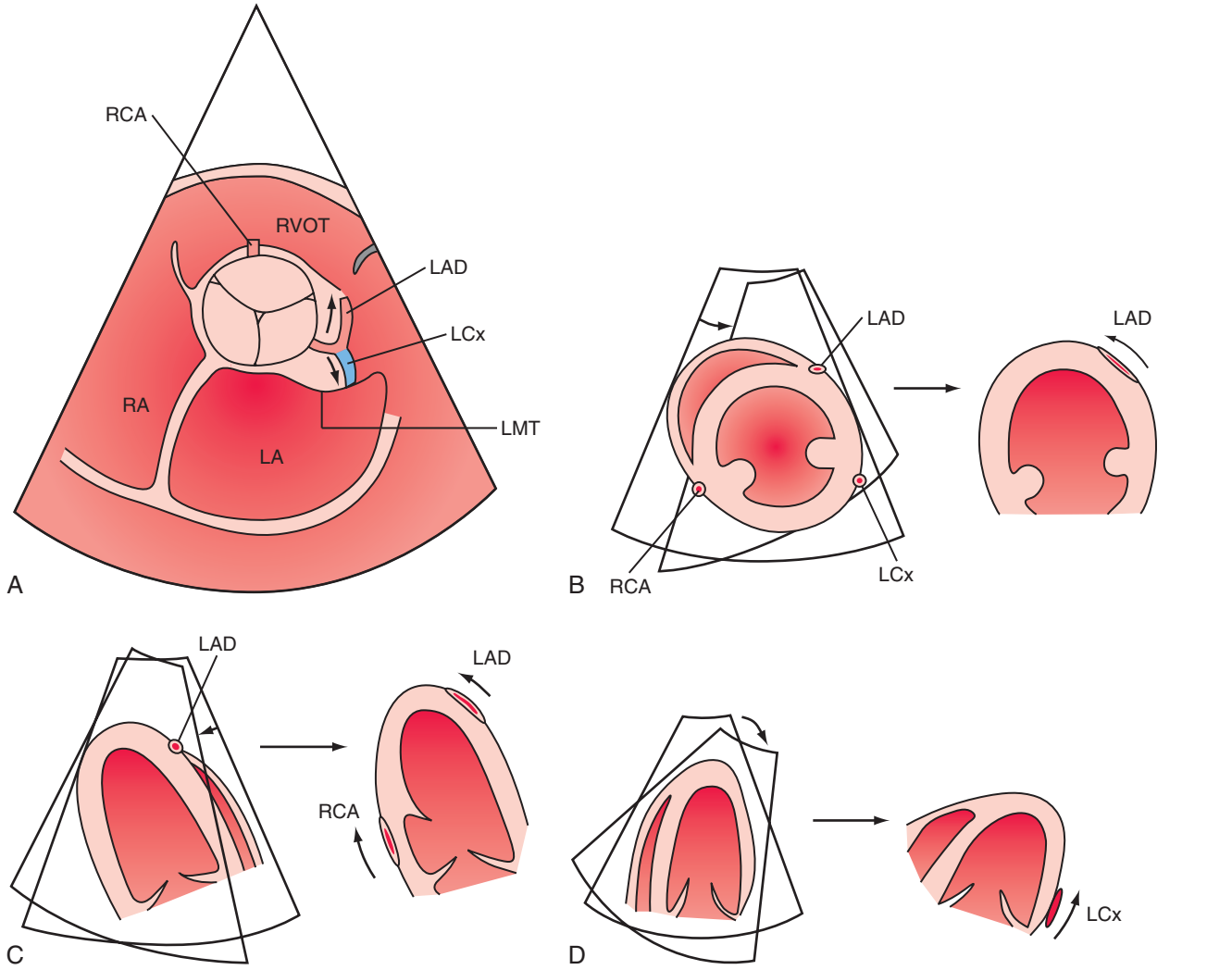



**Figure 17-2 Schematic illustrations of coronary flow detection by transthoracic Doppler echocardiography. A,** Proximal portion of left and right coronary arteries in short-axis view at the level of coronary sinus. The left main trunk (*LMT*) originates from the left coronary sinus, and the right coronary artery (*RCA*) originates from the right coronary sinus. **B,** Position of three coronary arteries in LV short-axis view. Cross-sectional coronary arteries can be observed by color Doppler. Left anterior descending artery (*LAD*) is positioned at anterior interventricular sulcus. LAD signal can be seen longer by counterclockwise rotation. Posterior descending artery (*RCA*) is seen at the position of posterior interventricular sulcus. Left circumflex artery (*LCx*) is seen in a varied position but generally can be found at lateral wall of the LV (3-o'clock to 5-o'clock position). **C,** Detection of distal portion of LAD artery by apical view. Posterior descending artery is visualized in posterior interventricular sulcus. In apical long-axis view, cross-sectional LAD flow can be found. The flow signal becomes longer by adjusting the transducer to look at the interventricular sulcus (clockwise rotation). **D,** Detection of LCx by apical view. The LCx is normally distinguished as a color flow signal running along the basal lateral wall in the modified four-chamber view. *RVOT*, Right ventricular outflow tract.

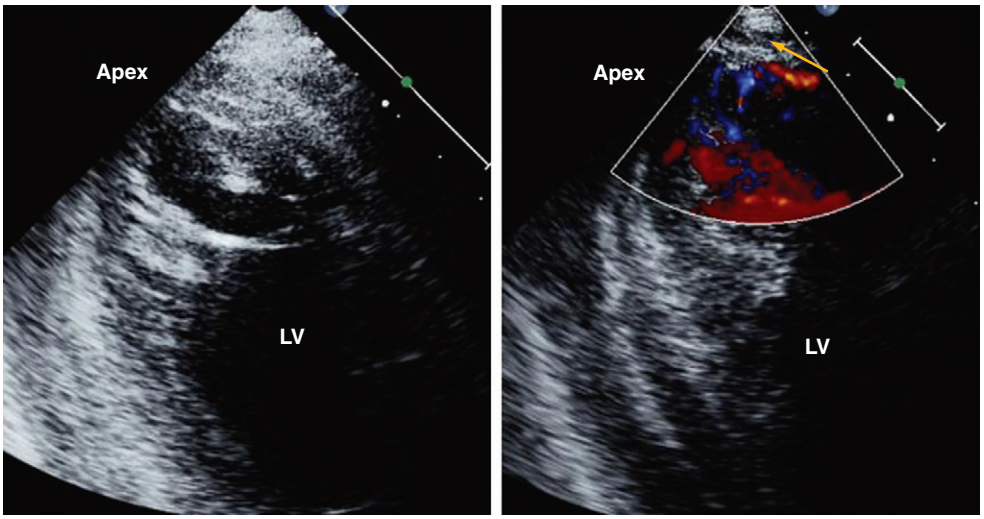



**Figure 17-3 Detection of the proximal portion of left and right coronary arteries (short-axis view at the level of coronary sinus).** The left main coronary artery (*LMT*) originates from the left coronary sinus, and the right coronary artery (*RCA*) originates from the right coronary sinus (*left* panel). Coronary flow signal in the LMT is observed by color Doppler (*right* panel). *Ao*, Aorta; *RVOT*, right ventricular outflow tract.

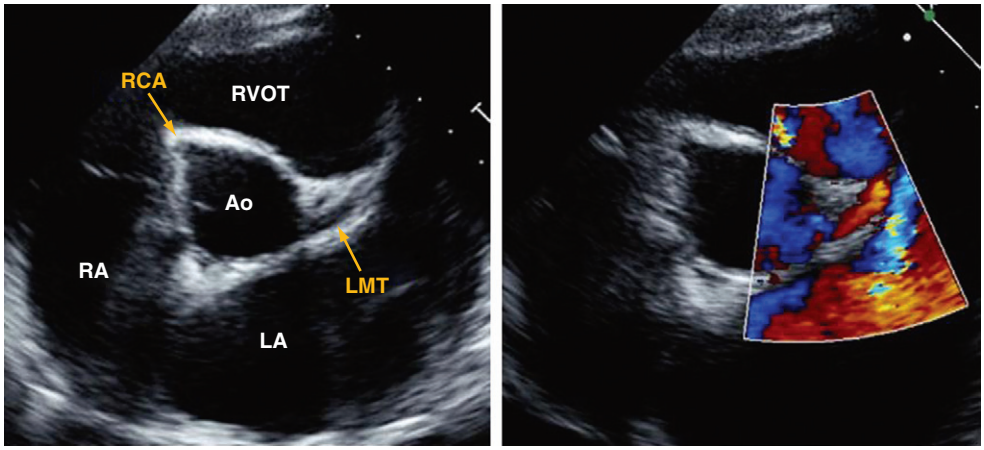



**Figure 17-4 Distal portion of the left anterior descending artery by color Doppler echocardiography.** In modified apical long-axis view, left anterior descending artery flow signal appears as *red* color signal in diastole.

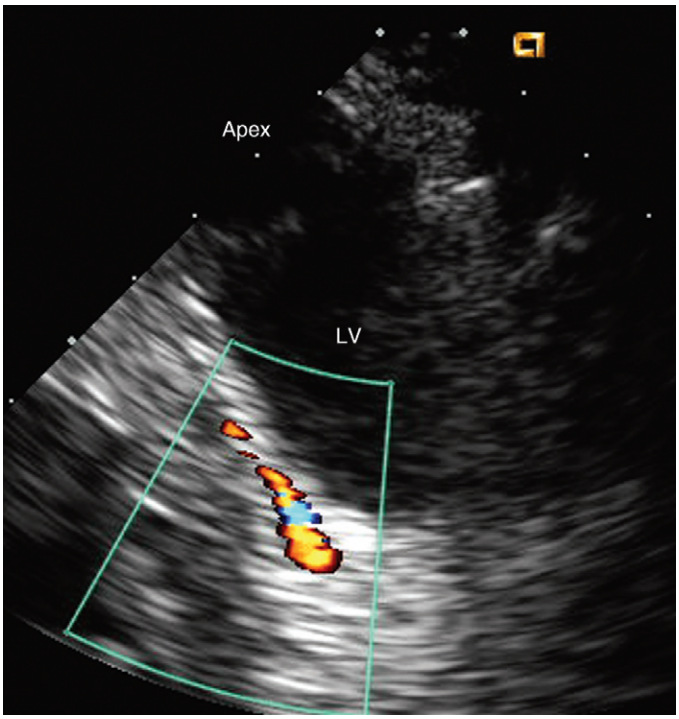



**Figure 17-5** Right coronary artery (posterior descending artery) by color Doppler echocardiography. In modified two-chamber view, posterior descending artery appears as *red* color signal in diastole.

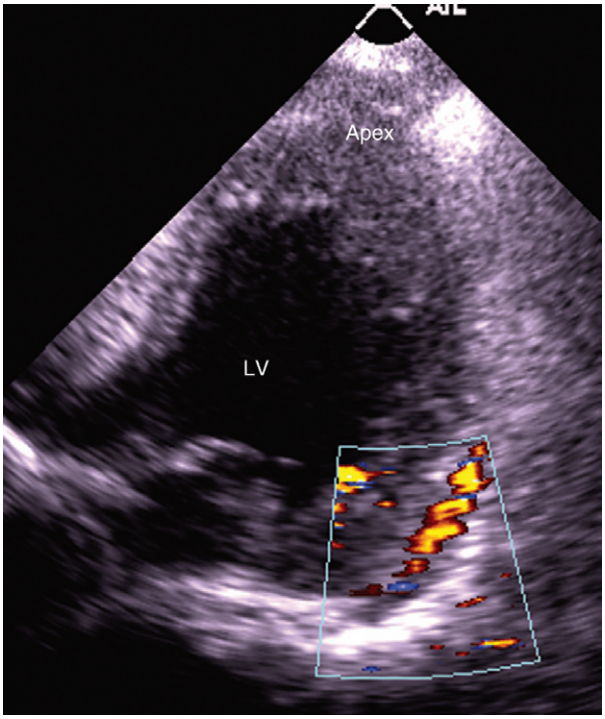



**Figure 17-6** Left circumflex artery by color Doppler echocardiography. Left circumflex artery flow signal is seen at the epicardial side in the lateral wall in modified four-chamber view.

Doppler TTE is derived from changes in the velocity of coronary blood flow, which has been shown to correlate with absolute CFR.

## Clinical Applications

### CORONARY FLOW VELOCITY RESERVE MEASUREMENT

CFR is expressed as a ratio of maximum flow to resting flow (Fig. 17-8). With a normal coronary artery, a vasodilatory stimulus results in an approximately fourfold increase in flow rate compared to baseline. With progressive coronary stenosis, baseline flow remains normal until the coronary artery is narrowed by 80% to 85% diameter stenosis. However, CFR begins to decrease at 40% to 50% diameter stenosis.[17] CFR decreases to two times baseline at approximately 75% diameter stenosis, which indicates myocardial ischemia.

Coronary flow velocity reserve can be alternatively assessed as the ratio of hyperemic to basal coronary flow velocity after drug-induced coronary vasodilatation. Measurements of coronary flow velocity reserve by Doppler TTE have already been established as feasible and accurate.[3,5,6]

After recording baseline spectral Doppler signals in the distal portion of the LAD artery, administer the vasodilator, either adenosine 140 mcg/kg/min as an intravenous infusion for about 1 minute or dipyridamole 0.56 mg/kg intravenously for about 4 minutes, to achieve maximum flow. Then spectral Doppler signals are recorded during hyperemic conditions

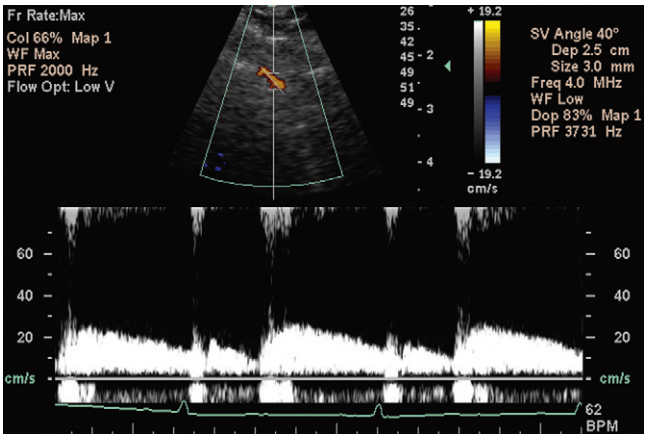



**Figure 17-7 Coronary flow velocity profile in normal subject.** Coronary flow velocity profile is characterized by biphasic flow pattern with small systolic and large diastolic components.

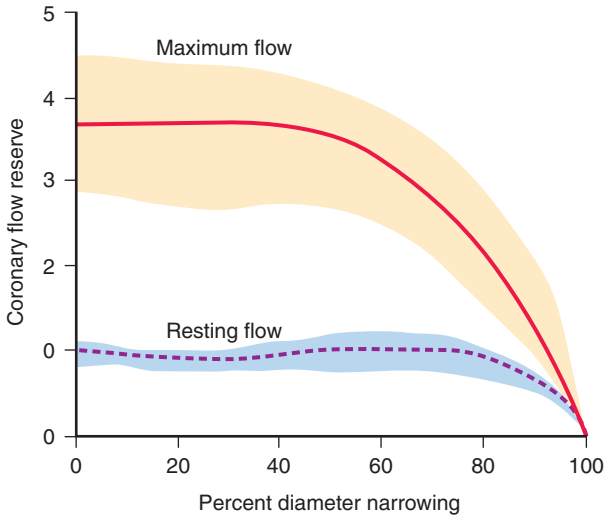



**Figure 17-8 Coronary flow reserve (CFR) and percent diameter stenosis.** With progressive coronary stenosis, baseline flow remains normal until the coronary artery is narrowed by 80% to 85% diameter stenosis. However, CFR begins to decrease at 40% to 50% diameter stenosis for a vasodilatory stimulus, increasing flow normally to four times baseline. CFR decreases to two times baseline at approximately 75% diameter stenosis. *(From Gould KL, Lipscomb K: Effects of coronary stenoses on coronary flow reserve and resistance.* Am J Cardiol *34:48-55, 1974.)*

(Fig. 17-9) with measurement of the mean diastolic velocity and peak diastolic velocity of each flow spectrum. Coronary flow velocity reserve by the transthoracic-Doppler technique is measured from only diastolic mean velocities and not mean velocities throughout the entire cardiac cycle because, in some cases, cardiac motion makes it difficult to obtain a complete Doppler spectral envelope throughout the cardiac cycle. However, previous studies have reported that the ratio of hyperemic to basal mean diastolic velocity and peak diastolic velocity was useful in the evaluation of functional coronary stenosis. Coronary flow velocity reserve is defined as the ratio of hyperemic to basal peak diastolic coronary flow velocity or the ratio of hyperemic to basal mean diastolic coronary flow velocity. Adenosine starts to act generally in 30 seconds, and the coronary flow velocity

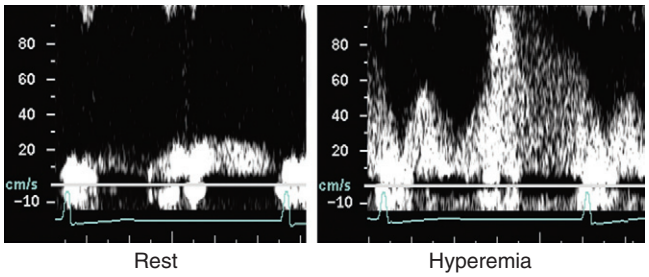



**Figure 17-9 Coronary flow velocity reserve measurement by pulsed-Doppler echocardiography in patient with a normal coronary artery.** Both systolic and diastolic flow velocity increase during hyperemia.

comes to maximum in 1 minute. Dipyridamole starts to act in 4 to 6 minutes and has a prolonged duration of action (about 30 minutes after administration). The short-acting effect is an advantage of adenosine. Although both vasodilators can cause flushing, headache, hypotension, or bradycardia, the adverse effects of adenosine are alleviated immediately after the infusion is finished.

In the clinical setting, some factors that are related to coronary risk factors have been known to affect CFR. Passive smoking has been reported to reduce CFR in healthy nonsmokers, not in active smokers.[18] Another study demonstrated that CFR was significantly higher in nonsmokers than in smokers, and interestingly, oral antioxidant vitamin C increased CFR in nonsmokers but not in smokers.[19] Patients with hypertension showed lower CFR than did normotensive controls[20]; CFR is reduced in diabetic patients, especially in patients with retinopathy[21,22]; and CFR decreased after a single high-fat meal in young healthy men.[23] Because of the noninvasive nature of transthoracic Doppler, it can be used for serial evaluation of drug effects on coronary microcirculation.[24-27] CFR is also reduced in metabolic syndrome[28] and nonalcoholic fatty liver disease.[29] Another study showed that in premenopausal women, CFR varies during the menstrual cycle, and in postmenopausal women, CFR increases after acute estrogen replacement.[30] Noninvasive CFR is expected to contribute to the evaluation of coronary microvascular function in various clinical situation other than ischemic heart disease, such as cardiomyopathy or heart failure.[31] Several papers have reported its usefulness in the assessment of cardiac allograft vasculopathy in patients after heart transplantation.[32,33]

## NONINVASIVE DIAGNOSIS OF CORONARY STENOSIS

### *Coronary Flow Velocity Reserve Measurement Approach*

Coronary flow velocity reserve defined as a mean diastolic velocity increase with hyperemia less than 2 had a sensitivity of 91% to 92% and a specificity of 75% to 86% for the presence of significant LAD artery stenosis.[34,35] Compared with thallium-201 single photon emission computed tomography (SPECT), a mean CFR derived from transthoracic Doppler greater than or equal to 2 predicted reversible perfusion defects, with a sensitivity and specificity of 92% and 90%, respectively.[36] CFR improves after coronary stenting,[37] and a CFR less than 2 had high sensitivity (91%) and specificity (95%) in the diagnosis of in-stent restenosis after coronary intervention.[38] Another paper

similarly reported that CFR less than 2 predicted restenosis determined by thallium-201 SPECT, with a sensitivity of 94% and a specificity of 100%.[39] Furthermore, Voci and colleagues[40] reported that a CFR less than 1, which may reflect coronary steal phenomenon, could discriminate high-risk patients with severe stenosis from patients with nonsevere stenosis. A CFR of 2 or less can be applied to the prediction of the outcome in patients with intermediate coronary stenosis. In the population of medically treated patients with intermediate LAD stenosis (51% to 75% diameter), 30-month event-free survival was higher in patients with normal CFR and lower in patients with decreased CFR (86% vs. 30%).[41]

For coronary stenosis in the right coronary territory, coronary flow velocity reserve measured in the posterior descending coronary artery is useful. Detection of the posterior descending artery is more difficult than that of the LAD artery, but the use of an intravenous contrast injection improves Doppler signal recording.[15] Using the cutoff value of 2 for coronary flow velocity reserve in the RCA, the sensitivity and specificity for detection of significant stenosis were 84% to 91% and 83% to 91%, respectively.[6,15,35] Coronary flow velocity reserve less than 2 in the LCx artery has been reported to have a sensitivity of 92% and specificity of 96% for reversible perfusion defect detected by SPECT.[16]

A Japanese group has tested the feasibility and usefulness of CFR measurements in the three major coronary arteries as a screening examination. They found that the noninvasive technique is a promising tool for the detection of coronary stenosis in patients with chest pain[42] and for the detection of restenosis after coronary intervention.[43] Although each coronary risk factor influences the result of coronary flow velocity reserve, a cutoff value less than 2 was still adequate in terms of the diagnosis of significant coronary stenosis. A cutoff value less than 2 for CFR had a sensitivity of 90%, a specificity of 93%, a positive predictive value of 77%, and a negative predictive value of 97% for the presence of significant coronary stenosis in a population that included patients with various coronary risk factors.[44]

### *Phasic Flow Characteristics and Coronary Stenosis*

Resting coronary flow pattern is characterized by a diastolic dominant biphasic flow. In severe coronary stenosis, diastolic flow decreases, and hence, diastolic to systolic flow velocity ratio decreases at rest.[45] Cutoff points of 1.6 for the ratio of peak diastolic to systolic velocity and 1.5 for mean velocities have high sensitivities and specificities in the detection of severe coronary stenosis (greater than 85%)[46] and of myocardial ischemia compared to thallium-201 SPECT.[47] The diastolic to systolic velocity ratio can be measured in the emergency setting as a simple screening of critical coronary stenosis.[48] Okura and colleagues[49] have reported that these ratio measurements were useful in the differentiation of the ischemic cardiomyopathy from the nonischemic dilated cardiomyopathy. In their study population, a peak or mean ratio less than 1.8 had a sensitivity of 77% and a specificity of 77% for detecting the presence of severe LAD.

## *Direct Measurements of the Coronary Flow Velocity in the Stenotic Site*

### Detection of Proximal Left Coronary Artery Stenosis

In the stenotic site of the coronary artery, color Doppler signal appears as "aliasing" or "mosaic flow." Although transesophageal echocardiography has an advantage in the assessment of left main coronary artery stenosis, mosaic flow and high velocity in the left main trunk can be observed by using transthoracic Doppler echocardiography. Significant left main stenosis can be diagnosed by a mosaic flow and/or peak diastolic velocity of at least 1.5 m/s (sensitivity of 85%, positive predictive value 82.5%).[50] In a similar study of a population with unstable angina, a velocity cutoff value of 47.5 cm/s or greater predicted significant coronary stenosis of the proximal left anterior descending or left main coronary artery with a sensitivity of 88% and specificity of 97%.[51] Okayama and co-workers[52] measured coronary flow velocity in the proximal and distal sites of the left coronary artery to calculate the distal averaged diastolic peak velocity to proximal averaged diastolic peak velocity ratio. A ratio less than or equal to 0.5 predicted significant coronary stenosis with a sensitivity of 91% and a specificity of 72% in their study. However, low success rate in the visualization of the left main coronary artery is a limitation of this technique.

### Prestenotic to Stenotic Flow Velocity Ratio

The location of the coronary artery stenosis can be identified based on "aliasing" of color Doppler. In the diagnosis of significant restenosis (greater than 50%) after coronary intervention in the LAD artery, a prestenotic-to-stenotic mean diastolic flow velocity ratio less than 0.45 had a sensitivity of 86% and a specificity of 93%.[53] Flow velocity measurements were possible for in-stent stenosis with high sensitivity and specificity as well.[54] Another study has investigated three major coronary vessels by color Doppler and pulsed-Doppler echocardiography. Overall sensitivity and specificity was 82% and 92%, respectively, for the detection of greater than 50% stenosis. The sensitivity and specificity were 73% and 92%, respectively, for the LAD artery, 63% and 96% for the RCA, and 38% and 99% for the LCx artery.[55]

### *Detection of Total Occlusion by Retrograde Coronary Flow*

Following occlusion of a major epicardial coronary artery, blood flow to the previously supplied myocardium must arrive via coronary collateral vessels. The retrograde blood flow velocity distal to a totally occluded coronary vessel represents collateral flow to the occluded region. Retrograde LAD flow by Doppler TTE had a sensitivity of 93% and a specificity of 100% for the detection of total LAD occlusion[56] (Fig. 17-10). Retrograde flow in the LAD or septal artery had a sensitivity of 96% and a specificity of 100% for the detection of total LAD occlusion.[57] Retrograde coronary flow detection is also useful in the RCA. Detection of reverse flow in the distal RCA and the inferior septal branches had a sensitivity of 100% and a specificity of 97.8% for identification of occluded RCA (Fig. 17-11).[58] Boshchenko and colleagues[59] have tested the diagnostic usefulness of detecting the total occlusion of coronary arteries by observing the coronary flow direction in the epicardial and intramyocardial collaterals in the three major coronary arteries. They found that the Doppler TTE was a sensitive and highly specific method for diagnosis of LAD and RCA occlusions. Transthoracic Doppler echocardiography can also evaluate intramyocardial collateral flow in patients with total occlusion of epicardial arteries. Pizzuto and co-workers[60] successfully measured collateral function by recording coronary flow velocity during adenosine stress (collateral flow reserve).

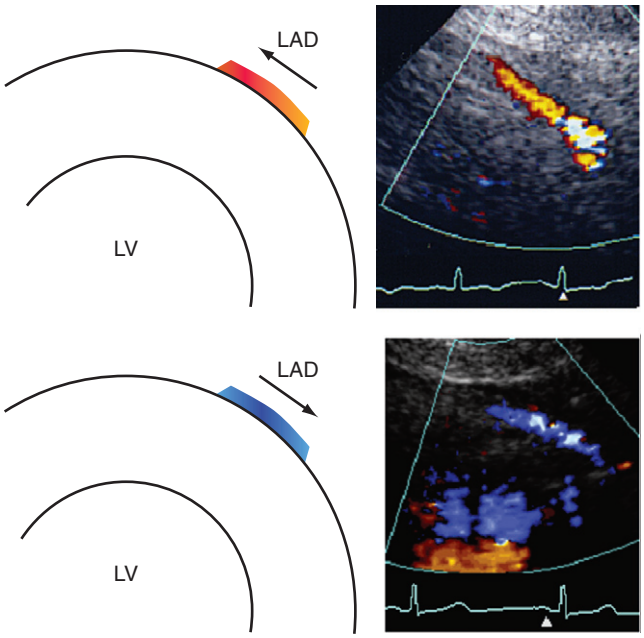



**Figure 17-10 Antegrade and retrograde flow signals.** Normal left anterior descending artery (*LAD*) flow (*upper panel*); retrograde left anterior descending artery flow in patient with total LAD occlusion (*lower panel*). In total LAD occlusion, retrograde coronary flow signal, which reflects the collateral flow, is observed as *blue* color. *(From Watanabe N, Akasaka T, Yamaura Y, et al: Noninvasive detection of total occlusion of the left anterior descending coronary artery with transthoracic Doppler echocardiography.* J Am Coll Cardiol *38:1328-1332, 2001.)*

### *Combination with Stress Echocardiography*

Coronary flow velocity reserve measurements are expected to contribute to the noninvasive diagnosis of coronary heart disease in combination with conventional dobutamine stress echocardiography (DSE). Transthoracic Doppler measurements of CFR with dobutamine have been proven to be comparable to CFR with adenosine in patients with a wide range of LAD diseases.[61] Coronary flow velocity reserve measurements are feasible during dobutamine stress[62] or before dobutamine stress[63] and provide useful additional information in the clinical diagnosis of coronary stenosis. Takeuchi and colleagues[64] have compared the diagnostic accuracy of the contrast-enhanced DSE and CFR measurements during the DSE in the diagnosis of LAD stenosis. They concluded that the diagnostic accuracy of CFR measurement was equivalent to wall motion assessment in the detection of LAD stenosis. Several studies have shown that CFR measurements can provide additional diagnostic or prognostic information over regional wall motion diagnosis by stress echocardiography. Rigo and co-workers[65] assessed the prognostic value of CFR in patients with known or suspected coronary artery disease and negative stress echo. In their study, CFR less than or equal to 1.92 was the best predictor of future events (area under the curve = 0.80, sensitivity = 77%, specificity = 85%), and the 3-year event-free survival was lower in patients with reduced CFR compared with normals (98% vs. 64%, P less than .0001).

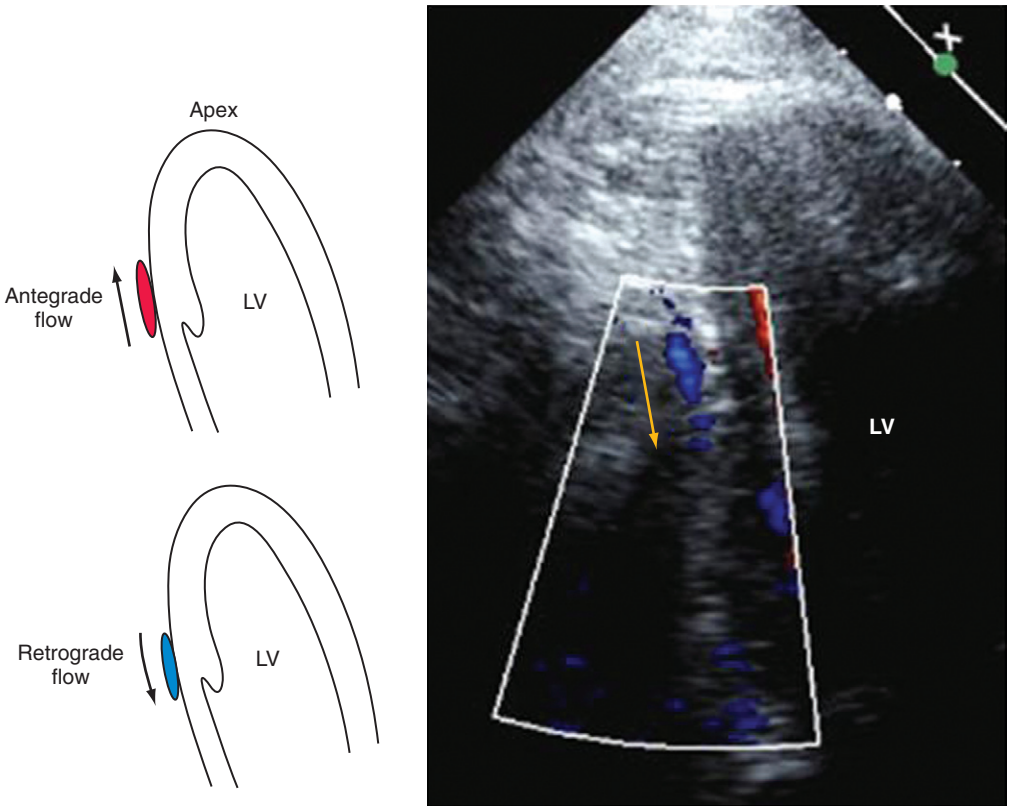



**Figure 17-11 Retrograde coronary flow signal in the distal right coronary artery (posterior descending artery).** Coronary flow signal is observed as *blue* color in patient with total RCA occlusion.

## CORONARY FLOW MEASUREMENTS IN ACUTE CORONARY SYNDROME

Suboptimal coronary reperfusion with thrombolysis in myocardial infarction (TIMI) grade 2 coronary blood flow in acute myocardial infarction adversely affects patient prognosis and requires additional procedures, such as thrombolysis or percutaneous coronary intervention. Doppler TTE enables a rapid noninvasive differentiation of TIMI 3 from TIMI 2 coronary reperfusion in patients with acute myocardial infarction in the acute phase before emergent coronary intervention. The diagnosis of TIMI 3 flow based on a diastolic peak distal LAD flow velocity of at least 25 cm/s by Doppler TTE had a sensitivity, specificity, and accuracy of 77%, 94%, and 89%, respectively.[66] Voci and colleagues[67] have proposed the "open perforator hypothesis" that presence of the perforator signals in the anterior-apical wall by color Doppler TTE reflects adequate myocardial reperfusion, and hence, perforators are early noninvasive markers of myocardial viability. In the coronary care unit, noninvasive transthoracic detection of coronary flow patterns is useful in the direct monitoring of coronary flow augmentation during intraaortic balloon pumping.[68] Evaluation of coronary flow by Doppler TTE gives important physiologic information in addition to the conventional diagnostic examination in acute coronary syndrome.

## CORONARY FLOW IN THE NO-REFLOW PHENOMENON

In no-reflow after coronary revascularization for acute myocardial infarction, coronary flow velocity shows a characteristic to-and-fro pattern, which consists of systolic reversal and rapid diastolic deceleration (Fig. 17-12). This low systolic flow velocity and rapid deceleration time of diastolic coronary blood flow spectrum immediately after primary coronary intervention reflects a greater degree of microvascular damage in the risk area, and evaluation of coronary flow profile after revascularization is useful in predicting recovery of regional left ventricular (LV) function. Optimal cutoff values to predict viable myocardium were 6.5 cm/s for average systolic velocity and 600 ms for diastolic deceleration time (sensitivity, 79% and 86%, respectively; specificity, 89% and 89%, respectively).[69,70] Doppler TTE allows recording of the temporal sequence of coronary flow pattern after coronary intervention. Serial evaluation of the coronary flow velocity profile showed that persistence of abnormal coronary flow pattern can predict LV remodeling after myocardial infarction.[71,72] Clinical studies using transthoracic Doppler echocardiography have proven that shorter diastolic deceleration time and/or lower CFR after percutaneous coronary intervention for the acute myocardial infarction can predict worse outcome of the LV function, myocardial damage, or cardiac events.[73-77]

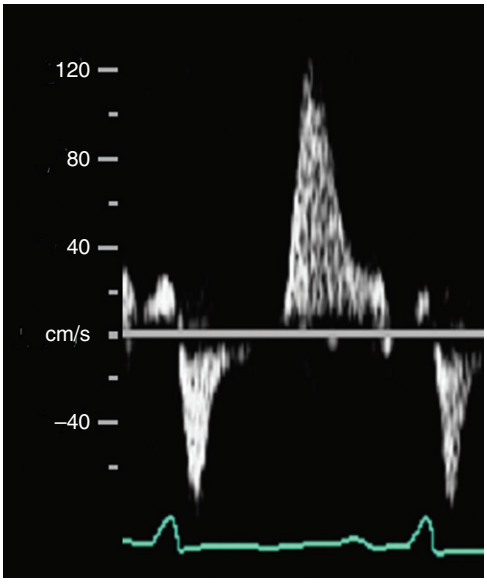



**Figure 17-12 To-and-fro pattern of coronary flow profile in no-reflow phenomenon.** Coronary flow velocity pattern in no-reflow is characterized by a systolic reversal flow followed by a diastolic flow with rapid deceleration. Short deceleration time is a predictor of long-term prognosis.

## IMPAIRED CORONARY CIRCULATION IN HYPERTROPHIC CARDIOMYOPATHY

CFR is reduced in hypertrophic cardiomyopathy (HCM).[78] Several reports have shown the unique coronary flow pattern in HCM, which is characterized by systolic flow reversal and high-velocity diastolic flow. Coronary flow abnormalities in HCM are related to myocardial thickness rather than the degree of outflow obstruction.[78-81] This characteristic is seen in intramyocardial small coronary arteries as well as in epicardial coronary arteries.[82] It has been reported that this unique to-and-fro pattern in the intramyocardial arteries is related to the myocardial ischemia and chest pain in HCM.[83] Serial measurements of the CFR in patients with HCM found that the administration of cibenzoline significantly improved CFR ($2.0 \pm 0.8$ to $3.0 \pm 1.0$), and reduction in the LV outflow tract pressure gradient ($55 \pm 30$ to $23 \pm 18$ mm Hg).[84] Noninvasive Doppler examination of the coronary circulation might contribute to further research in HCM.

## CORONARY FLOW RESERVE IN SYNDROME X AND CHEST PAIN SYNDROME

Several clinical studies have shown the microvascular disturbance in patients with syndrome X. Galiuto and associates[85] have reported that CFR in the LAD was significantly decreased in patients with syndrome X and even more in those with angina pectoris and ST-segment depression during adenosine testing. Lanza and colleagues[86] have evaluated CFR by transthoracic Doppler echocardiography in patients with syndrome X. They compared the data with myocardial perfusion defects detected during dobutamine stress test by cardiovascular magnetic resonance imaging (MRI). They proved the existence of the coronary microvascular dysfunction by reduced CFR that correlated with perfusion defects by MRI. CFR has also been evaluated in chest pain syndrome. Decreased CFR on LAD was associated with increased risk in chest pain syndrome and a normal result of stress echocardiography[87] or normal coronary angiography.[88]

# Alternative Approaches

There are advantages and disadvantages for each imaging modality in the assessment of coronary flow. The greatest advantage of Doppler TTE coronary imaging is that this examination is totally noninvasive and can be easily and repetitively

**TABLE 17-1 Alternative Approaches for Evaluation of the Coronary Arteries**

| | *Advantages* | *Disadvantages* |
|---|---|---|
| X-ray angiography | Full coverage of the coronary arteries; high resolution | Invasive; radiation exposure, needs nephrotoxic contrast agents |
| Transthoracic Doppler echocardiography | Noninvasive; no radiation exposure; portable; cost-effective; physiologic assessment of coronary stenosis (CFR measurement) | Limited sites of coronary detection; low success rate in RCA and LCx (need contrast agent); need vasodilator infusion in measuring CFR |
| Multislice CT | Noninvasive; relatively high resolution; anatomic assessment of coronary stenosis; tissue characterization; plaque volume measurements | Radiation exposure, motion artifacts; not available at calcified lesion; limited accuracy in the diagnosis of coronary stenosis; need a beta-blocker before examination; expensive; nephrotoxic contrast agents; not available in the heavily calcified lesion |
| MRI | Noninvasive; no radiation exposure; anatomic assessment of coronary stenosis; soft-tissue characterization; CFR measurement | Expensive; time consuming; slower acquisition, motion artifacts; interpretable segments are limited by the size of the artery; limited accuracy in the diagnosis of coronary stenosis |

*CFR*, Coronary flow reserve; *CT*, computed tomography; *LCx*, left circumflex artery; *MRI*, magnetic resonance imaging; *RCA*, right coronary artery.

performed at the bedside. The pulsed-Doppler technique is a simple and reliable method for detection of coronary flow profiles. Advantages and disadvantages of each coronary imaging examination are summarized in Table 17-1. An interesting clinical study by Pizzuto and colleagues[89] indicates that CFR can improve the diagnostic accuracy of computed tomographic coronary angiography to detect significant LAD stenosis.[89] In this era of noninvasive cardiac imaging, a combination of imaging modalities would be expected to provide a new standard. Assessment of coronary flow by Doppler echocardiography is a promising tool for an additional examination that can improve the diagnostic approach to all types of cardiac diseases.

## KEY POINTS

- For evaluation of coronary blood flow by Doppler echocardiography, it is important to choose a transducer with adequate frequency and set the color Doppler velocity range around ±20 cm/s.
- The coronary flow signal is mainly observed during diastole.
- The normal coronary flow pattern is characterized by diastolic dominant biphasic flow.
- CFR can be measured by adenosine or dipyridamole intravenous infusion.
- CFR decreases (ratio of hyperemia to rest less than 2) when significant coronary stenosis is present.
- In acute myocardial infarction, a coronary flow peak velocity < 25 cm/s predicts poor reperfusion with ≤ TIMI flow 2.
- CFR reflects intramyocardial coronary microcirculation. CFR is decreased when microvascular dysfunction is present.

## REFERENCES


1. Voci P, Testa G, Plaustro G: Imaging of the distal left anterior descending coronary artery by transthoracic color-Doppler echocardiography. *Am J Cardiol* 81:74G-78G, 1998.
2. Tries HP, Lambertz H, Lethen H: Transthoracic echocardiographic visualization of coronary artery blood flow and assessment of coronary flow reserve in the right coronary artery: a first report of 3 patients. *J Am Soc Echocardiogr* 15:739-742, 2002.
3. Hozumi T, Yoshida K, Akasaka T, et al: Noninvasive assessment of coronary flow velocity and coronary flow velocity reserve in the left anterior descending coronary artery by Doppler echocardiography: comparison with invasive technique. *J Am Coll Cardiol* 32:1251-1259, 1998.
4. Voudris V, Athanassopoulos G, Vassilikos V, et al: Usefulness of flow reserve in the left internal mammary artery to determine graft patency to the left anterior descending coronary artery. *Am J Cardiol* 83:1157-1163, 1999.
5. Caiati C, Montaldo C, Zedda N, et al: Validation of a new noninvasive method (contrast-enhanced transthoracic second harmonic echo Doppler) for the evaluation of coronary flow reserve: comparison with intracoronary Doppler flow wire. *J Am Coll Cardiol* 34:1193-1200, 1999.
6. Ueno Y, Nakamura Y, Takashima H, et al: Noninvasive assessment of coronary flow velocity and coronary flow velocity reserve in the right coronary artery by transthoracic Doppler echocardiography: comparison with intracoronary Doppler guidewire. *J Am Soc Echocardiogr* 15:1074-1079, 2002.
7. Lethen H, Flachskampf FA, Schneider R, et al: Frequency of deep vein thrombosis in patients with patent foramen ovale and ischemic stroke or transient ischemic attack. *Am J Cardiol* 80:1066-1069, 1997.
8. Meimoun P, Tribouilloy C: Non-invasive assessment of coronary flow and coronary flow reserve by transthoracic Doppler echocardiography: a magic tool for the real world. *Eur J Echocardiogr* 9:449-457, 2008.
9. Rigo F, Murer B, Ossena G, Favaretto E: Transthoracic echocardiographic imaging of coronary arteries: tips, traps, and pitfalls. *Cardiovasc Ultrasound* 6:7, 2008.
10. Takeuchi M, Lodato JA, Furlong KT, et al: Feasibility of measuring coronary flow velocity and reserve in the left anterior descending coronary artery by transthoracic Doppler echocardiography in a relatively obese American population. *Echocardiography* 22:225-232, 2005.
11. Caiati C, Montaldo C, Zedda N, Bina A, Iliceto S: New noninvasive method for coronary flow reserve assessment: contrast-enhanced transthoracic second harmonic echo Doppler [see comments]. *Circulation* 99:771-778, 1999.
12. Lambertz H, Tries HP, Stein T, Lethen H: Noninvasive assessment of coronary flow reserve with transthoracic signal-enhanced Doppler echocardiography. *J Am Soc Echocardiogr* 12: 186-195, 1999.
13. Bartel T, Muller S, Baumgart D, et al: Improved high-frequency transthoracic flow velocity measurement in the left anterior descending coronary artery after intravenous peripheral injection of Levovist. *J Am Soc Echocardiogr* 12: 252-256, 1999.
14. Caiati C, Zedda N, Montaldo C, Montisci R, Iliceto S: Contrast-enhanced transthoracic second harmonic echo Doppler with adenosine: a noninvasive, rapid and effective method for coronary flow reserve assessment [see comments]. *J Am Coll Cardiol* 34:122-130, 1999.
15. Watanabe H, Hozumi T, Hirata K, et al: Noninvasive coronary flow velocity reserve measurement in the posterior descending coronary artery for detecting coronary stenosis in the right coronary artery using contrast-enhanced transthoracic Doppler echocardiography. *Echocardiography* 21:225-233, 2004.
16. Fujimoto K, Watanabe H, Hozumi T, et al: New noninvasive diagnosis of myocardial ischemia of the left circumflex coronary artery using coronary flow reserve measurement by transthoracic Doppler echocardiography: comparison with

thallium-201 single photon emission computed tomography. *J Cardiol* 43:109-116, 2004.
17. Gould KL, Lipscomb K: Effects of coronary stenoses on coronary flow reserve and resistance. *Am J Cardiol* 34:48-55, 1974.
18. Otsuka R, Watanabe H, Hirata K, et al: Acute effects of passive smoking on the coronary circulation in healthy young adults. *Jama* 286:436-441, 2001.
19. Teramoto K, Daimon M, Hasegawa R, et al: Acute effect of oral vitamin C on coronary circulation in young healthy smokers. *Am Heart J* 148:300-305, 2004.
20. Bartel T, Yang Y, Muller S, et al: Noninvasive assessment of microvascular function in arterial hypertension by transthoracic Doppler harmonic echocardiography. *J Am Coll Cardiol* 39:2012-2018, 2002.
21. Nahser PJ, Jr, Brown RE, Oskarsson H, Winniford MD, Rossen JD: Maximal coronary flow reserve and metabolic coronary vasodilation in patients with diabetes mellitus. *Circulation* 91:635-640, 1995.
22. Akasaka T, Yoshida K, Hozumi T, et al: Retinopathy identifies marked restriction of coronary flow reserve in patients with diabetes mellitus. *J Am Coll Cardiol* 30:935-941, 1997.
23. Hozumi T, Eisenberg M, Sugioka K, et al: Change in coronary flow reserve on transthoracic Doppler echocardiography after a single high-fat meal in young healthy men. *Ann Intern Med* 136:523-528, 2002.
24. Kawata T, Daimon M, Hasegawa R, et al: Effect on coronary flow velocity reserve in patients with type 2 diabetes mellitus: comparison between angiotensin-converting enzyme inhibitor and angiotensin II type 1 receptor antagonist. *Am Heart J* 151:798 e9-e15, 2006.
25. Kawata T, Daimon M, Hasegawa R, et al: Effect of angiotensin-converting enzyme inhibitor on serum asymmetric dimethylarginine and coronary circulation in patients with type 2 diabetes mellitus. *Int J Cardiol* 132:286-288, 2009.
26. Zhang X, Yang Y, Li Z, et al: Noninvasive evaluation of coronary flow velocity reserve in homozygous familial hypercholesterolemia by transthoracic Doppler echocardiography. *Echocardiography* 27:985-989, 2010.
27. Kamezaki F, Tasaki H, Yamashita K, et al: Angiotensin receptor blocker improves coronary flow velocity reserve in hypertensive patients: comparison with calcium channel blocker. *Hypertens Res* 30:699-706, 2007.
28. Pirat B, Bozbas H, Simsek V, et al: Impaired coronary flow reserve in patients with metabolic syndrome. *Atherosclerosis* 201:112-116, 2008.
29. Yilmaz Y, Kurt R, Yonal O, et al: Coronary flow reserve is impaired in patients with nonalcoholic fatty liver disease: association with liver fibrosis. *Atherosclerosis* 211:182-186, 2010.
30. Hirata K, Shimada K, Watanabe H, et al: Modulation of coronary flow velocity reserve by gender, menstrual cycle and hormone replacement therapy. *J Am Coll Cardiol* 38:1879-1884, 2001.
31. Neishi Y, Akasaka T, Tsukiji M, et al: Reduced coronary flow reserve in patients with congestive heart failure assessed by transthoracic Doppler echocardiography. *J Am Soc Echocardiogr* 18:15-19, 2005.
32. Osto E, Tona F, Angelini A, et al: Determinants of coronary flow reserve in heart transplantation: a study performed with contrast-enhanced echocardiography. *J Heart Lung Transplant* 28:453-4560, 2009.
33. Tona F, Caforio AL, Montisci R, et al: Coronary flow velocity pattern and coronary flow reserve by contrast-enhanced transthoracic echocardiography predict long-term outcome in heart transplantation. *Circulation* 114:I49-I55, 2006.
34. Hozumi T, Yoshida K, Ogata Y, et al: Noninvasive assessment of significant left anterior descending coronary artery stenosis by coronary flow velocity reserve with transthoracic color Doppler echocardiography. *Circulation* 97:1557-1562, 1998.
35. Takeuchi M, Ogawa K, Wake R, et al: Measurement of coronary flow velocity reserve in the posterior descending coronary artery by contrast-enhanced transthoracic Doppler echocardiography. *J Am Soc Echocardiogr* 17:21-27, 2004.
36. Daimon M, Watanabe H, Yamagishi H, et al: Physiologic assessment of coronary artery stenosis by coronary flow reserve measurements with transthoracic Doppler echocardiography: comparison with exercise thallium-201 single piston emission computed tomography. *J Am Coll Cardiol* 37:1310-1315, 2001.
37. Pizzuto F, Voci P, Mariano E, et al: Assessment of flow velocity reserve by transthoracic Doppler echocardiography and venous adenosine infusion before and after left anterior descending coronary artery stenting. *J Am Coll Cardiol* 38:155-162, 2001.
38. Pizzuto F, Voci P, Mariano E, et al: Noninvasive coronary flow reserve assessed by transthoracic coronary Doppler ultrasound in patients with left anterior descending coronary artery stents. *Am J Cardiol* 91:522-526, 2003.
39. Hirata K, Watanabe H, Otsuka R, et al: Noninvasive diagnosis of restenosis by transthoracic Doppler echocardiography after percutaneous coronary intervention: comparison with exercise Tl-SPECT. *J Am Soc Echocardiogr* 19:165-171, 2006.
40. Voci P, Pizzuto F, Mariano E, et al: Usefulness of coronary flow reserve measured by transthoracic coronary Doppler ultrasound to detect severe left anterior descending coronary artery stenosis. *Am J Cardiol* 92:1320-1324, 2003.
41. Rigo F, Sicari R, Gherardi S, et al: Prognostic value of coronary flow reserve in medically treated patients with left anterior descending coronary disease with stenosis 51% to 75% in diameter. *Am J Cardiol* 100:1527-1531, 2007.
42. Murata E, Hozumi T, Matsumura Y, et al: Coronary flow velocity reserve measurement in three major coronary arteries using transthoracic Doppler echocardiography. *Echocardiography* 23:279-286, 2006.
43. Hyodo E, Hirata K, Hirose M, et al: Detection of restenosis after percutaneous coronary intervention in three major coronary arteries by transthoracic Doppler echocardiography. *J Am Soc Echocardiogr* 23:553-559, 2010.
44. Matsumura Y, Hozumi T, Watanabe H, et al: Cut-off value of coronary flow velocity reserve by transthoracic Doppler echocardiography for diagnosis of significant left anterior descending artery stenosis in patients with coronary risk factors. *Am J Cardiol* 92:1389-1393, 2003.
45. Crowley JJ, Shapiro LM: Noninvasive analysis of coronary artery poststenotic flow characteristics by using transthoracic echocardiography. *J Am Soc Echocardiogr* 11:1-9, 1998.
46. Higashiue S, Watanabe H, Yokoi Y, Takeuchi K, Yoshikawa J: Simple detection of severe coronary stenosis using transthoracic Doppler echocardiography at rest. *Am J Cardiol* 87:1064-1068, 2001.
47. Daimon M, Watanabe H, Yamagishi H, et al: Physiologic assessment of coronary artery stenosis without stress tests: noninvasive analysis of phasic flow characteristics by transthoracic Doppler echocardiography. *J Am Soc Echocardiogr* 18:949-955, 2005.
48. Tani T, Tanabe K, Kitai T, et al: Detection of severe stenosis and total occlusion in the left anterior descending coronary artery with transthoracic Doppler echocardiography in the emergency room. *Echocardiography* 26:15-20, 2009.
49. Okura H, Fuyuki H, Kubo T, et al: Noninvasive diagnosis of ischemic and nonischemic cardiomyopathy using coronary flow velocity measurements of the left anterior descending coronary artery by transthoracic Doppler echocardiography. *J Am Soc Echocardiogr* 19:552-558, 2006.
50. Anjaneyulu A, Raghu K, Chandramukhi S, et al: Evaluation of left main coronary artery stenosis by transthoracic echocardiography. *J Am Soc Echocardiogr* 21:855-860, 2008.
51. Nishimura K, Okayama H, Inoue K, et al: Usefulness of the MOSAIC (measurement of stenosis by aliasing coronary flow) method using transthoracic color Doppler echocardiography in unstable angina patients. *Int J Cardiol* 151: 170-174, 2011.
52. Okayama H, Nishimura K, Saito M, et al: Significance of the distal to proximal coronary flow velocity ratio by transthoracic Doppler echocardiography for diagnosis of proximal left coronary artery stenosis. *J Am Soc Echocardiogr* 21:756-760, 2008.
53. Hozumi T, Yoshida K, Akasaka T, et al: Value of acceleration flow and the prestenotic to stenotic coronary flow velocity ratio by transthoracic color Doppler echocardiography in noninvasive diagnosis of restenosis after percutaneous transluminal coronary angioplasty. *J Am Coll Cardiol* 35:164-168, 2000.
54. Watanabe N, Akasaka T, Yamaura Y, et al: Transthoracic Doppler echocardiography can detect coronary flow signals through the coronary stents—noninvasive direct visualization of in-stent coronary restenosis. *J Echocardiogr* 2:61-67, 2004.
55. Saraste M, Vesalainen RK, Ylitalo A, et al: Transthoracic Doppler echocardiography as a noninvasive tool to assess coronary artery stenoses—a comparison with quantitative coronary angiography. *J Am Soc Echocardiogr* 18:679-685, 2005.
56. Watanabe N, Akasaka T, Yamaura Y, et al: Noninvasive detection of total occlusion of the left anterior descending coronary artery with transthoracic Doppler echocardiography. *J Am Coll Cardiol* 38:1328-1332, 2001.
57. Hirata K, Watanabe H, Hozumi T, et al: Simple detection of occluded coronary artery using retrograde flow in septal branch and left anterior descending coronary artery by transthoracic Doppler echocardiography at rest. *J Am Soc Echocardiogr* 17:108-113, 2004.
58. Otsuka R, Watanabe H, Hirata K, et al: A novel technique to detect total occlusion in the right coronary artery using retrograde flow by transthoracic Doppler echocardiography. *J Am Soc Echocardiogr* 18:704-709, 2005.
59. Boshchenko AA, Vrublevsky AV, Karpov RS: Transthoracic echocardiography in the detection of chronic total coronary artery occlusion. *Eur J Echocardiogr* 10:62-68, 2009.
60. Pizzuto F, Voci P, Puddu PE, et al: Functional assessment of the collateral-dependent circulation in chronic total coronary occlusion using transthoracic Doppler ultrasound and venous adenosine infusion. *Am J Cardiol* 98:197-203, 2006.
61. Meimoun P, Sayah S, Tcheuffa JC, et al: Transthoracic coronary flow velocity reserve

assessment: comparison between adenosine and dobutamine. *J Am Soc Echocardiogr* 19:1220-1228, 2006.
62. Takeuchi M, Miyazaki C, Yoshitani H, et al: Assessment of coronary flow velocity with transthoracic Doppler echocardiography during dobutamine stress echocardiography. *J Am Coll Cardiol* 38:117-123, 2001.
63. Florenciano-Sanchez R, de la Morena-Valenzuela G, Villegas-Garcia M, et al: Noninvasive assessment of coronary flow velocity reserve in left anterior descending artery adds diagnostic value to both clinical variables and dobutamine echocardiography: a study based on clinical practice. *Eur J Echocardiogr* 6:251-259, 2005.
64. Takeuchi M, Miyazaki C, Yoshitani H, et al: Which is the better method in detecting significant left anterior descending coronary artery stenosis during contrast-enhanced dobutamine stress echocardiography: coronary flow velocity reserve or wall-motion assessment? *J Am Soc Echocardiogr* 16:614-621, 2003.
65. Rigo F, Cortigiani L, Pasanisi E, et al: The additional prognostic value of coronary flow reserve on left anterior descending artery in patients with negative stress echo by wall motion criteria. A Transthoracic Vasodilator Stress Echocardiography Study. *Am Heart J* 151:124-130, 2006.
66. Lee S, Otsuji Y, Minagoe S, et al: Noninvasive evaluation of coronary reperfusion by transthoracic Doppler echocardiography in patients with anterior acute myocardial infarction before coronary intervention. *Circulation* 108:2763-2768, 2003.
67. Voci P, Mariano E, Pizzuto F, Puddu PE, Romeo F: Coronary recanalization in anterior myocardial infarction: the open perforator hypothesis. *J Am Coll Cardiol* 40:1205-1213, 2002.
68. Takeuchi M, Nohtomi Y, Yoshitani H, et al: Enhanced coronary flow velocity during intra-aortic balloon pumping assessed by transthoracic Doppler echocardiography. *J Am Coll Cardiol* 43:368-376, 2004.
69. Kawamoto T, Yoshida K, Akasaka T, et al: Can coronary blood flow velocity pattern after primary percutaneous transluminal coronary angioplasty [correction of angiography] predict recovery of regional left ventricular function in patients with acute myocardial infarction? *Circulation* 100:339-345, 1999.
70. Yamamuro A, Akasaka T, Tamita K, et al: Coronary flow velocity pattern immediately after percutaneous coronary intervention as a predictor of complications and in-hospital survival after acute myocardial infarction. *Circulation* 106:3051-3056, 2002.
71. Hozumi T, Kanzaki Y, Ueda Y, et al: Coronary flow velocity analysis during short term follow up after coronary reperfusion: use of transthoracic Doppler echocardiography to predict regional wall motion recovery in patients with acute myocardial infarction. *Heart* 89:1163-1168, 2003.
72. Shintani Y, Ito H, Iwakura K, et al: Usefulness of impairment of coronary microcirculation in predicting left ventricular dilation after acute myocardial infarction. *Am J Cardiol* 93:974-978, 2004.
73. Rigo F, Varga Z, Di Pede F, et al: Early assessment of coronary flow reserve by transthoracic Doppler echocardiography predicts late remodeling in reperfused anterior myocardial infarction. *J Am Soc Echocardiogr* 17:750-755, 2004.
74. Okcular I, Sezer M, Aslanger E, et al: The accuracy of deceleration time of diastolic coronary flow measured by transthoracic echocardiography in predicting long-term left ventricular infarct size and function after reperfused myocardial infarction. *Eur J Echocardiogr* 11:823-828, 2010.
75. Ueda Y, Akasaka T, Hozumi T, et al: Transthoracic Doppler echocardiographic assessment of coronary flow velocity pattern in patient with acute myocardial infarction implies progression of myocardial damage. *J Am Soc Echocardiogr* 18:1163-1172, 2005.
76. Katayama M, Yamamuro A, Ueda Y, et al: Coronary flow velocity pattern assessed noninvasively by transthoracic color Doppler echocardiography serves as a predictor of adverse cardiac events and left ventricular remodeling in patients with acute myocardial infarction. *J Am Soc Echocardiogr* 19:335-340, 2006.
77. Saraste A, Koskenvuo JW, Saraste M, et al: Coronary artery flow velocity profile measured by transthoracic Doppler echocardiography predicts myocardial viability after acute myocardial infarction. *Heart* 93:456-457, 2007.
78. Yoshida K, Hozumi T, Takemoto Y, et al: Impaired coronary circulation in patients with apical hypertrophic cardiomyopathy: noninvasive analysis by transthoracic Doppler echocardiography. *Echocardiography* 22:723-729, 2005.
79. Akasaka T, Yoshikawa J, Yoshida K, et al: Phasic coronary flow characteristics in patients with hypertrophic cardiomyopathy: a study by coronary Doppler catheter. *J Am Soc Echocardiogr* 7:9-19, 1994.
80. Celik S, Dagdeviren B, Yildirim A, et al: Determinants of coronary flow abnormalities in obstructive type hypertrophic cardiomyopathy: noninvasive assessment by transthoracic Doppler echocardiography. *J Am Soc Echocardiogr* 17:744-749, 2004.
81. Celik S, Dagdeviren B, Yildirim A, et al: Comparison of coronary flow velocities between patients with obstructive and nonobstructive type hypertrophic cardiomyopathy: noninvasive assessment by transthoracic Doppler echocardiography. *Echocardiography* 22:1-7, 2005.
82. Watanabe N, Akasaka T, Yamaura Y, et al: Intramyocardial coronary flow characteristics in patients with hypertrophic cardiomyopathy: non-invasive assessment by transthoracic Doppler echocardiography. *Heart* 89:657-658, 2003.
83. Kim WS, Minagoe S, Mizukami N, et al: No reflow-like pattern in intramyocardial coronary artery suggests myocardial ischemia in patients with hypertrophic cardiomyopathy. *J Cardiol* 52:7-16, 2008.
84. Sekine T, Daimon M, Hasegawa R, et al: Cibenzoline improves coronary flow velocity reserve in patients with hypertrophic obstructive cardiomyopathy. *Heart Vessels* 21:350-355, 2006.
85. Galiuto L, Sestito A, Barchetta S, et al: Noninvasive evaluation of flow reserve in the left anterior descending coronary artery in patients with cardiac syndrome X. *Am J Cardiol* 99:1378-1383, 2007.
86. Lanza GA, Buffon A, Sestito A, et al: Relation between stress-induced myocardial perfusion defects on cardiovascular magnetic resonance and coronary microvascular dysfunction in patients with cardiac syndrome X. *J Am Coll Cardiol* 51:466-472, 2008.
87. Cortigiani L, Rigo F, Gherardi S, et al: Prognostic effect of coronary flow reserve in women versus men with chest pain syndrome and normal dipyridamole stress echocardiography. *Am J Cardiol* 106:1703-1708, 2010.
88. Lee DH, Youn HJ, Choi YS, et al: Coronary flow reserve is a comprehensive indicator of cardiovascular risk factors in subjects with chest pain and normal coronary angiogram. *Circ J* 74:1405-1414, 2010.
89. Pizzuto F, Voci P, Bartolomucci F, et al: Usefulness of coronary flow reserve measured by echocardiography to improve the identification of significant left anterior descending coronary artery stenosis assessed by multidetector computed tomography. *Am J Cardiol* 104:657-664, 2009.

# 18 Mitral Valve Anatomy, Quantification of Mitral Regurgitation, and Timing of Surgical Intervention for Mitral Regurgitation

JUDY HUNG, MD

**Mitral Valve Anatomy and Mechanisms of Mitral Regurgitation**
Embryology and Anatomy
Mechanism of Mitral Regurgitation
**Quantification of Mitral Regurgitation**
Color Doppler Methods
Volumetric Methods with Pulsed Doppler Imaging
Supportive Evidence in the Assessment of Mitral Regurgitation
Three-Dimensional Echocardiography
**Timing of Surgical Intervention for Mitral Regurgitation**
Pathophysiology
Determination of Mechanism

Mitral regurgitation (MR) is a common valvular disorder that is a significant cause of morbidity and mortality in cardiovascular disease.[1-9] Population studies have estimated the prevalence rate of mild or greater MR to be approximately 20%.[10-12] Approximately 30,000 patients in the United States undergo mitral valve surgery annually for significant (moderate or severe) MR.[13] MR can be categorized as primary (valvular) or secondary (ischemic or functional). Primary MR results from abnormalities of the mitral leaflets and chordal structures, such as prolapse, flail, or endocarditis. Secondary MR results from abnormalities of the left ventricle (LV), from either ischemic or myopathic remodeling of the ventricular myocardium that underlies the papillary muscles, which support the mitral valve apparatus. The LV abnormalities result in tethering of the mitral leaflets and incomplete leaflet coaptation. It is important to distinguish the mechanism of MR because therapy is based on whether MR is primary or secondary.

Accurate quantification of MR plays an important role in clinical practice. The introduction of Doppler techniques to echocardiography in the early 1980s transformed the diagnosis and management of mitral valve disease, providing accurate quantification of MR performed noninvasively. Clinical decision making in patients with significant MR, generally considered to be moderate or greater, relies on accurate assessment of both etiology and quantification of MR. This chapter reviews the mechanistic basis and quantification of MR and how these factors guide clinical decision making.

## Mitral Valve Anatomy and Mechanisms of Mitral Regurgitation

### EMBRYOLOGY AND ANATOMY

The mitral valve apparatus forms from delamination of the ventricular myocardium after formation of the atrioventricular valves from the endocardial cushions. The mitral valve apparatus includes the mitral annulus, mitral leaflets, chordae tendineae, and papillary muscles. A detailed knowledge of the anatomy of the mitral valve apparatus is important in understanding mitral valve function and the mechanism of both primary and secondary MR.

#### *Mitral Annulus*

The mitral annulus is a D-shaped fibrous structure formed from the fibrous skeleton of the heart that serves to anchor the leaflets. The mitral annulus has a bimodal or saddle shape, with the anterior and posterior points superiorly oriented (toward the left atrium [LA]) and the medial and lateral points inferiorly oriented (toward the LV; Fig. 18-1).[14] In vitro testing and computer modeling studies have shown that a bimodal shape is optimal for minimizing stress on the leaflets during mitral leaflet opening and closing.[15-18] The anteromedial portion of the mitral annulus, which forms the straight edge of the "D," shares a common wall with the aortic annulus at the attachment of noncoronary and left coronary cusps. This shared wall is called the intervalvular fibrosa (also termed aortomitral curtain) and

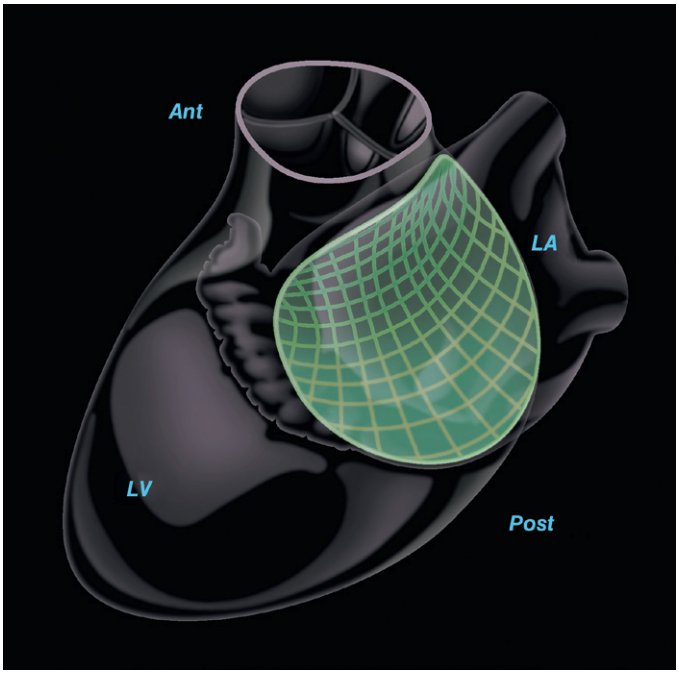



**Figure 18-1 3D reconstruction of the mitral valve annulus.** Image shows bimodal shape and orientation of the superior and inferior points. *Ant,* Anterior; *Post,* posterior.

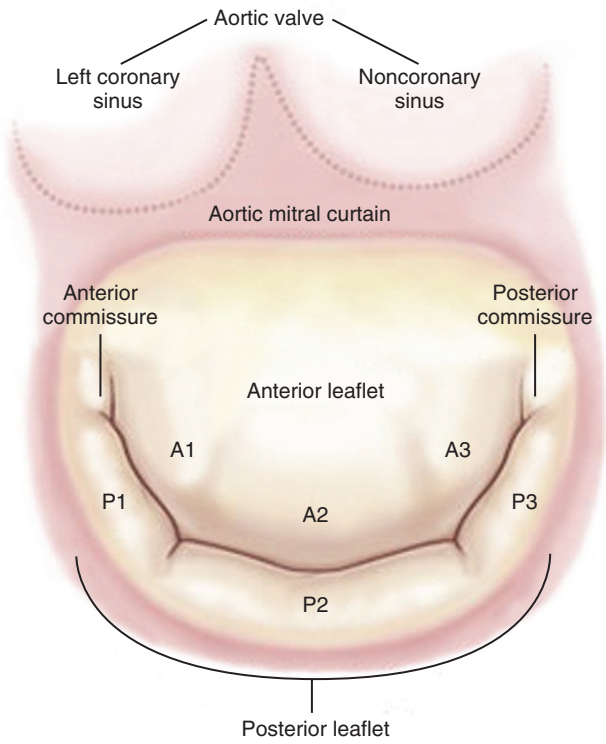



**Figure 18-2 Schematic of mitral valve from LA aspect.** The anterior leaflet is longer than the posterior leaflet but occupies less of the annular circumference. Each leaflet can be divided into three scallops, numbered from lateral to medial, which allows precise description of the location of valve dysfunction identified by echocardiographic imaging.

is more rigid than the posterior annulus as a result of these fibrous attachments. The posterior portion of the annulus accounts for a greater circumferential length than the anterior portion. Because the anterior annulus is relatively fixed compared with the posterior annulus, posterior dilation of the mitral annulus is predominant, although not exclusive; studies have shown that the anterior annulus does dilate, although not to as great an extent as the posterior annulus.[19] The mitral annular area is dynamic throughout the cardiac cycle and is influenced by LA contraction and filling mechanics throughout the cardiac cycle.

### *Mitral Leaflets*

The two leaflets of the mitral valve are referred to as anterior and posterior on the basis of their anatomic location. The broad anterior leaflet has a greater surface area and thickness than the posterior leaflet and accounts for most of the closing surface area of the mitral valve (Fig. 18-2). The anterior leaflet is attached to the anterior mitral annulus through fibrous continuity with the noncoronary and left aortic cusps. The posterior leaflet is crescent-shaped and has overall less surface area than the anterior leaflet, despite a greater circumferential attachment length to the mitral annulus. The shape of the posterior leaflet forms three scalloped segments that are separated by thin clefts between each segment. The anterior and posterior leaflets are attached at the posterior and anterior commissures. A common nomenclature for the leaflet segments divides each leaflet into three segments or scallops that are labeled 1 to 3, with 1 the anterolateral segment, 2 the middle segment, and 3 the posteromedial segment (see Fig. 18-2).

### *Chordae Tendinae and Papillary Muscles*

The mitral chordae tendinae, which typically number 25, are thin fibrous structures composed of collagen interwoven with elastin fibers, which extend from the papillary muscles to attach to the mitral leaflets. The chordae provide the critical functions of anchoring the mitral leaflets during systole, allowing for symmetric coaptation, and preventing prolapse of the leaflets into the LA.

The three types of mitral chordae are named primary, secondary, and tertiary. The primary chordae (also known as marginal chordae) extend from the papillary muscles in a branching pattern to attach along the coaptation line (margins) of the leaflet. These primary chordae are responsible for the primary role of the chordae, which is to maintain coaptation of the leaflets.[20] Rupture or elongation of the primary chordae results in loss of coaptation and development of prolapse or flail leaflet and invariably MR. The secondary chordae (also known as basal or strut chordae) attach at the mid body of the leaflets in the transition zone between the rough and smooth zone of the leaflets. Their main function is to provide the basic support length from the papillary muscle to the leaflet.[20] Secondary chordae are thicker and longer than primary chordae and do not have a branching pattern. Secondary chordae may rupture without compromising coaptation or development of severe MR. The body of each leaflet has a rough zone defined by where the primary chordae attach (the edge of the leaflets to approximately one third of the leaflet body) and a smooth zone (remainder of leaflet body). Tertiary chordae are small in number and arise from the basal myocardium, with attachment to the base of the leaflet to provide structural support.

The chordae are attached to the LV via the papillary muscles. During systole, the papillary muscles contract to facilitate closure of the leaflets via the chordae. The two papillary muscles in the LV are named by their location of origin: posteromedial and anterolateral. The anterolateral papillary muscle is somewhat a misnomer because it is actually located along the

posterolateral wall rather than the anterior wall. Each papillary muscle can have one head, multiple heads, or fused heads from which the chordae extend. Rarely, an accessory papillary muscle that arises from the anterior wall, often close to the septum, is present.[21] In case reports, accessory papillary muscles and associated chordae can insert directly onto the anterior leaflet, or even interventricular septum, resulting in mitral valve dysfunction.[22]

Equal numbers of chordae come from each papillary muscle to insert into each of the leaflets. Chordae that originate from the posteromedial papillary muscle attach to the medial half of each leaflet, and chordae from the anterolateral papillary muscle attach to the lateral half of each leaflet (Fig. 18-3).

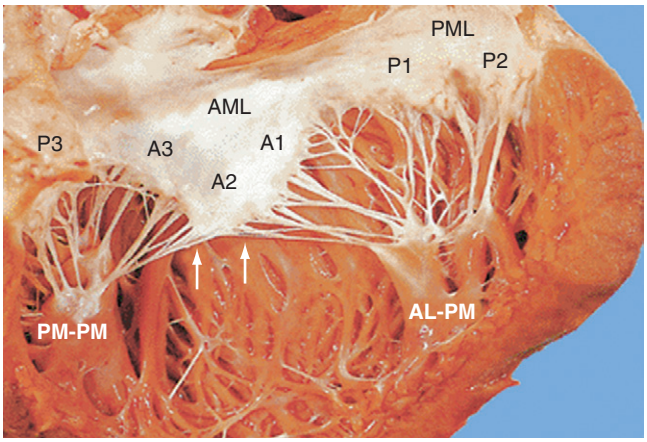



**Figure 18-3 Chordae originating from the posteromedial papillary muscle.** Chordae originating from the posteromedial papillary muscle (*PM-PM*) attach to the medial half of each leaflet (*A3* and half of *A2; P3* and half of *P2*), and chordae from the anterolateral papillary muscle (*AL-PM*) attach to the lateral half of each leaflet (*A1* and half of *A2; P1* and half of *P2*). Primary chordae (*white arrows*) have a branching pattern and insert at the edge of the leaflets. *AML,* Anterior mitral leaflet; *PML,* posterior mitral leaflet. *(Adapted from Mills SE, editor:* Histology for pathologists, *ed 3, Philadelphia, 2006, Lippincott Williams & Wilkins.)*

## MECHANISM OF MITRAL REGURGITATION

Mechanisms of MR can be broadly categorized as primary, in which valvular (leaflets and chordae) abnormalities result in MR, or secondary, in which mitral valve function is abnormal as a result of distortion of the geometric relationships of the mitral valve apparatus and the LV. In the latter, valvular structures are morphologically normal. Table 18-1 summarizes the etiologies of MR based on primary or secondary mechanism.

Mitral valve prolapse is the most common type of primary MR and is defined as displacement of the mitral leaflets during systole of at least 2 mm from the annular plane (Fig. 18-4).[14] Flail leaflet is defined as an eversion of the leaflet segment with loss of the normal concave shape of the leaflet (Fig. 18-5) and is associated with significant, frequently severe MR. Flail leaflet results almost always from rupture of the primary or marginal

**TABLE 18-1 Causes of Mitral Regurgitation**

| | |
|---|---|
| **Primary MR** | Valvular abnormality |
| Degenerative | Mitral valve prolapse, myxomatous changes<br>Ruptured chordae<br>Thickening/calcification |
| Infectious | Endocarditis, vegetations; leaflet perforations |
| Inflammatory | Systematic inflammatory disorders, valvulitis; Libman-Sacks lesions |
| Rheumatic | Leaflet thickening/restricted posterior leaflet mixed mitral disease: mitral stenosis/MR |
| Radiation | Leaflet thickening/restricted posterior leaflet mixed mitral disease: mitral stenosis/MR |
| Drugs | Leaflet thickening/restricted posterior leaflet mixed mitral disease: mitral stenosis/MR |
| Congenital | Cleft mitral valve/endocardial cushion defects |
| **Secondary MR** | Ventricular distortion of mitral apparatus from coronary artery disease or cardiomyopathy |

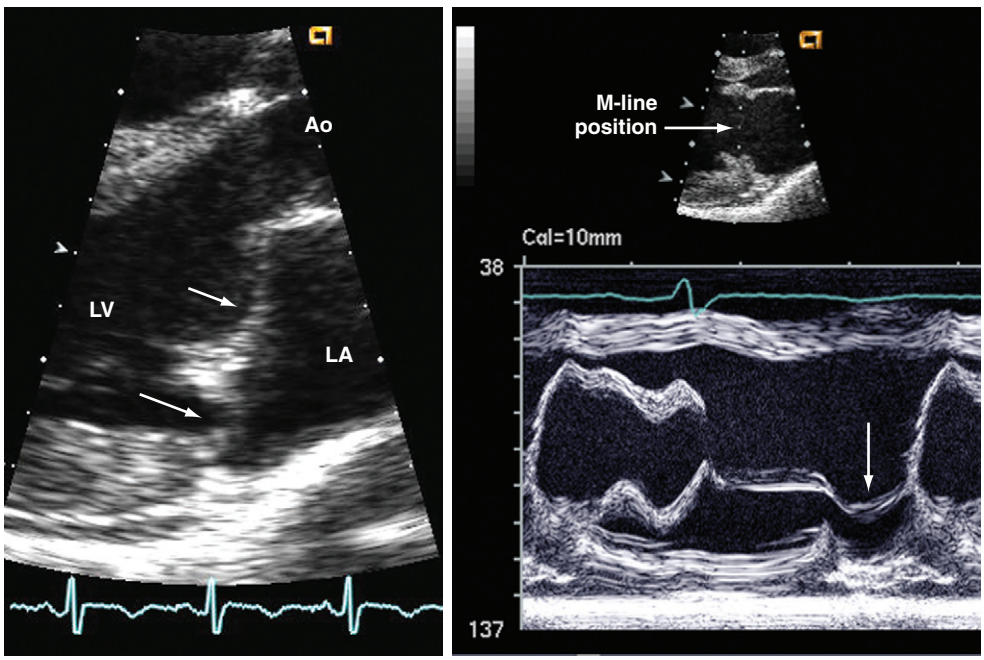



**Figure 18-4 Parasternal long-axis view (*left*) and M-mode recording (*right*) in a young woman with mitral valve prolapse.** Bileaflet prolapse is seen on 2D imaging (*arrows*), and the M-mode shows late systolic posterior motion of the leaflets (*arrow*). *Ao,* Aorta.

chordae. Rarely, elongation of the chordae without frank rupture can also result in flail leaflet. Both conditions lead to loss of leaflet coaptation with a gap at the coaptation line. The prevalence rate of mitral valve prolapse is approximately 2.4% in contemporary studies, and MR as a result of mitral valve prolapse accounts for most of the 10,000 isolated mitral valve surgeries performed annually in the United States.[13,23] With echocardiography, mitral valve prolapse encompasses a spectrum from minimal prolapse to flail leaflet. Leaflet thickness can vary from normal to diffusely thickened and redundant leaflets. The latter is also known as Barlow's disease of the mitral valve, named after Dr John Barlow, and is at the severe end of the spectrum of mitral valve prolapse.[24] Factors that are associated with worse prognosis in the mitral valve prolapse spectrum are leaflet thickness of more than 5 mm, moderate or greater MR, and LV ejection fraction of less than 50%.[4,25-27]

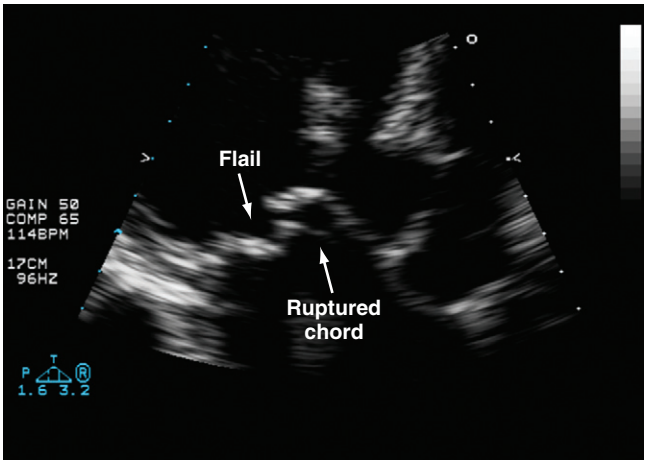



**Figure 18-5 Flail mitral leaflet.** Flail mitral leaflet (*arrow*) occurs when chordal disruption (*arrow;* either rupture or elongation) results in an eversion of the leaflet.

Other valvular causes of MR include endocarditis in which the mechanism includes destruction of leaflet, leaflet perforation, and inflammation with thickening of mitral leaflets that leads to poor coaptation. Less common causes are rheumatic disease (in developed countries) where the mechanism is the result of leaflet thickening and scarring and restricted posterior leaflet motion that prevents complete coaptation (Fig. 18-6), valvulitis from collagen-vascular disease, radiation, and drug-induced mitral valve disease. Calcific mitral annular disease in which annular calcification extends onto the leaflet bodies often results in mixed mitral valve disease with both stenosis and MR present. Congenital abnormalities of the mitral valve make up a small percentage of adult patients with MR. The most common congenital abnormality in the pediatric population that causes MR is mitral valve prolapse, with cleft mitral valve second most common.

Secondary MR results from ischemic or myopathic LV remodeling, which results in lateral displacement of the papillary muscles and tethering of the mitral leaflets and incomplete leaflet coaptation (Fig. 18-7). Secondary MR is a more common mechanism of MR than primary valvular etiologies because the prevalence of ischemic heart disease is much greater than primary mitral valvular disorders. The prevalence rate of development of mild or greater MR after myocardial infarction has been estimated to be up to 50% and is associated with worse prognosis.[5,6,28] Patients who present with congestive heart failure from systolic dysfunction have an approximately 50% incidence rate of moderate or greater MR.[7-9] Ischemic and functional MR are types of secondary MR. Ischemic MR specifically relates to MR that results from coronary artery disease. Papillary muscle rupture is an uncommon but dramatic type of ischemic MR, with 1.0% of patients with myocardial infarction having development of papillary muscle rupture.[29] Ischemic MR can also

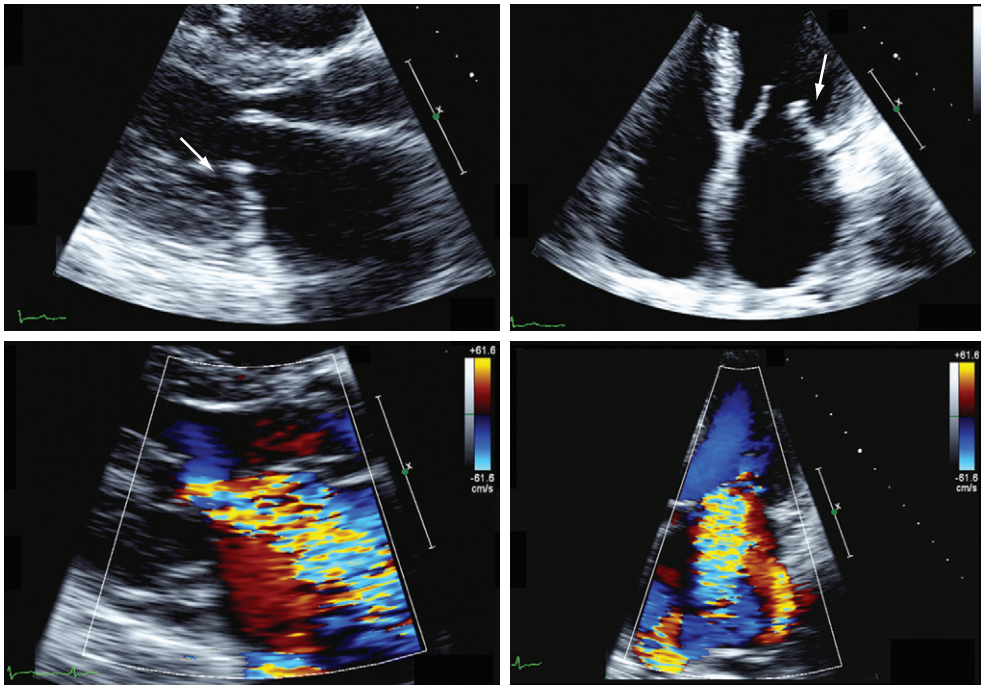


**Figure 18-6 Rheumatic mitral valve changes result in mitral regurgitation.** In rheumatic mitral valve disease, the posterior leaflet becomes rigid (*top panels, arrows*), which results in poor coaptation and mitral regurgitation (*bottom panels*).

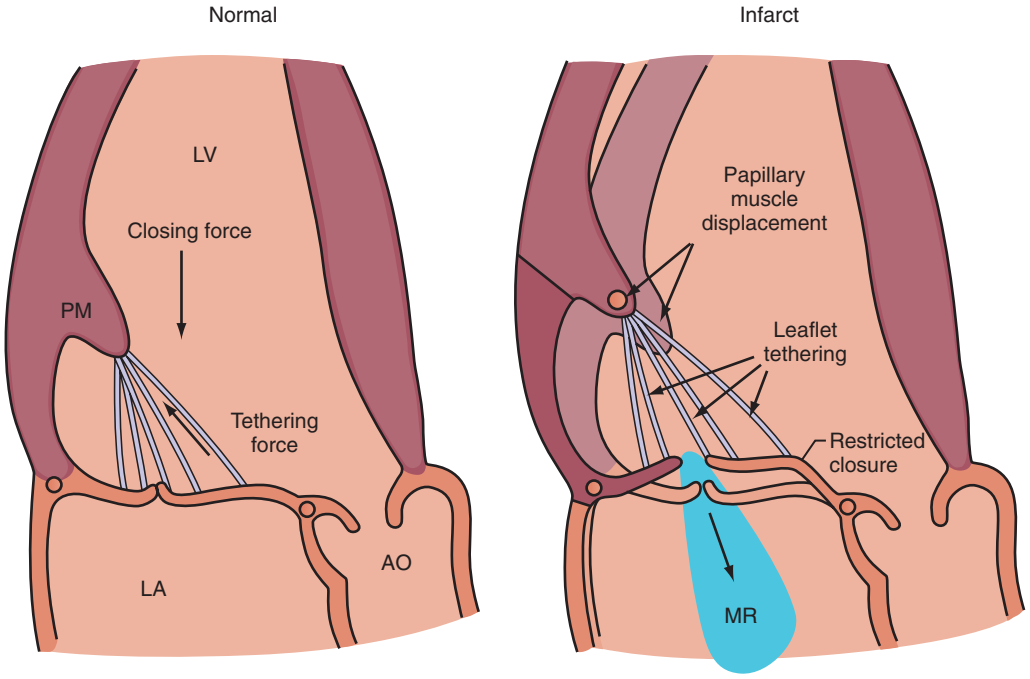



**Figure 18-7 Schematic of mechanism of secondary mitral regurgitation.** This diagram illustrates the mechanism of ischemic mitral regurgitation. *Left,* Balance of forces acting on mitral leaflets in systole. *Right,* Effect of papillary muscle displacement. *Dark shading* indicates inferobasal myocardial infarction. *(Modified from Liel-Cohen N, Guerrero JL, Otsuji Y, et al: Design of a new surgical approach for ventricular remodeling to relieve ischemic mitral regurgitation: insights from 3-dimensional echocardiography.* Circulation *101:2756-2763, 2000.) AO,* Aorta; *MR,* mitral regurgitation; *PM,* papillary muscle.

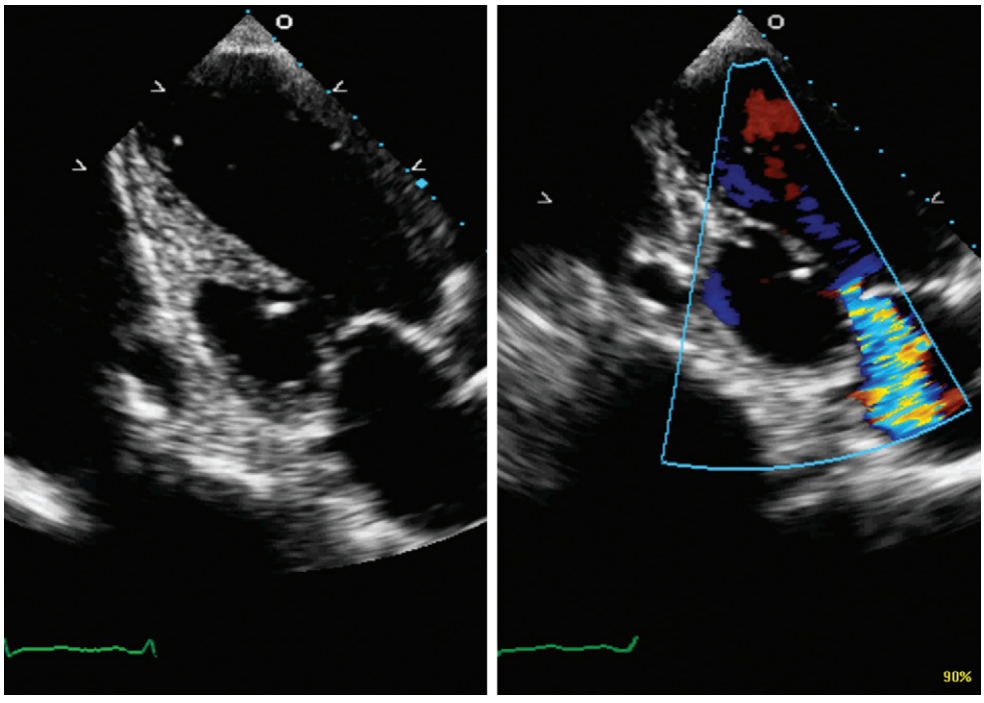



**Figure 18-8 Aneurysm of inferior wall from infarction.** *Left panel* shows aneurysm of inferior wall from infarction, which results in distortion of the LV wall leading to mitral leaflet tethering and restricted closure with development of mitral regurgitation (*right panel*).

develop from acute myocardial ischemia. The MR is in this case is usually transient, resolving once the acute ischemia subsides. By far the more common type of ischemic MR is a result of chronic LV remodeling after myocardial infarction that causes geometric distortion of the mitral valve apparatus.[30] Development of akinesis, scar, or aneurysm of the infarcted or ischemic myocardium underlying the papillary muscles results in lateral displacement of the affected papillary muscles, which in turn leads to tethering of the mitral leaflets and incomplete closure (Fig. 18-8). Echocardiographic features are apical tenting of the mitral leaflets, best imaged in the apical four-chamber view in mid systole; loss of normal convex shape into concave shape; and a bend noted in the anterior mitral leaflet from tethering of the anterior leaflet from a secondary (strut) chord (Fig.18-9). Because the papillary muscles are located along the inferior-posterolateral walls, the incidence of ischemic MR is greater in inferior myocardial infarctions than in anterior myocardial infarctions.[31] However, ischemic MR can develop with any large

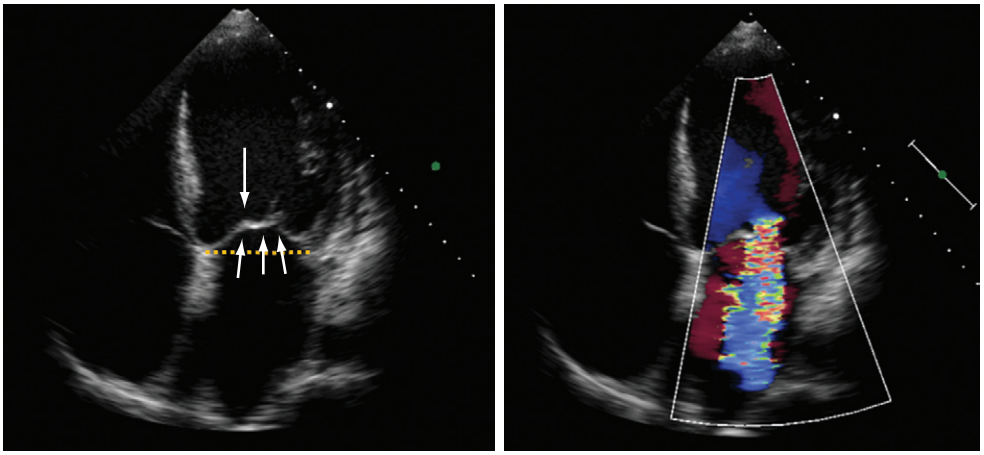


**Figure 18-9 Echocardiographic features of ischemic mitral regurgitation.** Features are apical tenting of the mitral leaflets (best imaged in the apical four-chamber in mid systole), where the mitral leaflets coapt apically instead of at the annular plane (*yellow dashed line*); loss of normal convex shape into concave shape (*small arrows*); and a bend (*large arrow*) noted in the anterior mitral leaflet from tethering of the anterior leaflet from secondary strut chords. These features result in ischemic mitral regurgitation (*right panel*).

myocardial infarction that results in significant LV dilation and remodeling to affect the mitral valve geometry.

Functional MR is a general term that indicates MR resulting from ventricular distortion of the mitral valve apparatus. This can be from a cardiomyopathy or coronary disease. However, functional MR is often used specifically to MR that develops from a cardiomyopathy, to distinguish from ischemic MR. From a mechanistic basis, ischemic (from coronary artery disease) and functional (from cardiomyopathy) MR are similar.

An alternate classification of MR mechanisms proposed by Alain Carpentier[32] is based on motion of the mitral leaflets. In type I, mitral leaflet motion is normal and the MR results from annular dilation. Type II MR is the result of excessive leaflet motion, such as prolapse or flail leaflet. Type III is from restricted leaflet motion and is subdivided into type IIIa and IIIb. In type IIIa, leaflets have restricted motion in both systole and diastole; rheumatic MR falls into this category. Ischemic and functional MR are grouped into type IIIb, where there is restricted motion during systole (Fig. 18-10).

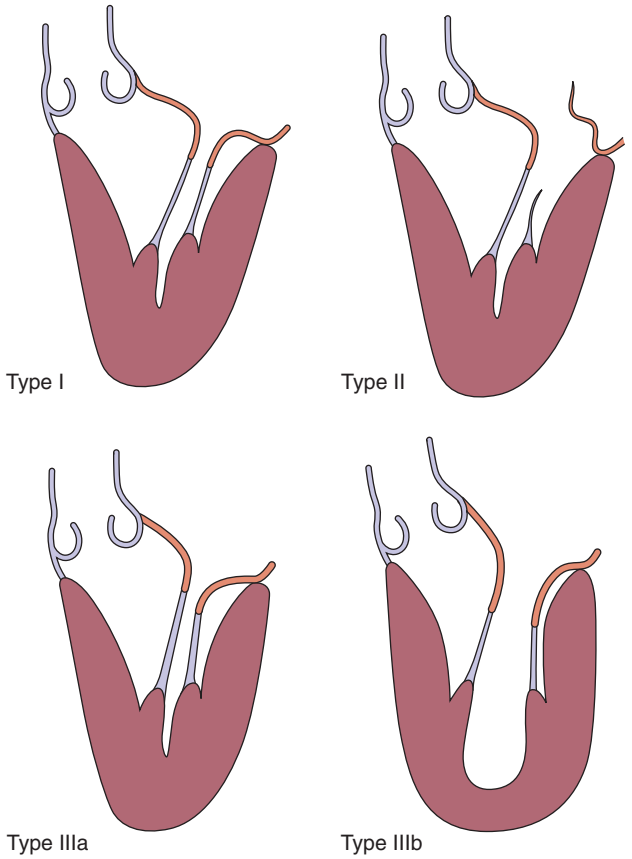



**Figure 18-10 Carpentier classification of mitral regurgitation.** In type I, mitral leaflet motion is normal and the MR results from annular dilation. Type II MR is the result of excessive leaflet motion, such as prolapse or flail leaflet. Type III is from restricted leaflet motion and is subdivided into type IIIa and IIIb. In IIIa, leaflets have restricted motion in both systole and diastole. Rheumatic MR falls into this category. Ischemic MR and functional MR are grouped into type IIIb, in which there is restricted motion during systole. (*From Adams DH, Filsoufi F: Another chapter in an enlarging book: Repair degenerative mitral valves.* J Thorac Cardiovasc Surg *125:1197-1199, 2003.*)

## Quantification of Mitral Regurgitation

Color Doppler techniques are the most commonly applied method for quantification of valvular regurgitation in clinical practice. The regurgitant color Doppler flow pattern has three components: the proximal flow convergence or proximal isovelocity surface area (PISA), the vena contracta, and the distal jet (Figure 18-11, *left* panel).[33] Principles of fluid dynamics can be applied to these components of regurgitant flow where flow can be considered to approach a finite orifice with flow distal to the orifice entering a constrained receiving chamber. The proximal flow convergence region occurs proximal to the regurgitant orifice (proximal to the leaflets). The vena contracta represents the narrowest point at the level or just distal to the leaflets and represents the effective orifice area and not the anatomic orifice area. The latter is defined as an orifice at the level of the leaflets, whereas the effective orifice area is defined by the narrowest point of the flow steam, which typically occurs just distal to the leaflets as flow continues to converge for a short distance beyond the anatomic orifice (Fig. 18-11, *right* panel).[33] The final component is the distal regurgitant jet, which represents the

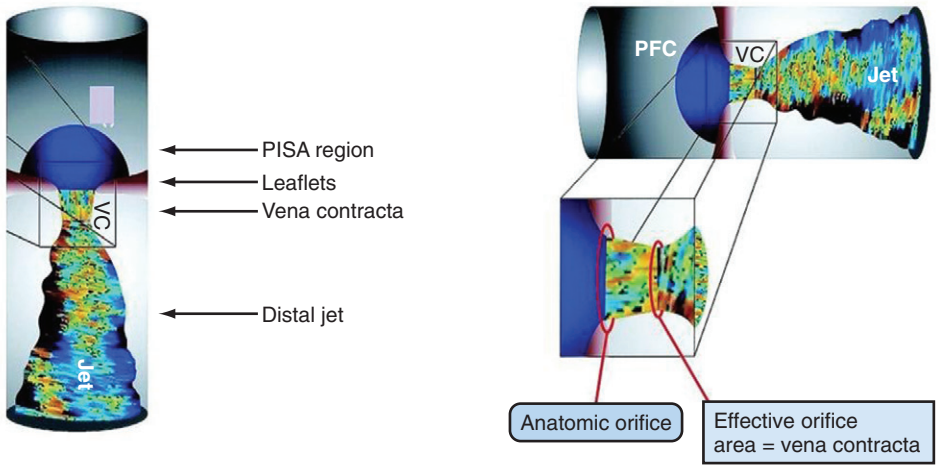



**Figure 18-11 The three components of a regurgitant jet (*left panel*).** The proximal isovelocity surface area (*PISA*) region, also referred to as proximal flow convergence (*PFC*) region; vena contracta (*VC*); and distal jet. *Right panel*: The effective regurgitant orifice area is the orifice area defined by the narrowest regurgitant flow stream and typically occurs distal to the anatomic orifice defined by the valve leaflets. *(Adapted from Roberts BJ, Grayburn P: Color flow imaging of the vena contracta in mitral regurgitation: technical considerations.* JASE *16:1002-1006, 2003.)*

regurgitant flow once it has passed the leaflets and into the receiving chamber. This distal jet is most readily detected and measured but also most subject to external influences present in the receiving chamber.

## COLOR DOPPLER METHODS

### *Distal Jet Area Method*

A standard method for assessment of MR is measurement of the distal MR jet area as it enters the LA.[34,35] The MR jet is defined as the turbulent mosaic color flow within the LA during systole that emanates from the mitral leaflets. Care should be taken to avoid including the low-velocity (nonturbulent) blood flows in the LA surrounding the turbulent jet because this falsely increases the MR jet area. The maximal jet area is traced in multiple views, and an average of the areas is calculated.

The distal jet area method is a relatively simple and commonly applied technique for the qualitative assessment of MR. However, a number of technical and physiologic factors should be taken into account. Assessment of the severity of MR with distal MR jet is based on the assumption that the color Doppler display of MR flow velocities can be a surrogate for MR regurgitant volume. On an empiric basis, this has been validated against angiographic standards. It is important to keep in mind limitations with the color display of the MR flow velocities as a substitute for mitral regurgitant volume. First of all, measurement of the regurgitant jet is taken as the maximal instantaneous valve, whereas regurgitant volume includes the time that the MR flow occurs. In addition, because MR flow occurs in a pulsatile manner, the flow rate is not constant; hence, the relationship between jet velocity and flow rate varies. Because the MR flow is entering a constrained chamber (LA), the behavior of the MR jet is influenced by a number of factors, including physical containment from the LA wall, entrainment of blood pool in the LA into the MR flow, and flow influences from the pulmonary veins.

Eccentric MR jets are subject to impingement from the LA wall, which can result in a decrease in the size of the mitral regurgitant jet. In addition, wall jets are subject to the Coandal effect, which is the tendency of flow to follow adjacent to or along a wall. This effect influences the direction, and ultimately the display, of the MR jet.[36,37] Eccentric jets in which the MR jet courses out of the plane of the ultrasound beam also are missed or underestimated. Because of the limitations with eccentric jets, the jet area method is probably best applied to centrally directed jets.[37,38] Machine settings can also influence the distal MR jet. Over gain, in which there is random color noise present, can overestimate the size of the jet. In contrast, too low gain settings underestimate the jet size. Low Nyquist settings can also overestimate the true MR jet as lower velocity blood flows present in the LA are merged into the true MR jet. In general, Nyquist limits should be at least 50 cm/s for color flow mapping of MR regurgitant jets.

Importantly, distal jet area is influenced by hemodynamic conditions.[38-43] Studies have shown that the size of the regurgitant jet depends to some extent on the driving pressure across the mitral valve, which is dictated by the LV systolic pressure to LA pressure gradient.[40,43] As this gradient is maximal at mid systole, the MR jet tends to be maximal at this time point in the cardiac cycle. Hemodynamic conditions that alter systemic arterial pressure or LA pressure can influence the overall jet size.[39,41]

Typically, the distal MR jet area is normalized relative to the LA area (Fig. 18-12). Comparison studies suggest that normalization for LA size correlates better than absolute jet area compared with angiographic standards.[37,44] The MR jet area and LA area are measured in the same systolic frame to obtain a ratio of jet area to LA area (see Fig. 18-11).[44,45] Fig. 18-13 shows examples of jet areas corresponding to mild, moderate, and severe MR. The maximal MR jet area is traced, and then this area divided by the LA area measured from the same frame. MR jet area to LA area ratios of less than 20% correspond to mild MR, whereas ratios of more than 40% correspond to severe MR (see Table 18-1).[38] Factors that affect the accuracy of the jet area to LA area method are that the jet area to LA area ratio method assumes a relatively linear relationship between jet area size and LA area. However, this is not always the case; in some situations, the actual MR volume is greater than suggested by the jet area/LA area, such as in cases of chronic MR where there has been extensive LA remodeling. Table 18-2 summarizes validation studies for distal jet area methods against comparable standards.

### *Vena Contracta Method*

The vena contracta is the narrowest portion of the mitral regurgitant jet and provides a simple linear measurement of the proximal MR jet.[33,45-51] The vena contracta can be considered to be a surrogate measure of the effective regurgitant orifice area because the vena contracta essentially represents the anterior-posterior dimension of the effective regurgitant orifice area. Measurement of the vena contracta is important to perform in views orthogonal to the coaptation line of the mitral leaflets, such as the parasternal long-axis or apical long-axis views, because this provides the optimal color resolution of the vena contracta as imaged in the anterior-posterior plane (Fig. 18-14). Views that display the MR jet along the coaptation line, such as the two-chamber view (medial-lateral dimension), falsely increase the width of the vena contracta (Fig. 18-15).

Because the vena contracta measurement inherently is within a narrow range, small differences in measurement can make a large impact on MR degree. Care must be taken to optimize the vena contracta region for measurement by magnifying and adjusting depth and sector settings for optimal color Doppler resolution. In addition, defining the "narrowest" portion of the MR jet can be difficult because, in some cases, the neck of the proximal MR jet is not easily seen or is obscured by the leaflets. Measurement of the width of the proximal jet either at the level of the leaflets or just distal to the coaptation line can sometimes

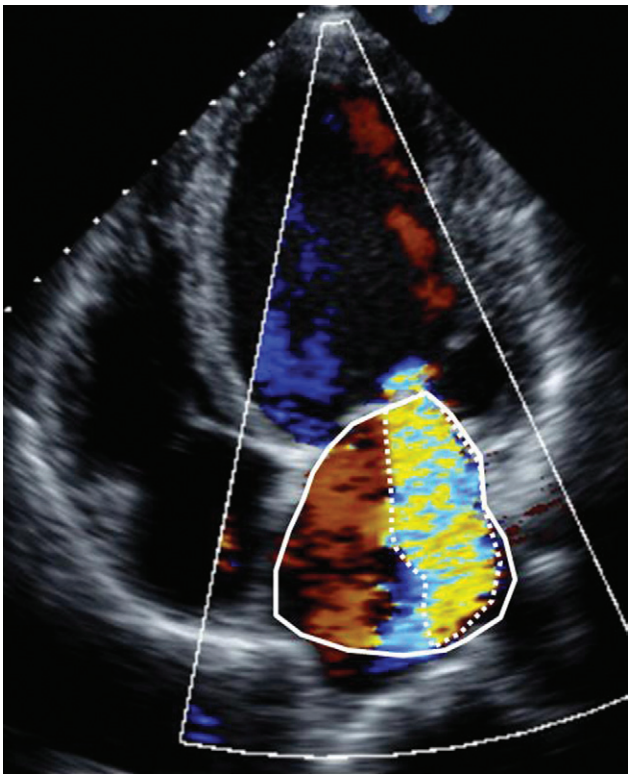


**Figure 18-12 Mitral regurgitation assessed with distal jet area to LA area ratio method.** Mitral regurgitation (MR) jet area is traced (*dashed line*) and divided by LA area (*solid line*).

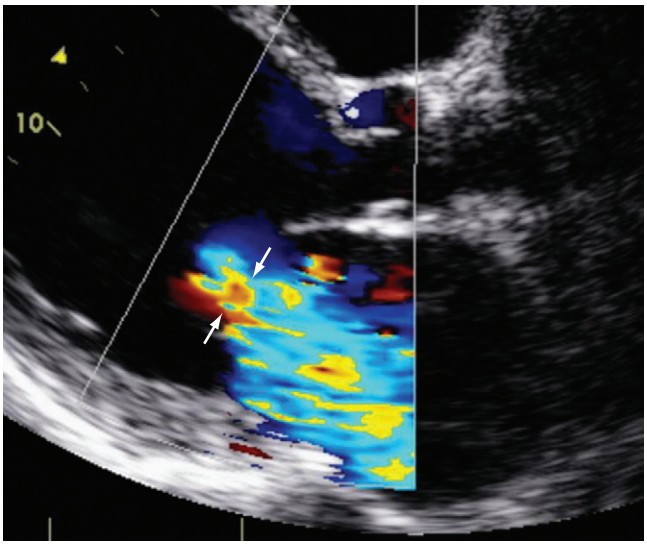



**Figure 18-14 The vena contracta (*arrows*) of the mitral regurgitant jet is the narrowest diameter of the mitral regurgitant jet at the level of or just distal to the leaflets.**

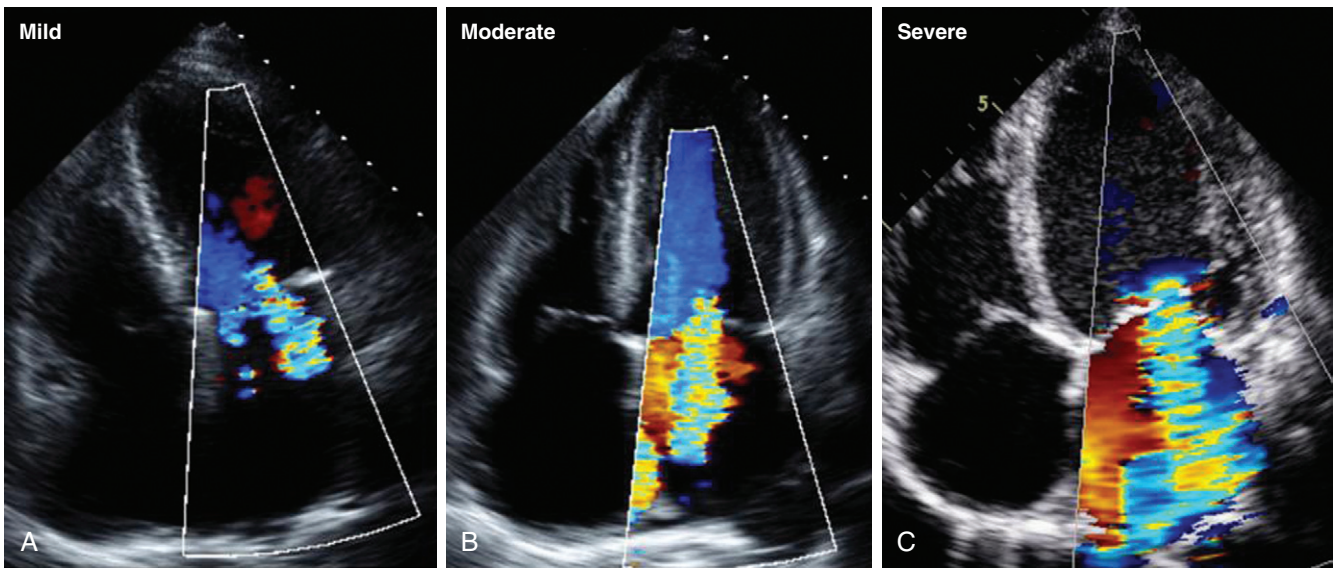



**Figure 18-13 Increasing degrees of mitral regurgitation as assessed with jet area method area to LA area ratio. A,** Mild: Jet area to LA ratio of less than 20%. **B,** Moderate: Jet area to LA ratio between 20% and 39%. **C,** Severe: Jet area to LA ratio of 40% or greater.

**TABLE 18-2 Summary of Methods for Mitral Regurgitation**

| *Study* | *Method* | *N* | *Comparison Standard* | *Results* |
|---|---|---|---|---|
| Omoto[35] | Jet area (absolute) | 72, both aortic and mitral regurgitation | Angiography | Descriptive data showing method of color flow imaging with good correlation with angiography. |
| Miyatake[34] | Jet area | 109 | Angiography | r = 0.87 |
| Helmcke | Jet area/LA area | 147 | Angiography | r = 0.78 |
| Spain[44] | Jet area | 47 | Angiography | r = 0.76 |
| Fehske[45] | Vena contracta | 78 | Angiography | r = 0.94<br>r = 0.83 (RV) |
| Heinle[51] | Vena contracta TEE | 35 | Pulsed Doppler Quantitation (RV) | r = 0.81 |
| Castello[77] | Jet area TEE | 80 | Angiography | r = 0.90 |
| Hall[50] | Vena contracta | 80 | Pulsed Doppler Quantitation (RV) | r = 0.85 |
| Mele | Vena contracta/proximal jet | 33<br>47 | Angiography<br>Pulsed-wave Doppler | r = 0.85 – 0.91<br>r = 0.86 |
| Omoto[35] | Jet area TEE | 37, patients with MR | Angiography | |
| Grayburn[49] | Vena contracta TEE | 80 | Angiography | Sensitivity, 100%<br>Single plane TEE: specificity, 83%; sensitivity, 95%<br>Multiplane TEE: sensitivity, 98% |
| Recusani[55] | PISA in vitro | | Electromagnetic flow meter | r = 0.94 – 0.99 (flow rate)<br>r = 0.795 – 0.96 (EROA) |
| Bargiggia[56] | PISA | 52 | Angiography<br>PISA flow rate | r = 0.91 versus (flow rate)<br>r = 0.93 (RV) |
| Utsunomiya[57] | PISA in vitro | 226 | Flow meter | |
| Dujardins | Pulsed Doppler | 180 | Angiography | EROA, r = 0.79<br>RV, r = 0.80<br>RF, r = 0.78 |
| Kizilbash | Pulsed Doppler | n = 22 | Magnetic resonance imaging | RF, r = 0.82 |
| Tribouilloy[69] | Pulsed Doppler | n = 27 | Angiography | RF with echo 45.8 mL ± 19.2%<br>versus<br>RF with angio, 41.3 ± 17.8% |
| Rokey[67] | Pulsed Doppler | n = 25 | Angiography | r = 0.91 |
| Blumlein[68] | Pulsed Doppler Quantification | 27 | Angiography<br>Scintigraphy | r = 0.82<br>r = 0.89 |
| Ascah[71] | Pulsed Doppler (canine experimental model) | 7 | Electromagnetic flow meter | r = 0.84 (RF) low<br>r = 0.83 (RF) |

*angio,* Angiography; *echo,* echocardiography; *EROA*, effective regurgitant orifice area; *PISA,* proximal isovelocity surface area; *RF,* regurgitant fraction.

References:
Helmcke F, Nanda NC, Hsiung MC, et al: Color Doppler assessment of mitral regurgitation with orthogonal planes. *Circulation* 75:175-183, 1987.
Mele D, Vandervoort P, Palacios I, et al: Proximal jet size by Doppler color flow mapping predicts severity of mitral regurgitation. Clinical studies. *Circulation* 91:746-754, 1995.
Dujardin KS, Enriquez-Sarano M, Bailey KR, et al: Grading of mitral regurgitation by quantitative Doppler echocardiography: calibration by left ventricular angiography in routine clinical practice. *Circulation* 96:3409-3415, 1997.
Kizilbash AM, Hundley WG, Willett DL, et al: Comparison of quantitative Doppler with magnetic resonance imaging for assessment of the severity of mitral regurgitation. *Am J Cardiol* 81:792-795, 1998.

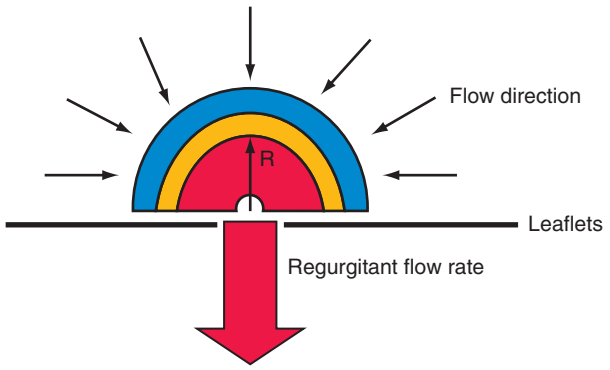



**Figure 18-15 Proximal isovelocity surface area.** Fluid dynamic theory predicts that as flow approaches a circular finite orifice, it forms a series of concentric hemispheric shells with gradually decreasing area and increasing velocity. *Arrows* refer to direction of flow as it approaches the proximal isovelocity surface area region. *R* is the radius of a hemispherical shell. With principle of conservation of mass, flow through the regurgitant orifice = flow through the isovelocity surface = $2\pi r^2 \times$ aliasing velocity.

circumvent this. The vena contracta is believed to be less influenced by physiologic loading conditions and thus may be more reproducible than jet area methods.[45] In vitro studies have shown that vena contracta is less dependent on hemodynamic factors than distal jet area.[46] Another potential advantage of vena contracta measurement over jet area may be in eccentric jets where the proximal jet is less affected by wall impingement. Table 18-2 summarizes validation studies of the vena contracta method against comparable standards.

Table 18-1 shows values for vena contracta corresponding to MR degree. Vena contracta measurements of less than 3 mm correspond to mild MR; 0.3 to 0.69 mm corresponds to moderate MR, and 0.7 mm or more corresponds to severe MR. A broad range for vena contracta is considered to be in the moderate range, which limits the vena contracta as a quantitative measure. Despite this, vena contracta remains a clinically useful semiquantitative measure of MR, which is simple in concept and measurement.

### *Proximal Isovelocity Surface Area Method*

The PISA method is based on the fluid dynamic principle that as flow approaches a circular finite orifice, it forms concentric hemispherical shells with gradually decreasing surface area and

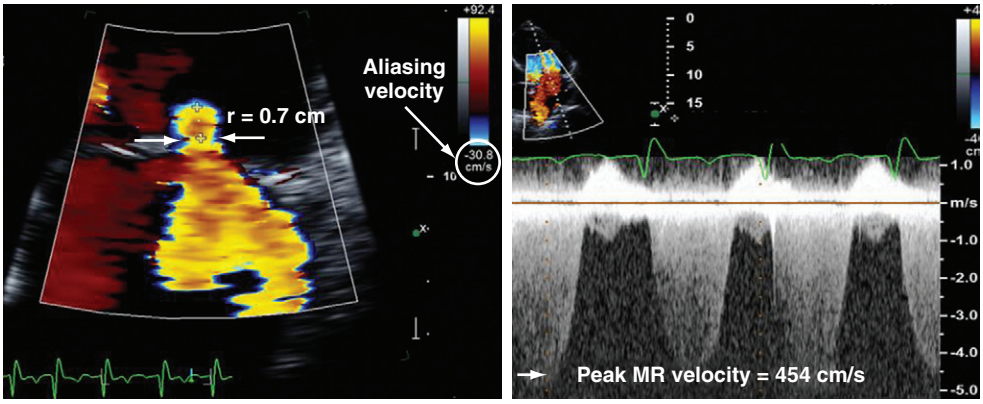



**Figure 18-16** **The proximal isovelocity surface area region (*left*) is displayed after baseline shifting and magnification.** The *arrows* point to the dropout in Doppler flow along the sides of the proximal isovelocity surface area region where the flow is perpendicular to the ultrasound beam. The radius of the proximal isovelocity surface area zone measures 0.7 cm. The aliasing velocity is 30.8 cm/s as displayed by the Nyquist limit. The peak regurgitant flow rate = $2 \times \Pi \times (0.7\ cm)^2 \times 30.8\ cm/s = 95\ mL/s$. The regurgitant orifice area = $95\ cm^3/sec \div 454\ cm/s = 0.21\ cm^2$.

increasing velocity (see Fig. 18-15).[52] This principle can be applied to mitral regurgitant flow, where the PISA region is the hemispheric shell that forms proximal to the mitral leaflets on the LV side and the finite orifice is the mitral regurgitant orifice at the level of the leaflets[42,52-58] With the conservation of mass principle, the flow rate of each of the isovelocity shells equals the flow rate at the regurgitant orifice. Assuming a hemispheric shape for the isovelocity shells, then flow rate = surface area of a hemisphere = $2\pi r^2 \times$ aliasing velocity, where $r$ is the radius of the hemispherical shell. The flow rate of the hemispheric shell equals the MR rate at the orifice with the conservation of mass principle. Once flow rate is calculated, the MR regurgitant orifice area and regurgitant volume can be derived with the following formulas: regurgitant orifice area = MR flow rate/peak MR velocity with continuous wave (CW; Fig. 18-16). As the regurgitant orifice area is calculated from an instantaneous peak flow rate, regurgitant orifice area obtained with the PISA method represents a maximal instantaneous regurgitation orifice area. For calculation of regurgitant volume, the effective regurgitant orifice area is divided by the time velocity integral of the MR: regurgitant volume = effective regurgitant orifice area × time velocity integral (MR jet). The regurgitant fraction is calculated as regurgitant volume divided by the stroke volume. Stroke volume can be calculated as: (end-diastolic volume—end-systolic volume)/end-diastolic volume. To optimize measurement of the radius r, baseline shifting of the Nyquist limit is recommended (Fig. 18-17). The baseline is shifted toward the direction of the regurgitant flow. The Nyquist limit should be relatively low compared with the regurgitant velocity or the hemispherical assumption can be invalid.[59] Thus, measurement of the radius of the PISA region at Nyquist limits much lower than flow rates is important. In general, 20 to 40 cm/s is the Nyquist limit range at which there is an optimal balance of maximal radius resolution and integrity of the PISA shape. Very low Nyquist limits overestimate the size of the PISA region, in which case, there is elongation in the axial dimension, and conversely high Nyquist limits minimize the PISA region, making accurate measurements difficult.[53,57,59-62] Mitral regurgitant flow rate and effective orifice area can be dynamic throughout systole depending on the etiology of MR,[63,64] which is an important consideration in the decision of at what time point during systole to measure the PISA radius. For example, with functional MR, there is typically a bimodal pattern with peak MR flow rates in early and late systole; MR flow rate is the least

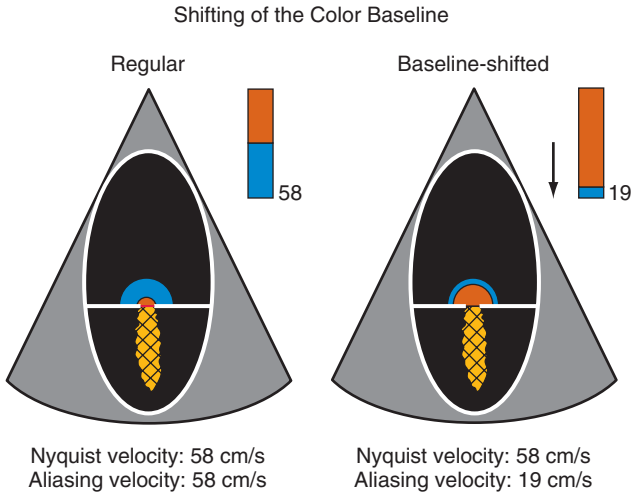



**Figure 18-17** **Baseline shifting of the Nyquist limit toward the direction of the regurgitant flow results in a larger proximal isovelocity surface area zone for optimal measurement of the proximal isovelocity surface area region radius (*right panel*).**

during mid systole. In patients with mitral valve prolapse, peak MR flow occurs mid to late systole. For rheumatic disease, the MR flow rate is constant during systole. PISA radius measurement should be avoided very early or very late in systole because these are times when the mitral leaflets are just closing or are about to open and the flow rate may not be at equilibrium. As a general rule, the PISA radius measurement should occur at the same time as the peak MR velocity (as measured with CW Doppler). This usually occurs at mid systole or at the T wave in the electrocardiogram pattern. In practice, precise alignment in time of the peak MR velocity with a PISA region suitable for accurate measurement can be difficult. In these situations, it is best to aim for accurate PISA region radius measurement at a time point that is closest to the peak MR velocity. Accuracy and reproducibility of the PISA method is highly dependent on careful attention to technique of acquisition and measurements. The PISA region should be magnified with sector and depth optimized for color Doppler resolution, with the PISA region and mitral leaflets encompassing most of the sector. Measurement of the PISA should be aligned parallel to flow rate direction because this optimizes Doppler resolution. MR regurgitant volumes of more than 0.40 $cm^2$ are consistent with severe

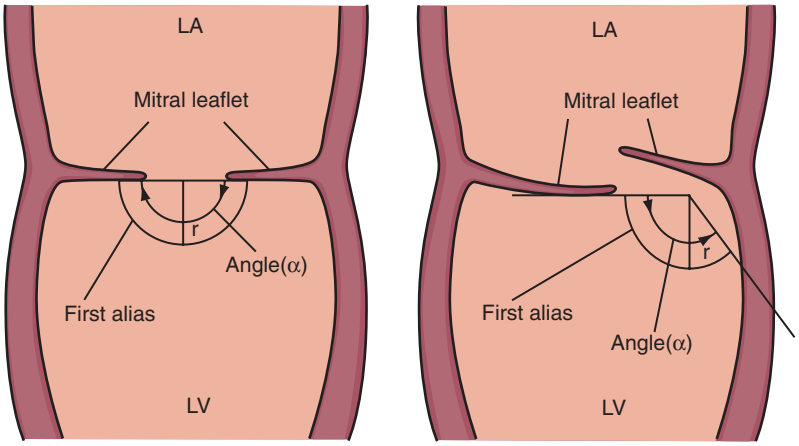



**Figure 18-18 Angle correction method for eccentric proximal isovelocity surface area.** These schematics show the radius (r) and convergence angle measurements of the proximal convergence field for central (*left*) and eccentric (*right*) convergence. The convergence angle is obtained by projecting the most distal point of the isovelocity contour onto the constraining wall. *(Adapted from Pu M, Vandervoort PM, Griffin BP, et al: Quantification of mitral regurgitation by the proximal convergence method using transesophageal echocardiography. Clinical validation of a geometric correction for proximal flow constraint.* Circulation *92:2169-2177, 1995.)*

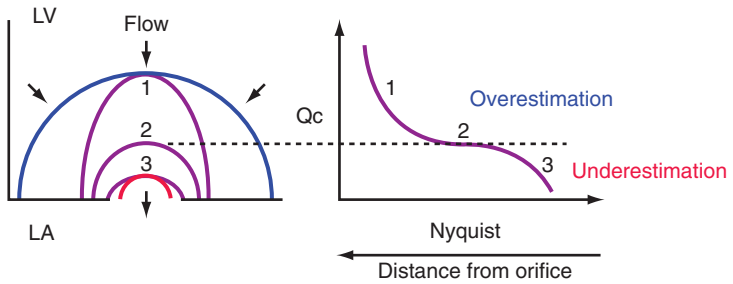



**Figure 18-19 Effect of proximal isovelocity surface area radius on proximal isovelocity surface area shape and flow calculation.** Schematic of isovelocity hemispheres proximal to a mitral regurgitant orifice (*left*) at three different distances from the orifice and corresponding plots of calculated flow rates (Qc) as a function of distance from the orifice. The *dashed line* represents the actual regurgitant flow rate. *(Adapted from Schwammenthal E, Nakatani S, He S, et al: New method for accurate calculation of regurgitant flow based on analysis of Doppler color flow maps of the proximal flow field: validation in a canine model of mitral regurgitation with initial application in patients.* J Am Coll Cardiol *27:161-172, 1996.)*

MR, whereas regurgitant volumes of less than 0.20 $cm^2$ are consistent with mild MR. Table 18-2 summarizes validation studies of the PISA method against comparable standards.

## Geometric Factors That Influence Proximal Isovelocity Surface Area Method

In theory, the PISA method provides an accurate quantitative measure of MR. However, some technical and practical aspects to the PISA method should be considered. The PISA region is influenced by the surrounding geometry of the orifice.[52] This principle is important in examination of eccentrically directed PISA regions, such as occur in flail mitral leaflet. This typically results in an overestimation of the PISA radius due to distortion of the PISA region from constraint from the LA wall, which results in a falsely increased radius.[54] To overcome this, an angle correction factor can be applied to the surface area calculation.[52] Angle correction is performed by multiplying the surface area calculation by $\alpha/180$, where $\alpha$ is the angle between the mitral leaflet and the end of the PISA region confined by the LA wall (Fig. 18-18).[65] Angle correction for eccentric PISA regions adds additional complexity to the MR flow rate calculation, creating additional opportunities for measurement error. Furthermore, accurate measurement of the $\alpha$ angle is not always possible because of LV wall confinement. The practical difficulties in applying angle correction have limited its use clinically.

## Technical Factors

One should measure the radius of the PISA region at Nyquist velocities, which are reliably displayed with color Doppler flow mapping. One major limitation of the PISA method has been that the calculated results vary widely when the radius is measured at different distances from the orifice because of varying three-dimensional (3D) shapes of the isovelocity surface. The contour of the PISA region changes depending on location of flow rate relative to the regurgitant orifice.[52,61,62] The contour flattens out close to the orifice, whereas the contour assumes an elongated or more oval shape furthest from the orifice. These variations in PISA contour result in systematic overestimation at flow rates farthest from the orifice and in underestimation closest to the orifice (Fig. 18-19). In addition, measurement of the radius should be avoided along the sides of the PISA region because flow here is perpendicular to the ultrasound beam, resulting in underestimation of the velocity component with frank dropout of flow display at angles perpendicular to flow. This dropout of color display where flow is perpendicular gives the PISA region a rounded appearance at its base. Figure 18-20 shows an ideal zone for PISA radius measurement to occur and zones in which to avoid measurement.

In vitro studies have shown that regurgitant orifice shape can impact the shape of the PISA region.[57] This important factor should be considered with application of the use of a hemispherical formula to the PISA contour because this assumes a circular regurgitant orifice. However, the regurgitant orifice may not be circular, particularly in view of the elliptical coaptation zone of the mitral leaflets, which may be especially important in functional MR where symmetric tethering of the mitral leaflets results in an elliptical regurgitant orifice. Hemispheric assumption of the PISA region underestimates the regurgitant flow rate, especially with rectangular regurgitant orifices.[57] Application of a hemielliptical formula to the PISA region has

shown improved accuracy MR quantification.[58,66] However, the hemielliptical surface area formula is complex, requiring measurement of three radii, which are orthogonally oriented, and integrated for surface area calculation. This adds considerable complexity to the PISA method and has limited clinical application of a hemielliptical formula for the PISA region.

The PISA region appears less influenced by changes in machine settings such as gain, wall filter, frame rate, and packet size compared with distal jet area methods.[53]

## VOLUMETRIC METHODS WITH PULSED DOPPLER IMAGING

Volumetric methods use pulse wave Doppler techniques to calculate flow rates and stroke volumes. The stroke volume across a valve annulus can be calculated as: time velocity integral across valve annulus multiplied by the cross-sectional area of the annulus. The MR regurgitant volume can be calculated from the flow across cardiac valves.[67-71] Although many combinations can be used, a common way to derive MR volume is: MR volume = mitral inflow minus aortic outflow (Fig. 18-21).

Mitral inflow volume is calculated as: (time velocity integral of mitral inflow) × (cross-sectional area) of the mitral annulus. The time velocity integral of mitral inflow should be measured at the level of the mitral annular plane because this is where the cross-sectional area is measured (Fig. 18-22). The cross-sectional area of the mitral annulus is assumed to be circular and calculated as $\pi r^2$, where $r$ is the diameter measured in the in apical four-chamber divided by 2. Anatomically, the mitral annulus is D-shaped, more like an ellipse than a circle. However, use of a circular assumption for the annulus is reasonable in patients who have at least moderate MR given the annular dilation that occurs with development of moderate or greater MR. Alternatively, the mitral annulus can also be calculated as an ellipse in which the area is $\pi ab$, with $a$ and $b$ being the diameters measured in the apical four-chamber and two-chamber views divided by 2. Aortic outflow is calculated as time velocity integral of aortic outflow × cross-sectional area of LV outflow tract. This method assumes that there is no aortic regurgitation; otherwise, pulmonary artery outflow can be used, assuming no significant pulmonary regurgitation. The MR regurgitant volume can also be obtained by calculating LV stroke volume and subtracting aortic outflow volume, assuming no aortic insufficiency is present. Table 18-2 summarizes validation of volumetric methods with pulsed Doppler against comparable standards.

Although straightforward in concept, volumetric methods are subject to increased variability related to the number of measurements necessary to calculate cardiac flows from pulsed Doppler and annular areas. For reproducible results, these methods generally require significant training. In addition, as the radius is squared in the area term, small errors in measurement are amplified,[67] and accurate resolution of the annulus is important to minimize measurement errors.

## SUPPORTIVE EVIDENCE IN THE ASSESSMENT OF MITRAL REGURGITATION

### *Pulmonary Venous Inflow Pattern*

The pulmonary venous inflow pattern provides confirmatory data in assessment of MR severity. Normal pulmonary venous inflow has forward flow during both systole and diastole, with

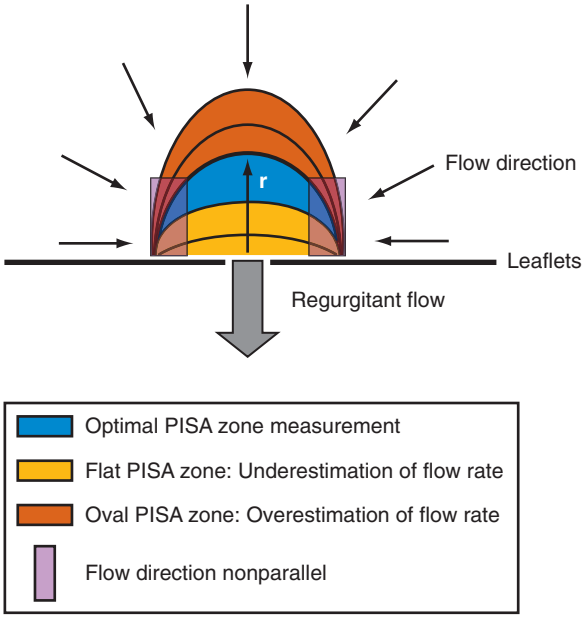



**Figure 18-20 The proximal isovelocity surface area (*PISA*) region is optimally measured where the region is hemispherical.** Flows farthest away from the orifice assume an elongated or oval contour and overestimate flows, whereas flows closest to the orifice assume a flat contour and underestimate flows. Measurement of the radius should be avoided along the sides of the PISA region because flow here is perpendicular to the ultrasound beam, which results in underestimation of the velocity component with frank dropout of flow display at angles perpendicular to flow.

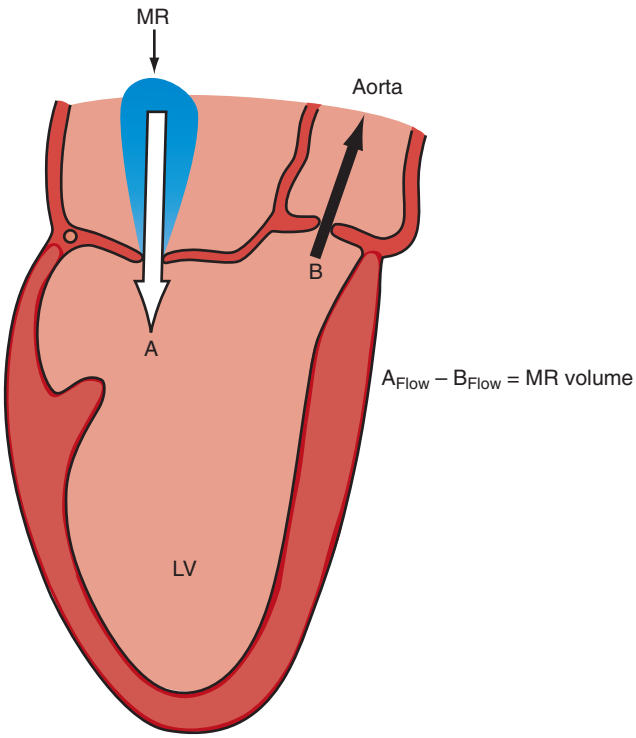



**Figure 18-21 Schematic shows volumetric method for calculation of mitral regurgitant (*MR*) volume.** Mitral inflow minus the aortic outflow equals the MR regurgitant volume, provided there is no significant aortic regurgitation.

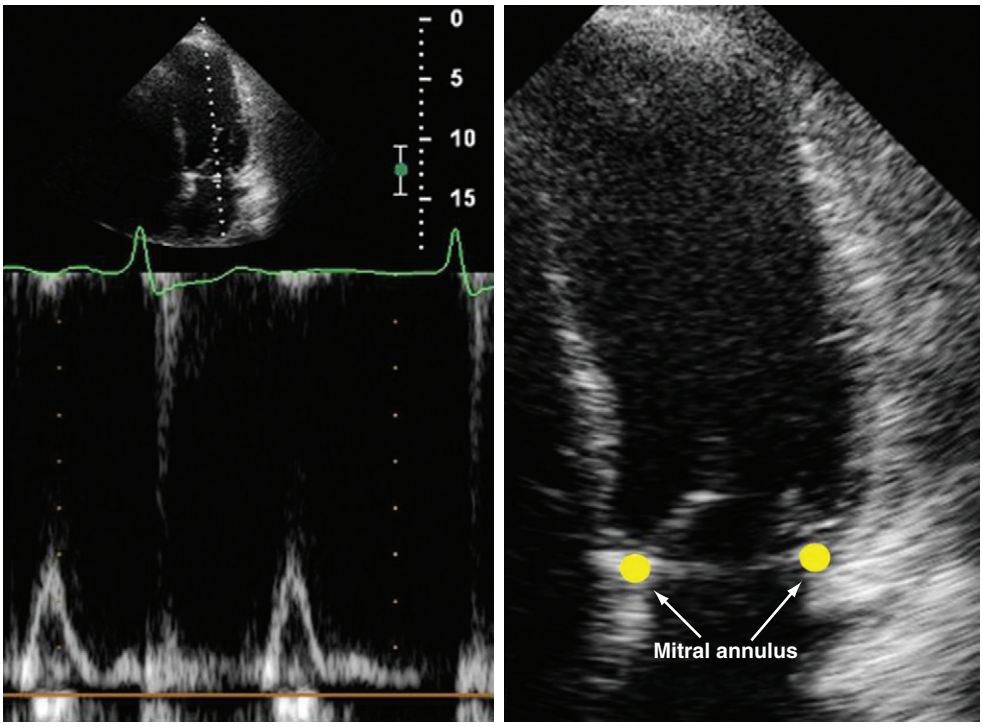



**Figure 18-22 Mitral inflow measured at the level of the mitral annulus (*left panel*).** *Right panel*: Diameter of the mitral annulus (*yellow dots*) measured in mid diastole.

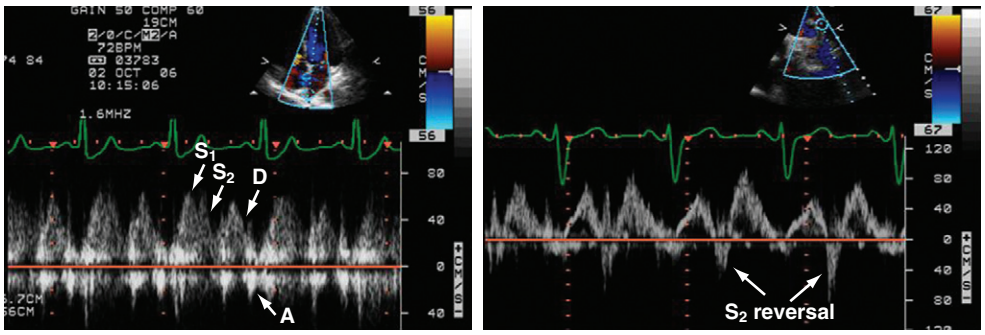



**Figure 18-23 Normal pulmonary venous pattern (*left panel*).** Pulmonary venous inflow into the LA occurs both in systole ($S_1$ and $S_2$) and diastole (*D*), with brief reversal of flow during atrial contraction (*A*). *Right panel*: Reversal of $S_2$ component (*arrows*) with severe mitral regurgitation.

a brief reversal of flow during atrial contraction (Fig. 18-23). Systolic flow (S wave) has two components: $S_1$ and $S_2$. The S wave is slightly larger than the D wave. Pulmonary veins are sampled in the apical four-chamber view with the sample volume placed approximately 1 cm from the orifice. Studies have shown feasibility of imaging the pulmonary venous inflow pattern with transthoracic imaging,[72-74] with a reported success rate of 95% for pulmonary venous systolic and diastolic flow velocity and 90% for the atrial reversal wave. Systolic flow reversal as detected with transthoracic imaging had a sensitivity of 61% and specificity of 92% for severe MR as measured with PISA method.[75] Limitations with transthoracic echocardiographic (TTE) imaging of the pulmonary venous inflow pattern occur where increased depth settings have resulted in inadequate pulsed-wave Doppler sampling.

Changes in the systolic pulmonary venous pattern can estimate the degree of MR severity. As MR increases, the systolic wave becomes blunted, decreasing to less than the D wave. As the MR volume increases, there is eventual reversal of first the $S_2$ wave (see Fig. 18-23, *right* panel) and then the entire S wave.[76] Changes in pulmonary venous pattern with increasing MR volume relates to initial blunting of the systolic wave from the propagation wave formed by the MR volume into the LA, with overt reversal of pulmonary systolic flow with increasing MR volume. Other studies have suggested that pulmonary venous inflow is best imaged with transesophageal echocardiographic (TEE) techniques. Studies with TEE have shown sensitivity of 82% to 90% and specificity of 100% for systolic flow reversal as indicative of severe MR.[77,78]

Systolic blunting of pulmonary veins without reversal of flow also provides confirmatory evidence of significant MR. However, the presence of systolic blunting is nonspecific as it can occur in a number of clinical situations where there is elevated LA pressures, such as in LV dysfunction or atrial fibrillation.[79,80] Consequently, the presence of systolic blunting is not a specific sign of MR severity and should be interpreted with this in mind.

On the other hand, systolic flow reversal is a fairly specific sign of severe MR. Flow reversal can be difficult to demonstrate with transthoracic imaging. In addition, the MR jet itself can flow directly into the pulmonary vein, contaminating the pulmonary venous Doppler signal. In eccentric MR jets, the right and left pulmonary veins can be differentially affected, depending on the direction of the jet. The best method is to pulse Doppler both right and left pulmonary veins to obtain a complete sampling.[76,81]

### *Continuous Wave Doppler Pattern*

Continuous wave Doppler of the MR jet provides an indirect assessment of MR severity. The more intense the CW signal of the MR, the greater number of red blood cell reflectors and hence, MR volume. In addition, the more complete the MR CW signal, the greater likelihood the MR is significant. Studies have shown that the signal intensity of the MR CW tracing correlates with MR severity compared with an angiographic standard.[82,83] Rapid equilibration of the LV-LA gradient that occurs with severe MR can result in a "V" shape pattern to the normal parabolic CW MR jet. CW intensity and pattern should be used as supportive evidence for MR severity because signal intensity and shape can vary greatly with machine settings and alignment of the CW beam along the regurgitant jet.

### *Other Supportive Factors*

Valve morphology can provide important clues in the assessment of MR. Apical tenting of the mitral leaflets is associated with functional MR, which develops in the setting of LV cardiomyopathy.[84-87] The presence of valvular vegetations, flail portion, and frank papillary muscle rupture are associated with severe MR. Increased LA and LV size are associated with significant MR, presumably from a volume effect in increasing chamber size. However, left-sided chamber enlargement results from a number of clinical situations, such as arrhythmias and cardiomyopathy, and thus is not specific for MR severity. An elevated right ventricular (RV) systolic pressure also suggests clinically important MR as a result of the regurgitant volume effect on the pulmonary vasculature. An increased E wave velocity is also supportive of significant MR.

## THREE-DIMENSIONAL ECHOCARDIOGRAPHY

3D echocardiography allows for direct planimetry of vena contracta area, a measure of the regurgitant orifice area. An advantage of 3D echocardiography is that it does not rely on geometric assumptions for measurement of regurgitant orifice area, which are necessary in two-dimensional (2D) regurgitant orifice area methods. For planimetry of the vena contracta area, a full-volume 3D color Doppler acquisition should be obtained 7 to 14 consecutive cardiac cycles with electrocardiographic gating. Sector size should be narrowed to maximize frame rate. With use of multiplanar reconstruction software available on commercial 3D analysis systems, two orthogonal image planes parallel to the regurgitant jet direction can be cropped across the regurgitant jet; then a third cropping plane oriented perpendicular to the jet direction can be aligned until the cross-sectional area at the level of the vena contracta is visualized. The frame with the largest vena contracta area in systole is measured with direct planimetry of the color Doppler flow signal (Fig. 18-24).[88]

Validation studies have shown that 3D guided direct planimetry of vena contracta area is feasible and correlates well with regurgitant orifice area derived with the volumetric Doppler approach.[88-90] More recently, Marsan and associates reported that 3D vena contracta area was highly accurate compared with MR volume measured with velocity-encoded cardiac magnetic resonance imaging in patients with functional MR.[89] An important limitation of 3D color-guided direct planimetry of vena contracta area is the relatively low 3D spatial resolution, particularly in the nonaxial planes. For optimization of spatial resolution, depth should be adjusted for maximal resolution and 3D data acquisitions should be performed with the highest number of cardiac cycles whenever possible. 3D color-guided planimetry of the vena contracta area is best applied for moderate or greater MR, given the limitations of 3D spatial resolution. This alternate measure of effective regurgitant orifice area can provide an alternative measure or complementary measure to 2D methods, especially in borderline cases.

Because there is no single reference standard for MR grading, and because each method has inherent limitations, the American Society of Echocardiography has recommended an integrated approach to grading MR, where multiple parameters are included rather than dependence on a single measurement in evaluation of severity of MR.[7] The integrative method includes quantitative and semiquantitative Doppler methods that include PISA method, vena contracta width, jet area to LA area ratio, and volumetric methods. In addition, supportive data such as pulmonary vein flow pattern and height of the E wave should be included in the grading of MR. Table 18-3 summarizes the echocardiographic criteria for quantification of MR.

# Timing of Surgical Intervention for Mitral Regurgitation

## PATHOPHYSIOLOGY

Mitral regurgitation results in a significant fraction of the LV ejection volume returning to the LA. To maintain the same forward stroke volume, the LV compensates by increasing the dilating and the ejection fraction, resulting in hyperdynamic LV function. Eventually, the LV becomes unable to compensate for the increased volume workload, and the LV ejection fraction begins to decrease while the LV end-systolic volume increases. The development of MR can be acute, such as in acute mitral valve endocarditis, or chronic, such as frequently occurs with mitral valve prolapse. In addition, acute MR can occur in the setting of chronic MR, such as with development of flail leaflet from ruptured chord in a patient with chronic MR from mitral valve prolapse. The presentation and pathophysiology of acute MR differs from that of chronic MR (Fig. 18-25). In acute MR, the LA cannot accommodate the sudden volume load because it has not had time to adapt. This results in acute pulmonary edema, elevated right-sided pressures, and severe dyspnea. The LV function becomes hyperdynamic to compensate but may not be able to dilate adequately to maintain forward stroke volume, resulting in decreased cardiac output and hypotension. Treatment for acute MR focuses on acute unloading with afterload agents if blood pressure allows or with insertion of an intraaortic balloon pump. These are often temporary measures because, ultimately, the primary treatment is surgical correction.

In chronic MR, the LV has time to remodel. The additional volume load on the LV leads to an eccentric hypertrophy pattern as part of the remodeling process. Histologic examination of the myocardium in this setting shows myocyte hypertrophy, predominantly through addition of sarcomeres in series, resulting in elongation of the myofibers. This remodeling process

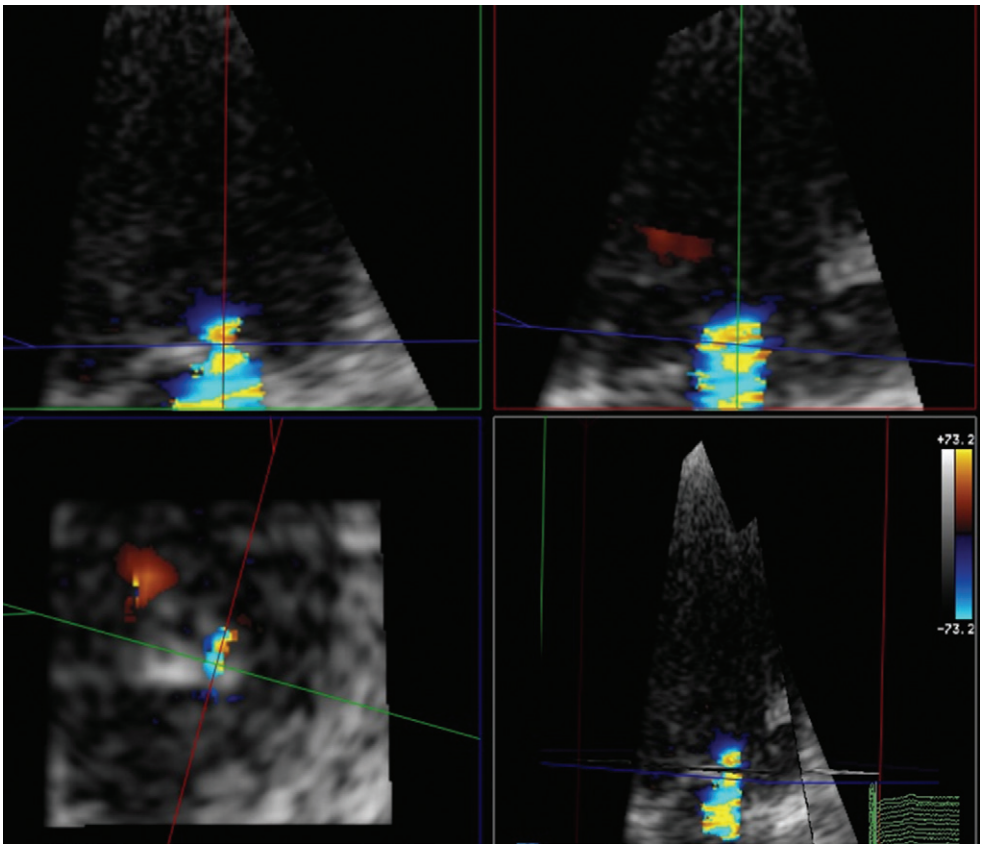



**Figure 18-24 3D guided direct planimetry of vena contracta area.** Two orthogonal image planes parallel to the regurgitant jet direction are displayed simultaneously (*top panels*). A third cropping plane, which is perpendicularly oriented to the jet direction, is moved along the jet direction until the cross-sectional area at the level of the vena contracta is visualized (*bottom right panel*).The vena contracta area is measured with direct planimetry of the color Doppler flow signal (*bottom left panel*). *(Adapted from Zeng X, Levine RA, Hua L, et al: Diagnostic value of vena contracta area in the quantification of mitral regurgitation severity by color Doppler 3D echocardiography.* Circ Cardiovasc Imaging *4:506-513, 2011. Epub Jul 5, 2011.)*

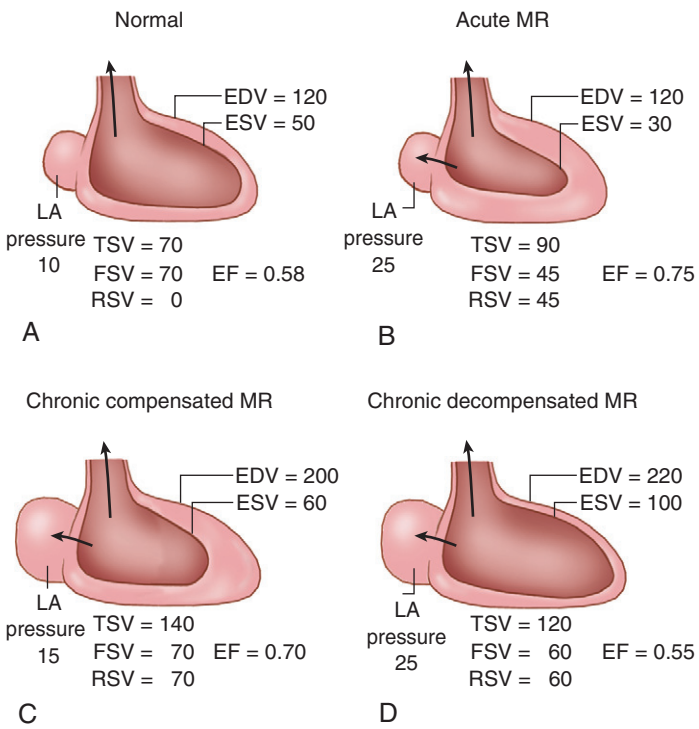



**Figure 18-25 Three phases of MR compared with normal physiology. A,** Normal physiology. **B,** In acute MR, an increase in preload and a decrease in afterload cause an increase in end-diastolic volume (*EDV*) and a decrease in end-systolic volume (*ESV*), producing an increase in total stroke volume (*TSV*). However, forward stroke volume (*FSV*) is diminished because 50% of the TSV regurgitates as the regurgitant stroke volume (*RSV*), resulting in an increase in *LA pressure*. **C,** In the chronic compensated phase, eccentric hypertrophy has developed and EDV is now increased substantially. Afterload has returned toward normal as the radius term of the Laplace relationship increases with the increase in EDV. Normal muscle function and a large increase in EDV permit a substantial increase in TSV from the acute phase. This, in turn, permits a normal FSV. LA enlargement now accommodates the regurgitant volume at lower LA pressure. Ejection fraction (*EF*) remains greater than normal. **D,** In the chronic decompensated phase, muscle dysfunction has developed, impairing ejection fraction, diminishing both TSV and FSV. The EF, although still normal" has decreased to 0.55, and LA pressure is reelevated because less volume is ejected during systole, causing a higher ESV. *(From Carabello BA: Progress in mitral and aortic regurgitation.* Curr Probl Cardiol *28:553, 2003.)*

**TABLE 18-3 Qualitative and Quantitative Parameters Useful in Grading of Mitral Regurgitation Severity**

| | *Mild* | *Moderate* | *Severe* |
|---|---|---|---|
| **Structural Parameters** | | | |
| LA size | Normal* | Normal or dilated | Usually dilated† |
| LV size | Normal* | Normal or dilated | Usually dilated† |
| Mitral leaflets or support apparatus | Normal or abnormal | Normal or abnormal | Abnormal/flail leaflet/ruptured papillary muscle |
| **Doppler Parameters** | | | |
| Color flow jet area‡ | Small central jet (usually <4 $cm^2$ or <20% of LA area) | Variable | Large central jet (usually >10 $cm^2$ or >40% of LA area) or variable size wall-impinging jet swirling in LA |
| Mitral inflow, pulsed wave | A wave dominant‖ | Variable | E wave dominant‖ (E usually 1.2 m/s) |
| Jet density, CW | Incomplete or faint | Dense | Dense |
| Jet contour, CW | Parabolic | Usually parabolic | Early peaking, triangular |
| Pulmonary vein flow | Systolic dominance¶ | Systolic blunting¶ | Systolic flow reversal§ |
| **Quantitative Parameters**** | | | |
| Vena contracta width (cm) | <0.3 | 0.3-0.69 | ≥0.7 |
| Regurgitant volume (mL/beat) | <30 | 30-44, 45-59 | ≥60 |
| Regurgitant fraction (%) | <30 | 30-39, 40-49 | ≥50 |
| EROA ($cm^2$) | <0.20 | 0.20-0.29, 0.30-0.39 | ≥0.40 |

Adapted from Zoghbi WA, Enriquez-Sarano M, Foster E, et al: Recommendations for evaluation of the severity of native valvular regurgitation with two-dimensional and Doppler echocardiography. *J Am Soc Echocardiogr* 16:777-802, 2003.

*EROA*, Effective regurgitant orifice area.

*Unless there are other reasons for LA or LV dilation. Normal 2D measurements: LV minor axis, ≤2.8 $cm/m^2$; LV end-diastolic volume, ≤82 $mL/m^2$; maximal LA anteroposterior diameter, ≤2 $cm/m^2$; maximal LA volume, ≤36 $mL/m^2$.[2,33,35]

†Exception: acute mitral regurgitation.

‡At a Nyquist limit of 50 to 60 cm/s.

§Pulmonary venous systolic flow reversal is specific but not sensitive for severe MR.

‖Usually more than 50 years of age or in conditions of impaired relaxation, in the absence of mitral stenosis or other causes of elevated LA pressure.

¶Unless other reasons for systolic blunting (e.g., atrial fibrillation, elevated LA pressure).

**Quantitative parameters can help subclassify the moderate regurgitation group into mild-to-moderate and moderate-to-severe.

results in LV dilation and augmented contraction, which results in hyperdynamic LV function providing a larger total ejection volume to maintain forward stroke volume. Similarly, the LA remodels by dilating to increase compliance to accommodate the MR volume. This lessens the transmitted pressure from backward flow of blood directly into the pulmonary circulation and results in less elevation of right-sided pressures and dyspnea.

Eventually, the LV is unable to compensate with the gradual replacement of myocyte mass with interstitial fibrosis as the remodeling process progresses (Fig. 18-26).[91] LV volumes increase further but cannot fully compensate, resulting in a decrease in LV ejection fraction, predominantly by a relatively greater increase in end-systolic volume. The forward stroke volume falls, and without intervention, onset of heart failure occurs. Patients with chronic severe MR can be asymptomatic for a long period of time, with studies reporting an average of 5 to 10 years from time of diagnosis before signs of symptoms or other indications for surgical intervention develop.[2,92,93]

Treatment with afterload unloading agents for chronic severe primary MR has not been shown to be of benefit.[94,95] Because the pathophysiology of MR is not one of increased afterload, treatment with these agents does not address the mechanistic derangement and in fact may mask the development of LV dysfunction by unloading the ventricle.

## DETERMINATION OF MECHANISM

Determination of the mechanism of MR is important because it dictates the therapeutic course, especially as treatment options for primary versus secondary MR are different.

For primary severe valvular MR, consensus guidelines support a class I indication surgical intervention with mitral valve repair or replacement when symptoms develop or when evidence of LV dysfunction is present.[96] Consensus guidelines support an LV ejection fraction of 0.60 or less or LV end-systolic dimension of 40 mm or more as cutoff values for the presence of LV decompensation in severe MR.

A natural history study of 229 patients with MR from isolated flail mitral leaflet diagnosed from 1980 to 1989 with clinical follow-up period from 1994 to 1995 showed that patients with flail mitral leaflet had decreased survival rates compared with the expected survival rates of an age-matched and gender-matched control group (Fig. 18-27).[1] The incidence rate of surgical intervention or death was 90% at 10 years from diagnosis (Fig. 18-28). Factors associated with increased postsurgical morbidity and mortality were an LV ejection fraction of 0.60 or less and or New York Heart Association functional class 3 to 4.[97,98]

Asymptomatic patients with severe MR with preserved LV function are an important but challenging group. Early mitral repair in asymptomatic patients with chronic severe MR and preserved LV function is a class 2a indication in selected cases, with a high likelihood of mitral valve repair (more than 90%) with low operative mortality rate (1% or less). One of the challenges is determination of whether patients are truly asymptomatic because decreased functional capacity may be attributed to deconditioning and age or manifested as nonspecific symptoms. In addition, some patients reduce their activity subtly in response and may not be aware of or recognize a reduction in functional capacity. In these cases, exercise testing echocardiography can provide objective evidence of functional capacity and, if performed with echocardiography, can also provide hemodynamic data such as right-sided pressures changes and valvular and ventricular function in response to exercise.

Mitral valve repair is associated with improved survival rates in patients compared with mitral valve replacement. If mitral valve repair is not possible, then mitral valve replacement should be performed with chordal preservation. An algorithm for management of severe chronic primary (valvular) MR is displayed in Figure 18-29.[96]

For secondary MR, the therapeutic approach is less clear. The development of MR (even mild) after myocardial infarction is associated with decreased survival (Fig. 18-30).[3,4] Yet it is unknown whether the procedure to reduce the MR severity results in a decrease in cardiovasular morbidity and mortality or improvement in total survival. Medical management should be aimed toward primary LV dysfunction. Specifically, angiotensin-converting enzyme inhibitors and beta-blockers have shown a reduction in MR in this patient population, as has cardiac resynchronization.[99-102]

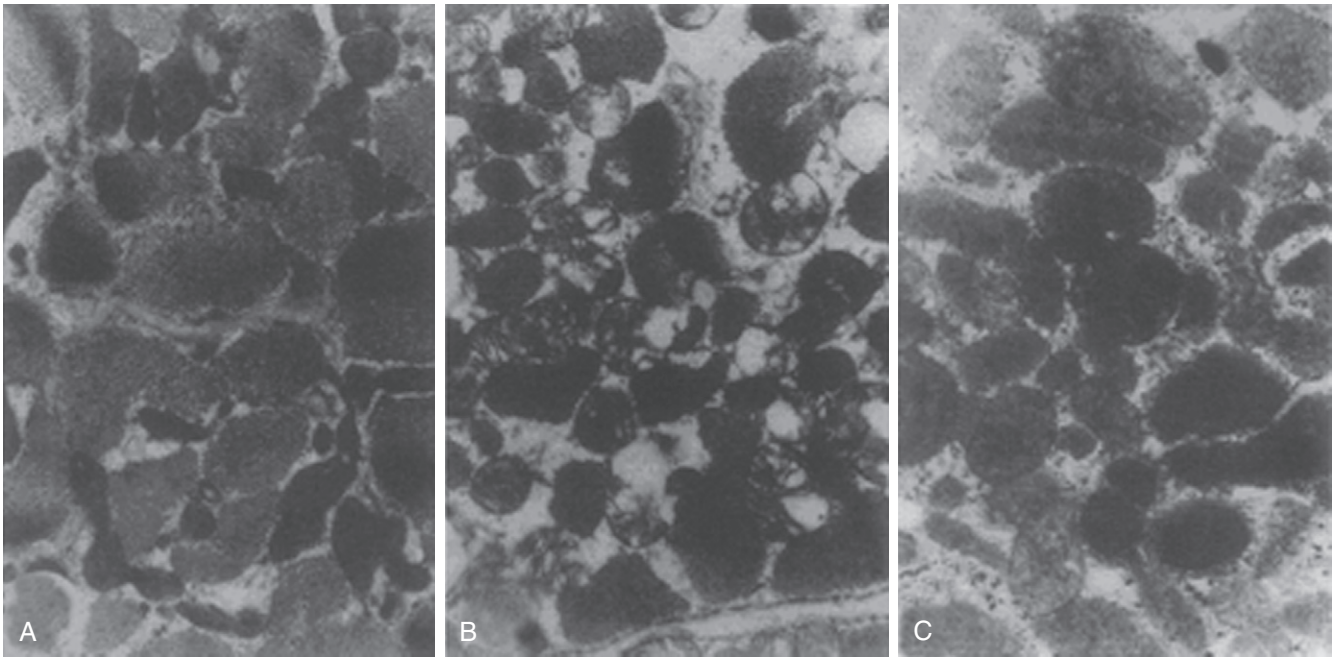



**Figure 18-26 Myocardial ultrastructures of normal dogs (A), dogs with severe mitral regurgitation (MR) (B), and dogs that had severe MR corrected surgically (C) are shown.** With severe MR, a loss of contractile elements is restored after surgery. *(From Spinale FG, Ishihara K, Zile M, et al: Structural basis for changes in left ventricular function and geometry because of chronic mitral regurgitation and after correction of volume overload.* J Thorac Cardiovasc Surg *106:1147-1157, 1993.)*

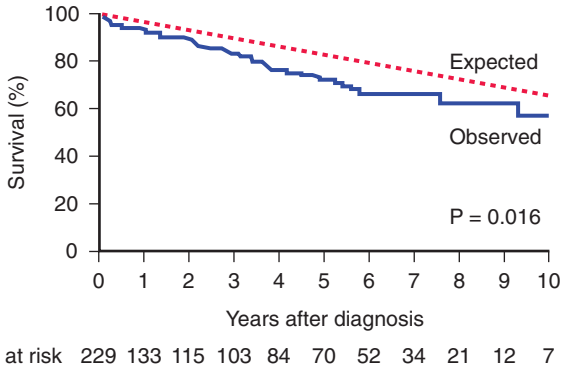



**Figure 18-27 Decreased survival of 229 patients with flail mitral leaflet with medial treatment alone compared with expected survival in an age-matched and gender-matched control group.** *(From Ling LH, et al: Clinical outcome of mitral regurgitation due to flail leaflet.* N Engl J Med *335:1417-1423, 1996.)*

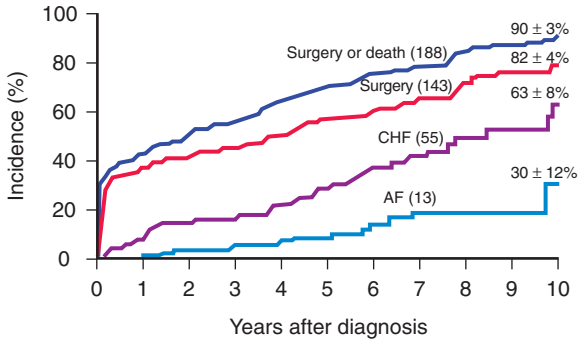



**Figure 18-28 Incidence rates of atrial fibrillation (*AF*), congestive heart failure (*CHF*), mitral-valve surgery, and surgery or death in adults with a flail mitral leaflet.** A total of 175 patients were initially at risk for atrial fibrillation, and 229 were initially at risk for the other endpoints. The numbers in parentheses are numbers of events for each endpoint. Plus-minus values are mean (±SE) event rates at 10 years. *(From Ling LH, et al: Clinical outcome of mitral regurgitation due to flail leaflet.* N Engl J Med *335:1417-1423, 1996.)*

Surgical mitral valve repair or replacement for ischemic MR is most often performed at time of coronary artery bypass graft surgery in patients with moderate to severe ischemic MR. Mitral valve repair seems preferable over replacement for ischemic MR in most patients; retrospective studies suggest improved survival in patients undergoing mitral valve repair compared with replacement.[103,104]

Much of the uncertainty regarding the therapeutic approach for secondary MR is the lack of consistent data that show improvement in survival or functional status in patient who undergo mitral valve repair at time of coronary artery bypass graft surgery.[105] Until recently, no prospective randomized trials have examined impact of mitral valve repair in patients undergoing coronary artery bypass graft surgery with moderate or greater MR. The Cardiothoracic Surgical Network (www.ctsnet.org) is currently conducting two randomized trials on this topic.[106] One examines the impact on end-systolic volume index of coronary artery bypass graft plus mitral valve repair or coronary artery bypass graft alone in patients with moderate ischemic MR. A second one examines the impact on end-systolic volume index of coronary artery bypass graft plus mitral valve repair or coronary artery bypass graft plus mitral valve replacement in patients with severe ischemic MR. Adding to the therapeutic uncertainty in ischemic MR is that there is a significant recurrence rate of MR of up to one third of patients after mitral valve repair.[107-109] This may result from progression of LV dilation or persistent tethering of the mitral leaflets despite ring annuloplasty.[110,111]

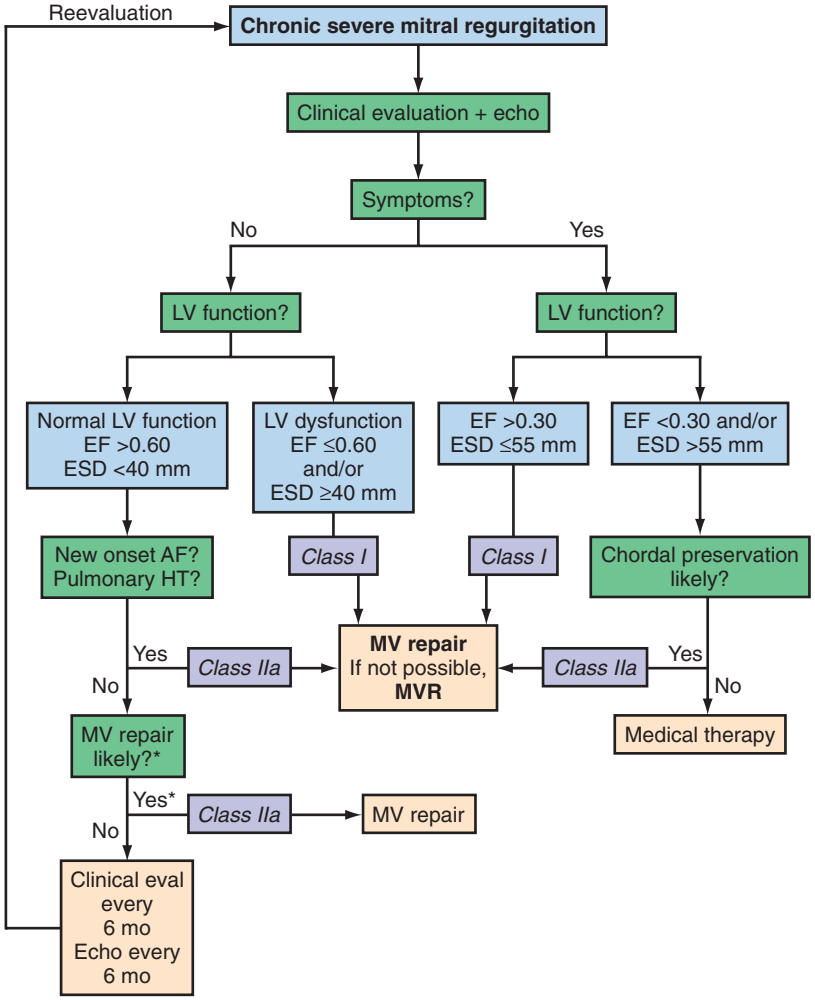



**Figure 18-29** **Algorithm for management of severe chronic primary mitral regurgitation.** *AF,* Atrial fibrillation; *EF,* ejection fraction; *ESD,* end-systolic dimension; *HT,* hypertension; *MV,* mitral valve; *MVR,* mitral valve replacement. *(From Bonow RO, et al: ACC/AHA guidelines for the management of patients with valvular heart disease.* Circulation *114:84-231, 2006.)*

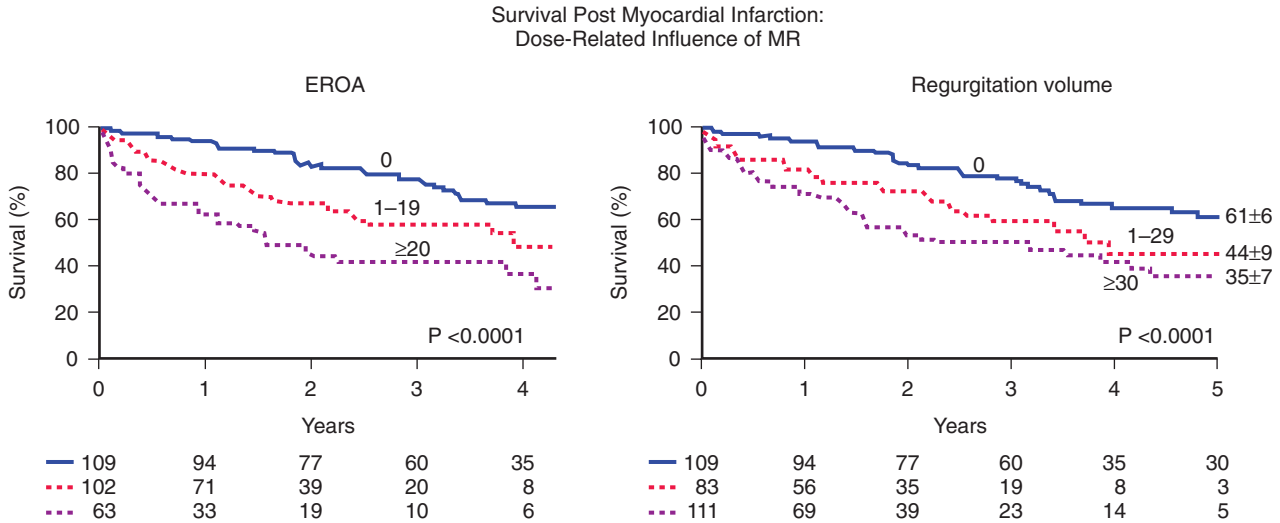



**Figure 18-30** **Mitral regurgitation and survival after myocardial infarction with patients stratified by mitral regurgitant severity based on effective regurgitation orifice area (*EROA; left*) or regurgitation volume (*right*).** *(From Grigioni F, et al: Ischemic mitral regurgitation: long-term outcome and prognostic implications with quantitative Doppler assessment.* Circulation *103:1759-1764, 2001.)*

## KEY POINTS

- The mitral valve apparatus consist of mitral annulus, mitral leaflets, chordae tendineae, and papillary muscles.
- The mitral annulus shape is bimodal with superior (high) points oriented anterior-posterior and inferior (low) points oriented medial-lateral.
- The anterior leaflet accounts for most of the leaflet closing surface area. The posterior leaflet is crescent shaped and scalloped with small clefts between the scallop segments.
- The primary or marginal chordae attach along the edges of the leaflets and function to produce a level coaptation plane. Rupture of the primary chordae is associated with flail leaflet and significant MR.
- The assessment of MR should be performed in an integrative manner, with Doppler methods and supportive evidence taken into account.
- Distal jet area and vena contracta methods provide semiquantitative methods for assessment of MR.
- With eccentric MR jets, jet area methods may underestimate MR degree because of wall impingement.
- Quantitation of MR is performed by calculating effective regurgitant orifice area or regurgitant volume or fraction with PISA or volumetric pulsed Doppler methods when technically possible in moderate or greater degrees of MR.
- Pulmonary venous Doppler pattern provides supportive evidence of MR severity, particularly the presence of pulmonary venous systolic flow reversal.
- Supportive evidence such as LA and LV chamber enlargement, LV hypertrophy, elevated RV pressures, and peak mitral E wave velocity should be included in the overall assessment of MR.
- Direct planimetry of vena contracta area (a measure of the effective regurgitant orifice area) is feasible with 3D color-guided echocardiography and can be useful in determination of MR degree and as complementary data to 2D methods, especially in cases where MR grade is in a border zone.
- Clinical decision making for management of MR is predicated on echocardiographic assessment of mechanism, severity of MR, and LV function.
- It is important to distinguish the mechanism of MR as primary (valvular etiology) or secondary (ventricular abnormality) because the approach to therapy is different.
- Development of MR can be acute, chronic, or acute on chronic.
- For severe primary MR, class 1 indications for surgical intervention are for development of symptoms or evidence of LV decompensation (LV ejection fraction of 0.6 or less or LV end-systolic diameter of 40 mm or more).
- Early mitral valve repair can be considered for asymptomatic patients with severe primary MR and preserved LV function if there is a high likelihood (more than 90%) of mitral valve repair and low operative mortality (less than 1%).
- Therapy for secondary MR should focus on medical management of the primary LV dysfunction with angiotensin-converting enzyme inhibitors and beta-blockers showing a decrease in MR in this patient population.

## REFERENCES


1. Ling LH, Enriques-Sarano M, Sweard JB, et al: Clinical outcome of mitral regurgitation due to flail leaflet. *N Engl J Med* 335:1417-1423, 1996.
2. Rosen SE, Borer JS, Hochreiter C, et al: Natural history of the asymptomatic/minimally symptomatic patient with severe mitral regurgitation secondary to mitral valve prolapse and normal right and left ventricular performance. *Am J Cardiol* 74:374-380, 1994.
3. Clemens JD, Horwitz RI, Jaffe CC, et al: A controlled evaluation of the risk of bacterial endocarditis in persons with mitral-valve prolapse. *N Engl J Med* 307:776-781, 1982.
4. Nishimura RA, Magoon MD, Shub C, et al: Echocardiographically documented mitral-valve prolapse. Long-term follow-up of 237 patients. *N Engl J Med* 313:1305-1309, 1985.
5. Lamas GA, Mitchell GF, Smith SC Jr, et al: Clinical significance of mitral regurgitation after acute myocardial infarction. Survival and Ventricular Enlargement Investigators. *Circulation* 96:827-833, 1997.
6. Grigioni F, Enriques-Sarano M, Zehr KJ, et al: Ischemic mitral regurgitation: long-term outcome and prognostic implications with quantitative Doppler assessment. *Circulation* 103:1759-1764, 2001.
7. Stevenson LW, Grover-McKay M, Brucken RC, et al: Effects of afterload reduction (diuretics and vasodilators) on left ventricular volume and mitral regurgitation in severe congestive heart failure secondary to ischemic or idiopathic dilated cardiomyopathy. *Am J Cardiol* 60:654-658, 1987.
8. Junker A, Thaysen P, Nielsen B, et al: The hemodynamic and prognostic significance of echo-Doppler-proven mitral regurgitation in patients with dilated cardiomyopathy. *Cardiology* 83:14-20, 1993.
9. Koelling TM, Aaronson KD, Cody RJ, et al: Prognostic significance of mitral regurgitation and tricuspid regurgitation in patients with left ventricular systolic dysfunction. *Am Heart J* 144:524-529, 2002.
10. Nkomo VT, Gardin JM, Skelton TN, et al: Burden of valvular heart diseases: a population-based study. *Lancet* 368:1005-1011, 2006.
11. Jones EC, Devereux RB, Roman MJ, et al: Prevalence and correlates of mitral regurgitation in a population-based sample (the Strong Heart Study). *Am J Cardiol* 87:298-304, 2001.
12. Singh JP, Evans JC, Levy D, et al: Prevalence and clinical determinants of mitral, tricuspid, and aortic regurgitation (the Framingham Heart Study). *Am J Cardiol* 83:897-902, 1999.
13. Gammie JS, Shubin S, Bartley G, et al: Trends in mitral valve surgery in the United States: results from the Society of Thoracic Surgeons Adult Cardiac Surgery Database. *Ann Thorac Surg* 87:1431-1439, 2009.
14. Levine RA, Triulzi MO, Harrigan P, et al: The relationship of mitral annular shape to the diagnosis of mitral valve prolapse. *Circulation* 75:756-767, 1987.
15. Jimenez JH, Liou SW, Padala M, et al: A saddle-shaped annulus reduces systolic strain on the central region of the mitral valve anterior leaflet. *J Thorac Cardiovasc Surg* 134:1562-1568, 2007.
16. Padala M, Hutchinson BS, Croft LR, et al: Saddle shape of the mitral annulus reduces systolic strains on the P2 segment of the posterior mitral leaflet. *Ann Thorac Surg* 88:1499-1504, 2009.
17. Kunzelman KS, Reimink MS, Cochran RP: Annular dilatation increases stress in the mitral valve and delays coaptation: a finite element computer model. *Cardiovasc Surg* 5:427-434, 1997.
18. Kunzelman KS, Cochran RP, Chuong C, et al: Finite element analysis of the mitral valve. *J Heart Valve Dis* 2:326-340, 1993.
19. Mihalatos DG, Joseph S, Gopal A, et al: Mitral annular remodeling with varying degrees and mechanisms of chronic mitral regurgitation. *J Am Soc Echocardiogr* 20:397-404, 2007.
20. He S, Weston MW, Lemmon J, et al: Geometric distribution of chordae tendineae: an important anatomic feature in mitral valve function. *J Heart Valve Dis* 9:495-503, 2000.
21. Kaiser LR, Spray TL, editors: *Mastery of cardiothoracic surgery*, ed 2. New York, 2007, Lippincott Williams & Wilkins, p. 1009.

22. Yoshikai M, Kado H, Yasuda R, et al: Anomalous papillary muscle causing tethering of the mitral valve. *J Heart Valve Dis* 16:608-610, 2007.
23. Freed LA, Levy D, Levine RA, et al: Prevalence and clinical outcome of mitral-valve prolapse. *N Engl J Med* 341:1-7, 1999.
24. Adams DH, Anyanwu AC, Rahmanian PB, et al: Large annuloplasty rings facilitate mitral valve repair in Barlow's disease. *Ann Thorac Surg* 82:2096-2101, 2006.
25. Marks AR, Choong CY, Sanfilippo AJ, et al: Identification of high-risk and low-risk subgroups of patients with mitral-valve prolapse. *N Engl J Med* 320:1031-1036, 1989.
26. Zuppiroli A, Mori F, Favilli S, et al: Arrhythmias in mitral valve prolapse: relation to anterior mitral leaflet thickening, clinical variables, and color Doppler echocardiographic parameters. *Am Heart J* 128:919-927, 1994.
27. Avierinos JF, Gersh BJ, Melton LJ III, et al: Natural history of asymptomatic mitral valve prolapse in the community. *Circulation* 106:1355-1361, 2002.
28. Bursi F, Enrique-Sarano M, Nkomo VT, et al: Heart failure and death after myocardial infarction in the community: the emerging role of mitral regurgitation. *Circulation* 111: 295-301, 2005.
29. Clements SD Jr, Story WE, Hurst JW, et al: Ruptured papillary muscle, a complication of myocardial infarction: clinical presentation, diagnosis, and treatment. *Clin Cardiol* 8:93-103, 1985.
30. Levine RA, Schwammenthal E: Ischemic mitral regurgitation on the threshold of a solution: from paradoxes to unifying concepts. *Circulation* 112:745-758, 2005.
31. Kumanohoso T, Otsuji Y, Yoshifuku S, et al: Mechanism of higher incidence of ischemic mitral regurgitation in patients with inferior myocardial infarction: quantitative analysis of left ventricular and mitral valve geometry in 103 patients with prior myocardial infarction. *J Thorac Cardiovasc Surg* 125:135-143, 2003.
32. Carpentier A: Cardiac valve surgery: the "French correction." *J Thorac Cardiovasc Surg* 86:323-337, 1983.
33. Roberts BJ, Grayburn PA: Color flow imaging of the vena contracta in mitral regurgitation: technical considerations. *J Am Soc Echocardiogr* 16:1002-1006, 2003.
34. Miyatake K, Izumi S, Okamoto M, et al: Semiquantitative grading of severity of mitral regurgitation by real-time two-dimensional Doppler flow imaging technique. *J Am Coll Cardiol* 7:82-88, 1986.
35. Omoto R, Yokote Y, Takamoto S, et al: The development of real-time two-dimensional Doppler echocardiography and its clinical significance in acquired valvular diseases. With special reference to the evaluation of valvular regurgitation. *Jpn Heart J* 25:325-340, 1984.
36. Chen CG, Thomas JD, Anconina J, et al: Impact of impinging wall jet on color Doppler quantification of mitral regurgitation. *Circulation* 84:712-720, 1991.
37. Enriquez-Sarano M, Tajik AJ, Bailey KR, et al: Color flow imaging compared with quantitative Doppler assessment of severity of mitral regurgitation: influence of eccentricity of jet and mechanism of regurgitation. *J Am Coll Cardiol* 21:1211-1219, 1993.
38. Zoghbi WA, Enriquez-Sarano M, Foster E, et al: Recommendations for evaluation of the severity of native valvular regurgitation with two-dimensional and Doppler echocardiography. *J Am Soc Echocardiogr* 16:777-802, 2003.
39. Maciel BC, Moises VA, Shandas R, et al: Effects of pressure and volume of the receiving chamber on the spatial distribution of regurgitant jets as imaged by color Doppler flow mapping. An in vitro study. *Circulation* 83:605-613, 1991.
40. Hoit BD, Jones M, Eidbo EE, et al: Sources of variability for Doppler color flow mapping of regurgitant jets in an animal model of mitral regurgitation. *J Am Coll Cardiol* 13:1631-1636, 1989.
41. Yellin EL, Yoran C, Sonnenblick EH, et al: Dynamic changes in the canine mitral regurgitant orifice area during ventricular ejection. *Circ Res* 45:677-683, 1979.
42. Rivera JM, Mele D, Vandervoort PM, et al: Physical factors determining mitral regurgitation jet area. *Am J Cardiol* 74:515-516, 1994.
43. Simpson IA, Valdes-Cruz LM, Sahn DJ, et al: Doppler color flow mapping of simulated in vitro regurgitant jets: evaluation of the effects of orifice size and hemodynamic variables. *J Am Coll Cardiol* 13:1195-1207, 1989.
44. Spain MG, Smith MD, Grayburn PA, et al: Quantitative assessment of mitral regurgitation by Doppler color flow imaging: angiographic and hemodynamic correlations. *J Am Coll Cardiol* 13:585-590, 1989.
45. Fehske W, Omran H, Manz M, et al: Color-coded Doppler imaging of the vena contracta as a basis for quantification of pure mitral regurgitation. *Am J Cardiol* 73:268-274, 1994.
46. Baumgartner H, Schima H, Kuhn P: Value and limitations of proximal jet dimensions for the quantitation of valvular regurgitation: an in vitro study using Doppler flow imaging. *J Am Soc Echocardiogr* 4:57-66, 1991.
47. Lesniak-Sobelga A, Olszowska M, Pienazek P, et al: Vena contracta width as a simple method of assessing mitral valve regurgitation. Comparison with Doppler quantitative methods. *J Heart Valve Dis* 13:608-614, 2004.
48. Zhou X, Jones M, Shiota I, et al: Vena contracta imaged by Doppler color flow mapping predicts the severity of eccentric mitral regurgitation better than color jet area: a chronic animal study. *J Am Coll Cardiol* 30:1393-1398, 1997.
49. Grayburn PA, Fehske W, Omran H, et al: Multiplane transesophageal echocardiographic assessment of mitral regurgitation by Doppler color flow mapping of the vena contracta. *Am J Cardiol* 74:912-917, 1994.
50. Hall SA, Brickner ME, Willett DL, et al: Assessment of mitral regurgitation severity by Doppler color flow mapping of the vena contracta. *Circulation* 95:636-642, 1997.
51. Heinle SK, Hall SA, Brickner ME, et al: Comparison of vena contracta width by multiplane transesophageal echocardiography with quantitative Doppler assessment of mitral regurgitation. *Am J Cardiol* 81:175-179, 1998.
52. Vandervoort PM, Thoreau DH, Rivera JM, et al: Automated flow rate calculations based on digital analysis of flow convergence proximal to regurgitant orifices. *J Am Coll Cardiol* 22:535-541, 1993.
53. Utsunomiya T, Ogawa T, Tang HA, et al: Doppler color flow mapping of the proximal isovelocity surface area: a new method for measuring volume flow rate across a narrowed orifice. *J Am Soc Echocardiogr* 4:338-348, 1991.
54. Rodriguez L, Anconina J, Flachskampf FA, et al: Impact of finite orifice size on proximal flow convergence. Implications for Doppler quantification of valvular regurgitation. *Circ Res* 70:923-930, 1992.
55. Recusani F, Bargiggia GS, Yoganathan AP, et al: A new method for quantification of regurgitant flow rate using color Doppler flow imaging of the flow convergence region proximal to a discrete orifice. An in vitro study. *Circulation* 83:594-604, 1991.
56. Bargiggia GS, Tronconi L, Sahn DJ, et al: A new method for quantitation of mitral regurgitation based on color flow Doppler imaging of flow convergence proximal to regurgitant orifice. *Circulation* 84:1481-1489, 1991.
57. Utsunomiya T, Ogawa T, Doshi R, et al: Doppler color flow "proximal isovelocity surface area" method for estimating volume flow rate: effects of orifice shape and machine factors. *J Am Coll Cardiol* 17:1103-1111, 1991.
58. Rivera JM, Vandervoort PM, Thoreau DH, et al: Quantification of mitral regurgitation with the proximal flow convergence method: a clinical study. *Am Heart J* 124:1289-1296, 1992.
59. Utsunomiya T, Doshi R, Patel D, et al: Calculation of volume flow rate by the proximal isovelocity surface area method: simplified approach using color Doppler zero baseline shift. *J Am Coll Cardiol* 22:277-282, 1993.
60. Enriquez-Sarano M, Miller FA Jr, Hayes SN, et al: Effective mitral regurgitant orifice area: clinical use and pitfalls of the proximal isovelocity surface area method. *J Am Coll Cardiol* 25:703-709, 1995.
61. Schwammenthal E, Chen C, Giesler M, et al: New method for accurate calculation of regurgitant flow rate based on analysis of Doppler color flow maps of the proximal flow field. Validation in a canine model of mitral regurgitation with initial application in patients. *J Am Coll Cardiol* 27:161-172, 1996.
62. Moises VA, Maciel BC, Hornberger LK, et al: A new method for noninvasive estimation of ventricular septal defect shunt flow by Doppler color flow mapping: imaging of the laminar flow convergence region on the left septal surface. *J Am Coll Cardiol* 18:824-832, 1991.
63. Schwammenthal E, Chen C, Benning F, et al: Dynamics of mitral regurgitant flow and orifice area. Physiologic application of the proximal flow convergence method: clinical data and experimental testing. *Circulation* 90:307-322, 1994.
64. Enriquez-Sarano M, Sinak LJ, Tajik AJ, et al: Changes in effective regurgitant orifice throughout systole in patients with mitral valve prolapse. A clinical study using the proximal isovelocity surface area method. *Circulation* 92:2951-2958, 1995.
65. Pu M, Vandervoort PM, Griffin BP, et al: Quantification of mitral regurgitation by the proximal convergence method using transesophageal echocardiography. Clinical validation of a geometric correction for proximal flow constraint. *Circulation* 92:2169-2177, 1995.
66. Hopmeyer J, He S, Thorvig KM, et al: Estimation of mitral regurgitation with a hemielliptic curve-fitting algorithm: in vitro experiments with native mitral valves. *J Am Soc Echocardiogr* 11:322-331, 1998.
67. Rokey R, Sterling LL, Zoghbi WA, et al: Determination of regurgitant fraction in isolated mitral or aortic regurgitation by pulsed Doppler two-dimensional echocardiography. *J Am Coll Cardiol* 7:1273-1278, 1986.
68. Blumlein S, Bouchard A, Schiller NB, et al: Quantitation of mitral regurgitation by Doppler echocardiography. *Circulation* 74:306-314, 1986.

69. Tribouilloy C, Shen WF, Slama MA, et al: Noninvasive measurement of the regurgitant fraction by pulsed Doppler echocardiography in isolated pure mitral regurgitation. *Br Heart J* 66:290-294, 1991.
70. Dujardin KS, Enrique-Sarano M, Bailey KR, et al: Grading of mitral regurgitation by quantitative Doppler echocardiography: calibration by left ventricular angiography in routine clinical practice. *Circulation* 96:3409-3415, 1997.
71. Ascah KJ, Stewart KJ, Jiang L, et al: A Doppler-two-dimensional echocardiographic method for quantitation of mitral regurgitation. *Circulation* 72:377-383, 1985.
72. Masuyama T: Transthoracic Doppler echocardiographic measurements of pulmonary venous flow velocity patterns: comparison with transesophageal measurements. *J Am Soc Echocardiogr* 8:61-69, 1995.
73. Jensen JL, Williams FE, Beilby BJ, et al: Feasibility of obtaining pulmonary venous flow velocity in cardiac patients using transthoracic pulsed wave Doppler technique. *J Am Soc Echocardiogr* 10:60-66, 1997.
74. Keren G, Bier A, Sherez J, et al: Atrial contraction is an important determinant of pulmonary venous flow. *J Am Coll Cardiol* 7:693-695, 1986.
75. Enriquez-Sarano M, Dujardin KS, Tribouilloy CM, et al: Determinants of pulmonary venous flow reversal in mitral regurgitation and its usefulness in determining the severity of regurgitation. *Am J Cardiol* 83:535-541, 1999.
76. Klein AL, Obarski TP, Stewart WJ, et al: Transesophageal Doppler echocardiography of pulmonary venous flow: a new marker of mitral regurgitation severity. *J Am Coll Cardiol* 18:518-526, 1991.
77. Castello R, Pearson AC, Lenzen P, et al: Effect of mitral regurgitation on pulmonary venous velocities derived from transesophageal echocardiography color-guided pulsed Doppler imaging. *J Am Coll Cardiol* 17:1499-1506, 1991.
78. Kamp O, Huitnik H, van Eenige MJ, et al: Value of pulmonary venous flow characteristics in the assessment of severity of native mitral valve regurgitation: an angiographic correlated study. *J Am Soc Echocardiogr* 5:239-246, 1992.
79. Appleton CP, Gallaway JM, Gonzalez MS, et al: Estimation of left ventricular filling pressures using two-dimensional and Doppler echocardiography in adult patients with cardiac disease. Additional value of analyzing left atrial size, left atrial ejection fraction and the difference in duration of pulmonary venous and mitral flow velocity at atrial contraction. *J Am Coll Cardiol* 22:1972-1982, 1993.
80. Bartzokis T, Lee R, Yeoh TK, et al: Transesophageal echo-Doppler echocardiographic assessment of pulmonary venous flow patterns. *J Am Soc Echocardiogr* 4:457-464, 1991.
81. Pieper EP, Hellemans IM, Hamer HP, et al: Value of systolic pulmonary venous flow reversal and color Doppler jet measurements assessed with transesophageal echocardiography in recognizing severe pure mitral regurgitation. *Am J Cardiol* 78:444-450, 1996.
82. Utsunomiya T, Patel D, Doshi R, et al: Can signal intensity of the continuous wave Doppler regurgitant jet estimate severity of mitral regurgitation? *Am Heart J* 123:166-171, 1992.
83. Jenni R, Ritter M, Eberli F, et al: Quantification of mitral regurgitation with amplitude-weighted mean velocity from continuous wave Doppler spectra. *Circulation* 79:1294-1299, 1989.
84. Godley RW, Wann LS, Rogers EW, et al: Incomplete mitral leaflet closure in patients with papillary muscle dysfunction. *Circulation* 63:565-571, 1981.
85. Otsuji Y, Gilon D, Jiang L, et al: Restricted diastolic opening of the mitral leaflets in patients with left ventricular dysfunction: evidence for increased valve tethering. *J Am Coll Cardiol* 32:398-404, 1998.
86. Yiu SF, Enriquez-Sarano M, Tribouilloy C, et al: Determinants of the degree of functional mitral regurgitation in patients with systolic left ventricular dysfunction: a quantitative clinical study. *Circulation* 102:1400-1406, 2000.
87. Nesta F, Otsuiji Y, Handschumacher MD, et al: Leaflet concavity: a rapid visual clue to the presence and mechanism of functional mitral regurgitation. *J Am Soc Echocardiogr* 16:1301-1308, 2003.
88. Zeng X, Levine RA, Hua L, et al: Diagnostic value of vena contracta area in the quantification of mitral regurgitation severity by color Doppler 3D echocardiography. *Circulation Cardiovasc Imaging* 4:506-513, 2011.
89. Marsan NA, Westenberg JJM, Ypenburg C, et al: Quantification of functional mitral regurgitation by real-time 3D echocardiography: comparison with 3D velocity-encoded cardiac magnetic resonance. *JACC Cardiovasc Imaging* 2:1245-1252, 2009.
90. Yosefy C, Hung J, Chua S, et al: Direct measurement of vena contracta area by real-time 3-dimensional echocardiography for assessing severity of mitral regurgitation. *Am J Cardiol* 104:978-983, 2009.
91. Carabello BA, Nakano K, Corin W, et al: Left ventricular function in experimental volume overload hypertrophy. *Am J Physiol* 256:H974–H981, 1989.
92. Enriquez-Sarano M, Avierinos JF, Messika-Zeitoun D, et al: Quantitative determinants of the outcome of asymptomatic mitral regurgitation. *N Engl J Med* 352:875-883, 2005.
93. Rosenhek R, Rader F, Klaar U, et al: Outcome of watchful waiting in asymptomatic severe mitral regurgitation. *Circulation* 113:2238-2244, 2006.
94. Tischler MD, Rowan M, LeWinter MM: Effect of enalapril therapy on left ventricular mass and volumes in asymptomatic chronic, severe mitral regurgitation secondary to mitral valve prolapse. *Am J Cardiol* 82:242-245, 1998.
95. Host U, Kelbaek H, Hildebrandt P, et al: Effect of ramipril on mitral regurgitation secondary to mitral valve prolapse. *Am J Cardiol* 80:655-658, 1997.
96. Bonow RO, Carabello BA, Kanu C, et al: ACC/AHA guidelines for the management of patients with valvular heart disease. *Circulation* 114:84-231, 2006.
97. Tribouilloy CM, Enriquez-Sarano M, Schaff HV, et al: Impact of preoperative symptoms on survival after surgical correction of organic mitral regurgitation: rationale for optimizing surgical indications. *Circulation* 99:400-405, 1999.
98. Enriquez-Sarano M, Tajik AJ, Schaff HV, et al: Echocardiographic prediction of survival after surgical correction of organic mitral regurgitation. *Circulation* 90:830-837, 1994.
99. Capomolla S, Bebo O, Gnemmi M, et al: Beta-blockade therapy in chronic heart failure: diastolic function and mitral regurgitation improvement by carvedilol. *Am Heart J* 139:596-608, 2000.
100. Linde C, Leclercq C, Rex S, et al: Long-term benefits of biventricular pacing in congestive heart failure: results from the MUltisite STimulation in cardiomyopathy (MUSTIC) study. *J Am Coll Cardiol* 40:111-118, 2002.
101. Breithardt OA, Sinha AM, Schwammenthal E, et al: Acute effects of cardiac resynchronization therapy on functional mitral regurgitation in advanced systolic heart failure. *J Am Coll Cardiol* 41:765-770, 2003.
102. Solis J, McCarty D, Levine RA, et al: Mechanism of decrease in mitral regurgitation after cardiac resynchronization therapy: optimization of the force-balance relationship. *Circulation Cardiovasc Imaging* 2:444-450, 2009.
103. Gillinov AM, Wierup PN, Blackstone EH, et al: Is repair preferable to replacement for ischemic mitral regurgitation? *J Thorac Cradiovasc Surg* 122:1125-1141, 2001.
104. Grossi EA, Goldberg JD, LaPietra A, et al: Ischemic mitral valve reconstruction and replacement: comparison of long-term survival and complications. *J Thorac Cardiovasc Surg* 122:1107-1124, 2001.
105. DiSalvo TG, Normand SL, Hauptman PJ, et al: Pitfalls in assessing the quality of care for patients with cardiovascular disease. *Am J Med* 111:297-303, 2001.
106. NHLBI: Cardiothoracic Surgical Trials Network. ctsn-dcc@inchoir.org. Accessed 2007.
107. Calafiore AM, Gallina S, Di Mauro M, et al: Mitral valve procedure in dilated cardiomyopathy: repair or replacement? *Ann Thorac Surg* 71:1146-1153, 2001.
108. Tahta SA, Oury JH, Maxwell JM, et al: Outcome after mitral valve repair for functional ischemic mitral regurgitation. *J Heart Valve Dis* 11:11-19, 2002.
109. McGee EC, Gillinov AM, Blackstone EH, et al: Recurrent mitral regurgitation after annuloplasty for functional ischemic mitral regurgitation. *J Thorac Cardiovasc Surg* 128:916-924, 2004.
110. Hung J, Papakostas L, Tahta SA, et al: Mechanism of recurrent ischemic mitral regurgitation after annuloplasty: continued LV remodeling as a moving target. *Circulation* 110:II85-II90, 2004.
111. Kuwahara E, Otsuji Y, Iguro Y, et al: Mechanism of recurrent/persistent ischemic/functional mitral regurgitation in the chronic phase after surgical annuloplasty: importance of augmented posterior leaflet tethering. *Circulation* 114:I529-I534, 2006.

# 19 Intraoperative Echocardiography in Surgical and Transcatheter Mitral Valve Repair

ANDREW O. ZURICK, MD | WILLIAM J. STEWART, MD | BRIAN P. GRIFFIN, MD

**Indications for Intraoperative Echocardiography**
**Technique of Intraoperative Echocardiography**
Echocardiographic Equipment
Intraoperative Echocardiography Examination
**Prepump Intraoperative Echocardiography in Patients Undergoing Valve Repair for Mitral Regurgitation**
Severity of Mitral Regurgitation
Mechanism of Mitral Regurgitation
**Determining the Need for Mitral Valve Surgery in Patients Undergoing Cardiac Surgery for Other Reasons**
**Postpump Intraoperative Echocardiography in Mitral Repair**
Timing
Intraoperative Findings
Incomplete Mitral Repair
Impact on Clinical Outcome
**Other Complications of Mitral Valve Repair**
Systolic Anterior Motion of the Mitral Valve
Suture Dehiscence, Perforation Jet Lesions, and Annuloplasty Dehiscence
LV Systolic Dysfunction
Tricuspid Regurgitation
Mitral Stenosis
**Mitral Valve Repair Involving Commissurotomy**
**TEE in Minimally Invasive and Robotic Mitral Valve Repair**
**TEE in Transcatheter Mitral Valve Repair**
Percutaneous Edge-to-Edge Repair of Mitral Regurgitation
Percutaneous Closure of Paravalvular Mitral Regurgitation

The advent of transesophageal echocardiography (TEE) and innovations in ultrasound technology have led to progressive improvement in the outcomes of valve procedures, especially surgical and transcatheter interventions on the mitral valve.

## Indications for Intraoperative Echocardiography

Intraoperative echocardiography (IOE) has both diagnostic and monitoring functions that are useful in valve surgery, especially valve-sparing operations. The diagnostic functions of IOE are used before cardiopulmonary bypass (prepump) to determine the mechanism and severity of the mitral valvular dysfunction, identify lesions of other valves, and refine the surgical mission. After cardiopulmonary bypass (postpump), the diagnostic strengths of IOE are used again to determine the success of the surgical mission. IOE is essential in performing mitral valve repair and many other types of innovative heart surgery. In addition to its use in valve surgery, the diagnostic function of IOE also is used in the surgical management of congenital heart disease,[1,2] hypertrophic cardiomyopathy,[3,4] reconstruction of the ascending aorta,[5,6] and many other surgeries (Box 19-1).[7] In addition, echocardiography in preparation for and during transcatheter procedures is now an increasingly important and essential role.

## Technique of Intraoperative Echocardiography

TEE is the most widely used technique for IOE. TEE became available in 1987 and progressively supplanted the epicardial route for most studies. Compared with epicardial echocardiography, TEE has the advantage of allowing image acquisition without interfering with the surgical field or procedure. Immediately after induction of anesthesia and endotracheal intubation, the TEE probe is inserted and left in place throughout the operation.

Although the technique of intraoperative TEE is similar to TEE in the echocardiography laboratory or the intensive care unit, there are additional potential pitfalls. First, it is occasionally difficult to pass the probe, particularly if the patient has been draped and the ether screen has been positioned. Usually, laryngoscope and direct vision succeed in placement of the probe, but sometimes this problem cannot be overcome.

Inadequate imaging occurs with the transesophageal approach for a number of reasons. Anatomic causes include a hiatal hernia or the presence of an echodense structure such as a mechanical valve prosthesis, which can cause shadowing of other cardiac structures. With all TEE studies, there is a "blind spot" approximately 2 to 4 cm in size in the middle portion of the ascending aorta caused by interposition of the trachea

**Box 19-1**

**INTRAOPERATIVE ASSESSMENT OF REPAIR AND RECONSTRUCTIVE VALVE OPERATIONS**

**Prepump**
Assess severity of stenosis/regurgitation.
Assess mechanism of regurgitation and potential reparability of valve.
Measure dimensions of annulus, chambers, and valves.
Assess whether lesions other than the primary lesion require surgery.
Determine biventricular function.

**Postpump**
Assess severity and mechanism of residual regurgitation/stenosis.
Detect systolic anterior motion of the mitral valve and LV outflow obstruction.
Determine change in severity of other valve lesions.
Assess biventricular function.
Detect iatrogenic complications.

between the esophagus and the ascending aorta. Interference from electrical apparatus such as electrocautery leads to distortion of two-dimensional (2D) imaging and often renders spectral and color Doppler signals impossible to interpret. Fortunately, imaging may be resumed once the electrocautery is discontinued. Also, while the patient is on cardiopulmonary bypass, the incomplete filling and the absence of cardiac motion cause suboptimal images until the heart is filled with blood again and starts to eject during rewarming.

## ECHOCARDIOGRAPHIC EQUIPMENT

Ideally, an ultrasound machine devoted solely to IOE should be available. In addition to interfacing with transesophageal and transthoracic transducers, the machine should be capable of recording M-mode, 2D imaging, three-dimensional (3D) imaging, and all Doppler modalities (see Chapter 2). Sterile sleeves and acoustic gel should be available for epicardial imaging.[8] Cables should be available to input the electrocardiographic signal from the operating room monitoring system into the ultrasound machine. Many institutions have the capability of transmitting images from the operating room to a server for digital storage of images, which can be reviewed in a remote site such as the echocardiography laboratory in order to allow oversight or second opinions to be obtained in selected cases.[9]

Real-time 3D echocardiography acquisition using transesophageal and transthoracic transducers is currently an important component of intraoperative echocardiographic diagnosis (see Chapter 4).

The mitral valve can now be viewed en face as a complex saddle-shaped, anatomic structure and rotated into the surgeon's view orientation as viewed from the left atrium (LA) (Fig. 19-1; Video 19-1; see ExpertConsult.com). Assessment of mitral valve morphology using real-time 3D TEE and offline reconstruction 3D TEE showed similar accuracy in defining mitral leaflet prolapse but greater interobserver agreement compared with 2D TEE.[10] Recent studies have demonstrated the feasibility of intraoperative assessment of the mitral valve morphology by real-time 3D TEE, with superior accuracy to standard 2D TEE in defining leaflet pathology when both were later compared to surgical findings.[11]

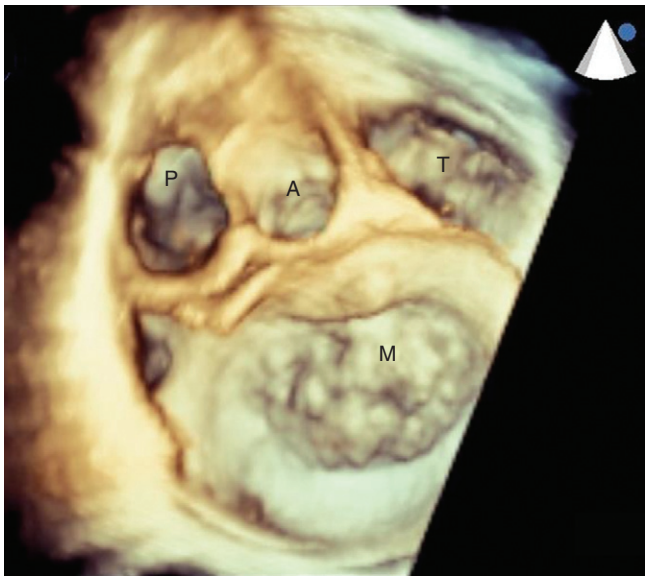



**Figure 19-1 3D TEE image of the atrioventricular and semilunar valves.** *A,* Aorta; *M,* mitral valve; *P,* pulmonic valve; *T,* tricuspid valve.

3D echocardiography has tremendous potential in the analysis of complex cardiac morphology, including the assessment of lesions in which mitral repair or reconstruction is being considered.[12] The complex 3D geometry of some valvular and congenital lesions is easier to display and understand using 3D echocardiography.[13,14] 3D reconstruction may allow more appropriate selection of patients, help determine the most appropriate surgical procedure, and potentially allow the surgeon to map out the reconstruction ahead of time in 3D computer space.[15-17] Importantly, 3D echocardiography allows additional slices to be derived at a later time from one stored volumetric data set. 3D data yielded incremental information to standard 2D TEE in up to 25% of patients.[18] 3D imaging can reconstruct structures such as the regurgitant orifice area[19] and the location of mitral valve prolapse.[20]

## INTRAOPERATIVE ECHOCARDIOGRAPHY EXAMINATION

Intraoperative TEE examinations should be performed in a standard comprehensive manner so that the acquisition of critical information is not omitted. It is important to do a complete TEE study, using imaging planes (Fig. 19-2) that allow long- and short-axis views of each intracardiac valve and chamber, as well as the great vessels.[21] Epicardial echocardiography is performed using a standard transthoracic transducer inside a sterile plastic sleeve with acoustic gel inside to eliminate the air. This technique is used in a minority of intraoperative cases, most commonly to evaluate the severity and location of atheroma in the ascending aorta, especially when it will affect the method of arterial cannulation for cardiopulmonary bypass. In cases where passage of the TEE probe is contraindicated or unsuccessful, a complete cardiac study can be obtained using four epicardial transducer positions as we have previously described.[8]

The entire prepump examination should be recorded to provide a durable record of the examination, especially as a reference for postpump studies and for medical-legal purposes. Storing key images in a cineloop facilitates rapid comparison at the end of the operation and in follow-up. In diagnostic (as

opposed to monitoring) studies, the structure of interest to the primary surgical mission should first be examined thoroughly in multiple planes, using imaging and Doppler modalities. If the echocardiographic study must thereafter be abbreviated because of pressing demands of the surgical agenda or the need to limit anesthetic and cross-clamp time, at least the primary concern, the raison d'étre of the echocardiographic study, has been addressed. Other structures of interest should then be examined, including long- and short-axis views of all four chambers, all four valves, and the great vessels. The entire aorta should be examined in all cases both prepump and postpump. We also advocate a routine intravenous contrast injection to look for intracardiac shunting.

Once the prepump study is completed, a written report of the examination detailing significant findings should be made. Although ultrasound has not been demonstrated to cause any significant damage to cardiac structures during prolonged examinations,[22] studies have shown that ultrasound waves can result in minor changes in pulmonary capillaries, so when imaging is not required, it is advisable to put the machine on freeze so that no ultrasound energy is transmitted. After cessation of cardiopulmonary bypass, a second comprehensive examination should be carried out and a second or updated report generated.

The intraoperative examination has several aspects that are different from a TEE or transthoracic echocardiography (TTE) study in the outpatient echocardiography laboratory:

1. The echocardiogram is performed simultaneously with the operation; therefore, the room conditions, including the lighting and the space for the machine, may be suboptimal. For example, radiofrequency interference from electrocautery or from other surgical equipment may mar the quality of echocardiographic images for long periods.

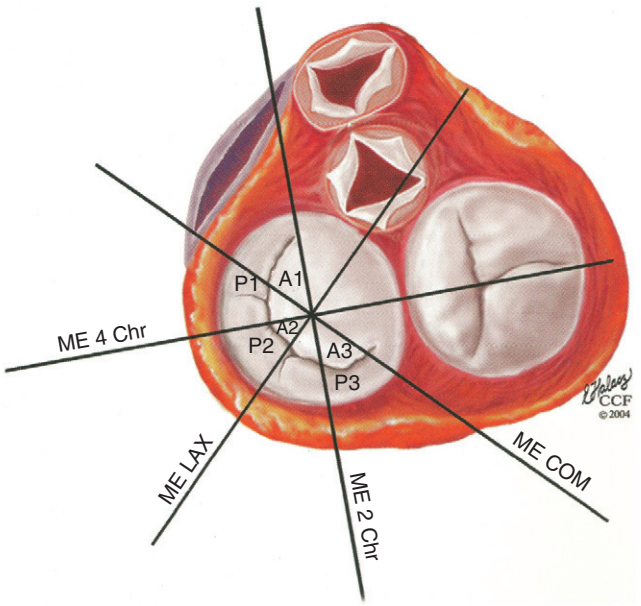



**Figure 19-2 Diagram oriented similarly to the transgastric short axis view of the mitral valve (posterior part of the heart toward the top of the screen).** The *solid lines* show the orientation of the midesophageal mitral valve planes as they can be rotated around the mitral circumference, including the midesophageal four-chamber view (*ME 4 Chr*) at about 0°, midesophageal commissural view (*ME COM*) at about 60°, the midesophageal 2 chamber view (*ME 2 Chr*) at about 90°, and the midesophageal long-axis view (*ME LAX*) at about 120°. *(Copyright CCF 2004.)*

2. The hemodynamic milieu may change quickly, and the echocardiographic appearance may differ from images acquired under "street conditions" outside the operating room. Changes in hemodynamics, such as intravascular volume, preload, and afterload, substantially affect the severity of valvular lesions and ventricular performance. If necessary, the hemodynamic situation should be manipulated to match preoperative conditions, in order to determine the true or potential severity of a valvular lesion.
3. The surgeon who requests the intraoperative study wants online interpretation. In fact, it is very tempting to "wing it" and give premature conclusions. Care must be maintained to make only diagnoses and conclusions that have been verified by examination from multiple imaging planes under appropriate imaging and hemodynamic conditions.

## Prepump Intraoperative Echocardiography in Patients Undergoing Valve Repair for Mitral Regurgitation

The prepump echocardiogram assessment of mitral regurgitation (MR) (Table 19-1) usually confirms findings made previously by preoperative echocardiography or cardiac catheterization. However, because of its improved resolution over TTE, TEE often improves on the accuracy and resolution of preoperative TTE of the component structures, the mitral valve, and the regurgitant jet. There are four main goals of IOE in mitral valve disease:

1. To assess the severity of MR and determine the need for mitral valve surgery
2. To assess the mechanism of MR and determine if a repair rather than prosthetic replacement is feasible and to determine the technique of repair
3. To determine the presence of other significant disease that may require surgical attention, such as tricuspid or aortic valve disease or intraluminal thrombi
4. To assess left and right ventricular function as a baseline with which to compare the postpump study

### SEVERITY OF MITRAL REGURGITATION

The severity of MR is assessed by IOE in the same manner as the use of echocardiography for other applications in other

**TABLE 19-1 Determination of the Mechanism of MR from Analysis of Jet Direction and Leaflet Mobility**

| | Leaflet Motion | | |
|---|---|---|---|
| *Jet Direction* | *Excessive* | *Restrictive* | *Normal* |
| Anterior | Prolapse/flail of posterior leaflet | | Perforation in posterior leaflet |
| Posterior | Prolapse/flail of anterior leaflet | Restriction of posterior > anterior leaflet | Apical tethering from LV dilation |
| Central | Prolapse/flail of both leaflets | Equal restriction of both leaflets | Apical tethering from LV dilation, annular dilation |
| Commissural | Rupture of commissural chordae or papillary muscle | | |
| Eccentric origin | | | Leaflet perforation or cleft |

parts of the hospital (see Chapter 18).[23-28] The intraoperative assessment of MR severity usually agrees with the preoperative assessment by contrast ventriculography or TTE[29,30]; however, it may reflect change, dependent on different loading conditions. In patients with ischemic MR, agreement between preoperative studies and the intraoperative assessment is less, possibly because the amount of regurgitation is more variable, dependent on hemodynamic conditions or differing degrees of ischemia. One study of patients with ischemic MR[31] showed that in 11% of patients, the preoperative and intraoperative assessments of MR severity differed by more than one grade, with discordance occurring in both directions. Discordance was more common in patients with clinical instability or those who received thrombolysis. MR resulting from any mechanism is a dynamic lesion, affected greatly by loading conditions. Reduction of afterload or intravascular volume at the time of the operation may reduce the true severity of the regurgitation. When less MR is found than expected, the intravascular blood volume should be expanded and systemic vascular resistance increased transiently using repeated boluses of intravenous phenylephrine, usually 100 mcg every 30 to 120 seconds. The velocity of MR, and therefore display of its jet by color Doppler, depends on the pressure difference between the LA and left ventricle (LV), which is higher with hypertension. The size of the jet in the LA is also variable based on changes in color gain (directly proportional) and pulse repetition frequency (inversely proportional) (see Chapter 18). Spatial mapping for the size of the MR jet in the LA should be performed at a Nyquist setting of 50 to 60 cm/s.

The transesophageal imaging window has advantages over transthoracic or epicardial imaging in the assessment of MR. A mitral prosthesis or severe mitral calcification causes acoustic shadowing of the regurgitant jet when the transducer is placed anteriorly, as in epicardial imaging or TTE. Excellent agreement, however, has been reported between the epicardial and transesophageal approaches in assessing MR.[32]

Semiquantitation of MR on a scale from 0 to 4+[23,24] is determined based on a weighted average of several criteria:

1. The size of the LA flow disturbance, based on the depth of penetration and area of the regurgitant jet in the LA cavity assessed in multiple imaging planes; a multiplane probe facilitates this process, especially in eccentric jets.
2. The geometry of the jet; eccentric jets tend to have a higher regurgitant volume than free jets of the same area.[25]
3. The size of the proximal convergence zone, by use of the proximal isovelocity surface area (PISA) technique. More severe regurgitation is associated with a larger radius of the proximal flow convergence.[26] Flow convergence can be used to calculate regurgitant flow, orifice area, and volume (see later).
4. The width of the proximal portion of the regurgitant jet ("vena contracta") on the LA side of the orifice is also useful and may be less load sensitive than mapping of the regurgitant jet in the atrium.[23]
5. The pulmonary venous pulsed Doppler tracing. Severe MR often leads to systolic reversal of flow in the pulmonary veins,[33] which is 69% sensitive and 98% specific in predicting a regurgitant orifice area of greater than 0.3 $cm^2$.[33] Blunting of pulmonary vein flow is somewhat reliable in predicting severe MR for patients in normal rhythm with normal LV function but is unreliable in patients with severe LV dysfunction or atrial fibrillation. A normal pulmonary vein flow pattern is useful in excluding severe MR and predicting a regurgitant orifice area of less than 0.3 $cm^2$. Importantly, in patients in whom the right and left pulmonary vein flow pattern is discordant (23% of patients), the more abnormal pattern is most predictive of MR severity.
6. Quantification of mitral regurgitant volume (RV) from the difference between Doppler echocardiography measurements of antegrade flow through the mitral and the aortic valves. Regurgitant fraction (RF) is the proportion of total mitral antegrade flow (MF) that is regurgitant:

$$RF\,(\%) = (RV/MF) \times 100$$

LV outflow tract flow and mitral valve flow can be assessed by the product of annular cross-sectional area derived from echocardiography and velocity derived from pulsed Doppler measurements at the same site. Mitral cross-sectional area is derived from two orthogonal diameters of the annulus, which is elliptical in shape.[34] This method has not been used routinely because of the time-consuming nature of the measurements required and the ease and general reliability of semiquantitative techniques (see Chapter 18).

The size of the regurgitant orifice area can be derived from Doppler echocardiography techniques in the operating room,[35] using either the antegrade flow difference method or the flow convergence method. The maximum regurgitant orifice area is calculated by dividing regurgitant flow rate by the maximum mitral regurgitant flow velocity ($V_{max}$) obtained from continuous-wave Doppler. The regurgitant orifice area is greater than 0.4 $cm^2$ in severe MR and greater than 0.30 $cm^2$ in moderately severe MR. It is hoped that 3D echocardiography will help with assessment of regurgitant orifice area in the future, though this is not feasible in most routine studies [36]

The flow convergence, or PISA, technique analyzes flow proximal (on the LV side) to the regurgitant orifice, assuming a hemispherical shape.[35,37] In this area, blood accelerates predictably as it moves toward the regurgitant orifice and forms a series of concentric shells of decreasing area and increasing velocity that are depicted clearly. The radius of these shells is easily measured on the color image because of the color aliasing of the accelerating flow. To the degree that the aliasing contours are shaped like a hemiellipse, the surface area of the hemiellipse can be calculated from $2\pi r^2$ for blood flow moving at velocity $v$ and at a radius $r$ from the regurgitant orifice, and the instantaneous flow rate $Q$ can be calculated from

$$Q = 2\pi r^2 v$$

The PISA method provides excellent estimation of regurgitant flow when the flow convergence is centrally located, elliptical, and well away from the walls. However, this method overestimates regurgitant flow when the proximal flow is constrained by the LV wall. Use of appropriate correction factors can compensate for this problem.[38] If the aliasing zone is hemispheric at an aliasing velocity of 40 cm/s, a simplified form of the PISA method can be used. Because 2 times $\pi$ times 40 divided by 500 is almost exactly 0.5, the mitral valve effective regurgitant orifice can be calculated from $1/2r^2$. This approximation also assumes that the peak mitral regurgitant jet velocity is 500 cm/s.

Other methods of assessing the severity of MR in the operating room include surgical palpation of the LA for the thrill of a mitral regurgitant jet, evaluation of the size of v waves on the LA pressure tracing, fluid filling of the arrested LV, and contrast

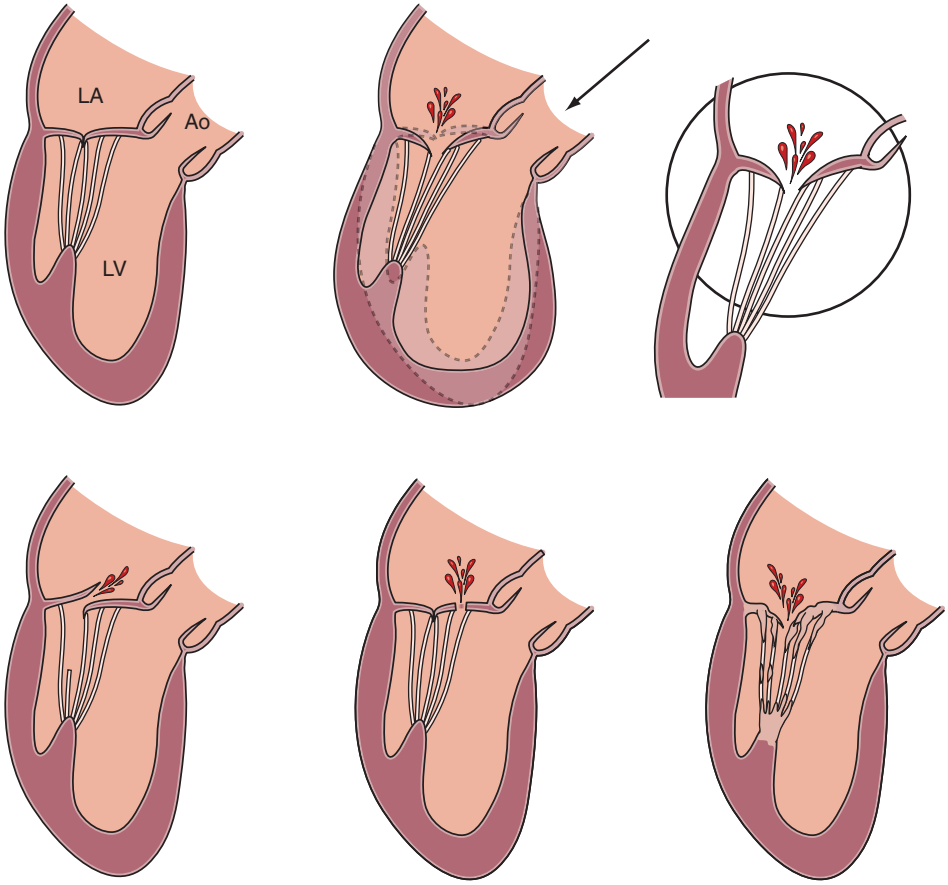



**Figure 19-3 Artist's drawings showing the morphology and echocardiographic demonstration of mechanisms of mitral regurgitation (MR).** A normal competent mitral valve is shown in the *upper left panel*. The *lower* three panels show "intrinsic valve mechanisms" of MR, including excessive leaflet motion (*lower left*) such as posterior leaflet flail due to ruptured chordae (Carpentier type 2), normal leaflet motion (*lower middle*) from a congenital cleft or leaflet perforation (Carpentier type 1), and restricted leaflet motion (*lower right*) due to fibrosis from rheumatic fever or chest radiation (Carpentier type 3A). Functional MR (FMR) is shown in the *upper middle panel*, with apical tethering of normal leaflets due to ischemic or nonischemic left ventricular systolic dysfunction (LVSD) (Carpentier type 3B) with outward displacement of the papillary muscles. The normal position of the leaflets, papillary muscle, and LV is shadowed behind the FMR anatomy. The *upper right panel* shows a close-up view of FMR.

echocardiography. These methods lack sensitivity and are not as reliable or as convenient as color flow Doppler techniques.[30,39,40]

## MECHANISM OF MITRAL REGURGITATION

Assessment of the cause and mechanism of MR[41] is of great importance in determining the suitability of the mitral valve for repair. Mitral valve repair is most likely in patients with MR due to myxomatous degeneration and is least likely in patients with regurgitation due to endocarditis or rheumatic valvular fibrosis. Repair is now successful in more than 90% of all patients with myxomatous disease. The probability of repair, however, is affected by the mechanism of regurgitation, especially whether the posterior leaflet, the anterior leaflet, or both leaflets are involved. Repair is most likely with posterior prolapse or flail, whereas isolated anterior leaflet prolapse is somewhat more difficult to repair.[42,43] Extensive chordal or leaflet disruption or the presence of mitral annular calcification also reduces the feasibility and likelihood of successful repair.[44]

### *An Organized Approach to Imaging the Mitral Valve*

To adequately assess the pathophysiologic mechanism responsible for MR, it is essential to perform a thorough examination of the mitral valve and mitral apparatus (Fig. 19-3) and to determine the origin and geometry of the regurgitant jet. The long-axis imaging planes are best for determining which mitral leaflet is involved. Long-axis views of the mitral valve are obtained by imaging from midesophageal TEE planes. Most basilar long-axis views around the entire multiplane sweep allow portions of both leaflets to be examined individually. The midesophageal intercommissural view[21] at approximately 50° to 60° in most patients, an imaging plane parallel to a line between the commissures, is very useful for determining which portion of the anterior or posterior leaflet is involved. Long-axis imaging at a multiplane angle of about 135° cuts perpendicular to this intercommissural line.

The short-axis views also are useful for determining which portion of the anterior or posterior leaflet is involved (Figs. 19-4 and 19-5). Useful views may be obtained from 3D echocardiography or from 2D planes recorded from the transgastric short-axis view.[45] A useful 3D volume set can be recorded from the midesophageal position by placing the border of the sampling zone for the "3D zoom view" just posterior to the mitral valve, so that no solid structures are within the data set posterior to the mitral valve. The derived data set, shaded for 3D viewing, is rotated around so it mimics the "surgeon's view" of the mitral valve (Fig. 19-6). Although 3D echocardiography is not as sensitive as 2D imaging in detection of small abnormalities,

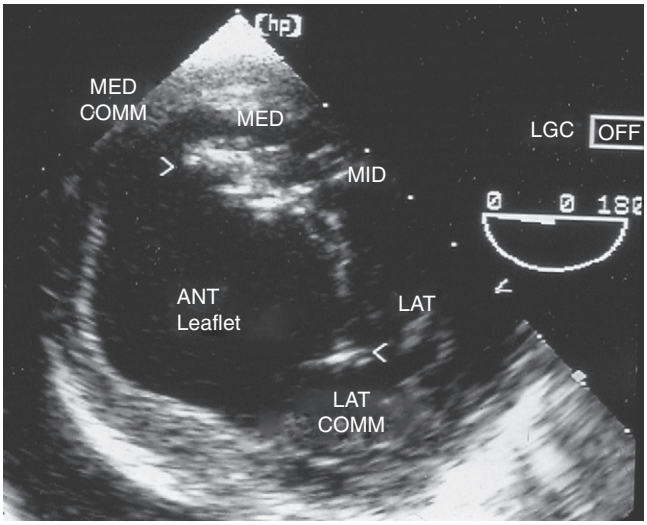



**Figure 19-4 The anatomy of the mitral valve in systole from a transverse transgastric short-axis view of the mitral valve.** The medial and lateral commissures (*MED COMM, LAT COMM*) and the positions of the medial (*MED*), middle (*MID*), and lateral (*LAT*) scallops of the posterior leaflet are shown. *ANT*, Anterior.

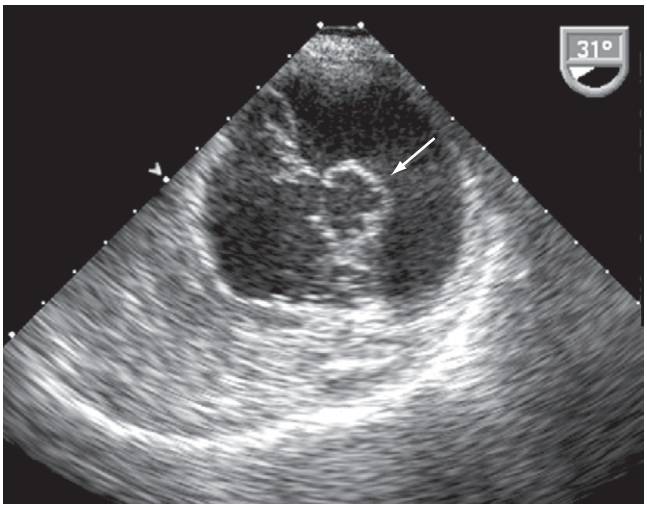



**Figure 19-5 P2 prolapse.** Transgastric short-axis view of the mitral valve in a patient with severe prolapse of the middle scallop of the posterior leaflet (*arrow*).

it facilitates understanding the exact locations and topographic relationships of the abnormalities.

The posterior leaflet has three divisions or scallops: the lateral, middle, and medial, respectively numbers P1, P2, and P3. The anterior leaflet is not scalloped but has a central portion known as the *bare area* between the insertions of the chordae from the anterolateral and posteromedial papillary muscles. Although there are no distinct scallops, the anterior leaflet is arbitrarily divided into segments that correspond to the segments of the posterior leaflet opposite them: the lateral, middle and medial segment, respectively A1, A2, and A3. In a similar way the posterior leaflet is also supported, about half each by chordae from the anterolateral and posteromedial papillary muscles. The papillary muscles lie below each mitral commissure. The papillary muscles and chordae usually are well visualized from the transgastric long-axis views of the LV.[46] In assessing the mitral valve and in providing the results to the surgeon, giving an accurate localization of the abnormality is important. A prospective study of 50 patients[47] used a segmental approach to the mitral valve, breaking each leaflet into three segments, and found that TEE was 96% accurate for localization compared with surgical findings. Other researchers have shown that localization of the defect to the posterior leaflet by TEE is 78% sensitive and 92% specific in myxomatous disease, with accuracy being least when the medial rather than the lateral or middle scallop is involved.[48] Assessment of the mechanism of MR is performed by analyzing the motion of the valve leaflets with 2D, and now more recently 3D echocardiography and the direction of the regurgitant jet with color flow imaging[49,50] (see Table 19-1). Four types of leaflet motion (see Fig. 19-3) may be associated with MR: (1) *normal motion* (Carpentier class 1) as seen with leaflet perforation, (2) *excessive motion* (Carpentier class 2) as seen with prolapse or flail valve such as chordal rupture or elongation, (3) *restricted motion* (Carpentier class 3) as seen in rheumatic mitral valve disease, and (4) *apical tethering of normal leaflets* (Carpentier class 3B) as seen in functional MR with ventricular and annular dilation.

IOE has been shown to be highly sensitive and specific in determining the mechanism of MR in patients undergoing mitral valve surgery. In a study of 286 patients undergoing mitral valve surgery in which the echocardiography mechanism was correlated with the surgical findings, echocardiography was highly accurate (86%) in determining the mechanism of MR.[49]

## Excessive Leaflet Motion (Carpentier Class 2)

Excessive leaflet motion occurs with elongation or disruption of any portion of the mitral valve or of the mitral apparatus,

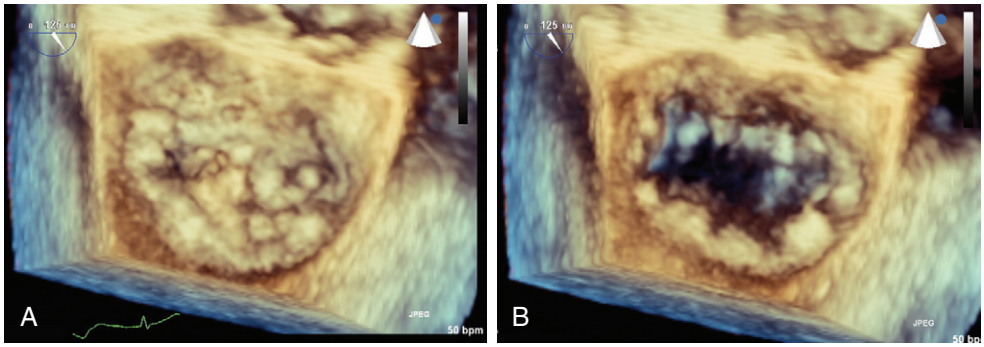



**Figure 19-6 3D TEE of the mitral valve.** The valve is viewed *en face* rotated to the "surgeon's view" shown in (**A**) systole and (**B**) diastole, demonstrating a P2 flail scallop.

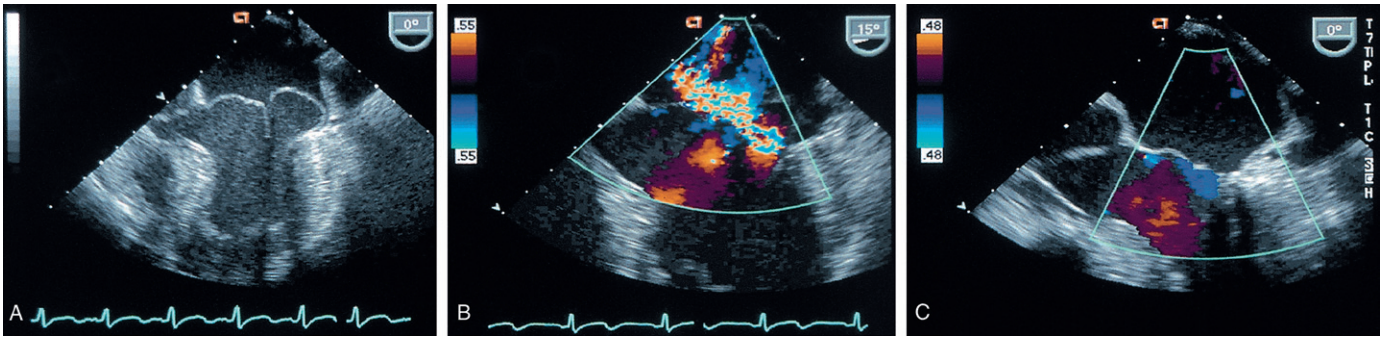



**Figure 19-7 Bileaflet prolapse.** The TEE four-chamber view shows prolapse (**A**) of the posterior, more than the anterior, leaflet causing severe MR (**B**) before mitral valve repair and no MR after successful mitral valve repair (**C**). The jet is deflected opposite the leaflet that has the most excessive leaflet motion.

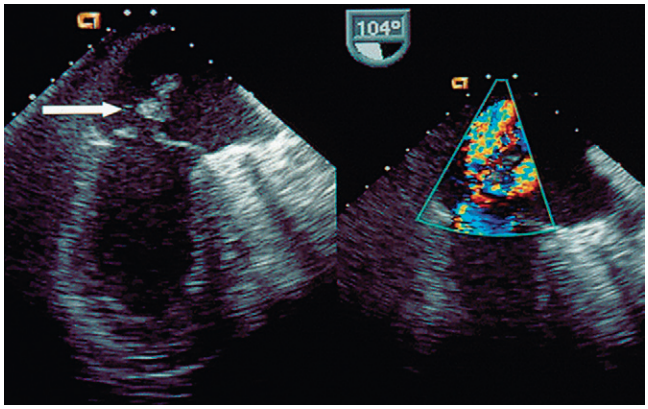


**Figure 19-8 Papillary muscle rupture with resulting severe mitral regurgitation (MR).** Ruptured portion of muscle is seen prolapsing into LA (*arrow*) in *left panel.* MR jet is seen in *right panel.*

including the papillary muscles and chordae. Myxomatous disease, endocarditis, and papillary muscle infarction all can lead to this abnormality. With excessive leaflet motion, the regurgitant jet is directed *away* from the affected leaflet. Thus, prolapse or flail of the posterior leaflet leads to an anteriorly directed jet (Fig. 19-7; see Fig. 29-6 and Video 19-2 at ExpertConsult.com). In bileaflet prolapse, the excessive motion is often asymmetric, and the jet direction is away from the more severely affected leaflet. When the amount of prolapse or flail is completely balanced between both leaflets, a central jet direction occurs. If the chordae to the commissures are ruptured, then a jet originating at the commissures is seen in the transgastric short-axis view. Jets originating at the commissure also are seen in infarction of a papillary muscle, most commonly the posteromedial one.[51] Excess motion with severe MR results when the head of a papillary muscle ruptures in an acute myocardial infarct. This type of rupture may be differentiated from acute chordal rupture by detecting a mass attached to the flail leaflet that is a portion of the muscle and by the appropriate clinical setting (Fig. 19-8).

Precise delineation of which portion of the valve has excess motion is important in planning the surgical repair. Rupture of the posterior chordae is the most common abnormality and is repaired by quadrilateral resection of the posterior leaflet (Fig. 19-9). Elongation of the chordae is repaired by chordal transfer or by implantation of artificial chordae. Papillary muscle elongation or disruption may be repaired by reimplanting, supporting, or shortening the affected muscle.[42] Postoperative prognosis is best in those with excessive leaflet motion.

### Restricted Leaflet Motion (Carpentier Class 3)

This pattern, involving leaflet thickening, is seen most commonly in rheumatic disease, but it also can result from ischemic heart disease, the chronic phase of lupus, radiation-induced valvular disease, or acquired disease caused by ergot derivatives or the fen-phen combination (fenfluramine and phentermine). If both leaflets are equally affected by the pathologic process, the jet direction is central. More commonly in rheumatic disease, the posterior leaflet is more severely affected than the anterior leaflet, and the relatively normal anterior leaflet "overrides" the restricted posterior leaflet. The direction of the regurgitant jet in this situation is posterior, *toward* the affected leaflet. The surgical approach to this condition includes débridement of the valve tissue and chordae, commissurotomy, and annuloplasty. This type of repair is more technically demanding, less often successful, and less durable because of postoperative progression of the fibrotic process.

### Apical Tethering of Normal Leaflets (Carpentier Class 3B)

In ischemic heart disease, the leaflets are usually structurally normal, but they are *tethered* and their motion is "relatively restricted," owing to apical displacement of the posteromedial papillary muscle. The leaflets themselves are not thickened but fail to coapt adequately (Fig. 19-10) because of tethering of the leaflets apically and outward by the LV enlargement. The surgical approach to this problem usually involves placement of an annuloplasty ring to reduce the size of the mitral annulus. Surgical treatment of ischemic regurgitation with apical tethering is less successful, and residual regurgitation is often more significant than after myxomatous valve repair.

Normal leaflet motion is commonly seen in patients with MR secondary to LV dilation of any cause, such as disease of other valves, dilated cardiomyopathy, or severe ischemic cardiomyopathy. We have previously termed this category *ventricular-annular dilation.* Ventricular enlargement causes displacement of the mitral coaptation point toward the apex with resultant impaired coaptation and leaflet "tenting." Annular dilation is seen in these patients, but it occurs in proportion to LV dilation, in contrast to myxomatous or rheumatic MR patients whose annulus size is often abnormally large. Annuloplasty with ring insertion is commonly used in the surgical management of these patients. An Alfieri stitch to support the valve also has been used instead of or in addition to the annuloplasty. There has been an upsurge in interest in the surgical management of severe MR in patients with dilated cardiomyopathy. Excellent functional improvement with a relatively low operative

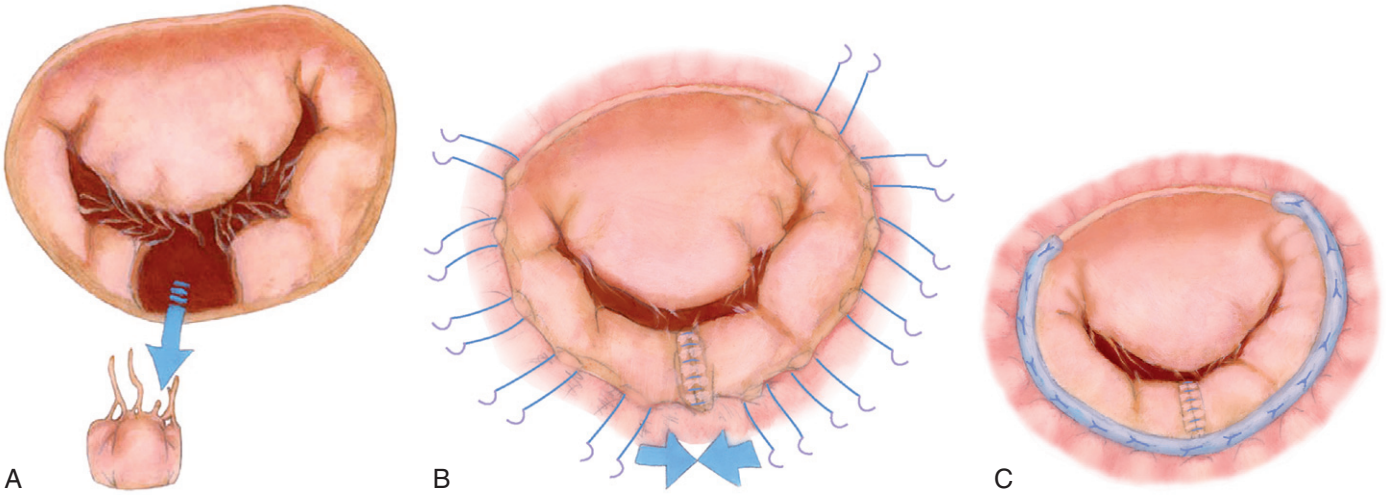



**Figure 19-9 Surgical mitral valve repair.** The first step is quadrilateral resection of the posterior leaflet (**A**) followed by repair of the posterior mitral valve leaflet, with placement of annular sutures (**B**), and then implantation of an annular ring (**C**). *(From Grewal KS, Malkowski MJ, Kramer CM, et al: Multiplane transesophageal echocardiographic identification of the involved scallop in patients with flail mitral valve leaflet: intraoperative correlation.* J Am Soc Echocardiogr *11:966-971, 1998.)*

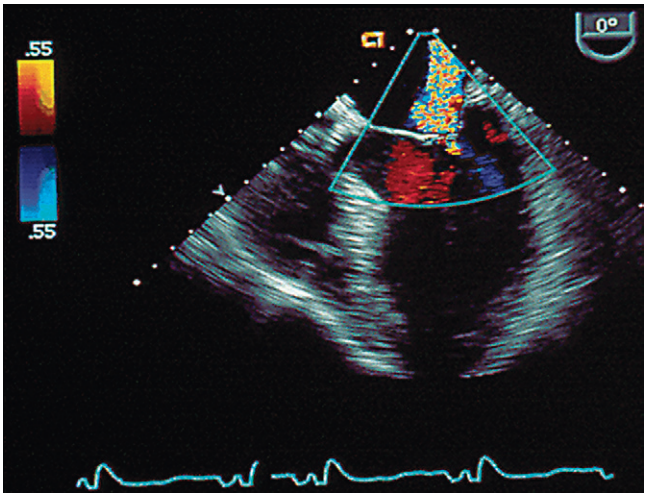



**Figure 19-10 Ischemic mitral regurgitation.** The TEE four-chamber view shows apical tethering, of normal mitral leaflets and a central to posteriorly directed jet of mitral regurgitation.

mortality has been reported even in selected patients with severe MR and severe LV dysfunction.

### Normal Leaflet Motion (Carpentier Class 1)

The least common type of MR occurs with normal leaflet motion either due to perforation of a valve leaflet, which occurs most commonly because of endocarditis, or because of a congenital cleft in the valve. Occasionally MR with normal leaflet motion is iatrogenic, after attempted repair. Typically, the jet origin is eccentric, arising from the midportion of the leaflets rather than from the coaptation line. The prejet flow acceleration also may be seen away from the coaptation line, along the affected leaflet. Leaflet perforation may be repaired in some instances by suture closure or with pericardial patch.[52]

One study of 248 patients undergoing mitral valve surgery showed that TEE was more than 90% accurate for defining the mechanism of regurgitation, localizing the origin of regurgitation, and detecting a flail segment. TEE was 88% accurate in detecting ruptured chordae. The TEE findings of valve function are highly predictive not only of valve reparability (Table 19-2), but also of long-term survival, which were independent of age, gender, ejection fraction, and coronary artery disease.[53]

**TABLE 19-2 Repairability and Durability of Repair for Mitral Regurgitation According to Mechanism and Morphology**

| *Carpentier Class* | *Morphology* | *>90% Repairable* | *Durable* |
|---|---|---|---|
| 1: Normal | Perforation | Yes | Variable |
| 2: Simple excessive | Flail, prolapse | Yes | Yes |
| 2: Complex excessive | Extensive flail, billowing, or calcium | No | Variable |
| 3A: Restricted | Fibrotic, retracted | No | Less |
| 3B: Apical tethering | Functional | Yes | Variable |

## Determining the Need for Mitral Valve Surgery in Patients Undergoing Cardiac Surgery for Other Reasons

IOE increasingly is used to determine the need for a mitral valve operation in patients undergoing aortic valve surgery or revascularization procedures; this is especially true in the assessment of patients in whom the severity of the MR preoperatively is significantly different by cardiac catheterization and echocardiography, when the severity of MR over time is variable (such as in ischemic heart disease), and when the MR is of moderate severity.

The following questions must be considered when determining the need for mitral valve surgery in addition to the primary surgery:

1. How severe is the MR?
2. Is there a primary abnormality of the mitral valve (such as a torn chord or prolapse)?
3. Will the MR change as a consequence of the primary operation?
4. Is the valve repairable or is prosthetic replacement necessary?

5. What is the additional risk imposed by the additional mitral valve procedure?

The final decision on what surgery is indicated is made by the surgeon; however, when the surgical plans are changed in the operating room, telephone consultation with the referring clinical doctor is advisable.

In many patients, especially those in whom the regurgitation is secondary to apical tethering from ischemic heart disease with LV dilation, the severity of the regurgitation may be variable. Sometimes, the severity of regurgitation detected at the time of operation is different from that recorded preoperatively. Frequently the difference in severity is due to a true physiologic change. Compared with ambulatory conditions, the loading conditions during surgery often entail a lower intravascular volume and less peripheral vasoconstriction, both of which may reduce the severity of valvular regurgitation and reduce stenotic valve gradients. On other occasions this discrepancy reflects the superior ability of esophageal and epicardial echocardiography to visualize MR compared to TTE.

In patient presenting with symptoms that might be due to MR, but severity is less than is expected or borderline, it is often useful to increase afterload with multiple boluses of phenylephrine (100 mcg every 30 to 120 seconds), and then to recheck the severity of regurgitation at a mean arterial pressure that is transiently as high as 120 mm Hg. Patients with 3+ or more MR at rest, or during this afterload stress test, are generally considered candidates for a mitral valve operation. The threshold for surgery on the mitral valve also is affected by other factors, including whether there is a primary structural abnormality of the valve. If the valve appears to be repairable, the threshold for surgery is lower, given the relatively low morbidity and mortality associated with repair as compared with valve replacement, whereas the threshold for surgery is higher in patients with valves that are not reparable. In patients undergoing surgery for aortic stenosis, improvement in the severity of the MR can be expected postoperatively; therefore, the threshold for concomitant mitral surgery is higher.[54,55] On any patient with valvular disease, a postpump assessment is made regardless of whether a surgical intervention on the mitral valve has been performed.

## Postpump Intraoperative Echocardiography in Mitral Repair

The most significant indication for IOE in mitral valve repair (see Box 19-1 and Table 19-3) is to determine the competency of the repair immediately after cardiopulmonary bypass. If the repair is inadequate, further repair or replacement can be performed immediately during the same thoracotomy.

### TIMING

To make a relevant assessment of valvular performance, postpump intraoperative echocardiographic assessment of valvular function should be done after loading conditions and ventricular function have reached their postoperative plateau, when the patient has returned to relatively normal loading conditions. The most appropriate time to image after repair is when the patient is off cardiopulmonary bypass, the intravascular volume is replete, and the loading conditions are similar to those in the ambulatory state. Imaging can be initiated earlier than that, after the aortic cross clamp is off and the LV is at least partially filled, but abnormal findings at this time may result from abnormal LV geometry. In particular, the surgeon should not act on these findings unless they are subsequently confirmed by further imaging after the cessation of cardiopulmonary bypass.

**TABLE 19-3 Management of Abnormal Findings on Doppler Echocardiography after Mitral Valve Repair**

| *Complication* | *Management* |
|---|---|
| Residual MR | Define mechanism. If ≤1+, accept. If 2+, give phenylephrine to recheck MR with increased afterload; if >2+, further surgery is required. |
| Systolic anterior motion with LVOT obstruction | Assess LVOT gradient and MR. Increase ventricular volume, stop positive inotropes. If these measures are not successful, further surgery is needed to revise repair. |
| Dehisced ring or leaflet perforation | Another pump run is needed to redo annuloplasty. |
| Residual mitral stenosis | Quantify severity. If mean gradient >5 mm Hg or area <1.5 $cm^2$, consider further surgery. |
| Significant tricuspid regurgitation | If 3+ or more, consider further repair. |
| Regional LV dysfunction | Assess intracardiac air; if not resolved after further time on pump, consider coronary bypass. |
| Global (right or left) ventricular dysfunction | Assess volume status, afterload, and response to medications. Assessment for coronary air emboli. |

*LVOT*, Left ventricular outflow tract; *MR*, mitral regurgitation.

### INTRAOPERATIVE FINDINGS

In most cases, with an experienced surgeon, mitral valve repair leads to a competent mitral valve with mild or no residual MR; however, there are potential complications of mitral valve repair that are readily recognized by postpump IOE. Many of these complications may not be apparent clinically or may take longer to accurately diagnose without echocardiography. If left untreated, these complications may interfere with the long-term success of the procedure and require early reoperation. Complications seen after mitral valve repair by IOE are shown in Table 19-3. In early experience with more than 6000 patients, the frequency of needing a second run of cardiopulmonary bypass in mitral repair was 7%, which was lower than the frequency of aortic repair (14.7%) and myectomy (17.9%), but greater than the frequency of tricuspid repair (5.1%), congenital heart disease (4.9%), and aortic aneurysm surgery (3.6%).

### INCOMPLETE MITRAL REPAIR

Significant residual MR is the most common postpump problem detected by IOE. Moderate (2+) or more MR, either at rest or following afterload challenge with phenylephrine as previously described, is generally considered excessive after mitral repair and is an indication for a further surgical procedure. The incidence of this complication varies with the cause of the valvular regurgitation, the complexity of the repair, the experience of the surgeon, and the threshold of the operative team to accept a suboptimal result. When residual MR is found, further repair of the valve may lead to an improved result with reduction or elimination of MR, particularly when the echocardiographer can define the mechanism of the residual regurgitation. In some patients, further repair is impossible or fails, and the patient requires a third pump run to implant a prosthesis.

If the regurgitation is mild (1+) or less on the postpump IOE, then the result is usually accepted, though individual surgeons vary in their willingness to accept even mild amounts of regurgitation. The severity of MR detected by immediate postpump

IOE correlates well with angiographic or TTE and TEE estimates of severity obtained later.[56,57] Rarely, changes in the early postoperative period such as progressive chordal rupture, suture dehiscence, or early postoperative endocarditis may cause acute worsening of the MR. Thus, IOE is a reliable measure of the severity of MR and the need for further intervention.

Other considerations in deciding whether residual MR should be accepted or subjected to another surgical procedure include the mechanism of the MR, the overall condition of the patient, and LV function. Postpump determination of the mechanism of the residual MR helps the surgeon to determine whether a further reparative procedure could lessen the regurgitation and yet conserve the valve. More MR than is usually desirable might be accepted when other surgical procedures such as aortic valve replacement or coronary artery bypass grafting have also been accomplished, particularly in elderly patients or those with significant LV dysfunction. For example, in patients with extensive mitral annular calcification, mitral prosthetic insertion may be technically more difficult and more hazardous for the patient than accepting a moderate amount of residual MR.[58]

In various studies of patients undergoing mitral valve repair, 4% to 11% have needed a second pump run. About half of these (for example, 3% of the total, less than half of the 8% in one study) had persistent MR that was greater than 2+.[29] In most of the patients in whom immediate failure of mitral repair is treated with a further run of cardiopulmonary bypass, further repair can be accomplished successfully, whereas a smaller percentage (10% to 15%) of the patients having a second pump run undergo mitral prosthetic implantation. In one study,[59] inadequate repair was associated with a degenerative cause of the MR and with the absence of an annuloplasty ring implantation at the time of initial repair. In another study,[60] the need for reoperation because of inadequate repair or systolic anterior motion (SAM) of the mitral valve was more common in patients with anterior mitral leaflet or bileaflet prolapse, as opposed to those with posterior prolapse. In still another study[61] with an 11% incidence of second pump runs, interscallop malcoaptation of the posterior leaflet was the most common cause of the initially persistent MR. In the previously cited large retrospective study by Click and colleagues,[62] the incidence of changes based on the postpump IOE was 6%, although only one third of those returned to cardiopulmonary bypass for further surgery.

### IMPACT ON CLINICAL OUTCOME

IOE has a positive impact on prognosis and the incidence of reoperation after mitral repair in large centers and in smaller community hospitals. Reoperations are lower when IOE is used,[63] and the percentage of valves that are repaired is improved by the use of IOE.[64]

The severity of residual MR after mitral valve repair, as assessed by IOE, is important for prognosis, as shown by several studies. In one of these studies,[64a] moderate or greater MR was associated with a higher incidence of congestive heart failure, repeat valve surgery, or postoperative death. In a study of ischemic MR,[31] residual regurgitation by postpump IOE was a strong predictor of survival after mitral valve repair. Postoperative recurrence of MR in ischemic heart disease, however, correlates more with the degree of apical tethering, annular dilation, and contractile impairment, rather than the technical success of the repair procedure.[65] In another study,[31] patients with 3+ MR as determined by postpump IOE who did not undergo a further pump run at the time of initial operation required reoperation within 5 days because of hemodynamic instability and the frequent inability to wean off mechanical ventilation.

Patients who undergo a second pump run for an initially inadequate repair have an in-hospital complication rate that is similar to that of patients who require a single pump run.[66,67] In one study,[68] residual MR of 1+ or 2+ did not increase hospital complications when compared with trivial or no regurgitation postoperatively. There was a trend for patients with 1+ or 2+ MR, however, to need more reoperations in late follow-up than those with trivial or no MR.

## Other Complications of Mitral Valve Repair

### SYSTOLIC ANTERIOR MOTION OF THE MITRAL VALVE

Significant LV outflow obstruction caused by SAM of the mitral valve has been recognized as a complication of surgery since the early days of mitral valve repair.[69,70] This abnormality simulates the physiology seen in hypertrophic obstructive cardiomyopathy, even though septal hypertrophy is absent. The SAM of the mitral valve after mitral repair in these patients is dynamic and is exacerbated by reducing the size of the ventricular chamber or augmenting contractility. SAM may cause pressure gradients of 100 mm Hg or more, severe hypotension, severe MR, and inability to wean the patient from cardiopulmonary bypass. In many cases, however, it is mild and is not the cause of congestive preload or decreased forward flow. Fortunately, this series of complications is readily recognized and quantified by an experienced echocardiographer on the postpump echocardiogram study (Fig. 19-11). If it is not recognized, in some patients it will cause postoperative problems and require reoperation. SAM was initially reported in 2% to 9% of patients undergoing mitral valve repair,[29,60,71] but it is now less common because of the ability to prevent it with better design of the initial repair procedure.

Several mechanisms have been proposed to explain SAM following mitral valve repair. These mechanisms include anterior displacement of the posterior ventricular wall, anterior displacement of the posterior mitral leaflet, and narrowing of the angle between the mitral and aortic valves.[72] It is clear that SAM occurs primarily in patients with degenerative mitral valve disease, those with large mitral leaflets, and in the presence of a hyperdynamic, small ventricle.[60] SAM is usually seen only after annuloplasty ring insertion, but it has been reported after a suture annuloplasty.[60] It is seen more commonly with stiff than with flexible annuloplasty rings.[60,71] One quantitative study[72] has shown that SAM is associated with anterior displacement of the mitral coaptation line. The anterior displacement is reduced or disappears after successful revision of the repair and elimination of SAM. The ratio of the length of the anterior and posterior leaflets during coaptation and the distance from the coaptation line to the septum, on preoperative TEE, were shown to be predictors of SAM. The smaller the ratio between anterior and posterior leaflet and the narrower the distance between the coaptation point and the septum, the greater the likelihood of SAM.[73]

When severe, SAM is easily recognized and may involve both leaflets. The LV outflow gradient and the severity of MR are important indicators of the hemodynamic severity. The best TEE view for measurement of the LV outflow gradient is the

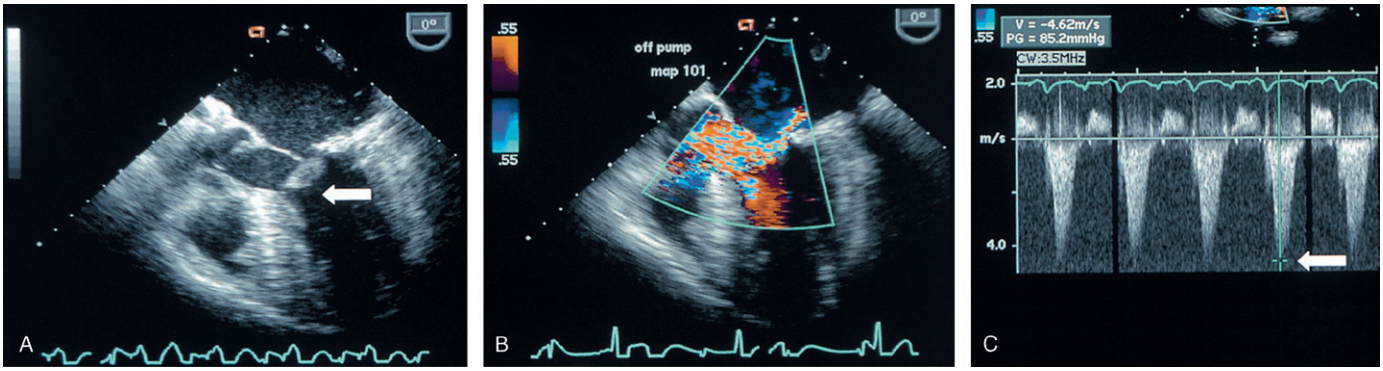



**Figure 19-11 Systolic anterior motion (SAM) of the anterior and posterior mitral valve leaflets at the end of the first pump run during mitral valve repair.** In the TEE four-chamber view, SAM is seen (**A,** *arrow*) leading to severe MR (**B**) and outflow obstruction. The maximal velocity measured in the outflow tract by continuous-wave Doppler (**C**) from the deep transgastric TEE view was 4.6 m/s, allowing estimation of an outflow tract pressure gradient of ≈85 mm Hg.

deep transgastric imaging window, which puts the heart in an orientation similar to a transthoracic apical five-chamber image and allows alignment of the continuous-wave Doppler cursor with the LV outflow tract jet. When this examination cannot be reliably performed with the transesophageal approach, the gradient can be measured with epicardial echocardiography. In many circumstances, the appearance on midesophageal images of marked SAM and significant persistent MR mandates a second pump run, without having to quantitate the gradient itself.

The initial management of patients with SAM and LV outflow obstruction after mitral repair should be to increase intracardiac volume by fluid repletion and to stop any positive inotropic agents that are being administered.[60] Systemic afterload can be supported by a pure alpha agonist (phenylephrine), avoiding any beta agonists such as dobutamine, dopamine, isoproterenol, or epinephrine. If these measures are inadequate to reduce the severity of SAM, another pump run to improve the SAM is indicated. A further procedure that may improve SAM is a sliding posterior leaflet advancement (sliding plasty), which reduces the anterior-posterior height of the posterior leaflet.

Sliding annuloplasty is currently used as a component of the primary operative procedure on patients who are considered at risk for developing SAM, particularly those with severe myxomatous leaflets with substantial redundancy, which has significantly reduced the incidence of this complication in those patients in whom it has been used.[74,75] If SAM persists despite these maneuvers, the final recourse is mitral prosthetic implantation. Patients in whom SAM is discovered by TTE days or longer after mitral valve repair, obviously a subset selected to have milder obstruction by successful weaning from bypass and extubation, may be treated medically with negative inotropic agents. Some patients show a late reduction in the LV outflow gradient, but obstruction may remain inducible by exercise, catecholamine infusions, or inhalation of amyl nitrite.[76]

## SUTURE DEHISCENCE, PERFORATION JET LESIONS, AND ANNULOPLASTY DEHISCENCE

Occasionally, suture dehiscence leads to significant MR after mitral valve repair. This complication was found by the post-pump IOE in 2% of operations in one series.[59] Kronzon and co-workers,[77] in a small case series of patients undergoing mitral valve repair or replacement, demonstrated that real-time 3D TEE provides additional information about the anatomic

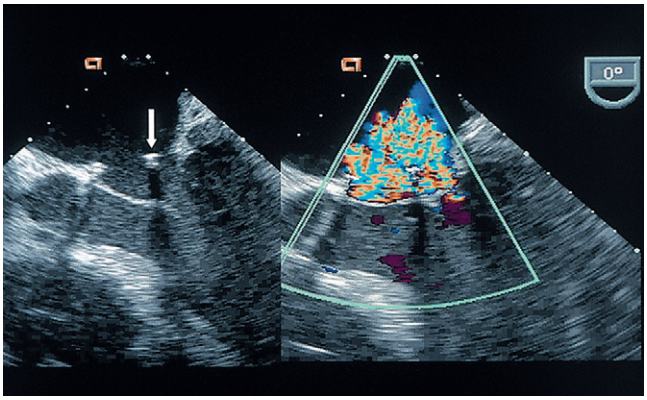


**Figure 19-12 Annular ring dehiscence.** Late failure of mitral repair due to annular ring dehiscence (*arrow, left panel*) leading to severe MR (*right panel*).

characteristics of mitral valve dehiscence and helps in planning appropriate corrective interventions. Dehiscence of a suture at the site of the leaflet resection or a suture line of the sliding plasty simulates a leaflet perforation mechanistically. This is now the most common cause of persistent MR after repair, and it is easily repaired on a second pump run. Another rare complication of mitral valve repair that can be detected by IOE is partial dehiscence of the annuloplasty ring. The annuloplasty ring shows increased mobility, and regurgitation may originate outside the ring (Fig. 19-12).

## LV SYSTOLIC DYSFUNCTION

Some reduction in LV function is often detected after mitral valve repair.[78,79] Early dysfunction after weaning from cardiopulmonary bypass may reflect the transient effects of cardioplegia and the suboptimal metabolic milieu. When dysfunction persists, it is most often global and may reflect the unmasking of LV dysfunction present preoperatively that had been concealed by the effects of increased ventricular preload and decreased afterload. In a minority of instances, a regional wall motion abnormality is detected, despite normal coronary vasculature preoperatively. This abnormality is usually caused by passage of air into a coronary vessel, most commonly a transient wall motion abnormality in the right coronary artery distribution, which usually but not always resolves without permanent infarction.[67,79a] Air within the LV cavity is readily detected by

echocardiography because it is echodense. The presence of large amounts of air on postpump IOE is an indication for increased surgical venting of the heart to prevent coronary embolization. Fortunately, most instances of air embolization of the coronary vessels resolve without significant long-term ventricular dysfunction. Because of its anterior position, air is more likely to travel to the right coronary artery in a supine patient, causing inferior wall motion abnormalities.

### TRICUSPID REGURGITATION

Tricuspid regurgitation is a common concomitant lesion to MR, More than moderate tricuspid regurgitation should treated with a ring annuloplasty at the time of mitral surgery. In all patients, whether tricuspid surgery is done or not, the amount of tricuspid regurgitation should be rechecked on the postpump intraoperative echocardiogram.[80] The success of the tricuspid surgery should be checked only after the intravascular volume status has been normalized.[81] Occasionally, tricuspid regurgitation that did not appear to be significant preoperatively may appear to be more severe on the postpump study and require a further pump run for tricuspid repair.

### MITRAL STENOSIS

In performing a mitral valve repair in a nonrheumatic valve, the surgeon may remove a significant portion of the leaflet or perform an annuloplasty that reduces the size of the mitral annular orifice. Despite these anatomic derangements, it is very unusual to have any significant stenosis in degenerative or ischemic mitral valve repair, because there is not any fusion of the mitral commissures or narrowing at the subvalvular level. The normal annulus area is 5 to 10 $cm^2$, varying with the size of the annuloplasty ring inserted. In contrast, residual stenosis of mild degree is common after rheumatic mitral valve repair because of the thickened leaflets and fusion of subvalvular chordae and commissures. The mitral valve gradient should be measured using continuous-wave Doppler after every mitral valve repair. A mean gradient in excess of 5 mm Hg should arouse suspicion of some degree of stenosis of the valve. Additional physiologic alterations with pharmacologic intervention may be needed to best demonstrate a transvalvular mitral valve gradient.

## Mitral Valve Repair Involving Commissurotomy

Mitral repair with open commissurotomy is used with decreasing frequency because of a progressive decline in the United States of the frequency of rheumatic valvular disease, and the recognition that repair of such valves is fraught with recurrence due to postoperative progression of the postinflammatory fibrosis. Balloon valvuloplasty is also a more common method of treating patients with isolated mitral stenosis. (See Chapter 21.) Nevertheless, mitral repair with open commissurotomy still has a place, especially in patients with mild or moderate valve calcification, or combined mitral stenosis and significant MR. It is especially useful when nonprosthetic outcomes are desirable, for example, in anticipation of future pregnancy. Before surgery, IOE is used to determine the severity of stenosis as a reference to assess the success of surgery. The severity of mitral stenosis is determined from the continuous-wave Doppler recording by planimetry of the diastolic velocity envelope, to measure the transmitral pressure gradient, and by measuring the pressure half-time.[82-84] An epicardial approach using a parasternal short-axis equivalent view may be used to obtain views suitable for planimetry of the mitral orifice itself, but most TEE short-axis views of the mitral valve from the transgastric window are not of sufficient quality for quantitative purposes. The mechanism of the stenosis, whether valvular or subvalvular, should also be determined. A splitability score generated in a manner similar to the transthoracic method used for percutaneous mitral valvuloplasty may help to determine the degree of valvular fibrosis and calcification and whether a valve-sparing procedure is feasible.[85] Because the surgeon can débride the valve under direct vision, open commissurotomy is sometimes possible even with a moderately high splitability score of 9 to 11, when a balloon valvuloplasty is not as likely to be effective or durable (see Chapter 21). The presence of MR and its mechanism, which is usually restricted leaflet motion, are also determined. It is important also to detect LA appendage thrombus preoperatively so that the surgeon can remove it.

On the postpump echocardiogram, the mitral valve gradient and area and MR are again assessed. The presence of residual MR of 2+ or greater, or a mitral valve area of less than 1.5 $cm^2$ by pressure half-time, is an indication for a further pump run, either to improve the repair or to implant a prosthesis. Frequently, when the patient has atrial fibrillation, a Maze procedure or pulmonary vein ablation will be performed. The LA appendage may be ligated in an effort to reduce the embolic risk, although in up to one third of patients, blood may still enter and leave the appendage.[86]

## TEE in Minimally Invasive and Robotic Mitral Valve Repair

Guidance by imaging is more important when the therapy involved is new or for some reason associated with more risks of mistaken objectives or faulty outcome. With the ongoing development of percutaneous leaflet repair and annuloplasty, along with minimally invasive valvular surgery, IOE continues to be a vital component in ensuring the success of these new techniques. (See Chapters 5 and 6.)

One such emerging arena is less invasive valve procedures. The vast majority (over 80%) of isolated minimally invasive mitral surgeries performed in the past 15 years have been done using a hemisternotomy, which involves a vertical incision about 8 to 10 cm long. This operation causes less chest trauma and bleeding and is associated with more rapid return to work, but it also involves less visual exposure of the heart, which is largely compensated for by intraoperative TEE.[17] In minimally invasive operations in which smaller incisions are used, surgical venting may be difficult or impossible. In this situation, resumption of cardiopulmonary bypass may be necessary for a period of time in order to allow slow resolution of the air.

Robotic heart surgery is a new field that requires very special techniques and technology. Again, robotic valve surgery relies heavily on IOE.[87] Recent studies have demonstrated the valuable adjunct role that TEE plays in the assessment of robotic MV repair. Wang and associates[28] recently performed intraoperative TEE in 22 consecutive patients at the General Hospital in Beijing, China, over a 2-year period and demonstrated that all patients (100%) had successful robotic MV repair with the use of intraoperative TEE.

## TEE in Transcatheter Mitral Valve Repair

Another innovation involves percutaneous valve procedures, which are done entirely via endovascular access. Percutaneous valve replacement has been developed, though only for the aortic and pulmonic valves thus far.[88-90] For severe MR, although endovascular valve replacement is not yet available, both direct and indirect percutaneous repair of the native mitral valve can now be accomplished.

The primary form of surgical mitral repair is annuloplasty. The placement of a ring or annuloplasty band in the mitral annulus, fixed by sutures, is the technique most commonly used. Percutaneous therapies for MR have paralleled many of these same surgical techniques. Percutaneous annuloplasty are under investigation through both direct and indirect approaches. Direct annuloplasty is significantly more challenging technically and associated with greater morbidity. A guide catheter must be passed retrogradely across the aortic valve and positioned within the LV on the undersurface of the posterior mitral leaflet. Current systems in development use either radiofrequency wires over which pledgets are passed and then connected via a string that is then plicated drawing the pledgets closer together, or Nitinol anchors that are placed directly in the mitral annulus and tethered together to draw the anchors closer together. Indirect annuloplasty fundamentally involves the placement of a device in the coronary sinus, which parallels the posterior mitral leaflet, and creates tension that is then transmitted to the mitral annulus. Given the relatively long history of implantation of devices in the coronary sinus, this approach is the less technically challenging. There are several limitations that are common to the indirect approach. Because of significant mechanical stresses causing significant torsional forces, there have been several cases of device fracture. Further, given the proximity of the circumflex coronary artery to the coronary sinus, compression is a potential concern. Alternative techniques for surgical mitral repair involve annuloplasty with leaflet resection and sliding annuloplasty.

### PERCUTANEOUS EDGE-TO-EDGE REPAIR OF MITRAL REGURGITATION

Though it is used less commonly for surgical repair, the edge-to-edge approximation technique is a leaflet maneuver first described by Alfieri and colleagues[91] in the early 1990s. A percutaneous method of direct mitral valve repair has been developed that uses this edge-to-edge approach via transseptal access[92] (Fig. 19-13). The MitraClip system consists of a guide catheter, a clip-delivery catheter, and an implantable dual-arm cobalt-chromium clip. The open clip can grasp the mitral leaflets via small grippers. When the edges of the two leaflets are attached, the intact chords to the anterior leaflet support the prolapsing posterior leaflet, or vice versa. TEE is essential for online assessment of the degree of reduction in MR in real time. The clip can be opened and closed multiple times for proper positioning, and if needed, a second clip can be placed if the reduction in MR is felt to be insufficient (Fig. 19-14). The EVEREST Phase I clinical trial evaluated 24 patients in whom the MitraClip was placed and followed them for 6 months.[93] In 13 of 14 patients where reduction of MR was 2+ or less after 1 month, the reduction was maintained at 6 months. The EVEREST II trial was a multicenter, randomized controlled trial that was designed to evaluate the benefits and risks of the MitraClip device for endovascular mitral valve repair compared with open surgery in patients with

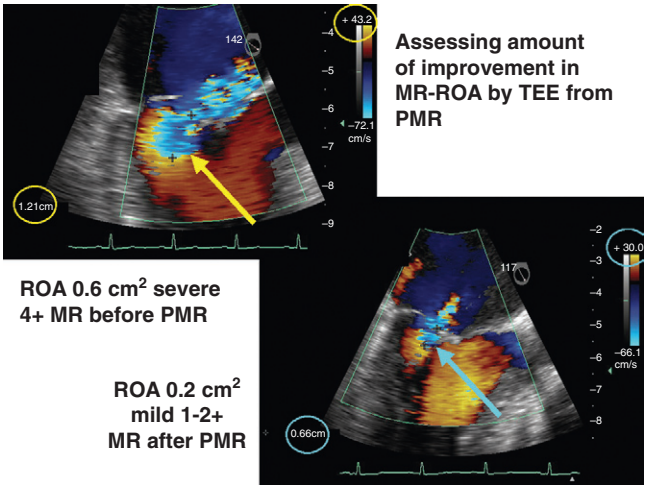



**Figure 19-13 Improvement in the amount of mitral regurgitation (MR) in a patient undergoing percutaneous mitral repair (PMR) is illustrated.** At *upper left*, the flow convergence zone is measured in a patient with severe prolapse of the posterior leaflet in a midesophageal TEE view from which the aliasing radius, at a Nyquist of 43 cm/s, permitted calculation of a regurgitant orifice area (*ROA*) of 0.6 $cm^2$. After percutaneous edge-to-edge repair (*lower right*), the MR has been reduced to mild or 1-2+ with an ROA of 0.2 $cm^2$, based on an aliasing radius of 0.66 cm at a Nyquist of 30 cm/s.

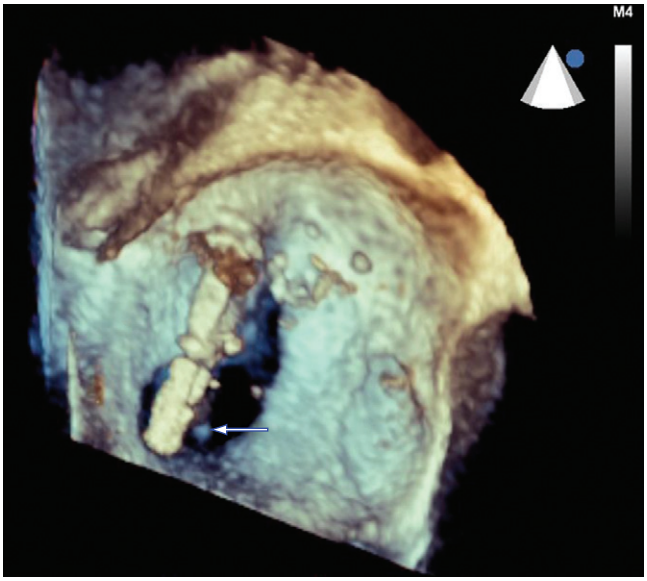



**Figure 19-14 3D TEE online still image of a patient with severe MR undergoing insertion of a percutaneous MitraClip via transseptal puncture.** The dual-arm cobalt-chromium clip (*arrow*) is seen at the end of the clip-delivery catheter.

moderate or severe MR.[94] A total of 279 patients were enrolled and evaluated for 12 months. The 1-year efficacy endpoint of the combined incidence of death, mitral valve surgery, or reoperation for mitral valve dysfunction was reached in nearly 75% of surgical patients and 66% of MitraClip patients, which met the noninferiority hypothesis for efficacy.

### PERCUTANEOUS CLOSURE OF PARAVALVULAR MITRAL REGURGITATION

Development of paravalvular leak is a well-known complication of mitral valve replacement surgery occurring in 1% to 5% of

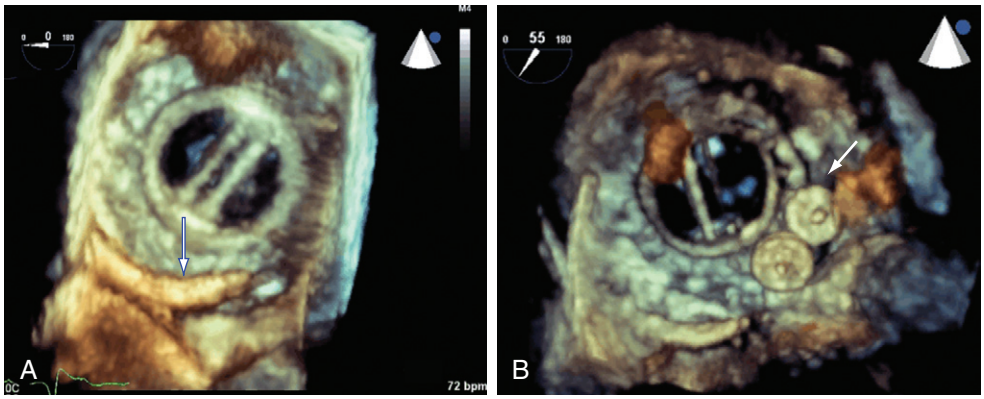



**Figure 19-15 3D TEE image of mechanical bileaflet mitral valve prosthesis in a patient with known paravalvular mitral regurgitation. A,** The transseptal sheath is seen within the LA (*arrow*) with guidewire positioned across the paravalvular orifice. **B,** Following percutaneous closure of the paravalvular leak using multiple Amplatzer occluder devices (*arrow*) within the defect.

patients.[95] Percutaneous transcatheter closure of mitral paravalvular leak has to date only achieved variable success ranging from 60% to 90% in the literature, as well as a need for repeat intervention in up to 40% of patients.[95] Part of the reason for the limited success rate in the percutaneous closure of paravalvular leaks stems from a major challenge, namely the ability to visualize the 3D nature of the defect (Fig. 19-15, Video 19-3 at ExpertConsult.com). Additionally, there is no one-size-fits-all device available for closure of these defects. Multiple devices approved by the U.S. Food and Drug Administration for closure of other cardiovascular defects are being used in an off-label fashion for this indication.[96] Advanced imaging guidance with 3D TEE is useful in guiding placement and defining the amount and location of paravalvular MR at each stage of the procedure.[97]

These percutaneous procedures are pushing the envelope of therapy for valvular heart disease, into cardiac interventional procedures in the catheterization laboratory. Imaging before, during, and after such procedures typically involves TEE.

## KEY POINTS

- IOE is useful before mitral valve repair to determine the mechanism and severity of the MR, determine the presence of other significant disease that may require surgical attention, establish baseline left and right ventricular function, and, after repair, to determine the success of the surgical procedure.
- The mechanism of MR, discerned from leaflet by 2D echocardiography and the jet direction by color Doppler, allows prediction of the feasibility of mitral valve repair and the surgical techniques of doing so.
- When residual MR is noted on the postpump TEE, further repair of the valve during a second pump run often improves the surgical result and has a positive impact on postoperative survival and freedom from reoperation.
- Real-time 3D TEE now provides incremental information and may allow more appropriate selection of patients. It may also help determine the most appropriate surgical procedure.

## REFERENCES


1. Gussenhoven EJ, van Herwerden LA, Roelandt J, et al: Intraoperative two-dimensional echocardiography in congenital heart disease. *J Am Coll Cardiol* 9:565-572, 1987.
2. Ungerleider RM, Greeley WJ, Sheikh KH, et al: Routine use of intraoperative epicardial echocardiography and Doppler color flow imaging to guide and evaluate repair of congenital heart lesions. *J Thorac Cardiovasc Surg* 100:297-309, 1990.
3. Marwick TH, Stewart WJ, Lever HM, et al: Benefits of intraoperative echocardiography in the surgical management of hypertrophic cardiomyopathy. *J Am Coll Cardiol* 20:1066-1072, 1992.
4. Stewart WJ, Schiavone WA, Salcedo EE, et al: Intraoperative Doppler echocardiography in hypertrophic cardiomyopathy: Correlations with the obstructive gradient. *J Am Coll Cardiol* 10:327, 1987.
5. Ribakove GH, Katz ES, Galloway AC, et al: Surgical implications of transesophageal echocardiography to grade the atheromatous aortic arch. *Ann Thorac Surg* 53:758-763, 1992.
6. Wiet SP, Pearce WH, McCarthy WJ, et al: Utility of transesophageal echocardiography in the diagnosis of disease of the thoracic aorta. *J Vasc Surg* 20:613-620, 1994.
7. Bryan AJ, Barzilai BN, Kouchoukos NT: Transesophageal echocardiography and adult cardiac operations. *Ann Thorac Surg* 59:773-779, 1995.
8. Stewart WJ, Currie PJ, Agler DA, Cosgrove DM: Intraoperative epicardial echocardiography: technique, imaging planes, and use in valve repair for mitral regurgitation. *Dynamic Cardiovasc Imaging* 1:166-173, 1987.
9. Lambert AS, Miller JP, Foster E, et al: The diagnostic validity of digitally captured intraoperative transesophageal echocardiography examinations compared with analog recordings: a pilot study. *J Am Soc Echocardiogr* 12:974-980, 1999.
10. Ahmed S, Nanda NC, Miller AP, et al: Usefulness of transesophageal three-dimensional echocardiography in the identification of individual segment/scallop prolapsed on the mitral valve. *Echocardiography* 20:203-209, 2003.
11. Sugeng L, Shernan SK, Weiner L, et al: Real-time three-dimensional transesophageal echocardiography in valve disease: comparison with surgical findings and evaluation of prosthetic valves. *J Am Soc Echocardiogr* 21:1347-1354, 2008.
12. Schwartz SL, Cao QL, Azevedo J, Pandian NG: Simulation of intraoperative visualization of cardiac structures and study of dynamic surgical anatomy with real-time three-dimensional echocardiography. *Am J Cardiol* 73:501, 1994.
13. Marx GR, Fulton DR, Pandian NG, et al: Delineation of site, relative size and dynamic

geometry of atrial septal defects by real-time three-dimensional echocardiography. *J Am Coll Cardiol* 25:482, 1995.
14. Levine RA, Handschumacher MD, Sanfilippo AJ, et al: Three-dimensional echocardiographic reconstruction of the mitral valve, with implications for the diagnosis of mitral valve prolapse. *Circulation* 80:589-598, 1989.
15. De Castro S, Salandin V, Cartoni D, et al: Qualitative and quantitative evaluation of mitral valve morphology by intraoperative volume-rendered three-dimensional echocardiography. *J Heart Valve Dis* 11:173-180, 2002.
16. Valocik G, Kamp O, Visser CA: Three-dimensional echocardiography in mitral valve disease. *Eur J Echocardiogr* 6:443-454, 2005.
17. Delabays A, Jeanrenaud X, Chassot PG, et al: Localization and quantification of mitral valve prolapse using three-dimensional echocardiography. *Eur J Echocardiogr* 5:422-429, 2004.
18. Abraham TP, Warner JG Jr, Kon ND, et al: Feasibility, accuracy and incremental value of intraoperative 3 dimensional transesophageal echocardiography in valve surgery. *Am J Cardiol* 80:1577-1582, 1997.
19. Breburda CS, Griffin BP, Pu M, et al: Three-dimensional echocardiographic planimetry of maximal regurgitant orifice area in myxomatous mitral regurgitation: Intraoperative comparison with proximal flow convergence. *J Am Coll Cardiol* 32:432-437, 1998.
20. De Castro S, Salandin V, Cartoni D, et al: Qualitative and quantitative evaluation of mitral valve morphology by intraoperative volume-rendered three-dimensional echocardiography. *J Heart Valve Dis* 11:173-180, 2002.
21. Shanewise JS, Cheung AT, Aronson S, et al: ASE/SCA guidelines for performing a comprehensive intraoperative multiplane transesophageal examination: recommendations of the American Society of Echocardiography Council for Intraoperative Echocardiography and the Society of Cardiovascular Anesthesiologists Task Force for Certification in Perioperative Transesophageal Echocardiography. *J Am Soc Echocardiogr* 12:884-900, 1999.
22. Urbanowicz JH, Kernoff RS, Oppenheim G, et al: Transesophageal echocardiography and its potential for esophageal damage. *Anesthesiology* 72:40-43, 1990.
23. Helmcke F, Nanda NC, Hsiung MC, et al: Color Doppler assessment of mitral regurgitation with orthogonal planes. *Circulation* 75:175-183, 1987.
24. Schiller NB, Foster E, Redberg RF: Transesophageal echocardiography in the evaluation of mitral regurgitation. The twenty-four signs of severe mitral regurgitation. *Cardiol Clin* 11:399-408, 1993.
25. Chen C, Thomas JD, Anconina J, et al: Impact of impinging wall jet on color Doppler quantification of mitral regurgitation. *Circulation* 84:714-720, 1991.
26. Bargiggia GS, Tronconi L, Sahn DJ, et al: A new method for quantification of mitral regurgitation based on color flow Doppler imaging of flow convergence proximal to regurgitant orifice. *Circulation* 84:1481-1489, 1991.
27. Klein AL, Stewart WJ, Bartlett J, et al: Effects of mitral regurgitation on pulmonary venous flow and left atrial pressure: An intraoperative transesophageal echocardiographic study. *J Am Coll Cardiol* 20:1345-1352, 1992.
28. Wang Y, Gao CQ, Wang JL, Yang M: The role of intraoperative transesophageal echocardiography in robotic mitral valve repair. *Echocardiography* 28:85-91, 2011.
29. Stewart WJ, Currie PJ, Salcedo EE, et al: Intraoperative Doppler color flow mapping for decision-making in valve repair for mitral regurgitation. Technique and results in 100 patients. *Circulation* 81:556-566, 1990.
30. Maurer G, Czer LS, Chaux A, et al: Intraoperative Doppler color flow mapping for assessment of valve repair for mitral regurgitation. *Am J Cardiol* 60:333-337, 1987.
31. Sheikh KH, Bengston JR, Rankin JS, et al: Intraoperative transesophageal Doppler color flow imaging used to guide patient selection and operative treatment of ischemic mitral regurgitation. *Circulation* 84:594-604, 1991.
32. Kleinman JP, Czer LS, DeRobertis M, et al: A quantitative comparison of transesophageal and epicardial color Doppler echocardiography in the intraoperative assessment of mitral regurgitation. *Am J Cardiol* 64:1168-1172, 1989.
33. Pu M, Griffin BP, Vandervoort PM, et al: The value of assessing pulmonary venous flow velocity for predicting severity of mitral regurgitation: A quantitative assessment integrating left ventricular function. *J Am Soc Echocardiogr* 12:736-743, 1999.
34. Pu M, Griffin BP, Vandervoort PM, et al: Intraoperative validation of mitral inflow determination by transesophageal echocardiography: Comparison of single, biplane and thermodilution techniques. *J Am Coll Cardiol* 26:1047-1053, 1995.
35. Vandervoort PM, Rivera JM, Mele D, et al: Application of color Doppler flow mapping to calculate effective orifice area. An in vitro study and initial clinical observations. *Circulation* 88:1150-1156, 1993.
36. Breburda CS, Griffin BP, Pu M, et al: Three-dimensional echocardiographic planimetry of maximal regurgitant orifice area in myxomatous mitral regurgitation: intraoperative comparison with proximal flow convergence. *J Am Coll Cardiol* 32(2):432-437, 1998.
37. Recusani F, Bargiggia GS, Yoganathan AP, et al: A new method for quantification of regurgitant flow rate using color Doppler flow imaging of the flow convergence region proximal to a discrete orifice: An in vitro study. *Circulation* 83:594-604, 1991.
38. Pu M, Vandervoort PM, Griffin BP, et al: Quantification of mitral regurgitation by the proximal flow convergence method using transesophageal echocardiography: clinical validation of a geometric correction for proximal flow constraint. *Circulation* 92:2169-2177, 1995.
39. Risk SC, DAmbra MN, Griffin B, et al: Left atrial V waves following mitral valve replacement are not specific for significant mitral regurgitation. *J Cardiothorac Vasc Anesth* 6:3-7, 1992.
40. Goldman ME, Mindich BP, Teichholz LE, et al: Intraoperative contrast echocardiography to evaluate mitral valve operations. *J Am Coll Cardiol* 4:1035-1040, 1984.
41. Stewart WJ: Choosing the "golden moment" for operation in the era of valve repair for mitral regurgitation. *ACC Heart House Learning Center Highlights* 10:2-4, 1995.
42. Cosgrove DM, Stewart WJ: Mitral valvuloplasty. *Curr Probl Cardiol* 14:359-415, 1989.
43. Iglesias I: Intraoperative TEE assessment during mitral valve repair for degenerative and ischemic mitral valve regurgitation. *Semin Cardiothorac Vasc Anesth* 11:301-305, 2007.
44. Chaudhry FA, Upadya SP, Singh VP, et al: Identifying patients with degenerative mitral regurgitation for mitral valve repair and replacement: a transesophageal echocardiographic study. *J Am Soc Echocardiogr* 17: 988-994, 2004.
45. Stewart WJ, Griffin B, Thomas JD: Multiplane transesophageal echocardiographic evaluation of mitral valve disease. *Am J Card Imaging* 9:121-128, 1995.
46. Fehske W, Grayburn PA, Omran H, et al: Morphology of the mitral valve as displayed by multiplane transesophageal echocardiography. *J Am Soc Echocardiogr* 7:472-479, 1994.
47. Foster GP, Isselbacher EM, Rose GA, et al: Accurate localization of mitral regurgitant defects using multiplane transesophageal echocardiography. *Ann Thorac Surg* 65:1025-1031, 1998.
48. Grewal KS, Malkowski MJ, Kramer CM, et al: Multiplane transesophageal echocardiographic identification of the involved scallop in patients with flail mitral valve leaflet: intraoperative correlation. *J Am Soc Echocardiogr* 11:966-971, 1998.
49. Stewart WJ, Currie PJ, Salcedo EE, et al: Evaluation of mitral leaflet motion by echocardiography and jet direction by Doppler color flow mapping to determine the mechanism of mitral regurgitation. *J Am Coll Cardiol* 20:1353-1361, 1992.
50. Grewal J, Mankad S, Freeman WK, et al: Real-time three-dimensional transesophageal echocardiography in the intraoperative assessment of mitral valve disease. *J Am Soc Echocardiogr* 22:34-41, 2009.
51. Izumi S, Miyatake K, Beppu S, et al: Mechanism of mitral regurgitation in patients with myocardial infarction: a study using real time two-dimensional Doppler flow imaging and echocardiography. *Circulation* 76:777-785, 1987.
52. Hendren WG, Morris AS, Rosenkranz ER, et al: Mitral valve repair for bacterial endocarditis. *J Thorac Cardiovasc Surg* 103:124-129, 1992.
53. Enriquez-Sarano M, Freeman WK, Tribouilloy CM, et al: Functional anatomy of mitral regurgitation: Accuracy and outcome implications of transesophageal echocardiography. *J Am Coll Cardiol* 34:1129-1136, 1999.
54. Tunick PA, Gindea A, Kronzon I: Effect of aortic valve replacement for aortic stenosis on severity of mitral regurgitation. *Am J Cardiol* 65:1219-1221, 1990.
55. Harris KM, Malenka DJ, Haney MF, et al: Improvement in mitral regurgitation after aortic valve replacement. *Am J Cardiol* 80:741-745, 1997.
56. Reichert SL, Visser CA, Moulijn AC, et al: Intraoperative transesophageal color-coded Doppler echocardiography for evaluation of residual regurgitation after mitral valve repair. *J Thorac Cardiovasc Surg* 100:756-761, 1990.
57. Saiki Y, Kasegawa H, Kawase M, et al: Intraoperative TEE during mitral valve repair: Does it predict early and late postoperative mitral valve dysfunction. *Ann Thorac Surg* 66:1277-1281, 1998.
58. Orszulak TA, Schaff HV, Danielson GK, et al: Results of reoperation for periprosthetic leakage. *Ann Thorac Surg* 35:584-589, 1983.
59. Marwick TH, Stewart WJ, Currie PJ, Cosgrove DM: Mechanisms of failure of mitral valve repair: An echocardiographic study. *Am Heart J* 122:149-156, 1991.
60. Freeman WK, Schaff HV, Khandheria EK, et al: Intraoperative evaluation of mitral valve regurgitation and repair by transesophageal echocardiography: Incidence and significance of systolic anterior motion. *J Am Coll Cardiol* 20:599-609, 1992.
61. Agricola E, Oppizzi M, Maisano F, et al: Detection of mechanisms of immediate failure by transesophageal echocardiography in quadrangular resection mitral valve repair technique for

severe mitral regurgitation. *Am J Cardiol* 91:175-179, 2003.
62. Click RL, Abel MD, Schaff HV: Intraoperative transesophageal echocardiography: 5-year prospective review of impact on surgical management. *Mayo Clinic Proceedings* 75:241-247, 2000.
63. Gillinov AM, Cosgrove DM, Blackstone EH, et al: Durability of mitral valve repair for degenerative disease. *J Thorac Cardiovasc Surg* 116:734-743, 1998.
64. Matsunaga A, Shah PM, Aidan A: Impact of intraoperative echocardiography/surgery team on successful mitral valve repair: a community hospital experience. *J Heart Valve Dis* 14:325-360, 2005.
64a. Sheikh KH, deBruijn NP, Rankin JS, et al: The utility of transesophageal echocardiography and Doppler color flow imaging in patients undergoing cardiac valve surgery. *J Am Coll Cardiol* 15:363, 1990.
65. Kongsaerepong V, Shiota M, Gillinov AM, et al: Echocardiographic predictors of successful versus unsuccessful mitral valve repair in ischemic mitral regurgitation. *Am J Cardiol* 98:504-508, 2006.
66. Northrup WF 3rd, DuBois KA, Kshettry VR: Morbidity and mortality of a failed attempt at mitral valve repair converted to replacement at the same operation. *J Heart Valve Dis* 12:700-706, 2003
67. Isada LR, Stewart WJ, Torelli J, et al: Morbidity and mortality is not affected by a second pump run for initially unsuccessful mitral valve repair [abstract]. *J Am Soc Echocardiogr* 5:312, 1992.
68. Fix J, Isada L, Cosgrove D, et al: Do patients with less than "echo-perfect" results from mitral valve repair by intraoperative echocardiography have a different outcome? *Circulation* 88:39-48, 1993.
69. Kronzon I, Cohen ML, Winer HE, Colvin SB: Left ventricular outflow obstruction: A complication of mitral valvuloplasty. *J Am Coll Cardiol* 4:825-828, 1984.
70. Kreindel MS, Schiavone WA, Lever HM, Cosgrove DM: Systolic anterior motion of the mitral valve after Carpentier ring valvuloplasty for mitral valve prolapse. *Am J Cardiol* 57:408-412, 1986.
71. Lee KS, Stewart WJ, Lever HM, et al: Mechanism of outflow tract obstruction causing failed mitral valve repair. Anterior displacement of leaflet coaptation. *Circulation* 88:24-29, 1993.
72. Mihaileanu S, Marino JP, Chauvaud S, et al: Left ventricular outflow obstruction after mitral repair (Carpentier's technique): Proposed mechanism of disease. *Circulation* 78:178-184, 1988.
73. Maslow AD, Regan MM, Haering JM, et al: Echocardiographic predictors of left ventricular outflow tract obstruction and systolic anterior motion of the mitral valve after mitral valve reconstruction for myxomatous valve disease. *J Am Coll Cardiol* 34:2096-2104, 1999.
74. Perier P, Clausnizer B, Mistarz K: Carpentier "sliding leaflet" technique for repair of the mitral valve: Early results. *Ann Thorac Surg* 57:383, 1994.
75. Jebara VA, Mihaileanu S, Acar C, et al: Left ventricular outflow tract obstruction after mitral valve repair. *Circulation* 88:30-34, 1993.
76. Schiavone WA, Cosgrove DM, Lever HM, et al: Long-term follow-up of patients with left ventricular outflow tract obstruction after Carpentier ring mitral valvuloplasty. *Circulation* 78:60-65, 1988.
77. Kronzon I, Sugeng L, Perk G, et al: Real-time 3-dimensional transesophageal echocardiography in the evaluation of post-operative mitral annuloplasty ring and prosthetic valve dehiscence. *J Am Coll Cardiol* 53:1543-1547, 2009.
78. Carabello BA: Mitral valve disease. *Curr Probl Cardiol* 18:423-478, 1993.
79. Starling MR, Kirsh MM, Montgomery DG, Gross MD: Impaired left ventricular contractile function in patients with long-term mitral regurgitation and normal ejection fraction. *J Am Coll Cardiol* 22:239-250, 1993.
79a. Obarski TP, Loop FD, Cosgrove DM, et al: Frequency of acute myocardial infarction in valve repairs versus valve replacement for pure mitral regurgitation. *Am J Cardiol* 65:887, 1990.
80. Wong M, Matsumura M, Kutsuzawa S, et al: The value of Doppler echocardiography in the treatment of tricuspid regurgitation in patients with mitral valve replacement. *J Thorac Cardiovasc Surg* 99:1003-1010, 1990.
81. Czer L, Maurer G, Bolger A, et al: Tricuspid valve repair: Operative and follow-up evaluation by Doppler color flow mapping. *J Thorac Cardiovasc Surg* 98:101-110, 1989.
82. Stoddard MF, Prince CR, Ammash NM, et al: Two-dimensional transesophageal echocardiographic determination of mitral valve area in adults with mitral stenosis. *Am Heart J* 127:1348-1353, 1994.
83. Stoddard MF, Prince CR, Tuman WL, et al: Angle of incidence does not affect accuracy of mitral stenosis area calculation by pressure half-time: Application to Doppler transesophageal echocardiography. *Am Heart J* 127:1562-1572, 1994.
84. Poh KK, Hong EC, Yang H, et al: Transesophageal echocardiography during mitral valve repair underestimates mitral valve area by pressure half-time calculation. *Int J Cardiol* 108:177-180, 2006.
85. Marwick T, Torelli J, Obarski T, et al: Assessment of the mitral valve splitability score by transthoracic and transesophageal echocardiography. *Am J Cardiol* 68:1106-1107, 1991.
86. Katz ES, Tsiamtsiouris T, Applebaum RM, et al: Surgical left atrial appendage ligation is frequently incomplete: A transesophageal echocardiographic study. *J Am Coll Cardiol* 36:468-471, 2000.
87. Sorrell VL, Rajeev AG, Nifong LW, et al: Intraoperative transesophageal echocardiography with a special focus on a patient undergoing advanced robotic-assisted procedures. *Echocardiography* 19(7 Pt 1):583-587, 2002.
88. Cribier A, Eltchaninoff H, Tron C, et al: Treatment of calcific aortic stenosis with the percutaneous heart valve: mid-term follow-up from the initial feasibility studies: the French experience. *J Am Coll Cardiol* 47:1214-1223, 2006.
89. Webb JG, Chandavimol M, Thompson CR, et al: Percutaneous aortic valve implantation retrograde from the femoral artery. *Circulation* 113:842-850, 2006.
90. McElhinney DB, Hellenbrand WE, Zahn EM, et al: Short- and medium-term outcomes after transcatheter pulmonary valve placement in the expanded multicenter US melody valve trial. *Circulation* 122:507-516, 2010.
91. Maisano F, Torracca L, Oppizzi M, et al: The edge-to-edge technique: a simplified method to correct mitral insufficiency. *Eur J Cardiothorac Surg* 13:240-245, 1998.
92. Feldman T, Cilingiroglu M. Percutaneous leaflet repair and annuloplasty for mitral regurgitation. *J Am Coll Cardiol* 57:529-537, 2011.
93. Feldman T, Wasserman HS, Herrmann HC, et al. Percutaneous mitral valve repair using the edge-to-edge technique: six-month results of the EVEREST Phase I clinical trial. *J Am Coll Cardiol* 46:2134-2140, 2005.
94. Mauri L, Garg P, Massaro JM, et al: The EVEREST II Trial: design and rationale for a randomized study of the Evalve MitraClip system compared with mitral valve surgery for mitral regurgitation. *Am Heart J* 160:23-29, 2010.
95. Pate GE, Al Zubaidi A, Chandavimol M, et al: Percutaneous closure of prosthetic paravalvular leaks: case series and review. *Catheter Cardiovasc Interv* 68:528-533, 2006.
96. Kim MS, Casserly IP, Garcia JA, et al: Percutaneous transcatheter closure of prosthetic mitral paravalvular leaks. Are we there yet? *J Am Coll Cardiol Interv* 2:81-90, 2009.
97. Balzer J, Kelm M, Kühl HP: Real-time three-dimensional transoesophageal echocardiography for guidance of non-coronary interventions in the catheter laboratory. *Eur J Echocardiogr* 10:341-349, 2009.

# 20 Aortic Valve Regurgitation: Quantitation of Disease Severity and Timing of Surgical Intervention

ARTUR EVANGELISTA, MD | PILAR TORNOS, MD

**Background**
**Etiology**
Leaflet Abnormalities
Aortic Root Abnormalities
Combined Valve and Aortic Root Abnormalities
**Aortic Regurgitation Severity**
Color Doppler Echocardiography
Volume Flow Calculations
Aortic Holodiastolic Flow Reversal
Continuous Wave Doppler Ultrasound
Integrating Doppler Indexes of Severity
Alternative Approaches
**Left Ventricle Size and Systolic Function**
Dimensions and Volumes
Contractile Reserve Evaluation
**Aortic Root and Ascending Aorta Evaluation**
Aortic Valve and Root Function
**Natural History and Serial Testing in Chronic AR**
**Management and Timing of Surgery**
Medical Treatment
Indications for Surgery
**Selecting and Guiding Surgical Treatment**
Functional Classification of AR
Role of Echocardiography
Surgical Implications
**Results of Surgery and Follow-up**
**Acute Aortic Regurgitation**
Acute Type A Aortic Dissection
Infective Endocarditis
Other Infrequent Causes of Acute Aortic Regurgitation

## Background

Aortic regurgitation (AR) is characterized by diastolic reflux of blood from the aorta into the left ventricle (LV). The clinical presentation is variable and depends on several factors, including acuity of onset, aortic and LV compliance, hemodynamic conditions, and severity of the lesion. Although chronic AR is generally well tolerated for many years, acute AR may lead to rapid decompensation and, if untreated, to early death. Doppler echocardiography is the primary modality for evaluation of the presence and severity of AR. However, two-dimensional (2D) and M-mode echocardiography are useful in evaluation of the mechanism of AR. The prevalence of AR depends on age, aortic root diameters, and ethnic group. The overall prevalence of chronic AR is 5% to 10%, with most cases being trace or mild; moderate or severe AR is less common (0.5% to 2.7%).[1,2] Precise determination of the severity of the regurgitation and its repercussions on LV function is essential for clinical management and appropriate timing of surgical intervention. Echocardiography has become the most frequently used noninvasive method for AR assessment, including not only the etiology, with evaluation of ascending aortic dilation, but also determination of the severity of regurgitation along with its effect on ventricular function.

## Etiology

AR results from numerous causes, with malcoaptation of the aortic leaflets due to abnormalities of the leaflets themselves or of the supporting structures, such as the aortic root and annulus, or both (Box 20-1). Although rheumatic heart disease remains the most common etiology in developing countries, ascending aortic diseases are becoming a more frequent cause in developed countries.[3,4]

Echocardiographic evaluation of the anatomy of aortic leaflets, annulus, and aortic root is important not only in defining the etiology but also in the prognosis and management of AR.

### LEAFLET ABNORMALITIES

There are several diseases that result in AR due to leaflet abnormalities:

1. Rheumatic disease is characterized by commissural fusion, thickening, and retraction of the aortic leaflets, which usually induces a central regurgitation jet.
2. Aortic valve sclerosis results in AR due to calcifications located in the central part of the cusps, which is more prevalent in the elderly population.
3. Congenital abnormalities include bicuspid and, more rarely, unicuspid or quadricuspid valves. In these congenital abnormal valves, abnormal stress on the leaflets modifies valve structure and causes AR, mainly due to valve prolapse. The long-axis view reveals an asymmetric closure line and systolic doming or diastolic prolapse of the leaflets. The short-axis view is more specific. The diagnosis is confirmed when only two leaflets are seen in systole with two commissures framing an elliptical systolic orifice[5-7] (Fig. 20-1). The diastolic image may mimic a trileaflet valve when a raphe is present. The most frequent abnormality is fusion of the right and left coronary cusps. Three-dimensional (3D) echocardiography may better define morphologic details of the

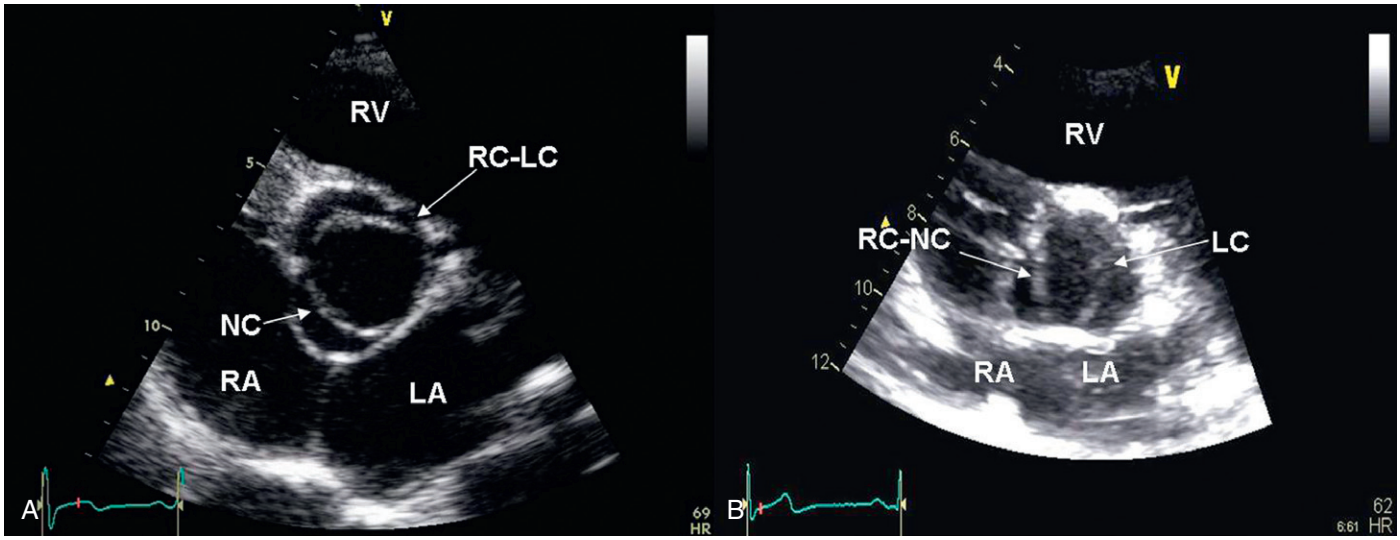



**Figure 20-1** **Parasternal short-axis view of a bicuspid aortic valve (BAV). A,** Fusion of the right and left coronary cusps (anterior-posterior BAV). **B,** Fusion of the right coronary and noncoronary cusps (right-left BAV).

**Box 20-1**

## ETIOLOGY OF CHRONIC AORTIC REGURGITATION

**Abnormalities of Aortic Leaflets**
Bicuspid aortic valve and other congenital abnormalities
Aortic valve sclerosis
Rheumatic heart disease
Myxomatous valve disease
Systemic inflammatory disorders
Antiphospholipid syndrome
Anorectic drugs
Subaortic stenosis

**Diseases of the Aortic Root**
Idiopathic aortic root dilatation
Aortoannular ectasia
Marfan syndrome
Ehlers-Danlos syndrome
Osteogenesis imperfecta
Aortic dissection
Syphilitic aortitis

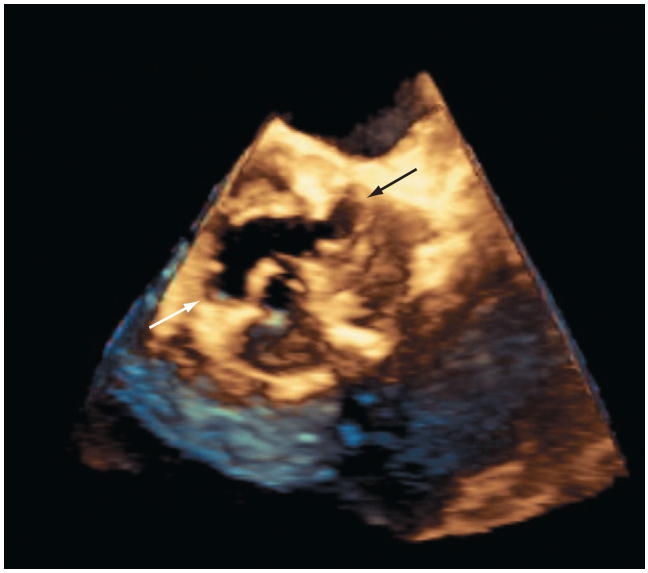


**Figure 20-2** **3D TEE image looking at the aortic side of a bicuspid aortic valve.** The two commissures (*arrows*) are seen with the slitlike valve opening in systole. The larger anterior leaflet has a prominent raphe.

bicuspid aortic valve (BAV)[8] (Fig. 20-2). Other congenital disorders such as ventricular septal defect or subvalvular aortic stenosis may also induce AR secondary to jet lesions.

4. Endocarditis results in acute AR either by leaflet perforation due to the infectious process (see Chapter 22) or to diastolic leaflet closure deformity caused by the presence of a valvular vegetation.[9]
5. Myxomatous valve disease can affect the aortic as well as the mitral valve. The leaflets are thickened and redundant with slight sagging into the LV outflow tract (LVOT) in diastole[10] (Fig. 20-3).
6. Less common abnormalities include congenital or iatrogenic leaflet fenestrations. In addition, leaflet thickening may be induced by drugs[11] or radiation, nonbacterial thrombotic endocarditis, lupus erythematosus, and other inflammatory diseases.[12]

## AORTIC ROOT ABNORMALITIES

AR may be caused, even when the leaflets themselves are normal, by alteration in the geometry of the structures supporting the leaflets. These conditions may now be more common than primary leaflet disease in patients undergoing surgical treatment for isolated AR in developed countries.[4] The aortic annulus is a complex crown-shaped structure where the leaflets attach to the aortic valve with the three points of the crown at the commissures and the three lowest points at the midsection of each leaflet (Fig. 20-4). Dilatation of this area at the base of the aortic root results in AR owing to inadequate coaptation of the stretched leaflets[13]. Aortic root dilatation may be due to a variety of causes[14] including chronic hypertension,[15] Marfan syndrome,[16] aortoannular ectasia (Fig. 20-5), Ehlers-Danlos syndrome, osteogenesis imperfecta, atherosclerotic aneurysms,

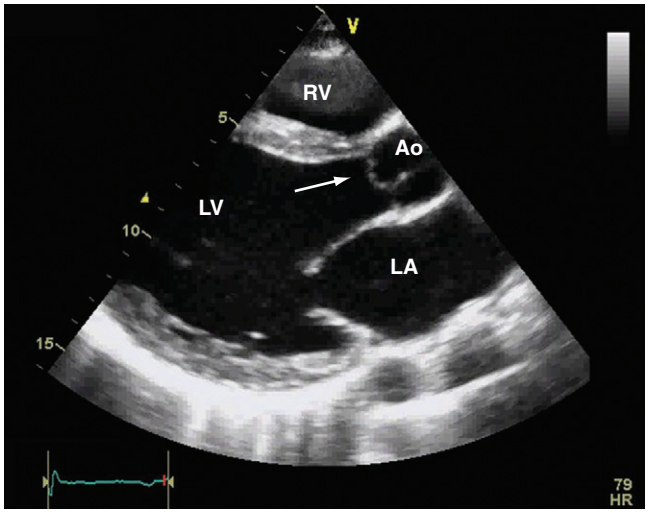



**Figure 20-3** Myxomatous aortic valve with a prolapse of right coronary cusp (*arrow*). Note that LV is severely dilated (end-diastolic diameter = 68 mm) due to chronic severe aortic regurgitation. *Ao*, Aorta.

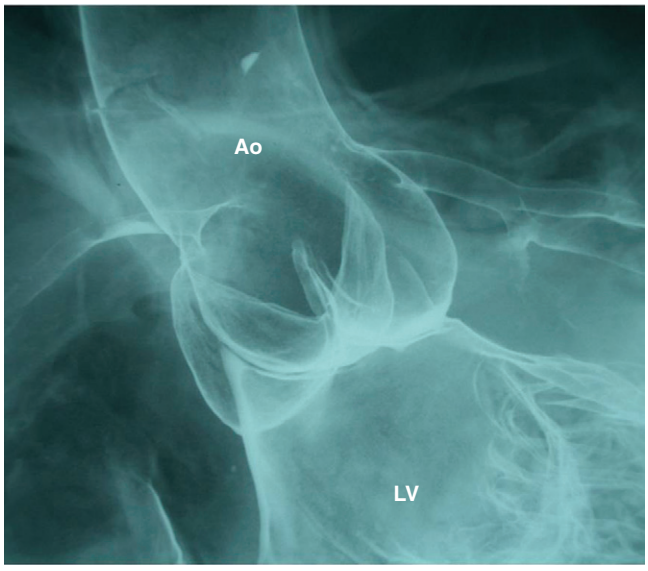



**Figure 20-4** **Aortic valve anatomy.** Radiograph of a valve outlined by contrast. *Ao*, Aorta. *(Courtesy Tim Fleming, MD.)*

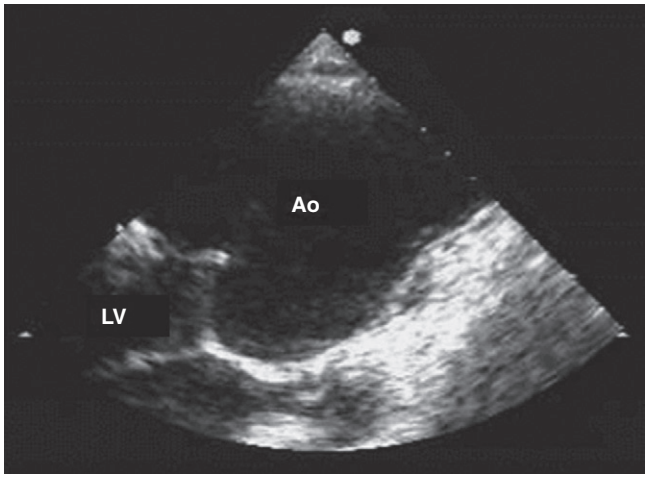



**Figure 20-5** **Annuloaortic ectasia** shown in parasternal long-axis view. *Ao*, Aorta.

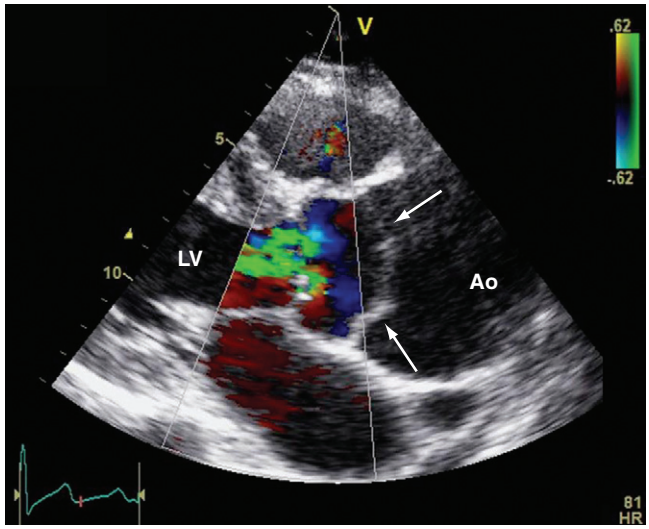



**Figure 20-6** **Acute aortic regurgitation secondary to type A aortic dissection.** *Arrows* show the intimal flap in aortic root by parasternal long-axis view. *Ao*, Aorta.

aortic dissection (Fig. 20-6), syphilitic aortitis, or various systemic inflammatory diseases.[14,17-19] (See Chapters 37 and 39.) Interestingly, in some studies, hypertension did not predict AR on multivariate analysis, thereby confirming the results of earlier studies showing hypertension to be associated with modest increases in aortic root size but not AR when age is included in the model.[15] Remarkably, Roberts and colleagues[4] analyzed the causes of pure AR in 268 patients undergoing isolated aortic valve replacement and showed that the cause was unclear by echocardiography, angiography, or histologic findings in more than 30% of cases. The group with unclear causes of AR was the oldest; 91% had hypertension, and 29% showed small calcific deposits in the valve cusp.

### COMBINED VALVE AND AORTIC ROOT ABNORMALITIES

Some diseases, such as BAV or ankylosing spondylitis, may share both leaflet and aortic root abnormalities. In fact, more than 50% of patients with BAV have echocardiographic evidence of aortic dilatation. Controversy exists as to whether aortic wall changes in BAV are caused by a congenital defect or whether they are due to the abnormal hemodynamic stress on the aortic wall secondary to abnormal helical systolic flow in the ascending aorta.[20,21] It has been suggested that type 1 BAV (fusion of right and left coronary cusp) is related to larger sinus diameter than type 2 (right and noncoronary fusion) and type 3 (left and noncoronary fusion). Type 2 morphology shows mid–ascending aortic dilatation[5] more frequently (see Fig. 20-1). However, other studies have not shown a significant relationship between aortic dimensions and morphologic valvular variables.[22] Finally, chronic severe AR of any etiology may lead to progressive enlargement of the aortic root and further worsening of AR over time.[23]

## Aortic Regurgitation Severity

### COLOR DOPPLER ECHOCARDIOGRAPHY

Color Doppler echocardiography is the key method for the diagnosis and quantification of AR in clinical practice.[24-26] Pulsed- and continuous-wave Doppler are used as complementary

methods. The regurgitant color Doppler flow pattern has three components: the proximal flow convergence or proximal isovelocity surface area (PISA), the vena contracta, and the distal jet.

1. *Color jet area and length* correlate only weakly with the degree of AR, mainly in acute or subacute AR, as they are particularly affected by the aortic-to-LV diastolic pressure gradient and LV compliance.[27-30] Despite these limitations, the difference between mild and significant AR may be estimated whenever the same instrument settings are used and complete visualization of the jet extension using different apical projections is used[31] (Fig. 20-7). When the AR jet is directed toward the mitral valve, the use of the apical long-axis view permits better visualization of the jet area. In our experience,[31] in chronic AR, a jet area less than 4 $cm^2$ or greater than 7 $cm^2$ is specific for mild or significant regurgitation, respectively. However, this method is associated with high intermachine variability.[31-33] In addition, in the presence of mitral stenosis or mitral valvular prosthesis, AR jet size is difficult to evaluate.[31,34]

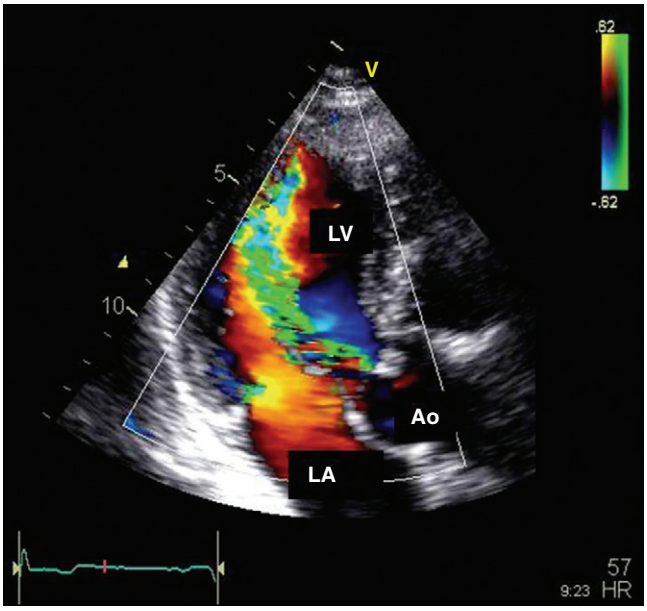



**Figure 20-7 Eccentric jet of aortic regurgitation directed toward mitral valve.** The jet is well visualized by apical three-chamber view. *Ao,* Aorta.

2. *Proximal regurgitant jet width* and its ratio to LVOT diameter is obtained from the long-axis views measured immediately below the aortic valve (at the junction of the LVOT and aortic annulus). A ratio less than 25% is consistent with mild AR, whereas a ratio greater than 65% is consistent with severe AR.[35] However, the absolute value of jet width has similar accuracy and better reproducibility than this ratio, indicating that jet width alone may be sufficient and more practical in the follow-up of patients. A jet width greater than 10 mm is indicative of severe AR and less than 7 mm of nonsignificant AR[31] (Fig. 20-8). This method has some limitations. Jet width should be measured perpendicular to the direction of the jet. However, eccentric jets directed predominantly toward the anterior leaflet of the mitral valve or the septum tend to occupy a small portion of the proximal outflow tract and may thus appear narrow and underestimate regurgitation severity.[31] Conversely, central jets tend to expand fully in the outflow tract (the spray effect) and may be overestimated. This method works best when the regurgitant orifice is relatively round in shape. When it is elliptical, as in BAV, jet width can lead to underestimation of AR severity.[25] The short-axis view is helpful in identifying regurgitant orifice shape (Fig. 20-9).
3. *Cross-sectional area of the jet* from the parasternal short-axis view and its ratio to the LVOT area are also indicators of AR severity. A ratio less than 25% is consistent with mild AR, whereas a ratio greater than 65% is consistent with severe AR.[24,25] In our experience an area greater than 1 $cm^2$ is indicative of severe AR[31] (see Fig. 20-9). The short-axis jet area has limitations because small changes in the level of the LVOT result in significant differences in jet area. In addition, image quality is suboptimal in more than 20% of cases in this view.

The combination of jet width greater than 10 mm with an apical color jet area greater than 7 $cm^2$ or cross-sectional area greater than 1 $cm^2$ has been considered a strong argument for severe AR. Unfortunately, concordance in severity grades among these Doppler methods was only 60%.[31]

4. *Vena contracta width* is one of the best methods for grading AR severity.[24,25] The vena contracta represents the smallest flow diameter at the aortic valve level, immediately below the flow convergence region. It provides, thus, an estimate of the size of the effective regurgitant orifice area (EROA) and is smaller than the regurgitant jet width in the LVOT. The vena contracta is measured in the parasternal long-axis view

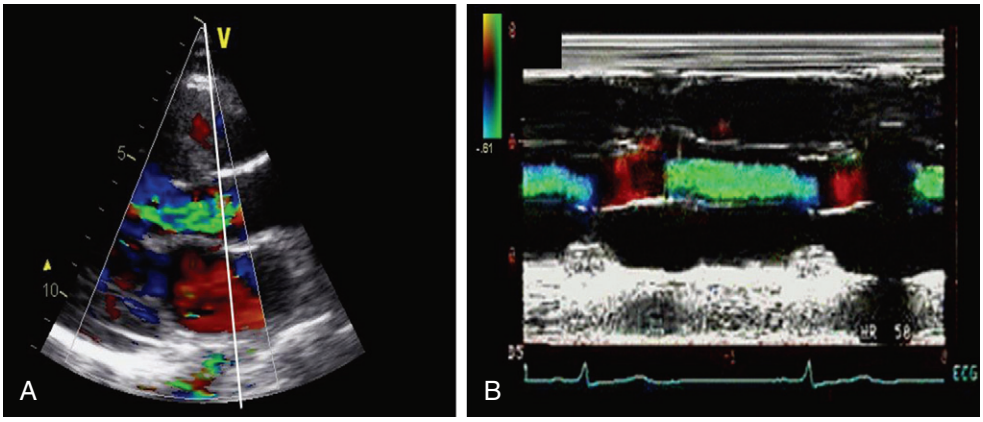



**Figure 20-8 Severe aortic regurgitation in parasternal long-axis view. A,** Color Doppler 2D. **B,** Color-coded M-mode depicting the time dependency of flow signal (*white line*) during the heart cycle.

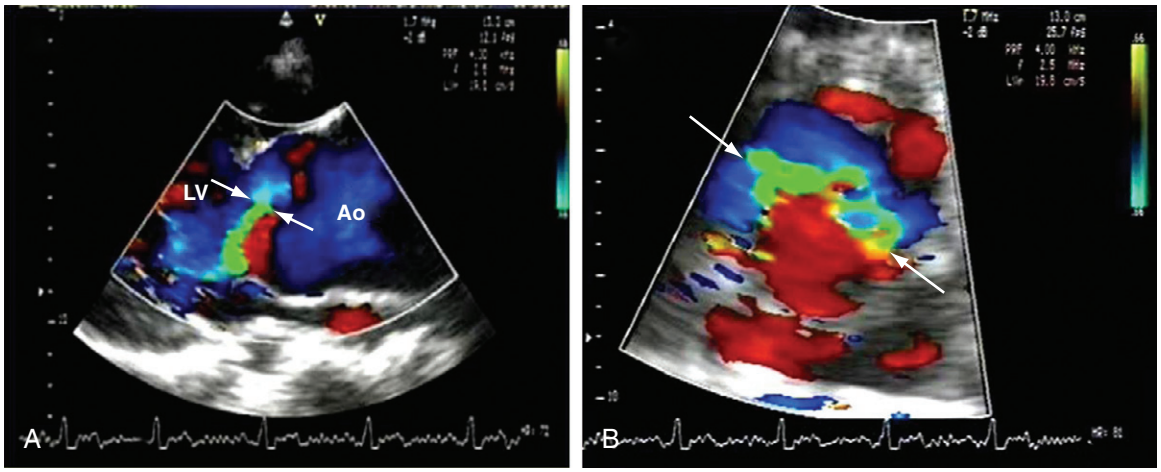



**Figure 20-9 Severe aortic regurgitation secondary to bicuspid aortic valve.** Although the vena contracta (**A,** *arrows*) of eccentric jet, directed toward mitral valve, is 5 mm, the short-axis view shows the elliptical shape (*arrows*) of the regurgitant orifice, suggesting a greater severity of AR (**B**). *Ao,* Aorta.

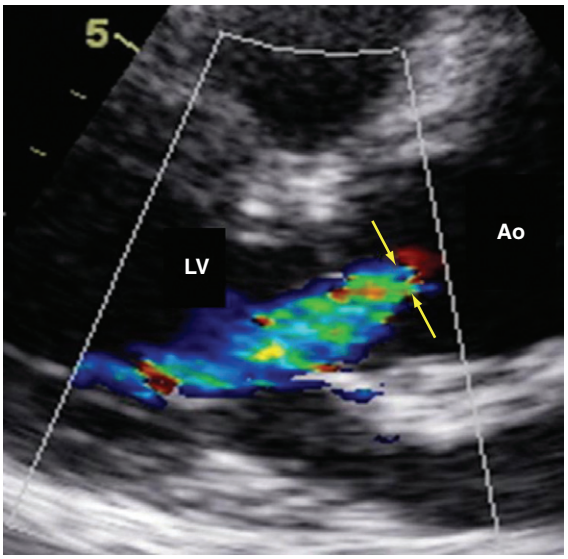



**Figure 20-10 Vena contracta of aortic regurgitation jet** (*arrows*). In the parasternal long-axis view, the vena contracta is the narrowest waist of the jet (7 mm in this example) just downstream from the aortic orifice. *Ao,* Aorta.

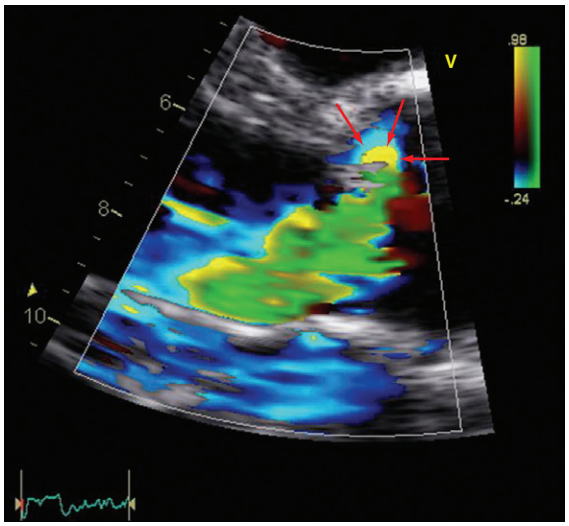



**Figure 20-11 Quantitative assessment of aortic regurgitation severity using the proximal isovelocity surface area (PISA) method.** Downward shift of zero baselines to obtain a hemispheric PISA.

(Fig. 20-10). A narrow color sector scan and zoom mode are recommended to optimize this measurement. Using a Nyquist limit of 50 to 60 cm/s, a vena contracta width of less than 3 mm correlates with mild AR, whereas a width greater than 6 mm indicates severe AR.[36,37] Because the vena contracta is often obscured by the leaflets, it can be difficult to measure accurately, mainly in calcified valves. The vena contracta method is also limited when the regurgitant orifice is elliptical or irregular. With 3D echocardiography, vena contracta areas less than 20 $cm^2$ and greater than 60 $cm^2$ have been proposed to define mild and severe AR, respectively.[38]

5. *The flow convergence method* is less commonly used to identify a clear proximal flow convergence in AR compared with mitral regurgitation. When feasible, the PISA method is less sensitive to loading conditions,[39-41] although this method is more technically demanding. The PISA region is imaged ideally in apical or right parasternal views (Fig. 20-11). The area of interest is expanded using the zoom mode, and the sector size is reduced as narrowly as possible to maximize the frame rate. The Nyquist limit should then be shifted in the direction of the AR jet to optimize measurements of the PISA radius. A clearly visible, hemispheric PISA is required for calculation. Peak flow is calculated as $2\pi r^2$ multiplied by the aliasing velocity ($V_{aliasing}$). The EROA is obtained by dividing the peak AR flow rate by the peak instantaneous AR velocity ($V_{AR}$) obtained by continuous-wave (CW) Doppler.

$$\text{EROA} = 6.28 \times r^2 \times V_{aliasing}/\text{peak } V_{AR}$$

The regurgitant volume is calculated from the EROA by multiplying by the velocity-time integral (VTI) of the AR jet. Possible accumulated errors of each variable of the equation for calculation of the regurgitant orifice do not render this method advisable for groups with limited experience in its routine use. Grading of AR severity classifies an EROA less than 10 $mm^2$ or an AR regurgitant volume less than 30 mL/beat as mild AR, and an EROA greater than 30 $mm^2$ or an AR regurgitant volume greater than 60 mL as severe AR.[41]

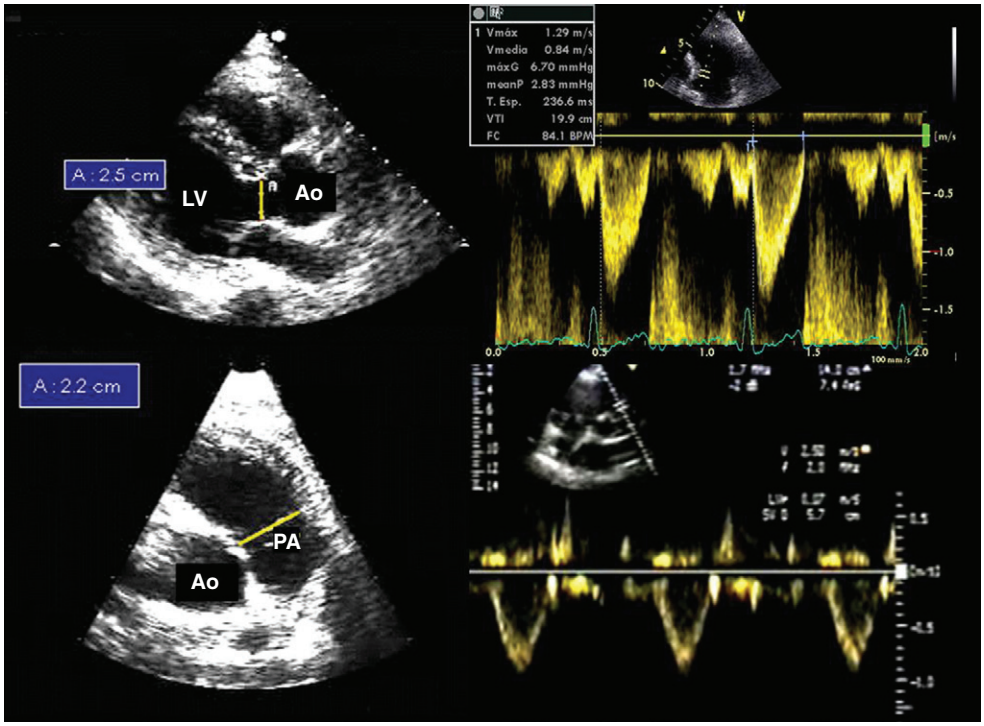



**Figure 20-12 Quantification of regurgitant fraction.** Stroke volume obtained in the left ventricular outflow tract (LVOT) (*top*) and RV outflow tract (*bottom*). Aortic annular diameter (*top right*) is 25 mm. Velocity-time integral (VTI) of LVOT (*top left*) is 20 cm; pulmonary annular diameter (*bottom right*) is 22 mm; VTI of RV outflow (*bottom left*) is 13 cm. LV outflow stroke volume is 98 mL, RV outflow stroke volume is 44 mL; thus, regurgitant volume is 54 mL and regurgitant fraction 55%. *Ao*, Aorta; *PA*, pulmonary artery.

When imaged from the apical window, the PISA method significantly underestimates AR severity in the presence of eccentric AR jets. In this situation, imaging the flow convergence zone from the parasternal long axis improves the accuracy of the PISA method.[24-26]

## VOLUME FLOW CALCULATIONS

*The pulsed Doppler volumetric method* can be used as an alternative method to quantify AR severity. The difference between LVOT flow volume and mitral or pulmonary flow volume facilitates estimation of regurgitant volume and regurgitant fraction.[31] Mitral inflow is calculated as VTI of mitral inflow (at annulus level) multiplied by the mitral annular area, assuming there is no more than mild MR. Mitral annular area is calculated as $\pi(D/2)^2$, in which D is the diameter of the mitral annulus measured in the apical four-chamber view in middiastole.[42] Measurement of stroke volume of right ventricular (RV) outflow is calculated as VTI of the RV outflow tract multiplied by the pulmonary annular area obtained from the parasternal short-axis view (Fig. 20-12). This approach is time consuming and is associated with drawbacks such as low reproducibility. In general, a regurgitant fraction greater than 50% indicates severe AR.[24,25]

## AORTIC HOLODIASTOLIC FLOW REVERSAL

*Diastolic flow reversal in descending aorta:* AR determined at the aortic isthmus level using the suprasternal view by pulsed Doppler is an easy method for identifying significant AR. A pulsed Doppler sample volume should be placed just distal to the origin of the subclavian artery, aligning it as far as possible along the major axis of the aorta. It is important for diastolic

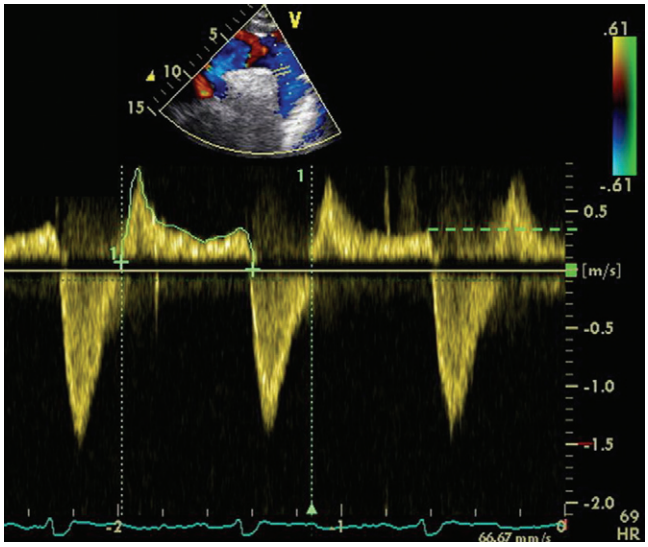



**Figure 20-13 Holodiastolic flow reversal in descending thoracic aorta with severe regurgitation.** Note that end-diastolic velocity is 35 cm/s.

flow reversal to occur throughout most of diastole, because there can be brief early diastolic flow in the ascending and descending aorta resulting from elastic recoil in a normal aortic Doppler pattern, particularly in young children and adults. As the degree of regurgitation increases, so do the duration and velocity of reversal flow.[43] End-diastolic velocity exceeding 20 cm/s is indicative of severe AR. In our experience, holodiastolic flow reversal with a diastolic VTI greater than 15 cm or with a similar value to the systolic antegrade VTI is a reliable qualitative sign of severe AR (Fig. 20-13). In addition,

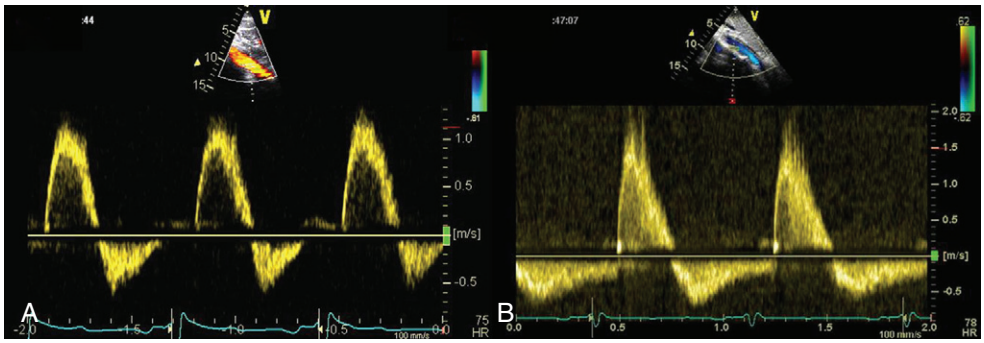



**Figure 20-14** **Abdominal aortic flow. A,** Brief diastolic flow in nonsevere aortic regurgitation (AR); **B,** pandiastolic flow reversal in severe AR.

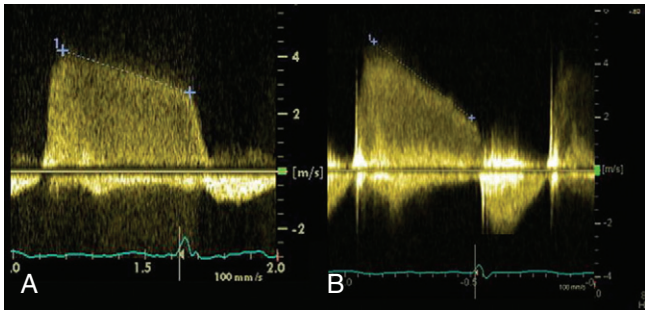



**Figure 20-15** **CW Doppler signal of aortic regurgitation (AR) with different diastolic deceleration slopes. A,** Moderate AR; **B,** severe-acute AR. Note that pressure half-time is significantly shorter in **B** than in **A.**

significant holodiastolic reversal in the abdominal aorta is also a specific sign of severe AR (Fig. 20-14).[24-27] However, these methods are influenced by heart rate, diastolic period duration, and aortic distensibility.

## CONTINUOUS WAVE DOPPLER ULTRASOUND

CW Doppler of the AR jet provides an indirect assessment of AR severity. The more intense the CW signal of the AR compared to systolic antegrade flow, the greater number of red blood cell reflectors and AR volume.

### *Deceleration Time of Regurgitant Flow*

The deceleration rate of the AR jet assessed by continuous wave Doppler provides supportive evidence when the degree of AR is assessed. The deceleration slope of the AR jet reflects the pressure difference between the aorta and the LV during diastole. It is classically best obtained from the apical five-chamber view (Fig. 20-15). The method is limited in mild AR and in the presence of eccentric jets because an adequate spectral envelope is not easy to obtain. Significant overlap exists between moderate and severe regurgitation.[31] The deceleration rate of the diastolic regurgitation jet and the derived pressure half-time (PHT) reflect both the degree of regurgitation and ventricular end-diastolic pressures. As the degree of AR increases, aortic diastolic pressure decreases and the LV end-diastolic pressure increases. The late diastolic jet velocity is thus reduced and the PHT shortened. A PHT of less than 200 ms is consistent with severe AR, whereas a value of greater than 500 ms suggests mild AR.[44-47] However, this method is influenced by chamber compliance, chamber pressure, peripheral resistance, or aortic compliance.[48,49] PHT assessment is less reliable in the setting of chronic AR in which the LV has been able to adapt to the chronic volume load.[48,49] PHT can underestimate AR in which LV end-diastolic pressure is elevated as a result of concurrent conditions such as LV systolic dysfunction. The use of PHT may be better in acute AR before changes in LV compliance occur with chronic volume load.[27]

## INTEGRATING DOPPLER INDEXES OF SEVERITY

The best way to evaluate AR severity is to integrate several Doppler methods. Based on literature data, a scheme of Doppler parameters for AR severity quantification has been proposed (Table 20-1, Fig. 20-16).[50-52] AR severity is easy to grade when results from the different parameters are congruent, particularly jet and vena contracta width and holodiastolic flow reversal in the proximal descending aorta and abdominal aorta.[31] When different parameters are contradictory, one must carefully seek technical and physiologic reasons for these discrepancies and rely on the components that have the best quality in the primary data. Quantitative parameters can help to subclassify the moderate regurgitation group into mild-to-moderate and moderate-to-severe and overcome certain limitations of some semiquantitative methods.[41] However, quantitative methods are more technically demanding, require adequate experience, and are also vulnerable to the accumulated errors of each variable when image quality is not perfect.[24,25]

## ALTERNATIVE APPROACHES

Transesophageal echocardiography (TEE) is the reference examination for AR quantification in nonechogenic patients (Fig. 20-17). Vena contracta imaging by TEE color flow mapping in the long axis (130°) is an accurate marker of AR severity.[53] In the absence of significant aortic annulus calcification, TEE permits planimetry of the regurgitant jet using color Doppler.[54,55]

Regurgitant vena contracta width greater than 6 mm and area greater than 7.5 $mm^2$, respectively, favor severe AR. Diastolic flow reversal at multiple sites in the descending aorta with biplane TEE may be useful to confirm severe AR.[55]

### *3D TTE*

Recent studies demonstrated the feasibility and accuracy of 3D TTE in quantifying AR (Fig. 20-18). Systematic cropping of the acquired 3D TTE data set is used to measure the vena contracta. The first step is to obtain the best AR jet in the long axis or from the apical view and, if the parasternal window is poor, by posterior-to-anterior cropping of the 3D TTE data set. The 3D TTE color Doppler data set is cropped from the aortic side to

**TABLE 20-1 Qualitative and Quantitative Parameters Useful in Grading Aortic Regurgitation Severity**

| *Structural Parameters* | *Mild* | *Moderate* | | *Severe* |
|---|---|---|---|---|
| LV size | Normal* | Normal or dilated | | Usually dilated† |
| Aortic leaflets | Normal or abnormal | Normal or abnormal | | Abnormal/flail, or wide coaptation defect |
| *Doppler Parameters* | | | | |
| Jet width in LVOT—color flow | Small in central jets | Intermediate | | Large in central jets; variable in eccentric jets |
| Jet density—CW | Incomplete or faint | Dense | | Dense |
| Jet deceleration rate—CW (PHT, ms)‡ | Slow >500 | Medium 500-200 | | Steep <200 |
| Diastolic flow reversal in descending aorta—PW | Brief, early diastolic reversal | Intermediate | | Prominent holodiastolic reversal |
| *Quantitative Parameters*§ | | | | |
| VC width, cm¶ | <0.3 | 0.3-0.6 | | >0.6 |
| | | *Mild to Moderate* | *Moderate to Severe* | |
| Jet width/LVOT width, %¶ | <25 | 25-45 | 46-64 | ≥65 |
| Jet CSA/LVOT CSA, %¶ | <5 | 5-20 | 21-59 | ≥60 |
| R Vol, mL/beat | <30 | 30-44 | 45-59 | ≥60 |
| RF, % | <30 | 30-39 | 40-49 | ≥50 |
| EROA, $cm^2$ | <0.10 | 0.10-0.19 | 0.20-0.29 | ≥0.30 |

Table adapted from Table 4 in Zoghbi WA, Enriquez-Sarano M, Foster E, et al: Recommendations for evaluation of the severity of native valvular regurgitation with two-dimensional and Doppler echocardiography. *J Am Soc Echocardiogr* 16:777-802, 2003.

*AR,* Aortic regurgitation; *CSA,* cross-sectional area; *EROA,* effective regurgitant orifice area; *LVOT,* left ventricular outflow tract; *PHT,* pressure half-time; *PW,* pulsed-wave Doppler; *R Vol,* regurgitant volume; *RF,* regurgitant fraction; *VC,* vena contracta.

*Unless there are other reasons for LV dilation. Normal 2D measurements: LV minor axis end-diastolic diameter ≤ 2.8 $cm/m^2$

†Exception: would be acute AR, in which chambers have not had time to dilate.

‡PHT is shortened with increasing LV diastolic pressure and vasodilator therapy and may be lengthened in chronic adaptation to severe AR.

§Quantitative parameters can subclassify the moderate regurgitation group into mild-to-moderate and moderate-to-severe regurgitation as shown.

¶At Nyquist limit of 50-60 cm/s.

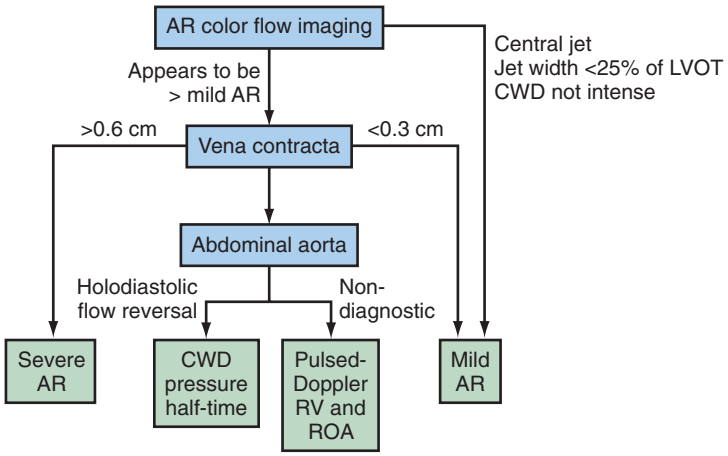



**Figure 20-16** Flow chart illustrating the clinical approach to evaluation of AR severity by echocardiography. *AR,* Aortic regurgitation; *CWD,* continuous-wave Doppler; *LVOT,* left ventricular outflow tract; *ROA,* regurgitant orifice area; *RV,* regurgitant volume. *(From Otto CM: Textbook of Clinical Echocardiography, ed 4. Philadelphia, 2009, Elsevier.)*

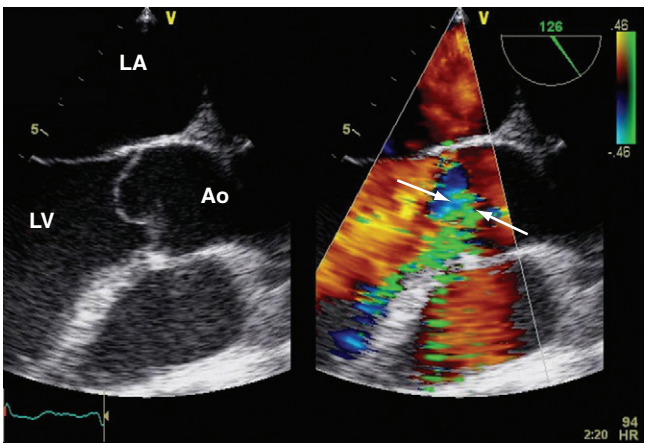



**Figure 20-17 Aortic valve prolapse.** TEE shows the presence of aortic leaflet prolapse (*left*), which leads to significant aortic regurgitation (*right*). Vena contracta (7 mm) of aortic regurgitant jet (*arrows*). *Ao,* Aorta.

the level of the vena contracta, just below the aortic leaflets, in a plane that is exactly perpendicular to the AR jet.[38,56] The image is tilted en face, and the cropped portion of the data set is added back to obtain the maximum area of vena contracta viewed in the short axis in systole. The vena contracta area can be multiplied by the VTI to accurately estimate the instantaneous regurgitant volume.

### *Magnetic Resonance Imaging*

Current recommendations consider cardiac magnetic resonance imaging (MRI) for the noninvasive evaluation of AR when echocardiography is not diagnostic (Fig. 20-19). Regurgitant volume can be calculated from the difference in the antegrade and retrograde flow volume rates in ascending aorta by phase-contrast sequences.[57-59] The good reproducibility of velocity cine MRI for the quantitative assessment of RV and RF indicates the potential of this technique for follow-up and monitoring of response to therapy.[52] Like echocardiography, MRI can also evaluate the presence of holodiastolic flow reversal in the descending aorta.

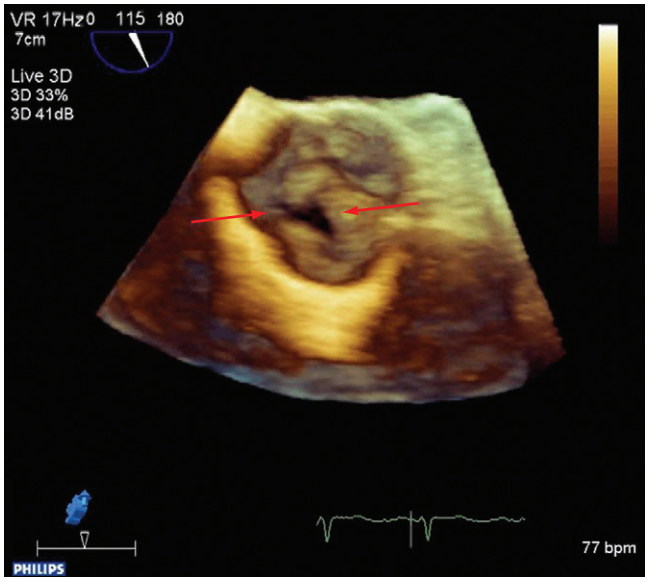



**Figure 20-18** 3D TTE showing the regurgitant orifice (*arrows*) in diastole.

## Left Ventricle Size and Systolic Function

### DIMENSIONS AND VOLUMES

Echocardiography is the diagnostic tool most widely used to assess LV dimensions, volumes, and ejection fraction (EF) (see Chapter 9). End-diastolic and end-systolic dimensions are measured using the LV minor axis from the parasternal long-axis view. 2D or 3D imaging is used to optimize alignment; however, the most accurate measurements with higher reproducibility are still taken using guided M-mode owing to the clear identification of endocardial borders[60] and excellent temporal resolution. M-mode may complement 2D images in separating structures such as trabeculae adjacent to the posterior wall, false tendons on the left side of the septum, and tricuspid apparatus or moderator band on the right side of the septum from the adjacent endocardium. However, even with 2D guidance, it may not be possible to align the M-mode cursor perpendicular to the long axis of the LV, which is mandatory to obtain a true minor axis (Fig. 20-20). Alternatively, chamber dimension and wall thickness can be acquired from the parasternal short axis at the mitral chordae level using direct measurements or targeted M-mode echocardiography, provided that the M-mode cursor can be positioned perpendicular to the septum and LV posterior wall. End-diastolic and end-systolic volumes are obtained according to Simpson's biplane rule using

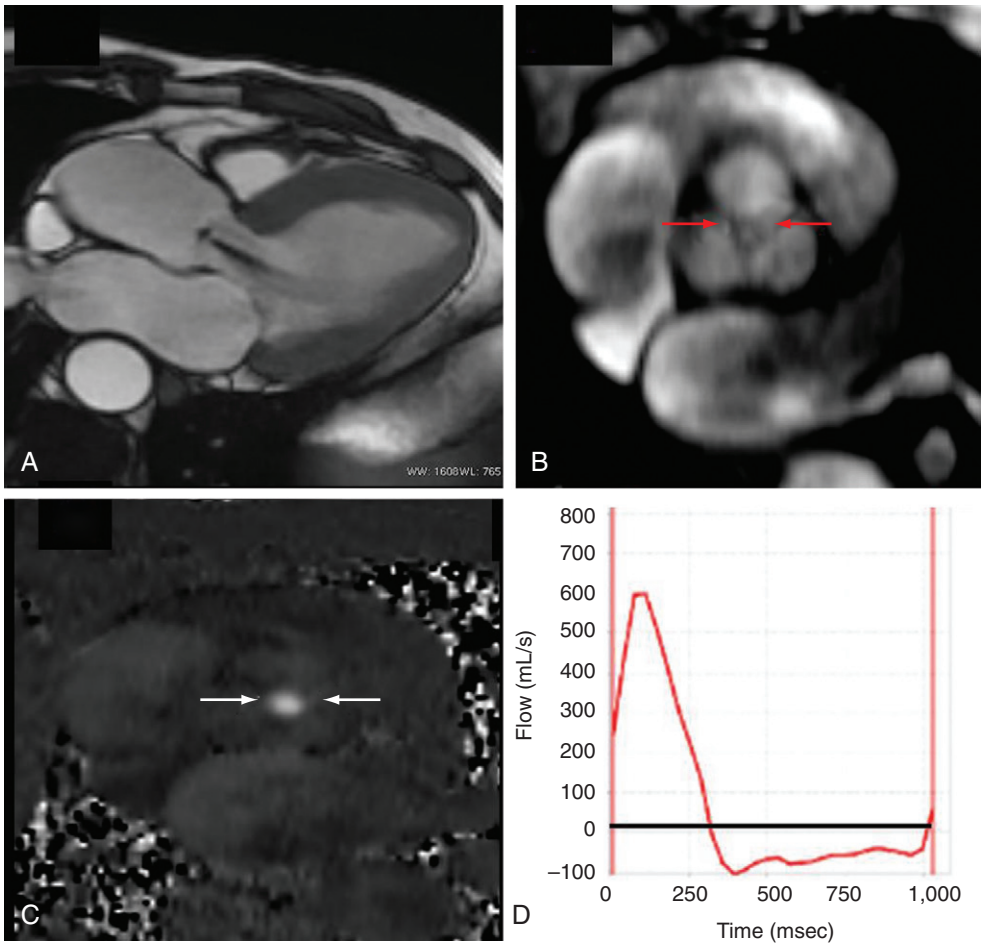



**Figure 20-19** **Cardiac magnetic resonance imaging in a patient with aortic regurgitation (AR). A,** Balanced steady-state free precession image. Oblique axial LV inflow/outflow view, showing grade 2 AR. **B,** Oblique axial plane in the aortic root, just above the aortic valve at the level of the coronary artery change (opening for ostia)(*arrows*). **C,** Phase-contrast velocity mapping. The central jet of AR is seen in white (*arrows*). **D,** Flow versus time plot for the ascending aorta. Antegrade flow was 121 mL/beat, retrograde flow was 43 mL/beat, and aortic regurgitant fraction was 36%.

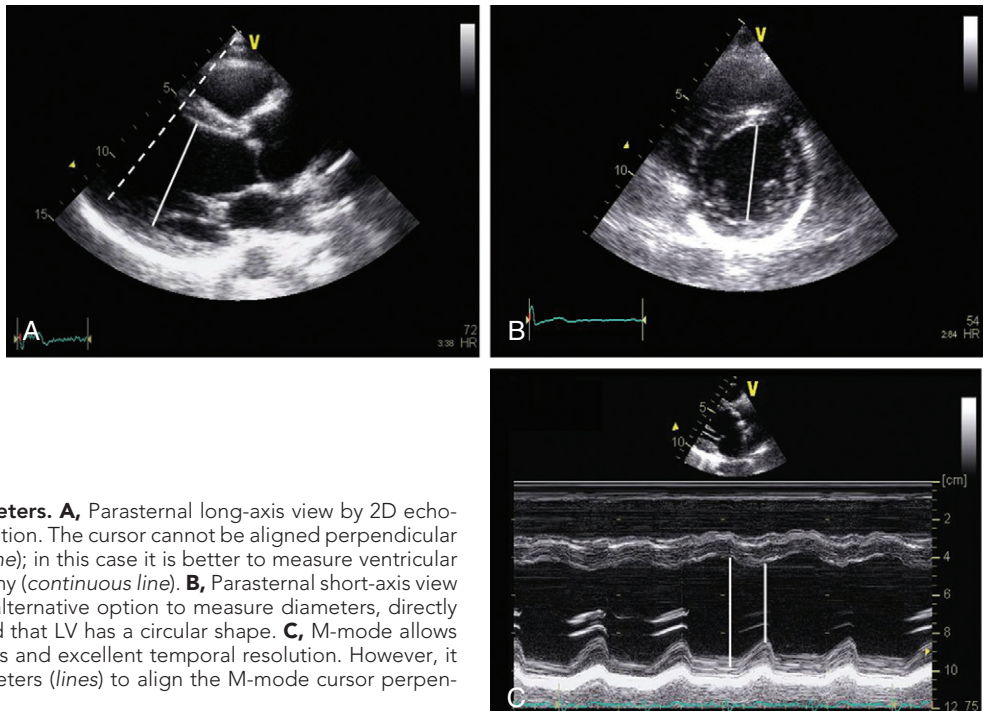



**Figure 20-20 Measurement of LV diameters. A,** Parasternal long-axis view by 2D echocardiography used to guide M-mode evaluation. The cursor cannot be aligned perpendicular to the septum and posterior wall (*dotted line*); in this case it is better to measure ventricular diameters directly from 2D echocardiography (*continuous line*). **B,** Parasternal short-axis view acquired at the mitral chordae level is an alternative option to measure diameters, directly or by M-mode echocardiography, provided that LV has a circular shape. **C,** M-mode allows a clear identification of endocardial borders and excellent temporal resolution. However, it is crucial for correct measurement of diameters (*lines*) to align the M-mode cursor perpendicular to the long axis of the LV.

the apical biplane approach. If image quality is suboptimal, left-sided contrast can be infused to enhance endocardial definition. It is important to emphasize that 2D echocardiographic methods have limitations that militate against their routine use for quantitation in the clinical setting. Apical images may foreshorten true LV length. On serial studies, a review of previous images minimizes measurement variability resulting from changes in the echocardiographic image plane, measurement site, or foreshortening of the apical view. Slight changes in measurements may not be clinically significant. Decision making is based on consistent directional changes on serial studies.[27] If measurements are approaching a value that would indicate surgical intervention, a repeat evaluation at a shorter time interval or confirmation by an alternative imaging technique is appropriate. LV wall stress may also be estimated from blood pressure and echocardiographic measurements. However, such wall stress measurements are difficult to reproduce, have methodologic and conceptual problems, and should not be used for diagnosis or management decision making in clinical practice.

Although LVEF is the fundamental parameter for evaluating LV contractility, new parameters obtained by tissue Doppler and strain rate imaging may be useful in borderline LVEF values; however, data remain scant. Two studies have shown peak systolic wave velocity less than 9 cm/s at the mitral annulus to be a predictor of complications and related to LV contractile reserve.[61,62] These studies suggested that in patients with asymptomatic chronic AR, estimation of LV long-axis contraction could unmask subnormal LV functional status at baseline that was prone to becoming more evident 12 months later. Recent studies suggested that the strain rate may be useful not only for estimating subclinical myocardial dysfunction but also for predicting postoperative LV systolic dysfunction.[63-65] Indexed volume by deformation could predict increasing LV dilatation. A cutoff value of the ratio of strain rate to end-diastolic volume less than 0.006 had 90% sensitivity and specificity. for detecting subclinical changes in deformation of the lateral wall, In another study,[64] systolic radial strain rate derived from tissue Doppler was a good predictor of postoperative LV dysfunction, with the cutoff value being 1.82 per second.

In cases with suboptimal echocardiographic images or unclear results, MRI may be indicated. MRI has become the gold standard in EF quantification.[26] Furthermore, measurement of LV and RV volumes provides the opportunity to obtain the regurgitant volume by their subtraction.

In cases with discrepancies between AR severity and LV function, other imaging techniques such as computed tomography (CT) or MRI could be useful to diagnose coronary artery disease or dilated cardiomyopathy.[66-69]

## CONTRACTILE RESERVE EVALUATION

Exercise testing may be useful when the relationship between symptoms and LV systolic function is uncertain. In this subset of patients, exercise testing may be very useful in eliciting symptoms or determining functional capacity.[69] Assessment of contractile reserve may be helpful in patients with severe AR and equivocal symptoms or borderline values in terms of LV EF (50% to 55%) or end-systolic diameter close to 50 mm or 25 mm/m$^2$. The absence of contractile reserve seems to be predictive of LV function after surgery.[70] The main limitation is the measurement variability in EF at exercise by echocardiography. Radionuclide ventriculography overcomes these limitations[71]; however, further studies are required for these findings to be used in clinical practice. Nevertheless, a decrease in EF during exercise should not be used as the only indication for surgical treatment in asymptomatic patients with normal LV systolic function at rest, because exercise EF is multifactorial and the strength of the evidence is limited. On the other hand, the change in EF with exercise is a relatively nonspecific response related to both severity of volume load and exercise-induced changes in preload and peripheral resistance.

## Aortic Root and Ascending Aorta Evaluation

Assessment of aortic root and ascending aorta dilatation is an important part of the evaluation of patients with AR. Echocardiography is accurate in the assessment and follow-up of aortic root size. MRI or CT scanning are recommended for ascending aorta evaluation in patients with an enlarged aorta detected by echocardiography, particularly when enlargement may indicate surgery.

### AORTIC VALVE AND ROOT FUNCTION

The aortic root may be defined as the portion of the aorta that supports the leaflets of the aortic valve, delineated superiorly by the sinotubular junction and inferiorly by the aortoventricular junction.[72] It is made up of the sinuses, leaflets, commissures, and interleaflet triangles. The sinotubular ridge is circular, composed primarily of elastic tissue, and supports the peripheral attachments of the valve leaflets. The valve leaflets are inserted into the aortic wall in semilunar fashion, and their closure determines a complete central coaptation. The level of coaptation is midway between the nadir of their insertion and the commissural areas.[73] The aorta-ventricular junction or base of the aortic root is defined by the nadirs of attachments of these leaflets and the inter-leaflet triangles (Fig. 20-21). The term *aortic annulus* is frequently used to describe this area; however, this term is not strictly accurate because it implies a circular structure. Approximately 45% of the circumference of the aortic root is attached to the muscular interventricular septum and 55% to fibrous tissue. This fibrous tissue is the membranous interventricular septum and the fibrous body that connects the anterior leaflet of the mitral valve to the aortic root.[74]

The function of the aortic root has been well described, because it acts as an individual hemodynamic entity.[72] The integrity of all components of this entity is essential for normal function. An aneurysm of the ascending aorta can cause dilatation of the sinotubular junction with consequent AR due to lack of coaptation of the cusp, but the aortic annulus remains normal. The mechanism of AR in patients with aortic root aneurysm is more difficult to define. Dilatation of the aortic root often starts at the level of the sinuses of Valsalva. As wall tension increases, the sinotubular junction begins to dilate. The aortic annulus may also dilate in these patients and further complicate the mechanism of AR by widening the fibrous subcommissural triangles.[75]

Echocardiography can offer dynamic evaluation of the AR mechanism.[13] Accurate aortic root measurement is important for understanding functional AR mechanisms and targeting the optimal time and strategy for aortic valve–sparing surgery. The following parameters should be measured:

- Aortic annulus: distance between insertion of the basal valve cusps into the aortic root
- Sinuses of valsalva: maximum diameter of the sinuses
- Sinotubular junction: dimension of the aortic root at the level of commissural cusp-tip insertion into the aortic wall
- Tubular tract: maximum diameter of the ascending aorta distal to the sinotubular junction (Fig. 20-22)
- Coaptation height: maximum distance between the first point of protodiastolic coaptation of the leaflet tips and the annulus plane corresponding to the basal insertion of the leaflets
- Tented area: the maximum area subtending the ventricular surface of the leaflets as far as the annular plane

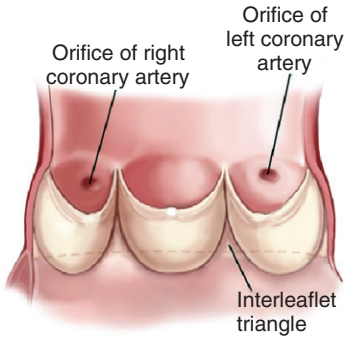



**Figure 20-21** Diagrammatic representation of the aortic valve and root that illustrates how the semilunar attachment of the valvar leaflets incorporates aortic wall in the intersinusal triangles, and the base of each of the coronary aortic sinuses. *(From Otto CM, Bonow RO:* Valvular Heart Disease, *ed 3. Philadephia, 2009, Elsevier, Fig. 12-1D, p. 188.)*

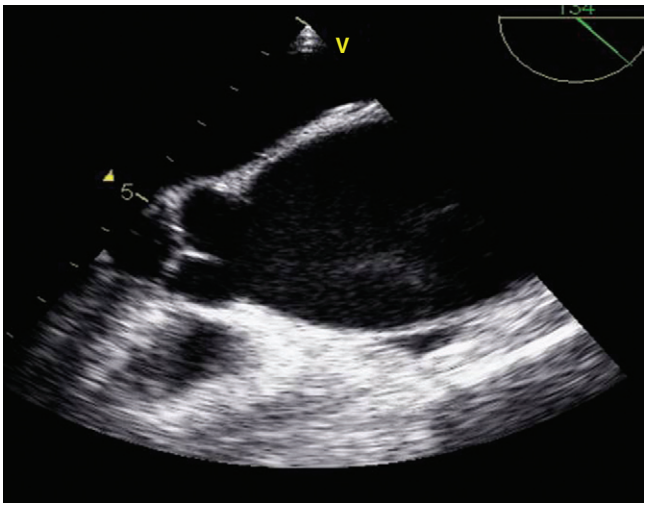



**Figure 20-22 TEE showing an ascending aorta aneurysm (50 mm) distal to the sinotubular junction.** Note the normal size of the sinuses of Valsalva.

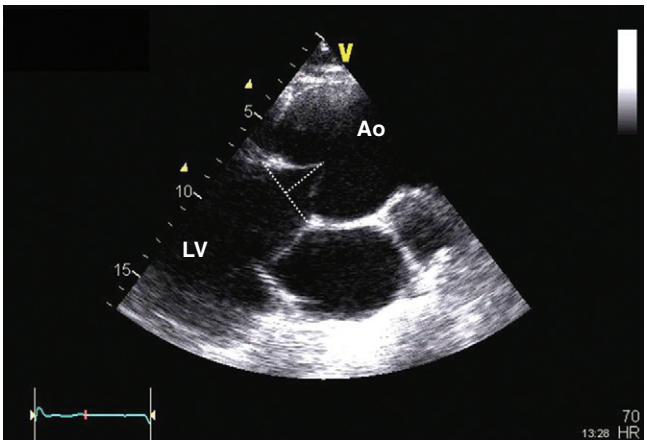



**Figure 20-23 Functional aortic regurgitation.** Parasternal long-axis view showing the aortic valve and the ascending thoracic aorta in a patient with diastolic cusp tenting with a coaptation height of 14 mm. *Ao*, Aorta.

The variable most strongly associated with functional AR severity is diastolic leaflet tenting, measured as coaptation height (Fig. 20-23). Sensitivity and specificity are over 95% using a cutoff value of 11 mm. In turn, tethering of the leaflets depends on the mismatch of sinotubular junction/

**TABLE 20-2 Studies of the Natural History of Asymptomatic Patients with Aortic Regurgitation[83-92]**

| Study | Number of Patients | Mean Follow-Up (yr) | Progression to Symptoms, Death, or LV Dysfunction Rate/Year (%) | Progression to Asymptomatic LV Dysfunction Rate/Year (%) | Mortality (Number of Patients) |
|---|---|---|---|---|---|
| Bonow[a,b] | 104 | 8.0 | 3.8 | 0.5 | 2 |
| Scognamiglio[f] | 30 | 4.7 | 2.1 | 2.1 | 0 |
| Siemienczuk[h] | 50 | 3.7 | 4.0 | 0.5 | 0 |
| Scognamiglio[g] | 74 | 6.0 | 5.7 | 3.4 | 0 |
| Tornos[j] | 101 | 4.6 | 3.0 | 1.3 | 0 |
| Ishii[e] | 27 | 14.2 | 3.6 | — | 0 |
| Borer[c] | 104 | 7.3 | 6.2 | 0.9 | 4 |
| Tarasoutchi[i] | 72 | 10 | 4.7 | 0.1 | 0 |
| Evangelista[d] | 31 | 7 | 3.6 | — | 1 |
| **Average** | **593** | **6.6** | **4.3** | **1.2** | **(0.18%/yr)** |

[a]Bonow RO, Lakatos E, Maron BJ, et al: Serial long-term assessment of the natural history of asymptomatic patients with chronic aortic regurgitation and normal left ventricular systolic function. *Circulation* 84:1625-1635, 1991.
[b]Bonow RO, Rosing DR, McIntosh CL, et al: The natural history of asymptomatic patients with aortic regurgitation and normal left ventricular function. *Circulation* 68:509-517, 1983.
[c]Borer JS, Hochreiter C, Herrold EM, et al: Prediction of indications for valve replacement among asymptomatic or minimally symptomatic patients with chronic aortic regurgitation and normal left ventricular performance. *Circulation* 97:525-534, 1998.
[d]Evangelista A, Tornos P, Sambola A, et al: Long-term vasodilator therapy in patients with severe aortic regurgitation. *N Engl J Med* 353:1342-1349, 2005.
[e]Ishii K, Hirota Y, Suwa M, et al: Natural history and left ventricular response in chronic aortic regurgitation. *Am J Cardiol* 78:357-361, 1996.
[f]Scognamiglio R, Fasoli G, Dalla VS: Progression of myocardial dysfunction in asymptomatic patients with severe aortic insufficiency. *Clin Cardiol* 9:151-156, 1986.
[g]Scognamiglio R, Rahimtoola SH, Fasoli G, et al: Nifedipine in asymptomatic patients with severe aortic regurgitation and normal left ventricular function. *N Engl J Med* 331:689-694, 1994.
[h]Siemienczuk D, Greenberg B, Morris C, et al: Chronic aortic insufficiency: factors associated with progression to aortic valve replacement. *Ann Intern Med* 110:587-592, 1989.
[i]Tarasoutchi F, Grinberg M, Spina GS, et al: Ten-year clinical laboratory follow-up after application of a symptom-based therapeutic strategy to patients with severe chronic aortic regurgitation of predominant rheumatic etiology. *J Am Coll Cardiol* 41:1316-1324, 2003.
[j]Tornos MP, Olona M, Permanyer-Miralda G, et al: Clinical outcome of severe asymptomatic chronic aortic regurgitation: a long-term prospective follow-up study. *Am Heart J* 130:333-339, 1995.

annulus diameters rather than the absolute dimension of the proximal aorta. A cutoff value greater than 1.6 strongly identifies diastolic leaflet tenting and is significantly associated with AR severity.[76,77]

## Natural History and Serial Testing in Chronic AR

Progression of AR involves a complicated interaction of several variables, including AR severity, aortic root disease, and the adaptive response of the LV. AR severity may worsen as a result of progressive leaflet deterioration and/or further dilatation of the aortic root.[78] Reimold and co-workers[79] showed that quantitative measurements of AR severity by echocardiography worsen over time. Padial and colleagues[80] showed that patients with more rapidly progressive increases in aortic root size also tend to have significant worsening of AR severity and LV dilatation.

Patients with chronic AR typically have slow LV dilatation and a prolonged asymptomatic phase. The LV adapts to the volume overload of chronic AR with a series of compensatory mechanisms, including an increase in end-diastolic volume and compliance and eccentric hypertrophy that accommodates the increased volume and maintains cardiac output without raising filling pressures. This compensated phase may last for decades. However, in most patients, the balance among afterload excess, preload reserve, and hypertrophy cannot be maintained indefinitely. Eventually, preload reserve is exhausted and/or hypertrophy becomes inadequate; thus, further increases in afterload result in a reduction in EF. This transition may be insidious, and some patients remain asymptomatic until severe LV dysfunction has developed. The decompensated stage is characterized by substantial and progressive LV enlargement, more spherical geometry, elevated LV diastolic pressures, increased systolic wall stress (i.e., afterload excess), and a decline in the EF.[81]

There are no large studies evaluating the natural history of asymptomatic patients in whom LV systolic function was normal. The current recommendations[69,82] derive from nine published series involving 593 patients with a mean follow-up period of 6.6 years[3,83-91] (Table 20-2). The rate of progression to symptoms and/or LV systolic dysfunction averaged 4.3% per year, development of asymptomatic LV dysfunction 1.2% per year, and sudden death 0.2% per year.[69] It should be emphasized that more than one fourth of patients who died or developed systolic dysfunction did so before the onset of symptoms.[84-86,90] LV size measured by echocardiography had a major predictive value. Patients with initial end-systolic dimension greater than 50 mm had a likelihood of death, symptoms, and/or LV dysfunction of 19% per year. In those with end-systolic dimension of 40 to 50 mm, this was 6% per year, and when the dimension was less than 40 mm, it was zero.[84] Thus, serial evaluation of asymptomatic patients by echocardiography is mandatory. On the other hand, 25% of asymptomatic patients with depressed systolic function developed symptoms per year.[83-94] In symptomatic patients with medical treatment, mortality over 10% to 20% per year has been reported.[89,93,94]

In asymptomatic patients with preserved systolic function, initial measurements of LV dimensions and function represent the baseline information with which future serial measurements can be compared. Patients with mild-to-moderate AR can be seen on a yearly basis and echocardiography performed every 2 to 3 years. All patients with severe AR and normal LV function should be seen for follow-up at 6 months after their initial examination. If LV diameter and/or EF show significant changes or become close to the threshold for intervention, follow-up should be continued at 6-month intervals.[69,82] Patients with stable parameters can be followed annually. In patients with dilated aorta, and especially in patients with Marfan syndrome or bicuspid valve, echocardiography should be performed on a yearly basis. CT or MRI are advisable when the

ascending aorta is not well visualized at the upper part of the sinotubular junction or when surgical indication may be based on aortic enlargement rather than LV size or function.[9]

## Management and Timing of Surgery

### MEDICAL TREATMENT

It has been hypothesized that reducing afterload by vasodilators will reduce LV wall stress, reduce LV dilatation, and delay the need for surgical treatment.[95-100] However, clinical and echocardiographic data supporting this approach have been inconclusive. Medical therapy is not able to significantly reduce regurgitant volume in chronic severe AR, because the regurgitant orifice area is relatively fixed and diastolic blood pressure is already low.[97] Only two randomized, controlled studies demonstrated significant reductions on LV end-diastolic diameters and an increase in EF with hydralazine or nifedipine.[87,95] However, a more recent randomized trial showed no benefit of therapy with enalapril or nifedipine compared to placebo[91] (Fig. 20-24). Thus, their use in not advised except in the presence of systemic hypertension (systolic blood pressure greater than 140 mm Hg) or overt heart failure en route to surgery.[69,82]

Beta blockers have been considered contraindicated in AR because cardiac output is maintained through an increase in heart rate, and lowering the heart rate may increase diastolic time and regurgitation volume.[69] However, a recent retrospective observational study[101] indicated that beta-blocker therapy was associated with better survival in patients with severe AR, mainly in the subgroup with higher heart rates. In patients with Marfan syndrome, beta-blockers can slow aortic root dilatation and reduce the risk of aortic complications. Preliminary findings suggest that ARA-II have an intrinsic effect on the aortic wall by preserving elastin fibers.[102-103] However, their clinical benefit remains to be proven by ongoing trials.[104,105]

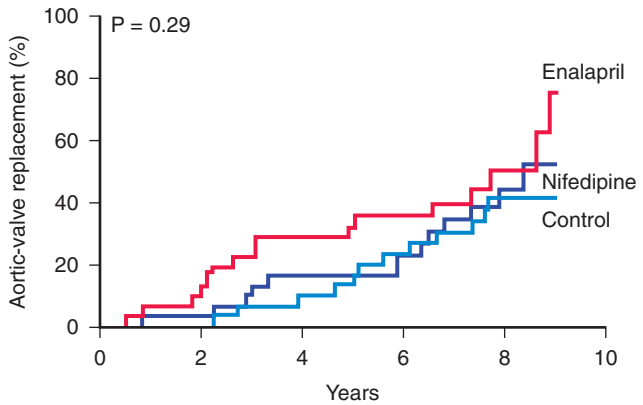



**Figure 20-24 Effect of vasodilator therapy on time to aortic valve replacement in adults with chronic aortic regurgitation (AR).** The Kaplan Meier curves show the percent of patients undergoing aortic valve replacement in a prospective, randomized, open label study of 95 adults with asymptomatic severe AR randomized to nifedipine (20 mg every 12 hours), enalapril (20 mg daily), or no treatment. *(From Evangelista A, Tornos P, Sambola A, Permanyer-Miralda G, Soler-Soler J: Long-term vasodilator therapy in patients with severe aortic regurgitation.* N Engl J Med *353(13):1342-1349, 2005.)*

### INDICATIONS FOR SURGERY

There are no randomized controlled trials to guide surgical decision making for adults with chronic AR. However, reasonable guidelines have been proposed on the basis of natural history, retrospective studies, and expert opinion.[69,80] Indication for surgery is based on three aspects: symptoms, LV function and size, and aortic dilatation. Determining LV function and dimensions should be paramount for the correct management of AR. A curvilinear relationship exists between the preoperative degree of LV dilation and postoperative EF[106] (Fig. 20-25). End-systolic ventricular size is less load dependent and thus a more robust predictor of outcome compared to end-diastolic measurements. Indexing for body surface area (BSA) could be recommended, particularly in patients of small body size and women.[94,107-109]

#### *Symptomatic Patients with LV Dysfunction*

Surgery should not be denied in symptomatic patients with severe LV dysfunction (EF less than 30%) or marked LV dilatation after careful ruling out of other possible causes. Postoperative outcome is worse in these patients,[110,111] and the likelihood of recovery of systolic function is lower than in patients operated on at an earlier stage. Patients with markedly low EF have higher long-term likelihood of postoperative heart failure; however, at 10 years only a minority of patients (25%) had this complication. Even in patients with NYHA functional class IV, improvement in LV function and clinical symptoms can be achieved, although mortality associated with aortic valve replacement approaches 10%.[110-112]

#### *Symptomatic Patients with Normal LV Systolic Function*

Surgical treatment is indicated in patients with normal LV systolic function, defined as EF greater than 50% at rest, who have NYHA functional class III or IV. In many cases of patients with NYHA functional class II dyspnea, the cause of symptoms is often unclear. Although a period of observation may be reasonable, an exercise imaging test could be helpful in identifying the causes of symptoms. Evaluation of new parameters obtained by tissue Doppler and strain rate imaging may be useful in borderline LVEF values.

#### *Asymptomatic Patients with Reduced Ejection Fraction*

Surgical treatment in asymptomatic patients is indicated in those with LV dysfunction (LVEF less than 50%). However, it is important to consider the variability of echocardiographic measurements, and exercise tests or other imaging techniques could be performed to confirm LV systolic dysfunction.

#### *Asymptomatic Patients with Normal Ejection Fraction*

Surgical treatment is also recommended in patients with normal EF and severe LV dilatation (end-diastolic dimension greater than 75 mm or end-systolic dimension greater than 55 mm).[69] Patients with severe AR in whom the degree of LV dilatation has not reached, but is approaching, these threshold values (end-diastolic dimension 70 to 75 mm or end-systolic dimension of 50 to 55 mm) should be followed with frequent echocardiograms every 4 months. In the ESC Guidelines, end-diastolic diameter greater than 70 mm or end-systolic diameter greater than 50 mm (or greater than 25 mm/m$^2$) are considered

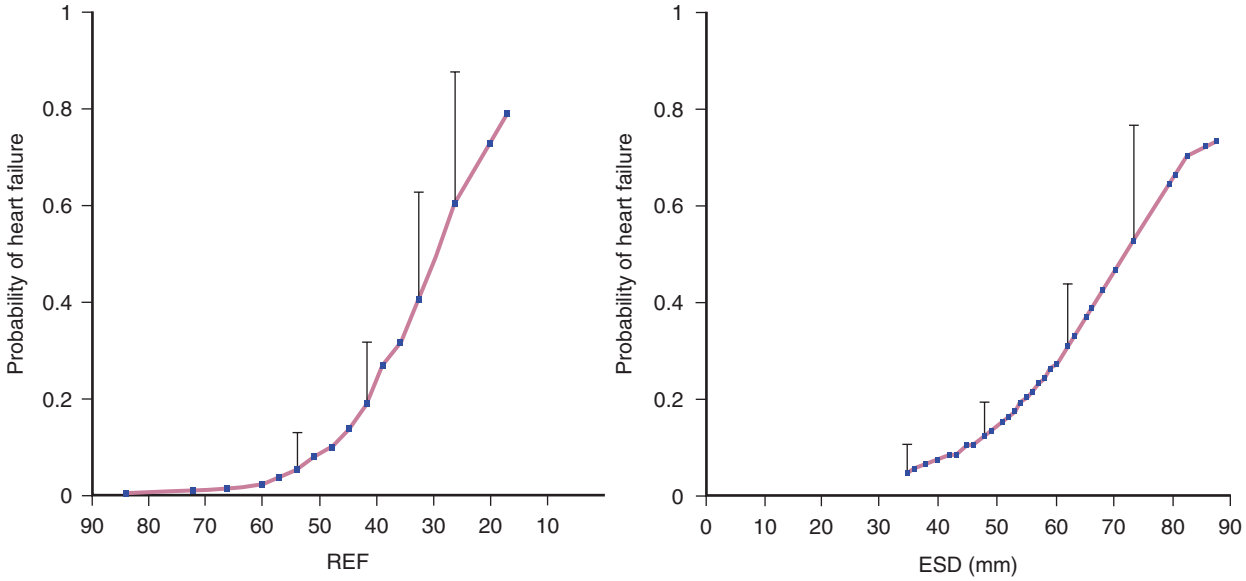



**Figure 20-25** Probability of heart failure during follow-up (*y*-axis) plotted against (*left*) preoperative radionuclide ejection fraction (REF) and (*right*) preoperative end-systolic diameter of LV in patients undergoing aortic valve replacement for severe aortic regurgitation. *(From Tornos MP, Olona M, Permanyer-Miralda G, et al: Heart failure after aortic valve replacement for aortic regurgitation: prospective 20-year study.* Am Heart J *136(4):681-687, 1998.)*

indications for surgery (class IIa)[82]. Despite preserved EF, a higher LV end-systolic volume index (45 mL/m$^2$ or higher) predicts more cardiac events within each AR grade.[13] Most patients with this severe LV dilatation and preserved EF have a high risk of outcome complications and reduced exercise tolerance. Some patients develop LV systolic dysfunction without marked LV dilatation. Women tend to develop symptoms and/or LV dysfunction with less LV dilatation than men. Anthropometric normalization of the LV end-diastolic dimension should be considered.[94,113] However, normalization for BSA may not be appropriate in patients with obesity. The use of height and a consideration of gender are likely to be more appropriate than BSA.[114]

Adherence to these guidelines for intervention in asymptomatic patients with evidence of LV dysfunction has been shown to improve long-term outcomes.[111] When ventricular dimensions of EF are used to recommend surgery, the variability in these measurements must be considered. Data are most convincing when serial studies, with side-by-side comparison of measurements, show a consistent directional change.

### *Concomitant Aortic Root Disease*

Dilatation of the ascending aorta is one of the most common causes of isolated AR. In these cases, AR is not severe, and surgical indications should be based more on aortic enlargement than on AR severity. Aortic root or ascending aorta dilatation greater than 55 mm should be a surgical indication, regardless of the degree of AR.[69] In cases of Marfan syndrome or bicuspid valves, smaller aortic diameters (at least 50 mm) have been proposed.[69,82] In Marfan patients with a family history of aortic dissection or with a rapid increase in aortic diameter (greater than 5 mm/year), aortic surgery is recommended when aortic root diameter is at least 45 mm.[82] Formulas based on patient height and the cross-sectional area of the aorta have been developed to define the thresholds for surgery, although they are less frequently used.[115,116] Indexing aortic diameters for BSA has been proposed for individuals with Turner syndrome.[117] This appears reasonable for all aortic aneurysms.[118,119]

The level of evidence for this aggressive approach is better defined in patients with Marfan syndrome than in patients with bicuspid valves.[7,20,120-124] In patients with BAV, indication for surgery in aortic diameters between 50 and 55 mm should be adapted according to patient age, body size, comorbidities, type of surgery, and presence of additional risk factors, including coarctation of the aorta, systemic hypertension, aortic valve stenosis, or rapid increase in aortic diameter at least 5 mm per year.

When valve replacement is required on the basis of AR severity, replacement of the ascending aorta should be considered when aortic diameter is greater than 50 mm, or greater than 45 mm depending on age, BSA, valvular disease etiology, presence of a BAV, and intraoperative shape and thickness of the ascending aorta.[125] Lower thresholds may be used for root replacement if repair of the aortic valve is planned in surgical centers with established expertise in repair of the aortic root and ascending aorta.[126]

## Selecting and Guiding Surgical Treatment

Treatment of isolated AR has traditionally consisted of valve replacement with a mechanical or biologic prosthesis. Replacement with a pulmonary autograft has been an operation reserved for special instances, primarily in children or very young adults.[127,128] Repair strategies for the regurgitant aortic valve have been developed in the past 20 years for different morphologies.[129-130] Potential advantages of aortic valve repair over replacement include a lower incidence of subsequent thromboembolic events, avoidance of long-term anticoagulation, and reduced risk of endocarditis. Aortic valve repair is increasingly favored over replacement with a prosthetic valve for a variety of lesions causing significant AR.[131-133] Despite these potential benefits, the durability of aortic repair procedures has been a matter of concern, with their success rate being varied and greatly dependent on the etiology and mechanisms of aortic valve dysfunction and experience of the surgeons.[130,131]

Aortic valve repair is possible in patients undergoing repair of aneurysms of the aorta or aortic root or in selected patients, such as those with bicuspid valves with prolapsing leaflets with minimal sclerosis. Dilatation of the aortic root, regardless of its etiology, has been treated by composite replacement of the valve and root/ascending aorta with a mechanical or biologic valve conduit.[134] Valve-sparing aortic replacement is increasingly being employed as an alternative. Supracoronary replacement of the ascending aorta can be used to treat aortic aneurysm when the sinuses of Valsalva are preserved.

The type of surgical treatment should also take patient age into consideration.[132] If valve repair or a valve-sparing intervention is considered, TEE may be performed preoperatively to define the anatomy of the cusps and ascending aorta.[13]

## FUNCTIONAL CLASSIFICATION OF AR

Analysis of the mechanism of AR influences patient management, particularly when the ascending aorta is dilated or when conservative surgery is considered. Several functional classifications have been proposed. The adapted Carpentier classification for AR is the most widely used[75]: type I, aortic root dilatation or leaflet perforation; type II, prolapse of one or more cusps; and type III, restricted motion as the consequence of rheumatic disease or secondary significant calcification (Fig. 20-26).

## ROLE OF ECHOCARDIOGRAPHY

The main roles of echocardiography are to evaluate regurgitation mechanisms, describe valve anatomy, and determine the feasibility of valve repair.[13] 2D TTE does not always show the lesion responsible for leaflet malcoaptation. Evaluation of the mechanisms of AR by TEE[13] follows the same principles:

1. Type I dysfunction: identified when the dimensions of a component of the aortic root, including the aortic annulus, sinuses of Valsalva, and sinotubular junction exceed the upper limits of published normal values and no other cause of AR is identified. Abnormalities in the type I group are further subdivided into type Ia, aneurysm of the ascending aorta (see Fig. 20-22); type Ib, aneurysm of the aortic root (see Fig. 20-23); type Ic, isolated dilatation of the annulus; and type Id, perforation of the leaflet due to either trauma or endocarditis.
2. Type II dysfunction: considered in the presence of an eccentric AR jet and either a cusp prolapse or cusp fenestration. Cusp prolapse is considered whenever the free edges of one or more of the aortic cusps override the plane of the aortic annulus. As in surgery, three subtypes of cusp prolapse are identified on TEE: cusp flail, whole cusp prolapse, and partial cusp prolapse. Cusp flail is defined as the complete eversion of a cusp into the LVOT in long-axis views. Partial cusp prolapse is considered whenever the distal part of a cusp is prolapsing into the LVOT. This is usually associated with clear bending of the cusp body on long-axis views, and with the presence of a small circular or oval structure near the cusp free edge on short-axis views. Whole-cusp prolapse is considered when the free edge of the entire body of the same cusp is billowing into the LVOT. Billowing of the cusp body is best seen on short-axis views of the LVOT, immediately beneath the valve, where it appears as a large circular or oval structure (see Fig. 20-17). Fenestration of a cusp free edge is considered in the presence of an eccentric AR jet, but with no definite evidence of cusp prolapse. Careful inspection of long-axis gray-scale and color Doppler images usually permits the identification of small defects near the free edge of the affected cusp.
3. Type III dysfunction: considered whenever quality or quantity of the cusp tissue are judged to be poor. Thickened and rigid valves with reduced motion, valves whose leaflet tissue has been destroyed by endocarditis, and severely calcified valves are included in this category.

Intraoperative TEE should be mandatory after repair to assess the functional result and identify patients at risk for early recurrence of AR.[135] The primary interest is in the

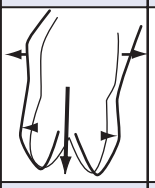
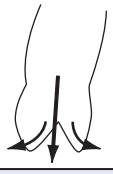
| AR Class | Type I Normal cusp motion with FAA dilatation or cusp perforation | | | | Type II Cusp prolapse | Type III Type II restriction |
|---|---|---|---|---|---|---|
| | Ia | Ib | Ic | Id | | |
| Mechanism |  |  |  |  |  |  |
| Repair techniques (Primary) | STJ remodeling<br>*Ascending aortic graft* | Aortic valve sparing:<br>*Reimplantation or Remodeling with SCA* | SCA | Patch repair<br>*Autologous or bovine pericardium* | Prolapse repair<br>*Plication*<br>*Triangular resection*<br>*Free margin*<br>*Resuspension*<br>*patch* | Leaflet repair<br>*Shaving*<br>*Decalcification*<br>*patch* |
| (Secondary) | SCA | | STJ annuloplasty | SCA | SCA | SCA |

**Figure 20-26** Repair-oriented functional classification of aortic regurgitation (AR) with description of disease mechanisms and repair techniques used. *FAA*, functional aortic annulus; *SCA*, subcomissural annuloplasty; *STJ*, sinotubular junction *(Redrawn from Boodhwani M, de Kaerchove L, Glineur D et al:* J Thorac Cardiovasc Surg *137:286-294, 2009.)*

number and location of jets and whether these are deflected. Jet deflection is a surrogate for cusp tissue redundancy and prolapse. A central nondeflected jet suggests restriction and cusp tissue deficiency relative to the root. The accuracy of TEE compared with surgical observation is high, even for identification of the various subtypes of aortic cusp prolapses. This identification is of paramount importance for the success of valve-sparing surgery since failure to identify and correct a preexisting cusp prolapse is a frequent cause of failure in valve-sparing operations.[136]

## SURGICAL IMPLICATIONS

In type I lesions, whenever the AR jet is central and perpendicular to the LVOT, absence of associated type II is supposed, and surgical correction is based on replacement of the ascending aorta and subcommissural annuloplasty (Fig. 20-27). If the AR jet is not perpendicular to the LVOT, a type II lesion must be suspected and treated. Direction of the jet toward the mitral valve or septum determines the responsible prolapsing cusp; in this case, concomitant surgical repair of type II is mandatory.[75]

In type Ib secondary to aortic root aneurysm, the indication for surgery is often diameter rather than AR severity. Even in patients with severe AR, one or more cusps remain nearly normal owing to the asymmetric nature of aortic root dilatation. After sparing surgery is achieved, by either remodeling or reimplantation procedures, a missed prolapse could be present and necessitate repair to avoid an immediate valve repair failure. Type Ib lesions with significant AR are best treated by reimplantation techniques.[74]

Among patients undergoing AR repair, those with Marfan syndrome or type III dysfunction are more likely to exhibit recurrent moderate to severe AR. The primary cause of failure, in patients with recurrent significant AR, is the persistence or induction of some degree of cuspal prolapse at the time of the initial operation. Immediate postrepair intraoperative TEE permits identification of certain functional and morphologic features associated with late repair failure, including the persistence of a residual AR jet, coaptation length less than 4 mm, coaptation level occurring below the level of the aortic annulus, and an enlarged aortic annulus. Pliability of each cusp is estimated as an apparent change in its area from systole to diastole and is termed the *tissue normality index* (TNI): TNI = (diastolic area − systolic cusp area)/diastolic cusp area. Adequacy of cusp tissue for coaptation is estimated by measuring the curvilinear height of anterior and posterior cusps in a plane parallel to the aortic orifice. A coaptation deficiency index (CDI) is calculated using the formula CDI = (conjoint cusp height + reference cusp height)/diastolic aortic "annulus" diameter. Redundant or sufficient cusp tissue offers greater potential for valve repair than restricted cusps with deficient tissue.[137] 3D echocardiography and gated high-resolution CT are promising technologies to improve aortic valve imaging.

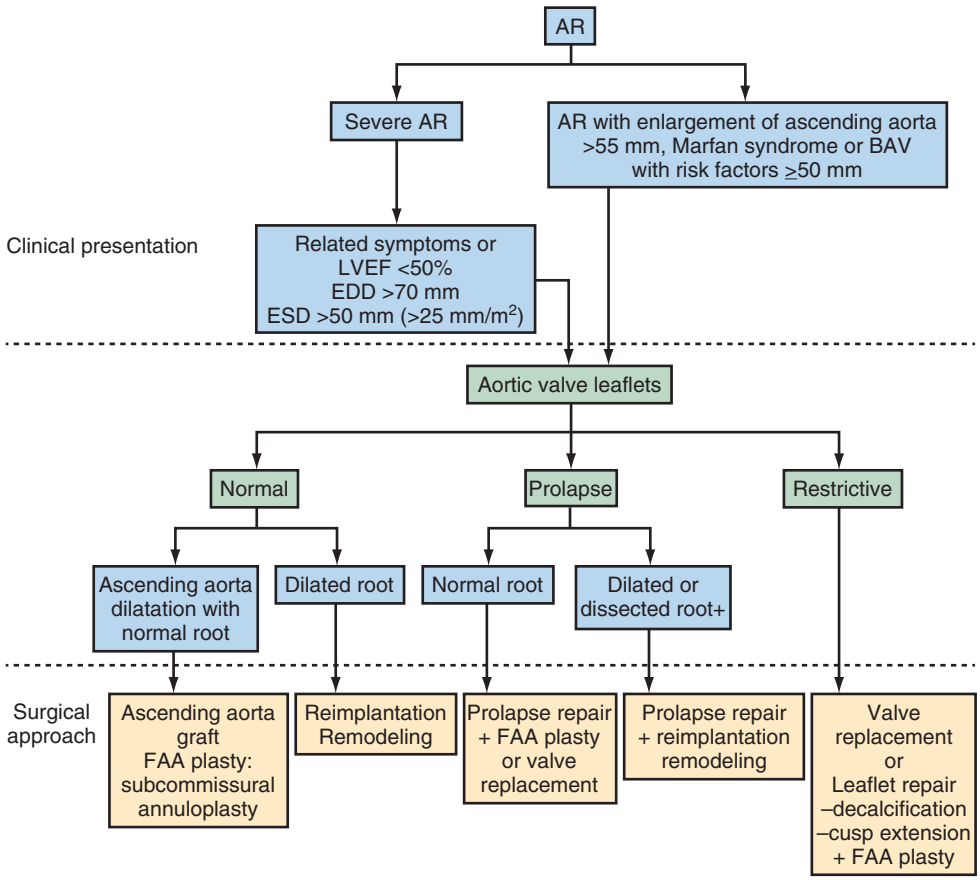



**Figure 20-27 Flow chart depicting management strategy for patients with chronic aortic regurgitation (*AR*).** *EDD*, End-diastolic dimension; *ESD*, end-systolic dimension; *FAA*, functional aortic annulus; *LVEF*, left ventricular ejection fraction.

## Results of Surgery and Follow-up

Operative mortality is low (1% to 4%) in isolated aortic valve surgery. In the presence of advanced age or impaired LV function, and in patients with concomitant coronary artery bypass grafting, operative mortality ranges from 3% to 7%.[138,139] In patients with ascending aortic aneurysm, an ascending aortic graft with prosthesis is associated with 1% to 10% mortality depending on symptoms, LV size and function, and AR severity, with the most important determinants being the skill and experience of the surgical team.[138-141] With the advent of conservative aortic valve surgery, including valve-sparing operations and aortic cusp repair, the management of severe AR has changed significantly. These operations have low operative mortality and good long-term durability. Data on reconstructive surgery from expert centers show hospital mortality of less than 2% for isolated valve repair and valve-sparing aortic replacement.[129-131,134] Mortality after pulmonary autograft is approximately 2% and thus apparently not increased despite the complexity of the operation.[140,141]

The incidence of valve-related complications after aortic valve reconstruction and valve-sparing aortic replacement at experienced centers is lower than those published for conventional valve replacement.[130,131] A linearized risk of reoperation of 1% per year has been published by experienced centers.[142,143]

After aortic valve replacement, close follow-up is recommended during the early and long-term postoperative course to evaluate prosthetic valve and LV function. An echocardiogram should be performed soon after surgery to assess the results. In the first weeks postsurgery, there is little change in LV systolic function. A better predictor of subsequent LV systolic function is the reduction in LV end-diastolic dimension, which declines significantly in the first 2 weeks postsurgery. After initial postoperative reevaluation, the patient should be seen and examined at 6 and 12 months and then on a yearly basis if the clinical course is uncomplicated.[69] After isolated surgery for a BAV, patients should have serial CT or MRI evaluation every 2 years. Patients who have ascending aorta replacement with or without aortic valve surgery should be evaluated annually with echocardiography to assess the size of the retained aortic root and should also undergo CT scans or MRI of the remaining thoracic and abdominal aorta every 3 to 5 years.

## Acute Aortic Regurgitation

In acute severe AR, the sudden large regurgitant volume is imposed on a normal-sized LV that has not had time to adapt to the volume overload. Thus, the acute increase in diastolic flow into a nondilated LV leads to a marked rise in end-diastolic pressure, and forward cardiac output is decreased. In severe cases, the increased ventricular filling pressures in conjunction with the decrease in aortic diastolic pressure lead to a rapid equalization of aortic and LV pressures at end-diastole.[144] Compensatory tachycardia tries to correct the decline in forward cardiac output; however, it is often insufficient, and patients may suffer cardiac shock. Pulmonary edema results from elevated LV end-diastolic pressure. Furthermore, coronary flow reserve is impaired, and subendocardial myocardial ischemia may result. The causes of acute AR are shown in Box 20-2.

Many of the physical signs of chronic AR are absent in the acute setting. Therefore, the diagnosis of acute severe AR can be difficult or underestimated. Physical signs include tachycardia, a sometimes difficult-to-hear diastolic murmur, and heart failure signs, but with normal pulse pressure and absence of peripheral signs of AR. The lack of physical signs of chronic severe AR renders acute AR difficult to identify, and the diagnosis is usually made by echocardiography.

Echocardiography is essential to confirm the presence and severity of AR, assess its cause, and determine the impact of acute AR on LV hemodynamics.

Echocardiographic findings of acute severe AR are shown in Box 20-3. In acute AR, premature mitral valve closure, before ventricular systole, results from the rapid rise in LV diastolic pressures from the aortic regurgitant volume and is indicative of acute severe AR. Premature mitral valve closure is best demonstrated by M-mode, because its greater temporal resolution compared to 2D imaging permits delineation of the early closure of the valve.[27] Quantitative measures of regurgitant severity that are useful in chronic AR are less useful in acute regurgitation. Hemodynamic data have demonstrated the variability in regurgitant orifice area and regurgitant volume depending on afterload and loading conditions.[41,79] TEE is indicated in most cases of acute AR to define the causes, mainly when acute dissection, endocarditis, or trauma are suspected or in other situations of uncertain etiology.

Patients with acute AR require emergent or urgent surgery to correct the underlying disease and relieve the acute volume overload of the LV. The type of surgery will depend on the underlying cause.

### ACUTE TYPE A AORTIC DISSECTION

AR frequently complicates acute type A aortic dissection, occurring in 41% to 76% of patients.[45] Although the need for early aortic surgery is well established, the optimal management of associated AR is controversial (see Chapter 36). For many years, aortic valve replacement was preferred; however, several

**Box 20-2**

**CAUSES OF ACUTE AORTIC REGURGITATION**

- Aortic dissection
- Native valve infective endocarditis
- Prosthetic valve infective endocarditis
- Trauma
- Spontaneous rupture or prolapse of an aortic cusp with bioprosthetic valve degeneration
- Leaflet perforation in the setting of connective tissue disorders
- Rupture of a fenestrated cusp
- Spontaneous dehiscence of valve commissures
- After surgical or catheter valvuloplasty

**Box 20-3**

**ECHOCARDIOGRAPHIC FINDINGS IN ACUTE AORTIC REGURGITATION**

- Vena contracta greater than 6 mm
- Pressure half-time less than 200 ms
- Holodiastolic flow reversal in abdominal aorta
- Premature mitral valve closure
- Normal left ventricular size and function

investigators have more recently reported favorable short- and long-term results with aortic valve preservation. TEE can define the mechanisms and severity of AR that complicate acute type A aortic dissection. These findings may help the surgeon to distinguish valve and geometry distortion amenable to repair from those with fixed abnormalities that require replacement. Five mechanisms of AR are identified by TEE, the first three of which are considered repairable without the need for valve replacement:

1. Incomplete closure of intrinsically normal leaflets due to leaflet tethering by a dilated sinotubular junction
2. Leaflet prolapse due to disruption of leaflet attachment by a dissection flap that extends below the sinotubular junction and into the aortic root
3. Prolapse of the dissection flap through intrinsically normal leaflets that disrupts leaflet coaptation (see Fig. 20-6)
4. BAV with associated leaflet prolapse unrelated to the dissection process
5. Degenerative leaflet thickening resulting in abnormal leaflet coaptation

Some patients have more than one mechanism of AR.

In the series of Movsowitz and co-workers,[145] the aortic valve was spared in 77% of 43 patients undergoing aortic surgery with excellent results. Therefore, TEE should play an important role in determining the optimal management of patients with type A aortic dissection and significant AR.

## INFECTIVE ENDOCARDITIS

Heart failure, caused by severe aortic or mitral regurgitation, is the most common complication of infective endocarditis and represents the most frequent indication for surgery (see Chapter 22). Heart failure is more often present when infective endocarditis affects the aortic rather than the mitral valve.[146,147] Moderate to severe heart failure is the leading predictor of in-hospital and 6-month mortality. Acute AR in the setting of infective endocarditis may occur as a result of leaflet rupture, leaflet perforation, or, more rarely, interference of the vegetation mass with leaflet closure. In patients with infective endocarditis on prosthetic valves, acute AR can occur as a result of large prosthetic dehiscence. In addition to the clinical signs of heart failure, TTE and TEE are of crucial importance for the diagnosis and evaluation of AR and for defining the presence of vegetations and perivalvular complications.

In acute severe AR due to infective endocarditis, patients need immediate antibiotics and aggressive medical management. If the hemodynamic situation does not immediately improve, emergency aortic valve replacement may be lifesaving. If the clinical situation stabilizes, patients may benefit from several days of antibiotic treatment before surgery, under strict clinical and echocardiographic surveillance.[148-150] The beneficial impact of surgery in patients with endocarditis and heart failure is clearly established.[151]

Intraoperative TEE and direct assessment of annular involvement are crucial for planning the surgical procedure. Assessment of the annulus is essential to ensure that it is intact and that there are no undrained abscesses.

## OTHER INFREQUENT CAUSES OF ACUTE AORTIC REGURGITATION

Acute AR can result from traumatic disruption of the aortic valve,[152,153] inflammation and perforation of leaflets in the setting of connective tissue diseases,[154] after surgical or catheter valvuloplasty,[155,156] or as a result of rupture of a fenestrated cusp[157] or spontaneous dehiscence of valve commisures.[158,159] Disrupted leaflets due to trauma or a fenestration can be repaired, but valvular replacement is the norm. As with other causes of AR, surgery should be tailored according to the intraoperative TEE and anatomic findings.

## KEY POINTS

- AR may be caused by abnormalities of the aortic leaflets, aortic root, or ascending aorta. Isolated AR most often is due to alterations in aortic geometry.
- Color Doppler proximal jet width with measurement of the vena contracta is the most useful method to quantify AR in clinical practice.
- Intermediate vena contracta values need confirmation by a more quantitative method, when feasible, optimally with integration of several Doppler methods.
- Measurement of diastolic flow reversal in the descending aorta is the strongest additional parameter for quantifying AR severity.
- CW Doppler density relative to antegrade flow is also useful, but pressure half-time is influenced by chamber compliance and pressures.
- The flow convergence method (PISA method) is less sensitive to loading conditions but is more technically demanding.
- Cardiac MRI provides quantitative assessment of regurgitant severity and LV function when echocardiography is nondiagnostic.
- Symptoms are the indication for surgical intervention in most patients with chronic AR, but some patients have impaired ventricular contractility in the absence of symptoms. LV diameters, volumes, and EF are the most useful parameters for clinical decision making. Indexed end-systolic diameter is recommended when BSA is less than 1.65 $cm^2$.
- Exercise echocardiography may be useful in patients with severe AR and equivocal symptoms or in patients with borderline values for LVEF (50% to 55%) or end-systolic diameter (close to 50 mm or 25 $mm/m^2$).
- Accurate aortic root measurements are important for understanding functional AR mechanisms and targeting the optimal time and strategy for aortic valve–sparing surgery.
- Conservative aortic valve surgery, including valve-sparing operations, and aortic cusp repair have improved the management of severe AR. Intraoperative TEE is mandatory after repair to assess the functional result and identify patients at risk for early AR recurrence.

## REFERENCES


1. Singh JP, Evans JC, Levy D, et al: Prevalence and clinical determinants of mitral, tricuspid, and aortic regurgitation (the Framingham Heart Study) [Published correction appears in *Am J Cardiol* 84:1143, 1999]. *Am J Cardiol* 83:897-902, 1999.
2. Lebowitz NE, Bella JN, Roman MJ, et al: Prevalence and correlates of aortic regurgitation in American Indians: the Strong Heart Study. *J Am Coll Cardiol* 36:461-467, 2000.
3. Tarasoutchi F, Grinberg M, Spina GS, et al: Ten-year clinical laboratory follow-up after application of a symptom-based therapeutic strategy to patients with severe chronic aortic regurgitation of predominant rheumatic etiology. *J Am Coll Cardiol* 41:1316-1324, 2003.
4. Roberts WC, Ko JM, Moore TR, et al: Causes of pure aortic regurgitation in patients having isolated aortic valve replacement at a single US tertiary hospital (1993-2005). *Circulation* 114:422-429, 2006.
5. Schaefer BM, Lewin MB, Stout KK, et al: The bicuspid aortic valve: an integrated phenotypic classification of leaflet morphology and aortic root shape. *Heart* 94:1634-1638, 2008.
6. Buchner S, Hülsmann M, Poschenrieder F, et al: Variable phenotypes of bicuspid aortic valve disease: classification by cardiovascular magnetic resonance. *Heart* 96:1233-1240, 2010.
7. Siu SC, Candice K, Silversides K: Bicuspid aortic valve disease. *J Am Coll Cardiol* 55:2789-2800, 2010.
8. Espinola-Zavaleta N, Muñoz-Castellanos L, Attié F, et al: Anatomic three-dimensional echocardiographic correlation of bicuspid aortic valve. *J Am Soc Echocardiogr* 16:46-53, 2003.
9. Evangelista A, González-Alujas MT: Echocardiography in infective endocarditis. *Heart* 90:614-617, 2004.
10. Iung B, Baron G, Butchart EG, et al: A prospective survey of patients with valvular heart disease. *Eur Heart J* 24:1231-1243, 2003.
11. Zanettini R, Antonini A, Gatto G, et al: Valvular heart disease and the use of dopamine agonists for Parkinson's disease. *N Engl J Med* 356:39-46, 2007.
12. Pardos-Gea J, Ordi-Ros J, Avegliano G, et al: Echocardiography at diagnosis of antiphospholipid syndrome provides prognostic information on valvular disease evolution and identifies two subtypes of patients. *Lupus* 19(5):575-582, 2010.
13. le Polain de Waroux JB, Pouleur AC, et al: Functional anatomy of aortic regurgitation. Accuracy, prediction of surgical repairability and outcome implications of transesophageal echocardiography. *Circulation* 116(suppl I): I264-I269, 2007.
14. Evangelista A: Aneurysm of ascending thoracic aorta. *Heart* 96:979-985, 2010.
15. Kim M, Roman MJ, Cavallini C, et al: Effect of hypertension on aortic root size and prevalence of aortic regurgitation. *Am Heart J* 28:47-52, 1996.
16. Leggert ME, Unger TA, O'Sullivan CK, et al: Aortic root complications in Marfan's syndrome: identification of a lower risk group. *Heart* 75(4):389-395, 1996.
17. Hagan PG, Nienaber CA, Isselbacher EM, et al: The International Registry of Acute Aortic Dissection (IRAD). New Insights Into an old disease. *JAMA* 283:897-903, 2000.
18. Evangelista A, Mukherjee D, Mehta RH, et al: Acute Intramural Hematoma of the aorta: a mystery in evolution. *Circulation*; 11:1063-1070, 2005.
19. Bossone E, Evangelista A, Isselbacher E, et al: International Registry of Acute Aortic Dissection Investigators. Prognostic role of transesophageal echocardiography in acute type A aortic dissection. *Am Heart J* 153(6):1013-1020, 2007.
20. Tadros TM, Klein MD, Shapira OM: Ascending aortic dilatation associated with bicuspid aortic valve. Pathophysiology, molecular biology, and clinical implications. *Circulation* 119:880-890, 2009.
21. Biner S, Rafique AM, Ray I, et al: Aortopathy is prevalent in relatives if bicuspid aortic valve patients. *J Am Coll Cardiol* 53:2288-2295, 2009.
22. Hope MD, Hope TA, Meadows AK, et al: Bicuspid aortic valve: four-dimensional MR evaluation of ascending aortic systolic flow patterns. *Radiology* 255:53-61, 2010.
23. Padial LR, Oliver A, Sagie A, et al: Two-dimensional echocardiographic assessment of the progression of aortic root size in 127 patients with chronic aortic regurgitation: role of the supraaortic ridge and relation to the progression of the lesion. *Am Heart J* 134:814-821, 1997.
24. Zoghbi WA, Enriquez-Sarano M, Foster E, et al: Recommendations for evaluation of the severity of native valvular regurgitation with two-dimensional and Doppler echocardiography. *J Am Soc Echocardiogr* 16:777-802, 2003.
25. Lancelloti P, Tribouilloy C, Hagendorff A, et al: European Association of Echocardiography recommendations for the assessment of valvular regurgitation. Part 1: aortic and pulmonary regurgitation (native valve disease). *Eur J Echocardiogr* 11:223-244, 2010.
26. Pierard LA, Moonen M, Lancellotti P: Valvular regurgitations. In Zamorano JL, Bax JJ, Rademakers FE, editors: *ESC Textbook of Cardiovascular Imaging*. London, 2010, Springer, pp 150-176.
27. Thomas JD, O'Shea JP, Rodriguez L, et al: Impact of orifice geometry on the shape of jets. An in vitro Doppler color flow study. *J Am Coll Cardiol* 176:901-908, 1991.
28. Switzer DF, Yoganathan AP, Nanda NC, et al: Calibration of color Doppler flow mapping during extreme hemodynamic conditions in vitro: a foundation for a reliable quantitative grading system for aortic incompetence. *Circulation* 4:837-846, 1987.
29. Taylor AL, Eichhorn EJ, Brickner ME, et al: Aortic valve morphology: an important in vitro determinant of proximal regurgitant jet width by Doppler color flow mapping. *J Am Coll Cardiol* 16:405-412, 1990.
30. Cape EG, Yoganathan AP, Levine RA: Increased heart rate can cause underestimation of regurgitant jet size by Doppler color flow mapping. *J Am Coll Cardiol* 21:1029-1037, 1993.
31. Evangelista A, García del Castillo H, Calvo F, et al: Strategy for optimal aortic regurgitation quantification by Doppler echocardiography: agreement among different methods. *Am Heart J* 139:773-781, 2000.
32. Fan P, Anayiotos A, Nanda NC, et al: Intramachine and intermachine variability in transesophageal color Doppler images of pulsatile jets. *Circulation* 89:2141-2149, 1994.
33. Smith MD, Grayburn PA, Michael D, et al: Observer variability in the quantitation of Doppler color flow jet areas for mitral and aortic regurgitation. *J Am Coll Cardiol* 11:579-584, 1988.
34. Reimold SC, Atkinson CM, Luna FB, Lee RT: Influence of jet impingement on color Doppler parameters of aortic regurgitation. *Echocardiography* 10:113-119, 1993.
35. Perry GJ, Helmcke F, Nanda NC, et al: Evaluation of aortic insufficiency by Doppler colour flow mapping. *J Am Coll Cardiol* 9:952-959, 1987.
36. Tribouilloy CM, Enriquez-Serrano M, Bailey KR, et al: Assessment of severity of aortic regurgitation using the width of the vena contracta: a clinical color Doppler imaging study. *Circulation* 102: 558-564, 2000.
37. Eren M, Eksik A, Gorgulu S, et al: Determination of vena contracta and its value in evaluating severity of aortic regurgitation. *J Heart Valve Dis* 11:567-575, 2002.
38. Fang L, Hsiung MC, Miller AP, et al: Assessment of aortic regurgitation by live three-dimensional transthoracic echocardiographic measurements of vena contracta area: usefulness and validation. *Echocardiography* 22:775-781, 2005.
39. Tribouilloy CM, Enriquez-Serrano M, Fett SL, et al: Application of the proximal flow convergence method to calculate the effective regurgitant orifice area in aortic regurgitation. *J Am Coll Cardiol* 32:1032-1039, 1998.
40. Pouleur AC, de Waroux JB, Goffinet C, et al: Accuracy of the flow convergence method for quantification of aortic regurgitation in patients with central versus eccentric jets. *Am J Cardiol* 102:475-480, 2008.
41. Detaint D, Messika-Zeitoun D, Maalouf J, et al: Quantitative echocardiographic determinants of clinical outcome in asymptomatic patients with aortic regurgitation: a prospective study. *JACC Cardiovasc Imaging* 1:1-11, 2008.
42. Xie GY, Berk MR, Smith MD, et al: A simplified method for determining regurgitant fraction by Doppler echocardiography in patients with aortic regurgitation. *J Am Coll Cardiol* 24:1041-1045, 1994.
43. Tribouilloy C, Avinée P, Shen WF, et al: End diastolic flow velocity just beneath the aortic isthmus assessed by pulsed Doppler echocardiography: a new predictor of the aortic regurgitant fraction. *Br Heart J* 65:37-40, 1991.
44. Samstad SO, Hegrenaes L, Skjaerpe T, et al: Half time of the diastolic aortoventricular pressure difference by continuous wave Doppler ultrasound: a measure of the severity of AR? *Br Heart J* 61:336-343, 1989.
45. Griffin BP, Flachskampf FA, Siu S, et al: The effects of regurgitant orifice size, chamber compliance, and systemic vascular resistance on aortic regurgitant velocity slope and pressure half-time. *Am Heart J* 122:1049-1056, 1991.
46. Vanoverschelde JL, Taymans-Robert AR, Raphael DA, et al: Influence of transmitral filling dynamics on continuous-wave Doppler assessment of aortic regurgitation by half-time methods. *Am J Cardiol* 64: 614-619, 1989.
47. Grayburn PA, Handshoe R, Smith MD, et al: Quantitative assessment of the hemodynamic consequences of aortic regurgitation by means of continuous wave Doppler Recordings. *J Am Coll Cardiol* 10:135-141, 1987.
48. Griffin BP, Flachskampf FA, Reimold SC, et al: Relationship of aortic regurgitant velocity slope and pressure half-time to severity of

aortic regurgitation under changing haemodynamic conditions. *Eur Heart J* 15:681-685, 1994
49. de Marchi SF, Windecker S, Aeschbacher BC, et al: Influence of left ventricular relaxation on the pressure half-time of aortic regurgitation. *Heart* 82:607-613, 1999.
50. Dolan MS, Castello R, St. Brain JA, et al: Quantitation of aortic regurgitation by Doppler echocardiography: a practical approach. *Am Heart J* 129:1014-1020, 1995.
51. Gottdiener JS, Panza JA, John Sutton M, et al: Testing the test: The reliability of echocardiography in the sequential assessment of valvular regurgitation. *Am Heart J* 144:115-121, 2002.
52. Zarauza J, Ares M, González Vilchez F, et al: An integrated approach to the quantification of aortic regurgitation by Doppler echocardiography. *Am Heart J* 136:1030-1041, 1998.
53. Willett DL, Hall SA, Jessen ME, et al: Assessment of aortic regurgitation by transesophageal color Doppler imaging of the vena contracta: Validation against an intraoperative aortic flow probe. *J Am Coll Cardiol* 37:1450-1455, 2001.
54. Sato Y, Kawazoe K, Kamata J, et al: Clinical usefulness of the effective regurgitant orifice area determined by transesophageal echocardiography in patients with eccentric aortic regurgitation. *J Heart Valve Dis* 6:580-586, 1997.
55. Sutton DC, Kluger R, Ahmed SU, et al: Flow reversal in the descending aorta: A guide to intraoperative assessment of aortic regurgitation withy transesophageal echocardiography. *J Thorac Cardiovasc Surg* 108:576-582, 1994.
56. Shiota T, Jones M, Tsujino H, et al: Quantitative analysis of AR: real-time 3-dimensional and 2-dimensional color Doppler echocardiographic method: a clinical and a chronic animal study. *J Am Soc Echocardiogr* 15:966-971, 2002
57. Dulce MC, Mostbeck GH, O'Sullivan M, et al: Severity of AR: interstudy reproducibility of measurements with velocity-encoded cine MR imaging. *Radiology* 185:235-240, 1992.
58. Chatzimavroudis G, Chatzimavroudis GP, Walker PG, et al: Slice location dependence of AR measurements with MR phase velocity mapping. *Magn Reson Med* 37:545-551, 1997.
59. Sondergaard L, Lindvig K, Hildebrandt P, et al: Quantification of AR by magnetic resonance velocity mapping. *Am Heart J* 125:1081-1890, 1993.
60. Lang RM, Bierig M, Devereux RB, et al: Recommendations for chamber quantification: a report from the American Society of Echocardiography's Guidelines and Standards Committee and the Chamber Quantification Writing Group, developed in conjunction with the European Association of Echocardiography, a branch of the European Society of Cardiology. *J Am Soc Echocardiogr* 18:1440-1463, 2005.
61. Vinereanu D, Ionescu AA, Fraser G: Assessment of left ventricular long axis contraction can detect early myocardial dysfunction in asymptomatic patients with severe aortic regurgitation. *Heart* 85:30-36, 2001.
62. Paraskevaidis IA, Kyrzopoulos S, Farmakis D, et al: Ventricular long-axis contraction as an earlier predictor of outcome in asymptomatic aortic regurgitation. *Am J Cardiol* 100:1677-1682, 2007.
63. Marciniak A, Sutherland GR, Marciniak M, et al: Myocardial deformation abnormalities in patients with aortic regurgitation: a strain rate imaging study. *Eur J Echocardiogr* 10:112-119, 2009.
64. Onishi T, Kawai H, Tatsumi K, et al: Preoperative systolic strain rate predicts postoperative left ventricular dysfunction in patients with chronic aortic regurgitation. *Circ Cardiovasc Imaging* 3:134-141, 2010.
65. Tayyareci Y, Yildirimturk O, Aytekin V, et al: Subclinical left ventricular dysfunction in asymptomatic severe aortic regurgitation patients with normal ejection fraction: a combined tissue Doppler and velocity vector imaging study. *Echocardiography* 27:260-268, 2010.
66. le Polain de Waroux JB, Pouleur AC, Goffinet C, et al: Combined coronary and late-enhanced multidetector-computed tomography for delineation of the etiology of left ventricular dysfunction: comparison with coronary angiography and contrast-enhanced cardiac magnetic resonance imaging. *Eur Heart J* 29:2544-2551, 2008.
67. McCrohon JA, Moon JC, Prasad SK, et al: Differentiation of heart failure related to dilated cardiomyopathy and coronary artery disease using gadolinium-enhanced cardiovascular magnetic resonance. *Circulation* 108:54-59, 2003.
68. Soriano CJ, Ridocci F, Estornell J, et al: Noninvasive diagnosis of coronary artery disease in patients with heart failure and systolic dysfunction of uncertain etiology, using late gadolinium-enhanced cardiovascular magnetic resonance. *J Am Coll Cardiol* 45:743-748, 2005.
69. Bonow RO, Carabello BA, Chatterjee K, et al: 2008 focused update incorporated into the ACC/AHA 2006 guidelines for the management of patients with valvular heart disease. *Circulation* 118:e523-e661, 2008.
70. Wahi S, Haluska B, Pasquet A, et al: Exercise echocardiography predicts development of left ventricular dysfunction in medically and surgically treated patients with asymptomatic severe aortic regurgitation. *Heart* 84:606-614, 2000.
71. Tamas E, Broqvist M, Olsson E, et al: Exercise radionuclide ventriculography for predicting post-operative left ventricular function in chronic aortic regurgitation. *JACC Cardiovasc Imaging* 2:48-55, 2009.
72. Underwood MJ, Khoury GE, Deronck D, et al: The aortic root: structure, function, and surgical reconstruction. *Heart* 83:376-380, 2000.
73. Kunzelman KS, Grande J, David TE, et al: Aortic root and valve relationships. *J Thorac Cardiovasc Surg* 107:162-170, 1994.
74. Fazel SS, David TE: Aortic valve-sparing operations for aortic root and ascending aortic aneurysms. *Curr Opin Cardiol* 22:497-503, 2007.
75. Khoury El, Glineur D, Rubay J, et al: Functional classification of aortic root/valve abnormalities and their correlation with etiologies and surgical procedures. *Curr Opin Cardiol* 20:115-121, 2005.
76. La Canna G, Maisano F, De Michele L, et al: Determinants of the degree of functional aortic regurgitation in patients with anatomically normal aortic valve and ascending thoracic aorta aneurysm. Transoesophageal Doppler echocardiography study. *Heart* 95: 130-136, 2009.
77. Evangelista A, Flachskampf, Erbel R, et al: Echocardiography in aortic diseases: EAE recommendations for clinical practice. *Eur J Echocardiogr* 11:645-658, 2010.
78. Bekeredjian R, Grayburn A: Valvular heart disease. Aortic regurgitation. *Circulation* 112:125-134, 2005.
79. Reimold S, Orav EJ, Come PC, et al: Progressive enlargement of the regurgitant orifice in patients with chronic aortic regurgitation. *J Am Soc Echocardiogr* 11:259-265, 1998.
80. Padial LR, Oliver A, Sagie A, et al: Two dimensional echocardiographic assessment of the progression of aortic root size in 127 patients with chronic aortic regurgitation: role of the supraaortic ridge and relation to the progression of the lesion. *Am Heart J* 134:814-821, 1997.
81. Gaasch WH, Sundaram M, Meyer TH: Managing asymptomatic patients with chronic aortic regurgitation. *Chest* 111:1702-1709, 1997.
82. Vahanian A, Baumgatner H, Bax J, et al: Guidelines on the management of valvular heart disease: the Task Force on the Management of Valvular Heart Disease of the European Society of Cardiology. *Eur Heart J* 28: 230-268, 2007.
83. Bonow RO, Rosing DR, McIntosh CL, et al: The natural history of asymptomatic patients with aortic regurgitation and normal left ventricular function. *Circulation* 68:509-517, 1983.
84. Bonow RO, Lakatos E, Maron BJ, et al: Serial long-term assessment of the natural history of asymptomatic patients with chronic aortic regurgitation and normal left ventricular systolic function. *Circulation* 84:1625-1635, 1991.
85. Scognamiglio R, Fasoli G, Dalla VS: Progression of myocardial dysfunction in asymptomatic patients with severe aortic insufficiency. *Clin Cardiol* 9:151-156, 1986.
86. Siemienczuk D, Greenberg B, Morris C, et al: Chronic aortic insufficiency: factors associated with progression to aortic valve replacement. *Ann Intern Med* 110:587-592, 1989.
87. Scognamiglio R, Rahimtoola SH, Fasoli G, et al: Nifedipine in asymptomatic patients with severe aortic regurgitation and normal left ventricular function. *N Engl J Med* 331:689-694, 1994.
88. Tornos MP, Olona M, Permanyer-Miralda G, et al: Clinical outcome of severe asymptomatic chronic aortic regurgitation: a long-term prospective follow-up study. *Am Heart J* 130:333-339, 1995.
89. Ishii K, Hirota Y, Suwa M, et al: Natural history and left ventricular response in chronic aortic regurgitation. *Am J Cardiol* 78:357-361, 1996.
90. Borer JS, Hochreiter C, Herrold EM, et al: Prediction of indications for valve replacement among asymptomatic or minimally symptomatic patients with chronic aortic regurgitation and normal left ventricular performance. *Circulation* 97:525-534, 1998.
91. Evangelista A, Tornos P, Sambola A, et al: Long-term vasodilator therapy in patients with severe aortic regurgitation. *N Engl J Med* 353:1342-1349, 2005.
92. Tarasoutchi F, Grinberg M, Spina GS, et al: Ten-year clinical laboratory follow-up after application of a symptom-based therapeutic strategy to patients with severe chronic aortic regurgitation of predominant rheumatic etiology. *J Am Coll Cardiol* 41:1316-1324, 2003.
93. Aronow WS, Ahn C, Kronzon I, et al: Prognosis of patients with heart failure and unoperated severe aortic valvular regurgitation and relation to ejection fraction. *Am J Cardiol* 74:286-288, 1994.
94. Dujardin KS, Enriquez-Sarano M, Schaff HV, et al: Mortality and morbidity of aortic regurgitation in clinical practice: a long-term

follow-up study. *Circulation* 99:1851-1857, 1999.
95. Greenberg BH, DeMots H, Murphy E, et al: Beneficial effects of hydralazine on rest and exercise hemodynamics in patients with chronic severe aortic insufficiency. *Circulation* 62:49-55, 1980.
96. Greenberg BH, DeMots H, Murphy E, et al: Mechanism for improved cardiac performance with arteriolar dilators in aortic insufficiency. *Circulation* 63:263-268, 1981.
97. Levine HJ, Gaasch WH: Vasoactive drugs in chronic regurgitant lesions of the mitral and aortic valves. *J Am Coll Cardiol* 28:1083-1091, 1996.
98. Sondergaard L, Aldershvile J, Hildebrandt P, et al: Vasodilatation with felodipine in chronic asymptomatic aortic regurgitation. *Am Heart J* 139:667-674, 2000.
99. Scognamiglio R, Fasoli G, Ponchia A, et al: Long-term nifedipine unloading therapy in asymptomatic patients with chronic severe aortic regurgitation. *J Am Coll Cardiol* 16:424-429, 1990.
100. Lin M, Chiang HT, Lin SL, et al: Vasodilator therapy in chronic asymptomatic aortic regurgitation: enalapril versus hydralazine therapy. *J Am Coll Cardiol* 24:1046-1053, 1994.
101. Shores J, Berger KR, Murphy EA, et al: Progression of aortic dilatation and the benefit of long-term β-adrenergic blockade in Marfan's syndrome. *N Engl J Med* 330:1335-1341, 1994.
102. Brooke BS, Habashi JP, Judge DP, et al: Angiotensin II blockade and aortic-root dilation in Marfan's syndrome. *N Engl J Med* 358:2787-2795, 2008.
103. Ahimastos AA, Aggarwal A, D'Orsa KM, et al: Effect of Perindopril on large artery stiffness and aortic root diameter in patients with Marfan syndrome. *JAMA* 298:1539-1547, 2007.
104. Lacro RV, Dietz HC, Wruck LM, et al: Rationale and design of a randomized clinical trial of beta-blocker therapy (atenolol) versus angiotensin II receptor blocker therapy (losartan) in individuals with Marfan syndrome. *Am Heart J* 154:624-631, 2007.
105. Radonic T, de Witte P, Baars MJH, et al: COMPARE study group. Losartan therapy in adults with Marfan syndrome: study protocol of the multi-center randomized controlled COMPARE trial. *Trials* 11:1-3, 2010.
106. Tornos P, Olona M, Permanyer-Miralda G, et al: Heart failure after aortic valve replacement for aortic regurgitation: Prospective 20-year study. *Am Heart J* 136:681-687, 1998.
107. Klodas E, Enriquez-Sarano M, Tajik AJ, et al: Surgery for aortic regurgitation in women: contrasting indications and outcomes compared with men. *Circulation* 94:2472-2478, 1996.
108. Enriquez-Sarano M, Tajik AJ Clinical practice: aortic regurgitation. *N Engl J Med* 351:1539-1546, 2004.
109. Sambola A, Tornos P, Ferreira-Gonzalez I, Evangelista A: Prognostic value of preoperative indexed end-systolic left ventricle diameter in the outcome after surgery in patients with chronic aortic regurgitation. *Am Heart J* 155:1114-1120, 2008.
110. Chaliki HP, Mohty D, Avierinos J-F, et al: Outcomes after aortic valve replacement in patients with severe aortic regurgitation and markedly reduced left ventricular function. *Circulation* 106:2687-2693, 2002.
111. Tornos P, Sambola A, Permanyer-Miralda G, et al: Long-term outcome of surgically treated aortic regurgitation: influence of guidelines adherence toward early surgery. *J Am Coll Cardiol* 47:1012-1017, 2006.
112. Bonow RO, Dodd JT, Maron BJ, et al: Long-term serial changes in left ventricular function and reversal of ventricular dilatation after valve replacement for chronic aortic regurgitation. *Circulation* 78: 1108-1120, 1988.
113. Mathew RK, Gaasch WH, Guilmette NE, et al: Anthropometric normalization of left ventricular size in chronic mitral regurgitation. *Am J Cardiol* 91:762-764, 2003.
114. Vasan RS, Larson MG, Levy D, et al: Distribution and categorization of echocardiographic measurements in relation to reference limits: the Framingham Heart Study: formulation of a height- and sex-specific classification and its prospective validation. *Circulation* 96:1863-1873, 1997.
115. Svensson LG, Kim K-H, Lytle BW, et al: Relationship of aortic cross-sectional area to height ratio and the risk of aortic dissection in patients with bicuspid aortic valves. *J Thorac Cardiovasc Surg* 126:892-893, 2003.
116. Svensson LG, Khitin L: Aortic cross-sectional area/height ratio timing of aortic surgery in asymptomatic patients with Marfan syndrome. *J Thorac Cardiovasc Surg* 123: 360-361, 2002.
117. Matura LA, Ho VB, Rosing DR, et al: Aortic dilatation and dissection in Turner syndrome. *Circulation* 116:1663-1670, 2007.
118. Davies RR, Gallo A, Coady MA, et al: Novel measurement of relative aortic size predicts rupture of thoracic aortic aneurysms. *Ann Thorac Surg* 81:169-177, 2006.
119. Eleftiarides JA, Farkas EA: Thoracic aortic aneurysm. Clinically pertinent controversies and uncertainties. *J Am Coll Cardiol* 55:841-857, 2010.
120. Gott VL, Greene PS, Alejo DE, et al: Replacement of the aortic root in patients with Marfan's syndrome. *N Engl J Med* 340:1307-1313, 1999
121. Tzemos N, Therrien J, Yip J, et al: Outcomes in adults with bicuspid aortic valves. *JAMA* 300: 1317-1325, 2008.
122. Davies RR, Kaple RK, Mandapati D, et al: Natural history of ascending aortic aneurysms in the setting of an unreplaced bicuspid aortic valve. *Ann Thorac Surg* 83:1338-1344, 2007.
123. Judge D, Dietz HC Marfan's syndrome. *Lancet* 366:1965-1976, 2005
124. Yasuda H, Nakatani S, Stugaard M, et al: Failure to prevent progressive dilation of ascending aorta by aortic valve replacement in patients with bicuspid aortic valve: comparison with tricuspid aortic valve. *Circulation* 108(suppl II):II291-II294, 2003.
125. Borger MA, Preston M, Ivanov J, et al: Should the ascending aorta be replaced more frequently in patients with bicuspid aortic valve disease? *J Thorac Cardiovasc Surg* 128:677-683, 2004.
126. Ergin MA, Spielvogel D, Apaydin A, et al: Surgical treatment of the dilated ascending aorta: when and how? *Ann Thorac Surg* 67:1834-1839, 1999.
127. Chiappini B, Absil B, Rubay J, et al: The Ross procedure: clinical and echocardiographic follow-up in 219 consecutive patients. *Ann Thorac Surg* 83:1285-1289, 2007.
128. Boodhwani M, de Kerchove L, Glineur D, et al: Repair-oriented classification of aortic insufficiency: Impact on surgical techniques and clinical outcomes. *J Thorac Cardiovasc Surg* 137:286-294, 2009.
129. Schèfers HJ, Kunihara T, Fries P, et al: Valve preserving root replacement in bicuspid aortic valves. *J Thorac Cardiovasc Surg* 140:S36-S40, 2010.
130. Boodhwani M, de Kerchove L, Glineur D, et al: Repair of regurgitant bicuspid aortic valves: a systematic approach. *J Thorac Cardiovasc Surg* 140:276-284, 2010.
131. Pacini D, Ranocchi F, Angeli E, et al: Aortic root replacement with composite valve graft. *Ann Thorac Surg* 76:90-98, 2003.
132. Hiratzka LF, Bakris GL, Beckman JA, et al: 2010 ACCF/AHA/AATS/ACR/ASA/SCA/SCAI/SIR/STS/SVM guidelines for the diagnosis and management of patients with thoracic aortic disease. *Circulation* 121:e266-e369, 2010.
133. Nash PJ, Vitvitsky E, Li J, et al: Feasibility of valve repair for regurgitant bicuspid aortic valves-an echocardiographic study. *Ann Thorac Surg* 79:1473-1479, 2005.
134. Schmittio JD, Mokashi SA, Chen FY, Chen EP: Aortic valve-sparing operation: state of the art. *Curr Opin Cardiol* 25:102-106, 2010.
135. Petterson GB, Crucean AC, Savage R, et al: Towards predictable repair of regurgitant aortic valve. A systematic morphology-directed approach to bicomissural repair. *J Am Coll Cardiol* 52:40-49, 2008.
136. David TE, Armstrong S, Maganti M, et al: Long-term results of aortic valve-sparing operations in patients with Marfan syndrome. *J Thorac Surg* 138:859-864, 2009.
137. le Polain de Waroux JB, Pouleur AC, Robert A, et al: Mechanisms of recurrent aortic regurgitation after aortic valve repair. *JACC Cardiovasc Imaging* 2:931-939, 2009.
138. Turina J, Milincic J, Seifert B, et al: Valve replacement in chronic aortic regurgitation. True predictors of survival after extended follow-up. *Circulation* 98:II100-II107, 1998.
139. Florath I, Rosendahl UP, Mortasawi A, et al: Current determinants of operative mortality in 1400 patients requiring aortic valve replacement. *Ann Thorac Surg* 76:75-83, 2003.
140. Takkenberg JJ, Klieverik LM, Schoof PH, et al: The Ross procedure: a systematic review and meta-analysis. *Circulation* 119:222-228, 2009.
141. Sievers H, Hanke T, Stierle U, et al: A critical reappraisal of the Ross operation: renaissance of the subcoronary implantation technique? *Circulation* 114:I504-I511, 2006.
142. Etz CD, Hamman TM, Rane, et al: Aortic root reconstruction with a bioprosthetic valved conduit: a consecutive series of 275 procedures. *J Thorac Cardiovasc Surg* 133:1455-1462, 2007.
143. Kindo M, Billaud P, Gerelli S, et al: Twenty-seven-year experience with composite valve graft replacement of the aortic root. *J Heart Valve Dis* 16:370-377, 2007.
144. Stout KK, Verrier E: Acute valvular regurgitation *Circulation* 119:3232-3241, 2009
145. Movsowitz HD, Levine RA, Higenberg AD, Isselbacher EM: Transesophageal echocardiography. Description of the mechanisms of aortic regurgitation in acute type A aortic dissection: implications for aortic valve repair. *J Am Coll Cardiol* 36:884-890, 2000.
146. Baddour LM, Wilson WR, Bayer AS, et al: Infective endocarditis: diagnosis, antimicrobial therapy and management of complications. *Circulation* 111:e394-e434, 2005.
147. Tornos P, Iung B, Permanyer-Miralda G, et al: Infective endocarditis in Europe: lessons from the Euro heart survey. *Heart* 91:571-575, 2005.
148. Habib G, Avierinos JF, Thuny F: Aortic valve endocarditis: is there an optimal surgical timing? *Curr Opin Cardiol* 22:77-83, 2007.

149. Habib G, Hoen B, Tornos P, et al: Guidelines on the prevention, diagnosis, and treatment of infective endocarditis (new version 2009): the Task Force on the Prevention, Diagnosis, and Treatment of Infective Endocarditis of the European Society of Cardiology (ESC). *Eur Heart J* 19:2369-2413, 2009.
150. Prendergast BD, Tornos P: Surgery for infective endocarditis: who and when? *Circulation* 121:1141-1152, 2010.
151. Vikram HR, Buenconsejo J, Hasbun R, Quagliarello VJ: Impact of valve surgery on 6-month mortality in adults with complicated, left-sided native valve endocarditis: a propensity analysis. *JAMA* 290:3207-3214, 2003.
152. Kaljusto ML, Vengen OA, Tønnessen T: Traumatic aortic valve rupture after a high-speed motor vehicle accident. *J Heart Valve Dis* 17:586-588, 2008.
153. Turk T, Vural H, Ata Y, Eris C, Yavuz S: Acute aortic insufficiency after blunt chest trauma: a case report. *J Cardiovasc Surg (Torino)* 48:359-361, 2007.
154. Hirata K, Kakazu M, Wake M, et al: Acute aortic valvular regurgitation secondary to avulsion of aortic valve commissure in a patient with pseudoxanthoma elasticum. *Intern Med* 39:940-942, 2000.
155. Brown DW, Dipilato AE, Chong EC, et al: Aortic valve reinterventions after balloon aortic valvuloplasty for congenital aortic stenosis intermediate and late follow-up. *J Am Coll Cardiol* 16:1740-1749, 2010.
156. Safar B, Milleron O, Mesnildrey P, Cattan S: Aortic regurgitation after cardiac catheterization. *JACC Cardiovasc Interv* 3:984-985, 2010.
157. Blaszyk H, Witkiewicz AJ, Edwards WD: Acute aortic regurgitation due to spontaneous rupture of a fenestrated cusp: report in a 65-year-old man and review of seven additional cases. *Cardiovasc Pathol* 8:213-216, 1999.
158. Nakamura E, Nakamura K, Niina K, et al: Acute aortic regurgitation resulting from dehiscence of the aortic valve commissures. *Ann Thorac Cardiovasc Surg* 16:294-296, 2010.
159. Kazuya A, Jun H, Naohito T, et al: Echocardiographic and surgical findings of spontaneous avulsion of the aortic valve commissure. *Circ J* 68:254-256, 2004.



# Echocardiography in the Patient Undergoing Catheter Balloon Mitral Valvotomy: Patient Selection, Hemodynamic Results, Complications, and Long-Term Outcomes

BERNARD IUNG, MD | ALEC VAHANIAN, MD

**Background**
**Basic Principles and Echocardiographic Approach**
Diagnosis
Evaluation of the Severity
Assessment of Consequences
Assessment of Valve Anatomy
Mitral Regurgitation
Associated Lesions
Thromboembolic Complications
Use of the Different Echocardiographic Techniques
**Technique, Quantitation, and Data Analysis**
Before Balloon Mitral Valvotomy
During Balloon Mitral Valvotomy
Early after Balloon Mitral Valvotomy
During Follow-up
**Clinical Utility**
Results of Balloon Mitral Valvotomy
Implications for Patient Selection
**Research Applications**
Stress Echocardiography
Evaluation of Valve Anatomy
**Potential Limitations, Future Directions**
**Alternative Approaches**

Echocardiography plays a key role in the assessment of mitral stenosis (MS). As in other heart valve diseases, it has superseded invasive investigations for assessing the severity and consequences of MS. Echocardiography is also used to analyze valve anatomy, which contributes to the selection of the most appropriate intervention. This has been of particular interest with the development of balloon mitral valvotomy (BMV). Growing experience from large series reporting results of BMV in a variety of patient subsets enables the type and timing of interventions for MS to be clarified in guidelines.

## Background

Unlike for other valve diseases, the main etiology of MS remains rheumatic heart disease, even in Western countries.[1] Despite the sharp decrease in the incidence of rheumatic fever in Western countries, rheumatic heart disease has not disappeared, in particular because of the presence of immigrants from countries where rheumatic fever remains endemic. The prevalence of MS has been estimated at 0.1% in a population-based based study in the United States,[1,2] and MS accounted for 9% of native valve diseases in Europe. The burden of rheumatic heart disease remains high in developing countries, where its prevalence is estimated at between 1 and 7 per 1000 in school-age children when using clinical screening, and between 20 and 30 per 1000 when using systematic echocardiographic screening.[3-5] In Western countries, MS affects older patients who have more severe impairment of valve anatomy than in countries where rheumatic fever remains endemic.[6,7]

In addition to epidemiologic changes, the management of MS has dramatically changed with the development of BMV since its first description in 1984.[8] The possibility of treating MS using a low-risk procedure progressively led to the extension of indications for interventional treatment. At the same time, technical refinements in ultrasonographic examinations have improved the possibility of assessing the severity of valve disease and its consequences noninvasively and describing the anatomic lesions.

## Basic Principles and Echocardiographic Approach

The aims of echocardiographic examination in MS can be summarized as follows: diagnosis, evaluation of the severity and consequences of valve lesions, and assessment of valve anatomy and of associated diseases.

### DIAGNOSIS

Transthoracic echocardiography (TTE) is mandatory for any clinical suspicion of MS. Given the decreased awareness of MS in Western countries and the difficulties of auscultatory diagnosis, MS might only be diagnosed when TTE is performed to

establish the cause of unexplained dyspnea or thromboembolic events.

The diagnosis of rheumatic MS relies mainly on two-dimensional (2D) echocardiography that shows leaflet thickening and decreased mobility, commissural fusion, and involvement of the subvalvular apparatus, as assessed using parasternal and apical views. The parasternal short-axis view is of particular importance in assessing commissural fusion. The same views are used for the detailed anatomic evaluation of the leaflets and subvalvular apparatus (see Assessment of Valve Anatomy, later). Anatomic analysis also enables rheumatic MS to be distinguished from rare congenital or degenerative MS.

## EVALUATION OF THE SEVERITY

The assessment of the severity of MS is based on the estimation of valve area (Table 21-1).[9,10] Gradient is not a reliable marker of the severity of valve stenosis because it is highly dependent on heart rate and cardiac output. Various techniques can be used to assess mitral valve area.

- Planimetry of the mitral orifice, using the transthoracic parasternal short-axis view, is the reference measurement because it is the only direct measurement of valve area and correlates closely with anatomic findings.[9,11] Planimetry does not involve hypotheses concerning loading conditions, compliance of cardiac chambers, or associated valve disease. However, planimetry requires particular expertise to ensure that the cross-sectional area corresponds to the leaflet tips.[9]
- The pressure half-time method is frequently used because it is easy to perform, provided the Doppler signal of transmitral flow is of good quality with a well-defined linear slope of the Doppler E wave. However, the pressure half-time depends not only on valve area but also on chamber compliance and associated aortic regurgitation.[12]
- The continuity equation is based on the ratio between stroke volume in the left or right ventricular outflow tract and velocity-time integral to the mitral flow.[13] Its accuracy is limited by potential errors on the numerous measurements and hypotheses on the circularity of left ventricular (LV) outflow tract and mitral annulus.[9] It is valid only in the absence of significant mitral regurgitation (MR), and it tends to give smaller estimations of valve area as compared with planimetry.[10]
- The proximal isovelocity surface area method is based on the hemispherical shape of the convergence of mitral flow as shown by color Doppler. This method can be used in the presence of significant MR. However, it is technically demanding and requires multiple measurements. The use of M-mode improves its accuracy, enabling simultaneous measurement of flow and velocity.[14]

**TABLE 21-1 Recommendations for Classification of Mitral Stenosis Severity**

| | Significant | | |
|---|---|---|---|
| | *Mild* | *Moderate* | *Severe* |
| **Specific Findings** | | | |
| Valve area ($cm^2$) | >1.5 | 1.0-1.5 | <1.0 |
| **Supportive Findings** | | | |
| Mean gradient (mm Hg)* | <5 | 5-10 | >10 |
| Systolic pulmonary artery pressure (mm Hg) | <30 | 30-50 | >50 |

Adapted from Baumgartner H, Hung J, Bermejo J, et al: Echocardiographic assessment of valve stenosis: EAE/ASE recommendations for clinical practice. *J Am Soc Echocardiogr* 22:1-23; quiz 101-102, 2009.

*At heart rates between 60 and 80 bpm and in sinus rhythm.

## ASSESSMENT OF CONSEQUENCES

Mean mitral gradient, as assessed by pulsed- or continuous-wave Doppler, gives information on the consequences of MS, because it is the main determinant of the increase of upstream pressures in left atrium (LA) and pulmonary circulation.

LA enlargement is due to chronic pressure overload. Time-motion measurement may be inaccurate because enlargement does not follow a spherical pattern in most cases. The assessment of LA volume using biplane area-length method should be preferred because it is more accurate and is strongly related to other markers of the thromboembolic risk.[15]

Systolic pulmonary artery pressure is estimated from the velocity of Doppler tricuspid flow. Diastolic and mean pulmonary artery pressures can be derived from pulmonary flow.

## ASSESSMENT OF VALVE ANATOMY

A detailed analysis of the different components of the mitral valve is necessary for diagnosis, but also contributes to the choice of the type of intervention (Fig. 21-1):

- Leaflet mobility is particularly well analyzed using the long-axis parasternal view.
- Leaflet thickening is considered significant if thickness if 5 mm or more.
- Leaflet calcification is suspected in the presence of increased echocardiographic brightness.
- The extent of commissural fusion is analyzed using the short-axis parasternal view.
- The impairment of subvalvular apparatus is analyzed from long-axis parasternal and apical views, which show thickening, fusion, or shortening of chordae.

The echocardiographic report should accurately describe the extent and location of each abnormality, with particular regard to commissural areas.

The definition of calcification using ultrasonographic criteria may be debated. Only acoustic shadowing is specific to calcification alone, whereas localized brightness can also be due to fibrosis. For this reason, certain teams require the confirmation of calcification using fluoroscopic examination.[16]

Different scoring systems combine the features of mitral valve anatomy. Their value and limitations in the prediction of the results of BMV and patient selection are addressed further.

## MITRAL REGURGITATION

The detection and quantitation of associated MR have important implications for the choice of intervention. Quantitative measurements should be combined and are preferred over methods using color flow mapping of the regurgitant jet in the LA.[17,18] The presence of MR does not alter the validity of the quantitation of MS, except in regard to the continuity equation.

## ASSOCIATED LESIONS

Dysfunction of the tricuspid valve is frequently associated with MS. It is most often functional tricuspid regurgitation, which is due to chronic increase in pulmonary artery pressure through right ventricular dilatation and lack of coaptation of tricuspid

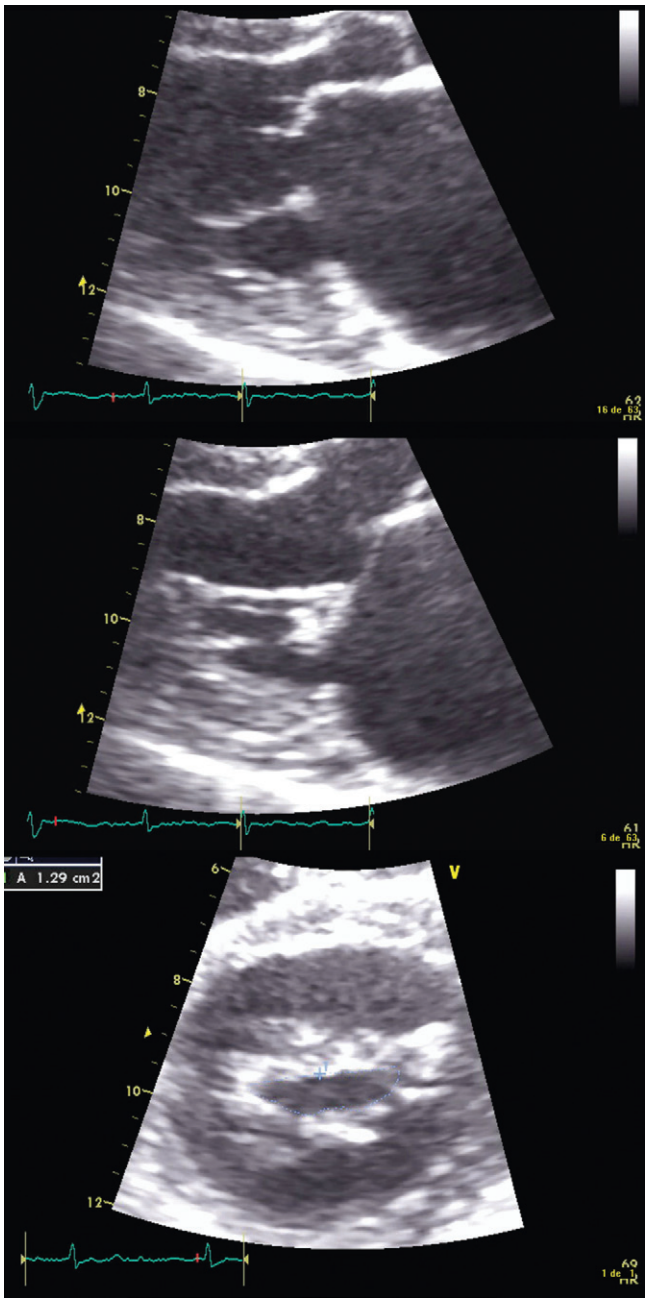



**Figure 21-1 Evaluation of valvular anatomy before balloon mitral valvotomy.** Favorable anatomic conditions. TTE. *Top:* Parasternal long-axis view showing pliable, noncalcified valve. *Middle:* Parasternal long-axis view showing moderate impairment of subvalvular apparatus. *Bottom:* Parasternal long-axis view showing moderate and homogeneous thickening of the leaflet tips and fusion of both commissures.

leaflets, despite normal valve anatomy. Whatever the method used, quantitation of tricuspid regurgitation is highly dependent on loading conditions.[17,18] This explains the current trend to rely more on the measurement of the tricuspid annulus than on the quantitation of regurgitation, particularly in regard to decision making for combining the correction of functional tricuspid regurgitation with left heart valve surgery.[19] However, the three-dimensional (3D) shape of the tricuspid annulus raises concerns regarding the reliability and reproducibility of the usual 2D measurements of the tricuspid annulus diameter.[20] Rheumatic tricuspid disease is far less frequent and is characterized by thickening and decreased mobility of tricuspid leaflets. Quantitation of tricuspid stenosis relies mainly on mean gradient.[9]

Associated rheumatic aortic valve disease is quantitated, if required, using standard techniques. Severe aortic stenosis may be associated with a low gradient because stroke volume is often decreased in MS. Thus, careful quantitation of the aortic valve area is needed, using the continuity equation and/or planimetry of the aortic valve with TTE or transesophageal echocardiography (TEE).[9]

LV enlargement and systolic dysfunction are unusual in MS, and the first reaction should be to search for an associated valvular regurgitation or coronary artery disease.

### THROMBOEMBOLIC COMPLICATIONS

The diagnosis of LA thrombosis relies on TEE, which has a much higher sensitivity than TTE, in particular for location in the left appendage. Echocardiography also plays an important role in risk stratification of thromboembolism. LA enlargement is a risk factor of thromboembolism. A LA volume greater than 60 mL/m$^2$ of body surface area is associated with the presence of surrogate markers of the thromboembolic risk.[15] LA spontaneous contrast is a strong predictor of thromboembolic risk in patients with MS.[21]

### USE OF THE DIFFERENT ECHOCARDIOGRAPHIC TECHNIQUES

A comprehensive evaluation of MS can be performed using TTE in most cases; TTE also plays an important role during the BMV procedure to monitor valve opening and to quantitate MR.

In the rare cases where TTE is of poor quality, TEE may be required. However, the main indication for TEE is the detection of LA thrombosis before BMV.

Other than for research purposes, the main indication for stress echocardiography is exercise echocardiography in asymptomatic patients.

## Technique, Quantitation, and Data Analysis

The respective parts of various features analyzed by echocardiography differ according to whether echocardiography is performed as an initial evaluation or to assess the results of an interventional procedure, immediately or during later follow-up.

### BEFORE BALLOON MITRAL VALVOTOMY

#### *Valve Function*

Moderate MS is defined by a valve area between 1.0 and 1.5 cm$^2$ and severe MS by a valve area less than 1.0 cm$^2$.[9] The threshold of 1.5 cm$^2$ is the most relevant in practice, because this is the value above which hemodynamics are not affected at rest,[22] and there is a consensus for considering intervention when mitral valve area is less than 1.5 cm$^2$.[23,24] It is advised to take the patient's body size into account. Although no value indexed on body surface area can be firmly established from the literature, it is generally admitted that MS is significant when index valve area is below 0.9 to 1.0 cm$^2$/m$^2$ body surface area.

The main pitfall when using planimetry is the overestimation of valve area because of inappropriate positioning of the measurement plane above the leaflet tips. The best way to avoid this

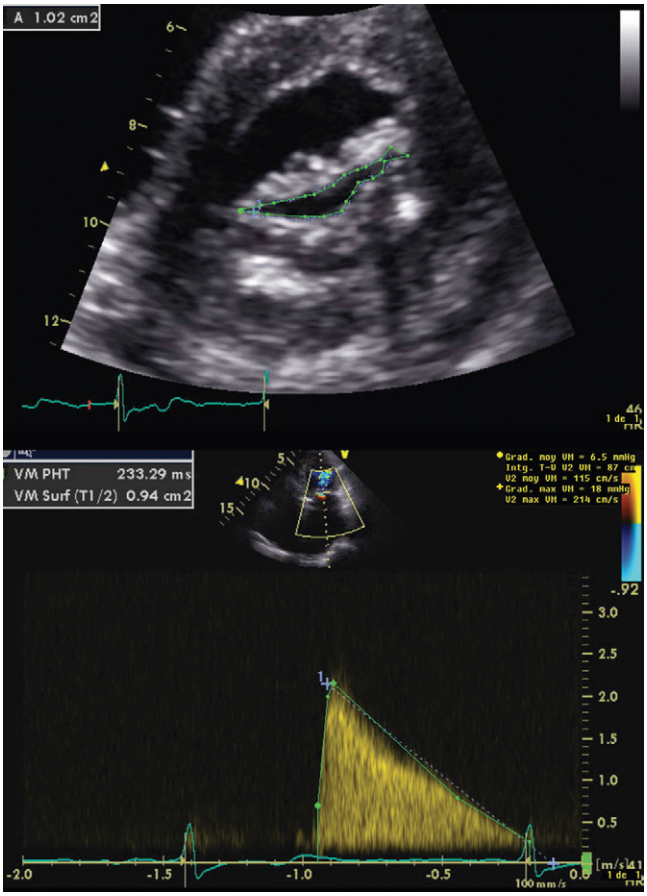



**Figure 21-2 Evaluation of mitral valve area before balloon mitral valvotomy.** Consistency between estimations using planimetry (valve area = 1.02 $cm^2$) (*Top:* TTE, parasternal short-axis view) and pressure half-time (*Bottom:* continuous-wave Doppler of the diastolic mitral flow, valve area = 0.94 $cm^2$). Mean gradient is 6.5 mm Hg.

is to scan slowly from the apex to the base and to select the narrowest orifice. Real-time 3D echocardiography is helpful to optimize the positioning of the measurement plan, which improves the accuracy of planimetry, in particular for less experienced echocardiographers.[25-27]

Technical difficulties inherent in planimetry justify the systematic use of the pressure half-time method, keeping in mind its limitations due to confounding factors. In our experience, its most important discrepancies with planimetry are observed in patients older than 60 and in those in atrial fibrillation, not only after but also before BMV.[28]

In current practice, 2D planimetry and the pressure half-time method are recommended in the standard evaluation of MS (Fig. 21-2). Other methods are used only if usual measurements are inconclusive or inconsistent with clinical data (Table 21-2).[9] The estimation of valve resistance is not considered as a relevant marker of stenosis severity.

### *Valve Anatomy*

Different approaches have been developed to combine the anatomic features of MS, aiming to predict the results of BMV and, therefore, to improve patient selection.

The most widely used scoring system is the Wilkins score, in which four components are graded from 1 to 4: leaflet mobility, thickness, calcification, and impairment of subvalvular apparatus (Table 21-3).[29] Another approach relies on a global assessment of mitral valve anatomy, with a classification into three groups according to the best surgical alternative: patients in group 1 are optimal candidates for closed-heart commissurotomy, patients in group 2 are more likely to be candidates for open-heart commissurotomy, and patients in group 3 are usually treated using prosthetic valve replacement (Table 21-4).[16,30] These two scores were developed at the beginning of the development of BMV.

A common limitation of these two scoring systems is the lack of information on the location of leaflet thickening and calcification, in particular in relation to the commissures, which may influence the results of BMV.[31-34] Another drawback of the current scoring systems is that the respective weights of each abnormality may be debated. In particular, the importance of subvalvular apparatus impairment is probably underestimated.[35]

At the present time, there are no large-scale comparative evaluations of the predictive value of different scoring systems, which could lead to recommending the use of a particular one. For the echocardiographer, the best solution is to use a method of analysis with which one is familiar and to include valve anatomy among other clinical and echocardiographic findings. The echocardiographic report should include a comprehensive description of mitral anatomy and not summarize it using a score alone.

### *Evaluation on Exercise*

Semisupine exercise echocardiography enables mitral gradient and systolic pulmonary artery pressure to be recorded for increasing levels of exercise. This approach is now favored over postexercise echocardiography, which is hampered by rapid changes in loading conditions and heart rate.[36,37]

Stroke volume and valve area are more difficult to obtain during exercise, and they are analyzed only for research purposes.

## DURING BALLOON MITRAL VALVOTOMY

Echocardiography also plays an important role in the catheterization laboratory, in particular with the Inoue technique (Fig. 21-3).[38,39] The main advantages of the Inoue balloon are its ease of use, partly related to self-positioning, and the possibility of performing stepwise inflations with a progressive increase in balloon diameter. TTE enables valve area, the degree of commissural opening, mean gradient, and MR to be assessed after each balloon inflation, leading to continued balloon inflation or stopping the procedure (Fig. 21-4). Planimetry should be used to monitor BMV, because the pressure half-time method is not reliable in this context and mean gradient is influenced by changes in loading conditions or heart rate.

Echocardiography is also helpful in the catheterization laboratory to promptly detect pericardial effusion, which is a rare but severe complication of transseptal catheterization.

In rare instances, TEE can be required during BMV, mainly to guide transseptal catheterization in difficult situations. Given the discomfort for the patient, the procedure is generally conducted under general anesthesia when TEE is used.

## EARLY AFTER BALLOON MITRAL VALVOTOMY

Even more than in other situations, planimetry using 2D echocardiography is the reference measurement of mitral valve area immediately after BMV. It enables the commissural opening to be visualized; valvular area tracing should include opened commissures (Fig. 21-5). The pressure half-time method is

**TABLE 21-2 Approaches to Evaluation of Mitral Stenosis**

| *Measurement* | *Units* | *Formula / Method* | *Concept* | *Advantages* | *Disadvantages* |
|---|---|---|---|---|---|
| **Valve area** | | | | | |
| Planimetry by 2D echocardiography | $cm^2$ | Tracing mitral orifice using 2D echocardiography | Direct measurement of anatomic MVA | Accuracy<br>Independence from other factors | Experience required<br>Not always feasible (poor acoustic window, severe valve calcification) |
| Pressure half-time | $cm^2$ | $220/T_{1/2}$ | Rate of decrease of transmitral flow is inversely proportional to MVA | Easy to obtain | Dependence on other factors (AR, LA compliance, LV diastolic function…) |
| Continuity equation | $cm^2$ | $MVA = CSA_{LVOT} \cdot VTI_{Aortic} / VTI_{Mitral}$ | Volume flows through mitral and aortic orifices are equal | Independence from flow conditions | Multiple measurements (sources of errors)<br>Not valid if significant AR or MR |
| PISA | $cm^2$ | $MVA = \pi r^2 \times (V_{aliasing} / \text{peak } V_{Mitral}) \times (\alpha/180°)$ | MVA assessed by dividing mitral volume flow by the maximum velocity of diastolic mitral flow | Independence from flow conditions | Technically difficult |
| **Mean gradient** | mm Hg | $\Delta P_{Mitral} = 4v^2_{Mitral}$ | Pressure gradient calculated from velocity using the Bernoulli equation | Easy to obtain | Dependent on heart rate and flow conditions |
| **Systolic pulmonary artery pressure** | mm Hg | $sPAP = 4v^2_{TR}$ + RA pressure | Addition of RA pressure and maximum gradient between RV and RA | Obtained in most patients with MS | Arbitrary estimation of RA pressure<br>No estimation of pulmonary vascular resistance |
| **Mean gradient and systolic pulmonary artery pressure at exercise** | mm Hg | $\Delta P_{Mitral} = 4v^2_{Mitral}$<br>$sPAP = 4v^2_{Tricuspid}$ + RA pressure | Assessment of gradient and sPAP for increasing workload | Incremental value in assessment of tolerance | Experience required<br>Lack of validation for decision-making |
| **Valve resistance** | dynes $s^{-1}.cm^{-5}$ | $MV_{res} = \Delta P_{Mitral} / (CSA_{LVOT} \cdot VTI_{Aortic} / DFT)$ | Resistance to flow caused by MS | Initially suggested to be less flow dependent, but not confirmed | No prognostic value<br>No clear threshold for severity<br>No additional value vs. valve area |

Level of recommendations: 1, appropriate in all patients (light green); 2, reasonable when additional information is needed in selected patients (green); 3, not recommended (dark green).

From Baumgartner H, Hung J, Bermejo J, et al: Echocardiographic assessment of valve stenosis: EAE/ASE recommendations for clinical practice. *J Am Soc Echocardiogr* 22:1-23; quiz 101-102, 2009.

*AR,* Aortic regurgitation; *CSA,* cross-sectional area; *DFT,* diastolic filling time; *LVOT,* left ventricular outflow tract; *MR,* mitral regurgitation; *MS,* mitral stenosis; *MVA,* mitral valve area; *MVres,* mitral valve resistance, *ΔP,* gradient; *sPAP,* systolic pulmonary artery pressure; *r,* radius of convergence hemisphere; *RA,* right atrium; *RV,* right ventricle; *T1/2,* pressure half-time; *TR,* tricuspid regurgitation peak velocity; *v,* velocity; *VTI,* velocity-time integral.

**TABLE 21-3 Assessment of Mitral Valve Anatomy According to the Wilkins Score**

| *Grade* | *Mobility* | *Thickening* | *Calcification* | *Subvalvular Thickening* |
|---|---|---|---|---|
| 1 | Highly mobile valve with only leaflet tips restricted | Leaflets near normal in thickness (4-5 mm) | A single area of increased echocardiographic brightness | Minimal thickening just below the mitral leaflets |
| 2 | Leaflet mid and base portions have normal mobility | Midleaflets normal, considerable thickening of margins (5-8 mm) | Scattered areas of brightness confined to leaflet margins | Thickening of chordal structures extending to one of the chordal length |
| 3 | Valve continues to move forward in diastole, mainly from the base | Thickening extending through the entire leaflet (5-8 mm) | Brightness extending into the mid portions of the leaflets | Thickening extended to distal third of the chords |
| 4 | No or minimal forward movement of the leaflets in diastole | Considerable thickening of all leaflet tissue (>8-10 mm) | Extensive brightness throughout much of the leaflet tissue | Extensive thickening and shortening of all chordal structures extending down to the papillary muscles |

The total score is the sum of the four items and ranges between 4 and 16.

From Wilkins GT, Weyman AE, Abascal VM, et al: Percutaneous balloon dilatation of the mitral valve: an analysis of echocardiographic variables related to outcome and the mechanism of dilatation. *Br Heart J* 60:299-308, 1988.

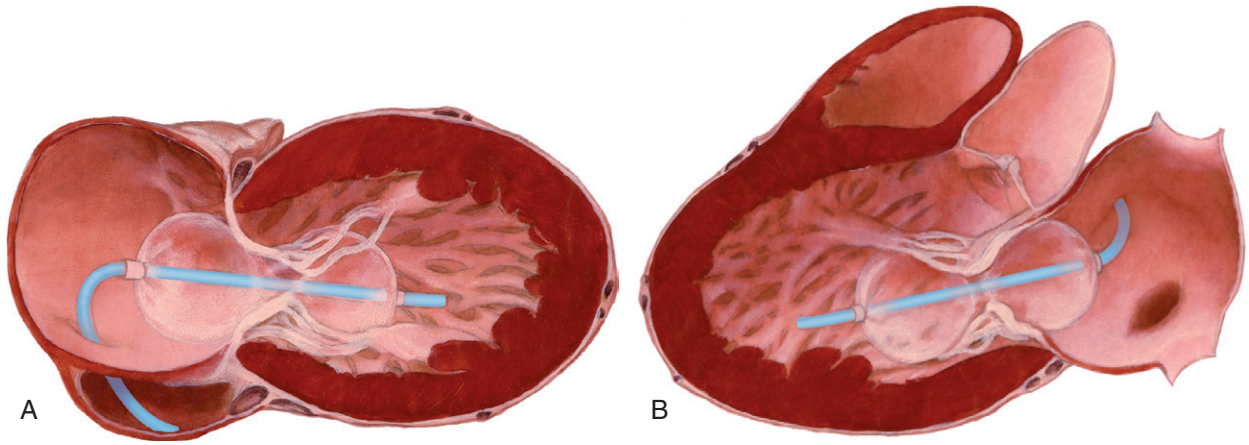



**Figure 21-3 Catheter balloon mitral valvotomy using the Inoue balloon.** The catheter is inserted through the atrial septum, and the balloon is inflated across the mitral valve. The waist of the balloon is positioned in the mitral orifice, and continuing inflation will ensure commissural opening. **A,** Right anterior oblique view. **B,** Left anterior oblique view.

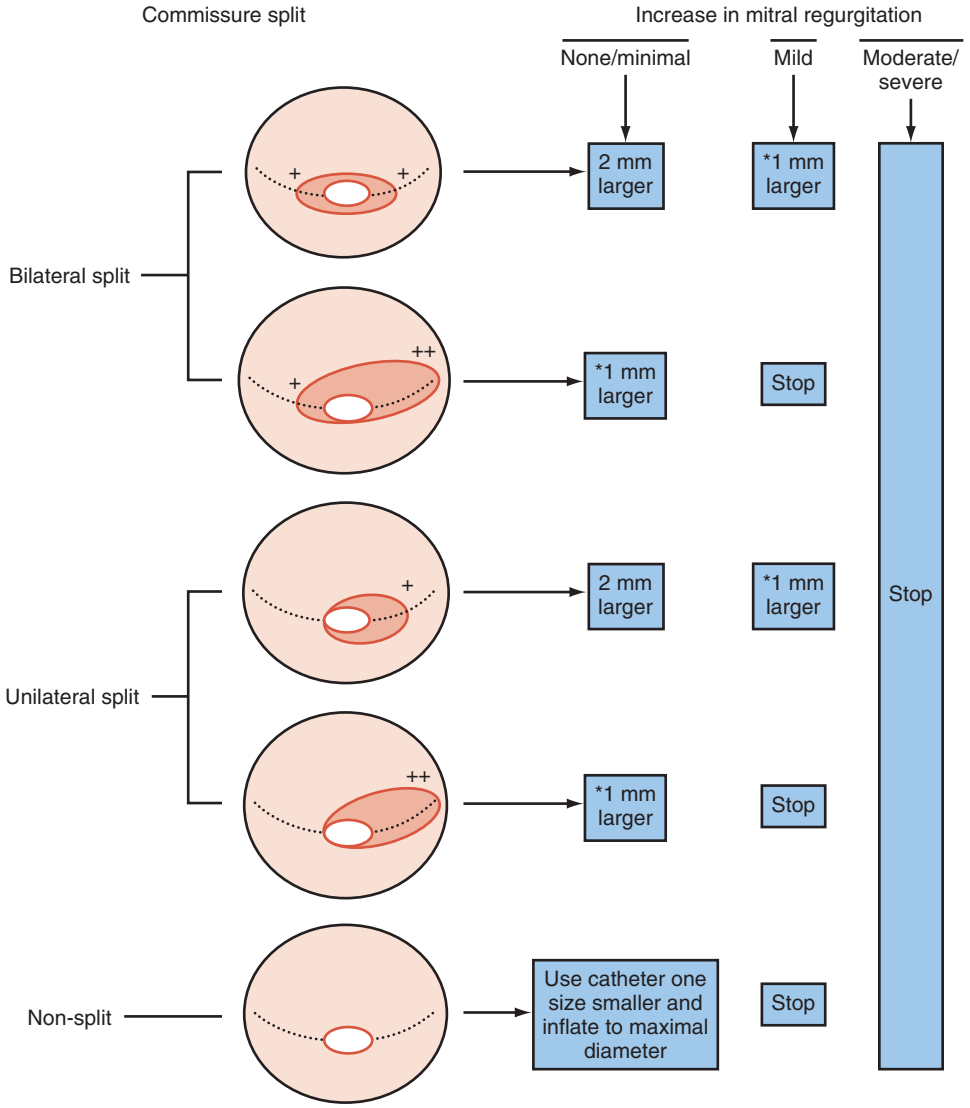



**Figure 21-4 Decision making during the stepwise dilation technique using the Inoue balloon, according to echocardiographic findings after each balloon inflation.** +, Incomplete split; ++, complete split; *, stop in cases of severely diseased valve or age greater than 65 years. *(From Vahanian A, Cormier B, Iung B: Mitral valvuloplasty. In Topol EJ, editor:* Textbook of interventional cardiology, *ed 5. Philadelphia, 2008, Saunders Elsevier, pp 879-893.)*

**TABLE 21-4 Assessment of Mitral Valve Anatomy According to the Cormier Score**

| *Echocardiographic Group* | *Mitral Valve Anatomy* |
|---|---|
| Group 1 | Pliable noncalcified anterior mitral leaflet and mild subvalvular disease (i.e., thin chordae ≥10 mm long) |
| Group 2 | Pliable noncalcified anterior mitral leaflet and severe subvalvular disease (i.e., thickened chordae <10 mm long) |
| Group 3 | Calcification of mitral valve of any extent, as assessed by fluoroscopy, whatever the state of subvalvular apparatus |

From Cormier B, Vahanian A, Michel PL, et al: [Evaluation by two-dimensional and Doppler echocardiography of the results of percutaneous mitral valvuloplasty]. *Arch Mal Coeur Vaiss* 82:185-191, 1989; Iung B, Cormier B, Ducimetiere P, et al: Immediate results of percutaneous mitral commissurotomy. A predictive model on a series of 1514 patients. *Circulation* 94:2124-2130, 1996.

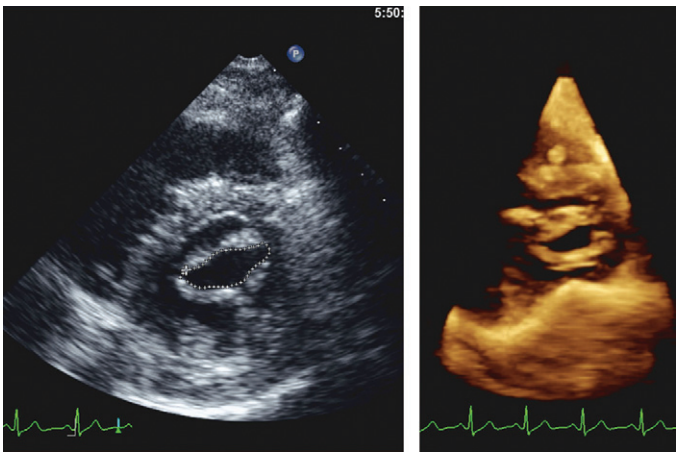


**Figure 21-5 Successful balloon mitral valvotomy (BMV) with bicommissural opening.** TTE, parasternal short-axis view. *Left:* After BMV (2D echocardiography). *Right:* After BMV (3D echocardiography).

inaccurate in this setting, the possible explanations being acute changes in cardiac chamber compliance or the presence of right-to-left shunt at the site of the transseptal puncture.[40] However, the pressure half-time method has a good specificity, although a low sensitivity, for identifying good valve opening, which may be helpful in technically difficult examinations.[28]

The echocardiographic assessment of the degree of opening of each commissure is strongly related to the quality of the immediate results of BMV and to late functional results.[41] The degree of commissural opening is thus an additional marker of the immediate results of BMV (Fig. 21-6). It is also useful as a baseline evaluation for the interpretation of echocardiographic follow-up. The assessment of the degree of commissural opening is improved by real-time 3D echocardiography.[26]

Although gradient is not a reliable marker of the severity of MS, it should be assessed after BMV because of its prognostic value on late functional results. In patients who had initial pulmonary hypertension, there is a frequent early decrease in pulmonary artery pressure, although it is generally more pronounced after several months.[42]

In most cases, there is little or no increase in MR after BMV. Moderate MR is often related to incomplete closure of free edges or commissures because of thickening and rigidity.[43] In these cases, color Doppler shows central and/or commissural small jets, and 2D echocardiography does not suggest traumatic lesion. If MR is severe (Fig. 21-7), its mechanism should be carefully assessed, using TEE if needed, looking at traumatic lesions. Traumatic MR is mainly caused by a noncommissural leaflet tear and is frequently associated with an absence of commissural opening, as shown by surgical or echocardiographic findings.[43,44] Lesions of the subvalvular apparatus are also frequent in traumatic MR, being mainly rupture of chordae, whereas partial or total papillary muscle rupture is rare (Fig. 21-8). These lesions cause particularly severe MR in patients with pliable leaflets.

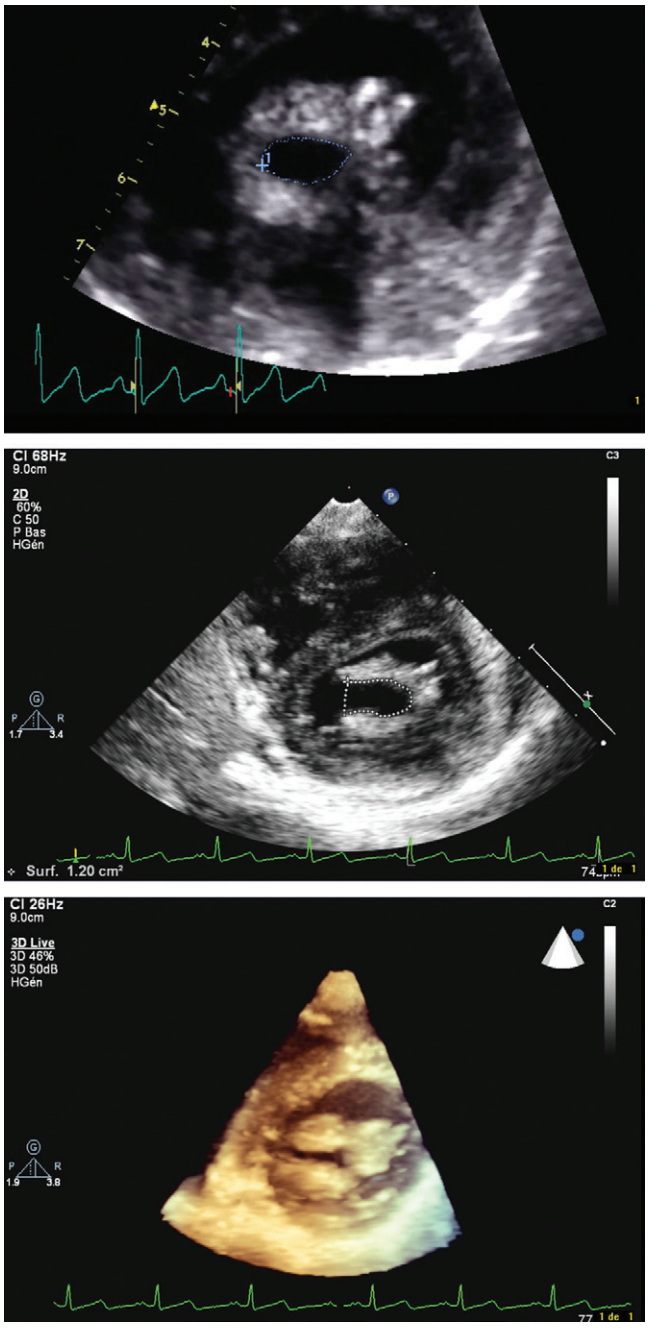



**Figure 21-6 Opening of the internal commissure after balloon mitral valvotomy (BMV) for very tight mitral stenosis in a 12-year-old boy.** TTE, parasternal short-axis view. *Top:* Planimetry before BMV (valve area 0.5 cm$^2$). *Middle:* Planimetry after BMV (2D echocardiography) (valve area 1.2 cm$^2$). *Bottom:* After BMV (3D echocardiography).

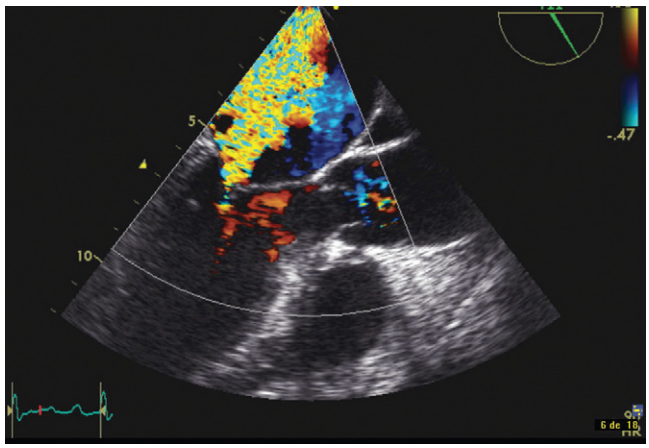


**Figure 21-7 TEE showing severe mitral regurgitation due to traumatic tear of the posterior leaflet.**

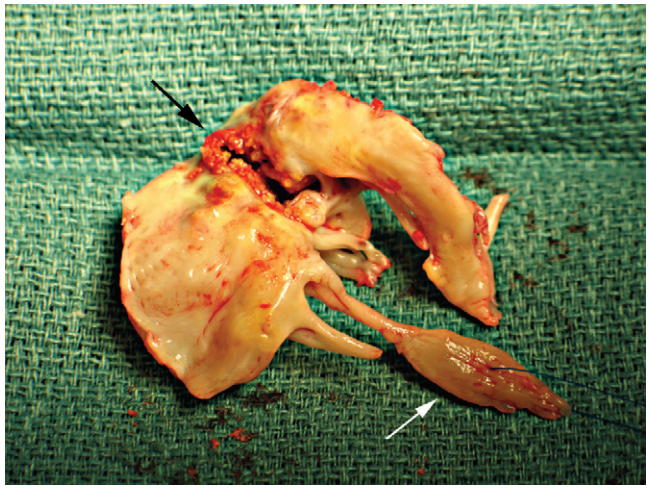


**Figure 21-8 Partial papillary muscle rupture** (*white arrow*) following balloon mitral valvotomy on a calcified mitral stenosis (calcification: *black arrow*).

Other findings from postprocedural echocardiography have less important consequences for patient management. Interatrial shunts can be visualized at the transseptal puncture site, in particular when using TEE. These are generally small shunts, which progressively disappear in the majority of cases.[45] The intensity of LA spontaneous contrast frequently decreases after successful BMV, and there is a further decrease until the sixth month.[46]

### DURING FOLLOW-UP

Echocardiographic follow-up assesses the usual features of valve function and its consequences.

The most frequent event is the occurrence of restenosis, which is generally defined as a valve area less than 1.5 $cm^2$ and greater than a 50% loss of the initial gain in valve area, although there is no standardized definition.[38,39,47] In patients with restenosis, the assessment of valve anatomy should pay particular attention to the degree of commissural fusion.

## Clinical Utility

Single- or multicenter series have analyzed immediate and late results of BMV and enable predictive factors to be identified, thereby contributing to an improvement in patient selection.

### RESULTS OF BALLOON MITRAL VALVOTOMY

#### *Failure and Complications*

The two main causes of failure are the impossibility of performing transseptal puncture or positioning the balloon across the mitral orifice. Failure rate is approximately 1% in series from experienced teams.[47-51] Higher rates were reported during early experience, which illustrates the importance of the learning curve.[30,52,53]

Severe complications are rare and, thus, need to be assessed using large series (Table 21-5).[47-52,54-59] In-hospital death occurs in less than 1% of patients, who are frequently in very poor clinical condition because of advanced age and/or severe hemodynamic impairment. Tamponade is a consequence of perforation by the transseptal needle or metallic guidewires. The risk of thromboembolic events is generally below 2%. Embolism leaving sequelae are mainly caused by fibrinothrombotic clots. They may occur despite systematic screening of LA thrombosis using TEE. Procedural complications are highly dependent on the experience of the interventional cardiologist, as shown by their relationship with the number of cases performed.[52] Technical simplifications inherent to the Inoue technique contribute to low complication rates, in particular tamponade, and partly account for the wide use of this technique.[22,60]

Severe traumatic MR is the most frequent severe complication of BMV, occurring in between 1% and 10% of cases. Attempts to identify predictive factors have not led to consistent results, which may be related to the small number of cases analyzed and differences in the methods used to define severe MR.[43,44,61-63] Severe MR is more frequent in patients with very tight MS and in those with severe impairment of leaflets and subvalvular apparatus, in particular when there is a heterogeneous distribution of leaflet abnormalities.[61] However, severe MR remains largely unpredictable in any given patient. Severe acute MR frequently requires surgery within weeks or months, but seldom in emergency.

#### *Immediate Results*

After BMV, there is approximately a doubling of mitral valve area in patients who underwent the different techniques (Table 21-6).[47-51,54-59,64-68] Series including heart catheterization demonstrated significant decreases in LA and pulmonary artery pressures and an increase in cardiac output. However, invasive investigations are now unlikely to be performed in routine assessment.

To simplify the interpretation and comparison of series, immediate results are also expressed following a binary endpoint, which is most often the association of final valve area 1.5 $cm^2$ or greater without MR greater than grade 2/4.

Mitral valve anatomy, as assessed by echocardiography whatever the scoring system used, is a strong predictor of immediate results of BMV.[30,49,54-58] The discriminant cutoff point of the Wilkins score has been set at 8 according to analyses

**TABLE 21-5 Severe Complications of Balloon Mitral Valvotomy**

| *Study* | *n* | *Age (years)* | *In-Hospital Death (%)* | *Tamponade (%)* | *Embolic Events (%)* | *Severe Mitral Regurgitation (%)* |
|---|---|---|---|---|---|---|
| Arora[50] (1987-2000) | 4850 | 27 | 0.2 | 0.2 | 0.1 | 1.4 |
| Chen*[48] (1985-1994) | 4832 | 37 | 0.1 | 0.8 | 0.5 | 1.4 |
| Iung[51] (1986-2001) | 2773 | 47 | 0.4 | 0.2 | 0.4 | 4.1 |
| Neumayer[57] (1989-2000) | 1123 | 57 | 0.4 | 0.9 | 0.9 | 6.0 |
| NHLBI Registry*[52] (1987-1989) | 738 | 54 | | | | |
| $n < 25$ | | | 2 | 6 | 4 | 4 |
| $25 \leq n < 100$ | | | 1 | 4 | 2 | 3 |
| $n \geq 100$ | | | 0.3 | 2 | 1 | 3 |
| Palacios[56] (1986-2000) | 879 | 55 | 0.6 | 1.0 | 1.8 | 9.4 |
| Jneid[59] (1986-2000) | 876 | 55 | 0.6 | 0.8 | 1.7 | 9.1 |
| Ben Farhat[49] (1987-1998) | 654 | 33 | 0.5 | 0.6 | 1.5 | 4.6 |
| Hernandez[47] (1989-1995) | 620 | 53 | 0.5 | 0.6 | — | 4.0 |
| Meneveau[54] (1986-1996) | 532 | 54 | 0.2 | 1.1 | — | 3.9 |
| Fawzy[58] (1989-2004) | 520 | 31 | 0 | 0.7 | 0.5 | 1.6 |
| Stefanadis*[55] (1988-1996) | 441 | 44 | 0.2 | 0 | 0 | 3.4 |

*Multicenter series.

**TABLE 21-6 Immediate Results of Balloon Mitral Valvotomy (BMV): Increase in Mitral Valve Area**

| Study | Patients n= | Age (years) | Mitral Valve Area ($cm^2$) | | Technique |
|---|---|---|---|---|---|
| | | | Before BMV | After BMV | |
| Arora[50] | 4850 | 27 | 0.7 | 1.9 | Inoue or double-balloon or metallic commissurotome |
| Chen[48] | 4832 | 37 | 1.1 | 2.1 | Inoue balloon |
| Iung[51] | 2773 | 47 | 1.0 | 1.9 | Inoue, single-, or double-balloon |
| Neumayer[57] | 1123 | 57 | 1.1 | 1.8 | Inoue balloon |
| Palacios[56] | 879 | 55 | 0.9 | 1.9 | Inoue or double-balloon |
| Jneid[59] | 876 | 55 | 0.9 | 1.9 | Inoue or double-balloon |
| Ben-Farhat[49] | 654 | 33 | 1.0 | 2.1 | Inoue or double-balloon |
| Hernandez[47] | 561 | 53 | 1.0 | 1.8 | Inoue balloon |
| Meneveau[54] | 532 | 54 | 1.0 | 1.7 | Inoue or double-balloon |
| Fawzy[58] | 520 | 31 | 0.9 | 2.0 | Inoue balloon |
| Eltchaninoff[68] | 500 | 34 | 0.9 | 2.1 | Metallic commissurotome |
| Stefanadis[55] | 441 | 44 | 1.0 | 2.1 | Modified single-, double-, or Inoue balloon (retrograde) |
| Kang[66] | 152 | 42 | 0.9 | 1.8 | Inoue balloon |
| (randomized comparison) | 150 | 40 | 0.9 | 1.9 | Double-balloon |

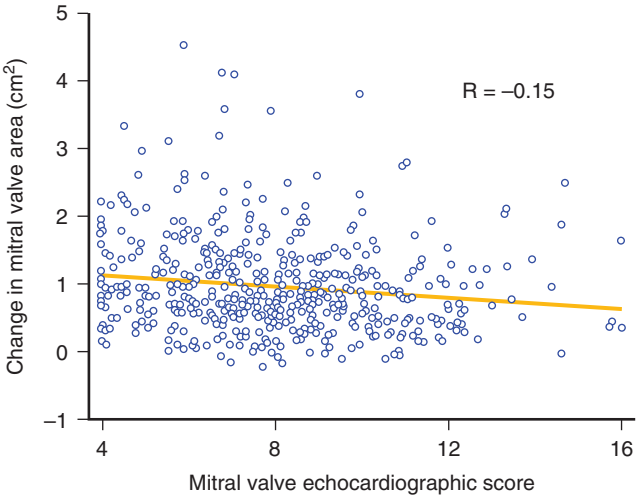



**Figure 21-9 Influence of mitral valve echocardiographic score on change in mitral valve area (by cardiac catheterization, $cm^2$) from before to immediately after balloon mitral valvotomy.** R value for all points is –0.15. *(From National Heart, Lung, and Blood Institute Balloon Valvuloplasty Registry Participants: Multicenter experience with balloon mitral commissurotomy. NHLBI Balloon Valvuloplasty Registry Report on immediate and 30-day follow-up results.* Circulation *85:448-461, 1992.)*

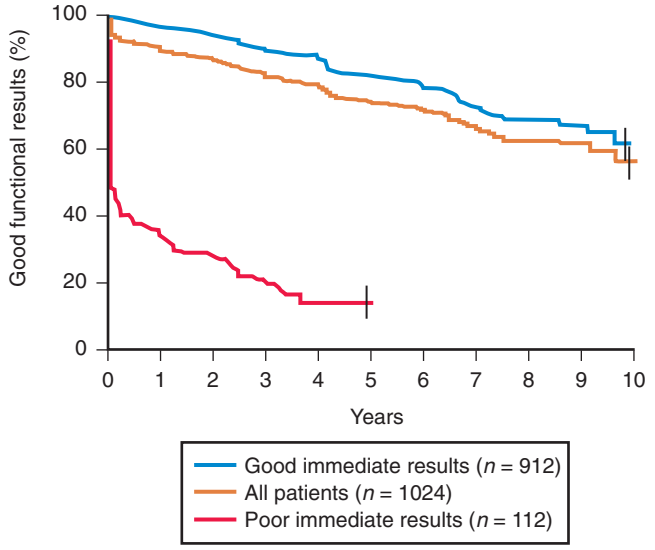



**Figure 21-10 Clinical outcomes stratified by BMV functional results.** Good functional results (survival considering cardiovascular-related deaths with no need for mitral surgery or repeat dilatation and in NYHA functional class I or II) after balloon mitral valvotomy in 1024 patients. *(From Iung B, Garbarz E, Michaud P, et al: Late results of percutaneous mitral commissurotomy in a series of 1024 patients.* Circulation *99:3272-3278, 1999.)*

of immediate results of BMV. However, all scoring systems are of limited predictive value, as shown by the low correlation (r = –0.15) between the Wilkins score and final valve area (Fig. 21-9).[69] Large series including patients with diverse characteristics have shown that other factors strongly influence immediate results of BMV.[30,69-71] Older age and smaller valve area not only are significant predictors of poor immediate results, but have similar or greater predictive strengths for valve calcification.[30,71] There were less consistent associations between poor immediate results and previous commissurotomy or baseline MR, which may be related to a differential effect according to other characteristics, as shown by significant interactions. In our experience, the interaction between age and previous commissurotomy means that previous commissurotomy is a factor in poor immediate results only in patients aged over 50 years.[30]

Consistently with the predictors identified, series including a majority of young patients with favorable anatomic conditions report particularly good immediate results.[48-50,58]

### *Late Results*

The assessment of late outcome following BMV is based on clinical endpoints in most series, because standardized echocardiographic follow-up raises obvious difficulties when a number of patients are followed over a long time period.

Late results should be interpreted according to the quality of immediate results. The majority of patients with residual stenosis or severe MR after BMV require surgery, the timing of which depends largely on comorbidities and the policy of the medical team. Conversely, cardiovascular events seldom occur following successful BMV, and most patients experience sustained functional improvement (Fig. 21-10). Mitral restenosis is the most frequent cause of late clinical deterioration, as it was after successful surgical commissurotomy.[47,63,72-74]

**TABLE 21-7 Late Results after Balloon Mitral Valvotomy**

| Study | n= | Age (years) | Maximum Follow-up (years) | Event-Free Survival (%) |
|---|---|---|---|---|
| Iung[75] | 1024 | 49 | 10 | 56† |
| Palacios[56] | 879 | 55 | 12 | 33† |
| Dean[77] (NHLBI registry) | 736 | 54 | 4 | 60* |
| Ben-Farhat[49] | 654 | 34 | 10 | 72† |
| Song[79] | 402 | 44 | 9 | 90* |
| Hernandez[47] | 561 | 53 | 7 | 69† |
| Meneveau[54] | 532 | 54 | 7.5 | 52† |
| Fawzy‡[58] | 520 | 31 | 17 | 31† |
| Stefanadis[55] | 441 | 44 | 9 | 75† |
| Cohen[76] | 146 | 59 | 5 | 51* |
| Orrange[78] | 132 | 44 | 7 | 65* |

*Survival without intervention.
†Survival without intervention and in New York Heart Association class I or II.
‡Patients with good immediate results.

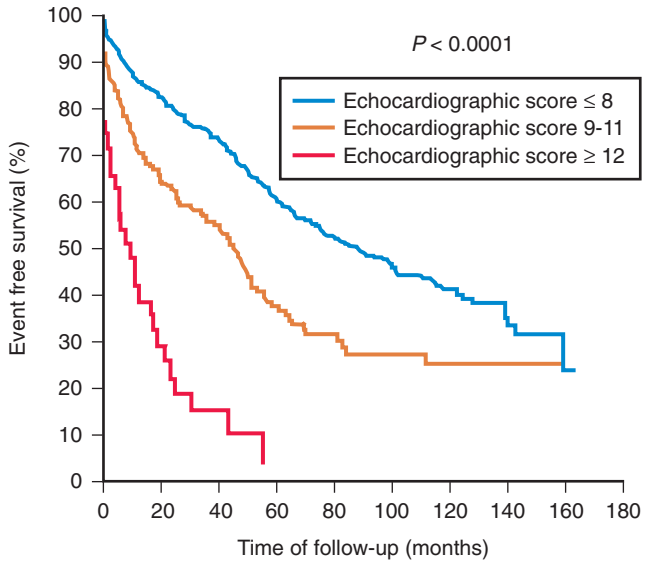



**Figure 21-11 Event-free survival (alive and free of mitral valve replacement or redo percutaneous mitral valvotomy) according to echocardiographic score.** *(From Palacios IF, Sanchez PL, Harrell LC, et al: Which patients benefit from percutaneous mitral balloon valvuloplasty? Prevalvuloplasty and postvalvuloplasty variables that predict long-term outcome.* Circulation *105, 1465-1471, 2002.)*

Overall, late results of BMV are satisfying; however, there is a wide range in clinical outcome (Table 21-7).[49,54-56,58,63,75-79] Apparent discrepancies are related to differences in patient characteristics. Series from developing countries include a majority of young patients with favorable anatomic conditions and report higher rates of event-free survival than series from Western countries which include older patients with less favorable anatomic conditions. Series comprising a wide range of patient characteristics enable predictive factors of late results to be identified. As for the prediction of immediate results, valve anatomy is a strong predictive factor of late clinical outcome, but it is only one factor among others (Fig. 21-11).[47,49,54-56,58,63,75-79] Besides impaired anatomy, baseline predictors of poor late outcome are higher age and the consequences of MS, such as a high functional class and the presence of atrial fibrillation (Table 21-8). These predictors are consistent with previous experience with surgical commissurotomy.[74]

**TABLE 21-8 Predictors of Poor Late Functional Results in 912 Patients Who Had Good Immediate Results after Balloon Mitral Valvotomy (Valve Area ≥ 1.5 cm² with No Regurgitation > Grade 2/4): Multivariate Analysis**

| Variable | Subgroups | Hazard Ratio and 95% Confidence Interval | p |
|---|---|---|---|
| **Before Procedure** | | | |
| Age (years) | <50 | 1 | 0.0008 |
| | 50-70 | 1.5 [1.2-2.0] | |
| | ≥70 | 2.4 [1.4-3.9] | |
| Functional class (NYHA) | I-II | 1 | <0.0001 |
| | III-IV | 2.7 [1.7-4.4] | |
| Rhythm | Sinus | 1 | <0.0001 |
| | Atrial fibrillation | 2.0 [1.4-2.7] | |
| Echocardiographic group | 1 | 1 | 0.003 |
| | 2 | 1.5 [1.1-1.9] | |
| | 3 | 2.2 [1.3-3.7] | |
| **After Procedure** | | | |
| Valve area (cm²) | ≥2.00 | 1 | 0.001 |
| | 1.75-2.00 | 1.4 [1.1-1.7] | |
| | 1.50-1.75 | 1.9 [1.3-2.8] | |
| Mean gradient (mm Hg) | ≤3 | 1 | <0.0001 |
| | 3-6 | 2.0 [1.6-2.5] | |
| | ≥6 | 4.0 [2.5-6.2] | |
| Mitral regurgitation | 0-1 | 1 | 0.04 |
| | 2 | 1.4 [1.0-2.0] | |

From Iung B, Garbarz E, Michaud P, et al: Late results of percutaneous mitral commissurotomy in a series of 1024 patients. *Circulation* 99:3272-3278, 1999.
*NYHA,* New York Heart Association.

Even in patients with good immediate results, the degree of valve opening has an impact on late outcome.[47,75,79] Besides postprocedural valve area, gradient is also a strong predictor of late clinical results, suggesting that it provides additional information.[75] The degree of commissural opening is strongly linked with postprocedural valve area and gradient but does not have an incremental prognostic value in multivariate analysis.[41] The persistence of a high gradient following BMV despite good valve opening can be related to limited valve reserve in relationship with a loss of pliability, which is likely to influence late restenosis.

Series including serial echocardiographic examinations showed a progressive decrease in mean mitral valve area over time, following a linear pattern.[47,72] The yearly decrease in valve area varies between series according to differences in patient characteristics, leading to inhomogeneous estimations of restenosis rates.[47,72] Conversely, there is generally no increase in mild-to-moderate MR.[47]

## *Particular Subgroups*

### Restenosis after Previous Commissurotomy

In patients with restenosis following prior closed- or open-heart commissurotomy, BMV is feasible and has the attraction of avoiding iterative surgery, providing restenosis is related to bicommissural fusion (Fig. 21-12).[80-82] Even if the results are less satisfying than in native valves, we reported a 48% rate of 8-year good functional results.[81] The possibility of deferring surgery by at least 8 years in half of the patients enables prosthesis-related complications to be postponed, because surgery consists of prosthetic valve replacement in most patients with restenosis. Young patients are likely to derive the greatest benefit from BMV for restenosis.[81]

Restenosis after previous BMV becomes more frequent. Repeat BMV can be performed in selected patients and gives

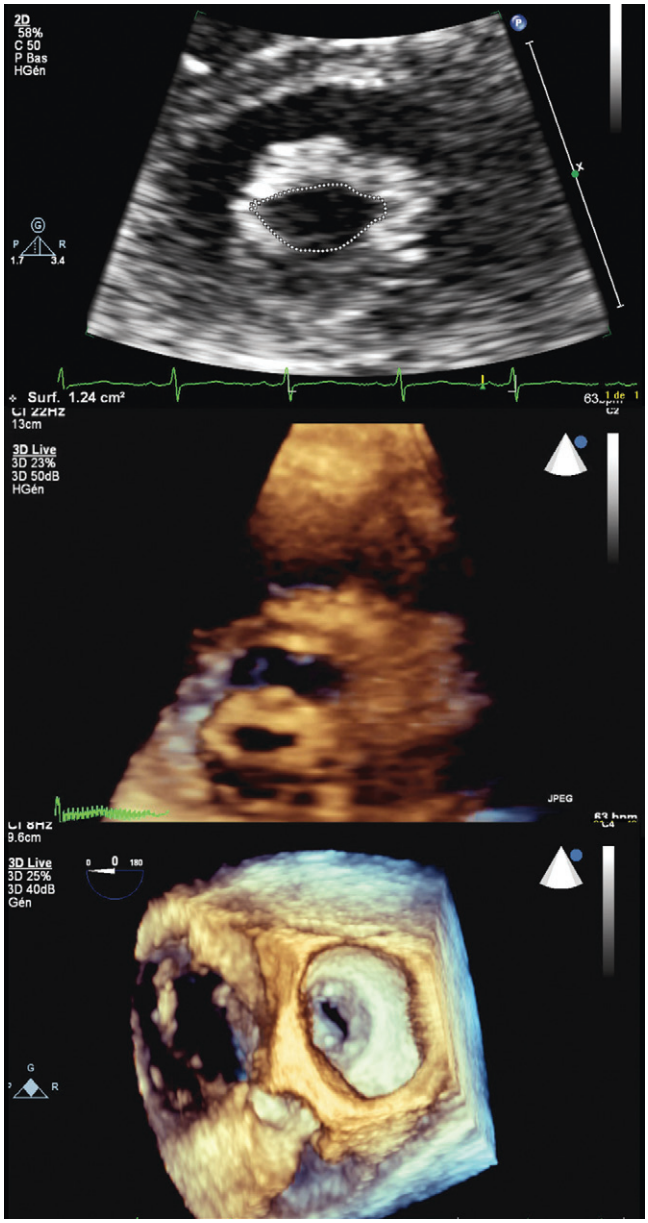



**Figure 21-12 Mitral restenosis after previous balloon mitral valvotomy, related to refusion of both commissures.** *Top:* TTE, parasternal short-axis, 2D echocardiography. *Middle:* TTE, parasternal short-axis, 3D echocardiography, view from the LV. *Bottom:* TEE, 3D echocardiography, view from the LA.

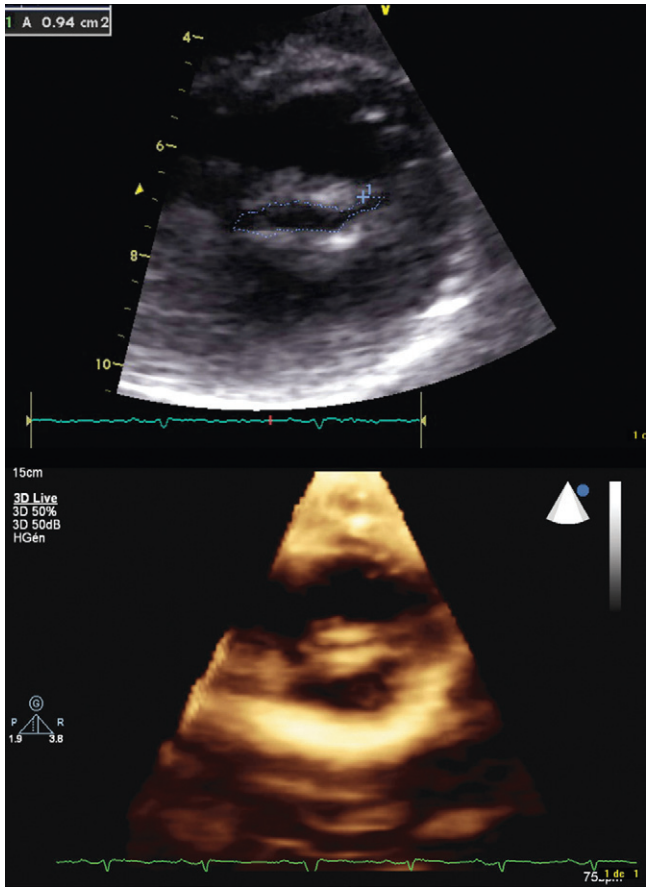



**Figure 21-13 Mitral restenosis after previous open-heart commissurotomy.** TTE, parasternal short-axis view. Both commissures are opened, and restenosis is due to rigidity of valvular and subvalvular apparatus. *Top:* 2D echocardiography. *Bottom:* 3D echocardiography, view from the LV.

good midterm clinical results, particularly in young patients with mild or no calcification,[82,83] whereas its efficacy is less convincing in older patients with calcified valves.[84-86]

Echocardiographic analysis of valve anatomy should carefully look at the extent of commissural refusion. Results of repeat BMV are less satisfying in patients who have incomplete commissural fusion.[85] Whatever the type of initial commissurotomy, BMV should not be considered in case of persistent opening of both commissures (Fig. 21-13).

## The Elderly

Theoretically, elderly patients are not good candidates for BMV because they combine predictive factors of poor immediate and late outcome, in particular, besides old age, frequent valve calcification, atrial fibrillation, and severe symptoms. Despite unfavorable anatomic conditions, good immediate results are frequently obtained, but subsequent deterioration occurs more rapidly than in younger patients.[87-89] However, these results should be weighed against the alternative of surgery, which is a high-risk option in this population. Even with unfavorable mitral anatomy, BMV can be considered as a palliative procedure in older patients with severely symptomatic MS.

Echocardiographic examination should pay particular attention to confirm the rheumatic etiology and distinguish it from degenerative MS. This disease is frequent in the elderly but seldom causes severe MS.[90] Degenerative MS is characterized by an extensive calcification of the mitral annulus, a stiffened anterior leaflet, and opened commissures (Fig. 21-14). Because there is no commissural fusion in these cases, degenerative MS is not amenable to BMV.

## Young Patients

Severe rheumatic MS may be encountered in young patients in countries where rheumatic fever is endemic. Two series have reported consistent results of BMV in patients aged below 20, who were followed up for 12 years.[91,92] Results tended to be better than in adults, and late functional results did not differ, with event-free survival rates ranging from 70% to 80% at 10 years. BMV is also a valid treatment of MS in children less than 12 years of age.[93]

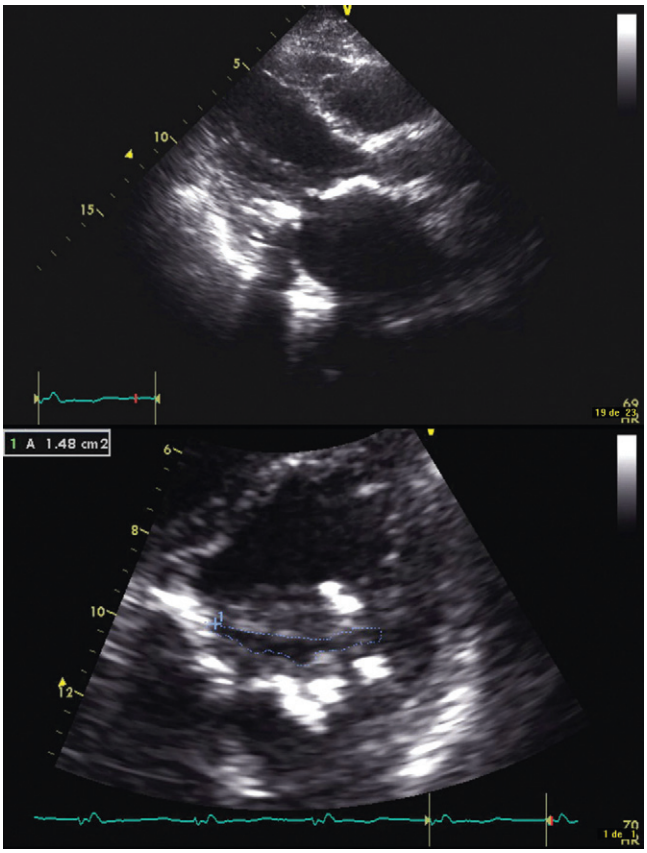



**Figure 21-14 Degenerative mitral stenosis.** Severe calcification of the posterior part of the mitral annulus, calcification of the external part anterior leaflet and absence of commissural fusion. *Top:* TEE, parasternal long-axis view. *Bottom:* Short-axis view.

### Pregnant Women

Hemodynamic changes during pregnancy worsen the clinical tolerance of MS, which may compromise the prognosis of both mother and fetus, in particular at delivery.[94] Therefore, intervention is required during pregnancy in women who remain symptomatic despite medical therapy. BMV can be safely performed during pregnancy, and fetal tolerance is good.[95,96] The increase of thromboembolic risk during pregnancy underscores the need for TEE, which is best performed under anesthesia just before the procedure to reduce the mother's discomfort.

## IMPLICATIONS FOR PATIENT SELECTION

### *Contraindications*

Contraindications to BMV are summarized in Box 21-1. Although cases of BMV using the Inoue balloon have been reported in patients with thrombosis located in the left appendage,[97] the experience remains limited. The potential hazards related to thrombus migration should lead to the consideration of persistent thrombus of LA, even when localized to the LA appendage, as a contraindication in most cases.[23,24] However, if the patient is in stable condition, the decision should be postponed until after repeat TEE following at least 2 months of optimal anticoagulant therapy. LA thrombosis has been shown to disappear in approximately 1 in 4 patients after 6 months of anticoagulant therapy, in particular when patients had a small thrombus and low grade LA spontaneous contrast.[98]

**Box 21-1**

**CONTRAINDICATIONS TO BALLOON MITRAL VALVOTOMY**

- Persistent LA thrombosis (including in the LA appendage)
- More than mild mitral regurgitation
- Massive or bicommissural calcification
- Severe concomitant aortic valve disease
- Severe organic tricuspid stenosis or severe functional regurgitation with enlarged annulus
- Severe concomitant coronary artery disease requiring bypass surgery

More than mild MR, or MR with a grade above 2/4 when using a semiquantitative approach, is a contraindication to BMV.[23,24] Although no study has validated thresholds based on quantitative echocardiography, this corresponds to an effective regurgitant orifice larger than 20 $mm^2$ and/or a regurgitant volume greater than 30 mL/beat. In patients who have borderline MR, BMV is more likely to be considered if valve anatomy is favorable.

Valve calcification contraindicates BMV in the rare cases where it is massive or localized in both commissures.[23,24]

Other contraindications are related to associated heart diseases needing surgical correction. Particular care should be taken to avoid underestimating the degree of aortic stenosis. Conversely, associated moderate aortic regurgitation without consequences on the LV does not contraindicate BMV, because its progression is slow.[99] Surgery is preferred if there is severe associated organic tricuspid disease or severe functional tricuspid regurgitation with major enlargement of the tricuspid annulus. In other cases, severe functional tricuspid regurgitation can decrease after BMV.[100]

### *Choice of Procedure*

There is now evidence supporting BMV as the procedure of choice in young patients. Young age is frequently associated with favorable valve anatomy, both features being strong predictors of good immediate and late results.[89] Randomized trials conducted in these homogeneous populations showed that mid- and long-term results of BMV were as good as those obtained with open-heart commissurotomy and similar to or better than those with closed-heart commissurotomy.[101-104] Moreover, the possibility of performing conservative treatment that can be repeated in selected patients is particularly attractive in young patients, including children and adolescents, to avoid iterative surgical interventions. However, a number of good candidates for BMV cannot benefit from the procedure for financial reasons in developing countries, which cannot always afford the cost of the balloon. This justifies attempts to lower the cost of the device, such as the Multi-Track system and the metallic commissurotome.[64,65,67] The possibility of reusing the metallic part of the percutaneous commissurotome significantly lowers the cost of the procedure.

The decision is more difficult in older patients, who have frequent impairment of the anatomy of the leaflets and subvalvular apparatus, and who represent the majority of patients with MS in Western countries.[1,51,88] They form a heterogeneous group for whom no randomized studies are available and comparative studies do not enable all potential confounding factors to be taken into account.[105] Patients should not be denied BMV

on the sole basis of unfavorable valve anatomy, given the low predictive value of valve anatomy alone. Good immediate and midterm results can be obtained in patients with unfavorable mitral anatomy, even with calcified valves.[89,106-109] Patient selection should rely on a global assessment, which can be aided by the use of predictive analyses and derived multivariate models enabling the results of BMV to be estimated according to individual patient characteristics.[23,71,110]

In patients with impaired valve anatomy, BMV can be considered in particular when their other characteristics are favorable, in particular age below 70 years, mitral valve area between 1.0 and 1.5 $cm^2$, moderate symptoms (NYHA class II), and sinus rhythm. Predictive models show a high likelihood of good immediate and late results in these patients.[30,75,81] This enables surgery to be postponed for several years, thereby affecting prosthesis-related complications, because the surgical alternative in these patients is valve replacement in most cases. This is illustrated by the simulation of midterm results of BMV in patients with calcified mitral valves according to the extent of calcification and other characteristics (Fig. 21-15).[109] Conversely, there is a much lower likelihood of sustained long-term improvement in old patients who have unfavorable mitral anatomy, tight stenosis, severe symptoms, and atrial fibrillation.[56,75] Moreover, the relevance of deferring surgery may be debatable in this age group. Thus, mitral surgery, often combined with tricuspid repair, can be considered as the first-line treatment provided the operative risk is acceptable. The choice between BMV and surgery in these difficult situations should also take into account the local expertise of interventional cardiologists and surgeons as well as the wishes of the patient.

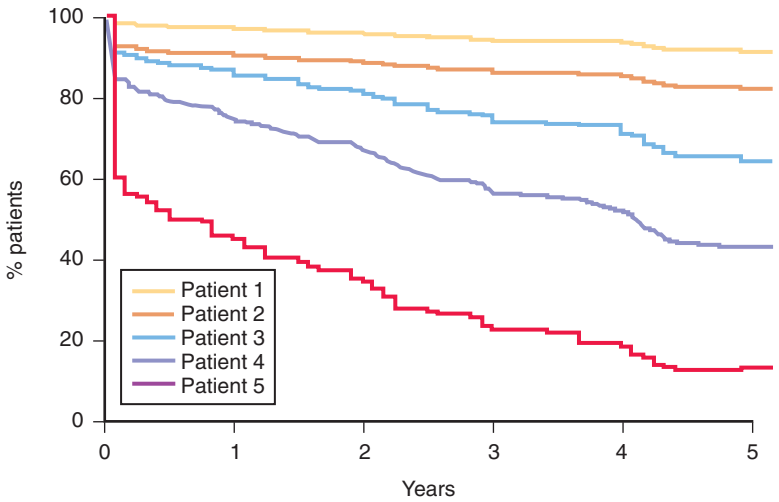
In Western countries, there is a trend for BMV to be performed in older patients with more severe impairment of valve anatomy.[51] In the Euro Heart Survey, surgical commissurotomy accounted for only 4% of the interventions performed for MS in 2001, whereas BMV was used in 34% of patients and prosthetic valve replacement in 62%.[1]

### *Timing of Procedure*

There is a consensus to advise intervention, whether it is percutaneous or surgical, in patients who have significant, that is, moderate or severe MS (valve area less than 1.5 $cm^2$) and symptoms.[23,24] Better insights into the prognosis of MS, with particular regard to the risk of thromboembolic complications or hemodynamic decompensation, and the availability of intervention at low risk have led to consideration of the indications for BMV at an earlier stage in selected patients. Intervention is generally not considered in mild MS because the variability of the progression does not support prophylactic BMV.[23,24,111] However, BMV can be considered in patients with borderline valve area in the presence of symptoms or pulmonary hypertension.[24]

The efficacy of BMV has been demonstrated on various markers of the thromboembolic risk in MS: LA spontaneous contrast, LA size and contractility, LA appendage flow velocity, and activation of coagulation in the LA.[46,112-114] Although the efficacy of BMV on the thromboembolic risk has not been demonstrated by randomized studies, a retrospective and prospective series showed that the performance of BMV was strongly associated with a decreased thromboembolic risk in patients with MS and atrial fibrillation.[115,116]

It is more difficult to evaluate the risk of acute hemodynamic complications in MS, apart from particular cases such as pregnancy. Exercise echocardiography is of potential interest because it provides additional information as compared with baseline evaluation. ACC/AHA guidelines recommend BMV, when anatomic conditions are favorable and systolic pulmonary artery pressure is greater than 60 mm Hg at peak exercise.[24] However, such thresholds are debatable because they can be reached in patients without heart disease, and their prognostic value in MS has not been validated in large series.[117,118] In addition, this is the reason why no particular recommendation is given in the ESC guidelines regarding the evolution of systolic pulmonary pressure at exercise.[23]




| Patient | Age (years) | NYHA class | Rhythm | Calcification | Valve area ($cm^2$) |
|---|---|---|---|---|---|
| 1 | <50 | II | Sinus | 1 | 1.25-1.5 |
| 2 | <50 | II | Sinus | 2 | 1-1.25 |
| 3 | 50-70 | III | Sinus | 2 | 1.25-1.5 |
| 4 | 50-70 | III | A. fib | 2 | 1.25-1.5 |
| 5 | ≥70 | III | A. fib | 3 | 0.75-1 |

**Figure 21-15 Long-term predicted outcome based on baseline clinical factors and procedural success.** Predicted probability of good immediate results (valve area ≥ 1.5 $cm^2$ without regurgitation > grade 2/4) and good late functional results (survival with no intervention and in NYHA functional class I or II) after balloon mitral valvotomy in calcified mitral stenosis, according to patient characteristics. The extent of calcification is graded from 1 (small nodule) to 4 (extensive calcification). *(From Iung B, Garbarz E, Doutrelant L, et al: Late results of percutaneous mitral commissurotomy for calcific mitral stenosis.* Am J Cardiol *85:1308-1314, 2000.)*

Recommendations on BMV according to current guidelines are summarized in Table 21-9.

## Research Applications

### STRESS ECHOCARDIOGRAPHY

Changes in the severity of MS and its consequences can be observed according to changes in hemodynamic conditions, as shown by exercise or pharmacologic stress combined with invasive measurements. They have been replaced by stress echocardiography, which has the advantage of allowing for repeated noninvasive measurements.

Exercise echocardiography is the most physiologic approach. Different series consistently showed an increase in mean gradient and systolic pulmonary artery pressure at submaximal effort or peak effort.[119-121] However, there is an important heterogeneity in the progression of mitral gradient and systolic pulmonary artery pressure on exercise, as well as stroke volume, which does not relate to baseline severity of MS.[119-121] A possible explanation comes from differences in the evolution of mitral valve area, as assessed by the continuity equation, and stroke volume. The increase in valve area on exercise is associated with an increase in stroke volume. Conversely, stroke volume does not increase when there is no significant change in valve area during exercise.[121,122] These two different patterns are not related to differences in baseline severity of MS, but to the impairment of valve anatomy.[122] A study[121] using exercise echocardiography to evaluate atrioventricular compliance demonstrated that systolic pulmonary artery pressure at rest, and even more so on exercise, was strongly correlated with atrioventricular compliance, but not with mitral valve area. Finally, the level of increase in systolic pulmonary artery pressure on exercise seems to be related to the type of limiting symptoms, whether they are dyspnea or fatigue.[120]

Most previous studies used treadmills and were based on postexercise data. Semisupine bicycle ergometry now enables hemodynamic changes to be assessed for each workload. Our experience suggests that the type of limiting symptom (dyspnea or fatigue) is more related to the pattern of increase of mitral gradient than to the level of mean gradient or systolic pulmonary artery pressure at peak exercise.[123]

Dobutamine stress echocardiography (DSE) is a less physiologic approach than exercise echocardiography in MS, but it is also associated with significant increases in mean gradient and systolic pulmonary artery pressure, as compared with resting values.[124] The only study thus far that has analyzed the relationship between findings from stress echocardiography and clinical outcome was based on DSE.[125] This study showed that mean mitral gradient during DSE was an independent predictor of clinical events during a 5-year follow-up, the cutoff value being 18 mm Hg. The incremental prognostic was particularly marked in patients who had a valve area between 1.0 and 1.5 $cm^2$.[125] Another study[126] using DSE showed a more important valve reserve, that is, a more important increase in valve area, in patients who had had previous commissurotomy as compared with those who had native MS.

Stress echocardiography is useful to refine the knowledge of the hemodynamic consequences of MS. However, at the present time, its implications for decision making need to be assessed by further prospective studies. This is particularly needed to validate thresholds of gradient and pulmonary artery pressure leading to the consideration of intervention in asymptomatic patients with MS in guidelines.

**TABLE 21-9 Recommendations for Balloon Mitral Valvotomy in Patients with Mitral Stenosis**

| *ACC / AHA Guidelines* | *ESC Guidelines* |
|---|---|
| **Symptomatic Patients** | |
| Symptomatic patients (NYHA functional class II, III, or IV), with moderate or severe MS* and valve morphology favorable for percutaneous balloon valvotomy in the absence of LA thrombus or moderate to severe MR **(IA)**<br>Patients with moderate or severe MS* who have a nonpliable calcified valve, are in NYHA functional class III-IV, and are either not candidates for surgery or are at high risk for surgery **(IIaC)**<br>Symptomatic patients (NYHA functional class II, III, or IV), with mitral valve area > 1.5 $cm^2$ if there is evidence of hemodynamically significant MS based on pulmonary artery systolic pressure > 60 mm Hg, pulmonary artery wedge pressure ≥ 25 mm Hg, or mean mitral valve gradient > 15 mm Hg during exercise **(IIbC)**<br>As an alternative to surgery for patients with moderate or severe MS* who have a nonpliable calcified valve and are in NYHA functional class III-IV **(IIbC)** | Patients with MS and valve area < 1.5 $cm^2$:<br>Symptomatic patients with favorable characteristics† for percutaneous mitral commissurotomy **(IB)**<br>Symptomatic patients with contraindications or high risk for surgery **(IC)**<br>As initial treatment in symptomatic patients with unfavorable anatomy but otherwise favorable clinical characteristics† **(IIaC)** |
| **Asymptomatic Patients** | |
| Asymptomatic patients with moderate or severe MS* and valve morphology favorable for percutaneous balloon valvotomy who have pulmonary hypertension (pulmonary artery systolic pressure > 50 mm Hg at rest or > 60 mm Hg with exercise) in the absence of LA thrombus or moderate to severe MR **(IC)**<br>Asymptomatic patients with moderate or severe MS* and valve morphology favorable for percutaneous balloon valvotomy who have new onset of atrial fibrillation in the absence of LA thrombus or moderate to severe MR **(IIbC)** | Asymptomatic patients with MS with valve area < 1.5 $cm^2$, favorable characteristics for percutaneous mitral commissurotomy and high thromboembolic risk or high risk of hemodynamic decompensation:<br>Previous history of embolism **(IIaC)**<br>Dense spontaneous contrast in the LA **(IIaC)**<br>Recent or paroxysmal atrial fibrillation **(IIaC)**<br>Systolic pulmonary pressure > 50 mm Hg at rest **(IIaC)**<br>Need for major noncardiac surgery **(IIaC)**<br>Desire for pregnancy **(IIaC)** |

From Vahanian A, Baumgartner H, Bax J, et al: Guidelines on the management of valvular heart disease: The Task Force on the Management of Valvular Heart Disease of the European Society of Cardiology. *Eur Heart J* 28:230-268, 2007; Bonow RO, Carabello BA, Chatterjee K, et al: 2008 focused update incorporated into the ACC/AHA 2006 guidelines for the management of patients with valvular heart disease: a report of the American College of Cardiology/American Heart Association Task Force on Practice Guidelines (Writing Committee to Revise the 1998 Guidelines for the Management of Patients with Valvular Heart Disease): endorsed by the Society of Cardiovascular Anesthesiologists, Society for Cardiovascular Angiography and Interventions, and Society of Thoracic Surgeons. *Circulation* 118:e523-661, 2008.

*ACC,* American College of Cardiology; *AHA,* American Heart Association; *ESC,* European Society of Cardiology; *NYHA,* New York Heart Association.

*See Table 21-1.

†Favorable characteristics for percutaneous mitral commissurotomy can be defined by the absence of several of the following: clinical characteristics—old age, history of commissurotomy, NYHA class IV, atrial fibrillation, severe pulmonary hypertension; anatomic characteristics—echocardiographic score ≥8, Cormier score 3 (calcification of mitral valve of any extent, as assessed by fluoroscopy), very small mitral valve area, severe tricuspid regurgitation.

### EVALUATION OF VALVE ANATOMY

Given the limitations of commonly used scoring systems for the prediction of the results of BMV, alternative approaches have been developed, in particular taking into account the location of valve abnormalities in relation to the commissures. Series have shown that commissural location of valve thickening and calcification influences immediate results of BMV.[31-33] However, no scoring system including these findings has been validated on large series in comparison with commonly used scoring systems. Another scoring system has been developed to predict the occurrence of severe MR, which is the most frequent complication following BMV.[61,62] It has the advantage of taking into account the heterogeneity of leaflet impairment and the presence of commissural fibrosis or calcification (Table 21-10). Nevertheless, its predictive value for immediate valve opening and late functional results has not been studied, and its usefulness in the prediction of severe MR has not been confirmed in large series.

Besides the location of valvular abnormalities, mechanical properties of valvular tissue probably influence immediate and late results of BMV. Resting atrioventricular compliance is closely related to upstream pressures; however, its impact on late outcome is not known.[127,128]

Thus, there are various approaches to refining the assessment of valve anatomy, combining more detailed scoring systems and evaluations of valvular mechanical properties. However, more complex analyses raise concerns regarding their applicability in current practice and their reproducibility. Moreover, it will be necessary to demonstrate their incremental predictive value on outcome, as compared with current validated multifactorial approaches.

## Potential Limitations, Future Directions

Despite technical refinements, there remain limitations in the feasibility or the relevance of certain echocardiographic analyses in MS.

Although planimetry is the reference measurement, it may not be feasible in patients with poor echocardiographic windows and/or in case of severe valve deformity, even with experienced operators. Other methods of measurement should be used, and their interpretation should take their own limitations into account.[129]

Doppler enables pulmonary artery pressure to be assessed in most patients. However, it is not possible to reliably assess capillary wedge pressure, and thus pulmonary vascular resistance, using ultrasonographic techniques. Pulmonary hypertension is passive in most patients, due to an increase in LA pressure with normal pulmonary vascular resistance. However, in certain patients, who frequently have long-standing disease, pulmonary vascular resistance is increased because of pulmonary vascular disease. The risk of surgery is higher in these patients, and BMV should be favored when feasible, because it provides functional improvement and progressive improvement in hemodynamics.[42,130] Estimation of pulmonary vascular resistance, using cardiac catheterization, is useful in patients who present with severe pulmonary hypertension seeming out of proportion with the degree of MS or pulmonary congestion as assessed by chest radiograph.

The limitations of anatomic scoring systems for the prediction of immediate and late results of BMV were reviewed earlier. Given the multiple determinants of the results of BMV, there is a low likelihood that any echocardiographic scoring system will ensure an optimal prediction of the results of BMV. A combined assessment using multislice computed tomography to quantitate valve calcification might be an interesting approach.

Future improvements in patient selection will probably come from the incorporation of improved anatomic evaluation using echocardiography and other imaging techniques, as well as other variables, such as stress hemodynamics indices, in multivariate models, rather than the optimization of a single scoring system.

## Alternative Approaches

Right and left heart cardiac catheterization enables valve area to be evaluated using the Gorlin formula. The Gorlin formula is sometimes considered as the reference method; however, this is mainly for historical reasons. Experimental as well as clinical data raise concerns regarding the validity of the Gorlin formula in cases of low output and immediately after BMV.[131,132] This explains why guidelines advise limiting invasive evaluation of the severity of MS to the rare situations where echocardiography is inconclusive or when there are discrepancies between different measurements and clinical evaluation.[23,24] Right heart catheterization is indicated in cases of suspected vascular pulmonary hypertension. In current practice, the main indication

**TABLE 21-10 Echocardiographic Score Proposed by Padial and Colleagues for the Prediction of Severe Mitral Regurgitation**

| *Grade* | *Anterior Leaflet* | *Posterior Leaflet* | *Commissural Calcification* | *Subvalvular Disease* |
|---|---|---|---|---|
| 1 | Leaflet near normal (4-5 mm) or with only a thick segment | Leaflet near normal (4-5 mm) or with only a thick segment | Fibrosis and/or calcium in only one commissure | Minimal thickening of chordal structures just below the valve |
| 2 | Leaflet fibrotic and/or calcified evenly; no thin area | Leaflet fibrotic and/or calcified evenly; no thin area | Both commissures mildly affected | Thickening of chordae extending up to one third of chordal length |
| 3 | Leaflet fibrotic and/or calcified with uneven distribution; thinner segments are mildly thickened (5-8 mm) | Leaflet fibrotic and/or calcified with uneven distribution; thinner segments are mildly thickened (5-8 mm) | Calcium in both commissures, one markedly affected | Thickening to the distal third of the chordae |
| 4 | Leaflet fibrotic and/or calcified with uneven distribution; thinner segments are near normal (4-5 mm) | Leaflet fibrotic and/or calcified with uneven distribution; thinner segments are near normal (4-5 mm) | Calcium in both commissures, both markedly affected | Extensive thickening and shortening of all chordae extending down the papillary muscle. |

The total score is the sum of the four items and ranges between 4 and 16.

From Padial LR, Freitas N, Sagie A, et al: Echocardiography can predict which patients will develop severe mitral regurgitation after percutaneous mitral valvulotomy. *J Am Coll Cardiol* 27:1225-1231, 1996.

for invasive investigations is the assessment of associated coronary disease using coronary angiography.[23,24] However, cardiac catheterization is still frequently performed, in particular as a systematic evaluation associated with coronary angiography, although this is not supported by guidelines.[1]

Magnetic resonance imaging and computed tomography are valid alternative noninvasive methods used to perform planimetry of the mitral valve. These methods could be useful when planimetry using 2D echocardiography is not feasible or not reliable.[133,134] Mitral gradient may also be assessed using velocity-encoded phase-contrast cine magnetic resonance imaging, but the reliability of this estimation is not certain.[135]

Experience with intracardiac echocardiography is limited (see Chapter 6). It is helpful to rule out LA thrombosis or to monitor transseptal puncture in difficult cases, thereby avoiding the use of TEE under general anaesthesia.[136,137] However, the high cost of the single-use device limits its use.

In conclusion, experience acquired with BMV for more than 20 years has confirmed its efficacy not only in young patients with favorable valve anatomy, but also in less optimal candidates. The prediction of the results of BMV is intrinsically multifactorial, which underscores the need for a complete assessment combining clinical and echocardiographic findings. Continuing evaluation of the results of BMV in large series or in selected subgroups is needed to improve decision making for the choice of the most appropriate procedure as well as its timing at different stages of the disease.

## KEY POINTS

- Planimetry using 2D echocardiography is the reference measurement for valve area and can be guided by 3D echocardiography.
- The use of cardiac catheterization should be limited to situations where noninvasive measurements are inconsistent or discordant with clinical findings.
- Patient selection should not overstress the assessment of valve anatomy, but it should take into account a number of clinical and echocardiographic variables, the predictive value of which has been validated in large series.
- BMV should be considered in patients who have MS with unfavorable anatomy, provided their other characteristics, in particular age, are favorable.
- Severe MR is the most frequent complication of BMV. It is difficult to predict in a given patient.
- The most frequent cause of late functional deterioration after BMV is mitral restenosis, the occurrence of which follows an approximately linear pattern.
- Exercise echocardiography is a promising method to refine indications for intervention in asymptomatic patients. However, there is still a need for validation through prognostic studies.
- BMV and surgery should not be considered as concurrent, but complementary techniques, which should be used at different times of the evolution of MS.

## REFERENCES


1. Iung B, Baron G, Tornos P, et al: Valvular heart disease in the community: a European experience. *Curr Probl Cardiol* 32:609-661, 2007.
2. Nkomo VT, Gardin JM, Skelton TN, et al: Burden of valvular heart diseases: a population-based study. *Lancet* 368:1005-1011, 2006.
3. Essop MR, Nkomo VT: Rheumatic and non-rheumatic valvular heart disease: epidemiology, management, and prevention in Africa. *Circulation* 112:3584-3591, 2005.
4. Carapetis JR: Rheumatic heart disease in Asia. *Circulation* 118:2748-2753, 2008.
5. Marijon E, Ou P, Celermajer DS, et al: Prevalence of rheumatic heart disease detected by echocardiographic screening. *N Engl J Med* 357:470-476, 2007.
6. Carroll JD, Feldman T: Percutaneous mitral balloon valvotomy and the new demographics of mitral stenosis. *JAMA* 270:1731-1736, 1993.
7. Marijon E, Iung B, Mocumbi AO, et al: What are the differences in presentation of candidates for percutaneous mitral commissurotomy across the world and do they influence the results of the procedure? *Arch Cardiovasc Dis* 101:611-617, 2008.
8. Inoue K, Owaki T, Nakamura T, Kitamura F, Miyamoto N: Clinical application of transvenous mitral commissurotomy by a new balloon catheter. *J Thorac Cardiovasc Surg* 87:394-402, 1984.
9. Baumgartner H, Hung J, Bermejo J, et al: Echocardiographic assessment of valve stenosis: EAE/ASE recommendations for clinical practice. *J Am Soc Echocardiogr* 22:1-23; quiz 101-102, 2009.
10. Messika-Zeitoun D, Iung B, Brochet E, et al: Evaluation of mitral stenosis in 2008. *Arch Cardiovasc Dis* 101:653-663, 2008.
11. Faletra F, Pezzano A Jr, Fusco R, et al: Measurement of mitral valve area in mitral stenosis: four echocardiographic methods compared with direct measurement of anatomic orifices. *J Am Coll Cardiol* 28:1190-1197, 1996.
12. Thomas JD, Wilkins GT, Choong CY, et al: Inaccuracy of mitral pressure half-time immediately after percutaneous mitral valvotomy. Dependence on transmitral gradient and left atrial and ventricular compliance. *Circulation* 78:980-993, 1988.
13. Nakatani S, Masuyama T, Kodama K, et al: Value and limitations of Doppler echocardiography in the quantification of stenotic mitral valve area: comparison of the pressure half-time and the continuity equation methods. *Circulation* 77:78-85, 1988.
14. Messika-Zeitoun D, Fung Yiu S, Cormier B, et al: Sequential assessment of mitral valve area during diastole using colour M-mode flow convergence analysis: new insights into mitral stenosis physiology. *Eur Heart J* 24:1244-1253, 2003.
15. Keenan NG, Cueff C, Cimadevilla C, et al: Usefulness of left atrial volume versus diameter to assess thromboembolic risk in mitral stenosis. *Am J Cardiol* 106:1152-1156, 2010.
16. Cormier B, Vahanian A, Michel PL, et al: [Evaluation by two-dimensional and Doppler echocardiography of the results of percutaneous mitral valvuloplasty]. *Arch Mal Coeur Vaiss* 82:185-191, 1989.
17. Zoghbi WA, Enriquez-Sarano M, Foster E, et al: Recommendations for evaluation of the severity of native valvular regurgitation with two-dimensional and Doppler echocardiography. *J Am Soc Echocardiogr* 16:777-802, 2003.
18. Lancellotti P, Moura L, Pierard LA, et al: European Association of Echocardiography recommendations for the assessment of valvular regurgitation. Part 2: mitral and tricuspid regurgitation (native valve disease). *Eur J Echocardiogr* 11:307-332, 2010.
19. Antunes MJ, Barlow JB: Management of tricuspid valve regurgitation. *Heart* 93:271-276, 2007.
20. Ton-Nu TT, Levine RA, Handschumacher MD, et al: Geometric determinants of functional tricuspid regurgitation: insights from 3-dimensional echocardiography. *Circulation* 114:143-149, 2006.
21. Black IW, Hopkins AP, Lee LC, Walsh WF: Left atrial spontaneous echo contrast: a clinical and echocardiographic analysis. *J Am Coll Cardiol* 18:398-404, 1991.
22. Chandrashekhar Y, Westaby S, Narula J: Mitral stenosis. *Lancet* 374:1271-1283, 2009.
23. Vahanian A, Baumgartner H, Bax J, et al: Guidelines on the management of valvular heart disease: The Task Force on the Management of Valvular Heart Disease of the European Society of Cardiology. *Eur Heart J* 28: 230-268, 2007.
24. Bonow RO, Carabello BA, Chatterjee K, et al: 2008 focused update incorporated into the ACC/AHA 2006 guidelines for the management of patients with valvular heart disease: a report of the American College of Cardiology/American Heart Association Task Force on Practice Guidelines (Writing Committee to Revise the 1998 Guidelines for the Management of Patients with Valvular Heart Disease): endorsed by the Society of Cardiovascular Anesthesiologists, Society for Cardiovascular Angiography and Interventions, and Society of

Thoracic Surgeons. *Circulation* 118:e523-e661, 2008.
25. Zamorano J, Cordeiro P, Sugeng L, et al: Real-time three-dimensional echocardiography for rheumatic mitral valve stenosis evaluation: an accurate and novel approach. *J Am Coll Cardiol* 43:2091-2096, 2004.
26. Messika-Zeitoun D, Brochet E, Holmin C, et al: Three-dimensional evaluation of the mitral valve area and commissural opening before and after percutaneous mitral commissurotomy in patients with mitral stenosis. *Eur Heart J* 28:72-79, 2007.
27. Sebag IA, Morgan JG, Handschumacher MD, et al: Usefulness of three-dimensionally guided assessment of mitral stenosis using matrix-array ultrasound. *Am J Cardiol* 96:1151-1156, 2005.
28. Messika-Zeitoun D, Meizels A, Cachier A, et al: Echocardiographic evaluation of the mitral valve area before and after percutaneous mitral commissurotomy: the pressure half-time method revisited. *J Am Soc Echocardiogr* 18:1409-1414, 2005.
29. Wilkins GT, Weyman AE, Abascal VM, et al: Percutaneous balloon dilatation of the mitral valve: an analysis of echocardiographic variables related to outcome and the mechanism of dilatation. *Br Heart J* 60:299-308, 1988.
30. Iung B, Cormier B, Ducimetiere P, et al: Immediate results of percutaneous mitral commissurotomy. A predictive model on a series of 1514 patients. *Circulation* 94:2124-2130, 1996.
31. Fatkin D, Roy P, Morgan JJ, Feneley MP: Percutaneous balloon mitral valvotomy with the Inoue single-balloon catheter: commissural morphology as a determinant of outcome. *J Am Coll Cardiol* 21:390-397, 1993.
32. Cannan CR, Nishimura RA, Reeder GS, et al: Echocardiographic assessment of commissural calcium: a simple predictor of outcome after percutaneous mitral balloon valvotomy. *J Am Coll Cardiol* 29:175-180, 1997.
33. Sutaria N, Shaw TR, Prendergast B, Northridge D: Transoesophageal echocardiographic assessment of mitral valve commissural morphology predicts outcome after balloon mitral valvotomy. *Heart* 92:52-57, 2006.
34. Rifaie O, Esmat I, Abdel-Rahman M, Nammas W: Can a novel echocardiographic score better predict outcome after percutaneous balloon mitral valvuloplasty? *Echocardiography* 26:119-127, 2009.
35. Turgeman Y, Atar S, Rosenfeld T: The subvalvular apparatus in rheumatic mitral stenosis: methods of assessment and therapeutic implications. *Chest* 124:1929-1936, 2003.
36. Pellikka PA, Nagueh SF, Elhendy AA, et al: American Society of Echocardiography recommendations for performance, interpretation, and application of stress echocardiography. *J Am Soc Echocardiogr* 20:1021-1041, 2007.
37. Sicari R, Nihoyannopoulos P, Evangelista A, et al: Stress echocardiography expert consensus statement: European Association of Echocardiography (EAE) (a registered branch of the ESC). *Eur J Echocardiogr* 9:415-437, 2008.
38. Vahanian A, Cormier B, Iung B: Mitral valvuloplasty. In Topol EJ, editor: *Textbook of interventional cardiology*, ed 5, Philadelphia, 2008, Saunders Elsevier, pp 879-893.
39. Iung B, Vahanian A: Rheumatic mitral valve disease. In Otto CM, Bonow RO, editors: *Valvular heart disease. A companion to Braunwald's heart disease*. Philadelphia, 2009, Saunders Elsevier, pp 221-243.
40. Chen CG, Wang YP, Guo BL, Lin YS: Reliability of the Doppler pressure half-time method for assessing effects of percutaneous mitral balloon valvuloplasty. *J Am Coll Cardiol* 13:1309-1313, 1989.
41. Messika-Zeitoun D, Blanc J, Iung B, et al: Impact of degree of commissural opening after percutaneous mitral commissurotomy on long-term outcome. *JACC Cardiovasc Imaging* 2:1-7, 2009.
42. Dev V, Shrivastava S: Time course of changes in pulmonary vascular resistance and the mechanism of regression of pulmonary arterial hypertension after balloon mitral valvuloplasty. *Am J Cardiol* 67:439-442, 1991.
43. Essop MR, Wisenbaugh T, Skoularigis J, et al: Mitral regurgitation following mitral balloon valvotomy. Differing mechanisms for severe versus mild-to-moderate lesions. *Circulation* 84:1669-1679, 1991.
44. Herrmann HC, Lima JA, Feldman T, et al: Mechanisms and outcome of severe mitral regurgitation after Inoue balloon valvuloplasty. North American Inoue Balloon Investigators. *J Am Coll Cardiol* 22:783-789, 1993.
45. Cequier A, Bonan R, Serra A, et al: Left-to-right atrial shunting after percutaneous mitral valvuloplasty. Incidence and long-term hemodynamic follow-up. *Circulation* 81:1190-1197, 1990.
46. Cormier B, Vahanian A, Iung B, et al: Influence of percutaneous mitral commissurotomy on left atrial spontaneous contrast of mitral stenosis. *Am J Cardiol* 71:842-847, 1993.
47. Hernandez R, Banuelos C, Alfonso F, et al: Long-term clinical and echocardiographic follow-up after percutaneous mitral valvuloplasty with the Inoue balloon. *Circulation* 99:1580-1586, 1999.
48. Chen CR, Cheng TO: Percutaneous balloon mitral valvuloplasty by the Inoue technique: a multicenter study of 4832 patients in China. *Am Heart J* 129:1197-1203, 1995.
49. Ben-Farhat M, Betbout F, Gamra H, et al: Predictors of long-term event-free survival and of freedom from restenosis after percutaneous balloon mitral commissurotomy. *Am Heart J* 142:1072-1079, 2001.
50. Arora R, Kalra GS, Singh S, et al: Percutaneous transvenous mitral commissurotomy: immediate and long-term follow-up results. *Catheter Cardiovasc Interv* 55:450-456, 2002.
51. Iung B, Nicoud-Houel A, Fondard O, et al: Temporal trends in percutaneous mitral commissurotomy over a 15-year period. *Eur Heart J* 25:701-707, 2004.
52. Complications and mortality of percutaneous balloon mitral commissurotomy. A report from the National Heart, Lung, and Blood Institute Balloon Valvuloplasty Registry. *Circulation* 85:2014-2024, 1992.
53. Tuzcu EM, Block PC, Palacios IF: Comparison of early versus late experience with percutaneous mitral balloon valvuloplasty. *J Am Coll Cardiol* 17:1121-1124, 1991.
54. Meneveau N, Schiele F, Seronde MF, et al: Predictors of event-free survival after percutaneous mitral commissurotomy. *Heart* 80:359-364, 1998.
55. Stefanadis CI, Stratos CG, Lambrou SG, et al: Retrograde nontransseptal balloon mitral valvuloplasty: immediate results and intermediate long-term outcome in 441 cases: a multicenter experience. *J Am Coll Cardiol* 32:1009-1016, 1998.
56. Palacios IF, Sanchez PL, Harrell LC, et al: Which patients benefit from percutaneous mitral balloon valvuloplasty? Prevalvuloplasty and postvalvuloplasty variables that predict long-term outcome. *Circulation* 105:1465-1471, 2002.
57. Neumayer U, Schmidt HK, Fassbender D, et al: Early (three-month) results of percutaneous mitral valvotomy with the Inoue balloon in 1,123 consecutive patients comparing various age groups. *Am J Cardiol* 90:190-193, 2002.
58. Fawzy ME, Shoukri M, Al Buraiki J, et al: Seventeen years' clinical and echocardiographic follow up of mitral balloon valvuloplasty in 520 patients, and predictors of long-term outcome. *J Heart Valve Dis* 16:454-460, 2007.
59. Jneid H, Cruz-Gonzalez I, Sanchez-Ledesma M, et al: Impact of pre- and postprocedural mitral regurgitation on outcomes after percutaneous mitral valvuloplasty for mitral stenosis. *Am J Cardiol* 104:1122-1127, 2009.
60. Bassand JP, Schiele F, Bernard Y, et al: The double-balloon and Inoue techniques in percutaneous mitral valvuloplasty: comparative results in a series of 232 cases. *J Am Coll Cardiol* 18:982-989, 1991.
61. Padial LR, Freitas N, Sagie A, et al: Echocardiography can predict which patients will develop severe mitral regurgitation after percutaneous mitral valvulotomy. *J Am Coll Cardiol* 27:1225-1231, 1996.
62. Padial LR, Abascal VM, Moreno PR, et al: Echocardiography can predict the development of severe mitral regurgitation after percutaneous mitral valvuloplasty by the Inoue technique. *Am J Cardiol* 83:1210-1213, 1999.
63. Hernandez R, Macaya C, Banuelos C, et al: Predictors, mechanisms and outcome of severe mitral regurgitation complicating percutaneous mitral valvotomy with the Inoue balloon. *Am J Cardiol* 70:1169-1174, 1992.
64. Bonhoeffer P, Esteves C, Casal U, et al: Percutaneous mitral valve dilatation with the Multi-Track System. *Catheter Cardiovasc Interv* 48:178-183, 1999.
65. Cribier A, Rath PC, Letac B: Percutaneous mitral valvotomy with a metal dilatator. *Lancet* 349:1667, 1997.
66. Kang DH, Park SW, Song JK, et al: Long-term clinical and echocardiographic outcome of percutaneous mitral valvuloplasty: randomized comparison of Inoue and double-balloon techniques. *J Am Coll Cardiol* 35: 169-175, 2000.
67. Cribier A, Eltchaninoff H, Koning R, et al: Percutaneous mechanical mitral commissurotomy with a newly designed metallic valvulotome: immediate results of the initial experience in 153 patients. *Circulation* 99:793-799, 1999.
68. Eltchaninoff H, Koning R, Derumeaux G, Cribier A: [Percutaneous mitral commissurotomy by metallic dilator. Multicenter experience with 500 patients]. *Arch Mal Coeur Vaiss* 93:685-692, 2000.
69. Multicenter experience with balloon mitral commissurotomy. NHLBI Balloon Valvuloplasty Registry Report on immediate and 30-day follow-up results. The National Heart, Lung, and Blood Institute Balloon Valvuloplasty Registry Participants. *Circulation* 85, 448-461, 1992.
70. Herrmann HC, Ramaswamy K, Isner JM, et al: Factors influencing immediate results, complications, and short-term follow-up status after Inoue balloon mitral valvotomy: a North American multicenter study. *Am Heart J* 124: 160-166, 1992.

71. Cruz-Gonzalez I, Sanchez-Ledesma M, Sanchez PL, et al: Predicting success and long-term outcomes of percutaneous mitral valvuloplasty: a multifactorial score. *Am J Med* 122(581):e511-589, 2009.
72. Wang A, Krasuski RA, Warner JJ, et al: Serial echocardiographic evaluation of restenosis after successful percutaneous mitral commissurotomy. *J Am Coll Cardiol* 39:328-334, 2002.
73. Heger JJ, Wann LS, Weyman AE, et al: Long-term changes in mitral valve area after successful mitral commissurotomy. *Circulation* 59:443-448, 1979.
74. Hickey MS, Blackstone EH, Kirklin JW, Dean LS: Outcome probabilities and life history after surgical mitral commissurotomy: implications for balloon commissurotomy. *J Am Coll Cardiol* 17:29-42, 1991.
75. Iung B, Garbarz E, Michaud P, et al: Late results of percutaneous mitral commissurotomy in a series of 1024 patients. Analysis of late clinical deterioration: frequency, anatomic findings, and predictive factors. *Circulation* 99:3272-3278, 1999.
76. Cohen DJ, Kuntz RE, Gordon SP, et al: Predictors of long-term outcome after percutaneous balloon mitral valvuloplasty. *N Engl J Med* 327:1329-1335, 1992.
77. Dean LS, Mickel M, Bonan R, et al: Four-year follow-up of patients undergoing percutaneous balloon mitral commissurotomy. A report from the National Heart, Lung, and Blood Institute Balloon Valvuloplasty Registry. *J Am Coll Cardiol* 28:1452-1457, 1996.
78. Orrange SE, Kawanishi DT, Lopez BM, et al: Actuarial outcome after catheter balloon commissurotomy in patients with mitral stenosis. *Circulation* 95:382-389, 1997.
79. Song JK, Song JM, Kang DH, et al: Restenosis and adverse clinical events after successful percutaneous mitral valvuloplasty: immediate post-procedural mitral valve area as an important prognostic factor. *Eur Heart J* 30:1254-1262, 2009.
80. Davidson CJ, Bashore TM, Mickel M, Davis K: Balloon mitral commissurotomy after previous surgical commissurotomy. The National Heart, Lung, and Blood Institute Balloon Valvuloplasty Registry participants. *Circulation* 86:91-99, 1992.
81. Iung B, Garbarz E, Michaud P, et al: Percutaneous mitral commissurotomy for restenosis after surgical commissurotomy: late efficacy and implications for patient selection. *J Am Coll Cardiol* 35:1295-1302, 2000.
82. Fawzy ME, Hassan W, Shoukri M, et al: Immediate and long-term results of mitral balloon valvotomy for restenosis following previous surgical or balloon mitral commissurotomy. *Am J Cardiol* 96:971-975, 2005.
83. Iung B, Garbarz E, Michaud P, et al: Immediate and mid-term results of repeat percutaneous mitral commissurotomy for restenosis following earlier percutaneous mitral commissurotomy. *Eur Heart J* 21:1683-1689, 2000.
84. Pathan AZ, Mahdi NA, Leon MN, et al: Is redo percutaneous mitral balloon valvuloplasty (PMV) indicated in patients with post-PMV mitral restenosis? *J Am Coll Cardiol* 34:49-54, 1999.
85. Turgeman Y, Atar S, Suleiman K, et al: Feasibility, safety, and morphologic predictors of outcome of repeat percutaneous balloon mitral commissurotomy. *Am J Cardiol* 95:989-991, 2005.
86. Kim JB, Ha JW, Kim JS, et al: Comparison of long-term outcome after mitral valve replacement or repeated balloon mitral valvotomy in patients with restenosis after previous balloon valvotomy. *Am J Cardiol* 99:1571-1574, 2007.
87. Iung B, Cormier B, Farah B, et al: Percutaneous mitral commissurotomy in the elderly. *Eur Heart J* 16:1092-1099, 1995.
88. Sutaria N, Elder AT, Shaw TR: Long term outcome of percutaneous mitral balloon valvotomy in patients aged 70 and over. *Heart* 83:433-438, 2000.
89. Shaw TR, Sutaria N, Prendergast B: Clinical and haemodynamic profiles of young, middle aged, and elderly patients with mitral stenosis undergoing mitral balloon valvotomy. *Heart* 89:1430-1436, 2003.
90. Pressman GS, Agarwal A, Braitman LE, Muddassir SM: Mitral annular calcium causing mitral stenosis. *Am J Cardiol* 105:389-391, 2010.
91. Gamra H, Betbout F, Ben Hamda K, et al: Balloon mitral commissurotomy in juvenile rheumatic mitral stenosis: a ten-year clinical and echocardiographic actuarial results. *Eur Heart J* 24:1349-1356, 2003.
92. Fawzy ME, Stefadouros MA, Hegazy H, et al: Long term clinical and echocardiographic results of mitral balloon valvotomy in children and adolescents. *Heart* 91:743-748, 2005.
93. Kothari SS, Ramakrishnan S, Kumar CK, et al: Intermediate-term results of percutaneous transvenous mitral commissurotomy in children less than 12 years of age. *Catheter Cardiovasc Interv* 64:487-490, 2005.
94. Hameed A, Karaalp IS, Tummala PP, et al: The effect of valvular heart disease on maternal and fetal outcome of pregnancy. *J Am Coll Cardiol* 37:893-899, 2001.
95. Iung B, Cormier B, Elias J, et al: Usefulness of percutaneous balloon commissurotomy for mitral stenosis during pregnancy. *Am J Cardiol* 73:398-400, 1994.
96. Oakley C, Child A, Iung B, et al: Expert consensus document on management of cardiovascular diseases during pregnancy. *Eur Heart J* 24:761-781, 2003.
97. Chen WJ, Chen MF, Liau CS, et al: Safety of percutaneous transvenous balloon mitral commissurotomy in patients with mitral stenosis and thrombus in the left atrial appendage. *Am J Cardiol* 70:117-119, 1992.
98. Silaruks S, Thinkhamrop B, Kiatchoosakun S, et al: Resolution of left atrial thrombus after 6 months of anticoagulation in candidates for percutaneous transvenous mitral commissurotomy. *Ann Intern Med* 140:101-105, 2004.
99. Vaturi M, Porter A, Adler Y, et al: The natural history of aortic valve disease after mitral valve surgery. *J Am Coll Cardiol* 33:2003-2008, 1999.
100. Song H, Kang DH, Kim JH, et al: Percutaneous mitral valvuloplasty versus surgical treatment in mitral stenosis with severe tricuspid regurgitation. *Circulation* 116:I246-I250, 2007.
101. Reyes VP, Raju BS, Wynne J, et al: Percutaneous balloon valvuloplasty compared with open surgical commissurotomy for mitral stenosis. *N Engl J Med* 331:961-967, 1994.
102. Turi ZG, Reyes VP, Raju BS, et al: Percutaneous balloon versus surgical closed commissurotomy for mitral stenosis. A prospective, randomized trial. *Circulation* 83:1179-1185, 1991.
103. Ben Farhat M, Ayari M, Maatouk F, et al: Percutaneous balloon versus surgical closed and open mitral commissurotomy: seven-year follow-up results of a randomized trial. *Circulation* 97:245-250, 1998.
104. Rifaie O, Abdel-Dayem MK, Ramzy A, et al: Percutaneous mitral valvotomy versus closed surgical commissurotomy. Up to 15 years of follow-up of a prospective randomized study. *J Cardiol* 53:28-34, 2009.
105. Song JK, Kim MJ, Yun SC, et al: Long-term outcomes of percutaneous mitral balloon valvuloplasty versus open cardiac surgery. *J Thorac Cardiovasc Surg* 139:103-110, 2010.
106. Feldman T, Carroll JD, Isner JM, et al: Effect of valve deformity on results and mitral regurgitation after Inoue balloon commissurotomy. *Circulation* 85:180-187, 1992.
107. Tuzcu EM, Block PC, Griffin B, et al: Percutaneous mitral balloon valvotomy in patients with calcific mitral stenosis: immediate and long-term outcome. *J Am Coll Cardiol* 23:1604-1609, 1994.
108. Hildick-Smith DJ, Taylor GJ, Shapiro LM: Inoue balloon mitral valvuloplasty: long-term clinical and echocardiographic follow-up of a predominantly unfavourable population. *Eur Heart J* 21:1690-1697, 2000.
109. Iung B, Garbarz E, Doutrelant L, et al: Late results of percutaneous mitral commissurotomy for calcific mitral stenosis. *Am J Cardiol* 85:1308-1314, 2000.
110. Vahanian A, Palacios IF: Percutaneous approaches to valvular disease. *Circulation* 109:1572-1579, 2004.
111. Gordon SP, Douglas PS, Come PC, Manning WJ: Two-dimensional and Doppler echocardiographic determinants of the natural history of mitral valve narrowing in patients with rheumatic mitral stenosis: implications for follow-up. *J Am Coll Cardiol* 19:968-973, 1992.
112. Stefanadis C, Dernellis J, Stratos C, et al: Effects of balloon mitral valvuloplasty on left atrial function in mitral stenosis as assessed by pressure-area relation. *J Am Coll Cardiol* 32:159-168, 1998.
113. Porte JM, Cormier B, Iung B, et al: Early assessment by transesophageal echocardiography of left atrial appendage function after percutaneous mitral commissurotomy. *Am J Cardiol* 77:72-76, 1996.
114. Peverill RE, Harper RW, Gelman J, et al: Determinants of increased regional left atrial coagulation activity in patients with mitral stenosis. *Circulation* 94:331-339, 1996.
115. Chiang CW, Lo SK, Ko YS, et al: Predictors of systemic embolism in patients with mitral stenosis. A prospective study. *Ann Intern Med* 128:885-889, 1998.
116. Liu TJ, Lai HC, Lee WL, et al: Percutaneous balloon commissurotomy reduces incidence of ischemic cerebral stroke in patients with symptomatic rheumatic mitral stenosis. *Int J Cardiol* 123:189-190, 2008.
117. Picano E, Pibarot P, Lancellotti P, et al: The emerging role of exercise testing and stress echocardiography in valvular heart disease. *J Am Coll Cardiol* 54:2251-2260, 2009.
118. Mahjoub H, Levy F, Cassol M, et al: Effects of age on pulmonary artery systolic pressure at rest and during exercise in normal adults. *Eur J Echocardiogr* 10:635-640, 2009.
119. Voelker W, Berner A, Regele B, et al: Effect of exercise on valvular resistance in patients with mitral stenosis. *J Am Coll Cardiol* 22:777-782, 1993.
120. Tunick PA, Freedberg RS, Gargiulo A, Kronzon I: Exercise Doppler echocardiography as an aid to clinical decision making in mitral valve disease. *J Am Soc Echocardiogr* 5:225-230, 1992.

121. Schwammenthal E, Vered Z, Agranat O, et al: Impact of atrioventricular compliance on pulmonary artery pressure in mitral stenosis: an exercise echocardiographic study. *Circulation* 102:2378-2384, 2000.
122. Dahan M, Paillole C, Martin D, Gourgon R: Determinants of stroke volume response to exercise in patients with mitral stenosis: a Doppler echocardiographic study. *J Am Coll Cardiol* 21:384-389, 1993.
123. Brochet E, Detaint D, Fondard O, et al: Early hemodynamic changes versus peak values: what is more useful to predict occurrence of dyspnea during stress echocardiography in patients with asymptomatic mitral stenosis? *J Am Soc Echocardiogr* 24:392-398, 2011.
124. Hecker SL, Zabalgoitia M, Ashline P, et al: Comparison of exercise and dobutamine stress echocardiography in assessing mitral stenosis. *Am J Cardiol* 80:1374-1377, 1997.
125. Reis G, Motta MS, Barbosa MM, et al: Dobutamine stress echocardiography for noninvasive assessment and risk stratification of patients with rheumatic mitral stenosis. *J Am Coll Cardiol* 43:393-401, 2004.
126. Okay T, Deligonul U, Sancaktar O, Kozan O: Contribution of mitral valve reserve capacity to sustained symptomatic improvement after balloon valvulotomy in mitral stenosis: implications for restenosis. *J Am Coll Cardiol* 22:1691-1696, 1993.
127. Li M, Dery JP, Dumesnil JG, et al: Usefulness of measuring net atrioventricular compliance by Doppler echocardiography in patients with mitral stenosis. *Am J Cardiol* 96:432-435, 2005.
128. Izgi C, Ozdemir N, Cevik C, et al: Mitral valve resistance as a determinant of resting and stress pulmonary artery pressure in patients with mitral stenosis: a dobutamine stress study. *J Am Soc Echocardiogr* 20:1160-1166, 2007.
129. Otto CM, Davis KB, Holmes DR Jr, et al: Methodologic issues in clinical evaluation of stenosis severity in adults undergoing aortic or mitral balloon valvuloplasty. The NHLBI Balloon Valvuloplasty Registry. *Am J Cardiol* 69:1607-1616, 1992.
130. Krishnamoorthy KM, Dash PK, Radhakrishnan S, Shrivastava S: Response of different grades of pulmonary artery hypertension to balloon mitral valvuloplasty. *Am J Cardiol* 90:1170-1173, 2002.
131. Segal J, Lerner DJ, Miller DC, et al: When should Doppler-determined valve area be better than the Gorlin formula? Variation in hydraulic constants in low flow states. *J Am Coll Cardiol* 9:1294-1305, 1987.
132. Petrossian GA, Tuzcu EM, Ziskind AA, et al: Atrial septal occlusion improves the accuracy of mitral valve area determination following percutaneous mitral balloon valvotomy. *Cathet Cardiovasc Diagn* 22:21-24, 1991.
133. Messika-Zeitoun D, Serfaty JM, Laissy JP, et al: Assessment of the mitral valve area in patients with mitral stenosis by multislice computed tomography. *J Am Coll Cardiol* 48:411-413, 2006.
134. Lanjewar C, Ephrem B, Mishra N, et al: Planimetry of mitral valve stenosis in rheumatic heart disease by magnetic resonance imaging. *J Heart Valve Dis* 19:357-363, 2010.
135. Morris MF, Maleszewski JJ, Suri RM, et al: CT and MR imaging of the mitral valve: radiologic-pathologic correlation. *Radiographics* 30:1603-1620, 2010.
136. Cafri C, de la Guardia B, Barasch E, et al: Transseptal puncture guided by intracardiac echocardiography during percutaneous transvenous mitral commissurotomy in patients with distorted anatomy of the fossa ovalis. *Catheter Cardiovasc Interv* 50:463-467, 2000.
137. Green NE, Hansgen AR, Carroll JD: Initial clinical experience with intracardiac echocardiography in guiding balloon mitral valvuloplasty: technique, safety, utility, and limitations. *Catheter Cardiovasc Interv* 63:385-394, 2004.

22

# Clinical Decision Making in Patients with Infective Endocarditis: The Role of Echocardiography

ZAINAB SAMAD, MD | ANDREW WANG, MD

Background
Basic Principles and Echocardiographic Approach
Technical Details, Quantitation and Data Analysis
Clinical Utility and Outcome Data
Utility in Diagnosis
Utility in Management
Utility in Follow-up
Research Applications
Potential Limitations and Future Directions
Alternative Approaches

## Background

Infective endocarditis (IE), a noncontagious infection of the endocardium and heart valves, has an incidence ranging from 2.6 to 11.6 per million[1,2] and a high in-hospital mortality rate of approximately 20% despite medical and surgical advances. The contemporary epidemiology of IE has changed significantly compared to earlier eras, and these changes have an important influence on the evaluation and outcome of this condition. In the large, prospective, multinational International Collaboration on Endocarditis (ICE) registry, the mean age of diagnosis of definite IE is the sixth decade, with approximately 2:1 male predominance and frequently occurring in the presence of comorbid conditions such as kidney disease and diabetes mellitus.[3] The major predisposition to IE is underlying degenerative valvular disease (particularly mitral valve disease), present in approximately 30% of cases, but a very low prevalence of underlying rheumatic heart disease.[3] The microbiology of the condition has shifted toward more virulent organisms, particularly *Staphylococcus aureus* as the most common cause, reflecting the growing influence of health care–associated infection as a cause of bacteremia.

The diagnosis and management of this condition has greatly improved with the advent of echocardiography. The first use of echocardiography in the diagnosis of IE was described in 1973 by Dillon and colleagues,[4] who applied M-mode echo to visualize evidence of vegetations. The high-frequency oscillations of vegetative lesions and/or destruction of aortic or mitral leaflet integrity could be documented using this technique (Fig. 22-1). M-mode, however, did not allow estimation of lesion size, morphology, and localization of specific leaflet involvement, which was provided by real-time, two-dimensional (2D) echocardiography first described by Gilbert and colleagues.[5] Over time, with the widespread use of 2D echocardiography and the improved spatial resolution offered by transesophageal echocardiographic (TEE) approaches,[6] echocardiography has become the diagnostic modality of choice in all cases of suspected IE. Echocardiography not only provides noninvasive evidence of endocardial infection but also offers important hemodynamic information regarding the presence and severity of valvular regurgitation and other structural complications, findings key to the management decision-making process in these patients. For these reasons, echocardiography is considered essential in all cases suspected of IE.[7]

## Basic Principles and Echocardiographic Approach

Clinical characteristics may identify the host at risk for IE and guide the use of echocardiography for diagnostic confirmation. IE is associated with fever in more than 90% of cases, and a similar percentage will have positive blood cultures for a microorganism associated with this condition.[3] Most patients present with symptom duration of less than 1 month.[3] Approximately half of patients will have evidence of a new or changing heart murmur reflecting valvular regurgitation or other endocardial damage, but a very small percentage will have peripheral manifestations of classical, subacute IE (Osler nodes, Janeway lesions, splinter hemorrhages, Roth spots).[3]

Historically, the association between infective lesions on the endocardium and the clinical manifestations of IE has been recognized for over a century. However, the clinical manifestations of the disease remained nonspecific and challenged accurate clinical diagnosis of the disease antemortem.[8] In 1977, Pelletier and Petersdorf[9] proposed case definitions for IE that relied mainly on clinical characteristics and, specifically, on the demonstration of continuous bacteremia. Although a first step in standardization of the diagnosis of IE, these criteria were highly specific but lacked sensitivity. In 1981, Von Reyn and colleagues[10] expanded on these clinical criteria and offered levels of diagnostic certainty (rejected, possible, probable, and definite) for suspected IE. These modifications improved sensitivity and specificity, but did not incorporate evidence of endocardial involvement by the relatively novel application of echocardiography at the time. Subsequently, in 1994, the Duke Criteria proposed by Durack and colleagues[11] incorporated visualization of endocardial involvement by echocardiography

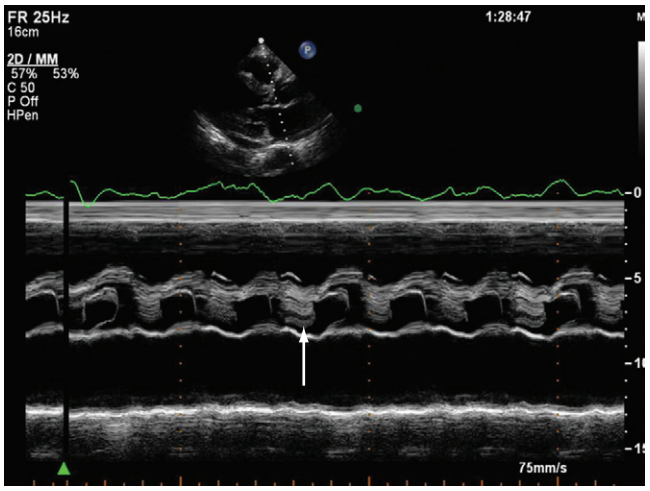



**Figure 22-1 M-mode echocardiogram recorded in a patient with aortic valve endocarditis.** Note mass of shaggy echoes (vegetation) in diastole.

with microbiologic and clinical criteria for the first time. Indeed, evidence of endocardial involvement, including new valvular regurgitation, intracardiac vegetation, paraannular abscess, or new dehiscence of prosthetic valve, became one of the two major diagnostic criteria for IE by the Duke case definition, along with microbiologic criteria.

Several comparative studies of the Von Reyn and Duke Criteria in various cohorts have subsequently established the superior sensitivity of the Duke criteria compared to earlier case definitions.[12-19] The negative predictive value of these criteria was more than 92% with a high sensitivity (100%) and specificity (88%).[20,21] Recent modifications of the Duke criteria (Box 22-1) have added greater specificity to the schema.[22]

## Technical Details, Quantitation, Data Analysis

Echocardiographic features of IE include vegetations, abscess, aneurysm, fistula, leaflet perforation, and valvular dehiscence (Table 22-1).[23] *Vegetations* occur at a region of endocardial denudation, often resulting from preexisting valvular disease (Figs. 22-2, 22-3, and 22-4). Disruption of the endocardial

**Box 22-1**

### THE MODIFIED DUKE CRITERIA AND CASE DEFINITIONS OF INFECTIVE ENDOCARDITIS

#### Modified Duke Criteria

**Major Criteria**

***Blood Culture Positive for Infective Endocarditis (IE)***

Typical microbes consistent with IE from 2 separate blood cultures: viridans streptococci, *Streptococcus bovis*, HACEK group, *Staphylococcus aureus*; community-acquired enterococci in absence of another focus; or

Microorganisms consistent with IE from persistently positive blood cultures defined as follows: at least 2 blood cultures drawn >12 hr apart or all of 3 or majority of >4 separate blood cultures

Single positive blood culture for *Coxiella burnetii* or antiphase IgG antibody titer >1:800

***Evidence of Endocardial Involvement***

Echocardiography positive for IE defined as follows:

Oscillating intracardiac mass on valve or supporting structure

Abscess

New partial dehiscence of prosthetic valve

New valvular regurgitation

***Minor Criteria***

Predisposition; predisposing heart condition or injection drug use

Fever, temperature >38°C

Vascular phenomena, major arterial emboli, septic pulmonary infarcts, mycotic aneurysm, intracranial hemorrhage, conjunctival hemorrhage, and Janeway lesions

Immunologic phenomena: glomerulonephritis, Osler's nodes, Roth's spots, rheumatoid factor

Microbiologic evidence: positive blood cultures but does not meet a major criterion as noted above, or serologic evidence of active infection with organism consistent with causing IE

#### Case Definitions

**Definitive Infective Endocarditis**

***Pathologic Criteria***

1. Microorganisms demonstrated by culture or histologic examination of a vegetation, a vegetation that has embolized or an intracardiac abscess specimen; or
2. Pathologic lesions; vegetation or intracardiac abscess confirmed by histologic examination showing active endocarditis

***Clinical Criteria***

1. 2 major criteria; or
2. 1 major and 3 minor criteria; or
3. 5 minor criteria

***Possible Infective Endocarditis***

1. 1 major criterion and 1 minor criterion; or
2. 3 minor criteria

***Rejected***

1. Firm alternate diagnosis explaining evidence of infective endocarditis; or
2. Resolution of infective endocarditis syndrome with antibiotic therapy for ≤4 days; or
3. No pathologic evidence of infective endocarditis at surgery or autopsy, with antibiotic therapy for <4 days; or
4. Does not meet criteria for possible infective endocarditis, as above

Adapted from Li JS, Sexton DJ, Mick N, et al: Proposed modifications to the Duke criteria for the diagnosis of infective endocarditis. *Clin Infect Dis* 30:633-638, 2000.

**TABLE 22-1 Pathologic Features of Infective Endocarditis: Echocardiographic Appearance and Clinical Significance**

| *Echocardiographic Finding* | *Pathology* | *Echocardiographic Appearance and Measurements* | *Pitfalls* | *Clinical Significance* |
|---|---|---|---|---|
| Vegetation | Collection of microorganisms embedded with platelets, fibrin and other inflammatory cellular material adherent to an endothelial surface within the heart | Irregularly shaped, discrete echogenic mass<br>Adherent to, yet distinct from cardiac surface<br>Oscillation of mass supportive, not mandatory<br>Measure maximum size | False (−):<br>Small size; sessile, not oscillating; degenerated valve; inappropriate gain setting<br>False (+):<br>Post-surgical changes; valve calcification; Libman-Sacks; Lambl's excrescence; thrombus; tumor | Size and location associated with embolic risk<br>Large size may suggest lower likelihood of cure with antibiotics alone |
| Abscess | A cavity with purulent exudates formed by liquefactive necrosis | Thickened area or mass within the myocardium or annular region<br>Appearance is nonhomogeneous with both echogenic and echolucent characteristics | False (−):<br>Absence of flow; early in abscess formation; gain settings; posterior mitral valve annulus when calcification present<br>False (+):<br>Postsurgical change after valve replacement, including paravalvular regurgitation; gain settings | May be associated with new conduction abnormality<br>Indication for surgery |
| Fistula | Abnormal connection between two distinct cardiac blood spaces through a nonanatomic channel | Left-to-right shunt visible on color Doppler imaging<br>Recorded loops should contain sweeps of the region of interest<br>Continuous-wave Doppler to show high-velocity jet across defect | False (−):<br>Small defect; masking by valvular regurgitation or flow turbulence<br>False (+):<br>Valvular regurgitation or other turbulent flow; no confirmation by high Doppler jet velocity across defect | Heart failure due to left-to-right shunting<br>Indication for surgery |
| Leaflet perforation | Defect in body of a valve leaflet with evidence of flow through defect | Color Doppler to document regurgitant flow through perforation<br>Multiple views to differentiate perforation from leaflet regurgitation<br>3DE may help locate precise location preoperatively<br>Quantify regurgitation | False (−):<br>High gain setting; small defect; regurgitant jet masks flow through perforation<br>False (+):<br>Echo dropout; commissure or cleft | Increases severity of regurgitation and possibility of heart failure |
| Prosthetic valve dehiscence | Rocking motion of prosthetic valve with excursion >15° in at least one direction | Regurgitant jets visible by color Doppler imaging<br>Quantify regurgitation | False (−):<br>No paravalvular regurgitation visualized<br>False (+):<br>Normal annulus motion during cardiac cycle | Paravalvular regurgitation may result in heart failure, hemolysis<br>Urgent indication for surgery |
| Cardiac implantable electronic device infection | Mobile mass seen on intracardiac device (lead) in setting of fever, bacteremia, and/or embolic events | Vegetation seen adherent to device lead<br>Careful search for vegetations throughout intracardiac course of device<br>Evaluate for concomitant valve infection | False (−):<br>Vegetation on extracardiac region of device<br>False (+):<br>Thrombus | Generally treated with device extraction and antibiotic therapy |

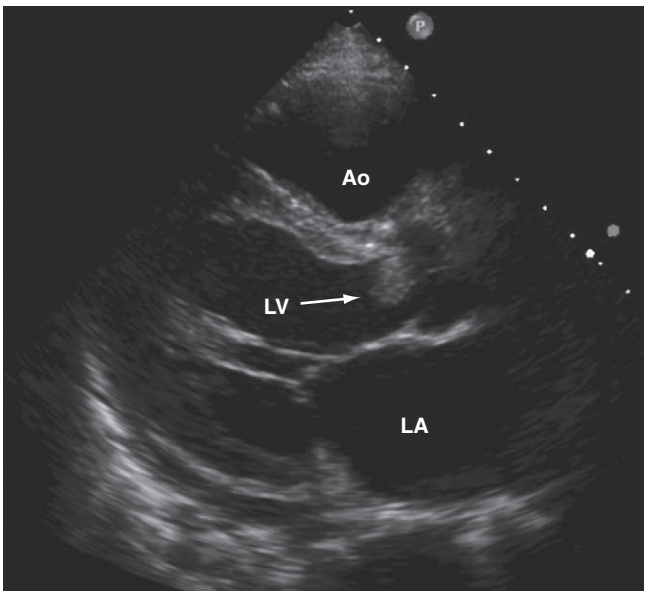



**Figure 22-2 2D TTE parasternal long-axis view recorded in a patient with aortic valve endocarditis.** *Arrow* points to a heterogeneous irregularly shaped mass attached to aortic valve leaflet prolapsing into the LV outflow tract. *Ao*, Aorta.

surface results in platelet adhesion and fibrin deposition, to which microorganisms adhere during transient bacteremia to form infected vegetation. Vegetations are visualized in nearly 90% of patients with definite IE.[3] By echocardiography, vegetations appear as irregularly shaped, discrete, oscillating, echogenic masses that are adherent to valves, chordate, or other endocardial surfaces in the path of turbulent jets passing through regurgitant valves or septal defects. They are typically located on the low-pressure side of high-velocity jets; hence, in cases of regurgitation, they are located on the atrial aspect of the mitral and tricuspid valves and on the ventricular aspect of the aortic and pulmonic valves. They often display the same echogenicity as midmyocardial structures and may be heterogenous with echodense or echolucent areas. Vegetations may also be found on noncardiac structures such as intracardiac devices. In the presence of vegetation, *perforation* of a valve leaflet may be visualized as a defect in the body of a valve leaflet with evidence of flow through the defect (Fig. 22-5).

Machine settings such as frame rate, sector arc size, gray scale, and focal zones must be optimized, and a careful examination including nonstandard views should be conducted to exclude the presence of vegetations. Increased gain settings and improper focal zones can make vegetations appear larger than actual size. On the other hand, color flow imaging may change pulse

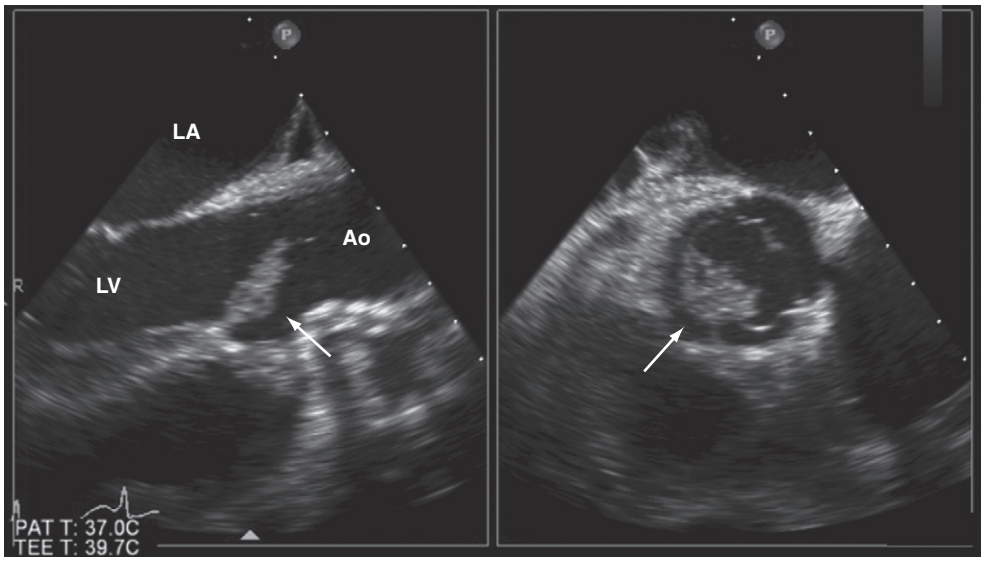



**Figure 22-3 TEE views of an aortic valve vegetation.** The 2D images show a heterogeneous mass, in the long-axis (*left*) and short-axis (*right*) views. Attachment of vegetation to the right coronary cusp is evident (*arrows*). *Ao*, Aorta.

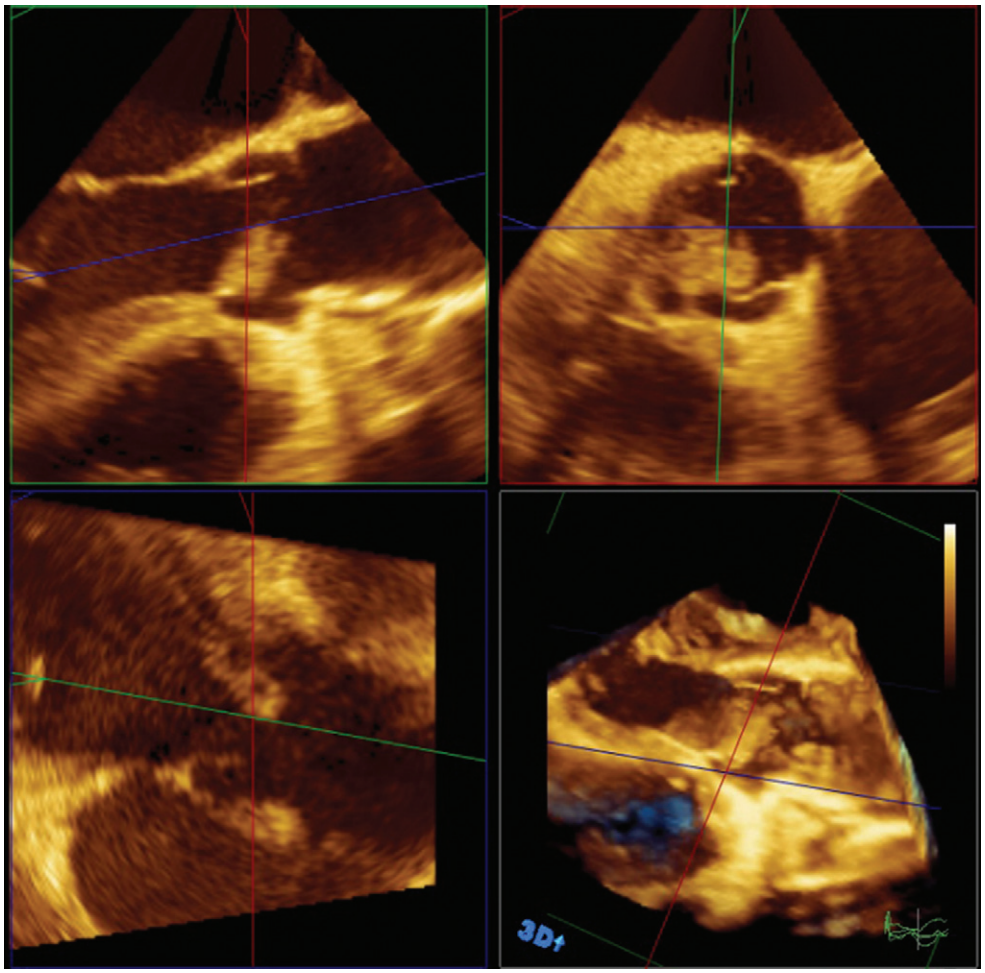



**Figure 22-4 3D TEE full-volume data set cropped to reveal aortic valve vegetation.** Anatomic relationships are displayed precisely.

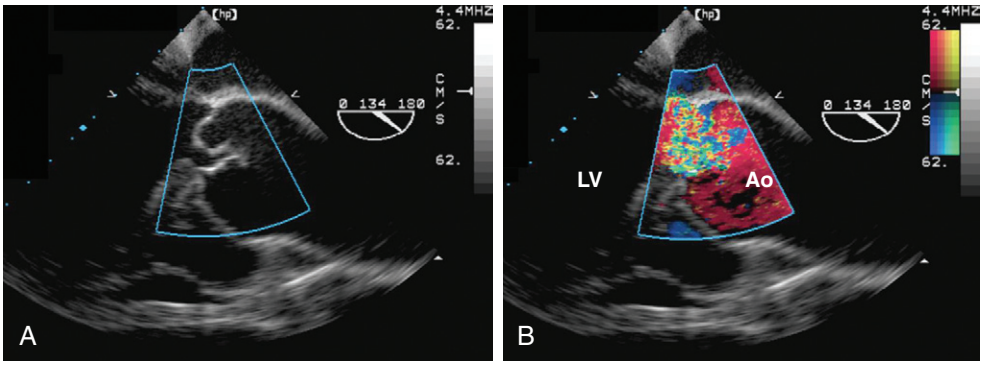



**Figure 22-5 Leaflet perforation and aortic regurgitation owing to endocarditis. A,** 2D TEE long-axis view of the aortic valve demonstrate loss of structural integrity and leaflet perforation. **B,** 2D TEE long-axis view of aortic valve with color Doppler demonstrating severe aortic regurgitation. *Ao,* Aorta.

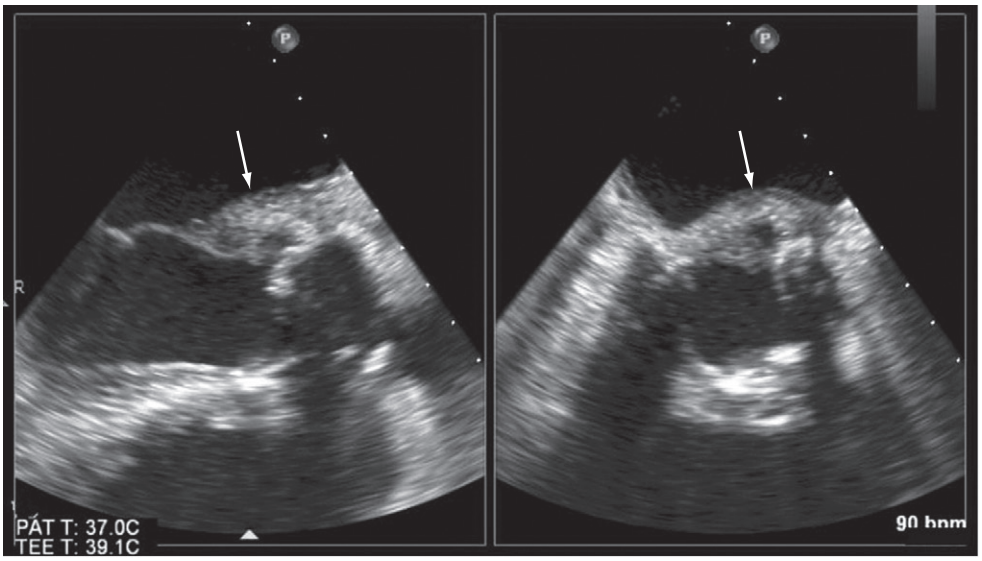



**Figure 22-6 Aortic root abscess owing to endocarditis.** 2D TEE orthogonal views of the aortic valve demonstrating thickening and heterogeneous echodensity of the aortic annulus (*arrows*). This is most prominent at the junction of the anterior mitral valve leaflet and aortic valve.

repetition frequency and impair visualization of the vegetation. The size of the vegetations should be measured within the resolution characteristics of the transducer so that machine settings can be duplicated for future comparative studies, if clinically indicated.

Vegetations may be present in patients with negative blood cultures, which is termed *culture-negative endocarditis* and represents approximately 10% of definite IE. Culture-negative endocarditis results from prior antibiotic therapy, fastidious organisms such as HACEK species, or unusual organisms such as *Coxiella burnetii* (Q fever) or *Bartonella quintana*. Vegetations also need to be differentiated from other masses with similar appearance on echocardiography such as Libman-Sacks (noninfective) endocarditis, degenerative change, Lambl's excrescences, thrombus, or tumors. Because there are no echocardiographic features that can reliably differentiate infective from noninfective endocardial lesions, the key to a proper diagnosis lies in integrating imaging data and clinical information. Visualization of distinct vegetation may be impaired by severe, underlying valvular degeneration, particularly prominent calcification of valve leaflets.

Tissue destruction in IE may result in other structural complications that can be identified on echocardiography. *Paravalvular abscess* complicated 30% to 40% of cases of IE in earlier reports[6] but were found in 14% of patients with definite IE in a larger, contemporary study[3] (Fig. 22-6). An abscess is a result of invasive infection that spreads generally along contiguous tissue planes, particularly with aortic valve infection. Development of a new atrioventricular conduction abnormality, worsening clinical picture, persistent bacteremia/fever in the setting of aortic valve endocarditis, injection drug use, infection with an invasive pathogen (staphylococcal), or prosthetic valves should prompt a search for an aortic root abscess.[24]

TEE is the diagnostic test of choice when an abscess is suspected clinically. An abscess is diagnosed by TEE as the visualization of a "thickened area" or "mass with a heterogeneous echogenic or echolucent appearance" within the myocardium or annular region.[6] On color Doppler imaging, flow within the area is supportive of the diagnosis. Abscesses complicating native valve IE most commonly involve the aortic valve annulus at the junction of aortic root and anterior mitral valve leaflet. Hence, they may extend into the adjacent interventricular septum, the right ventricular outflow tract, the interatrial septum, and the anterior mitral valve leaflet. Location of the abscess, particularly in the posterior annulus of the mitral valve when calcification is present, may limit its visualization by echocardiography.[25] In the ICE cohort, 22% of cases of definite aortic valve IE were complicated by a paravalvular abscess.[24]

These patients were more likely to have prosthetic valves and coagulase-negative staphylococcal infection. Surgical experience suggests an even higher prevalence of abscess formation not visualized by TEE.[25] New paravalvular regurgitation around a prosthetic valve may also suggest the presence of an abscess or infected sewing ring of the prosthesis.

If an abscess is identified, a careful examination is required to rule out extension into these areas, because this additional information has considerable implications for the type of reparative surgery to be undertaken. Loss of structural integrity of the valve, presence of valvular regurgitation and vegetations, and thickening of adjacent tissues help differentiate a native aortic valve abscess from fluid in the transverse pericardial sinus. These associated findings are also helpful in evaluating the presence of an abscess in patients with prosthetic valves in the aortic position. Postsurgical changes, including an echolucent space between a prosthetic valve sewing ring and the aortic root with or without paravalvular regurgitation, may pose a diagnostic dilemma in a patient with prosthetic valve and fever. In such cases, comparison with an intraoperative TEE, if available, may be very helpful to document the chronicity of the abnormality.

In rare cases, exposure of abscesses to high intravascular pressures and progressive burrowing infection may lead to *pseudoaneurysm formation* (color flow imaging demonstrating flow in echolucent space that is contiguous with the bloodstream). Because of further tissue invasion, these paravalvular cavities or pseudoaneurysms can form fistulous connections (aortoatrial or aortoventricular), leaflet perforation and even myocardial perforation. *Fistula formation* complicated 1.6% of cases of native valve IE and 3.5% of cases of prosthetic valve endocarditis in a cohort of 4681 cases of definite IE[26] (Fig. 22-7). These occurred with similar frequency in the three sinuses of Valsalva. Fistulas from the right or noncoronary sinus generally track or exit into the right ventricle, whereas fistulas from the left sinus exit to the left atrium.[27] TEE is the modality of choice to investigate these structural complications. Color flow Doppler imaging demonstrates flow turbulence, abnormal flow in echolucent spaces, and shunting of blood flow in cases of fistulous connections between cardiac chambers.

Progressive tissue destruction due to infection can also result in mitral chordal rupture in native valve IE and valvular dehiscence in prosthetic valve endocarditis. *Valvular dehiscence* is an uncommon, serious complication and portends poor outcome for the patient. On echocardiography, valvular dehiscence is defined as rocking motion of the valve with excursion of at least 15° in at least one direction (Fig. 22-8, *A*). This structural deterioration is often accompanied by severe, paravalvular regurgitation (Fig. 22-8, *B*).

In addition to these complications of IE, it is important to recognize that new valvular regurgitation may represent endocardial infection and is a major diagnostic Duke criterion for IE. Determining the mechanism of regurgitation as well as quantifying its severity is important: Severe regurgitation is poorly tolerated clinically because of acute onset without time for ventricular compensation and is an indication for surgical intervention.

In patients with mechanical prosthetic valves, a complete examination requires using a combination of transthoracic and transesophageal approaches. Transthoracic echocardiography (TTE) allows visualization of the ventricular aspect of the valve but is limited for examining the atrial aspect because of beam attenuation and shadowing. For the same reason, assessment of valvular regurgitation in case of mitral and triscuspid valve prosthesis is problematic with a transthoracic approach. Doppler echocardiography may be used to interrogate prosthetic valves for the presence of regurgitation using the velocity-time integral. TEE allows for much better assessment of valvular regurgitation and evaluation for vegetations on the atrial aspect of valve prostheses.

In patients with cardiac implantable electronic devices, there is substantial artifact generation, and TEE is superior to TTE in suspected infection in such devices.[28-30] Visualization of the lead in the proximal superior vena cava from TEE views may identify vegetations attached to cardiac implantable electronic device leads that are difficult to visualize by other modalities. During the examination, it is important to visualize the entire course of the prosthetic device throughout the vasculature and cardiac structures. A careful evaluation of the cardiac valves is also important because of the high rate of

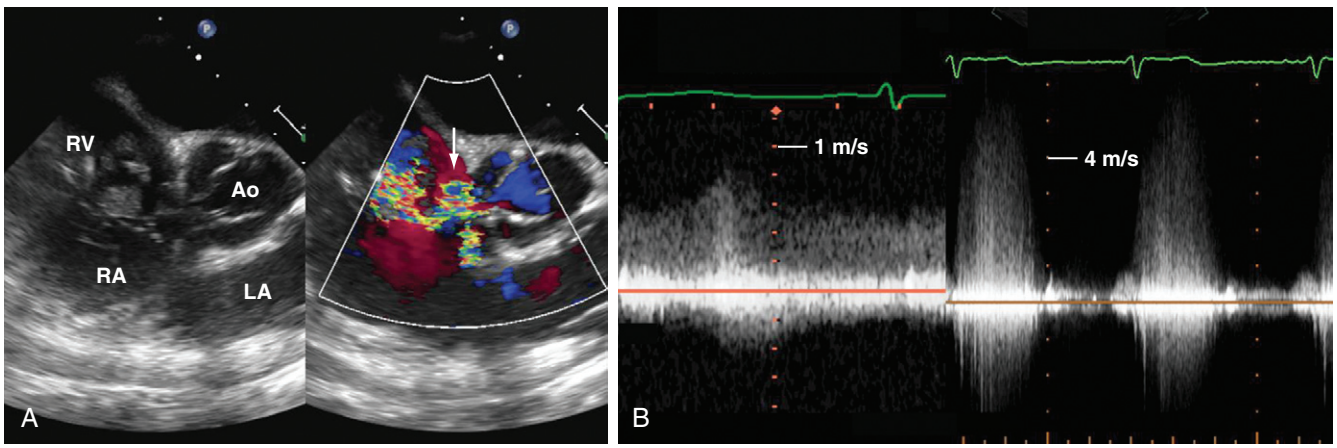



**Figure 22-7 Aortic to right ventricular fistula owing to endocarditis. A,** 2D and color Doppler TEE short-axis views of the aortic valve demonstrating a left-to-right shunt between the aorta and right ventricle. Also note large vegetations on the tricuspid valve and the bright echoes of an intracardiac device seen in the right atrium. *Ao*, Aorta. **B,** Continuous-wave Doppler recordings showing the difference in flow characteristics between an aorta-to-right-ventricle fistula showing continuous, low-velocity flow (*left*) and a perimembranous ventricular septal defect showing systolic, high-velocity flow (*right*).

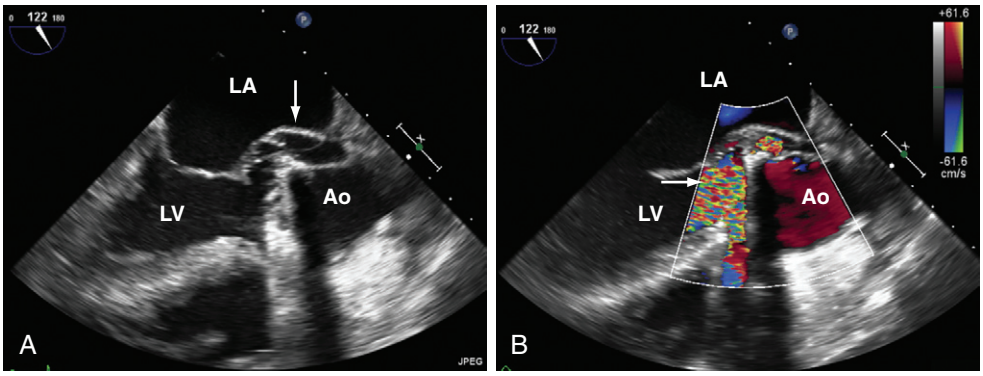



**Figure 22-8 Mechanical aortic valve prosthesis with paravalvular abscess and valve dehiscence. A,** 2D TEE long-axis view of a mechanical aortic valve recorded in systole. Note large, echolucent space (*arrow*) posterior to the valve. **B,** 2D color Doppler TEE image of the mechanical aortic valve demonstrating severe paravalvular regurgitation (*arrow*) due to valve dehiscence. *Ao*, Aorta.

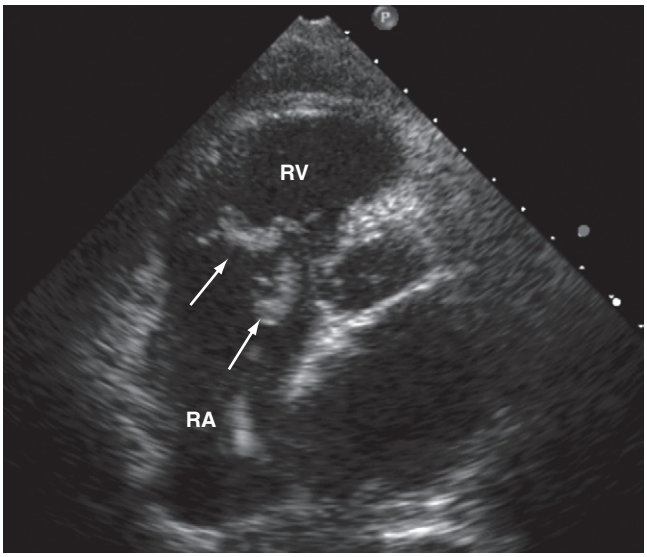



**Figure 22-9 2D TTE image of an infected cardiac implanted electronic device.** Note the presence of heterogeneous, echodense masses (*arrow*) on the anterior and septal tricuspid valve leaflets.

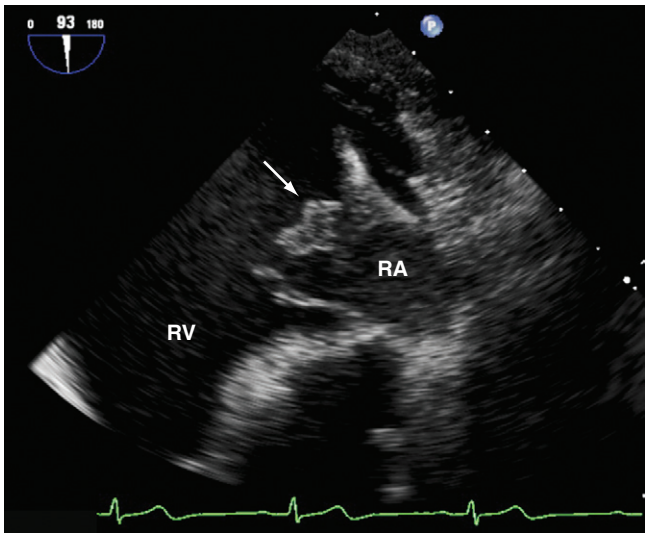



**Figure 22-10 2D TEE transgastric view of an infected cardiac implanted electronic device.** A heterogeneous, irregular mass (*arrow*) is seen attached to the intracardiac lead. Note the absence of involvement of the tricuspid valve.

concomitant valve infection, particularly tricuspid valve (Figs. 22-9 and 22-10).

## Clinical Utility and Outcome Data

### UTILITY IN DIAGNOSIS

#### *General Considerations*

The diagnostic yield of echocardiography is dependent on several variables including echocardiographic modality, vegetation size, vegetation location, native or prosthetic valve, presence of valve calcification (increases the sensitivity, but reduces the specificity of identifying vegetations), and preexisting valvular degeneration. With TTE, in approximately 15% of cases, variable sound transmission due to patient-related factors such as obesity, presence of lung disease, and chest wall deformities may limit diagnostic capability. Although vegetations as small as 2 to 5 mm can be detected, the sensitivity of TTE is low (approximately 40%) with such small lesions.[31] The sensitivity of TTE is highest for tricuspid valve infection because of the proximity to the chest wall. In a study of injection drug users with suspected right-sided IE,[32] TTE detected the presence of vegetations at the same rate as TEE; however, TEE was more effective at characterizing the vegetations. The diagnostic utility of TTE for suspected IE is highest in patients with intermediate to high likelihood of this disease[33] (e.g., a patient with a new or changed heart murmur and bacteremia). The limited sensitivity of TTE for the visualization of an intracardiac vegetation or abscess precludes "ruling out" the diagnosis of IE based on a negative study. Despite its poor sensitivity, TTE is often performed as the initial diagnostic study to assess for the presence and severity of valvular lesions and determine ventricular function. In a patient with a low pretest probability for IE and a normal TTE examination, a diagnosis other than IE should be pursued rather than proceeding to TEE examination (Fig. 22-11). TTE is also recommended for the reassessment of high-risk patients with definite IE (those with virulent organisms, clinical deterioration, persistent or recurrent fever, new murmur, or persistent bacteremia).

Although TTE and TEE have concordant results in approximately half of patients with suspected IE, TEE results in additional diagnostic information in a high percentage of patients.[34] TEE has several major advantages over TTE for the assessment of IE. These include better spatial resolution due to

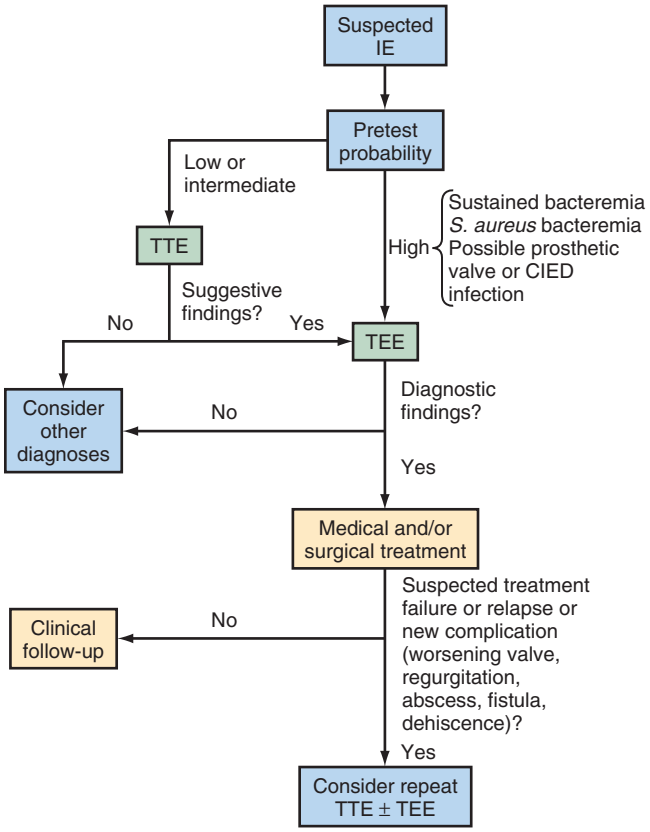



**Figure 22-11** Clinical applications of echocardiography in the evaluation and management of infective endocarditis (*IE*). *CIED*, Cardiac implantable electronic device.

**TABLE 22-2 Pretest Probability Estimates for Infective Endocarditis According to Patient Characteristics**

| *Clinical Feature* | *Estimate of Pretest Probability* |
|---|---|
| Viridans group streptococcal bacteremia | 14% (95% CI: 6-22%) |
| Unexplained bacteremia | 5-40% |
| Bacteremia and recent injection drug use | 31% (95% CI: 19-44%) |
| Admission with fever and recent injection drug use | 13% (95% CI: 7-19%) |
| Persistently positive blood cultures and predisposing heart disease | >50% |
| Persistently positive blood cultures and a new regurgitant murmur | >90% |
| Collective absence of vasculitic/embolic phenomena, central venous access, recent history of injection drug use, a prosthetic valve, and positive blood cultures | 0% |
| Firm alternate diagnosis or resolution of endocarditis syndrome within 4 days | <2% |
| Gram-negative bacteremia with clear noncardiac source of infection | <2% |

Adapted from Heidenreich PA, Masoudi FA, Maini B, et al: Echocardiography in patients with suspected endocarditis: a cost-effectiveness analysis. *Am J Med* 107:198-208, 1999; and Greaves K, Mou D, Patel A, Celermajer DS: Clinical criteria and the appropriate use of transthoracic echocardiography for the exclusion of infective endocarditis. *Heart* 89:273-275, 2003.

a higher-frequency transducer, lack of acoustic interference from adjacent structures such as the lungs and chest wall, and proximity to posterior structures such as the mitral valve and left atrium. TEE can detect vegetations as small as 1 to 2 mm and can detect vegetations 2 to 5 mm with a sensitivity of nearly 100%.[31] TEE should be performed in patients with a high clinical probability of IE and a negative TTE.[35]

Specific subsets of patients in whom TEE should be performed, even as the primary imaging modality (without preceding TTE) for diagnosis of IE, include (1) patients with prosthetic heart valves and suspected IE; (2) patients with persistent staphylococcal bacteremia without known source, or nosocomial staphylococcal bacteremia; and (3) patients with suspected infection in a cardiac implantable electronic device. Evidence suggests that TEE is also better than TTE for diagnosing native pulmonic valve IE,[36] although this is the least commonly infected valve and typically is associated with congenital heart disease as a predisposing condition. In patients with suspected culture-negative IE (approximately 10% of all cases of definite IE), TEE has higher sensitivity than TTE for visualizing diagnostic findings of endocardial involvement.[37]

Cost-effective analyses also support a diagnostic approach using echocardiography, particularly TEE. Heidenreich and coworkers[38] have shown that in suspected IE, a diagnostic strategy that focuses on TEE as the initial imaging modality is more cost effective than a staged procedure with TTE and is a superior strategy compared with empiric antibiotic therapy alone. In this study, TEE was optimal for patients who had a prior probability of IE that is observed commonly in clinical practice (4% to 60%) with a modestly reduced cost compared with the use of TTE as initial study.

It is important to note that the utility of a diagnostic tool such as echocardiography is optimal in the appropriate clinical context or pretest probability of disease (greater than 2% to 3%). Although there are few empiric data to quantify the pretest probability of disease, there is general consensus that certain characteristics increase the likelihood of disease (Table 22-2). Recent literature suggests that imaging technologies such as echocardiography can be overused in certain clinical scenarios, such as the evaluation of suspected IE. Kurupuu and colleagues[38a] have shown that 53% of echocardiograms could be avoided without loss of diagnostic accuracy by using a simple algorithm in patients with a low pretest probability of disease. Similarly, Greaves and associates[39] have shown that the absence of five simple clinical criteria was associated with a zero probability of a TTE demonstrating evidence of IE: (1) vasculitic/embolic phenomena, (2) central venous access, (3) a recent history of injection drug use, (4) prosthetic heart valve, and (5) positive blood cultures. Collectively, these studies have shown that in patients with very low pretest probability of disease, echocardiography may be avoided without the loss of diagnostic accuracy. Recommendations for the appropriate use of TTE and TEE in cases of suspected or known IE are provided in Tables 22-3 and 22-4. The evaluation of possible IE in specific clinical scenarios is discussed next.

### *Evaluation of the Patient with Bacteremia*

Because the clinical presentation of endocarditis is highly variable, early suspicion of IE is critical for an early diagnosis. A history of predisposing factors, including prosthetic valves, previous episode of endocarditis, congenital heart disease, and heart failure, or other stigmata of endocarditis with fever for more than 72 hours should prompt a search for the diagnosis with blood cultures and imaging.

Bacteremia with typical organisms including viridans streptococci, *Streptococcus bovis*, HACEK group, *S. aureus*, or

**TABLE 22-3 ACC/AHA Practice Guidelines and the Appropriateness Criteria for the Use of TTE in Suspected or Known IE**

| *Indications* | *Level of Evidence* |
|---|---|
| **Class I** | |
| 1. TTE to detect valvular vegetations with or without positive blood cultures is recommended for the diagnosis of infective endocarditis | B |
| 2. TTE is recommended to characterize the hemodynamic severity of valvular lesions in known infective endocarditis | B |
| 3. TTE is recommended for assessment of complications of infective endocarditis (e.g., abscesses, perforation, and shunts). | B |
| 4. TTE is recommended for reassessment of high-risk patients (e.g., those with virulent organisms, clinical deterioration, persistent or recurrent fever, new murmur, or persistent bacteremia) | C |
| **Class IIa** | |
| TTE is reasonable to diagnose infective endocarditis of a prosthetic valve in the presence of persistent fever without bacteremia or a new murmur | C |
| **Class IIb** | |
| TTE may be considered for the reevaluation of prosthetic valve endocarditis during antibiotic therapy in the absence of clinical deterioration | C |
| **Class III** | |
| TTE is not indicated to reevaluate uncomplicated (including no regurgitation on baseline echocardiogram) native valve endocarditis during antibiotic treatment in the absence of clinical deterioration, new physical findings, or persistent fever | C |
| *Appropriateness Criteria* | *Appropriateness Score (1-9)* |
| 1. Initial evaluation of suspected infective endocarditis with positive blood cultures or a new murmur | A (9) |
| 2. Transient fever without evidence of bacteremia or a new murmur | I (2) |
| 3. Transient bacteremia with a pathogen not typically associated with infective endocarditis and/or a documented nonendovascular source of infection | I (3) |
| 4. Re-evaluation of infective endocarditis at high risk for progression or complication or with a change in clinical status or cardiac exam | A (9) |
| 5. Routine surveillance of uncomplicated infective endocarditis when no change in management is contemplated | I (2) |

Adapted from Bonow RO, Carabello BA, Kanu C, et al: ACC/AHA 2006 guidelines for the management of patients with valvular heart disease. *Circulation* 114:e84-e231, 2006; and Douglas PS, Khandheria B, Stainback RF, et al: ACCF/ASE/ACEP/ASNC/SCAI/SCCT/SCMR 2007 appropriateness criteria for transthoracic and transesophageal echocardiography. *J Am Soc Echocardiogr* 20:787-805, 2007.

**TABLE 22-4 ACC/AHA Practice Guidelines and the Appropriateness Criteria for the Use of TEE in Suspected or Known IE**

| *Indications* | *Level of Evidence* |
|---|---|
| **Class I** | |
| 1. TEE is recommended to assess the severity of valvular lesions in symptomatic patients with infective endocarditis | C |
| 2. TEE is recommended to diagnose IE in patients with valvular heart disease and positive blood cultures if TTE is nondiagnostic | C |
| 3. TEE is recommended to diagnose complications of IE with potential impact on prognosis and management (e.g., abscess, perforation, and shunts) | C |
| 4. TEE is recommended as first-line diagnostic study to diagnose prosthetic valve endocarditis and assess for complications | C |
| 5. TEE is recommended for preoperative evaluation in patients with known IE unless the need for surgery is evident on TTE and unless preoperative imaging will delay surgery in urgent cases | C |
| 6. Intraoperative TEE is recommended for patients undergoing valve surgery for infective endocarditis | C |
| **Class IIa** | |
| TEE is reasonable to diagnose possible infective endocarditis in patients with persistent staphylococcal bacteremia without known source | C |
| **Class IIb** | |
| TEE might be considered to detect IE in patients with nosocomial staphylococcal bacteremia | C |
| *Appropriateness Criteria* | *Appropriateness Score (1-9)* |
| 1. Evaluation of valvular structure and function to assess suitability for, and assist in planning of, an intervention | A (9) |
| 2. To diagnose infective endocarditis with a low pretest probability (e.g., transient fever, known alternative source of infection, or negative blood cultures/atypical pathogen for endocarditis) | I (3) |
| 3. To diagnose infective endocarditis with a moderate or high pretest probability (e.g., staphylococcal bacteremia, fungemia, prosthetic heart valve, or intracardiac device) | A (9) |

Adapted from Bonow RO, Carabello BA, Kanu C, et al: ACC/AHA 2006 guidelines for the management of patients with valvular heart disease. *Circulation* 114:e84-e231, 2006; and Douglas PS, Khandheria B, Stainback RF, et al: ACCF/ASE/ACEP/ASNC/SCAI/SCCT/SCMR 2007 appropriateness criteria for transthoracic and transesophageal echocardiography. *J Am Soc Echocardiogr* 20:787-805, 2007.

Levels of evidence are defined as:
A, Data derived from multiple randomized clinical trials or metaanalysis.
B, Data derived from a single randomized study or from nonrandomized studies.
C, Consensus opinion of experts, cases studies or standards of care.
For the appropriateness score, A indicates the test is considered appropriate and I indicates it is inappropriate.

community-acquired enterococci in the absence of a primary focus constitute a major criterion for IE. Thus, bacteremia with typical organisms should be investigated for endocardial involvement with TTE. If the TTE is technically inadequate, nondiagnostic, or negative, TEE should be obtained.

*S. aureus* bacteremia of any origin or setting is a risk factor for IE, and thus the diagnosis should be ruled out by careful clinical evaluation and diagnostic testing. With virulent organisms such as *S. aureus,* which is capable of causing IE on apparently normal cardiac valves, the incidence of IE is high (approximately 30%).[40,41] Among 59 prospectively identified patients with *S. aureus* IE, the presumed source of the bacteremia was an intravascular catheter in 39%. Similarly, in a prospectively identified cohort of 922 patients with definite IE from 39 sites in 16 countries, *S. aureus* was the most common cause of IE, accounting for 35.7% of all cases, and it was associated

with a presumed intravascular catheter source in 39%.[42,43] These studies also underscore the association between catheter-associated bacteremia and IE. In cases where there is low clinical suspicion and blood culture data suggest skin contaminants (coagulase-negative *Staphylococcus*), a technically adequate TTE should be sufficient to exclude IE, and other diagnoses should be considered.

### *Evaluation of the Patient with Prosthetic Valves*

Prosthetic valves are a predisposing factor for IE and inevitably place the patient in a high risk group. Such valves were previously thought to account for only 1% to 5% of all IE cases. However, a recent prospective, multinational, observational cohort study[44] showed that of 2670 patients with IE, approximately 20% had definite prosthetic valve endocarditis. As compared to native valve IE, in-hospital mortality was high (23%) in this group of patients despite similar rates of complications and surgical intervention. These data emphasize the aggressive nature of prosthetic valve endocarditis and reiterate the need for an early diagnosis and intervention. *S. aureus* is the most the most common causative organism in prosthetic valve endocarditis. *S. aureus* infection and health care–associated infection were strong predictors of mortality in a large cohort.[44] In another study,[45] among patients with a prosthetic valve and *S. aureus* bacteremia, 50% were found to have endocarditis regardless of time since prosthetic valve implantation. Fever in a patient with prosthetic valves that is not otherwise explained along with risk factors such as bacteremia and indwelling catheters should heighten clinical suspicion and prompt an aggressive search for IE.

Prosthetic valve endocarditis also poses an imaging diagnostic challenge, because identification of the pathology that chiefly involves the paravalvular tissue and the usual complications such as paraprosthetic leaks, dehiscence, ring abscesses, and fistula formation can be masked by acoustic shadowing and reverberation artifacts caused by the prosthetic material. Vegetations on prosthetic valves cannot be reliably detected by TTE. TEE is preferred for the evaluation of suspected prosthetic valve IE and has been shown to have greater sensitivity for detecting vegetations than TTE.[46,47] Because of the greatly improved accuracy with TEE, it is recommended as a first-line diagnostic study to diagnose prosthetic valve endocarditis and assess for its complications.[48]

It should be noted that echocardiographic differentiation between tissue degeneration and small vegetations is sometimes not possible, even with TEE. In addition, paraprosthetic strands, which can be observed in early postoperative months, can cause false-positive interpretations.[49,50]

### *Evaluation of the Patient with a Cardiac Implantable Electronic Device*

An increase in the rate of cardiac device infections (permanent pacemakers, implantable cardioverter-defibrillators, prosthetic heart valves or material, and ventricular assist devices) has been observed in recent years. Cabell and colleagues[51] reported an increase from 0.94 to 2.11 per 1000 Medicare beneficiaries between 1990 and 1999. The rate of native valve IE, however, remained stable over that period (0.26 to 0.36 per 1000 beneficiaries).

Imaging with echocardiography, particularly TEE, is integral in evaluating patients with suspected infection of a cardiac implantable electronic device.[28-30] TEE examination is particularly useful among patients with *Staphylococcus aureus* bacteremia and presence of such a device, because the rate of underlying IE is significant.[40]

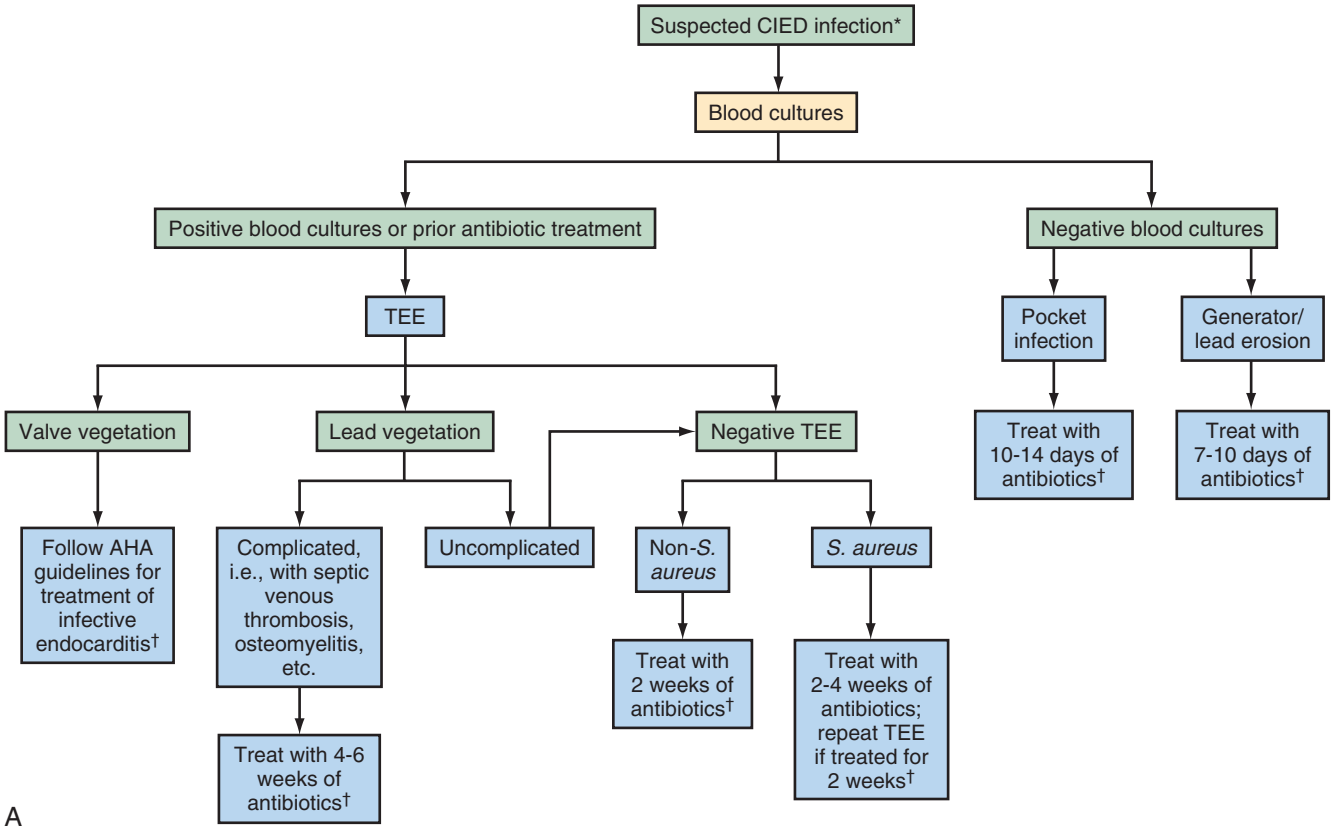
Importantly, failure to visualize a mass adherent to a lead with TEE does not exclude lead infection.[29] Conversely, visualization of a mass adherent to a cardiac lead by echocardiography may indicate either a thrombus or infected vegetation. Because it is impossible to distinguish between these two entities by echocardiography alone, and recognizing that 5% of adherent masses were deemed thrombus in one retrospective survey,[52] careful clinical judgment must be employed for the diagnosis of infection of a cardiac implantable electronic device. Masses that are detected in patients without positive blood cultures or other suggestive features for infection are likely to represent thrombus and, in isolation, do not indicate the need for lead extraction or antibiotic treatment without clinical suspicion for infection. Because of its poor sensitivity, TTE is less useful to rule out the diagnosis of infection of a cardiac implantable electronic device, particularly in adults. However, several prognostic features may be better defined on TTE than on TEE, such as pericardial effusion, ventricular dysfunction, pulmonary vascular pressure estimations, and quantitation of valvular regurgitation. Figure 22-12 depicts a suggested approach for the diagnosis and management of infection of a cardiac implantable electronic device using TEE. Importantly, complete CIED removal is recommended in cases of definite device or valve infection; pocket abscess, erosion, or draining sinus; and occult staphylococcal bacteremia.[29]

## UTILITY IN MANAGEMENT

Prompt diagnosis, initiation of appropriate antibiotics, and consideration of surgical intervention along with a cohesive, multidisciplinary approach forms the basis of management. From determining the duration of antibiotic therapy to identification of complications needing prompt surgery, echocardiography has an important role in the management of this complex disease, particularly with regard to prognostic factors that may require surgical intervention rather than medical therapy alone.

The Duke criteria were developed to provide a more sensitive case definition of IE, but their possible prognostic influence was evaluated in a single-center study[53] from our institution. In 267 patients with definite or possible IE by Duke criteria, early echocardiographic findings of IE, such as presence of vegetation and new valvular regurgitation as categorical variables, were not associated with in-hospital mortality.

Diagnostic imaging for evidence of IE typically occurs within the first few days after hospital admission with suspected IE, and approximately 90% of patients with definite IE have vegetations visualized. In this setting, vegetation characteristics such as size, mobility, attachment site, and shape and have been extensively studied as tools for risk stratification of patients with IE, particularly risk of embolic events. Vegetation size greater than 10 mm and increased mobility have been shown in several series to predict embolic events.[54,55] Embolic events in IE have been found to a strong, independent predictor of in-hospital mortality.[53] In one multicenter prospective study[56] of 384 patients with definite IE, vegetation length greater than 15 mm was independently associated with 1-year mortality (Fig. 22-13). In another recent observational study[57] of 132 patients with left-sided IE and approximately 40% with vegetation length of at least 15 mm, early surgery within 7 days of diagnosis was associated with a significantly lower



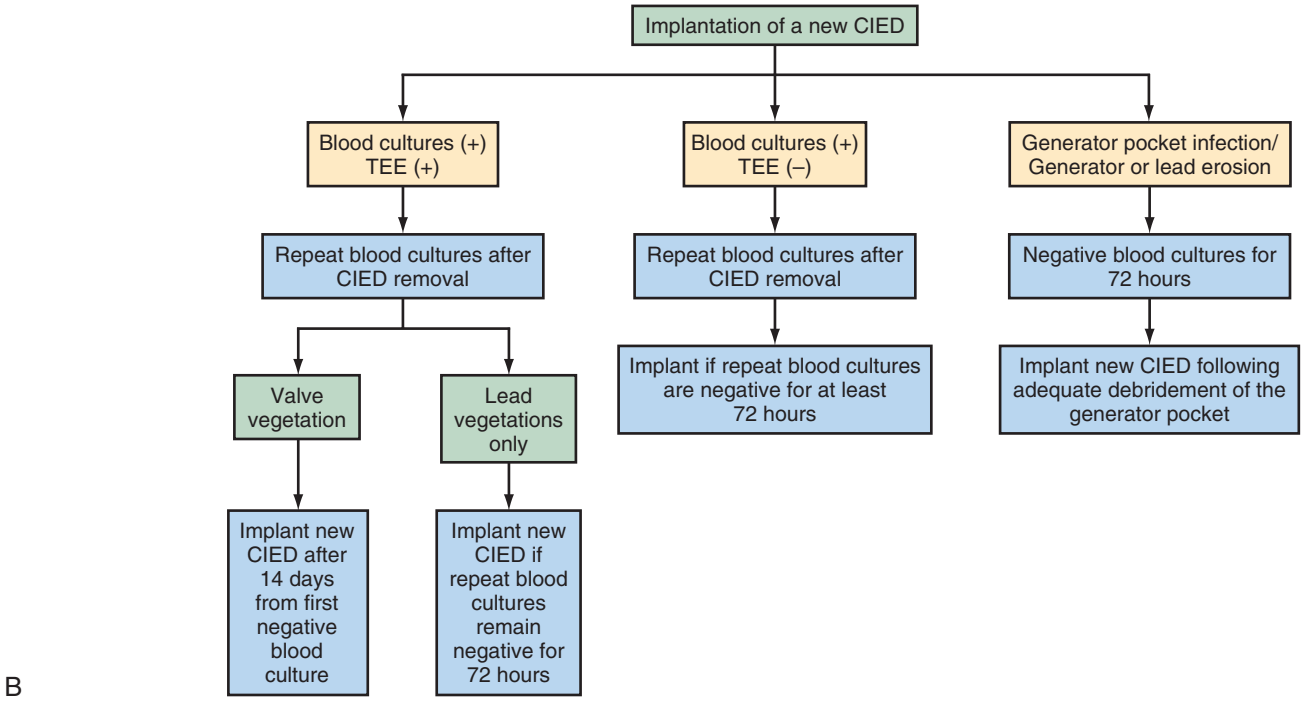




**Figure 22-12** **A,** Approach to management of adults with cardiac implantable electronic device (*CIED*) infection. **B,** Approach to implantation of a new device in patients after removal of an infected CIED. *(From Baddour LM, Epstein AE, Erickson CC, et al: Update on cardiovascular implantable electronic device infections and their management: a scientific statement from the American Heart Association. Circulation 121:458-477, 2010.)* *A history, physical examination, chest radiograph, electrocardiogram, and device interrogation are standard baseline procedures before CIED removal. †Duration of antibiotics should be counted from the day of device explantation. Treatment can be extended to 4 or more weeks if there are metastatic septic complications (i.e., osteomyelitis, organ or deep abscess, etc.) or sustained bloodstream infection despite CIED removal.

risk of embolic events compared to conventional treatment, with surgery deferred until complications occurred (Fig. 22-14). Therefore, current ACC/AHA guidelines recognize that surgery for native valve IE may be considered in patients who present with mobile vegetations more than 10 mm in size with or without emboli (class IIb recommendation, level of evidence C).

Although vegetation characteristics are clearly important in risk stratification, basing clinical decisions regarding surgery solely on this parameter is problematic, because of the considerable interobserver variability on echocardiographic features of vegetations. In a study by Heinle and colleagues,[58] complete observer agreement was achieved on vegetation size in only 73%, mobility in 57%, shape in 37%, and attachment in 40% of cases. These data also emphasize the need for careful standardization of exams. In addition, the risk of embolism has been found to decrease rapidly within the first week of antibiotic therapy (Fig. 22-15),[59] a beneficial effect of medical therapy that should be considered when considering surgery for the prevention of embolic events in IE.

After an embolic event has occurred, the residual presence of a vegetation poses a risk for recurrent embolism. However, routine surveillance for embolism in IE has demonstrated that approximately 50% of cases are associated with an embolic

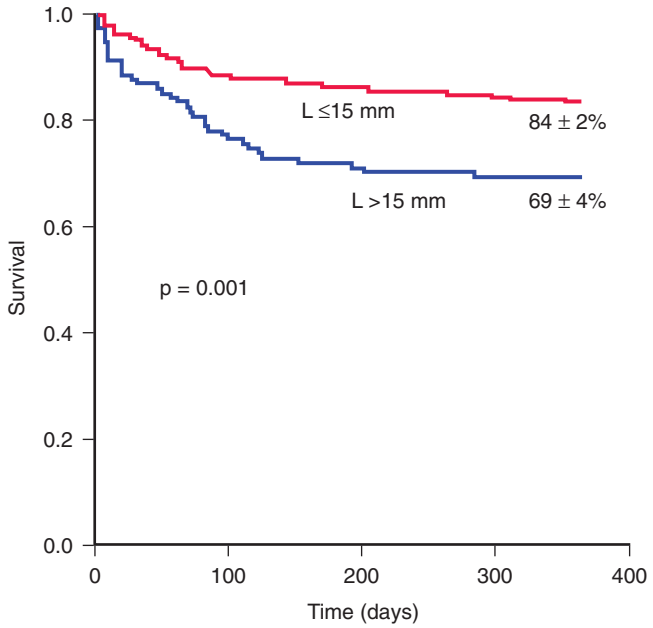



**Figure 22-13 Survival in infective endocarditis stratified by vegetation size.** *(From Thuny F, Di Salvo G, Belliard O, et al: Risk of embolism and death in infective endocarditis: prognostic value of echocardiography: a prospective multicenter study.* Circulation *112:69-75, 2005.) L,* Vegitation length.

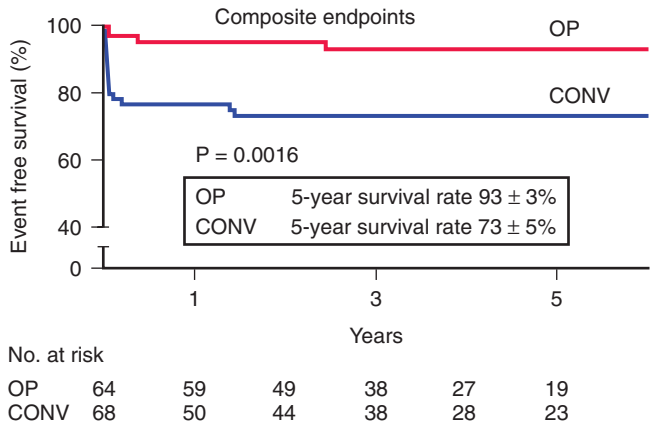



**Figure 22-14 Impact of early surgery on event-free survival in IE.** Patients treated with early surgery (*OP*) had lower rate of embolic events but similar mortality as patients treated with conventional (*CONV*) strategy of expectant surgery. *(From Kim D-HK, Lee M-Z, Yun S-C, et al: Impact of early surgery on embolic events in patients with infective endocarditis.* Circulation *122:S17-S22, 2010.)*

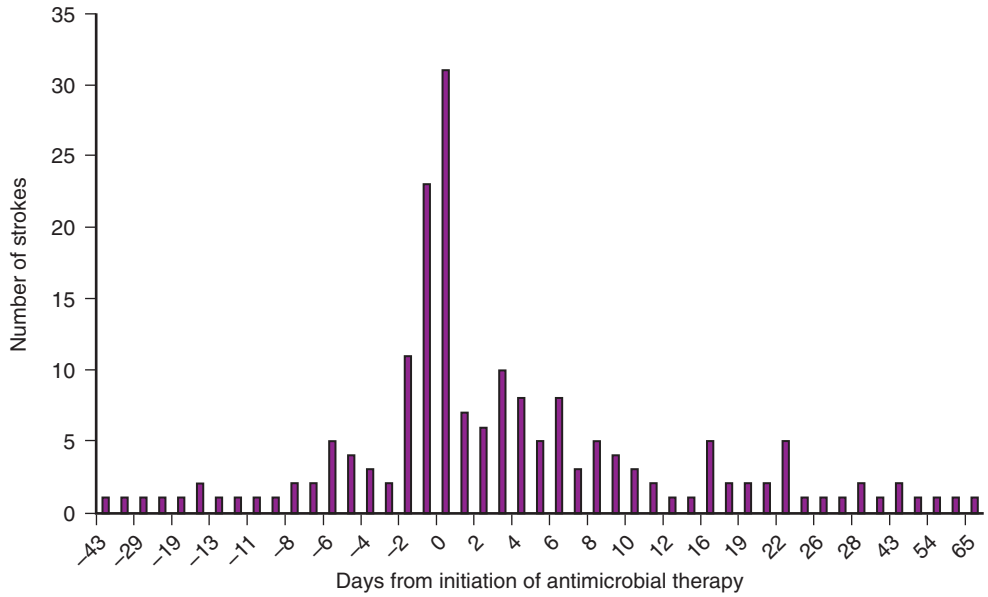



**Figure 22-15 Decrease in strokes in infective endocarditis as a function of duration of antibiotic therapy.** *(From Dickerman SA, Abrutyn E, Barsic B, et al: The relationship between the initiation of antimicrobial therapy and the incidence of stroke in infective endocarditis: an analysis from the ICE Prospective Cohort Study [ICE-PCS].* Am Heart J *154:1086-1094, 2007.)*

event (typically to brain, spleen, kidney, or lungs), and that most of these embolic events are clinically silent or asymptomatic. In this situation, the decision as to whether to proceed with cardiac surgery is again challenged by the subclinical nature of these events and the progressively lower risk of embolic events with antibiotic therapy. Conversely, asymptomatic brain infarcts have been associated with a poorer prognosis in IE and generally do not increase the risk of cardiac surgery in the absence of cerebral hemorrhage, abscess, or major neurologic impairment.[60] In comparison to TTE, TEE has improved ability to detect complications of IE such as paravalvular abscesses[6] or regurgitation, valvular perforation,[61] intracardiac shunt, and secondary involvement of the mitral-aortic intervalvular fibrosa.[62] The diagnosis of an abscess has significant prognostic and management implications. Rarely, antibiotic therapy may be used to treat an intracardiac abscess, though this treatment alone is generally reserved for patients who are poor surgical candidates. The vast majority of patients with an intracardiac abscess require cardiac surgery for débridement (class I recommendation, level of evidence C), and failure to diagnose an abscess by echocardiography is associated with delayed time to surgery.[25] In a recent study,[62a] the impact of early surgery on survival of patients with native valve IE was evaluated using propensity score and instrumental variable methods to adjust for treatment selection bias. In this prospective, multinational cohort, the investigators found a significant in-hospital mortality benefit associated with early surgery compared to medical therapy alone (12.1% versus 20.7%) and for those with paravalvular complications (intracardiac abscess or fistula formation—determined by echocardiography) (absolute risk reduction 17.3%, $P < 0.001$). In addition, surgery represents the gold standard for the confirmation of abscess visualized by echocardiography.

In IE complicated by fistula formation, the left-to-right shunting of blood flow generally augments the risk and/or severity of heart failure complicating IE. As a result, in-hospital mortality rate is very high (41%) despite the use of surgical therapy in the overwhelming majority of cases.[24] The development of cavitary fistulas thus heralds a poor outcome and should prompt urgent surgical intervention.

Finally, quantification of regurgitation severity and determining its impact on heart failure as a complication of IE are important prognostic factors. Acute regurgitation of IE that develops without the compensatory eccentric hypertrophy in chronic regurgitation is poorly tolerated clinically, potentially resulting in life-threatening pulmonary edema and cardiogenic shock. Acute aortic valve regurgitation is particularly ominous in its poor outcome and is an accepted criterion for surgical intervention. In patients with advanced heart failure symptoms (NYHA 3 or 4) complicating left-sided, native-valve IE, surgical therapy has clearly been shown to improve survival compared to medical therapy, whereas surgery for patients with no or mild heart failure appears to have little benefit for overall survival.[63] Even in patients without overt evidence of heart failure, severe regurgitation of either left-sided heart valve is a poor prognostic finding and an indication for surgical intervention. If severe mitral or aortic valve regurgitation is evident by echocardiography, close observation of the patient's hemodynamic status should be performed, often in an intensive care unit setting. In this situation, blood pressure that is lower than baseline or sinus tachycardia may herald acute decompensation even in the absence of more classic signs of heart failure. For these patients, use of intravenous afterload reduction agents (nitroprusside or nitroglycerine) may reduce the regurgitant volume and stabilize hemodynamic status. If severe heart failure or cardiogenic shock ensues, use of inotropic agents may be needed, and an intraaortic balloon pump can be used in severe mitral regurgitation as a bridge to cardiac surgery. Finally, new-onset atrial fibrillation is poorly tolerated in patients with acute, severe, valvular regurgitation; restoration of sinus rhythm with antiarrhythmic therapy and/or direct-current cardioversion may significantly improve hemodynamic stability.

In IE cases complicated by mechanical complications such as abscess, fistula, severe valvular regurgitation, or valve dehiscence, intraoperative TEE is indicated to assess complete repair of these defects. Indeed, an intraoperative TEE is now considered routine in most centers. Shapira and coworkers[64,65] analyzed the impact of TEE in 59 patients diagnosed with IE. In their experience, intraoperative TEE before cardiopulmonary bypass led to the modification of the surgical plan in 11.5% of cases. Intraoperatively, echocardiographic goals include assessment of not only the obviously dysfunctional valve but also the other valves and contiguous structures. Post–cardiopulmonary bypass images should confirm the adequacy of the repair or replacement and document the successful closure of fistulous tracts. Paravalvular leaks related to technical factors should be recognized and documented to avoid future uncertainty as to whether the leaks are the result of recurrent infection. During imaging after cardiopulmonary bypass, it is often necessary to augment afterload to reach representative ambulatory levels to avoid underestimation of regurgitant jet size and significance and to ensure that abnormal communications have been closed. It should be noted, however, that afterload augmentation may not always mimic actual awake physiology and may still lead to an inaccurate evaluation of the conscious postoperative state.[7,66]

Echocardiography has been used to analyze cost effectiveness in establishing the duration of treatment in the setting of acute IE as well as determining the need for a surgical intervention. Rosen and colleagues[66a] evaluated the cost effectiveness of TEE in establishing the duration of therapy for catheter-associated bacteremia. In this study, three management strategies were compared: (1) empirical treatment with 4 weeks of antibiotics (long course); (2) empirical treatment with 2 weeks of antibiotic therapy; and (3) TEE-guided therapy. In the TEE-guided strategy, a positive TEE dictated a long course of antibiotic therapy, and a negative TEE dictated a short course of therapy. The effectiveness of an empiric long-course strategy and a TEE-guided strategy were both superior to empiric short-course therapy. When costs were taken into account, the TEE-guided strategy was superior to the empiric long-course strategy, which cost more than $1.5 million per quality-adjusted life year saved. In a similar study, using a decision tree and Markov analysis, Liao and associates[67] showed that echocardiographically guided risk stratification to assess for complications that might benefit from early surgical intervention was a cost-effective treatment strategy, improving outcome for an incremental cost less than $50,000 per quality-adjusted life year saved.

Approximately 50% of patients with IE undergo cardiac valve surgery during the index hospitalization. Once the decision to proceed to surgery is made, it is important to provide the surgeon with an accurate assessment of valve anatomy for the purpose of operative planning. This preoperative assessment may be especially valuable when repair, rather than replacement, of a diseased mitral valve is considered. In addition, for patients with an aortic abscess, consideration of a homograft

replacement may be facilitated by accurate measurement of the annulus diameter. After valve surgery for IE, outpatient TTE is indicated early after surgery. The results of this study serve as a useful baseline hemodynamic assessment of the replaced or repaired valve's function as well as ventricular function for future comparisons, as clinically indicated.

### UTILITY IN FOLLOW-UP

There are no conclusive data to support serial echocardiographic examinations for surveillance in uncomplicated IE. The diagnostic value of TEE in monitoring the clinical course was evaluated in 83 patients with echocardiographic evidence of IE by Rohmann and colleagues.[68] Each patient in this cohort received at least two consecutive TEE studies. The study found that patients with an increase or no change in vegetation size had a higher incidence of complications after diagnosis and initiation of therapy, including valve replacement, embolic events, paravalvular abscess formation, and mortality, as compared to the cohort that demonstrated a decrease in vegetation size. Although these data suggest that multiple echocardiographic evaluations may be useful in determining the prognosis of patients with IE, there is great potential for inappropriate overuse of the test. Vieira and co-workers[69] evaluated the diagnostic contribution of repeated TTE and TEE examinations among patients with suspected IE. Over a 3-year period, they evaluated 262 patients with 266 episodes of suspected IE referred for echocardiography. They found that repeat echocardiography was frequent: TTEs were repeated at least once in 192 (72.2%) patients, whereas TEEs were repeated in 49 (18.4%) of patients. A mean of 2.4 TTE and 1.2 TEE examinations were performed for each episode of suspected IE. The second and third TTEs added diagnostic information in 34 (26.7%) and the second and third TEEs added diagnostic information in 25 (19.7%) of 127 episodes with definite IE. After the third TTE or TEE, no additional diagnostic information was obtained.

Therefore, a TTE or TEE as routine surveillance of uncomplicated IE when no change in management is contemplated is deemed inappropriate by the recently published appropriateness criteria for echocardiography. In patients with an established diagnosis of IE who develop worrisome clinical features such as a new atrioventricular block, persistent fever or bacteremia, progression of heart failure symptoms, or a change in cardiac murmur during or after the course of therapy, repeat echocardiography (TTE or TEE) to evaluate for structural complications is warranted (class I recommendation, level of evidence A). Because all patients with a history of IE remain at high risk for recurrent infection indefinitely, a TTE examination should be conducted to establish a new baseline for valve morphology and cardiac function, after completion of antimicrobial therapy (class IIb recommendation, level of evidence C).

## Research Applications

With the advent of real-time, three-dimensional (3D) TEE, which allows acquisition of full volume data, it is possible to precisely define anatomic structures, as well as vegetation characteristics and location. Cropping through the images may reveal structures and flows not visualized with TEE or TTE. 3D TEE appears to be a promising technique in examining prosthetic valves and patients with intracardiac devices. Initial experience using 3D TEE in patients with prosthetic valve endocarditis suggests that 3D TEE may provide additional information not readily appreciated on standard 2D TEE imaging.[70] Liu and associates[70a] performed 2D and real-time 3D TTE in 46 patients with definite IE. The sensitivity for both modalities was 91.6%, but specificity using real-time 3D echocardiography was higher (100% versus 88.2%, respectively). Although these data are encouraging, further research is needed to define the role of 3D echocardiography in the diagnosis as well as management of IE. In addition, from a clinical-outcome perspective, additional studies are needed to better define the prognostic influence of echocardiographic findings in IE and their severity over time after treatment.

## Potential Limitations and Future Directions

Echocardiography is an important tool for diagnosis of endocarditis when used in the correct clinical scenario with an appropriate pretest probability of disease. However, its overuse is associated with avoidable costs. False-positive results can lead to unnecessary treatment, potential complications, and increased medical costs. In addition, with an invasive procedure such as TEE, there is a small but definable risk to the patient of complications related to sedation and probe insertion, including aspiration, esophageal perforation, induction of cardiac arrhythmia, respiratory compromise, and patient discomfort. Approximately 10% of patients with IE will not have evidence of vegetation or other endocardial involvement at the time of diagnosis, perhaps because of the limitations of imaging. Treatment of these patients should be guided by the clinical suspicion for IE, particularly for patients with prosthetic heart valves and those who meet criteria for definite IE by other major and minor criteria.

## Alternative Approaches

Other imaging modalities such as cardiac magnetic resonance imaging with contrast appear promising for the detection of paravalvular abscesses, thrombus associated with vegetations, valvular complications, and aortocameral fistulas, although temporal resolution may limit their use for detection of vegetation (level of evidence C). The role of cardiac magnetic resonance imaging with contrast is also limited in the evaluation of patients with cardiac implantable electronic devices, and the procedure is often not feasible in critically ill patients. Cardiac computed tomography has also been used to detect aortic root abscesses, but radiation risk as well as temporal resolution are again limiting factors in its widespread use.

Clinical experience with these techniques in IE patients is limited, and their operating characteristics (sensitivity and specificity) in comparison to echocardiography are not well defined.[71-73] As a result, no other imaging modality for the visualization of endocardial involvement or complications of IE is an acceptable alternative to echocardiography in clinical practice.

## KEY POINTS

- Echocardiography is essential for the diagnosis and management of infective endocarditis.
- Echocardiographic findings that are major diagnostic criteria for endocarditis include vegetations, abscess, new partial dehiscence of prosthetic valve, and new valvular regurgitation.
- Echocardiography should be considered for patients with an intermediate or high pretest probability for endocarditis, including clinical features of fever, positive blood cultures, or new or changing regurgitant heart murmur.
- Approximately 90% of patients with definite endocarditis have evidence of vegetation by echocardiography.
- The sensitivity of TEE (greater than 95%) is superior to the sensitivity of TTE (40% to 60%) for the diagnosis of endocarditis.
- TEE is appropriate as the primary diagnostic test (without preceding transthoracic study) for patients with prosthetic heart valves, patients with staphylococcal bacteremia without known source or that is nosocomial in origin, and patients with possible infection of a cardiac implanted electronic device (permanent pacemaker or implantable cardioverter-defibrillator).
- Findings on echocardiography that suggest a poor prognosis for the patient with endocarditis include large vegetations (greater than 10 mm), severe valvular regurgitation (particularly aortic valve), abscess or fistula formation, or prosthetic valve dehiscence. Any of these findings should trigger prompt surgical evaluation for urgent valve surgery.
- TEE is an important tool for preoperative planning in patients undergoing valve surgery for endocarditis.
- In the absence of clinical findings suggesting relapse of endocarditis or worsening cardiac involvement (e.g., atrioventricular conduction block, changing heart murmur, or evidence of heart failure), routine, repeat echocardiography during or after the course of antibiotic therapy has little clinical utility.

## ACKNOWLEDGMENTS

*Images were provided by John H. Toptine, RCS, RDCS, and James G. Jollis, MD, from the Duke Echocardiography Laboratory. We appreciate Dr. Joseph A. Kisslo's critical insights regarding technical aspects of image acquisition in patients with IE.*

## REFERENCES

1. Delahaye F, Goulet V, Lacassin F, et al: Characteristics of infective endocarditis in France in 1991. A 1-year survey. *Eur Heart J* 16:394-401, 1995.
2. Berlin JA, Abrutyn E, Strom BL, et al: Incidence of infective endocarditis in the Delaware Valley, 1988-1990. *Am J Cardiol* 76:933-936, 1995.
3. Murdoch DR, Corey GR, Hoen B, et al: Clinical presentation, etiology, and outcome of infective endocarditis in the 21st century: the International Collaboration on Endocarditis—Prospective Cohort Study. *Arch Intern Med* 169:463-473, 2009.
4. Dillon JC, Feigenbaum H, Konecke LL, et al: Echocardiographic manifestations of valvular vegetations. *Am Heart J* 86:698-704, 1973.
5. Gilbert BW, Haney RS, Crawford F, et al: Two-dimensional echocardiographic assessment of vegetative endocarditis. *Circulation* 55:346-353, 1977.
6. Daniel WG, Mugge A, Martin RP, et al: Improvement in the diagnosis of abscesses associated with endocarditis by transesophageal echocardiography. *N Engl J Med* 324:795-800, 1991.
7. Baddour LM, Wilson WR, Bayer AS, et al: Infective endocarditis: diagnosis, antimicrobial therapy, and management of complications: a statement for healthcare professionals from the Committee on Rheumatic Fever, Endocarditis, and Kawasaki Disease, Council on Cardiovascular Disease in the Young, and the Councils on Clinical Cardiology, Stroke, and Cardiovascular Surgery and Anesthesia, American Heart Association: endorsed by the Infectious Diseases Society of America. *Circulation* 111:e394-e434, 2005.
8. Osler W: Gulstonian Lectures on Malignant Endocarditis: Lectures 1-3. *Lancet* 1:415-418, 1885.
9. Pelletier LL, Jr, Petersdorf RG: Infective endocarditis: a review of 125 cases from the University of Washington Hospitals, 1963-72. *Medicine (Baltimore)* 56:287-313, 1977.
10. Von Reyn CF, Levy BS, Arbeit RD, et al: Infective endocarditis: an analysis based on strict case definitions. *Ann Intern Med* 94:505-518, 1981.
11. Durack DT, Lukes AS, Bright DK: New criteria for diagnosis of infective endocarditis: utilization of specific echocardiographic findings. Duke Endocarditis Service. *Am J Med* 96:200-209, 1994.
12. Andres E, Baudoux C, Noel E, et al: The value of the Von Reyn and the Duke diagnostic criteria for infective endocarditis in internal medicine practice. A study of 38 cases. *Eur J Intern Med* 14:411-414, 2003.
13. Perez-Vazquez A, Farinas MC, Garcia-Palomo JD, et al: Evaluation of the Duke criteria in 93 episodes of prosthetic valve endocarditis: could sensitivity be improved? *Arch Intern Med* 160:1185-1191, 2000.
14. Stockheim JA, Chadwick EG, Kessler S, et al: Are the Duke criteria superior to the Beth Israel criteria for the diagnosis of infective endocarditis in children? *Clin Infect Dis* 27:1451-1456, 1998.
15. Heiro M, Nikoskelainen J, Hartiala JJ, et al: Diagnosis of infective endocarditis. Sensitivity of the Duke vs von Reyn criteria. *Arch Intern Med* 158:18-24, 1998.
16. Sekeres MA, Abrutyn E, Berlin JA, et al: An assessment of the usefulness of the Duke criteria for diagnosing active infective endocarditis. *Clin Infect Dis* 24:1185-1190, 1997.
17. Martos-Perez F, Reguera JM, Colmenero JD: Comparable sensitivity of the Duke criteria and the modified Beth Israel criteria for diagnosing infective endocarditis. *Clin Infect Dis* 23:410-411, 1996.
18. Olaison L, Hogevik H: Comparison of the von Reyn and Duke criteria for the diagnosis of infective endocarditis: a critical analysis of 161 episodes. *Scand J Infect Dis* 28:399-406, 1996.
19. Hoen B, Selton-Suty C, Danchin N, et al: Evaluation of the Duke criteria versus the Beth Israel criteria for the diagnosis of infective endocarditis. *Clin Infect Dis* 21:905-909, 1995.
20. Cecchi E, Parrini I, Chinaglia A, et al: New diagnostic criteria for infective endocarditis. A study of sensitivity and specificity. *Eur Heart J* 18: 1149-1156, 1997.
21. Dodds GA, Sexton DJ, Durack DT, et al: Negative predictive value of the Duke criteria for infective endocarditis. *Am J Cardiol* 77:403-407, 1996.
22. Li JS, Sexton DJ, Mick N, et al: Proposed modifications to the Duke criteria for the diagnosis of infective endocarditis. *Clin Infect Dis* 30:633-638, 2000.
23. Sachdev M, Peterson GE, Jollis JG: Imaging techniques for diagnosis of infective endocarditis. *Cardiol Clin* 21:185-195, 2003.
24. Anguera I, Miro JM, Cabell CH, et al: Clinical characteristics and outcome of aortic endocarditis with periannular abscess in the International Collaboration on Endocarditis Merged Database. *Am J Cardiol* 96:976-981, 2005.

25. Hill EE, Herijgers P, Claus P, et al: Abscess in infective endocarditis: the value of transesophageal echocardiography and outcome: a 5-year study. *Am Heart J* 154:923-928, 2007.
26. Anguera I, Miro JM, Vilacosta I, et al: Aortocavitary fistulous tract formation in infective endocarditis: clinical and echocardiographic features of 76 cases and risk factors for mortality. *Eur Heart J* 26:288-297, 2005.
27. Kang N, Wan S, Ng CS, Underwood MJ: Periannular extension of infective endocarditis. *Ann Thorac Cardiovasc Surg* 15:74-81, 2009.
28. Victor F, De Place C, Camus C, et al: Pacemaker lead infection: echocardiographic features, management, and outcome. *Heart* 81:82-87, 1999.
29. Baddour LM, Epstein AE, Erickson CC, et al: Update on cardiovascular implantable electronic device infections and their management: a scientific statement from the American Heart Association. *Circulation* 121:458-477, 2010.
30. Chu VH, Bayer AS: Use of echocardiography in the diagnosis and management of infective endocarditis. *Curr Infect Dis Rep* 9:283-290, 2007.
31. Khandheria BK: Suspected bacterial endocarditis: to TEE or not to TEE. *J Am Coll Cardiol* 21:222-224, 1993.
32. San Roman JA, Vilacosta I, Zamorano JL, et al: Transesophageal echocardiography in right-sided endocarditis. *J Am Coll Cardiol* 21:1226-1230, 1993.
33. Lindner JR, Case RA, Dent JM, et al: Diagnostic value of echocardiography in suspected endocarditis. An evaluation based on the pretest probability of disease. *Circulation* 93:730-736, 1996.
34. Roe MT, Abramson MA, Li J, et al: Clinical information determines the impact of transesophageal echocardiography on the diagnosis of infective endocarditis by the duke criteria. *Am Heart J* 139:945-951, 2000.
35. Erbel R, Rohmann S, Drexler M, et al: Improved diagnostic value of echocardiography in patients with infective endocarditis by transoesophageal approach. A prospective study. *Eur Heart J* 9:43-53, 1988.
36. Shapiro SM, Young E, Ginzton LE, Bayer AS: Pulmonic valve endocarditis as an underdiagnosed disease: role of transesophageal echocardiography. *J Am Soc Echocardiogr* 5:48-51, 1992.
37. Kupferwasser LI, Darius H, Muller AM, et al: Diagnosis of culture-negative endocarditis: the role of the Duke criteria and the impact of transesophageal echocardiography. *Am Heart J* 142:146-152, 2001.
38. Heidenreich PA, Masoudi FA, Maini B, et al: Echocardiography in patients with suspected endocarditis: a cost-effectiveness analysis. *Am J Med* 107:198-208, 1999.

38a. Kuruppu JC, Corretti M, Mackowiak, et al: Overuse of transthoracic echocardiography in the diagnosis of native valve endocarditis. *Arch Intern Med* 162(15):1715-1720, 2002.

39. Greaves K, Mou D, Patel A, Celermajer DS: Clinical criteria and the appropriate use of transthoracic echocardiography for the exclusion of infective endocarditis. *Heart* 89:273-275, 2003.
40. Fowler VG Jr, Li J, Corey GR, et al: Role of echocardiography in evaluation of patients with *Staphylococcus aureus* bacteremia: experience in 103 patients. *J Am Coll Cardiol* 30:1072-1078, 1997.
41. Abraham J, Mansour C, Veledar E, et al: *Staphylococcus aureus* bacteremia and endocarditis: the Grady Memorial Hospital experience with methicillin-sensitive *S. aureus* and methicillin-resistant *S. aureus* bacteremia. *Am Heart J* 147:536-539, 2004.
42. Fowler VG, Jr., Sanders LL, Kong LK, et al: Infective endocarditis due to *Staphylococcus aureus*: 59 prospectively identified cases with follow-up. *Clin Infect Dis* 28:106-114, 1999.
43. Fowler VG, Jr., Miro JM, Hoen B, et al: *Staphylococcus aureus* endocarditis: a consequence of medical progress. *JAMA* 293:3012-3021, 2005.
44. Wang A, Athan E, Pappas PA, et al: Contemporary clinical profile and outcome of prosthetic valve endocarditis. *JAMA* 297:1354-1361, 2007.
45. El-Ahdab F, Benjamin DK, Jr, Wang A, et al: Risk of endocarditis among patients with prosthetic valves and *Staphylococcus aureus* bacteremia. *Am J Med* 118:225-229, 2005.
46. Birmingham GD, Rahko PS, Ballantyne F 3rd: Improved detection of infective endocarditis with transesophageal echocardiography. *Am Heart J* 123:774-781, 1992.
47. Mugge A, Daniel WG, Frank G, Lichtlen PR: Echocardiography in infective endocarditis: reassessment of prognostic implications of vegetation size determined by the transthoracic and the transesophageal approach. *J Am Coll Cardiol* 14:631-638, 1989.
48. Bonow RO, Carabello BA, Kanu C, et al: ACC/AHA 2006 guidelines for the management of patients with valvular heart disease: a report of the American College of Cardiology/American Heart Association Task Force on Practice Guidelines (writing committee to revise the 1998 Guidelines for the Management of Patients with Valvular Heart Disease): developed in collaboration with the Society of Cardiovascular Anesthesiologists: endorsed by the Society for Cardiovascular Angiography and Interventions and the Society of Thoracic Surgeons. *Circulation* 114:e84-e231, 2006.
49. Lengyel M: The impact of transesophageal echocardiography on the management of prosthetic valve endocarditis: experience of 31 cases and review of the literature. *J Heart Valve Dis* 6:204-211, 1997.
50. Rozich JD, Edwards WD, Hanna RD, et al: Mechanical prosthetic valve-associated strands: pathologic correlates to transesophageal echocardiography. *J Am Soc Echocardiogr* 16:97-100, 2003.
51. Cabell CH, Heidenreich PA, Chu VH, et al: Increasing rates of cardiac device infections among Medicare beneficiaries: 1990-1999. *Am Heart J* 147:582-586, 2004.
52. Lo R, D'Anca M, Cohen T, Kerwin T: Incidence and prognosis of pacemaker lead-associated masses: a study of 1,569 transesophageal echocardiograms. *J Invasive Cardiol* 18:599-601, 2006.
53. Chu VH, Cabell CH, Benjamin DK, Jr, et al: Early predictors of in-hospital death in infective endocarditis. *Circulation* 109:1745-1749, 2004.
54. Di Salvo G, Habib G, Pergola V, et al: Echocardiography predicts embolic events in infective endocarditis. *J Am Coll Cardiol* 37:1069-1076, 2001.
55. Tischler MD, Vaitkus PT: The ability of vegetation size on echocardiography to predict clinical complications: a meta-analysis. *J Am Soc Echocardiogr* 10:562-568, 1997.
56. Thuny F, Di Salvo G, Belliard O, et al: Risk of embolism and death in infective endocarditis: prognostic value of echocardiography: a prospective multicenter study. *Circulation* 112:69-75, 2005.
57. Kim D-HK, Lee M-Z, Yun S-C, et al: Impact of early surgery on embolic events in patients with infective endocarditis. *Circulation* 122:S17-S22, 2010.
58. Heinle S, Wilderman N, Harrison JK, et al: Value of transthoracic echocardiography in predicting embolic events in active infective endocarditis. Duke Endocarditis Service. *Am J Cardiol* 74:799-801, 1994.
59. Dickerman SA, Abrutyn E, Barsic B, et al: The relationship between the initiation of antimicrobial therapy and the incidence of stroke in infective endocarditis: an analysis from the ICE Prospective Cohort Study (ICE-PCS). *Am Heart J* 154:1086-1094, 2007.
60. Cooper HA, Thompson EC, Laureno R, et al: Subclinical brain embolization in left-sided infective endocarditis: results from the Evaluation by MRI of the Brains of Patients with Left-sided Intracardiac Solid Masses (EMBOLISM) pilot study. *Circulation* 120:585-591, 2009.
61. De Castro S, Cartoni D, d'Amati G, et al: Diagnostic accuracy of transthoracic and multiplane transesophageal echocardiography for valvular perforation in acute infective endocarditis: correlation with anatomic findings. *Clin Infect Dis* 30:825-826, 2000.
62. Karalis DG, Bansal RC, Hauck AJ, et al: Transesophageal echocardiographic recognition of subaortic complications in aortic valve endocarditis. Clinical and surgical implications. *Circulation* 86:353-362, 1992.

62a. Lalani T, Cabell CH, Benjamin DK, et al: Analysis of the impact of early surgery on in-hospital mortality of native valve endocarditis: use of propensity score and instrumental variable methods to adjust for treatment-selection bias. *Circulation* 121(8):1005-1013, 2010.

63. Vikram HR, Buenconsejo J, Hasbun R, Quagliarello VJ: Impact of valve surgery on 6-month mortality in adults with complicated, left-sided native valve endocarditis: a propensity analysis. *JAMA* 290:3207-3214, 2003.
64. Shanewise JS, Cheung AT, Aronson S, et al: ASE/SCA guidelines for performing a comprehensive intraoperative multiplane transesophageal echocardiography examination: recommendations of the American Society of Echocardiography Council for Intraoperative Echocardiography and the Society of Cardiovascular Anesthesiologists Task Force for Certification in Perioperative Transesophageal Echocardiography. *J Am Soc Echocardiogr* 12:884-900, 1999.
65. Shapira Y, Vaturi M, Weisenberg DE, et al: Impact of intraoperative transesophageal echocardiography in patients undergoing valve replacement. *Ann Thorac Surg* 78:579-583; discussion 583-584, 2004.
66. Mestres CA, Fita G, Azqueta M, Miro JM: Role of echocardiogram in decision making for surgery in endocarditis. *Curr Infect Dis Rep* 12:321-328, 2010.

66a. Rosen AB, Fowler VG, Corey GR, et al: Cost effectiveness of transesophageal echocardiography to determine the duration of therapy for intravascular catheter-associated Staphylococcus aureus bacteremia. *Ann Intern Med* 130(10):810-820, 1999.

67. Liao L, Kong DF, Samad Z, et al: Echocardiographic risk stratification for early surgery with endocarditis: a cost-effectiveness analysis. *Heart* 94:e18, 2008.
68. Rohmann S, Erbel R, Darius H, et al: Prediction of rapid versus prolonged healing of infective endocarditis by monitoring vegetation size. *J Am Soc Echocardiogr* 4:465-474, 1991.

69. Vieira ML, Grinberg M, Pomerantzeff PM, et al: Repeated echocardiographic examinations of patients with suspected infective endocarditis. *Heart* 90:1020-1024, 2004.
70. Kort S: Real-time 3-dimensional echocardiography for prosthetic valve endocarditis: initial experience. *J Am Soc Echocardiogr* 19:130-139, 2006.
70a. Liu Y-W, Tsai W-C, Lin C-C, et al: Usefulness of real time three dimensional echocardiography for diagnosis of infective endocarditis. *Scandinavian Cardiovascular J* 43:318-323, 2009.
71. Cowan JC, Patrick D, Reid DS: Aortic root abscess complicating bacterial endocarditis. Demonstration by computed tomography. *Br Heart J* 52:591-593, 1984.
72. Allum C, Knight C, Mohiaddin R, Poole-Wilson P: Images in cardiovascular medicine. Use of magnetic resonance imaging to demonstrate a fistula from the aorta to the right atrium. *Circulation* 97:1024, 1998.
73. Akins EW, Slone RM, Wiechmann BN, et al: Perivalvular pseudoaneurysm complicating bacterial endocarditis: MR detection in five cases. *AJR Am J Roentgenol* 156:1155-1158, 1991.



# Aortic Stenosis: Disease Severity, Progression, Timing of Intervention, and Role in Monitoring Transcatheter Valve Implantation

RAPHAEL ROSENHEK, MD

**Imaging Aortic Stenosis**
Calcific Aortic Stenosis
Congenital Aortic Stenosis
Rheumatic Aortic Stenosis
Assessment of Aortic Valve Calcification
Aortic Root
Indirect Echocardiographic Findings Suggestive of Aortic Stenosis
Differential Diagnosis
**Quantification of Aortic Stenosis Severity**
Classical Echocardiographic Measures of Stenosis Severity
Other Measures of Severity
**Physiologic Variability in Measures of Stenosis Severity**
Exercise Hemodynamics in Valvular Aortic Stenosis
Changes in Aortic Valve Area with Changes in Volume Flow Rate
Change in Other Measures of Stenosis Severity with Change in Volume Flow Rate
Theoretical Considerations for a Measure of Stenosis Severity
**The LV Response to Valvular Aortic Stenosis**
Diastolic Function
Wall Stress and Concentric Hypertrophy
Gender Differences in the LV Response to Aortic Stenosis
Systolic Dysfunction
**Natural History, Progression, and the Role of Echocardiography in Clinical Decision Making**
Natural History of Aortic Stenosis
Progression of Aortic Stenosis
Risk Stratification
Timing of Surgery in Patients with Nonsevere Aortic Stenosis Undergoing Cardiac Surgery
Aortic Stenosis with Reduced LV Function or Flow
**Assessment of Interventional Risk and Choice of Procedure**
Preinterventional Assessment of Coronary Artery Disease
**Echocardiography in Transcatheter Aortic Valve Implantation**
Patient Selection
Valve Implantation

Aortic stenosis (AS) is the most frequent heart valve disease in developed countries, with an incidence of about 2% to 9% in elderly patients. Aortic sclerosis, which is the precursor of AS, is present in 29% of patients older than 65 years. With an ageing population, the widespread use of echocardiography and percutaneous treatment options, referrals of patients with AS are increasing.

Clinically, AS is suspected when a systolic murmur is detected or when compatible symptoms such as angina pectoris, exertional dyspnea, or syncope occur.

AS is coincidentally diagnosed in patients referred to echocardiography for other reasons. Echocardiography is the standard exam for diagnosis and quantification of AS, of associated valve lesions, and of implications for the left ventricle (LV). For an adequate interpretation, the limitations and pitfalls of the technique must be considered and are therefore treated in this chapter. The prognostic value of these echocardiographic findings is discussed, together with the natural history and progression of the disease, so as to be comprehensively included in an optimized management strategy. Echocardiography is essential in the screening of patients for transcatheter aortic valve implantation and the monitoring of the procedure.

## Imaging Aortic Stenosis

Calcific AS is the most common etiology of AS that is diagnosed, followed by rheumatic stenosis (which is in decline in Western societies) and congenital stenosis.[1] Roberts and Ko[2] report an incidence of bicuspid aortic valves of 53% in a large series of surgically excised stenotic aortic valves. These data suggest that in morphologically calcified aortic valves, an underlying congenital abnormality is not uncommon. At more advanced disease stages, also congenitally stenotic valves calcify, and mechanisms of calcification resemble those observed in calcific AS, making morphologic characterization of the aortic valve challenging.

### CALCIFIC AORTIC STENOSIS

AS is an active and progressive disease, showing parallels with atherosclerotic disease, such as inflammation, lipid infiltration, dystrophic calcification, and even ossification.[3] Thus, the historical concept that degenerative AS results from mechanical stress due to wear and tear of the aortic valve is outdated, and the term *calcific AS* is more appropriate. The stenotic valve

is indeed characterized by thickened and calcified cusps with reduced systolic opening and reduced leaflet motion (Fig. 23-1).

### CONGENITAL AORTIC STENOSIS

Congenitally stenotic aortic valves present as unicuspid, bicuspid, tricuspid, and quadricuspid valves.[4] Bicuspid valves, which account for the majority of these cases, are characterized by two cusps that are typically of different size, the larger cusp often containing a raphe (left over along the fusion line of two leaflets) (Fig. 23-2). A prominent raphe may make the differentiation from a tricuspid aortic valve difficult, and therefore the aortic valve opening should be displayed. Transesophageal echocardiography (TEE) may be required for an exact morphologic description.

Typically the leaflets in bicuspid aortic valves are oriented in an anterior-posterior or right-left manner.[5] Other malformations that are associated with a bicuspid aortic valve and that should be systematically ruled out are presence of an aortic coarctation, a persistent ductus arteriosus, or a ventricular septal defect. Unicuspid valves may present without an identifiable commissure (acommissural) or as unicommissural valves.

### RHEUMATIC AORTIC STENOSIS

Rheumatic AS is characterized by commissural fusion and thickening of the leaflet edges and sometimes leaflet retraction (Fig. 23-3). Not all the commissures are necessarily fused. Associated aortic regurgitation and mitral valve involvement are common in rheumatic disease.

### ASSESSMENT OF AORTIC VALVE CALCIFICATION

Aortic valve calcification is best assessed in a parasternal short-axis view. The degree of calcification can be classified into mild (isolated, small spots), moderate (multiple bigger spots), and severe calcification (extensive thickening/calcification of all cusps)[6] (Fig. 23-4). Because of its prognostic importance, the degree of aortic valve calcification should be routinely described. In the presence of severe calcification, an exact etiologic characterization of stenosis may be difficult.

### AORTIC ROOT

Echocardiography allows the assessment of the aortic annulus, aortic root, and ascending aorta. Aortic root dilation is present in about 50% of cases of bicuspid[7] but also unicuspid aortic valves.[8] Although the concept of a poststenotic dilatation due to hemodynamic factors is accepted, primary tissue abnormalities of the aortic media that are present in patients with congenitally malformed aortic valves contribute to further aortic dilation.[7]

### INDIRECT ECHOCARDIOGRAPHIC FINDINGS SUGGESTIVE OF AORTIC STENOSIS

Several indirect echocardiographic findings are suggestive of the presence of AS. Among them, an aliasing in the left ventricular (LV) outflow tract, LV hypertrophy, and, importantly, an increased aortic velocity should be noted.

### DIFFERENTIAL DIAGNOSIS

Although valvular AS accounts for most cases of LV outflow-tract obstruction, potential differential diagnoses include subvalvular or supravalvular stenosis and hypertrophic cardiomyopathy. Coexisting subvalvular obstruction, which may be present in addition to valvular AS should be ruled out.[9]

## Quantification of Aortic Stenosis Severity

A normally opening aortic valve is not obstructive to blood flow. It has an opening area of 3 to 4 $cm^2$ and the transvalvular flow is laminar with a peak velocity below 2 m/s. When the valve becomes stenotic, and thus obstructive to blood flow, a pressure drop occurs across the valve (Fig. 23-5). Aortic jet velocities increase with decreasing aortic valve area. When the aortic valve area becomes smaller than 1 $cm^2$, the increase of aortic jet velocity is most significant, indicative of the hemodynamic relevance of the obstruction. Several parameters have been proposed for the quantification of AS.[10] For an appropriate interpretation, understanding the theoretical background and the limitations of the respective measures is required. Some parameters, such as aortic jet velocity and aortic valve area have been extensively validated in clinical studies, whereas others are experimental. The integration of additional measures of severity can be helpful in selected cases.

### CLASSICAL ECHOCARDIOGRAPHIC MEASURES OF STENOSIS SEVERITY

#### *Doppler Measurements*

##### Transaortic Velocities and Gradients

Transaortic jet velocities are directly recorded by using a continuous-wave (CW) Doppler probe. Transvalvular gradients are derived from velocities using the Bernoulli equation, which is based on the conservation of energy principle in a closed system. In practice, accurate gradient calculations are performed using the simplified Bernoulli equation that ignores viscous losses and the effects of flow acceleration, both of which can generally be neglected in the clinical setting:

$$\Delta P = 4v^2$$

These Doppler-derived gradients have been shown to correlate well with invasively measured pressure gradients, both in the experimental and in the clinical setting.[11-16] Furthermore, the Doppler gradients also accurately reflect pressure gradient changes appearing with a change in flow rate.[11,12,17]

The simplified Bernoulli equation ignores the flow velocity proximal to the stenosis, which is an acceptable assumption when the transvalvular velocity is significantly greater than the proximal flow velocity. However, if this difference is less accentuated (i.e., in the presence of accelerated flow or less significant stenosis), the use of a more complete form of the Bernoulli equation is more appropriate, where $v_2$ and $v_1$ represent the transvalvular and the proximal flow velocities, respectively:

$$\Delta P = 4(v_2^2 - v_1^2)$$

The peak transaortic pressure gradient corresponds to the maximal pressure difference between the aorta and the LV. With increasing stenosis severity, the peak of the gradient occurs later during systole.[18]

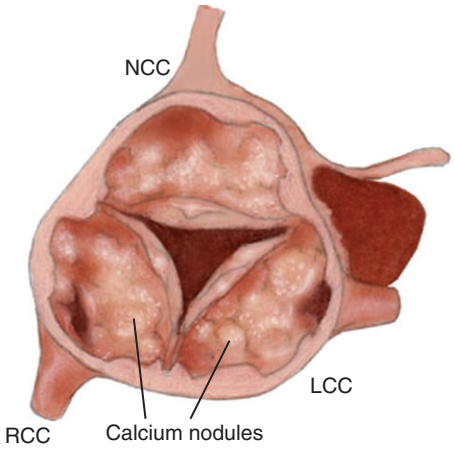



**Figure 23-1** Calcific aortic stenosis with thickened and calcified cusps in TEE short-axis view orientation. *LCC*, Left coronary cusp; *NCC*, noncoronary cusp; *RCC*, right coronary cusp.

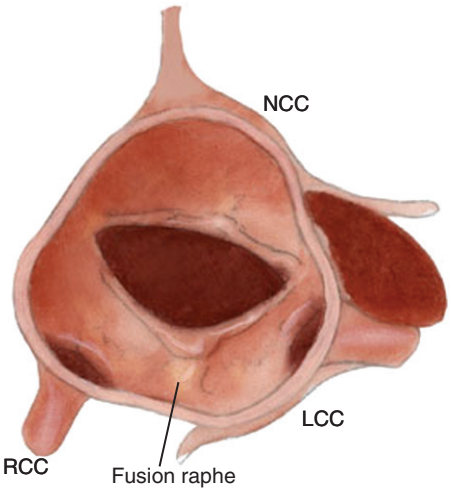



**Figure 23-2** Bicuspid aortic stenosis with anteroposterior orientation and raphe in TEE short-axis view orientation. *LCC*, Left coronary cusp; *NCC*, noncoronary cusp; *RCC*, right coronary cusp.

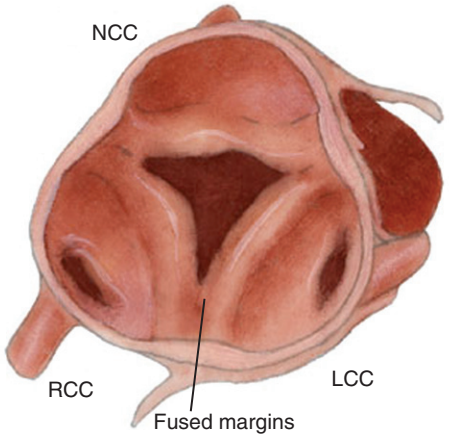



**Figure 23-3** Rheumatic aortic stenosis with commissural fusion, thickening of leaflet edges, and leaflet retraction in TEE short-axis view orientation. *LCC*, Left coronary cusp; *NCC*, noncoronary cusp; *RCC*, right coronary cusp.

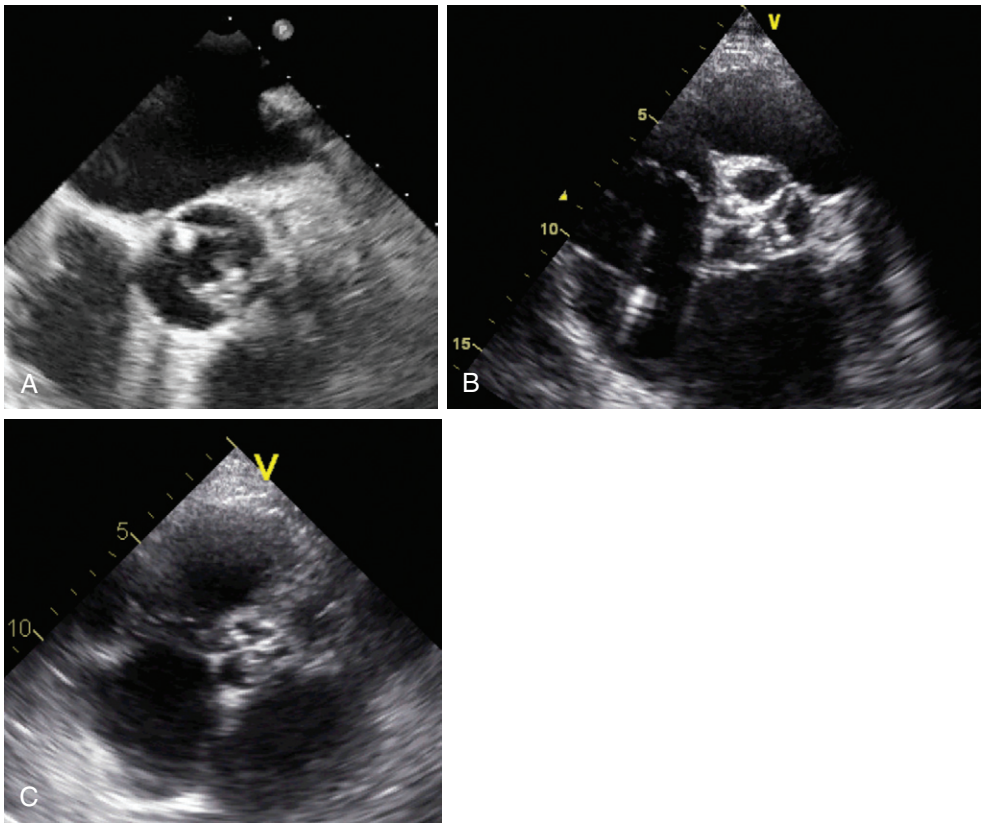



**Figure 23-4** **A,** Parasternal short-axis view of mildly calcified stenotic aortic valve showing isolated spots of calcification**. B,** Parasternal short-axis view of moderately calcified stenotic aortic valve showing multiple spots of calcification. **C,** Parasternal short-axis view of severely calcified stenotic aortic valve showing extensive calcification of all cusps.

The mean gradient is obtained by integrating the peak gradient over the duration of the entire systole. The relationship between peak and mean transaortic gradients is linear and can be expressed by the following equations (they apply to native aortic valve stenosis with its typical shape of the velocity curve over time only)[14,15,19]:

$$\text{Mean } \Delta P = (\text{Max } \Delta P/1.45) - 2.2 \quad \text{and}$$

$$\text{Mean } \Delta P = 2.4 \times V_{max}$$

This close relationship between mean and peak transaortic gradients on the one hand and peak aortic jet velocity on the other emphasizes the value of peak aortic jet velocity as a flow-dependent expression of stenosis severity in clinical decision making.

## Pitfalls

**Technical Considerations.** Care is required to record the maximal AS jet velocity, which requires aligning the Doppler probe with the jet direction. Any alignment error leads to an angle-dependent underestimation of the Doppler gradient. Multiple transducer positions (i.e., right parasternal, suprasternal, apical, and even subcostal) have to be used to obtain the peak signal, because the exact orientation of the aortic jet cannot be predicted from the two-dimensional (2D) image. The use of a small, dedicated CW Doppler transducer (so-called "pencil" probe) is mandatory to avoid a misclassification of AS severity, which may otherwise occur in about 20% of cases[20] (Fig. 23-6). The image window used to record peak transaortic velocity should be mentioned in the report. When determining rates of hemodynamic progression, measurements recorded from the same window must be used.

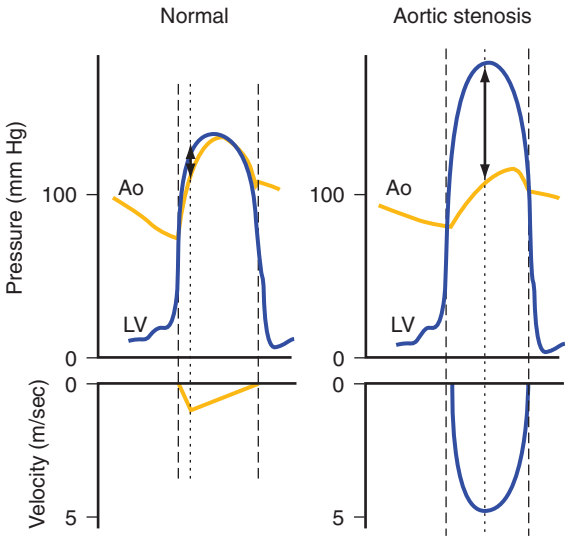



**Figure 23-5 Relationship of pressures to Doppler velocities in normal and aortic stenosis.** Note that maximum pressure gradient (*double-headed arrow*) corresponds to maximum Doppler velocity in both situations, but timing of the LV-to-Ao pressure gradient is quite different when valve obstruction is present. *Ao*, Aorta.

Even with an experienced operator and attention to technical details, there is some degree of measurement variability, so that a change in jet velocity of more than 0.2 m/s indicates actual progression of the disease in the absence of interval physiologic changes.[21]

**Other Signals.** While recording the Doppler signal, care has to be applied not to confound the signal with that of another form of obstruction or another flow signal such as that of mitral or tricuspid regurgitation. If the patient has atrial fibrillation, several consecutive beats need to be averaged to obtain a representative result.

**Pressure Recovery.** Pressure recovery may explain discrepancies between catheter and Doppler pressure gradients in patients with AS.[22-25] In valvular AS, a laminar high-velocity jet is present across the narrowed orifice.[26] The minimal cross-sectional area of the jet is called vena contracta: it has a smaller diameter and occurs distal to the anatomic valve orifice. Pressure is lowest and velocity is greatest at that level.

Distal to the vena contracta, the jet expands and decelerates. Because total energy remains constant according to Bernoulli's law, the velocity reduction is paralleled by an increase in aortic pressure. The Doppler gradient corresponds to the peak gradient at the site of the vena contracta and overestimates the catheter gradient that is measured farther downstream. In most cases the observed magnitude of pressure recovery is in the range of 10 mm Hg and does not affect clinical decision making.[22] However, pressure recovery may be significant in the presence of less severe AS and a small ascending aorta.[27] The phenomenon can be predicted from Doppler velocity, aortic valve area, and the size of the ascending aorta.[24] Thus, patients with severe AS and poststenotic aortic root dilation may show less pressure recovery than patients with mild-to-moderate stenosis and a small or normal aortic root dimension.

**Flow Dependence of Measurements.** Doppler measurements of AS severity are limited by their flow dependence. The presence of a high flow rate such as in hyperdynamic states or in the presence of significant aortic regurgitation may lead to an overestimation of AS severity. On the other hand, a low flow rate that can be observed in the presence of a depressed LV function or coexisting mitral regurgitation may lead to an underestimation of AS severity. Furthermore, there are intraindividual variations of aortic jet velocity due to changes in transaortic flow volume such as those occurring during exercise. If the patient is not in sinus rhythm—atrial fibrillation being common—there is a beat-to-beat variability in flow

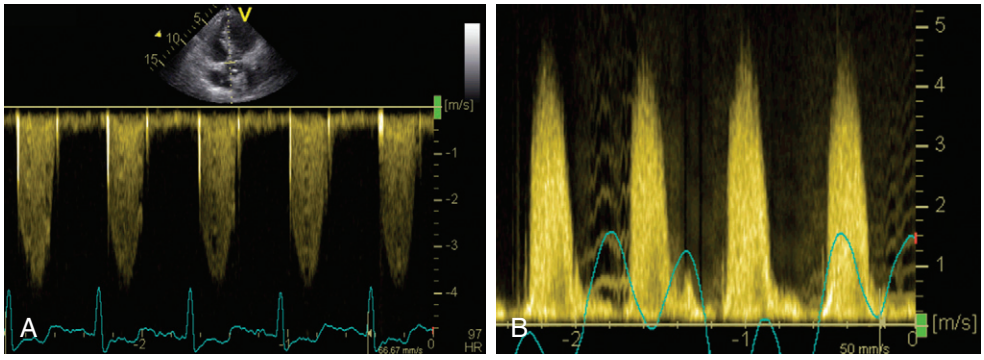



**Figure 23-6** CW Doppler tracings of aortic stenosis velocity obtained from apical (**A**) and right parasternal recording using dedicated CW probe (**B**) in the same patient. This example emphasizes importance of alignment of Doppler probe with aortic jet direction in order to record maximal signal and not to underestimate severity of stenosis.

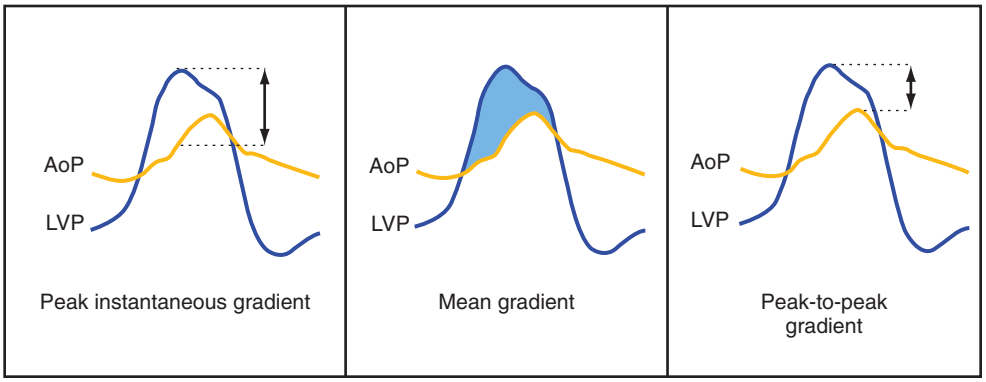



**Figure 23-7** Peak Doppler echocardiographic gradient corresponds to maximal difference between aortic pressure (*AoP*) and instantaneous LV pressure (*LVP*) (*left*). Mean gradients represent average pressure difference between aorta and LV over systolic ejection (*middle*). "Peak-to-peak" gradient corresponds to difference between peak aortic pressure and peak LV pressure (*right*).

measurements, and several consecutive beats need to be averaged.

It is therefore important to rely not only on a flow-dependent but also on a relatively flow-independent measure of AS severity: the calculated aortic valve area.

### Comparison with Catheter-Measured Gradients

Doppler and invasively measured mean gradients both represent the average pressure difference between the aorta and the LV over the systolic ejection period and should ideally be identical when simultaneously recorded in practice.

The peak Doppler echocardiographic gradient corresponds to the maximal instantaneous difference between the aortic and the LV pressure.

The catheter-derived "peak-to-peak" gradient, which cannot be determined by Doppler echocardiography, does not exist physiologically and corresponds to the difference between peak aortic pressure and peak LV pressure (Fig. 23-7).

### *Valve Area Calculation*

Calcific AS is characterized by stiff leaflets that open to a variable degree depending on the force applied on the valve. This limits attempts at direct measurement of aortic valve area and even applies to the situation where the surgeon applies direct force, inspecting the valve with the finger.

### Continuity Equation

The continuity equation method for the calculation of valve area[11,15,28-31] is based on the consideration that the same stroke volume crosses the LV outflow tract and the aortic valve.

Aortic valve area (AVA) is calculated as

$$AVA = (CSA_{LVOT} \times VTI_{LVOT})/VTI_{AS}$$

where $VTI_{LVOT}$ and $VTI_{AS}$ represent velocity time integrals at the levels of the LV outflow tract and the stenotic aortic valve, respectively, and $CSA_{LVOT}$ represents the cross-sectional area in the outflow tract.

A simplified form of the continuity equation in which velocities are measured instead of velocity-time integrals can be used in clinical routine where velocities in the LV outflow tract and across the aortic valve are measured:

$$AVA = (V_{LVOT} \times CSA_{LVOT})/V_{AS}$$

where $V_{LVOT}$ and $V_{AS}$ represent the velocities in LV outflow tract and at the level of the stenotic aortic valve, respectively.

The LV outflow tract flow velocity profile is measured from an apical approach using pulsed-wave (PW) Doppler ultrasound. The AS jet velocity profile is measured with CW Doppler from the echocardiographic window that yields the highest velocity signal (Fig. 23-8). Theoretically, volume flow rate can be measured at several intracardiac sites (pulmonary artery, mitral annulus, and LV outflow tract). Flow measurements just proximal to the stenotic aortic valve are technically feasible in nearly all adult patients, whereas volume flow-rate calculations at other intracardiac sites often are limited by image quality. Furthermore, when coexisting aortic regurgitation is present (encountered to some degree in more than 80% of adults with AS), volume flow measured across other valves may not equal the volume flow rate across the aortic valve.[21] Thus, in practice, the LV outflow tract is used for measurement of transaortic volume flow rate in nearly all cases. Volume flow measurement proximal to the stenotic aortic valve assumes that (1) the cross-sectional area of flow is circular in systole and flow fills the anatomic cross-sectional area, (2) the pattern of blood flow is laminar with uniform parallel stream lines of flow, (3) cross-sectional area and flow velocity are measured at the same site, and (4) the spatial flow velocity profile is relatively "flat" (same flow velocities in the center and at the edges of the flow stream) during ventricular ejection. The assumptions of a circular cross-sectional area with flow filling the anatomic area have been corroborated by short-axis 2D and color flow imaging in animal models and in patients with valvular obstruction.[15] Laminar flow is confirmed by recording a narrow band of velocities throughout ejection on the PW Doppler spectral tracing.

For the determination of $CSA_{LVOT}$, the LV outflow tract diameter is measured in midsystole from a 2D parasternal long-axis view, parallel and adjacent to the aortic valve plane. In this view the outflow tract is perpendicular to the ultrasound beam, and axial resolution provides a more accurate diameter measurement than the use of apical views. In practice, zooming in on the area of interest and confirmation of the diameter from an apical five-chamber view is recommended.

Continuity equation valve area calculations assume accurate recording of the maximum aortic jet velocity, as discussed earlier for pressure gradients. The area is then calculated assuming a circular outflow tract, although it is oval in most patients.

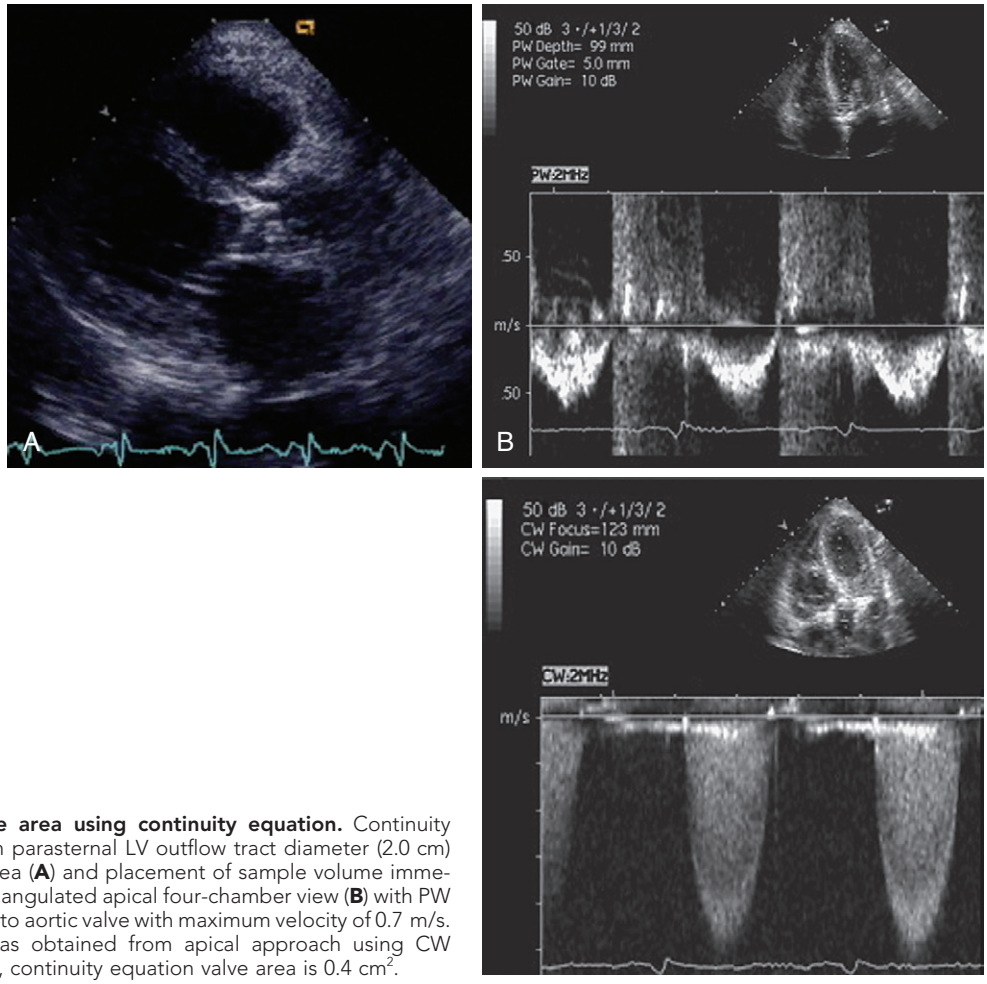



**Figure 23-8 Calculation of aortic valve area using continuity equation.** Continuity equation valve area is calculated based on parasternal LV outflow tract diameter (2.0 cm) for calculation of circular cross-sectional area (**A**) and placement of sample volume immediately proximal to aortic valve in anteriorly angulated apical four-chamber view (**B**) with PW Doppler recording of laminar flow proximal to aortic valve with maximum velocity of 0.7 m/s. Highest velocity aortic signal (5.2 m/s) was obtained from apical approach using CW Doppler (**C**) in this patient. In this example, continuity equation valve area is 0.4 $cm^2$.

In addition, the mean inter- and intraobserver variabilities of the outflow tract diameter measurement are in the range of 5% to 8%, resulting in a variability of about 0.15 $cm^2$ for a calculated valve area of 1.0 $cm^2$. In an individual patient, the outflow tract diameter remains relatively constant over time, such that a change of more than 0.1 $cm^2$ most likely represents an actual change in valve area over time.

For the calculation of the circular cross-sectional outflow tract area, the LV outflow tract diameter is measured in the parasternal long-axis view, immediately adjacent and parallel to the aortic valve plane in midsystole. To ensure that diameter and flow measurements are recorded from the same anatomic site, both measurements should be made as close to the aortic valve as possible. In theory, the tapering of the outflow tract and the acceleration of blood during systole, both of which result in blunt flow profiles at the entrance to large vessels, allow the assumption of a relatively "flat" spatial flow profile in the outflow tract. A direct examination of the spatial flow profile in the LV outflow tract proximal to the stenotic aortic valve was initially performed with conventional PW Doppler by recording flow at sequential sites across the outflow tract.[21,32] Another study, using color flow mapping in patients with AS both before and after aortic valve replacement, showed variable skewing in the spatial flow profile, with highest velocities most often encountered in the region from the center of the outflow tract toward the septum[33] (Fig. 23-9). Patients with predominant AS were found to have relatively flat flow profiles, whereas normal subjects and patients with aortic regurgitation had skewed velocity profiles with the highest velocities occurring anteroseptally.[34] For clinical practice, even when the flow profile is skewed to some extent, a reasonably accurate volume flow rate can be calculated if the recorded flow velocity reasonably approximates the spatial and temporal flow velocity in the outflow tract.

Ideally, the accuracy of Doppler transaortic volume flow measurements should be validated by comparison to an established standard of reference. This is difficult in clinical studies, because most patients with AS have coexisting aortic and/or mitral regurgitation. Even a hemodynamically "insignificant" regurgitation will lead to an inaccurate assessment of forward (Fick or thermodilution) and of total (angiographic) cardiac output, thereby inadequately representing the volume flow rate across the aortic valve. In the research setting, transaortic volume flow rate can be measured directly, using an electromagnetic or a transit time flow meter. In both acute and chronic models of valvular AS, Doppler transaortic volume flow rates have been shown to be accurate (Table 23-1)[15,17] with a standard error of the estimate of 2 to 4 mL for stroke volume and of 0.25 to 0.5 L/min for cardiac output over a wide range of flow rates (Fig. 23-10).

## Comparison of Valve Areas Calculated by the Continuity Equation and by the Gorlin Formula

Aortic valve areas calculated from invasive hemodynamic data using the formula of Gorlin and Gorlin,[35] which was published in 1951, have been used as the standard of reference for validation of continuity equation valve areas.[21,31,36]

Understanding the different underlying principles of these equations is important (Fig. 23-11). According to the formula by Gorlin and Gorlin, aortic valve area is calculated as

$$AVA = (\text{cardiac output}) \Big/ \left(HR \times SEP \times 44.3 \times \sqrt{\Delta P_{mean}}\right)$$

where $\Delta P_{mean}$ represents the manometrically measured mean pressure gradient, SEP is the systolic ejection period, and HR is the heart rate.

Accurate pressure gradient measurements depend on careful attention to frequency response, damping, and catheter positioning. The use of a double-lumen catheter as opposed to measurement of the femoral artery pressure as a surrogate for the aortic pressure provides more accurate results. Cardiac output should reflect transaortic volume flow rate. Although the Fick or thermodilution methods can be used to calculate cardiac output in isolated AS, an angiographically assessed cardiac output is more appropriate in the presence of aortic regurgitation. In the presence of both mitral and aortic regurgitation, an accurate invasive determination of the transaortic volume flow rate is not possible in the clinical setting.

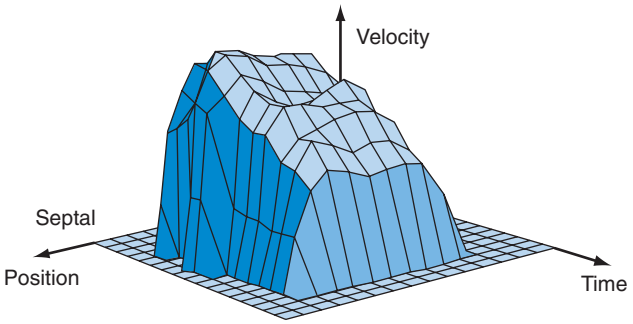



**Figure 23-9 3D plot of velocity distribution in LV outflow tract close to level of aortic annulus.** Velocity is plotted against position in LV outflow tract diameter and against time. There are 20-ms intervals along time axis and approximately 2 mm between each observation along diameter axis. *(From Wiseth R, Samstad S, Rossvoll O, et al: Cross-sectional left ventricular outflow tract velocities before and after aortic valve replacement: a comparative study with two-dimensional Doppler ultrasound.* J Am Soc Echocardiogr *6:279-285, 1993.)*

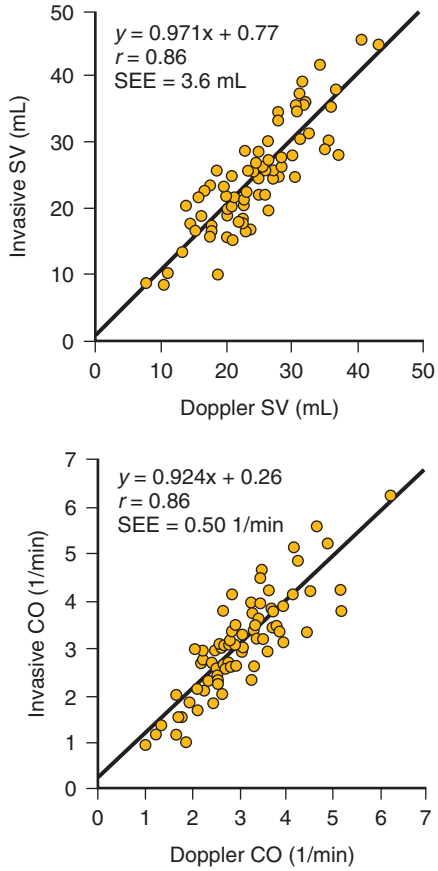



**Figure 23-10** Correlation of simultaneous echo-Doppler and ascending aortic transit time stroke volume (*SV*) and cardiac output (*CO*) during 75 separate interventions. *(From Burwash IG, Forbes AD, Sadahiro M, et al: Echocardiographic volume flow and stenosis severity measures with changing flow rate in aortic stenosis.* Am J Physiol *265:H1734-H1743, 1993.)*

**TABLE 23-1 In Vivo Studies of Simultaneous Invasive and Doppler Volume Flow Measurements from LV Outflow Tract at Aortic Annulus in Subjects with AS and Subjects without AS**

| *Model* | n | *Standard of Reference* | Cardiac Output r | Cardiac Output *Range, L/min* | Cardiac Output *SEE, L/min* | Stroke Volume r | Stroke Volume *Range, mL* | Stroke Volume *SEE, mL* | *Study* |
|---|---|---|---|---|---|---|---|---|---|
| Chronic valvular AS (closed- and open-chest dogs) altered volume flow rate | 75 | Transit time-flow | 0.86 | 0.9-6.2 | 0.50 | 0.86 | 9-45 | 3.6 | Burwash[17] |
| Acute valvular AS (open-chest dogs) altered volume flow rate | 52 | Electromagnetic flow | 0.90 | 0.9-3.2 | 0.25 | 0.88 | 5-26 | 2.4 | Otto[15] |
| Normal (open-chest dogs) altered volume flow rate | 33 | Roller pump | 0.98 | 0.5-5.0 | 0.30 | NA | NA | NA | Stewart |
| Patients (no AS) | 35 | Thermodilution | 0.91 | 2.1-9.5 | 0.63 | 0.95 | 24-87 | 6.4 | Lewis |
| Patients (no AS) | 31 | Thermodilution | 0.90 | 1.6-8.4 | 0.95 | NA | NA | NA | Labovitz |

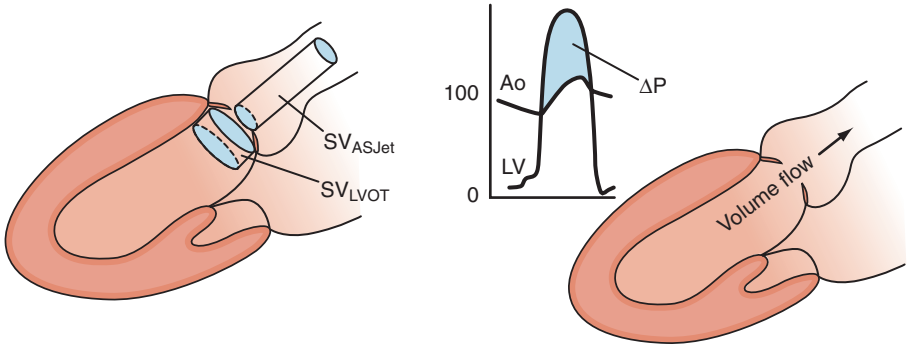
*AS*, Aortic stenosis; *SEE*, standard error of the estimate.

References

Stewart WJ, Jiang L, Mich R, et al: Variable effects of changes in flow rate through the aortic, pulmonary and mitral valves on valve area and flow velocity: impact on quantitative Doppler flow calculations. *J Am Coll Cardiol* 6:653-662, 1985.

Lewis JF, Kuo LC, Nelson JG, et al: Pulsed Doppler echocardiographic determination of stroke volume and cardiac output: clinical validation of two new methods using the apical window. *Circulation* 70:425-431, 1984.

Labovitz AJ, Buckingham TA, Habermehl K, et al: The effects of sampling site on the two-dimensional echo-Doppler determination of cardiac output. *Am Heart J* 109:327-332, 1985.




$SV_{LVOT} = SV_{ASJet}$

$CSA_{LVOT} \times VTI_{LVOT} = AVA \times VTI_{ASJet}$

$AVA = (VTI_{LVOT} \times CSA_{LVOT})/VTI_{ASJet}$

$Flow = AVA \times V \times C_C$

$V^2 = (C_V)^2 \times 2g \times \Delta P$

$V = C_V \times \sqrt{2g\,\Delta P}$

$AVA = Flow/(44.3 \times C_C \times C_V\sqrt{\Delta P})$

**Figure 23-11** Comparison of Gorlin and continuity-equation valve areas. *Ao*, Aorta; $AS_{Jet}$, aortic stenosis jet; *AVA*, aortic valve area; $C_C$, coefficient of orifice contraction; *CSA*, cross-sectional area; $C_V$, coefficient of velocity; *ΔP*, pressure gradient; *LVOT*, left ventricular outflow tract; *SV*, stroke volume; *V*, velocity of flow; *VTI*, velocity-time integral.

The Gorlin formula contains an empirically derived constant (C) incorporating the coefficient of contraction, reflecting the difference between the anatomic valve area and the area of the vena contracta; the coefficient of velocity, relating to the conversion of potential to kinetic energy; measurement of pressure in mm Hg; and an empiric "correction" factor. Both in vitro and in vivo studies suggest that the Gorlin constant may vary with changes in volume flow rate, orifice shape, and stenosis severity.[37,38]

When comparing Gorlin and continuity-equation valve areas, it is fundamental to bear in mind that they measure different parameters: The Gorlin formula examines the hydraulic load and calculates an anatomic orifice area, whereas the continuity equation describes the physiologic flow area of the vena contracta.[39,40] Thus, one cannot expect these two measurements to yield identical results. Pressure recovery is contributing to this discrepancy.[41] In terms of clinical decision making, their precision, reproducibility, and ability to predict patient outcome are more important than agreement or disagreement. As Gorlin and Gorlin[42] note:

> *We need not be frustrated when valve areas derived by two different methods are not the same. Rather, we should, like the princes of Serendip, seize upon the difference for what it reveals about the anatomy of the valve orifice as opposed to the physiology of the total obstructing valve tract under active pressure and flow conditions.*

## Definition of the Degree of Severity

Quantification of AS severity is fundamental in the clinical context. Conceptually AS severity can be considered as a continuum ranging from aortic sclerosis to hemodynamically significant disease. Thus, the actual measure of severity should be integrated in the decision-making process. The categorical differentiation between severe and nonsevere stenosis is of particular importance because of direct implications for patient management. Information from aortic jet velocity, mean gradient, and valve area should be integrated and is ideally concordant. In the past, "severe" or "critical" AS has been defined in terms of a specific valve area. Recent clinical studies have used a peak aortic jet velocity of 4 m/s or more to define severe AS.[6,43,44]

Cutoff values for the effective aortic valve area in the range of 0.8 to 1 $cm^2$ to define severe AS are encountered in the literature, but more recent guidelines recommend an area of 1 $cm^2$.[45,46] However, a marked overlap in hemodynamic severity between symptomatic and asymptomatic patients indicates that the "critical" degree of valve narrowing varies from patient to patient (Fig. 23-12). This observation has been confirmed in prospective studies showing that symptom onset occurs with a jet velocity lower than 4.0 m/s or may be delayed until the jet velocity is over 5.0 m/s. The variability of valve areas for a given aortic jet velocity is large.[47] In addition, even among patients with very advanced disease, defined by an aortic jet velocity of 5 m/s, valve areas ranged between 0.3 and 0.9 $cm^2$, further emphasizing the limited accuracy of calculated valve area in clinical routine use.[48] Nevertheless, a valve area below 1.0 $cm^2$ has a high sensitivity to identify patients with severe AS. In the presence of a preserved transaortic flow, peak aortic jet velocity is probably the most robust and predictive measure of severity. Because of the increasing likelihood of symptom development with increasing aortic jet velocities, the entity of very severe AS might be defined. In this context, using a threshold for the peak aortic jet velocity of 5 m/s or more has been suggested. The transaortic gradient almost doubles with an increase of peak aortic velocity from 4.0 to 5.5 m/s: Because of the quadratic relationship, the gradients corresponding to velocities of 4.0, 5.0, and 5.5 m/s are 64, 100, and 121 mm Hg, respectively. Although all of these velocities correspond to "severe" AS, it is obvious that the hemodynamic repercussions are different, further supporting the concept of a delineation of "very severe" AS.

It has been suggested that an aortic valve area indexed to body surface area of less than 0.6 $cm^2/m^2$ defines severe AS.[49] However, because of a distortion of indexed valve areas at the extremes of the spectrum of body surface area, such as in slim and small or in obese persons, the value is inherently limited. From a pragmatic approach, it is recommended to consider patient stature and build when quantifying AS severity. The quantification of AS needs to be individualized, particularly when the measured values are in the borderline zone between

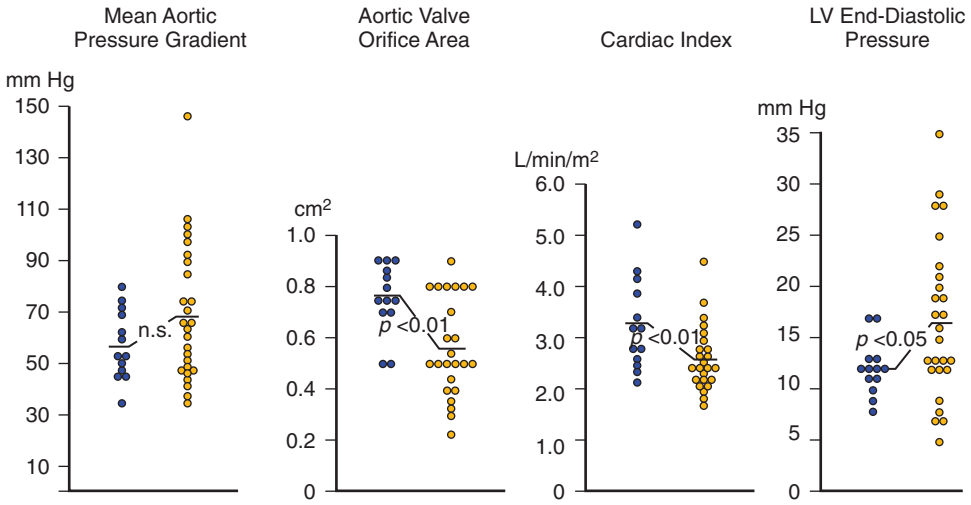



**Figure 23-12** Hemodynamically severe aortic stenosis: mean aortic pressure gradient, valve orifice area, cardiac index, and LV end-diastolic pressure in severely symptomatic (*open circles*) and asymptomatic or mildly symptomatic (*closed circles*) patients. Mean value (*horizontal line*) and statistical difference between both groups are indicated. *n.s.*, Not significant. *(From Turina J, Hess O, Sepulcri F, et al: Spontaneous course of aortic valve disease.* Eur Heart J *8:471-483, 1987.)*

moderate and severe stenosis. In this regard, consideration of the symptomatic status of the patient is essential.

The differentiation between different degrees of nonsevere stenosis (i.e., aortic sclerosis, mild and moderate stenosis) is less critical with regard to immediate therapeutic choices but is relevant to determine prognosis and schedule follow-up exams.[43,50,51] Mild AS is defined by a valve area of more than 1.5 $cm^2$, a mean gradient of less than 25 mm Hg, and an aortic jet velocity of less than 3.0 m/s.

## OTHER MEASURES OF SEVERITY

### *Velocity Ratio*

The velocity ratio is defined as the ratio of velocities in the LV outflow tract and across the aortic valve:

$$\text{Velocity ratio} = V_{LVOT}/V_{AS}$$

or

$$\text{Velocity time integral ratio} = VTI_{LVOT}/VTI_{AS}$$

Severe stenosis is defined by a velocity (or VTI) ratio of less than 0.25.

This measure has the theoretical advantages of being flow independent and of not requiring LV outflow tract measurements (in contrast to the continuity equation). However, its prognostic value has not been validated in large clinical series.

### *Aortic Valve Resistance*

Valve resistance (expressed in dynes-s-$cm^{-5}$) is calculated from invasive or Doppler data as[52,56,57]

$$\text{Resistance} = (\Delta P_{mean}/Q_{mean}) \times 1333$$

where $\Delta P_{mean}$ (in mm Hg) and $Q_{mean}$ (in mL/s) represent the mean transaortic pressure gradient and the mean volume flow rate, respectively, and 1333 is a conversion factor. The concept of valve resistance offers the advantage that no empirical constant is involved as compared to the Gorlin formula. Several investigators have observed a curvilinear relationship between valve resistance and valve area (with invasive and Doppler data).[52] This observation is supported by the mathematical derivation of the valve area and resistance concepts. In fact, the concepts of valve area and valve resistance are to some extent mutually exclusive. Valve area calculations with the Gorlin formula assume a quadratic relationship between pressure gradient and flow rate. Conversely, the valve resistance concept assumes a linear relationship between these two variables. Most clinical and experimental data support the concept of a quadratic, rather than linear, relationship between pressure gradient and flow rate across a stenotic valve[53] (Fig. 23-13). More complete modeling of the interaction among the LV, the valve, and the peripheral vasculature may enhance our understanding of the hemodynamics of valvular AS.[54] From several studies, it appears that valve resistance is flow dependent and thus does not offer a direct advantage over valve area calculations.[55,56] Because of a lack of consensus among studies as to whether it adds information to conventional measures of severity, valve resistance has not gained widespread clinical acceptance.[52,57]

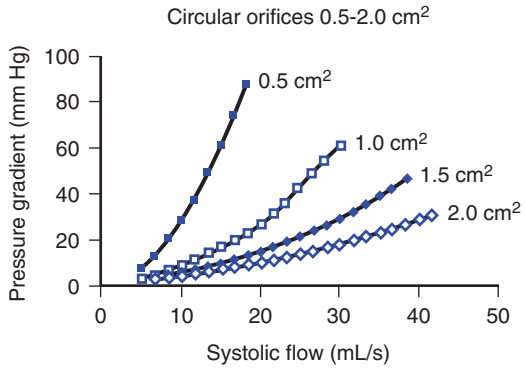



**Figure 23-13** Plot of square-law dependence of pressure gradient on flow demonstrated for circular stenoses with orifices from 0.5 to 2.0 $cm^2$. *(From Voelker W, Reul H, Nienhaus G, et al: Comparison of valvular resistance, stroke work loss, and Gorlin valve area for quantification of aortic stenosis. An in vitro study in a pulsatile aortic flow model.* Circulation *91:1196-1204, 1995.)*

### *Stroke Work Loss*

Based on the energy-loss concept, the amount of work expended by the LV to keep the aortic valve open during systole compared to the amount of work resulting in effective forward blood flow has been proposed as a potential measure of stenosis severity. This measure would reflect the intrinsic stiffness of the valve leaflets and thus be less dependent on volume flow rate.[58,59] For a stenotic aortic valve, the difference between work calculated from LV pressures and aortic pressures represents the amount of work "lost" in opening the stiff leaflets. When the aortic valve opens normally, this difference is not significant. Work is calculated by generating a power curve, multiplying instantaneous flow with pressure. Total potential stroke work is calculated by integrating power over the systolic ejection period[59] either using LV (for total work) or aortic (for effective work) pressures. The steady component of work is defined as mean systolic pressure multiplied by stroke volume; pulsatile work is defined as total minus steady work. Stroke work loss then represents the difference between LV and effective work and can be calculated for total, steady, and pulsatile components[58] as

$$\text{LV stroke work loss} = \text{LV work} - \text{effective work}$$

Because potential work increases with an increasing flow rate, the potential work loss across the stenotic valve is indexed for volume flow rate and expressed as the percent LV stroke work loss.

$$\%\ \text{LV stroke work loss} = (\text{stroke work loss}/\text{LV stroke work}) \times 100$$

Given that stroke work is the instantaneous product of pressure and flow, and stroke work loss is the difference of LV and aortic work, this proposed index of stenosis severity is likely to vary with volume flow rate if the actual degree of valve opening varies. Note that when the ratio of LV to aortic work is calculated, the terms for transaortic volume flow rate cancel each other, so that stroke work loss can be determined from Doppler pressure calculations alone. A new index of energy loss that takes body surface area into account and can be calculated from Doppler-derived data was evaluated in an experimental model[60] assessing fixed stenoses and bioprosthetic valves of two sizes at different flow rates.

### *Planimetry of the Aortic Valve Area*

The opening surface of a stenotic aortic valve represents a complex three-dimensional (3D) structure that cannot be reliably assessed with a planar 2D image. The presence of valvular calcification may further limit an accurate delineation of the valve orifice.[61]

Whereas some investigators have reported favorable correlations between planimetered stenotic orifice areas obtained on multiplane TEE and continuity equation valve areas and/or Gorlin valve areas,[62] others have found planimetry of the aortic orifice to be difficult and less accurate than continuity-equation valve areas obtained from transthoracic imaging.[63] However, valve area planimetry may be helpful when transthoracic imaging quality is poor, such as in ventilated patients.

### *3D Echocardiography*

3D echocardiography is increasingly integrated in commercial echocardiographic systems, and good imaging quality can be obtained, particularly when using a transesophageal approach. Recent series report the feasibility of the method in the majority of patients with a good correlation of the valve area derived by flow-derived methods or standard TEE.[64]

## Physiologic Variability in Measures of Stenosis Severity

### EXERCISE HEMODYNAMICS IN VALVULAR AORTIC STENOSIS

Exercise testing is contraindicated in symptomatic patients with valvular AS, because of the high risk of complications.[65] However, it can be safely performed in asymptomatic patients, where a number of studies have provided an insight into the relationship between hemodynamic severity and clinical symptoms[66,67] (Table 23-2). In asymptomatic patients with AS, exercise results in an appropriate rise in heart rate and cardiac output. The increase in cardiac output with upright exercise is mediated almost entirely by heart rate, with little change in stroke volume. However, even though stroke volume remains constant, transaortic volume flow rate is increased because of the shortening of the systolic ejection period. Thus, exercise results in an increase in peak aortic jet velocity, with a corresponding increase in the mean transaortic gradient as predicted by the Bernoulli equation.

The continuity equation predicts a linear relationship between maximum volume flow rate ($Q_{max}$) and maximum jet velocity ($V_{max}$) for any given valve area.[66] In clinical studies—where normally only two data points can be acquired—the slope of the change in $V_{max}$ relative to $Q_{max}$ parallels the slope predicted by the continuity equation in patients when the valve area remains constant with exercise. If the valve area increases with exercise, the observed slope is greater than that predicted for a fixed valve area.

### CHANGES IN AORTIC VALVE AREA WITH CHANGES IN VOLUME FLOW RATE

The effect of changes in volume flow rate on valve areas calculated using the Gorlin and the continuity equations has been examined in in vitro and animal models[68] and in patients with valvular AS (Fig. 23-14). These studies consistently show an increase in valve area with an increase in transaortic volume flow rate.[56,58,69-75] Although these apparent increases could be due to some extent to errors inherent to the valve area formulas, the concept that valve area itself, both anatomic and physiologic, varies with transaortic volume flow rate is supported by in vitro pulsatile flow model data[53] and video imaging of flow-dependent changes in valve opening.[76] The effects of flow-rate changes on valve area are not due to artifacts but can be explained by an actual increase in leaflet opening with increasing flow rates and to unsteady effects at low flow rates.[77] This finding is in agreement with the observation that even normal aortic valve leaflets open less when volume flow rate is decreased—for example, in patients with a dilated cardiomyopathy.

### CHANGE IN OTHER MEASURES OF STENOSIS SEVERITY WITH CHANGE IN VOLUME FLOW RATE

Some investigators have suggested that valve resistance is independent of flow rate,[78] whereas others have shown changes in valve resistance with changes in volume flow rate in in vitro models,[53] in animal models, and in patients with asymptomatic AS.[17,71] In part, the relative stability of valve resistance with changes in flow rate observed in some studies[52] may relate to the range of stenosis severity evaluated. Because of the

**TABLE 23-2 Physiologic Changes with Exercise in Adults with Valvular AS**

| | *Bache (1971)*[70] | *Ettinger (1972)** | *Otto (1992)*[66] | *Martin (1992)*[74] | *Burwash (1994)*[71] |
|---|---|---|---|---|---|
| n | 20 | 10 | 28 | 85 | 110 |
| Measurements | Invasive | Invasive | Doppler-echo | Invasive | Doppler-echo |
| Type of exercise | Supine bicycle | Supine bicycle | Treadmill | Supine bicycle | Treadmill |
| HR (bpm) | | | | | |
| Rest | 79 ± 3 | 87 ± 5 | 71 ± 17 | 71 ± 2 | 63 ± 14 |
| Exercise | 112 ± 5 | 109 ± 5 | 147 ± 28 | 98 ± 2 | 104 ± 23 |
| Systolic BP (mm Hg) | | | | | |
| Rest | 120 ± 3 | 118 ± 8 | 139 ± 15 | — | 143 ± 22 |
| Exercise | 136 ± 3 | 133 ± 8 | 155 ± 24 | — | 163 ± 29 |
| SV (mL) | | | | | |
| Rest | — | — | 98 ± 29 | — | 103 ± 30 |
| Exercise | — | — | 89 ± 32 | — | 96 ± 30 |
| $Q_{mean}$ (mL/s) | | | | | |
| Rest | 245 ± 14 | — | 300 ± 85 | 275 ± 8 | 319 ± 80 |
| Exercise | 318 ± 21 | — | 366 ± 159 | 325 ± 10 | 400 ± 140 |
| CO (L/min) | | | | | |
| Rest | 5.4 ± 0.3 | 8.6 ± 1.1 | 6.5 ± 1.7 | 6.0 ± 0.2 | 6.3 ± 1.7 |
| Exercise | 8.5 ± 0.6 | 9.2 ± 0.9 | 10.7 ± 4.4 | 9.3 ± 0.2 | 9.9 ± 3.8 |
| $\Delta P_{mean}$ (mm Hg) | | | | | |
| Rest | 59 ± 4 | 37 ± 9 | 39 ± 20 | 37 ± 2 | 30 ± 14 |
| Exercise | 74 ± 5 | 38 ± 11 | 52 ± 26 | 41 ± 2 | 41 ± 18 |
| $V_{max}$ (m/s) | | | | | |
| Rest | — | — | 4.0 ± 0.9 | — | 3.6 ± 0.8 |
| Exercise | — | — | 4.6 ± 1.1 | — | 4.3 ± 0.8 |

*BP*, Blood pressure; *CO*, cardiac output; $\Delta P_{mean}$, mean pressure gradient; *HR*, heart rate; $Q_{mean}$, mean volume flow rate; *SV*, stroke volume; $V_{max}$, peak aortic jet velocity.
*Ettinger PO, Frank MJ, Levinson GE: Hemodynamics at rest and during exercise in combined aortic stenosis and insufficiency. *Circulation* 45:267-276, 1972.

curvilinear relationship between resistance and valve area, for "larger" valve areas (right side of curve) resistance changes very little even with substantial changes in valve area, whereas for smaller valve areas (left side of curve) large changes in resistance are expected with only small changes in valve area.

Similarly, LV stroke work loss varies with changes in volume flow rate.[53,56,79] Overall, there is an inverse correlation between valve area and both total and steady LV stroke work loss. However, for a specific valve anatomy, work loss increases with an increase in stroke volume despite a concurrent increase in valve area. This suggests that for a given degree of leaflet stiffness, greater opening of the valve is achieved at the expense of greater work loss. Alternatively, because work includes both potential and kinetic energy, a decrease in the percentage of potential work converted to kinetic work would lead to this observation. In studies to date, only potential work has been measured because of the conceptual and technical difficulties in measurement of kinetic work. Changes in the effective frictional loss component with changes in volume flow rate also may affect calculated measures of stenosis severity.

### THEORETICAL CONSIDERATIONS FOR A MEASURE OF STENOSIS SEVERITY

Degenerative calcific aortic valve stenosis is characterized by thickened, stiff leaflets without commissural fusion. Given this anatomic substrate, it is not surprising that the degree of valve opening varies with the amount of "force" applied to the valve, whether this force is represented by the surgeon's finger, a balloon valvuloplasty catheter, or the rate and volume of blood ejected by the LV. Most proposed measures of stenosis severity, when examined in detail, vary with changes in volume flow rate. These measures include peak LV-to-aortic pressure gradient, mean transaortic pressure gradient, maximum Doppler aortic jet velocity, Gorlin valve area, continuity equation valve area, LV stroke work loss, and valve resistance. Despite this theoretical limitation, most clinical decisions can be made with a high degree of reliability using these imperfect indices of disease severity.

The ideal measure for AS quantification accurately reflects disease severity and even more importantly predicts clinical outcome, at the same time having an acceptable intra- and interobserver reproducibility. In addition, it should be noninvasive, easy to perform, readily available, and inexpensive. Doppler-echocardiographic measures of jet velocity and valve area meet these criteria. In the clinical setting, the impetus to derive a flow-independent measure of stenosis severity arises from the relatively unusual clinical situation in which there is coexisting LV systolic dysfunction and an anatomically abnormal aortic valve. Potential approaches to this clinical dilemma are discussed next.

Determination of hemodynamic progression is important, both in the clinical setting[6] and in research applications. Hemodynamic progression is related to clinical outcome, and its assessment is of interest for the identification of potential predictors of progression as well as of potential therapies aiming at preventing or slowing the hemodynamic progression of AS. In this context, measures of stenosis severity with a high reproducibility over time and between institutions are needed.

## The LV Response to Valvular Aortic Stenosis

### DIASTOLIC FUNCTION

The initial physiologic response to chronic pressure overload of the LV is impaired early diastolic relaxation as manifested

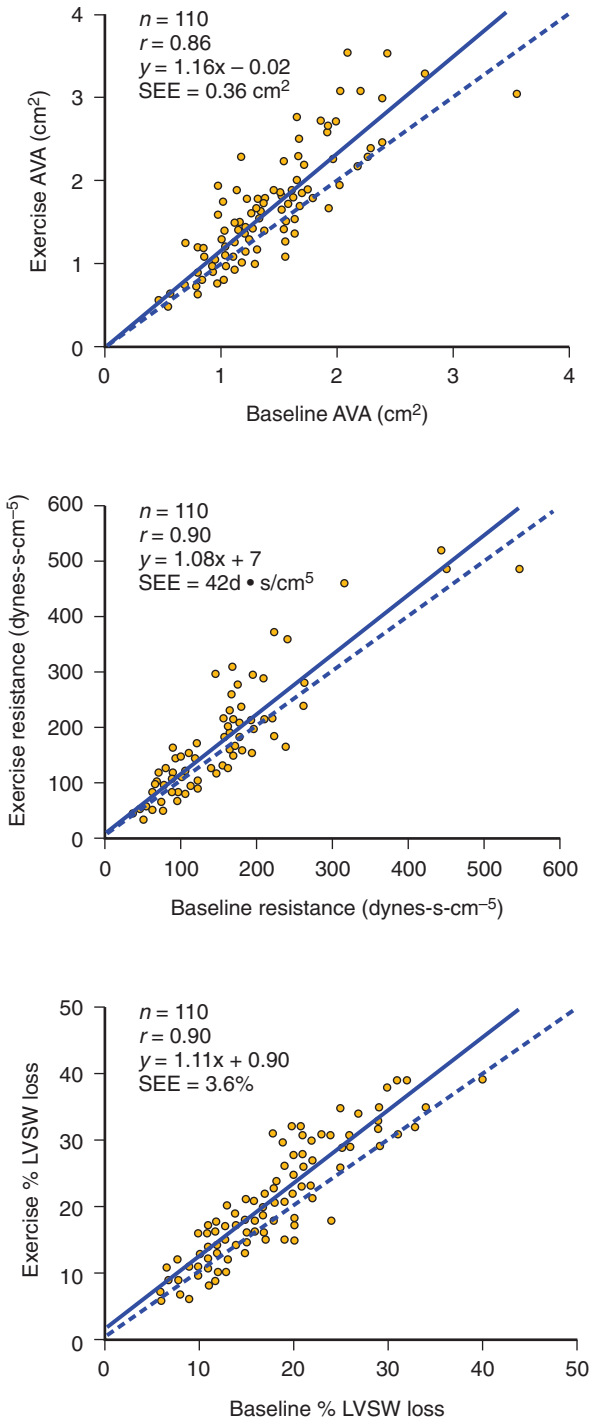



**Figure 23-14** Relation of rest and continuity equation aortic valve area (*AVA*) (*top*), aortic valve resistance (*middle*), and percent left ventricular stroke work (*LVSW*) loss (*bottom*) in 110 exercise studies. Slopes of regression lines (*solid line*) are greater than line of identity (*dashed line*), demonstrating increase in all three indexes with exercise. *SEE*, Standard error of estimate. *(From Burwash IG, Pearlman AS, Kraft CD, et al: Flow dependence of measures of aortic stenosis severity during exercise.* J Am Coll Cardiol *24:1342-1350, 1994.)*

by a prolonged time constant of relaxation, a lengthened isovolumic relaxation time, and a reduced early diastolic filling velocity, similar to the changes seen in patients with systemic hypertension.[80-83] Changes in diastolic function typically precede evidence of systolic dysfunction and thus may be present early in the disease course. Although some investigators suggest that Doppler measures of early and late diastolic filling velocities (or rates) may not be sensitive for detection of early diastolic dysfunction,[83] others propose that diastolic parameters can distinguish symptomatic from asymptomatic patients.[84] Tissue Doppler imaging has been reported to allow estimation the diastolic performance and LV filling pressures in these patients.[85] Using tissue Doppler imaging, diastolic dysfunction is even detected in patients with moderate AS.[86] Later in the disease course, decreased diastolic compliance plus a rightward shift on the passive diastolic pressure-volume relationship may result in a filling pattern characterized by a shortened isovolumic relaxation time, increased early diastolic filling velocity, rapid early deceleration slope, and reduced atrial contribution to diastolic filling, a pattern often referred to as "pseudonormalization."[82]

## WALL STRESS AND CONCENTRIC HYPERTROPHY

With increasing stenosis severity, concentric LV hypertrophy develops in response to chronically elevated LV systolic pressures. Normal wall stress is maintained given that wall stress is directly related to chamber pressure and dimension, but inversely related to wall thickness. LV hypertrophy is reliably assessed by calculation of LV mass, although simple chamber dimensions and diastolic wall thickness may be adequate for clinical evaluation.

LV hypertrophy in patients with AS is associated with abnormalities in coronary microcirculatory function.[87] This microcirculatory dysfunction may not necessarily be explained by the presence of hypertrophy itself but rather by an increased extravascular compression and a reduced diastolic perfusion time.[88]

In some individuals, the degree of hypertrophy appears out of proportion to AS severity. In these patients, other causes for hypertrophy should be considered, such as hypertension, coexisting hypertrophic cardiomyopathy, or an infiltrative myocardial process. The high prevalence of arterial hypertension in AS patients may explain some extent of hypertrophy, in particular when AS is not severe.[89] Genetic factors may also play a role in the degree of LV hypertrophy. Associations between polymorphisms of the angiotensin-converting enzyme gene and LV hypertrophy have been described.[90,91] Excessive hypertrophy was associated with an increased risk of cardiac events in patients with asymptomatic severe AS.[92] However, LV mass and tissue Doppler measures of LV systolic and diastolic function provided limited predictive information when considering the AS severity.[93]

## GENDER DIFFERENCES IN THE LV RESPONSE TO AORTIC STENOSIS

Significant gender differences in the LV response to the chronic pressure overload of AS have been reported.[94] In symptomatic patients referred for aortic valvuloplasty, women had higher transaortic gradients despite similar valve areas, higher relative wall thicknesses, and a higher prevalence of LV hypertrophy using gender-specific hypertrophy criteria. In addition, women had a lower functional status score for the same degree of aortic valve obstruction.[95] Another study observed higher peak LV pressures, higher ejection fractions, smaller LV end-diastolic dimensions, and a higher relative wall thickness in women with AS compared to men with the same condition.[96]

In a series of consecutive asymptomatic AS patients,[97] in the presence of comparable stenosis severity, women reported more functional limitation, had smaller LV end-diastolic and end-systolic volumes and mass index, but had a higher relative wall thickness and fractional shortening compared to men. In addition, women had a shorter treadmill exercise duration and a smaller increase in cardiac output with exercise even though heart rate and blood pressure responses were similar in men and women.[97]

The importance of gender differences in the LV response to chronic pressure overload are illustrated by the observation that after aortic valve replacement in patients with depressed LV systolic function (ejection fraction less than 45%), women had a greater improvement in ejection fraction after valve replacement, although survival was similar between men and women. The ejection fraction increased from 33% ± 8% to 48% ± 15% in women and from 32% ± 9% to 42% ± 15% in men (p less than 0.02).[98]

In summary, the degree of LV hypertrophy is variable in both men and women. However, women tend to have small ventricles with thick walls, low wall stress, and normal or hyperdynamic systolic function. In contrast, men tend to have LV dilation with normal wall thickness, increased wall stress, and depressed systolic function.

### SYSTOLIC DYSFUNCTION

Manifest LV systolic dysfunction due to valvular AS usually occurs late in the disease course. However, subclinical myocardial dysfunction identified by reduced myocardial strain has been described even in patients with mild AS with progressive impairment, with increasing degrees of AS severity, and in symptomatic patients.[99] Given the high ventricular afterload due to the stenotic valve, LV contractility typically remains normal despite a low ejection fraction. Relief of the high afterload with valve replacement leads to rapid normalization of systolic function in the majority of patients. However, LV systolic dysfunction may be caused by mechanisms other than AS, such as coronary artery or myocardial disease. Under these circumstances, LV function often fails to improve with valve replacement, and the outcome remains poor. In the setting of a moderate aortic valve gradient, distinguishing poor LV systolic function due to severe AS from that of concurrent ischemic or myocardial disease with only moderate aortic valve disease remains a difficult dilemma. One approach is to use a flow-independent measure of stenosis severity or to look at the change in stenosis severity with a change in volume flow rate. The theoretical alternate approach to use a load-independent measure of LV contractility to evaluate myocardial function has proven as elusive as a flow-independent measure of stenosis severity.[83]

## Natural History, Progression, and the Role of Echocardiography in Clinical Decision Making

### NATURAL HISTORY OF AORTIC STENOSIS

The natural history of AS is characterized by an asymptomatic phase of variable duration, during which the LV is subjected to increasing outflow obstruction and adaptive mechanisms[100-102] (Table 23-3). The occurrence of symptoms presents a change in the natural history of the disease. Patients with congenital AS may become symptomatic in early childhood or adolescence; patients with unicuspid valves are particularly likely to present with early symptoms. Later, these patients may also present with symptoms due to restenosis after a surgical valvotomy in childhood. In patients with a bicuspid AS, surgery is typically needed at age 50 to 70 years.[2,103,104] In the elderly patient with

**TABLE 23-3 Event-Free Survival of Asymptomatic Patients with Aortic Stenosis**

| *Study* | *Year* | *Entry Criteria* | n | *Age (years)* | *Follow-up (months)* | *AS Severity* | *Event-Free Survival* |
|---|---|---|---|---|---|---|---|
| Kelly[111] | 1988 | $V_{max}$ ≥3.5 | 51 | 63 ± 19 | 15 ± 10 | ΔP 68 ± 19 mm Hg | 60% at 2 yr |
| Pellikka[44] | 1990 | $V_{max}$ ≥4.0 | 143 | 72 (40 to 94) | 20 | $V_{max}$ 4.4 (4-6.4) m/s | 62% at 2 yr |
| Kennedy[112] | 1991 | Moderate AS at catheterization | 66 | 67 ± 10 | 35 | AVA 0.92 ± 0.13 $cm^2$ | 59% at 4 yr |
| Otto[43] | 1997 | Abnormal Valve with $V_{max}$ >2.6 m/s | 123 | 63 ± 16 | 30 | $V_{max}$ <3.0 m/s | 84% at 2 yr |
| | | | | | | $V_{max}$ 3-4 m/s | 66% at 2 yr |
| | | | | | | $V_{max}$ >4 m/s | 21% at 2 yr |
| Rosenhek[6] | 2000 | $V_{max}$ ≥4.0 | 128 | 60 ± 18 | 22 ± 18 | $V_{max}$ 5.0 ± 0.7 m/s | 67% at 1 yr |
| | | | | | | | 56% at 2 yr |
| | | | | | | | 33% at 4 yr |
| Rosenhek[51] | 2004 | Abnormal Valve with $V_{max}$ 2.5-3.9 m/s | 176 | 58 ± 19 | 48 ± 19 | $V_{max}$ 3.1 ± 0.4 m/s | 95% at 1 yr |
| | | | | | | | 75% at 2 yr |
| | | | | | | | 60% at 5 yr |
| Pellikka[123] | 2005 | $V_{max}$ ≥4.0 | 622 | 72 ± 11 | 65 ± 48 | $V_{max}$ 4.4 ± 0.4 m/s | 82% at 1 yr |
| | | | | | | | 67% at 2 yr |
| | | | | | | | 33% at 5 yr |
| Rossebø[142] | 2008 | $V_{max}$ 2.5-4.0 | 1873 | 68 ± 9 | 52 (median) | $V_{max}$ 3.1 ± 0.55 | Approx. 65% at 5 yr |
| Lancellotti[126] | 2010 | AVAi ≤0.6 $cm^2/m^2$ | 163 | 70 ± 10 | 20 ± 19 | ≤0.6 $cm^2/m^2$ | 50% at 2 yr |
| | | | | | | | 44% at 4 yr |
| Kang[127] | 2010 | $V_{max}$ ≥4.5 | 95 | 63 ± 12 | 58 (median) | 4.9 ± 0.4 | 71 ± 5% at 2 yr |
| | | | | | | | 47 ± 5% at 4 yr |
| | | | | | | | 28 ± 6% at 6 yr |
| Rosenhek[48] | 2010 | $V_{max}$ ≥5.0 | 116 | 67 ± 15 | 41 (median) | $V_{max}$ 5.0-5.5 m/s | 43% at 2 yr |
| | | | | | | $V_{max}$ ≥5.5 m/s | 25% at 2 yr |

*AS*, Aortic stenosis; *AVA*, aortic valve area; *AVAi*, indexed aortic valve area; *ΔP*, pressure gradient; $V_{max}$, peak aortic jet velocity.

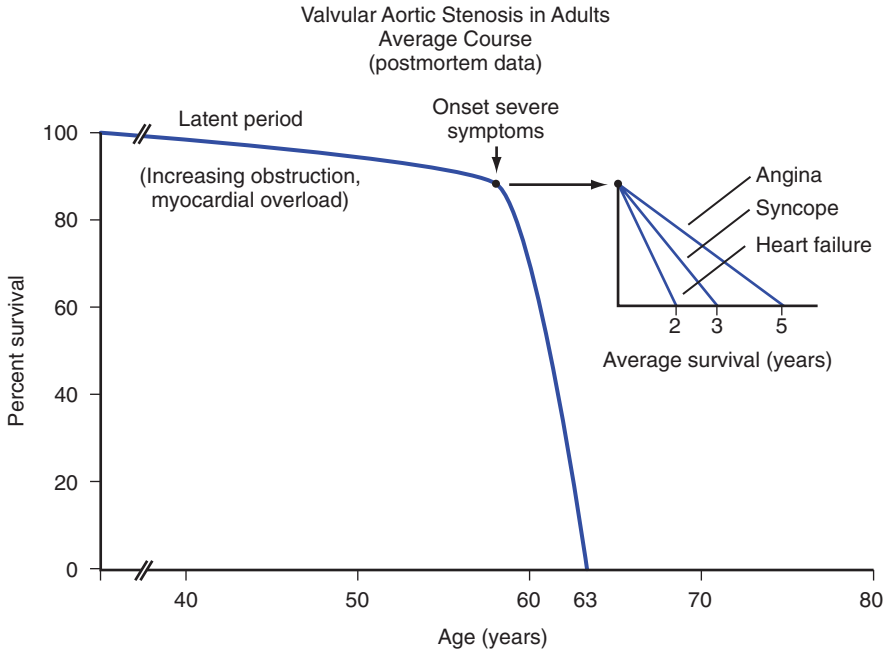



**Figure 23-15 Natural history of aortic stenosis.** Poor outcome is indicated by occurrence of symptoms. This graph reflects outcomes in the presurgical era based on autopsy data with primarily rheumatic valve disease. *(From Ross J Jr, Braunwald E: Aortic stenosis.* Circulation *38:61-67, 1968.)*

degenerative calcific valve disease, symptom onset may have occurred at an age of 50 years but typically occurs at age 60 to 90 years.[2]

Rheumatic valvular AS has a variable course with significant aortic valve obstruction (in conjunction with mitral valve involvement) occurring over a wide age range.

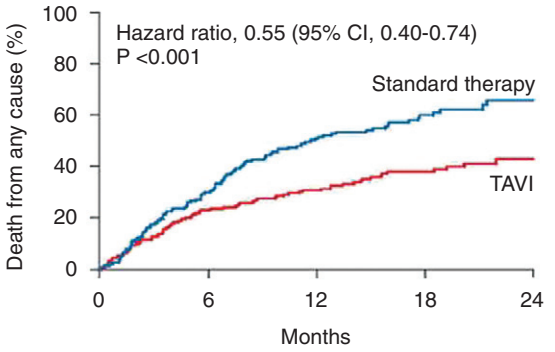
### *Asymptomatic versus Symptomatic Aortic Stenosis and Severe versus Nonsevere Aortic Stenosis*

With an ageing population, the incidence of calcific aortic valve disease is increasing. Furthermore, with the widespread use of echocardiography, the diagnosis is made more commonly in asymptomatic patients as coincidental finding or after suspicion due to a systolic murmur. Its spectrum ranges from severe symptomatic stenosis to aortic sclerosis without hemodynamic implications. In between are the asymptomatic patients with severe, moderate, and mild AS. The incidence of AS in the population of advanced age is estimated to be between 2% and 9%. Aortic sclerosis is present in up to 25% of patients over 65 years of age.[50,105,106]

The first step in the clinical decision-making process for the timing of intervention in a patient with valvular AS is a careful history as to whether symptoms (angina, exertional dizziness, exercise intolerance, or heart failure) are present or absent. Exercise testing may be appropriate and safe in apparently asymptomatic patients and may unmask latent symptoms in up to one third of these.[107,108] The greatest predictive value of exercise testing can be derived in physically active patients who are younger than 70 years.[108] It must be emphasized that exercise testing is contraindicated in symptomatic patients.

### *Symptomatic Aortic Stenosis*

The poor outcome of patients with severe symptomatic AS was well described in a postmortem analysis in 1968.[101] After symptom onset, the average survival has been reported to be less than 2 to 3 years (Fig. 23-15). Additional data were derived from studies of patients who refused surgical intervention.[100,109-114] In a recent contemporary series of symptomatic




| No. at risk | | | | | |
|---|---|---|---|---|---|
| TAVI | 179 | 138 | 122 | 67 | 26 |
| Standard therapy | 179 | 121 | 83 | 41 | 12 |

**Figure 23-16** Kaplan-Meier survival rates for inoperable symptomatic patients with severe aortic stenosis receiving conventional therapy (n = 179) versus transcatheter aortic valve implantation (*TAVI*) (n = 179). *CI*, Confidence interval. *(From Leon MB, Smith CR, Mack M, et al: Transcatheter aortic-valve implantation for aortic stenosis in patients who cannot undergo surgery.* N Engl J Med *363:1597-1607, 2010.)*

patients with severe AS who were managed conservatively because they were considered not to be candidates for surgery, the 1-year mortality was 50.7% as compared to 30.7% for patients receiving a transcatheter aortic valve implantation[115] (Fig. 23-16). Surprisingly, 83.8% of the patients that were managed "conservatively" underwent balloon aortic valvuloplasty in this series. In patients with severe, symptomatic AS, predictors of survival include the transaortic gradient or velocity, LV systolic function as assessed qualitatively on echocardiography, age, and gender.[116] Among symptomatic patients who are managed conservatively, higher levels of B-type natriuretic peptide (BNP) are associated with increased mortality.[117] Of note, patients with a higher transaortic gradient have a better prognosis, most likely because when severe stenosis is present,

a low gradient indicates a low transaortic stroke volume. On the other hand, current results of aortic valve replacement for acquired AS have been shown to be excellent.[110] Thus, it is generally accepted that surgery must be strongly recommended for patients with critical AS who develop symptoms. Only rarely does severe comorbid disease result in an unacceptably high operative morbidity and mortality. Nevertheless, about one third of patients with symptomatic severe AS are denied surgery.[118,119] Transcatheter aortic valve implantation techniques are an accepted treatment option for selected patients with high surgical risk or in whom surgery is contraindicated.

## *Asymptomatic Aortic Valve Disease*

### Aortic Sclerosis and Mild-to-Moderate Aortic Stenosis

A number of older studies have reported a relatively benign course of moderate AS, suggesting a stable course of the disease.[100,109,110] These data suggested that mild and moderate AS represent a relatively benign disease, although one study described a poor outcome of moderate AS, with 14 deaths attributed to AS among 66 patients followed for 35 months.[112] However, most of these studies date back to catheter era and are limited by small patient numbers and their retrospective nature.[100,109,110,112]

More recent studies have shed new light on the seriousness of the disease. A community-based study showed that the presence of aortic valve sclerosis is associated with a significantly increased cardiovascular and all-cause mortality in the absence of hemodynamic obstruction to blood flow.[50] Recent studies have also shown that mild-to-moderate AS is not a benign disease, with increased cardiovascular and noncardiac mortalities.[43,51] Thus, aortic sclerosis and mild-to-moderate AS must be viewed as indicators of poor overall prognosis.

In addition, the prognosis of these patients is influenced by hemodynamic disease progression. In fact, the progression of aortic sclerosis to AS affects about 16% of patients within a short time period.[120] The interval between observing aortic valve "sclerosis" and clinical evidence of severe AS may be as short as 5 years. The progression from mild to severe AS is also common and may be rapid.[51]

As long as AS is not severe, these patients can be managed conservatively. However, knowing that a rapid progression to severe AS may occur, it is important to instruct even patients with mild-to-moderate AS about potential symptoms of AS and the necessity to immediately report to a physician after their onset. Performing a repeat echocardiography is warranted after a change in symptomatic status to assess a potential hemodynamic disease progression.

### Asymptomatic Severe Aortic Stenosis

The management of asymptomatic patients with severe AS remains a matter of controversy. Overall, it is relatively safe to delay surgery in patients with severe AS until symptoms develop, following a watchful waiting strategy.[6] However, there are concerns when following such patients conservatively.[121] Among these concerns is the risk of sudden death, which may occur even in the absence of preceding symptoms. However, this appears to be an uncommon event, occurring at a rate of less than 1% per year during the asymptomatic disease phase.[6,43,48,108,111,122-127] (Table 23-4). Finally, sudden death may also occur after successful valve replacement, with an incidence of about 0.3% per year.[128,129]

### Asymptomatic Very Severe Aortic Stenosis

AS severity represented by peak aortic jet velocity is an important predictor of event-free survival across the spectrum of mild to severe AS.[43] Peak aortic jet velocity allows risk stratification among asymptomatic patients with severe stenosis.[48] Event-free survival rates at 3 years were 49%, 33%, and 11% for patients with peak aortic jet velocities between 4.0 and 5.0 m/s, between 5.0 and 5.5 m/s, or above 5.5 m/s, respectively (Fig. 23-17). Most patients with an aortic jet velocity greater than 5.0 m/s are already symptomatic at presentation, and those who are still asymptomatic have a high likelihood of a rapid symptom onset. These findings strongly support defining the entity of "very severe" AS. Kang and colleagues[127] reported a better outcome for 102 patients with asymptomatic AS with a peak aortic jet velocity of more than 4.5 m/s who underwent elective aortic valve replacement as compared to patients who were initially followed conservatively. However, this study was nonrandomized, and mortality in the group of patients who were initially

**TABLE 23-4 Incidence of Sudden Death in Patients with Aortic Stenosis**

| *Study* | *Year* | n | *Follow-up (months)* | *AS Severity at Entry ($V_{max}$ in m/s)* | *AS Severity (AVA in cm²)* | *Sudden Deaths* (n) | *Sudden Deaths (% per year)* |
|---|---|---|---|---|---|---|---|
| Kelly[111] | 1988 | 51 | 18 | ≥3.5 | | 0 | 0 |
| Faggiano[122] | 1992 | 37 | 24 | | 0.85 ± 015 | 0 | 0 |
| Otto[43] | 1997 | 114 | 30 | 3.6 ± 0.6 | | 0 | 0 |
| Rosenhek[6] | 2000 | 128 | 22 | ≥4.0 | | 1 | 0.4 |
| Amato[107] | 2001 | 66 | 15 | | ≤1.0 | 4 | 4.8 |
| Das[123] | 2005 | 125 | 12 | | ≤1.4 | 0 | 0 |
| Pellikka[123] | 2005 | 270 | 65 | ≥4.0 | | 11 | 0.75 |
| Rossebø[142] | 2008 | 1873 | 52 | 2.5-4.0 | | 40 | 0.5 |
| Monin[125] | 2009 | 211 | 22 | ≥3.0 | ≤1 | 2 | 0.5 |
| Lancellotti[126] | 2010 | 163 | 20 | | ≤0.6 cm²/m² | 3 | 1.1 |
| Kang[127] | 2010 | 95 | 59 | ≥4.5 | ≥0.75 | 9 | 1.9 |
| Marechaux[124] | 2010 | 135 | 20 | | ≤1.5 | 1 | 0.4 |
| Rosenhek[48] | 2010 | 116 | 41 | ≥5.0 | | 1 | 0.3 |
| Total | | 3384 | 31* | | | 72 | 0.8 |

*AS*, Aortic stenosis; *AVA*, aortic valve area; $V_{max}$, peak aortic jet velocity.
*Mean follow-up duration.

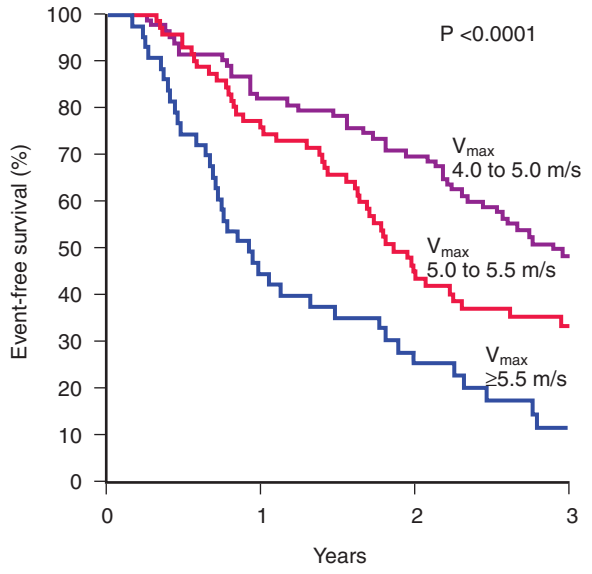



**Figure 23-17** Kaplan-Meier event-free survival rate for patients with peak aortic jet velocity ($V_{max}$) between 4.0 and 5.0 m/s (*purple line*; n = 82) versus between 5.0 and 5.5 m/s (*red line*; n = 72) versus ≥5.5 m/s (*blue line*; n = 44). *(From Rosenhek R, Zilberszac R, Schemper M, et al: Natural history of very severe aortic stenosis.* Circulation *121:151-156, 2010.)*

managed conservatively was unexpectedly high, with a mortality of 24% at 6 years.

## PROGRESSION OF AORTIC STENOSIS

Echocardiography, which is an accurate, noninvasive method to evaluate hemodynamic severity, has allowed large and detailed studies on the rate of hemodynamic progression.[6,51,122,130-136] Recent intervention studies, designed to assess the effects of statin therapy in halting or delaying the progression of AS, provide additional information on hemodynamic progression[137-143] (Table 23-5). Overall, these studies showed an average rate of increase in aortic jet maximum velocity ranges of 0.2 to 0.4 m/s/year, in mean pressure gradients of about 8 mm Hg per year, and a decrease in valve areas of about 0.15 $cm^2$ per year. However, there was marked individual variability in the rate of hemodynamic progression (see Figs. 23-7 and 23-8). Although Doppler-echocardiographic studies have the advantage of larger patient numbers and potentially less selection bias (a repeat echocardiographic study is likely to be requested more often than a repeat cardiac catheterization), many of these are retrospective with data extracted from ongoing clinical databases. Thus, patients with rapid progression, those developing symptoms, or those requiring surgical intervention may be overrepresented. Conversely, repeat studies may not have been performed in clinically stable patients. The prospective studies may avoid some of these biases.[6,43,139]

As the disease progresses, increasing obstruction to LV outflow most often is reflected by a decrease in valve area and an increase in jet velocity and pressure gradient. However, if there is a

**TABLE 23-5 Hemodynamic Progression of Valvular Aortic Stenosis**

| *Study* | *Year* | *Type of Study* | *Clinical Status at Entry* | n | *Mean Follow-up (yr)* | *Increase in Mean ΔP (mm Hg/yr)* | *Increase in $V_{max}$ (m/s/yr)* | *Decrease in AVA ($cm^2$/yr)* |
|---|---|---|---|---|---|---|---|---|
| **Echocardiographic Studies** | | | | | | | | |
| Otto[133] | 1989 | Prospective | Asymptomatic | 42 | 1.7 | 8 (−7 to 23) | 0.36 ± 0.31 | 0.1 (0-0.5) |
| Roger[136] | 1990 | Retrospective | AS on echo | 112 | 2.1 | | 0.23 ± 0.37 | |
| Faggiano[122] | 1992 | Prospective | AS on echo | 45 | 1.5 | | 0.4 ± 0.3 | 0.1 ± 0.13 (−0.7 to 0.1) |
| Peter[135] | 1993 | Retrospective | AS on echo | 49 | 2.7 | 7.2 | | |
| Brener[131] | 1995 | Retrospective | AS on echo | 394 | 6.3 | | | 0.14 |
| Otto[43] | 1997 | Prospective | Asymptomatic | 123 | 2.5 | 7 ± 7 | 0.32 ± 0.34 | 0.12 ± 0.19 |
| Bahler[130] | 1999 | Retrospective | AS on echo | 91 | 1.8 | 2.8 | 0.2 | 0.04 |
| Palta[134] | 2000 | Retrospective | AS on echo | 170 | 1.9 | | | 0.10 ± 0.27 |
| Rosenhek[6] | 2000 | Prospective | $V_{max}$ >4.0 m/s | 128 | 1.8 | Slow | 0.14 ± 0.18 | |
| | | | | | | Rapid | 0.45 ± 0.38 | |
| Rosenhek[51] | 2004 | Retrospective | $V_{max}$ 2.5-3.9 m/s | 176 | 3.8 | | 0.24 ± 0.30 | |
| **Echocardiographic Intervention Studies** | | | | | | | | |
| Novaro[140] | 2001 | Retrospective | AVA 1.0-1.8 $cm^2$ | 174 | 1.7 | Statin therapy | | 0.06 ± 0.16 |
| | | | | | | No statin | | 0.11 ± 0.18 |
| Bellamy[138] | 2002 | Retrospective | AVA <2.0 $cm^2$ | 156 | 3.7 | Statin therapy | | 0.04 ± 0.15 |
| | | | | | | No statin | | 0.09 ± 0.17 |
| Rosenhek[141] | 2004 | Retrospective | $V_{max}$ >2.5 m/s | 211 | 2.0 | Statin therapy | 0.1 ± 041 | |
| | | | | | | No statin | 0.39 ± 0.42 | |
| Cowell[139] | 2005 | Prospective | $V_{max}$ >2.5 m/s | 134 | 2.1 | Statin therapy | 0.2 ± 0.21 | 0.08 ± 0.11 |
| | | | | | | No statin | 0.2 ± 0.21 | 0.08 ± 0.11 |
| Moura[143] | 2007 | Prospective | AVA 1.0-1.5 $cm^2$ | 121 | 1.4 | Statin therapy | 0.4 ± 0.38 | 0.05 ± 0.12 |
| | | | | | | No statin | 0.24 ± 0.30 | 0.1 ± 0.09 |
| Rossebø*[142] | 2008 | Prospective | $V_{max}$ 2.5-4.0 m/s | 1873 | 5.4 | Statin 2.7 ± 0.1 | 0.15 ± 0.01 | 0.03 ± 0.01 |
| | | | | | | No statin 2.8 ± 0.1 | 0.16 ± 0.01 | 0.03 ± 0.01 |
| Chan[182] | 2010 | Prospective | $V_{max}$ 2.5-4.0 m/s | 269 | 3.5 | Statin 3.8 ± 4.4<br>No statin 3.9 ± 4.9 | Statin<br>No statin | 0.08 ± 0.21<br>0.07 ± 0.15 |

*AS*, Aortic stenosis; *AVA*, aortic valve area; *ΔP*, pressure gradient; *echo*, echocardiography; $V_{max}$, peak aortic jet velocity.
*Data expressed as mean ± standard error.

concurrent decrease in transaortic volume flow rate, a decrease in valve area alone may be seen with no change in jet velocity. This situation may occur secondary to comorbid disease (e.g., increasing mitral regurgitation or myocardial infarction) or decreasing LV function late in the disease course. On the other hand, an increase in jet velocity and pressure gradient with no change in valve area may be observed if transaortic stroke volume is increased in hyperdynamic states (e.g., anemia, fever, pregnancy) or with increasing aortic regurgitation.

## RISK STRATIFICATION

### *Rationale for Risk Stratification*

One concern when following patients with severe AS is the possibility of delayed symptom-onset reporting with the associated increased risk of mortality. Similar considerations apply to the issue of waiting lists for surgery, with estimated mortality rates for symptomatic patients of around 14% per year.[144] Operative mortality is also significantly lower for mildly symptomatic patients in whom surgery is electively scheduled as compared to an increased surgical risk for patients with advanced symptoms needing urgent surgery.

However, although the operative risk has dramatically decreased over recent decades, it must be considered to be in the range of 2% to 3% and may be as high as 5% to 10% in the elderly.[145] In an asymptomatic patient, this risk has to be outweighed by a proven benefit.

After valve replacement with a mechanical or bioprosthetic valve, valve-related complications such as thromboembolism, bleeding, endocarditis, valve thrombosis, paravalvular regurgitation, and valve failure occur at a rate of 2% to 3% per year. Death directly related to the prosthesis has been reported at a rate of up to 1% per year. The individual disease course is highly variable, and some patients may remain asymptomatic for many years. Early elective surgery is thus not generally recommended, and risk stratification may be required to identify patients likely to benefit from such an intervention.

### *Predictors of Hemodynamic Progression*

Hemodynamic progression of AS is highly variable for individual patients (Fig. 23-18). The exact rate of hemodynamic progression in an individual patient cannot be precisely anticipated (Fig. 23-19). Patterns of progression may be nonlinear with episodes of rapid progression following phases of steady and slow progression. Clinical factors such as elevated serum lipid levels, hypertension, smoking, and diabetes have been found to be associated with AS[146] but have not been convincingly proven to affect disease progression.

Most patients with a bicuspid stenotic valve require surgical intervention at a younger age than those with calcific AS.[104] However, this may relate to a disease onset at an early age. In the early disease phase, when bicuspid aortic valves are only mildly calcified, progression can be expected to be slower. Yet, these bicuspid valves also tend to calcify, and valve calcification predicts disease progression.[6,51,147] Other factors associated with disease progression are the severity of AS (advanced disease results in earlier symptom onset), age, and coronary artery disease[51]—these factors are directly associated with aortic valve calcification.

### *Predictors of Clinical Outcome*

Predictors of outcome are particularly relevant in asymptomatic patients with severe AS because they allow optimal

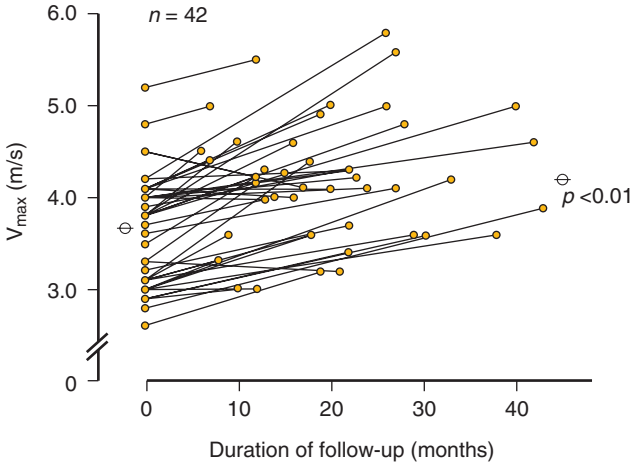



**Figure 23-18** Peak aortic jet velocity ($V_{max}$) plotted for initial and final Doppler studies in 42 asymptomatic patients. Group means indicated by the symbol ⊖. *(From Otto CM, Pearlman AS, Gardner CL: Hemodynamic progression of aortic stenosis in adults assessed by Doppler echocardiography.* J Am Coll Cardiol *13:545-550, 1989.)*

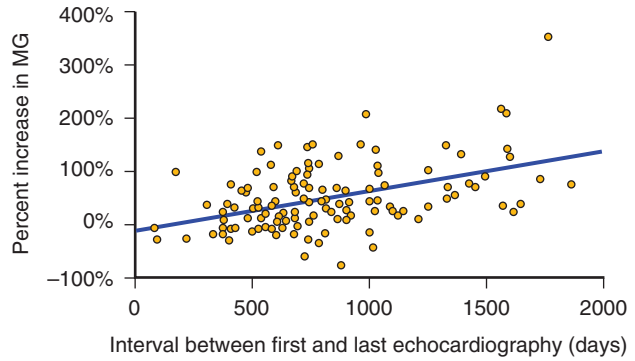



**Figure 23-19** Change in mean aortic gradient (*MG*) in 394 consecutive patients with aortic stenosis represented according to follow-up duration. Despite strong correlation predicting increase of gradient over time (r = 0.40, p < 0.0001), interindividual variability of hemodynamic progression can be appreciated. *(From Brener SJ, Duffy CI, Thomas JD, et al: Progression of aortic stenosis in 394 patients: relation to changes in myocardial and mitral valve dysfunction.* J Am Coll Cardiol *25:305-310, 1995.)*

scheduling of follow-up exams and the identification of candidates for early elective surgery.

Stenosis severity is one of the most robust predictors of outcome in patients with AS. Several studies have confirmed that the likelihood of aortic valve surgery is related to peak aortic jet velocity across the entire disease spectrum: Event rates are lowest in patients with mild stenosis, followed by moderate, severe, and very severe stenosis[6,43,48,51] (Fig. 23-20).

Significant valve calcification, rapid hemodynamic progression, and the presence of coronary artery disease predict high event rates in patients with mild to moderate AS.[51]

In a prospective study including 126 patients with asymptomatic severe AS, it was shown that moderate-to-severe aortic valve calcification detected by echocardiography was associated with an 80% rate of either symptom onset warranting aortic valve replacement or death within 4 years (Fig. 23-21). The finding that aortic valve calcification is associated with poor outcome was confirmed by a study assessing the degree of aortic valve calcification by electron-beam tomography.[148] Patients

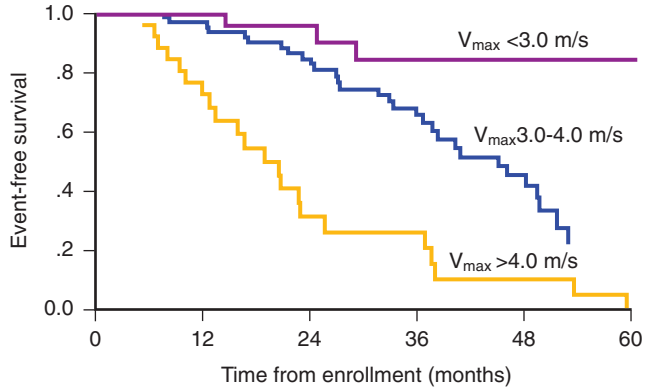



**Figure 23-20** Kaplan-Meier event-free survival of 123 asymptomatic patients with aortic stenosis according to their degree of severity expressed by peak aortic jet velocity ($V_{max}$) ($p < 0.0001$). *(From Otto CM, Burwash IG, Legget ME, et al: Prospective study of asymptomatic valvular aortic stenosis. Clinical, echocardiographic, and exercise predictors of outcome.* Circulation *95:2262-2270, 1997.)*

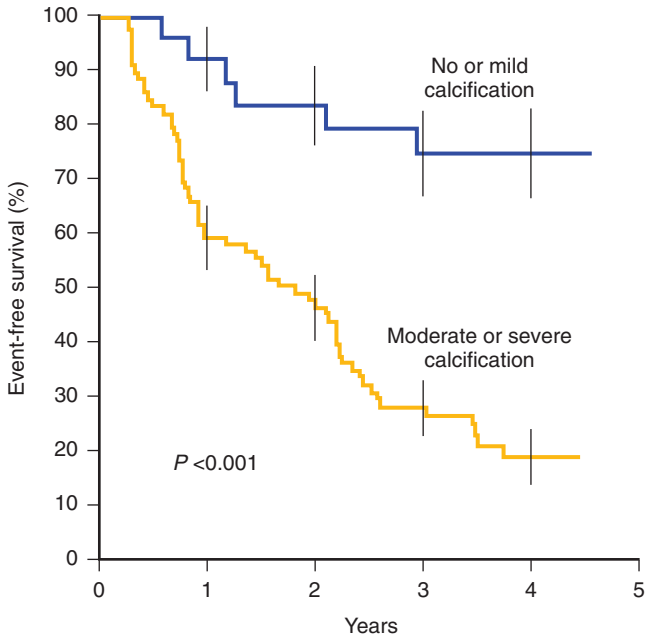



**Figure 23-21** Kaplan-Meier analysis of event-free survival among 25 patients with no or mild aortic valve calcification, as compared with 101 patients with moderate or severe calcification. Vertical bars indicate standard errors. All subjects in this study had initial aortic jet velocity of at least 4.0 m/s (mean 5.0 ± 0.6 m/s). *(From Rosenhek R, Binder T, Porenta G, et al: Predictors of outcome in severe, asymptomatic aortic stenosis.* N Engl J Med *343:611-617, 2000.)*

with calcified aortic valves are more likely to have a rapid hemodynamic progression.[51,147] The combined presence of a calcified aortic valve with a rapid hemodynamic progression (defined as an increase in peak aortic jet velocity of more than 0.3 m/s/year) characterizes a high-risk group with an event rate of 79% within 2 years[6] (Fig. 23-22). Although the echocardiographic determination of aortic valve calcification is semiquantitative, it has the advantage of being quickly and easily obtainable. Furthermore, the clinically relevant differentiation between no or mild calcification and moderate to severe calcification is easily performed. Ultimately, calcification is related to

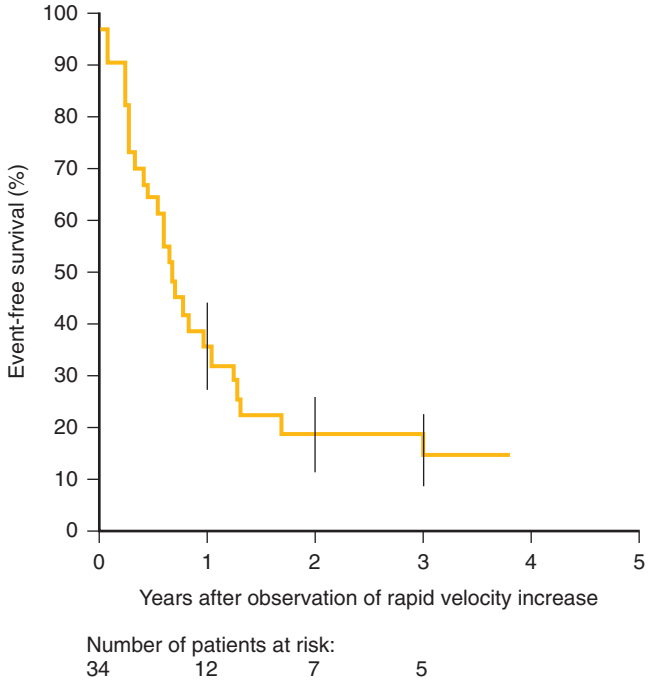



**Figure 23-22** Kaplan-Meier analysis of event-free survival among patients with moderately to severely calcified aortic valves and rapid hemodynamic progression defined by increase in peak aortic jet velocity of more than 0.3 m/s within 12 months. Vertical bars indicate standard errors. *(From Rosenhek R, Binder T, Porenta G, et al: Predictors of outcome in severe, asymptomatic aortic stenosis.* N Engl J Med *343:611-617, 2000.)*

hemodynamic progression, which in turn results in more severe stenosis as reflected by a higher transaortic jet velocity. Peak aortic jet velocity is probably the most robust and extensively studied predictor of outcome in asymptomatic patients with AS.[6,43,48,51,125]

Using exercise Doppler echocardiography in severe asymptomatic AS,[67] an exercise-induced increase of mean transaortic gradient of18 mm Hg or greater, an abnormal exercise test, and an aortic valve area of less than 0.75 $cm^2$ were independent predictors of events, with an incremental value when occurring together. The predictive value of an exercise-induced increase of mean transaortic gradient of 20 mm Hg or more among was confirmed in a group of 135 asymptomatic patients with at least moderate AS.[124]

There is an undisputed role for exercise testing in asymptomatic patients with severe AS for risk stratification and in unmasking symptoms. Patients who have a negative exercise test have a relatively good outcome.[107] Exercise testing has the best positive predictive value for active patients under the age of 70 years and may unmask latent symptoms, which are present in up to 30% of apparently asymptomatic patients.[108] The occurrence of an ST-segment depression, of abnormal blood pressure regulation, or of arrhythmias during exercise had a lower predictive value in this study.[108]

Finally, BNP levels have been shown to correlate with symptomatic status in patients with AS.[149] In asymptomatic patients, low BNP levels are associated with a good short-term outcome.[150,151] However, their positive predictive value needs to be viewed cautiously because of the nonspecificity of this measure and the fact that several cutoff values were proposed in different studies to indicate a poor outcome. Recently, Monin and colleagues[125] proposed a risk score for the identification of

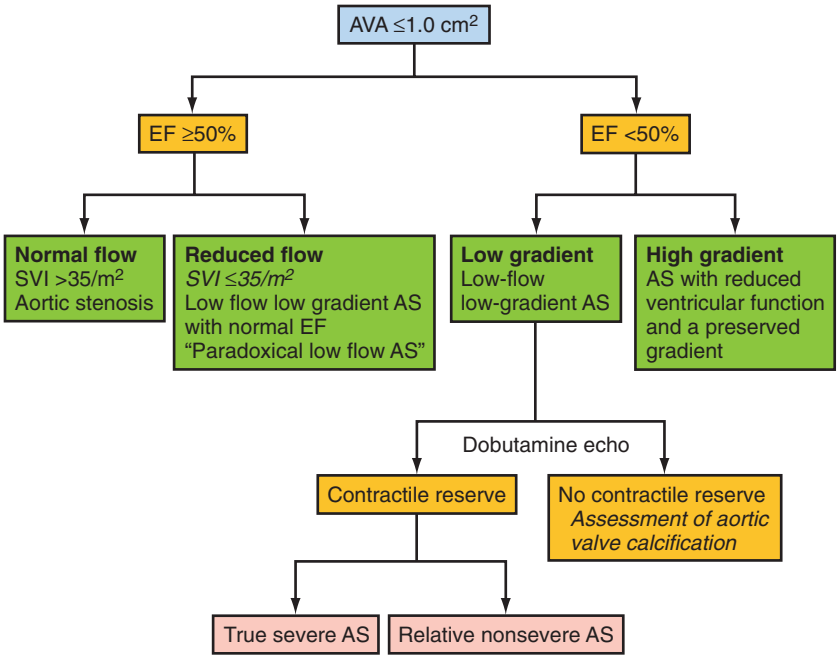



**Figure 23-23** Classification of aortic stenosis (*AS*) defined by calculated aortic valve area (*AVA*) ≤1.0 $cm^2$ according to ventricular function, transvalvular gradients, and flow. *EF*, Ejection fraction; *SVI*, stroke volume index.

high-risk patients that includes information on both stenosis severity and BNP levels.

Valvuloarterial impedance, which is a measure of global systemic load that integrates information on LV pressure burden from AS and systemic arterial compliance,[152] has been suggested to be of additional predictive value.[126]

## TIMING OF SURGERY IN PATIENTS WITH NONSEVERE AORTIC STENOSIS UNDERGOING CARDIAC SURGERY

It is evident that a severely stenotic aortic valve should be replaced at the time of cardiac surgery performed for another reason. The decision as to whether an aortic valve replacement should be performed in the presence of a valve that is not severely stenotic is more complex, given the interindividual variability of disease progression. "Prophylactic" valve replacement for moderate AS is considered to avoid repeat surgery that may be needed within less than 5 years.[153] However, the risks of combined surgery and of potential prosthesis-related complications have to be weighed against the likelihood and risk of two separate operations. The degree of severity, but also risk factors associated with hemodynamic progression, should be considered in this decision.[154,155] In this context, the degree of disease severity, valve calcification, and data on previous hemodynamic progression should be used to define patients likely to benefit from a combined procedure.

## AORTIC STENOSIS WITH REDUCED LV FUNCTION OR FLOW

Impaired LV function in patients with AS is generally associated with poor outcome. However, differentiation according to presence of either a preserved or a reduced transaortic gradient is fundamental in this setting (Fig. 23-23).

### *In the Presence of a Normal Transaortic Gradient*

It is recognized that patients with severe AS who have beginning systolic dysfunction should undergo valve replacement. These patients generally benefit from surgery with an improvement of LV function.

When LV function is significantly impaired, operative risk is significantly increased. However, improvement of LV function and of symptoms can be expected in the majority of patients. Patients with reduced systolic function and a history of prior myocardial infarction experience a particularly poor outcome following valve replacement.[156] Also, the presence of atrial fibrillation has been reported to predict a higher operative risk and worse postoperative outcome in patients with AS and reduced LV function.[157]

### *Low-Flow, Low-Gradient Aortic Stenosis*

The situation of low-flow, low-gradient AS is clinically challenging. It is defined by a small calculated valve area (less than 1 $cm^2$), which is a flow-independent measure of stenosis severity, and a mean transvalvular gradient in the range of 25 to 40 mm Hg in the presence of a reduced LV ejection fraction. In this setting, differentiation between restricted valve opening due to excessive leaflet stiffness and limited leaflet motion due to low transaortic stroke volume is warranted.

The risk of aortic valve replacement in the setting of low-flow, low-gradient AS is high, with an operative mortality in the range of 9% to 33%.[158-160] However, symptoms and LV function typically improve in the patients surviving surgery.[159,160]

Improvement after valve replacement is expected if LV systolic dysfunction is due to AS, but only to a limited extent when it is due to end-stage ischemic disease or a primary cardiomyopathy.

Stress echocardiography with low-dose dobutamine (maximal dose 20 mcg/kg/min) is useful for the evaluation and risk stratification of such patients. It allows the assessment of contractile reserve, defined by an increase in stroke volume of 20% or more.[161] In the presence of contractile reserve, true severe and relative AS can be differentiated.[162,163] If the ventricle fails to respond to inotropic stimulation (i.e., no increase in cardiac output), interpretation is difficult.[72,162,164]

In patients with relative or pseudosevere AS, the augmentation of transaortic volume flow rate results in a significant

increase (at least 0.2 $cm^2$) of valve area as the flexible leaflets open to a greater extent, while the transaortic gradient remains more or less unchanged. Conversely, when true severe AS is present, valve area will change little despite an increased transaortic volume flow due to stiff, rigid valve leaflets, and the transaortic gradients will increase significantly.

However, a small increase in aortic valve area can be seen in some patients with surgically confirmed severe AS and therefore does not exclude fixed valve disease.[165] Dobutamine infusion leads to a variable increase in transaortic flow rate; in some patients, normalized flow rates might not be reached. In an attempt to standardize these findings, the use of a projected effective orifice area (at a normal flow rate of 250 mL/s), which is determined by plotting (and extrapolating if necessary) the effective orifice area against transvalvular flow at the different exam stages, has been proposed to improve accuracy for distinguishing true severe from pseudosevere AS.[166]

In two small studies, 8 of 24[163] and 5 of 12[162] patients with contractile reserve had relative AS. In these studies, surgery led to an improved outcome in patients with true severe AS and preserved LV function. In a large multicentric study, patients with a contractile reserve had a significantly improved survival when they underwent surgery as compared to medically treated patients[161] (see Fig. 23-24). Patients without contractile reserve had poor overall survival, although a trend toward slightly improved outcome was described for patients undergoing surgery. In this study only 7 of 136 patients had relative AS. The failure of volume flow rate to increase may be due to a flow limitation of a severely stenotic valve or to an unresponsive myocardium. Importantly, despite a high operative risk, LV function and symptomatic status may even improve in patients without contractile reserve surviving aortic valve replacement surgery. This suggests that even in this subgroup, selected patients may benefit from surgery, which should thus not be generally precluded.[167-169] In the absence of contractile reserve, extensive aortic valve calcification may be indicative of severe AS.[170]

Although stress echocardiography may not always give all the expected answers in an unambiguous way, a pragmatic clinical approach to this patient group that includes looking at the valve, at the patient, and at the options might be helpful. A heavily calcified valve will be an argument in favor of valve replacement, whereas thin, flexible leaflets argue against valve surgery. Angiographic assessment of the coronary arteries is an integral part of the diagnostic workup.

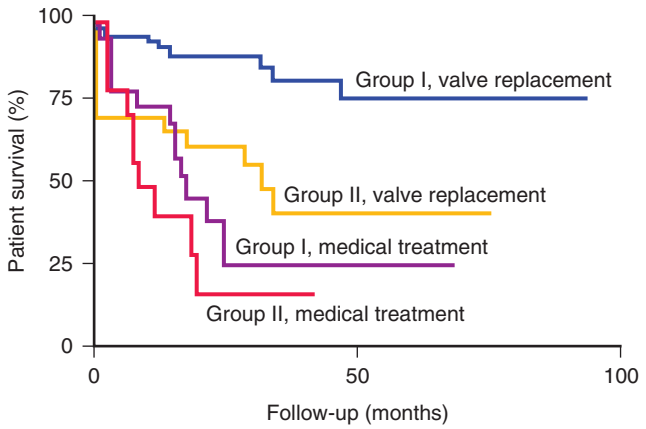



**Figure 23-24 Kaplan-Meier survival estimates of 136 consecutive patients with low-flow, low-gradient aortic stenosis.** Group I (n = 92) represents patients with contractile reserve determined by low-dose dobutamine echocardiography. Group II (n = 44) represents patients with absent contractile reserve. Survival estimates represented according to contractile reserve and treatment strategy (aortic valve replacement versus medical therapy). *(From Monin JL, Quere JP, Monchi M, et al: Low-gradient aortic stenosis: operative risk stratification and predictors for long-term outcome: a multicenter study using dobutamine stress hemodynamics.* Circulation *108:319-324, 2003.)*

### *Low-Flow, Low-Gradient Aortic Stenosis Despite Preserved Ejection Fraction (Paradoxical Low-Flow Aortic Stenosis)*

The concept of low-flow, low-gradient AS despite a preserved ejection fraction has been described.[171] Like classical low-flow, low-gradient AS, it is characterized by a small calculated aortic valve area, while the transaortic gradients correspond to nonsevere stenosis. In contrast to classical low-flow, low-gradient AS, however, ejection fraction is normal but stroke volume is nevertheless reduced (a stroke volume index of 35 $mL/m^2$ or less has been proposed to define a low stroke volume). This situation may be observed in the presence of severe LV hypertrophy with a small LV cavity or when a concomitant atrial septal defect with left-to-right shunting is present. Before diagnosing paradoxical low-flow AS, it is important to rule out potential underestimation of peak aortic jet velocity and measurement error in LV outflow tract area, both of which may also lead to a similar constellation of measurements. In the initial retrospective study, a worse outcome was described in patients with paradoxical low-flow AS who were managed conservatively as compared to those undergoing aortic valve replacement surgery. However, a recent analysis of data from the prospective SEAS cohort described an outcome that was comparable to moderate AS.[172] Although it is premature to draw final conclusions with regard to the management of these patients, decisions need to be individualized. In particular, it seems unlikely that asymptomatic patients would benefit from surgery.

## Assessment of Interventional Risk and Choice of the Procedure

The introduction of transcatheter aortic valve implantation techniques has expanded the options for the management of high-risk patients with AS. An optimal decision-making process depends on an interdisciplinary team approach including cardiac surgeons, interventional cardiologists, and noninterventional cardiologists.[173] In specific cases, additional consultation with an anesthesiologist, a geriatrician, or other specialties might be recommended. Currently available surgical risk scores do not reliably predict the risk of valve procedures in an individual patient and should thus only be used as part of an integrated approach.[174] An objective assessment of frailty should be integrated in the decision-making process.

### PREINTERVENTIONAL ASSESSMENT OF CORONARY ARTERY DISEASE

Coronary artery disease is frequent in patients with calcific AS. Concurrent coronary artery bypass grafting is recommended in the presence of significant coronary artery disease. If concomitant coronary artery disease is present at the time of aortic valve replacement for AS, operative mortality is significantly lower when additional coronary bypass grafting is performed (1.1% to 4.8%) in contrast to when valve replacement is performed alone (4.0% to 13.2%).[175,176] Also, risk of sudden death after

valve replacement is significantly higher when patients with coronary artery disease are not revascularized at the time of surgery.[177] Furthermore, the need for early reoperation for coronary artery disease is averted.

In AS patients with angina, the prevalence of significant coronary artery disease ranges from 40% to 80%. Preoperative coronary angiography is therefore definitely needed.

However, even in the absence of angina the prevalence of significant coronary artery disease ranges between 0% and 54% (average 16%). The appropriate diagnostic approach to these patients is less clear. Exercise treadmill testing is contraindicated in symptomatic patients with AS. It is of note that even in asymptomatic patients, ST-segment depression during exercise is often nondiagnostic for the presence of coronary artery disease and is possibly related to LV hypertrophy.[66,178] Multidetector computed tomography coronary angiography is becoming increasingly available as a noninvasive technique for the assessment of the coronary anatomy. Recently, several small studies have reported high negative predictive values for this technique to rule out the presence of significant coronary artery disease in patients with AS.[179,180] With further improvements in image quality, this technique might become an alternative to coronary angiography in patients at low to moderate risk for the presence of coronary artery disease. In patients with a moderate to high likelihood of coronary artery disease, conventional preoperative coronary angiography remains mandatory.

## Echocardiography in Transcatheter Aortic Valve Implantation

Transcatheter aortic valve implantation has become a treatment option for high-risk patients with AS. As discussed earlier, the choice of a management strategy in a specific patient should be based on a multidisciplinary approach. Echocardiography has a role both in the patient selection process and as a monitoring technique during valve implantation. The transcatheter valve can be implanted either retrogradely via a transfemoral access or surgically via the apex (see Chapter 5).

### PATIENT SELECTION

Several factors determine whether a patient is suitable for a transcatheter aortic valve implantation. Presently two valves, the CoreValve (Medtronic, Minneapolis) and the Edwards SAPIEN (Edwards LifeSciences, Irvine, Calif.) valves are commercially available. One of the most important factors is the sizing of the aortic annulus, which determines whether the available valve types are suitable and also affects the choice of prosthetic valve size. Although the aortic annulus can be visualized in transthoracic echocardiography, the use of TEE is recommended because it allows more accurate delineation of the annulus.[181] It further allows measurement of the distance from the aortic cusps to the coronary ostia. Furthermore, TEE permits a morphologic characterization of the thoracic aorta and thus the identification of aortic plaques. Nevertheless, computed tomography angiography of the aorta, which provides complementary information with regard to annulus size and aortic morphology, is routinely performed. The determination of aortic valve etiology is mandatory: A bicuspid aortic valve is a contraindication for transcatheter valve implantation because of the likelihood of noncircular deployment of the valve. However, it is not unlikely to miss the diagnosis of a bicuspid valve in the presence of a severely calcified valve, where an exact morphologic description is difficult. In the process of preinterventional patient evaluation, the basal interventricular septum should be assessed to detect a subaortic septal bulge that may interfere with an adequate valve deployment. Concomitant valve lesions are routinely assessed. In particular, the presence of concomitant mitral regurgitation may affect treatment decisions. When the mitral valve is morphologically normal, a reduction of regurgitation severity can be expected after aortic valve implantation and the resulting drop in LV afterload. However, when a structural lesion is present, regurgitation typically persists.

### VALVE IMPLANTATION

Intraprocedural TEE is complementary to fluoroscopy for the positioning of the balloon during valvuloplasty and also to confirm the position of the valve prosthesis before deployment. 3D TEE allows improved visualization of the prosthesis. Following prosthesis implantation, the valve position is confirmed and its function evaluated. In particular, the shape of stent expansion and the presence of aortic regurgitation, which is of prognostic relevance, can be assessed. Periinterventional TEE monitoring is particularly important for the identification of potential complications, such as incorrect valve positioning, pericardial effusion, cardiac tamponade, aortic dissection, or the rare event of annular rupture.

### KEY POINTS

- With an ageing population and widespread use of echocardiography, AS is increasingly diagnosed.
- Knowledge of the prognostic implications of echocardiographic findings in AS is essential for optimal management and should always be put in clinical context.
- Echocardiography is the method of choice for follow-up of patients with AS and allows:
  - The determination of the etiology of the stenosis (i.e., calcific, rheumatic, congenital)
  - The exclusion of other causes of obstruction to LV outflow (i.e., supravalvular AS, subvalvular AS, hypertrophic obstructive cardiomyopathy)
  - Identification of consequences of AS such as LV hypertrophy, impairment of LV systolic function, or presence of diastolic dysfunction as well as concomitant valve lesions
  - Quantification of the severity of the stenosis using flow-dependent (peak aortic jet velocity, mean gradient) and flow-independent (aortic valve area assessed by the continuity equation) variables
  - Measurement of hemodynamic progression
  - Risk stratification by integrating the information on stenosis severity, rate of hemodynamic progression and degree of aortic valve calcification
- Echocardiography plays a central role in management decisions, including surgical indications and scheduling control intervals.

## REFERENCES


1. Iung B, Baron G, Butchart EG, et al: A prospective survey of patients with valvular heart disease in Europe: the Euro Heart Survey on Valvular Heart Disease. *Eur Heart J* 24:1231-1243, 2003.
2. Roberts WC, Ko JM: Frequency by decades of unicuspid, bicuspid, and tricuspid aortic valves in adults having isolated aortic valve replacement for aortic stenosis, with or without associated aortic regurgitation. *Circulation* 111:920-925, 2005.
3. Otto CM: Calcific aortic stenosis—time to look more closely at the valve. *N Engl J Med* 359:1395-1398, 2008.
4. Waller B, Howard J, Fess S: Pathology of aortic valve stenosis and pure aortic regurgitation. A clinical morphologic assessment—part I. *Clin Cardiol* 17:85-92, 1994.
5. Schaefer BM, Lewin MB, Stout KK, et al: The bicuspid aortic valve: an integrated phenotypic classification of leaflet morphology and aortic root shape. *Heart* 94:1634-1638, 2008.
6. Rosenhek R, Binder T, Porenta G, et al: Predictors of outcome in severe, asymptomatic aortic stenosis. *N Engl J Med* 343:611-617, 2000.
7. Keane MG, Wiegers SE, Plappert T, et al: Bicuspid aortic valves are associated with aortic dilatation out of proportion to coexistent valvular lesions. *Circulation* 102:III35-III39, 2000.
8. Novaro GM, Mishra M, Griffin BP: Incidence and echocardiographic features of congenital unicuspid aortic valve in an adult population. *J Heart Valve Dis* 12:674-678, 2003.
9. Bach DS: Subvalvular left ventricular outflow obstruction for patients undergoing aortic valve replacement for aortic stenosis: echocardiographic recognition and identification of patients at risk. *J Am Soc Echocardiogr* 18:1155-1162, 2005.
10. Baumgartner H, Hung J, Bermejo J, et al: Echocardiographic assessment of valve stenosis: EAE/ASE recommendations for clinical practice. *Eur J Echocardiogr* 10:1-25, 2009.
11. Currie PJ, Hagler DJ, Seward JB, et al: Instantaneous pressure gradient: a simultaneous Doppler and dual catheter correlative study. *J Am Coll Cardiol* 7:800-806, 1986.
12. Currie PJ, Seward JB, Reeder GS, et al: Continuous-wave Doppler echocardiographic assessment of severity of calcific aortic stenosis: a simultaneous Doppler-catheter correlative study in 100 adult patients. *Circulation* 71:1162-1169, 1985.
13. Hatle L, Angelsen BA, Tromsdal A: Non-invasive assessment of aortic stenosis by Doppler ultrasound. *Br Heart J* 43:284-292, 1980.
14. Hegrenaes L, Hatle L: Aortic stenosis in adults. Non-invasive estimation of pressure differences by continuous wave Doppler echocardiography. *Br Heart J* 54:396-404, 1985.
15. Otto CM, Pearlman AS, Gardner CL, et al: Experimental validation of Doppler echocardiographic measurement of volume flow through the stenotic aortic valve. *Circulation* 78:435-441, 1988.
16. Stamm RB, Martin RP: Quantification of pressure gradients across stenotic valves by Doppler ultrasound. *J Am Coll Cardiol* 2:707-718, 1983.
17. Burwash IG, Forbes AD, Sadahiro M, et al: Echocardiographic volume flow and stenosis severity measures with changing flow rate in aortic stenosis. *Am J Physiol* 265:H1734-H1743, 1993.
18. Hatle L: Noninvasive assessment and differentiation of left ventricular outflow obstruction with Doppler ultrasound. *Circulation* 64:381-387, 1981.
19. Otto CM, Davis KB, Holmes DR Jr, et al: Methodologic issues in clinical evaluation of stenosis severity in adults undergoing aortic or mitral balloon valvuloplasty. The NHLBI Balloon Valvuloplasty Registry. *Am J Cardiol* 69:1607-1616, 1992.
20. Cueff de Monchy C, Lepage L, Boutron I, et al: Usefulness of the right parasternal view and non-imaging continuous-wave Doppler transducer for the evaluation of the severity of aortic stenosis in the modern area. *Eur J Echocardiogr* 10:420-424, 2009.
21. Otto CM, Pearlman AS, Comess KA, et al: Determination of the stenotic aortic valve area in adults using Doppler echocardiography. *J Am Coll Cardiol* 7:509-517, 1986.
22. Laskey WK, Kussmaul WG: Pressure recovery in aortic valve stenosis. *Circulation* 89:116-121, 1994.
23. Levine RA, Jimoh A, Cape EG, et al: Pressure recovery distal to a stenosis: potential cause of gradient "overestimation" by Doppler echocardiography. *J Am Coll Cardiol* 13:706-715, 1989.
24. Baumgartner H, Stefenelli T, Niederberger J, et al: "Overestimation" of catheter gradients by Doppler ultrasound in patients with aortic stenosis: a predictable manifestation of pressure recovery. *J Am Coll Cardiol* 33:1655-1661, 1999.
25. Voelker W, Reul H, Stelzer T, et al: Pressure recovery in aortic stenosis: an in vitro study in a pulsatile flow model. *J Am Coll Cardiol* 20:1585-1593, 1992.
26. Yoganathan AP: Fluid mechanics of aortic stenosis. *Eur Heart J* 9(Suppl E):13-17, 1988.
27. Niederberger J, Schima H, Maurer G, Baumgartner H: Importance of pressure recovery for the assessment of aortic stenosis by Doppler ultrasound. Role of aortic size, aortic valve area, and direction of the stenotic jet in vitro. *Circulation* 94:1934-1940, 1996.
28. Grayburn PA, Smith MD, Harrison MR, et al: Pivotal role of aortic valve area calculation by the continuity equation for Doppler assessment of aortic stenosis in patients with combined aortic stenosis and regurgitation. *Am J Cardiol* 61:376-381, 1988.
29. Otto CM: The difficulties in assessing patients with moderate aortic stenosis. *Heart* 82:5-6, 1999.
30. Teirstein P, Yeager M, Yock PG, Popp RL: Doppler echocardiographic measurement of aortic valve area in aortic stenosis: a noninvasive application of the Gorlin formula. *J Am Coll Cardiol* 8:1059-1065, 1986.
31. Zoghbi WA, Farmer KL, Soto JG, et al: Accurate noninvasive quantification of stenotic aortic valve area by Doppler echocardiography. *Circulation* 73:452-459, 1986.
32. Otto CM, Pearlman AS: Doppler echocardiography in adults with symptomatic aortic stenosis. Diagnostic utility and cost-effectiveness. *Arch Intern Med* 148:2553-2560, 1988.
33. Wiseth R, Samstad S, Rossvoll O, et al: Cross-sectional left ventricular outflow tract velocities before and after aortic valve replacement: a comparative study with two-dimensional Doppler ultrasound. *J Am Soc Echocardiogr* 6:279-285, 1993.
34. Sjoberg BJ, Ask P, Loyd D, Wranne B: Subaortic flow profiles in aortic valve disease: a two-dimensional color Doppler study. *J Am Soc Echocardiogr* 7:276-285, 1994.
35. Gorlin R, Gorlin SG: Hydraulic formula for calculation of the area of the stenotic mitral valve, other cardiac valves, and central circulatory shunts. I. *Am Heart J* 41:1-29, 1951.
36. Skjaerpe T, Hegrenaes L, Hatle L: Noninvasive estimation of valve area in patients with aortic stenosis by Doppler ultrasound and two-dimensional echocardiography. *Circulation* 72: 810-818, 1985.
37. Flachskampf FA, Weyman AE, Guerrero JL, Thomas JD: Influence of orifice geometry and flow rate on effective valve area: an in vitro study. *J Am Coll Cardiol* 15:1173-1180, 1990.
38. Segal J, Lerner DJ, Miller DC, et al: When should Doppler-determined valve area be better than the Gorlin formula?: Variation in hydraulic constants in low flow states. *J Am Coll Cardiol* 9:1294-1305, 1987.
39. Dumesnil JG, Yoganathan AP: Theoretical and practical differences between the Gorlin formula and the continuity equation for calculating aortic and mitral valve areas. *Am J Cardiol* 67:1268-1272, 1991.
40. Lemler MS, Valdes-Cruz LM, Shandas RS, Cape EG: Insights into catheter/Doppler discrepancies in congenital aortic stenosis. *Am J Cardiol* 83:1447-1450, 1999.
41. Garcia D, Dumesnil JG, Durand LG, et al: Discrepancies between catheter and Doppler estimates of valve effective orifice area can be predicted from the pressure recovery phenomenon: practical implications with regard to quantification of aortic stenosis severity. *J Am Coll Cardiol* 41:435-442, 2003.
42. Gorlin R, Gorlin WB: Further reconciliation between pathoanatomy and pathophysiology of stenotic cardiac valves. *J Am Coll Cardiol* 15:1181-1182, 1990.
43. Otto CM, Burwash IG, Legget ME, et al: Prospective study of asymptomatic valvular aortic stenosis. Clinical, echocardiographic, and exercise predictors of outcome. *Circulation* 95: 2262-2270, 1997.
44. Pellikka PA, Nishimura RA, Bailey KR, Tajik AJ: The natural history of adults with asymptomatic, hemodynamically significant aortic stenosis. *J Am Coll Cardiol* 15:1012-1017, 1990.
45. Vahanian A, Baumgartner H, Bax J, et al: Guidelines on the management of valvular heart disease: the Task Force on the Management of Valvular Heart Disease of the European Society of Cardiology. *Eur Heart J* 28: 230-268, 2007.
46. Bonow RO, Carabello BA, Chatterjee K, et al: 2008 focused update incorporated into the ACC/AHA 2006 guidelines for the management of patients with valvular heart disease: a report of the American College of Cardiology/American Heart Association Task Force on Practice Guidelines (writing committee to revise the 1998 guidelines for the management of patients with valvular heart disease). Endorsed by the Society of Cardiovascular Anesthesiologists, Society for Cardiovascular Angiography and Interventions, and Society of Thoracic Surgeons. *J Am Coll Cardiol* 52:e1-e142, 2008.
47. Minners J, Allgeier M, Gohlke-Baerwolf C, et al: Inconsistencies of echocardiographic criteria for the grading of aortic valve stenosis. *Eur Heart J* 29:1043-1048, 2008.
48. Rosenhek R, Zilberszac R, Schemper M, et al: Natural history of very severe aortic stenosis. *Circulation* 121:151-156, 2010.

49. Rahimtoola SH: Perspective on valvular heart disease: an update. *J Am Coll Cardiol* 14:1-23, 1989.
50. Otto CM, Lind BK, Kitzman DW, et al: Association of aortic-valve sclerosis with cardiovascular mortality and morbidity in the elderly. *N Engl J Med* 341:142-147, 1999.
51. Rosenhek R, Klaar U, Schemper M, et al: Mild and moderate aortic stenosis; natural history and risk stratification by echocardiography. *Eur Heart J* 25:199-205, 2004.
52. Cannon JD Jr, Zile MR, Crawford FA Jr, Carabello BA: Aortic valve resistance as an adjunct to the Gorlin formula in assessing the severity of aortic stenosis in symptomatic patients. *J Am Coll Cardiol* 20:1517-1523, 1992.
53. Voelker W, Reul H, Nienhaus G, et al: Comparison of valvular resistance, stroke work loss, and Gorlin valve area for quantification of aortic stenosis. An in vitro study in a pulsatile aortic flow model. *Circulation* 91:1196-1204, 1995.
54. Laskey WK, Kussmaul WG, Noordergraaf A: Valvular and systemic arterial hemodynamics in aortic valve stenosis. A model-based approach. *Circulation* 92:1473-1478, 1995.
55. Blais C, Pibarot P, Dumesnil JG, et al: Comparison of valve resistance with effective orifice area regarding flow dependence. *Am J Cardiol* 88:45-52, 2001.
56. Burwash IG, Pearlman AS, Kraft CD, et al: Flow dependence of measures of aortic stenosis severity during exercise. *J Am Coll Cardiol* 24:1342-1350, 1994.
57. Roger VL, Seward JB, Bailey KR, et al: Aortic valve resistance in aortic stenosis: Doppler echocardiographic study and surgical correlation. *Am Heart J* 134:924-929, 1997.
58. Sprigings DC, Chambers JB, Cochrane T, et al: Ventricular stroke work loss: validation of a method of quantifying the severity of aortic stenosis and derivation of an orifice formula. *J Am Coll Cardiol* 16:1608-1614, 1990.
59. Milnor W: *Cardiac dynamics*, Baltimore, 1982, Williams & Wilkins.
60. Garcia D, Pibarot P, Dumesnil JG, et al: Assessment of aortic valve stenosis severity: a new index based on the energy loss concept. *Circulation* 101:765-771, 2000.
61. Cormier B, Iung B, Porte JM, et al: Value of multiplane transesophageal echocardiography in determining aortic valve area in aortic stenosis. *Am J Cardiol* 77:882-885, 1996.
62. Tribouilloy C, Shen WF, Peltier M, et al: Quantitation of aortic valve area in aortic stenosis with multiplane transesophageal echocardiography: comparison with monoplane transesophageal approach. *Am Heart J* 128:526-532, 1994.
63. Bernard Y, Meneveau N, Vuillemenot A, et al: Planimetry of aortic valve area using multiplane transoesophageal echocardiography is not a reliable method for assessing severity of aortic stenosis. *Heart* 78:68-73, 1997.
64. Goland S, Trento A, Iida K, et al: Assessment of aortic stenosis by three-dimensional echocardiography: an accurate and novel approach. *Heart* 93:801-807, 2007.
65. Faggiano P, Gualeni A, Antonini-Canterin F, et al: Doppler echocardiographic assessment of hemodynamic progression of valvular aortic stenosis over time: comparison between aortic valve resistance and valve area. *G Ital Cardiol* 29:1131-1136, 1999.
66. Otto CM, Pearlman AS, Kraft CD, et al: Physiologic changes with maximal exercise in asymptomatic valvular aortic stenosis assessed by Doppler echocardiography. *J Am Coll Cardiol* 20:1160-1167, 1992.
67. Lancellotti P, Lebois F, Simon M, et al: Prognostic importance of quantitative exercise Doppler echocardiography in asymptomatic valvular aortic stenosis. *Circulation* 112:I377-382, 2005.
68. Kitabatake A, Fujii K, Tanouchi J, et al: Doppler echocardiographic quantitation of cross-sectional area under various hemodynamic conditions: an experimental validation in a canine model of supravalvular aortic stenosis. *J Am Coll Cardiol* 15:1654-1661, 1990.
69. Anderson FL, Tsagaris TJ, Tikoff G, et al: Hemodynamic effects of exercise in patients with aortic stenosis. *Am J Med* 46:872-885, 1969.
70. Bache RJ, Wang Y, Jorgensen CR: Hemodynamic effects of exercise in isolated valvular aortic stenosis. *Circulation* 44:1003-1013, 1971.
71. Burwash IG, Thomas DD, Sadahiro M, et al: Dependence of Gorlin formula and continuity equation valve areas on transvalvular volume flow rate in valvular aortic stenosis. *Circulation* 89:827-835, 1994.
72. Casale PN, Palacios IF, Abascal VM, et al: Effects of dobutamine on Gorlin and continuity equation valve areas and valve resistance in valvular aortic stenosis. *Am J Cardiol* 70:1175-1179, 1992.
73. Cochrane T, Kenyon CJ, Lawford PV, et al: Validation of the orifice formula for estimating effective heart valve opening area. *Clin Phys Physiol Meas* 12:21-37, 1991.
74. Martin TW, Moody JM Jr, Bird JJ, et al: Effect of exercise on indices of valvular aortic stenosis. *Cathet Cardiovasc Diagn* 25:265-271, 1992.
75. Montarello JK, Perakis AC, Rosenthal E, et al: Normal and stenotic human aortic valve opening: in vitro assessment of orifice area changes with flow. *Eur Heart J* 11:484-491, 1990.
76. Chambers JB, Sprigings DC, Cochrane T, et al: Continuity equation and Gorlin formula compared with directly observed orifice area in native and prosthetic aortic valves. *Br Heart J* 67:193-199, 1992.
77. Kadem L, Rieu R, Dumesnil JG, et al: Flow-dependent changes in Doppler-derived aortic valve effective orifice area are real and not due to artifact. *J Am Coll Cardiol* 47:131-137, 2006.
78. Bermejo J, Garcia-Fernandez MA, Torrecilla EG, et al: Effects of dobutamine on Doppler echocardiographic indexes of aortic stenosis. *J Am Coll Cardiol* 28:1206-1213, 1996.
79. Burwash IG, Dickinson A, Teskey RJ, et al: Aortic valve area discrepancy by Gorlin equation and Doppler echocardiography continuity equation: relationship to flow in patients with valvular aortic stenosis. *Can J Cardiol* 16:985-992, 2000.
80. Gallino RA, Milner MR, Goldstein SA, et al: Left ventricular filling patterns in aortic stenosis in patients older than 65 years of age. *Am J Cardiol* 63:1103-1106, 1989.
81. Hess OM, Ritter M, Schneider J, et al: Diastolic stiffness and myocardial structure in aortic valve disease before and after valve replacement. *Circulation* 69:855-865, 1984.
82. Otto CM, Pearlman AS, Amsler LC: Doppler echocardiographic evaluation of left ventricular diastolic filling in isolated valvular aortic stenosis. *Am J Cardiol* 63:313-316, 1989.
83. Villari B, Hess OM, Kaufmann P, et al: Effect of aortic valve stenosis (pressure overload) and regurgitation (volume overload) on left ventricular systolic and diastolic function. *Am J Cardiol* 69:927-934, 1992.
84. Archer SL, Mike DK, Hetland MB, et al: Usefulness of mean aortic valve gradient and left ventricular diastolic filling pattern for distinguishing symptomatic from asymptomatic patients. *Am J Cardiol* 73:275-281, 1994.
85. Bruch C, Stypmann J, Grude M, et al: Tissue Doppler imaging in patients with moderate to severe aortic valve stenosis: clinical usefulness and diagnostic accuracy. *Am Heart J* 148:696-702, 2004.
86. Steine K, Rossebo AB, Stugaard M, Pedersen TR: Left ventricular systolic and diastolic function in asymptomatic patients with moderate aortic stenosis. *Am J Cardiol* 102:897-901, 2008.
87. Rajappan K, Rimoldi OE, Dutka DP, et al: Mechanisms of coronary microcirculatory dysfunction in patients with aortic stenosis and angiographically normal coronary arteries. *Circulation* 105:470-476, 2002.
88. Rajappan K, Rimoldi OE, Camici PG, et al: Functional changes in coronary microcirculation after valve replacement in patients with aortic stenosis. *Circulation* 107:3170-3175, 2003.
89. Chambers J, Takeda S, Rimington H, et al: Determinants of left ventricular mass in aortic stenosis. *J Heart Valve Dis* 13:873-880, 2004.
90. Dellgren G, Eriksson MJ, Blange I, et al: Angiotensin-converting enzyme gene polymorphism influences degree of left ventricular hypertrophy and its regression in patients undergoing operation for aortic stenosis. *Am J Cardiol* 84:909-913, 1999.
91. Orlowska-Baranowska E, Placha G, Gaciong Z, et al: Influence of ACE I/D genotypes on left ventricular hypertrophy in aortic stenosis: gender-related differences. *J Heart Valve Dis* 13:574-581, 2004.
92. Cioffi G, Faggiano P, Vizzardi E, et al: Prognostic effect of inappropriately high left ventricular mass in asymptomatic severe aortic stenosis. *Heart* 97:301-307, 2011.
93. Stewart RA, Kerr AJ, Whalley GA, et al: Left ventricular systolic and diastolic function assessed by tissue Doppler imaging and outcome in asymptomatic aortic stenosis. *Eur Heart J* 31:2216-2222, 2010.
94. Carroll JD, Carroll EP, Feldman T, et al: Sex-associated differences in left ventricular function in aortic stenosis of the elderly. *Circulation* 86:1099-1107, 1992.
95. Douglas PS, Otto CM, Mickel MC, et al: Gender differences in left ventricle geometry and function in patients undergoing balloon dilatation of the aortic valve for isolated aortic stenosis. NHLBI Balloon Valvuloplasty Registry. *Br Heart J* 73:548-554, 1995.
96. Aurigemma GP, Silver KH, McLaughlin M, et al: Impact of chamber geometry and gender on left ventricular systolic function in patients > 60 years of age with aortic stenosis. *Am J Cardiol* 74:794-798, 1994.
97. Legget ME, Kuusisto J, Healy NL, et al: Gender differences in left ventricular function at rest and with exercise in asymptomatic aortic stenosis. *Am Heart J* 131:94-100, 1996.
98. Morris JJ, Schaff HV, Mullany CJ, et al: Gender differences in left ventricular functional response to aortic valve replacement. *Circulation* 90:II183-189, 1994.

99. Ng AC, Delgado V, Bertini M, et al: Alterations in multidirectional myocardial functions in patients with aortic stenosis and preserved ejection fraction: a two-dimensional speckle tracking analysis. *Eur Heart J* 32:1542-1550, 2011.
100. Frank S, Johnson A, Ross J Jr: Natural history of valvular aortic stenosis. *Br Heart J* 35:41-46, 1973.
101. Ross J Jr, Braunwald E: Aortic stenosis. *Circulation* 38:61-67, 1968.
102. Selzer A: Changing aspects of the natural history of valvular aortic stenosis. *N Engl J Med* 317:91-98, 1987.
103. Beppu S, Suzuki S, Matsuda H, et al: Rapidity of progression of aortic stenosis in patients with congenital bicuspid aortic valves. *Am J Cardiol* 71:322-327, 1993.
104. Pachulski RT, Chan KL: Progression of aortic valve dysfunction in 51 adult patients with congenital bicuspid aortic valve: assessment and follow up by Doppler echocardiography. *Br Heart J* 69:237-240, 1993.
105. Aronow WS, Kronzon I: Prevalence and severity of valvular aortic stenosis determined by Doppler echocardiography and its association with echocardiographic and electrocardiographic left ventricular hypertrophy and physical signs of aortic stenosis in elderly patients. *Am J Cardiol* 67:776-777, 1991.
106. Lindroos M, Kupari M, Heikkila J, Tilvis R: Prevalence of aortic valve abnormalities in the elderly: an echocardiographic study of a random population sample. *J Am Coll Cardiol* 21:1220-1225, 1993.
107. Amato MC, Moffa PJ, Werner KE, Ramires JA: Treatment decision in asymptomatic aortic valve stenosis: role of exercise testing. *Heart* 86:381-386, 2001.
108. Das P, Rimington H, Chambers J: Exercise testing to stratify risk in aortic stenosis. *Eur Heart J* 26:1309-1313, 2005.
109. Chizner MA, Pearle DL, deLeon AC Jr: The natural history of aortic stenosis in adults. *Am Heart J* 99:419-424, 1980.
110. Horstkotte D, Loogen F: The natural history of aortic valve stenosis. *Eur Heart J* 9(Suppl E):57-64, 1988.
111. Kelly TA, Rothbart RM, Cooper CM, et al: Comparison of outcome of asymptomatic to symptomatic patients older than 20 years of age with valvular aortic stenosis. *Am J Cardiol* 61:123-130, 1988.
112. Kennedy KD, Nishimura RA, Holmes DR Jr, Bailey KR: Natural history of moderate aortic stenosis. *J Am Coll Cardiol* 17:313-319, 1991.
113. O'Keefe JH Jr, Vlietstra RE, Bailey KR, Holmes DR Jr: Natural history of candidates for balloon aortic valvuloplasty. *Mayo Clin Proc* 62:986-991, 1987.
114. Turina J, Hess O, Sepulcri F, Krayenbuehl HP: Spontaneous course of aortic valve disease. *Eur Heart J* 8:471-483, 1987.
115. Leon MB, Smith CR, Mack M, et al: Transcatheter aortic-valve implantation for aortic stenosis in patients who cannot undergo surgery. *N Engl J Med* 363:1597-1607, 2010.
116. Otto CM, Mickel MC, Kennedy JW, et al: Three-year outcome after balloon aortic valvuloplasty. Insights into prognosis of valvular aortic stenosis. *Circulation* 89:642-650, 1994.
117. Nessmith MG, Fukuta H, Brucks S, Little WC: Usefulness of an elevated B-type natriuretic peptide in predicting survival in patients with aortic stenosis treated without surgery. *Am J Cardiol* 96:1445-1448, 2005.
118. Iung B, Cachier A, Baron G, et al: Decision-making in elderly patients with severe aortic stenosis: why are so many denied surgery? *Eur Heart J* 26:2714-2720, 2005.
119. Bach DS, Cimino N, Deeb GM: Unoperated patients with severe aortic stenosis. *J Am Coll Cardiol* 50:2018-2019, 2007.
120. Cosmi JE, Kort S, Tunick PA, et al: The risk of the development of aortic stenosis in patients with "benign" aortic valve thickening. *Arch Intern Med* 162:2345-2347, 2002.
121. Rosenhek R, Maurer G, Baumgartner H: Should early elective surgery be performed in patients with severe but asymptomatic aortic stenosis? *Eur Heart J* 23:1417-1421, 2002.
122. Faggiano P, Ghizzoni G, Sorgato A, et al: Rate of progression of valvular aortic stenosis in adults. *Am J Cardiol* 70:229-233, 1992.
123. Pellikka PA, Sarano ME, Nishimura RA, et al: Outcome of 622 adults with asymptomatic, hemodynamically significant aortic stenosis during prolonged follow-up. *Circulation* 111:3290-3295, 2005.
124. Marechaux S, Hachicha Z, Bellouin A, et al: Usefulness of exercise-stress echocardiography for risk stratification of true asymptomatic patients with aortic valve stenosis. *Eur Heart J* 31:1390-1397, 2010.
125. Monin JL, Lancellotti P, Monchi M, et al: Risk score for predicting outcome in patients with asymptomatic aortic stenosis. *Circulation* 120:69-75, 2009.
126. Lancellotti P, Donal E, Magne J, et al: Risk stratification in asymptomatic moderate to severe aortic stenosis: the importance of the valvular, arterial and ventricular interplay. *Heart* 96:1364-1371, 2010.
127. Kang DH, Park SJ, Rim JH, et al: Early surgery versus conventional treatment in asymptomatic very severe aortic stenosis. *Circulation* 121:1502-1509, 2010.
128. Easterling TR, Chadwick HS, Otto CM, Benedetti TJ: Aortic stenosis in pregnancy. *Obstet Gynecol* 72:113-118, 1988.
129. Keane JF, Driscoll DJ, Gersony WM, et al: Second natural history study of congenital heart defects. Results of treatment of patients with aortic valvar stenosis. *Circulation* 87:I16-27, 1993.
130. Bahler RC, Desser DR, Finkelhor RS, et al: Factors leading to progression of valvular aortic stenosis. *Am J Cardiol* 84:1044-1048, 1999.
131. Brener SJ, Duffy CI, Thomas JD, Stewart WJ: Progression of aortic stenosis in 394 patients: relation to changes in myocardial and mitral valve dysfunction. *J Am Coll Cardiol* 25:305-310, 1995.
132. Lester SJ, McElhinney DB, Miller JP, et al: Rate of change in aortic valve area during a cardiac cycle can predict the rate of hemodynamic progression of aortic stenosis. *Circulation* 101: 1947-1952, 2000.
133. Otto CM, Pearlman AS, Gardner CL: Hemodynamic progression of aortic stenosis in adults assessed by Doppler echocardiography. *J Am Coll Cardiol* 13:545-550, 1989.
134. Palta S, Pai AM, Gill KS, Pai RG: New insights into the progression of aortic stenosis: implications for secondary prevention. *Circulation* 101:2497-2502, 2000.
135. Peter M, Hoffmann A, Parker C, et al: Progression of aortic stenosis. Role of age and concomitant coronary artery disease. *Chest* 103: 1715-1719, 1993.
136. Roger VL, Tajik AJ, Bailey KR, et al: Progression of aortic stenosis in adults: new appraisal using Doppler echocardiography. *Am Heart J* 119: 331-338, 1990.
137. Aronow WS, Ahn C, Kronzon I, Goldman ME: Association of coronary risk factors and use of statins with progression of mild valvular aortic stenosis in older persons. *Am J Cardiol* 88:693-695, 2001.
138. Bellamy MF, Pellikka PA, Klarich KW, et al: Association of cholesterol levels, hydroxymethylglutaryl coenzyme-A reductase inhibitor treatment, and progression of aortic stenosis in the community. *J Am Coll Cardiol* 40:1723-1730, 2002.
139. Cowell SJ, Newby DE, Prescott RJ, et al: A randomized trial of intensive lipid lowering therapy in calcific aortic stenosis. *N Engl J Med* 352:2389-2397, 2005.
140. Novaro GM, Tiong IY, Pearce GL, et al: Effect of hydroxymethylglutaryl coenzyme a reductase inhibitors on the progression of calcific aortic stenosis. *Circulation* 104:2205-2209, 2001.
141. Rosenhek R, Rader F, Loho N, et al: Statins but not angiotensin-converting enzyme inhibitors delay progression of aortic stenosis. *Circulation* 110:1291-1295, 2004.
142. Rossebø AB, Pedersen TR, Boman K, et al: Intensive lipid lowering with simvastatin and ezetimibe in aortic stenosis. *N Engl J Med* 359:1343-1356, 2008.
143. Moura LM, Ramos SF, Zamorano JL, et al: Rosuvastatin affecting aortic valve endothelium to slow the progression of aortic stenosis. *J Am Coll Cardiol* 49:554-561, 2007.
144. Lund O, Nielsen TT, Emmertsen K, et al: Mortality and worsening of prognostic profile during waiting time for valve replacement in aortic stenosis. *Thorac Cardiovasc Surg* 44:289-295, 1996.
145. Brown JM, O'Brien SM, Wu C, et al: Isolated aortic valve replacement in North America comprising 108,687 patients in 10 years: changes in risks, valve types, and outcomes in the Society of Thoracic Surgeons National Database. *J Thorac Cardiovasc Surg* 137:82-90, 2009.
146. Stewart BF, Siscovick D, Lind BK, et al: Clinical factors associated with calcific aortic valve disease. Cardiovascular Health Study. *J Am Coll Cardiol* 29:630-634, 1997.
147. Messika-Zeitoun D, Bielak LF, Peyser PA, et al: Aortic valve calcification: determinants and progression in the population. *Arterioscler Thromb Vasc Biol* 27:642-648, 2007.
148. Messika-Zeitoun D, Aubry MC, Detaint D, et al: Evaluation and clinical implications of aortic valve calcification measured by electron-beam computed tomography. *Circulation* 110:356-362, 2004.
149. Gerber IL, Stewart RA, Legget ME, et al: Increased plasma natriuretic peptide levels reflect symptom onset in aortic stenosis. *Circulation* 107:1884-1890, 2003.
150. Bergler-Klein J, Klaar U, Heger M, et al: Natriuretic peptides predict symptom-free survival and postoperative outcome in severe aortic stenosis. *Circulation* 109:2302-2308, 2004.
151. Lim P, Monin JL, Monchi M, et al: Predictors of outcome in patients with severe aortic stenosis and normal left ventricular function: role of B-type natriuretic peptide. *Eur Heart J* 25:2048-2053, 2004.
152. Briand M, Dumesnil JG, Kadem L, et al: Reduced systemic arterial compliance impacts significantly on left ventricular afterload and function in aortic stenosis: implications for diagnosis and treatment. *J Am Coll Cardiol* 46:291-298, 2005.

153. Collins JJ Jr, Aranki SF: Management of mild aortic stenosis during coronary artery bypass graft surgery. *J Card Surg* 9:145-147, 1994.
154. Pereira JJ, Balaban K, Lauer MS, et al: Aortic valve replacement in patients with mild or moderate aortic stenosis and coronary bypass surgery. *Am J Med* 118:735-742, 2005.
155. Smith WT, Ferguson TB Jr, Ryan T, et al: Should coronary artery bypass graft surgery patients with mild or moderate aortic stenosis undergo concomitant aortic valve replacement? A decision analysis approach to the surgical dilemma. *J Am Coll Cardiol* 44:1241-1247, 2004.
156. Powell DE, Tunick PA, Rosenzweig BP, et al: Aortic valve replacement in patients with aortic stenosis and severe left ventricular dysfunction. *Arch Intern Med* 160:1337-1341, 2000.
157. Levy F, Garayalde E, Quere JP, et al: Prognostic value of preoperative atrial fibrillation in patients with aortic stenosis and low ejection fraction having aortic valve replacement. *Am J Cardiol* 98:809-811, 2006.
158. Brogan WC 3rd, Grayburn PA, Lange RA, Hillis LD: Prognosis after valve replacement in patients with severe aortic stenosis and a low transvalvular pressure gradient. *J Am Coll Cardiol* 21:1657-1660, 1993.
159. Connolly HM, Oh JK, Schaff HV, et al: Severe aortic stenosis with low transvalvular gradient and severe left ventricular dysfunction: result of aortic valve replacement in 52 patients. *Circulation* 101:1940-1946, 2000.
160. Pereira JJ, Lauer MS, Bashir M, et al: Survival after aortic valve replacement for severe aortic stenosis with low transvalvular gradients and severe left ventricular dysfunction. *J Am Coll Cardiol* 39:1356-1363, 2002.
161. Monin JL, Quere JP, Monchi M, et al: Low-gradient aortic stenosis: operative risk stratification and predictors for long-term outcome: a multicenter study using dobutamine stress hemodynamics. *Circulation* 108: 319-324, 2003.
162. deFilippi CR, Willett DL, Brickner ME, et al: Usefulness of dobutamine echocardiography in distinguishing severe from nonsevere valvular aortic stenosis in patients with depressed left ventricular function and low transvalvular gradients. *Am J Cardiol* 75:191-194, 1995.
163. Schwammenthal E, Vered Z, Moshkowitz Y, et al: Dobutamine echocardiography in patients with aortic stenosis and left ventricular dysfunction: predicting outcome as a function of management strategy. *Chest* 119:1766-1777, 2001.
164. Carabello BA: Do all patients with aortic stenosis and left ventricular dysfunction benefit from aortic valve replacement? *Cathet Cardiovasc Diagn* 17:131-132, 1989.
165. Lin SS, Roger VL, Pascoe R, et al: Dobutamine stress Doppler hemodynamics in patients with aortic stenosis: feasibility, safety, and surgical correlations. *Am Heart J* 136:1010-1016, 1998.
166. Blais C, Burwash IG, Mundigler G, et al: Projected valve area at normal flow rate improves the assessment of stenosis severity in patients with low-flow, low-gradient aortic stenosis: the multicenter TOPAS (Truly or Pseudo-Severe Aortic Stenosis) study. *Circulation* 113:711-721, 2006.
167. Quere JP, Monin JL, Levy F, et al: Influence of preoperative left ventricular contractile reserve on postoperative ejection fraction in low-gradient aortic stenosis. *Circulation* 113:1738-1744, 2006.
168. Tribouilloy C, Levy F, Rusinaru D, et al: Outcome after aortic valve replacement for low-flow/low-gradient aortic stenosis without contractile reserve on dobutamine stress echocardiography. *J Am Coll Cardiol* 53:1865-1873, 2009.
169. Levy F, Laurent M, Monin JL, et al: Aortic valve replacement for low-flow/low-gradient aortic stenosis operative risk stratification and long-term outcome: a European multicenter study. *J Am Coll Cardiol* 51:1466-1472, 2008.
170. Cueff C, Serfaty JM, Cimadevilla C, et al: Measurement of aortic valve calcification using multislice computed tomography: correlation with haemodynamic severity of aortic stenosis and clinical implication for patients with low ejection fraction. *Heart* 97:721-726, 2011.
171. Hachicha Z, Dumesnil JG, Bogaty P, Pibarot P: Paradoxical low-flow, low-gradient severe aortic stenosis despite preserved ejection fraction is associated with higher afterload and reduced survival. *Circulation* 115:2856-2864, 2007.
172. Jander N, Minners J, Holme I, et al: Outcome of patients with low-gradient "severe" aortic stenosis and preserved ejection fraction. *Circulation* 123:887-895, 2011.
173. Vahanian A, Alfieri O, Al-Attar N, et al: Transcatheter valve implantation for patients with aortic stenosis: a position statement from the European Association of Cardio-Thoracic Surgery (EACTS) and the European Society of Cardiology (ESC), in collaboration with the European Association of Percutaneous Cardiovascular Interventions (EAPCI). *Eur Heart J* 29:1463-1470, 2008.
174. Rosenhek R, Iung B, Tornos P, et al: ESC Working Group on Valvular Heart Disease position paper: assessing the risk of interventions in patients with valvular heart disease. *Eur Heart J* 2011. doi: 10.1093/eurheartj/ehr061
175. Iung B, Drissi MF, Michel PL, et al: Prognosis of valve replacement for aortic stenosis with or without coexisting coronary heart disease: a comparative study. *J Heart Valve Dis* 2:430-439, 1993.
176. Lund O, Nielsen TT, Pilegaard HK, et al: The influence of coronary artery disease and bypass grafting on early and late survival after valve replacement for aortic stenosis. *J Thorac Cardiovasc Surg* 100:327-337, 1990.
177. Czer LS, Gray RJ, Stewart ME, et al: Reduction in sudden late death by concomitant revascularization with aortic valve replacement. *J Thorac Cardiovasc Surg* 95:390-401, 1988.
178. Kveselis DA, Rocchini AP, Rosenthal A, et al: Hemodynamic determinants of exercise-induced ST-segment depression in children with valvar aortic stenosis. *Am J Cardiol* 55:1133-1139, 1985.
179. Gilard M, Cornily JC, Pennec PY, et al: Accuracy of multislice computed tomography in the preoperative assessment of coronary disease in patients with aortic valve stenosis. *J Am Coll Cardiol* 47:2020-2024, 2006.
180. Reant P, Brunot S, Lafitte S, et al: Predictive value of noninvasive coronary angiography with multidetector computed tomography to detect significant coronary stenosis before valve surgery. *Am J Cardiol* 97:1506-1510, 2006.
181. Messika-Zeitoun D, Serfaty JM, Brochet E, et al: Multimodal assessment of the aortic annulus diameter: implications for transcatheter aortic valve implantation. *J Am Coll Cardiol* 55:186-194, 2010.
182. Chan KL, Teo K, Dumesnil JG, Ni A, Tam J: Effect of lipid lowering with rosuvastatin on progression of aortic stenosis: results of the aortic stenosis progression observation measuring effects of rosuvastatin (ASTRONOMER) trial. *Circulation* 121:306-314, 2010.

# 24 Fluid Dynamics of Prosthetic Valves

AJIT P. YOGANATHAN, PhD | CHOON HWAI YAP, PhD

**Principles of Fluid Dynamics**
- Conservation of Mass
- Mechanical Energy
- Bernoulli's Equation
- The Control Volume Energy Analysis
- Mechanisms of Mechanical Energy Loss
- Mechanical Energy Conversion and Loss in a Stenosis

**Applications of Fluid Dynamics to Prosthetic Heart Valves**
- Pressure Drop
- Doppler Gradient
- Effective Orifice Area
- Regurgitant Volume
- Mechanical Energy Losses
- Novel Energy Loss Parameters
- In Vivo Evaluation of Prosthetic Valves

**Hemodynamics of Native Valves**

**Hemodynamics of Specific Prosthetic Valve Designs**
- Mechanical Valves
- Bioprostheses
- Transcatheter Valves

**Future Directions**

Doppler echocardiography has made noninvasive examination of prosthetic heart valve function a clinical reality. Unfortunately, there are still many imperfections in echocardiographic examinations due to acoustic shadowing, reflections caused by implanted valves, and limitations in ultrasound technology. Despite these limitations, a number of important parameters can be calculated or estimated to aid in the assessment of prosthetic heart valve function and performance. Once a valve has been implanted, its function is governed primarily by its hemodynamic characteristics. In order to understand the hemodynamic performance of prosthetic heart valves, it is necessary to have a solid background in the physical laws that govern their function. Therefore, the purpose of this chapter is to introduce cardiologists to the governing principles of fluid dynamics, relevant formulations used in prosthetic valve assessment, and fluid mechanical characteristics of specific prosthetic heart valves.

## Principles of Fluid Dynamics

### CONSERVATION OF MASS

The principle of conservation of mass is important in evaluating valve effective orifice area (EOA). Conservation of mass, or the continuity principle, is a mass balance over the boundaries of a volume of fluid. For example, this volume can be made to coincide with a section of an artery, with the left ventricle, or with the surface of a blood cell and may be made to move over time as well. Such a volume is called a *control volume*, and its boundaries are usually chosen to give information regarding an unknown flow rate, average velocity, or surface area flow into or out of the volume based on more easily measurable quantities. Examples of control volumes useful for determining aortic and mitral valve areas with conservation of mass are shown in Figure 24-1.

Conservation of mass within the control volume can be expressed in words as:

$$\text{Rate of mass accumulation} = \text{Rate of mass input} - \text{Rate of mass output} \quad (1)$$

In cardiovascular applications, we can assume that the density of blood is constant, because blood is composed mostly of water. Water is almost incompressible, and thermal expansion or contraction is insignificant because of the narrow range of body temperature. Because mass is the product of density and volume, mass conservation can be expressed as volume conservation:

$$\text{Rate of volume accumulation} = \text{Rate of volume input} - \text{Rate of volume output} \quad (2)$$

In mathematical form, this is

$$\frac{(V_f - V_i)}{t} = Q_{in} - Q_{out} \quad (3)$$

where $Q_{in}$ is the total flow rate into the control volume, $Q_{out}$ is the total flow rate out of the control volume, $V_i$ is the size of the control volume at the beginning of the observation, and $V_f$ is the size of the control volume after an observation at time $t$. There could be multiple sources of flow inlets and outlets, and thus

$$\frac{1}{t}(V_f - V_i) = (Q_{in(1)} + Q_{in(2)} + Q_{in(3)}) - (Q_{out(1)} + Q_{out(2)} + Q_{out(3)}) \quad (4)$$

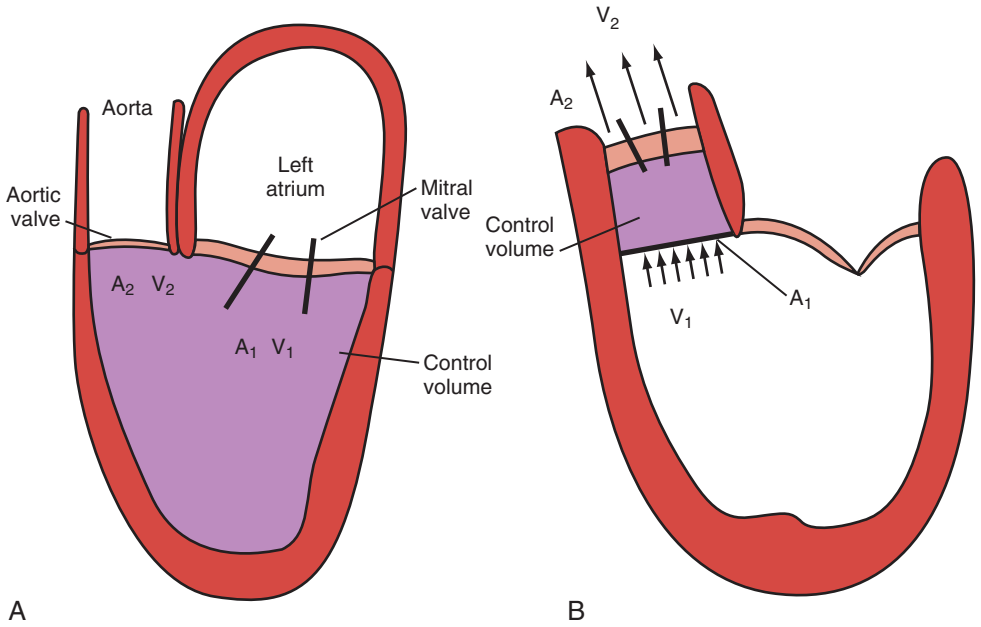



**Figure 24-1** Control volumes used for determining (**A**) mitral and (**B**) aortic valve area with conservation of mass. $V_1$ and $V_2$ represent average velocity of the blood flowing over areas $A_1$ and $A_2$.

If we further assume that the volume of the control volume does not change with time, the left side of Equation 3 is zero, and conservation of mass can be expressed as

$$Q_{in} = Q_{out} \tag{5}$$

This is approximately true in most blood vessels if we neglect expansion vessels under elevated pressure. Often, flow rate in circular, nonbranching vessels can be decomposed into an average axial velocity and a cross-sectional area (A). Equation 5 thus becomes:

$$\bar{v}_{in} A_{in} = \bar{v}_{out} A_{out} \tag{6}$$

Flow through a prosthetic aortic valve is an example of such a situation. The rate at which fluid mass moves toward the valve from upstream has to be equal to the rate at which fluid mass moves through the vena contracta or further downstream of the aorta. This principle is relied on to formulate the equations for calculating EOA using Doppler echocardiography.

## MECHANICAL ENERGY

Mechanical energy can be described as the ability to accelerate a mass of material over a certain distance. Energy per unit volume has the same dimensions as pressure. It is perhaps best to report energy in cardiovascular applications on a per-unit-volume basis, because the majority of the medical field is accustomed to working with the units of pressure. However, it is important to consider pressure as only one of several forms of mechanical energy.

Pressure ($p$) can be shown to be a form of mechanical energy per unit volume by recognizing that it represents a force ($F_p$) per unit area ($A$). If a force is applied to move a mass over a distance ($d$), it performs work, expending pressure energy ($E_p$). The area that the force acts on multiplied by the same distance represents a volume ($V$):

$$\frac{E_p}{V} = \frac{F_p d}{A d} = \frac{F_p}{A} = p \tag{7}$$

Pressure is not the only form of mechanical energy in the circulation. Acceleration due to gravity ($g$) creates another form of mechanical energy per unit volume. Gravity can accelerate a mass $m$ with a force $F_g$. If this force moves the mass over a vertical distance $h$, it too performs work and expends gravitational energy $E_g$. The energy per unit volume is obtained by substituting density $\rho$ for mass per unit volume.

$$\frac{E_g}{V} = \frac{F_g h}{V} = \frac{mgh}{V} = \rho g h \tag{8}$$

Finally, mechanical energy per unit volume exists in the circulation in the form of kinetic energy, or energy of movement. If a mass $m$ is moving at a velocity $v$, it contains kinetic energy equivalent to half the product of the mass and the square of the velocity:

$$\frac{E_k}{V} = \frac{\frac{1}{2} m v^2}{V} = \frac{1}{2} \rho v^2 \tag{9}$$

Again, the energy per unit volume is obtained by substituting density for mass per unit volume. Thus, there are three forms of mechanical energy in the circulation.

The primary source of mechanical energy in the circulation is the work performed by the left ventricle. Contraction of the ventricle creates an increase in pressure inside the ventricle. As Equation 7 implies, subsequent movement of a volume of fluid by this pressure results in the generation of mechanical energy. The energy generated by the ventricle is illustrated in Figure 24-2, which represents the pressure and volume within the ventricle during the course of one cardiac cycle. The curve between points *1* and *2* represents the period of diastolic filling, where the mitral valve is open and the ventricle fills. The mitral valve shuts at point *2*, and the period of isovolumic contraction begins. Between points *2* and *3*, the volume of blood in the ventricle remains constant, but the pressure rises considerably. The aortic valve opens at point *3*. This starts the period of systolic ejection, where blood is moved by the ventricle into the

aorta. At point *4*, the aortic valve closes and the period of isovolumic relaxation begins. During this period, the ventricular volume again remains constant, but the pressure falls. The fall in pressure returns the ventricle to its state at point *1*. The energy generated by the ventricle during one cardiac cycle is equivalent to the integral of the pressure-volume diagram (the shaded area in Fig. 24-2). The energy per unit volume generated by the ventricle is equivalent to the integral of the pressure-volume diagram divided by the stroke volume. This is roughly equivalent to the average increase in left ventricular pressure from diastole to systole. The ventricle thus creates energy in the form of pressure, but this energy is converted to gravitational and kinetic energy elsewhere in the circulation.

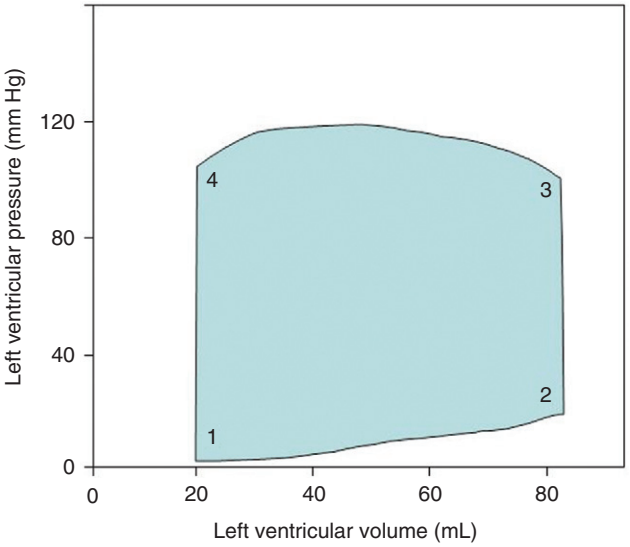



**Figure 24-2 Pressure-volume diagram for the left ventricle.** The shaded area represents the energy given to the flow by one stroke of the ventricle.

## BERNOULLI'S EQUATION

Pressure, gravitational, and kinetic energies in the circulation can be freely converted from one to another without energy loss. Bernoulli's equation for steady flow illustrates this. Bernoulli's equation for steady flow relates the relative amounts of pressure, gravitational, and kinetic energy per unit volume between two spatial locations along a path of a flow (locations 1 and 2, where location 2 is downstream of location 1), assuming that no energy is lost:

$$\frac{1}{2}\rho v_1^2 + \rho g h_1 + p_1 = \frac{1}{2}\rho v_2^2 + \rho g h_2 + p_2 \qquad (10)$$

Bernoulli's equation for steady flow states that the total mechanical energy per unit volume at locations 1 and 2 is the same but can exist in different forms. A decrease in pressure from location 1 to location 2 may be balanced by an increase in either fluid velocity or height without loss of energy. Therefore, a pressure drop is not mechanical energy loss if it is accompanied by an increase in either gravitational or kinetic energy. These energies can be converted back to pressure energy later.

Additional variables can be added to Bernoulli's equation for steady flow to account for the effects of unsteady flow and mechanical energy loss:

$$\frac{1}{2}\rho v_1^2 + \rho g h_1 + p_1 = \frac{1}{2}\rho v_2^2 + \rho g h_2 + p_2 + \int_1^2 \rho \frac{\partial v}{\partial t}\partial s + \Phi \qquad (11)$$

where $s$ represents the distance of the path between locations 1 and 2, and $\Phi$ represents loss of mechanical energy per unit volume. The added terms represents the contribution of acceleration of the fluid to the flow energy and the conversion of mechanical energy to heat, respectively, between locations 1 and 2. Rearranging Equation 11 to express energy loss in terms of the other parameters, we obtain

$$\Phi = (p_1 - p_2) + \frac{1}{2}\rho(v_1^2 - v_2^2) + \rho g(h_1 - h_2) - \int_1^2 \rho \frac{\partial v}{\partial t}\partial s \qquad (12)$$

## THE CONTROL VOLUME ENERGY ANALYSIS

A more detailed analysis of the energy of fluid flow through a valve can be conducted using the control volume approach. Bernoulli's equation describes energy conversion and loss along a streamline (line of fluid flow) and is a useful, simplified approach to analyze fluid energy in valves, while the control

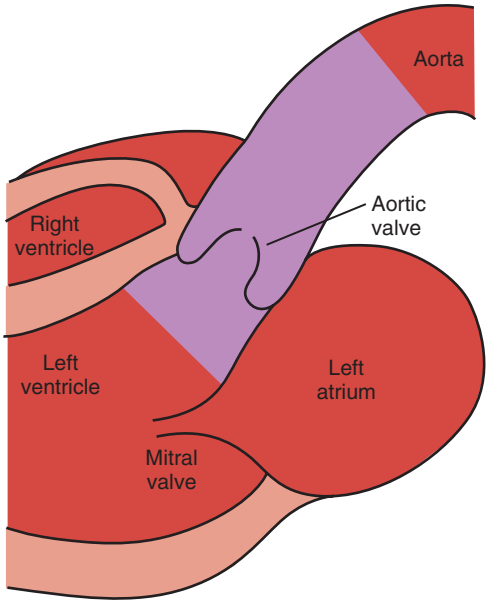



**Figure 24-3** Example of control volume for the analysis of energy loss in the aortic valve.

volume provides three-dimensional (3D) analysis of fluid energy at any time in the cardiac cycle. If we let the control volume be the blood volume around the valve, as shown in Figure 24-3, manipulation of the Navier-Stokes governing equations of fluid flow gives the following equation[1]:

$$\int S_{ij} T_{ij} dV = \int -P(u_i \cdot \hat{n}_i) dA - \int \rho u_i g_i dV - \frac{d}{dt}\int \frac{1}{2}\rho u_i^2 dV \qquad (13)$$

where $S$ is the shear stress, $T$ is the shear deformation, $P$ is pressure, $u$ is velocity, $A$ is the surface of the control volume, $\hat{n}$ is the normal direction at the surface of the control volume, $g$ is the gravitational force, and $V$ is the control volume. The subscripts $i$ and $j$ refer to any of the three Cartesian coordinate

axes, in accordance to Einstein's notation. Equation 13 can be described in words as

$$\begin{array}{c}\text{Energy}\\\text{dissipation}\end{array} = \begin{array}{c}\text{Energy supplied}\\\text{by pressure}\\\text{gradient}\end{array} - \begin{array}{c}\text{Energy}\\\text{converted to}\\\text{gravitational}\\\text{potential energy}\end{array} - \begin{array}{c}\text{Energy}\\\text{converted into}\\\text{kinetic energy}\end{array} \quad (14)$$

Pressure gradient across the valve, which is supplied by the heart muscles, is partially converted into kinetic energy, used to accelerate fluid, partially used to counter effects of gravity, and the remaining is lost as heat and sound.

## MECHANISMS OF MECHANICAL ENERGY LOSS

Mechanical energy can be converted to heat and sound through friction between blood moving at different velocities and between blood and the vessel walls. Heat and sound generated through friction is not readily converted back to mechanical energy, and this energy is said to be lost to the cause of blood circulation. These frictional losses take one of two forms: viscous losses and turbulent losses. Additional energy can be effectively lost in the circulation due to valvular leakage. These forms of energy loss are described next.

### *Viscous Losses*

As a result of frictional forces, fluid immediately adjacent to a solid boundary moves with the same velocity as the boundary. In the case of a stationary vessel, this means that fluid immediately adjacent to the vessel wall does not move, no matter how fast the surrounding flow is moving. As one moves away from the solid boundary, the velocity may increase. This leads to differences in fluid velocity with respect to radial distance within the vessel (Fig. 24-4). Fluid viscosity, the tendency of the fluid components or molecules to "stick" to each other, creates friction between the fluid components in close proximity if they move at different velocities. This is the mechanism of viscous energy loss. Viscous losses typically increase with flow rate and decrease dramatically with increasing vessel radius. This is why vasodilators are effective in relieving left ventricular workload.

### *Turbulent Losses*

Turbulent losses usually do not occur in the circulation but can be greater in magnitude than viscous losses when they do. Turbulence is characterized by chaotic spatial and temporal fluctuations in the direction and magnitude of fluid velocity. It is a result of the inertia of the flow being too great for frictional forces to stabilize fluid movement or to dampen unsteady secondary motions. The chaotic spatial and temporal velocity fluctuations result in excessive mixing of fluid, where individual tiny pockets of fluid will experience very high shear stresses with other pockets of fluid everywhere in the flow. Consequently, there will be high overall frictional energy loss, which is the essence of turbulence energy loss.

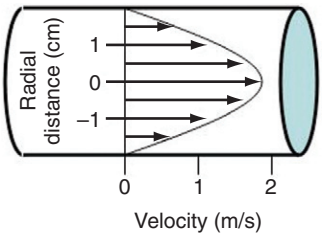



**Figure 24-4 Variations in velocity with respect to radial distance in a blood vessel.** These variations are a result of viscous forces.

In a straight vessel, fluid inertia disturbances may be initiated by small irregularities, or roughness, in the surface of the vessel. In laminar flow, these small inertial disturbances will quickly be damped out by viscous forces, and unsteady secondary flow and fluid mixing will be minimal. In turbulent flow, these inertial changes will be amplified because viscous forces are not strong enough to dampen them. The analogy is being tripped while one is walking versus running. It is harder to keep one's balance when tripped during running, because the inertia of the body's motion is difficult to control.

The tendency toward turbulence in a fluid flow depends on the ratio of inertial forces to frictional forces in the flow. The inertial force of a moving flow is the force required to bring the flow to rest, whereas the frictional force of such a flow is created by viscous shear stress acting on solid surfaces. In vessel flow, this ratio is approximated by the Reynolds number:

$$N_{Re} = \frac{D\bar{v}\rho}{\mu} \quad (15)$$

where $D$ is the inner diameter of the vessel, $v$ is the average velocity of the flow, $\rho$ is the fluid density, and $\mu$ is the fluid viscosity. A low Reynolds number will result in laminar flow; a high Reynolds number will result in turbulent flow. The point of transition between the two states, the critical Reynolds number, differs for different flow systems. For flow through a straight pipe, the critical Reynolds number is approximately 2000, and flow becomes fully turbulent at a Reynolds numbers of approximately 6000.[2] Flow through small, circular orifices creates a phenomenon known as a free jet. For steady free-jet flows, the critical Reynolds number is approximately 1000, with fully turbulent flow occurring at Reynolds numbers greater than 3000.[3,4] This transition point is lowered by sharp corners and bends in the flow, or rough solid surfaces. Further, for turbulence to occur, sufficient time must be allowed for the unsteadiness to amplify and grow. In pulsatile flows, however, if the frequency of pulses is too high, there may be insufficient time for turbulence to fully develop, making it harder to achieve turbulence. The critical Reynolds number thus increases.[5]

### *Valvular Regurgitation*

When valvular regurgitation occurs, the heart must compensate by expending more energy to pump additional blood through the valve during forward flow phase, such that the net of forward flow and regurgitation flow will still be sufficient for the body. Blood that leaks back through the valve will not contribute to circulation, and the energy used to pump it through the valve during forward flow phase can be viewed as being lost. In prosthetic valves, valvular regurgitation consists of the closing volume, paravalvular regurgitation, and perivalvular regurgitation. The closing volume is the amount of blood that will leak backwards through the valve at the end of forward flow before the valve can properly close (Fig. 24-5). Paravalvular regurgitation is the leakage of blood through the valve orifice. In the case of the bioprosthetic valve, calcification of the leaflets can lead to improper coaptation and thus paravalvular regurgitation. In mechanical valves, paravalvular regurgitation can occur through gaps in the closed valve. Perivalvular regurgitation occurs because of improper attachment of the prosthetic

valve with the heart tissues. For example, when prosthesis dehiscence occurs, blood will leak through the gap opened up by the dehiscence.

### MECHANICAL ENERGY CONVERSION AND LOSS IN A STENOSIS

To show how mechanical energy may be changed from one form to another or lost, we refer to an illustration depicting the changes in mechanical energy across an aortic stenosis. Figure 24-6 shows the overall energy conversion and losses, pressure energy, and kinetic energy as blood flow traverses the contraction, throat, and expansion sections of the stenosis.

The first section of the stenosis, from *1* to *2*, is a flow contraction. Because the continuity equation states that the velocity at *2* must be higher than that at *1*, kinetic energy increases from *1* to *2*. This increase in kinetic energy occurs at the expense of a large amount of pressure energy. A relatively small amount of total energy is actually lost in the flow contraction. Most of the lost energy in flow contraction is due to viscous losses. However, there may be a small amount of flow separation immediately following abrupt contractions. Flow separation occurs because the momentum of the flow causes it to continue to converge for a short period after the anatomic contraction (see Fig. 24-6). Such abrupt contractions have considerably more energy loss than gradual ones.

The second section of the stenosis, from *2* to *3*, represents a throat of constant cross-sectional area. In this section, the continuity equation states that the velocity at *2* and *3* are the same. Therefore, there is no loss in kinetic energy; the total energy lost in this section is completely pressure energy. It is worth noting that only in nonbranching vessels of constant cross-sectional area is pressure gradient equivalent to total energy loss per unit volume, and that usually only a small amount of total energy is lost in the stenosis throat. This energy loss is viscous in nature if the flow is laminar and completely turbulent in nature if the flow has enough momentum to enable its transition to turbulence.

Finally, in the expansion section of the stenosis, from *3* to *4*, a large amount of total energy is lost. All of this lost energy is kinetic in nature, which explains why the Doppler gradient correlates so strongly with total mechanical energy loss. However, the Doppler gradient does not completely specify total energy loss because a portion of the kinetic energy is converted into pressure. This is the cause of the *pressure recovery* phenomenon. The expansion section of the stenosis illustrates why pressure gradients can be misleading in the estimation of the lost driving force for flow. Although the pressure increased in the expansion section, the total energy loss was very large.

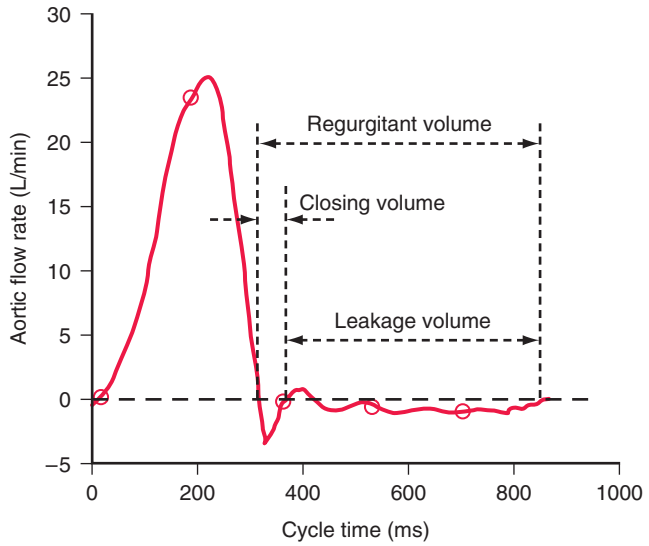



**Figure 24-5** Regurgitant, closing, and leakage volumes across an aortic valve.

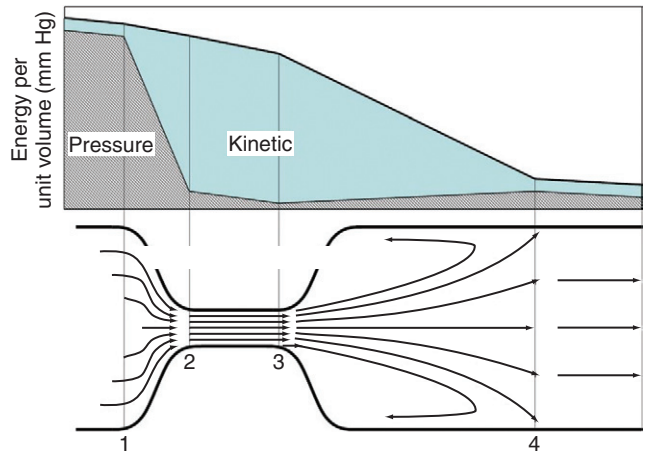



**Figure 24-6 Schematic of pressure and kinetic energy loss and conversion as flow traverses a stenosis.** The flow undergoes contraction from location *1* to location *2*. The throat of the stenosis lies between locations *2* and *3*, and the flow suddenly expands from location *3* to location *4*. *(From Yoganathan AP, He Z, Jones CS: Fluid mechanics of heart valves.* Annu Rev Biomed Eng *6:331-362, 2004.)*

## Applications of Fluid Dynamics to Prosthetic Heart Valves

### PRESSURE DROP

Pressure drop across a heart valve is commonly used to estimate the amount of energy lost by the flow in traversing the valve. Such pressure drops can be directly measured with invasive catheter techniques. Equation 16 shows that the pressure drop across a heart valve is equivalent to energy loss per unit volume if changes in the kinetic energy, gravitational energy, and local acceleration of the flow can be neglected. Because of the law of conservation of mass (see Equation 6), changes in kinetic energy are negligible if diameters of the vessels are the same at the locations of the upstream and downstream pressure measurements and if the downstream measurements are obtained at a location far enough from the valve to allow for pressure recovery. Changes in gravitational energy are negligible if the patient is supine, as there is little height difference between upstream and downstream measurement locations. If the patient is upright, every 5-cm difference in vertical height will result in approximately 3.9 mm Hg of pressure drop. Changes in local acceleration of the flow are negligible if measurements are obtained during peak flow rate across the valve (often called the peak gradient). This is because, at the peak flow rate, velocity is at the maximum turning point and is momentarily experiencing no acceleration. Effects of acceleration are also negligible if measurements are averaged over the forward flow portion of the valve cycle (often called the mean gradient). This is because fluid first accelerates and then decelerates back to the initial state over the forward flow phase; and thus, when the

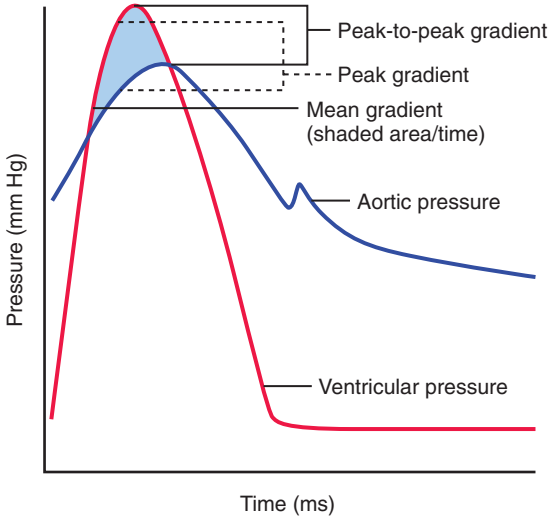



**Figure 24-7** Mean, peak, and peak-to-peak pressure differences across an aortic valve.

acceleration term is integrated over time, it becomes zero. However, it must be noted that *peak gradient* describes the energy loss during peak flow phase, whereas *mean gradient* describes the average energy loss over the entire forward flow period. Thus, peak gradient will always be higher than mean gradient. Pressure drop is also often reported in terms of a peak-to-peak gradient for convenience, as an approximation of the peak gradient. Differences between peak and peak-to-peak gradients are shown in Figure 24-7.

## DOPPLER GRADIENT

Although energy lost by the flow in traversing the valve can be estimated more directly with catheterization, such losses are now typically estimated noninvasively with the help of echocardiography. A simplified form of Equation 12 is used to estimate the amount of pressure converted to kinetic energy as the flow contracts from well upstream of the valve to the point of maximum flow contraction, by neglecting the small energy conversions to gravitational potential energy:

$$\Delta p = 4(v_{\max}{}^2 - v_{ups}{}^2) \tag{16}$$

where $\Delta p$ is the pressure drop ($p_1 - p_2$) during the flow contraction in mm Hg, $v_{ups}$ is the velocity upstream of the contraction during forward flow in cm/s, and $v_{\max}$ is the velocity at the point of maximum flow contraction during forward flow in cm/s. The constant 4 is used to account for the density of blood and unit conversions. This simplification assumes that mechanical energy loss and changes in gravitational energy and local acceleration are negligible as the flow contracts. Assumptions on changes in kinetic energy, effects of accelerations, the use of mean gradient versus peak gradient, and gravitational potential energy are the same as those discussed in the Pressure Drop section earlier.

The conversion from pressure to kinetic energy within the flow contraction of Figure 24-6 is therefore the quantity measured when estimating pressure gradient with Doppler echocardiography. Most of this converted energy will be lost after the expansion, because the kinetic energy upstream and that sufficiently downstream of the expansion are about the same according to Equation 6. However, because the Doppler gradient is measured between the upstream and the vena contracta point, it does not account for the pressure recovery, which occurs downstream of the vena contracta and may overestimate energy lost by the flow.

Another problem with the use of Doppler gradient is the placement of the transducer. If the transducer is placed obliquely with respect to the jet axis, the measured velocity will underestimate the true velocity of the jet,[6] and pressure gradient will be underestimated. Because the errors resulting from pressure recovery and oblique transducer placement tend to offset each other, Doppler ultrasound can at times match pressure measurements obtained from catheterization quite precisely. Nonetheless, there are instances when Doppler gradient gives significant errors.

Additional complications in the use of Doppler gradient to evaluate the total energy loss across mechanical prostheses arise because these valves have more than one orifice and because the resistance that each orifice offers to flow can be different. Velocity measurements made in the one orifice are therefore not representative of the gradient in either pressure or total energy as flow traverses the valve. The difference between Doppler and catheter gradients has been so notable for mechanical prostheses that empirically derived correction factors, dependent on valve design, have been suggested to the U.S. Food and Drug Administration (FDA).[7] Some studies claim that there is negligible difference between pressure gradients measured with catheter and Doppler, particularly with regard to mean gradients.[6] However, because of its potential problems, the use of Doppler to evaluate the performance of mechanical prostheses should be approached with caution. Often, Equation 16 is simplified further by assuming that upstream velocity is very small relative to the maximum velocity within the contraction:

$$\Delta p = 4v_{\max}{}^2 \tag{17}$$

In a very stenotic orifice, this equation will work well, because the velocity within the stenosis will indeed be much higher compared to the velocity upstream of the stenosis. This approximation should only be used in heavily calcified bioprosthetic valves.

## EFFECTIVE ORIFICE AREA

Evaluation of valve performance by pressure drop and Doppler gradient are heavily dependent on the flow rate across the valve. EOA does not represent the anatomic orifice area. Instead, it represents the cross-sectional area of the jet issuing from the valve at the point of its largest contraction (the vena contracta). The size of the EOA depends on the nature of the contraction as well as the size of the orifice itself. A sudden contraction will have a smaller EOA than a gradual contraction of the same orifice area. Although EOA has been considered to be an evaluation parameter of valve performance that is independent of cardiac output (CO) and heart rate (HR), in vivo[8,9] and in vitro[1] experiments have shown that it varies somewhat with flow rate. For bioprosthetic valves, higher flow causes the valve to open up a bigger valve orifice area by stretching the valve leaflets outward, allowing the jet flow area and thus EOA to be higher. For mechanical valves, changes in volumetric flow rate can lead to changes in the distribution of velocities across the diameter of the vena contracta,[10] leading to minor changes in the

computed EOA. However, the variation of EOA with flow is small, and so errors associated with the assumption of EOA invariance to flow rate are manageable.[11]

EOA can be estimated by applying the continuity equation (Equation 18) to echocardiography measurements of the upstream vessel area ($A_{ups}$), the temporal average of the velocity upstream of the contraction during forward flow, and the temporal average of the velocity at the point of maximum flow contraction during forward flow:

$$EOA = \frac{A_{ups} v_{ups}}{v_{\max}} \tag{18}$$

Pulsed-wave Doppler is used to measure the upstream velocity, whereas continuous-wave Doppler is used to measure the maximum velocity or the velocity within the vena contracta. If we assume *EOA* and $A_{ups}$ are constant over systole, we can use velocity-time integral (VTI) instead of velocities, which is the area under the curve of the velocity versus time plot. The upstream area is estimated with planimetry with B-mode echo. Thus, the clinically implemented equation is

$$EOA = \frac{A_{ups} VTI_{ups}}{VTI_{\max}} \tag{19}$$

The Gorlin formula can also be used to estimate EOA with catheter measurements. The Gorlin formula is a combination of Equation 6 and either Equation 16 or 17:

$$EOA = \frac{Q}{51.6\sqrt{\Delta p}} \tag{20}$$

where *EOA* is in $cm^2$, *Q* is the temporal average of the flow rate during forward flow in $cm^3$, and $\Delta p$ is the mean pressure drop across the valve during forward flow in mm Hg. The constant 51.6 in the denominator is used to account for the density of blood and unit conversions. It must be noted that the *EOA* differs from the aortic valve area initially described by Gorlin and Gorlin,[12] which is the geometric area of valve orifice traced by the free edge of the leaflets. The *EOA* is the area of flow slightly downstream of the aortic valve area, where flow contracted slightly. Thus, whereas a factor of 44.3 was used in the computation of aortic valve area, a factor of 51.6 should be used for *EOA*. *EOA* can be obtained through this method with either invasive cardiac catheterization or noninvasive echocardiographic examination. With the catheter approach, $\Delta p$ is directly measured with fluid-filled or sensor-mounted catheters, and *Q* is estimated by measuring the *CO* with the Fick method (thermodilution and dye dilution),[13] and the HR and systolic duration (*SD*):

$$Q = \frac{CO}{HR \cdot SD} \tag{21}$$

The catheter approach can be expected to overestimate the *EOA* because of the pressure recovery phenomenon. However, the catheter formulation, dubbed the energy loss coefficient, may be useful as a separate entity in evaluating the severity of aortic stenosis.

With the noninvasive echocardiography approach, *Q* is estimated by the upstream vessel area ($A_{ups}$) multiplied by the upstream velocity time integral ($VTI_{ups}$), and $\Delta p$ should be estimated by the Doppler gradient using Equation 16 or 17:

$$EOA = \frac{A_{ups} \cdot VTI_{ups}}{51.6\sqrt{\Delta p}} \tag{22}$$

Equation 16 or 17 will carry the same simplifying assumptions as those described in the sections on Doppler gradient and pressure Gradient and should be adapted for use with caution.

In the application of Equations 20 and 22, one subtlety should be kept in mind: all variables in the equations are averages during the systolic or diastolic forward flow period through the heart valve. Instantaneous values of pressure and flow rate cannot be used in these equations unless taken at peak flow rate. This is because the Gorlin formula is derived using Bernoulli's equation for steady flow and is, therefore, invalid in situations where there is a large net temporal acceleration or deceleration in the flow. For example, in the estimation of $\Delta p$ using the echocardiography method, one should use either the average of a few pressure gradients spaced equally over the forward flow phase or the time integration average of the pressure gradient data. For the estimation of *Q* in the echocardiography method, use of the velocity-time integral, which accounts for the velocities over the entire forward flow phase, is recommended.

Averages over the entire cycle may not be relevant either, especially if aortic regurgitation occurs concurrently.[14] Estimations of forward flow rate that do not involve echocardiography (Fick method, thermal and dye dilution) are averages over the entire cardiac cycle ($Q_{net}$). If no regurgitation is present, these methods can be used to estimate the average forward flow rate during systole. However, if aortic regurgitation is present, direct application of Gorlin's formula will result in an underestimation in *EOA*:

$$Q = \frac{Q_{net}}{(1 - RF)} \tag{23}$$

where *RF* represents the regurgitant fraction of the aortic valve.

In the in vitro setting, prosthetic valve *EOA* is measured with the Gorlin equation, because the direct measurement of pressures and flow is very easily achieved. Volumetric flow rate can be measured at high temporal resolution with commercial flow probes, and pressures can be measured through catheter-like tubes directly upstream and downstream of the valve, using commercial pressure gages. In vitro testing of prosthetic valves uses the following equation for calculating *EOA*[15]:

$$EOA = \frac{Q_{RMS}}{51.6\sqrt{\Delta p_{mean}}} \tag{24}$$

where *EOA* is in units of $cm^2$, $Q_{RMS}$ is the square root of the temporal mean of the square of volumetric flow rate in mL/s during the forward flow phase, and $\Delta p_{mean}$ is the temporal mean of the pressure drop across the valve during the forward flow phase in mm Hg.

A measure of a valve's resistance to forward flow that is based on *EOA* is the performance index. This is the ratio of EOA to the valve sewing ring area ($A_{sew}$):

$$PI = \frac{EOA}{A_{sew}} \tag{25}$$

It provides a measure of how well a valve design uses its total mounting area, the area the flow would experience without the valve. Although *EOA* is dependent on valve size, performance index effectively normalizes *EOA* for valve size.

## REGURGITANT VOLUME

Pressure drop, Doppler gradient, and *EOA* give quantitative estimates of the energy lost by the flow in traversing a valve during forward flow. Flow energy can also be lost due to leakage across the valve when the pressure gradient across the valve reverses. A small amount of flow leaks across the valve during valve closure. In addition, mechanical prosthetic valves are unable to form tight seals when closed, and regurgitant jets are present in these valves under normal conditions. Normal regurgitant flow is characterized by a closing volume during valve closure and leakage after closure. The regurgitant volume is the total volume of fluid through the valve per beat due to the retrograde flow. It is equal to the sum of the closing volume and the leakage volume. The closing volume is the volume of fluid flowing retrograde through the valve during valve closure. Any fluid volume accumulation after valve closure is due to leakage and is termed *leakage volume*.

Regurgitant volume of prosthetic valves is governed by valve type, size, and position. Bioprostheses have a small closing volume, but do not leak if functioning properly. Bileaflet mechanical designs tend to have greater regurgitant volume than tilting disk designs.[16] Larger valves leak more than smaller ones. Regurgitant volume is most problematic in positions where the pressure gradient during closure and leakage is high and where the duration of leakage is long. Energy losses due to regurgitant flow can exceed forward flow energy losses in large mitral prostheses.[16] Although prosthetic valves normally exhibit a very small amount of regurgitant flow, they can cause substantial regurgitation when they malfunction. To distinguish normal from abnormal valve function, it is important to differentiate between normal regurgitant volume and additional regurgitation due to disease. For in vitro evaluation of prosthetic valves, regurgitation volumes can be easily evaluated with commercial flow probes or velocimetry techniques such as particle image velocimetry or laser Doppler velocimetry. The energy loss due to regurgitation can be estimated using Equation 29, described later.

Most means of quantifying regurgitant volume use some form of a control volume and conservation of mass. For noninvasive quantification of regurgitation flow with echocardiography, perhaps the most commonly used method is the proximal isovelocity surface area method,[17-20] which is applicable for bioprosthetic valves. The principle of the proximal isovelocity surface area technique is based on the fact that a fluid entering a regurgitant orifice must accelerate to reach a peak velocity at the throat of the orifice. If the orifice is circular, this acceleration region should be axisymmetric about the center of the orifice. Thus, upstream of the regurgitant orifice, a series of hemispherical isovelocity contours can be defined within the flow field. Equation 5 states that for a control volume that does not change in size, the same amount of fluid that enters the volume must exit it as well. If the control volume is constructed to coincide with a hemispherical contour and the regurgitant orifice,

$$RV = 2\pi r^2 v_{ups} t \tag{26}$$

where $v_{ups}$ the temporal average of the velocity at a radial distance $r$ upstream of the regurgitant orifice during forward flow and $t$ represents the time during which regurgitation takes place during a single beat. The expression $2\pi r^2$ in this equation represents the surface area of the hemispherical shell surrounding the control volume.

## MECHANICAL ENERGY LOSSES

Pressure gradient and EOA parameters are indicative of the energy loss in valves. However, they are not direct measures of mechanical energy losses, which should be measured in joules per cycle or watts.

Direct measurement of mechanical energy losses is possible in vitro with both Equation 12 (the Bernoulli Equation analysis) and Equation 15 (the control volume analysis). When Equation 12 is integrated over one cardiac cycle, the final term on the right side of the equation becomes zero because of the periodicity or repetitive nature of the fluid flow. The gravitational potential energy term (the third term on the right side) is usually small and can be neglected. The remaining terms can be simplified to

$$\Phi_{cycle} = \int_{cycle} Q\left[\left(P_1 + \frac{1}{2}\rho v_1^2\right) - \left(P_2 + \frac{1}{2}\rho v_2^2\right)\right] dt \tag{27}$$

where $\Phi_{cycle}$ is the energy loss per cycle, $Q$ is the volumetric flow rate, and the subscripts *1* and *2* refer to upstream and downstream of the valve, respectively. Heinrich and colleagues[21] measured the energy loss per cardiac cycle for the St. Jude Medical bileaflet mechanical valve and the Medtronic Hall tilting disk mechanical valve and showed that there was no significant difference in the energy losses of these two valves. Energy loss was observed to increase with increased stroke volume and HR.

Equation 13 can be simplified to the following by assuming that energy conversion to gravitation potential energy is small:

$$\Phi_{inst} = Q \cdot (P_1 - P_2) - \frac{dKE}{dt} \tag{28}$$

where $\Phi_{inst}$ is the instantaneous energy loss, *KE* is the kinetic energy within the control volume, and the subscripts *1* and *2* refer to the control volume boundary upstream and downstream of the valve, respectively. By making suitable assumptions of the flow profile, Yap and co-workers[1] measured the instantaneous energy losses for a trileaflet valve and showed that most of the energy is lost during late systole, when there is adverse pressure gradient to decelerate forward flow and excessive mixing of fluid occurs from flow reversals. Energy loss was also observed to increase with stroke volume and HR.

To calculate energy loss as a result of valvular regurgitation, we assume that all the mechanical energy causing the regurgitation is lost:

$$\Phi_{regurg} = \int_{regurg} Q \cdot (P_1 - P_2) dt \tag{29}$$

where $\Phi_{regurg}$ is the total regurgitation energy loss over one cardiac cycle, $Q$ is the regurgitation volumetric flow rate, and the subscripts *1* and *2* refer to upstream and downstream of the regurgitation orifice, respectively (i.e., downstream and upstream of the valve, respectively). Azadani and associates[22] used this approach to estimate the regurgitation energy losses occurring in transcatheter valves and found that regurgitation energy loss can be as high as one third of the total energy loss associated with the valve.

Energy loss through valves during forward flow depends on the volumetric flow rate, the density of the fluid, the viscosity

of the fluid, the size of the valve (which can be represented by the body surface area), and the shape of the valve (for example, whether the valve is stenotic). Rigorous analysis with the Buckingham pi theorem indicates that energy loss can be nondimensionalized with density and the cube of flow rate and the square of body surface area.[23] When normalized by these scaling parameters, the energy loss is directly dependent on the Reynolds number and the shape of the valve:

$$\varepsilon \propto \rho \frac{Q^3}{BSA^2} \tag{30}$$

$$\frac{\varepsilon}{\rho \frac{Q^3}{BSA^2}} = f(N_{\mathrm{Re}}, S) \tag{31}$$

where $\varepsilon$ is energy dissipation, $\rho$ is density, $Q$ is flow rate, $BSA$ is body surface area, $N_{\mathrm{Re}}$ is the Reynolds number, and $S$ is the dimensionless shape factor.

Clinically, the direct measurement of energy loss is not widely used for assessing heart valves in vivo, even though energy efficiency parameters have the advantage of being a direct measure of the contribution of valve fluid dynamics to heart failure (heart failure can be interpreted as the failure of the heart to generate sufficient energy to overcome energy losses in the circulation). For example, Dasi and colleagues[23] discussed how end-stage aortic stenosis failure patients who have low flow and low gradients can have deceivingly normal EOAs, but with energy loss analysis, it becomes apparent that these patients have failing hearts. Atkins and co-workers[24] provided a review of mechanical energy loss analysis in heart valves.

## NOVEL ENERGY LOSS PARAMETERS

As Figure 24-6 implies, much more mechanical energy is lost in flow expansion than in flow contraction or in the throat regions of prosthetic valves. This is particularly true in tissue valves, because of the gradual nature of the flow contraction and the small throat region. The localization of energy loss to the flow expansion region simplifies the problem considerably by allowing energy losses occurring in aortic valve stenoses to be modeled by an abrupt expansion. The total energy loss per unit volume across an abrupt expansion can be derived using Equation 6, Equation 12, and a form of conservation of momentum[25]:

$$\Phi = 4v_{\max}{}^2 \left(1 - \left(\frac{EOA}{A_{aorta}}\right)\right)^2 \tag{32}$$

where $\Phi$ is in mm Hg and $v_{max}$ is the temporal average of the velocity at the point of maximum flow contraction, in cm/s. Equation 32, like recovered pressure, is thus a strong function of the EOA and the cross-sectional area of the aorta. As this area ratio approaches zero, the energy loss per unit volume in the expansion approaches the Doppler gradient. Thus, in cases of severe valvular stenosis, the Doppler gradient is equivalent to mechanical energy loss per unit volume. The advantage of using Equation 32 rather than pressure drop or Doppler gradient is that Equation 32 allows the estimation of energy lost by the flow in traversing the valve by noninvasive echocardiography while compensating for pressure recovery. In using this formulation in the aorta, the cross-sectional area of the expansion should be taken as the cross-sectional area of the aorta at the sinotubular junction, as the separated flow disappears after the flow has traversed the sinuses of Valsalva.

The energy loss in Equation 32, like pressure drop and Doppler gradient, is dependent on flow rate. It is desirable to have a parameter that is closely related to energy loss, but relatively independent of flow rate, for the evaluation of prosthesis function. Such a parameter can be derived by substituting Equation 32 for the Doppler gradient in Equation 20. This parameter has been dubbed the energy loss coefficient[26]:

$$ELCo = \frac{A_{aorta} EOA}{(A_{aorta} - EOA)} \tag{33}$$

where $EOA$ is measured by echocardiography, using either Equation 18 or Equation 20. The energy loss coefficient is equivalent to Equation 23 if $\Delta p$ in Equation 23 is measured with pressure transducers that are placed far enough downstream to account for energy recovery. The advantage of using the energy loss coefficient rather than $EOA$ is that the energy loss coefficient is based on recovered pressure.

## IN VIVO EVALUATION OF PROSTHETIC VALVES

The in vivo evaluation of prosthetic valves is done clinically when patients with prosthetic valve implants suffer from abnormal cardiac function. Prosthetic valve implants are all mildly stenotic, because prosthetic valves are usually implanted within aortic lumen space, which was previously space available for flow. In some cases, however, unusually high gradients despite normal prosthesis function are observed.[27] These are most likely cases of patient-prosthesis mismatch, where the implanted valve is too small to accommodate the CO required by the large size of the patient. Patients with hypertrophic hearts or calcific aortic stenosis are especially prone to patient-prosthesis mismatch, because it is difficult to insert the large prosthesis into constricted sites. Patient-prosthesis mismatch affects the patient's physical capacity as well as postoperative mortality.[28] To detect patient-prosthesis mismatch, the echocardiographic evaluation of the EOA of the prosthesis should be performed and compared to literature value of the EOA of the same model of prosthesis of the same size. If the EOA is lower than that reported in the literature, it is likely that there is prosthesis dysfunction. On the other hand, if the EOA is similar to that reported in the literature, and yet a high pressure gradient exists, patient-prosthesis mismatch is likely. In vitro investigation has shown that the indexed EOA is inversely related to mean pressure gradient, as shown in Figure 24-8. Further, in the case of a mismatch, where small indexed EOAs are present, exercising will lead to greater elevation in mean gradient than when the mismatch is not present.

# Hemodynamics of Native Valves

In order to effectively analyze flow through prosthetic heart valves in the mitral or aortic positions, it is important to

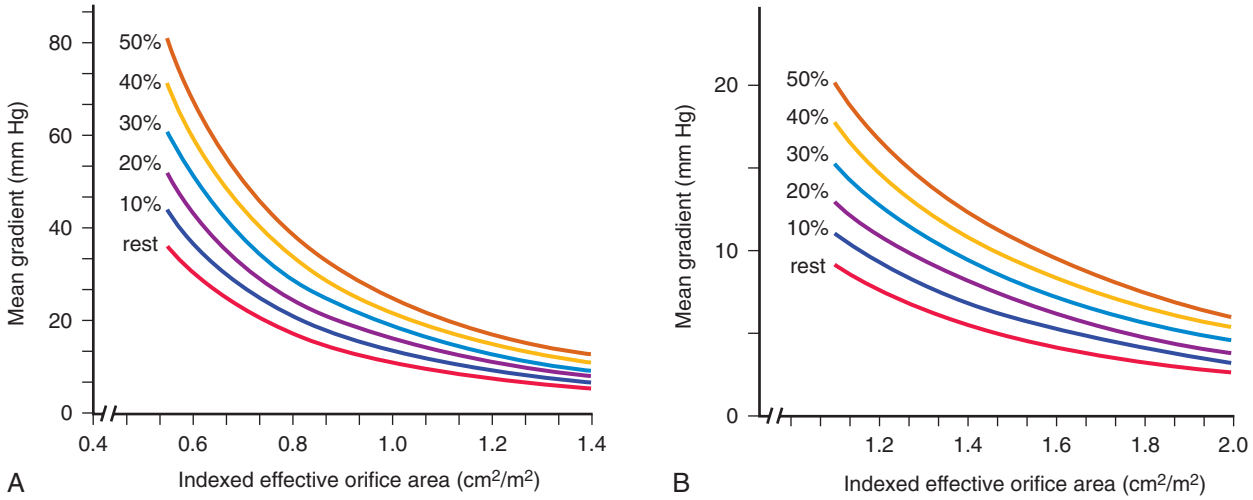



**Figure 24-8** Relationship between mean transprosthetic pressure gradients and indexed effective orifice area for (**A**) aortic bioprostheses and (**B**) mitral bioprostheses, studied in vitro in a physiologic pulse duplicator system assuming a normal cardiac index of 3.0 L/min/m$^2$ at rest, and 10% to 50% increase in stroke volume as may occur during exercise. *(Adapted from Dumesnil JG, Yoganathan AP: Valve prosthesis hemodynamics and the problem of high transprosthetic pressure gradients.* Eur J Cardiothorac Surg *6[Suppl 1]:S34-S37; discussion S38, 1992.)*

understand the conditions under which natural valves function. Figure 24-9 illustrates typical pressure and flow waveforms for healthy individuals at both the aortic and the mitral valves. During systole, the pressure difference required to drive the blood through the aortic valve is on the order of a few millimeters of mercury. Diastolic pressure differences across the aortic valve are much larger than systolic, the pressure usually being about 80 mm Hg. The valve closes near the end of the deceleration phase of systole with very little reverse flow. The blood flow through the mitral valve is biphasic during diastole, as shown in Figure 24-9. The first peak, the E-wave, is due to ventricular relaxation, whereas the second peak, the A-wave, is caused by contraction of the left atrium. This means that all valves in the mitral position open and close twice during each cardiac cycle. It is also evident that all cardiac valves are closed during both isovolumic contraction and isovolumic relaxation.

Measurements of the velocity profile just distal to the aortic valve have been performed with Doppler echocardiography in normal subjects.[26] The peak systolic velocity is 1.35 ± 0.35 m/s, and the velocity profile at the level of the aortic valve annulus is relatively flat. However, there is usually a slight skew toward the septal wall (less than 10% of the center-line velocity) caused by the orientation of the aortic valve relative to the long axis of the left ventricle. This skew in the velocity profile has been shown by many experimental techniques, including hot film anemometry,[29,30] Doppler ultrasound,[31] and magnetic resonance imaging.[32]

The flow patterns distal to the aortic valve also play an important role in proper valve function. During systole, vortices form behind each leaflet in the sinus region. In vitro studies have attempted to relate these vortices to effective valve closure.[33,34] It has been shown that the ventricular vortices are unnecessary for valve closure; however, they do ensure that the valve closes quickly, reducing leakage.[35]

The velocity profile at the mitral valve has been determined in detail in pigs and should be comparable to the velocity profile

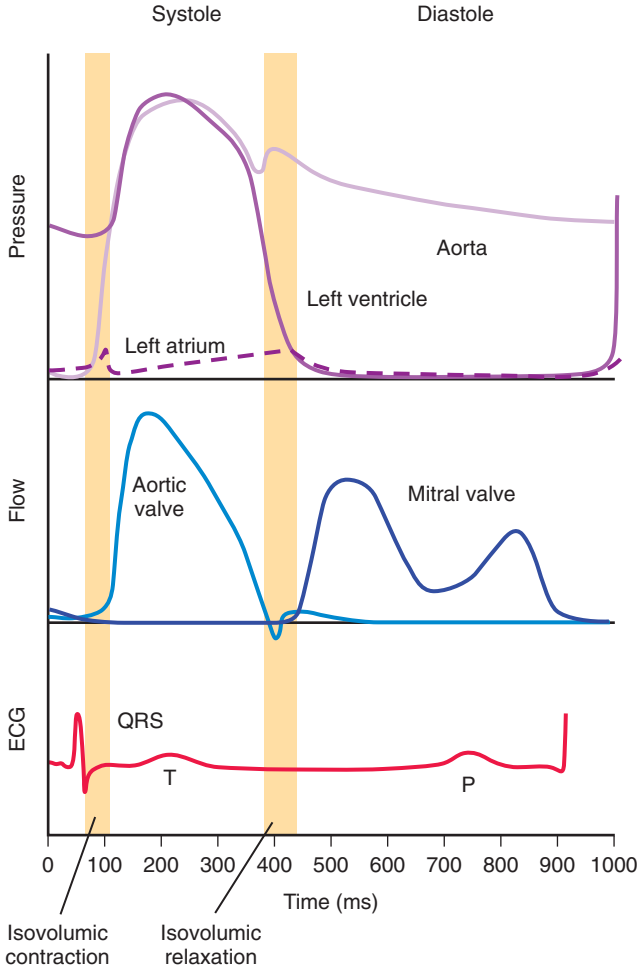



**Figure 24-9** Pressure and flow waveforms for the left heart.

in humans because of the similarity in cardiac anatomy.[36] Again, there is a slight skew to the profile, but there does not seem to be a preferred orientation. It is dependent on the particular geometry of the mitral valve, the diastolic flow patterns within the left ventricle, and the location at which the pulsed Doppler sample volume is placed. When the sample volume was placed at the mitral annulus, the peak early diastolic velocity was 63.6 ± 16.1 cm/s, whereas the late diastolic peak velocity was 53.7 ± 10.8 cm/s. When the sample volume was at the tip of the mitral valve leaflets, the peak early diastolic velocity was 82.9 ± 30.8 cm/s and the peak late diastolic velocity was 39.6 ± 14.2 cm/s.

Vortices develop in the left ventricle during diastole, as blood enters through the mitral valve. Bellhouse[28] proposed that the vortices helped to close the mitral valve at the end of diastole. Later work has shown that the vortices play a role in early closing of the mitral valve but late closure is dominated by left ventricular pressure.[37]

Because of the restrictive area of prosthetic valves, the peak velocities are usually higher, and the spatial velocity profiles are dramatically different from those in natural valves. The shear stresses in prosthetic valves will also be much larger because of the higher velocities and turbulence. The magnitude of the shear stress varies greatly depending on the type of prosthetic valve. It is important to note the differences and similarities between valve types in terms of shear stress magnitudes, peak velocities, and flow patterns so that an effective assessment of prosthetic valve function can be performed.

## Hemodynamics of Specific Prosthetic Valve Designs

Prosthetic heart valves have been successfully used in heart valve replacement over the past 40 years. Currently, heart valve prostheses can be classified into three primary categories: mechanical valves, biologic valves, and transcatheter valves. Mechanical valves are prosthetic valves manufactured from nonbiologic tissues. There are currently three basic designs or classifications of mechanical valves: ball and cage, tilting disk, and bileaflet. Biologic valves are prosthetic valves manufactured from animal tissues and can be further classified into three categories: stented, unstented, and homograft valves. Transcatheter valves are the newest addition to the prosthetic valve market. Although they are essentially biologic valves delivered through the catheter, these valves deserve a separate classification because of the novelty of their implantation mechanism. Figure 24-10 shows examples of each type of prosthesis.

Although significant progress has been made in the development of better prostheses through new materials and more physiologic valve designs, several problems associated with prosthetic valves have not been eliminated. Existing problems that can be related to the valve hemodynamics or local fluid mechanics are (1) thrombosis and thromboembolism, (2) hemolysis, (3) tissue overgrowth, (4) damage to endothelial lining, and (5) regurgitation. The presence of high shear stresses can lead to damage of formed blood elements, platelet activation, and initiation of biochemical processes affecting coagulation. Lethal damage to red cells can occur with fluid shear stresses as low as 800 dynes/cm$^2$.[38] However, these levels can be significantly lower, in the range of 10 to 100 dynes/cm$^2$, in the presence of foreign surfaces such as that presented by a valve prostheses.[39,40] In addition, platelet activation and damage have been shown to occur in shear stresses ranging from 100 to 500 dynes/cm$^2$.[41] The residence time of the cell in the damaging fluid environment is a significant factor in determining lethal stress levels that further complicates the mechanism for damage. Additionally, regions of flow separation and stagnation form local environments suitable for accumulation and growth of thrombi and fibrous/pannous tissue.[42]

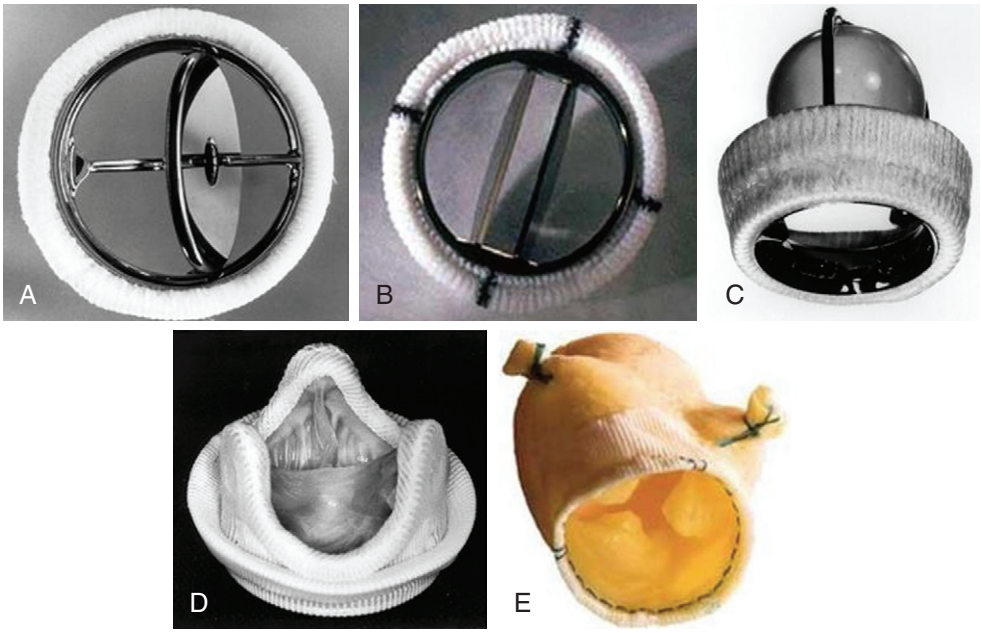



**Figure 24-10** **Major types of prosthetic heart valves. A,** Tilting disk; **B,** bileaflet; **C,** ball; **D,** stented bioprosthesis; **E,** stentless bioprosthesis.

The fluid mechanic performance of prosthetic heart valves is often assessed through in vitro testing to determine transvalvular pressure drops, regurgitant volumes (closure and leakage), distal and proximal velocity fields, and the locations and levels of turbulent stresses. The relationship between valve fluid mechanics and development of problematic function has been studied by numerous investigators over the past two decades. In vitro studies have concentrated on quantifying local fluid stress levels through flow measurement techniques such as laser Doppler anemometry, hot film anemometry, and ultrasound velocimetry. Table 24-1 summarizes the peak velocity and turbulent shear stress levels for many of the 27-mm aortic valves in clinical use. EOA and performance indices for such valves are provided in Tables 24-2 and 24-3.

The fluid mechanics of the various prosthetic valve designs are discussed in this section. Comparisons between the many

**TABLE 24-1 Peak Systolic Velocity and Turbulent Shear Stress Levels for Common 27 mm Aortic Valve Prostheses***

| *Valve Type* | *Valve* | *Measurement Location* | *Peak Velocity (cm/s)* | *Peak Turbulent Shear Stress (dynes/cm²)* |
|---|---|---|---|---|
| Ball-and-cage | Starr-Edwards 1260 | 12 mm downstream | 220 | 1850 |
| Tilting disk | Björk-Shiley Convexo-concave | 7 mm downstream | 200 | 3400 |
| | | 11 mm downstream | 200 | 1800 |
| | Björk-Shiley Monostrut | 8 mm downstream | 200 | 1250 |
| | | 11 mm downstream | 200 | 800 |
| | Medtronic-Hall | 13 mm downstream | 200 | 1500 |
| | Omnicarbon | 14 mm downstream | 225 | 2000 |
| Bileaflet | St. Jude Medical Standard | 13 mm downstream | 210 | 1500 |
| | Duramedics | 13 mm downstream | 210 | 2300 |
| | CarboMedics | 12 mm downstream | 228 | 1520 |
| Stented bioprosthesis | Carpentier-Edwards Porcine 2625 | 15 mm downstream | 370 | 4500 |
| | Carpentier-Edwards Porcine 2650 | 15 mm downstream | 200 | 2000 |
| | Carpentier-Edwards Pericardial 2900 | 17 mm downstream | 180 | 1000 |
| | Hancock MO Porcine 250 | 10 mm downstream | 330 | 2900 |
| | Hancock II Porcine 410 | 18 mm downstream | 260 | 2500 |
| | Ionescu-Shiley Standard Pericardial | 27 mm downstream | 230 | 2500 |
| | Hancock Pericardial | 18 mm downstream | 170 | 2100 |
| Nonstented bioprosthesis | Medtronic Freestyle† | Leaflet tips | 125 | |
| | | 10 mm from tips | 100 | |
| | TSPV† | Leaflet tips | 150 | |
| | | 10 mm from tips | 125 | |

*Heart rate = 70 bpm, cardiac output = 5 L/min, aortic pressure = 120/80 mm Hg.
†Data obtained from in vitro Doppler ultrasound measurements.

**TABLE 24-2 In Vitro Hemodynamic Data for Common Aortic Valve Prostheses***

| *Valve Type* | *Valve* | *Size* | *Regurgitant Volume (mL/beat)* | *EOA† (cm²)* | *PI* |
|---|---|---|---|---|---|
| Ball-and-cage | Starr-Edwards 1260 | 27 | 5.5 | 1.75 | 0.30 |
| | | 25 | 4.3 | 1.62 | 0.33 |
| | | 21 | 2.5 | 1.23 | 0.36 |
| Tilting disk | Björk-Shiley Convexo-concave | 27 | 8.5 | 2.59 | 0.45 |
| | | 25 | 7.3 | 2.37 | 0.48 |
| | | 21 | 5.5 | 1.54 | 0.45 |
| | Björk-Shiley Monostrut | 27 | 9.2 | 3.34 | 0.58 |
| | | 25 | 7.6 | 2.62 | 0.53 |
| | | 23 | 6.9 | 2.00 | 0.48 |
| | | 21 | 5.9 | 1.45 | 0.42 |
| | | 19 | 5.5 | 1.07 | 0.38 |
| | Medtronic-Hall | 27 | 9.6 | 3.64 | 0.64 |
| | | 25 | 8.4 | 3.07 | 0.62 |
| | | 23 | 7.3 | 2.26 | 0.54 |
| | | 20 | 6.2 | 1.74 | 0.51 |
| Bileaflet | St. Jude Standard | 27 | 10.8 | 4.09 | 0.71 |
| | | 25 | 9.9 | 3.23 | 0.66 |
| | | 23 | 8.3 | 2.24 | 0.54 |
| | | 21 | 6.8 | 1.81 | 0.52 |
| | | 19 | 6.8 | 1.21 | 0.43 |
| | St. Jude Regent | 29 | 13.5 | 4.98 | 0.75 |
| | | 27 | 12.3 | 4.40 | 0.77 |
| | | 25 | 11.2 | 3.97 | 0.81 |
| | | 23 | 10.3 | 3.47 | 0.83 |
| | | 21 | 9.0 | 2.81 | 0.81 |
| | | 19 | 7.6 | 2.06 | 0.73 |
| | | 17 | 6.3 | 1.56 | 0.69 |
| | CarboMedics | 27 | 7.5 | 3.75 | 0.65 |
| | | 25 | 6.1 | 3.14 | 0.64 |
| | | 23 | 6.51 | 2.28 | 0.55 |
| | | 21 | 3.4 | 1.66 | 0.48 |
| | | 19 | 3.0 | 1.12 | 0.40 |
| Stented bioprosthesis | Carpentier-Edwards Porcine 2625 | 27 | <3 | 1.95 | 0.34 |
| | | 25 | <2 | 1.52 | 0.31 |
| | | 21 | <2 | 1.28 | 0.37 |
| | Carpentier-Edwards Porcine 2650 | 27 | <2 | 2.74 | 0.48 |
| | | 25 | <2 | 2.36 | 0.48 |
| | | 21 | <2 | 1.38 | 0.40 |
| | | 19 | <2 | 1.17 | 0.41 |
| | Carpentier-Edwards Pericardial 2900 | 27 | <3 | 3.70 | 0.64 |
| | | 25 | <2 | 3.25 | 0.66 |
| | | 21 | <2 | 1.88 | 0.54 |
| | | 19 | <2 | 1.56 | 0.55 |
| | Hancock Porcine 242 | 27 | <3 | 2.14 | 0.37 |
| | | 25 | <2 | 1.93 | 0.39 |
| | | 23 | <2 | 1.73 | 0.42 |
| | | 21 | <2 | 1.31 | 0.38 |
| | | 19 | <2 | 1.15 | 0.41 |
| | Hancock MO Porcine 250 | 25 | <2 | 2.16 | 0.44 |
| | | 23 | <2 | 1.94 | 0.47 |
| | | 21 | <2 | 1.43 | 0.41 |
| | | 19 | <2 | 1.22 | 0.43 |
| | Hancock II Porcine 410 | 27 | <2 | 2.36 | 0.41 |
| | | 25 | <2 | 2.10 | 0.43 |
| | | 23 | <2 | 1.81 | 0.44 |
| | | 21 | <2 | 1.48 | 0.43 |
| | Ionescu-Shiley Standard Pericardial | 27 | <3 | 2.35 | 0.41 |
| | Medtronic Mosaic Porcine | 29 | <3 | 3.15 | 0.48 |
| | | 27 | <2 | 2.81 | 0.49 |
| | | 25 | <2 | 2.11 | 0.43 |
| | | 23 | <2 | 1.74 | 0.42 |
| | | 21 | <1 | 1.54 | 0.44 |
| | CarboMedics Mitroflow Pericardial | 29 | <4 | 3.71 | 0.56 |
| | | 23 | <3 | 2.12 | 0.51 |
| | | 19 | <2 | 1.34 | 0.47 |
| Nonstented Bioprosthesis | Medtronic Freestyle Porcine | 27 | <4 | 3.75 | 0.65 |
| | | 25 | <4 | 3.41 | 0.69 |
| | | 23 | <3 | 2.69 | 0.65 |
| | | 21 | <2 | 2.17 | 0.63 |
| | | 19 | <2 | 1.84 | 0.65 |

*EOA*, Effective orifice area; *PI*, performance index.
*Heart rate = 70 bpm; cardiac output = 5 L/min; aortic pressure = 120/80 mm Hg.
†EOA computed from Equation 24.

**TABLE 24-3 In Vitro Hemodynamic Data for Common Mitral Valve Prostheses***

| *Valve Type* | *Valve* | *Size* | *Regurgitant Volume (mL/beat)* | *EOA*† *(cm²)* | *PI* |
|---|---|---|---|---|---|
| Ball-and-cage | Starr-Edwards 1260 | 30 | | 1.99 | 0.28 |
| | | 28 | | 1.66 | 0.27 |
| | | 26 | | 1.56 | 0.29 |
| Tilting disk | Björk-Shiley Standard | 31 | | 3.40 | 0.45 |
| | | 29 | 6.7 | 2.79 | 0.42 |
| | | 25 | | 2.15 | 0.44 |
| | Björk-Shiley Convexo-concave | 29 | 10.1 | 2.96 | 0.45 |
| | | 27 | 8.3 | 2.28 | 0.40 |
| | | 25 | | 2.03 | 0.41 |
| | Medtronic-Hall | 31 | 10.0 | 3.53 | 0.47 |
| | | 29 | 10.0 | 3.53 | 0.53 |
| | | 27 | 8.9 | 2.73 | 0.47 |
| | | 25 | 7.2 | 2.23 | 0.45 |
| Bileaflet | St. Jude Medical Standard | 31 | 13.1 | 3.67 | 0.48 |
| | | 29 | 10.9 | 3.40 | 0.51 |
| | | 27 | 9.7 | 2.81 | 0.49 |
| Stented bioprosthesis | Hancock Porcine 342 | 35 | <4 | 2.72 | 0.28 |
| | | 33 | <4 | 2.54 | 0.30 |
| | | 31 | <4 | 2.36 | 0.31 |
| | | 29 | <4 | 2.11 | 0.32 |
| | | 27 | <2 | 1.77 | 0.31 |
| | | 25 | <2 | 1.63 | 0.33 |
| | Hancock II Porcine | 33 | <4 | 2.66 | 0.31 |
| | | 31 | <3 | 2.29 | 0.30 |
| | | 29 | <3 | 2.05 | 0.31 |
| | | 27 | <2 | 1.78 | 0.31 |
| | | 25 | <2 | 1.59 | 0.32 |
| | Carpentier-Edwards Porcine 6650 | 27 | <2 | 2.03 | 0.35 |
| | Carpentier-Edwards Porcine 6900 | 27 | <2 | 2.68 | 0.47 |
| | Carpentier-Edwards Porcine 6625 | 31 | <4 | 2.58 | 0.39 |
| | Edwards SAV | 33 | | 1.60 | |
| | | 31 | | 1.58 | |
| | | 29 | | 1.56 | |
| | | 27 | | 1.32 | |
| | | 25 | | 1.20 | |
| | Edwards Perimount | 33 | | 2.80 | |
| | | 31 | | 2.76 | |
| | | 29 | | 2.70 | |
| | | 27 | | 1.92 | |
| | | 25 | | 1.76 | |
| | Ionescu-Shiley Standard Pericardial | 31 | <5 | 3.00 | 0.40 |
| | | 27 | <2 | 1.77 | 0.31 |
| | | 25 | <2 | 1.61 | 0.33 |
| | Mosaic Porcine | 33 | <4 | 2.38 | 0.28 |
| | | 31 | <3 | 2.26 | 0.30 |
| | | 29 | <3 | 2.02 | 0.31 |
| | | 27 | <2 | 1.71 | 0.30 |
| | | 25 | <2 | 1.55 | 0.32 |
| | St. Jude Biocor Pericardial | 31 | | 2.53 | |
| | | 29 | | 1.48 | |
| | | 33 | | 2.04 | |
| | | 29 | | 1.96 | |
| Nonstented bioprosthesis | Mitral Valve Allograft‡ | 25 | | 3.38 | 0.69 |
| | | 23 | | 1.80 | 0.43 |

*EOA*, Effective orifice area; *PI*, performance index.
*Heart rate = 70 bpm; cardiac output = 5 L/min.
†EOA computed from Equation 24.
‡In vitro measurements at 5 L/min.

valve designs within each classification of prostheses are left to the many references dealing with the assessment of individual valves. Both antegrade and retrograde flow fields are described. All flow characteristics are referenced from in vitro experiments conducted in our laboratory unless otherwise specified. In most citations, the data are representative of 25- or 27-mm aortic prostheses tested under physiologic pulsatile flow conditions providing a CO of 5.0 to 6.0 L/min and an HR of 70 bpm. Exact test conditions (valve size, CO, HR, pressures) are noted for each citation.

## MECHANICAL VALVES

The three major mechanical valve designs or classes are the tilting disk, bileaflet, and ball and cage. These valves differ primarily in the type and function of the occluder. While these different designs influence the valvular fluid mechanics, all three designs share common flow structures such as well-defined jet flows, wakes with some degree of flow reversal, and turbulent shear layers (Figs. 24-11 to 24-16). The antegrade flow and regurgitant flow characteristics for each valve design are discussed in Table 24-4[43-54].

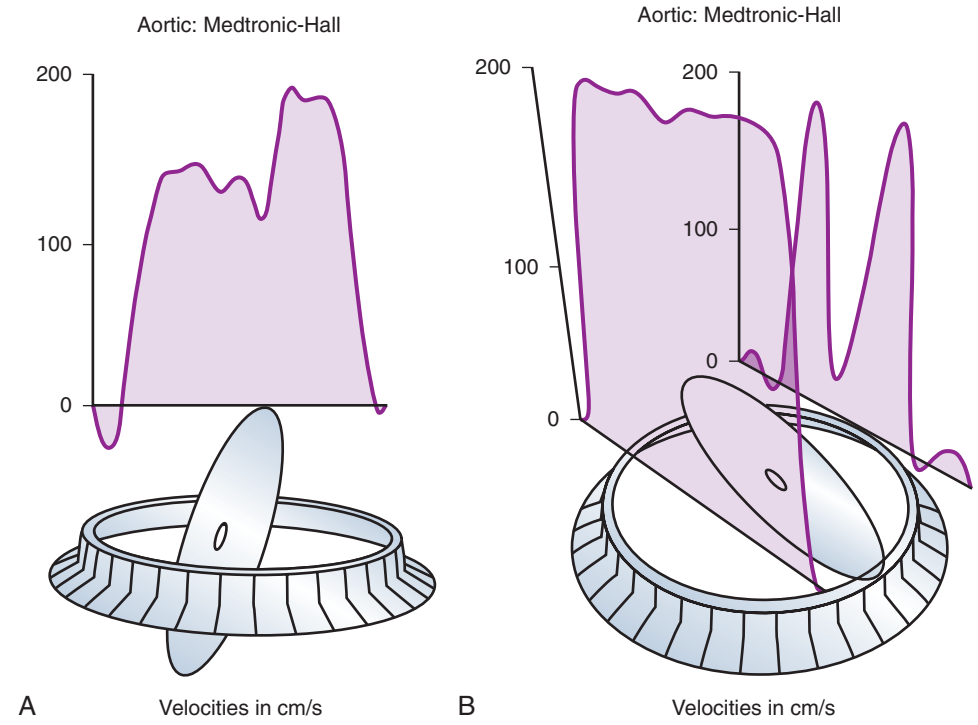



**Figure 24-11** **Velocity profiles downstream of a 27-mm Medtronic-Hall tilting disk valve at peak systole. A,** Centerline 15 mm downstream. **B,** Traversing major and minor orifices 13 mm downstream.

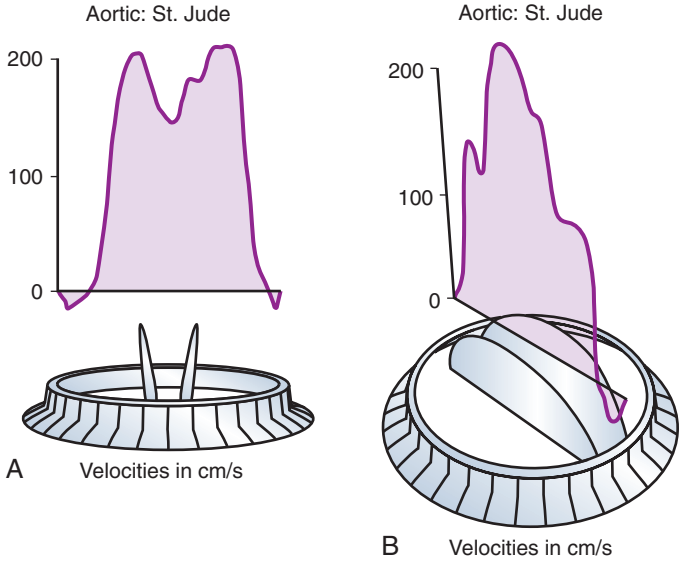



**Figure 24-12** Velocity profiles downstream of a 27-mm St. Jude Medical bileaflet valve at peak systole. **A,** Centerline 13 mm downstream. **B,** Traversing lateral and central orifices 13 mm downstream.

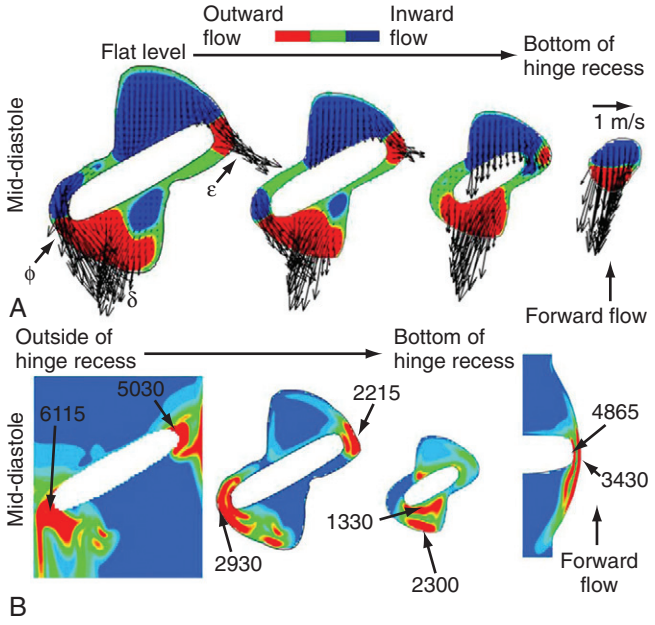



**Figure 24-13** **A,** Flow fields in at different depth in the hinge recess of the bileaflet mechanical valve during the leakage phase. **B,** Shear stresses at various locations near the hinge, obtained by computational fluid dynamics simulations. *(Simon HA, Ge L, Borazjani I, et al: Simulation of the three-dimensional hinge flow fields of a bileaflet mechanical heart valve under aortic conditions.* Ann Biomed Eng *38:841-853, 2010.)*

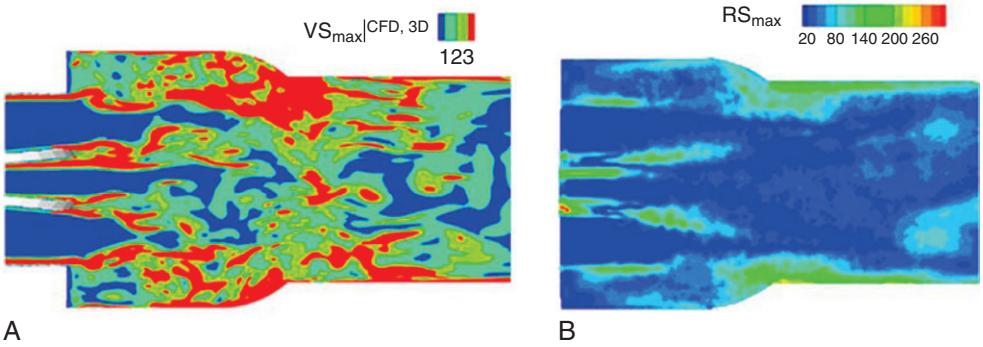



**Figure 24-14** **A,** Viscous shear stresses downstream of the bileaflet mechanical valve at peak flow time point, in N/m, obtained through three-dimensional computational fluid dynamics simulations. **B,** Turbulence shear stresses downstream of the bileaflet mechanical valve at the peak flow time point, in N/m, obtained through experimental measurements using a physiologic pulse duplicator system. *(Ge L, Dasi LP, Sotiropoulos F, Yoganathan AP: Characterization of hemodynamic forces induced by mechanical heart valves: Reynolds vs. viscous stresses.* Ann Biomed Eng *36:276-297, 2008.)*

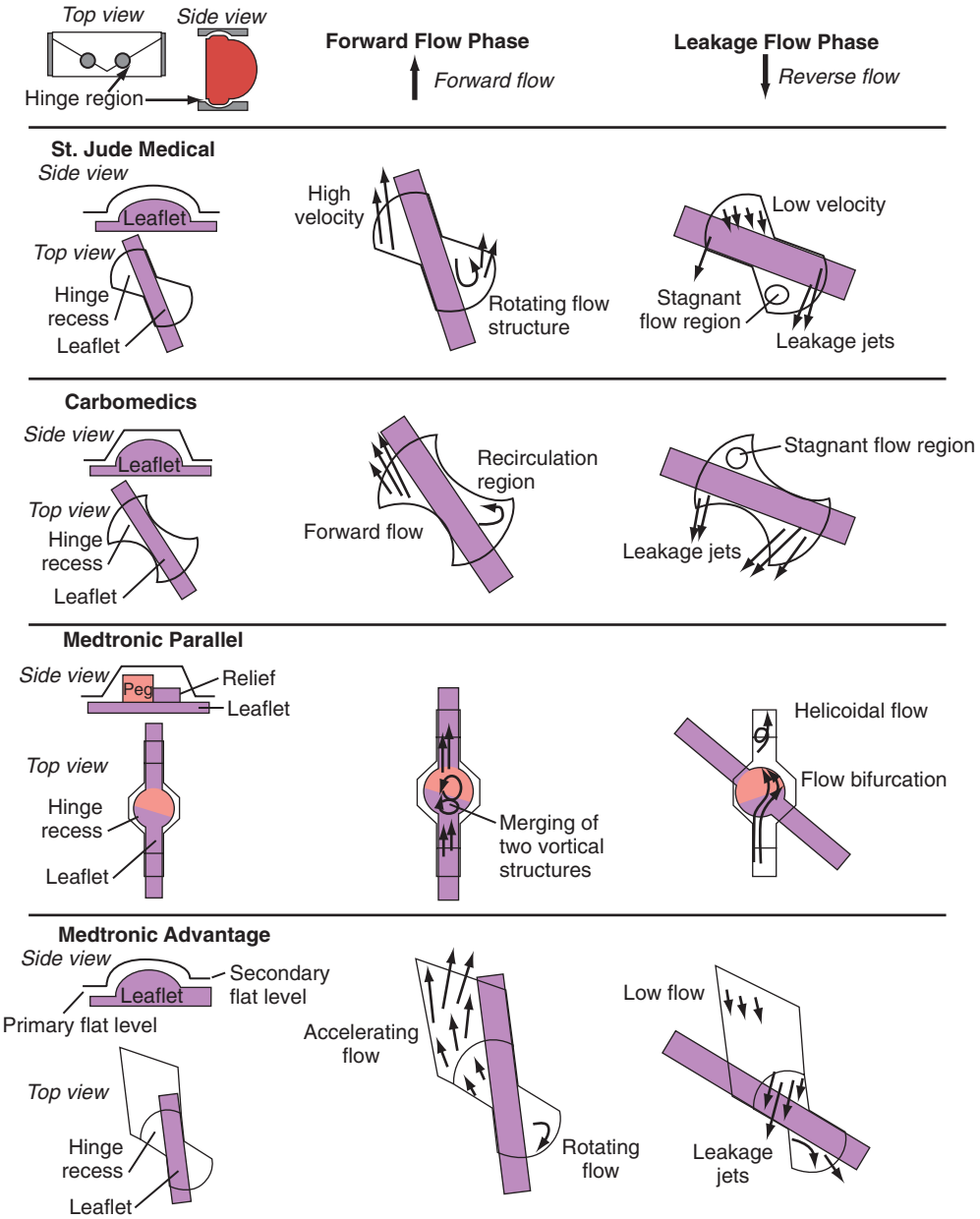



**Figure 24-15** Flow characteristics within the hinges of various bileaflet mechanical heart valves.[47,50-53]

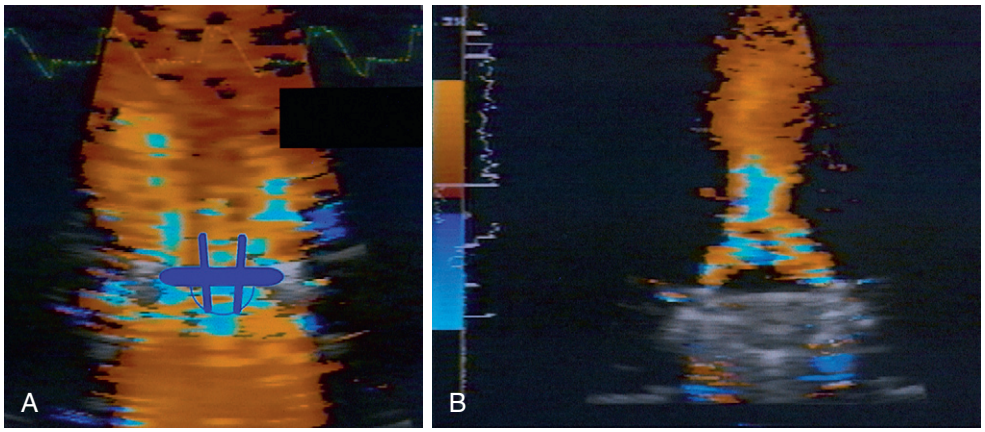



**Figure 24-16** **A,** 2D color Doppler flow mapping of downstream triple jet flow fields of a bileaflet valve design under physiologic pulsatile flow conditions. **B,** 2D color Doppler flow mapping of the leakage jet flow fields of a bileaflet valve design under physiologic pulsatile flow conditions.

**TABLE 24-4 Mechanical Valve Types, Function, and Fluid Mechanics**

| *Valve* | *Characteristics* | *Antegrade Flow* | *Normal Regurgitant Flow* | *Orientation* |
|---|---|---|---|---|
| Tilting disk valve | Consists of a circular occluder disk, which is free to rotate about a pivot axis (see Fig. 24-10, *A*). Metal struts are used to secure the disk within the valve housing. Typically, disk opens to 60° to 80° with respect to the annulus. | Valve opens two orifices on either side of the disk. The jet through the major orifice jet is semicircular in cross section with peak systolic velocities of approximately 2 m/s in the aortic position. If a strut support obstructs the minor orifice (Björk-Shiley and Medtronic-Hall valves), the minor orifice will have two jets. If two struts are present, there will be three jets, or if no strut is present (Omni Carbon valve), there will be one jet. Minor orifice jet velocities are 30% to 40% of major orifice jet velocities. An example of forward flow velocity profiles downstream of the tilting disk valve is shown in Figure 24-11. | Normal regurgitation flow is low due to reduced closing volume and leakage flow. | In the mitral position, the preferred orientation for tilting disk valves in the mitral position is with the major orifice oriented toward the left ventricular free wall, as opposed to the septum,[43] so as to minimize intraventricular turbulence and velocity reversals. In the aortic position, the preferred orientation is positioning the major orifice to the right posterior aortic wall. This orientation is found to minimize in turbulent stress magnitude and energy loss.[44,45] |
| Bileaflet valve | Consists of two semicircular leaflets typically made of pyrolytic carbon that are hinged to the valve housing (see Fig. 24-10, *B*). The leaflets divide the flow into three regions, two lateral major orifices and a central minor orifice. Pressure drops and EOAs are comparable to tilting disk valves. Variations in opening angle of leaflets are 75° to 90° among different designs. | Three jets emanate from the orifice as illustrated in Figure 24-12 and 24-14. Greater flow emerges from the lateral orifices than from the central orifice in most valves. Shear stress fields downstream of the St. Jude Medical bileaflet valve are shown in Figure 24-14, *A*.[46] Much of the shear stress occurs directly downstream of the leaflets, due to uneven velocities between the central orifice and lateral orifice. Reynolds shear stress analysis shows that turbulence in the same region (see Fig. 24-14, *B*). | The bileaflet design shows slightly larger regurgitant volumes than the tilting disk valve. Leakage flow occurs primarily through the hinges of the leaflets (see Fig. 24-16, *B*) and persists over diastole. Some leakage occurs through the gap between the two leaflets. Studies suggest that hinge leakage flow are mainly responsible for thrombosis.[47] Regurgitation flow are 2-3 m/s with very high turbulence stresses exceeding 3000 dynes/cm$^2$.[48,49] (See Fig. 24-13) There are multiple hinge designs with varying flow features, summarized in Figure 24-15.[47,50-53] | For the mitral position. Two possible orientation are "anatomic position," with the gap between the leaflets perpendicular to the line between the aortic outflow and mitral inflow tracts, and the "anti-anatomic position," where the leaflet gap is parallel to the aorto-mitral line. In vivo studies showed that the antianatomic position resulted in diastolic flow that moves toward the ventricular outflow tract, whereas the anatomic position resulted in diastolic flow that moves back toward the valve.<br>In the aortic position, Travis and colleagues[44] found that orienting the open valve leaflets to the proximal flow direction minimizes energy loss, whereas Kleine and co-workers[45] found that turbulence created by the valve is minimal when one lateral orifice faces the right posterior wall of the aorta. |
| Ball and cage valve | Consists of a silicone ball mounted into a wire cage, as illustrated in Figure 24-11, *C*. The cage is constructed of three wire struts separated by 120°. The ball travels 1-2 cm within the cage during opening. | The flow fields of these valves consist of annular jets that emerge from around the occluder or poppet. A large wake in the central part of the flow field is generated. Peak systolic velocities are about 2 m/s (see Fig. 24-17). Large regions of flow separation are responsible for thrombogenicity of the valves,[54] and the ball obstruction of flow results in lower pressure drop and EOA. | The normal regurgitant flow of the ball and cage design is composed mainly of the closing volume flow. The seating of the ball valve is generally very good, with little or no leakage flow. | |

*EOA*, Effective orifice area.

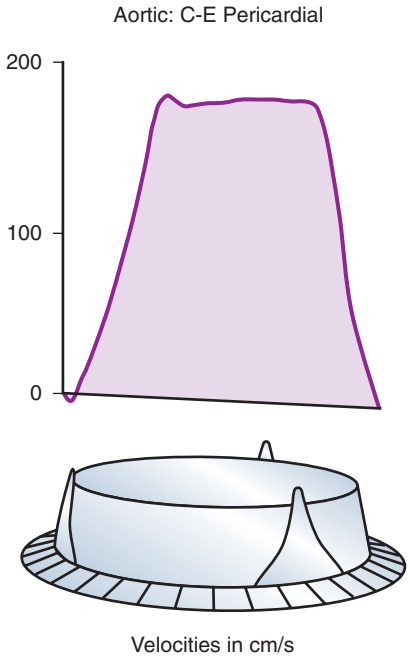



**Figure 24-17** Centerline velocity profile 17 mm downstream of a 27-mm Carpentier-Edwards pericardial valve at peak systole.

## BIOPROSTHESES

The three major tissue valve designs or classes are the stented xenograft, unstented xenograft, and homograft. These valves differ primarily in tissue type and structure. Tissue valves are less thrombogenic compared to mechanical valves and thus do not require anticoagulant treatment. However, these valves suffer from calcification of the leaflets and/or material fatigue leading to valve failure due to leaflet rupture or tearing. Calcification of the tissue is often a precursor to leaflet rupture and tearing, as these are often observed adjacent to calcified lesions. All bioprosthesis designs share the characteristics of flexible leaflets, a single orifice, and no leakage after valve closure (Fig. 24-17). The antegrade flow, regurgitant flow, and pressure drop characteristics for each valve type are summarized in Table 24-5.[55-57] The newest valve design, transcatheter valves, are discussed in more detail.

## TRANSCATHETER VALVES

The newest additions to the family of prosthetic valves are the transcatheter valves. Transcatheter valves are essentially bioprosthetic aortic valves mounted onto a collapsible stent, so that the valve can be collapsed onto a catheter and delivered through it in a minimally invasive manner Figure 24-18. These valves were introduced to target high risk-patient groups, such as old patients or those with diabetes, who are much less likely than others to survive an open-heart valve replacement treatment. The catheter delivery approach avoids cross-clamping and cardiopulmonary bypass and reduces procedure duration and thus risks. Although the outcome of transcatheter valve replacement has been shown to be poorer than that of traditional surgical

**TABLE 24-5 Bioprosthesis Valve Types, Function, and Fluid Mechanics**

| *Valve* | *Characteristics* | *Antegrade Flow* | *Normal Regurgitant Flow* | *Pressure Drops* |
|---|---|---|---|---|
| Stented xenograft | Most common valve: consist of three biologic leaflets made from the porcine aortic valve or bovine pericardium, mounted on a metal or polymeric stented ring. Various fixation methods are used. | All porcine stented valves are mildly stenotic in larger sizes and moderate to severely stenotic in small sizes. All valves have strong central jets (see Fig. 24-18). The newer generation valves have a flatter velocity profiles than earlier designs. | Regurgitant volumes are on the order of 1 mL/beat for most tissue valves. Regurgitation jets are normally nonexistent, and the presence of a jet indicates valve incompetence abnormality. | New generation of pericardial valves have pressure drops similar to those of tilting disk valves. |
| Unstented xenograft | Fashioned from porcine, bovine, and equine tissue and do not have rigid stents. Because of the complexity of the design, optimal performance is dependent on patient geometry and sizing of valve. | The flow accelerates uniformly through the valve, and downstream flow has a flat profile.[55] There is no appearance of a jet with steep velocity gradients, as is observed in stented bioprostheses. | Tests in our laboratory showed that unstented valves have comparable closing volumes to unfixed natural valves tested in the same flow loop. Good coaptation was observed with no leakage. The function of mitral heterografts is strongly dependent on the implantation technique. | The lack of stents and sewing cuffs allow larger valve sizes to be implanted for the same aorta size. Pressure drops are thus similar to those for mechanical prostheses.[55-57] |
| Homograft | Cryopreserved human valves; have been used for more than two decades in the aortic position. Aortic valve homografts are usually implanted as a complete aortic root, whereas mitral homografts are implanted with the leaflets, annulus, papillary muscles, and chordae tendineae intact. | Similar to those of the natural valves, although peak velocities are slightly higher because of the reduced EOAs resulting from the smaller area of the outflow tract. | Exhibit small closing volumes and little or no regurgitation due to leakage. Mitral homograft hemodynamics have the same dependency on implantation technique. For example, proper alignment of papillary muscles with valve annulus will eliminate regurgitation. | Has lower pressure drops and EOAs than mechanical and stented valves. |

*EOA*, Effective orifice area.

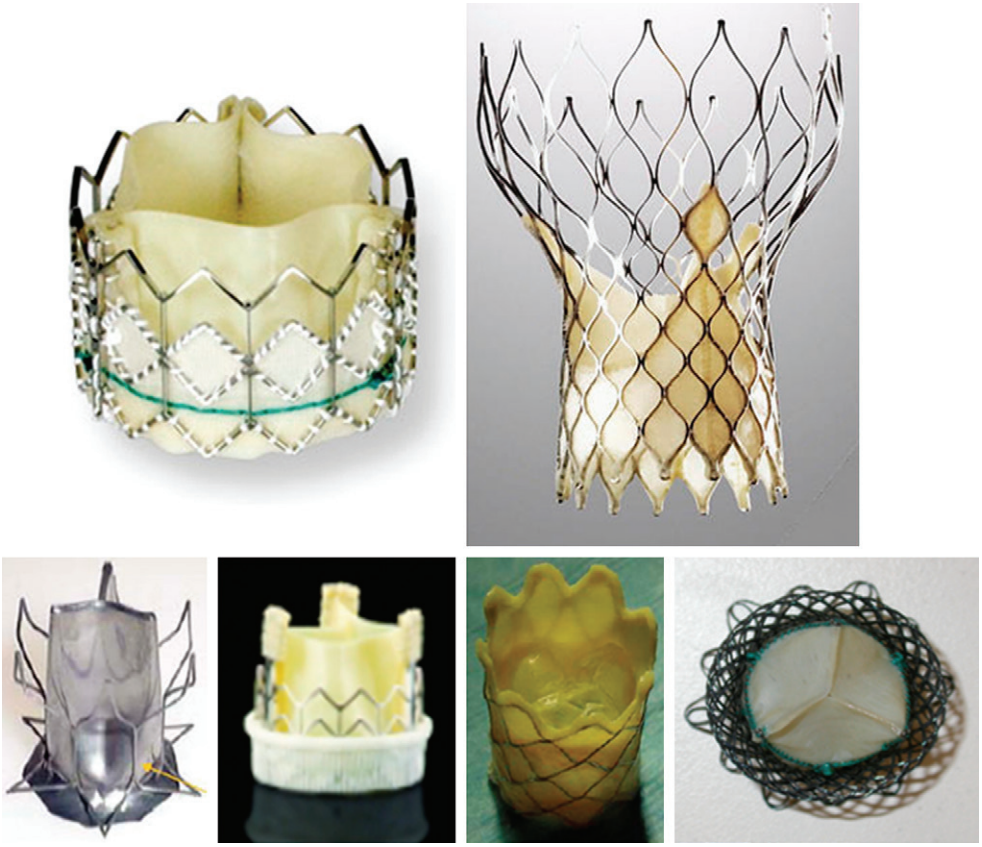


**Figure 24-18 Various designs of transcatheter valves.** *Top left*, Edwards Sapien valve; *top right*, Medtronic CoreValve. *Bottom*, Various other designs.

valve replacement, it appears to be better than other available options.[58]

Transcatheter valves can be delivered in a transfemoral or transapical manner. In the former, the catheter gains access to the diseased valve by entering through the femoral artery and backtracking through the aorta to the heart. In the latter, the catheter enters the left ventricle directly from the apex of the heart. Balloon valvuloplasty is first applied to the calcified aortic valve to open it up. The ventricle is then induced into a state of rapid pacing, and then the valve is deployed by expanding a second balloon from within the valve. There are multiple transcatheter valve designs, as shown in Figure 24-18. The leading designs are the Edwards Sapien valve and the Medtronic CoreValve. The Sapien valve is a trileaflet bovine pericardial valve mounted onto a stainless steel or cobalt-chromium frame. The CoreValve is a trileaflet porcine pericardial valve mounted in a Nitinol frame. The profile of the CoreValve stent is longer than that of the Sapien valve, because it extends slightly proximally and extends distally in a splayed-out manner to reach the aorta.

At the time of publication, no transcatheter valve design is currently approved by the FDA for clinical use in the United States. Other than their fluid dynamic performance, there are significant concerns in the biomechanics community about the long-term durability of transcatheter devices in comparison to surgically implanted prosthetic valves.

### *Antegrade Flow Fields*

Bench-testing of the transcatheter valve showed that they have EOA of about 1.8 $cm^2$ and mean pressure gradient of 8.3 mm Hg, which is comparable to stented bioprostheses.[22] Clinically, the EOAs of valves were shown to be between 1.5 and 1.8 $cm^2$, and pressure gradients were about 10 mm Hg.[59,60]

### *Normal Regurgitant Flow*

Unlike bioprosthetic valves, regurgitation in the transcatheter valve is very common. Mild to moderate regurgitation occurs in more than 50% of cases; severe regurgitation occurs in 5%.[59-62] Regurgitation in the transcatheter valve is mostly paravalvular, occurring between the valve and the native tissues rather than through the valve orifice. Because the implanted valve is merely pressed onto native tissues because of pressure exerted by the stents, a complete seal cannot be achieved in most cases, especially when the native aortic valve is heavily calcified and presents a very uneven surface for the transcatheter valve to fit onto. Perivalvular leakage can exert high shear stress on regurgitating blood and cause clots, which may explain the high incidence of vascular complication (10% to 15% of cases).[60,63]

## Future Directions

We foresee that future directions in prosthetic valve research will follow several courses: improved transcatheter valve technologies (delivery device designs as well as well valve designs); development of polymeric prostheses; tissue engineering bioprosthetic valves; invention of novel tissue fixation techniques; improving designs of mechanical valves; improving in vitro, computational, and animal testing protocols; and development of noninvasive diagnostic capabilities. Although transcatheter

valves enable noninvasive valve replacement, there are still concerns relating to durability and valve leakage. Currently, transcatheter valves are meant for use only in inoperable patients, because it cannot yet be shown that they provide better outcome in regular patients. Future improvements to the transcatheter valve may extend their application to regular patients. Polymeric prostheses may offer patients a durable alternative to mechanical and bioprostheses with little tendency for calcification or thromboembolic complications. The goal of tissue engineering research is to grow living human aortic valves in the laboratory, preferably using the patient's own tissue. Potential advantages involve total acceptance of the living tissue, with hemodynamic and cellular function similar to the normal human aortic valve, resulting in a lifetime equal to that of native valves. Tissue xenografts are currently fixed in glutaraldehyde, which stiffens the compliance of the valve material and hinders hemodynamic performance. Other fixative techniques may improve hemodynamic performance or increase the functional lifetime of xenografts. For mechanical valves, the focus will be on reducing their thrombogenic properties. This could possibly be accomplished by development of biocompatible surface coatings and materials, or by changing valve geometry to improve closure and leakage flow through these valves. A first step in this research should be in improved understanding of blood element damage, thromboembolic events, and thrombus formation. In vitro evaluation techniques and in vivo diagnostic techniques for bulk flow hemodynamics will focus more closely on mechanical energy loss, and more attention will be devoted to the small-scale, local hemodynamics that may give rise to thromboembolic complications.

## ACKNOWLEDGMENTS

The work reported on prosthetic heat valves was from our Cardiovascular Fluid Mechanics laboratory at Georgia Tech and has been supported by grants from the FDA, American Heart Association, the heart valve industry, and generous gifts from Tom and Shirley Gurley and the Lilla Boz Foundation.

## KEY POINTS

- Application of conservation of mass to a control volume allows the calculation of unknown flow rates, average velocities, or surface areas into or out of the volume based on measurable quantities.
- Mechanical energy per unit volume is a measure of the work available to drive flow.
- Pressure is one of several forms of mechanical energy, but there are others (kinetic and gravitational). These forms can be freely converted from one to another without loss. Pressure loss and mechanical energy loss per unit volume are not equivalent, as pressure can be recovered from a fall in either gravitational or kinetic energy.
- Effective means of reducing mechanical energy loss in the circulation include ensuring that any expansions in flow occur gradually, ensuring that bends and corners in the flow path are not sudden or sharp, and increasing vessel radius.
- The Doppler gradient measures the conversion of pressure to kinetic energy in flow across a valvular prosthesis. It does not measure mechanical energy loss, although it can be closely related to it.
- The EOA of a valvular prosthesis represents the cross-sectional area of a flow at its smallest contraction. It is equal to or smaller than the anatomic orifice area.
- Mechanical energy losses occur due to regurgitant flow as well as forward flow. Losses due to regurgitant flow can be greater than losses due to forward flow in large, mitral mechanical prostheses.

## REFERENCES

1. Yap CH, Dasi LP, Yoganathan AP: Dynamic hemodynamic energy loss in normal and stenosed aortic valves. *J Biomech Eng* 132:021005, 2010.
2. Batchelor G: *An introduction to fluid mechanics*, Cambridge, UK, 1994, Cambridge University Press.
3. Blevins R: *Applied fluid dynamics handbook*, New York, 1984, Van Nostrand Reinhold.
4. McNaughton KJ, Sinclair CG: Submerged jets in short cylindrical flow vessels. *J Fluid Mech* 25: 367-375, 1966.
5. Nerem RM, Seed WA: An in vivo study of aortic flow disturbances. *Cardiovasc Res* 6:1-14, 1972.
6. Knebel F, Gliech V, Walde T, et al: High concordance of invasive and echocardiographic mean pressure gradients in patients with a mechanical aortic valve prosthesis. *J Heart Valve Dis* 14:332-337, 2005.
7. Stewart SF, Herman BA, Nell DM, Retta SM: Effects of valve characteristics on the accuracy of the Bernoulli equation: a survey of data submitted to the U.S. FDA. *J Heart Valve Dis* 13:461-466, 2004.
8. Stewart WJ, Jiang L, Mich R, et al: Variable effects of changes in flow rate through the aortic, pulmonary and mitral valves on valve area and flow velocity: impact on quantitative Doppler flow calculations. *J Am Coll Cardiol* 6:653-662, 1985.
9. Burwash IG, Pearlman AS, Kraft CD, et al: Flow dependence of measures of aortic stenosis severity during exercise. *J Am Coll Cardiol* 24:1342-1350, 1994.
10. DeGroff CG, Shandas R, Valdes-Cruz L: Analysis of the effect of flow rate on the Doppler continuity equation for stenotic orifice area calculations: a numerical study. *Circulation* 97:1597-1605, 1998.
11. Garcia D, Pibarot P, Landry C, et al: Estimation of aortic valve effective orifice area by Doppler echocardiography: effects of valve inflow shape and flow rate. *J Am Soc Echocardiogr* 17:756-765, 2004.
12. Gorlin R, Gorlin SG: Hydraulic formula for calculation of the area of the stenotic mitral valve, other cardiac valves, and central circulatory shunts. I. *Am Heart J* 41:1-29, 1951.
13. Fagard R, Conway J: Measurement of cardiac output: Fick principle using catheterization. *Eur Heart J* 11 Suppl I:1-5, 1990.
14. Scotten LN, Walker DK, Dutton JW: Modified Gorlin equation for the diagnosis of mixed aortic valve pathology. *J Heart Valve Dis* 11:360-368; discussion 368, 2002.
15. Yoganathan AP, He Z, Jones SC: Fluid mechanics of heart valves. *Annu Rev Biomed Eng* 6:331-362, 2004.
16. Struber M, Campbell A, Richard G, Laas J: Hydrodynamic function of tilting disc prostheses and bileaflet valves in double valve replacement. *Eur J Cardiothorac Surg* 10:422-427, 1996.
17. Recusani F, Bargiggia GS, Yoganathan AP, et al: A new method for quantification of regurgitant flow rate using color Doppler flow imaging of the flow convergence region proximal to a discrete orifice. An in vitro study. *Circulation* 83:594-604, 1991.
18. Utsunomiya T, Doshi R, Patel D, et al: Regurgitant volume estimation in patients with mitral regurgitation: initial studies using color Doppler

"proximal isovelocity surface area" method. *Echocardiography* 9:63-70, 1992.
19. Utsunomiya T, Ogawa T, Doshi R, et al: Doppler color flow "proximal isovelocity surface area" method for estimating volume flow rate: effects of orifice shape and machine factors. *J Am Coll Cardiol* 17:1103-1111, 1991.
20. Utsunomiya T, Ogawa T, Tang HA, et al: Doppler color flow mapping of the proximal isovelocity surface area: a new method for measuring volume flow rate across a narrowed orifice. *J Am Soc Echocardiogr* 4:338-348, 1991.
21. Heinrich RS, Fontaine AA, Grimes RY, et al: Experimental analysis of fluid mechanical energy losses in aortic valve stenosis: importance of pressure recovery. *Ann Biomed Eng* 24:685-694, 1996.
22. Azadani AN, Jaussaud N, Matthews PB, et al: Energy loss due to paravalvular leak with transcatheter aortic valve implantation. *Ann Thorac Surg* 88:1857-1863, 2009.
23. Dasi LP, Pekkan K, de Zelicourt D, et al: Hemodynamic energy dissipation in the cardiovascular system: generalized theoretical analysis on disease states. *Ann Biomed Eng* 37:661-673, 2009.
24. Akins CW, Travis B, Yoganathan AP: Energy loss for evaluating heart valve performance. *J Thorac Cardiovasc Surg* 136:820-833, 2008.
25. Garcia D, Pibarot P, Dumesnil JG, et al: Assessment of aortic valve stenosis severity: A new index based on the energy loss concept. *Circulation* 101:765-771, 2000.
26. Garcia D, Jean GD, Louis-Gilles D, et al: Discrepancies between catheter and Doppler estimates of valve effective orifice area can be predicted from the pressure recovery phenomenon: practical implications with regard to quantification of aortic stenosis severity. *J Am Coll Cardiol* 41:435-442, 2003.
27. Dumesnil JG, Yoganathan AP: Valve prosthesis hemodynamics and the problem of high transprosthetic pressure gradients. *Eur J Cardiothorac Surg* 6(Suppl 1):S34-S37; discussion S38, 1992.
28. Bellhouse BJ, Talbot L: The fluid mechanics of the aortic valve. *J Fluid Mech* 35:721-735, 1969.
29. Paulsen PK, Hasenkam JM: Three-dimensional visualization of velocity profiles in the ascending aorta in dogs, measured with a hot-film anemometer. *J Biomech* 16:201-210, 1983.
30. Paulsen PK: Use of a hot-film anemometer system for cardiovascular studies, with special reference to the ascending aorta. *Dan Med Bull* 36:430-443, 1989.
31. Rossvoll O, Samstad S, Torp HG, et al: The velocity distribution in the aortic annulus in normal subjects: a quantitative analysis of two-dimensional Doppler flow maps. *J Am Soc Echocardiogr* 4:367-378, 1991.
32. Kilner PJ, Yang GZ, Mohiaddin RH et al: Helical and retrograde secondary flow patterns in the aortic arch studied by three-directional magnetic resonance velocity mapping. *Circulation* 88(5 Pt 1):2235-2247, 1993.
33. Bellhouse B, Bellhouse F: Fluid mechanics of model normal and stenosed aortic valves. *Circ Res* 25:693-704, 1969.
34. Bellhouse, BJ: Velocity and pressure distributions in the aortic valve. *J Fluid Mech* 37:587-600, 1969.
35. Reul H, Talukder N: Heart valve mechanics. In Hwang NHC, Gross DR, Patel DJ, editors: *Quantitative cardiovascular studies, clinical and research applications of engineering principles*. Baltimore, 1979, University Park Press, pp 527-564.
36. Kim WY, Bisgaard T, Nielsen SL, et al: Two-dimensional mitral flow velocity profiles in pig models using epicardial Doppler echocardiography. *J Am Coll Cardiol* 24:532-545, 1994.
37. Reul H, Talukder N, Muller EW: Fluid mechanics of the natural mitral valve. *J Biomech* 14:361-372, 1981.
38. Lu PC, Lai HC, Liu JS: A reevaluation and discussion on the threshold limit for hemolysis in a turbulent shear flow. *J Biomech* 34:1361-1364, 2001.
39. Mohandas N, Hochmuth RM, Spaeth EE: Adhesion of red cells to foreign surfaces in the presence of flow. *J Biomed Mater Res* 8:119-136, 1974.
40. Blackshear PL: Hemolysis at prosthetic surfaces. In Hair MR, editor: *Chemistry of biosurfaces*, New York, 1972, Marcel Dekker, pp 523-561.
41. Klaus S, Korfer S, Mottaghy K, et al: In vitro blood damage by high shear flow: human versus porcine blood. *Int J Artif Organs* 25:306-312, 2002.
42. Yoganathan AP, Wick TM, Reul H: The influence of flow characteristics of prosthetic heart valves on thrombus formation. In Butchart EG, Bodnar W, editors: *Current issues in heart valve disease: thrombosis, embolism and bleeding*. London, 1992, ICR, pp 123-148.
43. Jones M, McMillan ST, Eidbo EE, et al: Evaluation of prosthetic heart valves by Doppler flow imaging. *Echocardiography* 3:513-525, 1986.
44. Travis BR, Heinrich RS, Ensley AE, et al: The hemodynamic effects of mechanical prosthetic valve type and orientation on fluid mechanical energy loss and pressure drop in in vitro models of ventricular hypertrophy. *J Heart Valve Dis* 7:345-354, 1998.
45. Kleine P, Perthel M, Nygaard H, et al: Medtronic Hall versus St. Jude Medical mechanical aortic valve: downstream turbulences with respect to rotation in pigs. *J Heart Valve Dis* 7:548-555, 1998.
46. Ge L, Dasi LP, Sotiropoulos F, Yoganathan AP: Characterization of hemodynamic forces induced by mechanical heart valves: Reynolds vs. viscous stresses. *Ann Biomed Eng* 36:276-297, 2008.
47. Ellis JT, Travis BR, Yoganathan AP: An in vitro study of the hinge and near-field forward flow dynamics of the St. Jude Medical Regent bileaflet mechanical heart valve. *Ann Biomed Eng* 28:524-532, 2000.
48. Simon HA, Dasi LP, Leo HL, Yoganathan AP: Spatio-temporal flow analysis in bileaflet heart valve hinge regions: potential analysis for blood element damage. *Ann Biomed Eng* 35:1333-1346, 2007.
49. Ellis JT, Healy TM, Fontaine AA, et al: An in vitro investigation of the retrograde flow fields of two bileaflet mechanical heart valves. *J Heart Valve Dis* 5:600-606, 1996.
50. Saxena R, Lemmon J, Ellis J, Yoganathan A: An in vitro assessment by means of laser Doppler velocimetry of the Medtronic Advantage bileaflet mechanical heart valve hinge flow. *J Thorac Cardiovasc Surg* 126:90-98, 2003.
51. Leo HL, He Z, Ellis JT, Yoganathan AP: Microflow fields in the hinge region of the Carbo-Medics bileaflet mechanical heart valve design. *J Thorac Cardiovasc Surg* 124:561-574, 2002.
52. Gross JM, Shu MC, Dai FF, et al: A microstructural flow analysis within a bileaflet mechanical heart valve hinge. *J Heart Valve Dis* 5:581-590, 1996.
53. Ellis JT, Yoganathan AP: A comparison of the hinge and near-hinge flow fields of the St Jude Medical Hemodynamic Plus and Regent bileaflet mechanical heart valves. *J Thorac Cardiovasc Surg* 119:83-93, 2000.
54. Yoganathan AP, Reamer HH, Corcoran WH, et al: The Starr-Edwards aortic ball valve: flow characteristics, thrombus formation, and tissue overgrowth. *Artif Organs* 5:6-17, 1981.
55. Yoganathan AP, Eberhardt CE, Walker PG: Hydrodynamic performance of the Medtronic Freestyle Aortic Root Bioprosthesis. *J Heart Valve Dis* 3:571-580, 1994.
56. Nagy ZL, Fisher J, Walker PG, Watterson KG: The effect of sizing on the in vitro hydrodynamic characteristics and leaflet motion of the Toronto SPV stentless valve. *J Thorac Cardiovasc Surg* 117:92-98, 1999.
57. Eriksson MJ, Brodin LA, Dellgren GN, Radegran K: Rest and exercise hemodynamics of an extended stentless aortic bioprosthesis. *J Heart Valve Dis* 6:653-660, 1997.
58. Kapadia SR, Goel SS, Svensson L, et al: Characterization and outcome of patients with severe symptomatic aortic stenosis referred for percutaneous aortic valve replacement. *J Thorac Cardiovasc Surg* 137:1430-1435, 2009.
59. Webb JG, Pasupati S, Humphries K, et al: Percutaneous transarterial aortic valve replacement in selected high-risk patients with aortic stenosis. *Circulation* 116:755-763, 2007.
60. Vahanian A, Alfieri O, Al-Attar N, et al: Transcatheter valve implantation for patients with aortic stenosis: a position statement from the European Association of Cardio-Thoracic Surgery (EACTS) and the European Society of Cardiology (ESC), in collaboration with the European Association of Percutaneous Cardiovascular Interventions (EAPCI). *Eur Heart J* 29:1463-1470, 2008.
61. Clavel MA, Webb JG, Pibarot P, et al: Comparison of the hemodynamic performance of percutaneous and surgical bioprostheses for the treatment of severe aortic stenosis. *J Am Coll Cardiol* 53:1883-1891, 2009.
62. Grube E, Buellesfeld L, Mueller R, et al: Progress and current status of percutaneous aortic valve replacement: results of three device generations of the CoreValve Revalving system. *Circ Cardiovasc Interv* 1:167-175, 2008.
63. Vetter HO, Yoganathan AP, Fontaine AA, et al: Hydrodynamic characteristics of a new stentless mitral valve allograft: in vitro results. In Leipschs D, editor: *3rd International Symposium on Biofluid Mechanics*, Munich, 1994, VDI, pp 287-294.
64. Simon HA, Ge L, Borazjani I, et al: Simulation of the three-dimensional hinge flow fields of a bileaflet mechanical heart valve under aortic conditions. *Ann Biomed Eng* 38:841-853, 2010.

25

# Echocardiographic Recognition and Quantitation of Prosthetic Valve Dysfunction

PHILIPPE PIBAROT, DVM, PhD | JEAN G. DUMESNIL, MD

**Prosthetic Valve Complications and Dysfunction**
- Patient Prosthesis Mismatch
- Prosthetic Valve Thrombosis and Pannus
- Structural Valve Deterioration
- Infective Endocarditis
- Paravalvular Regurgitation

**Basic Principles and Parameters for the Doppler-Echocardiographic Evaluation of Prosthetic Valve Function**
- Timing of Echocardiographic Follow-up
- Clinical Data
- Recognition and Quantitation of Prosthetic Valve Stenosis
- Recognition and Quantitation of Prosthetic Valve Regurgitation
- Role of Stress Echocardiography
- Specific Considerations for Particular Types of Valve Substitutes

**Interpretation of Doppler-Echocardiographic Data**
- Interpretation of High Transprosthetic Gradients
- Special Considerations for Low–Flow-State Conditions
- Special Considerations for Perioperative Evaluation

**Utility of Doppler Echocardiography for Management of Specific Prosthetic Valve–Related Complications**
- Prosthetic Valve Thrombosis
- Prosthetic Valve Endocarditis
- Paravalvular Regurgitation

**Limitations, Alternative Approaches, and Future Directions**
- Quantitation of Prosthetic Valve Regurgitation
- Evaluation of Prosthetic Valve Leaflet Mobility
- Evaluation of Prosthetic Valve Endocarditis
- Evaluation of Transcatheter Valve Implantation

**Conclusion**

## Prosthetic Valve Complications and Dysfunction

Many prosthesis-related complications can be prevented or their impact minimized through optimal prosthesis selection in the individual patient, careful medical management, and close follow-up of prosthetic valve function after implantation. Doppler echocardiography is the method of choice for the evaluation of prosthetic valve function. This evaluation follows the same basic principles used for the evaluation of native valves with some important particularities and caveats specific to the prosthetic valves. These particularities are described in this chapter.

### PATIENT PROSTHESIS MISMATCH

Patient prosthesis mismatch (PPM) is not an intrinsic dysfunction of the prosthesis, per se. This problem indeed occurs when the effective orifice area (EOA) of a normally functioning prosthesis is too small in relation to the patient's body size (and thus cardiac output requirements), resulting in abnormally high postoperative gradients (see Clinical Case 25-1 at ExpertConsult.com). The most widely accepted and validated parameter for identifying PPM is the indexed EOA, that is, the EOA of the prosthesis divided by the patient's body surface area.[1-5] Table 25-1 shows the cutoff values of indexed EOA generally used to identify PPM and quantify its severity. Moderate PPM may be quite frequent both in the aortic (20% to 70%) and mitral (30% to 70%) positions, whereas the prevalence of severe PPM ranges from 2% to 10% in both positions.[4-7] PPM is associated with worse hemodynamics; less regression of left ventricular (LV) hypertrophy and pulmonary hypertension; worse functional class, exercise capacity, and quality of life; more cardiac events; and lower survival.[6-17] The impact of PPM, and especially severe PPM, on outcomes is more important in younger patients as well in those with poor LV function or severe LV hypertrophy.[8,16] Moreover, as opposed to most other risk factors, PPM can largely be prevented by using a prospective strategy at the time of operation.[18,19] Transthoracic echocardiography (TTE) is essential to make the differential diagnosis between PPM and intrinsic prosthetic valve dysfunction.

### PROSTHETIC VALVE THROMBOSIS AND PANNUS

Obstruction of prosthetic valves may be caused by thrombus formation (Fig. 25-1, *A*), pannus ingrowth (see Fig. 25-1, *B*) or a combination of both (see Clinical Case 25-2 at ExpertConsult.com). Pannus ingrowth alone may be encountered in both bioprostheses and mechanical valves. It may present as a slowly progressive obstruction due to a subvalvular annulus, in which case it may be difficult to visualize and thus to distinguish from progressive structural valve deterioration. Valve thrombosis is most often encountered in patients with mechanical valves and inadequate antithrombotic therapy. Thrombosis may also be seen in bioprosthetic valves, where it most often occurs in the early postoperative period. Pannus and

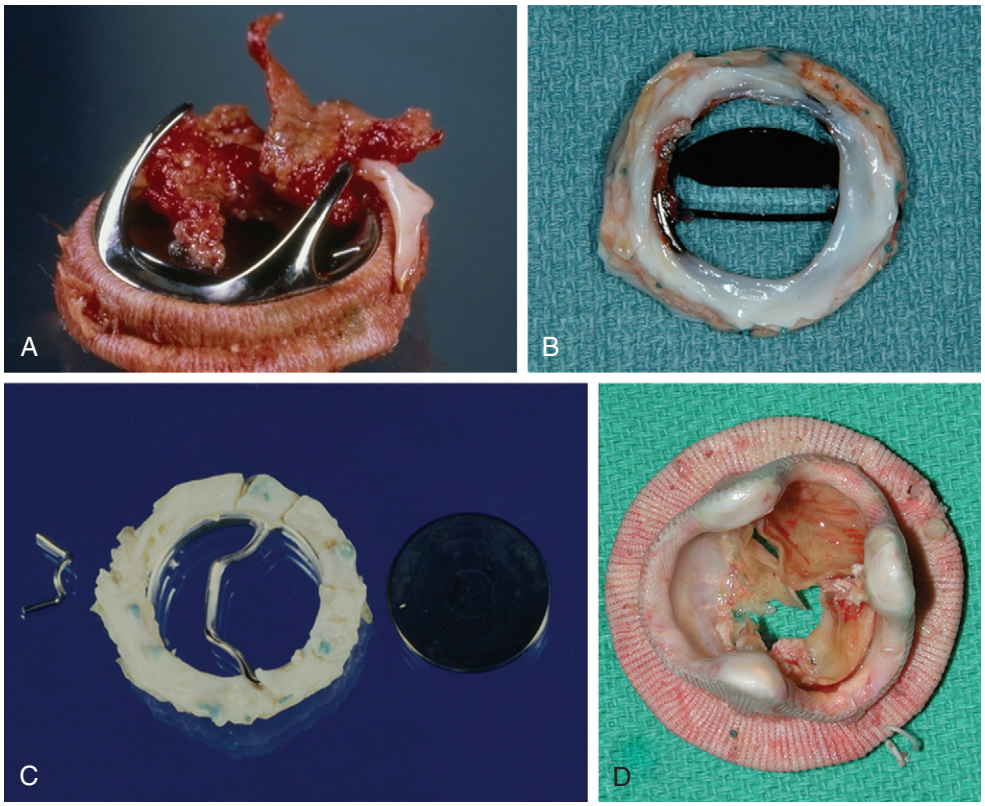



**Figure 25-1 Prosthetic valves explanted for severe dysfunction. A,** Obstructive thrombosis of a Lillehei-Kaster prosthesis. **B,** Pannus ingrowth interacting with leaflet opening in a St. Jude Medical bileaflet valve. **C,** Rupture of the outlet strut and leaflet escape in a Björk-Shiley prosthesis. **D,** Leaflet calcific degeneration and tear in a porcine bioprosthesis. (***A*** *and* ***C,*** *Courtesy Drs. Jacques Métras, Québec Heart & Lung Institute (QHLI), Québec;* ***B,*** *Christian Couture, QHLI;* ***D,*** *Gosta Petterson, Cleveland Clinic, Cleveland.)*

**TABLE 25-1 Criteria of Indexed Prosthetic Valve Effective Orifice Area ($cm^2/m^2$) for the Identification and Quantitation of Prosthesis-Patient Mismatch**

| | *Mild or Not Clinically Significant* | *Moderate* | *Severe* |
|---|---|---|---|
| Aortic position | >0.85 (0.8-0.9) | ≤0.85 (0.8-0.9) | ≤0.65 (0.6-0.7) |
| Mitral position | >1.2 (1.2-1.3) | ≤1.2 (1.2-1.3) | ≤0.9 (0.9) |

Numbers in parentheses represent the range of threshold values that have been used in the literature.

thrombosis may be present alone or in combination and cause acute or subacute valve obstruction. The incidence of obstructive valve thrombosis varies between 0.3% and 1.3% per patient-year in patients with mechanical valves.[20,21]

Pannus is usually encountered in patients with a normal anticoagulation profile and with subacute or chronic symptoms.[20] Valve thrombosis should be suspected in any patient with any type of prosthetic valve who presents with a recent increase in dyspnea or fatigue.[22] Suspicion should be higher if there has been a period of interrupted or subtherapeutic anticoagulation in the recent past. In such cases, echocardiography should be done promptly and include transesophageal echocardiography (TEE), particularly if the prosthesis is in the mitral position.

## STRUCTURAL VALVE DETERIORATION

Mechanical prostheses have an excellent durability, and structural valve deterioration is extremely rare with contemporary valves, although mechanical failure (e.g., strut fracture, leaflet escape, occluder dysfunction due to lipid adsorption) has occurred with some models in the past (see Fig. 25-1, *C*).

The rate of structural valve deterioration in bioprosthetic valves (see Fig. 25-1, *D*) increases over time, particularly after the initial 7 to 8 years after implantation. Structural valve deterioration is often characterized by calcific degeneration of valve leaflets. However, this process may also occur with no or minimal leaflet calcification in approximately 30% of the cases. Structural valve deterioration is, by far, the most frequent cause of bioprosthetic valve failure. With conventional stented bioprostheses, the freedom of structural valve failure is 70% to 90% at 10 years and 50% to 80% at 15 years.[21,23-26] Risk factors previously found to be associated with bioprosthetic structural valve deterioration include younger age, mitral valve position, renal insufficiency, and hyperparathyroidism.[23-25,27] Structural valve deterioration can result in prosthetic valve stenosis, regurgitation, or both. A meticulous baseline Doppler-echocardiographic evaluation of prosthetic valve morphology and function within the first year after prosthesis implantation and a regular follow-up thereafter are essential to early detection of structural valve deterioration.

## INFECTIVE ENDOCARDITIS

Prosthetic valve endocarditis is the most severe form of infective endocarditis and occurs in 1% to 6% of patients with valve prostheses accounting for 10% to 30% of all cases of infective endocarditis.[28] Prosthetic valve endocarditis is an extremely serious condition with high mortality rates (30% to 50%).[21,22] Echocardiography and particularly TEE plays a

key role in the diagnostic and prognostic assessment of prosthetic valve endocarditis. The diagnosis relies predominantly on the combination of positive blood cultures and echocardiographic evidence of prosthetic infection, including vegetations, paraprosthetic abscesses, or a new paravalvular regurgitation.[29]

## PARAVALVULAR REGURGITATION

Paravalvular regurgitation is typically due to infection, suture dehiscence, or fibrosis and calcification of the native annulus leading to inadequate contact between the sewing ring and annulus. Dehiscence of the prosthesis in the late postoperative period may be related to operative technical factors but is most often caused by endocarditis, in which case emergency surgical treatment is generally required.

Long-term prognosis is generally benign in patients with mild paravalvular regurgitation identified by perioperative echocardiography, with progression of regurgitation requiring reoperation in fewer than 1% of patients at follow-up beyond 1 to 2 years.[30] Hence, closer clinical and Doppler-echocardiographic follow-up appears justified in these patients, with surgical intervention warranted only for those who develop symptoms, hemolysis, and/or progressive LV dysfunction.[31] Paravalvular regurgitation is more common following transcatheter aortic valve implantation. Recent studies indeed report incidence of regurgitation of 30% to 80% with 5% to 14% being moderate or severe (Fig. 25-2, *C*).[32-34]

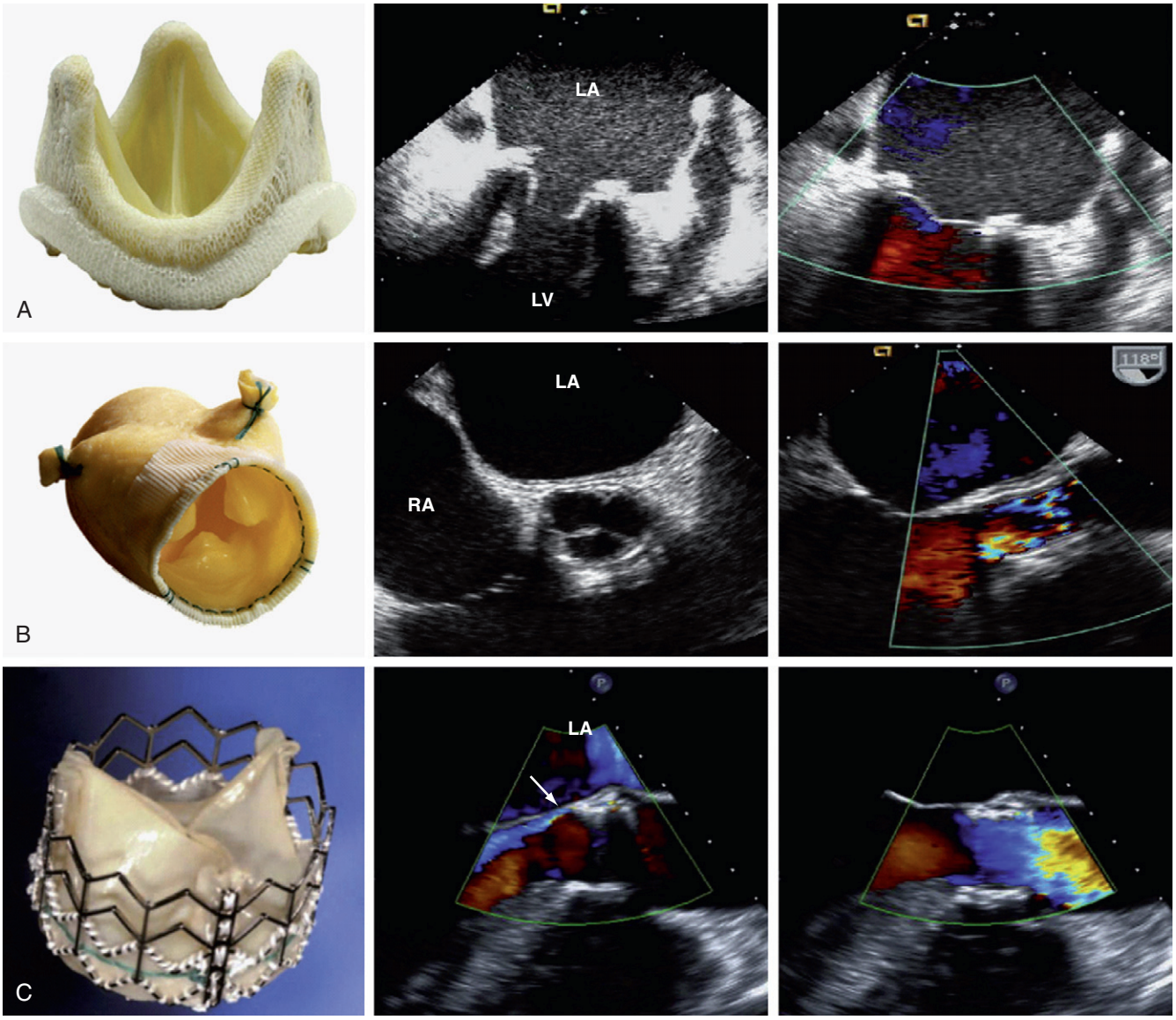



**Figure 25-2 Examples of stented (A), stentless (B), and percutaneous (C) biologic valves and their echocardiographic features in diastole (*middle*) and in systole (*right*) as seen by TEE.** The stentless valve is inserted by the root inclusion technique. Mild paravalvular aortic regurgitation in the percutaneous valve is shown by *arrow*. *(Reproduced with permission of the American Society of Echocardiography from Zoghbi WA, Chambers JB, Dumesnil JG, et al: Recommendations for evaluation of prosthetic valves with echocardiography and Doppler ultrasound: a report from the American Society of Echocardiography's Guidelines and Standards Committee and the Task Force on Prosthetic Valves.* J Am Soc Echocardiogr *22[9]:975-1014, 2009.)*

## Basic Principles and Parameters for the Doppler-Echocardiographic Evaluation of Prosthetic Valve Function

Doppler echocardiography is the method of choice to evaluate prosthetic valve function. This evaluation follows the same principles used for the evaluation of native valves with some important caveats described later. A complete echocardiography includes two-dimensional (2D) imaging of the prosthetic valve, evaluation of valve leaflet/occluder morphology and mobility, measurement of the transprosthetic gradients and EOA, estimation of the degree of regurgitation, evaluation of LV size and systolic function, and calculation of systolic pulmonary arterial pressure.

### TIMING OF ECHOCARDIOGRAPHIC FOLLOW-UP

Ideally, a baseline postoperative TTE study should be performed at the first visit, 2 to 4 weeks after hospital discharge, when the chest wound has healed, ventricular function has improved, and anemia with its associated hyperdynamic state has resolved.[35] However, if the patient is being transferred and/or may not return, it may be best to perform the study before hospital discharge, although image quality and reliability of measurements are often suboptimal. Routine follow-up clinical visits should be conducted annually after valve implantation, with earlier reevaluations and echocardiography if there is a change in clinical status. Routine echocardiography after a first postoperative study is not indicated for normally functioning prostheses unless there are other indications for echocardiography (e.g., follow-up of LV dysfunction) or clinical symptoms suggestive of valvular dysfunction or other cardiac pathology.[35] Annual echocardiography is recommended in patients with bioprosthetic valves after the first 5 years. In patients with mechanical valves, routine annual echocardiography is not indicated in the absence of a change in clinical status.

### CLINICAL DATA

The reason for the echocardiographic study and the patient's symptoms should be clearly documented. Furthermore, because the interpretation of Doppler-echocardiographic findings depends on the type and size of the replacement valve, this information and the date of surgery should be incorporated in the report. The exact type and model of prosthesis should clearly be recorded because the design and hemodynamic performance may differ substantially from one model generation to the other (e.g., St. Jude Standard vs. HP vs. Regent models). Blood pressure and heart rate should be measured. The heart rate of the cardiac cycles used for Doppler measurements is particularly important in mitral and tricuspid prosthetic valves, because the mean gradient is highly dependent on the duration of the diastolic filling period. Finally, the patient's height, weight, and body surface area should be recorded to assess whether PPM is present and to interpret the cardiac chamber size.

### RECOGNITION AND QUANTITATION OF PROSTHETIC VALVE STENOSIS

The appearance of a new murmur with new congestive heart failure symptoms in a patient with a prosthetic aortic valve should prompt an urgent TTE study and, if indicated, TEE.

**TABLE 25-2 Doppler-Echocardiographic Criteria for Detection and Quantitation of Prosthetic Aortic Valve Stenosis**

| | *Normal* | *Possible Stenosis* | *Significant Stenosis* |
|---|---|---|---|
| **Valve Structure and Motion** | | | |
| Mechanical or bioprosthesis | Normal | Often abnormal* | Abnormal* |
| **Doppler Quantitative Parameters** | | | |
| Peak velocity (m/s)† | <3 | 3-4 | >4 |
| Mean gradient (mm Hg)† | <20 | 20-35 | >35 |
| Doppler velocity index‡ | ≥0.30 | 0.25-0.29 | <0.25 |
| Effective orifice area ($cm^2$) | >1.2 | 0.8-1.2 | <0.8 |
| Effective orifice area vs. normal reference value | Reference ± 1 SD | < Reference − 1 SD | < Reference − 2 SD |
| Contour of the transprosthetic jet§ | Triangular, early peaking | Triangular to intermediate | Rounded, symmetric |
| Acceleration time (ms)§ | <80 | 80-100 | >100 |

See Table 25-4 to obtain the normal reference values of effective orifice area for the different models and sizes of prostheses.

Adapted in part from Zoghbi WA, Chambers JB, Dumesnil JG, et al: Recommendations for evaluation of prosthetic valves with echocardiography and Doppler ultrasound: a report from the American Society of Echocardiography's Guidelines and Standards Committee and the Task Force on Prosthetic Valves. *J Am Soc Echocardiogr* 22(9):975-1014, 2009, with permission of American Society of Echocardiography.

*SD*, Standard deviation.

*Abnormal mechanical valves: occluder that is immobile or with restricted mobility, thrombus or pannus; abnormal biologic valves: leaflet thickening/calcification, thrombus or pannus.

†These parameters are more affected by low or high flow states including low LV output and concomitant aortic regurgitation.

‡This parameter is dependent on the size of the LV outflow tract.

§These parameters are affected by LV function and chronotropy.

However, the initial suspicion of prosthetic valve stenosis may be the incidental finding of abnormally high flow velocities and gradients detected during a routine examination. Tables 25-2 and 25-3 present the Doppler-echocardiographic criteria for the recognition and quantitation of prosthetic valve stenosis.

#### *Leaflet Morphology and Mobility*

Echocardiographic imaging should identify the sewing ring, the valve occluder, and the surrounding area. Echocardiographic imaging of the ball or disk of mechanical valves is often difficult to obtain because of reverberations and shadowing caused by the valve components. Figures 25-2 and 25-3 show the echocardiographic features of normally functioning bioprosthetic and mechanical valves, respectively. The leaflets of tissue valves normally appear thin, with unrestricted motion and no evidence of prolapse. Stentless, homograft, or autograft valves may be indistinguishable from native valves.

TEE can provide improved image quality and thereby improved detection of cusp calcification and thickening; valvular vegetations due to endocarditis, thrombus, or pannus; and reduced leaflet/disk/ball mobility.[36] In the case of mechanical prostheses, evaluation of occluder mobility can be attempted with some degree of success, but in our experience, valve cinefluoroscopy is definitely the best, most economical, and least invasive technique that can be used for this purpose (see Chapter 5).

Prosthetic valve stenosis is generally associated with abnormal valve morphology and/or mobility (see Tables 25-2 and

**TABLE 25-3 Doppler-Echocardiographic Criteria for Detection and Quantitation of Prosthetic Mitral Valve Stenosis**

| | *Normal* | *Possible Stenosis* | *Significant Stenosis* |
|---|---|---|---|
| **Valve Structure and Motion** | | | |
| Mechanical or bioprosthesis | Normal | Often abnormal* | Abnormal* |
| **Doppler Quantitative Parameters** | | | |
| Peak velocity (m/s)†,‡ | <1.9 | 1.9-2.5 | >2.5 |
| Mean gradient (mm Hg)†,‡ | ≤5 | 6-10 | ≥10 |
| Doppler velocity index‡,§ | <2.2 | 2.2-2.5 | >2.5 |
| Effective orifice area ($cm^2$)‖ | ≥2 | 1-2 | <1 |
| Effective orifice area vs. normal reference value‖ | Reference ± 1 SD | <Reference − 1 SD | <Reference − 2 SD |
| Pressure half-time (ms)¶ | <130 | 130-200 | >200 |

See Table 25-5 to obtain the normal reference values of effective orifice area for the different models and sizes of prostheses.

Adapted in part from Zoghbi WA, Chambers JB, Dumesnil JG, et al: Recommendations for evaluation of prosthetic valves with echocardiography and Doppler ultrasound: a report from the American Society of Echocardiography's Guidelines and Standards Committee and the Task Force on Prosthetic Valves. *J Am Soc Echocardiogr* 22(9):975-1014, 2009, with permission of American Society of Echocardiography.

*SD*, Standard deviation.

*Abnormal mechanical valves: occluder that is immobile or with restricted mobility, thrombus or pannus; abnormal biologic valves: leaflet thickening/calcification, thrombus or pannus.

†The criteria proposed for these parameters are valid for near normal or normal diastolic volume (i.e., stroke volume: 50-90 mL) and heart rate (50-80 bpm).

‡These parameters are more affected by flow and chronotropy.

§These parameters are also abnormal in presence of significant mitral prosthesis regurgitation. This parameter is dependent on the size of the LV outflow tract.

‖These parameters are not valid when more than mild concomitant aortic or mitral regurgitation is present.

¶This parameter is influenced by chronotropy, LA compliance, and LV compliance.

25-3). In the cases of mechanical valves, the mobility of the occluder is usually reduced or absent (Fig. 25-4; also see Clinical Case 25-2). Thrombus, pannus, or vegetation are often visualized at the level of the prosthesis ring or hinge mechanism. In the case of bioprosthetic valves, prosthetic valve stenosis is most often associated with thickening, calcification, and reduced mobility of the leaflets (see Fig. 25-4 and Clinical Case 25-3). However, obstruction of the bioprosthesis may also be caused by thrombus, pannus, or vegetation.

### *Quantitative Parameters*

Quantitative parameters of prosthetic valve function include flow velocity, pressure gradients, EOA, and Doppler velocity index (DVI).

#### Transprosthetic Velocity and Gradient

The principles of interrogation and recording of flow velocity through prosthetic valves are similar to those used in evaluating native valve stenosis. This includes pulsed-wave (PW) and continuous-wave (CW) Doppler as well as color Doppler, using several windows for optimal recording and minimizing angulation between the Doppler beam and flow direction. CW Doppler evaluation of aortic prostheses must be performed from multiple transducer positions, including apical, right parasternal, right supraclavicular, and suprasternal notch. Measurements of prosthesis velocity and gradients are made from the transducer position yielding the highest velocities.[35]

One should however bear in mind that the fluid dynamics of the mechanical valves may differ substantially from those of the native valve (Figs. 25-3 and 25-5). The flow is eccentric in monoleaflet valves and composed of three separate jets in bileaflet valves. Because the direction of the transprosthetic jet may be eccentric, multiwindow examination should be carefully performed to detect the highest velocity signal in prosthetic aortic valves. Occasionally, an abnormally high jet gradient corresponding to a localized high velocity may be recorded by CW Doppler interrogation through the smaller central orifice of bileaflet mechanical prostheses in the aortic or mitral position (see Fig. 25-5).[37] This phenomenon may lead to an overestimation of gradient and a false suspicion of prosthesis dysfunction. In some rare cases, a double-envelope image may be observed with the superimposition of a high-velocity envelope corresponding to the flow through the central orifice and a lower-velocity envelope corresponding to the flow through the lateral orifices (Fig. 25-6).

Pressure gradient is calculated with the use of the simplified Bernoulli equation as follows: $\Delta P = 4 \times V_{Pr}^2$, where $V_{Pr}$ is the velocity of the peak transprosthetic flow jet in meters per second. In patients with aortic prostheses and high–flow-rate or narrow LV outflow tract (LVOT), the velocity proximal to the prosthesis may be increased and therefore not negligible. If proximal velocity ($V_{LVOT}$) is greater than 1.5 m/s, estimation of the pressure gradient is more accurately determined by including $V_{LVOT}$ in the equation: $\Delta P = 4 \times (V_{PrAv}^2 - V_{LVOT}^2)$.

Prosthetic valve stenosis is usually associated with increased transprosthetic peak flow velocity or mean gradient (at least 3 m/s or at least 20 mm Hg for aortic prostheses, and at least 1.9 m/s or at least 6 mm Hg for mitral prostheses) (see Tables 25-2 and 25-3). However, it is important to keep in mind that high velocity or gradient alone is not proof of intrinsic prosthetic obstruction and may be secondary to PPM, high-flow conditions, prosthetic valve regurgitation, or localized high central jet velocity in bileaflet mechanical valves (see Interpretation of High Transprosthetic Gradients for data interpretation and differential diagnosis). Significant prosthetic valve regurgitation may cause the flow rate across the prosthesis to increase, resulting in increased velocities and gradients.

The main limitation of transprosthetic velocity and gradients is that they are highly flow dependent. For instance, patients in a low cardiac-output state can exhibit normal transvalvular velocity and gradients despite the presence of significant prosthetic valve stenosis. Hence, other qualitative and quantitative indices that are less flow dependent should also be used to adequately assess prosthetic valve function.

#### Transprosthetic Jet Contour and Acceleration Time

The contour of the velocity through the prosthesis is a qualitative index that may be used to assess prosthetic aortic valve function in conjunction with the other quantitative indices. In a normal valve, the contour of the CW flow velocity generally has a triangular shape, with early peaking of the velocity and a short acceleration time, that is, the time from the onset of flow to maximal velocity (acceleration time less than 80 ms) (Fig. 25-7). With prosthetic valve obstruction, a more rounded velocity contour is seen, with the velocity peaking almost in midejection, prolonged acceleration time (greater than 100 ms) and ejection time, as well as the ratio of acceleration time to ejection time (greater than 0.4) (Fig. 25-7, and see Tables 25-2 and

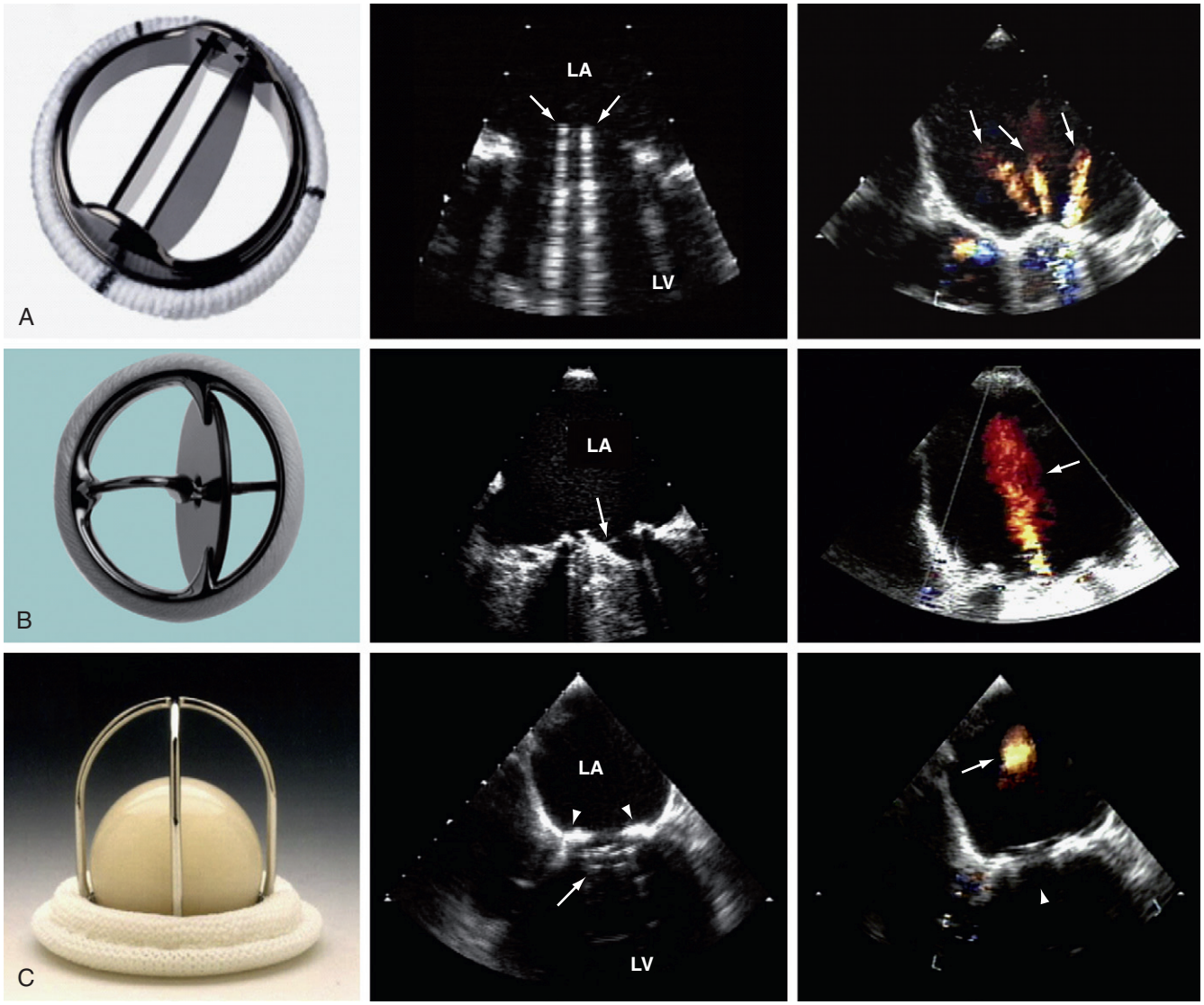



**Figure 25-3 Examples of bileaflet (A), monoleaflet (B), and caged-ball (C) mechanical valves and their transesophageal echocardiographic characteristics taken in the mitral position in diastole (*middle*) and in systole (*right*).** The *arrows* in diastole point to the occluder mechanism of the valve and in systole to the characteristic physiologic regurgitation observed with each valve. *(Reproduced with permission of the American Society of Echocardiography from Zoghbi WA, Chambers JB, Dumesnil JG, et al: Recommendations for evaluation of prosthetic valves with echocardiography and Doppler ultrasound: a report from the American Society of Echocardiography's Guidelines and Standards Committee and the Task Force on Prosthetic Valves.* J Am Soc Echocardiogr *22[9]:975-1014, 2009.)*

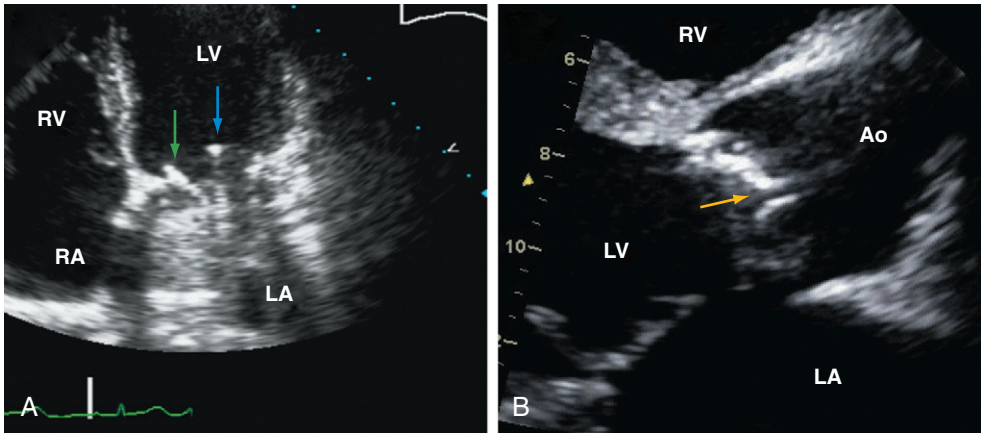



**Figure 25-4 Evaluation of prosthetic valve leaflet morphology and mobility. A,** Mitral bileaflet mechanical prosthesis in diastole with a fixed leaflet (*green arrow*); the other leaflet is still mobile (*blue arrow*). **B,** Thickening and reduced mobility of aortic bioprosthetic valve cusps (*yellow arrow*, systole). *Ao*, Aorta. (Image in panel **B** *courtesy Dr. John Chambers, Guy's and St. Thomas Hospitals, London.)*

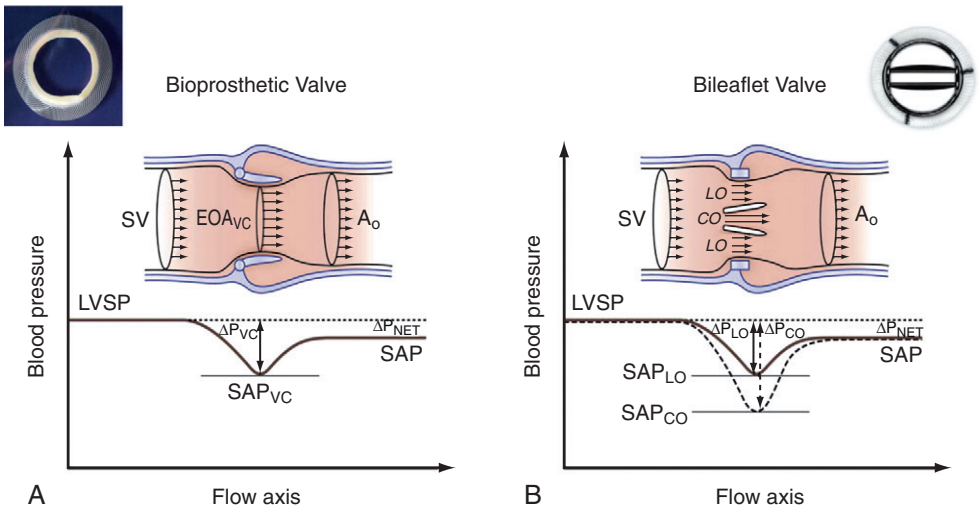



**Figure 25-5 Schematic representation of velocity and pressure changes from the LV outflow tract to the ascending aorta ($A_o$) in the presence of a stented bioprosthesis (A) and a bileaflet mechanical valve (B) illustrating the phenomena of pressure recovery and localized high gradient.** Because of pressure recovery, velocities are lower and systolic arterial pressure (*SAP*) is higher at the distal aorta than at the level of the vena contracta (*VC*). This is further exaggerated in the case of a bileaflet valve, in which the velocity is locally higher in the central orifice (*CO*) and thus pressure drop is higher at that level. Doppler gradients are estimated from maximal velocity at the level of the vena contracta and represent the maximal pressure drop, whereas invasive estimation of gradients usually reflect net pressure difference (*ΔP*) between LV systolic pressure (*LVSP*) and ascending aorta. *EOA*, Effective orifice area; *LO*, lateral orifice; *SAP*, systolic arterial pressure; *SV*, stroke volume in LV outflow tract; *VC*, vena contracta. *(Adapted with permission of the American Society of Echocardiography from Zoghbi WA, Chambers JB, Dumesnil JG, et al: Recommendations for evaluation of prosthetic valves with echocardiography and Doppler ultrasound: a report from the American Society of Echocardiography's Guidelines and Standards Committee and the Task Force on Prosthetic Valves.* J Am Soc Echocardiogr *22[9]:975-1014, 2009.)*

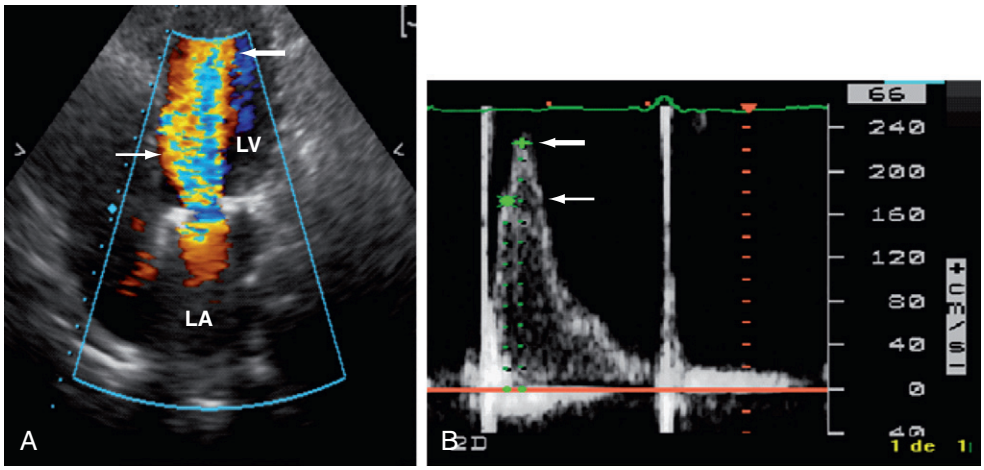



**Figure 25-6 Localized high gradient within the central orifice of a mitral bileaflet mechanical valve. A,** Visualization of lateral (*narrow arrow*) and central (*wide arrow*) jets on color Doppler image. **B,** Two Doppler envelopes are superimposed. The highest one, which presumably reflects the velocity within the central orifice, yields a value of peak gradient of 21 mm Hg, whereas the smallest one (lateral orifices) provides a gradient of 12 mm Hg. *(Adapted with permission of the American Heart Association from Pibarot P, Dumesnil JG: Prosthetic heart valves: selection of the optimal prosthesis and long-term management.* Circulation *119[7]:1034-1048, 2009.)*

25-3).[35] The advantage of these indices is that they are independent of Doppler beam angulation in relation to flow direction. The main limitation is that they are also influenced by LV systolic function and chronotropy. For example, a patient with a normally functioning aortic prosthesis and concomitant depressed myocardial contractility may nonetheless exhibit a rounded velocity contour with late velocity peaking, just as we have also witnessed in patients with severe PPM.

## Effective Orifice Area

The EOA of prosthetic aortic valves is calculated with the continuity equation, similar to native aortic valve area[38,39]:

$$EOA = (CSA_{LVOT} \times VTI_{LVOT})/VTI_{PrAv}$$

where $CSA_{LVOT}$ is the cross-sectional area of the LVOT, $VTI_{LVOT}$ the velocity-time integral obtained by PW Doppler in the LVOT,

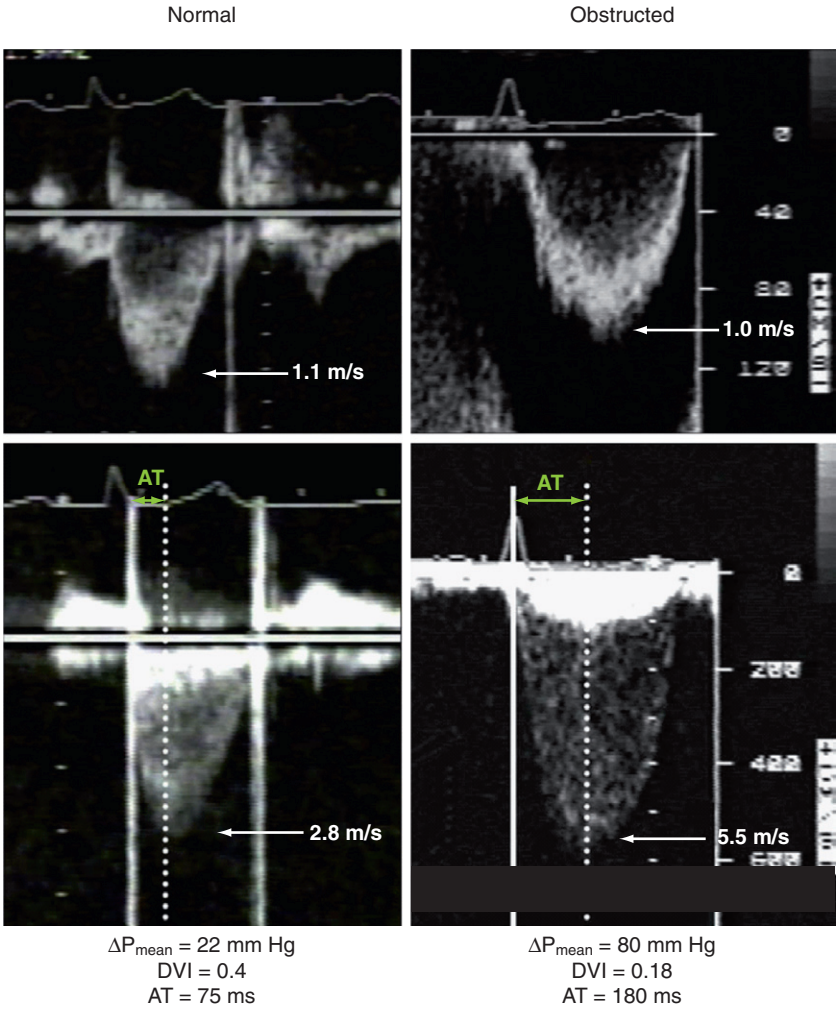



**Figure 25-7 Doppler recordings of a normal and obstructed prosthetic valve in the aortic position.** With obstruction, the velocity of the jet is increased along with changes in the contour of the jet velocity to that of a round, late-peaking profile. The acceleration time (*AT*) is increased. AT (in milliseconds) is measured as the duration from the onset of aortic ejection (*solid line*) to the maximal jet velocity (*dotted line*). Mean gradient ($\Delta P_{mean}$) is increased and the Doppler velocity index (*DVI*) is decreased with prosthetic obstruction. *(Reproduced with permission of the American Society of Echocardiography from Zoghbi WA, Chambers JB, Dumesnil JG, et al: Recommendations for evaluation of prosthetic valves with echocardiography and Doppler ultrasound: a report from the American Society of Echocardiography's Guidelines and Standards Committee and the Task Force on Prosthetic Valves.* J Am Soc Echocardiogr *22[9]:975-1014, 2009.)*

and $VTI_{PrAv}$ the velocity-time integral obtained by CW Doppler though the aortic prosthesis. When measuring the EOA of prosthetic aortic valves, a few specific caveats should be taken into consideration:

1. The cross-sectional area of the LVOT is derived from the diameter measurement just underneath the prosthesis from the parasternal long-axis zoomed view assuming a circular geometry (Fig. 25-8, *A*, *B*). This measurement is often difficult because of the reverberations and artifacts caused by the prosthesis stent or ring. Particular care should be taken not to mistake the inner border of the prosthesis stent/ring for the inner edge of the LVOT. One can use modified views (lower parasternal location) to keep the artifact from the prosthetic valve away from the LVOT. It is important to emphasize that the substitution of the LVOT diameter by the labeled prosthesis size in the continuity equation is not a valid method to determine the EOA of aortic prostheses.[40]
2. For the recording of LVOT velocity signal, care should be exercised in locating the PW Doppler sample volume adjacent to the prosthesis while avoiding the region of subvalvular acceleration (this usually requires a position 0.5 to 1 cm below the sewing ring (toward the apex). Color Doppler may be useful to guide the positioning of the PW Doppler sample. The Doppler waveform should be smooth, with minimal spectral broadening and a well-defined peak (see Fig. 25-8, *C*). An effort should be made to measure the LVOT VTI and LVOT diameter at about the same location.
3. The VTI across the prosthesis is obtained from the same signals that are used for measurement of prosthesis peak velocity and gradient (see Fig. 25-8, *D*).
4. The continuity equation method is also valid in presence of concomitant prosthetic aortic valve regurgitation because both the numerator and the denominator of the equation are increased in a similar proportion.

The EOA of mitral prostheses is calculated by the continuity equation using the stroke volume measured in the LVOT:

$$EOA = (CSA_{LVOT} \times VTI_{LVOT})/VTI_{PrMv}$$

where $VTI_{PrMv}$ is the velocity-time integral obtained by CW Doppler though the mitral prosthesis (Fig. 25-9). A few specific, important caveats should be taken into consideration for the estimation of EOA of prosthetic mitral valves:

1. The continuity equation method cannot be applied when there is more than mild concomitant mitral or aortic regurgitation.
2. The pressure half-time (PHT) method (similar to that used for native mitral valve stenosis) is not valid to estimate the valve EOA of mitral prostheses.[2,41] The PHT is highly influenced by chronotropy, left atrial (LA) compliance, and LV

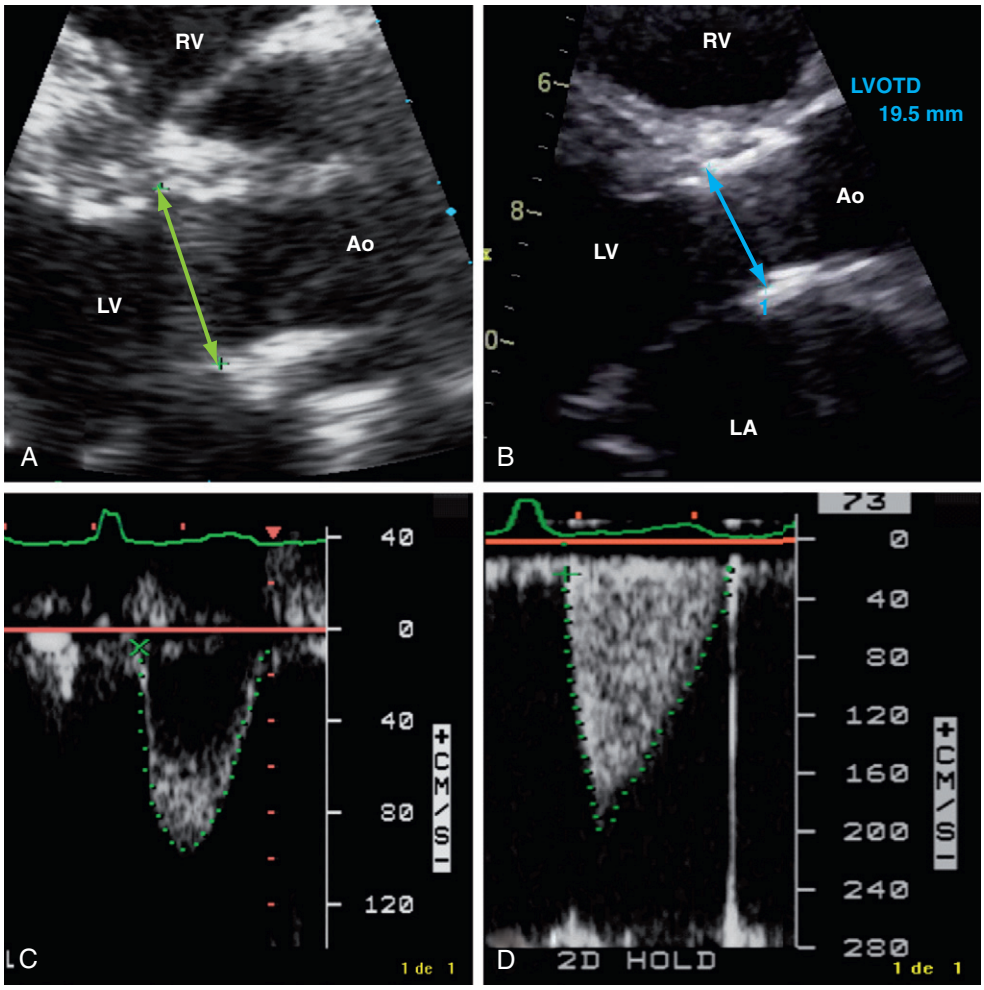



**Figure 25-8 Calculation of the effective orifice area of prosthetic valves in the aortic position using the continuity equation method.** The diameter of the LV outflow tract is measured just below the insertion of the prosthetic aortic valve (**A,** stented bioprosthesis; **B,** transcatheter bioprosthesis) from the junction of sewing ring and ventricular septum to the junction of the sewing ring and the base of the anterior mitral leaflet. Pulsed Doppler velocity recording is obtained in the LV outflow tract from the apical window (**C**). CW Doppler recording of the transprosthetic flow jet velocity is acquired from the apical five-chamber (**D**). *Ao*, Aorta.

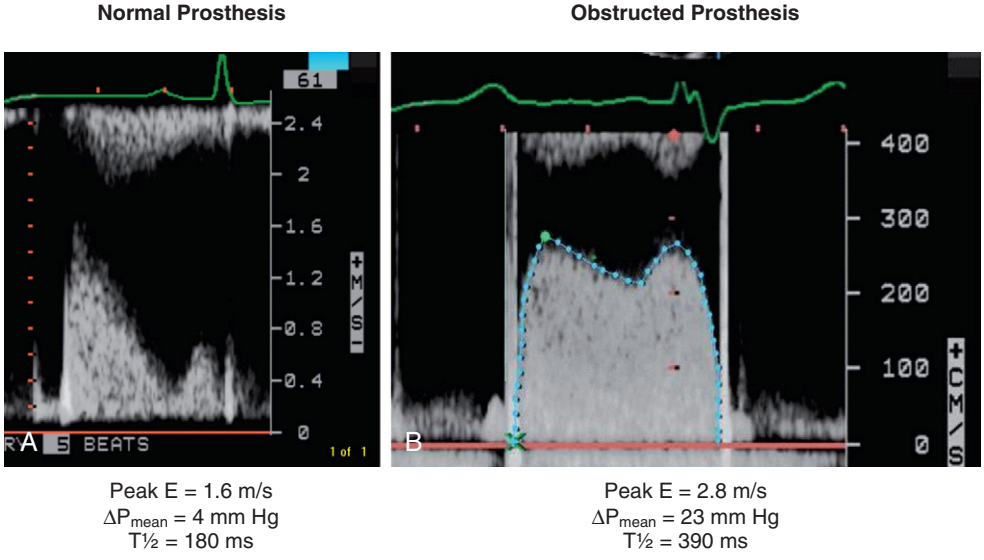



**Figure 25-9 Doppler findings with prosthetic mitral stenosis.** CW Doppler velocity recordings in a normal (**A**) and an obstructed (**B**) prosthetic valve in the mitral position. The peak E velocity, gradients, and pressure half-time ($T_{½}$) are elevated in the obstructed prosthetic valve.

compliance. Hence, patients with tachycardia or reduced atrioventricular compliance may exhibit a normal PHT despite the presence of significant prosthetic valve stenosis. Nonetheless, the pressure half time may be useful if it is significantly delayed (greater than 120 ms; see Table 25-3 and Fig. 25-9, *B*) or shows significant lengthening from one follow-up visit to the other despite similar heart rates.

Valve EOAs between 0.8 and 1.2 $cm^2$ and between 1.0 and 2.0 $cm^2$ suggest the presence of possible stenosis for aortic and mitral prostheses, respectively (see Tables 25-2 and 25-3), whereas values less than 0.8 $cm^2$ (aortic) and less than 1.0 $cm^2$ (mitral) indicate the presence of significant stenosis. These cutoff values proposed in the ASE guidelines,[35] however, have important limitation given that they overlap substantially with the normal reference values of EOA of several prosthesis models. In our experience, the recognition of prosthetic valve stenosis is better achieved by comparing the measured EOA to the normal reference value of EOA for the model and size of prosthesis implanted in the patient rather than applying fixed cutoff values to all patients regardless of the characteristics of their prosthesis.[42] Tables 25-4 and 25-5 show the normal reference values of EOA for the most commonly used prosthetic valves in the aortic and mitral position, respectively. If the measured EOA is less than the reference EOA minus one standard deviation, one should suspect possible stenosis. If the measured EOA is less than the reference minus two standard deviations, there is a high likelihood of significant stenosis (see Tables 25-2 and 25-3).

Given that its estimation requires the inclusion of several parameters in the continuity equation, the main limitation of the EOA is the susceptibility to measurement errors. In addition, although they are much less flow dependent than transprosthetic velocity or gradient, the anatomic and effective orifice areas may nonetheless vary, to some extent, with flow. The EOA may thus be "pseudoseverized" in the presence of low flow state (see Special Considerations for Low–Flow-State Conditions).

## Doppler Velocity Index

The DVI is a dimensionless ratio of the proximal velocity in the LVOT to the flow velocity through the aortic prosthesis: DVI = $V_{LVOT}/V_{PrAv}$. Time-velocity time integrals may also be used in place of peak velocities to calculate DVI = $VTI_{LVOT}/VTI_{PrAv}$. In the case of prosthetic mitral valves, the DVI is calculated by

**TABLE 25-4 Normal Reference Values of Effective Orifice Areas for the Prosthetic Aortic Valves**

| | Prosthetic Valve Size (mm) | | | | | | |
|---|---|---|---|---|---|---|---|
| | *19* | *21* | *23* | *25* | *27* | *29* | *Reference* |
| **Stented Bioprosthetic Valves** | | | | | | | |
| Mosaic | 1.1 ± 0.2 | 1.2 ± 0.3 | 1.4 ± 0.3 | 1.7 ± 0.4 | 1.8 ± 0.4 | 2.0 ± 0.4 | 5 |
| Hancock II | — | 1.2 ± 0.2 | 1.3 ± 0.2 | 1.5 ± 0.2 | 1.6 ± 0.2 | 1.6 ± 0.2 | 5 |
| Carpentier-Edwards Perimount | 1.1 ± 0.3 | 1.3 ± 0.4 | 1.50 ± 0.4 | 1.80 ± 0.4 | 2.1 ± 0.4 | 2.2 ± 0.4 | 5 |
| Carpentier-Edwards Magna | 1.3 ± 0.3 | 1.5 ± 0.3 | 1.8 ± 0.4 | 2.1 ± 0.5 | — | — | 83, 84 |
| Biocor (Epic) | 1.0 ± 0.3 | 1.3 ± 0.5 | 1.4 ± 0.5 | 1.9 ± 0.7 | — | — | 85, 86 |
| Mitroflow | 1.1 ± 0.2 | 1.2 ± 0.3 | 1.4 ± 0.3 | 1.6 ± 0.3 | 1.8 ± 0.3 | — | 87 |
| **Stentless Bioprosthetic Valves** | | | | | | | |
| Medtronic Freestyle | 1.2 ± 0.2 | 1.4 ± 0.2 | 1.5 ± 0.3 | 2.0 ± 0.4 | 2.3 ± 0.5 | — | 5 |
| St. Jude Medical Toronto SPV | — | 1.3 ± 0.3 | 1.5 ± 0.5 | 1.7 ± 0.8 | 2.1 ± 0.7 | 2.7 ± 1.0 | 5 |
| Prima Edwards | — | 1.3 ± 0.3 | 1.6 ± 0.3 | 1.9 ± 0.4 | — | — | 88, 89 |
| **Mechanical Valves** | | | | | | | |
| Medtronic-Hall | 1.2 ± 0.2 | 1.3 ± 0.2 | — | — | — | — | 5 |
| St. Jude Medical Standard | 1.0 ± 0.2 | 1.4 ± 0.2 | 1.5 ± 0.5 | 2.1 ± 0.4 | 2.7 ± 0.6 | 3.2 ± 0.3 | 5 |
| St. Jude Medical Regent | 1.6 ± 0.4 | 2.0 ± 0.7 | 2.2 ± 0.9 | 2.5 ± 0.9 | 3.6 ± 1.3 | 4.4 ± 0.6 | 90 |
| MCRI On-X | 1.5 ± 0.2 | 1.7 ± 0.4 | 2.0 ± 0.6 | 2.4 ± 0.8 | 3.2 ± 0.6 | 3.2 ± 0.6 | 91 |
| Carbomedics Standard and Top Hat | 1.0 ± 0.4 | 1.5 ± 0.3 | 1.7 ± 0.3 | 2.0 ± 0.4 | 2.5 ± 0.4 | 2.6 ± 0.4 | 5 |
| ATS Medical* | 1.1 ± 0.3 | 1.6 ± 0.4 | 1.8 ± 0.5 | 1.9 ± 0.3 | 2.3 ± 0.8 | — | 92 |

Effective orifice area is expressed as mean values ($cm^2$) available in the literature. Further studies are needed to validate these reference values.
Adapted with permission of the American Heart Association from Pibarot P, Dumesnil JG: Prosthetic heart valves: selection of the optimal prosthesis and long-term management. *Circulation* 119(7):1034-1048, 2009.
*For the ATS medical valve, the label valve sizes are 18, 20, 22, 24, 26 mm.

**TABLE 25-5 Normal Reference Values of Effective Orifice Areas for the Prosthetic Mitral Valves**

| | Prosthetic Valve Size (mm) | | | | | |
|---|---|---|---|---|---|---|
| | *25* | *27* | *29* | *31* | *33* | *Reference* |
| **Stented Bioprosthetic Valves** | | | | | | |
| Medtronic Mosaic | 1.5 ± 0.4 | 1.7 ± 0.5 | 1.9 ± 0.5 | 1.9 ± 0.5 | — | 6, 93 |
| Hancock II | 1.5 ± 0.4 | 1.8 ± 0.5 | 1.9 ± 0.5 | 2.6 ± 0.5 | 2.6 ± 0.7 | 7 |
| Carpentier-Edwards Perimount | 1.6 ± 0.4 | 1.8 ± 0.4 | 2.1 ± 0.5 | — | — | 6 |
| **Mechanical Valves** | | | | | | |
| St. Jude Medical Standard | 1.5 ± 0.3 | 1.7 ± 0.4 | 1.8 ± 0.4 | 2.0 ± 0.5 | 2.0 ± 0.5 | 6 |
| MCRI On-X* | 2.2 ± 0.9 | 2.2 ± 0.9 | 2.2 ± 0.9 | 2.2 ± 0.9 | 2.2 ± 0.9 | 6, 91, 94 |

Effective orifice area is expressed as mean values ($cm^2$) available in the literature. Further studies are needed to validate these reference values.
Adapted with permission of the American Heart Association from Pibarot P, Dumesnil JG: Prosthetic heart valves: selection of the optimal prosthesis and long-term management. *Circulation* 119(7):1034-1048, 2009.
*The ON-X valve has just one size for 27- to 29-mm and 31- to 33-mm prostheses. In addition, the strut and leaflets are identical for all sizes (25- to 33-mm); only the size of the sewing cuff is different.

dividing the VTI of the transprosthetic flow by that of LVOT flow: DVI = $VTI_{PrMv}/VTI_{LVOT}$. These parameters can be helpful to screen for valve obstruction, particularly when the cross-sectional area of the LVOT cannot be obtained.[43]

The DVI is reduced (less than or equal to 0.3) in presence of prosthetic aortic valve stenosis (see Table 25-2), whereas it is increased (greater than or equal to 2.2 m/s) in presence of prosthetic mitral valve stenosis (see Table 25-3). In presence of significant prosthetic valve stenosis, the DVI is generally less than 0.25 in the case of aortic prostheses and greater than 2.5 in the case of mitral prostheses.

The main limitations of the DVI are that it does not distinguish obstruction due to PPM from obstruction due to intrinsic dysfunction, and it is dependent on the size of the LVOT. For a given stroke volume and prosthetic valve EOA, the DVI will indeed be lower in a patient with a small LVOT than in a patient with a large LVOT. Hence, the cutoff values presented earlier (see Tables 25-2 and 25-3) may yield to overestimation or underestimation of prosthetic valve stenosis in the subsets of patients who are at the smaller or larger end of the LVOT size spectrum, respectively. Nonetheless, the observation of significant changes (decrease in case of aortic prostheses and increase in the case of mitral prostheses) in the DVI during serial echocardiographic follow-up is useful to detect the occurrence of prosthetic valve dysfunction.

#### Energy Loss Index and Influence of Pressure Recovery

Doppler echocardiography estimates the maximum pressure drop through the prosthesis from the maximum velocity recorded at the tip of the valve leaflets. However, several studies have reported that Doppler may overestimate the gradient across mechanical or bioprosthetic aortic valves when compared to catheter measurement.[44,45] As blood flow velocity decelerates between the aortic valve and the ascending aorta, part of the kinetic energy is reconverted back to static energy (i.e., pressure) because of the phenomenon called pressure recovery, and hence the net gradient between the LV and the ascending aorta (i.e., the gradient measured by catheter) is less than the maximum pressure gradient measured by Doppler (see Fig. 25-5, *A*).[45-49] The extent of pressure recovery is determined by the ratio between the valve EOA and the cross-sectional area of the downstream chamber, that is, the ascending aorta in the case of prosthetic aortic valves. Hence, pressure recovery generally becomes clinically relevant in patients with smaller aortas—those with an diameter at the sinotubular junction that is 30 mm or less.[47,48] In these patients, it thus becomes appropriate to account for pressure recovery by using the simple formula proposed by Garcia and collleagues[46] to calculate the energy loss coefficient: ELC = $(EOA \times A_A/A_A - EOA)$, where $A_A$ is the cross-sectional area of the aorta measured about 1 cm downstream of the sinotubular junction. The energy loss coefficient should be indexed for body surface area (i.e., energy loss index) to account for the change in cardiac output related to body size. An energy loss index less than 0.55 to 0.6 $cm^2/m^2$ suggests a significant prosthetic valve stenosis or PPM.[46] Not accounting for pressure recovery in patients with small aortas (i.e., smaller than 30 mm) may cause overestimation of prosthetic valve stenosis and/or PPM by Doppler echocardiography and lead to unwarranted investigations or interventions. The pressure recovery is generally negligible in the case of mitral prostheses because the downstream chamber (i.e., the LV) is large relative to the EOA of the prosthesis.

Hence, significant pressure recovery may occur downstream of aortic valves regardless of their type (native, bioprosthetic, or mechanical). This phenomenon should not, however, be confused with the phenomenon of localized high gradient that is specific to bileaflet mechanical valves (see Figs. 25-5, *B*, and 25-6). A localized high gradient may indeed be recorded through the central orifice of bileaflet mechanical valves, and this phenomenon may yield to substantial overestimation of gradient regardless of the position (aortic or mitral) of the prosthesis. The prevalence and magnitude of this phenomenon is not fully understood but is probably related to prosthetic valve size and design (ratio of the size of the central orifice to that of lateral orifices) and flow conditions.[42,49]

## RECOGNITION AND QUANTITATION OF PROSTHETIC VALVE REGURGITATION

The approach to detecting and grading prosthesis regurgitation is similar to that of native valves and involves multiple color Doppler views and measurements of several Doppler-echocardiographic indices.[50] However, care is needed to separate physiologic from pathologic prosthesis regurgitation. Mechanical prostheses indeed have a normal regurgitant volume known as leakage backflow. This "built-in" regurgitation theoretically prevents blood stasis and thrombus formation using a washing effect. As opposed to the pathologic regurgitant jets, the normal leakage backflow jets are characterized by being short in duration, narrow, and symmetric (see Fig. 25-3). In the case of pathologic regurgitation, it is also important to localize the origin of the regurgitant jet(s) in order to distinguish paravalvular from transvalvular regurgitation.

### *Prosthetic Aortic Valve Regurgitation*

#### Imaging Considerations

TTE generally provides a good visualization of the LV outflow tract and of both transvalvular and paravalvular prosthetic aortic regurgitation. Acoustic shadowing and occulting of regurgitant jets is less an issue for aortic prostheses than for mitral prostheses (Fig. 25-10).[35] The optimal views for the detection of prosthetic aortic valve regurgitant jets include the parasternal long-axis and short-axis views, the apical long-axis view, and the five-chamber view. Off-axis views may be helpful in determining the origin of the jets. Meticulous color flow Doppler interrogation should be performed in the parasternal long-axis view to localize and define the extent of a paravalvular leak. However, regurgitant jets may be occulted by acoustic shadowing, especially in the noncoronary sinus region.

TEE may be useful to identify the origin (paravalvular vs. transvalvular) of the regurgitant jets in technically difficult TTE studies and to identify the mechanism of regurgitation and the associated complications, such as flail bioprosthetic cusp; presence of pannus, thrombus, vegetations, or masses interacting with occluder closure; abscess formation; or prosthesis dehiscence (Figs. 25-11 and 25-12).[36] The long-axis view is useful for measuring LVOT diameter and jet width. Acoustic shadowing in the anterior region may limit the performance of TEE for evaluation of prosthetic aortic regurgitation at the midesophageal level. Importantly, the presence of a concomitant mitral prosthesis will cause significant shadowing and obscure the LVOT. In such cases it is crucial to evaluate the prosthesis from transgastric transducer positions.

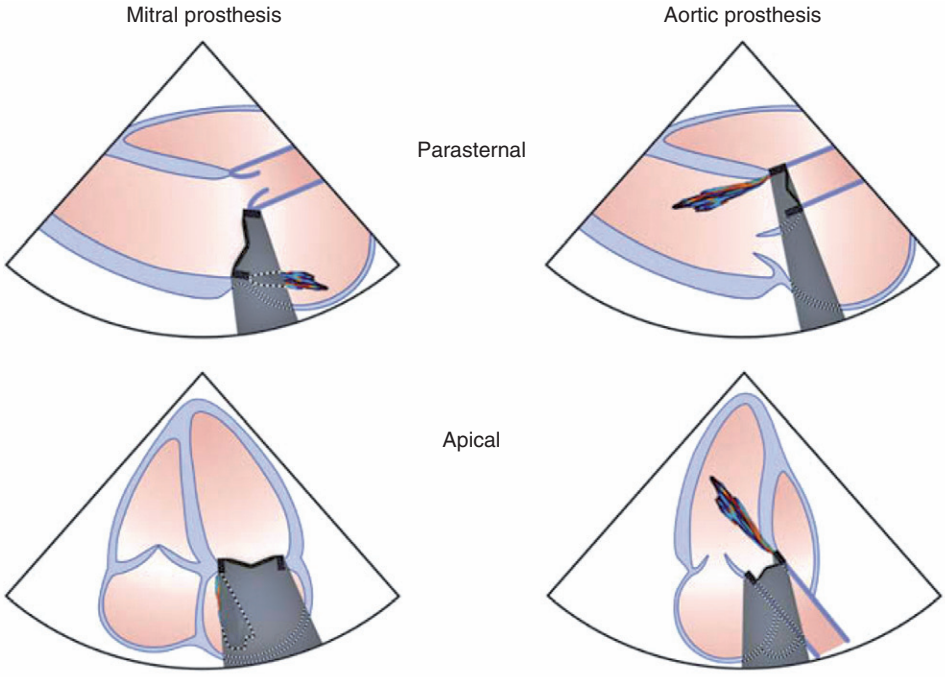



**Figure 25-10 Effect of position of mechanical prosthetic valve and of echocardiographic imaging view on shadowing and masking of regurgitation jet by Doppler.** Greater effect from TTE imaging is seen on prostheses in the mitral position compared to the aortic position. *(Reproduced with permission of the American Society of Echocardiography from Zoghbi WA, Chambers JB, Dumesnil JG, et al: Recommendations for evaluation of prosthetic valves with echocardiography and Doppler ultrasound: a report from the American Society of Echocardiography's Guidelines and Standards Committee and the Task Force on Prosthetic Valves.* J Am Soc Echocardiogr *22[9]:975-1014, 2009.)*

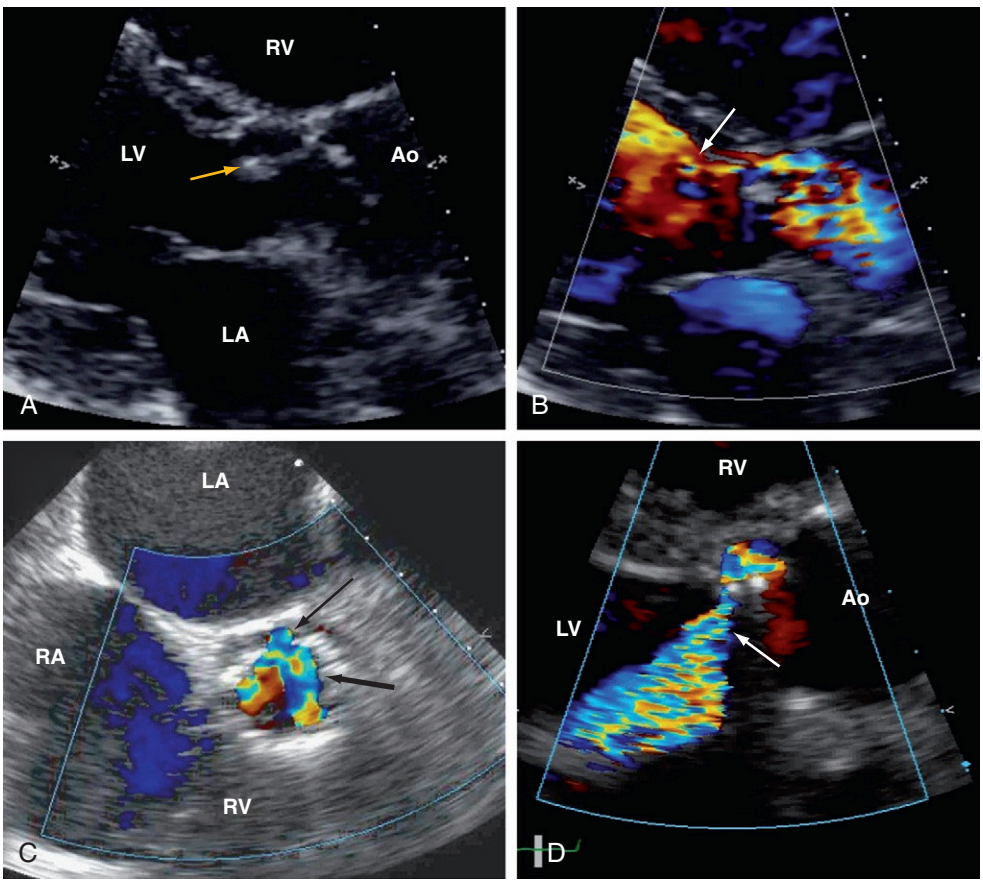



**Figure 25-11 Color Doppler images of transvalvular and paravalvular regurgitation.** The *white* or *black arrows* indicate the regurgitant jet(s). Avulsed cusp (*yellow arrow*, **A**) and resulting transvalvular regurgitant jet (*white arrow*, **B**) in an aortic bioprosthetic valve. **C,** TEE view of severe transvalvular regurgitation (*thick black arrow*; one of the cusps is blocked in open position) and mild paravalvular regurgitation (*thin black arrow*) in a transcatheter bioprosthetic aortic valve. **D,** Moderate paravalvular eccentric regurgitant jet in a stented bioprosthetic aortic valve. *Ao*, Aorta. (***A*** *and* ***B,*** *Courtesy Dr. Bibiana Cujec, Mazankowski Heart Institute, Edmonton, Alberta, Canada;* ***D,*** *courtesy Dr. John Chambers, Guy's and St Thomas Hospitals, London.)*

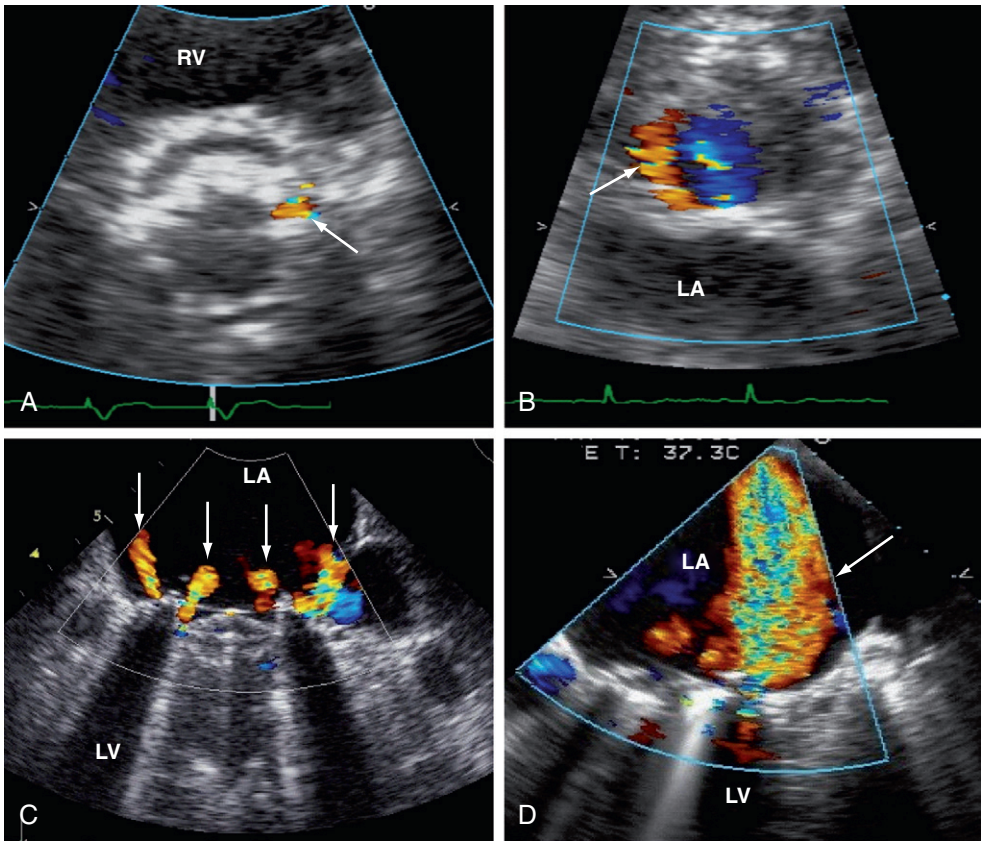



**Figure 25-12 Color Doppler images of transvalvular and paravalvular regurgitation.** Mild (less than 10% of circumference; **A**) and severe (more than 20% of circumference; **B**) paravalvular regurgitation in bioprosthetic aortic valves. **C,** Mild paravalvular regurgitant jets (*arrows*) and normal physiological regurgitant jets (*arrows*) in a mitral bileaflet mechanical valve. **D,** Severe paravalvular regurgitation (*arrow*) in mitral bileaflet mechanical valves. (***C*** *and* ***D,*** *Courtesy Dr. Arsène Basmadjan, Montreal Heart Institute, Montreal, Canada.)*

### Parameters of the Severity of Prosthetic Aortic Valve Regurgitation

The same principles and methods used for grading severity of native aortic valve regurgitation[50] can be used for prosthetic aortic regurgitation. It must be remembered, however, that there are very limited data on the application and validation of quantitative parameters such as the width of the regurgitant jet or of the vena contracta, the effective regurgitant orifice area, and the regurgitant volume in the context of prosthetic valves.[51,52] Given that all parameters of aortic regurgitation have important limitations and may be subject to measurement errors, a comprehensive, multiparametric approach is highly recommended (Table 25-6).

**Color Doppler parameters.** The ratios of regurgitant jet diameter to LVOT diameter from the parasternal long-axis view and of jet area to LVOT area from the parasternal short-axis view just below the prosthesis can be used to estimate the severity of central regurgitation. A ratio of jet diameter to LVOT diameter greater than 25% suggests moderate regurgitation and >65%, severe regurgitation (see Table 25-6). However, using this approach, regurgitation severity may be overestimated in the case of eccentric or crescent-shaped jets and underestimated in the case of jets impinging the wall of the LVOT or of anterior mitral valve (see Fig. 25-11, *B*, *D*). In contrast to native valves, the width of the vena contracta may be difficult to accurately measure in the long-axis view because of the shadowing caused by the prosthesis ring or stent.

For semiquantitative evaluation of the severity of paravalvular regurgitation, careful imaging of the neck of the jet in a short-axis view, at the level of the prosthesis sewing ring (surgically implanted prostheses) or stent (transcatheter bioprostheses), allows determination of the circumferential extent of regurgitation in the case of paravalvular regurgitation. A regurgitant jet occupying less than 10% of the sewing ring or stent circumference suggests mild, 10% to 20% suggests moderate, and more than 20% suggests severe regurgitation (see Table 25-6 and Fig. 25-12, *A*, *B*).[33,35] Rocking of the prosthesis is usually associated with greater than 40% dehiscence.[53]

The entrainment of the regurgitant (paravalvular or transvalvular) jet in the LVOT may lead to rapid broadening of the jet just after the vena contracta and thus to overestimation of regurgitant severity when using color Doppler parameters. Moreover, the estimation of regurgitation severity becomes more complex and less reliable when multiple jets are present. TEE may be helpful to better identify the origin (paravalvular vs. transvalvular) of the regurgitant jets and to better estimate the circumferential extent of paravalvular regurgitation.

**Spectral Doppler parameters.** Spectral Doppler parameters are useful to assess prosthetic aortic valve regurgitation because they are less sensitive to the prosthesis position and the associated shadowing and artifacts. The pressure half-time of the CW regurgitant jet signal is useful when the value is less than 200 ms, suggesting severe regurgitation, or greater than 500 ms, consistent with mild regurgitation (see Table 25-6). However,

**TABLE 25-6 Doppler-Echocardiographic Criteria for Severity of Prosthetic Aortic Valve Regurgitation (Central and Paravalvular)**

| | *Mild* | *Moderate* | *Severe* |
|---|---|---|---|
| **Valve Structure and Motion** | | | |
| Mechanical or bioprosthesis | Usually normal | Usually abnormal* | Usually abnormal* |
| **Doppler Parameters (Qualitative or Semiquantitative)** | | | |
| Jet width in central jets (%LVOT diameter): color Doppler† | Narrow (≤25) | Intermediate (26-64) | Large (>65) |
| Jet density: CW Doppler | Incomplete or faint | Dense | Dense |
| Jet deceleration rate (PHT, ms): CW Doppler‡ | Slow (>500) | Variable (200-500) | Steep (<200) |
| LV outflow vs. RV outflow Ratio: PW Doppler (ratio of stroke volumes or velocity-time integrals) | Slightly increased (>1.2) | Intermediate (>1.5) | Greatly increased (>1.8) |
| Diastolic flow reversal in the ascending aorta: PW Doppler | Absent or brief early diastolic | Intermediate | Prominent holodiastolic (end-diastolic velocity >18 cm/s) |
| Circumferential extent of paravalvular regurgitation (%)§ | <10 | 10-20 | >20 |
| **Doppler Parameters (Quantitative)** | | | |
| Vena contracta width (mm)† | <3 | 3-6 | >6 |
| Regurgitant volume (mL/beat) | <30 | 30-59 | ≥60 |
| Regurgitant fraction (%) | <30 | 30-49 | ≥50 |
| **Indirect Signs** | | | |
| LV size‖ | Normal | Normal/mildly dilated | Dilated |

Adapted in part from Zoghbi WA, Chambers JB, Dumesnil JG, et al: Recommendations for evaluation of prosthetic valves with echocardiography and Doppler ultrasound: a report from the American Society of Echocardiography's Guidelines and Standards Committee and the Task Force on Prosthetic Valves. *J Am Soc Echocardiogr* 22(9):975-1014, 2009, with permission of American Society of Echocardiography.

*PHT*, Pressure half time.

*Abnormal mechanical valves: immobile occluder, dehiscence or rocking (paravalvular regurgitation); abnormal biologic valves: leaflet thickening/calcification or prolapse, dehiscence or rocking (paravalvular regurgitation).

†Parameter applicable to central jets and is less accurate in eccentric jets.

‡This parameter is influenced by LV compliance.

§Applies only to paravalvular regurgitation.

‖Applies to chronic, late postoperative prosthetic aortic valve regurgitation in the absence of other etiologies.

intermediate values of pressure half-time (200 to 500 ms) are less specific because they are influenced by other variables such as heart rate and LV compliance. Proper care should also be given to obtaining a good-quality Doppler spectral envelope, which may not always be possible and might lead to gross over- or underestimations of in the case of frankly eccentric jets. The presence of holodiastolic flow reversal in the descending thoracic aorta is indicative of at least moderate AR; severe AR is suspected when the VTI of the reverse flow approximates that of the forward flow and when the end-diastolic velocity is greater than 18 cm/s.[54]

Regurgitant volume can be calculated as the difference between stroke volume at the LVOT (or 2D-derived total LV stroke volume) and the transmitral or pulmonary flow. Cutoff values for severity are similar to those for native aortic valve regurgitation.[50] The quantitative method based on proximal isovelocity surface area is difficult to apply to aortic prostheses. The ratio of the stroke volume measured in the LVOT to the stroke volume measured in the RV outflow tract (RVOT) may be helpful to assess aortic regurgitation severity (see Table 25-6). Given that the RVOT diameter is often difficult to measure, the ratio of the LVOT VTI to the RVOT VTI can be used alternatively, provided no dilation of LVOT or RVOT exist.

### Integrative, Multiparametric Approach for the Evaluation of Prosthetic Aortic Valve Regurgitation

Assessment of severity of prosthetic aortic valve regurgitation is generally much more complex than in native valves because of the high prevalence of paravalvular regurgitation and eccentric jets (see Figs. 25-11 and 25-12). The process of grading regurgitation severity should be comprehensive, integrative, and based on a multiparametric approach that includes the qualitative and semiquantitative parameters shown in Table 25-6. If the regurgitation is classified as mild or less using these parameters, no further measurement is needed. On the other hand, if there are parameters suggestive of more than mild AR and the quality of the data enables quantitation, it is recommended to measure quantitative parameters of regurgitation, including the vena contracta width, and the regurgitant volume and fraction. When the different parameters are concordant, it is easy to confirm the severity of the regurgitation. However, when there are discordances among the different parameters, one must look carefully for physiologic or technical reasons to explain these discrepancies and to rely on the parameters that have the best quality in terms of image/signal and that are the more accurate and reliable in the context of prosthetic valves. Importantly, one must also examine the indirect signs of prosthetic valve dysfunction (see later discussion under Indirect Signs and Consequences of Prosthetic Valve Regurgitation). Hence, in presence of severe chronic prosthetic valve regurgitation, one would expect to see a dilated LV.

## *Prosthetic Mitral Valve Regurgitation*

### Imaging Considerations

Assessment of prosthetic mitral regurgitation by TTE is problematic because the LA is largely occulted by the acoustic shadowing due to the metallic components of the prosthesis (see Fig. 25-10 and Clinical Case 25-2).[35] This problem is more frequent in mechanical valves than in bioprosthetic valves. In contrast, TEE provides excellent visualization of the LA and mitral regurgitant jet, but acoustic shadowing limits visualization of the LV. Thus, a comprehensive assessment of prosthetic mitral valve function often requires both TTE and TEE when valve dysfunction is suspected.

At TTE examination, the presence of "occult" mitral prosthesis regurgitation should be suspected when the following signs are present: presence of flow convergence on the LV side of the prosthesis during systole; increased mitral peak E wave velocity (greater than 2 m/s) and/or mean gradient (greater than 6 mm Hg); DVI greater than 2.2; unexplained or new worsening of pulmonary arterial hypertension; and a dilated and hyperkinetic LV (Table 25-7).[43] TEE should be systematically performed when there is a clinical or TTE suspicion of pathologic mitral regurgitation.[36] TEE is indeed superior to TTE in detecting prosthetic mitral regurgitation and determining its localization and mechanism.[55,56] On color Doppler, paravalvular leaks have a typical appearance of a jet that passes from the LV into the LA outside the prosthesis ring and often projects into the atrium in an eccentric direction (see Figs. 25-11 and 25-12).

**TABLE 25-7 Doppler-Echocardiographic Criteria for Severity of Prosthetic Mitral Valve Regurgitation (Central and Paravalvular)**

| | *Mild* | *Moderate* | *Severe* |
|---|---|---|---|
| **Valve Structure and Motion** | | | |
| Mechanical or bioprosthesis | Usually normal | Usually abnormal* | Usually abnormal* |
| **Doppler Parameters (Qualitative or Semiquantitative)** | | | |
| Color flow jet area | Small, central jet (usually <4 $cm^2$ or <20% of LA area) | Variable | Large central jet (usually >8 $cm^2$ or >40% of LA area) or variable size wall impinging jet swirling in LA |
| Flow convergence | None or minimal | Intermediate | Large |
| Jet density: CW Doppler | Incomplete or faint | Dense | Dense |
| Jet contour: CW Doppler† | Parabolic | Usually parabolic | Early peaking, triangular |
| Pulmonary venous flow: PW Doppler | Systolic dominance | Systolic blunting | Systolic flow reversal |
| Doppler velocity index: PW Doppler | <2.2 | 2.2-2.5 | >2.5 |
| **Doppler Parameters (Quantitative)** | | | |
| Vena contracta width (mm)‡ | <3 | 3-6 | >6 |
| Regurgitant volume (mL/beat) | <30 | 30-59 | ≥60 |
| Regurgitant fraction (%) | <30 | 30-49 | ≥50 |
| Effective regurgitant orifice area ($mm^2$) | <20 | 20-39 | ≥40 |
| **Indirect Signs** | | | |
| LV size§ | Normal | Normal/mildly dilated | Dilated |
| LA size | Normal | Normal/mildly dilated | Dilated |
| Pulmonary hypertension (SPAP ≥50 mm Hg at rest and ≥60 mm Hg at exercise) | Generally absent | Variable | Generally present |

Adapted in part from Zoghbi WA, Chambers JB, Dumesnil JG, et al: Recommendations for evaluation of prosthetic valves with echocardiography and Doppler ultrasound: a report from the American Society of Echocardiography's Guidelines and Standards Committee and the Task Force on Prosthetic Valves. *J Am Soc Echocardiogr* 22(9):975-1014, 2009, with permission of American Society of Echocardiography.

*Abnormal mechanical valves: immobile occluder, dehiscence or rocking (paravalvular regurgitation); abnormal biologic valves: leaflet thickening/calcification or prolapse, dehiscence or rocking (paravalvular regurgitation)

†This parameter is influenced by LV compliance.

‡Parameter applicable to central jets and is less accurate in eccentric jets.

§Applies to chronic, late postoperative prosthetic aortic valve regurgitation in the absence of other etiologies.

Multiple-plane examination is essential to determine the origin and extent of the regurgitant jet(s).

## Parameters of the Severity of Prosthetic Mitral Valve Regurgitation

Assessment of severity of prosthetic mitral regurgitation is complex because all quantitative parameters have important limitations and cannot be applied consistently in all patients. Hence, it is recommended to use a comprehensive approach that integrates the different findings and parameters obtained by TTE and TEE (see Table 25-7).

The estimation of regurgitant jet area in the LA is often difficult due to the shadowing and artifacts created by the prosthesis. A small thin jet (jet area less than 4 $cm^2$, less than 20% of the LA) usually reflects mild mitral regurgitation but can be grossly underestimated and should not be used to exclude severe regurgitation, whereas a large, wide jet (8 $cm^2$ or larger, more than 40% of the LA) is most often consistent with severe regurgitation.[35] A width of the vena contracta of less than 3, 3 to 6, and greater than 6 mm denotes mild, moderate, and severe regurgitation, respectively (see Table 25-7).[52] Significant swirling of the jet within the atrium as well as the presence of retrograde systolic flow in one or more of the pulmonary veins is specific for significant mitral regurgitation. TEE is superior to TTE to record the pulmonary venous flow in presence of a mitral prosthesis. The density and contour of the regurgitant jet CW Doppler signal may also be helpful to corroborate regurgitation severity (see Table 25-7).

The radius of the proximal flow convergence (i.e., proximal isovelocity surface area method) can be used in combination with recordings of mitral regurgitation velocity by CW Doppler to estimate effective regurgitant orifice area.[50,57] However, because mitral prosthetic regurgitation is often characterized by eccentric and/or multiple jets, the proximal isovelocity surface area method is difficult to achieve and may grossly under- or overestimate regurgitation severity. Given these important limitations, the volumetric method is often preferred to the proximal isovelocity surface area method for quantitation of mitral prosthesis regurgitation.[35] The calculation of regurgitant stroke volume consists in subtracting the LVOT stroke volume from the total LV stroke volume derived by 2D echocardiography. Total LV stroke volume may be obtained by the Simpson method. However, this method often underestimates the LV volumes and the LV stroke volume. Hence, one can alternatively estimate the total stroke volume by multiplying the LV ejection fraction calculated by the Simpson method by the LV end-diastolic volume obtained by the Teichholz formula (i.e., Dumesnil's method in reverse).[58] Three-dimensional (3D) echocardiography may also enhance the accuracy of the estimation of total LV stroke volume, especially when combined with enhancement of endocardial border with a contrast agent.[59] A LV ejection fraction above 60% with normal-sized or enlarged LV, along with a reduction of LVOT stroke volume, should raise the possibility that the mitral regurgitation is significant. Again, in light of the important challenges and limitations posed by quantitation of prosthetic mitral regurgitation, one should always have a comprehensive, multiparametric, and integrative approach (see Table 25-7).

### *Indirect Signs and Consequences of Prosthetic Valve Regurgitation*

The size and function of the LV and atrial chambers as well as the level of systolic pulmonary arterial pressure can be used to corroborate severity of prosthesis dysfunction and especially of prosthetic valve regurgitation. In particular, these measurements can be compared to previous measurements and are often the first sign to alert attention when the regurgitation is difficult to visualize. Although LV dilation is expected in the presence of hemodynamically significant prosthetic aortic or mitral valve regurgitation, LV volumes may also reflect the preoperative state, especially in cases of early postoperative prosthetic regurgitation. However, if LV volumes fail to decrease after valve replacement for aortic or mitral regurgitation or tend to increase after valve replacement for aortic or mitral stenosis, and in particular if the LV is hyperdynamic, a hemodynamically significant leak should be suspected among other factors. On the other hand, in the context of chronic aortic or mitral prosthesis regurgitation, the absence of dilation of LV and atrial chambers during follow-up is rather suggestive of a nonsignificant leak.

## ROLE OF STRESS ECHOCARDIOGRAPHY

Because normally and abnormally functioning prostheses can produce similar gradients at rest by TTE, stress echocardiography may be valuable in confirming or excluding the presence of hemodynamically significant prosthetic valve stenosis or PPM, especially when there is discordance between the patient's symptomatic status and the prosthetic valve hemodynamics measured at rest.[60-66] As opposed to normally functioning and well-matched prostheses or to bileaflet mechanical valves with localized high gradient, the presence of valve stenosis or significant PPM is generally associated with a marked increase in gradients and pulmonary arterial pressure, the occurrence of symptoms, and an impaired exercise capacity on stress exercise echocardiography.[60] In light of studies performed in the context of native or prosthetic valves, an absolute increase in mean gradient of at least 20 mm Hg in the aortic position and at least 12 mm Hg in the mitral position suggests severe prosthesis dysfunction or PPM.[61-69] A peak stress systolic pulmonary arterial pressure of 60 mm Hg or greater is consistent with the presence of a hemodynamically significant mitral prosthesis stenosis or regurgitation or mitral PPM.[60,61,69] Exercise testing is also useful to unmask symptoms in a significant proportion of patients with prosthetic valve dysfunction or PPM who claim to be asymptomatic.

## SPECIFIC CONSIDERATIONS FOR PARTICULAR TYPES OF VALVE SUBSTITUTES

### *Stentless Aortic Valve Substitutes*

Stentless substitutes include stentless bioprostheses, aortic homografts, and pulmonary autografts (the Ross operation). These substitutes are more likely than stented valves to have minor transvalvular regurgitant jets. In the early postoperative period, the stentless bioprostheses, particularly if implanted by the subcoronary technique, may exhibit higher than expected gradients, which often regress within the next 3 months, most likely because of regression of the edema between the prosthesis and the aortic wall and/or remodeling of the LVOT. In the late postoperative follow-up, the stentless substitutes are more likely than stented bioprostheses or mechanical valves to develop "functional" central aortic insufficiency due to dilation of the aortic root. This aspect thus needs particular attention, and it is recommended to regularly (i.e., every 2 years) measure the dimensions of the aortic root (annulus, sinus, and sinotubular junction levels) and ascending aorta, especially the diameter at the sinotubular junction. If dilation of the aorta and/or aortic insufficiency develops, closer follow-up is recommended.

### *Transcatheter Aortic Valves*

#### Valve Sizing and Positioning

In patients undergoing transcatheter aortic valve implantation, intraoperative TEE is particularly helpful (1) to accurately measure the aortic annulus size that is crucial to select the valve size, (2) to complement fluoroscopic imaging for positioning of the valve before deployment, and (3) to rapidly identify complications. The size of the transcatheter prostheses is selected according to the pre- or intraprocedural measurement of the aortic annulus diameter by TEE using a midesophageal long-axis view. The same view is used for valve positioning. The objective is to align the ventricular end of the valve prosthesis stent with the hinge point of the anterior leaflet of the mitral valve (Fig. 25-13).[70,71] Real-time 3D TEE may further facilitate valve positioning. Some investigators primarily use TEE instead of fluoroscopy to guide valve positioning and implantation in order to reduce the amount of contrast agent and thereby preserve kidney function.[70]

#### Late Postoperative Follow-up

One could use the same principles as for surgical prostheses. In particular, for the measurement of valve EOA, the LVOT diameter and velocity should be measured just underneath the stent (see Fig. 25-8, *B*). However, if the ventricular end of the stent sits too low in the LVOT, which may occur more frequently with self-expandable prostheses (such as the CoreValve), it may be preferable to measure the LVOT diameter and velocity within the proximal portion of the stent at approximately 5 to 10 mm below the bioprosthetic valve leaflets. As with surgical prostheses, the observation of significant changes in gradient, DVI, and EOA during serial evaluations as well as the comparison of the valve EOA measured by Doppler echocardiography during follow-up to the normal reference value may be useful to identify and quantify prosthetic valve stenosis (see Table 25-2). However, in the case of transcatheter valves, the normal reference EOA does not depend only on the model and label size of the prosthesis. It also depends on the size of the patient's aortic annulus, as this is the main factor limiting the expansion of the valve at implantation. It is too early to determine what will be the durability of the transcatheter valves. Gurvitch and co-workers[72] reported a slight deterioration of EOAs and gradients at 3-year follow-up. The severity of paravalvular regurgitations appears to remain stable during follow-up.

### *Prosthetic Pulmonary and Tricuspid Valves*

#### Prosthetic Tricuspid Valve

The tricuspid prosthesis flow velocities vary not only with the duration of the cycle but also with respiration. A minimum of five cardiac cycles should thus be averaged for the estimation of the Doppler-echocardiographic indices, whether the patient is in sinus rhythm or in atrial fibrillation. Prosthetic tricuspid valve stenosis should be suspected when prosthetic valve leaflet morphology and mobility are abnormal, peak velocity is greater

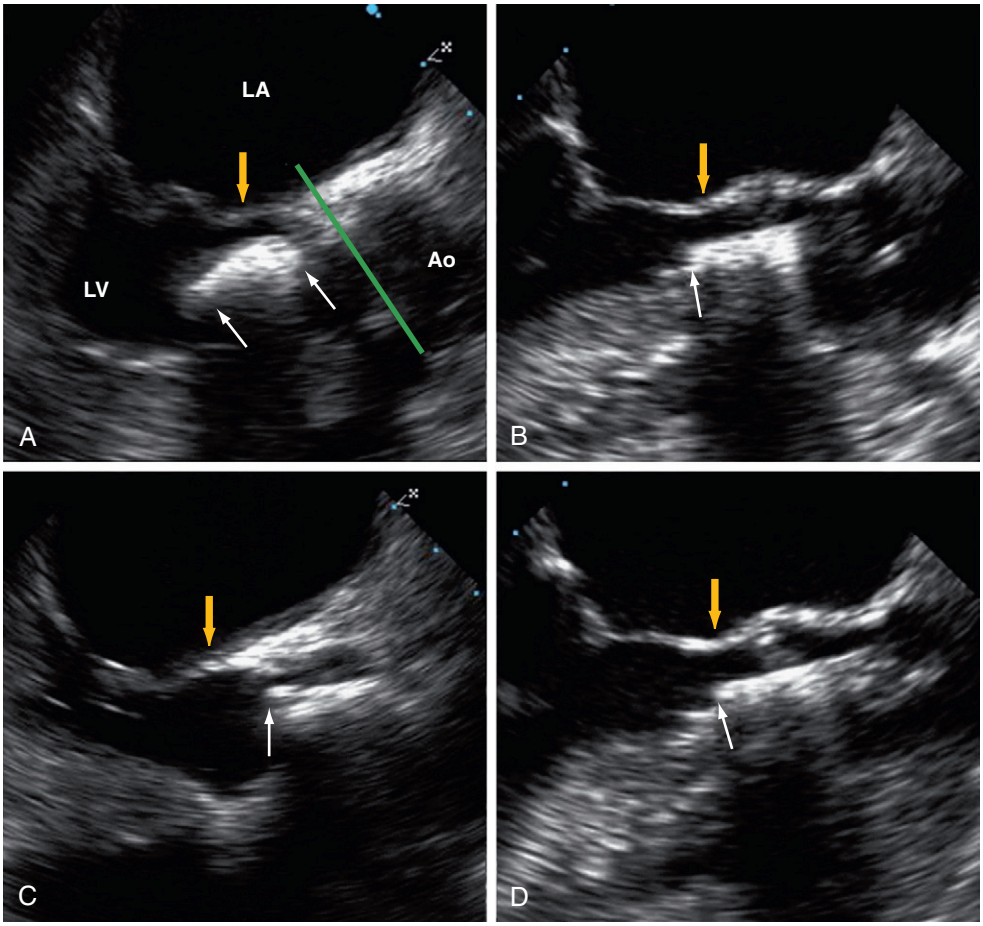



**Figure 25-13 Utility of TEE for positioning of transcatheter bioprosthetic aortic valves. A,** Prosthetic valve in the LV cavity showing the ventricular and aortic ends of the stent containing the valve (*white arrows*); *yellow arrow*, hinge point of the anterior mitral leaflet; *green line*, aortic annulus. **B,** "Too low" (ventricular) positioning of valve, (**C**) "too high" (aortic) positioning of valve, and (**D**) adequate positioning of valve, all using hinge point of anterior mitral leaflet (*yellow arrows*) as landmark for the ventricular end of the valve (*white arrows*). *Ao*, Aorta. *(Reproduced with permission of American College of Cardiology from Bagur R, Rodés-Cabau J, Doyle D, et al: Usefulness of TEE as the primary imaging technique to guide transcatheter transapical aortic valve implantation.* J Am Coll Cardiol *4[2]:115-124, 2011.)*

than 1.7 m/s, mean gradient is 6 mm Hg or greater, and/or pressure half-time is at least 230 ms.[35] The criteria for assessing severity of prosthetic tricuspid regurgitation are similar to those for native tricuspid valves.[35,50] TEE should be considered for all patients with clinical and/or TTE evidence of tricuspid prosthesis obstruction or regurgitation.

### Prosthetic Pulmonary Valve

Findings suspicious of prosthetic pulmonary valve stenosis include leaflet thickening or immobility, narrowing of forward color flow map, transvalvular peak velocity greater than 3 m/s for a prosthesis or greater than 2 m/s for a homograft, increase in peak velocity on serial studies, impaired RV function, or elevated RV systolic pressure. The severity of pulmonary prosthetic valve regurgitation is usually subjectively graded, using an integrative approach similar to native pulmonary regurgitation.[35,50]

## Interpretation of Doppler-Echocardiographic Data

### INTERPRETATION OF HIGH TRANSPROSTHETIC GRADIENTS

It is relatively frequent to measure a high gradient across a prosthetic valve and the differential diagnosis is much more complex than for native valves (see Clinical Cases 25-1, 25-2, and 25-3). Indeed, there are several potential causes of an elevated transprosthetic gradient. PPM is the most frequent cause of high gradient after valve replacement, the other potential causes being a central jet artifact in bileaflet prostheses, intrinsic valve dysfunction, high flow states, or technical errors.[35,42] Various algorithms aimed at better interpreting these high gradients have previously been proposed in the guidelines as well as by various authors including ourselves.[35,42,73] However, the acceptance of these algorithms by clinicians has varied, and they have been criticized for being either too complicated for routine clinical use or too simplistic to cover all possibilities. In a recent paper,[74] we thus proposed another alternative that is something of a compendium of previous algorithms and that can, we hope, answer both criticisms (Figs. 25-14 and 25-15).

#### *Prosthetic Aortic Valves*

After having excluded possible technical errors and given that PPM is the most frequent cause of high transprosthetic gradients after aortic valve replacement, the first step in the algorithm (see Fig. 25-14 and Clinical Case 25-1) would be to simply calculate the projected indexed EOA, that is, the ratio of EOA to body surface area, using the normal reference value of EOA for the type and size of prosthesis having been implanted (see Table 25-4). If the result is less than 0.85 $cm^2/m^2$, one can then surmise that PPM is present and that, depending on its degree of severity (see Table 25-1), it may be partially or totally responsible for the high gradient. In this context, it is important to keep in mind that both phenomena, PPM and intrinsic

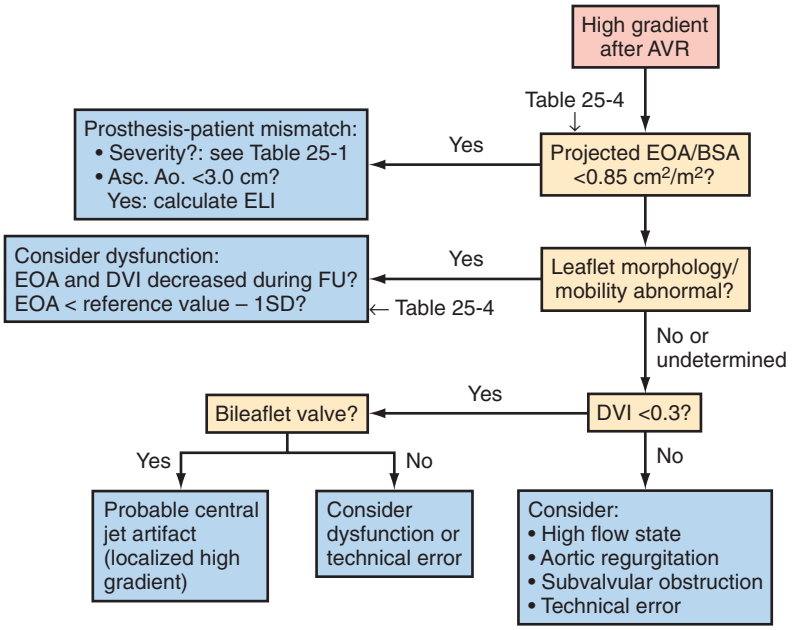



**Figure 25-14** Algorithm for interpreting abnormally high transprosthetic pressure gradients after aortic valve replacement (*AVR*). *BSA*, Body surface area; *DVI*, Doppler velocity index; *ELI*, energy loss index; *EOA*, effective orifice area; *FU*, follow-up; *SD*, standard deviation. *(Adapted from Dumesnil JG, Pibarot P: Prosthesis-patient mismatch: an update.* Curr Cardiol Rep *13[3]:250-257, 2011.)*

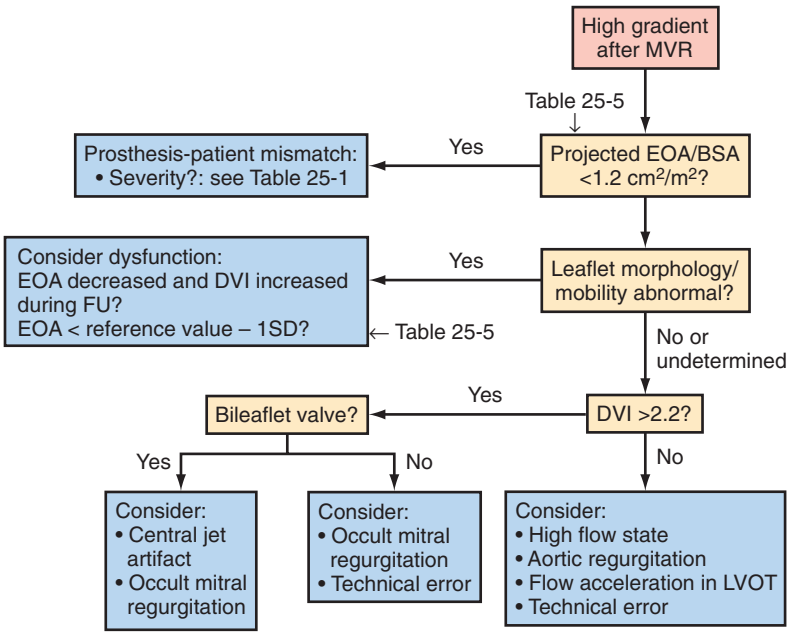



**Figure 25-15** Algorithm for interpreting abnormally high transprosthetic pressure gradients after mitral valve replacement (*MVR*). *BSA*, Body surface area; *DVI*, Doppler velocity index; *ELI*, energy loss index; *EOA*, effective orifice area; *FU*, follow-up; *SD*, standard deviation.

dysfunction, may coexist. To fully appreciate the clinical impact of the gradient, it should also be remembered that the net gradient is less in patients with a small aortic diameter (less than 3.0 cm) because of pressure recovery, and it might be useful in such cases to calculate the energy loss index.[46]

If PPM is not present or is not severe enough to totally explain the increased gradient, the next crucial step would be to thoroughly evaluate leaflet morphology and mobility. In the case of mechanical valves, TTE and even TEE often do not allow adequate visualization of leaflet(s) motion, and cinefluoroscopy should be performed in addition to echocardiography (see Fig. 25-14). If leaflet mobility is abnormal (see Fig. 25-4), dysfunction should be suspected. This can be corroborated if the EOA actually measured by echocardiography is much lower than the normal reference value for the same type and size of prosthesis (see Table 25-4) and/or has decreased progressively during follow-up. If, on the other hand, there is still uncertainty with regard to possible abnormal leaflet mobility, one can then proceed to calculate the DVI. If the DVI is less than 0.30 and the prosthesis is a bileaflet valve with normal leaflet mobility, the high gradient is in all likelihood due to a central jet artifact, that is, a localized high jet velocity through the central orifice (see Fig. 25-5). On the other hand, if the valve is not bileaflet, intrinsic dysfunction should be reconsidered as discussed previously, and the possibility of a technical error should also be envisioned. Finally, if the DVI is 0.30 or greater, possible etiologies for the high gradient include high flow states, aortic regurgitation, subvalvular obstruction, and, again, a technical error.

It should be noted that technical errors, particularly with regard to measurements in the LV outflow tract diameter, are frequent, and that this possibility should never be neglected.

### *Prosthetic Mitral Valves*

A similar algorithm can be used when confronted to a high gradient or velocity across a mitral prosthesis (see Fig. 25-15 and Clinical Cases 25-2 and 25-3). It should, however, be noted that the cutoff values of indexed EOA and DVI are different from those used for aortic prostheses. In the last step of the algorithm, if the leaflet mobility is considered to be normal or is undetermined and the DVI is less than 2.2, one should also suspect occult mitral transvalvular or paravalvular regurgitation, and TEE should be performed. This situation may also be related to the recording of a localized high gradient within the central orifice in the case of bileaflet mechanical valves (see Figs. 25-5 and 25-6).

## SPECIAL CONSIDERATIONS FOR LOW–FLOW-STATE CONDITIONS

It should be remembered that in patients with low flow states due to LV dysfunction, transprosthetic gradients may be only slightly or moderately elevated despite the presence of significant PPM or prosthesis dysfunction.[20,42] Gradients are indeed highly flow dependent and may thus be "pseudonormalized" in the presence of low flow states. The measurement of a low gradient in concomitance with a small EOA (less than 1.2 $cm^2$ and/or less than reference minus one standard deviation) should prompt further evaluation. As for the management of low-flow, low-gradient native aortic or mitral stenosis, dobutamine stress echocardiography (DSE) may be useful to differentiate a true from a pseudostenosis or mismatch in patients with prosthetic valves and low cardiac output. In the situation of pseudostenosis/PPM, the resting transprosthetic flow rate and thus the force applied on the leaflets are too low to completely open the valve. On DSE, these patients nonetheless have a substantial increase in valve EOA and no or minimal elevation in gradients with increasing flow rate. On the other hand, true stenosis or PPM is associated with no or minimal increase in EOA, a marked increase in gradient, and most often the occurrence of indirect signs (LV dysfunction, marked elevation in pulmonary arterial pressure, etc.) and symptoms. It should, however, be considered that DSE does not allow for the distinction between prosthesis stenosis and PPM. For this purpose, one should apply the algorithm presented in Figures 25-14 and 25-15 to the EOA and DVI values obtained after normalization of cardiac output on stress echocardiography.

## SPECIAL CONSIDERATIONS FOR PERIOPERATIVE EVALUATION

The most frequent causes of prosthesis dysfunction in the perioperative period are prosthetic valve thrombosis, entrapment of a valve leaflet by preserved chordae in mitral mechanical prosthesis, or entrapment or perforation/tear of a prosthetic valve leaflet by a suture. In transcatheter bioprostheses, suboptimal deployment, malpositioning, or migration of the prosthesis stent may cause prosthetic valve stenosis or regurgitation.

Small paravalvular regurgitant jets are frequently (10% to 25% of cases) seen on intraoperative TEE before cardiopulmonary bypass weaning[30,75] and may significantly decrease or resolve after the injection of protamine or in the days, weeks, or months after valve replacement as the healing process evolves. Moderate or severe paravalvular regurgitation is rare (1% to 2%) following aortic or mitral valve replacement and requires returning to cardiopulmonary bypass for immediate correction.

Because of LV remodeling, relative high output states, and the frequent occurrence of tachycardia, hemodynamic assessment of the prosthetic valve done in the immediate postoperative period cannot be considered as definitive. Moreover, the echocardiograms are technically challenging because of the location of the various incisions, and the quality of the images is often suboptimal. The main objective of a perioperative echocardiogram is to detect the presence of paravalvular or transvalvular regurgitation and obtain accurate measurements of peak and mean gradients as well as the EOA and DVI, when feasible and reliable. Several pitfalls may be encountered when performing these measurements in the immediate postoperative period: (1) Poor-quality images may yield to erroneous measurement of LVOT diameter; (2) LVOT flow velocity may be abnormally increased by high cardiac output or dynamic obstruction from temporary remodeling of the LVOT, hypovolemia, and/or perioperative use of inotropes; or (3) the presence of perivalvular edema or hematoma in a stentless bioprosthesis implanted with the subcoronary technique may result in a lower than expected EOA and higher gradient during the first few months after operation.

For these reasons, the recording of relatively high gradients in the immediate postoperative period should not be viewed with undue concern. The first step is to assess the presence and severity of PPM by calculating the projected indexed EOA (see Figs. 25-14 and 25-15). This step does not require any Doppler-echocardiographic measurement and can thus be done irrespective of the image quality and the patient's hemodynamic condition. If PPM is present, it may explain, in part or in totality, the high transprosthetic gradient. If PPM is absent, several of the aforementioned conditions and technical pitfalls must first be ruled out before concluding that prosthesis dysfunction has occurred. In particular, one must first determine if the gradient is not partially or principally related to a high flow velocity in the LVOT. Relief of the valvular obstruction in patients operated for aortic stenosis may result in some remodeling and temporary narrowing of the LVOT. The administration of inotropic agents during weaning from cardiopulmonary bypass may also contribute to this phenomenon. Therefore, unless the transvalvular gradients are very high or are associated with abnormality of leaflet motion, significant symptoms, or deterioration in LV function, a conservative approach with observation and repeat assessment 3 to 6 months later is advocated.

# Utility of Doppler Echocardiography for Management of Specific Prosthetic Valve–Related Complications

## PROSTHETIC VALVE THROMBOSIS

If prosthetic valve thrombosis is suspected, echocardiography should be performed promptly and include TEE (see Clinical Case 25-2).[20] A comprehensive TTE is performed first, with particular attention directed at evaluation of leaflet mobility and valve hemodynamic function and identification of thrombus and/or pannus. In the rare case of massive prosthetic valve thrombosis with hemodynamic instability, TEE will not be

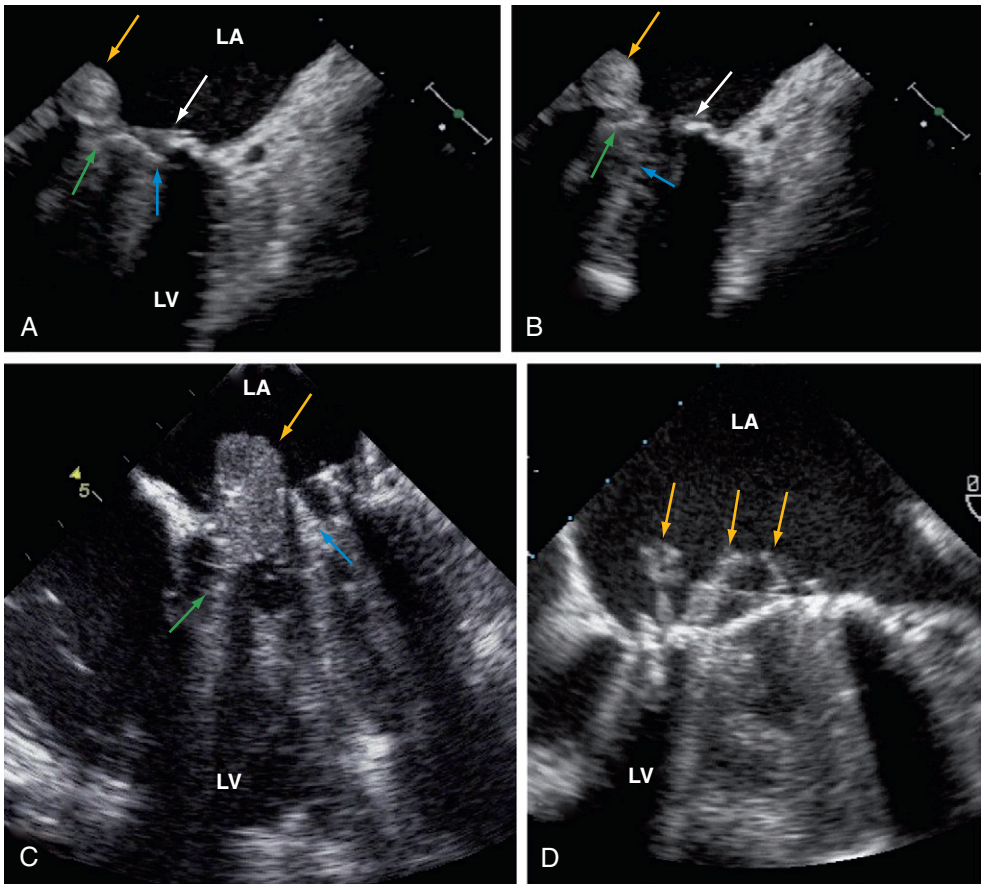



**Figure 25-16 Utility of TEE for diagnosis and treatment of prosthetic valve thrombosis.** Patient with obstructed mitral bileaflet mechanical valve in systole (**A**) and diastole (**B**). *Yellow arrow*: large thrombus; *white arrow*: pannus; *blue arrow*: mobile leaflet; *green arrow*: immobile leaflet. **C,** Mitral bileaflet mechanical valve obstructed by very large thrombus (*yellow arrow*). *Green arrow*: reverberation of immobile leaflet surrounded by thrombus; *blue arrow*: mobile leaflet with reverberation underneath. **D,** Multiple thrombi (*yellow arrows*) attached to mitral monoleaflet mechanical valve. (***A*** *and* ***B,*** *Courtesy Steven A. Goldstein, MD, Washington Hospital Center.* ***C*** *and* ***D,*** *Courtesy John Chambers, MD, Guy's and St. Thomas Hospitals, London.)*

needed, as this dramatic presentation constitutes a surgical emergency.[20] In most other cases, TEE will provide important incremental diagnostic information, which will also guide therapeutic management (Fig. 25-16; also see Clinical Case 25-2). TEE also has some limitations: aortic prostheses are more difficult to evaluate than mitral prostheses, and the ventricular side of a mitral prosthesis is more difficult to visualize than the atrial side.

Direct signs of prosthetic valve thrombosis include immobility or reduced leaflet mobility, and the presence of thrombus on either side of the prosthesis, with or without obstruction (see Fig. 25-4, *A*, and Fig. 25-16). It is important to differentiate thrombi from a fibrous pannus, which is usually annular in location and typically appears as a very dense immobile echo (see Fig. 25-16). Pannus formation is more frequent on aortic than on mitral prostheses and when observed on mitral prosthetic valves, they most often occur on the atrial side of the prosthesis (see Fig. 25-16, *A*, *B*). It is also important to differentiate small thrombi from strands or sutures. Strands are believed to be fibrin filaments, which appear as fine (1-mm), filamentous, mobile echoes of variable length (5 to 15 mm), most often observed on the atrial side of mitral prostheses.[20] Although the clinical relevance of these strands remains undetermined, there is no evidence that they are associated with an increased embolic risk.[20]

The most important factors to consider for therapeutic decision making (Fig. 25-17) are: (1) the presence of prosthetic valve obstruction; (2) the size and mobility of the thrombus; and (3) the clinical and hemodynamic condition of the patient.

In nonobstructive left-sided prosthetic valve thrombosis confirmed by TTE or TEE, first-line treatment consists of a short course of IV heparin with close echocardiographic follow-up plus adjustment of warfarin therapy and addition of aspirin (81 mg per day) (see Fig. 25-17).[20] However, if the medical treatment is unsuccessful, surgery should be considered in patients with large (length greater than 5 to 10 mm and/or area greater than 0.8 $cm^2$ as determined by TEE) or mobile thrombi. Thrombolysis with urokinase, streptokinase, or recombinant tissue plasminogen activator is recommended in other patients.[20,26,76] The presence of a large thrombus has been associated with a major increase in the risk of embolic complications following lytic treatment in the PRO-TEE registry.[77]

Urgent or emergent surgery (i.e., thrombectomy or valve replacement) is the treatment of choice in patients with obstructive valve thrombosis (see Fig. 25-17).[20] However, rescue thrombolysis should be considered in patients unlikely to survive surgery or when surgical treatment is unavailable and the patient cannot be transferred.[20,26,76] Thrombolysis may also be considered in patients with mild to moderate prosthetic valve

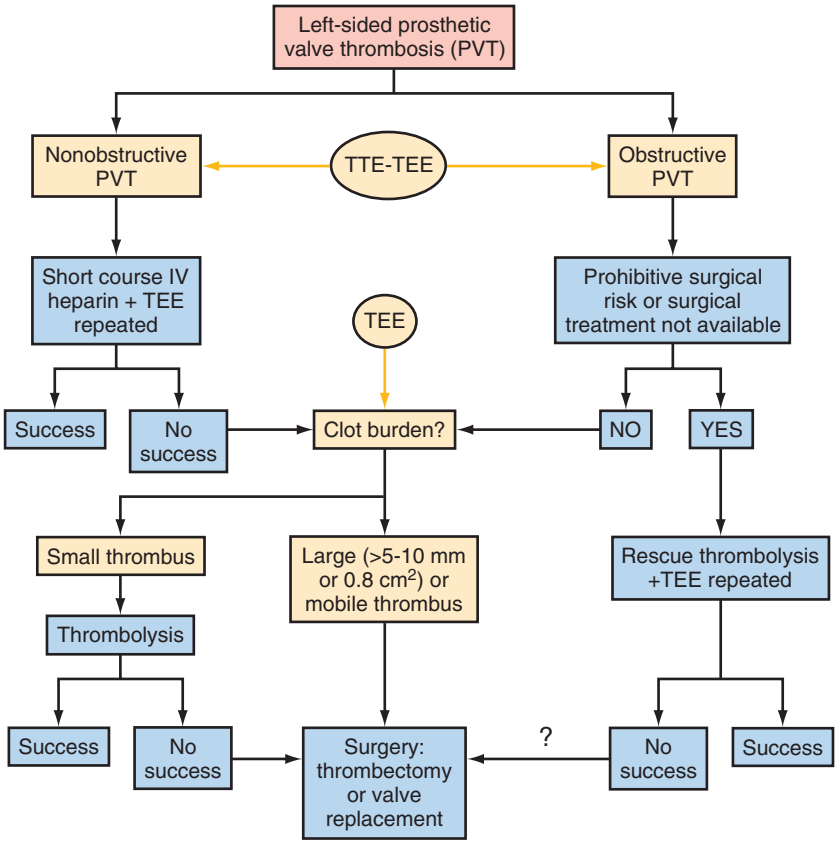



**Figure 25-17 Algorithm for the management of patients with left-sided prosthetic valve thrombosis (*PVT*).** *(Adapted with permission of American Heart Association from Pibarot P, Dumesnil JG: Prosthetic heart valves: selection of the optimal prosthesis and long-term management.* Circulation *119[7]:1034-1048, 2009.)*

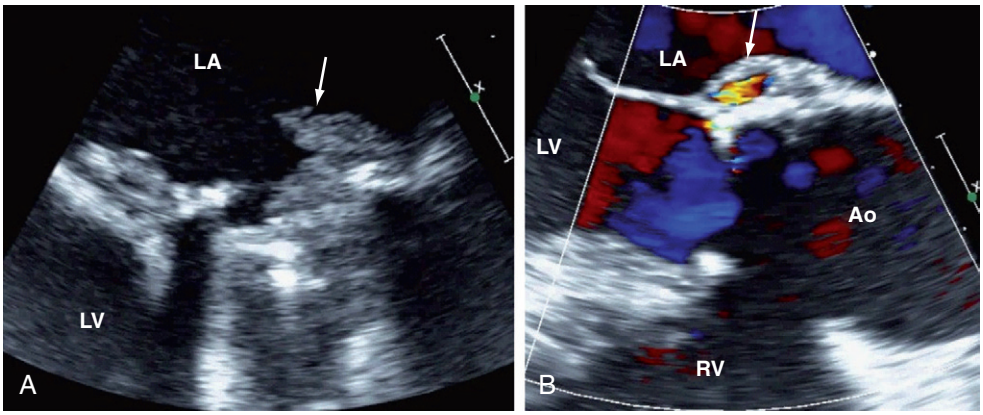



**Figure 25-18 Utility of TEE for diagnosis and treatment of prosthetic valve endocarditis. A,** Large vegetation (*arrow*) attached to a mitral bioprosthetic valve cusp and prolapsing in the LA during systole. **B,** Pseudoaneurysm (*arrow*) of aortic root in patient with bioprosthetic aortic valve. Color Doppler shows flow entering the pseudoaneurysm. *Ao*, Aorta. *(Courtesy Dr. Gilbert Habib, Hôpital La Timone, Marseille, France.)*

obstruction who are hemodynamically stable and have a small clot burden (see Fig. 25-17 and Clinical Case 25-2).

## PROSTHETIC VALVE ENDOCARDITIS

Prosthetic valve endocarditis represents one of the most frequent and severe form of infective endocarditis.[28] TEE is mandatory in prosthetic valve endocarditis because of its better sensitivity and specificity for the detection of vegetations, abscesses, and paravalvular lesions in this setting (Fig. 25-18).[36] When compared to native valve endocarditis, prosthetic valve endocarditis is characterized by a lower incidence of vegetations and higher incidence of abscesses and paravalvular complications. The sensitivity and specificity of both TTE and TEE are lower in prosthetic valve endocarditis than in native valve endocarditis.[28] Indeed, the components of the prosthetic valve may hinder the detection of vegetations and abscesses. Moreover, it may be difficult to differentiate a thrombus from a vegetation or bioprosthetic valve degeneration from infective lesions. Consequently, a negative echocardiogram is often observed in prosthetic valve endocarditis and does not rule out the diagnosis of infective endocarditis. If the initial TEE is negative but

suspicion for infective endocarditis remains, one should repeat within 7 to 10 days and/or use alternative imaging modality such as positron emission tomography or computed tomography (see Evaluation of Prosthetic Valve Endocarditis, later).

Infective endocarditis must be suspected in the presence of a new paraprosthetic regurgitation, even in the absence of a vegetation or abscess. TEE has a better sensitivity than TTE for this diagnosis, especially in mitral prosthetic valve endocarditis. Paravalvular complications are more frequent in aortic prosthetic valve endocarditis.[28] The anatomic involvement of infective endocarditis differs according to the type of prosthetic valve. In mechanical valves, the infection usually involves the junction between the sewing ring and the annulus, leading to paravalvular abscess, dehiscence, pseudoaneurysms, and fistula, whereas in bioprosthetic valve endocarditis, infection is more frequently located on the leaflets, leading to cusp tear, perforation, and vegetations (see Fig. 25-18).

Surgery should be considered in the following situations: failure of medical treatment; hemodynamically significant prosthesis regurgitation or obstruction, especially if associated with deterioration of LV function; large vegetations; paraprosthetic complications; and development of intracardiac fistulas.[22,26,29] Echocardiography is recommended for the perioperative and postoperative assessment of operated patients and for the follow-up of patients treated by medical therapy alone, because of the risk of late prosthetic dysfunction.[28]

### PARAVALVULAR REGURGITATION

Paravalvular regurgitation associated with development of symptoms, LV dysfunction, or hemolysis generally requires surgery. The paravalvular leaks can be repaired without valve replacement in approximately 50% of cases. Intraoperative TEE is mandatory to assess the results of leak correction. In patients with severe paravalvular mitral regurgitation refractory to aggressive medical therapy who are not candidates for surgical intervention, percutaneous implantation of an Amplatzer septal occluder device offers an alternative therapeutic option.[78] Contraindications to this alternative transcatheter procedure include very large paravalvular leak, valve rocking, more than two significant leaks, and active endocarditis. TEE is crucial to describe the location and extension of the paravalvular leak(s) and to guide and monitor the procedure.

## Limitations, Alternative Approaches, and Future Directions

### QUANTITATION OF PROSTHETIC VALVE REGURGITATION

One of the most difficult challenges in the Doppler-echocardiographic assessment of prosthetic valve function is the quantitation of prosthetic valve regurgitation, particularly when it is paravalvular, eccentric, and/or multijet. There is an urgent need for the development of new Doppler-echocardiographic methods that would allow accurate and reliable estimation of regurgitation severity, regardless of the location, direction, and number of regurgitant jet(s). The analysis of 3D color Doppler images and/or of the backscattered Doppler power signal may provide interesting avenues for future research in this regard.[79,80] Measurement of transprosthetic forward and backward flow by velocity-encoded cardiac magnetic resonance imaging may also be useful to quantitate prosthetic valve regurgitation, but the high cost and limited availability of this modality remains an important limitation.

**TABLE 25-8 Normal Maximum Opening Angles for Mechanical Prosthetic Valves**

| *Valve* | *Opening Angle (°)* |
|---|---|
| Medtronic-Hall | 75 |
| St. Jude Medical Standard | 85 |
| St. Jude Medical Regent | 85 |
| MCRI On-X | 85 |
| Carbomedics Standard and Top Hat | 78 |
| ATS Medical | 85 |

### EVALUATION OF PROSTHETIC VALVE LEAFLET MOBILITY

One of the main limitations of TTE and to a lesser extent of TEE is the limited sensitivity for the detection of abnormalities of leaflet morphology and mobility, especially in the context of mechanical valves. The assessment of leaflet mobility is crucial to make the differential diagnosis between intrinsic valve dysfunction versus central localized high gradient in bileaflet mechanical valves (see Figs. 25-14 and 25-15). It is also helpful to differentiate prosthetic valve dysfunction versus PPM when the measurement of valve EOA is not feasible or not reliable. Cinefluoroscopy is a simple, fast, and noninvasive method that allows adequate visualization of leaflets and measurements of leaflets opening and closing angles in patients with mechanical valves (Table 25-8; also see Clinical Case 25-2). When a patient with a bileaflet mechanical valve presents with a high transprosthetic gradient that cannot be explained based from the findings of TTE, it is recommended to proceed to cinefluoroscopic examination of leaflet mobility. If it is normal, the high gradient is most likely due to localized high gradient across the central orifice (artifact), and prosthesis dysfunction can be excluded. If it is abnormal, the presence of prosthesis dysfunction is confirmed, and TEE should be performed to detect the presence of thrombus, pannus, vegetation, and/or occult regurgitation. Multislice computed tomography may also be used to evaluate leaflet mobility (Fig. 25-19, *A*).

### EVALUATION OF PROSTHETIC VALVE ENDOCARDITIS

Early diagnosis of prosthetic valve endocarditis is crucial to improve the success of therapy and the survival of patients. Unfortunately, some patients may have negative blood cultures and negative TTE and TEE despite presence of active prosthetic valve endocarditis, especially in the initial stages of the pathologic process. Enhanced uptake of fluorine-18-fluorodeoxyglucose in the region of the valve documented by positron emission tomography–computed tomography may help to confirm the presence of endocarditis and prompt the initiation of therapy (see Fig. 25-19, *B*).[81]

### EVALUATION OF TRANSCATHETER VALVE IMPLANTATION

It is expected that the number of these procedures will rise dramatically in the near future. TTE and TEE, including real-time 3D, will play a major role in patient selection, procedure

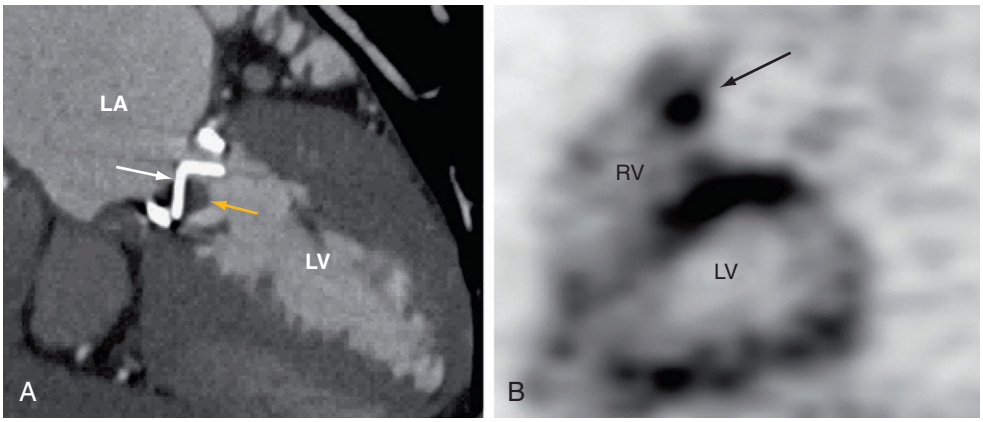



**Figure 25-19 Alternative imaging modalities to detect prosthetic valve dysfunction. A,** Multislice computed tomography for assessment of mechanical valve leaflet mobility. *White arrow*: immobile leaflet; *yellow arrow*: thrombus. **B,** Positron emission tomography to confirm endocarditis in patient with stented bioprosthetic valve in pulmonary position. Sagittal fluorine-18-fluorodeoxyglucose attenuation corrected view shows increased focal uptake in the prosthetic valve location (*black arrow*). (***A,*** *Courtesy Dr. Steven A. Goldstein, Washington Hospital Center.* ***B,*** *Adapted with permission of the Society of Thoracic Surgeons from Yedidya I, Stein GY, Vaturi M, et al: Positron emission tomography/computed tomography for the diagnosis of endocarditis in patients with pulmonic stented valve/pulmonic stent.* Ann Thorac Surg *91[1]:287-289, 2011.)*

guidance, and follow-up. Recently, transcatheter valves have also been implanted within failed bioprosthetic valves implanted surgically in the aortic, mitral, or pulmonary positions.[82] These emerging "valve-in-valve" procedures bring new challenges with regard to the role and use of Doppler echocardiography for selection of the appropriate size and model of transcatheter valve, and the assessment of prosthetic valve function in this particular context.

## Conclusion

Owing to its versatile, noninvasive, radiation-free nature and its low cost, Doppler echocardiography is undoubtedly the method of choice to identify and quantitate prosthetic valve dysfunction and assess its repercussions for cardiac function. However, the particular context of prosthetic valves poses some major challenges in terms of imaging and flow dynamics that push Doppler echocardiography to its limits. A comprehensive approach that integrates several direct and indirect parameters of valve function measured by TTE and TEE is key to appropriate assessment of prosthetic valve function, and other imaging modalities are often needed to complement or confirm the information obtained by Doppler echocardiography.

### KEY POINTS

- A comprehensive approach that integrates several direct and indirect Doppler-echocardiographic parameters of valve function is key to appropriately detect, quantitate, and manage prosthetic valve dysfunction
- Besides TTE, TEE provides important incremental information for the assessment and therapeutic management of prosthetic valve dysfunction and complications.
- Assessment of high transprosthetic gradient or velocity is much more complex than in native valves because there are several potential etiologies including PPM, prosthetic valve dysfunction, and localized high gradient.
- Assessment of severity of prosthetic valve regurgitation is generally much more complex than in native valves because of the high prevalence of paravalvular regurgitation and eccentric jets
- A high transprosthetic gradient or velocity does not necessarily imply prosthetic valve dysfunction. Conversely, a low gradient/velocity does not necessarily indicate absence of valve dysfunction.
- Evaluation of prosthetic leaflet morphology and mobility by TTE, TEE, or cinefluoroscopy is fundamental in making the differential diagnosis between prosthetic valve dysfunction and other potential causes of increased transprosthetic gradient.
- PPM is the most frequent cause of high gradient across prosthetic valves.
- TTE may underestimate the presence and severity of prosthetic mitral thrombosis and/or regurgitation because of reverberations and shadowing caused by the valve components. TEE is useful to unmask these "occult" abnormalities.

## ACKNOWLEDGMENTS

*The authors thank Drs. Marie-Annick Clavel, Haïfa Mahjoub, Bibiana Cujec, John Chambers, Steven Goldstein, Arsène Basmajan, Gilbert Habib, Gosta Petterson, Jacques Métras, and Christian Couture for their contribution to the preparation of this chapter.*

## REFERENCES

1. Rahimtoola SH: The problem of valve prosthesis-patient mismatch. *Circulation* 58:20-24, 1978.
2. Dumesnil JG, Honos GN, Lemieux M, Beauchemin J: Validation and applications of mitral prosthetic valvular areas calculated by Doppler echocardiography. *Am J Cardiol* 65:1443-1448, 1990.
3. Dumesnil JG, Honos GN, Lemieux M, Beauchemin J: Validation and applications of indexed aortic prosthetic valve areas calculated by Doppler echocardiography. *J Am Coll Cardiol* 16:637-643, 1990.
4. Pibarot P, Dumesnil JG: Prosthesis-patient mismatch: definition, clinical impact, and prevention. *Heart* 92:1022-1029, 2006.

5. Pibarot P, Dumesnil JG: Hemodynamic and clinical impact of prosthesis-patient mismatch in the aortic valve position and its prevention, *J Am Coll Cardiol* 36:1131-1141, 2000.
6. Magne J, Mathieu P, Dumesnil JG, et al: Impact of prosthesis-patient mismatch on survival after mitral valve replacement. *Circulation* 115: 1417-1425, 2007.
7. Lam BK, Chan V, Hendry P, et al: The impact of patient-prosthesis mismatch on late outcomes after mitral valve replacement. *J Thorac Cardiovasc Surg* 133:1464-1473, 2007.
8. Blais C, Dumesnil JG, Baillot R, et al: Impact of valve prosthesis-patient mismatch on short-term mortality after aortic valve replacement. *Circulation* 108:983-988, 2003.
9. Tasca G, Brunelli F, Cirillo M, et al: Impact of valve prosthesis-patient mismatch on left ventricular mass regression following aortic valve replacement. *Ann Thorac Surg* 79:505-510, 2005.
10. Ruel M, Rubens FD, Masters RG, et al: Late incidence and predictors of persistent or recurrent heart failure in patients with aortic prosthetic valves. *J Thorac Cardiovasc Surg* 127:149-159, 2004.
11. Tasca G, Mhagna Z, Perotti S, et al: Impact of prosthesis-patient mismatch on cardiac events and midterm mortality after aortic valve replacement in patients with pure aortic stenosis. *Circulation* 113:570-576, 2006.
12. Bleiziffer S, Eichinger WB, Hettich I, et al: Impact of prosthesis-patient mismatch on exercise capacity in patients after bioprosthetic aortic valve replacement. *Heart* 94:637-641, 2008.
13. Bleiziffer S, Ali A, Hettich IM, et al: Impact of the indexed effective orifice area on mid-term cardiac-related mortality after aortic valve replacement. *Heart* 96:865-871, 2010.
14. Kohsaka S, Mohan S, Virani S, et al: Prosthesis-patient mismatch affects long-term survival after mechanical valve replacement. *J Thorac Cardiovasc Surg* 135:1076-1080, 2008.
15. Mohty D, Malouf JF, Girard SE, et al: Impact of prosthesis-patient mismatch on long-term survival in patients with small St. Jude medical mechanical prostheses in the aortic position. *Circulation* 113:420-426, 2006.
16. Mohty D, Dumesnil JG, Echahidi N, et al: Impact of prosthesis-patient mismatch on long-term survival after aortic valve replacement: influence of age, obesity, and left ventricular dysfunction. *J Am Coll Cardiol* 53:39-47, 2009.
17. Ennker J, Rosendahl U, Albert A, et al: Stentless bioprostheses in small aortic roots: impact of patient-prosthesis mismatch on survival and quality of life. *J Heart Valve Dis* 14:523-530, 2005.
18. Castro LJ, Arcidi JMJ, Fisher AL, Gaudiani VA: Routine enlargement of the small aortic root: a preventive strategy to minimize mismatch. *Ann Thorac Surg* 74:31-36, 2002.
19. Bleiziffer S, Eichinger WB, Hettich I, et al: Prediction of valve prosthesis-patient mismatch prior to aortic valve replacement: which is the best method? *Heart* 93:615-620, 2007.
20. Roudaut R, Serri K, Lafitte S: Thrombosis of prosthetic heart valves: diagnosis and therapeutic considerations. *Heart* 93:137-142, 2007.
21. Vesey JM, Otto CM: Complications of prosthetic heart valves. *Curr Cardiol Rep* 6:106-111, 2004.
22. Butchart EG, Gohlke-Barwolf C, Antunes MJ, et al: Recommendations for the management of patients after heart valve surgery. *Eur Heart J* 26:2463-2471, 2005.
23. Schoen FJ, Levy RJ: Calcification of tissue heart valve substitutes: progress toward understanding and prevention. *Ann Thorac Surg* 79:1072-1080, 2005.
24. Ruel M, Kulik A, Rubens FD, et al: Late incidence and determinants of reoperation in patients with prosthetic heart valves. *Eur J Cardiothorac Surg* 25:364-370, 2004.
25. Jamieson WR, Cartier PC, Allard M, et al: Surgical management of valvular heart disease 2004. *Can J Cardiol* 20(Suppl E):7E-120E, 2004.
26. Bonow RO, Carabello BA, Kanu C, et al: ACC/AHA 2006 guidelines for the management of patients with valvular heart disease: a report of the American College of Cardiology/American Heart Association Task Force on Practice Guidelines (writing committee to revise the 1998 Guidelines for the Management of Patients With Valvular Heart Disease): developed in collaboration with the Society of Cardiovascular Anesthesiologists: endorsed by the Society for Cardiovascular Angiography and Interventions and the Society of Thoracic Surgeons. *Circulation* 114:e84-231, 2006.
27. Flameng W, Herregods MC, Vercalsteren M, et al: Prosthesis-patient mismatch predicts structural valve degeneration in bioprosthetic heart valves. *Circulation* 121:2123-2129, 2010.
28. Habib G, Badano L, Tribouilloy C, et al: Recommendations for the practice of echocardiography in infective endocarditis. *Eur J Echocardiogr* 11:202-219, 2010.
29. Horstkotte D, Follath F, Gutschik E, et al: Guidelines on prevention, diagnosis and treatment of infective endocarditis executive summary; the task force on infective endocarditis of the European society of cardiology. *Eur Heart J* 25:267-276, 2004.
30. O'Rourke DJ, Palac RT, Malenka DJ, et al: Outcome of mild periprosthetic regurgitation detected by intraoperative transesophageal echocardiography. *J Am Coll Cardiol* 38:163-166, 2001.
31. Akins CW, Bitondo JM, Hilgenberg AD, et al: Early and late results of the surgical correction of cardiac prosthetic paravalvular leaks. *J Heart Valve Dis* 14:792-799, 2005.
32. Clavel MA, Webb JG, Rodés-Cabau J, et al: Comparison between transcatheter and surgical prosthetic valve implantation in patients with severe aortic stenosis and reduced left ventricular ejection fraction. *Circulation* 122:1928-1936, 2010.
33. Leon MB, Smith CR, Mack M, et al: Transcatheter aortic-valve implantation for aortic stenosis in patients who cannot undergo surgery. *N Engl J Med* vol 1-11, 2010.
34. Sherif MA, Abdel-Wahab M, Stocker B, et al: Anatomic and procedural predictors of paravalvular aortic regurgitation after implantation of the Medtronic core valve bioprosthesis. *J Am Coll Cardiol* 56:1623-1629, 2010.
35. Zoghbi WA, Chambers JB, Dumesnil JG, et al: Recommendations for evaluation of prosthetic valves with echocardiography and Doppler ultrasound: a report from the American Society of Echocardiography's Guidelines and Standards Committee and the Task Force on Prosthetic Valves, developed in conjunction with the American College of Cardiology Cardiovascular Imaging Committee, Cardiac Imaging Committee of the American Heart Association, the European Association of Echocardiography, a registered branch of the European Society of Cardiology, the Japanese Society of Echocardiography and the Canadian Society of Echocardiography, endorsed by the American College of Cardiology Foundation, American Heart Association, European Association of Echocardiography, a registered branch of the European Society of Cardiology, the Japanese Society of Echocardiography, and Canadian Society of Echocardiography. *J Am Soc Echocardiogr* 22:975-1014, 2009.
36. Bach DS: Transesophageal echocardiographic (TEE) evaluation of prosthetic valves. *Cardiol Clin* 18:751-771, 2000.
37. Baumgartner H, Khan S, DeRobertis M, et al: Discrepancies between Doppler and catheter gradients in aortic prosthetic valves in vitro. A manifestation of localized gradients and pressure recovery. *Circulation* 82:1467-1475, 1990.
38. Otto CM, Pearlman AS, Comess KA, et al: Determination of the stenotic aortic valve area in adults using Doppler echocardiography. *J Am Coll Cardiol* 7:509-517, 1986.
39. Chafizadeh ER, Zoghbi WA: Doppler echocardiographic assessment of the St-Jude medical prosthetic valve in the aortic position using the continuity equation. *Circulation* 83:213-223, 1991.
40. Pibarot P, Honos GN, Durand LG, Dumesnil JG: Substitution of left ventricular outflow tract diameter with prosthesis size is inadequate for calculation of the aortic prosthetic valve area by the continuity equation. *J Am Soc Echocardiogr* 8:511-517, 1995.
41. Bitar JN, Lechin ME, Salazar G, Zoghbi WA: Doppler echocardiographic assessment with the continuity equation of St. Jude medical mechanical prostheses in the mitral valve position. *Am J Cardiol* 76:287-293, 1995.
42. Pibarot P, Dumesnil JG: Prosthetic heart valves: selection of the optimal prosthesis and long-term management. *Circulation* 119:1034-1048, 2009.
43. Fernandes V, Olmos L, Nagueh SF, et al: Peak early diastolic velocity rather than pressure half-time is the best index of mechanical prosthetic mitral valve function. *Am J Cardiol* 89:704-710, 2002.
44. Baumgartner H, Schima H, Kühn P: Discrepancies between Doppler and catheter gradients across bileaflet aortic valve prostheses. *Am J Cardiol* 71:1241-1243, 1993.
45. Aljassim O, Svensson G, Houltz E, Bech-Hanssen O: Doppler-catheter discrepancies in patients with bileaflet mechanical prostheses or bioprostheses in the aortic valve position. *Am J Cardiol* 102:1383-1389, 2008.
46. Garcia D, Pibarot P, Dumesnil JG, et al: Assessment of aortic valve stenosis severity: A new index based on the energy loss concept. *Circulation* 101:765-771, 2000.
47. Baumgartner H, Steffenelli T, Niederberger J, et al: "Overestimation" of catheter gradients by Doppler ultrasound in patients with aortic stenosis: a predictable manifestation of pressure recovery. *J Am Coll Cardiol* 33:1655-1661, 1999.
48. Garcia D, Dumesnil JG, Durand LG, et al: Discrepancies between catheter and Doppler estimates of valve effective orifice area can be predicted from the pressure recovery phenomenon: Practical implications with regard to quantification of aortic stenosis severity. *J Am Coll Cardiol* 41:435-442, 2003.
49. Bech-Hanssen O, Caidahl K, Wallentin I, et al: Aortic prosthetic valve design and size: relation to Doppler echocardiographic findings and pressure recovery—An in vitro study. *J Am Soc Echocardiogr* 13:39-50, 2000.
50. Zoghbi WA, Enriquez-Sarano M, Foster E, et al: Recommendations for evaluation of the severity of native valvular regurgitation with

two-dimensional and Doppler echocardiography. *J Am Soc Echocardiogr* 16:777-802, 2003.
51. Rallidis LS, Moyssakis IE, Ikonomidis I, Nihoyannopoulos P: Natural history of early aortic paraprosthetic regurgitation: a five-year follow-up. *Am Heart J* 138:351-357, 1999.
52. Vitarelli A, Conde Y, Cimino E, et al: Assessment of severity of mechanical prosthetic mitral regurgitation by transoesophageal echocardiography. *Heart* 90:539-544, 2004.
53. Effron MK, Popp RL: Two-dimensional echocardiographic assessment of bioprosthetic valve dysfunction and infective endocarditis. *J Am Coll Cardiol* 2:597-606, 1983.
54. Tribouilloy C, Avinee P, Shen W, et al: End diastolic flow velocity just beneath aortic isthmus assessed by pulsed Doppler echocardiography: a new predictor of aortic regurgitant fraction. *Br Heart J* 65:37-40, 1991.
55. Daniel LB, Grigg LE, Weisel RD, Rakowski H: Comparison of transthoracic and transesophageal assessment of prosthetic valve dysfunction. *Echocardiography* 7:83-95, 1990.
56. Alton M, Pasierski TJ, Orsinelli DA, Eaton GM, Pearson AC: Comparison of transthoracic and transesophageal echocardiography in evaluation of 47 Starr-Edwards prosthetic valves. *J Am Coll Cardiol* 20:1503-1511, 1992.
57. Lancellotti P, Moura L, Pierard LA, et al: European Association of Echocardiography recommendations for the assessment of valvular regurgitation. Part 2: mitral and tricuspid regurgitation (native valve disease). *Eur J Echocardiogr* 11:307-332, 2010.
58. Dumesnil JG, Dion D, Yvorchuk K, et al: A new, simple and accurate method for determining ejection fraction by Doppler echocardiography. *Can J Cardiol* 11:1007-1014, 1995.
59. Hung J, Lang R, Flachskampf F, et al: 3D echocardiography: a review of the current status and future directions. *J Am Soc Echocardiogr* 20:213-233, 2007.
60. Picano E, Pibarot P, Lancellotti P, et al: The emerging role of exercise testing and stress echocardiography in valvular heart disease. *J Am Coll Cardio* 54:2251-2260, 2009.
61. Jaffe WM, Coverdale HA, Roche AHG, et al: Rest and exercise hemodynamics of 20 to 23 mm allograft, Medtronic Intact (porcine), and St. Jude medical valves in the aortic position. *J Thorac Cardiovasc Surg* 100:167-174, 1990.
62. Eriksson MJ, Brodin LA, Dellgren GN, Radegran K: Rest and exercise hemodynamics of an extended stentless aortic bioprosthesis. *J Heart Valve Dis* 6:653-660, 1997.
63. Pibarot P, Dumesnil JG, Jobin J, et al: Hemodynamic and physical performance during maximal exercise in patients with an aortic bioprosthetic valve. Comparison of stentless versus stented bioprostheses. *J Am Coll Cardiol* 34:1609-1617, 1999.
64. Pibarot P, Dumesnil JG, Jobin J, et al: Usefulness of the indexed effective orifice area at rest in predicting an increase in gradient during maximum exercise in patients with a bioprosthesis in the aortic valve position. *Am J Cardiol* 83:542-546, 1999.
65. Fries R, Wendler O, Schieffer H, Schäfers H-J: Comparative rest and exercise hemodynamics of 23-mm stentless versus 23-mm stented aortic bioprostheses. *Ann Thorac Surg* 69:817-822, 2000.
66. Chambers J, Rimington H, Rajani R, et al: Hemodynamic performance on exercise: comparison of a stentless and stented biological aortic valve replacement. *J Heart Valve Dis* 13:729-733, 2004.
67. Reis G, Motta MS, Barbosa MM, et al: Dobutamine stress echocardiography for noninvasive assessment and risk stratification of patients with rheumatic mitral stenosis. *J Am Coll Cardiol* 43:393-401, 2004.
68. Maréchaux S, Hachicha Z, Bellouin A, et al: Usefulness of exercise stress echocardiography for risk stratification of true asymptomatic patients with aortic valve stenosis. *Eur Heart J* 31:1390-1397, 2010.
69. Magne J, Lancellotti P, Pierard LA: Exercise pulmonary hypertension in asymptomatic degenerative mitral regurgitation. *Circulation* 122:33-41, 2010.
70. Bagur R, Rodés-Cabau J, Doyle D, et al: Usefulness of TEE as the primary imaging technique to guide transcatheter transapical aortic valve implantation. *J Am Coll Cardiol* 4:115-124, 2011.
71. Jayasuriya C, Moss RR, Munt B: Transcatheter aortic valve implantation in aortic stenosis: the role of echocardiography. *J Am Soc Echocardiogr* 24:15-27, 2011.
72. Gurvitch R, Wood DA, Tay EL, et al: Transcatheter aortic valve implantation. Durability of clinical and hemodynamic outcomes beyond 3 years in a large patient cohort. *Circulation* 122:1319-1327, 2010.
73. Bach DS: Echo/Doppler evaluation of hemodynamics after aortic valve replacement: Principles of interrogation and evaluation of high gradients. *JACC Imaging* 3:296-304, 2010.
74. Dumesnil JG, Pibarot P: Prosthesis-patient mismatch: an update. *Curr Cardiol Rep* 13:250-257, 2011.
75. Davila-Roman VG, Waggoner AD, Kennard ED, et al: Prevalence and severity of paravalvular regurgitation in the artificial valve endocarditis reduction trial (AVERT) echocardiography study. *J Am Coll Cardiol* 44:1467-1472, 2004.
76. Vahanian A, Baumgartner H, Bax J, et al: Guidelines on the management of valvular heart disease: The Task Force on the Management of Valvular Heart Disease of the European Society of Cardiology. *Eur Heart J* 28:230-268, 2007.
77. Tong AT, Roudaut R, Ozkan M, et al: Transesophageal echocardiography improves risk assessment of thrombolysis of prosthetic valve thrombosis: results of the international PRO-TEE registry. *J Am Coll Cardiol* 43:77-84, 2004.
78. Sorajja P, Cabalka AK, Hagler DJ, et al: Successful percutaneous repair of perivalvular prosthetic regurgitation. *Catheter Cardiovasc Interv* 70:815-823, 2007.
79. Plicht B, Kahlert P, Goldwasser R, et al: Direct quantification of mitral regurgitant flow volume by real-time three-dimensional echocardiography using dealiasing of color Doppler flow at the vena contracta. *J Am Soc Echocardiogr* 21:1337-1346, 2008.
80. Buck T, Hwang SM, Plicht B, et al: Automated flow quantification in valvular heart disease based on backscattered Doppler power analysis: implementation on matrix-array ultrasound imaging systems. *Int J Cardiovasc Imaging* 24:463-477, 2008.
81. Yedidya I, Stein GY, Vaturi M, et al: Positron emission tomography/computed tomography for the diagnosis of endocarditis in patients with pulmonic stented valve/pulmonic stent. *Ann Thorac Surg* 91:287-289, 2011.
82. Webb JG, Wood DA, Ye J, et al: Transcatheter valve-in-valve implantation for failed bioprosthetic heart valves. *Circulation* 121:1848-1857, 2010.
83. Botzenhardt F, Eichinger WB, Guenzinger R, et al: Hemodynamic performance and incidence of patient-prosthesis mismatch of the complete supraannular Perimount Magna bioprosthesis in the aortic position. *Thorac Cardiovasc Surg* 53:226-230, 2005.
84. Edwards Lifesciences: Summary of safety and effectiveness data: Magna Ease Pericardial Aortic Bioprosthesis, U.S. Food and Drug Administration. April 2009.
85. Dellgren G, Eriksson MJ, Brodin LA, Radegran K: Eleven years' experience with the Biocor stentless aortic bioprosthesis: clinical and hemodynamic follow-up with long-term relative survival rate. *Eur J Cardiothorac Surg* 22:912-921, 2002.
86. St Jude Medical: Summary of safety and effectiveness data: SJM Biocor Valve and SJM Biocor Supra Valve, U.S. Food and Drug Administration. 2005 August 5.
87. CarboMedics Inc: Summary of safety and effectiveness data: Mitroflow aortic pericardial heart valve, U.S. Food and Drug Administration. 2007 October 23.
88. Dossche K, Vanermen H, Daenen W, et al: Hemodynamic performance of the PRIMA™ Edwards stentless aortic xenograft: early results of a multicenter clinical trial. *Thorac Cardiovasc Surg* 44:11-14, 1996.
89. Jin XY, Dhital K, Bhattacharya K, Pieris R, et al: Fifth-year hemodynamic performance of the prima stentless aortic valve. *Ann Thorac Surg* 66:805-809, 1998.
90. Bach DS, Sakwa MP, Goldbach M, et al: Hemodynamics and early clinical performance of the St. Jude Medical Regent mechanical aortic valve. *Ann Thorac Surg* 74:2003-2009, 2002.
91. Chambers J, Ely JL: Early postoperative echocardiographic hemodynamic performance of the On-X prosthetic heart valve: a multicenter study. *J Heart Valve Dis* 7:569-573, 1998.
92. Emery RW, Van Nooten GJ, Tesar PJ: The initial experience with the ATS Medical mechanical cardiac valve prosthesis. *Ann Thorac Surg* 75:444-452, 2003.
93. Eichinger WB, Botzenhardt F, Gunzinger R, et al: European experience with the Mosaic bioprosthesis. *J Thorac Cardiovasc Surg* 124:333-339, 2002.
94. Medical Carbon Research Institute. Summary of safety and effectiveness data On-X® prosthetic heart valve, models ONXM and ONXMC. Food and Drug Administration. 2002 March 6.

# 26 Doppler Echocardiography in Heart Failure and Cardiac Resynchronization

MARTIN ST. JOHN SUTTON, MD | THEODORE PLAPPERT, CVT

**Basic Principles**
- Definition of Heart Failure
- Prevalence of Heart Failure
- Etiology of Heart Failure

**Echocardiographic Diagnosis of Left Heart Failure**
- Acute Left Heart Failure
- Chronic Left Heart Failure
- Left Ventricular Remodeling to Heart Failure
- Systolic Versus Diastolic Heart Failure

**Echocardiographic Diagnosis of Right Heart Failure**
- Acute Right Ventricular Heart Failure
- Chronic Right Heart Failure
- Right Ventricular Remodeling to Heart Failure

**Echocardiography in Pharmacologic Therapy for Heart Failure**
- Pharmacologic Therapy

**Echocardiography for Mechanical Therapies in Heart Failure**
- Intraaortic Counterpulsation
- Ventricular Assist Devices
- Surgical Valve Repair or Replacement
- Cardiac Resynchronization Therapy
- New Techniques for Detection of Left Ventricular Dyssynchrony
- Heart Transplantation

**Summary**

## Basic Principles

### DEFINITION OF HEART FAILURE

Heart failure is a clinical syndrome characterized by easy fatigue, shortness of breath, exercise intolerance, fluid retention with lower extremity edema, and pulmonary congestion. Heart failure may be systolic as a result of abnormal myocardial excitation-contraction coupling or diastolic as a result of abnormal relaxation and increased myocardial passive stiffness. The symptomatic presentations of systolic and diastolic heart failure may be indistinguishable clinically, but the two etiologies can be determined with Doppler echocardiography by differences in left ventricular (LV) architecture and function. Differentiation between systolic and diastolic heart failure is important because the respective treatments and prognoses are different. Traditionally, diastolic heart failure has been regarded as a more benign form of heart failure than systolic heart failure. However, the annual mortality rate from diastolic heart failure is between 5% and 15%, and the hospitalization readmission rate for new onset heart failure is approximately 50% within the first 6 months.[1-4]

Systolic heart failure may be defined as the inability of the heart to supply the metabolic requirements of the body tissues. In systolic heart failure, myocardial shortening is impaired and results in a shift of the length-tension relationship to the right of the normal pressure-volume relationship (Fig. 26-1).[1,5]

Diastolic heart failure may be defined as the inability of the heart to receive blood from the body tissues at normal filling pressures.[4] In diastolic heart failure, the myocardial passive or resting length-tension relationship is displaced upwards and leftwards of the normal relationship (see Fig. 26-1). Thus, significant increases in LV diastolic pressure may occur with no detectable change in ventricular volume.[4,6] Myocardial relaxation is delayed or incomplete at the time of minimal LV diastolic pressure.[6]

The abnormal pressure-volume relations in systolic heart failure result in LV dilation and changes in both the composition and the material properties of the myocardium. This pattern of remodeling is known as "eccentric remodeling" and typifies systolic heart failure (Fig. 26-2). A chronically abnormal resting pressure-volume relationship is also associated with LV hypertrophy in which normal LV cavity size or volume is maintained, wall thickness is increased, and ejection performance is preserved. This latter form of "concentric remodeling" results in increased diastolic stiffness and incomplete or slowed relaxation that is characteristic of diastolic heart failure (see Fig. 26-2).

The purpose of this chapter is to show how Doppler echocardiography can be used in the clinical diagnosis of heart failure, to determine the etiology of heart failure and to distinguish systolic from diastolic heart failure. A second purpose of this chapter is to show how Doppler echocardiography can be used to assess of the efficacy of new treatments for heart failure and to guide the selection of novel pharmacologic agents or devices to optimize therapy.

### PREVALENCE OF HEART FAILURE

An estimated 30 million people worldwide are affected with chronic heart failure. Between five and six million patients with heart failure reside in the United States, and an additional 500,000 to 600,000 new cases are diagnosed each year.[7] This increase is the result of the greater availability of advanced diagnostic cardiac imaging capabilities. In a large proportion of these patients, the initial diagnosis of heart failure is made or confirmed by noninvasive imaging with Doppler echocardiography. Systolic heart failure is almost twice as common as diastolic heart failure and portends a much worse prognosis.[8]

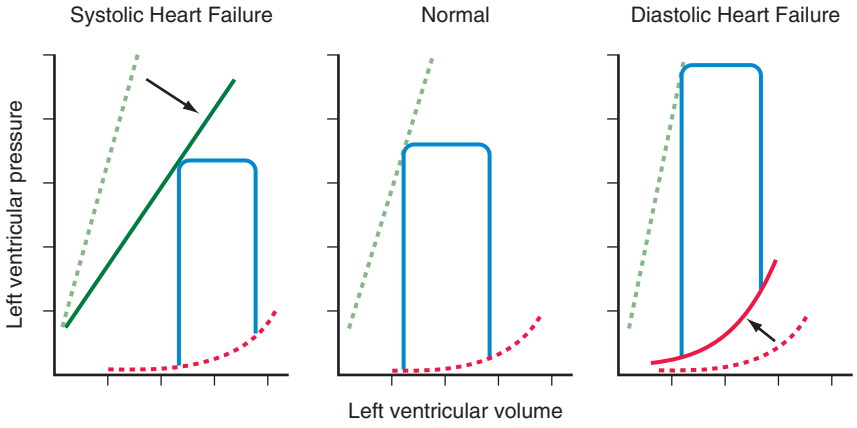



**Figure 26-1 LV pressure-volume loops in systolic heart failure (*left*), a normal control (*center*), and diastolic heart failure (*right*).** In systolic heart failure, a decrease is seen in the slope of the end-systolic pressure-volume relationship (decreased LV contractility); whereas in diastolic heart failure, the pressure-volume loop is shifted up and to the left (increased stiffness). *(From Aurigemma GP, Zile MR, Gaasch WH:* Circulation *113:296-304, 2006.)*

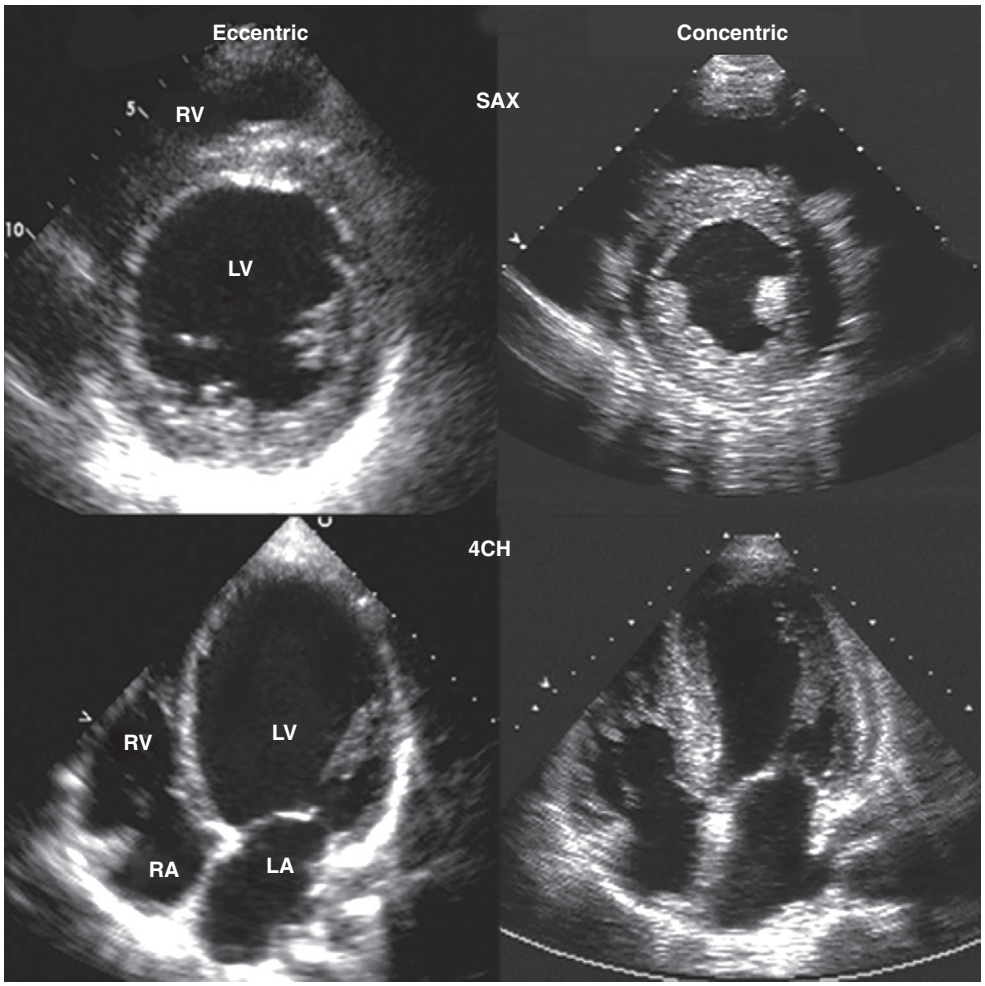



**Figure 26-2 LV short-axis (*top left*) and the apical four-chamber view (*bottom left*) of a patient with "eccentric" hypertrophy.** This is the result of a primary volume overload with a compensatory increase in wall thickness that fails to meet the increase in cavity radius. On the *right,* LV short axis *(top)* and apical four-chamber view *(bottom)* of a patient with "concentric" hypertrophy. This is the result of a primary pressure overload with an increase in wall thickness without significant increase in cavity radius. *SAX,* Short axis view; *4CH,* four-chamber view.

Heart failure increases with age so that currently 6% to 10% of persons older than 65 years have heart failure. Although the survival rate for women with heart failure has improved in the last two decades, the survival rate for men is unchanged in the same time period. The overall 5-year and 10-year survival rates in New York Heart Association Symptom Class III are 50% and 30%, respectively.

The total costs for the diagnostic related group for heart failure nationwide already exceeds 30 billion dollars per year. Included in this price tag are multiple hospital admissions, drugs, internal cardiac defibrillators, ventricular assist devices, cardiac resynchronization therapy (CRT), and heart transplants. These striking population statistics underscore the size of the problem of heart failure worldwide and the reason that

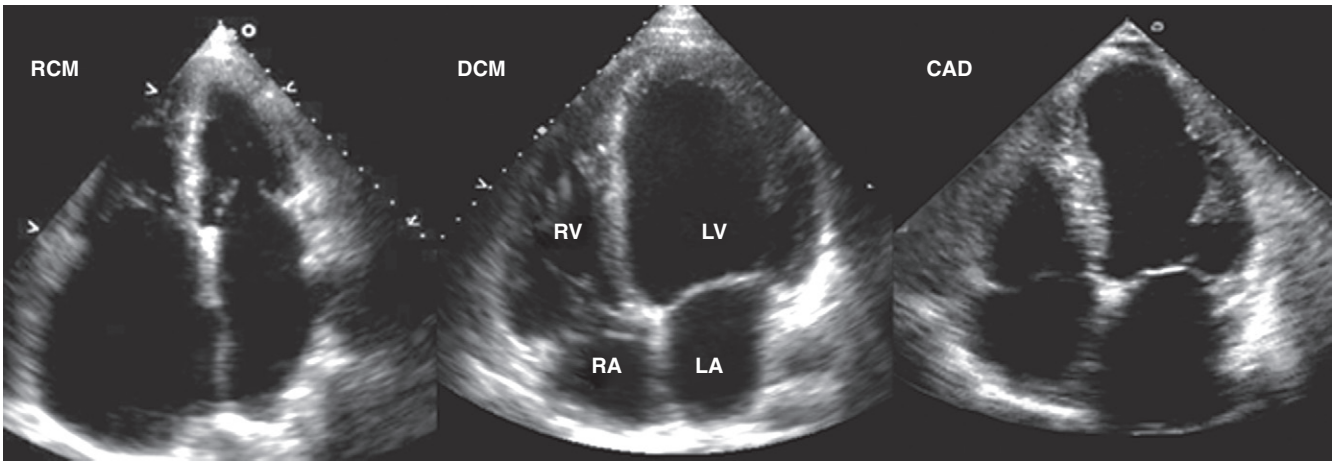



**Figure 26-3 Comparative imaging findings in restrictive cardiomyopathy (*RCM*), dilated cardiomyopathy (*DCM*) and coronary artery disease (*CAD*).** Apical four-chamber view of a patient with restrictive cardiomyopathy (*left*) that shows a small LV and biatrial dilation; apical four-chamber view of a dilated cardiomyopathy (*center*) with a dilated LV; and an apical four-chamber view of a patient with coronary artery disease (*right*) that shows apical dilation.

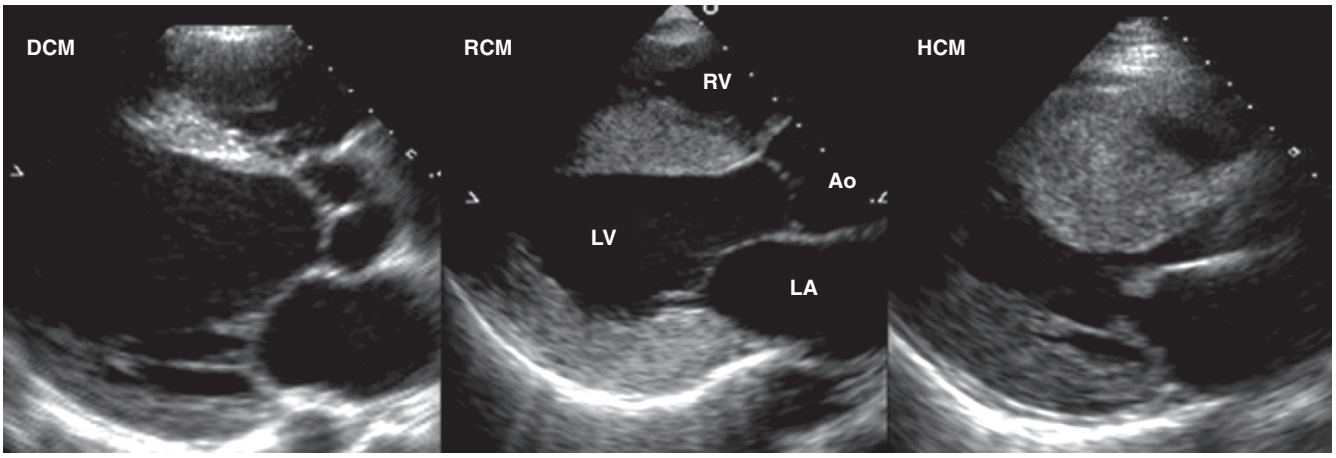



**Figure 26-4** Parasternal long-axis view of a patient with dilated cardiomyopathy shows an increase in internal diameter of the LV with normal wall thickness *(left);* parasternal long-axis view of a patient with amyloid restrictive cardiomyopathy (*center;* the walls are thick and highly reflective, and the LV diameter is normal); and parasternal long-axis view of a hypertrophic cardiomyopathy with asymmetric septal hypertrophy (*right;* the upper interventricular septum measures 4 cm with a small LV diameter). *Ao,* Aorta; *DCM,* dilated cardiomyopathy; *RCM,* restrictive cardiomyopathy; *HCM,* hypertrophic cardiomyopathy.

heart failure has become a high priority health care policy initiative.

### ETIOLOGY OF HEART FAILURE

Heart failure has many divergent causes, and their individual prevalence varies geographically. In the United States, Canada, and Europe, atherosclerotic coronary artery disease and myocardial infarction (MI) is the most common etiology, accounting for more than two thirds of all cases of chronic heart failure.[9] In West Africa, restrictive cardiomyopathy is the predominant etiology of heart failure. In Central and South America, heart failure is most frequently the result of an immunologic response to chronic infection with *Trypanosoma cruzi*. These three widely different etiologies of heart failure have their own individual structural and functional stigmata that can be easily recognized with Doppler echocardiography (Fig. 26-3). Other major causes of heart failure that can be diagnosed echocardiographically include chronic pressure overload from systemic hypertension; pressure or volume overload from valvular heart disease; and primary dilated, hypertrophic, and restrictive cardiomyopathies from genetically determined abnormalities of the sarcomeric contractile proteins or infiltrative diseases that change the extracellular matrix. Cardiac toxins are an infrequent cause of heart failure that include chronic excessive ingestion of alcohol and chemotherapeutic agents such as cytoxan and adriamycin, even in therapeutic doses for primary malignant solid and liquid tumors and as pretreatment for bone marrow transplant. Some of these conditions express consistent phenotypes that are pathognomonic and readily diagnosed with Doppler echocardiography (e.g., cardiac amyloid, hypertrophic cardiomyopathy, and dilated cardiomyopathy; Fig. 26-4).

## Echocardiographic Diagnosis of Left Heart Failure

### ACUTE LEFT HEART FAILURE

"The single most useful diagnostic test" in the evaluation of patients with heart failure is Doppler echocardiography for determination of whether abnormalities of the myocardium,

heart valves, or pericardium are present and which cardiac chambers are involved.[10] In patients with new-onset heart failure, the American College of Cardiology/American Heart Association practice guidelines recommend an initial Doppler echocardiographic algorithm to resolve three important issues.[10] The first issue is establishment of whether the LV ejection fraction is normal or decreased. The second issue is determination of whether LV structure is normal or abnormal and whether the LV is dilated, hypertrophied, or of normal size. The third issue is assessment of whether other structural abnormalities, such as valvular heart disease, pericardial disease, right ventricular (RV) abnormalities, or chronic pulmonary disease, could account for the clinical presentation of heart failure.

Common causes of acute onset of LV systolic heart failure include: (1) extensive acute MI; (2) acute LV volume overload from severe mitral regurgitation (MR) as a result of rupture of a papillary muscle after infarction (see Chapter 14); (3) severe ischemic MR with flash pulmonary edema from acute elevation of LV end-diastolic pressure; (4) postinfarction rupture of the interventricular septum (ventricular septal defect) with a large left-to-right shunt after infarction (see Chapter 14); (5) chordal rupture after MI or from endocarditis that causes a flail leaflet and severe MR; (6) acute severe MR as a result of rupture of a native valve or dehiscence of a prosthetic valve from vegetative endocarditis (see Chapter 25); (7) acute severe aortic regurgitation that results from avulsion of the aortic valve or dehiscence of a prosthetic aortic valve from endocarditis (see Chapter 22); (8) thrombotic encapsulation and occlusion of a mechanical aortic or mitral prosthetic valve as a result of inadequate oral anticoagulation status (see Chapter 25); (9) acute myocarditis; (10) exposure to oncologic cardiotoxic chemotherapeutic agents; and (11) acute destabilization of previously known or unknown chronic severe dilated cardiomyopathy. All of these conditions, except for the latter, present with either sudden massive increase in LV loading conditions, acute loss of contracting cardio-myocytes, or severe injury to the full complement of working myocardium.

Acute MI is diagnosed by history and confirmed with electrocardiographic changes and elevated cardiac enzymes. Echocardiography early after MI shows normal LV size with decreased global function and a variable sized regional wall motion abnormality in the territory of the occluded culprit coronary artery. Infarct size can be assessed with two-dimensional (2D) or three-dimensional (3D) echocardiography using a 17-segment model of the LV and scoring of regional wall motion in each segment from normal to akinetic. The average wall motion is calculated as a wall motion score index that correlates with the magnitude of the elevation of cardiac enzymes.

Sudden exacerbation of heart failure in the early periinfarction period may result from either rupture of the interventricular septum or acute severe MR from papillary muscle dysfunction or rupture. Although these two different lesions cannot be reliably distinguished clinically, Doppler echocardiography can unequivocally differentiate between the two lesions. These structural changes can be localized with color flow Doppler scan and their severity quantified as MR volume, the ratio of pulmonary blood flow to systemic blood flow (Qp/Qs), and the magnitude of shunt flow through the ventricular septal defect (see Chapter 14).

The remaining causes of acute heart failure listed previously are usually readily recognized with transthoracic Doppler echocardiography. Transesophageal echocardiography may be needed for diagnosis of vegetative endovascular infections that cause perforation or avulsion of native mitral or aortic valves (see Chapters 22 and 25) or dehiscence of a mechanical or biological aortic or mitral prosthesis. Transthoracic and transesophageal echocardiography are often necessary for diagnosis of acute severe MR associated with degenerative mitral valve disease as a result of rupture of redundant chordae that causes flail leaflets that fail to coapt normally and result in acute severe MR (see Chapter 18). The thickened yet highly mobile prolapsing myxomatous leaflets of degenerative mitral valve disease are easily recognized. Transesophageal echocardiography is invaluable for determining whether the valve can be repaired rather than replaced.

Acute left heart failure from use of high doses of oncologic agents results in severe global dysfunction that has a temporal cause-and-effect relationship to drug administration. In acute heart failure caused by adriamycin, transthoracic echocardiography shows that LV end-diastolic size is usually normal but the end-systolic size is increased so that resting sinus tachycardia is a prerequisite for maintaining resting cardiac output (Fig. 26-5).

## CHRONIC LEFT HEART FAILURE

The common causes of chronic left heart failure are coronary artery disease and MI, hypertensive heart disease, valvular disease, and cardiomyopathies. The different pathoetiologies in their late stages progress down a final common pathway to left-sided systolic heart failure characterized by structural and functional remodeling changes that lend themselves well to echocardiographic imaging. One finding that is almost universal in chronic systolic heart failure is the presence of LV dilation, which can be quantified echocardiographically either as cavity diameter at end-diastole and end-systole or as end-diastolic and end-systolic volumes with the modified Simpson's rule. The importance of LV volumes after infarction is their predictive value for adverse clinical outcome.[11] Increasing evidence shows that measurements of global longitudinal, radial, and circumferential myocardial strain with speckle tracking provide even greater predictive information regarding clinical outcomes after infarction and in dilated cardiomyopathies. Transthoracic 2D echocardiography has shown that progressive LV dilation occurs by a disproportionately greater increase in LV short-axis diameter than in LV long-axis diameter as exemplified by idiopathic dilated cardiomyopathy (Figs. 26-6 and 26-7). This pattern of remodeling confers on the LV a mechanically disadvantageous cavity shape that is more spherical compared with the configuration of the normal heart.[11] This change in LV shape is readily discernible with echocardiographic images of the LV in the apical two-chamber and apical four-chamber views (see Fig. 26-7). As the LV remodels to a larger volume, contractile function deteriorates because of inadequate hypertrophy that is unable to normalize end-systolic wall stress and leads to heart failure. In healthy subjects, the end-diastolic mass-to-volume relationship is virtually constant in normotensive hearts from early infancy through old age.

There are three important sequelae of the abnormal LV size and shape. First is the increase in loading conditions with the disproportionate LV mass-volume ratio associated with decreased contractile function. Second, LV dilation combined with the decreased contractile function results in low blood flow velocities within the LV, which predisposes to thrombus formation, especially in the apex of the LV cavity with regional wall motion abnormalities (Fig. 26-8). Thrombus may also occur in

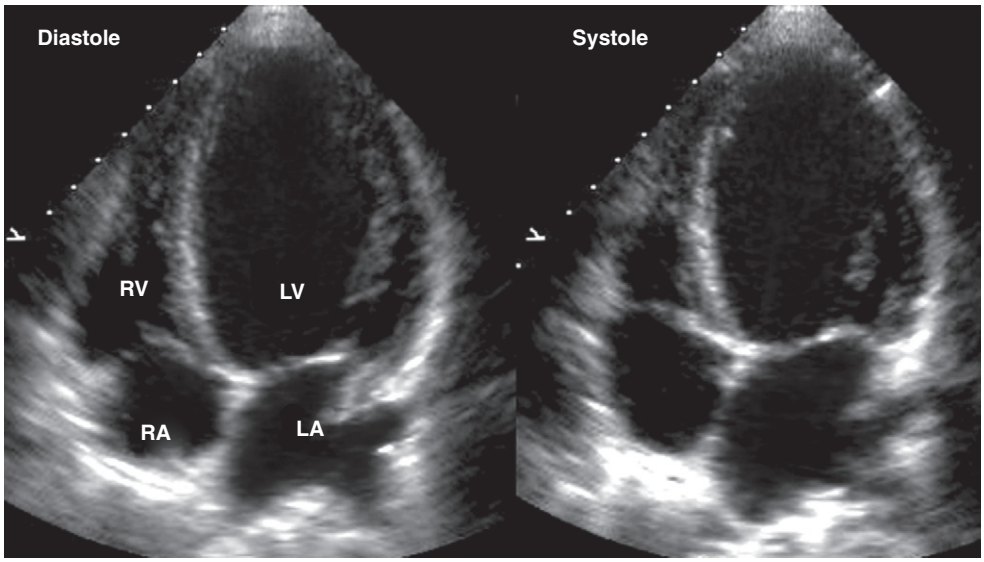



**Figure 26-5** Apical four-chamber view of a patient with adriamycin-induced cardiomyopathy that shows minimal LV dilation and little change in LV size from diastole (*left panel*) to systole (*right panel*), consistent with a very low stroke volume.

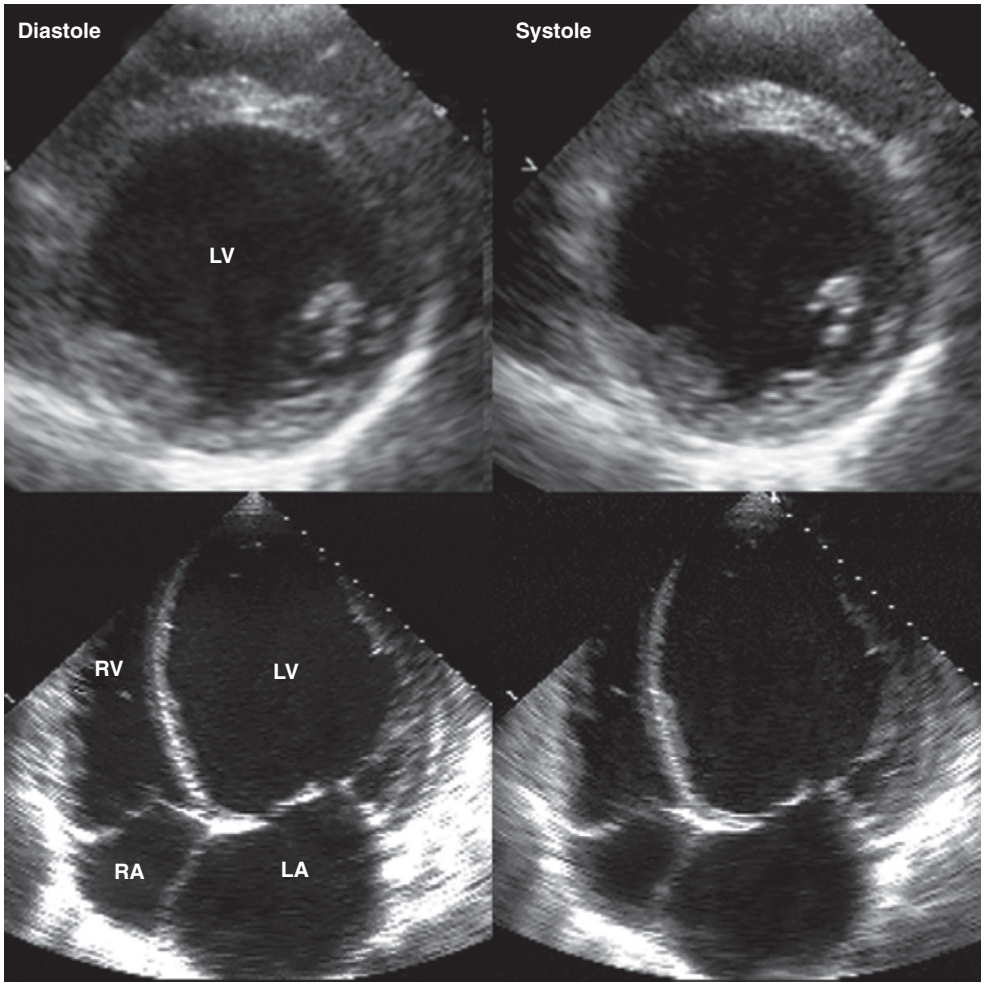



**Figure 26-6** Short-axis and four-chamber views of a dilated cardiomyopathy at end-diastole (*left*) and short-axis and four-chamber views of a dilated cardiomyopathy (*right*). Note the greater increase in the short-axis diameter as compared with the LV long-axis length in the four-chamber views.

the left atrial appendage as a result of low flow velocities. Both LV (see Fig. 26-8) and left atrial (LA) thrombus (Fig. 26-9) are potential sources of systemic embolism and especially stroke. Thrombus formation may be subtle and necessitate echocardiographic imaging with increased gain in orthogonal planes of the LV long axes with serial short-axis views with a high-frequency near-focus transducer. When doubt still remains as to the presence of LV thrombus, echocontrast studies are recommended to enhance endocardial definition (Fig. 26-10) so that the diagnosis of LV thrombus is unequivocal. The morphologic features of LV thrombus that correlate with increased embolic potential include mobility, large size, and convexity of the thrombus toward the LV cavity.

The third important consequence of LV dilation and change in LV shape is enlargement of the mitral annulus and distortion of the mitral valve and subvalve geometry. The spatial separation of the two papillary muscles caused by LV dilation increases the angle they subtend to the midpoint of the plane of the mitral annulus. This occurs without lengthening of the chordae and therefore reduces the area of leaflet coaptation that results in MR even though the mitral valve is intrinsically normal (Fig. 26-11). The anatomic relationships between the various components of the mitral valve apparatus are best appreciated with real-time 3D echocardiography in the short-axis and apical long-axis or four-chamber views (Fig. 26-12).

A different yet frequent cause of MR in heart failure relates to the presence of provocable ischemia in patients with advanced coronary artery disease. Serial quantitative Doppler echocardiographic studies of ischemic MR show its important adverse impact on survival.[12] MR is significantly more common and more severe in eccentric remodeling that occurs in systolic heart failure than in concentric remodeling in diastolic heart failure, in which LV cavity size is typically normal.

The severity of MR can be semiquantified with 2D transthoracic echocardiography as the ratio of color flow MR jet area averaged from orthogonal views and left atrial area. MR severity can be quantified as the effective regurgitant orifice area or regurgitant volume with proximal isovelocity surface area technique or with the diameter of the vena contracta (see Chapter 18). The significance of MR in systolic heart failure is that it results in an additional increase in load when loading conditions are already increased. Quantification of MR with proximal isovelocity surface area is advised.

After posteroinferior infarction, residual ischemia of the inferomedial papillary muscle may interfere with the timing and extent of shortening and cause MR. Hemodynamically important MR may escalate deterioration in contractile function. Ischemic MR may cause flash pulmonary edema triggered by transient increases in afterload associated with physical exertion. The poor prognosis of ischemic MR correlates closely with the severity of MR with Doppler echocardiography.[12] Rupture of a papillary muscle after MI may not be diagnosed initially but is usually suggested by the discrepancy between relatively normal LV size and function and the torrential MR. A search should be made to identify the papillary muscle heads and primary chordae that are disconnected from the muscle. This is a "must diagnose" because the severity of

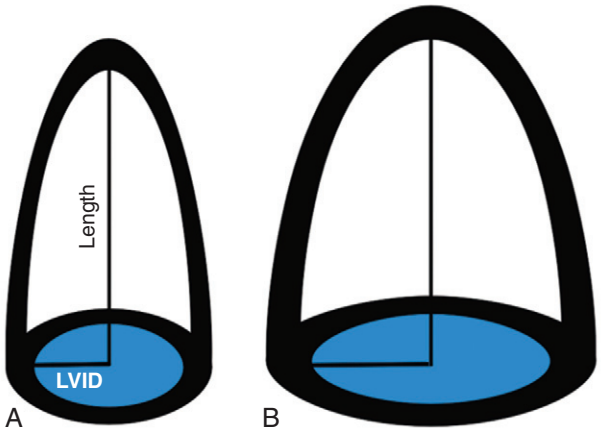



**Figure 26-7** Schematic representation of a normal LV shape (**A**) and a more spherical shape as a result of a greater increase of the minor diameter than in LV length (**B**) in dilated cardiomyopathy.

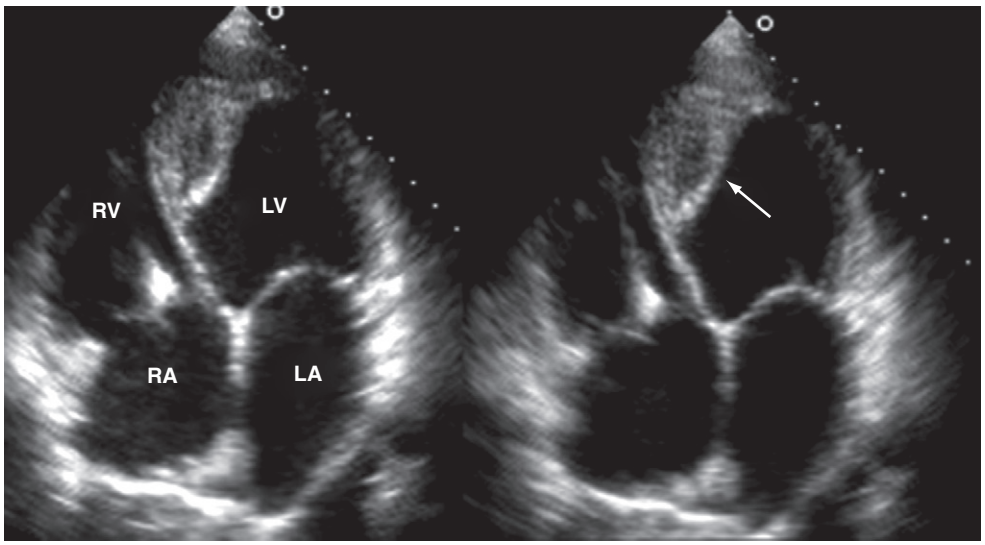



**Figure 26-8** **Echocardiographic appearance of LV thrombus.** Transthoracic apical four-chamber view that shows a large sessile LV cavity thrombus (*white arrow*) attached to the apical septum in an area of akinesis. A defibrillator electrode is present in the RV.

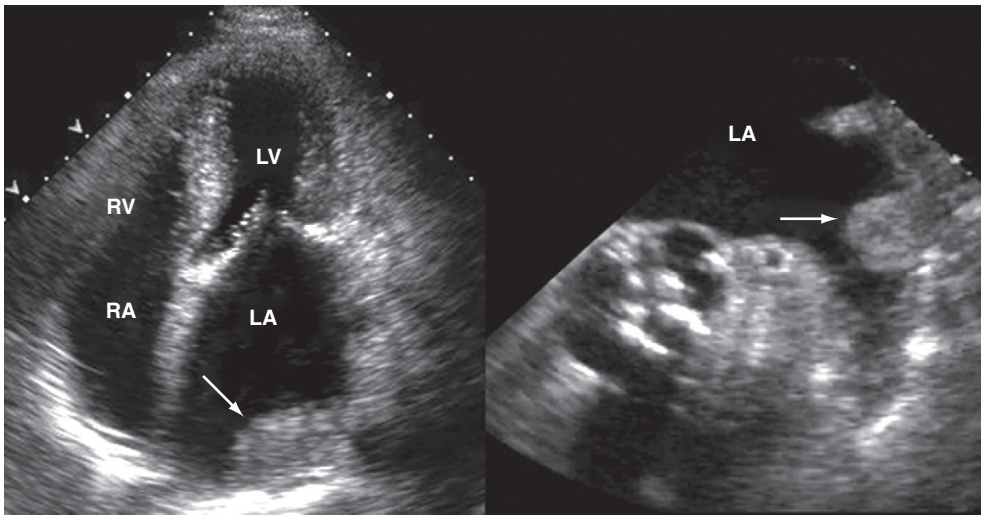



**Figure 26-9 Valvular heart disease with ventricular dysfunction**. Transthoracic echocardiogram of the four-chamber view of a patient with moderate LV dysfunction and heart failure symptoms with degenerative and calcific aortic and mitral valve disease (*left panel*). Note the large thrombus adherent to the roof of the markedly enlarged LA (*left panel*). A discrete immobile thrombus is visualized in the left atrial appendix that is a repository for the development of thrombus (*white arrow*). Calcification and narrowing of the aortic valve leaflets are also seen, consistent with at least mild aortic stenosis.

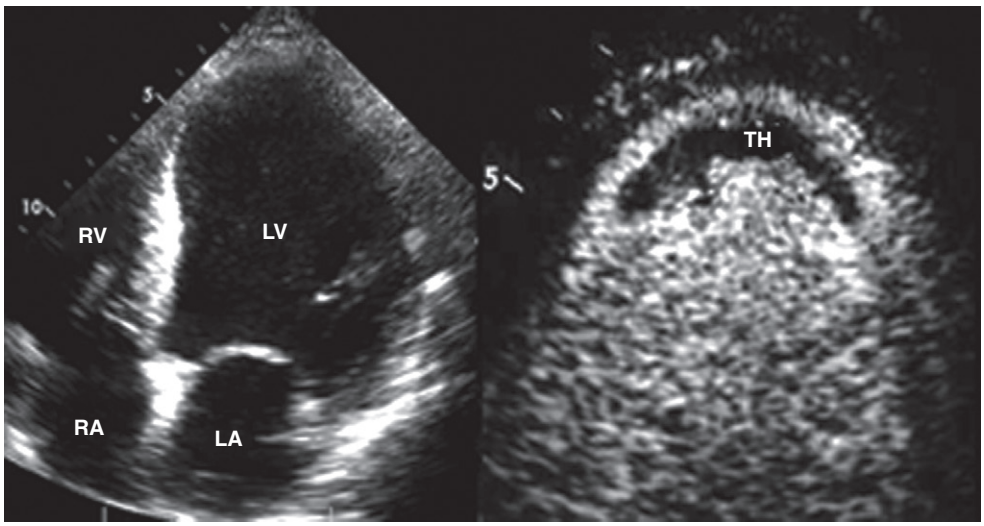



**Figure 26-10 Apical aneurysm.** Transthoracic 2D echocardiogram of an apical four-chamber view from a patient with ischemic cardiomyopathy that shows an apical aneurysm without any obvious thrombus present (*left panel*). However, when the endocardial definition is improved with intravenous contrast, a laminar thrombus becomes apparent (*right panel*). *TH*, Thrombus.

MR is poorly tolerated and irreversible cardiogenic shock may supervene.

## LEFT VENTRICULAR REMODELING TO HEART FAILURE

Left ventricular remodeling is a dynamic process that includes progressive LV dilation, distortion of LV shape, disruption of mitral valve geometry, development of MR, and deterioration in LV function. This type of remodeling is known as eccentric remodeling. These structural and functional changes and the transition to heart failure have been characterized by Doppler echocardiography.

Left ventricular remodeling is triggered by an imbalance between myocardial wall stress and the normal restraining forces exerted by the viscoelastic collagen matrix. Increased wall stress activates cell surface mechanoreceptors (integrins) that in turn activate myocardial matrix metalloproteinases that degrade the extracellular collagen matrix, thereby facilitating LV dilation. A new equilibrium is established between collagen degradation and collagen synthesis that stabilizes LV size and function. Progressive LV dilation leads to chronically elevated wall stress, which, if unchecked, results in heart failure. Thus, LV dilation begets increased wall stress that begets further LV dilation. LV dilation results in an increase in loading conditions that can be assessed as meridional and circumferential midwall stresses from echocardiographic measurements of LV cavity radius, length, and wall thickness. Cuff systolic blood pressure can be used to represent LV peak pressure.[13] A strong inverse relationship exists between end-systolic wall stress and ejection fraction, such that the greater the wall stress, the lower the LV ejection fraction. Increased myocardial wall stress is also a major stimulus for ventricular hypertrophy mediated by the angiotensin I receptor. When the hypertrophic response is

sufficient to normalize wall stress, the progressive deterioration in LV function is attenuated, LV geometry is stabilized, and function is preserved.

Insight into the structural and functional eccentric remodeling process and transition from stable LV function to systolic heart failure has been provided by Doppler echocardiography in a number of post-MI and heart failure clinical trials (SAVE and SOLVD).[11,14] Speckle tracking with 2D and 3D echocardiography provides a means of quantifying regional and global longitudinal, radial, and circumferential strain (Figs. 26-13 and 26-14) and also assessment of the temporal development of peak systolic velocities in opposing walls as a measure of dyssynchrony.

## SYSTOLIC VERSUS DIASTOLIC HEART FAILURE

The diagnostic criteria for diastolic heart failure are the combination of symptomatic heart failure and an LV ejection fraction of 50% or more to distinguish LV diastolic from systolic heart failure. Controversy exists with regard to nomenclature: "diastolic heart failure" versus "heart failure with preserved ejection fraction." There was concern initially as to whether Doppler indices provided sufficiently specific information about intrinsic passive diastolic properties of the myocardium and whether the information derived from LV filling dynamics equated with intrinsic myocardial diastolic dysfunction.[15] Other investigators have indicated that diastolic heart failure can be confidently diagnosed with the combined presence of impaired relaxation, decreased compliance, and increased LV filling pressures.[16]

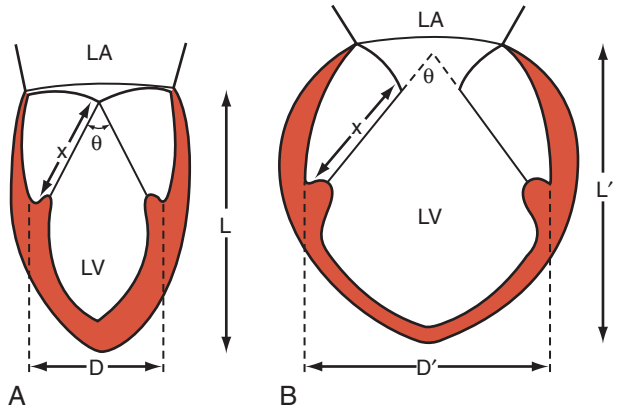



**Figure 26-11 Mechanism of functional mitral regurgitation.** Schematic that shows the LV architecture, the relations between the diameter and length of the LV and the geometry of the normal mitral valve (**A**), and the greater increase in LV diameter than the increase in LV length that confers an abnormal shape on the LV and also disrupts the mitral valve geometry that alters mitral leaflet coaptation area, leading to mitral regurgitation (**B**).

Diastolic heart failure has been less well characterized than systolic heart failure, until the last decade, when it became clear that LV diastolic dysfunction was responsible for 30% to 50% of all patients with heart failure and had an annual mortality rate of 5% to 15%. Patients with diastolic heart failure are similar to patients with systolic heart failure with regards to impaired quality of life, exercise capacity, demographic profiling, and neurohormonal activation. Neurohormonal activation in diastolic heart failure is similar to systolic failure with regard to norepinephrine levels, but plasma levels of brain natriuretic peptide and atrial natriuretic peptides are consistently greater in systolic heart failure.[17]

Diastolic dysfunction often precedes the onset of systolic dysfunction in hypertensive heart disease and in coronary artery disease. Factors that determine which patients have diastolic rather than systolic heart failure develop are largely unknown. Furthermore, diastolic heart failure may transition into systolic failure in its terminal stages, which confounds the arbitrary division between diastolic and systolic heart failure.

Diastolic heart failure occurs more commonly in elderly women, of whom more than 75% have a history of hypertension and approximately 40% have LV hypertrophy defined as a LV mass of more than 125 g/m$^2$.[2,16] The structural and functional concentric pattern of LV remodeling in diastolic heart failure is characterized echocardiographically by normal or near-normal LV end-diastolic volume, normal cavity shape, increased absolute and increased relative wall thicknesses (wall thickness/LV cavity radius), increased LV mass-volume ratio from a disproportionately greater increase in LV mass than volume, and preserved ejection fraction (more than 50%).[17] More specific Doppler echocardiographic findings in chronic diastolic heart failure include abnormal LV filling patterns (larger A wave velocity, a normal E wave deceleration time); prolonged

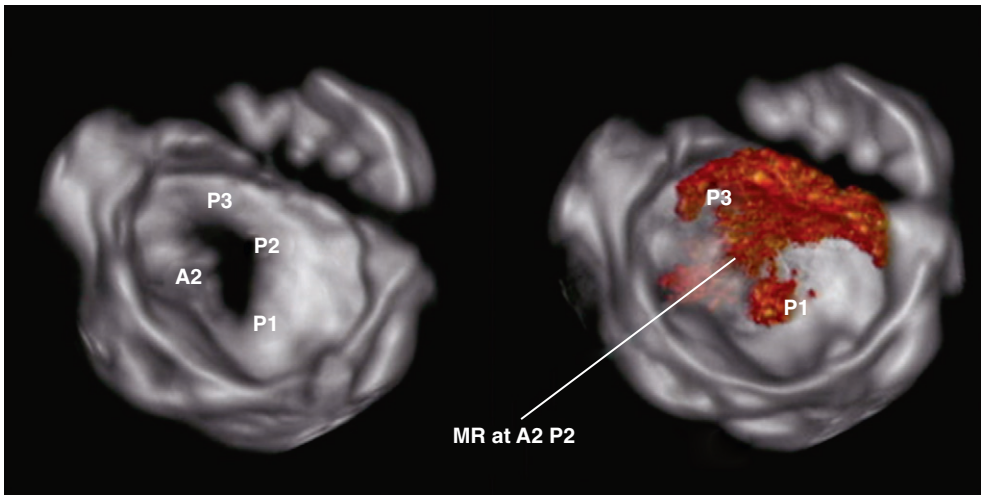



**Figure 26-12 Mitral valve prolapse.** Mitral valve visualized with 3D transesophageal echocardiography that shows prolapse of the P2 and A2 scallops (*left panel*) and the Doppler color flow jet of mitral regurgitant flow (*right panel*).

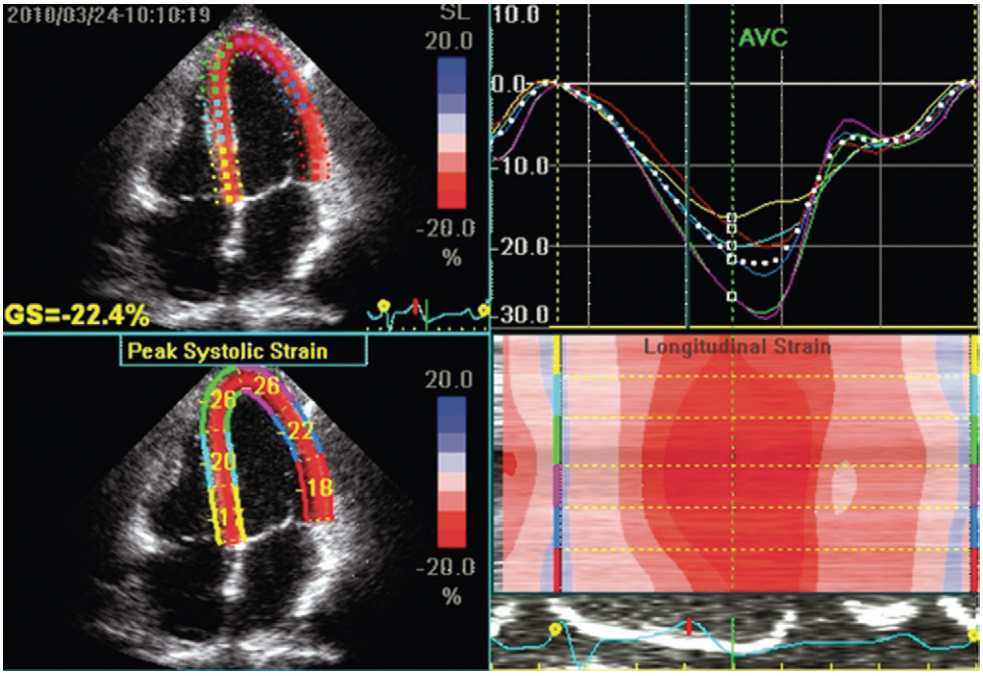



**Figure 26-13 Speckle tracking longitudinal strain.** Transthoracic echocardiogram in the apical four-chamber view with speckle tracking to quantify longitudinal strain with the average values in each myocardial segment (*right panels*). Continuous longitudinal myocardial strain recorded from four myocardial segments shows the high level of concordance between the segments that peak at the same time.

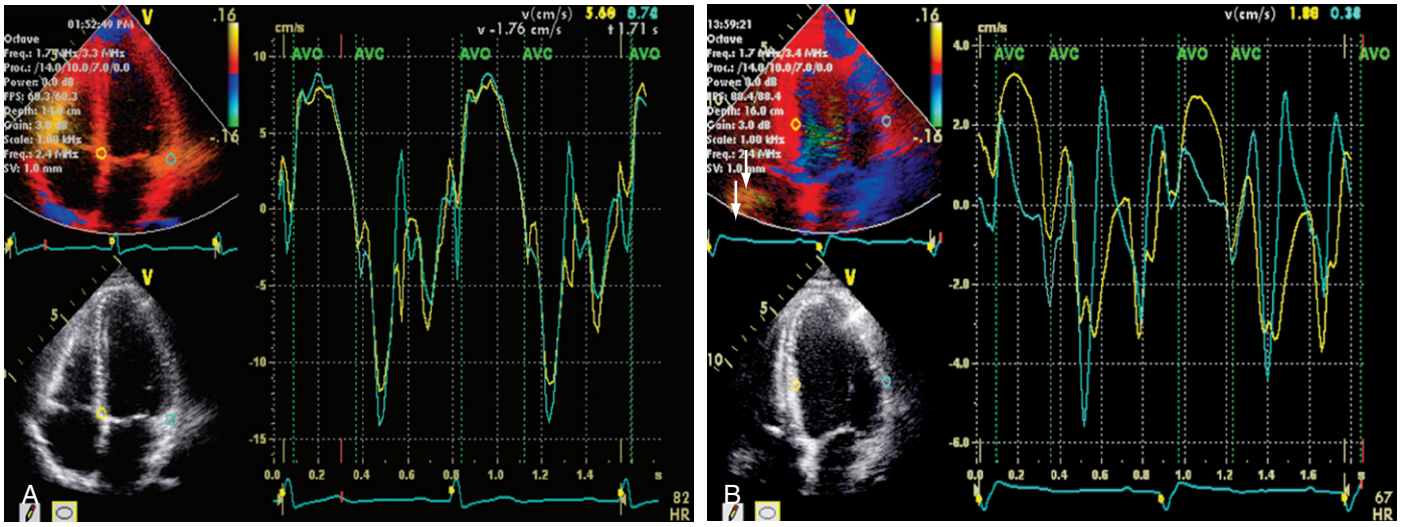



**Figure 26-14 Tissue Doppler myocardial velocity imaging. A,** Transthoracic echocardiogram of a normal LV with sample volumes placed in the proximal septum and in the lateral wall at the level of the mitral annulus (*left panel*) to obtain continuous myocardial velocities with tissue-Doppler imaging. Notice that the two tracings have similar magnitude throughout the whole cardiac cycle and track together in time such that the time interval between the onset of the QRS and acquisition of peak systolic myocardial velocity for the two sample volumes are virtually identical, occurring during ejection between aortic valve opening (*AVO*) and aortic valve closure (*AVC; right panel*). **B,** This recording has an identical format as the previous computer output but in an abnormal heart that shows the significant delay in the peak myocardial velocity in the lateral wall compared with the septum by more than 65 ms, a delay that defined the presence of ventricular dyssynchrony.

isovolumic relaxation time, which is the period between aortic valve closure and mitral valve opening; decreased propagation velocity in the LV inflow tract; and abnormal myocardial diastolic velocities with tissue-Doppler imaging (TDI); (see Chapter 11). TDI myocardial velocities and myocardial displacement reported in small cohorts of patients with diastolic heart failure are normal in more than 50%. Not all of the more specific Doppler echocardiographic parameters listed previously are abnormal in every patient with diastolic heart failure.

Detection of diastolic dysfunction is important because it is associated with a five-fold increase in mortality.[18] The earliest sign of diastolic dysfunction is impairment of relaxation from slowing of the rate of LV diastolic pressure decay. This early evidence for diastolic dysfunction can be detected noninvasively with prolongation of isovolumic relaxation time. Isovolumic relaxation time can be measured with the echocardiography transducer at the apex of the heart angled to record both aortic and mitral valve leaflet motion with Doppler scan and formerly with M-mode echograms recorded at a sweep speed of 200 cm/s.

Slow and prolonged myocardial relaxation are also detectable as altered mitral inflow velocities with a decreased peak velocity during passive filling (E wave), an increased E wave deceleration time, and an augmented peak velocity during active atrial systolic contraction (A wave) with a shortened duration. As the

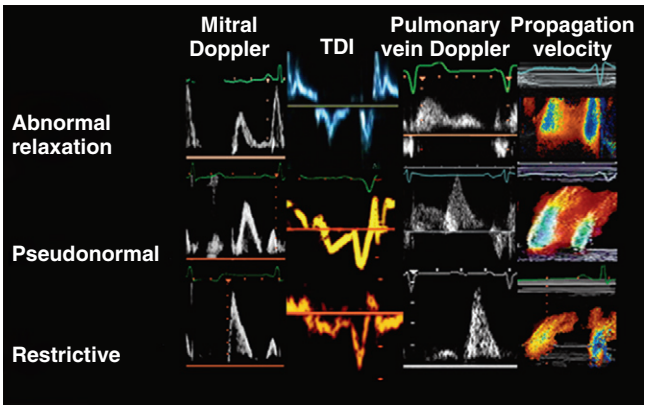



**Figure 26-15** Transmitral Doppler flow velocity, tissue Doppler imaging (TDI), pulmonary vein Doppler velocity and propagation velocity showing transition from abnormal relaxation through pseudo-normalization to restrictive physiology. *(From Zile MR, Brutsaert DL: Circulation 105:1387-1393, 2002.)*

duration of the peak A wave of the mitral inflow shortens, so the duration of the flow reversal in the pulmonary venous velocity profile increases until it finally exceeds the mitral peak A wave duration. Slowed or delayed LV relaxation can be diagnosed with TDI as reduced and delayed E′ velocity of the mitral annulus most frequently obtained from the septum and lateral wall.

The mitral diastolic flow propagation velocity recorded with color flow Doppler scan at the LV inflow correlates with tau (τ) and decreases progressively with increasing LV diastolic dysfunction. LV filling pressure or pulmonary capillary wedge pressure can be derived from the deceleration time of the E wave of the mitral inflow, and a value of less than 140 ms indicates a mitral inflow velocity profile consistent with restrictive physiology. Alternatively, LV diastolic pressure can be estimated from the ratio of E/E′ over a wide range of filling pressures and LV ejection fractions.[19] Chronic LV diastolic dysfunction may transition to heart failure, and in doing so, the mitral inflow, pulmonary venous, and TDI flow velocity profiles change from a pseudonormal pattern, which is reversible, to a restrictive physiology, which is irreversible (Fig. 26-15). Thus, diastolic heart failure can be diagnosed in symptomatic patients with normal LV size and ejection fraction and evidence for abnormal relaxation, diminished compliance, and increased LV diastolic filling pressure.[16]

Cardiac amyloid exemplifies the changes in cardiac architecture, LV diastolic function, and preservation of systolic function until late in the course of the disease. The LV cavity is typically normal size, and wall thickness is moderately to severely increased by deposition of noncontractile amyloid protein (immunoglobulin light chains) in the myocardial interstitium between the myofilaments. This protein deposition alters the material properties of the myocardium and causes increased chamber stiffness and abnormal mitral inflow velocity pattern consistent with restrictive physiology. The deceleration time is dramatically shortened, and the A wave of the mitral inflow is abbreviated and of low amplitude. The duration of the E wave deceleration time in cardiac amyloid is strongly predictive of clinical outcome.[20] In addition, the pulmonary venous velocity spectra show attenuation of the systolic wave. Marked reduction in the E′ wave of the mitral annulus is usually seen in the septum and in the lateral wall. These abnormal Doppler echocardiographic findings progress from the time of diagnosis to the restrictive physiology in the final stages of the disease (see Fig. 26-15).

Hypertrophic cardiomyopathy may present with classic symptoms of heart failure with supranormal systolic function and an ejection fraction of more than 70%. The LV cavity is small or normal with severe LV hypertrophy and asymmetric septal hypertrophy (see Chapter 27) or concentric hypertrophy typical of concentric remodeling. In cases with resting LV outflow tract obstruction, two echocardiographic features assist in diagnosis. Systolic anterior motion of the mitral valve narrows the LV outflow tract. The site of obstruction is shown by the onset of flow acceleration with color flow Doppler scan (see Chapter 27). Of note, diastolic septal thickness of more than 3.0 cm is associated with increased risk of sudden death and is one of the criteria for internal cardiac defibrillator placement. The second echocardiographic finding is the early systolic closure of the aortic valve that occurs at the end of ejection but may happen within the first half of systole. The peak and mean systolic LV outflow tract gradients should be measured at rest and after Valsalva's maneuver or isometric exercise (i.e., hand grip that usually increases the gradients to more than their resting values).

Ischemic cardiomyopathy can be detected with echocardiography because of: (1) the enlarged LV cavity; (2) the ejection fraction of less than 40%; (3) regional wall motion abnormalities; (4) loss of the normal uniform wall thickness; and (5) the near ubiquitous presence of MR.

## Echocardiographic Diagnosis of Right Heart Failure

### ACUTE RIGHT VENTRICULAR HEART FAILURE

Acute right heart failure and RV remodeling may occur over hours as compared with the time course of weeks to months in chronic RV failure. A sudden increase in RV afterload from a major pulmonary embolus causes acute RV dilation and usually severe reduction in systolic contractile function with hemodynamic compromise. This constellation of findings can be shown with Doppler echocardiography and the pathoetiologic mechanism ascertained (Fig. 26-16). Occasionally, mobile thrombus can be seen in transit through the right heart chambers or in the proximal pulmonary arteries (Fig. 26-17) with transthoracic or transesophageal echocardiography. RV function in major pulmonary embolism is severely depressed globally but usually recovers if reperfusion of the pulmonary circulation is reestablished and the increased load is rapidly attenuated with thrombolytic therapy, intravenous high-dose heparin, or acute surgical pulmonary arterial thrombectomy.

Acute RV dilation is associated with mild to moderate tricuspid regurgitation from disruption of the normal tricuspid valve geometry as a result of RV dilation. Pulmonary arterial systolic pressure can be estimated with the modified Bernoulli's formula ($4 \times$ peak [tricuspid regurgitation jet velocity]$^2$ + right atrial pressure). Right atrial pressure can be estimated from the degree of inferior vena cava collapse during normal respiration. The increase in pulmonary arterial systolic pressure is moderate rather than severe and characteristically does not exceed 55 mm Hg. Doppler echocardiography shows the time-dependent changes in RV remodeling in right heart systolic failure, the degree of secondary pulmonary hypertension, and often the pathoetiology of the RV failure.

Isolated RV infarction is a relatively rare cause of acute right heart failure that is important to recognize early and

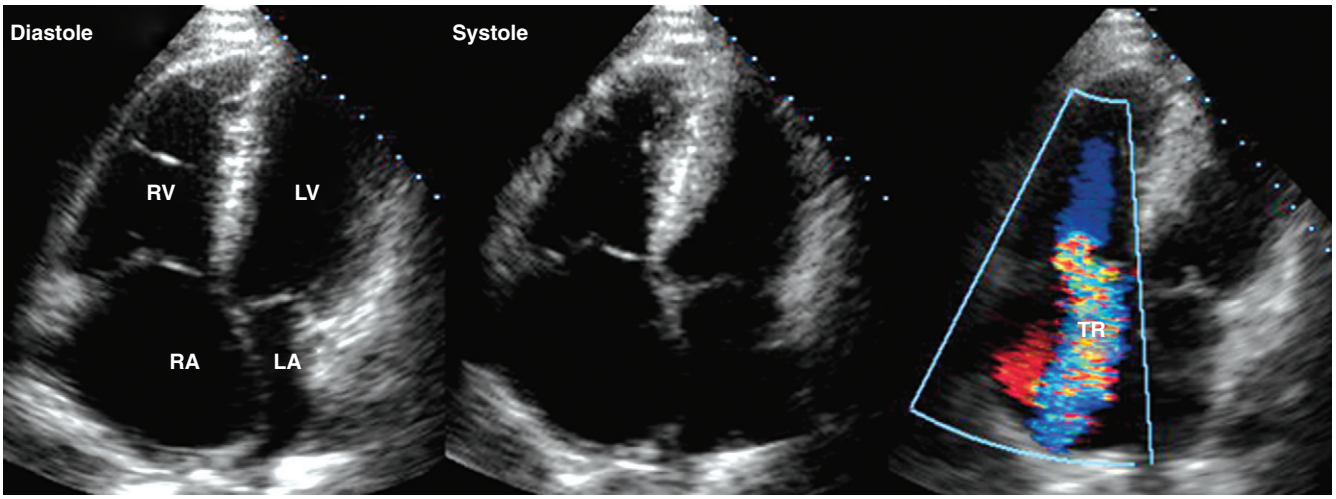



**Figure 26-16 Acute RV failure.** Transthoracic echocardiogram of the four-chamber view from a patient with acute RV strain at end-diastole (*left*) that shows a dilated overloaded RV. The RA is also dilated, and the interatrial septum bulges to the left at end systole (*center*). Color flow Doppler scan (*right*) shows severe tricuspid regurgitation (*TR*).

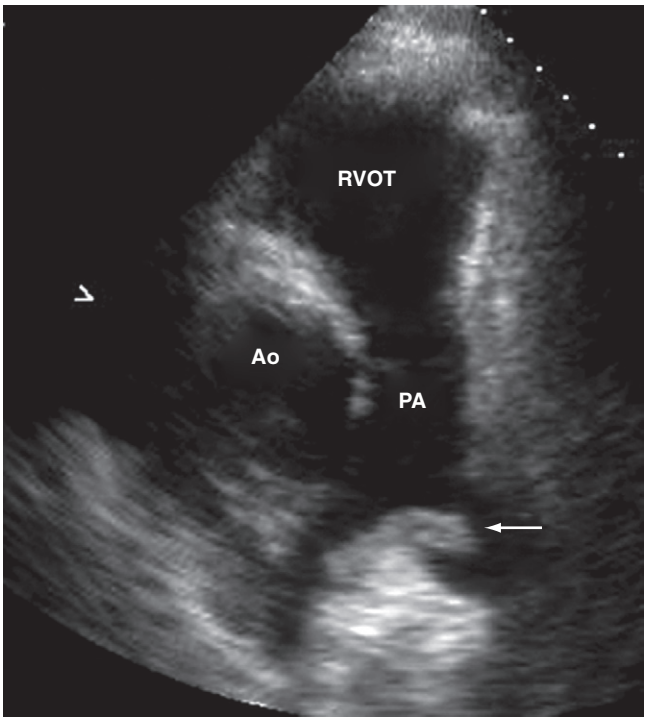



**Figure 26-17 Pulmonary embolus.** Transthoracic echocardiogram shows the main pulmonary artery in long-axis view and the bifurcation across which was a moderately large saddle embolus (*white arrow*).

begin treatment with intravenous fluid resuscitation and coronary reperfusion. The echocardiographic hallmark for diagnosis of RV infarction is unequivocal evidence of RV segmental wall motion abnormality. Usually, RV infarction is an extension of an inferoposterior LV MI as a result of proximal occlusion of a dominant right coronary artery (Fig. 26-18).

## CHRONIC RIGHT HEART FAILURE

In chronic systolic right heart failure, the RV dilates in response to chronically increased loading conditions when hypertrophy can no longer normalize the increase in wall stress. RV hypertrophy may be concentric or eccentric depending on whether the stimulus is pressure or volume overload. As the loading conditions increase, the interventricular septum bulges into the LV outflow tract and the RV shape changes to a more spherical configuration (see Chapter 33). RV diastolic pressure exceeds that in the LV and may result in abnormal LV diastolic filling and intracardiac shunting from right to left if a patent foramen ovale is present. Tricuspid regurgitation develops as the tricuspid subvalve geometry is disrupted by chamber dilation and accelerates the deterioration in RV function with progressive enlargement of the right atrium. As RV failure progresses, the RV continues to enlarge until it forms the apex of the heart. Echocardiographic measurements of RV end-systolic dimension and percent fractional area change in the apical four-chamber or subcostal four-chamber views are important predictors of adverse cardiovascular events.[21]

The configuration and internal architecture of the RV is not designed to generate chronically elevated systolic pressures. When RV systolic pressure exceeds 40 mm Hg, tricuspid regurgitation supervenes, which is associated with further RV dilation, such that a vicious cycle occurs that culminates in right heart failure. Echocardiography plays a key role not only in detection of right heart failure but also in differentiation of acute from chronic right heart failure in terms of LV cavity architecture and function.

Recently, echocardiographic measurements of the tricuspid annulus peak systolic excursion that reflect RV long-axis shortening have been shown to correlate with RV ejection function and predict clinical outcome.[22]

## RIGHT VENTRICULAR REMODELING TO HEART FAILURE

Until recently, few attempts were made to study RV remodeling because the unusual RV architecture cannot be represented by a simple or compound geometric algorithm that enables reproducible assessment of RV volumes and RV ejection fraction. Right ventricular remodeling is usually triggered by LV disease transmitted to the right heart chambers via the pulmonary venous circulation. The pulmonary arterioles react to chronic pressure and volume overload by developing medial hypertrophy that increases pulmonary vascular resistance and in turn

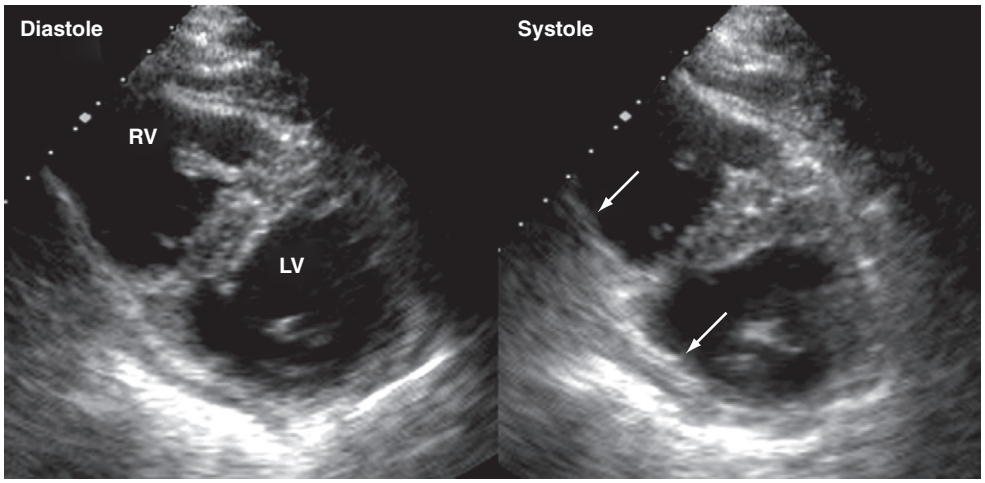



**Figure 26-18 RV infarction.** Parasternal LV short-axis view of a patient with a RV myocardial infarction in diastole (*left*) and in systole (*right*). Contiguous posterior infarction with RV involvement is seen (*white arrows*).

results in pulmonary arterial hypertension. Pulmonary hypertension induces RV hypertrophy that may temporarily normalize RV loading conditions and preserve near-normal RV cavity geometry and function for a prolonged period of time. However, unchecked RV afterload excess from chronic pulmonary hypertension causes progressive RV remodeling with dilation and hypertrophy in similar fashion to that which occurs in the LV (see Chapter 33).

## Echocardiography in Pharmacologic Therapy for Heart Failure

The primary aims in the treatment of chronic systolic heart failure are to provide symptomatic relief, improve quality of life, and ideally increase longevity. These aims may be achieved in part with prevention of progressive LV dilation, promotion of reverse remodeling, and improvement in ventricular function. Doppler echocardiography is the ideal method for tracking longitudinal changes in LV volume, shape, and function that result from treatment interventions. This technique has been used successfully in numerous prospective randomized chronic heart failure trials. New advanced technology with speckle tracking of the myocardium has provided a method for assessment of longitudinal, radial, and circumferential regional and global strain. Strain provides incremental information about myocardial function over and above that of LV volumes and LV ejection fraction.

### PHARMACOLOGIC THERAPY

Contemporary management of acute heart failure involves three fundamental principles. The first is aimed at maintenance of a normal blood pressure for organ perfusion with an increase in contractile performance (myocardial systolic shortening) with intravenous catecholamines in patients with hemodynamic compromise. The second medical strategy is reduction of LV loading conditions with vasodilator therapy. The third medical treatment strategy involves blocking neurohormonal activation with β-adrenergic receptor blockers plus angiotensin receptor blockers or angiotensin-converting enzyme inhibitors in combination with aldosterone antagonists.

Echocardiography has played a pivotal role in showing the efficacy of pharmacologic interventions and identifying individuals at increased risk for major complications in several randomized clinical trials. Echocardiography has clearly shown that serious adverse cardiovascular events, namely recurrent infarction, heart failure exacerbation, ventricular arrhythmias, and death, predominate in patients with progressive LV dilation.[23,24]

Serial echocardiography in patients with acute heart failure after MI provides unique information that is unattainable routinely with any other imaging technique and allows early risk stratification for optimization of individualized therapy. Numerous clinical post-MI and heart failure trials have shown that echocardiographic measurements of LV volumes, ejection fraction, and infarct size and RV systolic shortening predict clinical outcome (Fig. 26-19).[24-26] The prevalence of these adverse cardiovascular events increases directly with LV dilation assessed with echocardiography. Prevention of LV dilation and remodeling with angiotensin-converting enzyme inhibitors reduces the recurrence rate of heart failure. Echocardiographically determined LV volumes and percentage changes in systolic cavity area are powerful predictors of ventricular arrhythmias from the early postinfarction period through the 2-year follow-up (see Fig. 26-19).[21]

Serial echocardiographic measurements of LV size and function have shown the efficacy of angiotensin-converting enzyme inhibitors in infarct-related heart failure that is mediated through attenuating LV dilation by structural and functional reverse remodeling and blocking the neurohormonal activation.[23-26] Logistic regression analysis of baseline demographics for predictors of survival in post-MI and heart failure trials showed that echocardiographic LV end-systolic size was the most powerful predictor of survival after MI, even more than ejection fraction.[24] Similar randomized controlled trials of β-adrenergic receptor blocking agents in chronic systolic heart failure have used quantitative echocardiography to document efficacy.

## Echocardiography for Mechanical Therapies in Heart Failure

Surgical treatment has an important role in the management of acute heart failure and, similar to medical treatment, is based on two strategies. The first strategy is augmentation of cardiac output either with intraaortic balloon counterpulsation, LV or

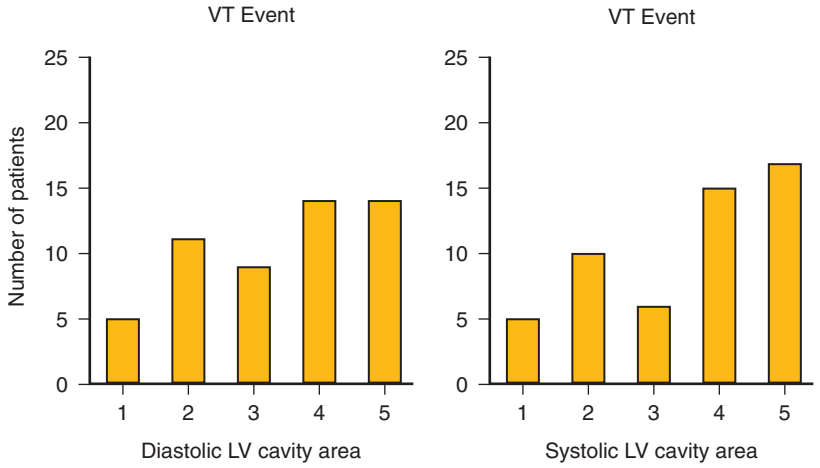



**Figure 26-19 Ventricular tachycardia after myocardial infarction.** A strong relationship is shown between LV size in diastole (*left*) and in systole (*right*) and ventricular tachycardia early after myocardial infarction. The same robust relationship was present at 2 years after myocardial infarction. *(From unpublished data.)*

RV assist device (Fig. 26-20), or acute heart transplantation. The second strategy is reduction of the acute elevation in LV loading conditions from MR with mitral valve repair or replacement and with aortic valve replacement for heart failure from acute or chronic severe valvular regurgitation.

## INTRAAORTIC COUNTERPULSATION

No randomized clinical trials with Doppler echocardiography have assessed the efficacy of intraaortic balloon counterpulsation in acute heart failure after MI where echocardiographic assessment was a primary or secondary endpoint. However, Doppler echocardiographic assessment of cardiac output is used routinely to measure the impact of intraaortic balloon counterpulsation on LV volumes, ejection fraction, and cardiac output. Forward stroke volume can be estimated as the product of the cross-sectional area of the flow stream and the time-velocity integral recorded from the LV outflow tract. Reliable Doppler echocardiographic measurements are critically important before and immediately after deployment of an intraaortic balloon counterpulsation and also during weaning from intraaortic balloon counterpulsation support, as the counterpulsation–to–native heart ratio is downgraded from 1:1 to 1:2 and 1:3. When cardiac output remains stable, withdrawal of intraaortic balloon counterpulsation can be achieved safely.

## VENTRICULAR ASSIST DEVICES

Placement of LV assist devices (LVAD) for severe acute heart failure or acute hemodynamic decompensation of chronic heart failure is becoming increasingly frequent.[27] Echocardiographic screening for significant aortic regurgitation and LV apical thrombus before insertion is important to avoid systemic embolization during insertion of the LV cannula. After insertion of a LVAD, which may provide pulsatile or nonpulsatile flow, the presettings of the LVAD pump are routinely evaluated with Doppler echocardiography over a range of flows. LV output is assessed by aligning the continuous wave Doppler scan parallel with the direction of blood flow through the sump drain at the LV apex. Stroke output is calculated as the product of the time-velocity integral and the cross-sectional area of the outlet cannula (see Fig. 26-20). Doppler echocardiographic assessment of LV outputs is reliable and correlates closely with LVAD flow rates. When divergence is found between the two estimates of flow, the Doppler flow is invariably lower; but if this occurs across a range of flow settings, it suggests partial obstruction of the LV outlet by thrombus either within or protruding into the LV apical cannula (Fig. 26-21).[28] Partial occlusion of the LV outlet cannula by either apical thrombus or myocardial trabeculations is identified by the presence of flow acceleration with color flow Doppler scan and a large systolic gradient across the LV apical outflow cannula (see Fig. 26-20). Recently, long-term or so-called destination LVAD therapy has been instituted for patients who need obligatory mechanical support and are not suitable candidates for orthotopic heart transplantation. These patients need regular corroboration between the pump flows and Doppler echocardiographic estimates of flow.

## SURGICAL VALVE REPAIR OR REPLACEMENT

Other surgical interventions for acute heart failure aim for reduction in systolic loading conditions, including mitral valve repair or replacement for acute severe MR after chordal rupture that results in a flail leaflet or papillary muscle rupture after MI. Similar reduction in afterload is the aim in patients with acute severe aortic regurgitation either from aortic valve endocarditis or from acute type A aortic dissection. In addition to establishing these individual diagnoses with either transthoracic or transesophageal assessment, baseline echocardiographic ejection fraction and LV size are the major determinants of survival and clinical outcome. Furthermore, Doppler echocardiography has been used to compare LV architecture (LV volume and mass) and function (ejection fraction) before and after surgery to determine whether any favorable structural changes have occurred that might explain the symptomatic improvement that occurs after successful surgery.

## CARDIAC RESYNCHRONIZATION THERAPY

Cardiac resynchronization therapy is a newly established therapy for patients with New York Heart Association symptom class II through IV heart failure, a prolonged QRS duration (more than 120 ms), and LV dyssynchrony. Prolonged QRS duration occurs in 30% to 50% of patients with heart failure and correlates directly with mortality.[29] The specific aim of CRT in heart failure is to alleviate symptoms and promote structural and functional reverse LV remodeling. This result is achieved with optimizing atrioventricular conduction,

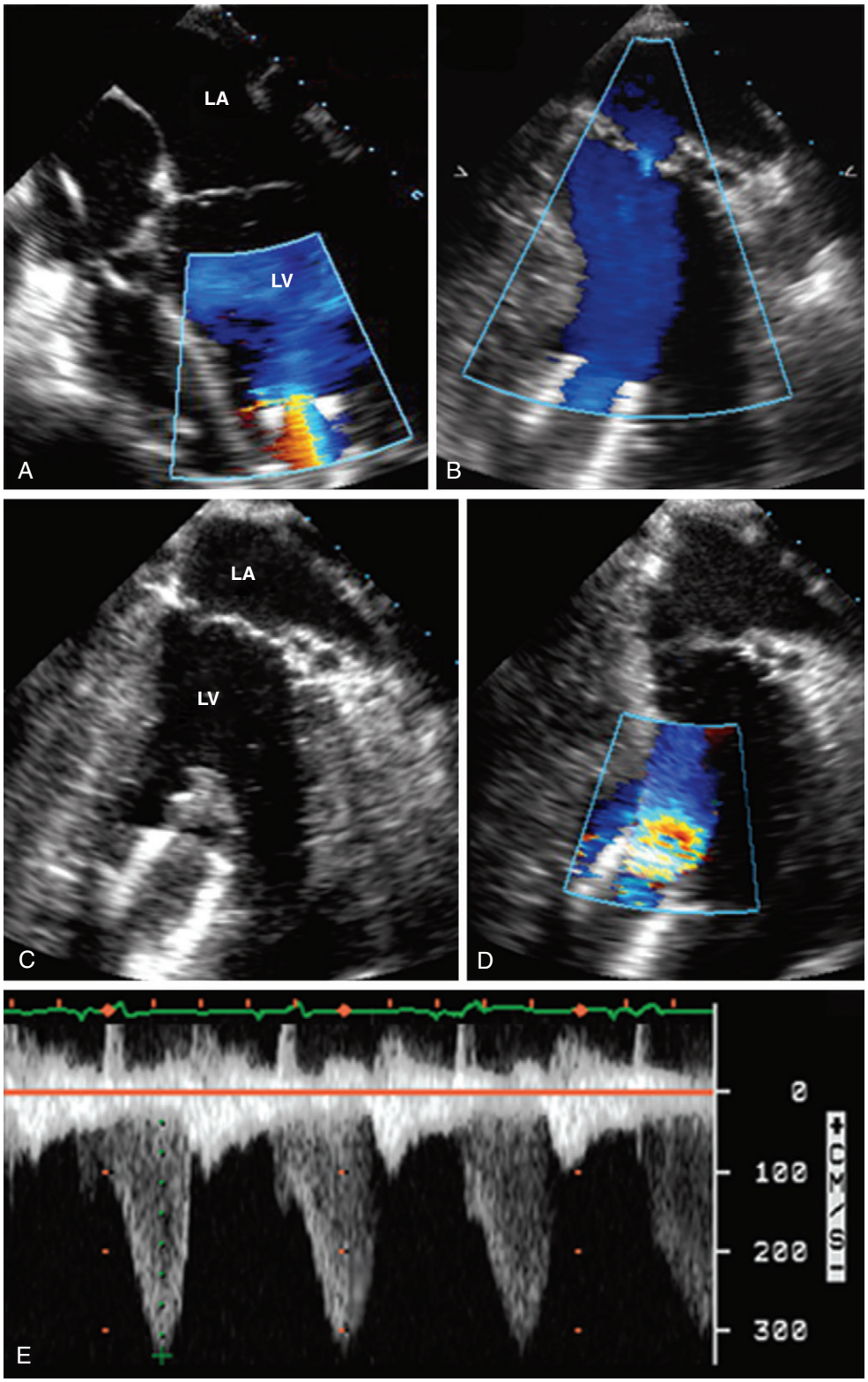



**Figure 26-20 Transesophageal echocardiogram of a patient with LV assist device.** The cannula is seen at the LV apex (**A** and **B**). A thrombus can be seen in the LV assist device cannula with color flow Doppler scan that shows obstruction (**C** and **D**). A systolic gradient was detected across the sump drain at the LV apex, corroborating the gradient obtained previously (**E**).

prolonging LV filling time, and synchronizing RV and LV contraction by minimizing interventricular and intraventricular mechanical delay.

Symptomatic benefit and improved exercise capacity have been consistent findings in CRT trials in most patients (65%)[30-36] already undergoing optimal medical heart failure therapy. Doppler echocardiography has played a crucial role in elucidating the mechanism of structural and functional LV reverse remodeling with CRT. Doppler echocardiography has also been used in an attempt to identify the 60% to 70% of

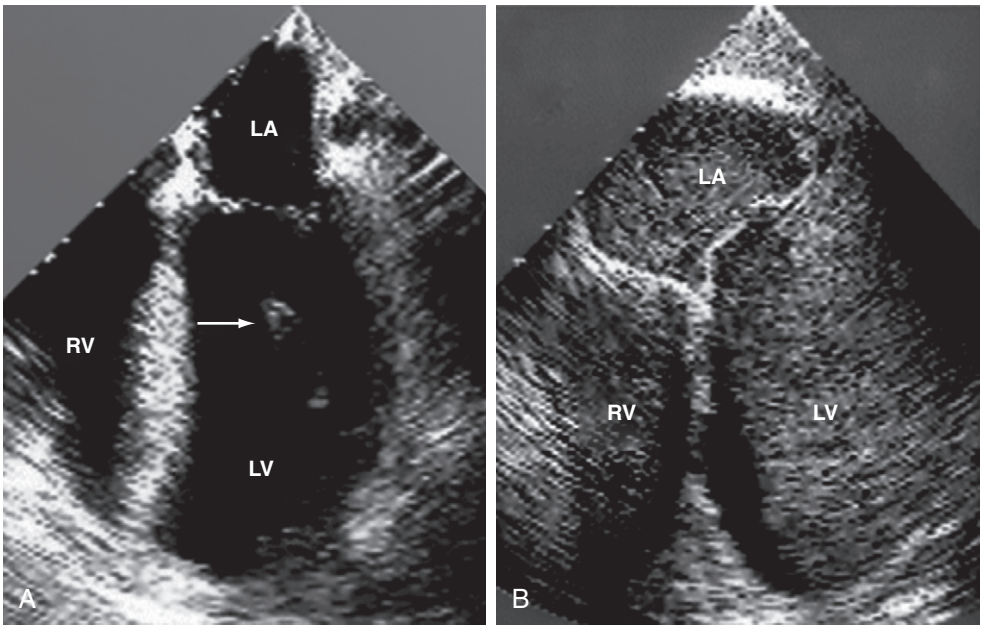



**Figure 26-21 Refractory right heart failure occurred 3 days after LV assist device placement.** At baseline, post device deployment was unremarkable except for a small mobile thrombus (**A**). On day 3, an emergency echocardiogram was performed that showed almost complete cardiac thrombosis from which the patient sustained a stroke and died soon after (**B**).

patients that are likely to respond to CRT before device implantation. The PROSPECT trial used advanced Doppler echocardiographic technology with the specific aim of discovering which Doppler echocardiographic parameter reliably identified patients with heart failure who have an optimal response to CRT before device implantation.[37] This trial failed to show that any single Doppler echocardiographic measurement predicted response to CRT. This negative PROSPECT trial resulted in a major loss of confidence in Doppler echocardiography by electrophysiologists. However, a number of recent studies have shown that the major reasons for the lack of response in 30% of patients with heart failure have been attributed to inappropriate LV lead position, the absence of dyssynchrony, or both of these factors. Of note, nonresponders to CRT, when treated aggressively with programmed medical therapy, achieved the same degree of symptomatic improvement and reverse remodeling as did the positive responders.[38] Internal cardiac defibrillator together with CRT affords additional survival benefit[35,39,40] by protecting against sudden death from ventricular arrhythmias.

Recently, large CRT trials[37-41] have used serial Doppler echocardiography to characterize LV structural and functional reverse remodeling and have shown for how long reverse remodeling is sustained. Most of these trials used echocardiographic assessment of LV end-diastolic and end-systolic diameters or LV volumes as secondary endpoints and showed that CRT results in significant decrease as early as 1 month[42,43] compared with control. Further reduction in LV volumes occurs by 6 months (Fig. 26-22), and these changes are sustained for at least 18 months[39-41] and potentially as long as 44 months when data are available from MADIT-CRT, RAFT, and REVERSE extension trials. The reduction in LV volumes with CRT results in a decrease in LV wall stress, which is a powerful stimulus for regression of LV mass. The decrease in LV mass was significant by 6 months but occurred at a slower rate than the reduction in LV volume.

Serial echocardiographic studies have shown that the sustained reductions in LV volume and mass with CRT result in alterations in LV architecture and restoration of mitral annular and subvalve geometry towards normal. Changes in the geometry of the mitral valve apparatus are associated with decreased MR. The severity of MR decreased significantly by 3 months and was maintained at 6 and 12 months (see Fig. 26-22). The favorable changes in LV load and architecture, together with the decrease in MR, are associated with progressive increase in LV ejection fraction at 3 and 6 months from baseline (see Fig. 26-22). Continuous CRT is required to sustain reverse LV remodeling.[44]

### *Changes in Diastolic Ventricular Function with Cardiac Resynchronization Therapy*

Cardiac resynchronization therapy studies have been conducted almost exclusively in patients with advanced systolic heart failure, but Doppler echocardiography has shown concomitant improvements in diastolic function.[43] CRT prolongs the duration of LV filling, separates the rapid filling phase from atrial systolic contraction, shortens interventricular mechanical delay, and coordinates regional and global ventricular contraction and relaxation. The prolonged LV diastolic filling time induced by CRT is not associated with changes in transmitral peak flow velocities during passive filling (E wave), during atrial contraction (peak A wave), the E/A ratio, or isovolumic relaxation time. The E wave deceleration time and the myocardial performance index improve by 3 months and improve further by 12 months.[43] However, patients with restrictive LV filling characterized by a short deceleration time and peak E wave velocity of more than 1.0 m/s exhibit little or no response to CRT.

Historically, exercise capacity in systolic heart failure has not correlated with changes in LV volume or ejection fraction. However, in the MIRACLE trial, the symptomatic benefits associated with CRT occurred predominantly in those patients with the greatest structural and functional LV remodeling.[30]

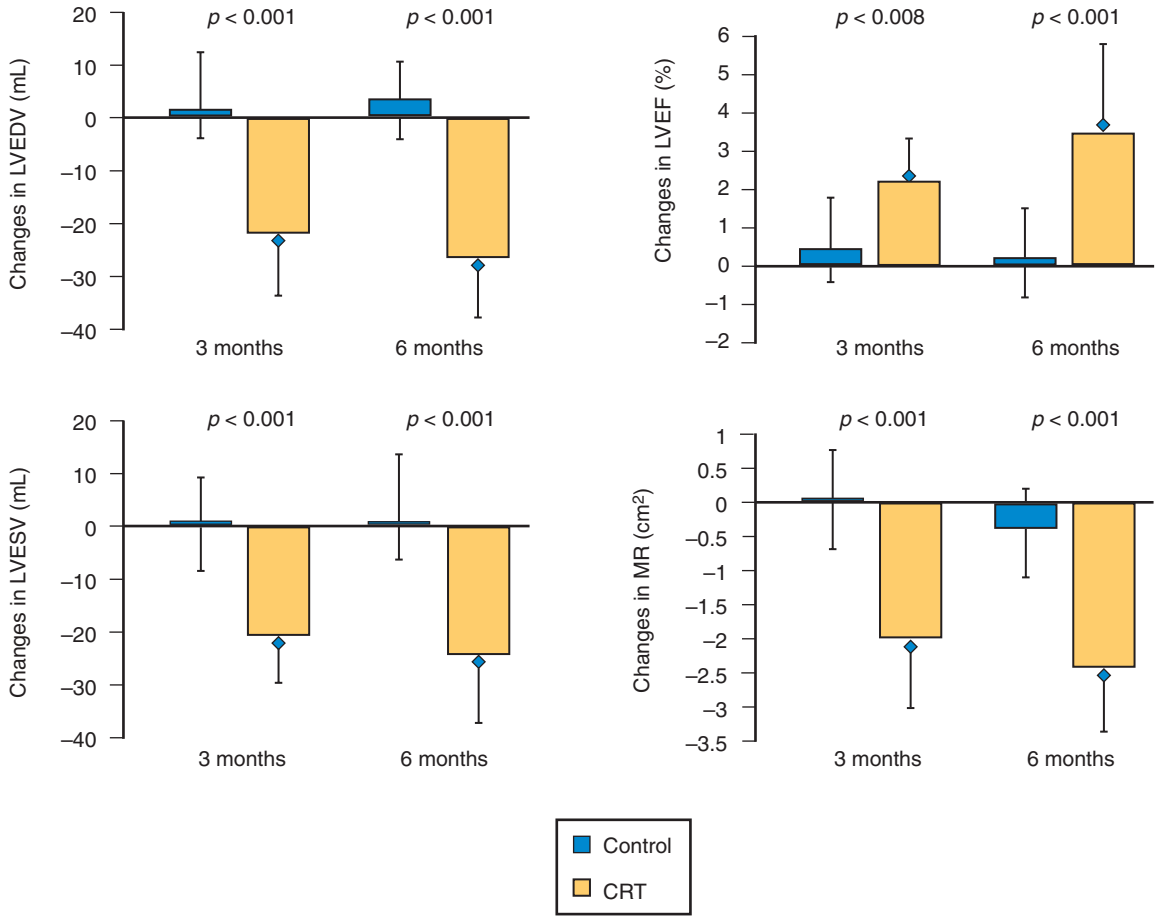



**Figure 26-22 Median changes in LV end-diastolic and end-systolic ventricular volumes, ejection fraction, and severity of mitral regurgitation.** All improved with cardiac resynchronization therapy as compared with optimized heart failure treatment at 3 and 6 months. *(With permission from St. John Sutton MG, Lee D, Rouleau JL, et al: Left ventricular remodeling and ventricular arrhythmias after myocardial infarction.* Circulation *107:2577-2582, 2003.)*

### *Responders and Nonresponders to Resynchronization Therapy*

The proportion of patients with New York Heart Association III/IV heart failure who respond to CRT (60% to 65%) by exhibiting LV reverse remodeling measured with Doppler echocardiography and symptomatic improvement is similar in patients with ischemic and nonischemic heart failure. Reduction in LV volumes and severity of MR and increase in LV ejection fraction are consistently two to three times greater in nonischemic than ischemic heart failure.[44,45] However, in spite of the two-fold to three-fold difference in LV volume reduction in the nonischemic cases at 6 months, both ischemic and nonischemic heart failure have similar improvement in symptoms and exercise capacity.

### *Predictors of Optimal Response to Resynchronization Therapy*

Between 60% and 70% of all patients for CRT exhibit reverse LV remodeling shown with echocardiography. The reasons for this short fall are not clear even 10 years after use was approved by the U.S. Food and Drug Administration. No baseline clinical demographics distinguish responders from nonresponders to CRT or predict an optimal response before device implantation. A number of possible mechanisms have been proposed. One theory is suboptimal placement of the RV or LV electrodes, especially in ischemic heart failure when myocardial scar may be subjacent to the LV electrode or when electrode placement is constrained by the anatomy of the coronary sinus. Prolonged QRS duration has been used as a surrogate for LV dyssynchrony even though the coefficient of correlation is weak ($r = 0.26$).[46-48] The presence of LV mechanical dyssynchrony is a prerequisite for optimal response to CRT, without which there is no substrate for improvement. However, prolonged QRS, and not ventricular dyssynchrony, is a guideline for use of CRT.

## NEW TECHNIQUES FOR DETECTION OF LEFT VENTRICULAR DYSSYNCHRONY

New advanced noninvasive imaging technology has recently been introduced for detection and semiquantification of regional (spatial) and temporal LV mechanical dyssynchrony or incoordinate contraction for identification of responders to CRT before device placement. Baseline clinical demographics, QRS duration, and echocardiographic measures of LV size or end-systolic volume, which are normally powerful predictors of clinical outcome, do not reliably predict response to CRT. What appears to be fundamental for a positive response to CRT is the presence of regional and global LV dyssynchrony that is associated with delayed electrical activation (prolonged QRS).

In the healthy heart, electrical activation results in synchronous long-axis and short-axis contraction. The concentric

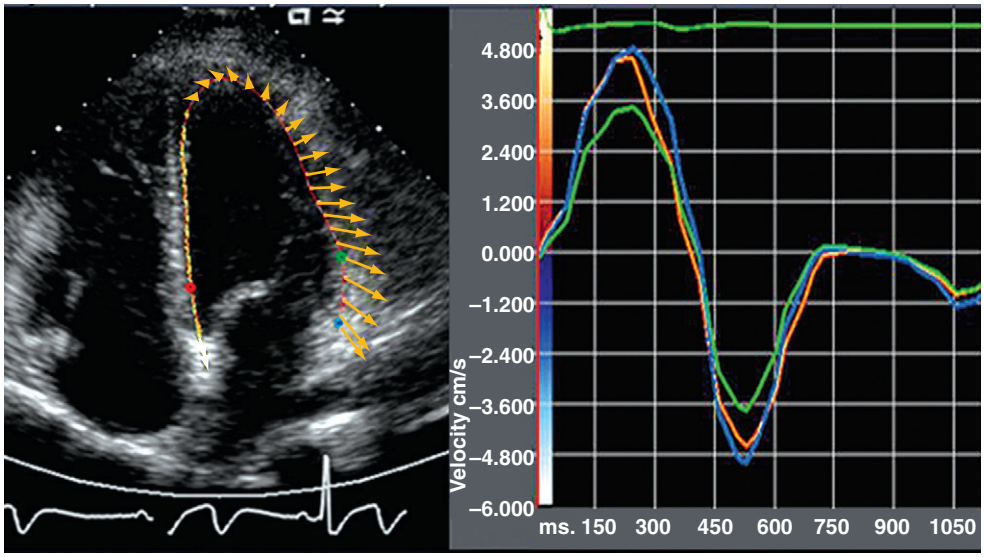



**Figure 26-23 Myocardial tracking in the four-chamber view from a healthy subject.** The continuous velocities of all LV segments should be aligned in time at the acme, the zero crossing point, and the nadir, indicating that the opposing walls in healthy subjects are completely synchronous.

inward wall motion can be appreciated visually in 2D and 3D echocardiograms of LV short-axis and LV apical four-chamber and two-chamber echocardiograms. Alternatively, myocardium can be tracked with velocity vector imaging or speckle tracking techniques (Fig. 26-23). LV dyssynchrony is the result of premature regional contraction before ejection or delayed regional contraction that stretches already contracting myocardium and thereby disrupts the normal coordinated sequence of activation and contraction that results in reduction in ejection fraction. The time interval between maximal posterior excursion of the septum and peak anterior excursion of the posterior LV wall with M-mode echocardiography LV wall has been used to identify dyssynchrony defined as a time delay of more than 130 ms.[49] This method is restricted to two opposing walls of the LV, and measurement of this time delay may not be possible when the septum is infarcted and does not thicken or move posteriorly. Several Doppler echocardiographic methodologies have been advocated for the diagnosis of dyssynchrony.

One of the most frequently used TDI methods for detection of LV dyssynchrony is measurement of the time interval from the onset of the QRS to the peak myocardial longitudinal systolic velocities in the basal and middle wall segments of opposing walls from the apical four-chamber, apical two-chamber, and apical long-axis views with color-coded or pulsed TDI (see Fig. 26-14). A delay in the time from the QRS to the peak velocity between segments in opposing walls of more than 65 ms is evidence for LV dyssynchrony and moreover predicts a favorable response to CRT. A more comprehensive assessment of LV dyssynchrony is the mechanical dyssynchrony index, which requires measurement of all six basal and middle segments in the three apical views and computation of the standard deviation of the time to peak systolic myocardial velocity that occurs during LV ejection. LV dyssynchrony can be detected throughout the LV as regional variation in the relative timing of contraction and automated time to peak velocities registered on the 2D echocardiographic images as color-coded overlays. This technique is commercially available and known as tissue synchronization imaging. These parameters are more robust estimates of LV dyssynchrony than measurement of the QRS duration, which has been used erroneously as a surrogate for dyssynchrony.

Regional deformation or strain defined as change in length through the cardiac cycle expressed as a ratio of resting length can be computed in the LV short axis (radial strain) and in the LV long axis (longitudinal strain) with speckle tracking techniques (Figs. 26-24 and 26-25). This can be used to detect LV dyssynchrony as delay in time to peak strain. These values can be displayed in simple graphics that enable dyssynchrony to be recognized. The topographic representation of dyssynchrony (see Figs. 26-14, 26-24, and 26-25) in terms of longitudinal and radial strain can be displayed in the format of a polar map. Speckle tracking of the myocardium and velocity vector imaging of the myocardium enable recording from multiple regions of myocardium simultaneously and analysis of timing of peak myocardial velocities (see Fig. 26-23). Strain rate imaging has thus far been disappointing as a measure of dyssynchrony on account of its limited reproducibility.

Real-time 3D echocardiography with the conventional 16-segment or 17-segment models of the LV can show LV dyssynchrony as regional variation in the timing of acquisition of minimal systolic and maximal diastolic volumes for each of the segments (Fig. 26-26). In addition, after resynchronization therapy, restoration of coordinated contraction occurs with minimal differences in the timing of onset of contraction and peak shortening among the 16 or 17 segments. Myocardial velocity information from real-time 3D echocardiography can also be displayed in a polar map format of the 16 or 17 LV segments, which when color-coded for time, provides a velocity map in real time that enables dyssynchrony to be easily identified visually (Fig. 26-27).

## HEART TRANSPLANTATION

Orthotopic heart transplantation is performed in patients with chronic and occasionally acute heart failure, which is refractory to medical therapy in approximately 2000 patients annually in

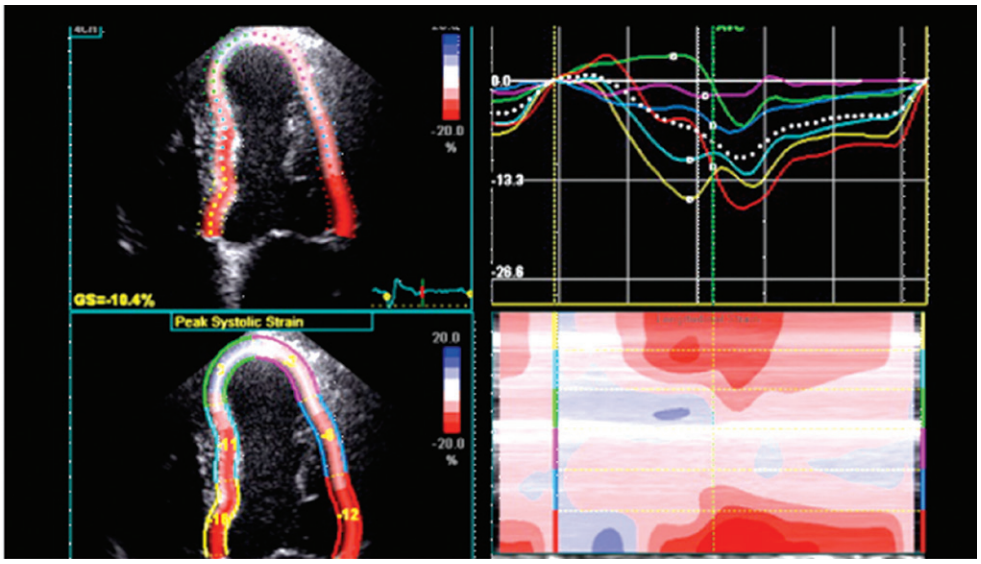



**Figure 26-24 Speckle tracking in the apical four-chamber view to measure global longitudinal strain and regional longitudinal strain from four myocardial segments from a patient with ischemic cardiomyopathy.** The two important findings are: first, the close time relations in acquisition of peak longitudinal strain from each segment is lost, suggesting the presence of ventricular dyssynchrony; and second, the magnitude of peak longitudinal by all segments is low and corroborated by the continuous recording of global strain. Compare with the normal tracing shown in Figure 26-13.

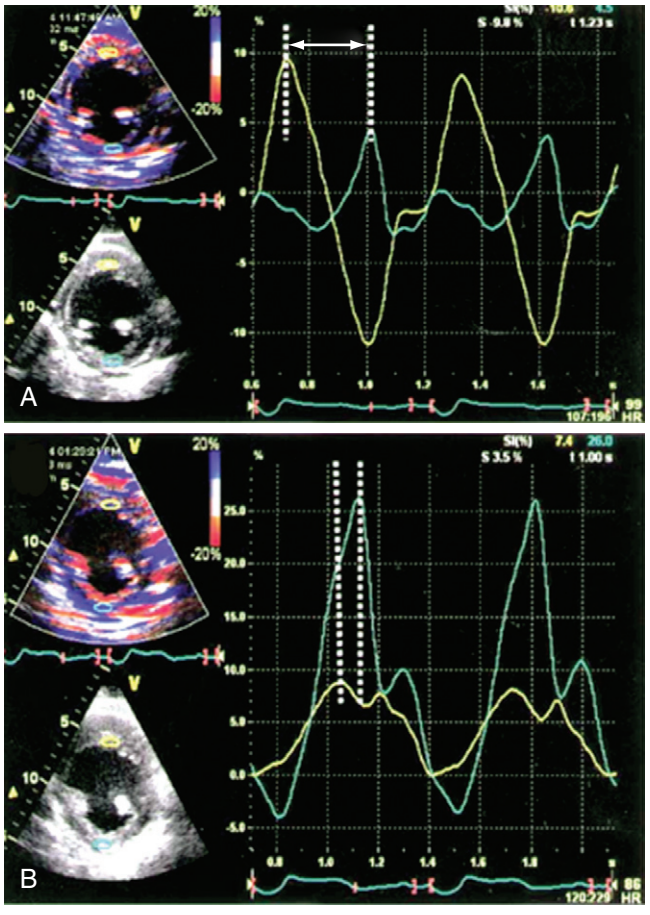



**Figure 26-25 A,** Radial strain imaging in a patient with ventricular dyssynchrony and a favorable response to cardiac resynchronization therapy. At baseline, the anterior septum had early peak strain development coincident with aortic valve opening (*AVO*), and the posterior wall development of peak radial strain occurred late coincident with aortic valve closure (*white arrows*) consistent with severe dyssynchrony. **B,** Time-strain plots after cardiac resynchronization therapy showed immediate improvement in the close time relations between peak strain developed by the same two myocardial walls, indicating immediate improvement in dyssynchrony. *(From Dohi K, Suffoletto MS, Schwartzman D, et al: Utility of echocardiographic radial strain imaging to quantify left ventricular dyssynchrony and predict acute response to cardiac resynchronization therapy.* Am J Cardiol *96:112-116, 2005.)*

the United States. This number of heart transplants has not increased in the last 5 years nationwide because of the scarcity of donors, the logistics and expense of organ procurement, and the subsequent immunosuppression therapy. Doppler echocardiography plays an important role in heart transplantation. The first role is in assessment of the donor heart for global and regional function and exclusion of all pathology. Second, after transplantation, Doppler echocardiography is used in the early postoperative period in all patients, especially those in whom early complications develop from rejection or severe pump failure and who need LVAD placement. The dramatic temporal and spatial changes in LV and RV structure and function in the transplanted heart have been well characterized with Doppler echocardiography[50] and are described in the chapter on heart transplantation (see Chapter 30).

## Summary

Recent advances in Doppler echocardiographic imaging have provided new insights into patient selection for novel heart failure therapies. LV volumes and ejection fraction can be computed and have proved to be powerful predictors of clinical outcomes in heart failure. The introduction of speckle tracking enables temporal and spatial quantification of regional and global myocardial strain that can be displayed as a polar map, and allows instantaneous visual recognition of the topography of abnormal longitudinal and radial strain distribution throughout the LV. CRT is now recognized as effective treatment in patients deemed refractory to traditional heart failure, although no significant benefit of CRT occurs in 30% of patients.

Current ongoing randomized CRT trials suggest that nonresponders to CRT with or without prolonged QRS duration have little or no ventricular dyssynchrony and have the worst prognosis.

Similar to surgical interventions and devices, pharmacologic agents are needed to do more than provide symptomatic relief by preventing development of heart failure and reversing rather than just attenuating the remodeling process. The efficacy and monitoring of new therapies are assessed by 2D and 3D echocardiographic imaging and quantitative Doppler echocardiography.

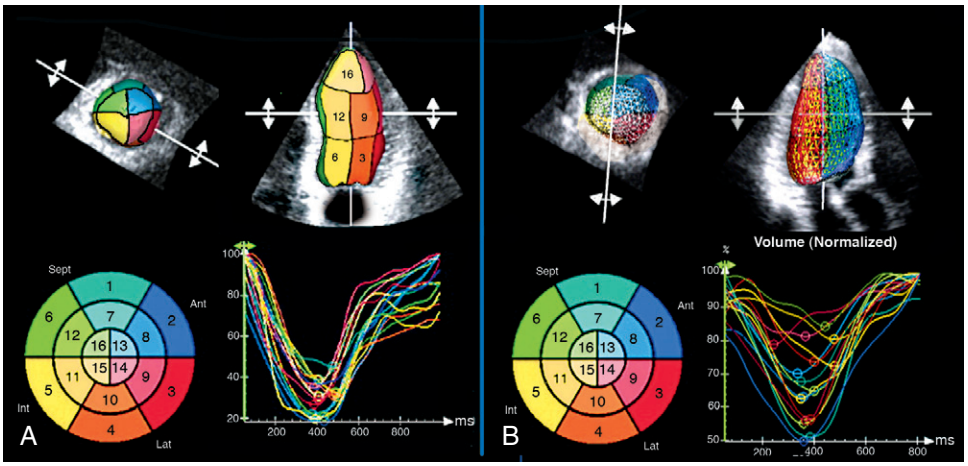



**Figure 26-26** **A,** Real-time 3D echocardiogram recordings from the apex enable the heart to be segmented with either a 16-segment or 17-segment model with continuous time-volume curves from each myocardial segment. In a normal heart, the minimal/end-systolic volumes from each segment occur at the same time (*bottom right*). **B,** By comparison with the normal heart in **A,** major differences in time of minimal/end-systolic volume for each segment (*bottom right*) are consistent with major dyssynchrony that is likely to improve with cardiac resynchronization therapy.

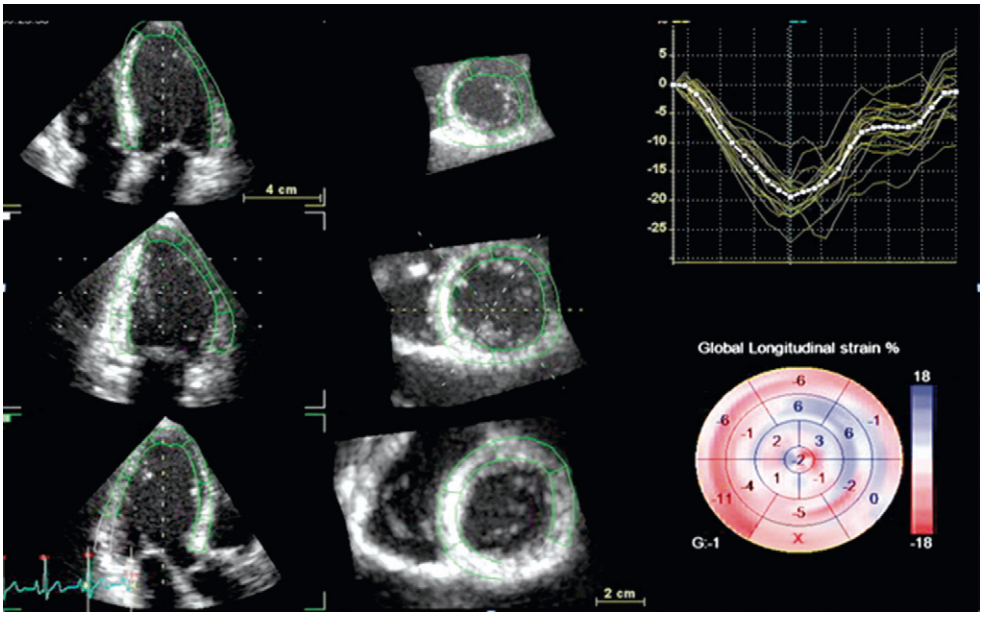



**Figure 26-27** Real-time 3D echocardiogram with speckle tracking provides instantaneous time-longitudinal strain plots for each segment and for global strain. The timing of peak strain enables dyssynchrony to be recognized and enables identification of patients likely to benefit from cardiac resynchronization therapy.

## KEY POINTS

- Echocardiography is the single most useful diagnostic test in evaluation of patients with heart failure.
- In chronic systolic heart failure, LV remodeling leads to a change in cavity shape because of the greater increase in the short-axis diameter than in LV long-axis diameter. As a result, the LV loses its ellipsoidal shape and becomes more spherical. LV shape is a predictor of clinical outcome.
- The four important sequelae to the abnormal LV size and shape are:
  - Increase in LV loading conditions.
  - Decrease in contractile function.
  - Predisposition to thrombus formation.
  - Mitral regurgitation from enlargement of the mitral annulus and distortion of the mitral valve and subvalvular geometry.
- Echocardiography plays a vital role in the diagnosis of right-sided heart failure and differentiation of acute from chronic right-sided heart failure in terms of RV cavity architecture and function.
- CRT is an established therapy for patients with New York Heart Association II to IV heart failure, prolonged QRS duration (more than 130 ms), and LV dyssynchrony.
- CRT reverses LV remodeling by optimizing atrioventricular conduction, prolonging LV filling time, and synchronizing RV and LV contraction.
- CRT studies have been conducted almost exclusively in patients with advanced systolic heart failure, but Doppler echocardiography has consistently shown concomitant improvements in diastolic function.
- Only 60% to 65% of patients with heart failure and QRS duration of more than 130 ms respond to CRT therapy.
- LV mechanical dyssynchrony is a prerequisite for response to CRT. Prolonged QRS duration correlates poorly with dyssynchrony and may be absent despite prolonged QRS duration.
- Longitudinal and radial strain and the 3D echocardiographic regional volume estimations may prove more robust estimates of LV dyssynchrony than QRS duration.

## REFERENCES


1. Aurigemma GP, Gaasch WH: Clinical practice. Diastolic heart failure. *N Engl J Med* 351:1097-1105, 2004.
2. Owan TE, Hodge DO, Herges RM, et al: Trends in prevalence and outcome of heart failure with preserved ejection fraction. *N Engl J Med* 355:251-259, 2006.
3. Kitzman DW, Little WC, Brubaker PH, et al: Pathophysiological characterization of isolated diastolic heart failure in comparison to systolic heart failure. *JAMA* 288:2144-2150, 2002.
4. Zile MR, Brutsaert DL: New concepts in diastolic dysfunction and diastolic heart failure: part I: diagnosis, prognosis, and measurements of diastolic function. *Circulation* 105:1387-1393, 2002.
5. Gorcsan J, 3rd, Gasior TA, Mandarino WA, et al: Assessment of the immediate effects of cardiopulmonary bypass on left ventricular performance by on-line pressure-area relations. *Circulation* 89:180-190, 1994.
6. Zile MR, Baicu CF, Gaasch WH: Diastolic heart failure: abnormalities in active relaxation and passive stiffness of the left ventricle. *N Engl J Med* 350:1953-1959, 2004.
7. Thom T, Haase N, Rosamond W, et al: Heart disease and stroke statistics: 2006 update: a report from the American Heart Association Statistics Committee and Stroke Statistics Subcommittee. *Circulation* 113:e85-e151, 2006.
8. Vasan RS, Larson MG, Benjamin EJ, et al: Congestive heart failure in subjects with normal versus reduced left ventricular ejection fraction: prevalence and mortality in a population-based cohort. *J Am Coll Cardiol* 33:1948-1955, 1999.
9. Gheorghiade M, Bonow RO: Chronic heart failure in the United States: a manifestation of coronary artery disease. *Circulation* 97:282-289, 1998.
10. Hunt SA, Abraham WT, Chin MH, et al: ACC/AHA 2005 guideline update of the diagnosis and management of chronic heart failure in the adult: a report of the American College of Cardiology/American Heart Association Task Force on Practice Guidelines (Writing Committee to Update the 2001 Guidelines for the Evaluation and Management of Heart Failure): developed in collaboration with the American College of Chest Physicians and the International Society for Heart and Lung Transplantation: endorsed by the Heart Rhythm Society. *Circulation* 112:e154-e235, 2005.
11. Pfeffer MA, Braunwald E, Moye LA, et al: Effect of captopril on mortality and morbidity in patients with left ventricular dysfunction after myocardial infarction. Results of the survival and ventricular enlargement trial. The SAVE Investigators. *N Engl J Med* 327:669-677, 1992.
12. Grigioni F, Enriquez-Sarano M, Zehr KJ, et al: Ischemic mitral regurgitation: long-term outcome and prognostic implications with quantitative Doppler assessment. *Circulation* 103;1759-1764, 2001.
13. Reichek N, Wilson JR, St John Sutton M, et al: Non-invasive determination of LV end-systolic stress: validation of the method and initial application. *Circulation* 65:99-108, 1982.
14. Effect of enalapril on mortality and the development of heart failure in asymptomatic patients with reduced left ventricular ejection fractions. The SOLVD Investigators. *N Engl J Med* 327:685-691, 1992.
15. Maurer MS, Spevack D, Burkhoff D, Kronzon I: Diastolic dysfunction: can it be diagnosed by Doppler echocardiography? *J Am Coll Cardiol* 44:1543-1549, 2004.
16. Oh JK, Katle L, Tajik AJ, Little WC: Diastolic heart failure can be diagnosed by comprehensive two-dimensional and Doppler echocardiography. *J Am Coll Cardiol* 47:500-506, 2006.
17. Kitzman DW, Little WC, Brubaker PH, et al: Pathophysiological characterization of isolated diastolic heart failure in comparison to systolic heart failure. *JAMA* 288:2144-2150, 2002.
18. Redfield MM, Jacobsen SJ, Burnett JC, Jr, et al: Burden of systolic and diastolic ventricular dysfunction in the community: appreciating the scope of the heart failure epidemic. *JAMA* 289:194-202, 2003.
19. Nagueh SF, Middleton KJ, Kopelen HA, et al: Doppler tissue imaging: a noninvasive technique for evaluation of left ventricular relaxation and estimation of filling pressures. *J Am Coll Cardiol* 30:1527-1533, 1997.
20. Klein AL, Hatle LK, Taliercio CP, et al: Prognostic significance of Doppler measures of diastolic function in cardiac amyloidosis. A Doppler echocardiography study. *Circulation* 83:808-816, 1991.
21. Zornoff LA, Skali H, Pfeffer MA, et al: Right ventricular dysfunction and risk of heart failure and mortality after myocardial infarction. *J Am Coll Cardiol* 39:1450-1455, 2002.
22. Forfia PR, Fisher MR, Mathai SC, et al: Tricuspid annular displacement predicts survival in pulmonary hypertension. *Am J Respir Crit Care Med* 174:1034-1041, 2006.
23. St John Sutton M, Lee D, Rouleau JL, et al: Left ventricular remodeling and ventricular arrhythmias after myocardial infarction. *Circulation* 107;2577-2582, 2003.
24. St John Sutton M, Pfeffer MA, Plappert T, et al: Quantitative two-dimensional echocardiographic measurements are major predictors of adverse cardiovascular events after acute myocardial infarction. The protective effects of captopril. *Circulation* 89:68-75, 1994.
25. Verma A, Meris A, Skali H, et al: Prognostic implications of left ventricular mass and geometry following myocardial infarction: the VALIANT (VALsartan in Acute myocardial iNfarcTion) echocardiographic study. *J Am Coll Cardiol Cardiovasc Imaging* 1:582-591, 2008.
26. Lewis EF, Velazquez EJ, Solomon SD, et al: Predictors of the first heart failure hospitalization in patients who are stable survivors of myocardial infarction complicated by pulmonary congestion and or left ventricular dysfunction: a VALIANT study. *Eur Heart J* 29:748-756, 2008.
27. Birks EJ, Tansley PD, Hardy J, et al: Left ventricular assist device and drug therapy for the reversal of heart failure. *N Engl J Med* 355:1873-1884, 2006.
28. Reilly MP, Wiegers SE, Cucchiara AJ, et al: Frequency, risk factors, and clinical outcomes of left ventricular assist device-associated ventricular thrombus. *Am J Cardiol* 86:1156-1159, A10, 2000.
29. Shamim W, Francis DP, Yousufuddin M, et al: Intraventricular conduction delay: a prognostic marker in chronic heart failure. *Int J Cardiol* 70:171-178, 1999.
30. Abraham WT, Fisher WG, Smith AL, et al: Multicenter InSync Randomized Clinical Evaluation. Cardiac resynchronization in chronic heart failure. *N Engl J Med* 346:1845-1853, 2002.
31. Cazeau S, Leclercq C, Lavergne T, et al: Effects of multisite biventricular pacing in patients with heart failure and intraventricular pacing in patients with heart failure and intraventricular conduction delay. *N Engl J Med* 344:873-880, 2001.
32. Stellbrink C, Breithardt OA, Franke A, et al: Impact of cardiac resynchronization therapy using hemodynamically optimized pacing on left ventricular remodeling in patients with congestive heart failure and ventricular conduction disturbances. *J Am Coll Cardiol* 38:1957-1965, 2001.
33. Young JB, Abraham WT, Smith AL, et al: Combined cardiac resynchronization and implantable cardioversion defibrillation in advanced chronic heart failure: the MIRACLE ICD trial. *JAMA* 289:2685-2694, 2003.
34. Bristow MR, Saxon LA, Boehmer J, et al: Cardiac-resynchronization therapy with or without an implantable defibrillator in advanced chronic heart failure. *N Engl J Med* 350:2140-2150, 2004.
35. Cleland JG, Daubert JC, Erdmann E, et al: The effect of cardiac resynchronization on morbidity and mortality in heart failure. *N Engl J Med* 352:1539-1549, 2005.
36. Linde C, Leclercz C, Rex S, et al: Long-term benefits of biventricular pacing in congestive heart failure: results from the Multisite Stimulation in cardiomyopathy (MUSTIC) study. *J Am Coll Cardiol* 40:111-118, 2002.
37. Chung ES, Leon AR, Tavazzi L, et al: Results of the predictors of response to CRT (PROSPECT) trial. *Circulation* 117:2608-2616, 2008.
38. Tang WH, Francis GS: Cardiac resynchronization therapy in patients with class I/II heart failure and a wide QRS: a cautionary note. *Circulation* 123:203-208, 2011.
39. Moss AJ, Hall WJ, Cannom DS, et al: Cardiac resynchronization therapy for the prevention of heart failure events. *N Engl J Med* 361:1329-1338, 2009.
40. Tang ASL, Wells GA, Talajic M, et al: Cardiac resynchronizaton therapy for mild to moderate heart failure. *N Engl J Med* 363:2385-2395, 2010.
41. Linde C, Abraham WT, Gold MR, et al: Randomized trial of resynchronization in mildly symptomatic heart failure patients and asymptomatic patients with left ventricular dysfunction and previous heart failure symptoms. *J Am Coll Cardiol* 52:1834-1843, 2008.
42. St John Sutton MG, Plappert T, Abraham WT, et al: Effect of cardiac resynchronization therapy on left ventricular size and function in chronic heart failure. *Circulation* 107:1985-1990, 2003.
43. Sutton MG, Plappert T, Hilpisch KE, et al: Sustained reverse left ventricular structural remodeling with cardiac resynchronization at one year is a function of etiology: quantitative Doppler echocardiographic evidence from the Multicenter InSync Randomized Clinical Evaluation (MIRACLE). *Circulation* 113:266-272, 2006.
44. Yu CM, Chau E, Sanderson JE, et al: Tissue Doppler echocardiographic evidence of reverse remodeling and improved synchronicity by simultaneously delaying regional contraction after biventricular pacing therapy in heart failure. *Circulation* 150:438-445, 2002.
45. St John Sutton M, Ghio S, Plappert T, et al: Cardiac resynchronization induces major structural and functional reverse remodeling in patients with New York Heart Association class I/II heart failure. *Circulation* 120:1858-1865, 2009.
46. Linde C, Abraham WT, GoldMR, et al: Cardiac resynchronization therapy in asymptomatic or

mildly symptomatic heart failure patients in relation to etiology: results from the REVERSE (**RE**synchronization re**VE**rses **R**emodeling in **S**ystolic Left v**E**ntricular Dysfunction) Study. *J Am Coll Cardiol* 56:1826-1831, 2010.
47. Bax JJ, Abraham T, Barold SS, et al: Cardiac resynchronization therapy: part 1: issues before device implantation. *J Am Coll Cardiol* 45:2153-2167, 2005.
48. Bax JJ, Abraham T, Barold SS, et al: Cardiac resynchronization therapy: part 2: issues during and after device implantation and unresolved questions. *J Am Coll Cardiol* 45:2168-2182, 2005.
49. Pitzalis MV, Iacoviello M, Romito R, et al: Ventricular asynchrony predicts a better outcome in patients with chronic heart failure receiving cardiac resynchronization therapy. *J Am Coll Cardiol* 45:65-69, 2005.
50. Bhatia SJ, Kirshenbaum JM, Shemin RJ, et al: Time course of resolution of pulmonary hypertension and right ventricular remodeling after orthotopic cardiac transplantation. *Circulation* 76:819-826, 1987.



# Echocardiography in the Evaluation and Management of Patients with Hypertrophic Cardiomyopathy

LYNNE WILLIAMS, PhD | ANNA WOO, MD | CHRISTIANE GRUNER, MD | HARRY RAKOWSKI, MD

**Epidemiology**
**Molecular Genetics**
**Diagnosis**
- Diagnostic Criteria
- Family Screening for Hypertrophic Cardiomyopathy

**Differential Diagnosis**
- Mimics of Hypertrophic Cardiomyopathy
- Storage Diseases
- Athlete's Heart
- Septal Hypertrophy in the Elderly

**Evaluation by Echocardiography**
- Left Ventricular Hypertrophy: Severity, Distribution, and Patterns of Hypertrophy
- Technical Factors and Echocardiographic Pitfalls

**Left Ventricular Outflow Tract Obstruction**
- Pathophysiology of Left Ventricular Outflow Tract Obstruction
- Mitral Leaflet Systolic Anterior Motion
- Doppler Assessment of Outflow Tract Obstruction in Hypertrophic Cardiomyopathy
- Latent Obstructive Hypertrophic Cardiomyopathy
- Technical Aspects of Doppler Evaluation in Hypertrophic Cardiomyopathy

**Mitral Regurgitation in Hypertrophic Cardiomyopathy**

**Subtypes of Hypertrophic Cardiomyopathy**
- Asymmetric Apical Hypertrophic Cardiomyopathy
- Midventricular Obstruction
- Hypertrophic Cardiomyopathy of the Elderly

**Evaluation of Diastolic Function**
- Factors Contributing to Impaired Diastolic Function in Hypertrophic Cardiomyopathy
- Techniques for the Assessment of Diastolic Function
- Tissue Doppler Imaging
- Asynchronous Contraction and Relaxation in Hypertrophic Cardiomyopathy

**Strain Imaging in Hypertrophic Cardiomyopathy**
**Prognostication by Echocardiography**
**Medical Therapy**
**Dual-Chamber Pacing**
**Septal Ethanol Ablation**
- Myocardial Contrast Echocardiography During Septal Ethanol Ablation
- Improved Outcomes with Contrast Echocardiography
- Clinical Results Following Septal Ethanol Ablation

**Surgical Myectomy**
- Intraoperative Echocardiography
- Outcomes Following Myectomy

**Comparison of Treatment Strategies for Obstructive Hypertrophic Cardiomyopathy**

Hypertrophic cardiomyopathy (HCM) has unique clinical, echocardiographic, and hemodynamic features.[1] Since the modern description of HCM five decades ago,[2,3] there have been significant advances in its diagnosis, the understanding of its complex pathophysiology, and the evolution of its management.[1] HCM is defined as a hypertrophied, nondilated left ventricle (LV) in the absence of another cardiac or systemic disease that is capable of producing the magnitude of wall thickening detected (Fig. 27-1).[4] Echocardiography has played a crucial role in determining the pathophysiology of HCM, quantitating its morphologic and hemodynamic severity, and assessing the acute and chronic responses to various therapies.[5]

Echocardiographic studies have also provided invaluable insight into the epidemiology,[6] inheritance,[7] and prognosis of HCM.[8,9] The ability to perform serial noninvasive studies makes echocardiography the modality of choice in the screening,[7,10] diagnosis,[4] and serial monitoring of patients with this condition. In recent years the role of echocardiography in this disorder has extended to intraprocedural decision making, with the use of intraoperative transesophageal echocardiography (TEE) during surgical myectomy[11] and the application of myocardial contrast echocardiography in the guidance of septal ethanol ablation.[12,13]

## Epidemiology

HCM was initially thought to be a rare disorder affecting young adults.[3] However, modern studies using echocardiography in the evaluation of subjects suggest a much higher prevalence of this condition. The Coronary Artery Risk Development in Adults (CARDIA) study, a prospective study of 4111 apparently healthy young adults from a general population, detected HCM by echocardiographic examination in 0.17% of subjects.[6] There was a similar prevalence of HCM in a large study of 33,735 young athletes undergoing preparticipation medical screening in Italy, with a total of 22 cases (0.07%) identified from this cohort.[10] The reported incidence of HCM has ranged from an incidence of 0.4 per 100,000 person-years from 1980 to 1981 in Western Denmark[14] to 2.5 per 100,000 person-years between the years 1975 and 1984 in Olmsted County, Minnesota.[15]

Recent studies of the incidence of HCM in children have reported an annual incidence of 0.42 per 100,000 in the United States[16] and 0.32 per 100,000 children in Australia.[17]

## Molecular Genetics

HCM is a genetic disorder with an autosomal dominant pattern of inheritance. This condition is thought to arise from a genetic defect involving one of the genes encoding proteins of the cardiac sarcomeric apparatus.[18,19] The initial genetic defect was described in the late 1980s, and since then more than 400 different mutations have been associated with HCM. Mutations in the genes encoding β-myosin heavy chain (*MYH7*) and myosin binding protein C (*MYBPC3*) account for 80% to 85% of cases with identified mutations in most series, with mutations in troponin T (*TNNT2*), troponin I (*TNNI3*), and α-tropomyosin (*TPM1*) comprising 10% to 15% of additional cases. These genes, along with the myosin light chains (*MYL2* and *MYL3*) and α-cardiac actin (*ACTC*), are the eight genes most commonly involved in HCM. Rarer genetic causes include mutations in α-myosin heavy chain (*MYH6*), titin (*TTN*), and cardiac troponin C (*TNNC1*). More recently, mutations in genes encoding the cardiac Z-disk proteins have been implicated in the pathogenesis of HCM.[20]

The extent to which the underlying genotype influences the phenotype of this condition remains unclear. Some studies have suggested that patients with *MYH7* mutations have a greater degree and an earlier onset of hypertrophy than those patients with non-*MYH7* defects.[21,22] No significant differences were found in the degree of hypertrophy among patients with different mutations of the *MYH7* gene.[23,24] In contrast, mutations of the *MYBPC* gene have been associated with delayed penetrance.[21,25] However, one large study found no difference in the degree and onset of hypertrophy when comparing patients with mutations involving the thick filament, thin filament, or *MYBPC* genes.[26]

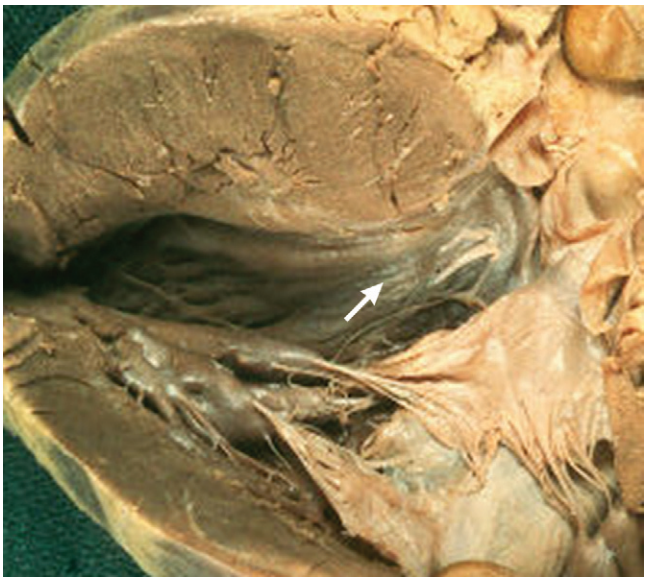


**Figure 27-1 Gross pathologic specimen of the heart from a patient with hypertrophic cardiomyopathy and LV outflow tract obstruction who died suddenly.** Note the asymmetric hypertrophy with a markedly thickened interventricular septum and narrow outflow tract between the basal septum and anterior mitral valve leaflet, which is thickened and fibrosed from repeated mitral leaflet-septal contact (*arrow*).

## Diagnosis

### DIAGNOSTIC CRITERIA

The diagnosis of HCM is based on the demonstration of LV hypertrophy in the absence of other causes, such as systemic hypertension or aortic stenosis (Fig. 27-2).[4] M-mode echocardiography assumed an early role in the diagnosis of HCM.[27,28] The echocardiographic finding of asymmetric septal hypertrophy, defined as a septal/posterior wall thickness ratio of 1.3 or greater, is strongly associated with HCM.[29] The septum is typically at least 15 mm in thickness.[1,29,30] Other findings associated with obstructive HCM, such as systolic anterior motion (SAM), have been detected in other conditions and are not considered

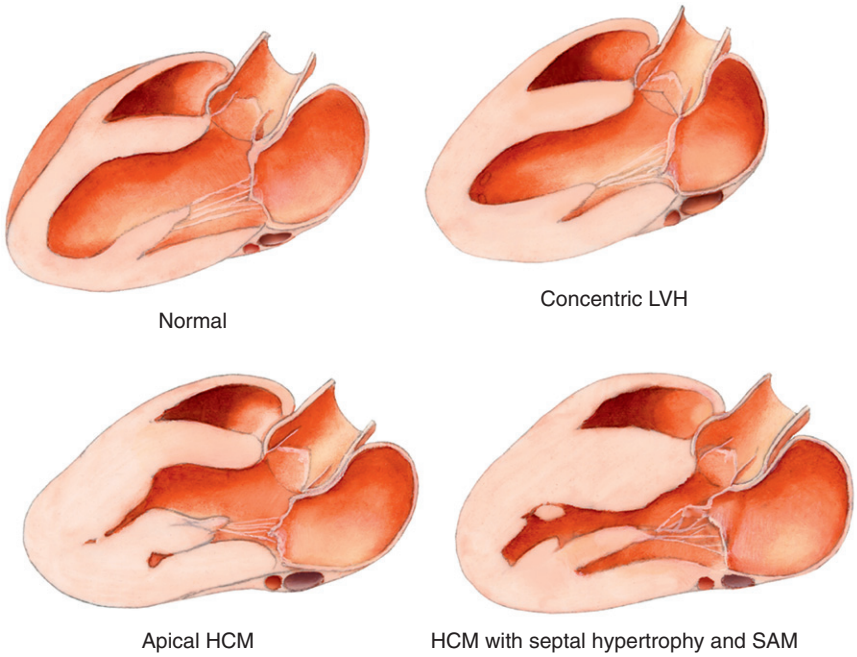



**Figure 27-2 Patterns of ventricular hypertrophy in hypertrophic cardiomyopathy patients.** Diagrammatic representation of the various forms of left ventricular hypertrophy (*LVH*), as viewed in a parasternal long-axis view. *Upper left*: Normal wall thickness in a normal subject. *Upper right*: Concentric pattern of LVH with similar increases in the wall thickness of the interventricular septum and the LV free wall. This is the predominant form of hypertrophy in patients with systemic hypertension or valvular aortic stenosis. *Lower left*: In contrast, patients with apical hypertrophic cardiomyopathy (*HCM*) have hypertrophy predominantly of the apical segments. Note that the basal interventricular septum is spared from hypertrophy and the distal LV cavity is small. Patients with apical HCM have near obliteration of the distal LV cavity during systole. *Lower right*: The more common form of HCM involves asymmetric hypertrophy of the interventricular septum. The LV free wall is normal or minimally thickened. Patients with the obstructive form of HCM typically have a narrow LV outflow tract, an anteriorly displaced mitral apparatus, and systolic anterior motion (*SAM*) of the anterior mitral leaflet.

pathognomonic for HCM.[31] The diagnosis of HCM is made in children when LV wall measurements are more than two standard deviations above the mean (corrected for age and body surface area).[32] Approximately 25% of patients have obstructive HCM, which has traditionally been defined as a left ventricular outflow tract (LVOT) gradient of at least 30 mm Hg at rest.[8]

### FAMILY SCREENING FOR HYPERTROPHIC CARDIOMYOPATHY

The first-degree relatives of patients with HCM should be screened for this condition.[1,33] Screening methods for family members include a history and physical examination, 12-lead electrocardiography, and echocardiography. Echocardiography is the most widely accepted screening test for HCM. Genetic testing is becoming more widely available, typically in academic centers.[1] Screening for HCM is recommended by at least 12 years of age (or earlier if a child is symptomatic, engaged in competitive sports, or has a malignant family history of premature death attributed to HCM).[33] Serial evaluations are then performed every 12 to 18 months until physical maturity is achieved (generally between ages 18 and 21). Because HCM may present in late adulthood, screening is generally recommended at 5-year intervals during adulthood.[33]

Genetic studies of patients with HCM have demonstrated that genotype-positive relatives of patients with HCM may have minimal or no hypertrophy evident on echocardiography.[21,24,25,33] Recent studies have shown that tissue Doppler imaging may identify genotype-positive patients before the onset of LV hypertrophy.[34,35] Reduced systolic and diastolic tissue Doppler velocities have a high sensitivity and high specificity in identifying mutation carriers (Table 27-1). Moreover, serial echocardiographic assessments of genotype-positive and initially phenotype-negative patients showed further reductions in tissue Doppler velocities and the development of overt hypertrophy during 2-year follow-up.[36]

## Differential Diagnosis

### MIMICS OF HYPERTROPHIC CARDIOMYOPATHY

There are multiple potential other causes for the echocardiographic abnormalities seen in HCM, often termed phenocopies (Box 27-1).[37,38] HCM caused by a genetic defect of the cardiac sarcomeric proteins needs to be distinguished from one of the congenital malformations/syndromes (e.g., Noonan or LEOPARD syndrome). Disproportionate hypertrophy of the ventricular septum may occur with right ventricular (RV) hypertrophy and D-transposition of the great arteries.[39] Other nongenetic causes of LV hypertrophy include athlete's heart (see later discussion), systemic hypertension, and aortic stenosis. Hypertrophy secondary to these disorders is usually concentric but may also be associated with a degree of focal septal hypertrophy and/or SAM.[30] Increased wall thickness not attributable to myocyte hypertrophy may be secondary to metabolic disorders (storage disorders—see later discussion), hypothyroidism,[40] or infiltrative cardiomyopathies (Fig. 27-3).[41] The increased wall thickness of patients with metabolic disorders or infiltrative cardiomyopathies typically occurs in a concentric pattern but may occasionally manifest as disproportionate septal thickening.

**TABLE 27-1 Test Characteristics of Tissue Doppler Findings for Diagnosis of Hypertrophic Cardiomyopathy**

| *Tissue Doppler Parameter* | *Sensitivity* | *Specificity* |
|---|---|---|
| S′ (lateral) <13 cm/s[35] | 100% | 93% |
| S′ (septal) <12 cm/s[35] | 100% | 90% |
| E′ (lateral) <14 cm/s[35] | 100% | 90% |
| E′ (septal) <13 cm/s[35] | 100% | 90% |
| Average E′ (from 4 corners) ≤13.5 cm/s[34] | 75% | 86% |
| Average E′ <15 cm/s + LVEF ≥ 68%[34] | 44% | 100% |

*E′*, Tissue Doppler early diastolic velocity; *LVEF*, left ventricular ejection fraction; *S′*, tissue Doppler systolic velocity.

### STORAGE DISEASES

Storage diseases should be considered in the workup of patients with unexplained increased LV wall thickness. Fabry disease was detected in 7 of 230 patients with LV hypertrophy (3% prevalence), with all of these patients having a concentric pattern of hypertrophy.[42] In male patients with a diagnosis of HCM, Fabry disease was detected in 6% of patients diagnosed at 40 years of age or older and in 1% diagnosed at 40 years of age or younger. The pattern of hypertrophy was concentric in 5 patients and asymmetric in 1 patient.[43] Approximately 50% to 60% of patients with Fabry disease present with cardiac symptoms, with one third dying from cardiac causes.[44] Most patients with cardiomyopathy exhibit concentric hypertrophy with preserved global ejection fraction and only mildly impaired diastolic function.[45] Characteristic of Fabry disease is the development of replacement fibrosis in the basal posterolateral wall, which in the late stage of the disease results in the coexistence of myocardial hypertrophy, myocardial thinning, and the presence of wall motion abnormalities in the fibrotic segments.[46]

Glycogen storage diseases may also mimic HCM. Mutations of the AMP-protein kinase $\gamma_2$ (*PRKAG2*) gene cause a glycogen storage cardiomyopathy, mutations of the lysosome-associated

**Box 27-1**

**DIFFERENTIAL DIAGNOSIS OF HYPERTROPHIC CARDIOMYOPATHY ON ECHOCARDIOGRAPHY**

**Syndromic Hypertrophic Cardiomyopathy**
Noonan syndrome
LEOPARD syndrome
Friedrich ataxia

**Disproportionate Ventricular Septal Hypertrophy**
RV hypertrophy
D-transposition of the great arteries

**Other Causes of Left Ventricular Hypertrophy**
Athlete's heart
Systemic hypertension
Aortic valve stenosis (and fixed subvalvular and supravalvular stenosis)

**Metabolic Disease**
Fabry disease
Glycogen storage disease
Mucopolysaccharide storage disease
Hypothyroidism

**Infiltrative Cardiomyopathy**
Amyloidosis
Sarcoidosis

LEOPARD stands for **L**entigines, **E**CG abnormalities, **O**cular hypertelorism, **P**ulmonary stenosis, **A**bnormal genitalia, **R**etardation of growth, **D**eafness.

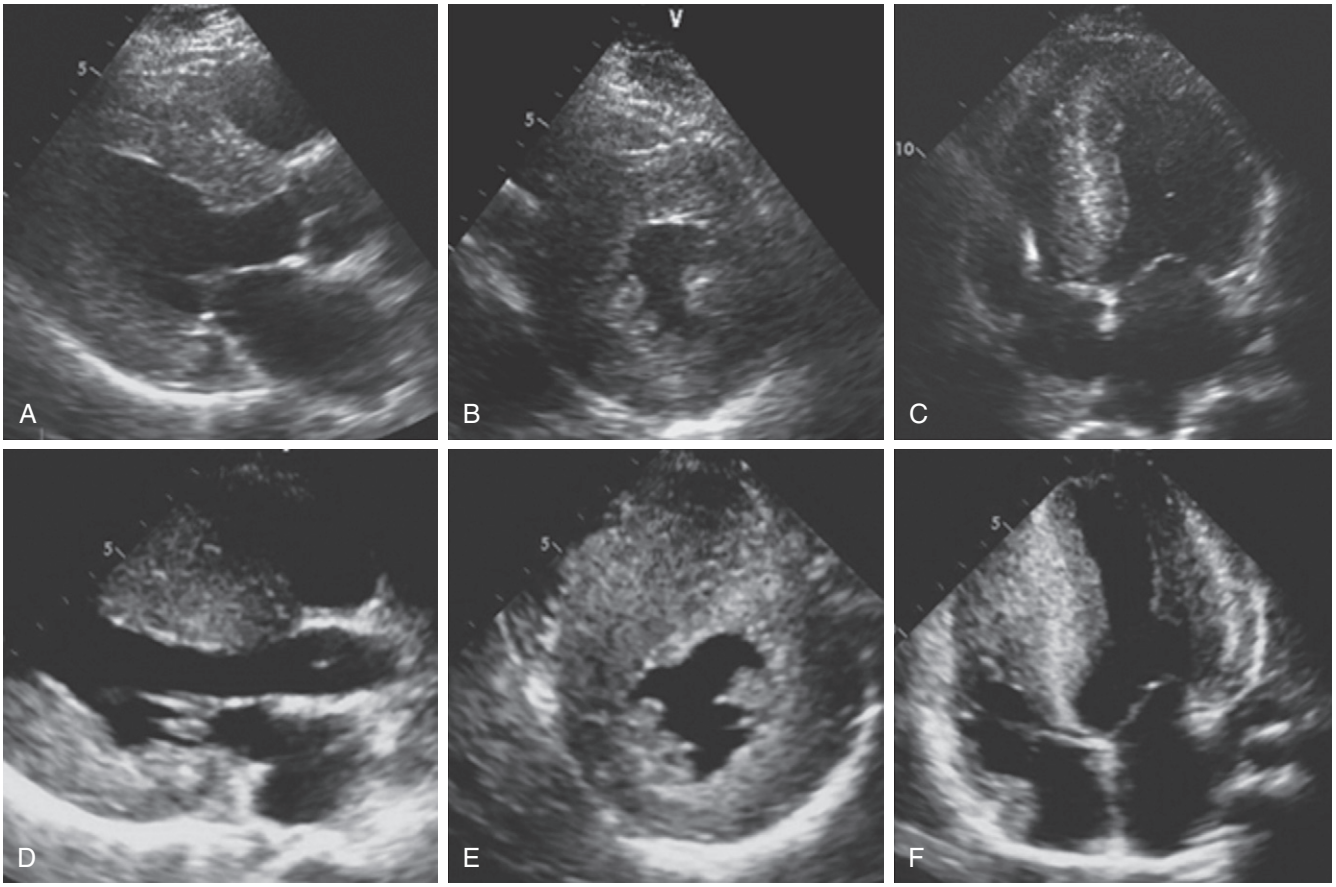



**Figure 27-3 Tissue Doppler findings in hypertrophic cardiomyopathy.** Tracings from a patient with mimics of hypertrophic cardiomyopathy. *Upper panel*: Parasternal long-axis (**A**), parasternal short-axis (**B**), and apical four-chamber (**C**) views from a patient with Fabry disease. These images demonstrate concentric LV hypertrophy. *Lower panel*: Parasternal long-axis (**D**), parasternal short-axis (**E**), and apical four-chamber (**F**) views from a patient with glycogen storage disease (type III). In this patient there is evidence of an asymmetric distribution of the hypertrophy.

membrane protein 2 (*LAMP2*) gene cause Danon disease, and mutations of the acid α-1,4-glucosidase gene cause Pompe disease.[47] In a cohort of 75 patients with unexplained hypertrophy, 40 patients (53%) were identified with sarcomeric protein gene mutations, 1 patient (1%) had a *PRKAG2* defect, and 2 patients (3%) had *LAMP2* mutations.[47] In another cohort of 24 patients with increased wall thickness and ventricular preexcitation, mutations of the *PRKAG2* and *LAMP2* genes were detected in 7 (29%) and 4 (17%) patients, respectively. None of these patients had the genetic defects causing Fabry or Pompe disease.[47]

## ATHLETE'S HEART

It is crucial to accurately diagnose HCM in individuals with LV hypertrophy participating in competitive sports given the potential risk of sudden cardiac death. HCM remains the most common cause of sudden death in young adults undertaking competitive sports. The diagnosis can be difficult in athletes with an advanced degree of physiologic hypertrophy. In dynamic exercise, the load on the heart is predominantly a volume overload, leading to dilatation of the LV cavity (and an increased LV end-diastolic dimension), associated with a proportional increase in wall thickness (eccentric hypertrophy). In static exercise, a pressure load can result in LV hypertrophy without an increase in LV cavity size (concentric hypertrophy). Although there is some variation in the study data, the largest study of elite athletes showed that only 2% develop an interventricular septal thickness greater than 13 mm,[48] with a wall thickness of 14 to 16 mm appearing to be the upper limit of physiologic hypertrophy. The distinction between athlete's heart and pathologic hypertrophy may be less of an issue in women because the LV wall thickness of elite female athletes is in the range of 6 to 12 mm, which does not exceed normal age-adjusted limits for wall thickness.[49] The pattern of hypertrophy tends to be symmetric, and true asymmetric LV hypertrophy is encountered only rarely in athletes.[50] The chamber size can also provide an invaluable clue. Outside the setting of "end-stage" HCM, the LV end-diastolic dimension is typically normal or reduced, whereas in athletes this dimension commonly exceeds 55 mm. About 5% of elite athletes have a diastolic dimension greater than 60 mm, well above the upper limit of normal. Power athletes such as weight lifters can develop thickening of the septum and posterior walls without an increase in cavity size. In these cases it is important to calculate true LV mass index to avoid making a spurious diagnosis of LV hypertrophy, because these athletes are often very large. LV systolic function is normal to supranormal in athletes, both at rest and on exercise. LV diastolic function is on average normal at rest, but is enhanced on exercise, favoring adequate filling of the ventricle at high heart rates. Tissue Doppler velocity imaging is extremely helpful in differentiating the two conditions. Whereas HCM patients demonstrate a reduction in both systolic and diastolic tissue Doppler velocities, athletes have normal or supranormal systolic and

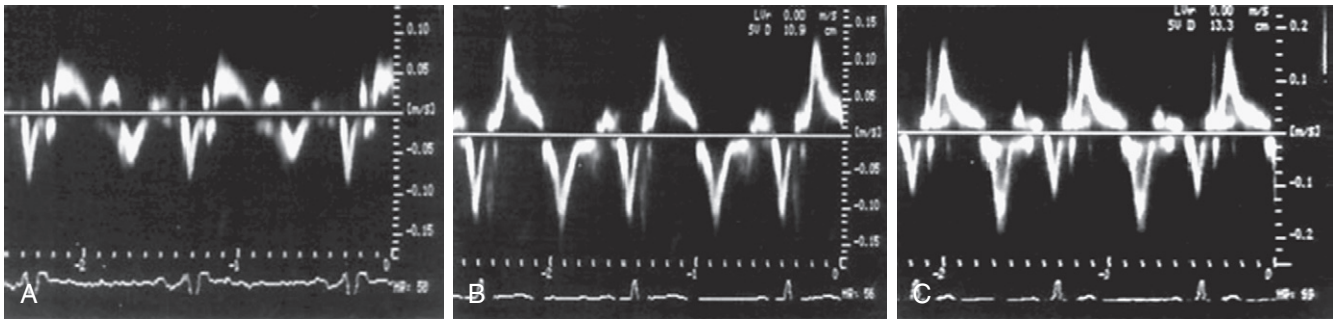



**Figure 27-4** Tissue Doppler velocity traces in a patients with hypertrophic cardiomyopathy (**A**), an athlete (**B**), and a healthy control (**C**). Note the significant reduction in both systolic and early diastolic velocities in the patient with hypertrophic cardiomyopathy in contrast to both the athlete and the healthy control.

**TABLE 27-2 Differentiation of Athlete's Heart from Hypertrophic Cardiomyopathy**

| | *Hypertrophic Cardiomyopathy* | *Athlete's Heart* |
|---|---|---|
| Unusual pattern of LVH | + | – |
| LV cavity ≤45 mm | + | – |
| LV cavity ≥55 mm | – | + |
| Abnormal LV filling | + | – |
| Female gender | + | – |
| Family history of HCM | + | – |
| Decreased wall thickness with deconditioning | – | + |

*HCM*, Hypertrophic cardiomyopathy; *LVH*, left ventricular hypertrophy.

diastolic function (Fig. 27-4).[51] A reflection of the diastolic dysfunction seen in HCM is left atrial (LA) enlargement. If LA size is normal, then LA pressure and LV end-diastolic pressure are very likely to be normal, making a diagnosis of athlete's heart more likely. The diagnosis of HCM is favored in the presence of the following: (1) a family history of HCM, (2) bizarre electrocardiographic patterns, (3) asymmetric hypertrophy (or other unusual patterns of hypertrophy), (4) an LV cavity size less than 45 mm, (5) LA enlargement, and (6) an abnormal LV filling profile (Table 27-2).[52] In some cases it may be necessary for the athlete to decondition. If regression of LV hypertrophy occurs, this is more suggestive of a diagnosis of athlete's heart rather than HCM.

### SEPTAL HYPERTROPHY IN THE ELDERLY

It may be difficult to distinguish between elderly patients with HCM and those with hypertensive heart disease. Elderly subjects may develop a sigmoid-shaped septum as an age-related phenomenon.[53] Terms that have been used to describe this finding are sigmoid septum, septal bulge, or discrete upper septal hypertrophy. It is controversial whether this finding should be considered a subtype of HCM or whether it represents a benign anatomic variant.[54,55] Other findings on echocardiographic examination that are more compatible with a septal bulge rather than HCM of the elderly include focal hypertrophy limited to less than a 3-cm length of the basal anterior septum, protrusion of the focal hypertrophy into the LVOT, a normal LV end-diastolic diameter, and the absence of characteristic echocardiographic findings of HCM.[55] Echocardiographic and clinical features of HCM in the elderly are discussed later in this chapter.

## Evaluation by Echocardiography

### LEFT VENTRICULAR HYPERTROPHY: SEVERITY, DISTRIBUTION, AND PATTERNS OF HYPERTROPHY

Two-dimensional (2D) echocardiography greatly increased the ability to detect the full extent, distribution, and severity of myocardial hypertrophy. Comprehensive echocardiographic assessment requires imaging of the LV from several transthoracic windows, including the parasternal long-axis view, serial parasternal short-axis views, and the apical windows. Measurements of the wall segments are obtained from cross-sectional parasternal short-axis views and are made at three levels: (1) basal (at the level of the mitral valve), (2) midventricular (at the level of the papillary muscles), and (3) apical.[5] The pattern of ventricular septal hypertrophy is variable and can be broadly divided into morphologic subtypes: reverse curvature, sigmoid, and neutral (Fig. 27-5). Reverse curvature morphology is characterized by a predominant midseptal convexity toward the LV cavity, with the cavity itself often having an overall crescent shape. In patients with sigmoid septal morphology the LV cavity is generally ovoid in shape, with the septum being concave to the LV cavity and a prominent basal septal bulge. Neutral septum HCM shows an overall straight septum that is neither predominantly convex nor concave toward the LV cavity.

Appropriate identification of these morphologic subtypes may be helpful because they appear to be closely related to the presence of an HCM-related genetic abnormality. In a recent study, the majority of patients (79%) with reverse curvature septum HCM harbored an identifiable HCM-associated mutation, compared with only a small proportion of patients with a sigmoid septum (8%).[56] Of those patients with apical hypertrophy, 30% were found to be genotype positive, with 41% of patients having a neutral septal morphology being genotype positive. These data have significant implications with respect to genetic counseling and the clinical application of genetic testing. Specifically, the possibility of echocardiography-guided genetic testing in HCM is evident.

### TECHNICAL FACTORS AND ECHOCARDIOGRAPHIC PITFALLS

There are important technical considerations in the echocardiographic assessment of HCM. The diagnosis of HCM is challenging, and diagnosis can only be 100% reliable when a genetic mutation has been identified. Echocardiographic assessment requires a comprehensive assessment in several imaging planes with careful attention to correct beam alignment in order to

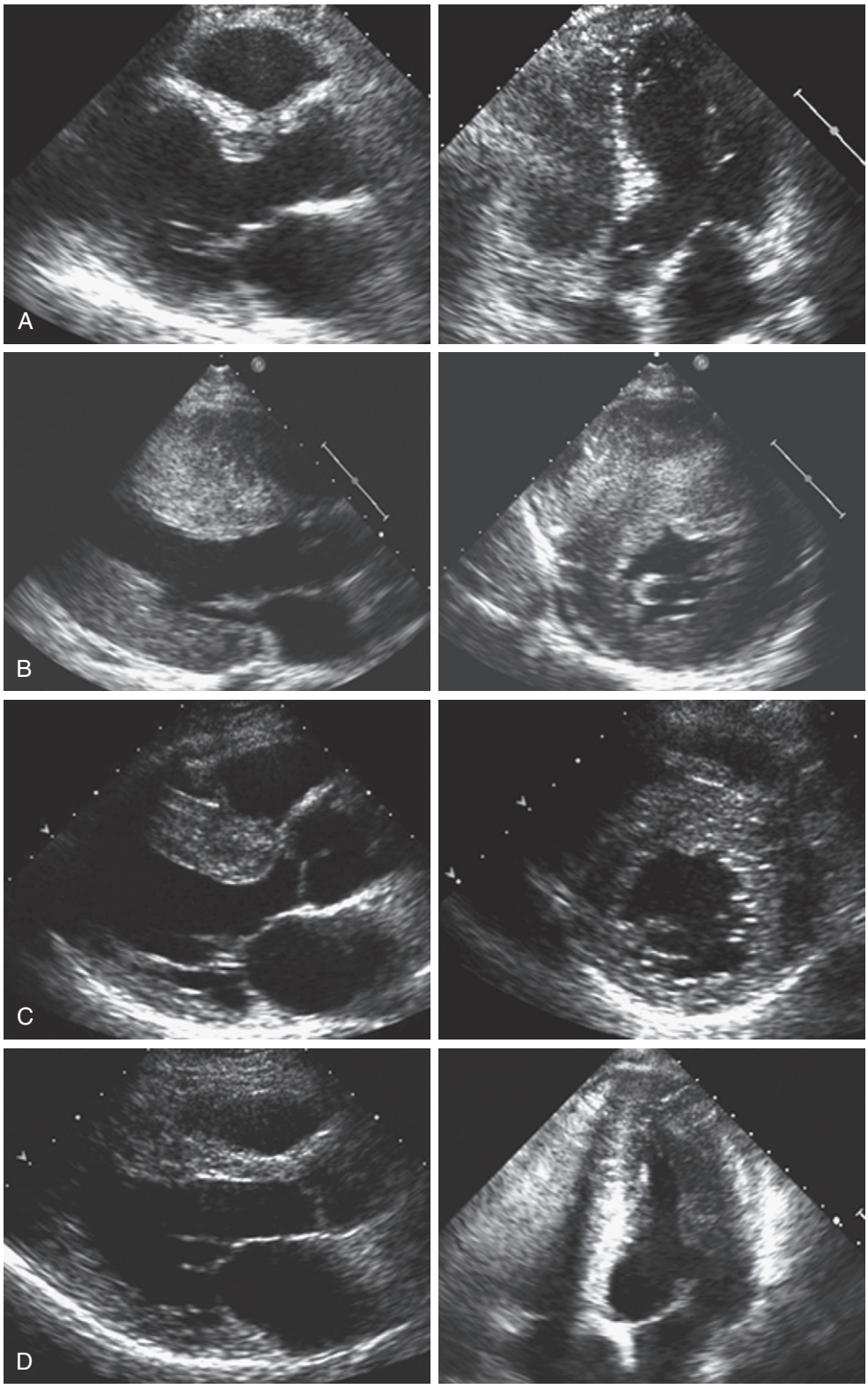



**Figure 27-5 Spectrum of morphologies in hypertrophic cardiomyopathy. A,** Sigmoid septum with hypertrophy confined to basal septum. **B,** Massive hypertrophy with reverse curvature pattern leading to crescent shape of LV cavity. **C,** Asymmetric septal hypertrophy with neutral septal morphology that is neither convex nor concave to LV cavity. **D,** Apical hypertrophy with hypertrophy confined to apex and normal wall thicknesses in basal segments.

minimize errors in the measurement of wall thickness and appropriate identification of hypertrophy with an unusual distribution.

### *Overdetection (False-Positive Diagnosis of Hypertrophic Cardiomyopathy)*

Oblique cuts of the LV can spuriously produce the appearance of asymmetric septal hypertrophy and overestimate wall thickness.[57] Similarly, the presence of an RV moderator band or an LV tendon may result in overestimation of septal thickness. Potential misdiagnosis may occur in hypertensive patients who have had an inferior myocardial infarction. In this setting, the septal/posterior wall ratio may exceed 1.3 simply because the septum is mildly hypertrophied and the posterior wall thinned as a result of prior infarction.

### *Underdetection (False-Negative Diagnosis of Hypertrophic Cardiomyopathy)*

2D echocardiographic studies have demonstrated that hypertrophy can be quite localized or eccentric in distribution.[58] More atypical forms of HCM, such as isolated lateral wall hypertrophy or asymmetric apical hypertrophy, may be missed from standard parasternal long-axis views, because the septum and anterior wall appear normal in thickness and there is no SAM of the mitral valve. The diagnosis of apical HCM by echocardiography may be missed in patients with difficult or suboptimal apical windows or if the apical segments are foreshortened. Wall thickness may be entirely normal, particularly in children and adolescents, in patients with specific gene mutations, and in end-stage HCM with a dilated impaired LV.

## Left Ventricular Outflow Tract Obstruction

### PATHOPHYSIOLOGY OF LEFT VENTRICULAR OUTFLOW TRACT OBSTRUCTION

M-mode echocardiographic studies have demonstrated narrowing of the LVOT,[59] SAM of the mitral valve,[28,30] and midsystolic notching of the aortic valve[60] and established the important role of echocardiography in the assessment of LVOT obstruction in patients with HCM. Advances in 2D echocardiography and Doppler techniques would provide additional insights into the mechanisms responsible for dynamic outflow tract obstruction (Box 27-2). Morphologic features of HCM that contribute to LVOT obstruction include narrowing of the outflow tract by septal hypertrophy,[61] intrinsic abnormalities of the mitral leaflets,[62,63] anterior displacement of the mitral apparatus,[63,64] and anterior malposition of the papillary muscles.[65]

**Box 27-2**

**FACTORS CONTRIBUTING TO DYNAMIC LEFT VENTRICULAR OUTFLOW TRACT OBSTRUCTION**

**Narrowing of Left Ventricular Outflow Tract**
Septal hypertrophy
Anterior displacement of the mitral apparatus
Anterior displacement of the papillary muscles

**Hydrodynamic Forces (Venturi and Drag Forces) Causing Systolic Anterior Motion**
Rapid early LV ejection
Elongated mitral leaflets

There tends to be a close relationship between the extent of LV hypertrophy and the presence of LVOT obstruction. The presence of resting outflow tract obstruction is associated with a higher hypertrophy point score.[66] The mitral leaflets in HCM are typically elongated[67] and coapt abnormally in the body of the leaflets rather than at the tips.[63,67] Patients with enlarged mitral valves have "typical" SAM and contact of the distal and central portions of the anterior mitral leaflet with the septum. In contrast, patients with normal-sized mitral valves have "atypical" SAM, involving greater portions of the body of the anterior mitral leaflet and related chordae tendinae, and with little bending of the anterior mitral leaflet.[68] The degree of anterior displacement of the mitral apparatus has been related to the degree of obstruction.[63,64] Furthermore, in HCM, the papillary muscle tips are displaced anteriorly and toward one another. This results in a decrease in the relative tension on the chordae tendinae to the body of the anterior mitral leaflet, producing relative chordal slack in the central and anterior leaflet portions.[67,69] Reduced chordal tension is more likely when the distance from the papillary muscle tips to the mitral leaflets is decreased by a combination of hypertrophy at the base of the papillary muscles and increased leaflet length.

### MITRAL LEAFLET SYSTOLIC ANTERIOR MOTION

Although the nature of the hydrodynamic forces on the anterior mitral leaflet remains controversial, it is believed that the anterior leaflet distal to the site of coaptation is subjected to Venturi and/or drag forces. Therefore, SAM occurs, and the tip of the anterior mitral valve leaflet typically develops a sharp anterior and superior angulation, leading to mitral leaflet-septal contact in early to midsystole (Fig. 27-6). There is a significant relationship between the development of SAM and the onset of the obstructive pressure gradient, which was demonstrated in patients undergoing simultaneous cardiac catheterization and M-mode echocardiographic studies (Fig. 27-7).[70] The presence of mitral leaflet-septal contact occurs almost simultaneously with the onset of the pressure gradient.

M-mode, 2D, and Doppler echocardiography are established noninvasive techniques in the assessment of the degree of LVOT obstruction in patients with HCM. An M-mode echocardiographic study classified the degree of SAM into three categories: (1) mild (SAM-septal distance greater than 10 mm), (2) moderate (SAM-septal distance less than 10 mm or brief mitral leaflet-septal contact), and (3) severe (prolonged SAM-septal contact, lasting more than 30% of echocardiographic systole).[30] There is a linear relationship between the time of onset of SAM and the severity of LVOT obstruction.[71]

### DOPPLER ASSESSMENT OF OUTFLOW TRACT OBSTRUCTION IN HYPERTROPHIC CARDIOMYOPATHY

Pulsed-wave (PW) and continuous-wave (CW) Doppler have been used to determine the pressure gradient across the LV outflow tract in patients with HCM. High–pulse-repetition frequency Doppler signals can be recorded sequentially from the LV apex to the outflow tract in order to establish the anatomic site of obstruction. Color flow mapping has been used to characterize the level of obstruction, either in the LVOT or in the midventricle.[72] It is important to identify those patients with midcavity obstruction, as this may be associated with apical aneurysm formation, which in turn carries a risk for systemic

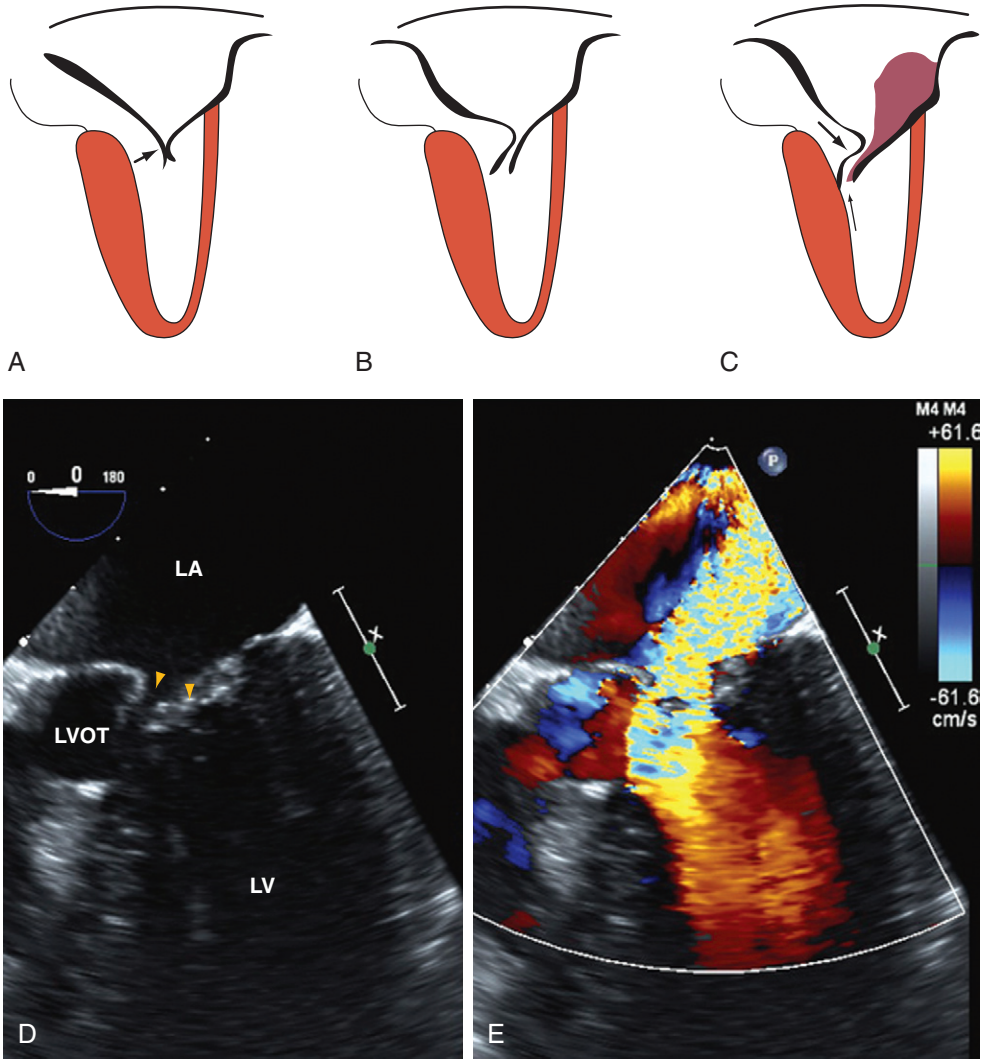



**Figure 27-6 Mechanism of dynamic outflow obstruction.** At the onset of systole (**A**), the coaptation point (*arrow*) is in the body of the mitral leaflets. During early systole (**B**) and midsystole (**C**), there is anterior and basal movement of the residual length of the anterior mitral leaflet (*thick arrow*) with septal contact and failure of leaflet coaptation. The resulting interleaflet gap (*thin arrow*) causes a posteriorly directed jet of mitral regurgitation into the LA cavity (*purple area*). Corresponding 2D transesophageal views (**D**) with color flow imaging (**E**) in a patient with obstructive hypertrophic cardiomyopathy show septal hypertrophy, anterior motion of anterior mitral valve leaflet, and color turbulence in left ventricular outflow tract (*LVOT*) with posteriorly directed mitral regurgitation. Failure of coaptation is demonstrated by *orange arrowheads*. *(Panels **A** to **C**, from Grigg LE, Wigle ED, Williams WG, et al: Transesophageal Doppler echocardiography in obstructive hypertrophic cardiomyopathy: clarification of pathophysiology and importance in intraoperative decision making.* J Am Coll Cardiol *20:42-52, 1992.)*

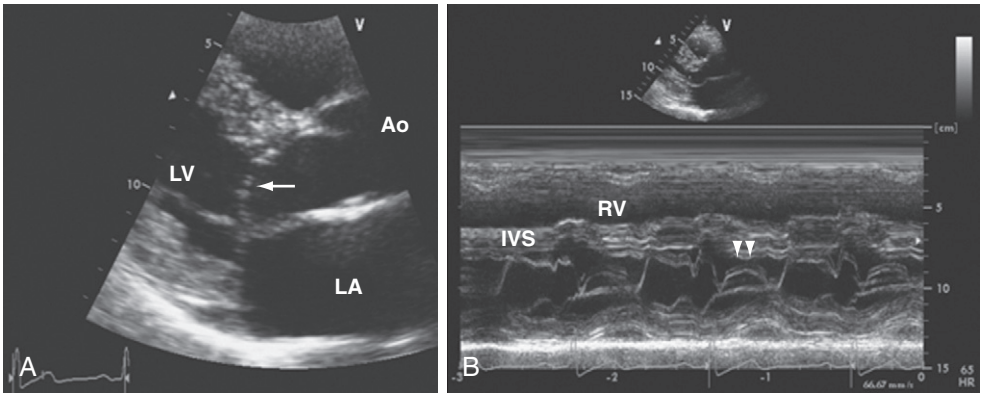



**Figure 27-7 2D and M-mode findings with dynamic outflow obstruction.** 2D parasternal long-axis (**A**) and M-mode (**B**) images obtained at level of mitral leaflet tips in patient with symptomatic obstructive hypertrophic cardiomyopathy. **A,** Anterior motion of the anterior mitral valve leaflet during systole (*arrow*). **B,** Corresponding finding marked by *arrowheads*. *Ao*, Aorta; *IVS*, interventricular septum.

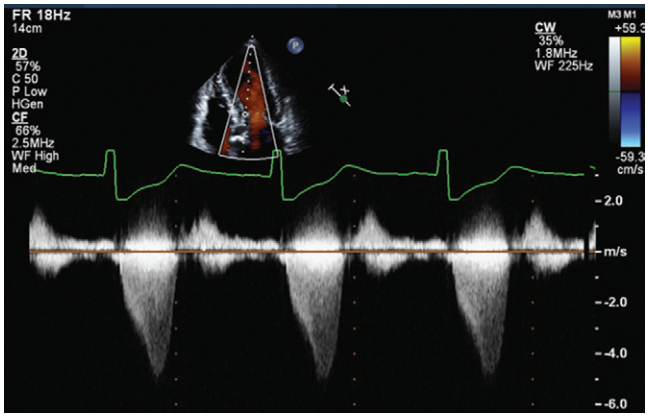



**Figure 27-8 CW Doppler recordings of left ventricular outflow tract (LVOT) in patient with symptomatic obstructive hypertrophic cardiomyopathy.** Evaluation revealed severe systolic anterior motion and posteriorly directed mitral regurgitation. Spectral profile has characteristic dagger shape. Peak velocity in LVOT is 4.3 m/s, corresponding to peak LVOT gradient of 74 mm Hg based on modified Bernoulli equation.

embolism and ventricular arrhythmias. In those patients with obstruction at the level of the outflow tract, the peak velocity increases as the sample volume approaches the site of mitral leaflet-septal contact. CW Doppler assessment from an apical approach with the beam directed across the outflow tract can be used to determine the peak velocity ($V_{max}$) at the site of obstruction. Patients with outflow tract obstruction have a characteristic spectral profile with an asymmetric leftward concave shape. This results from a relatively rapid initial rise in velocity followed by a more gradual increase in the outflow tract velocity to cause a peak in late systole (the typical dagger-shaped Doppler profile) (Fig. 27-8).[73] The peak gradient ($\Delta P$) can be estimated using the modified Bernoulli equation ($\Delta P = 4V^2$). There is an excellent correlation between the pressure gradient determined by CW Doppler measurements and that determined by high-fidelity micromanometer recordings during cardiac catheterization.[74]

## LATENT OBSTRUCTIVE HYPERTROPHIC CARDIOMYOPATHY

When categorizing patients with HCM, three distinct hemodynamic groups of patients should be distinguished: those with resting outflow tract obstruction (obstructive), those with provocable gradients but no obstruction at rest (latent obstruction), and those with no gradient either at rest or on provocation (nonobstructive). Dynamic LVOT obstruction is an important and frequent manifestation of HCM and can be a major cause of symptoms such as dyspnea, chest pain, presyncope, or syncope. Resting LVOT obstruction (LVOT gradient 30 mm Hg or greater) is present in around 25% to 30% of patients with HCM. However, a multicenter study using stress echocardiography has identified that with exercise, provocable outflow tract gradients are present in up to 70% of patients with HCM.[75] Resting LV outflow tract obstruction is associated with a higher risk of progressive heart failure and cardiovascular death, likely due to chronic elevation in LV intracavitary pressure and wall stress.[76] Outflow tract obstruction in HCM is by nature dynamic and affected by numerous hemodynamic changes that occur during daily life. This variability is dependent not only on heart rate, inotropic state, and systemic vascular resistance, but also on loading conditions. The echocardiographic features of patients with latent LVOT obstruction include a proximal septal bulge, a narrow LVOT diameter (2 cm or less), and a more oblique angle (35° or greater) between the ejection flow and the mitral valve.[77] Obstruction may be provoked by either physiologic or pharmacologic maneuvers that diminish LV preload (assumption of the upright posture, use of sublingual nitroglycerine, Valsalva maneuver), augment LV contractility (via dobutamine infusion or physiologically by upright exercise), or result in vasodilator stress (inhalation of amyl nitrate). The most commonly used methods for provoking latent obstruction include the Valsalva maneuver, the inhalation of amyl nitrate, intravenous inotropes, and exercise.

With the exception of exercise, these provocative maneuvers are considered to be nonphysiologic and unable to perfectly reproduce the conditions under which obstruction and symptoms occur during daily life. The ACC/ESC Clinical Expert Consensus Document on Hypertrophic Cardiomyopathy does not recommend the use of dobutamine to provoke outflow tract gradients, because it is capable of producing LVOT gradients even in normal hearts. The presence of an inducible gradient is of questionable clinical and physiologic significance in patients with HCM.[1] Amyl nitrite has been shown to be an effective tool for provoking latent obstruction, but there is a relatively poor correlation between the gradients induced by amyl nitrate and exercise. This difference may partly be explained by the routine discontinuation of beta blockers before exercise but not for Valsalva studies. In a study by Marwick and colleagues,[78] amyl nitrate appeared more effective in an older patient group (age greater than 65 years) with lesser degrees of septal hypertrophy and narrower LV outflow tracts. However, amyl nitrite is not widely available in all centers. Assumption of the upright posture has recently been shown to result in a 76% increase in gradients compared with the resting supine state, but was not as potent a maneuver as either Valsalva or exercise.[79] Upright exercise echocardiography has been shown to be the most potent provocative maneuver for the assessment of latent LVOT obstruction in several studies, as it combines both preload reduction and increased adrenergic drive. Exercise echocardiography can be performed safely in patients with HCM: major complications occurred in 1 of 263 patients undergoing treadmill exercise testing.[80]

## TECHNICAL ASPECTS OF DOPPLER EVALUATION IN HYPERTROPHIC CARDIOMYOPATHY

There are important technical considerations in the performance and interpretation of Doppler studies in patients with HCM. It was not possible to obtain a discernible signal from the LVOT in 16% of patients in one study comparing CW Doppler echocardiography to cardiac catheterization.[81] This inability to acquire a clear spectral display from the outflow tract may be secondary to inadequate transthoracic windows or distortion of LV geometry. In addition, it is imperative to distinguish the high-velocity systolic signal coming from the outflow tract from the signal of mitral regurgitation. The spectral profile of mitral regurgitation is characterized by an earlier onset, a more abrupt initial increase in velocity, and a higher peak velocity than that of an outflow tract signal. Systolic jets with a peak velocity of greater than 5.5 m/s (gradient greater than 120 mm Hg) are most likely secondary to mitral regurgitation rather than LVOT obstruction.[81] Further differentiation of

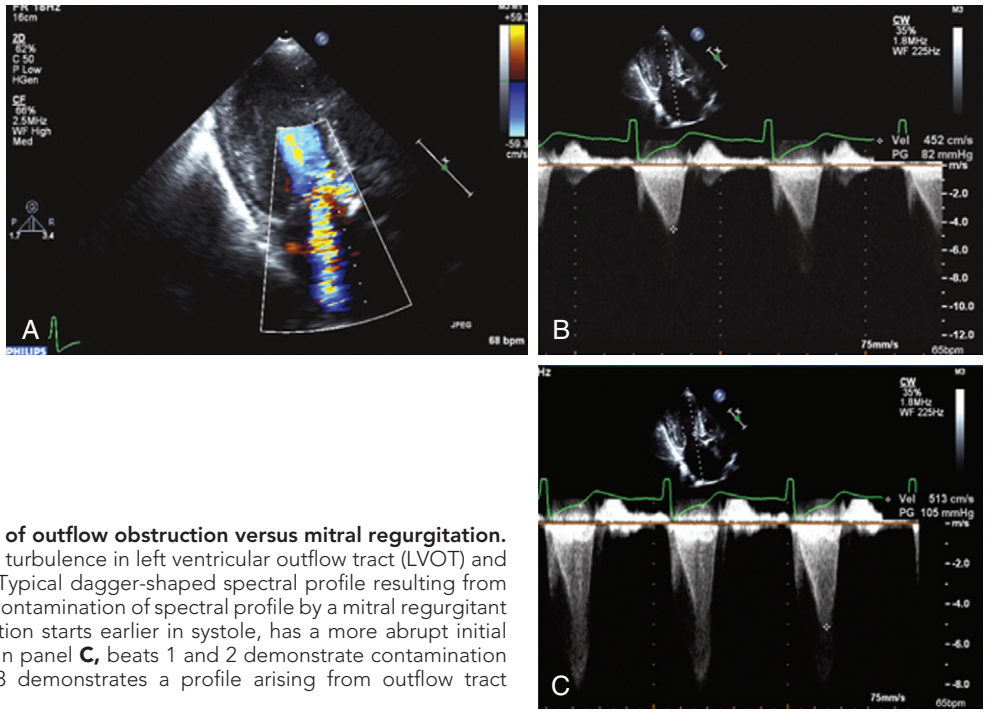



**Figure 27-9 CW Doppler characteristics of outflow obstruction versus mitral regurgitation.** **A,** Color Doppler imaging with evidence of turbulence in left ventricular outflow tract (LVOT) and fairly central jet of mitral regurgitation. **B,** Typical dagger-shaped spectral profile resulting from dynamic LVOT obstruction. **C,** Evidence of contamination of spectral profile by a mitral regurgitant jet. The spectral profile of mitral regurgitation starts earlier in systole, has a more abrupt initial rise in velocity and a higher peak velocity. In panel **C,** beats 1 and 2 demonstrate contamination from mitral regurgitation, whereas beat 3 demonstrates a profile arising from outflow tract obstruction alone.

these two jets can be accomplished by orienting the transducer more medially and anteriorly and away from the mitral regurgitant jet. Nevertheless, there may still be contamination of the high-velocity signal of outflow tract obstruction from the jet of mitral regurgitation (Fig. 27-9). This pitfall is particularly more common in patients with concomitant intrinsic mitral valve disease and a more centrally directed jet of mitral regurgitation. Despite optimal imaging, adjustments in instrument settings, and consideration of the differences in the timing and contour of these systolic jets, the distinction between these different Doppler signals may occasionally still be difficult.[82]

## Mitral Regurgitation in Hypertrophic Cardiomyopathy

Anterior mitral leaflet-septal contact and anterior displacement of the posterior leaflet results in failure of coaptation, creating a funnel-shaped gap in the leaflets through which mitral regurgitation develops, predominantly in mid- to late systole.[11] Patients with obstructive HCM and no independent mitral valve disease typically have a posteriorly directed jet of mitral regurgitation (Fig. 27-10).[11,83] Mitral regurgitation associated with obstructive HCM has been shown to be related to the degree of anterior leaflet SAM and to the length and mobility of the posterior leaflet, which determine the size of the interleaflet gap and the degree of midsystolic coaptation of the mitral leaflets.[84] These findings were corroborated by an intraoperative TEE study of 104 patients that demonstrated a significant correlation between the degree of mitral regurgitation, as assessed by color jet area and pulmonary venous flow pattern, and the degree of LVOT obstruction.[83] The presence of a nonposterior jet of mitral regurgitation suggests intrinsic mitral valve leaflet disease independent of SAM.

**Box 27-3**

### INTRINSIC MITRAL VALVE ABNORMALITIES IN PATIENTS WITH HYPERTROPHIC CARDIOMYOPATHY

- Degenerative changes
  - Mitral annular calcification
- Leaflet trauma
- Myxomatous mitral valve leaflets
- Papillary muscle abnormalities
  - Hypertrophied papillary muscles
  - Direct insertion of the papillary muscle into the anterior mitral valve leaflet
- Restrictive chordal and leaflet abnormalities
  - Shortened/calcified chordae
  - Abnormal chordal insertions
  - Thickened/tethered leaflets

Adapted from Kaple RK, Murphy RT, DiPaola LM, et al: Mitral valve abnormalities in hypertrophic cardiomyopathy: echocardiographic features and surgical outcomes. *Ann Thorac Surg* 85:1527-1536, 2008.

Independent mitral valve lesions can be identified by echocardiography and are usually related to mitral valve prolapse, ruptured chordae, mitral annular calcification, anomalous insertion of a papillary muscle into the anterior mitral leaflet, or leaflet trauma (Box 27-3).[85] Repeated mitral leaflet-septal contact is associated with fibrosis and thickening of the anterior mitral leaflet (and with subaortic septal endocardial fibrosis and thickening, previously described as a septal "callus"). Myectomy alone is generally successful in relieving posteriorly directed mitral regurgitation, without the requirement for associated mitral valve replacement.[83]

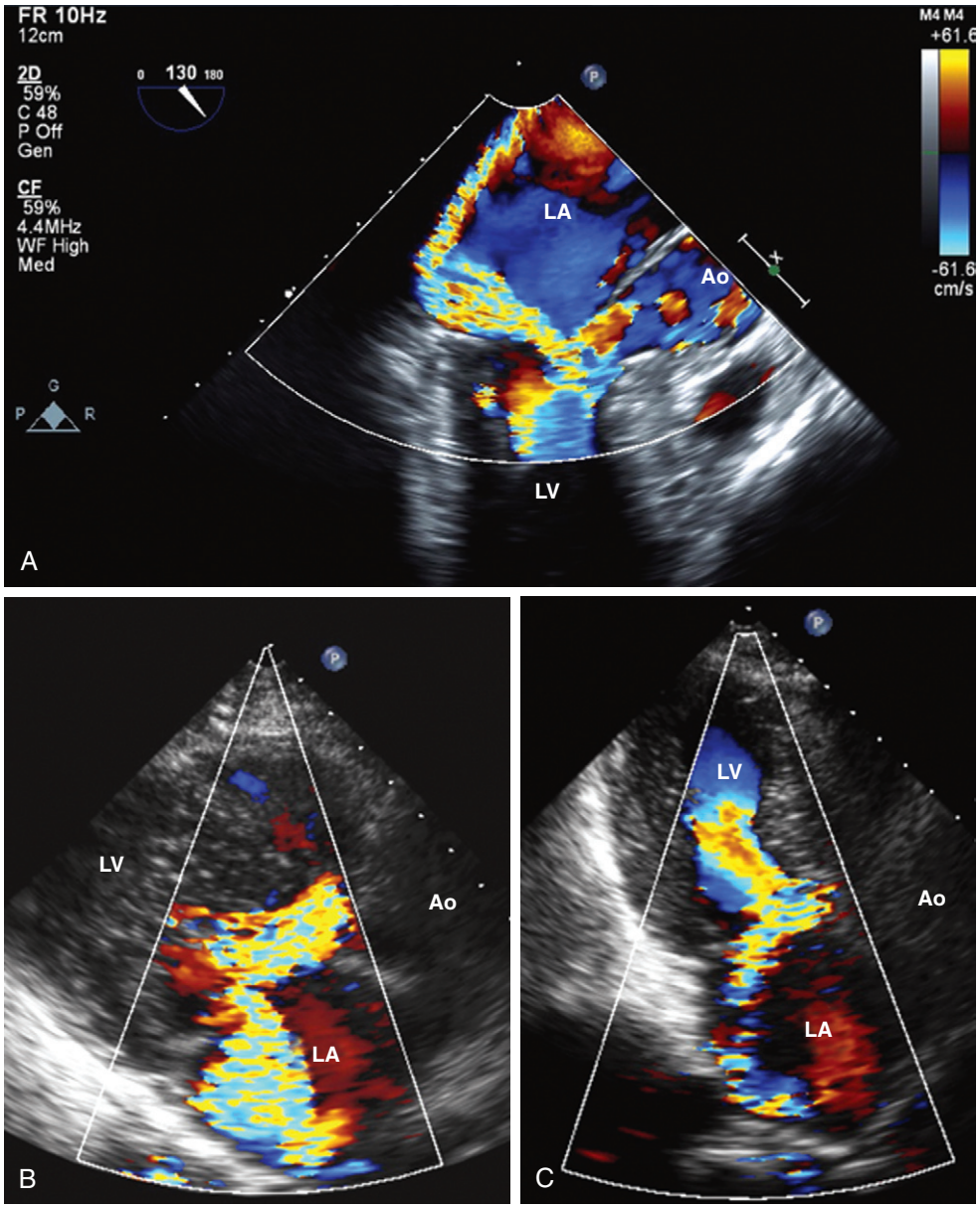



**Figure 27-10** **Color Doppler findings with dynamic outflow obstruction. A,** Midesophageal long-axis view at 130°. **B,** Transthoracic parasternal long-axis view. **C,** Transthoracic apical three-chamber view. Demonstration of posteriorly directed jet of mitral regurgitation secondary to systolic anterior motion of mitral valve causing dynamic outflow tract obstruction. *Ao*, Aorta.

## Subtypes of Hypertrophic Cardiomyopathy

### ASYMMETRIC APICAL HYPERTROPHIC CARDIOMYOPATHY

Asymmetric apical HCM was initially reported by Japanese investigators in the 1970s.[86,87] This unusual variant of HCM has subsequently been described in non-Asian populations.[88] The striking features of patients with apical hypertrophy include the presence of giant negative T waves (at least 10 mm) in the precordial electrocardiographic leads and an "ace of spades" configuration to the LV (Fig. 27-11). The diagnosis may be missed if acoustic windows are suboptimal and endocardial definition is poor. Contrast echocardiography may be useful in identifying cases of apical hypertrophy (Fig. 27-12). Echocardiography plays an important role in the assessment of the degree and extent of hypertrophy at the apex and the development of such complications as impaired diastolic filling, apical infarction, and aneurysm formation (Fig. 27-13) (which may result in ventricular tachycardia) and LA enlargement (which predisposes to atrial fibrillation). The long-term prognosis of patients with apical HCM is generally excellent (in the absence of apical aneurysm formation).[88]

### MIDVENTRICULAR OBSTRUCTION

The midventricular form of obstructive HCM, initially described in 1976,[89] is an uncommon variant of this condition. The features of this condition include an "hourglass"-shaped LV cavity, midventricular obliteration in systole, a distinct apical chamber, color turbulence at the midventricle, and a systolic pressure gradient at the midventricular level (Fig. 27-14).[72,90] The combination of color flow mapping, PW, and CW Doppler techniques is useful in localizing the level and severity of obstruction.

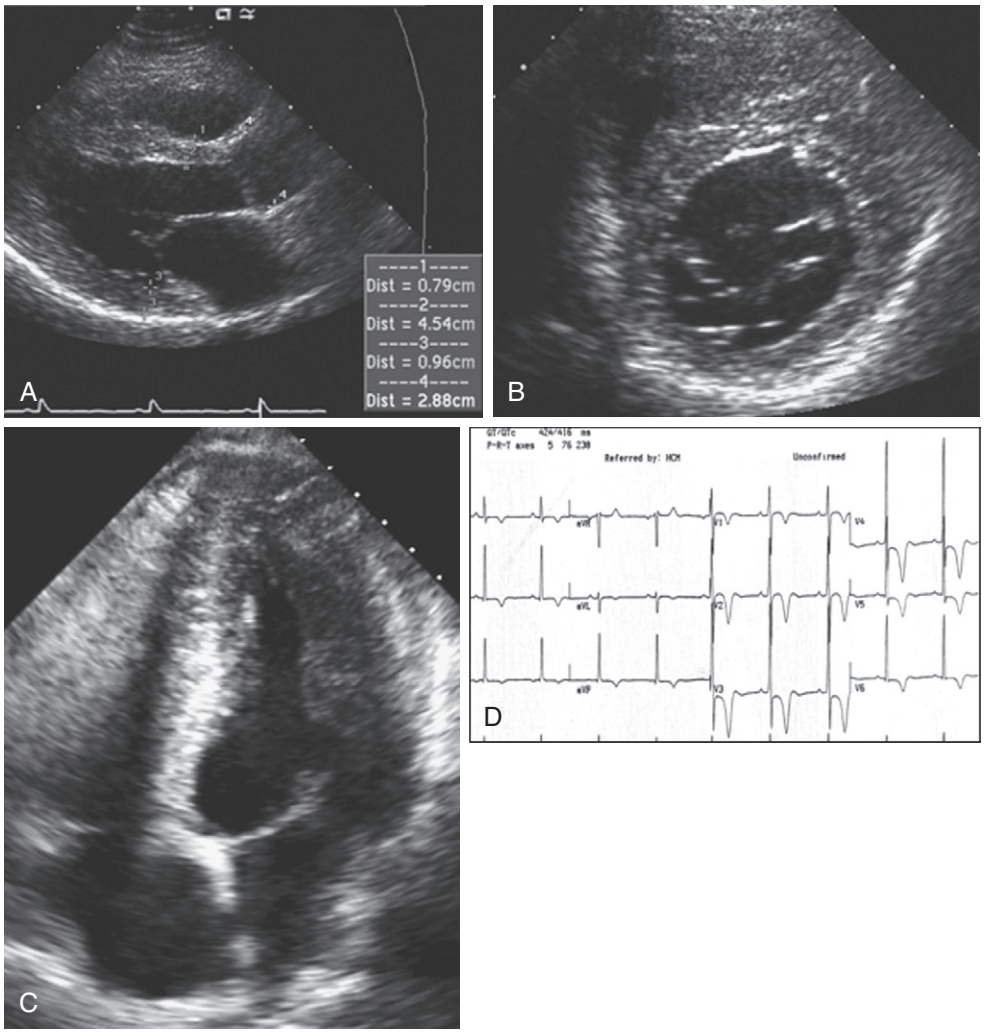



**Figure 27-11 Apical hypertrophic cardiomyopathy (HCM).** Parasternal long-axis view (**A**) and parasternal short-axis view at basal level (**B**). Wall thickness is normal in basal segments. Apical four-chamber view (**C**) shows hypertrophy of apical segments, resulting in typical "ace of spades" configuration of LV cavity. Corresponding electrocardiogram (**D**) demonstrates typical LV hypertrophy pattern seen in apical HCM, with giant negative T waves in chest leads.

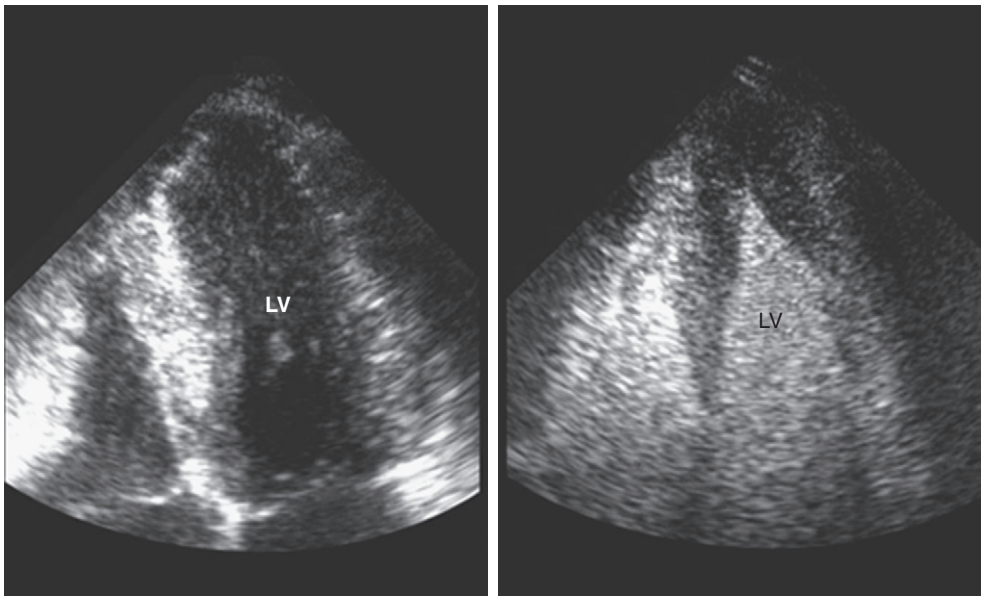



**Figure 27-12 Contrast echocardiography for diagnosis of apical hypertrophic cardiomyopathy.** In cases of suboptimal endocardial definition on TTE, injection of contrast agent may help to better visualize the apex. In addition, injection of contrast may be used to differentiate between apical hypertrophic cardiomyopathy and noncompaction of the LV.

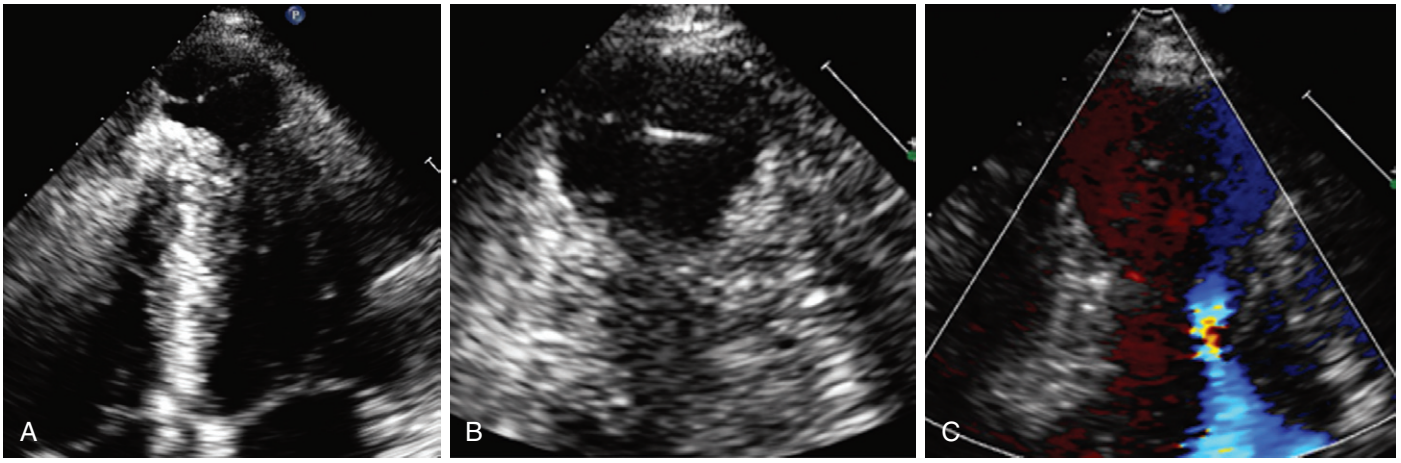



**Figure 27-13 Apical aneurysm in hypertrophic cardiomyopathy.** 2D echocardiographic images demonstrate apical aneurysm in a patient with apical hypertrophic cardiomyopathy. Note wall thinning in the apical segments (**A** and **B**). Color Doppler imaging may help assess for presence of thrombus in aneurysm (**C**). When using color Doppler, it is important to alter the Nyquist limit to account for low flow conditions in apical aneurysm.

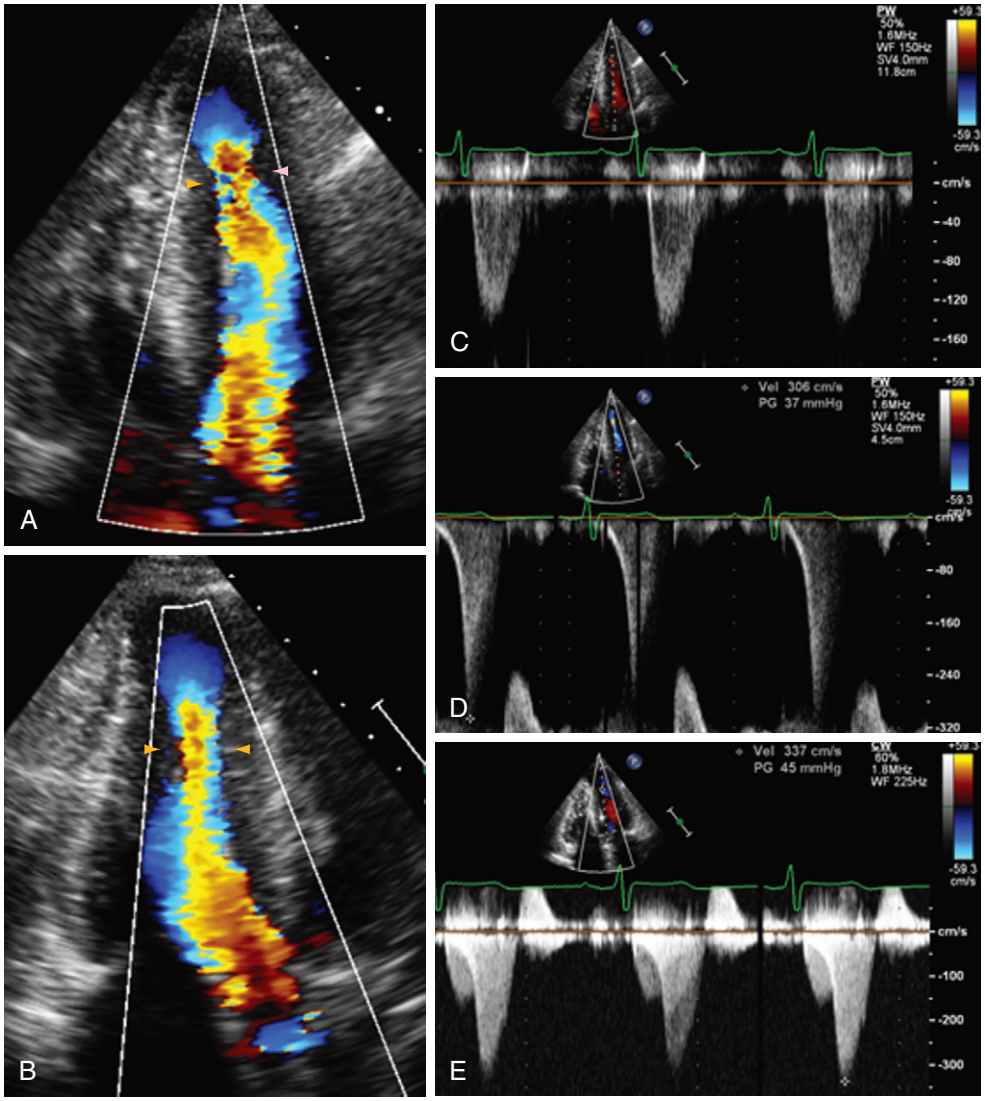



**Figure 27-14 Hypertrophic cardiomyopathy with midventricular obstruction.** 2D color Doppler echocardiographic images in apical five-chamber (**A**) and three-chamber (**B**) views demonstrate turbulent flow at level of midventricle (*yellow arrows*). PW Doppler traces demonstrate normal velocities in LV outflow tract (**C**), but evidence of obstruction at the midventricle (**D**). **E,** CW Doppler trace for assessment of peak velocity.

It is particularly important to identify those patients with mid-cavity obstruction, as this may be associated apical aneurysm formation, which is associated with systemic embolism, LV systolic dysfunction, and a risk of ventricular arrhythmias.[91]

### HYPERTROPHIC CARDIOMYOPATHY OF THE ELDERLY

HCM of the elderly is a subset of this condition with some distinguishing clinical and echocardiographic features.[92,93] The pattern of hypertrophy tends to be focal and localized to the basal anterior or posterior interventricular septum.[94] Elderly patients with HCM tend to have a milder degree of hypertrophy. The shape of the LV cavity in elderly patients is typically ovoid with normal septal curvature. In contrast, younger patients tend to have a crescent-shaped LV cavity and an abnormal convexity to the septum, characterized as a reversal of septal curvature.[95] Concomitant mitral annular calcification is a common feature of HCM in the elderly.[96]

The mechanisms leading to LVOT obstruction in HCM of the elderly are different from those seen in younger patients. Elderly patients have a relatively small heart and distorted geometry of the LVOT. Mitral annular calcification results in anterior displacement of the mitral apparatus, narrowing of the outflow tract, and less angulation of the mitral leaflets. Outflow tract obstruction, either at rest or with provocation, is associated with the majority of patients with HCM of the elderly.[95] Furthermore, the presence of mitral annular calcification distorts the mitral annulus and may lead to an independent jet of mitral regurgitation, which is often centrally directed and distinct from the posteriorly directed mitral regurgitant jet caused by SAM. However, in a recent study by Kubo and co-workers,[97] the authors demonstrated a significant correlation between the presence of reverse curvature morphology and genotype positivity (79%), compared with a low prevalence (8%) of mutations in those with sigmoid septal morphology. The previously mentioned echocardiographic features were described before the advent of genetic testing, and it is possible that LV hypertrophy of heterogeneous cause or age-related changes in morphology may have been included.

## Evaluation of Diastolic Function

### FACTORS CONTRIBUTING TO IMPAIRED DIASTOLIC FUNCTION IN HYPERTROPHIC CARDIOMYOPATHY

Diastolic filling of the LV is impaired in HCM and may result in dyspnea on exertion, elevated filling pressures, and progressive LA enlargement. Box 27-4 outlines the factors that contribute to diastolic filling in HCM. Impaired relaxation of the LV is secondary to increased contraction load, decreased relaxation loads, decreased inactivation, and increased nonuniformity. The early contraction load of outflow tract obstruction impairs and delays the onset of relaxation. The major relaxation loads, coronary and ventricular filling, are decreased. Calcium overload secondary to hypertrophy or ischemia leads to myofibril inactivation of actin-myosin cross-bridges. Relaxation is further impaired by the nonuniformity of load and inactivation in different segments of the LV. Chamber stiffness is directly proportional to the myocardial mass and the degree of myocardial fibrosis and is inversely proportional to the LV chamber volume.

**Box 27-4**

**FACTORS AFFECTING DIASTOLIC FUNCTION IN HYPERTROPHIC CARDIOMYOPATHY**

**Relaxation**
***Loads***
Contraction load
  Dynamic left ventricular outflow tract obstruction
Relaxation loads
  Late systolic loading
  End-systolic deformation (restoring forces)
  Coronary filling
  Ventricular filling
Inactivation
  Myocardial calcium overload
Nonuniformity of load and inactivation (nonuniformity of contraction and relaxation)

**Chamber Stiffness**
Myocardial mass
LV volume
Myocardial stiffness (fibrosis)

Adapted from Rakowski H, Sasson Z, Wigle ED: Echocardiographic and Doppler assessment of hypertrophic cardiomyopathy. *J Am Soc Echocardiogr* 1:31-47, 1988.

### TECHNIQUES FOR THE ASSESSMENT OF DIASTOLIC FUNCTION

Impaired LV relaxation is the predominant diastolic abnormality identified in patients with HCM, regardless of symptomatic status or the presence of LVOT obstruction.[98] The mitral inflow pattern typically demonstrates a prolonged isovolumic relaxation time, reduced early rapid filling (E), a prolonged deceleration time, and increased atrial filling (A). However, mitral inflow and pulmonary venous flow assessments correlate poorly with invasively measured filling pressures.[99,100] In addition, LV filling pressures can be assessed by calculating the E/E′ ratio (derived from the early diastolic tissue Doppler velocity from the lateral mitral annulus),[101] despite the correlation being only modest in the HCM patient population. There is a good correlation between LV filling pressures and the ratio of mitral inflow E velocity to flow propagation velocity ($V_P$).[101]

### TISSUE DOPPLER IMAGING

In addition to the assessment of LV filling pressures, tissue Doppler can provide important insights in the evaluation of patients with HCM. Reduced tissue Doppler early diastolic velocities have been detected in genotype-positive subjects without LV hypertrophy, suggesting that diastolic abnormalities may precede the onset of hypertrophy (see Diagnosis section).[34-36] Early diastolic velocities at the lateral and septal annulus are lower in patients with HCM compared to control subjects.[102] The E/E′ ratio was found to correlate inversely with peak oxygen consumption.[102] Patients with higher LA volumes had a higher E/E′ ratio, a higher incidence of diastolic filling abnormalities, and a higher incidence of serious cardiovascular events.[103] In addition, tissue Doppler has been used to monitor the response to invasive therapies. A significant increase in E′, suggestive of improved LV relaxation, was demonstrated in patients 6 months after septal ethanol ablation.[104] Similar improvements in diastolic function (as assessed by tissue Doppler and color M-mode Doppler) were demonstrated in patients undergoing septal ethanol ablation and myectomy.[105]

### ASYNCHRONOUS CONTRACTION AND RELAXATION IN HYPERTROPHIC CARDIOMYOPATHY

The inhomogeneity of relaxation seen in patients with HCM may result in LV intracavitary flow during isovolumic relaxation. Asynchronous relaxation in patients with asymmetric septal hypertrophy leads to earlier relaxation of the apex. Blood flow from the LV base to apex is detected during isovolumic relaxation and has been termed intracavitary "isovolumic relaxation time flow."[106] In contrast, patients with asymmetric apical HCM may have intracavitary apex-to-base flow, previously described as a paradoxical jet flow, with earlier relaxation of proximal LV segments.[107] Interventricular and intraventricular dyssynchrony are relatively common in HCM despite the absence of bundle branch block on the surface electrocardiogram. The degree of dyssynchrony appears to correlate with the degree of septal hypertrophy and the presence of LVOT obstruction.[108] A significant increase in LV dyssynchrony is seen in HCM patients compared with controls and patients with hypertensive heart disease, with no significant differences in dyssynchrony in those HCM patients with asymmetric septal hypertrophy versus those with apical HCM.[109]

## Strain Imaging in Hypertrophic Cardiomyopathy

Using gray-scale imaging, 2D deformation analysis allows spatial and temporal tracking of longitudinal, circumferential (representing systolic shortening), and radial (representing systolic thickening) myocardial deformation in order to quantify regional and global ventricular mechanics. Its ability to provide angle-independent measures of LV strain is advantageous. Studies in patients with HCM have demonstrated a reduction in longitudinal strain, an increase in circumferential strain, and a normal twist angle (despite a change in direction at the level of the midventricle), but a reduction in untwisting in diastole. Studies in the HCM population have shown evidence of reduced diastolic but preserved systolic strain in carriers of sarcomere mutations with no evidence of LV hypertrophy.[110] In overt disease, despite a preserved ejection fraction, there is a significant global reduction in longitudinal strain in association with a compensatory increase in circumferential strain.[111] These changes in systolic strain are mirrored by changes in the early diastolic strain rates in this patient group.[112] The longitudinal strain rate E/S ratio allows assessment of the relative extent of diastolic changes to systolic ones and has been shown to be reduced in HCM, most profoundly in those patients with obstruction.[112] Systolic contraction is dependent on twisting of the heart, with untwisting after systolic contraction being an important mechanism by which the heart recoils, in effect creating suction force that augments early diastolic filling. Although twist time is shortened in patients with HCM, the untwist time is prolonged, a finding that paralleled the severity of LV hypertrophy (Fig. 27-15).[113] Strain rate imaging has been shown to be useful in differentiating HCM from hypertensive LV hypertrophy, with the septum/posterior wall thickness ratio (greater than 1.3) and systolic strain ($\varepsilon_{sys}$) being the two parameters that were useful in distinguishing between these two disorders.[114] The combination of the septum/posterior wall thickness and $\varepsilon_{sys}$ discriminated HCM from hypertensive heart disease with a predictive accuracy of 96%.[114]

## Prognostication by Echocardiography

Echocardiography is increasingly providing important information regarding the long-term prognosis of patients with HCM. Spirito and colleagues[9] have demonstrated in a series of

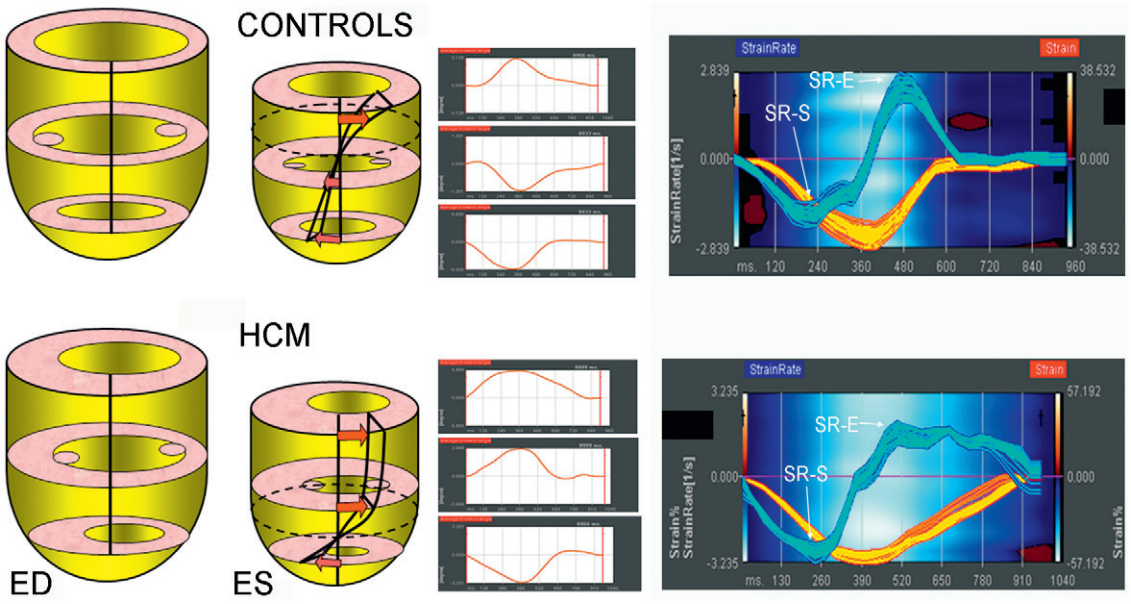



**Figure 27-15 LV rotation and twist, strain, and strain rate in hypertrophic cardiomyopathy (*HCM*) compared with controls.** Changes in rotation and twist of LV (*left*) in a patient with HCM. Principal difference is at midlevel, which rotates in opposite direction (clockwise) in patients with HCM compared with control subjects. Thus, in HCM, rotation of midventricle follows the base, in contrast with controls, where midventricle follows the apex. This may be consistent with the hypertrophied and rigid myocardium of HCM, which prevents a more gradual change of rotation from base to apex. Circumferential strain (*center panels*) and strain rate (*right*) show an increase in circumferential strain and systolic strain rate in patient with HCM. Reduction in diastolic strain rate in patient with HCM reflects underlying diastolic dysfunction. *ED*, Early diastole; *ES*, early systole; *SR-S*, strain rate in systole; *SR-E*, strain rate in early diastole.

about 500 patients that a wall thickness greater than 30 mm confers a long-term risk of sudden death of 20% at 10 years and 40% at 20 years. A further study of more than 600 patients again demonstrated the highest risk in patients with a wall thickness greater than 30 mm (with a relative risk of 1.31 for every further 5-mm increase in wall thickness).[115]

The presence of resting LVOT obstruction has also been associated with increased mortality.[8] In addition, McLeod and colleagues[116] have demonstrated a significantly lower rate of appropriate ICD discharges after septal myectomy compared with a nonoperated group with obstructive HCM. However, the positive predictive value of a resting LVOT gradient for the development of sudden cardiac death is particularly low (7%).[8] Finally, LA enlargement has been found to be a significant predictor of atrial fibrillation in patients with HCM[117] and of long-term survival in patients following surgical myectomy.[118]

## Medical Therapy

Medical management in HCM is optimized by monitoring the response to therapy with serial echocardiographic and Doppler studies. The three different classes of pharmacologic agents used for the treatment of obstructive HCM are beta blockers, disopyramide, and calcium channel blockers. The mechanism of benefit of these agents is thought to be a decrease in myocardial contractility, which results in decreased LV ejection velocity, the delayed onset of mitral leaflet SAM, and, consequently, decreased outflow tract obstruction and mitral regurgitation. In addition, beta blockers and calcium channel blockers relieve myocardial ischemia and reduce the heart rate, which prolongs diastole and relaxation and increases passive ventricular filling.[1] However, verapamil should be used with caution in patients with obstructive HCM because it can lead to vasodilatation and worsening outflow tract obstruction.[119] Disopyramide is a type IA antiarrhythmic agent with significant negative inotropic properties.[120] Cardiac symptoms and the magnitude of the LVOT gradient are significantly improved following the institution of disopyramide. In one multicenter study of 118 patients treated with disopyramide, two thirds of patients were maintained with disopyramide without the need for an invasive intervention.[121]

## Dual-Chamber Pacing

The interest in dual-chamber pacing in the reduction of outflow tract obstruction dates back to the 1960s, when it was noted that patients who developed a left bundle branch block after myectomy had a better clinical outcome than those patients with no interventricular delay. RV pacing results in a reduction in outflow tract obstruction via an alteration in the activation sequence of the interventricular septum, resulting in an increased outflow tract diameter and a reduction in SAM of the mitral valve. In addition, the resultant dyssynchrony results in a fall in LV contractility and stroke work.[122,123] Initial studies had suggested significant symptomatic improvement and LV mass regression with dual-chamber pacing.[124] However, the results of multiple subsequent studies have been less encouraging. Randomized crossover studies of dual-chamber pacing (treatment arm) versus atrial demand inhibited pacing (control arm) have shown an incomplete reduction in the LVOT gradient, no significant decrease in LV wall thickness, and no significant increase in peak myocardial oxygen consumption ($VO_2$) during follow-up.[125-127] The perceived decline in symptoms following pacemaker implantation may, in part, be due to a placebo effect.[127] These findings were corroborated by a nonrandomized study comparing dual-chamber pacing and septal myectomy, which showed a significantly greater improvement in the functional class, oxygen consumption, and LVOT gradient in the patients who underwent surgery.[128]

## Septal Ethanol Ablation

Septal ethanol ablation is an interventional technique that consists of the selective injection of ethanol into a septal perforator branch of the left anterior descending artery.[129] This leads to occlusion of the septal branch and localized infarction of the hypertrophied interventricular septum. The targeted infarction results in focal thinning of the septum, widening of the LVOT, and relief of LVOT obstruction.[130] The first clinical experience with septal ethanol ablation was reported in the 1990s. The selection of the appropriate septal branch to be injected was determined by the reduction in the LVOT gradient following transient occlusion of the targeted vessel by a balloon catheter. However, a key development in this technique was the use of intraprocedural echocardiography. Myocardial contrast echocardiography with transthoracic imaging has become essential for the guidance and monitoring of septal ethanol ablation.[12,13,131]

### MYOCARDIAL CONTRAST ECHOCARDIOGRAPHY DURING SEPTAL ETHANOL ABLATION

The intraarterial injection of an echo-enhancing agent allows for the specific localization of the vascular beds perfused by individual septal perforator branches of the left anterior descending artery. The vascular territory targeted by contrast echocardiography is the region of contact of the anterior mitral leaflet with the basal septum, which leads to LVOT obstruction. The site of leaflet-septal contact is typically adjacent to the zone of flow acceleration and color turbulence in the LVOT (Fig. 27-16).[12] Contrast agents that have been used during septal ethanol ablation have included sonicated human albumin (Albunex), Levovist, Optison, and most recently Definity. After the injection of the contrast agent, the segments of the interventricular septum supplied by the septal branch become opacified. The spatial extent of myocardial opacification can be determined from multiple transthoracic windows. The contrast effect of ethanol has the same distribution as that of the contrast agent, and intraarterial ethanol injection frequently results in increased echogenicity and reflectivity.

### IMPROVED OUTCOMES WITH CONTRAST ECHOCARDIOGRAPHY

Intraprocedural contrast echocardiography results in improved outcomes compared with the strategy of target vessel selection by probatory balloon occlusion.[12] The use of contrast echocardiography was associated with a shorter intervention time, a smaller amount of injected ethanol, a smaller infarct, and a significantly higher number of patients with more than 50% gradient reduction (92% versus 70%). The superiority of this echocardiographic approach persisted at 3-month follow-up, in terms of improvements in both the functional class and the magnitude of the LVOT gradient.[12]

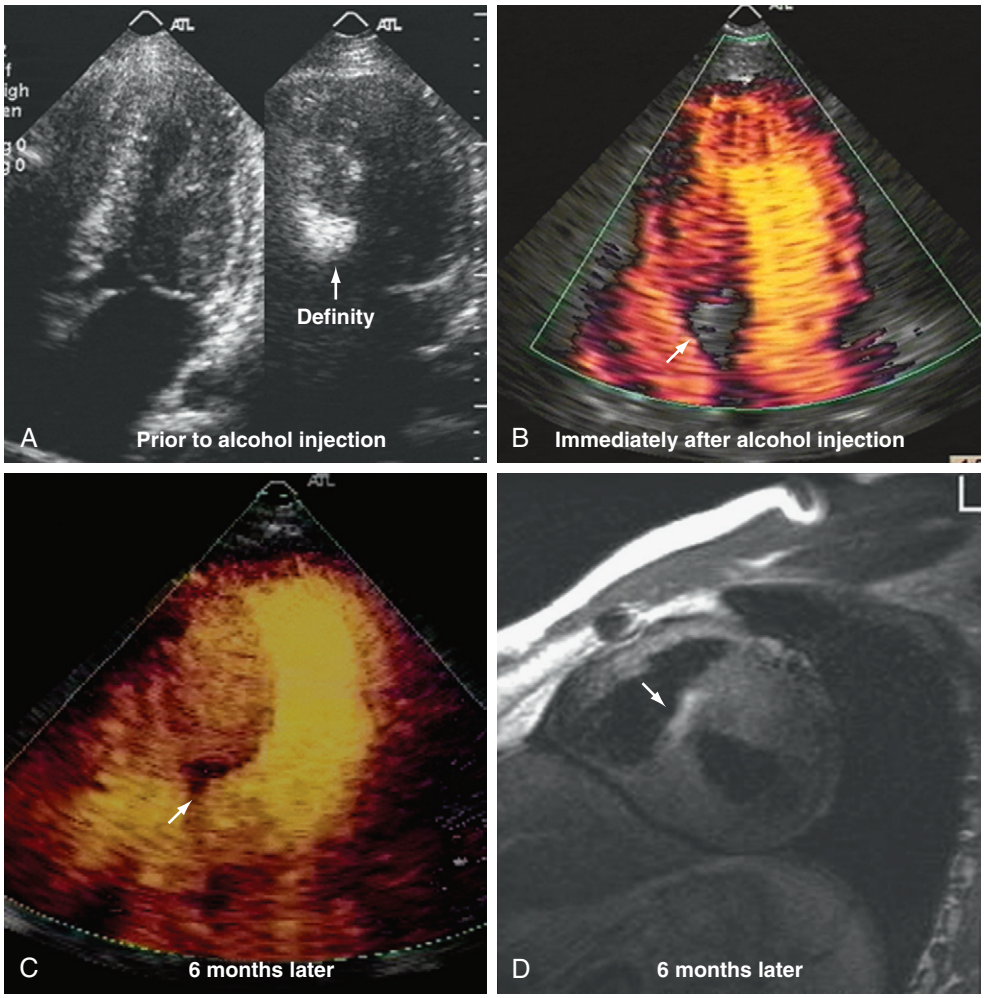



**Figure 27-16** **Intraprocedural myocardial contrast echocardiography during septal ethanol ablation. A,** Baseline echocardiogram prior to septal ethanol ablation (*left*). Following injection of echocardiographic contrast agent into first septal perforator of left anterior descending artery, contrast depot is identified in region of basal septum by transthoracic 2D apical imaging (*right*). **B,** Immediately after alcohol injection, venous injection of contrast demonstrates perfusion defect in basal septum (*arrow*). **C,** Repeat transthoracic apical view with contrast injection at 6 months postprocedure demonstrates thinning of basal septum and perfusion defect in basal septum (*arrow*). **D,** Corresponding cardiac magnetic resonance imaging at 6 months postprocedure demonstrating thinning of septum and evidence of scarring after gadolinium injection (*arrow*).

Contrast echocardiography is invaluable in detecting contrast opacification in regions remote from the site of mitral leaflet-septal contact. Echocardiographic guidance with a contrast agent can determine whether the selected septal branch supplies other territories such as the LV free wall or apex, RV free wall, or a papillary muscle (Fig. 27-17).[131,132] Contrast enhancement in nonseptal sites necessitates the selection of another vessel to be injected or abandonment of the procedure. Studies have shown that 7% to 11% of all procedures have been altered based on information obtained by contrast echocardiography.[131,133]

Furthermore, the size of the induced infarct, as determined by planimetry of the contrast-enhanced region, can provide incremental information regarding outcomes following septal ethanol ablation.[134] A septal infarction risk area of 3.5 $cm^2$ or greater has been associated with a higher risk of cardiovascular complications after the procedure (primarily pacemaker and defibrillator implantation), without necessarily improving the clinical and hemodynamic results of septal ethanol ablation.[134] In summary, myocardial contrast echocardiography optimizes septal ethanol ablation by permitting the targeted delivery of ethanol, by limiting the induced infarction to the culprit region of mitral leaflet-septal contact, and by minimizing procedural complications.

## CLINICAL RESULTS FOLLOWING SEPTAL ETHANOL ABLATION

Studies from multiple experienced centers have demonstrated that septal ethanol ablation can effectively reduce the LVOT gradient in patients with obstructive HCM.[135-138] Subsequent studies beyond 1 year following this procedure have shown ongoing symptomatic improvement.[139,140] Septal ethanol ablation results in an acute deterioration of basal septal function and a delay in LV ejection.[130] There is a gradual and continued decrease in the degree of LVOT obstruction,[135,138] with thinning of the infarcted septal segment and enlargement of the outflow tract.[141] Echocardiographic and Doppler studies are beneficial in the serial noninvasive follow-up of patients after septal ethanol ablation. Multiple studies have documented significant progressive reductions in basal septal thickness and the resting and provocable LVOT gradients.[135,138,142] These developments have been associated with favorable changes in the geometry of the LVOT.[130,141] In addition to the alleviation of LVOT

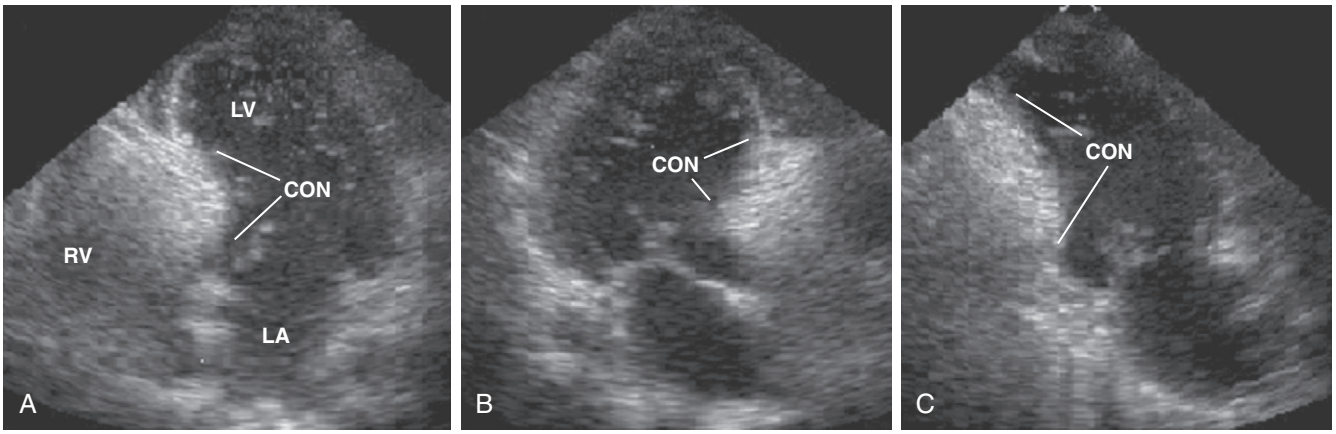



**Figure 27-17 Echocardiographic guidance of transcatheter septal ablation.** Intraprocedural myocardial contrast echocardiography during septal ethanol ablation is essential for guiding the targeted delivery of ethanol. After intraarterial injection of echocardiographic contrast (*CON*), transthoracic imaging from apical four-chamber view (**A**) and apical three-chamber view (**B**) shows opacification of basal and midposterior and anterior interventricular septum. However, apical two-chamber view (**C**) reveals contrast opacification of inferior wall. Selected vessel was not thought to be suitable for the injection of ethanol. No other septal perforator branches were identified; procedure was abandoned and patient referred for septal myectomy.

obstruction and septal remodeling, improvements in LV diastolic function have been demonstrated 6 months after this procedure.[104] These changes in diastolic function, as assessed by tissue and color M-mode Doppler, were sustained at 2 years of follow-up.[143] The long-term risk of late ventricular arrhythmias after induced infarction in patients with HCM remains unclear, although the majority of studies thus far have not demonstrated an increased risk of ventricular arrhythmias or of sudden death.[136,140,144]

## Surgical Myectomy

Septal myotomy or myectomy has been performed for the past four decades for the management of severe obstructive HCM refractory to maximally tolerated medical therapy. Septal myectomy acutely relieves outflow tract obstruction by widening of the LVOT, which leads to decreased SAM of the mitral valve and decreased dynamic outflow tract obstruction. Echocardiography is useful in the identification of patients suitable for surgical myectomy. The preoperative echocardiographic characteristics predictive of symptomatic benefit from surgical myectomy include asymmetric hypertrophy, severe SAM of the mitral leaflet(s), and a prolonged isovolumic relaxation time.[145] In addition, echocardiography plays an important role in detecting additional lesions requiring surgical management. Comprehensive preoperative echocardiographic imaging in patients referred for surgical myectomy includes the evaluation of independent mitral valve disease, concomitant aortic valve disease, and the assessment of additional levels of obstruction (midventricular or RV outflow tract).[11]

### INTRAOPERATIVE ECHOCARDIOGRAPHY

Surgical myectomy is performed from the transaortic approach and is technically challenging given the limited exposure and visualization of the hypertrophied septum. Before the introduction of intraoperative echocardiography, the extent and degree of septal hypertrophy was estimated by surgical palpation and by preoperative TTE studies. A key development in the surgical management of obstructive HCM has been the use of TEE imaging. Intraoperative echocardiography guides the surgical intervention(s), assesses immediate results, and excludes important complications.[11,146] Intraoperative TEE allows for detailed delineation of the depth, width and length of the required myectomy, the degree of SAM and LVOT obstruction, and the quantitation and mechanism(s) of mitral regurgitation.[11,83] Imaging from multiple transesophageal and transgastric views using a multiplane transducer allows for the careful assessment of the thickness of the anterior and posterior portions of the interventricular septum. The length of septal hypertrophy is measured from the base of the right coronary cusp of the aortic valve (Fig. 27-18). The targeted length of resection is 1 cm below the point of anterior mitral leaflet-septal contact. The LVOT gradient can be measured by transgastric imaging in the long-axis view with the CW Doppler beam aligned parallel to the LVOT. Following surgical excision of the basal septum, repeat echocardiographic imaging permits the instantaneous evaluation of the adequacy of the myectomy (Figs. 27-19 and 27-20).[11,146] Intraoperative echocardiography can determine if there is significant residual outflow tract obstruction (Fig. 27-21) or hemodynamically important residual mitral regurgitation. In addition, intraoperative echocardiography allows for the immediate detection of such operative complications as a ventricular septal defect[147] and LV dysfunction.[11] The value of intraoperative echocardiography was demonstrated in one study[148] showing that intraoperative TEE detected unexpected findings in 17% of cases before cardiopulmonary bypass and in 7% of cases after cardiopulmonary bypass. Intraoperative echocardiography prompted further surgical procedures in 4% of cases.

### OUTCOMES FOLLOWING MYECTOMY

Studies of the results of surgical myectomy from experienced tertiary referral centers have shown excellent early and long-term postoperative outcomes. Potential complications following myectomy include heart block, ventricular septal defect, aortic regurgitation, and arrhythmias. Aortic regurgitation is felt to be mainly secondary to the loss of aortic annular support after myectomy.[149] Echocardiographic studies performed at rest and with provocative maneuvers are important in the serial monitoring of patients following myectomy. Multiple studies

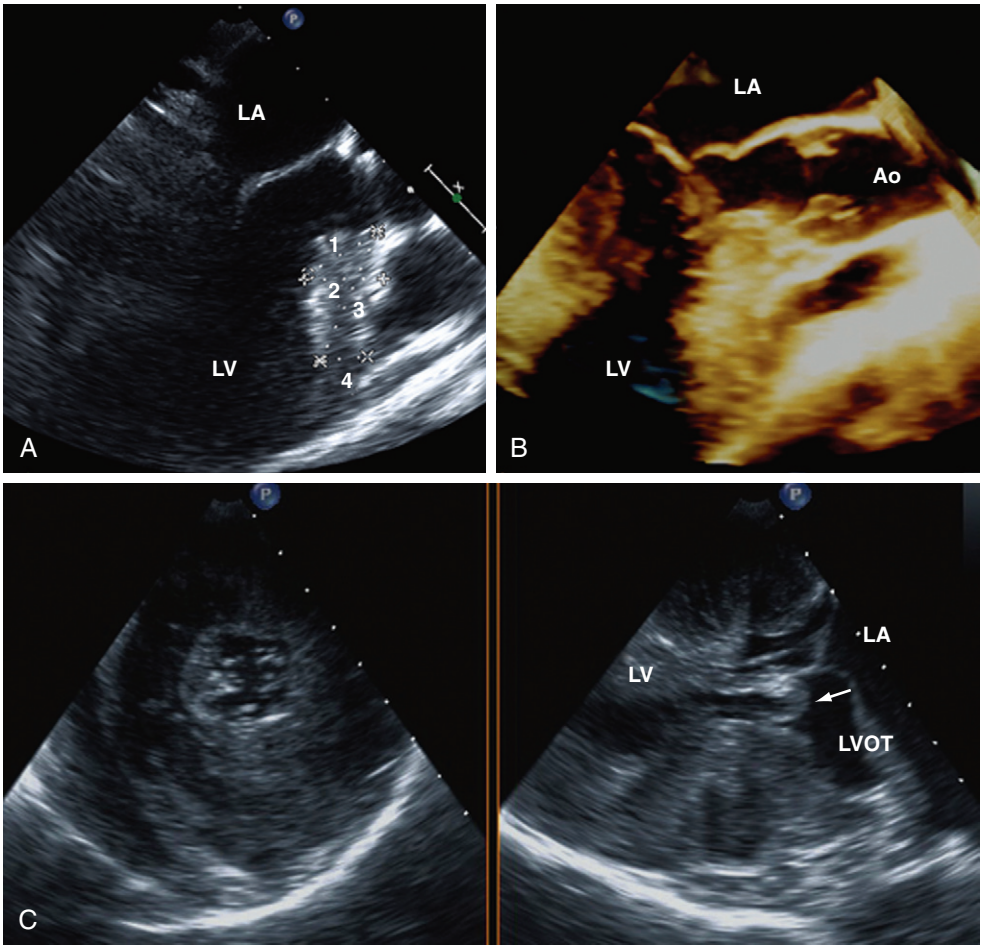



**Figure 27-18 Intraoperative transesophageal findings before surgical myectomy. A,** Midesophageal long-axis view at 120° demonstrating measurements required to determine the extent of surgical excision (*1*, distance from base of right coronary cusp to leaflet-septal contact point; *2*, maximal thickness of interventricular septum; *3*, distance from base of right coronary cusp to point of thinning of the septum; *4*, thickness of interventricular septum at point of thinning). **B,** 3D echocardiographic image of LV outflow tract in end-systole demonstrating systolic anterior motion (SAM) of mitral valve. **C,** Transgastric view in short-axis at basal level with X-plane, providing multiplanar views of LV. *Arrow*: SAM of mitral valve. *Ao*, Aorta; *LVOT*, left ventricular outflow tract.

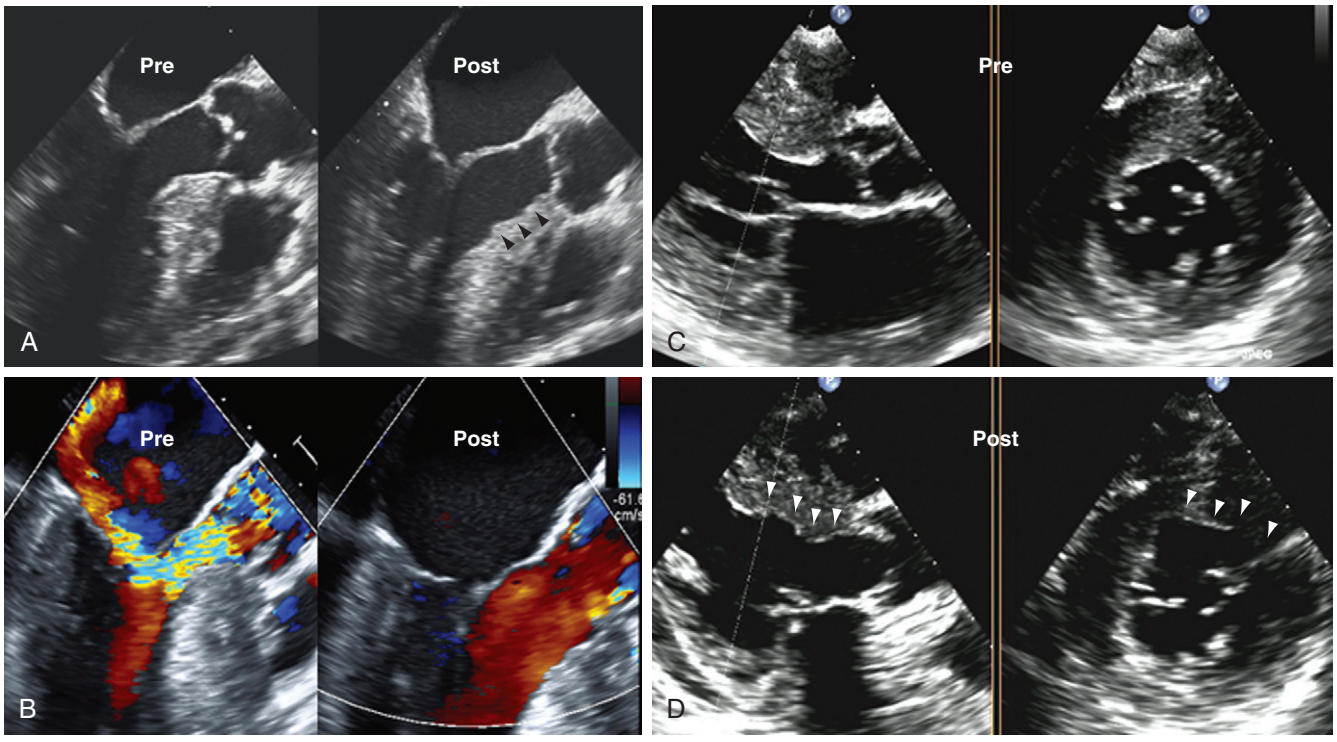



**Figure 27-19 Echocardiographic monitoring of surgical myectomy. A** and **B,** Midesophageal long-axis view at 120° on 2D and color Doppler imaging. Myectomy site shown by *black arrowheads*. Note that posteriorly directed mitral regurgitation jet has disappeared and there is laminar flow in the LV outflow tract. **C** and **D,** Epicardial echocardiography with X-plane imaging providing views corresponding to transthoracic long-axis and short-axis views. Myectomy site shown by *white arrowheads*. *Post*, Postmyectomy; *Pre*, premyectomy.

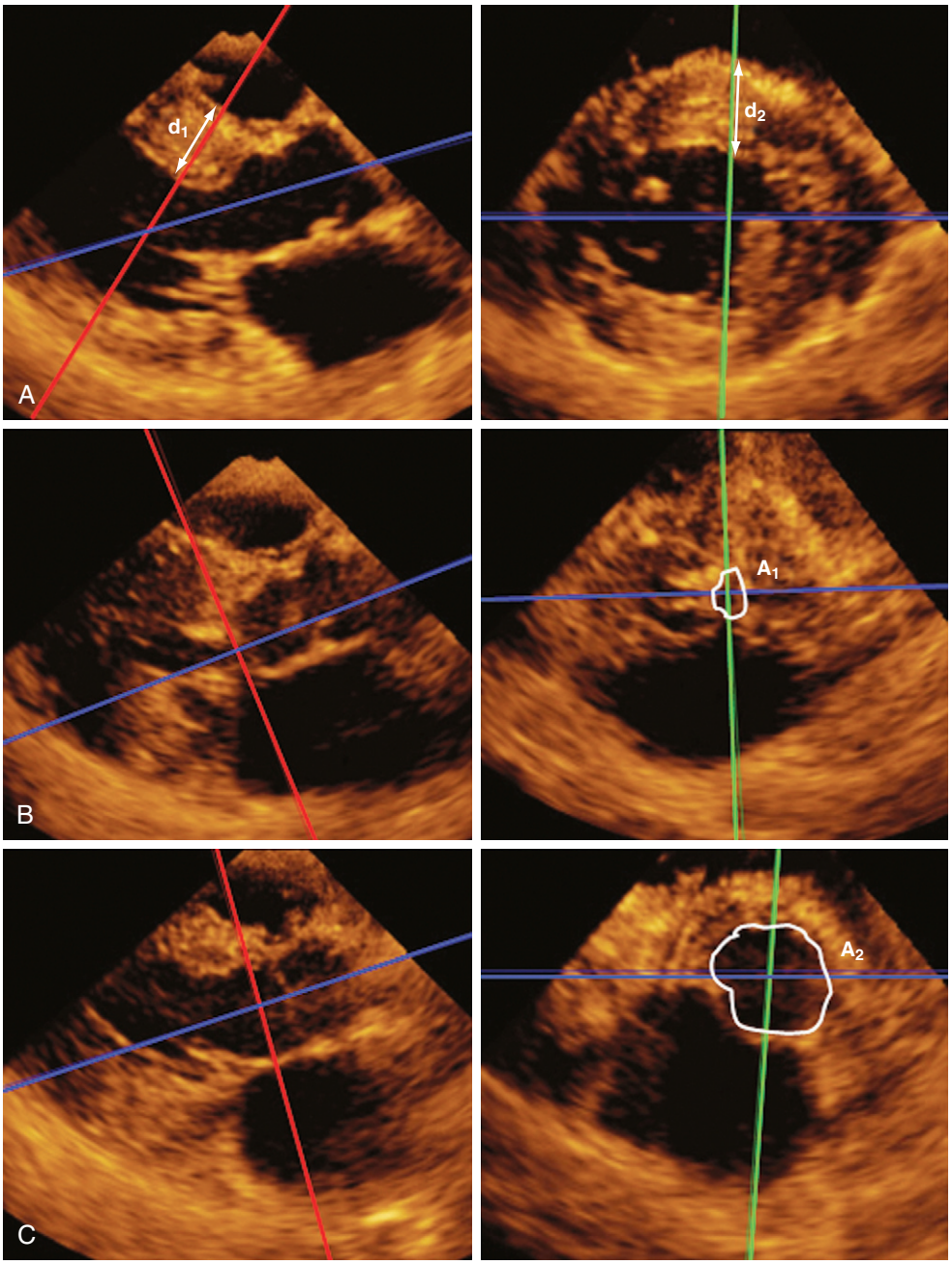



**Figure 27-20 3D epicardial echocardiographic images before and after surgical myectomy. A,** Maximal interventricular septal thickness of 20 mm ($d_1$ and $d_2$) in two perpendicular planes (*green* and *red*) before myectomy. **B,** LV outflow tract cross-sectional area (*red* plane at level of mitral leaflet tips) of 0.5 $cm^2$ (area $A_1$). **C,** Corresponding measurement after surgical myectomy, with impressive increase in cross-sectional area to 4.3 $cm^2$ (area $A_2$) (analyzed by 3D quantification software, Philips QLAB).

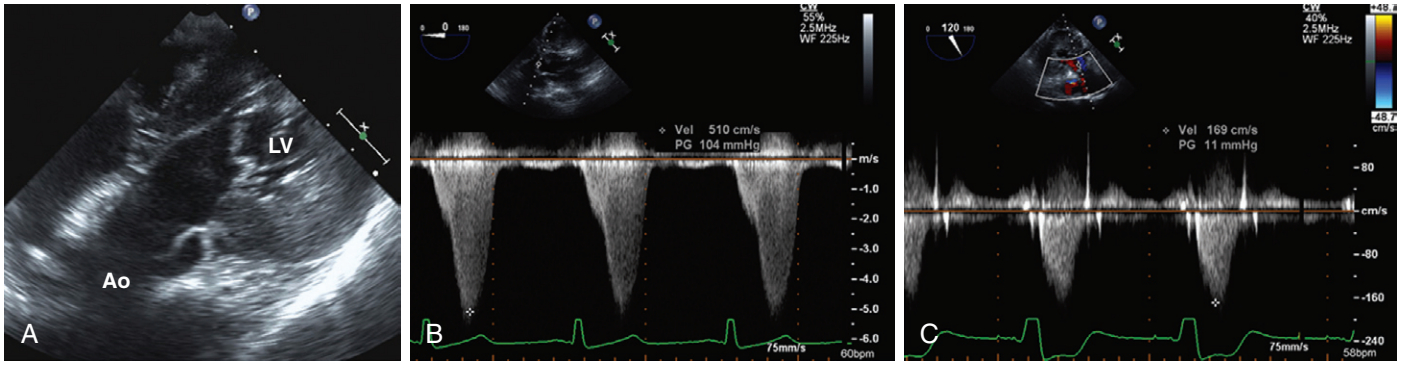



**Figure 27-21 TEE evaluation of outflow obstruction using CW Doppler during surgical myectomy. A,** Assessment of left ventricular outflow tract (LVOT) gradient in transesophageal deep transgastric view at 0°. **B,** CW Doppler across LVOT demonstrates significant resting gradient of 104 mm Hg before surgical myectomy. **C,** Significant reduction after the procedure, resulting in nonsignificant residual resting gradient of 11 mm Hg. *Ao*, Aorta.

**TABLE 27-3 Studies Comparing Invasive Strategies to Relieve Left Ventricular Outflow Tract Obstruction**

| Study | N Ablation/Myectomy | Follow-up (months) | Septal ethanol ablation (SEA) $\Delta P_{LVOT}$ (mm Hg) | Surgical myectomy (SM) $\Delta P_{LVOT}$ (mm Hg) | Pacemaker |
|---|---|---|---|---|---|
| Nagueh[156] (pre-2001) | 82 (41/41) | 12 | Pre 76 ± 23 Post 8 ± 15 | Pre 49 ± 16 Post 4 ± 7 | SEA: 22% SM: 2.4% |
| Qin[158] (1997-1999) | 51 (25/26) | 3 | Pre 64 ± 39 Post 24 ± 19 | Pre 62 ± 43 Post 11 ± 6 | SEA: 24% SM: 7.7% |
| Firoozi[157] (1997-2000) | 44 (20/24) | 12 | Pre 91 ± 18 Post 21 ± 12 | Pre 83 ± 23 Post 17 ± 12 | SEA: 15% SM: 4% |
| Ralph-Edwards[159] (1998-2003) | 102 (54/48) | 22-28 | Pre 74 ± 36 Post 15 | Pre 64 ± 27 Post 5 | |
| van der Lee[160] (1986-1999:SM) (1999-2003:SEA) | 72 (43/29) | 12 | Pre 101 ± 34 Post 23 ± 19 | Pre 100 ± 20 Post 17 ± 14 | SEA: 9% SM: 0% |
| Leonardi[144] (meta-analyses) | 4094 (2207/1887) | | Pre 76.8 Post 22 | Pre 67.3 Post 3 | SEA: 11% SM: 5% |
| Alam[161] (meta-analyses) | 351 (183/168) | | Pre 81.4 Post 18.2 ± 6.7 | Pre 77.4 Post 10.8 ± 6.3 | SEA: 18% SM: 3.4% |

Meta-analyses include the five cohorts above (in addition to other cohorts).
$\Delta P_{LVOT}$, Left ventricular outflow tract gradient before (pre) and after (post) procedure; *PPM*, permanent pacemaker; *SEA*, septal ethanol ablation; *SM*, septal myectomy.

have documented a significant reduction or abolition of the resting outflow tract gradient in the majority of patients following myectomy, resulting in substantial and lasting symptomatic improvement.[150-154] In addition, a recent study comparing invasive versus conservative management has demonstrated that invasive treatment results in improved overall, but not HCM-related, survival.[155]

## Comparison of Treatment Strategies for Obstructive Hypertrophic Cardiomyopathy

Multiple therapeutic options are currently available in the management of patients with obstructive HCM. Pharmacologic agents have variable effects in reducing the outflow tract gradient and in improving diastolic function. Patients with drug-refractory symptoms are candidates for dual-chamber pacing, septal ethanol ablation, or surgical myectomy. The initial enthusiasm for dual-chamber pacing as a treatment modality for LVOT obstruction has declined considerably. In terms of the outcomes of septal ethanol ablation compared with myectomy, there have been several nonrandomized studies that have compared these two treatment strategies.[144,156,158-161] No significant differences in cardiac mortality during early and midterm follow-up were identified. Patients who underwent septal ethanol ablation were more likely to develop atrioventricular block and require permanent pacing.[156,157,159] All these studies showed similar improvements in the functional class and in the resting LVOT gradients following both procedures (Table 27-3).[156-160] The greatest difference in the resting gradients between the two treatment groups occurred at 3 months after the procedure, when patients with septal ethanol ablation were more likely to have a larger resting outflow tract gradient.[158] This divergence likely emerged because myectomy offers immediate relief of the LVOT gradient, whereas the effect on the gradient with septal ethanol ablation is more gradual, with the maximal reduction in the gradient occurring at more than 1 year after the procedure.[138,140] In addition, the long-term benefits of myectomy have been well demonstrated, whereas the long-term sequelae of septal ethanol ablation have yet to be determined. Conditions that favor the selection of myectomy over septal ethanol ablation include the presence of coexisting disease (e.g., coronary artery disease, intrinsic disease of the mitral valve or subvalvular apparatus), the presence of coronary anatomy not amenable to septal ethanol ablation, the requirement for an acute reduction in the LVOT gradient, or the presence of extreme septal hypertrophy.

Septal ethanol ablation and surgical myectomy are challenging techniques. Importantly, both procedures need to be performed at centers with both technical and echocardiographic expertise. Comprehensive preprocedural echocardiographic assessment is essential for identifying patients with additional lesions that require surgical correction. The success of both septal ethanol ablation and myectomy depends on experienced intraprocedural echocardiographic guidance, with myocardial contrast echocardiography during septal ethanol ablation and TEE during myectomy. Intraprocedural echocardiographic guidance is indispensable for the identification of the culprit septal segments requiring chemical or surgical reduction, the immediate assessment of the LVOT gradient in response to septal infarction or myectomy, and the monitoring of potential complications.

## KEY POINTS

- The diagnostic feature of HCM on echocardiography is the finding of asymmetric septal hypertrophy, defined as a septal/posterior wall ratio of 1.3 or greater. The maximal wall thickness is typically at least 15 mm.
- Because there may be delayed penetrance of HCM, which has an autosomal dominant pattern of inheritance, serial screening (every 5 years) throughout adulthood is advised for the first-degree relatives of patients.
- The differential diagnosis of HCM is broad. Alternate causes of increased LV wall thickness include other causes of LV hypertrophy (e.g., hypertensive heart disease, athlete's heart), storage diseases (e.g., Fabry, glycogen storage diseases), and infiltrative cardiomyopathies (e.g., amyloidosis).
- 2D echocardiography with imaging from several transthoracic windows is used to determine the extent, distribution, and severity of LV hypertrophy.
- The pathophysiology of LVOT obstruction involves narrowing of the LVOT (due to septal hypertrophy, intrinsic abnormalities of the mitral leaflets, or anterior displacement of the mitral apparatus) and hydrodynamic forces causing SAM.
- The LVOT gradient can be measured with CW Doppler, where the pressure gradient = $4 \times V^2$ (V = LVOT velocity). The Doppler spectral profile is typically a dagger-shaped configuration.
- Subtypes of HCM that can be distinguished by echocardiography are asymmetric apical HCM, midventricular obstruction, latent obstructive HCM, and HCM of the elderly.
- Diastolic function in patients with HCM can be assessed with tissue Doppler imaging and color M mode Doppler.
- Septal ethanol ablation should be performed with myocardial contrast echocardiographic guidance, which allows for the targeted delivery of ethanol to the basal septum, avoids infarction of nonseptal sites, and minimizes complications.
- Intraoperative TEE during surgical myectomy provides detailed visualization of the septum and the mitral apparatus in order to guide the surgical resection and permits immediate assessment of the degree of residual outflow tract obstruction and mitral regurgitation.

## REFERENCES


1. Maron BJ, McKenna WJ, Danielson GK, et al: American College of Cardiology/European Society of Cardiology clinical expert consensus document on hypertrophic cardiomyopathy. A report of the American College of Cardiology Foundation Task Force on clinical expert consensus documents and the European Society of Cardiology Committee for practice guidelines. *J Am Coll Cardiol* 42:1687-1713, 2003.
2. Brock RC: Functional obstruction of the left ventricle. *Guys Hosp Rep* 106:221-238, 1957.
3. Teare RD: Asymmetrical hypertrophy of the heart in young adults. *Br Heart J* 20:1-8, 1958.
4. Maron BJ, Towbin JA, Thiene G, et al: Contemporary definitions and classification of the cardiomyopathies: an American Heart Association Scientific Statement from the Council on Clinical Cardiology, Heart Failure and Transplantation Committee; Quality of Care and Outcomes Research and Functional Genomics and Translational Biology Interdisciplinary Working Groups; and Council on Epidemiology and Prevention. *Circulation* 113:1807-1816, 2006.
5. Rakowski H, Sasson Z, Wigle ED: Echocardiographic and Doppler assessment of hypertrophic cardiomyopathy. *J Am Soc Echocardiogr* 1:31-47, 1988.
6. Maron BJ, Gardin JM, Flack JM, et al: Prevalence of hypertrophic cardiomyopathy in a general population of young adults: Echocardiographic analysis of 4111 subjects in the CARDIA study. *Circulation* 92:785-789, 1995.
7. Clark CE, Henry WL, Epstein SE: Familial prevalence and genetic transmission of idiopathic hypertrophic subaortic stenosis. *N Engl J Med* 289:709-714, 1973.
8. Maron MS, Olivotto I, Betocchi S, et al: Effect of left ventricular outflow tract obstruction on clinical outcome in hypertrophic cardiomyopathy. *N Engl J Med* 348:295-303, 2003.
9. Spirito P, Bellone P, Harris KM, et al: Magnitude of left ventricular hypertrophy and risk of sudden death in hypertrophic cardiomyopathy. *N Engl J Med* 342:1778-1785, 2000.
10. Corrado D, Basso C, Schiavon M, Thiene G: Screening for hypertrophic cardiomyopathy in young athletes. *N Engl J Med* 339:364-369, 1998.
11. Grigg LE, Wigle ED, Williams WG, et al: Transesophageal Doppler echocardiography in obstructive hypertrophic cardiomyopathy: clarification of pathophysiology and importance in intraoperative decision making. *J Am Coll Cardiol* 20:42-52, 1992.
12. Faber L, Seggewiss H, Gleichmann U: Percutaneous transluminal septal myocardial ablation in hypertrophic obstructive cardiomyopathy: Results with respect to intraprocedural myocardial contrast echocardiography. *Circulation* 98:2415-2421, 1998.
13. Nagueh SF, Lakkis NM, He ZX, et al: Role of myocardial contrast echocardiography during nonsurgical septal reduction therapy for hypertrophic obstructive cardiomyopathy. *J Am Coll Cardiol* 32:225-229, 1998.
14. Bagger JP, Baandrup U, Rasmussen K, et al: Cardiomyopathy in western Denmark. *Br Heart J* 52:327-331, 1984.
15. Codd MB, Sugure DD, Gersh BJ, Melton LJI: Epidemiology of idiopathic dilated and hypertrophic cardiomyopathy. A population-based study in Olmsted County, Minnesota. *Circulation* 80:564-572, 1989.
16. Lipshultz SE, Sleeper LA, Towbin JA, et al: The incidence of pediatric cardiomyopathy in two regions of the United States. *N Engl J Med* 348:1647-1655, 2003.
17. Nugent AW, Daubeney PEF, Chondros P, et al: The epidemiology of childhood cardiomyopathy in Australia. *N Engl J Med* 348:1639-1646, 2003.
18. Marian AJ: Clinical and molecular genetic aspects of hypertrophic cardiomyopathy. *Curr Cardiol Rev* 1:53-63, 2005.
19. Seidman CE: Hypertrophic cardiomyopathy: from man to mouse. *J Clin Invest* 106:S9-S13, 2000.
20. Kimura A: Molecular etiology and pathogenesis of hereditary cardiomyopathy. *Circ J* 72(Suppl A):A38-A48, 2008.
21. Niimura H, Bachinski LL, Sangwatanaroj S, et al: Mutations in the gene for cardiac myosin-binding protein C and late-onset familial hypertrophic cardiomyopathy. *N Engl J Med* 338:1248-1257, 1998.
22. Van Driest SL, Jaeger MA, Ommen SR, et al: Comprehensive analysis of the beta-myosin heavy chain gene in 389 unrelated patients with hypertrophic cardiomyopathy. *J Am Coll Cardiol* 44:602-610, 2004.
23. Solomon SD, Wolff S, Watkins H, et al: Left ventricular hypertrophy and morphology in familial hypertrophic cardiomyopathy associated with mutations of the beta-myosin heavy chain gene. *J Am Coll Cardiol* 22:498-505, 1993.
24. Woo A, Rakowski H, Liew JC, et al: Mutations of the beta myosin heavy chain gene in hypertrophic cardiomyopathy: critical functional sites determine prognosis. *Heart* 89:1179-1185, 2003.
25. Maron BJ, Niimura H, Casey SA, et al: Development of left ventricular hypertrophy in adults with hypertrophic cardiomyopathy caused by cardiac myosin-binding protein C gene mutations. *J Am Coll Cardiol* 38:315-321, 2001.
26. Van Driest SL, Vasile VC, Ommen SR, et al: Myosin binding protein C mutations and compound heterozygosity in hypertrophic cardiomyopathy. *J Am Coll Cardiol* 44:1903-1910, 2004.

27. Popp RL, Harrison DC: Ultrasound in the diagnosis and evaluation of therapy of idiopathic hypertrophic subaortic stenosis. *Circulation* 40:905-914, 1969.
28. Shah PM, Gramiak R, Kramer DH: Ultrasound location of left ventricular outflow obstruction in hypertrophic obstructive cardiomyopathy. *Circulation* 40:3-11, 1969.
29. Henry WL, Clark CE, Epstein SE: Asymmetric septal hypertrophy: echocardiographic identification of the pathognomonic anatomic abnormality of IHSS. *Circulation* 47:225-233, 1973.
30. Gilbert BW, Pollick C, Adelman AG, Wigle ED: Hypertrophic cardiomyopathy: Subclassification by M-mode echocardiography. *Am J Cardiol* 45:861-872, 1980.
31. Luckie M, Khattar RS: Systolic anterior motion of the mitral valve—beyond hypertrophic cardiomyopathy. *Heart* 94:1383-1385, 2008.
32. Humez FU, Houston AB, Watson J, et al: Age and body surface area related normal upper and lower limits of M-mode echocardiographic measurements and left ventricular volume and mass from infancy to early adulthood. *Br Heart J* 7:276-280, 1994.
33. Maron BJ, Seidman JG, Seidman CE: Proposal for contemporary screening strategies for families with hypertrophic cardiomyopathy. *J Am Coll Cardiol* 44:2125-2132, 2004.
34. Ho CY, Sweitzer NK, McDonough B, et al: Tissue Doppler imaging predicts the development of hypertrophic cardiomyopathy in subjects with subclinical disease. *Circulation* 105:2992-2997, 2002.
35. Nagueh SF, Bachinski LL, Meyer D, et al: Tissue Doppler imaging consistently detects myocardial abnormalities in patients with hypertrophic cardiomyopathy and provides a novel means for an early diagnosis before and independently of hypertrophy. *Circulation* 104:128-130, 2001.
36. Nagueh SF, McFalls J, Meyer D, et al: Assessment of diastolic function with Doppler tissue imaging to predict genotype in preclinical hypertrophic cardiomyopathy. *Circulation* 108:395-398, 2003.
37. Elliott P, McKenna WJ: Hypertrophic cardiomyopathy. *Lancet* 363:1881-1891, 2004.
38. Prasad K, Atherton J, Smith GC, et al: Echocardiographic pitfalls in the diagnosis of hypertrophic cardiomyopathy. *Heart* 82:III8-III15, 1999.
39. Riggs T, Hirschfeld S, Rajai H: The pediatric spectrum of dynamic left ventricular obstruction. *Am Heart J* 99:301-309, 1980.
40. Santos AD, Miller RP, Mathew PK, et al: Echocardiographic characterization of the reversible cardiomyopathy of hypothyroidism. *Am J Med* 68:675-682, 1980.
41. Klein AL, Oh JK, Miller FA, et al: Two-dimensional and Doppler echocardiographic assessment of infiltrative cardiomyopathy. *J Am Soc Echocardiogr* 1:48-59, 1988.
42. Nakao S, Takenaka T, Maeda M, et al: An atypical variant of Fabry's disease in men with left ventricular hypertrophy. *N Engl J Med* 333:288-293, 1995.
43. Sachdev B, Takenaka T, Teraguchi H, et al: Prevalence of Anderson-Fabry disease in male patients with late onset hypertrophic cardiomyopathy. *Circulation* 105:1407-1411, 2002.
44. Mehta A, Ricci R, Widmer U, et al: Fabry disease defined: baseline clinical manifestations of 366 patients in the Fabry Outcome Survey. *Eur J Clin Invest* 34:236-242, 2004.
45. Weidemann F, Strotmann JM, Breunig F, et al: Misleading terms in Anderson-Fabry disease. *Eur J Clin Invest* 38:191-196, 2008.
46. Weidemann F, Breunig F, Beer M, et al: The variation of morphological and functional cardiac manifestation in Fabry disease: potential implications for the time course of the disease. *Eur Heart J* 26:1221-1227, 2005.
47. Arad M, Maron BJ, Gorham JM: Glycogen storage diseases presenting as hypertrophic cardiomyopathy. *N Engl J Med* 352:362-372, 2005.
48. Pelliccia A, Maron BJ, Spataro A, et al: The upper limit of physiological cardiac hypertrophy in highly trained elite athletes. *N Engl J Med* 324:295-301, 1991.
49. Pelliccia A, Maron BJ, Culasso F, et al: Athlete's heart in women. *JAMA* 276:211-215, 1996.
50. Douglas PS, O' Toole ML, Katz SE, et al: Left ventricular hypertrophy in athletes. *Am J Cardiol* 80:1384-1388, 1997.
51. Cardim N, Cordeiro R, Correia MJ, et al: Tissue Doppler imaging and long axis left ventricular function: hypertrophic cardiomyopathy versus athlete's heart. *Rev Port Cardiol* 21:679-707, 2002.
52. Maron BJ, Pellicia A, Spirito P: Cardiac disease in young trained athletes: Insights into methods for distinguishing athlete's heart from structural heart disease, with particular emphasis on hypertrophic cardiomyopathy. *Circulation* 91:1596-1601, 1995.
53. Dalldorf FG, Willis PW: Angled aorta ("sigmoid septum") as a cause of hypertrophic stenosis. *Hum Pathol* 16:457-462, 1985.
54. Belenkie I, MacDonald RPR, Smith ER: Localized septal hypertrophy: Part of the spectrum of hypertrophic cardiomyopathy or an incidental echocardiographic finding? *Am Heart J* 115:385-390, 1988.
55. Krasnow N: Subaortic septal bulge simulates hypertrophic cardiomyopathy by angulation of the septum with age, independent of focal hypertrophy: an echocardiographic study. *J Am Soc Echocardiogr* 10:545-555, 1997.
56. Binder J, Ommen SR, Gersh BJ, et al: Echocardiography-guided genetic testing in hypertrophic cardiomyopathy: septal morphological features predict the presence of myofilament mutations. *Mayo Clin Proc* 81:459-467, 2006.
57. Fowles RE, Martin RP, Popp RL: Apparent asymmetric septal hypertrophy due to angled interventricular septum. *Am J Cardiol* 46:386-392, 1980.
58. Klues HG, Schiffers A, Maron BJ: Phenotypic spectrum and patterns of left ventricular hypertrophy in hypertrophic cardiomyopathy: morphologic observations and significance as assessed by two dimensional echocardiography in 600 patients. *J Am Coll Cardiol* 26:1699-1708, 1995.
59. Henry WL, Clark CE, Glancy DL, Epstein SE: Echocardiographic measurement of the left ventricular outflow gradient in idiopathic hypertrophic subaortic stenosis. *N Engl J Med* 288:989-993, 1973.
60. Boughner D, Schuld RL, Persaud JA: Hypertrophic obstructive cardiomyopathy: assessment by echocardiographic and Doppler ultrasound techniques. *Br Heart J* 37:917-923, 1975.
61. Spirito P, Maron BJ: Significance of left ventricular outflow tract cross-sectional area in hypertrophic cardiomyopathy: a two-dimensional echocardiographic assessment. *Circulation* 67:1100-1108, 1983.
62. Klues HG, Maron BJ, Dollar AL, Roberts WC: Diversity of structural mitral valve alterations in hypertrophic cardiomyopathy. *Circulation* 85:1651-1660, 1992.
63. Shah PM, Taylor RD, Wong M: Abnormal mitral valve coaptation in hypertrophic obstructive cardiomyopathy: proposed role in systolic anterior motion of the mitral valve. *Am J Cardiol* 48:258-262, 1981.
64. Henry WL, Clark CE, Griffith JM, Epstein SE: Mechanism of left ventricular outflow obstruction in patients with obstructive asymmetric septal hypertrophy (idiopathic subaortic stenosis). *Am J Cardiol* 35:337-345, 1975.
65. Reis R, Bolton MR, King JF, et al: Anterior-superior displacement of papillary muscles producing obstruction and mitral regurgitation in idiopathic hypertrophic subaortic stenosis. *Circulation* 49:181-188, 1974.
66. Rakowski H, Fulop J, Wigle ED: The role of echocardiography in the assessment of hypertrophic cardiomyopathy. *Postgrad Med J* 62:557-561, 1986.
67. Jiang L, Leving RA, King ME, Weyman AE: An integrated mechanism for systolic anterior motion of the mitral valve in hypertrophic cardiomyopathy based on echocardiographic observations. *Am Heart J* 113:633-644, 1987.
68. Klues HG, Roberts WC, Maron BJ: Morphologic determinants of echocardiographic patterns of mitral valve systolic anterior motion in obstructive hypertrophic cardiomyopathy. *Circulation* 87:1570-1579, 1993.
69. Sherrid MV, Chu CK, Delia E, et al: An echocardiographic study of the fluid mechanics of obstruction in hypertrophic cardiomyopathy. *J Am Coll Cardiol* 22:816-825, 1993.
70. Pollick C, Morgan CD, Gilbert BW, et al: Muscular subaortic stenosis: The temporal relationship between systolic anterior motion of the anterior mitral leaflet and the pressure gradient. *Circulation* 66:1087-1094, 1982.
71. Pollick C, Rakowski H, Wigle ED: Muscular subaortic stenosis: the quantitative relationship between systolic anterior motion and the pressure gradient. *Circulation* 69:43-49, 1984.
72. Schwammenthal E, Block M, Schwartzkopff B, et al: Prediction of the site and severity of obstruction in hypertrophic cardiomyopathy by color flow mapping and continuous wave Doppler echocardiography. *J Am Coll Cardiol* 20:964-972, 1992.
73. Bryg RJ, Pearson AC, Williams GA, Labovitz AJ: Left ventricular systolic and diastolic flow abnormalities determined by Doppler echocardiography in obstructive cardiomyopathy. *Am J Cardiol* 59:925-931, 1987.
74. Sasson Z, Yock PG, Hatle LK, et al: Doppler echocardiographic determination of the pressure gradient in hypertrophic cardiomyopathy. *J Am Coll Cardiol* 11:752-756, 1988.
75. Maron MS, Olivotto I, Zenovich AG, et al: Hypertrophic cardiomyopathy is predominantly a disease of left ventricular outflow tract obstruction. *Circulation* 2006-2232, 2006.
76. Yang WI, Shim CY, Kim YJ, et al: Left atrial volume index: a predictor of adverse outcome in patients with hypertrophic cardiomyopathy. *J Am Soc Echocardiogr* 22:1338-1343, 2009.
77. Nakatani S, Marwick TH, Lever HM, Thomas JD: Resting echocardiographic features of latent left ventricular outflow obstruction in hypertrophic cardiomyopathy. *Am J Cardiol* 78:662-667, 1996.
78. Marwick TH, Nakatani S, Haluska B, et al: Provocation of latent left ventricular outflow tract gradients with amyl nitrite and exercise in

hypertrophic cardiomyopathy. *Am J Cardiol* 75:805-809, 1995.
79. Joshi S, Patel UK, Yao S, et al: Standing and exercise Doppler echocardiography in obstructive hypertrophic cardiomyopathy: the range of gradients with upright activity. *J Am Soc Echocardiogr* 23:75-82, 2011.
80. Drinko JK, Nash PJ, Lever HM, Asher CR: Safety of stress testing in patients with hypertrophic cardiomyopathy. *Am J Cardiol* 93:1443-1444, 2004.
81. Panza JA, Petrone RK, Fananapazir L, Maron BJ: Utility of continuous wave Doppler echocardiography in the noninvasive assessment of left ventricular outflow tract pressure gradient in patients with hypertrophic cardiomyopathy. *J Am Coll Cardiol* 19:91-99, 1992.
82. Yock PG, Hatle L, Popp RL: Patterns and timing of Doppler-detected intracavitary and aortic flow in hypertrophic cardiomyopathy. *J Am Coll Cardiol* 8:1047-1058, 1986.
83. Yu EH, Omran AS, Wigle ED, et al: Mitral regurgitation in hypertrophic obstructive cardiomyopathy: relationship to obstruction and relief with myectomy. *J Am Coll Cardiol* 36:2219-2225, 2000.
84. Schwammenthal E, Nakatani S, He S, et al: Mechanism of mitral regurgitation in hypertrophic cardiomyopathy: mismatch of posterior to anterior leaflet length and mobility. *Circulation* 98:856-865, 1998.
85. Kaple RK, Murphy RT, DiPaola LM, et al: Mitral valve abnormalities in hypertrophic cardiomyopathy: Echocardiographic features and surgical outcomes. *Ann Thorac Surg* 85:1527-1536, 2008.
86. Sakamoto T, Tei C, Murayama M, et al: Giant T wave inversion as a manifestation of asymmetrical apical hypertrophy (AAH) of the left ventricle. Echocardiographic and ultrasonocardiotomographic study. *JpnHeart J* 17:611-629, 1976.
87. Yamaguchi H, Ishimura T, Nishiyama S, et al: Hypertrophic nonobstructive cardiomyopathy with giant negative T waves (apical hypertrophy): ventriculographic and echocardiographic features in 30 patients. *Am J Cardiol* 44:401-412, 1979.
88. Eriksson MJ, Sonnenberg B, Woo A, et al: Long-term outcome in patients with apical hypertrophic cardiomyopathy. *J Am Coll Cardiol* 39:638-645, 2002.
89. Falicov RE, Resnekov L, Bharati S, Lev M: Midventricular obstruction: a variant of obstructive cardiomyopathy. *Am J Cardiol* 37:432-437, 1976.
90. Kuhn H, Mercier J, Kohler E, et al: Differential diagnosis of hypertrophic cardiomyopathies: typical (subaortic) hypertrophic obstructive cardiomyopathy, atypical (mid-ventricular) hypertrophic obstructive cardiomyopathy and hypertrophic non-obstructive cardiomyopathy. *Eur Heart J* 4(Suppl F):93-104, 1983.
91. Maron MS, Finley JJ, Bos JM, et al: Prevalence, clinical significance, and natural history of left ventricular apical aneurysms in hypertrophic cardiomyopathy. *Circulation* 118:1541-1549, 2008.
92. Lewis JF, Maron BJ: Clinical and morphologic expression of hypertrophic cardiomyopathy in patients greater than or equal to 65 years of age. *Am J Cardiol* 73:1105-1111, 1994.
93. Whiting RB, Powell WJ Jr, Dinsmore RE, Sanders CA: Idiopathic hypertrophic subaortic stenosis in the elderly. *N Engl J Med* 285:196-200, 1971.
94. Chikamori T, Doi YL, Yonezawa Y, et al: Comparison of clinical features in patients greater than or equal to 60 years of age to those less than or equal to 40 years of age with hypertrophic cardiomyopathy. *Am J Cardiol* 66:875-878, 1990.
95. Lever HM, Karam RF, Currie PJ, Healy BP: Hypertrophic cardiomyopathy in the elderly. Distinctions from the young based on cardiac shape. *Circulation* 79:580-589, 1989.
96. Motamed HE, Roberts WC: Frequency and significance of mitral annular calcium in hypertrophic cardiomyopathy: analysis of 200 necropsy patients. *Am J Cardiol* 60:877-884, 1987.
97. Kubo T, Kitaoka H, Okawa M, et al: Hypertrophic cardiomyopathy in the elderly. *Geriatr Gerontol Int* 10:9-16, 2010.
98. Maron BJ, Spirito P, Green KJ, et al: Noninvasive assessment of left ventricular diastolic function by pulsed Doppler echocardiography in patients with hypertrophic cardiomyopathy. *J Am Coll Cardiol* 10:733-742, 1987.
99. Nagueh SF, Lakkis NM, Middleton KJ, et al: Doppler estimation of left ventricular filling pressures in patients with hypertrophic cardiomyopathy. *Circulation* 99:254-261, 1999.
100. Nishimura RA, Appleton CP, Redfield MM, et al: Noninvasive Doppler echocardiographic evaluation of left ventricular filling pressures in patients with cardiomyopathies: a simultaneous Doppler echocardiographic and cardiac catheterization study. *J Am Coll Cardiol* 28:1226-1233, 1996.
101. Nagueh SF, Lakkis NM, Middleton KJ, et al: Doppler estimation of left ventricular filling pressures in patients with hypertrophic cardiomyopathy. *Circulation* 99:254-261, 1999.
102. Matsumura Y, Elliott PM, Virdee MS, et al: Left ventricular diastolic function assessed using Doppler tissue imaging in patients with hypertrophic cardiomyopathy: relation to symptoms and exercise capacity. *Heart* 87:247-251, 2002.
103. Yang H, Woo A, Monakier D, et al: Enlarged left atrial volume in hypertrophic cardiomyopathy: a marker for disease severity. *J Am Soc Echocardiogr* 18:1074-1082, 2005.
104. Nagueh SF, Lakkis NM, Middleton KJ, et al: Changes in left ventricular diastolic function 6 months after nonsurgical septal reduction therapy for hypertrophic obstructive cardiomyopathy. *Circulation* 99:344-347, 1999.
105. Sitges M, Shiota T, Lever HM, et al: Comparison of left ventricular diastolic function in obstructive hypertrophic cardiomyopathy in patients undergoing percutaneous septal alcohol ablation versus surgical myotomy/myectomy. *Am J Cardiol* 91:817-821, 2003.
106. Sasson Z, Hatle L, Appleton CP, et al: Intraventricular flow during isovolumic relaxation: description and characterization by Doppler echocardiography. *J Am Coll Cardiol* 10:539-546, 1987.
107. Nakamura T, Matsubara K, Furukawa K, et al: Diastolic paradoxic jet flow in patients with hypertrophic cardiomyopathy: evidence of concealed apical asynergy with cavity obliteration. *J Am Coll Cardiol* 19:516-524, 1992.
108. D'Andrea A, Caso P, Severino S, et al: Association between intraventricular myocardial systolic dyssynchrony and ventricular arrhythmias in patients with hypertrophic cardiomyopathy. *Echocardiography* 22:571-578, 2005.
109. Nagakura T, Takeuchi M, Yoshitani H, et al: Hypertrophic cardiomyopathy is associated with more severe left ventricular dyssynchrony than is hypertensive left ventricular hypertrophy. *Echocardiography* 24:677-684, 2007.
110. Ho CY, Carlsen C, Thune JJ, et al: Echocardiographic strain imaging to assess early and late consequences of sarcomere mutations in hypertrophic cardiomyopathy. *Circ Cardiovasc Genet* 2:314-321, 2009.
111. Carasso S, Yang H, Woo A, et al: Systolic myocardial mechanics in hypertrophic cardiomyopathy: novel concepts and implications for clinical status. *J Am Soc Echocardiogr* 21:675-683, 2008.
112. Carasso S, Yang H, Woo A, et al: Diastolic myocardial mechanics in hypertrophic cardiomyopathy. *J Am Soc Echocardiogr* 23:164-171, 2010.
113. Takeuchi M, Borden WB, Nakai H, et al: Reduced and delayed untwisting of the left ventricle in patients with hypertension and left ventricular hypertrophy: a study using two-dimensional speckle tracking imaging. *Eur Heart J* 28:2756-2762, 2007.
114. Kato TS, Noda A, Izawa H, et al: Discrimination of nonobstructive hypertrophic cardiomyopathy from hypertensive left ventricular hypertrophy on the basis of strain rate imaging by tissue Doppler ultrasonography. *Circulation* 110:3808-3814, 2004.
115. Elliott PM, Gimeno B Jr, Mahon NG, et al: Relation between severity of left-ventricular hypertrophy and prognosis in patients with hypertrophic cardiomyopathy. *Lancet* 357:420-424, 2001.
116. McLeod CJ, Ommen SR, Ackerman MJ, et al: Surgical septal myectomy decreases the risk for appropriate implantable cardioverter defibrillator discharge in obstructive hypertrophic cardiomyopathy. *Eur Heart J* 28:2583-2588, 2007.
117. Olivotto I, Cecchi F, Casey SA, et al: Impact of atrial fibrillation on the clinical course of hypertrophic cardiomyopathy. *Circulation* 104:2517-2524, 2001.
118. Woo A, Williams WG, Choi R, et al: Clinical and echocardiographic determinants of long-term survival after surgical myectomy in obstructive hypertrophic cardiomyopathy. *Circulation* 111:2033-2041, 2005.
119. Epstein SE, Rosing DR: Verapamil: Its potential for causing serious complications in patients with hypertrophic cardiomyopathy. *Circulation* 64:437-441, 1981.
120. Pollick C: Muscular subaortic stenosis. Hemodynamic and clinical improvement after disopyramide. *N Engl J Med* 307:997-999, 1982.
121. Sherrid MV, Barac I, McKenna WJ, et al: Multicenter study of the efficacy and safety of disopyramide in obstructive hypertrophic cardiomyopathy. *J Am Coll Cardiol* 45:1251-1258, 2005.
122. Leclercq C, Gras D, Le Helloco A, et al: Hemodynamic importance of preserving the normal sequence of ventricular activation in permanent cardiac pacing. *Am Heart J* 129:1133-1141, 1995.
123. Nishimura RA, Hayes DL, Ilstrup DM, et al: Effect of dual-chamber pacing on systolic and diastolic function in patients with hypertrophic cardiomyopathy. Acute Doppler echocardiographic and catheterization hemodynamic study. *J Am Coll Cardiol* 27:421-430, 1996.
124. Fananapazir L, Epstein ND, Curiel RV, et al: Long-term results of dual-chamber (DDD) pacing in obstructive hypertrophic cardiomyopathy. Evidence for progressive symptomatic and hemodynamic improvement and

reduction of left ventricular hypertrophy. *Circulation* 90:2731-2742, 1994.
125. Kappenberger L, Linde C, Daubert C, et al: Pacing in hypertrophic obstructive cardiomyopathy. A randomized crossover study. PIC Study Group. *Eur Heart J* 18:1249-1256, 1997.
126. Maron BJ, Nishimura RA, McKenna WJ, et al: Assessment of permanent dual-chamber pacing as a treatment for drug-refractory symptomatic patients with obstructive hypertrophic cardiomyopathy. A randomized, double-blind, crossover study (M-PATHY). *Circulation* 99:2927-2933, 1999.
127. Nishimura RA, Trusty JM, Hayes DL, et al: Dual-chamber pacing for hypertrophic cardiomyopathy: a randomized, double-blind, crossover trial. *J Am Coll Cardiol* 29:435-441, 1997.
128. Ommen SR, Nishimura RA, Squires RW, et al: Comparison of dual-chamber pacing versus septal myectomy for the treatment of patients with hypertrophic obstructive cardiomyopathy: a comparison of objective hemodynamic and exercise end points. *J Am Coll Cardiol* 34:191-196, 1999.
129. Sigwart U: Non-surgical myocardial reduction for hypertrophic obstructive cardiomyopathy. *Lancet* 346:211-214, 1995.
130. Flores-Ramirez R, Lakkis NM, Middleton KJ, et al: Echocardiographic insights into the mechanisms of relief of left ventricular outflow tract obstruction after nonsurgical septal reduction therapy in patients with hypertrophic obstructive cardiomyopathy. *J Am Coll Cardiol* 37:208-214, 2001.
131. Faber L, Ziemssen P, Seggewiss H: Targeting percutaneous transluminal septal ablation for hypertrophic obstructive cardiomyopathy by intraprocedural echocardiographic monitoring. *J Am Soc Echocardiogr* 13:1074-1079, 2000.
132. Monakier D, Horlick E, Ross J, et al: Intra-coronary myocardial contrast echocardiography in a patient with drug refractory hypertrophic obstructive cardiomyopathy revealing extensive myocardium at risk for infarction with alcohol septal ablation. *Journal of Invasive Cardiology* 16:482-484, 2004.
133. Faber L, Seggewiss H, Welge D, et al: Echo-guided percutaneous septal ablation for symptomatic hypertrophic obstructive cardiomyopathy. *Eur J Echocardiography* 5:347-355, 2004.
134. Monakier D, Woo A, Puri T, et al: Usefulness of myocardial contrast echocardiographic quantification of risk area for predicting postprocedural complications in patients undergoing septal ethanol ablation for obstructive hypertrophic cardiomyopathy. *Am J Cardiol* 94:1515-1522, 2004.
135. Bhagwadeen R, Woo A, Ross J, et al: Septal ethanol ablation for hypertrophic obstructive cardiomyopathy: early and intermediate results in a Canadian referral center. *Can J Cardiol* 19:912-917, 2003.
136. Gietzen FH, Leuner CJ, Raute-Kreinsen U, et al: Acute and long-term results after transcoronary ablation of septal hypertrophy (TASH): Catheter interventional treatment for hypertrophic obstructive cardiomyopathy. *Eur Heart J* 20:1342-1354, 1999.
137. Lakkis NM, Nagueh SF, Kleiman NS, et al: Echocardiography-guided ethanol septal reduction for hypertrophic obstructive cardiomyopathy. *Circulation* 98:1750-1755, 1998.
138. Seggewiss H, Faber L, Gleichmann U: Percutaneous transluminal septal ablation in hypertrophic obstructive cardiomyopathy. *Thorac Cardiovasc Surg* 47:94-100, 1999.
139. Faber L, Meissner A, Ziemssen P, Seggewiss H: Percutaneous transluminal septal myocardial ablation for hypertrophic obstructive cardiomyopathy: long term follow up of the first series of 25 patients. *Heart* 83:326-331, 2000.
140. Fernandes VL, Nagueh SF, Wang W, et al: A prospective follow-up of alcohol septal ablation for symptomatic hypertrophic obstructive cardiomyopathy - the Baylor experience (1996-2002). *C* 28:124-130, 2005.
141. Schulz-Menger J, Strohm O, Waigand J, et al: The value of magnetic resonance imaging of the left ventricular outflow tract in patients with hypertrophic obstructive cardiomyopathy after septal artery embolization. *Circulation* 101:1764-1766, 2000.
142. Mazur W, Nagueh SF, Lakkis NM, et al: Regression of left ventricular hypertrophy after nonsurgical septal reduction therapy for hypertrophic obstructive cardiomyopathy. *Circulation* 103:1492-1496, 2001.
143. Jassal DS, Neilan T, Fifer MA, et al: Sustained improvements in left ventricular diastolic function after alcohol septal ablation for hypertrophic obstructive cardiomyopathy. *Eur Heart J* 27:1805-1810, 2006.
144. Leonardi RA, Kransdorf EP, Simel DL, Wang A: Meta-analyses of septal reduction therapies for obstructive hypertrophic cardiomyopathy: comparative rates of overall mortality and sudden cardiac death after treatment. *Circ Cardiovasc Interv* 3:97-104, 2010.
145. McCully RB, Nishimura RA, Bailey KR, et al: Hypertrophic obstructive cardiomyopathy: preoperative echocardiographic predictors of outcome after septal myectomy. *J Am Coll Cardiol* 27:1491-1496, 1996.
146. Marwick TH, Stewart WJ, Lever HM, et al: Benefits of intraoperative echocardiography in the surgical management of hypertrophic cardiomyopathy. *J Am Coll Cardiol* 20:1066-1072, 1992.
147. Siegman IL, Maron BJ, Permut LC, et al: Operative treatment in hypertrophic subaortic stenosis. Techniques, and the results of pre and postoperative assessments in 83 patients. *Circulation* 52:88-102, 1975.
148. Ommen S, Park SH, Click RL, et al: Impact of intraoperative transesophageal echocardiography in the surgical management of hypertrophic cardiomyopathy. *Am J Cardiol* 90: 1022-1024, 2002.
149. Sasson Z, Prieur T, Skrobik Y, et al: Aortic regurgitation: A common complication after surgery for hypertrophic obstructive cardiomyopathy. *J Am Coll Cardiol* 13:63-67, 1989.
150. Heric B, Lytle BW, Miller DP, et al: Surgical management of hypertrophic obstructive cardiomyopathy. Early and late results. *J Thorac Cardiovasc Surg* 110:195-206, 1995.
151. McCully RB, Nishimura RA, Tajik AJ, et al: Extent of clinical improvement after surgical treatment of hypertrophic obstructive cardiomyopathy. *Circulation* 94:467-471, 1996.
152. Merrill WH, Friesinger GC, Graham TP Jr, et al: Long-lasting improvement after septal myectomy for hypertrophic obstructive cardiomyopathy. *Ann Thorac Surg* 69:1732-1735, 2000.
153. Robbins RC, Stinson EB: Long-term results of left ventricular myotomy and myectomy for obstructive hypertrophic cardiomyopathy. *J Thorac Cardiovasc Surg* 111:586-594, 1996.
154. Schonbeck MH, Brunner-La Rocca HP, Vogt PR, et al: Long-term follow-up in hypertrophic obstructive cardiomyopathy after septal myectomy. *Ann Thorac Surg* 65:1207-1214, 1998.
155. Ball W, Ivanov J, Rakowski H, et al: Long-term survival in patients with resting obstructive hypertrophic cardiomyopathy: comparison of conservative versus invasive treatment. *J Am Coll Cardiol* 58:2313-2321, 2011.
156. Nagueh SF, Ommen S, Lakkis NM, et al: Comparison of ethanol septal reduction therapy with surgical myectomy for the treatment of hypertrophic obstructive cardiomyopathy. *J Am Coll Cardiol* 38:1701-1706, 2001.
157. Firoozi S, Elliott PM, Sharma S, et al: Septal myotomy-myectomy and transcoronary septal alcohol ablation in hypertrophic obstructive cardiomyopathy: a comparison of clinical, hemodynamic and exercise outcomes. *Eur Heart J* 23:1617-1624, 2002.
158. Qin JX, Shiota T, Lever HM, et al: Outcome of patients with hypertrophic obstructive cardiomyopathy after percutaneous transluminal septal myocardial ablation and septal myectomy surgery. *J Am Coll Cardiol* 38:1994-2000, 2001.
159. Ralph-Edwards A, Woo A, McCrindle BW, et al: Hypertrophic obstructive cardiomyopathy: comparison of outcomes after myectomy or alcohol ablation adjusted by propensity score. *J Thorac Cardiovasc Surg* 129:351-358, 2005.
160. van der Lee C, ten Cate FJ, Geleijnse ML, et al: Percutaneous versus surgical treatment for patients with hypertrophic obstructive cardiomyopathy and enlarged anterior mitral valve leaflets. *Circulation* 112:482-488, 2005.
161. Alam M, Dokainish HLNM: Hypertrophic obstructive cardiomyopathy—alcohol septal ablation vs. myectomy: a meta-analysis. *Eur Heart J* 30:1080-1087, 2009.

# 28 Restrictive Cardiomyopathy: Diagnosis and Prognostic Implications

TASNEEM Z. NAQVI, MD

**Definition of Restrictive Cardiomyopathy**
**Imaging**
**Echocardiographic Features**
Speckle Tracking
**Doppler Features**
**Cardiac Magnetic Resonance Imaging**
**Specific Restrictive Cardiomyopathies**
Amyloidosis
Hemochromatosis
Hypereosinophilic Syndrome and Endomyocardial Fibrosis
Sarcoidosis
Storage Disorders
Idiopathic Restrictive Cardiomyopathy
Drug-Induced Restrictive Cardiomyopathy
Postradiation Cardiomyopathy
Other Causes of Restrictive Cardiomyopathy
**Differentiating between Restrictive Cardiomyopathy and Constrictive Pericarditis**
**Echocardiography in Clinical Decision Making in Restrictive Cardiomyopathy**

## Definition of Restrictive Cardiomyopathy

Restrictive cardiomyopathy is an idiopathic or systemic myocardial disorder characterized by a primary abnormality of diastolic function leading to diastolic heart failure in the presence of normal or mildly abnormal systolic function. A recent consensus statement proposed replacement of the terms *systolic* and *diastolic heart failure* with HFrEF (heart failure with reduced ejection fraction) and HFpEF (heart failure with preserved ejection fraction), respectively, because diastolic dysfunction is highly prevalent in systolic heart failure,[1] and there is evidence to suggest reduced systolic tissue velocities in diastolic heart failure.[2] Primary diastolic dysfunction in HFpEF leads to abnormal ventricular filling, resulting in an increase in ventricular end-diastolic pressures and dilated atria. Biventricular volumes are either reduced or normal, and systolic function impairment manifest as reduced ejection fraction is seen in the late stages of the disease.[3]

Patients commonly present with congestive failure with fatigue, exercise intolerance, right-sided or left-sided heart failure, and atrial fibrillation.[4] An elevated jugular venous pressure with an x and prominent y descent, y descent only (late-stage), and Kussmaul sign may be present, although pulsus paradoxus is always absent. Depending on the stage of disease, an S4 (early) or S3 (late) may be present. Restriction can be isolated to either ventricle or show biventricular involvement[5] (Table 28-1). The prognosis of restrictive cardiomyopathies is generally poor, except for those with reversible causes such as hemochromatosis. Doppler echocardiography plays a key role in the diagnosis and management of this disease entity.

## Imaging

Guidelines on the diagnosis of HFpEF[1,2] require objective evidence of diastolic left ventricular (LV) dysfunction in addition to clinical features of heart failure and LV ejection fraction greater than 50%.[6] Thus, imaging modalities play a pivotal role in 2 of the 3 diagnostic criteria of HFpEF.[7]

## Echocardiographic Features

Echocardiographic assessment for restrictive cardiomyopathy includes measurement of LV wall thickness, LV mass, LV volumes, LV ejection fraction, and a comprehensive evaluation of diastolic function[8-10] (Table 28-2). More recently specific pattern of late gadolinium enhancement on magnetic resonance imaging (MRI) has been shown in restrictive cardiomyopathy of varying etiology. A number of important observations relative to this topic have been made recently, including the assessment of LV mass and volumes by three-dimensional (3D) echocardiography and assessment of myocardial function by two dimensional strain.

Restrictive cardiomyopathy is characterized by concentric remodeling with marked increase in wall thickness relative to cavity size and preservation of LV volumes (Figs. 28-1 and 28-2). Echocardiographic LV mass assessment by M-mode (see Fig. 28-2) has been replaced by two-dimensional (2D) methods. More recently, 3D echocardiographic measurement of LV mass has been shown to be more reproducible than 2D and to closely approximate cardiac MRI.[11] (See Chapters 4 and 9.) Assessment of LV volumes using biplane Simpson's method is used to measure LV volumes in the four- and two-chamber views. However, there is an inherent variability in ejection fraction measurement of ±5%, and lack of endocardial border visualization occurs in up to 30% of patients, precluding precise evaluation of LV ejection fraction. Use of contrast imaging improves accuracy of volume measurements by both 2D and 3D echocardiography.[12] More recently, 3D echocardiography has been shown to have superior reproducibility and closer approximation to MRI than 2D echocardiography in the measurement of LV ejection fraction.[13,14]

Atrial enlargement is often significant (see Fig. 28-1) and is associated with the grade of diastolic dysfunction. Mild,

**TABLE 28-1 Classification of Restrictive Cardiomyopathy**

| | |
|---|---|
| Noninfiltrative | Idiopathic<br>Scleroderma |
| Infiltrative | Amyloid heart disease<br>Immunoglobulin amyloidosis<br>Familial amyloidosis<br>Senile systemic amyloidosis<br>Secondary amyloidosis<br>Sarcoid<br>Gaucher disease<br>Hurler syndrome |
| Storage disease | Hemochromatosis<br>Glycogen storage disease<br>Fabry disease |
| Endomyocardial | Endomyocardial fibrosis<br>Hypereosinophilic syndrome<br>Carcinoid<br>Scleroderma<br>Ehlers-Danlos syndrome<br>Systemic lupus erythematosus<br>Metastatic malignancy<br>Radiation<br>Anthracycline toxicity<br>Drugs causing fibrous endocarditis (anthracyclines, serotonin, methysergide, ergotamine, mercurial agents, busulfan, chloroquine |

moderate, and severe diastolic dysfunction is often associated with left atrial (LA) volume index greater than 28 mL/m$^2$, greater than 35 mL/m$^2$, and greater than 40 mL/m$^2$, respectively. Simpson's biplane method or the area length method is used for assessment of LA volumes, and the two methods are closely correlated. More recently, 3D LA volumes have been shown to have less variability than 2D methods.[15]

## SPECKLE TRACKING

Speckle tracking technology is a newer echocardiographic method to evaluate segmental and global systolic LV function by tracking small myocardial regions of interest on 2D as well as 3D cineloops from frame to frame.[16] It allows assessment of subclinical LV and right ventricular (RV) systolic dysfunction even when the LV ejection fraction and segmental function appear preserved[17] and provides greater accuracy than LV ejection fraction in predicting events in patients with heart failure.[18] Radial, longitudinal, and circumferential myocardial deformation can be measured, because the technique is angle independent. (See Chapter 10.) It allows evaluation of basal clockwise and apical counterclockwise myocardial rotation and net LV twist. Longitudinal and radial systolic strains are reduced in diastolic heart failure, although LV twist is preserved.[19] Recent data suggest that in patients with elevated LV filling pressure and

**TABLE 28-2 Echocardiographic Features of Restrictive Cardiomyopathy**

| | |
|---|---|
| M-mode and color M-mode | Lack of septal bounce<br>Square root sign in the interventricular septum and the posterior wall motion<br>Presence of myocardial hypertrophy<br>Decreased velocity of flow propagation (Vp) |
| Two-dimensional findings | Preserved LV volumes<br>Preserved LV systolic function (early stages)<br>Biatrial enlargement<br>Myocardial hypertrophy without known cause<br>Myocardial speckling may be present<br>Atrial septal thickening<br>Homogenous atrioventricular valve thickening<br>May show small pericardial effusion<br>Occasionally ventricular thrombi or apical mass despite normal underlying wall motion |
| Mitral pulsed Doppler | Characterized by large E wave, small A wave; E/A ratio >2; short DT <150 ms; short IVRT <60 ms; no significant change in mitral E wave, deceleration time, or IVRT with phases of respiration<br>Abnormal relaxation pattern with E/A ratio <1 and prolonged deceleration time (DT) in early stages followed by pseudonormal and reversible restrictive before irreversible restrictive pattern<br>No significant respiratory variation |
| Tricuspid pulsed Doppler | Restrictive filling; increased E/A ratio and short DT. With inspiration, there is further shortening of the DT and minimal change in E/A ratio |
| Pulmonary vein | Dilated pulmonary veins<br>Diastolic dominant pattern and S/D ratio < 0.5<br>Increased velocity and duration of pulmonary vein reversal velocity ($a_{dur}$ > mitral inflow $A_{dur}$)<br>No change in D wave with respiration. |
| CWD mitral regurgitation | LV: $dP/dt$ and LAP[SBP − 4(MR velocity)$^2$] |
| CWD tricuspid regurgitation | PA systolic pressure [4 × (TR jet$^2$ (cm/s)] |
| CWD pulmonary regurgitation | PA diastolic pressure [4 × (PR jet$^2$ (cm/s)] plus RA pressure |
| Color Doppler findings | Mitral and tricuspid regurgitation due to leaflet or papillary muscle involvement. Tricuspid regurgitation may be secondary to pulmonary hypertension<br>Diastolic MR due to increased LV end-diastolic pressure |
| Mitral annulus TDI | E/E′ ratio to assess LV filling pressure. In restrictive cardiomyopathy, E′ is usually <8 cm/s and E/E′ is >15 because of elevated filling pressure |
| Tricuspid annulus TDI | RV function<br>RA pressure |
| Color M-mode examination | Vp is usually <45 cm/s in restrictive cardiomyopathy. E/Vp is >1.5 and can be used to assess LV filling pressure |
| Hepatic vein/flow | Dilated hepatic veins, S/D ratio <0.5<br>Prominent atrial and ventricular reversals which increase with inspiration and expiration |
| Inferior vena cava | Dilated with reduced respiratory variation |

*A*, Atrial transmitral filling velocity; $A_{dur}$, transmitral A velocity duration; $a_{dur}$, pulmonary vein atrial reversal duration; *CWD*, continuous-wave Doppler; *D*, diastolic flow; *dP/dt*, rate of ventricular pressure rise; *DT*, deceleration time; *E*, early transmitral filling velocity; *E′*, tissue Doppler early diastolic velocity; *IVRT*, isovolumetric relaxation time; *LAP*, left atrial pressure; *Vp*, propagation velocity; *MR*, mitral regurgitation; *PA*, pulmonary artery; *PR*, pulmonic regurgitation; *S*, systolic flow; *SBP*, systolic blood pressure; *TDI*, tissue-Doppler imaging; *TR*, tricuspid regurgitation.

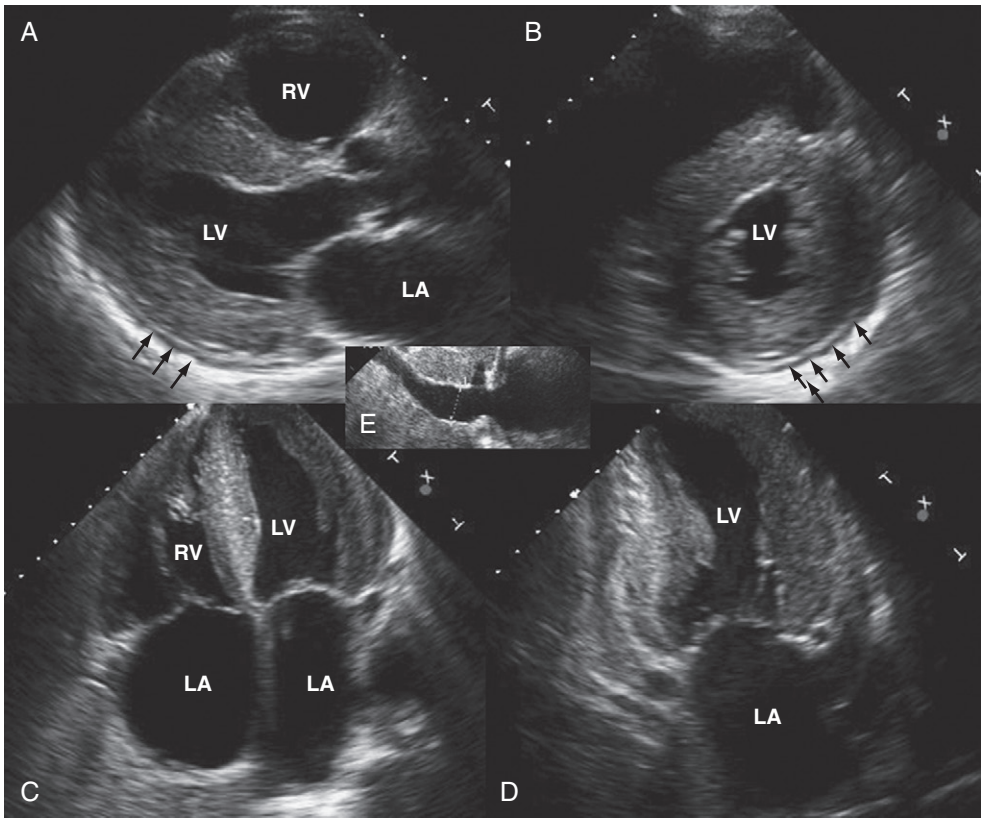



**Figure 28-1** **Cardiac amyloidosis. A,** Parasternal long-axis, (**B**) short-axis, (**C**) apical four-chamber, (**D**) apical two-chamber, and (**E**) subcostal views. Marked generalized hypertrophy is shown in all views. Note ground-glass appearance of myocardium, biatrial and RV enlargement, and small pericardial effusion (*arrows*) as well dilated inferior vena cava indicating elevated right atrial pressure.

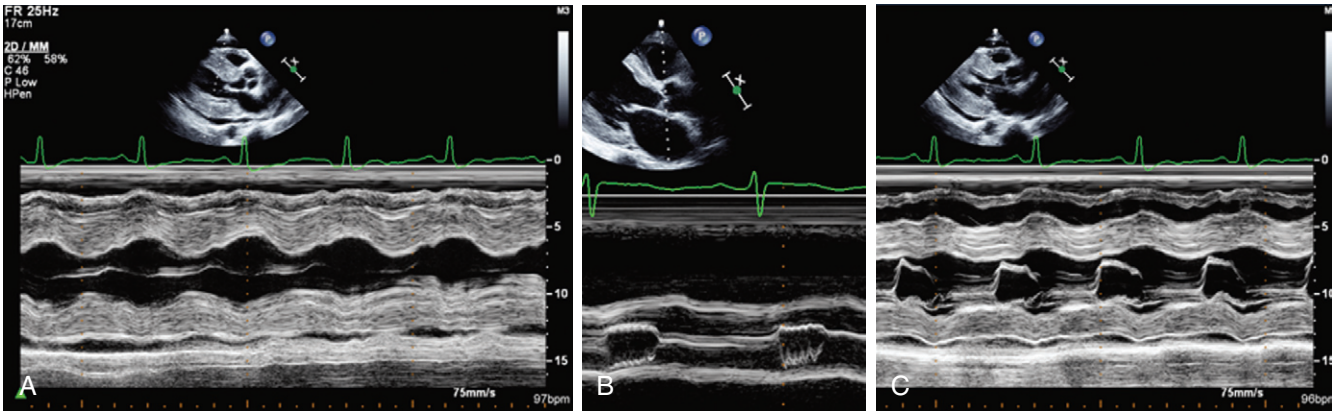



**Figure 28-2** **M-mode findings in senile cardiac amyloidosis. A,** Parasternal long-axis M-mode showing dilated RV and normal sized LV and marked increase in LV wall thickness. **B,** M-mode at aortic valve level showing deceased systolic opening time of aortic valve as well markedly reduced excursion of aortic root indicating reduced cardiac output and reduced atrial mechanical function. **C,** Reduced diastolic opening time of mitral valve consistent with reduced cardiac output.

preserved LV ejection fraction, significant abnormalities in myocardial mechanics are observed by speckle tracking with reduced longitudinal, radial, and circumferential strain rates, thus challenging the notion of HFpEF as an isolated diastolic dysfunction.[20] Other work has shown that although the deterioration of myocardial function begins in the longitudinal direction, patients with more advanced heart failure develop abnormalities in the radial and circumferential directions as well.[21]

## Doppler Features

Echocardiography is the gold standard for evaluation of diastolic LV and RV function.[22,23] (See Chapter 11.) Reports are, however, beginning to emerge of the feasibility of MRI and its modest correlation with Doppler echocardiography in evaluation of mitral inflow filling pattern in patients with cardiac amyloidosis.[24] However, the cardiac MRI technique remains time consuming and is not used clinically for assessment of diastolic function.

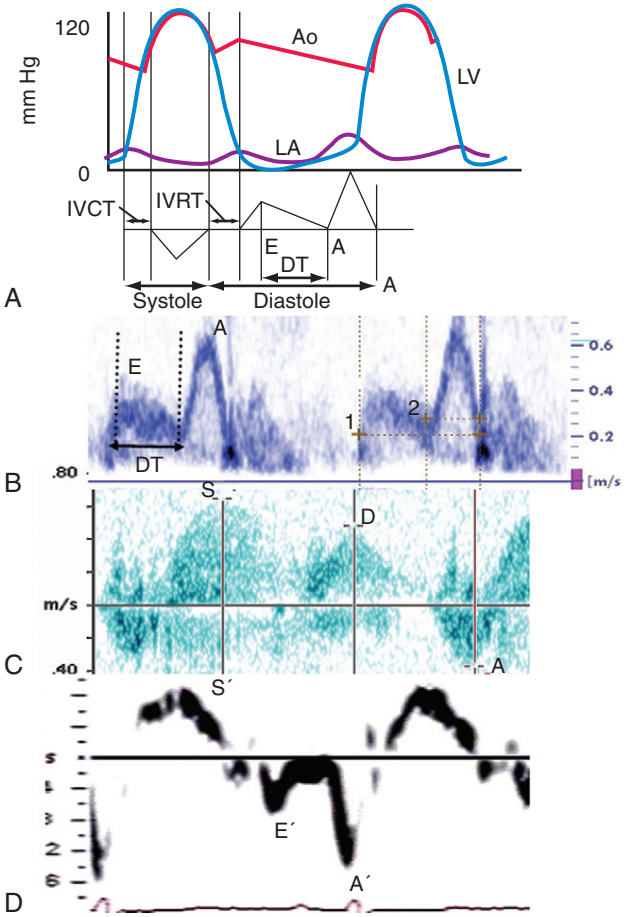



**Figure 28-3 Doppler findings with delayed LV relaxation.** LV, LA, and aortic (*Ao*) pressure tracings (**A**), mitral inflow PW Doppler (**B**), pulmonary vein PW Doppler (**C**), and mitral annular tissue Doppler (**D**) tracings are shown. Mitral inflow velocities were obtained by placing the PW Doppler sample volume between the tips of the mitral leaflets and Doppler tissue imaging by placing the PW Doppler sample volume at the lateral mitral annulus. *Large black horizontal arrows* depict duration of ventricular systole and ventricular diastole. Ventricular relaxation continues to occur in the latter third of diastole, causing E/A ratio less than 1 and prolonged mitral inflow deceleration time. Pulmonary vein flow pattern is systolic dominant, and there may be significant pulmonary vein atrial reversal. *D*, Diastolic; *DT*, deceleration time; *IVCT*, isovolumic contraction time; *IVRT*, isovolumic relaxation time; *S*, systolic.

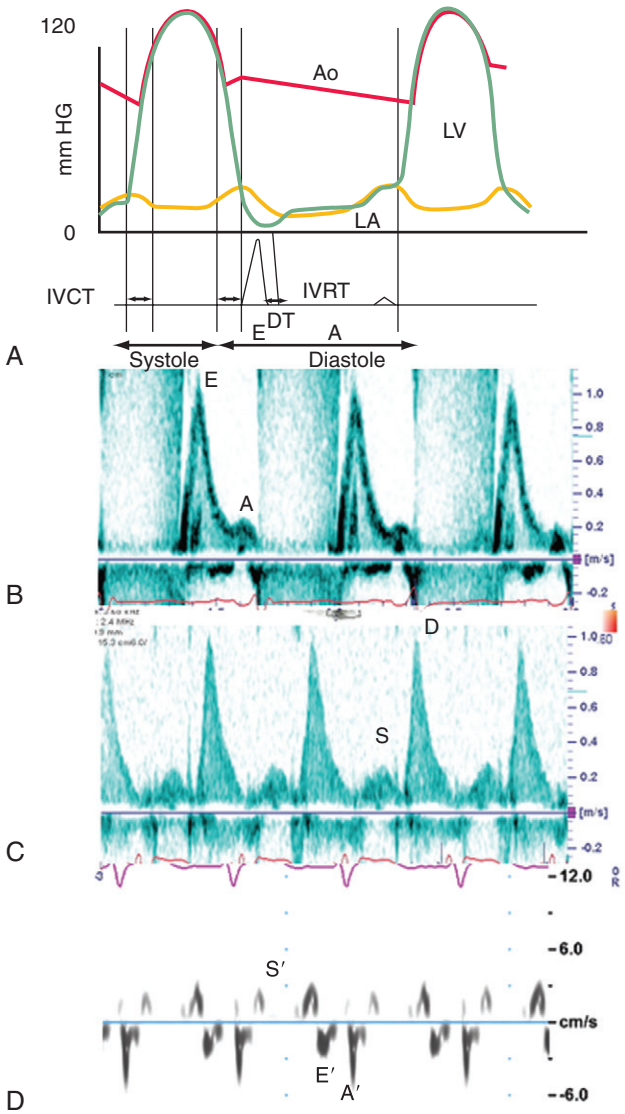



**Figure 28-4 Doppler findings with restrictive cardiomyopathy.** LV, LA, and aortic (*Ao*) pressure tracings (**A**), mitral inflow PW Doppler (**B**), pulmonary vein PW Doppler (**C**), and mitral annular tissue Doppler (**D**) show abnormal LV relaxation, abnormal LA and LV compliance, and elevated LA filling pressure. Mitral inflow velocities were obtained by placing the PW Doppler sample volume between the tips of the mitral leaflets and Doppler tissue imaging by placing the PW Doppler sample volume at the lateral mitral annulus. *Large black horizontal arrows* depict duration of LV systole and LV diastole. Early diastolic LV filling occurs due to the pressure gradient between LA and LV. Filling beyond first third of diastole is halted due to increase in LV diastolic pressure. Atrial contraction leads to a small filling A wave and marked pulmonary vein atrial reversal (unless in advanced stages when atrial pump failure occurs as shown in this example where no significant atrial reversal wave is seen despite a small mitral inflow A wave). Pulmonary vein PW Doppler shows marked S and D reversal with shortened pulmonary vein D-wave deceleration time. *D*, Diastolic; *DT*, deceleration time; *IVCT*, isovolumic contraction time; *IVRT*, isovolumic relaxation time; *S*, systolic.

### *Mitral Inflow Pulsed-Wave Doppler*

Diastolic features of restrictive cardiomyopathy show a spectrum of findings of increasing abnormality diastolic function, from normal diastolic function to abnormal relaxation (Fig. 28-3) and finally to a progressively abnormal chamber compliance leading to increase in LA and LV filling pressures (Figs. 28-4 and 28-5). In the early stages of the disease, mitral inflow filling pattern shows an abnormal relaxation pattern characterized by E/A ratio of less than 1, a prolonged mitral inflow E-wave deceleration time, and a prolonged isovolumic relaxation time (see Fig. 28-3). As the disease progresses and LA and LV diastolic compliance abnormality sets in, a pseudonormal phase is seen on mitral inflow that can reverse to an abnormal relaxation pattern on Valsalva maneuver.[25] With severe abnormalities of ventricular compliance, advanced diastolic dysfunction develops, characterized by a markedly increased E velocity. Deceleration time (DT) becomes short from rapid equalization of left atrioventricular pressure soon after early diastolic filling in a noncompliant ventricle (see Figs. 28-4 and 28-5). Because of poor LA function and limited late diastolic left atrioventricular pressure gradient from an elevated LV diastolic pressure, A-wave amplitude becomes small. Initially, this *restrictive mitral inflow pattern* is reversible on preload reduction with the Valsalva maneuver (Fig. 28-6) or nitroglycerin or diuretic administration. Finally, an irreversible restrictive pattern develops with no significant change with preload reduction (Fig. 28-7).

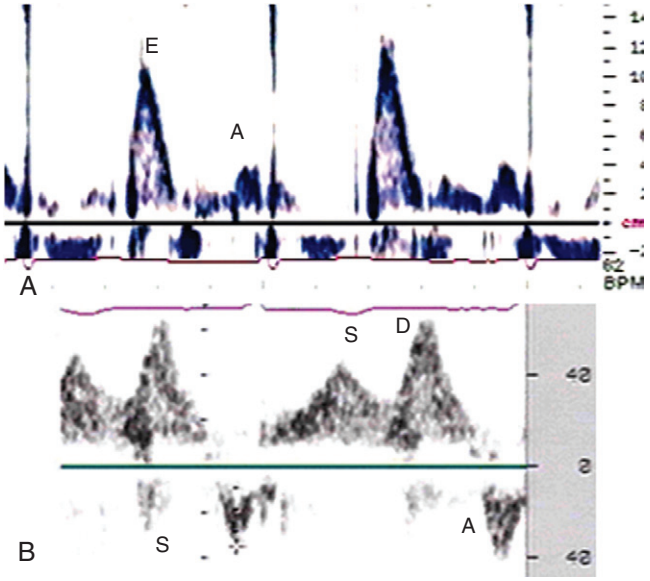



**Figure 28-5 Severely reduced LV diastolic compliance.** Restrictive mitral inflow (**A**) and pulmonary vein inflow (**B**) showing S and D reversal along with a prominent atrial reversal velocity and duration.

### *Pulmonary Vein Pulsed-Wave Doppler*

In the early stages of the disease, pulmonary vein flow may show a systolic dominant pattern with systolic-to-diastolic (D/S) ratio greater than 1 (see Fig. 28-3). Atrial reversal may be normal in early stages, and then as LA compliance abnormality sets in, progressively increasing A-wave velocity as well as duration develop (see Figs. 28-5 and 28-7). With progressively increasing compliance abnormality, decreased S and increased D waves on pulmonary vein Doppler occur (see Figs. 28-4, 28-5, and 28-7). The S wave becomes blunted due to decreased LA compliance, increased mean LA pressure,[26] and LV pressure.[27] Presence of significant mitral regurgitation may further blunt the S wave because of competing mitral regurgitation and pulmonary vein flow at the atrial inflow chamber.[28] In the presence of atrial fibrillation, marked blunting of pulmonary vein S wave with or without mitral regurgitation is the rule. The pulmonary-vein D wave that results from the pulmonary vein–LA pressure gradient created during atrioventricular filling in early LV diastole is dependent on the same factors that influence the early mitral velocity and its DT. Hence, in advanced stages of the disease a tall D wave with a shortened DT is seen (see Figs. 28-4 and

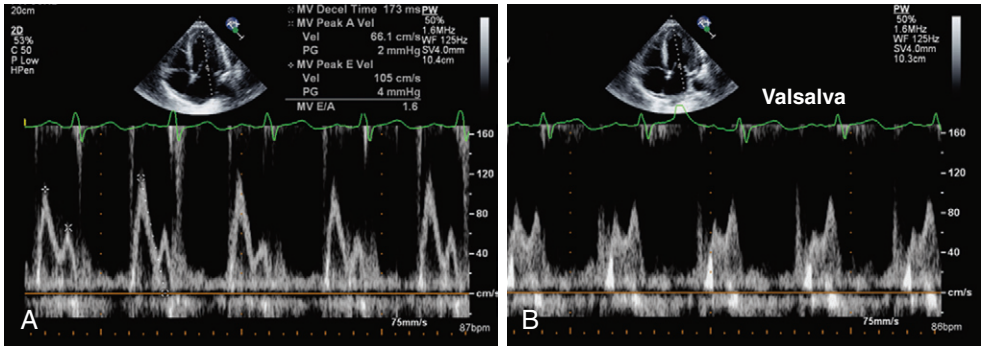



**Figure 28-6 Effect of Valsalva maneuver on mitral inflow filling pattern in a patient with restrictive cardiomyopathy.** Baseline E/A ratio is 1.6 (**A**) and reduced to 0.77 post Valsalva maneuver (**B**), indicating moderate diastolic dysfunction and reversible restrictive diastolic filling.

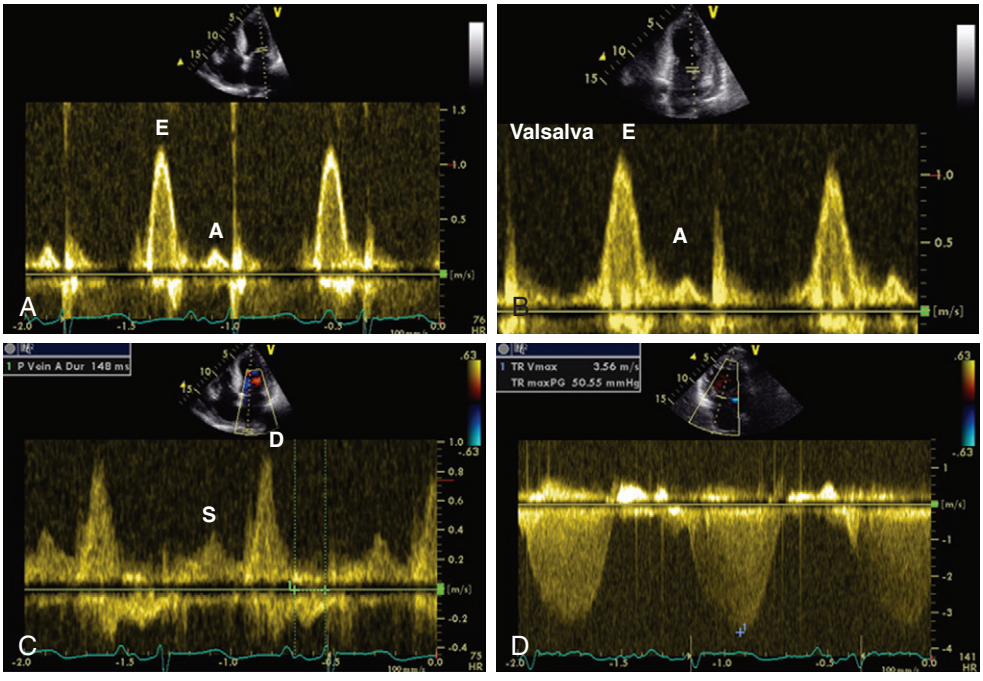



**Figure 28-7 Doppler characteristics of patients with restrictive cardiomyopathy. A,** Restrictive mitral inflow with increased E/A ratio and short mitral inflow E-wave deceleration time. **B,** No change in mitral inflow restrictive filling pattern with Valsalva maneuver, suggesting grade IV or advanced LV diastolic dysfunction. **C,** Restrictive pulmonary vein inflow with reversed S/D ratio and short pulmonary vein D-wave deceleration time. **D,** Increased pulmonary artery systolic pressure (RV-RA gradient of 3.56 m/s corresponding to a pressure gradient of 51 mm Hg in this case example).

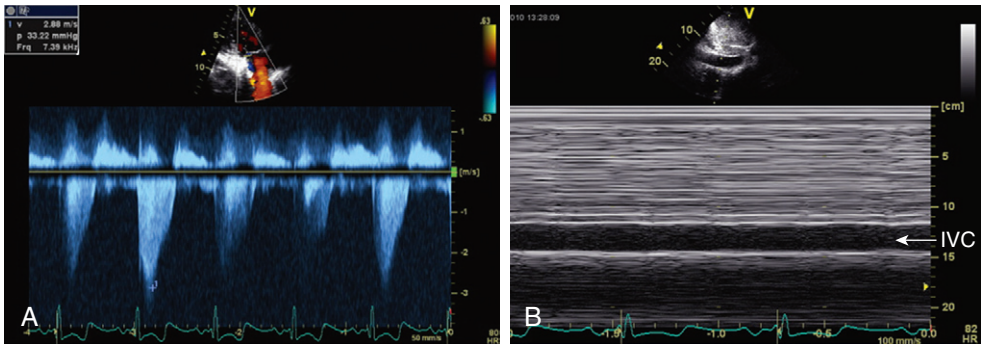



**Figure 28-8 Other Doppler features of restrictive cardiomyopathy. A,** V-shaped tricuspid regurgitation (TR) CW signal indicating elevated RA pressure. In addition, phasic change in tricuspid inflow and TR severity and gradient is noted. **B,** M-mode of the inferior vena cava (*IVC*) in the subcostal view showing dilated IVC without respiratory variation suggesting elevated RA pressure.

28-7). With abnormal LV relaxation and compliance, an increase in LV end-diastolic pressure leads to minimal atrioventricular filling on atrial contraction and a prominent and prolonged pulmonary vein A-wave reversal that becomes greater than the mitral inflow atrial duration. Finally, impairment of LA contraction due to mechanical atrial failure leads to a decrease in amplitude and duration of the pulmonary-vein A wave.[8]

Other pulsed-wave (PW) Doppler features include decreased tricuspid inflow DT on inspiration, D greater than S on the hepatic vein, and A-wave reversal in the hepatic vein on inspiration.

### *Color Doppler*

Moderate mitral and tricuspid valve regurgitation are often present. Because of a marked increase in LV end-diastolic pressure, diastolic mitral regurgitation may be seen, especially in the presence of first-degree heart block.

### *Continuous-Wave Doppler*

A characteristic V-shaped tricuspid regurgitation signal indicating elevated right atrial pressure may be seen (Fig. 28-8), along with mitral and tricuspid valve regurgitation on CW Doppler. Increased LV and RV *dP*/*dt* may be noted on CW Doppler signals.

### *Tissue Doppler*

#### Mitral Annulus

Unlike load dependence of mitral and pulmonary vein PW Doppler flow patterns, tissue Doppler imaging (TDI) of the septal and lateral mitral annulus allows more reliable and direct quantitation of myocardial relaxation.[29-31] With progressively increasing stages of the disease, the myocardial early motion wave shows a progressive decline in its amplitude so that the ratio of mitral inflow E wave to mitral annular E wave increases progressively (see Figs. 28-3 and 28-4). A markedly diminished velocity of diastolic motion is observed in patients with advanced restrictive cardiomyopathy (Fig. 28-9). In fact, decreased TDI velocities are used as a diagnostic method of differentiating between constrictive pericarditis (in which TDI velocities of mitral annulus are preserved) and restrictive cardiomyopathy when mitral annular E wave is less than 8 cm/s.[32] Systolic (S′) velocity of TDI of tricuspid annulus is a good measure of RV systolic function with a low-normal value of 10 cm/s.[33,34] A decrease in RV systolic and diastolic velocities is also often present and reflects a global impairment in myocardial relaxation (Fig. 28-10).

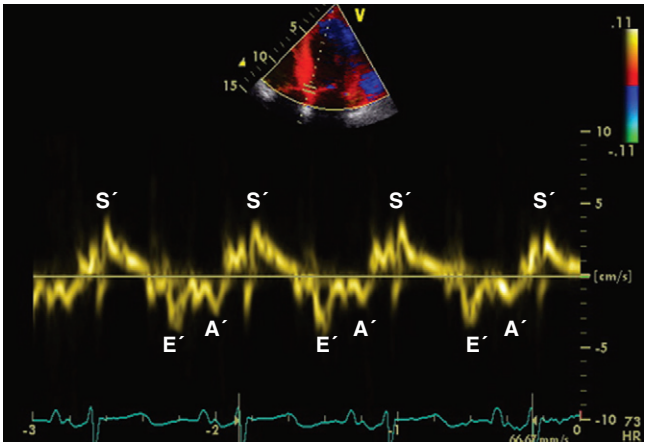



**Figure 28-9 Grade IV LV diastolic dysfunction.** Mitral septal annular tissue Doppler showing markedly reduced systolic (*S′*) as well as diastolic velocities (*E′* and *A′*).

#### Color M Mode

Patients with restrictive cardiomyopathy show a significantly slower slope of the first aliasing contour of velocity of propagation (Vp) on color M-mode. An E/Vp ratio greater than 1.5 can be used to assess elevated LV end-diastolic pressure[35] (Fig. 28-11).

## Cardiac Magnetic Resonance Imaging

Visual inspection of LV and RV architecture on MRI is able to identify patterns of regional or diffuse wall thinning and concentric or asymmetric hypertrophy. Pericardial thickness and calcification can be assessed to distinguish pericardial constriction from restrictive cardiomyopathy. Specific patterns of fibrosis and scarring are seen in different types of restrictive cardiomyopathies that may initially present with HFpEF.[36-39]

## Specific Restrictive Cardiomyopathies

Restrictive cardiomyopathies are associated with characteristic imaging features, although none is particularly sensitive or specific for the underlying etiology (see Table 28-1).[40] In most cases, careful consideration of the clinical context and endomyocardial biopsy may be required. Infiltrative processes and metabolic storage diseases including amyloidosis, hemochromatosis, sarcoidosis, Fabry disease, and glycogen storage diseases are the most frequent causes of restrictive cardiomyopathies. Less common forms of restrictive cardiomyopathies include

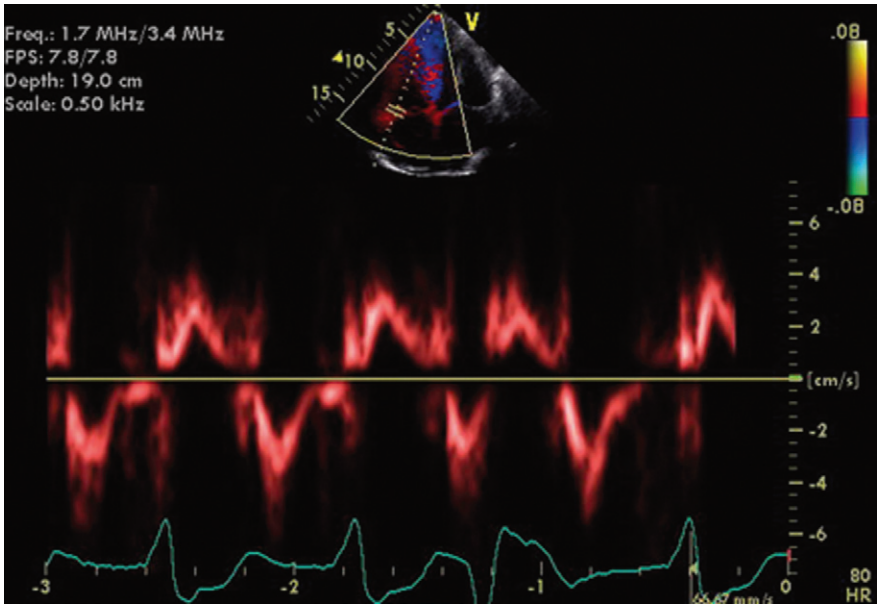



**Figure 28-10 Cardiac amyloidosis with atrial fibrillation.** Reduced systolic (S′) and diastolic (E′) tissue Doppler tricuspid annular velocities with the absence of A′ waves due to atrial fibrillation. Tissue Doppler PW sample volume is placed at the lateral tricuspid annulus in the four-chamber view.

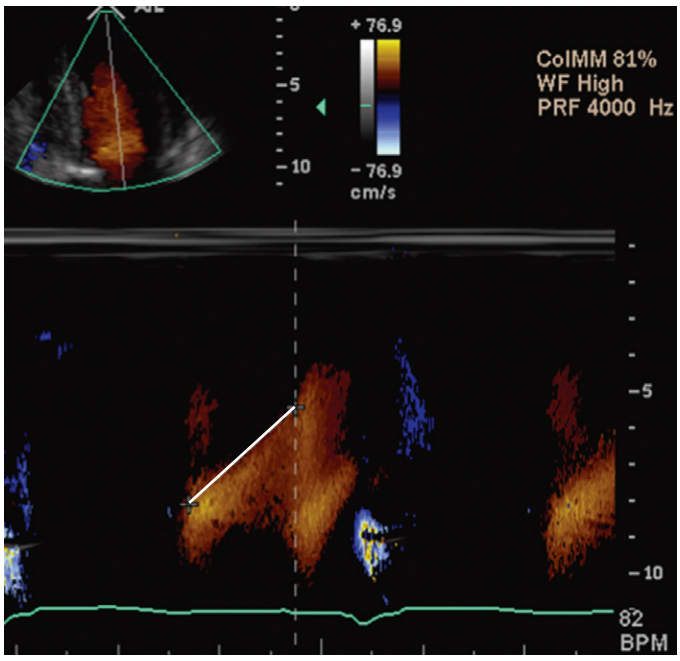



**Figure 28-11 Reduced E-wave propagation velocity with cardiac amyloidosis.** Markedly reduced velocity of E-wave propagation (Vp 13 cm/s) on color M-mode indicating markedly abnormal LV relaxation.

endocardial fibrosis associated with the hypereosinophilic syndrome (Loeffler cardiomyopathy), idiopathic restrictive cardiomyopathy scleroderma,[41,42] carcinoid syndrome,[43] and metastatic malignancy.[44]

## AMYLOIDOSIS

Amyloidosis is the most commonly encountered and recognized cause of restrictive cardiac disease. Four different types of amyloidosis have been described according to the underlying disease:

1. *Immunoglobulin amyloidosis:* Immunoglobulin amyloidosis constitutes about 85% of all newly diagnosed cases of amyloidosis. It includes primary amyloidosis, multiple myeloma, and other plasma cell dyscrasias such as B cell lymphoma and Waldenström macroglobulinemia.[45] The building block of the amyloid fibril is an immunoglobulin light-chain protein. Primary amyloidosis is a plasma cell disorder in which approximately 5% to 10% of bone marrow plasma cells have clonal dominance of a light chain isotype.[46] There is predominance of lambda versus kappa free light chains (3:1) in primary AL amyloidosis; in comparison, other plasma cell dyscrasias, such as multiple myeloma, usually have a lambda-to-kappa ratio of 1:2. Common presenting features include nephrotic syndrome, sensorimotor peripheral neuropathy, hepatomegaly, splenomegaly, and, less often, macroglossia.[47]
2. *Familial amyloidosis:* Familial amyloidosis, or hereditary amyloidosis, is less common than primary amyloidosis and is caused by an autosomal-dominant mutation, most frequently in the transthyretin gene.[48] Common features include peripheral neuropathy, renal impairment, autonomic dysfunction with mainly gastrointestinal symptoms, and cardiomyopathy.[49] Macroglossia does not occur, and renal involvement is less prevalent than it is in primary AL amyloidosis.
3. *Senile systemic amyloidosis:* Senile systemic amyloidosis affects approximately 25% of patients over the age of 80 and is derived from normal transthyretin.[50] This type of amyloidosis mainly involves the atria (91%) and less often is isolated in the aorta or involves the entire heart.[51] Senile cardiac amyloidosis is not always a benign condition and can result in heart failure, atrial fibrillation, and other conduction disturbances.[52] Isolated atrial involvement may occur.[53]
4. *Secondary amyloidosis:* Secondary amyloidosis is characterized by reactive amyloid fibrils, which are acute-phase reactants produced in response to systemic inflammation such as tuberculosis, leprosy, rheumatoid arthritis, familial

Mediterranean fever, inflammatory bowel syndrome, chronic lung diseases, and chronic infections.

### Cardiac Features

Restrictive cardiomyopathy is the main finding in cardiac amyloidosis. There is replacement of normal myocardial contractile elements by deposits of amyloid, leading to alterations in cellular metabolism, calcium transport, receptor regulation, and cellular edema. Injury can also occur from circulating light chains in the absence of amyloid fibril formation.[54] Amyloid myocardium becomes firm, rubbery, and noncompliant. Involvement of the cardiac conduction system can lead to fibrosis of sinoatrial and atrioventricular nodes as well as involvement of infra His fibers, leading to various types of heart block and arrhythmias.[55] Another cardiac manifestation can be cor pulmonale due to amyloid infiltration of pulmonary vasculature, causing significant pulmonary hypertension.[56] An infarction pattern in the absence of epicardial coronary disease is not uncommon as a result of amyloid deposition in the coronary microvasculature.[57]

Cardiac involvement is most common in immunoglobulin amyloidosis, occurring in about 50% of patients with congestive heart failure in about 25% of patients. Cardiac involvement is less common in other forms of primary amyloidosis and least common in secondary amyloidosis. Specific echocardiographic features occur in two third of patients[58] and in 91% of patients in a recent study and include thickening of the LV walls with low voltages on electrocardiography, increased myocardial reflectivity (the "speckled" or "granular" or "ground glass" pattern), biatrial enlargement, thickening of the interatrial septum, thickening of mitral and tricuspid valves, mitral and tricuspid regurgitation, presence of a small-to-moderate pericardial effusion and various abnormalities in diastolic filling and filling pressures depending on the stage of the disease (see Figs. 28-1 through 28-11), with restrictive filling pattern only in the advanced stages.[59] A marked reduction in tissue Doppler velocities, strain, and strain rate occurs in amyloidosis[60] even in early stages (see Fig. 28-9). Further studies are needed to define prognostic relevance of TDI and myocardial strain and strain rate[61] for earlier diagnosis of cardiac amyloid. Significant LV hypertrophy and wall motion abnormalities may be seen in patients with secondary amyloidosis.[62] Differential diagnosis of amyloidosis includes hypertrophic cardiomyopathy and other infiltrative cardiomyopathies. Decreased LV function strongly suggests absence of hypertrophic cardiomyopathy.

LA dysfunction preceding echocardiographic features of amyloidosis can be detected by atrial strain and rate. In 95 patients with amyloid LA ejection fraction was lower compared to controls ($40.4 \pm 13.6$ vs. $67.0 \pm 6\%$, $P = 0.01$). LA septal strain rate and strain were lower compared to controls ($0.8 \pm 0.5\ s^{-1}$ and $5.5 \pm 4\%$, respectively) compared with controls ($1.8 \pm 0.8\ s^{-1}$ and $14 \pm 4\%$, respectively, $P \leq 0.0001$).[63]

Endomyocardial biopsy remains the definitive diagnostic method for cardiac amyloidosis.[64] Transthoracic echocardiography has played a major role in the evaluation of amyloid deposition in the heart and is the procedure of choice for the noninvasive diagnosis of cardiac amyloid.[41] Increased myocardial echogenicity is useful for diagnosing cardiac amyloidosis. Especially in the presence of increased atrial thickness, specificity can reach 100%; however, this feature is evident only in the advanced stages of the disease. If the combined clinical[65] and echocardiographic picture suggests amyloidosis, then immunocharacterization of the underlying amyloid protein can be obtained less invasively from extracardiac tissue sites.[66] These sites include the tongue, subcutaneous fat pads, kidneys, bone marrow, gastric mucosa, and, less commonly, rectal mucosa.

### Other Diagnostic Approaches

A number of modalities besides echocardiography help arrive at a diagnosis of restrictive cardiomyopathy from amyloidosis. These are listed in Table 28-3.

Circulating free immunoglobulin light chains are found in over 98% of patients with primary amyloidosis and are used to determine prognosis and response to chemotherapy.[67] Serum levels of cardiac troponin (in response to myocardial injury) and pro–brain natriuretic peptide[68] (released in response to myocardial stress) are independent predictors of survival in patients with primary amyloidosis. Immunocharacterization of the underlying amyloid protein can be obtained by extracardiac tissue sites.[69] However, endomyocardial biopsy remains the definitive diagnostic method for cardiac amyloidosis. Nonbranching extracellular fibrils, interstitial eosinophilic amyloid deposits as homogenous waxy material on eosin hematoxylin staining, and apple-green birefringence Congo red staining under polarized light are the most common findings on pathology.[70] The characteristic fibrillar pattern of the amyloid deposits can be seen by electron microscopy and immunohistochemical staining can then be used to determine the type of amyloid deposit.[71] Combining a subcutaneous fat pad biopsy and Congo red staining of bone marrow has yielded a tissue diagnosis in 90% of patients with amyloidosis.[72] Electrocardiography shows a low voltage in up to 50% of patients with cardiac amyloidosis and, in conjunction with LV hypertrophy on echocardiography, should raise the suspicion for cardiac amyloidosis.[63]

Nuclear scintigraphy with $^{99}$Tc pyrophosphate[73] or indium-labeled serum amyloid protein can detect extensive cardiac involvement of cardiac amyloidosis.[74] Technetium pyrophosphate scan is positive in familial and senile amyloidosis (100% accuracy for diagnosis) and negative in primary amyloidosis (100% specificity).[74] Serum amyloid P component (SAP) is a normal circulating plasma protein that is deposited on amyloid fibrils because of its specific binding affinity for these fibrils. Scintigraphy after the injection of $^{123}$I-SAP can be used for diagnosing, locating, and monitoring the extent of systemic amyloidosis.[75]

The role of cardiac MRI has recently expanded in the diagnosis of cardiac amyloidosis. In patients with histologically verified cardiac amyloidosis, abnormal late gadolinium enhancement was found in 97% of patients and increased echocardiographic LV wall thickness in 91% patients.[76] Presence of late gadolinium enhancement on cardiac MRI in the absence of echocardiographic findings of cardiac amyloidosis is associated with worse clinical profile and disease severity.[77] Global subendocardial (Fig. 28-12, *A*) or transmural late gadolinium enhancement (see Fig. 28-12, *B*) along with reduced subendocardial to blood T1 difference on MRI has been reported to be very accurate in advanced stages of cardiac amyloidosis[39]; however, utility of cardiac MRI in early stages of the disease has not been evaluated (see Table 28-3).[77]

### Natural History

Onset of congestive heart failure is associated with poor prognosis, often with a survival less than 6 months. The prognosis varies according to the type of amyloidosis, the stage of the disease, and the age of the patient at the time of diagnosis. Primary amyloidosis has the worst prognosis, which

**TABLE 28-3 Other Approaches in the Diagnosis of Restrictive Cardiomyopathies**

| *Diagnostic Modalities* | *Findings* | *Limitations* |
|---|---|---|
| 2D/Doppler echocardiography | LV hypertrophy<br>Restrictive filling | Comorbidities of advanced age and coexisting hypertension renders LVH nonspecific. May be late findings with limited impact on guiding treatment or affecting prognosis. Nonreproducible measurements make regression difficult to follow.[80] Does not provide etiologic information in amyloidosis[60] |
| Systemic markers | Light chains, serum amyloid p component, troponin, and pro-BNP<br>In primary amyloidosis | |
| Biopsy<br>Tongue, subcutaneous fat pads, kidneys, bone marrow, gastric mucosa, rectal mucosa, and EMB | May reveal specific cause of restrictive cardiomyopathy<br>Eosinophilic interstitial deposits on H & E, apple-green birefringence on Congo red staining, and fibrillar protein on EM in cardiac amyloid | Procedural risk<br>Uncertainty about sampling error limits use in monitoring disease |
| Cardiac catheterization | Dip and plateau<br>RV systolic pressure usually >50 mm Hg<br>LVEDP often >5 mm Hg > RVEDP<br>RVEDP < one third of RV systolic pressure | |
| CT imaging | Pericardium of normal thickness | |
| MRI | High spatial resolution and tissue contrast definition. Pattern of late gadolinium enhancement is diffuse subendocardial or global transmural in over 83%. Suboptimal myocardial nulling (8%) and patchy focal LGE (6%) is less common in cardiac amyloidosis. LGE is subendocardial sparing and often involving basal inferolateral wall in Fabry disease, midwall within hypertrophied segments in patchy distribution most consistently at anterior and posterior junction of interventricular septum and right ventricular free wall in HCM. T2 noncontrast MRI valuable in quantitation of myocardial iron deposition in hemochromatosis. Subendocardial longitudinal relaxation time (T1) in amyloid patients is shorter than in controls. Prevalence of late gadolinium enhancement 50% in Fabry disease, 69% in cardiac amyloidosis and 80% in HCM | Risk of the development of nephrogenic systemic fibrosis from gadolinium, in patients with acute or chronic severe renal insufficiency (glomerular filtration rate <30 mL/min/1.73 $m^2$) and patients with renal dysfunction due to the hepatorenal syndrome |
| Nuclear scintigraphy with $^{99}$Tc pyrophosphate or indium-labeled systemic amyloid protein scan | Tc pyrophosphate scan differentiates between immunoglobulin light chain and transthyretin-related familial and senile amyloidosis. Strong uptake transthyretin-related amyloidosis with accuracy of 100%<br>Indium cardiac uptake in primary and multiorgan uptake in systemic amyloidosis | |

*BNP*, Brain natriuretic peptide; *CT*, computed tomography; *EM*, electron microscopy; *EMB*, endomyocardial biopsy; *HCM*, hypertrophic cardiomyopathy; *H & E*, hematoxylin-eosin (stain); *LGE*, late gadolinium enhancement; *LVEDP*, left ventricular end-diastolic pressure; *LVH*, left ventricular hypertrophy; *MRI*, magnetic resonance imaging; *RVEDP*, right ventricular end-diastolic pressure.

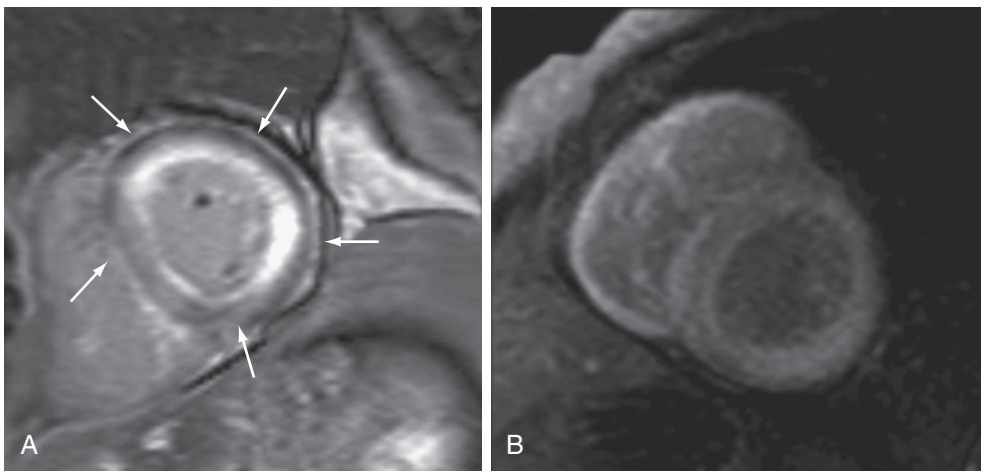



**Figure 28-12 Midventricular short-axis late gadolinium-enhanced magnetic resonance images showing two patients with systemic amyloidosis. A,** 76-year-old woman with histologic diagnosis of amyloidosis of periumbilical adipose tissue. Late enhancement in short-axis image shows intense subendocardial enhancement involving all LV walls (*arrows*). **B,** Global transmural late gadolinium enhancement in a homogenous pattern in the LV and RV. Blood pool has characteristic dark appearance commonly seen in cardiac amyloidosis. (***A,*** *Adapted from Belloni E, De Cobelli F, Esposito A, et al: MRI of cardiomyopathy.* Am J Roentgenol *191:1702-1710, 2008.* ***B,*** *Adapted from Syed IS, Glockner JF, Feng D, et al: Role of cardiac magnetic resonance imaging in the detection of cardiac amyloidosis.* JACC Cardiovasc Imaging *3:155-164(B), 2010.)*

is exacerbated by multisystem involvement and cardiac involvement in particular.[48] A marked increase in wall thickness, specifically mean LV and RV wall thickness of greater than 15 mm and 7 mm, respectively,[78] reduced LV systolic function, shortened mitral inflow DT of less than 150 ms,[79] increased early diastolic filling velocity to atrial filling (E/A) ratio, and Doppler-derived myocardial performance index (MPI)[80] have all been proposed as predictors of cardiac death. One study[81] found that the myocardial integrated back scatter of the posterior wall was a better predictor of cardiac and overall death compared to Doppler features. Another poor prognostic marker is RV dilation.[82] Late gadolinium enhancement has been shown

to offer prognostic value in the assessment of amyloidosis.[83] Histologically, the worst prognosis is connected with the presence of nodular deposits, thick perimyocytic layers of amyloid, and small myocyte diameters in endomyocardial biopsy.[84] The overall median survival after diagnosis is less than 2 years in most. Syncope indicates a poor prognosis as well and is often a precursor of sudden cardiac death.[85]

In secondary amyloidosis, the underlying chronic disease affects the prognosis, and hereditary amyloidoses vary in prognosis according to the specific mutation.[86] Heart rate variability assessed by Holter monitoring was found to be a possible predictor of mortality in patients with both primary and secondary amyloidosis involving the heart.[87] Impaired LV systolic function is more common in primary than other forms of amyloidosis[88]; primary amyloidosis also carries a worse prognosis compared to secondary amyloidosis.

### *Outcome Data*

The use of high-dose melphalan with rescue autologous peripheral blood stem cell transplantation has resulted in reversal of the clinical manifestations of AL amyloidosis in a significant proportion of patients who survived the procedure.[89-91]

## HEMOCHROMATOSIS

The clinical presentation of primary (hereditary) hemochromatosis (an autosomal recessive disorder) includes liver disease in 75% of cases, weakness and lethargy in 74%, skin hyperpigmentation in 70%, diabetes mellitus in 48%, arthralgia in 44%, impotence in 45%, electrocardiographic abnormalities in 31%, and heart failure and conduction disturbances in 15%.[92] The primary clinical feature of secondary hemochromatosis is high-output cardiac failure from anemia and hemosiderosis. Reversible restrictive cardiomyopathy has been described as a rare clinical feature of hemochromatosis.[93,94] An early echocardiographic study[95] in patients with anemia who developed cardiac secondary hemochromatosis due to transfusion described LV hypertrophy as characteristic of this disorder; however, a subsequent echocardiographic study[96] that examined echocardiographic features of patients with primary (hereditary) hemochromatosis compared to normal subjects found that hypertrophy is not a feature of hemochromatosis cardiomyopathy. One study[97] found increased echocardiographic integrated myocardial backscatter ($33 \pm 13$ vs. $21 \pm 6$, p less than 0.001) in 38 patients with thalassemia receiving chronic blood transfusion compared to 20 control subjects despite comparable fractional shortening but increased LV mass. The same group subsequently showed the myocardial backscatter in this group of patients is not related to prognosis over a $122 \pm 36$ month follow-up.[98] Decreased S′ of mitral annulus was found in treated subjects with hemochromatosis and S′ = 10.88 cm/s achieved a 56% sensitivity and 74% specificity for separating hemochromatosis from controls. Negative predictive value of S′ was only slightly greater than 50%; thus, additional imaging with cardiac MRI is still needed in the presence of normal S′.[99] Most of the echocardiographic studies[100] report a dilated cardiomyopathy with hemochromatosis. One study[101] found increased wall thickness that was reversible after iron chelation therapy. Increased thickness may be an early feature of the disease with progression to dilated cardiomyopathy in later stages. Serum ferritin is highly correlated with the amount of iron deposition and can therefore be used as an index for intracardiac iron load[102]; however, ferritin can be elevated in inflammation and fever.[103] T2 relaxation time on cardiac MRI has a linear correlation with the total iron content in the heart.[104]

## HYPEREOSINOPHILIC SYNDROME AND ENDOMYOCARDIAL FIBROSIS

Idiopathic hypereosinophilic syndrome is a leukoproliferative disorder characterized by idiopathic sustained peripheral blood eosinophilia (greater than $1.5 \times 10^9$/L) and (multi-) organ dysfunction caused by infiltration of eosinophils. Cardiac dysfunction is the most common cause of morbidity and mortality. Endocardial fibrosis and myocardial inflammation cause heart failure and ventricular mural thrombus formation.

Dyspnea, ascites, peripheral edema, and right heart failure are common clinical manifestations of the disease in patients with RV or biventricular involvement. Increased endocardial thickness suggestive of fibrosis with restricted leaflet motion of the atrioventricular valve is seen in endomyocardial fibrosis.[105] This disease is characterized by fibrosis of the endocardium and of the myocardium of the inlet region and LV apex. Involvement of the papillary muscles leads to regurgitation of mitral and tricuspid valves. Progressive shrinkage of the LV cavity occurs.[106] Ventriculography may show a polylobulated LV silhouette with linear calcific shadows at the "amputated" apex giving an appearance of a clenched fist[107] or a hissing snake.[108]

Echocardiographic findings include Merlon sign (basal hypercontractility), which contrasts with the abnormal apex.[109] On M-mode echocardiography, the initial rapid motion is followed by a flat endocardial reflection (the square root sign is seen in the septum and posterior wall). On 2D echocardiography, inversion of the normal ventricular-to-atrial size ratio is seen with obliterated ventricles and dilated atria. The LA is dilated with left-sided endomyocardial fibrosis, and the RA is dilated with right-sided endomyocardial fibrosis.[107] Marked biatrial enlargement is seen when both sides of the heart are involved. The apex of the involved ventricle shows layered thrombus in the early stages (Fig. 28-13), which is later obliterated by fibrosis. Apical thrombus does not alter the movement of the underlying myocardium. Different grades of pericardial effusion are also found. Echocardiography seems to be the only noninvasive method that can detect endomyocardial disease in its early stages.[110] Peripheral eosinophilia along with increased cardiac troponin T without other known etiology, which decreases after treatment, has been proposed to be an early marker of disease even before echocardiographic manifestations appear.[111]

A restrictive pattern is typical of the late stage of the disease. There is minimal change in mitral and tricuspid velocities as found in healthy patients, which differentiates endomyocardial fibrosis from constrictive pericarditis. Furthermore, a restrictive pattern is observed on both atrioventricular valves when both sides are involved with a markedly short tricuspid inflow DT. Pulmonary veins often show D dominance and a broad reversal A wave (the latter presented a low velocity when the wall of the LA is diseased). Hepatic veins showed a markedly deep diastolic forward wave throughout the respiratory cycle and a marked reversal with inspiration. Fibrous thickening of the endocardium, made up of collagen without elastic fibers and sometimes organized thrombus, is seen on endomyocardial biopsy. Normal thickness of mitral and tricuspid valve leaflets despite severe regurgitation, involvement of papillary muscles, obliteration of LV apex, and normal-sized to small ventricle in the presence of

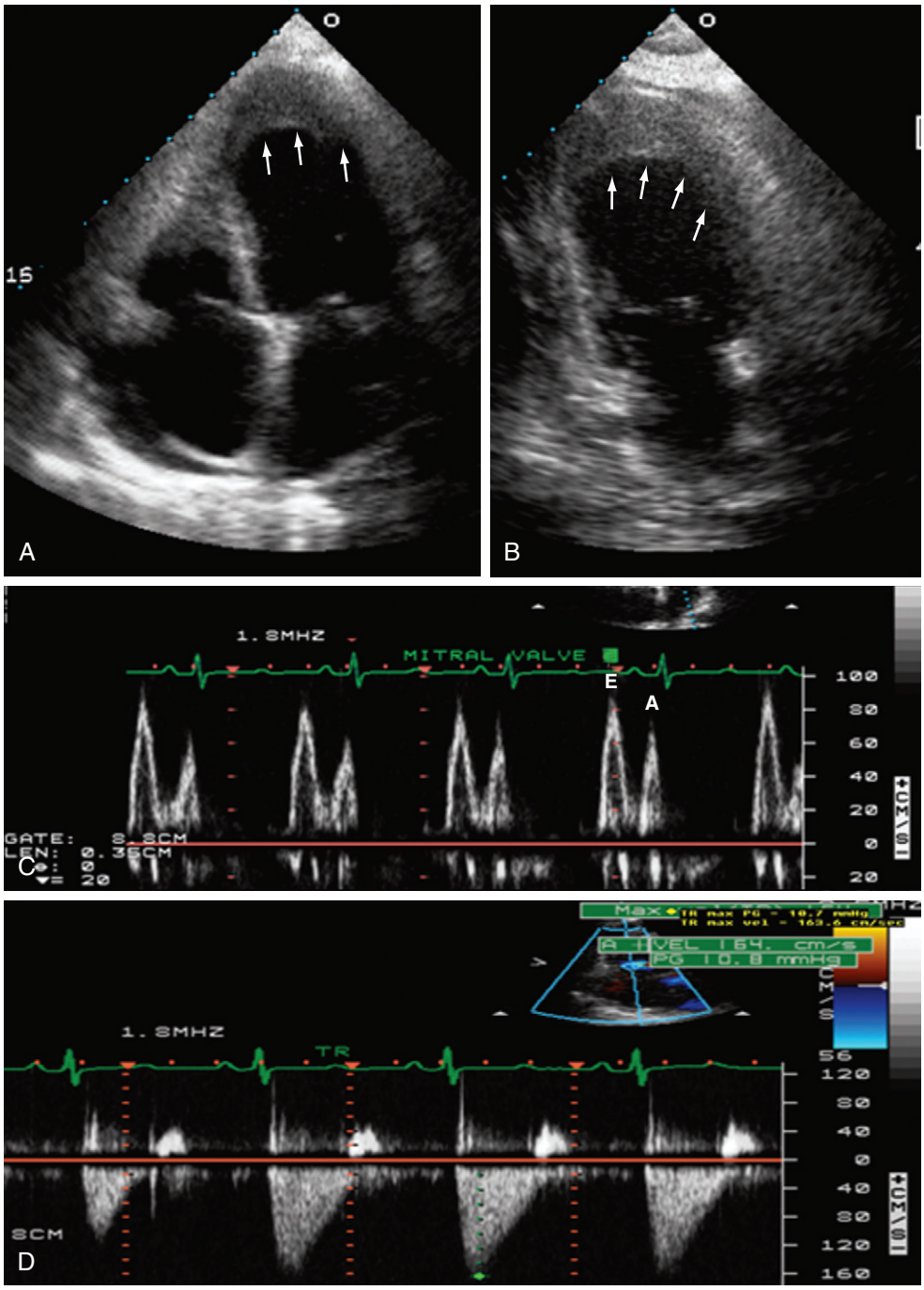



**Figure 28-13 Cardiac involvement in idiopathic hypereosinophilic syndrome.** TTE revealed the presence of deposits at the apex of the LV in apical four-channel and two-channel views (*white arrows*, **A** and **B**). **C,** Pseudonormal to restrictive filling pattern. **D,** Tricuspid regurgitation (TR) envelope by CW Doppler. V-shaped TR signal suggests markedly elevated RA pressure.

severe valvular regurgitation distinguish this condition from rheumatic heart disease.

Patients who present with right-sided endocardial fibrosis may have clinical features that can be confused with those of constrictive pericarditis. Presence of normal pericardial thickness, obliteration of RV apex, and markedly dilated RA distinguish it from constrictive pericarditis. Patients who develop an extensive LV apical thrombus after an acute myocardial infarction may mimic endomyocardial fibrosis; however, wall motion abnormalities in the classic distribution, history of myocardial infarction, and lack of eosinophilia aid in diagnosis (see Fig. 28-13). Obliteration of LV apex during both systole and diastole distinguishes endomyocardial fibrosis from apical hypertrophic cardiomyopathy where obliteration only occurs in systole. The presence of a normal-sized ventricle in the presence of gross cardiomegaly on chest radiography and normal-sized and normal LV systolic function distinguish it from dilated cardiomyopathy. Gigantic RA and apical obliteration of RV apex may suggest Ebstein anomaly; however, normal attachment of tricuspid leaflets and focal involvement of RV inflow and outflow regions distinguish right-sided endomyocardial fibrosis from Ebstein anomaly.

Asymptomatic patients are closely monitored with serum troponin level every 3 to 6 months and echocardiography and pulmonary function tests every 6 to 12 months. Early institution of alpha interferon, steroids, and hydroxyurea and favorable response to treatment may halt the fibrotic process and improve symptoms and prognosis in these patients. Imatinib mesylate (Novartis), a tyrosine kinase inhibitor, chemotherapeutic agents, and hematopoietic stem cell transplantation are used for resistant cases.[112] Valve replacement with bioprosthetic valves may be required in patients with severe regurgitant lesions. Risk of thrombosis with mechanical valves is very high in patients with hypereosinophilic syndrome despite therapeutic anticoagulation. Endocardiectomy may be required for patients with endomyocardial fibrosis, and thrombectomy may be required for individuals with thrombosis.

## SARCOIDOSIS

Sarcoidosis is a granulomatous disease of unknown etiology that has a predilection for certain ethnic groups such as African Americans. Pulmonary sarcoid is often the first manifestation of the disease.[113] Endomyocardial biopsy may assist in making a diagnosis with the finding of noncaseating granulomas. The histological diagnostic rate of cardiac sarcoidosis using endomyocardial biopsy has a low sensitivity of 19.2%[114] due to a patchy distribution of the pathology and predilection of granulomas for the cephalad portion of the septum that is less accessible to biopsy.

Cardiac involvement occurs in 25% of patients with systemic sarcoidosis but is clinically silent in the majority of patients.[115-117] In a comparative study[118] of cardiac sarcoidosis in Japanese, African Americans, and U.S. whites, the incidences of cardiac sarcoid granulomas were 67.8%, 21.2%, and 13.7%, respectively. A recent report in 69 patients, 30 with biopsy-proven sarcoid, without clinical evidence of heart disease found no differences in echocardiographic findings compared to 26 control subject except for a mildly reduced fractional shortening in patients with long-standing sarcoid.[119] In another study,[120] occult myocardial involvement was shown in patients with sarcoidosis without cardiac involvement. Of these 21 patients, 10 showed abnormal interventricular septal motion and abnormal LV ejection fraction during stress compared to control subjects. Diastolic dysfunction is not uncommon in patients with pulmonary sarcoid without any cardiac involvement.[121] Wall motion abnormalities, LV aneurysm, systolic dysfunction, dilated cardiomyopathy, conduction abnormalities, arrhythmias, and pericardial effusion are more common manifestations of cardiac sarcoidosis.[114] Sarcoid is an important diagnostic consideration in scar-related ventricular tachycardia.[122] Sudden death may be the first manifestation of cardiac sarcoidosis.[123] Sarcoid can be misdiagnosed as idiopathic or arrhythmogenic RV cardiomyopathy. Restrictive cardiomyopathy is more unusual, and diagnosis of sarcoid restrictive cardiomyopathy may be made only after characteristic findings of noncaseating granulomas on endomyocardial biopsy are documented.[124]

To date, no single cardiac investigation has been shown to reliably predict cardiac involvement. Valantine's group[125] reported that thinning, as well as wall motion abnormalities, at the base of the intraventricular septum characterizes the presence of cardiac sarcoidosis. The finding of reduced systolic thickening and excursions of the interventricular septum in about 10% of patients with cardiac sarcoid may be related to the frequent prevalence of sarcoid granulomas in the septum. Asymmetric septal hypertrophy, recorded in 10% of patients, may have had a similar origin.[126,127] Such abnormalities in the upper portion of the intraventricular septum may be considered a reliable diagnostic element of cardiac sarcoidosis, even though there is no further evidence of other organ involvement. One report found that more than 50% of patients with cardiac sarcoidosis had diastolic dysfunction and preserved systolic function.[128] One report described normal LV systolic function, marked biatrial enlargement, severe tricuspid regurgitation, and marked thickening of biatrial walls, appendages, and interatrial septum.[129] It may be considered that when thickening is present, the sarcoid lesions may be of a progressive nature, which is manifested with interstitial edema due to exudative or activated granuloma formation. In the advanced stages of disease, interstitial fibrosis may progress, and thus thinning of the ventricular wall may occur.

Because of low yield on endomyocardial biopsy,[115] the diagnosis is often made with a combination of electrocardiography, Holter monitoring, echocardiography, myocardial perfusion imaging, and, most recently, cardiac MRI.[130] Radionuclide scanning with thallium[131] or sestamibi[132] may show abnormal defects that reverse with dipyridamole.[133] In patients with normal coronaries and known cardiac sarcoid, presence of myocardial thallium defects may be used to guide response to therapy. One report found that Holter monitoring was associated with a sensitivity of 67% and a specificity of 80% for identification of cardiac involvement in patients with systemic sarcoidosis.[134] The plasma brain natriuretic peptide level is considered to be a useful noninvasive biomarker for identifying a possible cardiac involvement in sarcoidosis patients with a preserved LV ejection fraction.[135]

Unlike isolated pulmonary disease, cardiac involvement implies a poor prognosis. Patients with sarcoidosis are at increased risk of sudden death. Owing to the progress in antiarrhythmic drugs and pacemaker implantation, the primary cause of death in cardiac sarcoidosis has changed from sudden death to heart failure.

### *Outcome Data*

For symptomatic patients, medical therapy may include a trial of steroids and immunosuppressive therapy. An excellent response can be achieved with steroid therapy in the early acute inflammatory stage. Monoclonal antibodies against tumor necrosis factor may be employed in refractory cases. Heart block warrants a permanent pacemaker, whereas ventricular tachyarrhythmias are typically amiodarone unresponsive, requiring implantation of an implantable cardioverter-defibrillator. Heart transplantation is a suitable option for patients with end-stage disease.

## STORAGE DISORDERS[136]

### *Gaucher Disease*

Gaucher disease, the most common lysosomal storage disorder, is due to inherited deficiency of the lysosomal enzyme glucocerebrosidase.[137] Clinically, three phenotypes have been delineated on the basis of the presence and severity of central nervous system involvement[138]: type 1 (nonneuronopathic adult form), type 2 (acute neuronopathic form diagnosed classically in infants who are several months old), and type 3 (subacute neuronopathic juvenile form). Partial deficiency of acid beta-glucosidase is associated with parenchymal disease of the liver, spleen, and bone marrow with concomitant anemia and

thrombocytopenia in nonneuronopathic, type 1 Gaucher disease. Severe deficiency of glucocerebrosidase caused by severe mutations is additionally associated with neurological manifestations in the less common type 2 and type 3 subtypes.[139] The perinatal lethal form is very rare, and prominent features of the severe perinatal form are hepatosplenomegaly, associated with hydrops fetalis, generalized ichthyosis, and facial dysmorphy.[140]

Echocardiographic features of this disease in the nonneuropathic (adult) form include increase in LV mass with a septal muscular prominence, areas of apical akinesis, and pericardial changes.[141] Ascending aortic as well as aortic and mitral valve calcification has been described in a family.[142]

Enzyme replacement therapy in type 1 Gaucher disease regresses hepatosplenomegaly, anemia, thrombocytopenia, bone fractures, and bone crisis, whereas neurologic abnormalities and interstitial fibrosis do not respond to treatment.[143]

### *Glycogen Storage Disorder*

Pompe disease occurs due to an α-1,4-glucosidase deficiency, characterized by progressive deposition of glycogen in all tissues.[144] The disease has an autosomal recessive inheritance with a predicted frequency of 1 : 40,000. Pompe disease is associated with elevation of muscle enzymes creatine phosphokinase, lactate dehydrogenase, alanine aminotransferase, and aspartate aminotransferase in 90% to 95% of cases and is confirmed by measurement of α-glucosidase deficiency in leukocytes, fibroblasts, and/or in muscle tissue. The classic infantile form of the disease occurs in infants shortly after birth and is characterized by generalized hypotonia, failure to thrive, and cardiorespiratory failure. Muscular abnormalities and respiratory difficulties are the most common manifestations, followed by cardiac manifestations, pain, epilepsy, fatigue, feeding problems, underweight, macroglossia, abnormal speech, hepatosplenomegaly, abnormal mental development, and hyperparathyroidism.[145]

One review of 225 patients with adult-onset Pompe disease found echocardiographic evidence of hypertrophic cardiomyopathy in 5% of patients, cor pulmonale in 2%, and other cardiac abnormalities in another 4% of patients.[146] Cardiac hypertrophy was only found in subjects younger than 1 year. Echocardiographic features include severe thickening of the interventricular septum, free wall, and posterior LV wall[146] with a tumor-like appearance of the papillary muscles, a small LV cavity, and poor LV systolic function.[147] Case reports of apical hypertrophy causing artifacts on myocardial perfusion imaging and restrictive cardiomyopathy have been described.[148] Normal motion of the intraventricular septum and mitral valve leaflets and midsystolic closure of the aortic valve have been noted.[149] The combination of echocardiographic and electrocardiographic findings is helpful in the clinical diagnosis and recognition of the severity of cardiac involvement of this disease.

Patients with the infantile form of this disease usually die within the first year of life. The nonclassic or late-onset form of the disease may occur at any age in childhood or adulthood. It presents predominantly as a slowly progressive proximal myopathy (in 95% of patients), with or without respiratory difficulties (in 44%).[149,150]

Patients with later onset of disease have better prognosis.[146] Respiratory failure is the most common cause of death. Beneficial effects of recombinant human alpha glucosidase have been reported in patients with the classic infantile form[151] as well as in patients with the nonclassic or late-onset form of the disease.[152] Enzyme replacement therapy regresses cardiac hypertrophy and improves heart failure symptoms and skeletal muscle weakness and respiratory failure, whereas lower motor neuron disease is unresponsive to treatment.[153]

### *Fabry Disease*

Fabry disease is a rare X-linked recessive metabolic disorder caused by deficiency of the lysosomal enzyme α-galactosidase A.[154] Accordingly, hemizygous males have the most severe form of the disease and heterozygous females usually have a more benign presentation.[155] The enzymatic defect in this lysosomal storage disease leads to the accumulation of globotriaosylceramide in several organs including the skin, kidney, nervous system, cornea, and heart.

Cardiac involvement in Fabry disease may occur in conjunction with involvement of other organs or the disease may manifest only with cardiac involvement. Electrocardiographic features include a short PR interval, abnormalities of conduction, and LV hypertrophy.[156] Echocardiographic findings include aortic root dilatation, generalized asymmetric increase in myocardial wall thickness, myocardial dysfunction, ultimately dilated cardiac chambers, and valve dysfunction, especially of the mitral valve.[157] The increased ventricular wall thickness is the consequence of the deposition of globotriaosylceramide in cardiomyocytes and cellular hypertrophy. In female patients, the features are usually subclinical; however, more than half of heterozygous females may have cardiac hypertrophy on echocardiogram.[158] Endomyocardial biopsy and/or measurement of plasma α-galactosidase A activity are definitive diagnostic tests. Sarcoplasmic vacuolization is the classic finding on light microscopy of hematoxylin and eosin–stained tissue. On electron microscopy, concentric lamellar bodies are noted in the sarcoplasm of myocardial cells. In two recent studies, Fabry disease was diagnosed in 3% to 4% of men with concentric LV hypertrophy.[159,160] Asymmetric septal hypertrophy may be present in as many as 4% of patients with Fabry disease.

LV systolic function progressively deteriorates in untreated patients with Fabry disease. A large cross-sectional study[161] of a patient cohort from the Anderson Fabry disease clinical and genetic register showed that the median cumulative survival was 50 years (n = 51), which represents an approximately 20-year reduction of life span. Steep decline in survival occurs after age 35. Neuropathic pain (77%), sensorineural deafness (78%), renal failure (30%), cerebrovascular complications (24%), and low body mass index due to gastrointestinal complications were common.

Recently the availability of enzyme replacement therapy has been shown to result in clearing of vascular endothelial deposits of globotriaosylceramide.[162] Improvement in LV mass and systolic function has also been reported with enzyme replacement treatment.[163] A recent study[164] in 29 patients with mean age of 37 ± 13 years who were treated with 37-month enzyme replacement therapy demonstrated lack of progression of LV hypertrophy and some improvement in LV diastolic function with prolongation of mitral inflow E-wave DT and decreased E/E′ (lateral) ratio. Increased echogenicity in the posterobasal segment was present in 83% of patients, whereas binary appearance (increased echogenicity of the mid interventricular septum due to compartmentalization of glycosphingolipids) was found in only 20% of patients in this study. An earlier study[165] had found presence of binary appearance (Fig. 28-14) in 83% of patients with Fabry disease and had found its sensitivity and specificity at 94% and 100%, respectively, in detecting Fabry disease compared to patients with hypertrophic

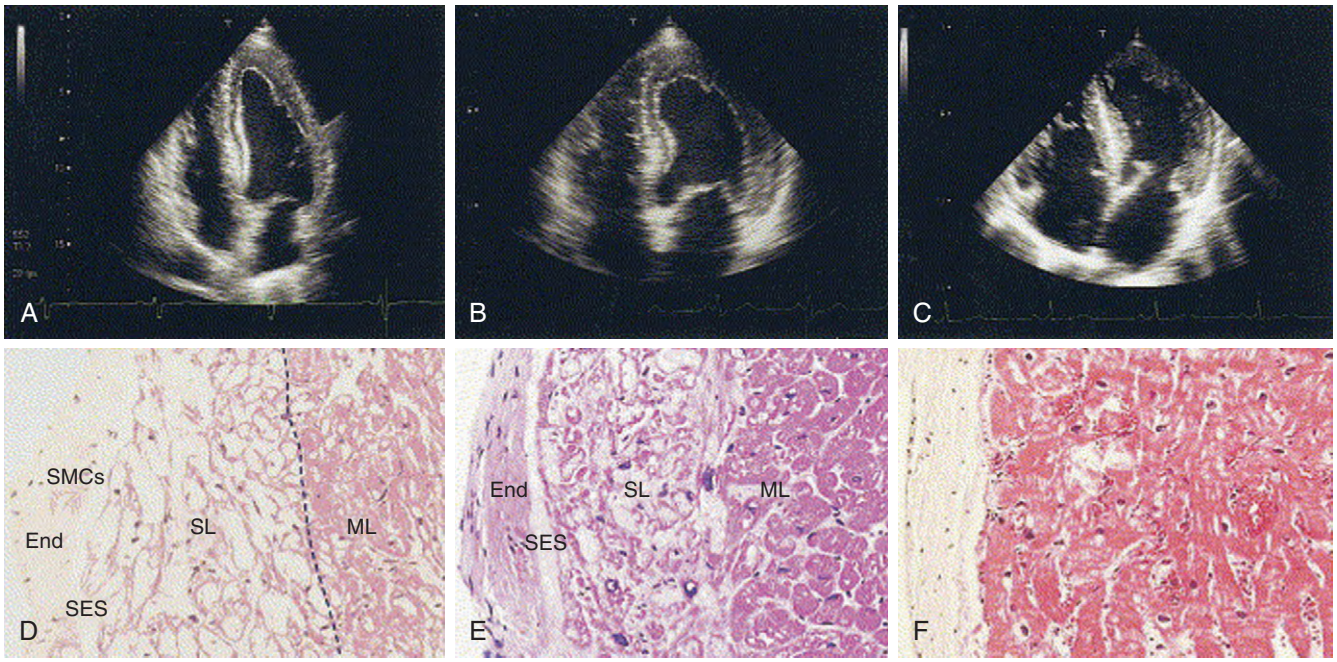



**Figure 28-14 Two-dimensional echocardiography in four-chamber apical view and LV endomyocardial biopsy from two patients with Fabry disease cardiomyopathy.** (**A, D** and **B, E,** respectively) and a patient with hypertrophic cardiomyopathy (**C, F**). Comparison of the three echocardiographic frames reveals the presence of a binary appearance of left ventricular endocardial border in the two Fabry patients (**A, B**). This echocardiographic finding reflects the glycosphingolipids compartmentalization involving a thickened endocardium (*End*) with enlarged and engulfed smooth muscle cells (*SMC*), a subendocardial empty space (*SES*), and a prominent involvement of subendocardial myocardial layer (*SL*), while the middle layer (*ML*) appears partially spared (**D, E**). The echocardiographic pattern is absent in hypertrophic cardiomyopathy (**C**), despite a similar thickening of the endocardium (**F**). *(From Pieroni M, Chimenti C, De Cobelli F, et al: Fabry's disease cardiomyopathy: echocardiographic detection of endomyocardial glycosphingolipid compartmentalization.* J Am Coll Cardiol *47:1663-1671, 2006.)*

cardiomyopathy and hypertensive and normal subjects. One study in patients with aortic stenosis, hypertrophic cardiomyopathy, and Fabry disease found a characteristic double peak sign on strain rate imaging in the 42 segments that showed late gadolinium enhancement. This pattern consisted of a sharp early first systolic peak (negative for longitudinal function and positive for radial function) followed by a rapid fall of strain rate close to the zero line and an additional second strain-rate peak during the isovolumic relaxation period (directed in the same direction as the first peak and at least 50% in magnitude compared with the first peak).[166]

## IDIOPATHIC RESTRICTIVE CARDIOMYOPATHY

Idiopathic restrictive cardiomyopathy occurs predominantly in elderly women. It is a rare entity distinguished from the other forms of restrictive cardiomyopathy by the presence of normal ventricular wall thickness. There have been a few reports of mutations in idiopathic restrictive cardiomyopathy, implicating the desmin and cardiac troponin I genes.[167] Linkage of genes to a region on chromosome 10 has been found in autosomal dominant restrictive cardiomyopathy in a family.[168] Idiopathic restrictive cardiomyopathy accounts for 2% to 5% of all cardiomyopathies in children.[169] Biatrial enlargement and no or minimal hypertrophy are evident, as in the idiopathic restrictive cardiomyopathy of the adult.

There is marked biatrial enlargement and presence of atrial fibrillation in the absence of valvular heart disease, hypertension, and ischemic heart disease. This disease is seen in individuals where other etiologies for cardiomyopathy have been excluded, such as connective tissue disease, carcinoid syndrome, amyloidosis, hemochromatosis, eosinophilic syndrome, malignancy, radiation exposure, cardiotoxic drug exposure, or history of alcohol abuse. Interstitial fibrosis is the predominant histologic finding. LV systolic function is preserved in more than two third of patients.[170] Compared to cardiac amyloidosis, long-axis function as measured by tissue Doppler imaging is often preserved in these patients.[171] Atrial fibrillation is common.[172] Endomyocardial biopsy shows mild to severe interstitial fibrosis and mild myocyte hypertrophy. The interstitial fibrosis found in this condition only rarely interferes with the shortening of myocardial fiber bundles but is sufficient to prevent ventricular dilation and thereby limit diastolic stretch.

The disease is characterized by increased mortality in adults, with 5- and 10-year survival rates of 64% and 37%, respectively.[172] LA dimension greater than 60 mm is associated with poor prognosis.[173] The disease carries a poor prognosis in children, with a median survival of 2 years.[173] The strongest predictor of survival in children with idiopathic restrictive cardiomyopathy is the extent of increase in LA-to-aortic ratio at presentation followed by pulmonary capillary wedge pressure and LV end-diastolic pressure. Symptoms at the time of presentation do not predict outcome.[174]

## DRUG-INDUCED RESTRICTIVE CARDIOMYOPATHY

Fibrous thickening of LV endocardium with features of restrictive cardiomyopathy occurs in anthracycline cardiotoxicity.[174] Ultrastructural abnormalities of the myocytes with myofibrillar loss and cytoplasmic vacuolation are seen in both anthracycline and chloroquine cardiotoxicity. Both restrictive features as well as concentric LV hypertrophy have been shown to be reversible

on chloroquine withdrawal.[175] Methysergide cardiotoxicity involves encasing of heart valves with fibrous tissue causing valvular regurgitation.

### POSTRADIATION CARDIOMYOPATHY

Radiation-induced heart disease, with its clinical manifestations, is becoming a growing problem. Its prevalence is increasing, keeping pace with the increased survival of many malignancies. The majority of patients with radiation induced heart disease are constituted by Hodgkin disease survivors, followed by non-Hodgkin disease, esophageal carcinoma, thymoma, lung cancer, breast cancer, and metastatic seminoma. Pericardial disease is the most well-known expression of radiation-induced heart disease, present clinically in 60% to 70% of patients receiving mediastinal irradiation.[176] The manifestations include acute pericarditis, pericardial effusion with or without tamponade, and constrictive pericarditis. Almost all patients who develop radiation-induced heart disease develop a pericardial effusion with relative sinus tachycardia 3 to 4 weeks postradiation, which may be transient. Six to 12 months after radiation, late damage is manifest as massive pericardial effusion followed by myocardial damage and coronary sclerosis depending on field and radiation dose. The mean time of presentation for constrictive pericarditis is 48 months. Follow-up of the irradiated patients by echocardiography, especially those who received more than 5000 rad to the heart area, is advisable.[177] Appropriate cardiac shielding and minimum possible radiation dose are preventive measures.

Late cardiac effects occur from mediastinal radiation.[178] Published observations on the effect of radiation of LV function differ. Gustavsson and colleagues[179] found a decrease of the LV shortening in 44% of patients and a decreased LV end-diastolic dimension in 28% of patients as well as evidence of diastolic dysfunction in 50% of patients. Others found decrease in LV systolic function in one third of patients and borderline value in another third;[180] still others[181] found no effect on LV function. The most conspicuous change is diffuse interstitial fibrosis seen chiefly in the RV, presumably because of the commonly used anterior radiation fields leading to congestive heart failure, and typically a restrictive cardiomyopathy. In an autopsy series, the endocardium was thickened from fibrous proliferation with some increase in elastic fibers mainly in the RV in 12 of 16 patients making the ventricular muscle less compliant and necessitating higher filling pressures to maintain stroke volume.[182] One series found cardiac involvement in 12 of 108 patients after irradiation for Hodgkin disease. Chronic pericardial disease and coronary artery disease were the most frequent manifestations.[183]

Coronary artery obstructive disease frequently involves ostial coronary segments and the left main coronary artery, and risk appears greater in those with known risk factors for coronary artery disease.[184] All patients undergoing chest irradiation require serial cardiac evaluation. Important risk factors for radiation-induced heart disease are previous chemotherapy, radiation exposure exceeding 4000 rad, and administration next to the heart and on the left side of the chest.[185] Doxorubicin treatment for acute lymphoblastic leukemia in children was found associated with chronic progressive cardiac dysfunction at 12-year follow-up and restrictive cardiomyopathy characterized by reduced cardiac mass, decreased LV dimension, and reduced wall thickness along with reduced LV systolic function. Although seen more commonly after high-dose doxorubicin treatment, cardiomyopathy was seen even after low-dose treatment.[186]

### OTHER CAUSES OF RESTRICTIVE CARDIOMYOPATHY

Connective tissue diseases such as scleroderma and systemic lupus erythematosus[187] and pseudoxanthoma elasticum[188] may produce features of restrictive cardiomyopathy. Calcified endocardial bands may be seen in those with restrictive cardiomyopathy due to pseudoxanthoma elasticum.[189]

## Differentiating between Restrictive Cardiomyopathy and Constrictive Pericarditis

The diagnosis of restrictive cardiomyopathy or constrictive pericarditis should be considered in any patient with a disproportionate degree of right heart failure in the setting of normal or mildly depressed LV systolic function and normal valvular function. Both constrictive pericarditis and restrictive cardiomyopathy are associated with increased intracardiac filling pressures; however, stiff pericardium versus stiff ventricle differentiate the two conditions and produce specific echocardiographic signs that help differentiate them.[190-193]

Pericardial calcification on chest radiography and thickened pericardium on computed tomography (CT) scan are diagnostic findings of constriction, although CT may have difficulty differentiating pericardial fluid from thickened pericardial tissue in some cases. MRI provides comprehensive images of the pericardium and is superior to both CT and echocardiography with respect to its ability to characterize pericardial effusions and pericardial masses. Although a pericardial thickness of 3 mm or more on transesophageal echocardiography is highly suggestive of constrictive pericarditis, echocardiography is not an accurate approach for evaluation of pericardial thickness.[194] In about 18% of patients with surgically proven constriction, pericardial thickness may not be increased on noninvasive imaging because of the patchy nature of pericardial involvement.[195] If pericardial thickness is normal on CT or MRI, biochemical tests to determine the etiology of restrictive cardiomyopathy such as serum/urine protein electrophoresis or iron studies should be performed, followed by endomyocardial biopsy. This will confirm the specific etiology of restrictive cardiomyopathy in about 39% of patients.[196]

The pathophysiologic feature that best separates constrictive pericarditis from restrictive cardiomyopathy is dissociation of intrathoracic and intracardiac pressure and increased ventricular interdependence (Table 28-4).[174,197,198] With constrictive pericarditis, negative chest pressure during inspiration is not transmitted to the cardiac chambers but is transmitted to the pulmonary venous bed. Thus, during inspiration, there is a higher decrease in pulmonary venous pressure relative to LV diastolic pressure, causing a decrease in transmitral gradient during the inspiratory phase.

In addition, ventricular interdependence is increased in constrictive pericarditis due to the constrained total cardiac volume and the lack of transmission of intrathoracic forces to the ventricular chambers. In contrast, ventricular interdependence is absent in restrictive cardiomyopathy because of involvement of the ventricular septum with a normal pericardium. In constrictive pericarditis, there is abrupt diastolic shift in the ventricular

**TABLE 28-4 Echocardiographic Features of Restrictive Cardiomyopathy and Constrictive Pericarditis**

| | *Restrictive Cardiomyopathy* | *Constrictive Pericarditis* |
|---|---|---|
| Pericardium | Normal | Thickened |
| Left ventricle | Small<br>May show systolic dysfunction<br>No septal bounce | Small<br>Usually intact, may be abnormal particularly after CABG or radiation<br>Septal bounce |
| Atria | Usually dilated | Usually nondilated |
| Mitral inflow | Increased E/A ratio, short DT<br>No significant respiratory variation of E velocity<br>Diastolic MR | Increased E/A ratio, short DT<br>>25% expiratory increase in E velocity<br>Diastolic MR |
| Tissue Doppler long velocities | Markedly reduced | Normal |
| Circumferential strain | Normal | Reduced |
| Peak radial strain LV base | Normal | Reduced |
| Net twist | Normal | Reduced |
| Basal longitudinal strain | Reduced | Normal |
| Apical untwisting velocities | Normal | Reduced |
| Pulmonary vein inflow | Decreased (0.5) S/D ratio<br>Prominent atrial reversal<br>No significant respiratory change | S/D ratio = 1<br>↓ in S and D* wave with inspiration |
| Tricuspid inflow | Mild respiratory variation | >25% inspiratory increase in E wave and TR velocity |
| Inferior vena cava | Dilated | Dilated |
| Hepatic veins | Blunted S/D ratio | Inspiration: minimal increase in S and D velocity; expiration: decreased diastolic flow and increase in reversals<br>>25% increase in atrial reversal in expiration compared to inspiration |
| Peak PA pressure | >40 mm Hg | <40 mm Hg |
| Color M-mode | Decreased Vp <45 cm/s | Normal or increased >100 cm/s |
| Mitral annular Doppler | Low velocity <8 cm/s | High velocity ≥8 cm/s |

*A*, Atrial transmitral filling velocity; *CABG*, coronary artery bypass graft; *D*, diastolic flow; *DT*, deceleration time; *E*, early transmitral filling velocity; *MR*, mitral regurgitation; *S*, systolic flow; *Vp*, propagation velocity.
*One study found significantly greater decrease of D wave only with respiration in constriction.[210]

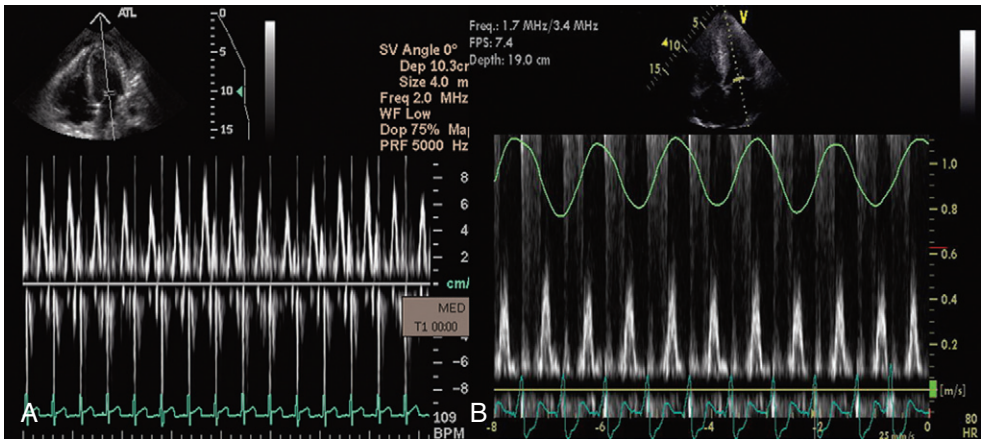



**Figure 28-15 Mitral inflow PW Doppler in a patient with constriction (A) and in a patient with cardiac amyloidosis (B).** Note marked respiratory changes with decrease in mitral inflow velocities during inspiration and increase during expiration in the patient with constriction and no significant respiratory change in the patient with cardiac amyloidosis.

septum toward the LV during inspiration and toward the RV in expiration.[199] Doppler echocardiography demonstrates exaggerated interventricular interdependence in constrictive pericarditis by showing marked respiratory variations in mitral (Fig. 28-15) and tricuspid flow Doppler. Characteristic respiratory variations in Doppler flow velocities in patients with constriction, not seen in patients with restriction, include a greater than 25% expiratory increase in mitral E velocity and an expiratory decrease in hepatic vein diastolic flow velocity, along with a greater than 25% increase in hepatic vein atrial reversal compared with inspiration; greater respiratory variation in pulmonary venous flows; and a pulmonary venous systolic flow velocity lower than diastolic velocity throughout respiration[200,201] (Fig. 28-16).

In some patients who have been aggressively diuresed, volume loading helps to bring out the specific features of constrictive pericarditis.[202] Alternatively, preload reduction helps to bring out the respiratory variation in volume-overloaded patients.[203] In some patients, there may be features of mixed restrictive cardiomyopathy and constrictive pericarditis, such as those with active myocarditis or with postradiation or other forms of cardiomyopathy. In patients with clinical as well as Doppler echocardiographic features of restrictive cardiomyopathy, constriction still must be excluded.

Recent observations using 2D speckle tracking have shown that deformation of the LV is constrained in the circumferential direction in constrictive pericarditis and in the longitudinal direction in restrictive cardiomyopathy.[204] Longitudinal tissue

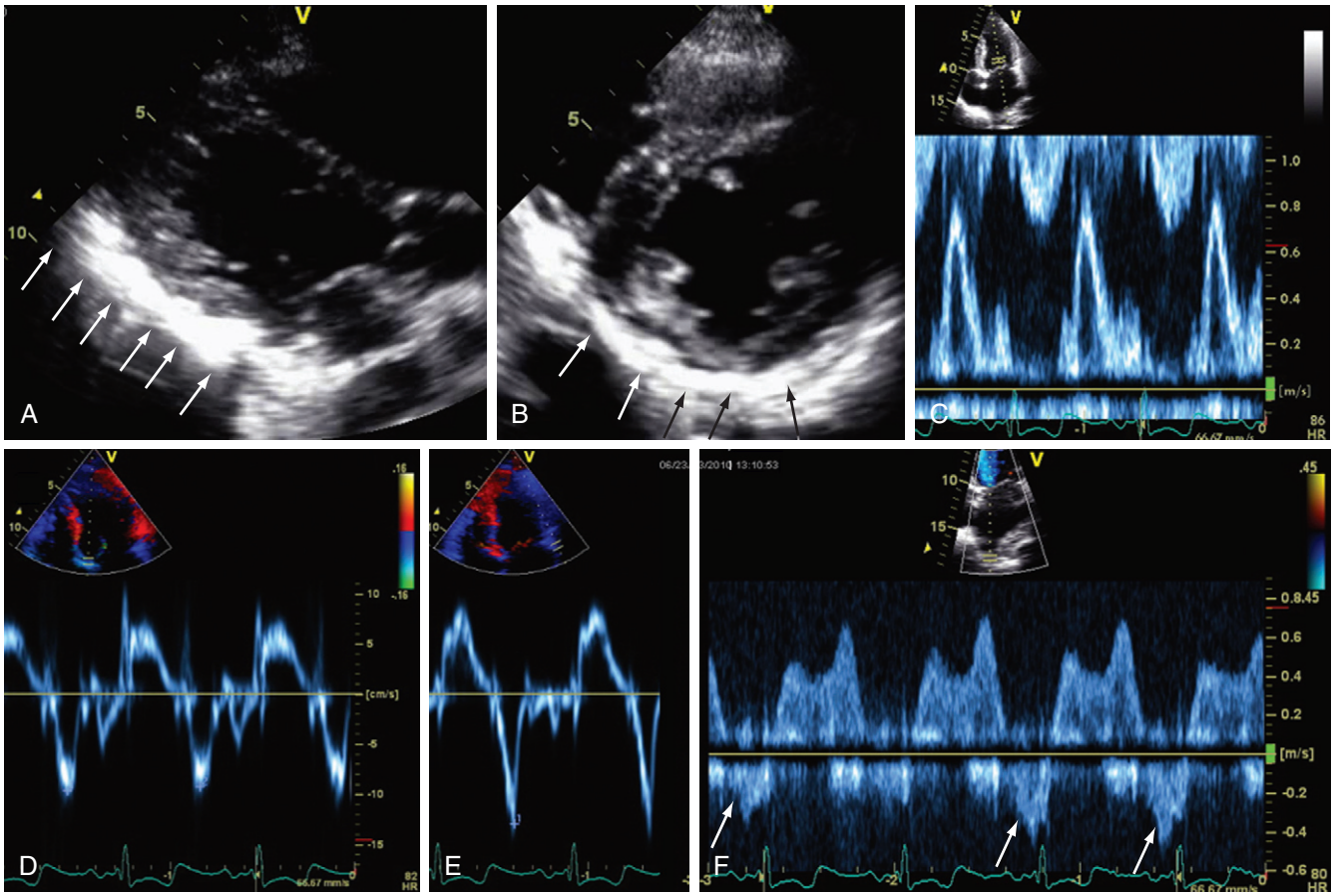



**Figure 28-16 Doppler and 2D imaging findings in constrictive pericarditis.** Parasternal long-axis (**A**) and short-axis (**B**) views showing pericardial calcification posterior to LV (*arrows*). Mitral inflow shows a higher E than A velocity with a steep deceleration slope (**C**) but tissue Doppler velocities of the septal (**D**) and lateral (**E**) mitral annulus are normal. Phasic increase in pulmonary vein flow reversal in expiration in **F** (*white arrows*). S:D reversal often seen in constriction is also shown.

Doppler velocity (E′) of 5 cm/s had 92% sensitivity and 90% specificity, peak untwisting velocity (Er) of −50°/s had 57% sensitivity and 95% specificity, and net LV twist of 10° had 83% sensitivity and 84% specificity in differentiating constrictive pericarditis from restrictive cardiomyopathy. The area under the receiver-operating characteristic curve was significantly higher for early diastolic longitudinal velocities as compared with early diastolic untwisting velocities ($P = 0.01$). Mean tissue Doppler velocities (averaged from the four basal LV walls) of greater than 5 cm/s distinguished all patients with constriction versus restriction, whereas overlap was noted for brain natriuretic peptide and basal septal PW TDI velocity.[205]

Early diastolic mitral annular velocity (E′) by tissue Doppler echocardiography can be used to differentiate constrictive pericarditis from restrictive cardiomyopathy.[35,206] Patients with constrictive pericarditis have a significantly higher E′ at septal annulus than those with primary restrictive cardiomyopathy or cardiac amyloidosis (12.3 vs. 5.1 cm/s, $P < 0.001$) (see Fig. 28-16). Specifically, an E′ cutoff value of 8 cm/s or greater is able to distinguish the two conditions with a high sensitivity and specificity (95% sensitivity and 96% specificity). Even in patients who do not manifest the diagnostic sign of greater than 25% variation of mitral inflow with inspiration in patients with constriction, mitral annular E′ velocity remains normal and helps differentiate constrictive pericarditis from restrictive cardiomyopathy.[207] Occasionally, when pericardial calcification and tethering involves the mitral annulus, E′ velocities may be reduced in constrictive pericarditis.[208] A recent study[209] found the utility of S′ velocity of septal and lateral mitral annulus in differentiating constriction versus restriction.[209] Receiver operating characteristic (ROC) analysis demonstrated an area under the curve of 0.889 (S′ septal), 0.823 (S′ lateral), 0.974 (E′ septal), and 0.915 (E′ lateral) for the differentiation of restrictive cardiomyopathy and constrictive pericarditis with a cutoff value of less than 8 cm/s.

Similar to an increased E′ mitral annular velocity, preserved diastolic function in patients with constriction is manifest by a rapid propagation slope on color M-mode of greater than 100 cm/s.[210] The myocardial velocity gradient, which is reduced in patients with restriction, also differentiates restrictive cardiomyopathy from constrictive pericarditis.[211] Even if mitral and pulmonary vein inflow are not diagnostic, TDI and color M-mode are able to correctly differentiate patients with constrictive pericarditis from those with restrictive cardiomyopathy.[207]

However, echocardiographic findings are not always diagnostic, and catheterization is often necessary for performing hemodynamic evaluation and obtaining endomyocardial biopsy specimens. The following three criteria have been proposed to differentiate the two conditions: (1) Equalization (less than 5 mm Hg difference between RV end-diastolic pressure and LV end-diastolic pressure) favors constriction.[212]

**TABLE 28-5 Echocardiographic Predictors of Outcome in Restrictive Cardiomyopathy**

| *Type of CMP* | *Study Findings* | *2D Echo Predictors* | *Other Features* | *References* |
|---|---|---|---|---|
| Amyloidosis | 132 patients with biopsy-proven systemic amyloidosis, median survival 1.1 years | Increased LV wall thickness >15 mm and reduced LV systolic function predicted decreased survival | | 78 |
| | 63 patients with biopsy-proven systemic amyloidosis, 32 deaths at a median 18 ± 12 month follow-up (78% cardiac deaths) | Shortened deceleration time of mitral inflow (<150 ms) and increased E/A ratio 2.1 were predictors of cardiac mortality | LV wall thickness and fractional shortening were not predictors of overall survival | 79 |
| | 45 patients with biopsy-proven systemic amyloidosis | Mitral inflow deceleration time, EF, and TEI on univariate analysis, MPI index on multivariate analysis. Median TEI index >0.77 vs ≤0.77 predictor of all cause mortality and cardiac death. | | 80 |
| | 208 patients with biopsy-proven primary amyloidosis, 32 cardiac deaths at 307 ± 156 days | Cycle-dependent variation of myocardial integrated backscatter (CV-IB) of the posterior LV wall is the strongest predictor of cardiovascular mortality. | Fractional shortening, mean LV wall thickness, and MPI index were not a predictor of cardiac death | 81 |
| | 37 patients with AL amyloidosis Patients with a dilated right ventricle (LV/RV area ratio <2) had a shorter median survival (4 months) compared with patients with an area ratio >2 | Right ventricular dilation | | 82 |
| Sarcoidosis | | LV dilation, reduced LVEF | | 116 |
| Idiopathic restrictive CMP | 94 patients with IRCMP. 5-year survival 64% | LA dimension >60 mm predictor of decreased survival | | 172 |

*CMP*, Cardiomyopathy; *DB*, decibel; *DT*, deceleration time; *EF*, ejection fraction; *IRCMP*, idiopathic restrictive cardiomyopathy; *LVEF*, left ventricular ejection fraction; *MPI*, myocardial performance index.

(2) Constriction is more often associated with modest elevations of RV systolic pressure (less than 50 mm Hg), whereas in restriction, RV systolic pressures frequently exceed 50 mm Hg.[213] (3) Constriction is associated with RV end-diastolic pressure exceeding one third the RV systolic pressure, whereas in restriction the ratio is characteristically less than one third. In one study that evaluated the value of these hemodynamic criteria,[214] the predictive accuracies of difference between right and LV end-diastolic pressures, RV systolic pressure, and the ratio of RV end-diastolic pressure to RV systolic pressure were 85%, 70%, and 76%, respectively.

## Echocardiography in Clinical Decision Making in Restrictive Cardiomyopathy

Echocardiography provides diagnostic and prognostic information in patients with restrictive cardiomyopathy (Table 28-5). Restrictive ventricular filling in the presence of mildly decreased or normal systolic function is strongly indicative of restrictive cardiomyopathy, particularly when associated with diffuse thickening of LV and RV walls (in the infiltrative forms and in the storage diseases) and biatrial enlargement. Echocardiography, however, is of limited value in determining the cause of restrictive cardiomyopathy.[215]

## KEY POINTS

- The primary abnormality in restrictive cardiomyopathy is diastolic dysfunction with increases in LV end-diastolic and LA filling pressures. LV systolic function is usually preserved until late stages of the disease. Patients may be asymptomatic in early stages and present with signs and symptoms of right heart failure, left heart failure, or low cardiac output.
- 2D, M-mode, and Doppler echocardiography remain the most useful clinical tools for diagnosis. Nuclear imaging is an adjunctive diagnostic modality. MRI shows specific patterns on T1- and T2-weighted images and shows specific late gadolinium enhancement patterns in infiltrative cardiomyopathies. Tissue diagnosis remains the gold standard for the diagnosis of infiltrative cardiomyopathies but carries a low sensitivity.
- Small LV cavity size with increased wall thickness, valvular, and interatrial septal thickening along with a granular, sparkling texture on echocardiography, and low voltage on electrocardiography are hallmarks of cardiac amyloidosis.
- Doppler signs of restrictive cardiomyopathy (in the absence of known coronary disease or hypertension) include: Mitral inflow E/A ratio greater than 2, short deceleration time (less than 150 ms), decreased pulmonary vein S/D ratio with blunted S, a large D wave with prominent atrial reversal, TDI E′ <8 cm/s, slow M-mode propagation, and increased pulmonary systolic pressure and RA pressure.
- A combination of diagnostic tests is often needed to differentiate restrictive cardiomyopathy from constrictive pericarditis. Tissue-Doppler imaging may help in differentiating between the two conditions.
- Prognosis of patients with restrictive cardiomyopathy is highly variable depending on underlying etiology.
- Restrictive cardiomyopathy should be considered in a patient post chest radiation who presents with heart failure of unknown etiology.
- Atrial arrhythmias and marked biatrial enlargement, in the absence of valvular and myocardial disease, are the most common presenting features in idiopathic restrictive cardiomyopathy in the elderly.
- Drug-induced cardiomyopathy and infiltrative cardiomyopathy in several storage disorders may be reversible on withdrawal of the culprit agent or by enzyme replacement therapy.

## REFERENCES


1. Bursi F, Weston SA, Redfield MM, et al: Systolic and diastolic heart failure in the community. *JAMA* 296:2209-2216, 2006.
2. Yu CM, Lin H, Yang H, et al: Progression of systolic abnormalities in patients with "isolated" diastolic heart failure and diastolic dysfunction. *Circulation* 105:1195-1201, 2002.
3. Richardson P, McKenna W, Bristow M, et al: Report of the 1995 World Health organization/International Society and Federation of Cardiology Task Force on the Definition and Classification of Cardiomyopathies. *Circulation* 93: 841-842, 1996.
4. Benotti JR, Grossman W, Cohn PF: Clinical profile of restrictive cardiomyopathy. *Circulation* 61:1206-1212, 1980.
5. Guadalajara J, Vera-Delgado A, Gaspar-Hernandez J, et al: Echocardiographic aspects of restrictive cardiomyopathy: their relation with pathophysiology. *Echocardiography* 15: 297-311, 1998.
6. Paulus WJ, Tschope C, Sanderson JE, et al: How to diagnose diastolic heart failure: a consensus statement on the diagnosis of heart failure with normal left ventricular ejection fraction by the Heart Failure and Echocardiography Associations of the European Society of Cardiology. *Eur Heart J* 28:2539-2550, 2007.
7. Leong DP, De Pasquale CG, Selvanayagam JB: Heart failure with normal ejection fraction: the complementary roles of echocardiography and CMR imaging. *J Am Coll Cardiol Imaging* 3:409-420, 2010.
8. Plehn JF, Southworth J, Cornwell GG, III. Brief report: atrial systolic failure in primary amyloidosis. *N Engl J Med* 327:1570-1573, 1992.
9. Tam JW, Shaikh N, Sutherland E: Echocardiographic assessment of patients with hypertrophic and restrictive cardiomyopathy: imaging and echocardiography. *Curr Opin Cardiol* 17:470-477, 2002.
10. Thamilarasan M, Klein AL: Restrictive cardiomyopathy: diagnostic and prognostic implications. In Otto CM, editor: *The practice of clinical echocardiography*, ed 2, Philadelphia, 2002, WB Saunders, pp 613-638.
11. Mor-Avi V, Sugeng L, Weinert L, et al: Fast measurement of left ventricular mass with real-time three-dimensional echocardiography: comparison with magnetic resonance imaging. *Circulation* 110:1814-1818, 2004.
12. Jenkins C, Moir S, Chan J, Rakhit D, et al: Left ventricular volume measurement with echocardiography: a comparison of left ventricular opacification, three-dimensional echocardiography, or both with magnetic resonance imaging. *Eur Heart J* 30:98-106, 2009.
13. Soliman OI, Kirschbaum SW, van Dalen BM, et al: Accuracy and reproducibility of quantitation of left ventricular function by real-time three dimensional echocardiography versus cardiac magnetic resonance. *Am J Cardiol* 102:778-783, 2008.
14. Sugeng L, Mor-Avi V, Weinert L, et al: Quantitative assessment of left ventricular size and function: side-by-side comparison of real-time three-dimensional echocardiography and computed tomography with magnetic resonance reference. *Circulation* 114:654-661, 2006.
15. Jenkins C, Bricknell K, Marwick TH: Use of real-time three-dimensional echocardiography to measure left atrial volume: comparison with other echocardiographic techniques. *J Am Soc Echocardiogr* 18:991-997, 2005.
16. Leitman M, Lysyansky P, Sidenko S, et al: Two-dimensional strain: a novel software for real-time quantitative echocardiographic assessment of myocardial function. *J Am Soc Echocardiogr* 17:1021-1029, 2004.
17. Ernande L, Rietzschel ER, Bergerot C, et al: Impaired myocardial radial function in asymptomatic patients with type 2 diabetes mellitus: a speckle-tracking imaging study. *J Am Soc Echocardiogr* 23:1266-1272, 2010.
18. Mignot A, Donal E, Zaroui A, et al: Global longitudinal strain as a major predictor of cardiac events in patients with depressed left ventricular function: a multicenter study. *J Am Soc Echocardiogr* 23:1019-1024, 2010.
19. Wang J, Khoury DS, Yue Y, et al: Preserved left ventricular twist and circumferential deformation, but depressed longitudinal and radial deformation in patients with diastolic heart failure. *Eur Heart J* 29:1283-1289, 2008.
20. Nguyen JS, Lakkis NM, Bobek J, et al: Systolic and diastolic myocardial mechanics in patients with cardiac disease and preserved ejection fraction: impact of left ventricular filling pressure. *J Am Soc Echocardiogr* 23:1273-1280, 2010.
21. Kosmala W, Plaksej R, Strotmann JM, et al: Progression of left ventricular functional abnormalities in hypertensive patients with heart failure: an ultrasonic two-dimensional speckle tracking study. *J Am Soc Echocardiogr* 21:1309-1317, 2008.
22. Oh J, Appleton C, Hatle L, et al: the noninvasive assessment of left ventricular diastolic function with two-dimensional and Doppler echocardiography. *J Am Soc Echocardiogr* 10:246-270, 1997.
23. Naqvi TZ: Diastolic function assessment by newer methods of Doppler echocardiography. *Rev Cardiovasc Med* 4:81-99, 2003.
24. Rubinshtein R, Glockner JF, Feng D, et al: Comparison of magnetic resonance imaging versus Doppler echocardiography for the evaluation of left ventricular diastolic function in patients with cardiac amyloidosis. *Am J Cardiol* 103:718-723, 2009.
25. Courtois M, Vered Z, Barzilai B, et al: The transmitral pressure-flow velocity relation: effect of abrupt preload reduction. *Circulation* 78:1459-1468, 1988.
26. Appleton CP, Gonzalez MS, Basnight MA: Relationship of left atrial pressure and pulmonary venous flow velocities: importance of baseline mitral and pulmonary venous flow patterns studied in lightly sedated dogs. *J Am Soc Echocardiogr* 7:264-275, 1994.
27. Nishimura RA, Abel MD, Hatle LK, Tajik AJ: Relation of pulmonary vein to mitral vein flow velocities by transesophageal Doppler echocardiography: effect of different loading conditions. *Circulation* 81:1488-1497, 1990.
28. Keren G, Sherez J, Megidish R, et al: Pulmonary venous flow pattern—its relationship to cardiac dynamics: a pulsed Doppler echocardiographic study. *Circulation* 71:1105-1112, 1985.
29. Nagueh SF, Middleton KJ, Kopelen HA, et al: Doppler tissue imaging: a noninvasive technique for evaluation of left ventricular relaxation and estimation of filling pressures. *J Am Coll Cardiol* 30:1527-1533, 1997.
30. Farias CA, Rodriguez L, Garcia MJ, et al: Assessment of diastolic function by tissue Doppler echocardiography: comparison with standard transmitral and pulmonary venous flow. *J Am Soc Echocardiogr* 12:609-617, 1999.
31. Naqvi TZ, Neyman G, Broydi A, Siegel RJ: Comparison of myocardial tissue Doppler with conventional transmitral flow Doppler in left ventricular hypertrophy. *J Am Soc Echocardiogr* 14:1153-1160, 2001.
32. Garcia MJ, Rodriguez L, Ares M, et al: Differentiation of constrictive pericarditis from restrictive cardiomyopathy: assessment of left ventricular diastolic velocities in longitudinal axis by Doppler tissue imaging. *J Am Coll Cardiol* 27:108-114, 1996.
33. Meluzin J, Spinarova L, Bakala J, et al: Pulsed Doppler tissue imaging of the velocity of tricuspid annular systolic motion; a new, rapid, and non-invasive method of evaluating right ventricular systolic function. *Eur Heart J* 22:340-348, 2001.
34. Rudski LG, Lai WW, Afilalo J, et al: Guidelines for the echocardiographic assessment of the right heart in adults: a report from the American Society of Echocardiography. *J Am Soc Echocardiogr* 23:685-713, 2010.
35. Garcia M, Thomas J, Klein A: New Doppler echocardiographic applications for the study of diastolic function. *J Am Coll Cardiol* 32:865-875, 1998.
36. Choudhury L, Mahrholdt H, Wagner A, et al: Myocardial scarring in asymptomatic or mildly symptomatic patients with hypertrophic cardiomyopathy. *J Am Coll Cardiol* 40:2156-2164, 2002.
37. Moon JC, Sachdev B, Elkington AG, et al: Gadolinium enhanced cardiovascular magnetic resonance in Anderson-Fabry disease. Evidence for a disease specific abnormality of the myocardial interstitium. *Eur Heart J* 24:2151-2155, 2003.
38. Maceira AM, Joshi J, Prasad SK, et al: Cardiovascular magnetic resonance in cardiac amyloidosis. *Circulation* 111;186-193, 2005.
39. Anderson LJ, Holden S, Davis B, et al: Cardiovascular T2-star (T2*) magnetic resonance for the early diagnosis of myocardial iron overload. *Eur Heart J* 22:2171-2179, 2001.
40. Klein AL, Oh JK, Miller FA, et al: Two-dimensional and Doppler echocardiographic assessment of infiltrative cardiomyopathy. *J Am Soc Echocardiogr* 1(1):48-59, 1988 Jan-Feb. Review.
41. Branea I, Stanciu L, Tomescu M, et al: The value of echocardiography in the early diagnosis of myocardial impairment due to connective tissue diseases. *Med Interne* 24:197-205, 1986.
42. Schurle DR, Evans RW, Cohlmia JB, Lin J: Restrictive cardiomyopathy in scleroderma. *J Kans Med Soc* 85:49-50, 1984.
43. Pellikka PA, Tajik AJ, Khandheria BK, et al: Carcinoid heart disease: clinical and echocardiographic spectrum in 74 patients. *Circulation* 87:1188-1196, 1993.
44. Roberts WC, Glancy DL, DeVita VT Jr: Heart in malignant lymphoma (Hodgkin's disease, lymphosarcoma, reticulum cell sarcoma and mycosis fungoides): a study of 196 autopsy cases. *Am J Cardiol* 22:85-107, 1968.
45. Benson MD: Amyloidosis. In Scriver CR, editor: *The metabolic and molecular bases of inherited disease, vol 1*, ed 8, New York, 2001, McGraw-Hill, pp 5345-5348.
46. Falk RH, Comenzo RL, Skinner M: The systemic amyloidoses. *N Engl J Med* 337:898-909, 1997.

47. Kyle RA, Gertz MA: Primary systemic amyloidosis: clinical and laboratory features in 474 cases. *Semin Hematol* 32:45-59, 1995.
48. Gertz MA, Kyle RA, Thibodeau SN: Familial amyloidosis: a study of 52 North American-born patients examined during a 30-year period. *Mayo Clin Proc* 67:428-440, 1992.
49. Dubrey SW, Davidoff R, Skinner M, et al: Progression of ventricular wall thickening after liver transplantation for familial amyloidosis. *Transplantation* 64:74-80, 1997.
50. Westermark P, Sletten K, Johansson B, Cornwell GG, 3rd. Fibril in senile systemic amyloidosis is derived from normal transthyretin. *Proc Natl Acad Sci U S A* 87:2843-2845, 1990.
51. Olson LJ, Gertz MA, Edwards WD, et al: Senile cardiac amyloidosis with myocardial dysfunction. Diagnosis by endomyocardial biopsy and immunohistochemistry. *N Engl J Med* 317:738-742, 1987.
52. Kyle RA, Spittell PC, Gertz MA, et al: The premortem recognition of systemic senile amyloidosis with cardiac involvement. *Am J Med* 101:395-400, 1996.
53. Kawamura S, Takahashi M, Ishihara T, Uchino F: Incidence and distribution of isolated atrial amyloid: histologic and immunohistochemical studies of 100 aging hearts. *Pathol Int* 45:335-342, 1995.
54. Hofer JF, Wimmer G: Severe heart failure from light chain cardiomyopathy (cardiac amyloidosis). *Z Kardiol* 92:90-95, 2003.
55. Reisinger J, Dubrey SW, Lavalley M, et al: Electrophysiologic abnormalities in AL (primary) amyloidosis with cardiac involvement. *J Am Coll Cardiol* 30:1046-1051, 1997.
56. Dingli D, Utz JP, Gertz MA: Pulmonary hypertension in patients with amyloidosis. *Chest* 120:1735-1738, 2001.
57. Neben-Wittich MA, Wittich CM, Mueller PS, et al: Obstructive intramural coronary amyloidosis and myocardial ischemia are common in primary amyloidosis. *Am J Med* 118:1287, 2005.
58. Falk R, Plehn J, Deering T, et al: Sensitivity and specificity of the echocardiographic features of cardiac amyloidosis. *Am J Cardiol* 59:418-422, 1987.
59. Klein AL, Hatle LK, Burstow DJ, et al: Doppler characterization of left ventricular diastolic function in cardiac amyloidosis. *J Am Coll Cardiol* 13:1017-1026, 1989.
60. Koyama J, Ray-Sequin PA, Falk RH: Longitudinal myocardial function assessed by tissue velocity, strain, and strain rate tissue Doppler echocardiography in patients with AL (primary) cardiac amyloidosis. *Circulation* 107:2446-2452, 2003.
61. Oki T, Tanaka H, Yamada H, et al: Diagnosis of cardiac amyloidosis based on the myocardial velocity profile in the hypertrophied left ventricular wall. *Am J Cardiol* 93:864, 2004.
62. Dubrey SW, Cha K, Simms RW, et al: Electrocardiography and Doppler echocardiography in secondary (AA) amyloidosis. *Am J Cardiol* 77:313-315, 1996.
63. Modesto KM, Dispenzieri A, Cauduro SA, et al: Left atrial myopathy in cardiac amyloidosis: implications of novel echocardiographic techniques. *Eur Heart J* 26:173-179, 2004.
64. Falk RH, Rubinow A, Cohen AS: Cardiac arrhythmias in systemic amyloidosis: correlation with echocardiographic abnormalities. *J Am Coll Cardiol* 3:107-113, 1984.
65. Kyle RA, Greipp PR: Amyloidosis: clinical and laboratory features in 229 cases. *Mayo Clin Proc* 58:665-683, 1983.
66. Arbustini E, Verga L, Concardi M, et al: Electron and immuno-electron microscopy of abdominal fat identifies and characterizes amyloid fibrils in suspected cardiac amyloidosis. *Amyloid* 9:108-114, 2002.
67. Lachmann HJ, Gallimore R, Gillmore JD, et al: Outcome in systemic AL amyloidosis in relation to changes in concentration of circulating free immunoglobulin light chains following chemotherapy. *Br J Haematol* 122:78-84, 2003.
68. Palladini G, Campana C, Klersy C, et al: Serum N-terminal pro-brain natriuretic peptide is a sensitive marker of myocardial dysfunction in AL amyloidosis. *Circulation* 107:2440-2445, 2003.
69. Arbustini E, Verga L, Concardi M, et al: Electron and immuno-electron microscopy of abdominal fat identifies and characterizes amyloid fibrils in suspected cardiac amyloidosis. *Amyloid* 9:108-114, 2002.
70. Picken MM: Amyloidosis—where are we now and where are we heading? *Arch Pathol Lab Med* 134:545-551, 2010.
71. Falk RH, Rubinow A, Cohen AS: Cardiac arrhythmias in systemic amyloidosis: correlation with echocardiographic abnormalities. *J Am Coll Cardiol* 3:107-113, 1984.
72. Gertz MA, Lacy MQ, Dispenzieri A: Amyloidosis; recognition, confirmation, prognosis, and therapy. *Mayo Clin Proc* 74;490-494, 1999.
73. Perugini E, Guidalotti PL, Salvi F, et al: Noninvasive etiologic diagnosis of cardiac amyloidosis using 99mTc-3,3-diphosphono-1,2-propanodicarboxylic acid scintigraphy. *J Am Coll Cardiol* 46:1076-1084, 2005.
74. Tanaka M, Hongo M, Kinoshita O, et al: Iodine-123 metaiodobenzylguanidine scintigraphic assessment of myocardial sympathetic innervation in patients with familial amyloid polyneuropathy. *J Am Coll Cardiol* 29:168-174, 1997.
75. Hawkins PN, Lavender JP, Pepys MB: Evaluation of systemic amyloidosis by scintigraphy with 123I-labeled serum amyloid P component. *N Engl J Med* 23:508-513, 1990.
76. Syed IS, Glockner JF, Feng D, et al: Role of cardiac magnetic resonance imaging in the detection of cardiac amyloidosis. *JACC Cardiovasc Imaging* 3:155-164, 2010.
77. Kwong RY, Falk RH: Cardiovascular Magnetic Resonance in Cardiac Amyloidosis. *Circulation* 111:122-124, 2005.
78. Cueto-Garcia L, Reeder GS, Kyle RA, et al: Echocardiographic findings in systemic amyloidosis: spectrum of cardiac involvement and relation to survival. *J Am Coll Cardiol* 6:737-743, 1985.
79. Klein AL, Hatle LK, Taliercio CP, et al: Prognostic significance of Doppler measures of diastolic function in cardiac amyloidosis: a Doppler echocardiography study. *Circulation* 83:808-816, 1991.
80. Tei C, Dujardin KS, Hodge DO, et al: Doppler index combining systolic and diastolic myocardial performance: clinical value in cardiac amyloidosis. *J Am Coll Cardiol* 28:658-664, 1996.
81. Koyama J, Ray-Sequin PA, Falk RH: Prognostic significance of ultrasound myocardial tissue characterization in patients with cardiac amyloidosis. *Circulation* 106:556-561, 2002.
82. Patel AR, Dubrey SW, Mendes LA, et al: Right ventricular dilation in primary amyloidosis: an independent predictor of survival. *Am J Cardiol* 80:486-492, 1997.
83. Maceira AM, Prasad SK, Hawkins PN, et al: Cardiovascular magnetic resonance and prognosis in cardiac amyloidosis. *J Cardiovasc Magn Res* 10:54-59, 2008.
84. Arbustini E, Merlini G, Gavazzi A, et al: Cardiac immunocyte-derived (AL) amyloidosis: an endomyocardial biopsy study in 11 patients. *Am Heart J* 130:528-536, 1995.
85. Chamarthi B, Dubrey SW, Cha K, et al: Features and prognosis of exertional syncope in light-chain associated AL cardiac amyloidosis. *Am J Cardiol* 80:1242-1245, 1997.
86. Dubrey SW, Cha K, Anderson J, et al: The clinical features of immunoglobulin light-chain (L) amyloidosis with heart involvement. *Q J Med* 91:141-157, 1998.
87. Reyners AK, Hazenberg BP, Reitsma WD, et al: Heart rate variability as a predictor of mortality in patients with AA and AL amyloidosis. *Eur Heart J* 23:157, 2002.
88. Moyssakis I, Triposkiadis F, Rallidid L, et al: Echocardiographic features of primary, secondary and familial amyloidosis. *Eur J Clin Invest* 29:484-489, 1999.
89. Comenzo RL, Vosburgh E, Falk RH, et al: Dose-intensive melphalan with blood stem-cell support for the treatment of AL (amyloid light-chain) amyloidosis: survival and responses in 25 patients. *Blood* 91:3662-3670, 1998.
90. Comenzo RL, Gertz MA: Autologous stem cell transplantation for primary systemic amyloidosis. *Blood* 99:4276-4282, 2002.
91. Moreau P, Leblond V, Bourquelot P, et al: Prognostic factors for survival and response after high-dose therapy and autologous stem cell transplantation in systemic AL amyloidosis: a report on 21 patients. *Br J Haematol* 101:766-769, 1998.
92. Niederau C, Strohmeyer G, Stremmel W: Epidemiology clinical spectrum and prognosis of hemochromatosis. *Adv Exp Med Biol* 356:293-302, 1994.
93. Cutler DJ, Isner JM, Bracey AW, et al: Hemochromatosis heart disease: an unemphasized cause of potentiallv reversible restrictive cardiomyopathy. *Am J Med* 60:923-928, 1980.
94. Barriales Alvarez V, Simarro Garcia C, Suarez Suarez E, et al: Restrictive cardiac involvement in a patient with dyserythropoietic anemia and secondary hemochromatosis. *Rev Esp Cardiol* 49:618-620, 1996.
95. Borer JS, Henry WL, Epstein SE: Echocardiographic observations in pabents with systemic infiltrative disease involving the heart. *Am J Cardiol* 39:184-188, 1977.
96. Olson LJ, Baldus WP, Tajik AJ: Echocardiographic features of idiopathic hemochromatosis. *Am J Cardiol* 60:885-889, 1987.
97. Lattanzi F, Bellotti P, Picano E, et al: Quantitative ultrasonic analysis of myocardium in patients with thalassemia major and iron overload. *Circulation* 87:748-754, 1993.
98. Jambrik Z, Derchi G, Picano E, et al: Lack of prognostic value of normalized integrated backscatter analysis of myocardium in patients with thalassemia major: a long-term follow-up study. *Echocardiography* 22:239-244, 2005.
99. Davidsen ES, Hervig T, Omvik P, Gerdts E: Left ventricular long-axis function in treated haemochromatosis. *Int J Cardiac Imaging* 25:237-247, 2009.
100. Candell-Riera J, Lu L, Se L, et al: Cardiac hemochromatosis: beneficial effects of iron removal therapy; an echocardiographic study. *Am J Cardiol* 52:824-829, 1983.

101. Cecchetti G, Binda A, Piperno A, et al: Cardiac alterations in 36 consecutive patients with idiopathic haemochromatosis: polygraphic and echocardiographic evaluation. *European Heart Journal* 12:224-230, 1991.
102. Jacobs A, Miller F, Worwood M, et al: Ferritin in the serum of normal subjects with iron deficiency and iron overload. *Br Med J* 206-211, 1972.
103. Crosby WH: Serum ferritin fails to indicate hemochromatosis: nothing gold cab stay. *N Engl J Med* 294:333-334, 1976.
104. Brittenham GM, Badman DG: Noninvasive measurement of iron: report of a NIDDK workshop. *Blood* 101:15-19, 2003.
105. Garcia-Pascual J, Gonzalez-Gallarza R, Jimenez M, et al:: Loffler's syndrome: pulmonary vein and transmitral Doppler flow analysis by transesophageal echocardiography-report of a case. *J Am Soc Echocardiogr* 13:690-692, 2000.
106. Hassan WM, Fawzy ME, Al Helaly S, et al: Pitfalls in diagnosis and clinical, echocardiographic, and hemodynamic findings in endomyocardial fibrosis. A 25-year experience. *Chest* 128:3985-3992, 2005.
107. Namboodiri KKN, Bohora S: Clenched fist appearance in endomyocardial fibrosis. *Heart* 92:720, 2006.
108. Pieroni M, Chimenti C, Frustaci A: Hissing snake left ventricle thrombotic phase of hypereosinophilic endomyocardial disease. *Eur Heart J* 27:778, 2006.
109. Berensztein C, Pineiro D, Marcotegui M, et al: Usefulness of echocardiography and Doppler echocardiography in endomyocardial fibrosis. *J Am Soc Echocardiogr* 13:385-392, 2000.
110. Zientek DM, King DL, Dewan SJ, et al: Hypereosinophilic syndrome with rapid progression of cardiac involvement and early echocardiographic abnormalities. *Am Heart J* 130:1295-1298, 1995.
111. Sato Y, Taniguchi R, Yamada T, et al: Measurement of serum concentrations of cardiac troponin T in patients with hypereosinophilic syndrome: a sensitive non-invasive marker of cardiac disorder. *Intern Med* 39:350, 2000.
112. Gleich GJ, Leiferman KM: The hypereosinophilic syndromes: current concepts and treatments. *Br J Haematol* 145:271-285, 2009.
113. Silverman KJ, Hutchins GM, Bulkley BH: Cardiac sarcoid: a clinicopathologic study of 84 unselected patients with systemic sarcoidosis. *Circulation* 58:1204-1211, 1978.
114. Uemura A, Morimoto S, Hiramitsu S, et al: Histologic diagnostic rate of cardiac sarcoidosis: evaluation endomyocardial biopsies. *Am Heart J* 138:299-302, 1999.
115. Angomachalelis N, Hourzamanis A: Diagnostic significance of two-dimensional echocardiography in sarcoid infiltrative cardiomyopathy. In Grassi C, Rizzato G, Pozzi E, editors: *Sarcoidosis and other granulomatous disorders*. Amsterdam, 1988, Elsevier Science, pp 503-504.
116. Burstow DJ, Tajik AJ, Bailey KR, et al: Two-dimensional echocardiographic findings in systemic sarcoidosis. *Am J Cardiol* 63:478-482, 1989.
117. Ohmori F, Tachibana T: Two-dimensional echocardiographic assessment of systemic sarcoidosis. *Sarcoidosis* 9(Suppl 1):241-244, 1992.
118. Iwai K, Sekiguti M, Hosoda Y, et al: Racial difference in cardiac sarcoidosis incidence observed at autopsy. *Sarcoidosis* 11:26-31, 1994.
119. Focardi M, Picchi A, Nikiforakis N, et al: Assessment of cardiac involvement in sarcoidosis by echocardiography. *Rheumatol Int* 29:1051-1055, 2009.
120. Rubinstein I, Fisman EZ, Rosenblum Y, et al: Left-ventricular exercise echocardiographic abnormalities in patients with sarcoidosis without ischemic heart disease. *Isr J Med Sci* 22:865-872, 1986.
121. Fahy GJ, Marwick T, McCreery CJ, et al: Doppler echocardiographic detection of left ventricular diastolic dysfunction in patients with pulmonary sarcoidosis. *Chest* 109:62-66, 1996.
122. Koplan BA, Soejima K, Baughman K, et al: Refractory ventricular tachycardia secondary to cardiac sarcoid: electrophysiologic characteristics, mapping, and ablation. *Heart Rhythm* 3:924-929, 2006.
123. Furushima H, Chinushi M, Sugiura H, et al: Ventricular tachyarrhythmia associated with cardiac sarcoidosis: its mechanism and outcome. *Clin Cardiol* 27:217-222, 2004.
124. Ratner SJ, Fenoglio JJ Jr, Ursell PC: Utility of endomyocardial biopsy in the diagnosis of cardiac sarcoidosis. *Chest* 90:528-533, 1986.
125. Valantine HA, Tazelaar HD, Macoviak J, et al: Cardiac sarcoidosis: Response to steroids and transplantation. *J Heart Transplant* 6:244-250, 1987.
126. Gregor P, Widimsky P, Sladkova T, et al: Echocardiography in sarcoidosis. *Jpn Heart J* 25:499-508, 1984.
127. Sekiguchi M, Yazaki Y, Isobe M, Hiroe M: Cardiac sarcoidosis: diagnostic, prognostic, and therapeutic considerations. *Cardiovasc Drugs Ther* 10:495-510, 1996.
128. Skold CM, Larsen FF, Rasmussen E, et al: Determination of cardiac involvement in sarcoidosis by magnetic resonance imaging and Doppler echocardiography. *J Intern Med* 252: 465-471, 2002.
129. Hourigan LA, Burstow DJ, Pohlner P, et al: Transesophageal echocardiographic abnormalities in a case of cardiac sarcoidosis. *J Am Soc Echocardiogr* 14:399-402, 2001.
130. Smedema JP, Snoep G, van Kroonenburgh MP, et al: The additional value of gadolinium-enhanced MRI to standard assessment for cardiac involvement in patients with pulmonary sarcoidosis. *Chest* 128:1629-1637, 2005.
131. Hirose Y, Ishida Y, Hayashida K, et al: Myocardial involvement in patients with sarcoidosis: an analysis of 75 patients. *Clin Nucl Med* 19:522-526, 1994.
132. Le Guludec D, Menad F, Faraggi M, et al: Myocardial sarcoidosis: clinical value of technetium-99m sestamibi tomoscintigraphy. *Chest* 106: 1675-1682, 1994.
133. Tellier P, Paycha F, Antony I, et al: Reversibility by dipyridamole of thallium-201 myocardial scan defects in patients with sarcoidosis. *Am J Med* 85:189-193, 1988.
134. Suzuki T, Kanda T, Kubota S, et al: Holter monitoring as a noninvasive indicator of cardiac involvement in sarcoidosis. *Chest* 106:1021-1024, 1994.
135. Date T, Shinozaki T, Yamakawa M, et al: Elevated plasma brain natriuretic peptide level in cardiac sarcoidosis patients with preserved ejection fraction. *Cardiology* 107:277-280, 2006.
136. Alizad A, Seward JB: Echocardiographic features of genetic diseases: part 2. Storage disease. *J Am Soc Echocardiogr* 13:164-170, 2000.
137. Brady RO, Kanfer JN, Shapiro D: Metabolism of glucocerebrosides. II. Evidence of an enzymatic deficiency in Gaucher's disease. *Biochem Biophys Res Commun* 18:221-225, 1965.
138. Beutler E, Grabowski GA: Gaucher disease. In Scriver CR, Sly WS, Childs B, et al, editors: *The metabolic and molecular bases of inherited disease,* vol. III, New York, 2001, McGraw-Hill, pp 3635-3668.
139. Germain DP: Gaucher's disease: a paradigm for interventional genetics. *Clin Genet* 65:77-86, 2004.
140. Mignot C, Gelot A, Bessieres B, et al: Perinatal-lethal Gaucher disease, *Am J Med Genet* 120A:338-344, 2003.
141. Saraclar M, Atalay S, Kocak N, Ozkutlu S: Gaucher's disease with mitral and aortic involvement: echocardiographic findings. *Pediatr Cardiol* 13:56-58, 1992.
142. Chabas A, Cormand B, Grinberg D, et al: Unusual expression of Gaucher's disease: cardiovascular calcifications in three sibs homozygous for the D409H mutation. *J Med Genet* 32:740-742, 1995.
143. Brady RO, Pentchev PG, Gal AE, et al: Replacement therapy for inherited enzyme deficiency: use of purified glucocerebrosidase in Gaucher's disease. *N Engl J Med* 291:989-993, 1974.
144. Garber AJ: Heritable disorders of carbohydrate metabolism. In Stein JH, editor: *Internal medicine*, ed 3, Boston, 1990, Little, Brown and Company, pp 2273-2278.
145. Winkel LP, Hagemans ML, van Doorn PA, et al: The natural course of non-classic Pompe's disease; a review of 225 published cases. *J Neurol* 252:875-884, 2005.
146. Gussenhoven WJ, Busch HF, Kleijer WJ, de Villeneuve VH: Echocardiographic features in the cardiac type of glycogen storage disease II. *Eur Heart J* 4:41-43, 1983.
147. Lorber A, Luder AS: Very early presentation of Pompe's disease and its cross-sectional echocardiographic features. *Int J Cardiol* 16:311-314, 1987.
148. Shi H, Cotton J, Starsiak MD, et al: Apical hypertrophy caused by glycogen storage disease creating artifacts in myocardial perfusion imaging. *Clin Nucl Med* 31:229-231, 2006.
149. Seward JB, Tajik AJ, Edwards WD, Hagler DJ: *Two-dimensional echocardiographic atlas. Vol 1. Congenital heart disease*. New York, 1987, Springer-Verlag, p 385.
150. van der Beek NA, Hagemans ML, van der Ploeg AT, et al: Pompe disease (glycogen storage disease type II): clinical features and enzyme replacement therapy. *Acta Neurol Belg* 106:82-86, 2006.
151. Klinge L, Straub V, Neudorf U, Voit T: Enzyme replacement therapy in classical infantile Pompe disease: results of a ten-month follow-up study. *Neuropediatrics* 36:6-11, 2005.
152. Winkel LP, Van den Hout JM, Kamphoven JH, et al: Enzyme replacement therapy in late-onset Pompe's disease: a three-year follow-up. *Ann Neurol* 55:495-502, 2004.
153. Amalifitano A, Bengur AR, Morse RP, et al: Recombinant human acid alpha-glucosidase enzyme therapy for infantile glycogen storage disease type II: results of a phase I/II clinical trial. *Genet Med* 3:132-138, 2001.
154. Brady RO, Gal AE, Bradley RM, et al: Enzymatic defect in Fabry's disease: ceramidetrihexosidase deficiency. *N Engl J Med* 276: 1163-1167, 1967.
155. Desnick RJ, Ioannou YA, Eng CM: Alpha galactosidase A deficiency: Fabry disease. In Scriver CR, Beaudet AL, Sly WS, Valle D, editors: *The metabolic and molecular bases of inherited disease,* ed 8, vol 3, New York, 2001, McGraw-Hill, pp 3733-3774.

156. Mehta J, Tuna N, Moller JH, et al: Electrocardiographic and vectorcardiographic abnormalities in Fabry's disease. *Am Heart J* 93:699-705, 1977.
157. Towbin JA, Roberts R: Cardiovascular diseases due to genetic abnormalities. In Schlant RC, Alexander RW, editors: *The heart arteries and veins*, ed 8, New York, 1994, McGraw-Hill, pp 1725-1759.
158. Kampmann C, Baehner F, Whybra C, et al: Cardiac manifestations of Anderson-Fabry disease in heterozygous females. *J Am Coll Cardiol* 40:1668-1674, 2002.
159. Nakao S, Takenaka T, Maeda M, et al: An atypical variant of Fabry's disease in men with left ventricular hypertrophy. *N Engl J Med* 333:288-293, 1995.
160. Sachdev B, Takenaka T, Teraguchi H, et al: Prevalence of Anderson-Fabry disease in male patients with late onset hypertrophic cardiomyopathy. *Circulation* 105:1407-1411, 2002.
161. MacDermot KD, Homes A, Miners AH: Anderson-Fabry disease: clinical manifestations and impact of disease in a cohort of 98 hemizygous males. *J Med Genet* 38:750-760, 2001.
162. Eng CM, Guffon N, Wilcox WR, et al: Safety and efficacy of recombinant human alpha galactosidase A replacement in Fabry disease. *N Engl J Med* 345:9-16, 2001.
163. Weidemann F, Breunig F, Beer M, et al: Improvement of cardiac function during enzyme replacement therapy in patients with Fabry disease: a prospective strain rate imaging study. *Circulation* 108:1299-1301, 2003.
164. Kovacevic-Preradovic T, Zuber M, Attenhofer Jost CH, et al: Anderson-Fabry disease: long-term echo-cardiographic follow-up under enzyme replacement therapy. *Eur J Echocardiogr* 9:729-735, 2008.
165. Pieroni M, Chimenti C, De Cobelli F, et al: Fabry's disease cardiomyopathy: echocardiographic detection of endomyocardial glycosphingolipid compartmentalization. *J Am Coll Cardiol* 47:1663-1671, 2006.
166. Weidemann F, Niemann M, Herrmann S, et al: A new echocardiographic approach for the detection of non-ischaemic fibrosis in hypertrophic myocardium. *Eur Heart J* 28:3020-3026, 2007.
167. Mogenson J, Kubo T, Duque M, et al: Idiopathic restrictive cardiomyopathy is part of the clinical expression of cardiac troponin I mutations. *J Clin Invest* 111:209-216, 2003.
168. Zhang J, Kumar A, Kaplan L, et al: Genetic linkage of a novel autosomal dominant restrictive cardiomyopathy locus. *J Med Genet* 42:663-665, 2005.
169. Lipschutz SE, Sleeper LA, Towbin JA, et al: The incidence of pediatric cardio-myopathy in two regions of the United States. *N Engl J Med* 348:1647-1655, 2003.
170. Kushwaha SS, Fallon JT, Fuster V: Restrictive cardiomyopathy. *N Engl J Med* 336:267-276, 1997.
171. Perugini E, Rapezzi C, Reggiani LB, et al: Comparison of ventricular long-axis function in patients with cardiac amyloidosis versus idiopathic restrictive cardiomyopathy. *Am J Cardiol* 95:146-149, 2005.
172. Ammash NM, Seward JB, Bailey KR, et al: Clinical profile and outcome of idiopathic restrictive cardiomyopathy, *Circulation* 101: 2490-2496, 2000.
173. Russo LM, Webber SA: Idiopathic restrictive cardiomyopathy in children. *Heart* 91:1199-1202, 2005.
174. Mortensen SA, Olsen HS, Baandrup U: Chronic anthracycline cardiotoxicity: haemodynamic and histopathological manifestations suggesting a restrictive endomyocardial disease. *Br Heart J* 55:274-282, 1986.
175. Naqvi TZ, Luthringer D, Marchevsky A, et al: Chloroquine Induced Cardiomyopathy—Echocardiographic Features. *J Am Soc Echocardiogr* 18:383-387, 2005.
176. Fajardo LF, Stewart JR, Cohn KE: Morphology of radiation induced heart disease. *Arch Pathol* 86:512-519, 1968.
177. Vallebona A: Cardiac damage following therapeutic chest irradiation. Importance, evaluation and treatment. *Minerva Cardioangiol* 48:79-87, 2000. Review.
178. Gottdiener JS, Katin MJ, Borer JS, et al: Late cardiac effects of therapeutic mediastinal irradiation: assessment by echocardiography and radionuclide angiography. *N Engl J Med* 308: 569-572, 1983.
179. Gustavsson A, Eskilsson T, Landberg T, et al: Late cardiac effects after mantle radiotherapy in patients with Hodgkin's disease. *Ann Oncol* 1:355-363, 1990.
180. Gomez GA, Park JJ, Panahon A, et al: Heart size and function after radiation therapy to the mediastinum in patients with Hodgkin's disease. *Cancer Treat Rep* 67:1099-1103, 1983.
181. Green DM, Gingell RL, Pearce J, et al: The effect of mediastinal irradiation on cardiac function of patients treated during childhood and adolescence for Hodgkin's disease. *J Clin Oncol* 5:239-245, 1987.
182. Brosius FC, Waller BF, Roberts WC: Analysis of 16 young (aged 15 to 33 years) necropsy patients who received over 3500 rads to the heart. *Am J Med* 70:519-530, 1981.
183. Piovaccari G, Ferretti RM, Prati F, et al: Cardiac disease after chest irradiation for Hodgkin's disease: incidence in 108 patients with long follow-up. *Int J Cardiol* 49:39-43, 1995.
184. King V, Constine LS, Clark D, et al: Symptomatic coronary artery disease after mantle irradiation for Hodgkin's disease. *Int J Radiat Oncol Biol Phys* 36:881-889, 1996.
185. Glanzmann C, Kaufmann P, Jenni R, et al: Cardiac risk after mediastinal irradiation for Hodgkin's disease. *Radiother Oncol* 46:51-62, 1998.
186. Lipshultz SE, Lipsitz SR, Sallan SE, et al: Chronic progressive cardiac dysfunction years after doxorubicin therapy for childhood acute lymphoblastic leukemia. *J Clin Oncol* 23:2629-2636, 2005.
187. Branea I, Stanciu L, Tomescu M, et al: The value of echocardiography in the early diagnosis of myocardial impairment due to connective tissue diseases. *Med Interne* 24:197-205, 1986.
188. Navarro-Lopez F, Llorian A, Ferrer-Roca O, et al: Restrictive cardio-myopathy in pseudoxanthoma elasticum. *Chest* 78:113-115, 1980.
189. Challenor VF, Conway N, Monro JL: The surgical treatment of restrictive cardio-myopathy in pseudoxanthoma elasticum. *Br Heart J* 59:266-269, 1988.
190. Palka P, Lange A, Donnelly E, et al: Differentiation between restrictive cardiomyopathy and constrictive pericarditis by early diastolic Doppler myocardial velocity gradient at the posterior wall. *Circulation* 102:655-662, 2000.
191. Klodas E, Nishimura R, Appleton C, et al: Doppler evaluation of patient with constrictive pericarditis: use of tricuspid regurgitation velocity curves to determine enhanced ventricular interaction. *J Am Coll Cardiol* 28:652-657, 1996.
192. Ha JW, Oh J, Ling L, et al: Annulus paradoxus: transmitral flow velocity to mitral annular velocity ratio is inversely proportional to pulmonary capillary wedge pressure in patients with constrictive pericarditis. *Circulation* 104:976-978, 2001.
193. Klodas E, Nishimura RA, Appleton CP, et al: Doppler evaluation of patients with constrictive pericarditis use of tricuspid regurgitation velocity curves to determine enhanced ventricular interaction, *J Am Coll Cardiol* 28:652-657, 1996.
194. Ling L, Oh J, Tei C: Pericardial thickness measured with transesophageal echocardiography: feasibility and potential clinical usefulness. *J Am Coll Cardiol* 29:1317-1323, 1997.
195. Talreja DR, Edwards WD, Danielson GK, et al: Constrictive pericarditis in 26 patients with histologically normal pericardial thickness. *Circulation* 108:1852-1857, 2003.
196. Schoenfeld M, Supple E, Dec W, et al: Restrictive cardiomyopathy versus constrictive pericarditis: role of endomyocardial biopsy in avoiding unnecessary thoracotomy. *Circulation* 75:1012-1017, 1987.
197. Asher CR, Klein AL: Diastolic heart failure: restrictive cardiomyopathy, constrictive pericarditis, and cardiac tamponade: clinical and echocardiographic evaluation. *Cardiol Rev* 10:218-229, 2002. Review.
198. Goldstein JA: Cardiac tamponade, constrictive pericarditis, and restrictive cardiomyopathy. *Curr Probl Cardiol* 29:503-567, 2004.
199. Hancock E: Differential diagnosis of restrictive cardiomyopathy and constrictive pericarditis. *Heart* 86:343-349, 2001.
200. Hatle L, Appleton C, Popp R: Differentiation of constrictive pericarditis and restrictive cardiomyopathy by Doppler echocardiography. *Circulation* 79:357-370, 1989.
201. Klein AL, Cohen GI, Pietrolungo JF: Differentiation of constrictive pericarditis from restrictive cardiomyopathy by Doppler transesophageal echocardiographic measurements of respiratory variations in pulmonary venous flow. *J Am Coll Cardiol* 22:1935-1943, 1993.
202. Abdalla IA, Murray RD, Lee JC, et al: Does rapid volume loading during transesophageal echocardiography differentiate constrictive pericarditis from restrictive cardiomyopathy? *Echocardiography* 19:125-134, 2002.
203. Oh JK, Tajik AJ, Appleton CP, et al: Preload reduction to unmask the characteristic Doppler feature of constrictive pericarditis. A new observation. *Circulation* 95:796-799, 1997.
204. Sengupta PP, Krishnamoorthy VK, Abhayaratna WP, et al: Disparate patterns of left ventricular mechanics differentiate constrictive pericarditis from restrictive cardiomyopathy. *JACC Cardiovasc Imaging* 1:29-38, 2008.
205. Sengupta PP, Krishnamoorthy VK, Abhayaratna WP, et al: Comparison of usefulness of tissue Doppler imaging versus brain natriuretic peptide for differentiation of constrictive pericardial disease from restrictive cardiomyopathy. *Am J Cardiol* 102:357-362, 2008.
206. Ha JW, Ommen SR, Tajik AJ, et al: Differentiation of constrictive pericarditis from restrictive cardiomyopathy using mitral annular velocity by tissue Doppler echocardiography. *Am J Cardiol* 94:316-319, 2004.
207. Ha JW, Oh JK, Ommen SR, et al: Diagnostic value of mitral annular velocity for constrictive pericarditis in the absence of respiratory varia-

tion in mitral inflow velocity. *J Am Soc Echocardiogr* 15:1468-1471, 2002.
208. Arnold MF, Voight JU, Kukulski T, et al: Does atrioventricular ring motion always distinguish constriction from restriction? A Doppler myocardial imaging study. *J Am Soc Echocardiogr* 14:391-395, 2001.
209. Butz T, Piper C, Langer C, et al: Diagnostic superiority of a combined assessment of the systolic and early diastolic mitral annular velocities by tissue Doppler imaging for the differentiation of restrictive cardiomyopathy from constrictive pericarditis. *Clin Res Cardiol* 99:207-215, 2010.
210. Rajagopalan N, Garcia MJ, Rodriguez L, et al: Comparison of new Doppler echocardiographic methods to differentiate constrictive pericardial heart disease and restrictive cardiomyopathy. *Am J Cardiol* 87:86-94, 2001.
211. Palka P, Lange A, Donnelly JE, Nihoyannopoulos P: Differentiation between restrictive cardiomyopathy and constrictive pericarditis by early diastolic Doppler myocardial velocity gradient at the posterior wall. *Circulation* 102:655-662, 2000.
212. Wood P: Chronic constrictive pericarditis. *Am J Cardiol* 7:48-61, 1961.
213. Yu PN, Lovejoy FW, Joos HA, et al: Right auricular and ventricular pressure patterns in constrictive pericarditis. *Circulation* 7:102-107, 1953.
214. Vaitkus PT, Kussmaul WG: Constrictive pericarditis versus restrictive cardiomyopathy: a reappraisal and update of diagnostic criteria. *Am Heart J* 122:1431-1441, 1991.
215. Lachmann HJ, Booth DR, Booth SE, et al: Misdiagnosis of hereditary amyloidosis as AL (primary) amyloidosis. *N Engl J Med* 346:1786-1791, 2002.

# 29 Pericardial Disease

BRADLEY I. MUNT, MD | ROBERT R. MOSS, MD | JASMINE GREWAL, MD

**Basic Principles**
- Anatomy of the Pericardium
- Pericardial Fluid
- Functions of the Pericardium
- Echocardiographic Evaluation for Pericardial Disease

**Constrictive Pericarditis**
- Pathophysiology
- Echocardiographic Diagnosis
- Constriction versus Restriction

**Pericardial Effusion**
- M-Mode and Two-Dimensional Echocardiography
- Factors Affecting the Appearance of Pericardial Effusions
- Determination of Pericardial Fluid Volume
- Clinical Considerations

**Pericardial Tamponade**
- Echocardiographic Evaluation
- The Role of Echocardiography in Patient Management
- Localized and Loculated Pericardial Fluid Collections
- Echocardiographically Guided Pericardiocentesis

**Acute Pericarditis**

**Effusive Constrictive Pericarditis**

**Pericardial Effusion as an Incidental Finding on Echocardiography**

**Congenital Disorders of the Pericardium**
- Congenital Absence of the Pericardium
- Pericardial Cysts

## Basic Principles

### ANATOMY OF THE PERICARDIUM

The pericardium consists of two layers that surround the heart and proximal segments of the aorta, pulmonary artery, pulmonary veins, and venae cavae. The outermost layer is a thick fibrous structure, which blends with the adventitia of the aorta and pulmonary arteries to provide firm support for the heart. This layer has supporting ligamentous attachments to the diaphragm, sternum, and vertebrae.[1,2] The inner layer is a serous membrane consisting of a single layer of mesothelial cells, which directly overlies the epicardial fat to form the visceral pericardium. This membrane reflects back on itself to line the inside of the fibrous layer and forms the parietal pericardium. The pericardial space is enclosed between the two layers of serous pericardium. This space is limited superiorly by the attachments of the fibrous pericardium to the great arteries. It is limited posteriorly by reflections of the pericardium as the pulmonary veins and venae cavae enter the atria (Fig. 29-1). These reflections result in the formation of two blind-ending tunnels or sinuses. The oblique sinus lies behind the left atrium (LA) and left ventricle (LV) and is limited superiorly by the pericardial reflection to the upper pulmonary veins, laterally by the reflections of the pericardium around the left pulmonary veins, and medially by the reflections of the pericardium around the right pulmonary veins and venae cavae. The transverse sinus lies above the pulmonary vein reflection and is bounded anteriorly by the great arteries and posteriorly by the LA roof (see Fig. 29-1). The main arterial supply of the pericardium is from a branch of the internal thoracic artery, the pericardiophrenic artery. Venous drainage is by the pericardiophrenic veins, which drain into the brachiocephalic veins. The phrenic nerve provides sensory innervation; the sympathetic trunks provide vasomotor innervation.

### PERICARDIAL FLUID

The pericardial space normally contains 10 to 50 mL of fluid that lubricates the contact between the two serosal layers of the pericardium.[3] This fluid is an ultrafiltrate of plasma and contains proteins, electrolytes, and phospholipids. It is believed to be formed in the visceral pericardium. The pericardial space drains via the thoracic and right lymphatic ducts. Any condition obstructing lymphatic flow or raising central venous pressure will lead to accumulation of pericardial fluid. Fluid will also accumulate in conditions increasing the normal pericardial permeability. The normal pericardium has a relatively small capacitance volume; acute accumulation of fluid will result in small increases in pericardial pressure until the capacitance has been exceeded. With additional increase in pericardial volume, a rapid rise in pericardial pressure and progressive hemodynamic disturbances will ensue (Fig. 29-2).[4]

### FUNCTIONS OF THE PERICARDIUM

The pericardium serves to reduce friction between the heart and the surrounding mediastinal structures and provides a barrier against the local spread of infection or malignancy to the heart.[2] The pericardium serves to distribute the pressure within the pericardial space to the cardiac structures enclosed within the pericardium and mediates ventricular coupling or interaction.[5] Understanding the role of the pericardium in pressure modulation and ventricular interaction is important to appreciate the hemodynamic effects and therefore the echocardiographic features of compressive pericardial disease.

#### *Pericardial Pressure*

The influences of pericardial restraint and pericardial pressure are important to bear in mind when assessing ventricular filling

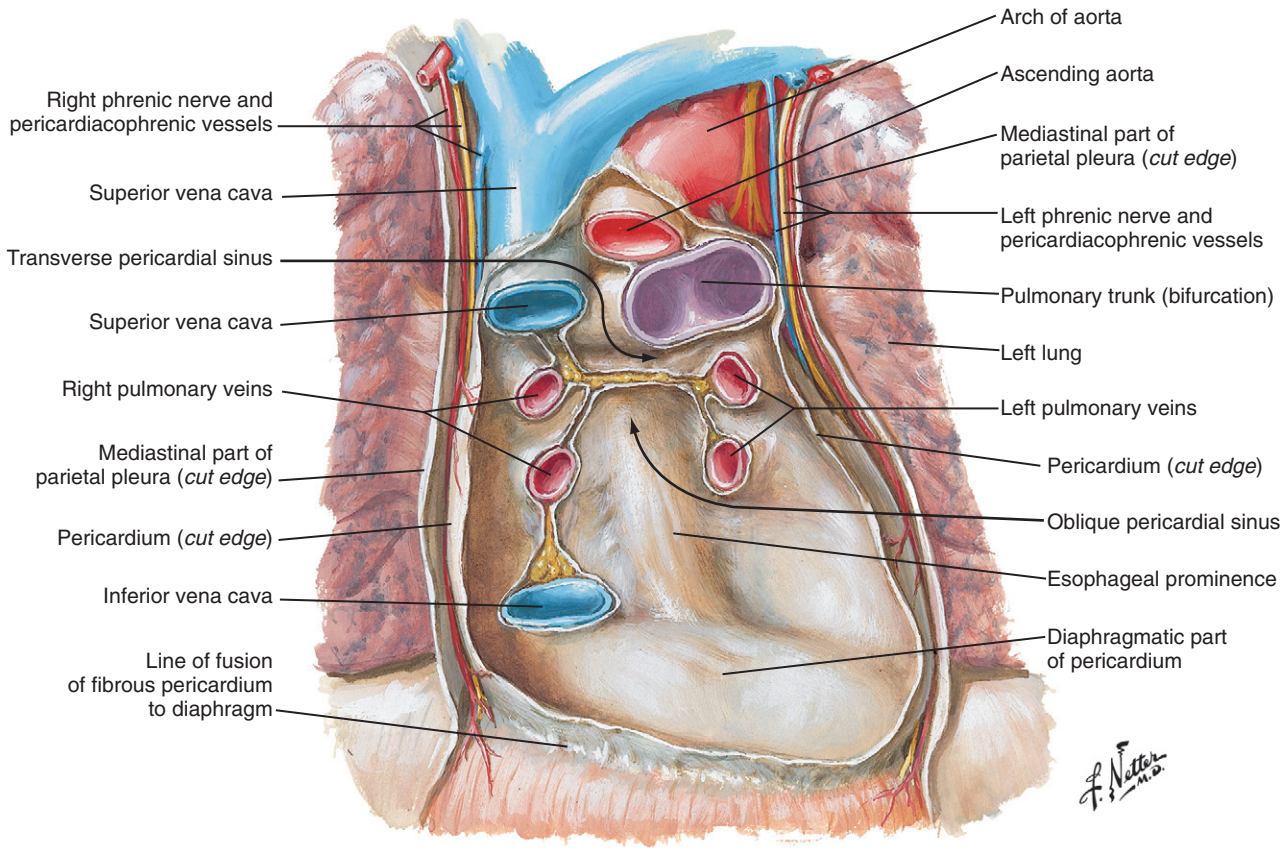



**Figure 29-1 Pericardial sac with heart removed: anterior view.** *(From Netter FH:* Atlas of human anatomy, *ed 1, Ciba-Geigy Pharmaceutical, 1989.)*

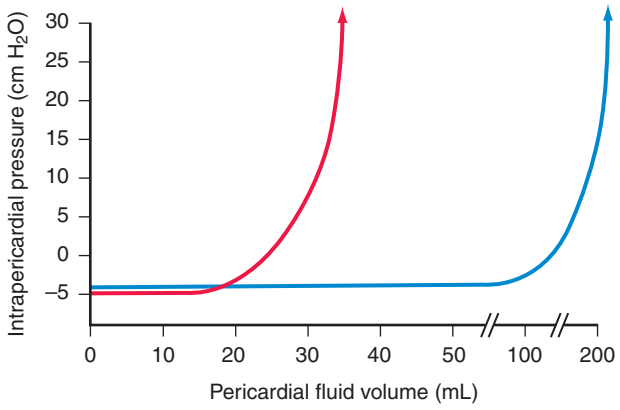



**Figure 29-2 Pericardial pressure-volume relationships in a patient with normal pericardial anatomy (*red line*) and a patient who has gradually developed a pericardial effusion (*blue line*).** *(From Edmunds HL:* Cardiac surgery in the adult, *New York, 1997, McGraw-Hill, p 1305.)*

and function. Over a century ago, Bernard concluded that the pericardium significantly constrained cardiac filling.[6] The concept of transmural pressure (the intracavity end-diastolic pressure minus the pericardial pressure) subsequently evolved to take into account this pericardial restraint. This concept is extremely important because transmural pressure is likely to be a closer representation of preload than the intracavity end-diastolic pressure. However, controversy exists as to the magnitude of this constraint because of difficulties in the accurate determination of pericardial pressure. Using a balloon to measure pericardial pressure, pericardial pressure approximates right atrial (RA) and right ventricular (RV) end-diastolic pressure. Others contend that balloon-based measurement techniques overestimate pericardial pressure and therefore underestimate true transmural pressure.[7]

### *Pericardial Restraint and Ventricular Interaction*

Because the pericardium is a relatively stiff structure, intrapericardial pressure rises rapidly as intrapericardial volume is increased acutely.[8] This increase in intrapericardial pressure may occur because of an accumulation of pericardial fluid or an increase in the volume of any intracardiac structure—particularly an increase in RV volume (Fig. 29-2). Shirato and colleagues[9] showed that acute volume loading in dogs with an intact pericardium caused a reduction in LV compliance. This is because an increase in intrapericardial volume (as a result of an increase in right-sided chamber volumes) increases intrapericardial pressure restraining LV filling. The opposite effects were seen with reductions in cardiac volume using nitroprusside. These effects were abolished by pericardectomy. Examples of ventricular interaction under different loading conditions have been seen in human studies (Fig. 29-3).[10]

The restraining effects of the pericardium are much less apparent in the chronic volume overloaded state because of adjustment in pericardial compliance[8] (see Fig. 29-2).

An increase in pericardial pressure resulting from pericardial fluid accumulation will also reduce transmural filling pressure

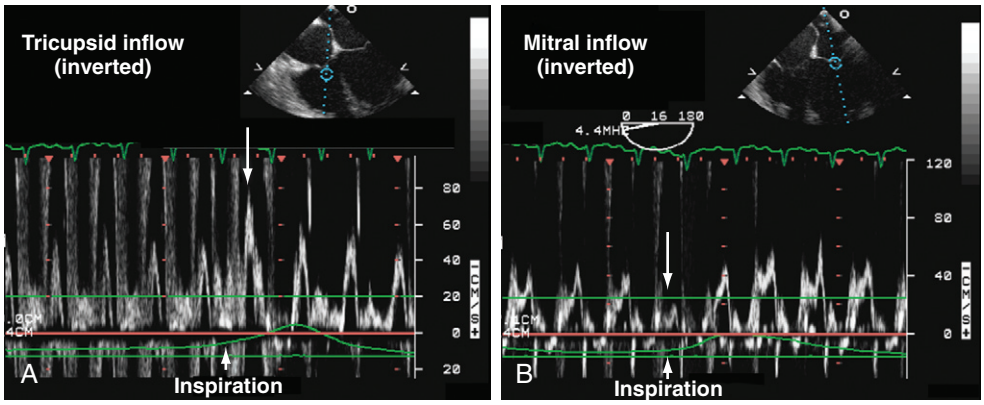



**Figure 29-3** **TEE images showing marked variation in mitral inflow velocities with respiration in a patient with dilated cardiomyopathy, RV enlargement, and volume overload. A,** Tricuspid inflow. **B,** Mitral Inflow. Note marked and opposite change in mitral and tricuspid flow velocities with first inspiratory beat (*arrow*). Marked ventricular interaction that simulates tamponade physiology can occur in settings other than pericardial effusion.

and shift ventricular pressure/volume relationships. Under conditions of raised pericardial volume and pressure or where the pericardium is stiff, there is enhanced potential for the LV and RV to interact and influence each other's diastolic function. Ventricular interaction can be either in series (i.e., the output of the right ventricle (RV) influencing left heart and LV filling), or in parallel, in which ventricular filling characteristics are changed by the side-by-side nature of the ventricles within a constrained pericardial volume. An understanding of the effects of ventricular interdependence is key to understanding the hemodynamic and therefore the echocardiographic features of compressive pericardial disease.

## ECHOCARDIOGRAPHIC EVALUATION FOR PERICARDIAL DISEASE

The pericardium covers the entire external surface of the heart and therefore is visualized from all standardized echocardiographic windows. The pericardium appears as a thin echogenic structure that is most obvious posteriorly. Normal pericardial thickness measures 1 mm or less. Normal pericardial fluid volume is minimal, and therefore the pericardial space is not appreciated in most normal subjects. Occasionally, a small amount of physiologic pericardial fluid may be seen in the posterior pericardial space. during ventricular systole. With the exception of some postsurgical pericardial effusions, the majority of pericardial processes are evident in the parasternal long-axis view.[11,12] When the clinical suspicion of a primary pericardial disease is low, therefore, a normal parasternal long-axis view has been considered adequate to rule out pericardial pathology. Unfortunately, in a recent series of patients who underwent pericardiocentesis for tamponade,[13] the diagnosis of pericardial effusion was not initially considered in 44% of patients before echocardiography. Accordingly, we advocate that the pericardial space be studied in all standard acoustic windows as part of the standard echocardiographic examination.

Because there is questionable correlation between measurements of pericardial thickness by transthoracic echocardiography (TTE) and pathologic examination,[14] we prefer computed tomography (CT) or magnetic resonance imaging (MRI) to evaluate the pericardium for thickening. These techniques also allow better visualization of adjacent thoracic structures.

**Box 29-1**

### ECHOCARDIOGRAPHIC IMAGING PROTOCOL IN SUSPECTED PERICARDIAL DISEASE

1. Full 2D examination with emphasis on the location, volume, and characteristics of the pericardial fluid and the characteristics of the pericardium. Views of RA and RV free walls are especially important. When recording digital images, extended loops (up to 10 beats) may be required to be recorded to capture changes related to the respiratory cycle.
2. M-mode examination with attention to imaging the RV free wall.
3. PW Doppler assessment of tricuspid (RV) inflow, mitral (LV) inflow, pulmonary vein flow, and hepatic vein flow. Superior vena cava flow can be imaged in selected patients. Long loops with respiratory tracking are recorded to appreciate respiratory changes in Doppler velocities.
4. Tissue-Doppler recordings of medial and lateral mitral annulus, with systolic (s′) and diastolic (E′ and A′) waves shown.
5. Careful 2D and M-mode imaging of the inferior vena cava and associated changes with respiration and a "sniff."
6. In postoperative patients, a detailed search for localized fluid collections and any resulting localized chamber compression.

Visualization of the RV and RA free walls, often with high–frame-rate M-mode or two-dimensional (2D) recordings of motion, is required to determine the hemodynamic significance of pericardial effusions. As well, pulsed-wave (PW) Doppler recordings of RV and LV inflow, with respiratory tracking and multiple complexes recorded, are needed as a minimum.

We strongly advocate that all patients with pericardial effusions undergo an initial comprehensive echocardiographic evaluation to rule out conditions that may modulate echocardiographic indicators of pericardial tamponade (such as atrial septal defects, RV hypertrophy), and detect coexisting cardiac conditions (Box 29-1). Follow-up examinations may be of a more directed, limited nature.

**Box 29-2**

**CAUSES OF PERICARDIAL INFLAMMATION**

**Idiopathic**

**Infectious Diseases**
Bacterial (including tuberculosis, *Chlamydia*, borreliosis, *Treponema pallidum*, *Haemophilus*, *Meningococcus*, *Pneumococcus*, *Gonococcus*)
Fungal (including *Candida*, histoplasmosis)
Viral (including coxsackie A9, B1-4, echo B, mumps, Epstein-Barr, cytomegalovirus, *Varicella*, rubella, human immunodeficiency virus, parvo B19)
Parasitic (including *Toxoplasma*, *Echinococcus*, *Entamoeba histolytica*)

**Trauma**
Blunt or penetrating trauma
Cardiac surgery

**Systematic Inflammatory Disorders**
Including rheumatoid arthritis, systemic lupus erythematosus, systemic sclerosis, Reiter syndrome

**Neoplasia**
Primary benign or malignant pericardial tumors
Secondary (including lung, breast, gastric, colon, leukemia, melanoma)

**Metabolic Disorders**
Including renal failure, hypothyroidism, Addison disease

**Miscellaneous**
Mediastinal irradiation
Pulmonary asbestosis

## Constrictive Pericarditis

A variety of disorders can cause pericardial inflammation and subsequent thickening, fibrosis, and calcification (Box 29-2). Pericardial inflammation and organization can lead to altered compliance characteristics of the pericardium (visceral, parietal, or with fusion of both layers). The underlying epicardium may also be abnormal. This results in impaired cardiac filling and characteristic echocardiographic signs. The echocardiographic recognition of pericardial constriction and its differentiation from other forms of diastolic heart failure (and in particular restrictive cardiomyopathy) remain among the essential challenges in echocardiography.

### PATHOPHYSIOLOGY

The thickened, fibrotic pericardium constricts the heart and reduces operative chamber compliance. Consequently, diastolic filling is impeded as the end-diastolic cardiac volume is limited by the pericardial volume. Early diastolic filling is usually not impaired (and in fact may be supranormal), whereas mid-diastolic and late-diastolic filling is impaired.

The pericardial thickening usually involves the whole pericardial surface (although the degree of thickening can vary) and leads to elevation and equalization of diastolic pressures in all four cardiac chambers, especially at end-diastole. In early diastole, ventricular filling can occur more rapidly than usual because of elevated atrial pressure. Once the pericardial volume is reached, however, filling halts abruptly, and there is little further increase in total chamber volume. This limitation to filling in mid and late diastole explains many of the M-mode, 2D, and Doppler abnormalities and leads to the typical square root sign seen with invasive hemodynamic measurement.[15]

One of the cardinal features of constriction is the dynamic changes in filling that occur throughout the respiratory cycle. At a physiologic level, these changes may be understood in terms of twin phenomena: the dissociation of intracardiac from intrathoracic pressures and ventricular interaction.[16] In the generally accepted model, thickened pericardium partially isolates the heart from the normal respiratory swings in intrathoracic pressure. Respiratory fluctuations in pulmonary venous pressure still occur (because portions of the pulmonary veins and the LA lie outside the pericardium), and a fall in pulmonary venous pressure with inspiration leads to a fall in LA filling without corresponding fall in the LV diastolic pressure.[4] The driving pressure across the mitral valve is therefore reduced. This prolongs the isovolumic relaxation time, reduces early diastolic transmitral flow velocity, and prolongs the deceleration time.[17] These changes can be useful diagnostically, as respiratory variations in flow are not characteristic of patients with other forms of diastolic heart failure such as restrictive cardiomyopathy. The pericardial limitation to filling also serves to exaggerate normal ventricular coupling/interaction. A reduction in LV filling with inspiration allows a compensatory increase in right-sided heart filling. This being said, it should be recognized that the interactions between the heart and the respiratory cycle in pericardial disease are complex and may also be modulated by abdominal venous pooling, blood volume, intraabdominal pressure, and their effects on the right side of the heart.[18,19] Irrespective of the primary driving forces, these respiratory fluctuations in left-sided and right-sided heart filling cause characteristic changes in mitral and tricuspid Doppler inflow patterns, ventricular dimensions, and hepatic vein flow dynamics.

### ECHOCARDIOGRAPHIC DIAGNOSIS

Given the challenges associated with the diagnosis of constriction, certain clinical scenarios should alert the cardiologist or sonographer and prompt the institution of a comprehensive imaging protocol appropriate to pericardial disease (see Box 29-1). Unexplained clinical evidence of right heart failure (especially in the setting of preserved LV ejection fraction) or unexplained hepatic dysfunction should arouse suspicion. Similarly, patients with a history of prior acute pericarditis or effusion, cardiac surgery, radiation, or systematic inflammatory disease are good candidates for careful pericardial evaluation.

#### *M-Mode and Two-Dimensional Abnormalities*

The abrupt cessation of flow in mid-diastole results in flattening of the motion of the posterior LV wall in mid and late diastole. This follows relatively normal motion in early diastole associated with rapid ventricular filling and is the M-mode equivalent of the square root sign. This sign is relatively sensitive, being reported in 85% of patients with constriction, but is not specific.[20] Abnormalities of interventricular septal motion are common in constriction. Septal position is influenced by pressure gradients between the LV and RV, and changes in septal position with respiration are exacerbated by the constricting effect of the rigid pericardium. Both parasternal M-mode and 2D echocardiography can demonstrate marked movement of the septum posteriorly with inspiration and the anteriorly with expiration, and consequent respiratory changes in LV and RV volumes.[21] An additional M-mode sign seen with constriction

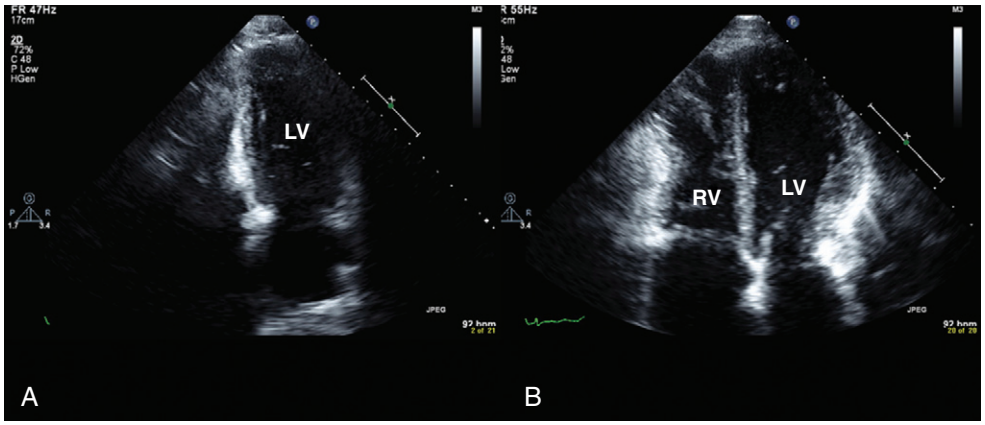



**Figure 29-4** **Pericardial thickening in surgically proven constriction. A,** Echogenic, thickened pericardium in relation to the mid and basal inferior wall of the LV. **B,** Similar pericardial thickening at mid-RV and basal lateral LV wall. Contour of RV is distorted. Cardiac MRI findings were similar. At surgery, pericardium was up to 1 cm in thickness.

is a "double component" of septal motion also known as the septal "bounce." A variety of abnormalities of septal motion after the onset of diastole have been reported,[21] with both initial anterior and posterior motion of the septum followed by restitution being described. Explanations advanced include phasic pressure differences between the LV and RV and, more recently, the effect of the tricuspid inflow jet on septal motion.[22] Tissue Doppler analysis of septal motion in the short-axis plane has revealed additional complexity: High-velocity early biphasic diastolic motion may be followed by multiple recoil waves (polyphasic diastolic septal fluttering).[23] Abrupt cessation of LV filling may sometimes be appreciated on 2D imaging as a perceptible "checking" of LV diastolic expansion.

Because of the interaction of ultrasound with thickened or calcified pericardium, suboptimal images are frequently obtained. Pericardial thickening and calcification can be appreciated using M-mode and 2D modalities (Fig. 29-4), although the sensitivity and specificity have been questioned. Early reports of M-mode sensitivity of almost 100% in diagnosing pericardial thickening[24] or diagnosing constrictive pericarditis from other findings[25] have not been confirmed in later studies.[20,26-28] A systematic overestimation of true thickness using TTE was found in dogs with experimental constrictive pericarditis.[14] These difficulties have been attributed to technical issues such as gain settings and resolution, fibrosis obscuring cardiac boundaries, and the nonuniform nature of pericardial thickening. A more recent study found that transesophageal echocardiography (TEE) was more accurate, with a sensitivity of 95% and specificity of 86% in the detection of thickened pericardium (using CT scanning as the gold standard).[29] It should be understood that while echocardiographic evaluation of the pericardium may arouse suspicion of the diagnosis, CT or MRI are the preferred imaging modalities for the diagnosis and measurement of pericardial thickening. It is also critical to recognize that surgically verified constriction has been noted in patients with normal pericardial thickness.[30] Adhesion of the epicardium to the pericardium with attendant loss of the usual sliding motion or tethering of the pericardium to surrounding anatomic structures may be appreciated on 2D imaging, especially from the subcostal view.

The inferior vena cava is also typically dilated with blunting of the normal inspiratory collapse, consistent with elevated right atrial pressure.[31]

### *Doppler Flow Abnormalities*

No single M-mode or 2D echocardiographic feature is diagnostic of constrictive pericarditis, nor is any combination. For this reason, careful analysis of Doppler imaging is an integral component in the diagnosis of constriction. In keeping with rapid early diastolic flow, the LV (mitral) inflow pattern typically shows a high E wave velocity, a short deceleration time, and a low A wave velocity. However, this restrictive filling pattern reflects elevated LA pressure and therefore is not specific to pericardial constriction. Of greater significance is the change in LV (mitral) and RV (tricuspid) inflow and hepatic vein flow patterns seen with respiration, which together form the cornerstone of the diagnosis of constriction. Several studies[17,32] have reported that in patients with pericardial constriction there is:

1. prolongation of the LV isovolumic relaxation time by greater than 25% with inspiration in all patients with constriction, whereas normal individuals changed by less than 5%;
2. reduction of greater than 25% in peak early LV inflow (E wave) velocity with inspiration in all patients compared with less than 5% in normal individuals;
3. larger expiratory decreases in RV inflow velocity than in normal individuals;
4. a 14% reduction in aortic velocity with inspiration versus a 4% reduction in normal individuals;
5. a 16% increase in pulmonary artery velocity with inspiration as compared to 5% in normal individuals;
6. changes in all parameters that were greatest in the first beat following inspiration as compared to changes two or three beats later in those patients with pulmonary disease;
7. an absence of these significant respiratory fluctuations after successful pericardectomy. In modern series, approximately 60% of patients have complete normalization of cardiac physiology postpericardectomy. There is a greater normalization of values in patients who become asymptomatic postpericardectomy.[33]

In the clinical setting, the major focus is on mitral inflow and hepatic vein Doppler; however, respiratory fluctuations in mitral inflow velocity are not invariably present. One study suggested normal respiratory fluctuations in 12% of patients with proven constriction,[32] whereas others have suggested that the proportion with less than 25% fluctuation in mitral E

velocity may be as high as 47%.[34] It is speculated that markedly elevated LA pressure forces mitral valve opening to occur on a steeper part of the LV curve, thus masking inspiratory changes in inflow velocity and isovolumic relaxation time.[32] This is supported by the finding that preload reduction in patients with constriction, and blunted respiratory change, unmasked the characteristic respiratory variation.[35]

Increased variation in flow through the right heart (with the resultant phasic changes in RV volume and pressure) also alters tricuspid regurgitation jet parameters. Increased RV preload increases the cavity pressure, increasing the regurgitation velocity and velocity-time integral (VTI). Klodas and colleagues[36] showed that in patients with constrictive pericarditis, there was a 13% increase in tricuspid regurgitation velocity with inspiration, as compared to an 8% drop in jet velocity in normal patients. Premature cessation of pulmonary regurgitant flow with inspiration has been reported in constriction.[37] Important abnormalities of hepatic vein flow have been described in association with constrictive pericarditis. Normal hepatic vein flow is biphasic and augments slightly with inspiration. There are brief flow reversals in late RV systole and atrial systole that are more prominent in expiration.[38] The predominant forward hepatic vein flow in constriction is typically during early diastole. This is the result of an elevated RA pressure inhibiting inflow during systole and driving flow across a high early diastolic transtricuspid gradient.[32] However, this pattern is not uniform, and systolic forward flow can also predominate. Expiration causes a reduction in diastolic forward flow along with significant diastolic flow reversals, although inspiratory flow reversals of lesser magnitude are sometimes also identified.[32] If the flow reversals are more prominent in inspiration, restriction is probably present. In a series of patients with surgically proven constrictive pericarditis, echocardiographic criteria based on respiratory variations in mitral and hepatic vein flow correctly diagnosed constriction in 22 of 25 patients.[32]

TEE-recorded pulmonary vein flow abnormalities and their role in distinguishing constriction from restriction have been described. Most notable are the higher systolic-to-diastolic filling ratio in constriction (as compared to restriction) and increased respiratory variation, in particular expiratory reduction in the diastolic flow component.[39]

Difficulty may occasionally arise in other clinical states where enhanced ventricular interaction is present and in which significant variation in mitral and tricuspid inflow velocities may occur. Typically constriction shows a fall in the mitral E wave velocity on the first inspiratory beat. In other settings, such as chronic obstructive pulmonary disease or marked obesity, a more gradual, phasic variation may be anticipated. Doppler interrogation of superior vena cava (SVC) flow is also useful. In chronic obstructive pulmonary disease, significant increases in superior vena cava flow velocity will be noted with inspiration. In constrictive pericarditis, minimal or no increase in superior vena caval flow velocity with inspiration is noted.[40]

### *Tissue-Doppler and Strain Imaging*

The advent of advanced Doppler and strain imaging has enhanced our understanding of myocardial mechanics in constriction. Most notably, tissue-Doppler imaging (TDI) may be useful in differentiating pericardial constriction from restriction and in solidifying the diagnosis when increased respiratory variation in mitral inflow Doppler is nondiagnostic or absent.[34] Early diastolic tissue velocities (E′) in patients with constriction are generally equivalent to those in normal controls[41] but may on occasion be supranormal. This is likely a result of the fact that whereas circumferential diastolic expansion of the heart is impeded in constriction, myocardial lengthening is relatively preserved. Most important, myocardial relaxation velocities (reflecting intrinsic myocardial disease) are usually lower in restriction than in constriction.[42] An E′ velocity 2 cm/s greater than predicted for age could differentiate patients with constriction from controls with a sensitivity of 76% and a specificity of 82%.[41] Similarly, a septal E′ cut-off value greater than 8 cm/s resulted in 95% sensitivity and 96% specificity for the diagnosis of constrictive pericarditis over a mixed group of cardiac amyloid and primary restrictive cardiomyopathy.[43] In constriction, septal E′ is more likely to exceed E′ at both lateral tricuspid and mitral annuli than in controls or restriction. This finding has been termed *annulus reversus* and may be due to tethering of the lateral wall[44,45] (Fig. 29-5). Annular mitral motion may precede mitral inflow in constriction, in contradistinction to the usual situation with restriction.[46]

Recent work has pointed to some limitations that exist in the use of TDI in differentiating constriction from restriction,[47] where myocardial dysfunction, marked segmental variation in myocardial velocities, and extensive mitral annular calcium can be problematic. It should be remembered that the two disease states can coexist in the same patients, especially after radiation therapy.[48]

Although less studied than tissue Doppler, rapid propagation of the mitral inflow wave by color M-mode has also been used to demonstrate relative preservation of early myocardial relaxation in constriction.[49]

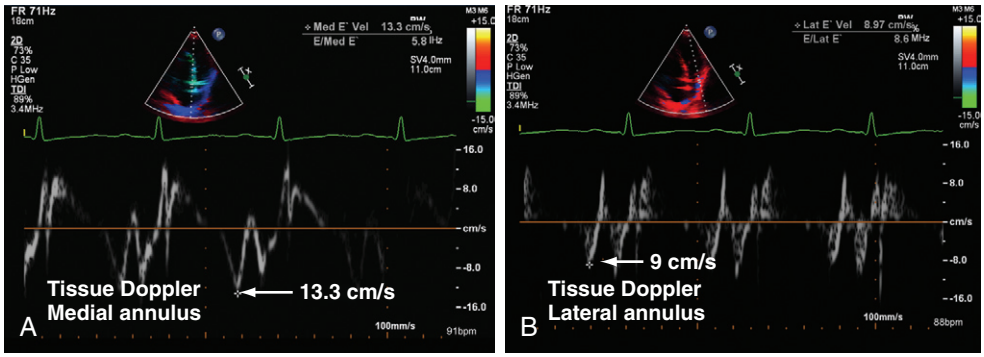



**Figure 29-5 Tissue-Doppler velocity recordings obtained from septal (medial) annulus (A) and lateral annulus (B).** Note that early diastolic septal annular velocity (E′) is supranormal, 13 cm/s. In contrast to the usual situation, lower E′ velocity is recorded at lateral annulus, termed *annulus reversus*. Patient also exhibits *annulus paradoxus*, low E/E′ ratio with elevated filling pressures. Patient subsequently had surgically confirmed pericardial constriction.

The use of speckle-tracking myocardial stain imaging is a new development that has already enhanced our understanding of myocardial mechanics but may in the future prove a useful diagnostic tool. Strain analysis confirms preserved longitudinal strain but abnormal circumferential strain in constriction compared to controls. Circumferential strain was also reduced in constriction compared to restrictive cardiomyopathy, and constrictive patients also showed significant abnormalities of torsional mechanics.[50]

### CONSTRICTION VERSUS RESTRICTION

A comparison of the echocardiographic features of constriction and restriction is presented in Chapter 28 (Table 28-4).

The echocardiographic evaluation of pericardial constriction and its distinction from restrictive cardiomyopathy remains a challenging task. Important diagnostic pitfalls may arise when localized constriction or mixed constriction and restriction or right-sided pathology can lead to heterogeneity of myocardial mechanics and atypical findings. Arrhythmias, especially atrial fibrillation, may make the interpretation of Doppler velocities difficult. The diagnosis of pericardial constriction relies on the integration of information acquired from high-quality 2D M-mode and Doppler imaging with a good understanding of the underlying clinical picture. Multimodality imaging is usually required and provides information that is complementary to echocardiography. On occasion, hemodynamic evaluation in an experienced cardiac catheterization lab will still be required.

## Pericardial Effusion

A wide variety of conditions, broadly divided into inflammatory, neoplastic, endocrine, and traumatic, can lead to an increase in the normal volume of pericardial fluid (see Box 29-2). Clinically, the consequences of this pericardial effusion are alterations in the physiology of cardiac function as intrapericardial pressure increases, reducing true (transmural) intracardiac filling pressures. Because right-sided pressures tend to be lower than left-sided pressure, direct effects of the pericardial fluid are usually first seen in right-sided chambers.[51]

### M-MODE AND TWO-DIMENSIONAL ECHOCARDIOGRAPHY

#### *Echocardiographic Appearance of Pericardial Fluid and Other Common Disorders Simulating Pericardial Effusion*

The hallmark of a pericardial effusion is visualization of an echolucent zone corresponding to a greater than physiologic volume of fluid in the pericardial space. If pericardial anatomy is relatively normal before fluid accumulation, fluid will first accumulate in the oblique sinus posterior to the left ventricle (LV)[11] (see Fig. 29-1) and is best viewed in the parasternal long-axis view. Once approximately 100 mL of fluid has accumulated in the pericardium, the fluid will tend to become circumferential, filling the entire pericardial space.

It is important to differentiate normal anatomic variants and nonpericardial processes from pericardial fluid. Left-sided pleural effusions appear posterior to the heart and should be distinguished from posterior pericardial effusion. Pericardial fluid will track anterior to the proximal descending thoracic aorta, whereas pleural effusions will not. When pericardial and pleural effusions coexist, the outline of the pericardium separating the fluid-filled spaces is often seen (Fig. 29-6). Occasionally, the use of a nonstandard imaging window through the pleural effusion may be helpful, and visualization of partially atelectatic lung in the fluid cavity confirms the diagnosis of pleural effusion.

Epicardial fat also leads to the appearance of an echolucent space within pericardium (Fig. 29-7). Unlike pericardial fluid, which tends to accumulate first in the posterior pericardial space, epicardial fat is generally more prominent anteriorly. This fat can occasionally cause diagnostic difficulty when

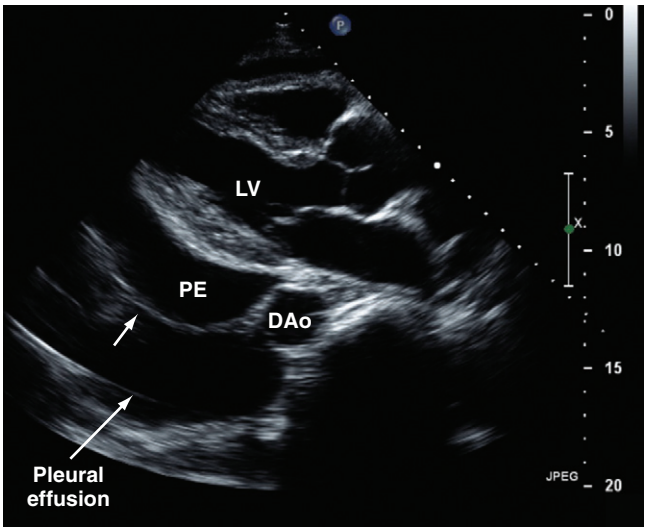



**Figure 29-6 Parasternal long-axis view of patient with both pericardial and pleural effusions.** Pericardial fluid tracks anteriorly to the descending thoracic aorta; pleural fluid is more posterior. Parietal pericardium is clearly seen separating fluid layers (*arrow*). A smaller amount of fluid is seen in the anterior pericardial space. *DAo,* Descending thoracic aorta; *PE,* pericardial effusion.

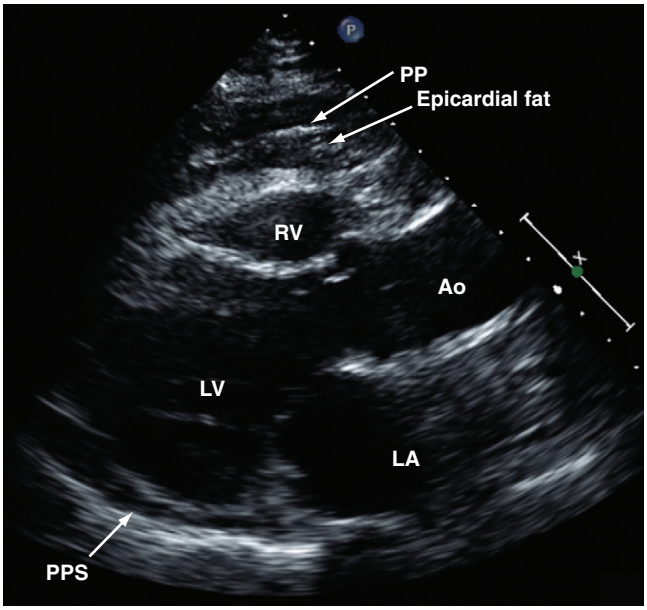



**Figure 29-7 TTE parasternal long-axis view.** Prominent echolucent zone is noted in the anterior pericardial space consistent with epicardial fat. Note the characteristic speckled appearance. There are in fact two fat layers, separated by parietal pericardium. Note also a smaller lucent zone in the posterior pericardial space, likely also due to epicardial fat. *Ao,* Aorta; *PP,* parietal pericardium; *PPS,* posterior pericardial space.

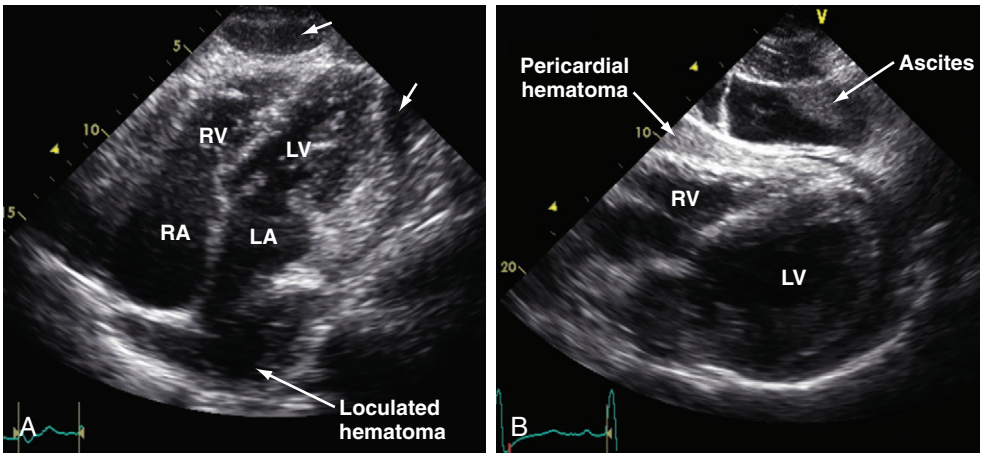



**Figure 29-8 Contrasting cases of pericardial hematoma. A,** Extensive pericardial hematoma (*arrows*) noted when the patient experienced hemodynamic collapse following an atrial septal defect repair. Contrast with **B,** where small layer of pericardial hematoma is noted on subcostal images. The fluid is relatively echogenic, consistent with blood in pericardial space. Patient experienced chest pain immediately following RV biopsy. Despite only a small volume of pericardial hematoma, severe hypotension was present. Ascites is also noted.

prominent posteriorly or when in unusual locations such as adjacent to the right atrium (RA). Epicardial fat will have echogenicity between that of the blood pool and myocardium[52,53] and tends to have a characteristic speckled appearance. Epicardial fat is more common in older, female, obese, and diabetic subjects, but correlation with severe obesity is not invariable.[54,55] MRI or CT imaging will resolve difficult cases.[56]

### FACTORS AFFECTING THE APPEARANCE OF PERICARDIAL EFFUSIONS

The echogenicity of the pericardial fluid will be influenced by features intrinsic to the fluid or related to the underlying pathologic process (e.g., tumor infiltration of the pericardium). In general, as the inflammatory nature of the fluid increases, so does its echogenicity. However, precise characterization may be elusive and tends to be more accurate with CT or MRI.[57,58]

### DETERMINATION OF PERICARDIAL FLUID VOLUME

2D (using a prolate ellipse model)[59] and especially three-dimensional (3D) echocardiography[60] has the ability to determine fluid volume. However, for clinical purposes, reporting of the effusion as minimal, small, moderate, or large is adequate. For circumferential pericardial effusions, we characterize any pericardial effusion with less than 5 mm of pericardial separation in diastole (corresponding to a fluid volume of 50 to 100 mL) as minimal, 5 to 10 mm of separation as small (corresponding to a fluid volume of 100 to 250 mL), 10 to 20 mm of separation as moderate (corresponding to a fluid volume of 250 to 500 mL), and greater than 20 mm separation as large (corresponding to a fluid volume greater than 500 mL). For any significant effusion, we report location, degree of loculation or septation, and the feasibility, risk, and suggested route for percutaneous intervention.

### CLINICAL CONSIDERATIONS

A common clinical scenario is a request for determination of the presence or absence of pericardial effusion and, if effusion is present, a determination of its size and hemodynamic effect. It should be remembered that an incompletely understood, complex interaction of factors influences the ultimate physiologic consequences of pericardial effusion and modulates the hemodynamic expression in any given patient. These include the pericardial pressure/volume relationship, the rapidity of fluid accumulation, underlying cardiac pathology (particularly hypertrophy and shunts), and systemic volume status.[61] It is well understood, for instance, that small acute pericardial effusions (occurring most commonly postintervention or traumatically) can lead to dramatic physiologic effects (Fig. 29-8), whereas moderate-sized or even large pericardial effusions that accumulate slowly can be hemodynamically well tolerated.[8] Localized cardiac compression may lead to dramatic hemodynamic consequences without producing classical echocardiographic indications of "tamponade."[62-65]

## Pericardial Tamponade

### ECHOCARDIOGRAPHIC EVALUATION

#### *Right Ventricular Compression, Inversion, or Collapse*

Perhaps the most useful echocardiographic indicator of a hemodynamically significant pericardial effusion is RV diastolic collapse. Echocardiographically, this is seen on M-mode or 2D recordings as a persistent inward motion of the RV free wall during diastole (Fig. 29-9). By the time this is noted in experimental preparations, there is already a significant reduction (approximately 20%) in forward cardiac output and elevation in heart rate without a change in mean arterial pressure.[66] There is no precise relationship between the duration or degree of RV diastolic collapse and the degree of elevation of intrapericardial pressure or the severity of the hemodynamic effect of the pericardial fluid.[67] Clinically, one can appreciate all degrees of this phenomenon, from a barely perceptible dip only seen with high–frame-rate recordings to complete collapse and obliteration of the RV throughout diastole.

Increases in intravascular volume,[68] RV pressure,[69] and increased chamber stiffness will all reduce the amount of RV diastolic collapse for any given increase in intrapericardial pressure. This means that in certain patients with pulmonary hypertension, RV hypertrophy, or RV volume overload (e.g., atrial

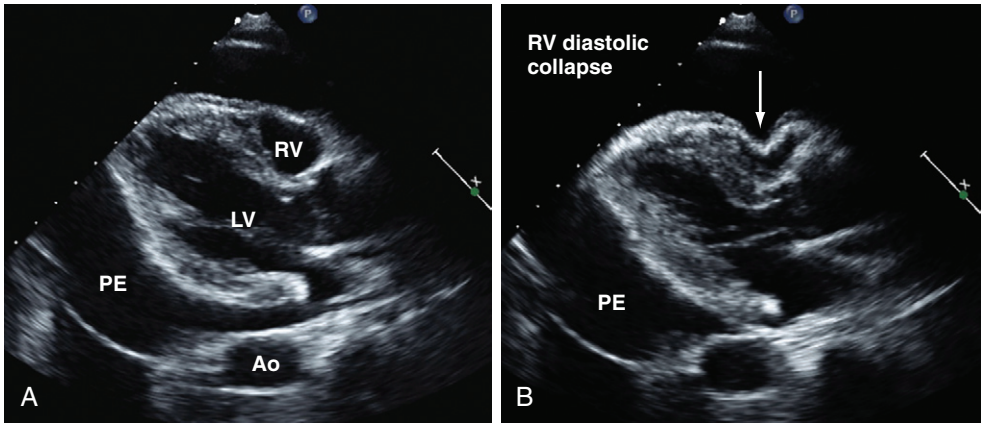



**Figure 29-9** **Parasternal long-axis image of a patient with large pericardial effusion (*PE*) and cardiac tamponade. A,** Late diastole; no RV collapse is evident. **B,** Marked RV collapse is present in early diastole (*arrow*). *Ao*, Aorta.

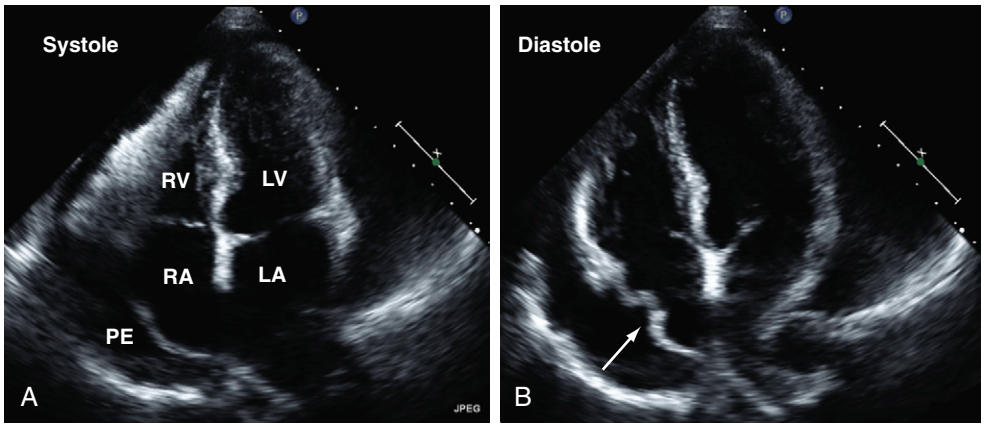



**Figure 29-10** **Apical four-chamber view of large pericardial effusion (*PE*) with transient RA collapse (*arrow*). A,** Systole. **B,** Diastole.

septal defects), RV diastolic collapse may not occur despite significant elevations in pericardial pressure.

Because the sensitivity and specificity and therefore the negative and positive predictive value of RV diastolic collapse depend on the definition of tamponade (Table 29-1),[31,51,62,70-72] we use a clinical approach to this finding. In a patient with clinical findings of tamponade, we would interpret RV diastolic collapse to indicate a significant hemodynamic contribution of the effusion to the patient's clinical state and require immediate therapy to remove pericardial fluid. In a patient without clinical tamponade, we would interpret RV diastolic collapse to indicate intrapericardial pressure at or above RV diastolic pressure and a potential for relatively acute hemodynamic deterioration. Although this is not viewed as an indication for immediate pericardial fluid removal, urgent action is indicated to reverse any factors worsening the hemodynamic effect of the effusion.

Large pleural effusions can cause RV diastolic collapse.[73] Where there is uncertainty as to the genesis of tamponade physiology, we drain the pleural effusion and then reevaluate the patient clinically and echocardiographically.

### *Right Atrial Compression, Inversion, or Collapse*

RA pressures are lower than RV pressures throughout most of the cardiac cycle. Because intrapericardial pressure is evenly distributed over the heart, one would surmise that RA compression would occur before RV compression as pericardial pressure is raised. This is borne out in imaging studies in which the RA and RV are continuously imaged during pericardiocentesis.[51] Subsequently, RA inversion, which tends to begin in late ventricular diastole but persists into early ventricular systole, is an extremely sensitive sign of cardiac tamponade[63] (Fig. 29-10). However, it is less specific than RV diastolic collapse (see Table 29-1). The depth of RA collapse bears an imprecise relationship to the hemodynamic effect of the fluid.[63,72] Conversely, the RA inversion time index (determined by counting the total number of frames showing atrial inversion divided by the total number of frames in the cycle) has been reported to have high sensitivity and specificity for the presence of clinical cardiac tamponade[72] (see Table 29-1). Marked elevation in RA pressure and ventricular pacing have the potential to influence the accuracy of this sign.[72]

### *Left Atrial Compression, Inversion, or Collapse*

Normally, mean LA pressure is higher than RA pressure. Therefore LA compression, inversion, or collapse is generally less sensitive but more specific than RA findings for tamponade.[62,63] (see Table 29-1). LA collapse may, however, be useful in settings of abnormally high right-sided pressures (e.g., pulmonary embolism) and may be the only sign of tamponade in the postoperative patient.[65]

Isolated LV diastolic collapse is occasionally seen with localized effusion, usually in the postsurgical setting.

**TABLE 29-1 Sensitivity, Specificity, Negative, and Positive Predictive Values of Echocardiographic Features of Pericardial Tamponade**

| *Study* | *Year* | *Echocardiographic Sign Evaluated* | *Patients (Total/Tamponade)* | *Definition of Tamponade* | *Sensitivity (%)* | *Specificity (%)* | *PPV (%)* | *NPV (%)* |
|---|---|---|---|---|---|---|---|---|
| Armstrong[70] | 1982 | RV diastolic collapse, M-mode, (posterior movement of the RV free wall in early and mid diastole as timed from the ECG) | 86/17 | Presence of a moderate to large pericardial effusion, plus at least two of the following: (1) elevated venous pressure, (2) systemic hypotension, (3) pulsus paradoxus and resolution of signs after pericardiocentesis | 76 | 84 | 54 | 93 |
| Armstrong[70] | 1982 | RV diastolic collapse, 2D (any indentation of the RV free wall during diastole) | 41/10 | Same as above | 100 | 87 | 71 | 100 |
| Engel[71] | 1982 | RV diastolic collapse, M-mode (persistent posterior motion of the RV free wall greater than 50 ms after mitral valve opening) | 37/21 | Pulsus paradoxus >10 mm Hg, elevated systemic venous pressure, and resolution of signs with pericardiocentesis | 81 | 94 | 89 | 80 |
| Gillam[72] | 1983 | RA collapse (inversion of the RA free wall at any point of the cardiac cycle) | 123/19 | Two or more of the following: (1) elevated jugular venous pressure, (2) relative hypotension, (3) pulsus paradoxus >10 mm Hg and resolution of the symptoms with pericardiocentesis | 100 | 82 | 50 | 100 |
| Gillam[72] | 1983 | RA diastolic collapse (RA inversion time index >0.34 [defined as the number of video fields demonstrating RA inversion divided by the total number of fields per cardiac cycle]) | 36/18 | Same as above | 94 | 100 | 100 | 95 |
| Kronzon[62] | 1983 | RA collapse, 2D (any reduction in RA size during diastole) | 29/9 | Clinical with relief after pericardiocentesis | 100 | 85 | 75 | 100 |
| Kronzon[62] | 1983 | LA collapse, 2D (posterior LA wall motion of at least 10 mm in diastole) | 29/9 | Same as above | 54 | 95 | 83 | 83 |
| Singh[51] | 1984 | RV diastolic collapse, 2D (persistent inward motion of the RV endocardial surface after opening of the mitral valve) | 16/12 | Equalization of RA, pulmonary capillary wedge, and intrapericardial pressures and elevation of these pressures to >10 mm Hg | 92 | 100 | 100 | 80 |
| Singh[51] | 1984 | RA collapse, 2D (RA free wall appears to be inverted at any point during the cardiac cycle) | 12/8 | Same as above | 63 | 100 | 100 | 57 |
| Singh[51] | 1984 | RV diastolic collapse, 2D (persistent inward motion of the RV endocardial surface after mitral valve opening) | 21/16 | Equalization of the intrapericardial, RA, and pulmonary wedge pressures with elevations of these pressures to >10 mm Hg | 93 | 100 | 100 | 83 |
| Himelman[31] | 1988 | Inferior vena cava plethora, 2D (a decrease in proximal vena cava diameter by >50% after a deep inspiration) | 115/33 | Either of the following: (1) elevation (mean >12 mm Hg) and equalization (≤5 mm Hg) of diastolic filling pressures; (2) systolic blood pressure <100 mm Hg that increased by >20 mm Hg after pericardiocentesis | 97 | 40 | 40 | 97 |
| Himelman[31] | 1988 | RA collapse, 2D (dynamic inversion of the RA wall occurring in late diastole or early systole) | 115/33 | Same as above | 55 | 66 | 39 | 78 |
| Himelman[31] | 1988 | RV diastolic collapse, 2D (early diastolic inversion of the RV free wall that varied with respiration) | 115/33 | Same as above | 48 | 68 | 38 | 77 |

Some of the values in the table differ from those reported in the original studies, as data from patients with "equivocal" tamponade have not been used. Sensitivity = true positives/(true positives + false negatives) and specificity = true negatives/(true negatives + false positives).

Data from references in the chart.

*ECG*, Electrocardiogram; *NPV*, negative predictive value (true negatives/[true negatives + false negatives]); *PPV*, positive predictive value (true positives/[true positives + false positives]).

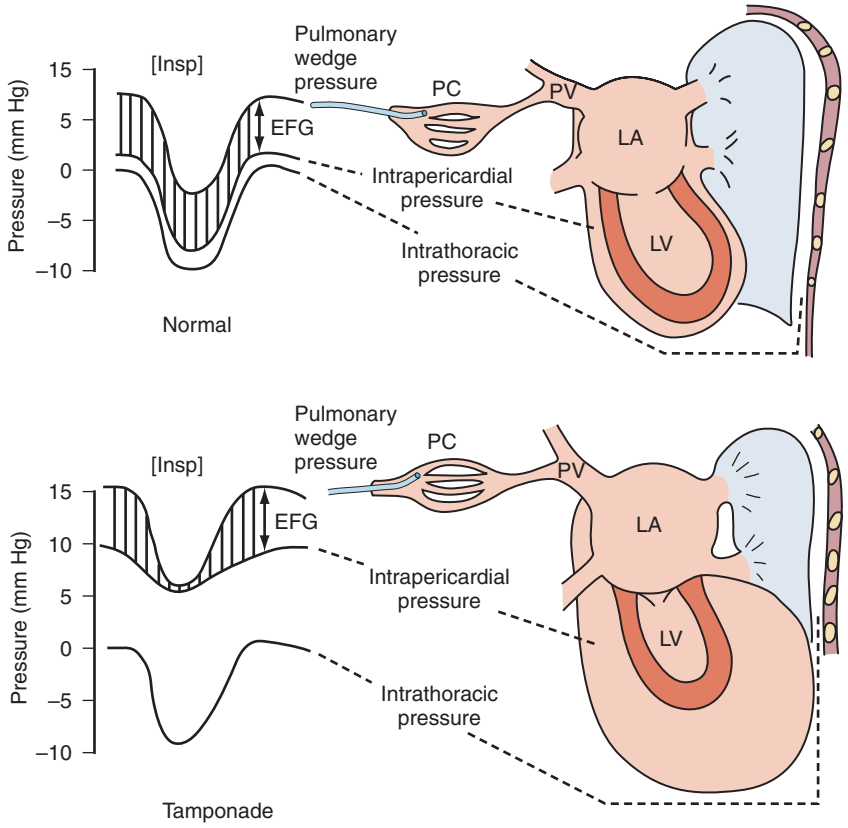



**Figure 29-11** *Top:* **Normal situation in which changes in intrathoracic pressure are transmitted to both pericardial sac and pulmonary veins.** Effective filling gradient (*EFG*) changes only slightly during respiration. *Bottom:* Cardiac tamponade. Changes in intrathoracic pressure are transmitted to pulmonary veins (*PV*) but not to pericardial sac. EFG falls during inspiration. *Insp*, Inspiration; *PC*, pulmonary capillaries. *(From Sharp JT, Bunnell IL, Holland JF, et al: Hemodynamics during induced cardiac tamponade in man.* Am J Med *29:640-646, 1960.)*

### *Phasic Respiratory Changes and Plethora of the Inferior Vena Cava*

Decreased phasic respiratory changes and plethora of the inferior vena cava have been reported in tamponade[31]; however, this is a nonspecific finding (see Table 29-1).

### *Doppler Echocardiography*

The determination of variations in intracardiac flows with respiration, specifically using PW Doppler, has been proven to aid clinical decision making in patients with pericardial effusions. Although tamponade bears certain similarities to the physiology of constriction, there are important differences. It should be recalled that, in tamponade, impedance to ventricular filling is pandiastolic and inspiratory augmentation of right-sided filling is somewhat preserved. Ventricular interaction and relative dissociation of intrathoracic from intrapericardial, and hence transmural, filling pressure are key to the understanding of both processes.[74]

During inspiration, normally intrathoracic, intrapericardial, and intracardiac pressures decrease in unison and to a similar extent. There is normally a small augmentation of right-sided transvalvular flows and a decrease in left-sided transvalvular flows accompanying inspiration.[75] Echocardiographically this is appreciated in normal subjects as minimal change in mitral E wave velocity with inspiration, and slightly more prominent respiratory changes in the right heart. The explanation for this is a combination of increased venous return secondary to decreased intrathoracic pressure, a fall in pulmonary vascular impedance, and ventricular interaction. With accumulation of pericardial fluid, there is a blunting of transmission of pressure changes from the intrathoracic compartment to the intrapericardial compartment.[75] As the pulmonary veins are intrathoracic (but extrapericardial), the pulmonary venous pressure falls with inspiration; however, the fall in pericardial pressure is blunted, resulting in a fall in driving pressure filling the LA and therefore a reduction in LV filling.[75] Respiratory augmentation remains intact on the right side, and RV filling increases during inspiration.[76] As pericardial fluid volume increases, available pericardial space becomes limited, enhancing the potential for ventricular interaction, which in turn amplifies the disparate patterns of left-sided and right-sided filling with respiration (Fig. 29-11). Although the magnitude of this flow disturbance is greater, and separation of values from normal occurs earlier with right-sided flows, in the clinical setting most attention has focused on the mitral inflow, because diagnostically adequate tricuspid inflow signals are obtained in around one third of patients.[38] In tamponade, there is characteristically an appreciable fall in mitral E wave velocity and VTI and lengthening of the isovolumic relaxation time on the first inspiratory beat. A summary of the magnitude and direction of flow disturbance in intracardiac flows are best illustrated in Figure 29-12 and summarized in Table 29-2.[38,76-78] Although most literature has concentrated on changes in transvalvular flow velocities, there is also a decrease in LV ejection time and LV inflow duration.[76]

Although some have noted a quantitative relationship between rise in pericardial pressure and the degree of respiratory variation in inflow velocities,[79] the relationship of the magnitude of this change to the severity of tamponade has been questioned.[80]

Interrogation of superior vena cava and hepatic vein flow may provide information that is complementary to analysis of mitral inflow velocities in equivocal cases. The superior vena cava is best imaged from the right supraclavicular window at a depth

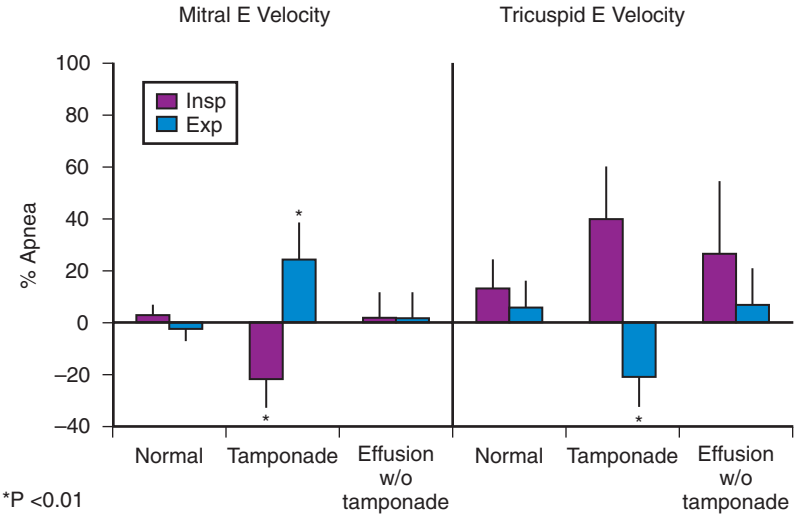



**Figure 29-12 Respiratory variation of mitral and tricuspid inflow velocities in cardiac tamponade, normal subjects, and patients with effusion without tamponade.** Mean percentage changes in mitral and tricuspid early filling velocities (*E*) with first beat of inspiration (*Insp*) and of expiration (*Exp*) are compared with mean apnea values. In comparison with normals and patients without tamponade, the mital E wave velocity in patients with tamponade decreases significantly with inspiration and increases with expiration. All patients exhibited an increase in tricuspid E wave velocity with inspiration, but only those with tamponade showed a decrease in expiratory E wave velocity. *(With permission from Burstow DJ, Oh JK, Bailey KR, et al: Cardiac tamponade: characteristic Doppler observations.* Mayo Clin Proc *64:312-324, 1989.)*

**TABLE 29-2 Respiratory Variation in Intracardiac Flows Reported in Normal Subjects, Pericardial Effusion without Tamponade, Tamponade, and Postpericardiocentesis**

| *Study/ Parameter* | *Year* | *Subjects* | Normal | | Tamponade | | Effusion without Tamponade | |
|---|---|---|---|---|---|---|---|---|
| | | | *Inspiration* | *Expiration* | *Inspiration* | *Expiration* | *Inspiration* | *Expiration* |
| **Pandian**[7] | 1985 | 9 dogs* 3 patients (all with tamponade) | | | | | | |
| Mitral mean flow velocity | | | ↓10 ± 2% | | ↓42 ± 3% | | ↓12 ± 1% | |
| Tricuspid mean flow velocity | | | ↑17 ± 2% | | ↑117 ± 19% | | ↑17 ± 3% | |
| **Leeman**[80] | 1987 | 19 (11 tamponade) | | | | | **Post-pericardiocentesis** | |
| Mitral VTI | | | ↓8% | | ↓35% | | ↓3% | |
| Tricuspid VTI | | | ↑9% | | ↑80% | | ↑11% | |
| Aortic VTI | | | ↓3% | | ↓33% | | ↓7% | |
| Pulmonary VTI | | | ↑9% | | ↑86% | | ↑11% | |
| **Appleton**[78] | 1988 | 27 (7 tamponade) | | | | | | |
| Mitral E velocity (cm/s) | | | 82 ± 17 | 85 ± 18 | 39 ± 12 | 68 ± 19 | 71 ± 12 | 77 ± 13 |
| Tricuspid E velocity (cm/s) | | | 64 ± 10 | 56 ± 9 | 60 ± 6 | 30 ± 9 | 60 ± 9 | 50 ± 8 |
| Aortic velocity (cm/s) | | | 109 ± 9 | 113 ± 9 | 80 ± 22 | 107 ± 26 | 103 ± 22 | 107 ± 22 |
| IVRT (ms) | | | 74 ± 15 | 72 ± 14 | 117 ± 39 | 64 ± 20 | 69 ± 15 | 67 ± 17 |
| **Burstow**[39] | 1989 | 28 (16 tamponade) | | | | | | |
| Mitral E velocity (cm/s) | | | 73 ± 12 | 74 ± 15 | 37 ± 12 | 59 ± 15 | 77 ± 19 | 78 ± 20 |
| | | | 55 ± 8 | 51 ± 7 | 51 ± 7 | 29 ± 5 | 54 ± 10 | 43 ± 11 |
| IVRT (ms) | | | 82 ± 7 | 79 ± 6 | 104 ± 17 | 75 ± 7 | 87 ± 10 | 84 ± 12 |

Data from references in the table.
*E*, Early diastolic filling wave of the left (mitral) or right (tricuspid) ventricle; *IVRT*, isovolumic relaxation time; *VTI*, velocity-time integral.
*Dogs were studies in three states: baseline, effusion without tamponade, and with tamponade.

of 5 to 7 cm. Normal superior vena cava flow patterns reflect phasic changes in RA pressure.[81] Doppler echocardiography of the superior vena cava in normal subjects reveals a biphasic, systolic flow pattern without significant flow reversals.[82] Patients with cardiac tamponade have been reported to show reduced, absent, or reversed diastolic flow with the first expiratory cardiac cycle, the Doppler counterpart of the loss of the Y descent and the prominent X descent.[76,83] In advanced tamponade, loss of diastolic filling throughout the respiratory cycle has been reported. Similar changes occur in hepatic vein flow, with marked expiratory loss of diastolic filling, along with expiratory diastolic flow reversals. Examples of abnormal Doppler flow recordings in cardiac tamponade are noted in Figure 29-13.

### *Tissue Doppler*

In eight patients with pericardial effusion and tamponade, E′ was reported to be lower than in age-matched and sex-matched control subjects, and unlike LV inflow (E wave), velocity did not show respiratory variation. E′ values returned to normal after pericardiocentesis.[41]

## THE ROLE OF ECHOCARDIOGRAPHY IN PATIENT MANAGEMENT

Echocardiographic signs of elevated pericardial pressure may precede the appearance of clinical tamponade (which we define as a fall in mean arterial pressure and a pulsus paradoxus greater

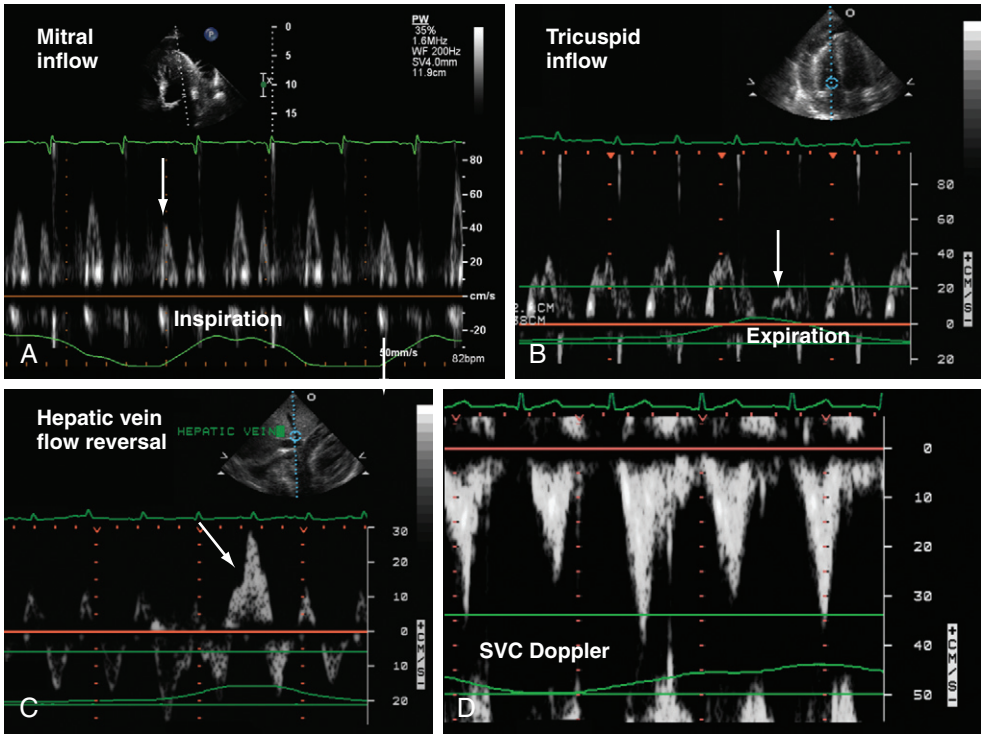



**Figure 29-13** **Doppler findings in cardiac tamponade. A,** Significant reduction in mitral inflow velocity is noted on first inspiratory beat (*arrow*). **B,** Marked fall in tricuspid inflow velocity is noted on first expiratory beat (*arrow*). **C,** Hepatic vein Doppler indicates marked flow reversal on first expiratory beat (*arrow*), after slight augmentation in forward velocities on inspiration. **D,** Superior vena cava Doppler in a patient with acute tamponade. Note loss of normal diastolic filling wave throughout respiratory cycle.

than 10 mm Hg as a result of raised pericardial pressure).[66] Given that the clinical transformation from stable to unstable can occur abruptly, echocardiography has come to play a pivotal role in the management of patients with pericardial effusion. It must be appreciated that the physiologic effects of an increasing pericardial effusion lie on a continuum, and therefore any separation into distinct stages is arbitrary. We find it useful, however to divide patients with pericardial effusions into three hemodynamic categories. First, those without echocardiographic evidence of hemodynamic compromise, (no RV collapse, no RA or LA collapse, physiologic changes in intracardiac flows with inspiration) we describe as "no evidence of hemodynamic effect." Second, those with any degree of RV diastolic collapse, prolonged (more than 35% of the cardiac cycle) RA collapse, or marked (greater than 25% LV or greater than 50% RV) early filling [E] velocity changes with inspiration, we report as showing "echocardiographic indications of 'tamponade.'" The use of quotation marks is to underscore the fact that tamponade is a clinical syndrome. Third, we report patients who fit into neither of the aforementioned categories as having "echocardiographic indicators of elevated pericardial pressure without echocardiographic features of 'tamponade.'" It cannot be overemphasized, however, that with localized cardiac compression or abnormal physiologic states, hemodynamic compromise may be present as a result of elevated pericardial pressure without any classic M-mode, 2D, or Doppler echocardiographic indicators of raised intrapericardial pressure.[63-65]

## LOCALIZED AND LOCULATED PERICARDIAL FLUID COLLECTIONS

In some cases, localized cardiac compression can occur rendering both the diagnosis of tamponade and attribution of the pericardial process to the clinical state difficult. This is especially challenging when hypotension occurs after cardiac surgery (see Fig. 29-12).[63-65] A high index of suspicion is especially appropriate in anticoagulated patients and following transvenous pacing lead removal. In this setting, traditional echocardiographic markers of tamponade may not be present. A careful search for localized chamber compression, localized collections of blood inside or adjacent to the pericardial space, and less usual features, such as LV or LA diastolic collapse,[84] must be performed. Transesophageal echocardiography may add incremental information, especially if imaging quality is poor.[85-87] Sometimes the most important role of the echocardiogram is to rule out other cardiac causes of the patient's clinical state. If doubt remains as to the presence or hemodynamic effect of a collection, alternative imaging techniques, catheter-based hemodynamic monitoring with volume manipulation, or even surgical exploration may be required for both diagnostic and therapeutic purposes.[65]

## ECHOCARDIOGRAPHICALLY GUIDED PERICARDIOCENTESIS

Before the advent of 2D echocardiography, percutaneous pericardiocentesis was viewed with trepidation. In cardiac catheterization laboratories, for instance, clinicians in large-volume centers achieved success rates of 86% in obtaining fluid, with death rates of 4%, and a further 4% risk of other major complications.[88] In contrast, echocardiographically guided series have indicated success rates of 97% or more, rare deaths, and total complication rates of 3% to 5%. Major complications have included cardiac laceration requiring surgery, hemothorax requiring thoracotomy, major pneumothoraces, and rare bacteremia or ventricular tachycardia. Less significant or

**Box 29-3**

**PERICARDIOCENTESIS CHECKLIST**

- Review indications, urgency of pericardiocentesis
- Review echo images, determine feasibility, select approach
- Review for bleeding diathesis, anticoagulant drugs, significant electrolyte disturbance, anemia,
- Consent
- Appropriate setting, monitoring (oxygen saturation, electrocardiogram, invasive or noninvasive blood pressure minimum)
- Intravenous access
- Check pericardiocentesis kit
- Check sedation, analgesia available

self-limiting complications include transient chamber entry, small pneumothoraces, vasovagal response, and minor arrhythmias.[89-91] It should be recalled that surgical approaches may be associated with significant morbidity.[92] Needle pericardiocentesis is generally not indicated in patients with pericardial effusions as a result of aortic dissection, penetrating trauma, or ruptured ventricular aneurysm where definitive surgical therapy is indicated.

In emergencies, the physicians at our institution prefer to have echocardiographic confirmation of an effusion, if at all possible. Most often, this occurs during percutaneous interventions or ablation procedures. When effusions are found, they use the information obtained to guide the percutaneous approach. This so-called rescue pericardiocentesis is successful in relieving tamponade in 99% of cases and may be the only and definitive therapy in 82% of cases.[93]

Although minor variations in approach to echocardiographically guided pericardiocentesis exist, certain basic principles apply.[90,91,94] We have evolved an institution approach, which is outlined next in point form.

1. **Preparation and orientation:** (See Box 29-3.) Outside of emergencies, we perform this procedure in our cardiac intensive care unit. Immediately before the procedure, we image the patient at the bedside to confirm that the correct approach (i.e., the most direct route to the largest collection of fluid) has been chosen. Attention is focused on avoiding both the internal thoracic arteries (located 0.5 to 2 cm lateral to the sternal edge) and intercostal vessels (inferior border of the rib). We then mark a proposed entry point with a permanent marker or reimage from this location to determine the depth to the fluid, the depth to the nearest cardiac structure, and the correct angle of approach. Most importantly, the angulation of the transducer in 3D space is carefully noted, as this will be subsequently replicated with the pericardiocentesis needle. We find it useful to form a mental map by drawing an imaginary line along the direction of the transducer and then noting its intersection with a remote anatomic structure, such as the point of the left shoulder or tip of the scapula. In our experience it is the inability to accurately reproduce this angle that causes most unsuccessful initial attempts. After a sterile field is established, local anesthesia is administered. Adequate topicalization along the line of approach is mandatory.
2. **Imaging:** A second operator or sonographer usually images from a window remote to the puncture site (usually parasternal or subcostal) to provide real-time visualization of the procedure. Alternatively, the imaging probe can be covered with a sterile sleeve and hence be manipulated by the operator. Imaging probes that allow needle insertion in the center of the imaging plane have been described.[95] Like other operators,[96] we favor the apical route as the safest and easiest approach, but other approaches may be more appropriate in certain situations or with loculated effusions.
3. **Pericardial puncture:** We then attach the pericardiocentesis needle to a 10-mL syringe with 5 mL of 1% lidocaine. The needle is advanced until pericardial fluid is obtained or a depth of needle is inserted that could contact a cardiac structure. Constant aspiration during the advancement of the needle followed by a slight pause for injection should be performed to guard against needle plugging. There is a characteristic "feel" or "pop" associated with contact of the needle with the pericardium and its puncture. Given the tomographic nature of 2D imaging and potential for imaging artifacts, care must be taken in interpretation of the image during this phase. In particular, the tip of the pericardiocentesis needle and its course are difficult to identify with imaging from a remote acoustic window. Indentation of the pericardium by the needle just before puncture is helpful if seen. Monitoring of the needle electrogram is no longer performed.
4. **Guidewire and catheter:** Once the pericardium is entered, there should be free flow of fluid into the syringe. If we are uncertain as to the position of the needle, if we aspirate blood, or in the case of small effusions, the intrapericardial position of the needle is confirmed with the injection of 1.0 to 5 mL of agitated saline via a three-way stopcock configuration. Visualization of the contrast in the pericardial space confirms correct needle position (Fig. 29-14, *A*). In larger effusions, the needle may be advanced incrementally, once pericardial fluid is obtained. A "J" guidewire is then introduced into the pericardial space. The wire is usually well seen in the pericardial space from the remote window. The track of the guidewire is dilated, and a pigtail catheter is placed over the wire into the pericardial space. Fluid is withdrawn for analysis. We do not routinely measure pericardial pressure; however, progressive disappearance of fluid from the pericardial space and resolution of signs of tamponade provides the final confirmation of successful pericardiocentesis. Once the majority of the fluid has been removed, the catheter is secured and a suction drain attached. Analysis of pericardial fluid should be ordered according to the clinical context.
5. **Subsequent catheter management:** The pericardial drain may be removed after the pericardial fluid has been fully aspirated. However, in most cases we leave the catheter in situ for 12 to 36 hours, removing once the drainage is minimal (less than 30 mL in 24 hours). In traumatic pericardial effusions occurring in the electrophysiology or catheterization lab, our practice is early removal, as recurrence in this setting is rare. Occasionally, the catheter is withdrawn slightly to avoid kinking or facilitate drainage. Small saline flushes are occasionally necessary to maintain patency. We generally avoid readvancing the catheter because of risk of infection.
6. **Troubleshooting:** See Table 29-3.

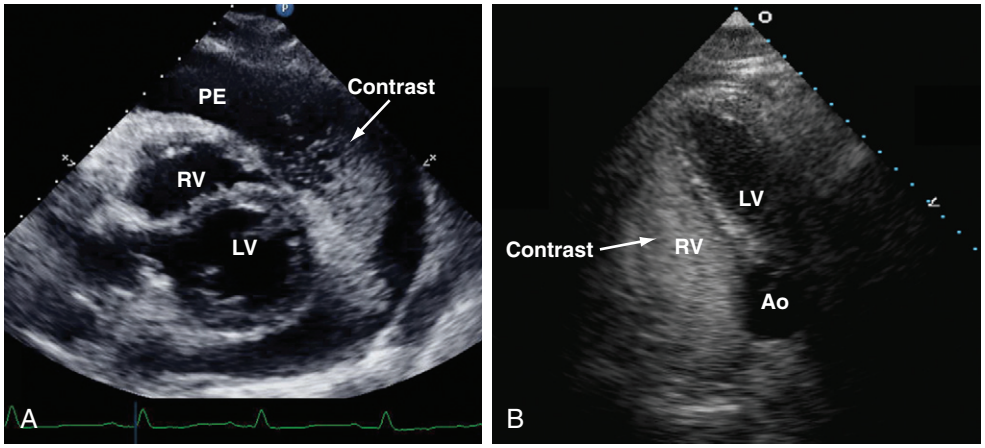



**Figure 29-14** **Use of bubble contrast in needle pericardiocentesis. A,** TTE parasternal short-axis view of saline bubble contrast in large pericardial effusion (*PE*) during pericardiocentesis. Saline contrast is seen in lateral pericardial space, confirming correct catheter position. **B,** Bedside off-axis apical five-chamber TTE. Emergency pericardiocentesis performed at bedside after patient became severely hypotensive following atrial fibrillation ablation procedure. Effusion was small and pericardiocentesis technically difficult. Bloody tap was obtained, and saline contrast was used to determine needle location. Saline contrast is seen to opacify the RV, confirming intracardiac needle position. After readjustment of needle orientation, pericardial space was entered and 150 mL of blood removed with marked hemodynamic improvement. *Ao*, Aorta.

## Acute Pericarditis

Acute pericarditis is caused by inflammation of the pericardium and can occur in isolation or secondary to an underlying systemic condition.[97,98] As an isolated entity, acute pericarditis is most commonly caused by a viral infection. In practice it is considered idiopathic when the viral agent is not identified.[99,100] Other causes include autoimmune disease; neoplastic invasion of the pericardium; uremia; acute myocardial infarction; and less commonly bacterial infections, previous cardiotomy, or aortic dissection.

Echocardiography remains the initial imaging modality of choice as it can rapidly and accurately assess the pericardium and underlying cardiac structure and function. In general, there is a paucity of echocardiographic findings. Patients with uncomplicated pericarditis will often have a normal echocardiogram.

The value of echocardiography in acute pericarditis lies in its unique ability to detect complications, at times aiding in the diagnosis of the underlying etiology or detecting other cardiac processes that may account for the patient's symptoms or clinical findings. Complications include pericardial effusion with or without hemodynamic effect, constrictive physiology, and/or myopericarditis. A large pericardial effusion or tamponade is a high-risk feature of pericarditis that warrants hospital admission and therefore is important to rule out either clinically or by echocardiography.[101] A transient constrictive phase during acute pericarditis has also been described,[102,103] and acute pericarditis may on occasion progress to overt constrictive pericarditis. In this setting echogenic inflammatory material may be noted in the pericardial space (Fig 29-15). Associated myocarditis can manifest as regional or global myocardial dysfunction. In occasional cases, tumor and/or neoplastic invasion of the pericardium may be seen. Myriad other cardiac diagnoses can mimic acute pericarditis, and the echocardiogram may be useful in this regard as well. One such scenario is in patients presenting with chest pain and electrocardiographic changes in which the differential diagnosis includes acute coronary syndrome and pericarditis. The finding of a regional wall motion abnormality in a coronary distribution without a significant effusion suggests that a diagnosis of acute coronary syndrome is more likely.

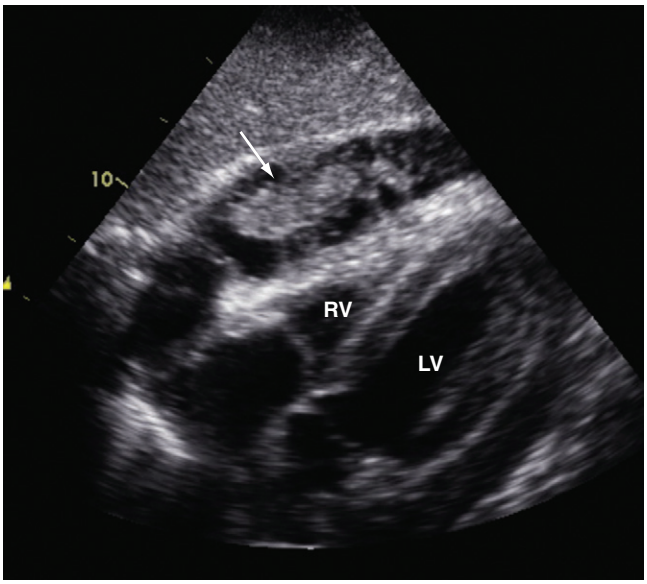



**Figure 29-15** **Subcostal view of a large pericardial effusion.** Extensive echogenic organized material is noted in pericardial space in relation to free wall of RV (*arrow*).

The finding of a pericardial effusion without a regional wall motion abnormality suggests that pericarditis is more likely.

An integrated multimodality imaging approach, in the form of cardiac CT and/or cardiac MRI in addition to TTE, may provide incremental value in more complicated cases of acute pericarditis. The complementary role of CT and MRI lies in their ability to clearly visualize pericardial thickening and inflammatory changes within the pericardium. An integrated approach can be considered in the case of therapeutic difficulty, recurrent pericarditis, development of constrictive physiology, or traumatic etiologies.

## Effusive Constrictive Pericarditis

Effusive constrictive pericarditis is an uncommon condition characterized by both a pericardial effusion and constrictive

**TABLE 29-3 Troubleshooting Pericardiocentesis**

| *Problem* | *Diagnosis* | *Action* |
|---|---|---|
| I can't hit the effusion. | Incorrect line of approach. Usually occurs with smaller, deeper pericardial effusions, especially with thick chest wall. | Recheck landmarks, reimage if uncertain. Check depth; consider long needle if deep fluid. Consider alternative window/approach. Use bubble contrast to confirm position in difficult tap. If repeated unsuccessful attempts, reconsider indication, consider surgical approach. |
| My catheter won't track over the guidewire. | Tip of catheter may not track guidewire because of tight tissue planes or thick skin. May be very thick, stiff pericardium. Guidewire may be kinked over periosteum, pleura, pericardium. | Ensure adequate skin "nick" at guidewire entry point. Consider redilatation over existing guidewire. If guidewire kinked, consider repuncture/replace guidewire. |
| I hit the effusion OK and advanced my guidewire, but now I can't aspirate pericardial fluid. | Catheter is no longer in the pericardial space, or the catheter is kinked. Occasionally dilator will displace wire from pericardial space if long tissue track or inadequate length of intrapericardial wire inserted. | Consider saline contrast to verify intrapericardial position. Usually repuncture is required (i.e., start again). |
| I keep aspirating blood from the catheter, but the effusion doesn't get any smaller. | Consider large hemorrhagic effusion. Consider intracardiac needle/catheter position. | If pulsatile flow, withdraw needle. Use saline contrast to rule out intracardiac needle/catheter placement. If dilators used and catheter intracardiac, consider surgical consult before removal of catheter. |
| I keep aspirating straw-colored fluid, but the effusion isn't getting any smaller. | Catheter in pleural effusion or ascites. | Recheck approach, depth. Give contrast bubbles if in doubt. |
| My patient is in severe pain after the pericardial catheter is placed. | Local irritation from pericardial catheter can occasionally cause intense pain; however, it may indicate more serious complication. | Check catheter position, ensure intrapericardial. Rule out other causes, including coronary artery injury, pleural catheter placement, myocardial tear. Consider nonsteroidal antiinflammatory drug, narcotic. Consider intrapericardial lidocaine. Consider early removal of catheter once effusion is drained. |
| My patient has acute shortness of breath. | Consider pneumothorax. | Chest radiograph if stable, intercostal catheter placement. |
| My patient is experiencing severe hypotension, hemodynamic collapse. | Consider vasovagal response, chamber laceration, tension pneumothorax, intrathoracic bleeding, acute myocardial infarction. | Repeat echocardiography, electrocardiogram, hematocrit. Therapy may include intrapleural drain, volume, atropine, thoracotomy. |
| The effusion recurred rapidly after the pericardial fluid was aspirated. | Needle pericardiocentesis without drainage catheter or catheter removed too soon. | Reaspirate and leave drain in situ 24-36 hours. Consider malignancy; consider surgical window. |
| The pericardial catheter has stopped draining, but there is still fluid around the heart. | Plugged or kinked catheter. Loculated pericardial fluid. | Continuous suction drainage helps prevent plugging. Consider small sterile saline flush/aspirate. Consider repuncture and guidewire placement of new catheter if significant residual pericardial fluid and/or echocardiographic signs of tamponade. |

pericarditis.[104] Based on a series of consecutive patients presenting with tamponade, the prevalence of effusive constriction is close to 8%.[104] Imaging of this entity should look for elements of pericardial effusion, a thickened pericardium or thick intrapericardial material, and evidence of constrictive physiology.[105,106] The hallmark of effusive constrictive pericarditis is persistence of constrictive physiology after removal of the pericardial fluid.[107] The hemodynamic findings may share common features of both pericardial tamponade and constriction.

The most common causes are idiopathic pericarditis and malignancy, but effusive constrictive pericarditis can also be seen after radiation, after pericardiotomy, and in tuberculosis pericarditis. The natural history of this condition is not well understood. However, in a subset of patients, constrictive pericarditis may be due to reversible inflammation, and there may be resolution of the constrictive physiology either spontaneously or following antiinflammatory treatment weeks to months after the effusion has been drained.[103]

## Pericardial Effusion as an Incidental Finding on Echocardiography

Occasionally a pericardial effusion will be noted as an incidental finding on an echocardiogram requested for another indication or as an ancillary finding during lung or abdominal imaging. Therapeutic pericardiocentesis is an absolute in the setting of cardiac tamponade. Among those with large pericardial effusions and no hemodynamic compromise, nearly one third will go on to develop tamponade.[108] Therefore, it is reasonable to perform a pericardiocentesis in the setting of a persistent large pericardial effusion (greater than 1 month) or those with nonspecific signs of tamponade such as RA collapse for less than one third of the cardiac cycle.[109] Small to moderate-sized pericardial effusions do not require drainage, provided that there is no evidence of hemodynamic compromise and the patient is asymptomatic. However, the question of diagnostic pericardiocentesis arises. This is not routinely recommended, given that the diagnostic yield is low. Instead, regardless of effusion size, a careful search for underlying disease likely to result in a pericardial effusion needs to be undertaken (see Box 29-2). In all cases, clinical and echocardiographic follow-up is imperative.

## Congenital Disorders of the Pericardium

### CONGENITAL ABSENCE OF THE PERICARDIUM

Congenital absence of the pericardium is a rare clinical entity found in approximately 1 in 10,000 autopsies. The defects,



**Figure 29-16 MRI image of patient with congenitally absent pericardium.** Abnormal position of heart in thorax explains unusual appearance of heart through usual imaging windows, including appearance of RV enlargement. Nonstandard imaging windows (axillary) are required in some patients.

classified as partial or complete, are most commonly partial, with two thirds of cases located on the left and the remainder on the right side.[110,111] Complete absence of the pericardium is rare and of minimal clinical importance. Leftward displacement of the heart is pronounced, and as a result, cardiac motion, especially of the LV posterior wall, is exaggerated. The right-sided chambers appear prominent, and there is abnormal septal motion.[112,113] Other echocardiographic signs include unusual apical imaging windows into the axilla and the appearance of compressed atria. At least one and usually two of these findings are reported in all patients with complete absence of the pericardium.[117] In contrast, partial absence of the pericardium often requires ancillary imaging techniques to fully delineate the nature and extent of the defect. In this regard, CT and MRI have proven to be especially useful (Fig. 29-16).[114,115]

Most patients are asymptomatic; however, closure of the defect can become necessary in symptomatic patients.[97] With significant leftward cardiac shift, patients may on occasion experience nonexertional chest pain or a prominent cardiac pulsation. Rarely, herniation of cardiac chambers through partial defects can occur, with reported cases of coronary artery obstruction resulting in sudden cardiac death,[116,117] LA strangulation,[118,119] herniation of the LA causing syncope,[120] or herniation of the LV or RV causing mitral or tricuspid regurgitation.[121] In addition, associated congenital defects should also be considered and include atrial septal defect, bicuspid aortic valve, patent ductus arteriosus, tetralogy of Fallot, and mitral stenosis in up to 30% of cases.[113,122] Reports of combined congenital pericardial and diaphragmatic defects also exist.[123]

## PERICARDIAL CYSTS

Pericardial cysts are rare, benign congenital lesions with an incidence of 1 in 100,000 and thought to be remnants of a defect in embryologic development of the pericardium. They are usually an incidental finding on chest radiography or TTE. The majority are located at the right costophrenic angle (70%), followed by the left costophrenic angle (20%), and the remainder are in either the anterior or posterior superior mediastinum.[124] The echocardiographic hallmark of a pericardial cyst is a round or oval echo-free structure adjacent to the cardiac border, most commonly near the RA, from which it is separated by a definite wall of echoes.[125,126] The presence of internal echoes suggesting a more solid structure should alert the clinician to the possibility of a less benign process. Color-flow and pulsed-Doppler assessment at a low velocity setting can be performed to ensure that there is no flow within the structure. Rarely, hydatid pericardial cysts[127] or a cardiac hemangioma[128] may have echocardiographic features mimicking pericardial cysts. Additional imaging with contrast CT can be performed if the diagnosis remains uncertain with echocardiography.[129,130] A pericardial cyst appears as a thin-walled, sharply defined homogenous mass with attenuation slightly higher than water, which fails to enhance with contrast on CT. Therapy is not required in the asymptomatic patient; however, there are numerous noninvasive treatments for pericardial cysts, including videoscopic resection, ethanol sclerosis, or needle aspiration and drainage if symptoms do develop. Symptoms commonly reported include chest pain and shortness of breath. Reported rare complications of pericardial cysts include cardiac tamponade,[131,132] hemorrhage,[124] or erosion of cardiac structures.[133,134]

### KEY POINTS

- An understanding of the effects of ventricular interdependence is key to understanding the hemodynamic and therefore echocardiographic features of compressive pericardial disease, such as tamponade or constriction.
- The diagnosis of pericardial constriction requires a careful integration of the results of M-mode Doppler and 2D imaging and a consideration of the clinical context. A good understanding of the uses and limitations of tissue Doppler imaging augments traditional tools for diagnosing constriction.
- Echocardiography is pivotal to management strategy and decision making in pericardial effusion.
- Traditional echocardiographic markers of cardiac tamponade may be absent in patients with localized pericardial effusions, especially in the postcardiac surgery setting.
- The presence of diastolic collapse of the free wall of the RV is a specific but not sensitive sign of pericardial tamponade.
- Percutaneous drainage of pericardial fluid may be safely performed with echocardiographic guidance.
- When an acute hemopericardium occurs, for instance in the setting of interventional cardiologic procedures, rapid and serious hemodynamic disturbance may ensue, despite the accumulation of a relatively small amount of fluid in the pericardial space.
- In acute pericarditis, the echocardiographic examination is commonly normal.
- The hallmark of effusive constrictive pericarditis is persistence of constrictive physiology following the removal of the pericardial fluid.
- In complex pericardial disease, or when echocardiographic images are suboptimal, integration of echocardiographic findings with findings from other imaging modalities may be required.

## REFERENCES


1. Holt J: The normal pericardium. *Am J Cardiol* 26:455-465, 1970.
2. Hoit B: Pericardial heart disease. *Curr Probl Cardiol* 22:353-400, 1997.
3. Spodick D: The normal and diseased pericardium: current concepts of pericardial physiology, diagnosis and treatment. *J Am Coll Cardiol* 1:240-251, 1983.
4. Goldstein J: Cardiac tamponade, constrictive pericarditis, and restrictive cardiomyopathy. *Curr Probl Cardiol* 29:503-567, 2004.
5. Baker A, Dani R, Smith ER, et al: Quantitative assessment of independent contributions of pericardium and septum to direct ventricular interaction. *Am J Physiol* 275:H476-H483, 1998.
6. Bernard H: The functions of the pericardium. *J Physiology* 22:43, 1898.
7. Slinker BK, Ditchey RV, Bell SP, et al: Right heart pressure does not equal pericardial pressure in the potassium chloride-arrested canine heart in situ. *Circulation* 76:357-362, 1987.
8. Freeman G, Le WM: Pericardial adaptations during chronic cardiac dilation in dogs. *Circ Res* 54:294-300, 1984.
9. Shirato K, Shabetai R, Bhargava V, et al: Alteration of the left ventricular diastolic pressure-segment length relation produced by the pericardium. Effects of cardiac distension and afterload reduction in conscious dogs. *Circulation* 57:1191-1198, 1978.
10. Atherton J, Moore T, Thomson HL, et al: Diastolic ventricular interaction in chronic heart failure [see comments]. *Lancet* 349:1720-1724, 1997.
11. Martin R, Rakowski H, French J, Popp RL: Localization of pericardial effusion with wide angle phased array echocardiography. *Am J Cardiol* 42:904-912, 1978.
12. Martin R, Bowden R, Filly K, Popp RL: Intrapericardial abnormalities in patients with pericardial effusion. Findings by two-dimensional echocardiography. *Circulation* 61:568-572, 1980.
13. Larose E, Ducharme A, Mercier LA, et al: Prolonged distress and clinical deterioration before pericardial drainage in patients with cardiac tamponade. *Can J Cardiol* 16:331-336, 2000.
14. Pandian N, Skorton D, Kieso RA, Kerber RE: Diagnosis of constrictive pericarditis by two-dimensional echocardiography: studies in a new experimental model and in patients. *J Am Coll Cardiol* 4:1164-1173, 1984.
15. Kern M, Aguirre F: Interpretation of cardiac pathophysiology from pressure waveform analysis: pericardial compressive hemodynamics, Part III. *Cathet Cardiovasc Diagn* 26:152-158, 1992.
16. Nishimura RA: Constrictive pericarditis in the modern era: a diagnostic dilemma. *Heart* 86:619-623, 2001.
17. Hatle L, Appleton C, Popp RL: Differentiation of constrictive pericarditis and restrictive cardiomyopathy by Doppler echocardiography [see comments]. *Circulation* 79:357-370, 1989.
18. Bilchick KC, Wise RA: Paradoxical physical findings described by Kussmaul: pulsus paradoxus and Kussmaul's sign. *Lancet* 359:1940-1942, 2002.
19. Takata M, Beloucif S, Shimada M, Robotham JL: Superior and inferior vena caval flows during respiration: pathogenesis of Kussmaul's sign. *Am J Physiol* 262:H763-H770, 1992.
20. Voelkel A, Pietro D, Folland ED, et al: Echocardiographic features of constrictive pericarditis. *Circulation* 58:871-875, 1978.
21. Gibson T, Grossman W, McLaurin LP, et al: An echocardiographic study of the interventricular septum in constrictive pericarditis. *Br Heart J* 38:738-743, 1976.
22. Angheloiu P, Rayarao G, Doyle M, et al: Can CMR characterize the etiology of septal bounce in patients with constrictive pericarditis. *J Am Coll Cardiol* 55:A27.E258, 2010.
23. Sengupta P, Mohan J, Mehta V, et al: Doppler tissue imaging improves assessment of abnormal interventricular septal and posterior wall motion in constrictive pericarditis. *J Am Soc Echocardiogr* 18:226-230, 2005.
24. Chandraratna P, Aronow W, Imaizumi T: Role of echocardiography in detecting the anatomic and physiologic abnormalities of constrictive pericarditis. *Am J Med Sci* 283:141-146, 1982.
25. Janos G, Arjunan K, Meyer RA, et al: Differentiation of constrictive pericarditis and restrictive cardiomyopathy using digitized echocardiography. *J Am Coll Cardiol* 1:541-549, 1983.
26. Hinds S, Reisner S, Amico AF: Diagnosis of pericardial abnormalities by 2D-echo: a pathology-echocardiography correlation in 85 patients. *Am Heart J* 123:143-150, 1992.
27. Morgan J, Raposo L, Clague JC, et al: Restrictive cardiomyopathy and constrictive pericarditis: non-invasive distinction by digitised M mode echocardiography. *Br Heart J* 61:29-37, 1989.
28. Engel P, Fowler N, Tei CW, et al: M-mode echocardiography in constrictive pericarditis. *J Am Coll Cardiol* 6:471-474, 1985.
29. Ling L, Oh J, Tei C, et al: Pericardial thickness measured with transesophageal echocardiography: feasibility and potential clinical usefulness. *J Am Coll Cardiol* 29:1317-1323, 1997.
30. Talreja D, Edwards W, Danielson GK, et al: Constrictive pericarditis in 26 patients with histologically normal pericardial thickness. *Circulation* 108:1852-1857, 2003.
31. Himelman RB, Kircher B, Rockey DC, Schiller NB: Inferior vena cava plethora with blunted respiratory response: a sensitive echocardiographic sign of cardiac tamponade. *J Am Coll Cardiol* 12:1470-1477, 1988.
32. Oh J, Hatle L, Seward JB, et al: Diagnostic role of Doppler echocardiography in constrictive pericarditis [see comments]. *J Am Coll Cardiol* 23:154-162, 1994.
33. De VP, Baumgartner W, Casale AS, et al: Current indications, risks, and outcome after pericardiectomy. *Ann Thorac Surg* 52:219-224, 1991.
34. Ha J, Oh J, Ommen SR, et al: Diagnostic value of mitral annular velocity for constrictive pericarditis in the absence of respiratory variation in mitral inflow velocity. *J Am Soc Echocardiogr* 15:1468-1471, 2002.
35. Oh J, Tajik A, Appleton CP, et al: Preload reduction to unmask the characteristic Doppler features of constrictive pericarditis. A new observation [see comments]. *Circulation* 95: 796-799, 1997.
36. Klodas E, Nishimura R, Appleton CP, et al: Doppler evaluation of patients with constrictive pericarditis: use of tricuspid regurgitation velocity curves to determine enhanced ventricular interaction [see comments]. *J Am Coll Cardiol* 28:652-657, 1996.
37. Gilman G, Ommen SR, Hansen WH, Higano ST: Doppler echocardiographic evaluation of pulmonary regurgitation facilitates the diagnosis of constrictive pericarditis. *J Am Soc Echocardiogr* 18:892-895, 2005.
38. Burstow DJ, Oh JK, Bailey KR, et al: Cardiac tamponade: characteristic Doppler observations. *Mayo Clin Proc* 64:312-324, 1989.
39. Klein A, Cohen G, Pietrolungo JF, et al: Differentiation of constrictive pericarditis from restrictive cardiomyopathy by Doppler transesophageal echocardiographic measurements of respiratory variations in pulmonary venous flow. *J Am Coll Cardiol* 22:1935-1943, 1993.
40. Boonyaratavej S, Oh J, Tajik AJ, et al: Comparison of mitral inflow and superior vena cava Doppler velocities in chronic obstructive pulmonary disease and constrictive pericarditis. *J Am Coll Cardiol* 32:2043-2048, 1998.
41. Sohn DW, Kim YJ, Kim HS, et al: Unique features of early diastolic mitral annulus velocity in constrictive pericarditis. *J Am Soc Echocardiogr* 17:222-226, 2004.
42. Garcia M, Rodriguez L, Ares M, et al: Differentiation of constrictive pericarditis from restrictive cardiomyopathy: assessment of left ventricular diastolic velocities in longitudinal axis by Doppler tissue imaging. *J Am Coll Cardiol* 27:108-114, 1996.
43. Ha J, Ommen S, Tajik J, et al: Differentiation of constrictive pericarditis from restrictive cardiomyopathy using mitral annulus velocity by tissue Doppler echocardiography. *Am J Cardiol* 94:316-319, 2004.
44. Reuss CS, Wilansky SM, Lester SJ, et al: Using "annulus reversus" to diagnose constrictive pericarditis. *Eur J Echocardiogr* 10:372-375, 2009.
45. Choi J, Chok J, Dong R, et al: Mitral and tricuspid annular velocities in constrictive pericarditis and restrictive cardiomyopathy: correlation with pericardial thickness on computed tomography. *J Am Coll Cardiol Img* 4: 567-575, 2011.
46. Choi EY, Ha JW, Kim JM, et al: Incremental value of combining systolic mitral annular velocity and time difference between mitral inflow and diastolic mitral annular velocity to early diastolic annular velocity for differentiating constrictive pericarditis from restrictive cardiomyopathy. *J Am Soc Echocardiogr* 20:738-743, 2007.
47. Sengupta P, Mohan J, Mehta V, et al: Accuracy and pitfalls of early diastolic motion of the mitral annulus for diagnosing constrictive pericarditis by tissue Doppler imaging. *Am J Cardiol* 93:886-890, 2004.
48. Yamada H, Tabata T, Jaffer SJ, et al: Clinical features of mixed physiology of constriction and restriction: echocardiographic characteristics and clinical outcome. *Eur J Echocardiogr* 8:185-194, 2006.
49. Rajagopalan N, Garcia MJ, Rodriguez L, et al: Comparison of new Doppler echocardiographic methods to differentiate constrictive pericardial heart disease and restrictive cardiomyopathy. *Am J Cardiol* 87:86-94, 2001.
50. Sengupta PP, Krishnamoorthy VK, Abhayaratna WP, et al: Disparate patterns of left ventricular mechanics differentiate constrictive pericarditis from restrictive cardiomyopathy. *JACC Cardiovasc Imaging* 1:29-38, 2008.
51. Singh S, Wann LS, Schuchard GH, et al: Right ventricular and right atrial collapse in patients

with cardiac tamponade—a combined echocardiographic and hemodynamic study. *Circulation* 70:966-971, 1984.
52. Rifkin R, Isner J, Carter BL, Bankoff MS: Combined posteroanterior subepicardial fat simulating the echocardiographic diagnosis of pericardial effusion. *J Am Coll Cardiol* 3:1333-1339, 1984.
53. Wada T, Honda M, Matsuyama S: Extra echo spaces: ultrasonography and computerised tomography correlations. *Br Heart J* 47:430-438, 1982.
54. Savage D, Garrison R, Brand F, et al: Prevalence and correlates of posterior extra echocardiographic spaces in a free-living population based sample (the Framingham study). *Am J Cardiol* 51:1207-1212, 1983.
55. Ansari A, Rholl AO: Pseudopericardial effusion: echocardiographic and computed tomographic correlations. *Clin Cardiol* 9:551-555, 1986.
56. Kanna B, Osorio F, Dharmarajan L: Pericardial fat mimicking pericardial effusion on two-dimensional echocardiography. *Echocardiography* 23:400-402, 2006.
57. Lopez-Sendon J, Garcia-Fernandez M, Corna-Canella I, et al: Identification of blood in the pericardial cavity in dogs by two-dimensional echocardiography. *Am J Cardiol* 53:1194-1197, 1984.
58. Imazio M, Spodick DH, Brucato A, et al: Controversial issues in the management of pericardial diseases. *Circulation* 121:916-928, 2010.
59. D'Cruz I, Hoffman P: A new cross sectional echocardiographic method for estimating the volume of large pericardial effusions. *Br Heart J* 66:448-451, 1991.
60. Vazquez de Prada JA, Jiang L, Handschumacher MD, et al: Quantification of pericardial effusions by three-dimensional echocardiography. *J Am Coll Cardiol* 24:254-259, 1994.
61. Reddy P, Curtiss EI, O'Toole JD, Shaver JA: Cardiac tamponade: hemodynamic observations in man. *Circulation* 58:265-272, 1978.
62. Kronzon I, Cohen M, Winer HE: Cardiac tamponade by loculated pericardial hematoma: limitations of M-mode echocardiography. *J Am Coll Cardiol* 1:913-915, 1983.
63. Kronzon I, Cohen ML, Winer HE: Diastolic atrial compression: a sensitive echocardiographic sign of cardiac tamponade. *J Am Coll Cardiol* 2:770-775, 1983.
64. Duvernoy O, Larsson S, Persson K, et al: Pericardial effusion and pericardial compartments after open heart surgery. An analysis by computed tomography and echocardiography. *Acta Radiol* 31:41-46, 1990.
65. Chuttani K, Tischler M, Pandian NG, et al: Diagnosis of cardiac tamponade after cardiac surgery: relative value of clinical, echocardiographic, and hemodynamic signs. *Am Heart J* 127:913-918, 1994.
66. Leimgruber P, Klopfenstein H, Wann LS, Brooks HL: The hemodynamic derangement associated with right ventricular diastolic collapse in cardiac tamponade: an experimental echocardiographic study. *Circulation* 68:612-620, 1983.
67. Gaffney F, Keller A, Peshock RM, et al: Pathophysiologic mechanisms of cardiac tamponade and pulsus alternans shown by echocardiography. *Am J Cardiol* 53:1662-1666, 1984.
68. Cogswell TL, Bernath GA, Wann LS, et al: Effects of intravascular volume state on the value of pulsus paradoxus and right ventricular diastolic collapse in predicting cardiac tamponade. *Circulation* 72:1076-1080, 1985.
69. Klopfenstein HS, Cogswell TL, Bernath GA, et al: Alterations in intravascular volume affect the relation between right ventricular diastolic collapse and the hemodynamic severity of cardiac tamponade. *J Am Coll Cardiol* 6:1057-1063, 1985.
70. Armstrong WF, Schilt BF, Helper DJ, et al: Diastolic collapse of the right ventricle with cardiac tamponade: an echocardiographic study. *Circulation* 65:1491-1496, 1982.
71. Engel PJ, Hon H, Fowler NO, Plummer S: Echocardiographic study of right ventricular wall motion in cardiac tamponade. *Am J Cardiol* 50:1018-1021, 1982.
72. Gillam L, Guyer D, Gibson TC, et al: Hydrodynamic compression of the right atrium: a new echocardiographic sign of cardiac tamponade. *Circulation* 68:294-301, 1983.
73. Kaplan L, Epstein S, Schwartz SL, et al: Clinical, echocardiographic, and hemodynamic evidence of cardiac tamponade caused by large pleural effusions. *Am J Respir Crit Care Med* 151:904-908, 1995.
74. Boltwood CM, Jr: Ventricular performance, related to transmural filling pressure in clinical cardiac tamponade. *Circulation* 75:941-955, 1987.
75. Sharp JT, Bunnell IL, Holland JF, et al: Hemodynamics during induced cardiac tamponade in man. *Am J Med* 29:640-646, 1960.
76. Appleton C, Hatle L, Popp RL: Cardiac tamponade and pericardial effusion: respiratory variation in transvalvular flow velocities studied by Doppler echocardiography. *J Am Coll Cardiol* 11:1020-1030, 1988.
77. Pandian N, Wang S, McInerny K, et al: Doppler echocardiography in cardiac tamponade: abnormalities in experimental and clinical tamponade (abstr). *J Am Coll Cardiol* 5:485, 1985.
78. Leeman D, Levine M, Come P: Doppler echocardiography in cardiac tamponade: exaggerated respiratory variation in transvalvular blood flow velocity integrals. *J Am Coll Cardiol* 11:572-578, 1988.
79. Picard M, Sanfilippo A, Newell JB, et al: Quantitative relation between increased intrapericardial pressure and Doppler flow velocities during experimental cardiac tamponade. *J Am Coll Cardiol* 18:234-242, 1991.
80. Gonzalez M, Basnight M, Appleton CP: Experimental pericardial effusion: relation of abnormal respiratory variation in mitral flow velocity to hemodynamics and diastolic right heart collapse [see comments]. *J Am Coll Cardiol* 17:239-248, 1991.
81. Sivaciyan V, Ranganathan N: Transcutaneous Doppler jugular venous flow velocity recording. *Circulation* 57:930-939, 1978.
82. Appleton CP, Hatle LK, Popp RL: Superior vena cava and hepatic vein Doppler echocardiography in healthy adults. *J Am Coll Cardiol* 10:1032-1039, 1987.
83. Zhang S, Kerins DM, Byrd BF 3rd: Doppler echocardiography in cardiac tamponade and constrictive pericarditis. *Echocardiography* 11:507-521, 1994.
84. Chuttani K, Pandian N, Mohanty PK, et al: Left ventricular diastolic collapse. An echocardiographic sign of regional cardiac tamponade. *Circulation* 83:1999-2006, 1991.
85. Kochar G, Jacobs L, Kotler MN: Right atrial compression in postoperative cardiac patients: detection by transesophageal echocardiography. *J Am Coll Cardiol* 16:511-516, 1990.
86. Jadhav P, Asirvatham S, Craven P, et al: Unusual presentation of late regional cardiac tamponade after aortic surgery. *Am J Card Imaging* 10:204-206, 1996.
87. Brooker R, Farah M: Postoperative left atrial compression diagnosed by transesophageal echocardiography. *J Cardiothorac Vasc Anesth* 9:304-307, 1995.
88. Krikorian J, Hancock E: Pericardiocentesis. *Am J Med* 65:808-814, 1978.
89. Callahan J, Seward J, Nishimura RA, et al: Two-dimensional echocardiographically guided pericardiocentesis: experience in 117 consecutive patients. *Am J Cardiol* 55:476-479, 1985.
90. Tsang T, Freeman W, Sinak LJ, Seward JB: Echocardiographically guided pericardiocentesis: evolution and state-of-the-art technique. *Mayo Clin Proc* 73:647-652, 1998.
91. Salem K, Mulji A, Lonn E: Echocardiographically guided pericardiocentesis—the gold standard for the management of pericardial effusion and cardiac tamponade. *Can J Cardiol* 15:1251-1255, 1999.
92. Alcan KE, Zabetakis PM, Marino ND, et al: Management of acute cardiac tamponade by subxiphoid pericardiotomy. *JAMA* 247:1143-1148, 1982.
93. Tsang T, Freeman W, Barnes ME, et al: Rescue echocardiographically guided pericardiocentesis for cardiac perforation complicating catheter-based procedures. The Mayo Clinic experience. *J Am Coll Cardiol* 32:1345-1350, 1998.
94. Pandian N, Brockway B, Simonetti J, et al: Pericardiocentesis under two-dimensional echocardiographic guidance in loculated pericardial effusion. *Ann Thorac Surg* 45:99-100, 1988.
95. Hanaki Y, Kamiya H, Todoroki H, et al: New two-dimensional, echocardiographically directed pericardiocentesis in cardiac tamponade. *Crit Care Med* 18:750-753, 1990.
96. Tsang TSM, Enriquez-Sarano M, Freeman WK, et al: Consecutive 1127 therapeutic echocardiographically guided pericardiocenteses: clinical profile, practice patterns, and outcomes spanning 21 years. *Mayo Clin Proc* 77:429-436, 2002.
97. Maisch B, Seferovic P, Ristic AD, et al: Guidelines on the diagnosis and management of pericardial diseases executive summary; the Task Force on the Diagnosis and Management of Pericardial Diseases of the European Society of Cardiology. *Eur Heart J* 25:587-610, 2004.
98. Troughton R, Asher C, Klein AL: Pericarditis. *Lancet* 363: 717-727, 2004.
99. Permanyer-Miralda G, Sagrista-Sauleda J, Soler-Soler J: Primary acute pericardial disease: a prospective series of 231 consecutive patients. *Am J Cardiol* 56:623-630, 1985.
100. Zayas R, Anguita M, Torres F, et al: Incidence of specific etiology and role of methods for specific etiologic diagnosis of primary acute pericarditis. *Am J Cardiol* 75:378-382, 1995.
101. Imazio M, Demichelis B, Parrini I, et al: Day-hospital treatment of acute pericarditis: a management program for outpatient therapy. *J Am Coll Cardiol* 43:1042-1046, 2004.
102. Oh J, Hatle L, Mulvagh SL, Tajik AK: Transient constrictive pericarditis: diagnosis by two-dimensional Doppler echocardiography. *Mayo Clin Proc* 68:1158-1164, 1993.
103. Haley J, Tajik A, Danielson GK, et al: Transient constrictive pericarditis: causes and natural history. *J Am Coll Cardiol* 43:271-275, 2004.
104. Sagrista-Sauleda J, Angel J, Sánchez A, et al: Effusive-constrictive pericarditis. *N Engl J Med* 350:469-475, 2004.
105. Baker CM, Orsinelli DA: Subacute effusive-constrictive pericarditis: diagnosis by serial

echocardiography. *J Am Soc Echocardiogr* 17: 1204-1206, 2004.
106. Zagol B, Minderman D, Munir A, D'Cruz I: Effusive constrictive pericarditis: 2D, 3D echocardiography and MRI imaging. *Echocardiography* 24:1110-1114, 2007.
107. Hancock E: Subacute effusive-constrictive pericarditis. *Circulation* 43:183-192, 1971.
108. Sagrista-Sauleda J, Angel J, Permanyer-Miralda G, Soler-Soler J: Long-term follow-up of idiopathic chronic pericardial effusion. *N Engl J Med* 341:2054-2059, 1999.
109. Little W, Freeman G: Pericardial disease. *Circulation* 113:1622-1632, 2006.
110. Tan R, Partridge J, Ilsley C, et al: Familial complete congenital absence of the pericardium. *Clin Radiol* 62: 85-87, 2007.
111. Tabakin BS, Hanson JS, Tampas JP, Calwell EJ: Congenital absence of the left pericardium. *Am J Roentgenol Radium Ther Nucl Med* 94: 122-128, 1965.
112. Connolly H, Click R, Schattenberg TT, et al: Congenital absence of the pericardium: echocardiography as a diagnostic tool. *J Am Soc Echocardiogr* 8:87-92, 1995.
113. Nasser W, Helmen C, Tavel ME, et al: Congenital absence of the left pericardium: clinical, electrocardiographic, radiographic, hemodynamic, and angiographic findings in six cases. *Circulation* 41:469-478, 1970.
114. Yamano T, Sawada T, Sakamoto K, et al: Magnetic resonance imaging differentiated partial from complete absence of the left pericardium in a case of leftward displacement of the heart. *Circ J* 68: 385-388, 2004.
115. Baim RS, MacDonald IL, Wise DJ, Lenkei SC: Computed tomography of absent left pericardium. *Radiology* 135: 127-128, 1980.
116. Amiri A, Weber C, Schlosser V, Meinertz TH: Coronary artery disease in a patient with a congenital pericardial defect. *Thorac Cardiovasc Surg* 37:379-381, 1989.
117. Saito R, Hotta F: Congenital pericardial defect associated with cardiac incarceration: case report. *Am Heart J* 100:866-870, 1980.
118. Vanderheyden M, De SJ, Nellens P, et al: Herniation of the left atrial appendage due to partial congenital absence of the left pericardium. *Acta Clin Belg* 51:91-93, 1996.
119. Finet G, Bozio A, Frieh JP, et al: Herniation of the left atrial appendage through a congenital partial pericardial defect. *Eur Heart J* 12:1148-1149, 1991.
120. Hoorntje JC, Mooyaart EL, Meuzelaar KJ: Left atrial herniation through a partial pericardial defect: a rare cause of syncope. *Pacing Clin Electrophysiol* 12:1841-1845, 1989.
121. Reginao E, Speroni F, Riccardi M, et al: Post-traumatic mitral regurgitation and ventricular septal defect in absence of left pericardium. *Thorac Cardiovasc Surg* 28:213-217, 1980.
122. Casey B, Neiman H, Gallagher T, et al: Syndrome of mesodermal defects involving the abdominal wall, diaphragm, sternum, heart and pericardium. *Br J Radiol* 48: 52-54, 1975.
123. Tosson R, Korbmacher B, Schulte HD: Combined congenital pericardial and diaphragmatic defects: a case report. *Cardiovasc Surg* 4:57-59, 1996.
124. Borges A, Gellert K, Dietel M, et al: Acute right-sided heart failure due to hemorrhage into a pericardial cyst [see comments]. *Ann Thorac Surg* 63:845-847, 1997.
125. Pezzano A, Belloni A, Faletra F, et al: Value of two-dimensional echocardiography in the diagnosis of pericardial cysts. *Eur Heart J* 4:238-246, 1983.
126. Bini R, Nath P, Ceballos R, et al: Pericardial cyst diagnosed by two-dimensional echocardiography and computed tomography in a newborn. *Pediatr Cardiol* 8:47-50, 1987.
127. Gürlek A, Dagalp Z, Ozyurda U: A case of multiple pericardial hydatid cysts. *Int J Cardiol* 36:366-368, 1992.
128. Landolphi DR, Belkin RN, Hjemdahl-Monsen CE, LaFaro RJ: Cardiac cavernous hemangioma mimicking pericardial cyst: atypical echocardiographic appearance of a rare cardiac tumor. *J Am Soc Echocardiogr* 10:579-581, 1997.
129. Patel J, Park C, Michaels J, et al: Pericardial cyst: case reports and a literature review. *Echocardiography* 21: 269-272, 2004.
130. Demos TC, Budorick NE, Posniak HV: Benign mediastinal cysts: pointed appearance on CT. *J Comput Assist Tomogr* 13: 132-133, 1989.
131. Bandeira FC, de Sá VP, Moriguti JC, et al: Cardiac tamponade: an unusual complication of pericardial cyst. *J Am Soc Echocardiogr* 9:108-112, 1996.
132. Bava G, Magliani L, Bertoli D, et al: Complicated pericardial cyst: atypical anatomy and clinical course. *Clin Cardiol* 21:862-864, 1998.
133. Williamson B, Spotnitz W, Gay SB, et al: Pericardial cyst. A rare mass abutting the aorta. *J Comput Tomogr* 12:264-266, 1988.
134. Chopra PS, Duke DJ, Pellett JR, Rahko PS: Pericardial cyst with partial erosion of the right ventricular wall. *Ann Thorac Surg* 51:840-841, 1991.

# 30 Cardiac Transplantation: Pretransplant and Posttransplant Evaluation

AUDREY H. WU, MD, MPH | THEODORE J. KOLIAS, MD

**Evaluation before Cardiac Transplantation**
Risk Assessment
Evaluation of the Donor Heart
**Structure and Function of the Cardiac Allograft**
Transplant Technique
Physiology of the Cardiac Allograft
Ventricular Systolic and Diastolic Function
Right Ventricular Structure and Function and Tricuspid Regurgitation
**Structure and Function of the Cardiac Allograft during Acute Rejection**
Changes in Systolic and Diastolic Function
Changes in Left Ventricular Mass or Wall Thickness
Echocardiographic Guidance for Endomyocardial Biopsy
**Early Postoperative Complications and Other Findings**
Early Postoperative Complications
Pericardial Effusion
**Posttransplant Monitoring**
Routine Follow-up
Diagnosis of Cardiac Allograft Vasculopathy

Improvements in medical management and advances in surgical techniques have increased the number of patients who survive with severe heart failure. Cardiac transplantation remains the treatment of choice for appropriate candidates with end-stage heart failure. More than 3000 cardiac transplants are performed worldwide annually. At the time of transplantation, roughly half of cardiac transplant recipients are treated with inotropic agents, whereas almost one quarter need some form of mechanical circulatory support, most frequently in the form of a left ventricular (LV) assist device. International registry data show that the mortality rate is greatest in the first 6 months after transplantation; the 1-year survival rate after cardiac transplantation is about 85%, with a 3% to 4% linear decrease annually thereafter and a median survival rate of 10.4 years for the cohort of patients who underwent transplantation in the 1992 to 2001 era. Survival rates have steadily improved since the early 1980s, despite the increasingly high-risk profile of the recipient population. Graft failure and infections account for a significant proportion of deaths in the first year after transplantation, whereas after 5 years, cardiac allograft vasculopathy (transplant coronary disease), late graft failure (likely a result of allograft vasculopathy), and malignancy disease are more common causes of death.[1]

## Evaluation before Cardiac Transplantation

### RISK ASSESSMENT

Box 30-1 summarizes echocardiographic markers of poor prognosis in the setting of advanced systolic heart failure. Although these generally are not included in widely used composite risk scores for heart failure (with the exception of ejection fraction), they are useful adjuncts to assessment of prognosis. In the context of evaluation before possible cardiac transplantation, right heart function and presence of pulmonary hypertension are of particular interest. Preoperative pulmonary hypertension, particularly if not medically reversible with vasodilators or if reversible at the expense of systemic hypotension, is associated with very high risk of short-term mortality, frequently as a result of right heart failure.[2] Although direct measurement of central hemodynamics with a pulmonary artery catheter is currently the gold standard, echocardiography has the advantage of being noninvasive and more widely available. Estimates of hemodynamic measurements with Doppler echocardiography have been shown to correlate closely with direct invasive measurements in patients with heart failure, with use of the following calculations for cardiac output (CO), right atrial (RA) pressure, pulmonary artery systolic pressure (PASP), pulmonary capillary wedge pressure (PCWP) and pulmonary vascular resistance (PVR)[3]:

$$CO = (HR)\,(VTI_{LVOT})\,(\pi)\,(D_{LVOT}/2)^2$$

$$\text{Mean RA pressure} = -1.263 + 0.01116 \times Ac,$$

where *Ac* is the acceleration rate ($cm/s^2$) of early tricuspid filling, D is diameter, HR is heart rate, LVOT is the left ventricular outflow tract, and VTI is the velocity time integral of flow

$$PASP = \text{RA pressure} + 4(V_{TR})^2,$$

where $V_{TR}$ is peak velocity of the tricuspid regurgitation signal.

$$PCWP = 32.16 + (-0.1045E) + (0.1345A) + (-0.17DT) + (4.95\,E/A), \text{ and}$$

$$PVR = [(PEP)/AcT/TT],$$

**Box 30-1**

## ECHOCARDIOGRAPHIC MARKERS FOR POOR PROGNOSIS AND POTENTIAL NEED FOR CARDIAC TRANSPLANTATION IN SYSTOLIC HEART FAILURE

- Left ventricular ejection fraction[1]
- Left ventricular cavity dilation[2]
- Doppler-derived measures of systolic and diastolic function
  - Restrictive mitral filling pattern (mitral deceleration time)[3]
  - Rate of change in pressure over time (dP/dt, –dP/dt)[4]
- Right ventricular function (tricuspid annular plane systolic excursion)[5]
- Tissue Doppler measures of systolic and diastolic function (systolic mitral annular velocity, mitral E/E')[6,7]
- Presence of severe mitral or tricuspid regurgitation[8]
- Speckle tracking measures of systolic function (strain)[9]

References
[1]Levy WC, Mozaffarian D, Linker DT, et al: The Seattle Heart Failure Model: prediction of survival in heart failure. *Circulation* 113:1424-1433, 2006.
[2]Lee TH, Hamilton MA, Stevenson LW, et al: Impact of left ventricular cavity size on survival in advanced heart failure. *Am J Cardiol* 72:672-676, 1993.
[3]Giannuzzi P, Temporelli PL, Bosimini E, et al: Independent and incremental prognostic value of Doppler-derived mitral deceleration time of early filling in both symptomatic and asymptomatic patients with left ventricular dysfunction. *J Am Coll Cardiol* 28:383-390, 1996.
[4]Kolias TJ, Aaronson KD, Armstrong WF: Doppler-derived dP/dt and –dP/dt predict survival in congestive heart failure. *J Am Coll Cardiol* 36:1594-1599, 2000.
[5]Ghio S, Recusani F, Klersy C, et al: Prognostic usefulness of the tricuspid annular plane systolic excursion in patients with congestive heart failure secondary to idiopathic or ischemic dilated cardiomyopathy. *Am J Cardiol* 85:837-842, 2000.
[6]Nikitin NP, Loh PH, Silva R, et al: Prognostic value of systolic mitral annular velocity measured with Doppler tissue imaging in patients with chronic heart failure caused by left ventricular systolic dysfunction. *Heart* 92:775-779, 2006.
[7]Dokainish H, Zoghbi WA, Lakkis NM, et al: Incremental predictive power of B-type natriuretic peptide and tissue Doppler echocardiography in the prognosis of patients with congestive heart failure. *J Am Coll Cardiol* 45:1223-1226, 2005.
[8]Koelling TM, Aaronson KD, Cody RJ, et al: Prognostic significance of mitral regurgitation and tricuspid regurgitation in patients with left ventricular systolic dysfunction. *Am Heart J* 144:524-529, 2002.
[9]Cho GY, Marwick TH, Kim HS, et al: Global 2-dimensional strain as a new prognosticator in patients with heart failure. *J Am Coll Cardiol* 54:618-624, 2009.

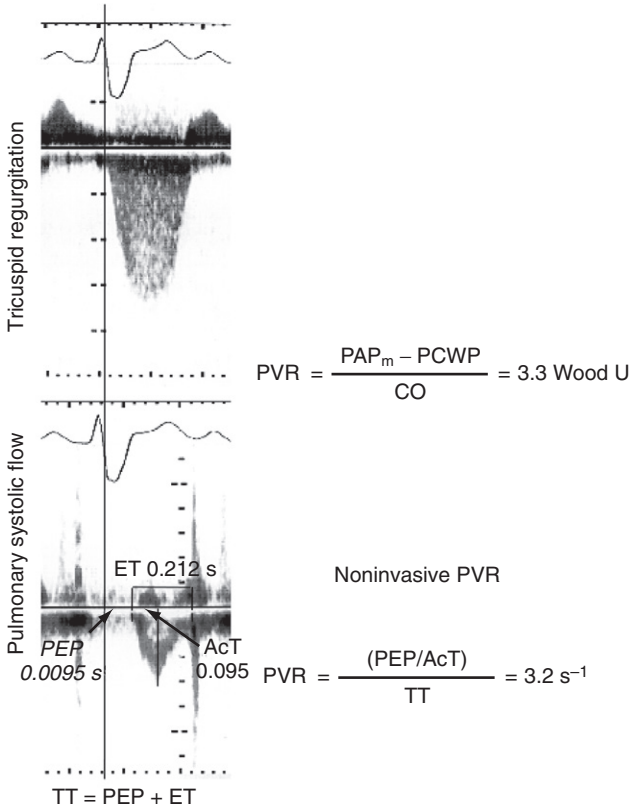



**Figure 30-1 Continuous wave Doppler recording of tricuspid regurgitant flow (*top*) and pulsed wave Doppler recording of pulmonary flow (*bottom*) in the same patient with invasive pulmonary vascular resistance of 3.3 Wood U.** *AcT,* Acceleration time; *CO,* cardiac output; *ET,* ejection time; *$PAP_m$,* pulmonary mean arterial pressure; *PCWP,* pulmonary capillary wedge pressure; *PEP,* preejection period; *PVR,* pulmonary vascular resistance; *TT,* total time. *(From Temporelli PL, Scapellato F, Eleuteri E, et al: Doppler echocardiography in advanced systolic heart failure.* Circ Heart Fail *3:387-394, 2010.)*

where E and A are LV diastolic filling velocities, *PEP* is preejection period, *AcT* is acceleration time, and *TT* is total systolic time, as measured with pulsed Doppler pulmonary systolic flow (Fig. 30-1).

## EVALUATION OF THE DONOR HEART

Echocardiography is necessary for the evaluation of potential donor hearts to help optimize the individual heart to undergo transplantation and, on a larger scale, to maximize use of this scarce resource. Once individuals with brain death are identified as potential heart donors, they typically are managed with the assistance of the regional donor procurement agency according to specific protocols to prepare the heart to undergo procurement and transplantation. In general, these protocols aim to optimize volume status and hemodynamics with volume resuscitation or diuretics, inotropes or vasopressors as needed, and hormonal manipulation with triiodothyronine, steroids and vasopressin,[4] frequently with the assistance of invasive hemodynamic monitoring with a pulmonary artery catheter.

Echocardiography is essential for assessment of structure and function of the donor heart. The evaluation for regional and global wall motion abnormalities, and for valvular or congenital abnormalities, is particularly important because these findings could potentially preclude use of the heart for transplantation. Estimates of the frequency of structural or functional abnormalities in potential donor hearts range from 10% to 45%. Although regional or global wall motion abnormalities may be present on initial assessment, in some cases, contractile function can be improved with medical therapy, particularly if the dysfunction is related to brain death or is catecholamine-induced. Serial echocardiograms can often confirm improvement in contractile function in the setting of hemodynamic and metabolic correction.[5] However, the lower the initial ejection fraction, the less likely the heart is able to be optimized for use for transplantation because this likely reflects intrinsic and irreversible causes for contractile dysfunction. Although early studies suggested suboptimal outcomes with the use of donor hearts with LV hypertrophy, more recent studies have found that transplant patients who received donor hearts with mild (interventricular septum or posterior wall 1.2 to 1.3 cm) or moderate (more than 1.3 to 1.7 cm) LV hypertrophy had similar short-term and long-term survival rates, up to 5 years after transplantation.[6]

## Structure and Function of the Cardiac Allograft

### TRANSPLANT TECHNIQUE

With the earlier biatrial technique for cardiac transplantation, bilateral atrial cuffs from the recipient were retained for direct anastomosis of the cardiac allograft. This approach produced large atrial cavities with long suture lines, which resulted in abnormal atrial geometry and function. In older series, mean measurements of left atrial (LA) diameter ranged from about 58 to 83 mm versus 41 to 42 mm for biatrial versus bicaval techniques, respectively.[7-9] Larger atrial size and atrial anatomic distortion have been implicated as contributors to mitral and tricuspid valve abnormalities and atrial thrombus formation.[10,11] The bicaval technique, with separate caval and pulmonary vein anastomoses, was developed to circumvent these problems. This approach did not become popular until the late 1980s and is currently the more commonly used technique.[12,13] Transplantation with the biatrial technique is associated with higher frequency of spontaneous contrast and atrial thrombi on echocardiography and also risk for systemic arterial embolism (roughly 15% incidence rate in one series).[7,14] Atrial thrombi are frequently located in areas not well seen on transthoracic echocardiography, such as the donor LA appendage or posterior wall, and require transesophageal echocardiography for visualization.[15] These echocardiographic findings and the elevated incidence of systemic embolism have not been observed with bicaval transplant recipients.[7,8,14] In addition to more normal atrial size and geometry, the bicaval technique results in more physiologic atrial function. Measures of atrial contractile function are significantly better in patients who underwent cardiac transplantation with the bicaval technique versus those who underwent transplantation with the biatrial technique and have been found to be comparable with those of normal controls.[16,17] Despite evidence for LA dysfunction, LA contraction appears to contribute significantly more to LV stroke volume than in nontransplant patients,[18] with the donor component of the LA contributing more to atrial emptying than the recipient atrial component.[19] Thus, the transplant patient may have poor tolerance for conditions in which the atrial contribution to cardiac output is compromised, such as with atrial tachyarrhythmias (Figs. 30-2 and 30-3).

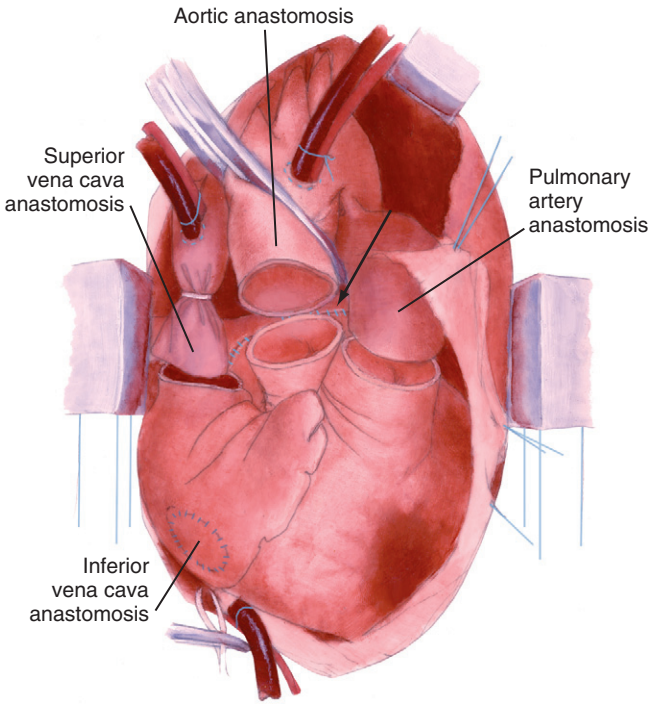



**Figure 30-2 Bicaval technique for heart transplantation.** The cardiac allograft is anastomosed to the recipient at the superior and inferior vena cavae, at the pulmonary artery and aorta, and at the LA.

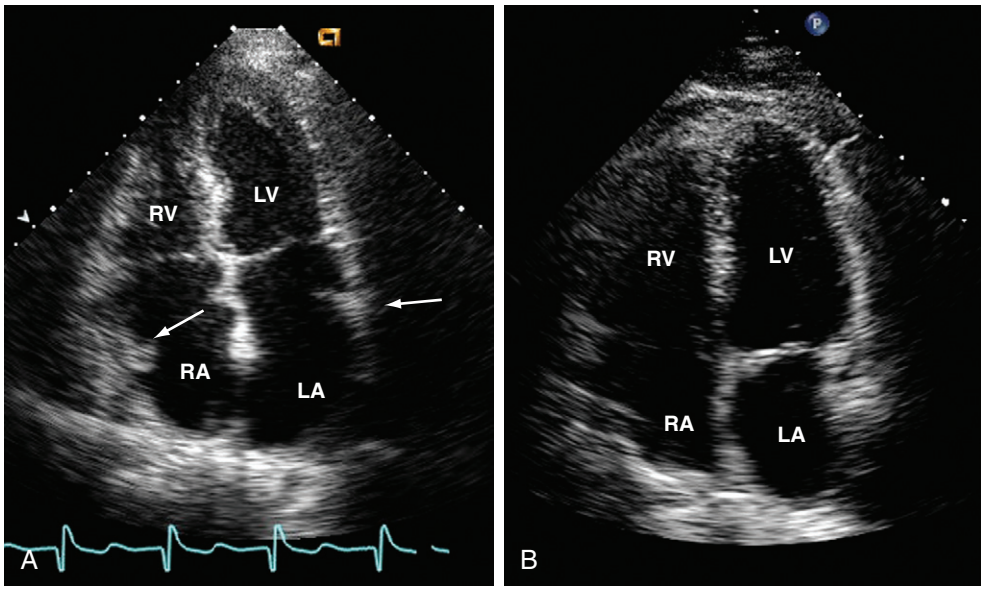



**Figure 30-3 Comparison of the echocardiographic appearance of cardiac allografts transplanted with the biatrial (A) versus bicaval (B) techniques.** In comparison with the bicaval technique, the biatrial technique results in much larger atria; prominent atrial suture lines are visible on echocardiogram (*arrows*).

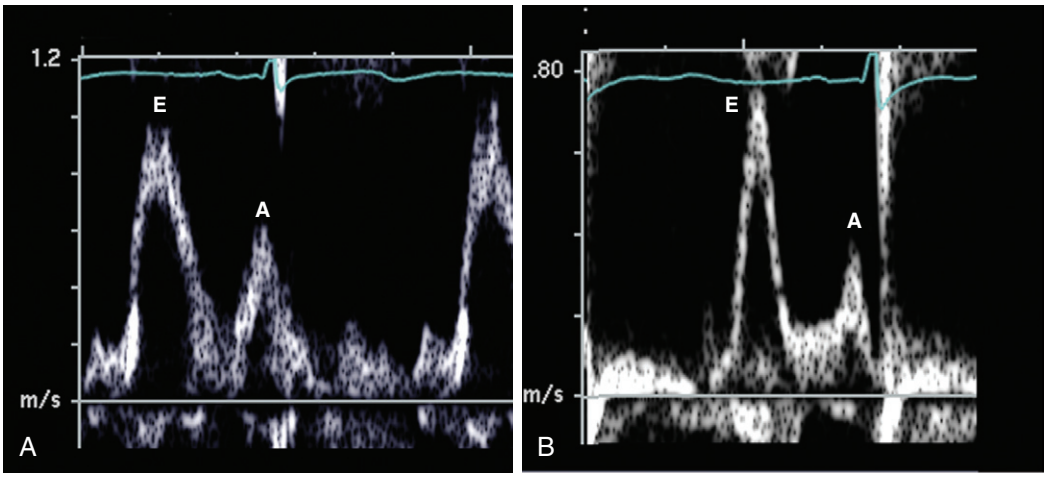



**Figure 30-4 Mitral valve inflow velocities show a normal E/A ratio and normal deceleration slope with normal diastolic function (A) compared with a pattern of "restrictive" filling with an increased E velocity with a steep deceleration slope and a reduced velocity (B).** *A,* Late transmitral flow velocity; *E,* early transmitral flow velocity.

## PHYSIOLOGY OF THE CARDIAC ALLOGRAFT

Although cardiac transplantation provides improved survival, functional capacity, and quality of life to patients with end-stage heart failure, the physiology of the cardiac allograft is not exactly the same as that of a normal nontransplanted heart. Hemodynamics immediately after cardiac transplantation are characterized by elevated filling pressures associated with impaired relaxation. This hemodynamic profile improves over the initial few weeks to months after transplantation and may continue to normalize over years but also may persist to a subtle degree.[20,21] Restrictive physiology early after transplantation may be the result of a combination of ischemic myocardial injury, recipient pulmonary hypertension, and volume overload, whereas persistent restrictive physiology may be attributed to donor-recipient size mismatch, ischemic fibrosis, increased afterload from systemic hypertension, or rejection. Because it is denervated, the cardiac allograft has an altered response to exercise, characterized by a slower early rise in heart rate and an overall blunted chronotropic response, with increases in cardiac output primarily the result of increases in stroke volume rather than heart rate.[21,22] Sympathetic reinnervation occurs over time and is associated with improved exercise capacity, including heart rate and ventricular contractile response to exercise.[23] Exercise capacity improves in the initial few years after transplantation but may never reach normal nontransplant levels.[24]

## VENTRICULAR SYSTOLIC AND DIASTOLIC FUNCTION

Early after transplantation, LV mass and end-diastolic volume increase; these changes may or may not persist for years, without adverse consequences to ejection fraction, although subtle decrements in systolic contractility may manifest early.[25-27] In the absence of complications that cause graft dysfunction, allograft ventricular systolic function generally remains normal as many as 10 to 15 years after transplant. LV hypertrophy is a common finding, as is postoperative septal motion.[27,28] Although systolic ventricular function remains largely normal, diastolic function is abnormal early after transplantation, the effects of which are frequently compounded by postoperative volume overload. A restrictive filling pattern may persist to some degree chronically in some patients or may reemerge during episodes of acute rejection. Early after transplantation, a restrictive filling pattern is present, characterized by shorter isovolumic relaxation time and E wave deceleration time and an increased E/A ratio (Fig. 30-4), with gradual evolution to a nonrestrictive pattern by 6 weeks after transplantation. Various clinical factors, such as preoperative pulmonary systolic pressures or pulmonary vascular resistance, duration of cardiopulmonary bypass, total ischemia time, or age of donor heart, did not significantly correlate with parameters of restrictive filling early after transplantation in one study.[29]

The incidence of diastolic dysfunction decreases over time, but diastolic abnormalities persist beyond the early postoperative period in a small proportion of patients. One estimate of the prevalence rates of diastolic dysfunction after cardiac transplantation was 22% at 6 weeks, 8% at 6 months, and 12% at 1 year. Right ventricular diastolic dysfunction (elevated right atrial pressure to stroke volume ratio) was associated with increased mortality.[30] In a series of 64 cardiac transplant recipients 1 year or more after transplant (mean, 5 years; range, 1 to 13 years) who underwent routine annual hemodynamic evaluation, 10 (15%) had a pattern of right and LV filling consistent with restrictive-constrictive physiology, with a characteristic dip-and-plateau hemodynamic tracing in early diastole. In general, transplant recipients with constrictive-restrictive hemodynamics had higher right-sided and left-sided filling pressures, shorter LV isovolumic relaxation times and E wave deceleration times, and higher mitral and tricuspid E/A ratios. Transplant recipients with constrictive-restrictive physiology had significantly more previous rejection episodes, a greater proportion had heart failure symptoms, and a significant proportion also had acute rejection diagnosed with biopsy performed concurrent with echocardiography.[31] Persistence of restrictive filling pattern up to 6 months after cardiac transplantation may be associated with reduced long-term survival.[32] The etiology of persistent diastolic dysfunction after transplantation is not fully defined but likely includes cumulative immune-mediated injury, fibrosis related to immune or nonimmune damage, and allograft vasculopathy. Newer techniques such as tissue Doppler imaging

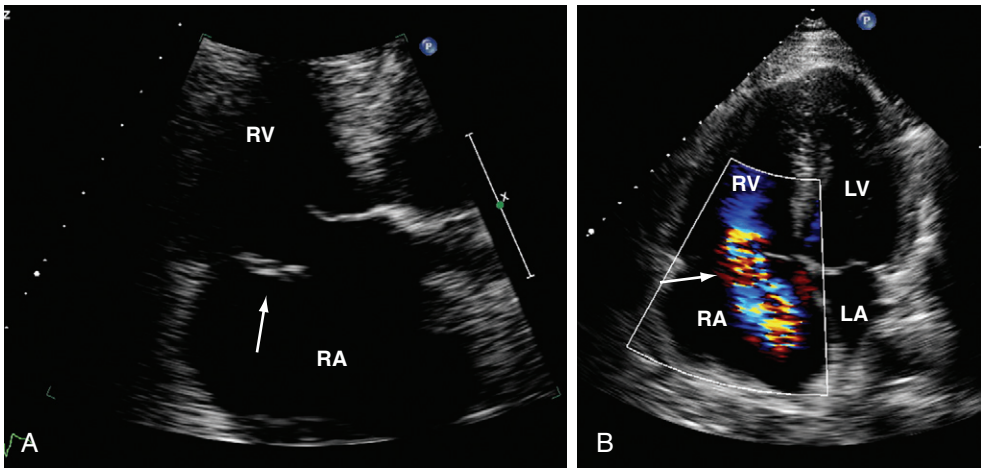



**Figure 30-5 Flail tricuspid valve leaflet with tricuspid regurgitation in a cardiac transplant recipient. A,** 2D imaging shows the flail leaflet (*arrow*). **B,** Color Doppler shows a wide jet (*arrow*) of tricuspid regurgitation.

have shown promise for assessment of early ventricular dysfunction caused by cardiac allograft vasculopathy.[33]

### RIGHT VENTRICULAR STRUCTURE AND FUNCTION AND TRICUSPID REGURGITATION

A significant proportion of patients with severe heart failure have pulmonary hypertension as a result of longstanding elevated left-sided filling pressures. Pulmonary hypertension frequently improves to normal or near-normal levels in the weeks to months after cardiac transplantation. The evolution of right-sided structure and function after transplantation parallels the resolution of pulmonary hypertension and volume overload,[34] although some right ventricular enlargement may persist long term.[35] Many patients at 10 to 15 years after transplantation have right atrial and right ventricular enlargement (right atrium, 40.7 ± 11.8 mm; right ventricle, 37.4 ± 8.3 mm, in one series). Despite the abnormalities in right-sided heart size and function, in the absence of severe tricuspid regurgitation, clinical signs and symptoms of heart failure are generally not present.[28]

Tricuspid regurgitation occurs early and late after cardiac transplantation. Early tricuspid regurgitation is more related to preoperative and postoperative pulmonary hypertension and right ventricular failure,[36] whereas valve injury from endomyocardial biopsies is often responsible for late tricuspid regurgitation (Fig. 30-5). Severity of tricuspid regurgitation on intraoperative transesophageal echocardiogram may be a marker for right ventricular dysfunction and appears to correlate with poor late survival. In one series of 181 patients, 20% of donor hearts at the time of transplantation had at least mild tricuspid regurgitation, which correlated strongly with presence of right ventricular dysfunction. The 5-year survival rate in this series was 85% for patients with no or trace intraoperative tricuspid regurgitation, versus 57% for those with mild to severe tricuspid regurgitation, even in the absence of overt right ventricular dysfunction on intraoperative transesophageal echocardiogram.[37] Donor tricuspid valve annuloplasty has not been found to have any significant effect on hemodynamics as measured with right heart catheterization and has not been shown to improve long-term survival.[38] At 10 years after transplantation, about 15% of patients may have severe tricuspid regurgitation. These patients are at increased risk for heart failure and may need tricuspid valve replacement.[39,40]

## Structure and Function of the Cardiac Allograft during Acute Rejection

Allograft rejection remains a significant limitation of cardiac transplantation. Acute cardiac allograft rejection is usually characterized by lymphocytic infiltration with or without myocyte necrosis, termed "cellular rejection."[41] A rarer, less well-understood type of rejection, termed "antibody-mediated rejection" (also called vascular or humoral rejection), involves endothelial cell activation and complement deposition that primarily involves the allograft vasculature.[42] Although the incidence rate of cellular rejection has drastically declined over the 1990s as a result of improvements in immunosuppression therapy, the incidence rate of noncellular rejection has remained stable.[43] Until recently, cardiac allograft rejection on endomyocardial biopsy was graded 0, 1A, 1B, 2, 3A, 3B, and 4 in order of increasing severity of lymphocyte infiltration and presence and amount of myocyte necrosis. In 2005, the classification was simplified into grades 0 (previous grade 0); 1R, mild rejection (previous 1A, 1B, 2); 2R, moderate rejection (previous grade 3A); and 3R, severe rejection (previous grades 3B and 4).[41] Echocardiographic abnormalities of the cardiac allograft during rejection may include changes in systolic and diastolic function and increases in LV wall thickness or mass. Currently, the gold standard for diagnosis of rejection is with endomyocardial biopsy, although this technique is limited by the risks inherent to an invasive procedure, sampling error, cost, and patient discomfort. More recently, gene expression profiling from peripheral blood samples has been tested as a noninvasive method for assessment for rejection. Although echocardiography alone has not been proven to be a definitive diagnostic method for detection of rejection, it has provided insight into the changes that occur during and around the time of rejection and may be a useful adjunct to diagnosis of rejection.

### CHANGES IN SYSTOLIC AND DIASTOLIC FUNCTION

New-onset systolic dysfunction in the setting of acute rejection is generally a late finding and indicates higher grade rejection, which is associated with hemodynamic compromise and clinical symptoms and with poorer prognosis.[44] The vast majority of rejection episodes are not associated with systolic impairment, and significant changes in echocardiographic systolic

function parameters are generally lacking. Abnormalities of diastolic filling are the earliest alterations to manifest in acute rejection.[31,45] Rejection of increasing severity has been associated with a progressive shortening of isovolumic relaxation time and pressure half-time and with an increase in peak early mitral flow velocity, although the latter has not been a consistent finding.[45-47] Measures of diastolic dysfunction generally return to baseline values after treatment of acute rejection.[47] However, in general, diastolic indices such as mitral E wave, deceleration time, isovolumic relaxation time, tissue Doppler early diastolic (E′) wave, and late diastolic (A′) wave are not sensitive enough for reliable diagnosis of acute rejection.[48]

Defined as the sum of isovolumic contraction time and isovolumic relaxation time divided by ejection time, the myocardial performance index is a single composite measurement of systolic and diastolic myocardial function. Although some studies have suggested a correlation between myocardial performance index and presence of acute rejection, sensitivity and specificity were low, and the relationship has not been a consistent finding. Concurrent decreases in isovolumic relaxation time and increases in isovolumic contraction time, which indicate development of abnormalities in diastolic and systolic function, respectively, with acute rejection resulted in an overall neutral effect on the myocardial performance index.[49,50]

Traditional Doppler-derived parameters of diastolic function, such as transmitral Doppler flow analysis, are influenced by variables other than ventricular diastolic function, such as ventricular loading conditions; and in transplant recipients specifically, the cardiac allograft may develop baseline diastolic filling abnormalities unrelated to acute rejection. Tissue-Doppler imaging is a technique for assessment of LV systolic and diastolic function with measurement of the systolic (S′) and the early (E′) and late (A′) diastolic velocities of the mitral annulus. Although late diastolic mitral annular velocity (A′) and mitral annular systolic velocity (S′) appear to be sensitive markers of acute severe rejection, they are not particularly specific.[51] Furthermore, the specificity is not significantly improved when both systolic and diastolic tissue-Doppler parameters are used. The combined peak systolic and peak diastolic velocity (peak-to-peak amplitude) of the tissue-Doppler mitral annular waveforms was significantly lower in patients experiencing any rejection (grade 1B or greater) and may be helpful in excluding presence of significant rejection.[52] Although tissue-Doppler measurements appear to be sensitive for detecting various degrees of acute rejection and for excluding rejection if measurements fall below receiver operating characteristic (ROC) determined cutoffs, they do not appear to be robust tools in differentiating impaired contraction or relaxation resulting from acute rejection rather than other causes. This poor specificity reflects confounding by the background diastolic filling abnormalities inherent to transplant physiology, which makes detection of early diastolic dysfunction as a result of acute rejection difficult. Newer modalities such as strain/strain rate imaging are being studied as methods to detect and monitor acute rejection.[53]

## CHANGES IN LEFT VENTRICULAR MASS OR WALL THICKNESS

Although older reports have suggested LV mass increases in the setting of acute cellular rejection,[54] this has not been a consistent finding,[55] and change in LV wall thickness alone has not proven to be a sensitive enough marker for diagnosis of cellular rejection.[56] Increased LV mass in the setting of rejection may be the result of increased interstitial edema or vascular leakage of fibrin. Significant increase in LV mass has been described during episodes of vascular rejection. In a series of 41 cardiac transplant patients, LV mass increased from a baseline of 109 ± 17 g to 151 ± 17 g during vascular rejection, although it did not significantly change during cellular rejection. Concurrently, LV wall thickness increased by nearly 20% during vascular rejection (1.3 ± 0.1 cm at baseline versus 1.6 ± 0.1 cm).[57]

## ECHOCARDIOGRAPHIC GUIDANCE FOR ENDOMYOCARDIAL BIOPSY

Endomyocardial biopsy remains the gold standard for diagnosing allograft rejection and following response to immunosuppressive treatment for rejection. The usual approach for introduction of the biopsy catheter is via the right internal jugular vein or, less frequently, the left internal jugular vein or femoral vein (Figs. 30-6 and 30-7). Traditionally, fluoroscopy has been used to guide the biopsy catheter tip to the interventricular septum to obtain biopsies. Echocardiography has been successfully used to guide endomyocardial biopsies with the benefits of lack of radiation exposure, portability, and provision of information on cardiac structure and function. Complication rates with echocardiography for biopsies are extremely low and comparable with those for fluoroscopic guided biopsies (about 0.4% of all biopsies attempts, or much lower with experienced operators).[58,59] One disadvantage is that initial insertion and advancement of the bioptome from the superior vena cava until entry into the right atrium is not directly visualized with echocardiography. The development of severe tricuspid regurgitation in the cardiac allograft is correlated with the total number of biopsies performed, presumably as a result of inadvertent damage to the tricuspid valve apparatus by the biopsy

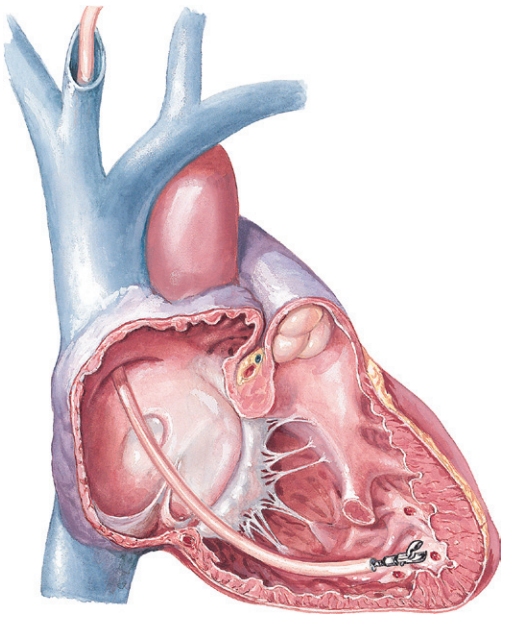


**Figure 30-6 Endomyocardial biopsy via right internal jugular vein approach.** A bioptome is advanced through the right atrium and tricuspid valve into the right ventricle. Samples are preferentially obtained from the interventricular septum to lessen the risk of cardiac perforation and tamponade, which is increased with biopsy of the right ventricular free wall.

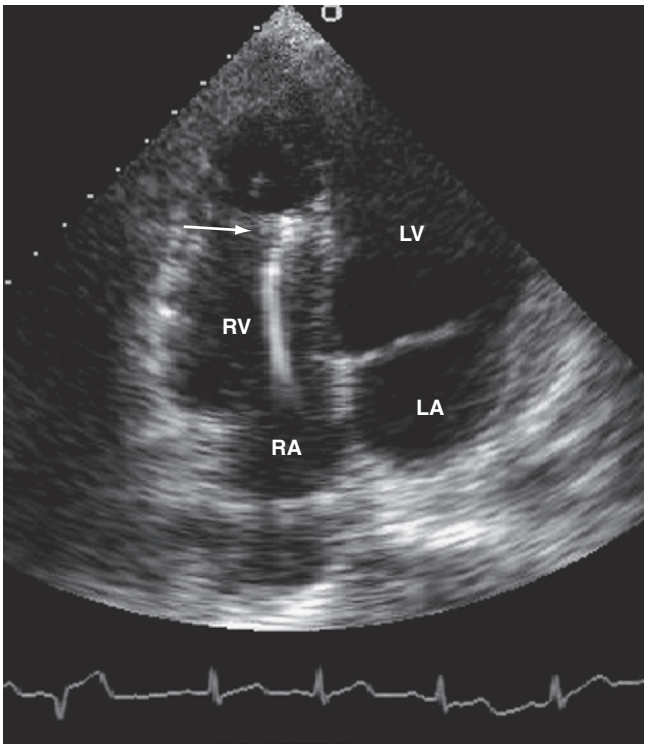



**Figure 30-7 Right ventricular biopsy of a cardiac allograft with echocardiographic guidance.** *Arrow* indicates tip of the bioptome, which is advanced through the right atrium and tricuspid valve into the right ventricle for biopsy from the interventricular septum.

catheter as it passes into the right ventricle.[60] Although measures such as use of a long sheath to introduce the bioptome directly into the right ventricle lessen the risk of development of tricuspid regurgitation, whether the routine use of echocardiography to guide biopsies lessens this risk has not been definitively established.

## Early Postoperative Complications and Other Findings

### EARLY POSTOPERATIVE COMPLICATIONS

Other than the routine use of intraoperative transesophageal echocardiography to monitor cardiac allograft function, echocardiography is generally not a significant part of routine monitoring of the recipient immediate after transplant, unless routine monitoring suggests a problem. Frequently, early indications of a problem or complication involving the cardiac allograft are detected via abnormalities in hemodynamics, either systemic blood pressure or heart rate, invasively measured central hemodynamics, or arrhythmias on telemetry monitoring. Early postoperative problems that may be diagnosed and evaluated with echocardiography include pericardial effusion or tamponade (discussed in more detail in the following section), right ventricular dysfunction, tricuspid valve regurgitation, and acute allograft failure.[61]

### PERICARDIAL EFFUSION

Estimates of occurrence of moderate to large-sized pericardial effusions that occur in the postoperative period range from 9% to 35%. The significant majority of these effusions do not appear to negatively impact short-term or intermediate-term outcomes, including hospital length of stay and survival, and there does not appear to be a correlation with occurrence of rejection.[62-64] The likelihood of development of pericardial effusion after cardiac transplantation may be higher in the absence of previous cardiac surgery or with undersized hearts.[62,63] The natural history of these effusions varies widely, with estimates of necessary intervention ranging from approximately 10% to 45% for pericardiocentesis and, in an older series, a minority for pericardiectomy.[63,64] Pericardial effusion that occurs more than 1 month after transplantation may be associated with less favorable implications. Some authors have found an association between late-onset persistent or increasing pericardial effusion with occurrence and severity of rejection.[65,66] Although pericardial fluid is usually sterile, given the altered immunity of these patients, infection and neoplasm should also be considered as possible causes.

**Box 30-2**

**STANDARD ECHOCARDIOGRAM FOR THE CARDIAC TRANSPLANT RECIPIENT**

The standard echocardiogram for the cardiac transplant recipient should include but is not necessarily limited to:

1. Standard 2D views, including parasternal long-axis and short-axis views and apical four-chamber, two-chamber, and long-axis views, for assessment of regional wall motion and overall systolic function.
2. Pulsed-wave Doppler recording of mitral inflow for assessment of diastolic function.
3. Tissue-Doppler measurement of septal and lateral mitral annular velocities for assessment of systolic and, especially, diastolic function.
4. 2D and color Doppler assessment of the valves, with particular attention to the tricuspid valve, which may have been traumatized by prior right ventricular biopsies.
5. Consideration of strain and strain rate analysis, either with Doppler-based or speckle tracking techniques, for more sensitive quantification of systolic function.

## Posttransplant Monitoring

### ROUTINE FOLLOW-UP

A general summary of consensus guidelines for routine follow-up care of the cardiac transplant recipient is shown in Figure 30-8. Echocardiography is primarily used for routine monitoring of cardiac allograft structure and function, including valvular abnormalities such as tricuspid regurgitation; as part of stress imaging for cardiac allograft vasculopathy surveillance; and as an adjunct to endomyocardial biopsy in the diagnosis of acute rejection. Elements of a standard echocardiogram of the cardiac transplant recipient are listed in Box 30-2. For patients with suspected acute rejection, an echocardiogram should be obtained with particular attention paid to identification of changes in measures of systolic and diastolic function. Comparison with prior echocardiograms obtained when no rejection was present may be helpful.

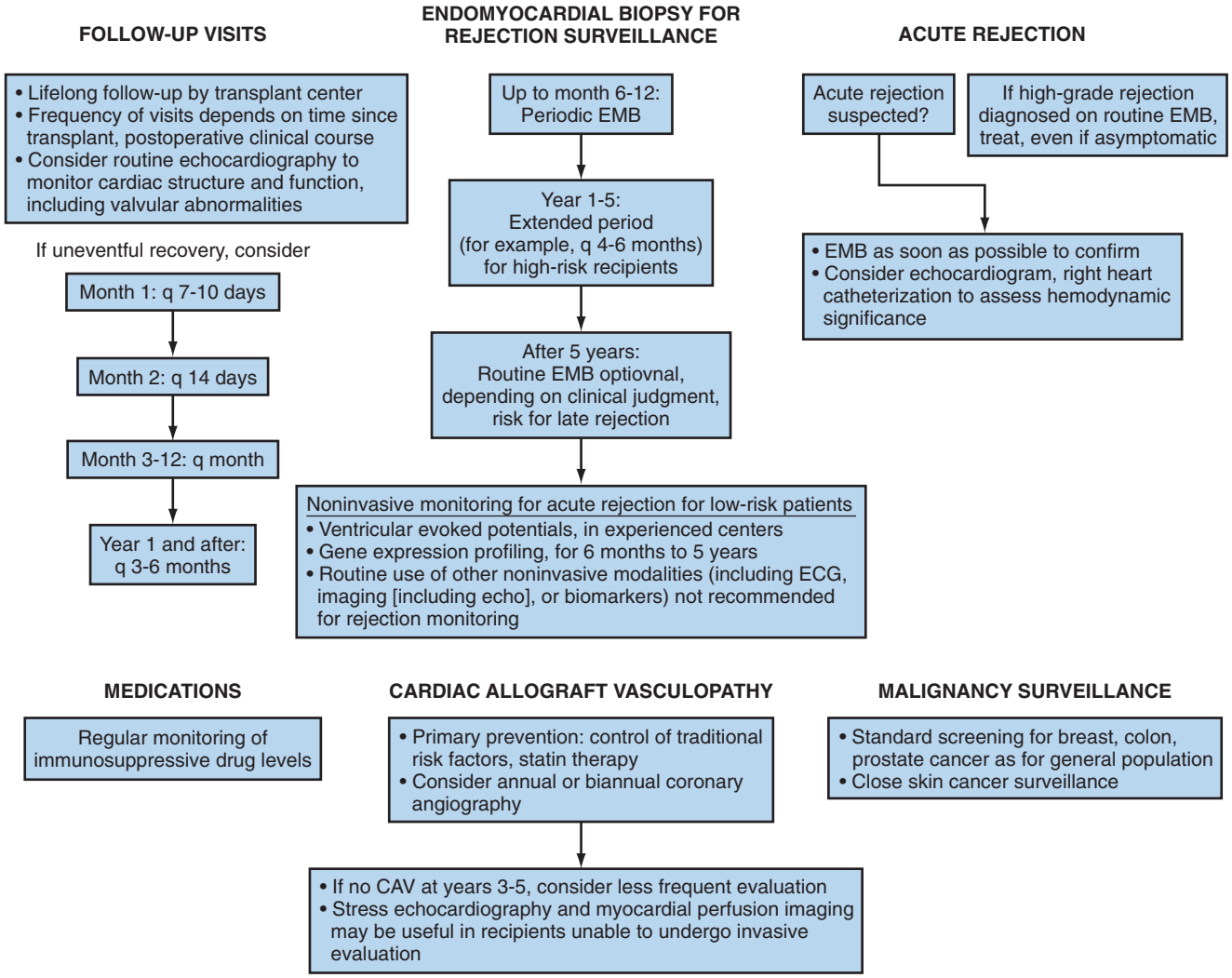



**Figure 30-8 Suggested guidelines for routine follow-up care of the cardiac transplant recipient.** In addition, chronic kidney disease, diabetes, hypertension and osteoporosis are managed as per general population with awareness of potential drug interactions with transplant medications. *CAV,* Cardiac allograft vasculopathy; *EMB,* endomyocardial biopsy. *(Adapted from Costanzo MR, et al: The International Society of Heart and Lung Transplantation guidelines for the care of heart transplant recipients.* J Heart Lung Transplant *29:914-956, 2010.)*

## DIAGNOSIS OF CARDIAC ALLOGRAFT VASCULOPATHY

Cardiac allograft vasculopathy is an entity distinct from native coronary disease of the nontransplanted heart and is one of the primary factors limiting the long-term functioning and life span of the allograft. Allograft vasculopathy is an accelerated form of intimal hyperplasia that likely results from both immune and nonimmune mechanisms. A classic finding is diffuse "pruning" of the smaller distal coronary vasculature, although discrete stenoses characteristic of native coronary disease may develop as well. In addition to transplant-specific immunologic risk factors, typical risk factors for native coronary disease, such as dyslipidemia and hypertension, also impact the development of cardiac allograft vasculopathy. Distinct from the de novo development of allograft vasculopathy, some component of atherosclerosis is also already present in the donor allograft, progression of which does not appear to be correlated with development of de novo vasculopathy.[67,68] Angiographic identification of transplant vasculopathy is associated with a fivefold greater risk of cardiac events, including myocardial infarction, heart failure, and sudden death.[69] As a result of cardiac denervation, clinical symptoms from cardiac allograft vasculopathy are frequently late and atypical, if at all.

### *Coronary Angiography with Intravascular Ultrasound*

Coronary angiography is relatively insensitive in detection of early transplant vasculopathy; up to three quarters of patients with intimal thickening with intravascular ultrasound (IVUS) have normal coronary angiograms.[70,71] Coronary angiography, which defines the luminal silhouette of the coronary artery, is not able to detect the often diffuse and concentric intimal hyperplasia that characterizes allograft vasculopathy. Because IVUS images vascular wall morphology, it has emerged as the gold standard for detection of transplant vasculopathy, particularly in its early stages. Extent of vasculopathy can be quantified according to intimal thickness and circumferential extent and also by change in measures of plaque burden over time. IVUS findings of allograft vasculopathy can be classified as Stanford class I (minimal: intimal thickness less than 0.3 mm and circumferential involvement less than 180 degrees), class II (mild: intimal thickness less than 0.3 mm and circumferential

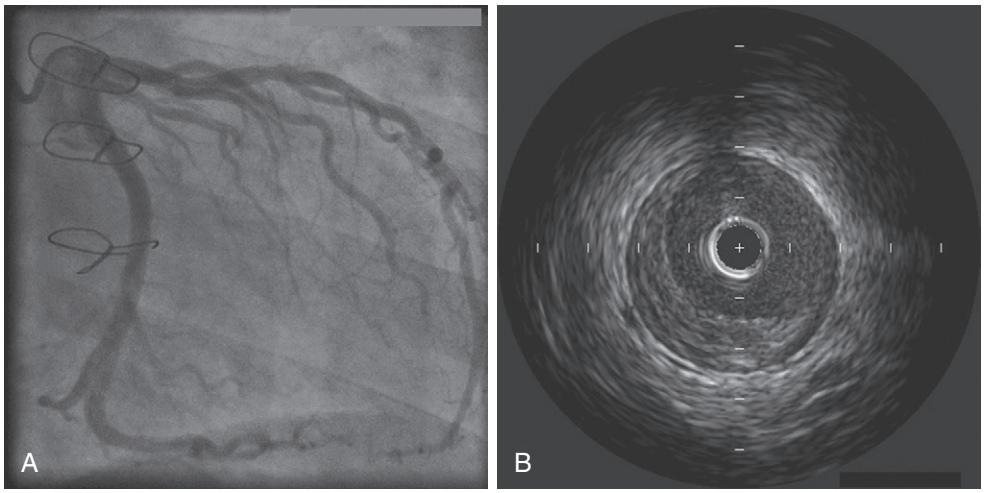



**Figure 30-9 The coronary angiogram (A) in this patient after transplant appears to show no significant narrowing of the lumen.** However, an intravascular ultrasound image in the mid left anterior descending coronary (**B**) shows a significant atherosclerotic plaque.

**TABLE 30-1 Comparative Test Characteristics for Diagnosis of Cardiac Allograft Vasculopathy**

| | *Sensitivity* | *Specificity* | *PPV* | *NPV* |
|---|---|---|---|---|
| **Dobutamine stress echocardiography, gold standard for diagnosis of CAV** | | | | |
| Angiography[a-c] | 64%-83% | 56%-95% | 40%-78% | 84%-90% |
| Intravascular ultrasound[a,d,e] | 72%-90% | 55%-88% | 75%-92% | 62%-79% |
| **Nuclear medicine–based myocardial perfusion scans**[f-h] | 63%-90% | 55%-78% | 42%-75% | 75%-96% |

*NPV,* negative predictive value; *PPV,* positive predictive value.

References

[a]Spes CH, Mudra H, Schnaack SD, et al: Dobutamine stress echocardiography for noninvasive diagnosis of cardiac allograft vasculopathy: a comparison with angiography and intravascular ultrasound. *Am J Cardiol* 78:168-174, 1996.

[b]Bacal F, Moreira L, Souza G, et al: Dobutamine stress echocardiography predicts cardiac events or death in asymptomatic patients long-term after heart transplantation: 4-year prospective evaluation. *J Heart Lung Transplant* 23:1238-1244, 2004.

[c]Derumeaux G, Redonnet M, Soyer R, et al: Assessment of the progression of cardiac allograft vasculopathy by dobutamine stress echocardiography. *J Heart Lung Transplant* 17:259-267, 1998.

[d]Spes CH, Klauss V, Mudra H, et al: Diagnostic and prognostic value of serial dobutamine stress echocardiography for noninvasive assessment of cardiac allograft vasculopathy: a comparison with coronary angiography and intravascular ultrasound. *Circulation* 100:509-515, 1999.

[e]Stork S, Behr TM, Birk M, et al: Assessment of cardiac allograft vasculopathy late after heart transplantation: when is coronary angiography necessary? *J Heart Lung Transplant* 25:1103-1108, 2006.

[f]Wu YW, Yen RF, Lee CM, et al: Diagnostic and prognostic value of dobutamine thallium-201 single-photon emission computed tomography after heart transplantation. *J Heart Lung Transplant* 24:544-550, 2005.

[g]Manrique A, Bernard M, Hitzel A, et al: Diagnostic and prognostic value of myocardial perfusion gated SPECT in orthotopic heart transplant recipients. *J Nucl Cardiol* 17:197-206, 2010.

[h]Elhendy A, Sozzi FB, van Domburg RT, et al: Accuracy of dobutamine tetrofosmin myocardial perfusion imaging for the noninvasive diagnosis of transplant coronary artery stenosis. *J Heart Lung Transplant* 19:360-366, 2000.

involvement more than 180 degrees), class III (moderate: intimal thickness 0.3 to 0.5 mm, or intimal thickness more than 0.5 mm and circumferential involvement less than 180 degrees), or class IV (severe: intimal thickness more than 1 mm, or intimal thickness more than 0.5 mm and circumferential involvement more than 180 degrees).[70] Severity of transplant vasculopathy progresses most rapidly in the first 2 years after transplantation.[72] Changes in the allograft vasculature in the first year after transplantation likely reflect the cumulative result of multiple insults, such as donor explosive brain death, early rejection, and cytomegalovirus infection, which influence the recipient's immune response to the allograft and thus the likelihood of development of vasculopathy. Early changes with IVUS during the first posttransplant year correlate with long-term prognosis. Progression of maximal intimal thickening of greater than or equal to 0.5 mm in the first year after transplantation is associated with a significantly higher risk of development of angiographic disease, nonfatal major adverse cardiac events, and death or graft loss in long-term follow-up (Fig. 30-9).[73,74]

### *Dobutamine Stress Echocardiography*

Dobutamine stress echocardiography is a valuable tool for detecting cardiac allograft vasculopathy and yielding prognostic information. With intracoronary IVUS as the gold standard, dobutamine stress echocardiography is highly sensitive and specific in detection of cardiac allograft vasculopathy. Positive dobutamine stress echocardiography is associated with increased risk of cardiac events, including myocardial infarction and heart failure, and risk for death.[75-77] Estimates of accuracy of dobutamine echocardiography for diagnosis of significant coronary allograft vasculopathy vary somewhat dependant on whether the gold standard being used is angiography or angiography with IVUS. In general, dobutamine stress echocardiography appears to agree better with IVUS–diagnosed disease and overall performs better than nuclear medicine myocardial perfusion scans (Table 30-1). In contrast, the sensitivity of stress echocardiography with exercise is somewhat limited by the blunted heart rate response to exercise that occurs from cardiac denervation; estimates of sensitivity of exercise echocardiography for diagnosis of cardiac allograft vasculopathy are as low as

15% to 20%.[78,79] Although worsening on serial dobutamine stress echocardiogram studies (interval increase in number of segments with wall motion abnormalities or in wall motion score by 1.0 or more) is variably accurate in diagnosis of angiographic/IVUS cardiac allograft vasculopathy,[77,80] worsening between interval dobutamine stress echocardiographic studies was still associated with a roughly sevenfold higher risk of events.[77] The addition of quantitative M-mode analysis or strain rate imaging to standard dobutamine stress echocardiography may also improve its diagnostic accuracy.[77,81]

## KEY POINTS

- Preoperative pulmonary hypertension, particularly if not medically reversible with vasodilators or if reversible at the expense of systemic hypotension, is associated with a very high risk of short-term mortality, frequently as a result of right heart failure, after cardiac transplantation.
- Currently, the bicaval technique of cardiac transplantation is more widely used than the older biatrial technique, with resultant lesser appearance of biatrial enlargement seen on echocardiography and better structural and functional preservation of the donor atria.
- Diastolic dysfunction is common immediately after cardiac transplantation and may be related to ischemic injury, recipient pulmonary hypertension, volume overload, or recipient-donor size mismatch. Diastolic dysfunction generally normalizes over weeks to months, or in some patients over years, but may also persist to a subtle degree.
- Persistence of a restrictive filling pattern may be associated with reduced long-term survival. A restrictive filling pattern may recur in the setting of acute rejection.
- Cardiac allograft systolic function generally remains normal as many as 10 to 15 years after transplant. LV hypertrophy and postoperative septal motion are common findings.
- Tricuspid regurgitation, sometimes severe enough to need corrective surgery, may be induced by inadvertent injury during routine endomyocardial biopsies.
- New onset systolic dysfunction in the setting of acute rejection generally indicates higher grade rejection with hemodynamic compromise. Diastolic abnormalities may manifest earlier, although they are not accurate enough to be the sole criteria for diagnosis of acute rejection.
- Cardiac allograft vasculopathy is an accelerated diffuse intimal hyperplasia that ultimately limits the long-term life span of the allograft in many cardiac transplant patients. The clinical presentation is frequently atypical as a result of denervation of the cardiac allograft. IVUS is currently the gold standard for diagnosis, although dobutamine stress echocardiography is also sensitive and specific and yields prognostic information.

## REFERENCES


1. Stehlik J, Edwards LB, Kucheryavaya AY, et al: The Registry of the International Society for Heart and Lung Transplantation: twenty-seventh official adult heart transplant report. *J Heart Lung Transplant* 29:1089-1103, 2010.
2. Costard-Jackle A, Fowler MB: Influence of preoperative pulmonary artery pressure on mortality after heart transplantation: testing of potential reversibility of pulmonary hypertension with nitroprusside is useful in defining a high risk group. *J Am Coll Cardiol* 19:48-54, 1992.
3. Temporelli PL, Scapellato F, Eleuteri E, et al: Doppler echocardiography in advanced systolic heart failure: a noninvasive alternative to Swan-Ganz catheter. *Circ Heart Fail* 3:387-394, 2010.
4. Rosendale JD, Kauffman HM, McBride MA, et al: Aggressive pharmacologic donor management results in more transplanted organs. *Transplantation* 75:482-487, 2003.
5. Zaroff JG, Babcock WD, Shiboski SC, et al: Temporal changes in left ventricular systolic function in heart donors: results of serial echocardiography. *J Heart Lung Transplant* 22:383-388, 2003.
6. Goland S, Czer LS, Kass RM, et al: Use of cardiac allografts with mild and moderate left ventricular hypertrophy can be safely used in heart transplantation to expand the donor pool. *J Am Coll Cardiol* 51:1214-1220, 2008.
7. Bouchart F, Derumeaux G, Mouton-Schleifer D, et al: Conventional and total orthotopic cardiac transplantation: a comparative clinical and echocardiographical study. *Eur J Cardiothorac Surg* 12:555-559, 1997.
8. Derumeaux G, Habib G, Schleifer DM, et al: Standard orthotopic heart transplantation versus total orthotopic heart transplantation. A transesophageal echocardiography study of the incidence of left atrial thrombosis. *Circulation* 92:II196-II201, 1995.
9. Kaye DM, Anderson ST, Federman J: Electrocardiographic and echocardiographic features of left atrial size after orthotopic cardiac transplantation. *Am J Cardiol* 70:1096-1099, 1992.
10. Angermann CE, Spes CH, Tammen A, et al: Anatomic characteristics and valvular function of the transplanted heart: transthoracic versus transesophageal echocardiographic findings. *J Heart Transplant* 9:331-338, 1990.
11. De Simone R, Lange R, Sack RU, et al: Atrioventricular valve insufficiency and atrial geometry after orthotopic heart transplantation. *Ann Thorac Surg* 60:1686-1693, 1995.
12. Aziz TM, Burgess MI, El-Gamel A, et al: Orthotopic cardiac transplantation technique: a survey of current practice. *Ann Thorac Surg* 68:1242-1246, 1999.
13. Davies RR, Russo MJ, Morgan JA, et al: Standard versus bicaval techniques for orthotopic heart transplantation: an analysis of the United Network for Organ Sharing database. *J Thorac Cardiovasc Surg* 140:700-708, e1-e2, 2010.
14. Riberi A, Ambrosi P, Habib G, et al: Systemic embolism: a serious complication after cardiac transplantation avoidable by bicaval technique. *Eur J Cardiothorac Surg* 19:307- 312, 2001.
15. Derumeaux G, Mouton-Schleifer D, Soyer R, et al: High incidence of left atrial thrombus detected by transoesophageal echocardiography in heart transplant recipients. *Eur Heart J* 16:120-125, 1995.
16. Freimark D, Czer LS, Aleksic I, et al: Improved left atrial transport and function with orthotopic heart transplantation by bicaval and pulmonary venous anastomoses. *Am Heart J* 130:121-126, 1995.
17. Traversi E, Pozzoli M, Grande A, et al: The bicaval anastomosis technique for orthotopic heart transplantation yields better atrial function than the standard technique: an echocardiographic automatic boundary detection study. *J Heart Lung Transplant* 17:1065-1074, 1998.
18. Boudoulas H, Starling RC, Vavuranakis M, et al: Left atrial volumes and function in orthotopic cardiac transplantation. *Am Heart J* 129:774-782, 1995.
19. Cresci S, Goldstein JA, Cardona H, et al: Impaired left atrial function after heart transplantation: disparate contribution of donor and recipient atrial components studied on-line with quantitative echocardiography. *J Heart Lung Transplant* 14:647-653, 1995.
20. Corcos T, Tamburino C, Leger P, et al: Early and late hemodynamic evaluation after cardiac transplantation: a study of 28 cases. *J Am Coll Cardiol* 11:264-269, 1988.
21. Cotts WG, Oren RM: Function of the transplanted heart: unique physiology and therapeutic implications. *Am J Med Sci* 314:164-172, 1997.
22. Young JB, Winters WL, Jr, Bourge R, Uretsky BF: 24th Bethesda conference: cardiac transplantation. Task Force 4: function of the heart

transplant recipient. *J Am Coll Cardiol* 22:31-41, 1993.
23. Bengel FM, Ueberfuhr P, Schiepel N, et al: Effect of sympathetic reinnervation on cardiac performance after heart transplantation. *N Engl J Med* 345:731-738, 2001.
24. Quigg R, Salyer J, Mohanty PK, Simpson P: Impaired exercise capacity late after cardiac transplantation: influence of chronotropic incompetence, hypertension, and calcium channel blockers. *Am Heart J* 136:465-473, 1998.
25. Antunes ML, Spotnitz HM, Clark MB, et al: Long-term function of human cardiac allografts assessed by two-dimensional echocardiography. *J Thorac Cardiovasc Surg* 98:275-284, 1989.
26. Tischler MD, Lee RT, Plappert T, et al: Serial assessment of left ventricular function and mass after orthotopic heart transplantation: a 4-year longitudinal study. *J Am Coll Cardiol* 19:60-66, 1992.
27. Globits S, De Marco T, Schwitter J, et al: Assessment of early left ventricular remodeling in orthotopic heart transplant recipients with cine magnetic resonance imaging: potential mechanisms. *J Heart Lung Transplant* 16:504-510, 1997.
28. Wilhelmi M, Pethig K, Nguyen H, et al: Heart transplantation: echocardiographic assessment of morphology and function after more than 10 years of follow-up. *Ann Thorac Surg* 74:1075-1079, 2002.
29. St Goar FG, Gibbons R, Schnittger I, et al: Left ventricular diastolic function. Doppler echocardiographic changes soon after cardiac transplantation. *Circulation* 82:872-878, 1990.
30. Tallaj JA, Kirklin JK, Brown RN, et al: Post-heart transplant diastolic dysfunction is a risk factor for mortality. *J Am Coll Cardiol* 50:1064-1069, 2007.
31. Valantine HA, Appleton CP, Hatle LK, et al: A hemodynamic and Doppler echocardiographic study of ventricular function in long-term cardiac allograft recipients. Etiology and prognosis of restrictive-constrictive physiology. *Circulation* 79:66-75, 1989.
32. Ross HJ, Gullestad L, Hunt SA, et al: Early Doppler echocardiographic dysfunction is associated with an increased mortality after orthotopic cardiac transplantation. *Circulation* 94: II289-II293, 1996.
33. Dandel M, Wellnhofer E, Hummel M, et al: Early detection of left ventricular dysfunction related to transplant coronary artery disease. *J Heart Lung Transplant* 22:1353-1364, 2003.
34. Hosenpud JD, Norman DJ, Cobanoglu MA, et al: Serial echocardiographic findings early after heart transplantation: evidence for reversible right ventricular dysfunction and myocardial edema. *J Heart Transplant* 6:343-347, 1987.
35. Bhatia SJ, Kirshenbaum JM, Shemin RJ, et al: Time course of resolution of pulmonary hypertension and right ventricular remodeling after orthotopic cardiac transplantation. *Circulation* 76:819-826, 1987.
36. Cladellas M, Oriol A, Caralps JM: Quantitative assessment of valvular function after cardiac transplantation by pulsed Doppler echocardiography. *Am J Cardiol* 73:1197-1201, 1994.
37. Anderson CA, Shernan SK, Leacche M, et al: Severity of intraoperative tricuspid regurgitation predicts poor late survival following cardiac transplantation. *Ann Thorac Surg* 78:1635-1642, 2004.
38. Fiorelli AI, Stolf NA, Abreu Filho CA, et al: Prophylactic donor tricuspid annuloplasty in orthotopic bicaval heart transplantation. *Transplant Proc* 39:2527-2530, 2007.
39. Chan MC, Giannetti N, Kato T, et al: Severe tricuspid regurgitation after heart transplantation. *J Heart Lung Transplant* 20:709-717, 2001.
40. Huddleston CB, Rosenbloom M, Goldstein JA, Pasque MK: Biopsy-induced tricuspid regurgitation after cardiac transplantation. *Ann Thorac Surg* 57:832-837, 1994.
41. Stewart S, Winters GL, Fishbein MC, et al: Revision of the 1990 working formulation for the standardization of nomenclature in the diagnosis of heart rejection. *J Heart Lung Transplant* 24:1710-1720, 2005.
42. Hammond EH, Yowell RL, Nunoda S, et al: Vascular (humoral) rejection in heart transplantation: pathologic observations and clinical implications. *J Heart Transplant* 8:430-443, 1989.
43. Subherwal S, Kobashigawa JA, Cogert G, et al: Incidence of acute cellular rejection and noncellular rejection in cardiac transplantation. *Transplant Proc* 36:3171-3172, 2004.
44. Mills RM, Naftel DC, Kirklin JK, et al: Heart transplant rejection with hemodynamic compromise: a multiinstitutional study of the role of endomyocardial cellular infiltrate. Cardiac Transplant Research Database. *J Heart Lung Transplant* 16:813-821, 1997.
45. Amende I, Simon R, Seegers A, et al: Diastolic dysfunction during acute cardiac allograft rejection. *Circulation* 81:III66-III70, 1990.
46. Valantine HA, Fowler MB, Hunt SA, et al: Changes in Doppler echocardiographic indexes of left ventricular function as potential markers of acute cardiac rejection. *Circulation* 76:V86-V92, 1987.
47. Desruennes M, Corcos T, Cabrol A, et al: Doppler echocardiography for the diagnosis of acute cardiac allograft rejection. *J Am Coll Cardiol* 12:63-70, 1988.
48. Mena C, Wencker D, Krumholz HM, McNamara RL: Detection of heart transplant rejection in adults by echocardiographic diastolic indices: a systematic review of the literature. *J Am Soc Echocardiogr* 19:1295-1300, 2006.
49. Toumanidis ST, Papadopoulou ES, Saridakis NS, et al: Evaluation of myocardial performance index to predict mild rejection in cardiac transplantation. *Clin Cardiol* 27:352-358, 2004.
50. Burgess MI, Bright-Thomas RJ, Yonan N, Ray SG: Can the index of myocardial performance be used to detect acute cellular rejection after heart transplantation? *Am J Cardiol* 92:308-311, 2003.
51. Stengel SM, Allemann Y, Zimmerli M, et al: Doppler tissue imaging for assessing left ventricular diastolic dysfunction in heart transplant rejection. *Heart* 86:432-437, 2001.
52. Mankad S, Murali S, Kormos RL, et al: Evaluation of the potential role of color-coded tissue Doppler echocardiography in the detection of allograft rejection in heart transplant recipients. *Am Heart J* 138:721-730, 1999.
53. Kato TS, Oda N, Hashimura K, et al: Strain rate imaging would predict sub-clinical acute rejection in heart transplant recipients. *Eur J Cardiothorac Surg* 37:1104-1110, 2010.
54. Sagar KB, Hastillo A, Wolfgang TC, et al: Left ventricular mass by M-mode echocardiography in cardiac transplant patients with acute rejection. *Circulation* 64:II217-II220, 1981.
55. Mannaerts HF, Balk AH, Simoons ML, et al: Changes in left ventricular function and wall thickness in heart transplant recipients and their relation to acute rejection: an assessment by digitised M mode echocardiography. *Br Heart J* 68:356-364, 1992.
56. Ciliberto GR, Mascarello M, Gronda E, et al: Acute rejection after heart transplantation: noninvasive echocardiographic evaluation. *J Am Coll Cardiol* 23:1156-1161, 1994.
57. Gill EA, Borrego C, Bray BE, et al: Left ventricular mass increases during cardiac allograft vascular rejection. *J Am Coll Cardiol* 25:922-926, 1995.
58. Miller LW, Labovitz AJ, McBride LA, et al: Echocardiography-guided endomyocardial biopsy. A 5-year experience. *Circulation* 78:III99-III102, 1988.
59. Bedanova H, Necas J, Petrikovits E, et al: Echo-guided endomyocardial biopsy in heart transplant recipients. *Transpl Int* 17:622-625, 2004.
60. Nguyen V, Cantarovich M, Cecere R, Giannetti N: Tricuspid regurgitation after cardiac transplantation: how many biopsies are too many? *J Heart Lung Transplant* 24:S227-S231, 2005.
61. Costanzo MR, Dipchand A, Starling R, et al: The International Society of Heart and Lung Transplantation Guidelines for the care of heart transplant recipients. *J Heart Lung Transplant* 29:914-956, 2010.
62. Quin JA, Tauriainen MP, Huber LM, et al: Predictors of pericardial effusion after orthotopic heart transplantation. *J Thorac Cardiovasc Surg* 124:979-983, 2002.
63. Hauptman PJ, Couper GS, Aranki SF, et al: Pericardial effusions after cardiac transplantation. *J Am Coll Cardiol* 23:1625-1629, 1994.
64. Al-Dadah AS, Guthrie TJ, Pasque MK, et al: Clinical course and predictors of pericardial effusion following cardiac transplantation. *Transplant Proc* 39:1589-1592, 2007.
65. Ciliberto GR, Anjos MC, Gronda E, et al: Significance of pericardial effusion after heart transplantation. *Am J Cardiol* 76:297-300, 1995.
66. Valantine HA, Hunt SA, Gibbons R, et al: Increasing pericardial effusion in cardiac transplant recipients. *Circulation* 79:603-609, 1989.
67. Kapadia SR, Nissen SE, Ziada KM, et al: Development of transplantation vasculopathy and progression of donor-transmitted atherosclerosis: comparison by serial intravascular ultrasound imaging. *Circulation* 98:2672-2678, 1998.
68. Li H, Tanaka K, Anzai H, et al: Influence of preexisting donor atherosclerosis on the development of cardiac allograft vasculopathy and outcomes in heart transplant recipients. *J Am Coll Cardiol* 47:2470-2476, 2006.
69. Uretsky BF, Murali S, Reddy PS, et al: Development of coronary artery disease in cardiac transplant patients receiving immunosuppressive therapy with cyclosporine and prednisone. *Circulation* 76:827-834, 1987.
70. St Goar FG, Pinto FJ, Alderman EL, et al: Intracoronary ultrasound in cardiac transplant recipients. In vivo evidence of "angiographically silent" intimal thickening. *Circulation* 85:979-987, 1992.
71. Pinto FJ, Chenzbraun A, Botas J, et al: Feasibility of serial intracoronary ultrasound imaging for assessment of progression of intimal proliferation in cardiac transplant recipients. *Circulation* 90:2348-2355, 1994.
72. Rickenbacher PR, Pinto FJ, Chenzbraun A, et al: Incidence and severity of transplant coronary artery disease early and up to 15 years after transplantation as detected by intravascular ultrasound. *J Am Coll Cardiol* 25:171-177, 1995.
73. Kobashigawa JA, Tobis JM, Starling RC, et al: Multicenter intravascular ultrasound validation study among heart transplant recipients: outcomes after five years. *J Am Coll Cardiol* 45:1532-1537, 2005.

74. Tuzcu EM, Kapadia SR, Sachar R, et al: Intravascular ultrasound evidence of angiographically silent progression in coronary atherosclerosis predicts long-term morbidity and mortality after cardiac transplantation. *J Am Coll Cardiol* 45:1538-1542, 2005.
75. Bacal F, Moreira L, Souza G, et al: Dobutamine stress echocardiography predicts cardiac events or death in asymptomatic patients long-term after heart transplantation: 4-year prospective evaluation. *J Heart Lung Transplant* 23:1238-1244, 2004.
76. Akosah KO, Olsovsky M, Kirchberg D, et al: Dobutamine stress echocardiography predicts cardiac events in heart transplant patients. *Circulation* 94:II283-II288, 1996.
77. Spes CH, Klauss V, Mudra H, et al: Diagnostic and prognostic value of serial dobutamine stress echocardiography for noninvasive assessment of cardiac allograft vasculopathy: a comparison with coronary angiography and intravascular ultrasound. *Circulation* 100:509-515, 1999.
78. Cohn JM, Wilensky RL, O'Donnell JA, et al: Exercise echocardiography, angiography, and intracoronary ultrasound after cardiac transplantation. *Am J Cardiol* 77:1216-1219, 1996.
79. Collings CA, Pinto FJ, Valantine HA, et al: Exercise echocardiography in heart transplant recipients: a comparison with angiography and intracoronary ultrasonography. *J Heart Lung Transplant* 13:604-613, 1994.
80. Derumeaux G, Redonnet M, Soyer R, et al: Assessment of the progression of cardiac allograft vasculopathy by dobutamine stress echocardiography. *J Heart Lung Transplant* 17:259-267, 1998.
81. Eroglu E, D'Hooge J, Sutherland GR, et al: Quantitative dobutamine stress echocardiography for the early detection of cardiac allograft vasculopathy in heart transplant recipients. *Heart* 94:e3, 2008.



# Cardiac Assist Devices: Normal Findings, Device Failure, and Weaning Parameters

JAMES N. KIRKPATRICK, MD

**Basic Principles of Cardiac Assist Devices and the Echocardiographic Approach**
Types of Cardiac Assist Devices
Preimplant Assessment
Periprocedural Guidance
Approach to Cardiac Assist Device Dysfunction
**Technical Details, Quantitation, and Data Analysis**
LVEDD and Septal Orientation
Ventricular Function
Aortic Valve Opening
Pericardium
Cannulae
Optimization
Weaning/Turndown
**Clinical Utility, Outcome Data**
**Potential Limitations, Future Directions**
**Alternate Approaches**

Cardiac assist devices are playing an increasingly important role in the treatment of heart failure. Early-generation ventricular assist devices (VADs) were used as a "bridge to recovery" to support patients expected to recover from reversible cardiac insults.[1,2] Indications soon expanded to include stabilization of patients before transplant ("bridge to transplant").[3-5] Technologic improvements reduced VAD size so that they could be implanted in the abdomen or chest, allowing patients to await transplant at home. The early devices, still used for temporary support, are the size of small refrigerators. The newest implantable pumps fit into the palm of one's hand.

The success of early VADs,[6] the limited number of donor hearts, and the large number of patients excluded from transplant candidacy because of age or comorbidities led to the use of VADs as permanent treatment. The 2001 REMATCH study demonstrated improvement in 2-year mortality and quality of life for patients randomized to permanent left ventricular assist device (LVAD) support versus medical therapy.[7] This use of LVADs as "destination therapy" has set the stage for more widespread use.[8,9]

In addition to bridge to recovery, bridge to transplant, and destination therapy, VADs are increasingly employed as "bridges to decision"—support of patients undergoing workup to determine transplant candidacy (Table 31-1). If rejected for transplant, these patients' devices become destination therapy. Conversely, some patients will unexpectedly recover ventricular function. In this case, VADs originally classified as bridge to transplant or destination therapy become bridge to recovery.

## Basic Principles of Cardiac Assist Devices and the Echocardiographic Approach

### TYPES OF CARDIAC ASSIST DEVICES

#### *Implanted Ventricular Assist Devices*

Most implanted VADs consist of a pump, an inflow cannula, an outflow cannula, a power supply, and a controller. The controller collects data from the pump and directs its action via a driveline. VADs can be classified according to the location of these components. Extracorporeal VADs have pumps and controllers outside the body. Patients with paracorporeal VADs have components strapped close to the body but not inside it. Intracorporeal VADs have implanted pumps, with drivelines connecting to a paracorporeal or extracorporeal controller (Table 31-2).

Cardiac assist devices can support the left ventricle (LVAD), the right ventricle (RVAD), or both ventricles (BiVAD) (Fig. 31-1). LVAD inflow cannulae are connected to the LV apex or the left atrium (LA). The outflow graft cannula can be attached to the ascending aorta or the descending aorta. RVADs involve right atrial (RA) or right ventricular (RV) inflow and pulmonary artery outflow cannulation.

Devices are also characterized by mechanism (see Table 31-2).[10] Early-generation cardiac VADs (still in use) use either a pneumatically compressed, distensible chamber or a pusher-plate mechanism to expel blood into the outflow cannula (see Fig. 31-1, *A*). Because of the size of the chamber, these pumps cannot be implanted in small patients. These early-generation devices mimic cardiac pulsatile action through one-way inlet and outlet valves. They can be set to pump at a fixed rate or to maintain a constant stroke volume (asynchronous with the heart rate). In this mode, they have been used in patients with refractory ventricular arrhythmias.[11] A third (rarely used) mode has pumping rate gated to the electrocardiogram.

The next VAD generation produces continuous flow. These devices have a rotating propeller and are called *axial-flow pumps*. Blood is drawn from the heart via the inflow cannula and propelled into the outflow graft cannula[12] (see Fig. 31-1, *B*). The speed of the propeller in revolutions per minute (rpm) and the pressure difference between inflow and outflow cannulae determine rate of flow. There is greater flow during systole, when the aortic-LV pressure difference drops (LV pressure rises with ventricular contraction) than during diastole (LV pressure falls with ventricular relaxation and the pressure difference increases). These devices are sometimes called "nonpulsatile" VADs, but residual ventricular function and nonuniform

**TABLE 31-1 INTERMACS* Strategy for Ventricular Assist Device at Implant**

| *Indication* | *N (%)* |
|---|---|
| Bridge to transplant | 458 (45) |
| Bridge to decision | 458 (42) |
| Destination therapy | 100 (9) |
| Bridge to recovery | 25 (2.3) |
| Other | 13 (1.2) |

*Interagency Registry for Mechanically Assisted Circulatory Support over 3 years, 1092 patients. Overall survival was 74% at 1 year and 55% at 2 years.[16]

pressure differences between the inflow and outflow cannulae produce some pulsatility. These axial continuous-flow pumps provide increased flow at lower pressures than pulsatile pumps.[12] They also tend to be more durable, because they lack valves (which wear out over time).[13,14] A 2009 trial of destination therapy LVADs demonstrated a benefit for axial flow over pulsatile devices in fewer strokes and device failures.[15] Preliminary registry results also suggest lower complication rates in continuous-flow versus pulsatile-flow devices in the first 6 months after implant.[16]

**TABLE 31-2 Examples of Ventricular Assist Devices**

| *Name (Company)* | *Pump Location* | *Mechanism* | *Cannulae* | *Specifications (Size/Flows/Rates)* | *Approved and/or Proposed Indications* |
|---|---|---|---|---|---|
| HeartMate XVE (Thoratec) | Anterior abdominal wall | Pulsatile | I = LV apex<br>O = Asc Ao | 1150 g<br>3-10 L/min at 180 bpm | FDA approved for BTT, destination therapy, CE mark for BTT and destination therapy |
| Novacor pumps (WorldHeart) (discontinued) | Anterior abdominal wall | Pulsatile | I = LV apex<br>O = Asc Ao | 1000 g<br>2-12 L/min at 120 bpm | FDA approval for BTT, CE mark |
| Excor pediatric (BerlinHeart) | Extracorporeal | Pulsatile | BiVAD<br>I = LV apex, RA<br>O = Asc Ao, PA | 6 different pump sizes from 10 to 80 mL | Investigational, CE mark pediatric |
| I-VAD (Thoratec) | Anterior chest | Pulsatile | BiVAD<br>I = LV apex, RA<br>O = Asc Ao, PA | 330 g<br>Up to 7.2 L/min at 110 bpm | FDA approved BTR (postcardiotomy), BTT, CE mark |
| p-VAD (Thoratec) | Paracorporeal | Pulsatile | BiVAD<br>I = LV apex, RA<br>O = Asc Ao, PA | 419 g<br>Up to 7.2 L/min at 110 bpm | FDA approved BTR (postcardiotomy), BTT, CE mark |
| HeartMateII (Thoratec) | Anterior abdominal wall | Axial | I = LV apex<br>O = Asc Ao | 400 g<br>3-10 L/min<br>6000-15,000 rpm | FDA approved for BTT, destination therapy, CE mark for BTT and destination therapy |
| Jarvik2000* (Jarvik Heart) | LV apex | Axial | I = LV apex<br>O = Asc Ao, DA | 90 g<br>8,000-12,000 rpm | Investigational DTT, CE mark |
| HeartAssist 5 (Micromed Cardiovascular) | Pericardium | Axial | I = LV apex<br>O = Asc Ao | 92 g<br>1-10 L/min<br>7500-12,500 rpm | CE mark pediatric and adult |
| Incor (BerlinHeart) | Pericardium | Axial | I = LV apex<br>O = Asc Ao | 200 g<br>3-10 L/min<br>5,000-10,000 rpm | HDE for BTT, CE mark |
| HeartWare* HVAD (Heartware) | Pericardium | Centrifugal | I = LV apex<br>O = Asc Ao | 145 g<br>Up to 10 L/min<br>2000-3000 rpm | FDA approved for BTT, CE mark |
| Duraheart* (Terumo Heart) | Anterior chest wall | Centrifugal | I = LV apex<br>O = Asc Ao | 540 g<br>2-8 L/min<br>1200-2400 rpm | Investigational, CE mark |
| Levacor (WorldHeart) | Anterior abdominal wall | Centrifugal | I = LV apex<br>O = Asc Ao | 440 g<br>Up to 10 L/min<br>1000-3000 rpm | Investigational BTT |
| Centrimag (Levitronix) | Extracorporeal | Centrifugal | I = LA or LV via RSPV, RA<br>O = Asc Ao, PA. Can use existing cannulae via connectors | 1700 g<br>Up to 9.9 L/min<br>1500-5500 rpm | FDA approved for support up to 6 hours and under HDE for RV support up to 30 days |
| Impella Recover 2.5 or 5 (Abiomed) | LVOT | PVAD | Single cannula placed retrograde across aortic valve | 5 g<br>2.5 L/min or 5 L/min<br>25,000-50,000 rpm or 10,000-31,000 rpm | FDA approved for support up to 6 hours, CE mark |
| TandemHeart (Cardiac Assist) | Extracorporeal | PVAD | Transseptal LA and femoral artery cannulation | 280 g<br>2-5 L/min<br>3000-7500 rpm | FDA approved for support up to 6 hours, CE mark |
| Abiocor (Abiomed) | | TAH | | 900 g<br>Up to 8 L/min | Investigational, HDE for biventricular failure in non-HT candidate, CE mark |
| Cardiowest (Syncardia) | | TAH | | 180 g<br>Up to 9.5 L/min | FDA approved for BTT, CE mark |

Company Headquarters: Thoratec (Pleasanton, Calif.), WorldHeart (Salt Lake City), BerlinHeart (Berlin), Jarvik Heart (New York), Micromed Cardiovascular (Houston), Heartware (Framingham, Mass.), TerumoHeart (Ann Arbor, Mich.), Levitronix (Waltham, Mass.), Abiomed (Danvers, Mass.), Cardiac Assist (Pittsburgh), Syncardia (Tucson).

*Asc Ao*, Ascending aorta; *BTR*, bridge to recovery; *BTT*, bridge to transplant; *CE* mark, "Conformité Européene" (product complies with essential requirements of relevant European health, safety and environmental protection legislation); *DA*, descending aorta; *HDE*, humanitarian device exemption; *HT*, heart transplant; *I*, inflow cannula location; *LVOT*, left ventricular outflow tract; *O*, outflow cannula location; *PA*, pulmonary artery; *PVAD*, percutaneous ventricular assist device; *RSPV*, right superior pulmonary vein; *RV*, right ventricle; *TAH*, total artificial heart.

*Pumps located in or near inflow cannula create imaging artifacts.

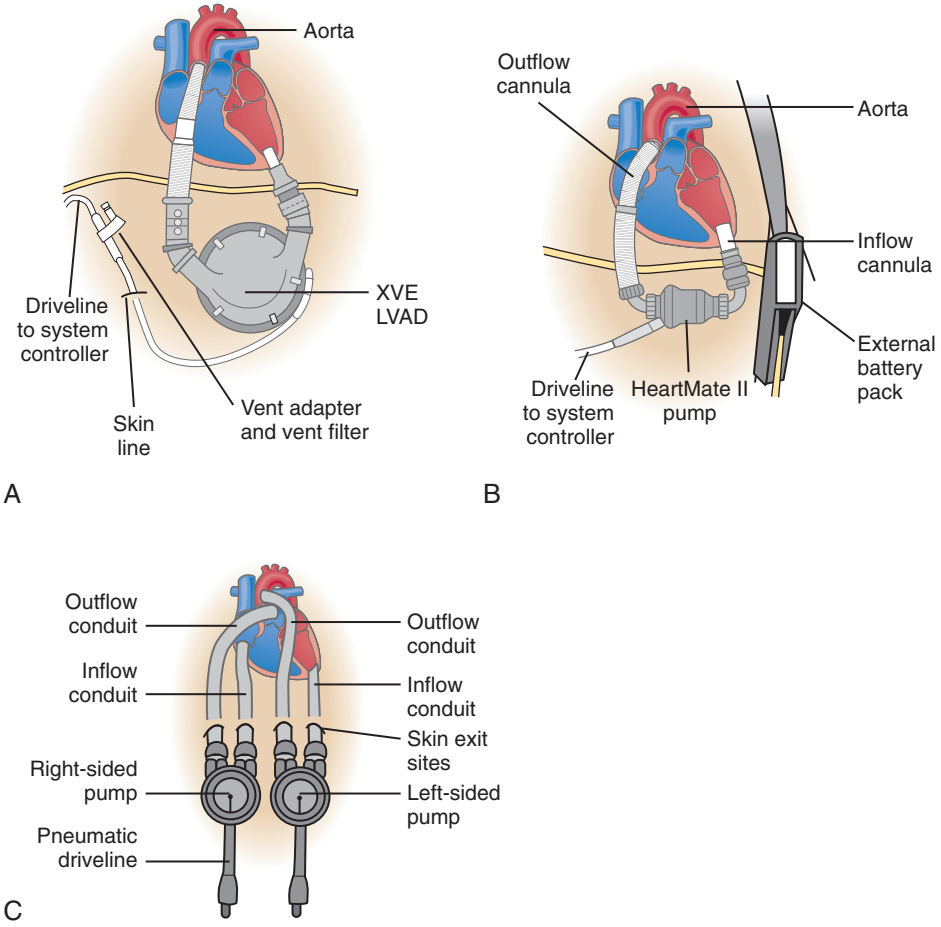



**Figure 31-1** **A,** Example of a pulsatile left ventricular assist device (LVAD) (Thoratec XVE, Thoratec, Pleasanton, Calif.). **B,** Example of a continuous-flow LVAD (HeartMate II, Thoratec). **C,** Example of a BiVAD (LVAD plus RV assist device).

The current generation of continuous-flow VADs employs centrifugal force to propel blood. Magnetic or hydrodynamic forces levitate and spin a disklike impeller, rather than a propeller. Like axial-flow pumps, centrifugal pumps have no valves, but they also lack bearings, and they may prove even more durable than axial-flow pumps. They also allow a greater degree of pulsatility than the axial-flow devices.[17-19]

### *Percutaneous Ventricular Assist Devices*

Percutaneous VADs are inserted via peripheral arteries and veins, usually in the catheterization laboratory, and can be placed quickly. Percutaneous VADs temporarily bridge patients to recovery, decision about transplant, or implanted VADs (see Table 31-2). Other indications include support during percutaneous coronary and valvular interventions.[20,21]

The Impella Recover (Abiomed, Danvers, Mass.) consists of an axial-flow pump (propeller) placed into the femoral artery, though the aorta, and across the aortic valve into the LV[22] (Fig. 31-2, *A*). The inflow port draws blood from the LV outflow tract and ejects it through the outflow port in the aorta. The Impella improves hemodynamic parameters in severe refractory cardiogenic shock, but early trials comparing it to the intraaortic balloon pump failed to demonstrate a mortality benefit.[23]

The TandemHeart (Cardiac Assist, Pittsburgh) has an extracorporeal centrifugal flow pump. The pump is connected to an inflow catheter placed into the LA across the interatrial septum and an outflow cannula in the distal aorta via the femoral artery[24] (see Fig. 31-2, *B*). The TandemHeart cannula can also be positioned in the RA (inflow) and the pulmonary artery (outflow) to support the RV. The TandemHeart improves cardiac index and pulmonary pressures in patients with decompensated heart failure after myocardial infarction and has also been used to stabilize patients with incessant ventricular tachycardia.[25]

### *Total Artificial Heart*

There are currently two available models of the total artificial heart. Both replace the ventricles with pulsatile pumps and metallic or plastic atrioventricular valves anastomosed to the native atria. The Syncardia temporary Total Artificial Heart (tTAH, Syncardia Inc, Tucson) pumping component is attached via drivelines to an extracorporeal controller and battery[26] (Fig. 31-3, *A*). The AbioCor (Abiomed, Danvers, Mass.) pump, controller, and battery are all implanted; the battery is recharged via a transcutaneous energy transfer system. (see Fig. 31-3, *B*) Only the Syncardia device is currently approved by the U.S. Food and Drug Administration (FDA) as bridge to transplant (see Table 31-2).

## PREIMPLANT ASSESSMENT

Specific criteria for placement of an LVAD as destination therapy include LV ejection fraction (EF) less than 25% to 30%, most often measured by echocardiography. Other criteria are

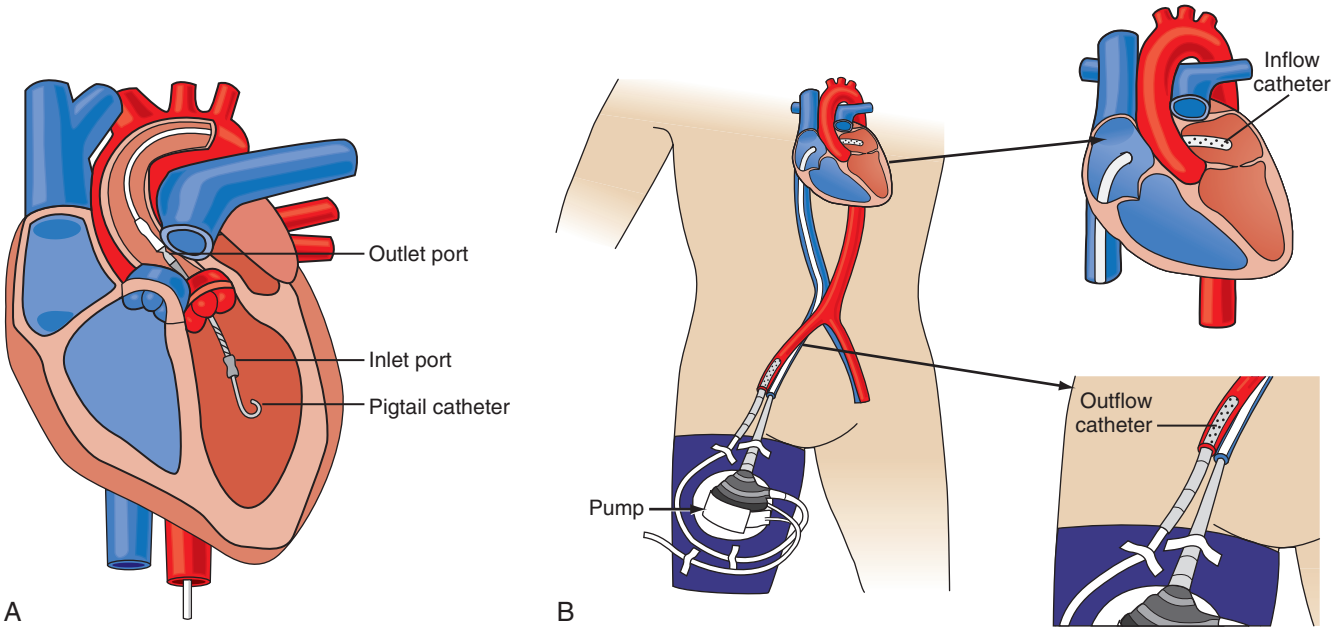



**Figure 31-2** **Percutaneous ventricular assist devices. A,** Impella Recover (Abiomed, Danvers, Mass.) consists of an axial-flow pump (propeller) inside a single 12F catheter that has a distal inflow port and a more proximal outflow port. The catheter is inserted into the femoral artery, through the aorta and across the aortic valve into the LV. A pigtail catheter is left in the central lumen for stabilization. The inflow port is positioned below the aortic valve to draw blood from the LV outflow tract. The outflow port is located in the ascending aorta. Flow is determined by the propeller speed and the aortic-LV pressure difference. The Impella can also be inserted through the chest into the ascending aorta, or into the pulmonary artery, from where it is advanced into the RV outflow tract to support the failing RV. **B,** The TandemHeart (Cardiac Assist, Pittsburgh) has an extracorporeal centrifugal flow pump connected to a 21F inflow cannula inserted in the femoral veins and advanced into the RA, across an interatrial septotomy, and into the LA. A separate 15-17F outflow cannula is inserted into one femoral artery and advanced into the distal aorta. Alternatively, a 12F outflow catheter can be inserted into each femoral artery. The TandemHeart cannula can also be positioned in the RA (inflow) and the pulmonary artery (outflow) to support the RV.

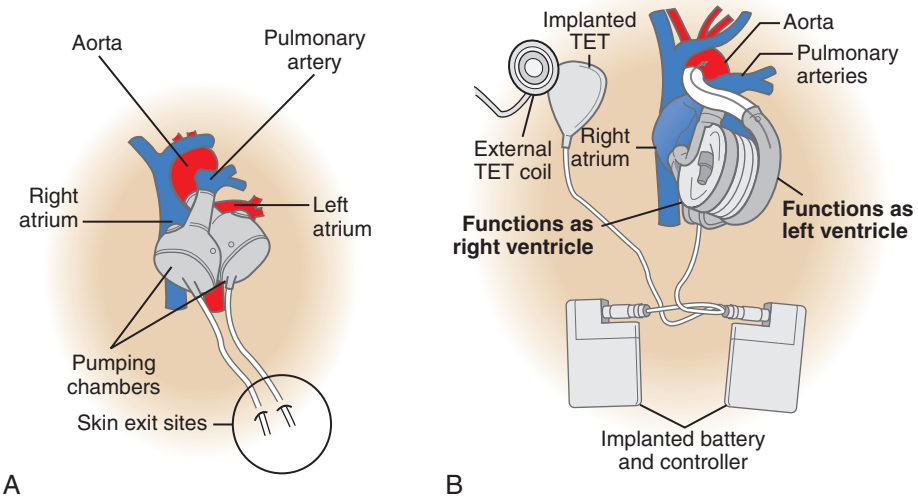



**Figure 31-3** **Total artificial hearts. A,** Syncardia. **B,** AbioCor. *TET*, Transcutaneous energy transmission.

detailed in Box 31-1.[27] Although the hemodynamic criteria refer to invasively determined measurements, echocardiography can provide noninvasive assessment of cardiac index and intracardiac pressures. In addition, echocardiography may identify pathology that warrants interventions other than or in addition to VAD implant, including valve repair or replacement.

Echocardiography identifies factors that complicate cardiac assist device placement or support use of one type of device over another[28] (Table 31-3). It is particularly important to detect thrombi that can embolize. Microbubble contrast may be necessary to exclude ventricular thrombi in patients with inadequate images, and transesophageal echocardiography (TEE)

**Box 31-1**

## CRITERIA FOR DESTINATION THERAPY VENTRICULAR ASSIST DEVICE

**Primary Criteria**

LV ejection fraction ≤25% to 30%
Refractory NYHA class IV heart failure symptoms while on maximal medical therapy, including need for continuous inotropic support
Peak maximal oxygen consumption <12 mL/kg/min
Patients usually have an estimated 1-year cardiac mortality of >50% and/or life expectancy without mechanical cardiac assistance of <2 years.[27,100]

**Additional Hemodynamic Criteria**

Cardiac index <2 L/min/$m^2$
Pulmonary capillary wedge pressure >20 mm Hg
Systolic blood pressure <80 mm Hg

**Box 31-2**

## PREOPERATIVE ECHOCARDIOGRAPHIC PREDICTORS OF POSTIMPLANT RV DYSFUNCTION

RV size
- RVEDD >85 mm
- RVEDV >200 mL
- RVESV >177 mL
- RV short-to-long axis ratio ≥0.6

RV function
- TAPSE <7.5 mm
- Qualitatively severe RV dysfunction

Moderate to severe tricuspid regurgitation
Hemodynamics (invasively determined, but measurable by echocardiography)
- Elevated RAP
- Low mean PAP
- Low cardiac output
- Low RV stroke work index
- Elevated PVR

*PAP*, Pulmonary artery pressure; *PVR*, pulmonary vascular resistance; *RAP*, right atrial pressure; *RVEDD*, right ventricular end-diastolic diameter; *RVEDV*, right ventricular end-diastolic volume; *RVESV*, right ventricular end-systolic volume; *TAPSE*, tricuspid annular planar systolic excursion.

**TABLE 31-3 Echocardiographic Findings That Complicate Ventricular Assist Device Implant**

| *Finding* | *Implications* |
|---|---|
| Thrombus in cardiac chamber | Thrombectomy<br>Placement of cannula in alternate chamber |
| Intracardiac shunting | Repair of shunt |
| Aortic aneurysms, tortuosity, atheromata | Graft repair of aneurysm<br>Placement of outflow graft cannula away from atheroma<br>Caution with Impella Recover |
| Aortic stenosis (≥ moderate) | Bioprosthetic valve replacement*<br>Impella Recover contraindicated |
| Aortic regurgitation (≥ moderate) | Bioprosthetic valve replacement*<br>Oversew valve cusps<br>Cannulation of descending aorta<br>Angle ascending aortic graft cannula away from aortic valve<br>Caution with TandemHeart (see text)<br>Impella Recover contraindicated |
| Mitral stenosis | Valvuloplasty<br>Bioprosthetic valve replacement*<br>Placement of inflow cannula in LA<br>Caution with Impella Recover |
| Mitral regurgitation | Repair or bioprosthetic valve replacement*<br>Caution with Impella Recover |
| RV failure | Caution with TandemHeart for LV support (requires the RV to provide adequate preload to the LA) |
| Ventricular septal defect | Caution with Impella Recover (right to left shunting) |
| Atrial septal defect | Caution with TandemHeart and LA cannulation (right to left shunting) |
| Interatrial septal aneurysm | Caution with TandemHeart and atrial cannulation (suckdown of aneurysm into cannula) |
| Heavy trabeculation, aneurysms/dyskinetic walls, redundant chords, prominent ridges, small inflow chamber | Orient inflow cannula away from potentially obstructing structures<br>Excise trabeculation<br>Excise aneurysm |
| Clotting diathesis | Avoid LA cannulation, caution with TandemHeart (stasis in bypassed LV)<br>Ensure aortic valve opening to "wash" aortic root<br>Higher INR target, additional antiplatelet agents |
| Pericardial effusion (chambers can collapse after decompression with VAD) | Effusion drainage |
| Peripheral vascular disease | Caution with Impella Recover<br>Caution with TandemHeart |

*INR*, International normalized ratio; *VAD*, ventricular assist device.
*Mechanical valves are generally not used in VAD patients because of concerns for thrombus formation despite anticoagulation.

should be used to examine left and right atrial appendages. Intracardiac shunting producing systemic hypoxemia and/or paradoxical emboli after LVAD placement should be repaired at the time of implant.[29] High LA pressure may prevent passage of agitated saline contrast across a patent foramen ovale (PFO), even after Valsalva. An LVAD will decompress the LV, lower LA filling pressure, and return more blood to the RA by increasing cardiac output, potentially opening the PFO.

Moderate or greater aortic regurgitation complicates the use of VADs.[30] Placement of an outflow cannula in the ascending aorta or an Impella Recover device across the aortic valve may worsen baseline aortic regurgitation, leading to circulation of blood from LV to VAD to aorta and back into the LV. High LV pressure and low diastolic pressure in the aortic root from severe aortic regurgitation can reduce coronary perfusion pressure, which is exacerbated by the fact that the TandemHeart draws blood from the LA and ejects it into the distal aorta (bypassing the coronary ostia). Preimplant grading of the degree of aortic regurgitation is complicated in end stage heart failure patients who commonly have low systemic pressure and high LV diastolic pressure (see Chapter 20). The low aortic-to-LV pressure gradient may artificially decrease the amount of regurgitation through an incompetent aortic valve.

Preimplant identification and characterization of RV dysfunction is vitally important[31-33] (Box 31-2) (see Chapter 33). RV failure is cause of morbidity and mortality in 10% to 30% of the LVAD population.[16,34,35] In patients with known RV dysfunction, planned early placement of an RVAD improves survival over delayed placement.[36] LVAD placement produces a higher cardiac output and increased venous return to the RV. An RV with preexisting dysfunction may fail in the setting of increased preload.[37,38] In addition, LVAD influence on septal motion reduces RV function and can worsen baseline tricuspid regurgitation.[39,40] On the other hand, decompression of the LV by a VAD can reduce pulmonary pressures and RV afterload, leading to an improvement in RV function.

## PERIPROCEDURAL GUIDANCE

Intracardiac echocardiography (ICE) or transesophageal echocardiography (TEE) provides real-time visualization to direct cannula placement away from potentially obstructing cardiac structures (see Chapters 5 and 6). The Impella device can be guided to position the inflow port in the LV outflow tract and the outflow port above the aortic valve. Echocardiography can guide transseptal puncture in TandemHeart insertion, preventing inadvertent puncture of the left or right atrial walls or the aortic root. As with other cardiac surgical procedures, TEE is useful in deairing the heart before coming off bypass. Air bubbles arise at cannula anastomosis sites and can embolize if not detected before the aortic crossclamp is removed. Anterior structures, including the ascending aorta, the RV, and anterior portions of the LV, should be examined for air bubbles[41] (Fig. 31-4).

## APPROACH TO CARDIAC ASSIST DEVICE DYSFUNCTION

Echocardiography is often required to elucidate the complicated processes and causes of VAD dysfunction[42-44] (Box 31-3).

### *Overfilling*

Regurgitation, obstruction and malfunction cause overfilling and pressure increase in the supported ventricle. In pulsatile VADs, failure of the one-way valves leads to regurgitation.[45] Cannula regurgitation can occur in continuous-flow devices when the systemic vascular resistance is elevated. Cannula obstruction can result from kinking, malposition, or thrombosis and can be partial, complete, or intermittent. VAD pumping mechanisms may become partially or completely obstructed, leading to increased shear stress and hemolysis. Pulsatile VADs with a special texture on the blood interface surface may be less thrombogenic, and the lower flows in third-generation VADs may be less likely to cause hemolysis. Finally, there can be primary failure of VAD components: battery, controller, or pump. These all cause the ventricle to dilate and the cardiac output to fall, and they may induce stasis and intracavitary thrombus formation.

### *Underfilling*

Underfilling of the supported ventricle shrinks the cavity size and can cause obstruction of the inflow cannula due to encroachment by normal cardiac structures, sometimes called *suckdown*. Trabeculations, papillary muscles, chordal structures, ridges, and septae are drawn into the orifice of the inflow cannula as chamber size decreases in conjunction with a rigid inflow cannula (Fig. 31-5). Obstruction of the orifice leads to a decrease in flow and reduced cardiac output, as well as arrhythmias.

Anything that reduces preload can predispose to obstruction of the inflow orifice, including dehydration, overdiuresis, sepsis, and tamponade. Bleeding is a special concern because some form of anticoagulation is advised for most VAD patients to prevent thrombosis. Up to one fourth of VAD patients may require reoperation for bleeding in the periimplant period.[46] In addition, continuous-flow VADs have been associated with increased risk of gastrointestinal bleeding, and a substantial number of patients cannot take anticoagulation for this reason.[47,48] It has been postulated that high shear stress through VADs depletes large von Willebrand factor monomers.[49-51]

### *Valvulopathy*

As described previously, relatively mild aortic regurgitation detected preimplant may worsen after LVAD placement.[16,52] Significant aortic regurgitation has been reported to arise months after implant. In addition, acquired aortic stenosis due to cusp fusion is an increasingly recognized complication of both pulsatile and continuous-flow devices.[53-55] The etiology is unknown, and echocardiographic examination of the valve leaflets reveals

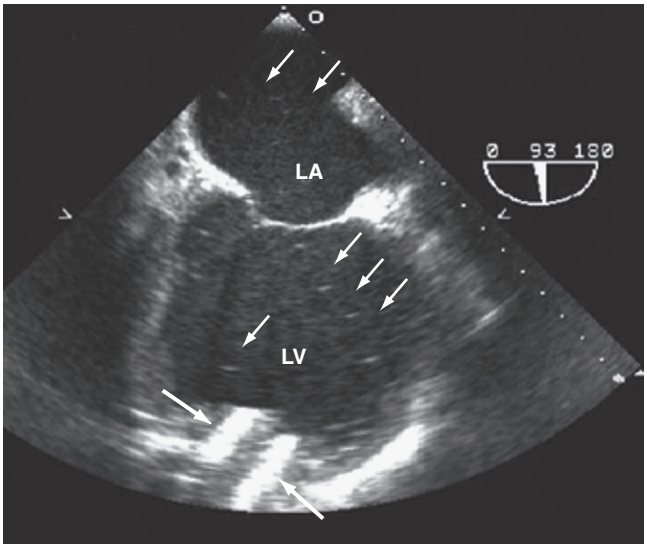



**Figure 31-4 Midesophageal TEE apex down two-chamber view.** Air bubbles (*small arrows*) in the LV and LA after placement of an LV apical inflow cannula (sides defined by *large arrows*). Echocardiography can detect bubbles arising at anastomotic sites. Ventricular chambers should be "de-aired" before coming off bypass.

**Box 31-3**

**ECHOCARDIOGRAPHIC FINDINGS IN VENTRICULAR ASSIST DEVICE DYSFUNCTION**

**Obstruction/Overfilling**
↑ LVEDD
Septum → RV
Spontaneous echo contrast
↑ Aortic valve opening
↑ cannula velocities
  Pulsatile: >2.3 m/s peak inflow, >2.1 m/s peak outflow*
  Continuous flow: >2 m/s peak
Inflow cannula regurgitation
  Pulsatile VAD peak outflow <1.8 m/s
  Flow reversal by color, spectral Doppler
Thrombus or vegetation obstructing cannula

**Underfilling**
↓ LVEDD
Septum → LV
↓ Aortic valve opening
Pericardial effusion with chamber collapse
Suckdown of cardiac structures into inflow cannula
↑ cannula velocities

*LVEDD*, Left ventricular end-diastolic diameter; *VAD*, ventricular assist device
*Few data exist on normal velocities, but for most continuous-flow devices, patients probably have peak velocities around 1 m/s.[84,101]

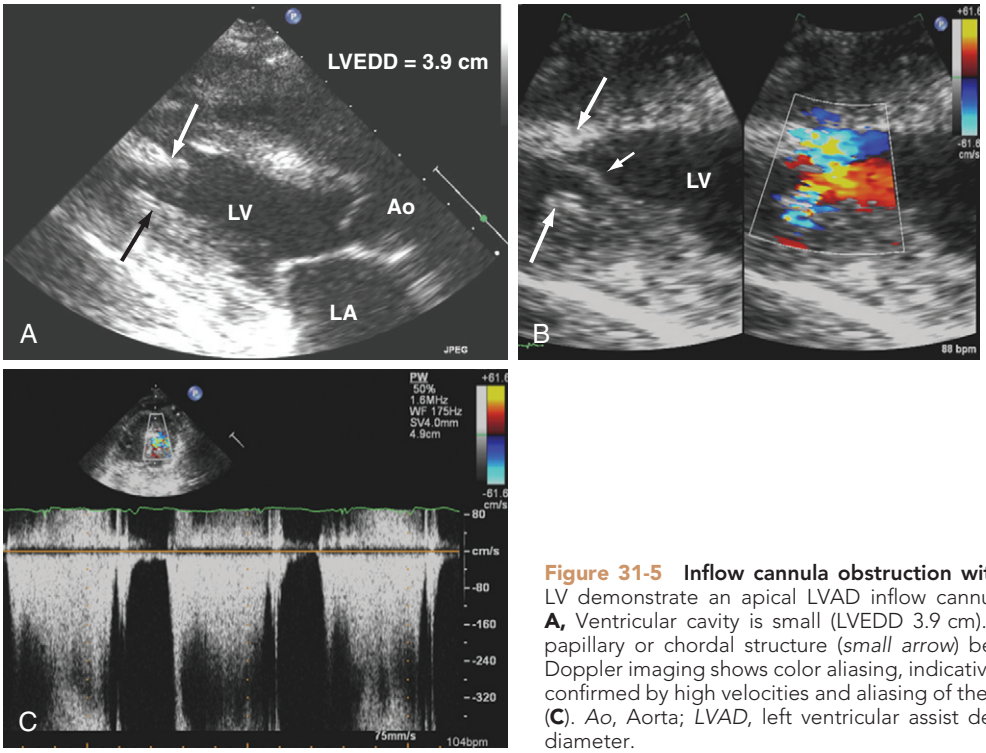



**Figure 31-5 Inflow cannula obstruction with small LV.** Parasternal long-axis views of LV demonstrate an apical LVAD inflow cannula (*large arrows* define sides of cannula). **A,** Ventricular cavity is small (LVEDD 3.9 cm). **B,** Zoomed view of the cannula shows a papillary or chordal structure (*small arrow*) being drawn into the cannula orifice. Color Doppler imaging shows color aliasing, indicative of high velocities from partial obstruction, confirmed by high velocities and aliasing of the PW spectral Doppler inflow cannula profile (**C**). *Ao*, Aorta; *LVAD*, left ventricular assist device; *LVEDD*, left ventricular end-diastolic diameter.

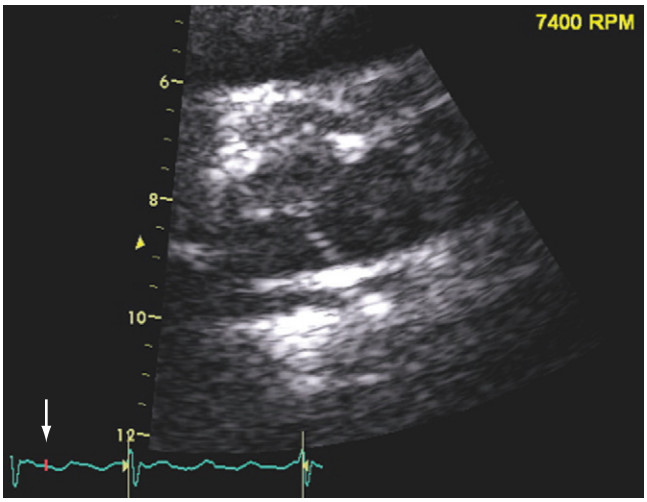



**Figure 31-6 Fused bioprosthetic aortic valve in a continuous-flow VAD patient, seen in zoomed parasternal short-axis view.** Shadowing off the struts creates a linear artifact on the right side of the image. *Arrow* demonstrates this still frame is taken in systole, when there should be some opening of the aortic leaflets at a relatively low propeller speed (for this patient with a Heartmate II device) of 7400 rpm. Despite being fused, the leaflets appear free of thickening or calcification.

relatively normal structure (Fig. 31-6). Both native and bioprosthetic cusps have been noted to fuse. Cusp fusion presents a significant problem in patients with VADs as bridge to recovery and may require balloon valvuloplasty. When the aortic valve does not open or opens minimally, there is a risk of thrombus formation in the aortic root, especially in continuous-flow VADs because of the lower, mostly nonpulsatile flows.[56]

Mitral regurgitation generally improves when an LVAD is placed, but the Impella Recover device may interfere with the chordal apparatus or the anterior mitral valve leaflet, leading to an increase in mitral regurgitation. Suckdown events that tether chordae or papillary muscles may have the same result. As noted earlier, tricuspid regurgitation can increase after LVAD placement because septal shift and annular distortion can lead to tethering on the septal leaflet.

Endocarditis on native valves or VAD components is another significant concern and one of the leading adverse events for cardiac assist devices. Infection is one of the top five causes of death in the VAD population.[16,57] Vegetations on intracorporeal VAD cannulae or pump components put patients at risk for obstruction and septic embolism. Device explant is often necessary.

### *Optimization*

In some cases, VAD pump function must be adjusted to address hemodynamic challenges. Reducing LVAD pumping rates, pumping volumes, or rotor speeds will increase preload. Higher preload may improve LV systolic function via Starling mechanisms, increasing ejection through the aortic valve. For continuous-flow devices, some degree of aortic valve opening is desirable to prevent cusp fusion and thrombus formation. Alternatively, reduced LVAD flow may overdistend the LV, leading to a reduction in residual function and symptoms of congestion.

Increasing LVAD pumping rates, pumping volumes, or rotor speeds will decrease ventricular preload, potentially alleviating distension and congestion. However, LV systolic function may fall and the aortic valve may cease to open, increasing risk of root thrombosis. Excessive reduction in pumping rates will produce underfilling and impingement of the inflow cannula.

Percutaneous VAD positioning may require guided adjustment. If the Impella migrates into the ventricle, the outflow portion may end up below the aortic valve (Fig. 31-7). If it migrates backward, the inflow portion may end up in the

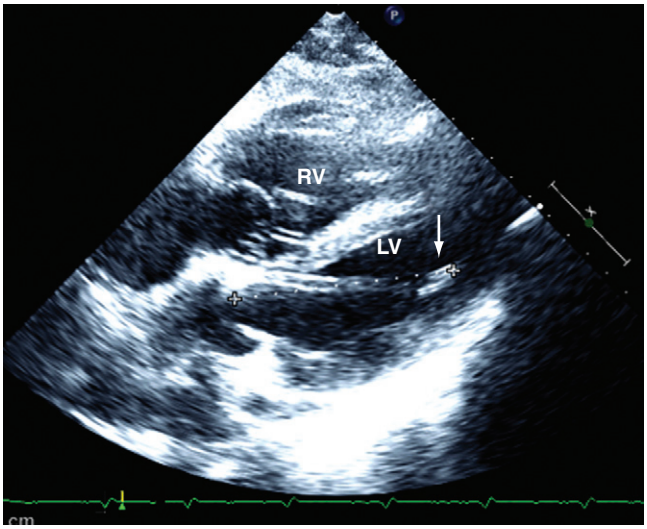



**Figure 31-7 Malposition of an Impella Recover device.** In this subcostal view, the end of the device (*arrow*) is imaged at least 8 cm below the aortic valve, twice the recommended distance of 3 to 4 cm. After appropriate initial placement, the device migrated apically. The outflow portion was located in the LV outflow tract, leading to device malfunction.

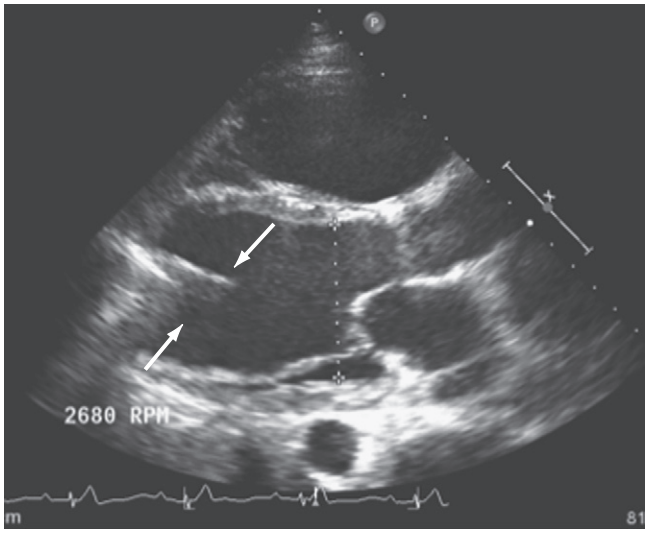



**Figure 31-8 LV size and appropriate septal position.** Parasternal long-axis view demonstrates normal LV size and a septum positioned neutrally between the LV and RV, indicative of adequate ventricular decompression. *Large arrows*: sides of continuous-flow left ventricular inflow device inflow cannula.

ascending aorta. Pressure sensors at each port can identify a problem, though loss of sensor signal has been reported.[58,59] A transseptally placed TandemHeart could move backward into the RA.

### *Ventricular Recovery*

VADs, especially percutaneous devices, are increasingly used to temporarily support patients with reversible causes of acute heart failure. In patients with chronic heart failure and VADs, ventricular unloading can produce reverse remodeling, including normalization of chamber sizes, regression of LV hypertrophy, recovery of beta receptor responsiveness, and normalization of calcium handing.[59-64] With decompression, however, reduced preload produces loss of systolic function due to reduced ventricular fiber stretch. Reductions in systolic function on VAD support are therefore not necessarily indicative of progression of myocardial dysfunction. LVAD-induced myocyte atrophy is controversial.[65] Improvements in systolic function may be a sign of overfilling or may portend resolution of an acute insult and/or reverse remodeling over time. Pulsatile LVADs may improve RV parameters, though not as rapidly,[66] and continuous-flow LVADs may lead to reductions in RV size but no improvement in RV function.[67] BiVAD/RVAD implant induces changes in RV function akin to the effect of an LVAD on the LV.[68] Early clinical results suggest that pharmacologic interventions may enhance VAD-induced recovery.[69-71]

Turning down VAD flows will lead to increases in afterload and preload. In patients with recovered heart function, increasing preload will lead to an improvement in ventricular function and maintenance of ventricular size. In patients who are dependent on VAD support, ventricles will fail and/or dilate because of inability to accommodate increased preload and afterload.

### *Ventricular Assist Device Flows*

Almost all of the currently available VADs calculate flows indirectly from changes in power consumption. Several VADs have mechanisms that directly measure flow, but they are limited in accuracy.[72] Reduced unloading in the setting of increased power consumption will set off a low-flow alarm, but the cause of the reduced flow cannot be assessed. In continuous-flow devices, changes in flow amplitude are used to calculate a *pulsatility index*.[73] Improvements in ventricular function will push blood through the inflow cannula, leading to increases in the pulsatility index from higher rotor speeds. However, the pulsatility index will also increase when there is intermittent cannula obstruction. Thus, VAD flow monitors provide a signal that dysfunction exists, but measurement of flows and definition of the cause of dysfunction require an imaging study.

## Technical Details, Quantitation, and Data Analysis

Standard echocardiographic imaging protocols provide structural, functional, and hemodynamic information about hearts supported by cardiac assist devices. Certain standard assessments deserve special emphasis, and specialized views to assess device components are necessary additions. Specific indication for the exam, device type, cannulation, mode, and pump settings should be noted on every examination, as should blood pressure (taken with a special cuff in patients with continuous-flow devices).

### LVEDD AND SEPTAL ORIENTATION

LV end-diastolic diameter (EDD) is a surrogate marker for filling status in VAD patients. It also reflects the position of the interventricular septum, which in turn reflects the interaction between the left and right ventricles. Optimal unloading of the LV has been reported with reductions in EDD of 20% to 30%.[74] In most VAD patients, the ideal position of the septum is neutral between the ventricles (parallel to the long axis of the LV) (Fig. 31-8). A neutral septum denotes adequate ventricular decompression. In the case of a dysfunctional LVAD and overfilling, the EDD size increases, in part because of a shift of the septum into the RV.

Cannula obstruction related to a small LV can manifest as a decrease in the LVEDD and septal bowing into the LV (Fig. 31-9). However, septal orientation toward the LV can also result from high right-sided pressures. Dyssynchrony from interventricular conduction delay, ischemic wall motion abnormalities, poststernotomy state, pericardial constriction, and RV pacing can also complicate assessment of septal position.

LVEDD measured in the two-dimensional (2D) parasternal long-axis view at the mitral valve leaflet tips[75] is generally reproducible, allowing detection of differences in size and septal position between serial studies, and in response to changes in VAD pump settings during optimization and weaning. Nonetheless, care must be taken to record images in the same plane each time. 2D directed M-mode can be used if the M-mode cursor can achieve perpendicular axis with respect to the ventricular walls. Although the direct measurement of LVEDD is most often used in the cardiac assist literature, it should probably be indexed to body surface area.[75] Assessment of septal position is subjective, with no validated quantitative measure currently available.

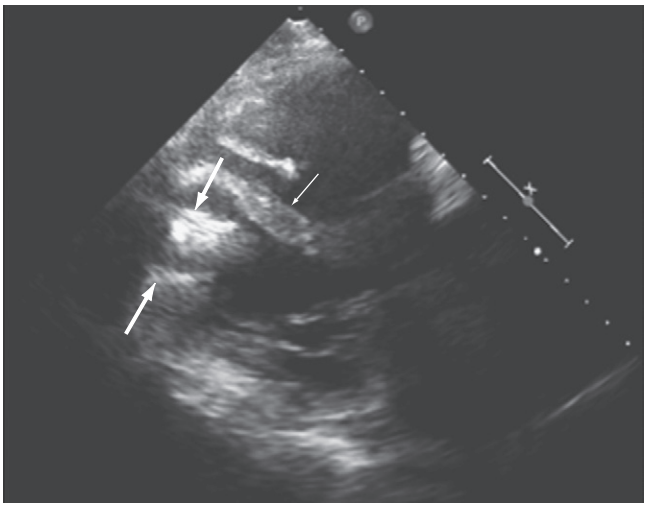


**Figure 31-9 Leftward septal bowing.** In a parasternal long-axis view, mild septal shift into LV is seen (*small arrow*), suggesting either LV underfilling or elevated right-sided pressures. *Large arrows*: sides of left ventricular assist device inflow cannula.

## VENTRICULAR FUNCTION

In the LVAD patient, it is often difficult to quantify LVEF using the biplane apical method,[75] because of artifact from the apical inflow cannula (see Chapter 9). Use of microbubble contrast to improve endocardial border definition in LVADs can be considered. Calculation of LVEF from linear measurements is confounded by LVAD effects on septal orientation and ventricular dimensions. The Quinones method, which calculates LVEF from measurements of multiple diameters in two views and does not account for motion of the apex (which may be akinetic in most VAD patients) is theoretically attractive but has not been well validated.[76,77]

Comprehensive imaging of RV function requires 2D assessment of size and systolic motion but also careful assessment of tricuspid regurgitation and measurement of right-sided hemodynamics.[78] Examination of the tricuspid valve should include assessment of leaflet flattening or prolapse, septal leaflet tethering, and annular dilatation (see Chapter 34). Noninvasive pulmonary vascular resistance, in particular, can be measured as a marker of LVAD effect on RV afterload.[79]

## AORTIC VALVE OPENING

Aortic valve opening is normally reduced because most of the LV output flows through the LVAD. Relative aortic valve opening can be a marker for both LVAD and ventricular contribution to cardiac output. The aortic valve may open minimally, briefly, and intermittently, or not at all when the ventricle is severely dysfunctional. In addition, the aortic-LV pressure difference opposes opening because the LV pressure is low as a result of decompression, and the LVAD outflow increases pressure in the aorta. Conversely, the aortic valve may open normally when there is ventricular recovery or LVAD dysfunction leading to high LV pressures. It has been proposed that the degree and frequency of aortic valve opening be assessed as complete opening, partial opening, intermittent opening, or complete closure.[77] Quantitation of the degree of opening can be obtained by planimetry of the open valve in the short-axis view, or by linear measurement of systolic cusp separation in the long-axis view. M-mode imaging at a low sweep speed gives a quantitative frequency of aortic valve opening as a percentage of recorded cardiac cycles (Fig. 31-10). Duration of opening can be measured by M-mode as time of opening or as a percentage of the R-R interval in which the valve is open.

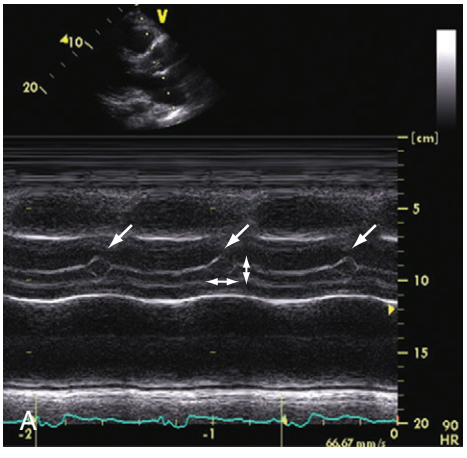



**Figure 31-10 Aortic valve opening. A,** M-mode tracing from parasternal long axis demonstrates reduced opening of aortic valve with each beat (*arrows*), consistent with normal left ventricular assist device (LVAD) function that prevents thrombus formation in aortic root. *Double-headed arrows* show duration and extent of opening, which can be measured to allow quantitative comparison between studies or at different LVAD pump settings. Increased opening can be a sign of overfilling or ventricular recovery. **B,** No aortic valve opening is seen, consistent with very low residual cardiac output, high LVAD pump flow, oversewn valve to prevent aortic regurgitation, or leaflet fusion.

## PERICARDIUM

2D imaging can visualize effusions or thrombus in the pericardial space compressing cardiac chambers, leading to underfilling and inflow cannula obstruction. Exaggerated Doppler flow variation across valves in the supported ventricle is generally unhelpful as a marker of intrapericardial pressure, because flow is affected by VAD function. The total artificial heart chambers are opaque to ultrasound, but the native atria, the superior and inferior vena cavae, and the pulmonary veins can be assessed for chamber collapse.

## CANNULAE

2D imaging, especially with TEE, can determine orientation of the cannulae and whether cardiac structures (such as trabeculations, septae and chordal structures) are sucked into the cannulae (see Fig. 31-5). 2D imaging should also assess for thrombi and vegetations on the cannulae. The LVAD inflow cannula in the LV should be imaged from all windows. Though the most parallel Doppler angle of insonation is often found in the apical views, the orientation of inflow cannulae can be variable, and the most parallel angle is sometimes found in the parasternal long-axis view or the subcostal view, especially if the cannula was placed via an inferior approach. VAD inflow cannulae placed in the left or right atrium may require TEE for visualization. The LVAD outflow cannula in the ascending aorta is often difficult to image by transthoracic echocardiography (TTE) and is best visualized from a right parasternal view or upper left parasternal view (Fig. 31-11, *A*). Using TEE, it is usually seen in the upper-midesophageal position (90-150 degrees) (see Fig. 31-11, *C*). The RVAD outflow cannula in the pulmonary artery can be seen in the short-axis view (Fig. 31-12).

The Impella Recover percutaneous VAD cannula is normally well seen from the parasternal long-axis view, but it may be necessary to angle the transducer off axis to ensure that the tip is visualized (see Fig. 31-7). Proper location of the inflow port (near the tip of the cannula) is 3 to 4 cm below the aortic valve. The outflow port should be 1.5 to 2 cm above the sinuses of Valsalva.[22]

Color Doppler examination of normal cannulae reveals laminar flow with minimal or no regurgitant flow. Aliasing of color flow may be seen at the inflow or outflow cannulae in cases of obstruction. The color Doppler jet can also help to direct angulation of the transducer to achieve a parallel alignment for spectral Doppler interrogation.

Pulsed-wave (PW) Doppler should be performed inside and immediately outside of the cannula orifice. Normal and abnormal Doppler profiles through inflow and outflow cannulae are illustrated in Figure 31-13 for pulsatile and continuous-flow devices. Partial obstruction will lead to increases in inflow and outflow velocities, depending on the site of obstruction[42,43] (see Box 31-3). Complete obstruction, as from thrombotic occlusion or kinking, leads to loss of Doppler signal or low velocities in the VAD cannulae.[80] Regurgitation can lead to low outflow velocities.[44] Continuous-wave (CW) Doppler interrogation is necessary to resolve high velocities, but, because of range ambiguity, the CW Doppler signal may become contaminated by other flows (e.g., LVAD inflow and aortic regurgitation).

Table 31-4 describes the formulas used to calculate the stroke volume through pulsatile VADs, flow through continuous-flow VADs, and VAD regurgitation using cross-sectional orifice area and PW Doppler velocity-time integral (VTI). Because continuous-flow VADs technically have no discrete stroke volume, VAD flows in liters per minute must be calculated indirectly using the residual output through the aortic valve and the output through the pulmonic valve, or directly by measuring the Doppler velocity time integral over 3 s (multiplied by 20 s to convert to minute flow rate).[81]

## OPTIMIZATION

LV EDD, septal position, and aortic valve opening are used to optimize VAD settings.[82] For a continuous-flow VAD, the rotor speed is adjusted until the septum is neutrally positioned at a near-normal LV EDD and the aortic valve opens to a small degree, for a brief period of time and/or at a reduced frequency.[83] The optimal opening characteristics to prevent aortic root thrombus and cusp fusion while signaling appropriate ventricular decompression have not been defined. Other targets of optimization can include mitral regurgitation, aortic regurgitation, pulmonary artery pressures, and Doppler-derived cannula flows (see Table 31-4). Optimization of RVAD and BiVAD function is not well described to date but could apply the same principles to RV size, septal positioning, and pulmonic valve opening.

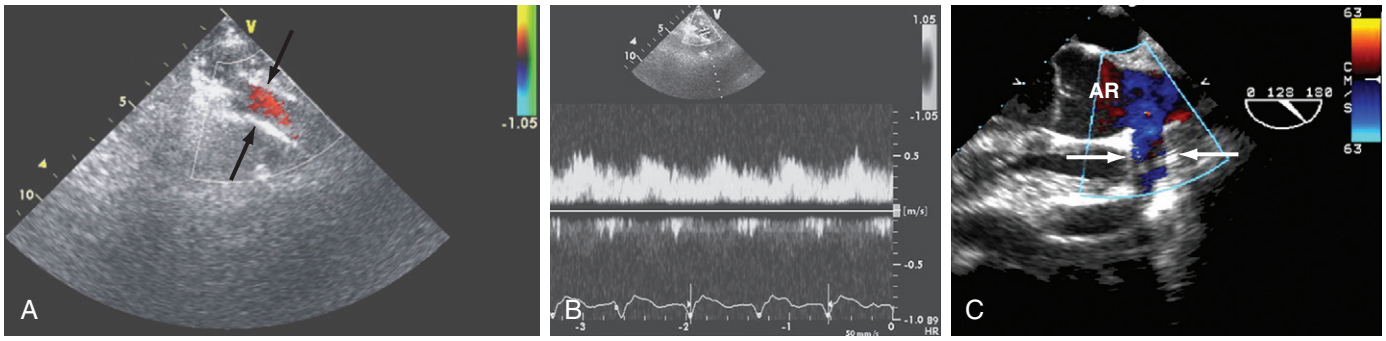



**Figure 31-11 Imaging left ventricular assist device (LVAD) outflow graft cannula. A,** LVAD outflow graft cannula can be visualized by TTE in many patients in right upper sternal border, but best imaging window depends on location of graft cannula, which can be variable. *Large arrows*: Sides of graft cannula. **B,** Although off axis with respect to axis of flow, PW Doppler profile demonstrates normal baseline flow with systolic peaks. **C,** Unlike inflow cannula (inserted through LV apical wall), outflow graft cannula is anastomosed end-to-side to ascending aorta. (See also Fig. 31-16, *B*.) Outflow graft cannula is usually very easily imaged by TEE from midesophageal position at 90° to 150°, depending on location of anastomosis. *Large arrows*: Sides of graft cannula. *AR*, Aortic root.

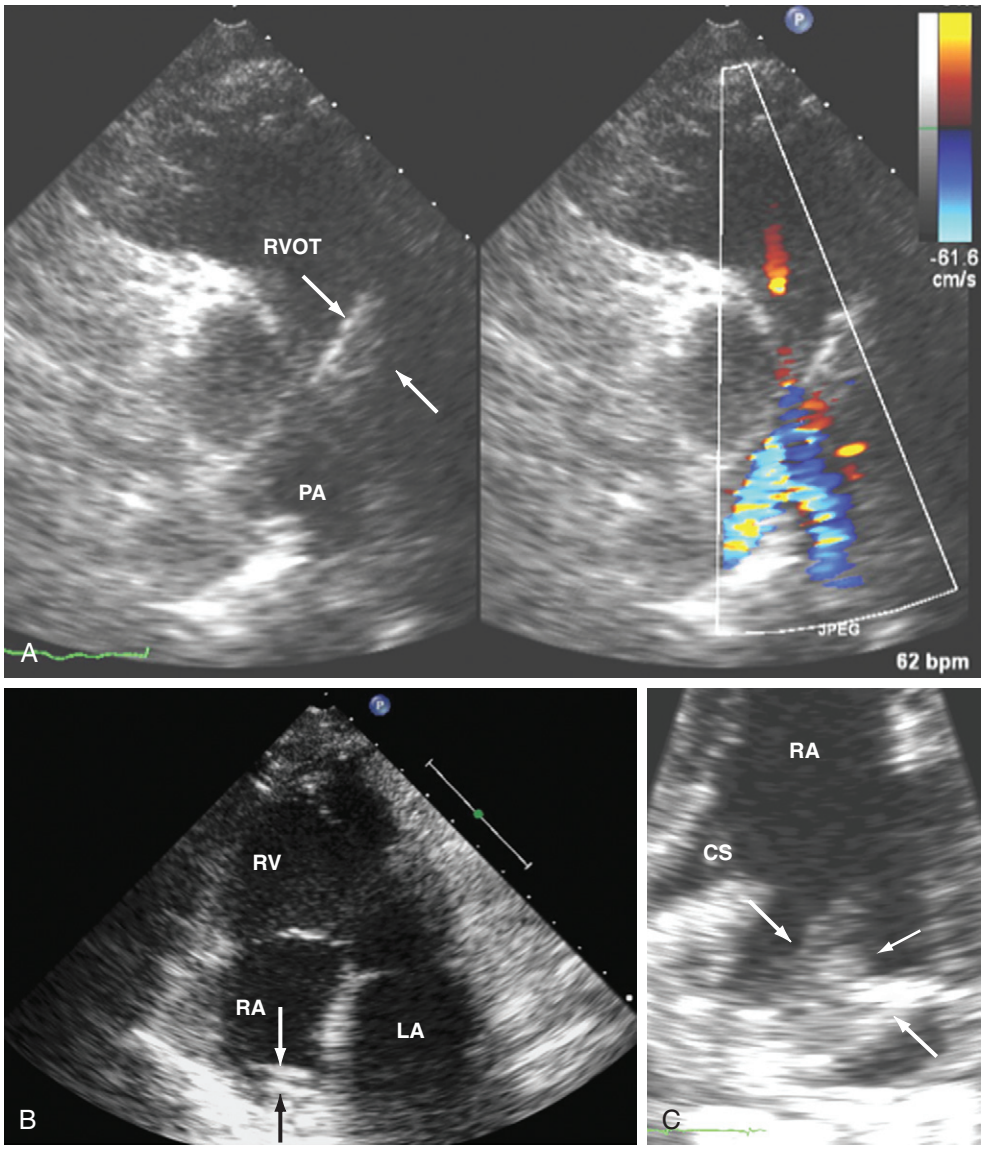



**Figure 31-12** **Imaging the right ventricular assist device (RVAD) cannulae. A,** The RVAD outflow cannula is often well seen in short-axis view in proximal main pulmonary artery (*PA*). *Large arrows, left*: Sides of cannula. *Right*: Color Doppler shows flow from cannula into main PA and left and right PA branches. Minimal pulmonic valve regurgitation is seen. **B,** RVAD inflow cannula is inserted into RA and is usually in far field by TTE (*large arrow*). **C,** Zoomed view of cannula from parasternal tricuspid inflow view demonstrates thrombus (*small arrow*) obstructing central lumen of cannula (sides denoted by *large arrows*). *CS*, Coronary sinus; *RVOT*, right ventricular outflow tract.

### WEANING/TURNDOWN

Before cardiac assist device explant, weaning is usually necessary to demonstrate the impact of reduced VAD support on cardiac structure and function. Protocols differ but generally involve echocardiography with or without invasive arterial and venous pressure monitoring. VAD support is decreased gradually, to avoid acute decompensation. Figure 31-14 provides an overview of echocardiographic parameters used during "turndown." If the results are favorable after turndown to minimal levels of support, some protocols call for exercise or dobutamine stress testing. Sometimes oxygen consumption measurement is added. Echocardiographic imaging at peak exercise is facilitated with supine bicycle stress. There may be adequate cardiac reserve to support the patient after LVAD explants if the LVEF improves, the aortic valve opens more, and stroke volume increases in response to dobutamine.[84]

Echocardiographic RVAD weaning protocols are less well described. As RVAD flows are decreased, RV failure or recovery may be predicted by central venous pressure, RV function, LV filling pressures, and tricuspid regurgitation.[23]

## Clinical Utility, Outcome Data

Echocardiography plays a major role in guiding care of VAD patients, but there are few outcome studies specifically evaluating the clinical utility of echocardiographic techniques.

Specific preimplant echocardiographic indices of RV structure and function have been reported to predict RV dysfunction post LVAD implant. (See Box 31-2.) However, only a few studies comprehensively evaluated echocardiographic techniques. Different studies tested different parameters, and most studies represent only single-center experiences.[32,35,85-87]

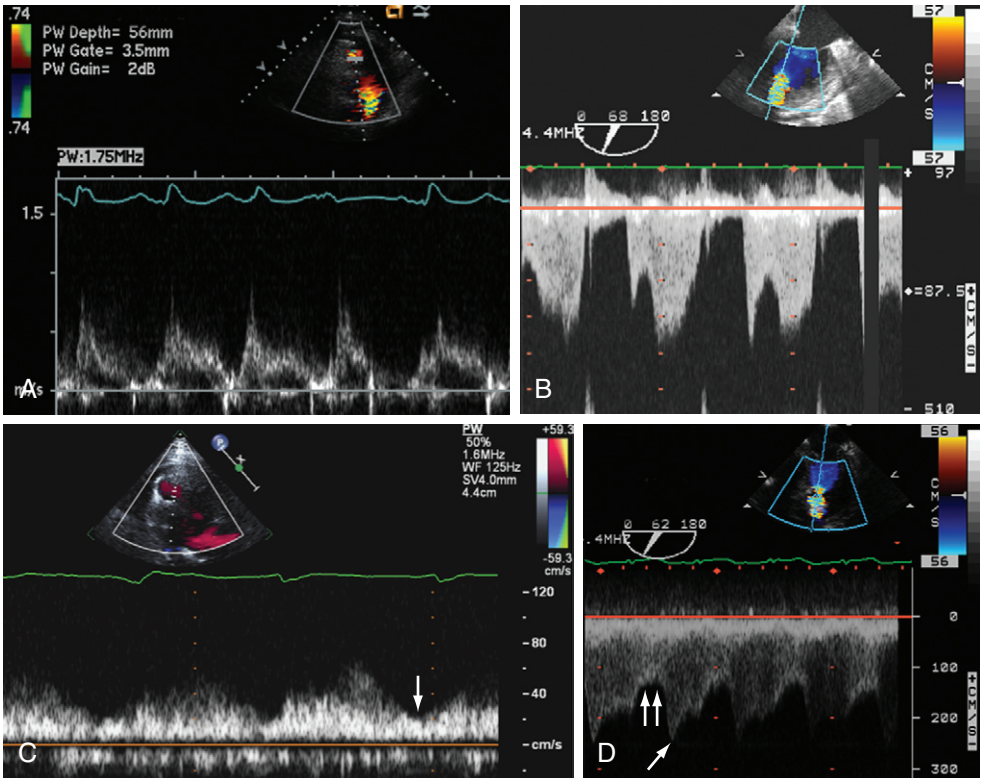



**Figure 31-13 VAD Doppler profiles.** **A,** Normal pulsatile left ventricular assist device (LVAD) inflow by PW Doppler (abnormal peak velocities >2.3 m/s). **B,** Elevated pulsatile LVAD inflow velocities by TEE (CW Doppler peak velocity measured at 3.5 m/s). **C,** Normal continuous LVAD inflow by PW Doppler. Peak velocities are 0.7 m/s, well below 2 m/s. Note continuous "background" flow during diastole (*arrow*). **D,** Increased continuous LVAD inflow velocities by TEE. *Single arrow*: CW Doppler peak velocity of 2.5 m/s. *Double arrows* show that "background" flow is also elevated at 1.3 m/s, suggesting inflow cannula obstruction.

**TABLE 31-4 Doppler Formulae for Ventricular Assist Device Flow Volumes**

| *Formulae* | *Measurements* |
|---|---|
| **Pulsatile VAD ($VAD_p$) stroke volume (SV)**<br>$SV_{VADp} = \pi(D_{can}/2)^2 \times VTI_{can}$ | $D_{can}$ = cannula diameter (usually 12-25 mm)<br>$VTI_{can}$ = VTI of the PW Doppler signal measured just within the cannula orifice |
| **Continuous flow LVAD ($VAD_c$)**<br>$SV_{VADc} = (\pi(D_{RVOT}/2)^2 \times VTI_{RVOT}) - (\pi(D_{LVOT}/2)^2 \times VTI_{LVOT})$ | $D_{RVOT}$ = RV outflow tract diameter<br>$VTI_{RVOT}$ = RV outflow tract VTI<br>$D_{LVOT}$ = LV outflow tract diameter<br>$VTI_{LVOT}$ = LV outflow tract VTI |
| $SV_{VADc} = VTI_{can3sec} \times 20 \times \pi(D_{can}/2)^2 \times C$ | C = correction factor for inflow cannula = (0.67)<br>$VTI_{can3sec}$ = 3 second tracing of VTI continuous flow in the VAD cannula |
| **Pulsatile VAD regurgitant volume (RV)**<br>$RV_{VADp} = (\pi(D_{IN}/2)^2 \times VTI_{IN}) - (\pi(D_{OUT}/2)^2 \times VTI_{OUT})$ | $VTI_{IN}$ = inflow cannula VTI<br>$VTI_{OUT}$ = outflow cannula VTI<br>$D_{OUT}$ = outflow cannula diameter<br>$D_{IN}$ = inflow cannula diameter |
| **Continuous flow VAD regurgitant volume (RV)**<br>$RV_{VADc} = (\pi(D_{asc}/2)^2 \times VTI_{asc}) - (\pi(D_{PA}/2)^2 \times VTI_{PA})$ | $D_{asc}$ = ascending aorta diameter<br>$D_{PA}$ = pulmonary artery diameter<br>$VTI_{asc}$ = ascending aorta VTI above the outflow cannula<br>$VTI_{PA}$ = pulmonary artery VTI |

*VTI*, Velocity time integral.

Even fewer studies have examined postimplant RV function and its effects on clinical parameters. Maeder and colleagues[38] showed that reduced mortality and improved renal function was associated with improved RV function after LVAD implant. Lam and co-workers[88] reported that a greater than 10% reduction in RV fractional area change postimplant portended worse quality of life and exercise capacity. Simon and associates[89] found that postimplant RV function was associated with lower maximum oxygen consumption.

Most of the studies investigating the use of echocardiographic measures to predict successful LVAD explant involve pulsatile devices.[90] An LVEDD less than 5.5 cm with LVEF greater than 45% at baseline (before turndown) predicted LV recovery in one study, with 87.5% of these patients exhibiting more than 5 years of "cardiac stability."[91] The peak systolic wall motion velocities by tissue Doppler imaging (Sm greater than or equal to 8) in both radial and longitudinal directions at the basal inferolateral wall also predicted recovery. A 2010 study from the same group reported 5-year survival free of heart-failure events was 92% for patients with an LVEF of at least 50% and 79% for those with an ejection fraction of 45% or more during "pump off" echocardiography.[92] Initial work has suggested that LVAD patients who respond favorably to exercise or dobutamine experience ventricular recovery allowing VAD explant.[84]

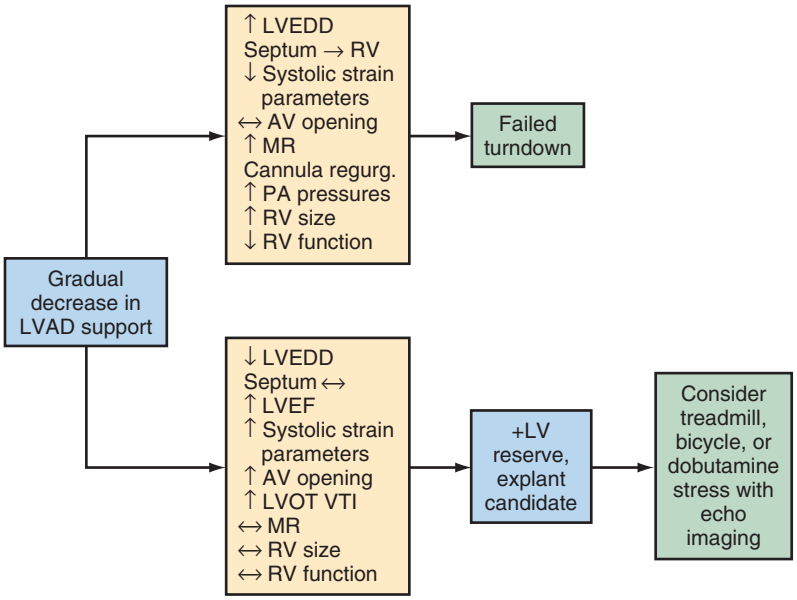



**Figure 31-14 LVAD weaning.** This flow chart outlines the echocardiographic parameters which can be used to determine whether a patient has experienced LV recovery and may be a candidate for device explant. The same parameters used during the "turndown" phase can be assessed during exercise or dobutamine stress, including LVEDD, septal orientation, LVEF, AV opening, LVOT VTI, degree of MR and RV size and function. Little data exists on the ability of any specific measures, but these parameters may form the basis for a "turndown score" to predict which patients are likely to be successfully explanted. *AV*, Aortic valve; *LVEDD*, left ventricular end-diastolic diameter; *LVEF*, left ventricular ejection fraction; *LVOT*, left ventricular outflow tract; *MR*, mitral regurgitation; *PA*, pulmonary artery; *VTI*, velocity-time integral.

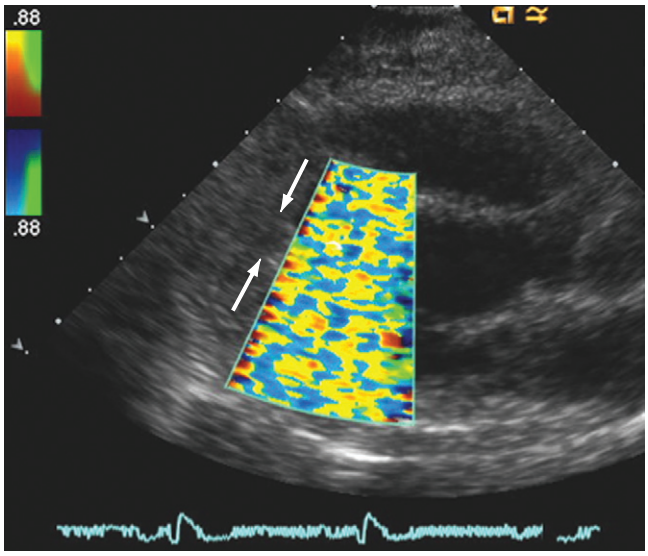



**Figure 31-15 Doppler artifact.** Ventricular assist devices with continuous-flow pumps located close to the heart (Jarvik 2000, HeartWare, Duraheart see Table 31-2) create Doppler artifacts, seen here filling entire Doppler sector in parasternal long-axis view. Artifact is located in mid-LV and precludes any assessment of flow into or out of inflow cannula (sides denoted by *large arrows*).

## Potential Limitations, Future Directions

Echocardiographic imaging is complicated in the postimplant state, when bandages, mechanical ventilation, and patient positioning compromise imaging windows. In addition to the attenuation artifacts created by LVAD inflow cannulae, significant artifacts are caused by continuous-flow rotor devices. VADs with continuous-flow pumps located very close to or in the inflow cannula (see Table 31-2) create Doppler distortion artifacts due to ultrasonic signals produced by the rotating propeller or disk (Fig. 31-15). It is possible to avoid Doppler sampling near the device and thus interrogate other cardiac structures with color and spectral Doppler. But inflow cannulae cannot be assessed for color aliasing or regurgitation, and cannula velocities cannot be measured.

Cannula orientation, orifice location, and proximity to ventricular structures are not always clear from 2D imaging planes. Real-time three-dimensional (3D) echocardiography may play a role in more precisely defining cannula position. 3D images of the LVAD inflow cannula and outflow cannulae are obtained from the midesophageal position (Fig. 31-16). 3D TEE also provides the best images of cannulae placed in the right and left atria. Real-time 3D imaging may facilitate visualization of the entire Impella Recover cannula, which tends to traverse 2D imaging planes. Real-time 3D echocardiography may also provide an assessment of RV size and function that accurately predicts which patients will experience RV failure after implant.[93]

Aortic stenosis from cusp fusion or degenerative disease is difficult to assess in the setting of an LVAD, because there is usually little flow through the valve. Detection and measurement of aortic stenosis requires a turndown procedure to elicit a greater degree of aortic valve opening. If increased preload fails to augment cardiac output, and the aortic valve opening remains reduced, dobutamine can be infused to attempt to stimulate cardiac output, as in the assessment of low-gradient aortic stenosis. Improvement in LV function without increased aortic valve opening signals cusp fusion (and should accompany increased flow through the LVAD).

Diastolic function is not well defined following cardiac assist device placement. Doppler inflow measures (E and A velocities), tissue Doppler relaxation velocities, and propagation velocity will be influenced by the LVAD inflow. A pulsatile LVAD in asynchronous mode and continuous-flow VADs draw blood to the LV apex independent of ventricular relaxation.

Although a favorable response to exercise and dobutamine stress testing may portend recovery to explant, a more precise and load-independent measure of intrinsic myocardial reserve is needed. Measures of myocardial deformation, including strain and strain rate, may provide a better way to predict recovery. Isovolumic acceleration measured by tissue Doppler or speckle tracking may also prove valuable[94] (see Chapter 10). Measures of myocardial deformation of the RV before LVAD implant may also improve the ability to predict which patients will require an RVAD.

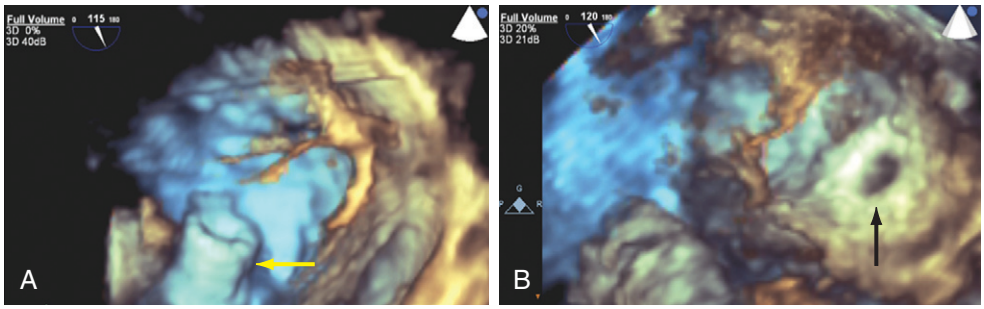



**Figure 31-16 3D imaging of LVAD cannulae. A,** Real-time 3D TEE in midesophageal position demonstrates normal positioning of inflow cannula (*arrow*) in LV apex (3D data set rotated to look inferiorly and posteriorly from anterior perspective). Orifice is unobstructed by any cardiac structures. **B,** Real-time 3D TEE in upper midesophageal position shows orifice of outflow graft cannula (*arrow*), as viewed from inside proximal ascending aorta. In contrast to inflow cannula, outflow graft cannula is anastomosed end-to-side to aorta.

## Alternate Approaches

Cardiac magnetic resonance imaging (MRI) provides highly accurate measures of ventricular volumes and function. In addition, MRI accurately measures RV size and function, potentially improving prediction of RV function post implant.[95] MRI can also accurately image the aorta and define pitfalls to Impella Recover and outflow cannula placement.[96] However, MRI cannot be used with current-generation VADs after implant.

Computed tomography (CT) can be used postimplant. Initial studies suggest a high sensitivity and specificity for the detection of cannula thrombosis and inflow cannula malposition.[97,98] Most cannulae do not cause significant CT artifact, and direct visualization of cannula orientation is easily achieved from data sets. The entire length of cannulae can be examined. CT also provides excellent preimplant imaging of the aorta.[99] The downsides to CT include radiation and nephrotoxicity of contrast—a concern in VAD patients, who often have compromised renal function.

Although preliminary studies suggest that Doppler-based estimation of pulmonary pressures and pulmonary vascular resistance is valid post-LVAD implant, validation in larger numbers of patients is needed. In the meantime, invasive measures of intracardiac hemodynamics may be necessary to establish accurate filling pressures, cardiac output, and pulmonary vascular resistance to guide therapy. Invasive hemodynamic measurements may also be necessary to assess the severity of valvular lesions, especially when echocardiographic images are limited.

### KEY POINTS

- Echocardiographic imaging and interpretation must take into account the type of cardiac assist device (e.g., LVAD, RVAD, BiVAD, percutaneous VAD, total artificial heart), location of cannulation sites (e.g., LV apex, ascending aorta), mechanism of action (pulsatile versus continuous-flow pumps), and settings (e.g., flows, rpm).
- Echocardiography plays a role before cardiac assist device implant to establish candidacy and identify specific obstacles to device placement, including thrombi, intracardiac shunts, aortic regurgitation, and RV dysfunction.
- During implant procedures, echocardiography guides device placement and deairing.
- After implant, echocardiography identifies causes and effects of cardiac assist device dysfunction including overfilling, underfilling inflow cannula obstruction, and valvulopathy.
- Optimization of cardiac assist device settings and monitoring of cardiac function during weaning/turndown studies involves 2D and Doppler assessments of LV diastolic dimensions and septal position, aortic valve opening, ventricular function, and mitral regurgitation.
- VAD stroke volumes can be calculated from cannula cross-sectional areas and pulsed Doppler VTI measurements at the cannula orifice.
- Preliminary work suggests that Doppler estimates of pulmonary pressures in cardiac assist device patients correlate with clinical outcomes.
- Real-time 3D echocardiography may overcome some of the limitations of cannula assessment by 2D echocardiography.
- CT shows promise in imaging cardiac assist device cannulae.

## REFERENCES

1. Hetzer R, Muller JH, Went Y, et al: Bridging-to-recovery. *Ann Thorac Surg* 71:S109-S113, 2001.
2. Boehmer JP, Popjes E: Cardiac failure: mechanical support strategies. *Crit Care Med* 34(Suppl):S268-S277, 2006.
3. Friedel N, Viazis P, Schiessler A, et al: Recovery of end-organ failure during mechanical circulatory support. *Eur J Cardiothorac Surg* 6:519-522, 1992.
4. Farrar DJ, Hill JD: Recovery of major organ function in patients awaiting heart transplantation with Thoratec ventricular assist devices. *J Heart Lung Transplant* 13:1125-1132, 1994.
5. Frazier OH, Rose EA, Oz MC, et al: Multicenter clinical evaluation of the HeartMate vented electric left ventricular assist system in patients awaiting heart transplantation. *J Thorac Cardiovasc Surg* 122:1186-1195, 2001.
6. Lietz K, Miller LW: Improved survival of patients with end-stage heart failure listed for heart transplantation. Analysis of Organ Procurement and Transplantation Network/U.S. United Network of Organ Sharing Data, 1990 to 2005. *J Am Coll Cardiol* 50:1282-1290, 2007.
7. Rose EA, Gelijns AC, Moskowitz AJ, et al: Randomized Evaluation of Mechanical Assistance for the Treatment of Congestive Heart

Failure (REMATCH) Study Group. Long-term mechanical left ventricular assistance for end-stage heart failure. *N Engl J Med* 345:1435-1443, 2001.
8. Lietz K, Long JW, Kfoury AG, et al: Outcomes of left ventricular assist device implantation as destination therapy in the post-REMATCH era: implications for patient selection. *Circulation* 116:497-505, 2007.
9. Westaby S, Frazier OH, Banning A: Six years of continuous mechanical circulatory support. *N Engl J Med* 355:325-327, 2006.
10. Alba AC, Delgado DH: The future is here: ventricular assist devices for the failing heart. *Expert Rev Cardiovasc Ther* 7:1067-1077, 2009.
11. Iqbal I, Ventura HO, Smart FW, Stapleton DD: Difficult cases in heart failure: left ventricular assist device implantation for the treatment of recurrent ventricular tachycardia in end stage heart failure. *Congest Heart Fail* 5:129-130, 1999.
12. Song X, Throckmorton AL, Untaroiu A, et al: Axial flow blood pumps. *ASAIO J* 49:355-364, 2003.
13. Miller LW, Pagani FD, Russell SD, et al: Use of a continuous-flow device in patients awaiting heart transplantation. *N Engl J Med* 357:885-896, 2007
14. John R, Kamdar F, Liao K, et al: Improved survival and decreasing incidence of adverse events using the HeartMate II left ventricular assist device as a bridge-to-transplant. *Ann Thorac Surg* 86:1227-1234, 2008.
15. Slaughter MS, Rogers JG, Milano CA, et al: Advanced heart failure treated with continuous-flow left ventricular assist device. *N Engl J Med* 361:2241-2251, 2009.
16. Kirklin J, Naftel D, Kormos R, et al: Second INTERMACS annual report: more than 1,000 primary left ventricular assist device implants. *J Heart Lung Transplant* 29:1-10, 2010.
17. Farrar DJ, Bourque K, Dague CP, et al: Design features, developmental status, and experimental results with the HeartMate III centrifugal left ventricular assist system with a magnetically levitated rotor. *ASAIO J* 53:310-315, 2007.
18. Pagani FD: Continuous-flow rotary left ventricular assist devices with "3rd generation" design. *Thorac Cardiovasc Surg* 20:255-263, 2008.
19. Wieselthaler GM, Strueber M, O'Drisoll GA, et al: Experience with the novel HeartWare HVAD with hydromagnetically levitated rotor in a multi-institutional trial. *J Heart Lung Transplant* 27:S245, 2008.
20. Kale P, Fang JC: Devices in acute heart failure. *Crit Care Med* 36(Suppl):S121-S128, 2008.
21. Sarkar K, Kini AS: Percutaneous left ventricular support devices. *Cardiol Clin* 28:169-184, 2010.
22. Catena E, Milazzo CE, Pittella G, et al: Echocardiographic approach in a new left ventricular assist device: Impella Recover 100. *J Am Soc Echocardiogr* 17:470-473, 2004.
23. Cheng JM, den Uil CA, Hoeks SE, et al: Percutaneous left ventricular assist devices vs intra-aortic balloon pump counterpulsation for treatment of cardiogenic shock: a meta-analysis of controlled trials. *Eur Heart J* 30:2102-2108, 2009.
24. Pretorius M, Hughes AK, Stahlman MB, et al: Placement of the TandemHeart percutaneous left ventricular assist device. *Anesth Analg* 103:1412-1413, 2006.
25. Thiele H, Lauer B, Hambrecht R, et al: Reversal of cardiogenic shock by percutaneous left atrial-to-femoral arterial bypass assistance. *Circulation* 104:2917-2922, 2001.
26. Copeland JG, Smith RG, Arabia FA, et al: Cardiac replacement with a total artificial heart as a bridge to transplantation. *N Engl J Med* 351:859-867, 2004.
27. Jessup M, Abraham WT, Casey DE, et al: 2009 focused update: ACCF/AHA Guidelines for the Diagnosis and Management of Heart Failure in Adults: a report of the American College of Cardiology Foundation/American Heart Association Task Force on Practice Guidelines: developed in collaboration with the International Society for Heart and Lung Transplantation. *J AmColl Cardiol* 53:1343-1382, 2009.
28. Chumnanvej S, Wood MJ, MacGillivray TE, Vidal Melo MF: Perioperative echocardiographic examination for ventricular assist device implantation. *Anesth Analg* 105:583-601, 2007.
29. Shapiro GC, Leibowitz DW, Oz MC, et al: Diagnosis of patent foramen ovale with transesophageal echocardiography in a patient supported with a left ventricular assist device. *J Heart Lung Transplant* 14:594-597, 1995.
30. John R, Mantz K, Eckman P, et al: Aortic valve pathophysiology during left ventricular assist device support. *J Heart Lung Transplant* 29:1321-1329, 2010.
31. Chen JM, Levin HR, Rose EA, et al: Experience with right ventricular assist devices for perioperative right-sided circulatory failure. *Ann Thorac Surg* 61:305-310, 1996.
32. Ochiai Y, McCarthy PM, Smedira NG, et al: Predictors of severe right ventricular failure after implantable left ventricular assist device insertion: analysis of 245 patients. *Circulation* 24:198-202, 2002.
33. Matthews JC, Koelling TM, Pagani FD, Aaronson KD: The right ventricular failure risk score a pre-operative tool for assessing the risk of right ventricular failure in left ventricular assist device candidates. *J Am Coll Cardiol* 51: 2163-2172, 2008.
34. Kormos RL, Teuteberg JJ, Pagani FD, et al: Right ventricular failure in patients with the HeartMate II continuous-flow left ventricular assist device: incidence, risk factors, and effect on outcomes. *J Thorac Cardiovasc Surg* 139: 1316-1324, 2010.
35. Catena E, Milazzo F: Echocardiography and cardiac assist devices. *Minerva Cardioangiol* 55:247-265, 2005.
36. Fitzpatrick JR III, Frederick JR, Hiesinger W, et al: Early planned institution of biventricular mechanical circulatory support results in improved outcomes compared with delayed conversion of a left ventricular assist device to a biventricular assist device. *J Thorac Cardiovasc Surg* 137:971-977, 2009
37. Farrar DJ, Compton PG, Hershon JJ, et al: Right heart interaction with the mechanically assisted left heart. *World J Surg* 9:89-102, 1985.
38. Maeder MT, Leet A, Ross A, et al: Changes in right ventricular function during continuous-low left ventricular assist device support. *J Heart Lung Transplant* 28:360-366, 2009.
39. Moon MR, Bolger AF, DeAnda A, et al: Septal function during left ventricular unloading. *Circulation* 95:1320-1327, 1997.
40. Buckberg GD: The ventricular septum: the lion of right ventricular function, and its impact on right ventricular restoration. *Eur J Cardiothorac Surg* 29(suppl):S272-S278, 2006.
41. Tingleff J, Joyce FS, Pettersson G: Intraoperative echocardiographic study of air embolism during cardiac operations. *Ann Thorac Surg* 60:673-677, 1995.
42. Scalia GM, McCarthy PM, Savage RM, et al: Clinical utility of echocardiography in the management of implantable ventricular assist device. *J Am Soc Echocardiogr* 13:754-763, 2000.
43. Catena E, Milazzo F, Montorsi E, et al: Left ventricular support by axial flow pump: the echocardiographic approach to device malfunction. *J Am Soc Echocardiogr* 18:1422, 2005.
44. Horton SC, Khodaverdian R, Chatelain P, et al: Left ventricular assist device malfunction: an approach to diagnosis by echocardiography. *J Am Coll Cardiol* 45:1435-1440, 2005.
45. Poirier VL: Inflow valve incompetence. *J Congestive Heart Fail Circ Support* 2:23-25, 2001.
46. Pagani FD, Miller LW, Russell SD, et al: Extended mechanical circulatory support with a continuous-flow rotary left ventricular assist device. *J Am Coll Cardiol* 54:312-321, 2009.
47. Crow S, John R, Boyle A, et al: Gastrointestinal bleeding rates in recipients of nonpulsatile and pulsatile left ventricular assist devices. *J Thorac Cardiovasc Surg* 137:208-215, 2009.
48. Letsou GV, Shah N, Gregoric ID, et al: Gastrointestinal bleeding from arteriovenous malformations in patients supported by the Jarvik 2000 axial-flow left ventricular assist device. *J Heart Lung Transplant* 24:105-109, 2005.
49. Klovaite J, Gustafsson F, Mortensen SA, et al: Severely impaired von Willebrand factor-dependent platelet aggregation in patient with a continuous-flow ventricular assist device (HeartMate II). *J Am Coll Cardiol* 53:2162-2167, 2009.
50. Geisen U, Heilmann C, Beyersdorf F, et al: Non-surgical bleeding in patients with ventricular assist devices could be explained by acquired von Willebrand disease. *Eur J Cardiothorac Surg* 33:679-684, 2008.
51. Meyer AL, Malehsa D, Bara C, et al: Acquired von Willebrand syndrome in patients with an axial flow left ventricular assist device. *Circ Heart Fail* 3:675-681, 2010.
52. Samuels LE, Thomas MP, Holmes EC, et al: Insufficiency of the native aortic valve and left ventricular assist system inflow valve after support with an implantable left ventricular assist system; signs, symptoms and concerns. *J Thorac Cardiovasc Surg* 122:380-381, 2001.
53. Connelly JH, Abrams J, Klima T, et al: Acquired commissural fusion of aortic valves in patients with left ventricular assist devices. *J Heart Lung Transplant* 22:1291-1295, 2003.
54. Mudd JO, Cuda JD, Halushka M, et al: Fusion of aortic valve commissures in patients supported by a continuous axial flow left ventricular assist device. *J Heart Lung Transplant* 27:1269-1274, 2008.
55. Baradarian S, Dembitsky WP, Jaski B, et al: Left ventricular outflow tract obstruction associated with chronic ventricular assist device support. *ASAIO J* 48:665-667, 2002.
56. Rose AG, Connelly JH, Park SJ, et al: Total left ventricular outflow tract obstruction due to left ventricular assist device induced sub-aortic thrombosis in 2 patients with aortic valve bioprosthesis. *J Heart Lung Transplant* 22:594-599, 2003.
57. Topkara VK, Kondareddy S, Malik F, et al: Infectious complications in patients with left ventricular assist device: etiology and

outcomes in the continuous flow era. *Ann Thorac Surg* 90:1270-1277, 2010.
58. Meyns B, Dens J, Sergeant P, et al: Initial experiences with the Impella device in patients with cardiogenic shock—Impella support for cardiogenic shock. *Thorac Cardiovasc Surg* 51:312-317, 2003.
59. Ogletree-Hughes ML, Stull LB, Sweet WE, et al: Mechanical unloading restores beta-adrenergic responsiveness and reverses receptor down-regulation in the failing human heart. *Circulation* 104:881-886, 2001.
60. Terracciano CM, Harding SE, Adamson D, et al: Changes in sarcolemmal Ca entry and sarcoplasmic reticulum Ca content in ventricular myocytes from patients with end-stage heart failure following myocardial recovery after combined pharmacological and ventricular assist device therapy. *Eur Heart J* 24:1329-1339, 2003.
61. Simon MA, Primack BA, Teuteberg J, et al: Left ventricular remodeling and myocardial recovery on mechanical circulatory support. *J Card Fail* 16:99-105, 2010.
62. Thohan V, Stetson SJ, Nagueh SF, et al: Cellular and hemodynamics responses of failing myocardium to continuous flow mechanical circulatory support using the DeBakey-Noon left ventricular assist device: a comparative analysis with pulsatile-type devices. *J Heart Lung Transplant* 24:566-575, 2005.
63. Klotz S, Danser AH, Burkhoff D: Impact of left ventricular assist device (LVAD) support on the cardiac reverse remodeling process. *Prog Biophys Mol Biol* 97:479-496, 2008.
64. Malliaras KG, Terrovitis JV, Drakos SG, Nanas JN: Reverse cardiac remodeling enabled by mechanical unloading of the left ventricle. *J Cardiovasc Transl Res* 2:114-125, 2009.
65. Soppa GK, Barton PJ, Terracciano CM, Yacoub MH: Left ventricular assist device-induced molecular changes in the failing myocardium. *Curr Opin Cardiol* 23:206-218, 2008.
66. Maybaum S, Mancini D, Xydas S, et al: Cardiac improvement during mechanical circulatory support: a prospective multicenter study of the LVAD Working Group. *Circulation* 115:2497-2505, 2007.
67. Palardy M, Nohria A, Rivero J, et al: Right ventricular dysfunction during intensive pharmacologic unloading persists after mechanical unloading. *J Card Fail* 16:218-224, 2009.
68. Klotz S, Naka Y, Oz MC, et al: Biventricular assist device induced right ventricular reverse structural and functional remodeling. *J Heart Lung Transplant* 24:1195-1201, 2005.
69. Yacoub MH: A novel strategy to maximize the efficacy of left ventricular assist devices as a bridge to recovery. *Eur Heart J* 22:534-540, 2001.
70. Birks EJ, Tansley PD, Hardy J, et al: Left ventricular assist device and drug therapy for the reversal of heart failure. *N Engl J Med* 355:1973-1984, 2006.
71. Klotz S, Danser AH, Foronjy RF, et al: The impact of angiotensin converting enzyme inhibitor therapy on the extracellular collagen matrix during left ventricular assist device support in patients with end-stage heart failure. *J Am Coll Cardiol* 49:1166-1174, 2007.
72. Slaughter MS, Bartoli CR, Sobieski MA, et al: Intraoperative evaluation of the HeartMate II flow estimator. *J Heart Lung Transplant* 28:39-43, 2009.
73. Griffith BP, Kormos RL, Borovetzv HS, et al: HeartMate II left ventricular assist system: from concept to first clinical use. *Ann Thorac Surg* 71(suppl):S116-S120, 2001
74. Xydas S, Rosen RS, Ng C, et al: Mechanical unloading leads to echocardiographic, electrocardiographic, neurohormonal, and histologic recovery. *J Heart Lung Transplant* 25:7-15, 2006.
75. Lang RM, Bierig M, Devereux RB, et al: Recommendations for chamber quantification: a report from the American Society of Echocardiography's Guidelines and Standards Committee and the Chamber Quantification Writing Group, developed in conjunction with the European Association of Echocardiography, a branch of the European Society of Cardiology. *J Am Soc Echocardiogr* 18:1440-1463, 2005
76. Quinones MA, Waggoner AD, Reduto LA, et al: A new simplified and accurate method for determining ejection fraction with two-dimensional echocardiography. *Circulation* 64:744-753, 1981.
77. Estep JD, Stainback RF, Little SH, et al: The role of echocardiography and other imaging modalities in patients with left ventricular assist devices. *JACC Cardiovasc Imaging* 3:1049-1064, 2010.
78. Rudski LG, Lai WW, Afilalo J, et al: Guidelines for the echocardiographic assessment of the right heart in adults: a report from the American Society of Echocardiography endorsed by the European Association of Echocardiography, a registered branch of the European Society of Cardiology, and the Canadian Society of Echocardiography. *J Am Soc Echocardiogr* 23:685-713, 2010.
79. Abbas AE, Fortuin FD, Schiller NB, et al: A simple method for noninvasive estimation of pulmonary vascular resistance. *J Am Coll Cardiol* 41:1021-1027, 2003.
80. Paluszkiewicz L, Gürsoy D, Spiliopoulos S, et al: HeartMate II ventricular assist device thrombosis—an echocardiographic approach to diagnosis: can Doppler evaluation of flow be useful? *J Am Soc Echocardiogr* 24:350.e1-4, 2011.
81. Schwarz KQ, Parikh SS, Chen X, et al: Noninvasive flow measurement of a rotary pump ventricular assist device using quantitative contrast echocardiography. *J Am Soc Echocardiogr* 23:324-329, 2010.
82. Kirkpatrick JN, Wiegers SE, Lang RM: Left ventricular assist devices and other devices for end-stage heart failure: utility of echocardiography. *Curr Cardiol Rep* 12:257-264, 2010.
83. Stainback RF, Croitoru M, Hernandez A, et al: Echocardiographic evaluation of the Jarvik 2000 axial-flow LVAD. *Tex Heart Inst J* 32:263-270, 2005.
84. Khan T, Delgado RM, Radovancevic B, et al: Dobutamine stress echocardiography predicts myocardial improvements in patients supported by left ventricular assist devices (LVADs): hemodynamic and histologic evidence of improvement before LVAD explantation. *J Heart Lung Transplant* 22:137-146, 2003.
85. Puwanant S, Hamilton KK, Klodell CT, et al: Tricuspid annular motion as a predictor of severe right ventricular failure after left ventricular assist device implantation. *J Heart Lung Transplant* 27:1102-1107, 2008.
86. Potapov EV, Stepanenko A, Dandel M, et al: Tricuspid incompetence and geometry of the right ventricle as predictors of right ventricular function after implantation of a left ventricular assist device. *J Heart Lung Transplant* 27:1275-1281, 2008.
87. Fitzpatrick JR, Frederick JR, Hsu VM, et al: Risk score derived from pre-operative data analysis predicts the need for biventricular mechanical circulatory support. *J Heart Lung Transplant* 27:1286-1292, 2008.
88. Lam KMT, Ennis S, O'Driscoll G, et al: Observations from non-invasive measures of right heart hemodynamics in left ventricular assist device patients. *J Am Soc Echocardiogr* 22:1055-1062, 2009.
89. Simon MA, Kormos RL, Murali S, et al: Myocardial recovery using ventricular assist devices: prevalence, clinical characteristics and outcomes. *Circulation* 112(Suppl I):I32-I36, 2005.
90. Gorcsan, J, Severyn D, Murali S, Kormos RL, et al: Non-invasive assessment of myocardial recovery on chronic left ventricular assist device: results associated with successful device removal. *J Heart Lung Transplant* 22:1304-1313, 2003.
91. Dandel M, Weng Y, Siniawski H, et al: Prediction of cardiac stability after weaning from left ventricular assist devices in patients with idiopathic dilated cardiomyopathy. *Circulation* 118(Suppl 1):S94-S105, 2008.
92. Dandel M, Weng Y, Siniawski H, et al: Heart failure reversal by ventricular unloading in patients with chronic cardiomyopathy: criteria for weaning from ventricular assist devices. *Eur Heart J* 32:1148-1160, 2011.
93. Niemann PS, Pinho L, Balbach T, et al: Anatomically oriented right ventricular volume measurements with dynamic three-dimensional echocardiography validated by 3-tesla magnetic resonance imaging. *J Am Coll Cardiol* 50:1668-1676, 2007.
94. Vogel M, Cheung MMH, Li J, et al: Noninvasive assessment of left ventricular force-frequency relationships using tissue Doppler-derived isovolumic acceleration validation in an animal model. *Circulation* 107:1647-1652, 2003.
95. Grothues F, Braun-Dulleaus R: Serial assessment of ventricular morphology and function. *Heart Fail Clin* 5:301-314, 2009.
96. Lohan DG, Krishnam M, Saleh R, et al: MR imaging of the thoracic aorta. *Magn Reson Imaging Clin North Am* 16:213-234, 2008.
97. Raman SV, Sahu A, Merchant AZ, et al: Noninvasive assessment of left ventricular assist devices with cardiovascular computed tomography and impact on management. *J Heart Lung Transplant* 29:79-85, 2010.
98. Acharya D, Singh S, Tallaj JA, et al: Use of gated cardiac computed tomography angiography in the assessment of left ventricular assist device dysfunction. *ASAIO J* 57:32-37, 2011.
99. Yu T, Zhu X, Tang L, et al: Review of CT angiography of aorta. *Radiol Clin North Am* 45:461-483, 2007.
100. Heart Failure Society of America: Executive summary: HFSA 2006 comprehensive heart failure practice guideline. *J Card Fail* 12:10-38, 2006.
101. Rasalingam R, Johnson SN, Bilhorn KR, et al: Transthoracic echocardiographic assessment of continuous-flow left ventricular assist devices. *J Am Soc Echocardiogr* 24:135-148, 2011.

# 32 Right Ventricular Anatomy, Function, and Echocardiographic Evaluation

CHRISTOPHER E. KURTZ, MD

**Right Heart Anatomy and Physiology**
**Basic Principles and Echocardiographic Approach**
Basic Approach to Assessment of the Right Heart
Transthoracic Imaging
Estimation of Right Heart Pressures
Transesophageal Imaging
**Technical Details, Quantitation, and Data Analysis**
Measures of Right Ventricular Size and Function
Reference Ranges, Quantitation and Data Analysis
**Clinical Utility and Outcome Data**
Outcome Data
Clinical Application
**Research Applications**
Three-Dimensional Echocardiography
Alternate Measures of Right Ventricular Systolic Function
Right Ventricular Diastolic Function
**Potential Limitations and Future Directions**
**Alternate Approaches**

The right ventricle (RV) plays an important role in the maintenance of normal circulatory function, and its assessment is valuable in a wide variety of cardiopulmonary diseases. However, clinical assessment of the RV has lagged behind that of other portions of the echocardiographic examination for several reasons—intense clinical focus on the left heart, historical lack of awareness of the clinical importance of RV function, the irregular shape of the RV, and a paucity of normative data.

Although practical challenges in assessment of the right heart persist, significant progress has been made, including generation of higher-quality normative data, validation of two-dimensional (2D) and Doppler measurements, and continued improvements in three-dimensional (3D) techniques. A guideline statement from the American Society of Echocardiography (ASE) dedicated solely to the assessment of the right heart was published in early 2010, highlighting these advances and underscoring the need for increased clinical attention to the right heart.

This chapter addresses the echocardiographic evaluation of right heart function, with attention to the value and limitations of objective measurements of RV size and function. The integration of echocardiographic findings into the diagnosis and treatment of specific disorders is discussed in greater detail in Chapters 33 (Echocardiographic Evaluation of the Patient with Pulmonary Hypertension) and 34 (Right-Sided Valve Disease in Adults).

## Right Heart Anatomy and Physiology

The right atrium (RA) forms the right heart border, lying superior, posterior, and rightward of the RV. The RA drains the superior vena cava superoposteriorly, the inferior vena cava (IVC) inferiorly, and the coronary sinus posteriorly, with the coronary sinus ostium between the IVC and the tricuspid valve annulus. The interatrial septum forms the posteromedial wall of the RA and contains the fossa ovalis lying between the caval orifices.

The tricuspid valve normally inserts on the septum approximately 2 mm more apical than the mitral valve. More apical insertion of the tricuspid valve may indicate Ebstein malformation, whereas insertion of the tricuspid valve at the same level as the mitral valve may be seen in atrioventricular canal defects. Each of the three tricuspid valve leaflets receives chordae from two of the three papillary muscles. The anterior papillary muscle is the largest of the three, arising from the anterior RV and fused with the moderator band. The posterior and septal papillary muscles are often multifid.

The RV forms the majority of the anterior and inferior borders of the heart and comprises two embryologically distinct regions, the inflow (sinus) portion and a funnel-shaped outflow portion—the conus or infundibulum (Fig. 32-1). The body of the RV is formed by the free wall and interventricular septum. The normal interventricular septum is convex toward the RV cavity, imparting a crescentic shape to the RV in short-axis views.

Unlike the left ventricle (LV), the RV is heavily trabeculated. A moderator band is present in approximately 75% of patients,[1] spanning the interventricular septum and the anterior free wall. The moderator band and tricuspid valve are always contained by the RV and may help distinguish the morphologic RV in patients with complex congenital heart disease.

The inflow and outflow portions of the RV are separated by the crista supraventricularis, a U-shaped muscular ridge that originates at the tricuspid annulus, extends to the interventricular septum, and bridges across the RV cavity by way of the moderator band to attach to the anterior wall of the RV and anterior papillary muscle. The crista functions as a contractile strut, transmitting septal contraction to the RV free wall—one

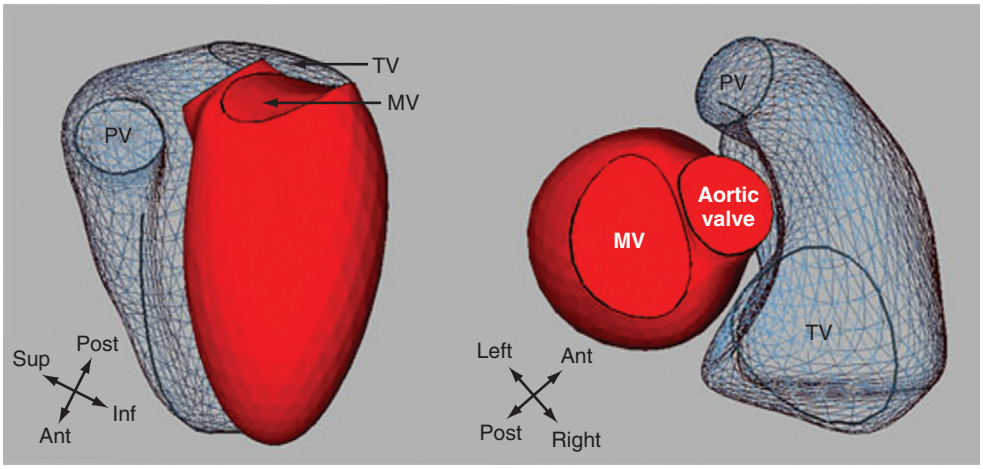



**Figure 32-1 Anatomy of normal RV.** *Left*: Left lateral view. *Right*: Basal view. Endocardial surfaces generated by reconstruction using 3D echocardiography and knowledge-based reconstruction. Hollow mesh is RV endocardial surface; solid red that of LV. RV is crescentic in short-axis section, with tricuspid and pulmonic valve orifices widely separated by crista supraventricularis. *Ant*, Anterior; *Inf*, inferior; *MV*, mitral valve; *Post*, posterior; *PV*, pulmonic valve; *Sup*, superior; *TV*, tricuspid valve. *(Images courtesy Dr. Florence H. Sheehan, University of Washington Cardiovascular Research and Training Center.)*

of many forms of ventricular interdependence. Via the crista, LV contraction narrows the tricuspid valve annulus and pulls the RV free wall toward the septum, promoting tricuspid valve competence and RV contraction. LV contraction normally accounts for an estimated 30% of pressure generation in the RV through the transmission of systolic forces from the LV to the RV.[2] Even an akinetic RV will generate some intracavitary systolic pressure as the LV "pulls" the RV free wall toward the septum. Experimental animal studies showed that damage to the RV alone did not alter central venous or systemic arterial pressure, but when a portion of the LV was also damaged via cautery, the animals rapidly succumbed to shock.[3]

The right coronary artery supplies the vast majority of the RV free wall (Fig. 32-2). A small anterior portion of the RV apex and the moderator band are supplied by the left anterior descending coronary artery, the latter via the moderator band artery, which arises from the first septal branch of the left anterior descending artery. In fewer than 10% of hearts, posterolateral branches of the left circumflex coronary artery supply a portion of the posterior RV free wall. The conus artery, arising from a separate coronary ostium in 30% of cases, supplies the infundibulum. Although coronary blood flow to the LV occurs predominantly in diastole, RV coronary blood flow occurs equally in systole and diastole because of lower intramural systolic pressure.[4] RV myocardial oxygen demand is much lower than that of the LV because of lower stroke work. Thus, the RV is far more tolerant of ischemia, and recovery of RV function following RV infarction is the rule rather than the exception. However, in the presence of pulmonary hypertension and RV hypertrophy, RV coronary flow becomes diastole-predominant[5] in like fashion to the LV and is much less tolerant of ischemia.[6]

Absent shunt, the RV generates the same stroke volume as the LV, but with one sixth the muscle mass. This is possible because of the low resistance of the pulmonary arterial vasculature. Because the normal RV is slightly larger than the LV, RV ejection fraction (EF) is normally lower than LV EF, typically between 45% and 70%.[7]

The pulmonary arterial vasculature consists of relatively thin and distensible large arteries without well-developed arterioles. Functionally, this translates to a pulse pressure that is one half, a mean arterial pressure that is one sixth, and vascular resistance one tenth that of the systemic circulation. In health, a transpulmonary gradient of only 5 mm Hg drives blood across the pulmonary circulation. Isovolumic RV contraction is brief compared to the LV,[8,9] and pulmonary artery flow continues throughout systole despite falling RV systolic pressure (the "hangout" period), due to blood inertia created by early RV ejection into a low-resistance vascular bed.

RV contraction is peristaltic, with initial activation of the RV inflow region followed in 30 to 40 ms by contraction of the conus region. Conus contraction contributes less than 15% of RV SV.[10] Whereas the LV shortens symmetrically in the transverse and longitudinal planes, normal RV contraction appears principally due to longitudinal shortening.[11] RV longitudinal shortening closely correlates with RV EF, whereas transverse RV shortening does not.[12] Similarly, longitudinal stroke work correlates with global RV stroke work, whereas circumferential regional RV stroke work does not.[13] Thus, normal RV contraction perhaps more closely resembles a piston than a bellows, which has important implications for strategies for quantifying RV systolic function noninvasively. However, chronic RV pressure or volume overload may result in relative hyperplasia of circumferential fibers[14]; in such chronically diseased RVs, circumferential contraction and free wall translation may have a greater relative contribution to systolic function.[15]

Diastolic function of the RV differs from that of the LV. The thin walls of the RV and its concave interventricular septum are relatively distensible, imparting high compliance to the RV (large changes in RV volume with only small changes in RV diastolic pressure). Thus, the RV may dilate significantly in response to acute pressure or volume overload, unlike the LV.

## Basic Principles and Echocardiographic Approach

### BASIC APPROACH TO ASSESSMENT OF THE RIGHT HEART

The complex shape of the RV makes assessment of its size and function difficult by any method, whether objective or subjective. Early studies estimated RV volume by modeling the RV as

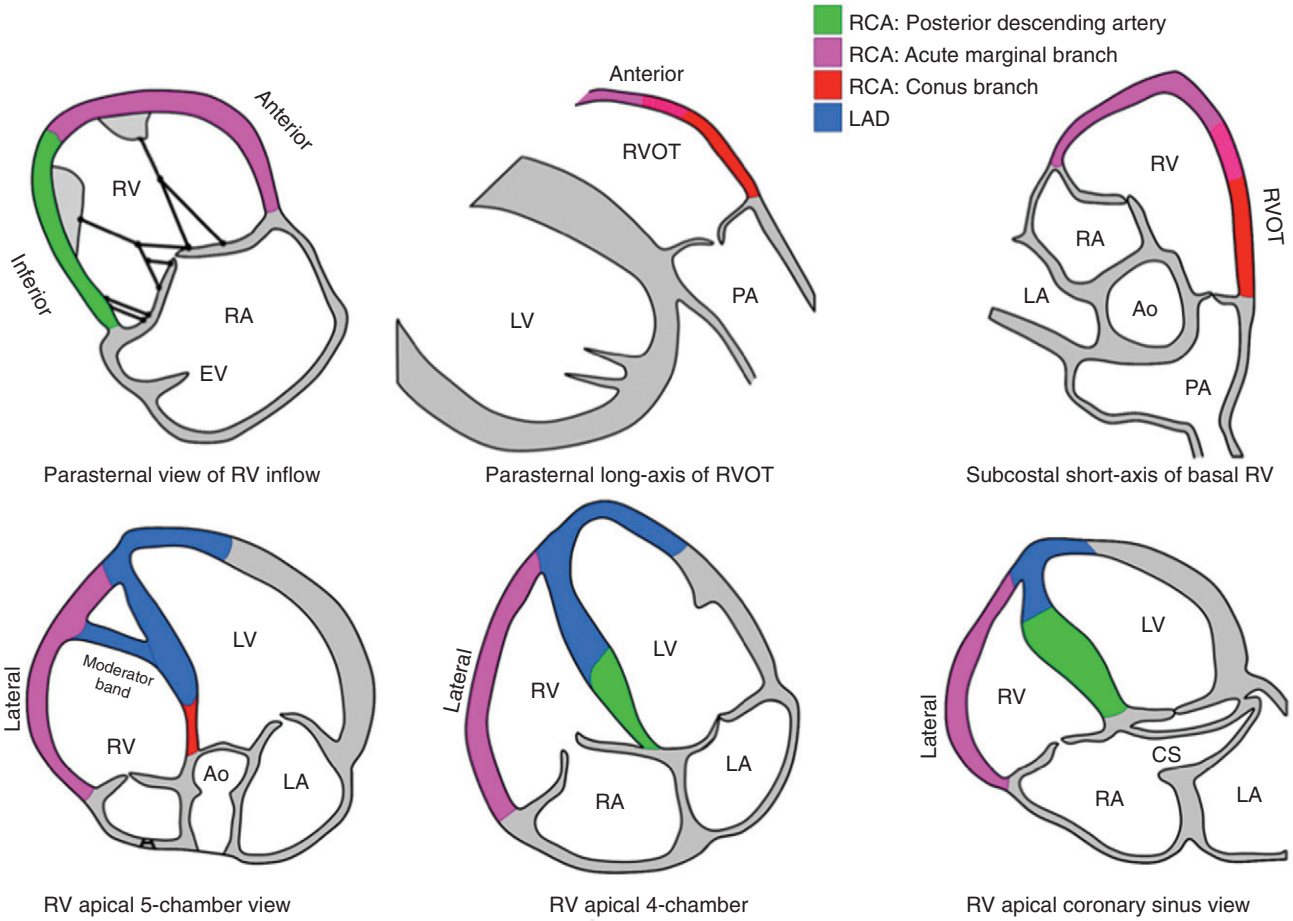



**Figure 32-2 Coronary supply of RV.** *Ao*, Aorta; *CS*, coronary sinus; *EV*, Eustachian valve; *LAD*, left anterior descending coronary artery; *PA*, pulmonary artery; *RCA*, right coronary artery; *RVOT*, right ventricular outflow tract. *(From Rudski LG, Lai WW, Afilalo J, et al: Guidelines for the echocardiographic assessment of the right heart in adults: a report from the American Society of Echocardiography endorsed by the European Association of Echocardiography, a registered branch of the European Society of Cardiology, and the Canadian Society of Echocardiography.* J Am Soc Echocardiogr *23:685-713, 2010.)*

a sum of prisms, with disk summation, or with area-length methods.[16] In brief, 2D methods of RV volume estimation are limited by geometric assumptions, resulting in only modest correlation with angiography and water displacement and significant underestimation of volumes compared to both 3D echocardiography and cardiac magnetic resonance imaging (MRI).[17] Thus, 2D-derived RV volumes and EF are not recommended for clinical use and are fading as a reference standard in research.

3D methods obviate geometric assumptions and are superior to 2D echocardiography for estimation of RV volumes and EF, but they are not yet routinely available in the community. Despite its limitations, 2D echocardiography therefore remains the principal clinical modality for assessment of the RV. Rather than attempting to calculate RV volume or EF from linear or area measurements, the clinician should compare 2D-derived measurements directly against normative values. These measurements should be considered together with visual estimation when classifying RV size and function. Because the RV lacks rotational symmetry and may remodel nonuniformly, individual 2D-derived indices of RV size may correlate poorly with RV volume, and multiple measurements should be taken when possible.

## TRANSTHORACIC IMAGING

Because RV dilation may occur regionally as well as globally, assessment of RV size requires visualization from multiple windows.

The apical four-chamber view is critical for assessment of the RV, providing the basal minor dimension (measured just apical to the tricuspid annulus, normal less than 42 mm; Fig. 32-3, *left* panel), and most 2D measures of RV systolic function: tricuspid annular plane systolic excursion (TAPSE), systolic tricuspid annular velocity (S′), fractional area change, and tissue right ventricular myocardial performance index. Most of these measurements rely heavily on good visualization of the RV free wall and lateral tricuspid annulus. If necessary, dedicated RV-focused apical four-chamber views should be obtained to ensure that the RV free wall and tricuspid annulus are well seen, away from the margin of the sector, and not shadowed. Anterior angulation or slight medial or lateral displacement of the transducer should be performed to allow this, though care must be taken to maintain a true four-chamber view (i.e., containing the crux and the true cardiac apex) to avoid misrepresenting RV size. If LV size is normal, RV size may be subjectively assessed using the ratio of RV to LV area: less than 0.66 is normal; 1.0 suggests at least moderate enlargement (Fig. 32-4). The RV apex may

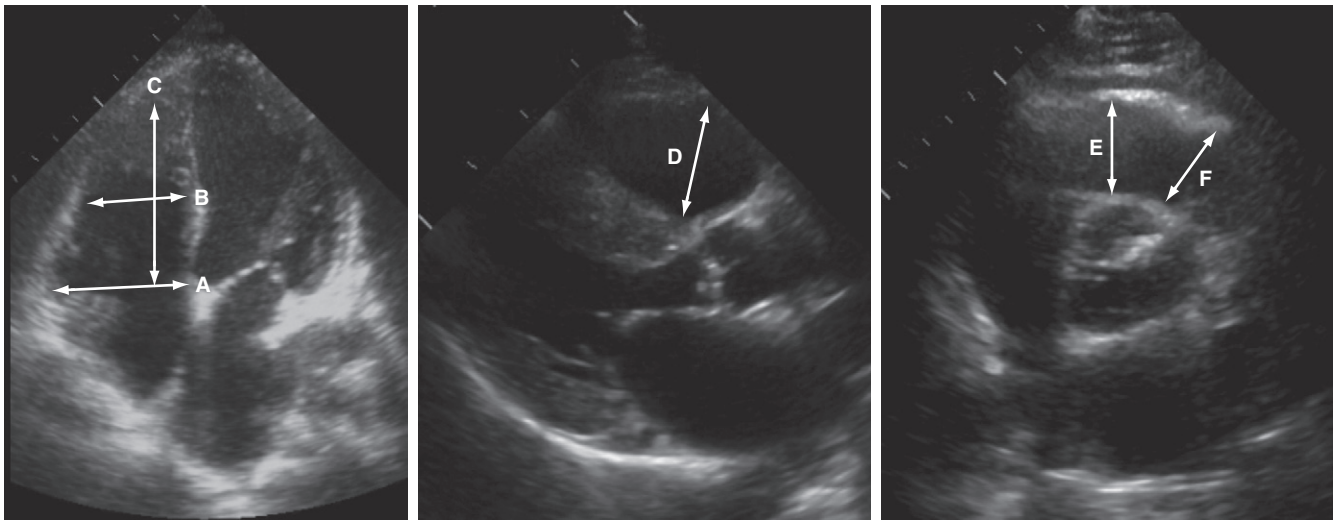



**Figure 32-3 Recommended parameters of RV size.** *Left*: Apical four-chamber view. *Center*: parasternal long-axis view. *Right*: parasternal short-axis view. *A*, Basal minor dimension; *B*, mid-cavity minor dimension; *C*, RV major (longitudinal) dimension; *D*, RVOT proximal diameter; *E*, RVOT proximal diameter; *F*, RVOT distal diameter; *RVOT*, right ventricular outflow tract.

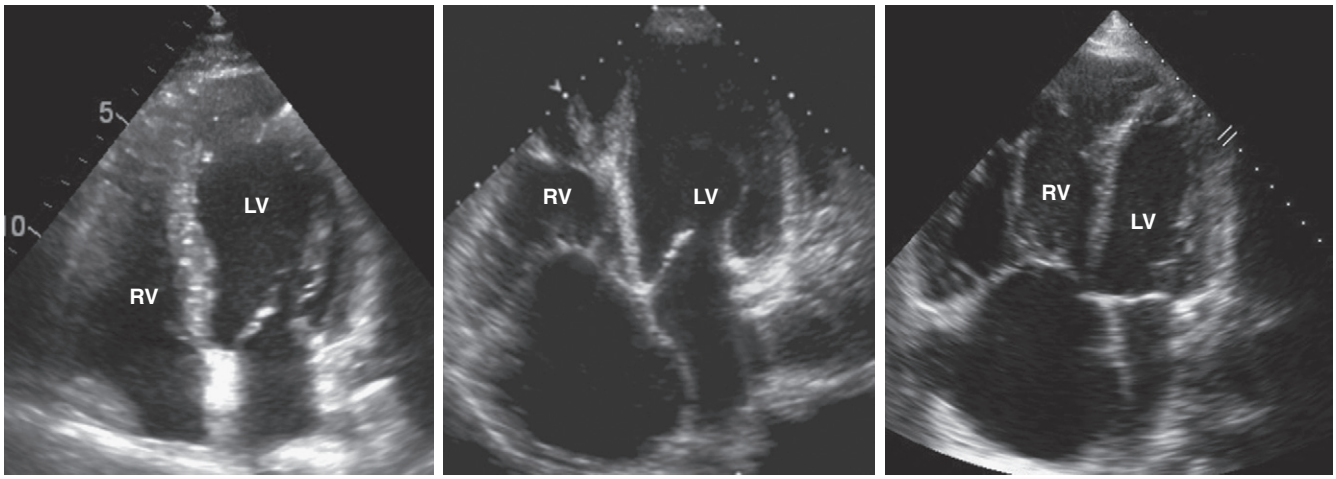



**Figure 32-4 Relative size of RV (compared to LV) in varying degrees of RV enlargement.** *Left*: Normal heart, ratio of RV area to LV area (RV:LV) approximately 0.6. *Center*: Moderate RV dilation; in this case, LV is dilated, and RV:LV is relatively low for the degree of absolute RV dilation at about 0.7-0.8. *Right*: Severe RV dilation, with RV:LV >1.5 and the RV is apex-forming.

appear "squared" if the RV is enlarged and may displace the LV to form the true apex if enlargement is severe.

If apical images are poor, the subcostal window may provide similar views of the RV (e.g., four-chamber and short-axis; Fig. 32-5). However, the difficulty in defining the anteroposterior plane needed to achieve a true four-chamber view from the subcostal window may result in foreshortening of the RV. RV wall thickness is best measured in the subcostal view, because the RV free wall is not in the near field (as in parasternal views) and is perpendicular to the ultrasound beam. The normal RV free wall is 2 mm thick, but a wall thickness of less than 5 mm is accepted as normal, because the RV free wall often cannot be resolved from the epicardium.[18,19]

The parasternal long-axis right ventricular outflow tract (RVOT) dimension is normally less than 60% of the LV dimension, but should be interpreted with care if obtained in supine position, as it can differ by up to 40% in the supine and left lateral decubitus positions. The parasternal RV inflow view shows more of the RV free wall and the anterior and posterior leaflets (the only standard view in which the posterior leaflet is

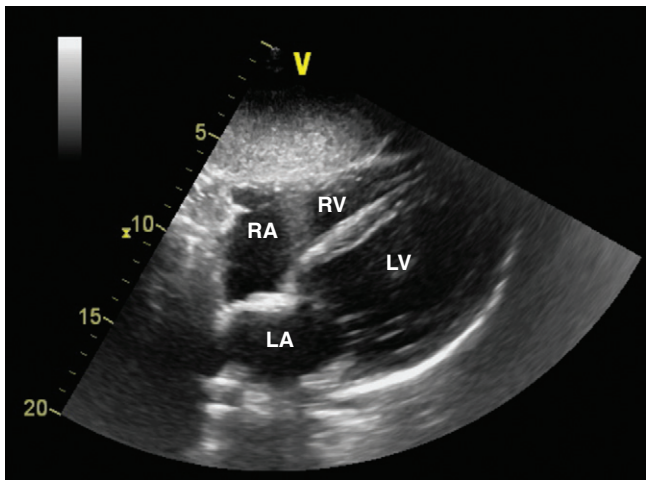



**Figure 32-5 Subcostal four-chamber view.**

seen), but the imaging plane can be highly variable and is unreliable for assessing systolic function. Although tricuspid regurgitation (TR) may be seen, the maximum jet velocity is not commonly obtained in parasternal views.

The basal parasternal short-axis view allows reliable measurement of the distal RVOT diameter (see Fig. 32-3, *right* panel). Parasternal short-axis views of the RV at midventricular levels may show septal flattening, which suggests volume overload if diastolic, pressure overload if systolic, and both if continuously present. However, beyond septal contour, the midventricular short-axis view is not reliable for assessment of RV size or systolic function, because cross-sectional area varies dramatically with the level of the short-axis plane, and the paucity of reference structures makes it difficult to reproduce planes from one study to another.

The basal short-axis view gives the best alignment for pulmonic valve velocity measurements, with trace or mild pulmonic regurgitation in most normal patients.[20] M-mode of the pulmonic valve may show notching of systolic leaflet excursion (the "flying W") in pulmonary hypertension due to a pressure wave reflected by the stiffened, abnormal pulmonary arterial bed, but specificity is limited, because this finding has also been described in pulmonary artery dilation with normal pulmonary artery pressures.[21] The spectral envelope of the pulmonary artery outflow is characteristically symmetric with a peak velocity of less than 0.8 m/s.[22] High-output states such as pregnancy, anemia, and cirrhosis may increase the velocity somewhat, but if peak velocity exceeds 1.2 m/s, pulmonic stenosis or left-to-right shunt should be suspected.

## ESTIMATION OF RIGHT HEART PRESSURES

Right atrial pressure (RAP) may be estimated echocardiographically.[23] The scheme most commonly used in clinical practice assesses the diameter of the IVC while the patient performs a "sniff" (Table 32-1). Normally, the IVC collapses as the intrathoracic pressure decreases. However, with elevated RAP, the IVC dilates and inspiratory collapse is less complete. Positive pressure ventilation makes the sniff method unreliable by altering the relationship between central venous pressure and IVC size.[24] If the IVC is poorly visualized and RA size is normal (end-systolic area 18 $cm^2$ or less), one may infer a normal RAP of 5 mm Hg. Errors made in estimation of RAP are propagated to echocardiographically calculated pulmonary artery pressures. This must be remembered especially in "torrential" TR, in which RAP may exceed 20 mm Hg by a considerable amount, leading to an underestimate of pulmonary artery pressure if 20 mm Hg is the maximum value used.

Absent pulmonic stenosis, pulmonary artery systolic pressure (PASP) may be estimated by the simplified Bernoulli equation[25]: $PASP = 4v^2_{TR} + RAP$, where $v_{TR}$ is the peak velocity of the TR jet by continuous-wave (CW) Doppler. When performed properly, this technique is highly reproducible and correlates closely with invasively derived PASP.[25-29] If pulmonic stenosis is present, peak pulmonary artery pressure may still be estimated by subtracting the gradient across the pulmonic valve from the peak RV systolic pressure. Pulmonary artery diastolic pressure (PADP) may be similarly be estimated: $PADP = 4v^2_{PR} + RAP$, where $v_{PR}$ is the end-diastolic pulmonary regurgitation velocity.[30] Mean pulmonary artery pressure (mPAP) may then be calculated: $mPAP = (2 \times PASP + PADP)/3$, where PASP and PADP are estimated as before. As with all Doppler-based measurements, interrogation from multiple windows is important to ensure parallel alignment with the TR jet and prevent underestimation of peak velocity and pressure. Only clearly visualized portions of the Doppler envelope should be measured to prevent overestimation of peak velocity (Fig. 32-6).

Invasively derived pulmonary vascular resistance (PVR) may be estimated by PVR (Wood units) $= 10 \times v_{TR}/VTI_{RVOT}$, where $v_{TR}$ is the peak TR jet velocity and $VTI_{RVOT}$ the velocity-time integral of the RVOT. This method may be helpful when it is

**TABLE 32-1 Echocardiographic Estimation of Right Atrial Pressure**

| *IVC Size* | *IVC Respiratory Change* | *RAP (mm Hg)* |
|---|---|---|
| Normal (≤21 mm) | >50% | 5 |
| Normal (≤21 mm) | <50% | 10 |
| Dilated (>21 mm) | >50% | 10 |
| Dilated (>21 mm) | <50% | 15 |
| Dilated (>21 mm) | None | 20 |

*IVC*, Inferior vena cava; *RAP*, right atrial pressure.

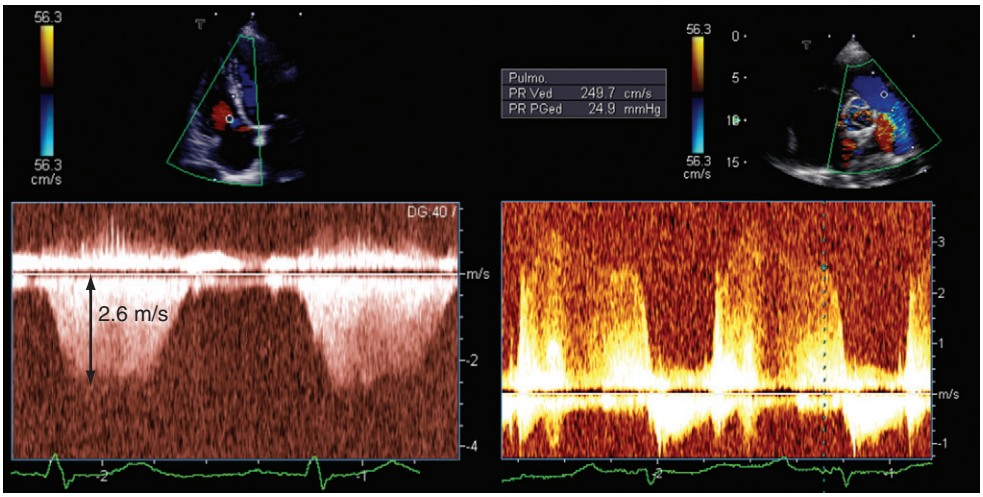



**Figure 32-6 Doppler estimation of pulmonary pressures.** *Left*: CW Doppler spectrum of tricuspid regurgitation, peak velocity 2.6 m/s, indicating systolic PA pressure = 27 mm Hg + RA pressure. Although the spectrum appears incomplete, velocity should not be "extrapolated" along a parabolic path beyond the visualized Doppler signal. *Right*: CW Doppler spectrum of pulmonic regurgitation (from a different patient), end-diastolic velocity 2.5 m/s, indicating PA diastolic pressure = 25 mm Hg + RA pressure. *PA*, Pulmonary artery; *RA*, right atrial.

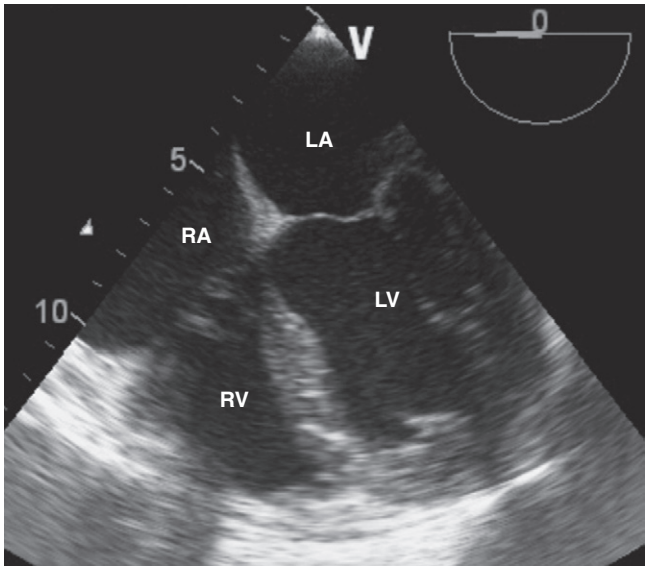



**Figure 32-7 Transesophageal modified four-chamber view.** From a standard four-chamber view, (with the LV apex centered), the transducer is turned towards the patient's right side to better visualize the right ventricle.

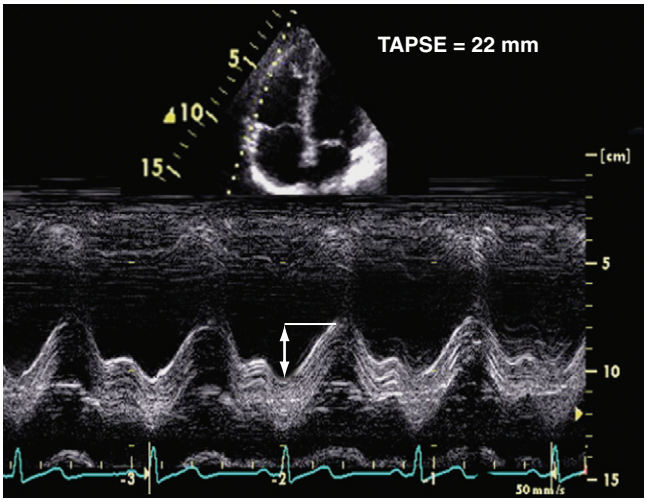



**Figure 32-8 Measurement of tricuspid annular plane systolic excursion (*TAPSE*).** The M-mode cursor is directed through lateral tricuspid annulus; apical view used to guide the cursor is shown at *top* of image.

unclear whether a modestly elevated PASP is due to increased PVR or increased cardiac output; however, it is imprecise, and catheter-derived hemodynamics remains the gold standard for diagnosis and serial clinical observation of clinically significant pulmonary hypertension.

### TRANSESOPHAGEAL IMAGING

The value of transesophageal echocardiography (TEE) in assessment of RV size and function is limited because of constraint of the transducer by the esophagus, and limited RV resolution due to its location in the far field. The modified four-chamber view (midesophageal, 0°; Fig. 32-7) foreshortens the RV considerably. Alignment with the TR jet is also difficult because of constraint of the transducer, making underestimation of the peak velocity common. Assessments of RV size and function and pulmonary artery pressures derived from transesophageal data should be interpreted with caution.

TEE is more useful for assessment of certain causes of RV dysfunction, particularly volume overload (e.g., atrial septal defects, anomalous pulmonary veins). The bicaval view (midesophageal, 90°) demonstrates the interatrial septum with high resolution, allowing interrogation by color Doppler or agitated saline contrast injection. The pulmonic valve and main pulmonary artery can be seen in the basal short-axis view (high esophageal, 60°), though visualization may be suboptimal because of their location in the far field, and the right and left pulmonary arteries are not reliably seen.

## Technical Details, Quantitation, and Data Analysis

### MEASURES OF RIGHT VENTRICULAR SIZE AND FUNCTION

#### *Linear and Area Measurements*

As with LV measurements, right heart chamber areas and dimensions should be traced from endocardium to endocardium. Trabeculations should be contained by traced chamber areas. RV basal dimension should be measured in the apical four-chamber view immediately below the tricuspid valve (see Fig. 32-3, *left* panel). The transducer should be rotated to the plane that maximizes the RV minor dimension, while still containing the LV apex and crux (neither the aortic root nor the coronary sinus should be seen). Proximal RVOT dimension should be measured at the largest anteroposterior dimension in the parasternal long-axis view, and distal RVOT dimension just below the pulmonic valve in the parasternal short-axis view.

#### *Tricuspid Annular Plane Systolic Excursion*

Tricuspid annular plane systolic excursion, sometimes referred to as tricuspid annular motion, is the distance moved by the tricuspid annulus from end-diastole to end-systole. TAPSE is obtained by M-mode in the apical four-chamber view (Fig. 32-8),[31] which is measured in most studies at the lateral annulus. TAPSE is gaining popularity because it is easy to perform, highly reproducible, requires no geometric assumptions, and correlates moderately with RV EF and RV fractional area change in a variety of patient populations.[12,31-33] It can also be obtained even when image quality is relatively poor, and it is relatively well studied and widely employed clinically. However, use of TAPSE as a surrogate for RV systolic function assumes that regional function (longitudinal translation at the tricuspid annulus) reflects global function. TAPSE may be reduced by factors other than RV global systolic dysfunction, including severe TR,[34] LV systolic dysfunction,[35] and prior cardiac surgery[36] or heart transplantation.[37] Severe TR reduces the correlation between TAPSE and RV EF (although the presence of severe TR itself suggests RV systolic dysfunction), whereas LV systolic dysfunction and cardiac surgery may reduce TAPSE independently of RV EF. TAPSE must be interpreted with caution when these conditions are present.

#### *Fractional Area Change*

Fractional area change is defined as [(RV end-diastolic area) – (RV end-systolic area)]/(RV end-diastolic area), obtained in the apical four-chamber view (Fig. 32-9). Fractional area change

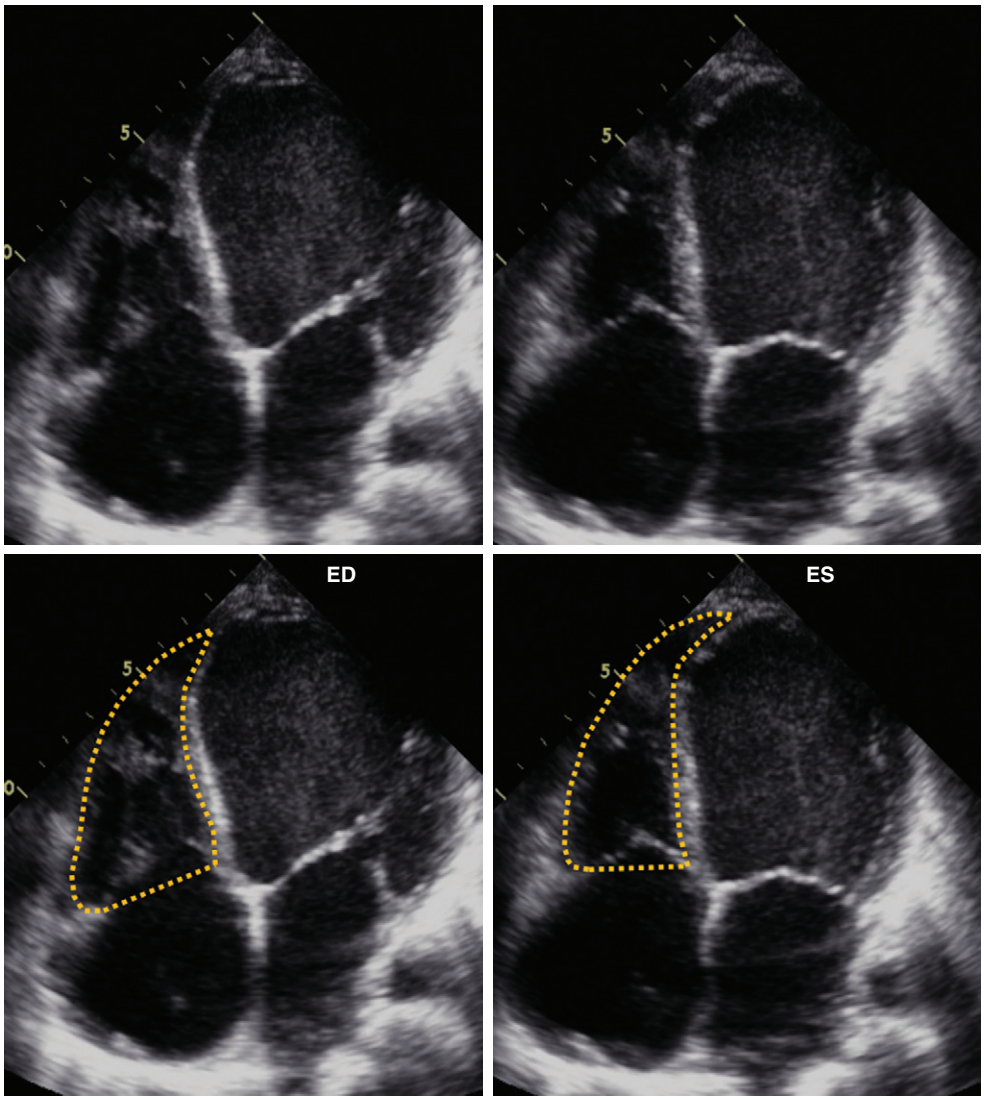



**Figure 32-9 Measurement of fractional area change from apical four-chamber view.** This patient had severe biventricular systolic dysfunction, with an RV fractional area change approximately 25%. *Left*: End-diastole (*ED*); *right*: end-systole (*ES*). *Top set of images* is identical to *bottom*, but shown without tracing to demonstrate location of borders. Trabeculations should be included in traced area.

does not require geometric assumptions and correlates well with RV EF.[38] However, measurement is often hampered by suboptimal endocardial definition, particularly of the RV free wall, and high interobserver and intraobserver variability. Care must be taken to select the true four-chamber view (containing the cardiac apex and the crux) to prevent foreshortening of the RV.

### *Peak Systolic Velocity of the Lateral Tricuspid Annulus*

Like TAPSE, the peak systolic velocity of the lateral tricuspid annulus (S′) reflects basal RV systolic motion. Echocardiographically, S′ is measured from the apical four-chamber view using tissue Doppler (Fig. 32-10), using instrument settings similar to those used for mitral tissue Doppler in assessment of LV diastolic function. S′ correlates with TAPSE[39] and shares most of its strengths and weaknesses: namely, a relatively large body of normative data, freedom from geometric assumptions, measurability in the face of suboptimal image quality, angle dependence, and blindness to systolic dysfunction in parts of the RV remote from the tricuspid annulus.

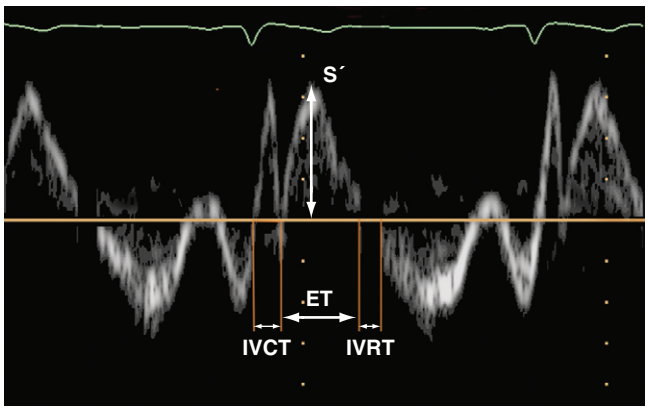



**Figure 32-10 Measurement of RV myocardial performance index.** Tissue Doppler of tricuspid annulus, with measurement of systolic peak velocity (*S′*) and elements of tissue-Doppler right index of myocardial performance. *ET*, Ejection time; *IVCT*, isovolumic contraction time; *IVRT*, isovolumic relaxation time.

### *Right Index of Myocardial Performance*

The myocardial performance index, also known as the Tei index or right ventricular myocardial performance index RV MPI, is a nongeometric combined measure of systolic and diastolic function: RV MPI = (IVRT + IVCT)/RVET, where IVRT is the RV isovolumic relaxation time, IVCT is the isovolumic contraction time, and RVET is the RV ejection time. Higher values correspond to worse ventricular function. IVRT, IVCT, and RVET can be measured by either tissue or pulsed Doppler. Because the RV inflow and outflow tracts are widely separated, two separate pulsed Doppler recordings must be made to obtain these variables in the right heart. Errors will be made if care is not taken to make measurements at comparable R-R intervals, especially if the rhythm is irregular; tissue Doppler RV MPI may often be easier to acquire (see Fig. 32-10).

RV MPI has been applied to congenital heart disease and evaluation of systemic RVs[40-42] and in adults with pulmonary hypertension. MPI has also been used to identify patients with early RV MPI dysfunction resulting from cardiac amyloidosis. In this study, nonsimultaneous recordings of pulmonary artery outflow and tricuspid valve inflow were used. The RV MPI in normal adult subjects was 0.28.[43] There is some concern that RV hypertrophy may shorten the IVRT leading to a paradoxically low MPI in the abnormal RV with hypertrophy.[44]

## REFERENCE RANGES, QUANTITATION AND DATA ANALYSIS

Parameters of RV size and their reference ranges are listed in Table 32-2 and were outlined in Figure 32-3. It should be noted that several of the ranges reported in the 2010 ASE guideline statement deviate substantially from the ranges in the 2005 ASE guideline statement on chamber quantitation,[45] which were based on very few studies.[46,47]

Selected parameters of RV systolic function and their reference ranges are outlined in Table 32-3. Although 2D methods for estimating RV EF per se have poor accuracy, individual one-dimensional, 2D, and nongeometric measures of RV systolic function do have some correlation with EF, and some have demonstrated enough individual correlation with clinical status in various diseases to be clinically useful as independent measures of systolic function. TAPSE is reproducible, easily acquired, and increasingly studied; we recommend it be measured in all comprehensive transthoracic examinations.

The 2010 ASE guideline statement does not advise any systematic method for incorporating multiple measures of RV size or function into a unified assessment (i.e., normal, or mildly, moderately, or severely abnormal). We recommend supplementing subjective assessments of both RV size and function with at least one objective measurement (we recommend RV basal minor dimension and TAPSE). Additional objective measurements should be used if initial assessments conflict or are ambiguous. Practical approaches are outlined in Figures 32-11 and 32-12, but others are possible. It should be remembered that these approaches, like the normative values themselves, are guidelines and are meant to supplement rather than replace clinical judgment.

**TABLE 32-2 Reference Values for Parameters of RV Size[7]**

| *Parameter* | *View* | *Patients (Studies)* | *Mean (LRV-URV)* |
|---|---|---|---|
| RV basal minor dimension (mm)* | A4C | 376 (10) | 33 (24-42) |
| RV mid-cavity minor dimension (mm) | A4C | 400 (12) | 28 (20-35) |
| RV major dimension (mm) | A4C | 359 (12) | 71 (56-86) |
| RV end-diastolic area ($cm^2$) | A4C | 623 (20) | 18 (10-25) |
| RV end-systolic area ($cm^2$) | A4C | 508 (16) | 9 (4-14) |
| RVOT proximal dimension (mm)* | PLAX | 405 (12) | 25 (18-33) |
| RVOT proximal dimension (mm) | PSAX | 193 (5) | 28 (21-35) |
| RVOT distal dimension (mm)* | PSAX | 159 (4) | 22 (17-27) |
| End-diastolic volume index ($mL/m^2$) | 3D | 426 (5) | 65 (40-89) |
| End-systolic volume index ($mL/m^2$) | 3D | 394 (4) | 28 (12-45) |
| RV wall thickness (mm)* | Subcostal | 180 (4) | 5 (4-5) |

Data from Rudski LG, Lai WW, Afilalo J, et al: Guidelines for the echocardiographic assessment of the right heart in adults: a report from the American Society of Echocardiography endorsed by the European Association of Echocardiography, a registered branch of the European Society of Cardiology, and the Canadian Society of Echocardiography. *J Am Soc Echocardiogr* 23:685-713, 2010.

*A4C*, Apical four-chamber; *LRV*, lower reference value (−2 standard deviations); *PLAX*, parasternal long-axis; *PSAX*, parasternal short-axis; *RVOT*, right ventricular outflow tract; *URV*, upper reference value (+2 standard deviations).

*Recommended for clinical use by the 2010 ASE guideline statement.

**TABLE 32-3 Reference Values for Parameters of RV Function[7]**

| *Parameter* | *View* | *Patients (Studies)* | *Mean (LRV-URV)* |
|---|---|---|---|
| S′ (cm/s)* | A4C | 2139 (43) | 15 (10-19) |
| TAPSE (mm)* | A4C | 2320 (46) | 23 (16-30) |
| FAC (%)* | A4C | 1276 (36) | 49 (35-63) |
| RV EF (%)† | 2D | 596 (12) | 58 (44-71) |
| RV EF (%)† | 3D | 524 (9) | 57 (44-69) |
| RV MPI (pulsed Doppler)* | A4C | 590 (8) | 0.28 (0.15-0.40) |
| RV MPI (tissue Doppler)* | A4C | 686 (17) | 0.39 (0.24-0.55) |

| *Index* | *S′** | *TAPSE** | *FAC** | *RV MPI (PW)** | *RV MPI (TDI)** | *RVEF (2D)* | *RVEF (3D)†* |
|---|---|---|---|---|---|---|---|
| Requires geometric assumptions | 0 | 0 | 0 | 0 | 0 | +++ | 0 |
| Angle-dependent | ++ | ++ | 0 | 0 | 0 | 0 | 0 |
| Load-dependent | + | ++ | ++ | + | + | ++ | ++ |
| Requires high spatial resolution | 0 | 0 | ++ | 0 | 0 | ++ | ++ |

Data from Rudski LG, Lai WW, Afilalo J, et al: Guidelines for the echocardiographic assessment of the right heart in adults: a report from the American Society of Echocardiography endorsed by the European Association of Echocardiography, a registered branch of the European Society of Cardiology, and the Canadian Society of Echocardiography. *J Am Soc Echocardiogr* 23:685-713, 2010.

*A4C*, Apical four-chamber; *EF*, ejection fraction; *FAC*, fractional area change; *LRV*, lower reference value (−2 standard deviations); *RV MPI*, right ventricular myocardial performance index; *S′*, systolic tricuspid annular peak velocity; *TAPSE*, tricuspid annular plane systolic excursion; *TDI*, tissue Doppler imaging; *URV*, upper reference value (+2 standard deviations).

*Recommended for clinical use by the 2010 ASE guideline statement.

†Recommended only for selected patients because of limited, heterogeneous normative data.

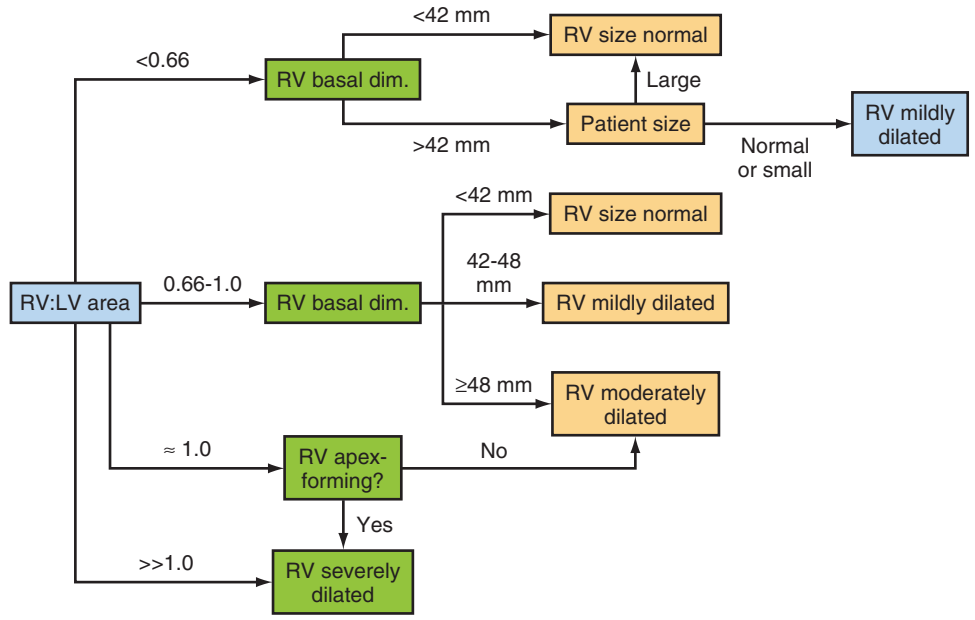



**Figure 32-11 Simplified algorithmic approach to assessment of RV size, beginning with visual assessment of relative RV size and incorporating basal minor dimension.** *dim.*, Dimension; *RV:LV area*, right ventricular to left ventricular area ratio.

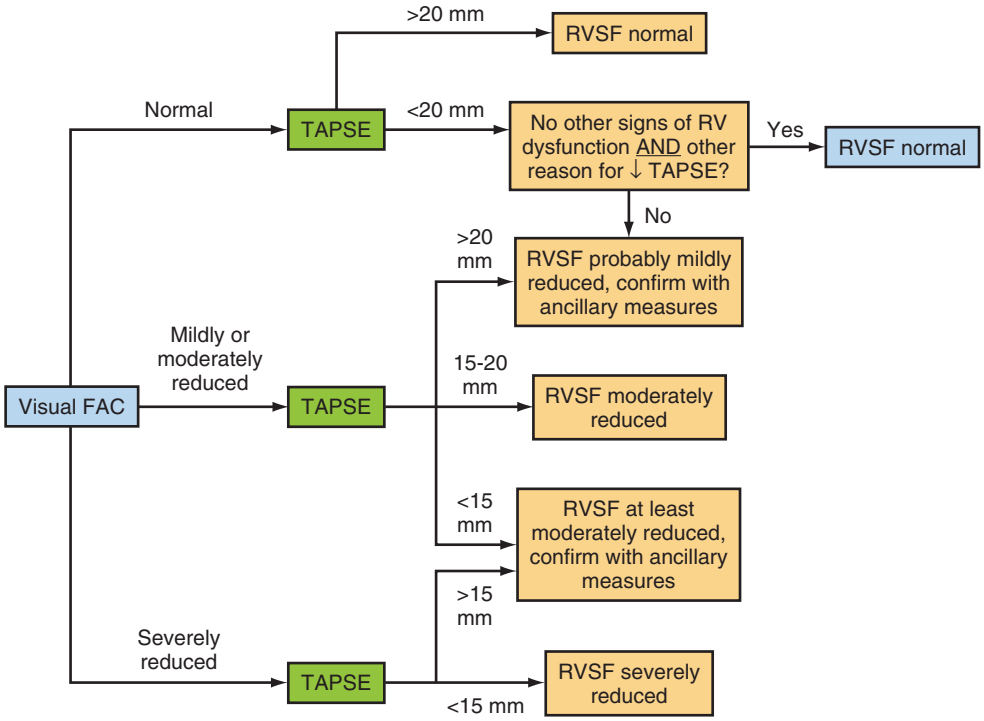



**Figure 32-12 Simplified algorithmic approach to assessment of RV systolic function, beginning with visually estimated fractional area change and incorporating TAPSE.** *FAC*, Fractional area change; *RVSF*, right ventricular systolic function; *TAPSE*, tricuspid annular systolic plane excursion.

## Clinical Utility and Outcome Data

### OUTCOME DATA

The impact of RV dilation and systolic dysfunction on clinical outcomes has been studied in a variety of conditions, both right-sided (e.g., pulmonary embolism, pulmonary hypertension, RV infarction) and systemic (myocardial infarction, LV systolic dysfunction, mitral regurgitation). RV dysfunction has been associated with obstructive sleep apnea,[48-50] but correlation with clinical outcomes has not yet been shown. Of the many indices that have been studied, TAPSE and RV fractional area change are emerging as the most widely used measures of RV systolic function. Selected studies showing the association of RV systolic dysfunction and clinical outcomes are summarized in Table 32-4.[32,33,51-57] Though limited because of variable methodology and moderate size, data show convincingly that

**TABLE 32-4 Selected Studies Showing Association of Clinical Outcomes with Echocardiographic Parameters of RV Size and Systolic Function**

| Year | Study | n | Population | Follow-up | Endpoint | Results | Adjusted for |
|---|---|---|---|---|---|---|---|
| 2000 | Ghio et al[33] | 140 | LVEF <35% | 25 months | Death or OHT | TAPSE ≤14 mm → HR 2.6, adjusted | Age, LVEF, sex, NYHA class, DT |
| 2008 | Dini et al[52] | 142 | LVEF ≤45%, MR VC ≥5 mm | 20 months | Death | TAPSE <16 mm → HR 2.6, adjusted | Age, LVEF, sex, CAD, NYHA class |
| 2008 | Puwanant et al[53] | 33 | LVAD | 6 months | RV failure | TAPSE <7.5 mm → 91% specific but only 46% sensitive for post-LVAD severe RV failure | Unadjusted |
| 2006 | Forfia et al[32] | 63 | PH (47 PAH) | 19 months | Death | Adjusted HR 1.16 for every 1-mm decrease in TAPSE in PAH cohort | Effusion, WHO class |
| 2002 | Zornoff et al[57] | 416 | LVEF ≤40%, 11 days post-MI | 31 months | Death | RV FAC <32% → HR 2.6, adjusted | Age, LVEF, sex, MI, DM, HTN, infarct size, smoking, treatment |
| 2008 | Anavekar et al[51] | 522 | LVSD or HF, 0.5-10 days post-MI | 25 months | Composite | Every 5% decrease in RV FAC → HR 1.53, adjusted; RV FAC independently associated with all-cause and cardiovascular mortality, HF, stroke | Age, LVEF, HF, Killip class, prior MI, first MI, angina, DM, AF, COPD, GFR |
| 2002 | Samad et al[54] | 194 | First MI | 24 months | Death | TAPSE <15 mm → increased mortality ($p < 0.02$) | Age, LVEF |
| 2005 | Skali et al[56] | 291 | 1 year post-MI | 22 months | Death | RV FAC <32% → HR 9.7, adjusted | Age, LVEF, sex, DM, blood pressure |
| 2005 | Scridon et al[55] | 141 | Acute pulmonary embolism | 1 month | Death | RVEDd/LVEDd > 0.9 → higher mortality (9% vs. 5% for no TnI leak, 38% vs. 23% for TnI >0.1 ng/mL) | Age, sex, hypotension |

*AF*, Atrial fibrillation; *CAD*, coronary artery disease; *COPD*, chronic obstructive pulmonary disease; *DM*, diabetes mellitus; *DT*, deceleration time; *GFR*, glomerular filtration rate; *HF*, heart failure; *HR*, hazard ratio; *HTN*, hypertension; *LVAD*, left ventricular assist device; *LVEDd*, left ventricular internal diastolic dimension; *LVEF*, left ventricular ejection fraction; *LVSD*, left ventricular systolic dysfunction; *MI*, myocardial infarction; *MR*, mitral regurgitation; *NYHA*, New York Heart Association; *OHT*, orthotopic heart transplant; *PAH*, pulmonary arterial hypertension; *PE*, pericardial effusion; *PH*, pulmonary hypertension; *RV FAC*, right ventricular fractional area change; *RVEDd*, right ventricular diastolic dimension; *TAPSE*, tricuspid annular plane systolic excursion; *TnI*, troponin I; *VC*, vena contracta; *WHO*, World Health Organization.

RV systolic function correlates with prognosis across a wide spectrum of pathology.

### CLINICAL APPLICATION

Although the foregoing data form a solid basis for further investigation, they are primarily observational. It remains unclear how to incorporate RV systolic dysfunction into practical clinical decision making beyond awareness of its negative prognostic implication, and generally heightened clinical concern and attention in its presence.

Prospective randomized trials evaluating indices of RV function as the basis for allocation of therapeutic interventions (similar to those exploring LV EF as the basis for therapies such as defibrillators, medications for treatment of systolic heart failure, valve replacement, and coronary revascularization) are not yet available. Such prospective trials are needed before guidelines can be created on the use of parameters such as TAPSE and RV fractional area change in clinical decision making.

## Research Applications

### THREE-DIMENSIONAL ECHOCARDIOGRAPHY

The strengths of 3D echocardiography are particularly suited to the assessment of the RV. Interested readers should consult Chapter 4 for a detailed review of 3D echocardiography in general, and a review by Horton and colleagues[58] for a discussion of its use in the assessment of the RV.

The principal advantage of 3D echocardiography is the ability to define the entire RV endocardial surface without geometric assumptions, which results in less underestimation of RV volumes and superior correlation with MRI as compared to 2D methods.[17,59] Although MRI has become the de facto standard for measurement of RV volumes, 3D echocardiography has shown comparable performance in vitro,[60-62] and 3D echocardiographic RV volumes and EF correlate closely with MRI-derived values in healthy individuals, pulmonary hypertension, congenital heart disease, and ischemic heart disease.[52,63-68] A recent metaanalysis of 23 small (n = 12-88) studies of healthy and diseased subjects confirmed that 3D echocardiography modestly underestimates RV end-diastolic volume compared to MRI, with greater underestimation of volumes in larger RVs[69] (Fig. 32-13).

Offline analysis remains relatively time consuming, but semiautomated border detection and other algorithms such as knowledge-based reconstruction (which allows generation of an endocardial surface based on a small number of user-identified points rather than fully traced endocardial borders) may speed the process.[70]

Normative data for 3D-derived RV volumes and EF are from relatively small studies with heterogeneous methods; however, upper reference limits of 89 and 45 mL/m$^2$ for RV end-diastolic and end-systolic volumes and a lower reference limit of 44% for RV EF are suggested by the ASE, based on pooled data.[7] 3D echocardiography appears reasonable for serial assessment of RV volumes within an individual patient (i.e., to assess for disease progression or response to treatment) but is not currently recommended by the ASE for routine assessment.

### ALTERNATE MEASURES OF RIGHT VENTRICULAR SYSTOLIC FUNCTION

Several other parameters of RV systolic function have been described but are as yet less suitable for clinical use because of limited normative data and/or practical limitations in acquisition.

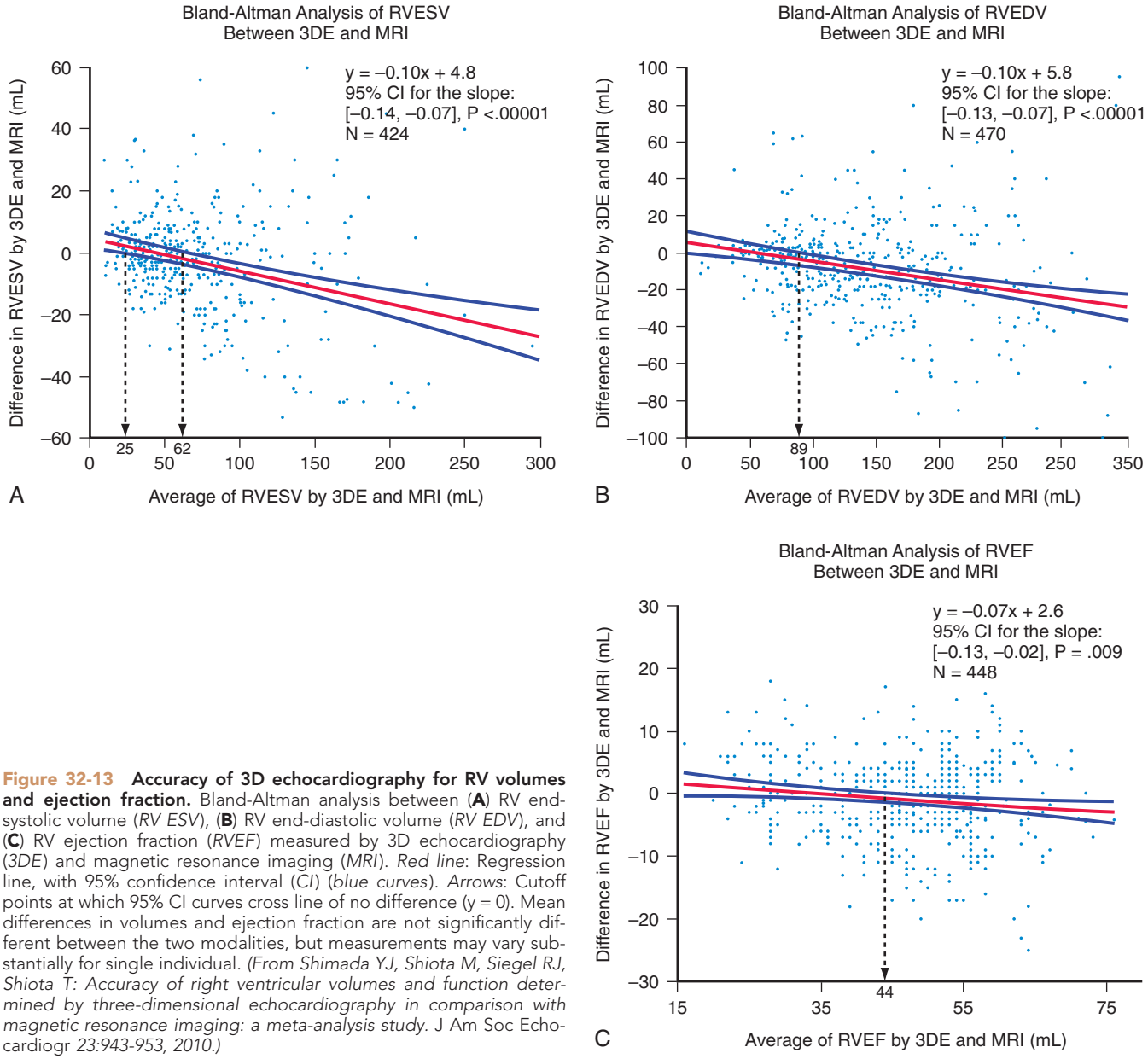



**Figure 32-13 Accuracy of 3D echocardiography for RV volumes and ejection fraction.** Bland-Altman analysis between (**A**) RV end-systolic volume (*RV ESV*), (**B**) RV end-diastolic volume (*RV EDV*), and (**C**) RV ejection fraction (*RVEF*) measured by 3D echocardiography (*3DE*) and magnetic resonance imaging (*MRI*). *Red line*: Regression line, with 95% confidence interval (*CI*) (*blue curves*). *Arrows*: Cutoff points at which 95% CI curves cross line of no difference (y = 0). Mean differences in volumes and ejection fraction are not significantly different between the two modalities, but measurements may vary substantially for single individual. *(From Shimada YJ, Shiota M, Siegel RJ, Shiota T: Accuracy of right ventricular volumes and function determined by three-dimensional echocardiography in comparison with magnetic resonance imaging: a meta-analysis study.* J Am Soc Echocardiogr *23:943-953, 2010.)*

### *dP/dt*

As RV contractility declines, the peak rate of pressure rise (*dP/dt*) decreases and can be estimated noninvasively by combining the simplified Bernoulli equation with measurements from the CW Doppler signal of TR. Because pressures are lower in the pulmonary vasculature, the time interval (*dt*) is measured between lower velocities than in the left heart, typically 1 to 2 m/s (*dP* = 12 mm Hg). Although *dP/dt* is free of geometric assumptions, it does require a complete TR spectral Doppler envelope and parallel alignment with the regurgitant jet. Normative data are very few, although the ASE suggests 400 mm Hg/s as a lower limit of normal. Indexing *dP/dt* to the peak RV systolic pressure theoretically reduces dependence on angle and preload.[71]

### *Strain and Strain Rate*

Myocardial strain (percent change in length) and strain rate (temporal derivative of strain) can be measured using tissue Doppler. Longitudinal strain and strain rate of the RV free wall have been shown to correlate with myocardial contractility[72] and with clinical events in PH.[73] However, acquisition is technically challenging, because the thin RV free wall yields a poor signal-to-noise ratio, and angle dependence may require medial displacement of the transducer from the cardiac apex to bring the ultrasound beam parallel to the RV free wall. Studies with normative values are relatively few and small, insufficient to give clinically useful reference ranges. 2D strain imaging using speckle tracking is a promising modality that allows assessment of strain and strain rate in multiple segments from a single clip

and partially overcomes the issue of angle dependence. However, normative data from this modality are even fewer than for one-dimensional strain. In general, systolic strain in the midwall of the RV is higher than either the basal or apical segments, and the RV demonstrates higher strain and strain rates compared to the LV[74].

### *Isovolumic Acceleration*

Isovolumic acceleration is defined as peak myocardial velocity during isovolumic contraction divided by the time from onset of contraction to peak velocity. This index is measured using tissue Doppler of the tricuspid annulus and may be less load dependent than other indices.[75] A lower reference limit of 2.2 m/s$^2$ based on pooled data is proposed by the ASE,[7] but limited data result in a wide 95% confidence interval (1.4 to 3.0), limiting its clinical utility.

## RIGHT VENTRICULAR DIASTOLIC FUNCTION

RV diastolic dysfunction, like RV systolic function, is associated with many clinical conditions, both "right-sided" (e.g., pulmonary hypertension, pulmonary embolism, right coronary ischemia) and systemic (left heart failure, heart transplantation, left-sided valve disease). There is not yet an established benefit to routine assessment of RV diastolic function; however, RV diastolic parameters may be useful adjuncts in assessment of right-sided filling pressures, or in identifying early disease when right-sided pathology is strongly suspected but RV size and systolic function appear normal.

Characterization of RV diastolic function is conceptually analogous to LV diastolic function. E/A and E/E′ are calculated from tricuspid inflow at the leaflet tips and tricuspid annular tissue Doppler. Ancillary measures are also similar, with hepatic vein diastolic flow predominance and RA dilation suggesting diastolic dysfunction. A reasonable clinical rubric for grading diastolic function is outlined in Table 32-5 and is largely in keeping with ASE guidelines. Tricuspid Doppler measurements should be taken from the apical four-chamber view during held end-expiration to avoid beat-to-beat variation in RV preload.

A few small studies suggest that E/E′ may be a promising measure of RAP. In two studies, E/E′ correlated well with RAP ($r \approx 0.8$).[76,77] Although E/E′ greater than 4 predicted RAP greater than 10 mm Hg with sensitivity and specificity of 88% and 85% in one study,[76] a cutoff of E/E′ greater than 8 was required to achieve similar test performance in patients after cardiac transplant.[77] Correlation of E/E′ with RAP may be better when RV systolic function is abnormal and worse early after cardiac surgery[76]. Diastolic parameters may also be confounded by TR (which may increase E velocity or blunt hepatic vein systolic flow) and tachycardia (which may decrease E/A by shortening diastole, or may cause E-A fusion).

**TABLE 32-5 Reference Values for Parameters of RV Diastolic Function[7]**

| *Parameter* | *Normal* | *Impaired Relaxation (Grade 1)* | *Pseudonormal (Grade 2)* | *Restrictive (Grade 3)* |
|---|---|---|---|---|
| *Trans-tricuspid E/A | 0.8-2.1 | <0.8 | 0.8-2.1 | >2.1 |
| *Tricuspid E/E′ | <6 | <6 | >6 | >6 |
| *RA size | Normal | Normal or dilated | Dilated | Dilated |
| Hepatic vein flow | Systolic-predominant | | Diastolic-predominant | Diastolic-predominant |
| Other parameters | | | | DT < 120 ms<br>Premature (late diastolic) PV opening |

*A*, Atrial contraction transtricuspid peak flow velocity; *DT*, deceleration time of the tricuspid valve; *E*, early diastolic transtricuspid peak flow velocity; *E′*, early diastolic tricuspid annulus velocity; *PV*, pulmonic valve.
*Recommended for clinical use by the 2010 ASE guideline statement.

## Potential Limitations and Future Directions

Although the pooled normative data published in the 2010 ASE guideline statement represent a significant step forward in our understanding of the right heart, several important limitations should be noted. None of the reported values are indexed to body size, and care must be taken when applying published values to large- or small-statured patients. Normative data on RV size and function are heterogeneous because of pooling (individual studies with average n = 20 to 50). Stratification of RV size and systolic function beyond normal and abnormal (e.g., mild, moderate, or severe) remains largely subjective. As discussed previously, prospective trials examining the benefit of using parameters of RV size and function to guide clinical decisions are lacking.

Future studies should address these limitations. Larger studies from a single center, or multiple centers with well-defined protocols for acquisition, should verify both raw and body-size-indexed normative values. Observational data suggesting worsened prognosis in the setting of RV systolic function should be extended with prospective trials examining treatment effect on populations selected using parameters of RV size and function.

3D echocardiography faces challenges similar to those faced by 2D echocardiography as described earlier. Although the superiority of 3D echocardiography in measurement of RV volumes and EF compared to 2D echocardiography is well established, 3D echocardiography is unlikely to be used routinely for assessment of the RV until a direct impact on clinical management is demonstrated.

## Alternate Approaches

MRI, computed tomography, and nuclear techniques have been applied to assessment of RV size and function. MRI has emerged as the de facto gold standard for right heart assessment. It has several advantages compared to echocardiography in assessment of the RV. MRI delineates the entire RV without geometric assumptions, is minimally affected by tissue and air interference, and has much higher myocardial-endocardial contrast, usually resulting in superior image quality (Fig. 32-14; compare to Fig. 32-9). Endocardial borders must still be generated through manual tracing, automated detection, or other methods. Like 3D echocardiography, MRI remains limited to a relatively few centers. It is not portable, may be limited by patient claustrophobia and the need to exclude metal from the imaging area, and cannot be used in patients with advanced renal failure because of the risk of nephrogenic systemic fibrosis. MRI can evaluate blood flow and calculate stroke volumes and cardiac output, but echocardiography and Doppler remain superior for evaluation of valve disease.

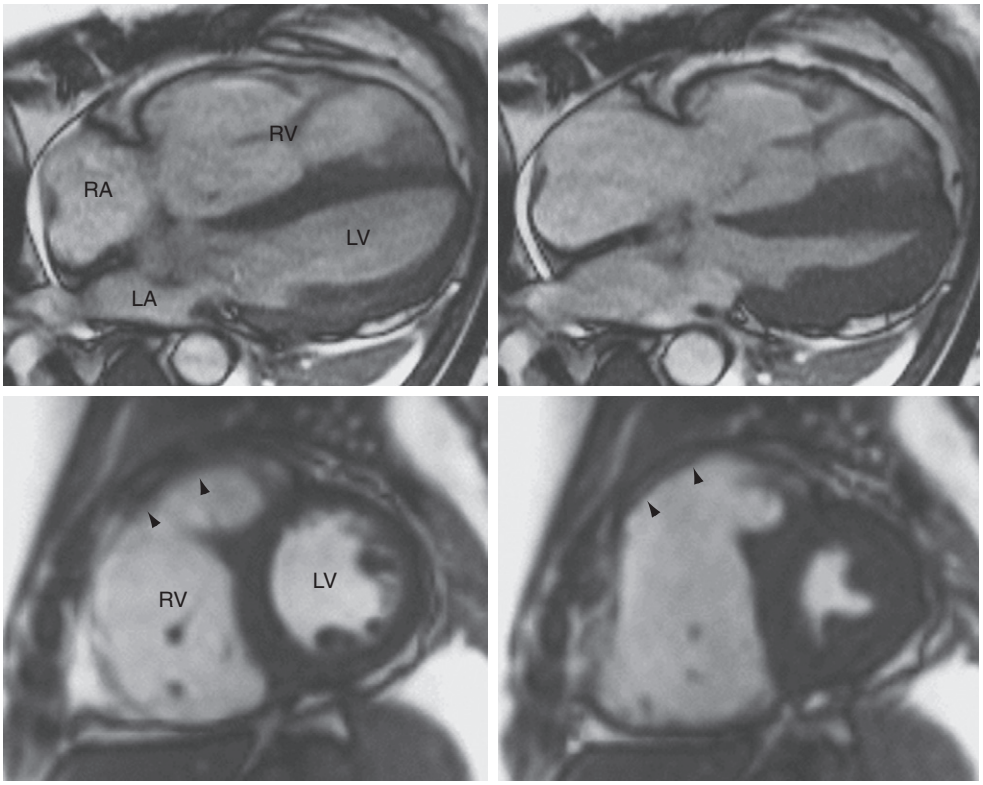



**Figure 32-14 Cardiac magnetic resonance imaging of heart affected by arrhythmogenic RV cardiomyopathy.** Global RV dysfunction is evident, as well as small dyskinetic aneurysm near RV outflow tract (*arrowheads*). *Top left*: Horizontal long-axis, end-diastole. *Top right*: Horizontal long-axis, end-systole. *Bottom left*: Short-axis, end-diastole. *Bottom right*: Short-axis, end-systole.

Cardiac computed tomography shares several of the strengths of MRI, including true 3D analysis independent of geometric assumptions and excellent myocardial-endocardial contrast, but radiation and potentially nephrotoxic contrast exposure have rendered it unpopular relative to MRI.

Nuclear imaging techniques with blood-pool imaging (e.g., first-pass or equilibrium radionuclide angiography) also measure RV EF without geometric assumptions. Correlation with correlation with MRI-derived RV EF is favorable,[78] but because nuclear imaging provides little other information about the right heart and requires radiation exposure, it is rarely used as a first-line modality for right heart assessment.

## ACKNOWLEDGMENTS

*The author acknowledges Paul R. Forfia, MD, and Susan E. Wiegers, MD, the authors of this chapter in* The Practice of Clinical Echocardiography, third edition.

## KEY POINTS

- Complex RV geometry mandates assessment of size and function from multiple echocardiographic views.
- 2D echocardiography remains the dominant clinical modality for assessment of RV size and function because of its widespread availability, but it does not yield accurate RV volumes or RV EF.
- "Standard" 2D transthoracic echocardiography views may not optimally demonstrate the right heart. Dedicated views of the RV (e.g., apical four-chamber view angled to bring the RV free wall and lateral tricuspid annulus toward the center of the field) should be used as needed.
- Normal reference values for recommended parameters of RV size (95th percentile upper limit) include basal minor dimension less than 42 mm, proximal RVOT diameter less than 33 mm (from the parasternal long-axis view), and distal RVOT diameter less than 27 mm (parasternal short-axis). If the LV is normal-sized, RV area greater than two-thirds LV area in the apical four-chamber view suggests RV enlargement.
- Normal reference values for recommended parameters of RV systolic function (95th percentile limit) include TAPSE greater than 16 mm, fractional area change greater than 35%, peak tricuspid annular velocity (S′) greater than 10 cm/s, and pulsed-Doppler right ventricular myocardial performance index (RV MPI) less than 0.40.

## KEY POINTS—cont'd

- TAPSE and fractional area change appear to correlate with clinical status in broad range of cardiovascular diseases. TAPSE is gaining clinical popularity because of its reproducibility and ease of acquisition and measurement. We recommend combining TAPSE with visual assessment when reporting RV systolic function. Prior cardiac surgery and LV dysfunction may reduce TAPSE independently of RV dysfunction. If TAPSE and visual assessment are discordant, other parameters (fractional area change, S′, RV PMI) help resolve the ambiguity.
- PASP is calculated by the peak velocity of the TR jet with the formula PASP = $4v_{TR}^2$ + RAP. The RAP is calculated by the degree of collapse of the IVC with inspiration or sniff. The diastolic pressure can be calculated from the pulmonary regurgitant jet velocity.
- 3D methods for assessment of RV size and function have shown promising results, but clinical use remains restricted by availability and limited normative and outcome data. MRI and 3D echocardiography show comparable performance for measurement of RV volumes and EF.

## REFERENCES


1. Markiewicz W, Sechtem U, Higgins CB: Evaluation of the right ventricle by magnetic resonance imaging. *Am Heart J* 113:8-15, 1987.
2. Santamore WP, Dell'Italia LJ: Ventricular interdependence: significant left ventricular contributions to right ventricular systolic function. *Prog Cardiovasc Dis* 40:289-308, 1998.
3. Bakos A: The question of the function of the right ventricular myocardium: an experimental study. *Fed Proc* 7:724-732, 1948.
4. Hess DS, Bache RJ: Transmural right ventricular myocardial blood flow during systole in the awake dog. *Circ Res* 45:88-94, 1979.
5. Lowensohn HS, Khouri EM, Gregg DE, et al: Phasic right coronary artery blood flow in conscious dogs with normal and elevated right ventricular pressures. *Circ Res* 39:760-766, 1976.
6. Forman MB, Wilson BH, Sheller JR, et al: Right ventricular hypertrophy is an important determinant of right ventricular infarction complicating acute inferior left ventricular infarction. *J Am Coll Cardiol* 10:1180-1187, 1987.
7. Rudski LG, Lai WW, Afilalo J, et al: Guidelines for the echocardiographic assessment of the right heart in adults: a report from the American Society of Echocardiography endorsed by the European Association of Echocardiography, a registered branch of the European Society of Cardiology, and the Canadian Society of Echocardiography. *J Am Soc Echocardiogr* 23:685-713; quiz 786-688, 2010.
8. Dell'Italia LJ, Santamore WP: Can indices of left ventricular function be applied to the right ventricle? *Prog Cardiovasc Dis* 40:309-324, 1998.
9. Maughan WL, Shoukas AA, Sagawa K, Weisfeldt ML: Instantaneous pressure-volume relationship of the canine right ventricle. *Circ Res* 44:309-315, 1979.
10. Geva T, Powell AJ, Crawford EC, et al: Evaluation of regional differences in right ventricular systolic function by acoustic quantification echocardiography and cine magnetic resonance imaging. *Circulation* 98:339-345, 1998.
11. Rushmer RF, Crystal DK, Wagner C: The functional anatomy of ventricular contraction. *Circ Res* 1:162-170, 1953.
12. Kaul S, Tei C, Hopkins JM, Shah PM: Assessment of right ventricular function using two-dimensional echocardiography. *Am Heart J* 107:526-531, 1984.
13. Leather HA, Ama R, Missant C, et al: Longitudinal but not circumferential deformation reflects global contractile function in the right ventricle with open pericardium. *Am J Physiol Heart Circ Physiol* 290:H2369-H2375, 2006.
14. Sanchez-Quintana D, Anderson RH, Ho SY: Ventricular myoarchitecture in tetralogy of Fallot. *Heart* 76:280-286, 1996.
15. Kind T, Mauritz GJ, Marcus JT, et al: Right ventricular ejection fraction is better reflected by transverse rather than longitudinal wall motion in pulmonary hypertension. *J Cardiovasc Magn Reson* 12:35, 2010.
16. Jiang L, Levine RA, Weyman AE: Echocardiographic assessment of right ventricular volume and function. *Echocardiography* 14:189-206, 1997.
17. Kjaergaard J, Petersen CL, Kjaer A, et al: Evaluation of right ventricular volume and function by 2D and 3D echocardiography compared to MRI. *Eur J Echocardiogr* 7:430-438, 2006.
18. Baker BJ, Scovil JA, Kane JJ, Murphy ML: Echocardiographic detection of right ventricular hypertrophy. *Am Heart J* 105:611-614, 1983.
19. Cacho A, Prakash R, Sarma R, Kaushik VS: Usefulness of two-dimensional echocardiography in diagnosing right ventricular hypertrophy. *Chest* 84:154-157, 1983.
20. Maciel BC, Simpson IA, Valdes-Cruz LM, et al: Color flow Doppler mapping studies of "physiologic" pulmonary and tricuspid regurgitation: evidence for true regurgitation as opposed to a valve closing volume. *J Am Soc Echocardiogr* 4:589-597, 1991.
21. Bauman W, Wann LS, Childress R, et al: Mid systolic notching of the pulmonary valve in the absence of pulmonary hypertension. *Am J Cardiol* 43:1049-1052, 1979.
22. Gardin JM, Burn CS, Childs WJ, Henry WL: Evaluation of blood flow velocity in the ascending aorta and main pulmonary artery of normal subjects by Doppler echocardiography. *Am Heart J* 107:310-319, 1984.
23. Kircher BJ, Himelman RB, Schiller NB: Noninvasive estimation of right atrial pressure from the inspiratory collapse of the inferior vena cava. *Am J Cardiol* 66:493-496, 1990.
24. Marangoni S, Vitacca M, Quadri A, et al: Noninvasive haemodynamic effects of two nasal positive pressure ventilation modalities in stable chronic obstructive lung disease patients. *Respiration* 64:138-144, 1997.
25. Yock PG, Popp RL: Noninvasive estimation of right ventricular systolic pressure by Doppler ultrasound in patients with tricuspid regurgitation. *Circulation* 70:657-662, 1984.
26. Berger M, Haimowitz A, Van Tosh A, et al: Quantitative assessment of pulmonary hypertension in patients with tricuspid regurgitation using continuous wave Doppler ultrasound. *J Am Coll Cardiol* 6:359-365, 1985.
27. Chan KL, Currie PJ, Seward JB, et al: Comparison of three Doppler ultrasound methods in the prediction of pulmonary artery pressure. *J Am Coll Cardiol* 9:549-554, 1987.
28. Currie PJ, Seward JB, Chan KL, et al: Continuous wave Doppler determination of right ventricular pressure: a simultaneous Doppler-catheterization study in 127 patients. *J Am Coll Cardiol* 6:750-756, 1985.
29. Stevenson JG: Comparison of several noninvasive methods for estimation of pulmonary artery pressure. *J Am Soc Echocardiogr* 2:157-171, 1989.
30. Masuyama T, Kodama K, Kitabatake A, et al: Continuous-wave Doppler echocardiographic detection of pulmonary regurgitation and its application to noninvasive estimation of pulmonary artery pressure. *Circulation* 74:484-492, 1986.
31. Hammarstrom E, Wranne B, Pinto FJ, et al: Tricuspid annular motion. *J Am Soc Echocardiogr* 4:131-139, 1991.
32. Forfia PR, Fisher MR, Mathai SC, et al: Tricuspid annular displacement predicts survival in pulmonary hypertension. *Am J Respir Crit Care Med* 174:1034-1041, 2006.
33. Ghio S, Recusani F, Klersy C, et al: Prognostic usefulness of the tricuspid annular plane systolic excursion in patients with congestive heart failure secondary to idiopathic or ischemic dilated cardiomyopathy. *Am J Cardiol* 85:837-842, 2000.
34. Hsiao SH, Lin SK, Wang WC, et al: Severe tricuspid regurgitation shows significant impact in the relationship among peak systolic tricuspid annular velocity, tricuspid annular plane systolic excursion, and right ventricular ejection fraction. *J Am Soc Echocardiogr* 19:902-910, 2006.
35. Lopez-Candales A, Rajagopalan N, et al: Right ventricular systolic function is not the sole determinant of tricuspid annular motion. *Am J Cardiol* 98:973-977, 2006.
36. Tamborini G, Muratori M, Brusoni D, et al: Is right ventricular systolic function reduced after cardiac surgery? A two- and three-dimensional echocardiographic study. *Eur J Echocardiogr* 10:630-634, 2009.
37. Doutreleau S, Talha S, Di Marco P, et al: Does tricuspid annular plane systolic excursion (TAPSE) or systolic velocity (Sm) allow an easier determination of right ventricular function after heart transplantation? *J Heart Lung Transplant* 26:302-303, 2007.
38. Anavekar NS, Gerson D, Skali H, et al: Two-dimensional assessment of right ventricular

function: an echocardiographic-MRI correlative study. *Echocardiography* 24:452-456, 2007.
39. Kukulski T, Hubbert L, Arnold M, et al: Normal regional right ventricular function and its change with age: a Doppler myocardial imaging study. *J Am Soc Echocardiogr* 13:194-204, 2000.
40. Morhy SS, Andrade JL, Soares AM, et al: Noninvasive assessment of right ventricular function in the late follow-up of the Senning procedure. *Cardiol Young* 15:154-159, 2005.
41. Norozi K, Buchhorn R, Alpers V, et al: Relation of systemic ventricular function quantified by myocardial performance index (Tei) to cardiopulmonary exercise capacity in adults after Mustard procedure for transposition of the great arteries. *Am J Cardiol* 96:1721-1725, 2005.
42. Salehian O, Schwerzmann M, Merchant N, et al: Assessment of systemic right ventricular function in patients with transposition of the great arteries using the myocardial performance index: comparison with cardiac magnetic resonance imaging. *Circulation* 110:3229-3233, 2004.
43. Kim WH, Otsuji Y, Yuasa T, et al: Evaluation of right ventricular dysfunction in patients with cardiac amyloidosis using Tei index. *J Am Soc Echocardiogr* 17:45-49, 2004.
44. Abdel Rahman MY, Abdul-Khaliq H, Vogel M, et al: Value of the new Doppler-derived myocardial performance index for the evaluation of right and left ventricular function following repair of tetralogy of Fallot. *Pediatr Cardiol* 23:502-507, 2002.
45. Lang RM, Bierig M, Devereux RB, et al: Recommendations for chamber quantification: a report from the American Society of Echocardiography's Guidelines and Standards Committee and the Chamber Quantification Writing Group, developed in conjunction with the European Association of Echocardiography, a branch of the European Society of Cardiology. *J Am Soc Echocardiogr* 18:1440-1463, 2005.
46. Foale R, Nihoyannopoulos P, McKenna W, et al: Echocardiographic measurement of the normal adult right ventricle. *Br Heart J* 56:33-44, 1986.
47. Schnittger I, Gordon EP, Fitzgerald PJ, Popp RL: Standardized intracardiac measurements of two-dimensional echocardiography. *J Am Coll Cardiol* 2:934-938, 1983.
48. Bayram NA, Ciftci B, Bayram H, et al: Effects of continuous positive airway pressure therapy on right ventricular function assessment by tissue Doppler imaging in patients with obstructive sleep apnea syndrome. *Echocardiography* 25: 1071-1078, 2008.
49. Romero-Corral A, Somers VK, Pellikka PA, et al: Decreased right and left ventricular myocardial performance in obstructive sleep apnea. *Chest* 132:1863-1870, 2007.
50. Tugcu A, Guzel D, Yildirimturk O, Aytekin S: Evaluation of right ventricular systolic and diastolic function in patients with newly diagnosed obstructive sleep apnea syndrome without hypertension. *Cardiology* 113:184-192, 2009.
51. Anavekar NS, Skali H, Bourgoun M, et al: Usefulness of right ventricular fractional area change to predict death, heart failure, and stroke following myocardial infarction (from the VALIANT ECHO Study). *Am J Cardiol* 101:607-612, 2008.
52. Dini FL, Fontanive P, Panicucci E, et al: Prognostic significance of tricuspid annular motion and plasma NT-proBNP in patients with heart failure and moderate-to-severe functional mitral regurgitation. *Eur J Heart Fail* 10:573-580, 2008.
53. Puwanant S, Hamilton KK, Klodell CT, et al: Tricuspid annular motion as a predictor of severe right ventricular failure after left ventricular assist device implantation. *J Heart Lung Transplant* 27:1102-1107, 2008.
54. Samad BA, Alam M, Jensen-Urstad K: Prognostic impact of right ventricular involvement as assessed by tricuspid annular motion in patients with acute myocardial infarction. *Am J Cardiol* 90:778-781, 2002.
55. Scridon T, Scridon C, Skali H, et al: Prognostic significance of troponin elevation and right ventricular enlargement in acute pulmonary embolism. *Am J Cardiol* 96:303-305, 2005.
56. Skali H, Zornoff LA, Pfeffer MA, et al: Prognostic use of echocardiography 1 year after a myocardial infarction. *Am Heart J* 150:743-749, 2005.
57. Zornoff LA, Skali H, Pfeffer MA, et al: Right ventricular dysfunction and risk of heart failure and mortality after myocardial infarction. *J Am Coll Cardiol* 39:1450-1455, 2002.
58. Horton KD, Meece RW, Hill JC: Assessment of the right ventricle by echocardiography: a primer for cardiac sonographers. *J Am Soc Echocardiogr* 22:776-792, 2009; quiz 861-772.
59. Jenkins C, Chan J, Bricknell K, et al: Reproducibility of right ventricular volumes and ejection fraction using real-time three-dimensional echocardiography: comparison with cardiac MRI. *Chest* 131:1844-1851, 2007.
60. Schindera ST, Mehwald PS, Sahn DJ, Kececioglu D: Accuracy of real-time three-dimensional echocardiography for quantifying right ventricular volume: static and pulsatile flow studies in an anatomic in vitro model. *J Ultrasound Med* 21:1069-1075, 2002.
61. Sheehan FH, Bolson EL: Measurement of right ventricular volume from biplane contrast ventriculograms: validation by cast and three-dimensional echo. *Catheter Cardiovasc Interv* 62:46-51, 2004.
62. Shiota T, Jones M, Chikada M, et al: Real-time three-dimensional echocardiography for determining right ventricular stroke volume in an animal model of chronic right ventricular volume overload. *Circulation* 97:1897-1900, 1998.
63. Grewal J, Majdalany D, Syed I, et al: Three-dimensional echocardiographic assessment of right ventricular volume and function in adult patients with congenital heart disease: comparison with magnetic resonance imaging. *J Am Soc Echocardiogr* 23:127-133, 2010.
64. Leibundgut G, Rohner A, Grize L, et al: Dynamic assessment of right ventricular volumes and function by real-time three-dimensional echocardiography: a comparison study with magnetic resonance imaging in 100 adult patients. *J Am Soc Echocardiogr* 23:116-126, 2010.
65. Nesser HJ, Tkalec W, Patel AR, et al: Quantitation of right ventricular volumes and ejection fraction by three-dimensional echocardiography in patients: comparison with magnetic resonance imaging and radionuclide ventriculography. *Echocardiography* 23:666-680, 2006.
66. van der Zwaan HB, Helbing WA, McGhie JS, et al: Clinical value of real-time three-dimensional echocardiography for right ventricular quantification in congenital heart disease: validation with cardiac magnetic resonance imaging. *J Am Soc Echocardiogr* 23:134-140, 2010.
67. Gopal AS, Chukwu EO, Iwuchukwu CJ, et al: Normal values of right ventricular size and function by real-time 3-dimensional echocardiography: comparison with cardiac magnetic resonance imaging. *J Am Soc Echocardiogr* 20:445-455, 2007.
68. Grapsa J, O'Regan DP, Pavlopoulos H, et al: Right ventricular remodelling in pulmonary arterial hypertension with three-dimensional echocardiography: comparison with cardiac magnetic resonance imaging. *Eur J Echocardiogr* 11:64-73, 2010.
69. Shimada YJ, Shiota M, Siegel RJ, Shiota T: Accuracy of right ventricular volumes and function determined by three-dimensional echocardiography in comparison with magnetic resonance imaging: a meta-analysis study. *J Am Soc Echocardiogr* 23:943-953, 2010.
70. Sheehan FH, Kilner PJ, Sahn DJ, et al: Accuracy of knowledge-based reconstruction for measurement of right ventricular volume and function in patients with tetralogy of Fallot. *Am J Cardiol* 105:993-999, 2010.
71. Kanzaki H, Nakatani S, Kawada T, et al: Right ventricular $dP/dt/P$(max), not $dP/dt$(max), noninvasively derived from tricuspid regurgitation velocity is a useful index of right ventricular contractility. *J Am Soc Echocardiogr* 15:136-142, 2002.
72. Jamal F, Bergerot C, Argaud L, et al: Longitudinal strain quantitates regional right ventricular contractile function. *Am J Physiol Heart Circ Physiol* 285:H2842-H2847, 2003.
73. Sachdev A, Villarraga HR, Frantz RP, et al: Right ventricular strain for prediction of survival in pulmonary arterial hypertension. *Chest* 139:1299-1309, 2011.
74. Weidemann F, Eyskens B, Jamal F, et al: Quantification of regional left and right ventricular radial and longitudinal function in healthy children using ultrasound-based strain rate and strain imaging. *J Am Soc Echocardiogr* 15:20-28, 2002.
75. Kjaergaard J, Snyder EM, Hassager C, et al: Impact of preload and afterload on global and regional right ventricular function and pressure: a quantitative echocardiography study. *J Am Soc Echocardiogr* 19:515-521, 2006.
76. Sade LE, Gulmez O, Eroglu S, et al: Noninvasive estimation of right ventricular filling pressure by ratio of early tricuspid inflow to annular diastolic velocity in patients with and without recent cardiac surgery. *J Am Soc Echocardiogr* 20:982-988, 2007.
77. Sundereswaran L, Nagueh SF, Vardan S, et al: Estimation of left and right ventricular filling pressures after heart transplantation by tissue Doppler imaging. *Am J Cardiol* 82:352-357, 1998.
78. Hornung TS, Anagnostopoulos C, Bhardwaj P, et al: Comparison of equilibrium radionuclide ventriculography with cardiovascular magnetic resonance for assessing the systemic right ventricle after Mustard or Senning procedures for complete transposition of the great arteries. *Am J Cardiol* 92:640-643, 2003.

# 33 Echocardiographic Evaluation of the Patient with Pulmonary Hypertension

PAUL ROBERT FORFIA, MD | SUSAN E. WIEGERS, MD

**Pulmonary Artery Pressure and Right Ventricular Afterload**
**Right Ventricular-Pulmonary Vascular Interaction**
**Pulmonary Vascular Disease**
Pulmonary Arterial Hypertension
Acute Pulmonary Embolism
Chronic Pulmonary Embolism
Pulmonary Venous Disease
**Pulmonary Hypertension as a Result of Chronic Respiratory Disease**
**Lung Transplantation**
**Pulmonary Hypertension without Pulmonary Vascular Disease**
Pulmonary Hypertension Related to Increased Cardiac Output
Systemic to Pulmonary Venous Shunts
**Pulmonary Hypertension Related to Left Heart Disease (Pulmonary Venous Hypertension)**
Differentiating Pulmonary Vascular (Arterial) from Pulmonary Venous Hypertension
Exercise Echocardiography

Pulmonary hypertension (PH) is defined as a mean pulmonary artery pressure (mPAP) of more than 25 mm Hg, which typically coincides with a pulmonary artery (PA) systolic pressure (PASP) of more than 40 mm Hg.[1,2] An increased mPAP is the hemodynamic consequence of perturbations in pulmonary blood flow (cardiac output [CO]), pulmonary vascular resistance (PVR), and left atrium (LA) pressure, as expressed in the following equation:

$$\text{mPAP} = \text{CO} \times \text{PVR} + \text{LA pressure}$$

where mPAP and LA pressure are measured in mm Hg, cardiac output in L/min, and PVR in mm Hg/L/min. Clinically PVR usually is expressed in Wood units, with a normal PVR less than 1.6 Wood units.

Many clinical diagnoses can cause or contribute to PH, including left heart disease with pulmonary venous hypertension (PVH; World Health Organization [WHO] group II), chronic respiratory conditions typically associated with hypoxia (WHO group III), chronic thromboembolic PH (CTEPH; WHO group IV), and miscellaneous/multifactorial causes (WHO group V). In addition, PH may arise from severe pulmonary vasculopathy in the absence of chronic left heart disease, respiratory disease, or prior pulmonary emboli, which is referred to as pulmonary arterial hypertension (PAH; WHO group I).[3] Given the highly diverse nature of PH, careful clinical and hemodynamic distinctions need to be made for the appropriate PH diagnosis. This is particularly true with discerning PAH from PVH because PH-specific therapy (i.e., prostacyclin analogues, endothelin receptor antagonists) intended for patients with PAH has either no effect or worsens the condition of a patient with left heart disease (Box 33-1).

The echocardiographic examination is central to the initial diagnosis of PH, and the serial assessment of PH. Fundamental to the diagnostic assessment is a variety of Doppler imaging–based pulmonary pressure estimations, as outlined in Chapter 32. However, many other ways exist to diagnose, infer, and assess PH and its hemodynamic causes aside from Doppler pressure estimation. Overreliance or exclusive focus on the Doppler pressure estimates and a failure to integrate other salient two-dimensional (2D) and Doppler findings into the overall echocardiographic interpretation greatly increase the risk of false-positive and false-negative diagnoses of PH. Conversely, a more integrated and pathophysiologic approach to the assessment not only enhances the diagnostic accuracy of PH but also allows for a much greater degree of pathophysiologic insight into an individual patient's PH.

## Pulmonary Artery Pressure and Right Ventricular Afterload

The level of pressure elevation does not correlate well with functional limitations or prognosis in PAH.[4] Similarly, right ventricular (RV) size, septal position, and RV systolic function vary widely at the same level of mean PAP, depending on the specific hemodynamic cause.[5] These observations relate to the fact that PAP is a relatively poor and incomplete measure of RV afterload. Afterload is the force that opposes RV ejection, and thus pulmonary blood flow, and is most completely described by PA input impedance. Input impedance is a composite measure of afterload that includes vascular resistance (PVR = mPAP – LA pressure/pulmonary blood flow), large PA stiffness, and the effects of these two factors on the magnitude and timing of reflected arterial waves arriving at the RV during systole.[6]

Thus PH can be present with normal pulmonary vessels when there is a high flow state or an elevated LA pressure, even when the pulmonary vessels themselves are normal. Conversely, abnormal changes in the pulmonary vessels themselves, or pulmonary vascular disease (PVD), may be present with only modest elevations in pulmonary pressure. Increased RV afterload is present in PH associated with PVD and is comparatively

**Box 33-1**

**PULMONARY HYPERTENSION DEFINITIONS AND WHO GROUPS**

**Pulmonary hypertension (PH):** an elevated pulmonary artery pressure of any cause
- **Group I. Pulmonary arterial hypertension (PAH):** PH due to severe pulmonary vasculopathy in the absence of an identifiable underlying cause
- **Group II. Pulmonary venous hypertension (PVH):** PH due to left sided heart disease
- **Group III.** PH due to chronic lung disease with hypoxia
- **Group IV.** Chronic thromboembolic pulmonary hypertension (CTEPH)
- **Group V.** Miscellaneous and other causes

Other definitions:
- **PASP**, pulmonary artery systolic pressure
- **mPAP**, mean pulmonary artery pressure
- **PVD**, pulmonary vascular disease (abnormal pulmonary vessels)

low in PH without PVD. PVR accounts for approximately 80% of total afterload in most clinical circumstances.[6] Increased PAP does increase afterload indirectly via increased PA stiffening, but to a relatively small degree. For example, in a patient with a large atrial septal defect but normal PVR, the RV can eject 15 L of flow through the lung (Qp), despite severe PH, and maintain normal RV systolic function. In this same patient, however, if the PVR increases from 2 mm Hg/L/min to 8 mm Hg/L/min, the Qp falls dramatically and frank RV dysfunction manifests.

The distinction between PAP and RV afterload has considerable practical value in the context of an echocardiographic evaluation of a patient with known or suspected PH. RV afterload, not PAP, is what impairs RV function and leads to the stereotypical triad of RV enlargement, interventricular septal flattening, and RV systolic dysfunction in PH. With this in mind, the clinician should remain highly suspicious for PH related to PVD if RV dilation, dysfunction, and septal bowing are present, even if the Doppler image–estimated PASP is reported as normal. This point cannot be overemphasized. Fisher et al[7] reported that more than 80% of subjects with severe PH that was related to an increased PVR and with PASP that was significantly underestimated with Doppler imaging possessed at least one of three features of the RV dysfunction triad on 2D examination. Conversely, if a patient has PH without significant rise in afterload (i.e., normal PVR), as in cases of high output PH or PH related to LA hypertension, RV structure and function remain comparatively normal, with the conspicuous absence of the RV dysfunction triad. Therefore, one can think of the RV as bearing witness to what is occurring within the pulmonary circulation. For these reasons, we consider PH associated with PVD ($PH_{+PVD}$) separately from PH in the relative absence of PVD ($PH_{\varnothing PVD}$).

## Right Ventricular-Pulmonary Vascular Interaction

The RV and the pulmonary circulation function as a coupled unit. In health, a normal pulmonary vasculature couples to an appropriately thin-walled, distensible RV that generates large amounts of blood flow without a resulting high pressure. As PVD develops, the PVR increases and the large arteries stiffen. As a result, the (formerly appropriate) nonmuscular RV is typically incapable of completely matching or of coupling its contractile performance to its new afterload.[8,9] This relative RV-PA uncoupling leads to a stereotypical triad of changes that occur at the level of the RV, including RV systolic dysfunction, increased size and altered shape of the RV, and varying degrees of systolic and diastolic bowing of the interventricular septum (Fig. 33-1). This triad of changes forms the basis of the echocardiographic diagnosis of $PH_{+PVD}$. The degree to which these changes occur is contingent on the degree of RV-PA uncoupling. Thus, at a PVR of 5 Wood units, a patient with depressed RV contractility has far more uncoupling to the vascular load than a patient with an intrinsically normal RV coupled to the same afterload. As such, the RV dysfunction triad helps to adjudicate and assess the physiologic and clinical significance of any given degree of PVD. The greater the RV impairment, the greater the clinical and physiologic significance of the $PH_{+PVD}$, no matter what the noninvasive (or invasive) pressure may be.

The RV outflow tract (RVOT) is a key anatomic and physiologic interface between the RV and pulmonary vasculature (Fig. 33-2, *A*). The pulsed-wave Doppler RV outflow velocity curve provides a wealth of physiologic information about RV and pulmonary vascular function. As such, analysis of the Doppler velocity signal represents perhaps the single most important aspect of the echocardiographic examination in a patient with known or suspected PH.

Early work from Kitabatake and associates[10] showed that the time to peak velocity, or acceleration time (AcT), of the RV outflow velocity curve provides an estimate of mPAP (Fig. 33-2, *C*). An average AcT of 137 ± 24 ms was seen in subjects with a mean PA pressure of 19 mm Hg or less, whereas AcTs of 97 ± 20 ms and 65 ± 14 ms were seen in patients with a mPAP of 20 to 39 mm Hg and 40 mm Hg or more, respectively. This method is relatively easy to perform and highly reproducible; and unlike pressure estimates based on tricuspid regurgitation (TR) velocity, Doppler recordings from the RVOT are available in virtually all patients. The AcT can provide useful corroborative information that aids in the accuracy of PH diagnosis; for example, in the presence of borderline PH by TR jet velocity, an AcT of more than 100 ms suggests there is no PH, whereas an AcT of less than 70 ms greatly increases the likelihood of significant PH.

In addition to AcT measurement, visual inspection of the shape of the RV outflow velocity signal has also been be used to qualitatively differentiate varying levels of PH. Prior work has shown that a rounded velocity curve with no evidence of Doppler "notching" has been associated with normal PA pressures, and that patients with mild-moderate PH more often have a triangular, or dagger-shaped, curve (often with late-systolic notching) and those with severe PH typically manifest prominent midsystolic notching of the Doppler velocity signal.[10] However, these same authors pointed out that only 53% of patients with PH evidenced a notched flow curve, which suggests that pressure is an associate cause but not the actual physiologic cause of this notching pattern.

The actual cause of Doppler notching is early arrival of reflected arterial waves from the pulmonary vasculature that leads to "real-time" impedance to RV ejection.[11] This was initially described in the setting of acute and chronic pulmonary emboli, related to proximal vascular obstruction.[12,13] However, Torbicki and colleagues[12] showed that the time to midsystolic

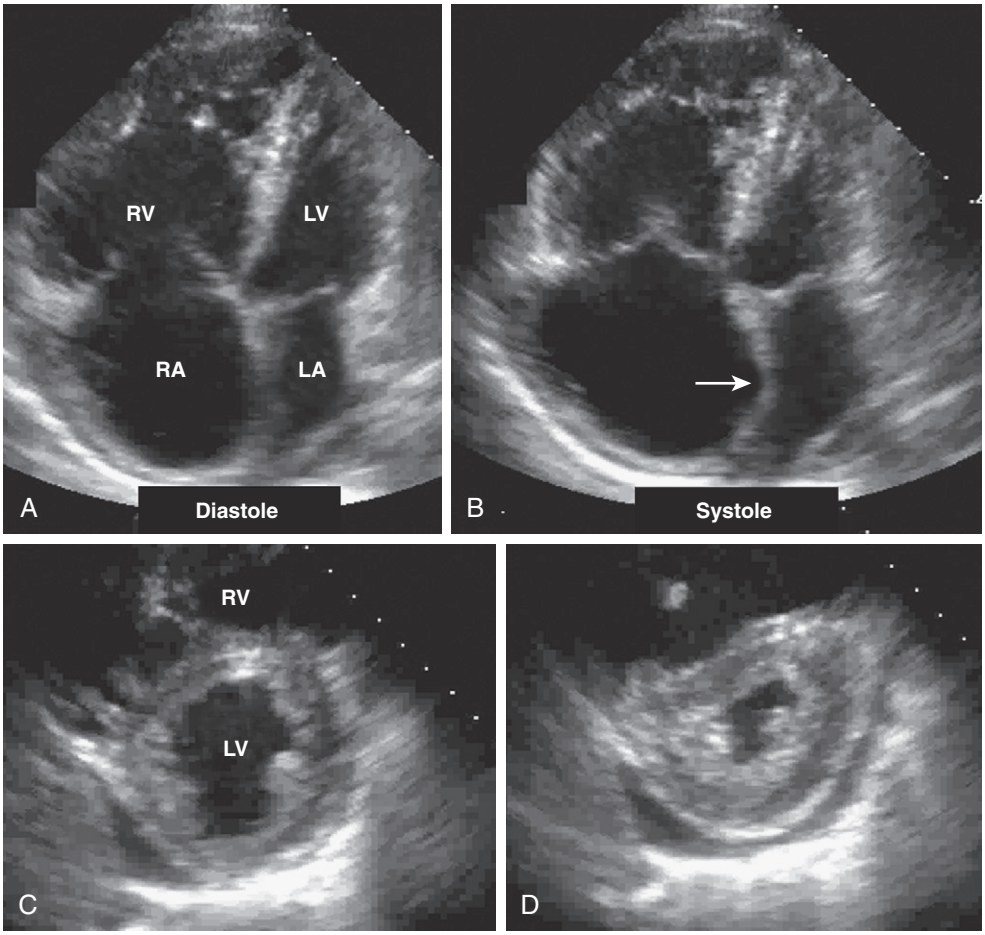



**Figure 33-1** **Apical four-chamber view in diastole (A) and systole (B) in a patient with idiopathic pulmonary arterial hypertension. A** and **B,** The RV is enlarged, and the interventricular septum bows to the left. Note the lack of significant fractional area change between diastole and systole, which indicates severe RV systolic dysfunction. The interatrial septum bows to the left as a result of severe RA hypertension (*arrow*). **C** and **D,** Parasternal short-axis view is shown in a similar patient in diastole (**C**) and systole (**D**). In diastole, the RV is noted to be enlarged, but the septal configuration is normal. In systole, severe septal bowing indicates markedly increased RV afterload (i.e., pulmonary vascular resistance). A moderate circumferential effusion is also present, a frequent finding in pulmonary arterial hypertension, especially with an increased right atrial pressure.

flow deceleration did not differ between patients with CTEPH and idiopathic PAH. Thus, analyses of the RV outflow velocity curve may be applied more broadly for detection of PVD.

Recent work was reported on a cohort of 79 patients (acute and chronic pulmonary embolic excluded) with undifferentiated PH and the hemodynamic differences seen on the basis of differences in the shape of the Doppler velocity curve.[5] In contrast to prior work, this study showed that the absence of Doppler notching did not necessarily indicate a lack of PH. Instead, the lack of Doppler notching (see Fig. 33-2, *C*) was strongly associated with a relative lack of PVD; when PH was present in these patients, it was the result of an increased LA pressure and a relatively normal PVR ($PH_{øPVD}$). In contrast, in the presence of increased PA stiffness and high PVR, reflected waves return to the RV during systole, impede RV ejection, and cause "notching" of the Doppler profile. A late systolic notch pattern typically coincides with moderate increases in the PVR (i.e., 3 to 6 Wood units; Fig. 33-3, *A*), most commonly seen in patients with milder degrees of PAH and in patients with chronic left heart disease or respiratory disease with concomitant PVD. A midsystolic notch pattern is especially abnormal and is the typical finding in patients with PAH and CTEPH. A midsystolic notch pattern is associated with an average PVR of more than 8 Wood units (Fig. 33-3, *B*); and a midsystolic notch pattern is 96% specific for a PVR of more than 5 Wood units. These findings indicate RV outflow velocity mid systolic notching is far more indicative of PVD (high PVR, low compliance) than high pulmonary pressure and help explain why notching is present in some, but not all, patients with PH.

In parallel with its associated RV afterload, the midsystolic notch pattern was associated with more advanced RV systolic dysfunction, lower tricuspid annular plane systolic excursion (TAPSE; Fig. 33-4, *B*), RV fractional area change, and the ratio of stroke volume index to RV end-diastolic area compared with normal patterns (no notching) and late-systolic notch groups. In contrast, patients with an elevated mPAP but normal pattern typically had either normal RV function or RV dysfunction associated with normal PVR and PA compliance. Taken together, these findings indicate that normal RV function without outflow notching suggests a relatively normal RV-PA interaction. In contrast, RV dysfunction in the presence of a notched outflow velocity curve strongly suggests an afterload-dependent mechanism, and RV dysfunction in the absence of RV outflow notching relates to primary afterload-independent RV dysfunction.

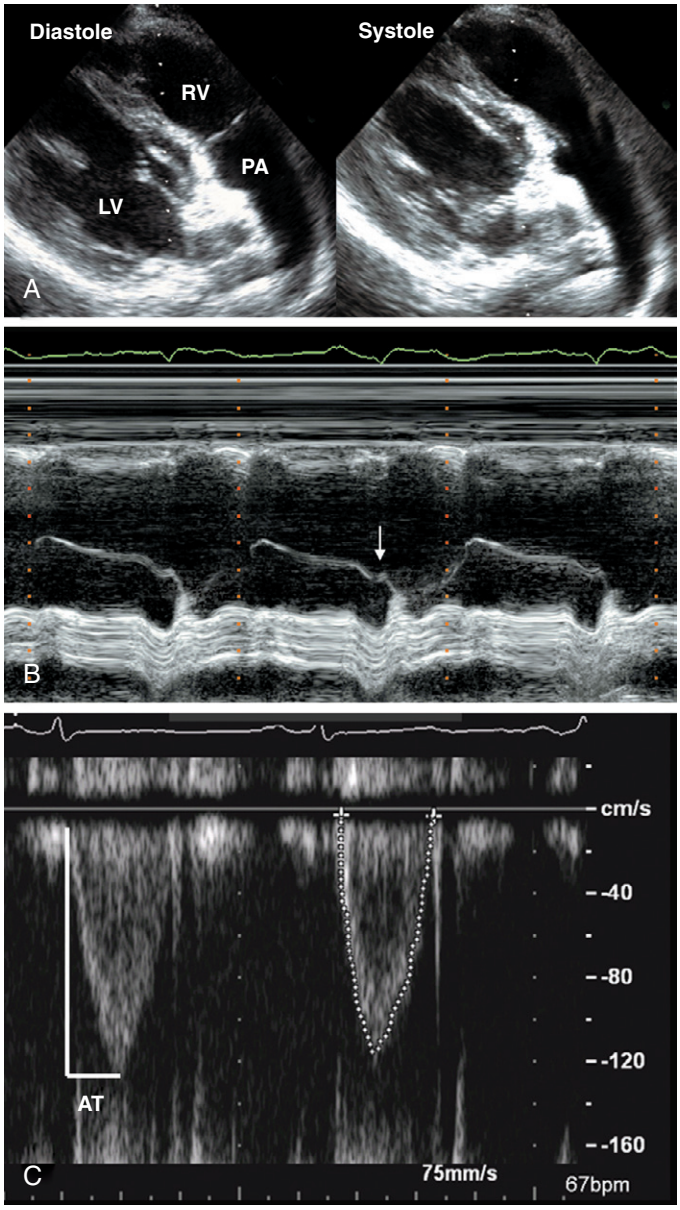



**Figure 33-2 A, Parasternal long-axis view of the pulmonary valve in diastole.** The RV outflow tract is clearly imaged in this view and is the best for pulsed wave Doppler sampling of the RV outflow tract flow velocity envelope (**C**). The PA bifurcation is out of plane. **B,** M-mode imaging of the pulmonary valve from the same view with normal movement of the valve leaflets away from the transducer in atrial systole. **C,** Normal (no notching pattern) pulsed wave flow velocity envelope taken in the RV outflow tract. The acceleration time (*AT*) is 110 ms, which is normal. Both findings strongly suggest normal pulmonary vascular resistance. If pulmonary hypertension is present in the absence of RV outflow tract Doppler notching, the increased PA systolic pressure is highly likely to arise from an increased LA pressure.

Thus, visual inspection of the RV outflow Doppler flow profile represents a simple rapid method of gleaning insight into the relative presence ("notched" pattern) or absence ("no notch" pattern) of PVD. This approach is extremely useful and applicable in clinical practice.

## Pulmonary Vascular Disease

Pulmonary vascular disease states are associated with varying degrees of increased PVR, loss of PA compliance, and pathologic arterial wave reflection. These changes within the pulmonary circulation impose a true afterload on the RV, such that specific 2D and Doppler "signatures" are highly prevalent in $PH_{+PVD}$, whereas such changes are relatively absent in $PH_{øPVD}$. The most prominent causes of $PH_{+PVD}$ are PAH and PH related to acute or chronic pulmonary emboli.

### PULMONARY ARTERIAL HYPERTENSION

Pulmonary arterial hypertension is the prototype of $PH_{+PVD}$ and can be familial or idiopathic (formerly referred to as primary PH) or associated with various predisposing conditions, including connective tissue disease (i.e., scleroderma), congenital systemic to pulmonary shunts, HIV infection, toxin-mediated pulmonary vascular injury, and other conditions.[3] Patients with PAH, by definition, have a mPAP of more than 25 mm Hg and an LA pressure of 15 mm Hg or less and universally have a PVR of more than 3 mm Hg/L/min (average PVR at index diagnosis, 8 to 10 mm Hg/L/min).[3,14,15] In addition to these hemodynamic criteria, a diagnosis of PAH requires the exclusion of chronic left heart disease, respiratory disease, and chronic pulmonary emboli. All approved forms of PH-specific therapy are particularly intended for patients with PAH. Importantly, the response to PH therapies and patient prognosis are linked to the relative stage of the disease at the time therapy is implemented.[4] This places a premium on early detection of PAH and, thus, on the importance of the echocardiographic examination, as this is one of the first noninvasive tests performed in the workup of a patient with suspected PAH. Echocardiography is a highly sensitive test for the detection of the physiology that underlies PAH, so long as the study is interpreted in an integrated manner, with due attention to RV size, shape, and function and other Doppler features that are nearly universally present in these patients. A normal or mildly elevated PASP Doppler estimate should not dissuade a suspected diagnosis of PAH when the other 2D and Doppler features of PAH are present.

In 1973, Goodman, Harrison, and Popp[16] reported the salient 2D echocardiographic findings of idiopathic PAH. All patients had RV dilation, and 50% had an RV:left ventricle (LV) dimension ratio of 1 or more. Patients commonly showed paradoxical septal motion, where the interventricular septum moved away from the center of the LV cavity in systole (Fig. 33-5). Aside from being a common echocardiographic feature in PAH, the relative loss of inward septal motion can account for a mild loss of LV systolic function in PAH, and thus, a low-normal or mildly reduced LV function can occur in PAH on this basis. Bossone and co-workers[17] published a larger observation series with idiopathic PAH and showed that 96% of patients had a Doppler-estimated pressure of more than 60 mm Hg at diagnosis; however, the overall correlation between Doppler and invasive pressure estimates was relatively low ($r$ = 0.31). Ninety-eight percent of subjects had RV enlargement, and 75% of subjects had qualitative evidence of RV systolic dysfunction. Systolic flattening of the interventricular septum occurred in 90% of subjects. Moderate or severe TR occurred in 80% of subjects, whereas mild to moderate mitral regurgitation was present in only one patient. A small or moderate-sized pericardial effusion was also noted in about 16% of subjects.[17]

In PAH, at least 70% of subjects manifest a transmitral Doppler E wave velocity to A wave velocity ratio (E:A ratio) of less than 1.0, consistent with grade I LV diastolic dysfunction. All subjects in this study had normal LA pressure with

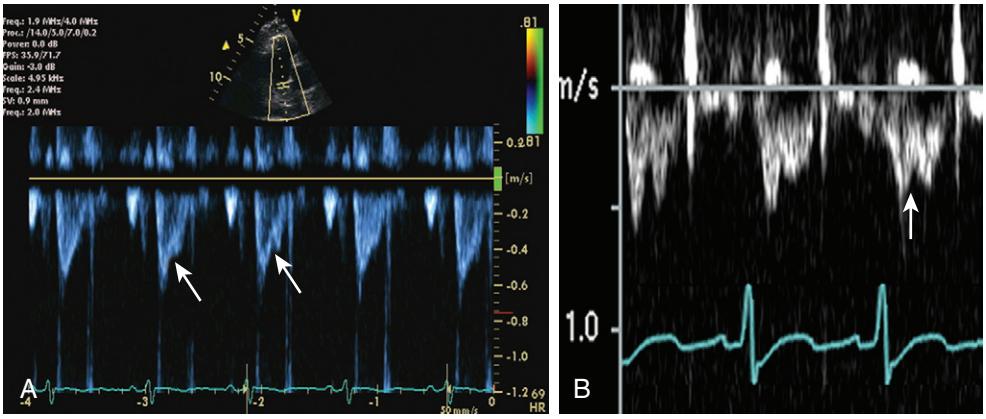



**Figure 33-3 A, Pulsed-wave Doppler signal from the RV outflow tract.** The Doppler signal displays late systolic notching (*arrow*), which typically coincides with a moderately shortened acceleration time (i.e., 70 t o 90 ms). Both findings suggest moderately increased pulmonary vascular resistance (i.e., 3 to 6 mm Hg/L/min). **B,** Pulsed-wave Doppler signal from the RV outflow tract. The Doppler signal displays midsystolic notching (*arrow*), which typically coincides with a severely shortened acceleration time (i.e., less than 70 ms). Both findings suggest a markedly elevated pulmonary vascular resistance (i.e., more than 6 mm Hg/L/min).

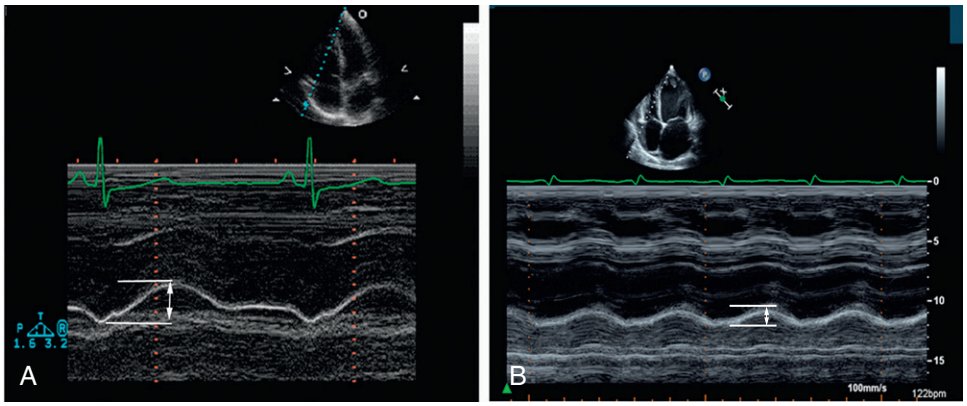



**Figure 33-4 A, M-mode imaging through tricuspid annulus recording of tricuspid annular plane systolic excursion in a patient with normal RV function.** The maximal excursion from diastole to systole is measured. The tricuspid annular plane systolic excursion is 2.4 cm. **B,** Tricuspid annular plane systolic excursion in a patient with severely reduced RV systolic function. The tricuspid annular plane systolic excursion is 1.3 cm.

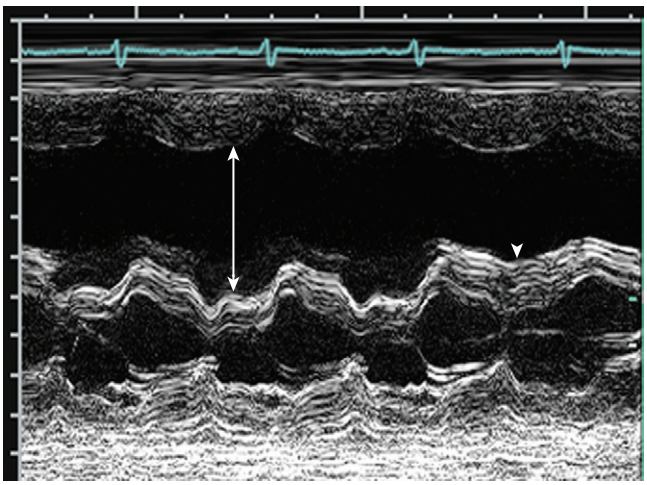


**Figure 33-5 M-mode imaging from the parasternal position in a patient with severe pulmonary arterial hypertension.** The RV:LV dimension ratio is greater than 1. The RV size increases with inspiration (*arrow*), with a resultant decrease in LV diameter. Paradoxical septal motion (*arrowhead*) is present.

right heart catheterization. In fact, grade I diastolic dysfunction in the vast majority of cases indicates normal LA pressure, reflecting the necessary redistribution of LV filling into late diastole that must occur when LV relaxation is impaired in the context of a normal LV filling pressure.[17,18] In clinical practice, the presence of any or all of the triad of findings of RV dysfunction, accompanied by grade I diastolic dysfunction, is a strong indicator of severe PH in the context of a normal LA pressure and high PVR. Arkles and associates[5] recently showed that a notched RV outflow velocity curve was seen in 100% of patients with an incident diagnosis of PAH, which coincides with prior data that show that 94% of subjects with PAH have an AcT of the RV outflow velocity curve less than 100 ms.[17] In our experience, the combination of a midsystolic notch RV outflow pattern with an E:A ratio of less than 1.0 is a highly sensitive and specific predictor of a markedly elevated PVR and a normal LA pressure.

Indices of right heart size, ventricular interdependence, and depressed RV function have been correlated with disease severity and patient outcome in patients with PAH.[4,19] In addition, studies have consistently shown that the presence and size of a

pericardial effusion predict poor outcome in patients with PAH.[20] Larger effusion size correlates with greater degrees of exercise intolerance, right atrium (RA) dilation, greater interventricular septal displacement, and more severe TR than in patients without an effusion.[19,21,22] The mechanism of the pericardial effusion in PAH most likely relates to slow progressive accumulation of intrapericardial fluid as a result of longstanding RA hypertension from decompensated right heart function. When the effusion is of moderate size or greater, the temptation is to intervene with percutaneous or surgical drainage. However, great caution should be exercised in this regard because drainage of pericardial effusions in patients with PAH has been associated with very poor outcomes, with death occurring within 12 to 24 hours of the procedure.[23] Importantly, the pericardial effusion is a marker of, but not the cause of, the right heart decompensation in this context. Thus, before pericardial drainage is considered, a right heart catheterization should be performed; if markedly elevated PVR, high RA pressure, and depressed cardiac index are found, the effusion is highly likely to be the direct result of afterload-induced RV failure. In the authors' experience, pericardial effusions in PAH almost invariably decrease in size or resolve over days or weeks as the RV failure is treated with pulmonary vasodilation therapy and diuresis.

Eysmann and colleagues[24] showed that a peak pulmonic flow velocity of more than 60 cm/s was predictive of a drop in PVR of more than 30% on acute vasodilator testing; no patient with a peak velocity of less than 60 cm/sec had a condition that was vasoreactive. Likewise, decreased LV and LA area, increasing RV:LV area ratio, and the degree of leftward septal bowing are also associated with an increased risk of systemic hypotension in response to calcium channel blocker therapy, likely reflecting the inability to sufficiently recruit RV stroke volume to overcome the drop in systemic vascular resistance.[25]

Other studies have focused on more direct assessment of RV systolic function. Tei et al[26] showed that the mean RV myocardial performance index (MPI) of patients with idiopathic PAH (0.83) was higher than in healthy controls (0.28) and that patients with an RV MPI of more than 0.83 had a less than 10% event-free survival rate at 5 years, versus more than 70% in those with an RV MPI of more than 0.83 (see Fig. 32-10).[27] A prospective study in patients with idiopathic PAH and PAH associated with connective tissue disease showed that a TAPSE of less than 1.8 cm was associated with lower invasively derived stroke volume index, higher RA pressure, greater RV dilation, right to left heart disproportion, and septal bowing and a higher incidence rate of pericardial effusion. Two-year survival rate estimates were 88% and 50% for patients with a TAPSE of 1.8 cm or more and less than 1.8 cm, respectively.[28] The prognostic value of TAPSE persisted after adjustment for several echocardiographic and invasive hemodynamic variables of known prognostic significance. The peak systolic tissue Doppler velocity is another practical measure of RV longitudinal function and is strongly correlated with TAPSE (see Fig. 32-10).

The typical changes in RV size, function, and septal position have been shown to improve in response to varying therapies. After 4 months of therapy with bosentan in patients with PAH, repeat echocardiographic examination showed improved RV MPI, reduced RV end-systolic area and RV:LV diastolic area ratio, improved early diastolic LV filling, and decreased pericardial effusion scores.[29] Similarly, after 3 months of intravenous epoprostenol infusion, RV size decreased, as did peak TR velocity and the noninvasive PVR estimate.[30]

Preliminary data from the authors' group have shown that after 6 months of PH-specific therapy, 78% of patients had increased TAPSE of more than 0.2 cm (mean, +0.5 cm), in association with significant improvements in 6-minute walk distance (median, +115 m), B-type natriuretic peptide levels (−210 pg/mL), and New York Heart Association functional class (−1.0 functional class). In those patients who reached a TAPSE of 2.0 cm or greater at 6 months, no deaths or right heart failure admissions were seen, as compared with two deaths and four right heart failure hospitalizations in those with a TAPSE of less than 2.0 cm on follow-up examination.[31] The increase in TAPSE in response to therapy is consistent with recent data that show that in PAH, PH-specific therapy leads to relatively selective improvement in longitudinal RV shortening, which suggests that long-axis shortening of the RV may represent the most afterload-responsive element of RV systolic function.[32]

Given the limited clinical and prognostic value of serial pressure assessment in PAH, along with concerns with the accuracy of Doppler-estimated PASP, most centers do not routinely follow or titrate therapy on the basis of changes in echocardiographic estimated PAP. Further study is needed to determine whether changes in various echocardiographic parameters have similar clinical and prognostic value as the invasive hemodynamic assessment of PVR and how such information can be used to determine favorable response and necessity of escalation of medical therapy or referral for lung transplant evaluation. It will also be important to determine whether certain threshold values exist (i.e., TAPSE, 2.0 cm or more) in PAH, such that TAPSE or other RV function measures may be added to the goal-directed therapeutic approach in PAH.

## ACUTE PULMONARY EMBOLISM

Acute pulmonary embolism and especially large proximal emboli lead to a sudden increase in the pulmonary vascular impedance without a marked rise in the PAP. This relates to the fact that the normal RV is typically incapable of generating a sufficient stroke volume to maintain a PASP of more than 60 mm Hg (mean pressure, 40 mm Hg) when suddenly uncoupled from a normal pulmonary vascular bed.[33,34] As a result, RV failure and cardiogenic shock may ensue despite a mean PA pressure between 20 and 40 mm Hg.[35] It follows that the degree of RV dysfunction predicts the extent of perfusion defects with ventilation/perfusion scan.[36] In contrast, small subsegmental pulmonary emboli that are not associated with a marked rise in PA impedance do not lead to abnormal echocardiographic findings, highlighting the fact that echocardiography cannot rule out an acute pulmonary embolism.[37] The relative degree of PH helps establish the chronicity of the embolic event, as the average transtricuspid flow velocity in acute proximal pulmonary emboli (3.0 m/s) is significantly lower than in patients with subacute pulmonary embolism (4.2 m/s).[34] In contrast, patients with acute pulmonary embolism with a PASP of more than 50 mm Hg at the time of diagnosis are at increased risk of persistent PH at 1-year follow-up.[38]

From a physiologic viewpoint, acute pulmonary embolism is an important and often dramatic clinical example that underscores the concept that PAP is a poor measure of RV afterload. RV dilation is almost universally present in the setting of a large pulmonary embolism, as the normally compliant RV rapidly distends in response to the increased vascular load. However, unlike in PAH or other forms of chronic PVD, RV hypertrophy is conspicuously absent. Another common finding in acute

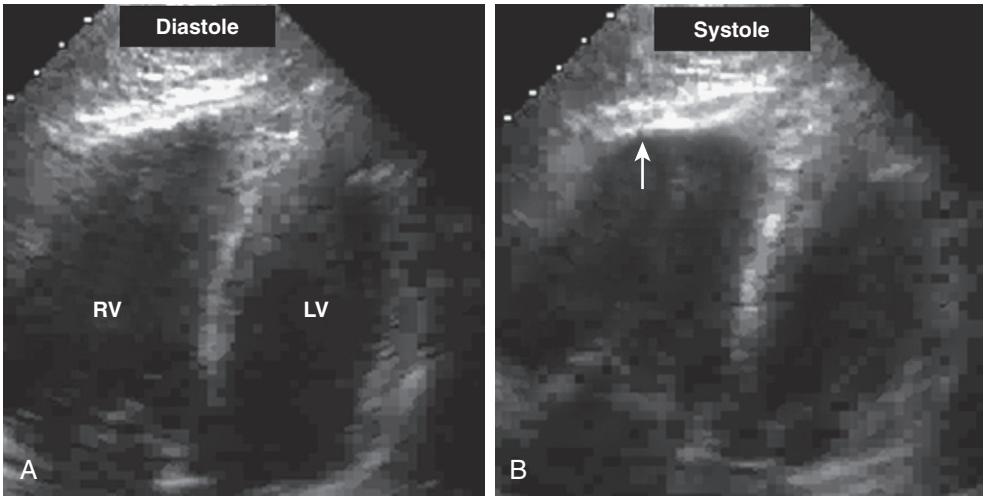



**Figure 33-6** **A, A close-up view of RV apex in diastole from the apical four-chamber view in a patient with acute pulmonary embolism.** The RV apex appears normal. **B,** Same view in systole. The RV free wall does not contract, but there is a hinge point (*arrow*) at the apex with some contraction; McConnell's sign is consistent with acute pulmonary embolism.

pulmonary embolism is McConnell's sign (Fig. 33-6), which is visually appreciated as RV dysfunction along the RV base and mid segments, with a hinge point or "buckling" of the RV free wall near the RV apex.[39] This relative sparing of RV apical wall motion likely is caused by tethering of the RV apex by a normal or hyperdynamic LV across the interventricular septum. Other studies have shown that the RV ejection fraction, RV stroke volume measured with pulsed Doppler imaging, and TAPSE are reduced in the setting of an acute pulmonary embolism.[40] A characteristic Doppler finding in acute pulmonary embolism is the "60/60 sign," which refers to a markedly shortened AcT (less than 60 ms) in the RV outflow velocity curve, because of the increased PA impedence, combined with a PASP of less than 60 mm Hg.[41] Similarly, midsystolic notching of RV outflow is a common finding in acute pulmonary embolism, relating to early arrival of reflected pressure waves from proximal vascular obstruction.

Another important finding to look for on the initial examination is right-sided heart thrombi and thrombi-in-transit, which complicate approximately 4% of cases with acute pulmonary emboli (Fig. 33-7).[42] Thrombi may be visualized within the RA and ventricle and occasionally are seen straddling the interatrial septum. Right heart thrombi are a high-risk feature, typically associated with prior massive pulmonary embolism, severe RV dysfunction, and high in-hospital mortality.[42] In such cases, thrombolysis or catheter-based versus surgical embolectomy is often warranted.[42,43]

The main PA and its bifurcation are well visualized with transesophageal echocardiography (TEE; Fig. 33-8). TEE has been shown to have comparable sensitivity (80% to 97%) and specificity (86% to 100%) with spiral computed tomographic (CT) scan for the detection of central pulmonary emboli. Thus, TEE may play a role in the diagnosis of central pulmonary emboli, perhaps best applied in the setting of clinical instability, where bedside assessment and monitoring with TEE may be preferred over transporting the patient out of the intensive care unit for spiral CT examination.[44]

The primary value of echocardiography in acute pulmonary embolism is in the risk assessment of the individual patient. Echocardiographic evidence of RV hypokinesis predicts a two-fold increase in mortality at 2 weeks and 3 months.[45-48] Even in patients with hemodynamically stable conditions, identification of RV dysfunction with echocardiography may be an indication for thrombolytic therapy.[49] Echocardiography should be rapidly performed in every patient in whom the diagnosis of acute pulmonary embolism is made.[50] Likewise, patients with severe RV dysfunction in whom thrombolysis is contraindicated, or those with severe RV dysfunction and shock, may need more aggressive surgical or catheter-based therapies.[51,52] In addition, significant PH at the time of diagnosis (RV systolic pressure, more than 50 mm Hg) predicts the presence of CTEPH at 1 year; thus, these patients should be referred to a PH center for monitoring and management after recovery from the acute event.[53]

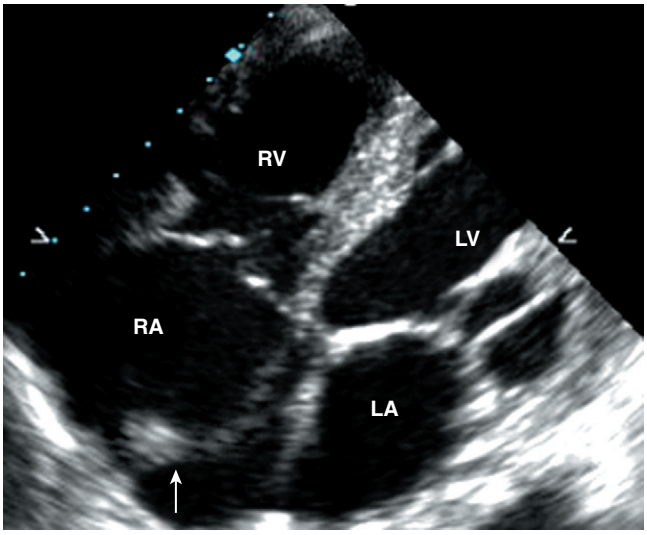



**Figure 33-7** **Venous thromboembolism.** In this off-axis four-chamber view, the RA and RV are dilated. A mass in the RA (*arrow*) represents a venous cast in transit. This cylindrical mass was highly mobile within the RA. RA hypertension is shown by the shift of the interatrial septum to the left. The patient had already sustained a pulmonary embolism but was a risk for another and probably lethal event. The patient was taken to the operating room immediately after these images were obtained.

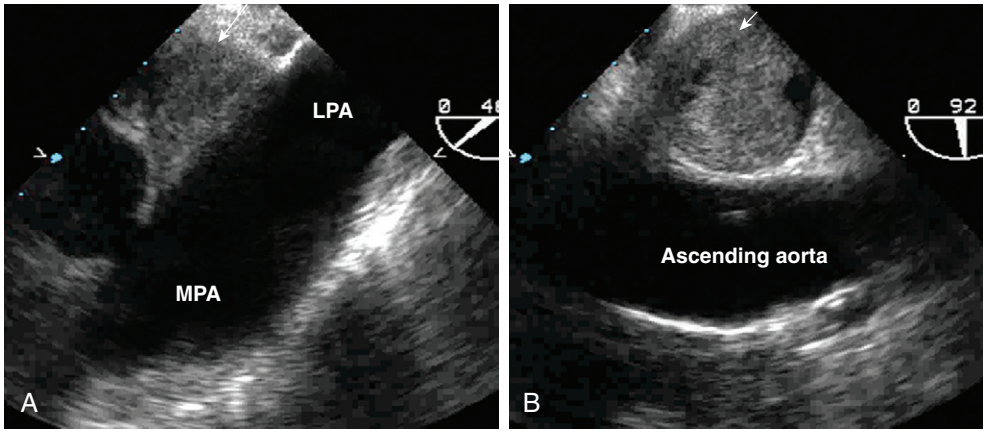



**Figure 33-8** **Pulmonary embolus. A,** TEE from the mid esophagus shows the pulmonary artery bifurcation. The right pulmonary artery is filled with thrombus and appears to be completely occluded. **B,** TEE from the same level in the transverse plane. The right pulmonary artery is filled with thrombus and is seen in the short-axis view. The ascending aorta is below the right pulmonary artery on the screen (anterior). *Asc Ao,* Ascending aorta; *LPA,* left PA; *MPA,* main PA.

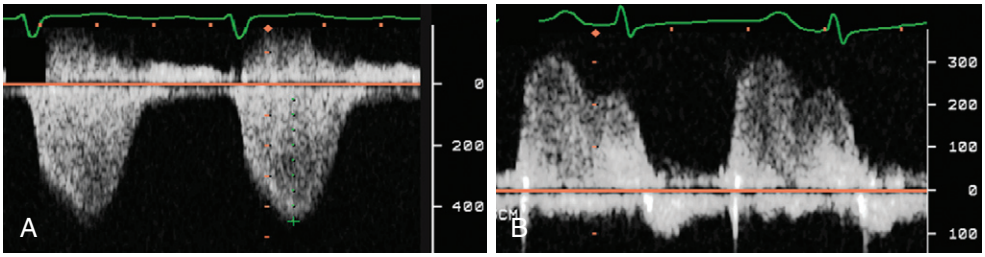



**Figure 33-9** **Pulmonary hypertension. A,** Continuous-wave Doppler image across the tricuspid valve in systole from the apical position. The peak velocity is 4 m/s. The RA pressure was estimated at 15 mm Hg. The pulmonary artery systolic pressure is 79 mm Hg. **B,** Continuous-wave Doppler across the pulmonic valve in diastole from the parasternal position. The peak velocity at end diastole is 2.4 m/s. The RA pressure estimate is 15 mm Hg. The pulmonary artery diastolic pressure is 38 mm Hg. The pulse pressure is thus calculated as 41 mm Hg (79 systolic minus 38 diastolic).

## CHRONIC PULMONARY EMBOLISM

Chronic thromboembolic PH is a relatively rare complication of prior acute pulmonary emboli that occurs in less than 5% of cases.[54,55] The major site of vascular impedance is often the proximal pulmonary vasculature because of the persistence of clot and vessel remodeling in the affected area. However, small vessel pulmonary arteriopathy is also known to occur in CTEPH, such that the degree of PVR elevation may be equal to or greater than that seen in idiopathic PAH.[56] The end result is often that the overall burden of PVD is comparable with that in PAH and, in some cases, worse because of the added hemodynamic load from the proximal obstruction. Thus, the typical triad of RV dysfunction, RV dilation, and septal bowing is present in CTEPH and is largely indistinguishable from the various forms of PAH. Nevertheless, hemodynamic differences between CTEPH and PAH can aid in differentiating the two conditions. Namely, in CTEPH, the presence of a discrete proximal obstruction leads to more exaggerated, earlier arrival of arterial reflected waves and thus a more pulsatile pulmonary vascular bed.[13] This increased pulsatility can be expressed as the fractional pulse pressure (FPP = PA pulse pressure/mean PA pressure); the typical FPP is 0.8 in PAH and 1.4 or more in CTEPH.[57,58] The FPP can also be estimated with Doppler imaging (Fig. 33-9), with a noninvasive FPP of 1.35 predicting CTEPH with a sensitivity of 95% and specificity of 100% over idiopathic PAH.[59]

Serial examinations after pulmonary endarterectomy have shown increases in RV fractional area change and reductions in RV size, decreased septal bowing, and improved early diastolic LV filling.[60,61] A study by Hardziyenka and co-workers[62] showed that patients with early arrival of arterial reflected waves, as measured by a shorter time to notching of the pulmonary flow velocity curve, were the only patients with CTEPH to benefit from endarterectomy. These findings prove that simple RV outflow velocity curve analysis is able to predict clinical response to surgery and that a requisite degree of pulmonary vascular impedance and arterial wave reflection is needed for sufficient RV-PA recoupling to occur after surgical intervention.

## PULMONARY VENOUS DISEASE

The prototype, and most severe form of pulmonary venous disease, is pulmonary venoocclusive disease (PVOD). This relatively rare entity may be idiopathic but has also been associated with toxin exposure, infectious agents including HIV, and autoimmune disease (see Chapter 37). In addition, PVOD or a PVOD-like state has also been reported repeatedly in sarcoid-associated pulmonary disease.[63,64] Given that the hemodynamics of PVOD are similar to PAH, with marked increases in the PVR and normal LA pressure, it follows that the echocardiographic findings in PVOD are essentially the same as in PAH. A diagnosis of PVOD should be suspected in a patient who shows echocardiographic features suggestive of PAH but with symptoms (orthopnea) and radiographic findings (pulmonary vascular congestion, pleural effusions) suggestive of left heart congestion.

Acquired pulmonary vein stenosis may be detected with echocardiography. Pulmonary vein stenosis should be suspected when the inflow velocity to the LA is greater than 1.1 m/s and the flow is turbulent with little variation in velocity.[65] Clinically, this should be suspected in a patient after pulmonary vein isolation for ablation of atrial fibrillation.[66] Although the presentation may be acute and fulminant, most commonly, patients present months after the procedure, with a symptom complex suggestive of left heart congestion yet *without* classic echocardiographic features of PAH, such as marked RV dilation, dysfunction, and septal bowing.[67,68] Intracardiac echocardiography guidance during the procedure may reduce the risk of injury.[69] Magnetic resonance imaging (MRI) may be necessary to confirm the presence of pulmonary vein stenosis and to guide in stenting. Patients should be monitored with follow-up echocardiography after stenting because restenosis may occur.[70] The right inferior pulmonary vein cannot be imaged with transthoracic echocardiography and TEE or repeated MRI may be necessary for surveillance. Pulmonary vein thrombosis and occlusion have also been reported after heart and lung transplantation.[71,72] Intraoperative TEE may reduce the incidence of pulmonary venous complications and help with hemodynamic monitoring during these complicated surgeries.[73-75]

## Pulmonary Hypertension as a Result of Chronic Respiratory Disease

The chronic respiratory disorders most commonly associated with PH include chronic obstructive pulmonary disease (COPD), interstitial lung disease (i.e., idiopathic pulmonary fibrosis), and disorders of alveolar hypoventilation, which include chronic neuromuscular disorders and sleep-disordered breathing. The pathogenesis of PH in COPD and interstitial lung disease is multifactorial and relates in part to parenchymal lung destruction and secondary loss of pulmonary vascular surface area. In addition, both acute hypoxic pulmonary vasoconstriction and the effects of chronic hypoxemia (and hypercapnia) on pulmonary vascular remodeling contribute to increased RV afterload in these conditions. Lastly, it is relatively common for patients with advanced lung disease to have an increased CO (as a result of adrenergic stimulation). Thus, the most common hemodynamic profile of PH in lung disease is that of mildly increased PVR (i.e., 2 to 4 Wood units), combined with mild or moderately increased CO. LA pressure is most often normal; however, this should be verified and not assumed. Given the modest increase in PVR, significant RV dysfunction and dilation is relatively uncommon in these patients. However, because of the chronicity of the conditions, RV hypertrophy is often present. Thus, the common constellation of findings in patients with chronic parenchymal lung disease includes mild to moderate PH; some degree of RV hypertrophy, typically with mild or lesser degrees of RV dilation; dysfunction; and septal flattening. The presence of PAH-like echocardiographic findings represents a departure from the norm in these patients and signifies a greater degree of PVD. The clinical circumstance under which the echocardiographic examination is performed is highly relevant in these patents because the hemodynamics in the setting of an acute respiratory exacerbation can differ greatly from those obtained under steady state conditions.[76] As a result, if the examination was initially performed in the context of an acute respiratory decompensation, the study should be repeated once the patient's condition is compensated and at the clinical baseline for more accurate assessment of the impact of the respiratory condition on the heart and pulmonary circulation.

Alveolar hypoventilation also predisposes to PH; however, intermittent hypoxemia (either nocturnal or daytime) is typically insufficient to result in chronic PH. Even in the setting of severe nocturnal desaturation, most patients with severe obstructive sleep apnea do not have significant PH. In contrast, PH is far more common in the setting of chronic daytime hypoxia and hypercarbia, as seen in patients with obesity-hypoventilation syndrome. As a result, the most significant predictors of PH in patients with sleep-disordered breathing are daytime $PO_2$ and $PCO_2$, and a lower forced expiratory capacity ($FEV_1$) and a higher body mass index.[77] Even in the setting of severe obesity and sleep apnea, RV systolic dysfunction and an increased PVR are not common, as shown in a cohort of patients at the time of referral for gastric bypass surgery.[78] As a result, PAH-like findings are uncommon in obstructive sleep apnea or obesity hypoventilation syndrome. When present, findings such as significant RV dilation, dysfunction, septal flattening, and a notched RV outflow pattern should greatly increase the suspicion for conditions such as PAH and CTEPH, as the pathophysiology of PH in obstructive sleep apnea is typically not sufficient to cause such findings.

Although most PH in the setting of respiratory disorders is precapillary, arising from an increased PVR and normal LA pressure, the presence of an increased LA pressure should not be overlooked as a contributor to PH in the setting of lung disease. This is especially true with comorbid conditions (i.e., COPD with hypertension and coronary artery disease) that may lead to the coexistence of both pulmonary and left-heart related causes of PH and is especially important given that pulmonary venous congestion is very poorly tolerated in the setting of significant lung disease and is a relatively easily reversible cause of dyspnea in these patients. An increased LA pressure is common in patients with morbid obesity and significant sleep-disordered breathing, given the high incidence rate of hypertensive heart disease and LV diastolic dysfunction in these patients.[79,80] In our experience, LA hypertension is the single most common cause of moderate or greater PH in patients with severe sleep-disordered breathing and also the most underappreciated.

Although most PH in the setting of parenchymal lung disease is rather modest and typically fits the previous hemodynamic profile, the degree of PH and the degree of PVR vary widely. Thus, the hemodynamic composition of PH within the context of chronic respiratory disorders is quite heterogeneous. As a result, the echocardiographic findings in this context can also vary widely.

A minority of patients with PH related to COPD or interstitial disease have severe PH as a result of a much greater degree of PVD. Approximately 1% to 5% of patients with COPD have hemodynamics comparable with patients with PAH, with an mPAP of more than 50 mm Hg in the context of a markedly elevated PVR and decreased cardiac index.[81,82] Interestingly, subjects with COPD and PAH-like hemodynamics are significantly more hypoxic than those with mild to moderate PH and have a $pCO_2$ less than 40 mm Hg; these arterial blood gas findings are more consistent with the findings of PAH than COPD. Moreover, these patients showed lesser degrees of airway obstruction than subjects without PVD. In the authors' experience, the echocardiographic examination of these patients mirrors their underlying physiology, and thus, they have similar

degrees of RV dilation, dysfunction, and septal flattening as patients with PAH.

Pulmonary sarcoid has a particular predilection for pulmonary vascular involvement, and thus, $PH_{+PVD}$ is seen in a significant minority of these patients. Other parenchymal lung disorders that present a higher risk of significant pulmonary vascular involvement include Langerhans cell histiocytosis and interstitial lung disease associated with scleroderma.[83-85] In each of these three diagnoses, the degree of PVD may occur in varying proportion to the severity of the parenchymal disease. Nevertheless, when the PVR is significantly elevated (i.e., 5 Wood units or more), the imaging and Doppler findings seen are typical for a patient with PAH or CTEPH, with comparable degrees of RV dilation, septal bowing, and RV systolic dysfunction. In addition, either late or midsystolic RV outflow notching is present and carries essentially the same pathophysiologic significance in these patients as described for patients with PAH. In patients with chronic lung disease and PH, subjects without a notched RV outflow velocity curve had an average mean and PASP of 30 mm Hg and 52 mm Hg, respectively, with a PVR of 3.2 Wood units. In contrast, subjects with a RV outflow notching had a mean and PASP of 48 mm Hg and 77 mm Hg, respectively, and a PVR of 8.0 Wood units. Moreover, RV function differed significantly, with relatively normal RV function (TAPSE, 2.0 cm) seen in the non notched group and moderate RV dysfunction observed in the RV outflow notching group (TAPSE, 1.6 cm).[86] Thus, the RV outflow notching pattern helped discern PH that was "proportionate" versus "disproportionate" to the degree of parenchymal lung disease.

As a word of caution, echocardiographic image quality can be suboptimal as increased lung volumes, obesity, and pulmonary fibrosis attenuate ultrasound penetration. Cardiac orientation is often abnormal, which may confound optimal Doppler alignment with the TR jet. These issues are well illustrated in a report of 374 patients with advanced lung disease who underwent right-sided heart catheterization and Doppler echocardiography less than 72 hours apart. Estimation of PASP was only possible in 44% of the population. There was only a modest overall correlation ($r = 0.69$) between invasively derived PASP and Doppler-estimated pressure, with 52% of the patients having a pressure estimate that was greater than 10 mm Hg from the catheter-derived value.[87] As a result, an integrated echocardiographic assessment is of particular importance in these patients. Appreciation of right heart size, septal position, and systolic function and careful inspection of the RV outflow pattern always provide a better assessment of PH in general and greatly offset the risks of overreliance on a single Doppler pressure estimate in these patients.

## Lung Transplantation

A decrease has been seen in the need for single or double lung transplantation as medical therapies for PAH have improved. Nevertheless, a minority of patients with PAH has progression despite maximal medical therapy and eventually needs lung transplantation. For the individual patient, lung transplantation may be lifesaving and markedly improve quality of life. In addition, the physiologic changes that occur after lung transplantation have provided important insight into the physiology of the RV-PA interaction that have helped improve medical therapy for those not in need or ineligible for transplantation.

Although RV dysfunction is nearly universally present in PAH, this is not primarily the result of intrinsic impairment of RV contractility. Instead, the ventricular dysfunction relates to chronic and severe mismatch between RV function and RV afterload. Pressure-volume loop studies have shown that intrinsic RV contractility (RV end-systolic elastance) is two-fold higher than in healthy subjects. However, this relative improvement in RV function is not sufficient to match the four-fold increase in RV afterload as compared with healthy subjects.[9] Restoration of afterload toward normal restores normal RV-PA coupling, and thus, RV function.[8] This is well demonstrated after lung transplantation. In a series of 17 patients with severe refractory idiopathic PAH, the average RV ejection fraction and cardiac index were 32% and 2.2 L/min/m$^2$ before transplantation. The average mean PA pressure was 61 mm Hg, and the PVR was 10 to 12 Wood units. All patients showed marked RV dysfunction, RV dilation, and right to left septal bowing. Three months after bilateral lung transplantation, there were significant reductions in RV diastolic dimensions and RV end-diastolic area and near complete resolution of TR. All patients had normal septal position on follow-up examination, and the average RV ejection fraction increased to 67%.[88] These findings underscore the concept that in the vast majority of patients with PAH, it is not impaired RV contractility per se, but rather excessive RV afterload that leads to RV failure. For these reasons, as long as RV afterload is massively elevated, there is no degree of pre–lung transplant RV dysfunction "cutoff" that precludes double lung transplantation.

## Pulmonary Hypertension without Pulmonary Vascular Disease

By definition, $PH_{øPVD}$ (i.e., normal PVR) must arise from either a rise in pulmonary blood flow or a rise in LA pressure. As such, $PH_{øPVD}$ occurs in the context of a relatively normal RV afterload, and therefore, the RV dysfunction triad of RV dilation, dysfunction, and septal flattening and RV outflow notching are conspicuously absent. Thus, the *lack* of typical Doppler findings of $PH_{+PVD}$ should serve as a critical clue to the presence of $PH_{øPVD}$, be it related to a high CO disease state, a congenital heart disease-related systemic to pulmonary shunt, or left heart disease.

### PULMONARY HYPERTENSION RELATED TO INCREASED CARDIAC OUTPUT

Because of the relative distensibility and low resistance nature of the pulmonary circulation, an increased CO alone is often insufficient to cause PH. The pulmonary flow required to cause significant PH is quite high. For example, with a PVR of 1.5 Wood units and a LA pressure of 10 mm Hg, the CO would need to be approximately 11 L/min to produce an mPAP of 25 to 30 mm Hg (mild PH). More typically, a high CO is paired with at least one other abnormality (i.e., an increased LA pressure) in the pulmonary circulation to cause PH.

An increased CO may be caused by increased inotropic stimulation, increased preload, or excessive reduction in LV afterload. An often underappreciated and relatively common cause of increased CO is the presence of a arteriovenous fistula or graft in the context of end-stage renal disease. Each can be associated with at least an additional liter of CO through their direct rerouting of blood flow and their indirect effect on lowering LV afterload. In isolation, they typically do not lead to PH; however, when combined with the common associates of LV

diastolic or systolic dysfunction, systemic hypertension, and generalized arteriosclerosis, PH is a common byproduct. In the authors' experience, the 2D examination typically shows some degree of RV dilation; however, systolic septal flattening and RV systolic dysfunction are notably absent. In fact, hyperdynamic RV function is more often present, given the excess preload returning to the right heart via the upper extremity veins. Moreover, stigmata of left heart disease are very frequently present, including LA enlargement, LV hypertrophy, and grade II or III LV diastolic dysfunction.[89]

Liver disease is another important cause of increased CO because of the presence of a markedly reduced systemic vascular resistance, at times combined with hypervolemia. Appreciation for the type of PH present in the setting of advanced liver disease is of great importance because the diagnostic and treatment strategies associated with portopulmonary hypertension (portoPH) are dramatically different from those associated with the vast majority of PH associated with liver disease. PortoPH is a form of PAH and is thus associated with a markedly increased PVR and shows echocardiographic findings similar to other forms of PAH. However, even amongst a cohort of 101 patients with advanced liver disease and a Doppler-estimated PASP of more than 50 mm Hg, 35% of subjects did not have portoPH and instead had PH related to increased CO or increased LA pressure.[90] The percentage of patients with flow-induced or left heart disease–related PH is likely to be even higher in a more general liver disease referral cohort. The echocardiographic findings between portoPH and high-flow, low-PVR causes of PH differ greatly. In the authors' experience, proper interpretation of the screening echocardiographic examination minimizes the risk of misclassification of the type of liver disease–associated PH and identifies those at risk of poor outcome with liver transplantation (portoPH) versus those with a poor outcome without liver transplantation (non-portoPH).

### SYSTEMIC TO PULMONARY VENOUS SHUNTS

Echocardiographic findings associated with congenital heart disease–related systemic to pulmonary shunts are discussed in Chapters 44 and 45. A variety of 2D and Doppler findings are associated with shunting at the venous, atrial, and ventricular levels. For the purpose of this discussion, we focus on the general principles of RV structure and function and basic shunt assessment.

In the setting of smaller shunts or larger shunts in the absence of PVD, the RV is primarily subject to an increased volume load. In the context of increased RV volume and normal RV afterload, RV function is typically increased on the basis of increased preload recruitable cardiac work (Starling effect). Thus, a dilated and hyperdynamic RV is an important initial clue to the presence of a left to right shunt. On short-axis imaging, bowing of the interventricular septum is often found, however, only appreciated in ventricular diastole. The degree of PH varies in proportion to the relative shunt fraction and increase in pulmonary blood flow. Herein lies another example of the disconnect between PA pressure and RV afterload, as the increased pressure is owed to, but not opposing, pulmonary blood flow.

Over time, excess pulmonary blood flow can lead to pulmonary endothelial dysfunction and PVD, with the degree of PVR reaching levels equal to or greater than that seen in other forms of PAH. In these conditions, the RV must accommodate the persistent volume load and the rise in PVR. However, the rise in RV afterload in the setting of a chronic systemic to pulmonary shunt occurs relatively slowly, often over decades. As a result, the structure and function of the RV in PAH associated with a chronic shunt often differ from other forms of PAH. Namely, the degree of RV hypertrophy is often greater than the degree of RV dilation.[91] Marked RV hypertrophy can often be appreciated by both wall thickening and excess RV trabeculations, and by a conspicuous moderator band; these findings alone can often help distinguish PAH related to an intracardiac shunt from other forms of PAH. RV dilation and dysfunction in the setting of a chronic shunting is especially worrisome and often coincides with very late stage disease.

Qualitative initial shunt assessment is often performed with rapid injection of agitated saline solution ("bubble study"), which opacifies the right heart chambers and allows for detection of both right to left shunts (early passage of bubbles from right to left) and left to right shunts (via a negative contrast jet created from the passage of blood into the opacified right heart chamber; Fig. 33-10). Shunt quantification with Doppler imaging is expressed by the ratio of pulmonary to systemic blood flow. Doppler flows in the RVOT (Qp) and LVOT (Qs) are assessed to derive the Doppler Qp:Qs ratio. The RVOT diameter is typically about 0.5 to 1.0 cm greater than the LVOT diameter; given that flow is equal to the product of cross-sectional area and velocity, it follows that the Doppler velocity time integral (VTI) in the RVOT is typically less than the VTI in the LVOT. Thus, a simple clue to a sizeable left to right shunt is when the RV outflow VTI is equal to or greater than the LV outflow VTI. A saline solution contrast study may reveal early passage of bubbles across a patent foramen ovale or atrial septal defect with shunt reversal (i.e., Eisenmenger syndrome) or a negative contrast jet in patients with left to right shunting (see Fig. 33-10). Shunt localization is performed by first assessing for 2D and color Doppler evidence of interatrial or interventricular septal defects. Of note, at least 20% of sinus venosus–related atrial septal defects may be missed with transthoracic Doppler examination and may require imaging with TEE, intracardiac echocardiography, or MRI for full characterization. Further shunt characteristics, such as blood flow direction, blood flow velocity, and estimated pressure gradients across shunts, can be performed with color, pulsed-wave, and continuous-wave Doppler examinations.

## Pulmonary Hypertension Related to Left Heart Disease (Pulmonary Venous Hypertension)

By far the most common cause of PH relates to passive elevation of the PAP from an increase in LA pressure. A variable degree of reactive pulmonary vascular remodeling may also occur, typically related to the severity and chronicity of the LA hypertension.[92,93] As a result, patients with PVH comprise a large percentage of patient referrals for PH evaluation. Thus, knowledge of the basic noninvasive manifestations of PVH is critically important in the initial approach to patients with undifferentiated PH.

It follows that the noninvasive predictors of PVH include 2D and Doppler findings that either reflect or predispose to LA hypertension and more direct Doppler estimates of increased LA pressure.[92-94] Importantly, the LV ejection fraction is a poor predictor of LA hypertension, and thus, a normal ejection fraction in no way provides reassurance that the LA pressure is normal.

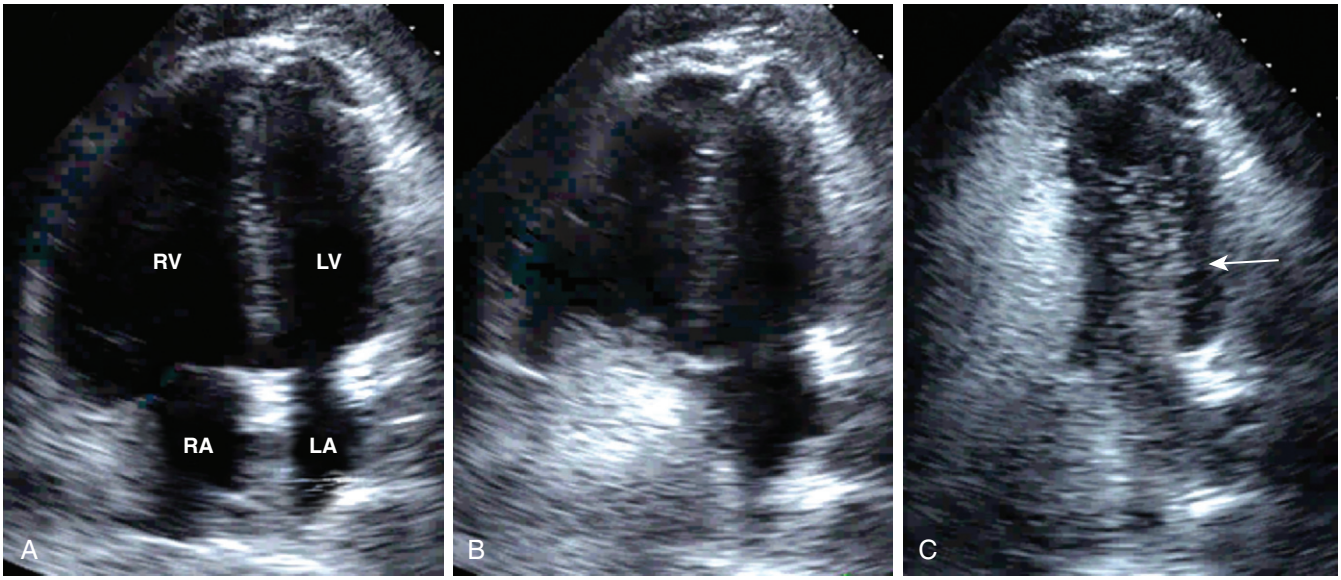



**Figure 33-10 A, Apical four-chamber image in a patient with dilated RV and moderate pulmonary hypertension as a result of idiopathic pulmonary fibrosis.** The patient's hypoxia was out of proportion to the lung disease. **B,** Agitated saline solution contrast entering the RA. **C,** Agitated saline solution contrast filling the RV and passing into the LA and subsequently the LV through a patent foramen ovale.

The 2D echocardiographic examination can provide compelling initial evidence that either supports or refutes the presence of LA hypertension. One of the first clues to past or present LA hypertension is LA enlargement, which should certainly not be considered a physiologic measurement of LA pressure. However, increasing LA size typically denotes chronically increased LA impedance and either the presence of, or predisposition for, increased LA pressure. LA enlargement is best appreciated in the parasternal long-axis view, with a LA dimension at end-systole of 4.0 cm or more generally being the accepted cutoff. However, the more reliable method is use of the biplane method of disks to measure LA volume. The apical four-chamber and apical two-chamber views are used, with care taken to avoid the pulmonary veins. The volumes are indexed to body surface area. Abnormal volume is considered more than 28 mL/m$^2$. Another important finding is the presence of LV hypertrophy; LV hypertrophy, even when mild, denotes chronic remodeling of the LV, typically the result of longstanding systemic hypertension. This is a significant form of structural left heart disease and is typically associated with increased LV chamber stiffness. Melenovsky and associates[94] showed that LA size (expressed as LA volume) and LV mass index, and the product of these two variables, were the strongest discriminates of nonsystolic heart failure from hypertensive heart disease without a history of heart failure. In the context of PVH as a result of elevated LA pressure, the interventricular septum typically maintains a normal configuration on short-axis imaging, convex toward the RV. In the apical four-chamber view, the ratio of RV:LV dimension (or area) typically remains less than 1.0, with the RV apex maintaining its sharp apical angle and with the LV forming the apex of the heart alone.

The Doppler examination also provides important physiologic information with respect to valvular function, diastolic function, and LA pressure assessment. As a general statement, moderate or greater dysfunction of either the aortic or the mitral valve is relatively uncommon when PVD is the primary source of the increased PA pressure. Of course, moderate or greater mitral stenosis is well known to cause severe PH, largely on the basis of passive pulmonary venous congestion. However, moderate or greater mitral regurgitation is also distinctly uncommon in the setting of PAH and provides fairly compelling evidence for a pulmonary venous source of PH.[17] Lastly, Doppler interrogation of the mitral valve inflow provides a key component to the patient with known or suspected PH. Grade II and III diastolic dysfunction are strongly suggestive of an increased LA pressure at the time of the examination and are uncommon findings in PAH.[5,17] In contrast, a PASP between 40 and 70 mm Hg (mean PA pressure, ~25 to 45 mm Hg) in the presence of pseudonormal or restrictive transmitral flow is strongly suggestive of PVH as the dominant source of PH. If this is coupled with normal septal position and normal RV size and shape, the diagnosis of PVH becomes almost certain. When PVH occurs in the context of some degree of PVD (e.g., in many patients with COPD), then the echocardiographic examination possesses 2D and Doppler features indicative of increased RV afterload and LA hypertension (i.e., LV hypertrophy and LA enlargement, grade II diastolic dysfunction), yet evidence of RV enlargement, RV dysfunction, and a late-systolic notching pattern in the RVOT Doppler profile.

## DIFFERENTIATING PULMONARY VASCULAR (ARTERIAL) FROM PULMONARY VENOUS HYPERTENSION

From the clinician's perspective, a useful initial diagnostic framework considers whether a patient's PH is from a pulmonary venous (postcapillary) or pulmonary arterial (precapillary) source. This approach is both rational and practical, given the prevalence of PVH and the fact that the diagnostic and therapeutic considerations for these patients differ considerably.

As outlined in the previous sections, a variety of echocardiographic parameters have significant diagnostic and prognostic value in PH. A transthoracic echocardiographic report customarily provides a list of normal and abnormal findings related to cardiac structure and function. Table 33-1 summarizes some of the salient 2D and Doppler features that aid in differentiating

**TABLE 33-1 Two-Dimensional, Doppler, and M-Mode Echocardiographic Features of Pulmonary Venous Hypertension and Pulmonary Arterial (and Related) Hypertension**

| *Pulmonary Venous Hypertension* | *Pulmonary Arterial* Hypertension* |
|---|---|
| **2D Imaging** | |
| Normal or dilated LV size | Normal or small LV size |
| LV hypertrophy | No LV hypertrophy |
| Variable LV ejection fraction | Normal or increased LV ejection fraction |
| Mitral annular calcification | No mitral annular calcification |
| Dilated LA size | Normal or small LA size |
| RV:LV ratio <1 | RV:LV ratio >1 |
| Sharp RV angle | Open/round RV angle |
| RV not apex forming | Apex-forming RV |
| Preserved septal shape (no flattening) | Septal flattening/D-shaped LV cavity |
| No pericardial effusion | Pericardial effusion |
| Normal RV function, TAPSE ≥2.0 cm | Reduced RV function, TAPSE <2.0 cm |
| **Doppler Imaging** | |
| E > A, type II or III (pseudonormal or restrictive diastolic filling pattern) | Normal or E < A, type I diastolic filling pattern |
| MR grade ≥2+, MR > TR | MR grade ≤1+, TR > MR |
| Variable PA systolic pressure (typically <70 mm Hg) | Variable PA systolic pressure (typically ≥ 70 mm Hg) |
| No systolic notching of flow velocity envelope in RV outflow tract | Mid-systolic notching of flow velocity envelope in RV outflow tract |
| Acceleration time of flow velocity envelope in RV outflow tract >95 ms | Acceleration time of flow velocity envelope in RV outflow tract <70 ms |
| TDI with RV S′ >10 cm/s | TDI with RV S′ <10 cm/s |
| **M-Mode Imaging** | |
| TAPSE ≥2.0 cm | TAPSE <2.0 cm |

*Pulmonary arterial causes to include pulmonary arterial hypertension (World Health Organization group I pulmonary hypertension), chronic thromboembolic pulmonary hypertension, and World Health Organization group III pulmonary hypertension with a normal LA pressure and pulmonary vascular resistance of more than 3 Wood units.

*A*, Atrial, or late diastolic inflow velocity; *E*, early diastolic inflow velocity; *MR*, mitral regurgitation; *TAPSE*, tricuspid annular systolic excursion; *TR*, tricuspid regurgitation.

the type of PH. This integrated assessment can help identify patients who need to be referred for invasive right heart catheterization.

Two examples of this integrated assessment are shown in Figures 33-11 and 33-12. All images in Figure 33-11 correspond to patient 1 (PVH), and the images in Figure 33-12 to patient 2 (PAH). In patient 1, the parasternal long-axis view (see Fig. 33-11, *A*) reveals LA enlargement and LV hypertrophy. The apical four-chamber view (see Fig. 33-11, *B*) also reveals LA enlargement and bowing of the interatrial septum to the right, which suggests higher LA than RA pressure. The LV ejection fraction is normal. The transmitral Doppler pattern reveals grade III diastolic dysfunction (see Fig. 33-11, *C*). The RV:LV ratio is less than 1.0 with a non–apex-forming RV and a relatively normal TAPSE (see Fig. 33-4, *A*). The RVOT Doppler pattern is not notched (see Fig. 33-11, *D*). This is highly suggestive of PVH without PVD. This patient would not likely be referred for invasive right heart catheterization at this stage because suspicion for PAH or an elevated PVR is low. Instead, the left heart condition would be managed and the patient's symptoms and PH monitored closely.

The parasternal long-axis view in patient 2 (see Fig. 33-12, *A*) shows normal LV wall thickness and LA size. Note the dilated coronary sinus, often indicative of high RA pressure (see Fig. 33-12, *A*, *arrow*). On the apical four-chamber view (see Figure 33-12, *B*), the RV:LV ratio is more than 1.0, with a rounded RV apical angle and an apex-forming RV. The LV ejection fraction is normal. The transmitral flow pattern reveals grade I diastolic dysfunction (see Fig. 33-12, *C*). The TAPSE (not shown) is reduced (1.7 cm), consistent with moderate RV dysfunction. The RVOT Doppler pattern has a midsystolic notching pattern (see Fig. 33-12, *D*), which has been shown to be 96% specific for a PVR of more than 5 Wood units.[5] The findings are highly consistent with PH of pulmonary vascular origin. This patient would be referred for urgent right heart catheterization, and the

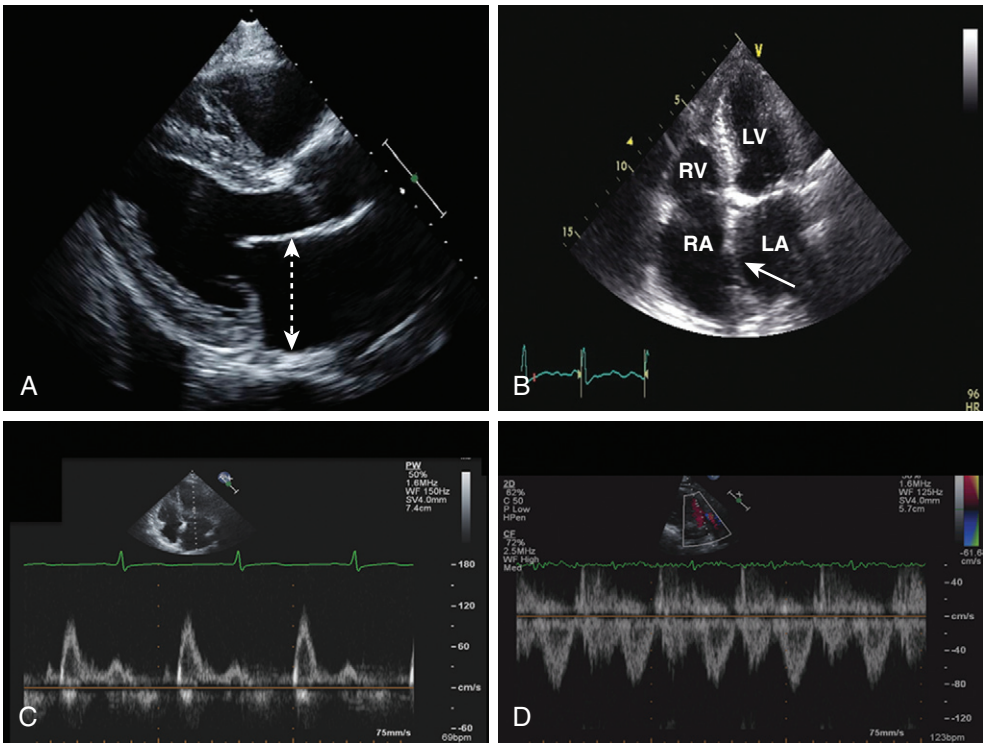



**Figure 33-11 Integrated 2D and Doppler echocardiographic assessment of a patient with pulmonary venous hypertension.** Note the LA enlargement (**A** and **B**) and the left to RA septal bowing (**B;** *arrow*). **C,** A restrictive transmitral flow pattern is shown. The pulsed wave Doppler of the RV outflow tract reveals no notching in the RV outflow velocity curve (**D**), consistent with a normal pulmonary vascular resistance

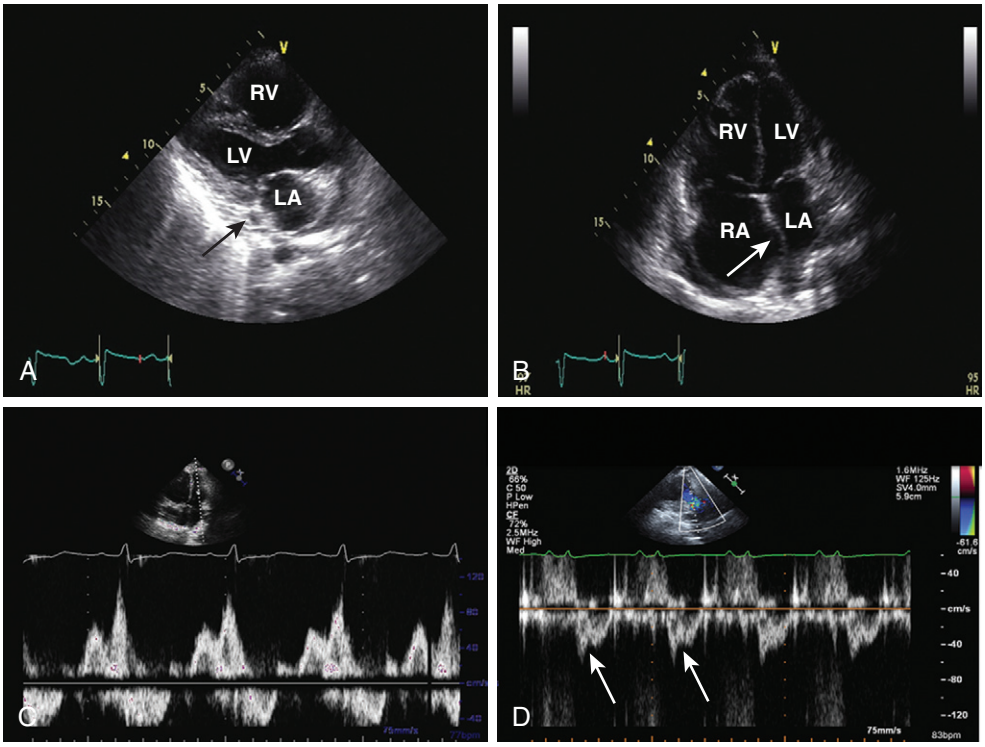



**Figure 33-12 Integrated 2D and Doppler echocardiographic assessment of a patient with pulmonary arterial hypertension.** Note normal LA size with a dilated coronary sinus (**A;** *arrow*) and right to LA septal bowing (**B**). **C,** A grade I diastolic dysfunction pattern is shown, and the pulsed wave Doppler of the RV outflow tract reveals a midsystolic notching in the RV outflow velocity signal (**D;** *arrows*), consistent with a high pulmonary vascular resistance.

needed imaging and functional studies would be completed to rule out underlying lung disease or CTEPH.

## EXERCISE ECHOCARDIOGRAPHY

Exercise stress echocardiography is used with increasing frequency in the assessment of patients with known or suspected PH and in the context of dyspnea of unclear etiology. In the former case, the presence or absence of exercise-induced PH is thought to increase the diagnostic sensitivity for the early stages of PVD; in the latter case, a rise in PASP is often thought to provide "proof" of PH as an important source of a patient's dyspnea. Although conceptually attractive, exercise stress echocardiographic assessment and interpretation has multiple important limitations that need be addressed to best apply this modality in clinical practice.

The first issue to address is whether a rise in PA pressure should occur with exercise. The time-honored teaching on this subject is that the PA pressure should not increase with exercise. However, studies do not support this and indicate that exercise-induced PH is more common than once appreciated. In 1966, Damato, Galante, and Smith[95] reported on the hemodynamic responses of 24 healthy male volunteers who underwent upright treadmill exercise with a PA catheter in place. The average peak oxygen consumption was 30 mL $O_2$/kg/min (~8 to 9 METS), which indicated normal but not elite exercise performance. At peak exercise, 10 of the 24 healthy subjects had a mPAP of more than 30 mm Hg, which met the definition of exercise-induced PH; the increases in PA pressure correlated with increasing CO, and the pressure-flow relationship and total pulmonary resistance remained normal in all subjects.[95] Bossone and colleagues[96] showed that highly conditioned college athletes routinely increased Doppler-estimated PASP to more than 50 mm Hg at peak exercise, whereas the healthy nonathletes typically did not exceed a PASP of 30 mm Hg. The degree of PASP elevation correlated best with changes in stroke volume, again indicating a normal pressure-flow relationship.

The second important limitation of exercise echocardiographic assessment of PA pressure is that changes in LA pressure are not accounted for during exercise. This is critical, given that exercise-induced PH (in health and in disease) most commonly arises from the interaction between an increased CO and a rise in the LA pressure.[97,98] To the contrary, Laskey and co-workers[99] showed that the PVR of patients with idiopathic PAH remained elevated during exercise but unchanged from resting values. Thus, exercise-induced pulmonary vasoconstriction is not typical, even in patients with established severe PVD. In the authors' experience with exercising patients with all forms of PH in the catheterization laboratory, a 1 to 2 Wood units increase in the PVR with exercise is quite unusual; and when it does occur, it is an abnormal finding that typically occurs in subjects with a significantly elevated baseline PVR.

The third limitation of exercise Doppler echocardiography is the accuracy of Doppler PASP assessment. Also, age likely exerts an important influence on the relative change in PA pressure with exercise because of age-related increases in pulmonary vascular stiffness; thus, exercise-induced PH, even at relatively low workloads, may be a part of the normal aging process, similar to the exaggerated increase in systemic arterial pressure with aging.[100] Lastly, the systemic blood pressure response to exercise should be factored into the interpretation of an exercise-induced rise in PA pressure. For example, a rise in PASP from 35 to 70 mm Hg in the context of a rise in systemic systolic pressure from 120 to 210 mm Hg indicates that the relative

proportion of pulmonary to systemic blood pressure has remained quite similar from rest to exercise, thus questioning the clinical significance of the rise in PA pressure in this context.

Taken together, one must exercise caution in the interpretation of a rise in Doppler-estimated PA pressure with exercise. A rise in PA pressure with exercise in many cases amounts to an association, but not a diagnosis, of the source of dyspnea in an individual patient. For many of these reasons, the recently published expert consensus document from the American College of Cardiology/American Heart Association recommends that at this time no treatment decisions for PH be made on the basis of exercise echocardiography.[1]

An alternative approach to exercise echocardiography may be a focus on the RV functional response to exercise, especially considering that impaired RV functional reserve is the mechanism of exercise limitation in PAH and other forms of PVD.[101] This approach may provide a more direct and clinically relevant answer as to whether a patient has clinically significant latent PVD or PH as the cause of dyspnea. If the RV function augments normally with exercise, the rise in PA pressure is likely flow mediated and of far less clinical significance. In contrast, a dilating and nonaugmenting RV seems to indicate an impedance-mediated process of greater clinical significance. In healthy subjects, TAPSE increases from approximately 2.5 cm at rest to 2.8 to 3.0 cm at peak exercise. Preliminary evidence suggests that the RV functional response to exercise (change in TAPSE) is linked to clinical outcome. In a relatively small cohort of patients with stable PAH, subjects either maintained a TAPSE similar to the resting TAPSE after graded supine ergometry or had a fall in TAPSE with exercise. A fall in TAPSE with exercise was strongly associated with adverse clinical events within 1 year of follow-up.[102] Importantly, a rise in the peak TR jet velocity after exercise was associated with better exercise-induced RV function and better clinical outcome. We suspect that more evidence will arise in the near future to support the notion that the focus of exercise echocardiography should be primarily on the RV functional response to exercise and away from the PASP change with exercise.

## KEY POINTS

- The pulmonary artery systolic pressure (PASP) is calculated by the peak velocity of the TR jet with the formula $PASP = 4v_{TR}^2 + RA$ pressure. The RA pressure is calculated from the collapse of the inferior vena cava during inspiration. The diastolic pressure can be obtained from the pulmonic regurgitation jet velocity at end diastole. The pulse pressure is the systolic minus the diastolic pressure.
- The RV shortens more in the longitudinal plane than in the transverse plane. TAPSE correlates well with RV function because it is a measure of longitudinal shortening. Assessment of free wall motion is not reliable, in itself, as a measure of RV function.
- The PASP depends on flow and LA pressure and on the afterload facing the RV (PVR). An elevated PASP is not synonymous with elevated afterload.
- The inspection of the RV outflow tract flow velocity envelope is an important part of the evaluation of a patient with elevated PASP. A short acceleration time (i.e., less than 80 ms) and a late or midsystolic notch are consistent with pulmonary hypertension (PH) from PVD; a normal acceleration time and flow velocity envelope without notching are not suggestive of elevated PVR no matter what the level of PASP.
- The classic triad of RV enlargement, decreased RV systolic function, and interventricular septal bowing into the LV suggests pulmonary vascular disease. The presence of these findings, even in the setting of a normal noninvasive PASP, should lead to further investigation.
- Chronic thromboembolic PH has similar echocardiographic features to idiopathic pulmonary arterial hypertension, but the pulmonary pulse pressure is usually greater than in other forms of PH.
- The most common cause of PH and RV dysfunction is LA hypertension. Increased LA volume, Doppler evidence of elevated LA pressure (grade II or III diastolic dysfunction), LV hypertrophy, and LV systolic dysfunction are present to varying degrees.
- Porto-pulmonary hypertension is a form of PAH. It is an important diagnosis in patients with end-stage liver disease because untreated it portends a poor prognosis with or without liver transplant. It must be distinguished from the far more common elevation in PAP in these patients from high CO.
- An integrated approach to the Doppler echocardiographic examination, which factors in both 2D and Doppler evidence that supports or refutes the presence of PVD, provides powerful insight into the hemodynamic basis of PH. This approach provides far greater physiologic information that the PASP assessment alone.

## REFERENCES


1. McLaughlin VV, Archer SL, Badesch DB, et al: ACCF/AHA 2009 expert consensus document on pulmonary hypertension a report of the American College of Cardiology Foundation Task Force on Expert Consensus Documents and the American Heart Association developed in collaboration with the American College of Chest Physicians; American Thoracic Society, Inc.; and the Pulmonary Hypertension Association. *J Am Coll Cardiol* 53:1573-1619, 2009.
2. McQuillan BM, Picard MH, Leavitt M, Weyman AE: Clinical correlates and reference intervals for pulmonary artery systolic pressure among echocardiographically normal subjects. *Circulation* 104:2797-2802, 2001.
3. Proceedings of the 4th World Symposium on Pulmonary Hypertension, February 2008, Dana Point, California. *J Am Coll Cardiol* 54:S1-S117, 2009.
4. McLaughlin VV, Presberg KW, Doyle RL, et al: Prognosis of pulmonary arterial hypertension: ACCP evidence-based clinical practice guidelines. *Chest* 126(1 Suppl):78S-92S, 2004.
5. Arkles JS, Opotowsky AR, Ojeda J, et al: Shape of the right ventricular Doppler envelope predicts hemodynamics and right heart function in pulmonary hypertension. *Am J Respir Crit Care Med* 183:268-276, 2011.
6. Kussmaul WG, Noordergraaf A, Laskey WK: Right ventricular-pulmonary arterial interactions. *Ann Biomed Engineering* 20:63-80, 1992.
7. Fisher MR, Forfia PR, Chamera E, et al: Accuracy of Doppler echocardiography in the hemodynamic assessment of pulmonary hypertension. *Am J Respir Crit Care Med* 179:615-621, 2009.
8. Kerbaul F, Brimioulle S, Rondelet B, et al: How prostacyclin improves cardiac output in right heart failure in conjunction with pulmonary

hypertension. *Am J Respir Crit Care Med* 175:846-850, 2007.
9. Kuehne T, Yilmaz S, Steendijk P, et al: Lange. Magnetic resonance imaging analysis of right ventricular pressure-volume loops: in vivo validation and clinical application in patients with pulmonary hypertension. *Circulation* 110:2010-2016, 2004.
10. Kitabatake A, Inoue M, Asao M, et al: Noninvasive evaluation of pulmonary hypertension by a pulsed Doppler technique. *Circulation* 68:302-309, 1983.
11. Furuno Y, Nagamoto Y, Fujita M, et al: Reflection as a cause of mid-systolic deceleration of pulmonary flow wave in dogs with acute pulmonary hypertension: comparison of pulmonary artery constriction with pulmonary embolisation. *Cardiovasc.Res* 25:118-124, 1991.
12. Torbicki A, Kurzyna M, Ciurzynski M, et al: Proximal pulmonary emboli modify right ventricular ejection pattern. *Eur Respir J* 13:616-621, 1999.
13. Castelain V, Hervé P, Lecarpentier Y, et al: Pulmonary artery pulse pressure and wave reflection in chronic pulmonary thromboembolism and primary pulmonary hypertension. *J Am Coll Cardiol* 37:1085-1092, 2001.
14. Galie N, Ghofrani HA, Torbicki A, et al: Sildenafil citrate therapy for pulmonary arterial hypertension. *N Engl J Med* 353:2148-2157, 2005.
15. Rubin LJ, Badesch DB, Barst RJ, et al: Bosentan therapy for pulmonary arterial hypertension. *N Engl J Med* 346:896-903, 2002.
16. Goodman DJ, Harrison DC, Popp RL: Echocardiographic features of primary pulmonary hypertension. *Am J Cardiol* 33:438-443, 1974.
17. Bossone E, Duong-Wagner TH, Paciocco G, et al: Echocardiographic features of primary ulmonary hypertension. *J Am Soc Echocardiogr* 12:655-662, 1999.
18. Nishimura RA, Tajik AJ: Evaluation of diastolic filling of left ventricle in health and disease: Doppler echocardiography is the clinician's Rosetta Stone. *J Am Coll Cardiol* 30:8-18, 1997.
19. Raymond RJ, Hinderliter AL, Willis PW, et al: Echocardiographic predictors of adverse outcomes in primary pulmonary hypertension. *J Am Coll Cardiol* 39:1214-1219, 2002.
20. Eysmann S, Palevsky HI, Reichek N, et al: Two-dimensional and Doppler echocardiographic and cardiac catheterization correlates of survival in primary pulmonary hypertension. *Circulation* 80:353-360, 1989.
21. Torbicki A, Kurzyna M: Pulmonary arterial hypertension: evaluation of the newly diagnosed patient. *Semin Respir Crit Care Med* 26:372-378, 2005.
22. Hinderliter AL, Willis PW, 4th, Long W, et al: Frequency and prognostic significance of pericardial effusion in primary pulmonary hypertension. PPH Study Group. Primary pulmonary hypertension. *Am J Cardiol* 84:481-484, 1999.
23. Hemnes AR, Gaine SP, Wiener CM: Poor outcomes associated with drainage of pericardial effusions in patients with pulmonary arterial hypertension. *South Med J* 101:490-494, 2008.
24. Eysmann SB, Palevsky HI, Reichek N, et al: Two-dimensional and Doppler-echocardiographic and cardiac catheterization correlates of survival in primary pulmonary hypertension. *Circulation* 80:353-360, 1989.
25. Ricciardi MJ, Bossone E, Bach DS, et al: Echocardiographic predictors of an adverse response to a nifedipine trial in primary pulmonary hypertension: diminished left ventricular size and leftward ventricular septal bowing. *Chest* 116:1218, 1999.
26. Tei C, Dujardin KS, Hodge DO, et al: Doppler echocardiographic index for assessment of global right ventricular function. *J Am Soc Echocardiogr* 9:838-847, 1996.
27. Yeo TC, Dujardin KS, Tei C, et al: Value of a Doppler-derived index combining systolic and diastolic time intervals in predicting outcome in primary pulmonary hypertension. *Am J Cardiol* 81:1157-1161, 1998.
28. Forfia PR, Fisher MR, Mathai SC, et al: Tricuspid annular displacement predicts survival in pulmonary hypertension. *Am J Respir Crit Care Med* 174:1034-1041, 2006.
29. Galiè N, Hinderliter AL, Torbicki A, et al: Effects of the oral endothelin-receptor antagonist bosentan on echocardiographic and doppler measures in patients with pulmonary arterial hypertension. *J Am Coll Cardiol* 41: 1380-1386, 2003.
30. Hinderliter AL, Willis PW 4th, Barst RJ, et al: Effects of long-term infusion of prostacyclin (epoprostenol) on echocardiographic measures of right ventricular structure and function in primary pulmonary hypertension. Primary Pulmonary Hypertension Study Group. *Circulation* 95:1479-1486, 1997.
31. Basil A, Liu T, Arkles J, et al: Serial changes in TAPSE correlate with functional assessment and clinical events in patients with PAH. *Am J Respir Crit Care Med* 179:A4882, 2009.
32. Brown SB, Raina A, Katz D, et al: Longitudinal shortening accounts for the majority of right ventricular contraction in normal subjects and in pulmonary arterial hypertension and improves after pulmonary vasodilator therapy. *Chest* 140:27-33, 2010.
33. Guyton AC, Lindsey AW, Gilluly JJ: The limits of right ventricular compensation following acute increase in pulmonary circulatory resistance. *Circ Res* 2:326-332, 1954.
34. Kasper W, Geibel A, Tiede N, et al: Distinguishing between acute and subacute massive pulmonary embolism by conventional and Doppler echocardiography. *Br Heart J* 70:352-356, 1993.
35. Jardin F, Dubourg O, Guéret P, et al: Quantitative two-dimensional echocardiography in massive pulmonary embolism: emphasis on ventricular interdependence and leftward septal displacement. *J Am Coll Cardiol* 10:1201-1206, 1987.
36. Ribeiro A, Juhlin-Dannfelt A, Brodin LA, et al: Pulmonary embolism: relation between the degree of right ventricle overload and the extent of perfusion defects. *Am Heart J* 135:868-874, 1998.
37. Miniati M, Monti S, Pratali L, et al: Value of transthoracic echocardiography in the diagnosis of pulmonary embolism: results of a prospective study in unselected patients. *Am J Med* 110:528-535, 2001.
38. Ribeiro A, Lindmarker P, Johnsson H, et al: Pulmonary embolism: one-year follow-up with echocardiography Doppler and five-year survival analysis. *Circulation* 99:1325-1330, 1999.
39. McConnell MV, Solomon SD, Rayan ME, et al: Regional right ventricular dysfunction detected by echocardiography in acute pulmonary embolism. *Am J Cardiol* 78:469-473, 1996.
40. Hsiao SH, Lee CY, Chang SM, et al: Pulmonary embolism and right heart function: insights from myocardial Doppler tissue imaging. *J Am Soc Echocardiogr* 19:822-828, 2006.
41. Kurzyna M, Torbicki A, Pruszczyk P, et al: Disturbed right ventricular ejection pattern as a new Doppler echocardiographic sign of acute pulmonary embolism. *Am J Cardiol* 90:507-511, 2002.
42. Torbicki A, Galiè N, Covezzoli A, et al: Right heart thrombi in pulmonary embolism: results from the International Cooperative Pulmonary Embolism Registry. *J Am Coll Cardiol* 41:2245-2251, 2003.
43. Pierre-Justin G, Pierard LA: Management of mobile right heart thrombi: a prospective series. *Int J Cardiol* 99:381-388, 2005.
44. Pruszczyk P, Torbicki A, Pacho R, et al: Noninvasive diagnosis of suspected severe pulmonary embolism: transesophageal echocardiography vs spiral CT. *Chest* 112:722-728, 1997.
45. Goldhaber SZ, Haire WD, Feldstein ML, et al: Alteplase versus heparin in acute pulmonary embolism: randomized trial assessing right-ventricular function and pulmonary perfusion. *Lancet* 341:507-511, 1993.
46. Goldhaber SZ, Visani L, De Rosa M: Acute pulmonary embolism: clinical outcomes in the International Cooperative Pulmonary Embolism Registry (ICOPER). *Lancet* 353:1386-1389, 1999.
47. Ribeiro A, Lindmarker P, Juhlin-Dannfelt A, et al: Echocardiography Doppler in pulmonary embolism: right ventricular dysfunction as a predictor of mortality rate. *Am Heart J* 134:479-487, 1997.
48. Kucher N, Rossi E, De Rosa M, Goldhaber SZ: Prognostic role of echocardiography among patients with acute pulmonary embolism and a systolic arterial pressure of 90 mm Hg or higher. *Arch Intern Med* 165:1777-1781, 2005.
49. Konstantinides S, Geibel A, Heusel G, et al: Heparin plus alteplase compared with heparin alone in patients with submasssivepulmonary embolism. *N Engl J Med* 347:1143-1150, 2002.
50. Goldhaber SZ: Thrombolysis for pulmonary embolism. *N Engl J Med* 347:1131-1132, 2002.
51. Sukhija R, Aronow WS, Lee J, et al: Association of right ventricular dysfunction with in-hospital mortality in patients with acute pulmonary embolism and reduction in mortality in patients with right ventricular dysfunction by pulmonary embolectomy. *Am J Cardiol* 95:695-696, 2005.
52. Leacche M, Unic D, Goldhaber SZ, et al: Modern surgical treatment of massive pulmonary embolism: results in 47 consecutive patients after rapid diagnosis and aggressive surgical approach [see comment]. *J Thorac Cardiovasc Surg* 129:1018-1023, 2005.
53. Ribeiro A, Lindmarker P, Johnsson H, et al: Pulmonary embolism: one-year follow-up with echocardiography Doppler and five-year survival analysis. *Circulation* 99:1325-1330, 1999.
54. Dartevelle P, Fadel E, Mussot S, et al: Chronic thromboembolic pulmonary hypertension. *Eur Respir J* 23:637-648, 2004.
55. Fedullo PF, Auger WR, Kerr KM, Rubin LJ: Chronic thromboembolic pulmonary hypertension. *N Engl J Med* 345:1465-1472, 2001.
56. Bresser P, Pepke-Zaba J, Jais X, et al: Medical therapies for chronic thromboembolic pulmonary hypertension: an evolving treatment paradigm. *Proc Am Thorac Soc* 3:594-600, 2006.
57. Nakayama Y, Nakanishi N, Sugimachi M, et al: Characteristics of pulmonary artery pressure waveform for differential diagnosis of chronic pulmonary thromboembolism and primary

pulmonary hypertension. *J Am Coll Cardiol* 29:1311-1316, 1997.
58. Tanabe N, Okada O, Abe Y, et al: The influence of fractional pulse pressure on the outcome of pulmonary thromboendarterectomy. *Eur Respir J* 17:653-659, 2001.
59. Nakayama Y, Sugimachi M, Nakanishi N, et al: Noninvasive differential diagnosis between chronic pulmonary thromboembolism and primary pulmonary hypertension by means of Doppler ultrasound measurement. *J Am Coll Cardiol* 31:1367-1371, 1998.
60. Casaclang-Verzosa G, McCully RB, Oh JK, et al: Effects of pulmonary thromboendarterectomy on right-sided echocardiographic parameters in patients with chronic thromboembolic pulmonary hypertension. *Mayo Clin Proc* 81:777-782, 2006.
61. Menzel T, Kramm T, Wagner S, et al: Improvement of tricuspid regurgitation after pulmonary thromboendarterectomy. *Ann Thorac Surg* 73:756-761, 2002.
62. Hardziyenka M, Reesink HJ, Bouma BJ, et al: A novel echocardiographic predictor of in-hospital mortality and mid-term haemodynamic improvement after pulmonary endarterectomy for chronic thrombo-embolic pulmonary hypertension. *Eur Heart J* 28:842-849, 2007.
63. Montani D, Price LC, Dorfmuller P, et al: Pulmonary veno-occlusive disease. *Eur Respir J* 33:189-200, 2009.
64. Nunes H, Humbert M, Capron F, et al: Pulmonary hypertension associated with sarcoidosis: mechanisms, haemodynamics and prognosis. *Thorax* 61:68-74, 2006.
65. Jander N, Minners J, Arentz T, et al: Transesophageal echocardiography in comparison with magnetic resonance imaging in the diagnosis of pulmonary vein stenosis after radiofrequency ablation therapy. *J Am Soc Echocardiogr* 18:654-659, 2005.
66. Packer DL, Keelan P, Munger TM, et al: Clinical presentation, investigation, and management of pulmonary vein stenosis complicating ablation for atrial fibrillation. *Circulation* 111:546-554, 2005.
67. Nilsson B, Chen X, Pehrson S, et al: Acute fatal pulmonary vein occlusion after catheter ablation of atrial fibrillation. *J Interv Card Electrophysiol* 11:127-130, 2004.
68. Arentz T, Jander N, von Rosenthal J, et al: Incidence of pulmonary vein stenosis 2 years after radiofrequency catheter ablation of refractory atrial fibrillation. *Eur Heart J* 24:963-969, 2003.
69. Marrouche NF, Martin DO, Wazni O, et al: Phased-array intracardiac echocardiography monitoring during pulmonary vein isolation in patients with atrial fibrillation: impact on outcome and complications. *Circulation* 107: 2710-2716, 2003.
70. Purerfellner H, Aichinger J, Martinek M, et al: Incidence, management, and outcome in signifi cant pulmonary vein stenosis complicating ablation for atrial fibrillation. *Am J Cardiol* 93:1428-1431, 2004.
71. Bottio T, Angelini A, Testolin L, et al: How an undiscovered extensive peripheral pulmonary venous thrombosis destroyed a heart transplant: a case report. *Transplant Proc* 36:1551-1553, 2004.
72. Reilly MP, Plappert TJ, Wiegers SE: Cerebrovascular emboli related to pulmonary venous thrombosis after lung transplantation. *J Am Soc Echocardiogr* 11:299-302, 1998.
73. Ben-Dor I, Kramer MR, Raccah A, et al: Echocardiography versus right-sided heart catheterization among lung transplantation candidates. *Ann Thorac Surg* 81:1056-1060, 2006.
74. Hofer CK, Zollinger A, Rak M, et al: Therapeutic impact of intraoperative transesophageal echocardiography during noncardiac surgery. *Anaesthesia* 59:3-9, 2004.
75. Huang YC, Cheng YJ, Lin YH, et al: Graft failure caused by pulmonary venous obstruction diagnosed by intraoperative transesophageal echocardiography during lung transplantation. *Anesth Analg* 91:558-560, 2000.
76. Anand IS, Chandrashekhar Y, Ferrari R, et al: Pathogenesis of congestive state in chronic obstructive pulmonary disease. Studies of body water and sodium, renal function, hemodynamics, and plasma hormones during edema and after recovery. *Circulation* 86:12-21, 1992.
77. Bady E, Achkar A, Pascal S, et al: Pulmonary arterial hypertension in patients with sleep apnea syndrome. *Thorax* 55:934-939, 2000.
78. Nakatsuka M: Pulmonary vascular resistance and right ventricular function in morbid obesity in relation to gastric bypass surgery. *J Clin Anesth* 8:205-209, 1996.
79. Hetzel M, Kochs M, Marx N, et al: Pulmonary hemodynamics in obstructive sleep apnea: frequency and causes of pulmonary hypertension. *Lung* 181:157-166, 2003.
80. O'Hearn DJ, Gold AR, Gold MS, et al: Lower extremity edema and pulmonary hypertension in morbidly obese patients with obstructive sleep apnea. *Sleep Breath* 13:25-34, 2009.
81. Thabut G, Dauriat G, Stern JB, et al: Pulmonary hemodynamics in advanced COPD candidates for lung volume reduction surgery or lung transplantation. *Chest* 127:1531-1536, 2005.
82. Chaouat A, Bugnet AS, Kadaoui N, et al: Severe pulmonary hypertension and chronic obstructive pulmonary disease. *Am J Respir Crit Care Med* 172:189-194, 2005.
83. Fartoukh M, Humbert M, Capron F, et al: Severe pulmonary hypertension in histiocytosis X. *Am J Respir Crit Care Med* 161:216-223, 2000.
84. Shorr AF, Helman DL, Davies DB, Nathan SD: Pulmonary hypertension in advanced sarcoidosis: epidemiology and clinical characteristics. *Eur Respir J* 25:783-788, 2005.
85. Trad S, Amoura Z, Beigelman C, et al: Pulmonary arterial hypertension is a major mortality factor in diffuse systemic sclerosis, independent of interstitial lung disease. *Arthritis Rheum* 54:184-191, 2006.
86. Prasanna V, Raina A, Arkles J, et al: Echo-Doppler scoring system identifies "proportionate" and "disproportionate" pulmonary hypertension in patients with chronic left heart disease and respiratory disease. *Am J Respir Crit Care Med* 183:A2294, 2011.
87. Arcasoy SM, et al: Echocardiographic assessment of pulmonary hypertension in patients with advanced lung disease. *Am J Respir Crit Care Med* 167:735-740, 2003.
88. Kasimirb MT, Seebachera G, Jakscha P, et al: Reverse cardiac remodelling in patients with primary pulmonary hypertension after isolated lung transplantation. *Eur J Cardiothoracic Surg* 26:776-781, 2004.
89. Casas-Aparicio G, Castillo-Martínez L, Orea-Tejeda A, et al: The effect of successful kidney transplantation on ventricular dysfunction and pulmonary hypertension. *Transplantation Proceedings* 42:3524-3528, 2010.
90. Krowka MJ, Swanson KL, Frantz RP, et al: Portopulmonary hypertension: results from a 10-year screening algorithm. *Hepatology* 44:1502-1510, 2006.
91. Hopkins WE: The remarkable right ventricle of patients with Eisenmenger syndrome. *Coron Artery Dis* 16:19-25, 2005.
92. Tribouilloy CM, Enriquez-Sarano M, Rossi A, et al: Determinants of the pulmonary artery pressure rise in left ventricular dysfunction. *Cardiologia* 42:1051-1058, 1997.
93. Forfia PR: Approach to patients with heart failure and pulmonary hypertension. *Curr Treat Options Cardiovasc Med* 9:302-309, 2007.
94. Melenovsky V, Borlaug BA, Rosen B, et al: Cardiovascular features of heart failure with preserved ejection fraction versus nonfailing hypertensive left ventricular hypertrophy in the urban Baltimore community: the role of atrial remodeling/dysfunction. *J Am Coll Cardiol* 49:198-207, 2007.
95. Damato AN, Galante JG, Smith WM: Hemodynamic response to treadmill exercise in normal subjects. *J Appl Physiol* 21:959-966, 1966.
96. Bossone E, Rubenfire M, Bach DS, et al: Range of tricuspid regurgitation velocity at rest and during exercise in normal adult men: implications for the diagnosis of pulmonary hypertension. *J Am Coll Cardiol* 33:1662-1666, 1999.
97. Wagner PD, Gale GE, Moon RE, et al: Pulmonary gas exchange in humans exercising at sea level and simulated altitude. *J Appl Physiol* 61:260-270, 1986.
98. West JB: Left ventricular filling pressures during exercise: a cardiological blind spot? *Chest* 113:1695-1697, 1998.
99. Laskey WK, Ferrari VA, Palevsky HI, Kussmaul WG: Pulmonary artery hemodynamics in primary pulmonary hypertension. *J Am Coll Cardiol* 21:406-412, 1993.
100. Kovacs G, Berghold A, Scheidl S, Olschewski H: Pulmonary arterial pressure during rest and exercise in healthy subjects. A systematic review. *Eur Respir J* 34:888-894, 2009.
101. Sun XG, Hansen JE, Oudiz RJ, Wasserman K: Exercise pathophysiology in patients with primary pulmonary hypertension. *Circulation* 104:429-435, 2001.
102. Hacobian M, Cohen MC, Atherton D, Wirth JA: Right ventricular exercise echocardiographic predictors of worsened clinical status in patients with pulmonary arterial hypertension. *Am J Resp Crit Care Med* 183:A4996, 2011.

# 34 Right-Sided Valve Disease

CHARLES J. BRUCE, MB, CHB | HEIDI M. CONNOLLY, MD

**Introduction**
**Tricuspid Valve Disease**
**Tricuspid Regurgitation**
Background
Basic Principles and Echocardiographic Approach to Diagnosis
Technical Details, Quantitation, and Data Analysis
Clinical Utility, Outcome Data
Research Applications
Potential Limitations, Future Directions
**Tricuspid Stenosis**
Background
Basic Principles and Echocardiographic Approach
Technical Details, Quantitation, and Data Analysis
Clinical Utility, Outcome Data
Alternate Approaches
**Pulmonic Valve Disease**
**Pulmonic Valve Stenosis**
Background
Basic Principles and Echocardiographic Approach
Technical Details, Quantitation, and Data Analysis
Clinical Utility, Outcome Data
Alternate Approaches
**Pulmonic Valve Regurgitation**
Background
Basic Principles and Echocardiographic Approach
Technical Details, Quantitation, and Data Analysis
Clinical Utility, Outcome Data
Alternate Approaches

## Introduction

Right-sided valvular disease has historically received less attention than left-sided valve disease, in part because of how well these valve lesions are initially tolerated and the associated protracted latent asymptomatic period. Moreover, because tricuspid regurgitation (TR) is often the result of left-sided valve disease and pulmonic regurgitation (PR) is often the result of an underlying congenital cardiac lesion, the underlying disorder tends to dominate the clinical picture. However, right-sided valve disease, even if the result of an underlying disorder, is not benign, and the impact of tricuspid valve (TV) and pulmonic valve disease on morbidity and mortality is increasingly recognized. In this era of increasing awareness and improved treatment options for patients with valve disease, clinicians must consider the diagnosis of right-sided valve disease, understand the pathophysiology, choose appropriate confirmatory testing, and refer patients for timely intervention to prevent clinical deterioration with associated adverse consequences. Echocardiography plays a critical role in facilitating this process.

## Tricuspid Valve Disease

The normal TV is characterized by three sail-like leaflets: the anterior, posterior, and septal (Figure 34-1). The anterior leaflet is the most anatomically constant of the three; the other leaflets vary more often in size and position. The leaflets are attached to the TV annulus, a nonplanar structure with an elliptical saddle shape.[1] Similar to the mitral valve leaflets, the TV leaflets are restrained by chordae tendinea attached to the papillary muscles usually arranged in three groups, which are in turn inserted into the right ventricle (RV) wall beneath each of the three commissures. TV chordae may also insert directly into the RV free wall, a feature that distinguishes the right and left ventricles.

## Tricuspid Regurgitation

### BACKGROUND

Differentiation of a primary valve abnormality from valve dysfunction as a result of pulmonary hypertension or primary right heart disease is an important first step in the evaluation of patients with TR. Primary anatomic abnormalities of the TV, such as TV prolapse or endocarditis, are infrequent causes of TR. Rather, TR is more commonly the result of pulmonary hypertension, which in turn is often the result of left-sided heart disease.

### BASIC PRINCIPLES AND ECHOCARDIOGRAPHIC APPROACH TO DIAGNOSIS

Echocardiography is currently the reference standard for diagnosis and evaluation of TR. Because of nonspecific symptoms and subtle physical examination findings, severe TR is most often an incidental diagnosis at the time of echocardiographic evaluation of left-sided heart disease.

The echocardiographic evaluation follows the same principles as evaluation of left-sided lesions (see Chapter 18) and not only confirms the presence and severity of TR but also provides important information regarding etiology. Noninvasive estimation of pulmonary artery (PA) pressure and assessment of the

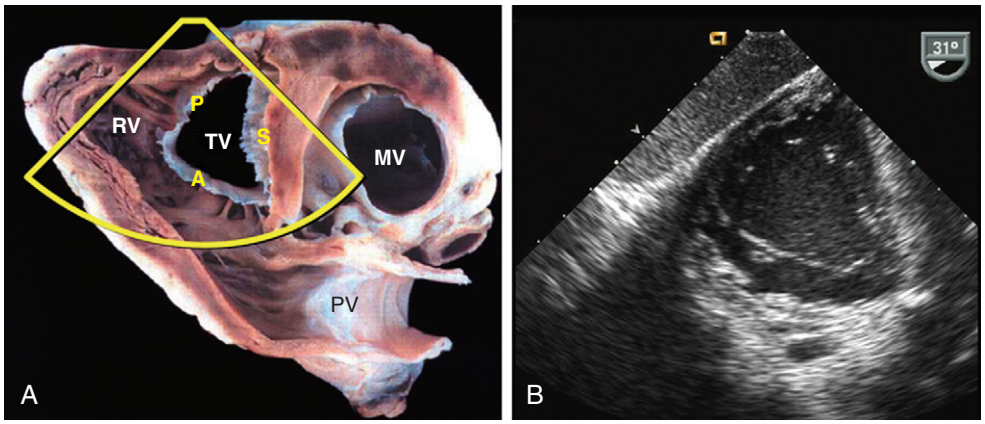



**Figure 34-1 Normal tricuspid valve anatomy. A,** Pathology image shows the RV with the tricuspid valve in a short-axis view. The pathologic section is oriented to replicate the transesophageal transgastric view obtained at a transducer angle of 31 degrees (**B**). Note the septal, anterior, and posterior leaflets. **B,** Transesophageal transgastric echocardiographic image with the same imaging plane (defined by the border in **A** shows the RV with tricuspid valve septal, anterior, and posterior leaflets. *A,* Anterior leaflet; *MV,* mitral valve; *P,* posterior leaflet; *PV,* pulmonic valve; *S,* septal leaflet. *(Pathologic image courtesy Dr William D. Edwards, Department of Laboratory Medicine and Pathology, Mayo Clinic College of Medicine.)*

consequences of TR on RV size and function are essential components of the echocardiographic examination. The approach to echocardiographic assessment of RV size and function and estimation of PA pressure are discussed in detail in Chapter 32.

## TECHNICAL DETAILS, QUANTITATION, AND DATA ANALYSIS

### *Determining the Etiology of Tricuspid Regurgitation*

Determination of the etiology requires careful assessment of TV leaflet morphology, annular dimension, subvalvular apparatus, and RV size and function (Box 34-1). Coexisting left-sided valvular heart disease or intracardiac shunt should be identified, and the presence of an intracardiac device (e.g., pacer or defibrillation lead) should prompt careful assessment of TV leaflet mobility. Also, assessment of the consequences of the valve abnormality on RV size and function is important.[2-4]

Transthoracic two-dimensional (2D) imaging of the TV involves ventricular inflow and short-axis views from the parasternal window and four-chamber views from both the apical and the subcostal windows. With 2D echocardiography, visualization of all three leaflets in one view is challenging.[5] The septal and anterior leaflets are consistently seen in the parasternal short-axis and apical four-chamber views.[6] Imaging with an anterior to posterior sweep in an apical four-chamber or subcostal view can overcome the limitation of reliable identification of the posterior leaflet. When the coronary sinus is seen, because this is a posterior structure, the posterior leaflet is identified. In addition, the posterior TV leaflet may occasionally be visualized from the parasternal short-axis view and from the RV inflow view with rotation of the transducer 90 degrees clockwise, resulting in a two-chamber view of the right heart. With transesophageal echocardiography (TEE), the TV is often best seen in the transgastric long-axis and short-axis views with the probe rotated towards the patient's right side (see Fig. 34-1). This view provides the only opportunity to visualize an en face view of the TV with 2D echocardiography. The TV can also be visualized from the mid esophageal four-chamber and basal short-axis views.[7]

Tricuspid regurgitation that is at least moderate or greater in severity is most frequently "functional" in nature. Functional

**Box 34-1**

**CAUSES OF TRICUSPID VALVE REGURGITATION**

**Congenital**
- Ebstein anomaly
- Tricuspid valve dysplasia
- Tricuspid valve hypoplasia
- Tricuspid valve cleft
- Double orifice tricuspid valve
- Unguarded tricuspid valve orifice

**Right Ventricular Disease**
- Right ventricular dysplasia
- Endomyocardial fibrosis
- Increased right heart pressure

**Acquired**
- Annular dilation
- Left-sided valvular heart disease
- Endocarditis
- Trauma
- Carcinoid heart disease
- Rheumatic heart disease
- Tricuspid valve prolapse
- Iatrogenic (radiation, drugs, biopsy, pacemaker, implanted cardiac defibrillator)

**Right Ventricular Dilation**
- Pulmonary hypertension
  - Primary pulmonary hypertension
  - Secondary to left-sided heart disease (valvular heart disease, cardiomyopathy, etc)
- Right ventricular volume overload
  - Atrial septal defect
  - Anomalous pulmonary venous drainage

TR by definition is not related to primary TV leaflet pathology but rather is the result of another disease process that causes RV dilation, distortion of the subvalvular apparatus, tricuspid annular ditation, or a combination of these.

On the basis of 2D imaging, the average normal annular diameter is 31 ± 1 mm, measured in a single plane from an apical four-chamber view. However, this measurement may be misleading because the tricuspid annulus is a dynamic structure and its dimensions change during the course of the cardiac cycle and in phases of respiration.[8,9] Furthermore, the tricuspid annulus

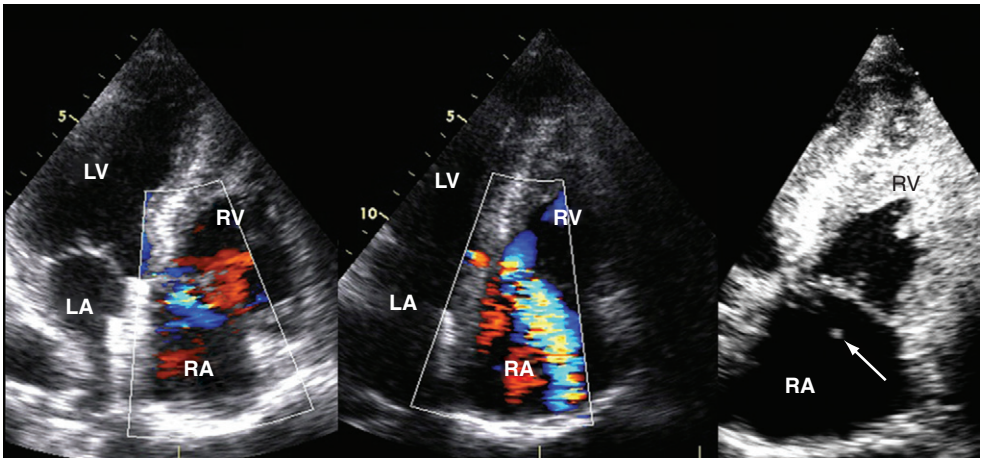



**Figure 34-2 Composite image showing a complication of endomyocardial biopsy.** In the *left image* (apical four-chamber view), mild tricuspid regurgitation is seen with color flow Doppler imaging. In the *center image*, obtained from the same view, an eccentric laterally directed jet of severe tricuspid regurgitation is seen. In the *right image*, a zoomed view of the tricuspid valve is seen. In addition, the severed tricuspid chordae is appreciated (*arrow*).

has a complex, three-dimensional (3D) saddle-like shape that make 2D assessment challenging. Three-dimensional echocardiography has shown that as functional TR worsens, the tricuspid annulus progressively becomes flatter and more circular, tending to dilate in the septal-lateral and posteroseptal to anterolateral dimensions.[1,8] Thus, 3D echocardiography holds promise in better definition of tricuspid annular dimensions and geometry, overcoming the inherent limitations of 2D imaging.

Causes of clinically significant TR are outlined in Box 34-1. Furthermore, a moderate or greater degree of TR, regardless of the primary etiology, usually engenders additional TR because of the adverse hemodynamic consequence of RV volume overload that results in a slow and inexorable clinical and hemodynamic deterioration.

Functional TR as a result of pulmonary hypertension is seen in patients with significant left-sided heart disease, commonly rheumatic in origin; in those with primary pulmonary hypertension; and in those with pulmonary disease that leads to cor pulmonale.[10] As a general rule, when systolic PA pressures increase beyond 55 mm Hg, TR can occur despite anatomically normal TV leaflets; whereas more than mild TR that occurs in the setting of lower systolic pulmonary pressures (less than 40 mm Hg) likely reflects a structural abnormality of the valve leaflets or the subvalvular apparatus.[2,11] Functional TR also results from tricuspid annular dilation in patients with RV enlargement from RV infarction, dilated cardiomyopathy, or left-to-right shunt, such as an atrial septal defect or anomalous pulmonary venous drainage.[12-14]

Primary TV pathology that leads to TR may result from blunt trauma or iatrogenic injury or from direct leaflet involvement by specific diseases. When the cause is by permanent pacemaker or internal cardiac defibrillator leads, the mechanism of valve injury is variable, related to lead entrapment in the tricuspid apparatus, direct leaflet perforation at the time of lead insertion, fibrotic adhesion of the lead to the leaflet, or avulsion or laceration of the TV leaflets on lead removal.[15] Because leaflet injury may be underappreciated in patients who have undergone lead implants, a high clinical index of suspicion is warranted, particularly when these patients present with worsening right heart failure.

Direct trauma from transvenous endomyocardial biopsy may occur, particularly in patients for cardiac transplantation who undergo repeated biopsies for rejection surveillance (Fig. 34-2).[16] Echocardiographic guidance during the biopsy may avert damage to the TV or subvalvular apparatus.

The TV leaflets and supporting structures may also be damaged indirectly with blunt chest trauma, most often after a motor vehicle accident that results in papillary muscle, valve, or chordal rupture. Routine use of echocardiography in the evaluation of victims of blunt chest trauma enhances detection of traumatic TR, overcoming the limitations of the history and physical examination.

Direct damage to the TV may occur as a result of infective and marantic endocarditis.[16,17] Right-sided infective endocarditis may be a manifestation of intravenous drug abuse.[2,18] It is also increasingly seen in patients with indwelling venous catheters used for dialysis or chemotherapy or with infected pacemaker or defibrillator devices. *Staphylococcus aureus* is responsible for 80% of these TV infections.[2] Infrequently, marantic or noninfective endocarditis may occur in the setting of connective tissue diseases, such as systemic lupus erythematosus, rheumatoid arthritis, or antiphospholipid antibody syndrome.[19] The TV may also be affected directly in as many as 30% to 50% of patients with rheumatic mitral valve disease.[20]

Serotonin active drugs may also induce TR by directly damaging the valve leaflets. This association was first described with the ergot alkaloids, ergotamine and methysergide, used for migraine therapy.[21] The anorectic drugs fenfluramine and dexfenfluramine, and pergolide and cabergoline, both dopamine agonists used in treatment of Parkinson disease and restless leg syndrome, may also induce TR with a similar mechanism.[22-24] The histopathologic changes seen in these drug-related valves include a fibroproliferative response that appears to be mediated by the 5-$HT_{2B}$ receptor.[25] These pathologic features are similar to those seen in carcinoid heart disease.

Carcinoid heart disease is a rare but distinctive form of valve disease that primarily affects the right-sided cardiac valves. Carcinoid is a tumor that arises from argentaffin cells. The primary tumor is usually located in the small bowel and metastasizes to the liver. The primary tumor and metastases produce active substances, including serotonin. Serotonin is recognized to be an agent involved in the development and progression of valve disease in patients with carcinoid syndrome.[26] Carcinoid heart disease involves a combination of TR (Fig. 34-3) with rare

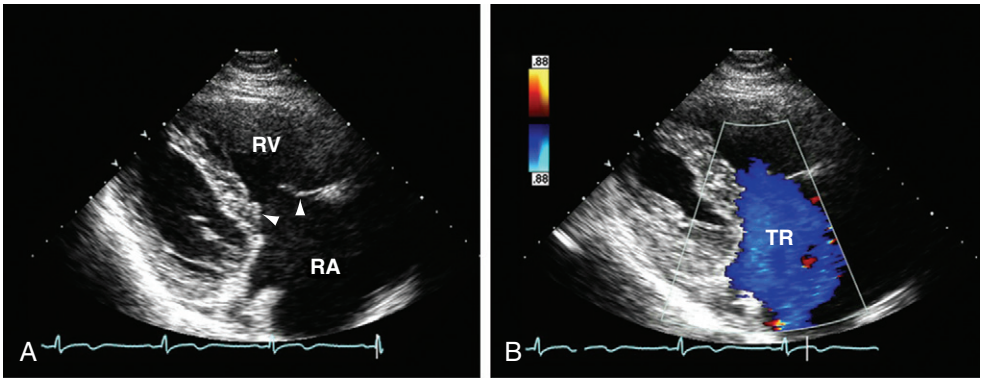
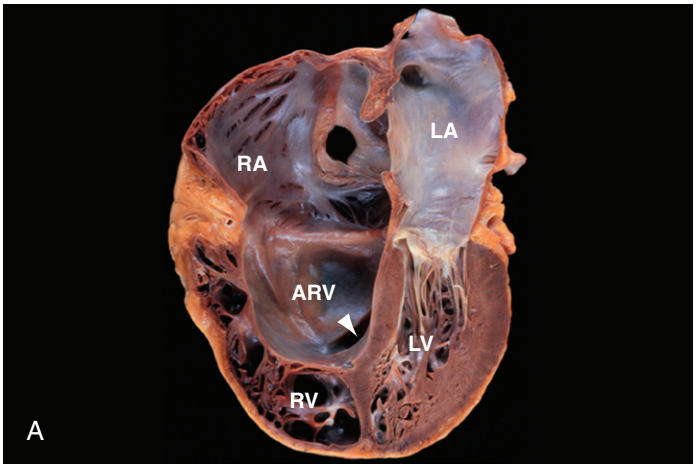
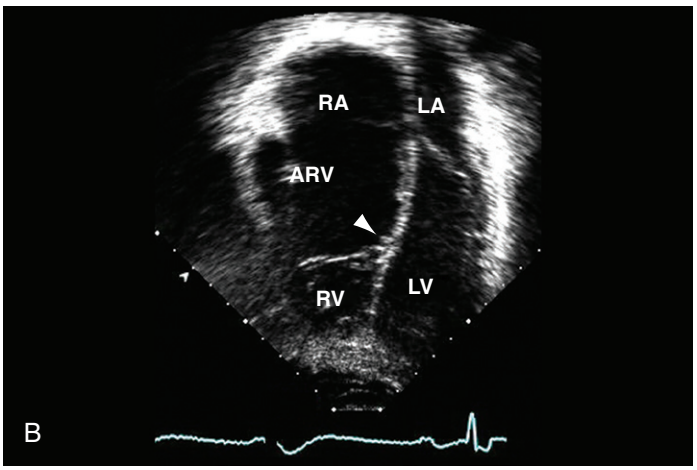



**Figure 34-3 Carcinoid heart disease.** **A,** Two-dimensional echocardiographic systolic image (RV inflow view) shows thickened septal and anterior tricuspid valve leaflets (*arrowheads*) and enlargement of the RV and RA. **B,** Color flow Doppler image shows severe tricuspid regurgitation (*TR*) in the same patient. Note laminar color flow (*blue*) filling an enlarged RA.



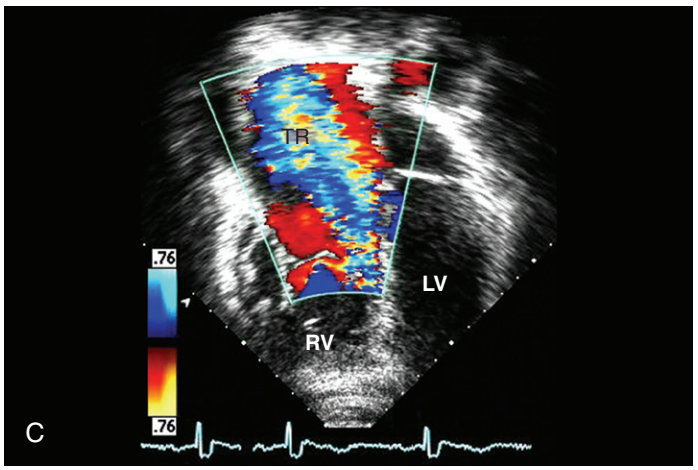




**Figure 34-4 Ebstein anomaly is characterized by apical displacement of the septal leaflet of the tricuspid valve (*arrowhead*) and variable tethering of the anterior leaflet.** The segment of RV myocardium between the leaflet insertion and the anatomic annulus is "atrialized" (*ARV*), as seen in the pathology specimen shown in the apical four-chamber "apex down" imaging format (**A**) and the 2D echocardiographic image shown in the same format (**B**). Because of associated valve disease, severe tricuspid regurgitation (*TR*) was noted with color flow imaging (**C**), resulting in a severely enlarged right heart chamber. *(Pathology image courtesy Dr. William D. Edwards, Department of Laboratory Medicine and Pathology, Mayo Clinic College of Medicine).*

stenosis and pulmonic stenosis (PS) and PR. Left-sided valvular abnormalities occur in approximately 10% of patients with carcinoid valve disease, characteristically as a result of shunting of blood from the right-to-left atrium through a patent foramen ovale or atrial septal defect and less commonly as a result of a bronchial carcinoid or active carcinoid disease with high levels of circulating serotonin.[27] Rarely, carcinoid valve disease occurs in patients without hepatic metastases; an ovarian carcinoid should be sought in this setting.[28]

Mediastinal radiation can directly damage the TV leaflets. The associated postinflammatory fibrosis and calcification that usually manifest 5 or more years after the radiation insult result in distortion of the leaflets that cause TR.[2,29,30] Assessment and treatment of TR in this setting may be complicated by concomitant dysfunction of other cardiac valves and pericardial, myocardial, and coronary artery involvement.

Endomyocardial fibrosis, which is prevalent in tropical Africa, causes fibrosis of the papillary muscle tip and thickening and shortening of the leaflets and chordae, which lead to regurgitation. This process may affect both mitral valves and TVs.

Congenital causes of TR are rare and include congenital TV prolapse, which may occur as an isolated abnormality or be associated with mitral valve prolapse and other connective tissue disorders.[31,32] The most common congenital cause of TR is Ebstein anomaly (Fig. 34-4).[33] In Ebstein anomaly, apical displacement of the septal and posterior TV leaflets into the RV and variable tethering of the anterior leaflet occur. The severity of TR depends on significant adherence of the leaflets to the RV

wall, the degree of annular tethering, and valve leaflet fenestrations. A patent foramen ovale or atrial septal defect occurs in more than 50% of patients with Ebstein anomaly. Other associations that should be considered include PS or ventricular septal defect.[34]

### *Determining the Severity of Tricuspid Regurgitation*

As many as 80% to 90% of patients referred for echocardiography have some degree of TR.[35] Thus, screening for significant TR often relies primarily on visual assessment of the jet area with color flow Doppler imaging. When this technique is used in research settings, the ratio of the jet area to the right atrial (RA) area is calculated. These areas are measured from the same view after ensuring the sector width allows visualization of the entire right atrium. A jet area of more than 10 $cm^2$ or a jet area-RA area ratio of 30% or more suggests severe TR.[4,7] However, although jet area has been reported to correlate with angiographic grading[36,37] and quantitative Doppler echocardiographic methods,[38] significant limitations are found with this approach. The regurgitant jet area, even corrected for the receiving chamber size, is strongly limited by its dependence on hemodynamic conditions,[39] instrument settings,[40] and jet interaction with the receiving chamber.[41] Accordingly, only a mediocre correlation exists between jet size and TR severity.[9,38,42-44] In addition, TR severity may be underestimated with color flow Doppler imaging when the jet is eccentric because the extent of the jet may not be appreciated in standard views.

Quantitative assessment of TR severity is possible with color flow Doppler to estimate the effective regurgitant orifice area with measuring the vena contracta. The vena contracta is the smallest regurgitant flow area immediately beyond the flow convergence region and before expansion of the turbulent regurgitant jet and corresponds hydrodynamically with the effective regurgitant orifice area. Imaging is usually performed from an apical view with use of the narrowest sector angle to optimize the imaging frame rate. The color gain should be adjusted step by step to obtain the maximal color gain level that does not introduce signal outside of flow areas. If necessary, the position of the transducer should be modified to optimize visualization of the flow convergence region and the regurgitant flow proximal and distal to the TV. With use of a zoom of the region of interest, the vena contracta is visualized (Fig. 34-5).[44] Measurements of the vena contracta width, made in mid systole, over four consecutive cardiac cycles should be averaged.[44] A vena contracta width of 6.5 mm or more identifies severe TR, with 89% sensitivity and 93% specificity. This measurement has a better correlation with the effective regurgitant orifice than that of TR jet area or jet-RA area ratio. On the basis of published guidelines for assessment of TR, when the vena contracta measures greater than 0.7 cm (with prioritization of specificity and positive predictive value), severe TR is present.[2,4,45,46]

Quantitative Doppler assessment is also feasible with the proximal isovelocity surface area (PISA) method, although this requires angle correction.[4] Color Doppler images of the proximal flow convergence of TR are obtained from an apical or paraapical view with a zoom of the region of interest. The position of the transducer should be modified to minimize the angle between the centerline of the flow convergence and the ultrasound beam. The color flow velocity scale is maximized and the baseline shifted downward until the flow convergence region is clearly visualized. After downshifting of the color baseline, the radius of the flow convergence is measured in mid systole and the corresponding aliasing velocity is noted. The ratio alpha/180 is then calculated, where alpha is the angle of the systolic inverted TV funnel (measured with a protractor from the same apical view), to account for the shape of the TV. With this angle correction, the midsystolic instantaneous regurgitant flow is then calculated as

$$\text{Rflow} = (2\pi \times r^2 \times \text{Vr}) \times (\text{alpha}/180)$$

where Rflow is the regurgitant flow, r is the radius, and Vr is the corresponding aliasing velocity. The effective regurgitant orifice area is then calculated as

$$\text{ERO} = \text{Rflow}/\text{V}$$

where ERO is the effective regurgitant orifice (Fig. 34-6). An effective regurgitant orifice of 0.4 $cm^2$ or more and a regurgitant

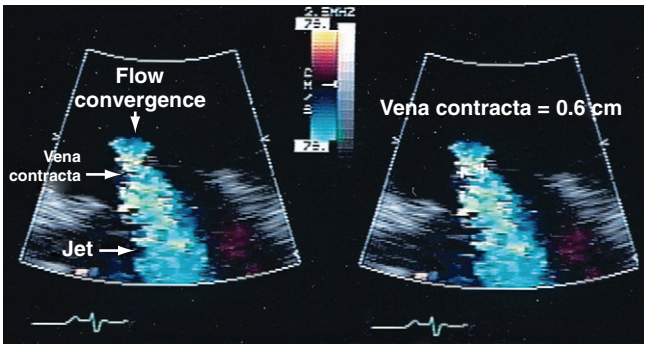



**Figure 34-5 Measurement of vena contracta.** Example of tricuspid regurgitant flow from the apical view with definition of the three components of the regurgitant flow (*left*) and measurement of the vena contracta width (*right; crosses*). *(With permission, from Tribouilloy CM, et al: Quantification of tricuspid regurgitation by measuring the width of the vena contracta with Doppler color flow imaging: a clinical study.* J Am Coll Cardiol *36:472-478, 2000.)*

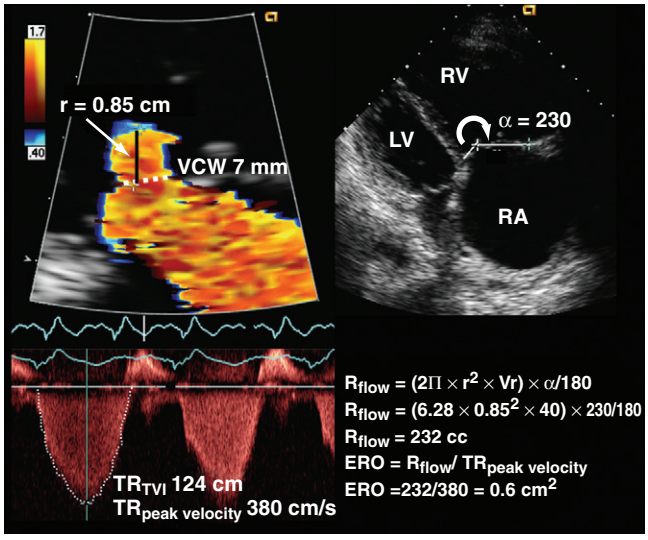



**Figure 34-6 Quantitative measurement of tricuspid regurgitation *(TR)* severity with the proximal isovelocity surface area method.** These images were obtained from a patient with severe pulmonary hypertension from pulmonary thromboembolic disease. The tricuspid regurgitation jet area is broad, and the vena contracta (*VC; top left panel, dashed line*) measures 0.7 cm, consistent with severe tricuspid regurgitation. The calculation of the effective regurgitant orifice *(ERO)* from the Doppler data as described in the text is illustrated. Note the angle correction illustrated in the *top right image*. In this patient, the effective regurgitant orifice is 0.6 $cm^2$, consistent with severe tricuspid regurgitation. *r,* Hemisphere radius.

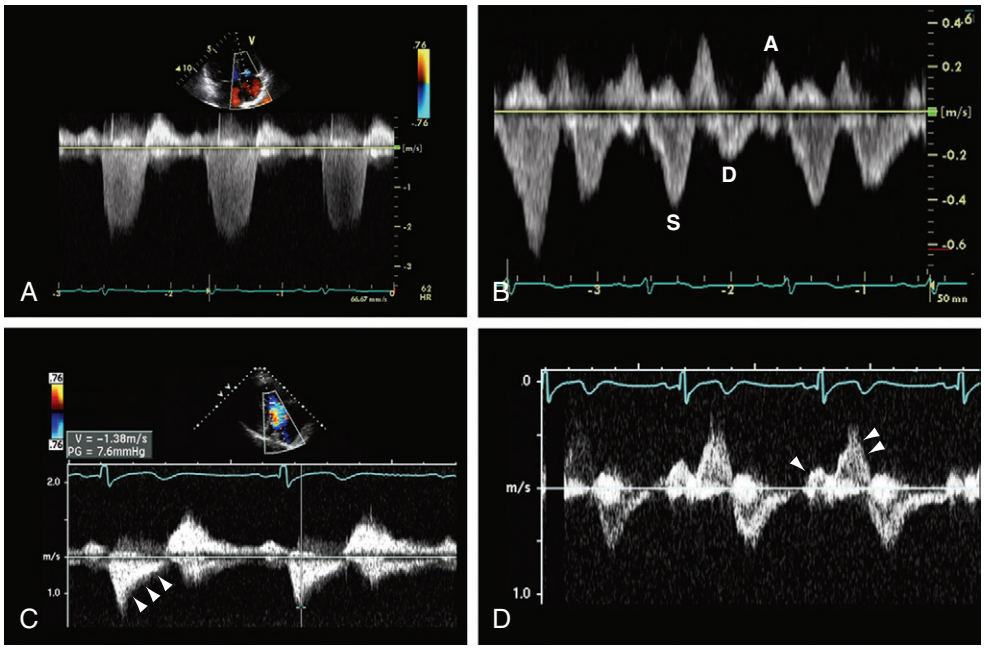



**Figure 34-7 Doppler findings in mild and severe tricuspid regurgitation. A,** Continuous wave Doppler signal across the tricuspid valve shows a low-velocity systolic jet (2 m/s) with a symmetrical rounded appearance consistent with mild tricuspid valve regurgitation. Measurement of the peak systolic velocity provides an indirect assessment of RV systolic pressure with the modified Bernoulli equation. **B,** Hepatic vein pulsed wave Doppler signal with accompanying electrocardiographic tracing shows normal hepatic vein flow in this patient with mild tricuspid regurgitation. Systolic flow *(S)* and diastolic flow *(D)* is seen emanating from the hepatic veins into the inferior vena cava (flow seen displayed below the baseline) and atrial reversal flow *(A)* representing normal flow refluxing into the hepatic veins resulting from atrial contraction. **C,** A dense systolic continuous wave Doppler signal is shown in a patient with severe tricuspid valve regurgitation. Severe tricuspid regurgitation results in a triangular or "dagger-shaped" *(arrowheads)* early peaking tricuspid regurgitant jet profile as a result of early equilibration of pressures between the RA and RV. **D,** Hepatic vein pulsed wave Doppler signal shows both atrial *(single arrowhead)* and systolic reversed flow *(double arrowhead)*, indicating elevation in RA pressure and severe tricuspid valve regurgitation in a patient in sinus rhythm. These systolic reversals reflect retrograde flow in the hepatic veins that can be appreciated clinically as a pulsatile liver. Hepatic vein systolic reversals may not be specific for severe tricuspid regurgitation when atrial fibrillation is present.

volume of 45 mL or more are considered diagnostic thresholds for severe TR.[7,43] Although the proximal isovelocity surface area method is quantitative,[18] it is not widely used in clinical practice because it is time consuming, requires technical experience in addition to angle correction, and is less well validated.

In general, the shape of the continuous wave TR Doppler signal is parabolic in patients with less than severe TR. In patients with severe TR, the continuous wave regurgitation jet may have a dense signal and a dagger-shaped appearance as a result of rapid equalization of pressures between the RA and the RV (Fig. 34-7).

Ancillary echocardiographic findings in patients with severe TR include increased tricuspid inflow velocity (1 m/s or more), inferior vena cava dilation of more than 2 cm, and systolic flow reversals in the hepatic veins.[4,46-48] The utility, advantages, and limitations of these measurements and the assessment and grading of TR severity are summarized in Tables 34-1 and 34-2.[4]

Recent research has highlighted the dynamic changes in TR severity with respiration. Large respiratory variations in TR occur with a striking inspiratory increase in vena contracta, effective regurgitant orifice, and regurgitant volume. This results principally from marked RV plasticity, inspiratory widening that results in annular enlargement and leads to less systolic annular coverage by the TV leaflets, and increased valvular tenting that contributes to mal coaptation. Thus, quantitative measurements of TR severity should take into account these large respiratory variations, avoiding the measurement of largest values and ensuring that measurements are included over the entire respiratory cycle (Fig. 34-8).[9]

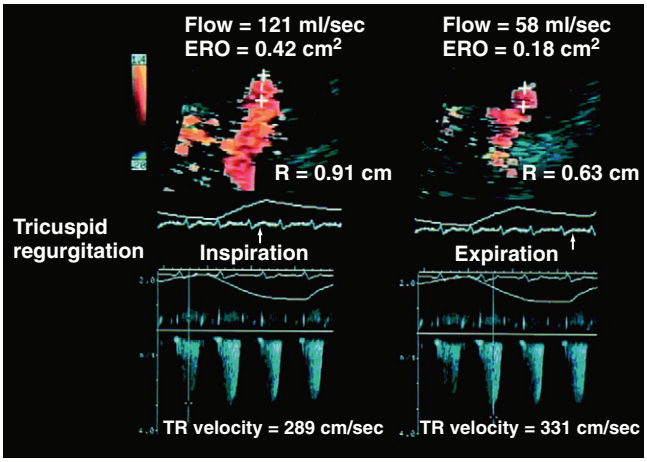



**Figure 34-8 Proximal flow convergence method: influence of respiration on tricuspid regurgitation severity.** Example of quantitative measurement of tricuspid regurgitation with inspiration and expiration. Shown are the measurements of regurgitant flow with the flow convergence method (*top*) and peak velocity with continuous wave Doppler imaging (*bottom*) with calculation of effective regurgitant orifice (*ERO*) in inspiration (*left*) and expiration (*right*). Respirometer curves ascend with inspiration and descend with expiration. During inspiration, maximal velocity decreases, regurgitant flow increases, and effective regurgitant orifice increases considerably. *(With permission, from Topilsky Y, et al: Pathophysiology of tricuspid regurgitation: quantitative Doppler echocardiographic assessment of respiratory dependence.* Circulation *122:1505-1513, 2010.)*

**TABLE 34-1 Echocardiographic and Doppler Parameters for Evaluation of Tricuspid Regurgitation: Utility, Advantages, and Limitations**

| *Parameter* | *Utility/Advantages* | *Limitations* |
|---|---|---|
| RV/RA/IVC size | Enlargement sensitive for chronic significant TR. Normal size virtually excludes significant chronic TR. | Enlargement seen in other conditions. May be normal in acute significant TR. |
| TV leaflet alterations | Flail valve specific for significant TR. | Other abnormalities do not imply significant TR. |
| Paradoxical septal motion (volume overload pattern) | Simple sign of severe TR. | Not specific for TR. |
| Jet area–color flow Doppler | Simple, quick screen for TR. | Subject to technical and hemodynamic factors. Underestimates severity in eccentric jets. |
| Vena contracta width | Simple, quantitative; separates mild from severe TR. | Intermediate values require further confirmation. |
| PISA method | Quantitative. | Validated in only a few studies. |
| Flow quantitation–pulse wave Doppler | Quantitative. | Not validated for determination of TR regurgitant fraction. |
| Jet profile–continuous wave Doppler | Simple, readily available. | Qualitative, complementary data. |
| Peak tricuspid E velocity | Simple, usually increased in severe TR. | Depends on RA pressure and RV relaxation, TV area, and atrial fibrillation; complementary data only. |
| Hepatic vein flow | Simple; systolic flow reversal is sensitive for severe TR. | Influenced by RA pressure, atrial fibrillation. |

With permission, from Zoghbi WA, et al: Recommendations for evaluation of the severity of native valvular regurgitation with two dimensional and Doppler echocardiography. *J Am Soc Echocardiogr* 16:777-802, 2003.
*IVC,* Inferior vena cava; *PISA,* proximal isovelocity surface area; *TR,* tricuspid regurgitation; *TV,* tricuspid valve.

**TABLE 34-2 Echocardiographic and Doppler Parameters Used in Grading of Tricuspid Regurgitation Severity**

| *Parameter* | *Mild* | *Moderate* | *Severe* |
|---|---|---|---|
| Tricuspid valve | Usually normal | Normal or abnormal | Abnormal, flail leaflet, poor coaptation |
| RV/RA/IVC size | Normal* | Normal or dilated | Usually dilated† |
| Jet area–central jets ($cm^2$)‡ | <5 | 5-10 | >10 |
| VC width (cm)§ | Not defined | Not defined, but <0.7 | >0.7 |
| PISA radius (cm)‖ | ≤0.5 | 0.6-0.9 | >0.9 |
| Jet density and contour–continuous wave | Soft and parabolic | Dense, variable contour | Dense, triangular with early peaking |
| Hepatic vein flow¶ | Systolic dominance | Systolic blunting | Systolic reversal |

With permission, from Zoghbi WA, et al: Recommendations for evaluation of the severity of native valvular regurgitation with two dimensional and Doppler echocardiography. *J Am Soc Echocardiogr* 16:777-802, 2003.
*IVC,* Inferior vena cava; *PISA,* proximal isovelocity surface area; *VC,* vena cava.
*Unless there are other reasons for RA or RV dilation. Normal 2D measurements from the apical 4-chamber view: RV medio-lateral end-diastolic dimension ≤4.3 cm, RV end-diastolic area ≤35.5 $cm^2$, maximal RA mediolateral and superoinferior dimensions ≤4.6 cm and 4.9 cm respectively, maximal RA volume ≤33 $ml/m^2$.
†Exception: acute TR.
‡At a Nyquist limit of 50-60 cm/s. Not valid in eccentric jets. Jet area is not recommended as the sole parameter of TR severity due to its dependence on hemodynamic and technical factors.
§At a Nyquist limit of 50-60 cm/s.
‖Baseline shift with Nyquist limit of 28 cm/s.
¶Other conditions may cause systolic blunting (e.g., atrial fibrillation, elevated RA pressure).

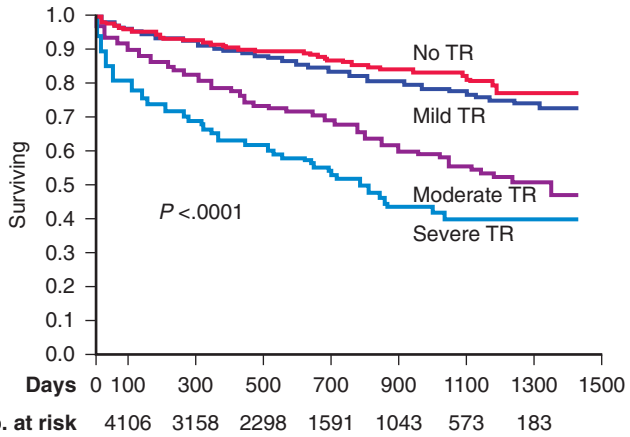



**Figure 34-9 Kaplan-Meier survival curves for all patients with tricuspid regurgitation (*TR*).** Survival is significantly worse in patients with moderate and severe tricuspid regurgitation.[51]

Also, note that the severity of TR can be difficult to appreciate or underestimated with TEE with Doppler techniques because of the limited views afforded and suboptimal beam alignment.

## CLINICAL UTILITY, OUTCOME DATA

Severe TR has an important impact on clinical outcome and survival. Patients with severe TR have a significant reduction in exercise capacity caused by impaired cardiac output response.[49] TR also has a negative impact on long-term survival, which was seen in patients with mitral stenosis after percutaneous balloon mitral valvuloplasty[50] and in a retrospective study of more than 5000 patients in whom increasing TR severity was associated with worse survival regardless of left ventricular ejection fraction or PA pressure. Moreover, severe TR was associated with a poor prognosis that was independent of age, biventricular systolic function, and RV size (Fig. 34-9).[51]

The independent effect of TR on prognosis was evaluated by Messika-Zeitoun and colleagues.[16] They reported the outcome of flail TV leaflets in patients who were seen at Mayo Clinic over a 20-year period.[16] The 60 patients with TV flail were divided into three groups depending on symptoms and associated cardiovascular disease. Half of the patients underwent operative intervention (27 repairs and 6 TV replacements). The natural history of TR from flail leaflets without associated cardiovascular disease showed an increased risk of atrial fibrillation, symptoms, heart failure, surgery, and death (Figure 34-10). Symptomatic improvement was noted in 88% of patients who underwent operation. The long-term survival rate of patients with unoperated TR caused by flail leaflets compared with the expected survival rate in a U.S. matched population showed excess mortality (4.5%; *P* less than .01). The effect of right-sided chamber enlargement in patients with severe TR, even in asymptomatic patients, was noteworthy in this series. The clinical outcome stratified according to degree of right-sided cardiac chamber enlargement showed a marked difference in events

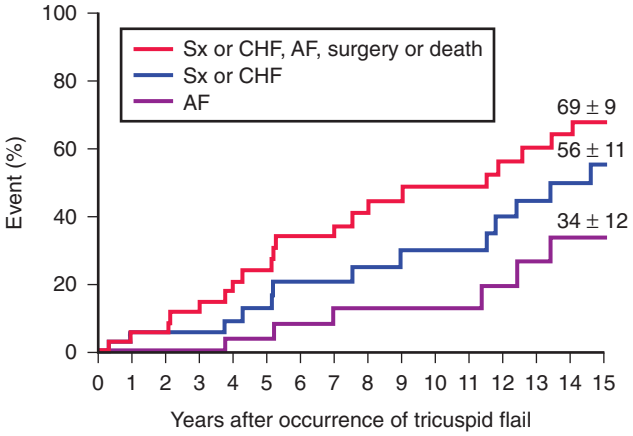



**Figure 34-10 Outcomes with severe tricuspid regurgitation due to a flail leaflet.** The Kaplan-Meier curves depict the incidence rate of new atrial fibrillation (2.8% yearly): class III or IV symptoms, or congestive heart failure (symptoms or *CHF*, 4.4% percent yearly); and the composite endpoint and first occurrence of symptoms or for heart failure, new atrial fibrillation (*AF*), tricuspid surgery, or death (6.5% per year).[16]

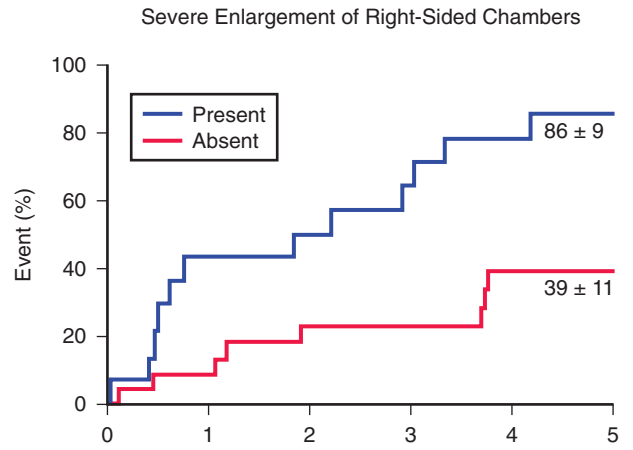



**Figure 34-11 Kaplan-Meier curves depict the incidence rate of combined endpoints of symptoms or heart failure, new atrial fibrillation, cardiac surgery, or death in patients with initial conservative management.** Note that patients with severe tricuspid regurgitation due too flail leaflet and severe right-sided cardiac chamber enlargement had a higher incidence rate of events.[16]

when severe enlargement of the right heart chambers was present (Fig. 34-11). An increase in morbidity was also noted even in asymptomatic patients with right heart enlargement. The operative risk for TV repair or replacement is low for these patients, and symptomatic improvement can be expected. Unfortunately, arrhythmia risks persist even after successful repair because surgery is mostly performed at an advanced stage.

The patient's clinical status and etiology of the TV abnormality usually determine the appropriate therapeutic strategy (Table 34-3).[2] If a correctable cause is identified, this is treated initially if possible.

Tricuspid valve surgery is the only demonstrated effective treatment for symptomatic TV regurgitation. At the authors' institution, where operative outcomes for TV disease are excellent, TV repair or replacement is recommended for patients with severe TR and:

1. Symptoms of reduced cardiac output, declining exercise capacity, or medically refractory right heart failure.

**TABLE 34-3 Management of Patients with Severe Tricuspid Regurgitation**

| *Level of Evidence* | *Class* |
|---|---|
| Tricuspid valve repair is beneficial for severe tricuspid regurgitation in patients with mitral valve disease that requires mitral valve surgery. | IB |
| 1. Tricuspid valve replacement or annuloplasty is reasonable for severe primary tricuspid regurgitation when it is symptomatic. | IIaC |
| 2. Tricuspid valve replacement is reasonable for severe tricuspid regurgitation as a result of diseased/abnormal tricuspid valve leaflets not amenable to annuloplasty or repair. | IIaC |
| Tricuspid annuloplasty may be considered for less than severe tricuspid regurgitation in patients undergoing mitral valve surgery when pulmonary hypertension or tricuspid annular dilation exists. | IIbC |
| 1. Tricuspid valve replacement or annuloplasty is not indicated in patients with tricuspid regurgitation who are asymptomatic and whose PA systolic pressure is less than 60 mm Hg in the presence of a normal mitral valve. | IIIC |
| 2. Tricuspid valve replacement or annuloplasty is not indicated in patients with mild primary tricuspid regurgitation. | IIIC |

Classification of recommendations and levels of evidence are expressed in the American College of Cardiology/American Heart Association 2006 Guidelines as follows:
**Class I:** Conditions for which there is evidence for and/or general agreement that the procedure or treatment is beneficial, useful, and effective.
**Class II:** Conditions for which there is conflicting evidence and/or a divergence of opinion about the usefulness/efficacy of a procedure or treatment.
**Class IIa:** Weight of evidence/opinion is in favor of usefulness/efficacy.
**Class IIb:** Usefulness/efficacy is less well established by evidence/opinion.
**Class III:** Conditions for which there is evidence and/or general agreement that the procedure/treatment is not useful/effective and in some cases may be harmful.
**Level of Evidence B:** Data derived from a single randomized trial or nonrandomized studies.
**Level of Evidence C:** Only consensus opinion of experts, case studies, or standard of care.

2. Mitral valve disease, or other cardiac disease that necessitates surgery.
3. Progressive RV enlargement or dysfunction.
4. Select asymptomatic patients, such as patients with traumatic TV flail with severe TR.

Surgery is also recommended in patients with moderate or more TR who are undergoing other cardiac surgery. The American College of Cardiology/American Heart Association guidelines for the timing of TV repair and replacement and those from the European Society of Cardiology are summarized in Tables 34-3 and 34-4 .[2,46] Predictors of long-term outcome after tricuspid valve replacement for severe tricuspid regurgitation include the Charlson comorbidity score, symptom severity, and the RV myocardial performance index.[46a]

Early surgery should be considered for patients with severe TR that results from blunt chest trauma because the long-term prognosis of flail TV leaflets is poor[16] and the likelihood of repair is high. When severe symptomatic TR is the result of leaflet perforation or lead impingement from a pacemaker lead, removal or repositioning of the lead may decrease the degree of TR.[52] If removal or repositioning is not feasible, TV repair or replacement should be performed.[15]

Carcinoid heart disease is best treated surgically with valve replacement to beneficially impact patient survival.[26] Indications for surgery include progressive symptoms and right heart failure. Asymptomatic patients with severe carcinoid heart disease may need valve replacement that enables partial hepatic resection or liver transplantation.

In patients with severe TR from pulmonary thromboembolic disease–related pulmonary hypertension, pulmonary thromboendarterectomy alone has been shown to reduce pulmonary hypertension and usually reduces TR without the need for

**TABLE 34-4 Indications for Intervention in Tricuspid Valve Disease (European Society of Cardiology 2007 Guidelines)**

| | *Class* |
|---|---|
| Severe TR in a patient undergoing left-sided valve surgery | IC |
| Severe primary TR and symptoms despite medical therapy without severe RV dysfunction | IC |
| Severe TS (±TR), with symptoms despite medical therapy* | IC |
| Severe TS (±TR), in a patient undergoing left-sided valve intervention* | IC |
| Moderate organic TR in a patient undergoing left-sided valve surgery | IIaC |
| Moderate secondary TR with dilated annulus (>40 mm) in a patient undergoing left-sided valve surgery | IIaC |
| Severe TR and symptoms, after left-sided valve surgery, in the absence of left-sided myocardial, valve, or RV dysfunction and without severe pulmonary hypertension (systolic PA pressure, >60 mm Hg) | IIaC |
| Severe isolated TR with mild or no symptoms and progressive dilation or deterioration of RV function | IIbC |

*TR,* Tricuspid regurgitation; *TS,* tricuspid stenosis.

*Percutaneous technique can be attempted as a first approach if TS is isolated.

Recommendation classes and levels of evidence:

**Class I:** Evidence and/or general agreement that a given treatment or procedure is beneficial, useful, and effective.

**Class II:** Conflicting evidence and/or a divergence of opinion about the usefulness/efficacy of a given treatment or procedure.

**Class IIa:** Weight of evidence/opinion is in favor of usefulness/efficacy.

**Class IIb:** Usefulness/efficacy is less well established by evidence/opinion.

**Level of Evidence A:** Data derived from multiple randomized clinical trials or meta-analyses.

**Level of Evidence B:** Data derived from a single randomized clinical trial or large non-randomized studies.

**Level of Evidence C:** Consensus of opinion of the experts and/or small studies, retrospective studies, registries.

concomitant TV annuloplasty, even when tricuspid annular dilatation is present.[53] In contrast, TR from severe primary pulmonary hypertension is usually treated with pulmonary vasodilator and diuretic therapy alone because of the high risk of morbidity and mortality related to valve replacement and poor overall prognosis.

The 2006 American College of Cardiology/American Heart Association Valvular Heart Disease Guidelines advocate TV annuloplasty at the time of left-sided valve surgery if the tricuspid annulus is dilated, even when only mild TR is present.[2] Interestingly, a number of observational studies have documented improvement in TR severity when percutaneous balloon mitral valvuloplasty is performed in patients with mitral stenosis, severe pulmonary hypertension, and significant functional TR.[54,55] Nevertheless, TV repair combined with mitral valve replacement is better than percutaneous balloon mitral valvuloplasty alone in patients with severe functional TR, especially if atrial fibrillation or RV enlargement in present.[56]

Unfortunately, the outlook is poor for patients who have previously undergone left-sided valvular heart disease surgery and subsequently present with symptomatic severe TR. Repeat surgery to specifically address the TR in these patients can be performed with an acceptable early mortality rate (8.8%). In the survivors, significant symptomatic improvement can be expected. However, the late mortality rate remains high (event-free survival rate, 41.6% ± 9.2%), predicted by age and the number of previous cardiac operations.[57] Video-assisted endoscopic minimal access procedures to correct atrioventricular valve disease after previous cardiac surgery were recently shown to be not only feasible but also accomplished with lower than predicted mortality, holding promise for treatment of these patients as an alternative to conventional redo open heart surgery.[58]

### RESEARCH APPLICATIONS

Although early experience with 3D echocardiography as a routine clinical tool has been disappointing, evaluation of TV morphology and annular geometry may be improved with newer transducers. Research to determine whether improved TV anatomy and functional assessment results in better patient selection or improved surgical outcomes is currently under way. The use of real-time 3D echocardiography may also be able to better define device lead complications and guide endocardial biopsy, improving safety of the procedure.

### POTENTIAL LIMITATIONS, FUTURE DIRECTIONS

Limitations exist regarding TR assessment with TEE. The TV is poorly visualized with TEE, principally because of its anterior location far from the transducer and in part because of the thinness of the leaflets. Also, the severity of TR can be difficult to appreciate or can be underestimated with TEE with Doppler techniques because of the limited views afforded and suboptimal beam alignment. These inherent limitations are unlikely to be overcome in the future.

The biggest promise for the future rests with the implementation of 3D echocardiography. With assessment of TR, a number of limitations are encountered with 2D echocardiography. Only two of the three TV leaflets are routinely imaged in a single 2D view. Also, the maximal dimensions and spatial geometry of the saddle-shaped tricuspid annulus cannot be easily measured with a single linear measurement. Lastly, the TV commissures and coaptation orifice cannot easily be assessed because an en face view of the TV is not readily available. Clinical research to determine whether 3D echocardiography will overcome these limitations is ongoing. As yet, no evidence shows that 3D assessment of TV anatomy and function results in better patient selection for operative intervention or improved surgical outcomes. Other challenges with regard to implementing 3D echocardiographic assessment include lack of standardized measures and specific software to facilitate tricuspid annulus and leaflet analysis. Lastly, real-time 3D echocardiography may be useful to guide transcatheter-based interventions for the treatment of TR in the future.

## Tricuspid Stenosis

### BACKGROUND

In developed countries, tricuspid stenosis (TS) is an exceptionally rare clinical condition, particularly because rheumatic heart disease accounts for about 90% of cases. Moreover, in patients with rheumatic mitral valve disease, only 3% to 5% have concurrent TS.[59,60] Unusual causes of TS include carcinoid heart disease,[61] congenital anomalies, infective endocarditis from large (often fungal) vegetations, and Whipple disease.[62] An RA myxoma might present with signs and symptoms that mimic obstruction at the TV level (Box 34-2).

### BASIC PRINCIPLES AND ECHOCARDIOGRAPHIC APPROACH

Echocardiography enables a definitive diagnosis of the severity of TS and provides clues to the etiology. Lesion severity is quantified with continuous wave Doppler to derive the mean gradient and valve area in valve stenosis.

**Box 34-2**

**ETIOLOGY OF TRICUSPID STENOSIS**

Rheumatic heart disease
Congenital tricuspid stenosis
Right atrial tumors
Carcinoid heart disease
Endomyocardial fibrosis
Valvular vegetations
Extracardiac tumors

Rheumatic involvement parallels the changes seen with rheumatic mitral valve disease, including commissural fusion and diastolic doming with thickened and shortened chordae. Even on echocardiography, findings can be subtle so that TV involvement may be overlooked unless specific attention is directed towards to TV anatomy and motion in patients with rheumatic mitral valve disease.

### TECHNICAL DETAILS, QUANTITATION, AND DATA ANALYSIS

Evaluation of the degree of TS includes calculation of:

1. The mean pressure gradient throughout both phases of respiration.
2. the pressure half-time valve area (the proposed constant to determine TV area is 190).[7,63]

Unlike the evaluation of mitral stenosis, short-axis 2D imaging of the valve orifice is rarely feasible.

Tricuspid stenosis is considered severe when the mean gradient is 7 mm Hg or more and the pressure half-time is 190 ms or longer.[7]

### CLINICAL UTILITY, OUTCOME DATA

Medical therapy for significant TS usually is ineffective because diuresis to improve systemic venous congestion further reduces cardiac output; thus, surgery should strongly be considered. If atrial fibrillation is present, ventricular rate control is important to promote diastolic filling. TS that requires surgery is most commonly the result of rheumatic heart disease and is best treated with valve replacement (see Table 34-4).[2,46]

Tricuspid valve balloon valvotomy has been advocated for TS of various causes. However, severe TR is a common consequence of this procedure, and results are poor when severe TR develops.[2,64,65]

### ALTERNATE APPROACHES

Tricuspid stenosis can be evaluated at catheterization with measurement of the transvalvular pressure gradient and calculation of valve area. According to the American College of Cardiology/American Heart Association guidelines,[2] severe TS is defined as a valve area of less than 1.0 $cm^2$. Nevertheless, because of the ease and accuracy of an echocardiographic assessment, cardiac catheterization is seldom necessary.[66-68]

## Pulmonic Valve Disease

Pulmonic valve disease is underappreciated and often overlooked because this valve is least commonly diseased. In the setting of RV pressure or volume overload, PS or PR should always be considered and specifically excluded with echocardiography.

## Pulmonic Valve Stenosis

### BACKGROUND

Valvular PS is usually an isolated congenital or genetic disorder and accounts for 80% to 90% of all RV outflow tract obstruction. The abnormal pulmonic valve may be classified as acommissural, unicommissural, bicuspid, or dysplastic (Fig. 34-12). Carcinoid syndrome and rheumatic valve disease may be associated with PS; in both conditions, PS generally occurs in conjunction with PR and TV or other valve disease. Congenital dysplastic pulmonic valve with PS, dysmorphic facial features, and variable intelligence characterize Noonan syndrome, an autosomal dominant disorder with variable penetrance.

Patients with mild and moderate PS are asymptomatic; they have minimal progression of disease and carry an excellent prognosis. Auscultatory findings include a pulmonic ejection sound that decreases in intensity with inspiration and a pulmonic ejection murmur that increases with inspiration. The electrocardiogram is normal in mild and moderate PS.[69]

Severe PS may be asymptomatic or cause fatigue and dyspnea. Systemic or suprasystemic RV pressures from PS may cause reduced exercise capacity, exertional lightheadedness, syncope, and eventually right-sided heart failure.[69] In severe PS, a jugular venous "a" wave and RV lift are common. A pulmonic ejection systolic murmur is audible and may be palpable at the upper left sternal border with radiation to the neck. With increasing PS severity, the ejection click moves closer to the first heart sound and eventually disappears; the second heart sound becomes widely split. A right-sided fourth heart sound may be heard. The electrocardiogram in severe PS is characterized by RA enlargement, right-axis deviation, RV hypertrophy, and RV strain pattern. Dilation of the main and left pulmonic arteries, diminished vascular lung markings, and occasionally, calcification of the pulmonic valve may be noted on the chest radiograph.

### BASIC PRINCIPLES AND ECHOCARDIOGRAPHIC APPROACH

Transthoracic echocardiography is the diagnostic test of choice for the initial diagnosis and follow-up of PS.[2] The echocardiographic examination follows the same basic principles as evaluation of aortic stenosis (see Chapter 23) and not only confirms the presence and severity of PS but also provides important information regarding etiology. Noninvasive estimation of RV pressure and assessment of RV size and function are essential components of the echocardiographic examination and are important in determination of management.

### TECHNICAL DETAILS, QUANTITATION, AND DATA ANALYSIS

Two-dimensional echocardiography shows thickened pulmonic valve cusps with systolic doming and reduced cusp mobility, which is usually best appreciated from the parasternal, the subcostal (Fig. 34-13), and occasionally, the anteriorly angulated apical views. The presence of subvalvular, annular, or supravalvular obstruction may also be noted with 2D echocardiography.

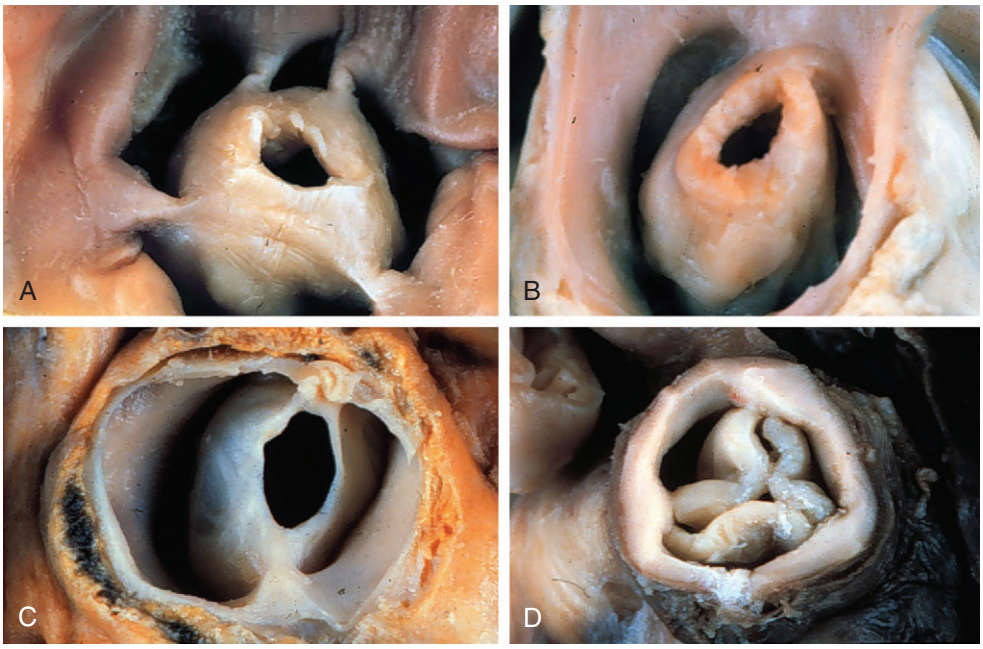



**Figure 34-12 Congenital pulmonic valve disease.** The abnormal pulmonic valve may be classified as acommisural (**A**) with prominent systolic doming of the valve cusps and an eccentric orifice; unicommissural (**B**); bicuspid with fused commissures (**C**); or dysplastic (**D**) with severely thickened and deformed valve cusps. *(Courtesy Dr. William D. Edwards, Department of Laboratory Medicine and Pathology, Mayo Clinic College of Medicine. With permission, from Otto CM, Bonow RO:* Valvular heart disease, *ed 3. Philadelphia, 2009, WB Saunders.)*

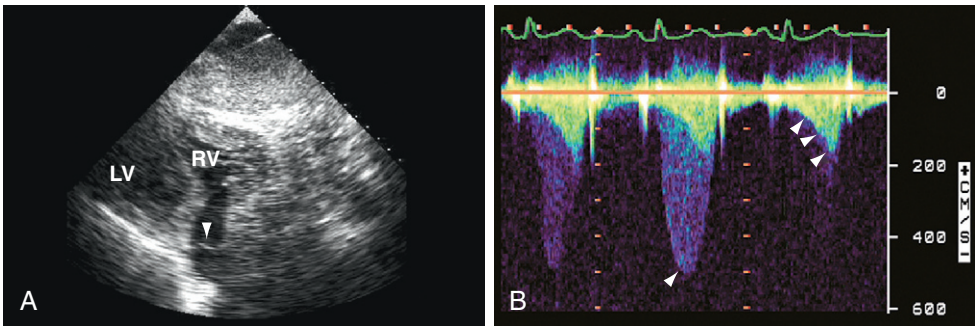



**Figure 34-13 Severe pulmonic valve stenosis. A,** Two-dimensional echocardiogram from a patient with severe pulmonic valve stenosis. The best alignment between the Doppler beam and the pulmonic flow signal was from a subcostal long-axis window with the transducer angled anteriorly. Marked RV hypertrophy was noted, and there was systolic doming of the pulmonic valve (*arrowhead*). **B,** From the same patient, the peak velocity recorded with continuous wave Doppler ultrasound scan for calculation of the transvalvular pressure gradient (*single arrowhead*) suggests a peak gradient of more than 100 mm Hg. Note the late peaking infundibular gradient (*three arrowheads*) from dynamic RV outflow tract obstruction. *(With permission, from Otto CM, Bonow RO:* Valvular heart disease, *ed 3. Philadelphia, 2009, WB Saunders.)*

RV wall thickness and function provides an indirect indicator of the degree of PS and adaptation of the RV to pressure overload. Poststenotic dilation of the pulmonic artery may become marked, with the degree of dilation unrelated to the degree of PS.

The severity of PS is determined with continuous wave Doppler peak transpulmonic velocity and gradient. The continuous wave Doppler spectrum of PS appears similar to the Doppler signal of aortic stenosis but is best obtained from the left upper parasternal or subcostal window. The maximal instantaneous gradient is generally reported for PS[70] and historically has been used to determine timing of PS intervention. Pulsed wave Doppler interrogation of the pulmonic annulus velocity should be obtained; if the proximal velocity is more than 1 m/s, then the modified Bernoulli equation ($\Delta P = 4[V_2^2 - V_1^2]$) is used to calculate the maximal instantaneous gradient. It is now recognized that the severity of PS is systematically overestimated with this technique. The mean PS gradient appears to correlate better with catheter-derived peak-to-peak gradients than the peak instantaneous PS gradient.[71] Ultimately, with determination of whether intervention is needed, correlation of the echocardiographic-Doppler gradient with other clinical findings is important.[72]

In the assessment of PS severity, integration of all available echocardiographic-Doppler data is important because the peak and mean gradients may be lower in patients with severe PS and reduced RV function, decreased cardiac output, and severe TR, which could potentially lead to an underestimate of PS severity. Pulmonic valve area is not generally reported with echocardiography because of inaccuracy in measurement of the RV outflow tract diameter. Pulsed-wave Doppler interrogation of the hepatic veins may show prominent atrial reversal, analogous to the jugular venous "a" wave noted in severe PS.

Severe PS is defined as a peak Doppler gradient of more than 50 mm Hg, moderate PS as a peak gradient of 30 to 50 mm Hg, and mild PS as a peak gradient of less than 30 mm Hg.[72]

Transesophageal echocardiography rarely provides improved visualization of the pulmonic valve compared with transthoracic echocardiography because of interposition of the bronchus between the transducer and the pulmonic valve, which causes shadowing, and because the pulmonic valve is in the far field of the imaging plane. The pulmonic valve is best visualized with the multiplane transesophageal probe rotated to about 90 degrees, resulting in a long-axis view of the RV outflow tract and pulmonic valve with the aortic valve in an oblique short-axis orientation. Alternatively, the pulmonic valve can be visualized in a transverse plane (0-degree rotation) with the probe at the level of the PA bifurcation to obtain an image that looks directly at the pulmonic valve from the bifurcation.

Three-dimensional echocardiography may allow improved visualization of the pulmonic valve morphology in select cases.[73]

## CLINICAL UTILITY, OUTCOME DATA

Patients with PS need lifelong informed clinical and echocardiographic follow-up. The frequency of follow-up depends on the severity of the lesion and results of the intervention performed. Patients with mild PS need to be seen once in 5 years with clinical and echocardiographic-Doppler examination. Patients with moderate PS should be seen with clinical and echocardiographic-Doppler examination every 2 to 5 years, and patients with severe PS who have not had intervention should be seen with testing annually.[69,72] Periodic clinical and echocardiographic follow-up is recommended for all patients after pulmonic balloon valvuloplasty or surgical management of PS, with specific attention given to the degree of PR and the impact of PR on the right heart. The frequency should be individualized based on the severity of hemodynamic abnormalities but should be at least every 5 years.

The event-free survival rate of PS is good and depends on the severity of obstruction. The long-term follow-up study of 592 patients with PS in the Second Natural History Study reported an overall survival rate at 25 years of 96%.[74] In this surgical series, event-free survival was related to preoperative pressure gradient.

Intervention in the Second Natural History Study involved surgical valvotomy. Reoperation was reported in only 4% of patients during a 10-year follow-up period.[74] In a subsequent longitudinal study of 90 consecutive patients with PS treated with operation, reoperation was required in 15%, primarily for PR (9%). At the last follow-up examination, moderate to severe PR was present in 37%, which emphasizes the importance of follow-up after PS intervention.[75]

Relief of PS is recommended for all patients with a peak instantaneous gradient of more than 60 mm Hg.[2,72] Additional recommendations for intervention are outlined in Table 34-5.[72] Percutaneous pulmonic balloon valvuloplasty is the procedure of choice for children and adults with severe or symptomatic PS and carries a low risk of morbidity, mortality, and restenosis.[2,69,72,76,77]

Pulmonic balloon valvuloplasty produces PS gradient relief with commissural splitting, and thus, patients with a dysplastic pulmonic valve generally have suboptimal results. In the Valvuloplasty and Angioplasty of Congenital Anomalies registry that involved 784 cases, the mean transvalvular gradient declined from 71 to 28 mm Hg in patients with typical PS and from 79 to 49 mm Hg in patients with a dysplastic PS.[78] Pulmonic balloon valvuloplasty is not recommended in patients with acquired PS related to carcinoid or rheumatic disease because of the nature of valve involvement, commonly associated PR, and concomitant valve involvement.

**TABLE 34-5 Recommendations for Intervention in Patients with Pulmonic Stenosis**

| *Level of Evidence* | *Class* |
|---|---|
| Balloon valvotomy is recommended for patients who are asymptomatic with a domed pulmonic valve and a peak instantaneous Doppler gradient greater than 60 mm Hg or a mean Doppler gradient greater than 40 mm Hg (in association with less than moderate PR). | IB |
| Balloon valvotomy is recommended for patients who are symptomatic with a domed pulmonic valve and a peak instantaneous Doppler gradient greater than 50 mm Hg or a mean Doppler gradient greater than 30 mm Hg (in association with less than moderate PR). | IC |
| Surgical therapy is recommended for patients with severe PS and an associated hypoplastic pulmonic annulus, severe PR, subvalvular PS, or supravalvular PS. Surgery is also preferred for most dysplastic pulmonic valves and for associated severe TR or the need for a surgical Maze procedure. | IC |
| Surgeons with training and expertise in congenital heart disease should perform operations for the RV outflow tract and pulmonic valve. | IB |
| Balloon valvotomy may be reasonable in patients who are asymptomatic with a dysplastic pulmonic valve and a peak instantaneous Doppler gradient greater than 60 mm Hg or a mean Doppler gradient greater than 40 mm Hg. | IIbC |
| Balloon valvotomy may be reasonable in selected patients who are symptomatic with a dysplastic pulmonic valve and peak instantaneous Doppler gradient greater than 50 mm Hg or a mean Doppler gradient greater than 30 mm Hg. | IIbC |
| Balloon valvotomy is not recommended for patients who are asymptomatic with a peak instantaneous Doppler gradient less than 50 mm Hg in the presence of normal cardiac output. | IIIC |
| Balloon valvotomy is not recommended for patients who are symptomatic with PS and severe PR. | IIIC |
| Balloon valvotomy is not recommended for patients who are symptomatic with a peak instantaneous Doppler gradient less than 30 mm Hg. | IIIC |

With permission, from Warnes C, Williams RB, Child J, et al: American College of Cardiology; American Heart Association Task Force on Practice Guidelines (Writing Committee to Develop Guidelines on the Management of Adults With Congenital Heart Disease); American Society of Echocardiography; Heart Rhythm Society; International Society for Adult Congenital Heart Disease; Society for Cardiovascular Angiography and Interventions; Society of Thoracic Surgeons. ACC/AHA 2008 guidelines for the management of adults with congenital heart disease. *J Am Coll Cardiol* 52:e1-e121, 2008.
*PR,* Pulmonic valve regurgitation; *PS,* pulmonic valve stenosis; *TR,* tricuspid regurgitation.

Severe PS often is associated with some degree of subvalvular muscular obstruction resulting from hypertrophy of the RV myocardium (see Figure 34-13). After relief of PS, infundibular obstruction may worsen transiently but then tends to regress over months with eventual resolution.[79,80] Acute severe muscular obstruction can cause "suicide" RV, which results in suprasystemic RV pressure with resultant cyanosis and hemodynamic instability. Beta-blocker therapy is recommended before pulmonic balloon valvuloplasty to prevent or reduce the severity of this complication; therapy generally is discontinued after 3 to 6 months.

A high frequency rate of PR has been reported after pulmonic balloon valvuloplasty; 57% of children had moderate or severe PR at the last follow-up.[81,82]

In patients who have unfavorable pulmonic valve morphology, hypoplastic pulmonic annulus, fixed subvalvar or supravalvar PS, severe PR, additional cardiac lesions that require operative intervention, or a poor result with pulmonic balloon valvuloplasty, surgical valvotomy or valve replacement may be preferred. The choice of pulmonic valve prosthesis type must be individualized.[83]

### ALTERNATE APPROACHES

Echocardiographic-Doppler assessment of PS severity remains challenging in patients with suboptimal echocardiographic image quality. Alternate imaging options, including 3D echocardiography with color flow mapping, may provide additional future data but require validation. Cardiac magnetic resonance imaging and cardiac computerized tomography can be performed to better define the level of obstruction; these techniques are particularly helpful when multiple levels of RV outflow obstruction are present in series.

Cardiac catheterization should be considered when discordant data are present, to confirm the extent, severity, and level of obstruction or to facilitate intervention.

## Pulmonic Valve Regurgitation

### BACKGROUND

In adults, pathologic PR most often is the consequence of prior interventions for congenital heart disease, such as tetralogy of Fallot repair with placement of an outflow tract patch[84] or valvotomy (surgical or balloon) for isolated congenital PS.[75] Additional causes of PR include pulmonary hypertension, rheumatic or carcinoid heart disease, trauma, endocarditis, and PA and annular dilation.

Patients with long-standing severe PR eventually have development of progressive RV dilation and reduced RV function. This development can lead to the inability to augment cardiac output with exercise, progressive TR from annular dilation, increased propensity to atrial and ventricular arrhythmias, and ultimately, right heart failure.

Patients with PR may have a parasternal lift as a result of RV enlargement. The murmur of PR is typically a soft, diastolic, decrescendo murmur best heard at the left upper sternal region. It begins after the pulmonic closure sound and may be accompanied by a pulmonic systolic ejection murmur. An increase in intensity of the murmur may be noted during inspiration or with pulmonary hypertension.

The dilated and dysfunctional RV associated with long-standing severe PR can cause QRS prolongation, ventricular arrhythmias, and sudden death. This mechanical-electric association has been documented in patients with transannular patch repair of tetralogy of Fallot.[85] Chest radiography may show cardiomegaly, involving the right-sided chambers and PA enlargement.

### BASIC PRINCIPLES AND ECHOCARDIOGRAPHIC APPROACH

Transthoracic echocardiography is the diagnostic test of choice for the initial diagnosis and follow-up of PR.[2] The echocardiographic examination follows the same principles as evaluation of aortic valve regurgitation (see Chapter 20), confirming the presence and severity of PR and also providing information regarding etiology. Noninvasive estimation of RV size and function are essential components of the echocardiographic examination, and are important in determination of management.

### TECHNICAL DETAILS, QUANTITATION, AND DATA ANALYSIS

The diagnosis of PR is usually made with echocardiography and graded with color Doppler imaging. A trivial or mild degree of PR is detectable in most healthy individuals.[35] Echocardiographic and Doppler parameters that are useful in the evaluation of PR are listed in Table 34-6.[4]

The mechanism of PR is usually determined with 2D echocardiographic evaluation of the RV outflow tract and pulmonic valve from the parasternal, the subcostal, and occasionally, the apical views. Identification of anatomic pulmonic valve abnormalities, such as absence of the pulmonic valve, flail cusp, or annular dilation, may help define the cause and delineate severity of PR. RV size and function provides an indirect indicator of the significance of PR and adaptation of the RV to volume overload.

Color Doppler imaging is the most common initial echocardiographic method used in identification of PR severity. When PR is unrestricted and the pulmonary pressures are low, the Doppler color-flow map may be laminar.[4,86] PR severity is generally determined by jet size and duration that in turn is affected by driving pressure, regurgitant volume, and the RV pressures. Pathologic PR is typically a wide holodiastolic jet (Fig. 34-14). In severe PR, equalization of PA and RV pressures early in diastole cause early and abrupt cessation of the color and continuous wave Doppler jet. Thus, reliance on the color flow jet alone may lead to underappreciation of the PR severity. It is therefore important to note the vena contracta width and continuous wave Doppler signal contour to recognize that severe PR is present.

The density and contour of the continuous wave Doppler signal and deceleration pressure half-time correspond to the degree of PR and RV pressures (Fig. 34-14, *C*).[87] Rapid continuous wave Doppler deceleration with a pressure half-time of less than 100 ms is suggestive but not specific for severe PR. Equal intensities of antegrade and retrograde flow across the pulmonic valve suggest severe PR but are influenced by RV diastolic properties and filling pressures. In severe PR, equalization of RV and PA pressures can occur before the end

**TABLE 34-6 Echocardiographic and Doppler Parameters Used in the Evaluation of Pulmonic Regurgitation Severity: Utility, Advantages, and Limitations**

| *Parameter* | *Utility/Advantages* | *Disadvantages* |
|---|---|---|
| RV size | RV enlargement sensitive for chronic significant pulmonic regurgitation. Normal size virtually excludes significant pulmonic regurgitation. | Enlargement seen in other conditions. |
| Paradoxical septal motion (volume overload pattern) | Simple sign of severe pulmonic regurgitation. | Not specific for pulmonic regurgitation. |
| Jet length–color flow | Simple. | Poor correlation with severity of pulmonic regurgitation. |
| Vena contracta width | Simple quantitative method that works well for other valves. | More difficult to perform; requires good images of pulmonary valve; lacks published validation. |
| Jet deceleration rate–continuous wave | Simple. | Steep deceleration not specific for severe pulmonic regurgitation. |
| Flow quantitation–pulsed wave | Quantitates regurgitant flow and fraction. | Subject to significant errors because of difficulties of measurement of pulmonic annulus and a dynamic RV outflow tract; not well validated. |

With permission, adapted from Zoghbi WA, Enriquez-Sarano M, Foster E, et al: Recommendations for evaluation of the severity of native valvular regurgitation with two-dimensional and Doppler echocardiography. *J Am Soc Echocardiogr* 16:777-802, 2003.

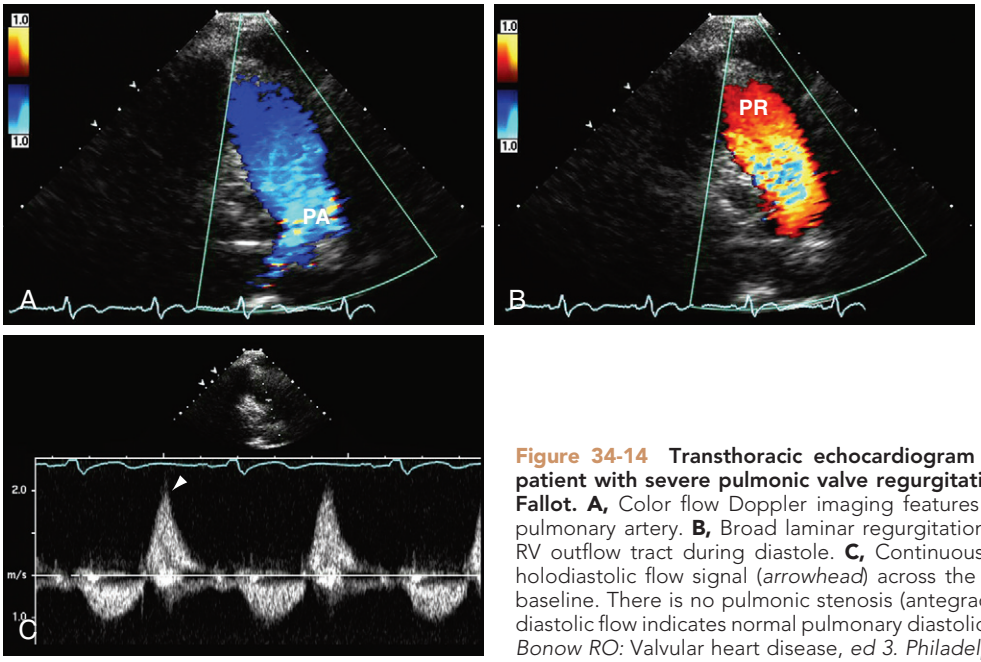



**Figure 34-14 Transthoracic echocardiogram images of the RV outflow tract from a patient with severe pulmonic valve regurgitation related to prior repair of tetralogy of Fallot. A,** Color flow Doppler imaging features show laminar flow during systole into the pulmonary artery. **B,** Broad laminar regurgitation jet of pulmonic regurgitation that fills the RV outflow tract during diastole. **C,** Continuous wave Doppler imaging shows an intense holodiastolic flow signal (*arrowhead*) across the pulmonic valve that decelerates rapidly to baseline. There is no pulmonic stenosis (antegrade velocity of 1.0 m/s), and the low-velocity diastolic flow indicates normal pulmonary diastolic pressures. *(With permission, from Otto CM, Bonow RO:* Valvular heart disease, *ed 3. Philadelphia, 2009, WB Saunders.)*

of diastole. The RV end-diastolic pressure may exceed the PA pressure during atrial contraction, resulting in antegrade flow across the pulmonic valve during atrial contraction. Pulsed wave Doppler scan determination of the ratio of the reverse-to-forward time velocity integral has been used to estimate the percent of PR flow.

Transesophageal echocardiography rarely provides improved visualization of the pulmonic valve compared with transthoracic echocardiography because of interposition of the bronchus between the transducer and the pulmonic valve that causes acoustic shadowing and because the pulmonic valve is an anterior structure located in the far field of the imaging plane. The pulmonic valve is best visualized with the multiplane transesophageal probe rotated to about 90 degrees, resulting in a long-axis view of the RV outflow tract and pulmonic valve with the aortic valve in an oblique short-axis orientation. This allows visualization of the PR jet size and vena contracta. Alternatively, the pulmonic valve can be visualized in a transverse plane (0-degree rotation) with the probe at the level of the PA bifurcation to obtain an image that looks directly at the pulmonic valve from the bifurcation. This view provides a parallel intercept angle that optimizes beam alignment for Doppler recordings. TEE is generally not performed for the diagnostic assessment of pulmonic valve disease.

Three-dimensional echocardiography may allow improved visualization of pulmonic valve morphology in select cases.[73]

A comprehensive multimodality echocardiographic evaluation of PR involves primarily a qualitative assessment that provides clinically useful estimates of PR severity and is feasible in most patients.[4] Information about right heart size and function is taken into account in the comprehensive approach to patients with PR (Table 34-7).

Insufficient data exist on the echocardiographic quantitation of PR to recommend routine use. Validation studies are lacking because of difficulties in imaging of the pulmonic valve and the low prevalence of severe PR. The vena contracta width is the smallest regurgitant flow area immediately beyond the flow convergence region and before expansion of the turbulent regurgitant jet, which corresponds with the effective regurgitant orifice area. The vena contracta appears to be a more accurate method of evaluation of the severity of PR with color Doppler imaging than regurgitant jet area; however, standards for PR vena contracta width have not been established.

Magnetic resonance imaging has become a common diagnostic tool used to assess PR severity and RV size and function in patients with PR. Two-dimensional and Doppler echocardiographic measurements that have been shown to be independent predictors of severe PR compared with cardiac magnetic resonance imaging include diastolic flow reversal in the main or branch PAs, PR jet width of 50% or more of the pulmonic annulus, and PR pressure half-time of less than 100 ms.[88] For assessment of PR severity after RV outflow tract reconstruction or pulmonic valve replacement, PR jet width-annulus ratio combined with diastolic flow reversal was found to be the most valuable echocardiographic measure with magnetic resonance imaging as a reference tool.[89]

## CLINICAL UTILITY, OUTCOME DATA

Most patients with mild degrees of PR have a benign clinical course. Chronic severe PR often is well tolerated for many years. However, the RV may dilate and develop systolic dysfunction, analogous to the effect of chronic aortic regurgitation on the left ventricle. Severe RV dilation is associated with an increased risk of sudden death, related primarily to arrhythmias.[85] No medical therapy has been shown to be effective in reducing the degree of PR or affecting the impact of PR on the RV. The impact of isolated late PR is increasingly recognized; PR not only affects RV size and function but also affects exercise capacity.[90] As the intervention options improve and the morbidity related to long-standing PR is increasingly recognized, indications for intervention are being refined.

Consensus Guidelines on the Management of Adults with Congenital Heart Disease recommend pulmonic valve replacement for severe PR and symptoms or decreased exercise tolerance (Table 34-8). Pulmonic valve replacement is also thought to be reasonable in adults with previous surgery for tetralogy of Fallot, severe PR, and: (1) moderate to severe RV

**TABLE 34-7 Echocardiographic and Doppler Parameters Used in Grading Pulmonic Regurgitation Severity**

| *Parameter* | *Mild* | *Moderate* | *Severe* |
|---|---|---|---|
| Pulmonic valve | Normal | Normal or abnormal | Abnormal |
| RV size | Normal* | Normal or dilated | Dilated |
| Jet size with color Doppler† | Thin (usually <10 mm in length) with a narrow origin | Intermediate | Usually large, with a wide origin; may be brief in duration |
| Jet density and deceleration rate–continuous wave Doppler‡ | Soft; slow deceleration | Dense; variable deceleration | Dense; steep deceleration, early termination of diastolic flow |
| Pulmonic systolic flow compared with systemic flow–pulsed wave Doppler§ | Slightly increased | Intermediate | Greatly increased |

With permission, adapted from Zoghbi WA, Enriquez-Sarano M, Foster E, et al: Recommendations for evaluation of the severity of native valvular regurgitation with two-dimensional and Doppler echocardiography. *J Am Soc Echocardiogr* 16:777-802, 2003.

*Unless there are other reasons for RV enlargement. Normal 2D measurements from the apical 4-chamber view; RV medio-lateral end-diastolic dimension ≤ 4.3 cm, RV end-diastolic area ≤ 35.5 $cm^2$

†At a Nyquist limit of 50-60 cm/s.

‡Steep deceleration is not specific for severe PR.

§Cut-off values for regurgitant volume and fraction are not well validated.

**TABLE 34-8 Recommendations for Surgery for Adults with Pulmonic Regurgitation**

| *Level of Evidence* | *Class* |
|---|---|
| Surgeons with training and expertise in congenital heart disease should perform operations in adults with previous repair of tetralogy of Fallot. | IC |
| Pulmonic valve replacement is indicated for severe PR and symptoms or decreased exercise tolerance. | IB |
| Coronary artery anatomy, specifically the possibility of an anomalous anterior descending coronary artery across the RV outflow tract, should be ascertained before operative intervention. | IC |
| Pulmonic valve replacement is reasonable in adults with previous repair of tetralogy of Fallot, severe PR, and any of the following: | |
| 1. moderate to severe RV dysfunction; | IIaB |
| 2. moderate to severe RV enlargement; | IIaB |
| 3. development of symptomatic or sustained atrial or ventricular arrhythmias; or | IIaC |
| 4. moderate to severe tricuspid regurgitation. | IIaC |

With permission, adapted from Warnes C, Williams RB, Child J, et al: American College of Cardiology; American Heart Association Task Force on Practice Guidelines (Writing Committee to Develop Guidelines on the Management of Adults With Congenital Heart Disease); American Society of Echocardiography; Heart Rhythm Society; International Society for Adult Congenital Heart Disease; Society for Cardiovascular Angiography and Interventions; Society of Thoracic Surgeons. ACC/AHA 2008 guidelines for the management of adults with congenital heart disease. *J Am Coll Cardiol* 52:e1-e121, 2008.

*PR,* Pulmonic regurgitation.

dysfunction; (2) moderate to severe RV enlargement; (3) development of symptomatic or sustained atrial or ventricular arrhythmias; and (4) moderate to severe TR.

In the authors' practice, pulmonic valve replacement for severe PR is also recommended for: (1) decline in functional aerobic capacity; (2) severe PR in a patient needing another cardiac operation; and (3) concern about risk of arrhythmia in patients with prolonged or increasing QRS duration (total QRS duration of 180 ms or more or QRS duration increase of 3.5 ms/y or more).[85]

Right ventricle size tends to decrease or normalize and functional status improves after pulmonic valve replacement for PR late after tetralogy of Fallot surgery.[91] Preoperative N-terminal-pro brain natriuretic peptide elevation and QRS prolongation may indicate patients with poorer outcome regarding RV function and volumes after surgery.[92] However, RV function may not fully recover after pulmonic valve replacement once marked enlargement and systolic dysfunction are evident.[93,94] When pulmonic valve replacement is recommended, the type of pulmonic valve prosthesis should be individualized.[83]

## ALTERNATE APPROACHES

Echocardiographic quantitation of PR remains challenging and not well validated. Future alternate imaging options, including 3D color flow mapping, may provide additional future data. Cardiac magnetic resonance imaging is considered the clinical gold-standard method for the noninvasive quantitation of PR and is commonly used to assess right-sided heart size and function in asymptomatic patients with severe PR to determine the optimal time of valve replacement. Cardiac catheterization is rarely performed to assess PR.

Pulmonic valve disease is underappreciated clinically and with echocardiography. In patients with RV pressure or volume overload, PS or PR should always be sought with multimodality echocardiographic imaging.

## KEY POINTS

- Moderate or more TR is most frequently "functional" in nature, that is, not related to primary tricuspid leaflet pathology but rather the result of another disease process that causes RV dilation, distortion of the subvalvular apparatus, tricuspid annular dilation, or a combination of these.
- Echocardiography is currently the reference standard for diagnosis and evaluation of tricuspid and pulmonic valve disease.
- An integrated assessment that incorporates 2D and Doppler qualitative and quantitative parameters is necessary to grade TR.
- Data suggest severe TR as a result of a flail leaflet is associated with adverse outcomes that favor early surgical repair.
- Severe TV regurgitation has an important impact on clinical outcome and survival in patients with concomitant cardiovascular disease.
- Tricuspid stenosis occurs infrequently and is essentially never seen in isolation.
- Pulmonic stenosis is most commonly an isolated congenital cardiac lesion.
- Pulmonic stenosis should always be considered in the setting of RV hypertension.
- Determination of PS severity requires comprehensive clinical and echocardiographic assessment.
- Pulmonic regurgitation is most commonly found in patients with prior intervention for congenital PS (balloon or surgical) or tetralogy of Fallot.
- Severe PR is often missed because of laminar color flow appearance and short duration.

## REFERENCES


1. Ton-Nu TT, Levine RA, Handschumacher MD, et al: Geometric determinants of functional tricuspid regurgitation: insights from 3-dimensional echocardiography. *Circulation* 114:143-149, 2006.
2. Bonow R, Carabello B, Kanu C, et al: American College of Cardiology/American Heart Association Task Force on Practice Guidelines; Society of Cardiovascular Anesthesiologists; Society for Cardiovascular Angiography and Interventions; Society of Thoracic Surgeons ACC/AHA 2006 guidelines for the management of patients with valvular heart disease. *Circulation* 114:e84-e231, 2006.
3. DePace N, Ross J, Iskandrian A, et al: Tricuspid regurgitation: noninvasive techniques for determining causes and severity. *J Am Coll Cardiol* 3:1540-1550, 1984.
4. Zoghbi WA, Enriquez-Sarano M, Foster E, et al: Recommendations for evaluation of the severity of native valvular regurgitation with two-dimensional and Doppler echocardiography. *J Am Soc Echocardiogr* 16:777-802, 2003.
5. Badano LP, Agricola E, Perez de Isla L, et al: Evaluation of the tricuspid valve morphology and function by transthoracic real-time three-dimensional echocardiography. *Eur J Echocardiogr* 10:477-484, 2009.
6. Anwar AM, Geleijnse ML, Soliman OI, et al: Assessment of normal tricuspid valve anatomy in adults by real-time three-dimensional echocardiography. *Int J Cardiovasc Imaging* 23:717-724, 2007.
7. Oh JK, Seward JB, Tajik AJ: *The echo manual*, ed 3, Philadelphia, 2006, Lippincott Williams & Wilkins.
8. Fukuda S, Gillinov AM, Song JM, et al: Echocardiographic insights into atrial and ventricular mechanisms of functional tricuspid regurgitation. *Am Heart J* 152:1208-1214, 2006.
9. Topilsky Y, Tribouilloy C, Michelena HI, et al: Pathophysiology of tricuspid regurgitation: quantitative Doppler echocardiographic assessment of respiratory dependence. *Circulation* 122:1505-1513, 2010.
10. Cohen S, Sell J, McIntosh C, et al: Tricuspid regurgitation in patients with acquired, chronic, pure mitral regurgitation. II. Nonoperative management, tricuspid valve annuloplasty, and tricuspid valve replacement. *J Thorac Cardiovasc Surg* 94:488-497, 1987.
11. Waller BF, Moriarty AT, Eble JN, et al: Etiology of pure tricuspid regurgitation based on anular circumference and leaflet area: analysis of 45 necropsy patients with clinical and morphologic evidence of pure tricuspid regurgitation. *J Am Coll Cardiol* 7:1063-1074, 1986.
12. Muller O, Shillingford J: Tricuspid incompentence. *Br Heart J* 16:195, 1954.
13. Salazar E, Levine H: Rheumatic tricuspid regurgitation. *Am J Med* 33:111, 1962.
14. Sepulveda G, Lukas D: The diagnosis of tricuspid insufficiency: clinical features in 60 cases with associated mitral valve disease. *Circulation* 11:552, 1955.
15. Lin G, Nishimura RA, Connolly HM, et al: Severe symptomatic tricuspid valve regurgitation due to permanent pacemaker or implantable cardioverter-defibrillator leads. *J Am Coll Cardiol* 45:1672-1675, 2005.
16. Messika-Zeitoun D, Thomson H, Bellamy M, et al: Medical and surgical outcome of tricuspid regurgitation caused by flail leaflets. *J Thorac Cardiovasc Surg* 128:296-302, 2004.
17. van Son JA, Danielson GK, Schaff HV, et al: Traumatic tricuspid valve insufficiency. Experience in thirteen patients. *J Thorac Cardiovasc Surg* 108:893-898, 1994.
18. Chan P, Ogilby JD, Segal B: Tricuspid valve endocarditis. *Am Heart J* 117:1140-1146, 1989.
19. Waller BF, Knapp WS, Edwards JE: Marantic valvular vegetations. *Circulation* 48:644-650, 1973.
20. Duran C: Tricuspid valve surgery revisited. *J Card Surg* 9:242-247, 1994.
21. Redfield MM, Nicholson WJ, Edwards WD, et al: Valve disease associated with ergot alkaloid use: echocardiographic and pathologic correlations. *Ann Intern Med* 117:50-52, 1992.
22. Pritchett AM, Morrison JF, Edwards WD, et al: Valvular heart disease in patients taking pergolide. *Mayo Clin Proc* 77:1280-1286, 2002.
23. Schade R, Andersohn F, Suissa S, et al: Dopamine agonists and the risk of cardiac-valve regurgitation. *N Engl J Med* 356:29-38, 2007.
24. Zanettini R, Antonini A, Gatto G, et al: Valvular heart disease and the use of dopamine agonists for Parkinson's disease. *N Engl J Med* 356:39-46, 2007.
25. Rothman RB, Baumann MH, Savage JE, et al: Evidence for possible involvement of 5-HT(2B) receptors in the cardiac valvulopathy associated with fenfluramine and other serotonergic medications. *Circulation* 102:2836-2841, 2000.
26. Moller JE, Pellikka PA, Bernheim AM, et al: Prognosis of carcinoid heart disease: analysis of 200 cases over two decades. *Circulation* 112: 3320-3327, 2005.
27. Connolly HM, Schaff HV, Mullany CJ, et al: Surgical management of left-sided carcinoid heart disease. *Circulation* 104:I36-I40, 2001.
28. Chaowalit N, Connolly HM, Schaff HV, et al: Carcinoid heart disease associated with primary ovarian carcinoid tumor. *Am J Cardiol* 93:1314-1315, 2004.
29. Adams MJ, Hardenbergh PH, Constine LS, et al: Radiation-associated cardiovascular disease. *Crit Rev Oncol Hematol* 45:55-75, 2003.
30. Crestanello JA, McGregor CG, Danielson GK, et al: Mitral and tricuspid valve repair in patients with previous mediastinal radiation therapy. *Ann Thorac Surg* 78:826-831, 2004.
31. Chandraratna P, Lopez J, Fernandez J, et al: Echocardiographic detection of tricuspid valve prolapse *Circulation* 51:823-826, 1975.
32. Weinreich D, Burke J, Bharati S, et al: Isolated prolapse of the tricuspid valve. *J Am Coll Cardiol* 6:475-481, 1985.
33. Attenhofer Jost CH, Connolly HM, Dearani JA, et al: Ebstein's anomaly. *Circulation* 115:277-285, 2007.
34. Celermajer D, Bull C, Till J, et al: Ebstein's anomaly: presentation and outcome from fetus to adult. *J Am Coll Cardiol* 23:170-176, 1994.
35. Klein A, Burstow D, Tajik A, et al: Age-related prevalence of valvular regurgitation in normal subjects: a comprehensive color flow examination of 118 volunteers. *J Am Soc Echocardiogr* 3:54-63, 1990.
36. Chopra HK, Nanda NC, Fan P, et al: Can two-dimensional echocardiography and Doppler color flow mapping identify the need for tricuspid valve repair? *J Am Coll Cardiol* 14:1266-1274, 1989.
37. Suzuki Y, Kambara H, Kadota K, et al: Detection and evaluation of tricuspid regurgitation using a real-time, two-dimensional, color-coded, Doppler flow imaging system: comparison with contrast two-dimensional echocardiography and right ventriculography. *Am J Cardiol* 57: 811-815, 1986.
38. Rivera JM, Vandervoort PM, Vazquez de Prada JA, et al: Which physical factors determine tricuspid regurgitation jet area in the clinical setting? *Am J Cardiol* 72:1305-1309, 1993.
39. Switzer DF, Yoganathan AP, Nanda NC, et al: Calibration of color Doppler flow mapping during extreme hemodynamic conditions in vitro: a foundation for a reliable quantitative grading system for aortic incompetence. *Circulation* 75:837-846, 1987.
40. Bolger AF, Eigler NL, Pfaff JM, et al: Computer analysis of Doppler color flow mapping images for quantitative assessment of in vitro fluid jets. *J Am Coll Cardiol* 12:450-457, 1988.
41. Cape EG, Yoganathan AP, Weyman AE, et al: Adjacent solid boundaries alter the size of regurgitant jets on Doppler color flow maps. *J Am Coll Cardiol* 17:1094-1102, 1991.
42. Grossmann G, Stein M, Kochs M, et al: Comparison of the proximal flow convergence method and the jet area method for the assessment of the severity of tricuspid regurgitation. *Eur Heart J* 19:652-659, 1998.
43. Rivera JM, Vandervoort PM, Morris E, et al: Visual assessment of valvular regurgitation: comparison with quantitative Doppler measurements. *J Am Soc Echocardiogr* 7:480-487, 1994.
44. Tribouilloy CM, Enriquez-Sarano M, Bailey KR, et al: Quantification of tricuspid regurgitation by measuring the width of the vena contracta with Doppler color flow imaging: a clinical study. *J Am Coll Cardiol* 36:472-478, 2000.
45. Baumgartner FJ, Milliken JC, Robertson JM, et al: Clinical patterns of surgical endocarditis. *J Card Surg* 22:32-38, 2007.
46. Vahanian A, Baumgartner H, Bax J, et al: Guidelines on the management of valvular heart disease: the Task Force on the Management of Valvular Heart Disease of the European Society of Cardiology. *Eur Heart J* 28:230-268, 2007.

46a. Topilsky Y, Khanna AD, Oh JK, et al: Preoperative factors associated with adverse outcome after tricuspid valve replacement. *Circulation* 123:1929-1939, 2011.

47. Pennestri F, Loperfido F, Salvatori MP, et al: Assessment of tricuspid regurgitation by pulsed Doppler ultrasonography of the hepatic veins. *Am J Cardiol* 54:363-368, 1984.
48. Sakai K, Nakamura K, Satomi G, et al: Evaluation of tricuspid regurgitation by blood flow pattern in the hepatic vein using pulsed Doppler technique. *Am Heart J* 108:516-523, 1984.
49. Groves P, Lewis N, Ikram S, et al: Reduced exercise capacity in patients with tricuspid regurgitation after successful mitral valve replacement for rheumatic mitral valve disease. *Br Heart J* 66:295-301, 1991.
50. Sagie A, Schwammenthal E, Newell J, et al: Significant tricuspid regurgitation is a marker for adverse outcome in patients undergoing percutaneous balloon mitral valvuloplasty. *J Am Coll Cardiol* 24:696-702, 1994.
51. Nath J, Foster E, Heidenreich PA: Impact of tricuspid regurgitation on long-term survival. *J Am Coll Cardiol* 43:405-409, 2004.
52. Bove E, Kavey R, Byrum C, et al: Improved right ventricular function following late pulmonary valve replacement for residual pulmonary insufficiency or stenosis. *J Thorac Cardiovasc Surg* 90:50-55, 1985.

53. Sadeghi HM, Kimura BJ, Raisinghani A, et al: Does lowering pulmonary arterial pressure eliminate severe functional tricuspid regurgitation? Insights from pulmonary thromboendarterectomy. *J Am Coll Cardiol* 44:126-132, 2004.
54. Hannoush H, Fawzy ME, Stefadouros M, et al: Regression of significant tricuspid regurgitation after mitral balloon valvotomy for severe mitral stenosis. *Am Heart J* 148:865-870, 2004.
55. Song JM, Kang DH, Song JK, et al: Outcome of significant functional tricuspid regurgitation after percutaneous mitral valvuloplasty. *Am Heart J* 145:371-376, 2003.
56. Song H, Kang DH, Kim JH, et al: Percutaneous mitral valvuloplasty versus surgical treatment in mitral stenosis with severe tricuspid regurgitation. *Circulation* 116(11 Suppl):I246-I250, 2007.
57. Staab ME, Nishimura RA, Dearani JA: Isolated tricuspid valve surgery for severe tricuspid regurgitation following prior left heart valve surgery: analysis of outcome in 34 patients. *J Heart Valve Dis* 8:567-574, 1999.
58. Casselman FP, La Meir M, Jeanmart H, et al: Endoscopic mitral and tricuspid valve surgery after previous cardiac surgery. *Circulation* 116:I270-I275, 2007.
59. Bousvaros G, Stubington D: Some auscultatory and phonocardiographic features of tricuspid stenosis. *Circulation* 29:26, 1964.
60. Kitchin A, Turner R: Diagnosis and treatment of tricuspid stenosis. *Br Heart J* 16:354, 1964.
61. Pellikka PA, Tajik AJ, Khandheria BK, et al: Carcinoid heart disease. Clinical and echocardiographic spectrum in 74 patients. *Circulation* 87:1188-1196, 1993.
62. Waller B, Howard J, Fess S: Pathology of tricuspid valve stenosis and pure tricuspid regurgitation: part III. *Clin Cardiol* 18:225-230, 1995.
63. Fawzy ME, Mercer EN, Dunn B, et al: Doppler echocardiography in the evaluation of tricuspid stenosis. *Eur Heart J* 10:985-990, 1989.
64. Onate A, Alcibar J, Inguanzo R, et al: Balloon dilation of tricuspid and pulmonary valves in carcinoid heart disease. *Tex Heart Inst J* 20:115-119, 1993.
65. Orbe LC, Sobrino N, Arcas R, et al: Initial outcome of percutaneous balloon valvuloplasty in rheumatic tricuspid valve stenosis. *Am J Cardiol* 71:353-354, 1993.
66. Guyer D, Gillam L, Foale R, et al: Comparison of the echocardiographic and hemodynamic diagnosis of rheumatic tricuspid stenosis. *J Am Coll Cardiol* 3:1135-1144, 1984.
67. Perez J, Ludbrook PJ, Ahumada G: Usefulness of Doppler echocardiography in detecting tricuspid valve stenosis. *Am J Cardiol* 55:601-603, 1985.
68. Shimada R, Takeshita A, Nakamura M, et al: Diagnosis of tricuspid stenosis by M-mode and two-dimensional echocardiography. *Am J Cardiol* 53:164-168, 1984.
69. Baumgartner H, Bonhoeffer P, De Groot N, et al: Task Force on the Management of Grown-up Congenital Heart Disease of the European Society of Cardiology (ESC). ESC Guidelines for the management of grown-up congenital heart disease (new version 2010). *Eur Heart J* 31:2915-2957, 2010.
70. Currie P, Hagler D, Seward J, et al: Instantaneous pressure gradient: a simultaneous Doppler and dual catheter correlative study. *J Am Coll Cardiol* 7:800-806, 1986.
71. Silvilairat S, Cabalka A, Cetta F, et al: Echocardiographic assessment of isolated pulmonary valve stenosis: which outpatient Doppler gradient has the most clinical validity? *J Am Soc Echocardiogr* 18:1137-1142, 2005.
72. Warnes C, Williams RB, Child TMJ, et al: American College of Cardiology; American Heart Association Task Force on Practice Guidelines (Writing Committee to Develop Guidelines on the Management of Adults With Congenital Heart Disease); American Society of Echocardiography; Heart Rhythm Society; International Society for Adult Congenital Heart Disease; Society for Cardiovascular Angiography and Interventions; Society of Thoracic Surgeons. ACC/AHA 2008 guidelines for the management of adults with congenital heart disease. *J Am Coll Cardiol* 52:e1-e121, 2008.
73. Lee K, Connolly H, Pellikka P: Carcinoid pulmonary valvulopathy evaluated by real-time 3-dimensional transthoracic echocardiography. *J Am Soc Echocardiogr* 21:407.e1-e2, 2008.
74. Hayes C, Gersony W, Driscoll D, et al: Second natural history study of congenital heart defects. Results of treatment of patients with pulmonary valvar stenosis. *Circulation* 87(2 suppl):I28-I37, 1993.
75. Roos-Hesselink J, Meijboom F, Sv Spitaels RT, et al: Long-term outcome after surgery for pulmonary stenosis (a longitudinal study of 22-33 years). *Eur Heart J* 27:482-488, 2006.
76. Chen C, Cheng T, Huang T, et al: Percutaneous balloon valvuloplasty for pulmonic stenosis in adolescents and adults. *N Engl J Med* 335:21-25, 1996.
77. Fawzy M, Awad M, Galal O, et al: Long-term results of pulmonary balloon valvulotomy in adult patients. *J Heart Valve Dis* 10:812-818, 2001.
78. Stanger P, Cassidy S, Girod D, et al: Balloon pulmonary valvuloplasty: results of the Valvuloplasty and Angioplasty of Congenital Anomalies Registry. *Am J Cardiol* 65:775-783, 1990.
79. Fawzy M, Galal O, Dunn B, et al: Regression of infundibular pulmonary stenosis after successful balloon pulmonary valvuloplasty in adults. *Cathet Cardiovasc Diagn* 21:77-81, 1990.
80. Teupe C, Burger W, Schrader R, et al: Late (five to nine years) follow-up after balloon dilation of valvular pulmonary stenosis in adults. *Am J Cardiol* 80:240-242, 1997.
81. Garty Y, Veldtman G, Lee K, et al: Late outcomes after pulmonary valve balloon dilatation in neonates, infants and children. *J Invasive Cardiol* 17:18-22, 2005.
82. Voet A, Rega F, de Bruaene A, et al: Long-term outcome after treatment of isolated pulmonary valve stenosis. *Int J Cardiol* 2010. DOI: [Epub ahead of print].
83. Bruce C, Connolly H: Right-sided valve disease. In: Otto C, Bonow R, editors: *Valvular heart disease*, ed 3, Philadelphia, 2009, Saunders Elsevier, p 452.
84. Oechslin E, Harrison D, Harris L, et al: Reoperation in adults with repair of tetralogy of fallot: indications and outcomes. *J Thorac Cardiovasc Surg* 118:245-251, 1999.
85. Therrien J, Siu S, Harris L, et al: Impact of pulmonary valve replacement on arrhythmia propensity late after repair of tetralogy of Fallot. *Circulation* 103:2489-2494, 2001.
86. Silversides C, Veldtman G, Crossin J, et al: Pressure half-time predicts hemodynamically significant pulmonary regurgitation in adult patients with repaired tetralogy of Fallot. *J Am Soc Echocardiogr* 16:1057-1062, 2003.
87. Buck T, Mucci R, Guerrero J, et al: The power-velocity integral at the vena contracta: a new method for direct quantification of regurgitant volume flow. *Circulation* 102:1053-1061, 2000.
88. Renella P, Aboulhosn J, Lohan D, et al: Two-dimensional and Doppler echocardiography reliably predict severe pulmonary regurgitation as quantified by cardiac magnetic resonance. *J Am Soc Echocardiogr* 23:880-886, 2010.
89. Puchalski M, Askovich B, Sower C, et al: Pulmonary regurgitation: determining severity by echocardiography and magnetic resonance imaging. *Congenit Heart Dis* 3:168-175, 2008.
90. Harrild D, Powell A, Tran T, et al: Long-term pulmonary regurgitation following balloon valvuloplasty for pulmonary stenosis risk factors and relationship to exercise capacity and ventricular volume and function. *J Am Coll Cardiol* 55:1041-1047, 2010.
91. Oosterhof T, van Straten A, Vliegen H, et al: Preoperative thresholds for pulmonary valve replacement in patients with corrected tetralogy of Fallot using cardiovascular magnetic resonance. *Circulation* 116:545-551, 2007.
92. Westhoff-Bleck M, Girke S, Breymann T, et al: Pulmonary valve replacement in chronic pulmonary regurgitation in adults with congenital heart disease: impact of preoperative QRS-duration and NT-proBNP levels on postoperative right ventricular function. *Int J Cardiol* 151:303-306, 2011.
93. Buechel E, Dave H, Kellenberger C, et al: Remodelling of the right ventricle after early pulmonary valve replacement in children with repaired tetralogy of Fallot: assessment by cardiovascular magnetic resonance. *Eur Heart J* 26:2721-2727, 2005.
94. Therrien J, Siu S, McLaughlin P, et al: Pulmonary valve replacement in adults late after repair of tetralogy of fallot: are we operating too late? *J Am Coll Cardiol* 36:1670-1675, 2000.

# 35 Role of Echocardiography in the Diagnosis and Management of Heart Disease in Pregnancy

KAREN K. STOUT, MD

**Normal Hemodynamic and Echocardiographic Changes with Pregnancy**
Normal Hemodynamic Changes
Technical Aspects of Doppler Cardiac Output Measurements
M-Mode and Two-Dimensional Echocardiographic Changes
Doppler Flows
Postpartum Changes
Normal Valvular Regurgitation
Similarity of Hemodynamic Changes with Exercise and during Pregnancy
**Doppler Echocardiographic Evaluation of Hemodynamics in Pregnancy**
Positional Hemodynamic Changes
Peripartum Period
Exercise Physiology
Systemic Diseases
**Pregnancy-Induced Hypertension and Preeclampsia**
Hemodynamics
Echocardiographic Findings
Impact on Prognosis and Treatment Plans
**Heart Disease in Pregnancy**
Pulmonary Vascular Disease
Congenital Heart Disease
Valvular Heart Disease
Cardiomyopathies
Other Heart Diseases
**Echocardiographic Monitoring in Pregnant Patients**
**Common Clinical Presentations**
Pulmonary Edema and Heart Failure
The Pregnant Patient with a Cardiac Murmur
Mitral Valve Prolapse
Palpitations and Arrhythmias in Pregnancy
**Limitations of Echocardiography and Alternative Approaches**

Echocardiography is often requested in pregnant women to evaluate preexisting heart disease or to assess women with cardiac symptoms or abnormal findings on physical examination. Many healthy women experience symptoms of fatigue, decreased exercise tolerance, or dyspnea during pregnancy. Clinical examination may be nondiagnostic, prompting a request for echocardiographic evaluation. Although a "flow murmur" is present in most pregnant women, this normal finding cannot always be clinically distinguished from a pathologic murmur. Diagnostic testing can differentiate between the normal alterations in cardiovascular physiology and anatomy resulting from pregnancy and from pathologic findings.

In pregnant patients with known cardiac disease, expected findings (and appropriate normal reference values) may be different from those in nongravid patients. Echocardiography may be used to monitor cardiovascular function during pregnancy and the peripartum period. In pregnant patients with concurrent systemic disease or with preeclampsia, echocardiography can provide important insights into the effect of the disease process on cardiovascular physiology and can assist in management of individual patients.

In this chapter, the normal hemodynamic and echocardiographic changes during pregnancy are reviewed and the role of echocardiography in management of pregnant women with known or suspected cardiac disease is summarized.

## Normal Hemodynamic and Echocardiographic Changes with Pregnancy

### NORMAL HEMODYNAMIC CHANGES

During normal pregnancy, plasma volume, erythrocyte volume, and cardiac output (CO) increase substantially over baseline values (Table 35-1 and Fig. 35-1). Many original studies of hemodynamic changes during pregnancy were based on right-sided heart catheterization with Fick or thermodilution CO data. These studies included small numbers of patients with evaluation of limited points during pregnancy.[1,2] More recent use of Doppler CO measurement techniques has greatly increased our understanding of the magnitude and timing of CO changes during pregnancy.[2-4]

CO increases during pregnancy by as much as 45% over baseline values.[4-7] Noninvasive Doppler measurements consistently show a definite rise in CO that occurs as early as 10 weeks gestation. Some studies suggest that maximum CO is reached at 24 weeks gestation with no further increase in later pregnancy (Fig. 35-2). Other studies (Figs. 35-3 and 35-4) show a continued increase in CO throughout pregnancy, with higher stroke volume accounting for much of the first-trimester increase, followed by a continued elevation in heart rate (and thus CO) in the last two trimesters. On average, heart rate

**TABLE 35-1 Normal Anatomic and Hemodynamic Changes of Pregnancy**

| | |
|---|---|
| **Anatomic** | |
| Aortic root | Slight increase in diameter (2-3 mm) |
| LV | Slight increase in end-diastolic dimension and slight decrease in end-systolic dimension |
| LA | Slight increase in size |
| **Hemodynamic** | |
| Cardiac output | Increased beginning in first trimester; maximum increase (at term) of 45% over baseline value |
| Stroke volume | Increased |
| Heart rate | Increased by 25% to 30% |
| Blood pressure | Unchanged |
| Systemic vascular resistance | Decreased |
| Pulmonary artery pressure | Unchanged |
| LV end-diastolic pressure | Unchanged |

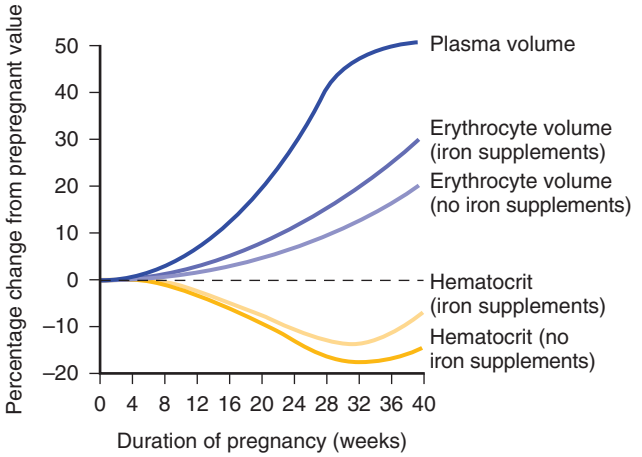



**Figure 35-1 Plasma and erythrocyte increase during pregnancy.** *(From Pitkin PM: Nutritional support in obstetrics and gynecology.* Clin Obstet Gynecol *19:489-513, 1976.)*

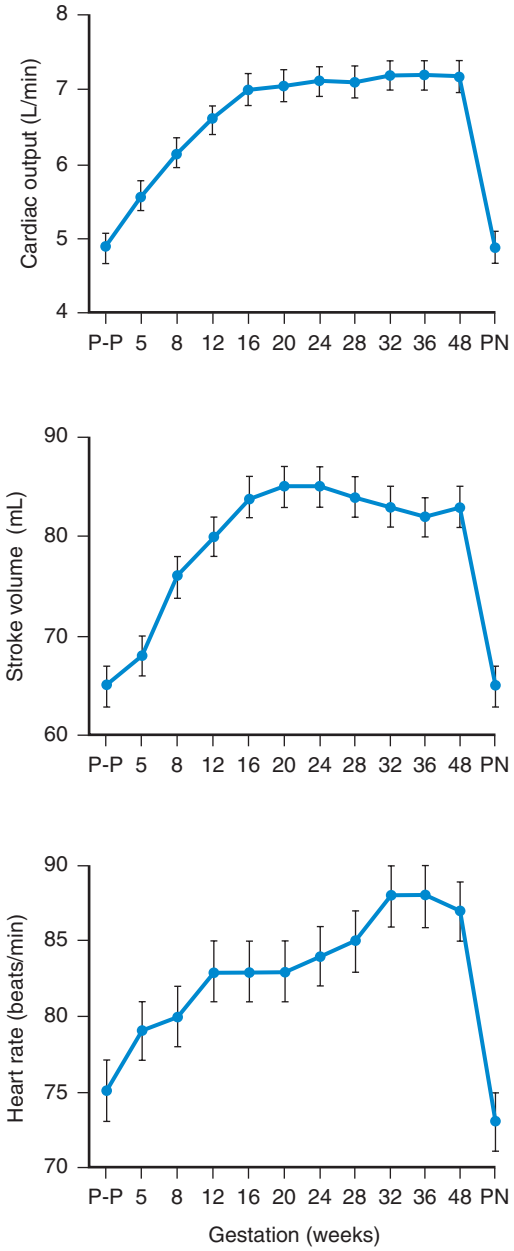



**Figure 35-2 Increase in cardiac output from the nonpregnant state throughout pregnancy.** *P-P*, Prepregnancy; *PN*, postnatal. (From Hunter S, Robson SC: Adaptation of the maternal heart in pregnancy. *Br Heart J* 68:540-543, 1992.)

increases 25% to 30% over baseline values during pregnancy[8] (Fig. 35-5).

The underlying etiology of increased CO with pregnancy is presumably hormonal, but the exact mechanism remains unclear.[9] Vasodilation may be mediated by nitric oxide[10] and hormones, such as relaxin.[11] An increase in venous tone during pregnancy contributes to preload augmentation.[4] In addition, decreased aortic stiffness reduces afterload.[6] Arterial capacitance increases during pregnancy, accounting for the decrease in total peripheral resistance.[12] This fall in systemic vascular resistance allows blood pressure to rise only slightly despite increased stroke volume (see Fig. 35-5). Some studies suggest that pregnancy is associated with an increased ventricular wall stress.[13] However, this view is challenged by other studies demonstrating a 30% decrease in wall stress.[4,14] Left ventricular (LV) contractility may to be depressed in pregnancy, based on measurement of the afterload adjusted velocity of circumferential fiber shortening.[13,14] LV systolic performance is maintained, despite this possible decrease in contractility, as a result of the altered loading conditions of pregnancy. However other studies suggest that there is no change in ventricular contractility.[1,12] Pulmonary pressures remain normal during pregnancy,[15] suggesting a similar decrease in pulmonary vascular resistance to balance the increased blood volume. Diastolic filling pressures in both the right-sided and left-sided heart also remain normal in pregnancy.[16]

## TECHNICAL ASPECTS OF DOPPLER CARDIAC OUTPUT MEASUREMENTS

Doppler measurement of CO in pregnancy is based on the same principles as in nonpregnant patients. Stroke volume (SV) is calculated from the cross-sectional area (CSA) of flow multiplied by the velocity-time integral (VTI) of flow at that site:

$$SV = CSA \times VTI$$

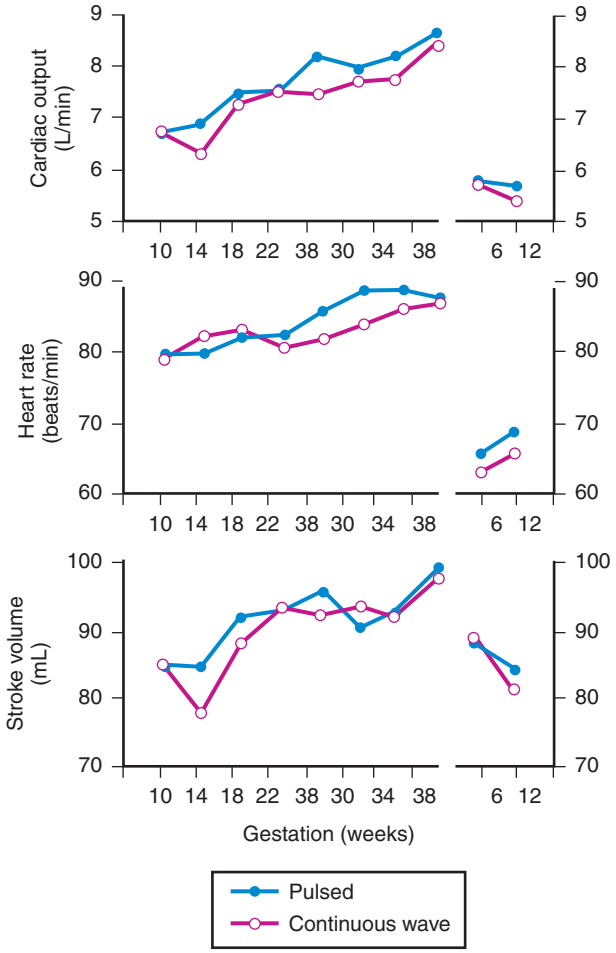



**Figure 35-3 Hemodynamic changes during pregnancy and postpartum.** *(From Mabie WC, DiSessa TG, Crocker LG, et al: A longitudinal study of cardiac output in normal human pregnancy.* Am J Obstet Gynecol *170:849-856, 1994.)*

Typically, the cross-sectional area is assumed to be circular and is calculated from a two-dimensional (2D) echocardiographic diameter measurement recorded with the ultrasound beam perpendicular to the flow diameter. The velocity-time integral is measured by either pulsed-wave (PW) or continuous-wave (CW) Doppler ultrasound, with the Doppler beam aligned parallel to the flow stream. As in nonpregnant patients, it is critical that (1) diameter is measured accurately, (2) the Doppler beam is aligned parallel to the direction of blood flow, and (3) diameter and velocity data are obtained almost simultaneously from the same intracardiac site. In addition, this method assumes that flow is laminar with a relatively flat (or blunt) flow-velocity profile and that flow fills the anatomic cross-sectional area. Although these assumptions appear to be warranted in nonpregnant patients according to numerous studies validating this approach,[17] the potential effect of the altered flow conditions during pregnancy warrants reevaluation. Specific concerns in pregnant patients include the possibility that the flow profile may not be blunt or may be asymmetric given the higher flow volumes. Possible changes in cross-sectional flow areas during pregnancy may also affect these measurements.

Validation of CO measurements in pregnancy has been performed by several groups of investigators using either of two

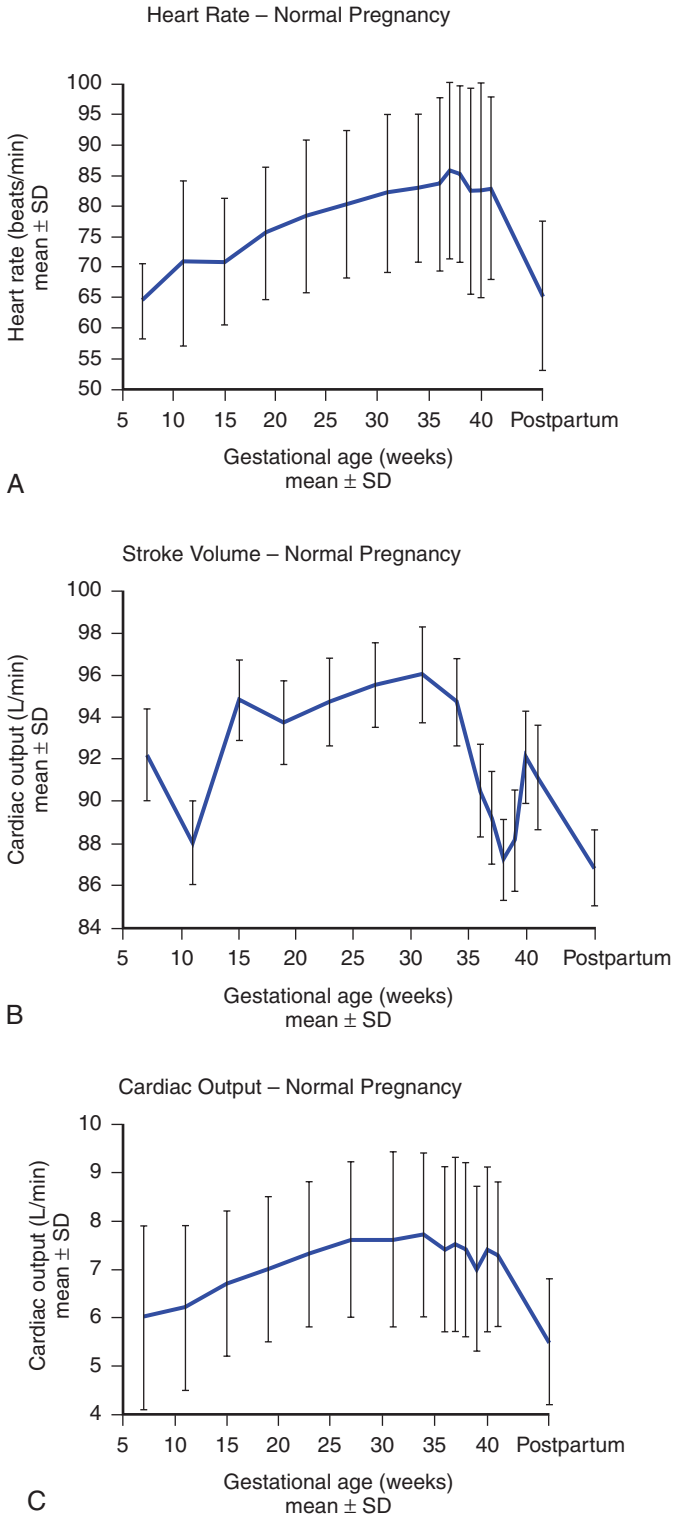



**Figure 35-4** Serial changes in heart rate (**A**), stroke volume (**B**), and cardiac output (**C**) recorded using Doppler echocardiography in a series of 89 women with no cardiac disease and a normal pregnancy. *SD,* Standard deviation. *(Data from Easterling TR, Benedetti TJ, Schmucker BC, Millard SP: Maternal hemodynamics in normal and preeclamptic pregnancies: a longitudinal study.* Obstet Gynecol *76:1061-1069, 1990.)*

basic Doppler approaches (Table 35-2). Some investigators have applied the technique of measuring ascending aortic flow with a CW Doppler probe from a suprasternal approach.[18,20] The cross-sectional area of flow is calculated from a carefully recorded A-mode aortic diameter measured at the sinotubular junction, the narrowest segment of the aorta, because the highest flow velocity (as obtained with CW Doppler) will correspond to the smallest flow area. Doppler COs calculated with this method correlated well with simultaneous thermodilution COs in pregnant women undergoing right-sided heart catheterization for clinical indications.[18] Of note, serial studies in pregnant women suggest that aortic root diameter increases during pregnancy,[21,22] so that repeat aortic diameter measurements are needed at each time point. This contrasts with the situation in nonpregnant adults in whom both left ventricular outflow tract (LVOT) and aortic diameters tend to remain relatively constant over time.

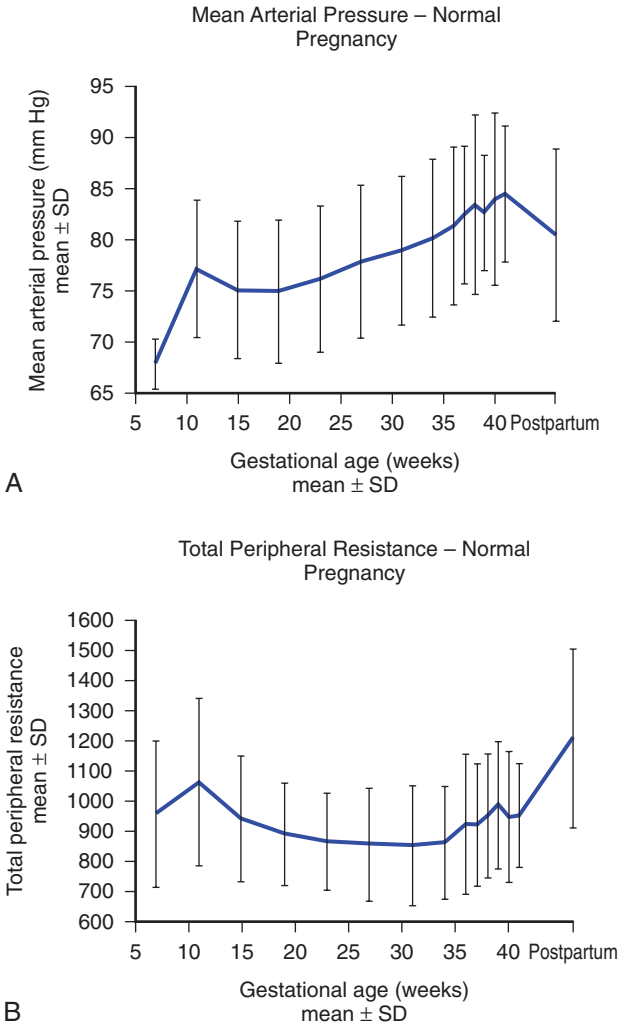



**Figure 35-5** Sequential changes in mean arterial pressure (**A**) and total peripheral resistance (**B**) in 89 women with no cardiac disease and a normal pregnancy. *SD*, Standard deviation. *(Data from Easterling TR, Benedetti TJ, Schmucker BC, Millard SP: Maternal hemodynamics in normal and preeclamptic pregnancies: a longitudinal study.* Obstet Gynecol *76:1061-1069, 1990.)*

Other investigators have measured CO in pregnant women using standard clinical cardiac ultrasound systems.[5,23-25] LVOT diameter is measured from a 2D parasternal long-axis view; LVOT flow is recorded via an apical approach using pulsed Doppler echocardiography, with the sample volume positioned just proximal to the aortic valve plane.[26] This method correlates well with simultaneous Fick COs in nonpregnant patients.[17] In a group of pregnant women, internal consistency between Doppler COs measured from diameter and flow data across the aortic, mitral, and pulmonic valves was demonstrated.[27]

Reproducibility, in addition to accuracy, is critical for the application of these methods in following individual patients during the course of pregnancy. Several studies suggest that both these methods can be performed reproducibly with an acceptable degree of recording and measurement variability in pregnant patients, with a coefficient of variation of 5% to 8%.[18,27] Although there is still concern that these methods have been validated against invasive standards in only small numbers of pregnant women, the data should still accurately reflect hemodynamic changes over time (if not absolute values) both in individuals and in groups of patients.

Compared with the 2D/pulsed Doppler approach, the advantage of the A-mode/CW method is that a smaller, less expensive, dedicated instrument can be used for CO measurements. Although optimal results require careful data acquisition, focused education and training of appropriate individuals allows more widespread application of this technique. Potential disadvantages include (1) the possibility of a nonperpendicular measurement of aortic root diameter (resulting in overestimation of CO), (2) a nonparallel intercept angle between the Doppler beam and the direction of aortic flow (resulting in underestimation of CO), and (3) failure to recognize abnormal aortic flow conditions (e.g., aortic stenosis or aortic regurgitation) that invalidate the Doppler method. When any of these problems are suspected, a standard clinical echocardiographic examination should be performed to resolve the difficulty.

**TABLE 35-2 Validation of Doppler Cardiac Output Measurements in Pregnancy**

| *Study* | *n* | *Gestational Age* | *Doppler Method* | *Standard of Reference* | *r* | *Regression Equation (L/min)* | *SEE (L/min)* |
|---|---|---|---|---|---|---|---|
| Easterling[18] | 23 | Third trimester | CWD | TD | 0.93 | Dop = 1.07 TD − 0.58 | — |
| | | | A-mode Ao | — | — | — | — |
| Robson[25] | 15 | Nonpregnant | PD asc Ao | Fick | 0.93 | Fick = 1.0 Dop + 0.8 | 0.4 |
| | | | 2D Ao-leaflets | — | — | — | — |
| Robson[25] | 40 | Pregnant | Ao | Doppler | — | — | — |
| | | Nonpregnant | MV vs. PA | MV | 0.96 | Ao = 1.02 MV − 0.96 | 0.37 |
| | | | — | PA | 0.96 | Ao = 0.97 PA + 0.40 | 0.47 |
| | | | — | — | 0.97 | MV = 0.92 PA + 0.62 | 0.34 |
| Lee[19] | 16 | Pregnant | LVOT | TD | 0.94 | TD = 0.74 LVOT + 1.91 | 0.64 |

*Ao*, Aorta; *asc*, ascending; *CWD*, continuous-wave Doppler; *Dop*, Doppler; *LVOT*, left ventricular outflow tract; *MV*, mitral valve; *PA*, pulmonary artery; *PD*, pulsed Doppler; *SEE*, standard error of estimate; *TD*, thermodilution.

**TABLE 35-3 Normal Echocardiographic Measurements in Pregnancy (Maximum Changes)**

| *Measurement* | *Modality* | *Mean ± SD* | *Gestational Age* | *Comparison Value* | *Time of Comparison* | *Reference* |
|---|---|---|---|---|---|---|
| Aortic root (mm) | M-mode | 30 ± 12 | Third trimester | 28 ± 3 | 2 months pp | Sadaniantz[22] |
| | A-mode | 25 ± 2 | Term | 24 ± 4 | 10 weeks | Easterling[21] |
| LVOT ($cm^2$) | 2D area | 3.5 ± 0.3 | Term | 3.2 ± 0.3 | 2 months pp | Vered[28] |
| LA dimension (mm) | 2D | 38 ± 4 | Term | 34 ± 5 | 2 months pp | Vered[28] |
| | M-mode | 36 | Term | 31 | Preconception | Sadaniantz[22] |
| | M-mode | 37 | Term | 33 | 24 weeks pp | Robson[29] |
| LV EDD (mm) | M-mode | 47 ± 4 | Term | 48 ± 4 | 12 weeks pp | Mabie[6] |
| | M-mode | 46 ± 3 | 24 to 32 weeks | 43 ± 3 | Nonpregnant controls | Rubler[30] |
| | M-mode | 51 ± 3 | Third trimester | 50 ± 4 | 2 months pp | Sadaniantz[22] |
| | M-mode | 48 | Third trimester | 45 | Preconception | Robson[26] |
| | M-mode | 49 | Term | 47 | 24 weeks pp | Robson[29] |
| | 2D | 52 ± 4 | Term | 50 ± 3 | 2 months pp | Vered[28] |
| LV ESD (mm) | M-mode | 32 | Term | 32 | 24 weeks pp | Robson[29] |
| | M-mode | 29 ± 3 | Term | 30 ± 2 | Nonpregnant controls | Rubler[30] |
| | 2D | 33 ± 4 | Term | 34 ± 5 | 2 months pp | Vered[28] |
| PWT (mm) | M-mode | 10 ± 1 | Term | 9 ± 1 | 12 weeks pp | Mabie[6] |
| | M-mode | 7 ± 1 | Third trimester | 6 ± 1 | 2 months pp | Sadaniantz[22] |
| | 2D | 8 ± 1 | Term | 7 ± 1 | 2 months pp | Vered[28] |
| LV mass (g) | M-mode | 175 ± 37 | Term | 135 ± 25 | 12 weeks pp | Mabie[6] |
| | M-mode | 203 | Term | 157 | 24 weeks pp | Robson[29] |
| | M-mode | 183 | Term | 120 | Preconception | Robson[26] |
| | M-mode | 186 ± 39 | Term | 151 ± 34 | 2 months pp | Vered[28] |
| FS (%) | M-mode | 40 ± 7 | Term | 33 ± 7 | 12 weeks pp | Mabie[6] |
| LV EDV (mL) | M-mode | 30 ± 5 | Term | 35 ± 5 | 2 months pp | Vered[28] |
| | 2D | 108 ± 14 | Term | 102 ± 13 | 2 months pp | Vered[28] |
| LV ESV (mL) | 2D | 44 ± 10 | Term | 44 ± 7 | 2 months pp | Vered[28] |
| EF (%) | 2D | 60 ± 4 | Term | 57 ± 4 | 2 months pp | Vered[28] |
| RV (mm) | M-mode | 20 ± 1 | Third trimester | 18 ± 1 | 2 months pp | Sadaniantz[22] |
| | M-mode | 19 ± 3 | 24 to 32 weeks | 15 ± 2 | Nonpregnant controls | Rubler[30] |
| Mitral annulus (mm) | 2D | 24 ± 5 | Third trimester | 21 ± 4 | 2 months pp | Sadaniantz[22] |
| Tricuspid annulus (mm) | 2D | 27 ± 3 | Third trimester | 18 ± 3 | 2 months pp | Sadaniantz[22] |

*EDD*, End-diastolic dimension; *EDV*, end-diastolic volume; *EF*, ejection fraction; *ESD*, end-systolic dimension; *ESV*, end-systolic volume; *FS*, fractional shortening; *LVOT*, left ventricular outflow tract; *pp*, postpartum; *PWT*, posterior wall thickness.

## M-MODE AND TWO-DIMENSIONAL ECHOCARDIOGRAPHIC CHANGES

The increased CO of pregnancy is reflected in changes in LV dimensions, volumes, and geometry (Table 35-3). M-mode studies show that LV end-diastolic dimension increases slightly (by 2 to 3 mm on average) and end-systolic dimension is unchanged, so that there is a slight increase in fractional shortening during pregnancy.[20,27,29,31] The change in LV diastolic dimension correlates with increased preload caused by changes in systemic venous tone.[30] LV wall thickness also increases slightly, with a corresponding increase in calculated LV mass. Similar changes in right ventricular (RV) dimensions have been noted.

With 2D echocardiography, a slight increase in end-diastolic volume and in ejection fraction is seen, with little change in end-systolic volume.[6,22,29,31,33,34] These findings are consistent with the altered loading conditions of an increased end-diastolic volume and decreased systemic vascular resistance and do not imply an increase in LV contractility. There are conflicting data on the changes in contractility with pregnancy.[4,14,16,31] There have been few studies evaluating LV geometry in normal pregnancy; however, no dramatic changes in ventricular shape have been observed.

Several investigators have found consistent increases in aortic and LVOT diameters during pregnancy, with the magnitude of this change averaging 1 to 2 mm.[20,35] Even this small average change is significant for accurate CO calculations, and given the wide range of values, some individuals have more pronounced changes in outflow tract geometry.

Left atrial (LA) anteroposterior dimension increases by about 4 mm. When compared with echocardiograms obtained several weeks postpartum, the maximal atrial size is seen at term.[22] Changes in atrial dimension in the peripartum period are associated with changes in serum atrial natriuretic peptide levels.[36] A small increase in mitral annulus diameter has been documented in conjunction with a much larger change in tricuspid annulus diameter.[22]

A small pericardial effusion is seen on echocardiography is as many as 25% of normal pregnant women, with a higher prevalence in women with preeclampsia.[36]

## DOPPLER FLOWS

Although enlargement in annular diameters partially compensate for the increased transvalvular volume flow of pregnancy, higher transvalvular flow velocities are also seen[24] (Table 35-4). Both the maximum aortic and LVOT flow velocity rises by approximately 0.3 m/s compared with the nongravid state. Less dramatic changes in transmitral velocities are seen with an increase in early (E) velocity of only 0 to 0.1 m/s and an increase in atrial (A) velocity of only 0.1 to 0.2 m/s. However, the relative increase in E and A velocities being unequal, the E/A ratio

**TABLE 35-4 Normal Doppler Flow Velocities in Pregnancy**

| *Measurement* | *Modality* | *Value* | *Gestational Age* | *Comparison Value* | *Time of Comparison* | *Reference* |
|---|---|---|---|---|---|---|
| Aorta (m/s) | CWD | 1.4 ± 0.2 | Term | 1.1 ± 0.2 | 12 weeks pp | Mabie[6] |
| LVOT (m/s) | PD | 1.3 ± 0.1 | Term | 1.0 ± 0.1 | 12 weeks pp | Mabie[6] |
| Mitral E (m/s) | MV-tips | 0.7 ± 0.2 | Third trimester | 0.8 ± 0.1 | 2 months pp | Sadaniantz[22] |
| | | 0.9 ± 0.1 | 6 to 12 weeks | 0.8 ± 0.1 | 12 weeks pp | Mabie[6] |
| Mitral A (m/s) | MV-tips | 0.6 ± 0.1 | Third trimester | 0.5 ± 0.1 | 2 months pp | Sadaniantz[22] |
| | | 0.6 ± 0.1 | 24 to 27 weeks | 0.5 ± 0.1 | 12 weeks pp | Mabie[6] |
| E/A | MV-tips | 1.5 ± 0.2 | Term | 1.8 ± 0.2 | 12 weeks pp | Mabie[6] |
| | | 1.3 ± 0.3 | Third trimester | 1.6 ± 0.4 | 2 months pp | Sadaniantz[22] |
| Heart rate (bpm) | | 84 ± 10 | Third trimester | 70 ± 16 | 2 months pp | Sadaniantz[22] |
| | | 89 ± 15 | 32 to 35 weeks | 69 ± 12 | 12 weeks pp | Mabie[6] |
| | | 87 | Term | 69 | 24 weeks pp | Robson[29] |
| | | 77 ± 10 | Term | 70 ± 7 | 2 months pp | Vered[28] |
| Cardiac output (L/min) | | 6.5 ± 1.5 | Term | 4.3 ± 0.6 | 2 months pp | Vered[28] |
| | | 7.6 | Term | 5.0 | 24 weeks pp | Robson[29] |

*CWD*, Continuous-wave Doppler; *LVOT*, left ventricular outflow tract; *MV*, mitral valve; *PD*, pulsed Doppler; *pp*, postpartum.

changes from the normal pattern in young women (higher E than A with an E/A ratio greater than 1.5) to a pattern of equalized or reversed E/A velocities (E/A ratio less than 1) later in pregnancy. Peak pulmonary venous A-wave velocity but not duration also increases during pregnancy.[6]

### POSTPARTUM CHANGES

Interestingly, the estimated magnitude of changes in hemodynamics and cardiac anatomy during pregnancy depends on whether the values obtained during pregnancy are compared to postpartum values or to values obtained in the same patient before pregnancy. It is often difficult to obtain data in the prepregnant time period (because women typically present to the physician after the onset of pregnancy), but a few studies have followed women prospectively starting from preconception. These studies found hemodynamic and anatomic changes of greater magnitude than studies that compared values obtained during pregnancy with postpartum data. This suggests that at least some of the changes of pregnancy may persist into the postpartum period or may be permanent. Although in the postpartum period hemodynamic and anatomic changes return rapidly toward baseline over 6 to 12 weeks (see Fig. 35-4),[5,26] the postpartum baseline may be different from the prepartum baseline. Specifically, aortic and LV dimensions, although remaining within normal adult limits, may remain larger than the prepregnant values in that individual. Analysis of these data is complicated by the small number of subjects studied, by the possibly confounding effects of breastfeeding or other factors, and by the measurement variability of the techniques. Further studies are needed because if there are significant, persistent changes after pregnancy, perhaps adult normal values not only should be indexed for body size and gender but also should consider parity.

### NORMAL VALVULAR REGURGITATION

As in nonpregnant patients, a small degree of valvular regurgitation is often found on Doppler echocardiography.[5,32,37] It is unlikely that these small regurgitant leaks are audible on auscultation or account for the presence of a murmur in pregnant patients. Early studies suggested an unusually high prevalence of tricuspid regurgitation in pregnant women.[32] With the recognition of the extremely high prevalence of small amounts of tricuspid, mitral, and pulmonic regurgitation in normal individuals, it is now apparent that the prevalence of physiologic degrees of valvular regurgitation in pregnant women is similar to that in nonpregnant normal adults.

### SIMILARITY OF HEMODYNAMIC CHANGES WITH EXERCISE AND DURING PREGNANCY

Many of the hemodynamic changes of pregnancy are similar to the normal changes seen with exercise. The increase in heart rate and CO and decrease in systemic vascular resistance are analogous to changes seen at a moderate level of physical exertion. In addition, the changes in cardiac anatomy seen with pregnancy are similar to those seen with repetitive activity in physically conditioned individuals. Specifically, the increases in LV end-diastolic dimensions, volume, and LV mass, with normal diastolic filling patterns, are analogous to the changes seen with regular physical activity in nonpregnant women and in men. Presumably, these changes represent a similar hemodynamic response to chronic elevation in volume flow rate. In contrast, the increase in aortic root dimension observed in pregnant women by several groups of investigators has not been seen with physical conditioning, suggesting that the mechanism of this effect is related to physical changes in the vessel wall, possibly mediated by hormonal effects.

## Doppler Echocardiographic Evaluation of Hemodynamics in Pregnancy

### POSITIONAL HEMODYNAMIC CHANGES

Doppler echocardiography can readily evaluate the effect of positional changes on hemodynamics. Orthostatic changes from sitting to standing positions are similar to the changes seen in nonpregnant individuals, with no significant differences between early and late pregnancy.[34] When a pregnant patient changes from a supine to a standing position, heart rate increases, stroke volume and CO decrease, and systemic vascular resistance rises, maintaining mean arterial pressure. During pregnancy, the supine position is associated with compression of the inferior vena cava by the gravid uterus, resulting in a decrease in venous return to the right atrium (RA) and a decline

in stroke volume and CO.[24] This supine decrease in CO can be reversed (or prevented) by placing the patient in a left lateral decubitus position. Accordingly, diagnostic echocardiographic studies should be performed with the pregnant patient in a left lateral decubitus position whenever possible. If optimal imaging requires a supine position, the length of time the patient is positioned on her back should be limited.

## PERIPARTUM PERIOD

Dramatic changes in loading conditions occur in the peripartum period related to the effects of (1) uterine contractions, (2) the pain associated with labor and delivery, (3) anesthetic medications, (4) the immediate blood loss associated with delivery (Fig. 35-6), and (5) the delivery of the placenta. Although these physiologic changes are well tolerated by healthy women, they can result in acute decompensation in women with underlying heart disease.

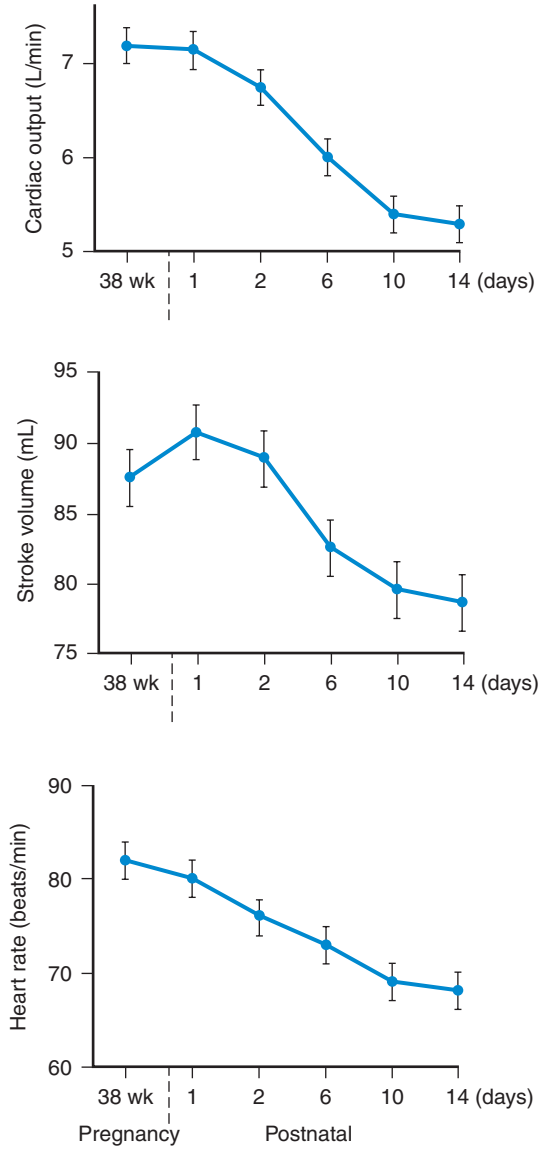



**Figure 35-6 Changes in heart rate and cardiac output after normal delivery.** *(From Hunter S, Robson SC: Adaptation of the maternal heart in pregnancy.* Br Heart J *68:540-543, 1992.)*

During labor, uterine contractions result in an acute increase in both heart rate and intravascular volume as uterine blood is forced into the circulation. The magnitude of CO rise during contractions increases as labor progresses, with an augmentation of as much as 20% in CO with each contraction.[38,39] There are also mild increases in pulmonary and LV pressures, which may be accentuated in patients with decreased LV compliance (e.g., those with aortic stenosis or LV hypertrophy). Despite the acute blood loss associated with delivery, stroke volume and CO actually rise after delivery of the placenta (by about 10%)[26] and remain elevated for about 24 hours.[26,38] Over the next several days to 2 weeks, CO declines by about 25% to 30% compared with the immediately prepartum value, related to a decrease in both heart rate and intravascular volume.

Volume changes associated with cesarean section and delivery are greater than those associated with vaginal delivery, so there is rarely hemodynamic advantage to this mode of delivery in patients with heart disease.[40]

The hemodynamic effects of pain include increased heart rate and systemic vascular resistance. In patients with cardiac disease, the hemodynamic effects of pain may lead to a decline in CO. The negative effects of pain can be eliminated by appropriate anesthesia. However, anesthesia-related changes in preload and afterload also affect cardiac function, especially in patients with heart disease. Thus, the choice of anesthetic agent and route of administration depends on the specific cardiovascular concerns in an individual patient.[40]

## EXERCISE PHYSIOLOGY

Exercise physiology in pregnant women is similar to that in nonpregnant women, except that the basal values are altered by pregnancy. Resting heart rate and stroke volume are elevated during pregnancy. With exercise, heart rate and CO rise appropriately.[41,42] Exercise in pregnant women at 32 weeks gestation was associated with a higher exercise heart rate, higher maximal oxygen consumption, and high atriovenous oxygen difference compared to 3 months postpartum.[43]

Conditioned pregnant women have a greater CO than sedentary women for any given heart rate, as is seen in nonpregnant, physically conditioned individuals.[44-48] However, the cardiovascular effects of aerobic conditioning are most evident during strenuous (not during mild or moderate) exercise in pregnant women.[49]

## SYSTEMIC DISEASES

Doppler echocardiography is a useful tool for examining the hemodynamic changes associated with systemic diseases in pregnant patients. For example, in hyperthyroid pregnant women, elevated CO and decreased systemic vascular resistance can be documented, and the resolution of these changes with therapy can be monitored.[50] Echocardiographic evaluation of the effects of beta-agonist tocolysis,[51] pheochromocytoma,[52] sickle cell disease,[53] and renal artery stenosis[54] has also been reported.

# Pregnancy-Induced Hypertension and Preeclampsia

## HEMODYNAMICS

There are four hypertensive conditions in pregnancy: preeclampsia, chronic hypertension, chronic hypertension with superimposed preeclampsia, and gestational hypertension.[55]

Preeclampsia is defined as systolic blood pressure greater than or equal to 140 mm Hg or diastolic blood pressure greater than or equal to 90 mm Hg and proteinuria greater than 0.3 g per 24 hours, developing after the 20th week of pregnancy in a previously normotensive woman. Eclampsia is the onset of seizures in a woman with preeclampsia. Gestational hypertension is hypertension after the 20th week of pregnancy in a previously normotensive woman, without proteinuria or signs of preeclampsia. Gestational hypertension may progress to preeclampsia but frequently resolves after delivery and has a more benign course than preeclampsia.[56] In a prospective study of 400 primigravid women, gestational hypertension developed in 24 and preeclampsia in 20 women.[57] Chronic hypertension is defined as systolic blood pressure greater than or equal to 140 mm Hg or diastolic blood pressure greater than or equal to 90 mm Hg that antedates pregnancy, develops before 20 weeks gestation, or persists longer than 12 weeks postpartum. If proteinuria develops after 20 weeks gestation in a woman with chronic hypertension, she is diagnosed with preeclampsia. Preeclampsia in a woman with preexisting hypertension and proteinuria is diagnosed if she develops severe hypertension (systolic greater than 160 mm Hg or diastolic greater than 110 mm Hg) in the last half of pregnancy.

The hemodynamics of preeclampsia and gestational hypertension are complex. There is a growing body of literature regarding the pathophysiology of preeclampsia.[23,47,58-60] Preeclampsia may be a heterogeneous disease with different hemodynamic subsets.[61] Investigators have identified that early in the disease course, CO is elevated, and later in the course, elevated systemic vascular resistance is seen associated with decreased CO and clinical decompensation.[57] For any given CO, mean arterial pressure is elevated in preeclamptic in comparison with normotensive pregnant women.[57,60,62] Central venous pressures, pulmonary capillary wedge pressures, and pulmonary artery pressures tend to be normal. The exception is decompensated patients with pulmonary edema, in whom central venous and pulmonary wedge pressures can be discrepant to the point that invasive hemodynamic monitoring is needed. However, because serum oncotic pressure is reduced even more than normal in preeclamptic pregnant patients, interstitial fluid in the lungs and pulmonary edema can occur at relatively low LA and pulmonary wedge pressures.

### ECHOCARDIOGRAPHIC FINDINGS

In the few studies that have compared cardiac structure in preeclamptic versus normotensive pregnant patients, there have been few or no differences in LV dimensions, volumes, fractional shortening, or LV mass (Table 35-5). Aortic root dimension appears to be slightly greater in preeclamptic than in normotensive pregnant patients and tends to be inversely related to total peripheral resistance.[21]

### IMPACT ON PROGNOSIS AND TREATMENT PLANS

The use of Doppler CO measurements and calculation of systemic vascular resistance in patients with pregnancy-induced hypertension and preeclampsia to tailor medical therapy is controversial. Some authors have described medication choice based on whether the patient has an elevated CO or elevated systemic vascular resistance.[63] For example, hypertension related to a high CO might respond to beta-blocker therapy, whereas elevated systemic vascular resistance might respond to vasodilator therapy. Importantly, maternal hemodynamics affect fetal growth: High-resistance hypertension is associated with lower birth weights.

Investigators identified women at risk of preeclampsia based on an elevated CO (greater than 7.4 L/min by Doppler echocardiogram) before 24 weeks gestation. In a subsequent double-blind, randomized trial of women with an elevated CO early in pregnancy, atenolol decreased the incidence of preeclampsia (1 of 28 versus 5 of 28, $p = 0.04$) but increased the risk of a low–birth-weight infant ($p = 0.02$).[64]

**TABLE 35-5 Echocardiographic Findings in Preeclampsia**

| *Study* | *Normal Pregnant Women* | *Women with PIH* | p *Value* |
|---|---|---|---|
| **EDD (mm)** | | | |
| Kuzniar* | 51.4 ± 2.2 | 49.2 ± 3.4 | 0.01 |
| Thompson† | 45 ± 2.3 | 44 ± 5.1 | NS |
| Veille‡ | 50 ± 4 | 48 ± 4 | NS |
| **ESD (mm)** | | | |
| Kuzniar* | 33.8 ± 2.6 | 32.3 ± 3.8 | NS |
| Thompson† | 28.7 ± 1.9 | 29.8 ± 4.7 | NS |
| **EDV (mL)** | | | |
| Kuzniar* | 128.5 ± 14.4 | 115.2 ± 18.8 | 0.01 |
| **ESV (mL)** | | | |
| Kuzniar* | 46.9 | 42.5 | NS |
| **FS (%)** | | | |
| Kuzniar* | 35 ± 3 | 35 ± 4 | NS |
| Thompson† | 36 ± 5 | 34 ± 4 | NS |
| Veille‡ | 32 ± 4 | 37 ± 7 | <0.02 |
| **Ao-Root** | | | |
| Easterling§ | 25 ± 0.2 | 27.3 ± 1 | 0.01 |
| **LV Mass** | | | |
| Thompson† | 147 ± 12 | 157 ± 16 | <0.01 |
| Veille‡ | 105 ± 14 | 117 ± 20 | <0.05 |

*Ao*, Aorta; *EDD*, end-diastolic dimension; *EDV*, end-diastolic volume; *EF*, ejection fraction; *ESD*, end-systolic dimension; *ESV*, end-systolic volume; *FS*, fractional shortening; *NS*, not significant; *PIH*, pregnancy-induced hypertension.

*Kuzniar J, Piela A, Skret A: Left ventricular function in preeclamptic patients: an echocardiographic study. *Am J Obstet Gynecol* 146:400-405, 1983 (25 normals, 42 PIH).

†Thompson JA, Hays PM, Sagar KB, Cruikshank DP: Echocardiographic left ventricular mass to differentiate chronic hypertension from preeclampsia during pregnancy. *Am J Obstet Gynecol* 155:994-999, 1986 (11 normals, 14 PIH).

‡Veille JC, Hosenpud JD, Morton MJ: Cardiac size and function in pregnancy-induced hypertension. *Am J Obstet Gynecol* 150:443-449, 1984 (17 normals, 23 PIH).

§Easterling TR, Benedetti TJ, Schmucker BC, et al: Maternal hemodynamics and aortic diameter in normal and hypertensive pregnancies. *Obstet Gynecol* 78:1073-1077, 1991 (89 normals, 9 PIH).

## Heart Disease in Pregnancy

Given the low prevalence of heart disease in women of childbearing age in the general population, few pregnant women have significant heart disease. Despite this low prevalence, heart disease is a leading cause of maternal morbidity and mortality. The prevalence of specific types of heart disease in pregnancy reflects both the geographic distribution of these diseases and the patterns of health care in the overall population.[65] For example, in the United States and Europe, the prevalence of rheumatic valvular disease in young women is decreasing, whereas that of surgically treated congenital heart disease with survival to adulthood is increasing. Several studies have demonstrated that severe complications related to chronic heart disease have increased, including one study demonstrating that although overall prevalence of heart disease in delivery hospitalizations in the United States had not changed from

1995-1997 to 2004-2006, the number of hospitalizations for severe cardiac complications tripled in that time and there was a linear increase in congenital heart disease, arrhythmias, and heart failure. These authors concluded that the severity of heart disease had increased and that specific diagnoses, such as congenital heart disease, were increasingly common.[66]

Although the incidence of significant heart disease is low, suspected cardiac disease is a common reason for echocardiographic evaluation of pregnant women. The most common symptoms and signs prompting a suspicion of cardiac disease are (1) evaluation of a murmur; (2) evaluation of cardiac symptoms, such as heart failure; and (3) a history of preexisting heart disease. It is important that the normal hemodynamic changes of pregnancy be distinguished from pathologic abnormalities when these patients are evaluated.

The echocardiographic diagnosis of significant heart disease in a pregnant woman can affect patient management in several ways.[67] First, the cardiac diagnosis may have important prognostic implications (morbidity and mortality) for both mother and fetus. Second, special or more intensive monitoring of the mother or fetus may be needed during pregnancy or in the peripartum period. Third, surgical or medical intervention may be needed either during or after pregnancy. Finally, the risk of congenital heart disease in the fetus may be increased, suggesting the need for fetal echocardiographic evaluation.

Several risk scores have been developed that allow stratification based not only on specific diagnosis, but on more broadly applicable clinical features such as systemic ventricular function, cyanosis, functional class, and prior history of events. Depending on the study, specific diagnoses also have been identified as risks for adverse outcomes, such as LV inflow or outflow obstruction (i.e., aortic or mitral stenosis) or tetralogy of Fallot with significant pulmonary regurgitation. A summary of the identified risks is found in Box 35-1. Echocardiography is an important component of the evaluation in such risk scores.[68,69] Recent data identified heart rate response to exercise as another important risk predictor in women with congenital heart disease who underwent cardiopulmonary exercise testing before pregnancy. There were 89 pregnancies in 83 women, with 18% suffering an adverse cardiac event such as heart failure or sustained arrhythmia during pregnancy. Peak heart rate and percentage of maximal heart rate were predictors of maternal cardiac events.[70]

Data such as this emphasize that although echocardiography and anatomic data are important in assessing risk, other data are necessary to provide a comprehensive preconceptional evaluation.

Additionally, there is data that events during pregnancy predict events in the years following pregnancy.[71] This group followed 318 women who had 405 pregnancies had found that 12% had cardiac events in the 5 years following delivery. Events before and during pregnancy predicted late events, with anatomic and functional risks similar to those identified in the risk scores developed to assess preconceptional risk (see Box 35-1).

The ACC/AHA Guidelines for the Management of Adults with Congenital Heart Disease[72] and the ACC/AHA Guidelines for the Management of Patients with Valvular Heart Disease[73] provide guidance on risk assessment, management, and the use of echocardiography in women with heart disease and are invaluable resources.

**Box 35-1**

**PREDICTORS OF CARDIAC EVENTS DURING PREGNANCY**

- Cardiac event before pregnancy
  - Heart failure, arrhythmia
- Functional status
  - NYHA class >2
- Cyanosis
- Left heart obstruction
  - Symptomatic or severe mitral stenosis
  - Severe aortic stenosis (aortic valve area <1.0 $cm^2$, aortic velocity >4.0 m/s)
  - Hypertrophic cardiomyopathy with LVOT ΔP >30 mm Hg
- Systemic ventricular dysfunction
  - Ejection fraction <40%
- Pulmonary hypertension
  - Systolic pressure >50% systemic
- Severe aortic or mitral regurgitation
  - NYHA class III or IV symptoms
- Smoking

Modified from references 68 and 69.
*LVOT*, Left ventricular outflow tract; *NYHA*, New York Heart Association.

## PULMONARY VASCULAR DISEASE

Elevated pulmonary artery pressures may be the result of primary pulmonary hypertension, pulmonary emboli, chronic lung disease, left-sided heart disease, or congenital heart disease with systemic-to-pulmonary shunting. Elevated pulmonary pressures of any cause are associated with poor maternal and fetal outcomes.

Initial concerns regarding the risk of pulmonary hypertension in pregnancy were raised by studies of women with Eisenmenger syndrome. Eisenmenger syndrome develops when a left-to-right shunt causes equalization of pulmonary and systemic vascular resistance, resulting in right-to-left shunting and cyanosis.[74] Women with Eisenmenger syndrome have cyanosis, arterial oxygen desaturation, and polycythemia. One of the largest single-center studies reported 70 pregnancies in 44 women with a maternal mortality of 52%. Over half of pregnancies delivered prematurely, and neonatal mortality was nearly 30%.[75] In a review of pulmonary vascular disease in pregnancy, 73 women with Eisenmenger syndrome had a maternal mortality of 36%, 27 with primary pulmonary hypertension had a mortality of 30%, and 25 with secondary pulmonary hypertension had a maternal mortality of 56%.[76] The neonatal survival was 88% in all groups, with all maternal deaths occurring within 35 days after delivery. Effective therapies for these conditions during pregnancy are not currently available, although small case reports describe pregnancies in patients receiving epoprostenol, sildenafil, or nitric oxide.[77,78] Despite the appeal of novel pulmonary vasodilators, maternal death is nonetheless reported following pregnancy treated with these medications.[79,80]

One series reported 9 women with 10 pregnancies who chose to continue pregnancy despite the increased risk and were managed with current pulmonary vasodilators and multidisciplinary pregnancy and delivery management. One woman who self-discontinued pulmonary vasodilators died 4 weeks after delivery, but the other women and their infants were alive after a median of 3.2 years.[81]

These data suggest that there may be mortality benefit to current pulmonary hypertension therapies combined with careful multidisciplinary management, although more data are needed to change current recommendations regarding the safety of pregnancy in these patients.

Doppler echocardiographic measurement of pulmonary pressures allows identification of women with pulmonary hypertension, quantitation of disease severity, and evaluation of the response to therapy. Doppler data are limited to assessment of pressures, not vascular resistance, and therefore may incompletely assess the extent of the underlying pathology.

## CONGENITAL HEART DISEASE

### *Acyanotic Patients with No Prior Surgical Procedures*[82]

The most common congenital defect newly diagnosed during pregnancy is an atrial septal defect (ASD). These patients are usually asymptomatic but have a prominent "flow murmur" prompting a request for echocardiography. 2D echocardiographic and Doppler diagnosis of atrial septal defects in pregnancy is straightforward (Fig. 35-7). Contrast echocardiography is not needed for detection of significant interatrial shunt and should be avoided to minimize embolic risks. Given the increased CO and ventricular volumes of pregnancy, evaluation of the shunt ratio can be problematic in borderline cases At least in theory the decreased systemic vascular resistance of pregnancy might result in increased systemic blood flow without affecting pulmonary blood flow, decreasing the pulmonic-to-systemic shunt ratio and leading to underestimation of the true magnitude of the atrial septal defect. However, accurate definition of the shunt ratio is not necessary during pregnancy because pregnancy is well tolerated if pulmonary pressures are normal, regardless of the size of the left-to-right shunt.[83]

Ventricular septal defects in acyanotic adults are typically small and associated with a loud systolic murmur. On Doppler examination, a high-velocity jet from LV to RV is seen with normal chamber dimensions and function. This lesion is also well tolerated, though one study suggests an increased risk of preeclampsia with unrepaired ventricular septal defect. The mechanism is not well understood.[84] Pregnancy does not significantly alter the echocardiographic findings. Large unrestrictive ventricular septal defects are uncommon in adulthood and almost always associated with Eisenmenger syndrome.

Occasionally, a previously undiagnosed patent ductus arteriosus becomes noticeable during pregnancy. The classic continuous machinery-like murmur may or may not be appreciated on auscultation if the murmur is soft. When a patent ductus arteriosus is not suspected a priori, findings of LA or LV enlargement in excess of the expected changes of pregnancy, diastolic flow reversal in the descending thoracic aorta in the absence of significant aortic regurgitation, or unexplained pulmonary hypertension should prompt a careful search for this possible diagnosis. On 2D imaging, the patent ductus is often difficult to visualize in adults, so that a directed Doppler examination is essential when this diagnosis is suspected. Diastolic flow reversal in the pulmonary artery is seen with both color flow imaging and pulsed Doppler techniques. The hemodynamic impact of a patent ductus arteriosus is similar to that of a ventricular septal defect and is also associated with Eisenmenger syndrome when large.

Other types of unoperated acyanotic congenital heart disease seen in pregnant patients include mild pulmonic stenosis and Ebstein's anomaly of the tricuspid valve. Both are well tolerated, provided there is no associated cyanosis.[85] Ebstein's anomaly may occur as an isolated anomaly with varying degrees of tricuspid regurgitation or may be associated with an atrial septal defect. The regurgitant jet may be directed at the atrial septum and in combination with impaired diastolic function may cause right-to-left shunting and cyanosis. In women with acyanotic Ebstein's anomaly, pregnancy is well tolerated.[86] Despite varying degrees of tricuspid regurgitation, no maternal deaths, strokes, heart failure, or arrhythmias were reported in 111 pregnancies in 44 women with Ebstein's anomaly.[87]

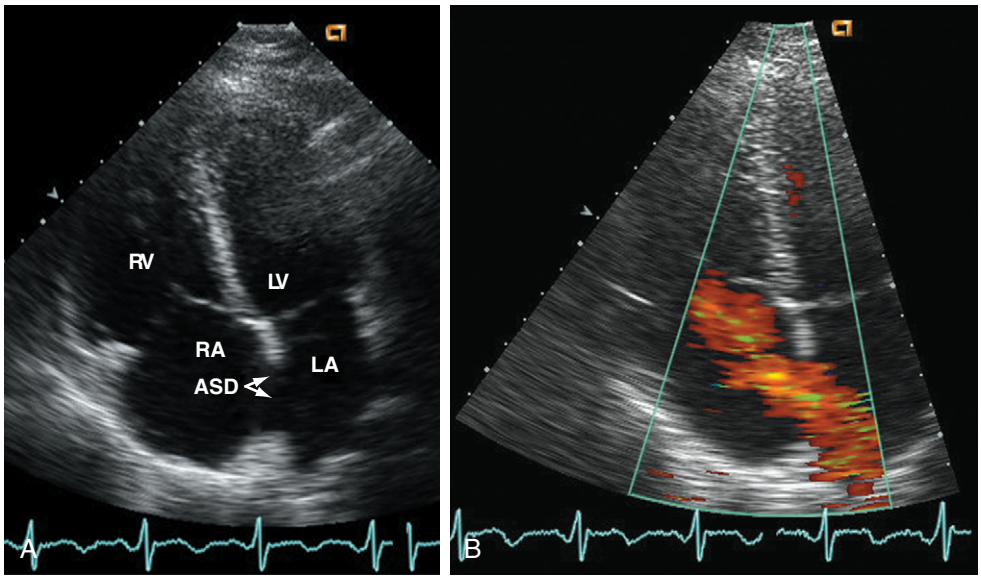



**Figure 35-7 A 24-year-old $G_1P_0$ woman at 14 weeks gestation is referred for echocardiography in evaluation of palpitations and a murmur.** Key findings from an apical four-chamber view included a secundum atrial septal defect (*ASD*) by 2D (**A**) imaging, left-to-right shunt by color Doppler (**B**), and RV and RV enlargement (**A**). Also found were normal pulmonary pressures and a 1.8:1 estimated left-to-right shunt . She was asymptomatic aside from the palpitations and went on to have an uneventful pregnancy with closure of her ASD via a percutaneous approach 4 months after delivery.

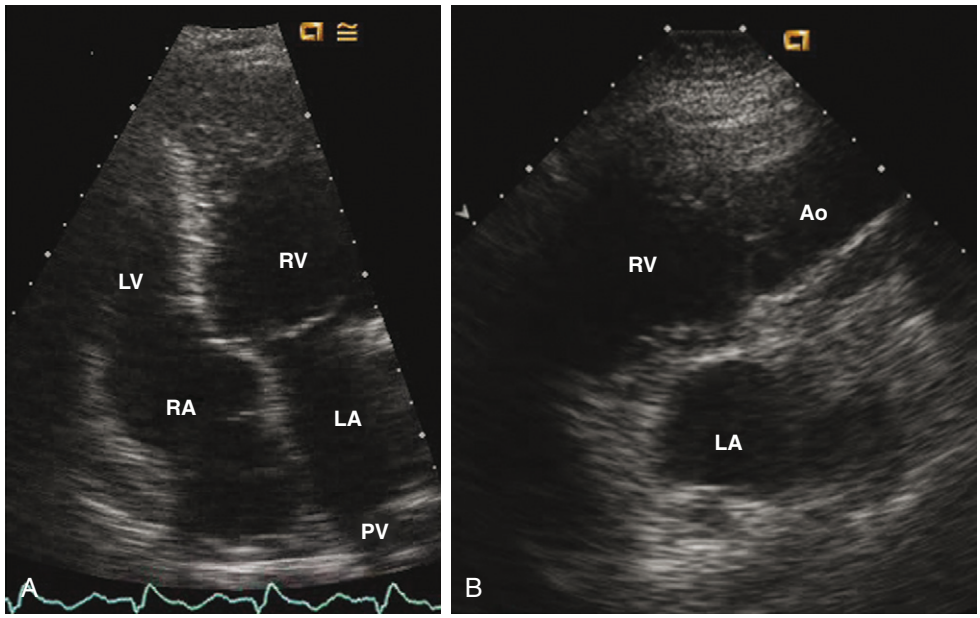



**Figure 35-8 A 34-year-old $G_3P_3$ woman with a history of congenitally corrected transposition of the great vessels returns for routine follow-up.** Her pregnancies had all been uneventful, and she has done well since her last delivery 2 years ago with minimal decrease in ventricular function. She required a pacemaker for complete heart block 1 year ago. On echocardiography, apical views demonstrate a hypertrophied anatomic RV that is rightward of the anatomic LV (**A**). An anterior aorta, typical of transposition of the great vessels, is seen on parasternal images (**B**). *Ao*, Aorta; *PV*, pulmonary vein.

Congenitally corrected transposition of the great arteries (CCTGA), also known as L-transposition with ventricular inversion (Fig. 35-8), is most often is associated with a normal physiologic pattern of blood flow through the heart and may first be recognized during pregnancy. Although there is physiologic blood flow through the heart, the anatomic RV is the systemic ventricle, and the tricuspid valve is the systemic atrioventricular valve. Associated defects are common, including ventricular septal defects, pulmonic stenosis, complete heart block, and regurgitation of the systemic atrioventricular valve, at times the result of Ebstein's anomaly of the tricuspid valve.

Outcome during pregnancy depends on the associated defects and systemic ventricular function in patients with CCTGA. Published summaries in a total of 87 women with 118 pregnancies demonstrated a live birth rate of 83%.[85,88,89] Complications during pregnancy included heart failure, increased cyanosis, endocarditis, stroke, and myocardial infarction (MI). Although there are few data regarding the fate of the systemic RV following pregnancy in CCTGA, studies of the systemic RV in patients with transposition of the great arteries corrected with an atrial-level switch (Mustard or Senning repair) may provide some insight. A study with longitudinal echocardiographic data of 16 women with 24 pregnancies demonstrated decline in systemic RV dysfunction during pregnancy in four patients (25%) with return to baseline in only one of those patients.[90] Patients with systemic RVs, including CCTGA, should have echocardiographic assessment during and after pregnancy.

### *Acyanotic Patients with Prior Surgical Procedures*

As medical therapy and cardiac surgery for congenital heart disease have advanced, the number of patients reaching adulthood has markedly increased. The majority of patients with complex congenital heart disease will have had at least one surgical repair in childhood. Additionally, the favored surgical repair of certain defects, such as transposition of the great arteries, has evolved over time and results in different anatomy and physiology depending on the era in which the repair was performed. When these patients become pregnant, echocardiographic evaluation can detect any residual structural or functional cardiac abnormalities, evaluate for long-term complications of the surgical procedure, and optimize patient management during pregnancy and in the peripartum period. Data on maternal and fetal outcomes in these patient populations are based on case series, with many series including multiple congenital abnormalities. As a consequence, although our understanding of pregnancy in congenital heart disease is increasing, recommendations based on large clinical trials are not available and recommendations must be tailored on an individual basis.

In patients with previous surgical procedures that completely correct the congenital abnormality, outcome in pregnancy is similar to that in normal women. For example, closure of an uncomplicated atrial or ventricular septal defect or patent ductus arteriosus ligation often result in normal cardiac anatomy and function, with a corresponding normal echocardiographic examination.[83] When mild abnormalities remain after corrective surgery for congenital heart disease, maternal outcome is also likely to be similar to that in women without heart disease, with the proviso that the echocardiographic examination should be directed toward potential residual abnormalities or late complications. With complex congenital heart disease and palliative or partially corrective surgical procedures, residual or recurrent anatomic/functional cardiac abnormalities occur commonly, resulting in an increased maternal risk. Echocardiographic evaluation is especially valuable in these patients both before pregnancy to assess the potential risk and during pregnancy to monitor cardiovascular function. In pregnant patients with complex congenital heart

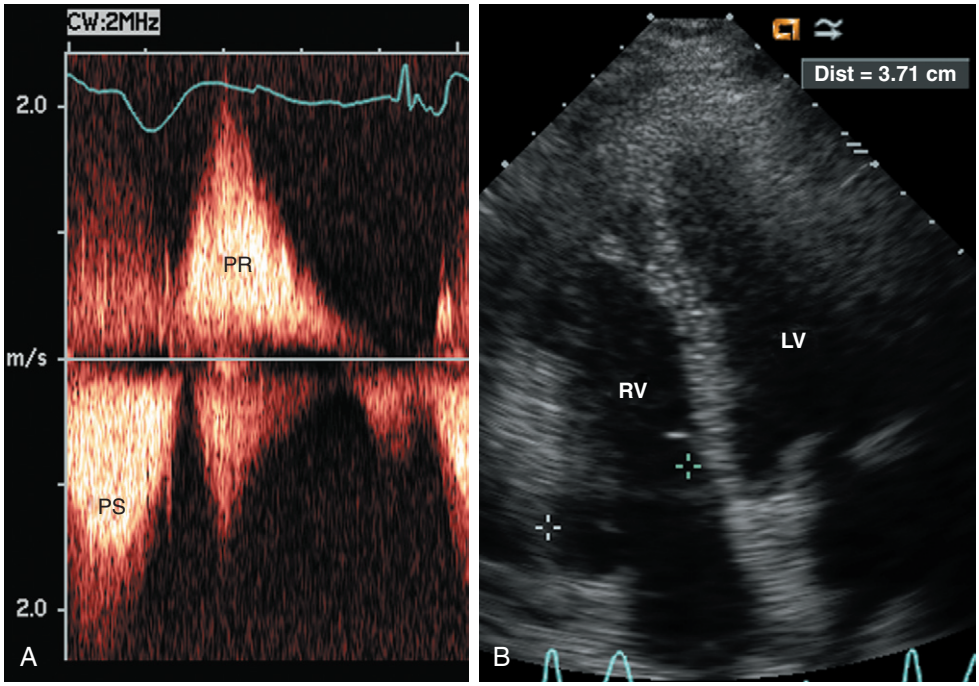



**Figure 35-9 A $G_0P_0$ 25-year-old woman with tetralogy of Fallot presents for preconception counseling.** She underwent initial Blalock-Taussig shunt palliation as an infant and subsequent complete repair with takedown of the Blalock-Taussig shunt at age 4. She is asymptomatic. An echocardiogram and cardiopulmonary exercise test are obtained. Key findings on echocardiography include significant pulmonic regurgitation (**A**), mild pulmonic stenosis (**A**), mild to moderate RV enlargement (**B**), and normal biventricular systolic function. Exercise testing demonstrated a mild reduction in exercise capacity. She was advised that pregnancy was likely to be well tolerated, and regular reassessment of her cardiac status during pregnancy was recommended. *PR*, Pulmonic regurgitation; *PS*, pulmonic stenosis.

disease, arrhythmias are a frequent cause of morbidity and mortality.[91]

## Tetralogy of Fallot

Patients with surgical repair of tetralogy of Fallot often have pulmonic regurgitation, recurrent or residual RV outflow tract obstruction, ventricular septal defect, or aneurysm of the RV outflow tract[92] (Fig. 35-9). Multiple series of pregnancies in patients with tetralogy of Fallot have been reported. Two series describe 92 women with 175 pregnancies. Cardiac complications included arrhythmias and symptomatic heart failure, which occurred in 8% of women and 4.5% of pregnancies.[93,94] There were no reported maternal deaths, but fetal complications included a high rate of spontaneous abortion. In one study, the risk of maternal and fetal complications was associated with LV dysfunction, severe pulmonary hypertension, and severe pulmonic regurgitation and RV dilation.[94]

Another more recent study evaluated 74 women with 157 pregnancies, with cardiovascular events in 8.1%, primarily supraventricular arrhythmias, with risks predicted by the use of cardiac medications before pregnancy.[95]

An echocardiographic evaluation of LV size and function during pregnancy in patients with tetralogy of Fallot followed 11 women with 17 pregnancies. An increase in LV end-diastolic diameter was noted in controls but not seen in patients with tetralogy of Fallot. A progressive increase in the Tei index as the pregnancy progressed was seen in patients with tetralogy of Fallot. Although this returned to normal postpartum, the progressive increase in Tei index was not seen in normal women.[96] This suggests that some of the normal echocardiographic findings in women without heart disease may not manifest in patients with congenital heart disease.

## Coarctation of the Aorta

Patients with a previous aortic coarctation repair may have residual or recurrent stenosis[97,98] (Fig. 35-10). Even in the absence of restenosis, these patients are at risk for late systemic hypertension, which may present initially as exercise-induced hypertension.[101] Women with a repaired coarctation and a residual gradient less than 20 mm Hg can have successful pregnancies, with one study reporting 29 births for 36 pregnancies.[90] A study of 50 women with coarctation found no significant maternal cardiovascular complications in 118 pregnancies. Thirty percent of women were hypertensive during pregnancy, and of those, 75% had a hemodynamically significant coarctation. The rate of spontaneous abortion and preeclampsia was similar to that of the general population.[102] Another series demonstrated that 24% of women with coarctation had hypertensive complications compared with 8% of women without coarctation. Women with coarctation had longer hospital stays and were more likely to have adverse cardiac outcomes.[103] These studies and other case reports suggest that hypertension during pregnancy is more common and needs to be controlled. Additionally, aneurysm in the area of prior repair or in the ascending aorta can be seen in patients with coarctation. These patients represent a higher risk group and consideration to aneurysm repair before pregnancy may be warranted. Echocardiographic evaluation may be insufficient to fully evaluate for aortic aneurysm in these patients, and other imaging modalities, such as magnetic resonance imaging or computed tomography, may be needed.[104]

## Fontan Repair

Following the initial description by Fontan and Baudet[105] of surgical atriopulmonary connection to alleviate cyanosis in

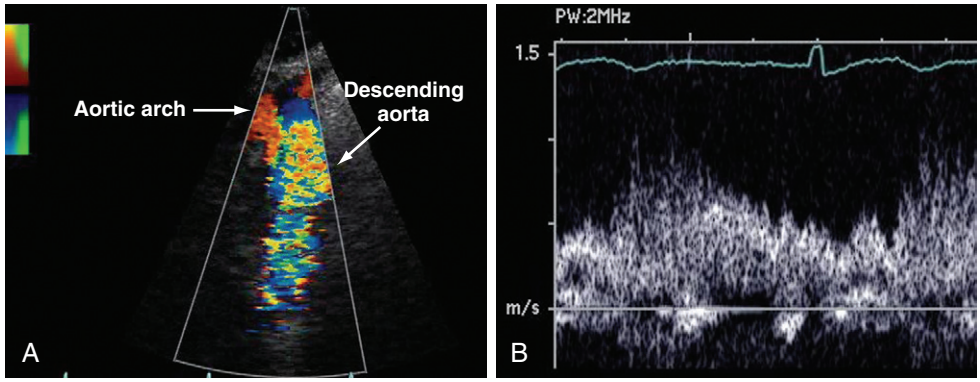



**Figure 35-10 A $G_1P_0$ 19-year-old woman underwent coarctation repair at age 6 months with subsequent repair of recoarctation at age 2 years.** She has a known mild residual coarctation and is now 7 weeks pregnant. By clinical examination, her right arm blood pressure is normal and she has a 10 mm Hg gradient by blood pressure measurements in the arms and legs. Key findings on echocardiography include narrowing by 2D and color Doppler (**A**) in the aortic arch and evidence of diastolic runoff in the abdominal aorta (**B**). CW Doppler is often an inaccurate measure of coarctation severity when using the Bernoulli equation; however, the finding of continuous forward flow is a better predictor of coarctation severity.[99,100] Further evaluation with computed tomography or gadolinium magnetic resonance imaging at 7 weeks gestation was not thought warranted, given the patient's normal blood pressure and attendant risks of radiation and gadolinium. She was followed closely during her pregnancy, and although her blood pressure and gradient increased minimally, fetal growth remained normal and she delivered a healthy girl by assisted vaginal delivery.

tricuspid atresia, modifications of the original repair have evolved, as have the underlying defects treated with a Fontan-type repair. The goal of the repair is to alleviate cyanosis in congenital defects that result in essentially single ventricle physiology. In this circulation, there is not a subpulmonic ventricle. Survival after Fontan repair is now 60% at 10 years, so that some women undergoing this procedure will reach childbearing age and may become pregnant.[91] Maternal survival has been documented, but fetal outcome is uncertain. In a series of 33 pregnancies in women with a Fontan repair, there were only 15 (45%) live births. However, there were no significant maternal complications and no deaths.[106] Another study of 38 women with Fontan repair identified 6 women with 10 pregnancies. They found a 50% spontaneous abortion rate, and of the 4 completed pregnancies, 50% of women had cardiac complications during the pregnancy including atrial arrhythmias and decline in New York Heart Association (NYHA) class. Fetal outcome of the live births was uniformly complicated, with all live infants delivered prematurely or small for gestational age, and there was one neonatal death.[107]

Another series of 6 women with 10 pregnancies had similar findings, with a high rate of miscarriage (50%) and cardiac events including a decline in functional status and atrial fibrillation.[108] Based on the limited data available, women with Fontan repairs may carry pregnancies to term. Maternal complications are generally related to supraventricular arrhythmias, especially in women with atriopulmonary anastomoses. However, the high rate of fetal loss and neonatal complications should be considered when counseling these patients.

## Transposition of the Great Arteries

Complete transposition of the great vessels (Fig. 35-11) requires surgical repair in childhood for survival and resolution of cyanosis. Initial repairs redirected blood flow at the atrial level, such that systemic venous return was directed to the LV and then the pulmonary artery and pulmonary venous return was directed to the RV and then the aorta (see Fig. 45-10). In the early and mid-1960s, Mustard and Senning each described a different surgical approach to atrial level switch procedures that bear their names.[109,110] By redirecting blood flow at the atrial level, these repairs leave the morphologic RV as the systemic ventricle.

Pregnancy in patients with a previous Mustard or Senning interatrial baffle repair (Fig. 35-12) for transposition of the great arteries has been reported in multiple series. One series of 28 women with 69 pregnancies found a decline in NYHA class during pregnancy in approximately one third of pregnancies.[111] Another reported 70 pregnancies in 40 women, with arrhythmias and heart failure complicating pregnancy and the postpartum period.[112] Multiple series have demonstrated a decline in systemic ventricular function that is permanent in some cases.[90,111,113] No maternal deaths were reported, but there was an increased rate of spontaneous abortion. In a study of asymptomatic patients who had excellent baseline prepregnancy functional status, none had significant maternal complications.[113] Specifically, none had significant baffle leaks or obstruction, significant systemic atrioventricular valve regurgitation, or systemic ventricular systolic dysfunction.

The available data suggest that in patients with significant functional cardiac abnormalities, maternal outcome is dependent on the specific underlying abnormalities (e.g., patients with systemic ventricular dysfunction are at risk for heart failure during pregnancy). Thus, echocardiographic evaluation is directed toward evaluation of the interatrial baffle (which may require transesophageal imaging), evaluation of systemic and venous ventricular function, detection and quantitation of systemic atrioventricular (tricuspid) valve regurgitation, and assessment of any other residual or acquired abnormalities.

Patients with transposition of the great arteries and ventricular septal defect may undergo a Rastelli repair, which baffles LV flow to the aorta through the ventricular septal defect and uses an RV-to-pulmonary artery conduit.[114] There are few data on pregnancy in the setting of Rastelli repair of transposition of the great arteries, and a series of 6 patients reports a 50% incidence of progressive LVOT obstruction during pregnancy.[115] Echocardiographic evaluation of these patients must focus on LVOT obstruction and dysfunction of the RV-to-pulmonary-artery conduit.

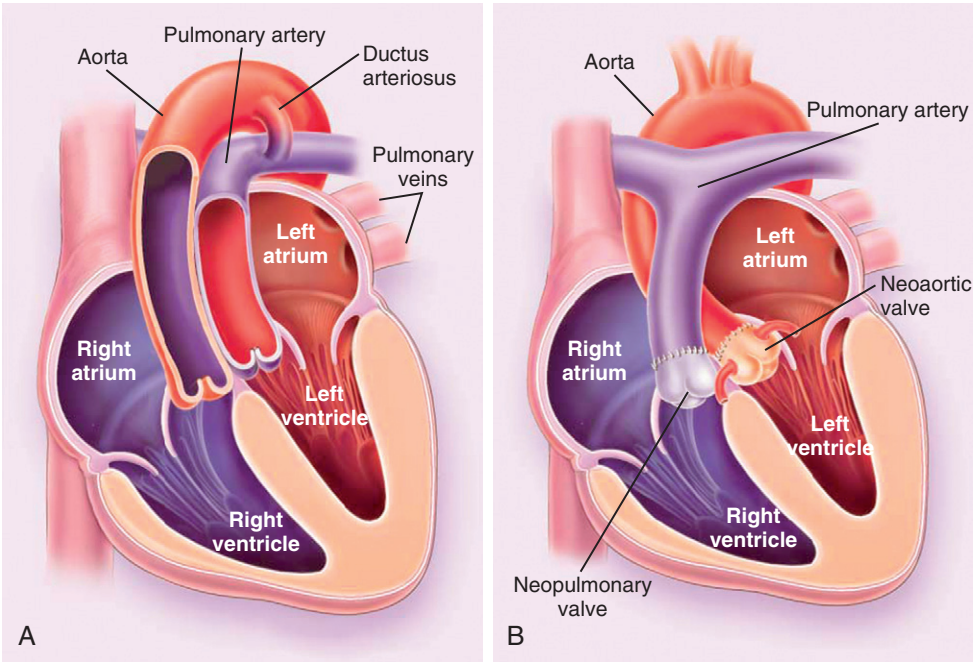



**Figure 35-11** Sketches of complete transposition of the great vessels (**A**) and an arterial switch repair (**B**). *(From Brickner EM, Hillis LD, Lange RA: Congenital heart disease in adults. Second of two parts.* N Engl J Med *342:334-342, 2000.)*

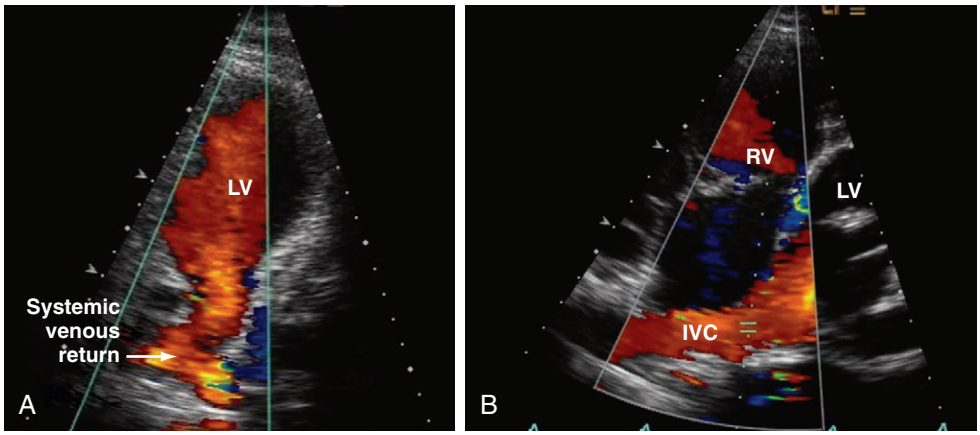



**Figure 35-12 A 28-year-old $G_2P_1$ woman with a history of transposition of the great vessels who underwent a Mustard repair in infancy presents at 10 weeks gestation.** Before pregnancy she was asymptomatic with normal exercise tolerance. Echocardiography demonstrated significant RV enlargement with mildly reduced systolic function. Long-standing, well-tolerated subpulmonic obstruction, in part as a result of systolic anterior motion of the mitral apparatus, was evident in parasternal views. Systemic (**A**) and pulmonary venous return (**B**) were unobstructed by 2D color flow, and PW Doppler. No baffle leaks were identified. Long-standing, mild tricuspid regurgitation was present. Her pregnancy was uneventful, and she delivered a healthy girl by an assisted vaginal delivery. Ventricular function remained unchanged following delivery. *IVC*, Inferior vena cava.

Currently, the preferred correction of transposition of the great arteries is the arterial switch operation as described by Jatene and colleagues[116] and later modified by LeCompte and associates[117] (see Fig. 35-11, *B*). This operation did not replace the Mustard and Senning repair until the early 1990s, and so the first patients with the arterial switch repair are just entering their reproductive years. Because the LV is the systemic ventricle, the anticipated problems relate less to ventricular function than issues related to the surgical repair, including ostial coronary stenoses, supravalvular and branch pulmonary stenosis, and supraaortic stenosis.

One series reports successful pregnancies in 9 women with 17 pregnancies with 2 pregnancy-related complications, 1 in a woman with LV dysfunction and 1 with a mechanical mitral valve. The series emphasized the importance of residua or other cardiac abnormalities in risks for adverse events.[118]

### *Cyanotic Heart Disease*

Eisenmenger physiology (Fig. 35-13) is characterized by equalization of pulmonary and systemic vascular pressures in association with a large systemic-to-pulmonary communication, such as a ventricular septal defect or atrioventricular canal defect.[119] During pregnancy and in the peripartum period, the decrease in systemic vascular resistance, in the setting of irreversible pulmonary hypertension, can result in increased right-to-left shunting and decreased pulmonary blood flow, with

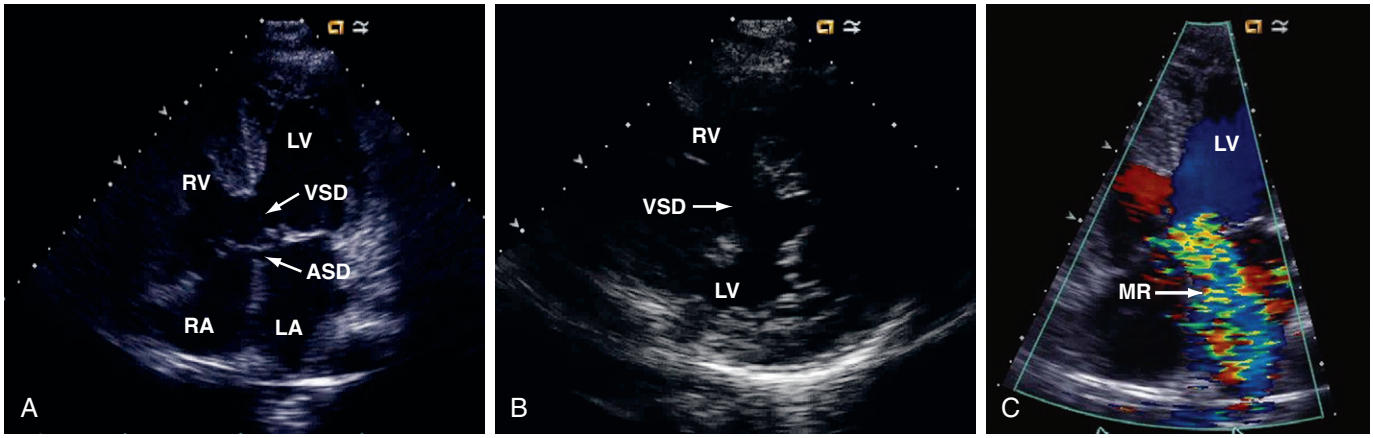



**Figure 35-13 Endocardial cushion defect with a large ventricular septal defect (*VSD*), atrial septal defect (*ASD*), and Eisenmenger physiology in a 19-year-old $G_1P_0$ pregnant woman with no previous cardiac diagnosis.** Apical four-chamber view (**A**) shows the ASD and VSD (*arrows*), and parasternal short-axis view shows the VSD (**B**). Color flow imaging (**C**) shows severe "mitral" (left-sided atrioventricular valve) regurgitation (*MR*). Despite relatively stable hemodynamics during pregnancy and delivery with careful hemodynamic monitoring, the patient had abrupt hemodynamic collapse 48 hours postpartum and died.

subsequent cardiovascular collapse resulting from hypoxia and hypotension.[120] Death usually occurs in the peripartum period, including cases reported 3 to 4 weeks postpartum. Maternal mortality is extremely high (between 30% and 70% in various series), and only 15% of infants are born at term, so pregnancy should be avoided in these patients.[74,121]

Pulmonary artery systolic pressure may be difficult to estimate in patients with Eisenmenger physiology as a result of an inadequate tricuspid regurgitation jet. The presence of pulmonary hypertension must therefore be inferred from findings of a large, nonrestrictive intracardiac communication or large systemic-to-pulmonary artery shunt, such as a patent ductus arteriosus, a short time to peak velocity in the pulmonary artery, midsystolic notching on the pulmonic valve M-mode, and the pattern of ventricular septal motion. If severe pulmonary hypertension is not clearly established, other confirmatory diagnostic tests should be considered in view of the grave prognosis associated with this condition. Rarely, a patient with previously unevaluated congenital heart disease is diagnosed during pregnancy with Eisenmenger physiology.

Cyanotic congenital heart disease without Eisenmenger physiology also connotes high maternal mortality and morbidity.[120,122] In 822 pregnancies in 416 cyanotic women, the rate of maternal cardiovascular complications was 32%, with one maternal death. Fetal outcome was also suboptimal; only 43% of pregnancies resulted in live births, 37% of which were premature. Factors that predict a poor outcome include functional status before pregnancy, arterial oxygen saturation, and blood hemoglobin. Other studies suggest that maternal outcome is also strongly related to the degree of RV pressure overload.[123] Thus, echocardiographic evaluation should include estimates of pulmonary systolic pressure and definition of the anatomic abnormalities and ventricular function.

For congenital heart disease with decreased pulmonary blood flow that cannot be physiologically repaired, palliative shunts to increase pulmonary blood flow are often used. These patients are cyanotic resulting from intracardiac shunting and decreased pulmonary blood flow, rather than from pulmonary hypertension and Eisenmenger syndrome. Few data exist on pregnancy in these patients. However, in a series of 41 pregnancies in 15 women with cyanosis after partial repair for complex pulmonary atresia, there were only 8 healthy children. Although there were no maternal deaths in this series or in a smaller study, maternal complications were high, including pulmonary embolism, heart failure, and arrhythmias.[107,109,123]

## VALVULAR HEART DISEASE

### *Valvular Stenosis*

In a pregnant patient, stenosis of a semilunar valve is usually the result of a congenitally abnormal valve.[110] Mild to moderate stenosis of the pulmonic valve is well tolerated, whereas severe pulmonic stenosis is rare in adults.[124] In contrast to patients with pulmonic valve stenosis, those with aortic valve stenosis, even if asymptomatic before pregnancy, may decompensate during pregnancy. In clinical series, the majority of pregnant patients with aortic stenosis have bicuspid valves.[125] Patients with a previous surgical commissurotomy may have significant restenosis[126]; one study estimated that about 20% of such patients require reoperation at a mean interval of 13 (range 3 to 26) years after the initial procedure.[127] Thus, depending on the patient's age at the initial commissurotomy, restenosis may be diagnosed during pregnancy.

As stroke volume increases across the stenotic valve with pregnancy, an increase in the pressure gradient measured by Doppler echocardiography is seen. Calculation of valve area with the continuity equation still provides accurate assessment of stenosis severity (Fig. 35-14). Some patients may become symptomatic during pregnancy as a result of increased metabolic demands in the setting of a limited ability to increase stroke volume across the valve.[126,128] These patients may develop angina or dyspnea during pregnancy even though they were asymptomatic before pregnancy. Reduced diastolic ventricular compliance secondary to LV hypertrophy can also lead to heart failure. Even when patients with aortic stenosis remain physiologically compensated during pregnancy, any superimposed hemodynamic alteration can lead to acute decompensation. For example, the high CO and heart rate associated with an infection or anemia may result in acute pulmonary edema resulting from a combination of an increased valve gradient and a shortened diastolic filling time.

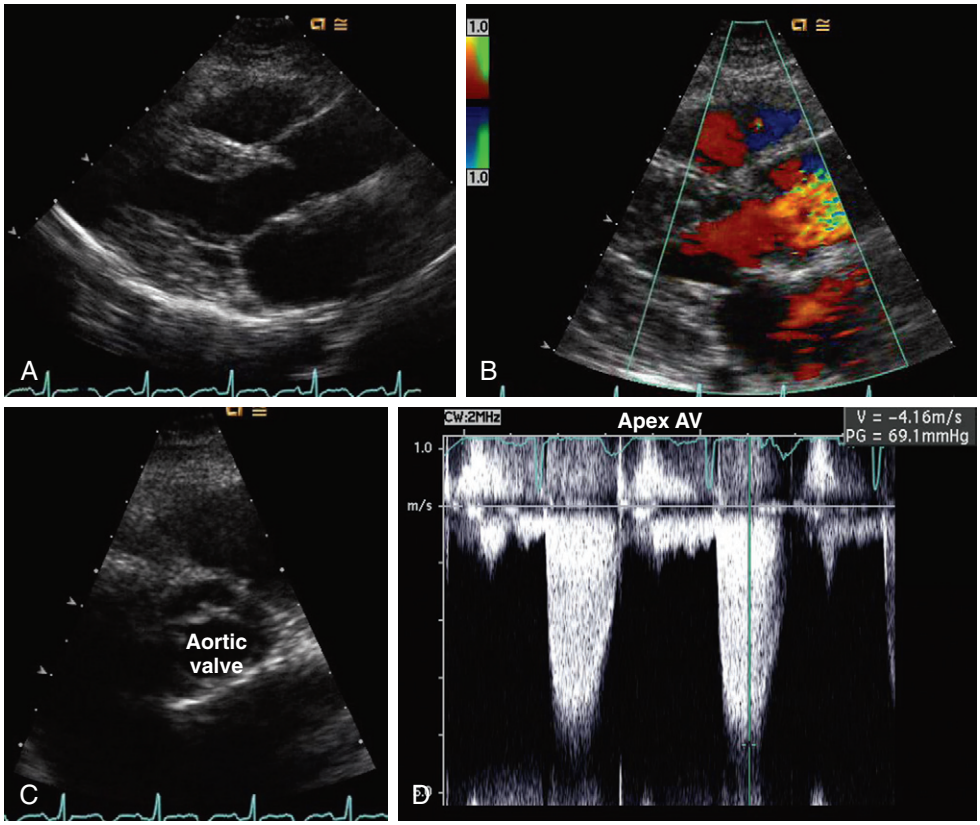



**Figure 35-14 Valvular aortic stenosis in a 25-year-old $G_1P_0$ pregnant woman who underwent an aortic valve commissurotomy 10 years previously.** The parasternal long-axis view (**A**) shows a congenitally abnormal aortic valve with reduced systolic opening. Color Doppler in this view (**B**) shows turbulent flow across the valve. Short-axis views confirm congenital aortic stenosis (**C**). The maximum jet across the aortic valve, recorded with CW Doppler from a high right parasternal position, shows maximum velocity of 4.1 m/s (**D**). There was mild coexisting aortic regurgitation. Aortic valve area, calculated by the continuity equation, was 1 $cm^2$. This patient was managed with placement of a pulmonary artery catheter and arterial line at the time of delivery. Because of fetal presentation, she underwent a cesarean section with epidural anesthesia, which was tolerated well.

The role of echocardiography in pregnant patients with aortic stenosis is to accurately delineate disease severity so that monitoring and therapy during pregnancy and in the peripartum period can be optimized (Fig. 35-15). In some patients the severity of stenosis may worsen during pregnancy, possibly related to the hormonal and metabolic changes. Most pregnant women with aortic stenosis can be managed medically, but balloon aortic valvuloplasty or valve replacement during pregnancy has been required in rare cases.[128-132] A series of 39 patients with 49 pregnancies divided groups based on stenosis severity. The mild to moderate stenosis group had no maternal complications, whereas pulmonary edema or arrhythmias occurred in 10% of pregnancies complicated by severe aortic stenosis. Interestingly, fetal complications, such as small for gestational age and prematurity, were found in both groups of patients, but more often in the mild to moderate stenosis group. Patients with severe stenosis were more likely to require valve replacement in the peripartum period than those with mild to moderate aortic stenosis, and a separate study by the same group showed that the likelihood of needing cardiac intervention was higher in those women who had undergone pregnancy than in those who had not.[128,133]

Some data exist using more novel echocardiographic modalities to identify patients at risk for adverse events. LV twist was increased in pregnant patients with aortic stenosis. Two of 10 women with aortic stenosis did not have an increase in LV twist, and both had symptomatic decline during pregnancy requiring balloon valvuloplasty.[134] As experience with novel echocardiographic modalities increases, there may be a role for some of these indices in assessing pregnant women and preconceptional risk.

Rheumatic mitral valve stenosis is often diagnosed during pregnancy (Fig. 35-16). If mitral stenosis is moderate in severity or if disease progression has been gradual, the patient may not have noted symptoms or exercise limitation before the pregnancy. Early in pregnancy the increased transmitral volume flow rate and the shortened diastolic filling time resulting from the increase in heart rate result in further elevation of LA pressures. This may result in pulmonary edema, depending on the severity of mitral valve obstruction. Because it is often difficult to appreciate the diastolic murmur of mitral stenosis in pregnant dyspneic patients, mitral stenosis should be considered in the differential diagnosis of all pregnant patients with heart failure or pulmonary congestion. Echocardiography reliably differentiates mitral stenosis from other causes of heart failure (e.g., cardiomyopathy or diastolic dysfunction) and will distinguish cardiac from noncardiac causes of respiratory distress. Echocardiographic measures of mitral stenosis severity, including 2D valve area, Doppler gradients, and pressure half-time valve area, remain valid in pregnancy, so that echocardiographic evaluation allows optimization of patient monitoring and therapy.

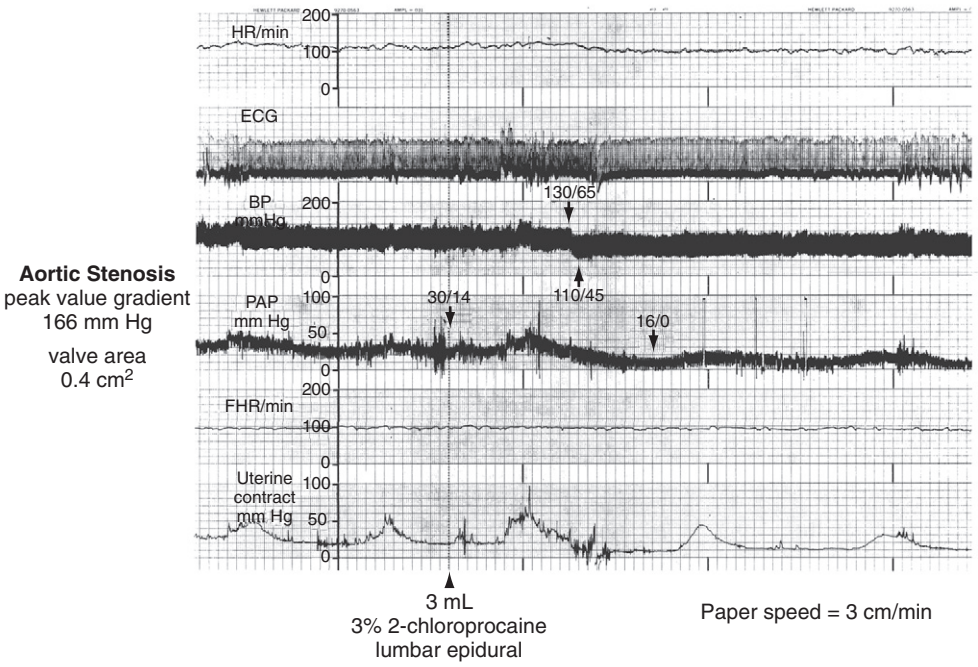



**Figure 35-15 Hemodynamic responses in a patient with severe valvular aortic stenosis showing increased vascular return associated with uterine contractions.** *BP*, Blood pressure; *ECG*, electrocardiogram; *FHR*, fetal heart rate; *HR*, heart rate; *PAP*, pulmonary artery pressure. *(From Easterling TR, Chadwick HS, Otto CM, Benedetti TJ: Aortic stenosis in pregnancy.* Obstet Gynecol *72:113-118, 1988. Reprinted with permission from The American College of Obstetricians and Gynecologists.)*

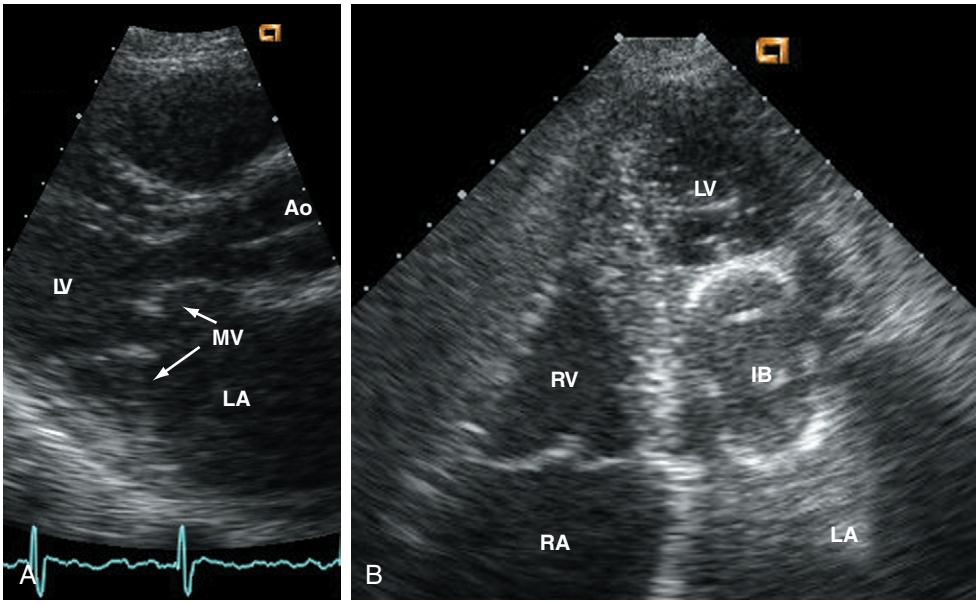



**Figure 35-16 A 35-year-old $G_2P_1$ woman presented with respiratory distress at 26 weeks gestation.** She was found to be in atrial fibrillation, and echocardiography demonstrated severe rheumatic mitral stenosis. 2D imaging is shown from a parasternal view (**A**). Despite efforts at medical stabilization, she remained in pulmonary edema. Balloon mitral valvuloplasty was performed using an Inoue balloon, seen from an apical view (**B**), and she symptomatically improved. She delivered at 35 weeks and required intravenous diuretics in the 48 hours after delivery to alleviate pulmonary edema. She subsequently recovered uneventfully. *Ao*, Aorta; *IB*, Inoue balloon; *MV*, mitral valve.

Usually, patients can be managed medically during pregnancy using beta-blockers to improve diastolic filling, even with severe mitral stenosis, although decompensation may require invasive monitoring in an intensive care unit setting.[135] In some severe cases, maternal or fetal complications may necessitate mechanical relief of stenosis during pregnancy, preferably with percutaneous balloon valvotomy.[136,137] Concerns regarding balloon angioplasty and pregnancy include both maternal risks of the procedure and the effects of radiation exposure on the fetus. One group reported 5-year follow-up of 22 women who underwent valvotomy during pregnancy at a mean gestation of 25 weeks. They demonstrated excellent maternal outcomes and no evidence of any clinical abnormalities in the children.[138] Echocardiography clearly plays a valuable role in assessing the

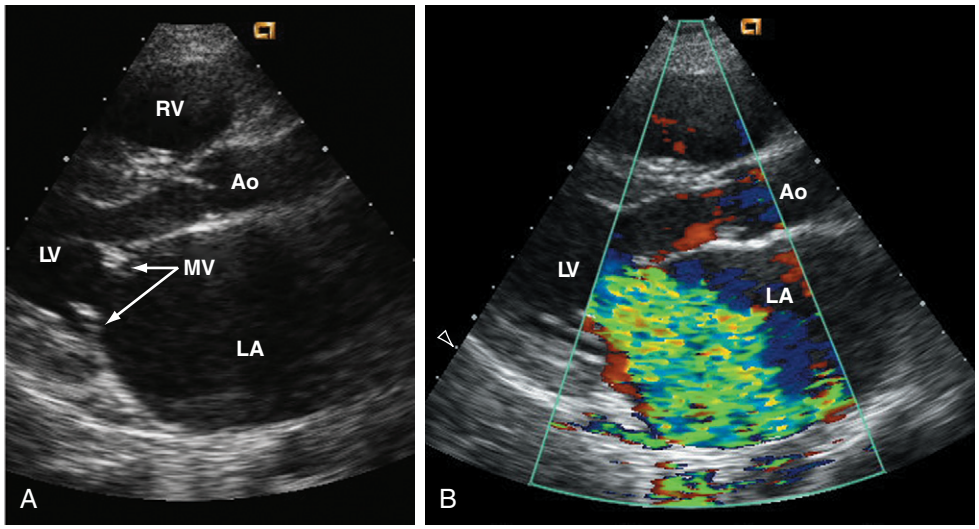



**Figure 35-17 A 34-year-old $G_3P_2$ woman presented at 28 weeks gestation with dyspnea with minimal exertion.** Failure of coaptation is seen on 2D imaging (**A**), and color Doppler shows severe mitral regurgitation (**B**). She was managed with diuretics and bedrest and delivered a healthy baby boy. After delivery she underwent mitral valve repair. *Ao*, Aorta; *MV*, mitral valve.

likelihood of complications and the expected result of percutaneous mitral valvotomy.[139] Echocardiographic monitoring also minimizes fluoroscopy time.[140]

### *Valvular Regurgitation*

Pathologic valvular regurgitation in pregnancy may be the result of a congenital abnormality (bicuspid aortic valve), previous bacterial endocarditis, rheumatic disease, or myxomatous valve disease (Fig. 35-17) or may be associated with more complex congenital heart disease. Standard 2D and Doppler echocardiographic methods for detection and evaluation of valvular regurgitation are applicable in the pregnant patient. Physiologically, it is plausible that pregnancy may result in a decrease in regurgitant severity as a result of the pregnancy-related afterload reduction. This potentially beneficial physiologic effect may be counterbalanced, to some extent, by the hormonal and vascular changes of pregnancy. Increased aortic root dimensions may increase aortic regurgitant severity, whereas increased laxity of valve tissues may lead to an increase in mitral regurgitant severity.

Valvular regurgitation is well tolerated during pregnancy by some patients. Others develop signs and symptoms of heart failure with pulmonary congestion, decreased exercise tolerance, orthopnea, and paroxysmal nocturnal dyspnea. Decompensation can occur in patients with chronic valvular regurgitation because of either (1) the increased CO demands of pregnancy or (2) worsening of the underlying valvular abnormality (e.g., chordal rupture in a patient with myxomatous mitral valve disease). Echocardiographic evaluation can distinguish between these possibilities and aid in optimizing therapy in the decompensated patient.

Quantitation of valvular regurgitant severity and evaluation of LV systolic function may be confounded by the anatomic and hemodynamic changes of pregnancy. In patients with severe aortic or mitral regurgitation, decreased systemic vascular resistance resulting from pregnancy can result in an apparent decrease in regurgitant severity and improvement in LV systolic function. In these patients, surgical intervention may be inappropriately delayed. Conversely, LV dimensions may be slightly larger than in the nonpregnant state, resulting in misdiagnosis in a patient with only moderate regurgitation. In either case, postpartum reevaluation of regurgitant severity and ventricular function will provide accurate data for clinical decision making.

### *Prosthetic Heart Valves*

The outcome of pregnancy is significantly affected by the presence of a prosthetic heart valve.[141-144] With mechanical valves, the risks of valve thrombosis (8% to 9%), embolic events (3% to 5%), serious bleeding (5%), heart failure (28%), and maternal death (4% to 8%) are high,[145] even with careful monitoring of anticoagulation.[146,147] With a bioprosthetic valve, there is less risk of maternal death (0% to 5%), but accelerated valve degeneration during pregnancy may occur and results in a high rate of heart failure (35%) and urgent repeat replacement of the valve in the early postpartum period (35%).[142] The effect of pregnancy in accelerating valve degeneration is controversial. Initial studies made the observation that women with prosthetic heart valves and more than one pregnancy have a lower 10-year graft survival rate for bioprosthetic valves (17%) than women with only one pregnancy (55%).[148] However, another study demonstrated no change in durability of bovine pericardial valves in women who bore children compared with a population who did not.[149] An evaluation of women who underwent pulmonic allograft replacement in the setting of a Ross repair for aortic valve disease did not demonstrate valvular degeneration of the pulmonic allograft.[150]

Echocardiography plays a critical role in identifying valve dysfunction and in assessing valve degeneration during pregnancy (Fig. 35-18). Assessment of prosthetic valves in women who are pregnant may be confounded by the normal hemodynamic changes of pregnancy. The increased heart rate and stroke volume affect Doppler evaluation of velocities and pressure gradients across prosthetic valves. Thus, the volume flow rate should be taken into consideration when evaluating prosthetic valves in pregnant women. The alterations in loading conditions may also affect the accuracy of the pressure half-time method.[151] Ideally, a baseline Doppler echocardiographic study in the prepartum period or early in pregnancy can be used to accurately assess changes later in pregnancy.

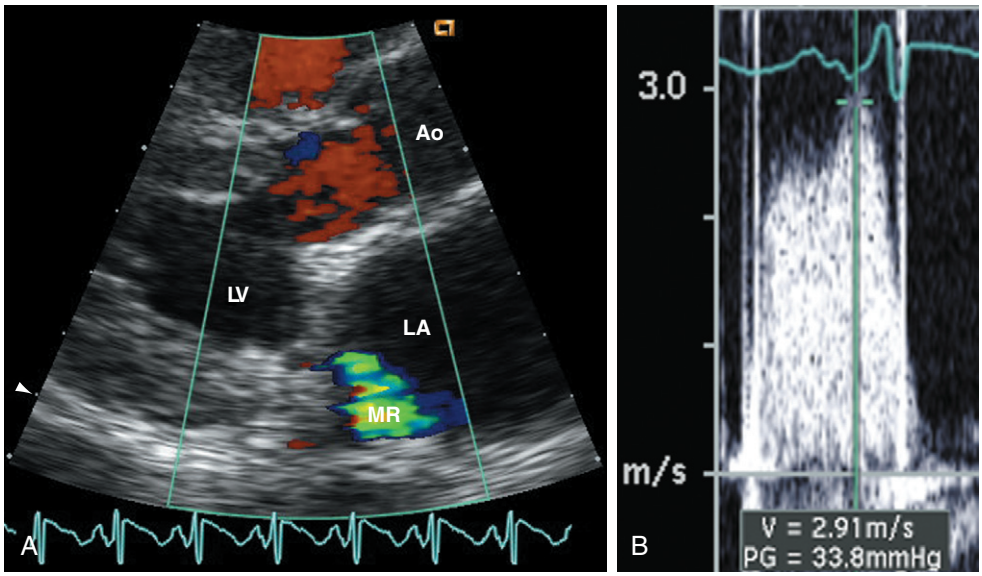



**Figure 35-18 A 24-year-old $G_1P_0$ woman with a St. Jude's mitral prosthesis placed at age 20 presented at 12 weeks gestation with dyspnea and exertional chest pain.** Her anticoagulation had been subtherapeutic. Echocardiography demonstrated more than the expected amount of mitral regurgitation (**A**) for this type of prosthesis by color Doppler and a peak gradient of 33 mm Hg and mean gradient of 20 mm Hg (**B**) by PW and CW Doppler. Despite aggressive anticoagulation and medical therapy, she did not improve. After discussion of the relative risks and benefits of thrombolytic therapy versus surgery, she was taken to the operating room for emergent valve replacement. She recovered uneventfully; however, the fetus did not survive. A subsequent pregnancy managed with therapeutic anticoagulation was uneventful, and she delivered a healthy baby. *Ao*, Aorta; *MR*, mitral regurgitation.

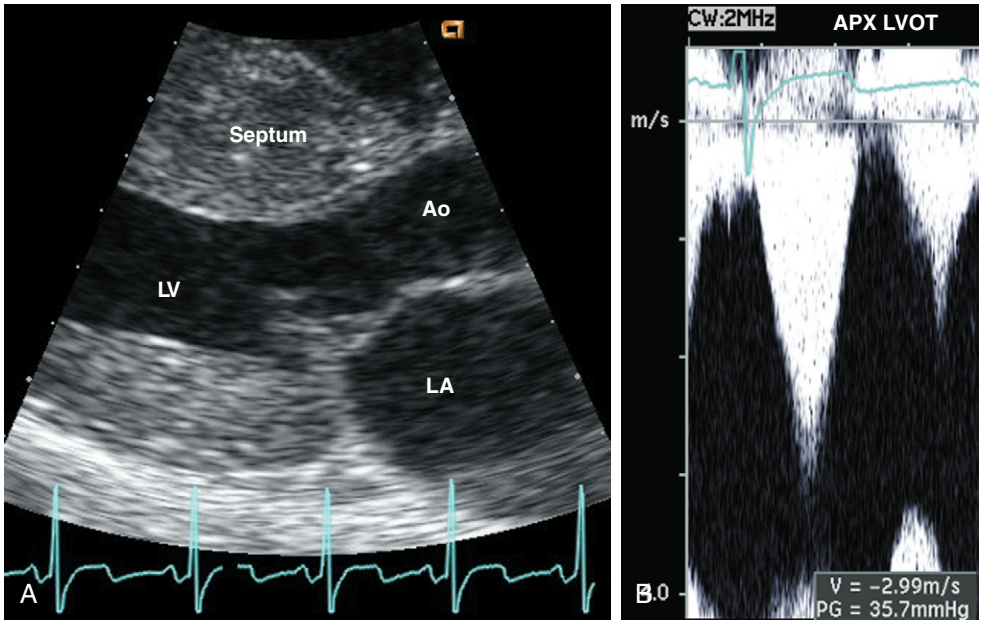



**Figure 35-19 A 21-year-old $G_1P_0$ woman with hypertrophic cardiomyopathy was seen throughout pregnancy. Before pregnancy, she had minimal symptoms of chest pain and exertional dyspnea.** Echocardiography demonstrated marked septal hypertrophy with posterior hypertrophy (**A**). Post-PVC peak gradient was approximately 3.0 m/s (**B**) and was stable from prior studies. Pulmonary pressures were normal. Her symptoms worsened during pregnancy but were controlled with diuretics and continued beta-blockers. She had an uneventful delivery and subsequently returned to her prepregnancy baseline. *Ao*, Aorta; *PVC*, premature ventricular contraction.

## CARDIOMYOPATHIES

The risk of pregnancy in a patient with a known cardiomyopathy is related to the severity of the underlying disease.[152] In familial types of cardiomyopathy, including hypertrophic (Fig. 35-19) and some forms of dilated cardiomyopathy, the genetic implications of the diagnosis also need to be taken into consideration. Echocardiography is used to confirm or exclude the diagnosis in patients considering pregnancy who are at risk for an inherited cardiomyopathy and to assess disease severity in patients with a known cardiomyopathy.[153]

Peripartum cardiomyopathy[152,154] was initially defined as heart failure presenting in the last month of pregnancy or

within 6 months of delivery, without other reason for cardiomyopathy.[155] More recently authors have suggested that the definition include LV dysfunction with an echocardiographic ejection fraction of less than 45%.[156] Others argue that the disease can be found earlier in pregnancy and that the "traditional" presentations represent a spectrum of disease that includes those patients with the earlier onset of cardiomyopathy. The diagnosis typically is established by echocardiography in the appropriate clinical setting. Despite overall improvement in therapy of heart failure, the mortality of peripartum cardiomyopathy remains greater than 20%.[157] The risk to women in subsequent pregnancies is high, particularly if the ejection fraction did not return to normal.[158] Dilated cardiomyopathy carries similarly high risks of adverse cardiac events, predicted by LV dysfunction and NYHA functional class.[159] Echocardiographic monitoring of disease severity, especially LV systolic function, helps optimize patient management.

Pregnancy in patients after cardiac transplantation has been described.[160,161] In one series of 29 organ recipients (26 heart and 3 heart-lung), 21% of women experienced a rejection episode during pregnancy, although only 3% had graft loss within 2 years of delivery. Fetal outcomes were notable for an 18% spontaneous abortion rate, higher than expected in the general population. Of live-born infants, 40% were premature and 40% had low birth weight.[162] As medical therapy for transplant patients evolves and the population requiring transplant includes more young women as a result of the increase in adults with congenital heart disease, one would expect an increase in the number of women bearing children following cardiac transplantation. Echocardiography can be used to evaluate for evidence of rejection during and after pregnancy.

## OTHER HEART DISEASES

### *Marfan Syndrome*

Pregnancy in patients with Marfan syndrome is associated with an increased risk of aortic dissection (Fig. 35-20). The mechanism of aortic dissection in pregnant women with Marfan syndrome presumably relates to (1) the underlying defect in aortic wall structure, (2) normal structural changes in the aortic wall with pregnancy, and (3) the increased stroke volume and LV *dP/dt* of pregnancy. Gestational hypertension may further aggravate the risk of dissection.[163]

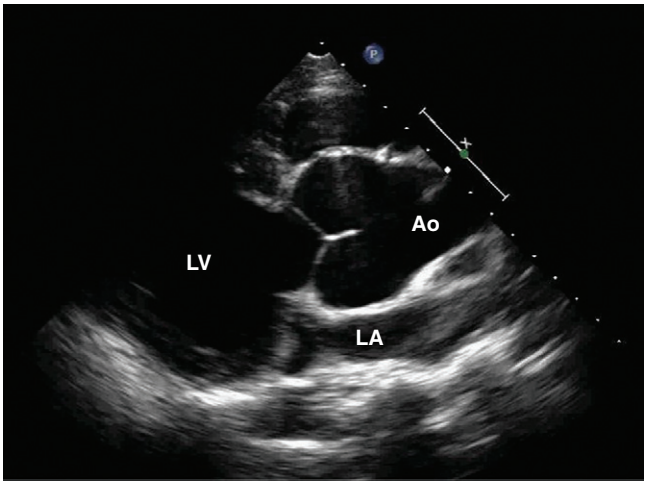



**Figure 35-20 A 23-year-old $G_1P_0$ woman with a history of Marfan syndrome presented at 6 weeks gestation with stable significant aortic enlargement with a maximal dimension of approximately 4.5 cm at the sinuses of Valsalva.** She was followed through pregnancy with serial echocardiograms with stable aortic dimensions. She had an assisted vaginal delivery and delivered a healthy baby girl who was noted to have some features suggestive of Marfan syndrome. *Ao*, Aorta.

As is the case with many cardiac disorders in pregnancy, there are difficulties in gleaning appropriate care recommendations based on the available literature. Initial series suggested a high risk of dissection: Of 35 women with Marfan syndrome and at least one pregnancy, 20 (63%) suffered an acute aortic dissection and 16 (50%) died during pregnancy.[164] Subsequent series suggested a maternal mortality rate of only 1%, especially when aortic diameter is only mildly increased.[165-169] However, in a study of 91 pregnancies in 36 women with Marfan syndrome, 4 of 36 (11%) had dissection related to pregnancy and 2 others required aortic surgery following delivery for a total aortic complication rate of 17%.[170]

As in nonpregnant patients, risk of aortic dissection increases with the degree of aortic dilation. Several studies have demonstrated an increase in the risk of dissection in women with aortic diameter greater than 4 cm.[167,168] One study evaluated 61 women, of whom 23 had had 31 pregnancies with known aortic root dimensions.[169] In this group, there were no complications in women with aortic diameters of 25 to 45 mm, with the only complication in a woman with a prior dissection. In addition to absolute diameter, change in aortic size during pregnancy has also been identified as a risk for dissection. Some patients with Marfan syndrome suffer aortic dissection with only mildly increased aortic root dimensions,[170,171] although a case report describes a woman with an aortic diameter of 8 cm who did not dissect during pregnancy.[172]

Echocardiography is extremely valuable in the preconceptional assessment of women with Marfan syndrome, as several authors have recommended prophylactic aortic root replacement when pregnancy is planned, if aortic root dilation is present.[173,174] Echocardiographic monitoring during pregnancy allows risk stratification by assessing both initial aortic diameter and progression in size increase over time. With careful echocardiographic evaluation of aortic root dimensions and geometry, review of the patient's family history, and consultation between the cardiologist and geneticist,[175] women with Marfan syndrome can be counseled about the potential risks before pregnancy, especially because the risk of dissection during pregnancy appears to be directly related to the degree of aortic root dilation. Treatment with beta-blockers[176,177] and careful peripartum anesthetic management[178] may improve the prognosis in pregnant patients with Marfan syndrome. Successful surgical repair during pregnancy of aortic dissection in Marfan syndrome has been reported.[179]

### *Aortic Dissection*

There is an increased risk of aortic dissection during pregnancy even in women without Marfan syndrome. Patients with connective tissue disorders such as Ehlers-Danlos syndrome are at higher risk, as are women with bicuspid aortic valve and dilated aortic root,[167] Turner syndrome,[180] and severe hypertension. Echocardiography is often the initial diagnostic test requested in these patients. Prompt recognition and surgical intervention can be lifesaving.[181]

### *Ischemic Heart Disease*

Acute coronary events and MI are rare in pregnancy, resulting from the low prevalence of coronary artery disease in women

of childbearing age. In women aged 15 to 44 years, the incidence of MI unrelated to pregnancy is 5 per 100,000 woman-years, and the rate of cerebrovascular events is 10.7 per 100,000 woman-years.[182] However, coronary dissection and thromboembolic events are unusual causes of MI disproportionately represented in pregnancy. A literature review of 125 cases of MI in pregnancy found the highest incidence in multigravid women over age 33 years. MI tended to occur in the third trimester, often during labor and delivery. Of the MIs, 43% were the result of atherosclerosis, 21% were thrombotic without evidence of underlying atherosclerosis, 16% were the result of coronary dissection, and in 29% coronary anatomy was normal, suggesting the possibility of coronary spasm.[182]

Another study identified 859 MIs related to pregnancy, which was a case event rate of 6.2 per 100,000. The case fatality rate was 5.1%, demonstrating that although rare, MI related to pregnancy carries a significant risk of mortality. In this study, classic risk factors for coronary artery disease, including hypertension, diabetes mellitus, and smoking, were significant. In addition, the risk was 30 times higher for women older than 40 years compared with women younger than 20 years.[183] As women delay childbirth, the incidence of MI in pregnancy may rise.[184] Though uncommon, rates of severe complications related to MI during pregnancy are high.[185] The usual criteria for MI apply in pregnancy and the puerperium, with the exception of myoglobin and creatinine kinase myocardial band, which may increase twofold in normal women within 30 minutes of delivery.[186] Troponin I is a more accurate marker in this setting. Segmental wall motion abnormalities on echocardiography should raise the possibility of ischemic heart disease.

Data regarding therapy of MI during pregnancy are limited. Thrombolytic therapy is contraindicated in pregnancy and the early postpartum period, so the optimal clinical approach to revascularization is percutaneous balloon angioplasty with or without placement of an intracoronary stent, although coronary bypass grafting surgery during pregnancy also has been described.[187] The use of clopidogrel can complicate delivery; therefore, stent selection is based on the anticipated delivery date and duration of clopidogrel therapy to protect from stent thrombosis.[188] Little is known about the risk of subsequent pregnancy for women with a pregnancy complicated by MI.

## Echocardiographic Monitoring in Pregnant Patients

In addition to monitoring disease severity and cardiovascular hemodynamics in pregnant patients, both transthoracic echocardiography (TTE) and transesophageal[140] echocardiography (TEE) have been used to monitor diagnostic and therapeutic procedures. One of the advantages of echocardiographic monitoring during pregnancy is the avoidance of exposure to ionizing radiation. Echocardiographic monitoring in pregnant women has been reported for electrophysiologic testing,[148] pacer implantation, and percutaneous balloon mitral valvotomy.[189]

## Common Clinical Presentations

### PULMONARY EDEMA AND HEART FAILURE

In the pregnant patient with acute respiratory distress, the initial differential diagnosis is cardiac and noncardiac causes, such as acute pulmonary embolism, pneumonia, or an acute viral syndrome. An echocardiographic study in these situations helps demonstrate normal cardiac anatomy and function, allowing attention to be focused on potential noncardiac causes of the illness. Conversely, a cardiac etiology can be quickly identified and evaluated, permitting appropriate therapeutic interventions.

**TABLE 35-6 Respiratory Distress in Pregnancy: Echocardiographic Differential Diagnosis**

| *Pathophysiology* | *Examples* |
|---|---|
| **Cardiac** | |
| ↓ LV (or systemic ventricle) systolic function | Peripartum cardiomyopathy |
| | Congenital heart disease |
| | Dilated cardiomyopathy |
| LV diastolic function | Hypertension |
| | Aortic stenosis |
| LV pressure overload | Aortic stenosis |
| | Hypertension |
| Impaired cardiac filling | Mitral stenosis |
| | Pericardial disease |
| LV (or systemic ventricle) volume overload | Aortic regurgitation |
| | Mitral regurgitation |
| | Tricuspid regurgitation in systemic RV |
| ↓ Pulmonary blood flow | Eisenmenger physiology |
| | Palliative systemic-to-pulmonary shunts |
| **Noncardiac** | |
| Capillary "leak" | Preeclampsia |
| | Adult respiratory distress syndrome |
| Infection | Pneumonia |
| | Viral syndrome |
| Pulmonary vascular obstruction | Pulmonary embolus |

From Vered Z, Poler SM, Gibson P, et al: Non-invasive detection of the morphologic and hemodynamic changes during normal pregnancy. *Clin Cardiol* 14:327-334, 1991.

Of the cardiac conditions presenting with pulmonary edema in the third trimester or in the peripartum period (Table 35-6), the most prevalent are mitral valve stenosis and peripartum cardiomyopathy. On physical examination, the diastolic rumbling murmur of mitral stenosis is difficult to appreciate and the patient herself is often unaware of a heart condition. The added hemodynamic burden of pregnancy may result in a previously asymptomatic patient being diagnosed with "sudden" and "unexplained" pulmonary edema. It is not unusual for the echocardiogram (ordered for other reasons) to be the first clue that valvular obstruction is present.

Peripartum cardiomyopathy may present with the insidious onset of heart failure symptoms or may be more abrupt in onset. In the latter case, it is likely that the patient has unrecognized heart failure symptoms that can be elicited in retrospect. The degree of LV systolic dysfunction is variable. Typically, clinical symptoms are first noted between 1 month antepartum and 1 month postpartum.[152,190] Echocardiographically, peripartum cardiomyopathy is indistinguishable from other forms of dilated cardiomyopathy.

### THE PREGNANT PATIENT WITH A CARDIAC MURMUR

A systolic murmur is a common finding during pregnancy, being reported in as many as 80% of women in some series.[191] This murmur typically is a "flow" murmur resulting from the increased volume flow rate of pregnancy. Depending on its location and timing, it most often originates from the pulmonic

valve, although some flow murmurs of pregnancy may be the result of high flow across the aortic valve. With the normal murmur of pregnancy, Doppler echocardiography shows no abnormal flow patterns, although antegrade velocities are increased, as expected in pregnancy.

One study of 103 women with no previous cardiac history referred for evaluation of a murmur during pregnancy found that 79% had a benign murmur on physical examination, and all of these individuals had normal results on Doppler echocardiography.[191] Benign ejection murmurs were soft and midsystolic. Even in the 14% with a loud or long ejection murmur, most had normal Doppler study results, with abnormalities seen in only 3 patients (1 mitral valve prolapse with mild mitral regurgitation, 1 nonobstructive hypertrophic cardiomyopathy, 1 bicuspid aortic valve). In contrast, in the 7% of patients with a pansystolic, late systolic, or diastolic murmur all had abnormal echocardiographic results. This group included 3 ventricular septal defects, 1 large atrial septal defect, one atrial septal defect in conjunction with rheumatic mitral regurgitation, 1 mitral valve prolapse, and 1 nonobstructive hypertrophic cardiomyopathy.

Although it is likely that the prevalence of specific cardiac diagnoses will vary with the population, this series clearly demonstrates the importance of careful patient selection in requesting echocardiography for evaluation of a murmur in pregnancy. To minimize the inappropriate use of echocardiography in pregnant women, one approach is to limit echocardiographic evaluation to pregnant women with a murmur only if they have (1) a history of underlying heart disease, (2) definite cardiac symptoms, (3) a grade 3/6 or greater systolic murmur, or (4) a diastolic murmur. Use of these criteria will avoid unnecessary echocardiography.

Conversely, it is critically important to perform an echocardiographic examination in patients with pathologic or possibly pathologic murmurs. Many cases of previously undiagnosed congenital heart disease, valvular stenosis, and valvular regurgitation are recognized during pregnancy. In addition to the prognostic information obtained by having the correct cardiac diagnosis, the echocardiographic data resulted in significant changes in patient management. Such changes included recommendation of endocarditis prophylaxis at delivery for structural heart disease, surgical closure of an atrial septal defect postpartum, and genetic counseling in patients with inherited diseases in the study described previously.[191]

Like other clinical guidelines, these criteria are not absolute, and given the negligible risk of echocardiography, it is preferable to err on the side of performing echocardiographic studies in normal women than to miss a case of significant heart disease in a pregnant patient. When a pathologic murmur is present, it is incumbent on the echocardiographer to make sure the referring physician is aware of the significance of this finding and to ensure appropriate assessment of maternal and fetal risk. In view of the multidisciplinary nature of care for pregnant women with heart disease and the impact of maternal heart disease on both mother and fetus, referral to a maternal-fetal specialist in a high-risk obstetrics clinic is needed for optimal care, particularly in patients with hemodynamically significant lesions. This consideration also applies to nonpregnant women with heart disease in whom appropriate counseling regarding the risks of pregnancy and contraceptive options is needed either to avoid unnecessary anxiety and delay in starting a family (if the maternal-fetal risk is low) or to avoid a high-risk complicated pregnancy (when the maternal-fetal risk is high). The echocardiographer often initiates communication with the maternal-fetal specialist.

### MITRAL VALVE PROLAPSE

Because a diagnosis of mitral valve prolapse is common in young women, concern is often raised that this diagnosis may affect the risk or management of pregnancy. Some series report a history of mitral valve prolapse in as many as 1.2% of all pregnancies.[192] No echocardiographic changes in the presence or degree of mitral prolapse[169] and no increase in maternal risk have been seen in pregnant patients with this diagnosis.[193,194] Many of these women have only minor abnormalities of leaflet anatomy or motion without significant valvular dysfunction. Thus, echocardiography plays an important role in reassuring both patient and referring physician that the risk of pregnancy is not affected by this diagnosis and that the management of pregnancy and the peripartum period can be considered routine, other than the need for endocarditis prophylaxis. In the patient with significant functional mitral valve disease—myxomatous leaflets and mitral regurgitation—echocardiography allows assessment of the degree of regurgitation and the LV response to chronic volume overload.

### PALPITATIONS AND ARRHYTHMIAS IN PREGNANCY

Most women experience an increased awareness of their heartbeat with occasional premature ventricular and atrial beats during pregnancy. Significant arrhythmias, associated with hypotension, dizziness, or shortness of breath, most often occur in patients with known underlying heart disease or a history of arrhythmias. The onset of symptomatic arrhythmia during pregnancy warrants echocardiographic evaluation, as in the nonpregnant patient, to evaluate for structural heart disease.

## Limitations of Echocardiography and Alternative Approaches

Echocardiography often provides all the information needed for patient management in pregnant women with heart disease, but in some situations other diagnostic approaches or imaging modalities may be needed. If TTE is inadequate because of poor ultrasound tissue penetration, TEE is appropriate and can be safely performed during pregnancy. Other useful imaging procedures in patients with congenital heart disease and valvular heart disease include radionuclide ventriculography, magnetic resonance imaging, computed tomographic imaging, and angiographic evaluation in the catheterization laboratory. In pregnant patients, the use of ionizing radiation with some of these techniques needs to be considered in the overall risk-benefit analysis of whether evaluation is needed during pregnancy or can be safely postponed to the postpartum period.

When direct and repeated measurements of pulmonary pressures, LV filling pressures, and CO are needed, invasive monitoring with an indwelling right-sided heart catheter is the procedure of choice. In patients with significant heart disease, invasive monitoring may be needed in the peripartum period to allow maintenance of optimal loading conditions under the changing volume and hemodynamic conditions of labor, delivery, and anesthesia.

## KEY POINTS

- Hemodynamic changes of pregnancy include increased cardiac output, increased heart rate, decreased systemic vascular resistance, and increased blood volume.
- Normal echocardiographic changes of pregnancy include an increased LV end-diastolic dimension with preserved systolic dimension, slight increase in aortic and LVOT diameters, and increased LA size.
- The most common cardiac conditions seen in pregnancy are valvular heart disease and congenital heart disease.
- Residual cardiac defects after surgical treatment of congenital heart disease may increase the risk of pregnancy, including:
  - Severe pulmonic regurgitation in patients with tetralogy of Fallot
  - Systemic ventricular systolic dysfunction after an interatrial baffle repair for transposition of the great arteries
- There is a higher risk of maternal and fetal complications with pregnancy in patients with:
  - Eisenmenger syndrome or severe pulmonary hypertension
  - Severe left-sided valvular stenosis (aortic stenosis or mitral stenosis)
  - Decreased systemic ventricular function (ejection fraction less than 40%)
  - Cyanotic heart disease including palliated complex congenital heart disease and Fontan repairs
  - Mechanical valve prostheses
  - Marfan syndrome, especially with a dilated ascending aorta
- Echocardiography before planned pregnancy is recommended in all women with congenital heart disease or valvular heart disease to assess prognosis, consider repair of any high-risk lesions, and optimize medical management.

## REFERENCES


1. Cole P, St. John Sutton M: Cardiovascular physiology in pregnancy. In Douglas PS, editor: *Cardiovascular health and disease in women*, Philadelphia, 1993, WB Saunders, pp 305-328.
2. Capeless EL, Clapp JF: Cardiovascular changes in early phase of pregnancy. *Am J Obstet Gynecol* 161:1449-1453, 1989.
3. Edouard DA, Pannier BM, London GM, et al: Venous and arterial behavior during normal pregnancy. *Am J Physiol* 274:H1605-H1612, 1998.
4. Gilson GJ, Samaan S, Crawford MH, et al: Changes in hemodynamics, ventricular remodeling, and ventricular contractility during normal pregnancy: a longitudinal study. *Obstet Gynecol* 89:957-962, 1997.
5. Hunter S, Robson SC: Adaptation of the maternal heart in pregnancy. *Br Heart J* 68:540-543, 1992.
6. Mabie WC, DiSessa TG, Crocker LG, et al: A longitudinal study of cardiac output in normal human pregnancy. *Am J Obstet Gynecol* 170:849-856, 1994.
7. Easterling TR, Benedetti TJ: Measurement of cardiac output by impedance technique. *Am J Obstet Gynecol* 163:1104-1106, 1990.
8. Mesa A, Jessurun C, Hernandez A, et al: Left ventricular diastolic function in normal human pregnancy. *Circulation* 99:511-517, 1999.
9. Duvekot JJ, Cheriex EC, Pieters FA, et al: Early pregnancy changes in hemodynamics and volume homeostasis are consecutive adjustments triggered by a primary fall in systemic vascular tone. *Am J Obstet Gynecol* 169:1382-1392, 1993.
10. Soubassi L, Haidopoulos D, Sindos M, et al: Pregnancy outcome in women with pre-existing lupus nephritis. *J Obstet Gynaecol* 24:630-634, 2004.
11. Carbillon L, Challier JC, Uzan S: Hemodynamical changes on the maternal side of the placental circulation in normal and complicated pregnancies. *Placenta* 25:834, 2004.
12. Poppas A, Shroff SG, Korcarz CE, et al: Serial assessment of the cardiovascular system in normal pregnancy: role of arterial compliance and pulsatile arterial load. *Circulation* 95:2407-2415, 1997.
13. Mone SM, Sanders SP, Colan SD: Control mechanisms for physiological hypertrophy of pregnancy. *Circulation* 94:667-672, 1996.
14. Geva T, Mauer MB, Striker L, et al: Effects of physiologic load of pregnancy on left ventricular contractility and remodeling. *Am Heart J* 133:53-59, 1997.
15. Robson SC, Hunter S, Boys RJ, et al: Serial changes in pulmonary haemodynamics during human pregnancy: A non-invasive study using Doppler echocardiography. *Clin Sci (Lond)* 80:113-117, 1991.
16. Clark SL, Cotton DB, Lee W, et al: Central hemodynamic assessment of normal term pregnancy. *Am J Obstet Gynecol* 161:1439-1442, 1989.
17. Otto CM, editor: *Textbook of clinical echocardiography*, ed 2, Philadelphia, 2000, Saunders.
18. Easterling TR, Carlson KL, Schmucker BC, et al: Measurement of cardiac output in pregnancy by Doppler technique. *Am J Perinatol* 7:220-222, 1990.
19. Lee W, Rokey K, Cotton DB: Noninvasive maternal stroke volume and cardiac output determinations by pulsed Doppler echocardiography. *Am J Obstet Gynecol* 158:505-510, 1988.
20. Easterling TR, Benedetti TJ: Techniques differ in use of Doppler ultrasonography. *Am J Obstet Gynecol* 161:1748-1749, 1989.
21. Easterling TR, Benedetti TJ, Schmucker BC, et al: Maternal hemodynamics and aortic diameter in normal and hypertensive pregnancies. *Obstet Gynecol* 78:1073-1077, 1991.
22. Sadaniantz A, Kocheril AG, Emaus SP, et al: Cardiovascular changes in pregnancy evaluated by two-dimensional and Doppler echocardiography. *J Am Soc Echocardiogr* 5:253-258, 1992.
23. Cotton DB, Lee W, Huhta JC, et al: Hemodynamic profile of severe pregnancy-induced hypertension. *Am J Obstet Gynecol* 158:523-529, 1988.
24. McLennan FM, Haites NE, Rawles JM: Stroke and minute distance in pregnancy: a longitudinal study using Doppler ultrasound. *Br J Obstet Gynaecol* 94:499-506, 1987.
25. Robson SC, Dunlop W, Moore M, et al: Combined Doppler and echocardiographic measurement of cardiac output: theory and application in pregnancy. *Br J Obstet Gynaecol* 94:1014-1027, 1987.
26. Robson SC, Hunter S, Boys RJ, et al: Hemodynamic changes during twin pregnancy. A Doppler and M-mode echocardiographic study. *Am J Obstet Gynecol* 161:1273-1278, 1989.
27. Robson SC, Boys RJ, Hunter S: Doppler echocardiographic estimation of cardiac output: analysis of temporal variability. *Eur Heart J* 9:313-318, 1988.
28. Vered Z, Poler SM, Gibson P, Wlody D, Pérez JE: Noninvasive detection of the morphologic and hemodynamic changes during normal pregnancy. *Clin Cardiol* 4:327-334, 1991.
29. Robson SC, Hunter S, Moore M, et al: Haemodynamic changes during the puerperium: a Doppler and M-mode echocardiographic study. *Br J Obstet Gynaecol* 94:1028-1039, 1987.
30. Rubler S, Damani PM, Pinto ER: Cardiac size and performance during pregnancy estimated with echocardiography. *Am J Cardiol* 40:534-540, 1977.
31. Rubler S, Schneebaum R, Hammer N: Systolic time intervals in pregnancy and the postpartum period. *Am Heart J* 86:182-188, 1973.
32. Laird-Meeter K, van de Ley G, Bom TH, et al: Cardiocirculatory adjustments during pregnancy—an echocardiographic study. *Clin Cardiol* 2:328-332, 1979.
33. Easterling TR, Schmucker BC, Benedetti TJ: The hemodynamic effects of orthostatic stress during pregnancy. *Obstet Gynecol* 72:550-552, 1988.
34. Hart MV, Morton MJ, Hosenpud JD, et al: Aortic function during normal human pregnancy. *Am J Obstet Gynecol* 154:887-891, 1986.

35. Pouta AM, Rasanen JP, Airaksinen KE, et al: Changes in maternal heart dimensions and plasma atrial natriuretic peptide levels in the early puerperium of normal and pre-eclamptic pregnancies. *Br J Obstet Gynaecol* 103:988-992, 1996.
36. Campos O, Andrade JL, Bocanegra J, et al: Physiologic multivalvular regurgitation during pregnancy: a longitudinal Doppler echocardiographic study. *Int J Cardiol* 40:265-272, 1993.
37. Limacher MC, Ware JA, O'Meara ME, et al: Tricuspid regurgitation during pregnancy: two-dimensional and pulsed Doppler echocardiographic observations. *Am J Cardiol* 55:1059-1062, 1985.
38. Robson SC, Dunlop W, Boys RJ, et al: Cardiac output during labour. *Br Med J (Clin Res Ed)* 295:1169-1172, 1987.
39. Lee W, Rokey R, Miller J, et al: Maternal hemodynamic effects of uterine contractions by M-mode and pulsed-Doppler echocardiography. *Am J Obstet Gynecol* 161:974-977, 1989.
40. Strickland RA, Oliver WC Jr, Chantigian RC, et al: Anesthesia, cardiopulmonary bypass, and the pregnant patient. *Mayo Clin Proc* 66:411-429, 1991.
41. Veille JC, Hellerstein HK, Bacevice AE Jr: Maternal left ventricular performance during bicycle exercise. *Am J Cardiol* 69:1506-1508, 1992.
42. Sady MA, Haydon BB, Sady SP, et al: Cardiovascular response to maximal cycle exercise during pregnancy and at two and seven months postpartum. *Am J Obstet Gynecol* 162:1181-1185, 1990.
43. Khodiguian N, Jaque-Fortunato SV, Wiswell RA, et al: A comparison of cross-sectional and longitudinal methods of assessing the influence of pregnancy on cardiac function during exercise. *Semin Perinatol* 20:232-241, 1996.
44. Pivarnik JM, Ayres NA, Mauer MB, et al: Effects of maternal aerobic fitness on cardiorespiratory responses to exercise. *Med Sci Sports Exerc* 25:993-998, 1993.
45. Pivarnik JM, Lee W, Clark SL, et al: Cardiac output responses of primigravid women during exercise determined by the direct Fick technique. *Obstet Gynecol* 75:954-959, 1990.
46. Van Hook JW, Gill P, Easterling TR, et al: The hemodynamic effects of isometric exercise during late normal pregnancy. *Am J Obstet Gynecol* 169:870-873, 1993.
47. Sibai BM, Mabie WC: Hemodynamics of preeclampsia. *Clin Perinatol* 18:727-747, 1991.
48. Guzman CA, Caplan R: Cardiorespiratory response to exercise during pregnancy. *Am J Obstet Gynecol* 108:600-605, 1970.
49. Wolfe LA, Preston RJ, Burggraf GW, et al: Effects of pregnancy and chronic exercise on maternal cardiac structure and function. *Can J Physiol Pharmacol* 77:909-917, 1999.
50. Easterling TR, Schmucker BC, Carlson KL, et al: Maternal hemodynamics in pregnancies complicated by hyperthyroidism. *Obstet Gynecol* 78:348-352, 1991.
51. Finley J, Katz M, Rojas-Perez M, et al: Cardiovascular consequences of beta-agonist tocolysis: an echocardiographic study. *Obstet Gynecol* 64:787-791, 1984.
52. Easterling TR, Carlson K, Benedetti TJ, et al: Hemodynamics associated with the diagnosis and treatment of pheochromocytoma in pregnancy. *Am J Perinatol* 9:464-466, 1992.
53. Veille JC, Hanson R: Left ventricular systolic and diastolic function in pregnant patients with sickle cell disease. *Am J Obstet Gynecol* 170:107-110, 1994.
54. Easterling TR, Brateng D, Goldman ML, et al: Renal vascular hypertension during pregnancy. *Obstet Gynecol* 78:921-925, 1991.
55. Roberts JM, Pearson G, Cutler J, et al: Summary of the NHLBI working group on research on hypertension during pregnancy. *Hypertension* 41:437-445, 2003.
56. Clinical Management Guidelines for Obstetrician-Gynecologists: Diagnosis and management of preeclampsia and eclampsia. *Obstet Gynecol* 99:159-167, 2002.
57. Bosio PM, McKenna PJ, Conroy R, et al: Maternal central hemodynamics in hypertensive disorders of pregnancy. *Obstet Gynecol* 94:978-984, 1999.
58. Broughton Pipkin F, Rubin PC: Pre-eclampsia—the "disease of theories." *Br Med Bull* 50:381-396, 1994.
59. Easterling TR: The maternal hemodynamics of preeclampsia. *Clin Obstet Gynecol* 35:375-386, 1992.
60. Easterling TR, Benedetti TJ, Schmucker BC, Millard SP: Maternal hemodynamics in normal and preeclamptic pregnancies: a longitudinal study. *Obstet Gynecol* 76:1061-1069, 1990.
61. Easterling TR, Watts DH, Schmucker BC, et al: Measurement of cardiac output during pregnancy: validation of Doppler technique and clinical observations in preeclampsia. *Obstet Gynecol* 69:845-850, 1987.
62. Easterling TR, Benedetti TJ, Carlson KC, et al: The effect of maternal hemodynamics on fetal growth in hypertensive pregnancies. *Am J Obstet Gynecol* 165:902-906, 1991.
63. Easterling TR, Benedetti TJ, Schmucker BC, et al: Antihypertensive therapy in pregnancy directed by noninvasive hemodynamic monitoring. *Am J Perinatol* 6:86-89, 1989.
64. Rutherford JD, Hands ME: Pregnancy with preexisting heart disease. In Douglas PS, editor: *Cardiovascular health and disease in women*, Philadelphia, 1993, WB Saunders, pp 329-336.
65. Clark SL: Cardiac disease in pregnancy. *Crit Care Clin* 7:777-797, 1991.
66. Kuklina E, Callaghan W: Chronic heart disease and severe obstetric morbidity among hospitalisations for pregnancy in the USA: 1995-2006. *BJOG* 118:345-352, 2011.
67. Hess DB, Hess LW: Management of cardiovascular disease in pregnancy. *Obstet Gynecol Clin North Am* 19:679-695, 1992.
68. Siu SC, Sermer M, Colman JM, et al: Prospective multicenter study of pregnancy outcomes in women with heart disease. *Circulation* 104:515-521, 2001.
69. Khairy P, Ouyang DW, Fernandes M, et al: Pregnancy outcomes in women with congenital heart disease. *Circulation* 113:517-524, 2006.
70. Lui GK, Silversides CK, Khairy P, et al: Heart rate response during exercise and pregnancy outcome in women with congenital heart disease. *Circulation* 123:242-248, 2011.
71. Balint OH, Siu SC, Mason J, et al: Cardiac outcomes after pregnancy in women with congenital heart disease. *Heart* 96:1656-1661, 2010.
72. Warnes CA, Williams RG, Bashore TM, et al, ACC/AHA 2008 Guidelines for the Management of Adults with Congenital Heart Disease: a report of the American College of Cardiology/American Heart Association Task Force on Practice Guidelines (writing committee to develop guidelines on the management of adults with congenital heart disease). *Circulation* 118:e714-e833, 2008.
73. Bonow RO, Carabello BA, Chatterjee K, et al: 2008 focused update incorporated into the ACC/AHA 2006 guidelines for the management of patients with valvular heart disease: a report of the American College of Cardiology/American Heart Association Task Force on Practice Guidelines (Writing Committee to revise the 1998 guidelines for the management of patients with valvular heart disease). Endorsed by the Society of Cardiovascular Anesthesiologists, Society for Cardiovascular Angiography and Interventions, and Society of Thoracic Surgeons. *J Am Coll Cardiol* 52:e1-e142, 2008.
74. Vongpatanasin W, Brickner ME, Hillis LD, et al: The Eisenmenger syndrome in adults. *Ann Intern Med* 128:745-755, 1998.
75. Gleicher N, Midwall J, Hochberger D, et al: Eisenmenger's syndrome and pregnancy. *Obstet Gynecol Surv* 34:721-741, 1979.
76. Weiss BM, Zemp L, Seifert B, et al: Outcome of pulmonary vascular disease in pregnancy: a systematic overview from 1978 through 1996. *J Am Coll Cardiol* 31:1650-1657, 1998.
77. Bendayan D, Hod M, Oron G, et al: Pregnancy outcome in patients with pulmonary arterial hypertension receiving prostacyclin therapy. *Obstet Gynecol* 106:1206-1210, 2005.
78. Lam GK, Stafford RE, Thorp J, et al: Inhaled nitric oxide for primary pulmonary hypertension in pregnancy. *Obstet Gynecol* 98:895-898, 2001.
79. Monnery L, Nanson J, Charlton G: Primary pulmonary hypertension in pregnancy: a role for novel vasodilators. *Br J Anesth* 87:295-298, 2001.
80. Goodwin TM, Gherman RB, Hameed A, et al: Favorable response of Eisenmenger syndrome to inhaled nitric oxide during pregnancy. *Am J Obstet Gynecol* 180:64-67, 1999.
81. Kiely DG, Condliffe R, Webster V, et al: Improved survival in pregnancy and pulmonary hypertension using a multiprofessional approach. *BJOG* 117:565-574, 2010.
82. Zuber M, Gautschi N, Oechslin E, et al: Outcome of pregnancy in women with congenital shunt lesions. *Heart* 81:271-275, 1999.
83. Horvath KA, Burke RP, Collins JJ Jr, et al: Surgical treatment of adult atrial septal defect: early and long-term results. *J Am Coll Cardiol* 20:1156-1159, 1992.
84. Yap SC, Drenthen W, Pieper PG, et al: Pregnancy outcome in women with repaired versus unrepaired isolated ventricular septal defect. *BJOG* 117:683-689, 2010.
85. Lundstrom U, Bull C, Wyse RK, et al: The natural and "unnatural" history of congenitally corrected transposition. *Am J Cardiol* 65:1222-1229, 1990.
86. Celermajer DS, Bull C, Till JA, et al: Ebstein's anomaly: presentation and outcome from fetus to adult. *J Am Coll Cardiol* 23:170-176, 1994.
87. Connolly HM, Warnes CA: Ebstein's anomaly: outcome of pregnancy. *J Am Coll Cardiol* 23:1194-1198, 1994.
88. Therrien J, Barnes I, Somerville J: Outcome of pregnancy in patients with congenitally corrected transposition of the great arteries. *Am J Cardiol* 84:820-824, 1999.
89. Connolly HM, Grogan M, Warnes CA: Pregnancy among women with congenitally corrected transposition of great arteries. *J Am Coll Cardiol* 33:1692-1695, 1999.

90. Guedes A, Mercier L-A, Leduc L, et al: Impact of pregnancy on the systemic right ventricle after a Mustard operation for transposition of the great arteries. *J Am Coll Cardiol* 44:433-437, 2004.
91. Driscoll DJ, Offord KP, Feldt RH, et al: Five- to fifteen-year follow-up after Fontan operation. *Circulation* 85:469-496, 1992.
92. Murphy JG, Gersh BJ, Mair DD, et al: Long-term outcome in patients undergoing surgical repair of tetralogy of Fallot. *N Engl J Med* 329:593-599, 1993.
93. Meijer JM, Pieper PG, Drenthen W, et al: Pregnancy, fertility, and recurrence risk in corrected tetralogy of Fallot. *Heart* 91:801-805, 2005.
94. Veldtman GR, Connolly HM, Grogan M, et al: Outcomes of pregnancy in women with tetralogy of Fallot. *J Am Coll Cardiol* 44:174-180, 2004.
95. Balci A, Drenthen W, Mulder BJ, et al: Pregnancy in women with corrected tetralogy of Fallot: occurrence and predictors of adverse events. *Am Heart J* 161:307-313, 2011.
96. Hidaka Y, Akagi T, Himeno W, et al: Left ventricular performance during pregnancy in patients with repaired tetralogy of Fallot: prospective evaluation using the Tei index. *Circ J* 67:682-686, 2003.
97. Kupferminc MJ, Lessing JB, Jaffa A, et al: Fetomaternal blood flow measurements and management of combined coarctation and aneurysm of the thoracic aorta in pregnancy. *Acta Obstet Gynecol Scand* 72:398-402, 1993.
98. Cohen M, Fuster V, Steele PM, et al: Coarctation of the aorta. Long-term follow-up and prediction of outcome after surgical correction. *Circulation* 80:840-845, 1989.
99. Carvalho JS, Redington AN, Shinebourne EA, Rigby ML, Gibson D: Continuous wave Doppler echocardiography and coarction of the aorta: gradients and flow patterns in the assessment of severity. *Br Heart J* 64:133-137, 1990.
100. Lim DS, Ralston MA: Echocardiographic indices of Doppler flow patterns compared with MRI or angiographic measurements to detect significant coarction of the aorta. *Echocardiography* 19:55-60, 2002.
101. Kimball TR, Reynolds JM, Mays WA, et al: Persistent hyperdynamic cardiovascular state at rest and during exercise in children after successful repair of coarctation of the aorta. *J Am Coll Cardiol* 24:194-200, 1994.
102. Beauchesne LM, Connolly HM, Ammash NM, et al: Coarctation of the aorta: outcome of pregnancy. *J Am Coll Cardiol* 38:1728-1733, 2001.
103. Krieger EV, Landsberg MJ, Economy KE, et al: Comparison of risk of hypertensive complications of pregnancy among women with versus without coarctation of the aorta. *Am J Cardiol* 107:1529-1534, 2011.
104. Therrien J, Thorne SA, Wright A, et al: Repaired coarctation: a cost-effective approach to identify complications in adults. *J Am Coll Cardiol* 35:997-1002, 2000.
105. Fontan F, Baudet E: Surgical repair of tricuspid atresia. *Thorax* 26:240-248, 1971.
106. Canobbio MM, Mair DD, van der Velde M, et al: Pregnancy outcomes after the Fontan repair. *J Am Coll Cardiol* 28:763-767, 1996.
107. Drenthen W, Pieper PG, Roos-Hesselink JW, et al: Pregnancy and delivery in women after Fontan palliation. *Heart* 92:1290-1294, 2006.
108. Drenthen, W, Pieper PG, Roos-Hesselink JW, et al: Pregnancy and delivery in women after Fontan palliation. *Heart*, 2006. DOI:10.1136/hrt.2005.085407.
109. Mustard WT: Progress in the total correction of complete transposition of the great vessels. *Vasc Dis* 3:177-179, 1966.
110. Senning A: Surgical treatment of transposition of the great vessels. *Mal Cardiovasc* 6:421-433, 1965.
111. Drenthen W, Pieper PG, Ploeg M, et al: Risk of complications during pregnancy after Senning or Mustard (atrial) repair of complete transposition of the great arteries. *Eur Heart J* 26:2588-2595, 2005.
112. Canobbi MM, Morris CD, Graham TP, Landzberg MJ: Pregnancy outcomes after atrial repair for transposition of the great arteries. *Am J Cardiol* 98:668-672, 2006.
113. Genoni M, Jenni R, Hoerstrup SP, et al: Pregnancy after atrial repair for transposition of the great arteries. *Heart* 81:276-277, 1999.
114. Rastelli GC, McGoon DC, Wallace RB: Anatomic correction of transposition of the great arteries with ventricular septal defect and subpulmonary stenosis. *J Thorac Cardiovasc Surg* 58:545-552, 1969.
115. Radford DJ, Stafford G: Pregnancy and the Rastelli operation. *Aust N Z J Obstet Gynaecol* 45:243-247, 2005.
116. Jatene AD, Fontes VF, Paulista PP, et al: Anatomic correction of transposition of the great vessels. *J Thorac Cardiovasc Surg* 72:364-370, 1976.
117. LeCompte Y, Zannini L, Hazan E, et al: Anatomic correction of the transposition of the great arteries. *J Thorac Cardiovasc Surg* 82:629-631, 1981.
118. Tobler D, Williams WG, Jegatheeswaran A, et al: Cardiac outcomes in young adult survivors of the arterial switch operation for transposition of the great arteries. *J Am Coll Cardiol* 56:58-64, 2010.
119. Ploeg M, Drenthen W, van Dijk A, et al: Successful pregnancy after an arterial switch procedure for complete transposition of the great arteries. *BJOG* 113:243-244, 2006.
120. Presbitero P, Somerville J, Stone S, et al: Pregnancy in cyanotic congenital heart disease. Outcome of mother and fetus. *Circulation* 89:2673-2676, 1994.
121. Yentis SM, Steer PJ, Plaat F: Eisenmenger's syndrome in pregnancy: maternal and fetal mortality in the 1990s. *Br J Obstet Gynaecol* 105:921-922, 1998.
122. Caruso A, de Carolis S, Ferrazzani S, et al: Pregnancy outcome in women with cardiac valve prosthesis. *Eur J Obstet Gynecol Reprod Biol* 54:7-11, 1994.
123. Connolly HM, Warnes CA: Outcome of pregnancy in patients with complex pulmonic valve atresia. *Am J Cardiol* 79:519-521, 1997.
124. Hameed AB, Goodwin TM, Elkayam U: Effect of pulmonary stenosis on pregnancy outcomes—a case-control study. *Am Heart J* 154:852-854, 2007.
125. Silversides CK, Colman JM, Sermer M, et al: Early and intermediate-term outcomes of pregnancy with congenital aortic stenosis. *Am J Cardiol* 91:1386-1389, 2003.
126. Lao TT, Sermer M, MaGee L, et al: Congenital aortic stenosis and pregnancy—a reappraisal. *Am J Obstet Gynecol* 169:540-545, 1993.
127. Horstkotte D, Loogen F: The natural history of aortic valve stenosis. *Eur Heart J* 9:57-64, 1988.
128. Easterling TR, Chadwick HS, Otto CM, Benedetti TJ: Aortic stenosis in pregnancy. *Obstet Gynecol* 72:113-118, 1988.
129. Lao TT, Adelman AG, Sermer M, et al: Balloon valvuloplasty for congenital aortic stenosis in pregnancy. *Br J Obstet Gynaecol* 100:1141-1142, 1993.
130. Brian JE Jr, Seifen AB, Clark RB, et al: Aortic stenosis, cesarean delivery, and epidural anesthesia. *J Clin Anesth* 5:154-157, 1993.
131. Sreeram N, Kitchiner D, Williams D, et al: Balloon dilatation of the aortic valve after previous surgical valvotomy: immediate and follow up results. *Br Heart J* 71:558-560, 1994.
132. Ben-Ami M, Battino S, Rosenfeld T, et al: Aortic valve replacement during pregnancy. A case report and review of the literature. *Acta Obstet Gynecol Scand* 69:651-653, 1990.
133. Tzemos N, Silversides CK, Colman JM, et al: Late cardiac outcomes after pregnancy in women with congenital aortic stenosis. *Am Heart J* 157:474-480, 2009.
134. Tzemos N, Silversides CK, Carasso S, et al: Effect of pregnancy on left ventricular motion (twist) in women with aortic stenosis. *Am J Cardiol* 101:870-873, 2008.
135. al Kasab SM, Sabag T, al Zaibag M, et al: Beta-adrenergic receptor blockade in the management of pregnant women with mitral stenosis. *Am J Obstet Gynecol* 163:37-40, 1990.
136. Ben Farhat M, Gamra H, Betbout F, et al: Percutaneous balloon mitral commissurotomy during pregnancy. *Heart* 77:564-567, 1997.
137. Gupta A, Lokhandwala YY, Satoskar PR, et al: Balloon mitral valvotomy in pregnancy: maternal and fetal outcomes. *J Am Coll Surg* 187:409-415, 1998.
138. Mangione JA, Lourenco RM, dos Santos ES, et al: Long-term follow-up of pregnant women after percutaneous mitral valvuloplasty. *Catheter Cardiovasc Interv* 50:413-417, 2000.
139. Ribeiro PA, Fawzy ME, Awad M, et al: Balloon valvotomy for pregnant patients with severe pliable mitral stenosis using the Inoue technique with total abdominal and pelvic shielding. *Am Heart J* 124:1558-1562, 1992.
140. Stoddard MF, Longaker RA, Vuocolo LM, et al: Transesophageal echocardiography in the pregnant patient. *Am Heart J* 124:785-787, 1992.
141. Pavankumar P, Venugopal P, Kaul U, et al: Pregnancy in patients with prosthetic cardiac valve. A 10-year experience. *Scand J Thorac Cardiovasc Surg* 22:19-22, 1988.
142. Sbarouni E, Oakley CM: Outcome of pregnancy in women with valve prostheses. *Br Heart J* 71:196-201, 1994.
143. Johnson JW, Longmate JA, Frentzen B: Excessive maternal weight and pregnancy outcome. *Am J Obstet Gynecol* 167:353-370; discussion 370-352, 1992.
144. Badduke BR, Jamieson WR, Miyagishima RT, et al: Pregnancy and childbearing in a population with biologic valvular prostheses. *J Thorac Cardiovasc Surg* 102:179-186, 1991.
145. Waller BF: *Pathology of the heart and great vessels*, New York, 1988, Churchill Livingstone.
146. Yinon Y, Siu SC, Warshafsky C, et al: Use of low molecular weight heparin in pregnant women with mechanical heart valves. *Am J Cardiol* 104:1259-1263, 2009.
147. McLintock C, McCowan LM, North RA: Maternal complications and pregnancy outcome in women with mechanical prosthetic

heart valves treated with enoxaparin. *BJOG* 116:1585-1592, 2009.
148. Lee CN, Wu CC, Lin PY, et al: Pregnancy following cardiac prosthetic valve replacement. *Obstet Gynecol* 83:353-356, 1994.
149. Salazar E, Espinola N, Roman L, et al: Effect of pregnancy on the duration of bovine pericardial bioprostheses. *Am Heart J* 137:714-720, 1999.
150. Dore A, Somerville J: Pregnancy in patients with pulmonary autograft valve replacement. *Eur Heart J* 18:1659-1662, 1997.
151. Rokey R, Hsu HW, Moise KJ Jr, et al: Inaccurate noninvasive mitral valve area calculation during pregnancy. *Obstet Gynecol* 84:950-955, 1994.
152. Homans DC: Peripartum cardiomyopathy. *N Engl J Med* 312:1432-1437, 1985.
153. Mabie WC, Hackman BB, Sibai BM: Pulmonary edema associated with pregnancy: echocardiographic insights and implications for treatment. *Obstet Gynecol* 81:227-234, 1993.
154. Nwosu EC, Burke MF: Cardiomyopathy of pregnancy. *Br J Obstet Gynaecol* 100:1145-1147, 1993.
155. Demakis JG, Rahimtoola SH: Peripartum cardiomyopathy. *Circulation* 44:964-968, 1971.
156. Hibbard JU, Lindheimer M, Lang RM: A modified definition for peripartum cardiomyopathy and prognosis based on echocardiography. *Obstetr Gynecol* 94:311-316, 1999.
157. Elkayam U, Tummala PP, Rao K, et al: Maternal and fetal outcomes of subsequent pregnancies in women with peripartum cardiomyopathy. *N Engl J Med* 344:1567-1571, 2001.
158. Habli M, O'Brien T, Nowack E, et al: Peripartum cardiomyopathy: prognostic factors for long-term maternal outcome. *Am J Obstet Gynecol* 199:415 e1-e5, 2008.
159. Grewal J, Siu SC, Ross HJ, et al: Pregnancy outcomes in women with dilated cardiomyopathy. *J Am Coll Cardiol* 55:45-52, 2009.
160. Carvalho AC, Almeida D, Cohen M, et al: Successful pregnancy, delivery and puerperium in a heart transplant patient with previous peripartum cardiomyopathy. *Eur Heart J* 13:1589-1591, 1992.
161. Scott JR, Wagoner LE, Olsen SL, et al: Pregnancy in heart transplant recipients: management and outcome. *Obstet Gynecol* 82:324-327, 1993.
162. Cowan SW, Coscia LC, Philips LZ, et al: Pregnancy outcomes in female heart and heart-lung transplant recipients. *Transplant Proceed* 34:1855-1856, 2002.
163. Chow SL: Acute aortic dissection in a patient with Marfan's syndrome complicated by gestational hypertension. *Med J Aust* 159:760-762, 1993.
164. Pyeritz RE: Maternal and fetal complications of pregnancy in the Marfan syndrome. *Am J Med* 71:784-790, 1981.
165. Pyeritz RE: The Marfan syndrome. *Am Fam Physician* 34:83-94, 1986.
166. Rosenblum NG, Grossman AR, Gabbe SG, et al: Failure of serial echocardiographic studies to predict aortic dissection in a pregnant patient with Marfan's syndrome. *Am J Obstet Gynecol* 146:470-471, 1983.
167. Immer FF, Bansi AG, Immer-Bansi AS, et al: Aortic dissection in pregnancy: analysis of risk factors and outcome. *Ann Thorac Surg* 76:309-314, 2003.
168. Lind J, Wallenburg HCS: The Marfan syndrome and pregnancy: a retrospective study in a Dutch population. *Eur J Obstet Gynecol Reprod Biol* 98:28-35, 2001.
169. Meijboom LJ, Drenthen W, Pieper PG, et al: Obstetric complications in Marfan syndrome. *Int J Cardiol* 110:53-59, 2006.
170. Lipscomb KJ, Smith JC, Clarke B, et al: Outcome of pregnancy in women with Marfan's syndrome. *Br J Obstet Gynaecol* 104: 201-206, 1997.
171. Legget ME, Unger TA, O'Sullivan CK, et al: Aortic root complications in Marfan's syndrome: identification of a lower risk group. *Heart* 75:389-395, 1996.
172. Mayet J, Steer P, Somerville J: Marfan syndrome, aortic dilatation, and pregnancy. *Obstet Gynecol* 92:713, 1998.
173. Treasure T: Elective replacement of the aortic root in Marfan's syndrome. *Br Heart J* 69:101-103, 1993.
174. Gott VL, Greene PS, Alejo DE, et al: Replacement of the aortic root in patients with Marfan's syndrome. *N Engl J Med* 340:1307-1313, 1999.
175. Pereira L, Levran O, Ramirez F, et al: A molecular approach to the stratification of cardiovascular risk in families with Marfan's syndrome. *N Engl J Med* 331:148-153, 1994.
176. Shores J, Berger KR, Murphy EA, et al: Progression of aortic dilatation and the benefit of long-term beta-adrenergic blockade in Marfan's syndrome. *N Engl J Med* 330:1335-1341, 1994.
177. Roman MJ, Rosen SE, Kramer-Fox R, et al: Prognostic significance of the pattern of aortic root dilation in the Marfan syndrome. *J Am Coll Cardiol* 22:1470-1476, 1993.
178. Gordon CF 3rd, Johnson MD: Anesthetic management of the pregnant patient with Marfan syndrome. *J Clin Anesth* 5:248-251, 1993.
179. Cola LM, Lavin JP Jr: Pregnancy complicated by Marfan's syndrome with aortic arch dissection, subsequent aortic arch replacement and triple coronary artery bypass grafts. *J Reprod Med* 30:685-688, 1985.
180. The Practice Committee of the American Society for Reproductive Medicine: Increased maternal cardiovascular mortality associated with pregnancy in women with Turner syndrome. *Fertil Steril* 83:1074-1075, 2005.
181. Snir E, Levinsky L, Salomon J, et al: Dissecting aortic aneurysm in pregnant women without Marfan disease. *Surg Gynecol Obstet* 167:463-465, 1988.
182. Petitti DB, Sidney S, Quesenberry CP Jr, et al: Incidence of stroke and myocardial infarction in women of reproductive age. *Stroke* 28:280-283, 1997.
183. James AH, Jamison MG, Biswas MS, et al: Acute myocardial infarction in pregnancy: a United States population-based study. *Circulation* 113:1564-1571, 2006.
184. Sullebarger JT, Fontanet HL, Matar FA, et al: Percutaneous coronary intervention for myocardial infarction during pregnancy: a new trend? *J Invasive Cardiol* 15:725-728, 2003.
185. Kuklina EV, Callaghan WM: Cardiomyopathy and other myocardial disorders among hospitalizations for pregnancy in the United States: 2004-2006. *Obstet Gynecol* 115:93-100, 2010.
186. Shivvers SA, Wians FH Jr, Keffer JH, et al: Maternal cardiac troponin I levels during normal labor and delivery. *Am J Obstet Gynecol* 180:122, 1999.
187. Ascarelli MH, Grider AR, Hsu HW: Acute myocardial infarction during pregnancy managed with immediate percutaneous transluminal coronary angioplasty. *Obstet Gynecol* 88:655-657, 1996.
188. Dwyer BK, Taylor L, Fuller A, et al: Percutaneous transluminal coronary angioplasty and stent placement in pregnancy. *Obstet Gynecol* 106:1162-1164, 2005.
189. Kultursay H, Turkoglu C, Akin M, et al: Mitral balloon valvuloplasty with transesophageal echocardiography without using fluoroscopy. *Cathet Cardiovasc Diagn* 27:317-321, 1992.
190. Carvalho A, Brandao A, Martinez EE, et al: Prognosis in peripartum cardiomyopathy. *Am J Cardiol* 64:540-542, 1989.
191. Mishra M, Chambers JB, Jackson G: Murmurs in pregnancy: an audit of echocardiography. *Bmj* 304:1413-1414, 1992.
192. Rayburn WF, LeMire MS, Bird JL, et al: Mitral valve prolapse. Echocardiographic changes during pregnancy. *J Reprod Med* 32:185-187, 1987.
193. Carvalho JS, Redington AN, Shinebourne EA, et al: Continuous wave Doppler echocardiography and coarctation of the aorta: gradients and flow patterns in the assessment of severity. *Br Heart J* 64:133-137, 1990.
194. Tan JL, Babu-Narayan SV, Henein MY, et al: Doppler echocardiographic profile and indexes in the evaluation of aortic coarctation in patients before and after stenting. *J Am Coll Cardiol* 46:1045-1053, 2005.



# Aortic Dissection and Trauma: Value and Limitations of Echocardiography

ANN F. BOLGER, MD

**Pathophysiology of Aortic Dissection**
Anatomy and Histology
Mechanical and Shear Stresses
Risk Factors
**Spectrum of Acute Aortic Syndromes**
Aortic Dissection
Intramural Hematoma
Penetrating Aortic Ulcer
Aortic Trauma
**Imaging Approaches to the Diagnosis of Acute Aortic Syndromes**
Transthoracic Echocardiography
Transesophageal Echocardiography
Computed Tomography
Magnetic Resonance Imaging
Choice of Imaging
**Transesophageal Echocardiography in Acute Aortic Syndromes**
Safety of Transesophageal Echocardiography
Diagnostic Features
Doppler Findings
Complications of Dissection
Inconclusive Transesophageal Echocardiographic Results
**Surgical Considerations**
Intraoperative Echocardiographic Monitoring
Aortic Regurgitation
Mitral Regurgitation
Perfusion of Distal Vascular Beds
**Endovascular Repair Considerations**
**Follow-up of Patients after Aortic Dissection**
Persistent Intimal Flaps
Progression of Disease
Pseudoaneurysm Formation
Recurrent Dissection
**Research Applications and Future Directions**
**Conclusions**

The mortality of acute type A aortic dissection escalates hourly,[1] reaching 50% by 48 hours. Immediate diagnosis and therapy are critical for survival. Two thousand new cases of acute dissection are reported in the United States per year[2]; the true incidence, including the large numbers of patients who die from unrecognized dissection, has been estimated at more than 10,000 per year.[3] Further, 10% to 30% of acute dissections occurring in the hospital may be misdiagnosed. It is a great clinical challenge that patients' presenting symptoms may be nonspecific or even misleading. Aortic dissection must be included in the differential diagnosis of chest pain in many patients at risk for dissection, and also when simultaneous acute involvement of multiple organ systems does not have a ready explanation.

Acute dissection of the aorta can create myocardial ischemia via compromise of the coronary arteries; Hirst and colleagues[4] found involvement of the coronary arteries on pathologic examination in 39 of 505 cases of acute dissection (7.7%). Many clinical signs of that coronary impairment are also seen in acute myocardial infarction due to acute coronary syndrome: pain (related to the dissection itself or to myocardial ischemia), electrocardiographic abnormalities consistent with ischemia (resulting from involvement of the coronary ostia in proximal dissection),[5] and elevated serum creatinine kinase levels.[6] Confusion of acute dissection with myocardial infarction not only delays appropriate treatment, but increases the risk of disastrous consequences from thrombolytics, aggressive antiplatelet regimens, or passage of coronary catheters in the course of left heart catheterization.[7] Given that the incidence of aortic dissection is far less than that of myocardial infarction and that ST segment elevation is a relatively rare finding in patients with aortic dissection, electrocardiographic changes without physical findings suggesting dissection will rarely mislead clinicians.[8] Maintenance of a high suspicion for dissection must be paired with highly reliable tests to avoid such infrequent but catastrophic misdiagnoses.

The optimal diagnostic test for acute aortic dissection, therefore, must be accurate, safe, and immediately applicable in a broad range of medical environments. The limited sensitivity of echocardiography for dissection from the transthoracic approach has been greatly improved by transesophageal echocardiography (TEE). Transesophageal examinations can be performed within minutes in the emergency department, operating room, or intensive care unit and provide high-quality images of the thoracic aorta as well as of other cardiac and vascular structures at risk. Time to transesophageal images often exceeds the time required for emergent computed tomography (CT) scanning in emergency departments, however, and the role of TEE in the immediate diagnosis of acute aortic syndromes has diminished. The specific advantages and limitations of TEE use in the management of patients with suspected aortic dissection or trauma have been carefully investigated at many centers and have refined TEE's ongoing role in the diagnosis, repair, and follow-up of acute aortic syndromes and trauma.

## Pathophysiology of Aortic Dissection

### ANATOMY AND HISTOLOGY

The diameter of the adult aorta tapers from a size of less than 2.1 cm/$m^2$ in the ascending aorta to less than 1.6 cm/ $m^2$ at the level of the aortic arch.[9] The size of aorta increases with age during adulthood at a rate of 1 to 2 mm/ year; aging is associated with a loss of compliance and increased wall stiffness.

The aortic wall comprises three layers: the intima, which is a single layer of vascular endothelium; the media, with concentric layers of smooth muscle cells, collagen, elastin, and extracellular matrix proteoglycans; and the peripheral adventitia, consisting of loose connective tissue that anchors the aorta in surrounding tissues. The vasa vasorum, which perfuse the aortic wall, are contained within the adventitia. Of the three layers of the aortic wall, the structure of the media dominates the wall's mechanical properties.[10] Medial smooth muscle directly influences wall stiffness by contraction. In addition, smooth muscle cells are the major source of the extracellular matrix components. These include the elastin fibers, which can be stretched to 300% of their resting length without rupturing[11] and are important contributors to the normal pulsatile behavior of the vessel. Elastin is less important to the overall strength of the aorta than collagen, however, which is both stiffer and much stronger than elastin.

The components of the media vary from vessel to vessel and change with age. In the aortas of older patients, the elastin content decreases and collagen increases, resulting in increased vascular stiffness.[12] The mechanical properties of the vasculature are also almost always disturbed in cases of systemic hypertension.[13]

### MECHANICAL AND SHEAR STRESSES

The aortic wall is subjected to mechanical stresses of several forms. Stress, which is expressed as force per unit area, may occur in radial, circumferential, or longitudinal directions. The normal intima bears little of the aorta's stress load. It is exposed to shear stresses, however, which are forces applied parallel to the vessel wall as a result of the viscous effects of blood flow. The amount of these shear stresses varies with the distribution of velocity across the vessel lumen and with local vessel geometry.

Circumferential stress predominantly affects the media. This type of stress ($\delta$) increases with the radial pressure from the aortic lumen (P) and the aortic radius (r) and decreases with increasing wall thickness (h):

$$\delta = Pr/2\,h$$

The danger of aortic dilation can therefore be understood: In dilated, thin-walled aortas, the circumferential stresses may be increased many times above normal. In addition, the geometry of the dilating aorta changes progressively from the normal cylinder to an ellipsoidal or even spherical shape. This slowly increases the circumferential stress but quickly exacerbates longitudinal stress. Most atraumatic aortic tears are caused by longitudinal stress, which explains why they are generally transverse in orientation.[14] The ascending aorta experiences additional longitudinal stress owing to the motion of the aortic annulus. Finally, dilated or aneurysmal vessels demonstrate marked stiffness, in part because of loss of elastin.[15] Combined aortic dilation, wall thinning, and shape change sets the stage for intimal rupture and the initiation of dissection.

Intimal and/or medial abnormalities of the aorta increase the resistance to both shear and circumferential stresses. Stress failures of both types may play a role in aortic dissection. Circumferential stress failure can occur when the stresses caused by intraluminal pressure are greatly magnified in the thin fibrous cap of an atheromatous lesion. If the lesion fractures and a small crack develops, the circumferential stress will cause it to extend through the wall.[10] Shear stress failure is due to inhomogeneity in the properties of the vessel wall. Even under normal conditions, mural stresses are greater on the inner than on the outer wall.[16] In the presence of atherosclerosis, incremental variations in the shear resistance between contiguous regions of diseased and normal wall occur. The progression of aortic dissection probably represents an example of shear failure, where the interface between two such aortic segments with different stiffness leads to separation of medial and intimal layers: the two layers slide relative to one another because the "glue" of the extracellular matrix cannot withstand the shear stress.[10]

Once initiated, dissections behave like a two-ply tube. The intima and the internal elastic lamina of the media form the inner layer, while the outer layer consists of the external elastic lamina and the adventitia. A velocity-dependent shear force will then further separate the two layers, creating a false lumen separated from the true lumen by the intima and internal elastic lamina (Fig. 36-1). Experimentally, it has been demonstrated that the work per unit area of tissue required to propagate a tear in the aorta is small ($15.9 \pm 0.9$ mJ $cm^{-2}$) and independent of the depth of the tear.[16]

Increasing recognition of intramural hematoma as one of the acute aortic syndromes has expanded our understanding of the precursors of dissection. In the case of hematoma formation, the inciting event is hemorrhage into the media from the vasa vasorum. This lesion may expand and rupture into the aortic lumen, creating what we recognize as an entry tear and allowing progression of the intimal detachment along the arterial tree. In other cases, the hematoma is contained but creates a risk of external rupture.

These concepts of shear and tensile failure are the basis for understanding why different patient populations are at increased

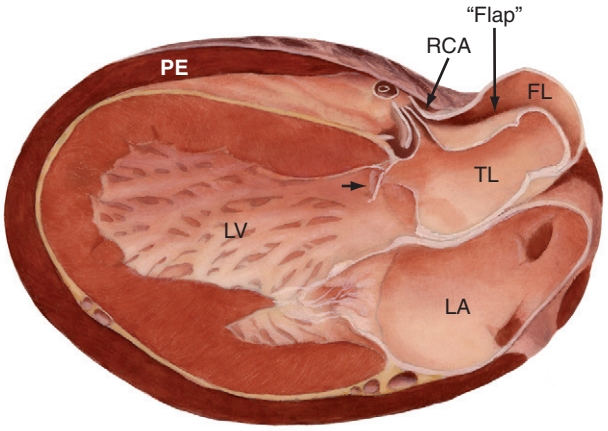



**Figure 36-1 Complications of aortic dissection.** The intimal flap is seen in the ascending aorta separating the true lumen (*TL*) from the false lumen (*FL*). The flap may extend into the right coronary artery (*RCA*), resulting in myocardial ischemia; may rupture into the pericardial space with a hemorrhagic pericardial effusion (*PE*) and tamponade physiology; or may disrupt the valve leaflet attachment with a flail leaflet (*small arrow*) and aortic regurgitation.

risk for aortic dissection. Medial elastic tissue degeneration resulting from hereditary defects of the arterial wall creates the substrate for dissection in patients with Marfan syndrome, Turner syndrome,[17] Noonan disease, Ehlers-Danlos syndrome, and osteogenesis imperfecta.[14,18] In these patients, as well as in other groups, dilation of the aorta is an important source of tensile failure and a precursor to dissection.

Both wall abnormalities (shear failure) and increased wall stress (tensile failure) owing to dilation are important in nonhereditary risk groups. Dissection occurring in hypertensive patients is generally based on high blood pressure, moderate aortic dilation, and medial muscular degeneration predisposing the internal layer to tear.[14] The contribution of shear stress in those patients is infrequent and unpredictable.

## RISK FACTORS

Hypertension and atherosclerosis are the predominant conditions that result in dissection. More infrequently, pregnancy, inflammatory disorders such as giant cell arteritis and Takayasu disease, or congenital collagen disorders such as Marfan syndrome, Turner syndrome, or Ehlers-Danlos are etiologic. Bicuspid aortic valve and/or aortic coarctation are other congenital causes.

Cocaine use, trauma, and iatrogenic disruption of the arterial structures during surgery or cardiac catheterization can also be the initiator (Box 36-1).[19-25]

### *Atherosclerosis*

Atherosclerosis is a highly prevalent disorder whose generalized and focal manifestations can predispose to dissection. True aortic aneurysms are due to atherosclerotic degeneration of the media and progress to involve all three layers of the vessel wall and to gradual dilation. Increasing risk accompanies enlarged diameters, rapid expansion, or symptoms. Formation of laminar thrombus within the aneurysm does not decrease the wall stress. The 1-year survival rate in patients with thoracic aortic aneurysms is less than 60%, and the 5-year survival rate approximately 20%. Up to 14% of patients presenting with dissection in the International Registry of Acute Aortic Dissection had preexisting aortic aneurysm.[26]

### *Trauma*

Trauma may create a spectrum of aortic injuries (see later discussion). Aortic dissection may occur in external, accidental trauma and be difficult to assess in the setting of major multisystem injuries. The region most prone to traumatic injury is the aortic isthmus, where relative tethering by the spinal arteries and ligamentum arteriosum resists abrupt deceleration more than the more mobile transverse arch.[27] Other vulnerable sites include the origin of the right brachiocephalic artery, particularly with vertical forces from falls, and the ascending aorta above the sinus of Valsalva.[28] Traumatic injuries to the aorta may result in intimal tears, recognizable on TEE as mobile flaps. Thrombus may be seen protruding into the lumen; in other cases, intramural hematoma without apparent intimal discontinuity is seen. Whereas very minor lesions such as minimal hematomas may regress spontaneously, the prognosis of significant aortic trauma is grave. Without repair, there is 30% mortality within the first 24 hours. Within 1 week, mortality is greater than 50%.[29] Prompt recognition is therefore critical to patient outcome. TEE has been shown to be safe and highly sensitive for aortic trauma after motor vehicle accidents, equivalent to angiography and more expeditiously applied.[30] TEE may also detect other signs of cardiac trauma, including wall motion abnormalities, pericardial effusion, and valvular regurgitation. When the suspicion of aortic rupture in the territory of the transverse arch remains high, CT may provide better images of those territories.

Other sources of trauma include the Heimlich maneuver for respiratory obstruction, and cardiovascular procedures. Operative sources of tears in the aorta include cannulation sites for cardiopulmonary bypass, aortic transections for valve or aortic segment replacement, and proximal anastomotic sites for coronary bypass grafts.[31,32] Very uncommonly, aortic catheterization for angiography may traumatize an atherosclerotic region and

**Box 36-1**

**PATIENT POPULATIONS AT RISK FOR AORTIC DISSECTION**

**Genetic Disorders (Medial Abnormalities)**
Marfan syndrome
Turner syndrome
Noonan disease
Ehlers-Danlos syndrome
Osteogenesis imperfecta

**Congenital Disorders**
Aortic coarctation
Unicuspid or bicuspid aortic valve

**Degenerative Disorders**
Hypertension
Atherosclerotic vascular disease
  Aortic ulcer
  Aortic aneurysm
Non–Marfan syndrome cystic medial necrosis

**Traumatic Causes**
Deceleration injury
Penetrating injury
Heimlich maneuver

**Postprocedural Causes**
Cardiac surgery
  Cannulation
  Cross-clamping
  Aortic valve replacement
Angioplasty
  Coronary
  Renal

**Inflammatory Disorders**
Syphilis
Giant cell arteritis

**Other Conditions**
Pregnancy
Weightlifting
Cocaine use
Discontinuation of beta blockers
Polycystic kidney disease

prompt dissection.[33] Angioplasty procedures of coronary or renal vessels can also initiate the process.[34] A history of these procedures may be important in alerting the clinician to the possibility of dissection in these patients.

### *Cocaine and Methamphetamine*

Cocaine stimulates central neural sympathetic outflow and blocks reuptake of catecholamines in the synaptic clefts. The resulting intense vasoconstriction; prothrombosis; and increase in heart rate, blood pressure, and myocardial contractility increase the risk of aortic dissection. In one series, 14 of 38 cases of aortic dissection were associated with cocaine use during the preceding 24 hours (average, 2 hours). The proportion of types A and B dissection was similar to than in nonusers of cocaine.[35] Methamphetamine use is increasing, and users may also experience a significant increase in their risk for acute aortic dissection. One retrospective series found that 20% of acute aortic dissections in patients under age 50 years were associated with methamphetamine.[36]

### *Pregnancy*

Although aortic dissection is mostly a disease of middle-aged or elderly males, women and children can also experience dissection. It has been claimed that half of all aortic dissections occurring in women younger than 40 years of age are associated with pregnancy, particularly during the third trimester, or the postpartum period.[37-39] This has been disputed by Oskoui and Lindsay,[40] who reviewed their own experience and published a series of 1253 dissections in consecutive patients (868 males and 385 females), with no cases occurring in pregnancy. They concluded that most women experiencing aortic dissection in pregnancy had other risk factors such as hypertension or Marfan syndrome, and that the apparent association could result from selective reporting and coincidental occurrence of dissection with the very common condition of pregnancy.

The most up-to-date information on acute aortic dissection in women from the International Registry of Acute Aortic Dissection implies that dissection generally affects women at a more advanced age than men and that they fare worse than their male counterparts with respect to rupture, hypotension, and surgical mortality.[26]

### *Genetic Diseases*

#### Marfan Syndrome

Of the genetic causes of aortic medial disease and aortic dissection, Marfan syndrome is the most common and best studied. Although a clinical diagnosis, Marfan syndrome may be confirmed by linkage to the dominantly inherited gene MFS-1 on 15q21 or by determination of the specific family mutation.[41] Histologic examination of the aortic wall in Marfan syndrome patients reveals fragmentation of aortic components, especially the elastic fibers,[42] and abnormal accumulation of collagenous and mucoid materials in the media.[43] Fragmentation of elastin-associated microfibrils also occurs in aortic valve leaflets.[44] The disruption and loss of elastic tissue of the media is attributed to a deficiency of fibrillin, a microfibrillar protein that scaffolds the elastic lamellae in the aortic wall.[45,46] These changes are greatest in the ascending aorta, which is subject to the greatest pulsatile expansion and therefore the highest stress in systole.[14] The alterations in aortic wall components are associated with abnormal functional properties: aortic elasticity is abnormal in patients with Marfan syndrome, irrespective of the aortic diameter.[47] A comparative study of aortic wall dynamics between Marfan syndrome patients and normal controls confirmed that in both groups, stiffness of the wall increases with age and aortic diameter, but at all ages the Marfan syndrome group exhibits a stiffer aorta than controls for a given diameter.[48] Furthermore, Marfan syndrome patients have large ascending aortic diameters, but not abdominal aortic size, after correction for body surface area.[47] Dissection occurs in Marfan syndrome patients because of this dilation in combination with wall weakness; mural stress increases dramatically with increasing radius and becomes self-perpetuating.[14]

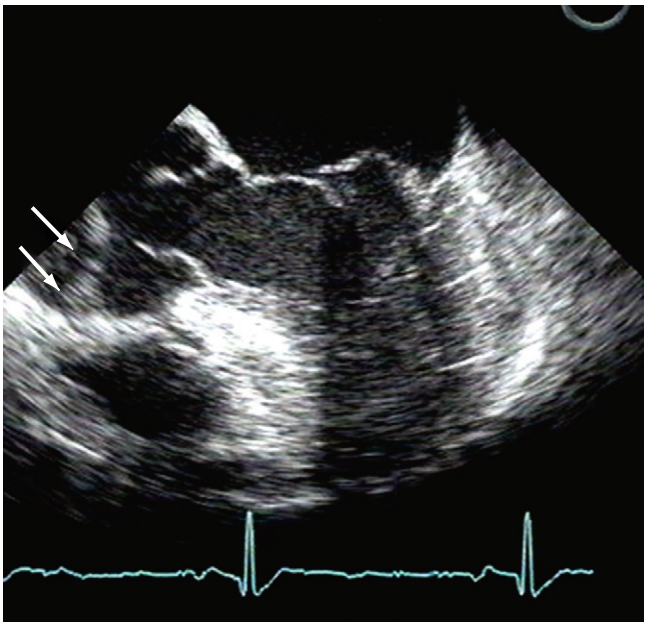


**Figure 36-2 Type A aortic dissection (*arrows* indicate intimal flap) in a patient with Marfan syndrome on transesophageal imaging.** Enlargement of the proximal aortic root and prolapse of the posterior mitral valve leaflet are also noted.

Echocardiographic evidence of aortic root dilation is present in 60% to 80% of Marfan syndrome patients (Fig. 36-2).[49] In one series, aortic dilation was generalized in 51% and localized in 28%.[50] Localized dilation did not appear to represent an earlier stage of aortic involvement, as the patient ages in both groups were identical, as was the duration of follow-up. It could not be determined whether generalized dilation reflected more severe underlying cystic medial necrosis from different specific mutations in fibrillin. Generalized dilation, however, was associated with higher rates of expansion as well as aortic regurgitation. In Marfan syndrome patients, aortic regurgitation has been associated with decreased survival.[25] The existence of mitral valve prolapse does not appear to be an independent predictor of outcome. The clinical course of Marfan syndrome patients with respect to progressive aortic dilation and dissection is variable.[50] Increased risk has been associated with older age,[51,52] male gender, aortic root diameters exceeding 60 mm,[50] aortic growth rate,[49,50] and a family history of dissection.[53] In one study, two groups of Marfan patients were identified according to the speed of their aortic root dilatation.[54] The speed of dilatation was not related to the use of beta blockers or the family history. The fast-growing group had significantly more type A dissection, as well as more elective root replacement, compared to subjects with slower dilatation. Of great

concern is the observation that aortic dissection can occur in Marfan syndrome patients even in the absence of aortic root dilation.[55]

Medical management of Marfan patients with aortic dilatation involves beta-blockers and observation of aortic root diameter to determine timing of elective surgery aimed at preventing aortic dissection. (See Chapter 39.) Long-term fatality rates are improved with prophylactic aortic root replacement; 5-year survival is approximately 97% for elective surgery versus only 51% with emergency surgery for dissection.[56] Operative mortality in experienced centers for elective surgery in Marfan patients is low (1.3% to 1.5% 30-day mortality versus 11.7% for emergency surgery).[57,58] In patients with normal aortic valve leaflets, elective aortic valve–sparing surgery may provide better clinical outcomes than aortic root replacement.[59] In this retrospective review, however, those undergoing aortic root replacement with aortic valve replacement had more cardiac comorbidities than the group in which valve-sparing surgery was possible. The size of aneurysm often determines the feasibility of valve-sparing surgery; hence, some centers recommend elective surgery when the aortic root reaches 50 mm.

### Bicuspid Aortic Valve

Bicuspid aortic valve is the most common congenital heart anomaly, with a prevalence of 1% to 2%. It has been estimated that patients with bicuspid valves have a ninefold increase in the risk of dissection compared to those with normal valves, and up to a 5% lifetime risk of dissection.[60] As with Marfan syndrome, aortic histology in bicuspid aortic valve patients demonstrates cystic medial necrosis, with significantly increased expression of metalloproteinase MMP2 and MMP9. It is important to remember that replacement of the malformed valve does not correct the patient's progressive aortic root dilatation or elevated dissection risk. Ascending aorta replacement is indicated when the aortic diameter exceeds 50 mm.[61]

### Turner Syndrome

The most common cause of aortic dissection in young women is Turner syndrome. This relatively common disorder is associated with short stature and congenital cardiovascular defects. These patients are at significantly increased risk for dissection at every age (1.4 in 100 patients with Turner syndrome, more than 100-fold increased from normal), but the risk appears highest during young adulthood and pregnancy.[62] The dissection risk is associated with ascending aortic dilation and is thought to be similar in etiology to the cystic medial necrosis of Marfan syndrome. Although bicuspid aortic valve and coarctation may also occur, their absence does not preclude dissection.[63]

### Familial Aortic Dissection

Twenty percent of patients with aortic dissection have a first-degree relative with a history of thoracic aneurysm or aortic aneurysm. The inherited risk for dissection appears to follow an autosomal dominant pattern, and surveillance of family members is warranted. [61]

## Spectrum of Acute Aortic Syndromes

It is now recognized that aortic dissection is part of a larger collection of acute aortic disorders (Box 36-2) which can share features of acuity, prognosis, treatment options, and etiology. Their separation is often temporal rather than etiologic: intramural hematoma and penetrating ulcer may progress to aortic dissection during their course.

**Box 36-2**

**ACUTE AORTIC SYNDROMES**

Aortic dissection
Intramural hematoma
Penetrating atherosclerotic ulcer
Traumatic aortic rupture

**TABLE 36-1 Nomenclature of Aortic Dissection**

| *Dissection Type* | *Classification* |
|---|---|
| Ascending aorta involved | Stanford type A<br>DeBakey I<br>DeBakey II<br>University of Alabama *ascending*<br>Massachusetts General Hospital *proximal* |
| Ascending aorta not involved | Stanford type B<br>DeBakey III<br>University of Alabama *descending*<br>Massachusetts General Hospital *distal* |

## AORTIC DISSECTION

Aortic dissection is defined by separation of the intima and internal media from the external media and adventitia of the aorta, with creation of an intimal flap that separates the true aortic lumen from a false lumen where active flow or thrombus can be seen. The etiologic event for dissection is a medial lesion that creates a hematoma in the aortic wall; a subsequent tear in the overlying tissue allows pulsatile aortic flow entry into the medial tissues. The primary entry tear is usually transverse and involves more than half of the circumference of the aorta. In 65% of cases it occurs within 3 cm of the coronary ostia. Ten percent of tears occur in the descending thoracic aorta and another 10% in the arch. Primary tears are rare in the abdominal aorta.[64] Whatever the location of the initial tear, dissections may progress distally, proximally, or occasionally in both directions.

### *Anatomic Classification*

There are several widely used classification systems for dissection (Table 36-1). The DeBakey classification divides dissections with involvement of the ascending aorta into type I, which extends into the transverse arch and distal aorta, and type II, which is confined to the ascending aorta. DeBakey type III dissections involve the descending aorta only.[65] The Stanford classification[66] was developed from a functional approach based on whether the ascending aorta is involved, regardless of the site of primary intimal tear and irrespective of the extent of distal propagation. This reflects clinical observations that the biologic behavior of the dissection, the clinical prognosis, and how the patient should be managed pivot almost exclusively on whether the ascending aorta is involved.[67-69] This system of nomenclature describes type A dissections as any with involvement of the ascending aorta (including DeBakey types I and II), and type B dissections as dissection limited to the descending aorta (DeBakey type III).

The clinical classification schemes just described do not emphasize the location of the primary entry tear or the extent of the distal propagation of the dissection. These two factors are

of less prognostic value and can be technically difficult to determine.[70,71] When identification of the entry site is possible, the culprit primary intimal tear is more easily resected. Although successful resection of the primary tear does not appear to affect early or late survival rates, it may decrease the incidence of late reoperation.[72]

Some cases of aortic dissection will present with multiple *primary* tears. Two separate dissections in the same patient may be more common than previously reported. Roberts and Roberts[73] reported that 3 of 40 necropsy patients had separate proximal and distal thoracic dissections. Although all fatal events were caused by rupture of the acute proximal dissections, a separate distal dissection may still pose a risk for late complications, and therefore recognizing two separate dissections may have important implications regarding follow-up and therapy.[74] Multiple distal *exit* tears, which decompress the false lumen, are extremely common.

### *Time Course*

Dissections are also differentiated with respect to their time course. Acute dissections are detected within 14 days of the onset of initial symptoms. Chronic dissections present more than 2 weeks after onset.[69,75] This division is arbitrary; it may primarily reflect the fact that the majority of type A dissection patients will die within 2 weeks if untreated. Chronic dissections may be detected because of symptoms or may be an incidental finding. They are differentiated from aortic aneurysms by the presence of an intimal flap and false lumen. These may not be easy to recognize when the false lumen is largely thrombosed. Pronounced atherosclerotic changes may be present in the false lumen in chronic dissections, even when the true lumen walls appear normal and hyperlipidemia is absent.[76]

### *Sequelae*

The sequelae of aortic dissection are many and varied. Obstruction of branch vessels may explain acute myocardial ischemia and infarction of cerebral, spinal, bowel, and renal territories. Aortic valve dehiscence with regurgitation, cardiac tamponade from retrograde extension into the pericardium, and frank aortic rupture are all highly morbid consequences.

## INTRAMURAL HEMATOMA

A small number of aortic dissections, estimated at 3% to 5%, occur without apparent intimal disruption.[6,77] The pathologic process in these cases of aortic intramural hematoma is rupture of the vasa vasorum into a region of medial degeneration, or possibly rupture of atherosclerotic plaque without an intimal tear. Patients with this form of disease tend to be older (mean age 70 years, versus 56 years for communicating dissection) and have frequently had long-term hypertension.

The clinical course of aortic intramural hematoma is similar to that of aortic dissection, with a high incidence of aortic dilation due to expansion of the false lumen, pleural and pericardial effusions, aortic regurgitation, aortic rupture, and progression to classical dissection. The early prognosis in aortic intramural hematoma patients may be slightly better than in those with acute "communicating" dissections; this may reflect the tendency for the noncommunicating medial space to heal with complete thrombus formation.[78] Many aortic intramural hematomas progress to typical dissection (in 33%) or to rupture (in 27%), however, and therefore usually require surgical rather than medical management.[79]

About half of patients progress despite medical treatment. Predictors of disease progression include involvement of the ascending aorta, a maximum aortic diameter of 50 mm or more, persistent pain, progressive thickening of the aortic wall, or expanding aortic diameter. The treatment of aortic intramural hematoma is similar to that of aortic dissection. If the aortic intramural hematoma is located in the ascending aorta, early surgical intervention with aortic graft replacement is often recommended. Mortality after surgery ranges from 10% to 50% at 30 days.[80,81,82] Another strategy that has been advocated is initial medical therapy with aggressive antihypertensive treatment and frequent imaging follow-up, with elective surgery for patients who develop complications.[83]

Early prognosis in those patients was somewhat better than in those with acute *communicating* dissections; this may reflect the tendency for the noncommunicating medial space to heal with complete thrombus formation.[84] These intramural hematomas may progress to typical dissection (in 33%) or to rupture (in 27%) and therefore usually require surgical rather than medical management.[79]

## PENETRATING AORTIC ULCER

Ulceration of an atheromatous plaque into the internal elastic lamina of the aorta creates a penetrating atheromatous ulcer.[85] Patients with such ulcers are typically older and have more cardiovascular risk factors and diffuse atherosclerosis. The ulcers are predominately located in the descending aorta, where atherosclerosis tends to be more severe. They can progress to aneurysm formation, intramural hematoma, dissection, or rupture. Controversy remains regarding medical versus surgical therapy for these lesions.[86,87]

## AORTIC TRAUMA

The intrathoracic aorta may be injured during penetrating or blunt trauma, particularly episodes that involve high-energy and/or marked deceleration, such as falls from over 10 feet or motor vehicle crashes at speeds over 40 miles per hour. The site most often affected is the aortic isthmus. The mechanism of injury is primarily rupture of the adventitia. This creates a high risk of lethal hemorrhage, which occurs in nearly 80% of blunt aortic injuries. In some cases mediastinal structures temporarily contain the rupture, but these will almost all rupture within 24 hours if untreated.[88,89]

Contrast-enhanced spiral CT of the chest is usually obtained early in trauma resuscitations. Its accuracy in diagnosis and exclusion of aortic injury generally places it ahead of TEE as an emergent modality. TEE is contraindicated with unstable injuries of the cervical spine or in the setting of suspected esophageal injury. TEE more often is applied in the operating room and during the intensive care unit course, where it can be performed serially if necessary.

TEE in patients with traumatic rupture of the aortic subadventitia will demonstrate flow on both sides of the wall. [90] The flap that is seen on TEE comprises the intima and media in separation from the adventitia. It may be limited to a few centimeters only, in contrast to the intimal flap of dissection which can extend longer distances in both directions.

Other aortic manifestations of trauma include dissection, intramural hematoma, and thrombus formation. False aneurysm originating at the site of the rupture may be seen.[90,91] Mediastinal hematomas can also be recognized[92,93] by noting an

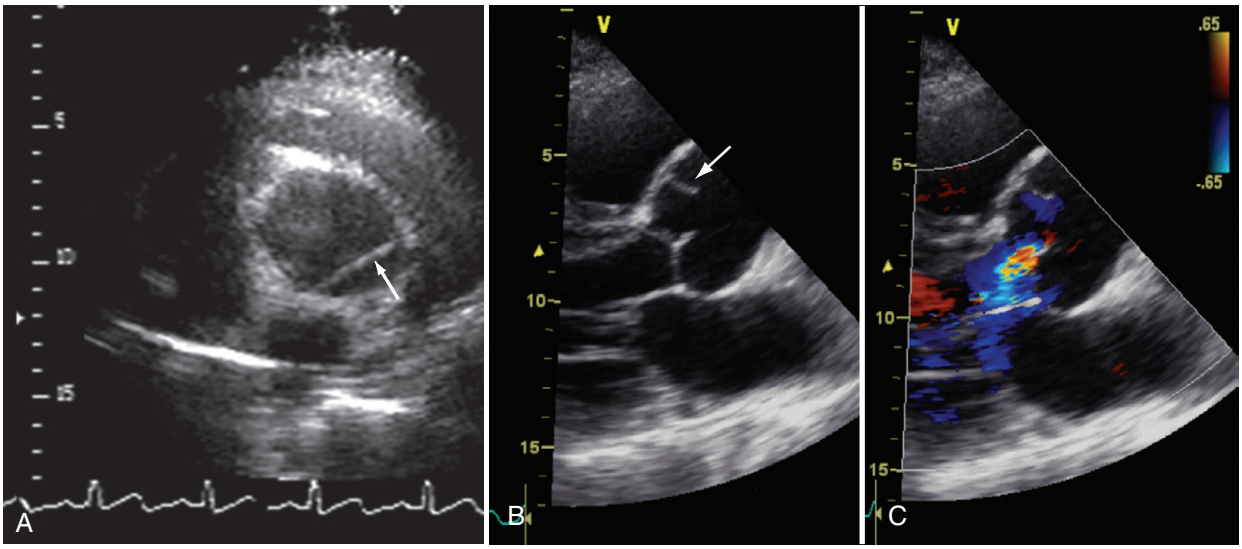



**Figure 36-3 Conventional transthoracic views are often the first clue to diagnosis of aortic dissection.** Parasternal short-axis views (**A**) demonstrate intimal flap in proximal aortic root (*arrow*). Long-axis views show the mobile flap (**B**) as well as the associated aortic regurgitation (**C**).

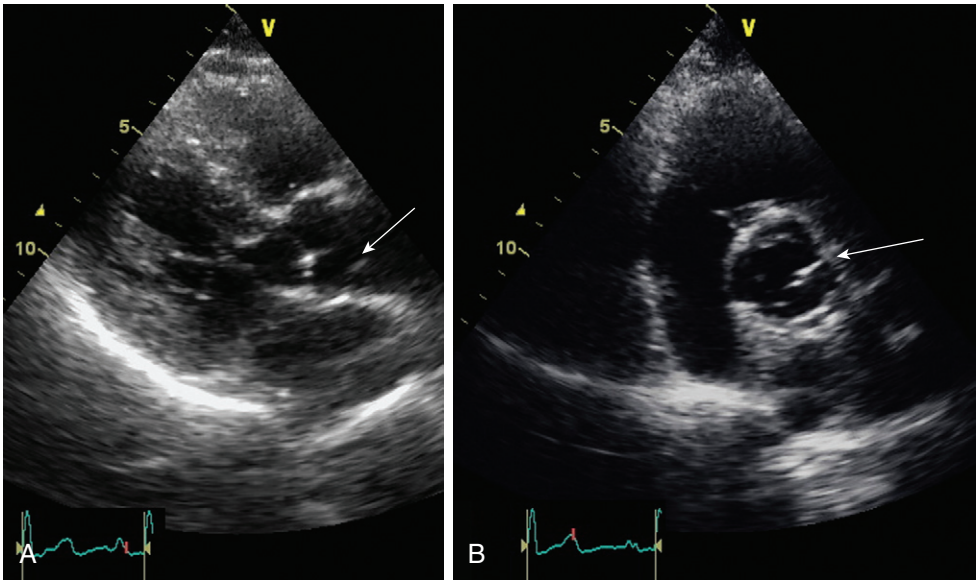



**Figure 36-4 Recognition of aortic dissection from transthoracic views often requires a high level of suspicion.** Linear structure near the posterior sinotubular ridge might be an artifact (**A,** *arrow*) but is more clearly seen on short-axis views (**B**). These inconclusive findings in a patient with clinical features of dissection merit clear communication to other care providers and rapid progression to another modality such as computed tomography or TEE. This patient had a type A dissection.

increased distance from the TEE probe face and the aortic lumen.

## Imaging Approaches to the Diagnosis of Acute Aortic Syndromes

### TRANSTHORACIC ECHOCARDIOGRAPHY

Time is of the essence when aortic dissection is suspected. Most emergency departments have ultrasound equipment that can be used by staff to quickly determine the presence of pericardial effusion using the standard FAST (Focused Assessment with Sonography for Trauma) examination. More expert users and dedicated echocardiography equipment can also be utilized to perform emergent transthoracic echocardiography (TTE) to rapidly define aortic valve competence, ventricular dysfunction, and regional wall motion abnormalities. Though these immediate scans are inherently restricted to available windows and have limited sensitivity, they can often provide the first images of mobile intimal flaps in the aortic root, arch or descending aorta (Figs. 36-3 through 36-6) that can guide earliest therapy and mobilize other resources.

### TRANSESOPHAGEAL ECHOCARDIOGRAPHY

The intrathoracic aorta is well visualized from esophageal windows (Fig. 36-7), with the exception of a well-recognized *blind spot* created by the interposition of the trachea between the esophagus and the heart, obscuring portions of the distal ascending aorta, superior transverse arch, and origins of the great vessels. As a result, a dissection limited to these areas could be missed by transesophageal imaging alone. This is of concern

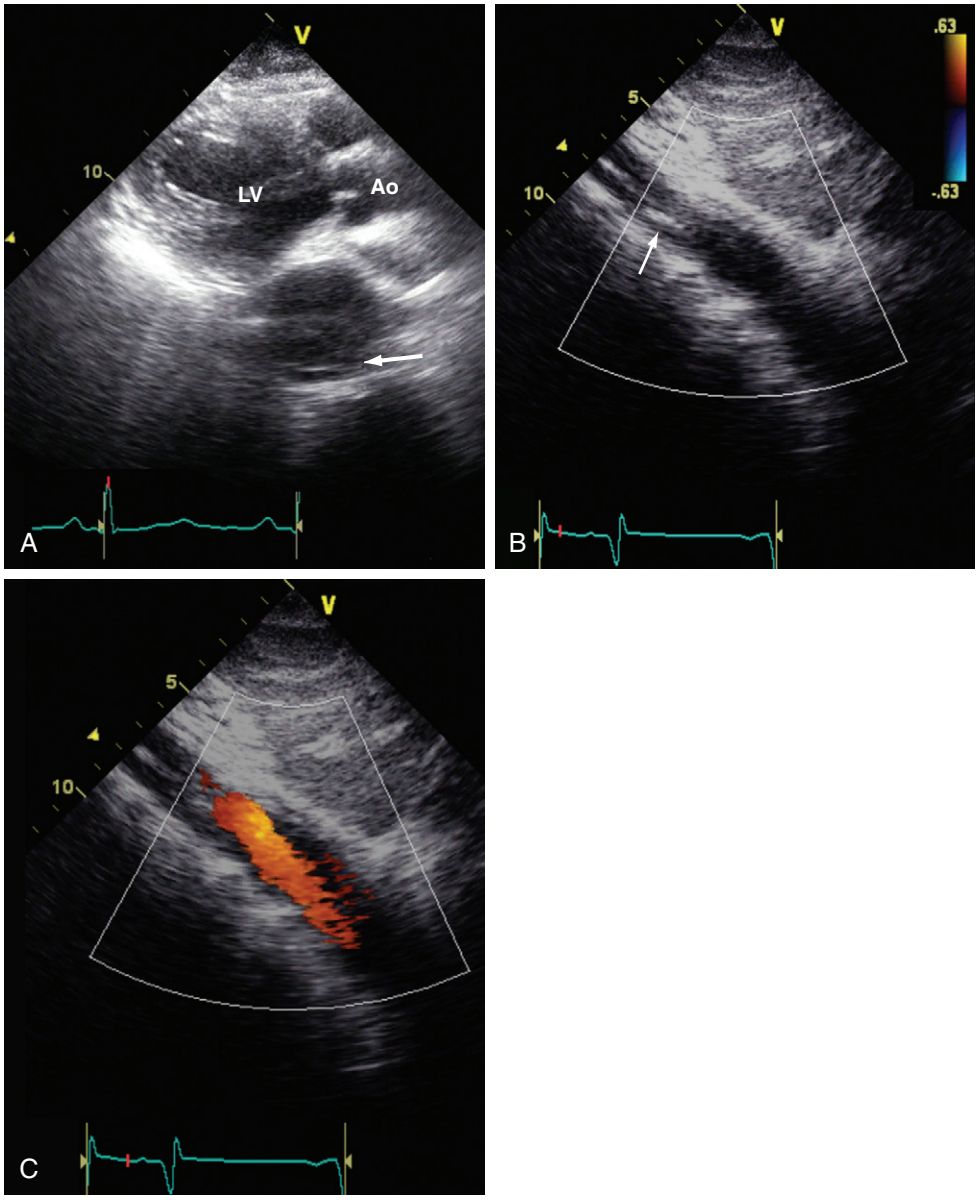



**Figure 36-5 Descending aortic dissection.** Transthoracic views can be helpful in some patients as shown by a parasternal long-axis view (**A**) showing enlarged descending thoracic aorta posterior to and compressing LA with a linear echo suggestive of a dissection flap (*arrow*). Subcostal view shows the flap (**B**) and flow in the true lumen (**C**). *Ao*, Aorta.

because the clinical behavior and therapeutic approach to the patient depend largely on whether the proximal aorta is involved in the dissection.[94] Despite this, the sensitivity and specificity of TEE for acute aortic dissection are high and well documented. More relevant considerations regarding emergent TEE for acute aortic syndromes are the delay to implementation (many sites will not have the personnel immediately available to perform this study, particularly off hours) and the conscious sedation that is required for alert patients. The potential for incomplete visualization of all thoracic aortic segments and therefore inconclusive results limits the use of emergent TEE where other highly reliable options are more readily available.

## COMPUTED TOMOGRAPHY

CT is a powerful and rapid tool for acute aortic syndromes (Fig. 36-8).The use of TEE in emergency departments for these cases has fallen well behind that of CT in centers where CT is immediately available. Extensive trauma where possible aortic involvement is the concern may often be better evaluated during the comprehensive CT scanning that those patients undergo. A concerted imaging strategy may well rely on more than one imaging modality, as the unique strengths of one method may offset the limitations of another. TEE may be the initial choice in patients with contraindications to CT contrast or magnetic resonance scanning, or be a subsequent choice when imaging artifacts in those tests render results inconclusive.

CT scans may demonstrate extension of dissection into great vessels that TEE views would not confirm. More often, CT is particularly useful in confirming that there is no demonstrable involvement of the distal ascending aorta. Another important role for CT is in clarifying inconclusive TEE results (see False Positives, later). The incidence of false-negative TEE studies has been minimal in large series,[76] and positive angiographic or CT results are rare when the initial TEE results are negative.

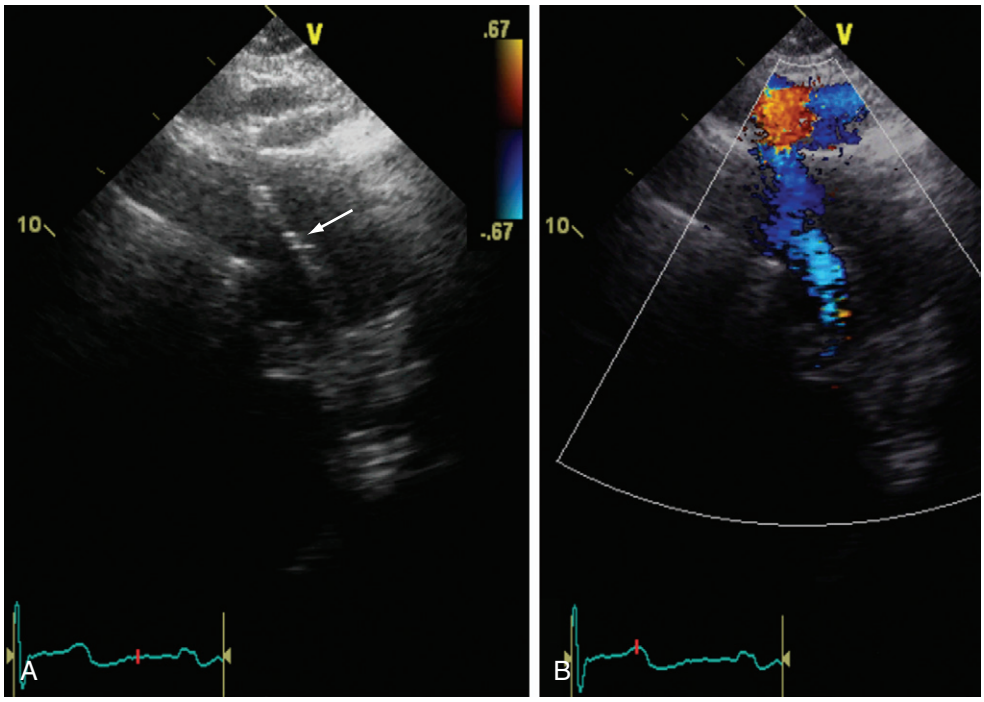



**Figure 36-6** **Aortic arch dissection flap.** Transthoracic suprasternal view (**A**) shows a clear intimal flap (*arrow*); there is no alternative diagnosis as its course does not mimic other surrounding structures. Color flow Doppler (**B**) shows systolic flow confined to the smaller true lumen, increasing confidence in the diagnosis.

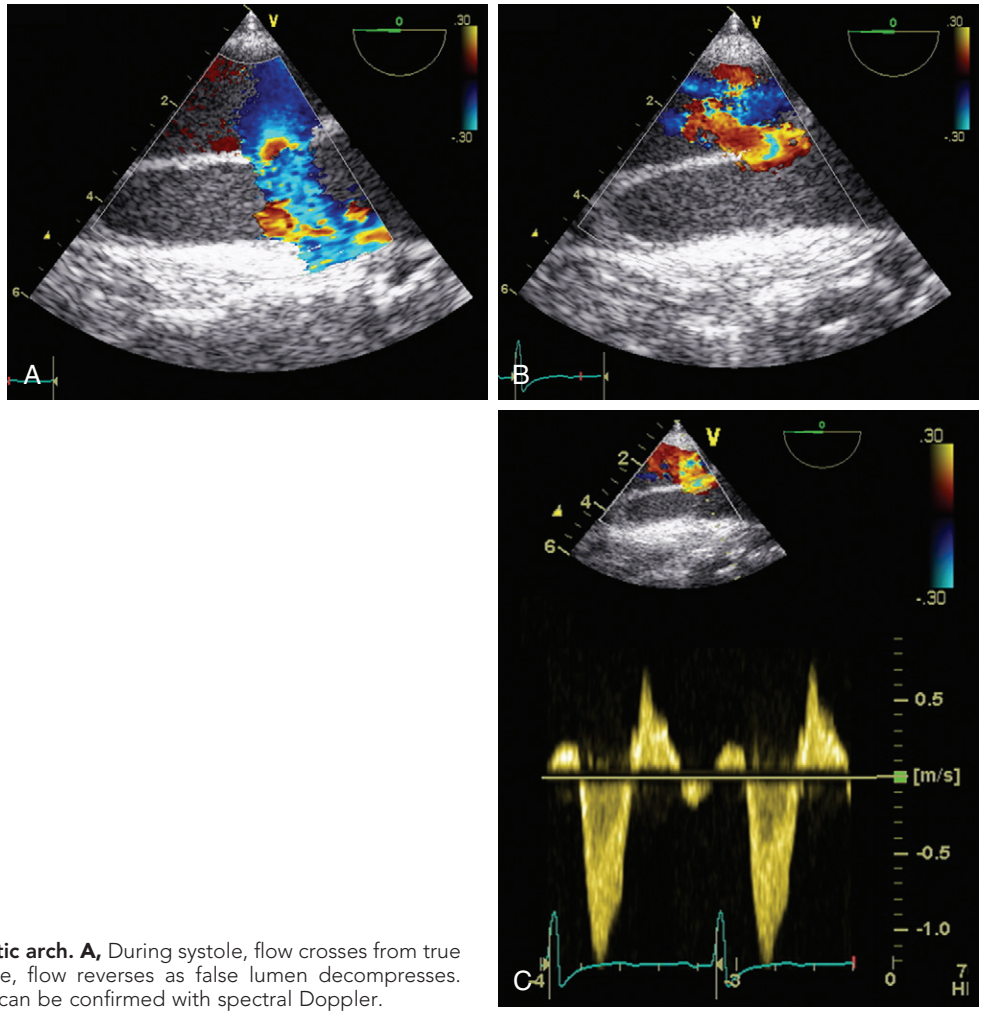



**Figure 36-7** **Entry tear in transverse aortic arch. A,** During systole, flow crosses from true lumen into false lumen. **B,** During diastole, flow reverses as false lumen decompresses. **C,** Alternating direction and timing of flow can be confirmed with spectral Doppler.

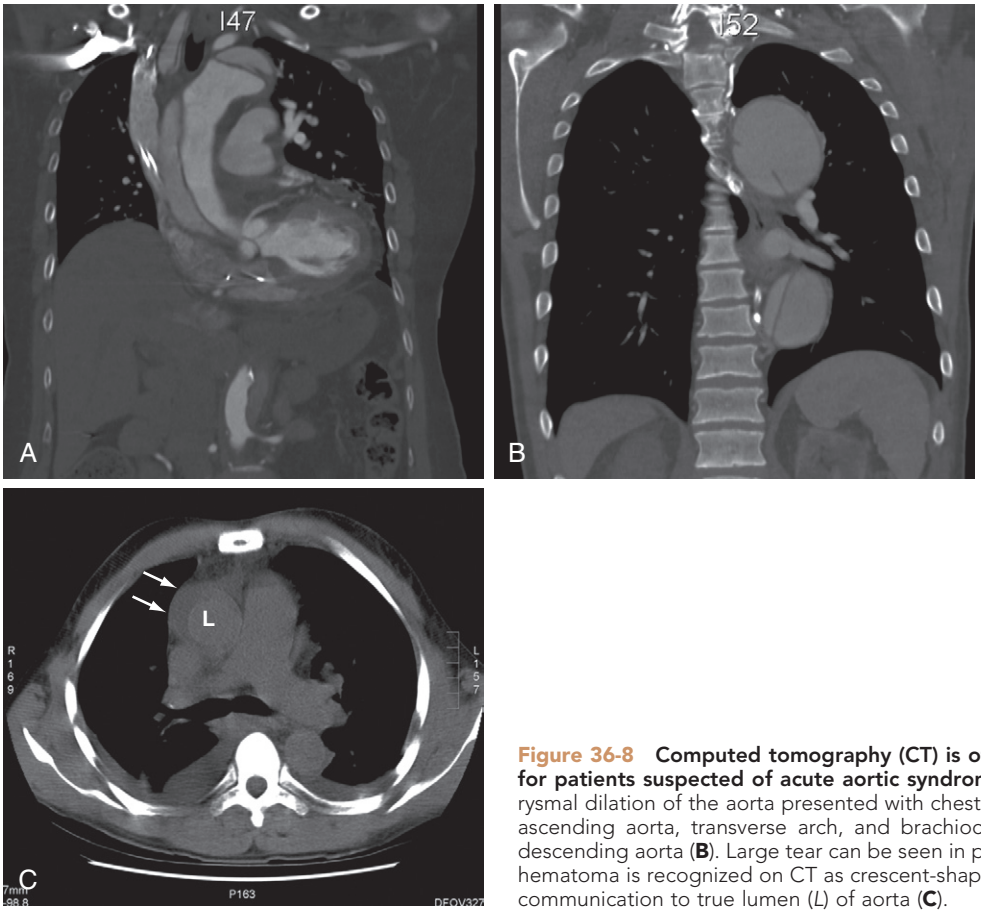



**Figure 36-8 Computed tomography (CT) is often used as an early diagnostic modality for patients suspected of acute aortic syndromes.** A patient with hypertension and aneurysmal dilation of the aorta presented with chest pain. Extensive dissection is seen involving ascending aorta, transverse arch, and brachiocephalic artery (**A**) and spiraling down the descending aorta (**B**). Large tear can be seen in proximal descending aorta. Aortic intramural hematoma is recognized on CT as crescent-shaped thickening of aortic wall (*arrows*) without communication to true lumen (*L*) of aorta (**C**).

## MAGNETIC RESONANCE IMAGING

The sensitivity of magnetic resonance imaging (MRI) for aortic dissection approaches 100% (Fig. 36-9).[95] However, pragmatic issues of imaging such acutely ill patients with trauma or need for hemodynamic monitoring or infusion of medications or those at risk for hemodynamic collapse continue to make CT or TEE preferable in acute settings unless the clinical suspicion is low or the patient is stable.

## CHOICE OF IMAGING

Echocardiography is only one of several diagnostic tests for acute aortic syndromes. The choice of one over the other, as well as the clinical confidence in positive or negative results, needs to be gauged relative to each test's performance (Table 36-2). A meta-analysis of 16 studies involving a total of 1139 patients reviewed the reliability of TEE, helical CT, and MRI.[96] The sensitivity and specificity of the three modalities were equivalent. After stratifying the patients for pretest likelihood of dissection (high-risk features included typical tearing chest pain in the back, hypotension, and pulse disparities), the positive likelihood ratio was highest for MRI, suggesting that this is the most powerful modality to confirm dissection in a patient with a high pretest likelihood of dissection. Helical CT had the lowest negative likelihood ratio of the three tests, suggesting that it is best at ruling out dissection in patients at lower risk. Angiography is a time-honored diagnostic method for aortic dissection that may identify the intimal flap and false lumen, as well as coronary and great vessel involvement. However, its sensitivity and specificity for dissection (88% and



**Figure 36-9 Gadolinium-enhanced magnetic resonance angiography (MRA) can be used to create 3D images of aorta and branches.** Follow-up of patients after acute dissection requires careful comparison of aortic dimensions; MRA is particularly useful for this. This demonstrates chronic dissection (*arrow* indicates intimal flap) that extends to level of renal arteries.

**TABLE 36-2 Imaging Modalities for Aortic Dissection**

| Modality | Sensitivity (%) | Specificity (%) | Positive Predictive Value (%) | Negative Predictive Value (%) | Accuracy (%) |
|---|---|---|---|---|---|
| TTE[67] | 77 | 93 | — | — | — |
| TTE[69] | 59 | 83 | — | — | — |
| TTE[68] | 83 | 63 | 80 | 70 | 75 |
| TEE[69] | 98 | 77 | — | — | — |
| TEE[1] | 98 | 97 | 98 | 97 | 97 |
| TEE[68] | 100 | 68 | 82 | 100 | 87 |
| Aortography[67] | 88 | 94 | 96 | 84 | — |
| Aortography[1] | 88 | 97 | 97 | 85 | 91 |
| MRI[68] | 100 | 100 | 100 | 100 | 100 |
| MRI[69] | 98 | 98 | — | — | — |
| CT[111] | 83 | 100 | 100 | 86 | — |
| CT[101] | 100 | 100 | — | — | 100 |

*CT*, Computed tomography; *MRI*, magnetic resonance imaging.

94%, respectively[97]) are limited by false lumen thrombosis, intramural hematomas, and equal flow in true and false lumens.[98,99] The last case is also an important limitation for CT studies, where differential flow may not be detectable even with dynamic CT imaging.[100] Ongoing improvements with multidetector, helical CT methods have improved the CT performance compared to early methods with lesser spatial and temporal resolution in assessing patients for aortic dissection.[101] Nevertheless, despite CT's high specificity (up to 100% in some series), a negative CT result in the presence of high clinical suspicion of dissection requires a second confirmatory test. This is also true for clinically discordant results from TEE or MRI as well.

## Transesophageal Echocardiography in Acute Aortic Syndromes

Multiple studies have documented that the specificity and sensitivity of TEE in the range of 98% and 99%, respectively. The recognized blind spot of TEE, involving the distal ascending aorta and superior aspect of the arch, is an important limitation, especially because entry tears in this region are important to clinical management. The goal of imaging the entire thoracic aorta may therefore require a combination of modalities and approaches, including transthoracic views (often from the suprasternal notch), transesophageal windows, and often direct epiaortic or epicardial views at the time of surgery (Fig. 36-10).

TEE has many discrete advantages in the diagnosis of acute aortic dissection, the most important of which is its documented accuracy. Erbel and colleagues,[102] reporting for the European Cooperative Study Group for Echocardiography on a series of 164 patients suspected of acute dissection, demonstrated sensitivity and specificity rates of 99% and 98%, respectively. Another large study by Nienaber and co-workers[103] compared TEE with MRI. Both TEE and MRI had perfect sensitivity; the 100% specificity of MRI exceeded the 68% specificity of TEE. The authors suggested that TEE's limited visualization of common ascending aorta pathology might have accounted for the higher rate of false-positive studies. In that study, strict criteria for diagnosing dissection were not applied (see later discussion); more stringent criteria could minimize false-positive results. TTE from the suprasternal notch provides additional views of this vulnerable area. The sequential use of TEE and CT, aortography, or MRI is clearly extremely powerful in clarifying suspicious or clinically incongruous results.[104,105]

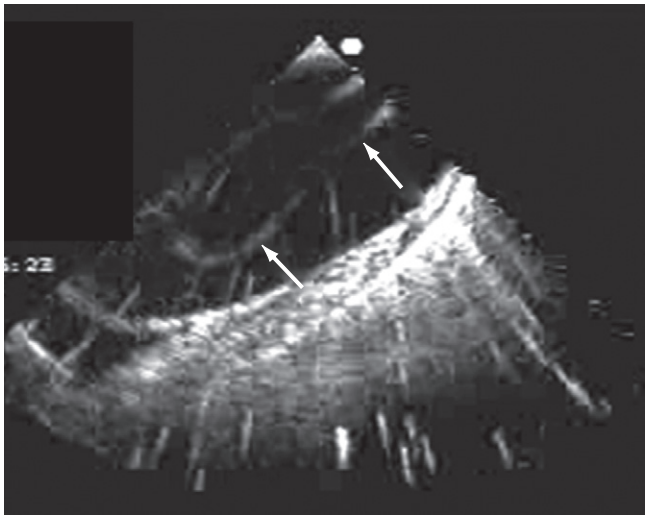


**Figure 36-10 Intraoperative epiaortic view of transverse aortic arch in patient with acute proximal aortic dissection.** Intima is widely dissected and highly mobile (*arrows*). Note linear streaking artifact from electrocautery.

TEE provides additional information about left and right ventricular wall motion and global function, and aortic and mitral valve competence. Importantly, with acute type A dissections, TEE is able to detect and determine the severity and mechanism of aortic valve regurgitation[106] and may influence the decision to replace or repair the valve.

An important advantage of TEE in cases of dissection is its rapid and safe performance in a wide range of clinical environments, including emergency departments, intensive care units, and the operating room. TEE requires minimal patient preparation, avoids the contrast and x-ray exposure associated with CT and angiography, and eliminates the time delays and practical encumbrances of MRI. Choice of a *best test* must always take into account the individual center's track record with each modality, as well as access issues.

## SAFETY OF TRANSESOPHAGEAL ECHOCARDIOGRAPHY

Safety of transesophageal examinations depends on adequate patient preparation with respect to pain, anxiety, and airway protection. (See Chapter 1.) Careful monitoring of the electrocardiogram and blood pressure is critical to avoiding adverse affects of TEE. In a study of 54 ambulatory patients, TEE was accompanied by an increase in systolic pressure in 77% of patients. This elevation was moderate (average increase of 16 mm Hg) in most patients, but some patients had acute increases of as much as 51 mm Hg.[107] Abrupt increases of blood pressure must clearly be avoided in any patient suspected of dissection. Serial blood pressure monitoring, pulse oximetry, intravenous sedation, topical anesthesia, and control of blood pressure with intravenous vasodilators and beta-blockers, if needed, are important to patient safety. With these precautions, the majority of patients can undergo esophageal intubation with minimal distress and good hemodynamic stability. Despite this, there has been a reported case of aortic rupture occurring during TEE in a patient with an acute dissection, which might have been elicited by retching and elevated blood pressure.[108] Other commonly reported adverse events during transesophageal studies that must be anticipated and avoided are nonsustained atrial and ventricular arrhythmias, excessive vagotonia with transient atrioventricular block, and arterial hypoxemia.[109]

## DIAGNOSTIC FEATURES

### *Dissection*

The diagnosis of aortic dissection is most secure when very specific criteria are met. Identification of an intimal flap, seen as a mobile, linear echo within the vascular lumen, and flow in the true and false channels on either side of the flap are highly sensitive features of dissection. The motion of the intimal flap toward the false lumen during systole may be a helpful feature. A thickening of the aortic wall in excess of 15 mm has also been used as a sign of dissection, suggesting thrombosis of a false channel, which makes the intimal flap difficult to recognize.[110] Strict adherence to these criteria can avoid confusion from imaging artifacts and manifestations of other types of disease and minimize false-positive results.[111] This is particularly important because most patients suspected of having an aortic dissection have evidence of vascular disease involving the thoracic aorta (Fig. 36-11). In one series of 40 patients evaluated for dissection, abnormal aortic findings (including atherosclerotic plaques, intravascular and extravascular masses, thrombi, and dilation) were found in 16 of 17 patients in whom aortic dissection and coronary artery disease were excluded as explanations for their chest pain.[112] Other underlying aortic abnormalities such as coarctation or prior surgical repair may affect clinical management, but they are also important potential sources of misdiagnosis.

### *Intramural Hematoma*

Transesophageal images demonstrate a thickened aortic wall with intramural echo-free spaces, an increased distance from the TEE probe to the inner aortic wall, and focal distortion of the transverse circular configuration of the aorta. Proposed echocardiographic criteria for aortic intramural hematoma include a crescent-shaped or circular thickening of the aortic wall 7 mm or more in thickness, extending 1 to 20 cm longitudinally, without an intimal flap or evidence of flow in the thickened aortic wall. TEE has a reported sensitivity of 100% and a specificity of 91% for the diagnosis of aortic intramural hematoma.[84]

### *Penetrating Ulcer*

Echocardiographic features of penetrating ulcers of the aorta include a crater-like outpouching of the aorta with jagged edges, associated with complex atheromatous plaque.

## DOPPLER FINDINGS

Color Doppler flow imaging during TEE is an excellent descriptor of the abnormal aortic flow patterns associated with acute dissection. Flow in the false channel is variable and complicated; the true lumen, which is often dwarfed by the false channel, is identified by forward systolic flow. With large proximal entry tears, flow in the nearby segments of the false lumen may have the same direction and timing as the true lumen flow and may reverse in diastole.[113,114] With smaller or more distal tears, false lumen flow is less similar to true lumen flow: It may be directed in the opposite direction, and peak velocity may occur later in the cardiac cycle, representing delay of flow into the false lumen. Many areas will show extremely slow, swirling flow with

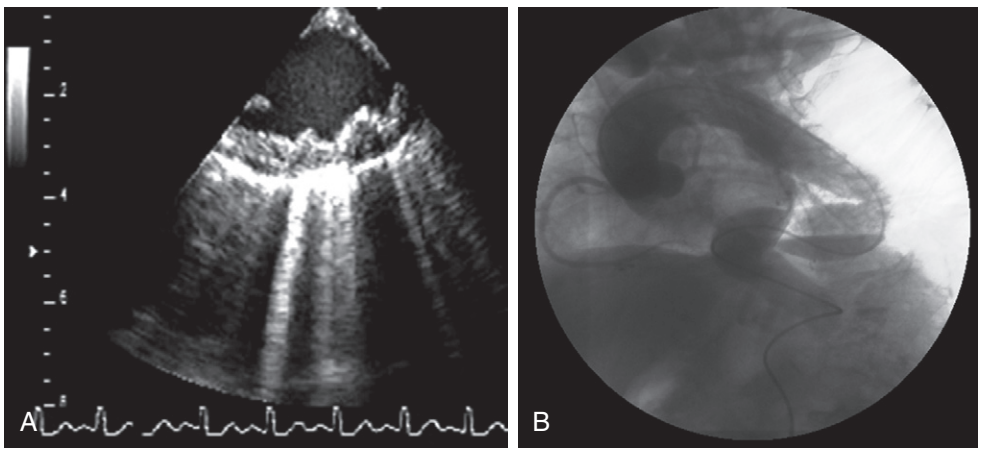



**Figure 36-11 Imaging artifacts and difficult views can be expected in the setting of severe atherosclerosis (A) and aortic tortuosity and/or ectasia (B).** Complementary methods such as computed tomography and magnetic resonance imaging may assist in difficult cases with low-confidence images.

spontaneous echo contrast or partial thrombosis. These segments tend to be remote from large entry or exit sites where high-velocity flow keeps these changes from occurring. Finally, areas of complete thrombosis are also seen, and care must be taken to ascertain that the hematoma is entirely intravascular and not actually the result of adventitial rupture, pseudoaneurysm formation, or intramural hematoma.

Multiple communications between the true and false lumens are often identified on careful scanning of the entire thoracic aorta. Some will represent entry sites with flow from the true toward the false channel, and others will be exit sites or have bidirectional flow (see Fig. 36-7). Exit tears, where flow reenters the true lumen from the false lumen, may occur at one or multiple sites. The exact location of a given tear can be estimated from the depth of probe insertion from the incisors, an arbitrary but convenient reference point. Recording this information at the time of the procedure and on the written report not only is helpful in the surgical correction of dissection, but also is extremely important for comparison with postoperative follow-up TEE studies, where many of the original tears may still be detectable.

Identification of the primary entry site must be deduced from location, size, and flow patterns. In some cases the primary tear cannot clearly be assigned to any one tear, either because of multiple tears as described earlier or, in some cases, because of the TEE blind spot. Adachi and associates[115] were able to identify the entry site in 50 of 57 patients with acute dissection. They were more successful in this with type B dissections (90%) than with type A (83%). As mentioned previously, identification of the primary tear is mostly important because ensuring that the surgical repair resects the primary entry site may decrease the incidence of late reoperation.

## COMPLICATIONS OF DISSECTION

An important goal of echocardiographic imaging in aortic dissection is identifying associated complications. Type A dissections may produce acute aortic regurgitation due to annular dilation or disruption of leaflet suspension. TEE can provide detailed morphologic information regarding the quality of the leaflet tissue and the mechanism of aortic regurgitation; these can help in the decision regarding valve resuspension versus replacement (see Chapter 20). This is a clear advantage and complementary feature to CT and MRI. Pericardial effusion and tamponade are manifestations of aortic rupture with dissection and are often readily identified on transthoracic views (Fig. 36-12). The Doppler manifestations of pericardial tamponade may be best obtained from external apical views and may obviate preoperative TEE in the interest of moving the patient emergently to the operating room (see Chapter 29). Other rupture syndromes can occur at different sites (Fig. 36-13). Uncontained rupture into the mediastinum or pleural space causes sudden death. Some ruptures are contained by the aortic adventitia, resulting in pseudoaneurysm formation or hematoma. In these cases TEE can detect the intimal breach as well as the extension of the hematoma into the surrounding tissues. An important proviso is to image the aorta at an adequate imaging depth so that such a hematoma can be recognized. These extravasations can be missed if the imaging field is restricted to the expected aortic contours; disastrous consequences can ensue if the site of the extravasation is not corrected along with the proximal aortic repair. Contrast may be useful in ruling out extravasation (Fig. 36-14).

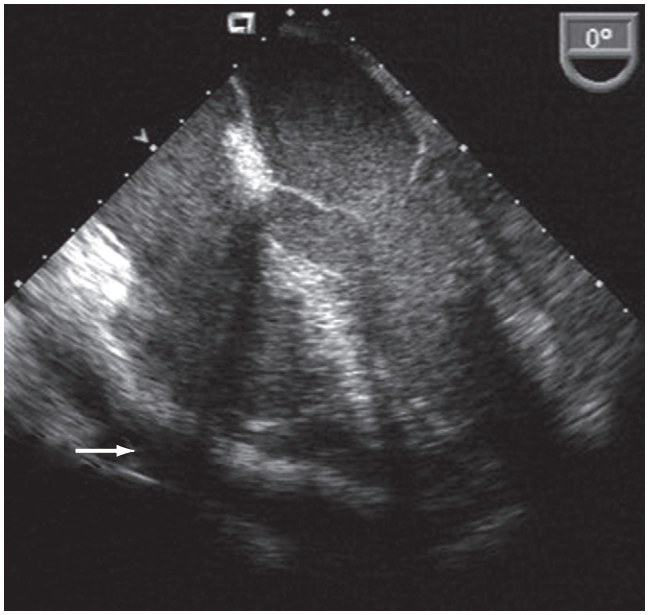



**Figure 36-12 Four-chamber TEE view in patient with type A dissection and pericardial effusion.** Contrast injection was performed and shows contrast in cardiac chambers, but not in the small pericardial effusion (*arrow*). This suggests that there is no active extravasation, which would have implied dissection with rupture. No tamponade physiology was detected.

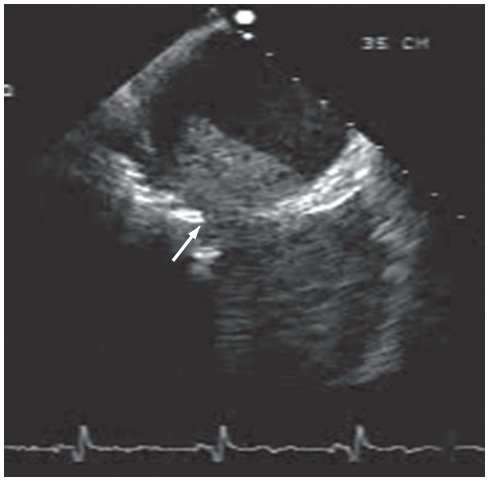



**Figure 36-13 Transesophageal view of descending aorta in patient after high-speed motor vehicle accident shows large thrombus in aortic lumen.** There is discontinuity of the posterior aortic wall (*arrow*) underlying the thrombus and extension of clot into periaortic tissues. This was confirmed to be a descending thoracic aortic rupture at emergent surgery.

### *Coronary Artery Involvement*

Involvement of coronary arteries by aortic dissection is an important issue, and one that raises the question of whether preoperative coronary angiography is mandatory. Involvement of one or both coronary arteries by acute aortic dissection has been estimated to occur in 10% to 20% of cases (Fig. 36-15).[116] In a series of 34 aortic dissection patients, Ballal and colleagues[117] detected coronary involvement with TEE in 6 of 7 surgically documented dissected coronaries. Of note, electrocardiographic changes were demonstrated in only 2 of the 6 patients with coronary involvement. Adequate views of the ostia and proximal vessel were obtained for 88% of left main arteries

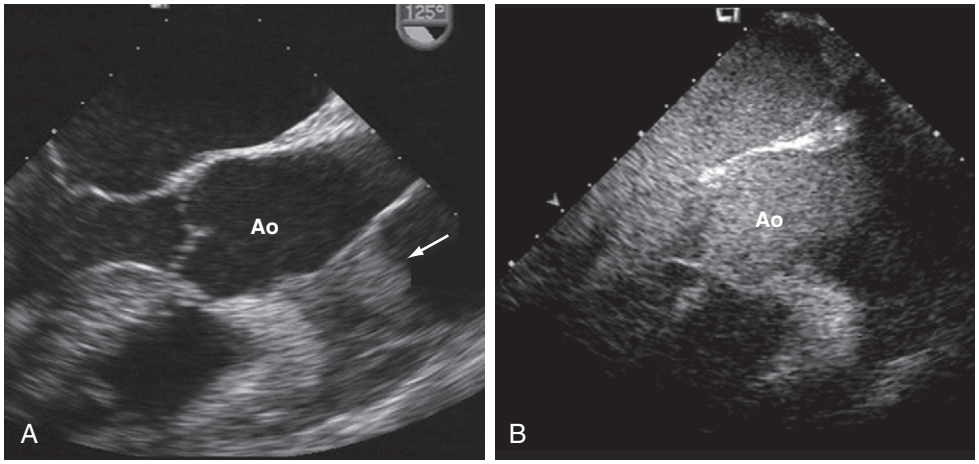



**Figure 36-14** **TEE view of the ascending aorta suggests an intimal flap with possible lumen rupture (A,** *arrow*). Contrast injection does not confirm extravasation outside aorta (**B**). *Ao*, Aorta.

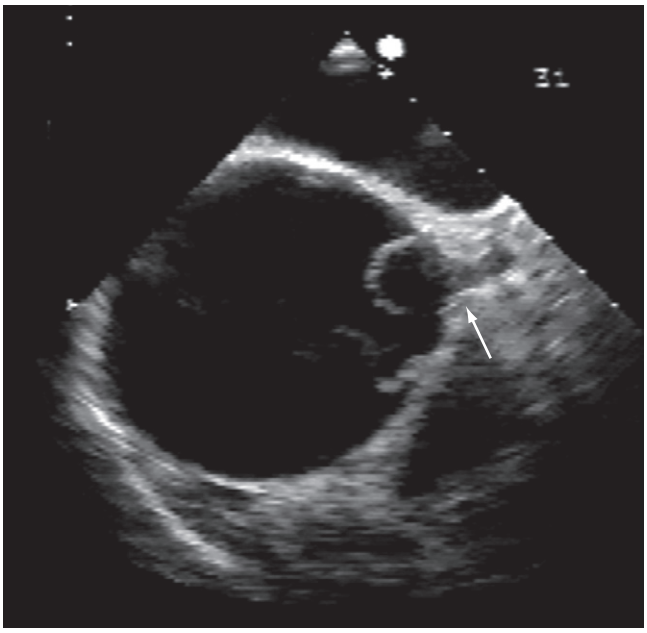


**Figure 36-15** **Short-axis TEE view of aortic root demonstrates an intimal flap in proximity to left coronary ostium (*arrow*).**

and 50% of right coronary arteries overall. Visualization of the ostia and proximal coronaries with TEE continues to improve. A separate but related issue is whether possible concomitant coronary artery disease, independent of coronary dissection, should prompt routine angiography. Given the underlying vascular disease that affects many patients with dissection, it is not surprising that coronary disease has been found in up to 43% of patients with aortic dissection. The benefits of addressing potentially important coronary stenoses must be weighed against the risk of delays and aortic manipulation during acute dissection and adjusted for the patient's baseline likelihood of coronary disease. A series of 122 patients from the Cleveland Clinic found no difference in the in-hospital mortality between patients who had emergency coronary arteriography before dissection repair and those who did not. Three-fourths of all coronary artery bypass grafting procedures performed in that series were done because of coronary dissection rather than obstruction due to coronary artery disease.[118]

### INCONCLUSIVE TRANSESOPHAGEAL ECHOCARDIOGRAPHIC RESULTS

The path of ultrasound through the esophageal wall and surrounding tissues may generate near-field artifacts that are often disconcertingly linear and run parallel to the aortic wall, mimicking an intimal flap. In patients with severe atherosclerotic disease, calcification in the wall can present similar artifacts and shadows. Abrupt aortic dilation can create a *shelf*, which can resemble a flap as well. Determining that these do not represent true intimal flaps depends on recognizing the minimal mobility of these structures and the homogeneity of flow on both sides of the line. The ability to change to a second imaging plane, as is possible with biplane or multiple-plane TEE probes, is extremely helpful in resolving the issue of artifactual flaps.[111,119] Multiple-plane imaging also allows better visualization of the proximal ascending aorta, where atherosclerosis and ectasia can be misinterpreted as dissection.[102]

Aneurysmal dilation of the aorta is another source of false-positive TEE studies for dissection.[120] Flow in aneurysmal areas is often low-velocity and swirling, similar to the flow in false channels. The absence of an intimal flap is important in avoiding misdiagnosis in this situation. The possibility that the intimal flap is not seen because the false channel has thrombosed must be excluded by carefully scanning up and down the aorta from the abnormal site. An intimal layer identified proximally or distally may be followed back to the suspicious dilated segment to suggest dissection.

## Surgical Considerations

The planning of surgical correction of aortic dissection is heavily influenced by many of the features discussed earlier. The extent of the dissection, the location of primary tears, and concomitant valvular regurgitation and coronary disease are all critically important to the surgical team. In addition, intraoperative ultrasound can address safe cannulation sites, aortic valve repair strategies, need for coronary reimplantation with root replacement, and confirmation of adequate cardiopulmonary bypass and even intraaortic balloon function (Box 36-3). Transesophageal imaging during surgery has the advantage of being unobtrusive (at least for the surgeon, if not for the anesthesiologist) and is commonly also used as an accurate monitor of left ventricular wall motion and volume status. The

Box 36-3

**OPERATIVE USES OF TRANSESOPHAGEAL ECHOCARDIOGRAPHY IN AORTIC DISSECTION**

**Pre–Cardiopulmonary Bypass Assessment**

***Aorta***
Intimal flap
Entry tear*
Intramural hematoma
Aortic rupture
Aortic pseudoaneurysm
Distal extent of extension
Additional tears
False lumen flow patterns, including thrombus
Branch vessel involvement*
  Coronary situs and dissection
  Involvement of origins of great vessels
Underlying pathology
  Atheromatous disease
  Coarctation
  Sites of previous repairs
Cannulation and cross-clamp sites*

***Aortic Valve***
Regurgitation
Suitability for repair versus replacement
Sizing for allograft replacement

***Mitral Valve***
Regurgitation
Suitability for repair versus replacement

***Left and Right Ventricle***
Wall motion abnormalities

***Pericardium***
Effusion

**Post–Cardiopulmonary Bypass Assessment**

***Aorta***
Confirm competency of proximal anastomosis
Establish baseline for false lumen flow and distal tears

***Aortic Valve***
Confirm competency of repaired valve

***Mitral Valve***
Confirm competency

***Left and Right Ventricle***
Wall motion

***Intraaortic Balloon***
Confirm position in true lumen

*Epicardial and/or epiaortic scanning may be important in fully defining these features.

long-term outcomes for surgery are very promising; a recent review found 96% and 90% survival at 1 and 3 years after surgery, respectively, for type A dissection.[121]

## INTRAOPERATIVE ECHOCARDIOGRAPHIC MONITORING

An additional tool for completing the scan of the aorta is intraoperative imaging from the epicardium or surface of the aorta (see Chapter 2). The unlimited number of acoustic windows from this approach allows careful interrogation of the aortic root, origins of the great vessels, cardiac valves, and left ventricular wall motion. The transesophageal blind spots in the ascending aorta and transverse arch can be thoroughly inspected from the epicardium, and potential aortic cannulation sites can be evaluated from the exterior aortic surface. Epicardial views give much greater freedom of visualization and measurement of the aortic valve and allow precise annular sizing before cardiopulmonary bypass to expedite selection of the valvular prosthesis. The position of the coronary ostia relative to the dissection and the annulus can be defined precisely with epicardial views, which may also aid in surgical decisions regarding valve-graft conduit placement or coronary ostial reimplantation.

The amount of time required for imaging in the surgical field can be limited to a few minutes, but this requires an experienced team with a surgeon or cardiologist familiar with the epicardial techniques and views. The combination of epicardial and transesophageal techniques ensures that a high-quality ultrasound image is acquired of all segments of the aorta above the diaphragm and eliminates any uncertainty regarding involvement of the ascending aorta. Post–cardiopulmonary bypass images from the epicardium can also be extremely helpful in reassessing proximal tears and interrogating suture lines between aorta and conduit.

Transesophageal views at the conclusion of cardiac surgery confirm aortic valve or prosthetic valve competency and allow prompt reinstitution of support if significant aortic regurgitation demands surgical revision. Intraaortic balloon pump position can be assessed with TEE; accidental placement of the balloon in the false lumen can be disastrous if not immediately recognized.[122] Finally, postoperative TEE images of the graft and native aorta create a baseline for subsequent follow-up studies.

## AORTIC REGURGITATION

Aortic valve regurgitation complicating aortic dissection has negative effects on outcome and may dictate important issues in surgical approach. Preservation of the native aortic valve is possible in 86% of type A dissection with excellent results.[123] If the aortic annulus is abnormal due to Marfan syndrome or annuloaortic ectasia, aortic valve replacement is preferred because of the limited long-term durability of aortic valve reconstruction in these patients. Initiation of cardioplegia for cardiopulmonary bypass usually depends on a competent aortic valve to allow antegrade perfusion of the coronaries; in the presence of significant aortic regurgitation, therefore, individual ostial cannulation or coronary sinus retroperfusion may be indicated. The specific causes of aortic regurgitation are also important[106]: Normal-appearing leaflets with a prolapsing cusp owing to avulsion of the leaflet base may be amenable to aortic repair with resuspension. Other cases may require aortic valve replacement. The specific involvement of the adjacent aortic root is also critical and may require a variable extent of prosthetic conduit. In some cases human aortic allografts are used, which have the advantage of supplying both natural aortic valve and root.

In proximal aortic involvement, the position and involvement of the coronary ostia are important. Ostial reimplantation

may be necessary; coronary bypass grafting may be unavoidable if the coronaries are dissected. Coronaries may be reattached by direct reimplantation with or without a surrounding button of aortic tissue, reattached to a piece of prosthetic conduit, or completely bypassed with saphenous vein or internal mammary artery grafts.

### MITRAL REGURGITATION

Mitral regurgitation is a different example of a valvular abnormality associated with aortic dissection. New regurgitation may result from wall motion abnormalities induced by coronary involvement in the dissection, or from acute left ventricular dilation induced by aortic regurgitation. In other cases mitral regurgitation is part of the underlying disorder, as is the case with Marfan syndrome with mitral valve prolapse. Identification of the etiologic factors in the mitral regurgitation (e.g., leaflet degeneration, ventricular dilation, or papillary muscle ischemia) will influence the need for repair or prosthetic replacement. Confirmation of results on early post–cardiopulmonary bypass images is important, especially when the decision is made to leave the mitral valve alone despite some regurgitation in hopes that correction of acute ischemia or dilation will remedy it.

### PERFUSION OF DISTAL VASCULAR BEDS

In the throes of acute aortic dissection, organs may be perfused by either the true or the false lumen flow. Organ underperfusion may occur if flow to the source lumen is compromised. During surgery, malperfusion may be caused by flow reversal when cardiopulmonary bypass is established by cannulation of the femoral artery, with obliteration of major communications between the two lumens from cross clamping, or with repair of the dissection itself. Neustein and colleagues[124] describe a case in which femoral cardiopulmonary bypass compressed the true lumen and created severe malperfusion once the dissection was repaired. Perfusion through the new ascending aortic graft allowed immediate reinstitution of forward flow.

## Endovascular Repair Considerations

Endovascular stenting is an important option and alternative to open surgery in selected patients with aortic trauma and dissection.[125] In traumatic rupture, it may be associated with lower mortality and incidence of complications such as spinal cord ischemia.[126] TEE may help guide endovascular stent placement[127] and detection of complications due to device deployment.[128] Echocardiography offers the best detection and delineation of endoleaks and is an important addition to angiography and intravascular ultrasound at the time of stent placement and at follow-up.[129] Intravascular ultrasound has also proved to be a valuable tool in this situation.

## Follow-up of Patients after Aortic Dissection

### PERSISTENT INTIMAL FLAPS

Despite successful surgical repair of aortic dissection, the aorta retains many abnormalities of structure and flow. Distal to the repair, the intimal flap and false lumen persist. The false lumen may fill with thrombus, or it may retain flow along with entry and exit flow through multiple fenestrations. One study detected persistent flap and false lumen in 100% of postrepair patients by MRI.[130] Persistent flow in the false lumen can be detected with TEE in the majority of patients after surgical repair. Mohr-Kahaly and co-workers[114] found persistence of the false lumen in 71% of their postoperative patients at a follow-up interval of 1 to 41 months, and in 82% of their medically treated patients. Dinsmore and Willerson[71] have suggested that long-term survival is poorer in patients with persistent flow in the false lumen. Thrombosis of the false channel seems to be protective, a "natural buttress against future or further extension of the dissection." TEE confirms that sites without communications develop low-velocity flow and thrombus, whereas healing changes are less likely to occur in regions with significant tears and persistent flow. TEE also demonstrates aggressive atherosclerotic changes and calcification of the neointima lining the false channel.

### PROGRESSION OF DISEASE

Patients with previous dissection may develop progressive abnormalities of both operated and nonoperated aortic segments. Of original dissections, 25% to 40% will enlarge over time, and the rate and extent of enlargement are primary factors driving the need for reoperation.[116] In addition, dilation of noncontiguous, nonoperated aortic segments develops in 17% of patients with prior acute type A dissections. Early recognition of this progressive downstream aortic pathology allows reoperation in hopes of preventing rupture or redissection.[131] The concern regarding disease progression commits these patients to routine follow-up studies indefinitely.

### PSEUDOANEURYSM FORMATION

Pseudoaneurysms form in 7% to 25% of patients with composite grafts, such as a Bentall procedure, secondary to hemorrhage at a suture line dehiscence.[132] Blood between the graft and aortic wall can create supravalvular aortic stenosis.[133] Both of these complications can be detected and completely delineated by TEE,[134] as well as by CT, angiography, and MRI.[135,136] Color flow Doppler will demonstrate blood flow into the echo-free space between the graft and the aortic wall. Other postoperative complications include endocarditis and development of a sinus of Valsalva aneurysm.[137]

### RECURRENT DISSECTION

Because the symptoms of acute redissection or expansion of a chronic dissection are nonspecific, the ability to reassess rapidly and compare the current findings with previous images is extremely important. Younger patients, those with Marfan syndrome, and those with primary tears involving the transverse arch are particularly prone to progression of their disease.[138] Because TEE may not be able to reproducibly measure the true transverse diameter of an ectactic aorta, suspicion of chronic expansion usually requires additional confirmatory tests such as CT or MRI. Excellent definition of the intimal flap, false channel thrombi and flow patterns, and consistent reference landmarks for serial sizing over time make MRI a highly reliable method. When recurrent chest pain or hemodynamic instability suggests acute redissection, TEE can rapidly define the new pathologic abnormality and its extent. Changes from baseline postoperative or postdissection images can be extremely helpful in clarifying the etiologic site and event.

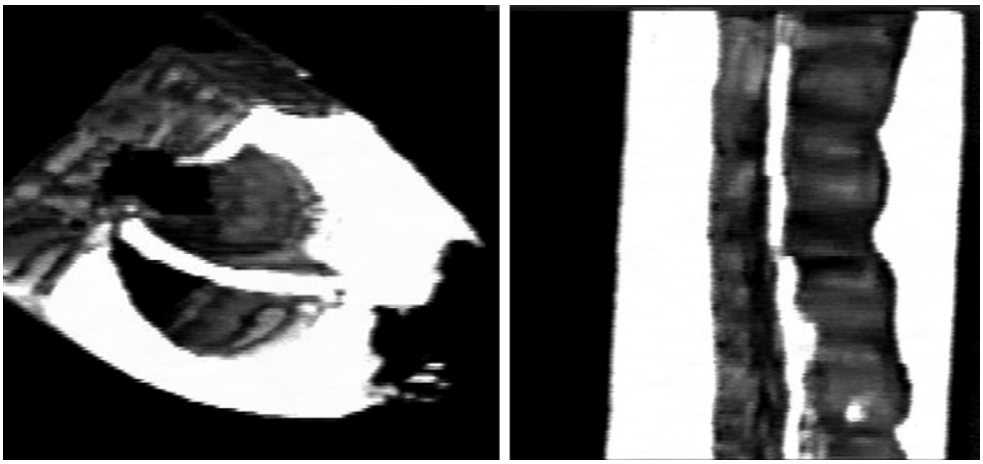


**Figure 36-16** 3D reconstructed views of the aorta in short-axis (*left*) and long-axis (*right*) orientations demonstrate intimal flap separating true and false lumens.

## Research Applications and Future Directions

TEE images provide excellent spatial resolution, and in combination with the high temporal resolution of M-mode methods they allow investigation of aortic distensibility in normal patients, in patients at risk for vascular disease, and after repair of aneurysms or dissection. These types of methods have documented decreases in elastic aortic properties after aortic surgery, which predispose patients to redissection.[139] Two-dimensional echocardiographic assessments of aortic distensibility have been shown to estimate changes in aortic mechanical properties resulting from increasing age[140]; Doppler estimates of pulse wave velocity are also being investigated as measures of aortic compliance.[141] Animal models for validation of these parameters include chronic models of accelerated atherogenesis, as well as acute aortic ischemia and decreased distensibility generated by removal of the vasa vasorum.[142] Multidimensional TEE images continue to inform regarding diagnosis and surgical planning (Fig. 36-16).

High-frequency ultrasonic integrated backscatter methods are also being applied to the aortic wall. Recchia and associates[143] detected sixfold decreases in backscatter and 15-fold decreases in anisotropy, suggesting marked disorganization of the three-dimensional (3D) aortic architecture in Marfan syndrome patients' aortas compared to those of normal patients. Tissue strain analysis based on speckle tracking and tissue Doppler are also being actively investigated alongside tonometry and peripheral vascular evaluations for the detection of aortic pathology. These types of functional and structural investigations may improve our recognition of aortic disease of many stages and refine our prediction of risk of dissection.

## Conclusions

The grim prognosis of patients with acute aortic dissection or traumatic aortic injury demands a rapid, highly sensitive, and efficient diagnostic approach. The use of imaging in the earliest minutes of patient evaluation continues to shift toward CT scanning. Echocardiography remains a mainstay in the emergent diagnosis, treatment, and follow-up of patients with acute aortic syndromes.

### KEY POINTS

- The immediate management and prognosis of acute aortic syndromes including dissection and intramural hematoma hinge on whether the ascending aorta is involved.
- Any dissection involving the ascending aorta is type A, irrespective of the site of the entry tear or direction of propagation.
- Mortality of type A aortic dissection is 1% per hour for the first 48 hours.
- TEE, MRI, and CT have similar clinical performance in assessing aortic dissection:
  - To rule out aortic dissection in a patient with low pretest probability, CT may be best but requires contrast and radiation exposure.
  - To confirm aortic dissection in a patient with high pretest probability, MRI may be best but is often inappropriate for unstable patients.
  - TEE can rapidly diagnose dissection and identify high-risk features, including pericardial effusion, aortic regurgitation, and wall motion abnormalities.
- Aortic intramural hematoma has the same prognosis and urgency as aortic dissection.
- Aortic dissection can occur without significant root enlargement in a patient with Marfan syndrome.
- Patients with bicuspid aortic valve remain at risk for progressive aortic dilation and dissection even after aortic valve replacement.
- After surgery for dissection, the intimal flap and false lumen usually persist distal to the graft, and multiple entry and exit tears may be seen.
- Aortic injury from severe blunt trauma or deceleration is usually rupture confined only by adventitia.

## REFERENCES


1. Chirillo F, Marchiori MC, Andriolo L, et al: Outcome of 290 patients with aortic dissection: a 12 year multicentre experience. *Eur Heart J* 11:311-319, 1990.
2. Demos TC, Posniak HV, Marsan RE: CT of aortic dissection. *Semin Roentgenol* 24:22-37, 1989.
3. Lilienfeld DE, Gunderson PD, Sprafka JM, et al: Epidemiology of aortic aneurysms: 1. Mortality trends in the United States, 1951-1981. *Arteriosclerosis* 7:637-643, 1987.
4. Hirst AE, Johns VJ, Kime SW: Dissecting aneurysm of the aorta. A review of 505 cases. *Medicine* 37:217-279, 1958.
5. Satler FL, Levine S, Kent KM, et al: Aortic dissection masquerading as acute myocardial infarction: implication for thrombolytics therapy without cardiac catheterization. *Am J Cardiol* 54:1134-1145, 1984.
6. Davidson E, Weinberger I, Rotenberg Z, et al: Elevated serum creatinine kinase levels: an early diagnostic sign of acute dissection of the aorta. *Arch Intern Med* 148:2184-2186, 1988.
7. Butler J, Davies AH, Westaby S: Streptokinase in acute aortic dissection. *Br Med J* 300:517-519, 1990.
8. Weiss P, Weiss I, Zuber M, Ritz R: How many patients with acute dissection of the thoracic aorta would erroneously receive thrombolytics therapy based on the electrocardiographic findings on admission? *Am J Cardiol* 72:1329-1330, 1993.
9. Erbel R, Eggebrecht H: Aortic dimensions and the risk of dissection. *Heart* 92:137-142, 2006.
10. Lee RT, Kamm RD: Vascular mechanics for the cardiologist. *J Am Coll Cardiol* 23:1289-1295, 1994.
11. Mukherjee DP, Kagan HM, Jordan RE, Franzblau C: Effect of hydrophobic elastin ligands on the stress-strain properties of elastin fibers. *Connect Tissue Res* 4:177-179, 1976.
12. Buntin CM, Silver FH: Noninvasive assessment of mechanical properties of peripheral arteries. *Ann Biomed Eng* 18:549-566, 1990.
13. Dzau VJ, Safar ME: Large conduit arteries in hypertension: role of the vascular renin-angiotensin system. *Circulation* 77:947-954, 1988.
14. Robicsek F, Thubrikar MJ: Hemodynamic considerations regarding the mechanism and prevention of aortic dissection. *Ann Thorac Surg* 58:1247-1253, 1994.
15. MacSweeney ST, Young G, Greenhalgh RM, Powell JT: Mechanical properties of the aneurysmal aorta. *Br J Surg* 79:1281-1284, 1992.
16. Carson MW, Roach MR: The strength of the aortic media and its role in the propagation of aortic dissection. *J Biomech* 23:579-588, 1990.
17. Rubin K: Aortic dissection and rupture in Turner syndrome [Letter]. *J Pediatr* 122:670, 1993.
18. Ashraf SS, Shaukat N, Masood M, et al: Type I aortic dissection in a patient with osteogenesis imperfecta. *Eur J Cardiothorac Surg* 7:665-666, 1993.
19. Biagini A, Maffei S, Baroni M, et al: Familiar clustering of aortic dissection in polycystic kidney disease. *Am J Cardiol* 72: 741-742, 1993.
20. Schor JS, Horowitz MD, Livingstone AS: Recreational weight lifting and aortic dissection: case report. *J Vasc Surg* 17:774-776, 1993.
21. Chauvel C, Cohen A, Albo C, et al: Aortic dissection and cardiovascular syphilis: report of an observation with transesophageal echocardiography and anatomopathologic findings. *J Am Soc Echocardiogr* 7:419-421, 1994.
22. Eber B, Tscheliessnigg KH, Anelli-Monti M, et al: Aortic dissection due to discontinuation of beta-blocker therapy. *Cardiology* 83:128-131, 1993.
23. Evans JM, Bowles CA, Bjornsson J, et al: Thoracic aortic aneurysm and rupture in giant cell arteritis. A descriptive study of 41 cases. *Arthritis Rheum* 37:1539-1547, 1994.
24. Gersbach P, Lang H, Kipfer B, et al: Impending rupture of the ascending aorta due to giant cell arteritis. *Eur J Cardiothorac Surg* 7:667-670, 1993.
25. Marsalese DL, Moodie DS, Lytle BW, et al: Cystic medial necrosis of the aorta in patients without Marfan's syndrome: Surgical outcome and long-term follow-up. *J Am Coll Cardiol* 16:68-73, 1990.
26. Nienaber CA, Fattori R, Mehta RH, et al; International Registry of Acute Aortic Dissection: Gender-related differences in acute aortic dissection. *Circulation* 109:3014-3021, 2004.
27. Pretre R, Chilcott M: Blunt trauma to the heart and great vessels. *N Engl J Med* 336:626-632, 1997.
28. Vlahakes GJ, Warren RL: Traumatic rupture of the aorta. *N Engl J Med* 332:389-390, 1995.
29. Parmley LF, Mattingly TW, Manion WC, et al: Nonpenetrating traumatic injury of the aorta. *Circulation* 17:1086-1101, 1958.
30. Smith MD, Cassidy JM, Souther S, et al: Transesophageal echocardiography in the diagnosis of traumatic rupture of the aorta. *N Engl J Med* 332:356-362, 1995.
31. Pieters FA, Widdershoven JW, Gerardy AC, et al: Risk of aortic dissection after aortic valve replacement. *Am J Cardiol* 72:1043-1047, 1993.
32. Katz ES, Tunick PA, Colvin SB, et al: Aortic dissection complicating cardiac surgery: Diagnosis by intraoperative biplane transesophageal echocardiography. *J Am Soc Echocardiogr* 6:217-222, 1993.
33. Sakamoto I, Hayashi K, Matsunaga N, et al: Aortic dissection caused by angiographic procedures. *Radiology* 191:467-471, 1994.
34. Dorsey DM, Rose SC: Extensive aortic and renal artery dissection following percutaneous transluminal angioplasty. *J Vasc Interv Radiol* 4:493-495, 1993.
35. Hsue PY, Salinas CL, Bolger AF, et al: Acute aortic dissection related to crack cocaine. *Circulation* 105:1592-1595, 2002.
36. Wako E, LeDoux D, Mitsumori L, Aldea GS: The emerging epidemic of methamphetamine-induced aortic dissections. *J Card Surg* 22:390-393, 2007.
37. Braunwald E: *Heart disease*, Philadelphia, 1992, WB Saunders, pp 1536-1551.
38. Nolte JE, Rutherford RB, Nawaz S, et al: Arterial dissections associated with pregnancy. *J Vasc Surg* 21:515-520, 1995.
39. Roberts WC: Aortic dissection: Anatomy, consequences and causes. *Am Heart J* 101:195-241, 1981.
40. Oskoui R, Lindsay J Jr: Aortic dissection in women less than 40 years of age and the unimportance of pregnancy. *Am J Cardiol* 73: 821-823, 1994.
41. Child AH: Marfan syndrome-current medical and genetic knowledge: how to treat and when. *J Card Surg* 12(2 Suppl):131-135, 1997.
42. McDonald GR, Schaff HV, Pyeritz RE, et al: Surgical management of patients with Marfan syndrome and dilatation of the ascending aorta. *J Thorac Cardiovasc Surg* 81:180-186, 1981.
43. Murdoch JL, Walker BA, Halpern BL, et al: Life expectancy and causes of death in the Marfan syndrome. *N Engl J Med* 286:804-808, 1972.
44. Gott VL, Laschinger JC, Cameron DE, et al: The Marfan syndrome and the cardiovascular surgeon. *Eur J Cardiothorac Surg* 10:149-158, 1996.
45. Pyeritz RE, McKusick VA: The Marfan syndrome diagnosis and management. *N Engl J Med* 300:772-777, 1979.
46. Hollister DW, Godfrey M, Sakai LY, Pyeritz RE: Immunohistologic abnormalities of the microfibrillar-fiber system in the Marfan syndrome. *N Engl J Med* 323:152-159, 1990.
47. Hirata K, Triposkiadis F, Sparks E, et al: The Marfan syndrome: abnormal aortic elastic properties. *J Am Coll Cardiol* 18:57-63, 1991.
48. Jeremy RW, Huang H, Hwa J, et al: Relation between age, arterial distensibility, and aortic dilatation in the Marfan syndrome. *Am J Cardiol* 74:369-373, 1994.
49. Come PC, Fortuin NJ, White RI, McKusick VA: Echocardiographic assessment of cardiovascular abnormalities in the Marfan syndrome. Comparison with clinical findings and with roentgenographic estimation of aortic root size. *Am J Med* 74:465-474, 1983.
50. Legget ME, Unger TA, Osullivan CK, et al: Aortic root complications in the Marfan's syndrome: Identification of a lower risk group. *Heart* 75:389-395, 1996.
51. Roman MJ, Rosen SE, Kramer-Fox R, Devereux RB: Prognostic significance of the pattern of aortic root dilation in the Marfan syndrome. *J Am Coll Cardiol* 22:1470-1476, 1993.
52. Gott VL, Pyeritz RE, Magovern GJ Jr, et al: Surgical treatment of aneurysms of the ascending aorta in the Marfan syndrome. Results of composite-graft repair in 50 patients. *N Engl J Med* 314:1070-1074, 1986.
53. Pyeritz RE: Predictors of dissection of the ascending aorta in Marfan syndrome [Abstract]. *Circulation* 84(Suppl II):II-351, 1991.
54. Meijboom LJ, Timmermans J, Zwinderman AH, et al: Aortic root growth in men and women with the Marfan's syndrome. *Am J Cardiol* 96:1441-1444, 2005.
55. Roberts WC, Honig HS: The spectrum of cardiovascular disease in the Marfan syndrome: A clinicomorphologic study of 18 necropsy patients and comparison to 151 previously reported necropsy patients. *Am Heart J* 104:115-135, 1982.
56. Groenink M, Lohuis TA, Tijssen JG, et al: Survival and complication free survival in Marfan's syndrome: implications of current guidelines. *Heart* 82:499-504, 1999.
57. Gott VL, Greene PS, Alejo DE, et al: Replacement of the aortic root in patients with Marfan's syndrome. *N Engl J Med* 340:1307-1313, 1999.
58. Coselli JS, LeMaire SA, Buket S: Marfan syndrome: the variability and outcome of operative management. *J Vasc Surg* 21:432-443, 1995.
59. Tambeur L, David TE, Unger M, et al: Results of surgery for aortic root aneurysm in patients with the Marfan syndrome. *Eur J Cardiothorac Surg* 17:415-419, 2000.
60. Erbel R, Eggebrecht H: Aortic dimensions and the risk of dissection. *Heart* 92:137-142, 2006.

61. Gleason TG: Heritable disorders predisposing to aortic dissection. *Semin Thorac Cardiovasc Surg* 17:274-281, 2005.
62. Gravholt CH, Landin-Wilhelmsen K, Stochholm K, et al: Clinical and epidemiological description of aortic dissection in Turner's syndrome. *Cardiol Young* 16:1-7, 2006.
63. Bondy CA: Aortic dissection in Turner syndrome. *Curr Opin Cardiol* 23:519-526, 2008.
64. Svensson LG, Labib SB: Aortic dissection and aortic aneurysm surgery. *Curr Opin Cardiol* 9:191-199, 1994.
65. DeBakey ME, McCollum CH, Crawford ES, et al: Dissection and dissecting aneurysms of the aorta: Twenty year follow-up of five hundred twenty seven patients treated surgically. *Surgery* 92:1118-1134, 1982.
66. Daily PO, Trueblood HW, Stinson EB, et al: Management of acute aortic dissections. *Ann Thorac Surg* 10:237-247, 1970.
67. Miller DC: Surgical management of aortic dissections: indications, perioperative management, and long term results. In Doroghazi RM, Slater EE, editors: *Aortic dissection*, New York, 1983, McGraw-Hill, pp 193-243.
68. Applebaum A, Karp RB, Kirklin JW: Ascending vs. descending aortic dissections. *Ann Surg* 183:296, 1976.
69. DeSanctis RW, Doroghazi RM, Austen WG, Bucklet MJ: Aortic dissection. *N Engl J Med* 317:1060-1067, 1987.
70. Miller DC: Acute dissection of the descending thoracic aorta. *Chest Surg Clin North Am* 2:347-378, 1992.
71. Dinsmore RE, Willerson JT: Dissecting aneurysms of the aorta. Angiographic features affecting prognosis. *Radiology* 105:567-572, 1972.
72. Miller DC: Improved follow-up for patients with chronic dissections. *Semin Thorac Cardiovasc Surg* 3:270-276, 1991.
73. Roberts CS, Roberts WC: Aortic dissection with the entrance tear in the descending thoracic aorta: analysis of 40 necropsy patients. *Ann Surg* 213:356-368, 1991.
74. Duch PM, Chandrasekaran K, Karalis DG, Ross JJ Jr: Improved diagnosis of coexisting types II and III aortic dissection with multiplane transesophageal echocardiography. *Am Heart J* 127:699-701, 1994.
75. Slater EE: Aortic dissection: Presentation and diagnosis. In Doroghazi RM, Slater EE, editors: *Aortic dissection*, New York, 1983, McGraw-Hill, pp 61-70.
76. Grossman CM, Dagostino AN: Advanced atherosclerosis in false channels of chronic aortic dissection. *Lancet* 342:1428-1429, 1993.
77. Eichelberger JP: Aortic dissection without intimal tear: Case report and findings on transesophageal echocardiography. *J Am Soc Echocardiogr* 7:82-86, 1994.
78. Erbel R, Oelert H, Meyer J, et al: Effect of medical and surgical therapy on aortic dissection evaluated by transesophageal echocardiography. Implications for prognosis and therapy. The European Cooperative Study Group on Echocardiography. *Circulation* 87:1604-1615, 1993.
79. Robbins RC, McManus RP, Mitchell RS, et al: Management of patients with intramural hematoma of the thoracic aorta. *Circulation* 88:II1-II10, 1993.
80. Nienaber CA, Sievers HH: Intramural hematoma in acute aortic syndrome: more than one variant of dissection? *Circulation* 106:284-285, 2002.
81. Dake MD: Aortic intramural haematoma: current therapeutic strategy. *Heart* 90:375-378, 2004.
82. Evangelista A, Mukherjee D, Mehta RH, et al; International Registry of Aortic Dissection (IRAD) Investigators: Acute intramural hematoma of the aorta: a mystery in evolution. *Circulation* 111:1063-1070, 2005.
83. Song JK, Kim HS, Kang DH, et al: Different clinical features of aortic intramural hematoma versus dissection involving the ascending aorta. *J Am Coll Cardiol* 37:1604-1610, 2001.
84. Willens HJ, Kessler KM: Transesophageal echocardiography in the diagnosis of diseases of the thoracic aorta: part 1. Aortic dissection, aortic intramural hematoma, and penetrating atherosclerotic ulcer of the aorta. *Chest* 116:1772-1779, 1999.
85. A.W. Stanson, F.J. Kazmier, L.H. Hollier et al: Penetrating atherosclerotic ulcers of the thoracic aorta: natural history and clinicopathologic correlations. *Ann Vasc Surg* 1:15-23, 1986.
86. Cooke JP, Kazimer FJ, Orszulak TA: The penetrating aortic ulcer: Pathology, diagnosis and management. *Mayo Clin Proc* 63:718-725, 1988.
87. Harris JA, Bis KG, Glover JL, et al: Penetrating atherosclerotic ulcers of the aorta. *J Vasc Surg* 19:90-98, 1994.
88. Parmley LF, Mattingly TW, Manion WC, et al: Nonpenetrating traumatic injury of the aorta. *Circulation* 17:1086-1101, 1958.
89. Legome E: General approach to blunt thoracic trauma in adults. In Basow DS, editor: *UpToDate*. Waltham, Mass., 2011, Elsevier.
90. Vignon P, Guéret P, Vedrinne JM, et al: Role of transesophageal echocardiography in the diagnosis and management of traumatic aortic disruption. *Circulation* 92:2959-2968, 1995.
91. Goarin JP, Catoire P, Jacquens Y, et al: Use of transesophageal echocardiography for diagnosis of traumatic aortic injury. *Chest* 112:71-80, 1997.
92. Le Bret F, Ruel P, Rosier H, et al: Diagnosis of traumatic mediastinal hematoma with transesophageal echocardiography. *Chest* 105:373-376, 1994.
93. Vignon P, Rambaud G, François B, et al: Quantification of traumatic hemomediastinum using transesophageal echocardiography: impact on patient management. *Chest* 113: 1475-1480, 1998.
94. Chan KL: Impact of transesophageal echocardiography on the treatment of patients with aortic dissection. *Chest* 101:406-410, 1992.
95. Laissy JP, Blanc F, Soyer P, et al: Thoracic aortic dissection: Diagnosis with transesophageal echocardiography versus MR imaging. *Radiology* 194:331-336, 1995.
96. Shiga T, Wajima Z, Apfel CC, Inoue T, Ohe Y: Diagnostic accuracy of transesophageal echocardiography, helical computed tomography, and magnetic resonance imaging for suspected thoracic aortic dissection: systematic review and meta-analysis. *Arch Intern Med* 166:1350-1356, 2006.
97. Erbel R, Engberding R, Daniel W, et al: Echocardiography in diagnosis of aortic dissection. *Lancet* 1:457-461, 1989.
98. Cigarroa JE, Isselbacher EM, DeSanctis RW, Eagle KA: Diagnostic imaging in the evaluation of suspected aortic dissection. Old standards and new directions. *N Engl J Med* 328:35-43, 1993.
99. Bansal RC, Chandrasekaran K, Ayala K, Smith DC: Frequency and explanation of false negative diagnosis of aortic dissection by aortography and transesophageal echocardiography. *J Am Coll Cardiol* 25:1393-1401, 1995.
100. Mugge A, Daniel WG, Laas J, et al: False-negative diagnosis of proximal aortic dissection by computed tomography or angiography and possible explanations based on transesophageal echocardiographic findings. *Am J Cardiol* 65:527-529, 1990.
101. Yoshida S, Akiba H, Tamakawa M, et al: Thoracic involvement of type A aortic dissection and intramural hematoma: diagnostic accuracy-comparison of emergency helical CT and surgical findings. *Radiology* 228:430-435, 2003.
102. Erbel R, Engberding R, Daniel W, et al: Echocardiography in diagnosis of aortic dissection. *Lancet* 1:457-461, 1989.
103. Nienaber CA, Spielmann RP, von Kodolitsch Y, et al: Diagnosis of thoracic aortic dissection: Magnetic resonance imaging versus transesophageal echocardiography. *Circulation* 85: 434-447, 1992.
104. Nienaber CA, von Kodolitsch Y, Nicolas V, et al: The diagnosis of thoracic aortic dissection by noninvasive imaging procedures. *N Engl J Med* 328:1-9, 1993.
105. Victor MF, Mintz GS, Kotler MN, et al: Two-dimensional echocardiographic diagnosis of aortic dissection. *Am J Cardiol* 48:1155-1159, 1981.
106. Movsowitz HD, Levine RA, Hilgenberg AD, et al: Transesophageal echocardiographic description of the mechanisms of aortic regurgitation in acute type A aortic dissection: implications for aortic valve repair. *J Am Coll Cardiol* 36:884-890, 2000.
107. Geibel A, Kasper W, Behroz A, et al: Risk of transesophageal echocardiography in awake patients with cardiac diseases. *Am J Cardiol* 62:337-339, 1988.
108. Silvey SV, Stroughton TL, Pearl W, et al: Rupture of the outer partition of aortic dissection during transesophageal echocardiography. *Am J Cardiol* 68:286-287, 1991.
109. Pearson AC, Castello R, Labovitz AJ: Safety and utility of transesophageal echocardiography in the critically ill patient. *Am Heart J* 119:1083-1089, 1990.
110. Iliceto S, Nanda NC, Rizzon P, et al: Color Doppler evaluation of aortic dissection. *Circulation* 75:748-755, 1987.
111. Appelbe AF, Walker PG, Yeoh JK, et al: Clinical significance and origin of artifacts in transesophageal echocardiography of the thoracic aorta. *J Am Coll Cardiol* 21:754-760, 1993.
112. Chan KL: Usefulness of transesophageal echocardiography in the diagnosis of conditions mimicking aortic dissection. *Am Heart J* 122:495-504, 1991.
113. Erbel R, Mohr-Kahaly S, Rennollet H, et al: Diagnosis of aortic dissection: The value of transesophageal echocardiography. *Thorac Cardiovasc Surg* 35:126-133, 1987.
114. Mohr-Kahaly S, Erbel R, Rennollet H, et al: Ambulatory follow-up of aortic dissection by transesophageal two-dimensional and color-coded Doppler echocardiography. *Circulation* 80:24-33, 1989.
115. Adachi H, Kyo S, Takamoto S, et al: Early diagnosis and surgical intervention of acute aortic dissection by transesophageal color flow mapping. *Circulation* 82(Suppl 4):19-23, 1990.
116. Crawford ES: The diagnosis and management of aortic dissection. *JAMA* 264:2537-2541, 1990.

117. Ballal RS, Nanda NC, Gatewood R, et al: Usefulness of transesophageal echocardiography in assessment of aortic dissection. *Circulation* 84:1903-1914, 1991.
118. Penn MS, Smedira N, Lytle B, et al: Does coronary angiography before emergency aortic surgery affect in-hospital mortality? *J Am Coll Cardiol* 35:889-894, 2000.
119. Adachi H, Omoto R, Kyo S, et al: Emergency surgical intervention of acute aortic dissection with the rapid diagnosis by transesophageal echocardiography. *Circulation* 84(Suppl 3):14-19, 1991.
120. Alter P, Herzum M, Maisch B: Echocardiographic findings mimicking type A aortic dissection. *Herz* 31:153-155, 2006.
121. Tsai TT, Evangelista A, Nienaber CA, et al; International Registry of Acute Aortic Dissection (IRAD): Long-term survival in patients presenting with type A acute aortic dissection: insights from the International Registry of Acute Aortic Dissection (IRAD). *Circulation* 114:I350-I356, 2006.
122. Nakatani S, Beppu S, Tanaka N, et al: Application of abdominal and transesophageal echocardiography as a guide for insertion of intraaortic balloon pump in aortic dissection. *Am J Cardiol* 64:1082-1083, 1989.
123. Mazzucotelli JP, Deleuze PH, Baufreton C, et al: Preservation of the aortic valve in acute aortic dissection: Long-term echocardiographic assessment and clinical outcome. *Ann Thorac Surg* 55:1513-1517, 1993.
124. Neustein SM, Lansman SL, Quintana CS, et al: Transesophageal Doppler echocardiographic monitoring for malperfusion during aortic dissection repair. *Ann Thorac Surg* 56:358-361, 1993.
125. Alsac JM, Boura B, Desgranges P, et al: Immediate endovascular repair for acute traumatic injuries of the thoracic aorta: a multicenter analysis of 28 cases. *J Vasc Surg* 48:1369-1374, 2008.
126. Xenos ES, Abedi NN, Davenport DL, et al: Meta-analysis of endovascular vs open repair for traumatic descending thoracic aortic rupture. *J Vasc Surg* 48:1343-1351, 2008.
127. Dobson G, Petrasek P, Alvarez N: Images in Anesthesia: transesophageal echocardiography enhances endovascular stent placement in traumatic trans-section of the thoracic aorta. *Can J Anaesth* 51:931, 2004.
128. Marty B, Tozzi P, Ruchat P, et al: An IVUS-based approach to traumatic aortic rupture, with a look at the lesion from inside. *J Endovasc Ther* 14:689-697, 2007.
129. Koschyk DH, Nienaber CA, Knap M, et al: How to guide stent-graft implantation in type B aortic dissection? Comparison of angiography, transesophageal echocardiography, and intravascular ultrasound. *Circulation* 112:I260-I264, 2005.
130. Laissy JP, Blanc F, Soyer P, et al: Thoracic aortic dissection: diagnosis with transesophageal echocardiography versus MR imaging. *Radiology* 194:331-336, 1995.
131. Heinemann M, Laas J, Karck M, Borst HG: Thoracic aortic aneurysms after acute type A aortic dissection: Necessity for follow-up. *Ann Thorac Surg* 49:580-584, 1990.
132. Barbetseas J, Crawford S, Safi HJ, et al: Doppler echocardiographic evaluation of pseudoaneurysms complicating composite grafts of the ascending aorta. *Circulation* 85:212-222, 1992.
133. Vilacosta I, Camino A, San Roman JA, et al: Supravalvular aortic stenosis after replacement of the ascending aorta. *Am J Cardiol* 70:1505-1507, 1992.
134. San Roman JA, Vilacosta I, Castillo JA, et al: Role of transesophageal echocardiography in the assessment of patients with composite aortic grafts for therapy in acute aortic dissection. *Am J Cardiol* 73:519-521, 1994.
135. Nath PH, Zollikofer C, Castaneda-Zuniga WR, et al: Radiological evaluation of composite aortic grafts. *Radiology* 131:43-51, 1979.
136. Pucillo AL, Schechter AG, Moggio RA, et al: Postoperative evaluation of ascending aortic prosthetic conduits by magnetic resonance imaging. *Chest* 97:106-110, 1990.
137. Simon P, Owen AN, Moidl R, et al: Sinus of Valsalva aneurysm: A late complication after repair of ascending aortic dissection. *Thorac Cardiovasc Surg* 42:29-31, 1994.
138. Haverich A, Miller DC, Scott WC, et al: Acute and chronic aortic dissections-determinant of long-term outcome for operative survivors. *Circulation* 72(Suppl 2):22-34, 1985.
139. Imawaki S, Maeta H, Shiraishi Y, et al: Decrease in aortic distensibility after an extended aortic reconstruction for Marfan's syndrome as a cause of postoperative acute aortic dissection DeBakey type I: a report of two cases. *Surg Today* 23:1010-1013, 1993.
140. Lacombe F, Dart A, Dewar E, et al: Arterial elastic properties in man: a comparison of echo-Doppler indices of aortic stiffness. *Eur Heart J* 13:1040-1045, 1992.
141. Lehmann ED, Hopkins KD, Gosling RG: Aortic compliance measurements using Doppler ultrasound: in vivo biochemical correlates. *Ultrasound Med Biol* 19:683-710, 1993.
142. Stefanadis CI, Karayannacos PE, Boudoulas HK, et al: Medial necrosis and acute alterations in aortic distensibility following removal of the vasa vasorum of canine ascending aorta. *Cardiovasc Res* 27:951-956, 1993.
143. Recchia D, Sharkey AM, Bosner MS, et al: Sensitive detection of abnormal aortic architecture in Marfan syndrome with high-frequency ultrasonic tissue characterization. *Circulation* 91:1036-1043, 1995.

# 37 Echocardiographic Findings in Systemic Diseases Characterized by Immune-Mediated Injury

CARLOS A. ROLDAN, MD

**Systemic Lupus Erythematosus**
Background
Associated Cardiovascular Involvement
**Primary Antiphospholipid Syndrome**
Background
Associated Cardiovascular Involvement
**Rheumatoid Arthritis**
Background
Associated Cardiovascular Involvement
**Ankylosing Spondylitis**
Background
Associated Cardiovascular Involvement
**Scleroderma**
Background
Associated Cardiovascular Involvement
**Polymyositis and Dermatomyositis**
Background
Associated Cardiovascular Involvement
**Mixed Connective Tissue Disease**
Background
Associated Cardiovascular Involvement

Rheumatologic diseases are chronic inflammatory states caused by autoimmunity. These diseases are more common in women than in men (with the exception of ankylosing spondylitis), usually manifest from the second through the fifth decade, and cause significant morbidity and mortality.

Although the heart is not the principal target organ of rheumatologic diseases, cardiovascular involvement is common and has serious consequences. The heart valves, myocardium, pericardium, coronary arteries, great vessels, and conduction system may be involved. Estimates of the prevalence of cardiac involvement vary widely because of differences in study design, study populations, and methods of cardiac evaluation.

Echocardiography plays a major role in the better understanding of the prevalence, incidence, characteristics, severity, evolution, and response to therapy of the cardiovascular diseases associated with rheumatologic diseases. The increasing application of real-time three-dimensional (3D) transthoracic echocardiography (TTE) and transesophageal echocardiography (TEE); tissue Doppler imaging, including myocardial strain; and contrast echocardiography will result in upward revision of prevalence and incidence rates, characterization, prognosis, and therapy of heart disease in patients with rheumatologic diseases. Also, echocardiography will play a major role in guiding and assessing the results of future pharmacotherapeutic trials and of percutaneous or surgical valve repair in these high-risk surgical candidates.

## Systemic Lupus Erythematosus

### BACKGROUND

Systemic lupus erythematosus (SLE) is a rheumatologic disease that affects predominantly the musculoskeletal and mucocutaneous systems. However, cardiovascular disease is the third most common cause of death in these patients, after infections and renal disease.

The most important forms of cardiac involvement in SLE are Libman-Sacks endocarditis, intracardiac thrombosis and thromboembolism, premature atherosclerosis, pericarditis, myocardial disease, and pulmonary hypertension.[1]

### ASSOCIATED CARDIOVASCULAR INVOLVEMENT

#### *Valve Disease*

Valve disease in SLE is subdivided into Libman-Sacks (inflammatory and thrombotic) or thrombotic vegetations, leaflet thickening with or without fibrosis, and valve regurgitation.[2,3] Mitral valve prolapse is more prevalent (up to 22%) in patients with lupus than in age-matched and gender-matched controls (5%).[4] About one third to half of patients with SLE may have valve vegetations or thickening, but the degree of associated valve regurgitation is usually mild to moderate and therefore clinically silent.[2,3] However, subclinical valve disease is

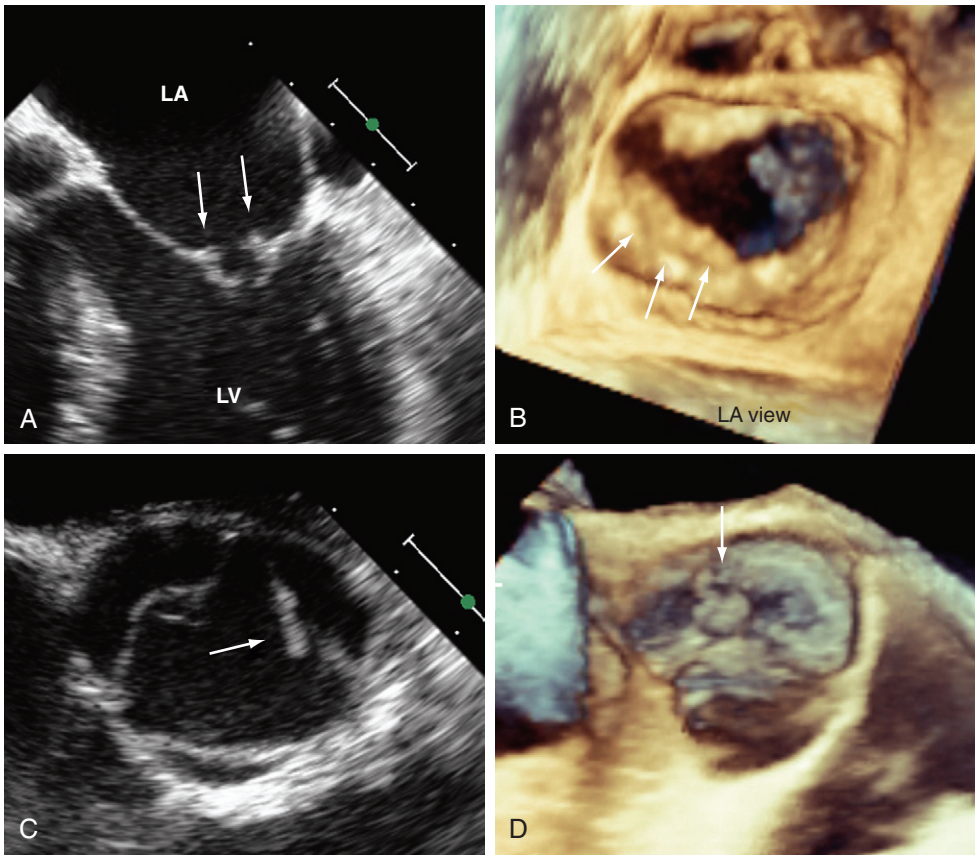



**Figure 37-1 Libman-Sacks vegetations of the mitral and aortic valves in a 27-year-old man with systemic lupus erythematosus. A,** This 2D TEE shows small, irregular-shaped, sessile, and soft tissue echoreflectant vegetations on the atrial side and coaptation point of the anterior and posterior mitral leaflets (*arrows*). Associated mild thickening of the leaflet tip is noted. Only mild mitral regurgitation was detected. **B,** This real-time 3D TEE of the mitral valve viewed from the atria and during diastole illustrates the tubular-shaped and sessile vegetation of the posterior mitral leaflet extending from P2 to P1 scallops (*arrows*). Similar characteristics of the anterior leaflet vegetation were best noted during systole. **C,** This 2D TEE shows a small, tubular-shaped, and homogeneously echo reflectant vegetation located at the tip on either the aortic or ventricular side of the left coronary cusp (*arrow*). **D,** This real-time 3D TEE of the aortic valve viewed from the aorta and during diastole shows the oval-shaped and soft tissue echoreflectant vegetation located on the tip and aortic side of the left coronary cusp (*arrow*). The aortic cusps are otherwise normal. No aortic regurgitation was shown.

commonly complicated by either subclinical or clinical cardioembolism and uncommonly by significant regurgitation from recurrent immune-mediated valvulitis or superimposed infective endocarditis.[3,5,6]

The pathogenesis of valve disease in SLE includes an immune-complex–mediated inflammation exacerbated by a commonly associated increased systemic and local thrombogenesis mediated by antiphospholipid antibodies, which include immunoglobulin G or immunoglobulin M anticardiolipin antibodies, lupus anticoagulant, and antibodies to plasma phospholipid-binding B2-glycoprotein I.[7,8] However, the temporal association of valve disease with activity and severity of SLE and the presence and levels of antiphospholipid antibodies is variable.[2,3,8,9] Libman-Sacks vegetations were originally described as cauliflower-like fibrous masses 2 to 4 mm in diameter that are located on any of the four cardiac valves. Active vegetations have central fibrinoid necrosis with fibroblastic proliferation and fibrosis surrounded by mononuclear and polymorphonuclear cellular infiltration, small hemorrhages, and platelet and fibrin thrombus.[10,11] Healed masses have central fibrosis, minimal or no inflammatory cell deposition, and no or hyalinized and endothelialized thrombus. Active, healed, and mixed masses can be seen in the same valve. Almost all patients with Libman-Sacks vegetations have a variable degree of leaflet fibrosis, but fibrosis is more prevalent than Libman-Sacks vegetations among unselected patients with SLE.

Echocardiographic studies have shown that Libman-Sacks vegetations are commonly less than 1 cm in diameter, vary in shape, have irregular borders, and have heterogeneous echodensity. The broad-based growths rarely move independently of the underlying valve structure. Lesions are more common on the mitral valve, are more commonly attached at the leaflet or cusp coaptation point, and typically are seen on the atrial side of the mitral valve and on either side of the aortic cusps (Figs. 37-1 to 37-4).[2,3,5,12] Rarely, vegetations are seen on the right-sided heart valves, atrial or ventricular endocardium, mitral or tricuspid subvalvular apparatus, or aortic root (see Question 37-1, Fig. 1, at ExpertConsult.com).[13] Echocardiographic studies estimate the prevalence rate of Libman-Sacks vegetations as less than 11% with TTE and 35% to 45% with TEE.[2,3,5,12,14] With TEE as the standard, TTE has a very low sensitivity and a low negative predictive value for detection of vegetations (11% and 57%, respectively).[15,16] The low detection of vegetations with TTE precludes assessment of its specificity and positive predictive value. Although real-time 3D TTE and TEE may improve the detection and characterization of Libman-Sacks vegetations, limited data are currently available.[17,18]

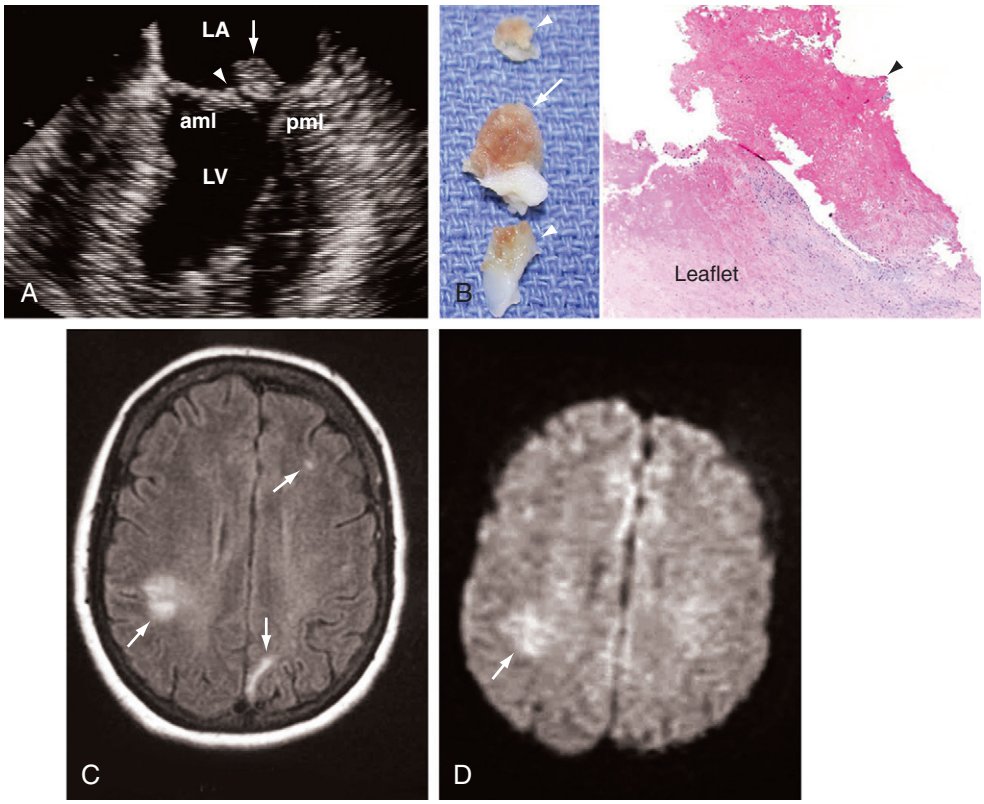



**Figure 37-2 Mitral valve Libman-Sacks vegetations in a 31-year-old woman with systemic lupus erythematosus and recurrent transient ischemic attacks. A,** This TEE shows a large vegetation on the atrial side and basal portion of the posterior mitral leaflet (*pml; arrow*) and a small vegetation on the atrial side of the anterior mitral leaflet (*aml; arrowhead*). Both leaflets had diffuse moderate thickening. Only mild mitral regurgitation was detected. The patient underwent mitral valve replacement as a result of recurrent transient ischemic attacks despite anticoagulation. **B,** Large vegetation (*arrow*) from the posterior leaflet and small vegetations (*arrowheads*) from the anterior leaflet. Histology of the leaflet revealed inflammation with mononuclear cells and fibrosis. Vegetations of predominant fibrinous material well adhered to the leaflet were shown (*arrowhead*). **C,** This fluid-attenuated inversion recovery magnetic resonance image shows a recent cerebral infarct in the right occipitoparietal white matter (*arrow on left*). Left occipital and frontal lobe small cerebral infarcts (*arrows on right*) are also shown. **D,** This diffusion-weighted image shows a large area of hyperintensity (focally restricted diffusion) and confirms a recent infarct in the right occipitoparietal white matter (*arrow*). The cerebral infarcts in the left occipital and frontal hyperintense lesions are not visible by diffusion-weighted image, indicating they are old infarcts.

Libman-Sacks vegetations and leaflet fibrosis are frequently accompanied by only mild to moderate valve regurgitation and therefore are usually clinically silent. However, significant complications, such as subclinical and clinical cardioembolism, commonly occur. Valve vegetations or thickening are more common in patients with asymptomatic or symptomatic focal ischemic brain injury on magnetic resonance imaging, in those with stroke or transient ischemic attack, and in those with nonfocal neurologic manifestations of cognitive dysfunction, acute confusional state, or seizures (Figs. 37-2 to 37-5).[3,5,19,20,21] Left-sided vegetations rarely embolize to the coronary arteries, and right-sided valve vegetations rarely embolize to the lungs or paradoxically embolize.[22,23] Also, transcranial Doppler imaging studies show higher rates of microembolic events in patients with valve disease and neurologic events.[24,25] In addition, in a series that correlated brain magnetic resonance imaging with pathology, a high association of valve vegetations or thickening with thromboembolic cerebrovascular injury was found.[26] Furthermore, Libman-Sacks endocarditis can be complicated with severe regurgitation that results from recurrent or acute valvulitis; noninfective valvulitic perforations, including bioprosthetic leaflets; noninfective mitral valve chordal rupture; or infective endocarditis in at least 20% of patients.[3,6,27,28] Infective endocarditis can mimic, accompany, or trigger a flare of SLE and can lead to severe valve dysfunction, congestive heart failure, and septic death. Similarly, a flare of SLE can mimic endocarditis (pseudoinfective endocarditis). The leaflet fibrosis (increased thickness and echoreflectance) that accompanies Libman-Sacks vegetations may cause reduced leaflet mobility, but valve stenosis is rare (less than 3%). In a TEE study, 48% of unselected patients with lupus younger than 60 years of age had abnormal leaflet thickness, defined as more than 3 mm.[2,3,12,16] With TEE as the standard, TTE has low sensitivity (53%), low specificity (50%), low negative predictive value (31%), and moderate positive predictive value (71%) for detection of valve thickening.[15,16] This limited diagnostic accuracy may explain the highly variable rates of valve thickening reported in studies with TTE. Shadowing caused by leaflet scarring is observed in 12% of patients. Annular, subvalvular, and right-sided heart involvement is rare.

The natural history of SLE-associated valve disease parallels that of the primary disease. With serial TEE, valve disease, especially valve vegetations, may appear de novo, resolve, change appearance, or progress (see Fig. 37-5).[3,12] Chronic inflammation may accelerate the progression of valve sclerosis into stenosis.[29] Also, patients with valve vegetations or with moderate to severe valve dysfunction have a threefold to fourfold higher combined incidence rate of stroke, peripheral embolism, need for valve surgery or repair, and death in a 2-year to 8-year follow-up period as compared with those without valve disease

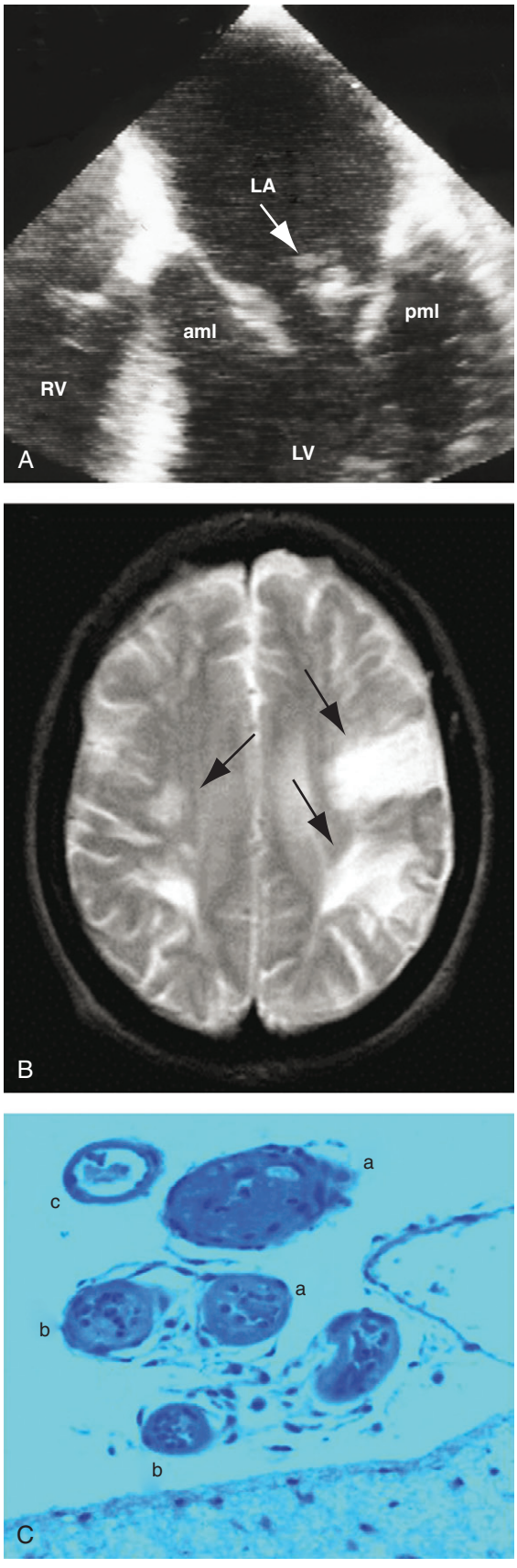



**Figure 37-3 Mitral valve Libman-Sacks vegetation in a 47-year-old woman with systemic lupus erythematosus and recurrent fatal stroke. A,** This TEE shows thickening of the mid and tip portions of the anterior (*aml*) and posterior (*pml*) mitral leaflets with a large vegetation on the midportion and atrial side of the posterior leaflet (*arrow*). **B,** This T2-weighted magnetic resonance imaging in the patient shows generalized cortical atrophy, multiple areas of old cerebral infarcts characterized by loss of both gray and white matter (large areas of hyperintensity; *arrows*) in a cortical or subcortical pattern, and multiple areas of deep white matter abnormality consistent with widespread ischemic cerebrovascular disease. **C,** Histopathology of the brain shows cerebral vessel occlusion by fibrin thrombi (*a*); intimal hyperplasia, vessel wall thickening, and platelet thrombi (*b*); and an occasional patent blood vessel (*c*).

or with mild valve disease.[3,5,6,28,30] The effect on valve vegetations of immunosuppressive therapy or long-term anticoagulation therapy is likely favorable but have not been tested in large controlled longitudinal series.

Rheumatic and SLE valve disease may have similar clinical, serologic, and echocardiographic findings.[31] In their chronic states, the echocardiographic characteristics of these two conditions may overlap. In patients greater than 60 years of age, the pattern of valve scarring characteristic of SLE may be obscured by changes that result from aging or atherosclerosis.[29] The echocardiographic appearances of Libman-Sacks, thrombotic, and infective vegetations also overlap (see Case 37-1 at Expert Consult.com).[3,11,32,33]

### *Intracardiac Thrombosis and Thromboembolism*

Patients with SLE are subject to intracardiac thrombosis and cerebral, peripheral arterial, and coronary artery thromboembolism. Pulmonary thromboembolism or rarely paradoxical embolism may occur in those with right heart lesions. These events occur independently of or are exacerbated by antiphospholipid antibody–induced thrombogenesis.[2,3,5,8,19,22,23,34] The most common substrates of high embolic potential are Libman-Sacks or thrombotic vegetations and less often intracardiac thrombi. Mitral valve vegetations are two to four times more common and are strong independent predictors of focal ischemic brain injury on magnetic resonance imaging, stroke or transient ischemic attack, and nonfocal neuropsychiatric manifestations.[5,19,20] Also, microembolism with transcranial Doppler ultrasound scan has been shown in patients with cerebral ischemic events.[24,25] In addition, postmortem series of patients with lupus frequently identify Libman-Sacks vegetations and thromboembolic ischemic brain injury.[26] Other uncommon embolic substrates in these patients are acute anterior myocardial infarction, more commonly resulting from coronary embolism or in situ thrombosis than from atherosclerotic disease; reduced left ventricular (LV) ejection fraction (less than 35%); and atrial fibrillation. Although paradoxical embolism has been reported, the prevalence and impact of patent foramen ovale have not been prospectively studied.[23] If substrates of high embolic potential are not identified on TTE, TEE should be performed.

### *Atherosclerotic Disease*

Controlled studies have shown that after controlling for traditional atherosclerotic risk factors, the prevalence rates of subclinical atherosclerosis in patients with lupus are two to four times higher than in matched controls.[1,35-37] Functional atherosclerosis in these patients is manifested as decreased coronary flow reserve with dipyridamole or adenosine echocardiography,

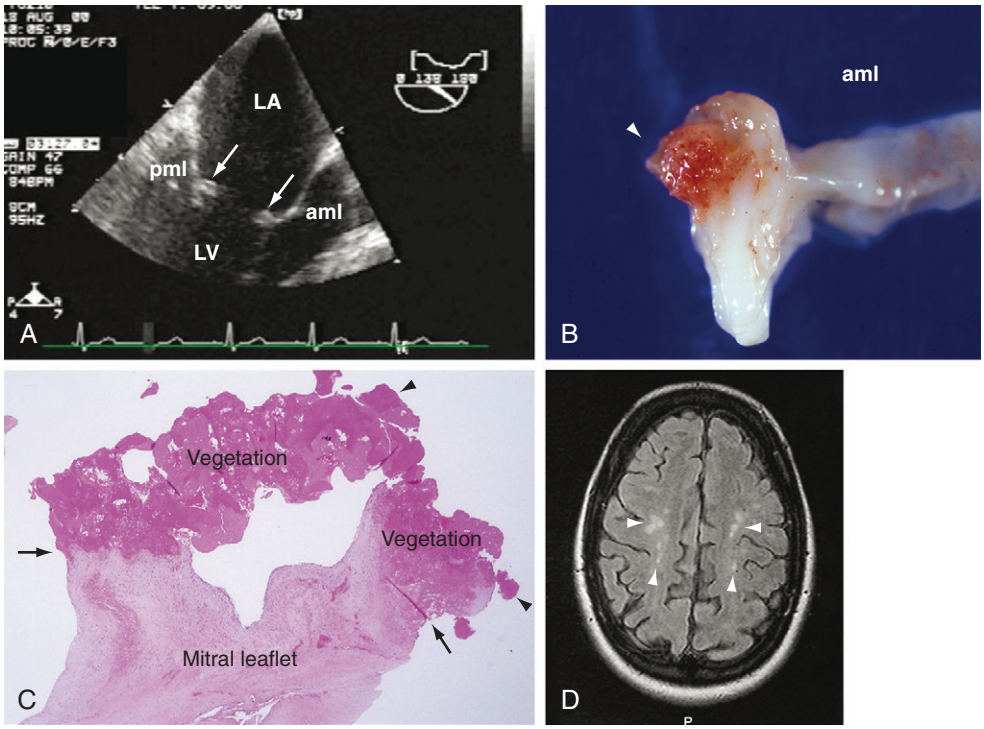



**Figure 37-4 Mitral valve Libman-Sacks vegetations in a 28-year-old woman with systemic lupus erythematosus and acute confusional state and cognitive dysfunction. A,** This TEE view shows small vegetations (*arrows*) on the atrial side and tip portions of the anterior (*aml*) and posterior (*pml*) mitral leaflets with associated leaflet thickening and decreased mobility. Patient underwent valve replacement because of associated symptomatic severe mitral regurgitation. **B,** Diffuse thickening with a Libman-Sacks vegetation on the atrial side and tip portion of the anterior leaflet is noted (*arrowhead*). **C,** Vegetation attached to the leaflets (*arrows*) shows amorphous eosinophilic fibrinous to granular deposits admixed with histiocytes, inflammatory cells, and superficial microthrombi (*arrowheads*). The mitral leaflet shows focal areas of myxoid degeneration and fibrinoid necrosis but no inflammation. **D,** This fluid-attenuated inversion recovery image shows multifocal hyperintensities in the subcortical white matter typical of small infarcts (*arrowheads*).

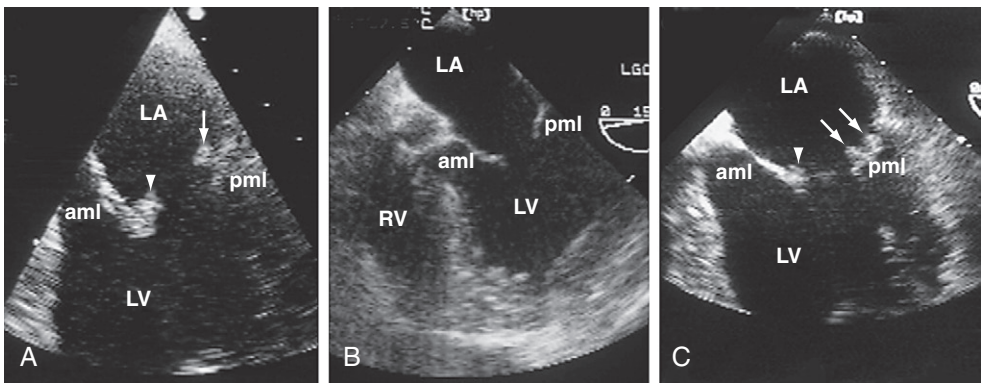



**Figure 37-5 Resolution and reappearance of mitral valve Libman-Sacks vegetations in a 37-year-old woman with systemic lupus erythematosus and a stroke. A,** This initial TEE shows two mitral valve vegetations: one on the atrial side of the tip of the anterior mitral leaflet (*aml; arrowhead*) and another on the midportion of the posterior leaflet (*pml; arrow*). Diffuse thickening of both mitral leaflets is also visible. Moderate mitral regurgitation is detected. **B,** Follow-up TEE obtained 2 months later shows resolution of both mitral valve vegetations and improvement in leaflet thickening. Mitral regurgitation was only mild. **C,** This TEE obtained 20 months later, when the patient had inactive systemic lupus erythematosus, shows reappearance of three mitral valve vegetations: one on the anterior mitral leaflet (*arrowhead*) and two on the posterior mitral leaflet (*arrows*). The thickening of both mitral leaflets has also worsened.

decreased peripheral arterial vasodilation, or increased carotid arteries and aortic stiffness. Premature subclinical atherosclerosis is also manifested as increased prevalence of coronary artery calcifications on computed tomography (31%) and increased carotid and aortic intima media thickening and plaques on carotid ultrasound scan (37%) and TEE (43%), respectively (Fig. 37-6).[35-40] Atherosclerotic aortic aneurysms have also been described.[41] Also, aortic and mitral valve sclerosis or calcification may be a manifestation of premature atherosclerosis.[29]

Clinically evident atherosclerosis is found in at least 10% of patients. Autopsy studies show a 25% prevalence rate of significant epicardial coronary atherosclerosis in patients with SLE. The proposed pathogenesis of atherosclerosis includes:

1. Activation of cellular and humoral immunity that causes cytotoxicity to the endothelium and vascular wall and results in increased vasoconstriction, thrombosis, neointimal and smooth muscle cell proliferation, medial hypertrophy, and ultimately plaque formation.

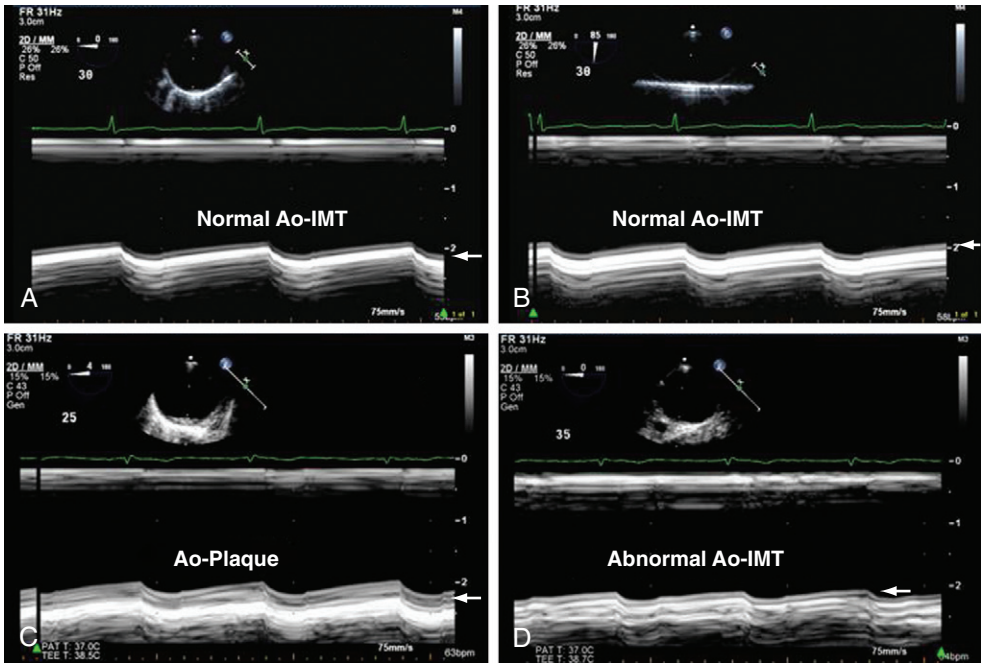



**Figure 37-6 Aortic atherosclerosis with TEE in patients with systemic lupus erythematosus.** Two-dimensional guided M-mode short-axis (**A**) and long-axis (**B**) TEE views of the anterior wall at the mid level (30 cm) of the descending thoracic aorta show normal intima media thickness (*IMT*) of less than 8 mm (*arrows*) in a 50-year-old woman with systemic lupus erythematosus. **C** and **D,** Two-dimensional guided M-mode short-axis TEE views of a 48-year-old woman with systemic lupus erythematosus show an aortic plaque of 3.3 mm at the proximal (25 cm; **C;** *arrow*) and abnormal intima media thickness of 1.2 mm at the distal (35 cm; **D;** *arrow*) descending thoracic aorta. *(Adapted from Roldan CA, Joson J, Sharrar J, Qualls CR, Sibbitt WL Jr: Premature aortic atherosclerosis in systemic lupus erythematosus: a controlled transesophageal echocardiographic study.* J Rheumatol *37:71-78, 2010.)*

2. Increased production of inflammatory cytokines and chemokines, which recruit inflammatory cells and promote vascular smooth cell proliferation, oxidative stress, endothelial apoptosis, and upregulation of adhesion molecules and chemokines.
3. Exacerbation of dyslipidemia, homocysteinemia, and insulin resistance by the disease itself and steroid therapy.

In patients with active SLE and vasculitis that affect other organs, angina and myocardial infarction may also rarely result from coronary arteritis.[22] In these patients, standard therapy for acute coronary syndrome, including percutaneous coronary interventions, and aggressive antiinflammatory therapy are beneficial.[42] Coronary embolism from a valve vegetation or in situ thrombosis warrants consideration when acute coronary syndrome occurs in a young patient with a cardioembolic substrate or antiphospholipid antibodies.

In patients with chest pain syndrome and regional wall motion abnormalities on echocardiography, coronary angiography most commonly reveals normal coronaries or nonobstructive coronary artery disease. In these patients frequently unable to exercise, stress echocardiography yields a low rate of abnormal results. Also, the clinical, electrocardiographic, serologic, and echocardiographic features of lupus myopericarditis or myocarditis mimic acute coronary syndrome. Therefore, coronary angiography may be warranted in patients with SLE with a suspected acute coronary syndrome.

### *Myocardial Disease*

Myocardial disease, manifested predominantly in the form of subclinical ventricular diastolic dysfunction, is common in patients with lupus and has multifactorial pathogenesis. One predominant cause is endothelial dysfunction–mediated microvascular coronary artery disease as determined by a decrease in coronary flow reserve by dipyridamole or adenosine Doppler TTE.[35] A highly prevalent (25% to 35%) arterial hypertension is the second most common cause.[35-40] In addition, premature peripheral arterial stiffness independent of hypertension may cause increased left ventricular (LV) afterload, LV mass, and diastolic dysfunction.[37,40,43,44] Small vessel vasculitis, coronary arteritis, and primary myocarditis are uncommon causes.[45] Rarely, acute lupus myocarditis manifested as clinical congestive heart failure with global or segmental LV dysfunction may be the initial manifestation of active SLE.[45] Finally, a chloroquine sulfate-induced dilated or restrictive cardiomyopathy has been recently reported.[46,47] Many controlled Doppler echocardiography series in asymptomatic patients without systemic or pulmonary hypertension and normal LV systolic function have shown a high prevalence rate (15% to 35%) of variable degrees of LV and right ventricular (RV) diastolic dysfunction.[48-50] Tissue-Doppler parameters and myocardial strain and strain rate are more sensitive than mitral inflow Doppler parameters in detection of early stages of ventricular diastolic and systolic dysfunction.[48-53] Subclinical LV diastolic and systolic dysfunction occur more frequently in patients with longer disease duration and in those with higher disease activity and severity.[49,53] Indicative of microvascular coronary artery disease, LV diastolic dysfunction has been associated with reversible, fixed, and mixed myocardial perfusion defects in young patients with active SLE and normal coronary arteries. In contrast to ventricular diastolic dysfunction, the prevalence rate of systolic dysfunction is less than 20% in unselected patients.[2,3,48,51-54] In summary, Doppler echocardiography is important in the detection of subclinical LV and RV diastolic and systolic dysfunction in patients with lupus. However, the clinical and prognostic implications of these findings need to be determined in longitudinal studies.

### *Pericarditis*

As many as 50% of patients with SLE have at least one episode of symptomatic pericarditis.[55] Most episodes are acute and frequently associated with active SLE. Cardiac tamponade and constrictive pericarditis are uncommon (less than 2%).[55-57] Rarely, acute pericarditis and cardiac tamponade can be the initial manifestation of SLE.[58] Because an effusion is not always present, the diagnosis of pericarditis rests on clinical manifestations, not the echocardiogram. However, echocardiography is of diagnostic value in these patients because pericardial chest pain can be mistaken as musculoskeletal or pleural pain.

An effusion without accompanying signs and symptoms of pericarditis in a patient with lupus results from mild pericarditis, hypoalbuminemia, or pulmonary hypertension with or without cor pulmonale.[59] Asymptomatic effusions are common incidental finding (~20%) in hospitalized patients with active SLE.

Echocardiography is the standard method for the evaluation of suspected SLE pericarditis to assess the size of an effusion and look for signs of tamponade. Tamponade is uncommon in SLE pericarditis, but the high morbidity rate of this complication and the potential for an atypical clinical presentation mandate careful evaluation. Echocardiographic indicators of tamponade should prompt intensive antiinflammatory and immunosuppressive therapy and pericardiocentesis. Echocardiographically guided diagnostic or therapeutic pericardiocentesis has been successfully performed in series of patients with lupus.

Rarely, constrictive or infectious pericarditis may complicate SLE pericarditis. Echocardiography is an effective screening method when constriction is under consideration. However, echocardiography is insensitive for the detection of mild or moderate pericardial thickening. Cardiac magnetic resonance imaging or computed tomography (CT) are preferred methods for assessment of pericardial thickness and are important confirmatory tests when the echocardiogram suggests constriction.

### *Pulmonary Hypertension*

Pulmonary hypertension occurs in at least 15% of patients with SLE. The most common causes include interstitial lung disease, vasculitis, and thromboembolism.[60,61] The association of pulmonary hypertension with Raynaud phenomenon also suggests a vasospastic etiology.[62] In fact, endothelin-1 receptor antagonists improve pulmonary arterial hypertension.[63] Resting and, in selected cases, exercise Doppler echocardiography is commonly used in the diagnosis and assessment of severity, causes, response to therapy, and follow-up of SLE-associated pulmonary hypertension.[60-62]

## Primary Antiphospholipid Syndrome

### BACKGROUND

Primary antiphospholipid syndrome (PAPS) is defined by:

1. Presence of antiphospholipid antibodies;
2. Venous or arterial thrombosis or complicated pregnancy (fetal loss, preeclampsia, and eclampsia); and
3. Lack of diagnostic criteria for other rheumatologic disease.

The diagnosis is established with one or more clinical criteria and one type of antiphospholipid antibodies on two or more occasions at least 6 weeks apart.[8] The pathogenesis of cardiovascular disease associated with PAPS may result from antiphospholipid antibody–induced functional and structural endothelial dysfunction, increased platelet aggregation, increased intrinsic and extrinsic coagulation pathways, and decreased fibrinolysis.[8,64] Cardiovascular disease occurs in 50% to 75% of patients with PAPS and is manifest as valve disease, intracardiac thrombosis and thromboembolism, pulmonary hypertension, nonobstructive coronary disease, and myocardial disease.[64-66]

### ASSOCIATED CARDIOVASCULAR INVOLVEMENT

#### *Valve Disease*

Valve disease is the most common cardiac manifestation of PAPS. The prevalence, distribution, characteristics, and clinical implications of valve disease in PAPS mimic those of SLE.[11,64-69] Valve disease manifests as valve vegetations, valve thickening, and less commonly, valve regurgitation. In controlled series with TTE, the prevalence rate of left-sided valve disease ranges from 30% to 40%, as compared with less than 5% in controls. With TEE, an even higher prevalence rate of valve disease (60% to 80%) is seen.[70,71] Echocardiographically, and probably histopathologically, vegetations associated with PAPS are indistinguishable from those associated with SLE (Fig. 37-7).[2,3,5,15,16,69-72] As in patients with SLE, valve lesions frequently persist unchanged (50% to 60%), appear de novo (20% to 30%), resolve (20%), uncommonly progress (less than 20%), or need valve replacement (less than 10%) during a 1- to 5-year follow-up period.[71,72] Left-sided valve lesions are associated with thromboembolism to the brain (50%), peripheral and coronary arteries (20% to 25%), and intraabdominal visceras.[70-72] The effect of anticoagulation therapy on valve lesions is generally beneficial, but the effect of antiinflammatory therapy is undefined. However, large controlled longitudinal therapeutic series are not available.[72,73]

#### *Intracardiac Thrombosis and Thromboembolism*

Patients with PAPS have a high prevalence rate (~60%) of left-sided and right-sided thrombotic valve vegetations and intracavitary thrombi.[64-72] Intracardiac thrombi include:

1. Thrombotic valve vegetations that consist of platelet or fibrin thrombi formed on structurally abnormal or rarely normal valves[64-73];
2. Left atrial (LA) appendage thrombi[74];
3. Atrial or ventricular wall or free-floating intracavitary thrombi[75,76];
4. Obstructive thrombi that create a functional tricuspid or mitral stenosis[77,78]; and
5. Thrombi associated with cardiac catheters, wires, or valve prosthesis.[78]

Right-sided heart thrombi are associated with deep venous thrombosis or pulmonary embolism and with right heart catheters or wires. Intracardiac thrombosis in patients with PAPS is predominantly associated with cerebral and peripheral arterial embolism, including the coronary arteries, and is uncommonly associated with pulmonary thromboembolism and rarely with paradoxical embolism. Valve vegetations and intracardiac thrombi are best detected with TEE. Expectedly, real-time 3D TEE may provide superior detection and characterization of valve vegetations and intracardiac thrombi in these patients, but limited data are currently available (see Fig. 37-7).

#### *Pulmonary Hypertension*

The prevalence rate of pulmonary hypertension on prospective echocardiographic series of patients with PAPS is at least 20% to 25% and results predominantly from chronic and recurrent

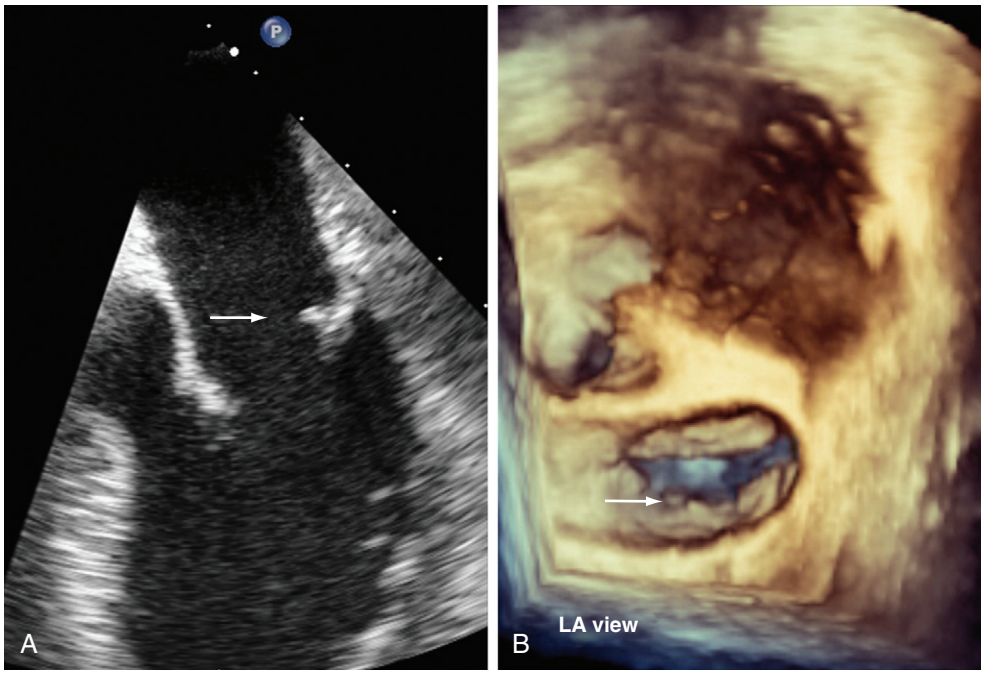



**Figure 37-7** **Mitral valve thrombotic vegetation in a 43-year-old man with primary antiphospholipid antibody syndrome and a stroke.** **A,** This 2D TEE shows a small, oval-shaped, sessile, heterogeneous echoreflectant vegetation with well-defined borders that is located on the mid to distal portions of the posterior mitral leaflet (*arrow*). Diffuse thickening of the posterior leaflet and thickening of the distal portion of the anterior leaflet is also noted. **B,** This real-time 3D TEE of the mitral valve viewed from the atria confirmed the characteristics of the vegetation as seen with 2D images and defined better the exact location of the vegetation at the tip and middle scallop of the posterior leaflet (*arrow*). The mitral valve vegetation resolved completely after several months of warfarin therapy.

pulmonary embolism and uncommonly from an abnormal vasospastic or in situ thrombotic vasculopathy.[72,75,78] Doppler echocardiography has an important role in the diagnosis, assessment of severity, response to therapy, and follow-up of PAPS-associated pulmonary hypertension.

### *Coronary Artery Disease*

Hemostatic abnormalities, possibly inflammation, and increased intake of oxidized low-density lipoprotein by activated macrophages in the coronary vessel wall cause endothelial damage and dysfunction, vasoconstriction, thrombosis, and atherosclerosis.[8,79,80] High prevalence rates of increased intima media thickness but no plaques of the carotid arteries are reported in these patients.[80,81] A high prevalence rate (20% to 35%) of myocardial infarction has been reported in patients with PAPS and results from microvascular disease, in situ coronary thrombosis, or coronary thromboembolism.[70,72,82,83] No series are found that systematically use resting or stress echocardiography for detection of epicardial coronary artery disease in patients with PAPS, but the sensitivity of these techniques is likely low given the low prevalence of epicardial atherosclerosis.

### *Myocardial Disease*

In small controlled cross-sectional studies of asymptomatic patients with PAPS, a high prevalence of LV diastolic dysfunction, predominantly impaired relaxation, is reported.[84] The mechanisms of diastolic dysfunction include microvascular coronary artery disease, thrombotic microangiopathy, and rarely, primary myocardial disease. Rarely, catastrophic PAPS may manifest as dilated cardiomyopathy with LV thrombus. RV diastolic dysfunction, predominantly impaired relaxation, is also common in patients with PAPS with pulmonary hypertension.[49]

## Rheumatoid Arthritis

### BACKGROUND

Rheumatoid arthritis is characterized by symmetric arthritis that involves any synovial joint but usually affects the metacarpophalangeal and proximal interphalangeal joints and wrists. Other manifestations of rheumatoid arthritis include rheumatoid nodules, systemic vasculitis, glomerulonephritis, pulmonary fibrosis, and cardiovascular disease.[85] Clinically apparent heart disease occurs in 25% to 40% of patients with rheumatoid arthritis. Heart disease is the third leading cause of death in patients with rheumatoid arthritis and accounts for nearly 40% of deaths.[86]

### ASSOCIATED CARDIOVASCULAR INVOLVEMENT

#### *Coronary Artery Disease*

After controlling for traditional atherogenic risk factors, the prevalence of coronary artery disease in patients with rheumatoid arthritis is two to three times higher than in matched controls.[87] Coronary arteritis is rare, whereas typical atherosclerotic epicardial coronary artery disease is common, often symptomatic, and associated with increased morbidity and mortality.[88] Estimates are that by age 65 to 70 years, 75% to 80% of patients with rheumatoid arthritis have angiographic evidence of coronary artery disease (30% with three vessels of coronary artery disease) and a high incidence of myocardial infarction (4.8 to 5.9 events per 1000 person-years). In addition, microvascular disease is common and correlates with levels of asymmetric dimethylarginine (an endogenous inhibitor of nitric oxide synthase).[89-91] Coronary artery disease accounts for at least 40% of the mortality of patients with rheumatoid arthritis.[88]

The pathogenesis of coronary artery disease in patients with rheumatoid arthritis is similar to that described for patients with SLE.[85,87,89-93] The rheumatoid arthritis–related clinical predictors of epicardial, microvascular, and inflammatory coronary artery disease include older age at onset of rheumatoid arthritis, longer duration of corticosteroid therapy, and long-standing disease (more than 10 years); active extraarticular, erosive polyarticular, and nodular disease; vasculitis; high titers of rheumatoid factor; high levels of haptoglobin, Von Willebrand factor, and plasminogen activator inhibitor; high levels of interleukins 1 and 6; and an erythrocyte sedimentation rate of more than 55 mm Hg. Compared with matched controls, a twofold increased risk is found for myocardial infarction, congestive heart failure, stroke, and cardiovascular mortality in patients with rheumatoid arthritis with elevated markers of inflammation and in those with reduced small and large arteries elasticity.[94-96] Patients with rheumatoid arthritis with an acute coronary syndrome have a higher recurrence rate of events and mortality than matched controls (58% versus 30% and 40% versus 15%, respectively).[97] Also, coronary artery bypass grafting surgical morbidity and mortality rates of patients with rheumatoid arthritis are two to four times higher than those of matched controls. In addition, a high prevalence rate (up to 61%) of subclinical coronary artery disease as determined with coronary artery calcification on computed tomography is seen in patients with established disease as compared with those with recent onset of the disease (43%) and matched controls (38%).[98] Furthermore, cyclooxygenase-2 selective inhibitors (which inhibit prostaglandin I-2, a vasodilator and inhibitor of platelet aggregation) and nonsteroidal anti-inflammatory drugs increase the risk of acute coronary syndromes in patients with rheumatoid arthritis.[99] Amelioration of inflammation with corticosteroids, cytotoxics, and disease-modifying antirheumatic drugs such as tumor necrosis factor–α blockers, inhibitors of interleukin 6, and statins decreases vascular inflammation and dysfunction and consequently the risk of adverse cardiovascular outcomes.[91,100,101]

Although rare, coronary vasculitis can affect small or medium-sized intramyocardial arteries. In patients with rheumatoid arthritis with an acute coronary syndrome from coronary arteritis, aggressive antiinflammatory and immunosuppressive therapy in conjunction with standard therapy, including coronary stents and surgical revascularization, has been successful (see Case 37-2 at ExpertConsult.com).

As in the general population, resting and stress echocardiography are useful in the detection of wall motion abnormalities in those with obstructive coronary artery disease but have decreased sensitivity for microvascular disease. Symptomatic patients with rheumatoid arthritis often have evidence of ischemia on resting and exercise echocardiography, and the presence of ischemia on exercise echocardiography portends a three times higher mortality rate than in matched controls with negative resting or exercise studies.[102] Also, dipyridamole or adenosine TTE can be used to assess coronary flow reserve in those with microvascular disease.

### *Pericarditis*

Echocardiographic studies have shown pericardial effusions in as many as 50% of patients with rheumatoid arthritis, but symptomatic pericarditis is less common. Pericarditis occurs in patients with active disease with similar clinical and serologic characteristics of those with coronary artery disease. Immunofluorescent staining of the pericardium reveals deposits of immunoglobulin G, immunoglobulin M, C3, and C1q, which indicates autoimmune injury. The pericardial effusion is exudative and bloody with a low glucose level, and it may contain rheumatoid factor. As in SLE pericarditis, tamponade and constriction are rarely reported. Also, asymptomatic pericardial effusions are seen in about 25% of patients and are associated with renal disease, hypoalbuminemia, and pulmonary hypertension.[103] The role of echocardiography in the diagnosis, management, and follow-up of rheumatoid effusions parallels its role in SLE pericarditis.[104]

### *Valve Disease*

Estimates of the clinical prevalence of valve disease in rheumatoid arthritis are undefined. The reported prevalence rate of valve abnormalities in unselected patients less than 60 years old is as low as 30% with TTE and nearly 60% with TEE.[85,105] Valve disease occur in five forms:

1. Valve nodules;
2. Healed valvulitis with residual leaflet fibrosis and regurgitation and rarely stenosis;
3. Acute chronic valvulitis;
4. Rarely acute valvulitis with Libman-Sacks–like vegetations; and
5. superimposed infective endocarditis.[85,105-107]

Acute and chronic valvulitis with resulting leaflet thickening or fibrosis is indistinguishable from that seen in SLE. Chronic inflammation may also promote accelerated leaflet fibrosis, calcification, and valve stenosis.[108] In contrast, valve nodules appear to be unique to rheumatoid arthritis. These nodules can also be seen on valve rings, papillary muscle tips, and atrial or ventricular endocardium.[109] Histologically, the valve nodules resemble subcutaneous nodules and may result from a process of focal vasculitis.

On TEE, rheumatoid valve nodules are detected in one third of patients; they usually appear as small (less than 0.5 $cm^2$) spheroid masses with homogeneous reflectance, typically appearing singly and on any portion of the leaflet.[105] The adjacent leaflet appears normal or shows mild sclerosis. This picture is unlike that of Libman-Sacks vegetations (compare Fig. 37-1 with Fig. 37-5 with Fig. 37-8). Acute valvulitis with superimposed Libman-Sacks–like vegetations can occur (Fig. 37-9). Valve thickening is detected in half of patients and is equally diffuse or localized (when localized affects any leaflet portion), is usually mild, involves equally the mitral and aortic valves, and involves rarely the annulus and subvalvular apparatus. Mild or worse valve regurgitation is seen in 20% to 25% of patients, but stenosis is rare (Fig. 37-10). However, in severe single or multiple acute valvulitis, diffuse leaflets thickening and moderate to severe valve regurgitation can occur (see Question 37-3 at ExpertConsult.com).

Rheumatoid valve disease is generally mild and asymptomatic, and it is less likely than SLE valve disease to result in clinically significant valve dysfunction. However, several uncommon severe manifestations of the disease have been described:

1. Valve thrombus overimposed on a valve nodule, Libman-Sacks–like vegetations, or superimposed valve strands complicated with systemic embolism (see Fig. 37-9)[105,110];
2. Acute or recurrent valvulitis that results in severe valve regurgitation and rarely stenosis (see Fig. 37-10)[109];
3. Acute severe valve regurgitation from rupture of a single or coalescent nodule or a large nodule that affects leaflet coapation[111];
4. Aortitis with aortic root dilation and aortic regurgitation; and
5. Superimposed infective endocarditis.[107]

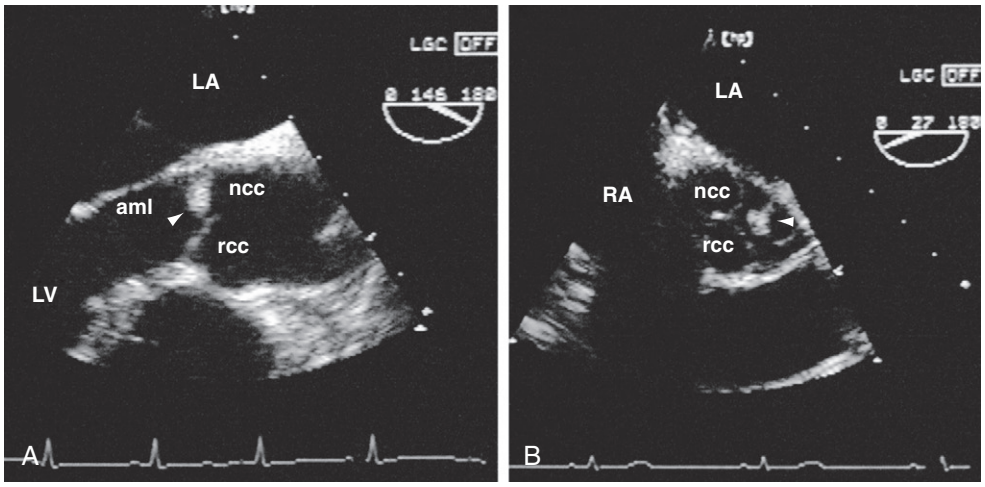



**Figure 37-8** **Rheumatoid aortic valve nodules in young asymptomatic patients. A,** This TEE view longitudinal to the outflow tract in a 48-year-old woman with rheumatoid arthritis shows an oval-shaped nodule with well-defined borders and homogeneous soft tissue echoreflectance within the midportion of the aortic noncoronary cusp (*ncc; arrowhead*). The appearance of the right coronary cusps is normal. Aortic valve regurgitation was not shown. **B,** This TEE short-axis view of the aortic valve in a 43-year-old man with rheumatoid arthritis shows a well-defined nodule with homogeneously increased echoreflectance within the tip and midportion of the left coronary cusp (*arrowhead*). Note the normal appearance of the uninvolved portions of the cusp and that of the noncoronary cusp and right coronary cusp (*rcc*). Mild aortic valve regurgitation was detected. *aml*, Anterior mitral leaflet.

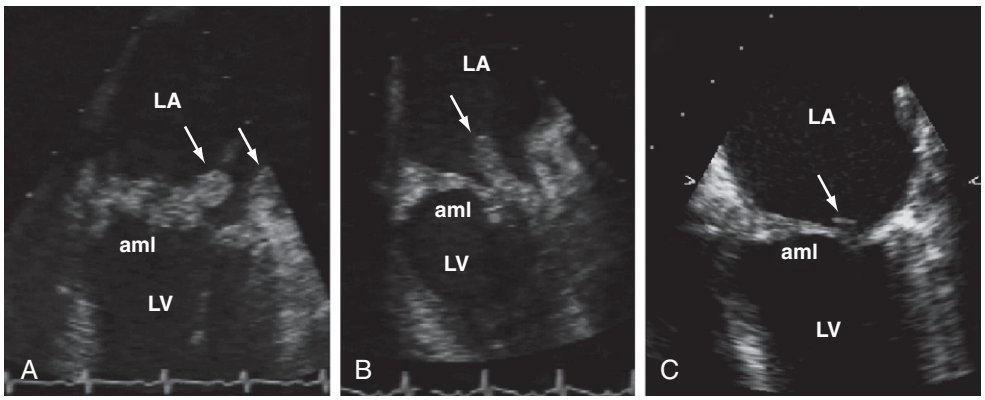



**Figure 37-9** **Severe mitral valvulitis with Libman-Sacks–like vegetations in a 52-year-old woman with severe rheumatoid arthritis and recurrent transient ischemic attacks. A,** This close-up four-chamber TEE view when patient presented with a transient ischemic attack shows severe and irregular thickening with soft tissue echoreflectance of the anterior and posterior mitral leaflets. Two large, multilobed masses, with irregular borders and with soft tissue echoreflectant, are noted on the atrial side of the anterior (*aml*) and posterior mitral leaflets (*arrows*). **B,** Close-up four-chamber TEE view after 3 months of warfarin, steroids, and tumor necrosis factor–α receptor inhibitors shows remarkable improvement of the thickening of the mitral leaflets, complete resolution of the anterior mitral leaflet vegetation, and reduction in size of the posterior mitral leaflet (*arrow*). **C,** Close-up four-chamber TEE view after 6 months of therapy shows further improvement in the thickening of the mitral leaflets and a very small residual vegetation on the atrial side and tip of the posterior mitral leaflet (*arrow*). Also, mitral regurgitation improved from moderate to trivial.

The short-term and long-term mortality rates of patients with rheumatoid arthritis with valve disease are significantly higher than those of matched controls. In small case series, the 30-day and 1-year morbidity and mortality rates of patients with rheumatoid arthritis undergoing valve replacement or rarely valve repair are two to three times higher than those of patients without rheumatoid arthritis.[109] Early diagnosis and aggressive antiinflammatory or immunosuppressive therapy may decrease the progression of the disease and improve patient survival. Therefore, TTE and TEE continue to play an important role in the diagnosis, characterization, management, and follow-up of rheumatoid valve disease.

### *Myocardial Disease*

Patients with rheumatoid arthritis have a high prevalence rate of subclinical and clinical LV and RV diastolic dysfunction as compared with matched controls (30% to 76% versus less than 20%, respectively) in multiple Doppler echocardiography series.[112-116] The pathogenetic factors for ventricular diastolic dysfunction are similar to those described in SLE.[90,91,113] Lower E′ and A′ velocities and increased E/E′ ratio with tissue Doppler imaging, lower color flow propagation velocity, decreased longitudinal myocardial strain and strain rate, and increased myocardial performance index are more sensitive than mitral or tricuspid inflow Doppler parameters. The clinical predictors of myocardial disease are similar to those described for coronary artery disease and valve disease. Also, large longitudinal series have shown a high incidence rate (35% to 40%) of clinical diastolic congestive heart failure independent of traditional risk factors for diastolic dysfunction. In these patients, diastolic congestive heart failure doubles the mortality risk as compared with matched controls with diastolic congestive heart failure but no

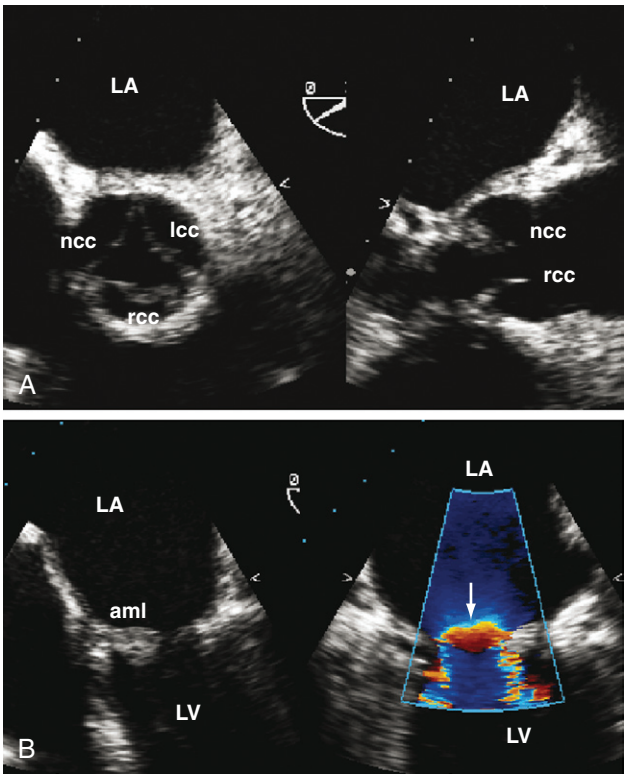



**Figure 37-10 Aortic and mitral stenosis in a patient with severe rheumatoid arthritis. A,** The short-axis and longitudinal TEE views of the aortic valve show diffuse soft tissue thickening and decreased mobility of the aortic cusps. An associated peak aortic valve gradient of 19 mm Hg consistent with mild aortic stenosis and mild aortic regurgitation was shown with continuous wave Doppler imaging. **B,** These close-up four-chamber TEE views of the mitral valve show severe soft-tissue thickening predominantly of the base and midportion of the mitral leaflets with significantly decreased mobility. Note the large acceleration zone with color Doppler imaging (*arrow*) of the mitral inflow that suggests mitral valve stenosis. Continuous wave Doppler imaging confirmed the presence of moderate mitral stenosis. Associated mild mitral regurgitation was also seen. This TEE was performed several months after patient had a flare of her disease associated with pancarditis. *aml,* Anterior mitral leaflet; *lcc,* left coronary cusp; *ncc,* noncoronary cusp; *rcc,* right coronary cusp.

rheumatoid arthritis.[117,118] The incidence rate of congestive heart failure decreases with tumor necrosis factor–α blocker therapy.[118] Pulmonary hypertension is the most common cause of RV diastolic dysfunction in patients with rheumatoid arthritis, but microvascular coronary artery disease and autoimmune mediated myocardial disease also play a role. Some patients with rheumatoid arthritis have myocarditis, myocardial nodules, or cardiac amyloidosis. Evidence of present or past myocarditis is revealed at autopsy in as many as 30% of patients, but decreased LV ejection fraction with echocardiography is less common. Myocarditis, associated with SS-A/SS-B autoantibodies can mimic non-ST and ST elevation myocardial infarction clinically, electrocardiographically, serologically, and echocardiographically.[119] Recently, a dilated or restrictive cardiomyopathy from chloroquine therapy has been reported.[120] Finally, rarely rheumatoid arthritis–associated myocardial amyloidosis can occur.

### *Pulmonary Hypertension*

Pulmonary hypertension with normal pulmonary venous pressure resulting from interstitial fibrosis, pulmonary vasculitis, or obliterative bronchiolitis is more common than left heart disease. In controlled series of asymptomatic patients, the prevalence rate of pulmonary hypertension by echocardiography is five times higher in patients with rheumatoid arthritis than in controls (21% versus 4%) and is even higher in those with symptoms or evidence of pulmonary disease.[121] The mortality rate is high within 1 year of diagnosis. Prompt diagnosis is vital because these conditions are responsive to immunosuppressive therapy.

Therefore, if pulmonary hypertension is identified, LA hypertension should be excluded and then the search for a treatable pulmonary cause should be pursued. When pulmonary hypertension is diagnosed in asymptomatic or symptomatic patients, echocardiography is useful not only for assessment of its severity and associated RV diastolic or systolic dysfunction and tricuspid regurgitation but also for assessment of the short-term and long-term response to therapy.

## Ankylosing Spondylitis

### BACKGROUND

Ankylosing spondylitis and other human leukocyte antigen-B27–related arthropathies are characterized by inflammation of the vertebral and sacroiliac joints. Arthritis of other joints, uveitis, and proximal aortitis and aortic valvulitis are common. Although arthritis may be disabling, the overall prognosis is good.

### ASSOCIATED CARDIOVASCULAR INVOLVEMENT

#### *Aortitis and Valve Disease*

Aortic root and valve disease in patients with ankylosing spondylitis is categorized as:

1. Proximal aortitis that leads to aortic root thickening, stiffness, dilation, and rarely aneurysm formation, all of which contribute to aortic regurgitation;
2. Aortic valvulitis that results in cusp thickening and retraction and also leads to aortic regurgitation;
3. Thickening of the aortomitral junction or "subaortic bump" that causes anterior mitral leaflet retraction with decreased mobility and asymmetric or incomplete mitral leaflet coaptation that leads to mitral regurgitation; and
4. Extension of the subaortic fibrotic process into the basal septum, atrioventricular node, proximal bundle of His, and bundle branches or fascicles that causes conduction disturbances.[122]

The reason for selective injury of the proximal aorta by this human leukocyte antigen-B27–mediated mononuclear cellular inflammatory process is unknown.

The prevalence of clinically manifested ascending aorta and aortic and mitral valve disease varies widely but is probably about 20%. Aortic or mitral regurgitation is generally mild to moderate. However, acute or healed aortitis, acute or healed aortic valvulitis, and superimposed infective endocarditis can lead to severe aortic regurgitation.[122-124]

In several echocardiographic studies, including TEE series, aortic root thickening or sclerosis (predominantly of the posterior wall), increased stiffness, and dilation range from 20% to 60%, 60%, and 25% to 50% of patients, respectively.[122,125,126] Aortic valve thickening seen in 40% of patients is manifested mainly as nodularities of the aortic cusps. Mitral valve thickening seen in one third of patients is manifested as basal thickening of the anterior mitral leaflet, forming the characteristic

subaortic bump. Valve regurgitation seen in almost half of patients was moderate in one third of them. Aortic root disease and valve disease are related to duration of the disease but are not temporally related to its activity, severity, or therapy (Figs. 37-11 and 37-12).[122,127] Mitral valve prolapse or myxomatous mitral leaflets with mild or moderate regurgitation is reported in 10% to 15% of patients.

The effect of corticosteroids or disease-modifying antirheumatic drug therapy on aortic root, valve disease, and conduction disturbances is uncertain. Because of the absence of multiorgan disease and infrequent use of corticosteroids or cytotoxics in patients with ankylosing spondylitis, the mortality rate during valve replacement is probably similar to that of the general population.

### *Conduction Abnormalities*

Atrioventricular and intraventricular conduction blocks occur in 20% or more of patients with ankylosing spondylitis.[128] Echocardiographic studies have shown an association of conduction abnormalities with aortic root thickening and subaortic bump, suggesting a role for extension of aortic root fibrosis into the proximal septum and atrioventricular node.[122,125,128] In a controlled tissue-Doppler echocardiography series, an increase in interatrial and intraatrial electromechanical coupling intervals has been demonstrated.[129] However, the clinical significance of these findings is uncertain.

### *Myocardial and Pericardial Disease*

Although the frequency of myocardial disease in patients with ankylosing spondylitis is higher than in the general population, it is generally subclinical and therefore more commonly incidentally detected. Patients with ankylosing spondylitis also have microvascular disease, which is associated with subclinical diastolic dysfunction.[130] In addition, the associated aortic stiffness may lead to increased LV afterload, LV mass, and diastolic dysfunction.[131] Few controlled Doppler echocardiography series in patients less than 50 years old with no clinical heart disease have uncommonly reported LV systolic dysfunction. In contrast, a 20% to 30% prevalence rate of diastolic dysfunction, predominantly impaired relaxation, has been reported. The prevalence rates of diastolic dysfunction are higher (up to 50%) with tissue-Doppler echocardiography.[129,132] In these studies, diastolic dysfunction was temporally unrelated to age, disease duration, or disease activity. Rarely, cardiac amyloidosis with diastolic congestive heart failure has been reported.

The prevalence of pericardial disease in patients with ankylosing spondylitis is rare, and the rate is probably similar to that of the general population (less than 2%). Echocardiographic studies report incidentally detected small pericardial effusions.

## Scleroderma

### BACKGROUND

In scleroderma, excessive connective tissue overproduction and accumulation, structural and functional microvascular disease, and immune-complex deposition affect the blood vessels, skin, joints, skeletal muscle, and multiple organs, including all structures of the heart. Thickening of the skin and Raynaud phenomenon affect more than 90% of patients. In the diffuse type, symmetric fibrosis of the skin of the face, trunk, and extremities is seen, with frequent involvement of internal organs. In the limited cutaneous type, the skin changes are limited to the extremities and face; internal organs are generally spared. This latter type is associated with the calcinosis, Raynaud phenomenon, esophageal hypomotility, sclerodactyly, and telangiectasia syndrome.

Cardiovascular disease occurs in as many as 50% of patients with scleroderma.[133] The predominant findings are functional and structural microvascular coronary artery disease, myocarditis, pulmonary and systemic hypertension-related heart disease, and pericarditis.[133-136] Atrial and ventricular arrhythmias and conduction abnormalities are less common but clinically relevant. Overall, pulmonary fibrosis and pulmonary arterial hypertension with or without cor pulmonale, congestive heart failure, and arrhythmias are the leading causes of death in patients with scleroderma.[137]

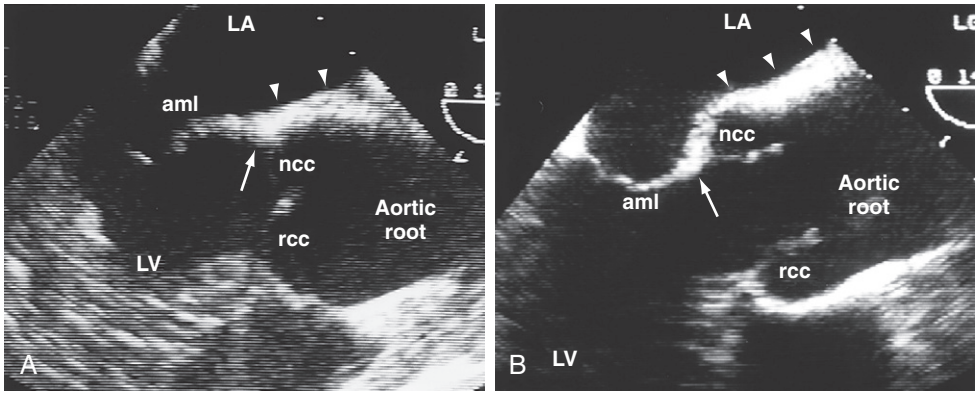



**Figure 37-11 Aortic root and aortic and mitral valves disease in patients with ankylosing spondylitis. A,** This TEE view longitudinal to the outflow tract in a 31-year-old man with progressive dyspnea of exertion and a diastolic murmur shows marked thickening of the posteromedial aortic root (*arrowheads*) extending to the basal portion of the noncoronary cusp (*ncc*) and into the base and midportions of the anterior mitral leaflet (subaortic bump; *arrow*). Mild thickening of the right coronary cusp (*rcc*) tip and mild aortic root dilation are also noted. Moderate to severe aortic regurgitation was shown. Therefore, the patient underwent an uncomplicated aortic valve replacement. **B,** This TEE view longitudinal to the outflow tract in a 43-year-old man shows severe sclerosis of the aortic root predominantly of the posteromedial wall (*arrowheads*) extending to the base of the anterior mitral leaflet (*aml*) to form the subaortic bump (*arrow*). Moderate aortic root dilation is present. The noncoronary (*ncc*) and right coronary cusp (*rcc*) show mild localized thickening of the middle and tip portions. Moderate aortic regurgitation was shown.

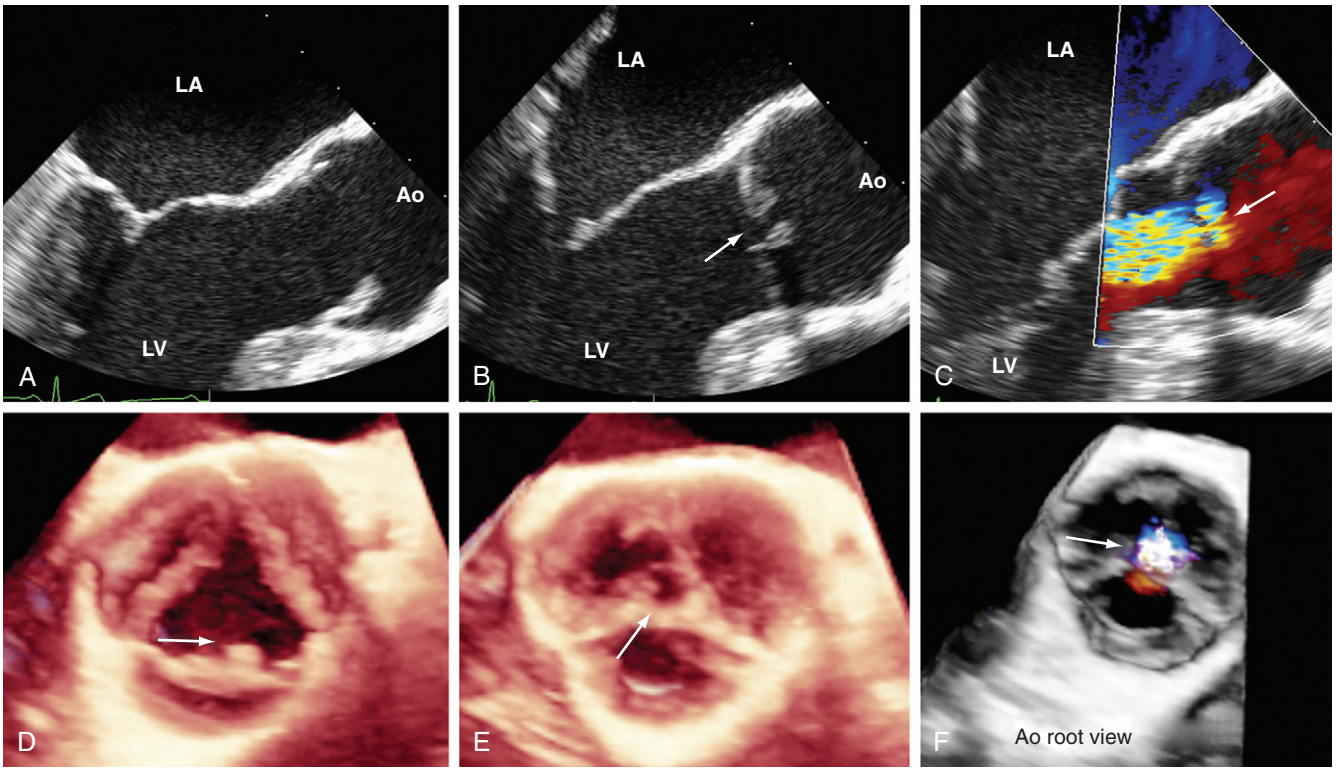



**Figure 37-12 Aortic valvulitis in a 37-year-old man with ankylosing spondylitis. A,** Two-dimensional TEE long-axis view during systole shows cusps thickening, retraction, and decreased doming mobility predominantly of the right coronary cusp. Also note aortic root sclerosis and mild thickening extending to the base of the anterior mitral leaflet (subaortic bump; *arrow*). **B,** Two-dimensional TEE long-axis view during diastole shows thickening predominantly of the tip portions and retraction of the aortic cusps leading to an incomplete coaptation (*arrow*). **C,** Two-dimensional TEE long-axis view with color Doppler imaging shows moderate aortic regurgitation based on a flow convergence zone of 3 mm (*arrow*), a vena contracta of 4 mm, and a jet height to LV outflow tract height ratio of 40%. **D,** Real-time 3D TEE of the aortic valve viewed from the aortic root and during systole defines better the moderate and diffuse thickening of the cusp tips and decreased mobility of all three cusps. Also a well-defined oval nodularity at the tip and ventricular side of the right coronary cusp is noted (*arrow*). **E,** During diastole, note the cusps retraction that leads to an incomplete central coaptation (*arrow*). **F,** With real-time 3D TEE of the aortic valve viewed from the aorta, the effective regurgitant orifice area and vena contracta area were 0.18 $cm^2$ and 0.19 $cm^2$ (*arrows*), respectively, confirming the severity of aortic regurgitation as moderate.

## ASSOCIATED CARDIOVASCULAR INVOLVEMENT

### *Coronary Artery Disease*

In scleroderma, the intramyocardial coronary arteries and arterioles are predominantly affected by two main mechanisms. The first is abnormally increased vasoconstriction that results from an immune-mediated inflammatory endothelial dysfunction. In these patients, high levels of asymmetric dimethylarginine, an endogenous inhibitor of nitric oxide synthase, have been reported, and intramyocardial coronary arterial spasm is highly associated with peripheral Raynaud phenomenon.[134,135,138] The second mechanism is obstructive microvascular disease that results from endothelial proliferation, intimal hypertrophy, intimal smooth muscle cell migration, fibrinoid necrosis, fibrosis, and ultimately, vessel narrowing. Consequently, focal or diffuse contraction band necrosis (from ischemia and reperfusion) and myocardial fibrosis occur. The prevalence of epicardial atherosclerotic disease is of less clinical relevance than microvascular disease. In fact, coronary angiography in asymptomatic patients with diffuse scleroderma shows normal or ectatic coronary arteries with slow flow indicative of increased intramyocardial coronary resistance; in those with typical or atypical angina, epicardial coronary artery disease is seen in more than 50% of patients, and in patients with myocardial infarction, normal epicardial arteries are seen in more than 30% of patients. Therefore, typical acute coronary syndrome, including myocardial infarction, is uncommon in these patients (less than 2%). Ischemic heart disease is most commonly manifested as subacute or chronic diastolic and uncommonly systolic congestive heart failure. However, acute ischemic congestive heart failure and sudden death rarely occur.

Because of predominant microvascular disease, echocardiographic findings typical of transmural ischemia or myocardial infarction are uncommon. In several prospective controlled series with Doppler TTE in asymptomatic young patients, reduction in coronary flow reserve (less than 2.5) during dipyridamole or adenosine infusion was detected in up to 50% of patients as compared with less than 5% of matched controls.[134,135] Reduction in coronary flow reserve is more common in the diffuse form of scleroderma and is related to the severity and duration of peripheral Raynaud phenomenon and duration and severity of the disease. As a result of microvascular disease, LV and RV diastolic and uncommonly systolic dysfunction can occur.[133,136,138] In contrast to typical atherosclerotic disease, areas of ischemic necrosis and fibrosis do not correspond to the regional distribution of a coronary artery and myocardial fibrosis is predominantly subendocardial and at the base and mid portions of both the LV and the RV. Occasionally, a transmural myocardial infarction from epicardial coronary vasospasm can occur, and its echocardiographic diagnosis relies on the same findings as those of atherosclerotic disease. The

cold pressor test with myocardial perfusion scanning and echocardiography shows transient wall motion abnormalities that correspond to reversible, fixed, or mixed perfusion abnormalities in patients with angiographically unremarkable epicardial coronary arteries. Symptoms and myocardial perfusion abnormalities improve with coronary vasodilator therapy.[139]

### *Myocardial Disease*

Myocardial disease is more common in patients with diffuse cutaneous involvement, anti-Scl70 and anticentromere antibodies, peripheral myopathy, and Raynaud phenomenon and in those with microvascular coronary artery disease.[133-137] Patchy myocyte contraction band necrosis (typical of ischemia and reperfusion) with myocardial fibrosis is characteristic of the disease and is reported in up to 80% in postmortem series. These data suggest that microvascular coronary artery disease is a common cause of scleroderma-associated myocardial disease. Also, patients with scleroderma commonly have septal infarction pattern, ventricular arrhythmias, or conduction abnormalities on electrocardiography, which are associated with fixed septal or anteroseptal perfusion abnormalities and correspond to areas of myocardial fibrosis on gadolinium-enhanced myocardial magnetic resonance imaging. Therefore, myocardial dysfunction in patients with scleroderma is also related to increased interstitial collagen deposition and fibrosis. Autoimmune-mediated myocarditis is uncommon. Independently of the pathogenesis, systolic congestive heart failure is associated with a high mortality rate (up to 80% at 1 year).[137]

In multiple controlled cross-sectional and longitudinal series with Doppler echocardiography, a high prevalence rate (30% to 50%) of LV and RV diastolic dysfunction is seen in unselected middle-aged patients with either diffuse or limited cutaneous disease as compared with less than 10% in controls.[135,136,138-144] Tissue-Doppler and myocardial strain and strain rate are more sensitive than mitral and tricuspid inflow patterns (60% versus 30%, respectively). Ventricular diastolic dysfunction correlates with higher levels of inflammatory markers and with the duration and severity of Raynaud phenomenon.[134,135,138,145] Right ventricular diastolic dysfunction is more common in those with pulmonary hypertension but also occurs in those without pulmonary or LA hypertension. A RV tissue-Doppler E velocity of less than 11 cm/s is found in select patients with pulmonary artery pressure greater than 35 mm Hg. Also, controlled Doppler echocardiographic series in middle-aged patients with normal LV ejection fraction, RV ejection fraction, and pulmonary artery pressure have shown significantly decreased tissue-Doppler systolic velocities of the mitral and tricuspid annulus in 15% to 20% of patients.[142-144] These findings also suggest subclinical LV and RV systolic dysfunction in these patients. Of clinical relevance, LV and RV diastolic dysfunction improve with vasodilators, including endothelin antagonists.[139] Finally, the short-term and long-term implications of subclinical diastolic and systolic dysfunction are still undefined.

### *Pulmonary Hypertension and Cor Pulmonale*

Interstitial lung disease and pulmonary arterial hypertension are major features and causes of mortality in scleroderma.[137] Pulmonary fibrosis can occur in as many as 80% and pulmonary hypertension in as many as 35% to 50% of patients in series with resting and exercise Doppler echocardiography and right heart catheterization.[146-148] The incidence of pulmonary hypertension is also high during a 3-year follow-up period of these patients.[149] Pulmonary arterial hypertension from inflammatory vasculopathy or pulmonary vasospasm is less common and is more often associated with the limited cutaneous type, Raynaud phenomenon, parameters of endothelial dysfunction, and anticentromere antibodies.[148,150,151] Abnormal pulmonary function tests, abnormal lung uptake of gallium and technetium-99 m sestamibi, and radiographic abnormalities often precede cor pulmonale on echocardiography. Patients with pulmonary hypertension have a decreased survival rate of 81%, 63%, and 56% at 1, 2, and 3 years, respectively, from the diagnosis and independent of the etiology of pulmonary hypertension.[137,152] Resting or exercise Doppler echocardiography are of important value in the detection and assessment of severity, pathogenesis, and response to therapy of pulmonary hypertension (see Question 37-4 at ExpertConsult.com).[146-148] A significant increase (20 mm Hg or more) from resting to peak exercise echocardiography is seen in up to 40% of patients with scleroderma with dyspnea of exertion or abnormal pulmonary function tests.[147,153] However, the sensitivity of Doppler echocardiography for detection of pulmonary hypertension as compared with right heart catheterization is moderate (about 60%) but highly specific (98%). Therefore, in patients with suspected symptomatic pulmonary hypertension, the ultimate diagnosis and therapeutic decisions may be best determined with right heart catheterization.

### *Pericarditis*

Clinically evident or symptomatic pericardial disease occurs in 4% to 17% of patients with scleroderma and manifests as acute pericarditis and rarely as cardiac tamponade or pericardial constriction.[154] This low clinical prevalence contrasts with that of postmortem and echocardiographic series, especially of asymptomatic pericardial effusions (30% to 50%). Asymptomatic pericardial effusions on echocardiography or computed tomography are common (up to 50%) in patients with pulmonary hypertension and hypoalbuminemia.[154] Symptomatic pericardial disease is two to four times more common in patients with the diffuse form than with the limited cutaneous form of the disease. Pericardial disease is rarely the initial manifestation of scleroderma.

### *Valve Disease*

Published data suggest that scleroderma rarely cause primary valve disease. Reports have described small masses similar to Libman-Sacks vegetations, aortitis, and aortic regurgitation and an unexplained increased frequency of mitral valve prolapse.[146,155,156] Because of the high prevalence of pulmonary hypertension and cor pulmonale, functional tricuspid regurgitation is common and predominantly of mild to moderate degree.

## Polymyositis and Dermatomyositis

### BACKGROUND

Polymyositis and dermatomyositis are clinically similar diseases characterized by autoimmune-mediated skeletal muscle inflammation that leads to symmetric proximal muscle weakness. Unlike polymyositis, dermatomyositis is accompanied by a rash on the face, neck, chest, and extensor surfaces of the extremities. Overlap syndromes frequently occur, in which features of

dermatomyositis or polymyositis are combined with those of SLE, rheumatoid arthritis, and scleroderma. Rarely, polymyositis or dermatomyositis can be associated with antiphospholipid antibody syndrome.

Myocarditis, pericarditis, and functional or structural microvascular coronary artery disease are the most common cardiac manifestations of polymyositis and dermatomyositis.[157] Epicardial atherosclerotic coronary artery disease, conduction disorders, valve dysfunction, and pulmonary hypertension are uncommon. As a result of the lack of controlled cross-sectional and longitudinal studies, reported prevalence rates of cardiovascular disease are highly variable. Although clinically manifested heart disease may occur in less than 25% of patients, it accounts for at least 10% of mortality.

### ASSOCIATED CARDIOVASCULAR INVOLVEMENT

#### *Myocardial Disease*

Myocardial disease is the result of a direct autoimmune myocardial inflammatory process and less likely of a functional microvascular coronary artery disease.[158] In postmortem series, as many as 50% of patients with polymyositis or dermatomyositis show histologic evidence of active or healed myocarditis. Although the clinical prevalence of myocarditis is unknown, approximately 10% to 20% of those who have myocarditis may have cardiomyopathy develop. Patients with myocarditis frequently have active skeletal myositis; as many as 50% of those with peripheral myositis, as indicated by uptake of technetium-99m pyrophosphate, also have myocardial uptake.[159] Rarely, a fulminant myocarditis with severe LV systolic dysfunction may be the initial manifestation of the disease. Also, acute myocarditis can mimic an acute coronary syndrome based on symptoms, non-ST and ST elevation, elevation of CPK-MB and troponin T from regenerating chronically inflamed muscles, and echocardiographic wall motion abnormalities.[160] Limited prospective echocardiographic studies suggest that few patients with polymyositis or dermatomyositis manifest wall motion abnormalities or a decreased LV ejection fraction during the course of their disease. In noncontrolled small series and a recent controlled Doppler echocardiography series, subclinical LV diastolic dysfunction as impaired relaxation was reported in 12% to 40% of patients.[158]

#### *Pericarditis*

The prevalence rate of clinically apparent pericardial disease in patients with polymyositis and dermatomyositis is low (~10%). Pericarditis is more frequent in patients with the overlap syndrome and in children. Pericarditis and cardiac tamponade can rarely be the initial manifestation of the disease.[161] Echocardiographic series have shown an up to a 25% prevalence rate of small and asymptomatic pericardial effusions. Cardiac tamponade and constriction are rare.

#### *Coronary Artery Disease, Valve Disease, and Pulmonary Hypertension*

Epicardial coronary artery disease with angina has been reported in 20% to 25% of patients. Microvascular disease may be as prevalent, but coronary arteritis is rare.[157]

Noninfective valve vegetations similar to those seen in SLE have been rarely reported.[162]

Pulmonary hypertension is uncommon, and its clinical and echocardiographic manifestations, treatment, and prognosis are similar to that of other rheumatologic diseases.

## Mixed Connective Tissue Disease

### BACKGROUND

Mixed connective tissue disease is an overlap syndrome with features of SLE, rheumatoid arthritis, scleroderma, and polymyositis. This disease is characterized by high titers of antibodies to nuclear ribonucleoprotein; patients also have speckled antinuclear antibodies and rheumatoid factor. Typical clinical features of this disease include Raynaud phenomenon, hand edema, polyarthritis, sclerodactyly, interstitial pulmonary fibrosis, myositis, and esophageal hypomotility. The true prevalence rate of heart disease in this disease is unknown, but it is highly variable (10% to 80%), with the highest rates of asymptomatic disease reported in echocardiographic series.[157] As for other rheumatologic diseases, the temporal correlation of heart disease with the severity and activity of the disease is variable.

### ASSOCIATED CARDIOVASCULAR INVOLVEMENT

#### *Pulmonary Hypertension*

Pulmonary hypertension is a common complication of mixed connective tissue disease and most frequently affects patients with features of scleroderma.[163] Proliferative vasculitis of the small and medium-sized pulmonary arteries and pulmonary fibrosis are the most common causes. Pulmonary arterial vasospasm and thromboembolism are uncommon. In those with a vasospastic etiology, a favorable short and long response to endothelin antagonists has been reported.[163] Echocardiography is essential in the diagnosis, stratification, and follow-up of these patients.

#### *Pericarditis*

Pericardial disease is common, but most patients have asymptomatic, small pericardial effusions on echocardiography. Clinical pericarditis has been reported in 25% to 30% of patients and rarely can be the initial manifestation of the disease.[164] Large pericardial effusion with tamponade rarely occurs and responds favorably to steroid or other immunosuppressive therapy (see Question 37-5 at ExpertConsult.com).[164,165]

#### *Valve Disease and Myocardial Disease*

No data associating specific forms of valve disease with mixed connective tissue disease have been reported. However, mitral valve prolapse has been reported in 20% to 25% of patients.[157] Myocarditis is uncommon and, when detected early, can be reversible with steroids and pulse cyclophosphamide therapy. On echocardiography, the spectrum of the disease ranges from diastolic dysfunction to global or regional LV systolic dysfunction and congestive heart failure.[166]

#### *Coronary Artery Disease*

As in other rheumatologic diseases, coronary artery disease in patients with mixed connective tissue disease is predominantly related to microvascular disease. Acute coronary syndromes may result from microvascular disease, coronary vasospasm, in situ thrombosis, coronary embolism from a valve vegetation, and rarely, arteritis.[167] Finally, acute myocarditis may mimic an acute coronary syndrome (Table 37-1).

**TABLE 37-1 Cardiovascular Involvement in Rheumatologic Diseases**

| *Disease* | *Type of Involvement* | *Frequency (%)** | *Key Characteristics* |
|---|---|---|---|
| Systemic lupus erythematosus (SLE) | Libman-Sacks vegetations | 10-35 | Characteristic, but not exclusive of systemic lupus erythematosus. Can be inflammatory, thrombotic, or mixed vegetations. Vegetations frequently change in appearance, resolve, appear de novo, or reappear. |
| | Leaflet fibrosis | 30-50 | Frequently diffuse. Associated calcification is uncommon. |
| | Valve regurgitation (mild or worse) | 30-50 | Can be severe with acute valvulitis or with overimposed infection. Valve stenosis is rare (<3%). |
| | Intracardiac thrombosis and cardioembolism | 15-20 | More commonly to the brain (50%-80%). |
| | Pericarditis | 10-50 | Antinuclear antibodies in pericardial fluid are diagnostic but not always present. Tamponade or constriction is rare. |
| | Asymptomatic effusion | 2-20 | Primary myocarditis is associated with cellular antigen Ro (SS-A) and La (SS-B) antibody. |
| | Myocarditis/cardiomyopathy | 1-20 | Most commonly nonobstructive. |
| | Coronary disease | | |
| | *Atherosclerotic* | 10-30 | Abnormal coronary vasodilation or microvascular disease. Microvascular thrombosis uncommon. |
| | *Functional* | 25-30 | Involves small and medium-sized vessels. |
| | *Arteritis* | Rare | A result of epicardial atherosclerosis, vasospasm, in situ thrombosis, or embolism. Arteritis is rare. |
| | Myocardial infarction | <10 | Predominantly impaired LV relaxation. |
| | Diastolic dysfunction† | 15-35 | Caused by interstitial lung disease, vasculitis, and thromboembolism. |
| | Pulmonary hypertension | 5-15 | |
| Primary antiphospholipid syndrome (PAPS) | Valve vegetations | 10-30 | All valve abnormalities, especially valve vegetations, have similar characteristics and evolution as to those of systemic lupus erythematosus. They are predominantly thrombotic but can be inflammatory or mixed. These vegetations also change in appearance over time, resolve, or reappear over time. |
| | Valve thickening | 40-60 | |
| | Valve regurgitation | 30-40 | |
| | Intracardiac thrombosis and cardioembolism | 15-20 | Includes thrombotic vegetations, adhered or free-floating intracavitary thrombi, atrioventricular valve thrombi with inflow obstruction mimicking stenosis, and echocardiographic pseudocontrast. |
| | Pulmonary hypertension | 20-25 | More commonly the result of pulmonary emboli, but pulmonary vasoconstriction or obstructive vasculopathy can occur. |
| | Coronary artery disease | 20-30 | Predominantly functional microvascular disease. |
| | Myocardial disease | 15-30 | Rarely primary inflammatory. Most commonly diastolic dysfunction from microvascular coronary artery disease. |
| Rheumatoid arthritis | Coronary artery disease | 40-60 | |
| | *Atherosclerotic* | >40 | Predominantly subclinical as detected with electron-beam computed tomography. |
| | *Functional* | >25 | Two to four times higher than the general population; severe obstructive disease uncommon. |
| | *Arteritis* | Uncommon | Abnormal coronary vasodilation or microvascular disease. |
| | Myocardial infarction | 10-15 | Difficult to diagnose clinically. |
| | Pericarditis | ≤10 | Most commonly the result of epicardial atherosclerosis. Rarely, coronary vasospasm, in situ thrombosis, or embolism. |
| | Asymptomatic effusion | 30-50 | Occurs in patients with active disease, high rheumatoid factor level, and nodular disease; pericardial fluid can have rheumatoid factor. |
| | Leaflet fibrosis | >30 | — |
| | Valve nodules | ~10 | Leaflet fibrosis is indistinguishable from that of systemic lupus. |
| | Valve regurgitation, mild or more | >30 | Characteristic of rheumatoid arthritis. |
| | Myocarditis/cardiomyopathy | <10 | Amyloid deposition is a rare cause. |
| | Diastolic dysfunction | 30-40 | Predominantly impaired LV relaxation. |
| | Pulmonary hypertension | ~20 | — |
| Ankylosing spondylitis | Proximal aortitis/valvulitis | 20-60 | Root sclerosis extending to base of anterior mitral leaflet and root dilation are characteristic of the disease. |
| | Aortic regurgitation, mild or more | 10-40 | Decreases anterior mitral leaflet mobility and causes regurgitation. |
| | Subaortic bump | 10-40 | — |
| | Conduction system disease | >20 | Extension of aortic root/annulus sclerosis into the proximal septum and atrioventricular node. |
| | Diastolic dysfunction | 20-30 | Predominantly impaired LV relaxation. |
| | Pericarditis | <5 | Primary immune mediated is uncommon. |
| | Asymptomatic effusion | <5 | — |
| | Myocarditis/cardiomyopathy | <5 | Primary immune-mediated myocarditis is rare. |
| Scleroderma | Coronary disease | | |
| | *Atherosclerotic* | <20 | — |
| | *Functional* | ~50 | Predominantly vasospastic or coronary Raynaud phenomenon. |
| | Myocarditis/cardiomyopathy | 10-50 | Most commonly related to recurrent intramyocardial ischemia/necrosis/fibrosis. Inflammatory uncommon. |
| | Diastolic dysfunction | 30-50 | Affects the LV and RV, and predominates as impaired relaxation. |
| | Pulmonary hypertension | 35-50 | Caused by pulmonary fibrosis, less commonly by vasculitis, vasospasm, or left heart disease. |
| | Pericarditis | 5-20 | — |
| | Asymptomatic effusion | 30-40 | — |
| | Valve disease | <10 | Nonspecific. Mitral valve prolapse is common. |
| Polymyositis/ dermatomyositis | Myocarditis/cardiomyopathy | >25 | Primary myocarditis more common in patients with myositis. Diastolic dysfunction occurs in 10% to 40% of patients. |
| | Pericarditis | ~10 | More frequent in children and in overlap syndrome. |
| | Asymptomatic effusion | 5-25 | Commonly nonobstructive atherosclerotic. |
| | Coronary artery disease | ~20 | Microvascular disease also common. Arteritis is rare. |
| | Valve disease | Unknown | Is nonspecific. Libman-Sacks–like vegetations are rare. |
| Mixed connective tissue disease (MCTD) | Pulmonary hypertension | ≤80 | More often resulting from proliferative vasculitis and pulmonary fibrosis. |
| | Pericarditis | 5-30 | — |
| | Asymptomatic effusion | Unknown | — |
| | Valve disease | Unknown | Nonspecific. High prevalence rate of mitral valve prolapse (20%-25%). |
| | Myocarditis/cardiomyopathy | <5 | — |
| | Coronary artery disease | Unknown | Predominantly microvascular disease. |

*Variability of rates is related to differences in patient population characteristics, study design, and diagnostic methods.
†Defined by Doppler echocardiographic criteria.

**TABLE 37-2 Key Echocardiographic Features of Valve Lesions in Selected Conditions**

| *Disease* | *Affected Structures* | *Key Characteristics* | *Functional Sequelae* |
|---|---|---|---|
| Systemic lupus erythematosus | Mitral valve more than aortic valve leaflets; rarely chordae, tricuspid valve, and pulmonary valve; spares annuli. | Libman-Sacks vegetations: masses usually <1 cm in diameter, with heterogeneous echocardiographic reflectance (but not calcified) and with irregular borders; usually rounded shape. Attached to leaflet with a broad base. Usually no independent motion. Lesions are located at any portion of leaflets, on atrial side of mitral valve and aortic vessel or ventricular side of aortic valve. Diffuse leaflet thickening or sclerosis common; calcification uncommon and mild. | Mild to moderate mitral regurgitation or aortic regurgitation is common, but stenosis is rare. High potential embolic source. |
| Primary antiphospholipid syndrome | Mitral valve more than aortic valve leaflets; rarely chordae, tricuspid valve, and pulmonary valve; spares annuli. | Libman-Sacks–like vegetations with similar characteristic to those described for systemic lupus erythematosus. | Mild to moderate mitral regurgitation or aortic regurgitation are common. High potential embolic source. |
| Rheumatoid arthritis | Mitral valve, aortic valve leaflets; rarely annuli and chordae; spares tricuspid valve and pulmonary valve. | Rheumatoid nodules: masses usually <1 cm in diameter, with homogeneous soft-tissue echocardiographic reflectance and irregular border; usually rounded shape. Any location within the leaflet; leaflet thickening/sclerosis generally mild or absent.<br>Libman-Sacks–like vegetations. | More than mild mitral regurgitation or aortic regurgitation is rare. Rupture of a nodule may lead to severe valve regurgitation. Rarely associated with cardioembolism.<br>Associated with acute or recurrent valvulitis. Similar characteristics to those associated with systemic lupus erythematosus. High embolic potential. Postvalvulitis stenosis is rare. |
| Ankylosing spondylitis | Proximal aorta, annulus and aortic valve, base of anterior mitral leaflet; posterior mitral valve leaflet, mitral annulus, and chordae spared. | Sclerosis, stiffness, and dilation of aortic root extend to the annulus. Aortic valve leaflet sclerosis is generally mild. Subaortic bump: a localized thickening of base of anterior mitral leaflet resulting from downward extension of aortic root and annular sclerosis. | Mild to moderate aortic regurgitation or mitral regurgitation are common. Stenosis not reported. |
| Rheumatic heart disease | 90% involvement of mitral valve or aortic valve; 10% tricuspid valve or pulmonary valve; annuli of valves and aortic root spared. | Mitral valve leaflet edges and chordae are most affected, and commissural fusion is common; with severe disease, sclerosis extends toward base of leaflet and may involve papillary muscles. Extensive calcification may occur. When localized, sclerosis may appear masslike, but very high echocardiographic reflectance is unlike other lesions, except degenerative. Aortic valve cusp edges are affected in a similar pattern. | Leaflet edge fusion and chordal shortening produce a tethered mitral leaflet motion; analogous doming motion of the aortic cusps may be seen. If fusion predominates, stenosis results; if leaflet retraction predominates, regurgitation results. |
| Degenerative disorders | Mitral valve and aortic valve annuli and leaflets; uncommonly involves chordae and tip of papillary muscles. | Sclerosis is concentrated at base of leaflets and annulus, with progressive extension toward leaflet mid portion; tip uncommonly involved. When localized, sclerosis may appear masslike or as nodules. Aortic valve nodules more commonly located at the base and commissural portions. | Annular calcification predominates for mitral valve, with leaflet sclerosis less common and usually limited to posterior leaflet. Mitral regurgitation rarely more than mild, and stenosis is rare and subclinical or mild. Aortic valve leaflet sclerosis and fusion lead to stenosis, and leaflet distortion leads to aortic regurgitation, generally mild. |
| Infective endocarditis | Acute: mass with homogeneous soft tissue reflectance and irregular borders; size and shape are highly variable, usually with narrow base, often pedunculated. Lesions almost always exhibit motion independent of underlying structure and almost always oscillatory. Mitral valve and tricuspid valve lesions prolapse into atria in systole; aortic valve and pulmonary valve lesions prolapse into outflow tracts in diastole. Lesions usually attached to distal third of leaflet. With aortic valve disease, additional vegetations may occur on anterior mitral leaflet and chordae.<br>Chronic: localized thickening or increased reflectance of leaflet or chordae. Lesion is not necessarily distal on leaflet. Fibrous tissue reflectance and calcification are common. | | Valve regurgitation is common and frequently severe; stenosis involving native valves is rare. Leaflet perforation or abscess formation occurs. Cardioembolism is common. |
| Valve or Lambl excrescences[168] | Detected with TEE, rarely with TTE. Similarly high frequency rate (35% to 40%) in healthy subjects, in patients with connective tissue diseases, and in patients with suspected cardioembolism. They are thin (0.6 to 2 mm in width), elongated (4 to 16 mm), hypermobile structures seen at or near the leaflets coaptation point, on the atrial side during systole for mitral and tricuspid valves and ventricular side during diastole for the aortic valve. Multivalvular involvement seen in 20% to 25% of subjects. | | Valve excrescences are not associated or cause valvular dysfunction, persist unchanged over time, and are not associated with antiphospholipid antibodies or with an increased risk of cardioembolism. |

## KEY POINTS

- Nonbacterial valve vegetations and leaflet fibrosis are seen in many patients with SLE, PAPS, and rheumatoid arthritis.
- Intracardiac thrombi, including thrombotic vegetations, are common in patients with SLE and PAPS and frequently lead to subclinical and clinical macroembolism or microembolism, predominantly to the brain.
- An increased prevalence of early coronary, carotid, and aortic atherosclerotic disease is found in patients with systemic inflammatory diseases, independent of traditional atherogenic risk factors.
- Chronic or recurrent systemic and local immune-mediated inflammation causes endothelial dysfunction that leads to abnormal coronary vasodilation or functional microvascular disease in patients with SLE, PAPS, and rheumatoid arthritis and especially in those with scleroderma.
- Subclinical LV and RV diastolic dysfunction is common in patients with rheumatologic disease and is predominantly the result of microvascular coronary artery disease.
- LV systolic dysfunction is uncommon in patients with systemic inflammatory disease and is usually multifactorial (microvascular or epicardial coronary artery disease, myocarditis, hypertension, or valve disease).
- Pericarditis is common in patients with SLE, rheumatoid arthritis, polymyositis, dermatomyositis, and mixed connective tissue disease.
- Pulmonary hypertension more commonly results from thromboembolism or vasculitis in SLE; from thromboembolism in PAPS; from interstitial lung disease or vasculitis in rheumatoid arthritis; and from interstitial lung disease, vasculitis, or vasospastic disease in scleroderma and mixed connective tissue disease.
- Libman-Sacks or thrombotic vegetations in SLE and PAPS, valve nodules in rheumatoid arthritis, and aortic root in association with aortic and mitral valve disease have distinctive echocardiographic features (Table 37-2).
- Although advances in echocardiography have upgraded the prevalence rates and characteristics of cardiovascular disease in rheumatologic diseases, the short-term and long-term clinical, prognostic, and therapeutic implications of common subclinical cardiovascular abnormalities are still uncertain and await large controlled cross-sectional and longitudinal studies.

## REFERENCES


1. Doria A, Iaccarino L, Sarzi-Puttini P, et al: Cardiac involvement in systemic lupus erythematosus. *Lupus* 14:683-686, 2005.
2. Roldan CA, Shively BK, Lau CC, et al: Systemic lupus erythematosus valve disease by transesophageal echocardiography and the role of antiphospholipid antibodies. *J Am Coll Cardiol* 20:1127-1134, 1992.
3. Roldan CA, Shively BK, Crawford MH: An echocardiographic study of valvular heart disease associated with systemic lupus erythematosus. *N Engl J Med* 335:1424-1430, 1996.
4. Evangelopoulos ME, Alevizaki M, Toumanidis S, et al: Mitral valve prolapse in systemic lupus erythematosus patients: clinical and immunological aspects. *Lupus* 12:308-311, 2003.
5. Roldan CA, Gelgand EA, Qualls CR, Sibbitt WL Jr: Valvular heart disease as a cause of cerebrovascular disease in patients with systemic lupus erythematosus. *Am J Cardiol* 95:1441-1447, 2005.
6. Einav E, Gitig A, Marinescu LM, et al: Valvulitis requiring triple valve surgery as an initial presentation of systemic lupus erythematosus. *J Am Soc Echocardiogr* 201315:e1-e3, 2007.
7. Afek A, Shoenfeld Y, Manor R, et al: Increased endothelial cell expression of alpha3beta1 integrin in cardiac valvulopathy in the primary (Hughes) and secondary antiphospholipid syndrome. *Lupus* 8:502-507, 1999.
8. Levine JS, Branch DW, Rauch J: The antiphospholipid syndrome. *N Engl J Med* 346:752-763, 2002.
9. Leszczynski P, Straburzynska-Migaj E, Korczowska I, et al: Cardiac valvular disease in patients with systemic lupus erythematosus. Relationship with anticardiolipin antibodies. *Clin Rheumatol* 22:405-408, 2003.
10. Libman E, Sacks B: A hitherto undescribed form of valvular and mural endocarditis. *Arch Intern Med* 33:701-737, 1924.
11. Eiken PW, Edwards WD, Tazelaar HD, et al: Surgical pathology of nonbacterial thrombotic endocarditis in 30 patients, 1985-2000. *Mayo Clin Proc* 76:1204-1212, 2001.
12. Omdal R, Lunde P, Rasmussen K, et al: Transesophageal and transthoracic echocardiography and Doppler-examinations in systemic lupus erythematosus. *Scand J Rheumatol* 30: 275-281, 2001.
13. Moaref AR, Afifi S, Rezaian S, Rezaian GR: Isolated tricuspid valve Libman-Sacks endocarditis and valvular stenosis: unusual manifestations of systemic lupus erythematosus. *J Am Soc Echocardiogr* 23:341.e3-341.e5, 2010.
14. Moyssakis I, Tektonidou MG, Vasilliou VA, et al: Libman-Sacks endocarditis in systemic lupus erythematosus: prevalence, associations, and evolution. *Am J Med* 120:636-642, 2007.
15. Roldan CA: Diagnostic value of transesophageal echocardiography in Libman-Sacks endocarditis. *Minerva Cardioangiol* 57:467-481, 2009.
16. Roldan CA, Qualls CR, Sopko KS, Sibbitt WL Jr: Transthoracic versus transesophageal echocardiography for detection of Libman-Sacks endocarditis: a randomized controlled study. *J Rheumatol* 35:224-229, 2008.
17. Plastiras SC, Pamboucas CA, Tzelepis GE, Toumanidis ST: Assessing mitral valve stenosis by real-time 3-dimensional echocardiography in systemic lupus erythematosus: a look inside the heart. *J Rheumatol* 36:1843-1845, 2009.
18. Plastiras SC, Pamboucas CA, Tektonidou M, Toumanidis ST: Real-time three-dimensional echocardiography in evaluating Libman-Sacks vegetations. *Eur J Echocardiogr* 11:184-185, 2010.
19. Roldan CA, Gelgand EA, Qualls CR, Sibbitt WL Jr: Valvular heart disease is associated with nonfocal neuropsychiatric systemic lupus erythematosus. *J Clin Rheumatol* 12:3-10, 2006.
20. Morelli S, Bernardo ML, Viganego F, et al: Left-sided heart valve abnormalities and risk of ischemic cerebrovascular accidents in patients with systemic lupus erythematosus. *Lupus* 12:805-812, 2003.
21. Roldan CA, Gelgand EA, Qualls CR, Sibbitt WL Jr: Valvular heart disease by transthoracic echocardiography is associated with focal brain injury and central neuropsychiatric systemic lupus erythematosus. *Cardiology* 108:331-337, 2007.
22. Nijjar PS, Mountis M, Amanullah AM: Acute myocardial infarction in a patient with systemic lupus erythematosus and normal coronary arteries. *Rev Cardiovasc Med* 8:36-40, 2007.
23. Zurick AO 3rd, Yang EH, Chang PP, et al: A 38-year-old Hispanic woman with paradoxical embolism and Libman-Sacks endocarditis involving the tricuspid valve. *J Am Soc Echocardiogr* 20:1316.e5-1316.e7, 2007.
24. Rademacher J, Sohngen D, Specker C, et al: Cerebral microembolism, a disease marker for ischemic cerebrovascular events in the antiphospholipid syndrome of systemic lupus erythematosus? *Acta Neurol Scand* 99:356-361, 1999.
25. Kumral E, Evyapan D, Keser G, et al: Detection of microemboli signals in patients with neuropsychiatric lupus erythematosus. *Eur Neurol* 47:131-135, 2002.
26. Sibbitt WL Jr, Brooks WM, Kornfeld M, et al: Magnetic resonance imaging and brain

histopathology in neuropsychiatric systemic lupus erythematosus. *Semin Arthritis Rheum* 40:32-52, 2010.
27. Tada H, Kawashiri MA, Watanabe G, Yamagishi M: Pictures in clinical medicine. Huge apertures in the aortic valve due to Libman-Sachs endocarditis. *Intern Med* 48:859, 2009.
28. Bouma W, Klinkenberg TJ, van der Horst IC, et al: Mitral valve surgery for mitral regurgitation caused by Libman-Sacks endocarditis: a report of four cases and a systematic review of the literature. *J Cardiothorac Surg* 23:13, 2010.
29. Molad Y, Levin-Iaina N, Vaturi M, et al: Heart valve calcification in young patients with systemic lupus erythematosus: a window to premature atherosclerotic vascular morbidity and a risk factor for all-cause mortality. *Atherosclerosis* 185:406-412, 2006.
30. Sasahashi N, Harada H, Saji Y, et al: Aortic valve replacement for aortic regurgitation in a patient with antiphospholipid antibody syndrome. *Gen Thorac Cardiovasc Surg* 55:293-296, 2007.
31. Blank M, Aron-Maor A, Shoenfeld Y: From rheumatic fever to Libman-Sacks endocarditis: is there any possible pathogenetic link? *Lupus* 14:697-701, 2005.
32. Blanchard DG, Ross RS, Dittrich HC: Nonbacterial thrombotic endocarditis: assessment by transesophageal echocardiography. *Chest* 102: 954-956, 1992.
33. Shively BK, Gurule FT, Roldan CA, et al: Diagnostic value of transesophageal compared with transthoracic echocardiography in infective endocarditis. *J Am Coll Cardiol* 18:391-397, 1991.
34. Cianciulli TF, Saccheri MC, Redruello HJ: Right atrial thrombus mimicking myxoma with pulmonary embolism in a patient with systemic lupus erythematosus and secondary antiphospholipid syndrome. *Tex Heart Inst J* 35:454-457, 2008.
35. Hirata K, Kadirvelu A, Kinjo M, et al: Altered coronary vasomotor function in young patients with systemic lupus erythematosus. *Arthritis Rheum* 56:1904-1909, 2007.
36. Roman MJ, Shanker BA, Davies AB, et al: Prevalence and correlates of accelerated atherosclerosis in systemic lupus erythematosus. *N Engl J Med* 349:2399-2406, 2003.
37. Roldan CA, Joson J, Sharrar J, et al: Premature aortic atherosclerosis in systemic lupus erythematosus: a controlled transesophageal echocardiographic study. *J Rheumatol* 37:71-78, 2010.
38. Dorai A, Schoenfeld Y, Pauletto P: Premature coronary disease in systemic lupus. *N Engl J Med* 350:1571-1575, 2004.
39. Greene ER, Lanphere KR, Sharrar J, Roldan CA: Arterial distensibility in systemic lupus erythematosus. *Conf Proc IEEE Eng Med Biol Soc* 1109-1112, 2009.
40. Roldan CA, Joson J, Qualls CR, et al: Premature aortic stiffness in systemic lupus erythematosus by transesophageal echocardiography. *Lupus* 19:1599-1605, 2010.
41. Augoustides JG, Pochettino A, Carpenter J: Surgical management of thoracoabdominal aortic aneurysm associated with systemic lupus erythematosus. *J Thorac Cardiovasc Surg* 136:215-216, 2008.
42. Lee CH, Chan MY: Dilemma of drug-eluting stent implantation in a patient with systemic lupus erythematosus. *Int J Cardiol* 114:e107-e108, 2007.
43. Pieretti J, Roman MJ, Devereux RB, et al: Systemic lupus erythematosus predicts increased left ventricular mass. *Circulation* 116:419-426, 2007.
44. Chow PC, Ho MH, Lee TL, et al: Relation of arterial stiffness to left ventricular structure and function in adolescents and young adults with pediatric-onset systemic lupus erythematosus. *J Rheumatol* 34:1345-1352, 2007.
45. Law WG, Thong BY, Lian TY, et al: Acute lupus myocarditis: clinical features and outcome of an oriental case series. *Lupus* 14:827-831, 2005.
46. Naqvi TZ, Luthringer D, Marchevsky A, et al: Chloroquine-induced cardiomyopathy-echocardiographic features. *J Am Soc Echocardiogr* 18:383-387, 2005.
47. Manohar VA, Moder KG, Edwards WD, Klarich K: Restrictive cardiomyopathy secondary to hydroxychloroquine therapy. *J Rheumatol* 36: 440-441, 2009.
48. Cacciapuoti F, Galzerano D, Capogrosso P, et al: Impairment of left ventricular function in systemic lupus erythematosus evaluated by measuring myocardial performance index with tissue Doppler echocardiography. *Echocardiography* 22:315-319, 2005.
49. Tektonidou MG, Ioannidis JP, Moyssakis I, et al: Right ventricular diastolic dysfunction in patients with anticardiolipin antibodies and antiphospholipid syndrome. *Ann Rheum Dis* 60:43-48, 2001.
50. Cheng CC, Huang WC, Chiou KR, et al: Tricuspid flow propagation velocity predicts exercise tolerance and readmission in patients with systemic lupus erythematosus. *J Am Soc Echocardiogr* 22:411-417, 2009.
51. Buss SJ, Wolf D, Korosoglou G, et al: Myocardial left ventricular dysfunction in patients with systemic lupus erythematosus: new insights from tissue Doppler and strain imaging. *J Rheumatol* 37:79-86, 2010.
52. Lee SW, Park MC, Park YB, Lee SK: E/E′ ratio is more sensitive than E/A ratio for detection of left ventricular diastolic dysfunction in systemic lupus erythematosus. *Lupus* 17:195-201, 2008.
53. Gin PL, Wang WC, Yang SH, et al: Right heart function in systemic lupus erythematosus: insights from myocardial Doppler tissue imaging. *J Am Soc Echocardiogr* 19:441-449, 2006.
54. Yip GW, Shang Q, Tam LS, et al: Disease chronicity and activity predict subclinical left ventricular systolic dysfunction in patients with systemic lupus erythematosus. *Heart* 95:980-987, 2009.
55. Cauduro SA, Moder KG, Tsang TS, Seward JB: Clinical and echocardiographic characteristics of hemodynamically significant pericardial effusions in patients with systemic lupus erythematosus. *Am J Cardiol* 92:1370-1372, 2003.
56. Stone D, Moberg P, Respicio G, et al: Pericarditis with cardiac tamponade in systemic lupus erythematosus. Development immediately following successful control of lupus flare. *Lupus* 19:890-891, 2010.
57. Nabibux MN, Dijkmans PA, Dijkmans BA: A swinging heart as complication of systemic lupus erythematosus. *Clin Rheumatol* 26:825-826, 2007.
58. Khouzam RN, Minderman D, Munir A, D'Cruz IA: Images in cardiovascular medicine. Cardiac tamponade with fibrin strands leading to the diagnosis of systemic lupus erythematosus. *Circulation* 116:e342-e344, 2007.
59. Sugiura T, Kumon Y, Kataoka H, et al: Asymptomatic pericardial effusion in patients with systemic lupus erythematosus. *Lupus* 18:128-132, 2009.
60. Galie N, Manes A, Farahani KV, et al: Pulmonary arterial hypertension associated to connective tissue diseases. *Lupus* 14:713-717, 2005.
61. Prabu A, Patel K, Yee CS, et al: Prevalence and risk factors for pulmonary arterial hypertension in patients with lupus. *Rheumatology (Oxford)* 48:1506-1511, 2009.
62. Kasparian A, Floros A, Gialafos E, et al: Raynaud's phenomenon is correlated with elevated systolic pulmonary arterial pressure in patients with systemic lupus erythematosus. *Lupus* 16:505-508, 2007.
63. Mok MY, Tsang PL, Lam YM, et al: Bosentan use in systemic lupus erythematosus patients with pulmonary arterial hypertension. *Lupus* 16:279-285, 2007.
64. Tenedios F, Erkan D, Lockshin MD: Cardiac involvement in the antiphospholipid syndrome. *Lupus* 14:691-696, 2005.
65. Lockshin MD, Tenedios F, Petri M, et al: Cardiac disease in antiphospholipid syndrome: recommendations for treatment. Committee consensus report. *Lupus* 12:518-523, 2003.
66. Qaddoura F, Connolly H, Grogan M, et al: Valve morphology in the antiphospholipid syndrome: echocardiographic features. *Echocardiography* 22:255-259, 2005.
67. Yamamoto H, Iwade T, Nakano R, et al: Images in cardiovascular medicine. Numerous small vegetations revealing Libman-Sacks endocarditis in catastrophic antiphospholipid syndrome. *Circulation* 116:e531-e535, 2007.
68. Vinales KL, Gopalan RS, Lanza LA, et al: Unusual case of nonbacterial thrombotic endocarditis attributable to primary antiphospholipid syndrome. *Circulation* 122:e459-e460, 2010.
69. Reisner SA, Brenner B, Haim N, et al: Echocardiography in non-bacterial thrombotic endocarditis: from autopsy to clinical entity. *J Am Soc Echocardiogr* 13:876-881, 2000.
70. Turiel M, Muzzupappa S, Gottardi B, et al: Evaluation of cardiac abnormalities and embolic sources in primary antiphospholipid syndrome by transesophageal echocardiography. *Lupus* 9:406-412, 2000.
71. Turiel M, Sarzi-Puttinin P, Peretti A, et al: Five year follow-up by transesophageal echocardiographic studies in primary antiphospholipid syndrome. *Am J Cardiol* 96:574-579, 2005.
72. Espinola Zavaleta N, Montes RM, Soto ME, et al: Primary antiphospholipid syndrome: a 5-year transesophageal echocardiographic follow-up study. *J Rheumatol* 31:2402-2407, 2004.
73. Nesher G, Ilany J, Rosenmann D, Abraham AS: Valvular dysfunction in antiphospholipid syndrome: prevalence, clinical features, and treatment. *Semin Arthritis Rheum* 27:27-35, 1997.
74. Yusuf S, Madden BP, Pumhrey CW: Left atrial thrombus caused by the primary antiphospholipid syndrome causing critical functional mitral stenosis. *Heart* 89:262, 2002.
75. Rawat SK, Mehta Y, Vats M, et al: Anesthetic management of right atrial mass removal and pulmonary artery thrombectomy in a patient with primary antiphospholipid antibody syndrome. *Ann Card Anaesth* 13:39-43, 2010.
76. Cianciulli TF, Saccheri MC, Lax JA, et al: Left ventricular thrombus mimicking primary cardiac tumor in a patient with primary antiphospholipid syndrome and recurrent systemic embolism. *Cardiol J* 16:560-563, 2009.

77. Mottram PM, Gelman JS: Mitral valve thrombus mimicking a primary tumor in the antiphospholipid syndrome. *J Am Soc Echocardiogr* 15:746-748, 2002.
78. Ebato M, Kitai H, Kumakura H, et al: Thrombus on the tricuspid valve in a patient with primary antiphospholipid syndrome after implantation of an inferior vena cava filter. *Circ J* 66:425-427, 2002.
79. Matsuura E, Lopez LR: Are oxidized LDL/b2-glycoprotein I complexes pathogenic antigens in autoimmune mediated atherosclerosis? *Clin Dev Immunol* 11:103-111, 2004.
80. Ames PRJ, Margarita A, Sokoll KB, et al: Premature atherosclerosis in primary antiphospholipid syndrome: preliminary data. *Ann Rheum Dis* 64:315-317, 2005.
81. Medina G, Casaos D, Jara LJ, et al: Increased carotid artery intima media thickness may be associated with stroke in primary antiphospholipid syndrome. *Ann Rheum Dis* 62:607-610, 2003.
82. Cervera R: Coronary and valvular syndromes and antiphospholipid antibodies. *Thromb Res* 114:501-507, 2004.
83. Lagana B, Baratta L, Tubani L, et al: Myocardial infarction with normal coronary arteries in a patient with primary antiphospholipid syndrome—case report and literature review. *Angiology* 52:785-788, 2001.
84. Paran D, Caspi D, Levartovsky D, et al: Cardiac dysfunction in patients with systemic lupus erythematosus and antiphospholipid syndrome. *Ann Rheum Dis* 66:506-510, 2007.
85. Gerli R, Goodson NJ: Cardiovascular involvement in rheumatoid arthritis. *Lupus* 14:679-682, 2005.
86. Nicola PJ, Crowson CS, Maradit-Kremers H, et al: Contribution of congestive heart failure and ischemic heart disease to excess mortality in rheumatoid arthritis. *Arthritis Rheum* 54:60-67, 2006.
87. Gonzalez-Gay MA, Gonzalez-Juanatey C, Martin J: Rheumatoid arthritis: a disease associated with accelerated atherogenesis. *Semin Arthritis Rheum* 35:8-17, 2005.
88. Sattar N, McInnes IB: Vascular comorbidity in rheumatoid arthritis: potential mechanisms and solutions. *Curr Opin Rheumatol* 17:286-292, 2005.
89. Turiel M, Atzeni F, Tomasoni L, et al: Non-invasive assessment of coronary flow reserve and ADMA levels: a case-control study of early rheumatoid arthritis patients. *Rheumatology (Oxford)* 48:834-839, 2009.
90. Ciftci O, Yilmaz S, Topcu S: Impaired coronary microvascular function and increased intima-media thickness in rheumatoid arthritis. *Atherosclerosis* 198:332-3337, 2008.
91. Ikonomidis I, Tzortzis S, Lekakis J, et al: Lowering interleukin-1 activity with anakinra improves myocardial deformation in rheumatoid arthritis. *Heart* 95:1502-1507, 2009.
92. Gerli R, Schillaci G, Giordano A, et al: CD4 T lymphocytes contribute to early atherosclerotic damage in rheumatoid arthritis patients. *Circulation* 109:2744-2748, 2004.
93. Csiszar A, Ungvari Z: Synergistic effects of vascular IL-17 and TNF-alpha may promote coronary artery disease. *Med Hypotheses* 63:696-698, 2004.
94. Maradit-Kremers H, Crowson CS, Nicola PJ, et al: Increased unrecognized coronary heart disease and sudden deaths in rheumatoid arthritis: a population-based cohort study. *Arthritis Rheum* 52:402-411, 2005.
95. Wolfe F, Freundlich B, Straus WL: Increase in cardiovascular and cerebrovascular disease prevalence in rheumatoid arthritis. *J Rheumatol* 30:36-40, 2003.
96. Wong M, Toh L, Wilson A, et al: Reduced arterial elasticity in rheumatoid arthritis and the relationship to vascular disease risk factors and inflammation. *Arthritis Rheum* 48:81-89, 2003.
97. Douglas KM, Pace AV, Treharne GJ, et al: Excess recurrent cardiac events in rheumatoid arthritis patients with acute coronary syndrome. *Ann Rheum Dis* 65:348-353, 2006.
98. Chung CP, Oeser A, Raggi P, et al: Increased coronary-artery atherosclerosis in rheumatoid arthritis: relationship to disease duration and cardiovascular risk factors. *Arthritis Rheum* 52:3045-3053, 2005.
99. Johnsen SP, Larson H, Tarone RE, et al: Risk of hospitalization for myocardial infarction among users of rofecoxib, celecoxib, and other NSAIDs: a population-based case-control study. *Arch Intern Med* 165:978-984, 2005.
100. Hurlimann D, Forster A, Noll G, et al: Anti-tumor necrosis factor-a treatment improves endothelial function in patients with rheumatoid arthritis. *Circulation* 106:2184-2187, 2002.
101. McCarey DW, McInnes IB, Madhok R, et al: Trial of atorvastatin in rheumatoid arthritis (TARA): double-blind, randomized placebo controlled trial. *Lancet* 363:2015-2021, 2004.
102. Saghir MK, Attenhofer Jost C, Warrington KJ, et al: Exercise echocardiography in rheumatoid arthritis: a case-control study. *J Am Soc Echocardiogr* 22:1228-1231, 2009.
103. Sugiura T, Kumon Y, Kataoka H, et al: Asymptomatic pericardial effusion in patients with rheumatoid arthritis. *Cardiology* 110:87-91, 2008.
104. Cauduro SA, Moder KG, Luthra HS, Seward JB: Echocardiographically guided pericardiocentesis for treatment of clinically significant pericardial effusion in rheumatoid arthritis. *J Rheumatol* 33:2173-2177, 2006.
105. Roldan CA, DeLong C, Qualls CR, Crawford MH: Characterization of valvular heart disease in rheumatoid arthritis by transesophageal echocardiography and clinical correlates. *Am J Cardiol* 100:496-502, 2007.
106. Anaya JM: Severe rheumatoid valvular heart disease. *Clin Rheumatol* 25:1-3, 2005.
107. Giladi H: A rare case of enterobacter endocarditis superimposed on a mitral valve rheumatoid nodule. *J Clin Rheumatol* 14:97-100, 2008.
108. Peyrou J, Saxer-Sekulic N, Lerch R, Müller H: Fast progression of aortic stenosis in rheumatoid arthritis. *Arch Cardiovasc Dis* 102:251-252, 2009.
109. Kang H, Baron M: Embolic complications of a mitral valve rheumatoid nodule. *J Rheumatol* 31:1001-1003, 2004.
110. Gonzalez-Juanatey C, Garcia-Porrua C, Testa A, Gonzalez-Gay MA: Potential role of mitral valve strands on stroke recurrence in rheumatoid arthritis. *Arthritis Rheum* 49:866-867, 2003.
111. Arakawa K, Yamazawa M, Morita Y, et al: Giant rheumatoid nodule causing simultaneous complete atrioventricular block and severe mitral regurgitation: a case report. *J Cardiol* 46:77-83, 2005.
112. Yazici D, Tokay S, Aydin S: Echocardiographic evaluation of cardiac diastolic function in patients with rheumatoid arthritis: 5 years of follow-up. *Clin Rheumatol* 27:647-650, 2008.
113. Liang KP, Myasoedova E, Crowson CS, et al: Increased prevalence of diastolic dysfunction in rheumatoid arthritis. *Ann Rheum Dis* 69:1665-1670, 2010.
114. Meune C, Wahbi K, Assous N, et al: Myocardial dysfunction in rheumatoid arthritis: a controlled tissue-Doppler echocardiography study. *J Rheumatol* 34:2005-2009, 2007.
115. Birdane A, Korkmaz C, Ata N, et al: Tissue Doppler imaging in the evaluation of the left and right ventricular diastolic functions in rheumatoid arthritis. *Echocardiography* 24:485-493, 2007.
116. Seyfeli E, Guler H, Akoglu S, et al: Right ventricular diastolic abnormalities in rheumatoid arthritis and its relationship with left ventricular and pulmonary involvement. A tissue Doppler echocardiographic study. *Int J Cardiovasc Imaging* 22:745-754, 2006.
117. Davis JM 3rd, Roger VL, Crowson CS, et al: The presentation and outcome of heart failure in patients with rheumatoid arthritis differs from that in the general population. *Arthritis Rheum* 58:2603-2611, 2008.
118. Wolfe F, Michaud K: Heart failure in rheumatoid arthritis: rates, predictors, and the effect of anti-tumor necrosis factor therapy. *Am J Med* 116:305-311, 2004.
119. Wu CH, Sung SH, Wu TC: Focal myocarditis mimicking myocardial infarction in a patient with rheumatoid arthritis. *Clin Rheumatol* 28:479-481, 2009.
120. Roos JM, Aubry MC, Edwards WD: Chloroquine cardiotoxicity: clinicopathologic features in three patients and comparison with three patients with Fabry disease. *Cardiovasc Pathol* 11:277-283, 2002.
121. Udayakumar N, Venkatesan S, Rajendiran C: Pulmonary hypertension in rheumatoid arthritis: relation with the duration of the disease. *Int J Cardiol* 127:410-412, 2008.
122. Roldan CA, Chavez J, Weist P, et al: Aortic root disease and valve disease associated with ankylosing spondylitis. *J Am Coll Cardiol* 32:1397-1404, 1998.
123. Yuan SM: Cardiovascular involvement of ankylosing spondylitis: report of three cases. *Vascular* 17:342-354, 2009.
124. Luckie M, Irion L, Khattar RS: Severe mitral and aortic regurgitation in association with ankylosing spondylitis. *Echocardiography* 26:705-710, 2009.
125. Yildirir A, Aksoyek S, Calguneri M, et al: Echocardiographic evidence of cardiac involvement in ankylosing spondylitis. *Clin Rheumatol* 21:129-134, 2002.
126. Krarup NH, Poulsen SH, Baandrup U, et al: Aorto-mitral inflammation in rheumatological disease: transoesophageal echocardiographic presentation. *Eur J Echocardiogr* 8:346-351, 2007.
127. Jimenez-Balderas FJ, Garcia-Rubi D, Perez-Hinojosa S, et al: Two-dimensional echo Doppler findings in juvenile and adult onset ankylosing spondylitis with long-term disease. *Angiology* 52:543-548, 2001.
128. Peters AJ, Wolde S, Sedney MI, et al: Heart conduction disturbance: an HLA-B27 associated disease. *Ann Rheum Dis* 50:348-350, 1991.
129. Acar G, Sayarlioglu M, Akcay A, et al: Assessment of atrial electromechanical coupling characteristics in patients with ankylosing spondylitis. *Echocardiography* 26:549-557, 2009.
130. Caliskan M, Erdogan D, Gullu H, et al: Impaired coronary microvascular and left ventricular diastolic functions in patients with ankylosing spondylitis. *Atherosclerosis* 196:306-312, 2008.

131. Moyssakis I, Gialafos E, Vassiliou VA, et al: Myocardial performance and aortic elasticity are impaired in patients with ankylosing spondylitis. *Scand J Rheumatol* 38:216-221, 2009.
132. Okan T, Sari I, Akar S, et al: Ventricular diastolic function of ankylosing spondylitis patients by using conventional pulsed wave Doppler, myocardial performance index and tissue Doppler imaging. *Echocardiography* 25: 47-56, 2008.
133. Kahan A, Coghlan G, McLaughlin V: Cardiac complications of systemic sclerosis. *Rheumatology (Oxford)* 48(Suppl 3):iii45-iii48, 2009.
134. Montisci R, Vacca A, Garau P, et al: Detection of early impairment of coronary flow reserve in patients with systemic sclerosis. *Ann Rheum Dis* 62:890-893, 2003.
135. D'Andrea A, Stisi S, Caso P, et al: Associations between left ventricular myocardial involvement and endothelial dysfunction in systemic sclerosis: noninvasive assessment in asymptomatic patients. *Echocardiography* 24:587-597, 2007.
136. Meune C, Allanore Y, Devaux JY, et al: High prevalence of right ventricular systolic dysfunction in early systemic sclerosis. *J Rheumatol* 31:1941-1945, 2004.
137. Tyndall AJ, Bannert B, Vonk M: Causes and risk factors for death in systemic sclerosis: a study from the EULAR Scleroderma Trials and Research (EUSTAR) database. *Ann Rheum Dis* 69:1809-1815, 2010.
138. Dimitroulas T, Giannakoulas G, Papadopoulou K, et al: Early detection of cardiac involvement in systemic sclerosis assessed by tissue-Doppler echocardiography: relationship with neurohormonal activation and endothelial dysfunction. *J Rheumatol* 37:993-999, 2010.
139. Allanore Y, Meune C, Vignaux O, et al: Bosentan increases myocardial perfusion and function in systemic sclerosis: a magnetic resonance imaging and tissue-Doppler echography study. *J Rheumatol* 33:2464-2469, 2006.
140. Rosato E, Maione S, Vitarelli A, et al: Regional diastolic function by tissue Doppler echocardiography in systemic sclerosis: correlation with clinical variables. *Rheumatol Int* 29:913-919, 2009.
141. Mele D, Censi S, La Corte R, et al: Abnormalities of left ventricular function in asymptomatic patients with systemic sclerosis using Doppler measures of myocardial strain. *J Am Soc Echocardiogr* 21:1257-1264, 2008.
142. Meune C, Avouac J, Wahbi K, et al: Cardiac involvement in systemic sclerosis assessed by tissue-doppler echocardiography during routine care: a controlled study of 100 consecutive patients. *Arthritis Rheum* 58:1803-1809, 2008.
143. Matias C, Isla LP, Vasconcelos M, et al: Speckle-tracking-derived strain and strain-rate analysis: a technique for the evaluation of early alterations in right ventricle systolic function in patients with systemic sclerosis and normal pulmonary artery pressure. *J Cardiovasc Med* 101:29-34, 2009.
144. Schattke S, Knebel F, Grohmann A, et al: Early right ventricular systolic dysfunction in patients with systemic sclerosis without pulmonary hypertension: a Doppler tissue and speckle tracking echocardiography study. *Cardiovasc Ultrasound* 22:3, 2010.
145. Shahin AA, Anwar S, Elawar AH, et al: Circulating soluble adhesion molecules in patients with systemic sclerosis: correlation between circulating soluble vascular cell adhesion molecule-1 (sVCAM-1) and impaired left ventricular diastolic function. *Rheumatol Int* 20: 21-24, 2000.
146. Serra W, Chetta A, Santilli D, et al: Echocardiography may help detect pulmonary vasculopathy in the early stages of pulmonary artery hypertension associated with systemic sclerosis. *Cardiovasc Ultrasound* 5:25, 2010.
147. Steen V, Chou M, Shanmugam V, et al: Exercise-induced pulmonary arterial hypertension in patients with systemic sclerosis. *Chest* 134:146-151, 2008.
148. Callejas-Rubio JL, Moreno-Escobar E, de la Fuente PM, et al: Prevalence of exercise pulmonary arterial hypertension in scleroderma. *J Rheumatol* 35:1812-1816, 2008.
149. Hachulla E, de Groote P, Gressin V, et al: The three-year incidence of pulmonary arterial hypertension associated with systemic sclerosis in a multicenter nationwide longitudinal study in France. *Arthritis Rheum* 60:1831-1839, 2009.
150. Kampolis C, Plastiras S, Vlachoyiannopoulos P, et al: The presence of anti-centromere antibodies may predict progression of estimated pulmonary arterial systolic pressure in systemic sclerosis. *Scand J Rheumatol* 37:278-283, 2008.
151. Peled N, Bendayan D, Shitrit D, et al: Peripheral endothelial dysfunction in patients with pulmonary arterial hypertension. *Respir Med* 102:1791-1796, 2008.
152. Mukerjee D, St George D, Coleiro B, et al: Prevalence and outcome in systemic sclerosis associated pulmonary arterial hypertension: application of a registry approach. *Ann Rheum Dis* 62:1088-1093, 2003.
153. Steen V, Chou M, Shanmugam V, et al: Exercise-induced pulmonary arterial hypertension in patients with systemic sclerosis. *Chest* 134:146-151, 2008.
154. Fischer A, Misumi S, Curran-Everett D, et al: Pericardial abnormalities predict the presence of echocardiographically defined pulmonary arterial hypertension in systemic sclerosis-related interstitial lung disease. *Chest* 131:988-992, 2007.
155. Pullicino P, Borg R, Agius-Musccat H, Nadassy V: Systemic embolism from mitral vegetation in scleroderma. *J R Soc Med* 82:502-503, 1989.
156. Uusimaa P, Krogerus ML, Airaksinen J, et al: Aortic valve insufficiency in patients with chronic rheumatic diseases. *Clin Rheumatol* 25:309-313, 2006.
157. Lundberg IE: Cardiac involvement in autoimmune myositis and mixed connective tissue disease. *Lupus* 14:708-712, 2005.
158. Schwartz T, Sanner H, Husebye T, et al: Cardiac dysfunction in juvenile dermatomyositis: a case-control study. *Ann Rheum Dis* 70:766-771, 2011.
159. Buchpiguel CA, Roizenblatt S, Lucenn-Fernandez MF: Radioisotopic assessment of peripheral and cardiac muscle involvement and dysfunction in polymyositis/dermatomyositis. *J Rheumatol* 18:1359-1363, 1991.
160. Bittenbring JT, Chen CH, Fries P, et al: Typical laboratory constellation of a non-ST-segment elevation myocardial infarction in polymyositis. *Dtsch Med Wochenschr* 135:2456-2458, 2010.
161. Martinez A, Vila LM, Rios-Olivares E: Predominance of CD4 T cells and Th2 cytokines in the pericardial fluid of a dermatomyositis patient with cardiac tamponade. *Clin Exp Rheumatol* 22:135, 2004.
162. Grillone P, Paolillo V, Presbitero P: Verrucous abacterial endocarditis and polymyositis. A possible association? *G Ital Cardiol* 26:1303-1307, 1996.
163. Naclerio C, D'Angelo S, Baldi S, et al: Efficacy of bosentan in the treatment of a patient with mixed connective tissue disease complicated by pulmonary arterial hypertension. *Clin Rheumatol* 29:687-690, 2010.
164. Bezerra MC, Saraiva F Jr, Carvalho JF, et al: Cardiac tamponade due to massive pericardial effusion in mixed connective tissue disease: reversal with steroid therapy. *Lupus* 13:618-620, 2004.
165. Kumar MS, Smith M, Pischel KD: Case report and review of cardiac tamponade in mixed connective tissue disease. *Arthritis Rheum* 55:826-830, 2006.
166. Végh J, Hegedus I, Szegedi G, et al: Diastolic function of the heart in mixed connective tissue disease. *Clin Rheumatol* 26:176-181, 2007.
167. Jang JJ, Olin JW, Fuster V: A teenager with mixed connective tissue disease presenting with acute coronary syndrome. *Vasc Med* 9:31-34, 2004.
168. Roldan CA, Shively BKS, Crawford MH: Valve excrescences: prevalence, evolution, and risk for cardioembolism. *J Am Coll Cardiol* 30:1308-1314, 1997.

# 38 Echocardiography in the Evaluation of Cardiac Disease Resulting from Endocrinopathies, Renal Disease, Obesity, and Nutritional Deficiencies

MARCUS F. STODDARD, MD

**Endocrinopathies**
- Diabetic Heart Disease
- Metabolic Syndrome
- Hypothyroidism
- Hyperthyroidism
- Acromegalic Heart Disease
- Primary Hyperparathyroidism
- Adrenal Diseases and Heart Disease

**Chronic Kidney Disease**
- Uremic Cardiomyopathy, Systolic Dysfunction, and LV Hypertrophy
- Diastolic Dysfunction
- Structural and Valvular Heart Disease
- Clinical Utility

**Obesity**
- Systolic Function
- Diastolic Function
- Structural Abnormalities
- Anorexigen Use, Valvulopathy, and Pulmonary Hypertension
- Clinical Utility

**Nutritional Deficiencies and Heart Disease**
- Vitamin and Trace Element Deficiencies
- Protein and Calorie Malnutrition

Endocrinopathies, renal diseases, nutritional deficiencies, and obesity have an adverse impact on cardiac function and structure and affect cardiovascular morbidity and mortality. These disorders may impair systolic and diastolic function, cause valvular regurgitation or stenosis, and lead to ventricular hypertrophy and dilation. Although the cardiac manifestations of these disorders are nonspecific, their detection has clinical relevance and significantly affects patient management. The emergence of strain imaging and tissue-Doppler echocardiography has allowed for early detection of myocardial disease. Conventional echocardiography and newer modalities play an important role in the timely detection of cardiac abnormalities from these diverse disease entities, particularly in asymptomatic patients.

## Endocrinopathies

### DIABETIC HEART DISEASE

Diabetes mellitus may cause a diabetic cardiomyopathy by impairing diastolic and systolic myocardial function via incompletely understood mechanisms independent of coronary artery disease or hypertension.[1] The mechanisms that cause diabetic cardiomyopathy are likely multifactorial and may relate to hyperglycemia, insulin resistance, diabetic microangiopathy of the coronary circulation, reduction in myocardial glucose supply and oxidation, impaired myocardial free fatty acid metabolism, abnormal regulation of intracellular calcium homeostasis, duration of diabetes, and type of diabetes. Diabetes is a major contributor to heart failure and occurs in 15% to 35% of heart failure patients.[2] In diabetic subjects, the risk of heart failure is higher in women than men. Cardiovascular prognosis is worse in heart failure patients with diabetes. Meta-analyses show that the relative risk for mortality is 28% higher in diabetic subjects with heart failure and systolic dysfunction as compared to their nondiabetic counterparts.[3] The impact of diabetes on outcome in patients with heart failure from diastolic dysfunction is less clear. In diabetic patients with diastolic dysfunction compared to those without, the cumulative probability of death at 5 years has been reported to be 30.8% versus 12.1%.[4] Diabetic cardiomyopathy begins in a preclinical phase as regional myocardial systolic and diastolic dysfunction that leads to global diastolic dysfunction, and progresses to left ventricular hypertrophy (LVH), fibrosis, dilatation, and global systolic dysfunction or reduced left ventricular (LV) ejection fraction. Detection of myocardial disease potentially on the basis of diabetes in its early stages, before structural changes such as hypertrophy or fibrosis occur, may affect intensity of treatment and disease progression.

#### *LV Systolic Dysfunction*

Regional impairment of LV myocardial systolic function is an early manifestation of diabetic heart disease assessed by strain, strain rate, and peak myocardial tissue-Doppler velocity imaging. It occurs before the onset of symptoms.[5-10] Regional contractility reserve is decreased in patients with diabetes as

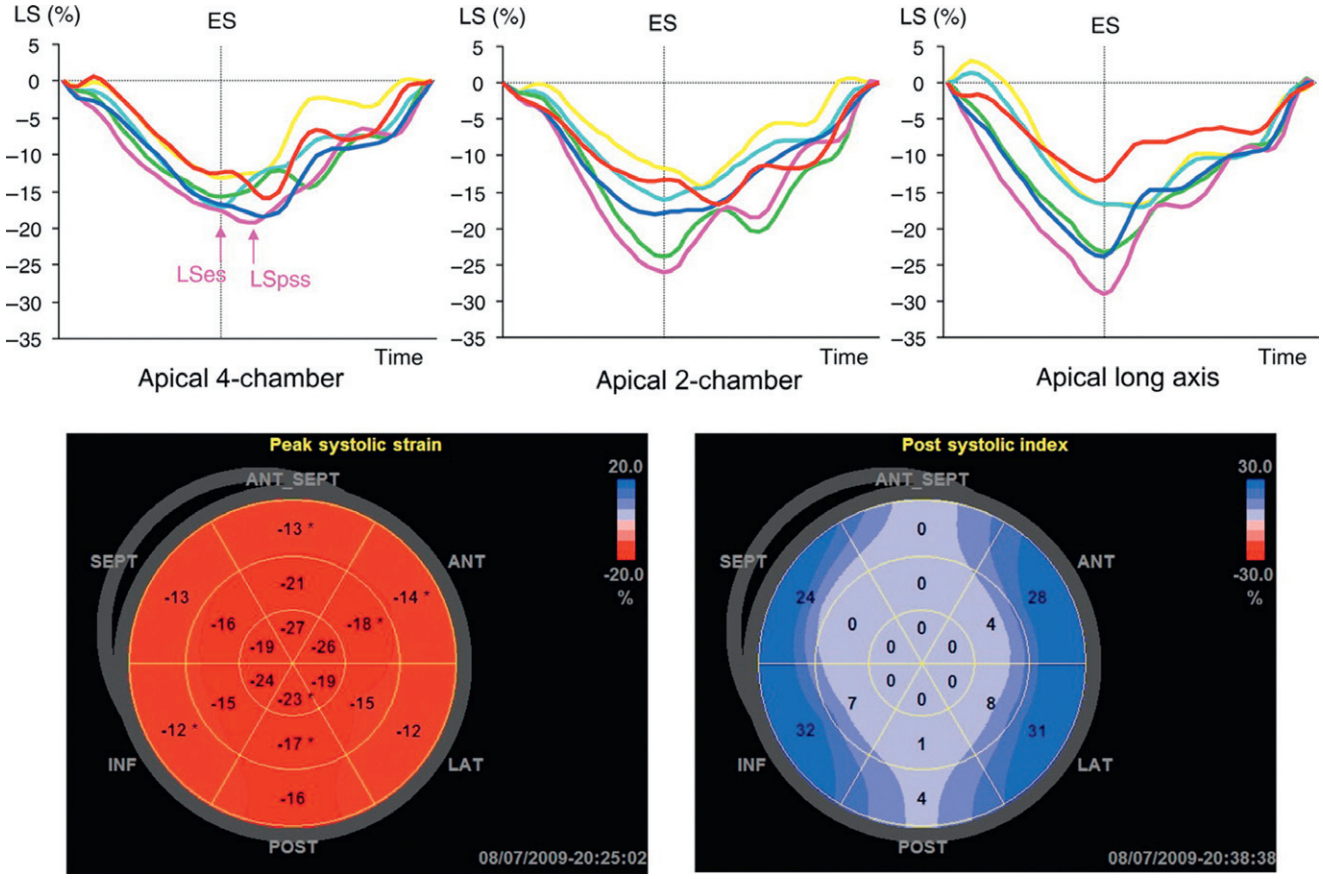



**Figure 38-1 Measurements of strain and post-systolic index in a diabetic patient.** *Upper three panels* show longitudinal regional strain curve of six segments from the apical four-chamber, two-chamber, and long-axis views. The *vertical line* denotes end-systole (*ES*). In addition to longitudinal strain values at end-systole (*LSes*), post-systolic peak longitudinal strain (*LSpss*) was measured, if the regional strain curve reached its peak after the aortic valve closure. *Lower panels* show parametric image of end-systolic strain and post-systolic index. Note that post-systolic index was observed in the basal part of the myocardium. *(Modified from Nakai H, Takeuchi M, Nishikage T, et al: Subclinical left ventricular dysfunction in asymptomatic diabetic patients assessed by two-dimensional speckle tracking echocardiography—correlation with diabetic duration.* Eur J Echocardiogr *10:926-932, 2009.)*

assessed by strain and peak strain rate imaging during dobutamine stress echocardiography.[11] Exercise may unmask potential abnormalities of systolic function unrelated to coronary artery disease that were not apparent at rest in diabetes.[12] Regional myocardial systolic dysfunction progresses to global impairment in systolic function as manifested by a reduced LV ejection fraction and associated remodeling.

LV longitudinal systolic strain and peak systolic tissue-Doppler velocity may be reduced in patients with diabetes, representing an early stage of systolic dysfunction that precedes abnormalities of more conventional echocardiographic indexes of systolic function (e.g., LV ejection fraction, ratio of preejection period to LV ejection time, or shortening fraction.[5-10,13] Nakai and co-workers[6] reported LV longitudinal systolic strain obtained as the average of 18 myocardial segments from apical four-, two-, and three-chamber views (Fig. 38-1) to be reduced in asymptomatic diabetic patients compared to controls (−17.6 ± 2.6% versus −20.8 ± 1.8%, $p < 0.001$). Ng and associates[7] noted similar findings, and that longitudinal systolic strain rate was lower in asymptomatic diabetic patients versus healthy subjects (−0.99 ± 0.17 $s^{-1}$ versus −1.07 ± 0.3 $s^{-1}$, $p = 0.009$). The influence of diabetes on radial systolic strain of the mid left ventricle (LV) is less consistent: Some investigators note normal systolic strain[6,7] and/or strain rates,[7] whereas other researchers report a decrease in systolic strain.[5] The myocardial performance index derived from conventional Doppler echocardiography may be abnormal during the early course of type 2 diabetes. Echocardiographic-based measurement of LV systolic torsion and contractile dyssynchrony offer promise in detection of diabetic myocardium in its early stages, but future studies validating their role are needed.[14]

In diabetic patients with long-term, complicated disease, systolic time intervals are frequently abnormal and include prolongation of LV preejection period and shortening of ejection time. Shortening fraction derived by M-mode echocardiography may be decreased in diabetic patients with long-standing disease. In young asymptomatic diabetic patients, abnormalities of LV shortening fraction and velocity of circumferential fiber shortening ($V_{cf}$) measured by M-mode echocardiography may become evident immediately after exercise. Divergent results have been reported in diabetic subjects on the response of peak systolic myocardial tissue velocity to dobutamine, with findings of a blunted increase[13] versus normal increase.[15]

Diabetes is a cause of LVH and concentric remodeling, which can be assessed for by M-mode and two-dimensional (2D) echocardiography.[16] Abnormal myocardial acoustic properties characterized by a reduction in the cyclic variation of ultrasound-integrated back-scatter and abnormal acoustic densitometry

can be detected in asymptomatic diabetic patients and reflect subclinical cardiomyopathic changes potentially attributable to collagen deposition or myocardial fibrosis in the heart.[10,17]

### *Right Ventricular Dysfunction*

Although data regarding the effect of diabetes on LV function and structure are robust, information is scant in regard to the right ventricle (RV). Studies show that diabetic patients have impaired regional and global relaxation (grade 1) of the RV, as evidenced by tricuspid valve peak early to atrial inflow velocity ratio less than 1.0, lateral tricuspid annular tissue-Doppler peak early to atrial velocity ratio less than 1.0,[18] and reduced peak early diastolic strain rate of base and apical RV free wall.[19] The potential influence of diabetes on RV systolic function is less well studied. Some studies support diabetes as a cause of impairment of RV systolic function,[19,20] whereas others do not.[18]

### *Valvular Function and Aortic Elastic Properties*

Type 2 diabetes accelerates the rate of progression in patients with moderate (i.e., valve area 1.0 to 1.5 $cm^2$) aortic stenosis.[21] Diabetic patients as compared to nondiabetic subjects showed a more rapid decrease in aortic valve area of $0.25 \pm 0.20$ versus $0.14 \pm 0.13$ $cm^2$/year ($p = 0.0016$).[21] In patients with severe aortic stenosis, the presence of diabetes leads to more adverse remodeling of the LV as characterized by greater LV mass and end-diastolic dimension than explained by afterload.[22] Elastic properties of the aorta are impaired in asymptomatic type 2 diabetic patients.[23] Aortic stiffness is increased and distensibility decreased as measured at the proximal ascending aorta using M-mode echocardiography.[23] Impaired aortic elastic function is associated with diastolic dysfunction in asymptomatic diabetic patients.[23]

### *Diastolic Dysfunction*

Conventional echocardiographic parameters of diastolic function (e.g., peak early filling velocity, peak early to atrial velocity ratio, deceleration time, inflow propagation rate, pulmonic vein systolic to diastolic peak velocity ratio, or isovolumetric relaxation time) largely reflect the impact of diabetes on diastolic function of the LV and/or RV chambers and as such are "global indexes" of diastolic function (Table 38-1). In well-controlled type 2 diabetic patients, 60% showed global diastolic dysfunction, with a pattern of impaired LV relaxation (grade 1) in 32% and pseudonormal (grade 2) in 28%.[24] Boyer et al.[25] reported grade 1 diastolic dysfunction in 46% of well-controlled type 2 diabetic patients. Pseudonormal diastolic function can be unmasked in diabetic patients with normal diastolic filling at rest by performance of Valsalva maneuver or isometric handgrip exercise Doppler echocardiography.[15] Restrictive diastolic filling in the absence of reduced LV ejection fraction (i.e., dilated cardiomyopathy) has not been convincingly shown as a feature of diabetic myocardial disease. However, before global diastolic function is impacted, a cumulative amount of regional myocardial diastolic dysfunction and/or dyssynchrony must occur.

**TABLE 38-1 Echocardiographic Findings in Diabetic Cardiomyopathy**

| *Myocardial Disease Stage* | *Diastolic Function* | *Systolic Function* | *Structure* |
|---|---|---|---|
| Early | **Strain/tissue-Doppler imaging:**<br>↓Peak global early LV diastolic SR (<1.0 $s^{-1}$)<br>↓MV annular E′ (<8 cm/s)<br>↓MV annular E′/A′ ratio (<1.0)<br>↓Diastolic reserve (i.e., blunted rise in annular E′ with supine bicycle exercise)<br>**Conventional Doppler indexes:**<br>Normal (E, E/A, IVRT, %AC, $V_p$) | **Strain/tissue-Doppler imaging:**<br>↓Global LV longitudinal strain (<–18%)<br>↓Peak global LV longitudinal systolic SR (<0.90 $s^{-1}$)<br>↓Systolic reserve (i.e., Blunted rise in annular S′ with supine bicycle exercise)<br>Possible ↓MV annular S′<br>Conventional 2D/3D echocardiography<br>Normal (rest LVEF, SF, $V_{cf}$)<br>**Conventional Doppler indexes:**<br>Normal (PEP/LVET) | **M-mode/2D echocardiography:**<br>Normal (LVM index, LV volume, LV wall thickness) |
| Middle | All strain and tissue-Doppler abnormalities of early stage<br>**Conventional Doppler/color M-mode Doppler:**<br>Grade 1 diastolic dysfunction:<br>↓E (<0.6 m/s)<br>↓E/A ratio (<1.0)<br>↓$V_p$ (<45 cm/s) via color M-mode<br>↑%AC, ↑IVRT (>90 ms), ↑DT (>250 ms)<br>Possible grade 2 diastolic dysfunction:<br>↑E/E′ (>15)<br>Normal (E, E/A, IVRT, %AC, $V_p$) | All strain and tissue-Doppler abnormalities of early stage<br>**Conventional 2D/3D echocardiography:**<br>Blunted rise in LVEF with exercise<br>Normal (rest LVEF, SF, $V_{cf}$)<br>Conventional Doppler indexes<br>PEP/LVET may be prolonged<br>↑Global LV Tei index (>0.50)<br>**Ultrasonic integrated back-scatter:**<br>↓Septal and posterior wall cyclic variation index | **M-mode/2D echocardiography:**<br>Possible ↑LVM index<br>Possible ↑LV wall thickness (concentric remodeling)<br>Possible ↑LA volume index (>28 $mL/m^2$ body surface area)<br>**Ultrasonic integrated back-scatter:**<br>↑Myocardial acoustic reflectivity |
| Late | All strain and tissue-Doppler abnormalities of early stage<br>Grade 2 diastolic dysfunction:<br>↑E/E′ (>15)<br>Normal (E, E/A, IVRT, %AC)<br>**Conventional Doppler:**<br>Grade 3 diastolic dysfunction if coexistent impaired LVEF:<br>↑E (<0.6 m/s)<br>↑E/A ratio (<1.0)<br>↓%AC, ↓IVRT (<60 ms)<br>↓DT (<150 ms)<br>↓$V_p$ (<45 cm/s) via color M-mode | All strain and tissue-Doppler abnormalities of early stage<br>All ultrasonic integrated back-scatter abnormalities of middle stage<br>**Conventional Doppler indexes:**<br>↑PEP/LVET (>0.50)<br>**Conventional 2D/3D echocardiography:**<br>LVEF, SF, $V_{cf}$ may be abnormal | **M-mode/2D echocardiography:**<br>Concentric remodeling<br>Concentric LVH<br>Eccentric LVH<br>LV enlargement<br>↑LVM index<br>↑LA volume index (>28 $mL/m^2$ body surface area)<br>**Ultrasonic integrated back-scatter:**<br>↑Myocardial acoustic reflectivity |

*DT*, Transmitral early diastolic deceleration time; *E*, peak transmitral early diastolic filling velocity; *E/A*, E/peak transmitral late diastolic filling velocity ratio; *E′*, peak early diastolic tissue-Doppler velocity; *E′/A′*, E′ to peak late diastolic tissue-Doppler velocity; *E/E′*, E to E′ ratio; *IVRT*, isovolumic relaxation time; *LVEF*, LV ejection fraction; *LVM*, LV mass; *MV*, mitral valve; *PEP/LVET*, LV preejection to LV ejection time ratio; *SF*, LV shortening fraction; *SR*, strain rate; *S′*, peak LV systolic tissue-Doppler velocity; $V_{cf}$, LV velocity of circumferential fiber shortening; $V_p$, LV inflow propagation rate; *%AC*, percent atrial contribution to LV filling.

Subclinical regional myocardial impairment of LV diastolic function is an early manifestation of diabetic cardiomyopathy independent of associated diseases, such as hypertension or coronary artery disease.[4] Studies using myocardial tissue-Doppler imaging have shown regional impairment of LV diastolic function at early stages in diabetes with a prevalence as high as 75%.[8,9,13,15,25,26] Importantly, progression to impaired global LV diastolic function as determined by Doppler echocardiography may occur after only a few years of diabetes. Although global LV diastolic function is more likely to be abnormal in diabetic patients with advanced disease manifestations, such as overt nephropathy, autonomic neuropathy, or retinopathy, it does occur in these patients with uncomplicated disease. Impairment of regional RV diastolic function is an early manifestation of diabetic heart disease and can be subclinical.[20]

Augmentation of regional myocardial relaxation (i.e., diastolic functional reserve) during dobutamine infusion[11] or exercise[27,28] as assessed by tissue-Doppler velocities, strain, and/or strain rate imaging is blunted in subjects with diabetes and occurs before the development of abnormalities in diastolic function at rest. Global or regional LV diastolic dysfunction determined by pulsed Doppler echocardiography or tissue-Doppler myocardial imaging, respectively, in type 2 diabetic subjects adversely reduces maximal exercise capacity and tolerance.[29-31]

Tissue-Doppler and strain imaging allow for a more direct appraisal of diastolic function at the regional myocardial level. As a result, these approaches are more sensitive for detection of diastolic dysfunction from diabetes and allow for its detection at a preclinical stage that precedes the earliest stage of global diastolic dysfunction (grade 1), that is, a "preglobal" (or pre–grade 1) diastolic dysfunction (Fig. 38-2). Supporting this concept is the study of Di Bonito and colleagues,[26] who showed that 50% of type 2 diabetics with uncomplicated and short-term (4 years or less) disease had a reduced (i.e., less than 1.0) ratio of peak early to atrial mitral annular tissue-Doppler (E′/A′), in the face of normal global indexes of diastolic function (see Chapter 11). The detection of diastolic dysfunction is enhanced by the addition of tissue-Doppler imaging parameters to that of conventional Doppler indexes (see Chapter 10). Individual diabetic patients may show an isolated abnormality in conventional or tissue-Doppler imaging indexes, which emphasizes the need for a comprehensive echocardiographic evaluation in the assessment of diastolic function. Tissue-Doppler echocardiography of peak septal mitral annular early diastolic velocity (E′) shows a blunted increase with supine bicycle exercise and may allow for early detection of diabetic myocardial disease.[27] Similarly, diabetes patients have a blunted decrease from rest to exercise in the time to onset of regional LV relaxation derived by strain imaging, a promising method to detect early diabetic myocardial disease.[28]

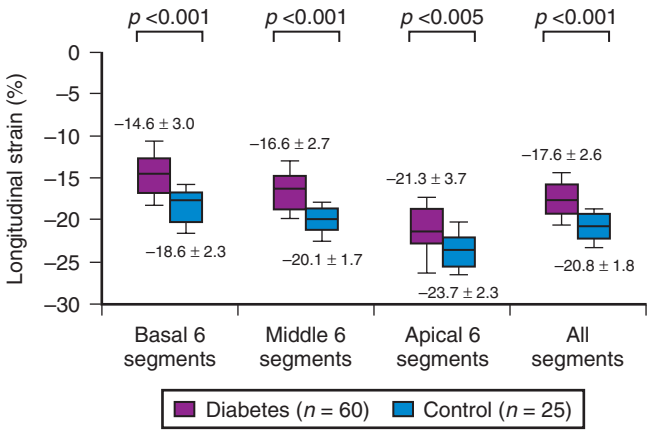



**Figure 38-2 LV longitudinal systolic strain values in diabetic patients (*purple boxes*) and control subjects (*blue boxes*) from basal, middle, and apical segments, and all segments averaged.** Systolic strain was reduced at each segment in diabetic patients. Numerical values are mean ± SD. *In each box, line in middle* equals median value, and *top and bottom of box* represent the 75th and 25th percentiles, respectively. *Upper and lower bars of each box* plot show the 90th and 10th percentiles, respectively. *(Modified from Nakai H, Takeuchi M, Nishikage T, et al: Subclinical left ventricular dysfunction in asymptomatic diabetic patients assessed by two-dimensional speckle tracking echocardiography—correlation with diabetic duration.* Eur J Echocardiogr *10:926-932, 2009.)*

2D speckle tracking has made echocardiographic strain imaging practical by eliminating many of the inherent limitations of color Doppler–based strain, such as dependency on angle of insonation, inability to correct for cardiac translational motion, and inability to measure radial or circumferential strain. Strain imaging is an important modality in the evaluation of diabetic patients with normal conventional indexes and tissue-Doppler parameters of diastolic function for early detection of diabetic myocardial disease.[7] Longitudinal early diastolic LV strain rate is decreased in asymptomatic patients with type 2 diabetes[7] (Fig. 38-3).

### *Interaction of Diabetes with Hypertension, Renal Insufficiency, Obesity, Aging, and Gender*

Diabetes and systemic hypertension are both independently associated with concentric LVH and concentric remodeling. The prevalence of concentric LVH and magnitude of relative wall thicknesses is greater in patients when these two diseases coexist as compared to when either exists in isolation.[32] Importantly, type 2 diabetes attenuates regression of LVH in patients treated for hypertension (Fig. 38-4).[33] LV diastolic function is more impaired in patients with coexisting diabetes and hypertension as compared to those subjects with only one of these diseases.[8] A novel application of strain rate imaging is assessment of left atrial (LA) function. In diabetic patients, hypertension augments impairment of LA conduit and booster function as assessed by peak early and late diastolic atrial strain rates, respectively.[33] LV diastolic dysfunction, independent of LVH, may markedly progress in patients with chronic kidney disease and diabetes.[34] LV diastolic dysfunction is significantly more prevalent in obese patients with as compared to those without diabetes.[35] Diabetes in the presence of obesity augments the increase in LV mass corrected for height.[36] The interaction of diabetes and obesity on increasing LV mass is further amplified by aging in women, but not in men.[36] Aging is an independent contributor to diastolic dysfunction in the normotensive type 2 diabetic patient.[37] There are gender differences in LV diastolic stiffness in diabetic patients.[2] Diabetes in women compared to men is associated with increased LV stiffness during supine bicycle exercise at 50 watts using a novel noninvasive echocardiographically derived index of elastance calculated as the ratio of peak mitral inflow to annular velocities divided by LV stroke volume.

### *Clinical Utility*

Echocardiography has emerged as an important, practical, and reliable modality for the early detection of diabetic myocardial

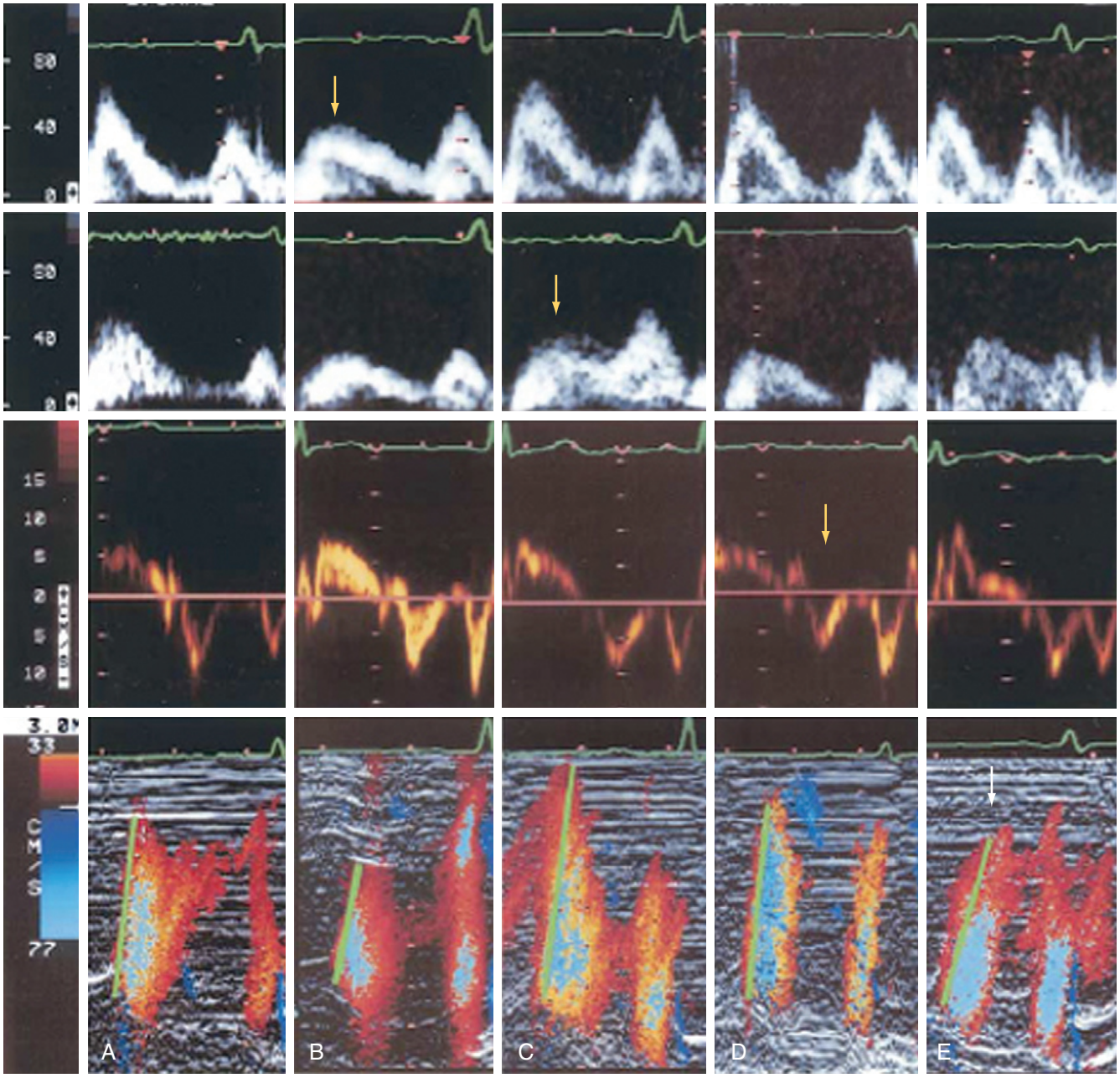



**Figure 38-3 Echocardiographic findings of diastolic function in five different patients with diabetes mellitus, designated as A, B, C, D, and E.** In order from *top*, rows represent resting pulsed Doppler mitral inflow, mitral inflow during the Valsalva maneuver, early diastolic tissue-Doppler velocity, and color M-mode inflow propagation rate, respectively. Patient A shows no diastolic dysfunction abnormalities. In patients B through E, only one of the diastolic parameters (*arrow*) was abnormal when the remaining measurements were normal. *(From Boyer JK, Thanigaraj S, Schechtman KB, Perez JE: Prevalence of ventricular diastolic dysfunction in asymptomatic, normotensive patients with diabetes mellitus.* Am J Cardiol *93:870-875, 2004.)*

disease, particularly when using tissue-Doppler and strain imaging,[5-9,13,15,25,26] and, when necessary, dobutamine or stress echocardiography.[11,27,28] Echocardiographic characterization of diastolic function yields insight into the status of myocardial pathology. It is proposed that in diabetic cardiomyopathy impaired relaxation (grade 1), pseudonormal (grade 2), or restrictive (grade 3) forms of diastolic dysfunction represent predominantly deranged myocardial metabolism with only mild fibrosis, a moderate degree of fibrosis, or severe fibrosis, respectively.[38] Preglobal diastolic dysfunction characterized by diastolic and/or systolic impairment of myocardium detectable by strain or tissue-Doppler imaging that precedes abnormalities of early diastolic filling (grade 1), or other global indexes such as isovolumic relaxation time or LV inflow propagation rate ($V_p$), may represent altered myocardial metabolism without fibrosis.[39] Diastolic dysfunction assessed by peak early mitral inflow velocity to early annular tissue-Doppler velocity (E/E′) ratio correlates with worsening glycemic control (Fig. 38-5).[40] Importantly, echocardiography is useful in demonstrating that therapeutic approaches may prevent or delay the progression of early diabetic myocardial disease. Diastolic and systolic dysfunction in diabetes improves with glycemic control as assessed

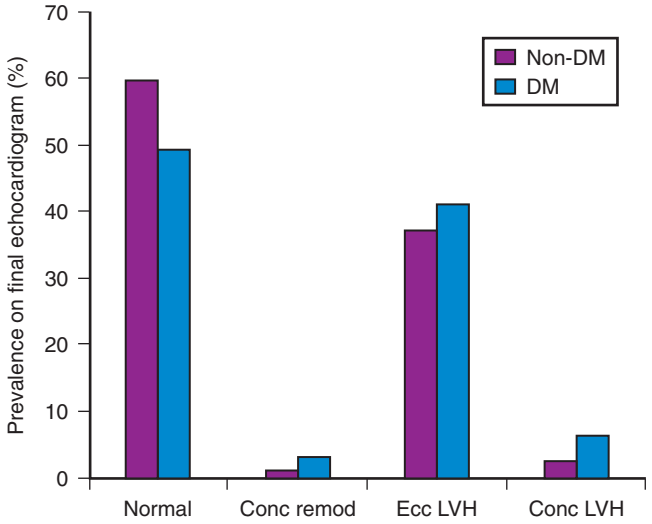



**Figure 38-4 LV geometry at time of final echocardiography in diabetic (*DM, blue bars*) and nondiabetic (*Non-DM, purple bars*) hypertensive patients in the LIFE study.** LV hypertrophy persisted at more than 3.5 years of follow-up more commonly in diabetic versus nondiabetic patients (47% versus 39%, $p$ <0.05) because of greater prevalence of concentric and eccentric LV hypertrophy. *Conc remod*, Concentric LV remodeling; *Ecc LVH*, eccentric LV hypertrophy; *Conc LVH*, concentric LV hypertrophy. *(From Gerdts E, Okin PM, Wachtell K, et al: Impact of diabetes on treatment-induced changes in left ventricular structure and function in hypertensive patients with left ventricular hypertrophy.* Nutr Metab Cardiovasc Dis *19:306-312, 2009.)*

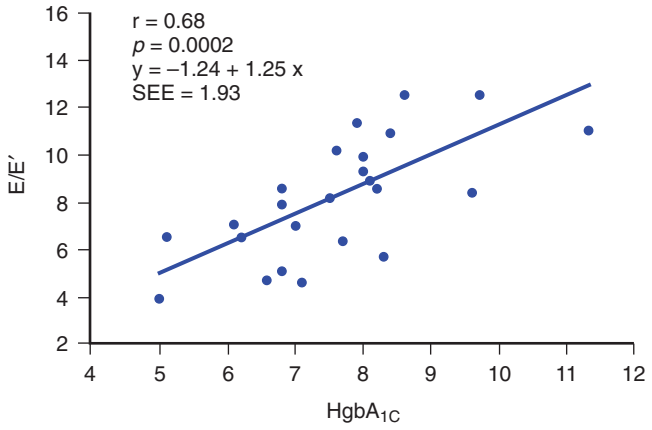



**Figure 38-5 Relation of hemoglobin $A_{1c}$ (*$HgbA_{1c}$*) to LV peak early mitral inflow velocity to early annular tissue-Doppler velocity ratio (*E/E′*) in type 1 diabetic patients.** Improved glycemic control is associated with better diastolic function. *SEE*, Standard error of estimate. *(Modified from Shishehbor MH, Hoogwerf BJ, Schoenhagen P, et al: Relation of hemoglobin A1c to left ventricular relaxation in patients with type 1 diabetes mellitus and without overt heart disease.* Am J Cardiol *91:1514-1517, 2003.)*

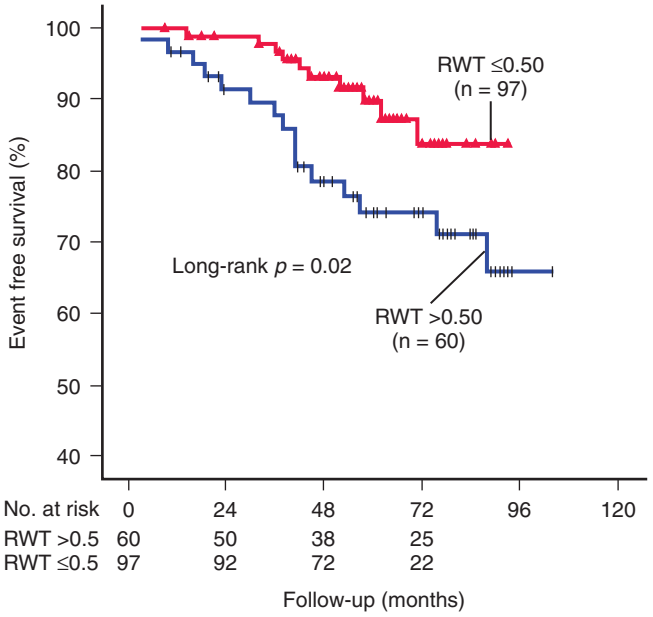



**Figure 38-6 Event-free survival curves without a cardiovascular event by relative wall thickness (*RWT*) >0.50 (4th quartile) or ≤0.50 (1st to 3rd quartiles) in nonobese type 2 diabetic patients.** Relative wall thickness greater than 0.50 was associated with greater events ($p$ = 0.18). *(Modified from Eguchi K, Ishikawa J, Hoshide S, et al: Differential impact of left ventricular mass and relative wall thickness on cardiovascular prognosis in diabetic and nondiabetic hypertensive subjects.* Am Heart J *154:79.e9-79.e15, 2007.)*

by early annular E′ and longitudinal systolic strain rate, respectively.[41,42] The potential benefits for cardiac function of individual treatments to achieve glycemic control in diabetes patients are not uniform. Metformin and rosiglitazone appear beneficial,[43,44] but pioglitazone does not.[45] Although vigorous training aiding in glycemic control may improve myocardial disease in diabetes patients as assessed by tissue-Doppler and strain,[46] conventional exercise training does not.[47] A randomized trial failed to demonstrate the benefit of glycemic control in diabetes on myocardial diastolic function, but studied only 39 patients.[48] Once diabetic myocardial disease is advanced or systolic heart failure ensues, the effectiveness of treatment for reversing the cardiomyopathic state is unproven.[49,50] In type 2 diabetes patients with hypertension, echocardiography determination of LV mass index greater than 142 g/m$^2$ in women, or greater than 164 g/m$^2$ in men, or a relative wall thickness greater than 0.50 is a predictor of cardiovascular events (Fig. 38-6).[51] The Framingham Heart Study estimates that in type 2 diabetes and no clinical coronary artery disease, each 50-g increase in LV mass index increases risk of cardiovascular disease in women by 57% and in men by 49%. Treatment may regress LVH in diabetes patients.[52] Fang and colleagues[53] reported that in unselected asymptomatic patients (n = 101) with diabetes, 22% had LVH, and in a subgroup (n = 66) without coronary artery disease or hypertrophy, 56% had myocardial diastolic or systolic dysfunction, or both as determined by tissue-Doppler velocities or strain. Brain natriuretic peptide was insensitive for detection of diabetic myocardial disease.[53] Echocardiographic screening of asymptomatic diabetic subjects for abnormalities in regional and global systolic and diastolic function, or LVH is advisable, particularly if there is the coexistence of diseases that potentiate the adverse effects of diabetes on cardiac structure and function, such as hypertension, chronic kidney disease, or obesity. Serial echocardiography would appear useful to gauge potential benefit of treatment.

## METABOLIC SYNDROME

The metabolic syndrome is a combination of three or more disorders that include fasting glucose level of 110 mg/dL or greater, central obesity, triglyceride level greater than 150 mg/

dL, high-density lipoprotein cholesterol level <40 mg/dL, and blood pressure at or above 130/80 mm Hg. It has an estimated prevalence of 75 million adults in the United States. It is not surprising that the metabolic syndrome is a risk factor for adverse cardiovascular complications, such as heart failure. Akin to diabetes, over the past 5 years substantial data has emerged confirming that abnormalities of LV diastolic and systolic function and structure occur with the metabolic syndrome.[54-61] It has not been completely determined whether these abnormalities are due to the metabolic syndrome per se, or due to specific individual components of the syndrome. Female compared to male gender in patients with metabolic syndrome is a greater risk factor for concentric remodeling or hypertrophy.[57,59] Dyssynchronous systolic contraction and impaired diastolic relaxation occur in the metabolic syndrome, and hypertension is not the most prominent determinant.[62] Briand and co-workers[63] have shown that metabolic syndrome doubles the rate of progression of aortic stenosis (−0.14 ± 0.13 $cm^2$/year versus −0.08 ± 0.08 $cm^2$/year, $p = 0.008$) and is associated with a substantially lower 3-year event-free survival (44 ± 8% versus 69 ± 6%, $p = 0.002$). In a separate study, these investigators have reported that metabolic syndrome is associated with a significantly faster rate of deterioration of bioprosthetic aortic valves.[64]

Abnormal echocardiography parameters of early LV myocardial disease that occur in subjects with metabolic syndrome include a reduced myocardial E′ or annular E′, decreased regional and global systolic and early diastolic strain rates, and regional systolic strain.[55,56] Grade 1 LV diastolic dysfunction characterized by a reduced transmitral E/A ratio may occur in 29% of subjects with metabolic syndrome.[54,55] The myocardial performance index or Tei index is adversely affected by metabolic syndrome and progressively worsens with more components of the disease (Fig. 38-7).[54,60]

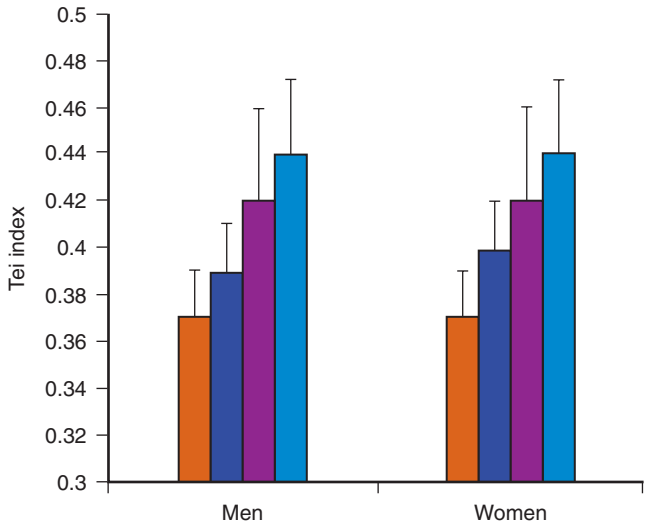



**Figure 38-7 The Tei index (mean ± SD) in men and women without (*orange bars*) metabolic syndrome, and with three (*dark blue bars*), four (*purple bars*), or five (*royal blue bars*) components of the metabolic syndrome.** Myocardial performance progressively worsens with increasing components of the metabolic syndrome. *(From Voulgari C, Moyssakis I, Papazafiropoulou A, et al: The impact of metabolic syndrome on left ventricular myocardial performance.* Diabetes Metab Rev *26:121-127, 2010.)*

## HYPOTHYROIDISM

Hypothyroidism occurs in 4.6% of adults in the United States and is subclinical in the vast majority of these individuals, whereby circulating free thyroid hormone concentrations are normal but thyroid stimulating hormone level is elevated. The Framingham Heart Study has shown hypothyroidism in 10.3% of individuals over age 60 years, and that it is over 2 times more common in women.[65] Thyroid dysfunction adversely affects LV function and structure and the pericardium (Table 38-2), with effects ranging from a subclinical level to frank heart failure.[66] RV systolic function may also be impaired in patients with overt hypothyroidism.[67] However, restoring normal thyroid homeostasis will often reverse adverse affects of thyroid disease, emphasizing the importance of detecting thyroid-induced heart disease.[68]

### *Systolic Dysfunction*

LV systolic dysfunction is a well-recognized feature of overt chronic hypothyroidism using conventional echocardiography measures, with signs including prolongation of the LV preejection period and a reduced ejection fraction, $V_{cf}$, and systolic ejection. More recently, Tiryakioglu and colleagues[69] reported that untreated patients with overt hypothyroidism compared to control subjects have reduced longitudinal systolic strain (16.4 ± 1.4% versus 20.6 ± 1.5%, $p < 0.001$) and peak strain rate (1.0 ± 0.1 $s^{-1}$ versus 1.4 ± 0.1 $s^{-1}$, $p < 0.001$) as determined from the average of all myocardial segments. Kaplan and co-workers[70] have used color Doppler–based tissue imaging to show that LV systolic dyssynchrony occurs more commonly in overt hypothyroidism compared to controls (84% versus 27%, $p < 0.001$) as defined when the standard deviation of time to peak myocardial velocity of the six basal and six midventricular segments exceeds 40 ms.

With subclinical hypothyroidism, LV systolic dysfunction, as evidenced by a reduced peak myocardial systolic velocity, is seen during exercise.[71-75] More sensitive measures of strain also show myocardial systolic dysfunction at rest in patients with subclinical hypothyroidism.[76] Aghini-Lombardi and associates[77] reported reduced systolic longitudinal strain of midseptal wall (−19.2 ± 4.2% versus −23.3 ± 5.4%, $p = 0.05$) and midlateral wall (−18.4 ± 3,7% versus −23.1 ± 5.6%, $p = 0.02$), as well as decreased peak strain rate of midseptal wall (−0.7 ± 0.2 $s^{-1}$ versus −1.2 ± 0.4 $s^{-1}$, $p = 0.05$) and midlateral wall (−1.05 ± 0.2 $s^{-1}$ versus −1.25 ± 0.2 $s^{-1}$, $p = 0.05$), in patients with subclinical hypothyroidism versus controls. The cyclic variation index, a measure of intrinsic contractility derived by integrated backscatter, is reduced in subclinical hypothyroidism.[78,77] The cyclic variation index of regional myocardial segments (e.g., septum or posterior wall) is the percent difference in integrated backscatter from end-diastole to end-systole. The cyclic variation index of the septum of less than 31% correctly discriminates subjects with subclinical hypothyroidism from controls in 86%, significantly better than conventional echocardiographic indexes.[77] Peak systolic tissue-Doppler velocity of the lateral or septal annulus at rest appears insensitive for myocardial dysfunction in subclinical hypothyroidism, as it may be normal despite abnormalities in global indexes of LV systolic (i.e., preejection period or increased preejection to LV ejection time ratio)[74,77] or diastolic (i.e., peak) function.[74,75,77,79]

The adverse effect of subclinical hypothyroidism on left and RV myocardial contractile function can be reversed or improved with thyroid replacement therapy.[79-81]

**TABLE 38-2 Echocardiographic Findings in Hypothyroidism**

| SUBCLINICAL HYPOTHYROIDISM | | |
|---|---|---|
| ***Systolic Dysfunction*** | ***Diastolic Dysfunction*** | ***Structural Abnormalities*** |
| **Strain/tissue-Doppler imaging:**<br>↓Global (<–18%), midseptal (<–17%), and midlateral (<–18%) wall LV longitudinal strain<br>↓Peak global (<0.90 $s^{-1}$), midseptal (<1.0 $s^{-1}$), and midlateral (<1.1 $s^{-1}$) wall LV longitudinal systolic SR<br>↓Systolic reserve (i.e., blunted rise in annular S′ with supine bicycle exercise)<br>**Ultrasonic integrated back-scatter**<br>↓Septal (<31%) and posterior wall cyclic variation index<br>**Conventional 2D/3D echocardiography:**<br>Normal LVEF | **Tissue-Doppler imaging:**<br>↓MV annular E′ (<8 cm/s)<br>↓Septal MV annular E′/A′ ratio (<1.0)<br>Conventional Doppler<br>Grade 1 diastolic dysfunction:<br>↓E (<0.6 m/s)<br>↓E/A ratio (<1.0)<br>↑IVRT (>90 ms) | **Ultrasonic integrated back-scatter:**<br>↑Myocardial acoustic reflectivity |
| **OVERT HYPOTHYROIDISM** | | |
| ***Systolic Dysfunction*** | ***Diastolic Dysfunction*** | ***Structural Abnormalities*** |
| All strain, tissue-Doppler, and ultrasonic integrated back-scatter abnormalities of subclinical hypothyroidism **plus**<br>**Conventional M-mode/2D/3D echocardiography:**<br>↓LVEF (<55%), ↓SF (<25%)<br>↓$V_{cf}$ (<1.0 circ/s)<br>**Conventional Doppler indexes:**<br>↑PEP/LVET (>0.50) | All strain, tissue-Doppler, and conventional Doppler abnormalities of subclinical hypothyroidism **plus**<br>↓Peak midseptal (<0.9 $s^{-1}$) and midlateral wall early LV diastolic SR<br>↓Peak mid-septal (<0.6 $s^{-1}$) and midlateral wall (<0.5 $s^{-1}$) wall LV diastolic SR | All ultrasonic integrated back-scatter abnormalities of subclinical hypothyroidism **plus**<br>**Conventional M-mode/2D echocardiography:**<br>LV hypertrophy<br>↑LVM index<br>LV enlargement<br>Dilated cardiomyopathy<br>Pericardial effusion |

*E*, Peak transmitral early diastolic filling velocity; *E/A*, E/peak transmitral late diastolic filling velocity ratio; *E′*, peak early diastolic tissue-Doppler velocity; *E′/A′*, E′ to peak late diastolic tissue-Doppler velocity; *E/E′*, E to E′ ratio; *IVRT*, isovolumic relaxation time; *LVEF*, LV ejection fraction; *LVM*, LV mass; *MV*, mitral valve; *PEP/LVET*, LV preejection to LV ejection time ratio; *SF*, LV shortening fraction; *SR*, strain rate; *S′*, peak LV systolic tissue-Doppler velocity; $V_{cf}$, LV velocity of circumferential fiber shortening.

### *Diastolic Dysfunction*

Overt hypothyroidism is typically associated with grade 1 diastolic dysfunction,[82-84] but grade 2 or pseudonormal diastolic dysfunction also may be seen.[69] Overt hypothyroidism impairs early and late regional and global diastolic peak longitudinal LV strain rates.[69,76,] In addition, tissue Doppler–derived E′ and the E′/A′ ratio are reduced,[84] and the myocardial performance index may be prolonged.[85]

In subclinical hypothyroidism, regional LV diastolic dysfunction has been consistently shown, as evidenced by a decrease in E′, or E′/A′ ratio as derived from pulsed-wave (PW) tissue-Doppler of the septal or lateral annulus.[73-75,77,79,81] Grade 1 global diastolic dysfunction may occur as shown by a decreased transmitral E and E/A ratio, or prolongation of isovolumic relaxation time derived from Doppler echocardiography.[73-75,77-79]

Importantly, impaired relaxation in subclinical and overt hypothyroidism may be reversed by thyroid hormone replacement.[72,78,80,83]

### *Pericardial and Structural Disease*

Echocardiographic[78] or ultrasonic tissue back-scatter[77,78,86,87] indexes of myocardial texture in adults with hypothyroidism are abnormal, consistent with histologic studies showing interstitial edema and fibrosis, and myofibril swelling.[77,78,86,87] These abnormalities of myocardial texture and septal hypertrophy may reverse with thyroid hormone treatment (Fig. 38-8).[86]

The incidence of pericardial effusion in hypothyroidism varies with severity of disease and occurs in 30% to 80% of patients with advanced disease and in 3% to 6% of patients with mild disease. However, cardiac tamponade due to pericardial effusion from hypothyroidism is rare.[88]

### *Clinical Utility*

Cardiac abnormalities of function and structure caused by subclinical hypothyroidism portend development of overt cardiac disease but are reversible with thyroid hormone replacement treatment.[80,79,81] Thus, early diagnosis is important and supports the need for thyroid hormone, although effective screening for myocardial dysfunction in these patients likely requires sophisticated echocardiographic techniques, such as strain, strain rate imaging, and tissue-Doppler imaging. This is particularly the case when conventional but less sensitive echocardiography methods for LV dysfunction are unremarkable. Otherwise, occult and reversible myocardial disease may go unrecognized.

Overt hypothyroidism causes diastolic and systolic heart failure, which is partially reversible.[82,83] However, making an accurate diagnosis of heart failure in the setting of overt hypothyroidism may be difficult because symptoms of heart failure are easily misdiagnosed as being attributable to hypothyroidism. Conventional echocardiographic findings of cardiac dysfunction support the diagnosis of heart failure and potentially affect the specific selection of medical therapy. Tissue-Doppler velocities and strain and strain rate imaging complement conventional echocardiography for these purposes, particularly for abnormalities in regional ventricular diastolic and systolic function.

Pericardial tamponade in overt hypothyroidism can easily be misdiagnosed as heart failure.[88] Both may present with dyspnea, jugular venous distention, enlarged cardiac silhouette, and peripheral edema. The diagnosis of cardiac tamponade is facilitated by the use of echocardiography.

## HYPERTHYROIDISM

### *Systolic Function*

Echocardiographic findings of systolic function in overt hyperthyroidism typically show increased LV ejection fraction or $V_{cf}$[89,90]; however, these findings are not uniform[91,92] (Table 38-3). Explanation for this difference in findings is unclear. Patients in these studies were untreated, newly diagnosed, and predominantly of female gender. However, etiologies of hyperthyroidism did differ (i.e., Graves disease, autonomous goiter, multinodular goiter, thyroid carcinoma). In addition, ejection fraction and $V_{cf}$ are load-dependent indexes. The increase in preload and decrease in afterload associated with

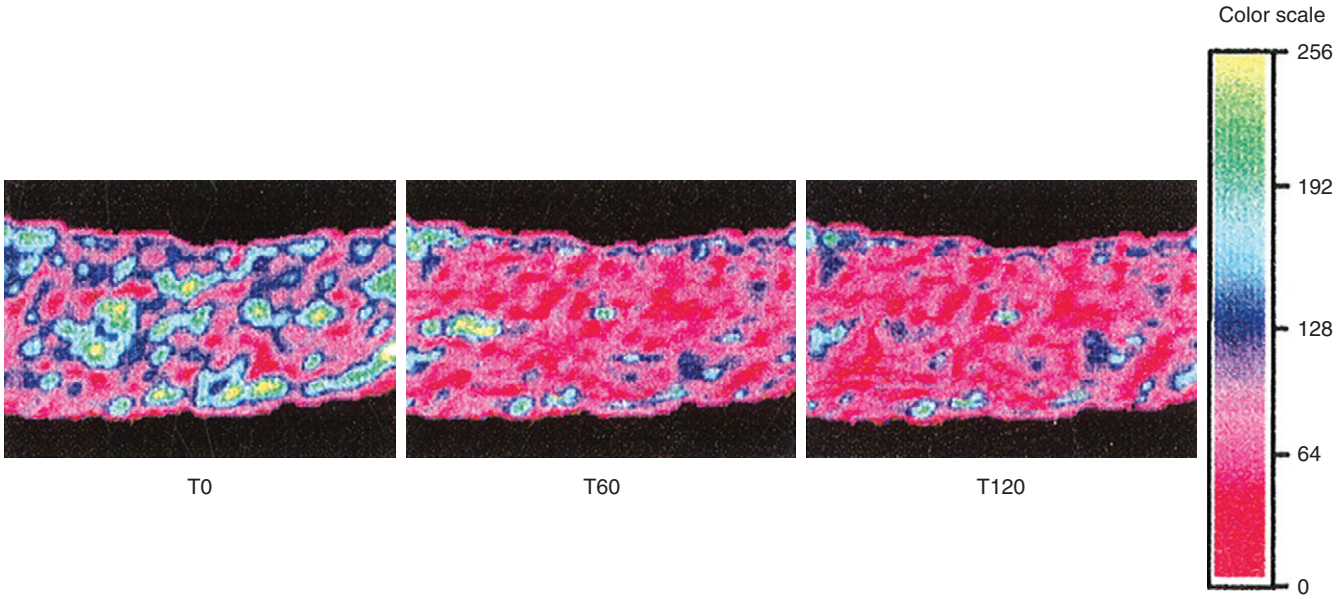



**Figure 38-8 Echocardiographic images from interventricular septum in representative patient with hypothyroidism obtained before (*T0*), 60 (*T60*), and 120 (*T120*) days after levothyroxine treatment.** An arbitrary color scale enhancing the changes in echoreflectivity was used. Abnormal amount of yellow before treatment denotes increased echoreflectivity, which progressively decreases after 60 and 120 days of treatment. *(From Ciulla MM, Paliotti R, Cortelazzi D, et al: Effects of thyroid hormones on cardiac structure: a tissue characterization study in patients with thyroid disorders before and after treatment.* Thyroid *11:613-619, 2001.)*

**TABLE 38-3 Echocardiographic Findings in Hyperthyroidism**

| *Systolic Function* | *Diastolic Function* | *Structural Abnormalities* |
|---|---|---|
| **Subclinical Hyperthyroidism** | | |
| **Strain/tissue-Doppler imaging in endogenous subclinical hyperthyroidism:**<br>↑Midseptal (>−30%) and midlateral (>27%) wall LV longitudinal strain<br>↑Peak midseptal (>1.5 $s^{-1}$) and midlateral (>1.5 $s^{-1}$) wall LV longitudinal systolic SR<br>**Ultrasonic integrated back-scatter in endogenous subclinical hyperthyroidism:**<br>↑Midseptal (>46%) and midlateral (>51%) wall cyclic variation index<br>**Strain/tissue-Doppler imaging in exogenous subclinical hyperthyroidism:**<br>↓Global LV longitudinal strain (<−17%)<br>**Conventional M-mode/2D echocardiography:**<br>↑ or normal LVEF<br>↑ or normal $V_{cf}$ | **Strain/tissue-Doppler imaging:**<br>↓Peak mid-septal (<0.8 $s^{-1}$) and mid-lateral (<0.5 $s^{-1}$) wall LV diastolic SR<br>↓Myocardial E′ (<6 cm/s) of basal LV<br>↓Septal MV annular E′/A′ ratio (<1.0)<br>**Conventional Doppler echocardiography:**<br>Grade 1 diastolic dysfunction:<br>↓E (<0.6 m/s)<br>↓E/A ratio (<1.0)<br>↑IVRT (>90 ms) | **Conventional M-mode/2D echocardiography:**<br>↑LVM index<br>Concentric LV hypertrophy |
| **Overt Hyperthyroidism** | | |
| *Systolic Function* | *Diastolic Function* | *Structural Abnormalities* |
| **Conventional M-mode/2D echocardiography:**<br>↑ (>70-75%) or normal LVEF<br>↑ or normal $V_{cf}$<br>Blunted rise in LVEF, stroke volume, cardiac output with exercise | **Conventional Doppler echocardiography:**<br>↑E (>1.5 m/s)<br>↑E/A ratio (>2.0)<br>↓IVRT (<60 ms)<br>↓E/A (noted in some patients)<br>**Strain/tissue-Doppler imaging (limited data):**<br>↓Myocardial E′ | **Conventional M-mode/2D/Doppler echocardiography:**<br>↑LVM index<br>Concentric LV hypertrophy<br>LV enlargement<br>Dilated cardiomyopathy<br>MVP (>16.5 to 25% with Graves disease)<br>MR (71% with Graves disease)<br>TR (63% with Graves disease) |

*E*, Peak transmitral early diastolic filling velocity; *E/A*, E/peak transmitral late diastolic filling velocity ratio; *E′*, peak early diastolic tissue-Doppler velocity; *E′/A′*, E′ to peak late diastolic tissue-Doppler velocity; *IVRT*, isovolumic relaxation time; *LVEF*, LV ejection fraction; *LVM*, LV mass; *MR*, mitral regurgitation; *MV*, mitral valve; *MVP*, mitral valve prolapse; *SR*, strain rate; *TR*, tricuspid regurgitation; $V_{cf}$, LV velocity of circumferential fiber shortening.

hyperthyroidism varies between patients, potentially contributing to divergence in results of studies.

During exercise patients with hyperthyroidism may display a decline or blunted increase in LV ejection fraction, stroke volume, heart rate, and cardiac output. Overt hyperthyroidism impairs cardiopulmonary exercise capacity, which is reversible by achieving a euthyroid state. Cardiomegaly, impaired global systolic function, and heart failure may ensue from overt hyperthyroidism, which can reverse after induction of a euthyroid state.[93] However, dilated cardiomyopathy persists in one third of these patients.[93] Takotsubo cardiomyopathy may occur from thyroid storm.[94] Although overt hyperthyroidism may enhance

RV systolic function,[68] in rare cases it may lead to RV volume overload and heart failure.[95] LV dyssynchronous systolic contraction occurs in overt hyperthyroidism.[96]

Subclinical hyperthyroidism is defined as normal free thyroid hormone levels in the face of lower than normal thyroid stimulating hormone concentration. It may be caused by endogenous thyroid disease or induced by thyroid hormone treatment (i.e., exogenous). Studies on the impact of subclinical hyperthyroidism on LV global and regional systolic function have shown seemingly divergent results. Several studies have shown exogenous or endogenous subclinical hyperthyroidism to increase global LV systolic function, but other researchers have reported no effect.[89,97,98] Similarly divergent results of regional systolic function have been reported.[99,100] Di Bello and colleagues[99] found enhanced longitudinal strain and systolic strain rate of the midseptal and lateral wall in patients with recently diagnosed and untreated endogenous subclinical hypothyroidism. However, Abdulrahman and co-workers[100] reported reduced longitudinal strain in patients with exogenous subclinical hyperthyroidism treated with suppressive therapy for at least 10 years. It is possible that the discrepancies in global and regional LV systolic function reported in patients with subclinical hyperthyroidism are partly explained by the duration of the illness, with early disease characterized by enhanced function that later normalizes and progresses to impaired systolic function.

### *Diastolic Function*

Most studies have shown that overt hyperthyroidism is associated with an increased transmitral E and/or shortened isovolumic relaxation time, findings that suggest enhanced global diastolic function.[89,90,101] However, limited data exist on less load-dependent indexes of diastolic function (e.g., diastolic strain rate or E′) in patients with overt hyperthyroidism.[101] It is unclear whether augmentation of myocardial diastolic function accounts for the enhanced early filling seen in these studies, because such changes could be on the basis of a decrease in systemic vascular resistance and/or increase in cardiac output, which also were reported to occur in these patients.[90] Others have reported a decrease transmitral E/A ratio[89] and reduced myocardial E′,[101] which suggests that overt hyperthyroidism is a cause of LV diastolic dysfunction in some patients. Yue and associates[101] noted a diagnosis of diastolic dysfunction in 31% (22 of 70) of patients with overt hyperthyroidism.

Exogenous[100,102] and endogenous[99] subclinical hyperthyroidism causes LV regional myocardial diastolic dysfunction as assessed by diastolic strain rate and tissue-Doppler velocity imaging. In patients with subclinical hyperthyroidism compared to controls, peak early diastolic strain rate derived by color Doppler tissue imaging is reduced of the midseptum ($0.8 \pm 0.4\ s^{-1}$ versus $1.4 \pm 0.6\ s^{-1}$, $p$ 0.001) and midlateral wall ($0.91 \pm 0.4\ s^{-1}$ versus $1.17 \pm 0.54\ s^{-1}$ $p$ 0.01).[99] Similarly, myocardial E′ obtained as the average of four basilar LV segments is reduced in subclinical hyperthyroidism ($5.7 \pm 1.3$ cm/s versus $9.0 \pm 1.6$ cm/s, $p$ <0.001).[99] Echocardiographic findings of global diastolic dysfunction in subclinical hyperthyroidism have been shown on the basis of conventional Doppler echocardiographic indexes, namely prolongation of isovolumic relaxation time and deceleration time of early filling and/or reduced peak transmitral E/A ratio.[99,100,102] For example, Smit and colleagues[102] reported in patients with subclinical hyperthyroidism compared to controls a decreased E/A ratio ($0.87 \pm 0.13$ versus $1.29 \pm 0.18$, $p$ <0.001), and prolonged deceleration time ($234 \pm 34$ ms versus $188 \pm 33$ ms, $p$ <0.001) and isovolumic relaxation time ($121 \pm 15$ ms versus $77 \pm 10$ ms, $p$ <0.001). Diastolic dysfunction, when present in exogenous subclinical hyperthyroidism, is partially reversible with achievement of a euthyroid state after medication titration.[102]

### *Structural Disease*

Increased LV mass and LVH, features of subclinical and overt hyperthyroidism, can be diagnosed by M-mode and 2D echocardiography.[89,98,102] Coexisting subclinical hyperthyroidism and hypertension are associated with substantially higher LV mass than when either disease is seen in isolation.[103]

Valvular heart disease, including mitral valve prolapse and hemodynamically significant mitral or tricuspid regurgitation, associated with overt hyperthyroidism can be assessed for clinical significance and progression with echocardiography. A prevalence as high as 16.5% to 25% of mitral valve prolapse in patients with Graves disease has been reported. The basis for this association remains unclear; however, prior studies support a possible autoimmune-mediated mechanism or potential genetic linkage between Graves disease and mitral valve prolapse. Mitral regurgitation occurs in 71% of patients with Graves disease, and tricuspid regurgitation may occur in 63% of such patients. Moderate or severe tricuspid regurgitation can be seen in 29% of these patients and is associated with congestive heart failure. Echocardiography has been used to demonstrate that pulmonary hypertension defined as peak pulmonary systolic pressure greater than 35 mm Hg may occur in as many as 41% of patients with overt hyperthyroidism.[105]

### *Clinical Utility*

Adverse cardiac effects from overt or subclinical hyperthyroidism are potentially reversible or improve with treatment.[93,102] Heart failure is the initial presentation of hyperthyroidism in approximately 6% of such patients.[93] In patients with overt hyperthyroidism, attributing exercise limitations to primary cardiac disease may be challenging on the basis of resting global systolic or diastolic function echocardiography indexes, which are typically enhanced. However, exercise echocardiography may be useful in unmasking a blunted improvement in systolic function with exercise and aid in treatment. The potential clinical usefulness of tissue-Doppler imaging in this setting is promising.[101] Future studies investigating strain and strain rate imaging in overt hypothyroidism are needed and may further guide the utility of echocardiography. Subclinical hyperthyroidism has a relevant clinical impact in that it adversely affects cardiac structure and function and impairs functional capacity. Subclinical hyperthyroidism patients with any of these manifestations should be treated by treating the primary thyroid disorder (e.g., thyroidectomy, radioiodine ablation, or antithyroid medications) if endogenous, by reducing thyroid hormone dose if exogenous, or by the use of beta-blockers. Screening for cardiac abnormalities with echocardiography, particularly using global indexes as well as sophisticated measures of regional diastolic function, is advisable. Last, overt hyperthyroidism should be included in the differential diagnosis of pulmonary hypertension.[104]

## ACROMEGALIC HEART DISEASE

Acromegaly is a rare pituitary disorder with a prevalence of 40 to 60 persons per million and incidence of 3 to 4 individuals per million caused by increased secretion of growth hormone.

**TABLE 38-4 Echocardiographic Findings in Acromegaly**

| *Structural Abnormalities* | *Systolic Function* | *Diastolic Dysfunction* |
|---|---|---|
| **Conventional M-mode/2D echocardiography:**<br>Concentric LV hypertrophy (more typical/>50% of patients)<br>Eccentric LV hypertrophy (less frequent)<br>Asymmetric septal hypertrophy (variable prevalence)<br>LV enlargement<br>↑LV mass (present in 38% to 81% of patients)<br>RV hypertrophy<br>Dilated cardiomyopathy (occurs in untreated and advanced disease)<br>**Ultrasonic integrated back-scatter:**<br>↑Derived collagen volume fraction<br>**Conventional Doppler echocardiography:**<br>Mitral regurgitation (progressive if disease uncontrolled/severe in 5%)<br>Aortic regurgitation (≥mild severity in 18% with inactive disease, but 31% if active disease) | **Strain/tissue-Doppler imaging:**<br>↓Septal (<−20%) and lateral (<−18%) wall LV longitudinal strain<br>↓Peak septal and lateral wall LV longitudinal systolic SR<br>↓Annular or myocardial S′ (inconsistently present)<br>↑Regional Tei index from lateral MV annulus (>0.50)<br>**Conventional M-mode/2D echocardiography in short-term acromegaly:**<br>↑LVEF<br>↑LV shortening fraction<br>↑Stroke volume<br>↑Cardiac output<br>**Conventional M-mode/2D/Doppler echocardiography in long-term acromegaly:**<br>↓ (<55%) or normal LVEF<br>↓LVEF—seen in 10% of high-output failure patients<br>↑Global LV Tei index (>0.60)<br>**Conventional 2D echocardiography:**<br>Blunted rise in LVEF with exercise<br>Ultrasonic integrated back-scatter<br>↓Cyclic variation index | **Strain/tissue-Doppler imaging:**<br>↓Peak septal and lateral wall LV diastolic SR<br>↓Peak myocardial or MV annular E′<br>↓Septal (<1.0) and lateral (<1.0) MV annular E′/A′ ratio<br>**Conventional Doppler echocardiography:**<br>Grade 1 diastolic dysfunction:<br>↓E (<0.6 m/s)<br>↓E/A ratio (<1.0)<br>↑IVRT (>90 ms)<br>↑DT (>250 ms) |

*DT*, Transmitral early diastolic deceleration time; *E*, peak transmitral early diastolic filling velocity; *E/A*, E/peak transmitral late diastolic filling velocity ratio; *E′*, peak early diastolic tissue-Doppler velocity; *E′/A′*, E′ to peak late diastolic tissue-Doppler velocity; *IVRT*, isovolumic relaxation time; *LVEF*, LV ejection fraction; *MV*, mitral valve; *SR*, strain rate; *S′*, peak LV systolic tissue-Doppler velocity.

Cardiovascular complications are a major cause of morbidity and mortality from acromegaly. Initially, patients show enhanced global systolic function, but progression to diastolic dysfunction and LV hypertrophy is typical, followed by systolic dysfunction and overt heart failure. In advanced, untreated acromegaly, a dilated cardiomyopathy may ensue with about 10% of patients presenting with heart failure. Before effective therapy, nearly 80% of patients died before age 60 years from cardiovascular complications.

### *Ventricular Hypertrophy*

Echocardiography is well suited to delineate the presence and severity of structural cardiac abnormalities due to acromegaly, which include increased LV mass,[105-110] concentric LVH,[108] eccentric LVH,[111] asymmetric septal hypertrophy, LV dilation, and RV hypertrophy (Table 38-4). LVH plays a significant role in the morbidity and mortality from this disease.[112-116] LVH is partially related to hypertension, an associated condition in acromegaly,[117] but it occurs in a substantial proportion of acromegalic patients in the absence of hypertension.[112] LV mass increases with short-term growth hormone hypersecretion[118] and regresses after effective chronic pharmacologic therapy.[105,113-116,119,120] In acromegaly, LVH is typically concentric, but eccentric hypertrophy whereby the increase in LV mass is predominantly on the basis of chamber dilatation does occur.[111] The reported prevalence of asymmetric septal hypertrophy in acromegaly is highly variable: Some studies report a rare association, whereas others describe a frequent association. LV chamber enlargement develops in acromegaly and may occur in the absence of associated conditions such as hypertension, coronary artery disease, or diabetes. The reported incidence of an increased LV mass in patients with acromegaly is 38% to 81%.[88,106] RV hypertrophy also occurs from acromegaly. Echocardiography is useful in documenting regression of hypertrophy with therapy for acromegaly.[105,113-115,119]

### *Diastolic Dysfunction*

LV diastolic dysfunction is present in over 50% of patients with acromegaly,[109,112-116] even in the absence of associated LVH, hypertension, premature coronary artery disease, and diabetes. Typically, there is a reduction of transmitral E and E/A ratio, an increase in peak atrial filling velocity, and a longer early diastolic deceleration time.[109,112-116] Isovolumic relaxation time, assessed by Doppler echocardiography, is prolonged.[112,113] Tissue-Doppler imaging of LV myocardium confirms regional diastolic dysfunction in acromegaly patients as evidenced by a decrease in myocardial E′ and annular E′/A′ ratio.[107-109,116,121,123] In these patients, early diastolic strain rate and peak annular velocity are reduced,[107-109,121,122] and grade 1 diastolic dysfunction is present.[109,112-116] Regional[108] and global[109] LV myocardial performance assessed by Tei index is reduced in acromegaly. Impaired LV diastolic function in acromegaly often improves with treatment.[105,113,115,116,123] Similar to the LV, abnormal regional and global RV diastolic function[107] is a feature of acromegaly.

### *Systolic Function*

In patients with short-term acromegaly uncomplicated by hypertension, coronary artery disease, or diabetes, global LV systolic function, as assessed by shortening fraction, stroke volume, and cardiac output, typically is enhanced. Global LV systolic dysfunction in acromegalic patients appears uncommon.[108,120,121] However, regional LV systolic dysfunction may be evident.[107,112,122,123] High-output heart failure with a modest reduction in LV ejection fraction occurs in 10% of newly diagnosed acromegaly.[124] Di Bello et al.[122] have shown untreated acromegaly patients have reduced longitudinal strain of septum (−19.8 ± 2.9% versus −27.9 ± 3.8%, $p$ <0.001) and lateral wall (−17.7 ± 2.2% versus −25.3 ± 2.6%, $p$ <0.001) and decreased peak strain rate of septum and lateral wall. Importantly, abnormalities of strain virtually normalized after 6 months of treatment with somatostatin analogs.[122] Reduced peak myocardial systolic velocity by PW tissue-Doppler imaging may be evident at rest with active acromegaly[107,112] but has not been consistently reported.[108] Exercise may show a blunted increase in LV ejection fraction, unmasking occult systolic dysfunction. Ultrasonic integrated back-scatter in patients with acromegaly shows reduced cyclic variation and increased derived collagen volume fraction, an index of myocardial fibrosis.[111,115]

### *Valvular Heart Disease*

Acromegaly is a cause of potentially significant mitral and aortic regurgitation.[125,126] Uncontrolled acromegaly is associated with progressive mitral regurgitation.[110] Severe mitral regurgitation has been noted in 5% of acromegaly patients.[126] Aortic regurgitation of a mild or greater severity occurs in 18% of patients with inactive acromegaly and increases to 31% if acromegaly is active.[125] Aortic root stiffness measured by transthoracic echocardiography[127] and aortic root sinotubular junction diameter[128] are increased in acromegaly and could contribute to the aortic regurgitation frequency and severity seen in this disease. The prevalence of significant aortic regurgitation increases with duration of disease, with significant aortic valve disease in only 10% of patients with 6 to 10 years of disease but in over 35% of those with a disease duration over 15 years.[126] Successful valvular surgery has been reported in acromegaly patients.[126,129] The echocardiographic manifestations of structural valvular disease in acromegaly include aortic and mitral valve fibrosis and calcification and mitral annular calcification.[125] Valvular pathology also includes myxoid degeneration.[129]

### *Clinical Utility*

Acromegalic heart disease begins subclinically but often portends serious morbidity and mortality.[123,124,130] Clinical studies show that suppression of growth hormone release by somatostatin analogs (e.g., octreotide acetate) in acromegalic patients significantly reduces LVH and improves abnormalities of global and regional diastolic and systolic function of the LH and RH.[105,113-116,119,120,122] A comprehensive echocardiographic evaluation of cardiac size and function in patients with acromegaly is of value to assess ventricular hypertrophy and cardiac dysfunction. Echocardiographic indexes of regional myocardial function, particularly of diastolic function, derived from strain and tissue-Doppler imaging appear very sensitive and should be employed. For example, tissue Doppler–derived LV E′/A′ was able to determine a greater severity of myocardial disease in patients with active versus well-controlled acromegaly.[109] Strain and tissue-Doppler imaging are useful in the serial evaluation of treated patients with acromegaly to detect cardiac involvement.[109,112,116,122]

Regional myocardial Tei index was found to be increased in patients with acromegaly (0.49 ± 13.4 versus 0.39 ± 5.2, $p$ = 0.005) and more sensitive for detection of diastolic dysfunction compared to conventional echocardiographic indexes (48% versus 36%).[108] Similarly, global Tei index is sensitive for detection of ventricular dysfunction in acromegaly.[109] However, E′/A′ (i.e., an index of regional function) compared to global Tei index is better for differentiating active from well-controlled acromegaly.[108] Prolongation of isovolumic relaxation time is the most sensitive of the conventional echocardiographic indexes of cardiac involvement in acromegaly and is useful for evaluation in the subclinical stage of the disease (Fig. 38-9). Regional and global Tei index should be used for detection of potential acromegalic heart disease when conventional echocardiography, strain, and tissue-Doppler imaging fail to confirm potential cardiac involvement from acromegaly. Ventricular hypertrophy and/or myocardial dysfunction signal the need for aggressive treatment to control growth hormone levels to improve heart disease in patients with acromegaly.[123,124,130] The use of more sophisticated but technically challenging echocardiographic techniques such as ultrasonic integrated back-scatter to assess for myocardial fibrosis and collagen volume await future investigations but are promising.[111,115]

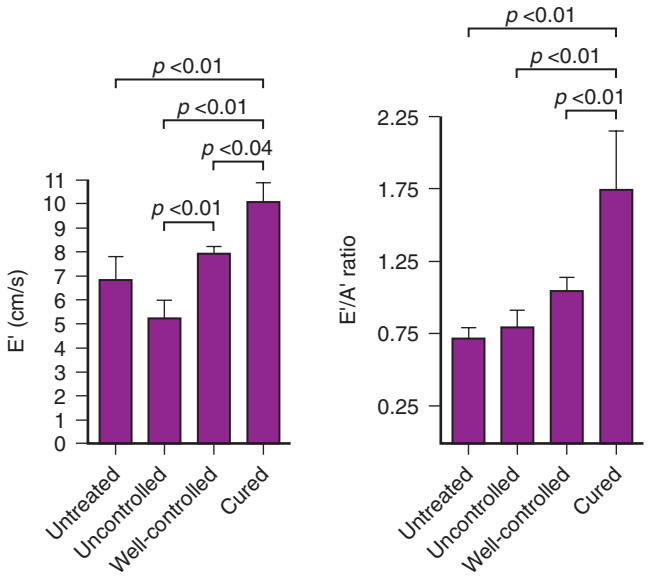



**Figure 38-9 Histogram demonstrating impact of acromegaly disease activity and treatment on LV regional diastolic function by tissue-Doppler echocardiography of peak early (*E′*) and peak early to atrial ratio (*E′/A′*) of septal annulus from four-chamber view.** Cured patients show normalized diastolic parameters, whereas untreated and uncontrolled subjects show impaired myocardial diastolic function. *(From van Thiel SW, Bax JJ, Biermasz NR, et al: Persistent diastolic dysfunction despite successful long-term octreotide treatment in acromegaly.* Eur J Endocrinol *153:231-238, 2005.)*

Acromegaly is a cause of significant mitral and/or aortic regurgitation, which can be clinically silent. Occasionally, surgical intervention is needed. Conventional color flow and spectral Doppler echocardiography are essential for the serial evaluation of patients with acromegaly and evidence of structural valvular disease, particularly with long-standing disease.[126]

## PRIMARY HYPERPARATHYROIDISM

Primary hyperparathyroidism is a recognized cause of increased cardiovascular morbidity and mortality from heart failure, stroke, and myocardial infarction in patients with moderate to severe or severe disease. The impact of milder forms of primary hyperparathyroidism on cardiovascular disease is controversial, with most studies finding no adverse effects.

### *Cardiac Calcification*

Hypercalcemia due to primary hyperparathyroidism may induce calcification of coronary arteries, valves, and myocardium. Aortic valve calcification occurs in 46% to 63% of primary hyperparathyroidism patients, and mitral valve or submitral annulus calcification has been reported in 33% to 49% of these patients. Aortic and mitral stenosis may result from primary hyperparathyroidism. Myocardial calcific deposits have been reported in 62% to 74% of patients with primary hyperparathyroidism. Myocardial calcification mainly involves the interventricular septum and may result in third-degree heart block. Successful parathyroidectomy appears to halt the progression of valvular calcification. Mild primary hyperparathyroidism appears not to show a propensity for valvular calcification.[131]

**TABLE 38-5 Echocardiographic Findings in Primary Hyperparathyroidism**

| *Structural Abnormalities* | *Normal or Enhanced Systolic Function* | *Diastolic Dysfunction* |
|---|---|---|
| **Conventional M-mode/2D/Doppler echocardiography:**<br>LV hypertrophy<br>↑LV mass<br>Hypertrophic cardiomyopathy phenotype<br>No increased LV mass in mild primary hyperparathyroidism<br>**Conventional M-mode/2D/Doppler echocardiography:**<br>Aortic valve calcification (in 46% to 63%)<br>Mitral valve and submitral annular calcification (in 33% to 49%)<br>Aortic stenosis<br>Mitral stenosis<br>Myocardial calcification—primarily of ventricular septum (in 62% to 74%)<br>No increased valvular or myocardial calcification in mild primary hyperparathyroidism | **Conventional M-mode/2D echocardiography:**<br>↑ or normal LVEF<br>↑ or normal LV Shortening fraction<br>**Tissue-Doppler imaging:**<br>Normal myocardial S′ | **Tissue-Doppler imaging:**<br>↓Peak lateral MV annular E′<br>↓Lateral MV annular E′/A′ ratio (<1.0)<br>↑Regional Tei index from lateral MV annulus (>0.50)<br>**Conventional Doppler echocardiography:**<br>Grade 1 diastolic dysfunction:<br>↓E (<0.6 m/s)<br>↓E/A ratio (<1.0)<br>↑IVRT (>90 ms)<br>↓$V_p$ (<45 cm/s) via color M-mode |

*E*, Peak transmitral early diastolic filling velocity; *E/A*, E/peak transmitral late diastolic filling velocity ratio; *E′*, peak early diastolic tissue-Doppler velocity; *E′/A′*, E′ to peak late diastolic tissue-Doppler velocity; *IVRT*, isovolumic relaxation time; *LVEF*, LV ejection fraction; *MV*, mitral valve; *S′*, peak LV systolic tissue-Doppler velocity; $V_p$, LV inflow propagation rate.

### *LV Structure and Function*

LVH is commonly associated with primary hyperparathyroidism and may be caused by excessive serum concentration of parathyroid hormone or intracellular calcium concentration[132] (Table 38-5). LVH develops independent of hypertension, a condition also associated with primary hyperparathyroidism. Partial regression of LVH may occur 6 months to 1 year after parathyroidectomy in these patients. Mild primary hyperparathyroidism appears unassociated with LVH.[131] Impaired myocardial relaxation and performance are associated with primary hyperparathyroidism as assessed by tissue-Doppler and Tei index, respectively. Grade 1 diastolic dysfunction characterized by reduced transmitral E, E/A, $V_p$, and prolonged isovolumic relaxation time are seen in primary hyperparathyroidism.[132,133] However, patients with mild primary hyperparathyroidism may display normal global and regional diastolic function.[131,134] Global LV systolic function is not impaired by primary hyperparathyroidism but may be slightly increased as assessed by LV ejection fraction or shortening fraction.[131,133,134] Similarly, regional myocardial systolic function assessed by peak myocardial systolic velocity is normal in patients with primary hyperparathyroidism.[133,134] Primary hyperparathyroidism reportedly may cause structural and function findings of hypertrophic cardiomyopathy. Alternatively, a reversible dilated cardiomyopathy and heart failure from severe hypocalcemia secondary to hypoparathyroidism is a recognized entity.[135]

### *Clinical Utility*

Echocardiography helps identify LVH, regional and global diastolic dysfunction, and valvular stenosis in patients with primary hyperparathyroidism. Parathyroidectomy may promote regression of myocardial hypertrophy, cessation of valvular calcification, and stabilization or improvement of diastolic dysfunction, all of which can be monitored by serial echocardiographic studies.[136]

## ADRENAL DISEASES AND HEART DISEASE

### *Cushing Syndrome*

Cushing syndrome is caused by excessive secretion of adrenocortical hormones, which causes hypertension, impaired glucose tolerance, diabetes, abdominal obesity, dyslipidemia, and hypercoagulability. These features of Cushing syndrome cause a fourfold increase in mortality rate from cardiovascular complications. Echocardiography shows LVH and asymmetric septal hypertrophy in 75% of patients with Cushing syndrome. LVH may be partly attributable to associated hypertension. Other findings in Cushing syndrome include the following:

- Asymmetric septal hypertrophy is common and severe, with interventricular septal thickness ranging from 1.6 to 3.2 cm and the ratio of septal to posterior wall thickness as high as 2.67.
- LV concentric remodeling occurs is independent of blood pressure.
- Regional and global LV diastolic dysfunction are seen.[137-141]
- Grade 1 global diastolic dysfunction is characterized by decreased transmitral E and E/A ratio, and prolonged deceleration time and isovolumic relaxation time.[137-140]
- Regional LV systolic dysfunction is present as demonstrated by strain measurements.[140]

LVH, regional and global diastolic dysfunction, and regional systolic dysfunction are reversible or improve with successful treatment of Cushing syndrome (Fig. 38-10).[140] A reversible dilated cardiomyopathy attributable to Cushing syndrome has been reported in a minority of patients.[142]

### *Primary Hyperaldosteronism*

Echocardiographic findings in patients with primary aldosteronism include:

- Concentric LVH
- Regional myocardial diastolic dysfunction as assessed by E′[143]
- Grade 1 global diastolic dysfunction[143]

However, LV systolic function does not appear to be impaired as assessed by LV ejection fraction or regional indexes, such as myocardial strain and peak systolic strain rate.[143] In primary hyperaldosteronism, myocardial ultrasonic integrated backscatter demonstrates decreased cyclic variation—findings consistent with greater myocardial collagen content and fibrosis.[144] Experimental data support the concept that excessive aldosterone, independent of its hypertensive effect, may induce ventricular hypertrophy and fibrosis.[145]

The frequency of concentric remodeling and diastolic dysfunction increases with longer duration of Cushing syndrome. These abnormalities may contribute to the high cardiovascular morbidity seen in patients with Cushing syndrome and suggest a role for echocardiography. Regression of LVH in Cushing syndrome after surgical treatment frequently occurs and may

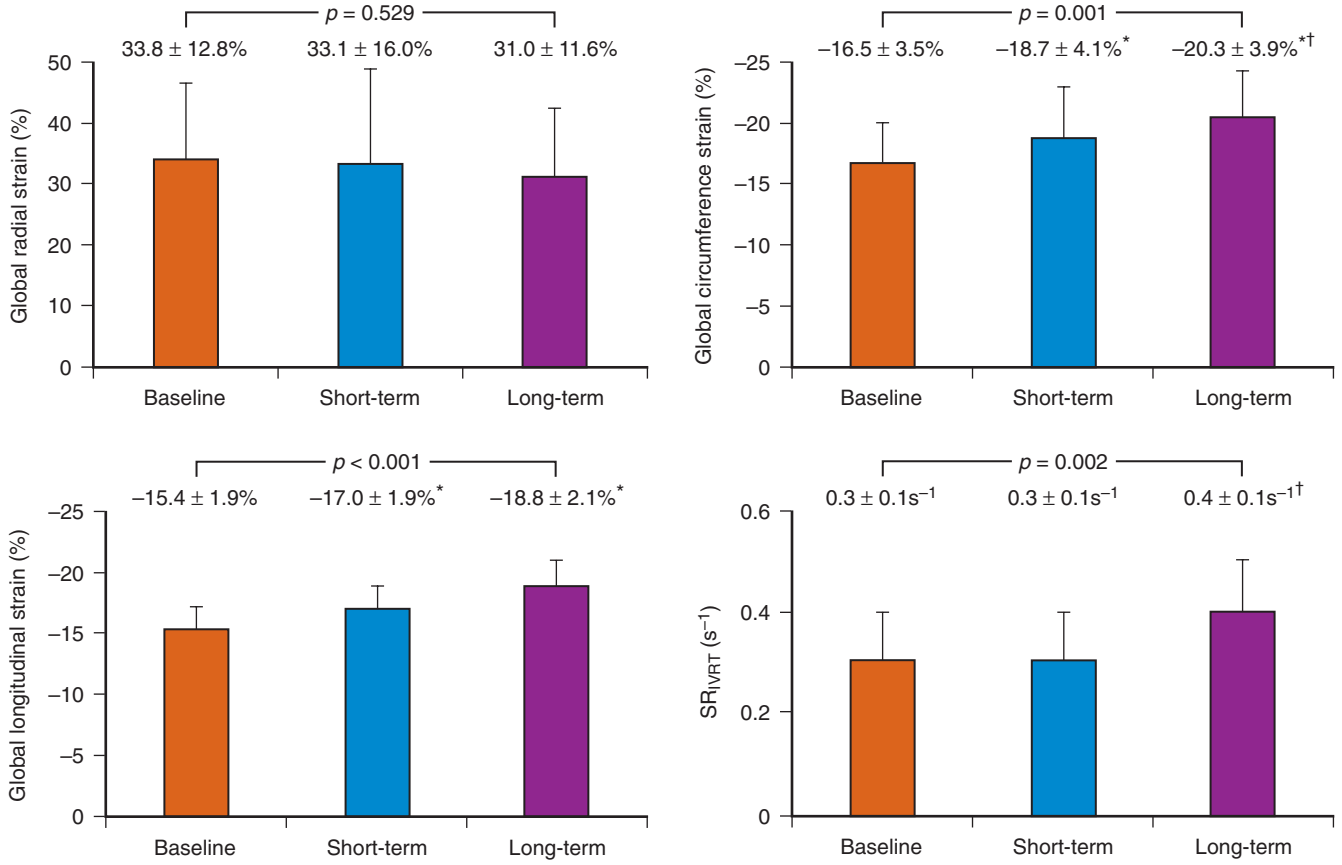



**Figure 38-10 Histograms showing reversibility of impaired LV global radial, circumferential, and longitudinal strain and strain rate at isovolumetric relaxation time ($SR_{IVRT}$) in 15 patients with Cushing syndrome after surgical treatment at short-term (median 1 month) and long-term (median 14 months) follow-up.** *(From Pereira AM, Delgado V, Romijn JA, et al: Cardiac dysfunction is reversed upon successful treatment of Cushing's syndrome.* Eur J Endocrinol *162:331-340, 2010.)*

**TABLE 38-6 Echocardiographic Findings in Chronic Kidney Disease**

| *Valvular Disease* | *Structural Abnormalities* | *Diastolic Dysfunction* | *Systolic Dysfunction* |
|---|---|---|---|
| **Conventional M-mode/2D/Doppler echocardiography:**<br>Aortic valve calcification (in 28% to 60% with ESRD)<br>Mitral annular calcification (in 10% to 36% on hemodialysis)<br>Aortic regurgitation (in 13% with CKD)<br>Mitral regurgitation (in 38% with CKD)<br>Aortic and mitral stenosis<br>Tricuspid and pulmonic insufficiency (secondary to pulmonary hypertension as opposed to calcification) | **Conventional M-mode/2D echocardiography:**<br>Concentric LV hypertrophy<br>Eccentric LV hypertrophy<br>Asymmetric LV hypertrophy<br>LV hypertrophy (in 70% with ESRD/in 34% to 78% with CKD)<br>LV hypertrophy—2.5 to 4× more common in women vs. men<br>LA enlargement<br>LV enlargement<br>Dilated cardiomyopathy (associated with secondary hyperparathyroidism)<br>**Ultrasonic integrated back-scatter:**<br>↑Myocardial acoustic reflectivity | **Strain/tissue-Doppler imaging:**<br>↓Global and mid (<1.2 $s^{-1}$) LV peak early diastolic SR<br>↑Regional Tei index<br>**Conventional Doppler echocardiography:**<br>Grade 1 diastolic dysfunction:<br>↓E (<0.6 m/s)<br>↓E/A ratio (<1.0)<br>↑IVRT (>90 ms)<br>Grade 2 (pseudonormal) and grade 3 (restrictive) diastolic dysfunction occur | **Strain imaging:**<br>↓Global (<−15%) and regional LV longitudinal strain<br>↓Peak global (<0.7 $s^{-1}$) and regional LV SR<br>**Conventional 2D echocardiography:**<br>↓LVEF (in 33% of new dialysis patients)<br>Global or regional myocardial stunning with hemodialysis |

*CKD*, Chronic kidney disease; *E*, peak transmitral early diastolic filling velocity; *E/A*, E/peak transmitral late diastolic filling velocity ratio; *ESRD*, end-stage renal disease; *IVRT*, isovolumic relaxation time; *LVEF*, LV ejection fraction; *SR*, strain rate.

be dramatic. Echocardiographic findings of severe LVH or hypertrophic cardiomyopathy without obvious cause should raise the clinical suspicion of glucocorticoid excess, possibly from Cushing syndrome. Regression of LVH may occur after surgical excision of an aldosterone-producing tumor in patients with primary hyperaldosteronism.

## Chronic Kidney Disease

Cardiovascular disease is a major cause of morbidity and mortality in patients with chronic kidney disease. In addition to a high prevalence of traditional risk factors, uremia-related risk factors contribute to cardiovascular disease, partly mediated from development of LVH, myocardial fibrosis, diastolic and systolic dysfunction, and valvular disease. Structural or valvular abnormalities of the heart detectable by echocardiography occur in most patients with end-stage renal disease and may include atrial or ventricular chamber enlargement; concentric or eccentric LVH; asymmetric septal hypertrophy; mitral annular calcification; valvular calcification; myocardial calcification; valvular regurgitation; aortic and mitral valve stenosis; and pericardial effusion (Table 38-6).[146-150]

## UREMIC CARDIOMYOPATHY, SYSTOLIC DYSFUNCTION, AND LV HYPERTROPHY

Chronic kidney disease contributes to and worsens structural and functional abnormalities of cardiac disease and may lead to heart failure. The multifactorial causes of heart failure from chronic kidney disease and uremia appear to include anemia, electrolyte and acid-base abnormalities, volume overload, hypertension, coronary artery disease, and uremic toxins. A specific uremic cardiomyopathy may ensue from these derangements and is characterized by cardiac enlargement, impaired LV systolic function, and ventricular hypertrophy.[151] A reduced LV ejection fraction is present in approximately one third of new dialysis patients. LVH is present in 70% of patients with end-stage renal disease and ranges from 34% to 78% in nonuremic chronic kidney disease.[146] Renal transplantation may reverse systolic dysfunction, decrease LV volume overload, and regress LVH, independent of blood pressure control.[152]

Global and regional LV myocardial systolic function is impaired in patients with early stages of chronic kidney disease,[153] moderately advanced chronic kidney disease,[154] and end-stage renal disease on hemodialysis[155] as assessed by peak longitudinal strain and strain rate. LV systolic dyssynchrony occurs with greater frequency in chronic kidney disease or end-stage renal disease patients.[156] It improves with hemodialysis.[147] Secondary hyperparathyroidism due to uremia is a cause of LV systolic dysfunction.[157] Dilated cardiomyopathy associated with advanced secondary hyperparathyroidism in patients on chronic dialysis improves 6 months after parathyroidectomy. LV myocardial systolic dysfunction occurs from mild secondary hyperparathyroidism.[157] Gender influences development of LVH in chronic kidney disease. LVH occurs 2.5 to 4 times more often in women compared to men with end-stage renal disease on hemodialysis.[158] In patients with hypertension, progression of chronic kidney disease from stage 2 to stage 5 is associated with increasing prevalences of concentric, eccentric, and "mixed" forms of LVH (Fig. 38-11).[148]

The systolic and diastolic dysfunction associated with chronic kidney disease and end-stage renal disease is detectable at a subclinical level using modern echocardiographic methods of strain, strain rate and tissue-Doppler velocity imaging. Edwards and colleagues[153] showed that in patients with early chronic kidney disease compared to controls, a reduced global LV longitudinal strain (−15 ± 4% versus −17 ± 3%, $p$ <0.01), peak systolic strain rate (0.88 ± 0.16 $s^{-1}$ versus 1.06 ± 0.31 $s^{-1}$, $p$ <0.05), and regional strain and strain rates. Gulel and associates[154] showed similar findings in patients with chronic kidney disease compared to controls as well as reduced mid-LV wall peak early diastolic strain rate (1.24 ± 0.58 $s^{-1}$ versus 2.02 ± 0.45 $s^{-1}$, $p$ <0.001).

Hemodialysis, a commonly used treatment in patients with end-stage renal disease, reduces intravascular volume and preload. The influence of preload reduction must be considered when diastolic function is being assessed in end-stage renal disease patients after dialysis. Conventional indexes (e.g., E and E/A) are sensitive to preload. E′ and myocardial Tei index appear less sensitive to preload reduction from hemodialysis, particularly when body weight postdialysis decreases by less than 2 to 3 kg.[159-162] The acute influence of hemodialysis on systolic function is complex and likely influenced by dialysate composition and temperature and by dialysis-induced changes in serum electrolytes, as well as by alteration in loading conditions. Systolic function acutely after hemodialysis, as assessed by echocardiographically derived shortening fraction, LV ejection fraction, $V_{cf}$, or ratio of fractional shortening to end-systolic stress, has shown divergent results. Systolic LV longitudinal strain decreases after hemodialysis.[163] The effect on strain rate is unclear. Hemodialysis may result in "stunned" myocardial segments, which may progress over 12 months to fixed dysfunctional segments.[164] Regional and global RV systolic dysfunction are impaired in hemodialysis patients with end-stage renal disease as assessed by tissue-Doppler indexes and ejection fraction, respectively.[165]

## DIASTOLIC DYSFUNCTION

LV regional and global diastolic dysfunction is associated with chronic kidney disease and end-stage renal disease.[154,155,166,167] In both these diseases, LVH is a common associated finding but is not a necessary feature to develop diastolic dysfunction. However, in end-stage renal disease, diastolic function worsens as LVF progresses.[167] The primary etiology of chronic kidney disease independently contributes to diastolic dysfunction, such as systemic hypertension or diabetes mellitus. Conventional Doppler indexes in chronic kidney disease patients may show grade 1 LV diastolic dysfunction with reduced transmitral E, E/A ratio, and prolonged isovolumic relaxation time,[167] as well as pseudonormal or restrictive patterns of diastolic dysfunction.

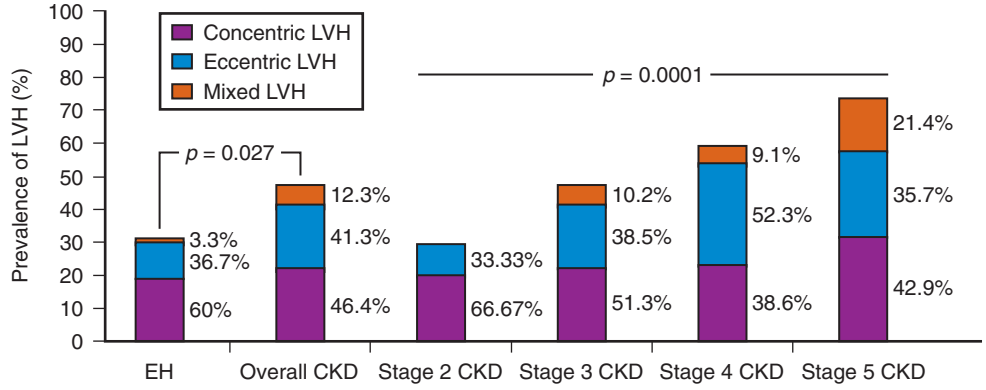



**Figure 38-11 Histograms showing prevalence of LV hypertrophy (*LVH*) in patients with essential hypertension (*EH*) and normal renal function and in patients with chronic kidney disease (*CKD*) of stages 2 to 5.** *Purple*, concentric LVH; *blue*, eccentric LVH; *orange*, "mixed" LVH. *(From Nardi E, Palermo A, Mulè G, et al: Left ventricular hypertrophy and geometry in hypertensive patients with chronic kidney disease.* J Hypertension *27:633-641, 2009.)*

## STRUCTURAL AND VALVULAR HEART DISEASE

Calcification of valves, cardiac skeleton, or myocardium is found in most patients with end-stage renal disease. It is caused by abnormalities in calcium and phosphorus metabolism.[149] Aortic valve calcification occurs in 28% to 60% of patients with end-stage renal disease.[149,150] Mitral annular calcification occurs in 10% to 36% of patients on dialysis and is associated with systemic inflammation.[168] Calcification from chronic kidney disease may occur in "atypical" areas, such as the base of both mitral leaflets and intervalvular fibrosa. Ultrasonic backscatter of myocardium in end-stage renal disease shows less homogeneity and greater reflectivity, reflecting myocardial calcification.

Aortic valve regurgitation occurs in 13% of chronic kidney disease patients, primarily due to calcification. Mitral regurgitation may occur in 38% of these patients and may be caused by mitral annular calcification or LV dilation. Tricuspid and pulmonic insufficiency occur with similar frequencies as that of mitral and aortic regurgitation, respectively, in patients with chronic kidney disease. However, tricuspid and pulmonic insufficiency occur secondary to increased pulmonary artery pressures as a consequence of significant mitral regurgitation and not valvular calcification.

Calcific aortic and mitral stenoses occur as a result of chronic kidney disease. Occasionally, they rapidly progress in patients with chronic kidney disease, possibly because of associated secondary hyperparathyroidism.[150] Chronic kidney disease may cause pericardial effusion, pericardial thickening, or cardiac tamponade.[168]

## CLINICAL UTILITY

Echocardiography is a useful noninvasive method of evaluating patients with chronic kidney disease and end-stage renal disease who present with symptoms suggestive of heart failure. An accurate clinical diagnosis of heart failure in these patients is challenging, because heart failure in such patients is often multifactorial. It could be on the basis of dilated cardiomyopathy, diastolic failure, inadequate ventricular hypertrophy, mitral or aortic valvular regurgitation, or stenosis. Pericardial effusion with secondary cardiac tamponade could mimic congestive heart failure. Conventional M-mode, 2D, and Doppler echocardiography techniques are useful in the diagnosis of the many structural and valvular abnormalities that may cause heart failure in the chronic kidney disease patient. In addition, tissue-Doppler imaging and strain rate imaging complement the conventional echocardiographic approaches in the comprehensive assessment of patients with chronic kidney disease for confirming associated myocardial disease. Myocardial tissue characterization with ultrasonic integrated back-scatter aids in the diagnosis of myocardial disease in patients with chronic kidney disease, but it has not been employed widely.

Echocardiography-derived measurements, when abnormal, are better predictors of prognosis than clinical evaluation or electrocardiographic findings in end-stage renal disease patients. These measurements include reduced LV ejection fraction and fractional shortening, increased LV volume, LVH, abnormal diastolic filling, increased E/E′ ratio, increased LA volume or diameter, and mitral annular calcification. End-stage renal disease patients with reduced LV systolic function and LV dilation have a poor prognosis, a mean survival of 7.8 months. Prospective studies in these patients show that improvement in echocardiography-derived systolic dysfunction and LVH or midwall fractional area change is associated with improved outcome over mean follow-up durations of 41 months[169] and 17 months,[170] respectively. LVH is a strong predictor of progression to dialysis in chronic kidney disease and is a major risk factor for morbidity and mortality in end-stage renal disease patients. Its complete regression may occur with intense and multifaceted therapy, making serial echocardiography useful in monitoring success of treatment.

In patients with end-stage renal disease, transmitral E/E′ ratio (an index of LV filling pressure), even when added to clinical parameters, LV mass index, and midwall fractional shortening, significantly improves prediction of overall mortality and cardiovascular death over 4 years (Fig. 38-12).[171] In chronic kidney disease patients with heart failure and systolic dysfunction, the presence of restrictive filling (grade 3 or 4) further adds to predicting cardiac death or need for urgent renal transplant over a mean follow-up duration of 16.5 months with a reported hazard ratio of 2.77 ($p = 0.019$).[172]

LA enlargement due to remodeling as determined by anterior-posterior diameter or volume is a practical and useful predictor of adverse outcome in chronic kidney disease and end-stage renal disease patients. Intuitively, it reflects the effects of multiple adverse cardiac abnormalities from chronic kidney disease, such as LVH, diastolic dysfunction, volume expansion, left-sided valvular disease, systolic dysfunction, hypertension, myocardial ischemia, and atrial fibrillation. However, even when all of these known factors are considered, LA enlargement remains an independent predictor of mortality. Chan and colleagues[173] reported in chronic kidney disease patients that an increased LA diameter indexed to body surface area independently adds to prediction of cardiovascular death. Similarly, LA volume indexed to body surface area greater than 32 mL/m$^2$ is a predictor of mortality.[174] In addition, serial monitoring for an increase in LA volume index to height by 1 mL/m$^2$ or more per year is associated with a 12% increase in relative risk for fatal and nonfatal cardiovascular events ($p < 0.001$).[175] Mitral annular calcification diagnosed by M-mode and/or 2D echocardiography is a predictor of mortality and coronary artery disease in patients with end-stage renal disease.[176]

Systemic hypotension complicating hemodialysis occurs often and is occasionally life threatening. Echocardiography is useful in identifying those patients predisposed to hemodialysis-induced hypotension. LA volume index greater than 35 mL/m$^2$ shows a 2.5-fold greater likelihood of hemodialysis-induced hypotension and was a better predictor of this occurrence as compared to LV systolic dysfunction.[177] Patients with impaired and short duration of early LV filling and/or reduced $V_p$ are at higher risk for hemodynamic instability during hemodialysis. $V_p$ less than 55 cm/s had a sensitivity of 47% and specificity of 86% for hemodialysis-induced hypotension.[178] During hemodialysis-induced hypotension refractory to conventional therapy, conventional and three-dimensional (3D) echocardiography helps assess potential causes of hypotension, such as intravascular volume depletion, impaired systolic function, or a hyperdynamic state with secondary intraventricular obstruction.[179]

Moderate or severe aortic valve calcification, as compared to none or mild, in end-stage renal disease patients identifies subjects prone to have a faster rate of progression in yearly aortic valve area diminution ($0.17 \pm 0.15$ cm$^2$/yr versus $0.04 \pm 0.07$ cm$^2$/yr, $p < 0.001$).[180] Serial echocardiography is useful to identify these high-risk patients and guide frequency of

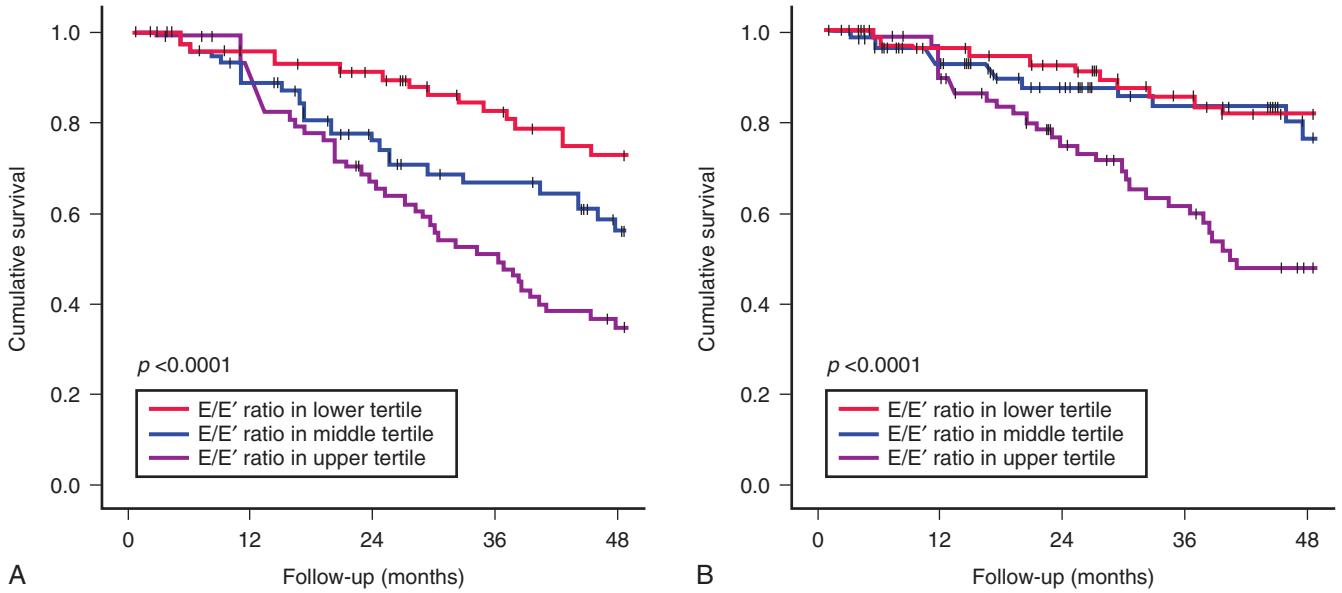



**Figure 38-12 Kaplan-Meier graphs of overall survival (A) and cardiovascular death (B) of patients with end-stage renal disease on basis of ratio of transmitral peak early filling to early diastolic tissue-Doppler velocity (*E/E′*) stratified by tertiles.** E/E′ defined as ≤14.43 for lower (*red line*), >14.43 to 21.73 for middle (*blue line*), and >21.73 for upper tertiles (*purple line*). Log-rank test showed significant differences between all tertiles for overall survival (**A**) and between upper versus middle or lower tertiles for cardiovascular death (**B**). *(From Wang AYM, Wang M, Lam CWK, et al: Left ventricular filling pressure by Doppler echocardiography in patients with end-stage renal disease.* Hypertension *52:107-114, 2008.)*

**TABLE 38-7 Echocardiographic Findings in Obesity**

| *Systolic Dysfunction* | *Diastolic Dysfunction* | *Structural Abnormalities* |
|---|---|---|
| **LV strain/tissue-Doppler imaging:** | **Strain/tissue-Doppler imaging:** | **Conventional M-mode/2D echocardiography:** |
| ↓Peak global LV longitudinal systolic SR (<0.90 $s^{-1}$) | ↓Peak LV early diastolic SR | Concentric LV hypertrophy (most common type of hypertrophy seen) |
| ↓LV myocardial or annular S′ | ↓MV annular E′ (<8.0 cm/s) | Concentric remodeling (more common in young females) |
| **Conventional M-mode/2D/Doppler echocardiography:** | **Conventional Doppler echocardiography:** | Eccentric LV hypertrophy |
| ↑ or normal LVEF (in early stages of obesity) | Grade 1 diastolic dysfunction: | ↑LV mass |
| ↑ or normal cardiac output and LV stroke volume (in early stages of obesity) | ↓E (<0.6 m/s) | ↑Septal and posterior wall diastolic thickness |
| ↓LVEF (in morbid obesity) | ↓E/A ratio (<1.0) | ↑LV end-diastolic diameter |
| ↓LV shortening fraction (in long-standing obesity) | ↑IVRT (>90 ms) | ↑LA diameter, area and volume |
| ↑PEP/LVET ratio | ≥Grade 2 (pseudonormal) diastolic dysfunction in 60% | ↑Aortic root diameter |
| Blunted rise in LVEF with exercise (in morbid obesity) | | ↑Epicardial fat layer thickness |
| **RV strain/tissue-Doppler imaging:** | | RV enlargement |
| ↓RV tricuspid annular S′ | | **Ultrasonic integrated back-scatter:** |
| ↓RV longitudinal strain and peak systolic SR | | ↑LV septal and lateral myocardial acoustic reflectivity |

*E*, Peak transmitral early diastolic filling velocity; *E/A*, E/peak transmitral late diastolic filling velocity ratio; *E′*, peak early diastolic tissue-Doppler velocity; *IVRT*, isovolumic relaxation time; *LVEF*, LV ejection fraction; *MV*, mitral valve; *PEP/LVET*, LV preejection to LV ejection time ratio; *SR*, strain rate; *S′*, peak LV systolic tissue-Doppler velocity.

evaluation, as aortic valve replacement is an effective treatment for aortic stenosis despite the presence of end-stage renal disease.[181]

Dobutamine stress echocardiography is useful to identify coronary artery disease in patients with chronic kidney disease or end-stage renal disease, and to predict mortality. Karagiannis and co-workers[182] reported in 2292 patients with chronic kidney disease followed for over 8 years. Dobutamine stress echocardiography–induced ischemia of more than four segments portended an 80% mortality over the course of the study.[182] Normal dobutamine stress echocardiography portended a risk of 10% for cardiac events at 15 months.[182] Early identification and aggressive risk factor modification of coronary artery disease are essential in the chronic kidney disease population.

The Kidney/Disease Outcome Quality Initiative guidelines recommends that patients undergoing hemodialysis echocardiography should be monitored for changes in cardiac structure and function at initiation of dialysis and every 3 years thereafter. This recommendation is supported by prospective studies.[183]

## Obesity

Obesity increases circulatory blood volume and cardiac output as a compensatory mechanism from high metabolic demands of excessive adipose. Moderate to severe obesity may lead to LV enlargement, eccentric LVH, and diastolic dysfunction in the absence of other obesity-related diseases, such as hypertension, coronary artery disease, obstructive sleep apnea, hypoventilation syndrome, and diabetes (Table 38-7). Systolic impairment

and heart failure may ensue, giving rise to an obesity cardiomyopathy.[184] Heart failure is a frequent cause of death in morbidly overweight persons.

## SYSTOLIC FUNCTION

Obesity causes increases in circulatory blood volume and cardiac output, which are proportional to excess body weight. The high-output state of morbid obesity occurs predominantly from increases in adipose tissue blood flow. Resting heart rate is only minimally affected, but stroke volume is increased. LV ejection fraction may be augmented or normal in the early stages of obesity.[176,185] However, systolic function curves or indexes, such as the stroke work index to LV end-diastolic pressure or preejection period to LV ejection time ratio, may be reduced in obese patients, consistent with depressed myocardial systolic function. In addition, even in the face of normal global LV systolic function, abnormalities in regional myocardial systolic function have been shown to exist in persons with obesity.[186-190] Wong and colleagues[186] demonstrated in overweight, mildly obese, or severely obese subjects with normal LV ejection fraction that regional myocardial systolic function is decreased as assessed by systolic strain or tissue-Doppler velocity. Others have confirmed these findings.[187-191]

Reduced LV ejection fraction and attenuation of the normal increase in LV ejection fraction with exercise may occur in morbidly obese persons. In such individuals, increased LV mass is associated with an attenuation of the normal increase in LV ejection fraction during exercise. RV regional and global systolic function may be impaired due to obesity.[191-193] Weight reduction in subjects with obesity is associated with improvement in systolic function.[192,193]

Echocardiography is a sensitive method for detection of myocardial systolic dysfunction from obesity when applying sophisticated methods of LV strain and strain rate.[186,188,189,191] Orhan and associates[191] reported in obese persons compared to controls decreased LV global longitudinal ($-1.07 \pm 0.14$ $s^{-1}$ versus $-1.38 \pm 0.12$ $s^{-1}$, $p < 0.001$) and regional strain (Fig. 38-13).[191] RV systolic dysfunction also is present in obese persons as demonstrated by tissue Doppler–derived RV peak systolic velocity ($6.5 \pm 2.4$ cm/s versus $10.2 \pm 1.5$ cm/s, $p < 0.001$), longitudinal strain ($-21.0 \pm 4.5\%$ versus $-28.8 \pm 4.2\%$, $p < 0.001$), and peak systolic strain rate ($1.4 \pm 0.4$ $s^{-1}$ versus $2.0 \pm 0.5$ $s^{-1}$, $p = 0.001$).[192]

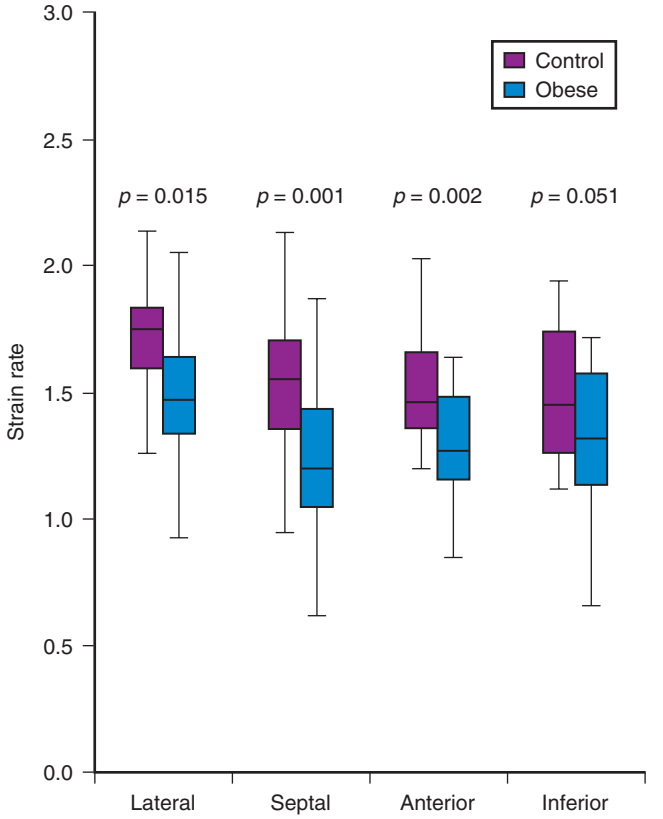



**Figure 38-13 Regional peak systolic longitudinal strain rates were lower in obese (*blue bars*) compared to controls (*purple bars*) measured from LV lateral, septal, anterior, and inferior basal walls.** *(From Orhan AL, Uslu N, Dayi SU, et al: Effects of isolated obesity on left and right ventricular function—a tissue-Doppler and strain rate imaging study.* Echocardiography *27:236-243, 2010.)*

## DIASTOLIC FUNCTION

Global LV diastolic dysfunction occurs in otherwise healthy obese persons as demonstrated by abnormalities of LV filling[185,194] and prolongation of isovolumic relaxation time.[185] LV diastolic dysfunction of at least a pseudonormal severity has been reported in 23% of obese persons without diabetes.[195] Regional myocardial diastolic function also is impaired in obese persons.[186,187,190] Findings include reduced E′ from tissue-Doppler ($10.1 \pm 1.7$ cm/s versus $8.0 \pm 2.2$ cm/s, $p < 0.01$)[191] and peak early LV diastolic strain rate. Impaired LV relaxation, compliance, or both occur in obese patients because of associated LVH. RV regional and global diastolic dysfunction occurs in obese persons, but the independent influence of coexisting diabetes and/or sleep apnea is difficult to quantify.[192,196,197] Weight reduction is associated with improvement in LV and RV diastolic dysfunction.[198]

LA enlargement ideally assessed by volume derived from 2D or 3D echocardiography can be on the basis of obesity, particularly in older subjects.[199] When LA enlargement is present despite normal conventional measures of global LV diastolic function (e.g., E/A ratio, isovolumic relaxation time, or $V_p$), pseudonormal diastolic dysfunction and elevated LA pressure should be suspected. This can be confirmed by an elevated E/E′ ratio, typically greater than 13 to 15.

RV systolic dysfunction is present in obese persons as demonstrated by tissue Doppler–derived RV peak early diastolic velocity ($6.8 \pm 2.4$ cm/s versus $10.3 \pm 2.5$ cm/s, $p < 0.001$).[192]

## STRUCTURAL ABNORMALITIES

Compared with normal-weight controls with similar blood pressure, obese patients show an increase in LA diameter, area, and volume, aortic root diameter, LV end-diastolic diameter, septal and posterior wall thickness, and LV mass[186-188,200-202] (see Table 38-7). Obesity causes predominantly concentric LVH but is also associated with concentric remodeling and eccentric LVH (Fig. 38-14).[201] Eccentric LVH in obesity is accounted for by chronic increased intravascular volume and partially explains the association between increasing LV mass and severity of obesity. Inadequate hypertrophy of the LV wall to normalize wall stress in the face of a dilated cavity occurs in some obese persons and may account for impaired myocardial systolic function. RV enlargement occurs in obesity and is partially explained by associated sleep apnea and pulmonary

hypertension. Weight loss induces significant reductions in LV end-diastolic diameter, end-systolic wall stress, LV mass, and RV size.[198,202,203] Ultrasonic integrated back-scatter of LV septum and posterior walls is increased in obese compared to controls, potentially on the basis of increased collagen content or myocardial fibrosis (Fig. 38-15).[204] Epicardial fat on the free wall of the RV is visceral fat that correlates with obesity-related insulin resistance and more commonly seen in obese persons.[205] Aerobic exercise and weight reduction decreases epicardial fat layer thickness.[206]

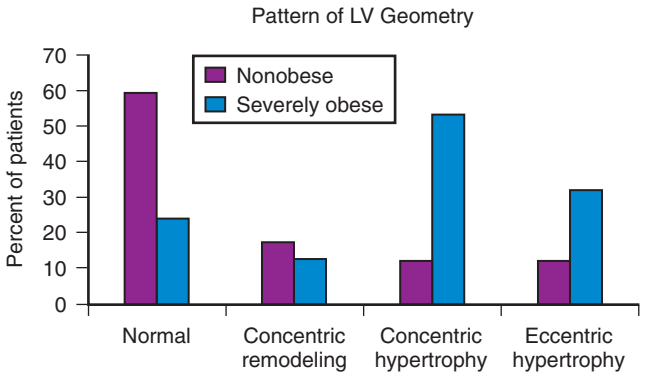
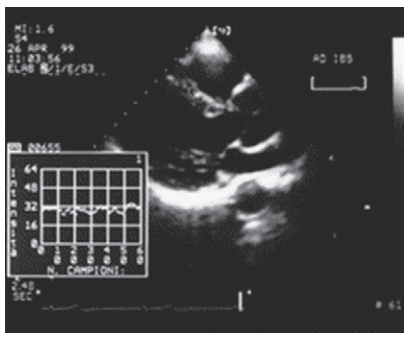


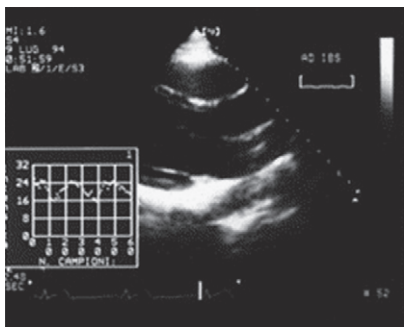

**Figure 38-14 Patterns of LV geometry in nonobese (n = 59; *purple bars*) and severely obese (n = 455; *blue bars*) subjects.** Concentric LV hypertrophy (LVH) is most frequent in obese subjects, but eccentric LVH represents a significant proportion. *(From Avelar E, Cloward TV, Walker JM, et al: Left ventricular hypertrophy in severe obesity—interactions among blood pressure, nocturnal hypoxemia, and body mass.* Hypertension *49:34-39, 2007.)*

## ANOREXIGEN USE, VALVULOPATHY, AND PULMONARY HYPERTENSION

Obesity is associated with serious cardiovascular health risks, such as heart failure, stroke, and systemic hypertension. Appetite-suppressant medications or anorexigens with diverse mechanisms of action are used in the treatment of obese subjects to promote weight reduction. Studies with matched control subjects and blinding of echocardiographic interpretations show a prevalence from 6.3% to 11.3% (unadjusted for background rates) of aortic valvular regurgitation in association with the use of anorexigens when the U.S. Food and Drug Administration (FDA) criteria (i.e., mild or greater aortic regurgitation) were met.[207] Studies have shown no association between anorexigen use and valvular heart disease when duration of treatment was less than 3 months.[208,209] Meta-analysis of four studies showed a statistically significant increase of moderate or greater mitral regurgitation in patients treated for greater than 90 days with fenfluramine or dexfenfluramine as compared to controls (i.e., 3.5% versus 1.8%). Structural abnormalities seen on echocardiography have been reported to include aortic or mitral leaflet thickening, diastolic doming of the anterior mitral leaflet and immobility of the posterior mitral leaflet, shortening and thickening of chordae tendineae, and retraction of aortic valve leaflets. Histopathologic and gross pathologic findings available in these subjects included fibrotic endocardial changes of valve leaflets and chordae tendineae with a "stuck on plaque" appearance and white glistening valves, which were indistinguishable from the features of carcinoid or ergotamine valvulopathy.

Aortic or mitral valvular regurgitation that meets the FDA criteria in severity, when present, appears far more likely to



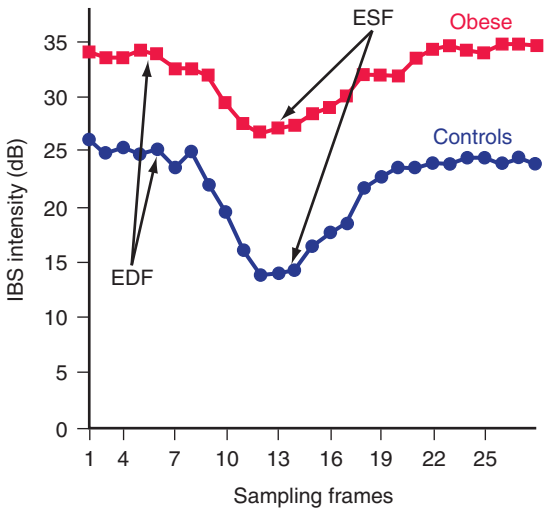




**Figure 38-15 Ultrasonic integrated back-scatter showing greater echoreflectivity of the myocardium in a representative obese patient versus healthy control person.** *EDF*, End-diastolic frames; *ESF*, end-systolic frames. *(From Di Bello V, Santini F, Cori AD, et al: Obesity cardiomyopathy—is it reality? An ultrasonic tissue characterization study.* J Am Soc Echocardiogr *19:1063-1071, 2006.)*

remain stable and/or to regress than to progress in obese subjects after cessation of the use of fenfluramine or dexfenfluramine.[210] Ideally, quantitative measures should be employed to assess regurgitation severity. The need for valve surgery from anorexigen valvulopathy is rare, particularly many years later in those not initially meeting FDA criteria of valvulopathy in proximity to fenfluramine or dexfenfluramine use.[211] The use of appetite suppressants, including dexfenfluramine or fenfluramine, for longer than 3 months showed an odds ratio of 23 (95% confidence index: 6.9 to 77) for primary pulmonary hypertension in obese individuals.[212] Echocardiography has an important role in the noninvasive estimation of pulmonary artery pressure in obese subjects when pulmonary hypertension on the basis of anorexigen use is suspected. Peak pulmonary systolic pressure, estimated by echocardiography, is greater than 35 mm Hg in nearly one third of otherwise normal obese individuals.[213] The prevalence of elevated pulmonary pressures in morbidly obese individuals living at moderate altitude may be in excess of 96%. These data suggest caution when ascribing mild elevation of pulmonary artery systolic pressure to anorexigen use in obese subjects.

### CLINICAL UTILITY

Although the echocardiographic findings of obesity are nonspecific, echocardiography is useful in the assessment of obese patients, particularly if there is long-standing heart failure or suspicion of the presence of heart failure. Appraisal of LV global and regional systolic function, diastolic function, chamber size, and hypertrophy, and RV function helps to guide medical therapy. Substantial weight reduction by the morbidly obese may improve LV and RV systolic and diastolic function, decrease LV chamber size, and reduce LV mass.[197,198,202,203]

Echocardiography is of benefit in obese subjects with suspected aortic or mitral valvulopathy on the basis of anorexigen use. The presence of aortic or mitral valvular thickening unexplained by other causes in combination with at least mild aortic regurgitation or at least greater than mild mitral regurgitation, respectively, should be present before a diagnosis of anorexigen-induced valvulopathy is entertained. Several quantitative measures should be employed to assess changes in severity of regurgitation over time, as reliance on qualitative assessments or any single method is unreliable and may lead to erroneous conclusions on the clinically relevant question of progression, stability, or regression in anorexigen-induced valvular heart disease.[214] Obesity is a cause of pulmonary hypertension and confirms a need for caution when attributing mild elevation of pulmonary artery systolic pressure as estimated by echocardiography to anorexigen use in obese subjects.[213]

## Nutritional Deficiencies and Heart Disease (Table 38-8)

### VITAMIN AND TRACE ELEMENT DEFICIENCIES

#### *Beriberi Heart Disease*

Thiamine deficiency may occur in many as 33% of patients with heart failure.[215] Diuretics increase urinary excretion of thiamine and is a cause of this deficiency. Body stores can be depleted in 2 to 3 weeks. Severe thiamine deficiency that persist for 3 months or longer may lead to beriberi. Heart disease in beriberi patients is characterized by biventricular failure and marked edema associated with a high cardiac output and arteriolar vasodilation. RV failure may predominate, but significant elevation of LV end-diastolic and pulmonary capillary wedge pressures occur. The disease has been virtually eliminated in the United States, but it can be seen in alcoholic persons who become thiamine deficient. The hemodynamic abnormalities are reversible with thiamine therapy but may not respond to inotropic agents or diuretics. The possibility of thiamine deficiency and beriberi heart disease should be considered in cases of refractory heart failure presumed to result from alcoholic cardiomyopathy.

#### *Keshan Heart Disease*

Keshan heart disease, first described in China, is a dilated cardiomyopathy characterized by myocardial fibrosis and necrosis. Selenium and vitamin E deficiency may be important in its development. Suspected cases of selenium deficiency and cardiomyopathy similar to this disease have been reported in the United States. Keshan disease is preventable by selenium supplementation in the diet.

#### *Other Vitamin Deficiencies*

Vitamin D deficiency is estimated to occur in 25% to 57% of adults in the United States. It has been linked to presence of valvular calcifications, mitral annular calcification, LV dilation, and possibly LVH.[216-218] Vitamin C deficiency may cause scurvy and heart abnormalities. The manifestations of cardiac involvement in scurvy may include dyspnea, chest pain, sudden death, PR interval prolongation, and ST-segment abnormalities. The direct effects of vitamin A or niacin deficiency on heart muscle in humans have not been established.

**TABLE 38-8 Echocardiographic Findings in Nutritional Deficiencies**

| *Beriberi Heart Disease (Thiamine Deficiency) Systolic Dysfunction/ Structural Abnormalities* | *Keshan Heart Disease (Selenium Deficiency) Systolic Dysfunction/Structural Abnormalities* | *Kwashiorkor (Protein-Calorie Malnutrition) Systolic Dysfunction/Structural Abnormalities* | *Vitamin D Deficiency Structural Abnormalities* |
|---|---|---|---|
| **M-mode/2D/Doppler echocardiography:**<br>↓LVEF<br>LV enlargement<br>RV enlargement<br>↑Cardiac output | **M-mode/2D echocardiography:**<br>↓LVEF<br>LV enlargement<br>Dilated cardiomyopathy | **M-mode/2D echocardiography:**<br>↓LV mass<br>Cardiac atrophy<br>↓LV shortening fraction<br>↓Mean $V_{cf}$<br>↓Cardiac output | Vitamin D deficiency occurs in 25% to 57% of adults in the United States<br>**M-mode/2D echocardiography:**<br>Associated with:<br>Valvular calcification<br>Mitral annular calcification<br>LV enlargement<br>Possible LV hypertrophy |

*LVEF*, LV ejection fraction; $V_{cf}$, LV velocity of circumferential fiber shortening.

## PROTEIN AND CALORIE MALNUTRITION

Protein-calorie malnutrition leads to kwashiorkor. Heart disease in this condition is shows atrophy of cardiac muscle fibers, interstitial edema, vacuolization of myocardial fibers, and low-output heart failure. The condition is rare in developed nations, but it contributes to heart disease in patients with chronic illnesses or anorexia nervosa. In children, LV diameter and mass assessed by M-mode echocardiography are decreased in protein-calorie malnutrition, proportional to the reduction in body size.[219] In children, LV systolic function may be decreased in protein-calorie malnutrition and manifested by a decrease in shortening fraction, mean $V_{cf}$, and systolic time interval, but these findings have not been consistently shown.[219]

## KEY POINTS

- Diabetes is associated with a cardiomyopathy characterized by impaired diastolic and systolic dysfunction, independent of coronary disease or hypertension.
  - Regional LV systolic dysfunction is an early manifestation of diabetic heart disease as measured by strain, strain rate, and tissue-Doppler velocity imaging.
  - Subclinical diastolic dysfunction also is evident by conventional Doppler and strain imaging.
  - An increased LV mass index is a predictor of adverse cardiovascular events in diabetic patients.
  - Aortic stenosis progression may be more rapid in diabetic subjects.
- Pericardial effusion may be seen in overt hypothyroidism or may be the first indication of thyroid dysfunction.
- Hyperthyroidism is associated with an increased LV ejection fraction at rest but a reduced increase in ejection fraction and stroke volume with exercise.
- Cardiovascular complications are common in patients with acromegaly, with early LV diastolic dysfunction followed by progression to systolic dysfunction and heart failure, often in associated with an increased LV mass index.
- In about 50% of patients with hyperparathyroidism, aortic valve and mitral annular calcification are present. Coronary artery calcification and myocardial calcium deposits also are common.
- Echocardiographic findings of severe LVH or hypertrophic cardiomyopathy without obvious cause should raise the clinical suspicion of glucocorticoid excess, possibly from Cushing syndrome.
- Chronic kidney disease results in impaired LV systolic and diastolic dysfunction. Concurrent hypertension leads to an increase in LV wall thickness and LV mass.
- Obesity results in increase in cardiac dimensions, LV diastolic dysfunction and RV systolic dysfunction.

## REFERENCES


1. Khavandi K, Khavandi A, Asghar O, et al: Diabetic cardiomyopathy—a distinct disease? *Best Pract Res Clin Endocrinol Metab* 23:347-360, 2009.
2. Cohen-Solal A, Beauvais F, Logeart D: Heart failure and diabetes mellitus: epidemiology and management of an alarming association. *J Cardiac Fail* 14:615-625, 2008.
3. Kamalesh M, Cleophas ATJ: Heart failure due to systolic dysfunction and mortality in diabetes: pooled analysis of 39,505 subjects. *J Cardiac Fail* 15:305-309, 2009.
4. From AM, Scott CG, Chen HH: The development of heart failure in patients with diabetes mellitus and pre-clinical diastolic dysfunction. *J Am Coll Cardiol* 55:300-305, 2010.
5. Ernande L, Rietzschel ER, Bergerot C, et al: Impaired myocardial radial function in asymptomatic patients with type 2 diabetes mellitus—a speckle-tracking imaging study. *J Am Soc Echocardiogr* 23:1266-1272, 2010.
6. Nakai H, Takeuchi M, Nishikage T, et al: Subclinical left ventricular dysfunction in asymptomatic diabetic patients assessed by two-dimensional speckle tracking echocardiography—correlation with diabetic duration. *Eur J Echocardiogr* 10:926-932, 2009.
7. Ng ACT, Delgado V, Bertini M, et al: Findings from left ventricular strain and strain rate imaging in asymptomatic patients with type 2 diabetes mellitus. *Am J Cardiol* 104:1398-1401, 2009.
8. Kosmala W, Kucharski W, Przewlocka-Kosmala M, Mazurek W: Comparison of left ventricular function by tissue Doppler imaging in patients with diabetes mellitus without systemic hypertension versus diabetes mellitus with systemic hypertension. *Am J Cardiol* 94:395-399, 2004.
9. Fang ZY, Schull-Meade R, Downey M, et al: Determinants of subclinical diabetic heart disease. *Diabetologia* 48:394-402, 2005.
10. Fang ZY, Yuda S, Anderson V, et al: Echocardiographic detection of early diabetic myocardial disease. *J Am Coll Cardiol* 41:611-617, 2003.
11. Galderisi M, de Simome G, Innelli P, et al: Impaired inotropic response in type 2 diabetes mellitus—a strain rate imaging study. *Am J Hypertens* 20:548-555, 2007.
12. Jellis CL, Jenkins C, Leano R, et al: Reduced end-systolic pressure-volume ratio response to exercise- a marker of subclinical myocardial disease in type 2 diabetes. *Circ Cardiovasc Imaging* 3:443-449, 2010.
13. Fang ZY, Najos-Valencia O, Leano R, Marwick TH: Patients with early diabetic heart disease demonstrate a normal myocardial response to dobutamine. *J Am Coll Cardiol* 42:446-453, 2003.
14. Korosoglou G, Humpert PM, Halbgewachs E, et al: Evidence of left ventricular contractile asynchrony by echocardiographic phase imaging in patients with type 2 diabetes mellitus and without clinically evident heart disease. *Am J Cardiol* 98:1525-1530, 2006.
15. Von Bibra H, Thrainsdottir IS, Hansen A, et al: Tissue Doppler imaging for the detection and quantitation of myocardial dysfunction in patients with type 2 diabetes mellitus. *Diab Vasc Dis Res* 2:24-30, 2005.
16. Devereux RB, Roman MJ, Paranicas M, et al: Impact of diabetes on cardiac structure and function: The strong heart study. *Circulation* 101:2271-2276, 2000.
17. Guo CY, Shen LH, Li HW, et al: Relation of hemoglobin A1c to myocardial acoustic densitometry and left ventricular diastolic function in patients with type 2 diabetes mellitus and without evident heart disease. *Diabetes Res Clin Pract* 83:365-370, 2009.
18. Kosmala W, Colonna P, Przewlocka-Kosmala M, Mazurek W: Right ventricular dysfunction in asymptomatic diabetic patients. *Diabetes Care* 27:2736-2738, 2004.
19. Kosmala W, Przewlocka-Kosmala M, Mazurek W, et al: Subclinical right ventricular dysfunction in diabetes mellitus—an ultrasonic strain/strain rate study. *Diabetic Medicine* 24, 656-663, 2007.
20. Tayyareci Y, Yurdakul S, Tayyareci G, et al: Impact of myocardial acceleration during isovolumic contraction in evaluating subclinical right ventricular systolic dysfunction in type 2 diabetes mellitus patients. *Echocardiography* 27,1211-1218, 2010.
21. Kamalesh M, Ng C, El Masry C, et al: Does diabetes accelerate progression of calcific aortic stenosis? *Eur J Echocardiogr* 10:723-725, 2009.
22. Lindman BR, Arnold SV, Madrazo JA, et al: The adverse impact of diabetes mellitus on left ventricular remodeling and function in patients

with severe aortic stenosis. *Circ Heart Fail* Feb 25, 2011.
23. Seyfeli E, Duru M, Saglam H, et al: *Int J Clin Pract* 62:1358-1365, 2008.
24. Poirier P, Bogaty P, Garneau C, et al: Diastolic dysfunction in normotensive men with well-controlled type 2 diabetes—importance of maneuvers in echocardiographic screening for preclinical diabetic cardiomyopathy. *Diabetes Care* 24:5-10, 2001.
25. Boyer JK, Thanigaraj S, Schechtman KB, Perez JE: Prevalence of ventricular diastolic dysfunction in asymptomatic, normotensive patients with diabetes mellitus. *Am J Cardiol* 93:870-875, 2004.
26. Di Bonito P, Moio N, Cavuto L, et al: Early detection of diabetic cardiomyopathy: usefulness of tissue Doppler imaging. *Diabet Med* 22:1720-1725, 2005.
27. Ha JW, Lee HC, Kang ES, et al: Abnormal left ventricular longitudinal functional reserve in patients with diabetes mellitus—implication for detecting subclinical myocardial dysfunction using exercise tissue Doppler echocardiography. *Heart* 93:1571-1576, 2007.
28. Mizuno R, Fujimoto S, Saito Y, et al: Exercise-induced delayed onset of left ventricular early relaxation in association with coronary microcirculatory dysfunction in patients with diabetes mellitus. *J Cardiac Fail* 16:211-217, 2010.
29. Poirier P, Garneau C, Bogaty P, et al: Impact of left ventricular diastolic dysfunction on maximal treadmill performance in normotensive subjects with well-controlled type 2 diabetes mellitus. *Am J Cardiol* 85:473-477, 2000.
30. Saraiva RM, Duarte DM, Duarte MP, et al: Tissue Doppler imaging identifies asymptomatic normotensive diabetes with diastolic dysfunction and reduced exercise tolerance. *Echocardiography* 22:561-570, 2005.
31. Fang ZY, Sharman J, Prins JB, Marwick TH: Determinants of exercise capacity in patients with type 2 diabetes. *Diabetes Care* 28:1643-1648, 2005.
32. Gerdts E, Okin PM, Wachtell K, et al: Impact of diabetes on treatment-induced changes in left ventricular structure and function in hypertensive patients with left ventricular hypertrophy. *Nutr Metab Cardiovasc Dis* 19:306-312, 2009.
33. Muranaka A, Yuda S, Tsuchihashi K, et al: Quantitative assessment of left ventricular and left atrial functions by strain rate imaging in diabetic patients with and without hypertension. *Echocardiography* 26:262-271, 2009.
34. Miyazato J, Horio T, Takiuchi S, et al: Left ventricular diastolic dysfunction in patients with chronic renal failure: impact of diabetes mellitus. *Diabet Med* 22:30-736, 2005.
35. Di Stante B, Galandauer I, Aronow WS, et al: Prevalence of left ventricular diastolic dysfunction in obese persons with and without diabetes mellitus. *Am J Cardiol* 95:1527-1528, 2005.
36. Kuperstein R, Hanly P, Niroumand M, Sasson Z: The importance of age and obesity on the relation between diabetes and left ventricular mass. *J Am Coll Cardiol* 37:1957-1962, 2001.
37. Masugata H, Senda S, Goda F, et al: Left ventricular diastolic dysfunction in normotensive diabetic patients in various age strata. *Diabetes Research and Clinical Practice* 79:91-96, 2008.
38. Fang ZY, Prins JB, Marwick TH: Diabetic cardiomyopathy—evidence, mechanisms, and therapeutic implications. *Endocrine Reviews* 25:543-567, 2004.
39. Diamant M, Lamb HJ, Groeneveld Y, et al: Diastolic dysfunction is associated with altered myocardial metabolism in asymptomatic normotensive patients with well-controlled type 2 diabetes mellitus. *J Am Coll Cardiol* 42:328-335, 2003.
40. Shishehbor MH, Hoogwerf BJ, Schoenhagen P, et al: Relation of hemoglobin A1c to left ventricular relaxation in patients with type 1 diabetes mellitus and without overt heart disease. *Am J Cardiol* 91:1514-1517, 2003.
41. von Bibra H, Siegmund T, Ceriello A, et al: Optimized postprandial glucose control is associated with improved cardiac/vascular function—comparison of three insulin regimens in well-controlled type 2 diabetes. *Horm Metab Res* 41:109-115, 2009.
42. Andersen NH, Hansen TK, Christiansen JS, et al: Changes in glycaemic control are related to the systolic function in type 1 diabetes mellitus. *Scand Cardiovasc J* 41:85-88, 2007.
43. Andersson C, Søgaard P, Hoffmann S, et al: Metformin is associated with improved left ventricular diastolic function measured by tissue Doppler imaging n patients with diabetes. *Eur J Endocrinol* 163:593-599, 2010.
44. Pala S, Esen O, Akcakoyun M, et al: Rosiglitazone, but not pioglitazone, improves myocardial systolic function in type 2 diabetic patients—a tissue Doppler study. *Echocardiography* 27:512-518, 2010.
45. Naka KK, Pappas K, Papathanassiou K, et al: Lack of effects of pioglitazone on cardiac function in patients with type 2 diabetes and evidence of left ventricular diastolic dysfunction—a tissue Doppler imaging study. *Cardiovasc Diabetol* 9:57, 2010.
46. Hordern MD, Coombes JS, Cooney LM, et al: Effects of exercise intervention on myocardial function in type 2 diabetes. *Heart* 95:1343-1349, 2009.
47. Loimaala A, Groundstroem K, Rinne M, et al: Exercise training does not improve myocardial diastolic tissue velocities in type 2 diabetes. *Cardiovasc Ultrasound* 5:32, 2007.
48. Jarnert C, Landstedt-Hallin L, Malmberg K, et al: A randomized trial of the impact of strict glycaemic control on myocardial diastolic function and perfusion reserve—a report from the DADD (Diabetes mellitus And Diastolic Dysfunction) study. *Eur J Heart Fail* 11:39-47, 2009.
49. Shah DD, Fonarow GC, Horwich TB. Metformin therapy and outcomes in patients with advanced systolic heart failure and diabetes. *J Cardiac Fail* 16:200-206, 2010.
50. Giles TD, Miller AB, Elkayam U, et al: Pioglitazone and heart failure—results from a controlled study in patients with type 2 diabetes mellitus and systolic dysfunction. *J Cardiac Fail* 14:445-452, 2008.
51. Eguchi K, Ishikawa J, Hoshide S, et al: Differential impact of left ventricular mass and relative wall thickness on cardiovascular prognosis in diabetic and nondiabetic hypertensive subjects. *Am Heart J* 154:79.e9-79.e15, 2007.
52. Cooper GJS, Young AA, Gamble GD, et al: A copper(II)-selective chelator ameliorates left-ventricular hypertrophy in type 2 diabetic patients—a randomized placebo-controlled study. *Diabetologia* 52:715-722, 2009.
53. Fang ZY, Schull-Meade R, Leano R, et al: Screening for heart disease in diabetic subjects. *Am Heart J* 149:349-354, 2005.
54. Masugata H, Senda S, Goda F, et al: Left ventricular diastolic dysfunction as assessed by echocardiography in metabolic syndrome. *Hypertens Res* 29:897-903, 2006.
55. de las Fuentes L, Brown AL, Matthews SJ, et al: Metabolic syndrome is associated with abnormal left ventricular diastolic function independent of left ventricular mass. *Eur Heart J* 28:553-559, 2007.
56. Gong H, Tan W, Fang N, et al: Impaired left ventricular systolic and diastolic function in patients with metabolic syndrome as assessed by strain and strain rate imaging. *Diabetes Res Clin Pract* 83:300-307, 2009.
57. Schillaci G, Pirro M, Pucci G, et al: Different impact of the metabolic syndrome on left ventricular structure and function in hypertension men and women. *Hypertension* 47:881-886, 2006.
58. Mulè G, Cusimano P, Nardi E, et al: Relationships between metabolic syndrome and left ventricular mass in hypertensive patients—does sex matter? *J Hum Hypertens* 22:788-795, 2008.
59. Mahmud A, Almuntaser I, Brown A, et al: Left ventricular structural and functional changes in the metabolic syndrome. *J Cardiometab Syndr* 4:81-88, 2009.
60. Voulgari C, Moyssakis I, Papazafiropoulou A, et al: The impact of metabolic syndrome on left ventricular myocardial performance. *Diabetes Metab Rev* 26:121-127, 2010.
61. Aijaz B, Ammar KA, Lopez-Jimenez F, et al: abnormal cardiac structure and function in the metabolic syndrome—a population-based study. *Mayo Clin Proc* 83:1350-1357, 2008.
62. Li SH, Yang B, Gong HP, et al: Impaired left ventricular synchronicity in patients with metabolic syndrome, regardless of hypertension. *J Hypertens* 27:869-875, 2009.
63. Briand M, Lemieux I, Dumesnil JG, et al: Metabolic syndrome negatively influences disease progression and prognosis in aortic stenosis. *J Am Coll Cardiol* 47:2229-2236, 2006.
64. Briand M, Pibarot P, Despres JP, et al: Metabolic syndrome is associated with faster degeneration of bioprosthetic valves. *Circulation* 114:I-512-I-517, 2006.
65. Pearce EN, Yang Q, Benjamin E, et al: Thyroid function and left ventricular structure and function in the Framingham Heart Study. *Thyroid* 20:369-372, 2010.
66. Rolondi N, Bauer DC, Cappola AR, et al: Subclinical thyroid dysfunction, cardiac function, and the risk of heart failure. *J Am Coll Cardiol* 52:1152-1159, 2008.
67. Arinc H, Gunduz H, Tamer A, et al: Evaluation of right ventricular function in patients with thyroid dysfunction. *Cardiology* 105:89-94, 2006.
68. Gerdes AM, Iervasi G: Thyroid replacement therapy and heart failure. *Circulation* 122:385-393, 2010.
69. Tiryakioglu SK, Tiryakioglu O, Ari H, et al: Left ventricular longitudinal myocardial function in overt hypothyroidism—a tissue Doppler echocardiographic study. *Echocardiography* 27: 505-511, 2010.
70. Kaplan S, Kiris A, Erem C, et al: Assessment of left ventricular systolic asynchrony in patients with clinical hypothyroidism. *Echocardiography* 27:117-122, 2010.
71. Akcakoyun M, Kaya H, Kargin R, et al: Abnormal left ventricular longitudinal functional reserve assessed by exercise pulsed wave tissue Doppler imaging in patients with subclinical hypothyroidism. *J Clin Endocrinol Metab* 94:2979-2983, 2009.
72. Arinc H, Gunduz H, Tamer A, et al: Tissue Doppler echocardiography in evaluation of

cardiac effects of subclinical hypothyroidism. *Int J Cardiovasc Imaging* 22:177-186, 2006.
73. Zoncu S, Pigliaru F, Putzu C, et al: Cardiac function in borderline hypothyroidism: a study by pulsed wave tissue Doppler imaging. *Eur J Endocrinol* 152:527-533, 2005.
74. Vitale G, Galderisi M, Lupoli GA, et al: Left ventricular myocardial impairment in subclinical hypothyroidism assessed by a new ultrasound tool: pulsed tissue Doppler. *J Clin Endocrinol Metab* 87:4350-4355, 2002.
75. Kosar F, Sahin I, Turan N, et al: Evaluation of right and left ventricular function using pulsed-wave tissue Doppler echocardiography in patients with subclinical hypothyroidism. *J Endocrinol Invest* 28:704-710, 2005.
76. Di Bello V, Talini E, Donne MGD, et al: New echocardiographic techniques in the evaluation of left ventricular mechanics in subclinical thyroid dysfunction. *Echocardiography* 26:711-719, 2009.
77. Aghini-Lombardi F, Di Bello V, Talini E, et al: Early textural and functional alterations of left ventricular myocardium in mild hypothyroidism. *Eur J Endocrinol* 155:3-9, 2006.
78. Di Bello V, Monzani F, Giorgi D, et al: Ultrasonic myocardial textural analysis in subclinical hypothyroidism. *J Am Soc Echocardiogr* 13:832-840, 2000.
79. Franzoni F, Galetta F, Tocchini L, et al: Effect of L-thyroxine treatment on left ventricular function in subclinical hypothyroidism. *Biomed Pharmacother* 60:431-436, 2006.
80. Monzani F, Di Bello V, Caraccio N, et al: Effect of levothyroxine on cardiac function and structure in subclinical hypothyroidism: a double blind, placebo-controlled study. *J Clin Endocrinol Metab* 86:1110-1115, 2001.
81. Turhan S, Tulunay C, Ozduman M, et al: Effects of thyroxine therapy on right ventricular systolic and diastolic function in patients with subclinical hypothyroidism—a study by pulsed wave tissue Doppler imaging. *J Clin Endocrinol Metab* 91:3490-3493, 2006.
82. Tielens ET, Pillay M, Storm C, et al: Changes in cardiac function at rest before and after treatment in primary hypothyroidism. *Am J Cardiol* 85:376-380, 2000.
83. Virtanen VK, Saha HH, Groundstroem KW, et al: Thyroid hormone substitution therapy rapidly enhances left-ventricular diastolic function in hypothyroid patients. *Cardiology* 96:59-64, 2001.
84. Kosar F, Sahin I, Aksoy Y, et al: Usefulness of pulsed-wave tissue Doppler echocardiography for the assessment of the left and right ventricular function in patients with clinical hypothyroidism. *Echocardiography* 23:471-477, 2006.
85. Doin FLC, Borges MDR, Campos O, et al: Effect of central hypothyroidism on Doppler-derived myocardial performance index. *J Am Soc Echocardiogr* 17:622-629, 2004.
86. Ciulla MM, Paliotti R, Cortelazzi D, et al: Effects of thyroid hormones on cardiac structure: a tissue characterization study in patients with thyroid disorders before and after treatment. *Thyroid* 11:613-619, 2001.
87. Romano M, Maciel L, Almeida-Filho O, et al: Myocardial ultrasonic tissue characterization in patients with thyroid dysfunction. *Cardiovasc Ultrasound* 8:15, 2010.
88. Wang JL, Hsieh MJ, Lee CH, et al: Hypothyroid cardiac tamponade—clinical features, electrocardiography, pericardial fluid and management. *Am J Med Sci* 340:276-281, 2010.
89. Petretta M, Bonaduce D, Spinelli L, et al: Cardiovascular haemodynamics and cardiac autonomic control in patients with subclinical and overt hyperthyroidism. *Eur J Endocrinol* 145:691-696, 2001.
90. Palmieri EA, Fazio S, Palmieri V, et al: Myocardial contractility and total arterial stiffness in patients with overt hyperthyroidism—acute effects of $\beta_1$-adrenergic blockade. *Eur J Endocrinol* 150:757-762, 2004.
91. Arikan S, Tuzcu A, Gokalp D, et al: Hyperthyroidism may affect serum N-terminal pro-B-type natriuretic peptide levels independently of cardiac dysfunction. *Clinical Endocrinol* 67:202-207, 2007.
92. Ertugrul DT, Yavuz B, Ata N, et al: Decreasing brain natriuretic peptide levels after treatment for hyperthyroidism. *Endocrine J* 56:1043-1048, 2009.
93. Siu CW, Yeung CY, Lau CP, et al: Incidence, clinical characteristics and outcome of congestive heart failure as the initial presentation in patients with primary hyperthyroidism. *Heart* 93:483-487, 2007.
94. Radhakrishnan A, Granato JE: An association between Takotsubo cardiomyopathy and thyroid storm. *Postgrad Med* 121:126-130, 2009.
95. Di Giovambattista R: Hyperthyroidism as a reversible cause of right ventricular overload and congestive heart failure. *Cardiovasc Ultrasound* 6:29, 2008.
96. Kırış A, Erem C, KırışG, et al: Intra-left ventricular systolic asynchrony in patients with overt hyperthyroidism. *Endocrine* 38:283-288, 2010 Oct.
97. Mercuro G, Panzuto MG, Bina A, et al: Cardiac function, physical exercise capacity, and quality of life during long-term thyrotropin-suppressive therapy with levothyroxine: effect of individual dose tailoring. *J Clin Endocrinol Metab* 85:159-164, 2000.
98. Sgarbi JA, Villaca FG, Garbeline B, et al: The effects of early antithyroid therapy for endogenous subclinical hyperthyroidism in clinical and heart abnormalities. *J Clin Endocrinol Metab* 88:1672-1677, 2003.
99. Di Bello V, Aghini-Lombardi F, Monzani F, et al: Early abnormalities of left ventricular myocardial characteristics associated with subclinical hyperthyroidism. *J Endocrinol Invest* 30: 564-571, 2007.
100. Abdulrahman RM, Delgado V, Ng ACT, et al: Abnormal cardiac contractility in long-term exogenous subclinical hyperthyroid patients as demonstrated by two-dimensional echocardiography speckle tracking imaging. *European J Endocrinol* 163:435-441, 2010.
101. Yue WS, Chong BH, Zhang XH, et al: Hyperthyroidism-induced left ventricular diastolic dysfunction: implication in hyperthyroidism-related heart failure. *Clin Endocrinol* 74:636-643, 2011.
102. Smit JWA, Eustatia-Rutten CFA, Corssmit EPM, et al: Reversible diastolic dysfunction after long-term exogenous subclinical hyperthyroidism—a randomized, placebo-controlled study. *J Clin Endocrinol Metab* 90: 6041-6047, 2005.
103. Tamer I, Sargin M, Sargin H, et al: The evaluation of left ventricular hypertrophy in hypertensive patients with subclinical hyperthyroidism. *Endocr J* 52:421-425, 2005.
104. Merce J, Ferras S, Oltra C, et al: Cardiovascular abnormalities in hyperthyroidism: a prospective Doppler echocardiographic study. *Am J Med* 118:126-131, 2005.
105. Pivonello R, Galderisi M, Auriemma RS, et al: Treatment with growth hormone receptor antagonist in acromegaly—effect on cardiac structure and performance. *J Clin Endocrinol Metab* 6:476-482, 2007.
106. Bogazzi F, Loambardi M, Strata E, et al: High prevalence of cardiac hypertrophy without detectable signs of fibrosis in patients with untreated active acromegaly—an in vivo study using magnetic resonance imaging. *Clin Endocrinol* 68:361-368, 2008.
107. Galderisi M, Vitale G, Bianco A, et al: Pulsed tissue Doppler identifies subclinical myocardial biventricular dysfunction in active acromegaly. *Clin Endocrinol* 64:390-397, 2006.
108. Baykan M, Erem C, Gedikli Ö, et al: Assessment of the Tei index by tissue Doppler imaging in patients with acromegaly—serum growth hormone level is associated with the Tei index. *Echocardiography* 25:374-380, 2008.
109. Akgul E, Tokgozoglu SL, Erbas T, et al: Evaluation of the impact of treatment of endothelial function and cardiac performance in acromegaly. *Echocardiography* 27:990-996, 2010.
110. van der Klaauw AA, Bax JJ, Roelfsema F, et al: Uncontrolled acromegaly is associated with progressive mitral valvular regurgitation. *Growth Hormone & IGF Research* 101-107, 2006.
111. Ciulla MM, Epaminonda P, Paliotti R, et al: Evaluation of cardiac structure by echoreflectivity analysis in acromegaly: effects of treatment. *Eur J Endocrinol* 151:179-186, 2004.
112. Mercuro G, Zoncu S, Colonna P, et al: Cardiac dysfunction in acromegaly: evidence by pulsed wave tissue Doppler imaging. *Eur J Endocrinol* 143:363-369, 2000.
113. Vianna CB, Vieira ML, Mady C, et al: Treatment of acromegaly improves myocardial abnormalities. *Am Heart J* 143:873-876, 2002.
114. Lombardi G, Colao A, Marzullo P, et al: Improvement of left ventricular hypertrophy and arrhythmias after lanreotide-induced GH and IGF-I decrease in acromegaly. A prospective multi-center study. *J Endocrinol Invest* 25:971-976, 2002.
115. Bogazzi F, Di Bello V, Palagi C, et al: Improvement of intrinsic myocardial contractility and cardiac fibrosis degree in acromegalic patients treated with somatostatin analogues: a prospective study. *Clin Endocrinol (Oxf)* 62:590-596, 2005.
116. van Thiel SW, Bax JJ, Biermasz NR, et al: Persistent diastolic dysfunction despite successful long-term octreotide treatment in acromegaly. *Eur J Endocrinol* 153:231-238, 2005.
117. Colao A, Baldelli R, Marzullo P, et al: Systemic hypertension and impaired glucose tolerance are independently correlated to the severity of the acromegalic cardiomyopathy. *J Clin Endocrinol Metab* 85:193-199, 2000.
118. Fazio S, Cittadini A, Biondi B, et al: Cardiovascular effects of short-term growth hormone hypersecretion. *J Clin Endocrinol Metab* 85:179-182, 2000.
119. Colao A, Marzullo P, Ferone D, et al: Cardiovascular effects of depot long-acting somatostatin analog Sandostatin LAR in acromegaly. *J Clin Endocrinol Metab* 85:3132-3140, 2000.
120. Bogazzi F, Lombardi M, Strata E, et al: Effects of somatostatin analogues on acromegalic cardiomyopathy—results from a prospective study using cardiac magnetic resonance. *J Endocrinol Invest* 33:103-108, 2010.
121. Leães CGS, Kramer CK, Pereira-Lima JFS, et al: Diastolic function study with conventional and pulsed tissue Doppler echocardiography

imaging in acromegalic patients. *Echocardiography* 26:651-656, 2009.
122. Di Bello V, Bogazzi F, Di Cori A, et al: Myocardial systolic strain abnormalities in patients with acromegaly: a prospective color Doppler imaging study. *J Endocrinol Invest* 29:544-550, 2006.
123. Bruch C, Herrmann B, Schmermund A, et al: Impact of disease activity on left ventricular performance in patients with acromegaly. *Am Heart J* 144:538-543, 2002.
124. Damjanovic SS, Neskovic AN, Petakov MS, et al: High output heart failure in patients with newly diagnosed acromegaly. *Am J Med* 112:610-616, 2002.
125. Colao A, Spinelli L, Marzullo P, et al: High prevalence of cardiac valve disease in acromegaly: an observational, analytical, case-control study. *J Clin Endocrinol Metab* 88:3196-3201, 2003.
126. Pereira AM, van Thiel SW, Lindner JR, et al: Increased prevalence of regurgitant valvular heart disease in acromegaly. *J Clin Endocrinol Metab* 89:71-75, 2004.
127. Nemes A, Gavallér H, Csajbók E, et al: Aortic stiffness is increased in acromegaly—a transthoracic echocardiographic study. *Int J Cardiol* 124:121-123, 2008.
128. van der Klaauw AA, Bax JJ, Smit JWA, et al: Increased aortic root diameters in patients with acromegaly. *Eur J Endocrinol* 159:97-103, 2008.
129. Cable DG, Dearani JA, O'Brien T, et al: Surgical treatment of valvular heart disease in patients with acromegaly. *J Heart Valve Dis* 9:828-831, 2000.
130. Bihan H, Espinosa C, Valdes-Socin H, et al: Long-term outcome of patients with acromegaly and congestive heart failure. *J Clin Endocrinol Metab* 89:5308-5313, 2004.
131. Walker MD, Fleischer JB, Di Tullio MR, et al: Cardiac structure and diastolic function in mild primary hyperparathyroidism. *J Clin Endocrinol Metab* 95:2172-2179, 2010.
132. Nappi S, Saha H, Virtanen V, et al: Left ventricular structure and function in primary hyperparathyroidism before and after parathyroidectomy. *Cardiology* 93:229-233, 2000.
133. Baykan M, Erem C, Erdogan T, et al: Assessment of left ventricular diastolic function and the Tei index by tissue Doppler imaging in patients with primary hyperparathyroidism. *Clin Endocrinol* 66:483-488, 2007.
134. Farahnak P, Ring M, Caidahl K, et al: Cardiac function in mild primary hyperparathyroidism and the outcome after parathyroidectomy. *Eur J Endocrinol* 163:461-467, 2010.
135. Kazmi AS, Wall BM: Reversible congestive heart failure related to profound hypocalcemia secondary to hypoparathyroidism. *Am J Med Sci* 333:226-229, 2007.
136. Nilsson IL, Aberg J, Rastad J, Lind L: Left ventricular systolic and diastolic function and exercise testing in primary hyperparathyroidism—effects of parathyroidectomy. *Surgery* 128:895-902, 2000.
137. Muiesan ML, Lupia M, Salvetti M, et al: Left ventricular structural and functional characteristics in Cushing's syndrome. *J Am Coll Cardiol* 41:2275-2279, 2003.
138. Baykan M, Erem C, Gedikli O, et al: Assessment of left ventricular diastolic function and Tei index by tissue Doppler imaging in patients with Cushing's syndrome. *Echocardiography* 25:182-190, 2008.
139. Bayram NA, Ersoy R, Aydin C, et al: Assessment of left ventricular functions by tissue Doppler echocardiography in patients with Cushing's disease. *J Endocrinol Invest* 32:248-252, 2009.
140. Pereira AM, Delgado V, Romijn JA, et al: Cardiac dysfunction is reversed upon successful treatment of Cushing's syndrome. *Eur J Endocrinol* 162:331-340, 2010.
141. Takagi S, Akiyo T, Tsuiki M, et al: Hypokalemia, diabetes mellitus, and hypercortisolemia are the major contributing factors to cardiac dysfunction in adrenal Cushing's syndrome. *Endocrine J* 56:1009-1018, 2009.
142. Peppa M, Ikonomaidis I, Hadjidakis D, et al: Dilated cardiomyopathy as the predominant feature of Cushing's syndrome. *Am J Med Sci* 338:252-253, 2009.
143. Stowasser M, Sharman J, Leano R, et al: Evidence for abnormal left ventricular structure and function in normotensive individuals with familial hyperaldosteronism type I. *J Clin Endocrinol Metab* 90:5070-5076, 2005.
144. Rossi GP, Di Bello V, Ganzaroli C, et al: Excess idosterone is associated with alterations of myocardial texture in primary aldosteronism. *Hypertension* 40:23-27, 2002.
145. Schmidt BM, Schmeider RE: Aldosterone-induced cardiac damage: focus on blood pressure independent effects. *Am J Hypertens* 16:80-86, 2003.
146. Levin A, Thompson C, Eithier J, et al: Left ventricular mass index increase in early renal disease—impact in decline in haemoglobin. *Am J Kidney Dis* 34:125-134, 1999.
147. Murata T, Dohi K, Onishi K, et al: Role of haemodialytic therapy on left ventricular mechanical dyssynchrony in patients with end-stage renal disease quantified by speckle-tracking strain imaging. *Nephrol Dial Transplant* 1-7, 2010.
148. Nardi E, Palermo A, Mulè G, et al: Left ventricular hypertrophy and geometry in hypertensive patients with chronic kidney disease. *J Hypertension* 27:633-641, 2009.
149. Tarrass F, Benjelloun M, Zamd M, et al: Heart valve calcification in patients with end-stage renal disease—analysis for risk factors. *Nephrology* 11:494-496, 2006.
150. Strozecki P, Odrowaz-Sypniewska G, Manitius J: Cardiac valve calcifications and left ventricular hypertrophy in hemodialysis patients. *Ren Fail* 27:733-738, 2005.
151. Vanholder R, Glorieux G, Lameire N, et al: Uremic toxins and cardiovascular disease. *Nephrol Dial Transplant* 18:463-466, 2003.
152. Zolty R, Hymes PJ, Vittorio TJ: Severe left ventricular systolic dysfunction may reverse with renal transplantation—uremic cardiomyopathy and cardiorenal syndrome. *Am J Transplantation* 8:2219-2224, 2008.
153. Edwards NC, Hirth A, Ferro CJ, et al: Subclinical abnormalities of left ventricular myocardial deformation in early-stage chronic kidney disease—the precursor of uremic cardiomyopathy. *J Am Soc Echocardiogr* 21:1293-1298, 2008.
154. Gulel O, Soylu K, Yuksei S, et al: Evidence of left ventricular systolic and diastolic dysfunction by color tissue Doppler imaging despite normal ejection fraction in patients on chronic hemodialysis program. *Echocardiography* 25:569-574, 2008.
155. Liu YW, Su CT, Huang YY, et al: Left ventricular systolic strain in chronic kidney disease and hemodialysis patients. *Am J Nephrol* 33:84-90, 2011.
156. Gedikli O, Baykan M, Kaynar K, et al: Assessment of left ventricular systolic synchronization in patients with chronic kidney disease and narrow QRS complexes. *Echocardiography* 26:528-533, 2009.
157. Iqbal A, Jorde R, Lunde P, et al: Left ventricular dysfunction in subjects with mild secondary hyperparathyroidism detected with pulsed wave tissue Doppler echocardiography. *Cardiology* 105:1-8, 2006.
158. Cheng LT, Gao YL, Tian JP, et al: Sex difference in the prevalence of left ventricular hypertrophy in dialysis patients. *Am J Nephrol* 29:398-405, 2009.
159. Hsiao SH, Huang WC, Sy CL, et al: Doppler tissue imaging and color M-mode flow propagation velocity—are they really preload independent? *J Am Soc Echocardiogr* 18:1277-1284, 2005.
160. Fijalkowski M, Koprowski A, Gruchala M, et al: Effect of preload reduction by hemodialysis on myocardial ultrasonic characterization, left atrial volume, and Doppler tissue imaging in patients with end-stage renal disease. *J Am Soc Echocardiogr* 19:1359-1364, 2006.
161. Su HM, Lin TH, Voon WC, et al: Impact of preload alterations by haemodialysis on the Tei index—comparison between pulsed flow and tissue Doppler analysis. *Acta Cardiol* 62:25-30, 2007.
162. Palecek T, Skalicka L, Lachmanava J, et al: Effect of preload reduction by hemodialysis on conventional and novel echocardiographic parameters of left ventricular structure and function. *Echocardiography* 25:162-168, 2008.
163. Choi JO, Shin DH, Cho SW, et al: Effect of preload on left ventricular longitudinal strain by 2D speckle tracking. *Echocardiogr* 25:873-879, 2008.
164. Burton JO, Jeffries HJ, Selby NM, et al: Hemodialysis-induced repetitive myocardial injury results in global and segmental reduction in systolic cardiac function. *Clin J Am Soc Nephrol* 4:1925-1931, 2009.
165. Paneni F, Gregori M, Ciavarella GM, et al: Right ventricular dysfunction in patients with end-stage renal disease. *Am J Nephrol* 32:432-438, 2010.
166. Hayashi SY, Rohani M, Lindholm B, et al: Left ventricular function in patients with chronic kidney disease evaluated by colour tissue Doppler velocity imaging. *Nephrol Dial Transplant* 21:125-132, 2006.
167. Nardi E, Cottone S, Mulè G, et al: Influence of chronic renal insufficiency on left ventricular diastolic function in hypertensives without left ventricular hypertrophy. *J Nephrol* 20:320-328, 2007.
168. Rao AK, Djamali A, Korcarz CE, et al: Mitral annular calcification is associated with reduced left ventricular function and inflammation in patients with chronic kidney disease. *J Am Soc Echocardiogr* 21:747-750, 2008.
169. Foley RN, Parfrey PS, Kent GM, et al: Serial change in echocardiographic parameters and cardiac failure in end-stage renal disease. *J Am Soc Nephrol* 11:912-916, 2000.
170. Zoccali C, Benedetto FA, Tripepi G, et al: Left ventricular systolic function monitoring in asymptomatic dialysis patients—a prospective cohort study. *J Am Soc Nephrol* 17:1460-1465, 2006.
171. Wang AYM, Wang M, Lam CWK, et al: Left ventricular filling pressure by Doppler echocardiography in patients with end-stage renal disease. *Hypertension* 52:107-114, 2008.
172. Burch C, Reinecke H, Rothenburger M, et al: Transmitral flow patterns and the presence of chronic kidney disease provide independent

and incremental prognostic information in patients with heart failure and systolic dysfunction. *J Am Soc Echocardiogr* 20:989-997, 2007.
173. Chan MY, Wong HB, Ong HY, et al: Prognostic value of left atrial size in chronic kidney disease. *Eur J Echocardiogr* 9:736-740, 2008.
174. Ozdogan O, Kayikcioglu M, Asci G, et al: Left atrial volume predicts mortality in low-risk dialysis population on long-term low-salt diet. *Am Heart J* 159:1089-1094, 2010.
175. Tripepi G, Benedetto FA, Mallamaci F, et al: Left atrial volume monitoring and cardiovascular risk in patients with end-stage renal disease—a prospective cohort study. *J Am Soc Nephrol* 18:1316-1322, 2007.
176. Sharma R, Pellerin D, Gaze DC, et al: Mitral annular calcification predicts mortality and coronary artery disease in endstage renal disease. *Atherosclerosis* 191:348-354, 2007.
177. Barberato SH, Misocami M, Pecoits-Filho R, et al: Association between left atrium enlargement and intradialytic hypotension—role of diastolic dysfunction in the hemodynamic complications during hemodialysis. *Echocardiogr* 26:767-771, 2009.
178. Rostoker G, Griuncelli M, Loridon C, et al: Left-ventricular diastolic dysfunction as a risk factor for dialytic hypotension. *Cardiology* 114:142-149, 2009.
179. Yang NI, Wang CH, Hung MJ, et al: Real-time three-dimensional echocardiography provides advanced haemodynamic information associated with intra-dialytic hypotension in patients with autonomic dysfunction. *Nephrol Dial Transplant* 25:249-254, 2010.
180. Kume T, Kawamoto T, Akasaka T, et al: Rate of progression of valvular aortic stenosis in patients undergoing dialysis. *J Am Soc Echocardiogr* 19:914-918, 2006.
181. Tanaka K, Tajima K, Takami Y, et al: Early and late outcomes of aortic valve replacement in dialysis patients. *Ann Thorac Surg* 89:65-71, 2010.
182. Karagiannis SE, Feringa HH, Elhendy A, et al: Prognostic significance of renal function in patients undergoing dobutamine stress echocardiography. *Nephrol Dial Transplant.* 23:601-607, 2008.
183. Covic A, Mardare NG, Ardeleanu S, et al: Serial echocardiographic changes in patients on hemodialysis: an evaluation of guideline implementation. *J Nephrol* 19(6):783-793, 2006.
184. Alpert MA: Obesity cardiomyopathy—pathophysiology and evolution of the clinical syndrome. *Am J Med Sci* 321:225-236, 2001.
185. Iacobellis G, Ribaudo MC, Leto G, et al: Influence of excess fat on cardiac morphology and function: study in uncomplicated obesity. *Obes Res* 10:767-773, 2002.
186. Wong CY, O'Moore-Sullivan, T, Leano R, et al: Alterations of left ventricular myocardial characteristics associated with obesity. *Circulation* 110:3081-3087, 2004.
187. Peterson LR, Waggoner AD, Schechtman KB, et al: Alterations in left ventricular structure and function in young healthy obese women: assessment by echocardiography and tissue Doppler imaging. *J Am Coll Cardiol* 43:1399-1404, 2004.
188. Tumuklu MM, Etikan I, Kisacik B, et al: Effect of obesity on left ventricular structure and myocardial systolic function—assessment by tissue Doppler imaging and strain/strain rate imaging. *Echocardiogr* 24:802-809, 2007.
189. Kuznetsova T, Herbots L, Richart T, et al: Left ventricular strain and strain rate in a general population. *Eur Heart J* 29:2014-2023, 2008.
190. Kosmala W, Wong C, Kuliczkowska J, et al: Use of body weight and insulin resistance to select obese patients for echocardiographic assessment of subclinical left ventricular dysfunction. *Am J Cardiol* 101:1334-1340, 2008.
191. Orhan AL, Uslu N, Dayi SU, et al: Effects of isolated obesity on left and right ventricular function—a tissue Doppler and strain rate imaging study. *Echocardiography* 27:236-243, 2010.
192. Wong CY, O'Moore-Sullivan T, Leano R, et al: Association of subclinical right ventricular dysfunction with obesity. *J Am Coll Cardiol* 47:611-616, 2006.
193. Maniscalco M, Arciello A, Zedda A, et al: Right ventricular performance in severe obesity—effect of weight loss. *Eur J Clin Invest* 37:270-275, 2007.
194. Pascual M, Pascual DA, Soria F, et al: Effects of isolated obesity on systolic and diastolic left ventricular function. *Heart* 89:1152-1156, 2003.
195. Di Stante B, Galandauer I, Aronow WS, et al: Prevalence of left ventricular diastolic dysfunction in obese persons with and without diabetes mellitus. *Am J Cardiol* 95:1527-1528, 2005.
196. Willens HJ, Chakko SS, Lowery MH, et al: Tissue Doppler imaging of the right and left ventricle in severe obesity (body mass index >35 kg/m$^2$). *Am J Cardiol* 94:1087-1090, 2004.
197. Willens HJ, Chakko SC, Byers P, et al: Effects of weight loss after gastric bypass on right and left ventricular function assessed by tissue Doppler imaging. *Am J Cardiol* 95:1521-1524, 2005.
198. de las Fuentes L, Waggoner AD, Mohammed S, et al: Effect of moderate diet-induced weight loss and weight regain on cardiovascular structure and function. *J Am Coll Cardiol* 54:2376-2381, 2009.
199. Stritzke J, Markus MRP, Duderstadt S, et al: The aging process of the heart—obesity is the main risk factor for left atrial enlargement during aging. *J Am Coll Cardiol* 54:1982-1989, 2009.
200. Otto ME, Belohlavek M, Romero-Corral A, et al: Comparison of cardiac structural and functional changes in obese otherwise healthy adults with versus without obstructive sleep apnea. *Am J Cardiol* 99:1298-1302, 2007.
201. Avelar E, Cloward TV, Walker JM, et al: Left ventricular hypertrophy in severe obesity—interactions among blood pressure, nocturnal hypoxemia, and body mass. *Hypertension* 49:34-39, 2007.
202. Garza CA, Pellikka PA, Somers VK, et al: Structural and functional changes in left and right ventricles after major weight loss following bariatric surgery for morbid obesity. *Am J Cardiol* 105:550-556, 2010.
203. Ikonomidis I, Mazarakis A, Papadopoulos C, et al: Weight loss after bariatric surgery improves aortic elastic properties and left ventricular function in individuals with morbid obesity—a 3-year follow-up. *J Hypertension* 25:439-447, 2007.
204. Di Bello V, Santini F, Cori AD, et al: Obesity cardiomyopathy—is it reality? An ultrasonic tissue characterization study. *J Am Soc Echocardiogr* 19:1063-1071, 2006.
205. Iacobellis G, Leonetti F. Epicardial adipose tissue and insulin resistance in obese subjects. *J Clin Endocrinol Metab* 90:6300-6302, 2005.
206. Kim MK, Tomita T, Kim MJ, et al: Aerobic exercise training reduces epicardial fat in obese men. *J Appl Physiol* 106:5-11, 2009.
207. Jollis JG, Landolfo CK, Kisslo J, et al: Fenfluramine and phentermine and cardiovascular findings: effect of treatment duration on prevalence of valve abnormalities. *Circulation* 101:2071-2077, 2000.
208. Weissman NJ, Tighe JF, Jr, Gottdiener JS, et al: An assessment of heart valve abnormalities in obese patients taking dexfenfluramine, sustained-release dexfenfluramine, or placebo. *N Engl J Med* 339:725-732, 1998.
209. Burger AJ, Sherman HB, Charlamb MJ, et al: Low prevalence of valvular heart disease in 226 phentermine-fenfluramine protocol subjects prospectively followed for up to 30 months. *J Am Coll Cardiol* 34:1153-1158, 1999.
210. Klein AL, Griffin BP, Grimm RA, et al: Natural history of valvular regurgitation using side-by-side echocardiographic analysis in anorexigen-treated subjects. *Am J Cardiol* 96:1711-1717, 2005.
211. Dahl CF, Allen MR, Urie PM, et al: Valvular regurgitation and surgery associated with fenfluramine use—an analysis of 5743 individuals. *BMC Medicine* 6:34, 2008.
212. Abenheim L, Moride Y, Brenot F, et al: Appetite suppressant drugs and the risk of primary pulmonary hypertension. *N Engl J Med* 335:609-616, 1996.
213. Weyman AE, Davidoff R, Gardin J, et al: Echocardiographic evaluation of pulmonary artery pressure with clinical correlates in predominantly obese adults. *J Am Soc Echocardiogr* 15:454-462, 2002.
214. Gottdiener JS, Panza JA, St, John Sutton M, et al: Testing the test: the reliability of echocardiography in the sequential assessment of valvular regurgitation. *Am Heart J* 144:115-121, 2002.
215. Hanninen SA, Darling PB, Sole MJ, et al: The prevalence of thiamin deficiency in hospitalized patients with congestive heart failure. *J Am Coll Cardiol* 47:354-361, 2006.
216. Dishmon DA, Dotson JL, Munir A, et al: Hypovitaminosis D and valvular calcification in patients with dilated cardiomyopathy. *Am J Med Sci* 337:312-316, 2009.
217. Artaza JN, Mehrotra R, Norris KC. Vitamin D and the cardiovascular system. *Clin J Am Soc Nephrol* 4:1515-1522, 2009.
218. Ameri P, Ronco D, Casu M, et al: High prevalence of vitamin D deficiency and its association with left ventricular dilation—an echocardiography study in elderly patients with chronic heart failure. *Nut Metab Cardiovascular Dis* 20:633-640, 2010.
219. Ocal B, Unal S, Zorlu P, et al: Echocardiographic evaluation of cardiac functions and left ventricular mass in children with malnutrition. *J Paediatr Child Health* 37:14-17, 2001.

# 39 Echocardiography in Patients with Inherited Connective Tissue Disorders

AARON K. OLSON, MD | MARK LEWIN, MD

**Forms of Connective Tissue Disorders**
Marfan Syndrome
Ehlers-Danlos Syndrome
Homocystinuria
Other Fibrillinopathies
Loeys-Dietz Syndrome
Bicuspid Aortic Valve
Turner Syndrome
Familial Thoracic Aortic Aneurysm and Dissection
**Histopathology**
**Echocardiographic Findings**
Aortic Dilation
Aortic Dissection
Other Aortic Arch Manifestations
Mitral Valve Prolapse
**Natural History**
Methods of Assessment
Limitations of Assessment
**Therapeutic Strategies**
Pharmacologic
Surgical
**Alternate Diagnostic Approaches**

## Forms of Connective Tissue Disorders

Although connective tissue disorders affect multiple organs, the impact on the cardiovascular system is considered the most dangerous. These disorders are known to cause progressive degeneration of the integument, joints, pleura, and eyes. Potential exists for both left and right heart involvement, but clinically important pathology is typically confined to the mitral valve, aortic valve, and the aorta itself.

As opposed to other forms of cardiovascular disease, many patients come to medical attention not because of symptoms referable to the cardiovascular system but rather because of findings associated with one of the noncardiac organ systems noted previously. In addition, identification of cardiovascular pathology may be noted on screening cardiac assessment as a result of the presence of a defined or suspected connective tissue disorder in another family member. Echocardiography is the mainstay of cardiac screening for the cardiac manifestations of connective tissue disorders. As with many other cardiac disorders, transesophageal echocardiography (TEE) complements transthoracic echocardiography (TTE) in developing a thorough set of data. In addition, other noninvasive imaging modalities (i.e., computerized tomography and magnetic resonance imaging) contribute to diagnosis in selected circumstances. Although Marfan syndrome (MFS) is the most common connective tissue disorder that leads to cardiovascular compromise, a number of other inherited and congenital conditions are known to affect the cardiac structures in similar ways (Box 39-1). These conditions are elucidated in this chapter. In addition, the spectrum of disease and the methods of assessment are highlighted.

### MARFAN SYNDROME

Marfan syndrome is a well-described heritable disorder of connective tissue with a broad phenotypic spectrum. Major clinical manifestations include the cardiovascular, ocular, and skeletal systems. The diagnosis is based on the Ghent nosology, which was recently revised by an international expert panel (Boxes 39-2 and 39-3).[1] The revised criteria place increased importance on the cardinal clinical features of aortic root dilation and dissection and ectopia lentis.

The evaluation of children and adolescents for MFS requires special consideration.[1] Serial evaluations are recommended because of their potential for evolving clinical features, which could progress so that a diagnostic criterion is eventually achieved. However, the practitioner should also be judicious in conferring this diagnosis because it may cause psychosocial stress, impact career decisions, and limit insurability. Young patients (younger than 20 years of age) with a fibrillin 1 (FBN1) mutation or a family history of MFS and aortic root measurements with a Z-score of less than 3 should have a diagnosis of "potential MFS" until follow-up evaluation shows further aortic dilation.

Marfan syndrome is inherited in an autosomal dominant manner, with 25% of patients representing sporadic new mutations without a family history.[2] Once an individual is diagnosed with MFS, first-degree relatives should be screened for the condition (with physical examination, accompanied by ophthalmologic assessment and echocardiography when clinically appropriate). The age-related penetrance is high, and both interfamilial and intrafamilial variability are well described. Molecular genetic testing of the fibrillin 1 gene (locus 15q21.1) reveals a causative mutation in about 70% to 90% of individuals with the clinical diagnostic criteria for MFS.[3]

Despite a considerable effort invested in defining genotype-phenotype correlations for MFS, few if any definitive correlations have emerged. Thus far, none have been shown to be specific enough to influence clinical management. Of those that have emerged, the patients with the most severe form of MFS (also termed infantile MFS) and an identifiable fibrillin 1 mutation tend to harbor mutations in the central portion of the gene,

**Box 39-1**

## INHERITED AND CONGENITAL DISORDERS ASSOCIATED WITH AORTIC DILATION OR MITRAL VALVE PROLAPSE

- Marfan syndrome
- Loeys-Dietz syndrome
- Ehlers-Danlos syndrome
- Homocystinuria
- Thoracic aortic aneurysm and dissection syndrome
- Familial thoracic aortic aneurysm
- MASS phenotype
- Bicuspid aortic valve
- Coarctation of the aorta
- Mitral valve prolapse syndrome
- Turner syndrome
- Osteogenesis imperfecta

*MASS*, *M*yopia, *M*itral valve prolapse, borderline *A*ortic enlargement, and nonspecific *S*kin/*S*keletal signs.

**Box 39-2**

## REVISED GHENT CRITERIA FOR THE DIAGNOSIS OF MARFAN SYNDROME

**In the Presence of Family History, Any of the Following Confirm the Diagnosis of Marfan Syndrome:**

- Ectopia lentis
- Systemic score ≥7
- Ao sinus dilation (Z-score ≥2 above age 20 years or Z-score ≥3 below age 20 years)

**In the Absence of Family History and without Discriminating Features of Another CTD:**

- Ao sinus dilation (Z-score ≥2) and ectopia lentis = Marfan syndrome
- Ao sinus dilation (Z-score ≥2 above age 20 years or Z-score ≥3 below age 20 years) and fibrillin 1 = Marfan syndrome
- Ao sinus dilation (Z-score ≥2) and systemic score ≥7 = Marfan syndrome
- Ectopia lentis and fibrillin 1 with known aortic dilation = Marfan syndrome

From Loeys BL, Dietz HC, Braverman AC, et al: The revised Ghent nosology for the Marfan syndrome. *J Med Genet* 47:476-485, 2010.
*Ao*, Aortic; *CTD*, connective tissue disorder.

**Box 39-3**

## SYSTEMIC SCORE IN MARFAN SYNDROME

- Wrist and thumb sign, 3 (wrist or thumb sign, 1)
- Pectus carinatum deformity, 2 (pectus excavatum or chest asymmetry, 1)
- Hind foot deformity, 2 (plain pes planus, 1)
- Pneumothorax, 2
- Dural ectasia, 2
- Protrusio acetabuli, 2
- Reduced upper segment/lower segment ratio and increased arm/height and no severe scoliosis, 1
- Reduced elbow extension, 1
- Scoliosis or thoracolumbar kyphosis, 1
- Facial feature (3/5), 1 (dolichocephaly, enophthalmos, downslanting palpebral fissures, malar hypoplasia, retrognathia)
- Skin stria, 1
- Myopia >3 diopters, 1
- Mitral valve prolapsed, 1

between exons 24 to 32.[4-6] Interestingly, mutations have been also found in this region in other patients with classic, atypically severe, and milder forms of MFS and other fibrillinopathies.[6-8] By way of contrast, mutations in fibrillin 1 that result in milder forms of a type 1 fibrillinopathy have also been described. These include mutations in the C-terminus region of fibrillin 1 that result in only the skeletal manifestations of MFS.[9] Mutations in exons 59 to 65 of fibrillin 1[10] and exons 1 to 10[11] have been associated with phenotypes that lack significant aortic involvement or with only late onset and relatively mild cardiovascular features.

## EHLERS-DANLOS SYNDROME

The multiple forms of Ehlers-Danlos syndrome (EDS) are each manifested by particular phenotypic features. The most common forms are type III, otherwise termed benign hypermobility syndrome; and the classic form, previously designated as types I and II but now recognized as forming a clinical continuum (involving hyperextensibility, fragile "cigarette paper" skin that heals poorly, scoliosis, and hernias). Between one quarter and one third of individuals with these types of Ehlers-Danlos syndrome have aortic dilation, but usually only to a mild degree. Aortic dissection is rare absent significant preexisting dilation.[12-14] The long-term prognosis regarding progression or development of aortic dilation is the subject of ongoing investigations.[12,13] Mitral valve prolapse is also encountered in these patients. Classic and type III Ehlers-Danlos syndrome are inherited in an autosomal dominant fashion and are caused by a disorder in synthesis of collagen.

Type IV or vascular form is considered the malignant form of Ehlers-Danlos syndrome in that there is an increased susceptibility to spontaneous vascular dissection. The median age of death is 48 years. Large vessel dissections can involve the aorta, but the cerebral and abdominal large arteries are also at risk.[15,16] The sites of arterial rupture are the thorax and abdomen (50%), head and neck (25%), and extremities (25%). Although uncommon, the vascular type of Ehlers-Danlos syndrome is a cause of stroke in young adults. The mean age of intracranial aneurysmal rupture, spontaneous carotid-cavernous sinus fistula, and cervical artery aneurysm is 28 years.[17] Hyperelastic tissues and hyperextensible joints are less frequent manifestations, but easy bruising, poor wound healing, and rupture of the gastrointestinal tract are commonly seen. Inheritance is autosomal dominant, with the defect occurring in the type III collagen gene *COL3A1*.[18]

All patients with Ehlers-Danlos syndrome (irrespective of particular type) should undergo screening echocardiographic assessment. Patients with types I, II, and IV (more commonly associated with cardiovascular manifestations) should be evaluated annually with echocardiography for a serial assessment of aortic dilation and mitral valve disease. Aortic regurgitation may also develop. The indications for surgical repair in classic and type III syndromes are similar to MFS and are discussed subsequently in the chapter. The fragile nature of the large vessels in the vascular form of Ehlers-Danlos syndrome increases surgical morbidity and mortality. Therefore, whether there is a role for early prophylactic repair of unruptured aneurysms in the vascular form of Ehlers-Danlos syndrome is unclear.[19] However, successful repairs of aneurysms and dissections can be achieved with careful surgical technique.[20] TEE should be approached with caution because of the potential for gastrointestinal involvement.

## HOMOCYSTINURIA

This disorder is defined as the presence of excessive homocysteine in the urine. The most common form of homocystinuria is caused by a metabolic disorder in which a deficiency of cystathionine β synthase results in an elevation of blood methionine and subsequent deposition of its precursor homocysteine in the urine. The inheritance occurs in an autosomal recessive pattern, with variable phenotypic expression even within the same family. Clinical findings can include developmental delay, ectopia lentis, coagulopathies, and many of the same skeletal features present in MFS, including scoliosis, arachnodactyly, tall stature, and pectus deformities. As opposed to the aortic dilation seen in patients with MFS, this entity is not generally present in homocystinuria. From a cardiovascular standpoint, these patients can have arterial and venous thromboses develop, which can lead to peripheral or cerebral vascular disease in both children and adults.[21] This is complicated by vascular injury, including medial degeneration of the aorta and large arteries, with intimal hyperplasia and fibrosis. There is resultant pulmonary embolism with associated right ventricular hypertension and ischemic coronary disease with the potential for myocardial infarction.

## OTHER FIBRILLINOPATHIES

Fibrillin 1 mutations have also been reported in distinct phenotypes that have overlap with MFS, including mitral valve prolapse syndrome, the MASS phenotype (*M*yopia, *M*itral valve prolapse, borderline *A*ortic enlargement, and nonspecific *S*kin/*S*keletal signs), apparently isolated ectopia lentis, predominant or isolated skeletal features of MFS, and familial aortic aneurysm or dissection.[3] Together, MFS and the MFS-related phenotypes have been termed the type 1 fibrillinopathies.

Congenital contractural arachnodactyly (also known as Beals syndrome), another connective tissue disorder similar to MFS, is caused by fibrillin-2 mutations. Differentiation between these two syndromes can be difficult because of the similar skeletal complications that include arachnodactyly, pectus deformities, and scoliosis. However, congenital contractural arachnodactyly usually presents with multiple joint contractures and crumpled ear helices. There is the occasional finding of aortic root dilation; in addition, eye involvement can be seen.[22]

## LOEYS-DIETZ SYNDROME

Loeys-Dietz syndrome is a recently described autosomal dominant connective tissue disease associated with arterial aneurysms and dissections and other systemic involvement.[23,24] Importantly, aortic dissection can occur at diameters smaller that those observed in MFS.[23,25] The genes for the transforming growth factor–β receptors 1 and 2 are the only currently known genes involved in this disorder.[24] Loeys-Dietz syndrome is characterized by the clinical triad of arterial tortuosity and aneurysms; hypertelorism; and bifid uvula or cleft palate or uvula with a wide base or prominent ridge. Aneurysms occur in the aortic root but are also commonly found in other arteries. The arterial tortuosity most commonly affects the head and neck vessels.

Specific diagnostic criteria for Loeys-Dietz syndrome have not been established. Typically, the diagnosis is rendered when a patient has findings from some of the commonly affected organ systems in addition to identification of a disease-causing mutation on genetic testing. The four main groups of clinical findings are vascular, skeletal, craniofacial, and cutaneous (Box 39-4).[23] We recommend genetic testing on patients with aortic root dilation who have any features from the other main groups of clinical findings. Some patients with aortic dilation and dissection have mutations in the transforming growth factor–β receptor 1 and 2 genes without other features of Loeys-Dietz syndrome. These patients fall in the category of thoracic aortic aneurysms and dissections and are discussed subsequently. Consideration should be given for genetic testing in families with multiple members with only aortic or other arterial dilation. Finally, it is reasonable also to consider genetic testing for transforming growth factor–β receptor 1 and 2 mutations in patients who have had aortic dissection at diameters less than 5 cm, unless another causative condition is identified.

Loeys-Dietz syndrome is often divided into two subtypes. Patients with Loeys-Dietz syndrome type I (around 75% of patients with Loeys-Dietz syndrome) do not typically have cutaneous abnormalities. Loeys-Dietz syndrome type II constitutes the remaining patients and does not typically have craniofacial findings, with the exception of isolated bifid uvula. Considerable overlap is found between the subtypes, and they are considered part of the same clinical continuum.

The most important complication in Loeys-Dietz syndrome is aortic root dilation and dissection. The mean age of death in the original case series was 26 years.[23] Nearly all patients had aortic root aneurysms that lead to dissection. As noted previously, dissection can occur at aortic dimensions that are not considered high risk in MFS (less than 5.0 cm), and dissections have been reported in infancy and early childhood. Around half of patients with Loeys-Dietz syndrome have dilation or tortuosity in the arterial tree away from the aortic root. Notably, these

**Box 39-4**

### CLINICAL FEATURES OF LOEYS-DIETZ SYNDROME

**Vascular**
- Aortic root dilation and dissection
- Distal arterial aneurysms and tortuosity

**Skeletal Manifestations**
- Pectus excavatum or carinatum
- Scoliosis
- Joint laxity
- Arachnodactyly
- Talipes equinovarus

**Craniofacial Features**
- Ocular hypertelorism
- Bifid uvula (or uvula with a wide base or prominent ridge)
- Cleft palate
- Craniosynostosis

**Cutaneous Features**
- Translucent skin
- Easy bruising
- Dystrophic scars

**Other**
- Females are at risk for uterine rupture during pregnancy

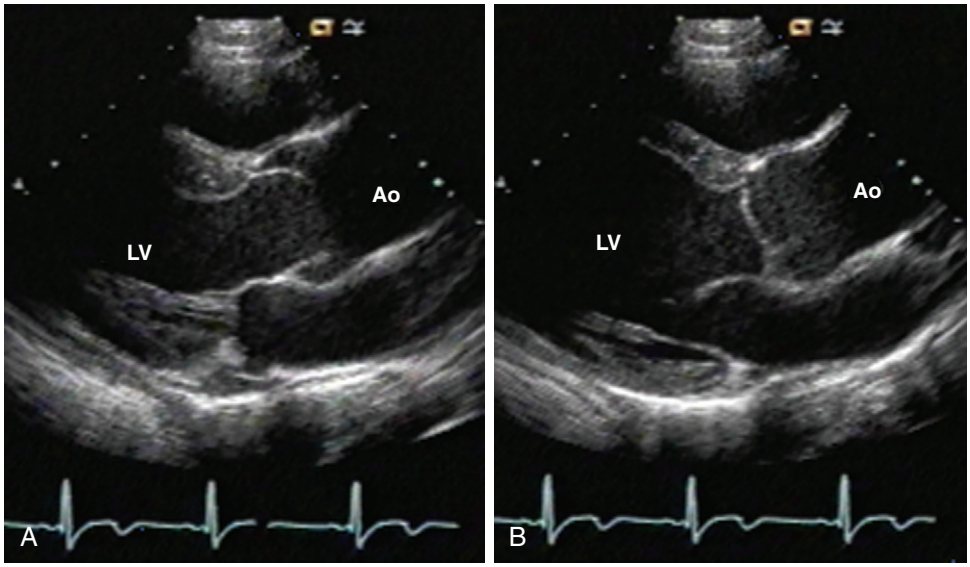



**Figure 39-1 Bicuspid aortic valve. A,** Parasternal long-axis view during systole shows doming of the aortic valve leaflets, effacement of the sinotubular junction, and dilation of the aortic root. **B,** Parasternal long-axis view during diastole shows eccentric valve leaflet closure and dilation of the sinus of Valsalva. *Ao,* Aorta.

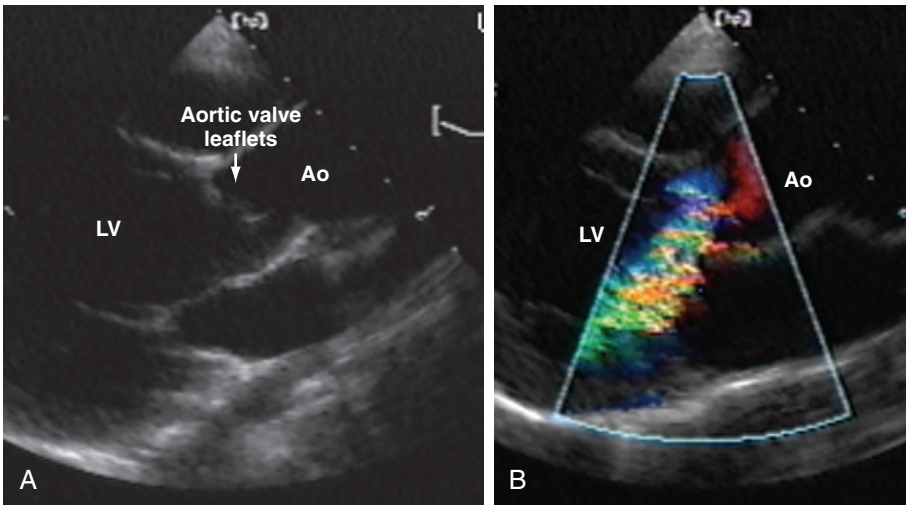



**Figure 39-2 A, A 10-year-old with Loeys-Dietz syndrome and severe aortic regurgitation from a bicuspid aortic valve and severe aortic root dilation.** Parasternal long-axis view of the thickened aortic valve leaflets, dilated LV, and aneurysm of the aortic root. **B,** Parasternal long-axis view of the severe jet of aortic regurgitation from the combined aortic valve and aortic root pathologic processes. *Ao,* Aorta.

distal lesions are not detected with echocardiogram. These vascular features differentiate the vascular disease in Loeys-Dietz syndrome from MFS. Additional cardiac malformations include patent ductus arteriosus, atrial septal defects, and bicuspid aortic valve.

## BICUSPID AORTIC VALVE

Bicuspid aortic valve is the most common form of congenital heart disease and affects between 0.5% and 2% of general population.[26] Clinical studies have identified a 9% prevalence rate of bicuspid aortic valve in first-degree relatives, which validates the inherited basis of this condition.[27,28] Interestingly, first-degree relatives have also been identified with aortic dilation in the absence of a bicuspid aortic valve.[29]

Patients with a bicuspid aortic valve are at increased risk of aortic aneurysm and dissection (Fig. 39-1). This appears to be a result of pathologic changes in the aortic wall that include decreased fibrillin-1, loss of elastic fibers, increased apoptosis, and altered smooth muscle cell alignment.[30] Patients with a bicuspid aortic valve have larger aortic annulus, sinus, and ascending aortic dimensions and an increased rate of aortic dilation over time (Fig. 39-2). Up to 15% of aortic dissections may occur in individuals with a bicuspid aortic valve.[31] Historically, the term poststenotic dilation was used as a hemodynamic explanation for the finding of aortic dilation in the presence of a bicuspid aortic valve. However, this relationship is now understood in fact to be the result of aortic pathology that is independent of the aortic valve disease itself.[32,33] The increased risk of aortic dissection in patients with a bicuspid valve is limited to a small group of the overall population of patients with a bicuspid valve.[34,35] Even after valve replacement, surgery for a bicuspid valve is a strong risk factor for subsequent aortic dissection. Thus it is likely that the concomitant finding of a bicuspid aortic valve and aortic aneurysm and dissection is a manifestation of what is the general class of systemic connective tissue disorders.[36]

Although multiple factors have been implicated in aortic dissection,[37] little is known of why or how a bicuspid aortic valve predisposes to aneurysm formation and dissection. In an

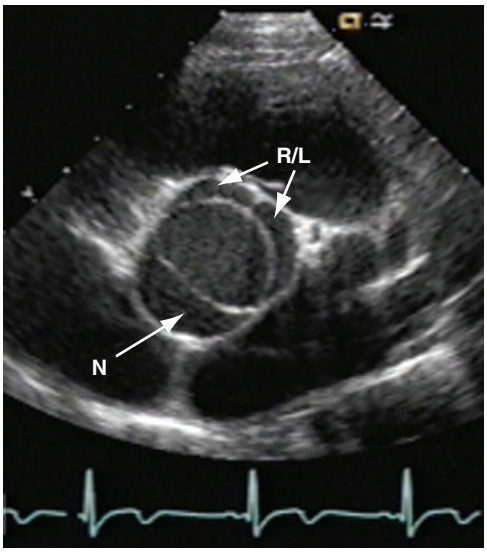



**Figure 39-3 Parasternal short-axis view of a patient with a dilated aortic root and associated bicuspid aortic valve.** The valve pathology is the result of fusion of the left (*L*) and right (*R*) coronary cusps. A raphe is noted between the left and right cusps. *N,* Noncoronary cusp.

attempt to address this question, Schaefer and associates[38] described differences in aortic dimensions and elasticity between different phenotypes. They found that subjects with type 1 bicuspid aortic valve (anterior-posterior leaflet orientation, with or without a raphe in the position demarcated by the left and right coronary cusps) had a larger dimension and increased wall stiffness at the sinuses of Valsalva (Fig. 39-3) than those with type 2 bicuspid aortic valve (right-left leaflet orientation, with or without a raphe in the position demarcated by the right and noncoronary cusps). The mechanism for these differences may be that the composition and elastic properties of the aortic wall are genetically related to aortic valve morphology. Hemodynamic differences may also contribute, with genetic upregulation altered by flow and force exerted on the aortic wall dependent on aortic valve morphology.

## TURNER SYNDROME

Patients with Turner syndrome are at high risk for the identification of left heart pathology, particularly a bicuspid aortic valve and coarctation of the aorta.[39] In addition, those with Turner syndrome have a higher incidence of systemic hypertension (even in the absence of anatomic cardiac pathology). Aortic dissection occurs in about 1.4% of patients with Turner syndrome,[40] and dissection often occurs at a young age (mean, 30 years).[41] Approximately 80% to 90% of those with aortic dissection have either systemic hypertension or a bicuspid aortic valve. Criteria with which to assign risk have been difficult to ascertain, particularly because most criteria are based on somatic growth (height, weight, body surface area). Because patients with Turner syndrome also have short stature, the general determinants of the relationship between somatic growth and expected aortic dimension remain problematic. For this reason, the definition of normal aortic size, especially in the presence or absence of potentially confounding factors (hypertension, bicuspid aortic valve, and coarctation of the aorta), is unclear. The general adult guidelines for the prediction of heightened risk for aortic dissection[42] in those with Turner syndrome and aortic dilation remain to be determined. In addition, the relative aortic dimensions when aggressive pharmacologic or surgical intervention should be instituted remain unclear. The presence of a generalized vasculopathy in those with Turner syndrome is well described and is characterized by aortic wall stiffness, arterial dilation, vessel wall thickening, and abnormal pulse wave propagation.[43] Because patients with Turner syndrome without aortic pathologic findings or systemic hypertension are found to have isolated aortic dilation, an intrinsic aortopathy is suggested to be a primary phenotypic feature of this condition.

A recent cross-sectional study of girls with Turner syndrome less than 18 years of age revealed a number of interesting echocardiographic findings.[44] When the group of subjects with Turner syndrome was compared with the control population, subjects with or without features that would be considered high risk (systemic hypertension, bicuspid aortic valve, coarctation or repaired coarctation of the aorta, or other organ system abnormalities, including renal or thyroid disease) had larger proximal aortas in almost all of the cases. The prevalence rates of individuals with Z-scores of 2 or more were 12% for the aortic annulus, 20% for the aortic root, 18% for the sinotubular junction, and 30% for the ascending aorta. These prevalence rates corresponded with increased relative risks of 4.8 to 12.0 times those of the control population. Even in the absence of a bicuspid aortic valve, patients with Turner syndrome had a larger aorta at the aortic root, sinotubular junction, and ascending aorta, suggesting that Turner syndrome alone predicts aortic dilation. The effect of a bicuspid aortic valve added incrementally to this independent effect of Turner syndrome on aortic dimension.

Although the data regarding aortic dilation in the presence of Turner syndrome raise obvious concerns regarding risk for dissection, additional work is needed to determine the gravity of this risk. Similarly, a better understanding as to the parameters relating dilation to dissection will allow us to develop treatment protocols appropriate to the specific features present in the individual patient with Turner syndrome. In the meantime, no global therapeutic guidelines are available. Most specialists caring for individuals with Turner syndrome therefore manage these patients in a manner similar to that of those with a bicuspid aortic valve.[45]

## FAMILIAL THORACIC AORTIC ANEURYSM AND DISSECTION

Up to 20% of patients without syndrome referred for repair of aortic aneurysm or dissection have a first-degree relative with a similar condition.[46,47] The diagnosis of familial thoracic aortic aneurysm and dissection is rendered based on the following criteria: progressive enlargement of the ascending aorta, positive family history of thoracic aortic aneurysm and dissection, and exclusion of syndrome causes of thoracic aortic aneurysm and dissection such as MFS, Loeys-Dietz syndrome, and Ehlers-Danlos syndrome. Recent work has indentified a genetic cause in some cases, with causative mutations thus far identified in genes for transforming growth factor–β receptors 1 and 2, smooth muscle cell–specific myosin heavy chain 11, and smooth muscle–specific alpha actin. Of note, patients with familial thoracic aortic aneurysm and dissection typically come to medical attention earlier than patients with spontaneous dissections or dilation but later than those with MFS or Loeys-Dietz syndrome.

## Histopathology

The fibrous structures of the heart are composed primarily of connective tissue proteins. These serve as a framework whereby the contractile myocardial tissue is structurally supported. Connective tissue also supports the underlying structure of the large blood vessels and valves. Collagen and elastin fibrils underlie the endocardial cells of the heart and blood vessels. Type I collagen fiber bundles make up the support structure for the atrioventricular valves and constitute the primary elements of the valvar fibrous rings. The major structural support of the large blood vessels is elastin and collagen types I and III; lesser amounts of types IV, V, and VI collagen also contribute to vessel wall integrity.

The aorta is comprised of three layers: the intima, media, and adventitia. The medial layer consists of concentric layers of smooth muscle cells, collagen, and elastin with extracellular matrix proteoglycans. In connective tissue disorders, dilation of the aortic root is caused by degenerative changes as a result of disruption and loss of elastin fibers, loss of smooth muscle cells, increase in collagen, and deposition of proteoglycans. This process has historically been termed cystic medial necrosis. However, because there is no true necrosis or cyst formation, the preferred terminology is medial degeneration. Molecular studies have identified some mechanisms that potentially underlie this process. Increased levels of matrix metalloproteinases, particularly matrix metalloproteinase-2 and matrix metalloproteinase-9, have been found in the medial layer of aortic aneurysms.[48-52] Matrix metalloproteinase-2 and matrix metalloproteinase-9 have elastolytic activity.

## Echocardiographic Findings

### AORTIC DILATION

The aortic root is comprised of the aortic valve annulus, the sinus of Valsalva, the sinotubular junction, and the ascending aorta. By convention, echocardiographic measurements of these regions are performed from the parasternal long-axis view at early systole (Fig. 39-4). The regions of the aortic arch are best viewed from the suprasternal notch (Fig. 39-5).

In addition, the aortic valve and ascending aorta may be imaged in children from the subcostal imaging plane (Fig. 39-6). In the presence of a connective tissue disorder, dilation may occur at any position along the aortic root and throughout the descending thoracic and abdominal aorta. However, the most typical sites of dilation encompass the sinus of Valsalva, sinotubular junction, and proximal ascending aorta. These sites develop the most significant pathology in that their position subjects them to the highest sheer stresses as a result of pulsatile expansion during systole.[53] Effacement of the sinotubular junction is a common finding, in which the sinotubular junction and proximal ascending aorta develop a flattened appearance and have essentially the same diameter as the sinus of Valsalva (see Fig. 39-6, *D*). The term *effacement* is qualitative and is not associated with defined measurements. In fact, effacement encompasses a spectrum of findings, initially manifest subtle changes in the natural tendency for the sinotubular junction to abruptly change direction and caliber at the onset of the proximal ascending aorta. As the severity of effacement progresses, there is a progressive transition to a morphologic pattern characterized by a constant caliber of vessel from the sinus of Valsalva through the proximal ascending aorta.

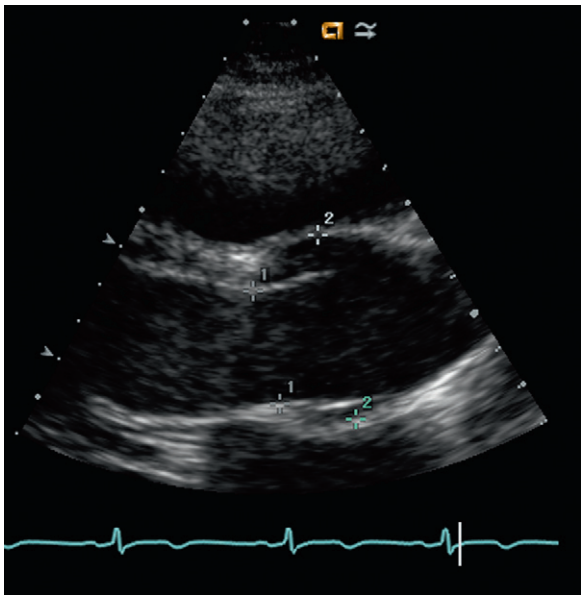


**Figure 39-4 Aortic sinus measurements.** Imaging of a 12-year-old with Marfan syndrome performed in the parasternal long-axis plane. The patient has severe dilation of the sinus of Valsalva (#2: 4.39 cm; 4.2 Z-scores) and normal aortic valve annulus (#1:2.7 cm; 1.6 Z-scores).

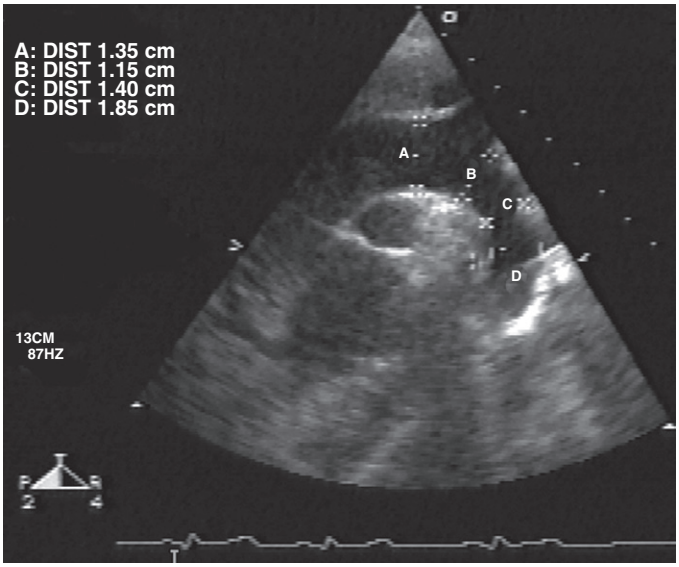



**Figure 39-5 Aortic arch imaging from the suprasternal long-axis imaging plane at end-systole.** Image shows the appropriate locations for measurement: the distal ascending aorta (*A*), just before the innominate artery; the transverse aorta (*B*), between the innominate artery and the left carotid artery; the aortic isthmus (*C*) just before the left subclavian artery; and the proximal descending aorta (*D*) just beyond the left subclavian artery.

In addition, as the severity of aortic root dilation worsens, aortic regurgitation can develop. This results from either asymmetric dilation of one or more cusps or generalized dilation at the aortic valve annulus. Either mechanism has the potential to alter the geometry of the aorta in such a manner that regurgitation develops (Figs. 39-7 and 39-8). In those situations in which the thoracic aorta cannot be imaged completely with TTE imaging, TEE should be used. Studies suggest that TEE is comparable with computed tomographic scan in defining thoracic aortic aneurysms.

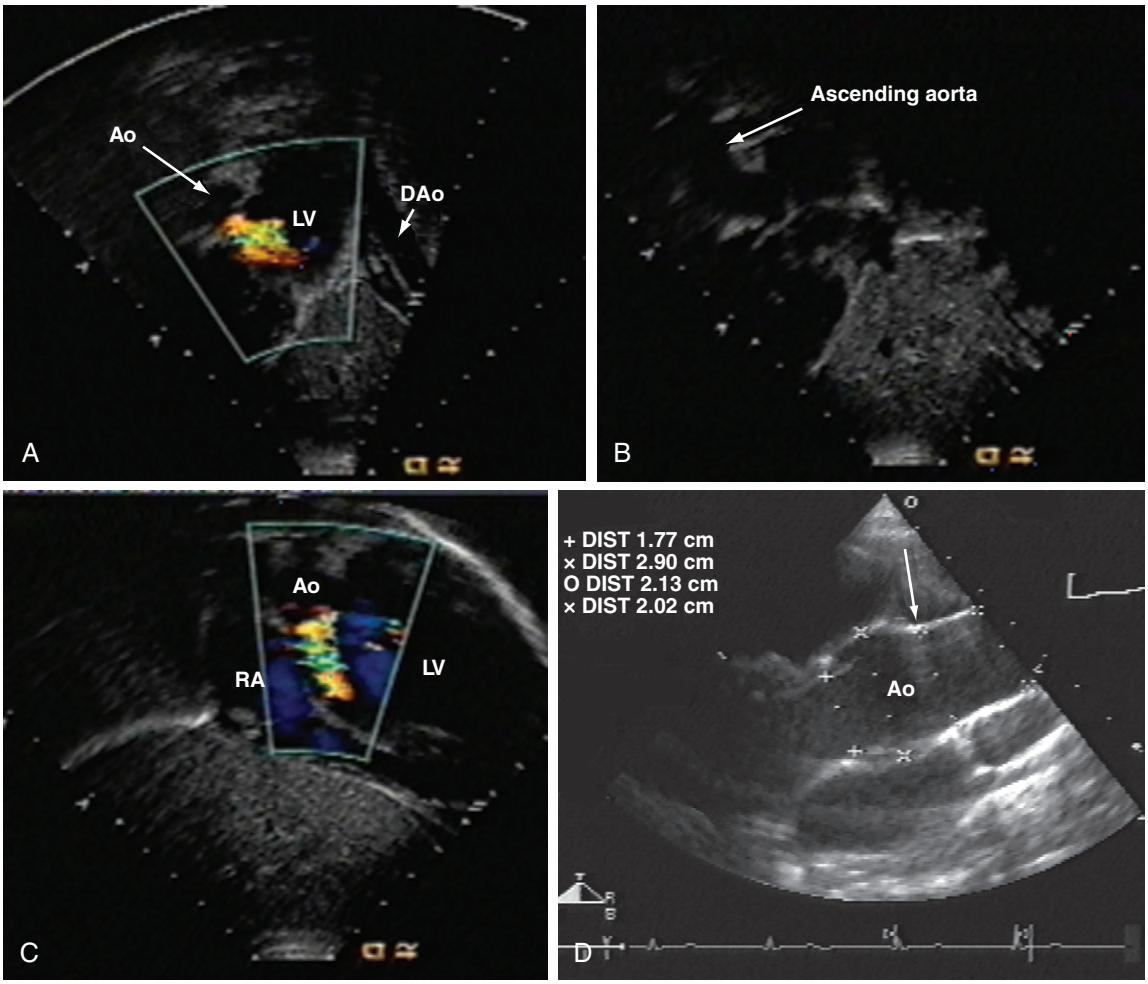



**Figure 39-6** **A 3-year-old with a transforming growth factor–β receptor mutation. A,** Subcostal short-axis imaging identifies moderate aortic regurgitation from dilation of the aortic root. **B,** Subcostal short-axis imaging allows visualization of the left ventricular outflow tract through the ascending aorta. **C,** Subcostal long-axis imaging of moderate aortic regurgitation. **D,** Image shows dilation of the aortic root resulting in effacement of the sinotubular junction *(arrow). DAo,* Descending aorta.

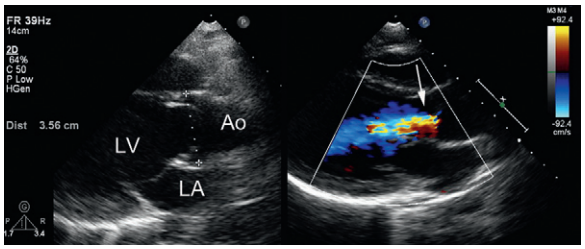



**Figure 39-7** **Aortic regurgitation due to aortic dilation.** *Left:* Parasternal long-axis imaging of a 16-year-old female with an mildly dilated aortic sinus of Valsalva, measuring 3.56 cm (2.8 Z-scores). *Right:* Color Doppler imaging demonstrating moderate aortic regurgitation (*arrow*) in the same patient. *Ao,* Aorta.

The normal adult abdominal aorta measures 2.0 cm at the level of the celiac trunk and 1.8 cm just below the renal arteries. Tapering occurs as the aorta approaches the level of the iliac arteries. Most abdominal aortic aneurysms form between the renal and iliac arteries. Clinically significant abdominal aortic aneurysms measure more than 4.0 cm in diameter. High degrees of sensitivity and specificity should be expected from abdominal ultrasound/echocardiography, but excessive body habitus can occasionally hamper complete visualization. In these cases, abdominal aortic angiography, computed tomographic scan, or aortic magnetic resonance imaging should provide data with which to achieve a definitive diagnosis.

Aortic aneurysms are classified as either true or false (pseudoaneurysm). A true aneurysm involves weakening and dilation of the entire vessel wall. A pseudoaneurysm occurs when a full thickness defect in the aortic wall allows blood to circulate out of the confines of the artery. The circulating blood is contained by the surrounding soft tissues. The most common etiologies for a true aneurysm include atherosclerosis, medial degeneration, and aortic dissection. Pseudoaneurysms are often the result of trauma or infection (e.g., endocarditis). Sinus of Valsalva aneurysm is associated with a number of secondary phenomena. The expansion of the aneurysm typically takes the path of least resistance into the right heart structures. Affected sites can include aortic valve leaflet distortion and aortic regurgitation, coronary artery occlusion, right ventricular outflow tract obstruction, tricuspid regurgitation, obstruction of the right pulmonary artery, and descending aortic obstruction.[54,55] With two-dimensional (2D) echocardiography, the dilated sinus can be elucidated.

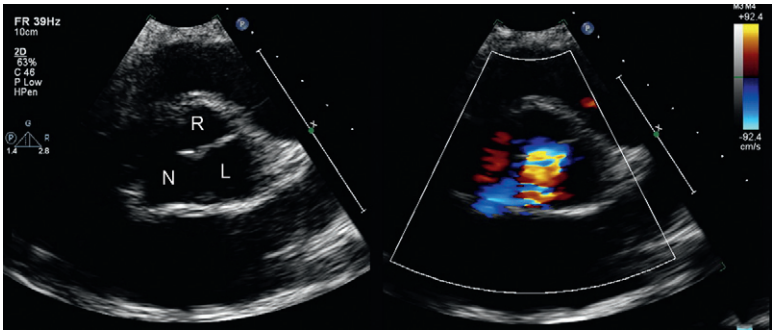



**Figure 39-8 Functional aortic regurgitation in short axis views.** *Left:* Parasternal short-axis imaging of the aortic valve in the patient from Figure 39-10 showing the right (*R*), left (*L*) and noncoronary (*N*) leaflets in diastole. *Right:* Color Doppler imaging showing the central aortic regurgitant jet.

## AORTIC DISSECTION

Patients with acute aortic dissection need emergent assessment and therapy. Prompt diagnosis is crucial to differentiate these patients from those with worrisome symptoms from more benign conditions. Mortality rate is estimated at about 1% per hour in the first 48 hours for those patients who survive to reach an acute care setting.[56] In addition to providing a diagnosis, the details of anatomy and physiology are vital to care. These include classification of the dissection, definition of the site of rupture, detection of extravasation, assessment of aortic regurgitation, and assessment of side-branch involvement.[57] TTE provides a rapid and readily accessible diagnostic tool and, in many cases, can answer all of the previous questions. TTE is frequently diagnostic in the detection of proximal aortic root dissection by revealing a progressively enlarging aortic root. In addition, the presence of a dissecting hematoma is oftentimes identified.[58] See Chapter 36 for a complete discussion of the echocardiographic features of aortic dissection.

## OTHER AORTIC ARCH MANIFESTATIONS

In addition to the natural history of aortic dilation and dissection that occurs in a subset of patients with connective tissue disorders, pathologic dilation can occur after aortic root surgery. In a study of patients with MFS, a retrospective analysis was performed based on presence or absence of prior elective aortic root surgery.[59] Multivariate analysis showed that a previous elective aortic root surgery was associated with a fourfold increased risk of subsequent dilation of the descending aorta. In addition, an increased descending aortic diameter was associated with a higher risk of aortic root dissection, independent of the diameter of the aortic root itself. These authors raised a cautionary flag in that only 37% of their patient population had complete measurements obtained at all aortic levels, suggesting the possibility that a large number of patients with a dangerous degree of aortic dilation are going undetected even when imaging studies are performed.

## MITRAL VALVE PROLAPSE

Mitral valve prolapse is defined as the displacement of abnormally thickened and redundant mitral valve leaflets into the left atrium during systole (Figs. 39-9 and 39-10). This geometric change in the integrity of the valve can result in poor coaptation and resultant mitral regurgitation. Mitral regurgitation eventually leads to left atrial and, subsequently, left ventricular dilation, which in-and-of itself worsens the degree of regurgitation.

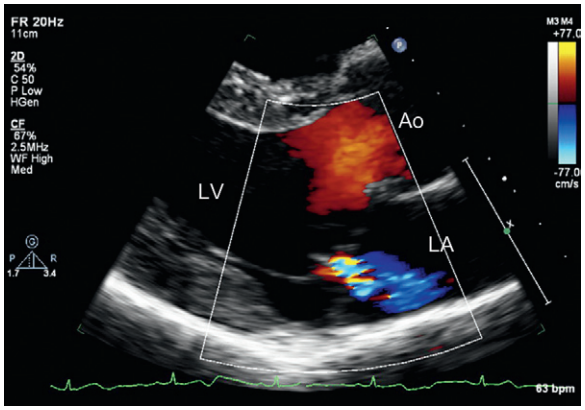



**Figure 39-9 Mitral valve prolapse.** Parasternal long-axis view of the mitral valve during systole shows redundant chordae, buckling of the anterior and posterior mitral valve leaflets, and resultant mitral valve prolapse and mitral regurgitation. The mitral valve leaflets are displaced in a posterosuperior direction into the LA. *Ao,* Aorta.

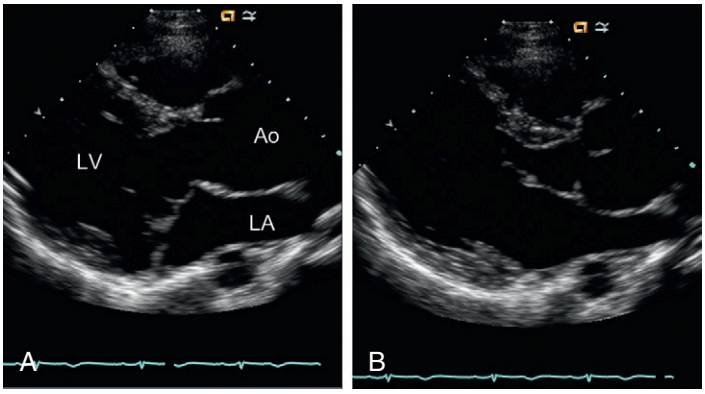



**Figure 39-10 Mitral valve prolapse. A,** Parasternal long-axis view of the mitral valve at end-systole shows buckling of the anterior and posterior mitral valve leaflets and resultant mitral valve prolapse. **B,** Parasternal long-axis view of the mitral valve at end-diastole shows thickening of the anterior and posterior mitral valve leaflet tips. *Ao,* Aorta.

Echocardiography is the current gold standard for the diagnosis and evaluation of mitral valve prolapse. Echocardiographic criteria have been established for the detailed assessment of the mitral valve; mitral valve prolapse is now defined as displacement of one or both leaflets by greater than 2 mm above the mitral annulus in the parasternal long-axis or apical long-axis view. Mitral valve prolapse is most accurately diagnosed from the parasternal views; apical imaging provides only confirmatory information and cannot be used for diagnosis without the presence of prolapse in the parasternal long-axis plane.

Mitral valve prolapse is further divided into classic and nonclassic forms: classic is defined as leaflet thickness of more than 5 mm; in the nonclassic form, the leaflets are less than 5 mm. Complications of endocarditis or the development of severe mitral regurgitation are more typically seen in the classic form of the disease.[60] The connective tissue disorders are more commonly associated with redundancy of the mitral valve leaflets, resulting in mitral valve prolapse. This is in distinction to mitral valve prolapse in the adult population caused by calcific disease in which the leaflets are less redundant but more thickened.

Evaluation of the valve has been greatly enhanced since the introduction of three-dimensional (3D) imaging. Although mitral valve prolapse is typically sporadic, it is also associated with disorders of connective tissues, including MFS, Ehlers-Danlos syndrome, osteogenesis imperfecta, and the MASS phenotype (defined previously). Because the association of MFS and mitral valve prolapse is common, the suspicion arose that isolated mitral valve prolapse might be the result of a mutation of fibrillin-1.[61] However, this association has never been established.

Mitral valve prolapse is the most prevalent valve abnormality in MFS, with a reported prevalence rate of greater than 35%.[62] It is important to recognize that surgical repair of mitral regurgitation can exacerbate aortic dilation after surgery as a result of the increased hemodynamic stresses on the aorta.

### *Left Ventricle*

Although aortic arch and mitral valve disease are most commonly seen in the presence of connective tissue disorders, abnormalities of left ventricular systolic and diastolic function are beginning to be elucidated.

#### Diastolic Function

With both cardiac magnetic resonance imaging and echocardiography, left ventricular diastolic function has been evaluated in a number of small studies. Impaired left ventricular diastolic function has been demonstrated with echocardiographic identification of an increase in deceleration time and an increase in isovolumic relaxation time; these findings were attributed to impaired elastic recoil.[63] An unusual pattern of transmitral flow was seen in which decreased ventricular compliance (decreased deceleration time) and reduced myocardial relaxation both occur.[64] With tissue-Doppler imaging, a prolongation of the early filling phase with reduced velocities at the mitral annulus (Ea) has been shown, which suggests that myocardial tissue relaxation is impaired.[65]

Echocardiographic data obtained in children as young as 3 years of age with MFS show early left ventricular diastolic function (relaxation) impairment.[63] More recently, in a study of 40 children and young adults with MFS compared with healthy age-matched controls, echocardiographic indices of left ventricular diastolic function (including prolonged deceleration time and isovolumic relaxation time and decreased mitral E/A ratio) also suggested impaired relaxation.[66] The presence early in life of increased myocardial stiffness, followed later in life by the development of aortic wall stiffness as the aorta distends,[67] may together contribute to the development of left ventricular systolic and diastolic dysfunction.

#### Systolic Function

Reduced systolic contractility in MFS has been thought to be solely a secondary phenomenon from associated aortic or mitral valve regurgitation. However, it has been suggested that, in the absence of valvular heart disease, subtle findings suggest that left ventricular systolic contractility is adversely affected. A small series from the Mayo Clinic showed no significant deterioration in ejection fraction and left ventricular end-systolic and end-diastolic dimensions; in addition, this study followed these parameters serially over a 10-year period without obvious changes developing longitudinally.[68] However, these findings differed from a more recent large-scale study of 234 adults with MFS. Although none of the patients met criteria for dilated cardiomyopathy, a small subset of the patients did show increased left ventricular end-systolic and end-diastolic dimensions, with an associated mild deterioration in ejection fraction.[69] In additional, meridional wall stress was similar between patients and controls; this suggests that, as opposed to an alteration in afterload causing left ventricular impairment, more likely the observed differences were from primary left ventricular contractile dysfunction.

The pathogenesis of left ventricular systolic and diastolic dysfunction in patients with MFS is incompletely understood but is likely the result of the primary structural and functional disorder in the fibrillin-1 protein. Microfibrils, which act as scaffolding for the formation of elastic fibers and contribute to their function, play an important role in mediating elastic recoil. These microfibrils contain the protein fibrillin-1 as one of their primary components. In that mutations in fibrillin-1 interfere with microfibril function, this in turn is predicted to lead to impairment of left ventricular diastolic elastic recoil.

### *Pulmonary Artery*

As opposed to the well-defined left heart pathology, abnormalities of the right heart are less well recognized. Dilation of the main pulmonary artery does occur, and serial echocardiographic measurements should be obtained. In the adult population, good correlation has been found between progressive dilation of the aortic root and main pulmonary artery.[70] However, dangerous pulmonary artery pathology from pulmonary artery aneurysm or dissection has not been reported, and the clinical significance of this finding requires further clarification. The population with associated pulmonary hypertension may be at risk given the expected abnormal increase in tensile stress thus placed on the pulmonary artery.

## Natural History

Of the connective tissue disorders described in this chapter, MFS is by far the best understood. Most patients with MFS present with ascending aortic dilation or dissection. Rarely does a patient present with a type B dissection of the descending thoracic aorta. However, there is evidence that identification of progressive descending aortic dilation predicts the eventual development of dissection in this region.[59] For this reason, even in the absence of significant ascending aortic dilation, recommendations have been made that serial assessment include careful monitoring of the entire aorta (from the level of the aortic valve to the abdominal aorta).

A distinct (and typically severe form) of MFS can be seen early in life; it is termed infantile MFS. Polyvalvar disease is common, most often resulting in mitral valve prolapse with associated marked mitral regurgitation and severe skeletal and pulmonary emphysematous changes. Congestive heart failure and respiratory compromise often lead to early death.[71]

The pregnant woman with MFS is at increased risk for aortic dissection, although the risk is low when the aorta is less than

**TABLE 39-1 Summary of Clinical and Echocardiographic Findings for the Most Common Forms of Connective Tissue Disorders**

| | *Affected Cardiac Structures* | *Characteristic Findings* | *Functional Sequelae* | *Prevalence* |
|---|---|---|---|---|
| Marfan syndrome | • Mitral valve<br>• Aortic root<br>• Ascending aorta | • Mitral valve prolapse<br>• Tricuspid valve prolapse<br>• Dilation of the aortic root | • Mitral regurgitation<br>• Aortic regurgitation<br>• Susceptibility to dissecting aortic aneurysm | 3:10,000 |
| Ehlers-Danlos, type IV | • Aortic root<br>• Large and small arteries | • Large and small arterial aneurysm<br>• Arteriovenous fistulae | • Aortic regurgitation<br>• Susceptibility to dissecting aortic aneurysm<br>• Dissection often spontaneous | ~1:250,000 |
| Bicuspid aortic valve | • Aortic valve<br>• Ascending aorta | • Aortic valve dysfunction<br>• Dilation of the ascending aorta | • Aortic regurgitation<br>• Aortic stenosis<br>• Ascending aortic dissection | ~1:100 |
| Loeys-Dietz syndrome | • Aortic arch | • Arterial tortuosity | • Aortic dissection (possibly at a smaller aortic diameter than with Marfan syndrome) | Unknown |
| Turner syndrome | • Aortic valve<br>• Ascending aorta<br>• Thoracic aorta | • Bicuspid aortic valve<br>• Coarctation of the aorta<br>• Dilation of the ascending aorta<br>• Hypertension | • Aortic stenosis<br>• Aortic regurgitation<br>• Ascending aortic dissection | ~1:2000-5000 live-born females |
| Thoracic aortic aneurysm and dissection syndrome | • Thoracic aorta | • Dilation of the aortic root<br>• Aneurysm of the thoracic aorta | • Ascending aortic dissection<br>• Descending thoracic aortic dissection | Unknown: aortic aneurysms result in 15,000 US deaths/y |

4.0 cm.[72] Echocardiograms should be performed serially throughout the pregnancy, especially during the third trimester when growth acceleration can occur.

In general, annual TTE assessment is recommended in patients with mild to moderate aortic dilation, so long as these findings have been stable. The major exception is for patients with Loeys-Dietz syndrome in whom TTE should be performed every 6 months and magnetic resonance angiograms (from head to pelvis) yearly. In young children, and in those who have severe disease, serial echocardiograms on a 6-month basis are recommended. Conversely, in individuals without aortic dilation, but with other features suggestive of a connective tissue disorder or a strong family history, echocardiograms are generally performed every few years until adulthood. Patients who manifest rapidly progressive disease and are thus approaching criteria for surgical intervention are followed at a minimum of every 6 months. This is generally accepted as growth approaching 5 mm every 6 months. Table 39-1 summarizes the clinical cardiac and echocardiographic features found in the most common connective tissue disorders. In addition, the prevalence of these connective tissue conditions in the general population is reviewed.

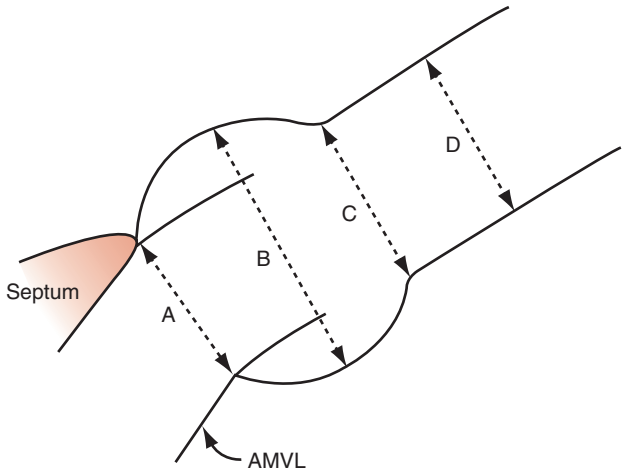



**Figure 39-11 Aortic root measurements on echocardiography.** Schematic shows the aortic valve annulus (*A*), sinus of Valsalva (*B*), sinotubular junction (*C*), and proximal ascending aorta (*D*), Measurements are obtained at early systole in children and at end-diastole in adults. *AMVL*, Anterior mitral valve leaflet.

## METHODS OF ASSESSMENT

Standard 2D imaging remains the screening tool for the assessment of valve morphology and for the measurement of aortic dimensions. The precision of this assessment is operator-dependent and is also mitigated by image quality (primarily because of issues of patient body habitus). Oblique measurements of the aorta can overestimate actual dimensions, as occurs for an aortic diameter that is not drawn perpendicular to the aortic flow center line. These measurements are typically acquired from the parasternal long-axis view, the long-axis view of the suprasternal notch, and the subcostal plane. Some laboratories measure the sinus of Valsalva with M-mode. Although this can provide reproducible and accurate measurement data, we recommend all measurements from 2D imaging with data acquired at early systole. The aortic valve annulus, sinus of Valsalva, and sinotubular junction (and the proximal aspect of the ascending aorta) are obtained from the parasternal long-axis view (Fig. 39-11), and the distal ascending aorta (just before the takeoff of the innominate artery), the transverse aortic arch, and the aortic isthmus are measured from the suprasternal notch (Fig. 39-12). In some individuals, the proximal descending aorta can be imaged from the parasternal window. In the pediatric population, it is common to obtain suitable images to visualize the distal thoracic aorta and abdominal aorta from the subcostal imaging plane (Figs. 39-13 and 39-14). Each of these areas should be imaged with aortic measurement in every patient who comes through the echocardiography laboratory.

Imaging of the valves can be enhanced with the acquisition of 3D data. With the availability of live 3D imaging, valve structure and function information can now be obtained in such a manner that immediate decisions can be made regarding the nature of the pathologic process. Although 3D imaging can also

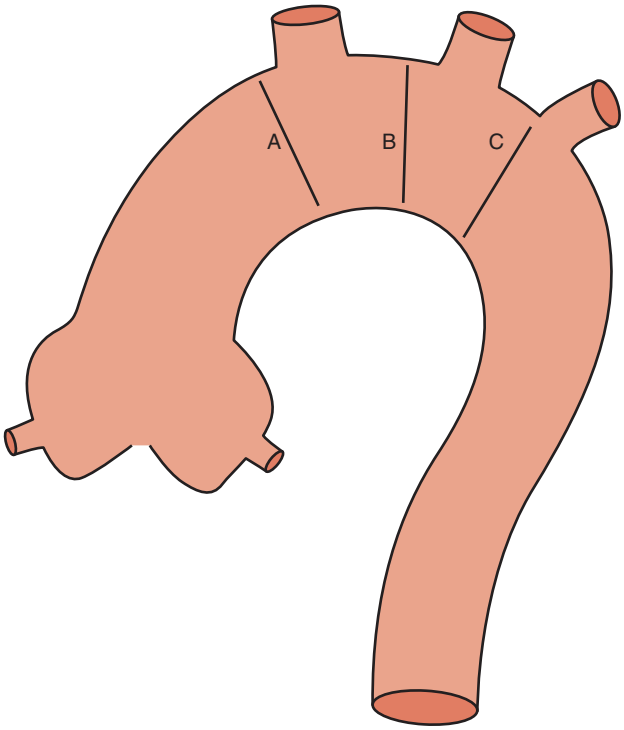



**Figure 39-12 Aortic arch measurements.** In the suprasternal long-axis–imaging plane measurements are obtained of the distal ascending aorta (*A*) just before the innominate artery, the transverse arch (*B*) between the innominate artery and the left carotid artery, and the aortic isthmus (*C*) just before the left subclavian artery.

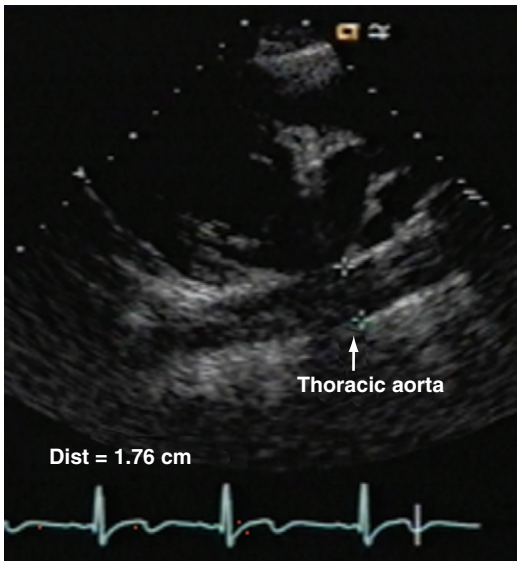



**Figure 39-13 Descending thoracic aorta.** Subcostal long-axis view shows the preferred location at which to measure the distal descending thoracic aorta.

be used for the acquisition of aortic arch images, this requires unique operator skills. Therefore, many laboratories obtain valve data with 3D imaging on a relatively frequent basis, but acquisition of 3D volume rendered images of the aortic arch are less common.

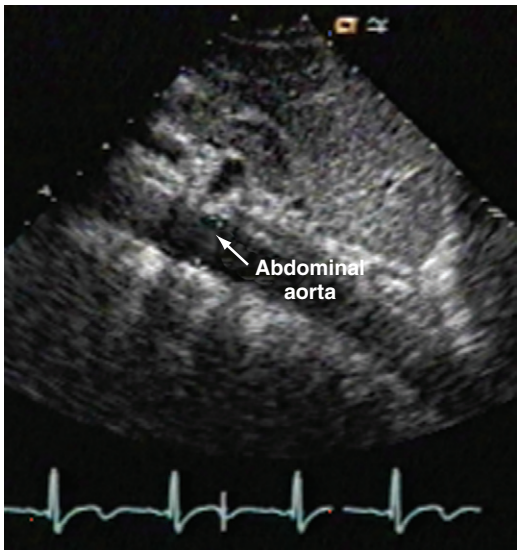



**Figure 39-14 Subcostal long-axis view.** Image shows the preferred location at which to measure the descending aorta inferior to the diaphragm.

Normalization of aortic measurements is an important aspect surrounding accurate data interpretation. Dependence on the accuracy of these normalized data is particularly acute in the pediatric population, where rapid changes occur during growth. Because of the prognostic significance of aortic measurements in patients with connective tissue disorders, aortic dimensions have been extensively studied with 2D echocardiography. Normal values have been reported for children and adults based on a range of indices, including age, body surface area, and height.[73-78]

In a study of 52 healthy infants and children (aged 1 month to 15 years) and 135 healthy adults (20 to 74 years), the aorta was measured at end-diastole in the parasternal long-axis view at four levels: aortic annulus, sinus of Valsalva, sinotubular junction, and proximal ascending aorta at its maximal dimension. Of note in this study, 2D measurements at the sinus of Valsalva were larger than those obtained with M-mode. When 2D values were normalized on M-mode nomograms, falsely diagnosed aortic dilation was found in 40% of healthy children and adults.[75]

Rigorous decisions are critical regarding which set of data is used as the standard in any individual echocardiography laboratory. Once a published dataset has been agreed on and implemented, all subsequent patient studies should be normalized with the same criteria. In the situation in which patients are plotted against differing normal datasets, wide variation in divergence from the norm can occur. As opposed to the use of published datasets, some groups have relied on either internally derived normal controls or unpublished data obtained from large institutional studies.[79]

The pediatric patient with marked aortic dilation oftentimes presents a difficult clinical dilemma. Although the aorta may be 50% to 75% larger than predicted when normalized for body surface area, little data are available to assign a definitive risk for the short-term development of aortic dissection. Each medical center approaches this problem in various ways, with no universally agreed-on algorithm. In an attempt to better

predict pediatric risk for aortic dissection, noninvasive assessment of aortic wall dysfunction has been undertaken. In 19 pediatric patients with MFS, transthoracic M-mode tracings were used to calculate aortic elastic properties.[80] Significant differences from control patients were seen, with patients with MFS showing decreased aortic distensibility, increased aortic wall stiffness indices, decreased systolic diameter increase, and decreased maximum systolic area increase. Although this study did not attempt to predict future risk, further work of this type may allow use to provide better prognostic data for the pediatric population with connective tissue disorders.

### LIMITATIONS OF ASSESSMENT

Although transthoracic 2D and M-mode assessment are the most common methods for assessment of the mitral valve and aorta in patients with connective tissue disorders, a number of limitations are associated with these methods. Data acquisition is equipment and operator dependent. Measurements of aortic dimensions are affected by patient body habitus, and significant overestimate can be introduced into these measurements if oblique measurements are obtained.

Transesophageal echocardiography is a value tool in assessment of the aorta in those patients with difficult transthoracic acoustic images. In addition to the routine use as a tool to obtain accurate measurements of the aortic root, TEE can also be used to evaluate properties of aortic distensibility. Measurement of aortic distensibility, stiffness index, and pulsed-wave velocity can be obtained with M-mode data from the TEE short-axis view. Tissue-Doppler imaging has been applied to the evaluation of thoracic aortic elasticity in patients with MFS. Acceleration time, maximal wall expansion velocity, and wall strain were calculated from tissue-Doppler imaging tracings in 31 patients with MFS. Data derived from TEE imaging found that tissue-Doppler imaging data were complementary to M-mode, together serving as a significant predictor of progressive aortic dilation and eventual dissection.[81]

## Therapeutic Strategies

### PHARMACOLOGIC

Pharmacologic strategies for the connective tissue diseases are based on studies for patients with MFS. For the past two decades, the standard of care in the treatment for MFS with associated aortic dilation has been β-adrenergic blockade. The validation for this approach is based on longitudinal follow-up data that assessed the progression of aortic dilation with and without β-blocker therapy showing a beneficial response in a subset of these patients.[82] Treated patients showed slower aortic root growth, less risk of the development of aortic dissection, less common need for aortic surgery, and less mortality. This therapeutic strategy has been shown in adults as well as children.[83] Although therapy does not necessarily result in avoidance of aortic surgery altogether, in general, surgical intervention is forestalled. In addition, the presence of significant aortic dilation has been shown to be less amenable to β-blocker therapy than is the case for the earlier treatment of the patient with milder aortic dilation.[82] Some studies have shown improved ascending aortic stiffness associated with β-blocker therapy in patients with MFS,[84,85] and others have shown no effect, or worsening of indices of aortic stiffness.[86] The initiation of β-blocker therapy is typically based on a confirmed clinical diagnosis of MFS (based on the revised Ghent criteria) and the attainment of quantitative aortic root dilation. This is generally defined as the presence of aortic sinus of Valsalva dimensions as measured with echocardiography or magnetic resonance imaging with more than 2.0 Z-scores from the mean for body surface area.

**TABLE 39-2 Three-Year Study of Angiotensin-Converting Enzyme Inhibitor versus β-Blocker Therapy for Marfan Syndrome**

| *Variable* | *Enalapril* | *β-Blocker* | *P Value* |
|---|---|---|---|
| Mean initial aortic diameter (mm) | 33 ± 8 | 31 ± 6 | .7 |
| Mean initial % predicted aortic size | 118 ± 18 | 118 ± 14 | .7 |
| Mean change in aortic diameter (mm) during the study | 0.1 ± 1.0 | 5.8 ± 5.2 | <.001 |
| Aortic stiffness index | 8.0 ± 2.9 | 18.4 ± 3.8 | <.05 |
| Aortic distensibility ($cm^2/dynes^{-1}$) | 3.0 ± 0.3 | 1.9 ± 0.4 | <.02 |
| Aortic root replacement | 2 | 7 | |

Adapted from Yetman AT, Bornemeier RA, McCrindle BW: Usefulness of enalapril versus propranolol or atenolol for prevention of aortic dilation in patients with the Marfan syndrome. *Am J Cardiol* 95:1125-1127, 2005.

In patients intolerant of β-blocker therapy, either because of associated reactive airways disease or other side effects (e.g., fatigue or dizziness from hypotension), other pharmacologic strategies have been used to delay progressive aortic dilation. These include calcium channel blockers[83] and angiotensin-converting enzyme inhibitors. In a 3-year longitudinal study of patients with MFS, comparing therapy with β-blockers versus angiotensin-converting enzyme inhibitors, patients treated with the latter were shown to have less aortic dilation (Table 39-2).[87] In addition, with echocardiographic measurements, both aortic stiffness index and aortic distensibility improved with angiotensin-converting enzyme inhibitor therapy.

Recent data have suggested a role for the angiotensin-1 receptor blocker (ARB) losartan. Studies have shown that myxomatous mitral valve disease, aortic dilation, and impaired pulmonary alveolar septation, all features of the murine model of MFS, are mediated by excessive transforming growth factor–β signaling. Losartan has been hypothesized to delay aortic dilation due to its effect in inhibiting transforming growth factor–β signaling in the aortic wall. Treatment with losartan in a mouse model of MFS, which carries a fibrillin-1 mutation, showed histologic improvement in aortic wall elastic matrix architecture. In addition, there was echocardiographic evidence of reduced aortic growth in the losartan-treated group.[88] A limited, nonrandomized clinical study suggested that losartan may slow the rate of aortic dilation in children, but the patient numbers are too small to judge at present.[89] A multicenter randomized blinded clinical trial comparing the β-blocker atenolol with losartan for the treatment of aortic dilation in MFS is currently being conducted by the Pediatric Heart Network and National Institutes of Health.[90] Hopes are that this study will provide important therapeutic guidance for the medical management of patients with MFS. Losartan therapy suggests an exciting new line of investigation in that it uses a strategy that is directed at disease pathogenesis and may be the first step towards actual disease prevention.

As noted previously, treatment guidelines for other connective tissue disorders with aortic aneurysm typically follow MFS

guidelines. However, the effectiveness of this strategy has not been evaluated (i.e., no clinical trials have been performed). The main exception is that patients with Loeys-Dietz syndrome are often treated with ARBs, including losartan as a first-line therapy rather than β-blockers.

### SURGICAL

In adults with MFS, the threshold for consideration of aortic root replacement occurs when the diameter reaches 5.0 cm (Fig. 39-15).[42,91] A clearly established risk exists when the aortic dimension exceeds 6.0 cm, with a fourfold increase in the cumulative risk of aortic dissection or rupture.[42] Factors that are used to modify these parameters downward include rapid aortic growth (more than 0.5 cm per year), a family history of early aortic dissection (particularly at less than 5 cm), females considering pregnancy (prophylactic aortic root replacement if the diameter is more than 4.0 cm), and the associated finding of moderate or severe aortic regurgitation. However, some patients (even in the absence of factors that would place them at higher risk) have aortic dissection develop at a diameter of less than 5 cm.[91] For this reason, patient education regarding the symptoms of aortic dissection is crucial. It should be noted that thresholds for surgical intervention are typically based on the external aortic diameters such as reported from magnetic resonance imaging or computed tomographic scan, rather than the internal diameter typically reported with echocardiograms. The external diameter is typically 0.2 to 0.4 cm larger than the internal diameter.

In the younger pediatric population with MFS (before adolescence), identification of aortic pathology of such severity that surgical intervention must be considered is relatively uncommon. However, when this situation does exist, decisions surrounding timing of aortic surgery are complicated by the lack of adequate data to predict when the risk of aortic dissection has reached unacceptable levels. We suggest that the preadolescent child with a connective tissue disorder is a candidate for surgery with the following conditions:

1. Maximal normalized aortic dimension of more than 8 to 10 standard deviations above the mean for body surface area
2. Accelerating aortic growth (more than 5 mm per 6 months)
3. Family history of early aortic dissection
4. Additional pathologic lesion requiring intervention (i.e., aortic regurgitation, mitral regurgitation from mitral valve prolapse)

The actual decision to proceed with aortic surgery in the pediatric population is frequently based on less well-defined theoretic concerns. Oftentimes, a maximal aortic dimension of more than 8 to 10 standard deviations from than the mean (as listed previously) is accepted.

Surgical indications for non-MFS connective tissue disorders are considerably less well understood and mostly based on small case series. In general, we recommend, based on the currently available literature, that surgery for patients with aortic diameters 5.0 cm or greater, rapid aneurysm progression (more than 0.5 cm per year), or aortic diameters of 4.5 cm if surgery is being performed on the aortic valve. There are a few exceptions to this practice, which are discussed subsequently. Patients with Loeys-Dietz syndrome and transforming growth factor–β receptor 1 or 2 mutations are at risk for aortic dissection at aortic diameters less than 5.0 cm. Therefore, current guidelines recommend aortic repair at a measurement between 4.0 and 4.2 cm internal diameter in adults.[19] For children with severe systemic manifestations of Loeys-Dietz syndrome, surgery should be considered once the aortic diameter exceeds the 99th percentile for age and the aortic valve annulus reaches 1.8 to 2.0 cm, which allows for the placement of a graft that can accommodate future somatic growth.[19,25] A small number of aortic dissections have also been reported in patients with alpha actin 2 or myosin heavy chain 11 mutations at diameters less than 5.0 cm. Therefore, surgical consideration in these patients may be reasonable at aortic diameters between 4.5 and 5.0 cm. Finally, given the high complication rate and tissue friability, whether early prophylactic repair of aortic aneurysms in Ehlers-Danlos syndrome type IV (vascular form) is indicated is unclear.

Surgical intervention for aortic dilation typically takes the form of either a composite graft and associated valve replacement (Bentall technique)[92] or procedures performed when the aortic valve remains competent and therefore the valve is spared.[93,94] The results of aortic replacement in adults are encouraging. In a report on 675 patients with MFS who underwent aortic replacement, a 1.5% operative mortality rate was seen in elective cases, as compared with 11.7% for emergency surgeries. Five-year and 10-year survival rates were 84% and 75%, respectively (Fig. 39-16).[91]

Although the success of aortic surgery has improved dramatically, postoperative complications remain. Pseudoaneurysm at the graft site or graft dehiscence is frequently difficult to detect with transthoracic imaging. In these situations, TEE has been clearly shown to provide additional diagnostic data.[6,95,96]

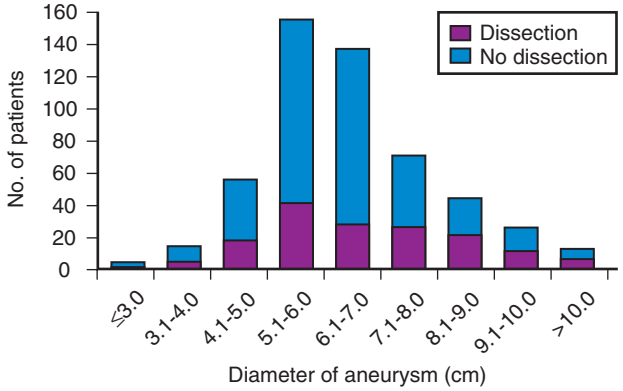
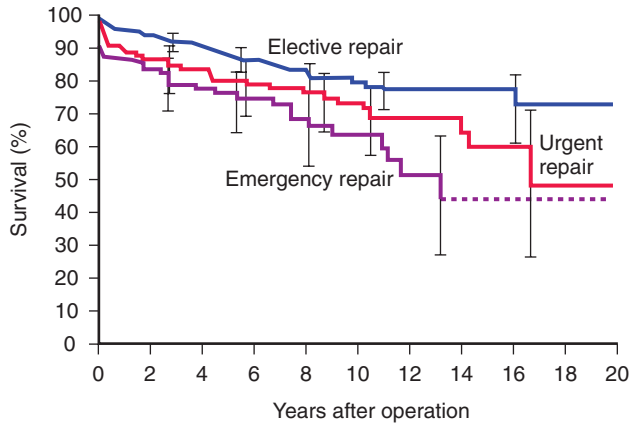



**Figure 39-15 Risk of aortic dissection in Marfan syndrome on the basis of aortic diameter.** Diameter of the aneurysm in 524 adult patients with Marfan syndrome, according to the presence of aortic dissection. *(From Gott VL, Greene PS, Alejo DE, et al: Replacement of the aortic root in patients with Marfan's syndrome.* N Engl J Med *340:1307-1313, 1999.)*

## Alternate Diagnostic Approaches

Magnetic resonance imaging and cardiac computed tomographic scan can be used in patients who have limited acoustic images or need detailed assessment in the situation where ambiguous data are present. This situation might include the patient with unusual tortuosity of the aortic arch, the question of dilation extending into the carotid arteries or circle of Willis, or an aortic dissection that cannot be entirely excluded. However, just as is the case with echocardiographic assessment, the accuracy of computed tomographic scan and magnetic




No. at risk

| | | | | | | | | | | | |
|---|---|---|---|---|---|---|---|---|---|---|---|
| Elective repair | 455 | 381 | 294 | 204 | 141 | 97 | 64 | 42 | 17 | 4 | 1 |
| Urgent repair | 117 | 88 | 74 | 62 | 53 | 41 | 23 | 16 | 8 | 4 | 3 |
| Emergency repair | 103 | 73 | 57 | 41 | 31 | 21 | 10 | 4 | 3 | 2 | 0 |

**Figure 39-16 Kaplan-Meier survival analysis of 675 patients with Marfan syndrome according to the urgency of surgery.** *(From Gott VL, Greene PS, Alejo DE, et al: Replacement of the aortic root in patients with Marfan's syndrome.* N Engl J Med *340:1307-1313, 1999.)*

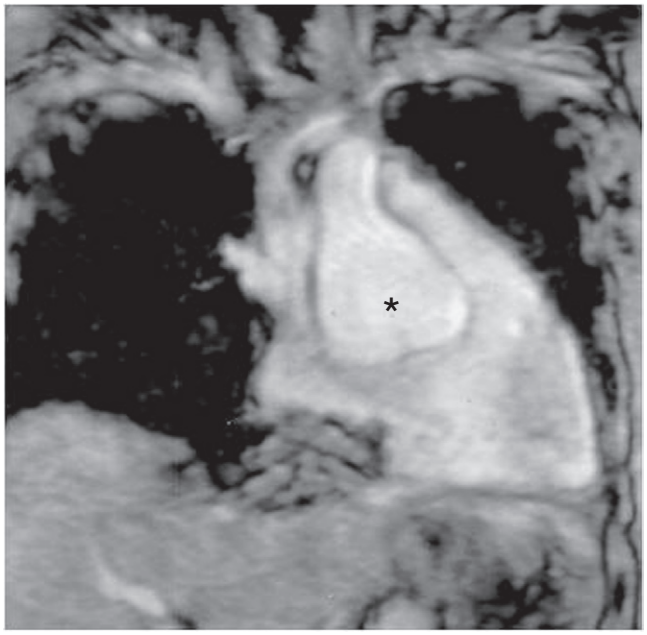



**Figure 39-17 Magnetic resonance imagining in a coronal plane.** Image shows a dilated aortic root in a patient with Marfan syndrome. *Location of the aortic root.

resonance imaging evaluation is reliant on availability of appropriate equipment and is operator dependent (Fig. 39-17).

Advances in magnetic resonance imaging have allowed for the evaluation of aortic elasticity in patients with MFS. The elasticity of the aorta has been found to be reduced in these patients. Magnetic resonance imaging velocity mapping of the aorta shows reduced aortic distensibility during systole and increased pulse wave propagation.[97] Use of magnetic resonance imaging velocity encoding shows a positive response to β-blocker therapy with a reduction in pulse wave propagation after β-blocker treatment. These techniques not only yield important information regarding the biophysical properties of the aorta in patients with connective tissue disorders but may also provide data to predict individual patient risk.[97]

## KEY POINTS

- A variety of disorders can lead to the connective tissue abnormalities, with many of these conditions manifesting similar cardiac features of aortic dilation and dissection and mitral valve prolapse.
- Although Marfan syndrome remains a clinical diagnosis primarily based on defined cardiac, skeletal, and ocular findings, refinement in genetic testing has improved diagnostic rates to close to 90%.
- In addition to the well-described fibrillin mutations associated with connective tissue disease, the role of transforming growth factor-β as a cause of these conditions is increasingly evident.
- In connective tissue disorders, dilation of the aortic root is caused by degenerative changes of smooth muscle cells, elastic fibers, and collagen, resulting in medial degeneration.
- Changes in mitral and aortic valve fibrous ring integrity, combined with dilation of the surrounding tissues causing alteration in valve geometry, result in the hemodynamic disturbances seen in the connective tissue disorders (predominantly regurgitation).
- In virtually all children and most adults, TTE is highly predictive of the pathologic changes in the mitral valve, aortic valve, and aorta associated with the connective tissue disorders.
- Transesophageal echocardiography and other imaging modalities (3D echocardiography, magnetic resonance imaging, and computed tomography) serve as adjunct modalities to diagnosis.
- In addition to valve and large vessel disease, the connective tissue disorders may also affect systolic and diastolic left ventricular function.
- When surgical intervention is contemplated for a bicuspid aortic valve in children and young adults and there is concomitant aortic dilation, careful consideration should be given to possible connective tissue conditions that might complicate the procedure and recuperation.
- In the growing child and teen, quantitative assessment of the aortic arch must incorporate the use of a well-validated nomogram to ensure clear understanding of the severity of dilation and rate of growth.

## REFERENCES


1. Loeys BL, Dietz HC, Braverman AC, et al: The revised Ghent nosology for the Marfan syndrome. *J Med Genet* 47:476-485, 2010.
2. Gray JR, Bridges AB, Faed MJ, et al: Ascertainment and severity of Marfan syndrome in a Scottish population. *J Med Genet* 31:51-54, 1994.
3. Ramirez F, Dietz HC: Marfan syndrome: from molecular pathogenesis to clinical treatment. *Curr Opin Genet Dev* 17:367, 2007.
4. Dietz H, Francke U, Furthmayr H, et al: The question of heterogeneity in Marfan syndrome. *Nat Genet* 9:228-231, 1995.
5. Schrijver I, Liu W, Brenn T, et al: Cysteine substitutions in epidermal growth factor-like domains of fibrillin-1: distinct effects on biochemical and clinical phenotypes. *Am J Hum Genet* 65:1007-1020, 1999.
6. Wang M, Price C, Han J, et al: Recurrent missplicing of fibrillin exon 32 in two patients with neonatal Marfan syndrome. *Hum Mol Genet* 4:607-613, 1995.
7. Dietz HC, Pyeritz RE: Mutations in the human gene for fibrillin-1 (FBN1) in the Marfan syndrome and related disorders. *Hum Mol Genet* 4:1799-1809, 1995.
8. Nijbroek G, Sood S, McIntosh I, et al: Fifteen novel FBN1 mutations causing Marfan syndrome detected by heteroduplex analysis of genomic amplicons. *Am J Hum Genet* 57:8-21, 1995.
9. Milewicz DM, Grossfield J, Cao SN, et al: A mutation in FBN1 disrupts profibrillin processing and results in isolated skeletal features of the Marfan syndrome. *J Clin Invest* 95:2373-2378, 1995.
10. Palz M, Tiecke F, Booms P, et al: Clustering of mutations associated with mild Marfan-like phenotypes in the 3' region of FBN1 suggests a potential genotype-phenotype correlation. *Am J Med Genet* 91:212-221, 2000.
11. Guo D, Hasham S, Kuang SQ, et al: Familial thoracic aortic aneurysms and dissections: genetic heterogeneity with a major locus mapping to 5q13-14. *Circulation* 103:2461-2468, 2001.
12. Leier CV, Call TD, Fulkerson PK, et al: The spectrum of cardiac defects in the Ehlers-Danlos syndrome, types I and III. *Ann Intern Med* 92:171-178, 1980.
13. McDonnell NB, Gorman BL, Mandel KW, et al: Echocardiographic findings in classical and hypermobile Ehlers-Danlos syndromes. *Am J Med Genet A* 140:129-136, 2006.
14. Wenstrup RJ, Meyer RA, Lyle JS, et al: Prevalence of aortic root dilation in the Ehlers-Danlos syndrome. *Genet Med* 4:112-117, 2002.
15. Pope FM, Kendall BE, Slapak GI, et al: Type III collagen mutations cause fragile cerebral arteries. *Br J Neurosurg* 5:551-574, 1991.
16. Bellenot F, Boisgard S, Kantelip B, et al: Type IV Ehlers-Danlos syndrome with isolated arterial involvement. *Ann Vasc Surg* 4:15-19, 1990.
17. North KN, Whiteman DA, Pepin BG, et al: Cerebrovascular complications in Ehlers-Danlos syndrome type IV. *Ann Neurol* 38:960-964, 1995.
18. Emanuel BS, Cannizzaro LA, Seyer JM, et al: Human alpha 1(III) and alpha 2(V) procollagen genes are located on the long arm of chromosome 2. *Proc Natl Acad Sci U S A* 82:3385-3389, 1985.
19. Hiratzka LF, Bakris GL, Beckman JA, et al: ACCF/AHA/AATS/ACR/ASA/SCA/SCAI/SIR/STS/SVM guidelines for the diagnosis and management of patients with Thoracic Aortic Disease: a report of the American College of Cardiology Foundation/American Heart Association Task Force on Practice Guidelines, American Association for Thoracic Surgery, American College of Radiology, American Stroke Association, Society of Cardiovascular Anesthesiologists, Society for Cardiovascular Angiography and Interventions, Society of Interventional Radiology, Society of Thoracic Surgeons, and Society for Vascular Medicine. *Circulation* 121:e266-e369, 2010.
20. Ascione R, Gomes WJ, Bates M, et al: Emergency repair of type A aortic dissection in type IV Ehlers-Danlos syndrome. *Cardiovasc Surg* 8:75-78, 2000.
21. Mudd SH, Skovby F, Levy HL, et al: The natural history of homocystinuria due to cystathionine beta-synthase deficiency. *Am J Hum Genet* 37:1-31, 1985.
22. Gupta PA, Wallis DD, Chin TO, et al: FBN2 mutation associated with manifestations of Marfan syndrome and congenital contractural arachnodactyly. *J Med Genet* 41:e56, 2004.
23. Loeys BL, Schwarze U, Holm T, et al: Aneurysm syndromes caused by mutations in the TGF-beta receptor. *N Engl J Med* 355:788-798, 2006.
24. Loeys BL, Chen J, Neptune ER, et al: A syndrome of altered cardiovascular, craniofacial, neurocognitive and skeletal development caused by mutations in TGFBR1 or TGFBR2. *Nat Genet* 37:275-281, 2005.
25. Williams JA, Loeys BL, Nwakanma LU, et al: Early surgical experience with Loeys-Dietz: a new syndrome of aggressive thoracic aortic aneurysm disease. *Ann Thorac Surg* 83:S757-S763;S785-S790, 2007.
26. Braverman AC, Güven H, Beardslee MA, et al: The bicuspid aortic valve. *Curr Probl Cardiol* 30:470-522, 2005.
27. Huntington K, Hunter AG, Chan KL: A prospective study to assess the frequency of familial clustering of congenital bicuspid aortic valve. *J Am Coll Cardiol* 30:1809-1812, 1997.
28. Clementi M, Notari L, Borghi A, et al: Familial congenital bicuspid aortic valve: a disorder of uncertain inheritance. *Am J Med Genet* 62:336-338, 1996.
29. Loscalzo ML, Goh DL, Loeys B, et al: Familial thoracic aortic dilation and bicommissural aortic valve: a prospective analysis of natural history and inheritance. *Am J Med Genet A* 143A:1960-1967, 2007.
30. Fedak PW, Verma S, David TE, et al: Clinical and pathophysiological implications of a bicuspid aortic valve. *Circulation* 106:900-904, 2002.
31. Ward C: Clinical significance of the bicuspid aortic valve. *Heart* 83:81-85, 2000.
32. Keane MG, Wiegers SE, Plappert T, et al: Bicuspid aortic valves are associated with aortic dilatation out of proportion to coexistent valvular lesions. *Circulation* 102:III35-III39, 2000.
33. Ferencik M, Pape LA: Changes in size of ascending aorta and aortic valve function with time in patients with congenitally bicuspid aortic valves. *Am J Cardiol* 92:43-46, 2003.
34. Roberts CS, Roberts WC: Dissection of the aorta associated with congenital malformation of the aortic valve. *J Am Coll Cardiol* 17:712-716, 1991.
35. Nistri S, Sorbo MD, Marin M, et al: Aortic root dilatation in young men with normally functioning bicuspid aortic valves. *Heart* 82:19-22, 1999.
36. Lewin MB, Otto CM: The bicuspid aortic valve: adverse outcomes from infancy to old age. *Circulation* 111:832-834, 2005.
37. Nienaber CA, Eagle KA: Aortic dissection: new frontiers in diagnosis and management: part I: from etiology to diagnostic strategies. *Circulation* 108:628-635, 2003.
38. Schaefer BM, Lewin MB, Stout KK, et al: Usefulness of bicuspid aortic valve phenotype to predict elastic properties of the ascending aorta. *Am J Cardiol* 99:686-690, 2007.
39. Lin AE, Lippe BM, Geffner ME, et al: Aortic dilation, dissection, and rupture in patients with Turner syndrome. *J Pediatr* 109:820-826, 1986.
40. Gravholt CH, Landin-Wilhelmsen K, Stochholm K, et al: Clinical and epidemiological description of aortic dissection in Turner's syndrome. *Cardiol Young* 16:430-436, 2006.
41. Carlson M, Silberbach M: Dissection of the aorta in Turner syndrome: two cases and review of 85 cases in the literature. *J Med Genet* 44:745-749, 2007.
42. Davies RR, Goldstein LJ, Coady MA, et al: Yearly rupture or dissection rates for thoracic aortic aneurysms: simple prediction based on size. *Ann Thorac Surg* 73:17-28, 2002.
43. Ostberg JE, Donald AE, Halcox JP, et al: Vasculopathy in Turner syndrome: arterial dilatation and intimal thickening without endothelial dysfunction. *J Clin Endocrinol Metab* 90:5161-5166, 2005.
44. Lopez L, Arheart KL, Colan SD, et al: Turner syndrome is an independent risk factor for aortic dilation in the young. *Pediatrics* 121:e1622-e1627, 2008.
45. Bonow RO, Carabello BA, Chatterjee K, et al: ACC/AHA 2006 guidelines for the management of patients with valvular heart disease: a report of the American College of Cardiology/American Heart Association Task Force on Practice Guidelines (writing Committee to Revise the 1998 guidelines for the management of patients with valvular heart disease) developed in collaboration with the Society of Cardiovascular Anesthesiologists endorsed by the Society for Cardiovascular Angiography and Interventions and the Society of Thoracic Surgeons. *J Am Coll Cardiol* 48:e1-e148, 2006.
46. Coady MA, Davies RR, Roberts M, et al: Familial patterns of thoracic aortic aneurysms. *Arch Surg* 134:361-367, 1999.
47. Biddinger A, Rocklin M, Coselli J, et al: Familial thoracic aortic dilatations and dissections: a case control study. *J Vasc Surg* 25:506-511, 1997.
48. Fedak PW, de Sa MP, Verman S, et al: Vascular matrix remodeling in patients with bicuspid aortic valve malformations: implications for aortic dilatation. *J Thorac Cardiovasc Surg* 126:797-806, 2003.
49. Ikonomidis JS, Jones JA, Barbour JR, et al: Expression of matrix metalloproteinases and endogenous inhibitors within ascending aortic aneurysms of patients with bicuspid or tricuspid aortic valves. *J Thorac Cardiovasc Surg* 133:1028-1036, 2007.
50. LeMaire SA, Pannu H, Tran-Fadulu V, et al: Severe aortic and arterial aneurysms associated with a TGFBR2 mutation. *Nat Clin Pract Cardiovasc Med* 4:167-171, 2007.
51. LeMaire SA, Ang X, Wilks JA, et al: Matrix metalloproteinases in ascending aortic aneurysms: bicuspid versus trileaflet aortic valves. *J Surg Res* 123:40-48, 2005.
52. Segura AM, Luna RE, Horiba K, et al: Immunohistochemistry of matrix metalloproteinases and their inhibitors in thoracic aortic aneurysms and aortic valves of patients with

Marfan's syndrome. *Circulation* 98:II331-II338, 1998.
53. Robicsek F, Thubrikar MJ: Hemodynamic considerations regarding the mechanism and prevention of aortic dissection. *Ann Thorac Surg* 58:1247-1253, 1994.
54. Engel PJ, Held JS, van der Bel-Kahn J, et al: Echocardiographic diagnosis of congenital sinus of Valsalva aneurysm with dissection of the interventricular septum. *Circulation* 63:705-711, 1981.
55. Shaffer EM, Snider AR, Beekman RH, et al: Sinus of Valsalva aneurysm complicating bacterial endocarditis in an infant: diagnosis with two-dimensional and Doppler echocardiography. *J Am Coll Cardiol* 9:588-591, 1987.
56. Khan IA, Nair CK: Clinical, diagnostic, and management perspectives of aortic dissection. *Chest* 122:311-328, 2002.
57. Erbel R, Alfonso F, Boileau C, et al: Diagnosis and management of aortic dissection. *Eur Heart J* 22:1642-1681, 2001.
58. Granato JE, Dee P, Gibson RS: Utility of two-dimensional echocardiography in suspected ascending aortic dissection. *Am J Cardiol* 56:123-129, 1985.
59. Engelfriet PM, Boersma E, Tijssen JG, et al: Beyond the root: dilatation of the distal aorta in the marfan syndrome. *Heart* 92:1238-1243, 2006.
60. Marks AR, Choong CY, Sanfilippo AJ, et al: Identification of high-risk and low-risk subgroups of patients with mitral-valve prolapse. *N Engl J Med* 320:1031-1036, 1989.
61. Dietz HC, Cutting GR, Pyeritz RE, et al: Marfan syndrome caused by a recurrent de novo missense mutation in the fibrillin gene. *Nature* 352:337-339, 1991.
62. van Karnebeek CD, Naeff MS, Mulder BJ, et al: Natural history of cardiovascular manifestations in Marfan syndrome. *Arch Dis Child* 84:129-137, 2001.
63. Savolainen A, Nisula L, Keto P, et al: Left ventricular function in children with the Marfan syndrome. *Eur Heart J* 15:625-630, 1994.
64. Porciani MC, Giurlani L, Chelucci A, et al: Diastolic subclinical primary alterations in Marfan syndrome and Marfan-related disorders. *Clin Cardiol* 25:416-420, 2002.
65. De Backer JF, Devos D, Segers P, et al: Primary impairment of left ventricular function in Marfan syndrome. *Int J Cardiol* 112:353-358, 2006.
66. Das BB, Taylor AL, Yetman AT: Left ventricular diastolic dysfunction in children and young adults with Marfan syndrome. *Pediatr Cardiol* 27:256-258, 2006.
67. Hirata K, Triposkiadis F, Sparks E, et al: The Marfan syndrome: abnormal aortic elastic properties. *J Am Coll Cardiol* 18:57-63, 1991.
68. Chatrath R, Beauchesne LM, Connolly HM, et al: Left ventricular function in the Marfan syndrome without significant valvular regurgitation. *Am J Cardiol* 91:914-916, 2003.
69. Meijboom LJ, Timmermans J, van Tintelen JP, et al: Evaluation of left ventricular dimensions and function in Marfan's syndrome without significant valvular regurgitation. *Am J Cardiol* 95:795-797, 2005.
70. Nollen GJ, van Schijndel KE, Timmermans J, et al: Pulmonary artery root dilatation in Marfan syndrome: quantitative assessment of an unknown criterion. *Heart* 87:470-471, 2002.
71. Gross DM, Robinson LK, Smith LT, et al: Severe perinatal Marfan syndrome. *Pediatrics* 84:83-89, 1989.
72. Lind J, Wallenburg HC: The Marfan syndrome and pregnancy: a retrospective study in a Dutch population. *Eur J Obstet Gynecol Reprod Biol* 98:28-35, 2001.
73. Tacy TA, Vermilion RP, Ludomirsky A: Range of normal valve annulus size in neonates. *Am J Cardiol* 75:541-543, 1995.
74. Rogé CL, Silverman NH, Hart PA, et al: Cardiac structure growth pattern determined by echocardiography. *Circulation* 57:285-290, 1978.
75. Roman MJ, Devereux RB, Kramer-Fox R, et al: Two-dimensional echocardiographic aortic root dimensions in normal children and adults. *Am J Cardiol* 64:507-512, 1989.
76. Nidorf SM, Picard MH, Triulzi MO, et al: New perspectives in the assessment of cardiac chamber dimensions during development and adulthood. *J Am Coll Cardiol* 19:983-988, 1992.
77. Sheil ML, Jenkins O, Sholler GF: Echocardiographic assessment of aortic root dimensions in normal children based on measurement of a new ratio of aortic size independent of growth. *Am J Cardiol* 75:711-715, 1995.
78. Daubeney PE, Blackstone EH, Weintraub RG, et al: Relationship of the dimension of cardiac structures to body size: an echocardiographic study in normal infants and children. *Cardiol Young* 9:402-410, 1999.
79. Colan S: *Normal echocardiographic values in infants and children.* Boston Children's Hospital. Unpublished data.
80. Baumgartner D, Baumgartner C, Mátyás G, et al: Diagnostic power of aortic elastic properties in young patients with Marfan syndrome. *J Thorac Cardiovasc Surg* 129:730-739, 2005.
81. Vitarelli A, Conde Y, Cimino E, et al: Aortic wall mechanics in the Marfan syndrome assessed by transesophageal tissue Doppler echocardiography. *Am J Cardiol* 97:571-577, 2006.
82. Shores J, Berger KR, Murphy EA, et al: Progression of aortic dilatation and the benefit of long-term beta-adrenergic blockade in Marfan's syndrome. *N Engl J Med* 330:1335-1341, 1994.
83. Rossi-Foulkes R, Roman MJ, Rosen SE, et al: Phenotypic features and impact of beta blocker or calcium antagonist therapy on aortic lumen size in the Marfan syndrome. *Am J Cardiol* 83:1364-1368, 1999.
84. Groenink M, de Roos A, Mulder BJ, et al: Changes in aortic distensibility and pulse wave velocity assessed with magnetic resonance imaging following beta-blocker therapy in the Marfan syndrome. *Am J Cardiol* 82:203-208, 1998.
85. Yin FC, Brin KP, Tinq CT, et al: Arterial hemodynamic indexes in Marfan's syndrome. *Circulation* 79:854-862, 1989.
86. Haouzi A, Berglund H, Pelikan PC, et al: Heterogeneous aortic response to acute beta-adrenergic blockade in Marfan syndrome. *Am Heart J* 133:60-63, 1997.
87. Yetman AT, Bornemeier RA, McCrindle BW: Usefulness of enalapril versus propranolol or atenolol for prevention of aortic dilation in patients with the Marfan syndrome. *Am J Cardiol* 95:1125-1127, 2005.
88. Habashi JP, Judge DP, Holm TM, et al: Losartan, an AT1 antagonist, prevents aortic aneurysm in a mouse model of Marfan syndrome. *Science* 312:117-121, 2006.
89. Brooke BS, Habashi JP, Judge DP, et al: Angiotensin II blockade and aortic-root dilation in Marfan's syndrome. *N Engl J Med* 358:2787-2795, 2008.
90. Lacro RV, Dietz HC, Wruck LM, et al: Rationale and design of a randomized clinical trial of beta-blocker therapy (atenolol) versus angiotensin II receptor blocker therapy (losartan) in individuals with Marfan syndrome. *Am Heart J* 154:624-631, 2007.
91. Gott VL, Greene PS, Alejo DE, et al: Replacement of the aortic root in patients with Marfan's syndrome. *N Engl J Med* 340:1307-1313, 1999.
92. Bentall H, De Bono A: A technique for complete replacement of the ascending aorta. *Thorax* 23:338-339, 1968.
93. Miller DC: Valve-sparing aortic root replacement in patients with the Marfan syndrome. *J Thorac Cardiovasc Surg* 125:773-778, 2003.
94. Sarsam MA, Yacoub M: Remodeling of the aortic valve anulus. *J Thorac Cardiovasc Surg* 105:435-438, 1993.
95. Yasuda H, Sakagoshi N, Lim YJ, et al: Pseudoaneurysm after Bentall operation diagnosed by transesophageal echocardiography. *Ann Thorac Surg* 78:1478, 2004.
96. Ballal RS, Gatewood RP Jr, Nanda NC, et al: Usefulness of transesophageal echocardiography in the assessment of aortic graft dehiscence. *Am J Cardiol* 80:372-376, 1997.
97. Groenink M, de Roos A, Mulder BJ, et al: Biophysical properties of the normal-sized aorta in patients with Marfan syndrome: evaluation with MR flow mapping. *Radiology* 219:535-540, 2001.

# 40 Aging Changes Seen on Echocardiography

MICHAEL A. CHEN, MD, PhD

**Background and Importance**
**Basic Principles and Echocardiographic Approach**
Normal Changes in Cardiac Structure
Normal Changes in Cardiac Function
**Clinical Outcome Data**
Valvular Heart Disease
Left Ventricular Hypertrophy
Left Atrial Size and Outcomes
Heart Failure
Coronary Artery Disease and Stress Testing
Cardiogenic Thromboembolism
Cardiac Amyloidosis
**Clinical Recommendations**

## Background and Importance

In the United States, by 2030, an estimated 72.1 million people will be age 65 or older (39.6 million in 2009), with 8.7 million of them over the age of 85 (5.6 million in 2009).[1] Cardiovascular disease is the leading cause of death and disability, and advanced age is a major risk factor for its development. Normal aging results in pervasive changes in cardiovascular structure and function, as well as alterations in other organ systems. Many normal age-related changes in cardiovascular structure and function are readily identifiable on echocardiography. This is also true of conditions that are pathologic, but common in the elderly.

## Basic Principles and Echocardiographic Approach

The echocardiographic techniques used to acquire images and other data are the same for the elderly as for younger persons.

### NORMAL CHANGES IN CARDIAC STRUCTURE

#### *Left Ventricular Wall Thickness and Chamber Dimensions*

Multiple studies have demonstrated increases in left ventricular (LV) wall thickness with age in patients without a history of hypertension or valvular or other cardiovascular disease[2-5] (Fig. 40-1). These cross-sectional studies involved from 53 to 136 normal healthy subjects and documented mild increases in LV wall thickness. For example, in a study by Gardin and colleagues,[2] 136 adults (78 men and 58 women aged 20 to 97 years) without evidence of cardiovascular disease were studied. The patients were stratified into six age groups, and significant increases in wall thickness with age were found. Comparing the youngest group (21 to 30 years) with the oldest group (more than 70 years), the mean septal wall thickness increased from 9.8 mm to 11.8 mm, and the mean posterior wall thickness increased from 10.1 mm to 11.8 mm. This represented increases of 20% and 18%, respectively.

#### *Left Ventricular Mass*

Based on data documenting increased wall thickness with increasing age, a number of prior echocardiographic studies, including a study of 700 healthy Japanese subjects aged 20 to 79 years, have suggested that there is an age related increase in LV mass (sometimes indexed for weight/height).[6-8]

The formula for LV (see Chapter 9) mass that is commonly used was derived by Devereux and co-workers[9]:

$$\text{LV mass} = 0.8 \times [1.04(\text{ST}_d + \text{LVID}_d + \text{PWT}_d)^3 - \text{LVID}_d{}^3] = 0.6\ \text{g}$$

where $ST_d$ is septal thickness at end-diastole, $LVID_d$ is LV internal dimension at end-diastole, and $PWT_d$ is LV posterior wall thickness at end-diastole.

In contrast to these findings, more recent studies of normal subjects using magnetic resonance imaging (MRI), including a study that was part of the Baltimore Longitudinal Study of Aging, have confirmed that MRI-derived wall thickness increases with age (particularly at the midventricle), with no change in the short-axis diastolic dimension (similar to prior echocardiographic data). On the other hand, LV length *declines* in both sexes over time. The resulting estimate of LV mass reveals no age relationship in women, although there is an age-related decline in men (due to a smaller increase in wall thickness). This suggests that with time, the LV becomes thicker and more spherical.[10,11]

The reason for the discrepancy in the findings between M-mode and two-dimensional (2D) echocardiographic data and MRI data lies in the algorithms used to calculate mass in the former techniques. These algorithms, such as the formula derived by Devereux and co-workers, assume an ellipsoid cavity and do not take into account changes in cavity shape. Thus, the calculations will be less accurate with cavities that are, for example, more spherical. Three-dimensional (3D) echocardiography has been shown to be a more accurate technique than 2D echocardiography in estimating LV mass in studies comparing the two techniques against weighing of the LV in both

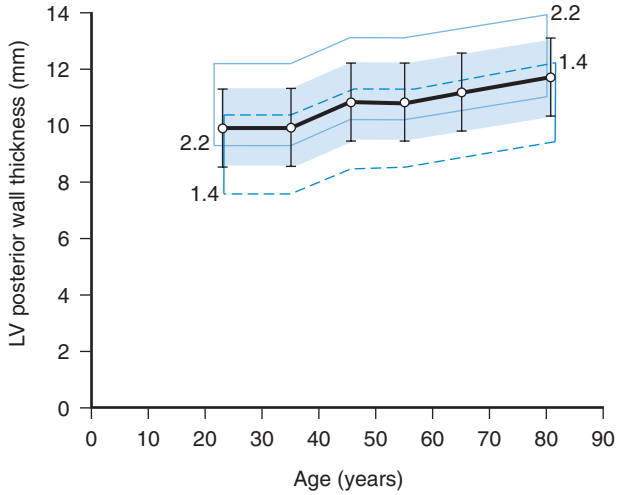



**Figure 40-1 Plot of LV posterior wall thickness in late diastole (mm) versus age in years.** For each age group the mean (*circle*) and 95% confidence interval (*blue shaded*) for normal values are depicted for a body surface area (BSA) of 1.8 $m^2$. The 95% confidence intervals are also shown for subjects with BSA values of 1.4 $m^2$ (*dashed lines*) and 2.2 $m^2$ (*solid lines*). *(From Gardin JM, Henry WL, Savage DD, et al: Echocardiographic measurements in normal subjects: evaluation of an adult population without clinically apparent heart disease.* J Clin Ultrasound *7:439-447, 1979. Copyright © 1979, John Wiley & Sons. Reprinted by permission John Wiley & Sons, Inc.)*

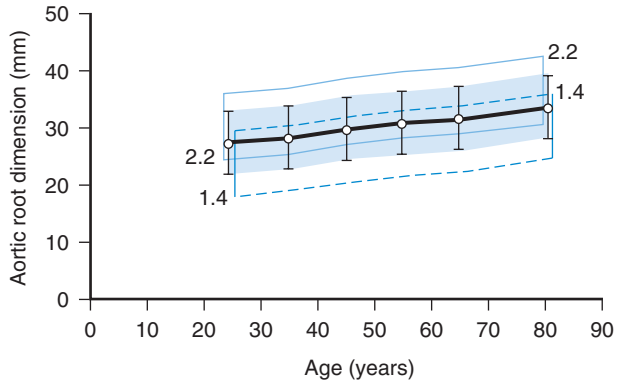



**Figure 40-2 Plot of aortic root dimension in late diastole (mm) versus age in years.** Mean value for each age group is depicted by a *circle* plotted at the mean age in the age group. The *bracket* and *shaded area* on either side of the circle represents the interval for normal values for a subject with a body surface area (BSA) of 1.8 $m^2$. The 95% prediction intervals are also shown for subjects with BSA values of 1.4 $m^2$ (*dotted lines*) and 2.2 $m^2$ (*solid lines*). *(From Gardin JM, Henry WL, Savage DD, et al: Echocardiographic measurements in normal subjects: evaluation of an adult population without clinically apparent heart disease.* J Clin Ultrasound *7:439-447, 1979. Copyright © 1979, John Wiley & Sons. Reprinted by permission John Wiley & Sons, Inc.)*

human and animal studies.[12-15] 3D echocardiography–derived LV mass estimates have also been shown to correlate well with MRI-derived estimates.[16-18]

### *Aortic Root Diameter*

A mild increase in the aortic root diameter is seen with age (Fig. 40-2). There is an approximately 6% increase in a normal population between the fourth and eighth decades.[3] A study of serial chest radiographs taken over 17 years noted an increase from 3.4 to 3.8 cm.[19] This enlargement may present an extra stimulus to the LV to hypertrophy, as it represents a larger blood volume that must be pushed forward.

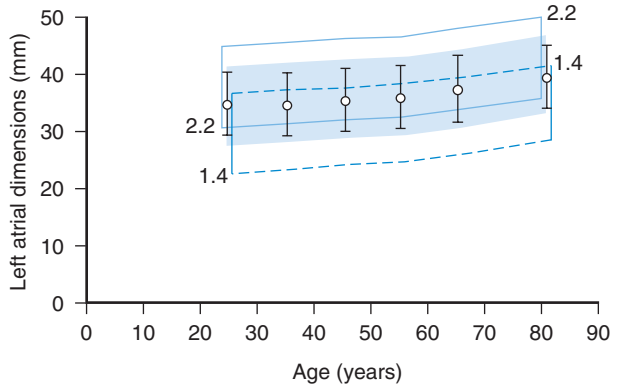



**Figure 40-3 Plot of LA dimension in late diastole (mm) versus age in years.** For each age group the mean and 95% prediction intervals for normal values are depicted for three different BSAs, as detailed in Figure 40-1. *(From Gardin JM, Henry WL, Savage DD, et al: Echocardiographic measurements in normal subjects: evaluation of an adult population without clinically apparent heart disease.* J Clin Ultrasound *7:439-447, 1979. Copyright © 1979, John Wiley & Sons. Reprinted by permission John Wiley & Sons, Inc.)*

### *Left Atrial Size*

There is a significant increase in size of the left atrium (LA) with age (Fig. 40-3). Because the LA is a 3D structure, many have argued that volume is a better way to evaluate LA enlargement rather than the 2D anterior-posterior diameter.[20,21] Some data suggest that the area-length method of calculating LA volume underestimates volume when compared with MRI,[22] whereas other data suggest that 3D echocardiography shows a good correlation with MRI.[23]

Recently, Aurigemma and colleagues,[24] using echocardiographic data from 230 subjects in the Cardiovascular Health Study who were free of cardiovascular disease and had a mean age of 75 ± 5 years, established reference ranges by gender for LA dimensions and volumes in this population. Table 40-1 shows the measurement ranges for LA parameters and clinical data regarding the patients in the study, and Table 40-2 shows the equations derived in the study that allow for estimation whether LA size is increased (i.e., above the 95th percentile for age/height/weight).

### *LV Dimensions*

In the studies that have documented increases in LV wall thickness, measurements of LV end-diastolic and end-systolic dimensions showed either a slight decrease to no change with age[2,3,6] (Table 40-3). Because LV stroke volume is the difference of LV end-diastolic and end-systolic volumes, supine resting LV stroke volume is also assumed to be unrelated to age.[25] MRI studies confirm the decreases in end-diastolic and end-systolic volumes, and these measurements correlate well with 3D echocardiography, although this method may underestimate volumes if trabeculations are not excluded from the analysis.[23,26]

### *Cardiac Chamber Dimensions*

Normal echocardiographic values are listed in Table 40-3. These normal changes should be taken into account when reporting abnormalities.

### *Cardiac Valves*

The four cardiac valves have been documented to change in morphology with age. These changes are most notable in the left-sided valves, and this is likely related to the higher pressures found in the associated chambers.

### Valve Circumference

Valve circumference has been found to increase with age.[27] In one study of 765 patients, the mean valve circumference, when indexed for body surface area, progressively rose through adult life, a trend that was greater for the semilunar than for the atrioventricular valves. Krovetz[28] reanalyzed data regarding aortic valve size and found that after approximately 18 to 21 years of age, the size of the aortic annulus increases in a near-linear fashion (Fig. 40-4).

**TABLE 40-1 Reference Ranges for LA Dimension and Volume and Selected Clinical Variables for the Subjects in the Cardiovascular Health Study**

| *Linear Dimensions* | *Sex* | *Mean* | *Range* | *Percentile 0.05* | *0.50* | *0.95* |
|---|---|---|---|---|---|---|
| Diameter, cm | Female | 3.0 ± 0.5 | 1.5-4.2 | 2.2 | 3.0 | 3.9 |
| | Male | 3.4 ± 0.6 | 2.1-4.8 | 2.4 | 3.3 | 4.4 |
| Length, cm | Female | 4.6 ± 0.7 | 2.8-6.1 | 3.6 | 4.6 | 5.7 |
| | Male | 4.8 ± 0.7 | 3.3-6.7 | 3.7 | 4.7 | 6.1 |
| Width, cm | Female | 3.6 ± 0.6 | 1.9-5.2 | 2.4 | 3.6 | 4.6 |
| | Male | 3.8 ± 0.6 | 2.4-5.1 | 2.6 | 3.7 | 4.7 |
| **Volume** | | | | | | |
| LA volume, mL | Female | 27.4 ± 10.0 | 8.7-53.9 | 12.3 | 26.4 | 46.7 |
| | Male | 32.0 ± 10.9 | 13.9-71.5 | 17.2 | 30.1 | 58.2 |
| *Clinical Data* | | | | | | |
| Age, yr | Female | 76.5 ± 4.9 | 68-91 | 70 | 76 | 85 |
| | Male | 77.3 ± 5.6 | 68-93 | 70 | 75 | 88 |
| Height, in | Female | 62.8 ± 2.2 | 57.9-68.1 | 58.4 | 63.0 | 66.2 |
| | Male | 67.9 ± 2.5 | 60.4-75.2 | 63.8 | 67.8 | 71.7 |
| Weight, lb | Female | 146 ± 29 | 84-233 | 96 | 144 | 193 |
| | Male | 173 ± 26 | 114-254 | 132 | 170 | 222 |
| BSA, $m^2$ | Female | 1.66 ± 0.17 | 1.27-2.07 | 1.37 | 1.66 | 1.93 |
| | Male | 1.89 ± 0.16 | 1.48-2.37 | 1.60 | 1.88 | 2.13 |
| BMI, $kg/m^2$ | Female | 25.9 ± 4.6 | 15.2-39.5 | 17.9 | 25.2 | 34.0 |
| | Male | 26.3 ± 3.2 | 18.4-37.6 | 21.6 | 26.0 | 31.7 |
| SBP, mm Hg | Female | 128 ± 18 | 84-181 | 99 | 126 | 158 |
| | Male | 130 ± 17 | 88-211 | 109 | 127 | 158 |
| DBP, mm Hg | Female | 68.4 ± 9.8 | 42-92 | 51 | 69 | 83 |
| | Male | 70.8 ± 9.6 | 49-110 | 56 | 70 | 87 |

From Aurigemma GP, Gottdiener JS, Arnold AM, et al: Left atrial volume and geometry in healthy aging: the Cardiovascular Health Study. *Circ Cardiovasc Imaging* 2:282-289, 2009. Copyright © 2009, Lippincott Williams & Wilkins. Adapted with permission Lippincott Williams & Wilkins.

*BSA*, Body surface area; *DBP*, diastolic blood pressure; *diameter,* LA dimension measured from anterior to posterior in the parasternal long-axis view; *length,* LA dimension measured from the annulus to superior LA wall in an apical four-chamber view; *SBP*, systolic blood pressure; *width,* LA dimension measured from medial to lateral in a four-chamber view.

### Valve Thickness

One autopsy study of 200 disease-free hearts demonstrated significant increases in mean thickness of the aortic and mitral valves with increasing age. This study showed that compared with subjects who were less than 20 years of age, those who were older than 60 years had valves that were twice as thick[29] (Table 40-4).

### Valvular Calcification

Aging is associated with thickening and calcification of the aortic valve cusps, also called aortic valve sclerosis, as well as the mitral and aortic valve annuli (termed *mitral annular calcification* and *aortic annular calcification*, respectively) (Figs. 40-5 and 40-6). Calcium is found at the bases of the aortic cusps and

**TABLE 40-3 Mean Values of Echocardiographic Parameters for Three Age Groups**

| *Parameter* | *Group I (25-44 yr)* | *Group II (45-64 yr)* | *Group III (65-84 yr)* |
|---|---|---|---|
| Mitral valve E-F slope (mm/s) | 102.3 ± 3.7 (52) | 79.0 ± 3.8 (35)* | 67.1 ± 5.2 (18)† |
| Aortic root, diastole (mm) | 30.9 ± 0.6 (45) | 32.0 ± 0.6 (34) | 32.9 ± 0.8 (17)‡ |
| LV wall thickness (mm) | | | |
| Systolic | 15.4 ± 0.5 (33) | 17.6 ± 0.7 (15) | 18.8 ± 0.6 (12)* |
| Diastolic | 8.7 ± 0.3 (33) | 9.8 ± 0.5 (16) | 10.7 ± 0.5 (13)* |
| Systolic/$m^2$ | 7.6 ± 0.3 (33) | 9.2 ± 0.3 (15)† | 10.0 ± 0.4 (12)† |
| Diastolic/$m^2$ | 4.3 ± 0.1 (33) | 5.0 ± 0.2 (16)* | 5.7 ± 0.2 (13)†,§ |
| LV dimension (mm) | | | |
| Systolic | 34.4 ± 1.1 (37) | 32.1 ± 0.89 (17) | 32.1 ± 1.4 (11) |
| Diastolic | 51.8 ± 1.03 (37) | 50.8 ± 1.3 (17) | 51.2 ± 1.4 (11) |
| Systolic/$m^2$ | 17.3 ± 0.5 (37) | 16.7 ± 0.5 (17) | 16.8 ± 0.6 (11) |
| Diastolic/$m^2$ | 26.0 ± 0.5 (37) | 26.4 ± 0.6 (17) | 27.0 ± 0.7 (11) |
| Fractional shortening | 0.34 ± 0.01 (37) | 0.36 ± 0.01 (17) | 0.37 ± 0.02 (11) |
| $V_{cf}$ (circ/s) | 1.17 ± 0.04 (37) | 1.23 ± 0.04 (17) | 1.30 ± 0.08 (11) |

Adapted from Gerstenblith G, Frederiksen J, Yin FC, et al: Echocardiographic assessment of a normal adult aging population. *Circulation* 56:273-278, 1977. Reproduced with permission. Copyright 1977 American Heart Association.

$V_{cf}$, Velocity of circumferential fiber shortening.

*$P$ <.01 as compared with group I. The number of subjects is given in parentheses next to the mean and standard error of the mean.

†$P$ <.001 as compared with group I.

‡$P$ <.05 as compared with group I.

§$P$ <.05 as compared with group II.

**TABLE 40-2 Reference Equations for Selected LA Parameters by Gender as Derived from the Subjects in the Cardiovascular Health Study**

| | *Predicted Value* | *Interval Width of Normal** | $R^2$ |
|---|---|---|---|
| **LA diameter (PLAX; cm)** | | | |
| Women | 3.82 + 0.015 age – 0.051 height (in) + 0.0085 weight (lb)<br>3.82 + 0.015 age – 1 .995 height (m) + 0.019 weight (kg) | 0.86 | 0.16 |
| Men | 1.79 + 0.024 age – 0.028 height (in) + 0.0095 weight (lb)<br>1.79 + 0.024 age – 1.095 height (m) + 0.021 weight (kg) | 0.82 | 0.15 |
| **LA length (SI; cm)** | | | |
| Women | 4.95 + 0.0006 age – 0.030 height (in) + 0.0105 weight (lb)<br>4.95 + 0.0006 age – 1.198 height (m) + 0.023 weight (kg) | 0.95 | 0.17 |
| Men | 4.01 + 0.035 age – 0.059 height (in) + 0.012 weight (lb)<br>4.01 + 0.035 age – 2.33 height (m) + 0.27 weight (kg) | 1.30 | 0.14 |
| **LA volume (mL)** | | | |
| Women | 47.7 + 0.150 age – 1.02 height (in) + 0.223 weight (lb)<br>47.7 + 0.150 age – 40.20 height (m) + 0.492 weight (kg) | 15.1 | 0.28 |
| Men | –20.6 + 0.524 age – 0.32 height (in) + 0.195 weight (lb)<br>–20.6 + 0.524 age – 12.60 height (m) + 0.431 weight (kg) | 20.6 | 0.18 |

From Aurigemma GP, Gottdiener JS, Arnold AM, et al: Left atrial volume and geometry in healthy aging: the Cardiovascular Health Study. *Circ Cardiovasc Imaging* 2:282-289, 2009. Copyright © 2009, Lippincott Williams & Wilkins. Adapted with permission Lippincott Williams & Wilkins.

*PLAX*, Parasternal long axis; *SI*, superior-inferior.

*Value to add to the predicted value to reach the upper limit of the normal range.

at the annulus, as well as at the margins of closure of the mitral leaflets on the atrial side and in the mitral valve annulus. The term *senile calcification syndrome* was coined to describe patients with aortic valve sclerosis, mitral annular calcification, and calcification of the epicardial coronary arteries.[19]

Various studies in elderly subjects have identified prevalence as high as approximately 50% for each of these lesions.[30-34] Although aortic valve sclerosis is equally common in men and women, mitral annular calcification is more frequently seen in women. The prevalence by age of mitral annular calcification in one study is listed in Table 40-5.

**TABLE 40-4 Aortic Valve Thickness for Age Ranges in 200 Normal Hearts***

| *Age (yr)* | *Range (mm)* | *Mean ± SD (mm)* |
|---|---|---|
| <20 | 0.35-1.55 | 0.67 ± 0.21 |
| 20-59 | 0.40-2.10 | 0.87 ± 0.27 |
| ≥60 | 0.55-3.50 | 1.42 ± 0.51 |

Adapted from Sahasakul Y, Edwards WD, Naessens JM, et al: Age-related changes in aortic and mitral valve thickness. Implication for two-dimensional echocardiography based on autopsy study of 200 normal hearts. *Am J Cardiol* 62:424-430, 1988. Reproduced with permission.

*SD*, Standard deviation.

*Thickness of all three cusps was measured, and the mean (± SD) was calculated.

## NORMAL CHANGES IN CARDIAC FUNCTION

### *LV Systolic Function*

Resting ejection fraction, percent fractional shortening, and cardiac output by echocardiography as well as by radionuclide ventriculography are unaffected by age in healthy normotensive people.[25,35,36] In order to maintain a normal ejection time in the setting of late systolic augmentation of aortic impedance, there is a prolonged contractile activation of the LV wall in the elderly.[36] This prolonged contractile activation means that when the mitral valve opens, myocardial relaxation is incomplete (relative to younger persons), and thus the early diastolic filling rate is lower in the elderly. Studies of rat and dog cardiac muscle have shown no change in contractile function (resting tension, peak isometric tension, maximal rate of tension development) with age.[36,37]

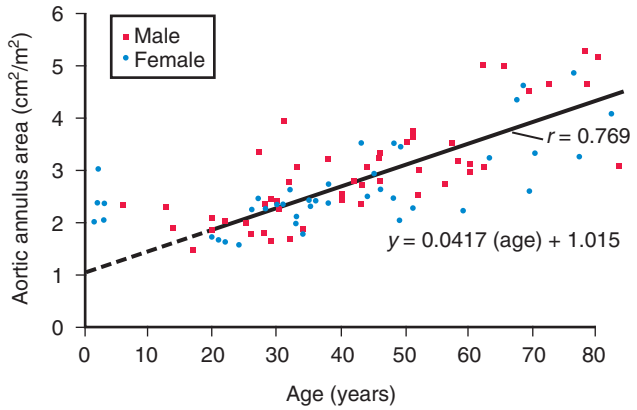



**Figure 40-4 Changes with age in the cross-sectional area of the aorta at the valve level.** Regression line shown is for patients over 20 years of age. Patients under 20 years of age, in general, have higher aortic annulus areas per square meter than predicted by the regression equation. *(From Krovetz LJ. Age-related changes in the size of the aortic valve annulus in man.* Am Heart J *90:569-574, 1975.)*

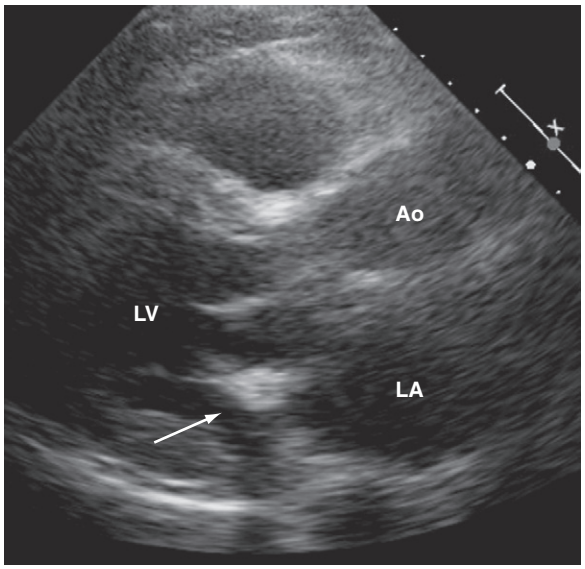



**Figure 40-6 Mitral annular calcification.** Note nodule of calcium on posterior annulus of mitral valve (*arrow*) in this parasternal long-axis view.

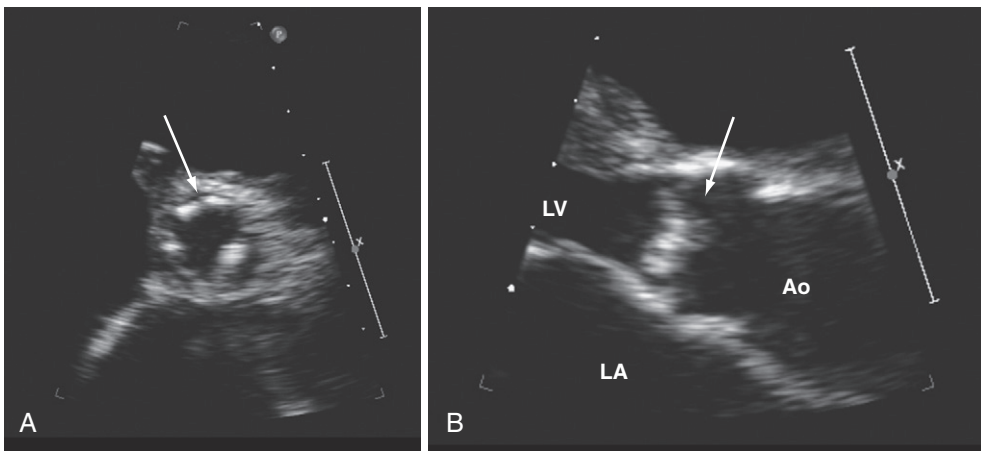



**Figure 40-5 Aortic sclerosis.** Note bright nodularity present on the aortic valve leaflets (*arrows*) in both short axis (**A**) in systole and long axis (**B**) in diastole.

**TABLE 40-5 Prevalence of Mitral Annular Calcification**

| *Age (yr)* | *Men* | *Women* |
|---|---|---|
| 62-70 | 4/22 (18)* | 7/35 (20)* |
| 71-80 | 13/42 (31) | 40/116 (34) |
| 81-90 | 44/75 (59) | 146/226 (64) |
| 91-100 | 19/22 (86) | 56/63 (89) |
| 101-103 | | 3/3 (100) |

Adapted from Aronow WS, Schwartz KS, Koenigsberg M: Correlation of atrial fibrillation with presence or absence of mitral annular calcium in 604 persons older than 60 years. *Am J Cardiol* 59:1213-1214, 1987.
*Number affected per total number, with the percentage affected given within parentheses.

**TABLE 40-6 Mean and Percentile Values of Doppler Diastolic Filling Indices for 114 Study Subjects Over 70 Years of Age**

| *Diastolic Indices* | *Mean* | Lower Percentiles | | Median Percentile | | Upper Percentiles | |
|---|---|---|---|---|---|---|---|
| | | *5%* | *10%* | *50%* | *75%* | *90%* | *95%* |
| E velocity (m/s) | 0.44 | 0.25 | 0.26 | 0.41 | 0.51 | 0.69 | 0.76 |
| A velocity (m/s) | 0.59 | 0.38 | 0.43 | 0.56 | 0.68 | 0.80 | 0.84 |
| E/A (ratio) | 0.76 | 0.48 | 0.52 | 0.70 | 0.86 | 1.05 | 1.21 |
| E/A VTI (ratio) | 1.36 | 0.79 | 0.90 | 1.33 | 1.57 | 1.76 | 1.94 |
| AFF (ratio) | 0.40 | 0.29 | 0.32 | 0.40 | 0.44 | 0.49 | 0.52 |
| AT (sec) | 0.06 | 0.02 | 0.03 | 0.05 | 0.07 | 0.08 | 0.09 |
| DT (sec) | 0.14 | 0.09 | 0.10 | 0.14 | 0.16 | 0.19 | 0.23 |

Modified from Sagie A, Benjamin EJ, Galderisi M, et al: Reference values for Doppler indexes of left ventricular diastolic filling in the elderly. *J Am Soc Echocardiogr* 6:570-576, 1993.
*AFF*, Atrial filling fraction; *A velocity*, peak velocity A; *AT*, acceleration time; *DT*, deceleration time; *E/A*, ratio of early to late peak velocities; *E/A VTI*, ratio of early to late time-velocity integrals; *E velocity*, peak velocity E.

### *LV Diastolic Function*

Although LV systolic performance in the aged is preserved, LV diastolic function changes markedly with age. Seminal work in this area showed a reduction in mitral valve E-F closure slope on M-mode echocardiography.[2,3] Later work utilizing pulsed Doppler examination confirmed that there was a reduction in early diastolic peak filling rate (peak E-wave velocity) of approximately 50% between 20 and 80 years of age. There is a concomitant increase with age in peak A-wave velocity, representing late LV filling resulting from atrial contraction. This atrial "kick" is powered by a modest age-related increase in LA size. It is reasonable to consider the augmented atrial contribution to LV filling to be a successful compensatory mechanism to the reduced early diastolic filling rate into the thicker, presumably less compliant ventricle.

A number of mechanisms have been proposed to explain the changes in diastolic function that occur with aging, and all likely play some role. These mechanisms include a lower rate of calcium accumulation by the sarcoplasmic reticulum.[38] Studies of whole animal hearts and isolated cardiac muscle have documented prolonged isovolumic relaxation and increased myocardial diastolic stiffness.[39] Sclerosis of the mitral leaflets with resultant prolonged diastolic filling time (late closure) has also been proposed as a possible mechanism, as has an increase in afterload.

Data from the Framingham Heart Study were used to establish reference values for various Doppler parameters for elderly patients, as depicted in Table 40-6.[40] These data were obtained by studying 114 men and women aged 70 to 87 years of age who were screened and found to be free of cardiovascular disease. Notably, the vast majority (87%) of these subjects had peak E/A velocity ratios less than 1.0; 75% had values less than 0.86; and 25% had values less than 0.62. Because normal young subjects have E/A velocities greater than 1.0, it may be inappropriate to use this as the normal standard against which to compare the diastolic function of an elderly person (Fig. 40-7; also see Chapter 11).

### *Cardiac Response to Pressor Stress*

The usual response of increases in blood pressure and heart rate in response to sustained, isometric handgrip is altered in healthy elderly as opposed to young persons. Heart rate does not increase as much in the older group, but blood pressure is increased more than in the young. Accompanying these changes are mild increases in echocardiographically measured LV diastolic and systolic dimensions that occur in the aged.[41,42] Similar changes in LV cavity size and blunted heart rate increase have been seen in response to phenylephrine infusion in healthy older versus younger volunteers.[43] It therefore appears that because of reduced contractile reserve in the aged heart in response to increased afterload, overall systolic performance is maintained by cavity enlargement (i.e., the Frank-Starling mechanism).

### *Cardiac Response to Exercise Stress*

Multiple studies have shown that maximum oxygen consumption declines with age. This finding is likely multifactorial and involves changes in cardiac output, pulmonary function, and muscle function, among other factors. There has also been a documented age-associated decline in maximum exercise cardiac output that is a result of the aforementioned blunted heart rate response to exercise. With exercise, stroke volume is maintained with aging. The mechanism by which this occurs is that larger LV end-diastolic volumes are achieved with exercise, which offsets the blunted capacity of the aging heart to reduce end-systolic volume. The larger LV end-diastolic volume is achieved to some degree as a result of the slower heart rate (longer diastolic filling time), as well as the larger end-systolic volume.[44]

Ejection fraction, however, does not increase as much in older healthy individuals as in younger ones, and they do not reach the same peak as in younger persons.[44] This results from a decreased ability to reduce their end-systolic volumes. These findings likely result from multiple mechanisms. These include reduced myocardial contractility, increased vascular afterload, diminished autonomic modulation of LV contractility and arterial afterload, and arterial-ventricular load mismatching.[45]

## Clinical Outcome Data

### VALVULAR HEART DISEASE

### *Aortic Valve Sclerosis*

Aortic valve sclerosis is one end of the spectrum of calcific aortic valvular disease. Early aortic sclerosis is characterized by mild focal (not diffuse) areas of leaflet thickening without restriction of outflow, At the other end of the spectrum is aortic stenosis, which may progress to severe calcification with restricted leaflet motion and obstruction to LV outflow. The lesions of early aortic sclerosis are complex focal subendothelial

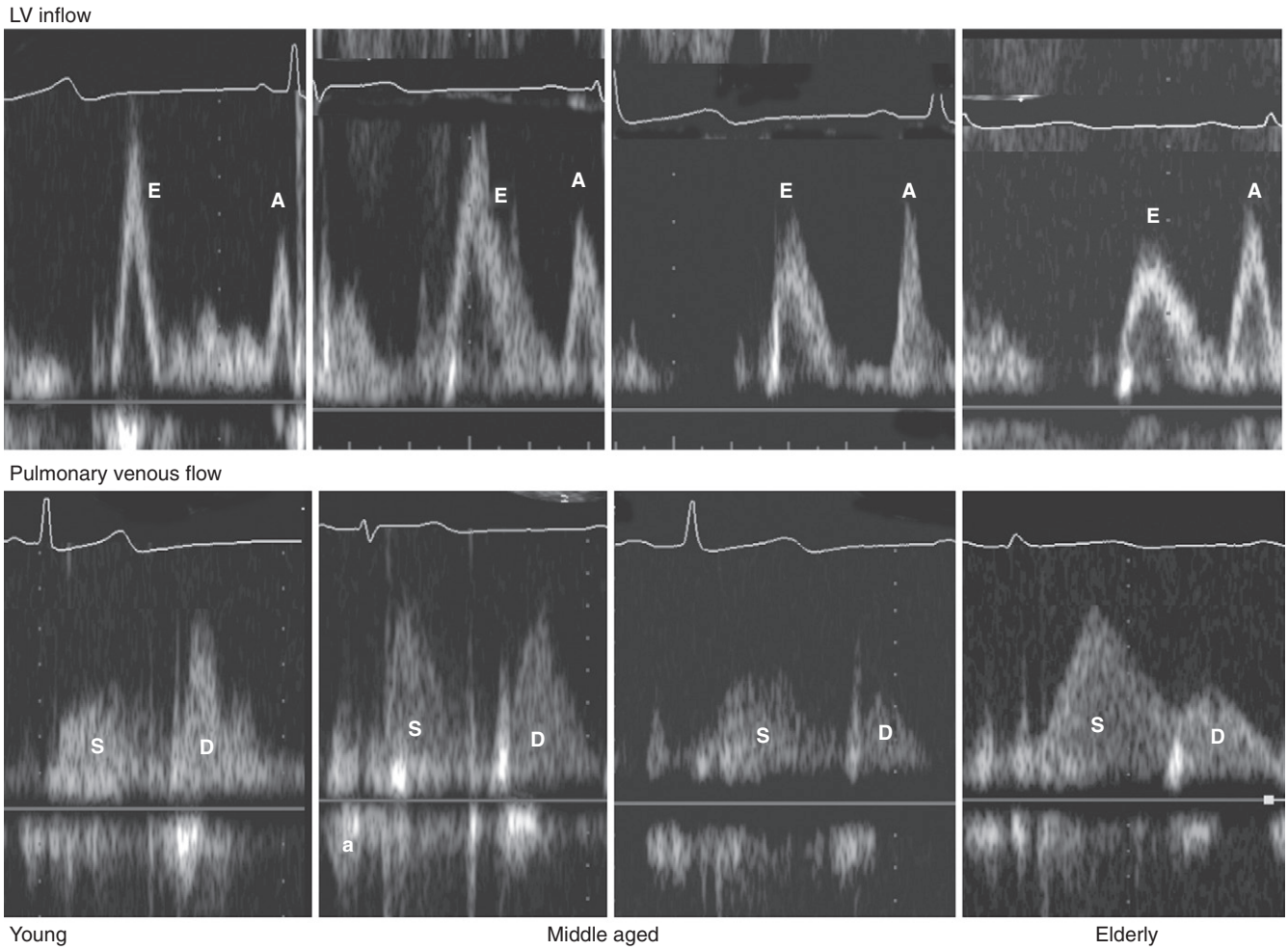



**Figure 40-7 Changes in LV and LA filling patterns with age.** Mitral inflow (*upper panels*) and pulmonary vein (*lower panels*) Doppler tracings from normal young, middle-aged, and elderly individuals. Normal progression of changes in LV filling is shown.

plaque-like lesions located on the aortic side of the valve leaflet that extend to the fibrosa layer. These lesions are probably reactions to increased mechanical or decreased shear stresses. Mechanical stresses are greatest on the aortic side near the attachments of the leaflets to the aortic root. Shear stress across the noncoronary cusp is lowest because of a lack of diastolic coronary blood flow, which probably explains why the noncoronary cusp is usually the first affected.[46] Patients with aortic stenosis who have bicuspid valves tend to present 20 years younger than patients with trileaflet valves, which supports the concept that mechanical stress (bileaflet valves are subject to a greater amount of such stress) is important in the pathogenesis of the disease.[46] The lesions of aortic valve sclerosis are active, with evidence of an accumulation of an inflammatory cell infiltrate, microscopic calcification, an accumulation of low-density lipoproteins and lipoprotein(a), and evidence of LDL oxidation.[47-50] As the process continues, calcification increases and there is active bone formation.[51] Ultimately, leaflet calcification can become so severe that opening of the valve is impaired, and hemodynamically significant aortic stenosis results. In longitudinal studies documenting progression from aortic valve sclerosis to aortic stenosis, moderate stenosis (jet velocity 3 to 4 m/s) was found in 3% of patients in one study and 5% in a second, and severe stenosis (jet velocity greater than 4 m/s) in 2.5% of patients in both studies.[52,53] Although the vast majority of patients will not progress to significant aortic stenosis, given the high prevalence of aortic valve sclerosis in the aging population, the sheer number of patients who could be affected is high, and thus its identification is important (see also Chapter 23).

### *Mitral Annular Calcification*

As noted, mitral annular calcification is characterized by calcification at the leaflet margins and in the annulus. It has been classified by its anatomic position. Anterior mitral annular calcification is defined by bright echodensities located at the level of the anterior mitral valve leaflet in systole and diastole and may extend from the annulus throughout the base of the heart into the mitral and aortic valves. Posterior mitral annular calcification is defined by similar echo signals anterior to the left posterior wall and merging with it.[54] Although many echocardiographers use personal subjective criteria to grade the severity of mitral annular calcification, a more systematic approach has also been used.[55] Mild mitral annular calcification can be defined as involving less than one third of the annular circumference (less than 3 mm in width) and are usually restricted to the angle between the posterior leaflet of the mitral valve and the LV posterior wall. In moderate mitral annular calcification, less than two thirds of the annular circumference is involved

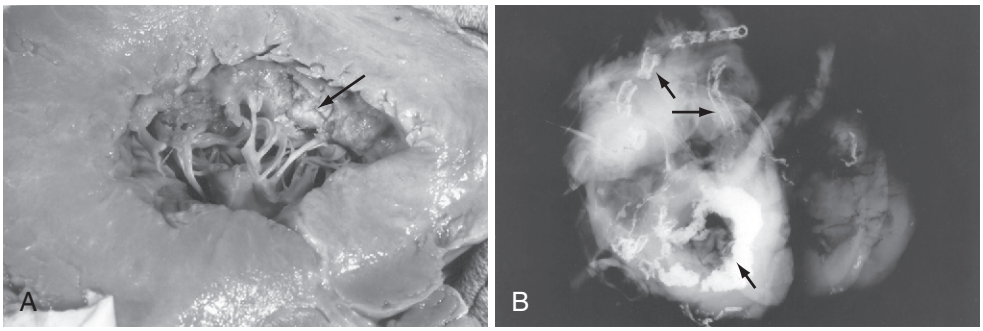



**Figure 40-8 Gross pathologic specimen depicting mitral annular calcification. A,** Ventricular aspect of mitral valve shows nodules of calcium deposited at annulus adherent to valve leaflet and chordae (*arrow*). **B,** Postmortem radiograph shows nearly "O"-shaped mitral annular calcification (*large arrow*) and calcified coronary arteries (*small arrows*).

(3 to 5 mm in width). In severe mitral annular calcification, more than two thirds of the circumference is affected (greater than 5 mm in width). It usually extends beneath the entire posterior mitral leaflet and may make a complete circle.

A rare variant of mitral annular calcification, called caseous calcification of the mitral ring, has been described. Echocardiographically, this entity is a large echodense structure with an echolucent center and smooth borders. Pathologically, it is composed of a mixture of calcium, cholesterol, and fatty acids.[56,57] It likely represents an active process, as in one longitudinal study, it was noted that some patients who had classic mitral annular calcification at baseline developed the appearance of caseous calcification, and some patients who had caseous calcification "reverted" back to the classic appearance.[58] Pathologically, in cases that have gone to surgery or autopsy, findings have included a calcified envelope surrounding caseous necrosis with cholesterol and fatty acids.[59] Others have found an amorphous eosinophilic acellular material surrounded by macrophages and lymphocytes.[57,60,61] Although the pathology is generally considered benign, it can be a nidus for infection[62] or thrombus and thus is a possible source of embolism.

### Mitral Annular Calcification and Valvular Dysfunction

There is a wide spectrum of calcification in mitral annular calcification and is probably progressive (Fig. 40-8). It usually begins with a small amount of calcium deposition at the basal insertion of the posterior mitral leaflet. Calcification of the annular connective tissue ensues and may form a ridge or ring that encircles the leaflets. As it progresses further, it may bulge into the LV cavity below the posterior leaflet and lift the leaflets toward the LA.[63,64] A larger extent of involvement may render the base of the posterior leaflet immobile and result in varying amounts of valvular regurgitation.[65] Actual leaflet calcification, however, is uncommon. The severity of mitral annular calcification seems to be correlated with the severity of associated mitral regurgitation when it is present.[65-67]

Mitral stenosis as a result of mitral annular calcification has also been described. In contrast to rheumatic mitral stenosis, where there is commissural fusion, in mitral annular calcification–associated mitral stenosis, the leaflets are not fused, but the increased flow velocities are a result of the decreased mitral annular excursion resulting from calcification.[68] Recent studies have suggested that mitral annular calcification, as the etiology of mitral stenosis, tends to be more mild in severity. However, it may be more common than previously thought and also is associated with risk factors for coronary artery disease.[69,70]

### Mitral Annular Calcification and Other Pathology

Mitral annular calcification is associated with LA well as LV enlargement.[55,71-73] In a prospective study of 976 elderly patients with and without mitral annular calcification, LA enlargement was 2.4 times more prevalent in patients with mitral annular calcification than in those without mitral annular calcification.[71]

### Mitral Annular Calcification and Conduction Abnormalities

Likely secondary to concomitant calcification within the conduction system (which may be contiguous as calcium extends from the annulus into the interventricular septum), mitral annular calcification is associated with conduction abnormalities such as atrioventricular block, sinoatrial node disease, bundle branch block, left anterior fascicular block, and nonspecific intraventricular conduction delay.[55,58,63,74]

### Mitral Annular Calcification and Atrial Fibrillation

Likely owing to the associated LA enlargement, atrial fibrillation is more common in patients with mitral annular calcification than in those without it. In various studies, the relative risk was increased from 1.4 to 12 times.[55,72,75,76]

### Mitral Annular Calcification and Thromboembolism

Mitral annular calcification is associated with a number of conditions that predispose to thromboembolic stroke, such as atrial fibrillation, mitral regurgitation and stenosis, LA enlargement, and heart failure. In addition, mitral annular calcification has been associated with aortic atheromata,[33,77] complex aortic debris,[78] and calcification of the thoracic aorta,[79] all of which could be sources of thromboembolic material. On the other hand, there is reason to suspect that mitral annular calcification itself may be involved in providing a source for thromboemboli. Although the calcification in mitral annular calcification is usually covered by a layer of endothelium, ulceration of the lining may expose the calcium and serve as a starting point for fibrin-platelet clot, which may embolize.[63,71] A number of studies designed to control for other factors have revealed an association of mitral annular calcification with cerebral embolization, with relative risks of 1.5 to 5.0.[55,71,75,80-84]

Studies have found mitral annular calcification to be an independent risk factor for stroke in patients who were in atrial fibrillation as well as those who were in sinus rhythm.[75] In the Strong Heart Study, mitral annular calcification, but not aortic valve sclerosis, was found to be a strong risk factor for incident stroke.[85] This has led to some advocating prophylactic

anticoagulation in patients with mitral annular calcification, regardless of rhythm.[86] Not all studies have found an association between mitral annular calcification and stroke, however.[87,88]

### Mitral Annular Calcification and Endocarditis

Abnormal valve morphology, hemodynamics, and endothelium have been implicated as predisposing the valve to infection (endocarditis).[71,63] In particular, patients with mitral annular calcification and chronic renal failure, seem to be at especially high risk.[89] Treatment of patients with antibiotics may also be less effective, as the avascular nature of the mitral annulus predisposes to periannular abscesses, and therefore some advocate antibiotic prophylaxis for patients with mitral annular calcification undergoing invasive procedures. However, the American Heart Association's most recent guidelines do not recommend prophylaxis for acquired aortic or mitral valve disease.[90,91]

### Mitral Annular Calcification and Renal Dysfunction

There has been increasing interest in studying the links between calcific valvular heart disease and renal dysfunction.[92] Data from the Cardiovascular Health Study[93] and the Framingham Offspring Study[94] have shown a relationship between chronic kidney disease and mitral annular calcification, but *not* with aortic valve sclerosis. On the other hand, data from the Multi-Ethnic Study of Atherosclerosis showed an association between impaired renal function and mitral annular calcification only among diabetics and did show a modest association between impaired renal function and aortic valve calcification.[95] The reasons for these differences have not yet been elucidated.

### *Aortic Valve Sclerosis and Mitral Annular Calcification: Cardiovascular Outcomes*

Several studies have found a strong association between mitral annular calcification and aortic valve sclerosis with adverse cardiovascular outcomes and mortality.[32,34,84,96-99] Otto and colleagues[34] found that in 5621 men and women 65 years of age or older who were participants in the Cardiovascular Health Study, aortic sclerosis (without hemodynamically significant outflow obstruction) was associated with an approximately 50% increase risk of death from cardiovascular causes and a 40% increase in the risk of myocardial infarction. In another study of 2358 elderly patients, those with aortic valve sclerosis had a risk of developing a new coronary event that was 1.8 times higher than those without it.[32] Lending support to the concept that calcific aortic valve disease and atherosclerotic vascular disease have a shared pathogenesis are data from Otto's study that older age, male gender, smoking, hypertension, and hyperlipidemia were associated with aortic sclerosis. Data from the Multi-Ethnic Study of Atherosclerosis have also linked mitral annular calcification with atherosclerotic vascular risk factors.[70] In the Northern Manhattan Study, 1655 subjects aged at least 40 years (average 68) without a history of myocardial infarction or stroke were followed for an average of approximately 7 years. The prevalence of mitral annular calcification was 27%, and after adjustment for traditional cardiovascular risk factors, mitral annular calcification was found to be a strong and independent predictor of myocardial infarction and vascular death (but not ischemic stroke). The risk increase was directly related to the severity of the calcification.[100]

Using data from the Cardiovascular Health Study, Barasch and co-workers[101] evaluated the prevalence and clinical outcomes of mitral annular calcification, aortic valve sclerosis, and aortic annular calcification. The 3929 subjects had a mean age of 76 years; 60% were women. In this study, mitral annular calcification was seen in 42% of subjects, aortic annular calcification in 44%, and aortic valve sclerosis in 54%. The rate of all three conditions being found in a single subject was 17%. Subjects with these conditions tended to be older, and those with mitral annular calcification had worse risk profiles (e.g., LV hypertrophy/mass, LA size, abnormal ejection fraction, carotid intimal media thickness, dyslipidemia, C-reactive protein) than those with aortic valve sclerosis and aortic annular calcification. In addition, this study showed that the severity of mitral annular calcification (estimated from 2D echocardiography, semiquantitatively) was associated with a higher prevalence of atherosclerotic vascular disease, independent of other risk factors. These conditions were associated with a significantly elevated risk of cardiovascular disease endpoints, and the strongest association was with the combined group (mitral annular calcification, aortic annular calcification, and aortic valve sclerosis) with heart failure (odds ratio 2.04, 95% confidence interval 1.34 to 3.09) (Figs. 40-9 and 40-10; Table 40-7).

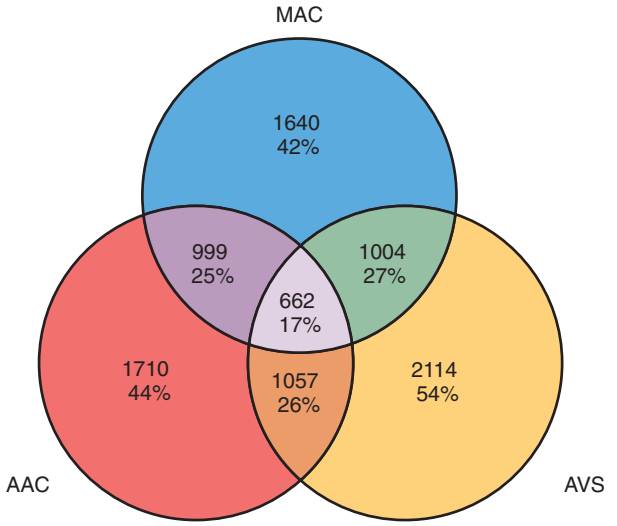



**Figure 40-9 Relationship between mitral annular calcification (*MAC*), aortic annular calcification (*AAC*), and aortic valve sclerosis (*AVS*) in 3929 participants in the Cardiovascular Health Study.** Numbers are total numbers of patients, and percentages refer to the percent of the total population of 3929 study participants. *(From Barasch E, Gottdiener JS, Larsen EKM, et al: Clinical significance of calcification of the fibrous skeleton of the heart and aortosclerosis in community dwelling elderly. The Cardiovascular Health Study (CHS).* Am Heart J *151:39-47, 2006. Reprinted with permission.)*

Although not definitively proven, a good deal of research has strongly suggested a relationship between calcification of the fibrous skeleton of the heart and aortic valve cusps and advanced atherosclerosis.[54,102-104] Inflammation and abnormalities of lipid metabolism have both been implicated in the development of both atherosclerosis and aortic valve calcification.[51,105-107] Other data have failed to support the association of inflammatory markers with calcific aortic valvular disease, however.[108]

## LEFT VENTRICULAR HYPERTROPHY

Data from both the Framingham Study and the Cardiovascular Health Study confirm that LV hypertrophy is a potent predictor of morbidity and mortality from coronary heart disease, heart failure, and stroke.[88,109,110]

The relationship between age and LV hypertrophy is complex. Evaluation of data from the Framingham Heart Study revealed

**TABLE 40-7 Odds Ratios (95% CI) for the Association of Valve Calcification with Major Cardiovascular Endpoints Adjusted for Age, Sex, and Race**

| | Odds Ratio (95% CI) | | | | |
|---|---|---|---|---|---|
| *Calcification Category* | *Myocardial Infarction* | *Stroke* | *Angina Pectoris* | *Heart Failure* | *Revascularization* |
| MAC | 1.70 (1.38-2.09) | 1.84 (1.40-2.41) | 1.29 (1.11-1.51) | 1.69 (1.31-2.17) | 1.50 (1.18-1.91) |
| AAC | 1.17 (0.95-1.54) | 1.13 (0.86-1.48) | 1.21 (1.03-1.42) | 1.75 (1.34-2.27) | 1.33 (1.04-1.71) |
| AVS | 1.27 (1.03-1.57) | 1.16 (0.88-1.53) | 1.24 (1.06-1.45) | 1.02 (0.79-1.31) | 1.07 (0.84-1.37) |
| MAC + AAC + AVS | 1.86 (1.32-2.62) | 1.95 (1.26-3.03) | 1.60 (1.24-2.07) | 2.04 (1.34-3.09) | 1.85 (1.21-2.84) |

The study involved the 3929 participants enrolled in the Cardiovascular Health Study.
From Barasch E, Gottdiener JS, Larsen EKM, et al: Clinical significance of calcification of the fibrous skeleton of the heart and aortosclerosis in community dwelling elderly. The Cardiovascular Health Study (CHS). *Am Heart J* 151:39-47, 2006. Reprinted with permission.
*AAC*, Aortic annular calcification; *AVS*, aortic valve sclerosis; *CI*, confidence interval; *MAC*, mitral annular calcification.

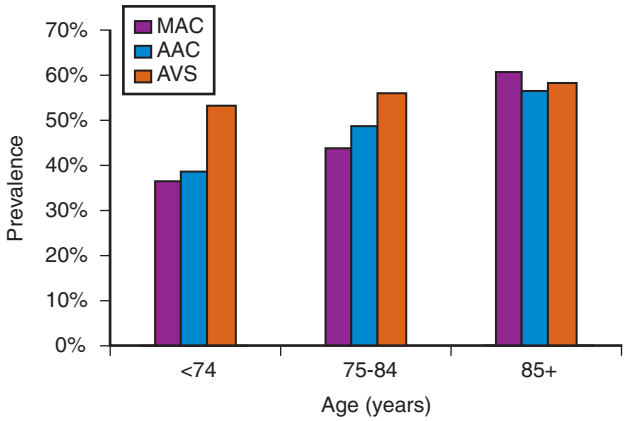



**Figure 40-10 Distribution of mitral annular calcification, aortic annular calcification, and aortic valve sclerosis in the three age groups of the 3929 participants enrolled in the Cardiovascular Health Study.** MAC: $P < 0.001$; AAC: $P < 0.001$; AVS: $P = 0.055$. *AAC*, Aortic annular calcification; *AVS*, aortic valve sclerosis; *MAC*, mitral annular calcification. *From Barasch E, Gottdiener JS, Larsen EKM, et al: Clinical significance of calcification of the fibrous skeleton of the heart and aortosclerosis in community dwelling elderly. The Cardiovascular Health Study (CHS).* Am Heart J *151:39-47, 2006. Reprinted with permission.*

**TABLE 40-8 Cumulative Cardiovascular Endpoints by LA Enlargement**

| | Enlarged LA (n = 461) | | Normal LA (n = 2343) | | |
|---|---|---|---|---|---|
| *Clinical Outcome* | *n* | *%* | *n* | *%* | *P* |
| First cardiovascular event | 86 | 18.7 | 282 | 12.0 | <.001 |
| Fatal and nonfatal CHD* | 52 | 11.2 | 169 | 7.2 | .003 |
| Fatal and nonfatal stroke | 15 | 3.3 | 51 | 2.2 | .186 |
| Fatal and nonfatal heart failure | 19 | 4.1 | 62 | 2.6 | .084 |
| Any cardiovascular death | 23 | 5.0 | 67 | 2.9 | .018 |

Data from the 2084 middle-aged and elderly participants in the Strong Heart Study.
Adapted from Kizer JR, Bella JN, Palmieri V, et al: Left atrial diameter as an independent predictor of first clinical cardiovascular events in middle-aged and elderly adults: The Strong Heart Study (SHS). *Am Heart J* 151:412-418, 2006. Reprinted with permission.
*CHD*, Coronary heart disease.
*Includes fatal and nonfatal myocardial infarction, sudden cardiac death, and other fatal and nonfatal coronary heart disease.

that age, height, systolic blood pressure, and body mass index were significant and independent predictors of LV mass in 4972 people aged 17 to 90 years. However, age was no longer a significant correlate of LV mass when people were screened out of the analysis who met one of the following conditions: evidence of cardiovascular disease on history, physical exam, electrocardiogram, chest radiography, or echocardiography; blood pressure greater than or equal to 140/90; on medications for cardiopulmonary disease; or at least 20% above or below recommended weight for height.[111] Thus, it seems that the increases in LV mass that are seen with age are often confounded by coexisting cardiopulmonary disease.

In the Seventh Report of the Joint National Committee on Prevention, Detection, Evaluation and Treatment of High Blood Pressure (JNC 7), the identification of LV hypertrophy in a patient with hypertension is considered evidence of target organ damage and thus is considered an indication for aggressive blood pressure management.[112]

## LEFT ATRIAL SIZE AND OUTCOMES

Elevated LA size has been shown to be a marker of cardiovascular risk. Largely from studies carried out in elderly populations, an enlarged LA is associated with an increased risk of atrial fibrillation, stroke, and death (including after myocardial infarction, in patients with mitral regurgitation, hypertension, and dilated cardiomyopathies).[113-119] Using data from the Strong Heart Study, Kizer and co-workers[120] showed that LA diameter (normal defined as less than 3.8 cm for women, less than 4.2 cm for men) was an independent predictor of incident cardiovascular events after adjustment for other factors (clinical, echocardiographic, inflammatory) (Table 40-8; Fig. 40-11). As noted, LA volume is emerging as a more robust measure of cardiovascular risk. In patients with mitral stenosis who are in sinus rhythm but have no history of embolism or thrombus, guidelines from the European Society of Cardiology as well as from the American College of Cardiology/American Heart Association suggest that anticoagulation can be considered if there is an enlarged LA or dense spontaneous echo contrast seen on echocardiography, albeit with lower level of evidence ratings.[91,121] Given this, Keenan and colleagues[122] compared measures of volume versus diameter in patients with mitral stenosis and showed that LA volume more strongly correlated with echocardiographic measures of thromboembolic risk (peak LA appendage emptying velocity, spontaneous LA contrast density during TEE) than LA diameter in patients with mitral stenosis (Fig. 40-12). These data would support using volumetric measurements over linear ones.

## HEART FAILURE

The reversal of early and late diastolic filling with age results in preserved end-diastolic and stroke volume (and therefore cardiac output), but a reduction in LV compliance may cause an elevated LV end-diastolic pressure in the elderly, especially with tachycardia (see Chapter 26). This would be expected to cause dyspnea to be more easily provoked and presumably forms the basis of heart failure in some patients.

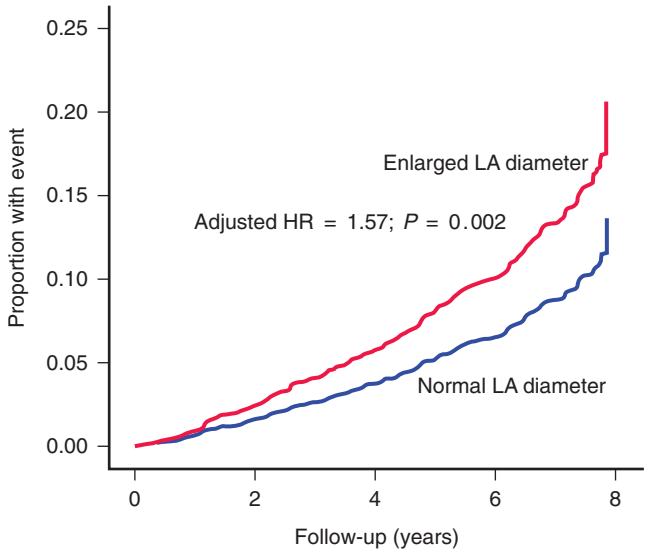



**Figure 40-11 Incidence of cardiovascular events by LA diameter in the Strong Heart Study, a study of 2084 middle-aged and elderly persons.** Adjusted Kaplan-Meier curves of first cardiovascular events according to presence or absence of LA enlargement. *HR*, Heart rate. *(Adapted from Kizer JR, Bella JN, Palmieri V, et al: LA diameter as an independent predictor of first clinical cardiovascular events in middle-aged and elderly adults: the Strong Heart Study [SHS].* Am Heart J *151:412-418, 2006. Reprinted with permission.)*

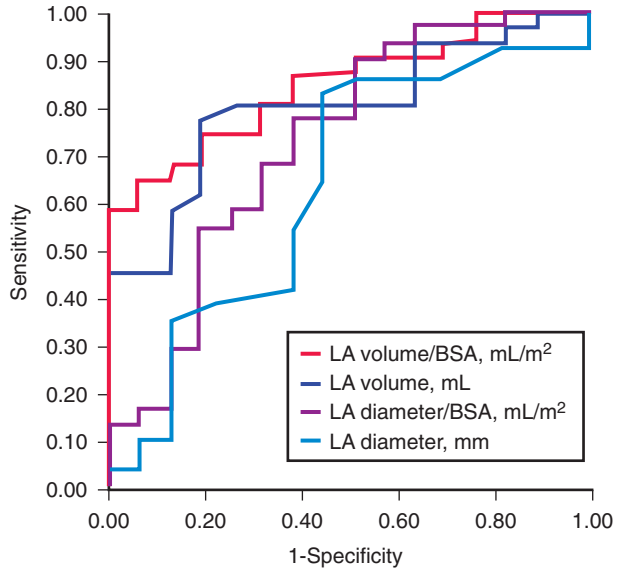



**Figure 40-12 LA size measurements as an index of thromboembolic risk.** Receiver operating characteristics curves of LA measurements (LA diameter, LA diameter indexed to body surface area [BSA], LA volume, and LA volume indexed to BSA) in diagnosing high thromboembolic risk (LA appendage emptying velocity <25 cm/s and/or dense spontaneous echocardiographic contrast). *(From Keenan NG, Cueff C, Cimadevilla C, et al: Usefulness of LA volume versus diameter to assess thromboembolic risk in mitral stenosis.* Am J Cardiol *106:1152-1156, 2010. Copyright © 2010, Elsevier. Reprinted by permission of Elsevier.)*

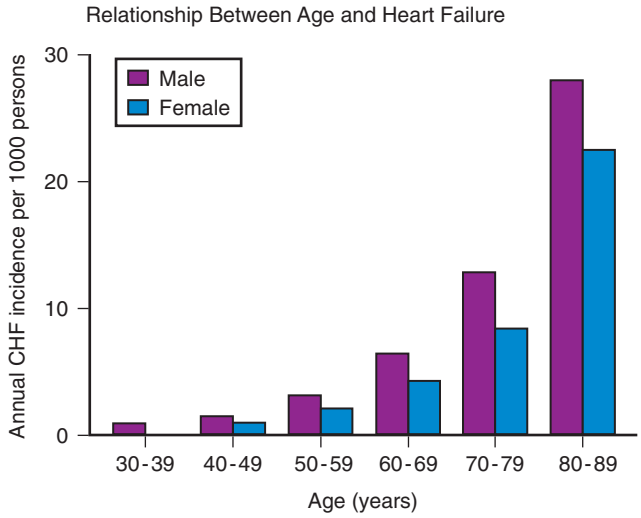



**Figure 40-13 Relationship between age, gender, and heart failure in Cardiovascular Health Study.** *(From Kitzman DW, Gardin JM, Gottdiener JS, et al: Importance of heart failure with preserved systolic function in patients 65 years of age.* Am J Cardiol *87:413-419, 2001.)*

**Box 40-1**

## EXAMPLES OF THE ETIOLOGY OF HEART FAILURE WITH PRESERVED EJECTION FRACTION

- Diastolic heart failure
  - Hypertension
  - Restrictive cardiomyopathy
  - Infiltrative cardiomyopathy
  - Hypertrophic cardiomyopathy
  - Noncompaction cardiomyopathy
- Right heart failure
  - Severe pulmonary hypertension
  - RV infarction
  - Arrhythmogenic RV dysplasia
  - Atrial septal defect
- Valvular heart diseases
  - Severe valvular stenosis
  - Severe valvular regurgitation
- Pericardial disease
  - Cardiac tamponade
  - Constrictive pericarditis
- Intracardiac mass
  - Atrial myxoma
  - Apical eosinophilic thrombus
- Pulmonary vein stenosis
- Congenital heart diseases

Adapted from Oh JK, Hatle L, Tajik AJ et al: Diastolic heart failure can be diagnosed by comprehensive two-dimensional and Doppler echocardiography. *J Am Coll Cardiol* 47:500-506, 2006. Reprinted with permission.

The syndrome of heart failure is common in the elderly and is increasingly prevalent with increasing age. In the Framingham Heart Study, the incidence of heart failure increased fivefold from age 40 to 70 years.[123] The Cardiovascular Health Study, which studied older men and women, found an increased prevalence of heart failure in women, from 4.1% at age 70 to 14.3% at age 85 (Fig. 40-13). The figures for men were 7.8% increasing to 18.4%.[124] Heart failure with normal or near-normal systolic function is also particularly prevalent in the elderly. Multiple population-based studies have suggested that 50% or more of elderly patients with heart failure have normal or near-normal systolic function. These studies have also documented that heart failure with preserved ejection fraction (HFpEF) is more common in women than in men.[21,125-128] Because women outnumber men in the older age group, the problem is even more prevalent with advancing age.

There are multiple etiologies of HFpEF, and several are listed in Box 40-1.[129] Evaluation of patients with heart failure by

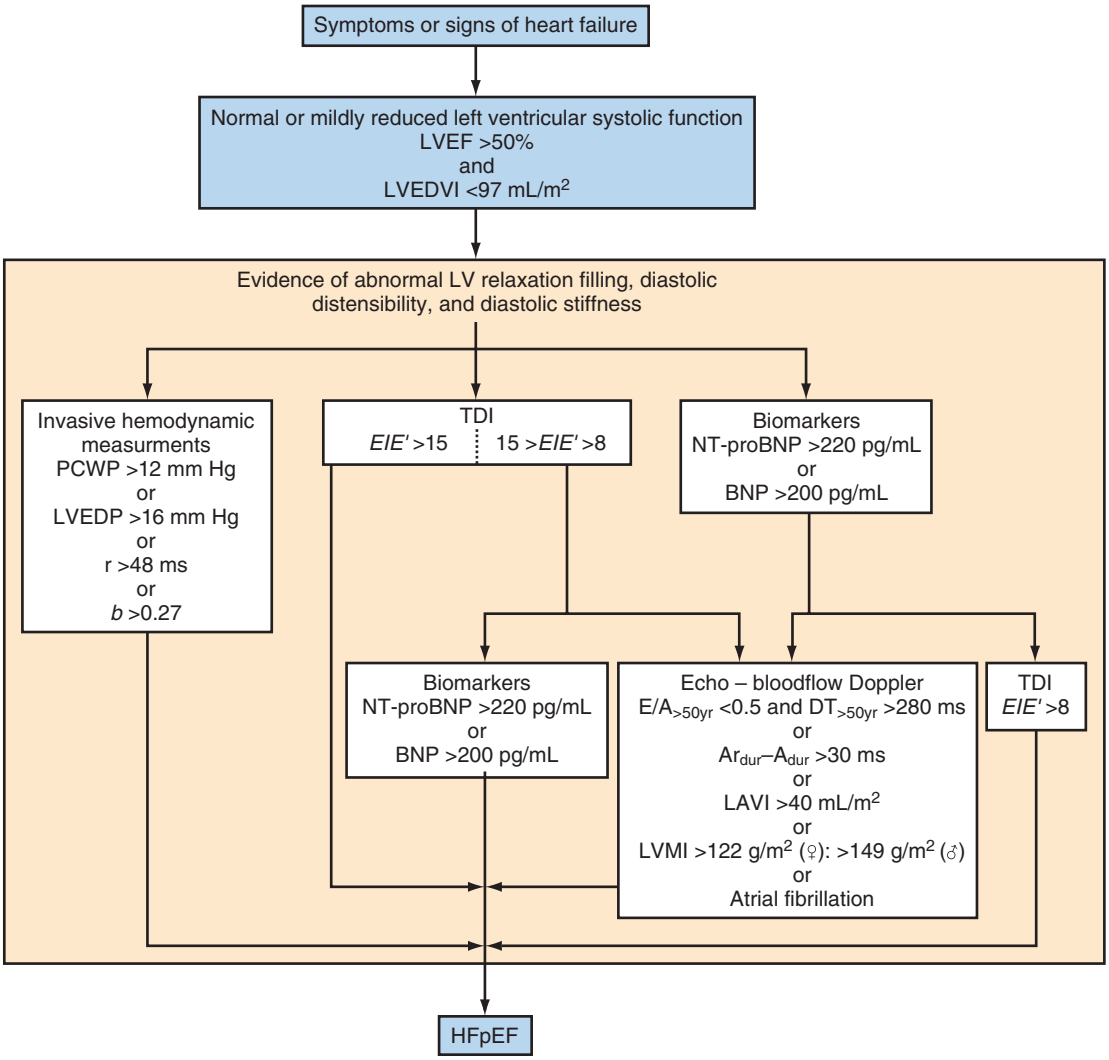



**Figure 40-14 Diagnostic flowchart for diagnosis of heart failure with preserved ejection fraction (HFpEF) in a patient suspected of having the condition.** $A_{dur}$, Duration of mitral valve atrial wave flow; *Ard*, duration of reverse pulmonary vein atrial systole flow; *b*, constant of LV chamber stiffness; *BNP*, brain natriuretic peptide; *DT*, deceleration time; *E*, early mitral valve flow velocity; *E′*, early tissue-Doppler lengthening velocity; *E/A*, ratio of early (E) to late (A) mitral valve flow velocity; *HFpEF*, heart failure with preserved ejection fraction; *LAVI*, left atrial volume index; *LVEDP*, LV end-diastolic pressure; *LVEDVI*, LV end-diastolic volume index; *LVMI*, LV mass index; *PCWP*, mean pulmonary capillary wedge pressure; *NT-proBNP*, N-terminal-pro brain natriuretic peptide; *t*, time constant of LV relaxation; *TDI*, tissue-Doppler imaging. *(From Paulus WJ, Tschope C, Sanderson JE, et al: How to diagnose diastolic heart failure: a consensus statement on the diagnosis of heart failure with normal LV ejection fraction by the Heart Failure and Echocardiography Associations of the European Society of Cardiology.* Eur Heart J *28:2539-2550, 2007. Copyright © 2007, Oxford University Press. Reprinted by permission of Oxford University Press.)*

echocardiography can lead to a diagnosis of the etiology of heart failure and as such can lead to more appropriate evaluation and treatment of the condition. It is important to recognize how prevalent heart failure is in the elderly, as well as the fact that patients with HFpEF also have impaired survival (although in some studies not to the same degree).[21,130,131] Furthermore, it has been shown that patients who do not have the syndrome of heart failure, but who have been found to have diastolic dysfunction, also have higher mortality than those with normal diastolic function.[132]

The current European Society of Cardiology consensus statement[133] on the diagnosis of heart failure with a normal ejection fraction include echocardiographic measures of abnormal diastolic function (Fig. 40-14).

## CORONARY ARTERY DISEASE AND STRESS TESTING

The identification of findings supportive of a diagnosis of coronary artery disease is very common in the elderly, as age is a major risk factor for coronary disease. Wall motion abnormalities, wall thinning, and aneurysm formation from prior myocardial infarction may be seen.

Stress echocardiography (exercise or pharmacologic) is a modality commonly used to evaluate for coronary artery disease and sometimes to evaluate myocardial viability (see also Chapters 15 and 16). The techniques used are the same for the elderly as for the younger patient. Age-adjusted normative values for target heart rate and exercise time are widely available. In addition, treadmill protocols that have a more

**TABLE 40-9 Sensitivity, Specificity, and Accuracy of Dobutamine and Adenosine Stress Echocardiography in the Detection of Coronary Artery Disease in the Elderly**

| | Sensitivity | | | | | |
|---|---|---|---|---|---|---|
| | *Overall* | *1-VD* | *2-VD* | *3-VD* | *Specificity* | *Accuracy* |
| Dobutamine | 86.5% (77/89) | 74% (14/19) | 88% (22/25) | 91% (41/45) | 84% (26/31) | 86% (103/120) |
| Adenosine | 66.3% (59/89) | 42% (8/19) | 76% (19/25) | 71% (32/45) | 90% (28/31) | 72.5% (87/120) |
| *P* value | <0.001 | o.227 | 0.124 | <0.01 | <0.001 | <0.001 |

Data in parentheses indicate number of patients.
This study enrolled 120 patients ≥70 years old with chest pain and known or suspected coronary artery disease who underwent both dobutamine and adenosine stress echocardiography, as well as coronary angiography.
From Anthopoulos LP, Bonou MS, Kardaras FG, et al: Stress echocardiography in elderly patients with coronary artery disease: applicability, safety and prognostic value of dobutamine and adenosine echocardiography in elderly patients. *J Am Coll Cardiol* 28(1):52-59, 1996. Reprinted with permission.
*1-VD*, One-vessel coronary artery disease; *2-VD*, two-vessel coronary artery disease; *3-VD*, three-vessel coronary artery disease.

gentle increase in speed or incline are common (e.g., the Modified Bruce, Naughton, and Balke protocols). Because many elderly have comorbid conditions that make exercise stress testing unattractive or impossible (e.g., chronic obstructive pulmonary disease, orthopedic/arthritic conditions, neuromuscular disorders, or peripheral vascular disease), the use of pharmacologic stress increases the number of patients eligible for stress testing in this age group. Vasodilators such as adenosine or dipyridamole and catecholamines (dobutamine) as pharmacologic stress agents are used in this population.

Studies in elderly patients referred for stress testing on clinical grounds, as well as in the post–myocardial infarction population, have demonstrated the value of exercise, adenosine, dipyridamole, and dobutamine echocardiography in predicting clinical outcomes.[134-138]

Some data suggest that dobutamine stress echocardiography (DSE) is more sensitive and accurate than, but as specific as, adenosine stress echocardiography (Table 40-9).

### *Safety*

The safety profile of these various types of stress testing in the elderly is good. Exercise echocardiography is similar to standard exercise testing with regard to safety, although some caution is needed as patients are guided back to the scanning bed from the treadmill. In one study of 454 patients, half at least 70 years old and half less than 70 years old, DSE was associated with higher rates in the elderly versus younger patients of asymptomatic hypotension (defined as a drop in systolic blood pressure of >20 mm Hg) of 37% versus 12%. There were also significantly higher rates of supraventricular tachycardia (7% versus 1%) and of premature ventricular contractions (74% versus 32%). There was a nonsignificant trend toward more frequent ventricular tachycardia (5% versus 2%) and of atrial fibrillation (3% versus 0.4%). The authors report that all arrhythmias resolved either with dobutamine infusion cessation or with administration of metoprolol.[139] Similar results were reported by Hiro and colleagues.[140] Newer protocols that call for early administration of atropine (when dobutamine infusion is at 20 mcg/kg/min if the heart rate is less than 100) during DSE have suggested a reduction in minor adverse effects, with similar diagnostic accuracy, including in an elderly population[141,142] (Fig. 40-15 and Table 40-10).

Dipyridamole and adenosine can cause bronchospasm, hypotension, and arrhythmias, and for the most part these effects do not seem to be age related.[143,144] However, elderly patients undergoing adenosine stress tests may be more likely to experience transient atrioventricular block. In one study of 120 patients 70 or more years old, this occurred in 6% of tests.[136]

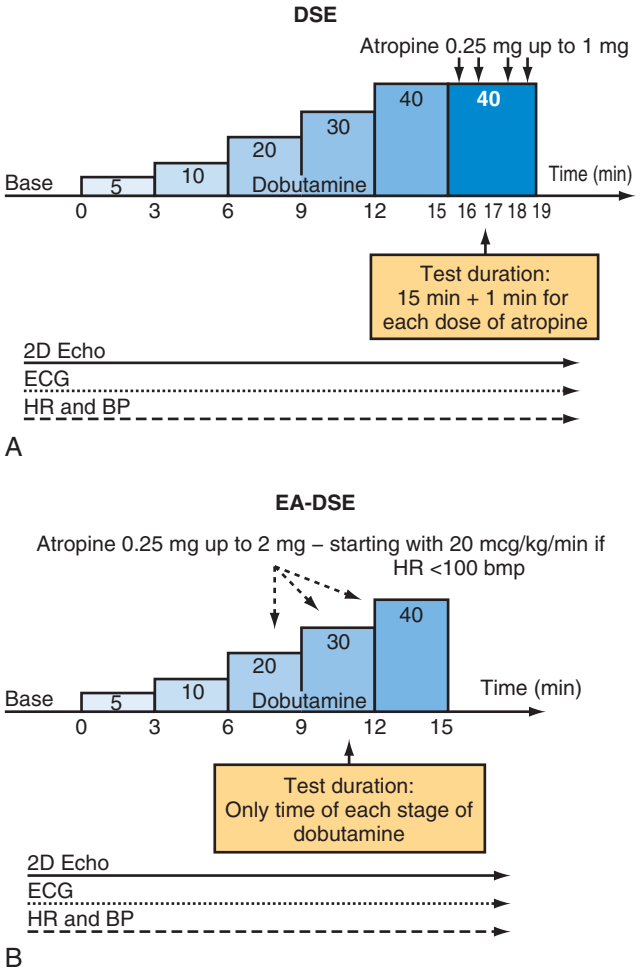



**Figure 40-15 Graphical depiction of (A) traditional dobutamine stress echocardiography (*DSE*) infusion protocol and (B) early atropine-dobutamine stress echocardiography (*EA-DSE*) protocol.** *2D Echo*, 2D echocardiography; *BP*, blood pressure; *ECG*, 12-lead electrocardiography; *HR*, heart rate. *(From Tsutsui JM, Osorio AF, Lario FA, et al: Comparison of safety and efficacy of the early injection of atropine during dobutamine stress echocardiography with the conventional protocol.* Am J Cardiol *94:1367-1372, 2004. Copyright © 2009, Elsevier. Reprinted by permission of Elsevier.)*

**TABLE 40-10 Dobutamine Stress Echocardiography: Conventional versus Early Administration of Atropine for the Detection of Coronary Artery Disease**

| *Diagnostic Parameter* | *DSE (n = 106)* | *EA-DSE (n = 106)* | P *Value* |
|---|---|---|---|
| Sensitivity | 53/62, 86% (77-94) | 57/68, 84% (75-93) | 0.10 |
| Specificity | 34/44, 78% (65-89) | 34/38, 90% (79-99) | 0.11 |
| Positive predictive value | 53/63, 84% (75-93) | 57/61, 93% (87-99) | 0.09 |
| Negative predictive value | 34/43, 79% (69-89) | 34/45, 76% (65-86) | 0.12 |
| Accuracy | 87/106, 82% (75-89) | 91/106, 86% (79-92) | 0.08 |

Data are number of patients, percentages (corresponding 95% confidence intervals).
From Tsutsui JM, Osorio AF, Lario FA, et al: Comparison of safety and efficacy of the early injection of atropine during dobutamine stress echocardiography with the conventional protocol. *Am J Cardiol* 94:1367-1372, 2004.
*DSE,* Dobutamine stress echocardiography; *EA-DSE,* early atropine administration during dobutamine stress echocardiography.

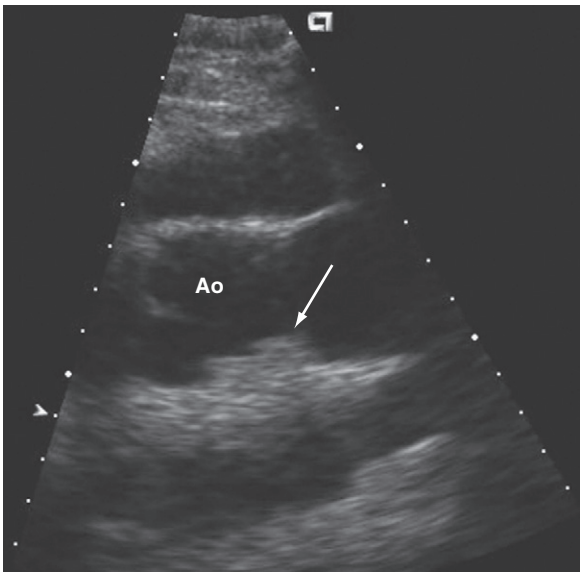



**Figure 40-16 Atherosclerotic plaque in the aortic root (*arrow*).** Long-axis view of the aortic valve and ascending aorta.

In another study it occurred in 18% of patients at least 75 years old versus 8% in those less than 75 years of age.[145]

Regadenoson is a new adenosine A(2A) specific receptor agonist that, because of its selective nature, is not associated with bronchospasm or atrioventricular node block as the nonspecific agents (adenosine and dipyridamole) are.[146] It is approved for use in stress myocardial perfusion (single photon emission computed tomography) imaging with a good tolerability and safety profile, including in the elderly,[147,148] and is being evaluated for use with atropine in stress echocardiography.[149] It may be an alternative stress echocardiography agent for patients with reactive airway disease and contraindications to dobutamine.

## CARDIOGENIC THROMBOEMBOLISM

Cardiac sources of embolism are thought to be responsible for ischemic strokes in as many as 30% of cases (see also Chapter 41).[150-152] Embolization of the components of mitral annular calcification as well as of atherosclerotic intraaortic debris is more common in elderly patients (see Figs. 40-6, 40-8, and 40-16). Aortic sclerosis has also been associated with the risk of stroke, but an independent association between aortic valve calcification and cerebral infarcts has been demonstrated only in the presence of aortic stenosis.[34,87,153] As noted previously, the association between mitral annular calcification and stroke is stronger.[85] As with younger patients, LV thrombus (usually associated with LV dysfunction), LA thrombus (usually associated with atrial fibrillation and/or flutter), vegetations, paradoxic emboli (across a patent foramen ovale), and myxoma are potential sources of embolism. Atrial fibrillation and flutter are more common in the elderly, although the prevalence of patent foramen ovale decreases with age. Many studies have demonstrated the higher sensitivity of transesophageal echocardiography (TEE) to detect potential sources of embolism, including in the elderly population.[154]

## CARDIAC AMYLOIDOSIS

Amyloid infiltration of the heart in the elderly has been described for decades and has been variously termed *senile amyloidosis of the heart* or *amyloidosis localized to the heart* (see also Chapter 28).[155,156] However, a more appropriate term is probably *systemic senile amyloidosis*, as evidence of small amyloid deposits has been found in the aorta, lung, gastrointestinal tract, liver, and kidney.[157,158] In addition to systemic senile amyloidosis, amyloid infiltration of the heart occurs in primary amyloidosis and amyloidosis associated with multiple myeloma, as well as secondary amyloidosis that is associated with chronic inflammation. The protein of senile amyloidosis is different from that of primary amyloidosis, and it portends a much better prognosis.[159] In one autopsy study of 244 patients who were greater than 60 years of age, amyloid was found in the heart in 50% of patients.[160] Although it infrequently causes clinical symptoms or signs,[161,162] it has been associated with atrial fibrillation, ventricular arrhythmias, and heart failure (usually when there is a large burden of involvement).[163,164] Studies have shown a male predominance in the primary systemic type, but an even greater predominance in the senile type.[159,164,165] In a study by Smith and colleagues[164] that compared patients with senile and primary amyloidosis, the male-to-female ratio was 5.5:1 for the senile group, and 1.6:1 for the primary group. The patients with senile amyloidosis were older with a mean age of 83 years, whereas only 4 of the 21 patients with primary amyloidosis were over 70 years old. Amyloid deposits can be found in the ventricular myocardium, as well as in the atrial mural endocardium. Less common sites of deposition in the senile type include the valves, Epicardium, and intramyocardial blood vessels.[166] Echocardiographic evidence of cardiac amyloidosis includes increased myocardial echogenicity with a "speckle" pattern, increased interatrial septal thickness, and valve thickening. The latter two characteristics are common in other conditions. Finding LV hypertrophy on echocardiography along with a low-voltage pattern on an electrocardiogram is suggestive of an infiltrative cardiomyopathy.

## Clinical Recommendations

1. Norms for chamber dimensions should be adjusted based on age.

2. Although valvular calcification is common (aortic valve sclerosis, aortic annular calcification, and mitral annular calcification), because its presence is associated with adverse outcomes, it should not be considered normal. Instead, cardiac calcification should be viewed as an important risk marker.
3. Diastolic filling parameters commonly change with age in a generally predictable manner, but do predispose patients to having adverse events/outcomes (e.g., atrial fibrillation, heart failure). Thus, they should not be considered normal, but rather the specific physiologic abnormalities should be described (e.g., impaired relaxation).
4. Although stress testing is generally safe to perform in the elderly population, practitioners should be aware that these patients are more likely than younger patients to experience supraventricular tachycardia, premature ventricular contractions, and asymptomatic hypotension with dobutamine, as well as transient atrioventricular block with adenosine.

## KEY POINTS

- Age is a major risk factor for cardiovascular disease, and many normal and pathologic changes that are common with age are readily detected on echocardiography.
- These changes in cardiac structure primarily affect the LV, LA, and valves.
- There are predictable changes in LV performance with age, particularly changes in diastolic function.
- Valvular calcification (including aortic valve sclerosis, aortic annular calcification, and mitral annular calcification) is common and is associated with adverse cardiovascular outcomes in the elderly.
- LV hypertrophy, elevated cardiac mass, and increased LA size also are associated with adverse cardiovascular outcomes.
- Heart failure and in particular diastolic heart failure are very common in the elderly.
- Pharmacologic stress testing is frequently requested in the elderly, and a heightened awareness of possible complications is advisable.

## REFERENCES


1. U.S. Department of Health and Human Services: Projected future growth of the older population. Administration on Aging., www.aoa.gov/AoARoot/Aging_Statistics/future_growth/future_growth.aspx#age. Accessed November 21, 2010.
2. Gardin JM, Henry WL, Savage DD, et al: Echocardiographic measurements in normal subjects: evaluation of an adult population without clinically apparent heart disease. *J Clin Ultrasound* 7:439-447, 1979.
3. Gerstenblith G, Frederiksen J, Yin FC, et al: Echocardiographic assessment of a normal adult aging population. *Circulation* 56:273-278, 1977.
4. Pearson AC, Gudipati CV, Labovitz AJ: Effects of aging on left ventricular structure and function. *Am Heart J* 121:871-875, 1991.
5. Henry WL, Gardin JM, Ware JH: Echocardiographic measurements in normal subjects from infancy to old age. *Circulation* 62:1054-1061, 1980.
6. Dannenberg AL, Levy D, Garrison RJ: Impact of age on echocardiographic left ventricular mass in a healthy population (the Framingham Study). *Am J Cardiol* 64:1066-1068, 1989.
7. Shub C, Klein AL, Zachariah PK, et al: Determination of left ventricular mass by echocardiography in a normal population: effect of age and sex in addition to body size. *Mayo Clin Proc* 69:205-211, 1994.
8. Daimon M, Watanabe H, Abe Y, et al: Normal values of echocardiographic parameters in relation to age in a healthy Japanese population: the JAMP study. *Circ J* 72:1859-1866, 2008.
9. Devereux RB, Alonso DR, Lutas EM, et al: Echocardiographic assessment of left ventricular hypertrophy: comparison to necropsy findings. *Am J Cardiol* 57:450-458, 1986.
10. Hees PS, Fleg JL, Lakatta EG, et al: Left ventricular remodeling with age in normal men versus women: novel insights using three-dimensional magnetic resonance imaging. *Am J Cardiol* 90:1231-1236, 2002.
11. Nikitin NP, Loh PH, de Silva R, et al: Left ventricular morphology, global and longitudinal function in normal older individuals: a cardiac magnetic resonance study. *Int J Cardiol* 108:76-83, 2006.
12. Sapin PM, Gopal AS, Clarke GB, et al: Three-dimensional echocardiography compared to two-dimensional echocardiography for measurement of left ventricular mass anatomic validation in an open chest canine model. *Am J Hypertens* 9:467-474, 1996.
13. Gopal AS, Keller AM, Shen Z, et al: Three-dimensional echocardiography: in vitro and in vivo validation of left ventricular mass and comparison with conventional echocardiographic methods. *J Am Coll Cardiol* 24:504-513, 1994.
14. Hubka M, Bolson EL, McDonald JA, et al: Three-dimensional echocardiographic measurement of left and right ventricular mass and volume: in vitro validation. *Int J Cardiovasc Imaging* 18:111-118, 2002.
15. Schmidt MA, Freidlin RZ, Ohazama CJ, et al: Anatomic validation of a novel method for left ventricular volume and mass measurements with use of real-time 3-dimensional echocardiography. *J Am Soc Echocardiogr* 14:1-10, 2001.
16. Gopal AS, Schnellbaecher MJ, Shen Z, et al: Freehand three-dimensional echocardiography for determination of left ventricular volume and mass in patients with abnormal ventricles: comparison with magnetic resonance imaging. *J Am Soc Echocardiogr* 10:853-861, 1997.
17. Mor-Avi V, Sugeng L, Weinert L, et al: Fast measurement of left ventricular mass with real-time three-dimensional echocardiography: comparison with magnetic resonance imaging. *Circulation* 110:1814-1818, 2004.
18. Oe H, Hozumi T, Arai K, et al: Comparison of accurate measurement of left ventricular mass in patients with hypertrophied hearts by real-time three-dimensional echocardiography versus magnetic resonance imaging. *Am J Cardiol* 95:1263-1267, 2005.
19. Ensor RE, Fleg JL, Kim YC, et al: Longitudinal chest x-ray changes in normal men. *J Gerontol* 38:307-314, 1983.
20. Tsang TS, Abhayaratna WP, Barnes ME, et al: Prediction of cardiovascular outcomes with left atrial size: is volume superior to area or diameter? *J Am Coll Cardiol* 47:1018-1023, 2006.
21. Badano LP, Albanese MC, De Biaggio P, et al: Prevalence, clinical characteristics, quality of life, and prognosis of patients with congestive heart failure and isolated left ventricular diastolic dysfunction. *J Am Soc Echocardiogr* 17:253-261, 2004.
22. Whitlock M, Garg A, Gelow J, et al: Comparison of left and right atrial volume by echocardiography versus cardiac magnetic resonance imaging using the area-length method. *Am J Cardiol* 106:1345-1350, 2010.
23. Nikitin NP, Constantin C, Loh PH, et al: New generation 3-dimensional echocardiography for left ventricular volumetric and functional measurements: comparison with cardiac magnetic resonance. *Eur J Echocardiogr* 7:365-372, 2006.
24. Aurigemma GP, Gottdiener JS, Arnold AM, et al: Left atrial volume and geometry in healthy aging: the Cardiovascular Health Study. *Circ Cardiovasc Imaging* 2:282-289, 2009.
25. Port S, Cobb FR, Coleman RE, et al: Effect of age on the response of the left ventricular ejection fraction to exercise. *N Engl J Med* 303:1133-1137, 1980.
26. Mor-Avi V, Sugeng L, Lang RM: Three-dimensional adult echocardiography: where the hidden dimension helps. *Curr Cardiol Rep* 10:218-225, 2008.
27. Kitzman DW, Scholz DG, Hagen PT, et al: Age-related changes in normal human hearts during the first 10 decades of life. Part II (maturity): a quantitative anatomic study of 765 specimens from subjects 20 to 99 years old. *Mayo Clin Proc* 63:137-146, 1988.
28. Krovetz LJ: Age-related changes in size of the aortic valve annulus in man. *Am Heart J* 90:569-574, 1975.

29. Sahasakul Y, Edwards WD, Naessens JM, et al: Age-related changes in aortic and mitral valve thickness: implications for two-dimensional echocardiography based on an autopsy study of 200 normal human hearts. *Am J Cardiol* 62:424-430, 1988.
30. Boon A, Lodder J, Cheriex E, et al: Mitral annulus calcification is not an independent risk factor for stroke: a cohort study of 657 patients. *J Neurol* 244:535-541, 1997.
31. Aronow WS, Schwartz KS, Koenigsberg M: Correlation of serum lipids, calcium and phosphorus, diabetes mellitus, aortic valve stenosis and history of systemic hypertension with presence or absence of mitral annular calcium in persons older than 62 years in a long-term health care facility. *Am J Cardiol* 59:381-382, 1987.
32. Aronow WS, Ahn C, Shirani J, et al: Comparison of frequency of new coronary events in older subjects with and without valvular aortic sclerosis. *Am J Cardiol* 83:599-600, A598, 1999.
33. Tolstrup K, Roldan CA, Qualls CR, et al: Aortic valve sclerosis, mitral annular calcium, and aortic root sclerosis as markers of atherosclerosis in men. *Am J Cardiol* 89:1030-1034, 2002.
34. Otto CM, Lind BK, Kitzman DW, et al: Association of aortic-valve sclerosis with cardiovascular mortality and morbidity in the elderly. *N Engl J Med* 341:142-147, 1999.
35. Rodeheffer RJ, Gerstenblith G, Becker LC, et al: Exercise cardiac output is maintained with advancing age in healthy human subjects: cardiac dilatation and increased stroke volume compensate for a diminished heart rate. *Circulation* 69:203-213, 1984.
36. Lakatta EG, Gerstenblith G, Angell CS, et al: Prolonged contraction duration in aged myocardium. *J Clin Invest* 55:61-68, 1975.
37. Yin FC, Weisfeldt ML, Milnor WR: Role of aortic input impedance in the decreased cardiovascular response to exercise with aging in dogs. *J Clin Invest* 68:28-38, 1981.
38. Froehlich JP, Lakatta EG, Beard E, et al: Studies of sarcoplasmic reticulum function and contraction duration in young adult and aged rat myocardium. *J Mol Cell Cardiol* 10:427-438, 1978.
39. Wei JY, Spurgeon HA, Lakatta EG: Excitation-contraction in rat myocardium: alterations with adult aging. *Am J Physiol* 246:H784-H791, 1984.
40. Sagie A, Benjamin EJ, Galderisi M, et al: Reference values for Doppler indexes of left ventricular diastolic filling in the elderly. *J Am Soc Echocardiogr* 6:570-576, 1993.
41. Petrofsky JS, Burse RL, Lind AR: Comparison of physiological responses of women and men to isometric exercise. *J Appl Physiol* 38:863-868, 1975.
42. Swinne CJ, Shapiro EP, Lima SD, et al: Age-associated changes in left ventricular diastolic performance during isometric exercise in normal subjects. *Am J Cardiol* 69:823-826, 1992.
43. Yin FC, Raizes GS, Guarnieri T, et al: Age-associated decrease in ventricular response to haemodynamic stress during beta-adrenergic blockade. *Br Heart J* 40:1349-1355, 1978.
44. Fleg JL, O'Connor F, Gerstenblith G, et al: Impact of age on the cardiovascular response to dynamic upright exercise in healthy men and women. *J Appl Physiol* 78:890-900, 1995.
45. Fleg J, Lakatta E: Normal aging of the cardiovascular system. In Aronow W, Fleg JL, editors: *Cardiovascular disease in the elderly*, New York, 2004, Marcel Dekker.
46. Freeman RV, Otto CM: Spectrum of calcific aortic valve disease: pathogenesis, disease progression, and treatment strategies. *Circulation* 111:3316-3326, 2005.
47. Otto CM, Kuusisto J, Reichenbach DD, et al: Characterization of the early lesion of "degenerative" valvular aortic stenosis. Histological and immunohistochemical studies. *Circulation* 90:844-853, 1994.
48. Olsson M, Dalsgaard CJ, Haegerstrand A, et al: Accumulation of T lymphocytes and expression of interleukin-2 receptors in nonrheumatic stenotic aortic valves. *J Am Coll Cardiol* 23:1162-1170, 1994.
49. O'Brien KD, Reichenbach DD, Marcovina SM, et al: Apolipoproteins B, (a), and E accumulate in the morphologically early lesion of "degenerative" valvular aortic stenosis. *Arterioscler Thromb Vasc Biol* 16:523-532, 1996.
50. Olsson M, Thyberg J, Nilsson J: Presence of oxidized low density lipoprotein in nonrheumatic stenotic aortic valves. *Arterioscler Thromb Vasc Biol* 19:1218-1222, 1999.
51. Mohler ER, 3rd, Gannon F, Reynolds C, et al: Bone formation and inflammation in cardiac valves. *Circulation* 103:1522-1528, 2001.
52. Cosmi JE, Kort S, Tunick PA, et al: The risk of the development of aortic stenosis in patients with "benign" aortic valve thickening. *Arch Intern Med* 162:2345-2347, 2002.
53. Faggiano P, Antonini-Canterin F, Erlicher A, et al: Progression of aortic valve sclerosis to aortic stenosis. *Am J Cardiol* 91:99-101, 2003.
54. Nair CK, Aronow WS, Sketch MH, et al: Clinical and echocardiographic characteristics of patients with mitral annular calcification. Comparison with age- and sex-matched control subjects. *Am J Cardiol* 51:992-995, 1983.
55. Nair CK, Thomson W, Ryschon K, et al: Long-term follow-up of patients with echocardiographically detected mitral annular calcium and comparison with age- and sex-matched control subjects. *Am J Cardiol* 63:465-470, 1989.
56. Marcu CB, Ghantous AE, Prokop EK: Caseous calcification of the mitral valve ring. *Heart Lung Circ* 15:187-188, 2006.
57. Harpaz D, Auerbach I, Vered Z, et al: Caseous calcification of the mitral annulus: a neglected, unrecognized diagnosis. *J Am Soc Echocardiogr* 14:825-831, 2001.
58. Deluca G, Correale M, Ieva R, et al: The incidence and clinical course of caseous calcification of the mitral annulus: a prospective echocardiographic study. *J Am Soc Echocardiogr* 21:828-833, 2008.
59. Kronzon I, Winer HE, Cohen ML: Sterile, caseous mitral annular abscess. *J Am Coll Cardiol* 2:186-190, 1983.
60. Kato M, Nakatani S, Okazaki H, et al: Unusual appearance of mitral annular calcification mimicking intracardiac tumor prompting early surgery. *Cardiology* 106:164-166, 2006.
61. de Vrey EA, Scholte AJ, Krauss XH, et al: Intracardiac pseudotumor caused by mitral annular calcification. *Eur J Echocardiogr* 7:62-66, 2006.
62. Eicher JC, De Nadai L, Soto FX, et al: Bacterial endocarditis complicating mitral annular calcification: a clinical and echocardiographic study. *J Heart Valve Dis* 13:217-227, 2004.
63. Fulkerson PK, Beaver BM, Auseon JC, et al: Calcification of the mitral annulus: etiology, clinical associations, complications and therapy. *Am J Med* 66:967-977, 1979.
64. Roberts WC, Perloff JK: Mitral valvular disease. A clinicopathologic survey of the conditions causing the mitral valve to function abnormally. *Ann Intern Med* 77:939-975, 1972.
65. Kaul S, Pearlman JD, Touchstone DA, et al: Prevalence and mechanisms of mitral regurgitation in the absence of intrinsic abnormalities of the mitral leaflets. *Am Heart J* 118:963-972, 1989.
66. Aronow WS, Kronzon I: Correlation of prevalence and severity of mitral regurgitation and mitral stenosis determined by Doppler echocardiography with physical signs of mitral regurgitation and mitral stenosis in 100 patients aged 62 to 100 years with mitral annular calcium. *Am J Cardiol* 60:1189-1190, 1987.
67. Labovitz AJ, Nelson JG, Windhorst DM, et al: Frequency of mitral valve dysfunction from mitral annular calcium as detected by Doppler echocardiography. *Am J Cardiol* 55:133-137, 1985.
68. Osterberger LE, Goldstein S, Khaja F, et al: Functional mitral stenosis in patients with massive mitral annular calcification. *Circulation* 64:472-476, 1981.
69. Akram MR, Chan T, McAuliffe S, et al: Nonrheumatic annular mitral stenosis: prevalence and characteristics. *Eur J Echocardiogr* 10:103-105, 2009.
70. Kanjanauthai S, Nasir K, Katz R, et al: Relationships of mitral annular calcification to cardiovascular risk factors: The Multi-Ethnic Study of Atherosclerosis (MESA). *Atherosclerosis* 213:558-562, 2010.
71. Aronow WS, Koenigsberg M, Kronzon I, et al: Association of mitral annular calcium with new thromboembolic stroke and cardiac events at 39-month follow-up in elderly patients. *Am J Cardiol* 65:1511-1512, 1990.
72. Savage DD, Garrison RJ, Castelli WP, et al: Prevalence of submitral (annular) calcium and its correlates in a general population-based sample (the Framingham Study). *Am J Cardiol* 51:1375-1378, 1983.
73. Nair CK, Sudhakaran C, Aronow WS, et al: Clinical characteristics of patients younger than 60 years with mitral annular calcium: comparison with age- and sex-matched control subjects. *Am J Cardiol* 54:1286-1287, 1984.
74. Nair CK, Sketch MH, Desai R, et al: High prevalence of symptomatic bradyarrhythmias due to atrioventricular node-fascicular and sinus node-atrial disease in patients with mitral annular calcification. *Am Heart J* 103:226-229, 1982.
75. Aronow WS, Ahn C, Kronzon I, et al: Association of mitral annular calcium with new thromboembolic stroke at 44-month follow-up of 2,148 persons, mean age 81 years. *Am J Cardiol* 81:105-106, 1998.
76. Fox CS, Parise H, Vasan RS, et al: Mitral annular calcification is a predictor for incident atrial fibrillation. *Atherosclerosis* 173:291-294, 2004.
77. Pujadas R, Arboix A, Anguera N, et al: Mitral annular calcification as a marker of complex aortic atheroma in patients with stroke of uncertain etiology. *Echocardiography* 25:124-132, 2008.
78. Rubin DC, Hawke MW, Plotnick GD: Relation between mitral annular calcium and complex intraaortic debris. *Am J Cardiol* 71:1251-1252, 1993.
79. Adler Y, Motro M, Shemesh J, et al: Association of mitral annular calcium on spiral computed tomography (dual-slice mode) with thoracic aorta calcium in patients with systemic hypertension. *Am J Cardiol* 89:1420-1422, 2002.

80. The effect of low-dose warfarin on the risk of stroke in patients with nonrheumatic atrial fibrillation. The Boston Area Anticoagulation Trial for Atrial Fibrillation Investigators. *N Engl J Med* 323:1505-1511, 1990.
81. Stein JH, Soble JS: Thrombus associated with mitral valve calcification. A possible mechanism for embolic stroke. *Stroke* 26:1697-1699, 1995.
82. Lin CS, Schwartz IS, Chapman I: Calcification of the mitral annulus fibrosus with systemic embolization. A clinicopathologic study of 16 cases. *Arch Pathol Lab Med* 111:411-414, 1987.
83. Aronow WS, Schwartz KS, Koenigsberg M: Correlation of murmurs of mitral stenosis and mitral regurgitation with presence or absence of mitral annular calcium in persons older than 62 years in a long-term health care facility. *Am J Cardiol* 59:181-182, 1987.
84. Benjamin EJ, Plehn JF, D'Agostino RB, et al: Mitral annular calcification and the risk of stroke in an elderly cohort. *N Engl J Med* 327:374-379, 1992.
85. Kizer JR, Wiebers DO, Whisnant JP, et al: Mitral annular calcification, aortic valve sclerosis, and incident stroke in adults free of clinical cardiovascular disease: the Strong Heart Study. *Stroke* 36:2533-2537, 2005.
86. Cheitlin MD, Aronow WS: Mitral regurgitation, stenosis, and annular calcification. In Aronow W, Fleg JL, editors: *Cardiovascular disease in the elderly*, New York, 2004, Marcel Dekker.
87. Boon A, Lodder J, Cheriex E, et al: Risk of stroke in a cohort of 815 patients with calcification of the aortic valve with or without stenosis. *Stroke* 27:847-851, 1996.
88. Gardin JM, McClelland R, Kitzman D, et al: M-mode echocardiographic predictors of six- to seven-year incidence of coronary heart disease, stroke, congestive heart failure, and mortality in an elderly cohort (the Cardiovascular Health Study). *Am J Cardiol* 87:1051-1057, 2001.
89. Schott CR, Kotler MN, Parry WR, et al: Mitral annular calcification. Clinical and echocardiographic correlations. *Arch Intern Med* 137:1143-1150, 1977.
90. Burnside JW, Desanctis RW: Bacterial endocarditis on calcification of the mitral annulus fibrosus. *Ann Intern Med* 76:615-618, 1972.
91. Bonow RO, Carabello BA, Chatterjee K, et al: 2008 Focused Update Incorporated into the ACC/AHA 2006 Guidelines for the Management of Patients with Valvular Heart Disease: a report of the American College of Cardiology/American Heart Association Task Force on Practice Guidelines (writing committee to revise the 1998 guidelines for the management of patients with valvular heart disease). Endorsed by the Society of Cardiovascular Anesthesiologists, Society for Cardiovascular Angiography and Interventions, and Society of Thoracic Surgeons. *J Am Coll Cardiol* 52:e1-142, 2008.
92. Jesri A, Braitman LE, Pressman GS: Severe mitral annular calcification predicts chronic kidney disease. *Int J Cardiol* 128:193-196, 2008.
93. Asselbergs FW, Mozaffarian D, Katz R, et al: Association of renal function with cardiac calcifications in older adults: the cardiovascular health study. *Nephrol Dial Transplant* 24:834-840, 2009.
94. Fox CS, Larson MG, Vasan RS, et al: Cross-sectional association of kidney function with valvular and annular calcification: the Framingham heart study. *J Am Soc Nephrol* 17:521-527, 2006.
95. Ix JH, Shlipak MG, Katz R, et al: Kidney function and aortic valve and mitral annular calcification in the Multi-Ethnic Study of Atherosclerosis (MESA). *Am J Kidney Dis* 50:412-420, 2007.
96. Fox CS, Vasan RS, Parise H, et al: Mitral annular calcification predicts cardiovascular morbidity and mortality: the Framingham Heart Study. *Circulation* 107:1492-1496, 2003.
97. Olsen MH, Wachtell K, Bella JN, et al: Aortic valve sclerosis relates to cardiovascular events in patients with hypertension (a LIFE substudy). *Am J Cardiol* 95:132-136, 2005.
98. Gondrie MJ, van der Graaf Y, Jacobs PC, et al: The association of incidentally detected heart valve calcification with future cardiovascular events. *Eur Radiol* 21:963-973, 2011.
99. Volzke H, Haring R, Lorbeer R, et al: Heart valve sclerosis predicts all-cause and cardiovascular mortality. *Atherosclerosis* 209:606-610, 2010.
100. Kohsaka S, Jin Z, Rundek T, et al: Impact of mitral annular calcification on cardiovascular events in a multiethnic community: the Northern Manhattan Study. *JACC Cardiovasc Imaging* 1:617-623, 2008.
101. Barasch E, Gottdiener JS, Larsen EK, et al: Clinical significance of calcification of the fibrous skeleton of the heart and aortosclerosis in community dwelling elderly. The Cardiovascular Health Study (CHS). *Am Heart J* 151:39-47, 2006.
102. Cao JJ, Thach C, Manolio TA, et al: C-reactive protein, carotid intima-media thickness, and incidence of ischemic stroke in the elderly: the Cardiovascular Health Study. *Circulation* 108:166-170, 2003.
103. Adler Y, Levinger U, Koren A, et al: Association between mitral annulus calcification and peripheral arterial atherosclerotic disease. *Angiology* 51:639-646, 2000.
104. Adler Y, Koren A, Fink N, et al: Association between mitral annulus calcification and carotid atherosclerotic disease. *Stroke* 29:1833-1837, 1998.
105. Ross R: Atherosclerosis: an inflammatory disease. *N Engl J Med* 340:115-126, 1999.
106. O'Brien KD, Shavelle DM, Caulfield MT, et al: Association of angiotensin-converting enzyme with low-density lipoprotein in aortic valvular lesions and in human plasma. *Circulation* 106:2224-2230, 2002.
107. Novaro GM, Sachar R, Pearce GL, et al: Association between apolipoprotein E alleles and calcific valvular heart disease. *Circulation* 108:1804-1808, 2003.
108. Agmon Y, Khandheria BK, Jamil Tajik A, et al: Inflammation, infection, and aortic valve sclerosis; Insights from the Olmsted County (Minnesota) population. *Atherosclerosis* 174:337-342, 2004.
109. Levy D, Garrison RJ, Savage DD, et al: Prognostic implications of echocardiographically determined left ventricular mass in the Framingham Heart Study. *N Engl J Med* 322:1561-1566, 1990.
110. Levy D, Garrison RJ, Savage DD, et al: Left ventricular mass and incidence of coronary heart disease in an elderly cohort. The Framingham Heart Study. *Ann Intern Med* 110:101-107, 1989.
111. Savage DD, Levy D, Dannenberg AL, et al: Association of echocardiographic left ventricular mass with body size, blood pressure and physical activity (the Framingham Study). *Am J Cardiol* 65:371-376, 1990.
112. Chobanian AV, Bakris GL, Black HR, et al: The Seventh Report of the Joint National Committee on Prevention, Detection, Evaluation, and Treatment of High Blood Pressure: the JNC 7 report. *JAMA* 289:2560-2572, 2003.
113. Tsang TS, Barnes ME, Bailey KR, et al: Left atrial volume: important risk marker of incident atrial fibrillation in 1655 older men and women. *Mayo Clin Proc* 76:467-475, 2001.
114. Barnes ME, Miyasaka Y, Seward JB, et al: Left atrial volume in the prediction of first ischemic stroke in an elderly cohort without atrial fibrillation. *Mayo Clin Proc* 79:1008-1014, 2004.
115. Tsang TS, Barnes ME, Gersh BJ, et al: Prediction of risk for first age-related cardiovascular events in an elderly population: the incremental value of echocardiography. *J Am Coll Cardiol* 42:1199-1205, 2003.
116. Moller JE, Hillis GS, Oh JK, et al: Left atrial volume: a powerful predictor of survival after acute myocardial infarction. *Circulation* 107:2207-2212, 2003.
117. Rossi A, Cicoira M, Zanolla L, et al: Determinants and prognostic value of left atrial volume in patients with dilated cardiomyopathy. *J Am Coll Cardiol* 40:1425, 2002.
118. Gerdts E, Wachtell K, Omvik P, et al: Left atrial size and risk of major cardiovascular events during antihypertensive treatment: losartan intervention for endpoint reduction in hypertension trial. *Hypertension* 49:311-316, 2007.
119. Le Tourneau T, Messika-Zeitoun D, Russo A, et al: Impact of left atrial volume on clinical outcome in organic mitral regurgitation. *J Am Coll Cardiol* 56:570-578, 2010.
120. Kizer JR, Bella JN, Palmieri V, et al: Left atrial diameter as an independent predictor of first clinical cardiovascular events in middle-aged and elderly adults: the Strong Heart Study (SHS). *Am Heart J* 151:412-418, 2006.
121. Vahanian A, Baumgartner H, Bax J, et al: Guidelines on the management of valvular heart disease: The Task Force on the Management of Valvular Heart Disease of the European Society of Cardiology. *Eur Heart J* 28:230-268, 2007.
122. Keenan NG, Cueff C, Cimadevilla C, et al: Usefulness of left atrial volume versus diameter to assess thromboembolic risk in mitral stenosis. *Am J Cardiol* 106:1152-1156, 2010.
123. Kannel WB: Epidemiological aspects of heart failure. *Cardiol Clin* 7:1-9, 1989.
124. Kitzman DW, Gardin JM, Gottdiener JS, et al: Importance of heart failure with preserved systolic function in patients > or = 65 years of age. CHS Research Group. Cardiovascular Health Study. *Am J Cardiol* 87:413-419, 2001.
125. Gottdiener JS, Arnold AM, Aurigemma GP, et al: Predictors of congestive heart failure in the elderly: the Cardiovascular Health Study. *J Am Coll Cardiol* 35:1628-1637, 2000.
126. Senni M, Tribouilloy CM, Rodeheffer RJ, et al: Congestive heart failure in the community: a study of all incident cases in Olmsted County, Minnesota, in 1991. *Circulation* 98:2282-2289, 1998.
127. Vasan RS, Larson MG, Benjamin EJ, et al: Congestive heart failure in subjects with normal versus reduced left ventricular ejection fraction: prevalence and mortality in a population-based cohort. *J Am Coll Cardiol* 33:1948-1955, 1999.
128. Bursi F, Weston SA, Redfield MM, et al: Systolic and diastolic heart failure in the community. *JAMA* 296:2209-2216, 2006.

129. Oh JK, Hatle L, Tajik AJ, et al: Diastolic heart failure can be diagnosed by comprehensive two-dimensional and Doppler echocardiography. *J Am Coll Cardiol* 47:500-506, 2006.
130. Philbin EF, Rocco TA, Jr, Lindenmuth NW, et al: Systolic versus diastolic heart failure in community practice: clinical features, outcomes, and the use of angiotensin-converting enzyme inhibitors. *Am J Med* 109:605-613, 2000.
131. Tsutsui H, Tsuchihashi M, Takeshita A: Mortality and readmission of hospitalized patients with congestive heart failure and preserved versus depressed systolic function. *Am J Cardiol* 88:530-533, 2001.
132. Redfield MM, Jacobsen SJ, Burnett JC, Jr., et al: Burden of systolic and diastolic ventricular dysfunction in the community: appreciating the scope of the heart failure epidemic. *JAMA* 289:194-202, 2003.
133. Paulus WJ, Tschope C, Sanderson JE, et al: How to diagnose diastolic heart failure: a consensus statement on the diagnosis of heart failure with normal left ventricular ejection fraction by the Heart Failure and Echocardiography Associations of the European Society of Cardiology. *Eur Heart J* 28:2539-2550, 2007.
134. Arruda AM, Das MK, Roger VL, et al: Prognostic value of exercise echocardiography in 2,632 patients > or = 65 years of age. *J Am Coll Cardiol* 37:1036-1041, 2001.
135. Smart S, Sagar K, Tresch D: Age-related determinants of outcome after acute myocardial infarction: a dobutamine-atropine stress echocardiographic study. *J Am Geriatr Soc* 50:1176-1185, 2002.
136. Anthopoulos LP, Bonou MS, Kardaras FG, et al: Stress echocardiography in elderly patients with coronary artery disease: applicability, safety and prognostic value of dobutamine and adenosine echocardiography in elderly patients. *J Am Coll Cardiol* 28:52-59, 1996.
137. Camerieri A, Picano E, Landi P, et al: Prognostic value of dipyridamole echocardiography early after myocardial infarction in elderly patients. Echo Persantine Italian Cooperative (EPIC) Study Group. *J Am Coll Cardiol* 22:1809-1815, 1993.
138. Sicari R, Pasanisi E, Venneri L, et al: Stress echo results predict mortality: a large-scale multicenter prospective international study. *J Am Coll Cardiol* 41:589-595, 2003.
139. Elhendy A, van Domburg RT, Bax JJ, et al: Safety, hemodynamic profile, and feasibility of dobutamine stress technetium myocardial perfusion single-photon emission CT imaging for evaluation of coronary artery disease in the elderly. *Chest* 117:649-656, 2000.
140. Hiro J, Hiro T, Reid CL, et al: Safety and results of dobutamine stress echocardiography in women versus men and in patients older and younger than 75 years of age. *Am J Cardiol* 80:1014-1020, 1997.
141. Tsutsui JM, Lario FC, Fernandes DR, et al: Safety and cardiac chronotropic responsiveness to the early injection of atropine during dobutamine stress echocardiography in the elderly. *Heart* 91:1563-1567, 2005.
142. Tsutsui JM, Osorio AF, Lario FA, et al: Comparison of safety and efficacy of the early injection of atropine during dobutamine stress echocardiography with the conventional protocol. *Am J Cardiol* 94:1367-1372, 2004.
143. Ranhosky A, Kempthorne-Rawson J: The safety of intravenous dipyridamole thallium myocardial perfusion imaging. Intravenous Dipyridamole Thallium Imaging Study Group. *Circulation* 81:1205-1209, 1990.
144. Lam JY, Chaitman BR, Glaenzer M, et al: Safety and diagnostic accuracy of dipyridamole-thallium imaging in the elderly. *J Am Coll Cardiol* 11:585-589, 1988.
145. Hashimoto A, Palmar EL, Scott JA, et al: Complications of exercise and pharmacologic stress tests: differences in younger and elderly patients. *J Nucl Cardiol* 6:612-619, 1999.
146. Al Jaroudi W, Iskandrian AE: Regadenoson: a new myocardial stress agent. *J Am Coll Cardiol* 54:1123-1130, 2009.
147. Thomas GS, Tammelin BR, Schiffman GL, et al: Safety of regadenoson, a selective adenosine A2A agonist, in patients with chronic obstructive pulmonary disease: a randomized, double-blind, placebo-controlled trial (RegCOPD trial). *J Nucl Cardiol* 15:319-328, 2008.
148. Leaker BR, O'Connor B, Hansel TT, et al: Safety of regadenoson, an adenosine A2A receptor agonist for myocardial perfusion imaging, in mild asthma and moderate asthma patients: a randomized, double-blind, placebo-controlled trial. *J Nucl Cardiol* 15:329-336, 2008.
149. Safety and Accuracy Study of Regadenoson Atropine Combination for Stress Echocardiography in Identification of Coronary Artery Disease (REGAT). http://clinicaltrials.gov/ct2/show/NCT00894179. Accessed December 2, 2010.
150. Sherman DG, Dyken ML, Fisher M, et al: Antithrombotic therapy for cerebrovascular disorders. *Chest* 95:140S-155S, 1989.
151. Ferro JM: Cardioembolic stroke: an update. *Lancet Neurol* 2:177-188, 2003.
152. Goldstein LB, Adams R, Alberts MJ, et al: Primary prevention of ischemic stroke: a guideline from the American Heart Association/American Stroke Association Stroke Council: cosponsored by the Atherosclerotic Peripheral Vascular Disease Interdisciplinary Working Group; Cardiovascular Nursing Council; Clinical Cardiology Council; Nutrition, Physical Activity, and Metabolism Council; and the Quality of Care and Outcomes Research Interdisciplinary Working Group: the American Academy of Neurology affirms the value of this guideline. *Stroke* 37:1583-1633, 2006.
153. Petty GW, Khandheria BK, Whisnant JP, et al: Predictors of cerebrovascular events and death among patients with valvular heart disease: a population-based study. *Stroke* 31:2628-2635, 2000.
154. Blum A, Reisner S, Farbstein Y: Transesophageal echocardiography (TEE) vs. transthoracic echocardiography (TTE) in assessing cardiovascular sources of emboli in patients with acute ischemic stroke. *Med Sci Monit* 10:CR521-523, 2004.
155. Josselson AJ, Pruitt RD, Edwards JE: Amyloid disease of the heart. *Med Clin North Am* 34:1137-1144, 1950.
156. Pomerance A: The pathology of senile cardiac amyloidosis. *J Pathol Bacteriol* 91:357-367, 1966.
157. Pitkanen P, Westermark P, Cornwell GG, 3rd: Senile systemic amyloidosis. *Am J Pathol* 117:391-399, 1984.
158. Cornwell GG, 3rd, Murdoch WL, Kyle RA, et al: Frequency and distribution of senile cardiovascular amyloid. A clinicopathologic correlation. *Am J Med* 75:618-623, 1983.
159. Kyle RA, Spittell PC, Gertz MA, et al: The premortem recognition of systemic senile amyloidosis with cardiac involvement. *Am J Med* 101:395-400, 1996.
160. Hodkinson HM, Pomerance A: The clinical significance of senile cardiac amyloidosis: a prospective clinico-pathological study. *Q J Med* 46:381-387, 1977.
161. Wright JR, Calkins E: Amyloid in the aged heart: frequency and clinical significance. *J Am Geriatr Soc* 23:97-103, 1975.
162. Shah PM, Abelmann WH, Gersh BJ: Cardiomyopathies in the elderly. *J Am Coll Cardiol* 10:77A-79A, 1987.
163. Johansson B, Westermark P: Senile systemic amyloidosis: a clinico-pathological study of twelve patients with massive amyloid infiltration. *Int J Cardiol* 32:83-92, 1991.
164. Smith TJ, Kyle RA, Lie JT: Clinical significance of histopathologic patterns of cardiac amyloidosis. *Mayo Clin Proc* 59:547-555, 1984.
165. Rapezzi C, Quarta CC, Riva L, et al: Transthyretin-related amyloidoses and the heart: a clinical overview. *Nat Rev Cardiol* 7: 398-408, 2010.
166. Lie JT, Hammond PI: Pathology of the senescent heart: anatomic observations on 237 autopsy studies of patients 90 to 105 years old. *Mayo Clin Proc* 63:552-564, 1988.



# Echocardiographic Evaluation of the Patient with a Systemic Embolic Event

MARCO R. DI TULLIO, MD

**Background**
Cardiac Embolism
Cardioembolic and Cryptogenic Stroke
**Basic Principles and Echocardiographic Approach**
**Technical Aspects**
Transesophageal Echocardiography versus Transthoracic Echocardiography in Cryptogenic Cerebral Ischemia
Safety of Transesophageal Echocardiography
**Clinical Utility and Outcome Data**
Myocardial Infarction, Left Ventricle Dysfunction, and Thrombus
Valvular Vegetations and Strands
Intracardiac Tumors
Left Atrial Thrombus and Spontaneous Echo-Contrast
Atrial Septum Abnormalities: Patent Foramen Ovale and Atrial Septal Aneurysm
Atherosclerotic Plaques in the Proximal Aorta
Echocardiography in the Catheterization Laboratory
**Research Applications**
**Potential Limitations and Future Approaches**
**Alternate Approaches**

## Background

### CARDIAC EMBOLISM

The heart and the aorta are potential sources of embolism to the systemic circulation. When the heart or the proximal segment of the aorta is the source for the embolism, the brain is the most frequent target. This circumstance, along with the fact that cerebral embolism often results in life-threatening or severely disabling consequences, makes the investigation for cardiac embolic sources especially aggressive after a cerebral embolic event, in an attempt to identify lesions that can be treated to prevent recurrences. Also, the largest amount of outcome data and information on means for reducing the incidence of recurrent embolic events in patients with cardioaortic embolic sources comes from the literature on embolic stroke. Therefore, this chapter mainly reviews the current knowledge on the diagnostic workup in patients with cerebral embolic events from a cardiac or aortic source. However, the same embolic sources (with the addition of those that originate from more distal segments of the aorta) and principles for investigating them also apply to embolic events that occur in any vascular territory of the systemic circulation.

### CARDIOEMBOLIC AND CRYPTOGENIC STROKE

Stroke is the third leading cause of death in the United States, after cardiac disease and cancer. Approximately 6,400,000 Americans 20 years of age or more have had a stroke.[1] Each year, approximately 795,000 people experience a stroke, as a first event in 80% of cases.[1] In addition, the number of transient ischemic attacks (TIAs), temporary episodes of neurologic dysfunction that have similar risk factors as stroke and often are prelude to it, is estimated at 200,000 to 500,000 per year.[1] The vast majority of strokes (87%) have an ischemic origin,[1] meaning that the etiology of the stroke consists of a blockage of the blood supply to the affected territory. The remainder is accounted for by intracerebral (10%) or subarachnoid (3%) hemorrhage.

Ischemic stroke has a cardioembolic source in approximately 20% of cases.[2] In addition, cases that have no apparent cause (also called cryptogenic strokes) often have clinical presentation and neuroimaging findings that are suggestive of an embolic event, but the embolic source is missing. In the Stroke Data Bank, a large observational study of more than 1800 patients with stroke, the classification of ischemic strokes into the three traditional diagnostic subtypes (large vessel atherosclerotic, cardioembolic, and small vessel disease) left approximately 40% of patients with no clear stroke etiology.[3] When forcibly reclassified into those three etiologic subtypes on the basis of the patient's clinical presentation and diagnostic workup, almost two thirds of cryptogenic strokes were considered of most likely cardioembolic origin.[3] The need for a better understanding of established cardioembolic sources and the identification of newer ones has indeed characterized the involvement of cardiologists, and especially echocardiographers, in the field of stroke diagnosis and prevention in the past 20 years. This effort has led to the reduction of the proportion of strokes labeled as cryptogenic,[4] often the alteration of the management of stroke, and the use of more rational and effective preventive strategies for decreasing the incidence of recurrent events.

## Basic Principles and Echocardiographic Approach

Transthoracic echocardiography (TTE) and, especially, transesophageal echocardiography (TEE) have been widely used for searching cardiac embolic sources and still represent the

mainstay for investigation in patients with stroke or TIA. TTE is performed in cases in which the cardiac chamber of interest can be optimally visualized, as in the case of the left ventricle (LV) in a search for an apical thrombus, or for the assessment of segmental wall motion abnormalities. Other examples of TTE use may include the assessment of left atrial (LA) size or of the presence of mitral annular calcification. TTE can also be indicated as a screening test for determination of whether to proceed to the more invasive TEE. In this latter category is the evaluation for presence of a patent foramen ovale (PFO) with TTE with contrast injection or the assessment for intracardiac masses or valvular vegetations in patients with low probability for these conditions. TEE, on the other hand, is preferred when TTE cannot clearly visualize the cardiac or aortic structures of interest and in all instances in which high-resolution imaging of such structures is needed. TEE is superior to TTE for the visualization of the atrial septum and the cardiac valves and allows, for example, a much more accurate diagnosis of PFO or infective endocarditis (IE). TEE also provides an accurate visualization of structures, such as the LA appendage or the proximal thoracic aorta, that are important targets of the investigation for embolic sources. The following section reviews the diagnostic accuracy of TTE and TEE for the detection of cardiac embolic sources and some technical aspects of their performance.

## Technical Aspects

### TRANSESOPHAGEAL ECHOCARDIOGRAPHY VERSUS TRANSTHORACIC ECHOCARDIOGRAPHY IN CRYPTOGENIC CEREBRAL ISCHEMIA

Several studies have compared the diagnostic yield of TEE and TTE in the investigation for potential cardiac embolic sources in patients with cryptogenic cerebral ischemia (stroke or TIA). TEE has been repeatedly shown to have greater sensitivity than TTE for this purpose. Initial studies in the 1990s reported on a greater than two-fold increase in detection rate of embolic sources with TEE compared with TTE.[5] This observation has been confirmed in recent years, when technologic advancements in the echocardiographic equipment may have narrowed the diagnostic gap between the two techniques. In 231 patients with cryptogenic stroke or TIA, a potential source of embolism was observed in 55% with TEE but in only 16% with TTE.[6] A major embolic source, with an absolute indication to anticoagulation therapy, was found in 20% of patients with TEE and in only 4% with TTE.[6] The great diagnostic yield of TEE was confirmed in a more recent study on 702 consecutive patients with ischemic stroke or TIA.[7] TEE revealed relevant findings in 52.6% of patients, with PFO (21.7%) or previously undiagnosed valvular disease (15.8%) the most common findings.[7] In another series of 503 patients with acute brain ischemia, TEE findings led to the initiation of systemic anticoagulation therapy in 65 of 212 patients (30.6%) with cryptogenic stroke.[8] Therefore, TEE has emerged as the most sensitive and clinically useful diagnostic technique for the search for cardiac and aortic embolic sources, and TTE is used as a screening technique and for specific indications that are highlighted later in the chapter. Table 41-1 shows a clinically useful classification of embolic sources and the appropriate diagnostic techniques for each of them.

**TABLE 41-1 Echocardiographic Evaluation of Cardioaortic Embolic Sources**

| | *Possibly Associated Conditions* | *Age Group* | *Best Diagnostic Test* |
|---|---|---|---|
| LV thrombus | Prior myocardial infarction, dilated cardiomyopathy | Any | TTE |
| LA thrombus or spontaneous echo-contrast | Atrial fibrillation, mitral valve disease | Any | TEE |
| Valvular vegetations | Infective endocarditis (fever, murmur, systemic symptoms), lupus erythematosus | Any | TEE or TTE (less sensitive) |
| Valvular disease | Variable | Any | TTE for initial evaluation; TEE for further assessment (especially for prosthetic valves) |
| Cardiac tumors (myxoma, fibroelastoma, secondary malignancies) | None, or nonspecific systemic symptoms | Any | TTE for screening; TEE if suspicion high despite nondiagnostic TTE |
| Patent foramen ovale | None | Any; more frequent in patients <55 years | TTE with contrast for screening; TEE if more detail is needed |
| Atrial septal aneurysm | None | Any; more frequent in patients <55 years | TTE for screening; TEE for better imaging |
| Valve strands | None | Any | TEE |
| Aortic plaques | Diffuse atherosclerosis | >60 years | TEE |

### SAFETY OF TRANSESOPHAGEAL ECHOCARDIOGRAPHY

Transesophageal echocardiography is a safe, although semiinvasive, diagnostic test. Major complications are uncommon and frequently occur in the setting of unsuspected esophageal disease. In a European series of more than 10,000 patients,[9] one death was observed. In an additional 2.7% of patients, the test could not be performed because of unsuccessful intubation (1.9%) or patient intolerance (0.8%). Similar results were obtained in a study from the Mayo Clinic on 15,381 consecutive patients, with two deaths (0.01%) and an overall incidence rate of complications of 1.7%.[10] More information on TEE performance and safety is provided in Chapter 1.

## Clinical Utility and Outcome Data

This section reviews the use of echocardiography for the investigation of specific embolic sources, the available data on the importance of each condition, and information on treatment to prevent recurrent events.

### MYOCARDIAL INFARCTION, LEFT VENTRICLE DYSFUNCTION, AND THROMBUS

Myocardial infarction (MI) and dilated cardiomyopathy are the conditions most frequently associated with LV thrombus formation, which may lead to cerebral embolism. In the first month after an acute MI, the incidence rate of stroke is between 2% and 3%; 50% of the events occur in the first 5 days (see Chapter 14).[11] In a study of 2160 patients with incident MI, the

incidence rate of stroke during the first month was 22.6 per 100 person-months, a 44-fold increase compared with controls.[12] The risk of stroke or TIA is elevated in the first 3 to 6 months; it declines thereafter but is still two-fold to three-fold higher than in controls during the first 3 years from the MI.[12]

The risk of stroke or TIA is mainly related to the formation of thrombus in the infarcted area. In a meta-analysis, the presence of echocardiographically confirmed mural thrombus carried a more than five-fold increase in stroke risk.[13] The frequency of thrombus formation is considered higher after anterior MI than after inferior MI. In a recent study of 642 patients with anterior MI, LV thrombus formed in 6.2%, without significant differences according to initial treatment modality (percutaneous coronary intervention, thrombolysis, or conservative management).[14]

Transthoracic echocardiography is commonly used for the detection of LV thrombus. In the presence of technically adequate images, TTE is at least as sensitive as TEE because most ventricular thrombi tend to form in the apical region of the ventricle (Fig. 41-1), which may or may not be optimally visualized with TEE. Therefore, the use of TEE to search for an LV thrombus should be reserved to patients with suboptimal TTE views. The use of a contrast agent for opacification of the LV chamber (Fig. 41-2) adds to the sensitivity of TTE and decreases the proportion of uncertain findings, further reducing the number of cases in which TEE may be needed. In a study on 123 patients with inconclusive TTE results, contrast injection revealed a thrombus in 14 and allowed its presence to be excluded in all others.[15] In 33 patients with suspected thrombus, contrast allowed its presence to be excluded in 13 (39%). Overall, the use of contrast led to a therapeutic change in a large number of patients, either as a treatment upgrade from antiplatelet agents to warfarin in cases with confirmed thrombus or as the avoidance of unnecessary anticoagulation therapy in others.[15]

Because most LV thrombi form in the apical region, apical views are usually the most useful TTE views for this diagnosis (see Fig. 41-1). Morphologic features of the thrombus, such as size, protrusion, and mobility, can be assessed and are important in evaluation of the thromboembolic potential. Whenever possible, the use of higher frequency transducers (3.5-MHz or 5-MHz) may further enhance the thrombus detection rate.

For patients with echocardiographically documented LV thrombus, prophylaxis with warfarin with a target international normalized ratio (INR) of 2.0 to 3.0 is recommended,[16] in addition to aspirin (75 to 162 mg), which is needed for secondary prevention of MI. Anticoagulation therapy should be lifelong in patients with atrial fibrillation; in patients in sinus rhythm with documented LV thrombus, at least 3 months of anticoagulation therapy is recommended,[17] with continuation

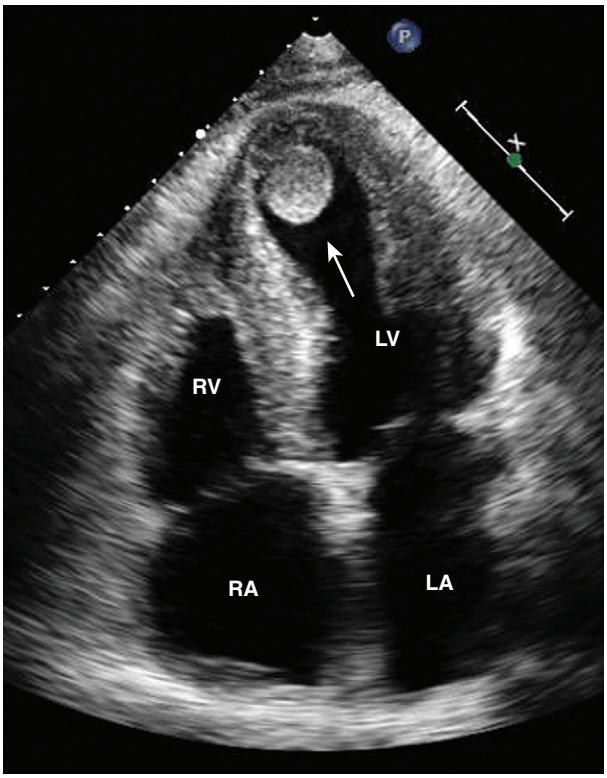



**Figure 41-1** **Example of large apical thrombus (*arrow*) with TTE.**

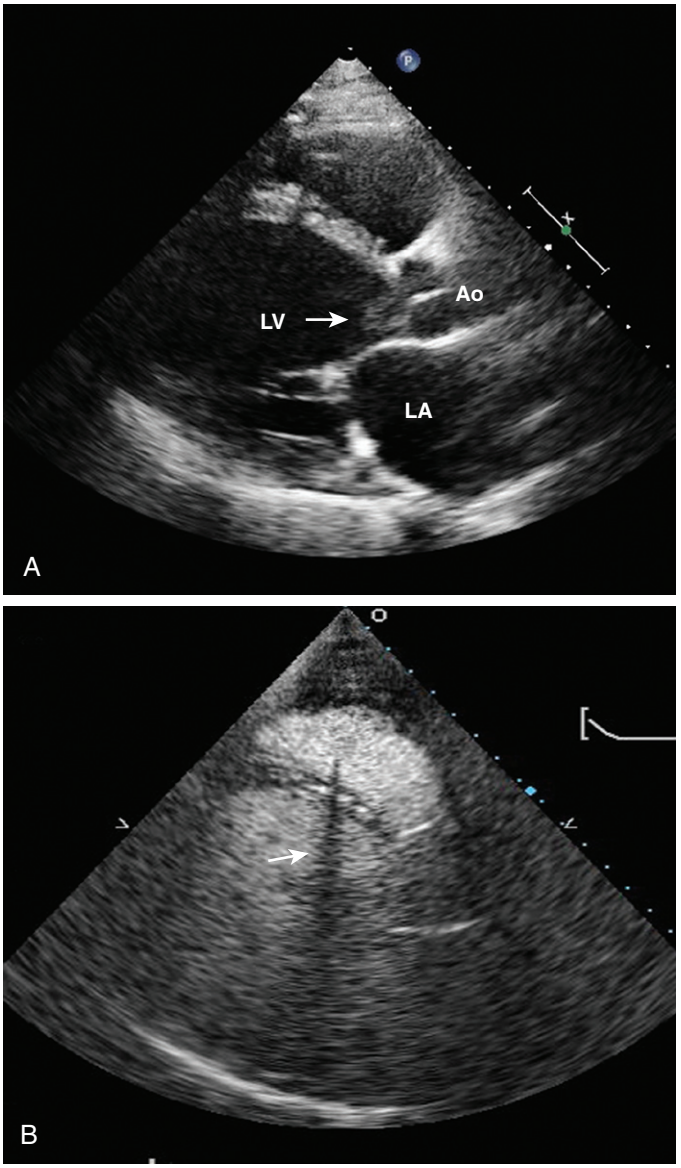



**Figure 41-2** **LV contrast utilization for the detection of intraventricular thrombus. A,** A faint echogenicity of uncertain significance (*arrow*) is visualized with TTE in the LV outflow tract. **B,** LV contrast injection shows the absence of any intracardiac mass in the LV outflow tract. A shadowing artifact from catheter in the RV is noted (*arrow*). *Ao*, Aorta.

of treatment based on follow-up echocardiographic findings (resolution or persistence of LV thrombus, severity of LV dysfunction). In 3404 patients who were randomized to systemic anticoagulation therapy or placebo after MI, anticoagulation therapy was associated with a 40% reduction in stroke risk over 3 years, and with an increase in the frequency of major hemorrhagic complications.[18] Long-term anticoagulation therapy is especially beneficial in patients with decreased LV function, whose risk of cerebrovascular events is particularly high.[19] However, the usefulness of systemic anticoagulation therapy in all patients with anterior MI, regardless of thrombus presence, appears questionable. In 2482 patients after anterior MI, 20% of whom were discharged on anticoagulation therapy, the use of such therapy for up to 90 days after the MI was not associated with a significant reduction in stroke risk in the following 4 years (hazard ratio [HR], 0.68; 95% confidence interval [CI], 0.37 to 1.26). Treatment with angiotensin-converting enzyme inhibitors (HR, 0.65; 95% CI, 0.44 to 0.95) and beta-blockers (HR, 0.60; 95% CI, 0.41 to 0.87), however, was.[20]

Only sparse information is available on the frequency of thrombus formation and the incidence of cerebral embolization in patients with dilated cardiomyopathy (see Chapter 26). The frequency of embolic events is thought to parallel the deterioration in LV function, but in the Study of Left Ventricular Dysfunction (SOLVD),[21] this relationship was observed only in women. Also, evidence shows that even mildly decreased LV systolic function may increase the stroke risk through unclear mechanisms.[22] Severe LV dysfunction may increase the risk of thromboembolic events, including stroke, as a result of the increased frequency of blood stagnation and therefore thrombus formation. An increased stroke incidence rate (up to 4% per year[23]) has been reported in patients with chronic heart failure, although this may be partly because of the frequent coexistence of atrial fibrillation. In patients with heart failure, the occurrence of a stroke is associated with a more than twofold increase in mortality rate.[12] Because heart failure is often accompanied by hypercoagulability,[24] antithrombotic treatment has been attempted to decrease the risk of embolic events. Although anticoagulation therapy is definitely indicated in patients with concomitant atrial fibrillation, its role in patients in sinus rhythm is controversial. In the largest treatment trial published to date, the Warfarin and Antiplatelet Therapy in Chronic Heart Failure (WATCH) trial, 1587 patient with symptomatic heart failure and LV ejection fraction were randomized to open label treatment with warfarin (target INR, 2.5 to 3.0), or to double-blind treatment with clopidogrel (75 mg daily) or aspirin (162 mg daily). During a mean follow-up period of 21 months, no significant differences were found between treatments in time to death, nonfatal MI, and nonfatal stroke.[25] Warfarin was associated with a reduction in nonfatal strokes ($P$ <.01 versus other treatments), but the number of events was small and the difference was offset by an increase in intracerebral bleeding.[25] The ongoing National Institute of Neurological Disorders and Stroke–sponsored Warfarin Aspirin in Reduced Cardiac Ejection Fraction (WARCEF) trial should soon provide new evidence on the efficacy of antithrombotic treatment in patient with reduced LV function.

## VALVULAR VEGETATIONS AND STRANDS

Vegetations on the mitral or aortic valve often embolize to the systemic circulation. The brain is frequently the target for the embolism, although the frequency of peripheral embolic events may be underestimated because these events are more easily misidentified. Neurologic complications occur in 20% to 40% of patients with IE (see Chapter 22).[26] In addition, silent brain infarcts on magnetic resonance imaging are found in approximately 50% of patients with IE.[27] In recent years, IE has become more often an acute rather than a subacute occurrence, and *Staphylococcus aureus* has become the most common etiologic organism.[28] Systemic embolism most commonly involves the spleen, the liver, the kidney, and the iliac or mesenteric arteries.[26] In a recent study of 2781 patients, stroke (16.9%), peripheral embolism (22.6%), and heart failure (32.3%) were the most frequently observed complications of IE. The frequency of embolic events in IE decreases rapidly after the initiation of effective antimicrobial treatment.[26] In a recent study of 1437 patients with left-sided IE, the incidence rate of stroke fell from 4.82 to 1.71 per 1000 patient-days between the first and second week of treatment and continued to decrease thereafter, regardless of valve or organism involved.[29] Overall, only 3.1% of patients had a stroke after the first week of therapy.[29] Early surgery may confer survival benefits, especially in patents at high risk of complications. In a recent study of 1552 patients with native valve IE (720 treated with surgery, and 832 with medical treatment), surgery was associated with a significant reduction in mortality rate (12.2% versus 20.1%; $P$ <.001).[30] Patients with stroke ($P$ = .02) or peripheral embolization ($P$ = .002) were among those who benefited the most from surgical treatment.[30] Therefore, the early identification of IE is of particular importance in patients with embolic events because of the potential repercussion on the choice of treatment.

Transesophageal echocardiography is the test of choice for the identification of valvular vegetations in IE (Fig. 41-3). TTE sensitivity for the diagnosis of IE is only about 58% to 63%,[31,32] although its specificity is high (98% to 100%).[31,32] More recent advancements in echocardiographic techniques, such as harmonic imaging, do not appear to have significantly improved the sensitivity of TTE for valvular vegetations.[33] The sensitivity of TEE is high (90% to 100%), as is its specificity (98% to 100%).[31,32] Echocardiographic characteristics of the vegetation that affect its embolic potential are size (more than 10 mm in diameter increases the risk), extension (more than one leaflet/valve), and mobility.[34,35] Table 41-2 shows the guidelines of the European Society of Cardiology[36] and the American Heart Association[37] for the use of echocardiography in IE. In cases that necessitate surgery, both the American Heart Association and the European Society of Cardiology endorse the use of intraoperative TEE. A negative TEE has a high negative predictive value for IE, with a range from 86% to 97%.[38] However, a TEE performed early in the course of the disease may be negative because the vegetation is still forming or is too small to be detected, hence the recommendation to repeat the test in cases in which the clinical suspicion of IE remains high.[36-38]

Vegetations on prosthetic valves are even more difficult to detect with TTE because the prosthesis itself may be interposed between the ultrasound beam and the vegetation, especially in case of mitral prostheses (see Chapter 25). The sensitivity of TTE for prosthetic IE is therefore low, whereas TEE has been reported to have 86% to 94% sensitivity and 88% to 100% specificity.[39] Therefore, TEE is recommended as the initial diagnostic test in all patients with suspected prosthetic valve endocarditis (Fig. 41-4).[40]

Valvular vegetations, or lesions that resemble them in echocardiographic appearance, may be found in patients without IE.

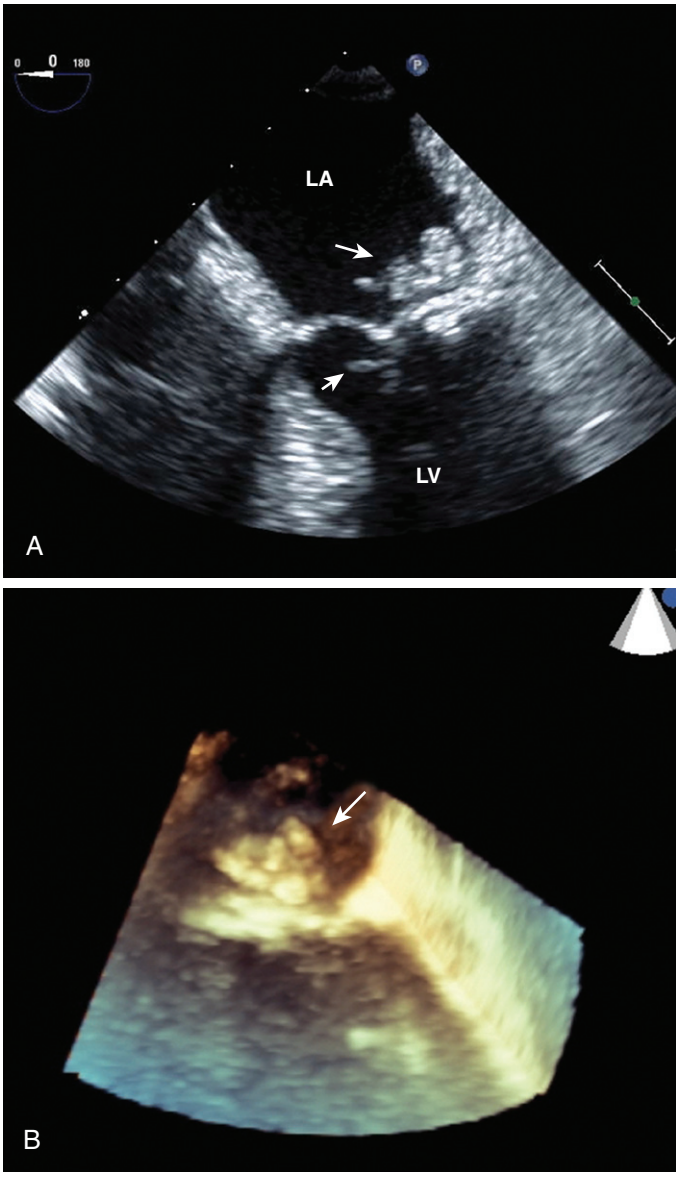



**Figure 41-3 TEE visualization of vegetation on the mitral valve. A,** A large vegetation (*arrow* in LA) is visualized on the atrial aspect of the posterior mitral leaflet. A small vegetation (*arrow* in LV) may be present on the chordal apparatus. **B,** 3D visualization of the same valvular vegetation (*arrow*) from an atrial point of view.

**TABLE 41-2 Guidelines for the Utilization of Echocardiography in Infective Endocarditis**

| | *American Heart Association 2005 (Endorsed by Infectious Diseases Society of America)* | *European Society of Cardiology 2009* |
|---|---|---|
| First diagnosis | TEE preferred; obtain TTE views for future comparison (TTE if TEE not immediately available, or in small children) | TTE, followed by TEE if TTE is negative but clinical suspicion of infective endocarditis is high |
| Repeat test | TEE after positive TEE as soon as possible in patients at high risk of complications (i.e., perivalvular extension)<br>TEE 7 to 10 days after initial TEE if:<br>1. No diagnosis of infective endocarditis but high clinical suspicion<br>2. Worrisome clinical course during treatment* | TTE or TEE in 7 to 10 days when first test is negative but clinical suspicion remains high<br>TEE in most patients with TTE-diagnosed vegetation (to measure size and evaluate for abscess)<br>TTE or TEE in case of new complications† |
| Completion of therapy | TTE to establish new baseline for valve morphology and function (TEE in case of complex anatomy) | TTE to establish new baseline for valve morphology and function |

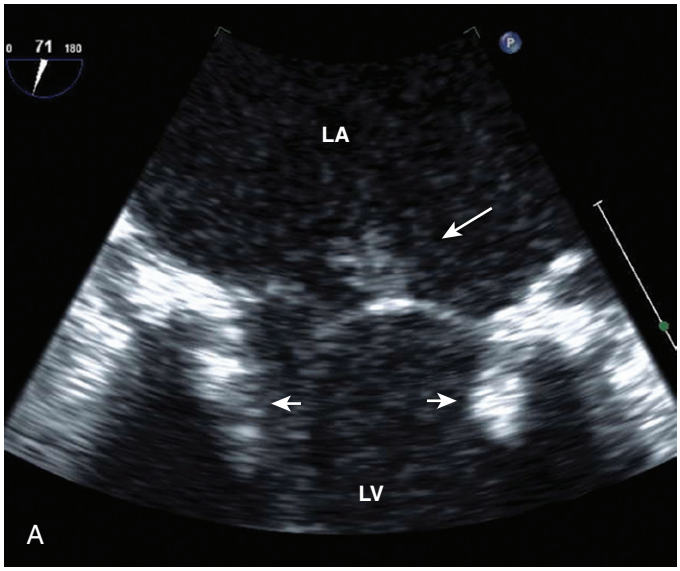
*Unexplained heart failure progression, change in murmur, or new atrioventricular block or arrhythmia.
†New murmur, embolism, persisting fever, heart failure, abscess, or atrioventricular block.

Degenerative or myxomatous valve disease, systemic lupus erythematosus (Libman-Sacks lesions, seen in as many as one in 10 patients with lupus[41]), rheumatoid disease, antiphospholipid syndrome, malignant disease (marantic endocarditis), chordal rupture, and small intracardiac tumors may all produce valvular lesions that may be indistinguishable from those of IE.[38] The clinical scenario and the results of other diagnostic tests are therefore crucial for the correct diagnosis (see Chapter 37).

Filamentous strands, also known as Lambl excrescences, are frequently observed with TEE on the mitral and aortic valve (Fig. 41-5), especially in the elderly. Often representing fibrinous material growing on the valve's edge, valve strands have been linked to an increased risk of stroke or TIA in case-control studies.[42-44] However, patients with valve strands incidentally found on TEE showed a subsequent incidence of only 1% to 2% in an average follow-up period of 4 years.[45] In elderly patients with a recent stroke, mitral valve strands were not associated with an increased risk of recurrence.[44] Therefore, the risk of cerebral embolic events associated with valve strands is unclear, as is the need for preventive treatment. In 619 patients with acute ischemic stroke who underwent TEE and were randomized to warfarin or aspirin treatment as part of the Patent Foramen Ovale in Cryptogenic Stroke Study (PICSS), strands were found on the aortic valve in 36 (5.8%) and on the mitral valve in 172 (27.8%). No increased risk of recurrent stroke was observed in patients with valve strands during a 2-year follow-up period (HR, 1.05; 95% CI, 0.70 to 1.57; $P = .82$).[46] Valve strands are often found on valve prostheses, especially in the mitral position. In 300 patients with 421 left-sided prosthetic heart valves, strands were observed in 49% of patients (38% of prostheses).[47] A lower level of anticoagulation therapy (INR less than 2.5) was significantly associated with strands frequency, suggesting that more aggressive anticoagulation therapy may be necessary in these patients.[47]

## INTRACARDIAC TUMORS

Primary intracardiac tumors are rare; they been found in less than 0.2% of unselected autopsy series.[48] When present, however, they are associated with a high frequency of embolic events (see Chapter 46). This appears especially true for the two most common varieties of tumor, myxomas and papillary fibroelastomas. Approximately 75% of all cardiac tumors are benign, and 50% are myxomas.[49] Three of four myxomas originate from the LA, especially the fossa ovalis area of the interatrial septum.[50] Estimates are that 30% to 40% of all myxomas eventually embolize,[50] to the cerebral circulation in more than 50% of cases. Tumor fragmentation, or embolization of superimposed thrombus, is considered a potential embolic mechanism. The morphologic features of the myxoma are an important determinant of its embolic risk. Large mobile myxomas or those with villous excrescences are more likely to embolize than those with



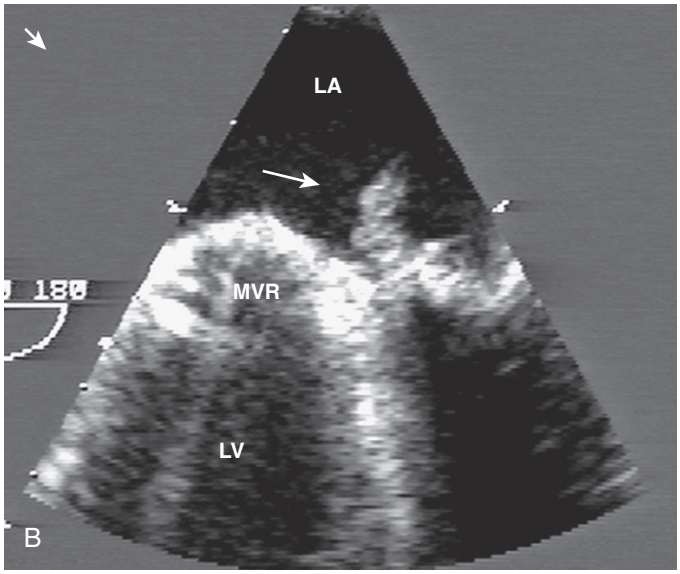




**Figure 41-4** **TEE visualization of vegetations on mitral prostheses. A,** A vegetation (*large arrow*) is visualized on the atrial aspect of a biological prosthesis. Note the native valve-like appearance of the leaflets and also the valvular supporting struts (*small arrows*). **B,** Large vegetation (*arrow*) on the lateral aspect of the annular ring of a mechanical prosthesis (*MVR*).

more solid polypoid aspects.[50] TTE can identify even relatively small myxomas (Fig. 41-6, *A*). TEE, however, can identify smaller tumors and help clarify morphologic aspects of importance for planning of the surgical resection, such as point of insertion into the cardiac wall and relation to adjacent structures (Fig. 41-6, *B*). Three-dimensional (3D) imaging (Fig. 41-6, *C*) may also help with the planning of the surgical approach because it more closely resembles the surgical view of the tumor. Surgical resection is recommended in all cases, especially when high-risk morphologic characteristics are present.

Papillary fibroelastomas are also frequently associated with cerebral embolism. Embolic events are often their first clinical manifestation because of their preferential location on highly mobile valve leaflets. Most fibroelastomas are diagnosed in the fourth or fifth decade of life, often after an episode of cerebral or cardiac ischemia.[51] In a review of 725 cases, the aortic valve was the most frequent location, followed by the mitral valve, whereas the LV was the most common extravalvular location.[52]

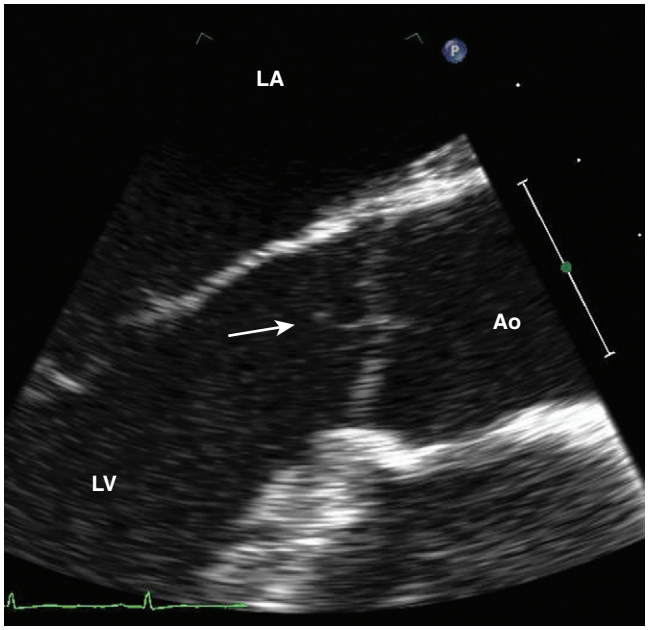



**Figure 41-5** **TEE visualization of filamentous strand (*arrow*) on the ventricular side of the aortic valve.**

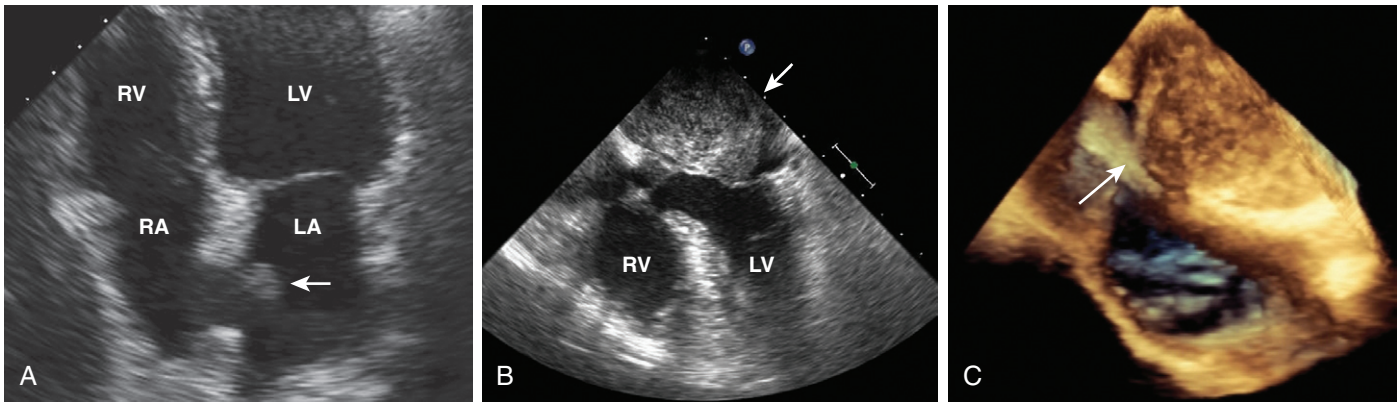



**Figure 41-6** **Left atrial myxoma. A,** TTE visualization of small myxoma (*arrow*) at the fossa ovalis area of the atrial septum. **B,** TEE visualization of large myxoma (*arrow*) almost filling the LA cavity and protruding towards the mitral valve. **C,** 3D imaging of the same tumor as in **B,** with clear visualization of the tumor insertion point in the fossa ovalis.

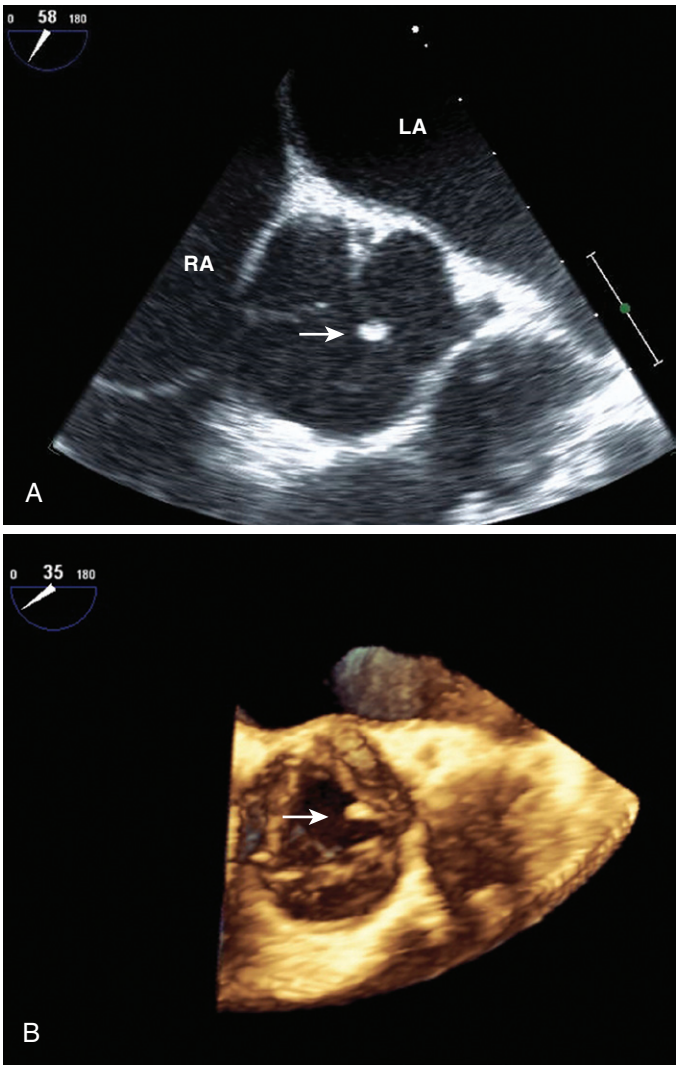



**Figure 41-7 TEE visualization of small papillary fibroelastoma on the aortic valve. A,** A small, brightly echolucent mass (*arrow*) suggestive of fibroelastoma is seen on the aortic aspect of the left coronary cusp (note the takeoff of the left main coronary artery on the right side of the screen). **B,** 3D imaging shows the small tumor (*arrow*) during the valve systolic opening.

Among morphologic characteristics, only mobility was an independent predictor of death or nonfatal embolization.[52] On the aortic valve, fibroelastomas are often located on the aortic side of the valve, unlike valvular vegetations, which tend to grow on the ventricular side. A clinically significant papillary fibroelastoma may be only a few millimeters large, which makes TEE a vastly better option than TTE for its visualization (Fig. 41-7). Although no controlled treatment studies are available, surgical resection appears indicated for all symptomatic fibroelastomas; in asymptomatic patients, oral anticoagulation therapy is usually used for nonmobile tumors; surgical resection should be strongly considered for mobile ones.[52]

Malignant primary tumors of the heart are rare, with an autopsy prevalence rate of 0.001% to 0.03%.[49] Sarcomas are the most common primary cardiac malignancies.[53] Cardiac obstruction, systemic or cerebral embolization, or systemic and constitutional symptoms are their modalities of presentation. Metastatic cardiac tumors are 20 to 40 times more frequent than primary tumors,[48] and the lungs constitute the most common primary location.[54] For the assessment of the associated embolic risk, the same considerations made for benign tumors on the usefulness of TEE and TTE apply. TEE is also invaluable in the assessment of tumor extension to adjacent structures and blood vessels, which may be critical for the decision about surgical treatment.

## LEFT ATRIAL THROMBUS AND SPONTANEOUS ECHO-CONTRAST

The presence of a thrombus in the LA is associated with significant risk of systemic embolization. LA thrombus, especially in the atrial appendage, is a frequent occurrence in the course of atrial fibrillation, although it is occasionally seen in patients in sinus rhythm with a recent cerebral ischemic event, especially when LV dysfunction coexists (see Chapter 42).[55]

Because of the proximity of the esophagus to the LA and the consequent possibility of use of high-frequency transducers, TEE is the test of choice to image the LA, and especially its appendage, which is difficult to image with TTE. With the use of modern omniplane transducers, the appendage can be imaged from a variety of angles, which allows a thorough investigation for the presence of thrombus. The presence of normal appendage trabeculations, the pectinate muscles, can be evaluated (Fig. 41-8, *A*). The sensitivity of TEE for thrombus detection is 90% to 95%, and its specificity is 95% to 100%.[56,57] An example of LA appendage thrombus is shown in Fig. 41-8, *B*. Three-dimensional imaging may also contribute to better thrombus visualization by providing alternate views (Fig. 41-8, *C*). The frequency of LA thrombus in atrial fibrillation is estimated at more than 20%.[58] In patients with a recent embolic event, the frequency is reported at 22% to 43%.[56,58] Although more frequent in chronic atrial fibrillation (27%), LA thrombus is also often observed in atrial fibrillation of less than 3 days duration (14%),[58] especially when accompanied by an embolic event (21% to 43%).[56,58]

Various conditions predispose to LA thrombus formation. A decreased LV systolic function has been shown to increase its likelihood, even in patients in sinus rhythm. In a study on 48 patients with stroke in sinus rhythm with LV ejection fraction of less than 45%, an atrial thrombus was found with TEE in 10 (21%).[59] LV ejection fraction of less than 35% was one of the two independent predictors of thrombus presence; the other predictor was LA appendage flow velocity of 55 cm/s or less.[59] The measurement of flow velocity in the appendage is indeed a useful clinical indicator of risk of thrombus formation. The appendage flow velocity can be obtained with pulsed Doppler interrogation of the inlet of the appendage in essentially all patients with TEE (Fig. 41-9, *A*) and occasionally with TTE. In patients with normal appendage function, velocities of 55 to 80 cm/s or higher are observed. The risk of thrombus formation appears to start rising with velocity of less than 55 cm/s[60] and increases as the velocity decreases. In the TEE substudy of the Stroke Prevention in Atrial Fibrillation III (SPAF III), a velocity of 20 cm/s or less was associated with increased frequency of thrombus (17%, versus 5% in patients with higher velocity; $P < .001$).[61] A decreased LA flow velocity is also a determinant of another important TEE finding that is associated with thrombus formation and thromboembolic risk: the presence of spontaneous echo-contrast (SEC). SEC is defined as dynamic, slow-swirling echoes that resemble a smoky haze within the body of the atrium or its appendage (Fig. 41-9, *B*). SEC represents increased echogenicity as a result of blood cell aggregation

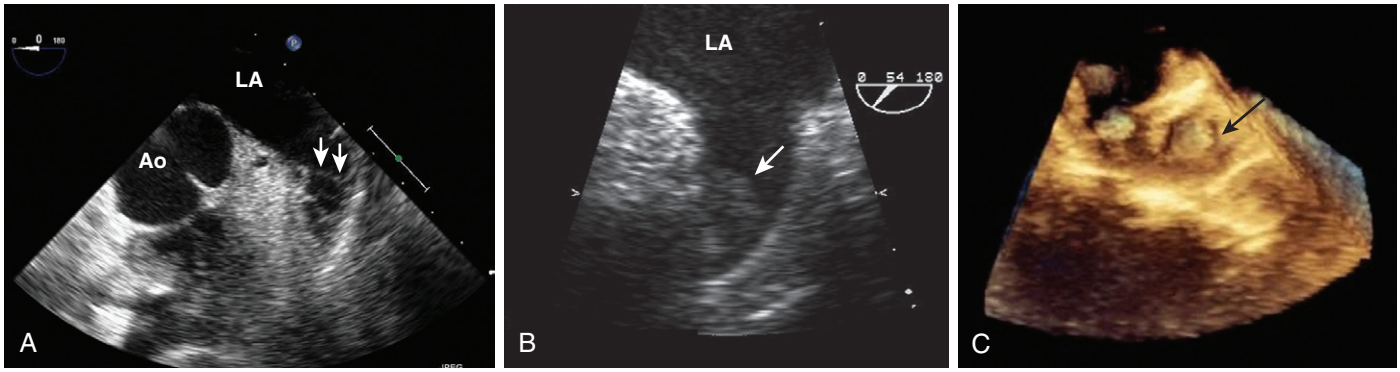



**Figure 41-8 Visualization of the LA appendage with TEE. A,** Prominent pectinate muscles (*arrows*) are visualized in the LA appendage. **B,** A thrombus (*arrow*) in the medial wall of the appendage near the apex. **C,** 3D imaging from an atrial viewpoint shows protrusion of the thrombus (*arrow*) towards the atrial chamber. *Ao,* Aorta.

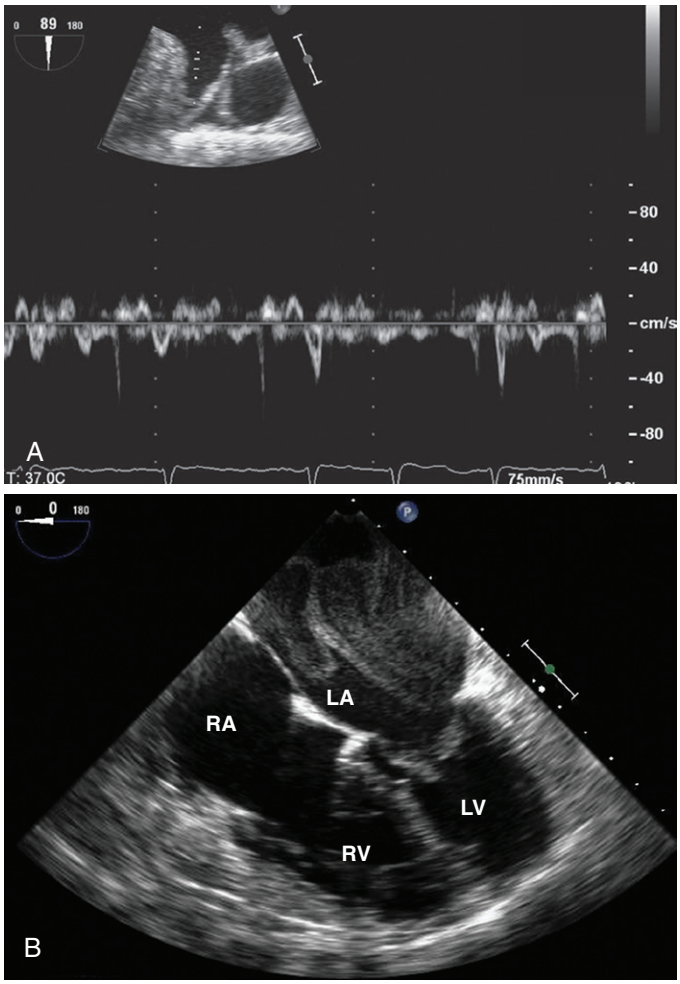



**Figure 41-9 Assessment of the LA appendage for embolic potential. A,** Pulsed Doppler interrogation of the appendage. Low emptying velocity (approximately 20 cm/s; see scale *on the right of the screen*) is shown. **B,** Example of dense spontaneous echo-contrast in the body of the LA.

at low shear rates and is therefore an indicator of stagnant blood or low flow states. SEC has been associated with severely decreased (lower than 25 cm/s)[62] but also mildly or moderately decreased (lower than 55 cm/s) appendage flow velocities.[60] SEC can be occasionally seen with TTE in low flow states (e.g., in the LV or aorta of patients with severely reduced LV function) but is better visualized with TEE because of the higher transducer frequency and, for the LA, the proximity to the chamber of interest. Accurate gain and compression settings are necessary to optimize the view and increase detection; relatively high gain settings may be necessary to maximize the detection rate, and white noise artifacts created by these settings may usually be identified because of their fixed, nonswirling appearance. The atrium and appendage should be imaged from different angles, and enough time should be spent in the imaging to ensure the capture of an often transient phenomenon such as SEC. LA SEC is present in more than 50% of patients with atrial fibrillation who undergo TEE. In a series of 272 patients, SEC was found in 161 (59%). During a mean follow-up period of 17.5 months, the rate of stroke or other embolic events was increased by four-fold in patients with SEC (12% per year versus 3% per year; $P = .002$).[63] SEC was also associated with increased mortality (25 versus 11 deaths; $P = .025$).[63] In the SPAF III study, the presence of SEC almost tripled the risk of stroke.[61] In a recent series of 295 patients with nonvalvular atrial fibrillation, the presence of atrial SEC or thrombus increased mortality by three-fold over a 5-year follow-up period,[64] although it was not an independent predictor of stroke or death in patients on anticoagulation therapy (odds ratio [OR], 1.55; 95% CI, 0.50 to 4.83).

The TEE-derived variables described previously (LA appendage thrombus and reduced flow velocity; SEC) may also aid in the choice of treatment for the prevention of thromboembolic events in patients with atrial fibrillation. Although prognostic scores such as CHADS(2) (Cardiac Failure, Hypertension, Age, Diabetes, Stroke or TIA [doubled]; Table 41-3) have been devised based on the probability of incident events,[65] some gray areas still exist. In general, oral anticoagulation therapy is recommended when the expected stroke risk is 5% per year or more; at the other end, aspirin may be chosen for patients when the expected stroke risk is lower than 2% per year. The intermediate risk group (3% to 4% risk per year) is more controversial.[66] The 2006 American College of Cardiology/American Heart Association/European Society of Cardiology guidelines for the management of patients with atrial fibrillation recommend the use aspirin 81 to 325 mg daily for patients with no risk factors and anticoagulation therapy with warfarin to an INR of 2 to 3 (target, 2.5) in patients with one high-risk factor (previous stroke, TIA, or embolism; mitral stenosis; prosthetic heart valve [if mechanical, INR of more than 2.5]) and in those

**TABLE 41-3 Use of TEE Before Cardioversion in Atrial Fibrillation: The ACUTE Study[69]**

| | *Conventional Treatment* (N = 603)* | *TEE-Guided Strategy (N = 609)* | P *Value* |
|---|---|---|---|
| Time to cardioversion (days) | 30.6 | 3.0 | <.001 |
| Successful cardioversion (%) | 65.2 | 71.1 | .03 |
| Hemorrhagic events (%) | 5.5 | 2.9 | .03 |
| Embolic events within 8 weeks (%) | 0.5 | 0.8 | .5 |

Both treatment groups received 4 weeks of oral anticoagulation therapy after cardioversion.
*ACUTE,* Assessment of Cardioversion Using Transesophageal Echocardiography.
*Three weeks of oral anticoagulation therapy before cardioversion.

with two or more moderate-risk factors (age 75 years or more; hypertension; heart failure; LV ejection fraction 35% or less; diabetes mellitus).[66] In patients with one moderate-risk factor, the choice between aspirin and warfarin was left to the physician's discretion. The use of TEE, and the detection of one of the high-risk echocardiographic indicators described previously, may tilt the therapeutic choice toward the use of anticoagulation therapy. In fact, even in the presence of a CHADS (2) score of 0 or 1, the annual stroke risk is not entirely negligible (1.9% to 2.8%); also, in a recent study on 295 patients with score 0 or 1, the prevalence of LA thrombus with TEE was 3% and that of dense SEC was 8%.[64] Therefore, 11% of patients with a low score had an indication for anticoagulation therapy when TEE was performed, which emphasizes the usefulness of TEE in the management of this patient group. Among newer therapeutic options, the oral thrombin inhibitor dabigatran has been shown to be at least as effective as warfarin in preventing strokes in atrial fibrillation and may therefore be a valid alternative to warfarin, without the need of frequent laboratory tests for monitoring of the anticoagulation intensity.[67] Other options, such as treatment with aspirin plus clopidogrel, have been proven inferior to warfarin in preventing stroke, although better than aspirin alone.[68]

The utility of TEE in atrial fibrillation goes beyond the assessment of thrombus or SEC. In the SPAF III TEE substudy, among multiple possible predictors of events, only SEC and complex aortic arch plaques (see subsequent discussion in the chapter for the definition) were found to be independently associated with recurrent vascular events.[61] Adjusted-dose warfarin treatment decreased the event rates by 75% in patients with atrial fibrillation and complex arch plaques (4.0% versus 15.8%; $P = .02$), and in patients in whom TEE failed to identify such plaques, the event rate was low (1.1% to 1.2% per year) regardless of treatment type.[61]

Transesophageal echocardiography may also used to exclude LA thrombus before cardioversion of atrial fibrillation, eliminating the need for several weeks of preprocedural anticoagulation therapy. In the Assessment of Cardioversion Using Transesophageal Echocardiography (ACUTE) study, the safety and efficacy of a TEE-based strategy to shorten anticoagulation therapy before electrical cardioversion was shown (see Table 41-3).[69]

Despite TEE's general superiority, TTE may be still a useful test in patients with atrial fibrillation because it allows the evaluation of the mitral valve and of the size of the LA, whose dilation is associated with increased risk of thrombus formation. TTE may also allow the detection of thrombus in the body of the LA. Finally, TTE may provide useful information in patients in whom TEE is not feasible or contraindicated. The combined use of two-dimensional (2D) and 3D TTE imaging identified all seven LA thrombi in a group of 91 patients with atrial fibrillation.[70]

## ATRIAL SEPTUM ABNORMALITIES: PATENT FORAMEN OVALE AND ATRIAL SEPTAL ANEURYSM

In the last two decades, the presence of a PFO has been associated with increased risk of ischemic stroke, especially when cryptogenic. The foramen ovale, a normal component of the fetal circulation, closes after birth but may remain partially open in 15% to 35% of healthy subjects.[71-74] An atrial septal aneurysm (ASA), a localized protrusion of the septum into either atrial chamber, has also been associated with an increased embolic risk. ASA is infrequently observed in the general population (approximately 1% to 4% of subjects)[75-78] but, when present, is associated with a PFO in more than 60% of cases.[79-87]

### *Detection of Patent Foramen Ovale*

An atrial septal defect is a fixed opening that allows the bidirectional shunting of blood, but a PFO is a functional opening that becomes patent when the pressure in the right atrium exceeds the pressure in the LA, as it happens at end-systole. Therefore, the diagnostic techniques for detection of a PFO are based on the demonstration of a right-to-left shunt, at rest or during maneuvers, such as coughing or Valsalva maneuver, which increase the right atrial pressure. TTE or TEE with contrast injection (agitated saline solution or polygelatin agents) is generally used. Five injections under different conditions (rest, Valsalva maneuver, cough) have been recommended.[88]

Transesophageal echocardiography has nearly 100% sensitivity and specificity for PFO detection when both color Doppler scan and contrast evaluation are performed.[89] The prevalence of PFO in a TEE study on a sample of the general population was found to be 24.3%,[76] similar to that observed in autopsy studies. With use of a longitudinal bicaval view, TEE often allows the direct visualization and measurement of the PFO opening (Fig. 41-10, *A*), the semiquantitative assessment of the shunt (with count of the shunting microbubbles; Fig. 41-10, *B*), and the differentiation from a shunt caused by transpulmonary recirculation, which can be excluded through the direct visualization of the pulmonary veins. TEE is very accurate in detection of the presence of an ASA (Fig. 41-11, *A*), generally diagnosed by the protrusion of the septum of at least 10 mm,[79,90] measured by adding the maximum excursions of the septum from the midline into either atrium.

Because TEE is a semiinvasive test that requires conscious sedation, its use is appropriate in cases that are diagnostically equivocal or when the morphologic characterization of the PFO is necessary (e.g., when PFO closure is entertained). For screening purposes, TTE with contrast is used. Contrast TTE (Fig. 41-10, *C*) has been reported to have lower sensitivity than TEE for PFO detection (50% to 60%),[91-98] but recent advances in imaging technique have improved its sensitivity (80% to 90%).[99,100] In a sample of the general population, the prevalence of PFO with contrast TTE was reported to be 14.9%,[77] lower than in the TEE-based study. The direct visualization of the PFO opening is not obtained with TTE; therefore, the distinction with intrapulmonary shunt is based on the timing of microbubbles appearance in the left-sided chambers (within three cardiac cycles from complete opacification of the right

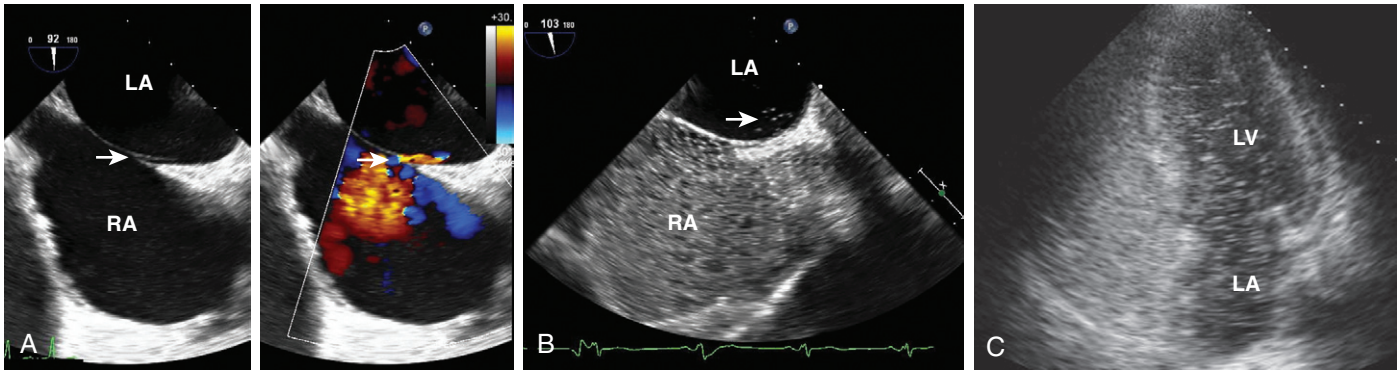



**Figure 41-10 Echocardiographic visualization of patent foramen ovale. A,** Visualization of patent foramen ovale with TEE. In bicaval view, the patent foramen ovale opening is visualized (*arrow, left panel*). Color flow Doppler imaging shows the presence of an interatrial shunt (*arrow, right panel*). **B,** Patent foramen ovale visualization with contrast TEE. Contrast material fills the RA, and a few microbubbles (*arrow*) are visualized as they enter the LA. **C,** Patent foramen ovale visualization with contrast TTE. The presence of a large right-to-left shunt is shown.

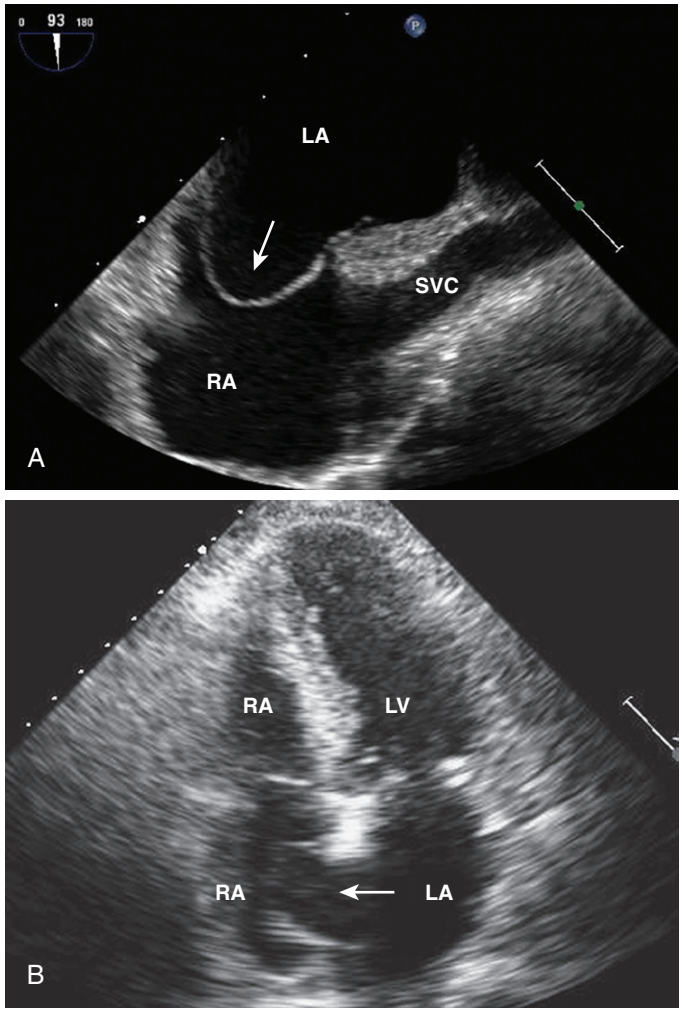



**Figure 41-11 Echocardiographic visualization of atrial septal aneurysm. A,** TEE visualization in longitudinal (bicaval) view. A large atrial septal aneurysm is visualized (*arrow*) that protrudes into the RA. **B,** TTE visualization. A large atrial septal aneurysm is visualized (*arrow*), again protruding into the RA. *SVC,* Superior vena cava.

atrium for PFO; delayed appearance in case of intrapulmonary shunt). Saline contrast with transmitral pulsed wave Doppler imaging has been used to quantify the PFO functional size.[101] An ASA can also be visualized with TTE (Fig. 41-11, *B*), although its sensitivity is lower than that of TEE.[79]

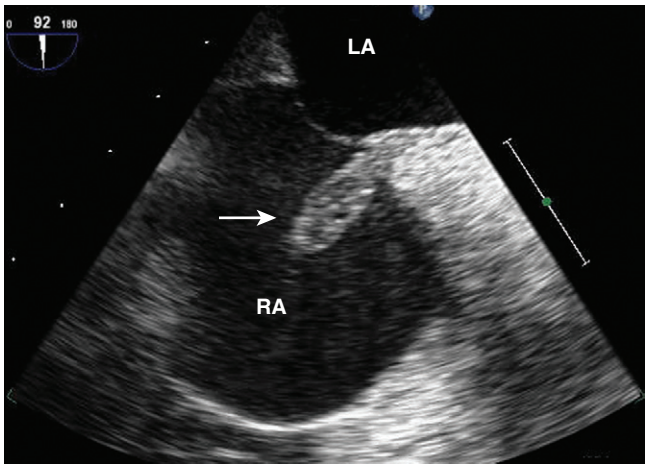



**Figure 41-12 TEE visualization of large thrombus (*arrow*) lodged in a patent foramen ovale.**

Transcranial Doppler imaging with contrast injection can also detect the presence of a PFO. Its sensitivity has been shown to be intermediate between that of TEE and TTE in some studies[92,94,95] but essentially equivalent to TEE in others.[96,98] Potentially important disadvantages of transcranial Doppler imaging are the impossibility to distinguish between PFO and intrapulmonary shunt and to assess for coexistence of an ASA.

### *Patent Foramen Ovale, Atrial Septal Aneurysm, and Stroke Risk*

Paradoxical embolization (i.e., embolization to the systemic circulation of a thrombus originating in the venous circulation) is the purported embolic mechanism associated with a PFO, a mechanism confirmed by the occasional detection of thrombus lodged in the PFO (Fig. 41-12). The relationship between PFO and cryptogenic stroke was first described in patients younger than 55[102] or 40[103] years of age and then extended to older patients, in whom such relationship has been more controversial, having been either supported[104] or negated.[105,106] Over the years, several studies with contrast TTE or TEE have confirmed the association between PFO and cryptogenic stroke in younger patients.[104,105,107-109] A recent large TEE study confirmed the existence of an association between PFO and stroke in the older age group.[109] After adjustment for age, aortic plaque thickness,

**TABLE 41-4 Relationship between Patent Foramen Ovale and Cryptogenic Stroke in Different Age Groups**

**A. Younger Patients**

| | | | Prevalence of Patent Foramen Ovale | | |
|---|---|---|---|---|---|
| *Study* | *N (Patients)* | *Age (years)* | *Cryptogenic* | *Control* | *P Value* |
| Lechat[102] | 26 | <55 | 54% (14/26) | 10% (10/100) | <.001 |
| Webster[103] | 34 | <40 | 56% (19/34) | 15% (6/40) | <.001 |
| Cabanes[107] | 64 | <55 | 56% (36/64) | 18% (9/50) | <.001 |
| de Belder[108]* | 39 | <55 | 13% (5/39) | 3% (1/39) | – |
| Di Tullio[104] | 21 | <55 | 47% (10/21) | 4% (1/24)† | <.001 |
| Hausmann[105] | 18 | <40 | 50% (9/18) | 11% (2/18) | <.05 |
| Handke[109] | 82 | <55 | 44% (36/82) | 14% (7/49)† | <.001 |
| **TOTAL** | **285** | | **45% (129/284)** | **11% (36/320)** | **<.001** |

**B. Older Patients**

| | | | Prevalence of Patent Foramen Ovale | | |
|---|---|---|---|---|---|
| *Study* | *N (Patients)* | *Age (years)* | *Cryptogenic* | *Control* | *P Value* |
| de Belder[108]* | 64 | >55 | 20% (13/64) | 5% (3/56) | <.001 |
| Di Tullio[104] | 24 | >55 | 38% (9/24) | 8% (6/77)† | <.001 |
| Hausmann[105] | 20 | >40 | 15% (3/20) | 23% (23/98) | NS |
| Jones[106] | 57 | >50 | 18% (10/57) | 16% (29/183) | NS |
| Handke[109] | 145 | >55 | 28% (41/145) | 12% (28/232)† | <.001 |
| **TOTAL** | **310** | | **25% (76/310)** | **14% (89/646)** | **<.001** |

*NS,* Not significant.
*Includes different stroke subtypes.
†Controls were patients with stroke of known cause.

hypertension, and coronary artery disease, PFO was strongly associated with cryptogenic stroke in both younger (OR, 3.70; 95% CI, 1.42 to 9.65; $P = .008$) and older patients (OR, 3.00; 95% CI, 1.73 to 5.23; $P < .001$).[109] Overall, the available evidence suggests an approximately four-fold increase in stroke risk from PFO in younger patients (Table 41-4, *A*) and a two-fold increase in older patients (Table 41-4, *B*).

### *Possible Associated Factors*

Because a PFO is present in approximately 25% of the general population but only a small fraction of individuals with a PFO will have a stroke, it is reasonable to believe that conditions may exist that increase the stroke risk. A recent meta-analysis of published studies suggested that the presence of a PFO may be an incidental rather than causative finding in one third of patients with cryptogenic stroke with a PFO,[110] again underscoring the possibility that associated factors may be important in increasing the embolic risk.

Anatomic characteristics of the atrial septum and of the right atrium have been suggested among potential cofactors. The width of the septal separation seen with TEE has been associated with increased stroke risk. Patients with presumed paradoxical embolization tend to have larger PFOs compared with controls, as assessed with contrast TTE,[103] TEE,[111-114] transcranial Doppler imaging,[93,115] and cardiac catheterization.[116] A PFO size of 2 mm or more[117] was more frequently seen in patients with stroke considered of embolic origin on the basis of brain imaging criteria,[117] and PFO size of more than 4 mm may be an independent risk factor for recurrent cerebrovascular events.[118] The degree of shunt, intended as the number of shunting microbubbles counted in the LA in a still frame, appears too subject to observer variability issues to be reliably used for risk stratification.

The presence of an ASA (see Fig. 41-11) has also been associated with an increased risk of stroke. Because ASA is frequently associated with a PFO and PFO size tends to be larger in patients with ASA,[87,119] the stroke risk is often considered to be the result of the coexistent PFO. However, the stroke risk in a meta-analysis was higher in subjects with PFO plus ASA than in those with either condition alone.[120] In stroke patients less than age 55 years who were treated with aspirin, the 4-year recurrent stroke rate with isolated PFO (2.3%) was similar to that with no PFO (4.2%) but was markedly higher (15.2%) with combined PFO and ASA.[121] A study with brain magnetic resonance imaging in 48 patients with cryptogenic stroke showed that patients with PFO and ASA had more multiple acute brain lesions than patients with PFO alone (53% versus 17%; $P = .01$), even after adjustment for PFO size, degree of shunt, and vascular risk factors.[122] Therefore, there may be more to the stroke risk associated with an ASA than the coexistence of a PFO. Other potential stroke mechanisms include in situ thrombosis formation, which appears infrequently,[79] and possibly a predisposition to the development of atrial arrhythmias,[123] which has also been questioned.[124]

A prominent Eustachian valve (the remnant of the right valve of the fetal sinus venosus that directs the blood from the inferior vena cava to the foramen ovale) has been found more frequently in patients with suspected paradoxical embolism,[125] but this has not been confirmed.[114] A Chiari network (threads and fibers that variably connect the Eustachian valve to other atrial structures) is present in approximately 2% of the general population[126] but is more frequently seen in patients with a PFO, ASA,[87] or unexplained arterial embolism.[126]

An increase in pressure in the right-sided cardiac chambers increases the likelihood of paradoxical embolization through a PFO. Pulmonary embolism,[127,128] right ventricular infarction,[129] and severe tricuspid regurgitation[130] have been associated with increased degree of shunting. Patients on mechanical LV assist device support also present an increased right-to-left shunting through the PFO, as a result of the decompression of the left-sided chambers.[131]

An increased prevalence of deep venous thrombosis has been reported[132] but not confirmed[133,134] in patients with cryptogenic stroke with a PFO. Pelvic vein thrombi were found more frequently in young patients with cryptogenic stroke than in those with defined causes of stroke.[135]

Prothrombotic states may increase the likelihood of thrombus formation and, therefore, paradoxical embolization. An increased prevalence of G20210A and factor V Leiden mutations has been reported in patients with cryptogenic stroke and PFO,[136-139] with the former mutation more frequent than the latter (8.2% versus 2.1%).[140] The association of either genotype with PFO increased the stroke risk by 4.7-fold.[140] An association between PFO size and presence of antiphospholipid antibodies has been suggested.[141] Recent surgery, trauma, or use of oral contraceptives may increase the likelihood of paradoxical embolization through a PFO.[142]

### *Prevention of Recurrent Embolism*

Because paradoxical embolization is the purported stroke mechanism from a PFO, antithrombotic treatment (systemic anticoagulation therapy with warfarin or use of antiplatelet agents such as aspirin) has been tested for preventive purpose. More recently, transcatheter closure of the PFO has also been used. The assessment of the relative efficacy of these approaches is hampered by the paucity of randomized clinical trials in the field. In the sole randomized double-blind trial of medical treatment, the previously mentioned PICSS, 630 patients with noncardioembolic stroke were randomized to aspirin 325 mg or warfarin (target INR, 1.4 to 2.8)[143] as part of the Warfarin Aspirin Recurrent Stroke Study.[144] After a 2-year follow-up period, no significant differences were observed in the rates of recurrent stroke or death among patients with or without PFO, both in the entire study group (14.8% versus 15.4%; HR, 0.96; 95% CI, 0.62 to 1.48; $P = .84$) and in the subgroup of patients with cryptogenic stroke (14.3% versus 12.7%; HR, 1.17; 95% CI, 0.60 to 2.37; $P = .65$). Although the comparison between treatment types was not the objective of the study, no significant differences in recurrent stroke or death rates were observed in patients treated with warfarin (9.5%) or aspirin (17.9%; HR, 0.52; 95% CI, 0.16 to 1.67; $P = .28$). PFO size and coexistence of an ASA also did not significantly affect the stroke risk.[143] Similar results were obtained in a more recent multicenter TEE study from Spain in 200 patients with stroke with a PFO treated with warfarin or antiplatelet agents, in which degree of right-to-left shunt or coexistence of an ASA were also not associated with an increased risk of recurrent stroke.[145]

Given the efficacy of antithrombotic treatment in prevention of recurrent events, the transcatheter closure of the PFO, which has all but replaced the formerly used surgical closure, would appear indicated only if its efficacy were to be found superior in randomized clinical trials or in patients with failure or contraindications to medical treatment. In the absence of results from such trials, transcatheter closure has had supporters[146] and critics.[147] The 2006 American Heart Association/American Stroke Association guidelines for the prevention of stroke in patients with ischemic stroke or TIA considered the data available at the time insufficient to make a recommendation for PFO closure in patients with a first stroke and a PFO.[148] PFO closure was recommended for consideration in patients with recurrent cryptogenic stroke despite medical therapy.[148] Otherwise, aspirin treatment was considered adequate in most patients, replaced by warfarin treatment in case of coexisting deep venous thrombosis or prothrombotic state. Five randomized trials that compare PFO closure and antithrombotic treatment are currently in different stages. In the first study to report its results, the CLOSURE I trial, no significant differences in recurrent stroke and death rates over a 2-year follow-up period were observed among 447 patients with stroke who had undergone PFO closure and 462 patients who were treated medically. For stroke, the incidence rate was 3.1% and 3.4%, respectively ($P = .77$).[149] Degree of shunt and presence of ASA did not significantly affect the results.

## ATHEROSCLEROTIC PLAQUES IN THE PROXIMAL AORTA

The presence of atherosclerotic plaques in the aorta is a risk factor for ischemic stroke and systemic embolization in the elderly. The association between proximal aortic plaques and ischemic stroke was first reported in a pathology study in which elderly patients who had died of a stroke had a much greater frequency of ulcerated aortic plaques than patients who had died of other neurologic diseases (26% versus 5%; age-adjusted OR, 4.0; 95% CI, 2.1 to 7.8).[150] The difference was especially significant for patients who had died of a cryptogenic stroke (61% versus 28%; adjusted OR, 5.7; 95% CI, 2.4 to 13.6) and persisted after adjustment for atrial fibrillation and carotid artery disease.[150] Only 3% of patients with ulcerated plaques were younger than 60 years, which suggests that this new stroke risk factor was only relevant to the elderly. TEE then provided an excellent opportunity to investigate the role of atherosclerotic plaques in vivo. TEE is the most sensitive and widely used technique for examination of the proximal portion of the aorta. The proximity of the esophagus to the aorta and the absence of interposed structures allow the use of high-frequency ultrasound transducers, which results in high-resolution images of the vessel. If ischemic stroke is the presenting clinical event, the portion of aorta proximal to the takeoff of the left subclavian artery is the focus of the examination, although the existence of retrograde diastolic flow has been shown in the aorta and the possibility of embolization to the brain from the initial segment of the descending aorta has been suggested.[151,152] The aorta can be accurately visualized with TEE from the aortic valve level to the initial curvature of the arch. The mid and distal segments of the aortic arch are also visible in all patients, whereas a small portion of the proximal arch cannot be visualized because of the interposition of the trachea. With TEE, an accurate assessment is possible of the presence and thickness of plaques (Fig. 41-13, *A*) and of the presence of ulcerations (Fig. 41-13, *B*) or superimposed thrombus (Figs. 41-13, *C*). TEE has been shown to be highly sensitive and specific for detection of aortic plaques[153,154] and superimposed thrombus (sensitivity, 91%; specificity, 90%).[154] TEE sensitivity for the detection of small plaque ulcerations, which may carry an additional embolic risk,[155-157] has been described as less than optimal (approximately 75%). The reproducibility of TEE measurements of aortic plaque thickness is very good, with agreement of 84% to 88% for the diagnosis of large (4 mm or more) plaques,[158] which are thought to carry higher stroke risk.[159]

With use of TEE, numerous case-control[155,157,159-162] and prospective studies[163-167] have confirmed the role of proximal arch plaques as risk factors for stroke and other embolic events (Table 41-5). Although the definition of large plaques has varied across the studies, the general consensus has been that a plaque thickness of 4 mm or more or 5 mm or more (measured perpendicular to the major vessel diameter; see Fig. 41-13, *A*) is associated with higher embolic risk. Unclear, however, is whether plaque thickness is directly related to the stroke mechanism or is rather a marker of diffuse atherosclerosis that portends the higher stroke risk. Smaller plaques (3 mm or more) have been

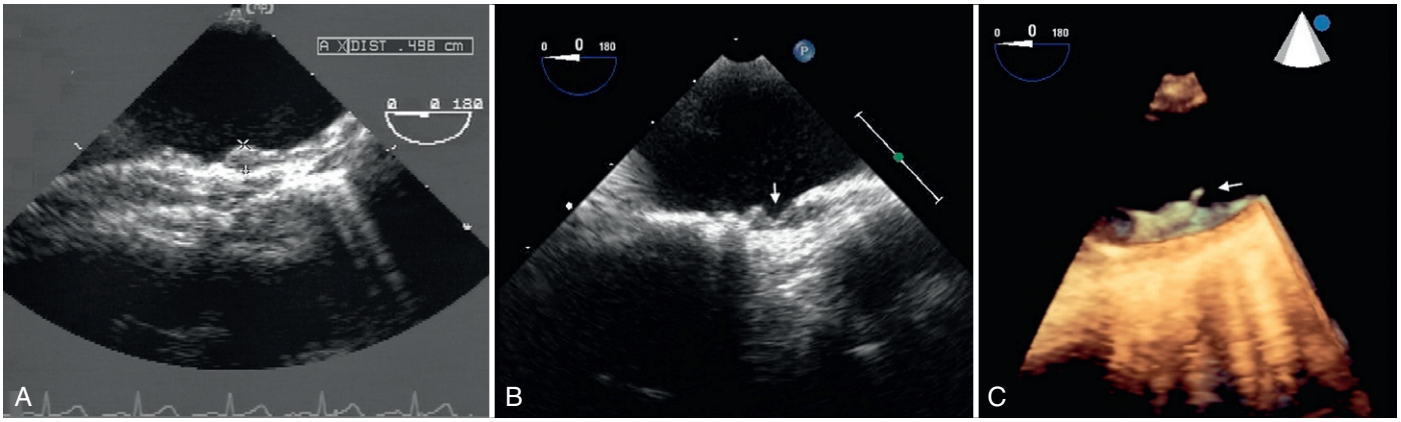



**Figure 41-13 TEE assessment of proximal aortic arch plaques. A,** A large plaque is present at mid arch, measuring approximately 5 mm in thickness. **B,** A large plaque is visualized at mid arch, with a large ulceration (*arrow*) in its intimal surface. **C,** 3D imaging of a large arch plaque. A small protruding component (*arrow*) is visualized, which was highly mobile in real-time imaging.

**TABLE 41-5 Aortic Arch Plaques and Risk of Ischemic Stroke**

**A. Studies Comparing Stroke Patients (Cases) to Matched Control Subjects**

| | | | | Prevalence of Aortic Plaque (%) | | |
|---|---|---|---|---|---|---|
| *Study* | *Cases/Controls (N)* | *Age (years)* | *Type of Plaque* | *Stroke Patients* | *Controls* | *Adjusted Odds Ratio* (95% Confidence Interval)* |
| Amarenco[159] | 250/250 | ≥60 | 1-3.9 mm | 46 | 22 | 4.4 (2.8-6.8) |
| | | | ≥4 mm | 14 | 2 | 9.1 (3.3-25.2) |
| Jones[157] | 215/202 | ≥60 | <5 mm, smooth | 33 | 22 | 2.3 (1.2-4.2) |
| | | | ≥5 mm, complex | 22 | 4 | 7.1 (2.7-18.4) |
| Di Tullio[155] | 106/114 | ≥40 | | 26 | 13 | 2.6 (1.1-5.9) |
| | 30/36 | <60 | ≥5 mm | 3 | 3 | 1.2 (0.7-20.2) |
| | 76/78 | ≥60 | | 36 | 18 | 2.4 (1.1-5.7) |
| Di Tullio[162] | 255/209 | ≥55 | ≥4 mm | 49 | 24 | 2.4 (1.3-4.6) |

**B. Prospective Studies of Stroke Patients with (AP+) and without (AP–) Aortic Plaque on TEE**

| *Study* | *AP+/AP– (N)* | *Follow-up (months)* | *Type of Plaque* | *AP+, Events (%)* | *AP, Events (%)* | *Adjusted Relative Risk† (95% Confidence Interval)* |
|---|---|---|---|---|---|---|
| Tunick[163] | 42/42 | 14 | ≥4 mm | 33 | 7 | 4.3 (1.2-15.0) |
| Mitusch[164] | 47/136 | 16 | ≥5 mm/mobile versus <5 mm | 13.7/year | 4.1/year | 4.3 (1.5-12.0) |
| FAPS[165] | 45/143 | 24-48 | ≥4 mm | 11.9/year<br>26.0/year‡ | 2.8/year<br>5.9/year‡ | 3.8 (1.8-7.8)<br>3.5 (2.1-5.9) |
| Fujimoto[167] | 67/216 | 40 | ≥4 mm versus <4 mm | 9.1 | 2.3 | 2.0 (0.9-4.2) |
| | 51/232 | 40 | ≥4 mm, extending to arch branches | 9.8 | 2.9 | 2.4 (1.1-5.2) |

*FAPS,* French Study of Aortic Plaques in Stroke.
*Adjusted for conventional stroke risk factors.
†Adjusted for traditional stroke risk factors.
‡Recurrent stroke and other embolic events combined.

shown to be associated with stroke in women,[168] which suggests that plaque thickness could be a marker of other conditions related to the stroke mechanism that may differ between men and women. On the other hand, plaque progression, defined as increase in thickness over time, has indeed been shown to be associated with increased incidence of vascular events. In 117 patients with stroke or TIA, plaque progression at 1 year was significantly associated with the incidence of vascular events (stroke, TIA, myocardial infarction, or death) over a median follow-up period of 1.7 years (51% versus 11%; $P < .0001$).[169]

The complex morphology of a plaque may be more directly related to the stroke mechanism in individual patients. Morphologic features such as ulceration or mobility have been linked with an increased stroke risk,[153-156,161,170,171] especially in the case of cryptogenic stroke. On the other hand, the presence of calcification within the plaque has been shown to decrease the risk of subsequent events, possibly because it may indicate a more stable lesion.[172] TEE is a very sensitive test for detection of such morphologic variants, and especially the presence of superimposed mobile components, which have been shown to represent thrombus.[171,173,174] Mobile components superimposed to an aortic plaque are infrequently seen in elderly patients with stroke, with a range from 1.6% to 8.7% in different studies.[153,156,157,159,161,162,175,176] However, when present, they represent a strong risk factor for brain embolization.[161] Occasionally, mobile thrombi without severe atherosclerotic changes can be seen in patients younger than 60 years who present with an embolic event (23 cases of 27,855 TEE examinations in a multicenter cardiology study).[177] These thrombi usually have an insertion site on small atherosclerotic plaques and appear to represent a rare variant of atherosclerotic disease associated with embolic events in younger patients.[177]

When the embolic event affects the systemic circulation, the entire aorta, rather than its proximal segment, should be the focus of the investigation. The frequency of atherosclerosis is, in fact, higher in the descending than in the proximal aorta.[170,178]

Besides being the site of origin of thromboembolism to the brain and the peripheral circulation, the atherosclerotic aorta can also give origin to atheroembolic phenomena, in which cholesterol crystal emboli are sent to various segments of the arterial circulation. Atheroembolism is generally characterized by small embolic particles that lodge in small arterioles[179] and may occur spontaneously or after vascular surgery, arteriography, or anticoagulation therapy.[180,181] Atheroembolism has a wide spectrum of clinical presentations, from clinically silent episodes only recognized during diagnostic procedures[182-184] to complex clinical pictures characterized by multiple organ involvement (brain, retina, kidneys, gastrointestinal tract, lower limbs).[185,186] The simultaneous or consecutive involvement of different body segments may, in fact, greatly facilitate a correct diagnosis in case of subtle or subacute clinical presentation. Occasionally, intraaortic tumors may be responsible for peripheral embolization.

### *Therapy and Prevention of Recurrent Events*

The detection of complex aortic plaques has therapeutic and preventive implications. Because most embolic events associated with large or complex proximal aortic plaques are thought to be thromboembolic in origin and because activation of the coagulation system has been shown in patients with acute stroke and large aortic arch plaques,[162] systemic anticoagulation therapy has been suggested to reduce the frequency of recurrent events. Anticoagulation therapy with warfarin appears indicated in patients with thrombus superimposed to the plaque,[187] who represent a small fraction of the total. In patients with large but nonmobile plaque, the best preventive option is debated. In 516 patients with acute ischemic stroke treated with aspirin or warfarin as part of the PICSS, antithrombotic treatment did not affect the incidence rate of recurrent stroke and death over a follow-up period of 2 years, as large plaques (4 mm or more) remained associated with an increased risk of events (adjusted HR, 2.12; 95% CI, 1.04 to 4.32), especially those with complex morphology (HR, 2.55; 95% CI, 1.10 to 5.89). The risk was highest among patients with cryptogenic stroke, both for large plaques (HR, 6.42; 95% CI, 1.62 to 25.46) and large-complex plaques (HR, 9.50; 95% CI, 1.92 to 47.10).[188] Further studies with larger patient populations are needed to evaluate the possibility of differences in efficacy between warfarin and aspirin or other antiplatelet agents in specific patient subgroups, such as patients with cryptogenic stroke. The combination of aspirin and clopidogrel is being tested against warfarin in patients with large plaques.[189] Statins have been shown to reduce the risk of recurrent events in patients with stroke in the Stroke Prevention by Aggressive Reduction in Cholesterol Levels (SPARCL) study,[190] but no separate data were available for patients with severe aortic plaques. Surgical endarterectomy for high-risk plaques has been shown to carry a significant risk of intraoperative stroke[191] and should be reserved for carefully selected cases.

Embolism from an atherosclerotic aorta can have devastating consequences during cardiac surgery. In 921 consecutive patients undergoing cardiac surgery,[192] the incidence rate of postoperative stroke was 8.7% in patients with atherosclerotic disease of the ascending aorta and 1.8% in patients without it ($P < .0001$), and aortic atherosclerosis was the strongest predictor. When the presence of severe atherosclerosis is known, modification of the cannulation of the aorta or use of off-pump procedures can drastically decrease the incidence of perioperative stroke.[193] TTE from a suprasternal window can be considered as a screening test. TEE or epiaortic ultrasound imaging of the aorta[194] at the time of surgery may also be performed for this purpose.

## ECHOCARDIOGRAPHY IN THE CATHETERIZATION LABORATORY

In recent years, the proliferation of transcatheter-based therapeutic procedures has resulted in a more frequent presence of echocardiographers in the catheterization laboratory, often to guide the performance and evaluate the results of the interventional procedures (see Chapter 5). From the standpoint of embolic risk, procedures that involve the left-sided cardiac chambers carry the highest risk. Percutaneous transvenous balloon valvuloplasty, alcohol septal ablation for hypertrophic cardiomyopathy, and cardiac electrophysiology procedures such as pulmonary veins isolation for atrial fibrillation are examples of procedures with potential embolic risk. More recently, closure of atrial septal defect or PFO, percutaneous mitral valve repair, percutaneous aortic valve replacement for aortic stenosis, and placement of LA appendage occlusion devices for stroke prevention in atrial fibrillation are becoming increasingly common, although some of these procedures are currently performed only as part of registries or clinical trials. All of these procedures carry a risk of periprocedural complications. For PFO closure, major complications from the device implantation (death, major hemorrhage, cardiac tamponade, and fatal pulmonary emboli) occurred in approximately 1.5% of the patients in a meta-analysis of 1355 patients, and less severe complications (atrial arrhythmias, device arm fractures, device embolization, device thrombosis, electrocardiographic changes, and arteriovenous fistula) were reported in 7.9%.[195] Lower complication rates have been reported in more recent studies, reflecting improved device construction and greater operator experience. In a multicenter European study on 430 patients (mean age, approximately 51 years), periprocedural complications occurred in 11.5% of patients, 0.2% of which were defined as major.[196] Transcatheter PFO closure may also be associated with a risk of intraprocedural or periprocedural embolization to the brain. Microembolic signals were detected with transcranial Doppler imaging during the procedure in 28 of 29 subjects.[197] Brain magnetic resonance imaging in 35 subjects documented the appearance of new microembolic lesions after the PFO closure in three of them (8.6%).[198]

Transesophageal echocardiography is commonly used to guide the deployment of the PFO closure device. However, intracardiac echocardiography is currently considered at least as effective as TEE for this purpose, with the added advantage of not requiring conscious sedation or additional echocardiography physician support (see Chapter 6). TTE can be used to evaluate the correct position of the closure device (Fig. 41-14, *A*) and the presence of some possible complications (e.g., septal erosion, pericardial effusion). Contrast study is used to evaluate any residual shunt, which is relatively common in the first months after the procedure and tends to close over time. TEE may be necessary for a better visualization of the device (Fig. 41-14, *B*) and the assessment of complications such as thrombus or vegetation (Fig. 41-14, *C*).

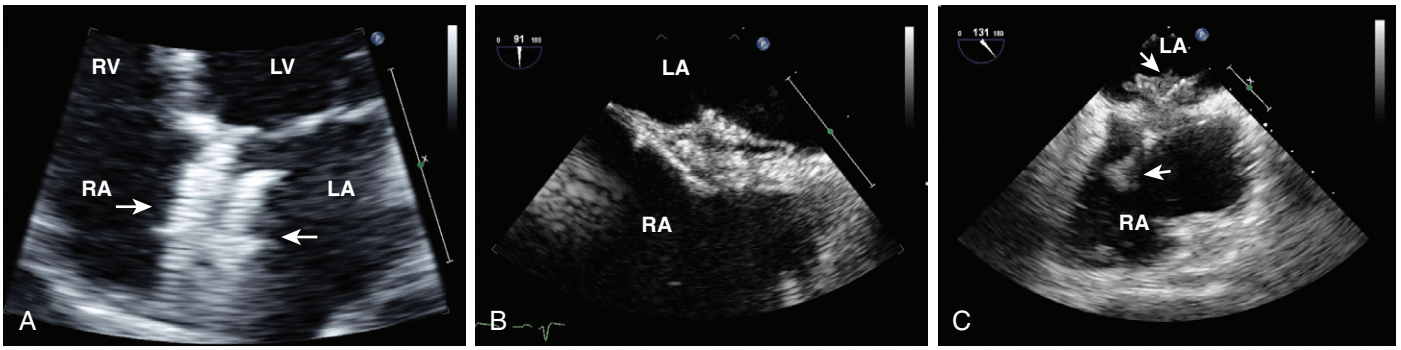



**Figure 41-14** **Echocardiographic visualization of patent foramen ovale closure device. A,** Visualization with TTE. The arms of the device (*arrows*) are clearly visualized on each atrial side. **B,** Visualization with TEE. The device arms are seen encasing the septum. **C,** TEE visualization of patent foramen ovale closure complication. Large echogenic masses (*arrows*) are seen on both sides of the device and were found to be infected thrombus at surgery.

## Research Applications

Most of the outcome data described in this chapter, and especially the data regarding new cardioembolic sources such as PFO or aortic plaques, has been obtained with the use of echocardiography, and TEE in particular. It is therefore conceivable that echocardiography will continue to play a primary role in future research in the field. The easy-to-perform and noninvasive TTE will likely remain the prime diagnostic technique for assessment of the relevance of a putative cardioembolic source in population studies. The possibility to perform and serially repeat high-resolution studies that TEE affords allows the monitoring of therapeutic interventions to reduce the risk of recurrent events, by using the changes in morphologic appearance of a lesion as a surrogate marker of embolic risk (e.g., the evaluation of the effects of statins or antithrombotic therapy on the size and morphologic appearance of an aortic plaque). Further research applications will probably be fostered by advancements in image quality and more extensive application of newer technologies, such as 3D imaging.

## Potential Limitations and Future Approaches

Despite the continuous improvement in image quality, the most important limitation of TTE for embolic source assessment remains the suboptimal visualization of the cardiac structures in some patients, an issue that has also limited the application of 3D echocardiography to the clinical practice. For TEE, the most important limitations are its semiinvasive nature, which requires the use of conscious sedation, and the still suboptimal ability to provide tissue characterization (e.g., thrombus versus vegetation versus tumor, or lipid versus thrombotic components in an aortic plaque). Some of these limitations may be overcome or lessened with future technical advancements. Also, a future direction of cardioembolic research may be the use of these imaging advancements to refine the assessment of embolic risk associated with some potential cardioembolic sources. The 3D assessment of the volume of an aortic plaque may provide a better estimate of its embolic potential than the mere measurement of its thickness; the 3D analysis of PFO morphology and adjacent atrial structures may allow a better prognostication of the likelihood of paradoxical embolization to occur. Better imaging transducers with smaller footprints may allow more accurate imaging of the aortic arch from a suprasternal approach, allowing the assessment of the atheroembolic risk before cardiac procedures and reducing the number the patients referred for TEE. This refinement of the evaluation of the risk associated with recently discovered cardioembolic sources, along with the possible discovery of newer ones, may represent one of the most important research applications of echocardiography to cardioembolic research in the years to come.

## Alternate Approaches

When TTE images are inadequate for diagnostic purposes, or when the suspected embolic source cannot be accurately investigated by it (e.g., LA appendage thrombus in atrial fibrillation), TEE provides the most logical and diagnostically sensitive alternative. In cases in which TEE cannot be performed, such as the presence of esophageal pathology or other contraindications, the choice of alternate imaging techniques depends on the a priori probability of a cardioembolic source. No real alternatives to echocardiography exist to assess for valvular vegetations in IE, which leaves the diagnosis to be made on clinical grounds. For intracardiac masses, computed tomography or magnetic resonance imaging may represent viable alternatives. Transcranial Doppler scan with contrast injection and more recently intracardiac echocardiography have been used to assess patients with suspected PFO. Magnetic resonance imaging has been shown to correlate well with TEE for aortic plaque determination[199] and to accurately define fibrotic and lipid plaque components in animal models.[200] Dual-helical computerized tomography showed sensitivity of 87%, specificity of 82%, and overall accuracy of 84% for the detection of aortic plaques in comparison with TEE.[201]

## KEY POINTS

- Approximately 20% of all ischemic strokes have a cardioembolic etiology. Cardioembolism may also be involved in a large proportion of so-called cryptogenic strokes, which still account for approximately 30% of all ischemic strokes.
- Transesophageal echocardiography (TEE) has far greater sensitivity than transthoracic echocardiography (TTE) for the detection of cardioembolic sources. TTE is a viable alternative for the assessment of LV thrombus and intracardiac masses and as a screening test for PFO (with contrast injection).
- TEE performance should be considered, especially in patients with a stroke with embolic features on neuroimaging but no obvious source of embolus on TTE.
- TEE should be performed in case of high suspicion of IE, even when TTE is negative. TEE is the test of choice for suspected prosthetic endocarditis.
- Intracardiac tumors, although rare, have high embolic potential. Their detection in the setting of an embolic event is an indication to surgical excision.
- In atrial fibrillation, TEE can be useful to evaluate the need for systemic anticoagulation therapy, particularly in patients with intermediate embolic risk.
- TTE with contrast injection is an adequate test for the detection of a PFO. TEE should be reserved for questionable or poorly visualized cases or when a more accurate morphologic assessment is needed (e.g., when PFO closure is entertained).
- Aortic arch plaques are a strong embolic risk factor in the elderly. TEE can identify morphologic features (ulceration, mobile components) that may suggest the need for more aggressive treatment (anticoagulation therapy).
- Unsuspected severe atherosclerosis of the proximal aorta is a strong risk factor for periprocedural stroke during cardiac catheterization or cardiac surgery. TTE from a suprasternal window may be an appropriate screening test to identify patients in need of TEE for further assessment.

## REFERENCES


1. Lloyd-Jones D, Adams RJ, Brown TM, et al: Heart disease and stroke statistics: 2010 update: a report from the American Heart Association. *Circulation* 121:e46-e215, 2010.
2. Furie KL, Kasner SE, Adams RJ, et al: Guidelines for the prevention of stroke in patients with stroke or transient ischemic attack: a guideline for healthcare professionals from the American Heart Association/American Stroke Association. *Stroke* 42:227-276, 2011.
3. Sacco RL, Ellenberg JH, Mohr JP, et al: Infarcts of undetermined cause: the NINCDS Stroke Data Bank. *Ann Neurol* 25:382-390, 1989.
4. Ay H, Furie KL, Singhal A, et al: An evidence-based causative classification system for acute ischemic stroke. *Ann Neurol* 58:688-697, 2005.
5. Pearson AC, Nagelhout D, Castello R, et al: Atrial septal aneurysm and stroke: a transesophageal echocardiographic study. *J Am Coll Cardiol* 18:1223-1229, 1991.
6. de Bruijn SF, Agema WR, Lammers GJ, et al: Transesophageal echocardiography is superior to transthoracic echocardiography in management of patients of any age with transient ischemic attack or stroke. *Stroke* 37:2531-2534, 2006.
7. Knebel F, Masuhr F, von HW, et al: Transesophageal echocardiography in patients with cryptogenic cerebral ischemia. *Cardiovasc Ultrasound* 7:15, 2009.
8. Harloff A, Handke M, Reinhard M, et al: Therapeutic strategies after examination by transesophageal echocardiography in 503 patients with ischemic stroke. *Stroke* 37:859-864, 2006.
9. Daniel WG, Erbel R, Kasper W, et al: Safety of transesophageal echocardiography. A multicenter survey of 10,419 examinations. *Circulation* 83:817-821, 1991.
10. Oh JK, Seward JB, Tajik AJ: *Transesophageal echocardiography. The echo manual*, ed 2, 1999, Lippincott Williams & Wilkins, pp 23-36.
11. Mooe T, Eriksson P, Stegmayr B: Ischemic stroke after acute myocardial infarction. A population-based study. *Stroke* 28:762-767, 1997.
12. Witt BJ, Brown RD Jr, Jacobsen SJ, et al: A community-based study of stroke incidence after myocardial infarction. *Ann Intern Med* 143:785-792, 2005.
13. Vaitkus PT, Barnathan ES: Embolic potential, prevention and management of mural thrombus complicating anterior myocardial infarction: a meta-analysis. *J Am Coll Cardiol* 22:1004-1009, 1993.
14. Osherov AB, Borovik-Raz M, Aronson D, et al: Incidence of early left ventricular thrombus after acute anterior wall myocardial infarction in the primary coronary intervention era. *Am Heart J* 157:1074-1080, 2009.
15. Siebelink HM, Scholte AJ, Van D, et al: Value of contrast echocardiography for left ventricular thrombus detection postinfarction and impact on antithrombotic therapy. *Coron Artery Dis* 20:462-466, 2009.
16. Smith SC Jr, Allen J, Blair SN, et al: AHA/ACC guidelines for secondary prevention for patients with coronary and other atherosclerotic vascular disease: 2006 update: endorsed by the National Heart, Lung, and Blood Institute. *Circulation* 113:2363-2372, 2006.
17. Antman EM, Anbe DT, Armstrong PW, et al: ACC/AHA guidelines for the management of patients with ST-elevation myocardial infarction; a report of the American College of Cardiology/American Heart Association Task Force on Practice Guidelines (Committee to Revise the 1999 Guidelines for the Management of Patients with Acute Myocardial Infarction). *J Am Coll Cardiol* 44:E1-E211, 2004.
18. Azar AJ, Koudstaal PJ, Wintzen AR, et al: Risk of stroke during long-term anticoagulant therapy in patients after myocardial infarction. *Ann Neurol* 39:301-307, 1996.
19. Loh E, Sutton MS, Wun CC, et al: Ventricular dysfunction and the risk of stroke after myocardial infarction. *N Engl J Med* 336:251-257, 1997.
20. Udell JA, Wang JT, Gladstone DJ, et al: Anticoagulation after anterior myocardial infarction and the risk of stroke. *PLoS One* 5:e12150, 2010.
21. Dries DL, Rosenberg YD, Waclawiw MA, et al: Ejection fraction and risk of thromboembolic events in patients with systolic dysfunction and sinus rhythm: evidence for gender differences in the studies of left ventricular dysfunction trials. *J Am Coll Cardiol* 29:1074-1080, 1997.
22. Hays AG, Sacco RL, Rundek T, et al: Left ventricular systolic dysfunction and the risk of ischemic stroke in a multiethnic population. *Stroke* 37:1715-1719, 2006.
23. Witt BJ, Brown RD Jr, Jacobsen SJ, et al: Ischemic stroke after heart failure: a community-based study. *Am Heart J* 152:102-109, 2006.
24. Yamamoto K, Ikeda U, Furuhashi K, et al: The coagulation system is activated in idiopathic cardiomyopathy. *J Am Coll Cardiol* 25:1634-1640, 1995.
25. Massie BM, Collins JF, Ammon SE, et al: Randomized trial of warfarin, aspirin, and clopidogrel in patients with chronic heart failure: the Warfarin and Antiplatelet Therapy in Chronic Heart Failure (WATCH) trial. *Circulation* 119:1616-1624, 2009.
26. Mylonakis E, Calderwood SB: Infective endocarditis in adults. *N Engl J Med* 345:1318-1330, 2001.
27. Cooper HA, Thompson EC, Laureno R, et al: Subclinical brain embolization in left-sided infective endocarditis: results from the evaluation by MRI of the brains of patients with left-sided intracardiac solid masses (EMBOLISM) pilot study. *Circulation* 120:585-591, 2009.
28. Murdoch DR, Corey GR, Hoen B, et al: Clinical presentation, etiology, and outcome of infective endocarditis in the 21st century: the International Collaboration on Endocarditis-Prospective Cohort Study. *Arch Intern Med* 169:463-473, 2009.
29. Dickerman SA, Abrutyn E, Barsic B, et al: The relationship between the initiation of antimicrobial therapy and the incidence of stroke in infective endocarditis: an analysis from the ICE Prospective Cohort Study (ICE-PCS). *Am Heart J* 154:1086-1094, 2007.

30. Lalani T, Cabell CH, Benjamin DK, et al: Analysis of the impact of early surgery on in-hospital mortality of native valve endocarditis: use of propensity score and instrumental variable methods to adjust for treatment-selection bias. *Circulation* 121:1005-1013, 2010.
31. Mugge A, Daniel WG, Frank G, et al: Echocardiography in infective endocarditis: reassessment of prognostic implications of vegetation size determined by the transthoracic and the transesophageal approach. *J Am Coll Cardiol* 14:631-638, 1989.
32. Erbel R, Rohmann S, Drexler M, et al: Improved diagnostic value of echocardiography in patients with infective endocarditis by transoesophageal approach. A prospective study. *Eur Heart J* 9:43-53, 1988.
33. Reynolds HR, Jagen MA, Tunick PA, et al: Sensitivity of transthoracic versus transesophageal echocardiography for the detection of native valve vegetations in the modern era. *J Am Soc Echocardiogr* 16:67-70, 2003.
34. Sanfilippo AJ, Picard MH, Newell JB, et al: Echocardiographic assessment of patients with infectious endocarditis: prediction of risk for complications. *J Am Coll Cardiol* 18:1191-1199, 1991.
35. Di SG, Habib G, Pergola V, et al: Echocardiography predicts embolic events in infective endocarditis. *J Am Coll Cardiol* 37:1069-1076, 2001.
36. Habib G, Hoen B, Tornos P, et al: Guidelines on the prevention, diagnosis, and treatment of infective endocarditis (new version 2009): the Task Force on the Prevention, Diagnosis, and Treatment of Infective Endocarditis of the European Society of Cardiology (ESC). Endorsed by the European Society of Clinical Microbiology and Infectious Diseases (ESCMID) and the International Society of Chemotherapy (ISC) for Infection and Cancer. *Eur Heart J* 30:2369-2413, 2009.
37. Baddour LM, Wilson WR, Bayer AS, et al: Infective endocarditis: diagnosis, antimicrobial therapy, and management of complications: a statement for healthcare professionals from the Committee on Rheumatic Fever, Endocarditis, and Kawasaki Disease, Council on Cardiovascular Disease in the Young, and the Councils on Clinical Cardiology, Stroke, and Cardiovascular Surgery and Anesthesia, American Heart Association: endorsed by the Infectious Diseases Society of America. *Circulation* 111:e394-e434, 2005.
38. Evangelista A, Gonzalez-Alujas MT: Echocardiography in infective endocarditis. *Heart* 90:614-617, 2004.
39. Lengyel M: The impact of transesophageal echocardiography on the management of prosthetic valve endocarditis: experience of 31 cases and review of the literature. *J Heart Valve Dis* 6:204-211, 1997.
40. Bonow RO, Carabello BA, Chatterjee K, et al: 2008 Focused update incorporated into the ACC/AHA 2006 guidelines for the management of patients with valvular heart disease: a report of the American College of Cardiology/American Heart Association Task Force on Practice Guidelines (Writing Committee to revise the 1998 guidelines for the management of patients with valvular heart disease). Endorsed by the Society of Cardiovascular Anesthesiologists, Society for Cardiovascular Angiography and Interventions, and Society of Thoracic Surgeons. *J Am Coll Cardiol* 52:e1-e142, 2008.
41. Moyssakis I, Tektonidou MG, Vasilliou VA, et al: Libman-Sacks endocarditis in systemic lupus erythematosus: prevalence, associations, and evolution. *Am J Med* 120:636-642, 2007.
42. Freedberg RS, Goodkin GM, Perez JL, et al: Valve strands are strongly associated with systemic embolization: a transesophageal echocardiographic study. *J Am Coll Cardiol* 26: 1709-1712, 1995.
43. Roberts JK, Omarali I, Di Tullio MR, et al: Valvular strands and cerebral ischemia. Effect of demographics and strand characteristics. *Stroke* 28:2185-2188, 1997.
44. Cohen A, Tzourio C, Chauvel C, et al: Mitral valve strands and the risk of ischemic stroke in elderly patients. The French Study of Aortic Plaques in Stroke (FAPS) Investigators. *Stroke* 28:1574-1578, 1997.
45. Roldan CA, Shively BK, Crawford MH: Valve excrescences: prevalence, evolution and risk for cardioembolism. *J Am Coll Cardiol* 30:1308-1314, 1997.
46. Homma S, Di Tullio MR, Sciacca RR, et al: Effect of aspirin and warfarin therapy in stroke patients with valvular strands. *Stroke* 35:1436-1442, 2004.
47. Kiavar M, Sadeghpour A, Bakhshandeh H, et al: Are prosthetic heart valve fibrin strands negligible? The associations and significance. *J Am Soc Echocardiogr* 22:890-894, 2009.
48. Reynen K: Frequency of primary tumors of the heart. *Am J Cardiol* 77:107, 1996.
49. Butany J, Nair V, Naseemuddin A, et al: Cardiac tumours: diagnosis and management. *Lancet Oncol* 6:219-228, 2005.
50. Reynen K: Cardiac myxomas. *N Engl J Med* 333:1610-1617, 1995.
51. Gegouskov V, Kadner A, Engelberger L, et al: Papillary fibroelastoma of the heart. *Heart Surg Forum* 11:E333-E339, 2008.
52. Gowda RM, Khan IA, Nair CK, et al: Cardiac papillary fibroelastoma: a comprehensive analysis of 725 cases. *Am Heart J* 146:404-410, 2003.
53. Neragi-Miandoab S, Kim J, Vlahakes GJ: Malignant tumours of the heart: a review of tumour type, diagnosis and therapy. *Clin Oncol (R Coll Radiol)* 19:748-756, 2007.
54. Ekmektzoglou KA, Samelis GF, Xanthos T: Heart and tumors: location, metastasis, clinical manifestations, diagnostic approaches and therapeutic considerations. *J Cardiovasc Med (Hagerstown)* 9:769-777, 2008.
55. Yahia AM, Shaukat A, Kirmani JF, et al: Prevalence and prediction of left atrial thrombus in patients with a recent cerebral ischemic event, who are in sinus rhythm: a single-center experience. *J Neuroimaging* 19:323-325, 2009.
56. Manning WJ, Silverman DI, Waksmonski CA, et al: Prevalence of residual left atrial thrombi among patients with acute thromboembolism and newly recognized atrial fibrillation. *Arch Intern Med* 155:2193-2198, 1995.
57. Agmon Y, Khandheria BK, Gentile F, et al: Echocardiographic assessment of the left atrial appendage. *J Am Coll Cardiol* 34:1867-1877, 1999.
58. Stoddard MF, Dawkins PR, Prince CR, et al: Left atrial appendage thrombus is not uncommon in patients with acute atrial fibrillation and a recent embolic event: a transesophageal echocardiographic study. *J Am Coll Cardiol* 25:452-459, 1995.
59. Handke M, Harloff A, Hetzel A, et al: Predictors of left atrial spontaneous echocardiographic contrast or thrombus formation in stroke patients with sinus rhythm and reduced left ventricular function. *Am J Cardiol* 96:1342-1344, 2005.
60. Handke M, Harloff A, Hetzel A, et al: Left atrial appendage flow velocity as a quantitative surrogate parameter for thromboembolic risk: determinants and relationship to spontaneous echocontrast and thrombus formation: a transesophageal echocardiographic study in 500 patients with cerebral ischemia. *J Am Soc Echocardiogr* 18:1366-1372, 2005.
61. The Stroke Prevention in Atrial Fibrillation Investigators Committee on Echocardiography: Transesophageal echocardiographic correlates of thromboembolism in high-risk patients with nonvalvular atrial fibrillation. *Ann Intern Med* 128:639-647, 1998.
62. Mugge A, Kuhn H, Nikutta P, et al: Assessment of left atrial appendage function by biplane transesophageal echocardiography in patients with nonrheumatic atrial fibrillation: identification of a subgroup of patients at increased embolic risk. *J Am Coll Cardiol* 23:599-607, 1994.
63. Leung DY, Black IW, Cranney GB, et al: Prognostic implications of left atrial spontaneous echo contrast in nonvalvular atrial fibrillation. *J Am Coll Cardiol* 24:755-762, 1994.
64. Kleemann T, Becker T, Strauss M, et al: Prevalence and clinical impact of left atrial thrombus and dense spontaneous echo contrast in patients with atrial fibrillation and low CHADS2 score. *Eur J Echocardiogr* 10:383-388, 2009.
65. Gage BF, Waterman AD, Shannon W, et al: Validation of clinical classification schemes for predicting stroke: results from the National Registry of Atrial Fibrillation. *JAMA* 285:2864-2870, 2001.
66. Fuster V, Ryden LE, Cannom DS, et al: ACC/AHA/ESC 2006 Guidelines for the Management of Patients with Atrial Fibrillation: a report of the American College of Cardiology/American Heart Association Task Force on Practice Guidelines and the European Society of Cardiology Committee for Practice Guidelines (Writing Committee to Revise the 2001 Guidelines for the Management of Patients With Atrial Fibrillation): developed in collaboration with the European Heart Rhythm Association and the Heart Rhythm Society. *Circulation* 114:e257-e354, 2006.
67. Connolly SJ, Ezekowitz MD, Yusuf S, et al: Dabigatran versus warfarin in patients with atrial fibrillation. *N Engl J Med* 361:1139-1151, 2009.
68. Wann LS, Curtis AB, January CT, et al: 2011 ACCF/AHA/HRS focused update on the management of patients with atrial fibrillation (updating the 2006 guideline): a report of the American College of Cardiology Foundation/American Heart Association Task Force on Practice Guidelines. *Circulation* 123:104-123, 2011.
69. Klein AL, Grimm RA, Murray RD, et al: Use of transesophageal echocardiography to guide cardioversion in patients with atrial fibrillation. *N Engl J Med* 344:1411-1420, 2001.
70. Karakus G, Kodali V, Inamdar V, et al: Comparative assessment of left atrial appendage by transesophageal and combined two- and three-dimensional transthoracic echocardiography. *Echocardiography* 25:918-924, 2008.
71. Penther P: Patent foramen ovale: an anatomical study. Apropos of 500 consecutive autopsies. *Arch Mal Coeur Vaiss* 87:15-21, 1994.

72. Schroeckenstein RF, Wasenda GJ, Edwards JE: Valvular competent patent foramen ovale in adults. *Minn Med* 55:11-13, 1972.
73. Hagen PT, Scholz DG, Edwards WD: Incidence and size of patent foramen ovale during the first 10 decades of life: an autopsy study of 965 normal hearts. *Mayo Clin Proc* 59:17-20, 1984.
74. Sweeney LJ, Rosenquist GC: The normal anatomy of the atrial septum in the human heart. *Am Heart J* 98:194-199, 1979.
75. Meissner I, Whisnant JP, Khandheria BK, et al: Prevalence of potential risk factors for stroke assessed by transesophageal echocardiography and carotid ultrasonography: the SPARC study. Stroke Prevention: Assessment of Risk in a Community. *Mayo Clin Proc* 74:862-869, 1999.
76. Meissner I, Khandheria BK, Heit JA, et al: Patent foramen ovale: innocent or guilty? Evidence from a prospective population-based study. *J Am Coll Cardiol* 47:440-445, 2006.
77. Di Tullio MR, Sacco RL, Sciacca RR, et al: Patent foramen ovale and the risk of ischemic stroke in a multiethnic population. *J Am Coll Cardiol* 49:797-802, 2007.
78. Kizer JR, Devereux RB: Clinical practice. Patent foramen ovale in young adults with unexplained stroke. *N Engl J Med* 353:2361-2372, 2005.
79. Mugge A, Daniel WG, Angermann C, et al: Atrial septal aneurysm in adult patients. A multicenter study using transthoracic and transesophageal echocardiography. *Circulation* 91:2785-2792, 1995.
80. Hanley PC, Tajik AJ, Hynes JK, et al: Diagnosis and classification of atrial septal aneurysm by two-dimensional echocardiography: report of 80 consecutive cases. *J Am Coll Cardiol* 6:1370-1382, 1985.
81. Schneider B, Hanrath P, Vogel P, et al: Improved morphologic characterization of atrial septal aneurysm by transesophageal echocardiography: relation to cerebrovascular events. *J Am Coll Cardiol* 16:1000-1009, 1990.
82. Zabalgoitia-Reyes M, Herrera C, Gandhi DK, et al: A possible mechanism for neurologic ischemic events in patients with atrial septal aneurysm. *Am J Cardiol* 66:761-764, 1990.
83. Pearson AC, Nagelhout D, Castello R, et al: Atrial septal aneurysm and stroke: a transesophageal echocardiographic study. *J Am Coll Cardiol* 18:1223-1229, 1991.
84. Silver MD, Dorsey JS: Aneurysms of the septum primum in adults. *Arch Pathol Lab Med* 102:62-65, 1978.
85. Mattioli AV, Bonetti L, Aquilina M, et al: Association between atrial septal aneurysm and patent foramen ovale in young patients with recent stroke and normal carotid arteries. *Cerebrovasc Dis* 15:4-10, 2003.
86. Burger AJ, Jadhav P, Kamalesh M: Low incidence of cerebrovascular events in patients with incidental atrial septal aneurysm. *Echocardiography* 14:589-596, 1997.
87. Homma S, Sacco RL, Di Tullio MR, et al: Atrial anatomy in non-cardioembolic stroke patients: effect of medical therapy. *J Am Coll Cardiol* 42:1066-1072, 2003.
88. Johansson MC, Helgason H, Dellborg M, et al: Sensitivity for detection of patent foramen ovale increased with increasing number of contrast injections: a descriptive study with contrast transesophageal echocardiography. *J Am Soc Echocardiogr* 21:419-424, 2008.
89. Schneider B, Zienkiewicz T, Jansen V, et al: Diagnosis of patent foramen ovale by transesophageal echocardiography and correlation with autopsy findings. *Am J Cardiol* 77:1202-1209, 1996.
90. Rodriguez CJ, Homma S, Sacco RL, et al: Race-ethnic differences in patent foramen ovale, atrial septal aneurysm, and right atrial anatomy among ischemic stroke patients. *Stroke* 34: 2097-2102, 2003.
91. Teague SM, Sharma MK: Detection of paradoxical cerebral echo contrast embolization by transcranial Doppler ultrasound. *Stroke* 22: 740-745, 1991.
92. Di Tullio M, Sacco RL, Venketasubramanian N, et al: Comparison of diagnostic techniques for the detection of a patent foramen ovale in stroke patients. *Stroke* 24:1020-1024, 1993.
93. Jauss M, Kaps M, Keberle M, et al: A comparison of transesophageal echocardiography and transcranial Doppler sonography with contrast medium for detection of patent foramen ovale. *Stroke* 25:1265-1267, 1994.
94. Karnik R, Stollberger C, Valentin A, et al: Detection of patent foramen ovale by transcranial contrast Doppler ultrasound. *Am J Cardiol* 69:560-562, 1992.
95. Job FP, Ringelstein EB, Grafen Y, et al: Comparison of transcranial contrast Doppler sonography and transesophageal contrast echocardiography for the detection of patent foramen ovale in young stroke patients. *Am J Cardiol* 74:381-384, 1994.
96. Klotzsch C, Janssen G, Berlit P: Transesophageal echocardiography and contrast-TCD in the detection of a patent foramen ovale: experiences with 111 patients. *Neurology* 44:1603-1606, 1994.
97. Di Tullio M, Sacco RL, Massaro A, et al: Transcranial Doppler with contrast injection for the detection of patent foramen ovale in stroke patients. *Int J Card Imaging* 9:1-5, 1993.
98. Nemec JJ, Marwick TH, Lorig RJ, et al: Comparison of transcranial Doppler ultrasound and transesophageal contrast echocardiography in the detection of interatrial right-to-left shunts. *Am J Cardiol* 68:1498-1502, 1991.
99. Clarke NR, Timperley J, Kelion AD, et al: Transthoracic echocardiography using second harmonic imaging with Valsalva manoeuvre for the detection of right to left shunts. *Eur J Echocardiogr* 5:176-181, 2004.
100. Daniels C, Weytjens C, Cosyns B, et al: Second harmonic transthoracic echocardiography: the new reference screening method for the detection of patent foramen ovale. *Eur J Echocardiogr* 5:449-452, 2004.
101. Kerr AJ, Buck T, Chia K, et al: Transmitral Doppler: a new transthoracic contrast method for patent foramen ovale detection and quantification. *J Am Coll Cardiol* 36:1959-1966, 2000.
102. Lechat P, Mas JL, Lascault G, et al: Prevalence of patent foramen ovale in patients with stroke. *N Engl J Med* 318:1148-1152, 1988.
103. Webster MW, Chancellor AM, Smith HJ, et al: Patent foramen ovale in young stroke patients. *Lancet* 2:11-12, 1988.
104. Di Tullio M, Sacco RL, Gopal A, et al: Patent foramen ovale as a risk factor for cryptogenic stroke. *Ann Intern Med* 117:461-465, 1992.
105. Hausmann D, Mugge A, Becht I, et al: Diagnosis of patent foramen ovale by transesophageal echocardiography and association with cerebral and peripheral embolic events. *Am J Cardiol* 70:668-672, 1992.
106. Jones EF, Calafiore P, Donnan GA, et al: Evidence that patent foramen ovale is not a risk factor for cerebral ischemia in the elderly. *Am J Cardiol* 74:596-599, 1994.
107. Cabanes L, Mas JL, Cohen A, et al: Atrial septal aneurysm and patent foramen ovale as risk factors for cryptogenic stroke in patients less than 55 years of age. A study using transesophageal echocardiography. *Stroke* 24:1865-1873, 1993.
108. de Belder MA, Tourikis L, Leech G, et al: Risk of patent foramen ovale for thromboembolic events in all age groups. *Am J Cardiol* 69:1316-1320, 1992.
109. Handke M, Harloff A, Olschewski M, et al: Patent foramen ovale and cryptogenic stroke in older patients. *N Engl J Med* 357:2262-2268, 2007.
110. Alsheikh-Ali AA, Thaler DE, Kent DM: Patent foramen ovale in cryptogenic stroke: incidental or pathogenic? *Stroke* 40:2349-2355, 2009.
111. Homma S, Di Tullio MR, Sacco RL, et al: Characteristics of patent foramen ovale associated with cryptogenic stroke. A biplane transesophageal echocardiographic study. *Stroke* 25:582-586, 1994.
112. Hausmann D, Mugge A, Daniel WG: Identification of patent foramen ovale permitting paradoxic embolism. *J Am Coll Cardiol* 26:1030-1038, 1995.
113. Van CG, Schulze D, Cosyns B, et al: Relation between patent foramen ovale and unexplained stroke. *Am J Cardiol* 71:596-598, 1993.
114. Goel SS, Tuzcu EM, Shishehbor MH, et al: Morphology of the patent foramen ovale in asymptomatic versus symptomatic (stroke or transient ischemic attack) patients. *Am J Cardiol* 103:124-129, 2009.
115. Serena J, Segura T, Perez-Ayuso MJ, et al: The need to quantify right-to-left shunt in acute ischemic stroke: a case-control study. *Stroke* 29:1322-1328, 1998.
116. Bridges ND, Hellenbrand W, Latson L, et al: Transcatheter closure of patent foramen ovale after presumed paradoxical embolism. *Circulation* 86:1902-1908, 1992.
117. Steiner MM, Di Tullio MR, Rundek T, et al: Patent foramen ovale size and embolic brain imaging findings among patients with ischemic stroke. *Stroke* 29:944-948, 1998.
118. Schuchlenz HW, Weihs W, Horner S, et al: The association between the diameter of a patent foramen ovale and the risk of embolic cerebrovascular events. *Am J Med* 109:456-462, 2000.
119. Fox ER, Picard MH, Chow CM, et al: Interatrial septal mobility predicts larger shunts across patent foramen ovales: an analysis with transmitral Doppler scanning. *Am Heart J* 145:730-736, 2003.
120. Overell JR, Bone I, Lees KR: Interatrial septal abnormalities and stroke: a meta-analysis of case-control studies. *Neurology* 55:1172-1179, 2000.
121. Mas JL, Arquizan C, Lamy C, et al: Recurrent cerebrovascular events associated with patent foramen ovale, atrial septal aneurysm, or both. *N Engl J Med* 345:1740-1746, 2001.
122. Bonati LH, Kessel-Schaefer A, Linka AZ, et al: Diffusion-weighted imaging in stroke attributable to patent foramen ovale: significance of concomitant atrial septum aneurysm. *Stroke* 37:2030-2034, 2006.
123. Berthet K, Lavergne T, Cohen A, et al: Significant association of atrial vulnerability with atrial septal abnormalities in young patients with ischemic stroke of unknown cause. *Stroke* 31:398-403, 2000.
124. Kizer JR: Patent foramen ovale and cryptogenic stroke. *Am J Med* 120:e13, 2007.
125. Schuchlenz HW, Saurer G, Weihs W, et al: Persisting eustachian valve in adults: relation to

patent foramen ovale and cerebrovascular events. *J Am Soc Echocardiogr* 17:231-233, 2004.
126. Schneider B, Hofmann T, Justen MH, et al: Chiari's network: normal anatomic variant or risk factor for arterial embolic events? *J Am Coll Cardiol* 26:203-210, 1995.
127. Lapostolle F, Borron SW, Surget V, et al: Stroke associated with pulmonary embolism after air travel. *Neurology* 60:1983-1985, 2003.
128. Kasper W, Geibel A, Tiede N, et al: Patent foramen ovale in patients with haemodynamically significant pulmonary embolism. *Lancet* 340:561-564, 1992.
129. Bansal RC, Marsa RJ, Holland D, et al: Severe hypoxemia due to shunting through a patent foramen ovale: a correctable complication of right ventricular infarction. *J Am Coll Cardiol* 5:188-192, 1985.
130. Harpaz D, Motro M, Kaplinsky E, et al: Right-to-left shunt through a patent foramen ovale caused by severe tricuspid regurgitation detected with color Doppler echocardiography. *J Am Soc Echocardiogr* 5:77-80, 1992.
131. Shapiro GC, Leibowitz DW, Oz MC, et al: Diagnosis of patent foramen ovale with transesophageal echocardiography in a patient supported with a left ventricular assist device. *J Heart Lung Transplant* 14:594-597, 1995.
132. Stollberger C, Slany J, Schuster I, et al: The prevalence of deep venous thrombosis in patients with suspected paradoxical embolism. *Ann Intern Med* 119:461-465, 1993.
133. Ranoux D, Cohen A, Cabanes L, et al: Patent foramen ovale: is stroke due to paradoxical embolism? *Stroke* 24:31-34, 1993.
134. Lethen H, Flachskampf FA, Schneider R, et al: Frequency of deep vein thrombosis in patients with patent foramen ovale and ischemic stroke or transient ischemic attack. *Am J Cardiol* 80:1066-1069, 1997.
135. Cramer SC, Rordorf G, Maki JH, et al: Increased pelvic vein thrombi in cryptogenic stroke: results of the Paradoxical Emboli from Large Veins in Ischemic Stroke (PELVIS) study. *Stroke* 35:46-50, 2004.
136. Chaturvedi S: Coagulation abnormalities in adults with cryptogenic stroke and patent foramen ovale. *J Neurol Sci* 160:158-160, 1998.
137. Pezzini A, Del ZE, Magoni M, et al: Inherited thrombophilic disorders in young adults with ischemic stroke and patent foramen ovale. *Stroke* 34:28-33, 2003.
138. Karttunen V, Hiltunen L, Rasi V, et al: Factor V Leiden and prothrombin gene mutation may predispose to paradoxical embolism in subjects with patent foramen ovale. *Blood Coagul Fibrinolysis* 14:261-268, 2003.
139. Lichy C, Reuner KH, Buggle F, et al: Prothrombin G20210A mutation, but not factor V Leiden, is a risk factor in patients with persistent foramen ovale and otherwise unexplained cerebral ischemia. *Cerebrovasc Dis* 16:83-87, 2003.
140. Botto N, Spadoni I, Giusti S, et al: Prothrombotic mutations as risk factors for cryptogenic ischemic cerebrovascular events in young subjects with patent foramen ovale. *Stroke* 38: 2070-2073, 2007.
141. Belvis R, Santamaria A, Marti-Fabregas J, et al: Patent foramen ovale and prothrombotic markers in young stroke patients. *Blood Coagul Fibrinolysis* 18:537-542, 2007.
142. Meacham RR III, Headley AS, Bronze MS, et al: Impending paradoxical embolism. *Arch Intern Med* 158:438-448, 1998.
143. Homma S, Sacco RL, Di Tullio MR, et al: Effect of medical treatment in stroke patients with patent foramen ovale: patent foramen ovale in Cryptogenic Stroke Study. *Circulation* 105: 2625-2631, 2002.
144. Mohr JP, Thompson JL, Lazar RM, et al: A comparison of warfarin and aspirin for the prevention of recurrent ischemic stroke. *N Engl J Med* 345:1444-1451, 2001.
145. Serena J, Marti-Fabregas J, Santamarina E, et al: Recurrent stroke and massive right-to-left shunt: results from the prospective Spanish multicenter (CODICIA) study. *Stroke* 39:3131-3136, 2008.
146. Windecker S, Meier B: Is closure recommended for patent foramen ovale and cryptogenic stroke? Patent foramen ovale and cryptogenic stroke: to close or not to close? Closure: what else! *Circulation* 118:1989-1998, 2008.
147. Messe SR, Kasner SE: Is closure recommended for patent foramen ovale and cryptogenic stroke? Patent foramen ovale in cryptogenic stroke: not to close. *Circulation* 118:1999-2004, 2008.
148. Sacco RL, Adams R, Albers G, et al: Guidelines for prevention of stroke in patients with ischemic stroke or transient ischemic attack: a statement for healthcare professionals from the American Heart Association/American Stroke Association Council on Stroke: co-sponsored by the Council on Cardiovascular Radiology and Intervention: the American Academy of Neurology affirms the value of this guideline. *Stroke* 37:577-617, 2006.
149. Furlan A, Massaro J, Mauri L, et al: CLOSURE I: a prospective, multicenter, randomized controlled trial to evaluate the safety and efficacy of STARFlex septal closure system versus best medical therapy in patients with a stroke or transient ischemic attack due to presumed paradoxical embolism through a patent foramen [abstract]. *Circulation* 122:2218, 2010.
150. Amarenco P, Duyckaerts C, Tzourio C, et al: The prevalence of ulcerated plaques in the aortic arch in patients with stroke. *N Engl J Med* 326:221-225, 1992.
151. Tenenbaum A, Motro M, Feinberg MS, et al: Retrograde flow in the thoracic aorta in patients with systemic emboli: a transesophageal echocardiographic evaluation of mobile plaque motion. *Chest* 118:1703-1708, 2000.
152. Harloff A, Strecker C, Frydrychowicz AP, et al: Plaques in the descending aorta: a new risk factor for stroke? Visualization of potential embolization pathways by 4D MRI. *J Magn Reson Imaging* 26:1651-1655, 2007.
153. Toyoda K, Yasaka M, Nagata S, et al: Aortogenic embolic stroke: a transesophageal echocardiographic approach. *Stroke* 23:1056-1061, 1992.
154. Vaduganathan P, Ewton A, Nagueh SF, et al: Pathologic correlates of aortic plaques, thrombi and mobile "aortic debris" imaged in vivo with transesophageal echocardiography. *J Am Coll Cardiol* 30:357-363, 1997.
155. Di Tullio MR, Sacco RL, Gersony D, et al: Aortic atheromas and acute ischemic stroke: a transesophageal echocardiographic study in an ethnically mixed population. *Neurology* 46:1560-1566, 1996.
156. Stone DA, Hawke MW, LaMonte M, et al: Ulcerated atherosclerotic plaques in the thoracic aorta are associated with cryptogenic stroke: a multiplane transesophageal echocardiographic study. *Am Heart J* 130:105-108, 1995.
157. Jones EF, Kalman JM, Calafiore P, et al: Proximal aortic atheroma. An independent risk factor for cerebral ischemia. *Stroke* 26:218-224, 1995.
158. Weber A, Jones EF, Zavala JA, et al: Intraobserver and interobserver variability of transesophageal echocardiography in aortic arch atheroma measurement. *J Am Soc Echocardiogr* 21:129-133, 2008.
159. Amarenco P, Cohen A, Tzourio C, et al: Atherosclerotic disease of the aortic arch and the risk of ischemic stroke. *N Engl J Med* 331:1474-1479, 1994.
160. Tunick PA, Perez JL, Kronzon I: Protruding atheromas in the thoracic aorta and systemic embolization. *Ann Intern Med* 115:423-427, 1991.
161. Di Tullio MR, Sacco RL, Savoia MT, et al: Aortic atheroma morphology and the risk of ischemic stroke in a multiethnic population. *Am Heart J* 139:329-336, 2000.
162. Di Tullio MR, Homma S, Jin Z, et al: Aortic atherosclerosis, hypercoagulability and stroke: the Aortic Plaques and Risk of Ischemic Stroke (APRIS) Study. *J Am Coll Cardiol* 52:855-861, 2008.
163. Tunick PA, Rosenzweig BP, Katz ES, et al: High risk for vascular events in patients with protruding aortic atheromas: a prospective study. *J Am Coll Cardiol* 23:1085-1090, 1994.
164. Mitusch R, Doherty C, Wucherpfennig H, et al: Vascular events during follow-up in patients with aortic arch atherosclerosis. *Stroke* 28:36-39, 1997.
165. The French Study of Aortic Plaques in Stroke Group: Atherosclerotic disease of the aortic arch as a risk factor for recurrent ischemic stroke. *N Engl J Med* 334:1216-1221, 1996.
166. Tanaka M, Yasaka M, Nagano K, et al: Moderate atheroma of the aortic arch and the risk of stroke. *Cerebrovasc Dis* 21:26-31, 2006.
167. Fujimoto S, Yasaka M, Otsubo R, et al: Aortic arch atherosclerotic lesions and the recurrence of ischemic stroke. *Stroke* 35:1426-1429, 2004.
168. Di Tullio MR, Sacco RL, Savoia MT, et al: Gender differences in the risk of ischemic stroke associated with aortic atheromas. *Stroke* 31:2623-2627, 2000.
169. Sen S, Hinderliter A, Sen PK, et al: Aortic arch atheroma progression and recurrent vascular events in patients with stroke or transient ischemic attack. *Circulation* 116:928-935, 2007.
170. Agmon Y, Khandheria BK, Meissner I, et al: Relation of coronary artery disease and cerebrovascular disease with atherosclerosis of the thoracic aorta in the general population. *Am J Cardiol* 89:262-267, 2002.
171. Khatibzadeh M, Mitusch R, Stierle U, et al: Aortic atherosclerotic plaques as a source of systemic embolism. *J Am Coll Cardiol* 27:664-669, 1996.
172. Cohen A, Tzourio C, Bertrand B, et al: Aortic plaque morphology and vascular events: a follow-up study in patients with ischemic stroke. FAPS Investigators. French Study of Aortic Plaques in Stroke. *Circulation* 96:3838-3841, 1997.
173. Tunick PA, Culliford AT, Lamparello PJ, et al: Atheromatosis of the aortic arch as an occult source of multiple systemic emboli. *Ann Intern Med* 114:391-392, 1991.
174. Tunick PA, Lackner H, Katz ES, et al: Multiple emboli from a large aortic arch thrombus in a patient with thrombotic diathesis. *Am Heart J* 124:239-241, 1992.
175. Nihoyannopoulos P, Joshi J, Athanasopoulos G, et al: Detection of atherosclerotic lesions in the aorta by transesophageal echocardiography. *Am J Cardiol* 71:1208-1212, 1993.

176. Ueno Y, Kimura K, Iguchi Y, et al: Mobile aortic plaques are a cause of multiple brain infarcts seen on diffusion-weighted imaging. *Stroke* 38:2470-2476, 2007.
177. Laperche T, Laurian C, Roudaut R, et al: Mobile thromboses of the aortic arch without aortic debris. A transesophageal echocardiographic finding associated with unexplained arterial embolism. The Filiale Echocardiographie de la Societe Francaise de Cardiologie. *Circulation* 96:288-294, 1997.
178. Russo C, Jin Z, Rundek T, et al: Aortic plaques and risk of vascular events in subjects without prior stroke. *Stroke* 40:2313-2318, 2009.
179. Soloway HB, Aronson SM: Atheromatous emboli to central nervous system. Report of 16 cases. *Arch Neurol* 11:657-667, 1964.
180. Ben-Horin S, Bardan E, Barshack I, et al: Cholesterol crystal embolization to the digestive system: characterization of a common, yet overlooked presentation of atheroembolism. *Am J Gastroenterol* 98:1471-1479, 2003.
181. Theriault J, Agharazzi M, Dumont M, et al: Atheroembolic renal failure requiring dialysis: potential for renal recovery? A review of 43 cases. *Nephron Clin Pract* 94:c11-c18, 2003.
182. Bruno A, Russell PW, Jones WL, et al: Concomitants of asymptomatic retinal cholesterol emboli. *Stroke* 23:900-902, 1992.
183. Bruno A, Jones WL, Austin JK, et al: Vascular outcome in men with asymptomatic retinal cholesterol emboli. A cohort study. *Ann Intern Med* 122:249-253, 1995.
184. Mouradian M, Wijman CA, Tomasian D, et al: Echocardiographic findings of patients with retinal ischemia or embolism. *J Neuroimaging* 12:219-223, 2002.
185. Gore I, Collins DP: Spontaneous atheromatous embolization. Review of the literature and a report of 16 additional cases. *Am J Clin Pathol* 33:416-426, 1960.
186. Hauben M, Norwich J, Shapiro E, et al: Multiple cholesterol emboli syndrome: six cases identified through the spontaneous reporting system. *Angiology* 46:779-784, 1995.
187. The Stroke Prevention in Atrial Fibrillation Investigators Committee on Echocardiography: Transesophageal echocardiographic correlates of thromboembolism in high-risk patients with nonvalvular atrial fibrillation. *Ann Intern Med* 128:639-647, 1998.
188. Di Tullio MR, Russo C, Jin Z, et al: Aortic arch plaques and risk of recurrent stroke and death. *Circulation* 119:2376-2382, 2009.
189. Donnan GA, Davis SM, Jones EF, et al: Aortic source of brain embolism. *Curr Treat Options Cardiovasc Med* 5:211-219, 2003.
190. Amarenco P, Goldstein LB, Szarek M, et al: Effects of intense low-density lipoprotein cholesterol reduction in patients with stroke or transient ischemic attack: the Stroke Prevention by Aggressive Reduction in Cholesterol Levels (SPARCL) trial. *Stroke* 38:3198-3204, 2007.
191. Stern A, Tunick PA, Culliford AT, et al: Protruding aortic arch atheromas: risk of stroke during heart surgery with and without aortic arch endarterectomy. *Am Heart J* 138:746-752, 1999.
192. van der LJ, Hadjinikolaou L, Bergman P, et al: Postoperative stroke in cardiac surgery is related to the location and extent of atherosclerotic disease in the ascending aorta. *J Am Coll Cardiol* 38:131-135, 2001.
193. Trehan N, Mishra M, Kasliwal RR, et al: Reduced neurological injury during CABG in patients with mobile aortic atheromas: a five-year follow-up study. *Ann Thorac Surg* 70:1558-1564, 2000.
194. Ura M, Sakata R, Nakayama Y, et al: Ultrasonographic demonstration of manipulation-related aortic injuries after cardiac surgery. *J Am Coll Cardiol* 35:1303-1310, 2000.
195. Khairy P, O'Donnell CP, Landzberg MJ: Transcatheter closure versus medical therapy of patent foramen ovale and presumed paradoxical thromboemboli: a systematic review. *Ann Intern Med* 139:753-760, 2003.
196. Luermans JG, Post MC, Schrader R, et al: Outcome after percutaneous closure of a patent foramen ovale using the Intrasepttrade mark device: a multi-centre study. *Catheter Cardiovasc Interv* 71:822-828, 2008.
197. Morandi E, Anzola GP, Casilli F, et al: Silent brain embolism during transcatheter closure of patent foramen ovale: a transcranial Doppler study. *Neurol Sci* 27:328-331, 2006.
198. Dorenbeck U, Simon B, Skowasch D, et al: Cerebral embolism with interventional closure of symptomatic patent foramen ovale: an MRI-based study using diffusion-weighted imaging. *Eur J Neurol* 14:451-454, 2007.
199. Fayad ZA, Nahar T, Fallon JT, et al: In vivo magnetic resonance evaluation of atherosclerotic plaques in the human thoracic aorta: a comparison with transesophageal echocardiography. *Circulation* 101:2503-2509, 2000.
200. Helft G, Worthley SG, Fuster V, et al: Atherosclerotic aortic component quantification by noninvasive magnetic resonance imaging: an in vivo study in rabbits. *J Am Coll Cardiol* 37:1149-1154, 2001.
201. Tenenbaum A, Garniek A, Shemesh J, et al: Dual-helical CT for detecting aortic atheromas as a source of stroke: comparison with transesophageal echocardiography. *Radiology* 208: 153-158, 1998.

# 42 The Role of Echocardiography in Atrial Fibrillation and Flutter

WARREN J. MANNING, MD

**Echocardiographic Assessment of Atrial Anatomy and Function**
Left Atrial Anatomy
Identification of Left Atrial Thrombi
Right Atrial Anatomy
Atrial Mechanical Function
Left Atrial Appendage Function
**Echocardiography and Atrial Fibrillation**
Prevalence of Atrial Fibrillation
Symptoms and Clinical Impact
Atrial Size and Atrial Fibrillation
Detection of Atrial Thrombi in Atrial Fibrillation
Mechanism of Thromboembolism after Cardioversion
Assessment of Return of Atrial Mechanical Function after Cardioversion
Evidence of Electrical Injury to the Atria
Spontaneous Echocardiographic Contrast
**Echocardiography and Atrial Flutter**
**Echocardiography and Guidance of Therapeutic Interventions in Atrial Fibrillation**
**Current and Future Areas of Investigation**

Technologic advances in two-dimensional (2D) and Doppler ultrasonography have led to the emergence of echocardiography as an integral tool in the evaluation and management of patients with cardiac dysrhythmias. Transthoracic echocardiography (TTE) and transesophageal echocardiography (TEE) provide detailed information about cardiac anatomy and function. Patients with ventricular tachyarrhythmias are routinely referred for echocardiographic examination for identification of suspected structural heart disease. Echocardiography may also play a role in characterization of ventricular dyssynchrony and response to cardiac resynchronization therapy (see Chapter 26).

In addition to ventricular arrhythmias, both TTE and TEE provide useful information in the evaluation and management of patients with atrial arrhythmias, particularly atrial fibrillation (AF). In this chapter, we review the detailed structural and functional information derived from TTE and TEE and how these data assist in the evaluation and management of patients with AF and atrial flutter.

## Echocardiographic Assessment of Atrial Anatomy and Function

### LEFT ATRIAL ANATOMY

TTE is a reliable and reproducible method to assess the anatomy of the body of the left atrium (LA). 2D directed M-mode echocardiography[1-3] in the parasternal long or short axis allows for the measurement of LA dimension (Fig. 42-1, *A*). Overall, this unidimensional index correlates well with angiographically derived LA area and volume[2,3] but may be disproportionately erroneous in common disease states associated with asymmetric atrial dilation, such as mitral valve disease[4] or situations in which the LA is deformed by extrinsic structures.

2D TTE provides more accurate assessment of atrial anatomy. The LA is well seen from both the parasternal and the apical windows. In many laboratories, LA anatomy is characterized by the M-mode or 2D dimension from the parasternal long or short axis and the LA length from the apical four-chamber view (see Fig. 42-1, *B*). However, because the LA is not spherically shaped and asymmetric enlargement may occur, 2D-derived LA volume provides a more accurate measure of LA size[5] and is advocated by the American Society of Echocardiography.[6] It more favorably compares with volumetric methods such as cardiovascular magnetic resonance and cardiac computed tomography.[7,8] With the biplane method,[9] maximum LA area and length are measured in the apical four-chamber ($A_{4C}$, $L_{4C}$) (see Fig. 42-1, *B*) and two-chamber ($A_{2C}$, $L_{2C}$) orientations with volume derived as:

$$\text{LA volume} = 1.7(A_{4C})(A_{2C})/[(L_{4C} + L_{2C})/2]$$

Population-based studies suggest LA volumes of 41.9 ± 11.9 mL or when normalized for body surface area, 22 ± 5 mL/m$^2$.[10] Increasing LA volume predicts development of AF in the general population[11] as well as after cardiac surgery[12] and in hypertrophic cardiomyopathy.[13,14] Biplane and Simpson's methods compare closely.[9] In situations in which there is focal atrial asymmetry, such as distortion of the LA from an extrinsic structure (e.g., mediastinal tumor, hiatal hernia, or descending thoracic aortic aneurysm), accurate calculation of LA volume may be improved by using a Simpson approach.

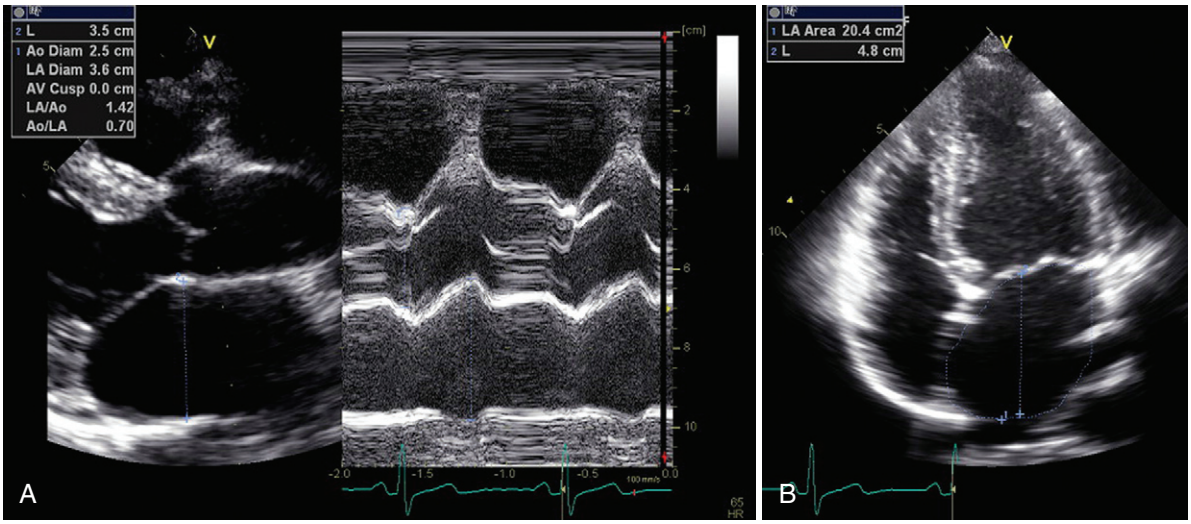



**Figure 42-1 Transthoracic echo (TTE). Parasternal long-axis view. A,** TTE image from parasternal long axis demonstrating measurement of the LA dimension from 2D and M-mode data. **B,** TTE from apical four-chamber view demonstrating measurement of LA length and LA area.

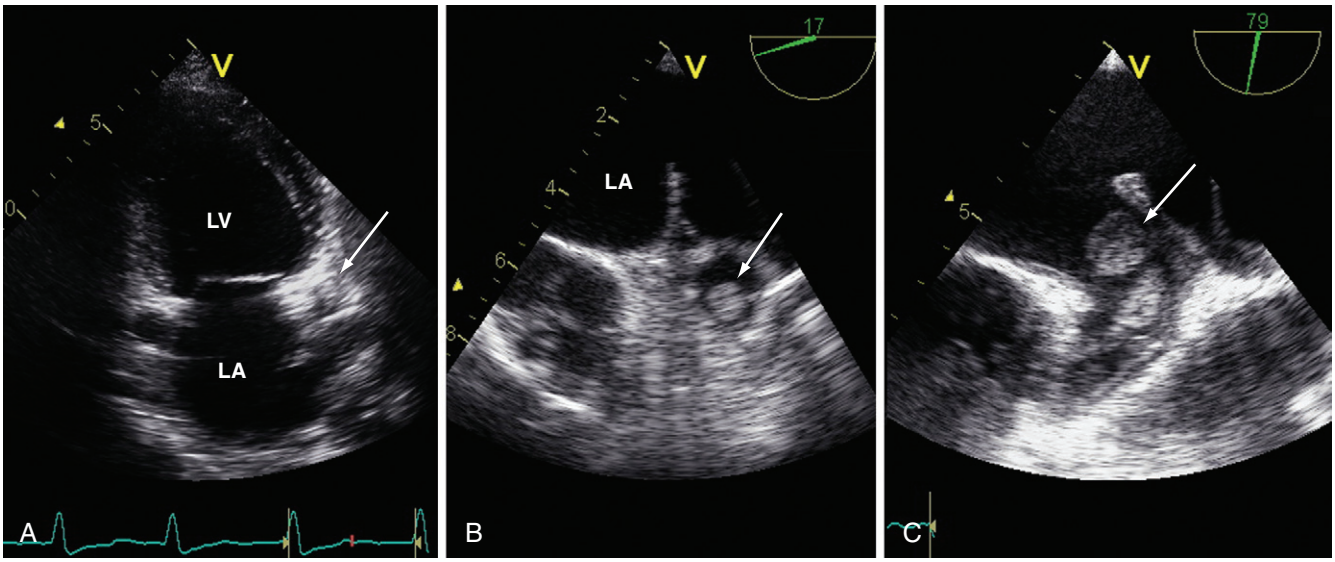



**Figure 42-2 Left atrial appendage thrombus. A,** TTE image taken from the apical two-chamber view demonstrating a thrombus (*arrow*) in the LA appendage. **B,** TEE in the same patient confirming the LA appendage thrombus. **C,** TEE in another patient demonstrating multiple thrombi in the LA appendage.

TEE is a well-tolerated but moderately invasive diagnostic imaging technique that allows for superior visualization of posterior structures such as the LA and LA appendage. Although TEE may be used to assess the body of the LA from orientations analogous to TTE imaging,[15] its greatest advantage over TTE is in evaluation of the anatomy and function of the left and right atrial appendages, structures poorly seen by TTE.

## IDENTIFICATION OF LEFT ATRIAL THROMBI

Anatomic imaging of the body of the LA may be readily obtained from 2D TTE, but identification or exclusion of LA and LA appendage thrombi is best performed by TEE. The sensitivity of TTE for detection of LA thrombi (Fig. 42-2, *A*) is only 39% to 63%,[16-18] with very limited success for identifying thrombi in the LA appendage. Even with modified views,[19] visualization of the LA appendage may be accomplished in less than 20% of patients.[20] Although identification of LA appendage thrombi using state-of-the-art TTE equipment has been described (see Fig. 42-2, *A*),[21] and echocardiographic contrast may be useful,[22] this has not been confirmed in a large series.

Imaging of the LA appendage is readily accomplished with multiplane TEE (Fig. 42-2, *B*). The normal length and neck width of the adult LA appendage in the horizontal and vertical imaging planes are 28 ± 5 mm and 16 ± 5 mm, respectively.[23] LA appendage anatomic indexes are dependent on imaging plane, with greater neck width and cross-sectional area when observed at a 135° imaging plane as compared with a 45° or 90° plane,[24] consistent with its shape idealized as a special ungula of a right circular cylinder.[25] The LA appendage commonly has multiple lobes and trabeculations (Fig. 42-3).

The accuracy of TEE for the identification of LA thrombi has been reported by several investigators and was initially based on older monoplane technology.[20,25-27] For nearly two decades, multiplane TEE technology has been the standard with superior visualization of the LA appendage. In our experience of nearly

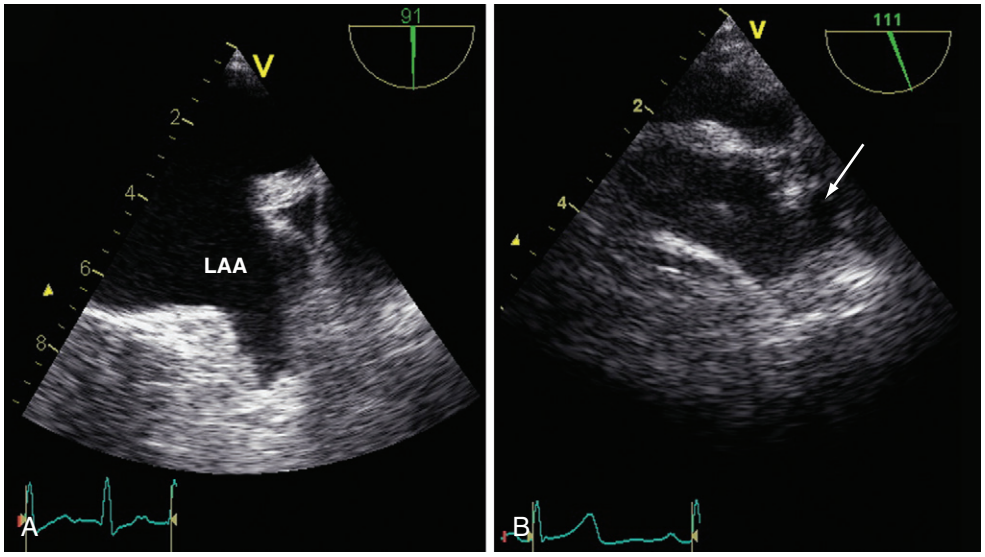



**Figure 42-3** **TEE of LA appendage. A,** Single-lobed LA appendage (*LAA*). **B,** LA appendage with an accessory lobe (*arrow*).

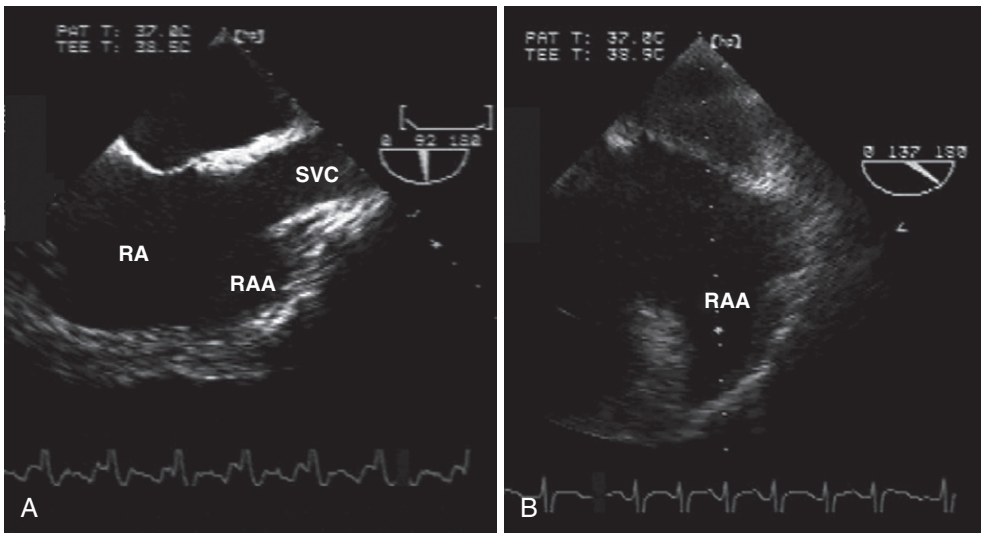



**Figure 42-4** **TEE of normal right atrial appendage (*RAA*). A,** 92° imaging plane. **B,** 137° imaging plane. *SVC*, Superior vena cava.

200 consecutive patients undergoing intraoperative TEE immediately before mitral valve surgery, TEE sensitivity and specificity for LA thrombi were 100% and 99%, respectively.[28] We have found the 90° imaging plane particularly advantageous for assessing the LA appendage for thrombus. Real-time three-dimensional (3D) TEE has been used to characterize LA appendage anatomy.[29] The accuracy of this technology for identification of LA appendage thrombus is currently unknown, though case reports and small series suggest a benefit (versus 2D multiplane TEE) when the appendage is heavily trabeculated.[30] For patients who are not candidates for conventional TEE, microprobe TEE or intracardiac echo[31,32] may be options, but these technologies have not been as well studied and few data are available on comparative accuracy.

## RIGHT ATRIAL ANATOMY

The right atrium has not been as well studied by either TTE or TEE. As is the case with the LA, 2D TTE provides a reasonably comprehensive assessment of right atrial (RA) volume. The primary transthoracic window is the apical four-chamber view, with RA area estimated using a length-diameter ellipsoid formula. Parasternal short-axis and subxiphoid windows provide complementary data. The RA appendage is rarely appreciated from TTE, but TEE at 90° (see Fig. 42-3) and 135° imaging orientations readily allow for visualization of this structure (Fig. 42-4).[33] RA appendage area and length are independent of transducer orientation with areas of 5.4 ± 2.4 $cm^2$ and lengths of 4.0 ± 0.9 cm reported for those in sinus rhythm.[33] Care must be taken to avoid mistaking normal structures (such as the Eustachian valve or Chiari network) for thrombi.[34]

TTE and TEE sensitivity and specificity data for identification of RA thrombi are relatively sparse. Schwartzbard and colleagues[35] reported on 20 patients with TEE evidence of RA thrombus, including 7 confirmed at surgery. TTE identified thrombus in only 6 patients (30%). All RA *appendage* thrombi were missed by TTE.

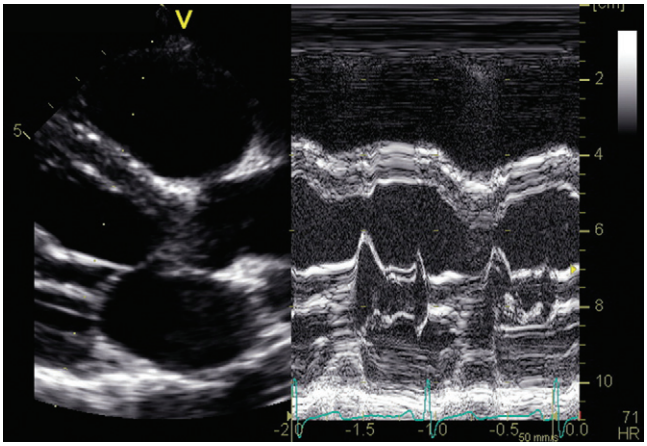



**Figure 42-5 TTE 2D guided M-mode demonstrating the normal motion of the mitral valve and atrial systole.** The height of the M-mode anterior leaflet A wave has been used as a measure of atrial mechanical function.

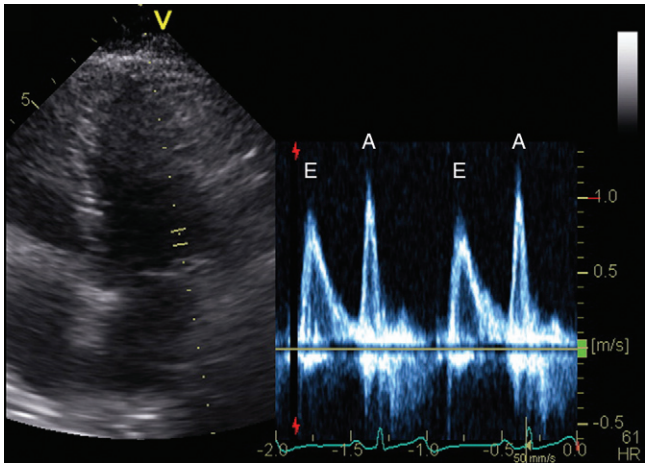



**Figure 42-6 TTE 2D guided spectral display of transmitral pulsed Doppler echocardiographic flow velocity.** *A,* Atrial filling wave; *E,* early filling wave.

## ATRIAL MECHANICAL FUNCTION

In addition to atrial anatomy, echocardiography is a powerful tool for evaluation of atrial systolic function. The atria are traditionally believed to have two primary functions: as passive conduits or reservoirs for oxygenated blood passing from the vena cava or pulmonary veins to the ventricles, and as booster pumps to augment passive diastolic ventricular filling.

Before the advent of echocardiography, assessment of atrial mechanical function had been limited to invasive catheter-based techniques,[36] an impractical approach for serial assessments. M-mode echocardiographic assessment of mitral valve motion (Fig. 42-5) can be used in patients with cardiac arrhythmias.[37] Normal anterior mitral leaflet excursion is 13 mm,[37,38] with depressed excursion seen with mitral stenosis, with low cardiac output, and with atrial mechanical dysfunction.

Transmitral Doppler has become recognized as an accurate technique for quantifying atrial mechanical function. In the absence of aortic regurgitation, left ventricular (LV) filling may be divided into passive and active phases. The initial (early, or E) wave in the transmitral Doppler flow profile represents passive ventricular filling, and the final (atrial, or A) wave represents active filling during atrial systole (Fig. 42-6). This transmitral Doppler flow profile can be influenced by a number of factors, including heart rate, loading conditions, and sample volume position. The most common indexes of interest include peak A-wave velocity, percent A-wave filling, and peak and percent E/A ratios. Peak E- and A-wave velocities vary considerably with sample position. In our laboratory, we assess the transmitral profile at its maximum (between the tips of the mitral leaflets).

In addition to the previously described quantitative measures of transmitral Doppler data, the transmitral Doppler profile may also be used to calculate atrial ejection force, defined as that force which the atrium exerts to propel blood into the left ventricle (LV).[39] The atrial ejection force is based on Newtonian mechanics and is proportional to the mitral orifice area and the square of the peak A-wave velocity. As with more traditional E-wave and A-wave indexes, atrial ejection force may be dependent on loading parameters. If calculation of atrial ejection force is desired, a pulsed Doppler sample position at the level of the mitral annulus would be geometrically more appropriate.

## LEFT ATRIAL APPENDAGE FUNCTION

Because the LA appendage is a blind pouch, volumetric ejection must equal inflow during each cardiac cycle. Pollick and Taylor[40] noted that patients with sinus rhythm who were free of atrial thrombus had a characteristic contractile LA appendage apex and a noncontractile base. 2D TEE-guided pulsed Doppler has allowed for further characterization of LA appendage systolic performance. The pulsed Doppler profile taken at the mouth of the LA appendage displayed characterizing ejection and filling phases (Fig. 42-7, *A*). In a healthy adult population, peak LA appendage ejection and filling velocities are 46 ± 18 cm/s and 46 ± 17 cm/s, respectively.[41] Investigators have subsequently characterized LA appendage flow patterns as having four distinct morphologic types (see Fig. 42-7): type I, sinus; type II, flutter (regularized sawtooth); type III, fibrillatory (irregular sawtooth) with ejection velocity greater than 0.2 m/s; and type IV, stagnant/absent flow with peak ejection velocity of greater than 0.2 m/s. In rare instances, there may be a discontinuity between the body of the atrium and appendage[42,43] with sinus pattern on transmitral flow but a fibrillatory pattern in the appendage or even a discrepancy among LA appendage lobes.[44] Although anatomic indexes appear to be dependent on imaging plane, Doppler indexes of LA appendage ejection and inflow are independent of imaging plane.[24] Spontaneous echocardiographic contrast, a marker for stasis, is typically seen with type III or IV appendage flow, whereas LA appendage thrombi are most commonly seen with type IV flow.[45,46] As with transmitral Doppler data, LA appendage flow velocities are dependent on Doppler sample position and loading conditions.[47]

RA appendage function has not been as well studied, but can also be readily assessed by TEE using pulsed Doppler in the 90° or 180° orientations. One report indicated normal RA appendage ejection velocity of 40 ± 16 cm/s, significantly lower than LA appendage ejection velocity.[33]

# Echocardiography and Atrial Fibrillation

## PREVALENCE OF ATRIAL FIBRILLATION

AF is a common arrhythmia, with an overall prevalence of 0.4% in the United States,[48] and is responsible for more than 180,000 hospital admissions annually.[48] Its prevalence increases sharply

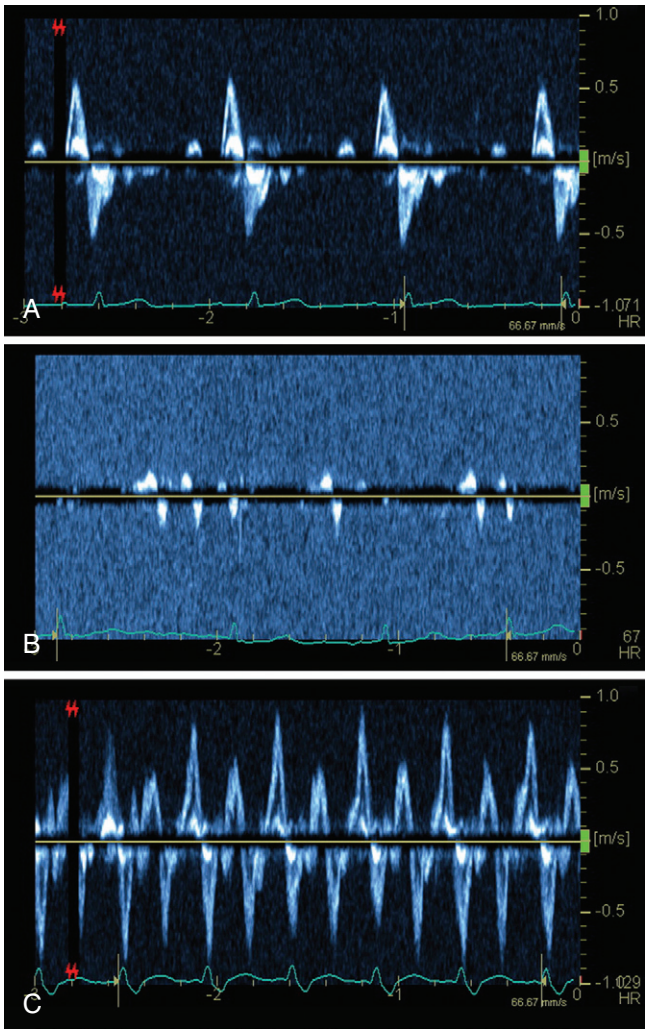



**Figure 42-7 TEE spectral display of pulsed Doppler echocardiographic flow velocity with the sample volume at the mouth of the LA appendage. A,** Patient in sinus rhythm. **B,** Patient with atrial fibrillation with minimal atrial appendage mechanical function. **C,** Patient with atrial flutter. Vertical calibration markings for each represent 0.1-m/s intervals.

with advancing age and is found in up to 4% of those over 60 years.[49] Data from the Framingham Heart Study suggest that an increased transmitral E/A was associated with an increased risk for the subsequent development of AF.[50] In an earlier Framingham Heart Study, the presence of permanent AF is associated with a near doubling of both overall and cardiovascular mortality.[51] Atrial flutter is a far less common sustained arrhythmia. Analogous detailed epidemiologic studies are not available.

## SYMPTOMS AND CLINICAL IMPACT

AF is characterized by a lack of organized atrial mechanical and electrical activity. This condition promotes stasis of blood within the atria and increases the risk of atrial thrombus formation. Thromboembolism associated with AF is believed to account for nearly half of all cardiac sources of emboli. In addition to the risk of thrombus formation, loss of organized atrial mechanical activity impairs the atrium's ability to act as a booster pump and thus impairs ventricular filling (and consequently cardiac output).[52] The mechanical function of the atria appears to be less severely impaired in atrial flutter, but thrombus formation remains a concern, particularly among patients with alternating AF and flutter or flutter in the setting of mitral stenosis or LV systolic dysfunction.

Important clinical issues related to AF include the following:

1. Thromboembolism, including cerebral and other systemic emboli and pulmonary emboli. These events are likely due to the migration of atrial thrombi during the period of AF or may relate to new thrombus formation during the peri-conversion period as a result of atrial stunning (see later). Among patients with nonvalvular AF, the vast majority (more than 90%) of atrial thrombi reside in the LA appendage (a structure best visualized by TEE). TEE evidence of spontaneous echocardiographic contrast and depressed atrial appendage ejection velocity (less than 0.2m/s) are markers for increased risk for both thrombus formation and for clinical thromboembolism.[46,53-55] Clinical markers for thromboembolism among patients with AF have been summarized by the CHADS2 scoring system (C = congestive heart failure, H = hypertension, A = age greater than 74 years, D = diabetes, S = stroke/neurologic event).[56] These same clinical risk factors have also been associated with increased risk of TEE evidence of LA thrombus.[57]
2. Hemodynamic decompensation, which may include depressed cardiac output, congestive heart failure, fatigue, and pulmonary edema. Decompensation is particularly common among patients with a noncompliant ventricle. Such a situation may occur with normal aging and with LV hypertrophy related to systemic hypertension or aortic stenosis. This hemodynamic deterioration is particularly common in the setting of a rapid ventricular rate, during which the diastolic filling period is preferentially shortened.
3. Palpitations, most commonly associated with AF and a rapid (greater than 100/min) ventricular response. Patients with controlled ventricular rates (less than 100/min) are often asymptomatic.
4. Tachycardia-induced cardiomyopathy, which may occur in patients with poorly controlled, rapid ventricular rates.

## ATRIAL SIZE AND ATRIAL FIBRILLATION

LA enlargement is common among patients with AF, particularly those with mitral valve disease and/or systemic hypertension. In addition, LA enlargement decreases the likelihood of long-term maintenance of sinus rhythm.[58,59] Aronow and co-workers[60] studied 588 patients and found LA enlargement in 57% of patients with permanent AF as compared with only 8% of those with sinus rhythm. Data from the Framingham Heart Study suggest that among those without a history of AF, LA enlargement is among the strongest predictors for the subsequent development of nonvalvular AF.[51] Several groups have reported that LA size increases with sustained AF.[61-63]

Although AF promotes further LA enlargement, data suggest that cardioversion of AF and long-term maintenance of sinus rhythm may reverse this process. Using M-mode techniques, DeMaria and associates[38] reported a decrease in LA dimension within 1 hour of cardioversion. We studied a group of 21 patients with AF of 5 months' duration.[64] Patients with persistent sinus rhythm had significantly smaller left atria 3 months after cardioversion as compared with precardioversion data. In contrast, the group of patients who reverted to AF had no change in LA size. Similarly, Gosselink[65] and Van Gelder,[66] with

their co-workers, reported on atrial size in 41 and 120 patients, respectively, with permanent AF undergoing precardioversion. At 6 months after cardioversion, both LA and RA volumes decreased among patients with persistent sinus rhythm, with no change in the group who reverted to AF. Similar results have also been seen 6 to 12 months after pulmonary vein isolation using 2D[67] and real-time 3D TEE LA volume methods.[68] These data strongly suggest that restoration of sinus rhythm may reverse the process of progressive LA and RA enlargement.

Because atrial enlargement may be deleterious and cardioversion to sinus rhythm may prevent or reverse such dilation, we think that avoidance of cardioversion should *not* be based solely on an absolute LA dimension or volume. Patients with permanent (more than 1 year) AF, rheumatic mitral valve disease, and prominent LA enlargement (dimension greater than 6.0 cm; volume greater than 44 mL/m$^2$), however, are far less likely to have long-term maintenance of sinus rhythm.[69]

## DETECTION OF ATRIAL THROMBI IN ATRIAL FIBRILLATION

AF is believed to be responsible for almost half of cardiogenic thromboembolism. Several large, multicenter, prospective randomized studies have confirmed the beneficial effect of chronic warfarin anticoagulation (international normalized ratio [INR] 2.0 to 3.0) or the oral thrombin inhibitor dabigatran (110 or 150 mg twice daily) in patients with nonvalvular AF[70-75] for clinical stroke prevention, with one retrospective study suggesting an INR of greater than 2.5 immediately before cardioversion to be particularly beneficial.[76] Because TTE is so limited for the assessment of atrial thrombi,[16-18] data on the prevalence of LA thrombi were not available until the introduction of TEE. Among patients presenting with AF of greater than 2 days' or unknown duration, we found atrial thrombi in 13%,[77,78] of which more than 92% were LA thrombi and nearly all involved the LA appendage. These data are similar to those reported by others,[79-85] but higher than the approximately 6% incidence of clinical thromboembolism following cardioversion without prolonged anticoagulation.[86-89] This apparent discrepancy may be because some thrombi may not migrate and some embolic events may be clinically silent.[90,91] Patients at particularly high risk for atrial thrombi (Table 42-1) include those with rheumatic mitral valve disease, depressed LV systolic function, recent thromboembolism,[92] and TEE evidence of severe LA spontaneous echocardiographic contrast and complex aortic debris.[55,91] Duration of AF and LA dimension are not predictive of LA thrombi.[71,72] The CHADS2 scoring system has also been associated with increased risk of TEE evidence of LA thrombus[57,93]: LA thrombi and spontaneous echocardiographic contrast are very rarely found in patients with a CHADS2 score of 0 with a progressive increase in atrial thrombi with increasing CHADS2 score (Fig. 42-8). Despite these provocative data, expedited cardioversion (without anticoagulation and screening TEE) or without a month of therapeutic warfarin is currently not recommended for the CHADS2 = 0 group. Similarly, preliminary data suggest that TEE evidence of LA appendage thrombi is not seen among those with a totally normal TTE.[94] In contrast to data suggesting that at least moderate mitral regurgitation is protective against clinical thromboembolism,[95,96] we have found that mitral regurgitation is not protective against LA thrombi (see Table 42-1) among those with new-onset AF.[77]

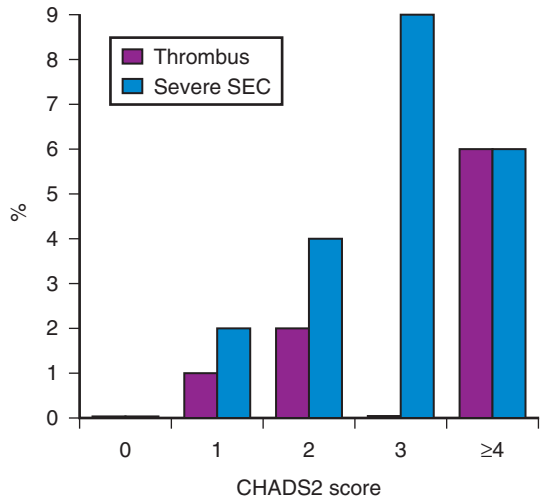



**Figure 42-8 Progressive relationship between *both* TEE evidence of LA appendage thrombus and severe spontaneous echocardiographic contrast (*SEC*) and increasing CHADS2 score.** *(Adapted from Puwanant S, Varr BC, Shrestha K, et al: Role of the CHADS2 score in the evaluation of thromboembolic risk in patients with atrial fibrillation undergoing transesophageal echocardiography before pulmonary vein isolation.* J Am Coll Cardiol *54:2032, 2009.)*

**TABLE 42-1 Characteristics of Patients at Risk for Atrial Thrombi***

| | *Entire Group* | *LA Thrombus* | *No LA Thrombus* | p *Value* |
|---|---|---|---|---|
| Total number | 533[†] | 70 | 463 | |
| Age (yr) | 71.6 ± 13.0 | 70.7 ± 14.0 | 71.7 ± 13.2 | .55 |
| Gender (% female) | 45.9 | 54.3 | 44.4 | .16 |
| First episode of AF (%) | 60.0 | 64.3 | 59.1 | .49 |
| Duration of AF (wk) | 4.4 ± 9.3 | 5.8 ± 15.4 | 3.9 ± 8.0 | .18 |
| History of thromboembolism (%) | 8.3 | 28.9 | 7.3 | .003 |
| LA SEC (%) | 48.0 | 85.5 | 36.9 | .0001 |
| LA dimension (cm) | 4.6 ± 0.7 | 4.7 ± 0.7 | 4.6 ± 0.7 | .29 |
| Mitral regurgitation (0-3+) | 1.3 ± 0.9 | 1.2 ± 0.6 | 1.3 ± 0.9 | .35 |
| LV dysfunction (%) | 40.9 | 60.7 | 38.1 | .002 |

Adapted from The Stroke Prevention in Atrial Fibrillation Investigators: Predictors of thromboembolism in atrial fibrillation: II. Echocardiographic features of patients at risk. *Ann Intern Med* 116:6-12, 1992.

*AF*, Atrial fibrillation; *SEC*, spontaneous echocardiographic contrast.

*Data presented are mean value ± SD.

[†]TEE could not be completed in six patients. Data for these six are excluded.

Immediate cardioversion is generally advocated for patients with AF of less than 2 days' duration,[97] under the assumption that the prevalence of atrial thrombi in this group was very low. This common teaching was challenged when Stoddard and colleagues[98] reported a 14% prevalence of atrial thrombi among patients with AF of less than 3 days' duration and a prevalence of 27% in those with a duration of at least 3 days in a predominantly male population. In contrast, we found clinical thromboembolism following cardioversion (without antecedent TEE or prolonged warfarin anticoagulation) of less than 1% among patients with AF of less than 2 days' duration.[99] Thus, prolonged warfarin or screening TEE is likely not needed in this group (unless there is a history of thromboembolism, severe LV systolic dysfunction, or mitral stenosis). Although we perform cardioversion of AF of less than 48 hours' duration without prolonged warfarin or screening TEE, we do initiate therapeutic anticoagulation at presentation (intravenous unfractionated heparin or low molecular weight heparin) rather than delaying anticoagulation until the patient has been in AF for 48 hours. If TEE is performed in this short-duration AF group, evidence of LA appendage thrombi is found in 1.4% to 4% of the group,[100] with thrombus and spontaneous echocardiographic contrast associated with depressed LV systolic function and enlarged LA.

As might be expected, atrial thrombi are more common among AF patients who present with acute thromboembolism. In our experience, residual LA thrombi are found in nearly 50% of these patients.[101] Because this group represents a very high clinical risk for whom chronic warfarin (or dabigatran) is indicated, we do not perform TEE to search for thrombi unless cardioversion is desired.

RA thrombi are far less common among patients with AF and represent less than 5% of all atrial thrombi identified by TEE.[77,78,102] RA spontaneous echocardiographic contrast is also distinctly unusual, seen in only 10% of AF patients,[77] and is highly predictive for RA thrombi.

### *Atrial Fibrillation and Predictors of Thromboembolism*

Compared with patients who present with new-onset AF and undergo TEE before cardioversion, risk factors of thromboembolism differ in patients with nonvalvular AF. Prior thromboembolism and LV systolic dysfunction are among the strongest independent predictors of clinical thromboembolism in patients with nonvalvular AF.[103] The TEE substudies of the Stroke Prevention in Atrial Fibrillation Investigators Committee (SPAF) III study[55] have extended echocardiographic indexes known to be associated with thromboembolism to include dense spontaneous echocardiographic contrast, depressed (less than 20 cm/s) LA appendage ejection velocity, LA thrombus, and complex (more than 4 mm thick and/or with mobile components) aortic atheroma. Importantly, the SPAF-III data suggest that these TEE indexes may identify high- and low-risk subgroups from among clinically high-risk patients (age, female gender, systemic hypertension, LV dysfunction, prior thromboembolism).[55] A subsequent study by Bernhardt and co-workers[104] confirmed the predictive power of these TEE measures for stroke.

### *Guidance of Early Cardioversion*

Cardioversion of AF is performed in an effort to improve cardiac function, relieve symptoms, and potentially decrease thrombus formation. However, data from several large prospective studies demonstrate no mortality or thromboembolic advantage to aggressive cardioversion and maintenance of sinus rhythm (versus chronic anticoagulation and rate control).[105-107] (For symptomatic patients who are difficult to rate control, however, cardioversion is still advocated.) Unfortunately, successful cardioversion of nonvalvular AF is associated with an approximately 6% incidence of clinical thromboembolism among patients who are not systematically anticoagulated for several weeks before cardioversion.[86-89] Because atrial thrombi are poorly detected by TTE, conventional care of patients with AF of unknown or prolonged (more than 2 days) duration had demanded that these patients receive several weeks of anticoagulation before cardioversion, with one study suggesting that an INR greater than 2.5 immediately before cardioversion further reduces risk.[76] Cardioversion is then followed by several weeks of anticoagulation while atrial mechanical function recovers[108] and for prophylaxis should the patient revert to AF. Although no randomized and only two prospective studies[79,82,109] have been reported, a month of precardioversion warfarin therapy decreases the risk of a clinical embolic event following cardioversion to less than 1.6%.[76,79,82,88,89] The majority of these clinical embolic events occur within the first 10 days after cardioversion (Fig. 42-9).[109,110] Use of warfarin, however, carries a risk of major (2%) and minor (10% to 20%) hemorrhagic complications.[79,82,111] In addition, many patients have a subtherapeutic INR during the month before cardioversion. For these individuals, the warfarin dose is increased and the "1-month clock" restarted, an approach supported by TEE studies demonstrating LA appendage thrombi in patients with a transient subtherapeutic INR.[112,113] Finally, conventional therapy leads to a delay in cardioversion for the large majority of patients who do not have an atrial thrombus, and a second hospitalization is needed for cardioversion.

## Rationale and Advantages

A TEE-guided approach to early and safe cardioversion (Fig. 42-10) has several advantages over traditional strategies for hospitalized patients with AF (Box 42-1). Currently, up to 8 weeks

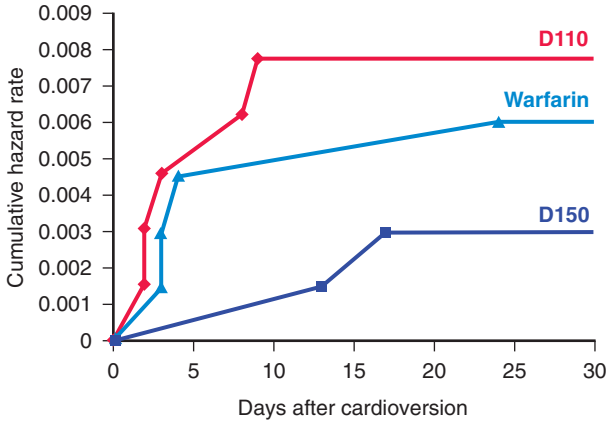



**Figure 42-9 Timing of thromboembolic events after cardioversion in patients receiving warfarin, dabigatran 110 mg twice daily (*D110*), and dabigatran 150 mg twice daily (*D150*).** Note that the vast majority of events are within the first 10 days after cardioversion. *(Reprinted from Nagarakanti R, Ezekowitz MD, Oldgren J, et al: Dabigatran versus warfarin in patients with atrial fibrillation: an analysis of patients undergoing cardioversion.* Circulation *123:131, 2011.)*

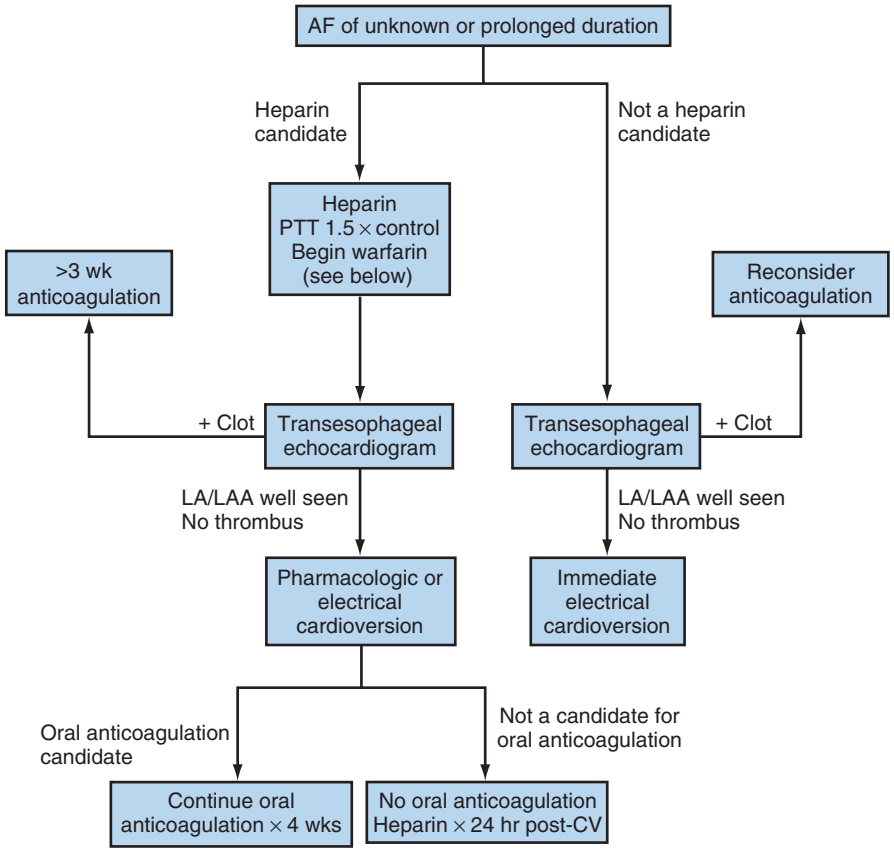



**Figure 42-10 Schematic of TEE-guided approach to early cardioversion.** Long term, either chronic warfarin or dabigatran can be used as guided by CHADS2 score. *AF*, Atrial fibrillation; *LAA*, left atrial appendage; *PTT*, partial thromboplastin time.

of oral anticoagulation is recommended with cardioversion,[97,114,115] including 1 month before and 1 month after cardioversion. This period of anticoagulation exposes patients to a significant risk of a hemorrhagic complication[79,82,111] by doubling the exposure to systemic anticoagulation (versus an expedited TEE approach). For uncertain reasons, the AF population appears to be at increased risk of hemorrhagic complications during the second month of anticoagulation.[79]

Early cardioversion offers physiologic advantages over traditional therapy. A shorter duration of precardioversion AF is among the strongest predictors for long-term maintenance of sinus rhythm.[59] Almost 60% of patients hospitalized for AF at our hospital[77,78] have been in AF for less than 1 month. For these individuals, traditional treatment of a month of precardioversion anticoagulation serves to more than double the total period of AF before cardioversion. The TEE-guided approach has been shown to be associated with fewer recurrences of AF[78] and to increased prevalence of sinus rhythm at 6 months postcardioversion.[116]

Early cardioversion may also lead to a more rapid return to normal atrial function. The recovery time for return of atrial mechanical function is directly related to the duration of precardioversion AF (Fig. 42-11).[108,117] Patients with AF for less than 2 weeks before cardioversion have complete return of atrial mechanical function within 24 hours of cardioversion, whereas those with AF of 2 to 6 weeks require a week. Those with

**Box 42-1**

## BENEFITS AND RISKS OF TEE-GUIDED CARDIOVERSION

**Benefits**

Shorter initial duration of atrial fibrillation (AF)
- Enhanced recovery of atrial mechanical function
- More rapid resolution of symptoms of congestive heart failure
- Increased likelihood that sinus rhythm will be maintained

No need to return for elective cardioversion after 1 month of warfarin or dabigatran anticoagulation

Shorter total duration of AF before cardioversion
- Fewer hemorrhagic complications
- Lower cost for warfarin medication and monitoring

Similar thromboembolic events than conventional therapy(?)

More cost-effective than conventional therapy (if TTE is not performed)

Identify high-risk population that requires lifelong warfarin or dabigatran regardless of clinical risk factors(?)

**Risks**

TEE may miss clinically relevant thrombi that subsequently migrate and cause stroke/thromboembolism

Morbidity associated with TEE

Cost of TEE

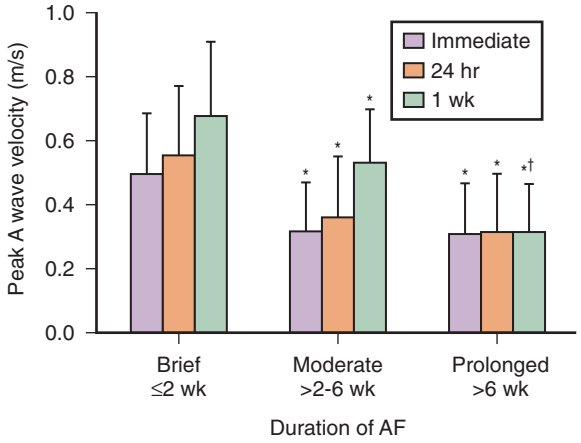



**Figure 42-11 Comparison of transmitral pulsed Doppler peak A-wave velocity among patients with brief (<2 weeks), moderate (2-6 weeks), and prolonged (>6 weeks) atrial fibrillation (AF) immediately after, at 24 hours, and at 1 week after cardioversion.** *$P$ <.05 vs. brief duration. †$P$ <.05 vs. moderate duration. *(From Manning WJ, Silverman DI, Katz SE, et al: Impaired left atrial mechanical function after cardioversion: Relationship to the duration of atrial fibrillation.* J Am Coll Cardiol *23:1537, 1994.)*

precardioversion AF for more than 6 weeks require up to 3 weeks for full atrial mechanical recovery.[108] With elimination of TTE, a TEE-guided procedure is cost effective.[118,119] The costs of the TEE approach include the cost of and morbidity of TEE and the risk that TEE will not be adequate to identify clinically relevant atrial thrombi.

## TEE-Guided Cardioversion Safety Data

We reported on our experience with a TEE-guided approach (see Fig. 42-6) to early cardioversion among 533 patients with AF of unknown or prolonged duration who underwent precardioversion TEE in the absence of prolonged chronic anticoagulation.[77,78,102] Seventy-six atrial thrombi were identified in 70 patients (13%). Of the 463 without TEE evidence of thrombi, 413 (89%) were successfully cardioverted, all without prolonged anticoagulation, and 1 (0.2%; 95% CI, 0 to 0.8%) experienced a clinical thromboembolic event. The only adverse event occurred in an elderly woman with mild rheumatic mitral stenosis who presented 1 week after cardioversion with a brachial artery embolus. She had been therapeutically anticoagulated between TEE and presentation with the adverse event.[78] None of the 70 patients with atrial thrombi were cardioverted, but 5 (7%) died during the index hospitalization. Repeat TEE to document resolution of atrial thrombi was recommended for all with atrial thrombi, with cardioversion only after documentation of thrombus resolution.

Other prospective studies using a similar anticoagulation regimen have shown similar results. Stoddard and co-workers[81] reported on 82 patients undergoing elective cardioversion of AF. Atrial thrombi were identified in 13% of patients. Of 71 patients without atrial thrombi, 66 underwent successful cardioversion, and no patient experienced a clinical embolic event. The pilot study data from the Assessment of Cardioversion Using Transesophageal Echocardiography (ACUTE) trial reported no thromboembolic complications among 47 patients treated with an anticoagulation strategy similar to ours.[79] The larger 1222-patient, multicenter, randomized ACUTE trial[82] directly compared conventional therapy of 4 weeks of precardioversion warfarin with a strategy of therapeutic anticoagulation followed by TEE and early cardioversion if no atrial thrombi are seen. At 8 weeks, equivalence was found for both approaches, though with 0.5% thromboembolic events in the conventional arm and 0.8% in the TEE arm. A subsequent prospective study by Strandberg and colleagues[83] using subcutaneous low molecular weight heparin and warfarin before TEE in 274 patients had a clinical stroke rate of 0.3%. Of note, nearly all of the adverse events in the ACUTE TEE arm occurred while the patient had either a subtherapeutic (less than 2.0) INR or was in AF. In contrast, the adverse events in the conventional therapy arm occurred in patients in sinus rhythm and with a therapeutic INR. These data highlight the importance of therapeutic post-cardioversion anticoagulation. Interestingly, the absence of an atrial thrombus on a prior TEE while in AF does not appear to preclude the need for a TEE if a patient returns with AF in the absence of chronic anticoagulation.[120] Six-month ACUTE data[121] showed that hemorrhagic complications were lower in the TEE arm (4.4% versus 7.5%, $P = 0.04$), but maintenance of sinus rhythm was similar (62.2% versus 58.1%).

Although these reports supporting an expedited TEE-guided approach using short-term precardioversion anticoagulation are encouraging, several adverse events have occurred among patients with a negative TEE for atrial thrombi who have undergone early cardioversion using monoplane TEE or in the absence of systemic anticoagulation.[122] Many underwent electrical cardioversion several days or weeks following TEE with no anticoagulation during the intervening period. For these patients, it is impossible to exclude the possibility that atrial thrombi may have formed between the TEE and cardioversion, or even after cardioversion. Impaired atrial mechanical function,[108,123] impaired atrial appendage function,[124,125] or new spontaneous contrast[81,125] have all been documented following cardioversion.

Although no data have been reported for conventional cardioversion approaches, a prospective study of 127 patients undergoing TEE-guided cardioversion reported no clinical embolic events, but cerebral magnetic resonance imaging (MRI) demonstrated that 4.7% of patients had new embolic lesions suggestive of a silent embolic event.[126]

As in our original report,[102] we strongly recommend that all patients undergoing a TEE-guided early cardioversion strategy be therapeutically anticoagulated with intravenous unfractionated heparin or warfarin at the time of TEE, continuing through cardioversion, and that warfarin (or dabigatran) anticoagulation be continued for at least 1 month after cardioversion. TEE should be performed (without preceding TTE to reduce costs[118]) immediately before cardioversion to adequately visualize the atria and appendages and to exclude the presence of atrial thrombi. Heightened vigilance for thrombi is necessary if there is prominent spontaneous echocardiographic contrast or poor (less than 0.2 m/s) atrial appendage ejection velocity or an increased CHADS2 risk score. Though of unproven efficacy,[127] if a thrombus is seen on TEE, we think that cardioversion should be deferred and the patient maintained on warfarin (or dabigatran 150 mg twice daily) for 4 weeks followed by repeat TEE to document thrombus resolution before cardioversion.[128] Patients with RA appendage thrombi should be treated in a similar manner. If the atrial appendage cannot be adequately cleared of thrombus, the patient should be treated conservatively with a month of therapeutic warfarin (or dabigatran) before cardioversion. The use of low-molecular-weight heparin or dabigatran precardioversion anticoagulation or as a bridge

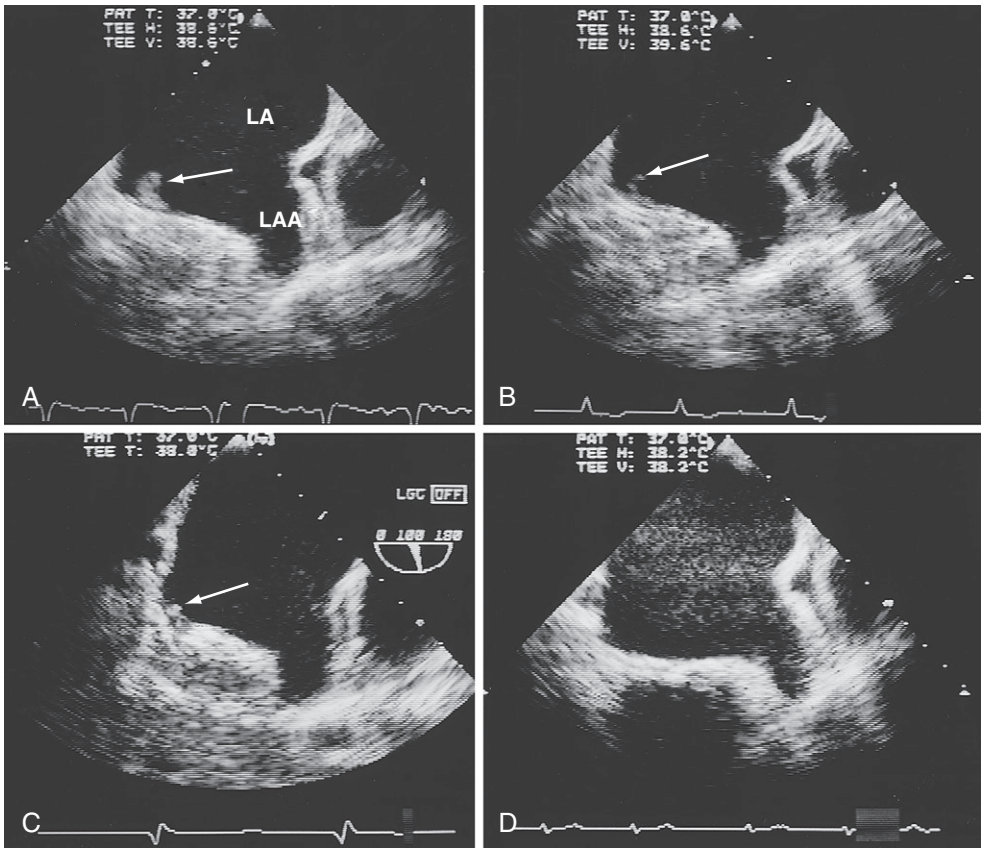



**Figure 42-12 Serial TEE studies showing the LA and LA appendage (*LAA*) viewed in the vertical plane with a 5-MHz biplane probe.** The thrombus (*arrow*) is in the body of the LA, closely associated with the mitral annulus in the posterior portion of the LA. **A,** Initial study demonstrating a mobile 12-mm thrombus. **B,** Thrombus persists but is smaller after 1 week of warfarin therapy. **C,** After 3 weeks of warfarin, the thrombus continues to be seen (*arrow*). **D,** Complete resolution of thrombus is seen after 5.5 weeks of warfarin. *(From Collins LJ, Silverman DI, Douglas PS, Manning WJ: Cardioversion of non-rheumatic atrial fibrillation: Reduced thromboembolic complications with 4 weeks of pre-cardioversion anticoagulation are related to atrial thrombus resolution.* Circulation *92:162, 1995, with permission.*Copyright 1995 American Heart Association.)

to therapeutic warfarin to expedite patient discharge has been less extensively studied, but appears to be a reasonable option with regards to safety and shortens hospitalization.[7,109,129,130] Further support for the use of pre-TEE anticoagulation comes from data demonstrating that clinical thromboembolism is less common among those with TEE evidence of a LA appendage thrombus if warfarin was initiated before the TEE.[131]

Although not directly supported by prospective clinical trials, it is our clinical practice to treat patients with AF who have TEE evidence of atrial thrombi with lifelong warfarin (INR 2 to 3) or dabigatran (150 mg twice daily), even if thrombus resolution has been documented and independent of CHADS2 score. We think that such an approach is prudent, given that the overall recurrence rate of AF is high, and these patients have already selected themselves as being at increased risk for atrial thrombus formation. [55] One prospective study with serial cranial MRI scans reported that more than half of patients with LA appendage thrombi on TEE suffered cerebral embolism and/or death during the succeeding 3 years.[132]

### *Resolution of Atrial Thrombi*

The use of several weeks of anticoagulation before cardioversion results in a reduction of cardioversion-related thromboembolism from 6% to <1%. The mechanism by which warfarin conveys this beneficial effect had been presumed to be thrombus organization and adherence to the atrial endocardium, thus reducing the likelihood of postcardioversion migration.[133] Consistent with this hypothesis, several investigators have reported that atrial thrombi in patients with rheumatic mitral valve disease may not resolve even after several months of warfarin.[134,135] In nonrheumatic, new-onset AF, a different mechanism appears responsible. We have found that after 4 weeks of warfarin, more than 80% of atrial thrombi have completely resolved[136] (Fig. 42-12). Similar data have been reported by others.[80,85,127,137,138] These data support the hypothesis that the mechanism of warfarin's benefit is related to thrombus resolution or silent migration and prevention of new thrombus formation (rather than thrombus organization and adherence). Although randomized data are not available and clinical reports in small groups are inconclusive,[127] we interpret these data as supportive of the need for follow-up TEE examination for documentation of thrombus resolution before cardioversion.[128]

## MECHANISM OF THROMBOEMBOLISM AFTER CARDIOVERSION

Although usually occurring within 72 hours, clinical thromboembolism has been reported up to 10 days following successful cardioversion in patients with maintained sinus rhythm.[109,110] Such adverse events have classically been attributed to migration of LA thrombi that were present at the time of cardioversion.[97,140] TEE has documented the new appearance of, or more pronounced, spontaneous echocardiographic contrast in the LA following electrical cardioversion.[81,125] In addition, more

depressed LA appendage ejection velocity is common after spontaneous or electrical cardioversion.[124,125] These findings have led to the hypothesis that atrial thrombi may form in the immediate postcardioversion period because of atrial injury or stunning. Indeed, LV stunning as a result of electrical cardioversion has been previously described,[141,142] and relatively impaired atrial mechanical function is seen after electrical (as compared with pharmacologic) cardioversion.[118,143] Finally, in rare instances, there may be a discontinuity between the body of the atrium and the appendage,[42,43] with a sinus pattern on the surface electrocardiogram and transmitral Doppler echocardiogram but a fibrillatory pattern in the appendage. Discordance among LA appendage lobes has also been reported.[44] Premature (less than 1 month postcardioversion) discontinuation of warfarin may thereby lead to new thrombus formation. These data all emphasize the importance of therapeutic (INR 2.0 to 3.0) warfarin (or dabigatran) anticoagulation during the pericardioversion and postcardioversion period. For patients who are not considered candidates for out-of-hospital warfarin or dabigatran, we recommend therapeutic anticoagulation with heparin for at least 24 hours after cardioversion.

## ASSESSMENT OF RETURN OF ATRIAL MECHANICAL FUNCTION AFTER CARDIOVERSION

The noninvasive nature of echocardiography makes it the ideal modality for the serial assessment of atrial function after cardioversion. DeMaria and colleagues[38] reported serial M-mode data of anterior mitral leaflet excursion before and after cardioversion among 35 patients with AF of 14 months' duration. One hour after cardioversion, prominent mitral "A" waves were found in 94% of subjects, although anterior leaflet excursion was less than that seen in normal subjects (7.5 mm versus 13 mm). These early data suggested that atrial mechanical contraction was reduced after cardioversion despite normal atrial depolarizations on electrocardiography. Two patients had no discernible atrial anterior mitral leaflet motion, and both of these patients reverted to AF within 1 week. They also found an increased LV end-diastolic dimension, with unchanged end-systolic dimension, consistent with an improvement in LV ejection fraction. Similarly, Orlando and co-workers[144] used M-mode echocardiography 5 hours after cardioversion and found that 4 of their 15 patients (27%) had no transmitral A wave. In their experience, neither the presence of an A wave nor its amplitude correlated with long-term maintenance of sinus rhythm.

Pulsed Doppler echocardiography permits serial noninvasive evaluation of flow across the mitral valve and accurately reflects the LA contribution to total LV filling. As reported by van Gelder and associates[145] and Viswanahan and colleagues,[146] these temporal changes in transmitral Doppler spectra parallel improvements in LV ejection fraction[148] and peak oxygen consumption.[145]

Shapiro and co-workers[123] reported transmitral Doppler data from a group of patients with AF of less than 2 days' duration. Peak A-wave velocities immediately after cardioversion were similar to those in a control (sinus) population. In contrast, patients with AF of more than 1 year before cardioversion had significantly smaller A-wave amplitude after cardioversion. We performed serial transmitral pulsed Doppler examination in 21 patients undergoing elective conventional cardioversion, with a duration of AF of 5 months.[60] Over 3 months of follow-up, there were significant increases in both peak A-wave velocity and percent atrial contribution to total LV filling. Neither index returned to normal until 3 weeks after cardioversion (see Fig. 42-11). Additional studies have confirmed that transmitral Doppler data are not predictive of the long-term maintenance of sinus rhythm.[144,147] Thus it appears that return of atrial mechanical function is not sufficient to allow for premature discontinuation of postcardioversion anticoagulation.

Atrial compartment surgery, or the maze procedure, has received considerable interest as an approach to prevent recurrent AF. Shyu and colleagues[148] studied 22 patients with chronic AF who underwent maze surgery. Over 70% of their group had no transmitral A wave 1 week after surgery, despite sinus rhythm on electrocardiography. Even after 2 months, 40% of their patients had not regained evidence of A waves. Of note, RA function appeared to recover more rapidly than LA function. Transient depression and then improvement in atrial mechanical function has also been demonstrated after pulmonary vein isolation.[149] Shortly after ablation for paroxysmal AF, LA minimal volumes increase, whereas maximal volumes are unchanged, resulting in a short-term decrease in LA ejection fraction. Subsequently, volumes and ejection fraction improve[150] with a 23% decline in LA area at 1 year.[151,152] Tissue Doppler myocardial (A′) velocities were similarly relatively depressed early after ablation.[150]

Studies of atrial mechanical function in patients with AF of an intermediate (3 days to 4 weeks) duration had been previously limited by the relative scarcity of such patients. This was due to the recommendation that patients with AF of more than 2 days' duration receive anticoagulation for a month before cardioversion. Our TEE cardioversion trial allowed us to evaluate atrial function among patients with this intermediate duration of AF. We found that both the immediate peak A velocity and the percentage A-wave filling were significantly lower in the groups with AF of moderate (more than 2 up to 6 weeks) and prolonged (more than 6 weeks) duration as compared with the patients only brief (2 weeks or less) duration of AF.[108] This depression in peak A velocity persisted until at least 1 week following cardioversion. In addition, 1 week after cardioversion, both peak A velocity and percentage A-wave filling were depressed in the group with prolonged duration as compared with the group with moderate-duration AF. As compared with 3-month postcardioversion data, full recovery of atrial mechanical function was achieved within 24 hours for patients with brief (less than 2 weeks) duration, within 1 week for moderate (2 to 6 weeks) duration, and within 1 month for prolonged (more than 6 weeks) duration AF. Twenty-seven patients (45%) reverted to AF during follow-up. Those reverting to AF had a longer AF duration before cardioversion (10.2 versus 5.3 weeks; $P = .04$). There were no differences between groups in LA dimension, patient age, mode of cardioversion, peak A-wave velocity, or percentage of A-wave filling.

Data suggest early atrial mechanical function post-electrical cardioversion may be modulated by angiotensin receptor blockers. Dagres and colleagues[153] studied 50 patients with AF of more than 4 weeks' duration undergoing elective electrical cardioversion, randomizing half to receive irbesartan. Immediately after cardioversion, LA appendage ejection velocities were less depressed in the irbesartan group and the prevalence of spontaneous echocardiographic contrast was lower (32% irbesartan versus 64% of controls). The clinical impact remains to be further explored.

### EVIDENCE OF ELECTRICAL INJURY TO THE ATRIA

LV myocardial injury as a result of electrical cardioversion has been previously described.[141,142] TEE data acquired with electrical cardioversion have shown new or more pronounced LA spontaneous echocardiographic contrast following electrical cardioversion[81,125] as well as depressed LA appendage ejection velocity.[124] We reported on transmitral Doppler data from 33 patients with AF of less than 5 weeks' duration following elective electrical or pharmacologic (primarily quinidine or procainamide) cardioversion.[143] Immediately following cardioversion, patients who underwent electrical cardioversion demonstrated lower transmitral peak A-wave velocity. This relative depression in atrial systolic function persisted at the 24-hour study but had resolved at 1 week. Similarly, Mattioli and colleagues[154] randomized 64 patients with AF (duration 1 day to 6 months) to either direct-current shock or pharmacologic cardioversion. Recovery of atrial mechanical function occurred sooner with pharmacologic cardioversion. Finally, Pollak and Falk[155] performed electrical cardioversion in 37 patients receiving sotalol or placebo. They found relatively depressed atrial function among the group receiving sotalol as compared with placebo.

### SPONTANEOUS ECHOCARDIOGRAPHIC CONTRAST

Spontaneous echocardiographic contrast, or *smoke*, refers to the presence of dynamic smokelike echoes in a cardiac cavity and is occasionally seen in the LA by TTE with mitral stenosis and AF. More commonly, TTE evidence of spontaneous echocardiographic contrast is seen in the LV apex with a high-frequency transducer in patients with an apical aneurysm. Spontaneous echocardiographic contrast likely represents stasis of blood within the cavity, but it may also reflect alterations in blood components such as platelets, red cells, and fibrinogen. Black and associates[156] found an association between spontaneous echocardiographic contrast and erythrocyte aggregation in low shear rate conditions. Aspirin and warfarin therapy do not appear to affect the presence of LA spontaneous echocardiographic contrast.[156] At least mild spontaneous echocardiographic contrast may be seen in over half of patients with AF[55,77,102] and in over 80% of patients with AF and LA appendage thrombi.[77] Among patients with nonvalvular AF, Chimowitz and co-workers[157] found that LA spontaneous echocardiographic contrast was associated with an increased risk of stroke, a finding also confirmed by Bernhardt for both clinical and silent strokes.[91] Black and associates[156] found that spontaneous echocardiographic contrast by TEE was an independent predictor of LA thrombus among patients with suspected cardioembolism. Although unproved, it seems likely that recovery of atrial mechanical function would decrease or abolish spontaneous echocardiographic contrast. The SPAF-III TEE substudy[55] suggests that warfarin anticoagulation decreases the risk of thromboembolism in patients with spontaneous echocardiographic contrast.

## Echocardiography and Atrial Flutter

Sustained atrial flutter is far less common than AF. As a result, there are fewer data regarding atrial function at baseline and following cardioversion. It has generally been accepted that the relatively preserved atrial mechanical function (see Fig. 42-7, *C*) with atrial flutter results in a lower risk of thromboembolism (as compared with AF). In a retrospective review, Arnold and colleagues[89] reported on 122 patients with atrial flutter at the time of cardioversion, including 74% who were not receiving anticoagulation. No patient experienced a clinical thromboembolic event. These data support the concept that patients with atrial flutter do not require anticoagulation before cardioversion. However, there have been reports of atrial thrombus identified during TEE study among patients with atrial flutter[85,158,159] and postcardioversion thromboembolism. A limitation of interpreting the literature on atrial flutter is the definition of the arrhythmia. For many studies, a patient is defined as having atrial flutter if it is the rhythm during the intervention or period of observation (e.g., at the time of TEE or cardioversion). Many patients may have alternating periods of AF and flutter, making clinical distinction of pure atrial flutter difficult. Irani and co-workers[160] performed TEE in 47 consecutive patients with atrial flutter (and without AF by history or Holter monitoring). They found that 11% of patients had LA thrombus, and 31% had LA spontaneous echocardiographic contrast, values similar to those found in patients with AF. Similar to our findings for AF, moderate or severe mitral regurgitation was not protective against thrombus formation for this group.

Jordaens and associates[161] studied 22 patients with atrial flutter with serial transmitral Doppler echocardiography after cardioversion. Analogous to data on AF, they found that 20% of patients had Doppler evidence of atrial standstill immediately after cardioversion. There was a progressive increase in peak A-wave velocity and percentage of A-wave filling over a 6-week period. Based on these data, our recommendation is to treat patients with atrial flutter in the same manner as those with isolated AF. We would generally treat conservatively patients who had atrial flutter in the setting of rheumatic mitral valve disease, a history of thromboembolism, or LV systolic dysfunction, with short-term anticoagulation and screening TEE or 1 month of anticoagulation before elective cardioversion.

## Echocardiography and Guidance of Therapeutic Interventions in Atrial Fibrillation

More than a decade ago, Haissaguerre and colleagues[162] demonstrated that the origin of AF was rapid electrical discharges originating in the pulmonary veins. Subsequently, pulmonary vein isolation has evolved as a moderately invasive percutaneous approach for primary antiarrhythmic therapy for AF by promoting long-term maintenance of sinus rhythm.[163] TEE is often used immediately before pulmonary vein isolation to exclude atrial thrombi as well as to guide transseptal puncture.[164,165] Intracardiac echocardiographic is a viable alternative for guiding transseptal puncture.[166] TEE studies demonstrate a 5% reduction in pulmonary vein diameter and an increase in peak velocity.[167] Decision analysis models suggest that it is cost effective with an absolute stroke risk reduction of 1.2%.[168] Other than LA appendage thrombus, TEE parameters do not appear to be predictive of stroke complications.[169] Postprocedure TTE is often performed to exclude pericardial effusion before resuming anticoagulant therapy.[170] Although TEE can also be used to monitor for pulmonary vein stenosis using both color and pulsed-wave Doppler,[171,172] this complication is

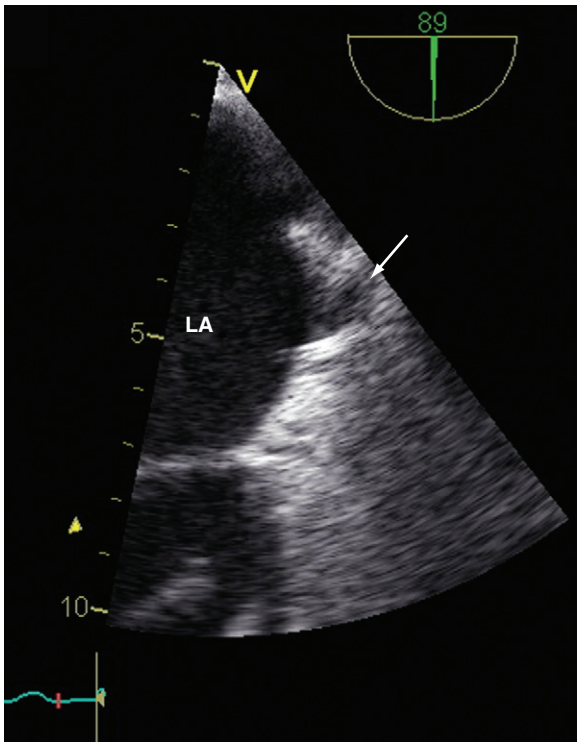



**Figure 42-13 TEE in a patient several months following surgical excision of the LA appendage.** Note the residual LA appendage with thrombus (*arrow*).

fortunately far less common today with use of ablation in the body of the atria (rather than within the pulmonary vein). In addition, use of TEE for identification of pulmonary vein stenosis has largely been supplanted by cardiac CT and/or magnetic resonance angiography because of their less invasive benefits.

Given the close association of LA appendage thrombi and clinical thromboembolism in AF, LA appendage surgical excision, suturing, and stapling[173] are being examined as potential alternatives for patients who are not candidates for warfarin (or dabigatran). Overall, surgical excision is more successful at fully excluding the LA appendage, with a success rate of 73% as compared with only 23% and 0% for suture and stapling, respectively (Fig. 42-13). LA appendage thrombus is common (up to 40%) among those with unsuccessful obliteration of the LA appendage.[173] LA appendage occlusion[174] is another alternative being explored. Each of these procedures is often intraoperatively guided (or confirmed) using 2D or 3D TEE or intracardiac echocardiography.[143]

## Current and Future Areas of Investigation

As the ability of echocardiography to provide detailed structural and functional information about the heart continues to grow, so likely will its role in the evaluation and optimal management of patients with AF. Among the areas of current and future investigation are:

1. Improved methods of assessment of atrial mechanical function with applications of tissue Doppler imaging.
2. Randomized prospective studies to further define the resolution of atrial thrombi using warfarin versus dabigatran (and/or other warfarin alternatives).
3. Prospective studies examining the frequency of silent cerebral embolism after cardioversion using conventional therapy (warfarin versus dabigatran).
4. Assistance in localization of structural abnormalities and foci of abnormal electrical activity, including assistance in radiofrequency ablation of arrhythmic foci.
5. Comparison of 2D and 3D TEE and intracardiac echocardiography for the identification of atrial appendage thrombi.
6. Identification of clinical or echocardiographic indexes that predict recurrence of AF or identify a group at low risk for thromboembolism so as to minimize postcardioversion anticoagulation.

### KEY POINTS

- LA volume (normalized for body surface area) is preferred for characterization of atrial size.
- Increased LA size is a risk factor for the development of AF.
- TEE is highly accurate for identification of atrial thrombi and superior to TTE.
- For patients with AF, TEE risk factors for clinical thromboembolism include LA appendage thrombus, severe spontaneous echocardiographic contrast, depressed (≤0.2 m/s) atrial appendage ejection velocity, and complex aortic plaque. The clinical CHADS2 risk score also correlates with thrombus risk.
- TEE will identify atrial thrombi in approximately 13% of patients presenting with new-onset AF of more than 2 days' duration. The vast majority of thrombi are within or involve the LA appendage.
- In concert with precardioversion therapeutic anticoagulation with unfractionated heparin, low molecular weight heparin, warfarin, or dabigatran, a TEE-guided strategy of early cardioversion is comparable to 1 month of precardioversion warfarin (INR 2.0-3.0) with a risk of clinical thromboembolism of <1%.
- After cardioversion, LA appendage mechanical function may be even more depressed. Depression of LA and LA appendage mechanical function may persist for several weeks after cardioversion, emphasizing the need for therapeutic warfarin (INR 2.0-3.0) or dabigatran for at least 1 month after cardioversion.
- For patients with new-onset, nonvalvular AF who have TEE evidence of atrial thrombi, more than 80% of the thrombi will resolve after 1 month of therapeutic warfarin.
- Recovery of atrial mechanical function after cardioversion is related to the duration of AF before cardioversion.
- Data for atrial flutter suggest that the incidences of atrial thrombi and thromboembolism are slightly reduced compared with AF, but that these patients should likely be treated with AF guidelines.
- TEE is increasingly used to guide interventional therapeutic procedures in the AF population, including pulmonary vein isolation and LA appendage exclusion.

## REFERENCES


1. Hirata T, Wolfe SB, Popp RL, et al: Estimation of left atrial size using ultrasound. *Am Heart J* 78:43-52, 1969.
2. Ten Cate FJ, Kloster FE, van Dorp WG, et al: Dimensions and volumes of the left atrium and ventricle determined by single beam echocardiography. *Br Heart J* 36:737-746, 1974.
3. Yabek SM, Isabel-Jones J, Bhatt DR, et al: Echocardiographic determination of left atrial volumes in children with congenital heart disease. *Circulation* 53:268-272, 1976.
4. Loperfido F, Pennestri F, Digaetano A, et al: Assessment of left atrial dimensions by cross-sectional echocardiography in patients with mitral valve disease. *Br Heart J* 50:570-578, 1983.
5. Lester SJ, Ryan EW, Schiller NB, Foster E: Best method in clinical practice and in research studies to determine left atrial size. *Am J Cardiol* 84:929-932, 1999.
6. Lang RM, Bierig M, Devereux RB, et al: Recommendations for chamber quantification: a report from the American Society of Echocardiography's Guidelines and Standards Committee and the Chamber Quantification Writing Group, developed in conjunction with the European Association of Echocardiography, a branch of the European Society of Cardiology. *J Am Soc Echocardiogr* 18:1440-1463, 2005.
7. Rodevan O, Bjornerheim R, Ljosland M, et al: Left atrial volumes assessed by three- and two-dimensional echocardiography compared with MRI estimates. *Int J Card Imaging* 15:397-410, 1999.
8. Vandenberg BF, Weiss RM, Kinzey J, et al: Comparison of left atrial volume by two-dimensional echocardiography and cine-computed tomography. *Am J Cardiol* 75: 754-757, 1995.
9. Ujino K, Barnes ME, Cha SS, et al: Two-dimensional echocardiographic methods for assessment of left atrial volume. *Am J Cardiol* 98:1185-1188, 2006.
10. Pritchett AM, Jacobsen SJ, Mahoney DW, et al: Left atrial volume as an index of left atrial size: a population based study. *J Am Coll Cardiol* 41:1036-1043, 2003.
11. Tsang TS, Barnes ME, Bailey KR, et al: Left atrial volume: important risk marker of incident atrial fibrillation in 1655 older men and women. *Mayo Clin Proc* 76:467-475, 2001.
12. Osranek M, Fatema K, Qaddoura F, et al: Left atrial volume predicts the risk of atrial fibrillation after cardiac surgery: a prospective study. *J Am Coll Cardiol* 48:779-786, 2006.
13. Tani T, Tanabe K, Ono M, et al: left atrial volume and risk of paroxysmal atrial fibrillation in patients with hypertrophic cardiomyopathy. *J Am Soc Echocardiogr* 17:644-648, 2004.
14. Losi MA, Betocchi S, Aversa M, et al: Determinants of atrial fibrillation development in patients with hypertrophic cardiomyopathy. *Am J Cardiol* 94:895-900, 2004.
15. Drexler M, Erbel R, Müller U, et al: Measurement of intracardiac dimensions and structures in normal young adult subjects by transesophageal echocardiography. *Am J Cardiol* 65:1491-1496, 1990.
16. Schweizer P, Bardos P, Erbel R, et al: Detection of left atrial thrombi by echocardiography. *Br Heart J* 45:148-156, 1981.
17. DePace NL, Soulen RL, Kotler MN, et al: Two dimensional echocardiographic detection of intraatrial masses. *Am J Cardiol* 48:954-960, 1981.
18. Shrestha NK, Moreno FL, Narciso FV, et al: Two-dimensional echocardiographic diagnosis of left atrial thrombus in rheumatic heart disease: a clinicopathologic study. *Circulation* 67:341-347, 1983.
19. Herzog CA, Bass D, Kane M, et al: Two-dimensional echocardiographic imaging of left atrial appendage thrombi. *J Am Coll Cardiol* 3:1340-1344, 1984.
20. Aschenberg W, Schlüter M, Kremer P, et al: Transesophageal two-dimensional echocardiography for the detection of left atrial appendage thrombus. *J Am Coll Cardiol* 7:163-166, 1986.
21. Omran H, Jung W, Rabahieh R, et al: Imaging of thrombi and assessment of left atrial appendage function: A prospective study comparing transthoracic and transoesophageal echocardiography. *Heart* 81:192-198, 1999.
22. Sallach JA, Puwanant S, Drinko JK, et al: Comprehensive left atrial appendage optimization of thrombus using surface echocardiography: the CLOTS multicenter pilot trial. *J Am Soc Echocardiogr* 22:1165-1172, 2009.
23. Cohen GI, White M, Sochowski RA, et al: Reference values for normal adult transesophageal echocardiographic measurements. *J Am Soc Echocardiogr* 8:221-230, 1995.
24. Chan SK, Kannam JP, Douglas PS, Manning WJ: Multiplane transesophageal echocardiographic assessment of left atrial appendage anatomy and function. *Am J Cardiol* 76:528-530, 1995.
25. Mügge A, Daniel WG, Hausmann D, et al: Diagnosis of left atrial appendage thrombi by transesophageal echocardiography: Clinical implications and follow-up. *Am J Cardiac Imag* 4:173-179, 1990.
26. Olson JD, Goldenberg IF, Pedersen W, et al: Exclusion of atrial thrombus by transesophageal echocardiography. *J Am Soc Echocardiogr* 5:52-56, 1992.
27. Hwang JJ, Chen JJ, Lin SC, et al: Diagnostic accuracy of transesophageal echocardiography for detecting left atrial thrombi in patients with rheumatic heart disease having undergone mitral valve operations. *Am J Cardiol* 72:677-681, 1993.
28. Manning WJ, Weintraub RM, Waksmonski CA, et al: Accuracy of transesophageal echocardiography for identifying left atrial thrombi: A prospective, intraoperative study. *Ann Intern Med* 123:817-822, 1995.
29. Nakajima H, Seo Y, Ishizu T, et al: Analysis of the left atrial appendage by three-dimensional transesophageal echocardiography. *Am J Cardiol* 106:885-892, 2010.
30. Latcu DG, Rinaldi JP, Saoudi N. Real-time three-dimensional transoesophageal echocardiography for diagnosis of left atrial appendage thrombus. *Eur J Echocardiogr* 10:711-712, 2009.
31. Stec S, Zaborska B, Sikora-Frac M, et al: First experience with microprobe transesophageal echocardiography in non-sedated adults undergoing atrial fibrillation ablation: feasibility study and comparison with intracardiac echocardiography. *Europace* 13:51-56, 2011.
32. Fukuda S, Shimada K, Kawasaki T, et al: Transnasal transesophageal echocardiography in the detection of left atrial thrombus. *J Cardiol* 54:425-431, 2009.
33. Subramaniam B, Riley MF, Panzica, PJ, Manning WJ. Transesophageal echocardiographic assessment of right atrial appendage anatomy and function: comparison with the left atrial appendage and implications for local thrombus formation. *J Am Soc Echocardiogr* 47:612-618, 2006.
34. Katz ES, Freedberg RS, Rutkovsky L, et al: Identification of an unusual right atrial mass as a Chiari Network by biplane transesophageal echocardiography. *Echocardiogr* 9:273-275, 1992.
35. Schwartzbard AZ, Tunick PA, Rosenzweig BP, et al: The role of transesophageal echocardiography in the diagnosis and treatment of right atrial thrombi. *J Am Soc Echocardiogr* 12:64-69, 1999.
36. Rowlands DJ, Logan WF, Howitt G: Atrial function after cardioversion. *Am Heart J* 74:149-160, 1967.
37. Gabor GE, Winsberg F: Motion of the mitral valves in cardiac arrhythmias: Ultrasonic cardiographic study. *Invest Radiol* 5:355-360, 1970.
38. DeMaria AN, Lies JE, King JF, et al: Echographic assessment of atrial transport, mitral movement and ventricular performance following electroversion of supraventricular arrhythmias. *Circulation* 51:273-282, 1975.
39. Manning WJ, Silverman DI, Katz SE, et al: Atrial ejection force: A new method for the assessment of atrial systolic function. *J Am Coll Cardiol* 22:221-225, 1993.
40. Pollick C, Taylor D: Assessment of left atrial appendage function by transesophageal echocardiography: Implications for the development of thrombus. *Circulation* 84:223-231, 1991.
41. Jue J, Winslow T, Fazio G, et al: Pulsed Doppler characterization of left atrial appendage flow. *J Am Soc Echocardiogr* 6:237-244, 1993.
42. Seto TB, Buchholz A, Douglas PS, Manning WJ: When the body and appendage of the left atrium disagree: "Focal" atrial fibrillation-implications for atrial thrombus formation and risk of thromboembolism. *J Am Soc Echocardiogr* 12:1097-1100, 1999.
43. Bellotti P, Spirito P, Lupi G, Vecchio C: Left atrial appendage function assessed by transesophageal echocardiography before and on the day after elective cardioversion for nonvalvular atrial fibrillation. *Am J Cardiol* 81:1199-1202, 1998.
44. Naqvi TZ, Rafie R, Cesario D. Electrical dissociation within the left atrium and left atrial appendage diagnosed with transesophageal echocardiography. *J Am Soc Echocardiogr* 23:e1-e4, 2010.
45. Rubin DN, Katz SE, Riley MF, et al: Evaluation of left atrial appendage anatomy and function in recent onset atrial fibrillation by transesophageal echocardiography. *Am J Cardiol* 78:774-778, 1996.
46. Fatkin D, Kelly RP, Feneley MP: Relations between left atrial appendage blood flow velocity, spontaneous echocardiographic contrast and thromboembolic risk in vivo. *J Am Coll Cardiol* 23:961-969, 1994.
47. Hoit BD, Shao Y, Gabel M: Influence of acutely altered loading conditions on left atrial appendage flow velocities. *J Am Coll Cardiol* 24:1117-1123, 1994.
48. Thom T, Haase N, Rosamond W, et al: AHA Statistical Update. Heart Disease and Stroke Statistics—2006 Update. A report from the

American Heart Association Statistics Committee and Stroke Statistics Subcommittee. *Circulation* 113:e85-151, 2006.
49. Lloyd-Jones DM, Wang TJ, Leip EP, et al: Lifetime risk for development of atrial fibrillation: the Framingham Heart Study. *Circulation* 110:1042-1046, 2004.
50. Vasan RS, Larson MG, Levy D, et al: Doppler transmitral flow indexes and risk of atrial fibrillation (the Framingham Heart Study). *Am J Cardiol* 91:1079-1083, 2003.
51. Vaziri SM, Larson MG, Benjamin EJ, Levy D: Echocardiographic predictors of nonrheumatic atrial fibrillation. The Framingham Heart Study. *Circulation* 89:724-730, 1994.
52. Morris JJ, Entman M, North WC, et al: The changes in cardiac output with reversion of atrial fibrillation to sinus rhythm. *Circulation* 31:670-678, 1965.
53. Zabalgoitia M, Halperin JL, Pearce LA, et al, for the Stroke Prevention in Atrial Fibrillation III Investigators: Transesophageal echocardiographic correlates of clinical risk of thromboembolism in nonvalvular atrial fibrillation. *J Am Coll Cardiol* 31:1622-1626, 1998.
54. Black IW, Hopkins AP, Lee LC, et al: Left atrial spontaneous echo contrast: A clinical and echocardiographic analysis. *J Am Coll Cardiol* 18:398-404, 1991.
55. The Stroke Prevention in Atrial Fibrillation Investigators Committee: Transesophageal echocardiographic correlates of thromboembolism in high-risk patients with nonvalvular atrial fibrillation. *Ann Intern Med* 128:639-647, 1998.
56. Gage BF, Waterman AD, Shannon W, et al: Validation of clinical classification schemes for predicting stroke: Results from the National Registry of Atrial Fibrillation. *JAMA* 285:2864-2870, 2001.
57. Puwanant S, Varr BC, Shrestha K, et al: Role of the CHADS2 score in the evaluation of thromboembolic risk in patients with atrial fibrillation undergoing transesophageal echocardiography before pulmonary vein isolation. *J Am Coll Cardiol* 54:2032-2039, 2009.
58. Höglund C, Rosenhamer G: Echocardiographic left atrial dimension as a predictor of maintaining sinus rhythm after conversion of atrial fibrillation. *Acta Med Scand* 217:411-415, 1985.
59. Dittrich HC, Erickson JS, Schneiderman T, et al: Echocardiographic and clinical predictors for outcome of elective cardioversion of atrial fibrillation. *Am J Cardiol* 63:193-197, 1989.
60. Aronow WS, Schwartz KS, Koenigsberg M: Prevalence of enlarged left atrial dimension by echocardiography and its correlation with atrial fibrillation and an abnormal P terminal force in lead V1 of the electrocardiogram in 588 elderly persons. *Am J Cardiol* 59:1003-1004, 1987.
61. Petersen P, Kastrup J, Brinch K, et al: Relation between left atrial dimension and duration of atrial fibrillation. *Am J Cardiol* 60:382-384, 1987.
62. Sanfillippo AJ, Abascal VM, Sheehan M, et al: Atrial enlargement as a consequence of atrial fibrillation: A prospective echocardiographic study. *Circulation* 82:792-797, 1990.
63. Suarez GS, Lampert S, Ravid S, et al: Changes in left atrial size in patients with lone atrial fibrillation. *Clin Cardiol* 14:652-656, 1991.
64. Manning WJ, Leeman DE, Gotch PJ, et al: Pulsed Doppler evaluation of atrial mechanical function after electrical cardioversion of atrial fibrillation. *J Am Coll Cardiol* 13:617-623, 1989.
65. Gosselink ATM, Crijns HJGM, Hamer HPM, et al: Changes in left and right atrial size after cardioversion of atrial fibrillation: Role of mitral valve disease. *J Am Coll Cardiol* 22:1666-1672, 1993.
66. Van Gelder IC, Crijns HJ, Van Gilst WH, et al: Decrease of right and left atrial sizes after direct current electrical cardioversion in chronic atrial fibrillation. *Am J Cardiol* 67:93-95, 1991.
67. Reant P, Lafitte S, Jais P, et al: Reverse remodeling of the left cardiac chambers after catheter ablation after 1 year in a series of patients with isolated atrial fibrillation. *Circulation* 112:2896-2903, 2005.
68. Delgado V, Videl B, Sitges M, et al: Fate of left atrial function as determined by real-time three-dimensional echocardiography study after radiofrequency catheter ablation for the treatment of atrial fibrillation. *Am J Cardiol* 101:1285-1290, 2008.
69. Brodsky MA, Allen BJ, Capparelli EV, et al: Factors determining maintenance of sinus rhythm after chronic atrial fibrillation with left atrial dilatation. *Am J Cardiol* 63:1065-1068, 1989.
70. The Boston Area Anticoagulation Trial for Atrial Fibrillation Investigators: The effect of low-dose warfarin on the risk of stroke in patients with non-rheumatic atrial fibrillation. *N Engl J Med* 323:1505-1511, 1990.
71. Petersen P, Godrfredsen J, Boysen GK, et al: Placebo-controlled, randomised trial of warfarin and aspirin for prevention of thromboembolic complications in chronic atrial fibrillation: the Copenhagen AFASAK study. *Lancet* 1:175-179, 1989.
72. Stroke Prevention in Atrial Fibrillation Study Group Investigators: Stroke Prevention in Atrial Fibrillation Study: Final results. *Circulation* 84:527-539, 1991.
73. Connolly SJ, Laupacis A, Gent M, et al: Canadian atrial fibrillation (CAFA) study. *J Am Coll Cardiol* 18:349-355, 1991.
74. Ezekowitz MD, Bridgers SL, James KE, et al: Warfarin in the prevention of stroke associated with nonrheumatic atrial fibrillation. Veterans Affairs Stroke Prevention in Nonrheumatic Atrial Fibrillation Investigators. *N Engl J Med* 327:1406-1412, 1993.
75. Connolly SJ, Ezekowitz MD, Yusuf S, et al: Dabigatran versus warfarin in patients with atrial fibrillation. *N Engl J Med* 361;1139-1151, 2009.
76. Gallagher MM, Hennessy BJ, Edwardsson N, et al: Embolic complications of direct current cardioversion of atrial arrhythmias: association with low intensity of anticoagulation at the time of cardioversion. *J Am Coll Cardiol* 40:926-933, 2002.
77. Manning WJ, Silverman DI, Keighley CS, et al: Transesophageal echocardiographically facilitated early cardioversion from atrial fibrillation using short-term anticoagulation: Final results of a prospective 4.5 year study. *J Am Coll Cardiol* 25:1354-1361, 1995.
78. Weigner MJ, Thomas LR, Patel U, et al: Transesophageal echocardiography facilitated early cardioversion from atrial fibrillation: Short-term safety and impact on maintenance of sinus rhythm at 1 year. *Am J Med* 110:694-702, 2001.
79. Klein AL, Grimm RA, Black IW, et al: Cardioversion guided by transesophageal echocardiography: The ACUTE Pilot Study. A randomized control trial. Assessment of cardioversion using transesophageal echocardiography. *Ann Intern Med* 126:200-209, 1997.
80. Corrado G, Tadeo G, Beretta S, et al: Atrial thrombi resolution after prolonged anticoagulation in patients with atrial fibrillation: A transesophageal echocardiography study. *Chest* 115:140-143, 1999.
81. Stoddard MF, Dawkins P, Prince CR, Longaker RA: Transesophageal echocardiographic guidance of cardioversion in patients with atrial fibrillation. *Am Heart J* 129:1204-1215, 1995.
82. Klein AL, Grimm RA, Murray RD, et al: Use of transesophageal echocardiography to guide cardioversion in patients with atrial fibrillation. *N Engl J Med* 344:1411-1420, 2001.
83. Strandberg M, Raatikainen MJ, Niemela M, et al: Clinical practicality and predictive value of transoesophageal echocardiography in early cardioversion of atrial fibrillation. *Europace* 8:408-412, 2006.
84. Wu LA, Chandrasekaran K, Friedman PA, et al: Safety of expedited anticoagulation in patients undergoing transesophageal echocardiographic-guided cardioversion. *Am J Med* 119:142, 2006.
85. Corrado G, Santarone M, Beretta S, et al: Early cardioversion of atrial fibrillation and atrial flutter guided by transesophageal echocardiography. A single centre 8.5-year experience. *Europace* 2:119-126, 2000.
86. Resnekov L, McDonald L: Complications in 220 patients with cardiac dysrhythmias treated by phased direct current shock, and indications for electroversion. *Br Heart J* 29: 926-936, 1967.
87. Lown B, Perlroth MG, Kaiddbey S, et al: "Cardioversion" of atrial fibrillation: A report on the treatment of 65 episodes in 50 patients. *N Engl J Med* 269:325-331, 1963.
88. Bjerkelund C, Ornig OM: The efficacy of anticoagulant therapy in preventing embolism related to D.C. electrical conversion of atrial fibrillation. *Am J Cardiol* 23:208-216, 1969.
89. Arnold AZ, Mick MJ, Mazurek RP, et al: Role of prophylactic anticoagulation for direct current cardioversion in patients with atrial fibrillation or atrial flutter. *J Am Coll Cardiol* 19:851-855, 1992.
90. Ezekowitz MD, James KE, Nazarian SM, et al: Silent cerebral infarction in patients with nonrheumatic atrial fibrillation. The Veterans Affairs Stroke Prevention in Nonrheumatic Atrial Fibrillation Investigators. *Circulation* 92:2178-2182, 1995.
91. Bernhardt P, Schmidt H, Hammerstingl C, et al: Patients with atrial fibrillation and dense spontaneous echo contrast at high risk. A prospective and serial follow-up over 12 months with transesophageal echocardiography and cerebral magnetic resonance imaging. *J Am Coll Cardiol* 45:1807-1812, 2005.
92. The Stroke Prevention in Atrial Fibrillation Investigators: Predictors of thromboembolism in atrial fibrillation: II. Echocardiographic features of patients at risk. *Ann Intern Med* 116:6-12, 1992.
93. McCready JW, Nunn L, Lambiase PD, et al: Incidence of left atrial thrombus prior to atrial fibrillation ablation: is pre-procedural transoesophageal echocardiography mandatory. *Europace* 12:927-932, 2010.
94. Sharifi M, Parhizgar A, Gupta P, et al: Is transesophageal echocardiography necessary before D.C. cardioversion in patients with a normal transthoracic echocardiogram? *Echocardiography* 24:397-400, 2007.
95. Blackshear JL, Pearce LA, Asinger RW, et al: Mitral regurgitation associated with reduced

thromboembolic events in high-risk patients with nonrheumatic atrial fibrillation. *Am J Cardiol* 72:840-843, 1993.
96. Nakagami H, Yamamoto K, Ikeda U, et al: Mitral regurgitation reduces the risk of stroke in patients with nonrheumatic atrial fibrillation. *Am Heart J* 136:528-532, 1998.
97. Pritchett ELC: Management of atrial fibrillation. *N Engl J Med* 326:1264-1271, 1992.
98. Stoddard MF, Dawkins PR, Prince CR, et al: Left atrial appendage thrombus is not uncommon in patients with acute atrial fibrillation and a recent embolic event: A transesophageal echocardiographic study. *J Am Coll Cardiol* 25:452-459, 1995.
99. Weigner MJ, Caulfield TA, Danias PG, et al: Risk for clinical thromboembolism associated with conversion to sinus rhythm in patients with atrial fibrillation lasting less than 48 hours. *Ann Intern Med* 126:615-620, 1997.
100. Kleeman T, Becker T, Strauss M, et al: Prevalence of left atrial thrombus and dense spontaneous echo contrast in patients with short-term atrial fibrillation < 48 hours undergoing cardioversion: value of transesophageal echocardiography to guide cardioversion. *J Am Soc Echocardiogr* 22:1403-1408, 2009.
101. Manning WJ, Silverman DI, Waksmonski CA, et al: Prevalence of residual left atrial thrombi among patients presenting with thromboembolism and newly recognized atrial fibrillation. *Arch Intern Med* 155:2193-2198, 1995.
102. Manning WJ, Silverman DI, Gordon SPF, et al: Cardioversion from atrial fibrillation without prolonged anticoagulation with use of transesophageal echocardiography to exclude the presence of atrial thrombi. *N Engl J Med* 328:750-755, 1993.
103. Gage BF, Waterman AD, Shannon W, et al: Validation of clinical classification schemes for predicting stroke: results from the National Registry of Atrial Fibrillation. *JAMA* 285:2864-2870, 2001.
104. Bernhardt P, Schmidt H, Hammerstingl C, et al: Patients at high risk with atrial fibrillation: a prospective and serial follow-up during 12 months with transesophageal echocardiography and cerebral magnetic resonance imaging. *J Am Soc Echocardiogr* 18:919-924, 2005.
105. Wyse DG, Waldo AL, DiMarco JP, et al: A comparison of rate control and rhythm control in patients with atrial fibrillation. The atrial fibrillation follow-up investigation of rhythm management (AFIRM) investigators. *N Engl J Med* 347:1825-1833, 2002.
106. Van Gelder IC, Hagens VE, Bosker HA, et al: A comparison of rate control and rhythm control in patients with recurrent persistent atrial fibrillation. *N Engl J Med* 347:1834-1840, 2002.
107. Carlsson J, Miketic S, Windeler J, et al: Randomized trial of rate-control versus rhythm-control in persistent atrial fibrillation: the Strategies of Treatment of Atrial Fibrillation (STAF) study. *J Am Coll Cardiol* 41:1690-1696, 2003.
108. Manning WJ, Silverman DI, Katz SE, et al: Impaired left atrial mechanical function after cardioversion: Relationship to the duration of atrial fibrillation. *J Am Coll Cardiol* 23:1535-1540, 1994.
109. Nagarakanti R, Ezekowitz MD, Oldgren J, et al: Dabigatran versus warfarin in patients with atrial fibrillation: an analysis of patients undergoing cardioversion. *Circulation* 123:131-136, 2011.
110. Berger M, Schweitzer P: Timing of thromboembolic events after electrical cardioversion of atrial fibrillation or flutter: A retrospective analysis. *Am J Cardiol* 82:1545-1547, 1998.
111. Weinberg DM, Mancini GBJ: Anticoagulation for cardioversion of atrial fibrillation. *Am J Cardiol* 63:745-746, 1989.
112. Shen X, Li H, Rovang K, et al: Prevalence of intra-atrial thrombi in atrial fibrillation patients with subtherapeutic international normalized ratios while taking conventional anticoagulation. *Am J Cardiol* 90:660-662, 2002.
113. Corrado G, Beretta S, Sormani L, et al: Prevalence of atrial thrombi in patients with atrial fibrillation/flutter and subtherapeutic anticoagulation prior to cardioversion. *Eur J Echocardiogr* 5:257-261, 2004.
114. Fuster V, Ryden LE, Cannom DS, et al: ACC/AHA/ESC 2006 Guidelines for the management of patients with atrial fibrillation - Executive summary. A report of the American College of Cardiology/American Heart Association Task Force on Practice Guidelines and the European Society of Cardiology Committee for Practice Guidelines (Writing Committee to Revise the 2001 Guidelines for the Management of Patients with Atrial Fibrillation). *Circulation* 114:700-752, 2006.
115. Singer DE, Albers GW, Dalen JE, et al: 7th ACCP Consensus Conference on Antithrombotic Therapy: Antithrombotic therapy in atrial fibrillation. *Chest* 126:429S-456S, 2004.
116. Klein AL, Grimm RA, Jasper SE, et al: Efficacy of transesophageal echocardiography-guided cardioversion of patients with atrial fibrillation at 6 months: a randomized controlled trial. *Am Heart J* 151:380-389, 2006.
117. Harjai KJ, Mobarek SK, Cheirif J, et al: Clinical variables affecting recovery of left atrial mechanical function after cardioversion from atrial fibrillation. *J Am Coll Cardiol* 30:481-486, 1997.
118. Seto TB, Taira DA, Tsevat J, et al: Cost-effectiveness of transesophageal echocardiographic-guided cardioversion: A decision analytic model for patients admitted to the hospital with atrial fibrillation. *J Am Coll Cardiol* 29: 122-130, 1997.
119. Klein AL, Murray RD, Becker ER, et al: Economic analysis of a transesophageal echocardiography-guided approach to cardioversion of patients with atrial fibrillation: the ACUTE economic data at eight weeks. *J Am Coll Cardiol* 43:1217-1224, 2004.
120. Shen X, Li H, Rovang K, et al: Transesophageal echocardiography before cardioversion of recurrent atrial fibrillation: does absence of previous atrial thrombi preclude the need of a repeat test? *Am Heart J* 146:741-745, 2003.
121. Klein AL, Grimm RA, Jasper SE, et al: Efficacy of transesophageal echocardiography-guided cardioversion of patients with atrial fibrillation at 6 months: a randomized controlled trial. *Am Heart J* 151:380-389, 2006.
122. Black IW, Fatkin D, Sagar KB, et al: Exclusion of atrial thrombus by transesophageal echocardiography does not preclude embolism after cardioversion of atrial fibrillation: A multicenter study. *Circulation* 89:25092513, 1994.
123. Shapiro EP, Effron MB, Lima S, et al: Transient atrial dysfunction after conversion of chronic atrial fibrillation to sinus rhythm. *Am J Cardiol* 62:1202, 1988.
124. Grimm RA, Stewart WJ, Maloney JD, et al: Impact of electrical cardioversion for atrial fibrillation on left atrial appendage function and spontaneous echo contrast: Characterization by simultaneous transesophageal echocardiography. *J Am Coll Cardiol* 22:1359-1366, 1993.
125. Fatkin D, Kuchar DL, Thorburn CW, et al: Transesophageal echocardiography before and during direct current cardioversion of atrial fibrillation: Evidence for atrial stunning as a mechanism of thromboembolic complications. *J Am Coll Cardiol* 23:307-316, 1994.
126. Bernhardt P, Schmidt H, Hammerstingl C, et al: Incidence of cerebral embolism after cardioversion of atrial fibrillation: a prospective study with transesophageal echocardiography and cerebral magnetic resonance imaging. *J Am Soc Echocardiogr* 18:649-653, 2005.
127. Saeed M, Rahman A, Afzal A, et al: Role of transesophageal echocardiography guided cardioversion in patients with atrial fibrillation, previous left atrial thrombus and effective anticoagulation. *Int J Cardiol* 113:401-405, 2006.
128. Seto TB, Taira DA, Manning WJ: Cardioversion in patients with atrial fibrillation and left atrial thrombi on initial transesophageal echocardiography: Should transesophageal echocardiography be repeated before elective cardioversion? A cost effectiveness analysis. *J Am Soc Echocardiogr* 12:508-516, 1999.
129. deLuca I, Sorino M, De Luca L, et al: Pre and post-cardioversion transesophageal echocardiography for brief anticoagulation therapy with enoxaparin in atrial fibrillation patients: a prospective study with a 1-year follow-up. *Int J Cardiol* 102:447-454, 2005.
130. Klein AL, Jasper SE, Katz WE, et al: The use of enoxaparin compared to unfractionated heparin for short-term antithrombotic therapy in atrial fibrillation patients undergoing TEE-guided cardioversion: Assessment of cardioversion using transesophageal echocardiography (ACUTE) II randomized multicenter pilot study. *Eur Heart J* 27:2858-2865, 2006.
131. Shen X, Li H, Nair CK, et al: Warfarin therapy initiated before is more beneficial than after transesophageal echocardiography detected left atrial thrombus. *Echocardiography* 24:14-19, 2007.
132. Bernhardt P, Schmidt H, Hammerstingl C, et al: Atrial thrombi—a prospective follow-up study over 3 years with transesophageal echocardiography and cranial magnetic resonance imaging. *Echocardiography* 23:388-394, 2006.
133. Goldman MJ: The management of chronic atrial fibrillation: Indications for and method of conversion to sinus rhythm. *Prog Cardiovasc Dis* 3:465, 1960.
134. Tsai LM, Hung JS, Chen JH, et al: Resolution of left atrial appendage thrombus in mitral stenosis after warfarin therapy. *Am Heart J* 121:1232-1234, 1991.
135. Pytlewski G, Panidis IP, Combs W, et al: Resolution of left atrial thrombus with warfarin by transesophageal echocardiography before percutaneous commissurotomy in mitral stenosis. *Am Heart J* 128:843-845, 1994.
136. Collins LJ, Silverman DI, Douglas PS, Manning WJ: Cardioversion of non-rheumatic atrial fibrillation: Reduced thromboembolic complications with 4 weeks of pre-cardioversion anticoagulation are related to atrial thrombus resolution. *Circulation* 92:160-163, 1995.
137. Jaber WA, Prior DL, Thamilarasan M, et al: Efficacy of anticoagulation in resolving left atrial and left atrial appendage thrombi: a transesophageal echocardiographic study. *Am Heart J* 140:150-156, 2000.
138. Thambidorai SK, Murray RD, Parakh K, et al: Utility of transesophageal echocardiography in

identification of thromboembolic milieu in patients with atrial fibrillation (an ACUTE ancillary study). *Am J Cardiol* 96:935-941, 2005.
139. Nair CK, Holmberg MJ, Aronow WS, et al: Thromboembolism in patients with atrial fibrillation with and without left atrial thrombus documented by transesophageal echocardiography. *Am J Ther* 16:385-392, 2009.
140. Parekh A, Jaladi R, Sharma S, et al: Images in cardiovascular medicine. The case of a disappearing left atrial appendage thrombus: direct visualization of left atrial thrombus migration, captured by echocardiography, in a patient with atrial fibrillation, resulting in a stroke *Circulation* 14:e513-e514, 2006.
141. Ehsani A, Ewy GA, Sobel BE: Effects of electrical countershock on serum creatine phosphokinase (CPK) isoenzyme activity. *Am J Cardiol* 37:12-18, 1976.
142. Yarbrough R, Ussery G, Whitley J: A comparison of the effects of A.C. and D.C. countershock on ventricular function in thoracotomized dogs. *Am J Cardiol* 14:504-512, 1964.
143. Manning WJ, Silverman DI, Katz SE, et al: Temporal dependence of the return of atrial mechanical function on the mode of cardioversion of atrial fibrillation to sinus rhythm. *Am J Cardiol* 75:624, 1995.
144. Orlando JR, van Herick R, Aronow WS, et al: Hemodynamics and echocardiograms before and after cardioversion of atrial fibrillation to normal sinus rhythm. *Chest* 76:521-526, 1979.
145. Van Gelder IC, Crijns HJGM, Blanksma PK, et al: Time course of hemodynamic changes and improvement of exercise tolerance after cardioversion of chronic atrial fibrillation unassociated with cardiac valve disease. *Am J Cardiol* 72:560-566, 1993.
146. Viswanathan K, Daniak S, Salamone K, et al: Effect of atrial fibrillation on improvement in left ventricular performance. *Am J Cardiol* 88:439-441, 2001.
147. Dethy M, Chassat C, Roy D, Mercier LA: Doppler echocardiographic predictors of recurrence of atrial fibrillation after cardioversion. *Am J Cardiol* 62:723-726, 1988.
148. Shyu KG, Cheng JJ, Chen JJ, et al: Recovery of atrial function after atrial compartment operation for chronic atrial fibrillation in mitral valve disease. *J Am Coll Cardiol* 24:392-398, 1994.
149. Donal E, Grimm RA, Yamada H, et al: Usefulness of Doppler assessment of pulmonary vein and left atrial appendage flow following pulmonary vein isolation of chronic atrial fibrillation in predicting recovery of left atrial function. *Am J Cardiol* 95:941-947, 2005.
150. Rodrigues AC, Scannavacca MI, Caldas MA, et al: Left atrial function after ablation for paroxysmal atrial fibrillation. *Am J Cardiol* 103:395-398, 2009.
151. Reant P, Lafitte S, Jais P, et al: Reverse remodeling of the left cardiac chambers after catheter ablation after 1 year in a series of patients with isolated atrial fibrillation. *Circulation* 112:2896-2903, 2005.
152. Donal E, Ollivier R, Weillard D, et al: Left atrial function assessed by transthoracic echocardiography in patients treated by ablation for a lone paroxysmal atrial fibrillation. *Eur J Echocardiogr* 11:845-852, 2010.
153. Dagres N, Karatasakis G, Panou F, et al: Pretreatment with irbesartan attenuates left atrial stunning after electrical cardioversion of atrial fibrillation. *Eur Heart J* 27:2062-2068, 2006.
154. Mattioli AV, Castelli A, Andria A, et al: Clinical and echocardiographic features influencing recovery of atrial function after cardioversion of atrial fibrillation. *Am J Cardiol* 82:1368-1371, 1998.
155. Pollak A, Falk RH: Aggravation of postcardioversion atrial dysfunction by sotalol. *J Am Coll Cardiol* 25:665-671, 1995.
156. Black IW, Hopkins AP, Lee LC, et al: Left atrial spontaneous echo contrast: A clinical and echocardiographic analysis. *J Am Coll Cardiol* 18:398-404, 1991.
157. Chimowitz MI, DeGeorgia MA, Poole RM, et al: Left atrial spontaneous echo contrast is highly associated with previous stroke in patients with atrial fibrillation or mitral stenosis. *Stroke* 24:1015-1019, 1993.
158. Orsinelli DA, Pearson AC: Usefulness of transesophageal echocardiography to screen for left atrial thrombus before elective cardioversion for atrial fibrillation. *Am J Cardiol* 72:1337-1339, 1993.
159. Bikkina M, Alpert MA, Mulekar M, et al: Prevalence of intraatrial thrombus in patients with atrial flutter. *Am J Cardiol* 76:186-189, 1995.
160. Irani WN, Grayburn PA, Afridi I: Prevalence of thrombus, spontaneous echo contrast, and atrial stunning in patients undergoing cardioversion of atrial flutter. *Circulation* 95:962-966, 1997.
161. Jordaens L, Missault L, Germonpré E, et al: Delayed restoration of atrial function after conversion of atrial flutter by pacing or electrical cardioversion. *Am J Cardiol* 71:63-67, 1993.
162. Haissaguerre M, Jais P, Shah DC, et al: Spontaneous initiation of atrial fibrillation by ectopic beats originating in the pulmonary veins. *N Engl J Med* 339:659-666, 1998.
163. Ouyang F, Tilz R, Chun J, et al: Long-term results of catheter ablation in paroxysmal atrial fibrillation: lessons from a 5-year follow-up. *Circulation* 122:2368-2377, 2010.
164. Yamashita E, Takamatsu H, Tada H, et al: Transesophageal echocardiography for thrombus screening prior to left atrial catheter ablation. *Circ J* 74:1081-1086, 2010.
165. Chierchia GB, Capulzini L, de Asmundis C, et al: First experience with real-time three-dimensional transoesophageal echocardiography-guided transseptal in patients undergoing atrial fibrillation ablation. *Europace* 10:1325-1328, 2008.
166. Mitchell-Heggs L, Lellouche N, Deal L, et al: Transseptal puncture using minimally invasive echocardiography during atrial fibrillation ablation. *Europace* 12:1435-1438, 2010.
167. De Piccoli B, Rossillo A, Zanella C, et al: Role of transoesophageal echocardiography in evaluating the effect of catheter ablation of atrial fibrillation on anatomy and function of the pulmonary veins. *Europace* 10:1079-1084, 2008.
168. Gula LJ, Massel D, Redfearn DP, et al: Impact of routine transesophageal echocardiography on safety, outcomes, and cost of pulmonary vein ablation: inferences drawn from a decision analysis model. *Europace* 12:1550-1557, 2010.
169. Chilukuri K, Mayer SA, Scherr D, et al: Transesophageal echocardiography predictors of periprocedural cerebrovascular accident in patients undergoing catheter ablation of atrial fibrillation. *Europace* 12:1543-1549, 2010.
170. Schaer BA, Maurer A, Sticherling C, et al: Routine echocardiography after radiofrequency ablation: to flog a dead horse. *Europace* 11:155-157, 2009.
171. Sigurdsson G, Troughton RW, Xu XF, et al: Detection of pulmonary vein stenosis by transesophageal echocardiography: comparison with multidetector computed tomography. *Am Heart J* 153:800-806, 2007.
172. Schneider C, Ernst S, Bahlmann E, et al: Transesophageal echocardiography: a screening method for pulmonary vein stenosis after catheter ablation of atrial fibrillation. *Eur J Echocardiogr* 7:447-456, 2006.
173. Kanderian AS, Gillinov AM, Pettersson GB, et al: Success of surgical left atrial appendage closure: assessment by transesophageal echocardiography. *J Am Coll Cardiol* 52:924-929, 2008.
174. Mraz T, Neuzil P, Mandysova E, et al: Role of echocardiography in percutaneous occlusion of the left atrial appendage. *Echocardiography* 24:401-404, 2007.



# General Echocardiographic Approach to the Adult with Suspected Congenital Heart Disease

MICHELLE GURVITZ, MD

**Basic Principles**
**Cardiac Position**
The Left-Sided Heart
The Right-Sided Heart
**Cardiac Morphology**
General
Atria
Atrioventricular Valves and Ventricles
Semilunar Valves and Great Arteries
**Cardiac Anatomy**
General
Determination of Atrial Situs and Venous Connections
Determination of Atrioventricular Valves and Ventricles
Determination of Semilunar Valves and Great Arteries
**Univentricular Heart**
General
Left Ventricular Type
Right Ventricular Type
Other Univentricular Physiology Hearts
**Color and Spectral Doppler Imaging**
General
Intracardiac Shunting
Great Arteries

The population of adults with congenital heart disease (CHD) is growing rapidly in the United States.[1-3] Adult patients with CHD have a variety of heart conditions, from simple "holes in the heart" to complex single ventricle anatomy. Some of these patients have undergone palliation or complete surgical repair, and others remain with their native heart condition or present de novo in adulthood. Many childhood patients have a long lapse in medical follow-up examinations and then present later in adulthood with complications of their underlying condition.[4-7] In all of these situations, echocardiography remains the mainstay of diagnosis for patients with CHD.[8-10] There are many approaches to echocardiographic imaging for adult patients with CHD; one of these methods is discussed in this chapter.

First, the positioning of the heart within the chest is addressed, followed by the definition and morphology of the cardiac chambers, valves, and great vessels. Further analysis is based on the segmental approach, which describes the alignments and relationships of the atria, ventricles, and great arteries. These fundamentals are necessary for recognition of the different morphologic cardiac components in the either usual or unusual anatomic arrangements. Next, the chapter reviews the more common anatomic arrangements that create normal hearts and congenital heart anomalies. This review is followed by a review of issues surrounding the assessment of the univentricular heart. Finally, there is a brief discussion on the use of color and spectral Doppler imaging for identification of shunts and valvular lesions in CHD.

Regardless of the specific disease, repair, technology, or technique at hand, the practitioner must keep certain general principles in mind in the imaging of patients with CHD.

- First, the presence of one congenital abnormality often means that more may exist. Completion of a comprehensive two-dimensional (2D) and Doppler evaluation is crucial in view of the possibility of more than one anomaly.
- Second, there may be exceptions to the "rules" of CHD and cardiac development. Thus, the physician must always describe what is present, even if that information seems inconsistent with what is known about conventional CHD lesions.
- Third, no physician or sonographer should hesitate to get a second opinion. Even the best congenital echocardiographers need assistance at times.
- Fourth, the larger body habitus of adults makes echocardiography more difficult than in children. Imaging may require other strategies to complement the echocardiography. These often include transesophageal echocardiography, magnetic resonance imaging, computerized tomography scanning, and cardiac catheterization.[11-15]

## Basic Principles

The cardiologist should expect that adult patients with CHD may not know specific information regarding their heart disease. Many of the patients may not familiar with the name of their heart condition or the particular aspects of surgical or catheter-based interventions. Some may understand it was a "hole in the heart" or a "narrow valve" or a "single pumping chamber," but many may not be able to describe it in any detail.[16,17]

The clinician, however, can derive a number of clues from basic patient information, and that information can help guide the physician and sonographer. This information includes:

1. Has the patient had surgery?
2. If so, how many surgeries? Were they sternotomies, thoracotomies, or both?

3. Is the patient's condition cyanotic?
4. Has the patient had any catheter-based interventional procedures?

For example, if the patient reports a "narrow valve," has had no surgeries but a catheter-based procedure, and has an acyanotic condition, one might expect aortic or pulmonary stenosis with a small chance of mitral valve disease. Of course, even with this information, the clinician has to keep an open mind in diagnosis of CHD because patients with CHD may have more than one condition. The echocardiography laboratory needs to be familiar with anatomic variations of CHD. However, although most congenital heart anomalies are well described in the pediatric cardiology literature, the nomenclature for some complex anatomic lesions remains disputed. For example, the segmental relationships of the cardiac structures have been variously classified from an embryologic perspective, a physiologic perspective, and even a surgical or interventional perspective.[18-21] In some cases, no universal agreement exists as to the definition of a ventricle, let alone complete segmental anatomy of certain conditions. Some of these controversies are discussed further this chapter. With these terminology disagreements in mind, this text focuses on identification and description of the cardiac chambers and great vessels, their anatomic alignment, and the position of the heart relative to the systemic venous system and other organs.

## Cardiac Position

The heart is normally positioned in the left chest with the apex pointing leftward. Depending on cardiac rotation in development, the heart may take other positions (or malpositions) that include location in the mid chest, the right chest, or even outside the chest (ectopia cordis).[22,23] The spatial position of a particular structure or organ in the body is known as the situs. The condition in which the heart and the other body organs are found in a usual arrangement is termed situs solitus. This includes a left-sided heart, left-sided stomach and spleen, and a right-sided liver. Departures from this normal organ arrangement are specially defined. For example, a complete inversion of the viscera, which results in a heart positioned in the right side of the thoracic cavity, with a rightward-pointing apex, and inversion of the abdominal organs and lungs, is called situs inversus totalis (Fig. 43-1).[18,20,21] Several other combinations can and do occur. For example, patients might have the heart positioned in the right chest but situs solitus of other organs or the heart positioned in the left chest with situs inversus of the other organs. Both of these situations are often associated with a structurally abnormal heart.[24] A small percentage of patients have an unusual and inconsistent arrangement of the viscera, with the heart positioned in either the mid chest or right or left thorax. This is often referred to as heterotaxy syndrome or asplenia and polysplenia syndromes.[25]

### THE LEFT-SIDED HEART

The normal position of the heart is in the left chest with an apex pointing leftward. In certain cases, because of anatomic abnormalities such as hypoplasia of the left lung, the heart may be located in the extreme left chest. This condition is called levoposition. In this situation, however, the heart usually maintains normal segmentation and connections. In some cases of situs inversus or heterotaxy, the heart may remain positioned in the left side of the chest but is then commonly associated with congenital heart defects.[24,25]

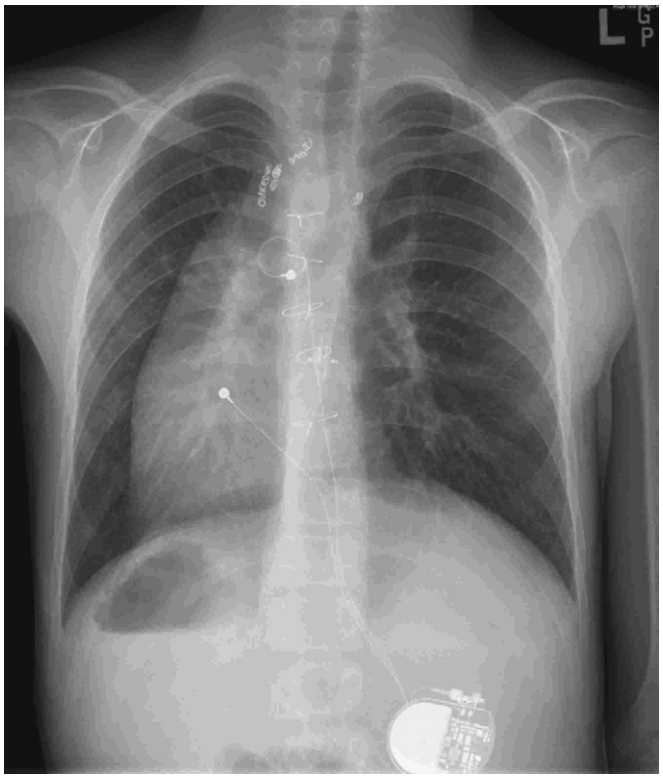


**Figure 43-1 Chest radiograph of a patient with situs inversus totalis.** The cardiac apex *points rightward.* The air bubble of the stomach is visualized in the *upper right abdomen.* The bronchi are also reversed, with a trilobed lung on the left and a bilobed lung on the right. A pacemaker is seen in the abdomen with leads to the atrium and ventricle. Of note, vascular coils are also noted in the *right upper chest.*

### THE RIGHT-SIDED HEART

#### *Anatomy*

A right-sided heart is known as dextrocardia with three basic types: dextroposition, mirror-image dextrocardia, and dextroversion (Fig. 43-2).[22,26]

Dextroposition occurs when mechanical considerations, such as right lung hypoplasia or severe scoliosis, displace the heart to the right side of the thorax. In these cases, the heart retains a leftward-pointing apex. The visceral and atrial positioning is most often situs solitus in this situation. The condition is usually not associated with intracardiac CHD. Mirror-image dextrocardia may be seen with complete situs inversus. In this condition, the heart is positioned in the right thorax with a rightward-pointing apex. The chamber and vessel relationships within the heart are usually normal, but the relative positions of the anatomic components are reversed or "mirror-image" in relation to the normal left-sided heart. A heart with mirror-image dextrocardia often has a right aortic arch and descending thoracic aorta.[23,27] Dextroversion describes a heart that has not rotated the cardiac apex to the left during embryologic development, resulting in a rightward apex with situs solitus or with unusual arrangements of the viscera. As with a leftward heart with situs inversus, these cases have an increased rate of intracardiac congenital heart defects. In some

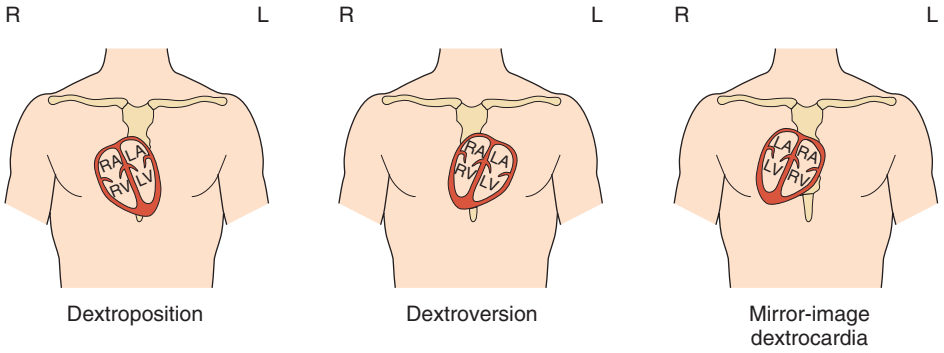



**Figure 43-2 Diagrammatic representation of the types of dextrocardia.** In dextroposition (in situs solitus), the entire heart is shifted to the right chest, either because of a space-occupying mass in the left chest or because of absence of the normal lung volume filling the right chest. Usually, the alignment of the major axis of the heart is normal (pointed toward the left) or rotated slightly vertically; however, the entire heart is shifted to the right of midline or to the retrosternal area. The parasternal long-axis and short-axis views are obtained with the usual orientation of the plane of sound but with the transducer positioned just to the right of the sternum. The apical views are also obtained with the usual orientation of the plane of sound but with the transducer positioned just to the right of the lower sternal border. In dextroversion (in situs solitus), there is failure of apical pivoting. The cardiac apex is to the right of midline, and the atria are usually in their normal positions or shifted slightly to the right. The major axis of the heart is aligned from the left shoulder toward the right hip. The parasternal long-axis view is obtained with the plane of sound oriented in the mirror-image direction of normal. Because the atria are usually normally positioned and the great arteries arise normally from the ventricles, the parasternal short-axis view is obtained with a normal orientation of the plane of sound. In mirror-image dextrocardia (situs inversus totalis), the heart is located in the mirror-image position of normal. Both atria are usually entirely to the right of the sternum, and the cardiac apex is usually in the right fifth or sixth intercostal space at the anterior axillary line; thus, the major axis of the heart is aligned between the left shoulder and right hip. The parasternal long-axis view is obtained from the right second or third intercostal space, with the plane of sound oriented in a mirror-image direction of normal (from left shoulder to right hip). The parasternal short-axis view is obtained from the same transducer location, with the plane of sound also oriented in the mirror-image direction of normal (from right shoulder to left hip). The apical views are obtained with the transducer positioned in the right fifth or sixth intercostal space in the anterior axillary line and with the plane of sound oriented in a mirror-image direction of normal.

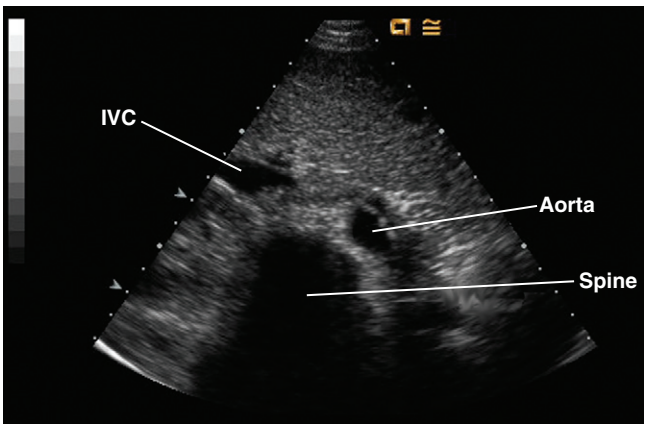



**Figure 43-3 Subcostal short-axis view in a patient with abdominal and atrial situs solitus.** The aorta is leftward and anterior of the spine. The inferior vena cava (*IVC*) is rightward and slightly more anterior.

studies, that correlation reaches 90% of patients with dextroversion having associated congenital heart defects.[25,28]

### *Imaging Approach*

In imaging of the patient with suspected dextrocardia or cardiac malposition, the first step is determination of abdominal situs and cardiac positioning. This is best done by starting with the subcostal view. In the normal subcostal short-axis view, the spine is positioned in the middle with the pulsatile aorta in cross section to the patient's left, just anterior to the spine. The collapsible inferior vena cava is seen in cross section to the patient's right and further anterior of the spine (Fig. 43-3). Ideally, before referral for an echocardiogram for suspected CHD, the patient has had a chest radiograph that shows the liver and stomach bubble and the positioning of the heart within the thorax. In dextroposition, the heart and its segmental connections usually remain normally positioned, albeit located to the right of the midline. The usual echocardiographic views can be used, but they should be adjusted for the rightward positioning and are frequently displaced to the right of the sternum.[23] In mirror-image dextrocardia with visceral and atrial situs inversus, the apex of the heart points toward the right leg and the long axis of the heart is oriented from left shoulder to right leg (Fig. 43-4). The intracardiac connections are often normally related; however, the morphologic right atrium and ventricle are positioned leftward of the morphologic left atrium and ventricle. The apex of the heart is usually positioned as inverted from normal and can be found in the right fifth or sixth intercostal space in the anterior axillary line.

Although further cardiac imaging in this condition can be confusing, the result is that the images either appear normal or are the mirror image of a normally positioned heart. For example, the parasternal long-axis view is obtained with the transducer oriented along the long axis of the heart from left shoulder toward right leg. Once recorded, the images look like those obtained in the usual parasternal long-axis view because there is no right-left orientation, only superior-inferior and anterior-posterior. The parasternal short-axis views are obtained in the orthogonal plane. In the short-axis view, right-left and anterior-posterior orientation is obtained so the image in a patient with dextrocardia looks like the "usual" view, only backwards or right-left inverted. The images obtained in the apical four-chamber view look "backward appearing," similar to the parasternal short-axis view, and they are obtained with the transducer positioned at the apex of the heart. The sonographer or physician should be careful not to invert the image so that it appears normal; this is confusing on later review of the study and misleading regarding the relationship of the heart within the thorax. The imaging positions for dextroversion are similar to that for mirror-image dextrocardia. Often, however, the heart

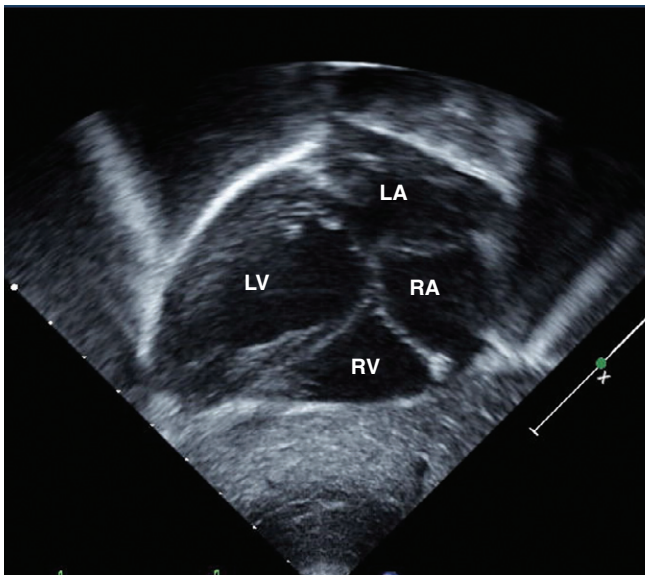



**Figure 43-4 Subcostal four-chamber view of a patient with mirror-image dextrocardia.** The left-sided ventricle has an inferiorly placed atrioventricular valve and is triangular in shape with a trabeculated apex, reflecting a morphologic right ventricle. The right-sided ventricle is more bullet-shaped and smooth walled and consistent with a morphologic left ventricle. The right-sided atrium appears to receive pulmonary veins and is consistent with a morphologic left atrium.

is not positioned as far rightward in the chest; moreover, this condition carries a much higher incidence rate of intracardiac congenital heart abnormalities. In any patient with dextrocardia, views of the aortic arch are obtained in the usual fashion in the suprasternal notch. In these conditions, identification of the presence of right-sided or left-sided arch, descending aorta, and the branching pattern of the head and neck vessels is important.

## Cardiac Morphology

### GENERAL

The heart's anatomic position and function do not always reflect the morphology of a chamber. For example, a left-sided ventricular chamber connected to an aortic outflow is not always a morphologic left ventricle (LV). In certain congenital heart defects, there are absent or atretic valves, chambers, or great vessels. In these cases, identification of the morphology of each chamber becomes more challenging. However, once one is familiar with the usual morphologic landmarks of the cardiac chambers and great arteries, the abnormal anatomic variants and unusual anatomic relationships found in many CHDs become easier to differentiate and recognize (Table 43-1).

### ATRIA

The right atrium is most easily characterized by its appendage, which is a broad-based and triangular structure that lies anterior to the chamber. Often a visible Eustachian valve arises from the orifice of the inferior vena cava, directed toward the mid portion of the interatrial septum. More specifically, the tissue of the valve runs along the inferior portion of the atrium and is directed toward the limbus or the inferior portion of the fossa ovalis (Fig. 43-5). The right atrium is also identified by connections with the suprahepatic portion of the inferior vena cava.

**TABLE 43-1 Morphologic Characteristics of Cardiac Chambers, Valves, and Great Arteries**

| *Morphologic Chamber* | *Identifying Features* |
|---|---|
| Right atrium | Receives inferior vena cava and has Eustachian valve<br>Broad-based and trabecular appendage |
| Left atrium | Receives pulmonary veins (usually)<br>Long and finger-like appendage |
| Tricuspid valve and RV | Atrioventricular valve is trileaflet and has septal attachments<br>Heavily trabeculaed chamber with moderator band<br>Discrete inflow and outflow portions |
| Mitral valve and LV | Atrioventricular valve is bileaflet and attaches to papillary muscles, not septum<br>Chamber is smooth walled |
| Aorta and aortic valve | Trileaflet semilunar valve<br>Gives rise to coronaries, head and neck vessels |
| Pulmonary artery and pulmonary valve | Trileaflet semilunar valve<br>Vessel bifurcates early into right and left branches |

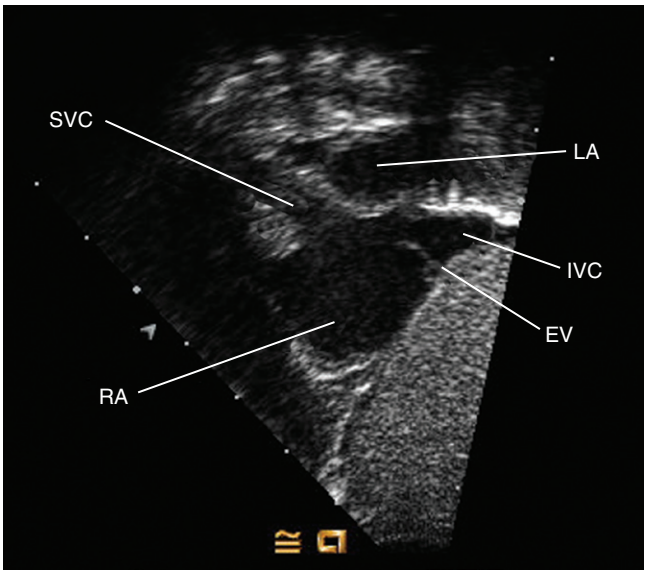



**Figure 43-5 Subcostal sagittal view in a patient with normal return of the superior vena cava (*SVC*) and inferior vena cava (*IVC*) to the right atrium.** The Eustachian valve (*EV*) is visualized near the origin of the inferior vena cava. The left atrium is also shown.

Even with abnormal connections of the superior vena cava, the suprahepatic portion of the inferior vena cava rarely connects anywhere except the morphologic right atrium.[29,30] Finally, the abdominal situs may also help identify atrial anatomy. The atrial situs usually follows the abdominal situs; in situs solitus, with the liver on the right and the stomach on the left, one expects a right-sided morphologic right atrium.[25,28] The left atrium is also best characterized by its appendage, which is a narrow and finger-like or windsock structure that lies anterior to the left atrium. The flap-valve of the foramen ovale, if present, should be found on the left surface of the interatrial septum and is a useful landmark. Finally, the practitioner should look for the connections of at least three individual pulmonary veins, with a minimum of at least one each from the right and left sides, entering an atrial chamber. This finding most always indicates a left atrium.[29,30] However, if the pulmonary veins come to a confluence and empty into an accessory vertical vein before entering an atrial chamber, that chamber is not necessarily a morphologic left atrium.

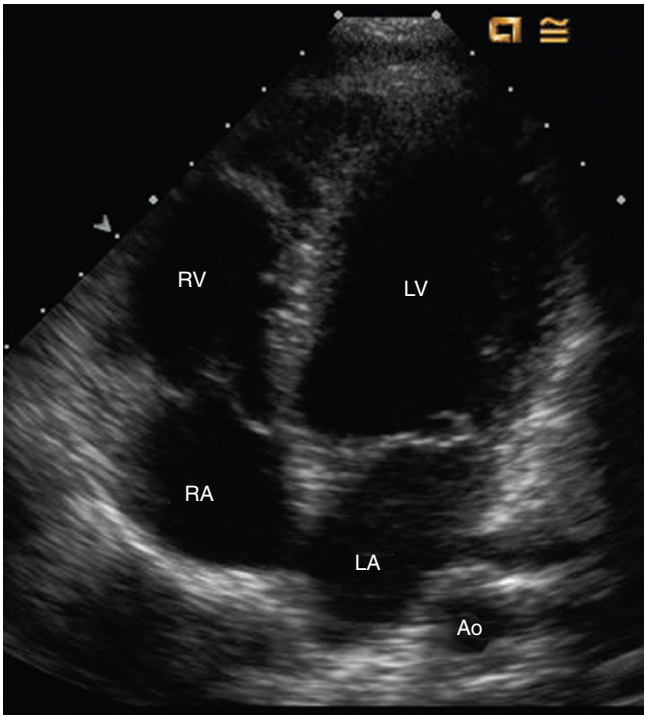



**Figure 43-6 Apical four-chamber view shows the normal relationships of the atria and ventricles.** The moderator band is well seen toward the apex of the trabeculated RV. The tricuspid valve is shown with one leaflet aimed toward the septum and is slightly apically displaced from the mitral valve. The LV is smooth walled. At least two pulmonary veins can be seen entering the left atrium. *Ao,* Aorta.

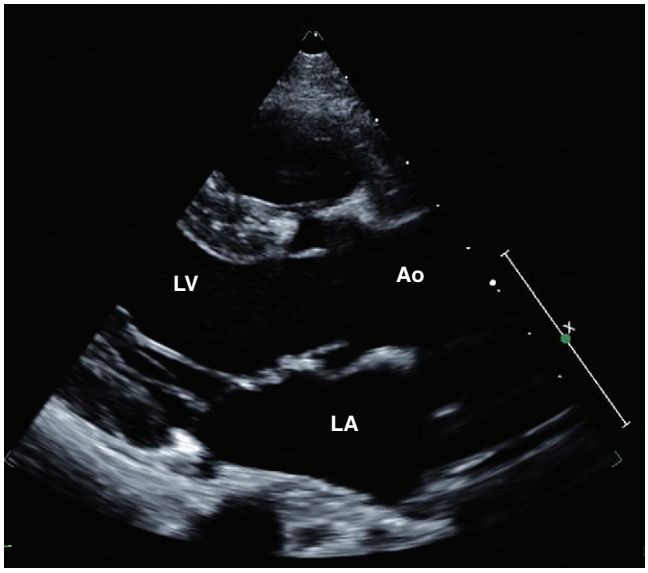



**Figure 43-7 Parasternal long-axis view shows the mitral valve apparatus attaching to papillary muscles away from the interventricular septum.** The mitral annulus is shown in continuity with the aortic valve. *Ao,* Aorta.

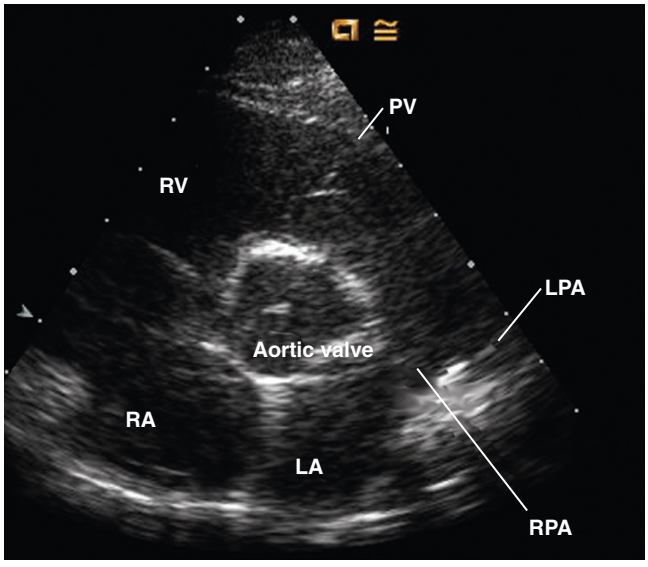



**Figure 43-8 Parasternal short-axis view shows the pulmonary valve anterior and slightly leftward of the aortic valve.** The main pulmonary artery is shown bifurcating into right and left branch pulmonary arteries (*RPA* and *LPA*). *PV,* Pulmonary valve.

## ATRIOVENTRICULAR VALVES AND VENTRICLES

When two atrioventricular valves and two ventricular chambers are found, the valves travel with the morphologically appropriate ventricle. Thus, identification of a tricuspid valve also identifies the right ventricle (RV); identification of a RV signals an associated tricuspid valve. The mitral valve likewise associates with the LV (Fig. 43-6). The tricuspid valve has three leaflets positioned as anterior, posterior, and septal. The leaflets are attached to a network of small papillary muscles on the RV free wall and the interventricular septum. Papillary muscles that arise from the septal surface are distinctive of the RV. As a result, papillary septal attachments are unique to the tricuspid valve and RV. If two distinct atrioventricular valves are present in the heart, then the tricuspid valve is usually the one more apically displaced.[29,30] The RV is also identified by its coarse trabeculations. A number of muscular bands within the chamber cross from the septal to the parietal surface. The most prominent of these is the moderator band, situated in the midcavitary portion of the ventricle (see Fig. 43-6). The relationship of inflow and outflow portions also differentiates the RV from the LV. The RV has a distinct outflow portion that consists of infundibular or conal muscular tissue. Consequently, the outflow semilunar valve and great artery are displaced from the inflow valve, unlike the morphologic LV. The mitral valve is the atrioventricular valve associated with the morphologic LV. The valve has two leaflets, one each in the anterior and posterior positions. Typically, little or no conal tissue separates the LV inflow and outflow, which allows for fibrous continuity of the mitral and LV outflow valve. The mitral valve apparatus is attached to two dominant papillary muscles: the superiorly positioned anterolateral papillary muscles and the more inferior posteromedial papillary muscles. Unlike the situation with the tricuspid valve, neither of the papillary muscles arises from the interventricular septum. The LV chamber itself is smooth walled and bullet shaped in comparison with the trabeculated and somewhat triangular RV. There is no separation of inflow and outflow, so there usually should be continuity between the mitral valve and the LV outflow valve (Fig. 43-7).[29,30]

## SEMILUNAR VALVES AND GREAT ARTERIES

The pulmonary valve is a trileaflet semilunar valve associated with a pulmonary artery (PA). The PA is identified as the great artery that arises from the heart and bifurcates early into right and left branches (Fig. 43-8). In the normal heart, the PA is

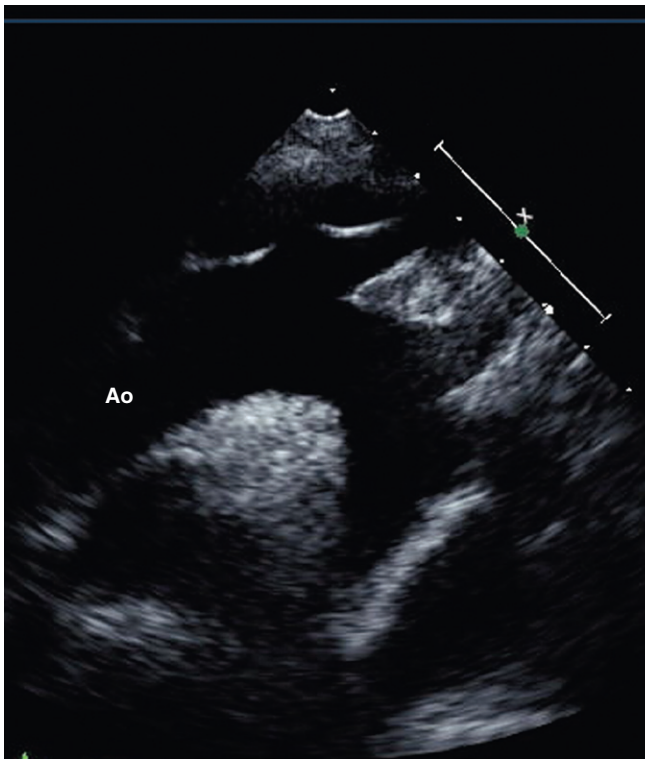



**Figure 43-9 Aortic arch visualized from the suprasternal notch view.** The head and neck vessels are shown arising from the transverse arch. *Ao*, Aorta.

found anterior to the aorta as it arises from the heart. But in CHD, this is not always the case. Thus, the best identification is usually a morphologic description of bifurcation of a vessel. Be aware, however, that there are exceptions. For example, conditions of isolated branch PA atresia are rare but do exist. The aortic valve is a semilunar three-leaflet valve associated with the aorta and aortic arch. The aorta gives rise to the origins of the right and left coronary arteries. The cusps or leaflets of the aortic valve are named right, left, and noncoronary: the right and left cusps are associated with the origins, respectively, of the right and left coronary arteries. About 1% to 2% of people in the United States are thought to have a bicuspid, or two-leaflet, aortic valve.[31] The aorta itself is identified as the great vessel that does not bifurcate early and from which the coronary arteries and head and neck arteries originate (Fig. 43-9). It is a rare case in which the coronary arteries do not arise from the aorta. Although the aortic arch normally arises leftward, it also can be rightward. When the aortic arch arises rightward, it can be associated with mirror-image branching of the head and neck vessels. The sidedness of the arch is most easily identified with evaluation of the direction of the first bifurcating head and neck vessel. If this first artery bifurcates rightward, then the aortic arch is usually leftward; and if the first artery goes leftward, then the aortic arch is most commonly a right arch. If there is no bifurcation of the first head and neck vessel, more involved abnormalities, such as aberrant subclavian arteries that arise from the more distal aorta and vascular rings, should be sought.[32-34] A number of variations on the positioning of the head and neck vessels can exist; they are best defined by tracing each vessel as far as possible in the suprasternal long-axis and short-axis views.

**TABLE 43-2 General Echocardiographic Approach**

| | |
|---|---|
| Abdominal situs | Solitus (liver on right, stomach on left)<br>Inversus (liver on left/transverse, stomach on the right) |
| Atrial anatomy and systemic venous connections | Solitus (right atrium on right side)<br>Inversus (right atrium on left side)<br>Ambiguous or indeterminate |
| Atrioventricular connection | Two atrioventricular valves<br>Common atrioventricular valve<br>Atrioventricular valve atresia<br>Straddling or overriding atrioventricular valve |
| Ventricular morphology and relationships | Dextro-loop (RV on right side)<br>Levo-loop (RV on left side)<br>Univentricular heart |
| Semilunar valves | Two semilunar valves<br>Common semilunar valve (truncus)<br>Semilunar valve atresia |
| Great artery relationships and connections | Concordant<br>Discordant<br>Double outlet (LV or RV)<br>Common outlet (truncus arteriosus)<br>Single outlet (great artery atresia) |

## Cardiac Anatomy

### GENERAL

#### *Segmental Approach*

The heart is anatomically described by the relationships of the atria, ventricles, and great arteries and the relationship of these to the systemic and pulmonary venous connections. Clinically, the segmental approach defines the heart by identifying these relationships within the patient (Table 43-2).

Generally, the easiest way to determine chamber and great vessel alignment is to follow the flow of blood through the heart. In the complete examination, three segments of the heart require description: the atria, the ventricles, and the great vessels. In the normal heart, the concordant arrangement has a right atrium aligned with a RV, the ventricle further aligned with a PA, and a left atrium aligned with LV, further aligned with the aorta. Any other alignment or arrangement between segments is considered discordant.[18,20,21,35]

In the segmental approach, the atria can take three possible configurations. Atrial situs solitus has a normal position, with a morphologic right atrium on the anatomic right side. Atrial situs inversus has reverse positioning, with a morphologic right atrium on the anatomic left side. Atrial situs ambiguous has atrial morphology too difficult to determine, which leaves the sidedness unclear. Often this involves what appears to be two right or two left atria. The atrial situs and abdominal visceral situs are usually similar.[20,21,35]

The ventricular segmental arrangement occurs in one of two positions determined embryologically by the bulboventricular looping of the heart. The first and normal orientation is the dextro-looped ventricles. In this case, the morphologic RV is located more anteriorly and on the anatomic right side. The second possibility is levo-looped, in which the morphologic RV is on the anatomic left side.[20,21,35]

The ventricles give rise to the outflow and great arteries. The description and segmentation of the great artery anatomy is the most confusing and somewhat controversial part of the segmental approach. The usual alignment of the great arteries has the aorta arising from the morphologic LV and the PA arising from the morphologic RV. In that arrangement, the aortic valve is aligned posterior and rightward of the pulmonary valve. In abnormal relations of the great vessels, the aorta arises from a

morphologic RV and the PA arises from a morphologic LV; both great vessels arise from a single ventricular chamber; or only a single outflow is present (truncus arteriosus or atresia of one of the great arteries).[20,21,35] Some definitions of abnormally related or transposed great vessels rely on the orientation of the vessels in relation to each other, noting that transposition occurs when the aorta is anterior to the PA. Other accepted definitions describe transposition as an abnormal alignment of the great vessel with the ventricle. In this definition, vessels are considered transposed if the aorta arises from the morphologic RV and the PA from the LV. Any other relationships of the great vessels to the ventricles, such as double-outlet ventricles, are considered malposed.[20,21,35] Because the morphology may depart in many ways from the normal arrangement, the clinician must describe the anatomy found in the patient, including the relationship of the great arteries to the ventricles and to each other.

### *Concordant and Discordant Arrangements*

Four atrioventricular and ventriculoarterial anatomic or segmental relationships are possible (Table 43-3). Concordance refers to the normal alignments, and discordance refers to abnormal alignments. First, there is normal cardiac alignment with atrioventricular and ventriculoarterial concordance. Second, there is atrioventricular concordance and ventriculoarterial discordance, or d-transposition of the great arteries (Fig. 43-10). Third, one can also have atrioventricular discordance with ventriculoarterial discordance, which is known as congenitally corrected transposition of the great arteries or L-transposition of the great arteries (Fig. 43-11). Fourth, there is atrioventricular discordance with ventriculoarterial concordance. This arrangement is rare; it can occur with different great artery arrangements and includes isolated ventricular inversion, isolated atrial noninversion, and anatomically corrected malposition of the great vessels. As one example, in isolated ventricular inversion, the morphologic right atrium is aligned with a morphologic LV, which is aligned with an aorta. Physiologically it is similar to D-transposition of the great arteries.[18,21,36]

### *Other Nonsegmental Abnormalities*

Apart from the segmental alignment of the heart, two areas of connections between these segments can also contribute to congenital abnormalities. The first is the atrioventricular connection, which consists of the atrioventricular valves and the inlet portion of the interventricular septum. The second is the ventriculoarterial connection, which consists of the semilunar valves and the outflow portion of the ventricular septum.

Abnormalities in the valves or the inlet and outflow regions of the heart require appropriate descriptions along with the segmental anatomy. For example, in common congenital heart anomalies such as a complete atrioventricular canal defect or tetralogy of Fallot, there is usually normal or concordant segmental alignments, but there are inlet or outflow abnormalities. General guidelines regarding such abnormal segmental alignment and segment connections are discussed subsequently.

## DETERMINATION OF ATRIAL SITUS AND VENOUS CONNECTIONS

In many patients with CHD, the segmental anatomy may be unclear or the diagnosis unknown. If so, the cardiac positioning in the thorax and apical direction are best analyzed beginning with the subcostal view. That view also helps determine the situs

**TABLE 43-3 Anatomic Alignments and Relationships**

| *Atrioventricular Connection* | *Ventriculoarterial Connection* | *Congenital Heart Defect* |
|---|---|---|
| Concordant | Concordant | Normal heart |
| Concordant | Discordant | d-TGA |
| Discordant | Discordant | Congenitally corrected TGA |
| Discordant | Concordant | Isolated ventricular inversion or anatomically corrected malposition |

*TGA*, Transposition of the great arteries.

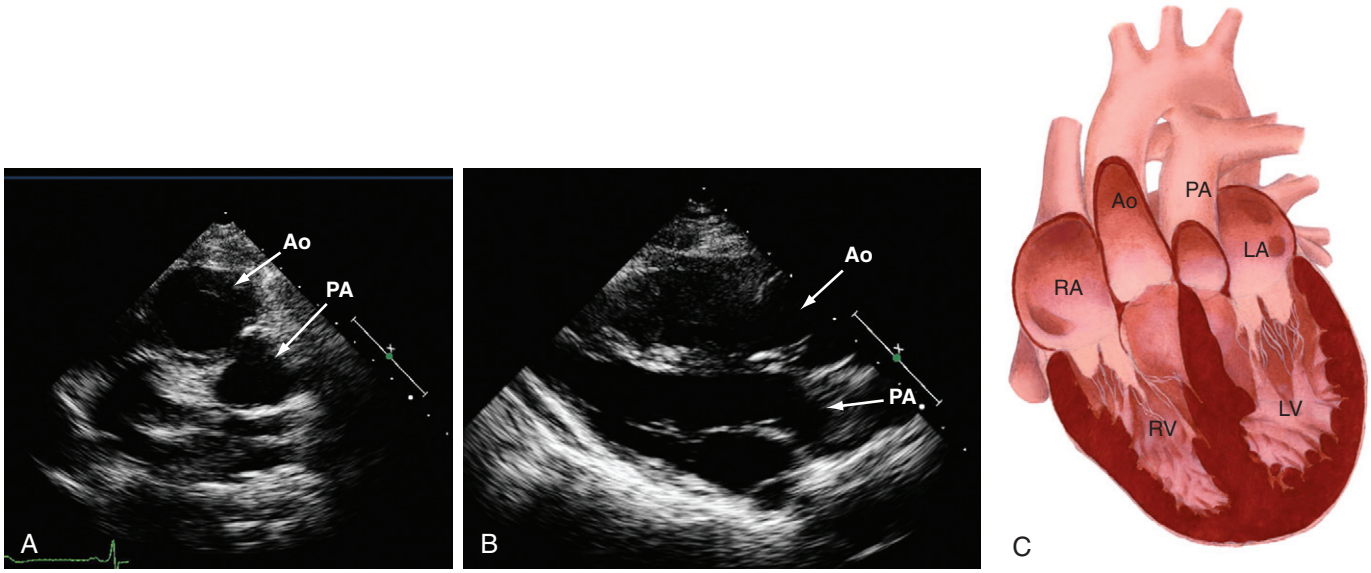



**Figure 43-10 The parasternal short-axis (A) and long-axis (B) views show the great arterial relationships in D-transposition of the great arteries. C,** The pulmonary artery (*PA*) is shown posterior to the aorta (*Ao*). The great vessels are shown as side-by-side in the parasternal long-axis view, which is a typical finding in D-transposition of the great arteries.

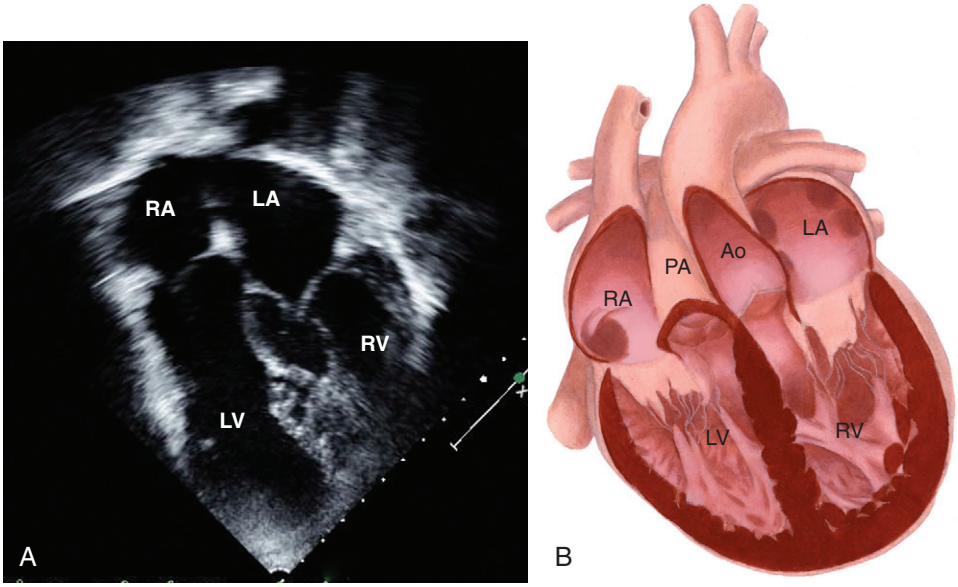



**Figure 43-11 The apical four-chamber view (A) shows the anatomy of L-transposition of the great arteries.** There is atrioventricular discordance. **B,** The morphologic LV is on the anatomic right side and is associated with a mitral valve. The morphologic RV is on the anatomic right side and is associated with a tricuspid valve with a mild Ebstein-like malformation.

of the liver, the position of the inferior vena cava and aorta in relation to the spine, and the relationship of the hepatic portion of the inferior vena cava drainage to the right atrium. In the subcostal short-axis view, the spine, liver, aorta, and inferior vena cava should be identified. In the usual arrangement, the aorta is on the patient's left, whereas the inferior vena cava is noted further anteriorly and rightward (see Figure 43-3). The liver is usually visualized on the patient's right, and often, the air of the stomach can be noted on the left. If the stomach and liver appear reversed, a diagnosis of complete situs inversus or heterotaxy syndrome should be considered. If the inferior vena cava is not present, an azygous or hemiazygous vein, positioned just to the right or left of the aorta, respectively, should be sought. Be aware that in certain cases the aorta may descend on the right side of the spine.[37] The connection of the inferior vena cava to the atrial chamber is often visible with sweeping anteriorly in the subcostal short-axis view. When the hepatic portion of the inferior vena cava is present, the chamber is almost always a morphologic right atrium (see Figure 43-5).[18,20,21] Visualization of the right atrial appendage in the subcostal short-axis view can also help confirm the anatomy, but the appendage may be difficult to see in adults with larger body habitus. The superior vena cava usually is visualized draining into a morphologic right atrium after the transducer is rotated into the subcostal sagittal view. This view may be difficult to obtain in some adults. The right-sided superior vena cava may also be seen in the suprasternal short-axis view aimed rightward of the aorta (Fig. 43-12). If the superior vena cava is not seen in these views or appears small or an innominate vein is absent, consider the diagnosis of a persistent embryologic left-sided superior vena cava. If the right superior vena cava is not visualized in any view entering the right atrium, and the patient has had heart surgery, the superior vena cava has possibly been attached directly to the right PA (Glenn shunt); this anatomy should be investigated. In some cases, particularly in patients with heterotaxy syndrome, both right and left superior vena cavas may be present.[25,28] A persistent left superior vena cava is




**Figure 43-12 The superior vena cava is well seen to the right of the aorta in the suprasternal short-axis view angled rightward.** The right pulmonary artery (*RPA*) is also visualized. *Ao,* Aorta; *SVC,* superior vena cava.

seen with failure of the embryologic left superior vena cava to regress. This has been reported to occur in 0.3% to 0.5% in the general population and in up to 4% to 5% of those with CHD.[24,38,39] A left superior vena cava often explains a coronary sinus that appears prominent in the apical view or is easily visualized in the parasternal long-axis view posteriorly in the

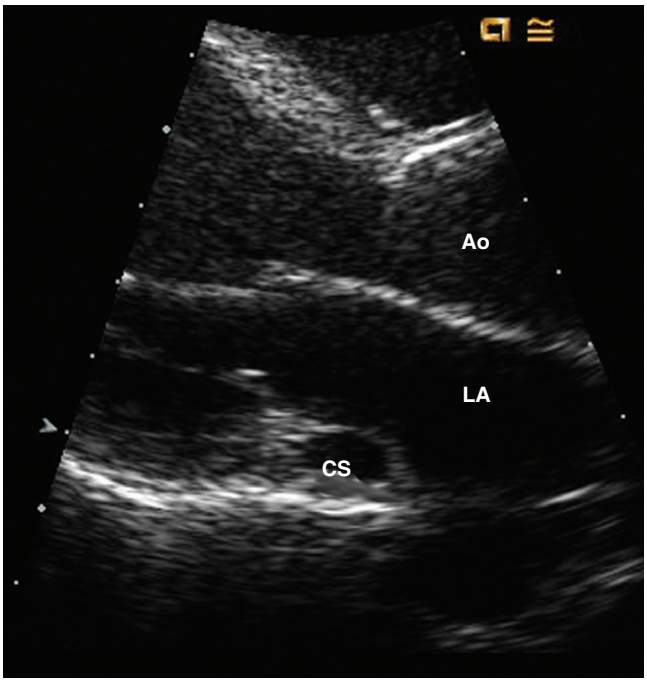



**Figure 43-13 Parasternal long-axis view shows a prominent coronary sinus (*CS*).** The most common association with this finding is a persistent left superior vena cava. *Ao,* Aorta.

left atrium (Fig. 43-13). (If no left superior vena cava is present, the dilated coronary sinus may also be explained by anomalous pulmonary venous drainage into the coronary sinus.) Although the left superior vena cava typically drains to the coronary sinus, it occasionally drains directly to the left atrium.

The subcostal sagittal view with aim leftward or the parasternal short-axis view often best shows the left superior vena cava draining into the coronary sinus near the level of the mitral annulus. In addition, the suprasternal short-axis view aimed to the left of the aorta, following inferiorly toward the coronary sinus, is also useful. Dual superior vena cavas are often best seen in the suprasternal short-axis view.[38,39] Drainage of all four individual pulmonary veins should be defined as well as possible to allow the clinician to evaluate a diagnosis of total or partial anomalous pulmonary venous return and to help determine the morphologic left atrium. Unrepaired total anomalous pulmonary venous return in an adult or older teen is very unusual because this almost always must be diagnosed and fixed in childhood. However, other abnormalities of the pulmonary veins might be diagnosed in adulthood, including partial anomalous venous return (one or two pulmonary veins returning to the systemic venous system or right atrium directly) and cor triatriatum.[40]

Identification of all four pulmonary veins on transthoracic imaging often is not possible in adults; typically, transesophageal imaging or another imaging modality is needed. In infants and children, the individual drainage of the pulmonary veins is best seen in the subcostal four-chamber view, the parasternal short-axis view, or a lower window in the suprasternal short-axis view. Color Doppler imaging is very helpful in identification of the orifice of the individual veins. If drainage of the individual pulmonary veins into the left atrium is not identified, and a right-to-left shunt is identified at the atrial level, a pulmonary venous confluence with a vertical vein connection to the systemic venous system should be sought. In this case of total anomalous pulmonary venous return, the confluence most often lies posterior to the left atrium and is visible in the parasternal long-axis, suprasternal, or subcostal view, depending on whether the drainage is intracardiac, supracardiac, or infracardiac, respectively. Pulmonary veins can also have mixed drainage, with individual veins seen draining to the left atrium, directly to the right atrium or the coronary sinus. In partial anomalous pulmonary venous return, usually two or three veins are seen entering the left atrium. The other veins, most commonly from the right side, usually enter the superior vena cava or the right atrium directly. This may occur in association with an atrial septal defect, particularly of the sinus venosus type. However, the partial anomalous pulmonary venous return is an isolated finding in 20% of cases.[40-42] Patients with partial anomalous pulmonary venous return often present as having right atrial and ventricular enlargement of uncertain etiology.

In rare cases, the pulmonary veins can drain to the left atrium but have incomplete integration with it. This condition is known as cor triatriatum and occurs when a membrane is present in the left atrium that separates and prevents some or all of the pulmonary veins from draining through the corresponding atrioventricular valve. Physiologically, this condition can be asymptomatic until adulthood if mild. However, the condition may mimic mitral stenosis and be symptomatic in childhood if severe.[43,44]

One further distinction regarding atrial anatomy should be mentioned. In rare conditions known as heterotaxy syndromes, the atrial and visceral situs are unusual and may be difficult to define. In some of these cases, the morphology of the two atria may look similar and the two chambers may resemble dual right or dual left atria. These findings are often associated with abnormal visceral anatomy. If dual atria are identified, other congenital heart defects should be sought. Abnormalities of the systemic and pulmonary veins and inflow and outflow anomalies, such as atrioventricular canal defect or double outlet RV, are commonly associated with heterotaxy syndromes.[25,28]

## DETERMINATION OF ATRIOVENTRICULAR VALVES AND VENTRICLES

Once the atrial arrangement has been identified, the alignment with the ventricle or ventricles is next to be defined. This is simplest with two ventricular chambers and two atrioventricular valves. As mentioned, the atrioventricular valve follows the chamber morphology. If there are two well-formed ventricular chambers, attempts are then made to morphologically distinguish a RV from a LV. In identification of ventricles, the evaluation for shape, trabeculations, and a moderator band is best done in the apical four-chamber view, with further use of the parasternal long-axis and short-axis views (see Fig. 43-6). If there are well-formed atrioventricular valves and interventricular septum, then the valve attachments to the interventricular septum may also help differentiate the morphology of the chambers. Only a morphologic RV has an atrioventricular valve with septal attachments. A single dominant ventricle or a univentricular heart poses further difficulties and is covered in more detail subsequently in the chapter. The atrioventricular valves require description and interrogation in their own right, not just in relation to the ventricles. The valves may be

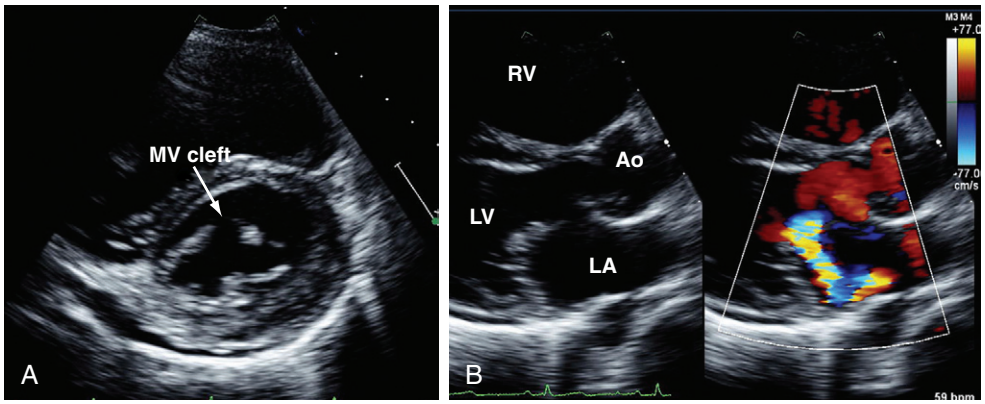



**Figure 43-14 Parasternal short-axis view at the level of the mitral valve shows a small cleft in the anterior leaflet.** Parasternal long-axis view shows mitral regurgitation through the cleft in the anterior leaflet. *MV,* Mitral valve.

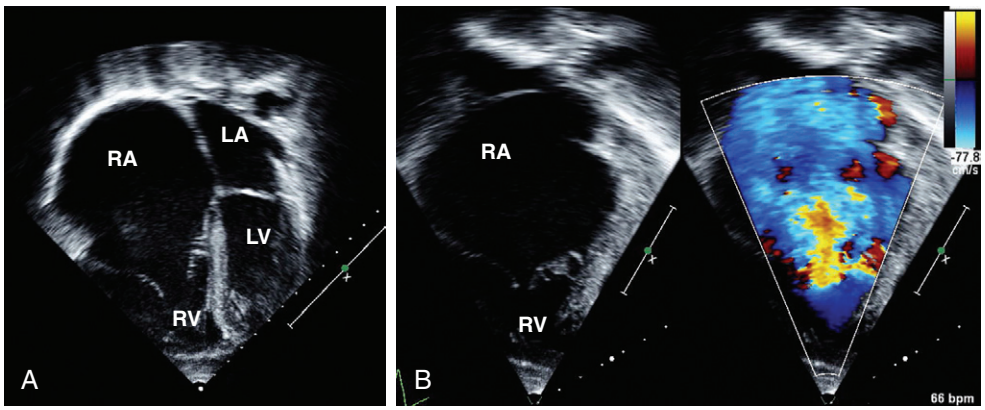



**Figure 43-15 Apical four-chamber view shows a patient with severe Ebstein anomaly of the tricuspid valve.** There is apical displacement of the tricuspid valve. The second image is focused on the right-sided chambers and shows severe tricuspid regurgitation.

morphologically abnormal or abnormally positioned even though the segments are concordant. The valve arrangements and attachments are well seen in the apical four-chamber, parasternal long-axis and short-axis, and subcostal sagittal views. Several arrangements or abnormalities of the atrioventricular valves can occur without corresponding abnormalities of segmentation or other chamber alignments. For example, there may be imperfect closure of the leaflets or abnormalities in the chordal apparatus of one of the two valves. On the mitral side, this can result in cleft, parachute, and arcade valves. A cleft is a separation in the valve leaflet that does not allow for full coaptation and results in mitral regurgitation. A parachute mitral valve involves a single dominant or asymmetric papillary muscle arrangement (Fig. 43-14). An arcade mitral valve is attached by short chords to multiple diminutive papillary muscle heads. The parachutes and arcades can be stenotic, regurgitant, or normally functioning.[45] On the tricuspid valve side, apical displacement and tethering of the septal and posterior leaflets results in Ebstein anomaly (Fig. 43-15).[46]

Another atrioventricular valve abnormality occurs when the patient has a common atrioventricular valve in place of two separate valves, as seen with atrioventricular septal defects. In that case, there is a primum atrial septal defect, an inlet ventricular septal defect, and a single atrioventricular valve with usually five leaflets that separate the atria from the respective ventricles. The most common leaflet arrangements of the single atrioventricular valve are: anterior and posterior bridging leaflets, right and left lateral leaflets, and a right accessory leaflet. Because of the common atrioventricular valve, the right and left sides are notably situated at the same level in the inlet; this differs from the usual position of mild apical displacement of the tricuspid valve relative to the mitral. The common valve may have attachments at the crest of the septum, or there may be no septal attachments at all.[47] In the adult, even if the atrioventricular septal defect has been repaired, the left and right atrioventricular valves remain at the same level.

The partial atrioventricular canal defect, which consists of a primum atrial septal defect and cleft mitral valve, can present unrepaired in adults.[48] The cleft can be best visualized with interrogation of the mitral valve in the parasternal short-axis view. Subaortic obstruction from the typical gooseneck deformity of the LV outflow tract or from accessory septal attachments should be considered in both repaired and unrepaired atrioventricular canal defects.

Other confusing atrioventricular alignments are presented by straddling, overriding, or atretic atrioventricular valves. With straddle or override, the affected atrioventricular valve is at least partially committed to the opposite ventricular chamber, either by the direction of the inflow (straddling) or by the alignment of the valve annulus (overriding).[49,50] When

only one atrioventricular valve is present, and it is not a common atrioventricular valve, the other valve is probably atretic or not fully formed. The most common form of this is atresia of the tricuspid valve with a resultant hypoplastic RV, usually known solely as tricuspid atresia. Congenital heart anomalies with atresia of one atrioventricular valve usually involve very complex anatomy and often a heart with a single dominant ventricular chamber.

With a very rare abnormality of criss-cross atrioventricular valves, the systemic and pulmonary venous flows cross to opposite ventricles in the unoperated heart or the right-sided atrium flows into the left-sided ventricle (and vice versa) without mixing oxygenated and deoxygenated blood. This is an embryologic rotational defect and can occur with atrioventricular and ventriculoarterial concordance or discordance. This defect should be suspected when two atrioventricular valves cannot be visualized in parallel in any of the routine views.[51-53]

### DETERMINATION OF SEMILUNAR VALVES AND GREAT ARTERIES

The relationship of the ventricles to the outflow valve and arteries is most easily described when there are two distinct ventricular chambers and two distinct arterial outflow vessels. In the normally positioned heart, the aortic valve and the origin of the aorta arise from the LV and are posterior and slightly rightward of the pulmonary valve and the PA origin arising from the RV outflow tract. The relationship of the great arteries to the ventricular chambers is well seen in the parasternal long-axis and short-axis views and in the apical four-chamber view (see Figs. 43-7 and 43-8).

From the parasternal long-axis view, the posterior vessel arising from the posterior ventricle should be followed to determine whether it gives rise to an aorta with head and neck vessels or a PA that turns further posteriorly and bifurcates early. These relationships can also be evaluated with sweeping anteriorly from the atrioventricular valves in the apical four-chamber view. The first vessel to come into view is the posterior great vessel; again, one can determine whether it is an aorta or PA on the basis of the early bifurcation or the presence of coronary and head and neck arteries. A great artery can be considered aligned with a ventricular chamber if half or more of that artery orifice is committed to the chamber. The alignment with the ventricular chamber can then be determined as concordant (e.g., aorta with LV) or discordant (e.g., PA with LV). The distinction between concordance and discordance becomes difficult when both great arteries arise from one chamber or there is only a single outflow. As with the atrioventricular valves, this anatomy still requires description. In some of the more recent classifications, these types of great artery relationships are termed malposed rather than transposed. In the double-outlet ventricle, both great arteries arise from a single ventricular chamber that is usually a morphologic RV. In a rare instance, the arteries arise from a morphologic LV. Many definitions and multiple anatomic variations comprise a diagnosis of double-outlet ventricles. In one definition, each great artery has some subarterial conal tissue; thus, neither is in fibrous continuity with the mitral valve. In the simpler definition of the double outlet RV, the anterior vessel arises completely from the RV and the posterior vessel may override the septum but is more than 50% committed from the RV.[53] Truncus arteriosus is another outflow tract abnormality. In this diagnosis, instead of two outflows from one ventricle, there is a single outflow that acts for both ventricles. The single outflow divides into both the aorta and either a main PA or individual branch PAs. As before, this is best diagnosed by following the outflow vessel in the apical four-chamber or parasternal long-axis and short-axis views to determine the branching patterns. In most cases, by the time a patient has reached adulthood, the truncus arteriosus has been repaired in childhood or the patient has severe cyanosis and development of Eisenmenger physiology. Once the individual great arteries have been identified, they must be traced distally as far as possible for examination for additional extracardiac congenital malformations. The imaging of the bifurcation of the normally positioned branch PAs is best performed in the parasternal short-axis view. The pulmonary valve can be seen giving rise to a main PA and the bifurcation of the right and left branches (see Fig. 43-8). The individual branches can also be visualized in the suprasternal notch views, with the right PA best seen in the suprasternal short-axis view (see Fig. 43-12), and the left PA can be seen by tilting slightly leftward of the standard suprasternal long-axis view. The PAs should be interrogated for absence or stenosis of a branch PA or other abnormalities such as a patent ductus arteriosus or aortopulmonary window. The aorta is visualized in multiple views to investigate as many of its segments as possible. The aortic valve and proximal ascending aorta are well seen in the usual parasternal long-axis view. The more distal aortic arch should be visualized from the suprasternal notch long-axis view. Often the entire transverse aortic arch and proximal portion of the descending thoracic aorta can be seen at this angle. It is an excellent view to interrogate for coarctation of the aorta or patent ductus arteriosus. When possible, the descending aorta should also be imaged from the subcostal views in both the short axis and long axis. Examination of abdominal aortic pulsatility can be helpful in determining a more distal coarctation or the severity of a more proximal coarctation.[54] Other extracardiac congenital abnormalities can be seen when imaging the aorta and branch PAs, including a patent ductus arteriosus and an aortopulmonary window. A patent ductus arteriosus is seen as a vascular connection that arises from the aorta, near the typical origin of a left subclavian artery, and enters the left PA. If the ductus is small, it may be difficult to see in 2D imaging but will be visible as continuous left to right shunting from the aorta to the PA with Doppler imaging. If the ductus is large and not discovered until adulthood, it is likely the patient will have elevated pulmonary vascular resistance or Eisenmenger physiology and there may be little residual shunting. An aortopulmonary window is usually seen as a connection between the main PA and the ascending aorta. It is best visualized in the parasternal short-axis view but may be difficult to discern in 2D images; often color and spectral Doppler images are required. As with a large ductus arteriosus, an aortopulmonary window may be hard to diagnose, even with Doppler imaging in adulthood, because the patients with unrepaired conditions have elevated PA pressures and have developed Eisenmenger physiology.

## Univentricular Heart

### GENERAL

As with congenital malformations previously discussed, the univentricular heart engenders its own debate over nomenclature.[18-21,29] Different terms are used to describe these hearts,

including primitive ventricles, univentricular hearts, and univentricular atrioventricular connections. Morphologically, the potential rudimentary chambers include those associated with an outflow vessel (outflow chamber) and those associated with neither an inflow nor outflow vessel (trabecular chamber). Some pathologists prefer to call these types of rudimentary chambers "ventricles" and describe the anatomy from an embryologic perspective. Others define a "ventricle" as a chamber that receives 50% of an inflow valve.[18] Still others describe the anatomy and morphology as found in the heart, such as double-inlet LV or unbalanced atrioventricular canal with hypoplastic LV. For purposes of this section, the univentricular heart refers to a heart in which the atrioventricular connection is predominantly related to a single ventricular chamber that is either morphologically right or left in origin. Occasionally, the morphology of the chamber cannot be determined; these instances should be referred to as univentricular heart of indeterminate type.[55,56] In the adult, the patient with a univentricular heart may present to the echocardiography laboratory either as unrepaired or with a palliative or reparative surgery. Unless one is familiar with all the different nomenclatures, the best practice often is simply to describe the chambers present and the relationship to the valves and great vessels. Determination of the morphology of the dominant ventricular chamber should focus on the anatomic landmarks, the atrioventricular connections, and the ventriculoarterial connections. Although two atrioventricular valves may enter a common chamber, such as in double-inlet LV, there can also be atresia of one of the valves or a common atrioventricular valve.[55-59] In the univentricular heart, the atrioventricular valves are often malformed in some way and may not carry the normal morphologic conditions of a mitral and tricuspid valve. These are more appropriately identified as right and left atrioventricular valves. Moreover, the ventriculoarterial connections can take any arrangement, including normally related, transposed, double outlet, and atresia of one of the vessels.[55-59]

## LEFT VENTRICULAR TYPE

The morphologic LV-type univentricular heart is the more common form of single ventricular chamber found in adults (Fig. 43-16). The rudimentary chamber is usually located at the base, anterior and superior to the ventricle, and often gives rise to the aortic outflow. The orientation of the chambers is most often levo-looped, with the LV somewhat rightward and the rudimentary chamber to the left; dextro-looping, however, also exists.[55-59] The connection between the ventricle and the rudimentary chamber is best seen in the subcostal, parasternal long-axis and short-axis views. In the long-axis view, the opening to the anterior rudimentary chamber is seen leading to an outflow vessel. In the coronal view, both the right and the left atrioventricular valves can be seen opening into the posterior ventricle and the rudimentary chamber is visualized anteriorly.

The atrioventricular valves can also be seen in the apical four-chamber view entering into a common chamber with no intervening inlet septum.[55,56,60] Although there are usually two separate atrioventricular valves, stenosis or atresia of one of the valves can occur, as can entry of a common valve (Fig. 43-17). In most of these patients, the great arteries are transposed, the aorta arises from the rudimentary chamber, and the PA arises from the morphologic LV.[55,56,60]

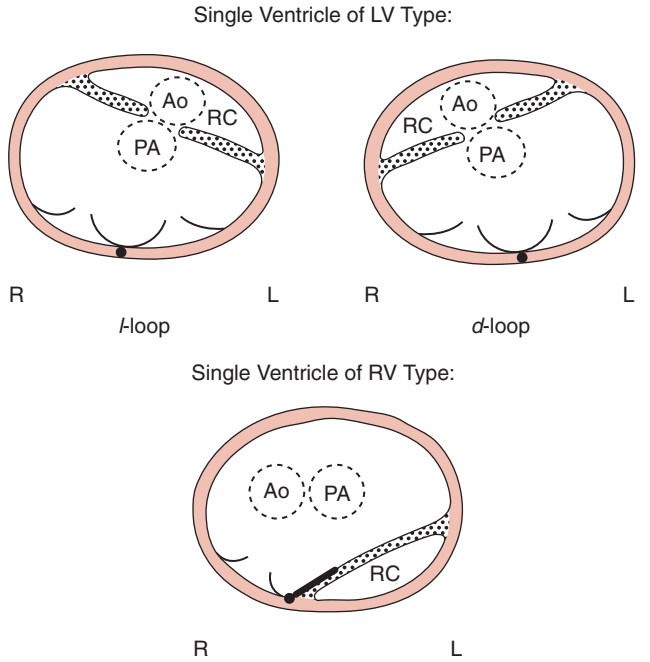



**Figure 43-16 Diagrammatic representation of the anatomic features used to diagnose the type of univentricular heart on 2D echocardiography.** The drawings represent parasternal short-axis projections. In single ventricle of the LV type, the trabecular septum (*stippled*) and rudimentary chamber (*RC*) are anterior to the atrioventricular valves. The trabecular septum runs to the acute or obtuse margin of the heart and not to the crux of the heart (*black circle*). Thus, there is no intervening septum at the crux of the heart between the atrioventricular valves. Most often, the rudimentary chamber is at the left basal aspect of the heart (levo-loop); however, it can also be located less frequently at the right basal aspect of the heart (dextro-loop). Most commonly, the ventriculoarterial connections are discordant with the aorta (*Ao*) arising from the rudimentary chamber and the pulmonary artery (*PA*) arising from the main ventricle (*depicted in the diagram*); however, any ventriculoarterial connection is possible. In single ventricle of the RV type, the rudimentary chamber and trabecular septum are posterior to the atrioventricular valves. The trabecular septum courses to the crux of the heart, and there is usually left atrioventricular valve atresia (*shown*). Most commonly, the ventriculoarterial connections are double outlet from the main ventricle (*shown*); however, any ventriculoarterial connection is possible.

## RIGHT VENTRICULAR TYPE

In adulthood, the less commonly seen condition is the single ventricular chamber of the RV type (see Fig. 43-16). In this case, the rudimentary chamber is located posterior and inferior to the morphologic RV.[55-61] This chamber may be located to the right (levo-loop) or to the left (dextro-loop) of the dominant RV. Some patients with a univentricular heart of the RV type and a common inlet may exhibit other features consistent with heterotaxy syndromes.[25]

The atrioventricular valves may be double inlet, single inlet with atresia of one valve, or a common inlet. The atrioventricular valve communications and the rudimentary chamber are best seen in the apical and subcostal four-chamber views because the valves lie more anteriorly and the rudimentary chamber lies more posteriorly. The rudimentary chamber usually does not give rise to any of the outflow vessels. Most often, the patient has a form of double-outlet RV, with both great arteries arising from the RV, or a single aorta with pulmonary atresia.

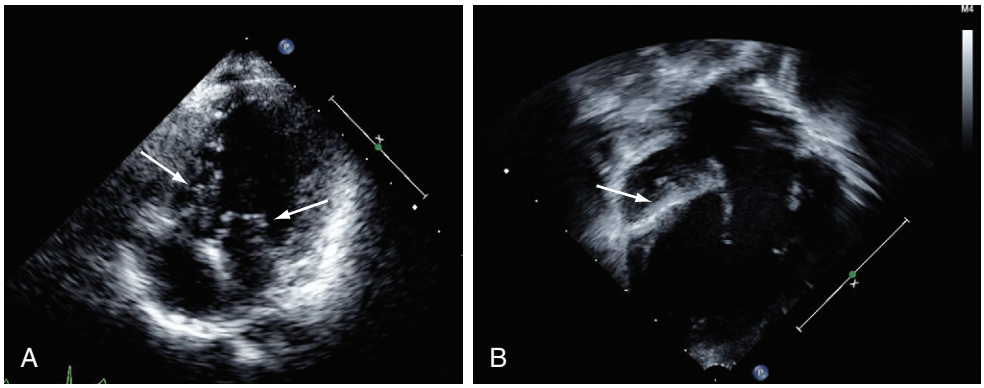



**Figure 43-17 Apical four-chamber views from patients with univentricular hearts of the LV type. A,** The transducer has been tilted posteriorly to image the inlets of the heart. This view is a posterior plane passing through both atrioventricular valve inlets and the crux of the heart; therefore, this plane lies posterior to the trabecular septum and rudimentary chamber. Note the "kissing" atrioventricular valve (*arrows*) with no intervening ventricular septum oriented to the crux of the heart. Both atrioventricular valves empty into the large posterior LV. **B,** Apical four-chamber view showing a univentricular heart with tricuspid atresia. There is a single ventricular chamber and a single left-sided atrioventricular valve. There is a membranous plate (*arrow*) where the right-sided atrioventricular valve would normally be located.

### OTHER UNIVENTRICULAR PHYSIOLOGY HEARTS

Special mention should be made of some subtle differences in describing a few of the univentricular lesions. For example, there are differences in describing a double inlet LV with right atrioventricular valve atresia, as opposed to diagnosing tricuspid atresia, or similarly, the differences between a univentricular heart of the RV type with absent left atrioventricular valve, as opposed to a hypoplastic left heart with mitral atresia. There are anatomic and embryologic differences in the development of these conditions. Visually, however, the differences may be difficult to determine. One echocardiographic distinction can be found in the positioning of the atria and the interventricular septum. In the cases of tricuspid atresia and hypoplastic left heart syndrome, the atria lies over the associated ventricular chamber and the ventricular septum is visualized up to the crux of the heart in the inlet septum. In the other cases of the univentricular heart, the inlet portion of the septum is often missing and the atria is seen over the dominant chamber, not the rudimentary chambers. However, in the adult who has often had multiple surgeries, these distinctions may be quite difficult.

## Color and Spectral Doppler Imaging

### GENERAL

Anatomy is obviously crucial, but it is only one part of the CHD evaluation. Color and spectral Doppler imaging are both critical tools in any comprehensive investigation of congenital heart lesions. In particular, Doppler imaging plays an important role in identification of intracardiac shunt lesions, such as ventricular septal defects; valve abnormalities, such as pulmonary stenosis; and residual embryologic vascular connections, such as a left superior vena cava to the coronary sinus. Similarly, the Doppler techniques help identify the direction of flow. These techniques also quantify flow in intracardiac shunting and valvular abnormalities.

### INTRACARDIAC SHUNTING

Once the anatomy and relationships of the chambers and great artery and venous connections have been determined, abnormalities between those chambers must be investigated.

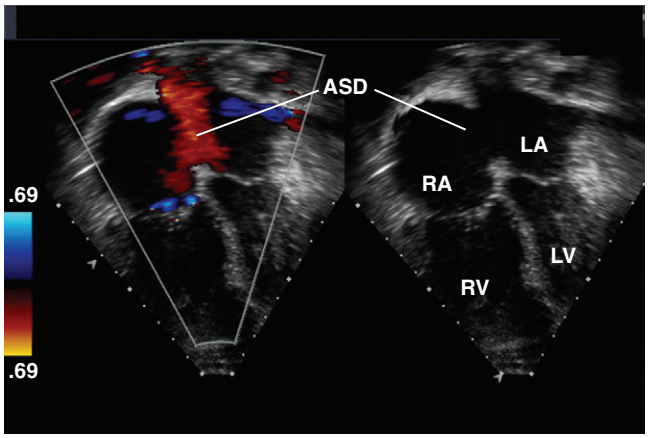



**Figure 43-18 Apical four-chamber view shows large secundum atrial septal defect (*ASD*).** There is also significant RA and RV enlargement.

- The interatrial and interventricular septa are closely examined for intracardiac shunting; and
- The atrioventricular and semilunar valves are interrogated for stenosis and regurgitation, regardless of the positioning within the heart.

Moreover, with univentricular hearts or single ventricles, determination of any connection between the ventricular chamber and rudimentary outflow chamber is crucial. It is important to determine whether there is obstruction in this region. Finally, the aorta and PAs are interrogated for stenosis at any point along the anatomic course. Atrial shunts are sought in the interatrial septum in multiple views. These views include the apical four-chamber, parasternal short-axis, and subcostal sagittal planes (Fig. 43-18). The subcostal view is often helpful because it shows the secundum septum and the venosus septa of the inferior vena cava and superior vena cava. However, in many adults, the subcostal images may not be clear. If an interatrial shunt is identified, the direction and velocity of flow between the interatrial chambers are reported. The degree of shunting can be estimated by the degree of RV enlargement. Alternatively, it can be determined quantitatively by calculating a pulmonary to systemic flow ratio, using the flow across the pulmonary valve and flow across the aortic valve in an otherwise structurally normal heart.[62]

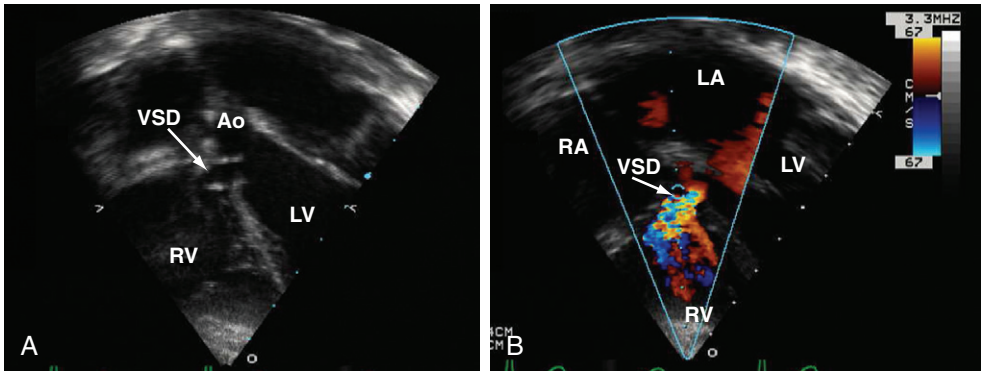



**Figure 43-19 Apical four-chamber views with and without color Doppler imaging show a perimembranous ventricular septal defect (*VSD*) with left-to-right shunting.** *Ao,* Aorta.

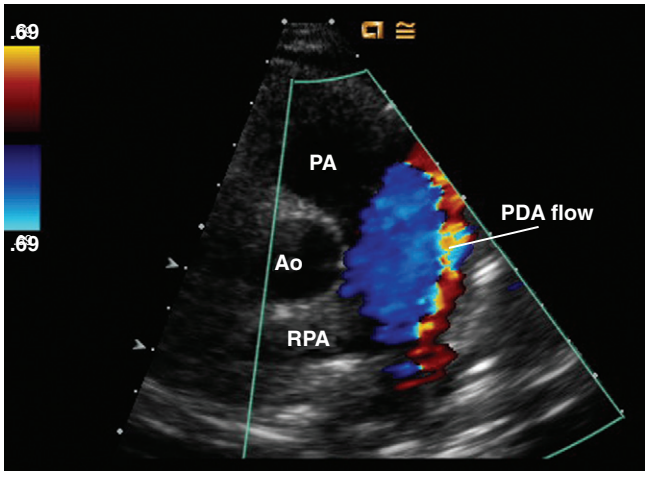



**Figure 43-20 Parasternal short-axis view with color Doppler imaging shows the left-to-right shunt (*red flow*) of the patent ductus arteriosus (*PDA*) into the main pulmonary artery (*PA*).** *Ao,* Aorta; *RPA,* right branch pulmonary artery.

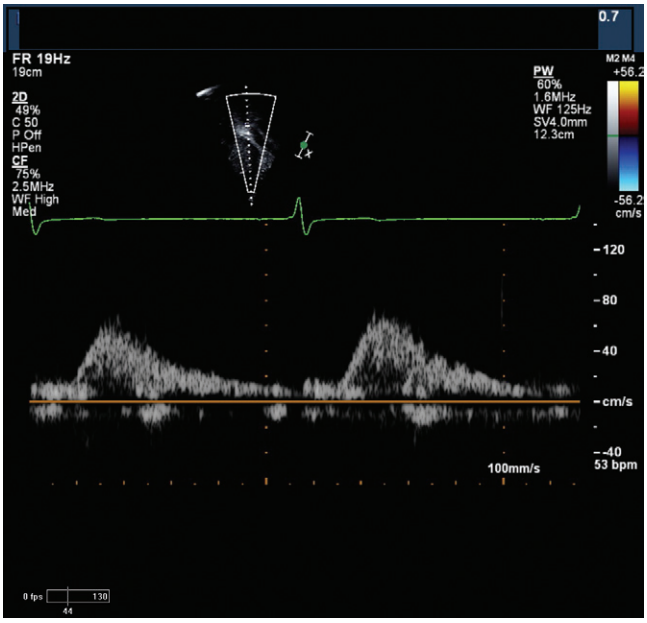



**Figure 43-21 Spectral Doppler profile of the descending aortic flow shows low peak velocity with an antegrade run-off into diastole.**

The interrogation for interatrial defects requires careful attention. With other signs of an intracardiac shunting, such as unexplained RV enlargement, the interrogation needs to include the venosus and primum portions of the septum. If the images are limited by body habitus, a saline solution bubble contrast study may be necessary.

Like the interatrial septum, the interventricular septum is interrogated in multiple views. These include the apical four-chamber, parasternal long-axis, and short-axis views (Fig. 43-19). For each view, imaging from the apex to the base of the septum is important. In the apical four-chamber and parasternal long-axis views, the transducer is aimed anteriorly and posteriorly to interrogate the outflow and inflow portions of the septum, respectively. The sector width should be narrow, and the color gain decreased, to identify smaller shunts. As with atrial level shunting, the direction and velocity of flow should be estimated with both color and spectral Doppler imaging. Note that with some serpiginous, or small, muscular defects, velocity interrogation may be inaccurate.

## GREAT ARTERIES

As with the normal heart, complete evaluation for valvular stenosis and regurgitation with color and spectral Doppler imaging is important. In CHD, several anomalies discussed in relation to the aortic arch and PA are better defined with Doppler interrogation. The aortic arch is best visualized in the suprasternal views. Color and spectral Doppler interrogation are investigated for flow acceleration, particularly in the area of the isthmus just at, or distal to, the left subclavian artery origin. Turbulence in this area may suggest a coarctation or a patent ductus arteriosus. The small ductus is identified as having continuous left to right shunting from the aorta into the PA (Fig. 43-20), whereas the larger ductus may have low velocity or bidirectional shunting if the patient has development of Eisenmenger physiology. In the case of a coarctation, there is increased velocity of flow across the narrowed area with persistent antegrade diastolic run-off. The downstream and abdominal aortic flow is also interrogated in the subcostal view to evaluate for blunting of pulsatile flow or persistent diastolic run-off (Fig. 43-21).

The branch PAs are best interrogated with Doppler imaging in the parasternal short-axis and suprasternal views for stenosis or other flow abnormality. If a patent ductus arteriosus is suspected, the diastolic flow into the PA from the aorta is often seen with color in these views. The PA branches can also be interrogated in the subcostal sagittal view if the patient has good subcostal images.

## KEY POINTS

- The segmental approach begins with the identification of the atrial and abdominal situs and continues with the identification of ventricular and arterial relationships.
  - The atria are defined by the appendages and by the systemic and pulmonary venous connections.
  - The right atrium has a broad appendage and is associated with the suprahepatic inferior vena cava.
  - The left atrium has a narrow appendage and is associated with the pulmonary venous return.
- The RV is recognized by the presence of a moderator band and association with a tricuspid valve, and the LV is bullet shaped and is associated with a mitral valve.
  - The tricuspid valve has three leaflets and attachments to the interventricular septum.
  - The mitral valve has two leaflets attached to papillary muscles opposite the interventricular septum.
  - In the normal heart, the tricuspid valve is more apically displaced.
- The great arteries are denoted by the bifurcation patterns as they exit the heart. Either vessel can be anterior or posterior, and either can be right or left.
  - The aorta bifurcates more distally and gives rise to the coronary arteries and head and neck vessels.
  - The PA bifurcates early into the right and left PA branches.
- Normal segmental alignment is when the right atrium is associated with the RV and the PA and the left atrium with the LV and the aorta.
- The most common abnormalities with discordant relationships are:
  - D-transposition of the great arteries with atrioventricular concordance and ventriculoarterial discordance; and
  - L-transposition of the great arteries or congenitally corrected transposition of the great arteries with atrioventricular discordance and ventriculoarterial discordance.
- Anatomic abnormalities of the atrioventricular and semilunar valves are common, even with normal segmentation.
  - Some of the more frequent findings include bicuspid aortic and pulmonary valves, Ebstein-like tricuspid valves, and cleft mitral valves.
  - Abnormalities can also include common, atretic, straddling, and overriding atrioventricular valves and common, overriding, and atretic semilunar valves.
- The univentricular heart refers to a heart in which the atrioventricular connection is predominantly related to a single ventricular chamber that is either morphologically right or left in origin.
  - In the LV type, the rudimentary chamber is usually anterior and superior and gives rise to the aorta.
  - In the RV type, the rudimentary chamber is usually inferior and posterior and is not associated with an outflow vessel.
- Full functional assessment with color and spectral Doppler imaging is required for:
  - All intracardiac valves for stenosis and regurgitation;
  - The atrial and interventricular septa for evidence of shunting; and
  - The aorta and pulmonary arteries for evidence of flow abnormalities and shunts.

## REFERENCES


1. Warnes CA, Liberthson R, et al: The 32nd Bethesda Conference Task Force 1: the changing profile of congenital heart disease in adult life. *J Am Coll Cardiol* 37:1171-1175, 2001.
2. Hoffman JI, Kaplan S, Liberthson RR: Prevalence of congenital heart disease. *Am Heart J* 147:425-439, 2004.
3. Niwa K, Perloff JK, Webb GD, et al: Survey of specialized tertiary care facilities for adults with congenital heart disease. *Int J Cardiol* 96:211-216, 2004.
4. Child JS, Collins-Nakai RL, Alpert JS, et al: Task force 3: workforce description and educational requirements for the care of adults with congenital heart disease. *J Am Coll Cardiol* 37:1183-1187, 2001.
5. Gurvitz MZ, Chang RK, Ramos FJ, et al: Variations in adult congenital heart disease training in adult and pediatric cardiology fellowship programs. *J Am Coll Cardiol* 46:893-898, 2005.
6. Reid GJ, Irvine MJ, McCrindle BW, et al: Prevalence and correlates of successful transfer from pediatric to adult health care among a cohort of young adults with complex congenital heart defects. *Pediatrics* 113:e197-e205, 2004.
7. Wacker A, Kaemmerer H, Hollweck R, et al: Outcome of operated and unoperated adults with congenital cardiac disease lost to follow-up for more than five years. *Am J Cardiol* 95:776-779, 2005.
8. Kaemmerer H, Stern H, Fratz S, et al: Imaging in adults with congenital cardiac disease (ACCD). *Thorac Cardiovasc Surg* 48:328-335, 2000.
9. Child JS: Echo-Doppler and color-flow imaging in congenital heart disease. *Cardiol Clin* 8:289-313, 1990.
10. Moodie DS: Diagnosis and management of congenital heart disease in the adult. *Cardiol Rev* 9:276-281, 2001.
11. Goo HW, Park IS, Ko JK, et al: Computed tomography for the diagnosis of congenital heart disease in pediatric and adult patients. *Int J Cardiovasc Imaging* 21:347-365, 2005.
12. Boxt LM: Magnetic resonance and computed tomographic evaluation of congenital heart disease. *J Magn Reson Imaging* 19:827-847, 2004.
13. Okuda S, Kikinis R, Geva T, et al: 3D-shaded surface rendering of gadolinium-enhanced MR angiography in congenital heart disease. *Pediatr Radiol* 30:540-545, 2000.
14. Hartnell GG, Cohen MC, Meier RA, Finn JP: Magnetic resonance angiography demonstration of congenital heart disease in adults. *Clin Radiol* 51:851-857, 1996.
15. Hirsch R, Kilner PJ, Connelly MS, et al: Diagnosis in adolescents and adults with congenital heart disease. Prospective assessment of individual and combined roles of magnetic resonance imaging and transesophageal echocardiography. *Circulation* 90:2937-2951, 1994.
16. Chessa M, De Rosa G, Pardeo M, et al: Illness understanding in adults with congenital heart disease. *Ital Heart J* 6:895-899, 2005.
17. Dore A, de Guise P, Mercier LA: Transition of care to adult congenital heart centres: what do patients know about their heart condition? *Can J Cardiol* 18:141-146, 2002.
18. Tynan MJ, Becker AE, Macartney FJ, et al: Nomenclature and classification of congenital heart disease. *Br Heart J* 41:544-553, 1979.
19. Jacobs ML, Mayer JE Jr: Congenital Heart Surgery Nomenclature and Database Project: single ventricle. *Ann Thorac Surg* 69(4 Suppl): S197-S204, 2000.
20. Van Praagh R: Terminology of congenital heart disease: glossary and commentary. *Circulation* 56:139-143, 1977.

21. Van Praagh R: Segmental approach to diagnosis. In Fyler D, editor: *Nadas' pediatric cardiology*, Philadelphia, 1992, Hanley and Belfus, pp 27-36.
22. Huhta JC, Hagler DJ, Seward JB, et al: Two-dimensional echocardiographic assessment of dextrocardia: a segmental approach. *Am J Cardiol* 50:1351-1360, 1982.
23. Snider AR, Serwer GA, Ritter SB: *Echocardiography in pediatric heart disease*, ed 2, St Louis, 1997, Mosby-Year Book, pp 560-562.
24. Perloff JK: *The clinical recognition of congenital heart disease*, ed 4, Philadelphia, 1994, Saunders.
25. Van Praagh S, Santini F, Sanders S: Cardiac malpositions with special emphasis on visceral heterotaxy. In Fyler D, editor: *Nadas' pediatric cardiology*, Philadelphia, 1992, Hanley and Belfus, pp 589-608.
26. Van Praagh R, Van Praagh S, Vlad P, et al: Anatomic types of congenital dextrocardia: diagnostic and embryologic implications. *Am J Cardiol* 13:510-531, 1964.
27. Garg N, Agarwal BL, Modi N, et al: Dextrocardia: an analysis of cardiac structures in 125 patients. *Int J Cardiol* 88:143-155, 2003.
28. Stanger P, Rudolph AM, Edwards JE: Cardiac malpositions: an overview based on study of sixty-five necropsy specimens. *Circulation* 56:159-172, 1977.
29. Van Praagh R, Van Praagh S: Morphologic anatomy. In Fyler D, editor: *Nadas' pediatric cardiology*, Philadelphia, 1992, Hanley and Belfus, pp 27-36.
30. Shinebourne EA, Macartney FJ, Anderson RH: Sequential chamber localization: logical approach to diagnosis in congenital heart disease. *Br Heart J* 38:327-340, 1976.
31. Roberts WC: The congenitally bicuspid aortic valve: a study of 85 autopsy cases. *Am J Cardiol* 26:72, 1970.
32. Celano V, Pieroni DR, Gingell RL, Roland JM: Two-dimensional echocardiographic recognition of the right aortic arch. *Am J Cardiol* 51:1507-1512, 1983.
33. Shrivastava S, Berry JM, Einzig S, Bass JL: Parasternal cross-sectional echocardiographic determination of aortic arch situs: a new approach. *Am J Cardiol* 55:1236-1238, 1985.
34. Snider AR, Serwer GA, Ritter SB: *Echocardiography in pediatric heart disease*, ed 2, St Louis, 1997, Mosby-Year Book, pp 476-478.
35. Van Praagh R: The importance of segmental situs in the diagnosis of congenital heart disease. *Semin Roentgenol* 20:254-271, 1985.
36. Van Praagh R, Durnin R, Jockin H, et al: Anatomically corrected malposition of the great arteries {S, D, L}. *Circulation* 51:20-31, 1975.
37. Snider AR, Serwer GA, Ritter SB: *Echocardiography in pediatric heart disease*, ed 2, St Louis, 1997, Mosby-Year Book, pp 558-560.
38. Tak T, Crouch E, Drake GB: Persistent left superior vena cava: incidence, significance and clinical correlates. *Int J Cardiol* 82:91-93, 2002.
39. Buirski G, Jordan SC, Joffe HS, Wilde P: Superior vena caval abnormalities: their occurrence rate, associated cardiac abnormalities and angiographic classification in a paediatric population with congenital heart disease. *Clin Radiol* 37:131-138, 1986.
40. Gustafson RA, Warden HE, Murray GF, et al: Partial anomalous pulmonary venous connection to the right side of the heart. *J Thorac Cardiovasc Surg* 98:861-868, 1989.
41. Wong ML, McCrindle BW, Mota C, Smallhorn JF: Echocardiographic evaluation of partial anomalous pulmonary venous drainage. *J Am Coll Cardiol* 26:503-507, 1995.
42. Snider AR, Serwer GA, Ritter SB: *Echocardiography in pediatric heart disease*, ed 2, St Louis, 1997, Mosby-Year Book, pp 474-475.
43. Alphonso N, Norgaard MA, Newcomb A, et al: Cor triatriatum: presentation, diagnosis and long-term surgical results. *Ann Thorac Surg* 80:1666-1671, 2005.
44. Slight RD, Nzewi OC, Buell R, Mankad PS: Cor triatriatum sinister presenting in the adult as mitral stenosis: an analysis of factors which may be relevant in late presentation. *Heart Lung Circ* 14:8-12, 2005.
45. Grenadier E, Sahn DJ, Valdes-Cruz LM, et al: Two-dimensional echo Doppler study of congenital disorders of the mitral valve. *Am Heart J* 107:319-325, 1984.
46. Anderson KR, Zuberbuhler JR, Anderson RH, et al: Morphologic spectrum of Ebstein's anomaly of the heart: a review. *Mayo Clin Proc* 54:174-180, 1979.
47. Anderson RH, Ho SY, Falcao S, et al: The diagnostic features of atrioventricular septal defect with common atrioventricular junction. *Cardiol Young* 8:33-49, 1998.
48. Gatzoulis MA, Hechter S, Webb GD, Williams WG: Surgery for partial atrioventricular septal defect in the adult. *Ann Thorac Surg* 67:504-510, 1999.
49. Pessotto R, Padalino M, Rubino M, et al: Straddling tricuspid valve as a sign of ventriculoatrial malalignment: a morphometric study of 19 postmortem cases. *Am Heart J* 138:1184-1195, 1999.
50. Rice MJ, Seward JB, Edwards WD, et al: Straddling atrioventricular valve: two-dimensional echocardiographic diagnosis, classification and surgical implications. *Am J Cardiol* 55:505-513, 1985.
51. Anderson KR, Lie JT, Sieg K, et al: A criss-cross heart. Detailed anatomic description and discussion of morphogenesis. *Mayo Clin Proc* 52: 569-575, 1977.
52. Hery E, Jimenez M, Didier D, et al: Echocardiographic and angiographic findings in superior-inferior cardiac ventricles. *Am J Cardiol* 63: 1385-1389, 1989.
53. de la Cruz MV, Cayre R, Arista-Salado Martinez O, et al: The infundibular interrelationships and the ventriculoarterial connection in double outlet right ventricle. Clinical and surgical implications. *Int J Cardiol* 35:153-164, 1992.
54. Shaddy RE, Snider AR, Silverman NH, Lutin W: Pulsed Doppler findings in patients with coarctation of the aorta. *Circulation* 73:82-88, 1986.
55. Rigby ML, Anderson RH, Gibson D, et al: Two dimensional echocardiographic categorisation of the univentricular heart. Ventricular morphology, type, and mode of atrioventricular connection. *Br Heart J* 46:603-612, 1981.
56. Huhta JC, Seward JB, Tajik AJ, et al: Two-dimensional echocardiographic spectrum of univentricular atrioventricular connection. *J Am Coll Cardiol* 5:149-157, 1985.
57. Beardshaw JA, Gibson DG, Pearson MC, et al: Echocardiographic diagnosis of primitive ventricle with two atrioventricular valves. *Br Heart J* 39:266-275, 1977.
58. Soto B, Pacifico AD, Di Sciascio G: Univentricular heart: an angiographic study. *Am J Cardiol* 49:787-794, 1982.
59. Ho SY, Zuberbuhler JR, Anderson RH: Pathology of hearts with a univentricular atrioventricular connection. *Perspect Pediatr Pathol* 12:69-99, 1988.
60. Snider AR, Serwer GA, Ritter SB: *Echocardiography in pediatric heart disease*, ed 2, St Louis, 1997, Mosby-Year Book, pp 343-351.
61. Shinebourne EA, Lau KC, Calcaterra G, Anderson RH: Univentricular heart of right ventricular type: clinical, angiographic and electocardiographic features. *Am J Cardiol* 46:439-445, 1980.
62. Snider AR, Serwer GA, Ritter SB: Echocardiography in pediatric heart disease, ed 2, St Louis, 1997, Mosby-Year Book, p 191.

# 44 Echocardiographic Evaluation of the Adult with Unoperated Congenital Heart Disease

ANNE MARIE VALENTE, MD | MARY ETTA E. KING, MD

**Valvular Abnormalities**
Bicuspid Aortic Valve
Pulmonic Valve Stenosis
Mitral Valve Anomalies
Tricuspid Valve Anomalies
**Left Ventricular Outflow Tract and Aorta**
Subaortic Stenosis
Supravalvular Aortic Stenosis
Sinus of Valsalva Aneurysms
Coarctation of the Aorta
**Septal Defects and Shunt Lesions**
Patent Foramen Ovale
Atrial Septal Defects
Anomalous Pulmonary Venous Connections
Ventricular Septal Defects
Patent Ductus Arteriosus
Coronary Artery Fistulas
**Complex Congenital Heart Disease**
Tetralogy of Fallot
Congenitally Corrected Transposition of the Great Arteries (CCTGA or L-Loop TGA)
Tricuspid Valve Atresia
Functional Univentricular Heart

Adults with congenital heart disease are increasingly coming to medical attention.[1] Caring for adults with congenital heart disease was formally recognized as a subspecialty within cardiology at the 22nd Bethesda Conference of the American College of Cardiology in 1990.[2] In 2001, the 32nd Bethesda Conference addressed the allocation of care of these patients and developed a system for grading the complexity of congenital heart disease lesions in adults (Box 44-1).[3] In managing adults with unoperated congenital heart disease, three clinical subgroups emerge: patients with mild or slowly progressive defects who do not require surgical intervention; patients who have eluded previous diagnosis and are still amenable to surgical or transcatheter intervention; and patients with abnormalities that are deemed inoperable. It is the task of the cardiologist to evaluate each patient thoroughly to determine optimal management. The American Heart Association and the American College of Cardiology have developed guidelines for management of adults with congenital heart disease, which includes adults who have not undergone prior surgical repair of certain congenital heart defects.[4]

Echocardiography has been a major advancement for cardiologists in diagnosing and evaluating the anatomic and physiologic status of the adult with congenital heart disease. The technique is not without challenge or difficulty, however. Echocardiographic windows may be limited by body habitus, including chest wall deformities and scoliosis. Congenital or acquired pulmonary disease and cardiac malpositions lend additional impediment to surface echocardiographic imaging. Transesophageal echocardiography (TEE) is useful in circumventing some of these difficulties and plays a major adjunctive role in evaluating and managing adults with congenital heart disease.[5-7] Increasingly, alternate imaging modalities, such as cardiac magnetic resonance imaging (MRI) and computed tomography (CT), are playing important roles in the complete evaluation of adults with congenital heart disease.[8,9]

This chapter includes the clinical features, echocardiographic evaluation, and management of many of the congenital heart defects that are encountered in the adult patient who has never undergone cardiac surgery. Additional discussion of complex congenital lesions can be found in Chapter 43 and of those with prior surgical procedures in Chapter 45.

## Valvular Abnormalities

### BICUSPID AORTIC VALVE

The congenitally bicuspid aortic valve is the most frequent of all congenital heart defects, occurring in approximately 1% to 2% of the U.S. population, and has a male predominance.[10] This is a highly heritable lesion, though a specific genetic abnormality has only been clearly defined for a small subset of families with autosomal dominant inheritance.[11,12] A bicuspid aortic valve is also associated with an increased risk of other left-sided obstructive lesions among relatives.[13] Morphologically, the bicuspid valve may have two equal cusps with a single central commissure, or the cusps may be disparate in size, with an eccentric commissure and the larger cusp containing a raphe.

Functionally, a bicuspid aortic valve may be nonstenotic and nonregurgitant, particularly in adolescents or young adults, of whom as many as one third have no significant functional impairment (see also Chapter 39). Progression of stenosis is common, however, even in valves with mild dysfunction. By the age of 60 years, 53% of bicuspid valves are stenotic, and by the age of 70 years, 73% are significantly stenotic (see Chapter 23).

**Box 44-1**

## ADULT CONGENITAL HEART LESIONS BY COMPLEXITY

**Simple Complexity**
Isolated congenital aortic valve disease
Isolated congenital mitral valve disease (e.g., except parachute valve, cleft leaflet)
Isolated patent foramen ovale or small atrial septal defect
Isolated small ventricular septal defect (no associated lesions)
Mild pulmonic stenosis
Previously ligated or occluded ductus arteriosus
Repaired secundum or sinus venosus defect without residua
Repaired ventricular septal defect without residua

**Moderate Complexity**
Aorto-LV fistulas
Anomalous pulmonary venous drainage, partial or total
Atrioventricular canal defects (partial or complete)
Coarctation of the aorta
Ebstein anomaly
Infundibular RV outflow obstruction of significance
Ostium primum atrial septal defect
Patent ductus arteriosus (not closed)
Pulmonic valve regurgitation (moderate to severe)
Pulmonic valve stenosis (moderate to severe)
Sinus of Valsalva fistula/aneurysm
Sinus venosus defect
Subvalvular or supravalvular aortic stenosis (except hypertrophic cardiomyopathy)
Tetralogy of Fallot
Ventricular septal defect with:
- Absent valve or valves
- Aortic regurgitation
- Coarctation of the aorta
- Mitral disease
- RV outflow tract obstruction
- Straddling tricuspid/mitral valve
- Subaortic stenosis

**Severe Complexity**
Conduits, valved or nonvalved
Cyanotic congenital heart disease (all forms)
Double-outlet ventricle
Eisenmenger syndrome
Fontan procedure
Mitral atresia
Single ventricle (also called double inlet or outlet, common or primitive)
Pulmonary atresia (all forms)
Pulmonary vascular obstructive diseases
Transposition of the great arteries
Tricuspid atresia
Truncus arteriosus/hemitruncus
Other abnormalities of atrioventricular or ventriculoarterial connection not included above (i.e., crisscross heart, isomerism, heterotaxy syndromes, ventricular inversion)

Adapted from Warnes CA, Liberthson R, Danielson GK Jr, et al: Task force 1: the changing profile of congenital heart disease in adult life. *J Am Coll Cardiol* 37(5):1170-1175, 2001 (the 32nd Bethesda Conference).

Of individuals older than 40 years who require aortic valve replacements, about 30% have evidence of a congenitally abnormal valve.[14] The mechanism of progressive valvular dysfunction appears to be a "wear-and-tear" process leading to fibrosis and calcification.

**Box 44-2**

## ASSOCIATED DEFECTS WITH BICUSPID AORTIC VALVE

Ventricular septal defect
Subaortic stenosis
Aortic coarctation or arch hypoplasia
Aortic dilation
Aortic aneurysm
Turner syndrome
Endocarditis

### *Associated Conditions*

Common associations with a bicuspid aortic valve are listed in Box 44-2. Congenitally bicuspid aortic valves have a known association with abnormalities of the aorta (see Chapter 39). Aortic coarctation occurs in a small percentage of patients with bicuspid aortic valve. Aortic dissection is another abnormality recognized for its association with bicuspid aortic valve. Reported studies have shown that 5% to 9% of patients with dissecting aortic aneurysms also have a bicuspid aortic valve.[15,16] Poststenotic dilatation of the ascending aorta has long been recognized in congenital aortic stenosis and has traditionally been attributed to mechanical impingement of a jet lesion eccentrically directed by the domed leaflets. However, the ascending aorta may be dilated even in functionally normal bicuspid valves, raising the possibility that aortic dilation may be caused by a developmental defect affecting both the valve and the aortic root.[17] In fact, an increase in vascular smooth muscle cell apoptosis and increased metalloproteinase activity has been described in the aortic walls of patients with bicuspid aortic valve, suggesting a genetic abnormality of the aortic wall. Periodic echocardiographic assessment of the ascending aorta is indicated in all patients with bicuspid aortic valve regardless of the functional status of the valve itself.

Another group of malformations associated with a bicuspid aortic valve is Shone complex. This complex comprises several levels of inflow or outflow obstruction to the left heart: supramitral ring, congenital mitral stenosis, discrete subaortic membrane, bicuspid aortic valve, and aortic coarctation.[18] Whereas most patients with this complex have undergone treatment in childhood, milder forms may be seen in the adult population, prompting careful assessment of the mitral valve structure, subaortic region, and aortic arch in the adult with bicuspid aortic valve.

Infectious endocarditis is a significant problem for patients with congenital aortic stenosis (see Chapter 22). Unfortunately, it may be the first mode of presentation for a patient with a previously undiagnosed bicuspid aortic valve. Natural history studies of young adults with congenital aortic stenosis found a 35-fold higher incidence of endocarditis in that group than the general population.[19] Progression of valvular infection to the surrounding aortic root may occur if there is a delay in diagnosis and treatment or in the presence of a particularly invasive organism. In a recent investigation of 310 consecutive patients with native aortic valve endocarditis, the presence of a bicuspid aortic valve was associated with a higher risk of abscess formation and more often required early surgical intervention.[20]

### *Echocardiographic Evaluation*

The distinctive echocardiographic features of congenitally bicuspid aortic valve include systolic doming in the parasternal

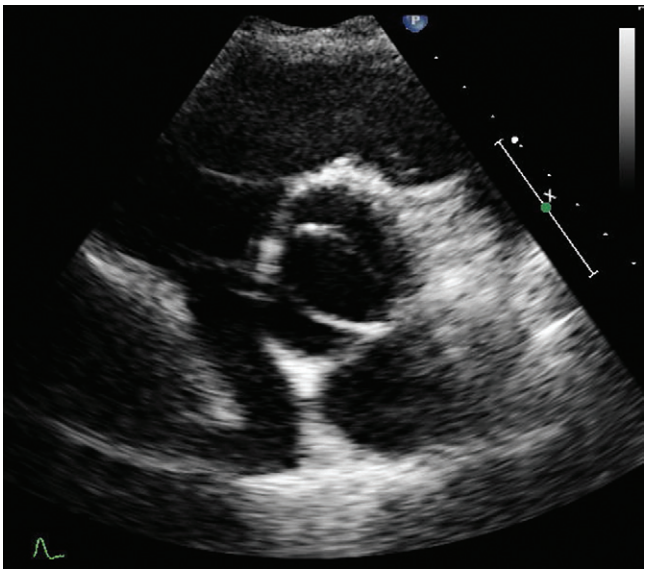


**Figure 44-1** Parasternal short-axis echocardiographic view of a bicuspid aortic valve.

long-axis views and demonstration of a single commissural line with two functional valve cusps in the parasternal short-axis views (Fig. 44-1). Particular care must be taken to assess the valve in systole and in diastole. In patients with asymmetric leaflets and a prominent raphe, the valve may appear tricuspid in diastole; however, the elliptical "football" shape of the systolic orifice indicates that the raphe is not a functional commissure. The valve leaflets often are thickened and fibrotic, more so with increasing age. When extensive calcification occurs, doming may no longer be noted, and the morphology of the cusps in the short-axis views may be difficult to distinguish from calcific stenosis of a tricuspid aortic valve.

Valvular stenosis should be evaluated with pulsed-wave (PW) and continuous-wave (CW) Doppler exactly as one would a stenotic trileaflet aortic valve. Because of the eccentric nature of the stenotic jet in congenital aortic stenosis, Doppler sampling from the right parasternal window may detect the highest systolic velocities and should always be attempted in addition to the usual apical and suprasternal notch sampling. In ongoing follow-up, serial aortic valve areas should be routinely calculated by the continuity equation in addition to peak and mean gradients. The development of left ventricular (LV) dysfunction may mask the progression of stenosis if valve gradients alone are used to assess the severity of stenosis.[21]

Valvular regurgitation is frequently present and may be the predominant functional abnormality in the adolescent and young adult. Careful echocardiographic inspection of the valve leaflets may give an indication as to whether the regurgitation is caused by fibrosis and retraction of the commissural margins of the leaflets, cusp prolapse, aneurysmal enlargement of the root and valve annulus, or valvular destruction secondary to endocarditis. Doppler color flow imaging readily detects the regurgitant flow and can be used for semiquantitation of the degree of aortic regurgitation. Serial assessment of the effect of regurgitation on ventricular size and function should be performed.

The subvalvular left ventricular outflow tract (LVOT) and mitral valve should be carefully investigated for congenital anomalies. Associated coarctation must be excluded, and the size and shape of the ascending aorta should be serially followed.

TEE may be useful if valve morphology is difficult to determine by transthoracic echocardiography (TTE) and if such information would guide a surgical attempt at valve repair. Additionally, more accurate aortic and pulmonary annular dimensions can be measured if a pulmonary autograft (Ross procedure) is planned or to guide the choice of a mechanical valve. Evaluation of endocarditis and aortic root abscess are also indications for a transesophageal study. Quantitative functional assessment of the valve usually is more accurate from the transthoracic approach, although transgastric views usually allow adequate Doppler alignment for valve gradients. Cardiac magnetic resonance angiography or CT can provide additional information regarding the entire aorta and should be considered when echocardiographic windows are nondiagnostic.

### *Management*

Confirmation of the presence of a bicuspid aortic valve and echocardiographic Doppler determination of the severity of stenosis and regurgitation assist in clinical management decisions. Patients with mild to moderate degrees of stenosis or regurgitation require more regular surveillance. The adolescent and young adult with bicuspid aortic valve should have echocardiographic Doppler study every year if the mean gradient is greater than 30 mm Hg, if the peak instantaneous gradient is greater than 50 mm Hg, if the aortic root or ascending aorta measures greater than 3.5 cm, or if root enlargement is progressing at 0.5 cm/year or more.[4,22] First-degree relatives of patients with a bicuspid aortic valve should be screened for its presence.[23] In a large cohort of 642 ambulatory adults with bicuspid aortic valve, 25% experienced a primary cardiac event during a mean follow-up of 9 years, yet the overall mortality rate was not significantly different from population estimates.[24] In a separate analysis of 212 asymptomatic bicuspid aortic valve patients in the community, there was a 42% incidence of cardiac medical or surgical events. Independent predictors of cardiac events included age greater than 50 years and valve degeneration at the time of diagnosis.[25]

Development of chest pain, syncope, heart failure, LV hypertrophy with strain, significant arrhythmia, or a mean Doppler gradient greater than 50 mm Hg are indications for further investigation and possible intervention. In the young adult with supple valve leaflets, balloon valvuloplasty often produces successful results in relieving aortic stenosis.[26,27] Aortic regurgitation, however, generally increases by at least one grade following this procedure in patients with mixed valve disease.[28] Indications for aortic balloon valvuloplasty include the lack of significant valve calcification and a peak-to-peak gradient of greater than 50 mm Hg in a symptomatic patient, or greater than 60 mm Hg in an asymptomatic patient. Intervention is reasonable in the asymptomatic adolescent or young adult with a peak-to-peak gradient of greater than 50 mm Hg when the patient is interested in participating in competitive athletics or wishes to become pregnant.[4]

With newer expertise in surgical aortic valve repair, current indications for surgical intervention in the adolescent and young adult with a bicuspid aortic valve may undergo closer scrutiny. Concerns about valve replacement and anticoagulation in young adults may be unnecessary if initial enthusiasm for aortic valve repair or the Ross procedure is maintained.[29-31] The Ross procedure involves translocation of the patient's native pulmonic valve into the aortic position and replacement of the pulmonic valve with an aortic homograft. The premature calcification and degeneration that have plagued the homograft

and heterologous bioprosthetic aortic valves are not a problem when the patient's own pulmonic valve is used in the aortic position. Some enlargement of the neoaortic sinuses has been observed in the early postoperative period, which does not appear to progress over time. The long-term outcome of an aortic homograft in the place of a translocated pulmonic valve is uncertain, but intermediate follow-up has shown reasonable durability, with a 9% failure rate and a 12% incidence of dysfunction in a large series of patients. The rate of freedom from dysfunction was 87% at 8 years. Use of a pulmonary homograft was associated with lower rates of failure and dysfunction.[32] A recent meta-analysis review of 39 reports of outcomes of the Ross procedure, including 12 adult series, revealed an autograft deterioration rate of 1.14% and right ventricular outflow tract (RVOT) deterioration rate of 0.65%/patient-year.[33]

## PULMONIC VALVE STENOSIS

Congenital valvular pulmonic stenosis is a common anomaly that has a slightly higher prevalence in women. The anomaly generally follows a benign course with increasing age. Because of the benign nature of this lesion, patients with pulmonic stenosis often escape detection during childhood and come to medical attention during their adult years. The second natural history study of congenital heart defects reported the outcomes of 464 adults with pulmonic stenosis and reported that those with mild pulmonic stenosis (peak gradient less than 25 mm Hg) have less than a 5% chance of requiring valvuloplasty during childhood and even less likelihood of requiring intervention in adulthood. Those with moderate degrees of stenosis (peak gradient of 25 to 50 mm Hg) have only a 20% likelihood of requiring an intervention.[34]

Adults with pulmonic stenosis most often have a supple but thickened valve with commissural fusion or a bicuspid valve. Calcification of the valve is uncommon, even in older patients. In a study of 325 patients with congenital pulmonic stenosis, doming was present in 31%, leaflet thickening in 24%, and calcification in 1% to 2%.[35] Poststenotic dilation of the main and branch pulmonary arteries (PA) is common. Pulmonic regurgitation is frequently present but is usually mild. Congenital pulmonic stenosis is often an isolated congenital heart lesion; however, it may be associated with other RVOT lesions, such as acquired infundibular stenosis, supravalvular or branch PA stenosis, or atrial septal defect (ASD). Abnormalities of the pulmonic valve and PA may be present in adults with certain genetic syndromes, such as Noonan syndrome, Williams syndrome, trisomies 13-15 and 18, and congenital rubella syndrome.[36] Specifically in Noonan syndrome, the frequency of pulmonic stenosis is approximately 25%, with 7% of these cases demonstrating a dysplastic pulmonic valve that may not be responsive to balloon angioplasty.[37]

### *Echocardiographic Evaluation*

Acquiring diagnostic two-dimensional (2D) images of the pulmonic valve in adults can be difficult due to the frequent interference of overlying lung tissue. The acoustic windows may be improved by positioning the patient in a high left lateral decubitus position and imaging during held expiration. Apical and subcostal views of the RVOT are also helpful in assessing the patient with pulmonic stenosis. Leaflet thickening may actually enhance echocardiographic visualization of the valve; the presence of poststenotic dilation of the main PA is a helpful clue in previously unsuspected valvular pathology. Classic valvular

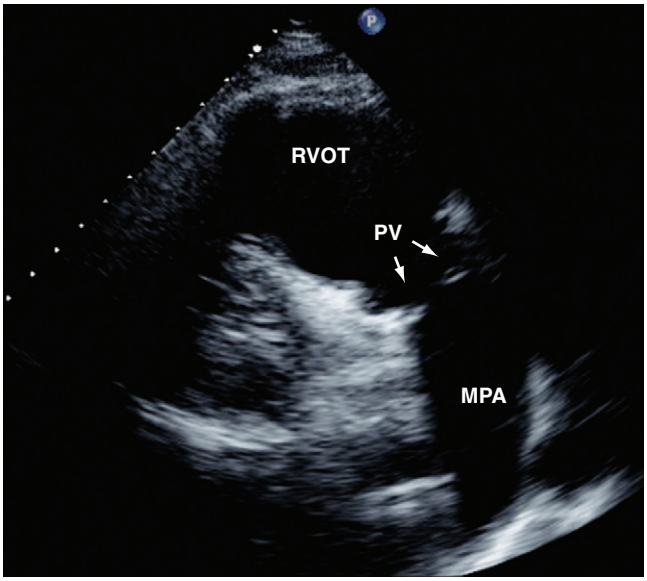



**Figure 44-2 Parasternal long-axis echocardiographic view of the *RVOT* in a patient with valvular pulmonic stenosis.** Valve leaflets are thickened and dome into pulmonary artery during systole (*arrows*). There is a poststenotic dilation of the main pulmonary artery. *MPA*, Main pulmonary artery; *PV*, pulmonic valve; *RVOT*, right ventricular outflow tract.

stenosis causes systolic doming of the leaflets (Fig. 44-2). PW Doppler demonstrates an increase in systolic velocity that begins at the valvular level, and CW Doppler allows estimation of the peak and mean transvalvular gradient. Color flow mapping distinctly delineates the turbulent jet of high-velocity flow into the main PA. Because of the horizontal substernal course of the RVOT, accurate peak Doppler flow velocities may be difficult to obtain from the parasternal approach. Sampling of the highest peak systolic velocity may be more accurate from the apical or subxiphoid approach. In older patients, long-standing valvular obstruction leads to significant RV hypertrophy including the infundibular portion of the ventricle. Dynamic infundibular obstruction thus adds to the valvular gradient over time. Doppler flow patterns sampled within the infundibulum typically demonstrate dagger-shaped, late-peaking systolic signal characteristics of dynamic obstruction.[35]

It is common to use the peak Doppler-derived gradient for assessment of severity of pulmonic stenosis. However, a recent investigation of 132 patients with congenital pulmonic stenosis indicated that Doppler peak gradients may overestimate the clinical severity of pulmonic stenosis, most likely because of pressure recovery effects, and the mean gradient more closely correlates with the measured peak-to-peak gradient by catheter methods.[38,39]

### *Management*

In general, the adult with mild pulmonic stenosis (peak systolic gradient less than 30 mm Hg) requires no specific intervention. Decisions regarding intervention in patients with higher gradients should be individualized based on symptomatology and echocardiographic findings. Box 44-3 summarizes the Class I recommendations for intervention in adults with pulmonic stenosis. Since the first successful report of balloon valvuloplasty for the treatment of pulmonic stenosis, it has now become the

**Box 44-3**

**CLASS I RECOMMENDATIONS FOR INTERVENTION IN ADULTS WITH CONGENITAL PULMONIC STENOSIS**

- Balloon valvuloplasty is recommended for asymptomatic patients with a domed pulmonic valve and a peak instantaneous Doppler gradient greater than 60 mm Hg or a mean Doppler gradient greater than 40 mm Hg (in association with less than moderate pulmonic regurgitation).
- Balloon valvuloplasty is recommended for symptomatic patients with a domed pulmonic valve and a peak instantaneous Doppler gradient greater than 50 mm Hg or a mean Doppler gradient greater than 30 mm Hg (in association with less than moderate pulmonic regurgitation).
- Surgical therapy is recommended for patients with severe pulmonic stenosis and an associated hypoplastic pulmonary annulus, severe pulmonic regurgitation, subvalvular pulmonic stenosis, or supravalvular pulmonic stenosis. Surgery is also preferred for most dysplastic pulmonic valves, and when there is associated severe tricuspid regurgitation or the need for a surgical Maze procedure.

Adapted from Warnes CA, Williams RG, Bashore TM et al. ACC/AHA 2008 guidelines for the management of adults with congenital heart disease. A report of the American College of Cardiology/American Heart Association Task Force on Practice Guidelines (writing committee to develop guidelines on the management of adults with congenital heart disease) developed in collaboration with the American Society of Echocardiography, Heart Rhythm Society, International Society for Adult Congenital Heart Disease, Society for Cardiovascular Angiography and Interventions, and Society of Thoracic Surgeons. *J Am Coll Cardiol* 52:e200, 2008.

treatment of choice for isolated pulmonic stenosis.[40,41] Echocardiographic evaluation is quite helpful, both for determining which patient is most likely to respond favorably and also to follow the results of the dilation. A small pulmonic valve annulus and markedly thickened, cartilaginous leaflets predict a poor response to balloon dilation. In addition, the patient who has acquired significant infundibular hypertrophy may demonstrate a high postprocedural gradient. Regression of hypertrophy does occur in a large percentage of patients after removal of the valvular component of obstruction and does not constitute a contraindication to balloon valvuloplasty.[42] In such cases with apparent residual obstruction, reassessment of Doppler gradients is recommended over the following 6 months before proceeding with a second procedure.

## MITRAL VALVE ANOMALIES

Adults with congenital anomalies of the mitral valve usually present with clinical findings of mitral regurgitation. Thus, when patients are referred for echocardiography of mitral regurgitation, one of several congenital problems in the mitral valve structure may be found. A cleft in the anterior leaflet occurs as either an isolated abnormality or a part of a complex involving defects in the atrioventricular (AV) septum. A double-orifice mitral valve results from abnormal fusion of the endocardial cushions during embryologic development. Patients with this anomaly may have two equal orifices or one large mitral orifice and a smaller vestigial one. Functionally, a double-orifice mitral valve may be either stenotic or regurgitant. A parachute mitral valve has abnormal attachments of the valve leaflets to the papillary muscles. Classically, one large centrally placed papillary muscle is present with all chordae from both leaflets converging on this muscle. Although this arrangement often creates significant inflow obstruction in childhood, the coexistence of redundant leaflet tissue and chordae with strategically placed commissures and clefts may produce a valve that functions with minimal obstruction.[43] A variety of other minor aberrant arrangements of the papillary muscles may be noted echocardiographically in adults that contribute to inadequate coaptation of the mitral valve leaflets during systole. For example, it is common to find an additional posterior papillary muscle with chordal attachments creating a bifid appearance of the posterior leaflet. Hypoplasia of the mural leaflet has been reported.[44] A papillary muscle on the high lateral or anterolateral wall (papillary muscle of Moulaert) may have chordal attachments from the anterior leaflet, resulting in a triangular mitral valve office.[45]

### *Echocardiographic Evaluation*

Echocardiographic assessment of congenital mitral anomalies uses all the usual windows for evaluating the mitral valve. The parasternal short-axis view defines the number of leaflets, a single or a double orifice, the presence of a cleft, and the number and location of the papillary muscles (Fig. 44-3). The orientation of the anterior leaflet cleft is toward the anterior septum in cases of isolated mitral valve cleft and toward the mid or inferior septum in patients with an associated AV canal defect. Long-axis or off-axis views may be needed to follow chordal attachments to their respective papillary muscles. PW, CW and color Doppler all are important to assess the functional significance of these structural anomalies. Doppler quantification of the severity of mitral stenosis and mitral regurgitation is discussed in Chapters 18 and 21. Abnormal flow patterns created by any of the congenital mitral valve lesions predispose to the development of infectious endocarditis. Mitral anomalies are sometimes first detected when a young adult is referred for an echocardiographic search for valvular vegetations in the setting of clinical endocarditis.[46]

### *Management*

Management of congenital mitral stenosis or mitral regurgitation in the adolescent or adult follows similar clinical guidelines to those in acquired mitral valve disease. Intervention for congenital mitral stenosis is indicated for symptomatic patients with a mean mitral valve gradient of 10 mm Hg and for asymptomatic patients with pulmonary hypertension with a mean gradient of at least 10 mm Hg.[47] Balloon mitral valvotomy has been attempted in congenital mitral stenosis but carries a significant risk of valve disruption and should only be attempted in selected cases by centers with experience with this lesion.[48] Intervention for patients with congenital mitral regurgitation should be reserved for those patients with symptomatic severe mitral regurgitation or asymptomatic patients with severe mitral regurgitation and LV dysfunction.[47] With the increasing success of mitral valve repair, delaying surgical treatment to avoid a prosthetic valve has become less imperative.[49,50] Preoperative or intraoperative TEE determination of exact leaflet anatomy and the mechanism of valve dysfunction has been a vital factor in predicting the successful repair.[51] TEE features of interest include the presence and degree of calcification or fibrosis, adequacy and mobility of individual leaflets, site and direction of the regurgitant jet, and presence of leaflet clefts and papillary muscle anomalies.

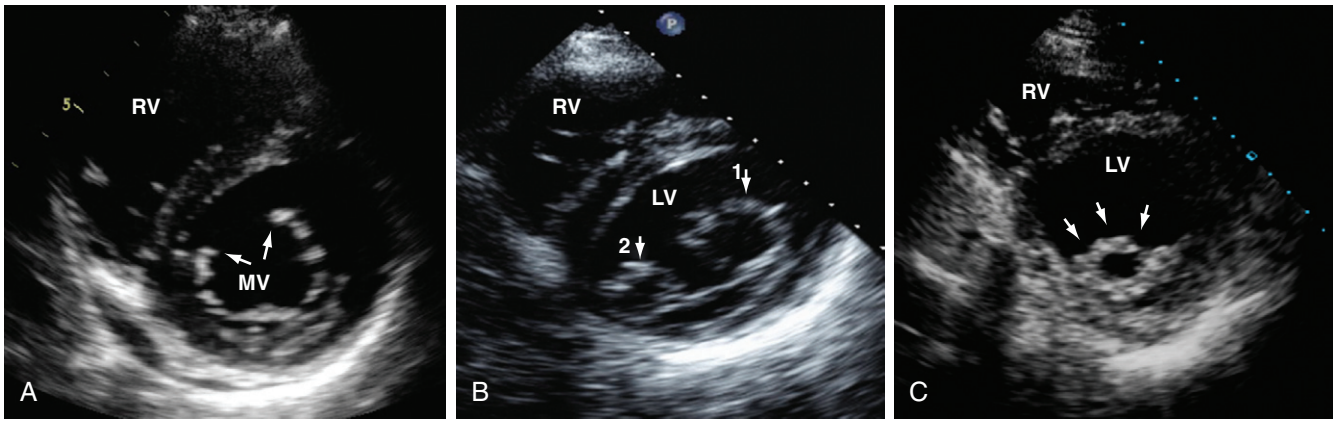



**Figure 44-3 Congenital mitral valve abnormalities.** Parasternal short-axis echocardiographic views of the LV at the mitral valve level. **A,** Cleft anterior leaflet (arrows) from patient with partial atrioventricular canal defect. **B,** Double-orifice mitral valve. Note discrepancy in orifice size: Orifice *1* is larger than orifice *2*. **C,** Parachute mitral valve with the anterior and posterior leaflets inserting into the posteromedial papillary muscle (*arrows*). *MV,* Mitral valve.

## TRICUSPID VALVE ANOMALIES

There are several congenital abnormalities that affect the tricuspid valve. The dysplastic tricuspid valve with inflow obstruction and regurgitation is part of the spectrum of hypoplastic right heart. Another congenital abnormality of the tricuspid valve occurs from involvement of the tricuspid leaflets in the septal aneurysm that forms around a perimembranous ventricular septal defect (VSD), resulting in tricuspid regurgitation. The most widely recognized congenital anomaly of the tricuspid valve is Ebstein anomaly. This malformation involves failure of delamination of the septal and posterior leaflets of the tricuspid valve resulting in apical displacement of these leaflets with an enlarged, redundant anterior leaflet. Downward displacement of the functional valve orifice results in an enlarged right atrium (RA) and an atrialized portion of the right ventricle (RV). The functional RV is frequently hypoplastic and functionally impaired. There may be underdevelopment of the infundibular portion of the RV and the PA. An ASD or patent foramen ovale is present in the majority of patients.[52] The clinical presentation of this anomaly is quite variable, ranging from severe cyanosis in the newborn to tricuspid regurgitation and arrhythmia in the adult. Tachyarrhythmias are common, with up to 20% of patients with Ebstein anomaly also demonstrating accessory pathways consistent with Wolff-Parkinson-White syndrome.[53] Diagnosis of Ebstein anomaly in the adolescent or adult is commonly made during echocardiographic evaluation of clicks and murmurs heard on auscultation or as part of clinical investigation for the cause of tachyarrhythmias. Rarely, a patient with unexplained cyanosis or paradoxical embolism is discovered to have Ebstein anomaly.

### *Echocardiographic Evaluation*

Echocardiography is ideally suited for the anatomic delineation of the tricuspid valve. The parasternal inflow view of the right heart, when properly aligned, demonstrates the apical displacement of the posterior leaflet and the elongated sail-like anterior leaflet arising normally from the tricuspid valve annulus. The apical four-chamber plane is optimal for defining the origin of the septal leaflet, the degree of adherence of the anterior leaflet to the free wall, and the size of the atrialized RV (Fig. 44-4). Off-axis apical views may be needed to assess the full extent of the functional RV, because the displacement of the tricuspid leaflets often orients the inflow axis more toward the RV outflow tract. It should be noted that apical displacement of the leaflet coaptation point alone can be seen in conditions that dilate the tricuspid annulus and create incomplete closure of the leaflets, such as an ASD with RV volume overload. These conditions differ from Ebstein anomaly in that the tricuspid valve leaflets all arise normally from the annular plane. To classify a displaced septal leaflet as diagnostic of Ebstein anomaly, the measured distance between the mitral leaflet insertion and the origin of the tricuspid septal leaflet in the apical view should be greater than 8 mm/m$^2$.[54]

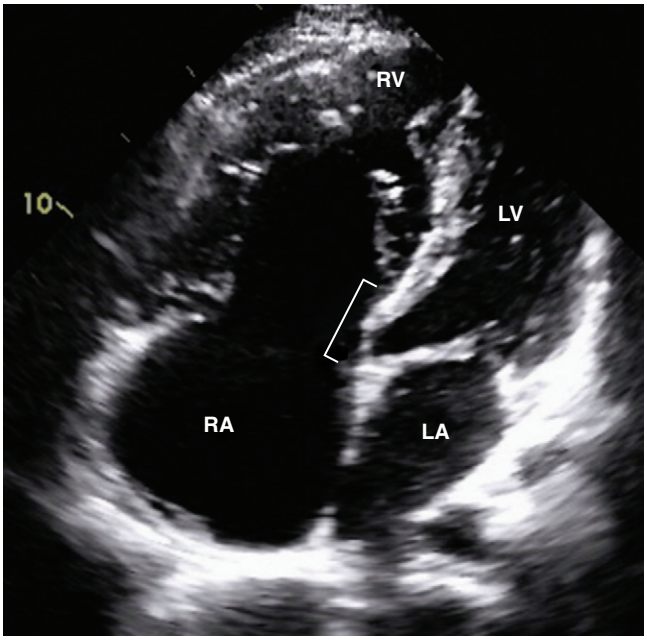



**Figure 44-4 Apical four-chamber echocardiographic view in a patient with Ebstein malformation of the tricuspid valve.** Note marked enlargement of RA with small functional RV. Septal leaflet of the tricuspid valve is apically displaced from the tricuspid valve annular plane (*bracket*).

Echocardiographic evaluation of Ebstein anomaly should also note the relative sizes and contractility of the atrialized and the functional RV. Color flow Doppler detects tricuspid regurgitation, which may be severe or can be present as multiple eccentric jets through commissures in the funnel-like valve

orifice. Inflow obstruction is rarely manifested as an elevated transvalvular gradient; instead, the displaced valve leaflets provide a resistance to forward flow that elevates systemic venous pressure and drives flow right to left across the atrial communication. Careful 2D imaging of the interatrial septum and color Doppler interrogation should demonstrate an atrial septal communication in most patients. Agitated saline contrast injection may be useful if imaging is suboptimal or the shunt is not apparent by color Doppler. TEE provides additional information about the leaflet origins and chordal attachments and better direct imaging of the interatrial septum in adults with difficult TTE studies.

In some individuals with Ebstein malformation, late development of clinical heart failure occurs as a result of LV dysfunction.[55] In some cases, this may be due to myocardial noncompaction.[56] In others, compression of the LV by massive right heart enlargement impairs diastolic filling. With significant distortion of the LV cavity by the enlarged right heart, calculation of the LV volumes and ejection fraction by the simpler echocardiographic methods is difficult. Qualitative estimation of LV function and measures of diastolic function, however, can provide useful clinical information regarding LV performance. Nongeometric indices of ventricular function, such as the myocardial performance index, have also been useful in this patient group.[57] Cardiac MRI is a useful imaging modality to evaluate the RV volume and function (Fig. 44-5).

### *Management*

Patients with Ebstein malformation frequently remain asymptomatic, leading full and active lives despite marked structural abnormality of the tricuspid valve and RA enlargement. Although some centers have suggested that tricuspid valve repair should be considered in the asymptomatic patient if the cardiothoracic ratio is greater than 65%, many centers restrict intervention to those with progressive cyanosis, severe tricuspid regurgitation, ventricular failure, paradoxical embolism, or intractable arrhythmia. Surgical repair of the abnormal tricuspid valve is preferred to valve replacement if the anatomy is favorable, with good results reported.[58] Echocardiographic assessment of the size, mobility, and degree of displacement of the leaflets, attachments of the leaflets to the RV free wall, and function of the RV is critical for the selection of patients most suitable for valve repair.

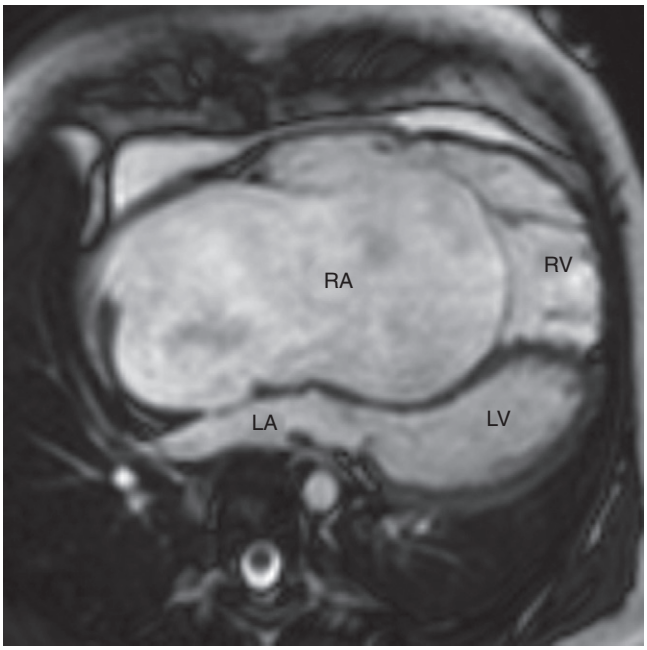



**Figure 44-5** Steady-state free precession cardiac magnetic resonance image in the four-chamber view in patient with Ebstein anomaly.

## Left Ventricular Outflow Tract and Aorta

### SUBAORTIC STENOSIS

Subaortic obstruction in the adult occurs in several forms. A discrete subaortic membrane is a developmental anomaly that is rarely seen in neonates but appears in older children and adults. It has been postulated that turbulent flow in the LV outflow tract stimulates the growth of "rest" tissue in the region of the perimembranous septum, creating discrete outflow obstruction.[59] Discrete subaortic stenosis is usually formed by a thin fibrous membrane attached circumferentially or along a portion of the circumference of the LVOT. It may lie immediately adjacent to the base of the aortic leaflets or be attached more distally near the junction of the muscular and perimembranous portion of the interventricular septum. Occasionally, the entire circumferential structure is composed of muscle, creating a muscular subaortic collar. In older patients, what began as a discrete membrane may be complicated by the development of subaortic hypertrophy. The muscular hypertrophy obscures the thinner membrane, thus masking the true pathophysiology of the obstruction. Long-segment tubular narrowing of the LVOT is more commonly seen in children and usually requires surgical attention before adulthood.

Discrete subaortic stenosis may occur in association with other left-sided obstructive lesions including supramitral ring, bicuspid aortic valve, and coarctation, or as part of a complex including perimembranous VSD and obstructive muscle bundles in the RV.[60] With increasing age, the VSD may close spontaneously, leaving the patient with a discrete obstruction of the LVOT and a muscular collar in the RV. Late development of discrete subaortic stenosis has been described in patients who have undergone surgical repair of AV canal defects.[61]

### *Echocardiographic Evaluation*

Echocardiographic detection of a subaortic membrane is typically made in the parasternal long-axis views of the LV outflow tract in which a linear structure protrudes from the left surface of the interventricular septum and the base of the anterior mitral valve leaflet is tented up by the tension of the circumferential membrane (Fig. 44-6). In some cases, the membrane is difficult to visualize unless the ultrasound beam is directly incident to the plane of the membrane. Low parasternal or apical long-axis views are thus more likely to detect the fine linear structure. When the membrane originates immediately beneath the aortic valve, its detection requires appreciation of subtle abnormality in the excursion of the aortic cusps and observation of a persistent structure in systole when the aortic cusps open into the sinus of Valsalva. Unexplained turbulence and increased flow velocities by Doppler across an apparently normal aortic valve are also a clue to the presence of a high discrete subaortic membrane. Systolic flow acceleration by PW or color Doppler occurs proximal to the aortic valve. Aortic

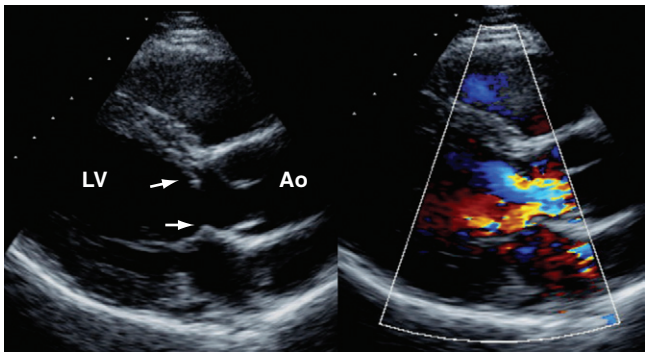



**Figure 44-6 Parasternal long-axis echocardiographic view of the LV in a patient with discrete subaortic stenosis.** Subaortic membrane (*arrows*) is a linear density protruding from upper left septal surface and anterior mitral valve leaflets. Color flow Doppler demonstrates acceleration of blood flow proximal to the aortic valve. *Ao*, Aorta.

**Box 44-4**

**CLASS I RECOMMENDATIONS FOR INTERVENTION IN ADULTS WITH ISOLATED SUBAORTIC STENOSIS**

- A peak instantaneous gradient of greater than 50 mm Hg or a mean gradient of 30 mm Hg on Doppler echocardiography
- Progressive aortic regurgitation and an LV end-systolic dimension of greater than 50 mm or an LV ejection fraction less than 55%

Adapted from Warnes CA, Williams RG, Bashore TM et al. ACC/AHA 2008 guidelines for the management of adults with congenital heart disease. A report of the American College of Cardiology/American Heart Association Task Force on Practice Guidelines (writing committee to develop guidelines on the management of adults with congenital heart disease) developed in collaboration with the American Society of Echocardiography, Heart Rhythm Society, International Society for Adult Congenital Heart Disease, Society for Cardiovascular Angiography and Interventions, and Society of Thoracic Surgeons. *J Am Coll Cardiol* 52:e191, 2008.

regurgitation is commonly found in these patients as a result of long-standing subaortic flow disturbance or from infectious endocarditis.

Initial and serial assessment of the outflow tract pressure gradients by Doppler is important because of the progression of both the severity of obstruction and the degree of aortic regurgitation.[62] As with other lesions, TEE may be helpful in the patient with limited transthoracic windows to delineate the exact nature of the LVOT obstruction. This approach is particularly useful in cases with mixed or multiple-level obstruction. Both midesophageal views of the subaortic area and transgastric images of the LVOT are useful for obtaining diagnostic information.[63]

### *Management*

Subaortic stenosis is often a progressive lesion, which can lead to aortic valve damage, ventricular dysfunction, and worsening aortic regurgitation. Risks factors for progression include a peak Doppler gradient across the subaortic stenosis of greater than 30 mm Hg, if the membrane is immediately adjacent to the aortic valve or if there is extension of the membrane onto the mitral valve.[64] The indications for surgical intervention are somewhat controversial. The Class I adult congenital heart disease (ACHD) guidelines for surgical intervention in subaortic stenosis are listed in Box 44-4. Varying outcomes have been reported following surgical resection of subaortic membranes. Some have argued that resection of the membrane preserves the aortic valve from further trauma and prevents progressive aortic regurgitation.[65] However, others report a less predictable course, with up to 55% developing a recurrent membrane over 6 months to 24 years.[66] Still other series have documented that some patients exhibit very slow progression of LVOT obstruction and aortic regurgitation in adulthood.[67] Therefore, caution should be taken in recommending surgery for the asymptomatic patient with only mild hemodynamic abnormalities. When surgical excision is indicated, intraoperative TEE is useful to monitor the success of membrane removal and detect complications, such as mitral valve perforation or iatrogenic creation of a VSD.[68]

Percutaneous balloon dilation has been attempted in patients with discrete subaortic membranes with a substantial reduction in the gradient that persists over 5 years in 48% of patients without significant change in the degree of aortic regurgitation.[69] However, the appropriate selection of patients suitable for percutaneous intervention is essential, and favorable factors include a thin discrete membrane less than 3 mm in width, a sufficient distance between the membrane and the aortic valve to permit a subaortic chamber, and the absence of more than grade 2 aortic regurgitation. Potential damage to the mitral and aortic valves and incomplete relief of obstruction has limited the applicability of this technique, and in many adults with acquired secondary muscular outflow obstruction, percutaneous dilation is unlikely to produce satisfactory results.

## SUPRAVALVULAR AORTIC STENOSIS

Supravalvular aortic stenosis is an uncommon lesion involving a fixed narrowing at the level of the sinotubular junction, which results in an "hourglass" appearance of the aorta (70%), diffuse hypoplasia of the entire ascending aorta (20%) or a discrete supravalvular perimembranous stenosis (10%).[70] This may occur as an isolated abnormality, or as part of Williams syndrome.[71] Other features of Williams syndrome include cognitive disorders, short stature, a "cocktail personality," "elfin facies," and systemic hypertension. A familial autosomal dominant form of supravalvular aortic stenosis that is not associated with developmental delay has also been described.[72] Genetic studies have suggested that the underlying cause of supravalvular aortic stenosis is a mutation of the elastin gene on chromosome 7q11.23, which leads to an arteriopathy of varying severity that is most uniformly expressed in the supravalvular aorta.[73]

Functionally, supravalvular aortic stenosis may occur as an incidental finding with a systolic murmur, often best appreciated in the suprasternal notch. In other cases, the lesion is progressively obstructive or part of a diffuse process affecting the aorta, coronary ostia, brachiocephalic origins, and pulmonary arterial tree. Box 44-5 lists the common associations found with supravalvular aortic stenosis. The aortic valve may be bicuspid or may be distorted by the supravalvular constriction or incorporated into the stenosing ring. Coronary artery issues are not uncommon, and are due to the fact that the coronary ostia are proximal to obstruction, and exposed to high systolic pressures and limited diastolic flow, which may lead to coronary ostial and vessel abnormalities. Pathologic studies on adults with supravalvular aortic stenosis have revealed diffuse or focal intimal and medial fibrosis, hyperplasia, or dysplasia of the

**Box 44-5**

**ASSOCIATED DEFECTS WITH SUPRAVALVAR AORTIC STENOSIS**

Bicuspid aortic valve
Coronary artery abnormalities (ostial stenosis, ostial occlusion, dilation)
Brachiocephalic artery stenosis
Multilevel right-sided obstructive lesions (especially with Williams syndrome)
Renal artery stenosis

coronary arteries.[74] These processes may lead to myocardial ischemia. When progressive obstruction and failure of normal aortic growth occurs, LV hypertrophy and typical symptoms of aortic stenosis develop.

### *Echocardiographic Evaluation*

Echocardiographic detection of supravalvular stenosis relies on careful inspection of the sinotubular junction and proximal ascending aorta, which is possible with cranial angulation in the right or left parasternal windows, or from the suprasternal notch views. The diameter of the normal aorta at the sinotubular junction equals or slightly exceeds that of the aortic annulus. The tubular portion of the ascending aorta should never be smaller than the aortic annulus.[75]

Echocardiographic Doppler study should determine the type of supravalvular lesion and the severity of stenosis. Although routine echocardiographic study now includes imaging the ascending aorta above the sinuses of Valsalva, this portion of the aorta is frequently not imaged, and the diagnosis of supravalvular aortic stenosis may be missed. The impetus to look specifically for this lesion may be a high-velocity turbulent flow detected by CW Doppler across a normal-appearing aortic valve. Accurate assessment of the supravalvular gradient by Doppler is best determined from the right parasternal or suprasternal windows, rather than the apical view. Doppler estimates of the severity of stenosis correlate poorly, however, with catheter-obtained gradients and often overestimate the true degree of obstruction due to pressure recovery in the tubular or long-segment stenosis.[76]

Careful assessment of the aortic arch and brachiocephalic vessels is essential, as there may be ascending or transverse aortic hypoplasia, coarctation, or stenosis of the origins of the head and neck vessels. Additionally, particularly in patients with Williams syndrome, branch pulmonary arteries and renal arteries should be evaluated for evidence of stenosis. An alternative imaging modality, such as cardiac MRI or computed tomography, is often desirable to complete the evaluation. The recently published ACHD guidelines advocate for one of these modalities to complement the echocardiographic assessment in the adult with unoperated supravalvular aortic stenosis. Additionally, these guidelines advocate for periodic screening for myocardial ischemia in these patients.[4]

### *Management*

The decision for surgical intervention for supravalvular aortic stenosis is similar to that for valvular obstruction—significant outflow gradient with LV hypertrophy or symptoms. Box 44-6 lists the Class I guidelines for intervention in adults with supravalvular aortic stenosis. The morphology

**Box 44-6**

**CLASS I RECOMMENDATIONS FOR INTERVENTION IN ADULTS WITH SUPRAVALVAR AORTIC STENOSIS**

- Symptoms and/or mean gradient greater than 50 mm Hg or peak instantaneous gradient by Doppler echocardiography greater than 70 mm Hg
- Surgical repair is recommended for adults with lesser degrees of supravalvular obstruction and the following:
  - Symptoms (i.e., angina, dyspnea, or syncope)
  - LV hypertrophy
  - Desire for greater degrees of exercise or a planned pregnancy
  - LV systolic dysfunction
- Interventions for coronary artery obstruction in patients with Supravalvular aortic stenosis should be performed in ACHD centers with demonstrated expertise in the interventional management of such patients

Adapted from Warnes CA, Williams RG, Bashore TM et al. ACC/AHA 2008 guidelines for the management of adults with congenital heart disease. A report of the American College of Cardiology/American Heart Association Task Force on Practice Guidelines (writing committee to develop guidelines on the management of adults with congenital heart disease) developed in collaboration with the American Society of Echocardiography, Heart Rhythm Society, International Society for Adult Congenital Heart Disease, Society for Cardiovascular Angiography and Interventions, and Society of Thoracic Surgeons. *J Am Coll Cardiol* 52:e193, 2008.
*ACHD*, Adult congenital heart disease.

of the supravalvular narrowing dictates the type of repair required, varying from patch aortoplasty to partial root replacement. Reconstruction of the coronary ostia or bypass grafting may be required, depending on the anatomy. Associated branch PA stenosis may need to be addressed concurrently. Abnormalities of the aortic valve leaflets may persist after repair and merit clinical and echocardiographic surveillance. The reported surgical outcomes following supravalvular aortic stenosis repair are favorable, with a low mortality and need for reintervention, providing that the associated lesions are addressed at the time of surgery.[77,78]

## SINUS OF VALSALVA ANEURYSMS

The aortic sinus is the part of the aortic root that is delineated proximally by the attachments of the aortic valve leaflet and distally by the sinotubular ridge.[79] Congenital aneurysms of the aortic sinuses of Valsalva are thought to result from a weakness in the aortic media at its junction with the annulus fibrosis. A small diverticulum or finger-like protrusion extends most commonly from the right coronary sinus and arises above the aortic annulus, in contrast to a prolapse of the aortic cusp that occurs below the annular level. The RV is the most common termination site. Aneurysms of the noncoronary sinus usually enter the RA.[80] Over time, the aneurysm may enlarge to become a "windsock," potentially causing obstructive problems in the RV outflow tract or tricuspid valve. Rarely, sinus of Valsalva aneurysms burrow into the interventricular septum and cause AV conduction defects. Protrusion into the LVOT may create outflow tract obstruction.[81] Sinus of Valsalva aneurysms can occur in isolation or with other anomalies, such as VSD, subaortic stenosis, tetralogy of Fallot, or aortic valve abnormalities.[82]

Congenital sinus of Valsalva aneurysms come to clinical attention most typically during adolescence and young adulthood when the protruding structure ruptures into the receiving

chamber. Acute rupture of a large aneurysm causes retrosternal or epigastric pain and severe dyspnea from heart failure. By contrast, perforation of a small aneurysm may go unnoticed until a continuous murmur is auscultated or worsening symptoms of heart failure bring the patient to medical attention. Coronary artery compression by a sinus of Valsalva aneurysm is an unusual mode of presentation.[83]

### *Echocardiographic Evaluation*

Sinus of Valsalva aneurysms may be an incidental finding on echocardiographic study, but they are more often discovered during echocardiographic-Doppler evaluation of a continuous murmur with the suspected diagnosis of patent ductus arteriosus or coronary artery fistula.[84,85] Parasternal long-axis and short-axis views of the aortic sinuses demonstrate the finger-like windsock extending from the base of the sinus toward the site of termination (Fig. 44-7). The originating sinus may be somewhat enlarged, but the native morphology of the root and valve is usually not significantly distorted. It is important to determine that the aneurysm originates from the aortic sinuses above the plane of the aortic valve to distinguish this lesion from the more common aneurysm of the perimembranous interventricular septum. Delineation of a normal coronary artery origin and lumen size distinguishes it from a coronary artery fistula. Acquired aortic fistulas after endocarditis can be differentiated because they lack the extended aneurysmal channel seen with a congenital sinus of Valsalva aneurysm. Color flow Doppler demonstrates continuous turbulent flow within the aneurysm and into the receiving chamber. In patients with a significant left-to-right shunt, cardiac chamber dilation is dependent on the site of termination. Aneurysms that terminate below the tricuspid valve (i.e., RV) result in LA and LV dilation, whereas those that terminate pre–tricuspid valve (RA) result in RV dilation. Aortic regurgitation, often mild, is expected because of distortion of the aortic cusp and aortic root enlargement as a result of long-standing volume overload. Severe aortic regurgitation should raise the suspicion of an aneurysm rupture into the LV outflow tract or endocarditis.

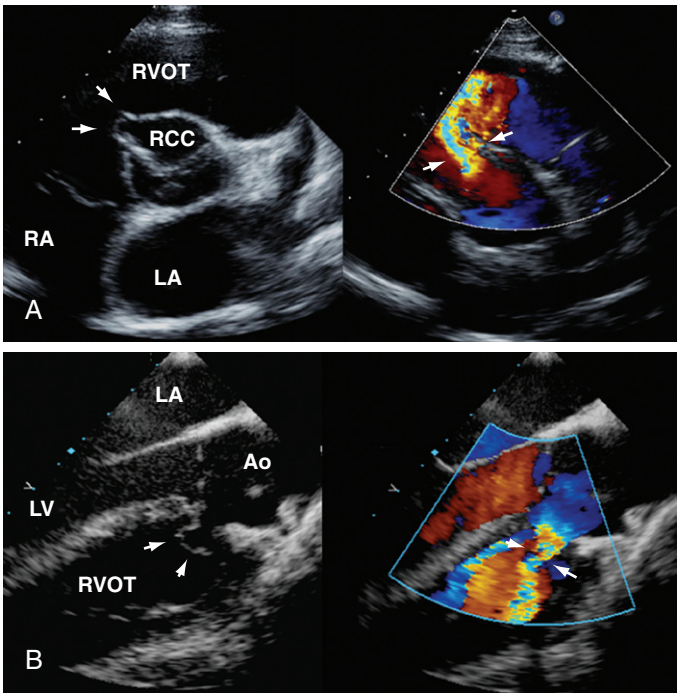



**Figure 44-7 A, Parasternal short-axis echocardiographic view in a patient with a ruptured sinus of Valsalva aneurysm.** Aneurysm of the right coronary cusp (*RCC*) creates a "windsock" protruding into the RV outflow tract (*RVOT*) (*arrows*). Color flow Doppler demonstrates turbulent shunt flow (*arrows*) from aorta into RVOT. **B,** TEE view from this patient further demonstrating this anatomy. *Ao*, Aorta.

### *Management*

Small unruptured aneurysms found incidentally can be followed expectantly. Larger aneurysms or those adversely affecting surrounding structures should be electively excised. Ruptured sinus of Valsalva aneurysms require surgical closure to prevent late congestive symptoms caused by volume overload and to decrease the susceptibility to infectious endocarditis. Surgical repair is highly successful. However, certain risk factors have been associated with poorer outcomes, including presence of infective endocarditis, long cross-clamp time, LV fistula, reoperation, aortic regurgitation, or aortic dehiscence.[86] In one large series of 129 patients with sinus of Valsalva aneurysms, perioperative mortality rate was 3.9%, and the etiology of the 23 late deaths included myocardial infarction, cardiac failure, dissection, and stroke.[87]

## COARCTATION OF THE AORTA

Native coarctation of the aorta in the adolescent and adult is most often discovered during an investigation of systemic hypertension. Weak or absent femoral pulses, LV hypertrophy on electrocardiogram (ECG), or systolic or continuous murmurs auscultated on the back are clues to the diagnosis.

The anatomic lesion most commonly found in the adult is a discrete narrowing of the aortic lumen just inferior to the left subclavian artery origin and opposite the ductus arteriosus or ligamentum arteriosum. Poststenotic dilation of the descending aorta is often present.

Functionally, patients seen as adults are usually asymptomatic because the degree of obstruction created by the coarctation may be mild or moderate, or the obstruction is moderated by the development of collateral vessels between the high-pressure aortic branches proximal to the coarctation and the low-pressure descending aorta.

Approximately 50% of patients with coarctation of the aorta have a bicuspid aortic valve.[88] Other associated cardiac defects include patent ductus arteriosus, VSD, and mitral valve abnormalities. As previously mentioned, it is particularly common in conditions with multiple left-sided obstructive lesions, such as Shone syndrome. Additionally, at least 10% of patients with Turner syndrome have aortic coarctation. The natural history of untreated coarctation of the aorta includes early mortality (mean age 31 years) with complications of cerebrovascular accidents from berry aneurysm rupture, aortic dissection, and endarteritis.[89]

### *Echocardiographic Evaluation*

Echocardiographic diagnosis of coarctation relies on 2D visualization of the anatomy of the aortic arch and Doppler detection of the flow disturbance in the descending aorta. Although the aorta can be imaged in part from a variety of parasternal views, suprasternal notch or right parasternal windows often provide the best visualization of the area of interest. The area of coarctation is often challenging to visualize in the adult, and patient positioning measures to optimize the suprasternal view are important. In the long-axis view of the aortic arch, the

brachiocephalic vessels should be identified and followed distally if possible. Immediately distal to the left subclavian artery, an infolding or posterior shelf of the coarctation narrows the aortic lumen. Poststenotic dilation of the descending thoracic aorta is common.

Color flow Doppler detects a narrowed flow stream at the point of coarctation and systolic flow acceleration, with continuation of flow into diastole in cases of significant obstruction. In fact, when 2D imaging is indistinct, the color flow turbulence may be a clue to the site of obstruction. CW Doppler in patients with discrete obstruction demonstrates a typical pattern of increased systolic flow velocity and a continued gradient in diastole. Doppler gradients (ΔP) estimated from the peak systolic velocity ($V_2$) of the CW Doppler signal usually overestimate the catheter-measured gradients. Better correlations have been shown when the velocity proximal to the coarctation ($V_1$) is included in the modified Bernoulli equation

$$\Delta P = 4\left(V_2^2 - V_1^2\right)$$

or when both the peak systolic velocity and pressure half-time of the diastolic gradient are considered.[90,91] Long-segment narrowing of the aorta without discrete obstruction causes acceleration of flow, giving high peak velocities by CW Doppler. Conversion of these velocities into systolic gradients mistakenly predicts significant coarctation. The lack of a diastolic gradient helps to distinguish flow acceleration from true obstruction. Doppler flow patterns in the descending abdominal aorta are extremely useful in detecting upstream obstruction.[92] Patients with tubular narrowing but without a discrete obstruction demonstrate a normal pattern of abdominal aortic flow: rapid systolic upstroke, relatively laminar flow signal, and no continuation of flow into diastole. With coarctation, the flow profile has a delay in the systolic upstroke, turbulence in systole, and variable degrees of diastolic antegrade flow (Fig. 44-8). Routinely including the Doppler profile of abdominal aortic flow in the clinical examination is an excellent method to screen for unsuspected coarctation. Adults with coarctation may have considerable tortuosity of the transverse arch, making both visualization and alignment for accurate Doppler detection of the gradient impossible. In such cases, a high degree of suspicion is generated by abnormal flow in the abdominal aorta, directing a more diligent search from off-axis views or with stand-alone CW Doppler probe.

Although Doppler flow patterns are relatively easy to obtain in most adults with coarctation, direct imaging of the anatomy of the transverse arch and descending aorta is frequently limited. Alternative imaging modalities are often necessary to further define the details of the obstruction and guide management decisions. TEE can detect the site and configuration of the obstruction. Long-axis views allow quantitation of luminal narrowing; however, Doppler gradients are difficult to obtain because the affected region of the aorta generally lies perpendicular to the interrogating Doppler beam.[93] In addition, visualization of the branch vessels and collaterals is limited with TEE, thus making alternative imaging modalities more useful (Fig. 44-9). The ACHD guidelines recommend that every patient with coarctation (repaired or not) should have at least one cardiac MRI exam or CT scan for complete evaluation of the thoracic aorta and intracranial vessels.[4]

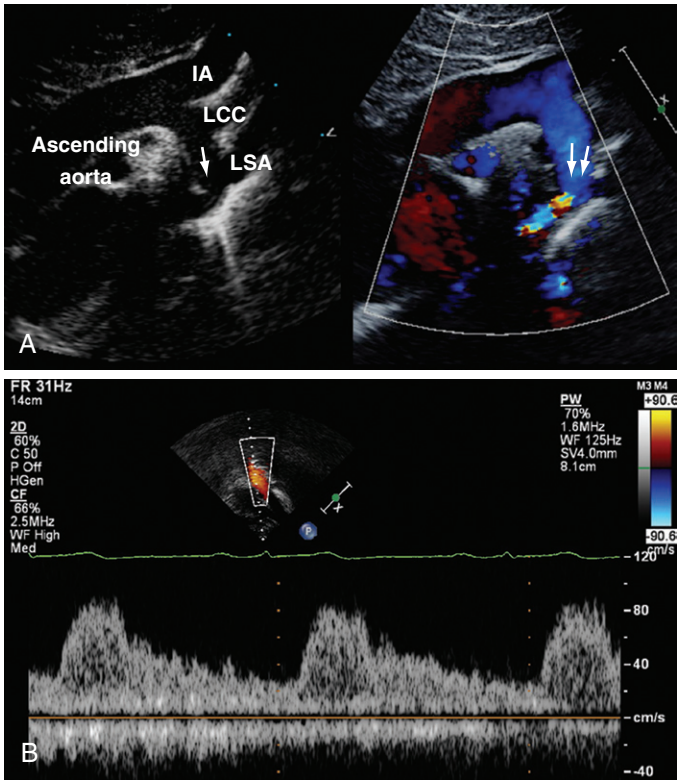



**Figure 44-8** **A, Suprasternal long-axis echocardiographic view of aortic arch demonstrates discrete coarctation at isthmus (*arrow*).** Color flow Doppler reveals aliasing and turbulence beginning at site of discrete obstruction (*double arrows*). **B,** Pulsed-wave Doppler signal in descending abdominal aorta reveals blunting of systolic upstroke and turbulent continuous flow during diastole indicative of significant obstruction to flow located more proximally in aorta. *IA,* Innominate artery; *LCC,* left common carotid artery; *LSA,* left subclavian artery.



**Figure 44-9** **Steady-state free precession cine MRI in oblique sagittal view of aortic arch in adult with discrete aortic coarctation (*arrow*).**

*Management*

Indications for intervention in the adult with coarctation include a peak-to-peak coarctation gradient greater than or equal to 20 mm Hg or the presence of significant coarctation and collateral flow by imaging. The choice of percutaneous catheter intervention versus surgical repair of a native discrete coarctation is sometimes controversial and should be discussed by a team involving ACHD cardiologists, interventionalists, and surgeons. Surgery is often recommended in cases of long-segment coarctation or concomitant hypoplasia of the transverse aortic arch. Percutaneous catheter intervention is indicated for recurrent, discrete coarctation and a peak-to-peak gradient of at least 20 mm Hg.

Balloon angioplasty of native coarctation in adults often results in significant relief of the gradient and improvement in systemic hypertension.[94] In an analysis of 970 percutaneous angioplasty procedures for coarctation, 81% of patients with native coarctation and 75% of those with recurrent aortic obstruction experienced early successful relief of obstruction without a major complication.[95] Small saccular aneurysms may occur at the site of dilation. The long-term outcome of these iatrogenic aneurysms is unknown. Intravascular echocardiography performed immediately after dilation can demonstrate an intimal tear that commonly occurs during balloon angioplasty.[96]

Intravascular stents are now routinely used in the treatment of aortic coarctation. Early and intermediate follow-up suggests excellent relief of stenosis without a significant incidence of stent migration, fracture, restenosis, or thromboembolic complications.[97] In one series of 153 patients with aortic coarctation who had undergone intravascular stenting procedures, serious injuries to the aortic wall were uncommon, and these investigators advocated for predilation of the coarctation site before stent placement.[98]

Coarctation in the adult can be surgically repaired with low operative mortality and good intermediate outcome. Attention to the degree of collateral formation is important to ensure adequate perfusion during cross-clamping and to prevent spinal cord injury. Prosthetic bypass grafts or other alternatives to mobilization and end-to-end anastomosis may be required in adults with less elastic tissue or with unfavorable anatomy such as hypoplasia of the transverse arch.

Residual hypertension is very common and occurs despite the absence of residual obstruction.[99] Patients with repaired aortic coarctation may have a normal resting blood pressure, yet demonstrate an exaggerated systolic blood pressure response to exercise.[100] There is increasing evidence that patients with aortic coarctation exhibit impaired vascular reactivity.[101] Lifelong cardiology follow-up is recommended for all patients with aortic coarctation. Box 44-7 lists the recommendations for key issues to evaluate in follow-up.

**Box 44-7**

**RECOMMENDATIONS FOR FOLLOW-UP IN ADULTS WITH COARCTATION OF THE AORTA**

- Lifelong cardiology follow-up is recommended for all patients with aortic coarctation (repaired or not), including consultation with a cardiologist with expertise in ACHD
- Patients who have undergone surgical repair or percutaneous intervention for coarctation of the aorta should have at least annual follow-up
- Even if the coarctation repair appears satisfactory, late postoperative thoracic aortic imaging should be performed to assess for aortic dilatation or aneurysm formation
- Patients should be observed closely for the appearance of resting or exercise-induced systemic arterial hypertension, which should be treated aggressively after recoarctation is excluded
- Evaluation of the coarctation repair site by MRI/CT should be performed at intervals of 5 years or less, depending on the specific anatomic findings

Adapted from Warnes CA, Williams RG, Bashore TM et al. ACC/AHA 2008 guidelines for the management of adults with congenital heart disease. A report of the American College of Cardiology/American Heart Association Task Force on Practice Guidelines (writing committee to develop guidelines on the management of adults with congenital heart disease) developed in collaboration with the American Society of Echocardiography, Heart Rhythm Society, International Society for Adult Congenital Heart Disease, Society for Cardiovascular Angiography and Interventions, and Society of Thoracic Surgeons. *J Am Coll Cardiol* 52:e196, 2008.

*ACHD*, Adult congenital heart disease; *CT*, computed tomography; *MRI*, magnetic resonance imaging.

## Septal Defects and Shunt Lesions

### PATENT FORAMEN OVALE

The most frequent atrial communication is a patent foramen ovale, which is prevalent in approximately 25% of adults.[102] During embryologic development, the atrial septum forms with a septum primum extending inferiorly toward the endocardial cushions. Concurrently, the septum secundum forms, and the defect in this structure, the foramen ovale, allows blood to flow from the fetal RA to left atrium (LA). Following birth, fusion of the two septa often occurs, closing the foramen completely in 75% of patients.

However, in the remaining individuals with incomplete fusion, the flap of septum primum covering the fossa ovalis may open transiently with changes in the transatrial pressure gradient, allowing communication of blood between the two atria. Additionally, this thin perimembranous layer may have small septal perforations or develop into a septal aneurysm with or without an atrial shunt.

Improved detection of patent foramen ovale has generated great interest in the association of this defect with cerebrovascular events, migraine headaches, and other conditions, such as sleep apnea. Although there is no definite consensus as to the risk of stroke implied by the presence of a patent foramen ovale, it is clear that the potential for a right-to-left embolus exists when there is any form of communication in the interatrial septum.

### ATRIAL SEPTAL DEFECTS

ASDs are one of the most common congenital heart lesions discovered in adults. The most common type of ASD is the secundum defect, followed by primum defects, and then sinus venosus defects. A much rarer type of defect is the coronary sinus septal defect, in which the roof of the coronary sinus is partially or completely absent, allowing left-to-right shunt from the LA into the coronary sinus and into the RA. The various types of ASDs are depicted in Figure 44-10.

Patients with shunting at the atrial level are often asymptomatic until middle to late adult years. Physical exam findings may

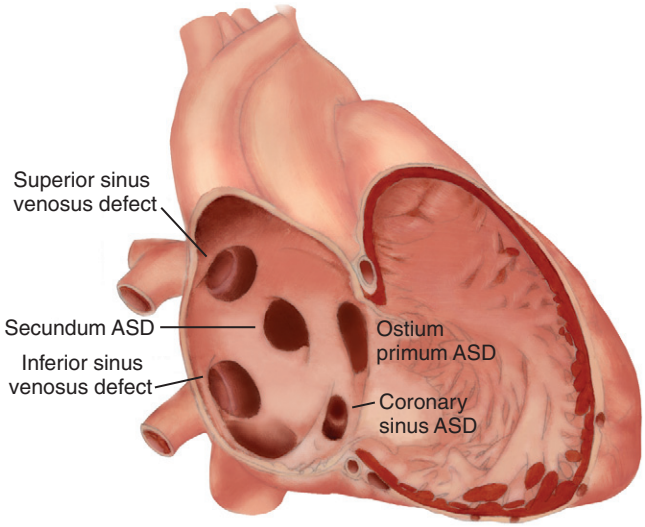



**Figure 44-10 Diagrammatic representation of interatrial septum as viewed from cutaway view of right heart to demonstrate various defect locations.** Superior and inferior sinus venosus defects are located near entry of superior vena cava and inferior vena cava, respectively. Secundum atrial septal defect (*ASD*) is centrally positioned. Primum ASD is inferiorly located near atrioventricular valves and coronary sinus septal defect.

**TABLE 44-1 Associated Defects with Atrial Septal Defect**

| *Type of Defect* | *Associated Lesion* |
|---|---|
| Secundum atrial septal defect | Mitral valve prolapse, pulmonic stenosis, partial anomalous pulmonary venous return |
| Primum atrial septal defect | Cleft mitral valve, inlet ventricular septal defect, septal aneurysm |
| Sinus venosus defect | Partial anomalous pulmonary venous return |
| Coronary sinus septal defect | Unroofed coronary sinus, left superior vena cava, partial anomalous pulmonary venous return |

include a widely split second heart sound and a systolic ejection murmur of increased flow across the pulmonic valve. Symptoms often develop during the third decade of life and beyond and include fatigue, exercise intolerance, dyspnea with exertion, and atrial arrhythmias. RV failure, pulmonary arterial hypertension, and paradoxical embolism are rare modes of presentation for older patients with unrepaired ASDs.[103,104]

### *Echocardiographic Evaluation*

Patients with ASDs require echocardiographic assessment of the anatomic abnormality of the atrial septum, the hemodynamic effect of shunt flow, and the presence of any associated defects (Table 44-1). Imaging of the atrial septum is best performed with subxiphoid views when possible. The apical four-chamber view is unreliable because false-positive dropout often occurs in the midatrial septum. An off-axis four-chamber view obtained by sliding midway between the apical and subxiphoid views, however, yields a more perpendicular interface between the interrogating ultrasound beam and the interatrial septum. Parasternal short-axis and right parasternal views are supplemental windows for imaging the atrial septum. The septum primum covering the fossa ovalis is thinner than either the superior or inferior limbic bands of the septum secundum. Mobility of the septum primum or aneurysmal deformity (greater than 1 cm deviation from the plane of the basal septum) raises the suspicion for a patent foramen ovale. True ASDs should have a distinct edge visible at the blood-tissue interface. All aspects of the atrial septum should be inspected, including the superior rim, with visualization of the superior vena caval entry. Right parasternal views are particularly helpful in imaging this area. When the atrial defect can be imaged directly, measurement of its dimensions in orthogonal planes, the septal rims, and its size relative to the entire atrial septal length should be made.

PW and color flow Doppler add diagnostic power to the transthoracic examination. The passage of flow across an apparent atrial defect confirms the presence of an atrial communication. When the right heart pressures are normal, a clear stream of flow occurs in late systole with accentuation in diastole. Elevation of right heart pressures decreases the transseptal pressure gradient, and shunt flow then may be difficult to distinguish from other low-velocity atrial flows.

Contrast echocardiography plays an important diagnostic role in cases in which the imaging and Doppler findings are equivocal. With rapid intravenous injection of several milliliters of agitated saline (or saline mixed with a small amount of the patient's blood), highly reflective microbubbles appear in the right side of the heart. Contrast passes into the LA within three to five cardiac cycles in the presence of an interatrial communication. Even when left-to-right shunting is predominant, there is a period of transient right-to-left shunting during which contrast can pass into the LA. The right-to-left pressure gradient can be augmented by having the patient cough or perform a Valsalva maneuver. A negative contrast effect occurs with left-to-right shunts when unopacified blood enters the densely opacified RA. Negative contrast is a less reliable diagnostic feature, however, because flow from the inferior vena cava or coronary sinus may create the same appearance. Sensitivities of 92% and above have been reported for detection of ASDs by contrast TTE.[105,106] It has been suggested that injection from the leg may improve the sensitivity of the contrast technique because the Eustachian valve tends to direct inferior vena cava flow across the fossa ovalis.[102]

TTE study also helps to define the hemodynamic effects of shunt flow. RA and RV enlargement and dilation of the main PA are expected with shunts of 1.5:1 or greater. The pulmonary veins are prominent, but the LA is usually normal in size unless there is a primum ASD present, with cleft mitral valve and mitral regurgitation. The interventricular septum in the short-axis views is flattened in diastole and moves paradoxically toward the RV in systole.

Specific quantification of shunt volume by echocardiographic-Doppler techniques has been attempted by several methods, all of which remain semi-quantitative in clinical use. PW Doppler determination of cardiac output has been validated with a high degree of accuracy in the experimental setting.[107] The ratio of PW Doppler–determined cardiac output across the pulmonic and aortic valves gives an estimate of pulmonary-to-systemic flow ratio ($Q_p/Q_s$). This technique is not accurate if the flow across either valve is influenced by something other than the intracardiac shunt, such as valvular stenosis, subvalvular obstruction, or significant valvular regurgitation. Application of this method to the clinical arena has been less successful, partly because of the difficulty of obtaining accurate dimensions of the pulmonary annulus in adults.

When color flow mapping became a part of the echocardiographic diagnostic armamentarium, there was initial enthusiasm for its quantitative potential. Planimetry of the area of the flow stream within the RA has been compared with shunt volumes, but with poor correlation. Better correlation has been shown when the diameter of the color flow stream at the atrial defect is compared with shunt ratios. However, this remains semiquantitative, with considerable overlap between patients with small, moderate, and large shunts. This result might be expected because the color flow diameter simply reflects the anatomic dimension of the atrial defect, and although it bears a gross relationship to the size of the shunt, factors such as RV compliance and PA pressures cause variation in the volume of shunt for a given ASD size.

Estimation of PA pressure is an important part of the echocardiographic assessment of atrial shunts. The pressure is easily and reliably determined by applying the modified Bernoulli equation to the peak velocity of the tricuspid regurgitation jet to obtain the pressure difference between the RA and RV.[108] If the patient does not have tricuspid regurgitation, other subjective signs of pulmonic hypertension may be present. For example, the interventricular septum is flattened in systole if the RV systolic pressure is greater than half the systemic pressure. Systolic notching on the pulmonic valve M-mode or the PA Doppler flow profile also indicates significant elevation in PA pressure. Applying the modified Bernoulli equation to the end-diastolic velocity of the pulmonic regurgitation jet provides quantitative information about the PA diastolic pressure.

The drainage of all the pulmonary veins should be established in any patient with an ASD. Anomalous return of the right superior and middle lobe veins is found in the majority of patients with sinus venosus defects and a small percentage of patients with secundum ASDs. From an anatomic standpoint, sinus venosus defects are not true ASDs, as they do not allow direct communication between the RA and LA, but rather the interatrial communication is through one or more pulmonary veins. These defects frequently result in significant RV volume overload.[109] Echocardiographic Doppler detection of sinus venosus defects in adults is difficult but can be attempted with long-axis and short-axis right parasternal views of the superior vena cava and occasionally can be appreciated in subcostal views of the superior vena cava. A turbulent flow stream entering the superior vena cava laterally and posteriorly represents the pulmonary vein inflow. In a superior sinus venosus defect, the right pulmonary veins drain to the superior vena cava either at the junction or more distally along the course of the superior vena cava (Fig. 44-11). A less common defect is the RA type, or inferior sinus venosus defect. This is also difficult to image and may be mistaken for an inferiorly located secundum ASD. The RA type sinus venosus defect is characterized by anomalous drainage of the right inferior and/or middle pulmonary veins into the inferior aspect of the RA or inferior vena cava. Right parasternal views that focus on the inferior vena caval entry to the RA may be helpful to search for the anomalous pulmonary venous inflow.

Primum ASD is an endocardial cushion defect, actually considered a type of partial AV canal defect with two separate AV valves and no VSD (Fig. 44-12). This type of ASD is usually accompanied by a cleft in the mitral valve, and patients may present with significant mitral regurgitation.

TEE has proven to be superior to TTE study in adult patients for detecting patency of the foramen ovale, secundum ASDs, sinus venosus defects, and anomalous pulmonary venous return.[110-112] Particularly in the case of patent foramen ovale and secundum ASD, TEE is very useful for defect sizing and determining specific anatomic details, such as presence of acceptable septal rims for percutaneous closure. With real time three-dimensional (3D) TEE it is possible to create an en face view of the interatrial septum in which the rims of the defect can be seen in one view (Fig. 44-13).




**Figure 44-11 Steady-state free precession cine MRI in axial view of superior sinus venosus defect.** Posterior wall of superior vena cava (*SVC*) is absent, allowing oxygenated blood from right superior pulmonary vein (*RPV*) to return to right side of heart. *Ao*, Aorta.

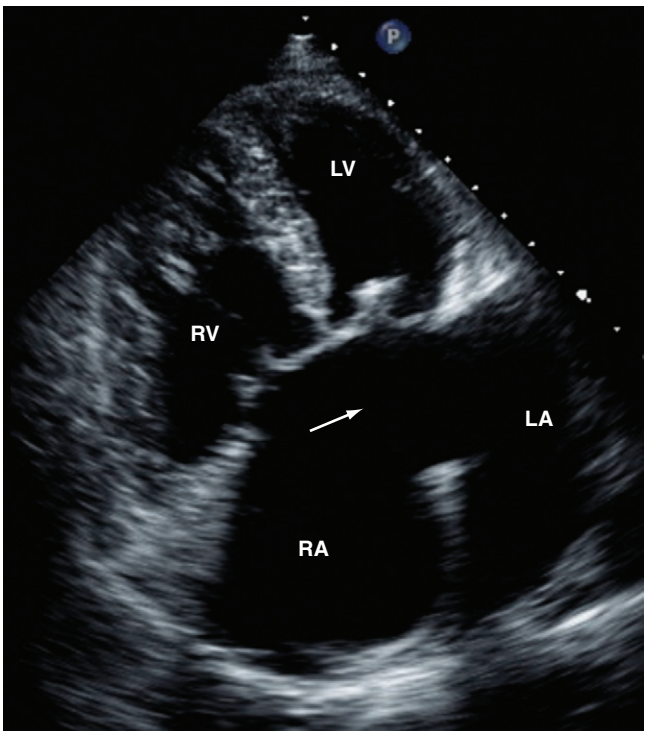



**Figure 44-12 Apical four-chamber echocardiographic view from a patient with a primum atrial septal defect (*arrow*).**

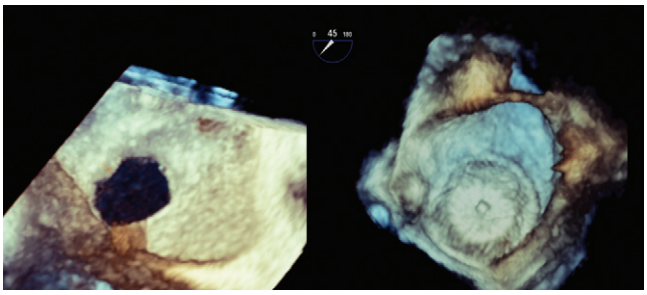


**Figure 44-13** 3D TEE image of en face view of a secundum atrial septal defect (*left*) and similar view following percutaneous device closure of defect (*right*).

The interatrial septum is easily imaged with the probe in the midesophageal position. At 0°, the crux of the heart is well seen, and ostium primum and secundum atrial defects are apparent. From the 90° bicaval view, the superior vena cava entry into the RA is clearly defined and superior sinus venosus defects can be detected. The flaplike opening of the patent foramen ovale can also be appreciated in this view. ASDs vary in shape, making the measurements of the defect in two orthogonal views important. The pulmonary veins can be identified from both the transverse and longitudinal planes.

Color flow mapping confirms the presence of shunting, and saline contrast injection may be useful. However, it is important to recognize that contrast injections may yield false-negative results with TEE imaging. Criteria necessary for an adequate contrast injection include the simultaneous presence of both leftward bulging of the interatrial septum and dense contrast filling of the RA, adjacent to the interatrial septum.[113]

### *Management*

Patients with an isolated ASD and evidence of RA or ventricular enlargement should have elective closure of the defect regardless of presence of symptoms. Small ASDs with a diameter less than 5 mm and no evidence of RV overload do not require closure unless associated with paradoxical embolism. Closure of larger ASDs is indicated to prevent long-term complications, such as atrial arrhythmias, reduced exercise tolerance, tricuspid regurgitation, right-to-left shunting and embolism during pregnancy, overt cardiac failure, or pulmonary vascular disease that may develop in up to 5% to 10% of affected patients.[4] Surgical mortality for this lesion is quite low, and long-term follow-up reveals improvement in symptoms, stabilization of pulmonary hypertension, and near-normal long-term survival rates in patients repaired before the age of 25 years.[114-116]

There is some divergence of opinion regarding closure of ASDs in older adults. One natural history study found no difference in survival or symptoms and no difference in the incidence of new arrhythmias, stroke, emboli, cardiac failure, or progressive pulmonary hypertension between medically and surgically treated patients over the age of 25 years.[117] A subsequent large series of adults over the age of 40 years, however, demonstrated a significant reduction in mortality and dramatic improvement in functional class after ASD closure compared with a similar group managed medically. The risk of atrial arrhythmias and attendant embolic complications was not altered by ASD closure.[118] Thus, with low surgical morbidity and mortality and with the availability of transcatheter closure devices, closure of ASDs with a significant shunt is recommended regardless of age.[119]

At present, patients with an incidentally detected patent foramen ovale do not require intervention. The occurrence of an embolic stroke or peripheral embolus in the patient with a patent foramen ovale and no other obvious embolic source may be considered justification for anticoagulation or for surgical or device closure, particularly in a younger adult. However, the results of several ongoing clinical trials are needed to determine if anticoagulation or antiplatelet agents alone are as effective as patent foramen ovale closure in preventing recurrent embolic events (see Chapter 41).

Many secundum ASDs in adults may be referred for percutaneous closure. Several transcatheter closure devices have been designed and are approved by the U.S. Food and Drug Administration for this purpose, such as the Amplatz Septal Occluder (AGA Medical, Golden Valley, Minn.) and the Helex ASD device (W.L. Gore, Flagstaff, Ariz.). The basic device is a flexible wire framework, covered with fabric or filled with foam, that folds inside a catheter delivery system. One portion of the device is extruded on the LA side of the ASD, the delivery sheath is withdrawn across the defect, and the other side of the device is employed along the RA side. Newer generation devices have a thick central core that allows the device to be self-centering within the defect. This characteristic provides better immediate closure rates and permits closure of larger ASDs because less overlap is required to ensure that the device remains well seated. For any of the current devices, the best results are achieved when the defect is centrally located in the interatrial septum because extension of the device beyond the edges of the defect may impinge on the AV valves or extend into the superior vena cava, right superior pulmonary vein, or coronary sinus. Therefore, sinus venosus and primum defects are not suitable for device closure with current technology.

Echocardiography plays an essential role in the selection of patients most suitable for device closure. Assessment of defect size, the overall length of the interatrial septum, the amount of septal rim around the defect, and the degree of mobility or aneurysm of the septum primum are all important factors in evaluating a patient for device closure. Although TTE can provide some of this information, TEE generally is more accurate in adults. The balloon-stretched diameter is the most reliable measurement in selecting a device size, as some traction is placed on the atrial septum in the process of placing the device. Thus, in clinical practice, TTE is used to diagnose the shunt at the atrial level, characterize the location of the defect and its approximate size, determine shunt size, and detect any associated defects. If device closure is considered, TEE before or during catheterization can further define the anatomy, and the balloon-stretched diameter can be measured. TEE guidance in the catheterization laboratory has greatly facilitated the optimal placement of the closure device parallel to the plane of the interatrial septum and centered across the defect (see Chapter 5). In addition, deployment in the atrial appendage or within the mitral valve orifice can be avoided under direct TEE observation. The fully deployed device can then be observed for a period of time before the procedure is completed to ensure that it remains in a good position (Fig. 44-14). Color flow Doppler and contrast echocardiography determine residual patency immediately after deployment. Some centers prefer the use of intracardiac echocardiography to monitor device placement (see Chapter 6). The ultrasound-tipped catheter can be inserted intravenously with local anesthesia

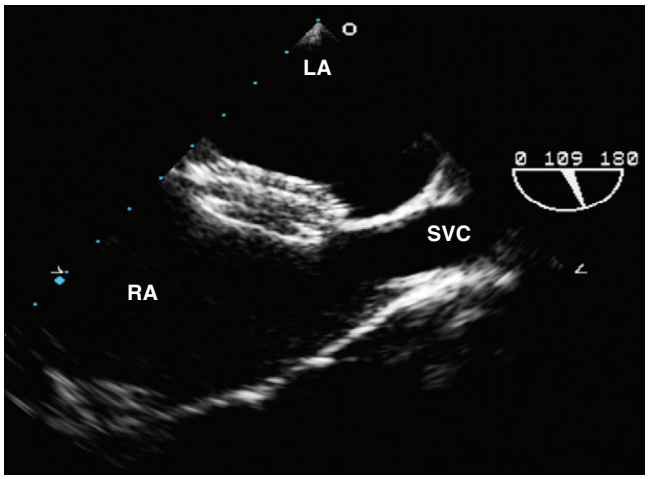



**Figure 44-14 TEE image of interatrial septum with Amplatzer occluder device in place.** *SVC,* Superior vena cava.

and manipulated by the interventionalist, avoiding the need for anesthesia and a separate TEE procedural staff. In experienced hands, intracardiac echocardiographic monitoring has been shown to be equally reliable for delineating the ASD or patent foramen ovale and for assessing device deployment.[120]

Follow-up studies of device closure of ASDs have shown a high rate of successful placement. Residual patency rates are small, with a continued decrease in shunting over time. Although a number of complications have been reported (device embolization, malposition, device erosion through the atrial wall or aorta, endocarditis, and thrombotic emboli), the complication rate is low.[121,122] Endothelialization of the device is thought to occur within 6 months when properly aligned flush with the native septum.[123]

## ANOMALOUS PULMONARY VENOUS CONNECTIONS

Connection of some or all of the pulmonary veins to the systemic circulation results in a left-to-right shunt and RV volume overload. Embryologically, these anomalies are the result of persistence of early fetal connections between the developing lung buds and the systemic venous pathways, with subsequent failure of incorporation of the common pulmonary venous confluence with the LA. Total anomalous pulmonary venous return almost always presents in infancy or early childhood, because of the marked hemodynamic derangement. However, there are rare reports of patients with this condition surviving to adulthood.[124,125] Partial anomalous pulmonary venous connections are occasionally discovered in adults with unexplained right heart dilation. Although there are a myriad possible anomalous connections (Fig. 44-15), the right pulmonary veins are more often involved than the left veins.[126] Commonly, the right pulmonary veins enter the superior vena cava, the superior vena cava–RA junction, or directly into the RA, with or without an associated sinus venosus defect. Anomalous right pulmonary venous connection of the right inferior pulmonary veins is frequently associated with scimitar syndrome, so named because the radiographic appearance of the anomalous pulmonary venous connection to the inferior vena cava resembles a Turkish sword. Anomalous drainage of the left pulmonary veins usually terminates via an ascending vertical vein into the innominate vein.

The clinical presentation of this anomaly is similar to that of an ASD, with a pulmonic flow murmur, RV volume overload, dyspnea, and exercise intolerance. In theory, the amount of left-to-right shunt with partial anomalous pulmonary venous connections should be small because each pulmonary vein carries only 25% of the total pulmonary blood flow. However, the lower resistance encountered in the RA causes preferential shunting of flow to the pulmonary segments that drain anomalously, thereby creating a larger left-to-right shunt.

### *Echocardiographic Evaluation*

As mentioned previously, partial anomalous pulmonary venous connections should be suspected whenever a sinus venosus defect is present and should be carefully considered in patients with a secundum ASD as well. The presence of right heart enlargement without an atrial shunt or other obvious cause of an RV volume overload is also a signal to inspect the pulmonary venous return carefully. Pulmonary venous entry to the LA should be sought in the parasternal short-axis views of the LA, the apical four-chamber view, the subxiphoid views of the LA, and the suprasternal "crab view" of the LA using color flow Doppler to demonstrate the venous inflow streams. If some of the pulmonary veins do not appear to enter the LA, attention should be directed to the known systemic venous entry points. Suprasternal or right parasternal views of the superior vena cava and innominate vein may demonstrate enlargement and more vigorous flow if this is the pathway for the anomalous drainage. Alternatively, the inferior vena cava or coronary sinus may be dilated if pulmonary venous flow is diverted into these systemic venous channels. Direct visualization of the pulmonary vein entry is often difficult in the adult patient by TTE but is occasionally possible when the potential sites of entry are carefully inspected using color Doppler. In experienced hands, TEE is accurate in diagnosing partial anomalous pulmonary venous connections and delineating the sites of anomalous entry.[126] MRI and CT are excellent adjuncts to echocardiography for visualizing pulmonary venous anatomy.[127,128]

### *Management*

Partial anomalous drainage of a single pulmonary vein usually does not create a significant hemodynamic disturbance and often does not require intervention. Anomalous pulmonary veins that cause RV volume overload, or that occur in association with an ASD, should undergo surgical correction. The surgical repair is individualized for the type of anomalous drainage, but whenever possible, anomalous veins are redirected to the LA via a baffle with closure of any associated septal defects.

## VENTRICULAR SEPTAL DEFECTS

VSDs are the most common congenital anomaly recognized at birth, but they account for only about 10% of cases of congenital heart disease in the adult. This decrement in prevalence is in part the result of a high rate of spontaneous closure during the first years of life.[129] In addition, moderate and large lesions generally cause symptoms of heart failure, dyspnea, and failure to thrive in childhood, requiring medical and surgical intervention before adulthood. The VSDs that persist into adult years, therefore, are either small defects, larger defects that have diminished in size, or large defects with irreversible pulmonary vascular disease. Spontaneous closure of VSDs after adolescence is very uncommon. Associated defects are listed in Table 44-2.

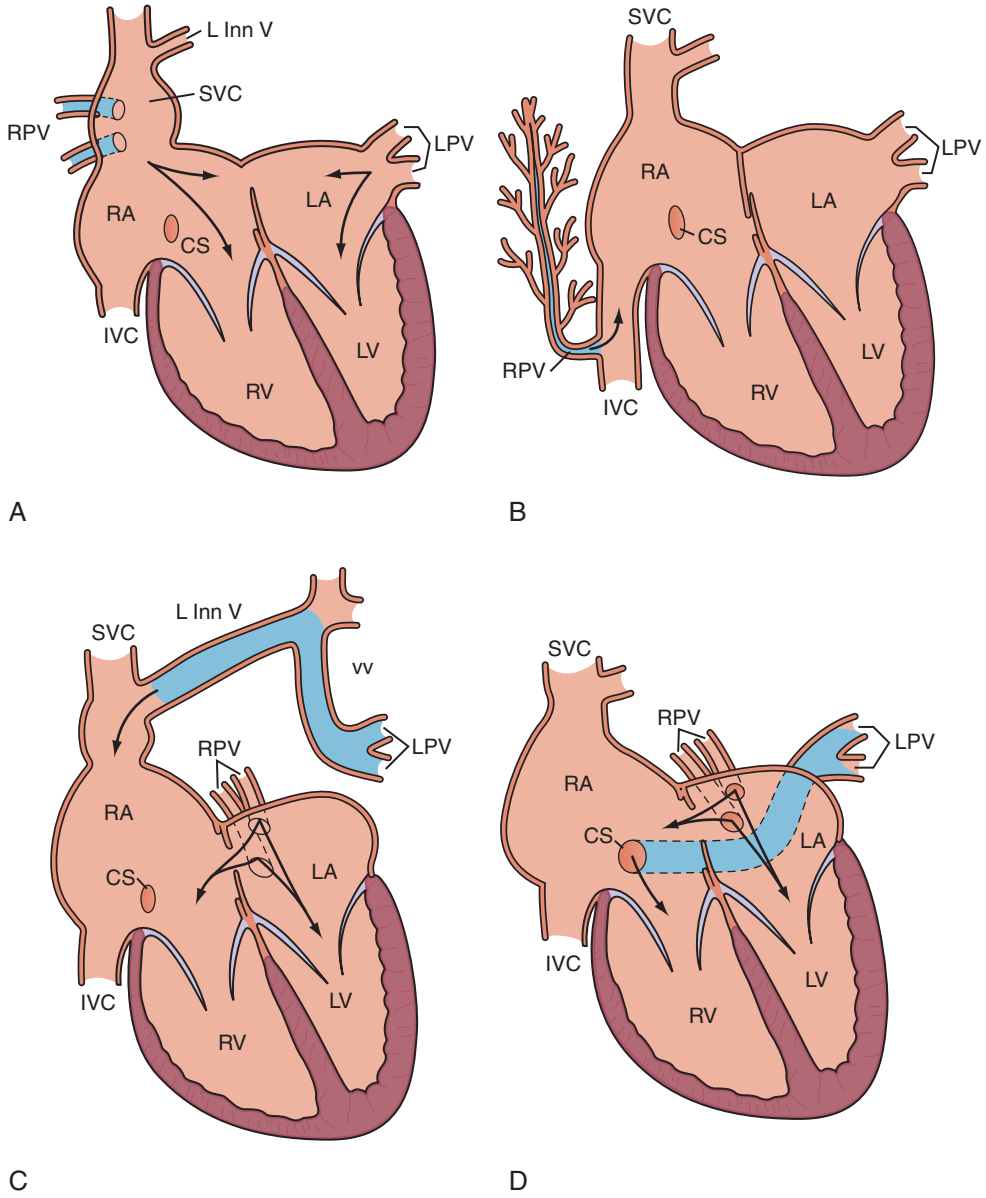



**Figure 44-15** **Diagrammatic depiction of several different types of partial anomalous pulmonary venous return. A,** Right pulmonary veins (*RPV*) drain to superior vena cava (*SVC*). **B,** Right pulmonary veins drain to inferior vena cava (*IVC*). **C,** Anomalous drainage of left pulmonary veins (*LPV*) via ascending vertical vein (*vv*) to left innominate vein (*L Inn V*). **D,** Drainage of left pulmonary veins to coronary sinus (*CS*). *(From Adams FH, Emmanoulides GC, Riemenschneider TA, editors:* Heart disease in infants, children, and adolescents, *ed 4. Williams & Wilkins, 1989, Baltimore, p 583.)*

**TABLE 44-2 Associated Defects with Ventricular Septal Defect**

| *Type of Ventricular Septal Defect* | *Associated Lesion* |
|---|---|
| Perimembranous ventricular septal defect | Septal aneurysm, subaortic stenosis, double-chambered RV |
| Conal septal ventricular septal defect | Aortic valve prolapse |
| Inlet ventricular septal defect | Cleft mitral valve, cleft tricuspid valve, primum atrial septal defect |

**TABLE 44-3 Ventricular Septal Defect Nomenclature**

| *CHS* | *Van Praagh* | *Anderson* | *Other* |
|---|---|---|---|
| Perimembranous | Conoventricular* | Perimembranous outlet | Subaortic |
| Subarterial | Conal septal | Juxtaarterial | Supracristal |
| Inlet | AV canal | Perimembranous | Inlet |
| Muscular | Muscular | Muscular | |

References:
Jacobs JP, Burke RP, Quintessenza JA, Mavroudis C: Congenital Heart Surgery (CHS) Nomenclature and Database Project: ventricular septal defect. *Ann Thorac Surg* 69(4 Suppl):S25-S35, 2000.
Van Praagh R, Geva T, Kreutzer J: Ventricular septal defects: how shall we describe, name and classify them? *J Am Coll Cardiol* 14:1298-1299, 1989.
Anderson RH, Lenox CC, Zuberbuhler JR: The morphology of ventricular septal defects. *Perspect Pediatr Pathol* 8:235-268, 1984.
*AV,* Atrioventricular.
*Not all conoventricular defects are in the perimembranous septum.

There are four anatomic types of VSDs, with multiple synonyms for each type (Table 44-3). The most common location for adult VSDs is the perimembranous ventricular septum (VSD locations, Fig. 44-16). Shunt flow passes from the LV outflow tract to the RV just beneath the septal leaflet of the tricuspid valve. Perimembranous septal aneurysm formation may occur by fibrous tissue proliferation and incorporation of

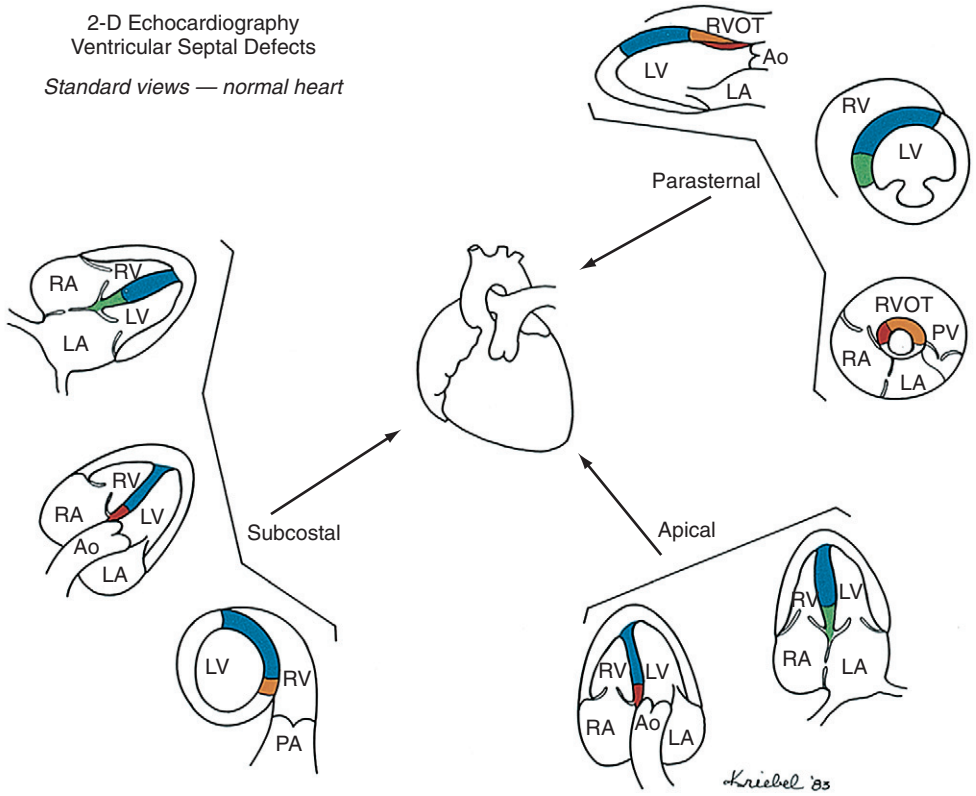



**Figure 44-16 Standard 2D echocardiographic views with color coding of the location of the common types of ventricular septal defects.** Perimembranous septum is coded in *red*, supracristal or infundibular septum in *orange*, inlet septum in *green*, and muscular septum in *blue*. *Ao*, Aorta; *PA*, pulmonary artery; *PV*, pulmonic valve; *RVOT*, right ventricular outflow tract. *(From Levine RA, Gillam LD, Guyer DE, et al: Echocardiography: principles and clinical applications. In Eagle KA, Haber E, DeSanctis RW, Austen WG, editors:* The practice of cardiology, *ed 2, Boston, 1989, Little, Brown and Company, p 1554.)*

the septal tricuspid valve leaflet. The aneurysm limits shunt flow and occasionally closes the defect entirely (Fig. 44-17). Aneurysms may become quite large and have been noted to cause turbulence and obstruction in the RV outflow tract. Distortion of the septal leaflet from incorporation into the septal aneurysm may create a communication from the LV outflow tract into the RA, a Gerbode defect. Over time, this defect leads to RA and RV volume overload and atrial arrhythmias. In some perimembranous VSDs, the support of the right aortic cusp is undermined, leading to prolapse of this cusp into the defect. Progressive aortic regurgitation often becomes a more important hemodynamic issue than the ventricular shunt. Subaortic membranes may also develop in association with perimembranous VSDs. Another important associated finding in patients with perimembranous VSDs is double-chamber RV. A low-lying obstructive muscle bundle develops between the inlet and outlet portions of the RV and may lie either proximal or distal to the VSD. This RV outflow obstruction results in RV hypertension, which may be mistaken for pulmonary hypertension from the VSD shunt if the muscle bundle is not detected.

Muscular VSDs are the next most common type of septal defect. The smaller muscular defects often close spontaneously, and the ones that persist into adulthood are generally quite large, sometimes multiple, and associated with pulmonary vascular obstructive disease (Eisenmenger syndrome). These patients may present with cyanosis from reversal of shunt flow. Pulmonary hypertension is avoided in a few individuals by the development of muscular hypertrophy of the RVOT, a sort of natural pulmonary banding referred to as the Gasul

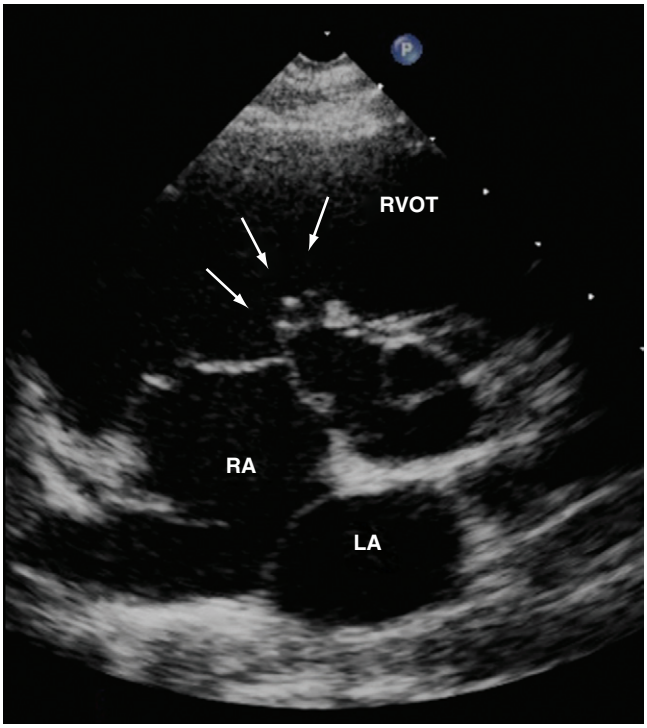



**Figure 44-17 Parasternal short-axis echocardiographic view from patient with perimembranous ventricular septal defect and perimembranous septal aneurysm.** The aneurysm protrudes into the right ventricular outflow tract (*RVOT*) and has associated tricuspid valve septal leaflet tissue.

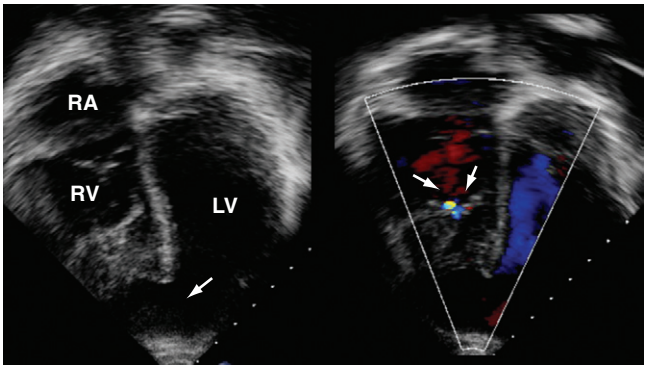



**Figure 44-18 Four-chamber echocardiographic view from patient with large apical muscular ventricular septal defect (VSD) (*arrow*).** Color flow Doppler reveals small area of aliasing (*arrows*) that represents turbulent flow from RV apex through moderator band, which has hypertrophied and effectively closed the large apical VSD shunt.

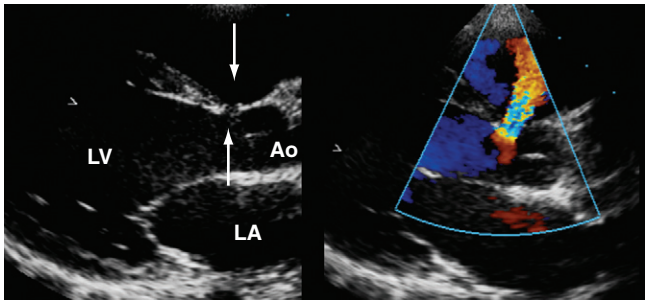



**Figure 44-19 Parasternal long-axis echocardiographic view from a patient with a perimembranous septal defect (*arrows*).** Color flow Doppler reveals shunt flow. *Ao*, Aorta.

phenomenon.[130] Hypertrophy of the moderator band also can restrict shunt flow across sizable apical muscular defects, and when this occurs, the LV and the RV apex become one chamber, giving the cardiac apex an aneurysmal appearance (Fig. 44-18).

Conal septal defects are found more commonly in patients of Asian descent and are frequently associated with aortic regurgitation. Prolapse of the right or left coronary cusp into the VSD may actually decrease the VSD shunt while creating more severe aortic regurgitation.[131] Occasionally, the aortic sinus is extruded through the defect and ruptures, causing a fistula from the aorta to the RV outflow tract.

Defects in the inlet septum are usually the result of a defect in formation of the AV septum. The formation of this portion of the septum is intimately associated with the development of the AV valves and the crux of the heart; therefore, associated AV valve anomalies and a primum ASD are common. Clefts in either the mitral or tricuspid valves may occur. The tricuspid valve occasionally straddles the inlet VSD, with chordal insertions that cross the defect into the left ventricle (LV). When the VSD is small, dense chordal tissue crossing the defect may effectively obstruct flow, limiting the shunt size. Fibrous aneurysms also occur with AV septal defects, decreasing or closing the ventricular septal communication. In most cases, however, an inlet VSD is large and rarely closes spontaneously. AV septal defects are frequently seen in adults with Down syndrome.

### *Echocardiographic Evaluation*

The interventricular septum is a complex fibrous and muscular structure requiring careful interrogation of all aspects by 2D imaging and color Doppler to detect VSDs. Perimembranous VSDs (Fig. 44-19) are best seen in the parasternal long-axis and short-axis views as echo dropout beneath the aortic valve and near the attachment of the septal leaflet of the tricuspid valve. Apical or subcostal five-chamber views also demonstrate the position of the defect in relation to the LV outflow tract and tricuspid valve. Associated abnormalities of the right aortic cusp, subaortic region, and septal aneurysm formation should be delineated. Interrogation for the presence of an obstructive muscle bundle in the RV must be performed. The conal septal VSD can be appreciated in the parasternal long-axis view at the base of the heart, located immediately proximal to the pulmonic valve. If the right aortic cusp has become distorted and prolapses into the VSD, the defect itself may not be detected without color or PW Doppler. Muscular septal defects may be located anywhere within the trabecular septum. Careful scrutiny of parasternal short-axis sweeps and apical, off-axis apical, and subcostal views is required to detect muscular defects. Inlet VSDs are most apparent in apical or subcostal four-chamber views directed posteriorly toward the crux of the heart.

Assessment of the LA and LV chamber size and function is important. Long-standing volume overload is associated with enlargement of left heart structures and may cause LV failure in the adult. In the clinical setting of endocarditis, vegetations can be detected on the aortic valve, the perimembranous septal aneurysm, or the tricuspid valve septal leaflet. Endarteritis at the site of the jet lesion within the RV or RV outflow tract is usually not detectable by 2D imaging unless vegetations are extensive.

Color flow mapping greatly enhances the sensitivity of detection of all forms of VSDs. Left-to-right shunts are readily detected as turbulent jets crossing the septum into the RV when the PA pressures are normal. Ambiguity may occur when there is little difference between left and right heart pressures because shunt flow is low in velocity and difficult to distinguish from other low-velocity flow within the right heart. PW and CW Doppler studies are helpful to confirm the timing and velocity of shunt flow. With small perimembranous and conal septal VSDs, low-velocity diastolic shunt flow may precede the high-velocity systolic jet, presumably owing to the slight differences in late diastolic pressures between the RV and LV. This diastolic flow is sometimes mistaken clinically for aortic regurgitation or another aortic runoff lesion such as a sinus of Valsalva fistula or coronary artery fistula.

CW Doppler measurement of the VSD peak jet velocity allows estimation of RV systolic pressures, and consequently PA systolic pressures. By applying the modified Bernoulli equation, one can calculate the pressure gradient between the left and RV from the VSD peak velocity. Subtracting this gradient from the cuff systolic blood pressure yields the RV systolic pressure (Fig. 44-20). Alignment as parallel as possible to the direction of the VSD jet prevents underestimation of the gradient between the ventricles. Sampling from multiple windows or off-axis views may be required to achieve the best alignment.

Shunt quantification by PW Doppler can be performed in the same way as with ASDs. Measurement of cardiac output across the pulmonic and aortic valves is made, and the pulmonic-to-systemic flow ratio ($Q_p/Q_s$) is computed. The turbulence created in the PA by shunt flow from nearby perimembranous and conal septal defects may make measurement of the pulmonary velocity-time integral inaccurate.

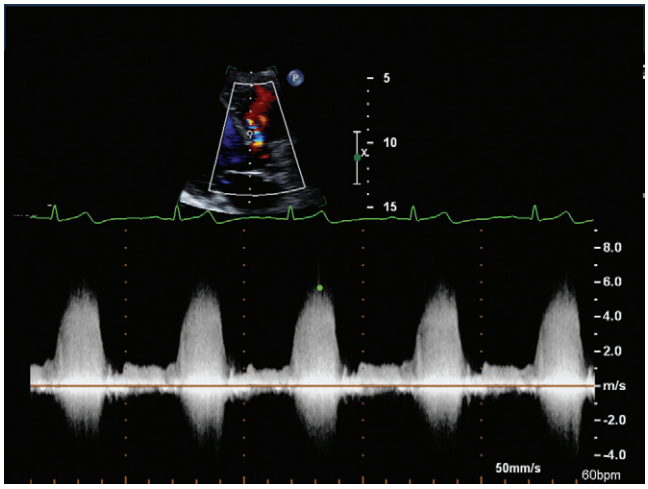



**Figure 44-20 CW Doppler spectral tracing of a ventricular septal defect shunt flow.** RV systolic pressure can be estimated by subtracting LV to RV pressure difference from systolic blood pressure. In this example, transseptal pressure gradient is $4V^2 = 4(5)^2 = 100$ mm Hg. With systolic blood pressure of 130 mm Hg, estimated RV systolic pressure is normal at 30 mm Hg.

An alternative method for deriving shunt ratios involves calculating the volumetric shunt flow across the VSD and adding it to the systemic cardiac output to get the pulmonary flow:

$$Q_p = Q_s + \text{VSD shunt}$$

The VSD shunt volume is the product of the cross-sectional area of the color flow jet at the defect and the velocity-time integral of the CW Doppler systolic flow signal. In one study, this method had better correlation with shunt ratios determined by the Fick method than the standard PW Doppler calculation of $Q_p/Q_s$.[132] It may prove particularly useful in patients with pulmonic stenosis or in whom the pulmonary annulus or pulmonary flow profile is difficult to measure.

### *Management*

The outcome of asymptomatic adults with small VSDs that have not been closed during childhood is excellent.[133,134] Surgical intervention for the adult with a small VSD with no significant LV volume overload and normal PA pressures is not necessary. Periodic follow-up is important, to reassess ventricular size and function and to follow PA pressures. Closure of a small VSD may be indicated when intervention is needed for associated abnormalities, such as significant aortic regurgitation or RV outflow tract obstruction. Surgical closure of a VSD is indicated for patients with a $Q_p/Q_s$ of greater than 2.0 and clinical evidence of LV volume overload or a history of infective endocarditis.[4]

Patients with large VSDs and irreversible pulmonary vascular obstructive disease should be managed medically. In select cases, small VSDs in adults may be closed percutaneously. Indications include residual defects after surgical closure, a history of bacterial endocarditis, or a hemodynamically significant left-to-right shunt. Appropriate placement requires a sufficient distance from the aortic valve or the AV valves to avoid damaging these structures. Acquired heart block, device embolization, and endocarditis have all been described as infrequent complications following device placement.[135,136]

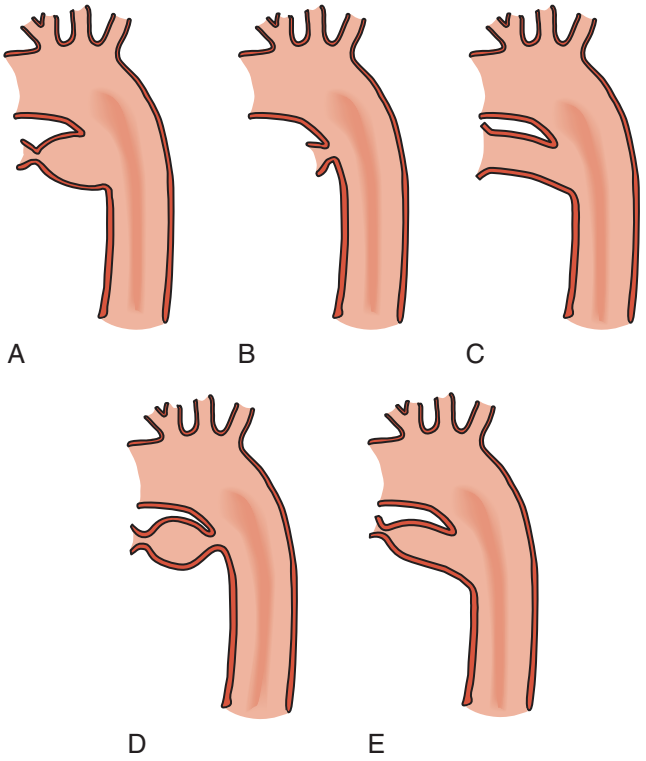



**Figure 44-21 Various shapes of patent ductus arteriosus as seen angiographically.** Ductus is shown arising from lesser curvature of aortic arch. Its configuration varies from window-like communication to long tortuous channel (**A** to **E**). Knowledge of ductal shape is important in choosing best method of transcatheter closure. *(Modified from Krichenko A, Benson L, Burrows P, et al: Angiographic classification of the isolated, persistently patent ductus arteriosus and implications for percutaneous catheter occlusion.* Am J Cardiol *63:878, 1989. Reprinted by permission of the publisher. Copyright 1989 by Excerpta Medica Inc.)*

## PATENT DUCTUS ARTERIOSUS

The ductus arteriosus is a normal fetal cardiac structure that functionally closes within the first days of life. It arises from the PA bifurcation near the origin of the left PA and inserts into the lesser curvature of the descending thoracic aorta. Ductal shape is quite variable, sometimes being a long, tortuous channel or a conical connection or even a short window-like communication (Fig. 44-21). The ductus arteriosus normally closes spontaneously within the first 24 to 48 hours of life. Persistence beyond the neonatal period is abnormal, and spontaneous closure after the first year of life is distinctly uncommon. This lesion is found only in about 2% of adults with congenital heart disease. It is usually an isolated anomaly, but it can occur in association with complex lesions, VSD, or coarctation. The ductal tissue becomes more friable and calcified with increasing age. Aneurysms of the ductus arteriosus or the closed ductal diverticulum also occur and may rupture.

The clinical presentation of an adult with a patent ductus arteriosus depends on the size of the shunt. Trivial shunts may be clinically silent, detected by an echocardiographic Doppler study that was requested for an unrelated lesion. Small ductal shunts produce a continuous murmur at the left upper sternal border, which can be confused with the murmur of a coronary artery fistula, mixed aortic valve disease, or a VSD with aortic regurgitation. Patients with moderate or large shunts develop heart failure and atrial arrhythmias from the long-standing LV

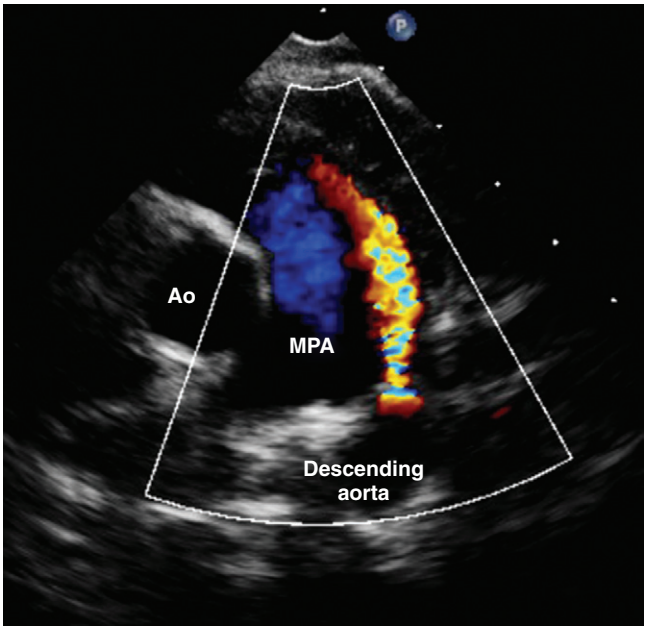



**Figure 44-22 Parasternal short-axis echocardiographic view of base of heart demonstrating small patent ductus arteriosus.** Stream of left-to-right shunt flow is show in color as it passes from descending thoracic aorta to the main pulmonary artery (*MPA*). *Ao*, Aorta.

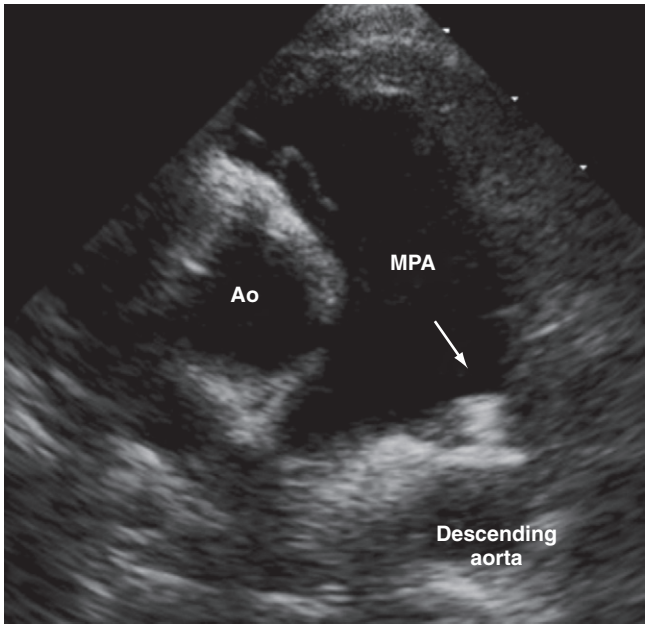



**Figure 44-23 Parasternal short-axis echocardiographic image from patient following patent ductus arteriosus occluder device closure.** Occluder device (*arrow*) is seen near origin of left pulmonary artery. *Ao*, Aorta; *MPA*, main pulmonary artery.

volume overload. With the onset of pulmonary hypertension and reversal of the shunt, the murmur decreases in intensity or disappears and differential cyanosis of the extremities may be noted.

### *Echocardiographic Evaluation*

2D imaging of the ductus arteriosus is accomplished with ease in the neonate and young child, but it becomes more challenging in older adolescents and adults. The direct view of the ductal channel is best obtained in a high left parasternal window at the PA bifurcation where the left PA crosses the descending thoracic aorta. The main PA appears to "trifurcate" with the third channel being the ductus. Visualization is possible in the suprasternal notch views of the aorta focused on the lesser curvature of the aorta opposite to the left subclavian artery. Diagnosis of a patent ductus arteriosus in the adult usually is made with color flow Doppler imaging rather than direct 2D imaging. The left-to-right flow stream appears as a red jet in diastole entering the main PA near the left PA origin (Fig. 44-22). Although patent ductus arteriosus shunt flow is continuous, the systolic component is usually washed along with the systolic flow in the main PA. If flow can be visualized within the ductus itself, however, a continuous Doppler signal is present. As the PA pressure rises, the velocity of the patent ductus arteriosus shunt decreases, and it becomes more difficult to distinguish a discrete patent ductus arteriosus jet from other low-velocity flows within the dilated pulmonary vessel. Adults with a dilated main PA often have a low-velocity retrograde flow in late systole from swirling of flow within the enlarged vessel. PW Doppler can distinguish this from ductal flow by the difference in timing. Continuous flow into the PA also is seen with coronary artery fistulas and with an aortopulmonary window. Demonstration of the color Doppler flow stream emanating from the bifurcation and originating within the descending thoracic aorta should confirm that the shunt comes from a patent ductus arteriosus.

CW Doppler sampling of ductal shunt flow is important for estimation of PA pressure. When the ultrasound beam is aligned from the high left parasternal window directly into the mouth of the patent ductus arteriosus, systolic and diastolic flow velocity can be recorded. Applying the modified Bernoulli equation, the peak systolic velocity of the patent ductus arteriosus jet can be used to calculate the systolic gradient between the aorta and the PA. Subtracting this gradient from the cuff systolic aortic blood pressure yields the PA systolic pressure.

### *Management*

Indications for patent ductus arteriosus closure include LA and/or LV enlargement, net left-to-right shunting, or prior endocarditis.[4] A patent ductus arteriosus discovered in the adult is often friable and calcified, and percutaneous device closure is often feasible. If the patent ductus arteriosus is associated with other cardiac lesions that require surgical correction, the ductus may be closed at the time of surgery; however, percutaneous closure before surgery may also be entertained. Percutaneous closure of a patent ductus arteriosus in an adult is usually technically successful, with a low rate of complications.[137] Several types of devices are currently in use, including a pluglike occluder within the ductus, umbrella devices that occlude the orifices at each end of the ductus, and coils that are extruded within the ductus and thrombose the channel.[138] TEE guidance of device placement has not played as critical a role for the ductus arteriosus as for ASD closure. The difficulty in imaging the anatomic details of the ductus arteriosus by TEE limits the usefulness of this modality, and fluoroscopic monitoring alone is sufficient for accurate placement.

TTE Doppler assessment after device closure is quite helpful to ensure appropriate device position and assess residual shunting. The highly reflective device can be appreciated by 2D imaging of the pulmonary bifurcation and along the lesser curvature of the aorta (Fig. 44-23). Malpositioning of the patent ductus arteriosus devices can result in protrusion of a portion of the occluder into the aortic lumen or into the main PA.[139] Feasibility and efficacy of device or coil occlusion of the patent ductus arteriosus are excellent. Complication rates are low but include device or coil embolization, hemolysis, and left PA stenosis.

## CORONARY ARTERY FISTULAS

A coronary artery fistula is an abnormal communication of a coronary artery with a cardiac chamber, great vessel, or other vascular structure without passing through the myocardial capillary bed. Most coronary artery fistulas are congenital, resulting from persistence of embryonic channels between cardiac chambers and the developing coronary circulation. Coronary artery fistulas are rare, reported in 0.2% of coronary angiograms, and are often discovered incidentally.[140] The clinical presentation depends on the site of termination of the fistula and the degree of shunting. Over 90% of coronary artery fistulas terminate in the right heart—RV, RGA, PA, coronary sinus, or superior vena cava. A continuous murmur is caused by shunting from the aorta to the right heart. When the fistula communicates to the LV, the murmur is audible only in diastole. Shunting is usually modest; in a review of a single-center experience with coronary artery fistulas, the median pulmonary-to-systemic flow ratio was 1.3 : 1.[141] Signs of RV volume overload and heart failure may appear later in life from the long-standing left-to-right shunt. The shunt is rarely large enough to cause severe pulmonary hypertension. Angina related to myocardial ischemia has been reported in a small number of patients as a result of "coronary steal" as the fistula diverts flow from the normal coronary circulation.[142]

### *Echocardiographic Evaluation*

Echocardiographic Doppler diagnosis of coronary artery fistula begins with the detection of enlargement of the proximal coronary artery involved in the abnormal communication. The affected coronary vessel is diffusely enlarged and can often be traced to the site of termination with knowledge of the expected coronary course and the usual sites of fistulous communication. Aneurysmal lakes develop near the communication with the receiving chamber or vessel, appearing as large sonolucent regions (Fig. 44-24). Enlargement of the heart chambers give an indication of the amount of left-to-right shunting.

Color flow Doppler demonstrates continuous flow with the involved coronary artery and helps to localize the exit site.[143,144] When a small fistula from the left coronary artery to PA is present, a tiny stream of continuous flow may be found incidentally in the proximal main PA. Larger fistulas are diagnosed by scanning the RA, RV, and LV for a continuous turbulent flow signal.

TEE can also detect coronary enlargement and visualize the enlarged and aneurysmal channels of the fistula. It is particularly helpful intraoperatively to assess residual fistulous flow and segmental wall motion after ligation of the feeding coronary vessel.[145]

Contrast echocardiography has been used in conjunction with angiography to detect fistulous communication when there are multiple entry sites of a coronary artery fistula.[146] If the fistula terminates in both the RV and LV, angiographic contrast may stream preferentially to the lower-pressure chamber. Faint opacification of the LV easily may be overlooked. With injection of agitated saline into the arterial catheter, however, even a trace of contrast in the LV is obvious echocardiographically.

### *Management*

Small, clinically silent fistulas do not require closure. Patients with fistulas that are large enough to cause coronary dilation should be followed clinically for development of symptoms of myocardial ischemia or ventricular volume overload. Coronary angiography is generally necessary to completely evaluate the coronary circulation for coexistent atherosclerotic disease and for complete anatomic delineation of the fistula. Closure of large fistulas may be approached surgically or with transcatheter coil occlusion or devices, depending on the specific anatomy of the lesion.[147,148]

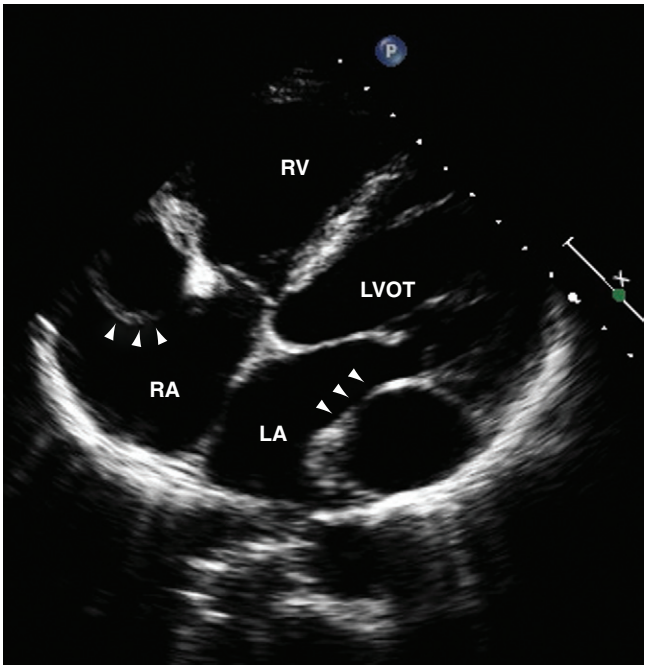



**Figure 44-24 Off-axis apical four-chamber echocardiographic view from patient with coronary artery fistula demonstrating large venous lakes (*arrowheads*) seen along atrial surfaces.** *LVOT,* Left ventricular outflow tract.

# Complex Congenital Heart Disease

Adults who survive with complex congenital heart defects represent a small but intriguing fraction of an adult cardiology practice. In the current surgical era, the vast majority of patients with complex lesions have had palliative surgeries during childhood (see Chapter 45). The rare patient reaches adulthood without prior intervention and seeks medical attention for symptoms that may be typical of acquired heart disease—heart failure, angina, arrhythmias, endocarditis—only to be found to have complex congenital heart disease when an echocardiographic study is performed. A brief consideration is given here to some of the complex lesions that permit natural survival into adulthood.

## TETRALOGY OF FALLOT

Originally described by Stensen in 1671, the anatomic features of "la maladie bleue" as detailed by Fallot in 1888 included a large VSD, an overriding aorta, pulmonic stenosis, and RV hypertrophy (Fig. 44-25). Approximately 15% of patients have an ASD (pentalogy of Fallot) and 25% have a right aortic arch. Anomalous origin of the left anterior descending coronary artery or bilateral left anterior descending vessels occur in up to 9% of patients, which may complicate the patch repair of the RV outflow tract as the anomalous vessel passes over it.[149,150]

Physiologically, the clinical picture with tetralogy of Fallot is that of a VSD with RV outflow obstruction of variable severity. Most patients develop severe cyanosis within the first year of

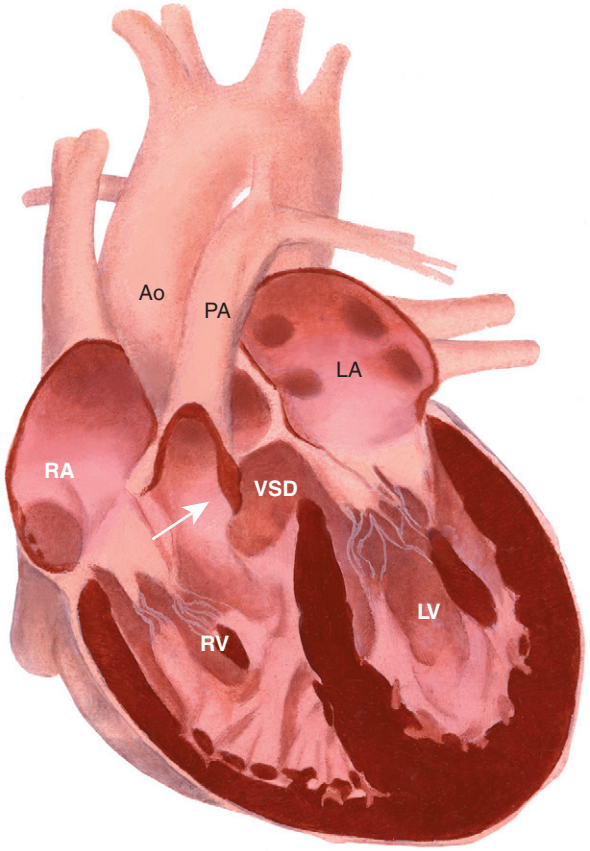



**Figure 44-25 Anatomic features of tetralogy of Fallot.** There is a large subaortic ventricular septal defect (*VSD*), aorta (*Ao*) straddling ventricular defect, and deviation of conal septum (*arrow*) into RV outflow tract creating subpulmonic stenosis.

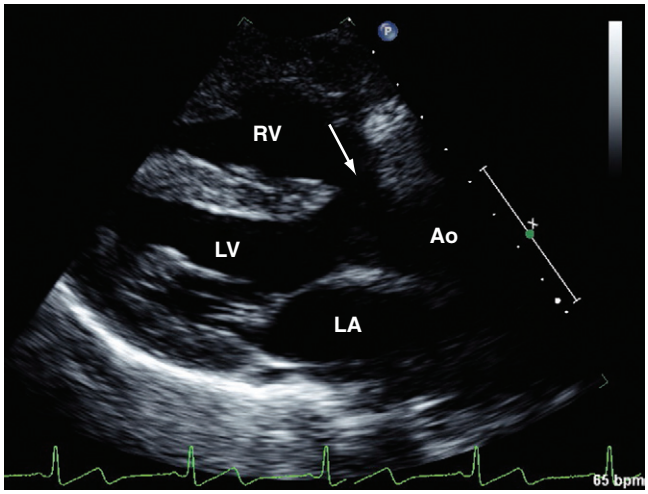



**Figure 44-26 Parasternal long-axis view from patient with tetralogy of Fallot demonstrating large conoventricular septal defect (*arrow*) and aortic (*Ao*) override of interventricular septum.**

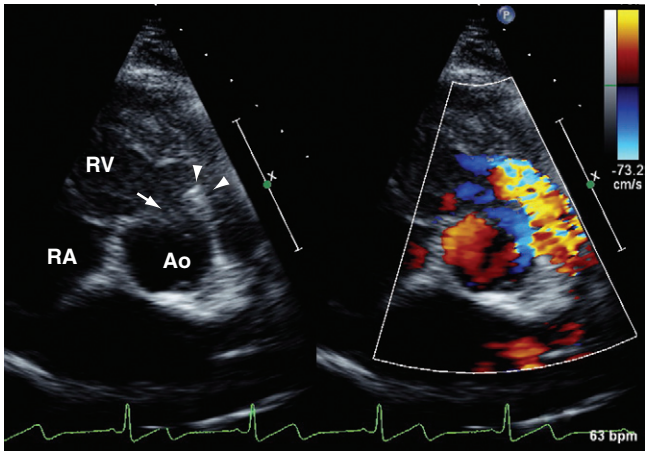



**Figure 44-27 Parasternal short-axis views from patient with tetralogy of Fallot demonstrating anterior deviation of conal septum (*arrowheads*).** *Arrow* indicates ventricular septal defect. Color flow Doppler reveals acceleration of blood flow at this level. *Ao*, Aorta.

life, requiring surgical palliation or correction. Only 11% of patients will survive to adulthood without intervention.[151] With only a modest degree of pulmonic stenosis, patients may survive with few symptoms into adult years. Paradoxically, the other group of late survivors without surgery includes patients with complete obstruction to blood flow. This subgroup of patients, those with pulmonic valve atresia and VSD, has multiple aortic-to-pulmonary arterial collaterals that supply the pulmonary circulation with only a modest amount of systemic desaturation. Morbidity and mortality in this group of patients is commonly due to symptoms from chronic hypoxia and secondary erythrocytosis and includes cerebrovascular accidents, brain abscess, endocarditis, and arrhythmias.

### *Echocardiographic Evaluation*

Echocardiographic Doppler evaluation can accurately define the characteristic features of tetralogy of Fallot. The conoventricular VSD usually is large and lies immediately beneath the dilated overriding aortic root (Fig. 44-26). In the parasternal views of the LV, the size of the VSD can be appreciated. The direction and velocity of shunt flow across the defect are easily determined in these planes by color flow and PW Doppler imaging. Unless the VSD has become restrictive over time, the shunt is low velocity and predominantly right-to-left. Parasternal short-axis views of the RVOT and aorta demonstrate the typical anterior deviation of the conal septum and narrowing of the RVOT (Fig. 44-27). A small pulmonary annulus, valvular pulmonic stenosis, and hypoplasia of the main and branch pulmonary arteries also are visible in this view. The systolic gradient across the stenotic outflow tract should be measured by CW Doppler imaging. In patients with native or acquired pulmonary atresia, the RVOT is filled with muscle and ends blindly with no visible pulmonic valve leaflets and no detectable flow by PW Doppler. When the parasternal views are not able to visualize the PA because of chest wall or lung interference, scanning from the suprasternal notch or high left subclavicular area may provide the necessary access to the branch pulmonary arteries. The proximal right PA is measurable in nearly all patients with confluent pulmonary arteries. Suprasternal or high parasternal views of the ascending aorta are most accurate for measuring the right PA, which passes behind the aorta as a small cross-sectional lumen in the long-axis plane. Aortopulmonary collaterals can be detected but are not fully delineated by 2D echocardiography. Apical and subcostal five-chamber views depict the large VSD and the overriding aorta. Aortic root dilation and regurgitation can also be evaluated at this point in the examination. Moving the scan plane even more anteriorly from the five-chamber view brings the RVOT into view. This approach may provide better alignment of the Doppler cursor for sampling the RV outflow tract gradient.

In the cross-sectional views of the aortic root at the base of the heart, attempts should be made to visualize the coronary arteries. Enlargement of the right coronary orifice hints at a larger blood supply through this vessel, perhaps caused by the anomalous origin of the left anterior descending coronary artery. Careful attention should be directed to the cross-sectional lumen seen anterior to the RV outflow tract in the high parasternal views and to anteriorly coursing vessels arising from the proximal right coronary artery. Although some success has been reported with TTE study of the coronary arteries in adults with tetralogy of Fallot,[152] an alternative imaging modality is often needed in preoperative adults.

Transesophageal imaging in tetralogy of Fallot can provide nearly all the important diagnostic information. Malalignment of the conal septum is apparent in the midesophageal longitudinal views of the RV outflow tract or from the transgastric approach. The pulmonic valve anatomy and the sizes of the main and right PA can be determined from the transverse views in the midesophagus or high esophagus. The left PA is often more difficult to image. The VSD and overriding aorta can be appreciated in transverse views from the midesophagus and from transgastric views.

### *Management*

Some adults with tetralogy of Fallot will be candidates for complete repair. Surgery for this lesion can be accomplished in the adult with acceptable mortality and with gratifying relief of cyanosis and improvement in functional class. In the subgroup with pulmonary atresia, decisions regarding surgical correction are based on the confluence and size of the PAs and the size and distribution of aortopulmonary collaterals.

## CONGENITALLY CORRECTED TRANSPOSITION OF THE GREAT ARTERIES (CCTGA OR L-LOOP TGA)

Also known as "physiologically corrected transposition of the great arteries," this is a malformation in which the great arteries are transposed but the ventricles are inverted and discordant relative to the atria (Fig. 44-28; see also Fig. 43-11). In the absence of associated lesions, L-loop TGA (Fig. 44-29) may not be clinically recognized and is compatible with a normal life span.[153,154] Complete heart block is increasingly prevalent with increasing age.[155] Several associated lesions may be present and are listed in Box 44-8.

Even with associated lesions, L-loop TGA is often compatible with survival into adulthood. The limiting factor is often the degree of systemic RV dysfunction and tricuspid regurgitation.[156,157] Severe tricuspid regurgitation is associated with poor long-term outcomes in this patient population.

### *Echocardiographic Evaluation*

The anatomic features and echocardiographic diagnosis of this lesion are reviewed in Chapter 43. Clinical echocardiographic-Doppler follow-up in patients with L-loop TGA is directed toward monitoring systemic RV function and systemic AV valve regurgitation. Ventricular shunting and pulmonary outflow obstruction also require serial assessment. Standard geometric models for assessing LV volumes and ejection fraction do not accurately model the unusual shape of the systemic RV; therefore the Simpson's rule method using two orthogonal apical planes may be a more accurate echocardiographic method for calculating systemic ventricular volume and function in this

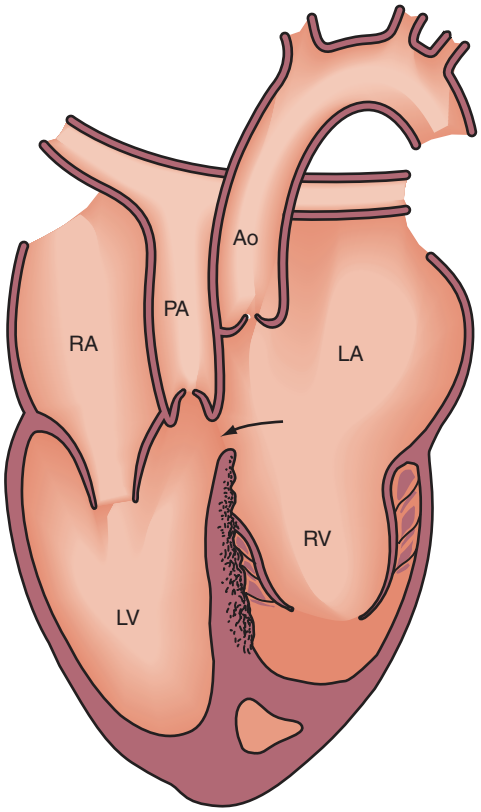



**Figure 44-28 Anatomic features of congenitally corrected transposition.** Aorta (*Ao*) lies anterior and to left of pulmonary artery (*PA*). It arises from morphologic RV, which is left sided. Most commonly associated lesions include pulmonic stenosis, ventricular septal defect (*arrow*), and Ebstein-like malformation of left-sided tricuspid valve. *(From King ME: Complex congenital heart disease II: a pathologic approach. In Weyman AE, editor:* Principles and practice of echocardiography, *ed 2, Philadelphia, 1994, Lea & Febiger, p 1038.)*

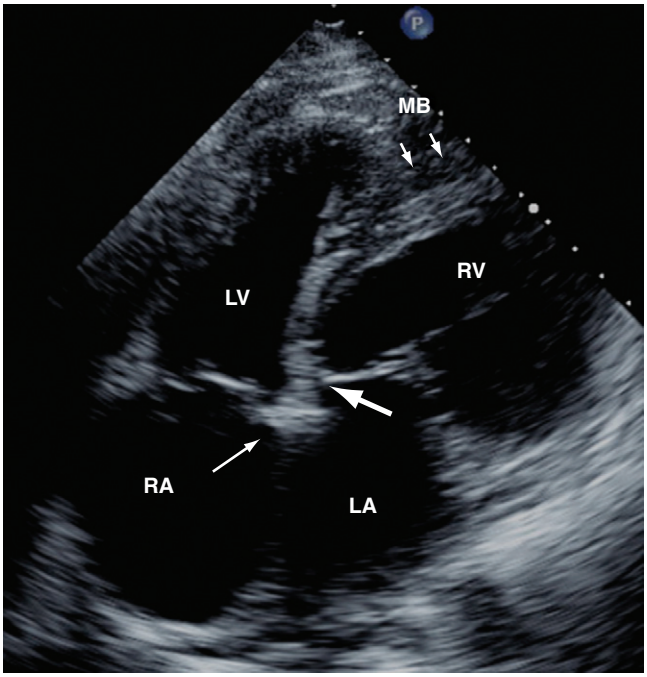



**Figure 44-29 Congenitally corrected transposition of the great arteries.** Off-axis apical four-chamber echocardiographic view shows that the anatomic RV has tricuspid valve (*large arrow*), which is more apically positioned than the mitral valve (*small arrow*). Prominent moderator band (*MB*) is visualized in RV (*double arrows*).

**Box 44-8**

**ASSOCIATED DEFECTS WITH CONGENITALLY CORRECTED TRANSPOSITION OF THE GREAT ARTERIES**

Ventricular septal defect
Pulmonary outflow obstruction
Ebstein malformation of the tricuspid valve
Dextrocardia
Ventricular noncompaction
Atrioventricular conduction abnormalities

group. Three-dimensional echocardiography does not require geometric assumptions and is an alternative modality for evaluating this anatomy.[158] Magnetic resonance imaging is also useful in following systemic RV function.[159,160] An alternative nongeometric means of serially following systemic ventricular function in this group of patients is the myocardial performance index, which uses Doppler measures of isovolumic time intervals and ejection time.[161]

### *Management*

The diagnosis of L-loop TGA may be made for the first time in adulthood; in one cohort the initial diagnosis was made in adulthood in 66% of patients, 17% of whom were more than 60 years of age at the time of diagnosis.[154] The asymptomatic adult patient with L-loop TGA requires no intervention. The incidence of complete heart block increases with age, and caution must be taken during any invasive cardiac procedures. The electrocardiogram demonstrates deep Q waves in the right precordial leads that can be mistaken for ischemic injury. The prevalence of systemic RV failure is difficult to determine, as the definition of systemic RV failure is widely variable in the literature, and this group is often discussed in combination with people who have undergone atrial switch procedures for complete (D-loop) transposition of the great arteries (see Fig. 43-10 and Chapter 45). Medical management of systemic RV dysfunction is appropriate, although studies are limited documenting the benefits of medical therapies proven for LV dysfunction, such as angiotensin-converting enzyme inhibitors or angiotensin receptor blockers.[162]

Patients with associated VSD and pulmonic stenosis should be managed in a similar fashion to those with normally related great arteries. If pulmonary outflow tract obstruction is severe enough to require operative correction, or if the systemic tricuspid valve requires surgical attention, the options for repair are either physiologic or anatomic. Physiologic repair would entail simply repairing or replacing the tricuspid valve, closing the VSD, or bypassing the pulmonic stenosis with an LV-PA conduit. This, however, leaves the anatomic RV as the systemic ventricle, which is problematic for long-term survival. Anatomic repair requires a double switch procedure, with an atrial switch, a Rastelli procedure to connect the LV to the aorta, and an RV-PA conduit. This anatomic approach is a more extensive surgery, and the result is an anatomic LV as the systemic ventricle and unloading of the RV with its abnormal tricuspid valve. In order for this anatomic surgery to be successful, the LV must be adequately trained to accept systemic pressures (through native pulmonic stenosis or placement of a PA band). This is most often performed in a young age group. The choice of surgical approach must be individualized to the patient's anatomy and physiology.[163,164]

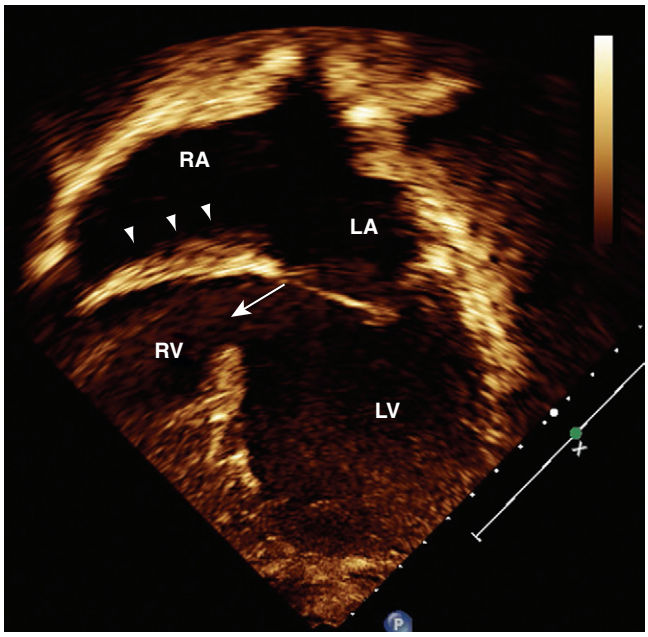



**Figure 44-30 Apical four-chamber echocardiographic view from patient with tricuspid atresia.** Atretic tricuspid valve is a thick, fibrous ridge (*arrowheads*) at base of enlarged RA. Ventricular septal defect (*arrow*) is present, which leads into a tiny RV chamber.

Adults with L-loop TGA should have regular follow-up with a cardiologist who has expertise in ACHD. Echocardiographic Doppler study and/or cardiac MRI should be performed yearly or at least every other year by staff trained in imaging complex congenital heart disease.[4]

## TRICUSPID VALVE ATRESIA

Tricuspid valve atresia constitutes 1% to 3% of all congenital heart defects, and fewer than 10% of patients survive beyond childhood without surgery.[165] In this malformation, the atrioventricular valve of the morphologic RV is absent or imperforate. The RV is variably underdeveloped and there is compensatory left heart enlargement. An atrial septal communication is present to allow egress of blood from the blind RA, and a VSD of variable size is usually present. Most commonly, the great vessels are normally related, but in up to 35% of cases, they are malposed, with or without obstruction to pulmonary blood flow. The physiology in the adult is that of a central mixing lesion creating cyanosis, with VSD and pulmonic stenosis, or VSD and pulmonary vascular disease. The adult with uncorrected tricuspid atresia is susceptible to multiorgan dysfunction due to the complications from chronic cyanosis.

### *Echocardiographic Evaluation*

In the place of the tricuspid valve, a thick band of fibromuscular tissue is recognized by 2D imaging (Fig. 44-30). No evidence of flow can be demonstrated by color or PW Doppler. The RA is enlarged, often with a prominent Eustachian valve. The size of the RV is related to the size of the VSD during fetal development. It may be vestigial and slitlike with a small VSD, or nearly normal in size with a large VSD. Progressive restriction of the VSD may occur.[166] When the great vessels are normally related, progressive VSD closure creates further obstruction to pulmonary blood flow. In patients with transposed great arteries, the systemic blood flow is jeopardized.

Thus, serial determination of the VSD size by 2D imaging and VSD gradient by Doppler is an important part of the echocardiographic evaluation.

The LV in this anomaly is enlarged, and systolic function may be impaired from long-standing volume overload. Quantitative assessment of ventricular function is performed by the usual echocardiographic methods and is an important factor in determining surgical options.

Echocardiographic study in the patient with tricuspid atresia also must focus on the presence, size, and origin of the aorta and PA. The orientation and relative size of the great arteries and associated abnormalities of the valvular and subvalvular region all can be appreciated from parasternal windows. Apical and subcostal images are particularly useful in establishing ventriculoarterial relationships and measuring gradients across the semilunar valves and outflow tracts.

The interatrial septum in the adult with uncorrected tricuspid atresia generally has a large, unrestricted ASD. Apical, subcostal, or right parasternal windows optimally should delineate the atrial septum and demonstrate right-to-left shunting by PW and color Doppler.

### *Management*

Patients with tricuspid atresia and restricted pulmonary blood flow may be candidates for a Fontan procedure, which diverts systemic venous return directly to the PA. The optimal candidate must have good LV function, no significant mitral regurgitation, and normal branch PA anatomy and pulmonary resistance. Natural survivors with tricuspid atresia and pulmonary vascular disease who are not amenable to surgical correction may be considered for heart-lung transplantation.[167]

## FUNCTIONAL UNIVENTRICULAR HEART

The basic element of the functional univentricular heart is communication of both AV valves, or a single common AV valve, with a single ventricular chamber.

Natural survival of adolescents and adults with this complex congenital anomaly depends on fortuitous streaming of oxygenated and unoxygenated blood and protection of the pulmonary circulation by an optimal degree of pulmonic stenosis.

### *Echocardiographic Evaluation*

The important aspects to ascertain echocardiographically in patients with this anomaly are listed in Box 44-9.

### *Management*

Adults with functional univentricular heart who are well balanced may not require surgical intervention, as long-term survival in the unoperated state in some cases equals that of corrective surgery.[168] Particularly, adults with double-inlet LV and well-balanced circulation may survive into their sixth decade of life with good functional capacity and preserved ventricular function.[169] However, operative strategies aimed at relieving the complications from cyanosis and preservation of late ventricular function may be entertained.[170] This consideration of a "late Fontan" surgery requires adequate PA size and confluence, low PA resistance, competent systemic AV valves, good ventricular function with low end-diastolic pressure, and unobstructed ventricular outflow. Palliative surgeries may also be considered, such as cavopulmonary or aortopulmonary shunts, in cases where the foregoing criteria are not met.[171]

**Box 44-9**

**IMAGING CHECKLIST IN THE EVALUATION OF ADULTS WITH FUNCTIONAL UNIVENTRICULAR PHYSIOLOGY**

- Presence and location of an accessory chamber
- Number and functional status of the atrioventricular valves
- Number and orientation of the great vessels and their relation to the main or accessory chamber
- Presence and severity of outflow tract obstruction
- Functional performance of the systemic ventricle
- Nature and adequacy of venous return in the case of atresia of one of the atrioventricular valves

**KEY POINTS**

- Adults with congenital heart disease may escape detection during childhood because their lesion is mild or slowly progressive, because their physiology is well balanced or protected, or because of poor access to medical care.
- The mode of presentation of the adult with unoperated congenital heart disease is often similar to that of adults with acquired heart disease—heart failure, arrhythmia, murmur, hypertension, or endocarditis.
- Bicuspid aortic valve is the most common form of congenital heart disease in the adult and requires continued follow-up for progressive stenosis or regurgitation and aortic root dilation.
- Despite marked structural abnormality, patients with Ebstein anomaly are often able to live active lives, but may experience adverse events such as tachyarrhythmias, paradoxical emboli, progressive tricuspid regurgitation, and heart failure.
- Discrete subaortic stenosis may be masked by development of septal hypertrophy, requiring careful TTE and TEE studies to elicit the correct pathophysiology.
- Aortic coarctation may be missed by transthoracic imaging, but PW Doppler in the abdominal aorta may alert the examiner to the flow disturbance more proximally in the aorta.
- Doppler gradients in supravalvular aortic stenosis and long-segment aortic coarctation often overestimate the true gradient because of flow acceleration in a tubular vessel with pressure recovery.
- Sinus venosus defects are the most frequently missed septal defect by TTE resulting from incomplete imaging of the most superior aspect of the septum; TEE or cardiac MRI is often required to detect the defect and partial anomalous pulmonary venous drainage.
- In the cyanotic adult with unoperated congenital heart disease, detecting the presence of pulmonic stenosis at any level may convert the clinical status from inoperable to surgically treatable.
- Alternative imaging modalities, such as cardiac MRI and CT, are important adjuncts to echocardiography in the complete assessment of the adult with congenital heart disease.

## REFERENCES


1. Marelli AJ, Mackie AS, Ionescu-Rittu I, et al: Congenital heart disease in the general population: changing prevalence and age distribution. *Circulation* 115:163-172, 2007.
2. Congenital heart disease after childhood: an expanding patient population. 22nd Bethesda Conference, Maryland, October 18–19, 1990. *J Am Coll Cardiol* 18:311-342, 1991.
3. Warnes CA, Liberthson R, Danielson GK Jr, et al: Task force 1: the changing profile of congenital heart disease in adult life. *J Am Coll Cardiol* 37:1170-1175, 2001.
4. Warnes CA, Williams RG, Bashore TM, et al: ACC/AHA 2008 Guidelines for the Management of Adults with Congenital Heart Disease: a report of the American College of Cardiology/American Heart Association Task Force on Practice Guidelines (writing committee to develop guidelines on the management of adults with congenital heart disease). *Circulation* 118:e714-e833, 2008.
5. Marelli AJ, Child JS, Perloff JK: Transesophageal echocardiography in congenital heart disease in the adult. *Cardiol Clin* 11:505-520, 1993.
6. Miller-Hance WC, Silverman NH: Transesophageal echocardiography (TEE) in congenital heart disease with focus on the adult. *Cardiol Clin* 18:861-892, 2000.
7. Sreeram N, Sutherland GR, Geuskens R, et al: The role of transoesophageal echocardiography in adolescents and adults with congenital heart defects. *Eur Heart J* 12:231-240, 1991.
8. Babu-Narayan SV, Gatzoulis MA, Kilner PJ: Non-invasive imaging in adult congenital heart disease using cardiovascular magnetic resonance. *J Cardiovasc Med (Hagerstown)* 8:23-29, 2007.
9. Cook SC, Raman SV: Unique application of multislice computed tomography in adults with congenital heart disease. *Int J Cardiol* 119:101-106, 2007.
10. Huntington K, Hunter AG, Chan KL: A prospective study to assess the frequency of familial clustering of congenital bicuspid aortic valve. *J Am Coll Cardiol* 30:1809-1812, 1997.
11. Cripe L, Andelfinger G, Martin LJ, et al: Bicuspid aortic valve is heritable. *J Am Coll Cardiol* 44:138-143, 2004.
12. Garg V, Muth AN, Ransom JF, et al: Mutations in NOTCH1 cause aortic valve disease. *Nature* 437:270-274, 2005.
13. McBride KL, Pignatelli R, Lewin M, et al: Inheritance analysis of congenital left ventricular outflow tract obstruction malformations: segregation, multiplex relative risk, heritability. *Am J Med Genet A* 134A:180-186, 2005.
14. Fenoglio JJ Jr, McAllister HA Jr, DeCastro CM, et al: Congenital bicuspid aortic valve after age 20. *Am J Cardiol* 39:164-169, 1977.
15. Roberts CS, Roberts WC: Dissection of the aorta associated with congenital malformation of the aortic valve. *J Am Coll Cardiol* 17:712-716, 1991.
16. Sabet HY, Edwards WD, Tazelaar HD, Daly RC: Congenitally bicuspid aortic valves: a surgical pathology study of 542 cases (1991 through 1996) and a literature review of 2,715 additional cases. *Mayo Clin Proc* 74:14-26, 1999.
17. Keane MG, Wiegers SE, Plappert T, et al: Bicuspid aortic valves are associated with aortic dilatation out of proportion to coexistent valvular lesions. *Circulation* 102:III35-III39, 2000.
18. Shone JD, Sellers RD, Anderson RC, et al: The developmental complex of "parachute mitral valve," supravalvular ring of left atrium, subaortic stenosis, and coarctation of aorta. *Am J Cardiol* 11:714-725, 1963.
19. Gersony WM, Hayes CJ, Driscoll DJ, et al: Bacterial endocarditis in patients with aortic stenosis, pulmonary stenosis, or ventricular septal defect. *Circulation* 87:I121-I126, 1993.
20. Tribouilloy C, Rusinaru D, Sorel C, et al: Clinical characteristics and outcome of infective endocarditis in adults with bicuspid aortic valves: a multicentre observational study. *Heart* 96:1723-1729, 2010.
21. Otto CM, Pearlman AS, Comess KA, et al: Determination of the stenotic aortic valve area in adults using Doppler echocardiography. *J Am Coll Cardiol* 7:509-517, 1986.
22. Hiratzka LF, Bakris GL, Beckman JA, et al: 2010 ACCF/AHA/AATS/ACR/ASA/SCA/SCAI/SIR/STS/SVM guidelines for the diagnosis and management of patients with thoracic aortic disease: a report of the American College of Cardiology Foundation/American Heart Association Task Force on Practice Guidelines, American Association for Thoracic Surgery, American College of Radiology, American Stroke Association, Society of Cardiovascular Anesthesiologists, Society for Cardiovascular Angiography and Interventions, Society of Interventional Radiology, Society of Thoracic Surgeons, and Society for Vascular Medicine. *Circulation* 121:e266-e369, 2010.
23. Hiratzka LF, Bakris GL, Beckman JA, et al: 2010 ACCF/AHA/AATS/ACR/ASA/SCA/SCAI/SIR/STS/SVM guidelines for the diagnosis and management of patients with thoracic aortic disease. A report of the American College of Cardiology Foundation/American Heart Association Task Force on Practice Guidelines, American Association for Thoracic Surgery, American College of Radiology, American Stroke Association, Society of Cardiovascular Anesthesiologists, Society for Cardiovascular Angiography and Interventions, Society of Interventional Radiology, Society of Thoracic Surgeons, and Society for Vascular Medicine. *J Am Coll Cardiol* 55:e27-e129, 2010.
24. Tzemos N, Therrien J, Yip J, et al: Outcomes in adults with bicuspid aortic valves. *JAMA* 300:1317-1325, 2008.
25. Michelena HI, Desjardins VA, Avierinos J-F, et al: Natural history of asymptomatic patients with normally functioning or minimally dysfunctional bicuspid aortic valve in the community. *Circulation* 117:2776-2784, 2008.
26. Bonow RO, Carabello BA, Chatterjee K, et al: ACC/AHA 2006 guidelines for the management of patients with valvular heart disease: a report of the American College of Cardiology/American Heart Association Task Force on Practice Guidelines (writing committee to revise the 1998 Guidelines for the Management of Patients with Valvular Heart Disease): developed in collaboration with the Society of Cardiovascular Anesthesiologists: endorsed by the Society for Cardiovascular Angiography and Interventions and the Society of Thoracic Surgeons. *Circulation* 114:e84-e231, 2006.
27. Rosenfeld HM, Landzberg MJ, Perry SB, et al: Balloon aortic valvuloplasty in the young adult with congenital aortic stenosis. *Am J Cardiol* 73:1112-1117, 1994.
28. Justo RN, McCrindle BW, Benson LN, et al: Aortic valve regurgitation after surgical versus percutaneous balloon valvotomy for congenital aortic valve stenosis. *Am J Cardiol* 77:1332-1338, 1996.
29. Ross D, Jackson M Davies J: The pulmonary autograft–a permanent aortic valve. *Eur J Cardiothorac Surg* 6:113-116, 1992; discussion 117.
30. Savoye C, Auffray JL, Hubert E, et al: Echocardiographic follow-up after Ross procedure in 100 patients. *Am J Cardiol* 85:854-857, 2000.
31. Kouchoukos NT, Masetti P, Nickerson NJ, et al: The Ross procedure: long-term clinical and echocardiographic follow-up. *Ann Thorac Surg* 78:773-781, 2004; discussion 773-781.
32. Niwaya K, Elkins RC, Knott-Craig CJ, et al: Normalization of left ventricular dimensions after Ross operation with aortic annular reduction. *Ann Thorac Surg* 68:812-818, 1999; discussion 818-819.
33. Takkenberg JJ, Klieverik LM, Schoof PH, et al: The Ross procedure: a systematic review and meta-analysis. *Circulation* 119:222-228, 2009.
34. Hayes CJ, Gersony WM, Driscoll DJ, et al: Second natural history study of congenital heart defects. Results of treatment of patients with pulmonary valvar stenosis. *Circulation* 87:I28-I37, 1993.
35. Nishimura RA, Pieroni DR, Bierman FZ, et al: Second natural history study of congenital heart defects. Pulmonary stenosis: echocardiography. *Circulation* 87:I73-I79, 1993.
36. Lin AE, Basson CT, Goldmuntz E, et al: Adults with genetic syndromes and cardiovascular abnormalities: clinical history and management. *Genet Med* 10:469-494, 2008.
37. Burch M, Sharland M, Shinebourne E, et al: Cardiologic abnormalities in Noonan syndrome: phenotypic diagnosis and echocardiographic assessment of 118 patients. *J Am Coll Cardiol* 22:1189-1192, 1993.
38. Silvilairat S, Cabalka AK, Cetta F, et al: Outpatient echocardiographic assessment of complex pulmonary outflow stenosis: Doppler mean gradient is superior to the maximum instantaneous gradient. *J Am Soc Echocardiogr* 18:1143-1148, 2005.
39. DeGroff C: Response to: "Echocardiographic assessment of isolated pulmonary valve stenosis: which outpatient Doppler gradient has the most clinical validity?" *J Am Soc Echocardiogr* 19:364, 2006.
40. Teupe CH, Burger W, Schräder R, et al: Late (five to nine years) follow-up after balloon dilation of valvular pulmonary stenosis in adults. *Am J Cardiol* 80:240-242, 1997.
41. Kan JS, White RI Jr, Mitchell SE, et al: Percutaneous balloon valvuloplasty: a new method for treating congenital pulmonary-valve stenosis. *N Engl J Med* 307:540-542, 1982.
42. McCrindle BW: Independent predictors of long-term results after balloon pulmonary valvuloplasty. Valvuloplasty and Angioplasty of Congenital Anomalies (VACA) Registry Investigators. *Circulation* 89:1751-1759, 1994.
43. Hakim FA, Kendall CB, Alharthi M, et al: Parachute mitral valve in adults—a systematic overview. *Echocardiography* 27:581-586, 2010.
44. Bär H, Siegmund A, Wolf D, et al: Prevalence of asymptomatic mitral valve malformations. *Clin Res Cardiol* 98:305-309, 2009.
45. Moulaert AJ, Oppenheimer-Dekker A: Anterolateral muscle bundle of the left ventricle, bulboventricular flange and subaortic stenosis. *Am J Cardiol* 37:78-81, 1976.

46. Li W, Somerville J: Infective endocarditis in the grown-up congenital heart (GUCH) population. *Eur Heart J* 19:166-173, 1998.
47. Bonow RO, Carabello BA, Chatterjee K, et al: 2008 focused update incorporated into the ACC/AHA 2006 guidelines for the management of patients with valvular heart disease: a report of the American College of Cardiology/American Heart Association Task Force on Practice Guidelines (writing committee to revise the 1998 guidelines for the management of patients with valvular heart disease): endorsed by the Society of Cardiovascular Anesthesiologists, Society for Cardiovascular Angiography and Interventions, and Society of Thoracic Surgeons. *Circulation* 118:e523-e661, 2008.
48. Moore P, Adatia I, Spevak PJ, et al: Severe congenital mitral stenosis in infants. *Circulation* 89:2099-2106, 1994.
49. Chauvaud S, Fuzellier JF, Houel R, et al: Reconstructive surgery in congenital mitral valve insufficiency (Carpentier's techniques): long-term results. *J Thorac Cardiovasc Surg* 115:84-92, 1998; discussion 92-93.
50. McCarthy JF, Neligan MC Wood AE: Ten years' experience of an aggressive reparative approach to congenital mitral valve anomalies. *Eur J Cardiothorac Surg* 10:534-539, 1996.
51. Marwick TH, Stewart WJ, Currie PJ, Cosgrove DM, et al: Mechanisms of failure of mitral valve repair: an echocardiographic study. *Am Heart J* 122:149-156, 1991.
52. Anderson KR, Zuberbuhler JR, Anderson RH, et al: Morphologic spectrum of Ebstein's anomaly of the heart: a review. *Mayo Clin Proc* 54:174-180, 1979.
53. Attenhofer Jost CH, Connolly HM, Edwards WD, et al: Ebstein's anomaly—review of a multifaceted congenital cardiac condition. *Swiss Med Wkly* 135:269-281, 2005.
54. Seward JB: Ebstein's anomaly: Ultrasound imaging and hemodynamic evaluation. *Echocardiography* 10:641-664, 1993.
55. Celermajer DS, Bull C, Till JA, et al: Ebstein's anomaly: presentation and outcome from fetus to adult. *J Am Coll Cardiol* 23:170-176, 1994.
56. Attenhofer Jost CH, Connolly HM, O'Leary PW, et al: Left heart lesions in patients with Ebstein anomaly. *Mayo Clin Proc* 80:361-368, 2005.
57. Eidem BW, Tei C, O'Leary PW, et al: Nongeometric quantitative assessment of right and left ventricular function: myocardial performance index in normal children and patients with Ebstein anomaly. *J Am Soc Echocardiogr* 11:849-856, 1998.
58. Dearani JA, Danielson GK: Surgical management of Ebstein's anomaly in the adult. *Semin Thorac Cardiovasc Surg* 17:148-154, 2005.
59. Gewillig M, Daenen W, Dumoulin M, et al: Rheologic genesis of discrete subvalvular aortic stenosis: a Doppler echocardiographic study. *J Am Coll Cardiol* 19:818-824, 1992.
60. Ward CJB, Culham JAG, Patterson MWH, Sandor GSS: The trilogy of double-chambered right ventricle, perimembranous ventricular septal defect and subaortic narrowing—a more common association than previously recognized. *Cardiol Young* 5:140-146, 1995.
61. Bergin ML, Warnes CA, Tajik AJ, et al: Partial atrioventricular canal defect: long-term follow-up after initial repair in patients > or = 40 years old. *J Am Coll Cardiol* 25:1189-1194, 1995.
62. Shem-Tov A, Schneeweiss S, Motro M, Neufeld HN: Clinical presentation and natural history of mild discrete subaortic stenosis. Follow-up of 1–17 years. *Circulation* 66:509-512, 1982.
63. Movsowitz C, Jacobs LE, Eisenberg S, et al: Discrete subaortic valvular stenosis: the clinical utility and limitations of transesophageal echocardiography. *Echocardiography* 10:485-487, 1993.
64. McMahon CJ, Gauvreau K, Edwards JC, Geva T: Risk factors for aortic valve dysfunction in children with discrete subvalvar aortic stenosis. *Am J Cardiol* 94:459-464, 2004.
65. Douville EC, Sade RM, Crawford FA Jr, Wiles HB: Subvalvar aortic stenosis: timing of operation. *Ann Thorac Surg* 50:29-33, 1990; discussion 33-34.
66. de Vries AG, Hess J, Witsenburg M, et al: Management of fixed subaortic stenosis: a retrospective study of 57 cases. *J Am Coll Cardiol* 19:1013-1017, 1992.
67. Oliver JM, González A, Gallego P, et al: Discrete subaortic stenosis in adults: increased prevalence and slow rate of progression of the obstruction and aortic regurgitation. *J Am Coll Cardiol* 38:835-842, 2001.
68. Rattes MF, Sochowski RA, Baird M, Chan KL: Intraoperative transesophageal echocardiographic demonstration of mitral leaflet tear following resection of a subaortic membrane. *Can J Cardiol* 8:785-787, 1992.
69. Suarez de Lezo J, Pan M, Medina A, et al: Immediate and follow-up results of transluminal balloon dilation for discrete subaortic stenosis. *J Am Coll Cardiol* 18:1309-1315, 1991.
70. Morrow AG, Waldhausen JA, Peters RL, et al: Supravalvular aortic stenosis: clinical, hemodynamic and pathologic observations. *Circulation* 20:1003-1010, 1959.
71. Williams JC, Barratt-Boyes BG Lowe JB: Supravalvular aortic stenosis. *Circulation* 24:1311-1318, 1961.
72. Logan WF, Wyn Jones E, Walker E, et al: Familial supravalvar aortic stenosis. *Br Heart J* 27:547-559, 1965.
73. Stamm C, Friehs I, Ho SY, et al: Congenital supravalvar aortic stenosis: a simple lesion? *Eur J Cardiothorac Surg* 19:195-202, 2001.
74. van Son JA, Edwards WD, Danielson GK: Pathology of coronary arteries, myocardium, and great arteries in supravalvular aortic stenosis. Report of five cases with implications for surgical treatment. *J Thorac Cardiovasc Surg* 108:21-28, 1994.
75. Weyman AE, Caldwell RL, Hurwitz RA, et al: Cross-sectional echocardiographic characterization of aortic obstruction. 1. Supravalvular aortic stenosis and aortic hypoplasia. *Circulation* 57:491-497, 1978.
76. Tani LY, Minich LL, Pagotto LT, et al: Usefulness of Doppler echocardiography to determine the timing of surgery for supravalvar aortic stenosis. *Am J Cardiol* 86:114-116, 2000.
77. Scott DJ, Campbell DN, Clarke DR, et al: Twenty-year surgical experience with congenital supravalvar aortic stenosis. *Ann Thorac Surg* 87:1501-1507, 2009; discussion 1507-1508.
78. McElhinney DB, Petrossian E, Tworetzky W, et al: Issues and outcomes in the management of supravalvar aortic stenosis. *Ann Thorac Surg* 69:562-567, 2000.
79. Menahem S, Johns JA, del Torso S, et al: Evaluation of aortic valve prolapse in ventricular septal defect. *Br Heart J* 56:242-249, 1986.
80. Sakakibara S, Konno S: Congenital aneurysm of the sinus of Valsalva. Anatomy and classification. *Am Heart J* 63:405-424, 1962.
81. Rothbaum DA, Dillon JC, Chang S, Feigenbaum H: Echocardiographic manifestation of right sinus of Valsalva aneurysm. *Circulation* 49:768-771, 1974.
82. Vural KM, Sener E, Tasdemir O, Bayazit K: Approach to sinus of Valsalva aneurysms: a review of 53 cases. *Eur J Cardiothorac Surg* 20:71-76, 2001.
83. Hiyamuta K, Ohtsuki T, Shimamatsu M, et al: Aneurysm of the left aortic sinus causing acute myocardial infarction. *Circulation* 67:1151-1154, 1983.
84. Matsumoto M, Matsuo H, Beppu S, et al: Echocardiography diagnosis of ruptured aneurysm of sinus of Valsalva. Report of two cases. *Circulation* 53:382-389, 1976.
85. Desai AG, Sharma S, Kumar A, et al: Echocardiographic diagnosis of unruptured aneurysm of right sinus of Valsalva: an unusual cause of right ventricular outflow obstruction. *Am Heart J* 109:363-364, 1985.
86. Au W-K, Chiu S-W, Mok C-K, et al: Repair of ruptured sinus of Valsalva aneurysm: determinants of long-term survival. *Ann Thorac Surg* 66:1604-1610, 1998.
87. Takach TJ, Reul GJ, Duncan JM, et al: Sinus of Valsalva aneurysm or fistula: management and outcome. *Ann Thorac Surg* 68:1573-1577, 1999.
88. Liberthson RR, Pennington DG, Jacobs ML, Daggett WM: Coarctation of the aorta: review of 234 patients and clarification of management problems. *Am J Cardiol* 43:835-840, 1979.
89. Campbell M: Natural history of coarctation of the aorta. *Br Heart J* 32:633-640, 1970.
90. Marx GR, Allen HD: Accuracy and pitfalls of Doppler evaluation of the pressure gradient in aortic coarctation. *J Am Coll Cardiol* 7:1379-1385, 1986.
91. Carvalho JS, Redington AN, Shinebourne EA, et al: Continuous wave Doppler echocardiography and coarctation of the aorta: gradients and flow patterns in the assessment of severity. *Br Heart J* 64:133-137, 1990.
92. Sanders SP, MacPherson D, Yeager SB: Temporal flow velocity profile in the descending aorta in coarctation. *J Am Coll Cardiol* 7:603-609, 1986.
93. Ryan K, Sanyal RS, Pinheiro L, et al: Assessment of aortic coarctation and collateral circulation by biplane transesophageal echocardiography. *Echocardiography* 9:277, 1992.
94. Rao PS: Coarctation of the aorta. *Curr Cardiol Rep* 7:425-434, 2005.
95. McCrindle BW, Jones TK, Morrow WR, et al: Acute results of balloon angioplasty of native coarctation versus recurrent aortic obstruction are equivalent. Valvuloplasty and Angioplasty of Congenital Anomalies (VACA) Registry Investigators. *J Am Coll Cardiol* 28:1810-1817, 1996.
96. Harrison JK, Sheikh KH, Davidson CJ, et al: Balloon angioplasty of coarctation of the aorta evaluated with intravascular ultrasound imaging. *J Am Coll Cardiol* 15:906-909, 1990.
97. Hornung TS, Benson LN, McLaughlin PR: Interventions for aortic coarctation. *Cardiol Rev* 10:139-148, 2002.
98. Qureshi AM, McElhinney DB, Lock JE, et al: Acute and intermediate outcomes, and evaluation of injury to the aortic wall, as based on 15 years experience of implanting stents to treat aortic coarctation. *Cardiol Young* 17:307-318, 2007.
99. Presbitero P, Demarie D, Villani M, et al: Long term results (15–30 years) of surgical repair of aortic coarctation. *Br Heart J* 57:462-467, 1987.
100. de Divitiis M, Pilla C, Kattenhorn M, et al: Ambulatory blood pressure, left ventricular mass, and conduit artery function late after

successful repair of coarctation of the aorta. *J Am Coll Cardiol* 41:2259-2265, 2003.
101. Barton CH, Ni Z Vaziri ND: Enhanced nitric oxide inactivation in aortic coarctation-induced hypertension. *Kidney Int* 60:1083-1087, 2001.
102. Seward JB, Tajik AJ, Spangler JG, Ritter DG: Echocardiographic contrast studies: initial experience. *Mayo Clin Proc* 50:163-192, 1975.
103. Balint OH, Samman A, Haberer K, et al: Outcomes in patients with pulmonary hypertension undergoing percutaneous atrial septal defect closure. *Heart* 94:1189-1193, 2008.
104. Bartz PJ, Cetta F, Cabalka AK, et al: Paradoxical emboli in children and young adults: role of atrial septal defect and patent foramen ovale device closure. *Mayo Clin Proc* 81:615-618, 2006.
105. Fraker TD Jr, Harris PJ, Behar VS, Kisslo JA: Detection and exclusion of interatrial shunts by two-dimensional echocardiography and peripheral venous injection. *Circulation* 59:379-384, 1979.
106. Grenadier E, Alpan G, Keidar S, et al: M-mode and two-dimensional contrast echocardiography in adult patients with atrial septal defects. *Clin Cardiol* 6:588-594, 1983.
107. Stewart WJ, Jiang L, Mich R, et al: Variable effects of changes in flow rate through the aortic, pulmonary and mitral valves on valve area and flow velocity: impact on quantitative Doppler flow calculations. *J Am Coll Cardiol* 6:653-662, 1985.
108. Yock PG, Popp RL: Noninvasive estimation of right ventricular systolic pressure by Doppler ultrasound in patients with tricuspid regurgitation. *Circulation* 70:657-662, 1984.
109. Valente AM, Sena L, Powell AJ, et al: Cardiac magnetic resonance imaging evaluation of sinus venosus defects: comparison to surgical findings. *Pediatr Cardiol* 28:51-56, 2007.
110. Hausmann D, Daniel WG, Mügge A, et al: Value of transesophageal color Doppler echocardiography for detection of different types of atrial septal defect in adults. *J Am Soc Echocardiogr* 5:481-488, 1992.
111. Kronzon I, Tunick PA, Freedberg RS, et al: Transesophageal echocardiography is superior to transthoracic echocardiography in the diagnosis of sinus venosus atrial septal defect. *J Am Coll Cardiol* 17:537-542, 1991.
112. Belkin RN, Pollack BD, Ruggiero ML, et al: Comparison of transesophageal and transthoracic echocardiography with contrast and color flow Doppler in the detection of patent foramen ovale. *Am Heart J* 128:520-525, 1994.
113. Johansson MC, Eriksson P, Guron CW, Dellborg M: Pitfalls in diagnosing PFO: characteristics of false-negative contrast injections during transesophageal echocardiography in patients with patent foramen ovales. *J Am Soc Echocardiogr* 23:1136-1142, 2010.
114. Horvath KA, Burke RP, Collins JJ Jr, Cohn LH: Surgical treatment of adult atrial septal defect: early and long-term results. *J Am Coll Cardiol* 20:1156-1159, 1992.
115. Murphy JG, Gersh BJ, McGoon MD, et al: Long-term outcome after surgical repair of isolated atrial septal defect. Follow-up at 27 to 32 years. *N Engl J Med* 323:1645-1650, 1990.
116. Liberthson RR, Boucher CA, Strauss HW, et al: Right ventricular function in adult atrial septal defect. Preoperative and postoperative assessment and clinical implications. *Am J Cardiol* 47:56-60, 1981.
117. Shah D, Azhar M, Oakley CM, et al: Natural history of secundum atrial septal defect in adults after medical or surgical treatment: a historical prospective study. *Br Heart J* 71:224-227, 1994; discussion 228.
118. Konstantinides S, Geibel A, Olschewski M, et al: A comparison of surgical and medical therapy for atrial septal defect in adults. *N Engl J Med* 333:469-473, 1995.
119. Gatzoulis MA, Redington AN, Somerville J, Shore DF: Should atrial septal defects in adults be closed? *Ann Thorac Surg* 61:657-659, 1996.
120. Boccalandro F, Baptista E, Muench A, et al: Comparison of intracardiac echocardiography versus transesophageal echocardiography guidance for percutaneous transcatheter closure of atrial septal defect. *Am J Cardiol* 93:437-440, 2004.
121. Rao PS: Catheter closure of atrial septal defects. *J Invasive Cardiol* 15:398-400, 2003.
122. Hein R, Büscheck F, Fischer E, et al: Atrial and ventricular septal defects can safely be closed by percutaneous intervention. *J Interv Cardiol* 18:515-522, 2005.
123. Kreutzer J, Ryan CA, Gauvreau K, et al: Healing response to the Clamshell device for closure of intracardiac defects in humans. *Catheter Cardiovasc Interv* 54:101-111, 2001.
124. Feng Q, Wu S Yu G: Surgical treatment of a 56-year-old woman with an intracardiac type of total anomalous pulmonary venous connection. *Thorac Cardiovasc Surg* 58:175-176, 2010.
125. Modi A, Vohra HA, Brown I, Langley SM: Successful surgical correction of total anomalous pulmonary venous drainage in the sixth decade. *Ann Thorac Surg* 86:1684-1686, 2008.
126. Ammash NM, Seward JB, Warnes CA, et al: Partial anomalous pulmonary venous connection: diagnosis by transesophageal echocardiography. *J Am Coll Cardiol* 29:1351-1358, 1997.
127. Greil GF, Powell AJ, Gildein HP, Geva T: Gadolinium-enhanced three-dimensional magnetic resonance angiography of pulmonary and systemic venous anomalies. *J Am Coll Cardiol* 39:335-341, 2002.
128. Ho M-L, Bhalla S, Bierhals A, Gutierrez F: MDCT of partial anomalous pulmonary venous return (PAPVR) in adults. *J Thorac Imaging* 24:89-95, 2009.
129. Kidd L, Driscoll DJ, Gersony WM, et al: Second natural history study of congenital heart defects. Results of treatment of patients with ventricular septal defects. *Circulation* 87:I38-I51, 1993.
130. Gasul BM, Dillon RF, Vria V, Hait G: Ventricular septal defects; their natural transformation into the cyanotic or noncyanotic type of tetralogy of Fallot. *JAMA* 1957. 164:847-853.
131. Tohyama K, Satomi G Momma K: Aortic valve prolapse and aortic regurgitation associated with subpulmonic ventricular septal defect. *Am J Cardiol* 79:1285-1289, 1997.
132. Sabry AF, Reller MD, Silberbach GM, et al: Comparison of four Doppler echocardiographic methods for calculating pulmonary-to-systemic shunt flow ratios in patients with ventricular septal defect. *Am J Cardiol* 75:611-614, 1995.
133. Gabriel HM, Heger M, Innerhofer P, et al: Long-term outcome of patients with ventricular septal defect considered not to require surgical closure during childhood. *J Am Coll Cardiol* 39:1066-1071, 2002.
134. Soufflet V, Van de Bruaene A, Troost E, et al: Behavior of unrepaired perimembranous ventricular septal defect in young adults. *Am J Cardiol* 105:404-407, 2010.
135. Holzer R, Balzer D, Amin Z, et al: Device closure of muscular ventricular septal defects using the Amplatzer muscular ventricular septal defect occluder: immediate and mid-term results of a U.S. registry. *J Am Coll Cardiol* 43:1257-1263, 2004.
136. Hijazi ZM: Device closure of ventricular septal defects. *Catheter Cardiovasc Interv* 60:107-114, 2003.
137. Celermajer DS, Sholler GF, Hughes CF, Baird DK: Persistent ductus arteriosus in adults. A review of surgical experience with 25 patients. *Med J Aust* 155:233-236, 1991.
138. Moore JW, Levi DS, Moore SD, et al: Interventional treatment of patent ductus arteriosus in 2004. *Catheter Cardiovasc Interv* 64:91-101, 2005.
139. Ottenkamp J, Hess J, Talsma MD, Buis-Liem TN: Protrusion of the device: a complication of catheter closure of patent ductus arteriosus. *Br Heart J* 68:301-303, 1992.
140. Hobbs RE, Millit HD, Raghavan PV, et al: Coronary artery fistulae: a 10-year review. *Cleve Clin Q* 49:191-197, 1982.
141. Valente AM, Lock JE, Gauvreau K, et al: Predictors of long-term adverse outcomes in patients with congenital coronary artery fistulae. *Circ Cardiovasc Interv* 3:134-139, 2010.
142. Cottier C, Kiowski W, von Bertrab R, et al: Multiple coronary arteriocameral fistulas as a cause of myocardial ischemia. *Am Heart J* 115:181-184, 1988.
143. Sanders SP, Parness IA, Colan SD: Recognition of abnormal connections of coronary arteries with the use of Doppler color flow mapping. *J Am Coll Cardiol* 13:922-926, 1989.
144. Shakudo M, Yoshikawa J, Yoshida K, et al: Noninvasive diagnosis of coronary artery fistula by Doppler color flow mapping. *J Am Coll Cardiol* 13:1572-1577, 1989.
145. Krishnamoorthy KM, Rao S: Transesophageal echocardiography for the diagnosis of coronary arteriovenous fistula. *Int J Cardiol* 96:281-283, 2004.
146. Cooper MJ, Bernstein D, Silverman NH: Recognition of left coronary artery fistula to the left and right ventricles by contrast echocardiography. *J Am Coll Cardiol* 6:923-926, 1985.
147. Armsby LR, Keane JF, Sherwood MC, et al: Management of coronary artery fistulae. Patient selection and results of transcatheter closure. *J Am Coll Cardiol* 39:1026-1032, 2002.
148. Cheung DL, Au WK, Cheung HH, et al: Coronary artery fistulas: long-term results of surgical correction. *Ann Thorac Surg* 71:190-195, 2001.
149. Dabizzi RP, Caprioli G, Aiazzi L, et al: Distribution and anomalies of coronary arteries in tetralogy of Fallot. *Circulation* 61:95-102, 1980.
150. Fellows KE, Smith J Keane JF: Preoperative angiocardiography in infants with tetrad of Fallot. Review of 36 cases. *Am J Cardiol* 47:1279-1285, 1981.
151. Bertranou EG, Blackstone EH, Hazelrig JB, et al: Life expectancy without surgery in tetralogy of Fallot. *Am J Cardiol* 42:458-466, 1978.
152. Berry JM Jr, Einzig S, Krabill KA, Bass JL: Evaluation of coronary artery anatomy in patients with tetralogy of Fallot by two-dimensional echocardiography. *Circulation* 78:149-156, 1988.
153. Lieberson AD, Schumacher RR, Childress RH, et al: Corrected transposition of the great vessels in a 73-year-old man. *Circulation* 39:96-100, 1969.
154. Beauchesne LM, Warnes CA, Connolly HM, et al: Outcome of the unoperated adult who

presents with congenitally corrected transposition of the great arteries. *J Am Coll Cardiol* 40:285-290, 2002.
155. Huhta JC, Maloney JD Ritter DG et al: Complete atrioventricular block in patients with atrioventricular discordance. *Circulation* 67: 1374-1377, 1983.
156. Graham TP Jr, Bernard YD, Mellen BG, et al: Long-term outcome in congenitally corrected transposition of the great arteries: a multi-institutional study. *J Am Coll Cardiol* 36:255-261, 2000.
157. Prieto LR, Hordof AJ, Secic M, et al: Progressive tricuspid valve disease in patients with congenitally corrected transposition of the great arteries. *Circulation* 98:997-1005, 1998.
158. Enar S, Singh P, Douglas C, et al: Live/real time three-dimensional transthoracic echocardiographic assessment of transposition of the great arteries in the adult. *Echocardiography* 26:1095-1104, 2009.
159. Benson LN, Burns R, Schwaiger M, et al: Radionuclide angiographic evaluation of ventricular function in isolated congenitally corrected transposition of the great arteries. *Am J Cardiol* 58:319-324, 1986.
160. Winter MM, Bernink FJP, Groenink M, et al: Evaluating the systemic right ventricle by CMR: the importance of consistent and reproducible delineation of the cavity. *J Cardiovasc Magn Reson* 10:40, 2008.
161. Eidem BW, O'Leary PW, Tei C, Seward JB: Usefulness of the myocardial performance index for assessing right ventricular function in congenital heart disease. *Am J Cardiol* 86:654-658, 2000.
162. Dore A, Houde C, Chan KL, et al: Angiotensin receptor blockade and exercise capacity in adults with systemic right ventricles: a multicenter, randomized, placebo-controlled clinical trial. *Circulation* 112:2411-2416, 2005.
163. Mavroudis C, Backer CL: Physiologic versus anatomic repair of congenitally corrected transposition of the great arteries. *Semin Thorac Cardiovasc Surg Pediatr Card Surg Annu* 6:16-26, 2003.
164. Alghamdi AA, McCrindle BW Van Arsdell GS: Physiologic versus anatomic repair of congenitally corrected transposition of the great arteries: meta-analysis of individual patient data. *Ann Thorac Surg* 81:1529-1535, 2006.
165. Dick M, Fyler DC, Nadas AS: Tricuspid atresia: clinical course in 101 patients. *Am J Cardiol* 36:327-337, 1975.
166. Rao PS: Further observations on the spontaneous closure of physiologically advantageous ventricular septal defects in tricuspid atresia: surgical implications. *Ann Thorac Surg* 35:121-131, 1983.
167. Pigula FA, Gandhi SK, Ristich J, et al: Cardiopulmonary transplantation for congenital heart disease in the adult. *J Heart Lung Transplant* 20:297-303, 2001.
168. Hager A, Kaemmerer H, Eicken A, et al: Long-term survival of patients with univentricular heart not treated surgically. *J Thorac Cardiovasc Surg* 123:1214-1217, 2002.
169. Ammash NM, Warnes CA: Survival into adulthood of patients with unoperated single ventricle. *Am J Cardiol* 77:542-544, 1996.
170. Burkhart HM, Dearani JA, Mair DD, et al: The modified Fontan procedure: early and late results in 132 adult patients. *J Thorac Cardiovasc Surg* 125:1252-1259, 2003.
171. Gatzoulis MA, Munk M-D, Williams WG, Webb GD: Definitive palliation with cavopulmonary or aortopulmonary shunts for adults with single ventricle physiology. *Heart* 83:51-57, 2000.

# 45 Echocardiographic Evaluation of the Adult with Postoperative Congenital Heart Disease

JAMIL A. ABOULHOSN, MD | JOHN S. CHILD, MD

**General Postoperative and Postinterventional Congenital Heart Disease Issues**
- Atrial and Ventricular Incisions and Devices
- Anatomic and Valvular Residua and Sequelae
- Ventricular Function
- Conduits, Patches, and Prosthetic Materials

**Palliative Procedures**
- Pulmonary Artery Banding
- Palliative Aortopulmonary Shunts
- Glenn Shunts

**Corrective Procedures for "Simple" Lesions**
- Atrial Septal Defects
- Ventricular Septal Defects
- Patent Ductus Arteriosus
- Bicuspid Aortic Valve
- Subaortic Stenosis
- Coarctation of the Aorta
- Ebstein Anomaly
- Pulmonic Stenosis
- Anomalies of the Coronary Arteries

**Repair of "Complex" Malformations**
- Atrial Switch Surgery
- Arterial Switch Surgery
- Total Anomalous Pulmonary Venous Connection
- Fontan Atrial Surgery
- Atrioventricular Septal Defects
- Biventricular Repairs
- Tetralogy of Fallot
- Complete Transposition of the Great Arteries
- Congenitally Corrected Transposition of the Great Arteries
- Double-Outlet Right Ventricle

The incidence of moderate and severe forms of congenital heart disease is approximately 6 per 1000 live births (19 per 1000 if a bicuspid aortic valve is included).[1] In the past 60 years, advances in diagnosis and in catheter and surgical treatment have resulted in nearly 1 million adult survivors with congenital heart disease in the United States.[2-6] Most surgically modified congenital heart diseases leave behind (residua) or cause (sequelae) problems ranging from trivial to serious.[6,7] An explosion in transcatheter interventions for congenital heart disease over the past three decades has obviated the need for surgery in an ever-growing list of native and postoperative lesions.

The evaluation and management of adult congenital heart disease requires detailed knowledge of the

1. Original anatomy and physiology;
2. Dynamic changes in anatomy and physiology that occur with time;
3. Effects of "adult" diseases (e.g., systemic arterial hypertension, coronary artery disease) or conditions (e.g., pregnancy) on that physiology;
4. Types of operative repair (both past and present) for each complex of lesions;
5. Presence and extent of possible postoperative residua, sequelae, and complications;
6. Types of transcatheter interventions and devices, their echocardiographic appearance, expected sequelae, and potential complications; and
7. Proper selection, performance, and interpretation of modalities required for anatomic imaging and hemodynamic assessment.[8]

It is impractical to repetitively catheterize these individuals; combined two-dimensional (2D), three-dimensional (3D), and Doppler echocardiography is often more useful than angiography in providing details of valvular anatomy and in visualizing patches and ventricular wall thickness.[8] In patients who have undergone transcatheter interventions, echocardiography can noninvasively evaluate device position (Fig. 45-1), residual shunting, and device impingement on valves, veins, and other structures. It can also assess for the presence of pericardial effusion and tamponade physiology following device placement.[9] Transthoracic, transesophageal, and intracardiac echocardiographic techniques are complementary and can be invaluable tools in the selection, procedural guidance, and long-term follow-up of transcatheter interventions.[9-11]

Transesophageal echocardiography (TEE) images areas often not seen on transthoracic echocardiography (TTE) and provides more complete depiction of complex anatomy.[8,12,13] It allows good visualization of the origins of the coronary arteries, main pulmonary artery branches, and entire aorta. TEE is essential in the evaluation of the atrial septum, characterization of septal defects, and assessment of rim adequacy and adjacent structures when considering device closure; the addition of 3D capability further improves the accuracy and utility of TEE in the guidance of device closure.[14-16] TEE is the standard for intra- and postoperative evaluation of complex congenital heart disease surgery.[8,12,13] In the postoperative care unit, TEE elucidates causes of general complications (e.g., hypotension, tamponade, ventricular dysfunction) or complications of specific congenital heart disease surgeries such as the Fontan procedure

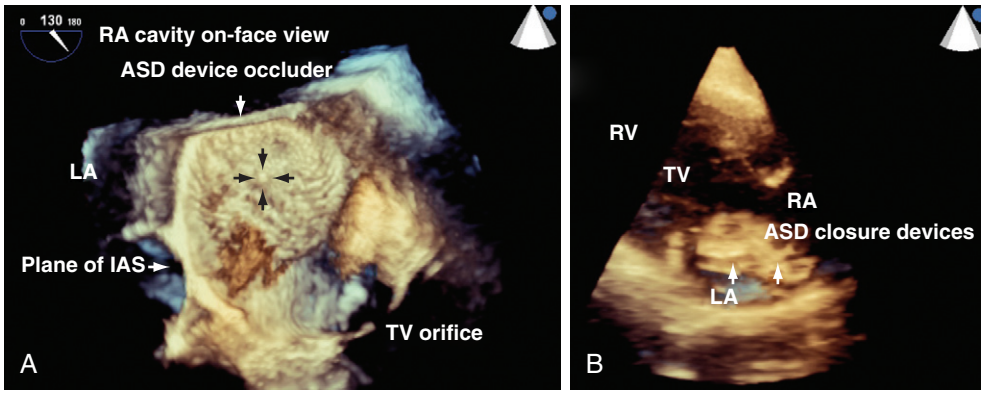



**Figure 45-1** **A, Live 3D TEE demonstrating an Amplatzer Septal Occluder straddling the intraatrial septum (*IAS*) as seen from the RA side. B,** 3D TTE of two Amplatzer Septal Occluders as seen from a parasternal RV inflow view. *ASD*, Atrial septal occluder; *TV*, tricuspid valve.

(e.g., lateral tunnel thrombus). TEE is widely used to guide transcatheter interventions, including closure of atrial and ventricular septal defects, aortic valvuloplasty, mitral valvotomy, pulmonary venous angioplasty and stenting, and Fontan fenestration creation or closure.

Intracardiac echocardiography is gaining popularity as an alternate means of structural imaging for procedural guidance.[11] The advantages of intracardiac echocardiography over TEE include the ability of a single operator to perform both the catheterization/intervention and the crucial guiding echocardiography. However, the major disadvantage is a more limited scope of imaging (typically from the right atrial location in intracardiac echocardiography as opposed to the length of the esophagus and the transgastric views by TEE).

## General Postoperative and Postinterventional Congenital Heart Disease Issues

### ATRIAL AND VENTRICULAR INCISIONS AND DEVICES

Electric instability may occur after atrial or ventricular incisional scars or aneurysms, or after insertion of intracardiac patches or conduits with possible disruption of the conduction system[6,7,17,18] (Table 45-1). Patients with intraatrial baffles or conduits (e.g., Mustard and Fontan procedures) frequently suffer atrial arrhythmias; superimposed pressure overload on a ventriculotomy site may cause ventricular arrhythmias.[7] Because certain subgroups of postoperative congenital heart disease often require pacemaker therapy, there are concerns about diminished ventricular contractility over the long term with pacing via one ventricle (usually the right).[19,20] Thus, ventricular resynchronization by biventricular or multisite pacing may be of value and is amenable to evaluation by Doppler echocardiography.[21,22] Transcatheter device closure of atrial septal defect (ASD) is associated with an early risk of atrial arrhythmias and/or sinus dysrhythmia.[23] The risk of heart block is low, and patients rarely require pacemaker implantation. The risk of heart block is higher in patients who undergo transcatheter closure of membranous/perimembranous ventricular septal defects (VSDs), with published rates ranging from 1% to 17%. The risk is highest in infants and young children.[24-28] Transcatheter device closure of muscular VSD does not carry a significant risk of heart block given the lack of proximity to the bundle of His.[29] However, all VSD devices do carry the risk of ventricular arrhythmias, mostly noted at or early after time of device placement and consisting largely of isolated premature ventricular contractions without clinical morbidity or mortality.

**TABLE 45-1 General Postoperative Issues in Congenital Heart Disease**

| *Postoperative Issue* | *Examples* |
|---|---|
| Electric instability | Atrial arrhythmias after intraatrial baffle procedures<br>Ventricular arrhythmias after ventriculotomy<br>Heart block and ventricular arrhythmias following device closure of VSD<br>Atrial dysrhythmias following device closure of ASD |
| Residual anatomic defects | Bicuspid aortic valve in patient with aortic coarctation<br>Residual mitral regurgitation after cleft leaflet or primum ASD repair<br>Pulmonic regurgitation after tetralogy of Fallot repair<br>Dilated aortic root<br>Residual shunt post surgical or device closure of ASD and/or VSD<br>Pulmonic and aortic valve regurgitation post balloon valvuloplasty |
| Impaired ventricular function | Chronic volume overload due to valve regurgitation<br>Anatomic RV functioning as the systemic ventricle<br>Single functioning ventricle<br>Coronary artery kinking post aortic root repair or replacement or post RV to PA conduit stenting |
| Prosthetic materials | Degeneration of septal patches, intracardiac and extracardiac conduits<br>Prosthetic valve dysfunction<br>Thrombus formation<br>Risk of infective endocarditis<br>Obstruction or leaking of conduits<br>Device embolization or migration<br>Device erosion into adjacent tissue (aorta or atrial wall) |

*ASD*, Atrial septal defect; *PA*, pulmonary artery; *VSD*, ventricular septal defect.

### ANATOMIC AND VALVULAR RESIDUA AND SEQUELAE

Postoperative anatomic and valvular sequelae and residua must be sought.[6,7] Bicuspid aortic valves, common with aortic coarctation, continue to pose risks of progressive stenosis, regurgitation, and endocarditis despite coarctation repair. Variations on a parachute mitral valve, also associated with coarctation and other stenoses in sequence on the left-sided circulation, are detected by imaging a decreased interpapillary muscle distance and Doppler evidence of inflow obstruction. Repair of an ostium

primum ASD with cleft mitral leaflet may leave residual mitral regurgitation or the sequel of mitral stenosis; subaortic stenosis due to anomalous chordal attachments should be sought. Transcatheter static balloon pulmonic valvuloplasty has supplanted surgery as the treatment of choice in isolated pulmonic valve stenosis.[30] Although effective at relieving stenosis, this technique can result in pulmonic regurgitation.[31,32] Similarly, balloon valvuloplasty of stenotic bicuspid aortic valves carries the risk of creating aortic regurgitation with resultant left ventricular (LV) volume overload.[33] In repaired tetralogy of Fallot, pulmonic regurgitation is a sequel to valvotomy or transannular incision and patch. Mild to moderate low-pressure pulmonic regurgitation is common and well tolerated. Severe pulmonic regurgitation may cause right ventricular (RV) dilation and tricuspid regurgitation, particularly if there is residual RV outflow obstruction. Muscular VSDs may have been missed and should be sought by color flow imaging. Residual shunting is common immediately following device occlusion of atrial or ventricular septal defects, patent ductus arteriosus, and many other congenital cardiac or extracardiac communications. However, with currently available devices that combine Nitinol and polyester, the majority of these residual shunts close within days to weeks of device implantation. The likelihood of complete VSD closure of perimembranous or muscular VSDs after device closure is less given the high-velocity shunt present at the ventricular level[27,29] (Fig. 45-2). A dilated aortic root or trunk may occur in tetralogy of Fallot, transposition of the great arteries, or single ventricle in association with pulmonic stenosis, and late aortic regurgitation is common in adults. Aortic aneurysms or pseudoaneurysms are not uncommon in patients with coarctation of the aorta following surgical repair (most commonly seen in those with patch augmentation) or following balloon angioplasty.[34,35] The rate of aneurysm or pseudoaneurysm formation is much lower when stents are employed and is essentially nonexistent with the use of covered stents.[36,37] Atrioventricular valve regurgitation, common preoperatively in Fontan patients, may progress postoperatively.

### VENTRICULAR FUNCTION

Valvular lesions pose a risk for endocarditis and, if severe, affect long-term ventricular performance.[38] Operative myocardial preservation often was faulty in earlier decades. The later in life the patient is operated, the less the regression of ventricular hypertrophy. Long term, a subaortic right ventricle (RV) operating at systemic pressures or a single functioning ventricle in a "univentricular" heart—even after a Fontan—may have an irreversible decline in contractility. Ventricular function may suffer if a prosthetic patch or conduit origin is large, if an incisional aneurysm acts as a "windkessel," or if valvular or conduit obstruction and regurgitation or large shunt overloads the heart. Procedures that involve manipulation or reimplantation of the coronary arteries carry the risk of coronary artery kinking, torsion, or obstruction with resultant downstream myocardial infarction and/or ischemia. This is an important clinical consideration in patients with complete transposition of the great arteries who have undergone the arterial switch operation, those who have undergone the Ross procedure, or those with anomalous coronary arterial anatomy who have undergone arteriotomy, reimplantation, or bypass. Transcatheter stent placement within an RV-to-pulmonary-artery conduit carries the risk of coronary compression (typically left main or proximal left anterior descending).

### CONDUITS, PATCHES, AND PROSTHETIC MATERIALS

Septal patches, prosthetic valves, and conduits may degenerate.[7,8] Foreign bodies such as pacer wires or mechanical valvular prostheses risk thrombus formation or endocarditis (Fig. 45-3). Bioprosthetic valves and conduits often develop obstruction and/or regurgitation due to degenerative changes and calcification or by intimal ingrowth, particularly in adolescents and young adults. External conduits may be kinked by compression between the heart and sternum. Obstruction can occur at the exit from the ventricle, at a bioprosthetic valve, or at the distal insertion site. An internal conduit may develop leaks, internal obstruction, or kinking, or it may partially obstruct the chamber within which it sits. Some conduits have unusual courses due to altered great artery relationships; therefore, multiple precordial and subcostal transducer positions or multiplane TEE may be required for an adequate anatomic-hemodynamic evaluation. Continuous-wave (CW) Doppler is directed into the conduit from multiple angles to predict the pressure gradient; most conduits curve, and the proper angle to record the true peak velocity may be difficult to obtain.[8] CW Doppler of atrioventricular valve regurgitation quantitates ventricular systolic pressure and estimates significant conduit stenosis. Transcatheter devices carry a small risk of erosion into adjacent structures. This is of greatest concern with large ASD occluders and may result in aortic root to atrial fistulas and/or hemopericardium. The risk of device embolization is low and highly operator dependent. Appropriate device sizing, device testing before deployment, and observation after device deployment reduce the risk of this dreaded complication. Device retrieval is feasible and effective in the majority of cases. Rarely, device embolization results in large pulmonary embolism, stroke, or limb ischemia. When imaging a patient with a history of device placement, every effort should be made to locate and interrogate the device. Intracardiac devices should be clearly visible by TTE. If they are not visualized on routine postprocedural surveillance (we typically perform this 12 to 24 hours after transcatheter device implantation), then we recommend further imaging to locate the device (fluoroscopy, computed tomographic [CT] angiography, or magnetic resonance imaging [MRI]). Devices or coils placed in the great arteries or extracardiac veins (e.g., patent ductus arteriosus occluder) may not be readily visible by TTE in the adult patient.

## Palliative Procedures

### PULMONARY ARTERY BANDING

Pulmonary artery banding may be used to decrease the volume and pressure effects of a large shunt at the ventricular level to avoid heart failure or pulmonary hypertension (Fig. 45-4). The band site is evaluated by echocardiographic anatomic imaging, the best band placement being the midportion of the pulmonary artery. A band that is too close to the valve may interfere with valve function, and a band that has slipped onto the bifurcation may cause branch artery stenosis. Inadequate banding allows pulmonary hypertension (Table 45-2). Band stenosis gradient is quantitated by aligning the CW Doppler beam with the color flow jet via the iatrogenic stenosis (see Fig. 45-4). Because most lesions that require banding have large VSDs, pulmonary artery systolic pressure can be

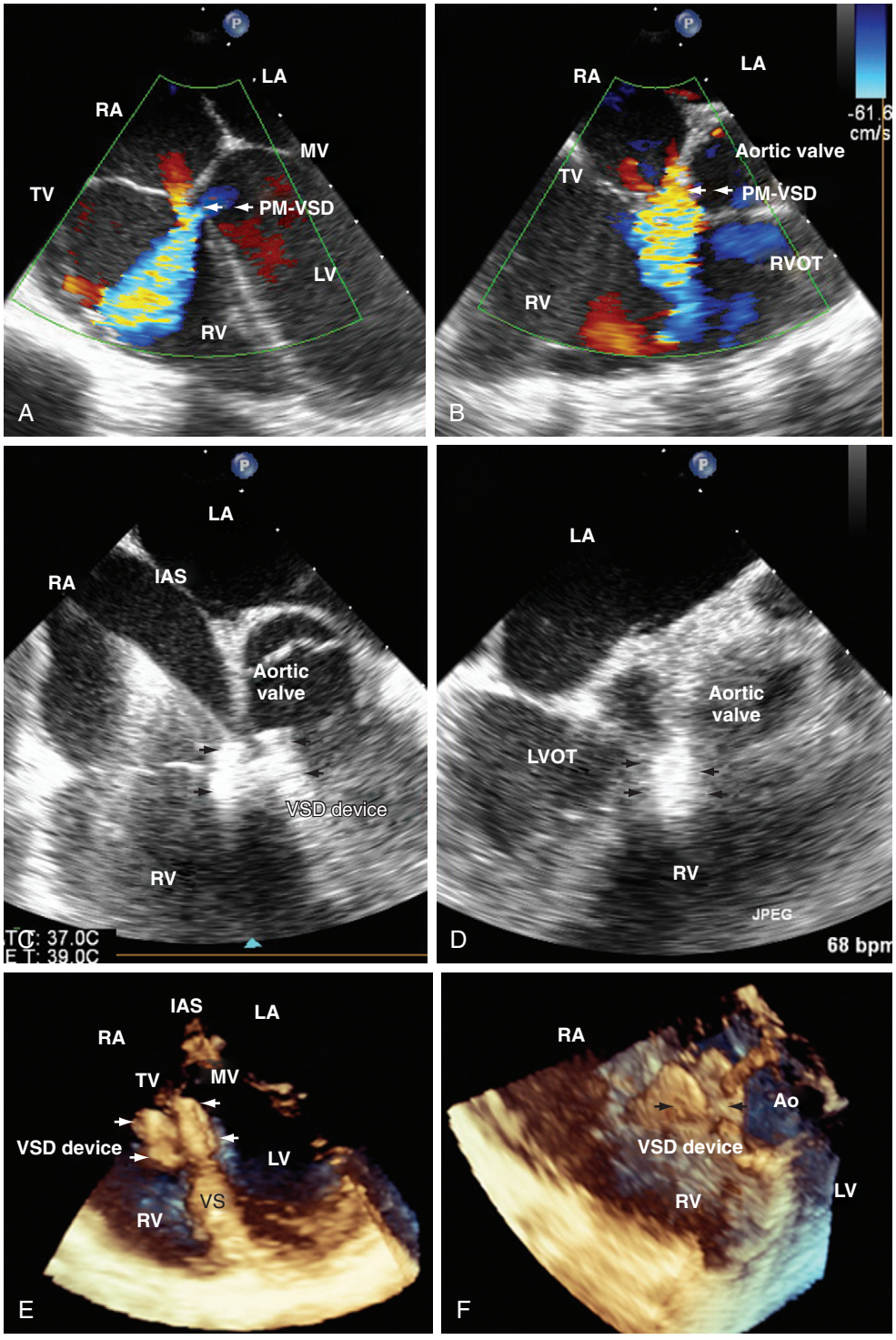



**Figure 45-2** **A** and **B, X-plane simultaneous orthogonal images from TEE with 2D and color flow Doppler demonstrating a moderate degree of high-velocity left-to-right systolic shunting across a perimembranous ventricular septal defect (*PM-VSD*). C** and **D,** Muscular VSD device attached to a cable is straddling the VSD just below the aortic valve. **E** and **F,** Live 3D TEE after VSD device release demonstrates its relationship to the mitral valve (*MV*), tricuspid valve (*TV*), and aortic valve. *IAS*, Intraatrial septum; *LVOT*, left ventricular outflow tract; *RVOT*, right ventricular outflow tract.

estimated as systolic systemic blood pressure minus the peak pressure gradient across the band (provided that there is no LV outflow tract obstruction). Transcatheter pulmonary artery "banding" is feasible with the use of flow restrictors. These are essentially occlusion devices with fenestrations that allow for continued but lessened flow. There is very little experience with such devices in adult congenital heart disease patients. Clinical investigation has focused on a neonatal population with single-ventricle physiology and excessive pulmonary blood flow.

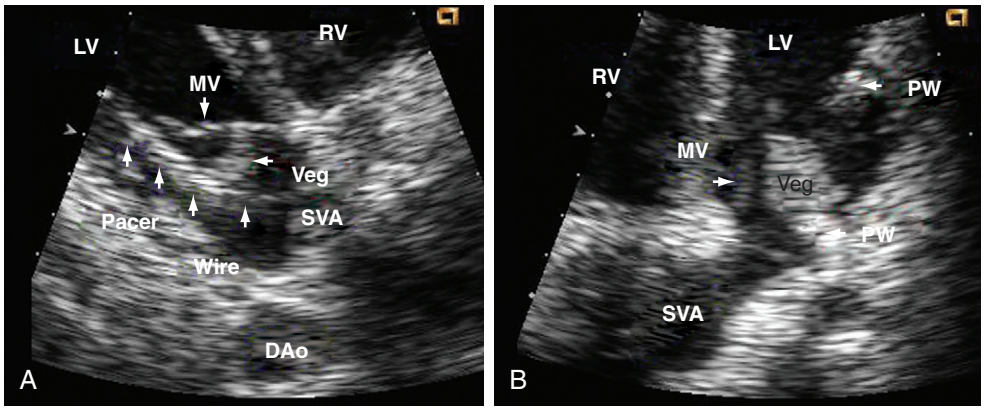



**Figure 45-3 Complete transposition of the great arteries late post Mustard with pacemaker previously inserted for sick sinus syndrome.** Patient presented with fevers and bacteremia. TTE views (**A,** modified parasternal long-axis view; **B,** zoomed portion of four-chamber apical view) reveal a vegetation (*Veg*) on the pacer wire (*PW*), which passes via the systemic venous atrium (*SVA*) from the superior vena cava to the LV. Vegetation resolved after 6 weeks of antibiotic therapy. *DAo*, Descending aorta; *MV*, mitral valve.

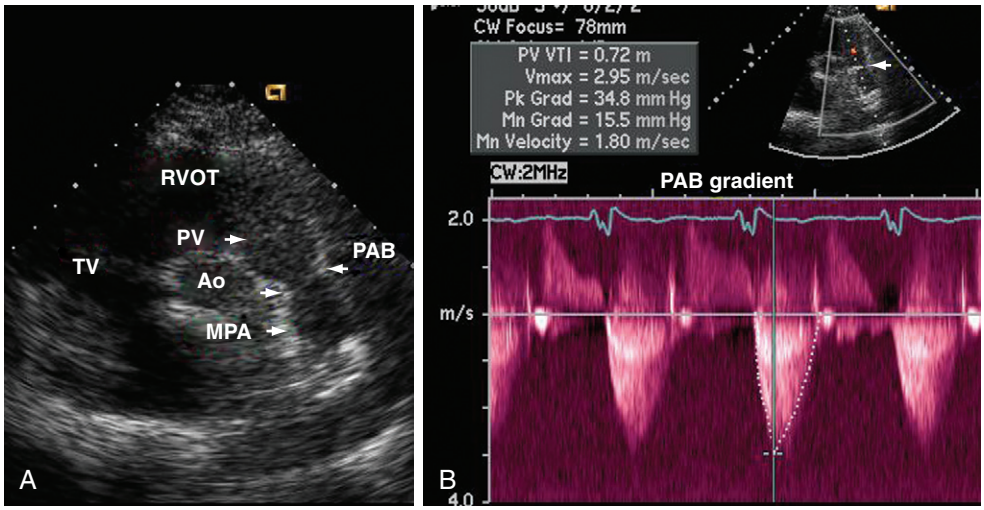



**Figure 45-4 Pulmonary artery band (*PAB*).** This patient had a previous PAB as a neonate before subsequent repair of an atrioventricular septal defect as an infant. **A,** Parasternal long-axis TTE view shows that PAB was not completely removed. **B,** Accompanying CW Doppler study reveals residual "stenosis" with a mean systolic gradient of 15.5 mm Hg. *Ao*, Aorta; *MPA*, main pulmonary artery; *RVOT*, right ventricular outflow tract; *TV*, tricuspid valve.

**TABLE 45-2 Palliative Procedures for Congenital Heart Disease**

| *Name of Procedure* | *Description* | *Complications* |
|---|---|---|
| Pulmonary artery banding | Constriction of main pulmonary artery | Inadequate band with consequent pulmonary vascular disease<br>Branch pulmonary artery stenosis<br>Pulmonic valve dysfunction |
| Waterston shunt | Ascending aorta to right pulmonary artery | Pulmonary hypertension due to too large a shunt |
| Potts shunt | Descending aorta to left pulmonary artery | Kinking of branch pulmonary arteries |
| Blalock-Taussig shunt | Subclavian artery to branch pulmonary artery | Inadequate shunt to maintain pulmonary blood flow |
| Modified Blalock-Taussig shunt | Gore-Tex graft from subclavian artery to pulmonary artery | Excessive shunt resulting in pulmonary hypertension |
| Glenn shunt | Superior vena cava to right pulmonary artery with division of main pulmonary artery | Postoperative cyanosis due to increased collaterals from superior to inferior vena cava or pulmonary arteriovenous fistulas |
| Bidirectional Glenn shunt | Superior vena cava to both (undivided) pulmonary arteries | Postoperative cyanosis due to increased collaterals from superior to inferior vena cava or pulmonary arteriovenous fistulas |

## PALLIATIVE AORTOPULMONARY SHUNTS

Palliative systemic arterial to pulmonary arterial shunts are performed for congenital heart disease characterized by decreased pulmonary arterial flow (e.g., tetralogy of Fallot) (Fig. 45-5). The shunts from the high-pressure aorta to the low-pressure pulmonary artery can be evaluated for patency by CW Doppler, which should reveal nonlaminar flow in both systole and diastole toward the pulmonary artery in the absence of pulmonary hypertension.

The Waterston (ascending aorta to right pulmonary artery) and Potts (descending aorta to left pulmonary artery) shunts are discrete side-to-side connections. Potts and Waterston anastomoses are now rarely performed because of problems with

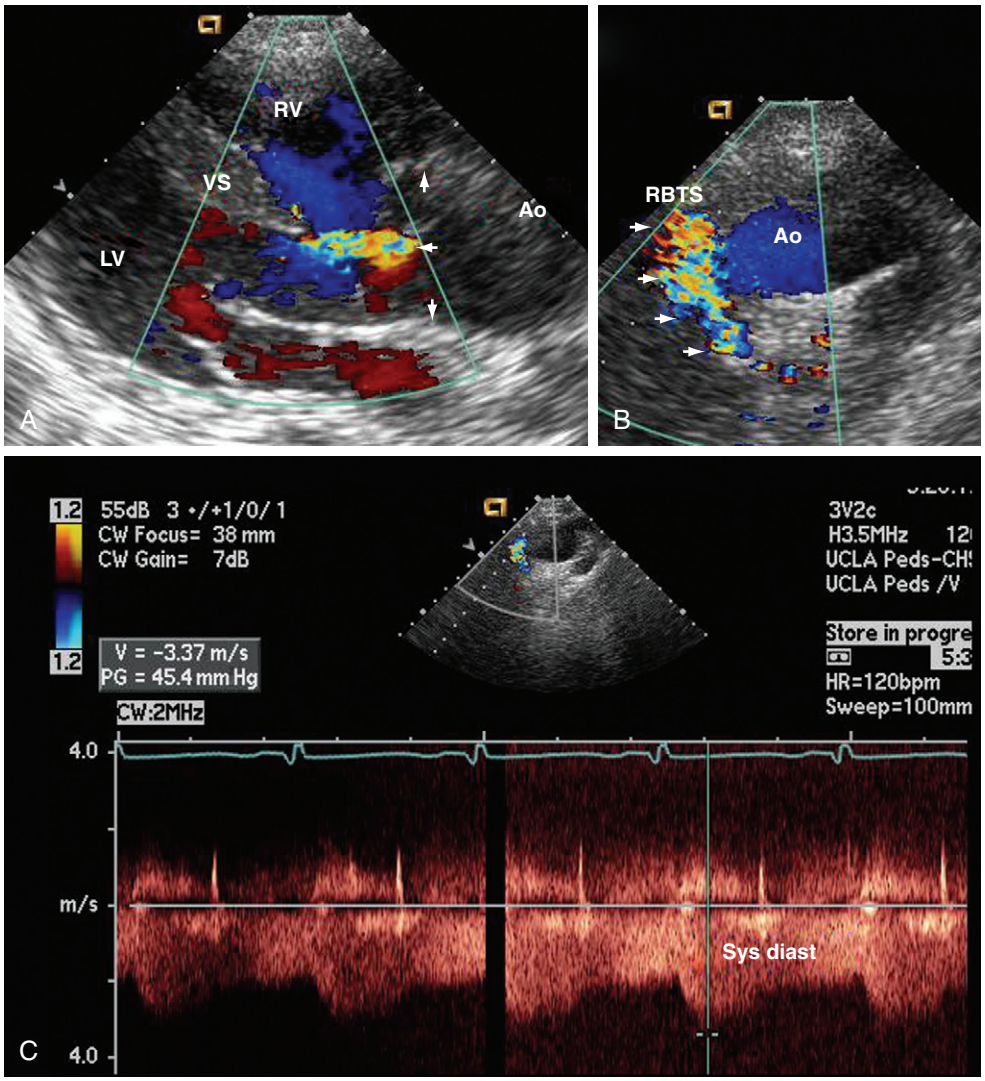



**Figure 45-5** **Right Blalock-Taussig shunt (*RBTS*) palliation in tetralogy of Fallot. A,** Underlying tetralogy anatomy of aorta overriding (*vertical arrows*) malaligned defect of ventricular septum (*VS*). Color flow shows jet of aortic regurgitation. **B,** Suprasternal notch view of RBTS descending (*horizontal arrows*) rightward along the transverse aorta (*Ao*). **C,** CW Doppler of RBTS with "continuous" high-velocity flow with peaking in systole (*Sys*) but persisting throughout diastole (*diast*), indicating low pulmonary vascular resistance.

precise control of size and possible pulmonary hypertension or kinking of branch pulmonary arteries, which may complicate further repair. TTE imaging of these anastomoses is often difficult in adults and may require TEE, where proper Doppler alignment with color flow imaging makes it possible to calculate the Bernoulli equation gradient. Pulmonary artery systolic pressure is estimated by subtracting the peak systolic pressure gradient from the brachial artery systolic peak pressure. As pulmonary artery pressures rise, diastolic flow decreases more than systolic flow; diminutive diastolic flow indicates increased diastolic pulmonary pressure.

A classic Blalock-Taussig shunt is a direct end-to-side anastomosis between a subclavian artery and a branch pulmonary artery, usually on the side opposite the aortic arch (see Fig. 45-5). A modified Blalock-Taussig shunt uses a 4- to 5-mm Gore-Tex tube or vein graft from the aorta or subclavian artery to the pulmonary artery. Imaging of a Blalock-Taussig shunt uses suprasternal and supraclavicular views augmented by color flow imaging. Estimation of pulmonary artery pressure may be unreliable in a long, curving connection. A low gradient may be seen in the presence of adequate flow and normal pulmonary artery pressures. The flow should be virtually continuous; thus, it must be distinguished from a patent ductus (see Fig. 45-5). If the shunt is small or occluded, flow decreases or is lost. Doppler is helpful in the early postoperative period in a patient who continues to have cyanosis, in order to assess adequacy of the shunt versus other causes of postoperative cyanosis (e.g., atelectasis). If the shunt is too large and results in pulmonary hypertension (fortunately an uncommon event), the diastolic flow decreases first, with decreased systolic flow later as pulmonary vascular resistance rises to equal systemic resistance.

## GLENN SHUNTS

A classic Glenn shunt is anastomosis of the end of the superior vena cava to the side of the right pulmonary artery divided from the main pulmonary artery and superior vena caval ligation as it enters the right atrium (RA). A bidirectional Glenn allows superior vena cava flow to both pulmonary arteries, causing improved systemic oxygen saturation without

ventricular volume overload, useful as definitive palliation or as a staging for subsequent Fontan procedures in complex congenital heart disease not amenable to biventricular repair. Echocardiographic imaging from right supraclavicular or suprasternal notch windows can show the course of the superior vena cava and the size of the connection to the right pulmonary artery. TEE imaging in at 90° to 110° alignment identifies the RA and upper stump of the superior vena cava and then, with rotation of the probe rightward, the superior vena cava–right pulmonary artery connection. Combined color flow and spectral Doppler evaluate anastomosis patency.[8,12,13]

Recurrent late postoperative cyanosis may be via collateral venous flow from the superior vena cava to the inferior vena cava or from pulmonary arteriovenous fistulas. Echocardiographic contrast detects these extracardiac shunts; after injection into an arm vein, late flow into the left atrium (LA) identifies pulmonary arteriovenous fistulas, whereas prompt appearance in the RA reveals azygous-venous collaterals to the inferior vena cava.[2] Fistulas and venous collaterals are amenable to catheter-directed coil embolization or device closure.

## Corrective Procedures for "Simple" Lesions

Simple lesions are isolated shunts, obstructive malformations, or regurgitant lesions. Complex malformations have two or more simple lesions, often with malpositions of veins, chambers, or great arteries and associated cyanosis.[8] Corrective procedures for simple lesions are listed in Table 45-3.

### ATRIAL SEPTAL DEFECTS

ASDs are among the most common unoperated and postoperative congenital heart defects. A secundum ASD, the most common, has conventionally been closed by direct surgical repair with good results even in adults more than 40 years old.[39-41] Recently, transcatheter device closure for secundum defects of appropriate size and rim for current devices has been successful with a low rate of complications (see Fig. 45-1).[23,42-45] Both TEE and intracardiac echocardiography are valuable in guiding proper insertion of ASD closure devices.[46,47] Echocardiographic exam after ASD closure searches for residual shunting, associated mitral abnormalities, pulmonary hypertension, and degree of resolution of right heart chamber enlargement.[8,48] Immediate residual shunting through the device is common after transcatheter ASD closure and usually resolves over a period of weeks to months as the device endothelializes. Surgical patch leaks are infrequently seen, provided that severe pulmonary hypertension was not present. A previously sizable shunt will have a decrease in but not necessarily normalization of RV size and increased LV size plus improved RV and LV myocardial performance index.[48] LV diastolic dysfunction, especially restrictive physiology, bears special consideration in the older adult with a secundum ASD; device or surgical closure of the defect results in increased LV preload and therefore increased filling pressure of a poorly compliant ventricle.[49] In patients with evidence of elevated LA pressure at baseline, test occlusion of the defect with continuous LA pressure assessment may reveal further increase in LA pressure and warrant device fenestration and further medical therapy (e.g., intravenous diuretic use).[50] TTE with color flow Doppler can be effective in monitoring device appearance and position as well as fenestration patency following the procedure.

Sinus venosus ASD, often associated with anomalous pulmonary venous connections to the superior vena cava, often requires TEE for precise diagnosis (Fig. 45-6). Repair requires patching of the defect with autologous pericardium so as to also baffle the anomalous pulmonary venous drainage to the LA via the ASD. TEE is valuable to evaluate the adequacy of patch closure of the defect with attention to possible superior vena caval or pulmonary venous obstruction (Fig. 45-7).

Atrioventricular canal–type ASD is considered in the section on "complex" repairs. A coronary sinus ASD, the rarest form, consists of partial or complete absence of the coronary sinus

**TABLE 45-3 Corrective Procedures for "Simple" Congenital Heart Lesions**

| *Lesion* | *Corrective Procedure* | *Complications and Residual Abnormalities* |
|---|---|---|
| Atrial septal defect | Suture repair, patch closure, or transcatheter closure | Residual shunting<br>Associated mitral valve abnormalities<br>Persistent pulmonary hypertension<br>Right heart chamber enlargement |
| Ventricular septal defect | Surgical repair (via right transatrial approach) | Residual patch leak<br>Arrhythmias if ventricular incision needed |
| Patent ductus arteriosus | Surgical ligation or catheter device closure | Residual shunting (more likely if calcified) |
| Bicuspid aortic valve | Surgical or balloon valvuloplasty<br>Pulmonic autograft<br>Valve replacement | Associated lesions (ventricular septal defect, coarctation)<br>Restenosis<br>Prosthetic valve dysfunction |
| Subaortic stenosis | Excision of membrane or fibromuscular ridge | Aortic regurgitation<br>Iatrogenic ventricular septal defect<br>Mitral valve injury<br>Recurrent stenosis |
| Coarctation of aorta | Multiple repair procedures | Residual or recurrent coarctation<br>LV hypertrophy<br>Associated lesions (e.g., bicuspid aortic valve, supramitral ring) |
| Ebstein anomaly | Surgical repair | Residual tricuspid regurgitation<br>Associated lesions (patent foramen ovale, atrial septal defects, pulmonic stenosis, ventricular septal defects) |
| Pulmonic stenosis | Balloon dilation<br>Surgical repair | Residual stenosis<br>Pulmonic regurgitation<br>Dynamic RV outflow obstruction (early postoperative) |
| Coronary artery anomalies | Various repair procedures | LV dysfunction<br>Mitral regurgitation |

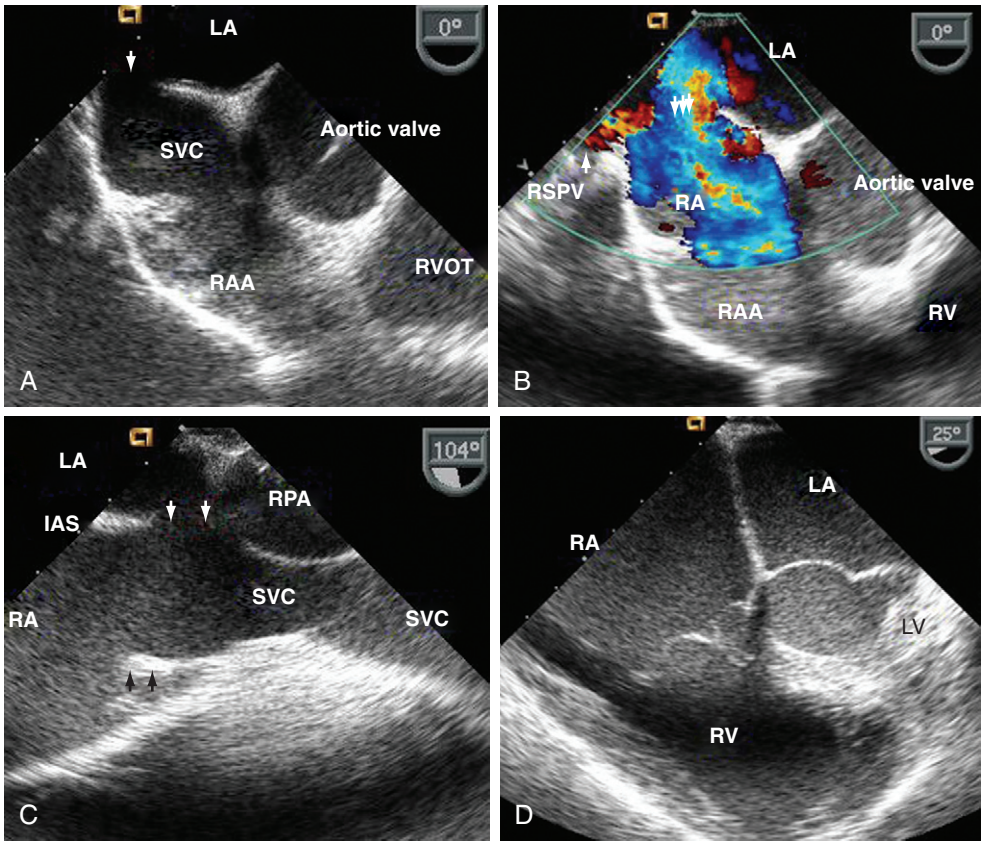



**Figure 45-6** **Sinus venosus atrial septal defect on preoperative multiplane TEE. A,** The horizontal plane demonstrates a communication (*arrow*) between LA and superior vena cava (*SVC*) at its entrance into RA at the level of the RA appendage (*RAA*). **B,** TEE color flow imaging shows a shunt from LA into SVC and RA. Also shows entrance of partial anomalous pulmonary venous connection of right superior pulmonary vein (*RSPV*) into RA rather than LA. **C,** Vertical plane of defect (*white arrows*) between LA and SVC; mouth of SVC to RA is seen on vertical plane with crista terminalis (*black arrows*). **D,** Horizontal plane below level of defect demonstrates severely dilated RA and RV. *IAS*, Interatrial septum; *RPA*, right pulmonary artery; *RVOT*, right ventricular outflow tract.

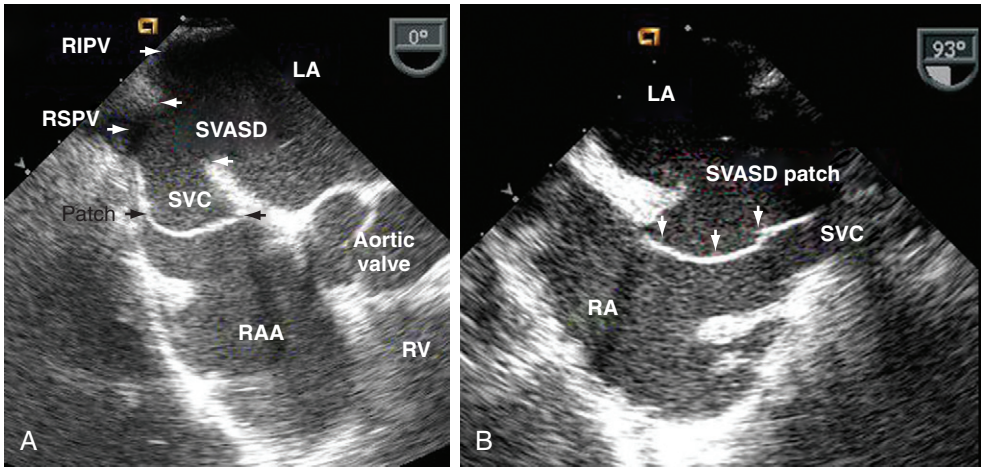



**Figure 45-7** **Sinus venosus atrial septal defect (*SVASD*) with partial anomalous pulmonary venous connection.** Intraoperative TEE in patient from Figure 45-6 after patch repair (*SVASD patch*) of defect where patch redirects right superior pulmonary vein (*RSPV*) flow to LA via defect that is left open. Superior vena cava (*SVC*) is mildly narrowed but patent. Right inferior pulmonary vein (*RIPV*) is seen to enter LA normally.

with connection of the LA to the RA via the usual location of the coronary sinus ostium, usually with a persistent left superior vena cava that joins the roof of the LA.[24] A coronary sinus ASD may be associated with complete atrioventricular septal defects or tricuspid atresia (and may first be detected after a Fontan repair).

## VENTRICULAR SEPTAL DEFECTS

VSD, a common congenital lesion alone or in combination with other anomalies, may occur anywhere in the ventricular septum. VSD may be classified as perimembranous, muscular, inlet, outlet, or malaligned. VSD may be characterized as

restrictive or nonrestrictive according to whether there is a significant systolic pressure gradient from LV to RV. In adults, substantial left-to-right shunt due to a nonrestrictive VSD is rare as a result of pulmonary vascular disease (Eisenmenger syndrome). Spontaneous closure of perimembranous VSD occurs frequently, mainly by adherence of septal tricuspid leaflet tissue but occasionally by prolapse of an aortic cusp into the defect. Tricuspid regurgitation may develop. Aortic regurgitation (especially with outlet supracristal defects) may occur; operative closure of the VSD usually prevents progression. Small defects risk infective endocarditis. Once endocarditis occurs, it may be argued that closure of the VSD will diminish subsequent risk. Nine of 296 patients who underwent closure of isolated VSD developed endocarditis; 3 of the 9 had no known residual shunt.[51]

A simple VSD is closed by right transatrial approach to avoid electrical and mechanical consequences of ventricular incisions. Multiple muscular VSDs may require left ventriculotomy for visualization, with the risks of ventricular arrhythmia and ventricular dysfunction. Investigation for patch leaks is imperative, preferably in the operating room at the time of closure to allow re-repair at that time. Color flow imaging after closure of a large VSD may show previously undetected smaller defects. Transcatheter device closure has been helpful for multiple muscular VSDs, for persistent postoperative VSD in complex conotruncal malformations, and for acquired postinfarction VSD and recently has been applied to perimembranous VSD.[24] TEE or intracardiac echocardiography during the procedure decreases fluoroscopy time, determines the device position relative to the defect and adjacent valves, and detects residual shunting.

## PATENT DUCTUS ARTERIOSUS

Patent ductus arteriosus is ordinarily detected in childhood, but undiagnosed cases are seen each year during routine echocardiography for other reasons. Operative closure of patent ductus arteriosus in the young leaves few residua; in adults, calcification is common and can tear during ligation. Catheter device closure is effective provided the size is less than 7 mm and previous endarteritis at the site has not occurred, which could weaken the vessel wall. TEE is useful in verifying complete uncomplicated closure. Color flow imaging search for residual shunting is essential to confirm success or the need for further device closure and for advice on antiinfective endocarditis prophylaxis.

## BICUSPID AORTIC VALVE

Bicuspid aortic valve, the most common congenital cardiac malformation, may initially be functionally normal, but with time most develop significant stenosis or regurgitation.[52,53] Associated lesions (e.g., VSD, aortic coarctation) should be sought. There is an associated tissue defect of the aortic wall with a tendency to aneurysm and ascending aortic dissection.[54]

Surgical or balloon catheter valvuloplasty can palliate young adults but can may cause aortic regurgitation. Most patients ultimately require valve replacement with a mechanical or bioprosthetic valve (homograft or heterograft or Ross procedure) or repair (Fig. 45-8). The Ross procedure (pulmonary autograft to the aortic position, heterograft or homograft to the pulmonary position, with or without reimplantation of the coronary arteries) reduces bioprosthetic degeneration in the aortic position, decreases the reoperation rate, and avoids long-term anticoagulation. Bioprosthetic pulmonic valve degeneration is often well tolerated, but late valve replacement is likely.

Concerns about pulmonary root autografts in the aortic position include potential for dilation of the wall of the pulmonary artery with continued exposure to systemic arterial pressure and the development of progressive "neoaortic" valvular regurgitation. Because cardiopulmonary bypass time is longer than for simple valve replacement, meticulous attention to myocardial preservation and to the technique of coronary reimplantation is required. Precise measurement of the pulmonary and aortic annuli to ensure parity and demonstration of only mild or no pulmonic regurgitation are helpful in deciding on the Ross procedure. Intraoperative TEE achieves these goals and verifies valvular and myocardial function and normal flow at coronary reimplantation sites.

## SUBAORTIC STENOSIS

Subaortic stenosis, most commonly due to a discrete fibromuscular ridge, may be isolated or may complicate perimembranous VSDs before or after closure.[55-57] Aortic valve regurgitation is more likely the closer the membrane is to the aortic valve. Excision of the membrane or fibromuscular ridge in association with focal septal myectomy is the treatment of choice to reduce the likelihood of recurrence. If associated aortic regurgitation is moderate or less, surgical repair may avoid replacement. Intraoperative TEE verifies relief of obstruction, lack of mitral injury, absence of iatrogenic VSD, and only mild or absent aortic regurgitation.[8] Surveillance for recurrence with stenosis and development or progression of aortic regurgitation is mandatory.

## COARCTATION OF THE AORTA

There are many survivors of coarctation surgical repair; the numbers of those treated with catheter balloon dilatation or stenting are steadily increasing (Fig. 45-9).[58,59] Residua, sequelae, or complications are frequent and require lifelong follow-up.[6,60-64] Bicuspid aortic valve, aortic medial defects, abnormal medium-sized arterial reactivity, and intracranial aneurysms are commonly associated with coarctation, suggesting a common developmental abnormality with diffuse arteriopathy.[6,65-69] Repairs include resection of coarctation with end-to-end anastomosis, patch, or subclavian flap aortoplasty or interposition conduit (see Fig. 45-9). If the condition is symptomatic, repair is best done in infancy. Otherwise, timing is "elective," but the later in life repair is performed, the more likely persistent hypertension and accelerated coronary artery disease. Suprasternal notch echocardiographic views are useful for imaging of residual or recurrent coarctation narrowing or aneurysm formation. Color flow imaging shows the narrowed site with proximal acceleration; CW Doppler is necessary to show the systolic gradient.[8] Continued diastolic forward flow through the zone of narrowing denotes significant obstruction (see Fig. 45-9). Exercise Doppler echocardiography is useful for follow-up of repaired coarctation to detect exercise-related hypertension and coarctation gradients. TEE is more effective than surface echocardiography in evaluating the extent and degree of coarctation. Doppler peak systolic velocity in the descending aorta correlates better with residual narrowing of the aortic isthmus or distal aortic arch than does the systolic blood pressure gradient between the upper and lower limbs.

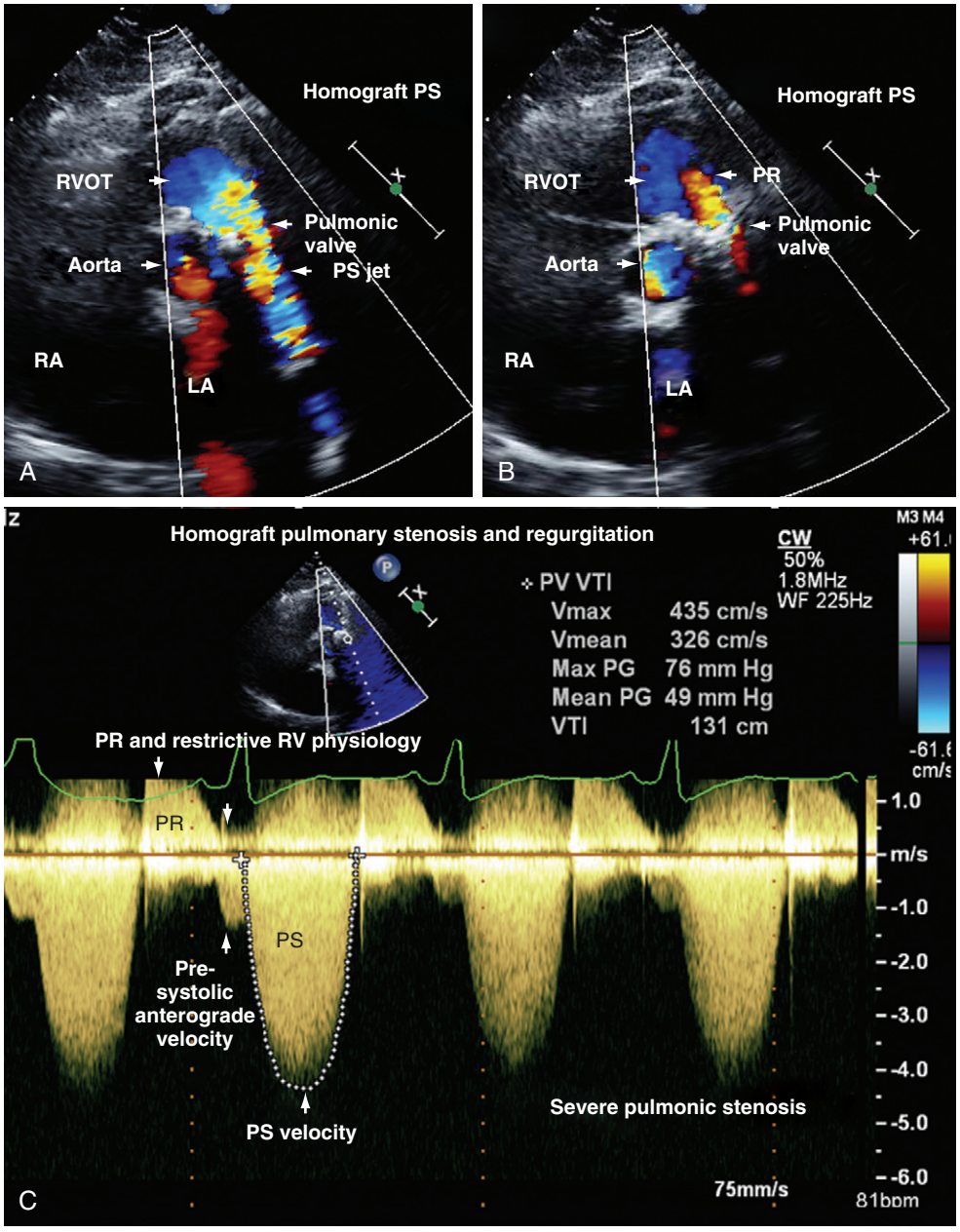



**Figure 45-8** **Homograft pulmonic stenosis. A,** TTE, systolic parasternal short-axis frame with color Doppler across stenotic pulmonary homograft in patient who has undergone Ross procedure. Note that the pulmonic stenosis jet (*PS jet*) is within the homograft and at pulmonic valve level. **B,** Diastolic frame demonstrating moderate pulmonic valve regurgitation (*PR*). **C,** CW Doppler demonstrating severe pulmonic stenosis (*PS*) with a peak and mean gradient of 76 mm Hg and 49 mm Hg, respectively. There is also evidence of moderate pulmonic regurgitation (*PR*) and restrictive RV physiology as evidenced by presystolic anterograde flow in the right ventricular outflow tract (*RVOT*).

Peak velocities greater than 2.5 m/s effectively detect greater than 25% narrowing. Prolongation of anterograde flow during diastole indicates a significant morphologic abnormality, such as restenosis or aneurysmal dilation.

LV hypertrophy and function should be quantified; associated left-sided obstructive lesions (e.g., bicuspid aortic valve, supramitral ring) must be sought. Postoperative endarteritis is rare but can result in a pseudoaneurysm. Balloon catheter dilation and stenting are often applied to recurrent or residual postoperative coarctation, but are effective and safe in native coarctation.[58] Balloon angioplasty alone carries a higher risk of aneurysm/pseudoaneurysm formation or dissection when compared to stenting. The use of covered stents essentially nullifies these risks, as well as the very low but dreaded risk of aortic rupture. Intravascular or transesophageal echocardiography during balloon dilation or stenting and intraoperatively is useful to show a good result and detect tear or dissection.[8]

## EBSTEIN ANOMALY

Ebstein anomaly has significant morbidity due to arrhythmias and right heart failure and even sudden death, possibly due to ventricular arrhythmias arising in the pathology of the atrialized RV.[70-73] It is characterized by apical displacement of the septal tricuspid leaflet with adherence of the septal and posterior tricuspid leaflets to the underlying myocardium, resulting

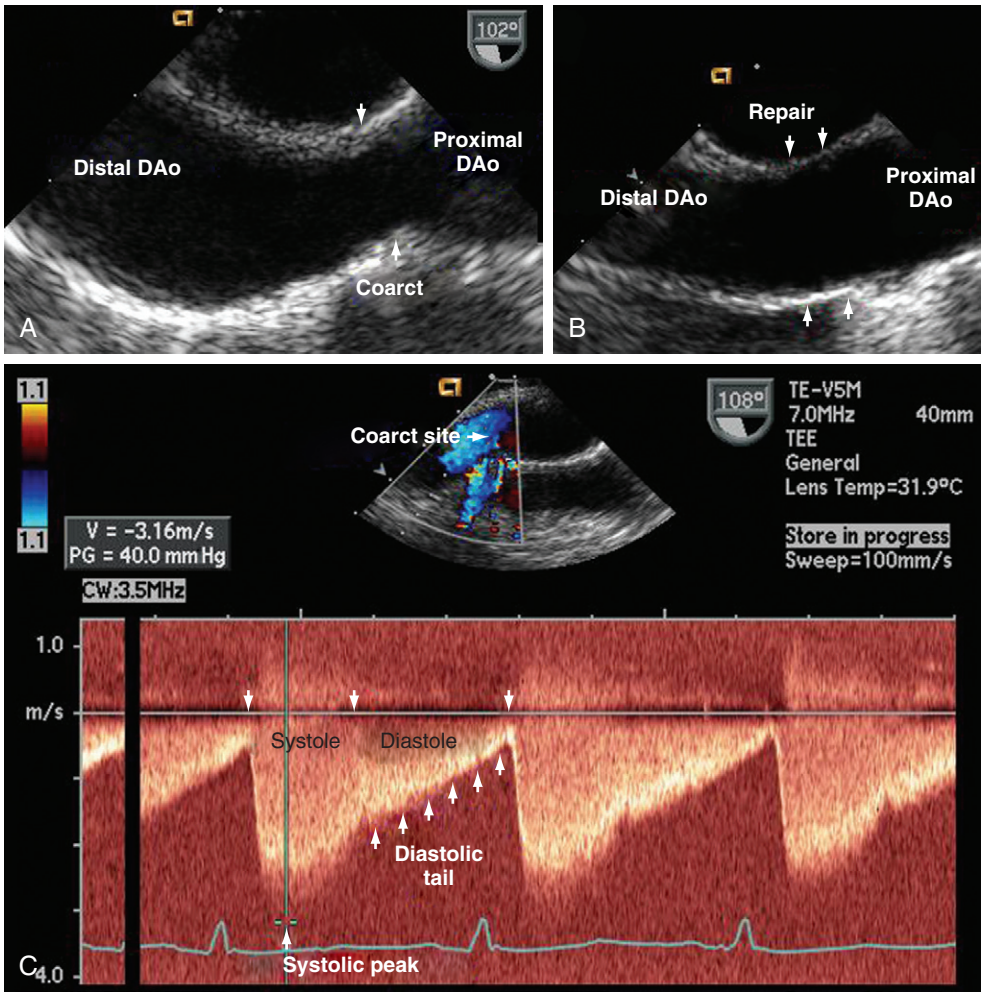



**Figure 45-9 Aortic coarctation. Intraoperative TEE. A,** Prerepair coarctation anatomy (*Coarct*) with dilatation of distal portion of descending aorta (*DAo*) that was nonpulsatile in contrast to excessively pulsatile proximal DAo. **B,** After coarctation repair (resection and end-to-end anastomosis), there is no residual stenosis. **C,** CW Doppler before coarctation repair that is not able to be precisely aligned with true angle of the coarctation. Thus peak recorded velocity of 3.16 m/s is underestimate of true peak instantaneous systolic gradient. Regardless, the continued diastolic tail reveals that this is significantly obstructive coarctation.

in downward displacement of the functional annulus and an "atrialized RV chamber" in its inflow portion. The anterior leaflet is redundant and may have abnormal fenestrations or tethering to ventricular myocardium. The true tricuspid annulus is dilated; tricuspid regurgitation is usual. Comprehensive echocardiographic definition of the tricuspid anatomy is usually adequate for diagnosis and prediction of suitability for repair and avoids the need for preoperative catheterization.[8,12,74,75] Associated anomalies include patent foramen ovale, ASD, pulmonic valve stenosis or atresia, VSDs, and tetralogy of Fallot. LV function can be decreased.[76] Tricuspid valve repair and annuloplasty with RV plication and RA reduction are preferable to valve replacement.[7,77-84] An anterior leaflet that is elongated, untethered, and freely mobile is necessary for best repair; a dysplastic, tethered, or fenestrated valve is undesirable. Intraoperative TEE verifies satisfactory reduction in tricuspid regurgitation without stenosis, repair of associated defects, and adequacy of myocardial preservation.

## PULMONIC STENOSIS

Pulmonic stenosis may be subvalvular, valvular, or supravalvular. Management requires elucidation of severity and site of stenosis and of associated abnormalities such as VSD or ASD. Some adults are still seen with previous surgical valvuloplasty for isolated valvular pulmonic stenosis. Balloon catheter dilatation is now usual in isolated valvular stenosis, but less so with dysplastic valves.[7] Immediately after valvuloplasty, the severely hypertrophied RV outflow tract may develop dynamic subpulmonic stenosis manifest by late-peaking high velocities that typically regress over time. Follow-up of residual stenosis or sequelae of pulmonic regurgitation is required.

Double-chambered RV, a variation of subpulmonic stenosis, due to aberrant muscle bundles at the junction of the inlet and outlet portions of the RV proximal to the infundibulum, is often associated with VSD and occasionally subaortic stenosis.[8] Only the inlet RV is under pressure from the "pulmonic stenosis" and, despite hypertrophy of that portion, the electrocardiogram shows remarkably low-voltage RV forces. Resection of the obstructing muscle bundles is indicated when there is more than mild stenosis.

## ANOMALIES OF THE CORONARY ARTERIES

Coronary artery anomalies include abnormal origin of the right, left main, or left coronary artery branches from one

coronary cusp or the other; associated abnormal courses of the anomalous artery; and abnormal connections to other vessels or chambers (e.g., coronary arteriovenous fistula or anomalous origin of the left coronary artery from the pulmonary artery).[7,8,12] Some of these anomalies are benign; others may result in myocardial ischemia, ventricular dysfunction, arrhythmias, and sudden death. Abnormalities of the course of the coronary arteries seen in tetralogy of Fallot or transposition complexes are important in relation to the technique of surgical repair. Echocardiography, particularly TEE, has had success in identifying coronary abnormalities.

Anomalous origin of the left coronary artery from the pulmonary artery is often associated with myocardial ischemia, congestive heart failure, mitral regurgitation, and arrhythmias. Surgical approaches include simple ligation of the left coronary artery at its attachment to the pulmonary trunk, saphenous vein or internal mammary artery bypass grafting, direct reimplantation of the coronary to the aorta, and (via a surgically created aortopulmonary window) fashioning of a tunnel that directs blood flow from the aorta to the left coronary ostium. Postoperative imaging of this connection in the operating room is necessary. Long-term echocardiographic evaluation includes quantitation of global and regional LV function and degree of mitral regurgitation.

## Repair of "Complex" Malformations

### ATRIAL SWITCH SURGERY

Atrial switch surgery (e.g., Mustard and Senning) is the reason most born with complete transposition of the great arteries are adolescents and young adults today (Table 45-4).[7] A combination of atrial septal tissue, pericardium, or synthetic material is used to fashion a baffle that reroutes systemic venous return to the subpulmonary morphologic left ventricle (LV) and pulmonary venous return to the subaortic morphologic RV (Figs. 45-10, 45-11, and 45-12). The atrial cavity is therefore divided into two portions: an anterior chamber receiving the systemic venous return and a posterior chamber receiving the pulmonary venous return. Sequelae and complications include dysrhythmias (sinus node dysfunction and atrial arrhythmias are frequent) and conduction disturbances, baffle leaks or obstruction, vena caval and pulmonary venous obstruction, tricuspid regurgitation, dysfunction of the RV, and even sudden death.[6,18,85-90] RV dysfunction may be due to ischemia or fibrosis.[91-93] Residual defects may include pulmonic stenosis, LV outflow tract obstruction, VSD patch leaks, and pulmonary hypertension.

Transthoracic Doppler echocardiography from multiple windows routinely allows imaging of the intraatrial pulmonary venous and systemic venous portions of the atrial switch (see Figs. 45-10, 45-11, and 45-12).[8] Presystolic flow reversal with atrial contraction into the hepatic venous confluence and superior vena cava provides indirect evidence of caval anastomotic patency. If echocardiographic contrast injected into a peripheral arm vein promptly enters the systemic venous atrium, the superior vena caval anastomosis is patent. In obstruction at the superior vena caval connection, azygous or other venous collaterals to the inferior vena cava will cause contrast to first enter the inferior vena cava and then the systemic venous atrium. Tricuspid regurgitation may occur with or without diminished RV function. Long-term performance of the systemic RV is often abnormal, especially in the VSD repair subgroup. In addition to evaluating RV size and ejection fraction, measuring RV myocardial performance index is useful.[8,94] TEE may be needed for accurate imaging of the entrance site of all four pulmonary veins and for imaging of the caval junctions with the systemic venous baffle.[12,13] Peripheral venous contrast injections help

**TABLE 45-4 Corrective Procedures for "Complex" Malformations**

| *Lesion* | *Corrective Procedure* | *Complications and Residual Abnormalities* |
|---|---|---|
| Transposition of the great arteries (TGA) | Atrial switch surgery (Mustard procedure) | Rhythm and conduction disturbances<br>Baffle leaks and obstruction<br>Vena caval and pulmonary venous obstruction<br>Tricuspid regurgitation<br>RV dysfunction |
| TGA | Arterial switch procedure | Supravalvular pulmonic stenosis<br>Supravalvular aortic stenosis (less common)<br>Regional wall motion abnormalities of the LV |
| Tricuspid atresia or double-inlet single ventricle | Fontan repair (RA to pulmonary artery or RV) | Cavoatrial shunting, atrial septal shunting, thrombus, RA-to-pulmonary-artery obstruction |
| Atrioventricular canal defects | Patching of atrial and/or ventricular septal defects combined with valve repair | Residual mitral regurgitation<br>Iatrogenic mitral stenosis<br>Subaortic stenosis<br>Patch leaks |
| Tetralogy of Fallot | VSD patch and relief of infundibular pulmonic stenosis | Pulmonic regurgitation<br>RV aneurysms (with older repairs)<br>Residual RV outflow obstruction<br>Ventricular septal patch leaks |
| TGA with ventricular septal defect (VSD) and pulmonic stenosis | Rastelli repair (conduit from RV to pulmonary artery with VSD patch directing subaortic flow) | VSD patch leak, subaortic obstruction<br>Prosthetic valve dysfunction |
| TGA with VSD and subaortic stenosis | Damus-Kaye-Stansel procedure | VSD patch leak<br>Pulmonic regurgitation |
| Congenitally corrected TGA | Various repairs, depending on associated defects | Left-sided atrioventricular valve regurgitation<br>Heart block<br>Systemic (anatomic right) ventricular systolic dysfunction |
| Double-outlet RV | Rastelli repair | Obstruction of LV to aortic baffle<br>Residual VSDs<br>Obstruction in right-sided conduit |

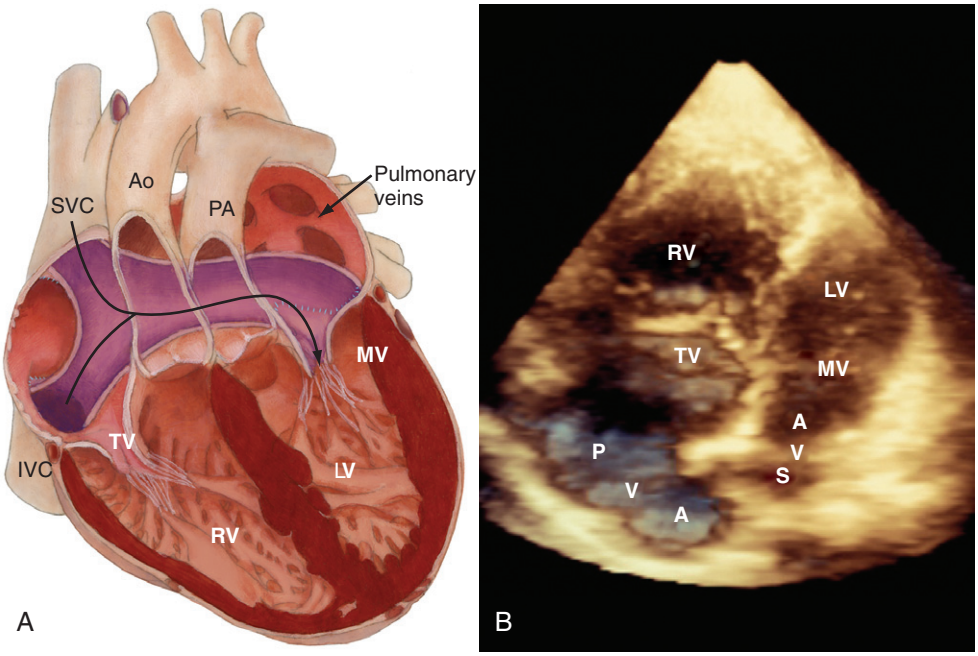



**Figure 45-10** **Complete transposition of great arteries (D-TGA) after atrial switch repair (Mustard or Senning). A,** Deoxygenated systemic venous return via superior vena cava (*SVC*) and inferior vena cava (*IVC*) is directed via intraatrial baffle (*curved arrow*), across mitral valve (*MV*), into subpulmonic LV and thereafter to pulmonary artery (*PA*) for oxygenation in lungs. Oxygenated blood returns from lungs via left-sided pulmonary veins that are baffled to tricuspid valve (*TV*). Oxygenated blood crosses TV into RV, which is connected to aorta (*Ao*). **B,** 3D echocardiography, apical four-chamber view, demonstrating widely patent pulmonary venous atrium (*PVA*) directing pulmonary venous return to TV and systemic RV. Systemic venous atrium (*SVA*) is typically not as well visualized as PVA.

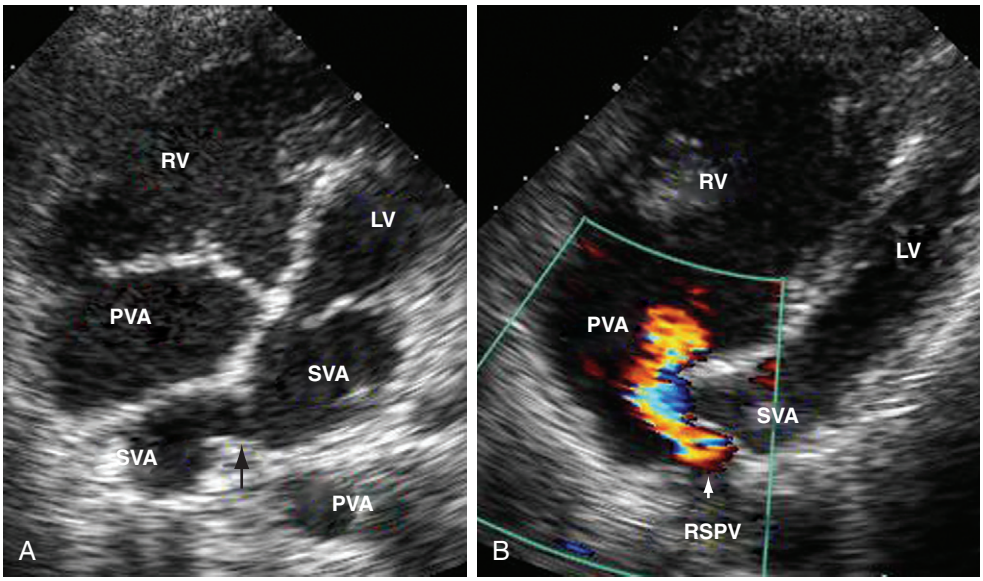



**Figure 45-11** **Pulmonary venous baffle stenosis in complete transposition of great arteries (D-TGA) late after Mustard procedure. A,** The TEE apical 2D four-chamber view shows the systemic venous atrium (*SVA*) with minimal narrowing in midportion (*arrow*); pulmonary venous atrium (*PVA*) wraps around SVA and thus is seen only in two parts. SVA connects vena cavae with LV via a portion of previous LA, and PVA connects posterior LA and pulmonary veins to RV via a portion of previous RA. **B,** Color flow imaging of PVA demonstrates color flow acceleration at narrowing of origin of right superior pulmonary vein (*RSPV*). PVA now courses obliquely across SVA, which is only incompletely seen. In both images, subaortic systemic RV is dilated.

detect baffle leaks. With TEE, obstructed caval-baffle, midbaffle, or pulmonary venous baffle sites are diagnosed by an increased peak velocity of continuous systolic and diastolic flow in combination with documented turbulent flow. TEE and/or intracardiac echocardiography are used in the catheterization laboratory to guide transcatheter interventions to relieve stenosis and/or to close baffle leaks.

## ARTERIAL SWITCH SURGERY

Because of late problems after atrial switch surgery, the arterial switch operation is preferred when possible. Issues include supravalvular aortic or pulmonary artery stenosis at the great arterial anastomoses as well as abnormalities of the proximal coronary arterial anastomoses with potential kinking and abnormal myocardial perfusion.[95-99] Postoperative

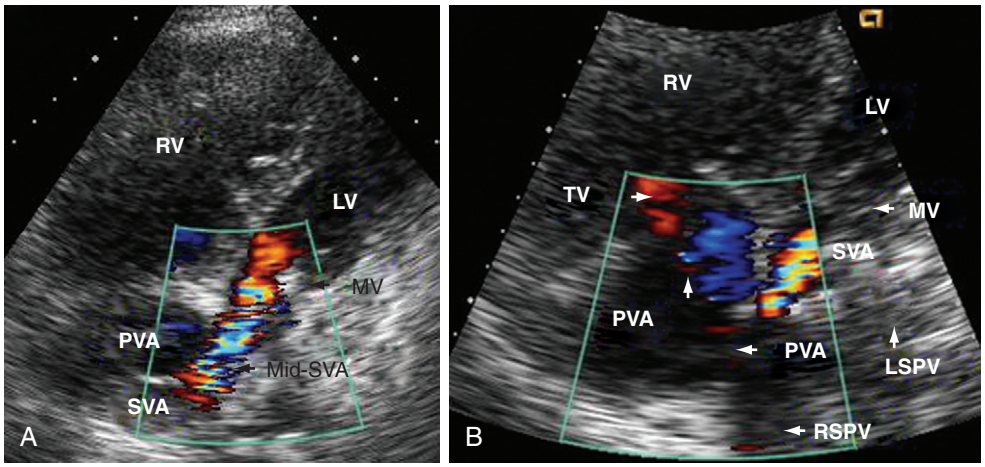



**Figure 45-12 Systemic venous return baffle obstruction in complete transposition of great arteries (D-TGA) late after Mustard procedure.** **A,** The TEE apical view shows the narrowed superior limb of systemic venous atrium (*SVA*) with color flow acceleration. **B,** Pulmonary venous atrium (*PVA*) is widely patent, and entry of pulmonary veins is well seen. *LSPV*, Left superior pulmonary vein; *MV*, mitral valve; *RSPV*, right superior pulmonary vein; *TV*, tricuspid valve.

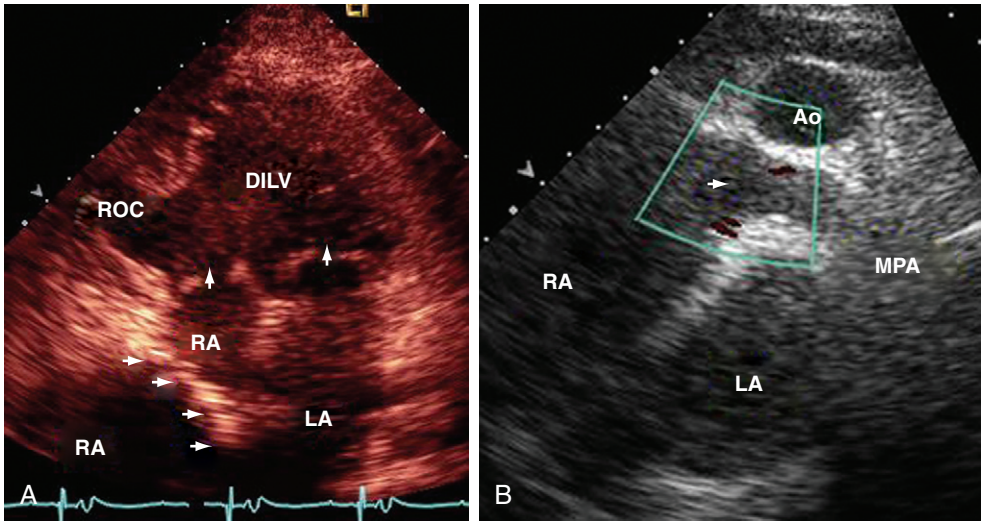



**Figure 45-13 A, TTE of double-inlet left ventricle (*DILV*) with hypoplastic RV forming right outflow chamber (*ROC*).** There is a modified RA to pulmonary artery (PA) Fontan with RA divided by a patch (*arrows*). Note inflow from both RA and LA to single ventricle. **B,** RA-to-PA connection from suprasternal notch view. *Ao*, Aorta; *MPA*, main pulmonary artery.

echocardiography plays an important role in evaluating the arterial anastomoses. Supravalvular pulmonic stenosis is the most frequent complication of the arterial switch operation. Neoaortic root dilatation as well as adequacy of the neoaortic (anatomic pulmonic) valve is a long-term concern. Proximal coronary artery torsion or kinking can be confirmed by intraoperative echocardiography. Myocardial perfusion defects are relatively common after the arterial switch operation; coronary events after the operation are not uncommon, usually occur early, and may be a cause of sudden death.[98,100] Regional wall motion abnormalities have been seen after two-stage repairs and correlate with myocardial perfusion defects.[101]

## TOTAL ANOMALOUS PULMONARY VENOUS CONNECTION

Total anomalous pulmonary venous connection is due to lack of development of communication of the common pulmonary vein and the LA. Most adults arrive already diagnosed and corrected with connection of the common pulmonary vein to the LA and closure of the obligatory ASD. After repair of total anomalous pulmonary venous connection, color flow and pulsed Doppler provide useful information regarding the presence of pulmonary venous obstruction.

## FONTAN ATRIAL SURGERY

Fontan-type atrial surgery, used when biventricular repair is not possible (e.g., tricuspid atresia or double-inlet single ventricle or complex straddling of atrioventricular valves, or crisscross relationships and superior-inferior ventricles—where two functioning ventricles cannot be established) has frequent short- and long-term morbidity and mortality.[102-105] The several variants of the Fontan repair all result in complete or near-complete (hemi-Fontan) separation of the pulmonary and systemic circulations. The RA was an integral part of the original Fontan anatomy. Many adults still living had the old-style direct RA–pulmonary artery anastomosis (Fig. 45-13).[103] In the past two decades, various modifications of the Fontan operations have been used. The RA-to-pulmonary-artery Fontan has been

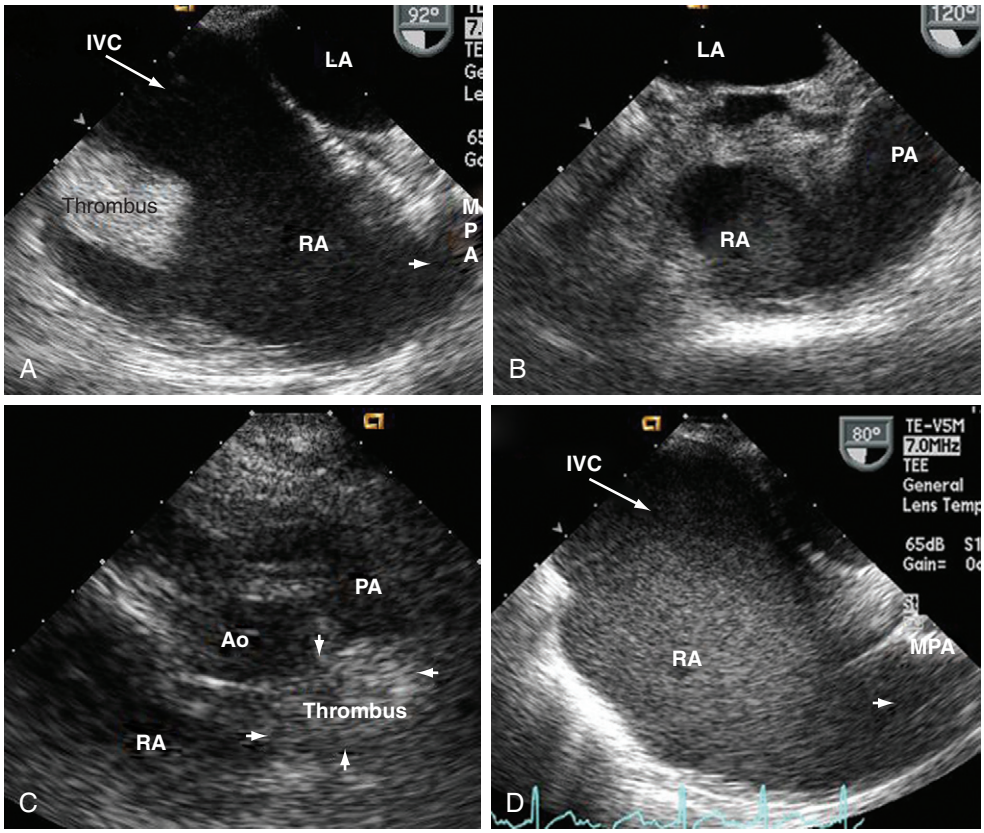



**Figure 45-14** **A, 2D TEE in patient with RA to main pulmonary artery (*MPA*) Fontan.** Note large thrombus near entry of inferior vena cava (*IVC*) to RA. **B,** Short-axis view demonstrating widely patent RA-to-PA connection. **C,** Patient desaturated dramatically the next day and urgent 2D TTE demonstrated embolization of large RA thrombus to RA-to-PA connection. **D,** TEE following treatment with thrombolytic therapy and anticoagulation for 4 weeks demonstrates complete resolution of thrombotic material in RA and RA-to-PA connection. *Ao*, Aorta.

abandoned, mainly because of the unacceptably high risk of arrhythmias and thromboembolism (Fig. 45-14). The two most widely encountered contemporary Fontans are the extracardiac conduit and the lateral or intraatrial tunnel (Fig. 45-15). In high-risk Fontan patients, an adjustable ASD or fenestration may be performed (see Fig. 45-15, *B*).[106,107] In double-inlet single ventricle, a direct atriopulmonary connection with patch exclusion of the right atrioventricular valve was a common modification of the Fontan procedure. The current total cavopulmonary connection is more hemodynamically efficient.[108] The total cavopulmonary connection is either an extracardiac tube connecting inferior vena cava to right pulmonary artery plus connection of superior vena cava to pulmonary artery, or an intracardiac tube or lateral tunnel using the lateral wall of the RA to bring the inferior vena cava to the pulmonary artery with the superior vena cava attached to the right pulmonary artery (see Fig. 45-15).[108-112] In adults whose Fontan circulation is failing or atrial arrhythmias are difficult to control, conversion to either a modern total cavopulmonary connection often with a modified maze procedure with RA size reduction is considered.[113] Patch exclusion of the RA may result in right atrioventricular valve regurgitation. Postoperative subaortic stenosis (dynamic or fixed—at the bulboventricular foramen in single ventricle, at the subaortic conus in tricuspid atresia with transposed great arteries) must be sought (Fig. 45-16).[8,12,13,114] The most common complications in the atrial portion of the Fontan circulation include cavoatrial shunting, atrial septal shunting, thrombus, and RA-to-pulmonary-artery obstruction; atrial arrhythmias are frequent.[102,103,105,111,112] Surgical sequelae purposely left behind in high-risk patients include atrial fenestrations and adjustable ASDs.[107] These communications are often closed later in the catheterization laboratory under TEE or intracardiac echocardiographic guidance.[115,116]

In adults, RA-RV conduits are occasionally seen by TTE examination but RA-pulmonary connections can be difficult to visualize (see Figs. 45-13 and 45-14).[8,12,13] Evaluation of ventricular hypertrophy and systolic and diastolic is important as they are determinants of long-term outcome.[117,118] Multiplane TEE consistently images the Fontan anastomosis, although not always with the necessary alignment to allow accurate spectral Doppler assessment of peak velocity profiles.[8,12,13]

In the Fontan patient, an important determinant of outcome is the systolic and diastolic function of the systemic ventricle and its atrioventricular valve, both of which are readily evaluated by transthoracic Doppler echocardiography studies.[2,12,13,119,120] TEE is useful when directed at suspected complications or known residua of the Fontan atrial anatomy (baffle shunts, thrombi, stenotic connections).

With no functioning subpulmonary RV in most with the Fontan repair, pulmonary artery flow shows a bi- or triphasic pattern with diastolic velocities equal to or greater than systolic, with accentuation of diastolic velocity at the time of RA contraction in those with RA-PA variants; this is not as appreciated in total cavopulmonary shunts (Fig. 45-17).[121] Inspiration augments pulmonary artery flow velocities (see Fig. 45-17), and pulmonary and systemic venous flow profiles remain relatively

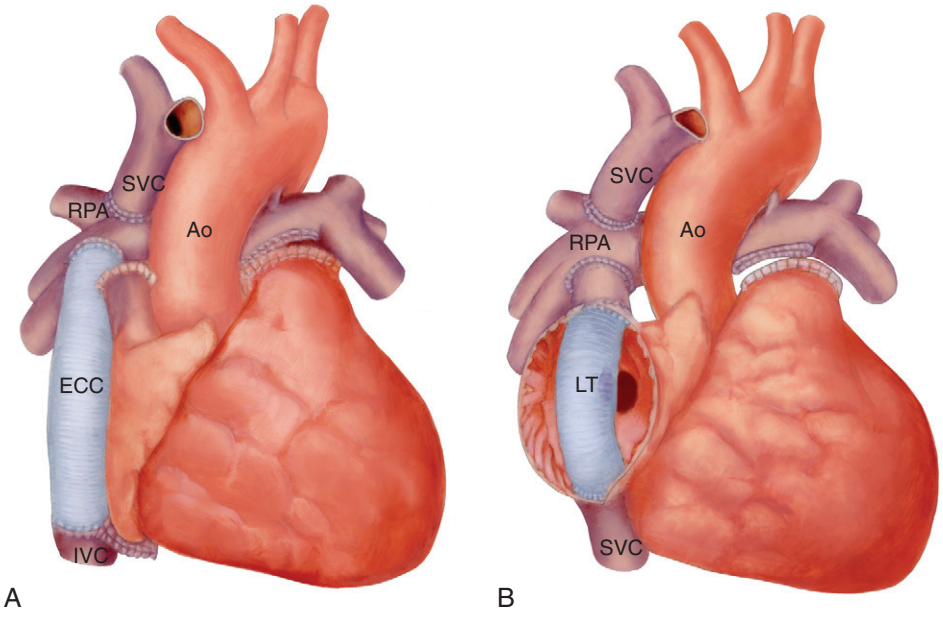



**Figure 45-15 Two most commonly employed Fontan modifications in the current era. A,** Extracardiac conduit (*ECC*) from inferior vena cava (*IVC*) to right pulmonary artery (*RPA*). Glenn connection from superior vena cava (*SVC*) to pulmonary artery is noted. **B,** Lateral tunnel (*LT*) Fontan running within RA with fenestration and atrial septal defect (*ASD*) left in place or created. *Ao*, Aorta.

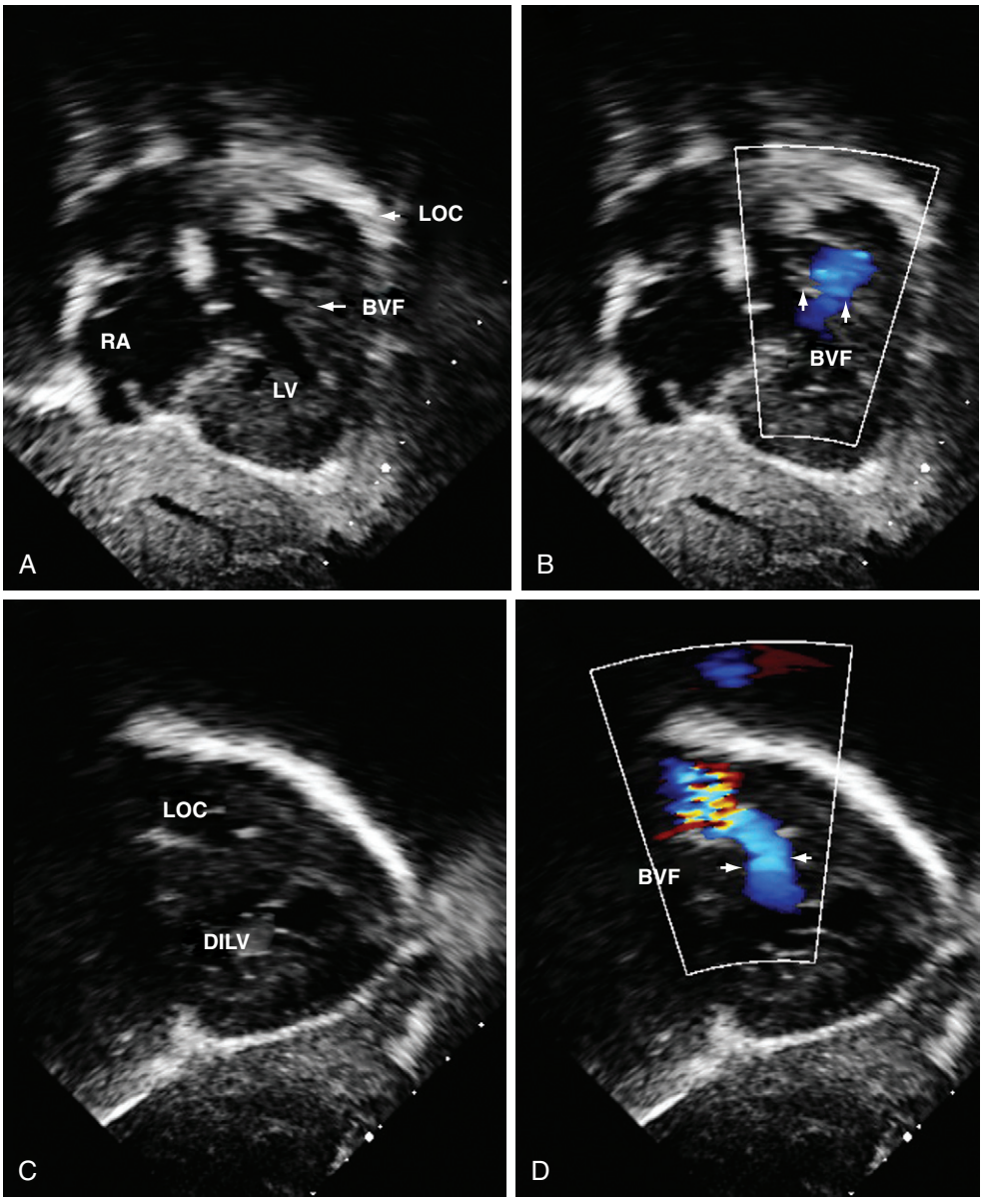



**Figure 45-16 Double-inlet LV (DILV).** Modified subcostal views show a narrowed bulboventricular foramen (*BVF*) into hypoplastic morphologic RV that forms left outlet chamber (*LOC*) This results in flow acceleration and subaortic stenosis.

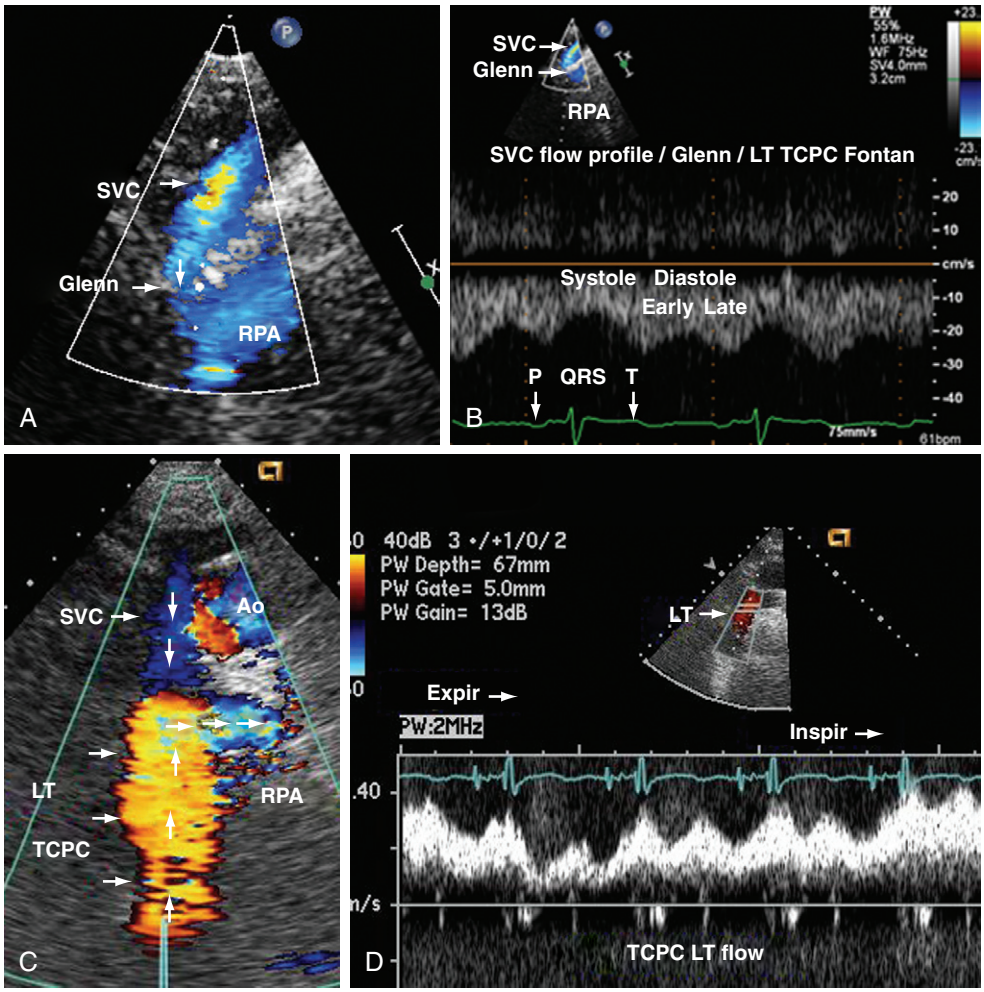



**Figure 45-17** **Single ventricle physiology with a total cavopulmonary connection (*TCPC*) using a lateral tunnel (LT) from inferior vena cava to the PA plus a Glenn anastomosis from the superior vena cava (*SVC*) to right pulmonary artery (*RPA*). A,** Suprasternal notch view with color Doppler demonstrating SVC-to-RPA Glenn connection. **B,** Pulsed-wave (PW) Doppler demonstrates continuous flow that is accentuated in early and late diastole. **C,** Color Doppler from suprasternal notch view clearly demonstrating flow from EC and Glenn into RPA. **D,** PW Doppler within ECC-to-RPA connection demonstrates continuous flow that is accentuated with inspiration. *Ao*, Aorta.

normal in patients with normal left (or single) ventricular function. Abnormal systemic ventricular performance is reflected in a reduced pulmonary arterial flow pattern velocity with decreased change on inspiration and a predominantly systolic profile.

Intraoperative TEE ensures patent connections and helps in sizing any surgical ASD or fenestration. Postoperative TEE may be required in the intensive care unit in Fontan patients to search for known complications (e.g., increasing pulmonary artery pressures with decreased cardiac output and "right heart failure" due to lateral tunnel Fontan thrombus embolization). TEE and intracardiac echocardiography can be used in the interventional catheterization laboratory to guide postoperative closure of surgical ASDs or fenestration.

## ATRIOVENTRICULAR SEPTAL DEFECTS

Atrioventricular septal or canal defects (AVSD) are a group of anomalies that share a defect at the site of the atrioventricular septum and abnormalities of the atrioventricular valves.[8,12,13,119] They are considered "complex" lesions because of the usual association of two or more abnormalities. These defects may be partial (partial endocardial cushion or primum ASDs, cleft mitral leaflet, and/or inlet VSD) or complete and will usually have been corrected in childhood or adolescence. The usual partial AVSD in adults is a primum ASD plus an anterior mitral leaflet cleft with abnormal chordal attachments to the LV outflow tract and variable degrees of mitral regurgitation. Repair requires primum ASD patching and mitral valve repair. Complete AVSDs, rarely first diagnosed in adults, are seen in patients surviving to adulthood after childhood repair. A complete AVSD has a large septal defect with interatrial and interventricular components plus a common atrioventricular valve that connects both atria and both ventricles.

Follow-up imaging examines adequacy of mitral repair, amount of regurgitation, and presence of iatrogenic mitral stenosis or subaortic stenosis. Subaortic stenosis may be due to a discrete fibromuscular narrowing or abnormal LV outflow tract attachments of anomalous chords and leaflet tissue, or may develop postoperatively because of reduction of LV outflow size as the cleft in the mitral leaflet is apposed.[8] Owing to combined preoperative RV and LV volume overload, the size and function of both ventricles must be quantified postoperatively. Occasionally, tricuspid regurgitation can be substantial, and tricuspid valvular repair requires postoperative evaluation. In addition, in complete AVSD repairs, the VSD patch must be evaluated.

Some patients, especially those with Down syndrome, can have pulmonary vascular disease; tricuspid and pulmonic regurgitant jets should quantify pulmonary artery pressure. To minimize significant residual defects (e.g., valvular regurgitation, patch leaks), intraoperative TEE should be used.[8,12,13]

## BIVENTRICULAR REPAIRS

Biventricular repairs result in two well-formed functional ventricles with a subpulmonic ventricle and a subaortic ventricle that are able to provide a circulation in series without an admixture of venous and systemic blood. Most complex congenital cardiac malformations amenable to biventricular repair are cyanotic and consist of a mixture of septal defects; obstructive and regurgitant valvular, subvalvular, or supravalvular lesions; and malpositions of the cardiac chambers and great arteries.[7] Anatomic substrates that are typical candidates include tetralogy of Fallot, pulmonary atresia with VSD, transposition complexes of the great arteries, and double-outlet ventricles.[7,8] The basic theme includes patch closure of a VSD and reconstitution of ventricular to pulmonary arterial blood flow (Fig. 45-18). If pulmonic stenosis cannot be directly repaired for anatomic or conduction system reasons, the pulmonary artery must be ligated or the valve oversewn and a conduit placed from the ventricle to pulmonary artery (see Fig. 45-18). Long-term postoperative survival is affected by age at operation, degree of relief of the loading conditions imposed on the ventricular myocardium, myocardial protection during operation, electrophysiologic sequelae, and the durability of prosthetic materials, especially valved or nonvalved conduits.

## TETRALOGY OF FALLOT

Tetralogy of Fallot is the most common complex congenital malformation with cyanosis at birth in which patients live to adulthood.[7] Tetralogy of Fallot is due to anterior deviation of the outlet septum with infundibular narrowing and a malaligned VSD. Echocardiography shows the malaligned VSD with aortic override plus a spectrum of RV outflow tract and pulmonary artery obstructive lesions from mild to complete pulmonary atresia (see Fig. 45-5).[8,12,13,119] Numerous associated defects must be identified for proper surgical and postoperative management—for example, ASDs, endocardial cushion abnormalities, Ebstein malformation, muscular VSDs, absent pulmonic valve or left pulmonary artery, abnormal origin of one pulmonary artery from the aorta, systemic and pulmonary

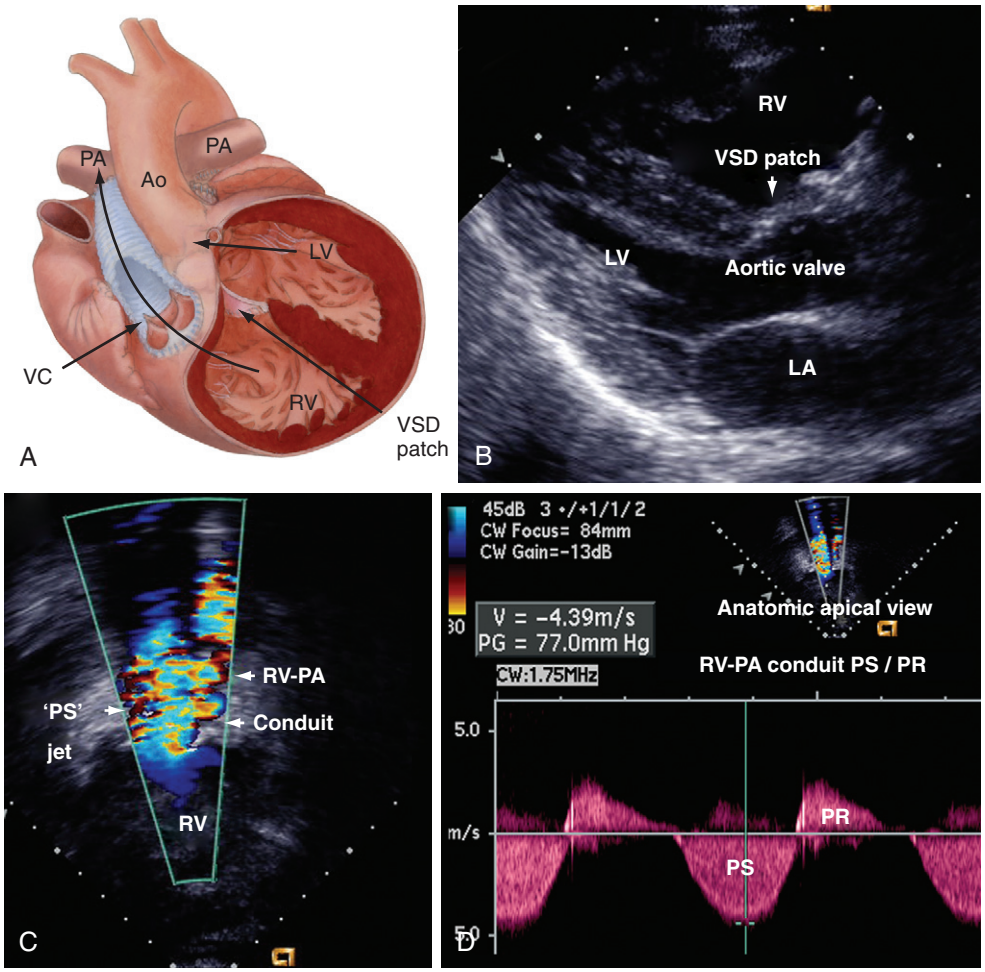



**Figure 45-18 A, Rastelli repair in patient with double-outlet RV with severe pulmonic stenosis involves patching of ventricular septal defect (*VSD*) to form internal tunnel from LV to aortic valve.** Valved conduit (*VC*) is placed from RV to pulmonary artery (*PA*). **B,** TTE parasternal long-axis view demonstrating VSD patch and internal tunnel from LV to aortic valve. **C,** Short-axis subcostal color flow Doppler demonstrating flow acceleration consistent with pulmonic stenosis (*PS*) within anteriorly located RV-to-PA conduit. **D,** CW Doppler from subcostal position demonstrates severe PS with estimated peak instantaneous systolic gradient of 77 mm Hg along with moderate pulmonic regurgitation (*PR*).

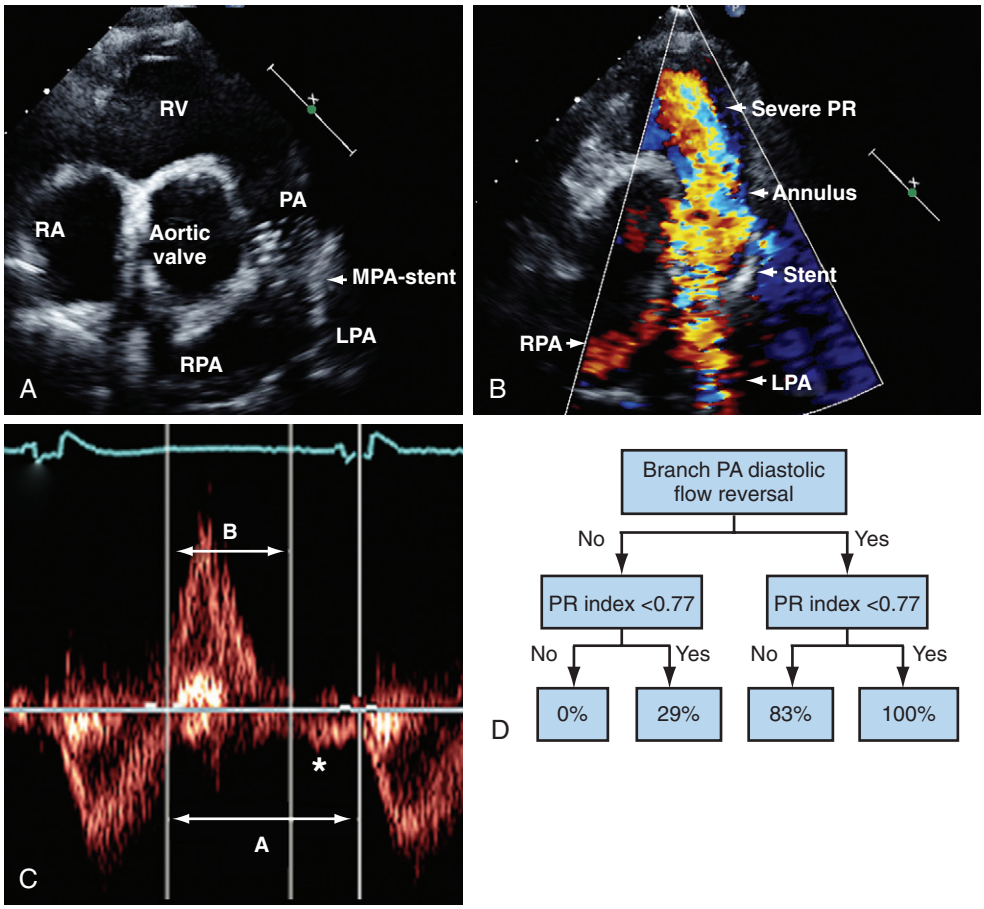



**Figure 45-19** **Tetralogy of Fallot with pulmonary atresia status post transannular patch placement from RV to pulmonary artery (*PA*). A,** TEE parasternal short-axis view shows residual stenosis of distal main pulmonary artery (*MPA*) that was treated with stent without obstructing right pulmonary artery (*RPA*) or left pulmonary artery (*LPA*) ostia. **B,** Color Doppler in diastole demonstrates severe pulmonic regurgitation (*PR*) with branch pulmonary artery flow reversal (*RPA* and *LPA*). Note that stent is well above level of pulmonic valve annulus. **C,** The PR index is the ratio of the duration of regurgitant flow (*arrow* in B) to the total duration of diastole (*arrow* in A). In this case, the PR index is <0.77, suggesting severe PR. End-diastolic forward flow (*) is sign of restrictive RV physiology. **D,** Flow chart for the likelihood of severe PR on velocity encoded MRI imaging, based on the presence of diastolic flow reversal in the branch pulmonary arteries and a PR index less than 0.77. When both are present, the likelihood of severe PR is 100%; if neither is present, the likelihood of severe PR is 0%. *(With permission from Renella P, Aboulhosn J, Lohan DG, et al: Two-dimensional and Doppler echocardiography reliably predict severe pulmonic regurgitation as quantified by cardiac magnetic resonance.* J Am Soc Echocardiogr *23:880-886, 2010.)*

venous anomalies, discrete subaortic stenosis, right-sided aortic arch, aortopulmonary window, aortopulmonary collaterals, and coronary artery anomalies.[8]

Tetralogy of Fallot repair includes patch closure of the VSD and usually an RV outflow tract incision to relieve infundibular stenosis. The RV incision at times must extend through the pulmonary annulus thus requiring a transannular patch. Pulmonic valve, trunk, or branch artery stenosis should be relieved (Fig. 45-19). If there is extreme pulmonic stenosis or pulmonary atresia, a valved conduit connects the RV to the pulmonary artery. After tetralogy of Fallot repair, long-term concerns focus on the RV and its outflow tract, the pulmonic valve and pulmonary artery, the LV, the aortic valve and ascending aorta, and electrophysiologic residua and sequelae (see Fig. 45-19).[6,7,17,122-158]

When tetralogy of Fallot is repaired in the first 5 years of life, late RV function remains normal in the absence of significant RV outflow obstruction provided low-pressure pulmonic valve regurgitation is only mild to moderate. Severe pulmonic regurgitation (see Fig. 45-19) causes RV enlargement and failure and tricuspid regurgitation, particularly if there is any residual RV outflow tract, pulmonic valve, or pulmonary artery (e.g., branch stenosis) obstruction (see Fig. 45-19; Fig. 45-20). Postoperative RV outflow tract scars and aneurysms may be present and lead to risk of ventricular arrhythmias and sudden death. 2D echocardiography with color flow and spectral Doppler examines the RV outflow and pulmonary artery anatomy for obstruction or regurgitation (see Fig. 45-19)[159]; CW Doppler tricuspid regurgitant jet velocities reflect RV systolic pressure.[8] VSD leaks, usually eccentric, may occur anywhere along the patch and require color flow imaging for detection. RV restrictive physiology late after repair of tetralogy is common as detected by Doppler hemodynamics. The A wave contributes to forward pulmonary flow and shortens the duration of pulmonic regurgitation, resulting in less RV enlargement and better exercise tolerance (see Fig. 45-19).[8,118,133,138,160] When severe pulmonic regurgitation results in impaired exercise performance, increasing RV size with decreasing RV systolic function, and increasing tricuspid regurgitation, pulmonic valve replacement is necessary. Aerobic capacity has been shown to improve after pulmonic valve replacement for severe pulmonic regurgitation after previous tetralogy of Fallot repair even if

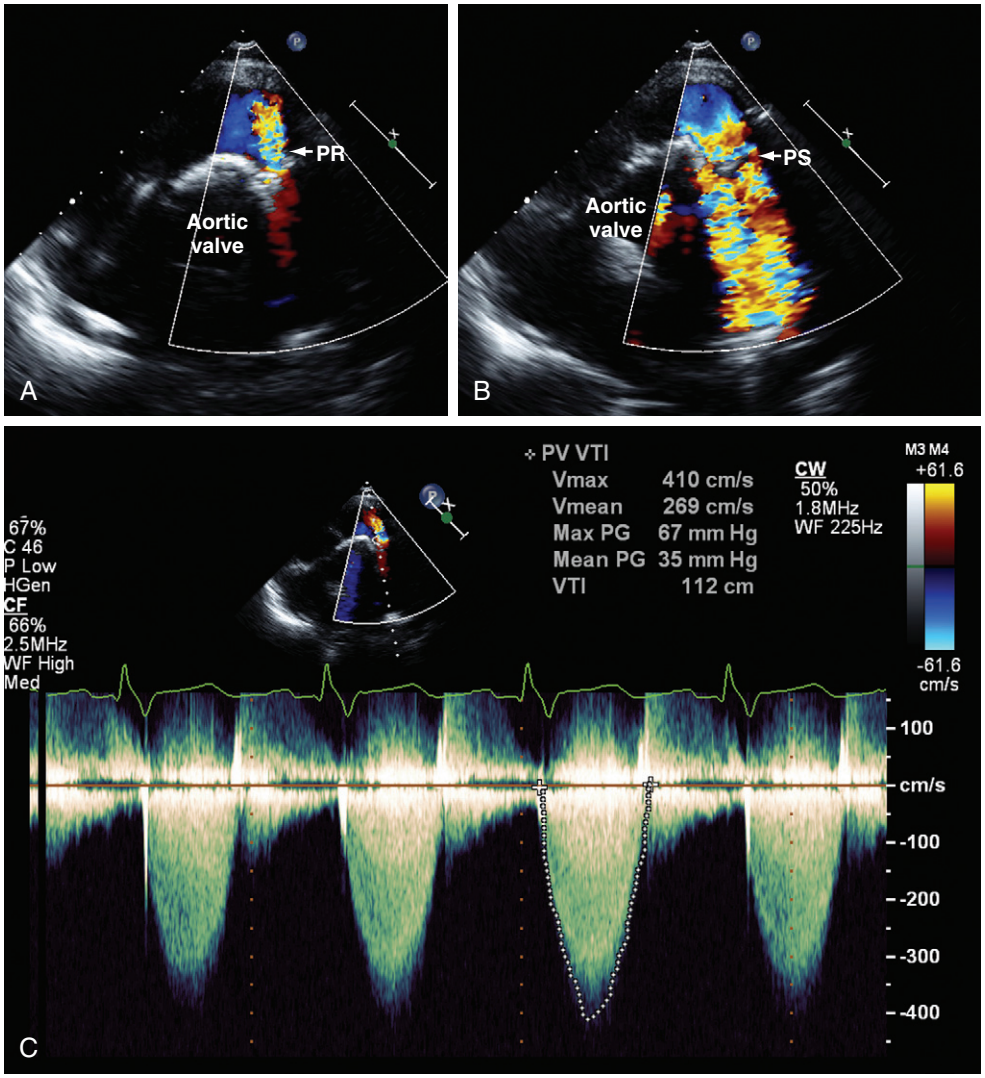



**Figure 45-20** **Bioprosthetic pulmonic valve dysfunction 14 years after tetralogy of Fallot surgery. A,** Residual moderate pulmonic regurgitation (*PR*) seen with color Doppler in a TTE parasternal view. **B,** Residual pulmonic stenosis (*PS*) with color flow acceleration at level of bioprosthetic valve. **C,** CW Doppler demonstrates estimated peak instantaneous systolic gradient of 67 mm Hg.

the RV size and function does not. The use of transcatheter pulmonic valve replacement is expected to increase dramatically as this technology becomes more widely available (Fig. 45-21).

Late postoperative LV function in tetralogy of Fallot is related to age at the time of repair and to previous volume overload from palliative shunt procedures. Patients with severe cyanotic tetralogy of Fallot have decreased left heart volumes and decreased LV ejection fractions related to the reduced pulmonary arterial blood flow. Repair in the first 2 years of life allows LV mass and volume to normalize; with repair after 2 years of age, left heart volumes increase but LV function remains subnormal. Medial aortic disease can cause a dilated aortic root or trunk; aortic regurgitation is common and at times has resulted in biventricular failure.[54] Any combination of persistent VSD patch leaks, ventricular-to-pulmonary outflow obstruction, and significant valvular regurgitation may cause serious ventricular overload. Inadequate operative myocardial preservation or the preexistence of volume overload (as with large palliative shunts before more complete hemodynamic repair) may cause ventricular failure over the long term.[7]

## COMPLETE TRANSPOSITION OF THE GREAT ARTERIES

Transposition complexes have each great artery arising from the wrong ventricle (ventriculoarterial discordance) (see Chapter 43). This definition is independent of the spatial relationships of the great arteries and the presence or absence of a subaortic infundibulum. In complete transposition of the great arteries (D-TGA), each atrium connects to its anatomically appropriate ventricle (atrioventricular concordance), but that ventricle gives rise to an anatomically inappropriate great artery (ventriculoarterial discordance). The aorta arises from the RV (with aortic-mitral discontinuity) and usually sits to the right of and anterior to the pulmonary artery, which emerges from the LV. This results in two separate and parallel circulations, and some communication between the two circulations must exist or be made iatrogenically after birth to sustain life.[7]

Echocardiographic imaging must define the course of each of the great arteries and

1. Identify the size and location of a VSD;
2. Confirm the presence and severity of pulmonic stenosis;

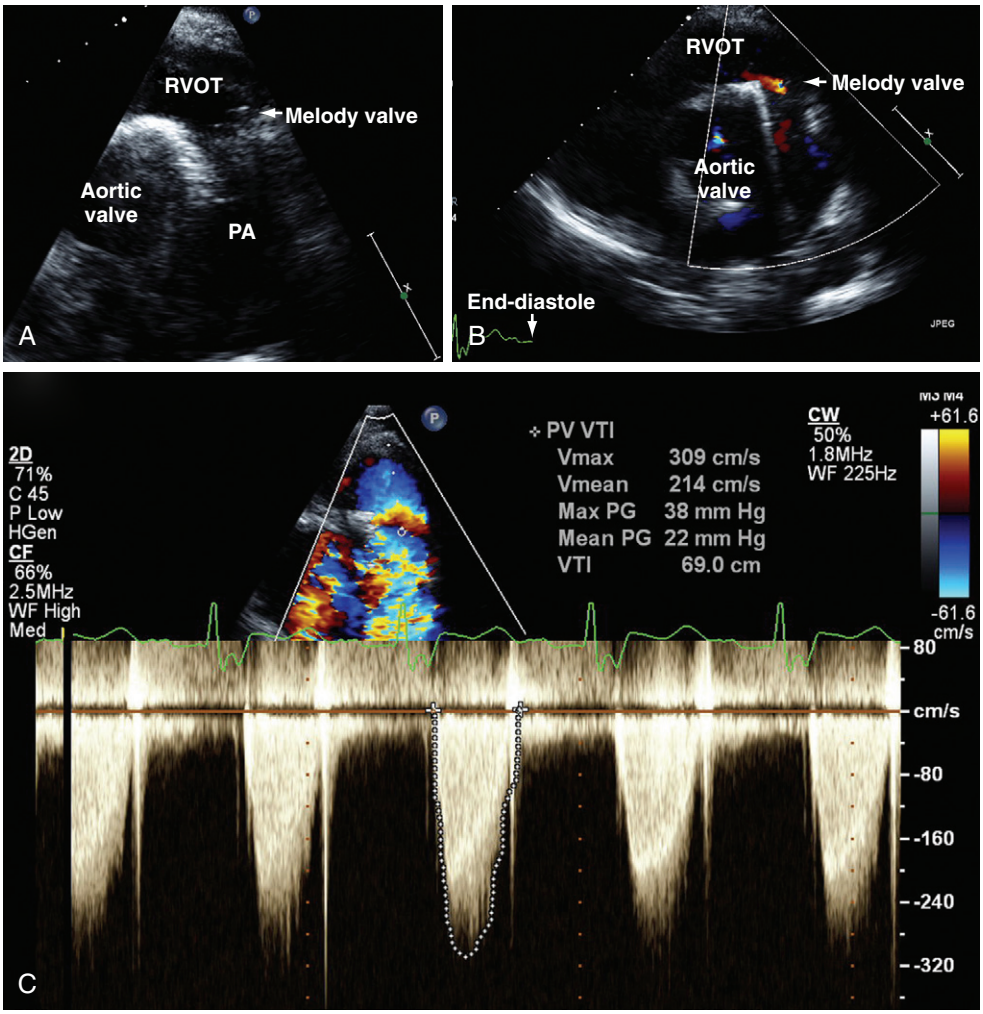



**Figure 45-21** **Transcatheter pulmonic valve replacement with 22-mm Melody valve in patient described in Figure 20. A,** Leaflets of Melody valve are seen are seen coapting appropriately in diastole. **B,** Color Doppler in diastole demonstrating minimal pulmonic regurgitation. **C,** CW Doppler demonstrating mild to moderate residual flow acceleration with peak instantaneous gradient of 38 mm Hg, a reduction of ~50% compared to pre-Melody assessment. *PA*, Pulmonary artery; *RVOT*, right ventricular outflow tract.

3. Detect other shunts; and
4. Evaluate the presence and severity of valvular regurgitation.[8,12,13]

Dynamic subvalvular pulmonic stenosis can be due to systolic anterior mitral motion into the LV outflow tract or dynamic subpulmonic septal contraction with obstruction versus fixed subvalvular stenosis. The pulmonic valve may be the site of obstruction. The location of the obstruction affects surgical planning; if not addressed, these problems contribute to postoperative morbidity and mortality.

Long-term outcome of surgical intervention for D-TGA, with or without VSD and pulmonic stenosis, depends on the type of repair.[4-6] In the past, most patients underwent intraatrial baffle procedures (e.g., Mustard or Senning), causing persistence of a systemic subaortic RV and tricuspid valve (see Figs. 45-10 and 45-11). In contrast, the arterial switch operation is now used and the LV is the systemic ventricle. Rastelli repair, whether for transposition of the great arteries (TGA) or for double-outlet right ventricle with VSD and pulmonic stenosis, uses an external conduit from RV to pulmonic artery and an intraventricular "tunnel" via the VSD from LV to aorta (see Fig. 45-18). An internal tunnel may develop a patch leak or obstruction due to kinking, or it may partially obstruct the chamber through which it transits. Long-term concerns include durability of a bioprosthesis, patency of conduits, VSD patch leaks, and postoperative electrophysiologic residua and sequelae.[7]

The Damus-Kaye-Stansel procedure, as applied to D-TGA with a VSD without pulmonic stenosis but with subaortic stenosis, consists of end-to-side anastomosis of the proximal pulmonary artery to aorta, oversewing of the aortic valve or proximal aorta, and a VSD patch. The RV is connected to the distal main pulmonary artery, now separated from the proximal main pulmonary artery, by a valved conduit. A variation of the Damus-Kaye-Stansel procedure is used in single ventricle with TGA and "subaortic stenosis" (bulboventricular foramen obstruction). Imaging of the pulmonic arterial to aortic anastomosis establishes lack of obstruction, pulmonary regurgitation, conduit patency, or VSD patch leaks.

## CONGENITALLY CORRECTED TRANSPOSITION OF THE GREAT ARTERIES

Congenitally corrected transposition of the great arteries (CCTGA) consists of discordant atrioventricular and ventriculoarterial connections with ventricular inversion (RA enters the LV via a mitral valve, LA enters the RV via a tricuspid valve; LV

gives rise to the pulmonary artery, RV gives rise to the aorta). The atrioventricular valves follow their ventricles, revealing the left-sided systemic ventricle as the anatomic RV and vice versa. Echocardiographic crux anatomy shows the left atrioventricular valve more apically placed than the right atrioventricular valve, identifying tricuspid and mitral valves, respectively. The aorta leaves the RV leftward and anterior (L-TGA) and LV connects to a rightward and posterior pulmonary trunk, well shown on short-axis parasternal views or angulated apical or subcostal views.[7,8] Associated anomalies include ASD, Ebstein-like abnormality of the left-sided tricuspid valve and tricuspid regurgitation (physiologically equivalent to mitral regurgitation), VSD, and subvalvular (fixed or dynamic) or valvular pulmonic stenosis. A large VSD with significant pulmonic stenosis or severe systemic atrioventricular valve regurgitation prompts consideration of surgery. A Rastelli procedure may be used in CCTGA with a VSD and subvalvular pulmonic stenosis. The LV may be connected to the pulmonic artery via a valved conduit, whereas the RV supplies the aorta once the VSD is patched. The subpulmonary stenosis is often not resected because of the high incidence of complete heart block.

Three issues materially influence long-term postoperative survival:

1. Progressive tricuspid regurgitation;
2. High incidence of heart block often caused by operation; and
3. Progressive decrease in systemic subaortic morphologic RV function.[6,7,161,162]

Atrioventricular valve regurgitation is common preoperatively, is difficult to repair (often requiring replacement instead), may progress postoperatively, poses a continuing risk of endocarditis, and may affect long-term ventricular performance.

## DOUBLE-OUTLET RIGHT VENTRICLE

Double-outlet right ventricle, a heterogeneous category, has both great arteries committed to the RV; the VSD may be committed to the aorta (subaortic, infracristal), to the pulmonary artery (subpulmonic, supracristal), to both (doubly committed, subarterial), or to neither. The VSD location affects the streaming characteristics of blood, the degree of cyanosis, and the capacity for and type of repair.[7] The presence or absence of pulmonic stenosis or increased pulmonary vascular resistance is a determinant of outcome. Double-outlet right ventricle with a subpulmonary VSD and an RV or biventricular pulmonary trunk (Taussig-Bing anomaly) may clinically resemble complete TGA with a nonrestrictive VSD. Cyanosis is usually mild initially but progresses as pulmonary vascular resistance rises. Favorable regulation of pulmonary blood flow occasionally establishes adequate but not excessive flow, with consequent amelioration of LV volume overload.

Echocardiography must address the spatial relationships between the great arteries, the outflow tract for each artery, the location and type of VSD, and the relationship of the VSD to the aorta. Associated anomalies must be sought (e.g., malpositions or atrioventricular canal or septal defects).

Rastelli repair for double-outlet RV with subaortic VSD and pulmonic stenosis consists of an external RV-to-pulmonary-artery conduit and an intraventricular LV to the aorta via the VSD tunnel (see Fig. 45-18). The intraventricular course of the LV to the aortic baffle can be long and kinking may occur; this is best evaluated intraoperatively with TEE. An RV-to-pulmonary artery valved conduit can develop obstruction. In double-outlet RV of a tetralogy of Fallot type with normally related great arteries and a subaortic VSD, the repair may use a septal patch and primary repair of the site of pulmonic stenosis without resort to a conduit. Residual defects in the native ventricular septum or around the patch may be more frequent in repair of double-outlet RV than in tetralogy of Fallot, presumably because the distance from the VSD to the aorta is greater and more complex as a result of both the proximity of tricuspid valve tissue and anomalies of the ventricular septal musculature. "Intramural" residual interventricular defects seen after repair of conotruncal malformations, most commonly double-outlet RV, are found around the anterior portion of the patch between the neosystemic outflow tract and RV and require careful color flow imaging to detect. In such cases, device occluder placement has reduced the shunt; successful surgical closure may require removal and reattachment of the anterior portion of the patch.

### KEY POINTS

- Advances in surgical and catheter treatments have resulted in more adults than children with congenital heart disease in the United States.
- Many adult echocardiographic laboratories are unprepared for the full range of previously operated or complex congenital heart disease. Echocardiographic studies in these patients should be done where expertise is best, whether in an adult or a pediatric laboratory.
- Echocardiographic imaging with color and spectral Doppler recordings provides comprehensive anatomic, functional, and hemodynamic details in adults with congenital heart disease.
- For best results, imaging and hemodynamic study requires detailed knowledge of: (1) the anatomic and hemodynamic faults of the original defect; (2) the types of operative repairs (both past and present) available for each complex of lesions; and (3) the potential residua, sequelae, and complications of the "old" and "new" repairs.
- Echocardiographic data are integrated with other imaging and hemodynamic modalities (MRI, CT, and cardiac catheterization) for optimal management of adults with congenital heart disease.

## REFERENCES


1. Hoffman JI, Kaplan S: The incidence of congenital heart disease. *J Am Coll Cardiol* 39:1890-1900, 2002.
2. Hoffman JI, Kaplan S, Liberthson RR: Prevalence of congenital heart disease. *Am Heart J* 147:425-439, 2004.
3. Warnes CA, Liberthson R, Danielson GK, et al: Task force 1: the changing profile of congenital heart disease in adult life. Care of the adult with congenital heart disease. Presented at the 32nd Bethesda Conference, Bethesda, Md., October 2-3, 2000. *J Am Coll Cardiol* 37:1170-1175, 2001.
4. Graham TP, Jr: The year in congenital heart disease. *J Am Coll Cardiol* 45:1887-1899, 2005.
5. Graham TP, Jr: The year in congenital heart disease. *J Am Coll Cardiol* 43:2132-2141, 2004.

6. Warnes CA: The adult with congenital heart disease: born to be bad? *J Am Coll Cardiol* 46:1-8, 2005.
7. Perloff JK, Child JS: *Congenital heart disease in adults*, ed 2, Philadelphia, 1998, WB Saunders.
8. Child JS: Transthoracic and transesophageal echocardiographic imaging: anatomic and hemodynamic assessment. In Perloff JKCJ, editor: *Congenital heart disease in adults*, ed 2, Philadelphia, 1998, WB Saunders, pp 91-128.
9. Tomar M, Radhakrishanan S: Role of echocardiography in catheter intervention in congenital heart defects. *Indian Heart J* 60:D1-21, 2008.
10. Rhodes JF, Jr, Qureshi AM, Preminger TJ, et al: Intracardiac echocardiography during transcatheter interventions for congenital heart disease. *Am J Cardiol* 92:1482-1484, 2003.
11. Hijazi ZM, Shivkumar K, Sahn DJ: Intracardiac echocardiography during interventional and electrophysiological cardiac catheterization. *Circulation* 2009;119:587-596.
12. Child JS: Congenital heart disease. In Roelandt JRTC, Pandian NG, editors: *Multiplane transesophageal echocardiography*, New York, 1996, Churchill Livingstone, pp 173-198.
13. Child JS: Atria and related structures. In Roelandt JRTC, Pandian NG, editors: *Multiplane transesophageal echocardiography*, New York, 1996, Churchill Livingstone, pp 139-154.
14. Abdel-Massih T, Dulac Y, Taktak A, et al: Assessment of atrial septal defect size with 3D-transesophageal echocardiography: comparison with balloon method. *Echocardiography* 22:121-127, 2005.
15. Saric M, Perk G, Purgess JR, Kronzon I: Imaging atrial septal defects by real-time three-dimensional transesophageal echocardiography: step-by-step approach. *J Am Soc Echocardiogr* 23:1128-1135, 2010.
16. Kijima Y, Taniguchi M, Akagi T, et al: Torn atrial septum during transcatheter closure of atrial septal defect visualized by real-time three-dimensional transesophageal echocardiography. *J Am Soc Echocardiogr* 23:1222 e1225-1228, 2010.
17. Perloff JK, Natterson PD: Atrial arrhythmias in adults after repair of tetralogy of Fallot. *Circulation* 91:2118-2119, 1995.
18. Williams RG, Pearson GD, Barst RJ, et al: Report of the National Heart, Lung, and Blood Institute Working Group on research in adult congenital heart disease. *J Am Coll Cardiol* 47:701-707, 2006.
19. Nahlawi M, Waligora M, Spies SM, et al: Left ventricular function during and after right ventricular pacing. *J Am Coll Cardiol* 44:1883-1888, 2004.
20. Barber BJ, Batra AS, Burch GH, et al: Acute hemodynamic effects of pacing in patients with Fontan physiology: a prospective study. *J Am Coll Cardiol* 46:1937-1942, 2005.
21. Bacha EA, Zimmerman FJ, Mor-Avi V, et al: Ventricular resynchronization by multisite pacing improves myocardial performance in the postoperative single-ventricle patient. *Ann Thorac Surg* 78:1678-1683, 2004.
22. Janousek J, Tomek V, Chaloupecky VA, et al: Cardiac resynchronization therapy: a novel adjunct to the treatment and prevention of systemic right ventricular failure. *J Am Coll Cardiol* 44:1927-1931, 2004.
23. Masura J, Gavora P, Podnar T: Long-term outcome of transcatheter secundum-type atrial septal defect closure using Amplatzer septal occluders. *J Am Coll Cardiol* 45:505-507, 2005.
24. Fu YC, Bass J, Amin Z, et al: Transcatheter closure of perimembranous ventricular septal defects using the new Amplatzer membranous VSD occluder: results of the U.S. phase I trial. *J Am Coll Cardiol* 47:319-325, 2006.
25. Masura J, Gao W, Gavora P, et al: Percutaneous closure of perimembranous ventricular septal defects with the eccentric Amplatzer device: multicenter follow-up study. *Pediatr Cardiol* 26:216-219, 2005.
26. Zuo J, Xie J, Yi W, et al: Results of transcatheter closure of perimembranous ventricular septal defect. *Am J Cardiol* 106:1034-1037, 2010.
27. Carminati M, Butera G, Chessa M, et al: Transcatheter closure of congenital ventricular septal defects: results of the European Registry. *Eur Heart J* 28:2361-2368, 2007.
28. Fischer G, Apostolopoulou SC, Rammos S, et al: The Amplatzer Membranous VSD Occluder and the vulnerability of the atrioventricular conduction system. *Cardiol Young* 17:499-504, 2007.
29. Bacha EA, Cao QL, Galantowicz ME, et al: Multicenter experience with perventricular device closure of muscular ventricular septal defects. *Pediatr Cardiol* 26:169-175, 2005.
30. Rome JJ. Balloon pulmonary valvuloplasty. *Pediatr Cardiol* 19:18-24; discussion 25-16, 1998.
31. Harrild DM, Powell AJ, Tran TX, et al: Long-term pulmonary regurgitation following balloon valvuloplasty for pulmonary stenosis risk factors and relationship to exercise capacity and ventricular volume and function. *J Am Coll Cardiol* 55:1041-1047, 2010.
32. McCrindle BW: Independent predictors of long-term results after balloon pulmonary valvuloplasty. Valvuloplasty and Angioplasty of Congenital Anomalies (VACA) Registry Investigators. *Circulation* 89:1751-1759, 1994.
33. Ewert P, Bertram H, Breuer J, et al: Balloon valvuloplasty in the treatment of congenital aortic valve stenosis—a retrospective multicenter survey of more than 1000 patients. *Int J Cardiol* 149:182-185, 2011.
34. Aboulhosn J, Child JS: Left ventricular outflow obstruction: subaortic stenosis, bicuspid aortic valve, supravalvar aortic stenosis, and coarctation of the aorta. *Circulation* 114:2412-2422, 2006.
35. Brown ML, Burkhart HM, Connolly HM, et al: Late outcomes of reintervention on the descending aorta after repair of aortic coarctation. *Circulation* 122:S81-S84, 2010.
36. Holzer R, Qureshi S, Ghasemi A, et al: Stenting of aortic coarctation: acute, intermediate, and long-term results of a prospective multi-institutional registry—Congenital Cardiovascular Interventional Study Consortium (CCISC). *Catheter Cardiovasc Interv* 76:553-563, 2010.
37. Lucas V: Large diameter covered stent treatment of aortic coarctation. *Catheter Cardiovasc Interv* 75:407, 2010.
38. Child JS, Perloff JK, Kubak B: Infective endocarditis: risks and prophylaxis. In Perloff JK, Child JS, editors: *Congenital heart disease in adults*, ed 2, Philadelphia, 1998, WB Saunders, pp 129-143.
39. Konstantinides S, Geibel A, Olschewski M, et al: A comparison of surgical and medical therapy for atrial septal defect in adults. *N Engl J Med* 333:469-473, 1995.
40. Attie F, Rosas M, Granados N, et al: Surgical treatment for secundum atrial septal defects in patients >40 years old. A randomized clinical trial. *J Am Coll Cardiol* 38:2035-2042, 2001.
41. Attenhofer Jost CH, Connolly HM, Danielson GK, et al: Sinus venosus atrial septal defect: long-term postoperative outcome for 115 patients. *Circulation* 112:1953-1958, 2005.
42. Krumsdorf U, Ostermayer S, Billinger K, et al: Incidence and clinical course of thrombus formation on atrial septal defect and patient foramen ovale closure devices in 1,000 consecutive patients. *J Am Coll Cardiol* 43:302-309, 2004.
43. Chessa M, Carminati M, Butera G, et al: Early and late complications associated with transcatheter occlusion of secundum atrial septal defect. *J Am Coll Cardiol* 39:1061-1065, 2002.
44. Du ZD, Hijazi ZM, Kleinman CS, et al: Comparison between transcatheter and surgical closure of secundum atrial septal defect in children and adults: results of a multicenter nonrandomized trial. *J Am Coll Cardiol* 39: 1836-1844, 2002.
45. Vida VL, Barnoya J, O'Connell M, et al: Surgical versus percutaneous occlusion of ostium secundum atrial septal defects: results and cost-effective considerations in a low-income country. *J Am Coll Cardiol* 47:326-331, 2006.
46. Hijazi ZM, Cao Q, Patel HT, et al: Transesophageal echocardiographic results of catheter closure of atrial septal defect in children and adults using the Amplatzer device. *Am J Cardiol* 85:1387-1390, 2000.
47. Mullen MJ, Dias BF, Walker F, et al: Intracardiac echocardiography guided device closure of atrial septal defects. *J Am Coll Cardiol* 41:285-292, 2003.
48. Salehian O, Horlick E, Schwerzmann M, et al: Improvements in cardiac form and function after transcatheter closure of secundum atrial septal defects. *J Am Coll Cardiol* 45:499-504, 2005.
49. Masutani S, Taketazu M, Mihara C, et al: Usefulness of early diastolic mitral annular velocity to predict plasma levels of brain natriuretic peptide and transient heart failure development after device closure of atrial septal defect. *Am J Cardiol* 104:1732-1736, 2009.
50. Holzer R, Cao QL, Hijazi ZM: Closure of a moderately large atrial septal defect with a self-fabricated fenestrated Amplatzer septal occluder in an 85-year-old patient with reduced diastolic elasticity of the left ventricle. *Catheter Cardiovasc Interv* 64:513-518; discussion 519-521, 2005.
51. Moller JH, Patton C, Varco RL, Lillehei CW: Late results (30 to 35 years) after operative closure of isolated ventricular septal defect from 1954 to 1960. *Am J Cardiol* 68:1491-1497, 1991.
52. Fedak PWM, Verma S, David TE, et al: Clinical and Pathophysiological Implications of a Bicuspid Aortic Valve. *Circulation* 106:900-904, 2002.
53. Lewin MB, Otto CM: The bicuspid aortic valve: adverse outcomes from infancy to old age. *Circulation* 111:832-834, 2005.
54. Niwa K, Perloff JK, Bhuta SM, et al: Structural Abnormalities of Great Arterial Walls in Congenital Heart Disease: Light and Electron Microscopic Analyses. *Circulation* 103:393-400, 2001.
55. Gersony WM: Natural history of discrete subvalvar aortic stenosis: management implications. *J Am Coll Cardiol* 38:843-845, 2001.
56. Van Arsdell G, Tsoi K: Subaortic stenosis: at risk substrates and treatment strategies. *Cardiol Clin* 20:421-429, 2002.

57. Oliver JM, Gonzalez A, Gallego P, et al: Discrete subaortic stenosis in adults: increased prevalence and slow rate of progression of the obstruction and aortic regurgitation. *J Am Coll Cardiol* 38:835-842, 2001.
58. Carr JA: The results of catheter-based therapy compared with surgical repair of adult aortic coarctation. *J Am Coll Cardiol* 47:1101-1107, 2006.
59. Carr JA, Amato JJ, Higgins RS: Long-term results of surgical coarctectomy in the adolescent and young adult with 18-year follow-up. *Ann Thorac Surg* 79:1950-1955; discussion 1955-1956, 2005.
60. Vriend JW, Mulder BJ: Late complications in patients after repair of aortic coarctation: implications for management. *Int J Cardiol* 101:399-406, 2005.
61. Vriend JW, Zwinderman AH, de Groot E, et al: Predictive value of mild, residual descending aortic narrowing for blood pressure and vascular damage in patients after repair of aortic coarctation. *Eur Heart J* 26:84-90, 2005.
62. Toro-Salazar OH, Steinberger J, Thomas W, et al: Long-term follow-up of patients after coarctation of the aorta repair. *Am J Cardiol* 89:541-547, 2002.
63. Stewart AB, Ahmed R, Travill CM, Newman CG: Coarctation of the aorta life and health 20-44 years after surgical repair. *Br Heart J* 69:65-70, 1993.
64. Cohen M, Fuster V, Steele PM, et al: Coarctation of the aorta. Long-term follow-up and prediction of outcome after surgical correction. *Circulation* 80:840-845, 1989.
65. Warnes CA: Bicuspid aortic valve and coarctation: two villains part of a diffuse problem. *Heart* 89:965-966, 2003.
66. Boyum J, Fellinger EK, Schmoker JD, et al: Matrix metalloproteinase activity in thoracic aortic aneurysms associated with bicuspid and tricuspid aortic valves. *J Thorac Cardiovasc Surg* 127:686-691, 2004.
67. Celermajer DS, Greaves K: Survivors of coarctation repair: fixed but not cured. *Heart* 88:113-114, 2002.
68. von Kodolitsch Y, Aydin MA, Koschyk DH, et al: Predictors of aneurysmal formation after surgical correction of aortic coarctation. *J Am Coll Cardiol* 39:617-624, 2002.
69. Vriend JW, de Groot E, Mulder BJ: Limited effect of early repair on carotid arterial wall stiffness in adult post-coarctectomy patients: in response to the article by Heger M, Willfort A, Neunteufl T, et al. Vascular dysfunction after coarctation repair is related to the age at surgery. *Int J Cardiol* 100:335-336, 2005.
70. Attie F, Rosas M, Rijlaarsdam M, et al: The adult patient with Ebstein anomaly. Outcome in 72 unoperated patients. *Medicine (Baltimore)* 79:27-36, 2000.
71. Celermajer DS, Bull C, Till JA, et al: Ebstein anomaly: presentation and outcome from fetus to adult. *J Am Coll Cardiol* 23:170-176, 1994.
72. Tede NH, Shivkumar K, Perloff JK, et al: Signal-averaged electrocardiogram in Ebstein anomaly. *Am J Cardiol* 93:432-436, 2004.
73. Zuberbuhler JR, Allwork SP, Anderson RH: The spectrum of Ebstein anomaly of the tricuspid valve. *J Thorac Cardiovasc Surg* 77:202-211, 1979.
74. Shiina A, Seward JB, Edwards WD, et al: Two-dimensional echocardiographic spectrum of Ebstein anomaly: detailed anatomic assessment. *J Am Coll Cardiol* 3:356-370, 1984.
75. Shiina A, Seward JB, Tajik AJ, et al: Two-dimensional echocardiographic–surgical correlation in Ebstein anomaly: preoperative determination of patients requiring tricuspid valve plication vs replacement. *Circulation* 68:534-544, 1983.
76. Benson LN, Child JS, Schwaiger M, et al: Left ventricular geometry and function in adults with Ebstein anomaly of the tricuspid valve. *Circulation* 75:353-359, 1987.
77. Chauvaud S: Ebstein malformation. surgical treatment and results. *Thorac Cardiovasc Surg* 48:220-223, 2000.
78. Augustin N, Schmidt-Habelmann P, Wottke M, et al: Results after surgical repair of Ebstein anomaly. *Ann Thorac Surg* 63:1650-1656, 1997.
79. Augustin N, Schreiber C, Lunge R: Valve preserving treatment of Ebstein anomaly: perioperative and follow-up results. *Thorac Cardiovasc Surg* 48:316, 2000.
80. Knott-Craig CJ, Overholt ED, Ward KE, Razook JD: Neonatal repair of Ebstein anomaly: indications, surgical technique, and medium-term follow-up. *Ann Thorac Surg* 69:1505-1510, 2000.
81. Knott-Craig CJ, Overholt ED, Ward KE, et al: Repair of Ebstein anomaly in the symptomatic neonate: an evolution of technique with 7-year follow-up. *Ann Thorac Surg* 73:1786-1792; discussion 1792-1783, 2002.
82. Mair DD, Seward JB, Driscoll DJ, Danielson GK: Surgical repair of Ebstein anomaly: selection of patients and early and late operative results. *Circulation* 72:II70-76, 1985.
83. Quaegebeur JM, Sreeram N, Fraser AG, et al: Surgery for Ebstein anomaly: the clinical and echocardiographic evaluation of a new technique. *J Am Coll Cardiol* 17:722-728, 1991.
84. Pressley JC, Wharton JM, Tang AS, et al: Effect of Ebstein anomaly on short- and long-term outcome of surgically treated patients with Wolff-Parkinson-White syndrome. *Circulation* 86:1147-1155, 1992.
85. Kammeraad JA, van Deurzen CH, Sreeram N, et al: Predictors of sudden cardiac death after Mustard or Senning repair for transposition of the great arteries. *J Am Coll Cardiol* 44:1095-1102, 2004.
86. Sarkar D, Bull C, Yates R, et al: Comparison of long-term outcomes of atrial repair of simple transposition with implications for a late arterial switch strategy. *Circulation* 100:II176-181, 1999.
87. Wilson NJ, Clarkson PM, Barratt-Boyes BG, et al: Long-term outcome after the Mustard repair for simple transposition of the great arteries. 28-year follow-up. *J Am Coll Cardiol* 32:758-765, 1998.
88. Puley G, Siu S, Connelly M, et al: Arrhythmia and survival in patients >18 years of age after the Mustard procedure for complete transposition of the great arteries. *Am J Cardiol* 83:1080-1084, 1999.
89. Gelatt M, Hamilton RM, McCrindle BW, et al: Arrhythmia and mortality after the Mustard procedure: a 30-year single-center experience. *J Am Coll Cardiol* 29:194-201, 1997.
90. Gatzoulis MA, Walters J, McLaughlin PR, et al: Late arrhythmia in adults with the Mustard procedure for transposition of great arteries: a surrogate marker for right ventricular dysfunction? *Heart* 84:409-415, 2000.
91. Babu-Narayan SV, Goktekin O, Moon JC, et al: Late gadolinium enhancement cardiovascular magnetic resonance of the systemic right ventricle in adults with previous atrial redirection surgery for transposition of the great arteries. *Circulation* 111:2091-2098, 2005.
92. Millane T, Bernard EJ, Jaeggi E, et al: Role of ischemia and infarction in late right ventricular dysfunction after atrial repair of transposition of the great arteries. *J Am Coll Cardiol* 35:1661-1668, 2000.
93. Lubiszewska B, Gosiewska E, Hoffman P, et al: Myocardial perfusion and function of the systemic right ventricle in patients after atrial switch procedure for complete transposition: long-term follow-up. *J Am Coll Cardiol* 36:1365-1370, 2000.
94. Salehian O, Schwerzmann M, Merchant N, et al: Assessment of systemic right ventricular function in patients with transposition of the great arteries using the myocardial performance index: comparison with cardiac magnetic resonance imaging. *Circulation* 110: 3229-3233, 2004.
95. Losay J, Hougen TJ: Treatment of transposition of the great arteries. *Curr Opin Cardiol* 12:84-90, 1997.
96. Losay J, Touchot A, Serraf A, et al: Late Outcome After Arterial Switch Operation for Transposition of the Great Arteries. *Circulation* 104:121I-126, 2001.
97. Schwartz ML, Gauvreau K, del Nido P, et al: Long-term predictors of aortic root dilation and aortic regurgitation after arterial switch operation. *Circulation* 110:II128-132, 2004.
98. Legendre A, Losay J, Touchot-Kone A, et al: Coronary events after arterial switch operation for transposition of the great arteries. *Circulation* 108:II186-190, 2003.
99. Oskarsson G, Pesonen E, Munkhammar P, et al: Normal coronary flow reserve after arterial switch operation for transposition of the great arteries: an intracoronary Doppler guidewire study. *Circulation* 106:1696-1702, 2002.
100. Rickers C, Sasse K, Buchert R, et al: Myocardial viability assessed by positron emission tomography in infants and children after the arterial switch operation and suspected infarction. *J Am Coll Cardiol* 36:1676-1683, 2000.
101. De Caro E, Ussia GP, Marasini M, Pongiglione G: Transoesophageal atrial pacing combined with transthoracic two dimensional echocardiography: experience in patients operated on with arterial switch operation for transposition of the great arteries. *Heart* 89:91-95, 2003.
102. van den Bosch AE, Roos-Hesselink JW, Van Domburg R, et al: Long-term outcome and quality of life in adult patients after the Fontan operation. *Am J Cardiol* 93:1141-1145, 2004.
103. Gates RN, Laks H, Drinkwater DC, Jr, et al: The Fontan procedure in adults. *Ann Thorac Surg* 63:1085-1090, 1997.
104. Gersony DR, Gersony WM: Management of the postoperative Fontan patient. *Progr Pediatr Cardiol* 17:73-79, 2003.
105. Veldtman GR, Nishimoto A, Siu S, et al: The Fontan procedure in adults. *Heart* 86:330-335, 2001.
106. Thompson LD, Petrossian E, McElhinney DB, et al: Is it necessary to routinely fenestrate an extracardiac Fontan? *J Am Coll Cardiol* 34:539-544, 1999.
107. Laks H, Pearl JM, Haas GS, et al: Partial Fontan: advantages of an adjustable interatrial communication. *Ann Thorac Surg* 52:1084-1094; discussion 1094-1085, 1991.
108. de Zelicourt DA, Pekkan K, Wills L, et al: In vitro flow analysis of a patient-specific intraatrial total cavopulmonary connection. *Ann Thorac Surg* 79:2094-2102, 2005.

109. Pearl JM, Laks H, Stein DG, et al: Total cavopulmonary anastomosis versus conventional modified Fontan procedure. *Ann Thorac Surg* 52:189-196, 1991.
110. Kuroczynski W, Kampmann C, Choi YH, et al: The Fontan-operation: from intra- to extracardiac procedure. *Cardiovasc Surg* 11:70-74, 2003.
111. Azakie A, McCrindle BW, Van Arsdell G, et al: Extracardiac conduit versus lateral tunnel cavopulmonary connections at a single institution: impact on outcomes. *J Thorac Cardiovasc Surg* 122:1219-1228, 2001.
112. Mavroudis C, Backer CL, Deal BJ, et al: Total cavopulmonary conversion and maze procedure for patients with failure of the Fontan operation. *J Thorac Cardiovasc Surg* 122:863-871, 2001.
113. Aboulhosn J, Williams R, Shivkumar K, et al: Arrhythmia recurrence in adult patients with single ventricle physiology following surgical Fontan conversion. *Congenit Heart Dis* 5:430-434, 2010.
114. Lan YT, Chang RK, Laks H: Outcome of patients with double-inlet left ventricle or tricuspid atresia with transposed great arteries. *J Am Coll Cardiol* 43:113-119, 2004.
115. Bhole V, Wright JG, De Giovanni JV, et al: Transcatheter interventions in the early postoperative period after the Fontan procedure. *Catheter Cardiovasc Interv* 77:92-98, 2010.
116. Gomez C, Lloyd T, Mosca R, et al: Fontan fenestration closure in the catheterization laboratory—echocardiographic evaluation of residual right to left shunts. *Am J Cardiol* 82:1304-1306, A1310-1301, 1998.
117. Border WL, Syed AU, Michelfelder EC, et al: Impaired systemic ventricular relaxation affects postoperative short-term outcome in Fontan patients. *J Thorac Cardiovasc Surg* 126:1760-1764, 2003.
118. Tede NH, Child JS: Diastolic dysfunction in patients with congenital heart disease. *Cardiol Clin* 18:491-499, 2000.
119. Child JS: Echo-Doppler and color-flow imaging in congenital heart disease. *Cardiol Clin* 8:289-313, 1990.
120. Cheung YF, Penny DJ, Redington AN: Serial assessment of left ventricular diastolic function after Fontan procedure. *Heart* 83:420-424, 2000.
121. Di Sessa TG, Child JS, Perloff J, et al: Systemic venous and pulmonary arterial flow patterns after Fontan's procedure for tricuspid atresia or single ventricle. *Circulation* 70:898-902, 1984.
122. Niwa K, Siu SC, Webb GD, Gatzoulis MA: Progressive aortic root dilatation in adults late after repair of tetralogy of Fallot. *Circulation* 106:1374-1378, 2002.
123. Warnes CA, Child JS: Aortic root dilatation after repair of tetralogy of Fallot: pathology from the past? *Circulation* 106:1310-1311, 2002.
124. Roest AAW, de Roos A, Lamb HJ, et al: Tetralogy of Fallot: postoperative delayed recovery of left ventricular stroke volume after physical exercise—assessment with fast MR Imaging. *Radiology* 226:278-284, 2003.
125. Roos-Hesselink J, Perlroth MG, McGhie J, Spitaels S: Atrial arrhythmias in adults after repair of tetralogy of Fallot. Correlations with clinical, exercise, and echocardiographic findings. *Circulation* 91:2214-2219, 1995.
126. Murphy JG, Gersh BJ, Mair DD, et al: Long-term outcome in patients undergoing surgical repair of tetralogy of Fallot. *N Engl J Med* 329:593-599, 1993.
127. Mahle WT, Parks WJ, Fyfe DA, Sallee D: Tricuspid regurgitation in patients with repaired tetralogy of Fallot and its relation to right ventricular dilatation. *Am J Cardiol* 92:643-645, 2003.
128. Lucron H, Marcon F, Bosser G, et al: Induction of sustained ventricular tachycardia after surgical repair of tetralogy of Fallot. *Am J Cardiol* 83:1369-1373, 1999.
129. Khairy P, Landzberg MJ, Gatzoulis MA, et al: Value of programmed ventricular stimulation after tetralogy of Fallot repair: a multicenter study. *Circulation* 109:1994-2000, 2004.
130. Joffe H, Georgakopoulos D, Celermajer DS, et al: Late ventricular arrhythmia is rare after early repair of tetralogy of Fallot. *J Am Coll Cardiol* 23:1146-1150, 1994.
131. Helbing WA, Roest AA, Niezen RA, et al: ECG predictors of ventricular arrhythmias and biventricular size and wall mass in tetralogy of Fallot with pulmonary regurgitation. *Heart* 88:515-519, 2002.
132. Hokanson JS, Moller JH: Significance of early transient complete heart block as a predictor of sudden death late after operative correction of tetralogy of Fallot. *Am J Cardiol* 87:1271-1277, 2001.
133. Helbing WA, Niezen RA, Le Cessie S, et al: Right ventricular diastolic function in children with pulmonary regurgitation after repair of tetralogy of Fallot: volumetric evaluation by magnetic resonance velocity mapping. *J Am Coll Cardiol* 28:1827-1835, 1996.
134. Hazekamp MG, Kurvers MMJ, Schoof PH, et al: Pulmonary valve insertion late after repair of Fallot's tetralogy. *Eur J Cardiothorac Surg* 19:667-670, 2001.
135. Harrison DA, Siu SC, Hussain F, et al: Sustained atrial arrhythmias in adults late after repair of tetralogy of Fallot. *Am J Cardiol* 87:584-588, 2001.
136. Gatzoulis MA: Tetralogy of Fallot. In Gatzoulis MA, Webb GD, Daubeney PEF, editors: *Diagnosis and management of adult congenital heart disease*, St. Louis, 2003, Churchill Livingstone, pp 315-326.
137. Gatzoulis MA, Balaji S, Webber SA, et al: Risk factors for arrhythmia and sudden cardiac death late after repair of tetralogy of Fallot: a multicentre study. *Lancet* 356:975-981, 2000.
138. Gatzoulis MA, Clark AL, Cullen S, et al: Right ventricular diastolic function 15 to 35 years after repair of tetralogy of Fallot. Restrictive physiology predicts superior exercise performance. *Circulation* 91:1775-1781, 1995.
139. El Rahman MYA, Abdul-Khaliq H, Vogel M, et al: Relation between right ventricular enlargement, QRS duration, and right ventricular function in patients with tetralogy of Fallot and pulmonary regurgitation after surgical repair. *Heart* 84:416-420, 2000.
140. Eidem BW, O'Leary PW, Tei C, Seward JB. Usefulness of the myocardial performance index for assessing right ventricular function in congenital heart disease. *Am J Cardiol* 86:654-658, 2000.
141. Dittrich S, Vogel M, Dahnert I, et al: Surgical repair of tetralogy of Fallot in adults today. *Clin Cardiol* 22:460-464, 1999.
142. Dodds GA, III, Warnes CA, Danielson GK: Aortic valve replacement after repair of pulmonary atresia and ventricular septal defect or tetralogy of Fallot. *J Thorac Cardiovasc Surg* 113:736-741, 1997.
143. Discigil B, Dearani JA, Puga FJ, et al: Late pulmonary valve replacement after repair of tetralogy of Fallot. *J Thorac Cardiovasc Surg* 121:344-351, 2001.
144. Daliento L, Folino AF, Menti L, et al: Adrenergic nervous activity in patients after surgical correction of tetralogy of Fallot. *J Am Coll Cardiol* 38:2043-2047, 2001.
145. Chandar JS, Wolff GS, Garson A, Jr, et al: Ventricular arrhythmias in postoperative tetralogy of Fallot. *Am J Cardiol* 65:655-661, 1990.
146. Chaturvedi RR, Shore DF, Lincoln C, et al: Acute right ventricular restrictive physiology after repair of tetralogy of Fallot: association with myocardial injury and oxidative stress. *Circulation* 100:1540-1547, 1999.
147. Bricker JT: Sudden death and tetralogy of Fallot. Risks, markers, and causes. *Circulation* 92:158-159, 1995.
148. Bacha EA, Scheule AM, Zurakowski D, et al: Long-term results after early primary repair of tetralogy of Fallot. *J Thorac Cardiovasc Surg* 122:154-161, 2001.
149. Ghai A, Silversides C, Harris L, et al: Left ventricular dysfunction is a risk factor for sudden cardiac death in adults late after repair of tetralogy of Fallot. *J Am Coll Cardiol* 40:1675-1680, 2002.
150. Geva T, Sandweiss BM, Gauvreau K, et al: Factors associated with impaired clinical status in long-term survivors of tetralogy of Fallot repair evaluated by magnetic resonance imaging. *J Am Coll Cardiol* 43:1068-1074, 2004.
151. Abd El Rahman MY, Hui W, Yigitbasi M, et al: Detection of left ventricular asynchrony in patients with right bundle branch block after repair of tetralogy of Fallot using tissue-Doppler imaging-derived strain. *J Am Coll Cardiol* 45:915-921, 2005.
152. Davlouros PA, Kilner PJ, Hornung TS, et al: Right ventricular function in adults with repaired tetralogy of Fallot assessed with cardiovascular magnetic resonance imaging: detrimental role of right ventricular outflow aneurysms or akinesia and adverse right-to-left ventricular interaction. *J Am Coll Cardiol* 40:2044-2052, 2002.
153. Davos CH, Davlouros PA, Wensel R, et al: Global impairment of cardiac autonomic nervous activity late after repair of tetralogy of Fallot. *Circulation* 106:69I-75, 2002.
154. Frigiola A, Redington AN, Cullen S, Vogel M: Pulmonary regurgitation is an important determinant of right ventricular contractile dysfunction in patients with surgically repaired tetralogy of Fallot. *Circulation* 110:II153-157, 2004.
155. Tulevski II, Hirsch A, Dodge-Khatami A, et al: Effect of pulmonary valve regurgitation on right ventricular function in patients with chronic right ventricular pressure overload. *Am J Cardiol* 92:113-116, 2003.
156. Vliegen HW, van Straten A, de Roos A, et al: Magnetic resonance imaging to assess the hemodynamic effects of pulmonary valve replacement in adults late after repair of tetralogy of Fallot. *Circulation* 106:1703-1707, 2002.
157. Babu-Narayan SV, Kilner PJ, Li W, et al: Ventricular fibrosis suggested by cardiovascular magnetic resonance in adults with repaired tetralogy of Fallot and its relationship to adverse markers of clinical outcome. *Circulation* 113:405-413, 2006.
158. Giannopoulos NM, Chatzis AC, Bobos DP, et al: Tetralogy of Fallot: influence of right ventricular outflow tract reconstruction on late outcome. *Int J Cardiol* 97:87-90, 2004.
159. Renella P, Aboulhosn J, Lohan DG, et al: Two-dimensional and Doppler echocardiography

reliably predict severe pulmonary regurgitation as quantified by cardiac magnetic resonance. *J Am Soc Echocardiogr* 23:880-886, 2010.

160. van Straten A, Vliegen HW, Lamb HJ, et al: Time course of diastolic and systolic function improvement after pulmonary valve replacement in adult patients with tetralogy of Fallot. *J Am Coll Cardiol* 46:1559-1564, 2005.
161. Graham TP, Jr, Bernard YD, Mellen BG, et al: Long-term outcome in congenitally corrected transposition of the great arteries: a multi-institutional study. *J Am Coll Cardiol* 36:255-261, 2000.
162. Beauchesne LM, Warnes CA, Connolly HM, et al: Outcome of the unoperated adult who presents with congenitally corrected transposition of the great arteries. *J Am Coll Cardiol* 40:285-290, 2002.

# 46 Cardiac Tumors

CHARLES J. BRUCE, MD

**Background**
- Classification of Cardiac Masses
- Diagnostic Approach

**Cardiac Myxomas**
- Clinical Setting
- Location
- Gross Appearance
- Echocardiographic Features
- Other Imaging Modalities
- Differential Diagnosis

**Papillary Fibroelastoma**
- Clinical Setting
- Gross Pathology
- Location
- Clinical Manifestations:
- Echocardiographic Diagnosis
- Other Imaging Modalities
- Differential Diagnosis

**Other Benign Cardiac Tumors**
- Lipoma and Lipomatous Hypertrophy
- Hemangioma
- Rhabdomyoma
- Cardiac Fibroma
- Cardiac Paraganglioma

**Malignant Primary Cardiac Tumors**
- Sarcoma
- Primary Cardiac Lymphoma
- Mesotheliomas

**Secondary or Metastatic Malignant Tumors of the Heart**
- Direct Extension
- Hematogenous Spread
- Lymphatic Spread
- Intraluminal Venous Extension

**Differential Diagnosis**

**Newer Echocardiographic Techniques**

## Background

Although cardiac tumors are rare, with an autopsy frequency of only 0.001% to 0.03%,[1,2] they represent an important group of cardiovascular abnormalities because an early and accurate diagnosis may permit a curative procedure or, in some circumstances, may even avoid unnecessary surgery.[3-5] Before the introduction of two-dimensional (2D) echocardiography in the 1970s, ante mortem diagnosis of cardiac tumors was exceptionally unusual.[6] However, with the advent of 2D transthoracic echocardiography, the ability to identify cardiac tumors ante mortem has been possible. Moreover, ante mortem diagnosis of cardiac masses and tumors has steadily increased. This has been brought about by improvements in imaging technology that include higher frequency transthoracic imaging transducers, harmonic imaging, and refinements in transesophageal echocardiography (TEE), including multiplane TEE and three-dimensional (3D) imaging.[7,8] Echocardiography is well suited as the initial imaging modality in patients suspected of having a cardiac tumor because it is a simple noninvasive technique with widespread availability and relatively low cost (Box 46-1). Computed tomographic (CT) scan and magnetic resonance imaging (MRI) provide additional diagnostic information and should be seen as ancillary complementary techniques[9] because they can provide information for staging and treatment planning, particularly when surgical resection is being considered.[10]

Patients with cardiac tumors may present with cardiovascular-related or constitutional symptoms. However, more often than not, a cardiac mass is discovered incidentally during an echocardiographic examination performed for an unrelated indication. These incidental masses usually represent thrombi or vegetations and often occur in a particular clinical milieu with associated unique concomitant echocardiographic abnormalities.[5] If a mass is indeed a tumor, it is most likely malignant as a result of a known malignant process elsewhere, usually from the breast or lung or malignant melanoma. Much less likely, the mass represents a primary cardiac tumor. In this case, it is most likely benign, with a nearly 50% likelihood of being a myxoma. Malignant primary cardiac tumors are very rare and represent only approximately a quarter of primary cardiac tumors. These are most often a variety of sarcoma.

Clinical symptoms and signs are often determined by location of the tumor rather than its histologic type.[11,12] Thus, the clinical significance of a "benign" tumor may be just as important as a "malignant" type. Benign tumors may be locally invasive and impair myocardial contractility or cause valve dysfunction presenting with heart failure or conduction system disease or fatal arrhythmias. Systemic or pulmonary tumor embolization is an important and relatively common complication that occurs in up to a quarter of cases and is related to specific structural and anatomic tumor characteristics. Tumors of the aortic valve and left atrium (LA) pose the highest embolic risk. In addition, and somewhat paradoxically, patients with minimal symptoms, hemodynamic alterations, and smaller tumors have higher embolic complications than patients with larger symptomatic tumors.[13] Often, tumors present with pericardial effusions with or without tamponade; others may present with constitutional or systemic symptoms.

The benefit of echocardiography lies in its ability to show precise anatomic details and pathology. It delineates the morphologic appearance, location, and motion of tumors and determines the hemodynamic consequences of the tumor, if any.[14] The sensitivity of echocardiography is greatest for endocardial lesions, where the contrast between the tumor and the

**Box 46-1**

**ECHOCARDIOGRAPHY IN THE EVALUATION, DIAGNOSIS, AND TREATMENT OF CARDIAC TUMORS**

**A. Evaluation of Cardiac Masses**
Normal variant anatomy
Nontumor masses and disorders that mimic tumors
- Thrombi
- Vegetation
- Infiltrative disorder
- Device hardware

**B. Diagnosis of Tumor**
Morphology
- Location
- Attachment site
- Mobility
- Size
- Shape

Hemodynamic impact

**C. Guiding Interventions**
Percutaneous biopsy
Pericardiocentesis
Intraoperative assessment before and after cardiopulmonary bypass

echolucent chamber is greatest, permitting accurate characterization of the size and mobility of the mass. Intramyocardial lesions are less well appreciated, and pericardial tumors are the most difficult to detect, mainly because of the increased pericardial echo density and its far-field position. MRI and CT scan offer benefits over echocardiography in defining lesions in these locations[15] and are also helpful in staging tumors, assessing degree of mural infiltration, and detecting pericardial involvement and presence of tumor extension or metastases (Table 46-1). MRI and CT scan are also particularly good at evaluating tumor vascularity and fat composition.

Transthoracic echocardiography and TEE have unique attributes and limitations in evaluation of cardiac tumors. Although the availability of transthoracic echocardiography is widespread and it is simpler to perform, multiplane TEE generates higher resolution images of structures, particularly near the esophagus. It is thus not only better suited to detection of tumors in the superior vena cava, right atrium, pulmonary arteries, LA, and descending thoracic aorta but also helpful in distinguishing these masses from thrombi and vegetations.[16,17] Overall, TEE has better sensitivity and specificity than transthoracic echocardiography, especially in identification of smaller tumors.[18] It is also particularly useful in distinguishing true pathology from normal or normal variant cardiac anatomy (e.g., a prominent crista terminalis or lipomatous hypertrophy of the interatrial septum).[4] However, TEE is not as good at identification of left ventricular (LV) apical masses; if this is a clinical concern, transthoracic echocardiography should be performed.[16,19]

The following discussion reviews the clinical scope of cardiac tumors and their incidence. A clinical classification and a diagnostic approach are presented, and the echocardiographic and pathologic correlation of the most common individual tumors is addressed in descending order of their prevalence. Alternative and complementary imaging techniques are also briefly discussed. Finally, conditions that mimic cardiac tumors and newer emerging echocardiographic technologies with potential for better evaluation of cardiac tumors are also discussed.

**TABLE 46-1 Diagnostic Techniques for the Diagnosis of Cardiac Tumors**

| | *Echocardiography* | *Computed Tomography* | *Magnetic Resonance Imaging* |
|---|---|---|---|
| **Primary Benign** | | | |
| Myxoma | +++++ | +++ | +++ |
| Lipoma | +++ | +++++ | +++++ |
| Fibroelastoma | +++++ | ++ | ++ |
| Rhabdomyoma | +++++ | +++ | +++ |
| Fibroma | ++++ | ++++ | +++ |
| **Primary Malignant** | | | |
| Sarcomas | +++ | ++++ | +++++ |
| Mesotheliomas | ++ | +++++ | ++++ |
| Lymphomas | ++ | ++++ | +++++ |
| **Secondary Tumors** | | | |
| Direct extension | +++ | +++++ | +++++ |
| Venous extension | ++++ | ++++ | +++++ |
| Metastatic spread | ++ | +++++ | ++++ |

+, Of limited use; ++, may be of use; +++, useful; ++++, very useful; +++++, preferred diagnostic tool.

## CLASSIFICATION OF CARDIAC MASSES

A classification of cardiac masses is presented in Table 46-2, and diagnostic approach is presented in Figure 46-1. The most likely etiology of a cardiac mass is thrombus or vegetation. The clinical setting provides diagnostic clues. For example, thrombi are most likely associated with atrial fibrillation or a LV apical infarct, and vegetations may be seen in patients with native valve disease or prosthetic valves. However, if a cardiac mass really represents a tumor, its etiology can often be determined with consideration of four factors:

1. the histology-based likelihood
2. the age of the patient at time of presentation
3. the tumor location; and
4. noninvasive tissue characterization

With this approach, and integration of the clinical data, an accurate diagnosis and treatment strategy is usually possible without the need for percutaneous or open surgical biopsy.

### *Histology-Based Likelihood*

Secondary malignant disease of the heart and pericardium is considerably more common than primary cardiac malignant disease; in some estimates, it is 30 to 1000 times more common.[2] In a random autopsy series, the frequency of metastatic involvement is 0.4%; and in patients with diagnosed cancer cardiac involvement, it is as high as 20%.[9] Spread to the heart is generally via direct tumor extension, venous/lymphatic spread, or arterial metastasis. The most common underlying malignant diseases with secondary cardiac involvement are carcinoma of the lung, breast, esophagus, stomach, and kidneys and melanoma, lymphoma, and leukemia.

Primary cardiac tumors are much rarer than secondary malignant lesions. Almost 90% of primary cardiac tumors excised surgically are benign, with nearly 80% of these tumors representing myxomas.[6] In a report of 323 consecutive patients undergoing surgical resection of primary cardiac tumors between 1957 and 2006 at the Mayo Clinic, 94% of tumors were benign, and 50% of these were myxomas. The remaining benign

**TABLE 46-2 Cardiac Masses**

| Neoplastic | | | Nonneoplastic | Other |
|---|---|---|---|---|
| *Primary* | | *Secondary* | | |
| **Benign** | **Malignant** | **Direct extension** | **Hamartomas** | Thrombus |
| Myxoma | Sarcoma | Breast | Rhabdomyoma | Vegetation |
| PFE* | Lymphoma | Lung | Fibroma | CAT |
| Lipoma | | Esophagus | PFE* | Normal structure |
| | | Mediastinal tumor | **Age-related growths** | Image artifact |
| | | **Hematogenous** | Lipomatous hypertrophy | |
| | | Melanoma | **Reactive proliferation** | |
| | | Lung | Lambl excrescence | |
| | | Breast | PFE† | |
| | | GU | | |
| | | GI | | |
| | | **Venous** | | |
| | | Renal | | |
| | | Adrenal | | |
| | | Thyroid | | |
| | | Lung | | |
| | | Hepatoma | | |
| | | **Lymphatic** | | |
| | | Lymphoma | | |
| | | Leukemia | | |

*CAT,* Calcified amorphous tumor; *GI,* gastrointestinal; *GU,* genitourinary; *PFE,* papillary fibroelastoma.
*PFE arising de novo.
†PFE arising in setting of HOCM or after endocardial injury.

tumors in descending order of frequency included papillary fibroelastomas (26%), fibromas (6%), lipomas (4%), and others, including calcified amorphous tumors, hemangiomas, teratomas, unilocular developmental cysts, and rhabdomyomas.[7] Although papillary fibroelastoma traditionally have been considered less frequent than myxoma, it is increasingly recognized in our clinical experience that papillary fibroelastoma may in fact now represent the most common form of benign cardiac tumor. This fact underscores the increasing ante mortem diagnosis of cardiac masses resulting from the widespread use of echocardiography and the enhanced images newer echocardiographic technology affords.

In contrast to benign primary cardiac tumors, only about 10% of primary cardiac tumors excised at surgery are malignant, of which more than 90% are sarcomas. The remaining few are represented by lymphomas.[7] To illustrate just how rare malignant primary cardiac tumors are, only 34 patients were identified at the Mayo Clinic between 1975 and 2007. All had sarcomas, and the commonest histologic type was angiosarcoma (41%).[8]

## DIAGNOSTIC APPROACH

### *Age at Presentation*

Because the incidence rate of cardiac tumors varies with age (Table 46-3), age at presentation provides a clue to the diagnosis. For example, rhabdomyomas and fibromas are the most common benign cardiac tumors in children.

### *Location*

Particular cardiac tumors have a predilection for certain locations (Fig. 46-2), which enables characterization by their location. Myxomas most commonly arise in the LA, usually from a stalk attached to the atrial septum. Sarcomas can also present as a LA mass and are commonly mistaken for a myxoma before surgery.[8] Angiosarcomas, in particular, tend to arise in the right atrium. Rhabdomyomas and fibromas are located within the ventricles. Papillary fibroelastomas are generally located on cardiac valves. Metastatic disease often affects the pericardium by direct invasion, present within the cardiac muscle if spread hematogenously and emanating from the pulmonary veins or inferior vena cava by intraluminal spread.

### *Noninvasive Tissue Characterization*

Echocardiography provides limited but useful information regarding tissue characteristics (Table 46-4), including echogenicity of the mass and whether calcification is present. Vascularity can also be assessed with color flow Doppler imaging and echocardiographic contrast. Strain imaging also has potential in identification of the noncontractile nature of masses, such as fibromas. CT scan provides information regarding vascularity by contrast enhancement, presence of calcification, and presence of fat. MRI also provides information regarding vascularity, presence of fat, degree of tissue edema, and possibly iron content.

## Cardiac Myxomas

Three quarters of all primary cardiac tumors are benign, and nearly half of these are myxomas. Myxomas occur in all age groups, most frequently between the third and sixth decades of life (with an approximate incidence rate of 45% in adults and 15% in children).[20] Women are more commonly affected.[21-26] Although myxomas usually occur sporadically as an isolated tumor in the LA, familial myxomas have been reported (accounting for 7% of myxomas).[27-30] The familial myxomas occur as an inherited autosomal dominant disorder, in combination with two or more of the following conditions: skin myxomas (single or multiple), cutaneous lentiginosis, myxoid fibroadenomas of the breast, pituitary adenomas, primary adrenocortical micronodular dysplasia with Cushing syndrome, and testicular tumors (characteristically large cell calcifying Sertoli cell tumors). Although multiple acronyms (LAMB and NAME) have been used to describe these associations in the past, these syndromes are now grouped under the broader category of Carney complex, named after the physician who first described the familial nature of the disorder.[31] These patients tend to be younger and may have the germ-line mutation PRKAR1A.[32]

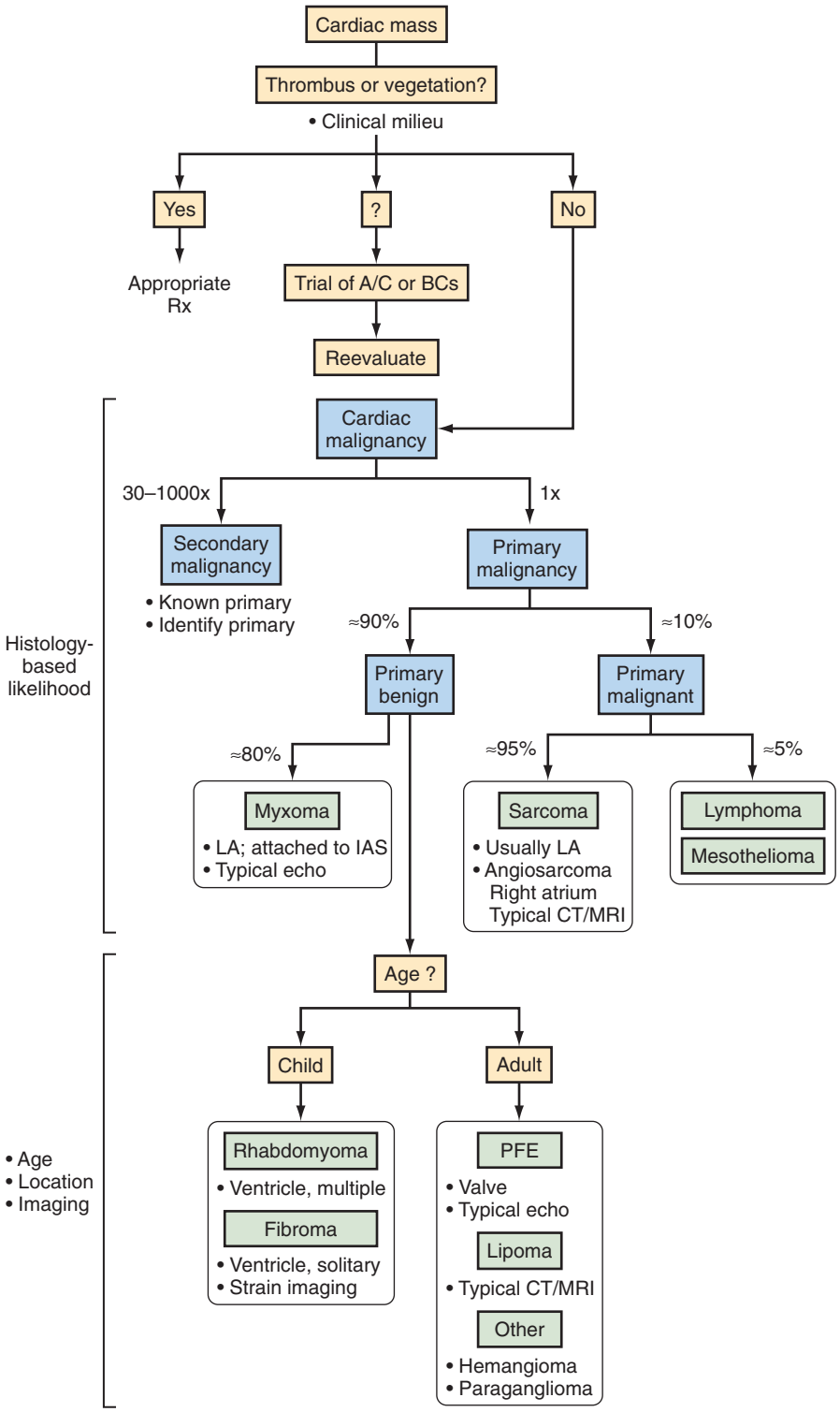



**Figure 46-1 Diagnostic algorithm for evaluation of a cardiac mass based on histology-based likelihood, age, location, and imaging characteristics.** *A/C,* Anticoagulation; *BCs,* blood cultures; *CT,* computed tomography; *IAS,* interatrial septum; *MRI,* magnetic resonance imaging; *PFE, papillary fibroelastoma*; *Rx,* treatment.

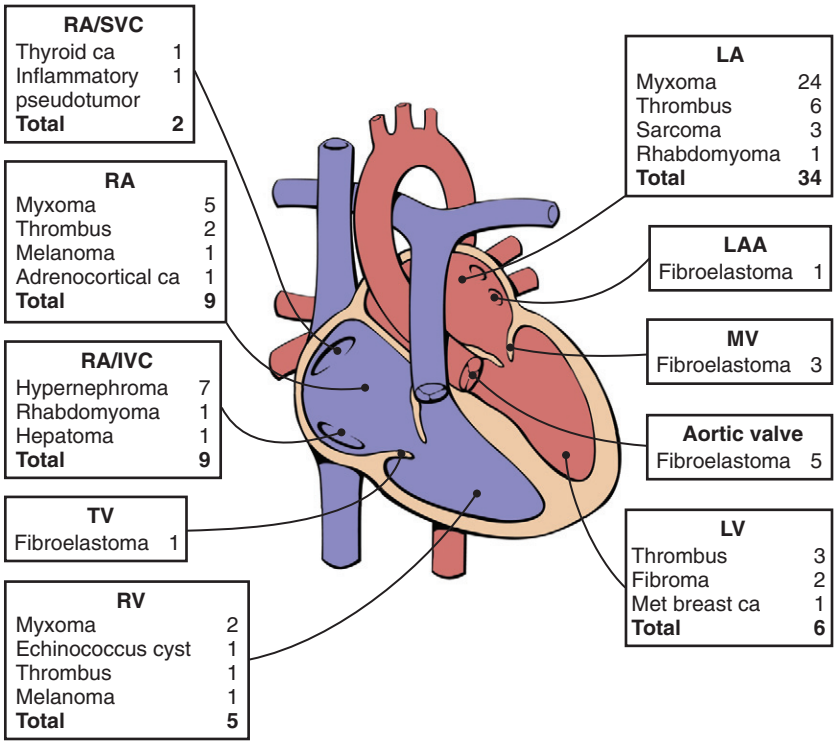



**Figure 46-2 Diagram shows the distribution and pathologic characteristics of cardiac masses according to intracardiac attachment site.** *ca,* Carcinoma; *IVC,* inferior vena cava; *LAA,* left atrial appendage; *met,* metastatic; *MV,* mitral valve; *SVC,* superior vena cava; *TV,* tricuspid valve. *(With permission from Dujardin KS, Click RL, Oh JK: The role of intraoperative transesophageal echocardiography in patients undergoing cardiac mass removal.* J Am Soc Echocardiogr *13:1080-1083, 2000.)*

**TABLE 46-3 Approximate Incidence Rate of Benign Tumors of the Heart in Adults and Children**

| | Incidence (%) | |
|---|---|---|
| | Adults | Children |
| Myxoma | 45 | 15 |
| Lipoma | 20 | – |
| Papillary fibroelastoma | 15 | – |
| Angioma | 5 | 5 |
| Fibroma | 3 | 15 |
| Hemangioma | 5 | 5 |
| Rhabdomyoma | 1 | 45 |
| Teratoma | <1 | 15 |

Adapted from Shapiro LM: Cardiac tumours: diagnosis and management. *Heart* 85:218-222, 2001.

They are also more likely to have multiple myxomas and have an increased risk of recurrence after resection.[21]

## CLINICAL SETTING

The clinical features of myxomas, like most cardiac tumors, are determined by their location, size, and mobility. These characteristics are easily addressed with echocardiography. Most patients present with one or more features of the triad of embolism, intracardiac obstruction, and constitutional symptoms. Dyspnea may occur as a result of atrioventricular valve obstruction. Occasionally, there are no symptoms, particularly with small tumors. Myxomas may recur after surgical resection. The overall risk of recurrence after resection is 13%, but it is much more common with familial myxomas than with sporadic tumors (22% versus 3%). The hazard of recurrence increases linearly for 4 years after resection, after which risk of recurrence is low. On the basis of this observation, semiannual surveillance echocardiographic follow-up examination has been recommended for 4 years after surgery.[33]

## LOCATION

Cardiac myxomas usually develop in the atria, with 75% originating in the LA and 15% to 20% in the right atrium. They characteristically arise from or near the interatrial septum at the border of the fossa ovalis membrane.[11,22-24,34] Occasionally they may grow through the fossa ovalis and into both atria. Myxomas may also originate (in descending order of frequency) from the posterior atrial wall, anterior atrial wall, and atrial appendage. Three percent to 4% of myxomas originate in the LV, and 3% to 4% in the right.[20,34] Tumors are usually solitary. Multiple tumors or atypical locations suggest familial myxoma. Myxomas of the heart valves have been reported but are extremely rare (Figs. 46-3 and 46-4).

## GROSS APPEARANCE

The gross appearance of cardiac myxomas is variable. The tumors range in size from 1 to 15 cm in diameter but most frequently measure 5 to 6 cm in diameter.[20] Myxomas are generally polypoid and often pedunculated, frequently arise from a narrow stalk, and are rarely sessile. They are usually round or ovoid in shape with a smooth or gently lobulated surface (Fig. 46-5). The mobility of the tumor depends on its consistency, which varies in part depending on the extent of attachment and the length of its stalk. Polypoid myxomas are usually compact and show little tendency towards spontaneous fragmentation. The less common villous or papillary myxomas have a surface that consists of multiple fine villous extensions that are fragile and tend to break off. The risk of embolization is greatest with these tumors (Table 46-5).[35-38] Adding to their embolic potential, they frequently have organized thrombi on their surface.

**TABLE 46-4 Features of Benign Primary Cardiac Tumors**

| *Type of Tumor* | *Patient Age at Diagnosis* | *Associated Syndromes* | *Most Common Location* | *Typical Morphologic Characteristics* | *Echocardiographic Features* | *CT Features* | *MRI Features* |
|---|---|---|---|---|---|---|---|
| Myxoma | 30-60 years (younger if associated with Carney complex) | Carney complex | Interatrial septum at fossa ovalis, LA more common than right | Gelatinous, attached to stalk; calcification common; hemorrhage or necrosis common | Mobile tumor, narrow stalk | Heterogeneous, low attenuation | Heterogeneous, bright on T2WI; heterogeneous enhancement |
| Papillary fibroelastoma | Middle-aged, elderly | None | Cardiac valves | Small (<1 cm), frond-like, narrow stalk; calcification rare; no hemorrhage or necrosis | "Shimmering" edges | Usually small pedunculated mass; may have calcifications and frond-like appearance when large | Usually small pedunculated mass; may have frond-like appearance when large |
| Lipoma | Variable | Multiple fatty lesions in tuberous sclerosis may be lipomas or angiomyolipomas | Pericardial space or any cardiac chamber | Large, broad-based; no calcification, hemorrhage, or necrosis | Usually hypoechoic in the pericardial space, echogenic in a cardiac chamber | Homogeneous fat attenuation (low attenuation) | Homogeneous fat signal intensity (increased T1); no enhancement |
| Hemangioma | All ages; mean, fourth decade | None | Anywhere; one third in RV, one third in LV; one fourth in right atrium | Multilobulated, unilocular, cystic, <1-8 cm | "Solid" echodense | Intense central contrast enhancement | Rapid enhancement increased T2WI signal |
| Rhabdomyoma | Infants, children <4 years | Tuberous sclerosis | LV, RV in walls on aortic valves outflow tract | Mural pedunculated multiple, variable size, spontaneous regression | Brighter than surrounding myocardium | Hypodense on contrast CT | Isointense to myocardium T2WI; hyperintense to myocardium T2WI |
| Fibroma | Infants, children, young adults | Gorlin syndrome | Ventricles | Large, intramural; calcification common; no hemorrhage or necrosis | Intramural, calcified | Low attenuation, calcified | Isointense on T1WI; dark on T2WI; usually little to no enhancement |
| Paraganglioma | Young adults | Many possible but almost always sporadic | LA, coronary arteries, aortic root | Broad-based, infiltrative or circumscribed; calcification rare; hemorrhage or necrosis common | Echogenic, relatively immobile | Low attenuation; avidly enhancing | Typically isointense or heterogeneous on T1WI, bright on T2WI; marked enhancement |

Adapted from Araoz PA, Mulvagh SL, Tazelaar HD, et al: CT and MR imaging of benign primary cardiac neoplasms with echocardiographic correlation. *Radiographics* 20:1303-1319, 2000.
*CT,* Computed tomography; *MRI,* magnetic resonance imaging; *T1WI,* T1-weighted images; *T2WI,* T2-weighted images.

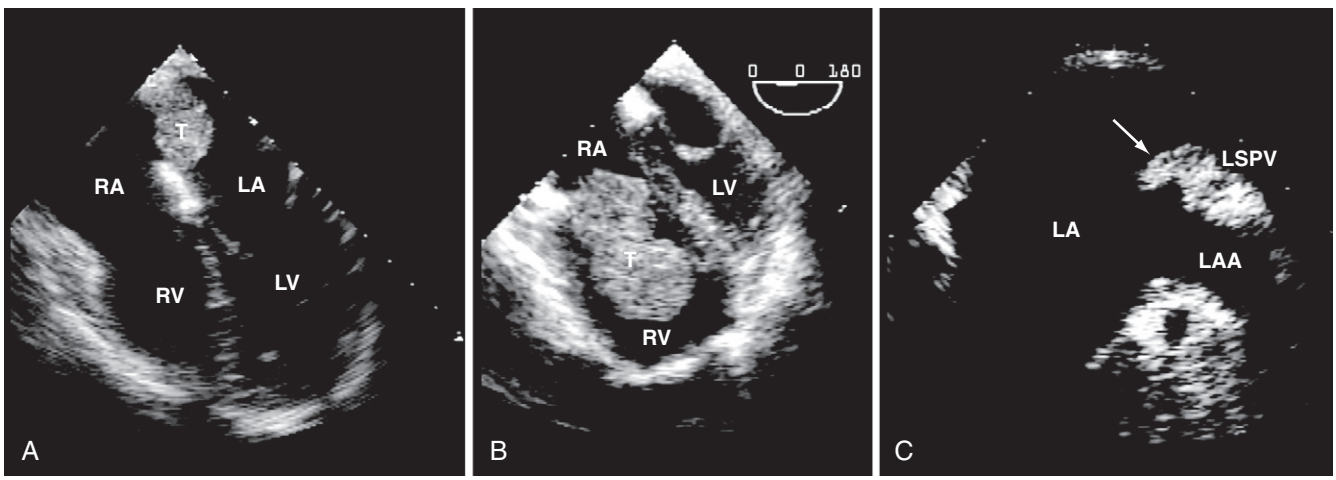



**Figure 46-3 Locations of myxomas. A,** TEE four-chamber view shows a 3.5-cm lobulated LA myxoma (*T*) arising from the fossa ovalis membrane. A mass at this location typically represents an atrial myxoma. At surgery, several "streamers" were attached to the tumor, not seen on echocardiography. **B,** A TEE four-chamber view shows a RV myxoma (*T*) measuring 7 × 4 cm that arises from the anterior tricuspid valve leaflet. This tumor extended through the RV outflow tract and pulmonic valve (not shown). Myxomas arising from unusual locations or from multiple sites should raise suspicion of Carney complex (see Figure 46-2). **C,** TEE in a 70-year-old woman presenting with a stroke. An 8-mm LA myxoma (*arrow*) is seen attached to the "Q tip" (junction of the left superior pulmonary vein [*LSPV*] and LA appendage orifice [*LAA*]). A lesion at this location may be confused with a thrombus. The mass did not resolve with anticoagulation therapy. At surgery, an additional smaller friable lesion was identified inferior to the primary lesion shown.




**Figure 46-4 A 19-year-old woman presented with a stroke.** On examination, there were cutaneous myxomas and lentigines of the lips (*bottom panel*). A TEE shows multiple intracardiac myxomas. Tumors are seen in the LA near the fossa ovalis (*double arrow*) and related to the anterior tricuspid valve leaflet (*single arrow*). A LV myxoma attached to the anterior septum is also present but is poorly seen in this still frame image (*top panel, arrowhead*). At surgery, an additional small RV apical myxoma was also identified with a thoracoscope. This was not appreciated on preoperative or intraoperative echocardiography. This patient was diagnosed with Carney complex. A repeat echocardiogram 4 years after tumor excision showed no recurrence. This case also stresses the importance of a careful search for additional lesions.

**TABLE 46-5 Morphologic Features of Myxomas Related to Embolism**

| | Emboli | | |
|---|---|---|---|
| *Morphologic Features* | *Yes (n = 10)* | *No (n = 27)* | P *Value* |
| Villous surface | 90 | 37 | .007 |
| Diameter (mm) | 48 ± 17 | 62 ± 26 | .132 |
| Gross calcifications | 0 | 15 | .557 |

Values given as percentage or mean plus or minus standard deviation, unless otherwise specified.

Adapted from Acebo E, Val-Bernal JF, Gomez-Roman JJ, Reveulta JM: Clinicopathologic study and DNA analysis of 37 cardiac myxomas: a 28-year experience.*Chest* 123:1379-1385, 2003.

Internally, myxomas often contain cysts and areas of necrosis and hemorrhage. Calcification has been observed but is rare, found only in 10% to 20% of cases.[20,39] Occasionally, myxomas may become infected.[40-43]

## ECHOCARDIOGRAPHIC FEATURES

Echocardiography accurately defines the location, size, shape, attachment, and mobility of the myxoma.[20,38] Multiple myxomas may be missed, particularly if the imager is distracted by finding the index tumor. Careful evaluation of all cardiac chambers is necessary to exclude multiple tumors. The characteristic narrow stalk is the most important distinguishing feature, followed by tumor mobility and distensibility.[9] When these features of a LA mass are seen, a diagnosis of cardiac myxoma can be made with a high degree of confidence,[44] especially if the stalk originates from the atrial septum. The internal echocardiographic appearance may be homogeneous or have central areas of hyperlucency, which represent necrotic foci and hemorrhage.[45,46] Internal areas of calcification may be present. Depending on their size and mobility, myxomas may result in LV or right ventricular (RV) inflow obstruction, the degree of obstruction sometimes varying with body position (see Fig. 46-5). TEE may provide additional important information in detecting the precise site of insertion and morphologic features of atrial and ventricular myxomas. It is also more sensitive for identification of small tumors (1 to 3 mm in diameter) and satellite tumors.[16,18,44,47-49]

## OTHER IMAGING MODALITIES

Tumor mobility, tumor distensibility and the thin delicate stalk are not as well seen with CT scan or MRI.[9] However, unlike echocardiography, CT scan and MRI can differentiate tissue composition, for better identification of solid, liquid, hemorrhagic, and fatty space-occupying tumors. CT scan and MRI findings of cardiac myxomas are variable, usually reflecting their gross pathologic features. Because of their gelatinous consistency, they have heterogeneous low attenuation at CT scan and calcification, if presence is also seen. They have markedly increased signal intensity on T2-weighted MRIs.[50,51] Presence of calcification or hemosiderin may result in areas of decreased signal intensity. Contrast enhancement is usually heterogeneous, reflecting the presence of necrotic areas.[9,52]

## DIFFERENTIAL DIAGNOSIS

Differentiation of cardiac myxoma from vegetations or thrombi is important. Usually, the echocardiographic appearance of a cardiac myxoma is quite distinctive. Sometimes, however, the diagnosis may be less certain, particularly when the myxoma has an unusual location or attachment, such as the LA appendage. In these instances, the clinical scenario (atrial fibrillation), associated echocardiographic findings (impaired ventricular function, LA enlargement, and spontaneous echocardiographic contrast), and CT/MRI findings are helpful in distinguishing thrombus from tumor. Sometimes, if the mass is small, a diagnostic trial of anticoagulation therapy can be attempted and imaging repeated to confirm resolution.

# Papillary Fibroelastoma

The true prevalence of papillary fibroelastomas is unknown. The reported prevalence of papillary fibroelastoma varies and is likely underreported because this condition is asymptomatic and thus underrepresented in surgical series, sometimes not appearing at all.[53] However, in a surgical series from the Mayo Clinic[39] and the Armed Forces Institute of Pathology,[53] papillary fibroelastomas accounted for 10% of primary cardiac tumors and were thus the second most common primary cardiac tumor.[5] Also, with the advent of echocardiography

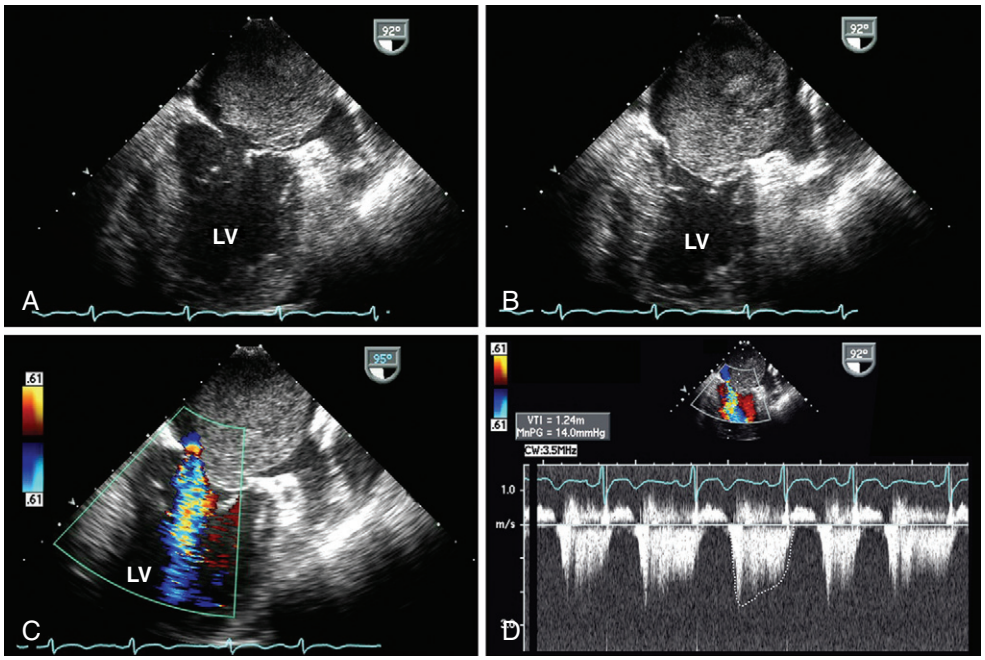



**Figure 46-5 A 64-year-old woman presented with exertional and resting chest heaviness and shortness of breath for 3 months.** The TEE shows the typical echocardiographic appearance of a large LA myxoma. **A,** A systolic frame shows a large 5 × 7 cm ovoid mass in the LA arising from a narrow stalk attached to the fossa ovalis (*not shown*). **B,** A diastolic frame shows the myxoma prolapsing through the mitral valve resulting in functional mitral valve stenosis (**C** and **D**). The mean gradient across the mitral valve is 14 mm Hg.

and improving imaging techniques, cardiac papillary fibroelastoma is detected earlier and increasingly reported.[6] These benign endocardial papillomas predominantly affect the cardiac valves and account for three quarters of all cardiac valvular tumors.[5] Patients with papillary fibroelastomas are often asymptomatic (30%) and diagnosed incidentally.[5,54] However, the clinical consequences of papillary fibroelastomas are significant and have been increasingly recognized as causes of stroke, transient ischemic attack, systemic embolism, and sudden cardiac death.[5,54]

## CLINICAL SETTING

Cardiac papillary fibroelastomas occur in all age groups but are predominantly identified in adulthood, particularly between the fourth and eighth decades of life.[5,54] The mean age of detection is approximately 60 years, which may reflect the increased use of echocardiography in older patients. Men and women are equally affected. There is a strong association with hypertrophic obstructive cardiomyopathy, and surgical, radiation, and hemodynamic.[33] The natural history of these tumors has not been characterized because serial studies with echocardiography have not been performed. They are considered generally slow-growing tumors but are clinically important because they may serve as a nidus for thrombus formation and potential thromboembolism.

## GROSS PATHOLOGY

Grossly, papillary fibroelastomas are small, usually less than 1 cm in diameter (mean, 9 cm), but they can be as large as 7 cm.[5] When these tumors occur in the cardiac chambers, they are larger than those found on the aortic and mitral valves.[54] These tumors have a characteristic flower-like appearance with multiple papillary fronds attached to the endocardium by a short pedicle; when immersed in saline solution, they exhibit the typical "sea anemone" appearance.[54,55] The papillary fronds are narrow, elongated, and branching and merge imperceptibly into the substance of the valve. Sometimes, the gross appearance of the characteristic papillary structure may be obscured by attached thrombi.[53,56] Calcification rarely occurs and has been reported in only two cases.[56]

## LOCATION

Papillary fibroelastomas usually develop on cardiac valves (75% to 90%) but may arise anywhere in the heart, originating from the LV, ostium of the right and left coronary arteries, LA appendage, atrial and ventricular septum, right atrium, LV outflow tract, Eustachian valve, and Chiari network. They have also been found in the right atrial appendage and RV outflow tract (Fig. 46-6).

Left-sided valves are affected 95% of the time, with aortic valve involvement slightly more common than mitral valve.[5,54] Valvular papillary fibroelastomas usually arise from the mid portion of the valve rather than the free edge (a distinguishing characteristic from Lambl excrescences; see subsequent discussion). Those that originate from the semilunar valves most often project into the arterial lumen but sometimes project into the ventricular cavity or even prolapse across the valve in diastole. Those that originate on the atrioventricular valves project into the atria. Rarely, they may arise from the subvalvular apparatus of the mitral and tricuspid valves.[57,58] Papillary fibroelastomas are usually solitary but can occur at multiple sites (9%).[5,54]

## CLINICAL MANIFESTATIONS

Nearly 50% of papillary fibroelastomas are discovered incidentally during echocardiography for unrelated reasons or during

evaluation of a cardiac source of embolism.[13,33] Like most cardiac tumors, their clinical presentation depends on many factors, including tumor location, size, growth rate, and tendency for embolization. The most common clinical presentations include cerebral and systemic embolization and coronary artery occlusion. Patients may also present with heart failure and sudden cardiac death. Embolism is thought to occur from superimposed thrombi or fragmentation of the papillary fronds themselves (sometimes both) because, on occasion, confirmed tumor fragments have been isolated in embolic material.[5,54]

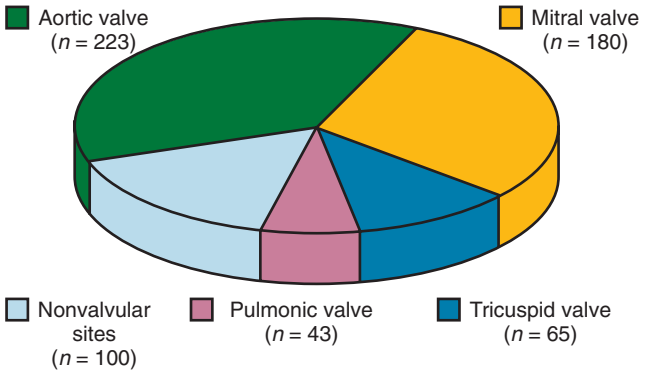



**Figure 46-6 Location of cardiac papillary fibroelastoma in 611 patients.** *(With permission from Gowda RM, Khan IA, Nair CK, et al: Cardiac papillary fibroelastoma: a comprehensive analysis of 725 cases.* Am Heart J *146:404-410, 2003.)*

## ECHOCARDIOGRAPHIC DIAGNOSIS

Papillary fibroelastomas are easily detected with echocardiography. Although transthoracic echocardiography can readily detect these tumors, the superior resolution of TEE makes this the definitive imaging modality for confirmation of the characteristic appearance of these usually small, highly mobile tumors and plays a central role in the search for multiple lesions.[5,59,60]

On 2D echocardiography, papillary fibroelastomas are characterized by a small, mobile, pedunculated valvular or, less commonly, endocardial mass, which on many occasions, flutters or prolapses into the cardiac chamber during systole or diastole (Fig. 46-7). Usually they have a well-defined "head," but they may appear as elongated strand-like projections. Characteristically, they have a stippled edge with a "shimmer" or "vibration" at the interface of the tumor with the surrounding blood, a finding that may distinguish them from thrombi.[5,61] Rather than being pedunculated and mobile, the tumors may be sessile. Sometimes, the tumors may be missed because they are small, the examination is not performed carefully enough because the clinical index of suspicion is low, or they are masked by an associated lesion or degenerative valvular disease.[54] If a papillary fibroelastoma is suspected as a source of embolism, a TEE should be performed. A proposed treatment algorithm based on imaging characteristics is presented in Fig. 46-8.

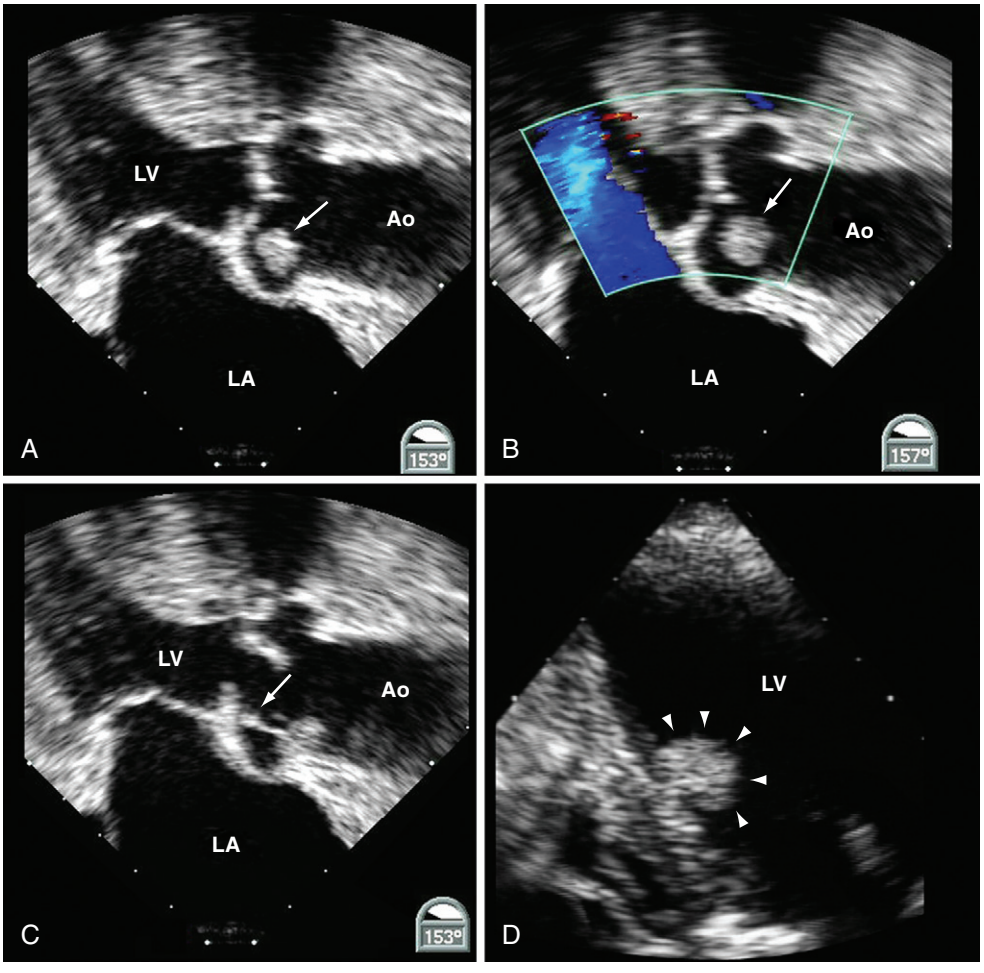



**Figure 46-7 An incidental mass was identified in an 80-year-old woman undergoing a routine transthoracic echocardiogram.** The TEE shows a 14 × 10 mm globular mass with an irregular border (*arrows,* **A** and **B**) attached to the aortic surface of the aortic valve noncoronary cusp by a thin stalk (*arrow,* **C**). Apart from aortic valve sclerosis, there were no associated valvular abnormalities or evidence of valvular destruction. **D,** Multiple papillary fibroelastomas were seen on transthoracic echocardiography in a 33-year-old woman with Hodgkin lymphoma and radiation-induced heart disease. In this zoomed apical two-chamber view image, one papillary fibroelastoma is seen attached to the endocardial surface of the mid inferior LV wall. The fimbriated surface can be appreciated (*small arrows*) Although papillary fibroelastomas are most commonly found on valves, they may arise anywhere in the heart. *Ao,* Aorta.

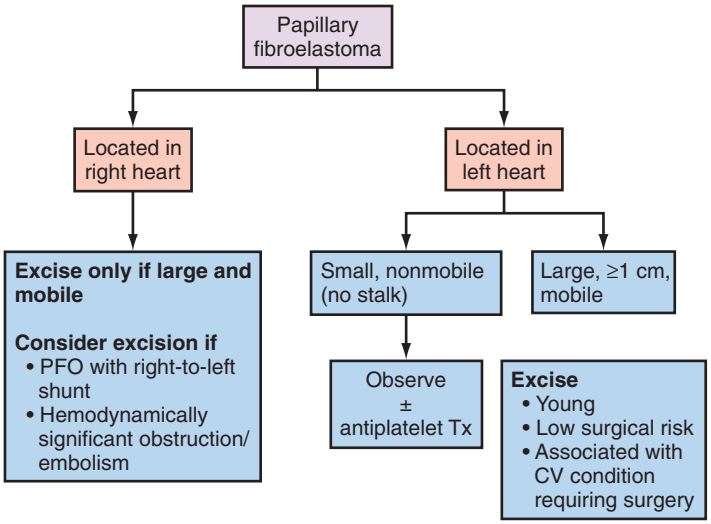



**Figure 46-8 Proposed management of papillary fibroelastomas based on echocardiography findings.** *CV,* Cardiovascular; *PFO,* patent foramen ovale; *Tx,* therapy.

## OTHER IMAGING MODALITIES

Although CT scan and MRI are getting faster and better at evaluation of cardiac valves, they are still less useful than echocardiography. The temporal and spatial resolution is often still inadequate because most of these tumors are small and attached to moving valves. The main disadvantage of MRI is susceptibility to motion artifact.[5,9]

## DIFFERENTIAL DIAGNOSIS

Again, the differential diagnosis includes thrombi, vegetations, other heart tumors, degenerative valvular calcification, and Lambl excrescences (Fig. 46-9). Lambl excrescences may be difficult to distinguish from papillary fibroelastomas.[62] These filiform fronds, first described by Lambl in 1856,[63] occur by definition at the sites of valve closure and are thought be the result of wear and tear lesions that originate as small thrombi on the endocardium of the contact margins of the valves at the site of minor endothelial damage, akin to the frayed edges of an old shirt cuff. In atrioventricular valves, Lambl excrescences are found at the site of valve closure on the atrial surface, but on semilunar valves, they can occur anywhere on the valve. Unlike papillary fibroelastomas, they usually do not occur on the arterial side of the semilunar valves or on the mural endocardium.[5] Unlike papillary fibroelastomas, Lambl excrescences are much

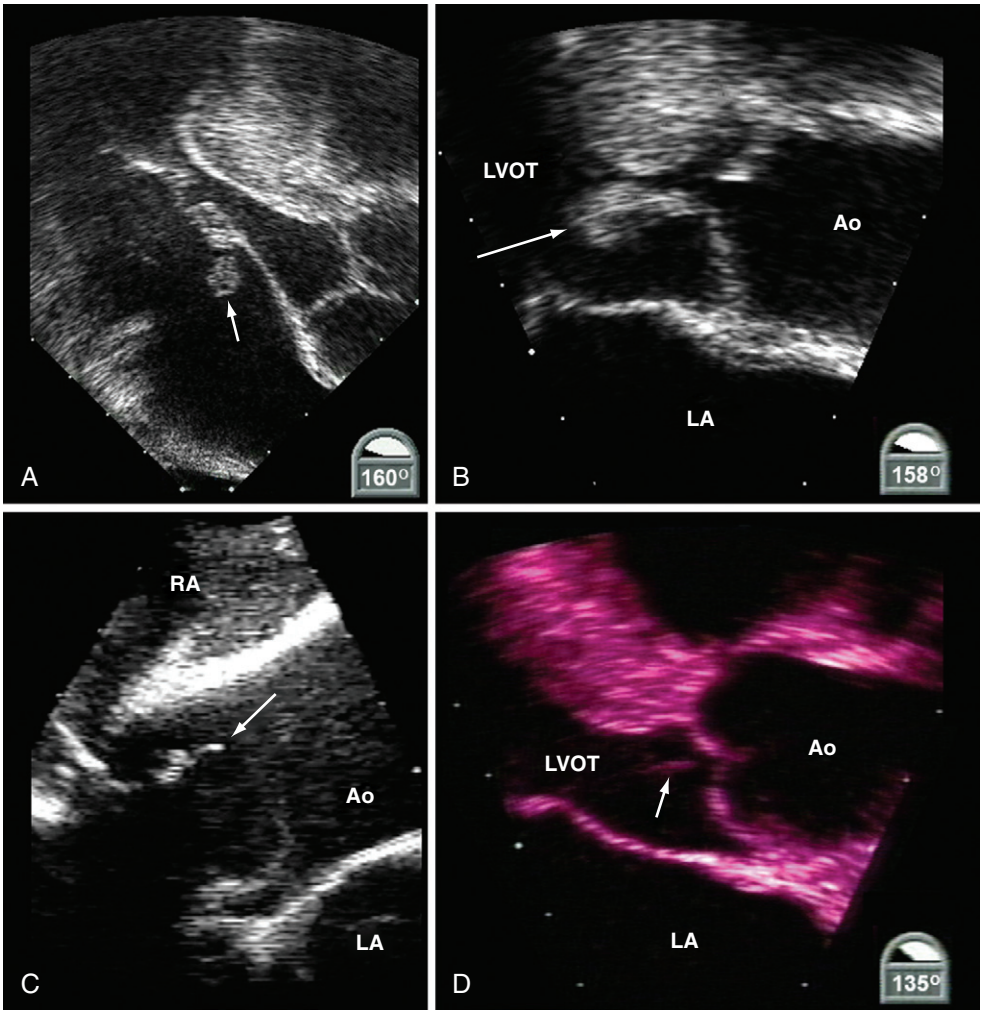



**Figure 46-9 Vegetations and Lambl excrescences may be confused with papillary fibroelastomas.** The *upper panels* show vegetations of the mitral (**A**) and aortic (**B**) valves in two patients with culture-positive enterococcal faecalis endocarditis. The vegetation on the aortic valve (*arrow*) is attached to the left ventricular outflow tract (*LVOT*) aspect of the aortic valve. It is highly mobile and, like the mitral vegetation, is associated with valve destruction and severe aortic regurgitation (*not shown*). Unlike papillary fibroelastomas, these vegetations do not have a characteristic thin stalk and fimbriated shimmering edge. Papillary fibroelastomas are usually not associated with valve destruction. Examples of a Lambl excrescence are shown attached to the aortic valve (*arrows*) in systole (**C**) and diastole (**D**). This fine filamentous highly mobile strand-like structure prolapses through the valve into the LV outflow tract in diastole. Unlike a papillary fibroelastoma, there is no globular "head" component at its distal end, and unlike a vegetation, apart from associated degenerative valve disease, overt valve destruction is unusual. *Ao,* Aorta.

more common, reported in up to 85% of adults, with multiple tumors present in more than 90% of cases. Papillary fibroelastomas, in contrast, are typically larger and more gelatinous and are present on valves away from the valvular lines of closure. They may also be found on endocardial surfaces of the atria and ventricles.[64-68] Despite these reported differences, noninvasively distinguishing these two abnormalities can sometimes be difficult.

## Other Benign Cardiac Tumors

### LIPOMA AND LIPOMATOUS HYPERTROPHY

Lipomatous hypertrophy of the atrial septum is a benign condition and is not a true tumor. It is discussed here because it is often confused with a lipoma. Lipomatous hypertrophy is defined as "any deposit of fat in the atrial septum at the level of the fossa ovalis which exceeds 2 cm in transverse dimension."[53] Lipomatous hypertrophy involves the interatrial septum, sparing the fossa ovalis membrane[53] and resulting in a characteristic dumbbell shape (Fig. 46-10). It results from adipose cell hyperplasia and is associated with increasing age and obesity.[69,70] It is a nonneoplastic condition and may be associated with atrial arrhythmias. It may very rarely result in superior vena cava obstruction.[71] Echocardiographically, the atrial septum may measure up to 3 cm in thickness and appears hyperechoic. Unlike lipomatous hypertrophy, lipomas are much less common. Unfortunately, the number of reported cases is not clear from the literature because some series do not differentiate between lipomas and lipomatous hypertrophy.[53] These homogeneous fatty encapsulated tumors usually arise from the epicardial surface, most often from a broad pedicle, and grow into the pericardial space.[9] Subendocardial lipomas are often small and sessile, whereas subepicardial lipomas tend to be larger. Subendocardial lipomas may also grow as broad-based pedunculated masses protruding into the cardiac chambers. Lipomas are usually asymptomatic but may cause symptoms from local compression (rarely, lipomas become quite large, weighing as much as 4.8 kg)[72] or cause arrhythmias; they occasionally may arise from the interatrial septum and extend into the LA cavity, mimicking a cardiac myxoma. Lipomas, unlike myxomas, however, have a broad base of attachment and are not as mobile as myxomas.[73,74] An unusual observation is that the echocardiographic appearance of lipomas varies depending on their particular location. In the pericardial space, they may appear echogenic or entirely hypoechoic or have hypoechoic regions.[75-77] Intracavitary lipomas, on the other hand, are homogeneous and hyperechoic.[74,78] The reason for this difference is not known (Fig. 46-11).[9]

If diagnostic uncertainty exists, with respect to identification of lipomatous hypertrophy or lipoma, CT scan and MRI are diagnostic because of their high specificity in identifying fat.[9,79-81] In fact, because the dumbbell appearance is so characteristic for lipomatous hypertrophy and noninvasive imaging is so specific for fat, a percutaneous tissue biopsy or surgical biopsy is unnecessary.[82]

### HEMANGIOMA

Hemangiomas are benign vascular tumors that represent only 2.8% to 10% of primary cardiac tumors.[83,84] They can arise anywhere in the heart and have been found in both ventricles and both atria, on the epicardial surface, and in the pericardium.[85-89] These tumors are seen more frequently in

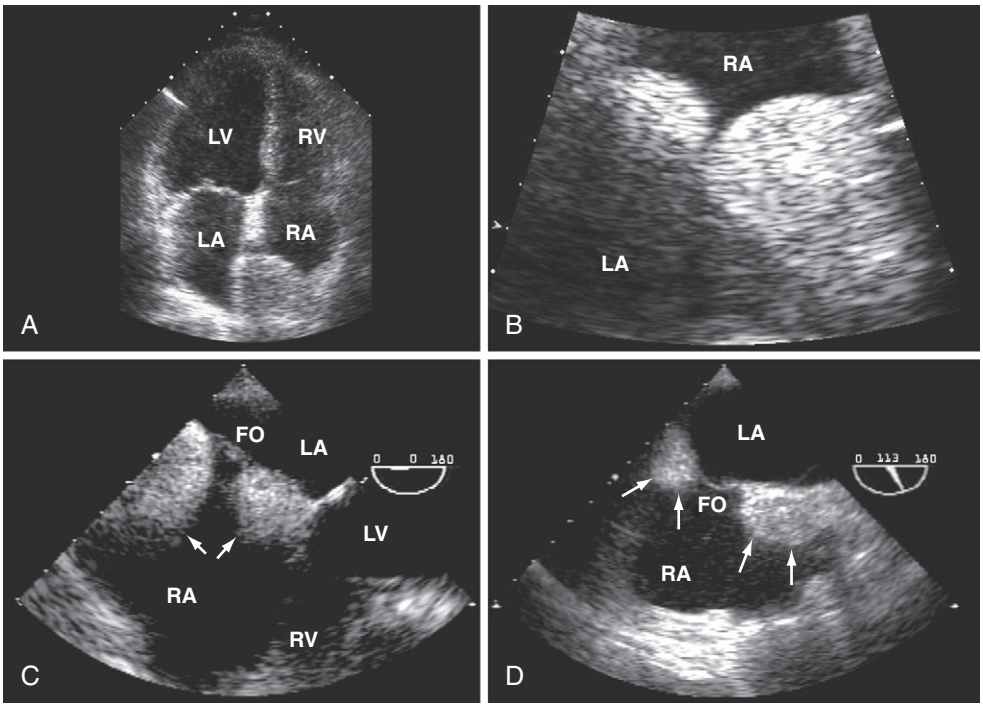



**Figure 46-10** **Typical appearance of exuberant lipomatous hypertrophy of the atrial septum. A,** Transthoracic echocardiogram, apical four-chamber view, shows a dumbbell-shaped mass in relation to the interatrial septum. The fossa ovalis membrane, which is characteristically spared in this condition, is thin, with most of the hypertrophy involving the superior limbus, resulting in a "mass-like" lesion in the roof of the right atrium. **B,** A zoomed image from a subcostal transthoracic echocardiographic view in the same patient. **C** and **D,** TEE views of lipomatous hypertrophy (*arrows*). Again, characteristically, the fossa ovalis membrane is spared. *FO,* Fossa ovalis membrane.

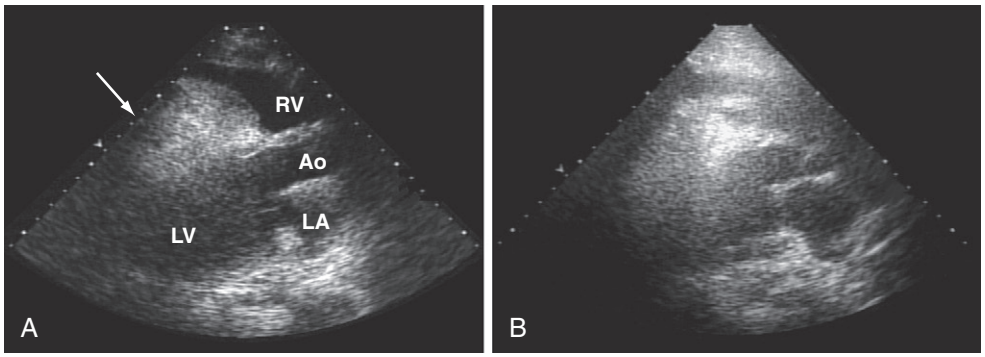



**Figure 46-11 Parasternal long-axis view images from a transthoracic echocardiogram in a 40-year-old woman with syncope and ventricular tachycardia are shown. A,** A large, poorly defined hyperechoic homogeneous intracardiac mass (*arrow*). involving the anterior interventricular septum is present. This mass also involved the anterior wall and extended to the apex. The size of the mass could not be accurately assessed because of acoustic shadowing, typical for a lipoma in this location (**B**). There was no evidence of significant outflow tract or valvular obstruction. MRI of the heart was diagnostic and showed the typical appearance of a lipoma. *Ao,* Aorta.

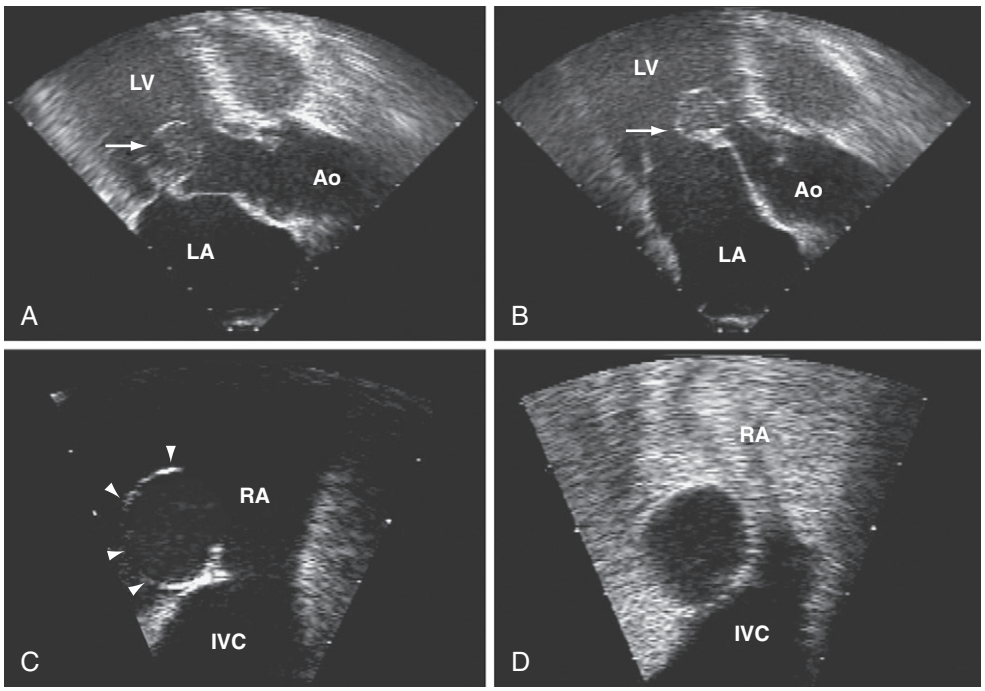



**Figure 46-12 Examples of cardiac hemangioma.** An incidental finding noted on transthoracic echocardiography in a 53-year-old man with ischemic heart disease led to this TEE (**A** and **B**). A 2-cm thin-walled echolucent mass (*arrow*) consistent with a hemangioma is seen attached to the ventricular aspect of the anterior mitral valve leaflet. Echocardiographic contrast administered intravenously is seen within the tumor, confirming its vascular nature. **C** and **D,** Another example of a hemangioma measuring 1.7 × 1.5 cm involving the Eustachian valve at the inferior vena cava–right atrial junction. The outline of the hemangioma is clearly demarcated with administration of agitated saline contrast injection via an antecubital vein. *Ao,* Aorta; *IVC,* inferior vena cava.

males than females, presenting at all ages, with a mean age at diagnosis of 43 years.[90] These tumors are usually asymptomatic and are discovered incidentally with echocardiography, CT scan, or MRI or at autopsy.[91] Symptoms depend on anatomic location and size of the tumor. They may cause arrhythmias, pericardial effusions, congestive heart failure, RV outflow tract obstruction, coronary insufficiency, and sudden cardiac death.[86] From a review of 56 reported cases, the localization of these tumors is approximately a third in the RV, a third in the LV, and a quarter in the right atrium. Other locations include the interatrial septum and interventricular septum and LA in 10% of cases. In a third of cases, multiple extensive tumors are present. The size of cardiac hemangiomas ranges from less than 1 cm to more than 8 cm.[86] Morphologically, the tumors have been variably described as a solid echodense bulge of the interventricular septum, a large multilobulated mass, or a unilocular mass with a cystic structure.[88] Although echocardiography can detect the tumor and its location, unfortunately no uniform diagnostic echocardiographic criteria exist (Fig. 46-12).[88] TEE provides incremental information regarding the accurate localization of the tumor and estimation of intracardiac and extracardiac extension and determination of the attachment site. It is also useful in assessment of whether there is extension of right atrial tumors into the great veins.[17] Cardiac catheterization and MRI are considered superior complementary diagnostic techniques. Cardiac catheterization reveals a characteristic "tumor blush"

that results from the tumor vascularity, and MRI can show the increased vascularity of the hemangioma with rapid enhancement during first pass gadolinium contrast infusion.[92-95]

The natural history of cardiac hemangiomas is poorly documented. Nevertheless, because the hemodynamic consequences of the tumor cannot be predicted, resection is recommended when feasible.

## RHABDOMYOMA

This intramyocardial tumor is the most frequent cardiac neoplasm of childhood, representing 60% of pediatric cardiac tumors,[15] and is often diagnosed in the first year of life, and increasingly in utero with the use of fetal echocardiography (Fig. 46-13).[83,85,86,89,96,97] There is a well-described and common association with rhabdomyoma and tuberous sclerosis, an autosomal dominant syndrome characterized by hamartomas in several organs, epilepsy, mental deficiency, and characteristic skin lesions. In fact, nearly 50% of infants with tuberous sclerosis are reported to have a rhabdomyoma.[98-100]

These tumors are almost always multiple and occur with equal frequency in the LV and RV, growing in the ventricular walls or on the atrioventricular valves. They vary in size from a few millimeters to a few centimeters and may be pedunculated, often obstructing ventricular inflow or outflow. Hemorrhage and calcification are uncommon.[53] Echocardiographically, they appear well circumscribed and slightly brighter than the surrounding normal myocardium (Fig. 46-14).[15]

Rhabdomyomas appear hypodense on contrast CT scan, isointense to myocardium on T1-weighted images, and hyperintense on T2-weighted images.[101] In contrast, fibromas (also a common childhood cardiac tumor; see subsequent discussion) appear as dark solitary masses, often with calcification on T2-weighted images.[102]

A characteristic and peculiar feature of rhabdomyomas is spontaneous regression (Fig. 46-15). The tumors usually regress in size or number or both in most patients less than 4 years of age. This phenomenon occurs less so in older patients, which probably accounts for their higher incidence in children and why, if found in adults, they are usually smaller than those

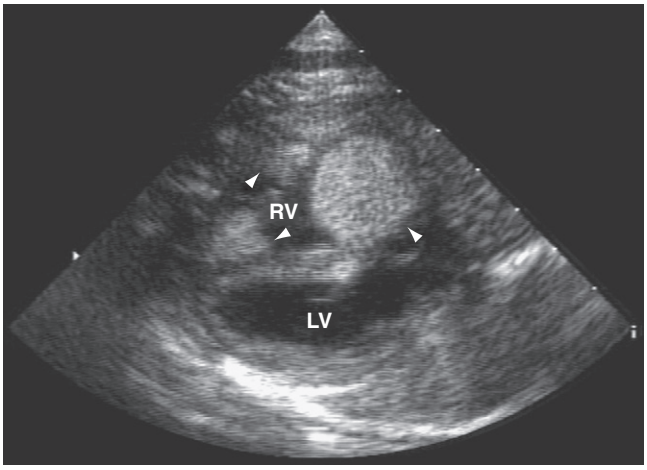



**Figure 46-13 Rhabdomyoma.** This fetal echocardiogram, longitudinal axis view, shows multiple well-circumscribed large and small tumors (*arrowheads*), typical for rhabdomyomas. These masses result in near obliteration of the RV cavity.

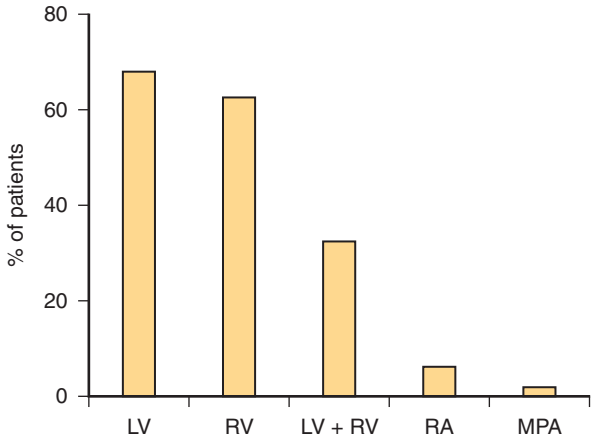



**Figure 46-15 Echocardiographic location of cardiac rhabdomyoma in the various cardiac chambers in 47 patients with tuberous sclerosis.** Some patients had tumors in more than one cardiac chamber. *MPA,* Main pulmonary artery. *(With permission Nir A, Tajik AJ, Freeman WK, et al: Tuberous sclerosis and cardiac rhabdomyoma.* Am J Cardiol *76:419-421, 1995.)*

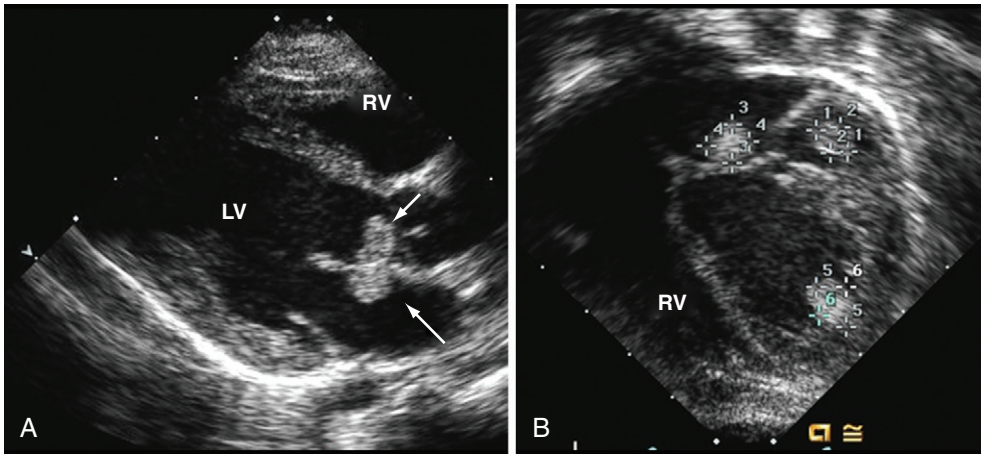



**Figure 46-14 A transthoracic echocardiogram, parasternal long-axis view (A) and oblique short-axis view (B), shows multiple intracardiac tumors attached to the endocardial surface within the LV, LA (*long arrow*), and left ventricular outflow tract (LVOT, *short arrow*).** The tumor in the LVOT resulted in mild outflow tract obstruction. An additional tumor was present in the RV (*not shown*). The patient was a 10-month-old child with tuberous sclerosis, seizures, and Wolf-Parkinson-White syndrome. These lesions in this clinical setting are typical for rhabdomyomas, and their size can be expected to regress with time.

typically seen in children.[100] These tumors are associated with a higher incidence of ventricular preexcitation and Wolff-Parkinson-White syndrome and may increase the risk of arrhythmia.[100] Because spontaneous tumor resolution is common, management is expectant in asymptomatic patients. Occasionally, surgical resection is necessary if the tumors are large and result in structural or hemodynamic complications.[103-107]

### CARDIAC FIBROMA

Cardiac fibroma is a congenital neoplasm that typically affects children, a third of whom are younger than 1 year at presentation. Like rhabdomyomas, they may also be detected in utero. It is the most common resected cardiac neoplasm in children and the second most common benign primary cardiac tumor found at autopsy in children.[53,108] Fibromas have been rarely reported in adults.[109] Males and females are equally affected, with a mean age at presentation of 13 years. There is an increased prevalence of cardiac fibromas in Gorlin syndrome, an autosomal dominant condition associated with multiple basal cell carcinomas, jaw cysts, skeletal anomalies, and tendency for development of neoplasms in several organ systems.[110-112] Patients with fibromas usually present with arrhythmias, heart failure, cyanosis, syncope, chest pain, or sudden death. One third may be asymptomatic.[53,108]

Cardiac fibromas are usually located in the ventricles and most often involve the LV free wall, the intraventricular septum, the RV, and rarely, the atria.[113,114] The tumors are characteristically solitary (unlike rhabdomyoma), circumscribed, and often centrally calcified without cystic change, necrosis, or hemorrhage (although this may be present in large tumors).[39,53,115-117] The typical echocardiographic appearance is of a discreet, often obstructive, echogenic, noncontractile mass that ranges in size from 1 to 10 cm in diameter (mean, 5 cm) in a ventricular wall.[53] The tumor may be nodular and discreet and may even mimic hypertrophic cardiomyopathy or ventricular septal hypertrophy (Fig. 46-16).[113,117-119]

With CT scan, fibromas appear as homogenous masses with soft tissue attenuation that may be either infiltrative or sharply marginated. Calcification is often seen. On MRI, they are homogeneous and hypointense on T2-weighted images and isointense relative to muscle on T1-weighted images. They show little or no contrast material enhancement.[9,116] MRI also shows the extent of myocardial infiltration, which can guide tumor resection.[120]

Surgery appears to be the optimal treatment in patients with symptomatic resectable tumors. The role of surgery in the patient with asymptomatic tumors is less clear because cardiac fibromas can remain dormant for many years and even regress.[116] However, because of fatal arrhythmias, surgery is often recommended, despite absence of symptoms. Transplantation is considered for large and unresectable tumors.

### CARDIAC PARAGANGLIOMA

Cardiac paraganglioma is an exceeding rare tumor, with only 30 cases reported before 1992 and 20 cases in the subsequent 10 years. Patients may present with symptoms of catecholamine excess or compression of adjacent structures. Echocardiography, particularly TEE, identifies ovoid, well-demarcated tumors characteristically within the atrioventricular groove adjacent to the epicardial arteries near the tricuspid and mitral annuli (Fig. 46-17).[121] MRI, CT scan, and nuclear medicine techniques for localizing extraadrenal paragangliomas are also useful in detecting and characterizing these tumors.

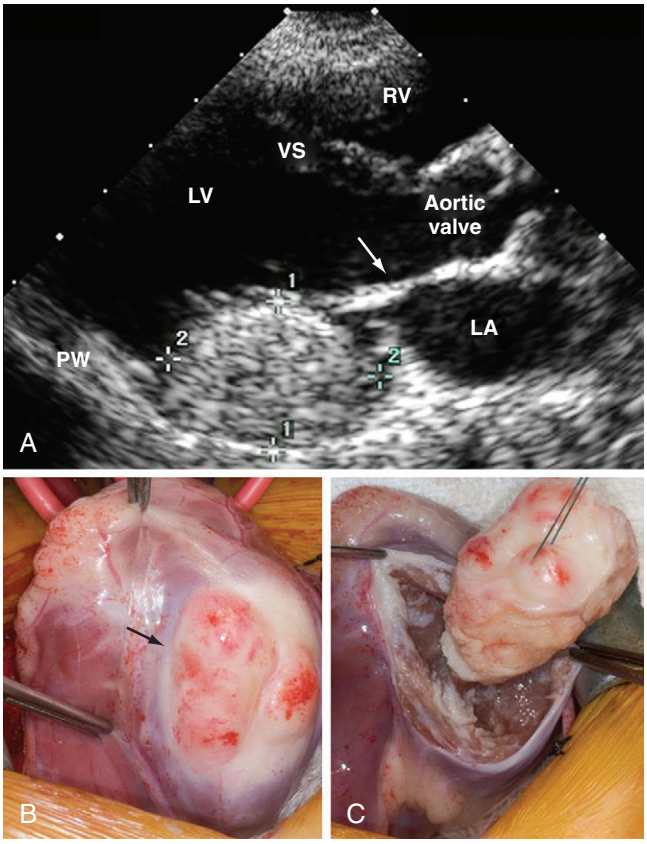



**Figure 46-16 Fibroma.** This 3-year-old girl presented with a cardiac mass diagnosed at 18 months of age when an incidental heart murmur was appreciated. She was entirely asymptomatic. **A,** A transthoracic echocardiogram, parasternal long-axis view. A large solitary homogeneous echodense mass measuring 3.5 cm × 4 cm is seen within the posterior wall, just beneath the mitral valve (*white arrow*), extending from the base to the apex of the LV. The mass did not involve the atrioventricular groove or papillary muscles. Surgery was recommended because of the risk of ventricular arrhythmias and sudden death. **B** and **C,** At surgery a white mass was visualized in the posteroinferior aspect of the free wall of the LV (*black arrow*). The tumor was completely shelled out without difficulty with sharp dissection and without having to enter the LV cavity. *(With permission from Bruce CJ: Cardiac tumours: diagnosis and management.* Heart *97:151-160, 2011.)*

## Malignant Primary Cardiac Tumors

Malignant primary tumors are rare. Metastatic disease or secondary cardiac malignant disease, on the other hand, is 30 times more common. Only approximately 15% of primary cardiac tumors are malignant. The vast majority (95%) of these primary malignant tumors are sarcomas, and the remaining 5% is made up of primary cardiac lymphomas and mesotheliomas.[122]

### SARCOMA

Sarcomas are most frequently diagnosed between the third and fifth decades of life and are found equally in men and women. Although they can arise at any part of the heart, they more commonly affect the left side of the heart, most commonly the LA.[123] The clinical course is dismal, rapidly progressive with death from widespread local infiltration, intracavitary

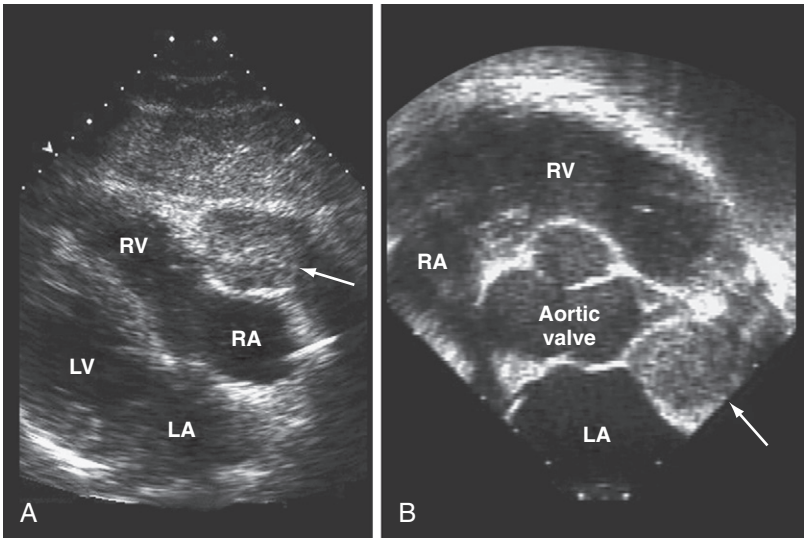



**Figure 46-17 Cardiac paragangliomas. A,** Transthoracic echocardiogram, subcostal view, shows an echogenic, ovoid well-demarcated intrapericardial 6 × 5 cm mass in the right atrioventricular groove producing mass effect but without invading the right atrial wall (*arrow*). There is no associated pericardial effusion. **B,** Transthoracic echocardiogram in a different patient, parasternal short-axis view, shows a mass (*arrow*) adjacent to the aortic valve, immediately beneath the aortic arch and adherent to the left pulmonary artery. Masses in these locations (**A** and **B**) are characteristic of this rare tumor.

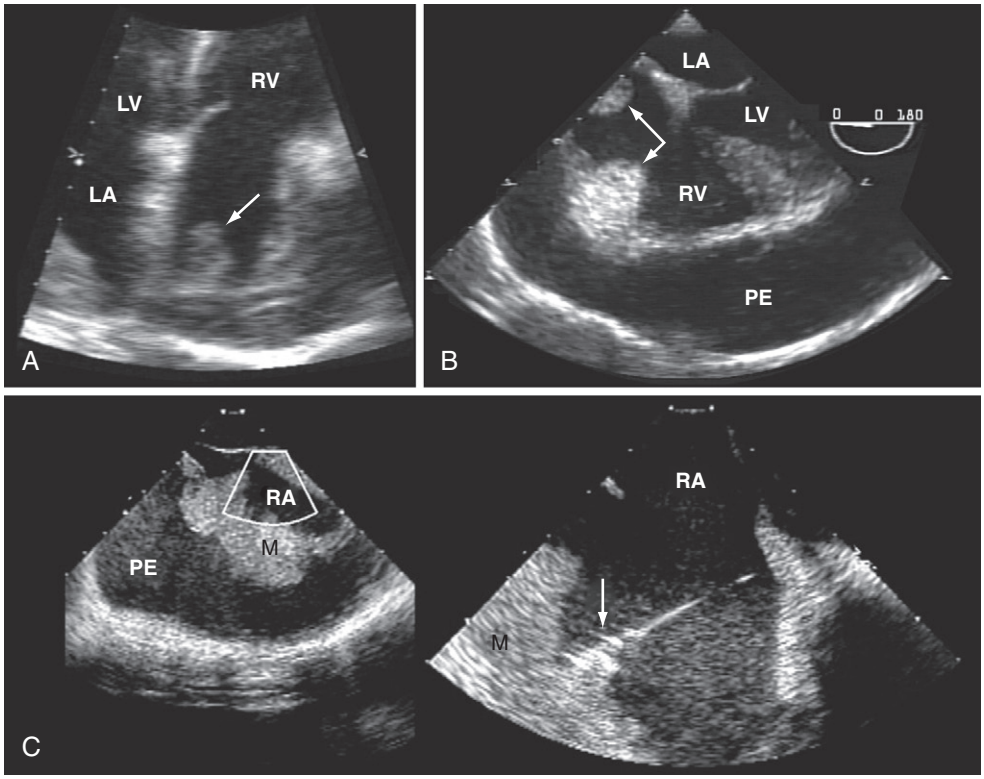



**Figure 46-18 A 33-year-old woman presented with pleuritic chest pain. A,** Transthoracic echocardiogram, apical four-chamber zoomed view, shows an irregular mass in the right atrium (*arrow*) with an associated posterior pericardial effusion predominantly located around the RV. **B,** A TEE image shows the same right atrial mass (*arrows*). Associated abnormal thickening of the right atrial wall and atrioventricular groove is appreciated. **C,** Intracardiac ultrasound imaging guides percutaneous pericardial effusion drainage and biopsy of the tumor. The intracardiac ultrasound probe tip is located within the body of the right atrium. The bioptome (*arrow*) is seen facilitating biopsy of tumor tissue and avoiding the uninvolved thin right atrial wall. Pathology confirmed angiosarcoma. *M,* Mass; *PE,* pericardial effusion.

obstruction, or metastases, often already present at the time of initial presentation. Although sarcomas can be differentiated histologically, their echocardiographic characteristics are not significantly unique to permit a reliable noninvasive histologic distinction (Figs. 46-18 and 46-19). Furthermore, to date, there is no conclusive evidence that histologic classification of sarcomas has any bearing on outcome or treatment.[124,125]

Angiosarcomas are the most common histologic subtype, with a male to female ratio of about two to one. Unlike other sarcomas, they usually arise in the right atrium or pericardium. The presenting signs and symptoms are nonspecific and may include right-sided heart failure, symptoms of pericardial involvement, or vena caval obstruction.[19,126,127] Echocardiography usually shows a broad-based right atrial mass near the inferior vena cava. Epicardial, endocardial, and intracavitary extension is common. On CT scan and MRI, they have avid, arterial phase enhancement that permits a definitive diagnosis. At surgery, local spread of the tumor to

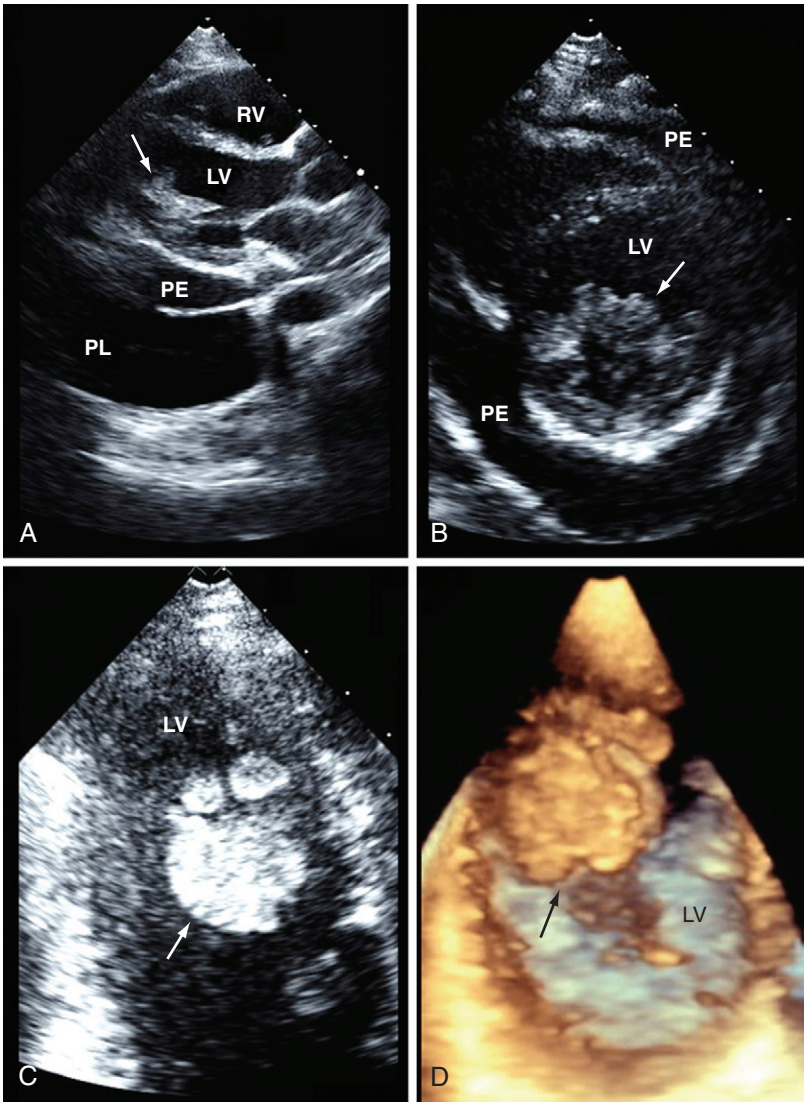



**Figure 46-19 Sarcoma.** This 48-year-old man presented with progressive dyspnea and syncope. A transthoracic echocardiogram was performed, and the parasternal long-axis view (**A**) and short-axis view (**B**) are shown. A large, 4 cm × 2 cm × 2 cm complex multilobulated intracavitary LV mass is readily appreciated on the short-axis view (*arrow*) and is less well appreciated on the accompanying long-axis view (*arrow*). Large pleural and pericardial effusions are also seen. Pericardial tamponade developed that necessitated emergency pericardiocentesis. A total of 800 mL of frankly bloody fluid was aspirated. The presence of hemorrhagic pleural and pericardial effusions with this echocardiographic appearance is suspicious for malignant disease. **C** and **D,** Zoomed 2D view of the complex mobile intraventricular mass arising from the apex of the LV with corresponding 3D image. Whole body CT scan documented widespread metastases. The cardiac tumor was considered unresectable. *PE,* Pericardial effusion; *PL,* plural effusion. *(With permission from Bruce CJ: Cardiac tumours: diagnosis and management.* Heart *97:151-160, 2011.)*

the pleural mediastinum is often found. Pulmonary metastases are frequent, and survival after diagnosis rarely exceeds 6 months.

Rhabdomyosarcomas account for 20% of sarcomas.[128] Multiple sites of myocardial involvement are common without predilection to any particular cardiac location.[31] Fibrosarcomas, histiosarcomas, and osteosarcomas constitute the remaining histologic subtypes of sarcomas. Osteosarcomas characteristically develop near the junction of the pulmonary veins and can extend into these vessels, a feature readily appreciated with TEE.[4]

## PRIMARY CARDIAC LYMPHOMA

The diagnosis of primary cardiac lymphoma requires the following:

1. Absence of lymphoma outside the pericardial sac (after a complete autopsy examination); and
2. The bulk of the tumor residing within the pericardium or cardiac symptoms that arise from lymphomatous cardiac infiltration at the time of initial diagnosis.

Although the incidence is exceedingly rare (1% of primary cardiac tumors in the Armed Forces Institute of Pathology Series report),[129] the incidence of cardiac lymphoma is increasing because of lymphoproliferative disorders related to viral infections (Epstein-Barr virus and HIV) and immunocompromise in transplant cases.[130-136] Cardiac lymphomas usually present during the fourth decade, with a slight predominance in men. All areas of the heart can be involved, including the pericardium. The lymphoma may become intracavitary and produce obstruction. The lesions appear as nodules and rarely as polypoid growths on the endocardial surface. Although echocardiography is a sensitive imaging technique, a definitive tissue diagnosis is still required.[137]

## MESOTHELIOMAS

Pericardial mesotheliomas are malignant tumors of the pericardium, which present clinically either as pericarditis, a pericardial effusion, or both. Some may present with features of constrictive pericarditis and signs of right heart failure (Fig. 46-20).[15] These tumors are more common in adults. Unlike pleural mesotheliomas, there is no association with asbestosis. Although solitary pericardial mesotheliomas occur, more frequently, they cover most of the parietal and visceral surface of the pericardium, encasing the heart. In contrast to sarcomas,

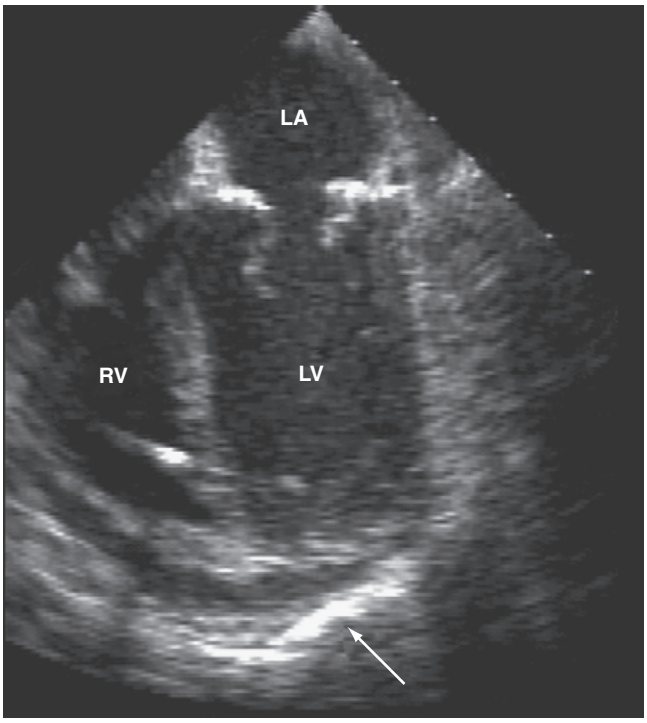



**Figure 46-20 Pericardial mesothelioma.** A TEE, four-chamber view, in a 47-year-old man with Hodgkin disease treated with radiation and chemotherapy presenting with a clinical diagnosis of constrictive pericarditis is shown. The pericardium is thickened (*arrow*), and there is a small associated pericardial effusion. The visceral pericardium also appears thick. At surgery, the pericardium was thick and friable. Histology confirmed pericardial mesothelioma.

invasion into the myocardium is only superficial. CT scan and MRI define tumor extent and degree of myocardial invasion.

## Secondary or Metastatic Malignant Tumors of the Heart

Whereas primary tumors of the heart are rare, secondary tumors are common. Among unselected autopsies, the incidence rate is about 4% and may be as high as 20% in patients dying of malignant disease.[138,139] Malignant tumors spread to the heart by direct extension, usually from mediastinal tumors, hematogenous spread, lymphatic spread, or intraluminal extension from the inferior vena cava.[140] Metastatic involvement can be either localized or diffuse. The nodules may be found in discreet locations or encase the epicardial surface. Pericardial effusion or cardiac tamponade may often be the initial presentation of secondary cardiac involvement. The noninvasive imaging appearance of metastatic deposits seldom distinguishes the tumor type. Rather, a careful evaluation for the primary tumor or a detailed history of malignancy disease provides the strongest clue.[126]

### DIRECT EXTENSION

Most secondary tumors of the heart arise contiguously from tumors in the chest cavity, most commonly breast, lung, or esophageal carcinoma. The initial clinical manifestation of these tumors is usually from pericardial involvement, and consequently, the most common echocardiographic finding in these patients is a pericardial effusion with or without cardiac tamponade.[15]

### HEMATOGENOUS SPREAD

Metastatic spread to the heart is usually hematogenous, with right-sided and left-sided metastases equally reported.[15] Ninety percent of metastases are clinically silent.[31]

Malignant melanoma, although a less common tumor than lung or breast carcinoma, is well recognized as having the highest rate of cardiac metastasis of any tumor,[141] with as many as 50% of all autopsy cases having cardiac involvement.[141] Moreover, more cases of cardiac involvement are being diagnosed as a result of rising melanoma incidence and increasing survival. Melanoma can involve any cardiac chamber and any cardiac structure, but most metastases are located in the myocardium, and valvular involvement is rare (Fig. 46-21). Glancy and Roberts[142] found cardiac involvement in 45 of 70 cases of metastatic melanoma. Most had multiple small metastases throughout the heart, with the right atrium most commonly involved. Intracavitary metastases from malignant melanoma make up most published cases and are usually discovered incidentally.[141] In patients with a history of melanoma who have cardiac symptoms, cardiac involvement can be ascertained with either transthoracic echocardiography or TEE, although TEE is better suited in identification of smaller lesions and definition of mobility and attachment.[16,143,144] MRI also shows site of mural attachment but defines extension of tumor into adjacent mediastinal structures better than TEE.[141] It also produces a characteristic hyperintense signal on T1-weighted images because of paramagnetic scavenging by melanin.[141]

Malignant carcinoid heart disease usually manifesting with characteristic valvular abnormalities may rarely present with metastatic cardiac disease typified by intramyocardial masses. These usually occur in the setting of known carcinoid syndrome (Fig. 46-22).[145]

### LYMPHATIC SPREAD

Most patients with cardiac metastases from lymphomas or leukemias have concomitant involvement of the mediastinal lymph nodes. Stagnated lymph flow allows for retrograde extension of the tumor. Lymphomas form discreet endomyocardial masses, which are usually clinical silent.

### INTRALUMINAL VENOUS EXTENSION

Tumors may propagate within blood vessels returning to the heart, most commonly originating from abdominal tumors via the inferior vena cava to the right heart. Renal cell carcinoma, adrenal carcinoma, hepatocellular carcinoma, and uterine leiomyosarcoma are the most common tumors that reach the heart in this manner.[15] Of these, renal cell carcinoma is the most common. These tumors usually appear as large elongated masses inside and emanating from the inferior vena cava and entering the right atrium, sometimes extending into the RV (Fig. 46-23).[4,146] These intraluminal tumors may be distinguished from simple thrombi because they have a rather more "mass-like" appearance, unlike thrombi, which usually appear as thin, elongated venous casts.[147]

Diagnostically, TEE is useful because it provides excellent visualization of venous inflow to the heart. It can also guide complete en bloc resection of the abdominal and intraluminal tumor and enable real-time monitoring of tumor embolization (see Figure 46-23).[4,148-150] On occasion, these tumors may also cross a patent foramen ovale, appearing as a thrombus in transit.

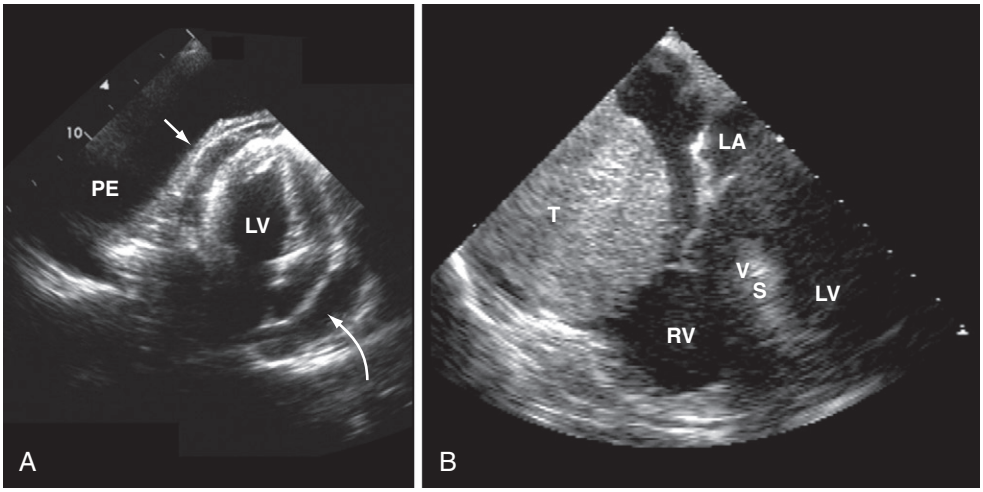



**Figure 46-21 Metastatic melanoma to the pericardium. A,** In the TTE four-chamber apical view, the pericardium around the LV is thickened with an irregular surface and texture (*arrow*). There is a moderate to large pericardial effusion around the RV and right atrium (*curved arrow*) and large pleural effusion (*PE*). **B,** A TEE in a 72-year-old man with a history of melanoma presenting with fatigue shows a 4 × 6 cm polypoid tumor (*T*) arising from the right atrium and prolapsing into the RV. Importantly, the tumor does not arise from the atrial septum, a factor potentially distinguishing it from a myxoma. It did not arise from the inferior vena cava (*not shown*). At surgery, the tumor was black in color, and pathology confirmed metastatic melanoma. *VS,* Ventricular septum.

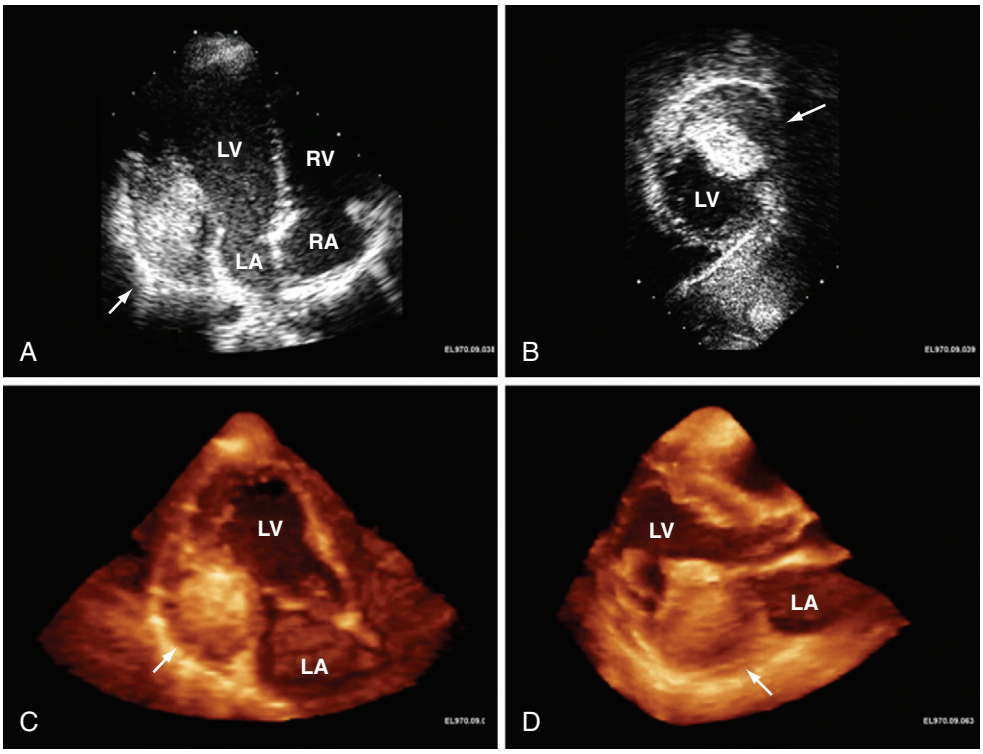



**Figure 46-22 Metastatic carcinoid tumor with atypical cardiac involvement. A,** Apical four-chamber view shows the relationship of the tumor to the atrioventricular groove, distorting the mitral annulus and mitral leaflet (*arrow*). **B,** Parasternal short-axis image at the basal LV level shows the large metastatic tumor located in the lateral wall (*arrow*). **C** and **D,** 3D images show the relationship of the tumor to the mitral valve apparatus.

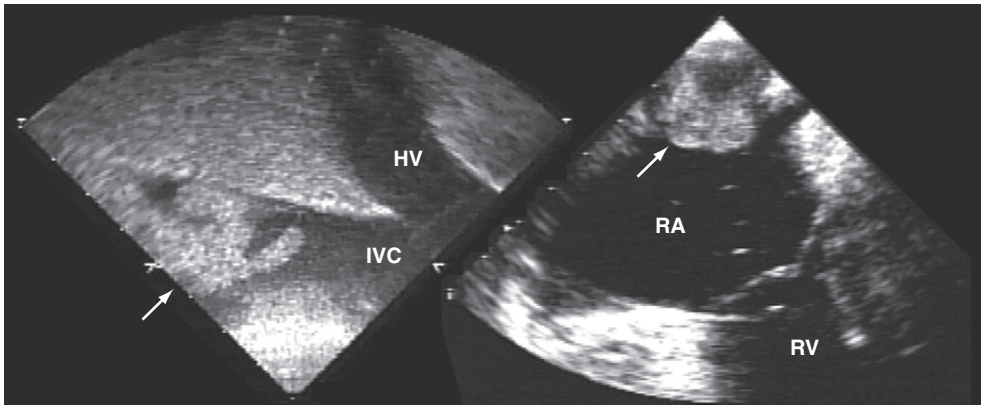



**Figure 46-23 Examples of classic venous extension of tumor thrombus from the kidney into the inferior vena cava characteristic for hypernephroma (renal cell carcinoma).** A complex tumor thrombus is seen within the lumen of the inferior vena cava (*arrow, left image*). The most distal extent of the tumor is 2 cm proximal to the origin of the hepatic vein. No intracardiac tumor was present in this patient. The *right image* shows tumor extension from the inferior vena cava into the right atrium (*arrow*). Both these tumors were successfully removed via a cavotomy with intraoperative TEE guidance. Transesophageal imaging confirmed complete removal of the tumor thrombus without embolization. *HV,* Hepatic vein; *IVC,* inferior vena cava.

In cases of intraluminal leiomyosarcoma, multiple points of attachment in the inferior vena cava may help distinguish these tumors from renal cell carcinoma or hepatoma. Thyroid carcinoma has been described growing along the superior vena cava into the right atrium,[151] and carcinoma of the lung may also extend into the LA intraluminally directly from the pulmonary veins.[15,147,152]

## Differential Diagnosis

When confronted with a suspected "mass," as always, it is important to integrate all the clinical information (e.g., age and history of malignancy disease) with all the echocardiographic information. The most likely etiology of an intracardiac mass is a thrombus, followed by vegetation. Primary cardiac tumors are rare, with metastatic involvement of the heart more frequent and usually occurring in the setting of previously diagnosed malignancy disease. Often, a cardiac mass is diagnosed when in fact the "mass" really represents an unusual tomographic plane of a normal cardiac structure or normal variant of cardiac anatomy. It is important to distinguish these findings from cardiac tumors. Box 46-2 includes the most common normal or variants of normal cardiac anatomy that are often confused with abnormal masses or tumors. Apart from the clinical history, associated echocardiographic findings also provide important clues as to the etiology of the "mass." For example, thrombi and vegetations have characteristic echocardiographic features, but in addition, they can often be distinguished from one another and from other cardiac masses by their particular intracardiac location (e.g., LA appendage or ventricular apex versus valve leaflets) and the "company they keep" (e.g., atrial fibrillation, LA enlargement, mitral valve disease, valvular destruction, and bacteremia). Thrombi seldom occur as an isolated finding. Ventricular thrombi usually occur in the setting of coronary artery disease with associated akinetic or dyskinetic myocardial segments, most commonly an aneurysmal LV apex with concomitant LV dysfunction. Atrial thrombi usually occur within the LA appendage in patients with atrial fibrillation, mitral valve disease, and LA enlargement. Ancillary features of sluggish blood flow, such as spontaneous echo contrast and reduced LA appendage emptying velocities, may be present. Another useful clinical strategy for determination of whether a mass is a thrombus or a tumor is to perform a serial echocardiographic evaluation after a period of systemic anticoagulation therapy. Thrombi usually resolve after 4 weeks of anticoagulation therapy, whereas tumors either increase in size or remain unchanged despite anticoagulation therapy (Fig. 46-24).

Vegetations may be confused with cardiac tumors (Fig. 46-25). However, apart from papillary fibroelastomas, primary tumors of the cardiac valves are exceedingly rare. Vegetations appear as mobile echogenic masses attached to valves and are usually diagnosed in the setting of known or suspected valve disease and bacteremia. Occasionally, when vegetations are seen in the absence of a bacteremia, other clinical features such as rheumatologic disease or underlying malignant disease may signify Libman-Sacks endocarditis. Valvular vegetations in the setting of infective endocarditis are also usually accompanied by features of valvular destruction and consequent regurgitation. Nonvalvular vegetations occur at sites of turbulence and may be attached to the ventricular endocardial surface in patients with hypertrophic obstructive cardiomyopathy and in patients with septal defects.

**Box 46-2**

### ECHOCARDIOGRAPHIC FINDINGS THAT MAY BE CONFUSED WITH CARDIAC TUMORS

**Normal or Normal-Variant Cardiac Structures**
- Right atrium
- Crista terminalis
- Eustachian valve
- Chiari network
- Left atrium
- Floor of left upper pulmonary vein adjacent to the LA appendage ("Q-tip")
- Right ventricle
- Moderator band
- Left ventricle
- Papillary muscles

**Nontumor Cardiac Pathology**
- Intracardiac
  - Thrombi
  - Valves
  - Vegetations (infective and marantic)
  - Lambl excrescence
  - Flail or prolapsing leaflet
  - Severed mitral valve apparatus after mitral valve replacement
  - Fatty tricuspid valve annulus
  - Mitral annular calcification
- Myocardium
  - Asymmetric ventricular hypertrophy
  - Noncompaction of the left ventricle
  - Hypereosinophilic syndrome
- Atrial septum
  - Lipomatous hypertrophy
  - Atrial septum aneurysm
- Extracardiac
  - Compression of LA by aorta
  - Coronary aneurysm or fistula
  - Potential space of the transverse sinus
  - Left lower lobe atelectasis
  - Hematoma
  - Hiatal hernia
  - Pericardial fat infiltration
  - Mediastinal tumor

**Intracardiac Hardware**
- Pacing leads
- Pulmonary artery catheter
- Central line catheter

Infiltrative disorders that involve the heart may mimic cardiac tumors. These include cardiac involvement by sarcoidosis,[153] Wegener granulomatosis,[154] hypereosinophilic syndrome,[155] and tuberculosis. Also, specific pathologic cardiac disorders reported to have been confused with cardiac tumors[156] include cardiac varices,[157] coronary artery fistula,[158] coronary artery aneurysm,[158,159] atrial septal aneurysm,[160,161] intramyocardial hematoma[162] after percutaneous intervention, blood cysts,[163] and pericardial cysts.[164]

Normal cardiac structures potentially confused with tumors include the crista terminalis (Fig. 46-26), Eustachian valve, Chiari network, lipomatous hypertrophy of the atrial septum, and the ridge of tissue seen between the left superior pulmonary

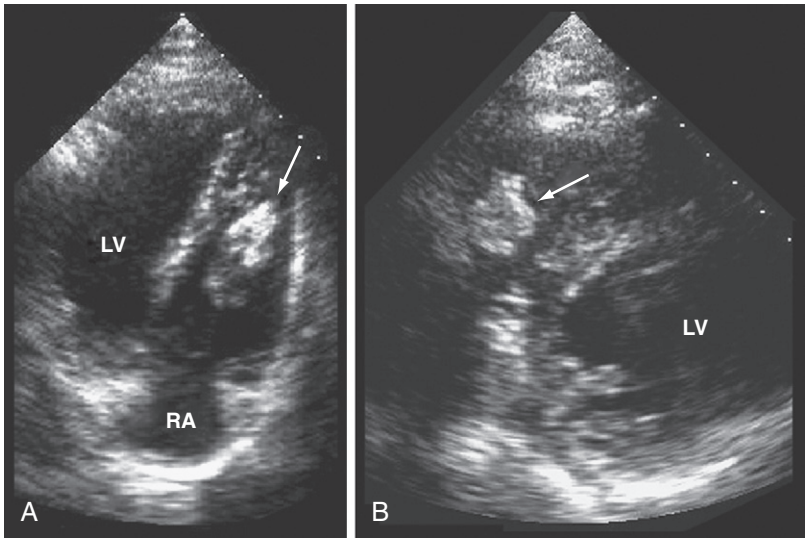



**Figure 46-24 Intracardiac thrombus.** A transthoracic echocardiogram (**A,** apical four-chamber view; **B,** parasternal short-axis view) in a 20-year-old with pulmonary embolism shows a calcified thrombus in the RV apex (*arrow*). The etiology of the mass was indeterminate and did not resolve after a month of systemic anticoagulation therapy. Surgical excision was advised. Histology showed a calcified amorphous tumor or thrombus with a mixed inflammatory infiltrate and associated calcification.

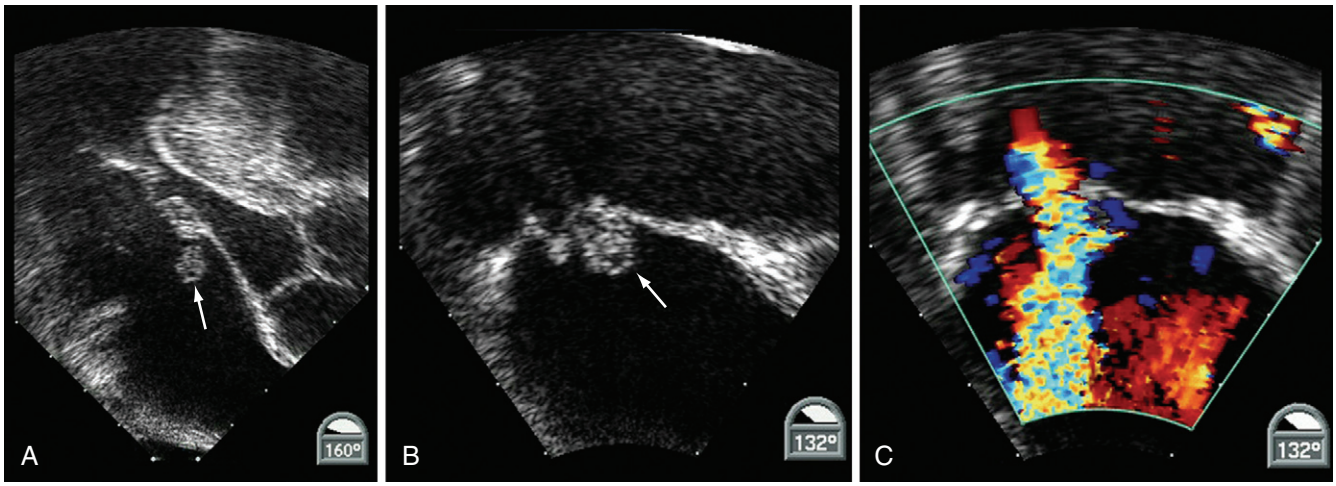



**Figure 46-25 Vegetations may be confused with papillary fibroelastomas.** These TEE images show distinguishing characteristics of endocarditis. A mobile 6 × 7 mm globular vegetation (*arrow*) is attached to the atrial aspect of the anterior mitral valve leaflet tip, seen in diastole (**A**) and systole (**B**). Color flow imaging of the mitral valve (**C**) shows severe mitral regurgitation from destruction of the mitral valve as the result of a perforation of the anterior leaflet. This characteristic mass lesion, associated with valvular destruction and positive blood cultures, is consistent with a diagnosis of a vegetation and thus infective endocarditis.

vein and LA appendage on TEE commonly referred to as the "Q-tip." Even a diaphragmatic hernia may be confused with a cardiac tumor. This can be readily identified by having the patient drink a carbonated beverage while being imaged and confirming the presence of gas bubbles in the stomach. Knowledge of these normal cardiac structures and normal variants of cardiac anatomy is important to avoid unnecessary additional evaluation, biopsy, or operation (see Box 46-2).

## Newer Echocardiographic Techniques

Although transthoracic echocardiography is an excellent screening tool, because of the limited image frequency of the transducer, detection of small tumors is insensitive. Transthoracic imaging has improved with the advent of tissue harmonic imaging, particularly in obese patients or those with chronic lung disease, and this has probably contributed to the increasing diagnosis of cardiac tumors ante mortem. Nevertheless, TEE is more sensitive than transthoracic echocardiography in diagnosis of small tumors, particularly papillary fibroelastomas. The reported diagnostic sensitivity for detection of mass lesions with transthoracic echocardiography and TEE is 93% and 97%, respectively.[165] TEE is also more sensitive in detection of abnormalities that involve the posterior cardiac structures, particularly the atria, interatrial septum, and pulmonary veins. Intracardiac ultrasound scan, with a variable frequency (5 to 10 MHz) phased array transducer affixed to the end of a deflectable catheter, provides very high-resolution images of intracardiac structures. These imaging catheters have been used to guide intracardiac tumor biopsy (see Fig. 46-18). However,

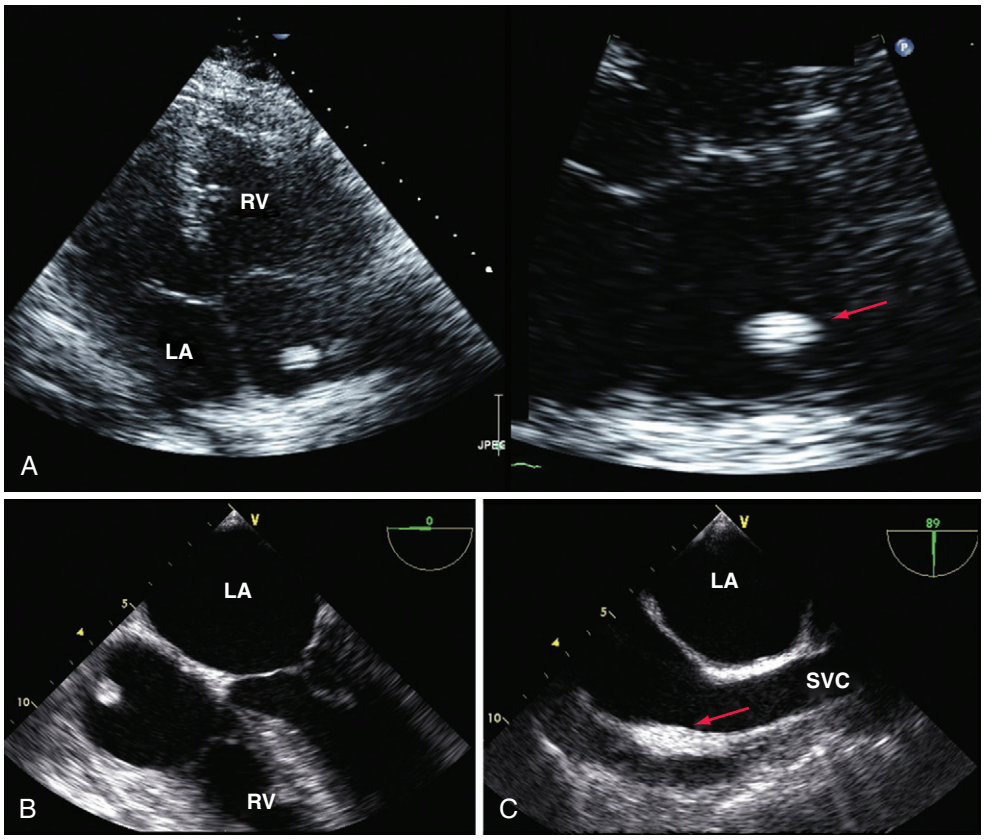



**Figure 46-26 Prominent crista terminalis. A,** An apical four-chamber view shows an echogenic circular "mass" in the right atrium. Zoomed view depicts the "mass" (*red arrow*). **B,** TEE, 0-degree mid-esophageal view, shows the same structure. **C,** Rotating the transducer to 90 degrees provides an orthogonal view of the circular structure demonstrating its longitudinal extent (*red arrow*), typical for a prominent crista terminalis.
*SVC,* Superior vena cava.

because this is an invasive tool, more widespread application for cardiac tumor diagnosis is limited.[166,167]

From both a diagnostic and therapeutic standpoint, echocardiography not only has an important and established role in invasive procedures related to diagnostic biopsy of cardiac masses but also has a role in the therapeutic and diagnostic drainage of suspected malignant pericardial effusions. Open thoracotomy, cardiopulmonary bypass and resection, or open biopsy remains the diagnostic standard.[167-172] However, in patients with right-sided lesions (most commonly malignant) who may be too ill, have unresectable disease, or only need a diagnostic tissue biopsy before chemotherapy, TEE or intracardiac echocardiography can be especially useful to guide percutaneous biopsy. Real-time visualization of the procedure enhances safety, minimizing risk of inadvertent damage to delicate surrounding structures and increasing diagnostic yield by directing the bioptome to the tumor tissue directly, as compared with use of fluoroscopy alone. For pericardial effusions, concomitant transthoracic echocardiography complements percutaneous pericardiocentesis. This approach has been well described and not only enhances safety of the procedure but also permits immediate hemodynamic assessment after pericardiocentesis and serial assessment after ongoing pericardial drainage.

Intraoperative TEE is also an important tool in guiding surgical intervention. In a report from the Mayo Clinic on patients undergoing cardiac surgery primarily for resection of mass lesions, intraoperative TEE added diagnostic information that resulted in modification of the surgical procedure, both before and after cardiopulmonary bypass in 16% of cases. In fact, this study and others have documented the importance of confirming that the mass is indeed present immediately before the skin incision to avoid unnecessary surgery for tumors that may have embolized in the period between initial detection and surgery.[173,174]

In recent years, 3D transthoracic echocardiography and TEE have evolved into a new clinical diagnostic tool in cardiac imaging.[175-178] With use of this technique, anatomy and pathology can be appreciated without having to perform "mental reconstruction" of the problem, permitting morphologic, volume, and spatial assessment of masses and tumors in vivo (Fig. 46-27).[179] It also permits noninvasive "sectioning" of the mass to better evaluate its morphologic and spatial characteristics, thereby reportedly helping guide preoperative decision making.[175,179] Unlike CT scan and MRI, a hemodynamic assessment can be performed at the same time.

Although 3D reconstruction can be derived from both transthoracic and transesophageal studies, transthoracic imaging yields poor quality images if poor acoustic windows are encountered. This can be overcome with TEE provided the probe is stabilized during held respiration and the study is gated to heart rate.[180] 3D TEE also permits volume quantification of intracardiac mass lesions. These volume assessments have been shown to correlate well with in vitro measured volumes of surgical specimens.[181] Currently, transthoracic 3D image resolution and quality is suboptimal for detection of small tumors. Therefore, standard 2D imaging techniques should still be used to identify cardiac tumors.

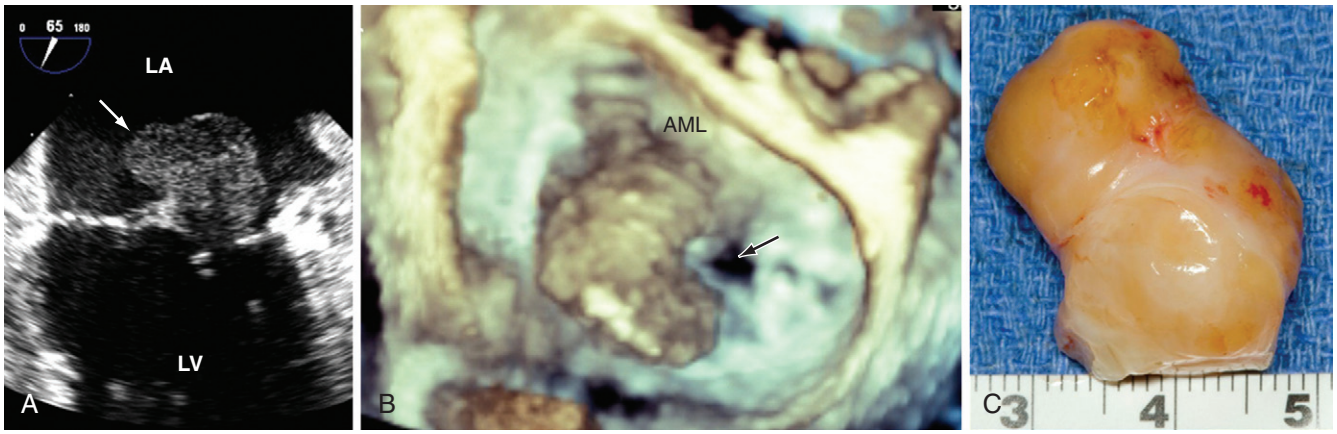



**Figure 46-27 Comparison of 2D and 3D imaging of a cardiac tumor with corresponding excised gross pathology.** This 57-year-old man with history of non-Hodgkin lymphoma presented with recently diagnosed Hodgkin lymphoma. A transthoracic echocardiogram before chemotherapy (**A**) documented an intracardiac mass; thus, a TEE was performed. Although the mass is appreciated well on 2D TEE (*arrow*), its volume and geometry, and broad base of attachment to the base of the anterior mitral leaflet (*AML*), are readily appreciated with 3D TEE. **B,** In the 3D image, the mitral valve is viewed from above (surgeon's view) and the *arrow* points to the mitral orifice. Histology of the tumor (**C**) confirmed nodular sclerosing Hodgkin lymphoma.

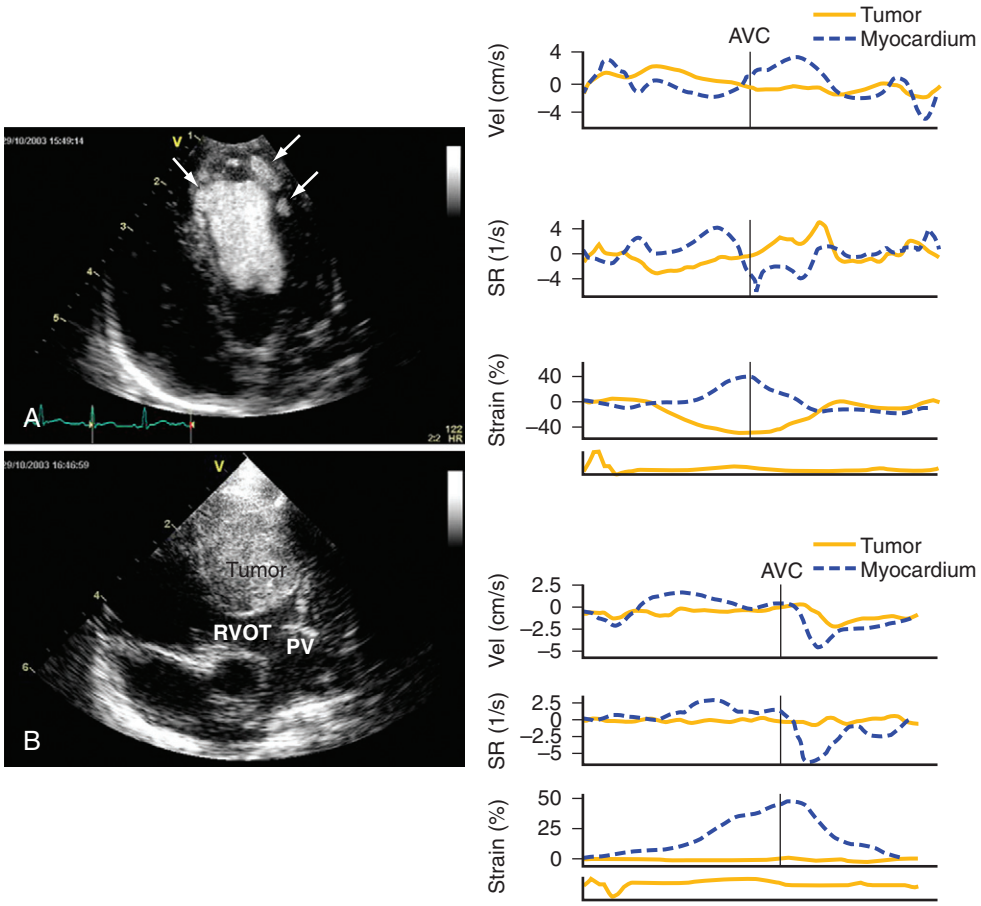



**Figure 46-28 Newer echocardiographic-based strain analysis applied to cardiac tumor diagnosis. A,** An apical four-chamber view shows three cardiac tumors in the LV (*arrows*) consistent with rhabdomyomas. Corresponding longitudinal color Doppler myocardial imaging curves are shown recorded from the tumor and adjacent interventricular septum. The *upper, mid,* and *lower curves* show myocardial velocity, strain rate, and strain, respectively. In early systole, the tumor moves and deforms in the same direction as the surrounding myocardium. Later in systole, the myocardium squeezes the soft mass in the opposite direction. **B,** Parasternal short-axis view shows a fibroma attached to the RV free wall extending toward the right ventricular outflow tract (*RVOT*). In this case, the fibroma neither moves nor deforms. These tissue Doppler characteristics may potentially be used to differentiate the rhabdomyoma from fibroma. *PV,* Pulmonic valve. *(With permission Ganame J, D'Hooge J, Mertens L: Different deformation patterns in intracardiac tumors.* Eur J Echocardiogr *6:461-464, 2005.)*

Analysis of myocardial motion with tissue Doppler imaging has also been used to characterize differences in tissue velocity of tumors versus normal myocardial tissue. Strain imaging, derived from either tissue velocity data or speckle tracking algorithms, is less susceptible to translational motion. It identifies contracting from noncontracting tissue and thus may be potentially helpful in distinguishing noncontractile tumors and thrombi from normal contracting myocardium. This concept has already been explored to identify and distinguish fibromas and rhabdomyomas.[182,183] Fibromas are composed of fibroblasts and collagen, and rhabdomyomas are composed of altered myocytes. Consequently, the fibroma has less deformability than the rhabdomyoma or the surrounding normal myocardium. Echocardiographic derived strain data can identify this deformation or lack thereof, providing additional diagnostic information to identify and distinguish these tumors (Fig. 46-28). This technique can also be used with tagged MRI, but it is labor intensive.[184]

Although the concept that unique ultrasound-tissue interaction holds potential in identification of abnormal from normal cardiac tissue, and despite being extensively explored in carefully controlled experiments, ultrasound-based tissue characterization has not proved practical or robust enough to be useful clinically.[185-187]

Echocardiographic contrast imaging may be useful in evaluation of cardiac tumors by enhancing border definition, better outlining tumor location and site of attachment, and also distinguishing vascular from avascular structures (e.g., thrombi) with assessment of myocardial perfusion.[188] Perfusion imaging has improved significantly with advances in second generation contrast agents and new imaging techniques, such as power modulation.[189-191] Both qualitative and quantitative differences in gray scale have been reported in various cardiac masses with this technique.[190] Malignant and highly vascular tumors showed greater enhancement than adjacent myocardium, whereas myxomas showed partial perfusion and quantitatively less enhancement than surrounding myocardium. Thrombi showed no perfusion. In this study, perfusion imaging also identified pericardial malignant disease, an area less well appreciated with standard noncontrast imaging. Although promising, a limitation of this method in clinical practice is that it is time consuming, requiring off-line analysis of time intensity curves. Also, the technique requires skill and experience in contrast administration and image acquisition.

Targeted microbubble delivery represents an exciting frontier. Echocardiographic contrast bubbles are being engineered to target tumors to "unmask" them, making them easier to identify and characterize and also potentially to serve as vehicles for targeted therapy delivery. A study in a tumor-bearing mouse model has evaluated the use of contrast microbubbles targeted to tumor vasculature via conjugation with the tumor-binding peptide arginine-arginine-leucine. With this technique, the investigators were able to distinguish normal tissue and tumor tissue in vivo. This pioneering work may open the possibility of ultrasonic molecular imaging of tumor angiogenesis in the clinical setting, thereby permitting improved noninvasive identification of tumors, assessment of malignant potential, and monitoring of tumor response.[192]

## ACKNOWLEDGMENTS

*The author thanks Bridgette A. Wagner for her assistance with this chapter.*

## KEY POINTS

- Cardiac tumors are rare. Incidental cardiac masses usually represent thrombi or vegetations. Three quarters of primary cardiac tumors are benign.
- Myxomas are the most common benign primary cardiac tumor and occur sporadically as an isolated tumor in the LA, usually attached to the fossa ovalis by a thin stalk. Multiple tumors or atypical locations suggest familial myxoma.
- Papillary fibroelastomas, characterized by a small mobile pedunculated "anemone"-like mass with a stippled edge, are the most common valvular tumors.
- Lipomatous hypertrophy of the atrial septum may be confused with an intracardiac tumor. It results in a dumbbell-shaped intraatrial septum with characteristic sparing of the fossa ovalis membrane. The diagnosis can be confirmed with MRI or CT scan.
- Rhabdomyomas are the most frequent cardiac neoplasm in childhood. They are almost always multiple, occurring in both the LV and the RV, and can be expected to spontaneously regress in size in most patients less than 4 years of age. They are seen in 50% of infants with tuberous sclerosis.
- Cardiac fibromas are the most common resected cardiac tumor in childhood. These characteristically solitary circumscribed tumors are usually located in the ventricles.
- Only 15% of primary cardiac tumors are malignant, the vast majority of which (95%) are sarcomas. Sarcomas do not have a characteristic echocardiographic appearance. They are most commonly found in the right atrium. Widespread local infiltration is usually present, and the clinical course is dismal.
- Secondary cardiac malignant disease or metastatic disease is 30 times more common than primary cardiac tumors. Malignant tumors spread to the heart by direct extension and hematogenous, lymphatic, and intraluminal spread. Malignant melanoma has the highest rate of cardiac metastasis of any tumor. Renal cell carcinoma is the most common tumor to spread to the heart by the inferior vena cava.
- Multiple tumors may be missed, particularly if the imager is distracted by finding the index tumor. Careful evaluation of all cardiac chambers is necessary to exclude multiple tumors.
- When confronted with a suspected "mass," it is important to integrate all the clinical information to make the most accurate noninvasive diagnosis.

## REFERENCES


1. Reynen K: Frequency of primary tumors of the heart. *Am J Cardiol* 77:107, 1996.
2. Lam KY, Dickens P, Chan AC: Tumors of the heart. A 20-year experience with a review of 12,485 consecutive autopsies. *Arch Pathol Lab Med* 117:1027-1031, 1993.
3. Piazza N, Chughtai T, Toledano K, et al: Primary cardiac tumours: eighteen years of surgical experience on 21 patients. *Can J Cardiol* 20:1443-1448, 2004.
4. Goldman JH, Foster E: Transesophageal echocardiographic (TEE) evaluation of intracardiac and pericardial masses. *Cardiol Clin* 18:849-860, 2000.
5. Gowda RM, Khan IA, Nair CK, et al: Cardiac papillary fibroelastoma: a comprehensive analysis of 725 cases. *Am Heart J* 146:404-410, 2003.
6. Howard RA, Aldea GS, Shapira OM, et al: Papillary fibroelastoma: increasing recognition of a surgical disease. *Ann Thorac Surg* 68:1881-1885, 1999.
7. Fyke FE, 3rd, Seqard JB, Edwards WD, et al: Primary cardiac tumors: experience with 30 consecutive patients since the introduction of two-dimensional echocardiography. *J Am Coll Cardiol* 5:1465-1473, 1985.
8. Endo A, Ohtahara A, Kinugawa T, et al: Characteristics of 161 patients with cardiac tumors diagnosed during 1993 and 1994 in Japan. *Am J Cardiol* 79:1708-1711, 1997.
9. Araoz PA, Mulvagh SL, Tazelaar HD, et al: CT and MR imaging of benign primary cardiac neoplasms with echocardiographic correlation. *Radiographics* 20:1303-1319, 2000.
10. Tatli S, Lipton MJ: CT for intracardiac thrombi and tumors. *Int J Cardiovasc Imaging* 21:115-131, 2005.
11. Vander Salm TJ: Unusual primary tumors of the heart. *Semin Thorac Cardiovasc Surg* 12:89-100, 2000.
12. Colucci WS: Primary tumors of the heart. In Braunwald W, Libby P, editors: *Heart disease*, ed 6, Philadelphia, 2001, WB Saunders.
13. Elbardissi AW, Dearani JA, Daly RC, et al: Embolic potential of cardiac tumors and outcome after resection: a case-control study. *Stroke* 40:156-162, 2009.
14. Parissis JT, Zezas S, Sfiras N, et al: An atypical left atrial myxoma causing intracavitary pressure gradient and typical diastolic transmitral flow of severe mitral stenosis. *Int J Cardiol* 102:165-167, 2005.
15. Salcedo EE, Cohen GI, White RD, et al: Cardiac tumors: diagnosis and management. *Curr Probl Cardiol* 17:73-137, 1992.
16. Mugge A, Daniel WG, Haverich A, et al: Diagnosis of noninfective cardiac mass lesions by two-dimensional echocardiography. Comparison of the transthoracic and transesophageal approaches. *Circulation* 83:70-78, 1991.
17. Leibowitz G, Keller NM, Daniel WG, et al: Transesophageal versus transthoracic echocardiography in the evaluation of right atrial tumors. *Am Heart J* 130:1224-1227, 1995.
18. Samdarshi TE, Mahan EF, 3rd, Nanda NC, et al: Transesophageal echocardiographic diagnosis of multicentric left ventricular myxomas mimicking a left atrial tumor. *J Thorac Cardiovasc Surg* 103:471-474, 1992.
19. Herrmann MA, Shankerman RA, Edwards WD, et al: Primary cardiac angiosarcoma: a clinicopathologic study of six cases. *J Thorac Cardiovasc Surg* 103:655-664, 1992.
20. Reynen K: Cardiac myxomas. *N Engl J Med* 333:1610-1617, 1995.
21. Pinede L, Duhaut P, Loire R: Clinical presentation of left atrial cardiac myxoma. A series of 112 consecutive cases. *Medicine (Baltimore)* 80:159-172, 2001.
22. Kuon E, Kreplin M, Weiss W, et al: The challenge presented by right atrial myxoma. *Herz* 29:702-709, 2004.
23. Keeling IM, Oberwalder P, Anelli-Monti M, et al: Cardiac myxomas: 24 years of experience in 49 patients. *Eur J Cardiothorac Surg* 22:971-977, 2002.
24. Jelic J, Milicic D, Alfirevic I, et al: Cardiac myxoma: diagnostic approach, surgical treatment and follow-up. A twenty years experience. *J Cardiovasc Surg (Torino)* 37:113-117, 1996.
25. Centofanti P, Di Rosa E, Deorsola L, et al: Primary cardiac tumors: early and late results of surgical treatment in 91 patients. *Ann Thorac Surg* 68:1236-1241, 1999.
26. Selkane C, Amahzoune B, Chavanis N, et al: Changing management of cardiac myxoma based on a series of 40 cases with long-term follow-up. *Ann Thorac Surg* 76:1935-1938, 2003.
27. Akbarzadeh Z, Esmailzadeh M, Yousefi A, et al: Multicentric familial cardiac myxoma. *Eur J Echocardiogr* 6:148-150, 2005.
28. Carney JA, Gordon H, Carpenter PC, et al: The complex of myxomas, spotty pigmentation, and endocrine overactivity. *Medicine (Baltimore)* 64:270-283, 1985.
29. Vidaillet HJ, Jr, Seward JB, Fyke FE, 3rd, et al: "Syndrome myxoma": a subset of patients with cardiac myxoma associated with pigmented skin lesions and peripheral and endocrine neoplasms. *Br Heart J* 57:247-255, 1987.
30. Edwards A, Bermudez C, Piwonka G, et al: Carney's syndrome: complex myxomas. Report of four cases and review of the literature. *Cardiovasc Surg* 10:264-275, 2002.
31. Shapiro LM: Cardiac tumours: diagnosis and management. *Heart* 85:218-222, 2001.
32. Szucs RA, Rehr RB, Yanovich S, et al: Magnetic resonance imaging of cardiac rhabdomyosarcoma. Quantifying the response to chemotherapy. *Cancer* 67:2066-2070, 1991.
33. Elbardissi AW, Dearani JA, Daly RC, et al: Survival after resection of primary cardiac tumors: a 48-year experience. *Circulation* 118:S7-S15, 2008.
34. Percell RL, Jr, Henning RJ, Siddique Patel M: Atrial myxoma: case report and a review of the literature. *Heart Dis* 5:224-230, 2003.
35. Heath D: Pathology of cardiac tumors. *Am J Cardiol* 21:315-327, 1968.
36. Schanz U, Schneider J: [Endocardial myxoma. Current aspects of its histopathogenesis.] *Schweiz Med Wochenschr* 114:850-857, 1984.
37. Prichard RW: Tumors of the heart; review of the subject and report of 150 cases. *AMA Arch Pathol* 51:98-128, 1951.
38. Acebo E, Val-Bernal JF, Gomez-Roman JJ, et al: Clinicopathologic study and DNA analysis of 37 cardiac myxomas: a 28-year experience. *Chest* 123:1379-1385, 2003.
39. Tazelaar HD, Locke TJ, McGregor CG: Pathology of surgically excised primary cardiac tumors. *Mayo Clin Proc* 67:957-965, 1992.
40. Schweiger MJ, Hafer JG, Jr, Brown R, et al: Spontaneous cure of infected left atrial myxoma following embolization. *Am Heart J* 99:630-634, 1980.
41. Graham HV, von Hartitzsch B, Medina JR: Infected atrial myxoma. *Am J Cardiol* 38:658-661, 1976.
42. Joseph P, Himmelstein DU, Mahowald JM, et al: Atrial myxoma infected with *Candida*: first survival. *Chest* 78:340-343, 1980.
43. Quinn TJ, Codini MA, Harris AA: Infected cardiac myxoma. *Am J Cardiol* 53:381-382, 1984.
44. Obeid AI, Marvasti M, Parker F, et al: Comparison of transthoracic and transesophageal echocardiography in diagnosis of left atrial myxoma. *Am J Cardiol* 63:1006-1008, 1989.
45. Thier W, Schluter M, Krebber HJ, et al: Cysts in left atrial myxomas identified by transesophageal cross-sectional echocardiography. *Am J Cardiol* 51:1793-1795, 1983.
46. Rahilly GT, Jr, Nanda NC: Two-dimensional echographic identification of tumor hemorrhages in atrial myxomas. *Am Heart J* 101:237-239, 1981.
47. Dittmann H, Voelker W, Karsch KR, et al: Bilateral atrial myxomas detected by transesophageal two-dimensional echocardiography. *Am Heart J* 118:172-173, 1989.
48. Engberding R, Daniel WG, Erbel R, et al: Diagnosis of heart tumours by transoesophageal echocardiography: a multicentre study in 154 patients. European Cooperative Study Group. *Eur Heart J* 14:1223-1228, 1993.
49. Perez de Isla L, de Castro R, Zamorano JL, et al: Diagnosis and treatment of cardiac myxomas by transesophageal echocardiography. *Am J Cardiol* 90:1419-1421, 2002.
50. Masui T, Takahashi M, Miura K, et al: Cardiac myxoma: identification of intratumoral hemorrhage and calcification on MR images. *A J R Am J Roentgenol* 164:850-852, 1995.
51. Lie JT: Petrified cardiac myxoma masquerading as organized atrial mural thrombus. *Arch Pathol Lab Med* 113:742-745, 1989.
52. Restrepo CS, Largoza A, Lemos DF, et al: CT and MR imaging findings of malignant cardiac tumors. *Curr Probl Diagn Radiol* 34:1-11, 2005.
53. Burke A: *Tumors of the heart and great vessels. Atlas of tumor pathology*, Washington, DC, 1996, Armed Forces Institute of Pathology; pp 1-98.
54. Sun JP, Asher CR, Yang XS, et al: Clinical and echocardiographic characteristics of papillary fibroelastomas: a retrospective and prospective study in 162 patients. *Circulation* 103:2687-2693, 2001.
55. Burn CG, Bishop MB, Davies JN: A stalked papillary tumor of the mural endocardium. *Am J Clin Pathol* 51:344-346, 1969.
56. Paelinck B, Vermeersch P, Kockx M: Calcified papillary fibroelastoma of the tricuspid valve. *Acta Cardiol* 53:165-167, 1998.
57. Bottio T, Basso C, Rizzoli G, et al: Case report: fibroelastoma of the papillary muscle of the mitral valve: diagnostic implications and review of the literature. *J Heart Valve Dis* 11:288-291, 2002.
58. Fabricius AM, Heidrich L, Gutz U, et al: Papillary fibroelastoma of the tricuspid valve chordae with a review of the literature. *Cardiovasc J S Afr* 13:122-124, 2002.
59. Brown RD, Jr, Khandheria BK, Edwards WD: Cardiac papillary fibroelastoma: a treatable cause of transient ischemic attack and ischemic stroke detected by transesophageal echocardiography. *Mayo Clin Proc* 70:863-868, 1995.
60. Kanarek SE, Wright P, Liu J, et al: Multiple fibroelastomas: a case report and review of the literature. *J Am Soc Echocardiogr* 16:373-376, 2003.

61. Klarich KW, Enriquez-Sarano M, Gura GM, et al: Papillary fibroelastoma: echocardiographic characteristics for diagnosis and pathologic correlation. *J Am Coll Cardiol* 30:784-790, 1997.
62. Daveron E, Jain N, Kelley GP, et al: Papillary fibroelastoma and Lambl's excrescences: echocardiographic diagnosis and differential diagnosis. *Echocardiography* 22:461-463, 2005.
63. Lambl V: Papillare excrescenzen an der semilunar-klappe der aorta. *Wien Med Wochenschr* 6:244-247, 1856.
64. McAllister HJ: Papillary fibroelastoma: tumors of the cardiovascular system. *AFIB Atlas of Tumor Pathology* 15:20-25, 1978.
65. Boone SA, Campagna M, Walley VM: Lambl's excrescences and papillary fibroelastomas: are they different? *Can J Cardiol* 8:372-376, 1992.
66. Paraf F, Berrebi A, Chauvaud S, et al: [Mitral papillary fibroelastoma in a HIV infected patient.] *Presse Med* 28:962-964, 1999.
67. Shirani J, Metveyeva P, Losada M, et al: Transient loss of vision as the presenting symptom of papillary fibroelastoma of aortic valve. *Cardiovasc Pathol* 6:237-240, 1997.
68. Okada K, Sueda T, Orihashi K, et al: Cardiac papillary fibroelastoma on the mitral valve. *J Card Surg* 16:335-337, 2001.
69. Basu S, Folliguet T, Anselmo M, et al: Lipomatous hypertrophy of the interatrial septum. *Cardiovasc Surg* 2:229-231, 1994.
70. Zeebregts CJ, Hensens AG, Timmermans J, et al: Lipomatous hypertrophy of the interatrial septum: indication for surgery? *Eur J Cardiothorac Surg* 11:785-787, 1997.
71. Breuer M, Wippermann J, Franke U, et al: Lipomatous hypertrophy of the interatrial septum and upper right atrial inflow obstruction. *Eur J Cardiothorac Surg* 22:1023-1025, 2002.
72. Lang-Lazdunski L, Oroudji M, Pansard Y, et al: Successful resection of giant intrapericardial lipoma. *Ann Thorac Surg* 58:238-241, 1994.
73. Vanderheyden M, De Sutter J, Wellens F, et al: Left atrial lipoma: case report and review of the literature. *Acta Cardiol* 53:31-32, 1998.
74. Mousseaux E, Idy-Peretti I, Bittoun J, et al: MR tissue characterization of a right atrial mass: diagnosis of a lipoma. *J Comput Assist Tomogr* 16:148-151, 1992.
75. Mullen JC, Schipper SA, Sett SS, et al: Right atrial lipoma. *Ann Thorac Surg* 59:1239-1241, 1995.
76. King SJ, Smallhorn JF, Burrows PE: Epicardial lipoma: imaging findings. *A J R Am J Roentgenol* 160:261-262, 1993.
77. Doshi S, Halim M, Singh H, et al: Massive intrapericardial lipoma, a rare cause of breathlessness. Investigations and management. *Int J Cardiol* 66:211-215, 1998.
78. Kamiya H, Ohno M, Iwata H, et al: Cardiac lipoma in the interventricular septum: evaluation by computed tomography and magnetic resonance imaging. *Am Heart J* 119:1215-1217, 1990.
79. Kozelj M, Angelski R, Pavcnik D: Lipomatous hypertrophy of the interatrial septum: diagnosis by echocardiography and magnetic resonance imaging. A case report. *Angiology* 46:863-866, 1995.
80. Restrepo CS, Largoza A, Lemos DF, et al: CT and MR imaging findings of benign cardiac tumors. *Curr Probl Diagn Radiol* 34:12-21, 2005.
81. Tuna IC, Julsrud PR, Click RL, et al: Tissue characterization of an unusual right atrial mass by magnetic resonance imaging. *Mayo Clin Proc* 66:498-501, 1991.
82. Nadra I, Dawson D, Schmitz SA, et al: Lipomatous hypertrophy of the interatrial septum: a commonly misdiagnosed mass often leading to unnecessary cardiac surgery. *Heart* 90:e66, 2004.
83. McAllister HJ: Tumors of the cardiovascular system. *Atlas tumor pathology*, Washington DC, 1978, Armed Forces Institute of Pathology.
84. Alsaileek A, Tepe SM, Alveraz L, et al: Diagnostic features of cardiac hemangioma on cardiovascular magnetic resonance, a case report. *Int J Cardiovasc Imaging* 22:699-702, 2006.
85. Lapenna E, De Bonis M, Torracca L, et al: Cavernous hemangioma of the tricuspid valve: minimally invasive surgical resection. *Ann Thorac Surg* 76:2097-2099, 2003.
86. Kojima S, Sumiyoshi M, Suwa S, et al: Cardiac hemangioma: a report of two cases and review of the literature. *Heart Vessels* 18:153-156, 2003.
87. Matsumoto Y, Watanabe G, Endo M, et al: Surgical treatment of a cavernous hemangioma of the left atrial roof. *Eur J Cardiothorac Surg* 20:633-635, 2001.
88. Landolphi DR, Belkin RN, Hjemdahl-Monsen CE, et al: Cardiac cavernous hemangioma mimicking pericardial cyst: atypical echocardiographic appearance of a rare cardiac tumor. *J Am Soc Echocardiogr* 10:579-581, 1997.
89. Hangler HB, Vorderwinkler KP, Fend F, et al: Intramural right atrial myocardial hemangioma treated by emergency surgery. *Eur J Cardiothorac Surg* 11:782-784, 1997.
90. Sarjeant JM, Butany J, Cusimano RJ: Cancer of the heart: epidemiology and management of primary tumors and metastases. *Am J Cardiovasc Drugs* 3:407-421, 2003.
91. Perk G, Yim J, Varkey M, et al: Cardiac cavernous hemangioma. *J Am Soc Echocardiogr* 18:979, 2005.
92. Fukuzawa S, Yamamoto T, Shimada K, et al: Hemangioma of the left ventricular cavity: presumptive diagnosis by magnetic resonance imaging. *Heart Vessels* 8:211-214, 1993.
93. Moniotte S, Geva T, Perez-Atayde A, et al: Images in cardiovascular medicine. Cardiac hemangioma. *Circulation* 112:e103-e104, 2005.
94. Brizard C, Latremouille C, Jebara VA, et al: Cardiac hemangiomas. *Ann Thorac Surg* 56:390-394, 1993.
95. Brodwater B, Erasmus J, McAdams HP, et al: Case report. Pericardial hemangioma. *J Comput Assist Tomogr* 20:954-956, 1996.
96. Freedom RM, Lee KJ, MacDonald C, et al: Selected aspects of cardiac tumors in infancy and childhood. *Pediatr Cardiol* 21:299-316, 2000.
97. Kagan KO, Schmidt M, Kuhn U, et al: Ventricular outflow obstruction, valve aplasia, bradyarrhythmia, pulmonary hypoplasia and non-immune fetal hydrops because of a large rhabdomyoma in a case of unknown tuberous sclerosis: a prenatal diagnosed cardiac rhabdomyoma with multiple symptoms. *Bjog* 111:1478-1480, 2004.
98. Bass JL, Breningstall GN, Swaiman KF: Echocardiographic incidence of cardiac rhabdomyoma in tuberous sclerosis. *Am J Cardiol* 55:1379-1382, 1985.
99. Smith HC, Watson GH, Patel RG, et al: Cardiac rhabdomyomata in tuberous sclerosis: their course and diagnostic value. *Arch Dis Child* 64:196-200, 1989.
100. Nir A, Tajik AJ, Freeman WK, et al: Tuberous sclerosis and cardiac rhabdomyoma. *Am J Cardiol* 76:419-421, 1995.
101. Fujita N, Caputo GR, Higgins CB: Diagnosis and characterization of intracardiac masses by magnetic resonance imaging. *Am J Card Imaging* 8:69-80, 1994.
102. Grebenc ML, Rosado de Christenson ML, Burke AP, et al: Primary cardiac and pericardial neoplasms: radiologic-pathologic correlation. *Radiographics* 20:1073-1103; quiz 1110-1112, 2000.
103. Bosi G, Lintermans JP, Pellegrino PA, et al: The natural history of cardiac rhabdomyoma with and without tuberous sclerosis. *Acta Paediatr* 85:928-931, 1996.
104. Smythe JF, Dyck JD, Smallhorn JF, et al: Natural history of cardiac rhabdomyoma in infancy and childhood. *Am J Cardiol* 66:1247-1249, 1990.
105. Becker AE: Primary heart tumors in the pediatric age group: a review of salient pathologic features relevant for clinicians. *Pediatr Cardiol* 21:317-323, 2000.
106. Jacobs JP, Konstantakos AK, Holland FW, 2nd, et al: Surgical treatment for cardiac rhabdomyomas in children. *Ann Thorac Surg* 58:1552-1555, 1994.
107. Jozwiak S, Kawalec W, Dluzewska J, et al: Cardiac tumours in tuberous sclerosis: their incidence and course. *Eur J Pediatr* 153:155-157, 1994.
108. Beghetti M, Gow RM, Haney I, et al: Pediatric primary benign cardiac tumors: a 15-year review. *Am Heart J* 134:1107-1114, 1997.
109. Kanemoto N, Usui K, Fusegawa Y: An adult case of cardiac fibroma. *Intern Med* 33:10-12, 1994.
110. Coffin CM: Congenital cardiac fibroma associated with Gorlin syndrome. *Pediatr Pathol* 12:255-262, 1992.
111. Herman TE, Siegel MJ, McAlister WH: Cardiac tumor in Gorlin syndrome. Nevoid basal cell carcinoma syndrome. *Pediatr Radiol* 21:234-235, 1991.
112. Gorlin RJ: Nevoid basal-cell carcinoma syndrome. *Medicine (Baltimore)* 66:98-113, 1987.
113. Parmley LF, Salley RK, Williams JP, et al: The clinical spectrum of cardiac fibroma with diagnostic and surgical considerations: noninvasive imaging enhances management. *Ann Thorac Surg* 45:455-465, 1988.
114. de Ruiz M, Potter JL, Stavinoha J, et al: Real-time ultrasound diagnosis of cardiac fibroma in a neonate. *J Ultrasound Med* 4:367-369, 1985.
115. Ferguson HL, Hawkins EP, Cooley LD: Infant cardiac fibroma with clonal t(1;9)(q32;q22) and review of benign fibrous tissue cytogenetics. *Cancer Genet Cytogenet* 87:34-37, 1996.
116. Burke AP, Rosado-de-Christenson M, Templeton PA, et al: Cardiac fibroma: clinicopathologic correlates and surgical treatment. *J Thorac Cardiovasc Surg* 108:862-870, 1994.
117. Basso C, Valente M, Poletti A, et al: Surgical pathology of primary cardiac and pericardial tumors. *Eur J Cardiothorac Surg* 12:730-738, 1997.
118. Veinot JP, O'Murchu B, Tazelaar HD, et al: Cardiac fibroma mimicking apical hypertrophic cardiomyopathy: a case report and differential diagnosis. *J Am Soc Echocardiogr* 9:94-99, 1996.
119. Grinda JM, Mace L, Dervanian P, et al: Obstructive right ventricular cardiac fibroma in an adult. *Eur J Cardiothorac Surg* 13:319-321, 1998.
120. Gutberlet M, Abdul-Khaliq H, Stiller B, et al: Giant fibroma in the left ventricle of an infant: imaging findings in magnetic resonance

imaging, echocardiography and angiography. *Eur Radiol* 12:S143-S148, 2002.
121. Osranek M, Bursi F, Gura GM, et al: Echocardiographic features of pheochromocytoma of the heart. *Am J Cardiol* 91:640-643, 2003.
122. Roberts WC: Primary and secondary neoplasms of the heart. *Am J Cardiol* 80:671-682, 1997.
123. Donsbeck AV, Ranchere D, Coindre JM, et al: Primary cardiac sarcomas: an immunohistochemical and grading study with long-term follow-up of 24 cases. *Histopathology* 34:295-304, 1999.
124. Burke A: Primary malignant cardiac tumors. *Semin Diagn Pathol* 25:39-46, 2008.
125. Simpson L, Kumar SK, Okuno SH, et al: Malignant primary cardiac tumors: review of a single institution experience. *Cancer* 112:2440-2446, 2008.
126. Butany J, Nair V, Naseemuddin A, et al: Cardiac tumours: diagnosis and management. *Lancet Oncol* 6:219-228, 2005.
127. Janigan DT, Husain A, Robinson NA: Cardiac angiosarcomas. A review and a case report. *Cancer* 57:852-859, 1986.
128. Castorino F, Masiello P, Quattrocchi E, et al: Primary cardiac rhabdomyosarcoma of the left atrium: an unusual presentation. *Tex Heart Inst J* 27:206-208, 2000.
129. McAllister HA Jr: Primary tumors and cysts of the heart and pericardium. *Curr Probl Cardiol* 4:1-51, 1979.
130. Holladay AO, Siegel RJ, Schwartz DA: Cardiac malignant lymphoma in acquired immune deficiency syndrome. *Cancer* 70:2203-2207, 1992.
131. Burtin P, Guerci A, Boman F, et al: Malignant lymphoma in the donor heart after heart transplantation. *Eur Heart J* 14:1143-1145, 1993.
132. Kelsey RC, Saker A, Morgan M: Cardiac lymphoma in a patient with AIDS. *Ann Intern Med* 115:370-371, 1991.
133. Pousset F, Le Heuzey JY, Pialoux G, et al: Cardiac lymphoma presenting as atrial flutter in an AIDS patient. *Eur Heart J* 15:862-864, 1994.
134. Le Heuzey JY, Pousset F, Pialoux G: [Apropos of a case of malignant cardiac lymphoma in HIV infection.] *Arch Mal Coeur Vaiss* 89:269, 1996.
135. Denis J, Hery B, Crepin V, et al: [Malignant tumoral lymphoma of the heart in human immunodeficiency virus infection: diagnosis by echocardiography.] *Arch Mal Coeur Vaiss* 88:507-510, 1995.
136. Pettelot G, Gibelin P, Blanc P, et al: [Complete regression of cardiac non-Hodgkin's lymphoma after 23 months with chemotherapy.] *Arch Mal Coeur Vaiss* 89:379-381, 1996.
137. Tighe DA, Anene CA, Rousou JA, et al: Primary cardiac lymphoma. *Echocardiography* 17:345-347, 2000.
138. Cohen GU, Perry TM, Evans JM: Neoplastic invasion of the heart and pericardium. *Ann Intern Med* 42:1238-1245, 1955.
139. Biran S, Hochman A, Levij IS, Stern S: Clinical diagnosis of secondary tumors of the heart and pericardium. *Dis Chest* 55:202, 1959.
140. Longo R, Mocini D, Santini M, et al: Unusual sites of metastatic malignancy: case 1. Cardiac metastasis in hepatocellular carcinoma. *J Clin Oncol* 22:5012-5014, 2004.
141. Gibbs P, Cebon JS, Calafiore P, et al: Cardiac metastases from malignant melanoma. *Cancer* 85:78-84, 1999.
142. Glancy DL, Roberts WC: The heart in malignant melanoma. A study of 70 autopsy cases. *Am J Cardiol* 21:555-571, 1968.
143. Obeid AI, al Mudamgha A, Smulyan H: Diagnosis of right atrial mass lesions by transesophageal and transthoracic echocardiography. *Chest* 103:1447-1451, 1993.
144. Reeder GS, Khandheria BK, Seward JB, et al: Transesophageal echocardiography and cardiac masses. *Mayo Clin Proc* 66:1101-1109, 1991.
145. Pandya UH, Pellikka PA, Enriquez-Sarano M, et al: Metastatic carcinoid tumor to the heart: echocardiographic-pathologic study of 11 patients. *J Am Coll Cardiol* 40:1328-1332, 2002.
146. Lee TM, Chen MF, Liau CS, et al: Role of transesophageal echocardiography in the management of metastatic tumors invading the left atrium. *Cardiology* 88:214-217, 1997.
147. Kullo IJ, Oh JK, Keeney GL, et al: Intracardiac leiomyomatosis: echocardiographic features. *Chest* 115:587-591, 1999.
148. Swenson JD, Hullander RM, Nolan JF, et al: Renal cell carcinoma in the inferior vena cava demonstrated by transesophageal echocardiography. *J Cardiothorac Vasc Anesth* 7:335-336, 1993.
149. Singh I, Jacobs LE, Kotler MN, et al: The utility of transesophageal echocardiography in the management of renal cell carcinoma with intracardiac extension. *J Am Soc Echocardiogr* 8:245-250, 1995.
150. Hasnain JU, Watson RJ: Transesophageal echocardiography during resection of renal cell carcinoma involving the inferior vena cava. *South Med J* 87:273-275, 1994.
151. Kim RH, Mautner L, Henning J, et al: An unusual case of thyroid carcinoma with direct extension to great veins, right heart, and pulmonary arteries. *Can Med Assoc J* 94:238-243, 1966.
152. Podolsky LA, Jacobs LE, Ioli A, et al: TEE in the diagnosis of intravenous leiomyomatosis extending into the right atrium. *Am Heart J* 125:1462-1464, 1993.
153. Joffe, II, Lampert C, Jacobs LE, et al: Cardiac sarcoidosis masquerading as a metastatic tumor: the role of transthoracic and transesophageal echocardiography. *J Am Soc Echocardiogr* 8:933-937, 1995.
154. Herbst A, Padilla MT, Prasad AR, et al: Cardiac Wegener's granulomatosis masquerading as left atrial myxoma. *Ann Thorac Surg* 75:1321-1323, 2003.
155. Eroglu E, Di Salvo G, Herbots L, et al: Restrictive left ventricular filling in hypereosinophilic syndrome as a result of partial cavity obliteration by an apical mass: a strain/strain rate study. *J Am Soc Echocardiogr* 16:1088-1090, 2003.
156. Ker J, Van Beljon J: Diaphragmatic hernia mimicking an atrial mass: a two-dimensional echocardiographic pitfall and a cause of postprandial syncope. *Cardiovasc J S Afr* 15:182-183, 2004.
157. Harrity PJ, Tazelaar HD, Edwards WD, et al: Intracardiac varices of the right atrium: a case report and review of the literature. *Int J Cardiol* 48:177-181, 1995.
158. Choi BJ, Chang HJ, Choi SY, et al: A coronary artery fistula with saccular aneurysm mimicking a right atrial cystic mass. *Jpn Heart J* 45:697-702, 2004.
159. Anfinsen OG, Aaberge L, Geiran O, et al: Coronary artery aneurysms mimicking cardiac tumor. *Eur J Echocardiogr* 5:308-312, 2004.
160. Malaterre HR, Cohen F, Kallee K, et al: Giant interatrial septal aneurysm mimicking a right atrial tumor. *Int J Card Imaging* 14:163-166, 1998.
161. Pappas KD, Arnaoutoglou E, Papadopoulos G: Giant atrial septal aneurysm simulating a right atrial tumour. *Heart* 90:493, 2004.
162. Cheng HW, Hung KC, Lin FC, et al: Spontaneous intramyocardial hematoma mimicking a cardiac tumor of the right ventricle. *J Am Soc Echocardiogr* 17:394-396, 2004.
163. Timperley J, Mitchell AR, Becher H: Primary cardiac lymphoma. *Eur J Echocardiogr* 4:327-330, 2003.
164. Padder FA, Conrad AR, Manzar KJ, et al: Echocardiographic diagnosis of pericardial cyst. *Am J Med Sci* 313:191-192, 1997.
165. Meng Q, Lai H, Lima J, et al: Echocardiographic and pathologic characteristics of primary cardiac tumors: a study of 149 cases. *Int J Cardiol* 84:69-75, 2002.
166. Bruce CJ, Packer DL, Seward JB: Intracardiac Doppler hemodynamics and flow: new vector, phased-array ultrasound-tipped catheter. *Am J Cardiol* 83:1509-1512, A9, 1999.
167. Bruce CJ, Nishimura RA, Rihal CS, et al: Intracardiac echocardiography in the interventional catheterization laboratory: preliminary experience with a novel, phased-array transducer. *Am J Cardiol* 89:635-640, 2002.
168. Segar DS, Bourdillon PD, Elsner G, et al: Intracardiac echocardiography-guided biopsy of intracardiac masses. *J Am Soc Echocardiogr* 8:927-929, 1995.
169. Malouf JF, Thompson RC, Maples WJ, et al: Diagnosis of right atrial metastatic melanoma by transesophageal echocardiographic-guided transvenous biopsy. *Mayo Clin Proc* 71:1167-1170, 1996.
170. Lynch M, Clements SD, Shanewise JS, et al: Right-sided cardiac tumors detected by transesophageal echocardiography and its usefulness in differentiating the benign from the malignant ones. *Am J Cardiol* 79:781-784, 1997.
171. Burling F, Devlin G, Heald S: Primary cardiac lymphoma diagnosed with transesophageal echocardiography-guided endomyocardial biopsy. *Circulation* 101:E179-E181, 2000.
172. Jurkovich D, de Marchena E, Bilsker M, et al: Primary cardiac lymphoma diagnosed by percutaneous intracardiac biopsy with combined fluoroscopic and transesophageal echocardiographic imaging. *Catheter Cardiovasc Interv* 50:226-233, 2000.
173. Dujardin KS, Click RL, Oh JK: The role of intraoperative transesophageal echocardiography in patients undergoing cardiac mass removal. *J Am Soc Echocardiogr* 13:1080-1083, 2000.
174. Ofori CS, Sharma BN, Moore LC, et al: Disappearing cardiac masses: the importance of intraoperative transesophageal echocardiography. *J Heart Valve Dis* 3:688-689, 1994.
175. Borges AC, Witt C, Bartel T, et al: Preoperative two- and three-dimensional transesophageal echocardiographic assessment of heart tumors. *Ann Thorac Surg* 61:1163-1167, 1996.
176. Espinola-Zavaleta N, Morales GH, Vargas-Barron J, et al: Three-dimensional transesophageal echocardiography in tumors of the heart. *J Am Soc Echocardiogr* 15:972-979, 2002.
177. Lokhandwala J, Liu Z, Jundi M, et al: Three-dimensional echocardiography of intracardiac masses. *Echocardiography* 21:159-163, 2004.
178. Mehmood F, Nanda NC, Vengala S, et al: Live three-dimensional transthoracic echocardiographic assessment of left atrial tumors. *Echocardiography* 22:137-143, 2005.

179. Handke M, Schochlin A, Schafer DM, et al: Myxoma of the mitral valve: diagnosis by 2-dimensional and 3-dimensional echocardiography. *J Am Soc Echocardiogr* 12:773-776, 1999.
180. Veiga Mde F, Lopes MG, Pinto FJ: Dynamic three-dimensional reconstruction of the heart by transesophageal echocardiography. *Arq Bras Cardiol* 72:559-568, 1999.
181. Ahmed S, Nanda NC, Miller AP, et al: Volume quantification of intracardiac mass lesions by transesophageal three-dimensional echocardiography. *Ultrasound Med Biol* 28:1389-1393, 2002.
182. Ganame J, D'Hooge J, Mertens L: Different deformation patterns in intracardiac tumors. *Eur J Echocardiogr* 6:461-464, 2005.
183. Pauliks LB, Miller S, Banerjee A: Intracardiac fibroma in nevoid-basal cell carcinoma (gorlin) syndrome: tissue characterization by strain rate imaging. *Echocardiography* 23:79-80, 2006.
184. Bouton S, Yang A, McCrindle BW, et al: Differentiation of tumor from viable myocardium using cardiac tagging with MR imaging. *J Comput Assist Tomogr* 15:676-678, 1991.
185. Green SE, Joynt LF, Fitzgerald PJ, et al: In vivo ultrasonic tissue characterization of human intracardiac masses. *Am J Cardiol* 51:231-236, 1983.
186. Xiao G, Brady M, Noble JA, et al: Segmentation of ultrasound B-mode images with intensity inhomogeneity correction. *IEEE Trans Med Imaging* 21:48-57, 2002.
187. Hao X, Bruce CJ, Pislaru C, et al: Characterization of reperfused infarcted myocardium from high-frequency intracardiac ultrasound imaging using homodyned K distribution. *IEEE Trans Ultrason Ferroelectr Freq Control* 49:1530-1542, 2002.
188. Lepper W, Shivalkar B, Rinkevich D, et al: Assessment of the vascularity of a left ventricular mass using myocardial contrast echocardiography. *J Am Soc Echocardiogr* 15:1419-1422, 2002.
189. Campani R, Calliada F, Bottinelli O, et al: Contrast enhancing agents in ultrasonography: clinical applications. *Eur J Radiol* 27:S161-S170, 1998.
190. Kirkpatrick JN, Wong T, Bednarz JE, et al: Differential diagnosis of cardiac masses using contrast echocardiographic perfusion imaging. *J Am Coll Cardiol* 43:1412-1419, 2004.
191. Tousek P, Orban M, Schomig A, et al: Images in cardiovascular medicine. Real-time perfusion echocardiography of an intracardiac mass. *Circulation* 107:2390, 2003.
192. Weller GE, Wong MK, Modzelewski RA, et al: Ultrasonic imaging of tumor angiogenesis using contrast microbubbles targeted via the tumor-binding peptide arginine-arginine-leucine. *Cancer Res* 65:533-539, 2005.

# INDEX

Page numbers followed by *f* indicate figures; *t*, tables; *b*, boxes.


## A

Abscess, paravalvular, in infective endocarditis, 410t, 412-413, 412f
Acromegalic heart disease, 742-744, 743t, 744f
Acute chest pain in emergency department, 236-246
  coronary angiography in, urgent, assessment of need for, 242
  diagnostic challenge of, 236
  echocardiography in
    in chest pain cause evaluation, 243, 243f, 244t
    in chest pain units, clinical algorithms and, 240-241, 240b
    clinical applications of, 239-243
    cost effectiveness of, 241-242
    future developments in, 244, 244f
    goals of, 236, 237b
    image acquisition in, 237, 238f-239f
    image interpretation in, 238-239, 240f
    limitations of, 243
    in long-term clinical outcome analysis, 242-243, 242f
    myocardial contrast, 239, 241f
      clinical use of, 239-240, 241f
    personnel availability limiting, 243
    in risk stratification, 242-243, 242f
    stress, 237-238
    technical aspects of, 237-239
  triage of patients with, 239, 239t
Acute coronary syndrome (ACS)
  diagnostic challenge of, 236
  echocardiographic evaluation for, limitations of, 243
Acute ischemia, physiology of, echocardiography and, 236-237
Acute ischemia/risk area detection in emergency setting, 52-53
Acute myocardial infarction
  complications of, detecting, 251-260, 251b, 251t
    acute mitral regurgitation as, 252-253, 253f
    infarct expansion as, 257-259, 258f
    left ventricular thrombus as, 259-260, 260f-261f
    pericardial effusion as, 252
    pericarditis as, 252
    pseudoaneurysm as, 256-257, 257f-258f
    true aneurysm formation as, 257-259, 258f-259f
    ventricular free wall rupture as, 255-256, 256f
    ventricular septal rupture as, 253-255, 254f-256f
  diagnosis of, echocardiography in, 248, 248t
  hemodynamic classification of, using Doppler echocardiography, 251-252
  localization of, 248-250, 249f
  right ventricular, 250-251, 250b
  risk stratification after, 260-263
    coronary flow reserve in, 262-263
    left atrial volume in, 262
    left ventricular diastolic function in, 261-262, 261t
    left ventricular remodeling in, 262
    left ventricular systolic function in, 260-261
    mitral regurgitation in, 263, 263f
    regional wall motion score in, 261
    stress echocardiography in, 262
Adenosine stress echocardiography, in coronary artery disease diagnosis, 301
Afterload
  definition of, 160-161
  right ventricular, pulmonary artery pressure and, 629-630
Aging, 774-790. *See also* Elderly.
  aortic root diameter changes in, 775, 775f
  aortic valve sclerosis in, 778-779
Aging *(Continued)*
  cardiac amyloidosis in, 786
  cardiac chamber dimensions in, 775, 776t
  cardiac function changes in, 777-778, 778t, 779f
  cardiac response to exercise stress in, 778
  cardiac response to pressor stress in, 778
  cardiac structural changes in, normal, 774-777
  cardiogenic thromboembolism in, 786, 786f
  clinical outcome data in, 778-786
  coronary artery disease in, stress testing and, 784-786, 785f, 785t-786t
  heart failure in, 782-784, 783b, 783f-784f
  left atrial size changes in, 775, 775f, 776t
    outcomes and, 782, 782t, 783f
  left ventricular changes in
    in chamber dimensions, 774
    in diastolic function, 778, 778t, 779f
    in dimensions, 775, 776t
    hypertrophy as, 781-782
    in mass, 774-775
    in systolic function, 777
    in wall thickness, 774, 775f
  mitral annular calcification in, 779-781, 780f
  valvular heart disease in, 778-781, 780f-782f, 782t
Alcohol septal ablation, for hypertrophic cardiomyopathy, 109-110, 110f
Alferi edge-to-edge mitral repair, 106, 107f-108f
Alveolar hypoventilation, pulmonary hypertension from, 637
Amyloidosis
  cardiac, in aging, 786
  diastolic function assessment in, 211, 212f
  restrictive cardiomyopathy in, 548-551, 550f
Aneurysm(s)
  atrial septal, echocardiography in, 800-801
  sinus of Valsalva, 854-855, 855f
  thoracic aortic, familial, 762
  true, formation of, complicating acute myocardial infarction, 257-259, 258f-259f
Angiography
  coronary, with intravascular ultrasound in cardiac allograft vasculopathy diagnosis, 592-593, 593f
  intravascular ultrasound versus, 133-134
Ankylosing spondylitis, 722-723, 723f-724f, 727t-728t
Annuloplasty, coronary sinus, for mitral regurgitation, 106-107
Annulus paradoxus, 213
Annulus reversus, 213
Anorexigen use in obesity, 751-752
Anthracycline, restrictive cardiomyopathy induced by, 555-556
Antiphospholipid syndrome, primary, 718-719, 719f
Aorta
  acute syndromes involving
    diagnosis of, imaging approaches to, 698-702
    spectrum of, 696-698, 696b
    transesophageal echocardiography in, 702-705, 702f
  ascending, perioperative and periinterventional imaging of, intracardiac echocardiography in, 125, 126f
  coarctation of, 855-857, 856f, 857b
  congenital disorders of, determination of, 840
  descending, measurements of, 767, 768f
  dilation of, in connective tissue disorders, 763-764, 763f-765f
  dissection of, 692-711. *See also* Aortic dissection.
  elastic properties of, in diabetic heart disease, 735
  intramural hematoma of, 697
Aorta *(Continued)*
    diagnosis of, transesophageal echocardiography in, 703
    transesophageal echocardiography in, 15
  morphology of, 834-835, 835f
  proximal, atherosclerotic plaque in, systemic embolic events and, 802-804, 803f, 803t
  pseudoaneurysms of, percutaneous closure of, 111
  rupture of, traumatic, transesophageal echocardiography in, 15
  thoracic. *See* Thoracic aorta.
  trauma to, 697-698
    blunt, transesophageal echocardiography in, 15
  ulcer of, penetrating, 697
    diagnosis of, transesophageal echocardiography in, 703
    transesophageal echocardiography in, 15
Aortic arch
  measurements of, 767, 768f
  morphology of, 834-835, 835f
Aortic arch views, in transesophageal echocardiography, 10-11, 10f
Aortic dissection, 692-711
  anatomic classification of, 696-697, 696t
  anatomy and, 693
  atherosclerosis and, 694
  bicuspid aortic valve and, 696
  cocaine use and, 695
  complications of, 704-705, 704f
  in connective tissue disorders, 765
  diagnosis of
    choice of imaging modality in, 701-702, 702t
    computed tomography in, 699, 701f
    magnetic resonance imaging in, 701, 701f
    transesophageal echocardiography in, 698-699, 700f, 703, 703f
    transthoracic echocardiography in, 698, 698f-700f
  endovascular repair considerations for, 707
  familial, 696
  follow-up of patients after, 707
  genetic diseases and, 695-696
  histology and, 693
  Marfan syndrome and, 695-696, 695f
  mechanical stresses of, 693-694
  methamphetamine use and, 695
  pathophysiology of, 693-696
  in pregnancy, 683
  pregnancy and, 695
  progression of, 707
  pseudoaneurysm formation in, 707
  recurrent, 707
  risk factors for, 694-696, 694b, 695f
  sequelae of, 697
  shear stresses of, 693-694, 693f
  surgical considerations for, 705-707, 706b
    intraoperative echocardiographic monitoring in, 706
  thoracic, familial, 762
  3D echocardiography in, 87
  time course of, 697
  transesophageal echocardiography in, 15, 702-705, 702f
    in diagnosis, 698-699, 700f, 703, 703f
    Doppler findings in, 703-704
    future directions for, 708
    research applications of, 708, 708f
    safety of, 703
  trauma and, 694-695, 694b
  Turner syndrome and, 696

Aortic regurgitation (AR), 367-388
  aortic root abnormalities in, 368-369, 369f
  aortic root and ascending aorta evaluation in, 377-378, 377f
  chronic, natural history and serial testing in, 378-379, 378t
  complicating aortic dissection, 706-707
  etiology of, 367-369, 368b
  functional classification of, 381, 381f
  leaflet abnormalities in, 367-368, 368f-369f
  left ventricle size and systolic function in, 375-376, 376f
  medical treatment of, 379, 379f
  in pregnant patients, 681
  in preimplant assessment for ventricular assist device, 601
  quantitation of severity of, 369-374
    alternative approaches to, 373-374, 374f
    aortic holodiastolic flow reversal in, 372-373, 372f-373f
    color Doppler echocardiography in, 369-372, 370f-371f
    continuous wave Doppler ultrasound in, 373, 373f
    integrating Doppler indexes in, 373, 374f, 374t
    magnetic resonance imaging in, 374, 375f
    3D transtracheal echocardiography in, 373-374, 375f
    volume flow calculations in, 372, 372f
  surgery for
    implications of, 382, 382f
    indications for, 379-380, 380f
    management and timing of, 379-380
    results and follow-up of, 383
    role of echocardiography in, 381-382
    selecting and guiding, 380-382
  3D echocardiography of, 81-82
  transesophageal echocardiography in, 13
Aortic root
  diameter of, changes in, with aging, 775, 775f
  imaging of, 426
  measurements of, 767, 767f
Aortic stenosis (AS)
  asymptomatic, 439-440, 439t, 440f
    versus symptomatic, 438
  calcific, imaging of, 425-426, 427f
  congenital, imaging of, 426, 427f
  in diabetic heart disease, 735
  imaging of, 425-426
  indirect echocardiographic findings suggestive of, 426
  interventional risk with, assessment of, 436-437
  natural history of, 437-440, 437t, 438f
  nonsevere, patients with, timing of cardiac surgery in, 443
  in pregnant patients, 678-679, 679f-680f
  progression of, 440-441, 440t
  with reduced left ventricular function or flow, 443-444, 443f-444f
  rheumatic, imaging of, 426, 427f
  risk stratification for, 441-443, 441f-442f
  severity of
    degree of, definition of, 432-433, 433f
    quantification of, 426-434, 428f
      aortic valve resistance in, 433, 433f
      Doppler measurements in, 426-429, 428f-429f
      physiologic variability in, 434-435, 435t, 436f
      planimetry of aortic valve area in, 434
      stroke work loss in, 434
      theoretical considerations for, 435
      3D echocardiography in, 434
      valve area calculation in, 429-432, 430f-432f, 431t
      velocity ratio in, 433
  supravalvular, 853-854, 854b
  symptomatic, 438-439, 438f
    versus asymptomatic, 438
  3D echocardiography of, 81
  transaortic velocities and gradients in, 426-427
  transcatheter aortic valve implantation in, echocardiography in, 445
  transesophageal echocardiography in, 13
  valvular, left ventricular response to, 435-437
Aortic valve
  basal views of, in transesophageal echocardiography, 4-7, 4t, 6f-8f
  bicuspid, 761-762, 761f-762f, 846-849. *See also* Bicuspid aortic valve.
  calcification of, assessment of, 426, 427f
  congenital disorders of, determination of, 840
  disease of. *See also* Aortic regurgitation (AR); Aortic stenosis (AS).
    in rheumatoid arthritis, 720, 721f
    3D echocardiography of, 81-82, 81f
  echocardiographic guided interventions for, 104-105
  morphology of, 834-835
  opening of, with ventricular assist devices, 605, 605f
  prosthetic
    high transprosthetic gradients in, interpretation of, 479t, 486-488, 487f
    implantation of, transcatheter. *See* Transcatheter aortic valve implantation (TAVI).
    regurgitation
      evaluation of, integrative, multiparametric approach for, 481f-482f, 483
      imaging considerations in, 480, 481f-482f
      recognition and quantitation of, 480-483
      severity of, parameters of, 481f-482f, 482-483, 483t
    stentless, Doppler evaluation of, 485
    3D echocardiography of, 82, 82f
  repair or replacement of, for heart failure, 508
  sclerosis of, in aging, 778-779, 781, 781f-782f, 782t
  transcatheter implantation of, echocardiography in, 445
  transesophageal echocardiography of, 13
Aortic views, in transesophageal echocardiography, 4t, 10-11, 10f
Aortitis, in ankylosing spondylitis, 722-723, 724f
Aortopulmonary shunts, palliative, issues resulting from, 880-881, 880t, 881f
AR. *See* Aortic regurgitation (AR).
Arrhythmias, in pregnancy, 685
Arterial switch surgery, issues resulting from, 887t, 888-889
Artery(ies). *See also specific artery, e.g.* Pulmonary artery (PA).
  great. *See* Great arteries.
Arthritis, rheumatoid, 719-722, 721f-722f. *See also* Rheumatoid arthritis.
Artificial hart, 598t, 599, 600f
AS. *See* Aortic stenosis (AS).
ASD. *See* Atrial septal defect (ASD).
Asymmetric apical hypertrophic cardiomyopathy, 527, 528f-529f
Atherosclerosis
  aortic dissection risk and, 694
  carotid artery, contrast-enhanced ultrasound in detection of, 60
  in systemic lupus erythematosus, 715-717, 717f
Atherosclerotic plaque
  intravascular ultrasound assessment of, 138, 139f
  in proximal aorta, systemic embolic events and, 802-804, 803f, 803t
Athlete's heart, hypertrophic cardiomyopathy differentiated from, 520-521, 521f, 521t
Atrial fibrillation
  atrial size and, 815-816
  atrial thrombi detection in, 816-820, 816f-820f, 816t
  cardioversion of
    electrical injury to atria from, 822
    guidance of, 817-820, 817f-818f, 818b
    thromboembolism mechanism after, 820-821
  catheter-based therapy of, 3D echocardiography guiding, 84-85
  mitral annular calcification and, in aging, 780
  prevalence of, 814-815
  symptoms and clinical impact of, 815
  therapeutic interventions in, guidance of, echocardiography and, 822-823, 823f
  thromboembolism predictors and, 817
  transesophageal echocardiography in, 15-16
Atrial flutter, 822
Atrial septal defect (ASD)
  closure of
    intracardiac echocardiography guiding, 120-122, 121b, 121f
    3D echocardiography guiding, 84
  congenital, 857-861, 858f
    echocardiographic evaluation of, 858-860, 858t, 859f-860f
    management of, 860-861, 861f
  corrective procedures for, issues resulting from, 882-883, 882t, 883f
  echocardiographic guided interventions for, 99-101, 103f
  transesophageal echocardiography in, 15, 798f, 799-802, 800f
  transthoracic echocardiography in, 799-802, 800f
Atrial septum
  aneurysms of, echocardiography in, 800-801
  defect of. *See* Atrial septal defect (ASD).
  imaging of, in transesophageal echocardiography, 4t, 5f-6f, 8
Atrial situs, congenital disorders of, determination of, 836-838
Atrial switch surgery, issues resulting from, 887-888, 887t, 888f-889f
Atrial systole, 197
Atrial volume, 3D echocardiography of, 76-77
Atrioventricular septal defects (AVSDs), corrective procedures for, issues resulting from, 887t, 892-893
Atrioventricular valves
  congenital disorders of, determination of, 838-840, 839f
  morphology of, 834, 834f
Atrium(ia)
  congenital defects of, corrected, issues with, 877, 877t
  electrical injury to, from cardioversion, 822
  left. *See* Left atrial *entries; Left atrium.*
  mechanical function of, 814, 814f
    return of, after cardioversion, assessment of, 821
  morphology of, 833, 833f
  right. *See* Right atrium.
  size of, atrial fibrillation and, 815-816
Automated border detection (ABD)
  active-appearance models of, 228-230, 230f
  classification and, 230, 231f
  in digital images. *See also* Digital images.
  in echocardiography, 222-223
    acquisition for, 222-223
    contour definitions and consistency for, 223
    detection technique choice for, 223
    image quality and, 222-223
    practical considerations for, 222-223, 223b
    problems and pitfalls of, 222
  future promise of, 230-231
  geometric modeling in, 225-226
  intelligent ultrasound systems in, 231
  methods of
    feature-driven, 223-224, 224f
    object-based, 225-226
    overview of, 223-230, 224t
    population-based, 228-230, 230f
    rules for, 222
    structure-based, 224-225, 225f
  pattern matching in, 226-227, 226f-227f
  3D active surface detection in, 227-228, 228f-229f
  tissue tracking in, 224-225, 225f


## B


Bacteremia, in infective endocarditis, evaluation of, 415-417
Ball and cage valves, 460f, 462, 465t
Balloon aortic valvuloplasty, echocardiographic guidance of, 104-105
Balloon mitral valvotomy (BMV), 389-407
  complications of, 396, 396t
  contraindications to, 400, 400b
  echocardiography in
    after procedure, early, 392-396, 394f-395f
    during follow-up, 396

Balloon mitral valvotomy (BMV) *(Continued)*
guiding procedure, 105, 106f
before procedure, 391-392, 392f, 393t-394t
during procedure, 392, 393f-394f
failure of, 396
imaging during, intracardiac echocardiography in, 127
results of, 396-400
in elderly, 399, 400f
immediate, 396-397, 397f, 397t
late, 397-398, 397f-398f, 398t
in pregnant women, 400
in restenosis after previous commissurotomy, 398-399, 399f
in young patients, 399
timing of, 401-402, 402t
Balloon tricuspid valvotomy, echocardiographic guidance of, 109
Beriberi heart disease, 752, 752t
Bicuspid aortic valve, 761-762, 761f-762f, 846-849
aortic dissection risk and, 696
conditions associated with, 847, 847b
corrective procedures for, issues resulting from, 882t, 884, 885f
echocardiographic evaluation of, 847-848, 848f
management of, 848-849
Bileaflet valves, 460f, 461t-462t, 462, 463f-465f, 465t
Bioprostheses, 460f, 461t-462t, 466, 466f, 466t
Biopsy, endomyocardial, after cardiac transplantation, 590-591, 590f-591f
Biventricular repairs, issues resulting from, 887t, 893, 893f
Blalock-Taussig shunt, palliative, issues resulting from, 880t, 881, 881f
Blood flow, coronary, 318-328
in acute coronary syndrome diagnosis, 325
assessment of, alternative approaches to, 325-326, 326t
clinical applications of, 321-325
coronary artery anatomy and, 318, 319f
coronary flow velocity reserve measurement of, 321-322, 322f
in coronary stenosis diagnosis, 322-323
Doppler evaluation of, 318-319
in detection of flow, 319, 320f-321f
technical aspects of, 318
no-reflow phenomenon in, 325, 325f
in noninvasive diagnosis of coronary stenosis, 322-324, 324f
profile of, assessment of, 319-321, 322f
retrograde, in total occlusion detection, 323, 324f
to right ventricle, 615, 616f
BMV. *See* Balloon mitral valvotomy (BMV).

## C

CAD. *See* Coronary artery disease (CAD).
Calcific aortic stenosis, imaging of, 425-426, 427f
Calcification
aortic valve, assessment of, 426, 427f
cardiac, in primary hyperparathyroidism, 744
mitral annular, in aging, 779-781, 780f-782f, 782t
valvular, in aging, 776-777, 777f, 778t
Cardiac amyloidosis, in aging, 786
Cardiac assist devices, 597-612
artificial hearts as, 598t, 599, 600f
ventricular assist devices as. *See* Ventricular assist device (VAD).
Cardiac chamber dimensions in aging, 775, 776t
Cardiac embolism, 791
Cardiac output (CO)
increased
in pregnancy, 664-665, 665f-666f, 665t
pulmonary hypertension related to, 638-639
in intraoperative ventricular function monitoring, 26-28
measurement of, in pregnancy, Doppler, technical aspects of, 667t, 668-669
in monitoring separation from cardiopulmonary bypass, 32-33, 33t
Cardiac resynchronization therapy, in heart failure, 508-511, 511f
Cardiac synchrony, 190-192
disorders of. *See* Dyssynchrony.
Cardiac tamponade, transesophageal echocardiography in, 16
Cardiac transplantation, 585-596
acute rejection in, structure and function of cardiac allograft during, 589-591
changes in left ventricular mass or wall thickness in, 590
changes in systolic and diastolic function in, 589-590
endomyocardial biopsy in, 590-591, 590f-591f
cardiac allograft in
in acute rejection, 589-591
physiology of, 588
structure and function of, 587-589
vasculopathy in, posttransplant, diagnosis of, 592-594, 593f, 593t
complications of, early postoperative, 591
donor heart evaluation before, 586
evaluation before, 585-586, 586b, 586f
exercise echocardiography applications in, 281-282
for heart failure, 512-513
monitoring after, 591-594, 591b, 592f
pericardial effusion after, 591
pregnancy after, 683
right ventricular structure and function after, 589
risk assessment before, 585-586, 586b, 586f
technique of, 587, 587f
tricuspid regurgitation after, 589, 589f
ventricular function monitoring during, 37, 38f
ventricular systolic and diastolic function after, 588-589, 588f
Cardiac tumors, 902-928
background on, 902-904
benign
cardiac myxomas as, 904-908. *See also* Myxomas, cardiac.
features of, 907t
fibroma as, 907t, 915, 915f
hemangioma as, 907t, 912-914, 913f
lipoma as, 907t, 912, 912f-913f
papillary fibroelastoma as, 908-912. *See also* Papillary fibroelastoma.
paraganglioma as, 907t, 915, 916f
rhabdomyoma as, 907t, 914-915, 914f
classification of, 903-904, 904t, 905f
diagnostic approach to, 903t, 904, 906f, 906t-907t
differential diagnosis of, 920-921, 920b, 921f-922f
direct extension of, 918
hematogenous spread of, 918, 919f
intraluminal venous extension of, 918-920, 919f
lymphatic spread of, 918
malignant
metastatic (secondary), 918-920, 919f
primary, 915-918
lymphoma as, 917
mesotheliomas as, 917-918, 918f
sarcoma as, 915-917, 916f-917f
newer echocardiographic techniques for, 921-924, 923f
transesophageal echocardiography in, 15, 795-797, 796f-797f
transthoracic echocardiography in, 795-797, 796f
Cardioembolic event, transesophageal echocardiography in, 14-15
Cardioembolic stroke, 791
Cardiogenic thromboembolism, in aging, 786, 786f
Cardiology, handheld echocardiography in, 152-153, 152f
Cardiomyopathy
dilated
diastolic function assessment in, 210-211
exercise echocardiography applications in, 281
hypertrophic, 517-541. *See also* Hypertrophic cardiomyopathy (HCM).
LV function quantitation in, 156, 158f
peripartum, 682-683
in pregnancy, 682-683, 682f
restrictive, 542-564. *See also* Restrictive cardiomyopathy.
uremic, 747, 747f
Cardiopulmonary bypass, separation from, monitoring of, 32-33
cardiac output in, 32-33, 33t
intracardiac air in, 32, 33f
CARDIOsphere, in ultrasound contrast imaging, 46
Cardioversion, of atrial fibrillation
atrial mechanical function after, assessment of return of, 821
electrical injury to atria from, 822
guidance of, 817-820, 817f, 818b
thromboembolism mechanism after, 820-821
Carotid artery atherosclerosis, contrast-enhanced ultrasound in detection of, 60
Catheter-based interventions, intracardiac, 3D echocardiography guidance of, 83-85
Catheterization
laboratory of future for, 113-114
transapical, echocardiographic guidance of, 98
transseptal, echocardiographic guidance of, 98, 99f
Central venous pressure air aspiration catheter positioning, intraoperative transesophageal echocardiography in, 29, 34
CHD. *See* Congenital heart disease (CHD).
Chest pain, acute, in emergency department, 236-246. *See also* Acute chest pain in emergency department.
Chest pain syndrome, coronary flow reserve in, 325
Chest pain units, echocardiography in, 240-241, 240b
Children, balloon mitral valvotomy in, 399-400
Chloroquine, restrictive cardiomyopathy induced by, 555-556
Chronic obstructive pulmonary disease (COPD), pulmonary hypertension in, 637-638
Cineangiography, in structural heart disease interventions, 97
Circumferential stress, calculation of, 159
CO. *See* Cardiac output (CO).
Coarctation of aorta, 855-857, 856f, 857b
corrective procedures for, issues resulting from, 882t, 884-885, 886f
Cocaine use, aortic dissection risk and, 695
Color Doppler echocardiography
in congenital heart disease evaluation, 842-843, 843f
M-mode
clinical use of, 207
in diastolic function evaluation, 206-207
in filling pressures estimation, 207
flow propagation velocity and hemodynamics in, 206-207
image acquisition in, 206, 206f
prognosis and, 207
in restrictive cardiomyopathy, 547, 548f
in mitral regurgitation quantification, 336-341, 337f, 338t
in myocardial velocity imaging, 177-178, 178f-180f
Commissurotomy, mitral valve repair involving, 362
Computed tomography (CT)
in aortic dissection diagnosis, 699, 701f
in guidance of structural heart disease interventions, 111-113
Conduction abnormalities, in ankylosing spondylitis, 723
Conduit, in congenital heart disease repair, issues from, 878
Congenital aortic stenosis, imaging of, 426, 427f
Congenital heart disease (CHD)
"complex" malformations in, corrective procedures for, 887-897, 887t, 888f-896f
palliative procedures for, issues resulting from, 878-882, 880f-881f, 880t
postoperative, 876-901
evaluation and management of, knowledge required for, 876
general issues in, 877-878, 877t
in pregnant patient
in acyanotic patients
with no prior surgical procedures, 673-674, 673f-674f
with prior surgical procedures, 674-677
coarctation of aorta as, 675, 676f
cyanotic heart disease as, 677-678, 678f
Fontan repair of, 675-676

Congenital heart disease (CHD) *(Continued)*
tetralogy of Fallot as, 675, 675f
transposition of great arteries as, 676-677, 677f
simple lesions in, corrective procedures for, 882-887, 882t, 883f, 885f-886f
suspected, echocardiographic approach to, 830-845
basic principles of, 830-831
cardiac anatomy and, 835-840, 835t-836t, 836f-839f
cardiac morphology and, 833-835, 833f-835f, 833t
cardiac position and, 831-833, 831f-833f
color and spectral Doppler imaging and, 842-843, 842f-843f
univentricular heart in, 840-842, 841f-842f
3D echocardiography of, 82-83, 83f
transesophageal echocardiography in, 16
unoperated, 846-875
complex, 867-871
by complexity, 847b
congenitally corrected transposition of great arteries as, 869-870, 869f, 870b
of left ventricular outflow tract and aorta, 852-857
septal defects and shunt lesions as, 857-867
tetralogy of Fallot as, 867-869, 868f
valvular, 846-852
Connective tissue disorders, 758-773
alternate diagnostic approaches to, 770-771, 771f
aortic dilation in, 763-764, 763f-765f
aortic dissection in, 765
assessment limitations in, 769
assessment methods in, 767-769, 767f-768f
bicuspid aortic valve as, 761-762, 761f-762f
diastolic function in, 766
echocardiographic findings in, 763-766, 763f-765f
Ehlers-Danlos syndrome as, 759
familial thoracic aortic aneurysm and dissection as, 762
fibrillinopathies as, 760
forms of, 758-762, 759b
histopathology of, 763
homocystinuria as, 760
left ventricle in, 766
Loeys-Dietz syndrome as, 760-761, 760b
Marfan syndrome as, 758-759, 759b
mitral valve prolapse in, 765-766, 765f
natural history of, 766-769, 767t
pharmacologic strategies for, 769-770, 769t
pulmonary artery in, 766
surgical strategies for, 770, 770f-771f
systolic function in, 766
therapeutic strategies for, 769-770, 769t
Turner syndrome as, 762
Conservation of mass, in fluid dynamics, 450-451, 451f-452f
Constrictive pericarditis, 568-571
causes of, 568b
Doppler flow abnormalities in, 569-570
echocardiographic diagnosis of, 568-571
effusive, 579-580
M-mode abnormalities in, 568-569, 569f
pathophysiology of, 568
restrictive cardiomyopathy compared with, 557t, 571
restrictive cardiomyopathy differentiated from, 556-559, 557f-558f
strain imaging in, 570-571
tissue-Doppler imaging in, 570-571, 570f
2D abnormalities in, 568-569, 569f
Continuity equation method, for aortic valve area calculation, 429-430, 430f-431f, 431t
Gorlin formula compared with, 431-432, 432f
Continuous infusion imaging, 50
Continuous wave Doppler
in mitral regurgitation quantification, 343
in restrictive cardiomyopathy, 547, 547f
Contractile function, definition of, 157-159
Contractility
definition of, 159, 161
in intraoperative ventricular function monitoring, 29
Control volume, in fluid dynamics, 450-451, 451f-452f
in energy analysis, 452-453
Cor pulmonale, in scleroderma, 725
Coronary artery(ies)
anatomy of, 318, 319f
anomalies of, corrective procedures for, issues resulting from, 882t, 886-887
in aortic dissection, transesophageal echocardiography in visualization of, 704-705, 705f
blood flow in, 318-328. *See also* Blood flow, coronary.
fistulas of, 867, 867f
left circumflex, blood flow detection in, 319, 321f
left main
blood flow detection in, 319, 320f
disease of, assessment of, intravascular ultrasound in, 135, 135f
stenosis of, diagnosis of, noninvasive, 322-324, 324f
Coronary artery disease (CAD)
in aging, stress testing and, 784-786, 785f, 785t-786t
diagnosis of
nonexercise stress echocardiography in, accuracy of, 301-303, 302f, 302t
pharmacologic stress echocardiography versus perfusion scintigraphy in, 312, 312t
diagnostic challenge of, 236
exercise echocardiography in, applications of
in initial diagnosis, 279
in known coronary artery disease, 279-280
prognostic, 280, 280f
in women, 280-281, 281t
LV function quantitation in, 156, 157f
in mixed connective tissue disease, 723-725, 727t
in polymyositis and dermatomyositis, 726, 727t
preinterventional assessment of, in aortic stenosis, 444-445
in primary antiphospholipid syndrome, 719, 727t
in rheumatoid arthritis, 719-720, 727t
in scleroderma, 724-725, 727t
stable, nonexercise stress echocardiography in prognostic evaluation in, 304-305, 305t
transesophageal echocardiography in, 16
ultrasonic contrast detection of, 53-58, 55f, 55t
during dobutamine or exercise stress echocardiography, 54-56, 56f-57f, 57t
vasodilator stress perfusion imaging in, 53-54, 55f, 55t
Coronary blood flow, 318-328. *See also* Blood flow, coronary.
Coronary care unit, echocardiography in, 247-267
in acute myocardial infarction, 248-251
in complication detection, 251-260, 251b, 251t
diagnostic role of, 248, 248t
in localization of infarction, 248-250, 249f
right ventricular, 250-251, 250b
applicable modes of, 247-248
Coronary flow reserve, in risk stratification after acute myocardial infarction, 262-263
Coronary sinus, in transesophageal echocardiography, transgastric view of, 4t, 10, 10f
Coronary sinus annuloplasty, for mitral regurgitation, 106-107
Coronary sinus cannulation positioning, intraoperative transesophageal echocardiography in, 36, 37f
Critically ill ICU patient, transesophageal echocardiography in, 16
Cryptogenic cerebral ischemia, transesophageal echocardiography versus transthoracic echocardiography in, 792, 792t
Cryptogenic stroke, 791
patent foramen ovale and, 800-801, 800f, 801t
Cushing syndrome, heart disease in, 745, 746f
Cysts, pericardial, 581

## D

Definity, in ultrasound contrast imaging, 46
Dehiscence
annuloplasty, complicating mitral valve repair, 361, 361f
Dehiscence *(Continued)*
suture, complicating mitral valve repair, 361
valvular, in infective endocarditis, 410t, 413, 414f
Dermatomyositis, 725-726, 727t-728t
Descending thoracic aorta, view of, in transesophageal echocardiography, 5f, 10
Diabetic heart disease, 733-738
aging and, 736
aortic elastic properties in, 735
diastolic dysfunction in, 735-736, 735t, 736f-737f
echocardiography in, clinical utility of, 736-738, 738f
gender and, 736
hypertension and, 736, 738f
left ventricular systolic dysfunction in, 733-735, 734f
obesity and, 736
renal insufficiency and, 736
right ventricular dysfunction in, 735
valvular function in, 735
Diastole
in left ventricular physiology, 188-189, 189f
physiology of, 197, 198f
Diastolic dysfunction
in chronic kidney disease, 747
definition of, 198-200, 199f, 199t
in diabetic heart disease, 735-736, 735t, 736f-737f
in hypothyroidism, 740
Diastolic function, 197-217
in acromegaly, 743
basic principles of, 197-200
in connective tissue disorders, 766
determinants of, 197-198
echocardiographic evaluation of, 200-210, 200t, 201f
clinical utility of, 210-213
in hypertension and hypertensive heart disease, 211-212
in ischemic cardiac disease, 212
in myocardial diseases, 210-211, 212f
in pericardial disease, 212
in restrictive versus constrictive physiology, 213, 213f
Doppler techniques in, 201-207
color M-mode Doppler as, 206-207, 206f
tissue-Doppler imaging as, 203-206
prognosis and, 205-206
left atrial volume index in, 207, 208t
new ASE/EAE guidelines on, 210, 210f-211f
strain imaging in, 207-209, 208f
torsion echocardiography in, 209
in hyperthyroidism, 741t, 742
in obesity, 750
stages of, 201f
Digital images, 218-233
automated analysis of, 218-219
future promise of, 230-231
intelligent ultrasound systems in, 231
automated border detection in. *See* Automated border detection (ABD).
brightness level manipulations of, 220, 220f
cardiac, interpretation of, 221-222
characteristics of, 219
compression of, 219
enhancement of, 218
in medical image processing, 219-220
filtering of, 220
interpretation pyramid for, 221-222, 221f, 221t
level manipulations of, 219-220
medical, processing of, 219-222
overview of, 218
processing of, 218-219
definition of, 218
pseudocoloring of, 220
storage formats for, 219
Digital Imaging and Communications in Medicine (DICOM), 219
Dilated cardiomyopathy
diastolic function assessment in, 210-211
exercise echocardiography applications in, 281-282
Dipyridamole stress echocardiography, in coronary artery disease diagnosis, 301

Displacement, myocardial, tissue Doppler imaging of, 179f-180f, 181, 190
Distal jet area method, in mitral regurgitation quantification, 336, 337f, 338t
Distal vascular beds, perfusion of, complicating aortic dissection, 707
Dobutamine stress echocardiography (DSE)
in cardiac allograft vasculopathy diagnosis, 593-594, 593t
in coronary artery disease detection, 54-56, 56f-57f, 57t
in coronary artery disease diagnosis, 301
in coronary stenosis diagnosis, 324
in myocardial viability assessment, 306-307, 307f
Donor heart, evaluation of, 586
Doppler echocardiography
color. *See* Color Doppler echocardiography.
in congenital heart disease evaluation, 842-843, 842f-843f
continuous wave
in mitral regurgitation quantification, 343
in restrictive cardiomyopathy, 547, 547f
of coronary blood flow, 318-319
in detection, 319, 320f-321f
technical aspects of, 318
in diastolic filling pattern assessment, 201-207
exercise, 274
in hemodynamic classification of myocardial infarction, 251-252
intravenous microbubbles enhancing, 59
in pericardial tamponade, 575-576, 575f-577f, 576t
in pregnancy
in cardiac output measurement, technical aspects of, 667t, 668-669
in hemodynamic evaluation, 669-670, 670f
in restrictive cardiomyopathy, 544-547, 545f-548f
in right heart evaluation, 203
spectral, in congenital heart disease evaluation, 842-843, 843f
stress, nonexercise, 310-311, 310f
tissue, 177-183. *See also* Tissue-Doppler imaging (TDI).
transesophageal, 12
in acute aortic syndromes, 703-704
dP/dt
in intraoperative ventricular function monitoring, 29-30, 30f
in right ventricular systolic function evaluation, 624
Drug delivery, microbubbles in, 56f, 60-61
Drug-eluding stents (DES), in restenosis reduction, 139, 140f
Drugs, restrictive cardiomyopathy induced by, 555-556
DSE. *See* Dobutamine stress echocardiography (DSE).
Dyssynchrony, left ventricular mechanical, mechanisms of, 191

## E

E′, relationship to active relaxation in tissue-Doppler imaging for diastolic function evaluation, 204-205
Ebstein anomaly, 851-852, 851f-852f
corrective procedures for, issues resulting from, 882t, 885-886
Echocardiography
in guidance of structural heart disease interventions, 95-117. *See also* Structural heart disease (SHD), interventions for, echocardiographic guidance of.
handheld, 146-154. *See also* Handheld echocardiography.
instruments for, types of, 146-147, 147t-148t
intracardiac, 118-129. *See also* Intracardiac echocardiography (ICE).
3D, 67-94. *See also* 3D echocardiography.
Effusion, pericardial, 571-572. *See also* Pericardial effusion.
Effusive constrictive pericarditis, 579-580
Ehlers-Danlos syndrome, 759
Ejection, in left ventricular physiology, 183t, 187
Ejection fraction
hemodynamic determinants of, 167
in intraoperative ventricular function monitoring, 28-29, 29f
in left ventricular systolic function assessment, 166-167
Elderly. *See also* Aging.
balloon mitral valvotomy in, 399-401, 400f-401f
diabetic heart disease in, 736
hypertrophic cardiomyopathy of, 530
septal hypertrophy in, hypertrophic cardiomyopathy differentiated form, 521
Electronic device, cardiac implantable
evaluation of patient with, 417, 418f
infected, imaging of, 410t, 413-414, 414f
Embolic events, systemic, 791-810. *See also* Systemic embolic events.
Embolism
cardiac, 791
cardiogenic, transesophageal echocardiography in, 14-15
Emergency department
acute chest pain in, 236-246. *See also* Acute chest pain in emergency department.
handheld echocardiography in, 151, 151b
End-diastolic area, in intraoperative ventricular function monitoring, 25-26, 26f
End-systolic area, in intraoperative ventricular function monitoring, 25-26
Endocarditis
infective, 408-424. *See also* Infective endocarditis (IE).
mitral annular calcification and, in aging, 781
3D echocardiography in, 86-87, 87f
Endocrinopathies, heart disease in, 733-746
in acromegaly, 742-744, 743t, 744f
in adrenal diseases, 745-746
in Cushing syndrome, 745, 746f
in diabetes mellitus, 733-738. *See also* Diabetic heart disease.
in hyperaldosteronism, 745-746
in hyperthyroidism, 740-742, 741t
in hypothyroidism, 739-740, 740t, 741f
in metabolic syndrome, 738-739, 750f
in primary hyperparathyroidism, 744-745, 745t
Endomyocardial biopsy, after cardiac transplantation, 590-591, 590f-591f
Endomyocardial fibrosis, restrictive cardiomyopathy in, 551-553
Esophageal intubation, for transesophageal echocardiography, 3-4
Exercise
hemodynamic changes in, pregnancy changes similar to, 669
physiology of, in pregnant women, 670
Exercise echocardiography, 268-291
appropriate use of, 278-279
in cardiac transplantation, applications of, 281-282
comparison of, with other stress modalities, 277-279, 277t, 278f
coronary artery disease applications of
for initial diagnosis, 279
in known coronary artery disease, 279-280
prognostic, 280, 280f
in women, 280-281, 281t
cost effectiveness of, 278
diagnostic accuracy of, 276-277, 276f, 277t
in dilated cardiomyopathy, applications of, 281-282
Doppler, 274
equipment for, 272
exercise stressors used in, 270-272, 271b, 272t
future directions for, 283-286, 284f-285f
in hypertrophic cardiomyopathy, applications of, 281, 282f
imaging in, 273-274
interpretation of, 275-276, 275t
methodology for, 272-276
personnel for, 274-275, 275b
physiologic principles of, 268-270, 269f-271f
procedure for, 272-273, 273b, 273f
in pulmonary hypertension, 642-643
quality assurance for, 278-279
Exercise echocardiography *(Continued)*
in risk stratification prior to noncardiac surgery, 281
room layout for, 274, 274f
safety of, 278, 279b
3D, 285-286
in valvular heart disease, applications of, 282-283, 283f
Exercise-stimulating agents, in nonexercise stress echocardiography, 293-294
technical aspects of, 299-300
Exercise stress, cardiac response to, in aging, 778
Exercise stress echocardiography
as alternative to nonexercise stress echocardiography, 311, 311f
in coronary artery disease detection, 54-56, 57t

## F

Fabry disease
hypertrophic cardiomyopathy differentiated from, 519
restrictive cardiomyopathy, 554-555, 555f
Familial aortic dissection, 696
Familial thoracic aortic aneurysm and dissection, 762
Femoral venous cannula positioning, intraoperative transesophageal echocardiography in, 37, 37f
Fibrillinopathies, 760
Fibroelastoma, papillary, 908-912. *See also* Papillary fibroelastoma.
Fibroma, cardiac, 907t, 915, 915f
Fistula(s)
coronary artery, 867, 867f
formation of, in infective endocarditis, 410t, 413, 413f
management of, 420
Fluid dynamics, of prosthetic valves, 450-469. *See also* Prosthetic valve fluid dynamics.
Fluoroscopy, in structural heart disease interventions, 97, 97t
Fontan atrial surgery, issues resulting from, 887t, 889-892, 889f-892f
Foramen ovale, patent. *See* Patent foramen ovale (PFO).
Four-chamber views, in transesophageal echocardiography, 4t, 5f-6f, 8-9, 8f
Fractional shortening, in left ventricular systolic function assessment, 167-168, 167f
Frank-Starling mechanism, 160

## G

Gaucher disease, restrictive cardiomyopathy, 553-554
Gender
diabetic heart disease and, 736
left ventricular response to aortic stenosis and, 436-437
Gene delivery, microbubbles in, 56f, 60-61
Genetic diseases, aortic dissection risk and, 695-696
Genetics, molecular, of hypertrophic cardiomyopathy, 518
Glenn shunts, palliative, issues resulting from, 880t, 881-882
Global systolic function, in intraoperative ventricular function monitoring, 26-30
Glycogen storage disorder
hypertrophic cardiomyopathy differentiated from, 519-520
restrictive cardiomyopathy, 554
Gorlin formula, in aortic valve area calculation, continuity equation method compared with, 431-432, 432f
Great arteries
color and spectral Doppler evaluation of, 843, 843f
congenital disorders of, determination of, 840
morphology of, 834-835, 835f
transposition of
congenitally corrected, 869-870, 869f, 870b
corrective procedures for, issues resulting from, 887-888, 887t

## H

Hand-carried ultrasound (HCU) devices, 146. *See also* Handheld echocardiography.
Handheld echocardiography, 146-154
  accuracy of, 147-148, 149f
  background on, 146-148
  in cardiology, 152-153, 152f
  clinical applications of, 151-153
  education and training guidelines and requirements for, 150-151
    for emergency physicians, 151
    for intensivists, 151
    for medical residents, 150-151
    for medical students, 150
    recommendations on, 151
  in emergency department, 151, 151b
  future directions for, 153
  in intensive care unit, 151
  in internal medicine, 150f, 152
  reliability of, 147-148
  ultrasound "stethoscope" in, 148-150, 149f-150f, 150b
HCM. *See* Hypertrophic cardiomyopathy (HCM).
Heart
  anatomy of, 835-840
    atrial situs in, 836-838
    atrioventricular valves in, 838-840, 839f
    concordant and discordant arrangements in, 836, 836f-837f, 836t
    great arteries in, 840
    nonsegmental abnormalities in, 836
    segmental approach to, 835-836, 835t
    semilunar valves in, 840
    venous connections in, 836-838, 837f-838f
    ventricles in, 838-840
  artificial, 598t, 599, 600f
  athlete's hypertrophic cardiomyopathy differentiated from, 520-521, 521f, 521t
  calcification of, in primary hyperparathyroidism, 744
  donor, evaluation of, 586
  function of, changes in aging, 777-778, 778t, 779f
  left-sided, 831
  morphology of, 833-835, 833f-835f, 833t
  position of, 831-833, 831f
  response of
    to exercise stress in aging, 778
    to pressor stress in aging, 778
  right, Doppler evaluation of, 203
  right-sided, 831-833, 832f-833f
  transplantation of, 585-596. *See also* Cardiac transplantation.
  tumors of, 902-928. *See also* Cardiac tumors.
  univentricular, 840-842, 841f-842f
    functional, 871, 871b
  valves of. *See also* Valve *entries*.
    calcification of, in aging, 776-777, 777f, 778t
    changes in, in aging, 775-776, 777t
Heart disease
  congenital. *See* Congenital heart disease (CHD).
  hypertensive, diastolic function assessment in, 211-212
  ischemic, diastolic function assessment in, 212
  nutritional deficiencies and, 752-753, 752t
  in pregnancy, 664-689. *See also* Pregnancy; Pregnancy, heart disease in.
  structural, 95-97. *See also* Structural heart disease (SHD).
Heart failure (HF), 496-516
  in aging, 782-784, 783b, 783f-784f
  cardiac resynchronization therapy for, 508-511, 511f
  definition of, 496, 497f
  diastolic, 198-200, 199f, 199t
  end-stage, cardiac transplantation for, 585. *See also* Cardiac transplantation.
  etiology of, 498, 498f
  heart transplantation for, 512-513
  intraaortic counterpulsation for, 508
  left
    acute, 498-499, 500f
    chronic, 499-505, 500f-503f
Heart failure (HF) *(Continued)*
    echocardiographic diagnosis of, 498-505
    systolic versus diastolic, 503-505, 505f
  left ventricular dyssynchrony in, detection techniques for, 511-512, 512f-514f
  left ventricular remodeling to, 502-503, 504f
  mechanical therapies in, echocardiography for, 507-513, 509f
  pharmacologic therapy for, 507, 508f
    echocardiography in, 507
  in pregnancy, 684
  prevalence of, 496-498
  right
    chronic, 506
    echocardiographic diagnosis of, 505-507
  right ventricular, acute, 505-506, 506f-507f
  right ventricular remodeling to, 506-507
  surgical valve repair or replacement for, 508
  ventricular assist devices for, 508, 510f. *See also* Ventricular assist devices.
Heart murmur, in pregnancy, 684-685
Heart rate, diastolic function and, 198
Hemangioma, cardiac, 907t, 912-914, 913f
Hematoma, of aorta, intramural, 697
  diagnosis of, transesophageal echocardiography in, 703
Hemochromatosis, restrictive cardiomyopathy in, 551
Homocystinuria, 760
Hyperaldosteronism, primary, heart disease in, 745-746
Hypereosinophilic syndrome, restrictive cardiomyopathy in, 551-553, 552f
Hyperparathyroidism, primary, heart disease in, 744-745, 745t
Hypertension
  in diabetic heart disease, 736, 738f
  diastolic function assessment in, 211-212
  pregnancy-induced, 670-671, 671t
  pulmonary, 629-645. *See also* Pulmonary hypertension (PH).
Hypertensive heart disease, diastolic function assessment in, 211-212
Hyperthyroidism, heart disease in, 737f, 740-742
Hypertrophic cardiomyopathy (HCM), 517-541
  alcohol septal ablation for, 109-110, 110f
  asymmetric apical, 527, 528f-529f
  athlete's heart differentiated from, 520-521, 521f, 521t
  condition mimicking, 519, 519b
  diagnosis of, 518-519, 518f
  diastolic function assessment in, 211
  diastolic function evaluation in, 530-531, 530b
  differential diagnosis of, 519-521, 519b, 520f-521f, 521t
  Doppler evaluation in, technical aspects of, 525-526, 526f
  dual-chamber pacing in, 532
  echocardiographic evaluation of, 521-523
  of elderly, 530
  epidemiology of, 517-518
  exercise echocardiography applications in, 281, 282f
  family screening for, 519, 519t
  impaired coronary circulation in, 325
  latent obstructive, 525
  medical therapy in, 532
  midventricular obstructive, 527-530, 529f
  mitral regurgitation in, 526, 526b, 527f
  molecular genetics of, 518
  obstructive, treatment strategies for, compared, 537, 537t
  outflow tract obstruction in, Doppler assessment of, 523-525, 525f
  in pregnancy, 682, 682f
  prognostication in, by echocardiography, 531-532
  septal ethanol ablation in, 532-534, 533f-534f
  septal hypertrophy in elderly differentiated from, 521
  storage diseases differentiated from, 519-520
  strain imaging in, 531, 531f
  subtypes of, 527-530
  surgical myectomy in, 534-537, 535f-536f
  3D echocardiography in, 86
Hypertrophy, septal, in elderly, hypertrophic cardiomyopathy differentiated from, 521
Hypothyroidism, heart disease in, 739-740, 740t, 741f

## I

ICE. *See* Intracardiac echocardiography (ICE).
ICU patients, critically ill, transesophageal echocardiography in, 16
IE. *See* Infective endocarditis (IE).
Image acquisition, in echocardiographic chest pain evaluation in ED, 237, 238f-239f
Image interpretation, in echocardiographic chest pain evaluation in ED, 238-239, 240f
Imagify, in ultrasound contrast imaging, 46, 47f-48f
Immune-mediated injury, systemic diseases characterized by, 712-732. *See also* Rheumatologic diseases.
Implantable electronic device, cardiac
  evaluation of patient with, 417, 418f
  infected, imaging of, 410t, 413-414, 414f
Infective endocarditis (IE), 408-424
  acute aortic regurgitation from, 384
  background of, 408
  clinical decision making in
    alternative approaches to, 421
    echocardiographic approach to, 408-424
      in diagnosis, 414-417, 415f, 415t-416t, 418f
      in follow-up, 421
      future directions for, 421
      limitations of, potential, 421
      in management, 417-421, 419f
      quantitation of, 413
      research applications of, 421
      technical details of, 409-414
  prosthetic valve, 471-472
    evaluation of, alternative approaches to, 491, 492f
    management of, Doppler echocardiography in, 490-491, 490f
  transesophageal echocardiography in, 14
Inferior vena cava, plethora of, in pericardial tamponade, 574t, 575
Intensive care unit, handheld echocardiography in, 151
Internal medicine, handheld echocardiography in, 150f, 152
Interventional procedures, transesophageal echocardiographic monitoring of, 16-17
Intraaortic balloon pump positioning, intraoperative transesophageal echocardiography in, 34-35, 35f
Intraaortic counterpulsation, for heart failure, 508
Intracardiac air, in monitoring separation from cardiopulmonary bypass, 32, 33f
Intracardiac echocardiography (ICE), 118-129
  developments in, 118
  in device closure of interatrial communications guidance, 120-122, 121b, 121f
  equipment and handling procedures for, 118-120, 119b, 119f-120f, 119t
  in guidance of structural heart disease interventions, 111, 112f-113f
  limitations of, 127-128, 128t
  in percutaneous left atrial appendage closure monitoring, 122, 122f
  in periinterventional imaging
    of ascending aorta, 125, 126f
    of descending thoracic aorta, 125-127, 126f-127f
    of mitral valve, 127
  in perioperative imaging of ascending aorta, 125, 126f
  in radiofrequency pulmonary vein ablation guidance, 122-123, 122f-123f
  standardized views using, 120t
  in transcatheter aortic valve implantation monitoring, 123-125, 123f-125f
Intracardiac masses, 3D echocardiography in, 88
Intracardiac tumors. *See* Cardiac tumors.
Intramural hematoma, of aorta, 697
  diagnosis of, transesophageal echocardiography in, 703

Intraoperative echocardiography (IOE), in mitral valve repair, 351-366. *See also* Mitral valve repair, intraoperative echocardiography in.
Intravascular device positioning, intraoperative transesophageal echocardiography in, 34-37
Intravascular ultrasound (IVUS), 130-145
  angiography versus, 133-134
  in atherosclerotic plaque assessment, 138, 139f
  in bioabsorbable stent evaluation, 140
  in bioabsorbable stent implantation guidance, evaluation of results of, 140-142
  clinical application of, 134-142
  gray-scale, 130, 131f
  image formation with, 130-132, 131f
  image interpretation with, 132, 132f
  in in-stent restenosis treatment evaluation, 140, 141f-142f
  integration of, into practice, 134
  in interventional complications assessment, 138
  in left main coronary artery disease assessment, 135, 135f
  in lesion length assessment, 135-136
  in lesion morphology assessment, 136-138, 136f-138f
  in no-reflow prediction during interventional procedures, 138
  practical recommendations for, 142
  radiofrequency, 133, 133f
  in reference lumen dimensions assessment, 135-136, 135f
  in restenosis reduction, 139-140, 140f
  safety of, 131f, 134
  standard acquisition protocol for, 134
  in stenosis severity assessment, 134-135
  technical background on, 130-134
Intubation, esophageal, for transesophageal echocardiography, 3-4
Ischemic cascade, 269, 269f
Ischemic heart disease
  acute chest pain in emergency department in, 236-246
  acute ischemia in, physiology of, 236-237
  coronary care unit for, 247-267. *See also* Coronary care unit.
  diastolic function assessment in, 212
  echocardiographic evaluation for, limitations of, 243
  in pregnancy, 683-684
Isovolumic acceleration, in right ventricular systolic function evaluation, 625
Isovolumic contraction, in left ventricular physiology, 186-187
Isovolumic relaxation
  in diastole, 197
  in left ventricular physiology, 188
IVUS. *See* Intravascular ultrasound (IVUS).

## K

Keshan heart disease, 752, 752t
Kidney. *See* Renal *entries*.
Kwashiorkor, heart disease in, 753

## L

Leaflet fibrosis, in systemic lupus erythematosus, 713-714
Leaflet perforation, in infective endocarditis, 409-410, 412f, 431t
Left anterior descending (LAD) coronary artery, blood flow detection in, 319, 321f
Left atrial appendage
  function of, 814, 815f
  percutaneous closure of
    echocardiographic guidance of, 110-111
    intracardiac echocardiographic monitoring of, 122, 122f
Left atrial appendage flow, in transesophageal echocardiography, 12
Left atrial pressure monitoring in operating room, 23-25, 25f
Left atrial strain evaluation, 209
Left atrial thrombus(i)
  detection of, in atrial fibrillation, 816-820, 816f-820f, 816t
  transesophageal echocardiography of, 14-15, 791, 793f, 795f, 797-799, 798f
Left atrial volume index, in diastolic function evaluation, 207, 208t
Left atrium
  anatomy of, 811-812, 812f
  compression, inversion, or collapse of, 573, 574t
  function of, diastolic function and, 198
  size of
    in aging, outcomes and, 782, 782t, 783f
    atrial fibrillation and, 815-816
    changes in, with aging, 775, 775f, 776t
  volume of, in risk stratification after acute myocardial infarction, 262
Left bundle branch block (LBBB), effect of, on left ventricular function, 191-192, 191f-192f
Left circumflex (LCx) coronary artery, blood flow detection in, 319, 321f
Left heart disease, pulmonary hypertension related to, 639-643
Left main coronary artery (LMCA)
  blood flow detection in, 319, 320f
  disease of, assessment of, intravascular ultrasound in, 135, 135f
Left ventricle
  cavity of, opacification of, improved, microbubbles in, 58-59
  compliance of, diastolic function and, 198, 198f
  in connective tissue disorders, 766
  diastolic function of, changes in, in aging, 778, 778t, 779f
  dimensions of, changes in, with aging, 774-775, 776t
  dyssynchrony of
    in heart failure, detection techniques for, 511-512, 512f-514f
    mechanical, mechanisms of, 191
    3D echocardiography in, 85-86, 87f
  filling of, monitoring of, in operating room, 23-26
  filling pressures for, estimation of, 205, 205f
  free wall of, rupture of, complicating acute myocardial infarction, 255-256, 256f
  function of
    effect of left bundle branch block on, 191-192, 191f-192f
    3D echocardiography of, 72-74
    with ventricular assist devices, 605
  geometry of, assessment of, 2D echocardiography in, 164-165
  hypertrophy of
    in acromegaly, 743, 743t
    in aging, 781-782
    in chronic kidney disease, 747, 747f
    in obesity, 750-751, 751f
    pressure overload, LV function quantitation in, 156
    volume overload, LV function quantitation in, 156, 158f
  mass of
    assessment of
      M-mode echocardiography in, 161-162, 161f, 165b
      2D echocardiography in, 164, 165b
    changes in
      with aging, 774-775
      in cardiac allograft during acute rejection, 590
    3D echocardiography of, 74-75, 76t
  opacification of, contrast echocardiography for, 308
  outflow tract of. *See* Left ventricular outflow tract (LVOT).
  percutaneous interventions in, echocardiographic guidance of, 109-110, 110f
  physiology of
    diastole in, 188-189, 189f
    ejection in, 183t, 187
    isovolumic contraction in, 186-187
    isovolumic relaxation in, 188
    normal, 186-189, 187f-189f
  in primary hyperparathyroidism, 745, 745t
  pseudoaneurysm of, percutaneous closure of, 110
Left ventricle *(Continued)*
  quantitative evaluation of, 156-176
    definitions and theoretical considerations on, 157-161, 159b, 159f
    potential limitations of, 173-174
    of structure
      Doppler echocardiography in, 165-166, 165f
      M-mode echocardiography in, 161-164, 161f, 162t, 163f
      magnetic resonance imaging in, 166
      2D echocardiography in, 164-165, 165b
    of systolic function, 166-173, 166b
      ejection fraction in, 166-167
      fractional shortening in, 167-168, 167f-168f
      myocardial performance index in, 168, 168f
      pressure-volume analysis in, 170-173, 172f-173f
      stress-shortening relations in, 168-170, 169f-172f
  remodeling of
    to heart failure, 502-503, 504f
    for mitral regurgitation, 107-108
    in risk stratification after acute myocardial infarction, 262
  response of, to valvular aortic stenosis, 435-437
  rotation and twist of, speckle tracking echocardiography of, 185-186, 186f-187f
  systolic dysfunction in, in diabetic heart disease, 733-735, 734f
  systolic function of
    changes in, in aging, 777
    in risk stratification after acute myocardial infarction, 260-261
  torsion of. *See* Torsion, left ventricular.
  in transesophageal echocardiography
    four-chamber views of, 4t, 5f, 8
    transgastric views of, 4t, 5f, 9, 9f-10f
  volume of
    assessment of
      M-mode echocardiography in, 162, 162t, 165b
      2D echocardiography in, 164, 165b
    3D echocardiography of, 72-74, 73t, 75f
  wall motion of, regional, in risk stratification after acute myocardial infarction, 261
  wall thickness of
    assessment of, M-mode echocardiography in, 161f, 162-164, 163f
    changes in
      with aging, 774, 775f
      in cardiac allograft during acute rejection, 590
Left ventricular assist device (LVAD), positioning of, intraoperative transesophageal echocardiography in, 35-36, 36f
Left ventricular diastolic function monitoring in operating room, 25, 25f
Left ventricular end-diastolic diameter, in ventricular assist devices, 604-605
Left ventricular hypertrophy (LVH), severity, distribution, and patterns of, 521, 522f
Left ventricular outflow tract (LVOT)
  congenital anomalies of, 852-857
  in intraoperative ventricular function monitoring, 26-27, 27f
  obstruction of, 523-526
    in hypertrophic cardiomyopathy, Doppler assessment of, 523-525, 525f
    pathophysiology of, 523, 523b
  in transesophageal echocardiography, four-chamber views of, 4t, 6f, 9
Left ventricular thrombus, complicating acute myocardial infarction, 259-260, 260f-261f
Left ventricular-type univentricular heart, 841, 841f-842f
Left ventricular vent positioning, intraoperative transesophageal echocardiography in, 37
Left ventricular volumes, in intraoperative ventricular function monitoring, 26
Lesion length, assessment of, intravascular ultrasound in, 135-136
Lesion morphology, assessment of, intravascular ultrasound in, 136-138, 136f-138f

Libman-Sacks vegetations, in systemic lupus erythematosus, 713, 713f-716f
Lipoma, 907t, 912, 912f-913f
Loeys-Dietz syndrome, 760-761, 760b
Lung transplantation
for pulmonary arterial hypertension, 638
ventricular function monitoring during, 37, 38f
LVOT. *See* Left ventricular outflow tract (LVOT).
Lymphoma, 917

## M

M-mode echocardiography
changes on, in pregnancy, 668, 668t
in left ventricular mass assessment, 161-162, 161f, 165b
in left ventricular relative wall thickness assessment, 161f, 162-164, 163f
in left ventricular volume assessment, 162, 162t, 165b
Magnetic resonance imaging (MRI)
in aortic dissection diagnosis, 701, 701f
cardiac
in guidance of structural heart disease interventions, 113
in restrictive cardiomyopathy, 547
in connective tissue disorder diagnosis, 770-771, 771f
Malnutrition, protein-calorie, heart disease and, 753
Marfan syndrome, 758-759, 759b
aortic dissection risk and, 695-696, 695f
pregnancy in patients with, 683, 683f
Meridional stress, calculation of, 159
Mesotheliomas, 917-918, 918f
Metabolic syndrome, heart disease in, 738-739, 768f
Methamphetamine use, aortic dissection risk and, 695
MI. *See* Myocardial infarction (MI).
Microbubbles
in carotid artery atherosclerosis detection, 60
characteristics of, 45-46, 46t
in contrast perfusion imaging of other organs, 59-60
diagnostic applications of, 58-60
in Doppler enhancement, 59
in drug and gene delivery, 56f, 60-61
for improved left ventricular cavity opacification, 58-59
in molecular imaging with contrast ultrasound, 60
targeted delivery of, in cardiac tumor diagnosis, 924
therapeutic applications of, 60-61
in thrombolysis, 56f, 60-61
Midventricular obstruction, hypertrophic cardiomyopathy with, 527-530, 529f
Midwall stress-shortening analysis, 169-170, 169f-172f
Mitral annulus, 330-331, 331f
calcification of, in aging, 779-781, 780f-782f, 782t
remodeling of, for mitral regurgitation, 107-108
Mitral inflow
Doppler recordings of, in diastolic filling assessment, 201-202, 202f
at peak Valsalva maneuver, 202, 203f
Mitral regurgitation (MR), 330-350
acute, complicating acute myocardial infarction, 252-253, 253f
causes of, 332t
complicating aortic dissection, 707
congenital, 850
in hypertrophic cardiomyopathy, 526, 526b, 527f
interventions for, echocardiographic guidance of, 105-108
coronary sinus annuloplasty as, 106-107
percutaneous edge-to-edge mitral repair as, 106, 107f-108f
percutaneous left ventricular and mitral annulus remodeling as, 107-108
in left heart failure, mechanism of, 501, 503f
mechanism of, 332-335, 332f-335f, 332t
mitral valve repair for, 353-358. *See also* Mitral valve repair, intraoperative echocardiography in, prepump, for mitral regurgitation.
paravalvular, percutaneous closure of, 363-364, 364f
percutaneous edge-to-edge repair of, 363, 363f
Mitral regurgitation (MR) *(Continued)*
in pregnant patients, 681, 681f
quantification of, 335-343
color Doppler methods in, 336-341, 337f, 338t
continuous wave Doppler pattern in, 343
distal jet area method of, 336, 337f, 338t
proximal isovelocity surface area method of, 338-341, 338f-339f, 338t
geometric factors influencing, 340, 340f
technical factors of, 340-341, 340f-341f
pulmonary venous inflow pattern in, 341-343, 342f
supportive evidence in, 341-343
3D echocardiography in, 343, 344f, 345t
vena contracta method of, 337-338, 337f-338f, 338t
volumetric methods of, with pulsed Doppler imaging, 341, 341f-342f
in risk stratification after acute myocardial infarction, 263, 263f
surgical intervention for, timing of, 343-346
determination of mechanism in, 345-346, 346f-347f
pathophysiology in, 343-345, 344f, 346f
3D echocardiography of, 78-81, 79f-80f
transesophageal echocardiography in, 13
Mitral stenosis (MS)
alternative approaches to, 403-404
background on, 389
balloon mitral valvotomy for, 389-407. *See also* Balloon mitral valvotomy (BMV).
complicating mitral valve repair, 362
congenital, 850
echocardiographic approach to, 389-391
in assessment of consequences, 390
associated lesions and, 390-391
in diagnosis, 389-390
future directions for, 403
mitral regurgitation and, 390
potential limitations of, 403
research applications of, 402-403, 402t-403t
in severity evaluation, 390, 390t
techniques in, 391
thromboembolic complications and, 391
in valve anatomy assessment, 390, 391f, 403, 403t
in pregnant patients, 679-681, 680f
3D echocardiography of, 77-78, 78f-79f
transesophageal echocardiography in, 13
Mitral valve
anatomy of, 330-335
echocardiographic assessment of, before balloon mitral valvotomy, 390, 391f
evaluation of, in predicting BMV results, 403, 403t
in mitral stenosis, in predicting BMV results, 392, 393t-394t
chordae tendinae of, 331-332, 332f
congenital anomalies of, 850, 851f
congenital disorders of, determination of, 838-839, 839f
disease of. *See also* Mitral regurgitation (MR); Mitral stenosis (MS).
in rheumatoid arthritis, 720, 721f
3D echocardiography of, 77-81
embryology of, 330-335
in intraoperative ventricular function monitoring, 28
leaflets of, 331, 331f
systolic anterior motion of, in left ventricular outflow tract obstruction, 523, 524f
morphology of, 834, 834f
papillary muscles of, 331-332, 332f
periinterventional imaging of, intracardiac echocardiography in, 127
prolapse of
in connective tissue disorders, 765-766, 765f
in left heart failure, 501, 503f
mitral regurgitation from, 332-333, 332f
in pregnancy, 685
prosthetic
high transprosthetic gradients in, interpretation of, 487f, 488
Mitral valve *(Continued)*
regurgitation
imaging considerations in, 481f-482f, 483-484, 484t
recognition and quantitation of, 483-484
severity of, parameters of, 484, 484t
repair of, 351-366. *See also* Mitral valve repair.
in transesophageal echocardiography
four-chamber views of, 4t, 5f, 8-9
transgastric views of, 4t, 9, 10f
transesophageal echocardiography of, 13
Mitral valve repair, 351-366
for heart failure, 508
intraoperative echocardiography in, 351-366
annuloplasty dehiscence complicating, 361, 361f
complications of, 360-362
equipment for, 352, 352f
examination for, 352-353, 353f
indications for, 351, 352b
involving commissurotomy, 362
left ventricular systolic function complicating, 361-362
mitral stenosis complicating, 362
need for, in patients undergoing cardiac surgery for other reasons, determining, 358-359
perforation jet lesions complicating, 361
postpump, 359-360
impact on clinical outcome, 360
incomplete mitral repair in, 359-360
intraoperative findings in, 359, 359t
timing of, 359
prepump, for mitral regurgitation, 353-358, 353t
apical tethering of normal leaflets in, 357-358, 358f
excessive leaflet motion in, 356-357, 357f-358f
mechanism of regurgitation in, 355-358
normal leaflet motion in, 358, 358t
organized approach to mitral valve imaging in, 355-358, 355f-356f
restricted leaflet motion in, 357
severity of regurgitation in, 353-355
suture dehiscence complicating, 361
systolic anterior motion of mitral valve complicating, 360-361, 361f
technique of, 351-353
tricuspid regurgitation complicating, 362
minimally invasive and robotic, transesophageal echocardiography in, 362
transcatheter, transesophageal echocardiography in, 363-364, 363f-364f
Mixed connective tissue disease, 726, 727t-728t
Molecular genetics, of hypertrophic cardiomyopathy, 518
Molecular imaging, with contrast ultrasound, 60
MS. *See* Mitral stenosis (MS).
Multimodality imaging, in guidance of structural heart disease interventions, 113
Myectomy, surgical, for hypertrophic cardiomyopathy, 534-537, 535f-536f
Myocardial contrast echocardiography, in acute chest pain evaluation in ED, 239, 241f
clinical use of, 239-240, 241f
Myocardial disease(s)
in ankylosing spondylitis, 723
diastolic function assessment in, 210-211, 212f
in hypothyroidism, 740, 741f
in mixed connective tissue disease, 726
in polymyositis and dermatomyositis, 726
in primary antiphospholipid syndrome, 719
in rheumatoid arthritis, 721-722
in scleroderma, 725
in systemic lupus erythematosus, 717
Myocardial infarction (MI)
acute. *See* Acute myocardial infarction.
diagnostic challenge of, 236
nonexercise stress echocardiography in prognostic evaluation after, 305, 306t
pericarditis and pericardial effusion after, 252
transesophageal echocardiography in, clinical utility and outcome data with, 792-794
transthoracic echocardiography in, clinical utility and outcome data with, 792-794

Myocardial ischemia, 189-190, 190f
exercise ECG testing in diagnosis of, 269, 269f
Myocardial performance index, 168, 168f
Myocardial perfusion
contrast echocardiography in assessment of, 308-309, 308f-309f
3D echocardiography in, 87-88
Myocardial velocities, tissue Doppler imaging of
color Doppler in, 177-178, 178f-180f
limitations of, 178-179
Myocardial viability
assessment of
in acute and chronic setting, 53, 54t
nonexercise stress echocardiography in, 305-308
diagnosis of, pharmacologic stress echocardiography versus perfusion scintigraphy in, 307f, 311-312, 313t
Myocardium
displacement of, tissue Doppler imaging of, 179f-180f, 181
mechanics of, 177-196
cardiac synchrony and, 190-192
left ventricular physiology and, 186-189, 187f-189f
mechanical dispersion and, 192-193, 193f
right ventricular function and, 193-194
speckle tracking echocardiography in evaluation of, 183-186. *See also* Speckle tracking echocardiography (STE).
tissue-Doppler imaging in evaluation of, 177-183. *See also* Tissue-Doppler imaging (TDI).
relaxation of, diastolic function and, 198
stunned, 269-270
Myxomas, cardiac, 904-908
clinical setting of, 906
differential diagnosis of, 908
echocardiographic features of, 908
features of, 907t
gross appearance of, 906-908, 908t, 909f
imaging modalities for, 908
location of, 906, 907f-908f

## N

Nutritional deficiencies, heart disease and, 752-753, 752t

## O

Obesity
in diabetic heart disease, 736
heart disease in, 749-752, 749t, 750f-751f
Operating room, ventricular function monitoring in, 23-44. *See also* Ventricular function, intraoperative, monitoring of.
Optisom, in ultrasound contrast imaging, 46

## P

PA. *See* Pulmonary artery (PA).
Pacing stress, in nonexercise stress echocardiography, 294
in coronary artery disease diagnosis, 302
technical aspects of, 300-301
PAH. *See* Pulmonary arterial hypertension (PAH).
Palpitations, in pregnancy, 685
Pannus, prosthetic valve, 470-471, 471f
Papillary fibroelastoma, 908-912
clinical manifestations of, 909-910
clinical setting of, 909
differential diagnosis of, 911-912, 911f
echocardiographic diagnosis of, 910, 910f-911f
features of, 907t
gross pathology of, 909
imaging modalities for, 911
location of, 909, 910f
PAPS (primary antiphospholipid syndrome), 718-719, 719f
Paraganglioma, cardiac, 907t, 915, 916f
Paravalvular regurgitation, management of, Doppler echocardiography in, 491
Patent ductus arteriosus (PDA), 865-866, 865f
corrective procedures for, issues resulting from, 882t, 884
echocardiographic evaluation of, 866, 866f
management of, 866, 866f
percutaneous device closure of, intracardiac echocardiography imaging in, 127, 127f
Patent foramen ovale (PFO), 857
cryptogenic stroke and, 800-802, 800f, 801t
echocardiographic guided interventions for, 101-102, 104f
transesophageal echocardiography in, 799-801, 800f
transthoracic echocardiography in, 799-801, 800f
PDA. *See* Patent ductus arteriosus (PDA).
Percutaneous closure
of aortic pseudoaneurysms, 111
of left atrial appendage, 110-111
Percutaneous edge-to-edge mitral repair, 106, 107f-108f
Percutaneous pulmonic valve implantation, 109
Perfusion scintigraphy, pharmacologic stress echocardiography versus, 311-312, 312t-313t
Pericardial disease, 565-584
in ankylosing spondylitis, 723
echocardiographic evaluation for, 567, 567b
pericardial effusion in, 571-572, 571f. *See also* Pericardial effusion.
pericardial tamponade in, 572-578. *See also* Pericardial tamponade.
transesophageal echocardiography in, 16
Pericardial effusion, 571-572
after cardiac transplantation, 591
appearance of, factors affecting, 572
clinical considerations on, 572, 572f
in hypothyroidism, 740
as incidental finding, 580
M-mode echocardiography in, 571-572, 571f
pericardial fluid volume in, determining, 572
pericardial tamponade from, 572-578. *See also* Pericardial tamponade.
postinfarction, 252
3D echocardiography in, 88
2D echocardiography in, 571-572, 571f
Pericardial fluid, 565, 566f
localized and loculated collections of, 576f, 577
Pericardial tamponade, 572-578
Doppler echocardiography in, 566f, 575-576, 575f-577f
inferior vena cava in, plethora of, 574t, 575
left atrial compression, inversion, or collapse in, 573, 574t
patient management in, echocardiography in, 576-577
guiding pericardiocentesis, 577-578, 578b, 579f
in localized and loculated pericardial fluid collection detection, 576f, 577
phasic respiratory changes in, 574t, 575
right atrial compression, inversion, or collapse in, 573, 573f, 574t
right ventricular compression, inversion, or collapse in, 572-573, 573f, 574t
Pericardiocentesis, echocardiographically guided, 577-578, 578b, 579f, 580t
Pericarditis
acute, 579, 579f
causes of, 568b
constrictive, 568-571. *See also* Constrictive pericarditis.
in mixed connective tissue disease, 726
in polymyositis and dermatomyositis, 726
postinfarction, 252
in rheumatoid arthritis, 720
in scleroderma, 725
in systemic lupus erythematosus, 718
Pericardium
anatomy of, 565, 566f
congenital absence of, 580-581, 581f
congenital disorders of, 580-581, 581f
cysts of, 581
diastolic function and, 198
disease of, 565-584. *See also* Pericardial disease.
functions of, 565-567
Pericardium *(Continued)*
inflammation of, 568-571. *See also* Pericarditis.
pressure-volume relationships in, 565-567, 566f
ventricular assist devices and, 606
PFO. *See* Patent foramen ovale (PFO).
PH. *See* Pulmonary hypertension (PH).
Pharmacologic stress echocardiography, 292-317. *See also* Stress echocardiography, nonexercise.
Pharmacologic therapy, for heart failure, 507, 508f
echocardiography in, 507
Plaque, atherosclerotic
intravascular ultrasound assessment of, 138, 139f
in proximal aorta, systemic embolic events and, 802-804, 803f, 803t
Polymyositis, 725-726, 727t-728t
Posterior descending coronary artery, blood flow detection in, 319, 321f
Postpartum hemodynamic and cardiac anatomy changes, 669
Potts shunt, palliative, issues resulting from, 880-881, 880t
Preeclampsia, 670-671, 671t
Pregnancy
alternative approaches in, 685
aortic dissection risk and, 695
arrhythmias in, 685
balloon mitral valvotomy in, 400
Doppler echocardiography in
in cardiac output measurement, technical aspects of, 667t, 668-669
in hemodynamic evaluation, 669-670, 670f
transvalvular flows in, 668-669, 669t
echocardiographic monitoring in, 684
heart disease in, 664-689
aortic dissection as, 683
cardiomyopathies as, 682-683, 682f
congenital, 673-678. *See also* Congenital heart disease (CHD), in pregnant patient.
ischemic, 683-684
Marfan syndrome as, 683, 683f
predictors of, 672b
valvular, 678-681
prosthetic heart valves for, 681, 682f
valvular regurgitation as, 681, 681f
valvular stenosis as, 678-681, 679f-680f
heart failure in, 684
heart murmur in, 684-685
hemodynamic changes in
Doppler echocardiographic evaluation of, 669-670, 670f
exercise changes similar to, 669
normal, 664-665
hypertension induced by, 670-671, 671t
limitations of echocardiography in, 685
mitral valve prolapse in, 685
palpitations in, 685
pulmonary edema in, 684, 684t
pulmonary vascular disease in, 672-673
Preload, definition of, 160
Pressor stress, cardiac response to, in aging, 778
Pressure-volume analysis, in left ventricular systolic function assessment, 170-173, 172f-173f
Primary antiphospholipid syndrome (PAPS), 718-719, 719f, 727t-728t
Prosthetic materials, in congenital heart disease repair, issues from, 878, 880f
Prosthetic valve(s)
aortic, 3D echocardiography of, 82, 82f
endocarditis of, management of, Doppler echocardiography in, 490-491, 490f
evaluation of patient with, 417
fluid dynamics of, 450-469. *See also* Prosthetic valve fluid dynamics.
function/dysfunction of, 470-494
Doppler-echocardiographic evaluation of, 473-486
clinical data in, 473
data interpretation in, 486-488
Doppler velocity index in, 473t-474t, 479-480
effective orifice area in, 476-479, 478f, 479t
energy loss index in, 480

Prosthetic valve(s) *(Continued)*
leaflet morphology and mobility in, 472f, 473-474, 475f
limitations, alternative approaches, and future directions of, 491-492, 491t, 492f
in management of specific prosthetic valve-related complications, 488-491
pressure recovery influence on, 480
in prosthetic pulmonary valve, 486
in prosthetic tricuspid valve, 485-486
in prosthetic valve regurgitation
aortic, 480-483, 481f-482f, 483t
indirect signs and consequences of, 485
mitral, 481f-482f, 483-484, 484t
recognition and quantitation of, 480-485
in prosthetic valve stenosis recognition and quantitation, 473-480, 473t-474t
leaflet morphology and mobility in, 472f, 473-474, 475f
quantitative parameters in, 473t-474t, 474-480, 476f-478f, 479t
quantitatve parameters in, 474-480
in stentless aortic valve substitutes, 485
stress echocardiography in, 485
timing of, 473
in transcatheter aortic valves, 485, 486f
transprosthetic jet contour and acceleration time in, 473t-474t, 474-476, 477f
transprosthetic velocity and gradient in, 473t-474t, 474, 476f
infective endocarditis as, 471-472
paravalvular regurgitation as, 472, 472f
patient-prosthesis mismatch as, 470, 471t
structural valve deterioration as, 471, 471f
thrombus and pannus as, 470-471, 471f
in vivo evaluation of, 458, 459f
leaflet mobility in, alternative approaches to evaluating, 491, 491t, 492f
paravalvular leaks in, repair of, 108
in pregnant patients, 681, 682f
pulmonic, percutaneous implantation of, 109
regurgitation quantitation in, alternative approaches to, 491
thrombosis in, management of, Doppler echocardiography in, 488-490, 489f-490f
transcatheter valve-in-valve implants for, 108
transesophageal echocardiography of, 13-14
Prosthetic valve fluid dynamics, 450-469
Bernoulli equation in, 452
in bioprostheses
stented, 460f, 461t-462t, 466, 466f, 466t
unstented, 460f, 461t-462t, 466, 466t
conservation of mass in, 450-451, 451f-452f
control volume energy analysis in, 452-453
Doppler gradient in, 455
effective orifice area in, 455-456
mechanical energy in, 451-452, 452f
loss(es) of, 457-458
conversion and, in stenosis, 454, 454f
mechanisms of, 453-454, 453f
novel parameters of, 458
in mechanical valves, 460f, 461t-462t, 462, 463f-464f, 465t
ball and cage, 460f, 462, 465t
bileaflet, 460f, 461t-462t, 462, 463f-465f, 465t
tilting disk, 460f, 461t-462t, 462, 463f, 465t
native valve hemodynamics and, 458-460, 459f
pressure drop in, 454-455, 455f
principles of, 450-454
regurgitant volume in, 457
in transcatheter valves, 466-467, 467f
Protein-calorie malnutrition, heart disease and, 753
Proximal coronary artery
blood flow detection in, 319
left, stenosis of, detection of, 323
Proximal isovelocity surface area (PISA) method, of mitral regurgitation quantification, 338-341, 338f-339f, 338t
geometric factors influencing, 340, 340f
technical factors of, 340-341, 340f-341f
Pseudoaneurysm(s)
aortic, percutaneous closure of, 111
complicating acute myocardial infarction, 256-257, 257f-258f
formation of, after grafts for aortic dissection, 707
in infective endocarditis, 413
of left ventricle, percutaneous closure of, 110
Pulmonary arterial hypertension (PAH), 632-634, 633f
lung transplantation for, 638
pulmonary venous hypertension differentiated from, 640-642, 641f-642f, 641t
Pulmonary artery catheter positioning, intraoperative transesophageal echocardiography in, 34, 35f
Pulmonary artery (PA)
banding of, issues resulting from, 878-879, 880f, 880t
congenital disorders of, determination of, 840
in connective tissue disorders, 766
in intraoperative ventricular function monitoring, 27, 28f
morphology of, 834-835
Pulmonary artery pressure (PAP)
in pulmonary hypertension, 629
right ventricular afterload and, 629-630
Pulmonary artery systolic pressure, estimation of, 618, 618f
Pulmonary bifurcation view, in transesophageal echocardiography, 8, 8f
Pulmonary edema, in pregnancy, 670f, 684
Pulmonary embolism, acute, pulmonary hypertension and, 634-635, 635f-636f
Pulmonary hypertension (PH), 629-645
acute pulmonary embolism and, 634-635, 635f-636f
arterial, 632-634, 633f
causes of, 629
chronic pulmonary embolism and, 636, 636f
from chronic respiratory disease, 637-638
definition of, 629, 630b
exercise echocardiography in, 642-643
with increased cardiac output, 638-639
in mixed connective tissue disease, 726
in obesity, 751-752
in polymyositis and dermatomyositis, 726
in primary antiphospholipid syndrome, 718-719
pulmonary venous disease and, 636-637
related to left heart disease, 639-643
in rheumatoid arthritis, 722
in scleroderma, 725
in systemic lupus erythematosus, 718
without pulmonary vascular disease, 638-639
Pulmonary thromboembolism, in systemic lupus erythematosus, 715
Pulmonary valve
congenital disorders of, determination of, 840
morphology of, 834-835
prosthetic, Doppler-echocardiographic evaluation of, 486
Pulmonary vascular disease, 632-637
in pregnancy, 672-673
Pulmonary vascular resistance, estimation of, 618-619
Pulmonary vasculature, right ventricular interaction with, 630-632, 631f-633f
Pulmonary vein(s)
connections of, anomalous, 861, 862f
corrective procedures for, issues resulting from, 887t, 889
disease of, pulmonary hypertension in, 636-637
radiofrequency ablation of, intracardiac echocardiographic guidance of, 122-123, 122f-123f
Pulmonary vein flow
in diastolic filling assessment, 202-203, 204f
in transesophageal echocardiography, 12
Pulmonary venous hypertension, 639-643
pulmonary vascular hypertension differentiated from, 640-642, 641f-642f, 641t
Pulmonary venous inflow pattern, in mitral regurgitation quantification, 341-343, 342f
Pulmonic regurgitation (PR), 658-660, 658t, 659f, 660t
Pulmonic stenosis (PS), 655-658, 656f, 849-850, 849f, 850b
assessment of
alternate approaches to, 658
clinical utility and outcome data of, 657, 657t
basic principles and echocardiographic approach to, 655
corrective procedures for, issue resulting from, 882t, 886
technical data, quantitation, and data analysis on, 655-657, 656f
Pulmonic valve
disease of, 655. *See also* Pulmonic regurgitation (PR); Pulmonic stenosis (PS).
3D echocardiography of, 82
prosthetic, implantation of, percutaneous, 109
transesophageal echocardiography of, 13
Pulmonic valvotomy, 109
Pulsatility index, with ventricular assist devices, 604
Pulsed Doppler echocardiography
in myocardial velocity imaging, 178, 181f
in volumetric methods of mitral regurgitation quantification, 341, 341f-342f

## R

Radiation, restrictive cardiomyopathy after, 556
Radiofrequency intravascular ultrasound, 133, 133f
Reconstruction techniques, using 3D echocardiography, 67
Regional wall motion, in intraoperative ventricular function monitoring, 30-31, 32f
Renal disease
chronic, heart disease in, 746-749, 746t, 749f
mitral annular calcification and, in aging, 781
Renal insufficiency, in diabetic heart disease, 736
Respiratory disease, chronic, pulmonary hypertension from, 637-638
Restenosis
in-stent
after intravascular ultrasound-guided bioabsorbable stent implantation, 140-142
treatment of, intravascular ultrasound evaluation of, 140, 141f-142f
reduction of, intravascular ultrasound in, 139-140, 140f
Restrictive cardiomyopathy, 542-564
in amyloidosis, 548-551, 550f
classification of, 543t
constrictive pericarditis compared with, 557t, 571
constrictive pericarditis differentiated from, 556-559, 557f-558f, 557t
definition of, 542
diagnostic approaches to, 550t
Doppler features of, 544-547, 545f-548f
drug-induced, 555-556
echocardiographic features of, 542-544, 543t, 544f
in clinical decision making, 559, 559t
in endomyocardial fibrosis, 551-553
in Fabry disease, 550f, 554-555
in Gaucher disease, 553-554
in glycogen storage disorder, 554
in hemochromatosis, 551
in hypereosinophilic syndrome, 551-553, 552f
idiopathic, 555
imaging of, 542
postradiation, 556
in sarcoidosis, 553
speckle tracking echocardiography in, 543-544
in storage disorders, 553-555
Resynchronization therapy, in heart failure, 508-511, 511f
Rhabdomyoma, 907t, 914-915, 914f
Rheumatic aortic stenosis, imaging of, 426, 427f
Rheumatoid arthritis, 719-722
coronary artery disease in, 719-720, 727t
myocardial disease in, 721-722
pericarditis in, 720
pulmonary hypertension in, 722
valve disease in, 720-721, 721f-722f, 728t

Rheumatologic diseases, 712-732
ankylosing spondylitis as, 722-723, 723f-724f
cardiovascular involvement in, 727t
dermatomyositis as, 725-726
mixed connective tissue disease as, 726
polymyositis as, 725-726
primary antiphospholipid syndrome as, 718-719, 719f
rheumatoid arthritis as, 719-722, 721f-722f. *See also* Rheumatoid arthritis.
scleroderma as, 723-725
systemic lupus erythematosus as, 712-718. *See also* Systemic lupus erythematosus (SLE).
Right atrial pressure, estimation of, 618, 618t
Right atrium
anatomy of, 614, 791-792, 796f
compression, inversion, or collapse of, 573, 573f, 574t
physiology of, 614
size of, atrial fibrillation and, 815-816
Right heart. *See also* Right atrium; Right ventricle.
echocardiographic assessment of
basic approach to, 615-616
pressures in, estimation of, 618-619, 618f, 618t
Right-sided valve disease, 646-662. *See also* Pulmonic valve; Tricuspid valve.
Right ventricle, 614-628
anatomy and physiology of, 614-615, 615f-616f
compression, inversion, or collapse of, 572-573, 573f, 574t
diastolic function of, evaluation of, 625, 625t
double-outlet, corrective procedures for, issues resulting from, 897
dysfunction of
in diabetic heart disease, 735
in preimplant assessment for ventricular assist device, 601, 601b
echocardiographic evaluation of
alternate approaches to, 625-626, 626f
basic approach to, 615-616
clinical application of, 623
future directions for, 625
outcome data for, 622-623, 623t
potential limitations of, 625
reference ranges, quantitation and data analysis for, 617f, 621, 621t
research applications of, 623-625, 624f, 625t
technical details of, 619-621
transesophageal imaging in, 619, 619f
transthoracic imaging in, 616-618, 617f
function of
in intraoperative ventricular function monitoring, 30, 31f
measures of, 619-621, 619f-620f
pericardial interaction with, 566-567, 567f
pulmonary vascular interaction with, 630-632, 631f-633f
remodeling of, to heart failure, 506-507
size of, measures of, 619-621, 619f-620f
systolic function of, alternate measures of, 623-625
volume of, 3D echocardiography of, 75-76
Right ventricular assist device positioning, intraoperative transesophageal echocardiography in, 36
Right ventricular infarction, echocardiographic diagnosis of, 250-251, 250b
Right ventricular outflow tract, in intraoperative ventricular function monitoring, 27-28
Right ventricular overload, pulmonary artery pressure and, 629-630
Right ventricular-type univentricular heart, 841

## S

Sarcoid, pulmonary, pulmonary hypertension in, 638
Sarcoidosis, restrictive cardiomyopathy, 553
Sarcoma, 915-917, 916f-917f
Scintigraphy, perfusion, pharmacologic stress echocardiography versus, 311-312, 312t-313t
Scleroderma, 723-725, 727t-728t
Semilunar valves
congenital disorders of, determination of, 840
morphology of, 834-835
Senile amyloidosis of heart, 786
Septal defects, congenital, 857-867
Septal ethanol ablation, in hypertrophic cardiomyopathy, 532-534, 533f-534f
Septal hypertrophy in elderly, hypertrophic cardiomyopathy differentiated from, 521
SHD. *See* Structural heart disease (SHD).
Shunt lesions, congenital, 857-867
Shunting, intracardiac, color and spectral Doppler imaging of, 842-843, 842f-843f
Shunts, aortopulmonary, palliative, issues resulting from, 880-881, 880t, 881f
Sinus of Valsalva aneurysms, 854-855, 855f
SLE. *See* Systemic lupus erythematosus (SLE).
Speckle tracking, in exercise echocardiography, 284-285, 285f
Speckle tracking echocardiography (STE)
in diastolic function assessment, 209
of left ventricular rotation and twist, 185-186, 186f-187f
physical principles of, 183-186, 183f-184f
in regional function analysis, 244
in restrictive cardiomyopathy, 543-544
of strain, 183-185, 184f, 185t
limitations of, 185
Spectral Doppler imaging, in congenital heart disease evaluation, 842-843, 843f
Spondylitis, ankylosing, 722-723, 723f-724f
Starling law of the heart, 160
STE. *See* Speckle tracking echocardiography (STE).
Stenosis
coronary, diagnosis of, noninvasive, 322-324, 324f
recurrence of. *See* Restenosis.
severity of, assessment of, intravascular ultrasound in, 134-135
valvular. *See specific valve, e.g.* Mitral stenosis (MS).
Stent(s)
bioabsorbable
implantation guidance by intravascular ultrasound, evaluation of results of, 140-142
intravascular ultrasound evaluation of, 140
drug-eluding, in restenosis reduction, 139, 140f
malapposition of, late-acquired, intravascular ultrasound assessment of, 139-140
restenosis in, treatment of, intravascular ultrasound evaluation of, 140, 141f-142f
size selection for, intravascular ultrasound in, 135-136, 135f
Stent fracture, very late stent thrombosis and, 140, 141f
Stent thrombosis
after intravascular ultrasound-guided bioabsorbable stent implantation, 140-142
late malapposition and, 139-140
very late, stent fracture and, 140, 141f
Stented bioprosthetic valves, 460f, 461t-462t, 466, 466f, 466t
Stentless bioprosthetic valves, 460f, 461t-462t, 466, 466t
Strain
definition of, 181, 181f
imaging of, 181-182, 181f
in diastolic function evaluation, 207-209, 208f
in hypertrophic cardiomyopathy, 531, 531f
in myocardial ischemia, 189, 190f
in right ventricular systolic function evaluation, 624-625
speckle tracking echocardiography in, 183-185, 184f, 185t, 284-285
tissue Doppler imaging in, 182-183
Strain echocardiography
diastolic function assessment by, 207-208, 208f
in regional function analysis, 244, 244f
Strain rate
calculation of, 181
definition of, 284-285
in right ventricular systolic function evaluation, 624-625
Stress
cardiac response to, in aging, 778
definition of, 159
mechanical, in aortic dissection, 693-694
shear, in aortic dissection, 693-694, 693f
Stress echocardiography
in acute chest pain evaluation in ED, 237-238
coronary artery disease in aging and, 784-786, 785f, 785t-786t
exercise stressors used in, 270-272, 271b, 272t
in mitral stenosis, research applications of, 402
nonexercise, 292-317
alternatives to, 311-312
basic principles of, 293-298
combined approaches to, 294
contrast
in left ventricular opacification, 308
in myocardial perfusion assessment, 308-309, 308f, 309t
in coronary artery disease diagnosis, accuracy of, 301-303, 302f, 302t
in disease significance assessment, 303-305, 303f
dobutamine. *See* Dobutamine stress echocardiography (DSE).
Doppler, 310-311, 310f
echocardiographic approach to, 295-298
image acquisition in, 295, 295f
image processing in, 295
qualitative interpretation in, 295-298, 296f-299f, 296t
in evaluation of therapy, 305
exercise-stimulating agents in, 293-294
technical aspects of, 299-300
future of, 313
image quality in, new technologies for, 308-309, 308f-309f
indications for, 292-293, 293b
interpretation of, quantitative approaches to, 309-310, 310f
mechanism of action of nonexercise stressors in, 293
in myocardial viability assessment, 305-308
agents used for, 293
clinical significance of, 305-306
dobutamine echocardiography in, 306-307, 307f
in global function and outcome recovery prediction, 307-308
new technologies in, 308-311
pacing stress for exercise stimulation in, 294
perfusion scintigraphy versus, 307f, 311-312, 312t-313t
pharmacology and physiopathology of, 293-294
in prediction of cardiac events in patients undergoing major noncardiac surgery, 304, 304f
prognostic evaluation using, 304
after myocardial infarction, 305, 306t
of stable coronary disease patients, 304-305, 305t
in risk stratification after acute myocardial infarction, 262
technical aspects of, 298-301
3D, 85, 86f, 309, 309f
vasoactive agents in, 293-294
pharmacologic. *See* Stress echocardiography, nonexercise.
in prosthetic valve function evaluation, 485
Stress-shortening relations, in left ventricular systolic function assessment, 168-170, 169f-172f
Stroke
cardioembolic, 791
cryptogenic, 791
patent foramen ovale and, 800-802, 800f, 801t
Stroke volume, in intraoperative ventricular function monitoring, 28-29, 29f
Structural heart disease (SHD)
definition of, 95
examples of, 96f
interventions for, 95-96, 96t
cardiac magnetic resonance imaging guiding, 113
catheterization laboratory of future for, 113-114
cineangiography in, 97
computed tomographic guidance of, 111-113
echocardiographic guidance of, 95-117
for aortic valve disorders, 104-105
for assisting with access routes, 97-98

Structural heart disease (SHD) *(Continued)*
for atrial septal defects, 99-101, 103f
for closure of aortic pseudoaneurysms, 111
for closure of intracardiac communications, 99-104
for closure of left atrial appendage, 110-111
in left ventricle, 109-110, 110f
limitations and alternate approaches to, 111-113
for mitral regurgitation, 105-108
modalities for, 97, 98f
for patent foramen ovale, 101-102, 104f
for prosthetic valves, 108
for recognizing and analyzing catheters and devices, 98, 99t, 100f
for right heart valve disease, 109
for septal defects, 99t
for transapical catheterization, 98
for transcatheter mitral valve replacement, 109
for transseptal catheterization, 98, 99f
for valves, 102t
for ventricular septal defects, 102-104
fluoroscopy in, 97, 97t
intracardiac ultrasound guidance of, 111, 112f-113f
multimodality imaging guiding, 113
for other abnormalities, 102t
Stunned myocardium, 269-270
Subaortic stenosis, 852-853, 853b, 853f
corrective procedures for, issues resulting from, 882t, 884
Supravalvular aortic stenosis, 853-854, 854b
Surgical myectomy, for hypertrophic cardiomyopathy, 534-537, 535f-536f
Surgical procedures
for congenital heart disease, problems after, 876-901. *See also* Congenital heart disease (CHD), postoperative.
noncardiac
cardiac events in patients undergoing, nonexercise stress echocardiography predicting, 299, 304f
risk stratification prior to, exercise echocardiography in, 281
transesophageal echocardiographic monitoring of, 16-17
Sympathomimetic agents, in nonexercise stress echocardiography, 299-300
Syndrome X, coronary flow reserve in, 325
Systemic embolic events, 791-810
atherosclerotic plaque in proximal aorta and, 802-804, 803f, 803t
transesophageal echocardiography in
alternate approaches to, 805
in catheterization laboratory, 804, 805f
clinical utility and outcome data with, 792-794
indications for, 791-792
in intracardiac tumors, 795-797, 796f-797f
in left atrial thrombus, 797-799, 798f
limitations and future approaches, 805
in myocardial infarction, 792-794
in patent foramen ovale, 799-801, 800f
research applications of, 805
safety of, 792
technical aspects of, 792, 792t
in valvular vegetations, 794-795, 795f, 795t
transthoracic echocardiography in
alternate approaches to, 805
in catheterization laboratory, 804, 805f
clinical utility and outcome data with, 792-794
indications for, 791-792
in intracardiac tumors, 795-797, 796f
limitations and future approaches, 805
in myocardial infarction, 792-794
in patent foramen ovale, 799-801, 800f
research applications of, 805
technical aspects of, 792t, 796f
in valvular vegetations, 794-795, 795t
Systemic lupus erythematosus (SLE), 712-718
atherosclerotic disease in, 715-717, 717f
cardiovascular involvement in, 712-718, 727t
Systemic lupus erythematosus (SLE) *(Continued)*
intracardiac thrombosis and thromboembolism in, 715
myocardial disease in, 717
pericarditis in, 718
pulmonary hypertension in, 718
valve disease in, 712-715, 728t
Systolic dysfunction
in chronic kidney disease, 747
in hypothyroidism, 739, 740t
Systolic function
in acromegaly, 743
in connective tissue disorders, 766
definition of, 157-159
in hyperthyroidism, 737f, 740-742
in obesity, 750, 750f

## T

TAVI. *See* Transcatheter aortic valve implantation (TAVI).
TDI. *See* Tissue-Doppler imaging (TDI).
TEE. *See* Transesophageal echocardiography (TEE).
Teleechocardiography, for acute chest pain in emergency department, 244
Tetralogy of Fallot, 867-869, 868f
corrective procedures for, issues resulting from, 887t, 893-895, 894f-896f
Thoracic aorta
aneurysm of, familial, 762
descending
dissection of, type B, intracardiac echocardiographic imaging of, 125-126
periinterventional imaging of, intracardiac echocardiography in, 125-127, 126f-127f
view of, in transesophageal echocardiography, 5f, 10
dissection of, familial, 762
measurements of, 767, 768f
Three-dimensional (3D) echocardiography, 67-94
advantages and disadvantages of, 71, 72f
of aortic dissection, 87
of aortic regurgitation, 81-82
of aortic stenosis, 81, 434
of aortic valve
disease of, 81-82, 81f
prosthetic, 82, 82f
of atrial volume, 76-77
of congenital heart disease, 82-83, 83f
of endocarditis, 86-87, 87f
evidence-based applications of, 72-88
future considerations for, 88-89, 88f
of hypertrophic cardiomyopathy, 86
for intracardiac catheter-based intervention guidance, 83-85, 84f-85f
of intracardiac masses, 88
of left ventricle
for dyssynchrony, 85-86
mass of, 74-75, 76t
volume and function of, 72-74, 73t, 75f
of mitral regurgitation, 78-81, 79f-80f
in mitral regurgitation quantification, 343, 344f, 345t
of mitral stenosis, 77-78, 78f-79f
of mitral valve disease, 77-81
of myocardial perfusion, 87-88
overview of, 67
of pericardial effusion, 88
of pulmonic valve disease, 82
reconstruction technique using, 67
of right ventricle, volume of, 75-76, 77t
of right ventricular evaluation, 623, 624f
in stress echocardiography, 85, 86f
technical considerations for, 67-71
transesophageal, 11-12, 11f, 11t
transthoracic, in cardiac tumor diagnosis, 922, 923f
of tricuspid valve disease, 82, 82f
of valvular heart disease, 77-82
volumetric technique using, 67-69, 68f-71f
work flow, 71-72, 74f
Thromboembolism
after cardioversion, mechanism of, 820-821
cardiogenic, in aging, 786, 786f
mitral annular calcification and, in aging, 780-781
predictors of, atrial fibrillation and, 817
in primary antiphospholipid syndrome, 718
in systemic lupus erythematosus, 715
Thrombolysis, microbubbles in, 61, 62f
Thrombosis
intracardiac
in primary antiphospholipid syndrome, 718, 719f
in systemic lupus erythematosus, 715
prosthetic valve, management of, Doppler echocardiography in, 488-490, 489f-490f
Thrombus(i)
left atrial
detection of, in atrial fibrillation, 816-820, 816f-820f, 816t
transesophageal echocardiography of, 14-15, 797-799, 798f
left ventricular
complicating acute myocardial infarction, 259-260, 260f-261f
transesophageal echocardiography in, 792-794
transthoracic echocardiography in, 792-794, 793f
prosthetic valve, 470-471, 471f
Thyroid disorders, heart disease in, 739-742, 740t-741t, 741f
Tilting disk valves, 460f, 461t-462t, 462, 463f, 465t
Tissue Doppler echocardiography (TDE), in pericardial tamponade, 576
Tissue-Doppler imaging (TDI)
angle dependency limiting
in strain-rate imaging, 182
in velocity imaging, 178
cardiac translation limiting, 179
in cardiac tumor diagnosis, 923f, 924
in clinical routine, preferred modalities for, 183, 183t
of deformation, 181-182
in diastolic function evaluation, 203-206
in hypertrophic cardiomyopathy, 530
in intraoperative ventricular function monitoring, 29, 30f
load dependency limiting, 179
movement of sample volume relative to myocardium limiting, 178
of myocardial displacement, 179f-180f, 181
in myocardial ischemia, 190, 191f
of myocardial movement, 183
of myocardial velocity, 177-181
by color Doppler, 177-178, 178f-180f
limitations of, 178-179
by pulsed Doppler, 178, 181f
physical principles of, 177-183
in regional function analysis, 244, 244f
in restrictive cardiomyopathy, 547, 547f-548f
reverberations limiting
in strain-rate imaging, 182-183
in velocity imaging, 178
signal noise limiting, 182
of strain and strain rate, 182-183
techniques of, 204
tethering effects limiting, 179
Torsion, left ventricular
definition of, 185
validation of, by speckle tracking, 209
Torsion echocardiography, in diastolic function assessment, 209
TR. *See* Tricuspid regurgitation (TR).
Transapical catheterization, echocardiographic guidance of, 98
Transcatheter aortic valve implantation (TAVI)
echocardiographic guidance of, 84, 105
echocardiographic sizing and positioning of, 485, 486f
intracardiac echocardiography monitoring, 123-125, 123f-125f
late postoperative follow-up of, 473t, 478f, 485
3D echocardiography guiding, 84, 105
2D echocardiography guiding, 105

Transcatheter valve-in-valve implants, 108
evaluation of, alternative approaches to, 491-492
Transcatheter valves, 466-467, 467f
Transesophageal echocardiography (TEE), 2-22
in acute aortic syndromes, 702-705, 702f
Doppler findings in, 703-704
inconclusive results with, 705
safety of, 703
aortic arch views in, 10-11, 10f
in aortic dissection
hematoma and rupture, 15
operative uses of, 706b
in aortic dissection diagnosis, 698-699, 700f, 703, 703f
aortic views in, 4t, 10-11, 10f
in atrial fibrillation, 15-16
in atrial septal abnormalities, 15
basal views in, 4-8, 4t
of aortic valve, 6f-8f
of atrial septum, 5f-6f, 8
pulmonary bifurcation, 8, 8f
in cardiac tumor detection, 921-922
in cardiac tumors, 15
in cardioembolic events, 14-15
in cardioversion in atrial fibrillation, 817-820, 818b, 818f
complications of, 17-18, 17b
in congenital heart disease, 16
contraindications to, 17, 17b
in coronary artery disease, 16
in critically ill ICU patient, 16
descending thoracic aorta view in, 5f, 10
Doppler, 12
in intraoperative ventricular function monitoring, 26
esophageal intubation for, 3-4
four-chamber views in, 4t, 5f-6f, 8-9, 8f
image format for, 4
indications for, 12-17, 13b
in infective endocarditis, 14, 414-417, 415f, 416t
intraoperative
in cardiac tumor intervention and evaluation, 922
in mitral valve repair, 351-352, 352f
in intraoperative ventricular function monitoring, 23-44. *See also* Ventricular function, intraoperative, monitoring of.
left atrial appendage flow in, 12
in minimally invasive and robotic mitral valve repair, 362
in monitoring during surgical and interventional procedures, 16-17
in native valve disease, 13
patient preparation for, 2-3
performance of, 2-4
cognitive and technical skills for, 3b
in pericardial disease, 16
in postoperative congenital heart disease visualization, 876-877, 877f
pulmonary vein flow in, 12
in right ventricle assessment, 619, 619f
standard imaging planes for, 4-11, 4t, 5f-6f
in systemic embolic events, 791-792. *See also* Systemic embolic events, transesophageal echocardiography in.
3D imaging in, 11-12, 11f, 11t
in transcatheter mitral valve repair, 363-364, 363f-364f
transgastric views of, 9-10
Transmitral flow, in diastolic filling assessment, 201-202, 202f
Transplantation. *See* Cardiac transplantation; Lung transplantation.
Transposition of the great arteries (TGA)
complete, corrective procedures for, issues resulting from, 887t, 895-896
congenitally corrected, 869-870, 869f, 870b
issues resulting from, 887t, 896-897
corrective procedures for, issues resulting from, 887-888, 887t
Transseptal catheterization, echocardiographic guidance of, 98, 99f
Transthoracic echocardiography (TTE)
in aortic dissection diagnosis, 698, 698f-700f
in infective endocarditis, 414-417, 415f, 416t
in mitral stenosis diagnosis, 389-390
in right ventricle assessment, 616-618, 617f
in systemic embolic events, 791-792. *See also* Systemic embolic events, transthoracic echocardiography in.
3D, in cardiac tumor diagnosis, 922, 923f
Trauma
to aorta, 697-698
aortic dissection risk and, 694-695, 694b
Tricuspid balloon valvotomy, 109
Tricuspid regurgitation (TR), 646-654
after cardiac transplantation, 589, 589f
assessment of
future directions for, 654
limitations of, 654
basic principles and echocardiographic diagnosis of, 646-647
clinical utility and outcome data on, 652-654, 652f-653f, 653t-654t
complicating mitral valve repair, 362
congenital, 851-852
etiology of, determining, 647-650, 647b, 648f-649f
research applications of, 654
severity of, determining, 650-652, 650f-651f, 652t
Tricuspid stenosis (TS), 654-655, 655b
Tricuspid valve
anatomy of, 646, 647f
atresia of, 870-871, 870f
congenital anomalies of, 851-852, 851f-852f
determination of, 838-839, 839f
disease of, 646. *See also* Tricuspid regurgitation (TR); Tricuspid stenosis (TS).
3D echocardiography of, 82, 82f
morphology of, 834, 834f
prosthetic, Doppler-echocardiographic evaluation of, 485-486
transesophageal echocardiography of, 13
TS. *See* Tricuspid stenosis (TS).
TTE. *See* Transthoracic echocardiography (TTE).
Tumors, cardiac, 902-928. *See also* Cardiac tumors.
Turbulent losses, in fluid dynamics, 453
Turner syndrome, 762
aortic dissection and, 696
Twist, left ventricular, definition of, 185
Two-dimensional (2D) echocardiography
changes on, in pregnancy, 668, 668t
in left ventricular geometry assessment, 164-165
in left ventricular mass assessment, 164, 165b
in left ventricular volume assessment, 164, 165b

## U

Ulcers, of aorta, penetrating, 697
diagnosis of, transesophageal echocardiography in, 703
Ultrasound, intravascular, 130-145. *See also* Intravascular ultrasound (IVUS).
Ultrasound contrast imaging, 45-66
in acute ischemia/risk area detection in emergency setting, 52-53
artifacts in, 50-51
in carotid artery atherosclerosis detection, 60
clinical applications of, 52-58
continuous infusion, 50, 50f-51f
contrast agents for, 46, 47f-48f
in coronary artery disease detection, 53-58, 55f, 55t
during dobutamine or exercise stress echocardiography, 54-56, 56f-57f, 57t
large arteriolar imaging in, 58
real-time myocardial contrast echocardiography in, 58, 58f
vasodilator stress perfusion imaging in, 53-54, 55f, 55t
in drug and gene delivery, 56f, 60-61
harmonic high–mechanical-index intermittent imaging in, 46-48
harmonic power Doppler in, 48
image processing in, 50-51
Ultrasound contrast imaging *(Continued)*
low–mechanical-index imaging schemes in, 48-49, 49f, 49t
microbubbles in, 45-46, 46t. *See also* Microbubbles.
molecular, 60
in myocardial perfusion assessments, artifacts in, 56-58, 57f-58f
in myocardial viability assessment in acute and chronic setting, 53, 54t
perfusion imaging techniques in, 46-49
perfusion imaging techniques of, for other organs, 59-60
qualitative and quantitative methods of analysis in, 49-51
safety of, 51-52, 52t
technical equipment for, 50-51
therapeutic applications of, 60-61
in thrombolysis, 56f, 61
Ultrasound "stethoscope,", 148-150, 149f-150f, 150b
Univentricular heart, 840-842, 841f-842f
functional, 871, 871b
Uremic cardiomyopathy, 747, 747f

## V

VAD. *See* Ventricular assist device (VAD).
Valve disease
in ankylosing spondylitis, 722-723, 723f, 728t
congenital, corrected, residua and sequelae of, 877-878, 879f
in mixed connective tissue disease, 726, 728t
in polymyositis and dermatomyositis, 726, 728t
in primary antiphospholipid syndrome, 718, 719f, 728t
in rheumatoid arthritis, 720-721, 721f-722f, 728t
right-sided, 646-662. *See also* Pulmonic valve; Tricuspid valve.
in scleroderma, 725, 728t
in systemic lupus erythematosus, 712-715, 728t
Valve hemodynamics
native, 458-460, 459f
prosthetic, of specific designs, 460-467, 460f, 461t-462t
Valvotomy
balloon
mitral, 389-407. *See also* Balloon mitral valvotomy (BMV).
tricuspid, echocardiographic guidance of, 109
pulmonic, echocardiographic guidance of, 109
Valvular heart disease
in acromegaly, 744
in aging, 778-781, 780f-782f, 782t
aortic, 81-82, 81f
catheter-based therapy of, 3D echocardiography guiding, 84, 85f
in chronic kidney disease, 748
congenital, 846-852
bicuspid aortic valve as, 846-849
mitral valve anomalies as, 850, 851f
pulmonic valve stenosis as, 849-850, 849f, 850b
tricuspid valve anomalies as, 851-852, 851f-852f
exercise echocardiography applications in, 282-283, 283f
in hyperthyroidism, 742
infective endocarditis as, 408-424. *See also* Infective endocarditis (IE).
mitral, 77-81
mitral valve repair for, 351-366. *See also* Mitral valve repair.
in pregnancy, 678-681
prosthetic valve fluid dynamics in, 450-469. *See also* Prosthetic valve fluid dynamics.
prosthetic valves for. *See* Prosthetic valves.
pulmonic, 3D echocardiography of, 82
regurgitation as
aortic, 81-82, 367-388. *See also* Aortic regurgitation (AR).
in infective endocarditis, management of, 420
mitral, 78-81, 79f-80f, 330-350. *See also* Mitral regurgitation.

Valvular heart disease *(Continued)*
stenosis as
aortic, 81, 425-449. *See also* Aortic stenosis (AS).
mitral, 77-78, 78f-79f, 389-407. *See also* Mitral stenosis (MS).
3D echocardiography of, 77-82
transesophageal echocardiography of, 13
tricuspid, 3D echocardiography of, 82, 82f
Valvular regurgitation(s)
in fluid dynamics, 453-454, 454f
in pregnancy, 669, 681, 681f
Valvular stenosis, in pregnancy, 678-681, 679f-680f
Valvulopathy
in obesity, 751-752
in ventricular assist device dysfunction, 602-603, 603f
Valvuloplasty, balloon aortic, echocardiographic guidance of, 104-105
Vasculopathy, cardiac allograft, diagnosis of, 592-594, 593f, 593t
Vasoactive agents, in nonexercise stress echocardiography, 293-294
Vasoconstrictor protocols, for nonexercise stress echocardiography, 300
Vasodilator stress
with adenosine echocardiography in CAD diagnosis, 301
protocols for, for nonexercise stress echocardiography, 300
Vasodilator stress perfusion imaging in coronary artery disease detection, 53-54, 55f, 55t
Vegetations
in infective endocarditis, 409-412, 410f-412f, 410t
management of, 417-420, 419f
Libman-Sacks, in systemic lupus erythematosus, 713, 713f-716f
thrombotic valve, in primary antiphospholipid syndrome, 718, 719f
valvular
transesophageal echocardiography in, 794-795, 795f, 795t
transthoracic echocardiography in, 794-795, 795t
Velocities
myocardial, imaging of
in myocardial ischemia, 189-190, 190f
by tissue Doppler
color, 177-178, 178f-180f
pulsed, 178, 181f
transvalvular flow, in pregnancy, Doppler imaging of, 668-669, 669t
Velocity propagation index (Vp), as preload independent index for relaxation, limitations of, 207
Vena contracta method, of mitral regurgitation quantification, 337-338, 337f-338f, 338t
Venous connections, cardiac, congenital disorders of, determination of, 836-838, 837f-838f
Venous shunts, systemic to pulmonary, 639, 640f
Ventricle(s). *See also* Left ventricle; Right ventricle.
congenital disorders of
corrected, issues with, 877, 877t
determination of, 838-840
morphology of, 834, 834f
recovery of, ventricular assist devices and, 604
Ventricular assist device (VAD), 597-612
alternate approaches for, 610
cannulae and, 606, 606f-608f, 608t
clinical utility and outcome data for, 607-608
dysfunction of, approach to, 602-604, 602b, 603f-604f
flows with, 604
future directions for, 609
for heart failure, 508, 510f
implanted, 597-599, 598t, 599f
periprocedural guidance for, 602, 602f
limitations of, 609, 609f-610f
optimization of, 606
percutaneous, 598t, 599, 600f
preimplant assessment for, 599-601, 601b, 601t
technical details, quantitation, and data analysis for, 604-607
weaning/turndown of, 607, 609f
Ventricular function
intraoperative, monitoring of, 23-44
cardiac output in, 26-28
in cardiopulmonary bypass, separation from, 32-33
cardiac output in, 32-33, 33t
intracardiac air in, 32, 33f
in central venous pressure air aspiration catheter positioning, 34, 35f
contractility in, 29
in coronary sinus cannulation positioning, 36, 37f
dP/dt in, 29-30, 30f
ejection fraction in, 28-29, 29f
end-diastolic area in, 25-26, 26f
end-systolic area in, 25-26
in femoral venous cannula positioning, 37, 37f
global systolic function in, 26-30
in heart transplantation, 37, 38f
in intraaortic balloon pump positioning, 34-35, 35f
in intravascular device positioning, 34-37
left atrial pressure in, 23-25, 25f
Ventricular function *(Continued)*
in left ventricular assist device positioning, 35-36, 36f
left ventricular diastolic function in, 25, 25f
left ventricular filling in, 23-26
left ventricular outflow tract in, 26-27, 27f
in left ventricular vent positioning, 37
left ventricular volumes in, 26
mitral valve in, 28
in noncardiac surgery, 33, 34t
in off-pump coronary bypass surgery, 33, 34f
practical considerations for, 28
in pulmonary artery catheter positioning, 34, 35f
pulmonary artery in, 27, 28f
regional wall motion in, 30-31, 32f
in right ventricular assist device positioning, 36
right ventricular function in, 30, 31f
right ventricular outflow tract in, 27-28
stroke volume in, 28-29, 29f
tissue Doppler imaging in, 29, 30f
transesophageal Doppler technology in, 26
transesophageal echocardiography in Doppler, 26
impact on postoperative outcomes and cost-effectiveness, 26f-29f, 34t, 37-42, 40t
in probe placement, problems in, 23, 24f
in specific clinical entities, 32-37
in postoperative congenital heart disease, 878
Ventricular septal defect (VSD), 861-865, 862t, 863f-864f
corrective procedures for, issues resulting from, 882t, 883-884
echocardiographic evaluation of, 864-865, 864f-865f
echocardiographic guided interventions for, 102-104
management of, 865
Ventricular septal rupture, complicating acute myocardial infarction, 253-255, 254f-256f
Viscous losses, in fluid dynamics, 453, 453f
Vitamin deficiencies, heart disease and, 752, 752t
Volumetric methods, of mitral regurgitation quantification, with pulsed Doppler imaging, 341, 341f-342f
Volumetric techniques, using 3D echocardiography, 67-69, 68f-71f
VSD. *See* Ventricular septal defect (VSD).

## W

Waterson shunt, palliative, issues resulting from, 880-881, 880t